EIGHTH EDITION

MANUAL OF MOLECULAR AND CLINICAL LABORATORY IMMUNOLOGY

EDITORS
Barbara Detrick
John L. Schmitz
Robert G. Hamilton

MANUAL OF MOLECULAR AND CLINICAL LABORATORY IMMUNOLOGY

EIGHTH EDITION

EIGHTH EDITION

MANUAL OF MOLECULAR AND CLINICAL LABORATORY IMMUNOLOGY

EDITED BY

BARBARA DETRICK
Johns Hopkins University, School of Medicine, Baltimore, Maryland

JOHN L. SCHMITZ
University of North Carolina, School of Medicine, Chapel Hill, North Carolina

ROBERT G. HAMILTON
Johns Hopkins University, School of Medicine, Baltimore, Maryland

ASM PRESS
WASHINGTON, DC

Library of Congress Cataloging-in-Publication Data

Names: Detrick, Barbara, editor. | Schmitz, John L. (John Leo), editor. | Hamilton, Robert G., editor.
Title: Manual of molecular and clinical laboratory immunology / edited by Barbara Detrick, John L. Schmitz, and Robert G. Hamilton.
Description: 8th edition. | Washington, DC : ASM Press, [2016] | ?2016
Identifiers: LCCN 2016012270 (print) | LCCN 2016014573 (ebook) | ISBN 9781555818715 | ISBN 9781555818722 ()
Subjects: LCSH: Immunodiagnosis—Handbooks, manuals, etc. | Immunology—Handbooks, manuals, etc. | Molecular immunology—Handbooks, manuals, etc.
Classification: LCC RB46.5 .M36 2016 (print) | LCC RB46.5 (ebook) | DDC 616.07/9—dc23
LC record available at http://lccn.loc.gov/2016012270

doi:10.1128/9781555818722

Printed in Canada

10 9 8 7 6 5 4 3 2 1

Address editorial correspondence to: ASM Press, 1752 N St., N.W., Washington, DC 20036-2904, USA.
Send orders to: ASM Press, P.O. Box 605, Herndon, VA 20172, USA.
Phone: 800-546-2416; 703-661-1593. Fax: 703-661-1501.
E-mail: books@asmusa.org
Online: http://estore.asm.org

Contents

section D

Flow Cytometry / 145

VOLUME EDITOR: JOHN L. SCHMITZ
SECTION EDITOR: MAURICE R. G. O'GORMAN

section E

Functional Cellular Assays / 259

VOLUME EDITOR: BARBARA DETRICK
SECTION EDITOR: STEVEN D. DOUGLAS

section F

Cytokines and Chemokines / 321

VOLUME EDITOR: BARBARA DETRICK
SECTION EDITOR: JOHN J. HOOKS

Editorial Board

Contributors

ROSHINI SARAH ABRAHAM
Mayo Clinic, Laboratory Medicine and Pathology, Hilton 210e, 200 1st St. SW, Rochester, MN 55905

MARIA E. AGUERO-ROSENFELD
NYU Langone Medical Center, Rm. H374A, 560 First Ave., New York, NY 10016

CEM AKIN
Brigham and Women's Hospital, Department of Medicine, Rheumatology, Immunology, 75 Francis Street, Boston, MA 02115

MOHSIN ALI
Icahn School of Medicine at Mount Sinai, Department of Medical Education, One Gustave L. Levy Place, New York, NY 10029

BURT ANDERSON
Department of Molecular Medicine, Morsani College of Medicine, University of South Florida, 12901 Bruce B. Downs Blvd., Tampa, FL 33612

LUIS EDUARDO COELHO ANDRADE
Escola Paulista de Medicina, Universidade Federal de Sao Paulo, Rheumatology Division, Rua Botucatu 740, Vila Clementino, Sao Paulo, SP 04023-062, and Fleury Laboratories, Immunology Division, Av. Valdomiro de Lima 508, São Paulo, SP 04344-070, Brazil

AFTAB A. ANSARI
Department of Pathology and Laboratory Medicine, Emory University School of Medicine, Atlanta, GA 30322

WILLIAM M. BALDWIN III
Department of Immunology, 9500 Euclid Ave., Cleveland, OH 44022

HENRY H. BALFOUR, JR.
University of Minnesota Medical School, Laboratory Medicine & Pathology, and Pediatrics, MMC 609, 420 Delaware St. SE, Minneapolis, MN 55455

GIUSEPPE BARBESINO
Thyroid Unit, Massachusetts General Hospital – Harvard Medical School, 15 Parkman St., Boston, MA 02114

DAVID R. BARNIDGE
Department of Laboratory Medicine and Pathology, Mayo Clinic, Rochester, MN 55905

LEE ANN BAXTER-LOWE
Children's Hospital Los Angeles, 4650 Sunset Blvd., #32, Los Angeles, CA 90027

ANGELIQUE BIANCOTTO
CHI/NHLBI, National Institutes of Health, 10 Center Drive, Bldg. 10 Room 7N110a, Bethesda, MD 20892

LUCAS S. BLANTON
University of Texas Medical Branch-Galveston, Department of Internal Medicine, 301 University Blvd., Galveston, TX 77555

MARY B. BROWN
Department of Infectious Diseases and Pathology, College of Veterinary Medicine, University of Florida, P.O. Box 110880, 2015 S.W. 16th Ave., Gainesville, FL 32611

SARAH K. BROWNE
NIAID, NIH, Immunopathogenesis Section, Bldg. 10 - CRC Rm. B3-4233, 10 Center Drive, Bethesda, MD 20014

YENAN T. BRYCESON
Center for Hematology and Regenerative Medicine, Department of Medicine, Karolinska Institutet, Karolinska University Hospital Huddinge, S-14186 Stockholm, Sweden, and Institute of Clinical Sciences, University of Bergen, N-5021 Bergen, Norway

MICHAEL RAYMOND BUBB
Division of Rheumatology, University of Florida, 1600 S.W. Archer Rd D2-39, P.O. Box 100221, Gainesville, FL 32610

C. E. BUCHNER
Genalyte, Inc., 10520 Wateridge Circle, San Diego, CA 92121

C. LYNNE BUREK
Johns Hopkins University, Department of Pathology, SOM, 720 Rutland Ave., Baltimore, MD 21205

RUFUS W. BURLINGAME
Genalyte, Inc., Diagnostic Assay Development, 10520 Wateridge Circle, San Diego, CA 92121

ROBERT L. BURTON
University of Alabama at Birmingham, 845 19th St. S, BBRB612, Birmingham, AL 35294

FREDERIC D. BUSHMAN
Perelman School of Medicine, University of Pennsylvania, Department of Microbiology, 3610 Hamilton Walk, Philadelphia, PA 19104

BREANNA CARUSO
National Institute of Neurological Disorders and Stroke, National Institutes of Health, 9000 Rockville Pike, Rockville, MD 20892

PATRIZIO CATUREGLI
Johns Hopkins University, Department of Pathology, SOM, 720 Rutland Ave., Baltimore, MD 21205

ANGELA CERIBELLI
Rheumatology and Clinical Immunology, Humanitas Clinical and Research Center, Via A. Manzoni 56, 20089, Rozzano (Milan), Italy

CHI-CHAO CHAN
Laboratory of Immunology, National Eye Institute, National Institutes of Health, Bldg. 10 Rm 10N109, 10 Center Drive, Bethesda, MD 20814

EDWARD K. L. CHAN
Department of Oral Biology, University of Florida, P.O. Box 100424, Gainesville, FL 32610

ANITA CHANDRA
Department of Clinical Biochemistry and Immunology, Box 109, Addenbrooke's Hospital, Hills Road, Cambridge CB2 0QQ, United Kingdom

ANN DUSKIN CHAUFFE
Division of Rheumatology, University of Florida, 1600 S.W. Archer Rd D2-39, P.O. Box 100221, Gainesville, FL 32610

SAMUEL C. C. CHIANG
Center for Hematology and Regenerative Medicine, Department of Medicine, Karolinska Institutet, Karolinska University Hospital Huddinge, S-14186 Stockholm, Sweden

A. BERNARD COLLINS
Massachusetts General Hospital, Pathology, 503 Warren Bldg., 14 Fruit St., Boston, MA 02114

LINDA COOK
University of Washington, Laboratory Medicine, 1616 Eastlake Ave. E, Suite 320, Seattle, WA 98102

SARAH COOLEY
University of Minnesota, Hematology, Oncology and Transplantation, 420 Delaware St. SE, Mayo Mail Code 806, Minneapolis, MN 55455

ROSS L. COPPEL
Faculty of Medicine, Nursing and Health Sciences, Monash University, Clayton, Victoria, Australia 3800

WILSON DE MELO CRUVINEL
Pontifícia Universidade Católica de Goiás, School of Medical, Pharmaceutical and Biomedical Sciences, Avenida Universitária 1440, Setor Universitário, Goiânia, GO, 74.605-010, Brazil

KELLY A. CURTIS
Division of HIV/AIDS Prevention, National Center for HIV/AIDS, Viral Hepatitis, STD, and TB Prevention, Centers for Disease Control and Prevention, Atlanta, GA 30329

DARSHANA DADHANIA
Weill Cornell Medical College, Division of Nephrology & Hypertension, 525 E. 68th St., Box 3, New York, NY 10065

BETHANY L. DALE
Immunogenetics Laboratory, Johns Hopkins University School of Medicine, 2041 E. Monument St., Baltimore, MD 21205

DANIEL C. DANILA
Memorial Sloan Kettering Cancer Center, 1275 York Ave., New York, NY 10065

ALESSSANDRA DE REMIGIS
Johns Hopkins University, Department of Pathology, Rutland Ave., Baltimore, MD 21205

WILLIAM MARCIEL DE SOUZA
Virology Research Center, School of Medicine of Ribeirao Preto of University of Sao Paulo, Ribeirao Preto, São Paulo, Brazil

LUDOVICA DE VINCENTIIS
Johns Hopkins University, Department of Pathology, Rutland Ave., Baltimore, MD 21205

HEBA DEGHEIDY
FDA, Center for Biologics Evaluation and Research, WO52/72 RM 3209, 10903 New Hampshire Ave., Silver Spring, MD 20993

ALESSANDRA DELLAVANCE
Fleury Laboratories, Research and Development Department, Avenida Valdomiro de Lima 508, São Paulo, SP 04344-070, Brazil

BARBARA DETRICK
Immunology Laboratory, Department of Pathology, Johns Hopkins University, School of Medicine, 600 N. Wolfe St., Baltimore, MD 21287

JOSEPH A. DiGIUSEPPE
Hematopathology and Special Hematology Laboratory, Department of Pathology & Laboratory Medicine, Hartford Hospital, 80 Seymour St., Hartford, CT 06102

STEVEN D. DOUGLAS
The Children's Hospital of Philadelphia, University of Pennsylvania, Suite 1208 Abramson Research Building, 34th & Civic Center Blvd., Philadelphia, PA 19104

ELIZABETH R. DUFFY
Boston University School of Medicine, Pathology and Laboratory Medicine, 670 Albany St., Boston, MA 02118

JAMIE DUKE
The Children's Hospital of Philadelphia, 3401 Civic Center Blvd., Philadelphia, PA 19104

BRUCE E. DUNN
Medical College of Wisconsin, 8701 Watertown Plank Road, Milwaukee, WI 53226

GEORGE S. EISENBARTH
[Deceased]

MELISSA ELDER
University of Florida, Pediatrics, 1600 S.W. Archer Road, Gainesville, FL 32610

DEBORAH FERRIOLA
The Children's Hospital of Philadelphia, 3401 Civic Center Blvd., Philadelphia, PA 19104

LUIZ TADEU MORAES FIGUEREIDO
Virology Research Center, School of Medicine of Ribeirao Preto of University of Sao Paulo, Ribeirao Preto, São Paulo, Brazil

DAVID M. FLEISCHER
Children's Hospital Colorado, Pediatrics, Aurora, CO 80045

MARTIN FLEISHER
Memorial Sloan Kettering Cancer Center, 1275 York Ave., New York, NY 10065

THOMAS A. FLEISHER
Department of Laboratory Medicine, Clinical Center, National Institutes of Health, Bldg. 10 Rm. 2C306, 10 Center Drive, Bethesda, MD 20814

JUAN FLORES-MONTERO
Centro de Investigación del Cáncer (Instituto de Biología Molecular y Celular del Cáncer, CSIC-USAL), Instituto Biosanitario de Salamanca (IBSAL), Servicio General de Citometría (NUCLEUS-Universidad de Salamanca), Salamanca, 37007, Spain

PAULO LUIZ CARVALHO FRANCESCANTONIO
Pontifícia Universidade Católica de Goiás, School of Medical, Pharmaceutical and Biomedical Sciences, Avenida Universitária 1440, Setor Universitário, Goiânia, GO, 74.605-010, Brazil

MARVIN J. FRITZLER
University of Calgary, Cumming School of Medicine, Calgary, Alberta T2N 4N1, Canada

DENNIS GALANAKIS
State University of New York, Stony Brook, NY 11794

M. ERIC GERSHWIN
Division of Rheumatology/Allergy and Clinical Immunology, Genome and Biomedical Sciences Facility Suite 6510, School of Medicine, University of California at Davis, Davis, CA 95616

EMANUELA M. GHIA
UCSD, Moores Cancer Center, 3855 Health Science Drive, M/C 0820, La Jolla, CA 92093

PATRICIA C. GICLAS
National Jewish Health, Diagnostic Complement Laboratory, 1400 N. Jackson St., Denver, CO 80206

KIMBERLY C. GILMOUR
Immunology, Camelia Botnar Laboratories, Great Ormond Street Hospital for Children NHS Foundation Trust, London WC1N 3JH, United Kingdom

ELIZABETH A. GODBEY
Department of Pathology, Columbia University Medical Center, New York, NY 10032

PETER D. GOREVIC
Division of Rheumatology, The Mount Sinai Medical Center, Annenberg Building; Room 21-056, Box 1244, New York, NY 10029

KIM Y. GREEN
Caliciviruses Section, Laboratory of Infectious Diseases, National Institute of Allergy and Infectious Diseases, 9000 Rockville Pike, Building 50, Room 6318, Bethesda, MD 20892

PAMELA A. GUERRERIO
Food Allergy Research Unit, Laboratory of Allergic Diseases, National Institute of Allergy and Infectious Diseases, 4 Memorial Dr., Building 4, Room 228B, MSC0430, Bethesda, MD 20892

ROBERT G. HAMILTON
Johns Hopkins University School of Medicine, Dermatology, Allergy and Clinical Immunology Reference Library, 5501 Hopkins Bayview Circle, Baltimore, MD 21224

SHUHONG HAN
University of Florida, Division of Rheumatology & Clinical Immunology, PO Box 100221, Gainesville, FL 32610-0221

J. G. HANLY
Dalhousie University and Nova Scotia Health Authority (Central Zone), Departments of Medicine and Pathology, Nova Scotia Rehabilitation Center, 1341 Summer St., Halifax, NS B3H 4K4, Canada

RONALD J. HARBECK
National Jewish Health, 1400 Jackson Street, Denver, CO 80206

NEIL HARRIS
University of Florida, Department of Pathology, 1600 SW Archer Rd, Gainesville, FL 32610

CHOLI HARTONO
Weill Cornell Medical College, Nephrology, 505 E. 70th St., Helmsley 2nd Floor, New York, NY 10021

HARRY R. HILL
University of Utah, Department of Pathology, Pediatrics and Medicine, 50 N. Medical Drive, Room 5B-114, Salt Lake City, UT 84132

MICHITO HIRAKATA
Medical Education Center, Graduate Medical Education Center, Keio University School of Medicine, Tokyo, Japan

RICHARD L. HODINKA
University of South Carolina School of Medicine Greenville and Greenville Health System, Room 210, Health Science Administration Building, 701 Grove Rd., Greenville, SC 2960

KRISTIN A. HOGQUIST
Center for Immunology, University of Minnesota, 2-186 MBB, 2101 6th St. SE, Minneapolis, MN 55455

STEVEN M. HOLLAND
National Institutes of Health, LCID, CRC B3-4141, MSC 1684, Bethesda, MD 20892

JOHN J. HOOKS
National Institutes of Health, Immunology & Virology Section, NEI, Bldg. 10 Rm. 10N248, 10 Center Drive, Bethesda, MD 20814

D. CRAIG HOOPER
Thomas Jefferson University, Jefferson Center for Neurovirology, 1020 Locust St, Philadelphia, PA 19107

AMY P. HSU
National Institutes of Health, Laboratory of Clinical Infectious Disease, National Institute of Allergy and Infectious Diseases, Bldg. 10 CRC Rm B3-4233, 10 Center Drive, Bethesda, MD 20892

RICHARD L. HUMPHREY
Johns Hopkins Hospital, Pathology, 600 North Wolfe St., Baltimore, MD 21287

ANDREA ILLINGWORTH
Dahl Chase Diagnostic Services, 417 State St., Suite 540, Bangor, ME 04401

SABINA A. ISLAM
Center for Immunology and Inflammatory Diseases, Division of Rheumatology, Allergy and Immunology, Massachusetts General Hospital, Boston, MA 02114

ANNETTE M. JACKSON
Immunogenetics Laboratory, Johns Hopkins University School of Medicine, 2041 E. Monument Street, Baltimore, MD 21205

STEVEN JACOBSON
National Institute of Neurological Disorders and Stroke, National Institutes of Health, 9000 Rockville Pike, Rockville, MD 20892

ELAINE S. JAFFE
Laboratory of Pathology, Center for Cancer Research, National Institutes of Health, 10 Center Dr./Rm. 3S235, MSC-1500, Bethesda, MD 20892

JEFFREY A. JOHNSON
Division of HIV/AIDS Prevention, National Center for HIV/AIDS, Viral Hepatitis, STD, and TB Prevention, Centers for Disease Control and Prevention, Atlanta, GA 30329

JERRY A. KATZMANN
Mayo Clinic and Mayo Foundation, Laboratory Medicine and Pathology, 200 First St. SW, Rochester, MN 55905

MICHAEL KEENEY
Hematology/Flow Cytometry, London Health Sciences Centre, Victoria Hospital, 800 Commissioners Road E, London, Ontario, N6A5W9 Canada

DAVID F. KEREN
University of Michigan, 5228 Medical Science I, 1301 Catherine, Ann Arbor, MI 48109

THOMAS S. KICKLER
Johns Hopkins University School of Medicine, 1800 Orleans Street, Sheikh Zayed B2-120Q, Baltimore, MD 21287

KAREN E. KING
Johns Hopkins Hospital, Transfusion Medicine, 1800 Orleans St., Baltimore, MD 21287

THOMAS J. KIPPS
UCSD, Moores Cancer Center, 3855 Health Science Drive, M/C 0820, La Jolla, CA 92093

AMY D. KLION
National Institutes of Health, Laboratory of Parasitic Diseases, NIAID, Bldg. 4, Rm. B1-28, Bethesda, MD 20892

VIJAYA KNIGHT
National Jewish Health, National Jewish Health Advanced Diagnostic Laboratories, Division of Pathology, Department of Medicine, 1400 Jackson St., Denver, CO 80206

DOUGLAS B. KUHNS
Clinical Services Program, P.O. Box B, Leidos Biomedical Research, Inc., Frederick National Laboratory for Cancer Research, Frederick, MD 21702

D.S. KUMARARATNE
Department of Clinical Biochemistry and Immunology, Box 109, Addenbrooke's Hospital, Hills Road, Cambridge CB2 0QQ, United Kingdom

MARK KUNKEL
The Children's Hospital of Philadelphia, 3401 Civic Center Blvd., Philadelphia, PA 19104

MASATAKA KUWANA
Department of Allergy and Rheumatology, Nippon Medical School, 1-1-5 Sendagi, Bunkyo-ku, Tokyo 113-8602, Japan

ROBERT S. LANCIOTTI
Arbovirus Diseases Branch, Centers for Disease Control & Prevention, 3150 Rampart Road (CSU Foothills Campus), Fort Collins, CO 80521

MARIE LOUISE LANDRY
Yale University, Laboratory Medicine and Internal Medicine, P.O. Box 208035, New Haven, CT 06520

TERRI LEBO
National Jewish Health, Advanced Diagnostic Laboratories, 1400 Jackson St., Denver, CO 80206

HOWARD M. LEDERMAN
Pediatric Allergy & Immunology, Johns Hopkins Hospital - CMSC 1102, 600 N Wolfe St, Baltimore, MD 21287-3923

DIANE S. LELAND
Department of Pathology and Laboratory Medicine, Indiana University School of Medicine, IU Health Pathology Laboratory Building, Room 6027F, 350 W 11th St, Indianapolis, IN 46202

PATRICK S. C. LEUNG
Division of Rheumatology/Allergy and Clinical Immunology, Genome and Biomedical Sciences Facility Suite 6510, School of Medicine, University of California at Davis, Davis, CA 95616

ARNOLD I. LEVINSON
Perelman School of Medicine, University of Pennsylvania School of Medicine, Room 316 Blockley Hall, 423 Guardian Drive, Philadelphia, PA 19104

YI LI
University of Florida, Division of Rheumatology & Clinical Immunology, PO Box 100221, Gainesville, FL 32610-0221

CURT LIND
The Children's Hospital of Philadelphia, 3401 Civic Center Blvd., Philadelphia, PA 19104

MARK D. LINDSLEY
Mycotic Diseases Branch, Centers for Disease Control and Prevention, 1600 Clifton Road, Mailstop G-11, Atlanta, GA 30333

ROBERT P. LISAK
Wayne State University Medical Center, Neurology, 4201 St. Antoine St., Detroit, MI 48201

CHRISTINE M. LITWIN
Department of Pathology and Laboratory Medicine, Medical University of South Carolina, 171 Ashley Ave., Charleston, SC 29425

SHELDON E. LITWIN
Department of Medicine, Medical University of South Carolina, 114 Doughty St., Charleston, SC 29425

DONNA P. LUCAS
Johns Hopkins University, Immunogenetics Laboratory, 2041 E. Monument St., Baltimore, MD 21205

ANDREW D. LUSTER
Center for Immunology and Inflammatory Diseases, Division of Rheumatology, Allergy and Immunology, Massachusetts General Hospital, Boston, MA 02114

HOLDEN T. MAECKER
Stanford University, Institute for Immunity, Transplantation, & Infection, Stanford University Medical School, 299 Campus Drive, Stanford, CA 94305

CHERYL L. MAIER
Department of Pathology and Laboratory Medicine, Emory University School of Medicine, Atlanta, GA 30322

MICHAEL P. MANNS
Department of Gastroenterology and Hepatology, Zentrum Innere Medizin, Medizinische Hochschule Hannover, Hannover, Germany

REBECCA MARSH
Division of Bone Marrow Transplantation and Immune Deficiency, Cincinnati Children's Hospital Medical Center, 3333 Burnet Ave., Cincinnati, OH 45229

JOHN MASSINI
University of Florida, Division of Rheumatology & Clinical Immunology, PO Box 100221, Gainesville, FL 32610-0221

RAYA MASSOUD
National Institute of Neurological Disorders and Stroke, National Institutes of Health, 9000 Rockville Pike, Rockville, MD 20892

J. PHILIP McCOY, JR.
National Institutes of Health, NHLBI, 10 Center Drive, Bethesda, MD 20892

BENJAMIN D. MEDOFF
Center for Immunology and Inflammatory Diseases, Pulmonary and Critical Care Unit, Massachusetts General Hospital, Harvard Medical School, Boston, MA 02114

DIANA METES
University of Pittsburgh Medical Center, Thomas E Starzl Transplantation Institute, BST E1549, 200 Lothrop St., Pittsburgh, PA 15213

DIMITRI MONOS
The Children's Hospital of Philadelphia, 3401 Civic Center Blvd., Philadelphia, PA 19104

MARTINA MURPHY
University of Florida, Hematology/Oncology, 1600 SW Archer Rd., Gainesville, FL 32610

THANGAMANI MUTHUKUMAR
Weill Cornell Medical College, Division of Nephrology & Hypertension, 525 E. 68th St., Box 3, New York, NY 10065

MOON H. NAHM
University of Alabama at Birmingham, 845 19th St. S, BBRB 614, Birmingham, AL 35294

STANLEY J. NAIDES
Immunology, Quest Diagnostics Nichols Institute, 33608 Ortega Highway, San Juan Capistrano, CA 92675

HUBERT G. M. NIESTERS
University Medical Centre Groningen, Department of Medical Microbiology, Division of Clinical Virology, Hanzeplein 1, Groningen, The Netherlands

TIMOTHY B. NIEWOLD
Mayo Clinic, Department of Immunology and Division of Rheumatology, 200 1st Street SW, Rochester, MN 55905

DOUGLAS F. NIXON
Dept. of Microbiology, Immunology and Tropical Medicine, School of Medicine & Health Sciences, The George Washington University, Ross Hall 736, 2300 Eye Street, NW, Washington, D.C. 20037

ROBERT NUSSENBLATT
Laboratory of Immunology, National Eye Institute, National Institutes of Health, Bldg. 10 Rm 10N109, 10 Center Drive, Bethesda, MD 20814

THOMAS B. NUTMAN
Laboratory of Parasitic Diseases, National Institute for Allergy and Infectious Diseases, National Institutes of Health, 4 Center Drive, Room B1 03, Bethesda, MD 20892

MAURICE R. G. O'GORMAN
Keck School of Medicine, University of Southern California, and the Children's Hospital of Los Angeles, Pathology and Pediatrics, 4650 Sunset Blvd #43, Los Angeles, CA 90027

ALBERTO ORFAO
Centro de Investigación del Cáncer (Instituto de Biología Molecular y Celular del Cáncer, CSIC-USAL), Instituto Biosanitario de Salamanca (IBSAL), Servicio General de Citometría (NUCLEUS-Universidad de Salamanca), Salamanca, 37007, Spain

S. MICHELE OWEN
National Center for HIV/AIDS, Viral Hepatitis, STD, and TB Prevention, Centers for Disease Control and Prevention, Atlanta, GA 30329

GABRIEL I. PARRA
Caliciviruses Section, Laboratory of Infectious Diseases, National Institute of Allergy and Infectious Diseases, 9000 Rockville Pike, Building 50, Room 6316, Bethesda, MD 20892

R. STOKES PEEBLES, JR.
Vanderbilt University, Medicine, T-1218 MCN, Vanderbilt University Medical Center, Nashville, TN 37232

JOSÉ JUAN PÉREZ
Departmento de Hematología, Hospital Universitario de Salamanca, Instituto Biosanitario de Salamanca (IBSAL); Centro de Investigación del Cáncer (Instituto de Biología Molecular y Celular del Cáncer, CSIC-USAL), Salamanca, 37007, Spain

ROBERT B. PETERSEN
Case Western Reserve University, Department of Pathology, 5-126 Wolstein Building, 2103 Cornell Road, Cleveland, OH 44106

SUHAS H. PHADNIS
Medical College of Wisconsin, Pathology, 9200 W. Wisconsin Ave., Milwaukee, WI 53005

FANNY POJERO
Centro de Investigación del Cáncer (Instituto de Biología Molecular y Celular del Cáncer, CSIC-USAL), Instituto Biosanitario de Salamanca (IBSAL), Servicio General de Citometría (NUCLEUS-Universidad de Salamanca), Salamanca, 37007, Spain

YVONNE POSEY
Beaumont Hospital – Royal Oak, Clinical Pathology, 3601 W. 13 Mile Road, Royal Oak, MI 48073

DEBRA LONG PRIEL
Clinical Services Program, P.O. Box B, Leidos Biomedical Research, Inc., Frederick National Laboratory for Cancer Research, Frederick, MD 21702

CALMAN PRUSSIN
Laboratory of Allergic Diseases, National Institute of Allergy and Infectious Diseases, National Institutes of Health, Building 10, Room 11N238, Bethesda, MD 20892-1881

NOEMÍ PUIG
Departmento de Hematología, Hospital Universitario de Salamanca, Instituto Biosanitario de Salamanca (IBSAL); Centro de Investigación del Cáncer (Instituto de Biología Molecular y Celular del Cáncer, CSIC-USAL), Salamanca, 37007, Spain

RONALD L. RABIN
Center for Biologics Evaluation and Research, U.S. Food and Drug Administration, 10903 New Hampshire Avenue, Silver Spring, MD 20993

MARK RAFFELD
Laboratory of Pathology, Center for Cancer Research, National Institutes of Health, 10 Center Dr./Rm. 3S235, MSC-1500, Bethesda, MD 20892

ALEX J. RAI
Department of Pathology, Columbia University Medical Center, New York, NY 10032

RAJA RAJALINGAM
University of California at San Francisco, Immunogenetics and Transplantation Laboratory, Department of Surgery, 45 Castro St., Main Hospital Level B, CPMC Davis Campus, San Francisco, CA 94114

AMY RASLEY
Host-Pathogen Laboratory Group, Lawrence Livermore National Laboratory, Livermore, CA 94550

LAURA Z. RASSENTI
UCSD, Moores Cancer Center, 3855 Health Science Drive, M/C 0820, La Jolla, CA 92093

ELAINE F. REED
UCLA, Pathology, Rehab 1520, 1000 Veteran Avenue, Immunogenetics Center, Los Angeles, CA 90095

WESTLEY H. REEVES
University of Florida, Division of Rheumatology & Clinical Immunology, PO Box 100221, Gainesville, FL 32610-0221

NANCY L. REINSMOEN
HLA and Immunogenetics Laboratory, Comprehensive Transplant Center, Cedars-Sinai Health Systems, HLA and Immunogenetics Lab-SSB 197, 8723 Alden Drive, Los Angeles, CA 90048

RYAN F. RELICH
Department of Pathology and Laboratory Medicine, Indiana University School of Medicine, IU Health Pathology Laboratory Building, Room 6027E, 350 W 11th St, Indianapolis, IN 46202

DANIEL G. REMICK
Boston University School of Medicine, 670 Albany St., Boston, MA 02118

LYNNSEY RENN
Center for Biologics Evaluation and Research, U.S. Food and Drug Administration, 10903 New Hampshire Avenue, Silver Spring, MD 20993

ADRIANA RICCIUTI
Johns Hopkins University, Department of Pathology, Rutland Ave., Baltimore, MD 21205

ANNELIES RIEZEBOS-BRILMAN
University Medical Centre Groningen, Department of Medical Microbiology, Division of Clinical Virology, Hanzeplein 1, Groningen, The Netherlands

KIMBERLY RISMA
Division of Allergy/Immunology, Cincinnati Children's Hospital Medical Center, 3333 Burnet Ave., Cincinnati, OH 45229

E. RENE RODRIGUEZ
Department of Pathology, 9500 Euclid Ave., Cleveland, OH 44022

JOHN T. ROEHRIG
Centers for Disease Control and Prevention, Atlanta, GA (Retired)

NOEL R. ROSE
Johns Hopkins University, Department of Pathology, SOM, 720 Rutland Avenue, Baltimore, MD 21205

JOHN M. ROUTES
Department of Pediatrics and Department of Microbiology and Molecular Genetics, Medical College of Wisconsin, Milwaukee, WI 53226

RICHARD RUBENSTEIN
SUNY Downstate Medical Center, Departments of Neurology and Physiology/Pharmacology, 450 Clarkson Ave., Brooklyn, NY 11203

DALIA A. A. SALEM
CCR, NCI, NIH, Laboratory of Pathology, Building 10, Mail Stop 1500, Room 3S 241, Bethesda, MD 20892

LUZALBA SANOJA
Centro de Investigación del Cáncer (Instituto de Biología Molecular y Celular del Cáncer, CSIC-USAL), Instituto Biosanitario de Salamanca (IBSAL), Servicio General de Citometría (NUCLEUS-Universidad de Salamanca), Salamanca, 37007, Spain

CARAH B. SANTOS
National Jewish Health, 1400 Jackson St., K731A, Denver, CO 80206

MINNIE M. SARWAL
University of California San Francisco, Division of Transplant Surgery, G893, 513 Parnassus Ave., San Francisco, CA 94143

MINORU SATOH
Department of Clinical Nursing, School of Health Sciences, University of Occupational and Environmental Health, Japan, 1-1 Isei-ga-oka, Yahata-nishi-ku, Kitakyushu, Fukuoka, 807-8555, Japan

HOWARD I. SCHER
Memorial Sloan Kettering Cancer Center, 1275 York Ave., New York, NY 10065

D. SCOTT SCHMID
Centers for Disease Control and Prevention, NCIRD/DVD/MMRHLB, 1600 Clifton Rd NE, Atlanta, GA 30333

JOHN L. SCHMITZ
University of North Carolina, Department of Pathology & Laboratory Medicine, School of Medicine, Rm. 1035 East Wing, UNC Hospitals, Chapel Hill, NC 27514

JOHN T. SCHROEDER
Johns Hopkins University, Medicine, Division of Allergy and Immunology, Unit Office 2, 5501 Hopkins Bayview Circle, Baltimore, MD 21224

H. NIDA SEN
Laboratory of Immunology, National Eye Institute, National Institutes of Health, Bldg. 10 Rm 10N109, 10 Center Drive, Bethesda, MD 20814

CHRISTINE SEROOGY
University of Wisconsin, Pediatrics, 1111 Highland Ave., 4139 WIMR, Madison, WI 53705

BARBARA L. SHACKLETT
Dept. of Medical Microbiology and Immunology, School of Medicine, University of California at Davis, 3146 Tupper Hall, 1 Shields Ave., Davis, CA 95616

ROSEMARY SHE
Keck Medical Center of USC, Pathology, 1441 Eastlake Ave., Suite 2424, Los Angeles, CA 90089

R. SUE SHIREY
Johns Hopkins Hospital, Transfusion Medicine, 1800 Orleans St., Baltimore, MD 21287

TARA SIGDEL
University of California San Francisco, Division of Transplant Surgery, 513 Parnassus Avenue, S-1268 Medical Sciences Building, San Francisco, CA 94143

PAUL SIKORSKI
Johns Hopkins University, Immunogenetics Laboratory, 2041 E. Monument St., Baltimore, MD 21205

JERRY W. SIMECKA
Department of Cell Biology and Immunology, University of North Texas Health Science Center, RES 402A 3500 Camp Bowie Blvd., Fort Worth, TX 76107

JAY E. SLATER
Center for Biologics Evaluation and Research, U.S. Food and Drug Administration, 10903 New Hampshire Avenue, Silver Spring, MD 20993

MAREK SMIEJA
McMaster University, Department of Pathology & Molecular Medicine, L424-St. Joseph's Healthcare Hamilton, 50 Charlton Ave E, Hamilton, ON L8N 4A6, Canada

RICHARD J. H. SMITH
Iowa Institute of Human Genetics, Molecular Otolaryngology and Renal Research Laboratories, University of Iowa, Iowa City, IA 52242

R. NEAL SMITH
Massachusetts General Hospital, Pathology, 501B Warren Bldg., 14 Fruit St., Boston, MA 02114

MELISSA R. SNYDER
Mayo Clinic, Hilton 2-10D, 200 First St. SW, Rochester, MN 55905

LORI J. SOKOLL
Department of Pathology, The Johns Hopkins University School of Medicine, Baltimore, MD 21205

JEREMY SOKOLOVE
VA Palo Alto Health Care System, 3801 Miranda Ave, Palo Alto, CA 94304-1207, and Division of Immunology and Rheumatology, Stanford University School of Medicine, Stanford, CA 94305

LORI SOMA
University of Washington, Department of Laboratory Medicine, NW120, Box 357110, 1959 Pacific St., Seattle, WA 98195-7110

DAVID J. SPEICHER
Griffith University, Menzies Health Institute Queensland, Gold Coast Campus, Queensland 4222, Australia

ANDREA K. STECK
Barbara Davis Center for Childhood Diabetes, University of Colorado School of Medicine, Aurora, CO 80045

MARYALICE STETLER-STEVENSON
CCR, NCI, NIH, Laboratory of Pathology, Building 10, Mail Stop 1500, Room 3S 235G, Bethesda, MD 20892

JAMES R. STONE
Massachusetts General Hospital, Pathology, 185 Cambridge Street, Boston, MA 02114

JOHN H. STONE
Harvard Medical School, Division of Rheumatology, 25 Shattuck St, Boston, MA 02115

MANIKKAM SUTHANTHIRAN
Weill Cornell Medical College, Division of Nephrology & Hypertension, 525 E. 68th St., Box 3, New York, NY 10065

D. ROBERT SUTHERLAND
Laboratory Medicine Program, Toronto General Hospital/ University Health Network, 200 Elizabeth St., Room 11E416, Toronto, Ontario, M5G2C4 Canada

ELIZABETH SYKES
Beaumont Hospital – Royal Oak, Clinical Pathology, 3601 W. 13 Mile Road, Royal Oak, MI 48073

CARMELA D. TAN
Department of Pathology, 9500 Euclid Ave., Cleveland, OH 44022

YI-WEI TANG
Memorial Sloan-Kettering Cancer Center, Clinical Microbiology Service, 1275 York Ave., S328, New York, NY 10065

STEFFEN THIEL
Aarhus University, Department of Medicine, Bartholin Building, Wilhelm Meyers Allé 4, Aarhus, 8000, Denmark

RENEE TSOLIS
Department of Medical Microbiology and Immunology, University of California, Davis, CA 95616

JEROEN VAN BERGEN
Department of Immunohematology and Blood Transfusion, Leiden University Medical Center, 2333 ZA Leiden, The Netherlands

CORETTA C. VAN LEER-BUTER
University Medical Centre Groningen, Department of Medical Microbiology, Division of Clinical Virology, Hanzeplein 1, Groningen, The Netherlands

PRIYANKA VASHISHT
Mayo Clinic, Department of Immunology and Division of Rheumatology, 200 1st St. SW, Rochester, MN 55905

RENATO VEGA
Johns Hopkins University, Immunogenetics Laboratory, 2041 E. Monument St., Baltimore, MD 21205

JAMES W. VERBSKY
Department of Pediatrics and Department of Microbiology and Molecular Genetics, Medical College of Wisconsin, Milwaukee, WI 53226

PRIYA S. VERGHESE
Pediatric Kidney Transplantation, University of Minnesota, Children's Hospital, 2450 Riverside Ave., MB 687, Minneapolis, MN 55454

MARÍA BELÉN VIDRIALES
Departmento de Hematología, Hospital Universitario de Salamanca, Instituto Biosanitario de Salamanca (IBSAL); Centro de Investigación del Cáncer (Instituto de Biología Molecular y Celular del Cáncer, CSIC-USAL), Salamanca, 37007, Spain

KEN B. WAITES
Department of Pathology, University of Alabama at Birmingham, WP 230, 619 S. 19th St., Birmingham, AL 35249

DAVID H. WALKER
University of Texas Medical Branch-Galveston, Department of Pathology, 301 University Blvd., Galveston, TX 77555

NOREEN M. WALSH
Dalhousie University and Nova Scotia Health Authority (Central Zone), Department of Pathology and Laboratory Medicine, Mackenzie Building, Room 721, 5788 University Ave., Halifax, Nova Scotia B3H1V8, Canada

GUIQING WANG
New York Medical College, Department of Pathology, 100 Woods Road, Westchester Medical Center Rm. 1J-04, Valhalla, NY 10595

JIAN WANG
Department of Endocrinology, Jinling Hospital, Nanjing, China

JEFFREY S. WARREN
University of Michigan, Pathology, 5242 MSI, 1301 Catherine St., Ann Arbor, MI 48109

ADRIANA WEINBERG
Department of Pediatrics, Medicine and Pathology, University of Colorado Health Sciences Center, 4200 E. Ninth Ave., Campus Box C 227, Denver, CO 80262

THERESA L. WHITESIDE
University of Pittsburgh Cancer Institute, Research Pavilion at the Hillman Cancer Center, 5117 Centre Ave. Suite 1.27, Pittsburgh, PA 15213

PATRICIA P. WILKINS
Division of Parasitic Diseases & Malaria, Center for Global Health, Centers for Disease Control and Prevention, 1600 Clifton Road, Atlanta, GA 30333

HUGH J. WILLISON
B330, GBRC, 120 University Place, University of Glasgow, Glasgow, Scotland, G12 8TA, United Kingdom

THOMAS WISNIEWSKI
New York University School of Medicine, Department of Neurology, Psychiatry and Pathology, Alexandria ERSP, Rm. 802, 450 E. 29th St., New York, NY 10016

BRENT WOOD
University of Washington Medical Center, Hematopathology, Seattle, WA 98109

ROBERT A. WOOD
Johns Hopkins University, Baltimore, MD 21287

LIPING YU
Barbara Davis Center for Childhood Diabetes, University of Colorado School of Medicine, Aurora, CO 80045

CONSTANCE M. YUAN
CCR, NCI, NIH, Laboratory of Pathology, Building 10, Mail Stop 1500, Room 2A33, Bethesda, MD 20892

ANDREA A. ZACHARY
Johns Hopkins University, Immunogenetics Laboratory, 2041 E. Monument St., Baltimore, MD 21205

ADRIANA ZEEVI
University of Pittsburgh Medical Center, Clinical Laboratory Building, Room 4033, 3477 Euler Way, Pittsburgh, PA 15213

QIUHENG JENNIFER ZHANG
UCLA Immunogenetics Center, Department Pathology & Laboratory Medicine, 15-20 Rehab, 1000 Veteran Ave., Los Angeles, CA 90024

Acknowledgment of Previous Contributors
The *Manual of Molecular and Clinical Laboratory Immunology* is by its nature a continuously revised work which refines and extends the contributions of previous editions. Since its first edition in 1976, many eminent scientists have contributed to this important reference work. The American Society for Microbiology and its Publications Board gratefully acknowledge the contributions of all of these generous authors over the life of this *Manual*.

Foreword: How It Began

In 1971, I was working at the University of Oxford's Sir William Dunn School of Pathology in the laboratory of James Gowans, the investigator who first definitively showed that the lymphocyte was the source of specific adaptive immunity. I was busily cannulating the thoracic ducts of rats in order to harvest T lymphocytes when I was informed that a transatlantic telephone call was coming in. My first reaction was fear of bad news. Rather, it was a phone call from Earle Spaulding. I knew Earle as the chairman of microbiology at Temple and active in the Eastern Pennsylvania branch of the American Society for Microbiology (ASM). He explained that he was calling as a member of the editorial group of the *Manual of Clinical Microbiology* (MCM), at that time in its first edition. His particular concern was the chapter on immunology, which devoted 100 pages to various serologic tests for infectious organisms with no mention of noninfectious diseases. Earle felt strongly that the field of immunologic diagnosis was growing exponentially and deserved a separate, companion manual. The MCM editorial board agreed, providing I was willing to accept the position of Editor-in-Chief.

I was delighted to receive the invitation. I had recently chaired a "blue ribbon" committee of the American Association of Immunologists (AAI) on the future of clinical immunology. We concluded that there was no space for a new patient-centered clinical specialty, but great need for improved, expanded laboratory support. A comprehensive manual would serve as a great stimulus to the whole field of laboratory-based clinical immunology. I accepted the offer with two qualifications. First, I needed a co-editor, particularly someone well versed at a practical level in immunology related to infectious diseases. Second, I asked that such a manual be cosponsored by the AAI. Both qualifications were agreed to by the ASM Publications Board.

The person I had in mind as co-Editor-in-Chief was Herman Friedman. I knew Herman from contacts arising from our joint interest in allergy research. I knew he understood the practice of laboratory immunology and was one of the few immunologists who actually researched the immunology of infection. Herman readily agreed to partner with me on the *Manual*, and so began a close collaboration that continued for three subsequent editions of the *Manual*, ended only by his untimely death. The AAI also accepted an offer of collaboration and appointed a liaison committee to work with us.

We were off and running, but we had no idea of how to proceed. There had never been a manual describing the entire laboratory practice of immunology. Part of our mission was to include the many applications of immunology devoted to detection and analysis of a wide variety of diseases, not only those induced by microorganisms. Should we approach the subjects disease by disease or method by method? We finally decided to compromise by beginning the book with invited chapters on the common methods used in the immunology laboratory, then continuing with sections covering their application to the main categories of disease. We included a final section on laboratory administration and quality control.

Having developed particular sections, we then sought the most experienced and highly qualified individuals to serve as section editors. Because of the cross-cutting matrix arrangement, there was major concern that some topics would be dealt with twice or even three times. We therefore decided to organize a "stakeholders meeting," at which all of the section editors met at ASM in Washington, DC, with proposed outlines of their sections. Going through each one systematically, we identified topics where overlap occurred and ensured that everything important was included once, but not more. We also made a fundamental decision that the book would be complete and free-standing. The methods would be described in sufficient detail that the laboratory worker could actually prepare the materials, perform the tests, and interpret the results without consulting other references. It should be understood that, at that time, most laboratory reagents

were prepared within the laboratory and were generally not available as commercial kits. This format required that we keep descriptions terse and the reference lists short.

When the first edition of the *Manual of Clinical Immunology* was published in 1976, we felt it warranted some type of celebration. Herman suggested that we should organize a meeting to mark the birth of the book and to bring together the leaders in clinical laboratory immunology, including our authors and section editors. Eventually, this led to the formation of the Association of Medical Laboratory Immunologists and the American Board of Medical Laboratory Immunology.

The *Manual* continues to be published at regular intervals to the present, as the editorial lineup has evolved. Barbara Detrick and Robert G. Hamilton joined me as Editors for the Sixth Edition, and Dr. Detrick has continued to lead the *Manual* for the Seventh and the present Eighth Edition. I hope the series will go on for many years. Although the *Manual*'s name has changed and the format is altered, the overall aim is still to improve the care of patients with infectious malignant inflammatory and immune-mediated disorders. With the ready availability of validated kits, the job of the clinical laboratory immunologist has shifted toward working with clinical colleagues on the significance and interpretation of laboratory tests.

I'm proud to have been involved in the genesis of this *Manual*. It would not have been possible without the continued support of ASM, the cooperation of AAI, the persistence of succeeding volume and section editors, the contributions of hundreds of practicing clinical laboratory immunologists, and the foresight of a few visionary microbiologists of the 1970 era who realized that immunology had become a discipline and specialty of its own. It never would have happened if Herman Friedman had not joined with me in accepting the challenge. I hope that he will long be remembered for his numerous contributions to immunology.

NOEL R. ROSE, MD, Ph.D.

Preface

For over 40 years, the *Manual of Clinical Laboratory Immunology* has been the leading reference source, both in the United States and abroad, to advance the field of laboratory immunology, to foster the best contemporary and most cutting-edge methodologies, and to translate basic immunologic principles into appropriate laboratory tests.

Since the publication of the 7th edition of this *Manual*, remarkable progress has been made in the field of immunology, and these notable advancements have been reflected in the clinical immunology arena as well. The scope of clinical immunology is exceptionally broad and encompasses nearly every medical specialty, including such areas as transplantation, rheumatology, oncology, infectious disease, allergy, hematology, and neurology, to name a few. Because of its strategic position in the hospital setting, it is critical that the clinical immunology laboratory should have a guide to follow with regard to accurate and appropriate laboratory procedures. As the field of clinical immunology continues to expand, we look to the laboratory director as a key person to gather the new basic information and integrate it into useful clinical procedures as well as to serve as a pivotal contact for communication with the various disciplines. In addition to keeping abreast with the most updated testing systems, the goal for this *Manual* is that it must not only serve the needs of today's clinical immunology laboratory but also look to the future, where even more dramatic progress in diagnosis and treatment can be anticipated.

In an effort to capture the new dimensions in this field and to reflect the continuous evolution of clinical immunology, significant changes have been introduced into the 8th edition of the *Manual of Molecular and Clinical Laboratory Immunology*. Several sections of the *Manual* have been notably updated to reflect the latest laboratory approaches in molecular assays as well as the shift to automated testing, kit-based diagnostics, and new technical tools: themes that are carried throughout the book. New chapters have been introduced to highlight these changes. For example, section D, Flow Cytometry, describes the latest applications of these techniques, such as polychromatic flow cytometry and mass cytometry; section F reviews fresh information on the clinical applications of cytokines and chemokines; the infectious disease sections H, I, and J include the newest strategies used in infectious disease diagnosis and treatment, including the HIV and syphilis algorithms; section K, Immunodeficiency Diseases, presents the recent newborn screening programs for severe combined immune deficiency; and section P, Transplantation Immunology, outlines the usefulness of next-generation sequencing in the human leukocyte antigen (HLA) laboratory.

Once again, this *Manual* is offered not just in print but also electronically as either an EPUB file or a PDF. This special feature will allow a larger audience to review and use the *Manual*.

As we produce the 8th edition of this *Manual*, it is appropriate to celebrate its success. Noel Rose, the *Manual*'s first Editor-in-Chief, has provided a foreword reflecting on how the field has changed over the past 5 decades.

Since the publication of this *Manual* is a joint effort of many dedicated individuals, I wish to acknowledge the outstanding commitment and invaluable support of our volume editors, section editors, and chapter authors, all of whom, as internationally renowned experts in their areas, have contributed their extraordinary experience, energy, and time to the success of this edition. Also, I would like to extend my appreciation to the ASM editorial staff, in particular Ellie Tupper, Senior Production Editor, and Christine Charlip, Director, ASM Press, who have provided their valuable experience and support to complete this edition.

BARBARA DETRICK, Ph.D.
Editor in Chief

Author and Editor Conflicts of Interest

Cem Akin (coauthor on chapter 85) has consultancy agreements with Novartis and Patara Pharma and receives research funding from Dyax.

Barbara Detrick (Editor in Chief, coauthor on chapter 106) serves as a consultant to Siemens Healthcare Diagnostics, Inc., Abbott Laboratories, and INOVA Diagnostics, Inc.

Deborah Ferriola (coauthor on chapter 113) receives royalties from Omixon. Omixon has licensed the protocol we developed for HLA typing by NGS from the Children's Hospital of Philadelphia and makes it available as a commercial product named "Holotype HLA." Omixon is mentioned in this chapter as a company that provides software analysis tools for the genotyping of HLAs using NGS data. It is not mentioned as a company that commercializes HLA typing products/kits, because at the time of writing Omixon had not developed this activity.

Marvin J. Fritzler (coauthor on chapter 88) has been a consultant to or received research gifts in kind from Inova Diagnostics Inc., Euroimmun GmbH, Mikrogen GmbH, Dr. Fooke Laboratorien GmbH, ImmunoConcepts, GSK Canada, Amgen, Roche, and Pfizer. He is the Director of Mitogen Advanced Diagnostics Laboratory.

Andrea Illingworth (coauthor on chapter 18) has received unrestricted Educational Grant funding and speaker honoraria from Alexion Pharmaceuticals.

Michael Keeney (coauthor on chapters 18 and 19) is a consultant for Beckman Coulter, Canada, and Alexion Pharma, Canada. He has received unrestricted Educational Grant funding and speaker honoraria from Alexion Pharmaceuticals.

Masataka Kuwana (chapter 91) holds a patent on an anti-RNA polymerase III antibody measuring kit.

Curt Lind (coauthor on chapter 113) receives royalties from a licensing agreement between Omixon Biocomputing and the Children's Hospital of Philadelphia and is an employee of Thermo Fisher Scientific, Transplant Diagnostics.

Robert P. Lisak (coauthor on chapter 99) is on an advisory board for Syntimmune.

Dimitri Monos (coauthor on chapter 113) receives royalties from Omixon. Omixon has licensed the protocol we developed for HLA typing by NGS from the Children's Hospital of Philadelphia and makes it available as a commercial product named "Holotype HLA." Omixon is mentioned in this chapter as a company that provides software analysis tools for the genotyping of HLAs using NGS data. It is not mentioned as a company that commercializes HLA typing products/kits, because at the time of writing Omixon had not developed this activity.

Stanley J. Naides (chapter 62) is a full-time employee of Quest Diagnostics Nichols Institute and receives a salary, stock, and stock options from Quest Diagnostics.

Timothy Niewold (coauthor on chapter 38) has received research grants from Janssen Inc. and EMD Serono Inc.

Maurice R. G. O'Gorman (chapter 20) is a BD Biosciences consultant and contractee.

Paul Sikorski (coauthor on chapter 114) is an employee of One Lambda, Inc., a Thermo Fisher Scientific brand.

Marek Smieja (coauthor on chapter 63) has done small studies with Copan and GenMark.

Melissa R. Snyder (chapter 103) participates on the Strategic Advisory Committee with INOVA Diagnostics.

Kathleen E. Sullivan (section editor) is a Baxter grant recipient and an Immune Deficiency Foundation consultant.

D. Robert Sutherland (coauthor on chapters 18 and 19) has received speaker fees and consulting fees from Alexion Pharmaceuticals.

Yi-Wei Tang (coauthor on chapter 57) has received research funds from Roche Molecular Dignostics and the Luminex Corporation.

Brent Wood (coauthor on chapter 22) has received research funding and honoraria for Advisory Board participation from Seattle Genetics and Amgen and honoraria from Abbvie for Advisory Board participation.

Andrea A. Zachary (coauthor on chapter 114) is a consultant for BiologicTx and Genentech and is a Scientific Advisory Board member for Immucor.

General Methods *section A*

VOLUME EDITOR: ROBERT G. HAMILTON
SECTION EDITOR: THOMAS A. FLEISHER

Introduction

THOMAS A. FLEISHER

1

The "-omics" revolution has begun. Since the publication of the previous edition of *Manual of Molecular and Clinical Laboratory Immunology*, there have been major technological advances that are facilitating the application of genomics, proteomics, and microbiomics to better understand human health and disease. These disciplines are truly complementary, as genomics is directly linked to proteomics, and these new technologies are providing an improved understanding of the functional consequences related to alterations in the genome that lead to changes in the protein products of genes. The major advancements in next-generation sequencing have made characterization of the human microbiome a reality. Major efforts in microbiomics currently are focused on evaluation of the human bacterial community in health and disease. These three disciplines find common ground in the field of immunology, in which the genome provides the triggering instructions for protein products that are critically important for immune function and host defense. Alterations in the genetic code are now known to contribute to an ever-growing list of defects in immune function that result in susceptibility to microbial disease. In addition, altered immune function leading to inflammatory disease will be further clarified with these powerful new tools. Early lessons in the study of the human microbiota have revealed that commensal bacteria interact directly with the immune system to aid and model immunity. They also provide advantage to the host in settings of health and contribute to pathogenesis in circumstances of disease. The future of clinical immunology at a diagnostic and therapeutic level increasingly will rely on these techniques and further advances that will evolve more and more rapidly.

The laboratory methods available to evaluate proteins and the nucleotide code form the substance of chapters 2 and 3. Chapter 4 by Abraham and Barnidge focuses on specific protein quantitation using current qualitative and quantitative methods as well as the applications of mass spectrometry to generate a more accurate reflection of the constituent protein components in a sample. The promise of new biomarkers that may aid in diagnostic and/or therapeutic monitoring has yet to be realized, but advances in proteomics technology suggest that these applications should become a reality in the near future. The field of genomics has exploded with readily available next-generation sequencing techniques that have clarified genetic causes for a number of newly characterized immune disorders. This trend will continue: currently based primarily on genomic applications focused on exome sequencing, but within the very near future the approach will move to whole-genome sequencing. The technology for next-generation sequencing continues to be refined, and there is every reason to believe that faster, less expensive, and more accurate whole-genome sequencing will result. Chapter 2 by Hsu provides an overview of the standard Sanger-based sequencing, with clinical examples to help exemplify successful application of this method. This chapter also provides an overview of next-generation sequencing and reviews clinical applications of this methodology. More-extensive discussions of next-generation sequencing applied in health and disease can be found in reviews by Gonzaga-Jaurequi et al. (1) and Manolio et al. (2). A newer component of the technological revolution in biologic systems is focused on evaluating the microbial constituents—the microbiome—that are the commensal "partners" of every living host. Chapter 3 by Bushman provides a clear overview of the basic principles that have propelled the field of microbiomics and how this is likely to provide insight into understanding human health and disease. A recent review focusing on the microbiome of the human gastrointestinal tract provides additional insights into this important and emerging field (3).

The combination of genomics, proteomics, and microbiomics, three complementary disciplines, has substantial impact on the field of clinical immunology. Discovery of new genes provides insight that is further clarified by studying the protein products of these genes both at a basic characterization and a functional level. The developments in the field of microbiomics are revealing that the environment of each individual makes significant contributions to the immunologic system and that perturbations among our microbial "partners" can significantly influence human health and disease. Familiarity with these developing areas is necessary as they move more and more into mainstream laboratory testing linked to patient diagnosis and care.

REFERENCES

1. **Gonzaga-Jaurequi C, Lupski JR, Gibbs RA.** 2012. Human genome sequencing in health and disease. *Annu Rev Med* **63:**35–61.

doi:10.1128/9781555818722.ch1

2. **Manolio TA, Chisholm RL, Ozenberger B, Roden DM, Williams MS, Wilson R, Bick D, Bottinger EP, Brilliant MH, Eng C, Frazer KA, Korf B, Ledbetter DH, Lupski JR, Marsh C, Mrazek D, Murray MF, O'Donnell PH, Rader DJ, Relling MV, Shuldiner AR, Valle D, Weinshilboum R, Green ED, Ginsburg GS.** 2013. Implementing genomic medicine in the clinic: the future is here. *Genet Med* **15:**258–267.
3. **Tyler AD, Smith MI, Silverberg MS.** 2014. Analyzing the human microbiome: a "how to" guide for physicians. *Am J Gastroenterol* **109:**983–993.

Molecular Methods for Diagnosis of Genetic Diseases Involving the Immune System

AMY P. HSU

2

Disorders of the immune system affect a significant number of individuals, with prevalence estimates (per 100,000) determined by registries ranging from 5.6 in Australia (1) to 4.979 in France, 2.6 in The Netherlands, and down to 1.377 in Germany (2). Accurate diagnosis of immune system disorders may allow early intervention prior to extensive illness for severe disease, or more specific treatment in the case of later-diagnosed or milder disease. This chapter explores some of the current molecular methodologies for detecting disorders of the immune system and highlights specific pitfalls that may hinder accurate diagnosis.

SAMPLES

Study of the immune system is aided by the accessibility of an appropriate sample. A single 8-cc tube of blood may be lysed to extract DNA and/or RNA from all the blood cells together. Alternatively, whole blood may be processed to separate peripheral blood mononuclear cells (PBMCs) from granulocytes, followed by DNA or RNA isolation from a subset of cells. If obtaining a blood sample is not possible, then small amounts of DNA may be isolated from buccal swabs, tissue biopsy samples, saliva, or cell lines such as fibroblasts or Epstein-Barr virus-transformed B-cell lines. A secondary sample may be utilized if the patient has already undergone hematopoietic stem cell transplant, in which case a non-hematopoietic-cell sample is required. Buccal swab samples are easily obtained, are room temperature stable, and may be shipped to a testing lab. DNA from a buccal sample is often used for diagnosing family members of an affected individual. Care must be taken, however, if a patient has already received a bone marrow transplant because the cells obtained from a buccal sample may contain a large percentage of neutrophils and thus produce a false-negative result. DNA extraction involves lysing of the nucleated cells either mechanically or with a detergent-based lysis solution, removal of lipids and proteins, followed by DNA purification through alcohol precipitation or column capture. RNA isolation is similar, although care must be taken to avoid RNA degradation by RNases. There are numerous off-the-shelf kits available for small-scale DNA and RNA isolation, as well as instruments for medium- to large-scale isolation.

PCR

One of the fundamental techniques in molecular genetics is the use of PCR. This technique allows the specific amplification of a segment of DNA defined by the forward and reverse primer pair used in the reaction. The double-stranded DNA template is denatured, and oligonucleotide primers in the 20- to 35-bp range anneal to the template at the location complementary to the sequence of the primer. A polymerase enzyme is then used to add individual deoxynucleotides to the 3′ end of the primer to continue copying the template molecule. After a specified time, the temperature rises to denature the template-copy strand, and both then become available for primer binding. The cycle then repeats itself, resulting in an exponential amplification of the target region.

Sanger sequencing has been the gold standard for genetic diagnosis in recent decades. The technique is similar to standard PCR; however, only one primer is used, either forward or reverse, and included in the PCR mix is a percentage of fluorescently labeled dideoxynucleotides (ddNTPs). When the polymerase incorporates a ddNTP, the extension ceases, resulting in a fragment labeled with a fluorochrome dependent on the identity of the final nucleotide. This is repeated through multiple cycles. The resulting product is cleaned to remove unincorporated, labeled ddNTPs and then electrophoresed through a polymer-filled capillary to separate the fragments based on size. The resulting chromatogram is actually a display of time on the *x* axis versus intensity on the *y* axis, with the color of the peak being the third dimension. Because smaller fragments migrate through the polymer faster, they are detected first and longer fragments are seen later (Fig. 1).

Peak heights from one base to the next are not necessarily even; there is some variability within the local sequence, and certain base combinations result in higher or lower peaks. In general, however, the shorter fragments seen at the beginning of the sequence readout have higher signal strengths and well-defined peaks (Fig. 1A), while larger, later fragments have shorter, broader peaks and less resolution in homopolymer runs, seen in the three red peaks in the middle panel. Good-quality sequence should have well-defined peaks with little to no baseline noise compared with the lower tracing in Fig. 1A, in which the baseline is high

doi:10.1128/9781555818722.ch2

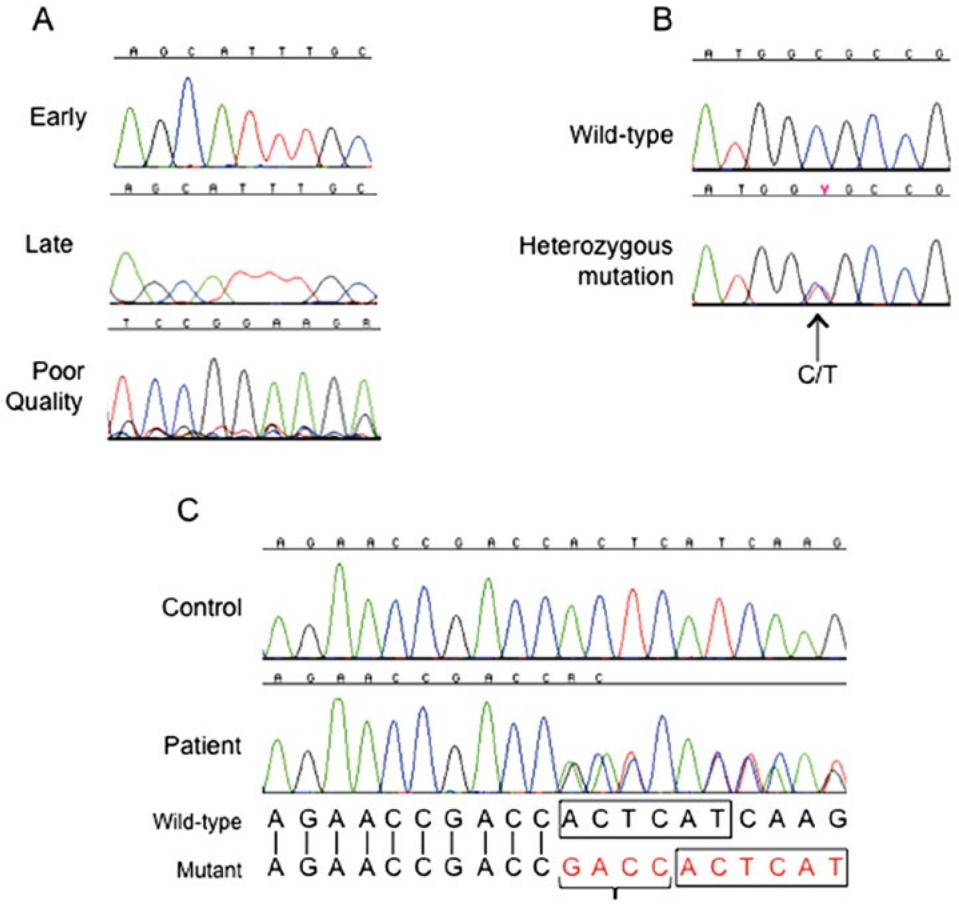

FIGURE 1 Sanger sequence chromatograms. (A) Normal sequence displaying a single base call at each location. The top row demonstrates sequence from early in the chromatogram, ~150 bp into the sequence, while the middle row is the same location but near the end of the chromatogram, at ~750 bp. The bottom chromatogram shows readable sequence but significant nonspecific baseline noise, making interpretation less than ideal. (B) An example of wild-type sequence compared to a heterozygous mixed base. The wild-type blue (C) peak has decreased in height, and the red (T) allele overlays the same location. (C) An example of wild-type sequence (top tracing) compared to 4-bp duplication (bottom tracing). The bases listed below the tracing demonstrate how to determine the variation causing the heterozygous peaks. Bases in black are wild type, while bases in red signify the mutant allele. Boxed bases correspond between wild type and mutant, allowing identification of the inserted bases indicated by a bracket.

with apparent nonspecific sequence. Poor sequence quality renders interpretation difficult.

SANGER SEQUENCE ANALYSIS

The product of a Sanger sequence reaction is a series of fragments of varying size with the final base labeled with an identifying fluorochrome. Each fragment is the product of one allele, while the resulting chromatogram is the sum of the fragments. Patients heterozygous for a single nucleotide polymorphism (SNP), a variant occurring in the general population that is usually not pathogenic, or a point mutation, a change from one nucleotide to another that is pathogenic and often specific to a patient or related individuals, have a chromatogram showing individual peaks with one site containing two peaks of roughly equal height. When compared with a chromatogram from an individual who is homozygous at the variant site, the peaks have decreased amplitude, because the signal is being split between two nucleotides in the heterozygous patient versus two copies of the same nucleotide in the homozygous patient. Figure 1B shows the control sequence on top, while the lower sequence has a decreased blue peak corresponding to the wild-type C allele and the presence of a red T peak as well at the same location. This is a mutation in the coding region of *GATA2* at cDNA 1081 that results in an amino acid change. It is named according to the Human Genome Variation Society nomenclature (3) as c.1081C>T. It indicates a change at base 1081 of the cDNA using the initiating ATG as base 1, and that the wild-type or major allele has cytosine while the mutation or minor allele has thymidine at that site. The protein nomenclature, p.R361C (preceded with a "p"), shows that the wild-type arginine at amino acid position 361 has been replaced with a cysteine.

In addition to single nucleotide changes, Sanger sequencing also detects small insertions or deletions. These may range from one to hundreds of nucleotides, but they must be wholly contained within the PCR product used as a sequence

template to be detected. In the case of Fig. 1C, two sequences align, with the left-hand portion being identical between the control and patient chromatograms. The tracings change from clean, individual peaks to double peaks in the patient. This has a very different appearance from the tracing in Fig. 1A with poor sequence quality. In this case, the peaks are still well defined, with no additional baseline. To determine the mutation resulting in the double sequence, it is helpful to write the bases on two lines, using the top line for the wild-type sequence seen in the top tracing and the mutant bases underneath seen in red. When the two sequences are compared, it becomes apparent that they differ by the insertion of the bracketed red bases, GACC, which is a duplication of the four preceding bases. After the duplication, the sequence matches the wild type, as shown by the boxed bases that are the same between wild type and mutant. Occasionally when the mutant allele is written out, it is determined to be a complex mutation containing both an insertion and deletion.

NEXT-GENERATION SEQUENCING

While Sanger sequencing is still the gold standard for molecular genetic diagnostics, decreasing cost and increased throughput are driving the use of next-generation sequencing (NGS). A further impetus for the use of NGS is the identification of disease genes in rare diseases in which only a few individuals are diagnosed with mutations in the gene. With targeted gene sequencing, the patient's phenotype or infection is used to suggest candidate genes to evaluate for mutations. For narrow, well-defined phenotypes such as infection with a mycobacteria species, this approach has identified ~80 to 90% of patient disease genes (S. M. Holland, personal communication), while in large-scale newborn screening, targeted sequencing has identified specific genetic lesions for T-B+ SCID in ~85% of patients (J. M. Puck, personal communication). In other cases with unusual presentations, pursuing Sanger sequencing of candidate genes can become expensive and time-consuming and still not identify a causative genetic lesion. Many laboratories are moving to NGS platforms as research tests, with suspected mutations confirmed by Sanger sequencing.

There are currently three main benchtop platforms available: the Illumina MiSeq, the Ion Torrent PGM, and the Roche 454 GS Junior. Each instrument is capable of generating sufficient data to perform exome sequencing or targeted resequencing of a defined panel of multiple genes, ranging from tens to a few hundred. All of the platforms have a workflow that includes fragmentation of the input sample, size selection, cleanup, and adapter ligation. The MiSeq then undergoes a cluster generation and sequencing on the instrument, while the 454 GS Junior and PGM have an emulsion PCR, bead recovery, and enrichment prior to sequencing. The library preparation allows for amplified input of numerous target regions compared with the single amplified fragment for Sanger sequencing. Coupled with the high-volume capture of the three instruments, it is easy to see the appeal for clinical usage. As of September 2013, the capital costs of the instruments ranged between $65,000 and $125,000, with the cost increased for a laboratory interested in higher throughput needing ancillary instrumentation such as robotics to take advantage of the capacity of the machines (4). Each instrument has its own advantages. Which platform is optimal for any given laboratory is based on the currently available configurations and the goals of the laboratory. Capacity will continue to increase at an astonishing rate, making comparisons virtually obsolete by the time they are published; however, recently reported performances for the three main platforms (5) are shown in Table 1. The broad conclusions drawn at the time of the analysis are that the MiSeq has the highest throughput and the lowest substitution error rate, at 0.1 per 100 bases; the 454 GS Junior has the longest reads; and the Ion Torrent is the fastest, with the highest reads per run, although it is less accurate when calling homopolymers of any length, with accuracy declining as the homopolymer stretch increases.

Data obtained from NGS need to undergo stringent analysis to obtain variant calls. There are numerous software packages available online or as part of genomics software suites (reviewed in reference 6 and elsewhere). While the choice of software is individual, all follow the same basic pipeline. For this discussion, the publicly available Genome Analysis Toolkit (GATK) pipeline is used as a model (7, 8). Because the reads are much shorter (100 to 500 bp) than those obtained by Sanger sequencing (800 to 1,000 bp) and the read outputs are pooled so they come from mixed locations, the reads must be mapped to a framework. In the case of patient samples, this would be the current human genome reference sequence. Each read aligns to a region, resulting in a pileup of fragments per region—this provides the read depth or coverage of a given target sequence. Once the data are mapped, the alignment is converted to the standard Sequence Alignment/Map (SAM) format (9), containing chromosome, start and stop bases of the alignment, strand, mismatch information, and probability scores. The SAM format can be converted to a compressed, indexed binary format called BAM, allowing for fine-tuning of the alignment. The mapped reads are filtered to remove duplicate reads, preventing overrepresentation of a variant or wild type due to repeat sequencing of one clone from the library preparation. Next, insertions and deletions (indels), which may align differently depending on the size of the indel and the strand sequenced, can be made consistent across all the reads in a region through the use of a realignment tool. This allows more confident detection of small indel variations. Lastly, just as individual peak heights vary in Sanger

TABLE 1 Comparison of three major NGS platforms

Platform	Price comparison					Run comparison			
	Cost per run	Minimum predicted throughput (Mb)	Run time (h)	Cost/Mb	Mb per h	Total bases	Mean read length (bases)	Indel error frequency (per 100 bases)	Assembled contig alignment to reference
454 GS Junior	$1,100	35	8	$31.00	4.4	71 Mb	522	0.38	3.72% unmapped
Ion Torrent PGM (316 chip)	$ 425	100	3	$ 4.25	33.3	300 Mb	122	1.5	4.6% unmapped
MiSeq	$ 750	1,500	27	$ 0.50	55.5	1.6 Gb	141	<0.001	3.95% unmapped

sequencing due to nucleotide neighbors, there is a similar variation in sequencing by synthesis. The quality scores of the alignment need to be recalibrated using base quality score recalibration to more accurately reflect the probability of mismatch to the reference. These scores are used in downstream variant calling that may identify a disease-causing mutation. At this point, the data are a BAM file that can be utilized for variant calling.

The goal of sequencing is to identify regions differing from the reference sequence. In Sanger sequencing, this is a visual process in which a peak is altered in height or fluorochrome detected, as seen in Fig. 1, and the investigator can decide if the variation is real or an artifact of the sequence reaction. In a similar manner, the BAM file needs to be analyzed to determine appropriate variants and sensitive enough not to miss calls, but specific enough to weed out most artifacts. There are several online tools available for variant detection, with new methods being published frequently (reviewed in reference 10). Here we use GATK's HaplotypeCaller as an example. The BAM file is analyzed for local regions of possible variation, and those regions undergo a *de novo* alignment to fine-tune the site. The local realignment can determine both single nucleotide variations as well as indels. The output of a variant detection script is a VCF file that provides a list of all changes identified and verified in the data set. As should be apparent at this point, unlike Sanger sequencing, the labor-intensive portion of generating NGS is not the bench science but the computational and bioinformatics demand of data analysis. As pointed out by McCourt et al. (11), moving forward, molecular diagnostic laboratories will have a basic requirement for molecular diagnostic bioinformaticians.

RT-PCR

Some mutations result in alteration of the primary RNA transcript, leading to errors in splicing, polyadenylation, or mRNA stability. Not all of these variants are detected by genomic sequence of the coding exons. In cases in which a patient's phenotype strongly suggests a specific gene, analysis of the RNA transcript may provide an answer. There is an extra step, however, in processing the patient sample. Because genomic DNA is double stranded, the use of two primers, one forward and one reverse, leads to exponential amplification of the target region. RNA, on the other hand, is single stranded and must first be made double stranded by reverse transcriptase PCR (RT-PCR). This is performed from total RNA using an oligo(dT) primer that will bind to the poly(A) tail of the mRNA. This process results in double-stranded mRNA, with random hexamer primers that will bind to any RNA molecule with the appropriate complementary hexamer or with a gene-specific primer that will bind only to a specific target. Once the RNA has been converted to double-stranded cDNA, amplification of a transcript of interest proceeds as in genomic DNA.

One measure of RNA is message abundance. This has been examined by the use of Northern blots, which entails running the RNA on an agarose gel to separate it by size. It is then transferred to a membrane support and probed with a complementary probe and detection label (either by radioactivity or a biotin-streptavidin reaction). The blot is then exposed to X-ray film or a capture screen, respectively. Densitometry may be used to obtain a relative quantitation of a specific transcript compared to a housekeeping gene, if the blot is stripped and reprobed, or compared to a healthy individual's control on the same blot. The initial gel or blot image can also provide information regarding the size of the transcript or the presence of multiple splice forms.

qPCR

An alternative method for measuring RNA transcripts is the use of quantitative RT-PCR (qPCR), in which the cDNA is amplified with a set of primers and the production of product is measured in "real time" via a scanning detector. This can be accomplished with the use of an intercalating dye such as SYBR green that will bind to double-stranded product and produce a fluorescent emission that accumulates over successive cycles. Alternatively, a fluorescent reporter probe can be used that binds between the two amplification primers. The reporter probe contains both a reporter and quencher molecule, which prevents fluorescence while the two are in close proximity. As extension from the amplification primer occurs, the exonuclease activity of the polymerase causes degradation of the probe separating the quencher from the reporter, allowing emission that is detected during scanning. As with SYBR green, as subsequent cycles of PCR occur, the intensity of the signal from the released fluorophore increases. The output of a qPCR assay is a logarithmic plot of fluorescence intensity versus cycle number (Fig. 2). Analysis of a qPCR assay is performed by quantifying each well to determine at which cycle the fluorescence exceeds a threshold value (C_T). Quantifying input copy number may be performed through the use of a standard curve with a titrated sample of known concentration and plotting of the experimental concentration (C_T) on the standard curve. Alternatively, a relative quantitation may be obtained by comparing the C_T of the target gene to a reference gene, usually a housekeeping gene. The difference in threshold cycles between target and reference transcripts provides a measure termed the ΔC_T. The difference in the ΔC_T between the experimental (treated or disease) and reference (untreated or healthy control) samples provides the $\Delta\Delta C_T$. Because PCR provides exponential amplification, the final calculation for quantification of input becomes $2^{-\Delta\Delta C_T}$. The derivation of this formula is well covered by Livak and Schmittgen (12).

TRECs

T-cell excision circles (TRECs) are formed during T-cell receptor V(D)J recombination and are biomarkers for newly produced naive T cells (13). Once this residual, circular DNA fragment is produced in an immature thymic T cell, it is not replicated during cell division. This dilutes the TREC concentration as naive T cells migrate to the periphery and expand in response to antigen. While relative quantitation is useful for looking at expression levels of target transcripts, genomic qPCR was adopted to quantitate total TRECs from newborn babies (14). It has become the gold-standard method for performing this analysis (15). Low or absent TRECs are a phenotypic indicator of poor or declining thymic output and usually severe T-cell lymphopenia, a marker of SCID or other severe defects in T-cell development. Many states are now screening for the presence of TRECs using dried blood spots obtained from all infants in the United States at birth. Reports from Wisconsin (16, 17) and California (18) have documented genetic diagnosis of infants who were initially discovered during newborn screening for TRECs, allowing medical intervention prior to the onset of illness.

ARRAYS

Microarray-based comparative genomic hybridization was initially utilized to screen for variations within cancer samples. It has been adapted by clinical laboratories, however, to screen for variations in DNA copy number, both deletions

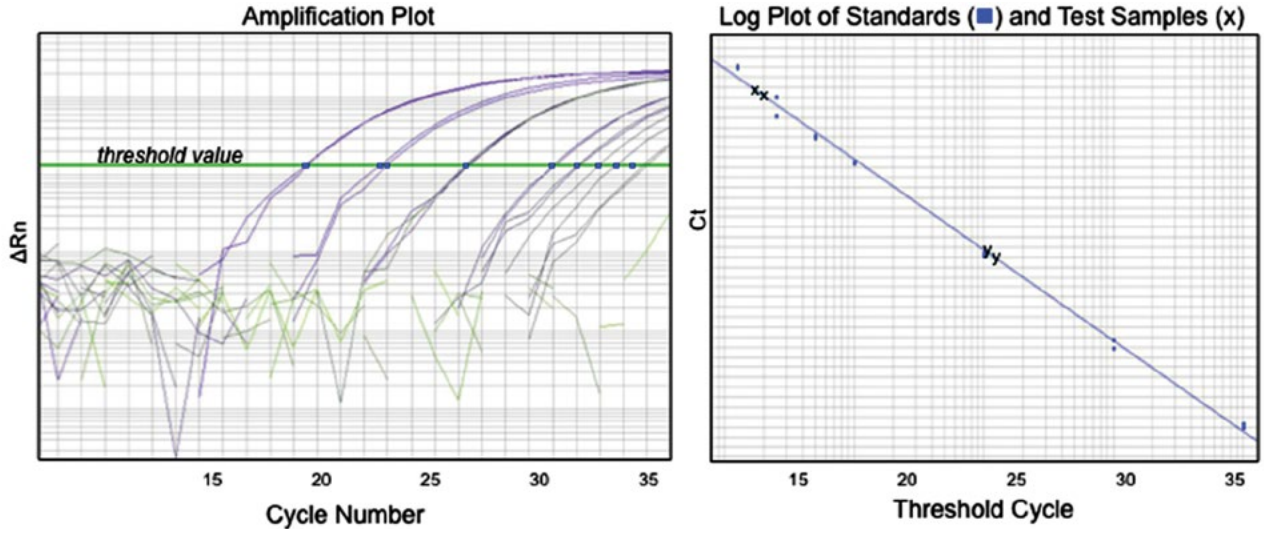

FIGURE 2 Real-time qPCR plot. (Left) Amplification plot of duplicate dilutions of a known standard TREC plasmid. The *x* axis is PCR cycle number; the *y* axis is ΔRn, which is Rn (the ratio of the reporter signal normalized to a constant fluorescent signal) minus the value of Rn at baseline; the green line is threshold value. Threshold cycle (C_T) is defined as the cycle number at which the amplification plot crosses the designated ΔRn threshold (blue dots). (Right) Logarithmic plot of the same standards as well as two duplicate unknown samples, *x* and *y*, for which the C_T value, and therefore copy number or concentration, can be derived by comparison with the standard curve. (Figure courtesy of Jennifer M. Puck.)

and insertions of 200 to 500 bp or larger. High-resolution comparative genomic hybridization, first described by Urban et al. (19), uses oligonucleotide probes spanning targeted genomic regions and spotted to a glass slide. DNA samples from a control and patient are fluorescently labeled, each with a different dye, and the resulting labeled DNA is hybridized to the array. After hybridization, the slide is scanned and the fluorescence intensity of each dye signal is calculated for each oligonucleotide probe on the slide. In regions where each sample hybridizes equally, the ratio of the signal between the two samples will be 1 because each has the same number of copies of the target region. If the patient sample contains a deletion on one chromosome, then the signal from that sample will be 0.5 times the signal of the control. Likewise, if there is a duplication of a region, the signal will be increased. As the probes are tiled across the target region, the ratios are plotted on a log 2 scale, so equivalent ratios will be plotted on the zero axis. If multiple consecutive probes have an aberrant signal, either high or low, then the analysis software will highlight the region as an insertion or deletion, respectively, as shown in Fig. 3. Similar to DNA arrays, which look for genomic variation, microarrays may be used with total RNA from a specific tissue to examine differences in RNA transcript levels between two tissue types or healthy versus diseased tissues. Mapping increased or decreased RNA transcripts may aid in defining pathways involved in disease pathogenesis.

ANALYSIS OF VARIATIONS

Regardless of whether a variant is identified by Sanger sequencing or NGS, once a change is recognized, then the consequence of the variant on the transcript or protein needs to be evaluated to determine if the change may be disease related. Single base changes can be mapped to the consensus coding sequence to determine if an amino acid codon is changed. SNPs resulting in an altered codon for the same amino acid as the consensus are referred to as

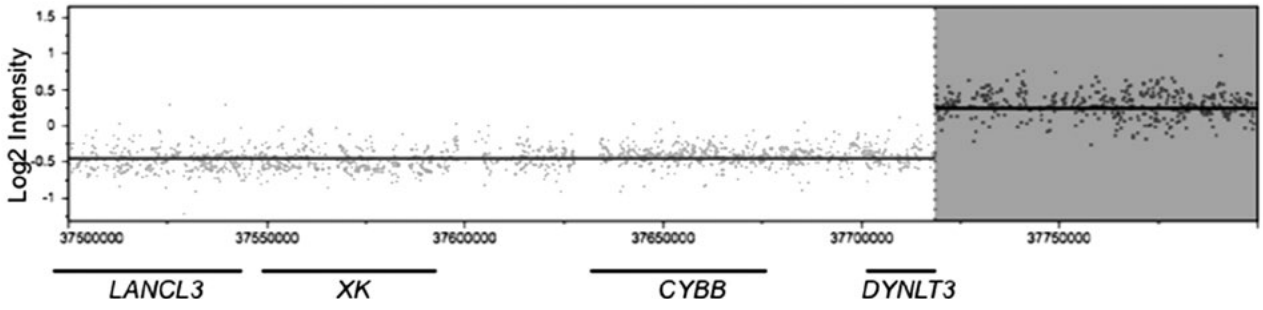

FIGURE 3 High-resolution comparative genomic hybridization array spanning 375,000 bases of the region surrounding *CYBB* on the X chromosome. Plots are log 2 of the intensity of the patient sample compared to all samples run on the array. Panel A demonstrates one female patient with a large deletion encompassing *LANCL3*, *XK*, *CYBB*, and *DYNLT3* as evidenced by the contiguous −0.5 intensity signal, which then resolves to 0, indicating the presence of two alleles.

"synonymous," while those causing amino acid substitutions are "nonsynonymous" SNPs. If a SNP is disease causing, then a nonsynonymous SNP is termed a "missense mutation," while a base change that results in a termination codon is referred to as a "nonsense mutation." At a given nucleotide, patients may be homozygous, meaning their two alleles have the same nucleotide at the site; or heterozygous, meaning they have two different bases at the site, indicating the presence of two identifiable alleles. A third possibility is that they may be hemizygous, meaning they have only one copy at that location. This is most often seen in the case of X or Y chromosome genes in males, although a deletion of one allele also results in hemizygosity. Sanger sequence chromatograms from homozygous and hemizygous individuals are indistinguishable, so care must be taken especially when reporting X chromosome genetic variations.

Identified variants need to be examined for suggested deleterious effects in light of the phenotype of the patient and possible inheritance patterns. Missense changes may be analyzed by examining the sequence homology within a protein family as well as across species, predicted structure-based alterations, mRNA and protein features, as well as conservation of the region identified by multiple alignments and phylogenetics. Historically, this was performed by aligning protein sequences across species or within the protein family to estimate conservation of the specific amino acid. Examining amino acid properties of the substituted amino acid versus the wild type could strengthen the prediction. Currently, there are numerous bioinformatics analysis programs available online to predict whether a change is deleterious. Several of these programs are listed in Table 2. The left-hand section of the table lists analyses that may be performed on single changes, while the two columns farthest to the right highlight two programs, wANNOVAR (20) and dbNSFP (21), for higher-throughput data such as NGS. The table shows which analyses the programs include. The second group is especially helpful for filtering the large number of variations identified with NGS.

Nonsense mutations, those resulting in a premature termination codon, can have different effects depending on the location within the transcript. Late stop codons, occurring in the last exon or near the end of the penultimate exon, usually result in a stable mRNA transcript, which may be translated into a truncated protein. The shortened protein may cause disease in a dominant-negative fashion by interfering with partner chains. This has been seen in autoimmune lymphoproliferative syndrome, in which the shortened FAS protein is capable of assembling into the stable trimer receptor. However, it is lacking the intracellular death domain critical for downstream signaling. The presence of one mutant allele results in only one in eight receptors being fully wild type. This is insufficient to transduce the apoptosis signal (22, 23). Transcripts containing a premature termination codon, such that splicing occurs more than 50 to 55 bp after the mutation, usually result in nonsense-mediated decay, a mechanism by which the cell degrades erroneous mRNA molecules (24; reviewed in reference 25). Loss of transcript or protein product from one allele may be seen in autosomal recessive diseases, in which case a mutation should be seen on the second allele as well. Alternatively, in tightly regulated genes, loss of one allele may result in haploinsufficiency, in which half the level of protein product is not sufficient. Haploinsufficiency in immune disorders has been reported in autoimmune lymphoproliferative syndrome due to insufficient FAS protein on the cell surface (26), as well as in GATA2 deficiency leading to MonoMAC syndrome (27).

In addition to changes within the coding sequence, many mutations occur at consensus splice sites immediately flanking the coding exons. Traditionally, splicing has been thought of in terms of the three core splicing signals: 5′ splice sites (5′ss), 3′ splice sites (3′ss), and the intronic branch point near the 3′ end of the intron. Figure 4 shows the conserved motifs associated with intron removal. Most easily identified are those changes altering the invariant GT or AT splice sites immediately flanking the exon. However, the entire motif may be critical to appropriate spliceosome formation. Wang and Burge (28) and Ward and Cooper (29) provide reviews of the motifs for recognition of splice sites and exon identity as well as components of the spliceosome. For example, a mutation at the first or last base of an exon, even if predicted to be synonymous, often leads to loss of correct splicing of that exon, as do mutations at the +5 site of an intron. For introns with short polypyrimidine tracts, a mutation that changes one of the pyrimidines to a purine may result in exon skipping, as seen in DOCK8 (dedicator of cytokinesis 8) deficiency (30). In addition to the three core splicing signals, there is an increased recognition of splicing regulatory elements (SREs) that occur in both exons and introns. SREs are composed of elements that enhance or inhibit splicing and are named by their location and effect on the transcript; exonic splicing enhancers (ESEs), exonic splicing silencers (ESSs), intronic splicing enhancers (ISEs), and intronic splicing silencers (ISSs) all act by recruiting factors to increase or decrease exon recognition and spliceosome recruitment. Many mutations predicted to result in missense or nonsense substitutions are being shown to affect SRE sequences and alter proper splicing of the exon (31). The third section of Table 2 indicates current websites available to screen for splicing mutations.

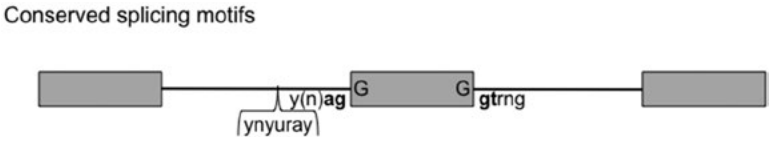

FIGURE 4 Conserved splicing motifs. Gray boxes indicate exons; solid lines are introns. 3′ss begins with the branch point located between 15 and 40 bases 5′ to the exon, noted in brackets, with the loose motif of YNYURAY. Y represents pyrimidines (C or T); N is any base; U is uracil, the RNA equivalent of T, R is A or G. Following the branch point sequence is the polypyrimidine tract, Y(n), where n ranges from 5 to 20 bases of mostly pyrimidines, followed by the 5′ss invariant AG (bold) as the last two bases. The first base of the exon is usually a G. At the end of the exon, the final base is again usually a G, followed by the invariant GT (bold) at the start of the intron. The 5′ss motif is GTRNG.

TABLE 2 Online resources for variation analysis

Resource			Contained in	
			wANNOVAR (20)	dbNSFP (21)
A. Analysis of missense changes				
Program (reference)	Information used	Prediction model		
PolyPhen2 (43)	Eight sequence-based and three structure-based predictive features	Naive Bayes classifier	Yes	Yes
SIFT (44)	Sequence homology based on PSI-BLAST	Position-specific scoring matrix	Yes	Yes
MutationTaster (45)	Conservation, splice site, mRNA features, protein features	Naive Bayes classifier	Yes	Yes
LRT (likelihood ratio test) (46)	Sequence homology	Likelihood ratio test of codon neutrality	Yes	Yes
Mutation Assessor (47)	Sequence homology of protein families and subfamilies within and between species	Combinatorial entropy formalism	No	Yes
FATHMM (48)	Sequence homology	Hidden Markov models	No	Yes
SiPhy (49)	Multiple alignments	Inferring nucleotide substitution pattern per site	No	Yes
GERP++ (50)	Multiple alignments and phylogenetic tree	Maximum likelihood evolutionary rate estimation	Yes	Yes
phyloP (51)	Multiple alignments and phylogenetic tree	Distributions of the number of substitutions based on phylogenetic hidden Markov model	Yes	Yes
B. Variation databases				
Database	Contents	Website		
dbSNP	Reported genomic variations	http://www.ncbi.nlm.nih.gov/SNP/	Yes	No
ESP6500	Allele frequency in 6,500 NHLBI ESP[a] exomes	http://evs.gs.washington.edu/EVS/	Yes	No
1000G (52)	Allele frequency in 1000 Genomes Project	http://www.1000genomes.org/	Yes	No
C. Splicing signals analysis				
Program	Splicing signals analyzed	Website		
Human Splicing Finder (32)	5′ss, 3′ss, ESE, ESS, ISE, ISS, mutation analysis	http://www.umd.be/HSF3	No	No
SROOGLE (53)	5′ss, 3′ss, ESE, ESS	http://sroogle.tau.ac.il/	No	No
Automated Splice Site and Exon Definition Analyses (ASSEDA)	5′ss, 3′ss, prediction of exon definition	http://ossify.sg.csd.uwo.ca	No	No
ESE Finder (54, 55)	ESE	http://rulai.cshl.edu/cgi-bin/tools/ESE3/esefinder.cgi?process=home	No	No
RESCUE-ESE (56)	ESE	http://genes.mit.edu/burgelab/rescue-ese/	No	No
PESX (57)	ESE, ESS	http://cubio.biology.columbia.edu/pesx/pesx/	No	No

[a]NHLBI ESP, National Heart, Lung, and Blood Institute Exome Sequencing Project.

DIAGNOSIS

Bioinformatics tools may be utilized to screen variants identified by sequence. However, on some level, the effect of the change needs to be demonstrated and correlated with the patient's phenotype. If a male infant presents with SCID, lacking T cells and NK cells but having adequate numbers of B cells, then the most likely diagnosis would be X-linked SCID and *IL2RG* would be the first gene sequenced. A mutation identified within the coding region that is predicted to be deleterious would fit the phenotype of the patient and correlate with other, previously identified mutations. There are some special cases that need to be considered and will be demonstrated by specific case studies below.

A young male patient presenting with granulomas and conical teeth, often seen with NF-κB essential modulator (NEMO) deficiency, was sequenced for *IKBKG*. Genomic sequencing revealed an apparent heterozygous change in exon 5, c.597G>A, which did not alter the encoded amino acid. Given the phenotype of the patient, which was strongly suggestive of an *IKBKG* mutation, intracellular NEMO protein was examined by flow cytometry. While the healthy control had a fluorescence index (FI) of 30.6, the patient had an FI of only 12.6, demonstrating reduced levels of intracellular NEMO protein. Full-length *IKBKG* cDNA was generated by RT-PCR, revealing a smaller fragment in the patient than in the control sample. Sequencing of the PCR product revealed a 153-bp in-frame deletion corresponding to exon 5 containing the c.597G>A change (Fig. 5). The 153-bp deletion is expected to result in a stable mRNA that should be translated into a protein missing 51 amino acids. Using the Human Splicing Finder website (32), the original c.597G>A mutation was predicted to cause both the loss of an exonic splicing enhancer and the creation of an hnRNP A1 silencer motif. The exonic binding of a silencer in place of a splicing enhancer has been recognized to mediate silencing of exon sequencing (33). Mutations such as this, in which the protein is present but not fully functional, are termed "hypomorphic."

A second patient with infections related to NEMO deficiency, *Haemophilus influenza* pericarditis in childhood and disseminated *Mycobacterium avium* as an adult, was screened by genomic PCR. The patient was reported to be

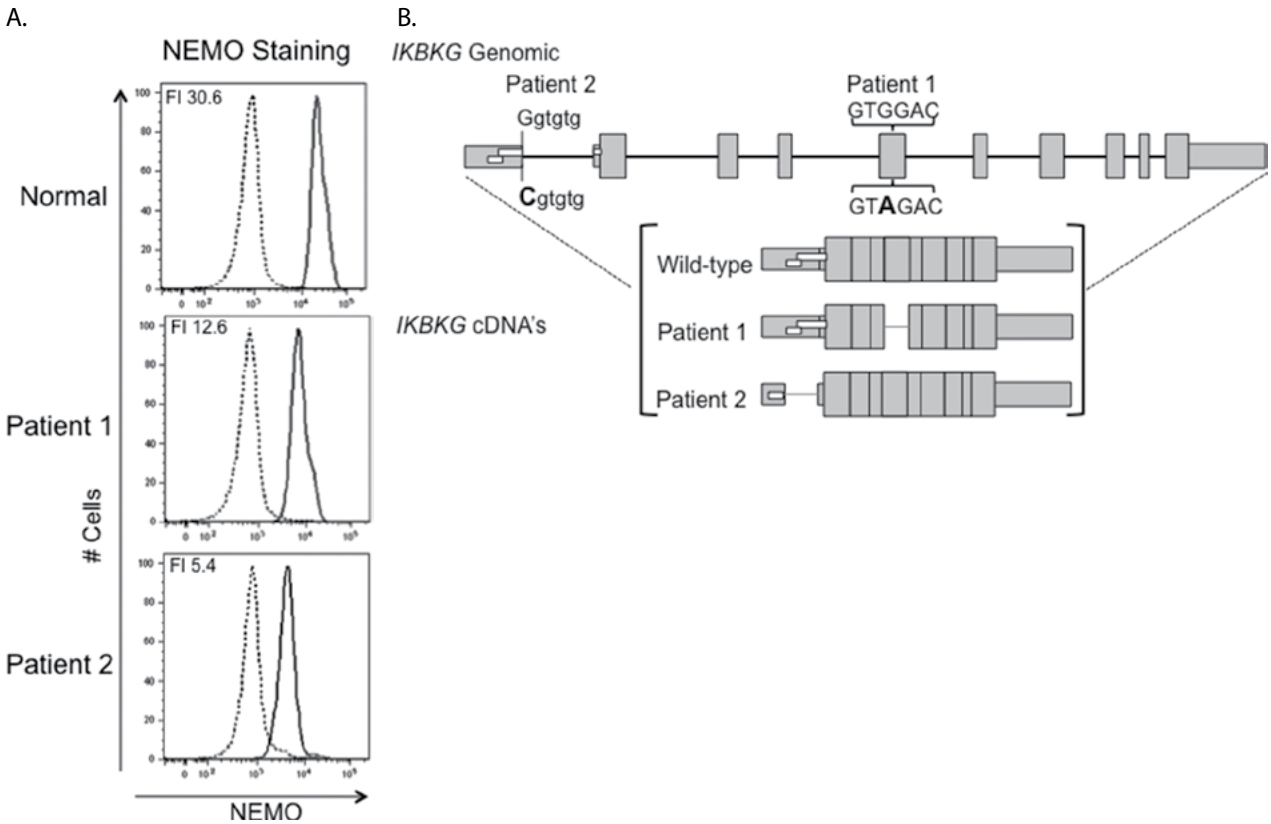

FIGURE 5 Analysis of NEMO variants. (A) Intracellular flow cytometry for NEMO protein. The dotted line is isotype control; the solid line is specific NEMO staining. The top panel is the normal control, showing an FI of 30.6. The middle panel is patient 1, with all cells showing specific staining but with a reduced intensity and an FI of 12.6. The bottom histogram is patient 2, again demonstrating that all cells contain NEMO protein, but less than both the control and patient 1, with an FI of 5.4. (B) The top panel shows the genomic organization of *IKBKG*, the gene encoding NEMO. Gray boxes are exons, narrow boxes are untranslated, and small white box insets are uORFs. Locations of patient genomic mutations are noted, with wild-type sequence above the genomic structure, mutant motif below, and the single base mutation in bold. The lower panel depicts the structure of the cDNA, showing aberrant splicing. Patient 1 has a 153-bp deletion of exon 5, noted by the thin line in the middle of the cDNA. Patient 2 has a deletion of a portion of the 5′ untranslated region, including one of the two uORFs.

wild type for the coding exons of *IKBKG*. Again, due to the phenotype of the patient, intracellular NEMO staining was performed, which demonstrated reduced, but not absent, NEMO protein levels. The patient had an FI of 5.4, compared with the 30.6 seen in the healthy control. Full-length cDNA was generated by RT-PCR, and Sanger sequencing revealed a 110-bp deletion at the 3′ end of the noncoding exon 1. Genomic sequencing of the exon revealed a G>C mutation at the last base of the exon. This caused a loss of the 5′ss of intron 1 and usage of an alternative, cryptic 5′ss contained within exon 1, resulting in the deletion seen in the cDNA. Contained within the untranslated exon are two upstream open reading frames (uORFs). Disruption of uORFs has been shown to alter uORF-mediated control of protein expression (34), suggesting that the deletion in the 5′ untranslated region seen in this patient leads to his decreased intracellular protein level and that his disease is caused by insufficient levels of NEMO protein.

A third male patient with possible NEMO deficiency was screened for mutations in the X-linked gene *IKBKG*. Genomic DNA was isolated, and PCR amplification of the 10 *IKBKG* exons was performed. Sanger sequencing demonstrated a single nucleotide change, c.761C>T, causing the substitution of glutamine for arginine at amino acid position 254, p.R254Q. This mutation has been seen previously in an unrelated family and is predicted to be deleterious by PolyPhen2 (unpublished data). Due to the genomic structure of the *IKBKG* locus, which is flanked by an inverted pseudogene of *IKBKG* exons 4 to 10, the genomic mutation appeared to be heterozygous. The sequencing was repeated using RT-PCR performed on RNA isolated from PBMCs. The primers were designed to amplify the full coding sequence of *IKBKG*. When the resulting PCR product was sequenced, only wild-type bases were seen throughout the coding region. This demonstrated that the mutation had occurred in the pseudogene and not in the transcript-producing *IKBKG* locus. Changes in the coding region that appear silent, mutations in the untranslated exons, and the presence of a pseudogene demonstrate the importance of performing cDNA analysis for *IKBKG* mutation screening.

There are some mutations that may be predicted to be benign. However, given the location within the protein or the clinical phenotype of the patient, they may warrant further analysis. A patient presented with an IPEX (immune dysregulation, polyendocrinopathy, enteropathy, X-linked)-like phenotype but without an identified mutation in *FOXP3*. Because there were other patients in this cohort with identified *STAT1* mutations, all exons of *STAT1* were sequenced and a single base change was seen that resulted in an amino acid substitution within the coiled-coil domain of STAT1, p.V266I. All of the algorithms from Table 1 predicted the amino acid change to be benign or neutral; however, there is a known mutation at the adjacent amino acid, A267V, causing an autosomal dominant gain-of-function mutation associated with disseminated coccidioidomycosis (35). Signal transduction studies performed using cells from the patient with V266I demonstrated that, similar to other mutations in the coiled-coil domain, this patient had increased and prolonged phosphorylation of STAT1 in response to cytokine stimuli (36).

Another class of mutations that may be initially dismissed by *in silico* analysis involves variations detected within a gene with autosomal recessive inheritance. To present with a disease phenotype, the patient requires two mutant alleles. Often the parents will be healthy because they have one normal allele and one mutant allele. Deleterious variations therefore may be seen at low frequency in the general population. With the explosion of whole-exome sequencing, every variation may now be deposited into the NCBI curated database, dbSNP, and be assigned an "rs" identifier number. Additionally, there is an active effort by NCBI to extract variants from the literature and enter them, which may result in errors due to mutations later being retracted or corrected. Currently, many mutant alleles are present in dbSNP, albeit with a low or absent population frequency, and automated analysis of NGS variants returns dbSNP identifiers. Assuming that presence in the "healthy" population excludes an allele from being pathogenic, this may result in a disease-causing mutation being filtered out. Large-scale data analysis is a balance between sensitivity and specificity, and care must be taken if a variant is identified in a logical candidate gene to not dismiss it based solely on *in silico* predictions.

Sometimes patients are seen with mild phenotypes reminiscent of a recognized disease. In this case, sequencing of the target gene should be performed and examined carefully. There are numerous cases in the literature in which a mutation is identified in an affected individual and screening of the family members reveals one parent as being a mosaic for the mutation, having a small percentage of cells with the mutation and the remaining cells being wild type. This has been reported in hyper-IgE syndrome due to mutations in *STAT3* in two unrelated families. In each case, the mutation seen in the children was identified in PBMCs from the father but at low levels (37). In this case, the mutation was identified by Sanger sequencing and the mutant peak, while heterozygous in the children, appeared as a minor peak in the father (Fig. 6A). Had the father been sequenced in isolation, the mutation may have been overlooked as nonspecific background. This is even though the wild-type peak is diminished in comparison with the normal control, as seen by the decreased height of the wild-type G (black) peak when compared with the C (blue) peak preceding it. The change in peak height is one sign that a portion of the sequence is derived from an altered nucleotide sequence rather than background nonspecific sequence.

A similar case is seen in a male patient with a presentation of leaky SCID, with reduced numbers of T cells and NK cells but normal numbers of B cells. Mutation of *IL2RG* is the most common genetic defect in SCID. Screening revealed two peaks at c.260T>C, which caused the substitution of proline for leucine at amino acid 87 (p.L87P). This mutation is predicted to be deleterious, and the patient's mother is heterozygous for it, indicating germ line inheritance. Closer examination of the sequence tracing, however, reveals a small wild-type peak in the patient (Fig. 6B). Because he has only one X chromosome, this change is suggestive of a reversion mutation—a change occurring in somatic cells that results in correction or modification of the mutation. In this case, it returned to the wild-type nucleotide. The most common single nucleotide change seen in the human genome is a C>T substitution that occurs in the context of a CG dinucleotide. In this patient, the mutation created a CG dinucleotide that subsequently underwent a C>T reversion event in a lymphocyte precursor. This reversion allowed for the development of T cells and the leaky phenotype observed (unpublished data). Both the mosaic and reversion patients demonstrate the importance of considering patient phenotype and family inheritance whenever possible. Given errors in amplification by PCR enzymes and natural occurrences of somatic variations, the low-level presence of the mosaic mutations and wild-type reversion may be filtered out in exome sequence data.

The phenotype of the patient, those characteristics or infections that bring him to seek medical attention, is a key

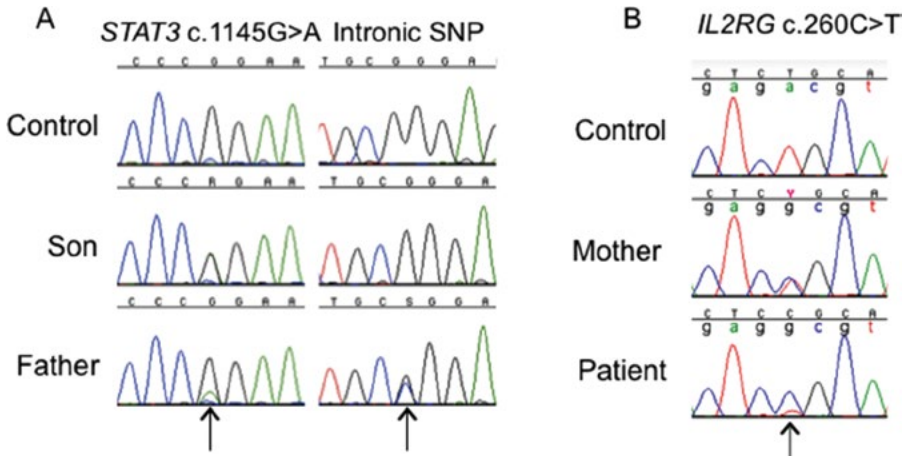

FIGURE 6 (A) Sanger sequence chromatograms from a patient demonstrating mosaicism for a *STAT3* mutant allele. The left column shows coding sequence; the right column, the intronic SNP 132 bp 3′ to the mutation but contained within the same PCR product. The top row is from a healthy control, demonstrating the wild-type G at c.1145 and homozygous G at the intronic SNP. The middle row is from the affected son, with heterozygous peaks at the site of the mutation, c.1145G>A, and homozygous G at the SNP. The bottom row is from the father, showing a reduced peak height of the wild-type G allele (black) compared with the healthy control and the presence of a small green peak corresponding to the mutant allele (arrow) but at less than heterozygous levels. This is in contrast to his intronic SNP, which demonstrates heterozygosity (arrow). (B) Sequence tracings of the X-linked *IL2RG* gene. The top tracing is from a healthy control, showing only wild-type sequence. The middle tracing is from the patient's mother, who is heterozygous for the c.260C>T mutation, showing the reduced T peak (red) and the presence of the mutant C peak (blue). The bottom tracing, from a male patient with the inherited mutant C allele from his mother, shows a small, wild-type T peak (red) underneath (arrow).

factor when evaluating genes for mutations. The patient's clinical presentation often suggests a need for specific, targeted gene or pathway evaluation using Sanger sequencing or whole-exome sequencing to discover variants. However, there are patients with a disease phenotype in whom no mutation can be identified, even when all exons and coding and noncoding regions are sequenced. In this case, if the phenotype of the patient matches a recognized disease gene, then screening for variations in cDNA may be helpful. Three unrelated patients presented with infections characteristic of chronic granulomatous disease (CGD). By the standard dihydrorhodamine flow cytometric assay for CGD, all three patients had reduced activity. This was reflected by an abnormal neutrophil oxidative burst. Sequencing of *CYBB*, the most frequently mutated gene causing CGD, failed to reveal a causal variation. RNA was isolated from patients' neutrophils, and full-length cDNA was generated by RT-PCR. Sequencing of the PCR product revealed an insertion in the cDNA between exons 3 and 4 in one patient, between exons 5 and 6 in a second, and between exons 6 and 7 in the third. Sequencing of the genome between the two exons in each case revealed that the inserts were derived from intronic sequences and were cryptic exons included due to a point mutation that created a strong 5′ss. As seen in Fig. 7, the cryptic exons in the first two patients resulted in a frameshift, which would indicate a loss of mRNA stability and subsequent protein production. The third patient had an insertion of 120 bp that was not predicted to disrupt mRNA stability and resulted in a 40-amino-acid in-frame insertion (unpublished data). Two additional patients with similar mutations have been reported by Noack et al. (38) and Rump et al. (39). None of these mutations would be identified by standard Sanger or whole-exome sequencing because the deep

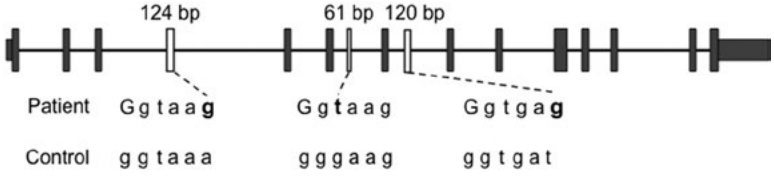

FIGURE 7 *CYBB* genomic structure showing exons (black boxes) and introns (black line). Below is intronic sequence from three patients, demonstrating the intronic point mutation (bold) in each that creates a cryptic 5′ss allowing for inclusion of a cryptic exon (white boxes). Wild-type sequence for each site is shown below the patients' mutant sequences. The insertion of the cryptic exon results in a frameshift for the first two patients, while the third, with an insertion of 120 bp, is predicted to have a 40-amino-acid insertion.

introns would not be screened again. This emphasizes the need for cDNA analysis.

One final example comes from a group of patients with MonoMAC syndrome (40), which is an autosomal dominant disease caused by mutations in the hematopoietic stem cell transcription factor GATA2. Missense mutations have been identified in the C-terminal region of the protein encoding the highly conserved second zinc finger involved in binding to the GATA motif on DNA. Additional mutations result in the loss of mRNA transcript from one allele, which is caused by a frameshift insertion or deletion mutation or premature stop codons. This indicates that a reduced level of GATA2 transcript or protein is sufficient to cause disease. Among patients with phenotypic MonoMAC syndrome, there were several without identified mutations after all exons and flanking splice sites had been sequenced. Similar to the patients without identified *CYBB* mutations, full-length *GATA2* cDNA screening was performed. In two patients, although they displayed heterozygosity by genomic sequence for known SNPs found within the exons, cDNA sequence demonstrated the presence of one predominant allele (Fig. 8A). Further work needs to be performed to elucidate the genetic lesion leading to loss of expression of the allele in these patients. Haploinsufficiency of *GATA2*

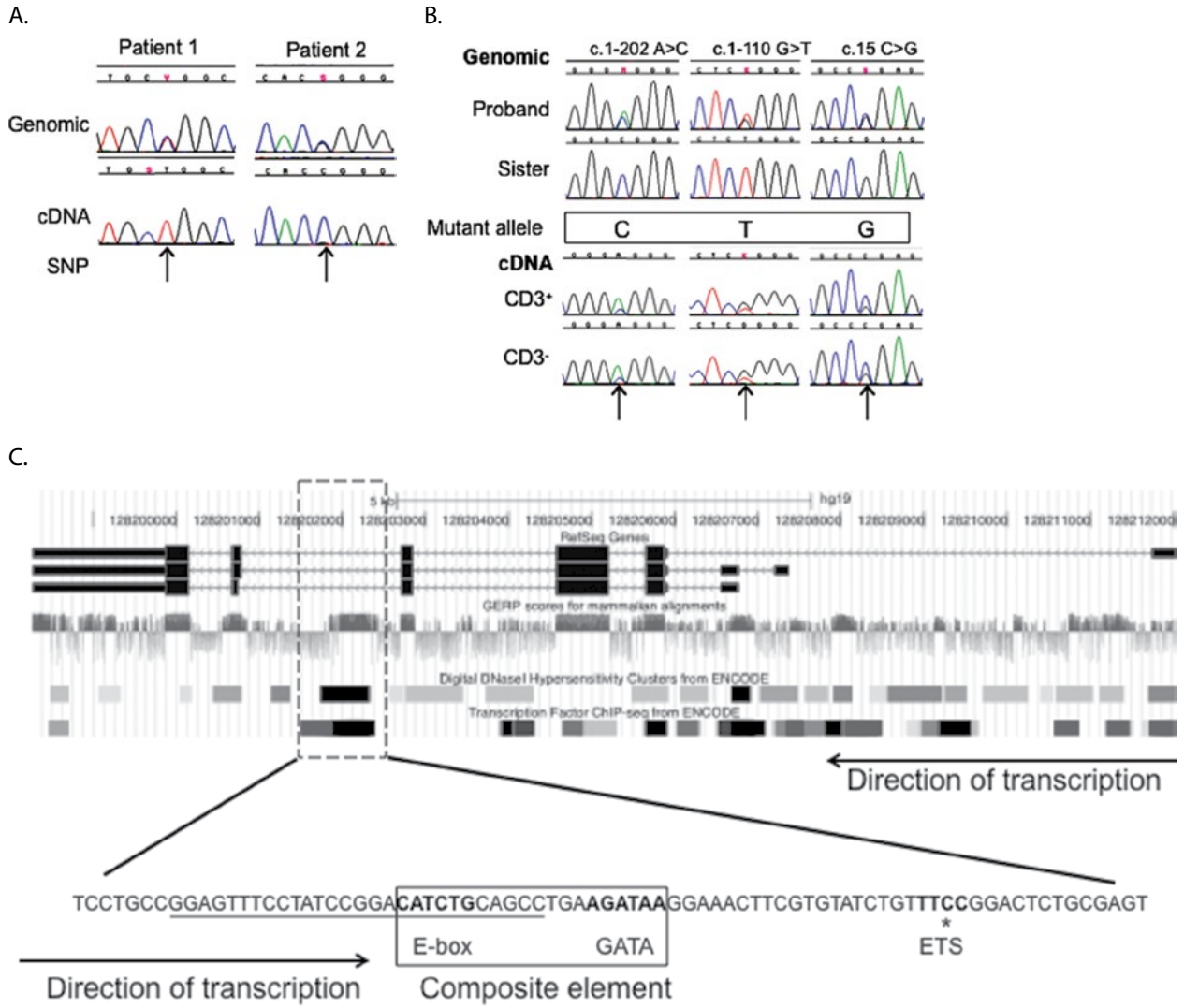

FIGURE 8 Reduced *GATA2* allelic expression in MonoMAC syndrome. (A) The top row shows genomic sequence from two patients demonstrating heterozygosity for a SNP within the cDNA transcript of *GATA2*. The bottom row shows cDNA sequence from full-length RT-PCR. In patient 1, only the T allele is present (arrow), indicating loss of the transcript containing the C allele, while patient 2's sequence contains the C allele with only a small peak of the G allele (arrow). These sequences demonstrate uniallelic expression leading to haploinsufficiency of *GATA2*. (B) At the top is genomic sequence from two affected sisters; the proband is heterozygous for three known SNPs found within the cDNA, while her sister is homozygous, allowing determination of the shared mutant allele haplotype (boxed bases). At the bottom is *GATA2* cDNA sequence from the proband's $CD3^+$ and $CD3^-$ PBMCs, revealing decreased levels of the mutant allele as represented by peak height (arrows). (C) *GATA2* genomic locus showing three reported isoform structures. The dashed box indicates a conserved intron 5 region with a high GERP score, DNase I hypersensitivity, and strong transcription factor binding. Zoom of bases highlights the E-box/GATA composite element (boxed); the 28-base deletion seen in the first patient (underlined sequence); and the ETS motif with a C>T mutation seen in five patients (asterisk), including the sisters shown in panel B.

has been demonstrated in patients with mutations causing mRNA instability. This suggests that the molecular basis of the disease in these two patients is likely a loss of expression of one *GATA2* allele. In another group of MonoMAC patients, reduced but not absent expression from one allele was recognized by cDNA analysis. Figure 8B shows genomic sequence from one patient and her sister, both affected with MonoMAC. The proband is heterozygous for three known SNPs found within the cDNA, while her sister is homozygous for the same SNPs. This allows determination of the mutant allele haplotype, as both sisters must have inherited the mutation. Subsequent screening of *GATA2* cDNA in the proband shows decreased peak height of the mutant allele compared with the heterozygous peaks seen in the genomic sequence. Examination of the genomic structure of *GATA2* from the UCSC Genome Browser reveals a region within intron 5 notable for high levels of conservation, DNase I sensitivity, and evidence of multiple transcription factor binding (Fig. 8C). Located with this is a composite element recognized as critical for *GATA2* expression (41). Screening of the conserved intronic region revealed a 28-base deletion encompassing a portion of the composite element in one patient, while a single point mutation at the nearby ETS transcription factor family motif was identified in the other patients. Functional constructs demonstrated reduced expression caused by each mutation (27, 42) and correlated with the reduced allelic expression seen in the patients. The data from these patients demonstrate another class of mutations, those resulting in reduced expression in a protein in which haploinsufficiency may cause disease. This condition is recognized primarily by screening for uniallelic expression by cDNA.

Figure 9 provides a framework for analysis of patients with immune disorders. First, the clinical phenotype needs to be defined. Clinical presentation including age, gender, TREC levels in infants, and medical history provides certain clues. The infection history of the patient also can suggest a target gene or pathway. Lastly, clinical laboratory assays such as lymphocyte phenotyping and functional flow cytometric assays can further refine a working diagnosis. If there is a specific pathway or gene suggested based on clinical presentation, then targeted Sanger sequencing of that gene may identify a genetic lesion. In the absence of a limited candidate gene list, then NGS via a medium-scale, targeted approach, such as using a panel of genes screened by Ion Torrent, or a large-scale whole-exome analysis may be performed. After bioinformatics processing of the data, a filtered list of candidate variations is obtained, which then

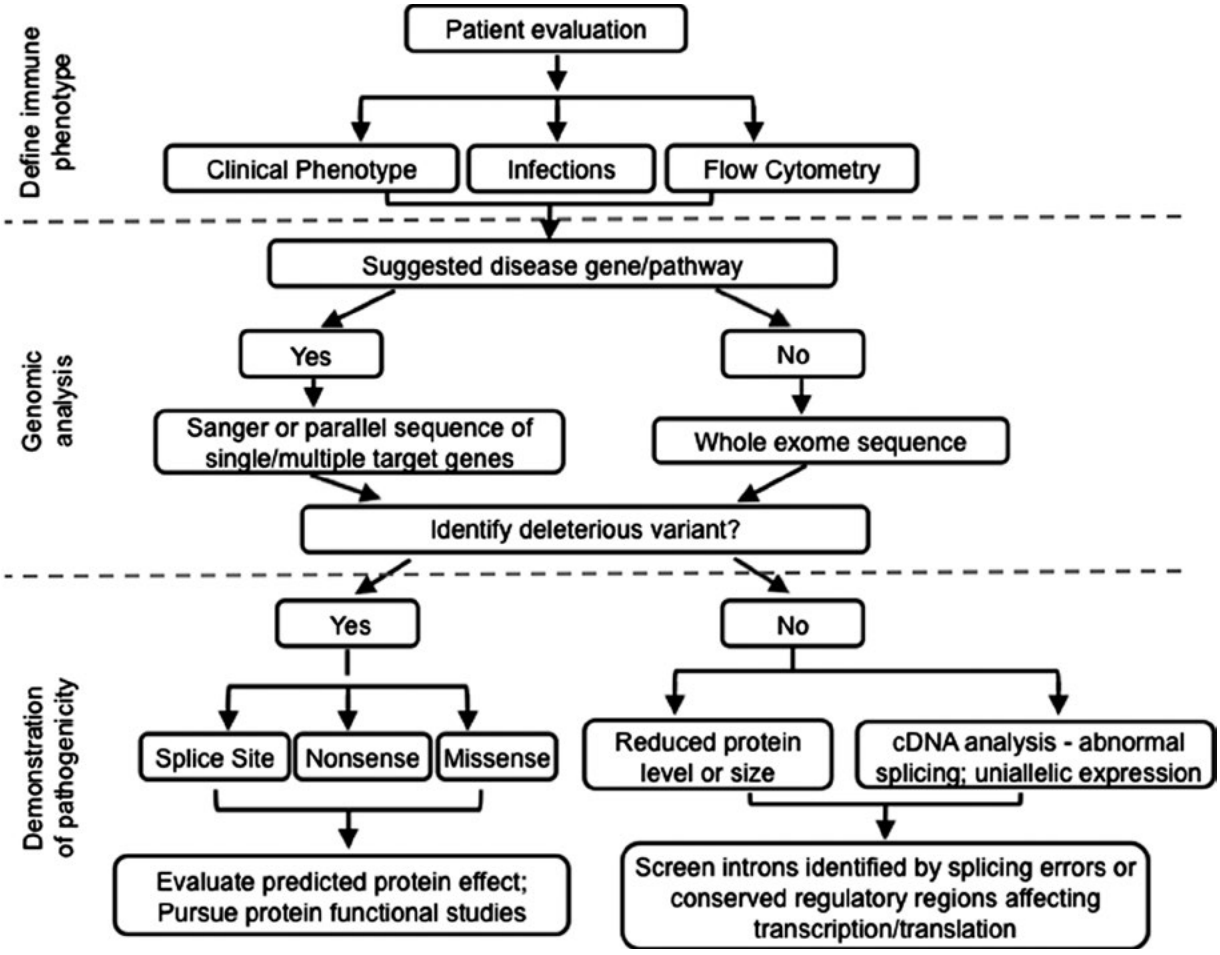

FIGURE 9 Framework for molecular and genetic diagnosis in immunocompromised patients, beginning with defining of patient phenotype, proceeding to performing genomic analysis, and concluding with inferred or demonstrated pathogenicity of mutation.

are examined to see if they are consistent with regard to the patient's phenotype. Variations resulting in loss of canonical splice sites or nonsense or missense changes should be evaluated for the predicted protein effect and confirmed with functional studies of the protein. In the case in which a deleterious variant is not identified, if a target gene is suspected, then screening for altered protein size or levels or aberrant cDNA caused by splicing defects or uniallelic expression may be useful. Recognition of the possibility of mutations in the untranslated exons and conserved regions within and flanking the gene is also important for defining genetic lesions. While methods to detect variations will continue to improve in both sensitivity and throughput, understanding how to analyze variations and their potential effect on transcript and protein will continue to be necessary to diagnose genetic lesions involved in defects of the immune system.

REFERENCES

1. **Kirkpatrick P, Riminton S.** 2007. Primary immunodeficiency diseases in Australia and New Zealand. *J Clin Immunol* **27:**517–524.
2. **Gathmann B, Binder N, Ehl S, Kindle G, ESID Registry Working Party.** 2012. The European internet-based patient and research database for primary immunodeficiencies: update 2011. *Clin Exp Immunol* **167:**479–491.
3. **Taschner PE, den Dunnen JT.** 2011. Describing structural changes by extending HGVS sequence variation nomenclature. *Hum Mutat* **32:**507–511.
4. **Quail MA, Smith M, Coupland P, Otto TD, Harris SR, Connor TR, Bertoni A, Swerdlow HP, Gu Y.** 2012. A tale of three next generation sequencing platforms: a comparison of Ion Torrent, Pacific Biosciences and Illumina MiSeq sequencers. *BMC Genomics* **13:**341. doi:10.1186/1471-2164-13-341.
5. **Loman NJ, Misra RV, Dallman TJ, Constantinidou C, Gharbia SE, Wain J, Pallen MJ.** 2012. Performance comparison of benchtop high-throughput sequencing platforms. *Nat Biotechnol* **30:**434–439.
6. **Lee HC, Lai K, Lorenc MT, Imelfort M, Duran C, Edwards D.** 2012. Bioinformatics tools and databases for analysis of next-generation sequence data. *Brief Funct Genomics* **11:**12–24.
7. **McKenna A, Hanna M, Banks E, Sivachenko A, Cibulskis K, Kernytsky A, Garimella K, Altshuler D, Gabriel S, Daly M, DePristo MA.** 2010. The Genome Analysis Toolkit: a MapReduce framework for analyzing next-generation DNA sequencing data. *Genome Res* **20:**1297–1303.
8. **DePristo MA, Banks E, Poplin R, Garimella KV, Maguire JR, Hartl C, Philippakis AA, del Angel G, Rivas MA, Hanna M, McKenna A, Fennell TJ, Kernytsky AM, Sivachenko AY, Cibulskis K, Gabriel SB, Altshuler D, Daly MJ.** 2011. A framework for variation discovery and genotyping using next-generation DNA sequencing data. *Nat Genet* **43:**491–498.
9. **Li H, Handsaker B, Wysoker A, Fennell T, Ruan J, Homer N, Marth G, Abecasis G, Durbin R, 1000 Genome Project Data Processing Subgroup.** 2009. The Sequence Alignment/Map (SAM) format and SAMtools. *Bioinformatics* **25:**2078–2079.
10. **Pabinger S, Dander A, Fischer M, Snajder R, Sperk M, Efremova M, Krabichler B, Speicher MR, Zschocke J, Trajanoske Z.** 2014. A survey of tools for variant analysis of next-generation genome sequencing data. *Brief Bioinform* **15:**256–278.
11. **McCourt CM, McArt DG, Mills K, Catherwood MA, Maxwell P, Waugh DJ, Hamilton P, O'Sullivan JM, Salto-Tellez M.** 2013. Validation of next generation sequencing technologies in comparison to current diagnostic gold standards for BRAF, EGFR and KRAS mutational analysis. *PLoS One* **8:**e69604. doi:10.1371/journal.pone.0069604.
12. **Livak KJ, Schmittgen TD.** 2001. Analysis of relative gene expression data using real-time quantitative PCR and the $2^{-\Delta\Delta C_T}$ method. *Methods* **25:**402–408.
13. **Hazenberg MD, Verschuren MC, Hamann D, Miedema F, van Dongen JJ.** 2001. T cell receptor excision circles as markers for recent thymic emigrants: basic aspects, technical approach, and guidelines for interpretation. *J Mol Med (Berl)* **79:**631–640.
14. **Chan K, Puck** JM. 2005. Development of population-based newborn screening for severe combined immunodeficiency. *J Allergy Clin Immunol* **115:**391–398.
15. **Puck JM.** 2012. Laboratory technology for population-based screening for severe combined immunodeficiency in neonates: the winner is T-cell receptor excision circles. *J Allergy Clin Immunol* **129:**607–616.
16. **Routes JM, Grossman WJ, Verbsky J, Laessig RH, Hoffman GL, Brokopp CD, Baker MW.** 2009. Statewide newborn screening for severe T-cell lymphopenia. *JAMA* **302:**2465–2470.
17. **Verbsky JW, Baker MW, Grossman WJ, Hintermeyer M, Dasu T, Bonacci B, Reddy S, Margolis D, Casper J, Gries M, Desantes K, Hoffman GL, Brokopp CD, Seroogy CM, Routes** JM. 2012. Newborn screening for severe combined immunodeficiency; the Wisconsin experience (2008–2011). *J Clin Immunol* **32:**82–88.
18. **Kwan A, Church JA, Cowan MJ, Agarwal R, Kapoor N, Kohn DB, Lewis DB, McGhee SA, Moore TB, Stiehm ER, Porteus M, Aznar CP, Currier R, Lorey F, Puck JM.** 2013. Newborn screening for severe combined immunodeficiency and T-cell lymphopenia in California: results of the first 2 years. *J Allergy Clin Immunol* **132:**140–150.
19. **Urban AE, Korbel JO, Selzer R, Richmond T, Hacker A, Popescu GV, Cubells JF, Green R, Emanuel BS, Gerstein MB, Weissman SM, Snyder M.** 2006. High-resolution mapping of DNA copy alterations in human chromosome 22 using high-density tiling oligonucleotide arrays. *Proc Natl Acad Sci U S A* **103:**4534–4539.
20. **Chang X, Wang K.** 2012. wANNOVAR: annotating genetic variants for personal genomes via the web. *J Med Genet* **49:**433–436.
21. **Liu X, Jian X, Boerwinkle E.** 2013. dbNSFP v2.0: a database of human non-synonymous SNVs and their functional predictions and annotations. *Hum Mutat* **34:**E2393–E2402.
22. **Fisher GH, Rosenberg FJ, Straus SE, Dale JK, Middleton LA, Lin AY, Strober W, Lenardo MJ, Puck JM.** 1995. Dominant interfering Fas gene mutations impair apoptosis in a human autoimmune lymphoproliferative syndrome. *Cell* **81:**935–946.
23. **Jackson CE, Fischer RE, Hsu AP, Anderson SM, Choi Y, Wang J, Dale JK, Fleisher TA, Middelton LA, Sneller MC, Lenardo MJ, Straus SE, Puck JM.** 1999. Autoimmune lymphoproliferative syndrome with defective Fas: genotype influences penetrance. *Am J Hum Genet* **64:**1002–1014.
24. **Nagy E, Maquat LE.** 1998. A rule for termination-codon position within intron-containing genes: when nonsense affects RNA abundance. *Trends Biochem Sci* **23:**198–199.
25. **Isken O, Maquat LE.** 2007. Quality control of eukaryotic mRNA: safeguarding cells from abnormal mRNA function. *Genes Dev* **21:**1833–1856.
26. **Hsu AP, Dowdell KC, Davis J, Niemela JE, Anderson SM, Shaw PA, Rao VK, Puck JM.** 2012. Autoimmune lymphoproliferative syndrome due to *FAS* mutations outside the signal-transducing death domain: molecular mechanisms and clinical penetrance. *Genet Med* **14:**81–89.
27. **Hsu AP, Johnson KD, Falcone EL, Sanalkumar R, Sanchez L, Hickstein DD, Cuellar-Rodriguez J, Lemieux JE,**

Zerbe CS, Bresnick EH, Holland SM. 2013. GATA2 haploinsufficiency caused by mutations in a conserved intronic element leads to MonoMAC syndrome. *Blood* **121:**3830–3837, S1–S7.
28. **Wang Z, Burge CB.** 2008. Splicing regulation: from a parts list of regulatory elements to an integrated splicing code. *RNA* **14:**802–813.
29. **Ward AJ, Cooper TA.** 2010. The pathobiology of splicing. *J Pathol* **220:**152–163.
30. **Zhang Q, Davis JC, Lamborn IT, Freeman AF, Jing H, Favreau AJ, Matthews HF, Davis J, Turner ML, Uzel G, Holland SM, Su HC.** 2009. Combined immunodeficiency associated with *DOCK8* mutations. *N Engl J Med* **361:**2046–2055.
31. **Sterne-Weiler T, Howard J, Mort M, Cooper DN, Sanford JR.** 2011. Loss of exon identity is a common mechanism of human inherited disease. *Genome Res* **21:**1563–1571.
32. **Desmet FO, Hamroun D, Lalande M, Collod-Béroud G, Claustres M, Béroud C.** 2009. Human Splicing Finder: an online bioinformatics tool to predict splicing signals. *Nucleic Acids Res* **37:**e67. doi:10.1093/nar/gkp215.
33. **Zhu J, Mayeda A, Krainer AR.** 2001. Exon identity established through differential antagonism between exonic splicing silencer-bound hnRNP A1 and enhancer-bound SR proteins. *Mol Cell* **8:**1351–1361.
34. **Barbosa C, Peixiero I, Romão L.** 2013. Gene expression regulation by upstream open reading frames and human disease. *PLoS Genet* **9:**e1003529. doi:10.1371/journal.pgen.1003529.
35. **Sampaio EP, Hsu AP, Pechacek J, Bax HI, Dias DL, Paulson ML, Chandrasekaran P, Rosen LB, Carvalho DS, Ding L, Vinh DC, Browne SK, Datta S, Milner JD, Kuhns DB, Long Priel DA, Sadat MA, Shiloh M, De Marco B, Alvares M, Gillman JW, Ramarathnam V, de la Morena M, Bezrodnik L, Moreira I, Uzel G, Johnson D, Spalding C, Zerbe CS, Wiley H, Greenberg DE, Hoover SE, Rosenzweig SD, Galgiani JN, Holland SM.** 2013. Signal transducer and activator of transcription 1 (*STAT1*) gain-of-function mutations and disseminated coccidioidomycosis and histoplasmosis. *J Allergy Clin Immunol* **131:**1624–1634.
36. **Uzel G, Sampaio EP, Lawrence MG, Hsu AP, Hackett M, Dorsey MJ, Noel RJ, Verbsky JW, Freeman AF, Janssen E, Bonilla FA, Pechacek J, Chandrasekaran P, Browne SK, Agharahimi A, Gharib AM, Mannurita SC, Yim JJ, Gambineri E, Torgerson T, Tran DQ, Milner JD, Holland SM.** 2013. Dominant gain-of-function *STAT1* mutations in FOXP3^{WT} IPEX-like syndrome. *J Allergy Clin Immunol* **131:**1611–1623.
37. **Hsu AP, Sowerwine KJ, Lawrence MG, Davis J, Henderson CJ, Zarember KA, Garofalo M, Gallin JI, Kuhns DB, Heller T, Milner JD, Puck JM, Freeman AF, Holland SM.** 2013. Intermediate phenotypes in patients with autosomal dominant hyper-IgE syndrome caused by somatic mosaicism. *J Allergy Clin Immunol* **131:**1586–1593.
38. **Noack D, Heyworth PG, Newburger PE, Cross AR.** 2001. An unusual intronic mutation in the *CYBB* gene giving rise to chronic granulomatous disease. *Biochim Biophys Acta* **1537:**125–31.
39. **Rump A, Rösen-Wolff A, Gahr M, Seidenberg J, Roos C, Walter L, Günther V, Roesler J.** 2006. A splice-supporting intronic mutation in the last bp position of a cryptic exon within intron 6 of the *CYBB* gene induces its incorporation into the mRNA causing chronic granulomatous disease (CGD). *Gene* **371:**174–181.
40. **Hsu AP, Sampaio EP, Khan J, Calvo KR, Lemieux JE, Patel SY, Frucht DM, Vinh DC, Auth RD, Freeman AF, Olivier KN, Uzel G, Zerbe CS, Spalding C, Pittaluga S, Raffeld M, Kuhns DB, Ding L, Paulson ML, Marciano BE, Gea-Banacloche JC, Orange JS, Cuellar-Rodriguez J, Hickstein DD, Holland SM.** 2011. Mutations in *GATA2* are associated with the autosomal dominant and sporadic monocytopenia and mycobacterial infection (MonoMAC) syndrome. *Blood* **118:**2653–2655.
41. **Wozniak RJ, Boyer ME, Grass JA, Lee Y, Bresnick EH.** 2007. Context-dependent GATA factor function: combinatorial requirements for transcriptional control in hematopoietic and endothelial cells. *J Biol Chem* **282:**14665–14674.
42. **Johnson KD, Hsu AP, Ryu MJ, Wang J, Gao X, Boyer ME, Liu Y, Lee Y, Calvo KR, Keles S, Zhang J, Holland SM, Bresnick EH.** 2012. *cis*-Element mutated in *GATA2*-dependent immunodeficiency governs hematopoiesis and vascular integrity. *J Clin Invest* **122:**3692–3704.
43. **Adzhubei IA, Schmidt S, Peshkin L, Ramensky VE, Gerasimova A, Bork P, Kondrashov AS, Sunyaev SR.** 2010. A method and server for predicting damaging missense mutations. *Nat Methods* **7:**248–249.
44. **Sim NL, Kumar P, Hu J, Henikoff S, Schneider G, Ng PC.** 2012. SIFT web server: predicting effects of amino acid substitutions on proteins. *Nucleic Acids Res* **40**(Web Server issue)**:**W452–W457.
45. **Schwarz JM, Rödelsperger C, Schuelke M, Seelow D.** 2010. MutationTaster evaluates disease-causing potential of sequence alterations. *Nat Methods* **7:**575–576.
46. **Chun S, Fay JC.** 2009. Identification of deleterious mutations within three human genomes. *Genome Res* **19:**1553–1561.
47. **Reva B, Antipin Y, Sander C.** 2011. Predicting the functional impact of protein mutations: application to cancer genomics. *Nucleic Acids Res* **39:**e118. doi:10.1093/nar/gkr407.
48. **Shihab HA, Gough J, Cooper DN, Stenson PD, Barker GL, Edwards KJ, Day IN, Gaunt TR.** 2013. Predicting the functional, molecular, and phenotypic consequences of amino acid substitutions using hidden Markov models. *Hum Mutat* **34:**57–65.
49. **Garber M, Guttman M, Clamp M, Zody MC, Friedman N, Xie X.** 2009. Identifying novel constrained elements by exploiting biased substitution patterns. *Bioinformatics* **25:**i54–i62.
50. **Davydov EV, Goode DL, Sirota M, Cooper GM, Sidow A, Batzoglou S.** 2010. Identifying a high fraction of the human genome to be under selective constraint using GERP++. *PLoS Comput Biol* **6:**e1001025. doi:10.1371/journal.pcbi.1001025.
51. **Pollard KS, Hubisz MJ, Rosenbloom KR, Siepel A.** 2010. Detection of nonneutral substitution rates on mammalian phylogenies. *Genome Res* **20:**110–121.
52. **Clarke L, Zheng-Bradley X, Smith R, Kulesha E, Xiao C, Toneva I, Vaughan B, Preuss D, Leinonen R, Shumway M, Sherry S, Flicek P, 1000 Genomes Project Consortium.** 2012. The 1000 Genomes Project: data management and community access. *Nat Methods* **9:**459–462.
53. **Schwartz S, Hall E, Ast G.** 2009. SROOGLE: webserver for integrative, user-friendly visualization of splicing signals. *Nucleic Acids Res* **37**(Web Server issue)**:** W189–W192.
54. **Smith PJ, Zhang C, Wang J, Chew SL, Zhang MQ, Krainer AR.** 2006. An increased specificity score matrix for the prediction of SF2/ASF-specific exonic splicing enhancers. *Hum Mol Genet* **15:**2490–2508.
55. **Cartegni L, Wang J, Zhu Z, Zhang MQ, Krainer AR.** 2003. ESEfinder: a web resource to identify exonic splicing enhancers. *Nucleic Acids Res* **31:**3568–3571.
56. **Fairbrother WG, Yeh RF, Sharp PA, Burge CB.** 2002. Predictive identification of exonic splicing enhancers in human genes. *Science* **297:**1007–1013.
57. **Zhang XH, Chasin LA.** 2004. Computational definition of sequence motifs governing constitutive exon splicing. *Genes Dev* **18:**1241–1250.

The Human Microbiome and Clinical Immunology

FREDERIC D. BUSHMAN

3

Humans, in many respects, are not single organisms, but more like coral reefs, complex assemblages of myriad diverse creatures. The human microbiota, the bugs living in association with humans, contains more cells than comprise the human body itself (1). Like the fish on a reef, the microbes interact with each other, sometimes competing and sometimes collaborating, to form a complex and resilient food web. Some of the population promote the growth and development of the reef, while others consume the reef material, turning the hard corals to sand.

This chapter reviews the nature of the human microbiome, with emphasis on methods for microbiome research and the pitfalls that have ruined many studies in the field. However, despite the challenges, the output from the field has been spectacular (2–7), and the technology emerging from microbiome research holds tremendous promise for translation to clinical applications. A few of the possible future directions are described at the end of the chapter.

WHAT IS METAGENOMIC ANALYSIS?

Microorganisms often live in mixed communities, and it is clear that the global composition and function of mixed communities can be relevant to human health. For example, actions of human microbial communities have been implicated in all the major causes of human mortality (1), including heart disease (8, 9), cancer (10), and diabetes (11). Loss of normal control of the microbiome in immunodeficient states is associated with pathogenesis of opportunistic infections, and the tools of metagenomic analysis can report the composition and nature of those communities in unprecedented detail.

Complicating analysis of the human microbiome, only a small minority of all the microbes on earth have been subjected to culture in the laboratory, so traditional culture-based methods are often not suitable for studies of mixed microbial communities. A new approach is made possible by the remarkable new "deep sequencing" methods, which allow determination of millions or even billions of bases of DNA sequence in a single instrument run.

Bacterial genomes range in size from ~500 kb to many megabases, and the genomes of fungi are larger still (12). Thus, sequencing all the genomes in a mixed community, which may contain hundreds of types of microbes, is still a daunting task. Furthermore, in a typical biomedical study, the goal is often to compare a set of healthy control samples to a set of samples from a disease state. For example, one might compare stool samples from a cohort of healthy children to samples from a cohort of immunocompromised children. It is typically not feasible to complete the sequences of all microbes in each sample, but it is possible to collect a deep sequence sample of each community. Sequences can then be aligned to databases and the types of microbes present inferred from database annotation. If total DNA is analyzed, then the gene types present (e.g., genes for adenine biosynthetic enzymes and virulence factors) can be assessed as well. One can then compare results for the collection of healthy control samples to the immunocompromised subject samples and identify differences associated with disease. Such an analysis, based on large-scale but incomplete characterization of mixed communities by sequencing, has come to be called "metagenomics."

METHODS FOR METAGENOMICS RESEARCH

In this section, we review the DNA isolation, library preparation, and sequencing approaches used in metagenomic studies. The overall lesson is that details of the analytical approach used are driven quite strongly by the exact question posed—relatively small differences in the goals of the study can mean dramatic differences in the metagenomic methods needed for analysis. Several examples of types of questions and approaches to their investigation are presented toward the end of this chapter.

Nucleic Acid Purification

First, a set of samples must be acquired and nucleic acid purified for sequencing. Many nucleic acid purification kits are available from commercial suppliers, and many can be used successfully (13). A key control for any study is to run DNA-free water samples through the purification procedure side by side with the samples of interest. Some commercial kits contain substantial quantities of contaminating 16S DNA, which can be ruinous if the starting amount of nucleic acid is low in the samples of interest. Commercial kits are also available that yield both DNA and RNA from the same sample, allowing assay of both.

Methods for lysis are worked out to allow capture of many organisms in a sample, but the methods represent a compromise between convenience and complete sampling. Some

doi:10.1128/9781555818722.ch3

Gram-positive bacteria and fungi have tough cell walls and are known to be harder to lyse than typical bacteria. Spores are tougher still, and any study for which data on spores are important requires targeted evaluation of methods for lysis. Unfortunately, it is possible that harsh lysis methods may degrade nucleic acid from the first-to-lyse organisms before the toughest are cracked open.

Stepping back, a general lesson is that it is important to carefully formulate the question under study, and if possible to check the performance of the methods chosen in addressing the question posed.

DNA Sequencing

The development of the astounding new DNA-sequencing methods has made possible the explosion of work on the human microbiome. For example, using the new Illumina HiSeq technology, one can acquire hundreds of billions of bases of sequence information in a single instrument run. The availability of such vast amounts of sequence data allows characterization of mixed microbial communities in unprecedented detail.

The automation of the Sanger sequencing chemistry was a breakthrough in its day, driving the completion of the first drafts of human genome sequence in 2001. These instruments could generate 384 reads of ~500 bases each, or ~200 kb of sequence per run, under favorable circumstances.

The first of the massively parallel deep sequencing methods to be commercialized was the Roche 454 pyrosequencing method (14). This allowed collection of ~500,000 sequence reads of ~350 bases per instrument run, or close to 200 million bases. All of these next-generation sequencing methods have higher error rates than the original Sanger sequencing method. The Roche 454 platform is particularly error prone at homopolymer sequences, so that the numbers of bases in the homopolymer runs are commonly miscounted.

While impressive, the newer Solexa/Illumina method is, at this writing, the most widely used and produces the most data per instrument run (15). The HiSeq instruments can generate >250 billion bases of sequence information in a single run in the form of paired 250-base reads. The ABI SOLiD system also delivers amounts of sequence in this range.

Additional companies are also developing still more remarkable technologies. Pacific Biosciences has marketed a third-generation instrument capable of generating long reads on single molecules (16) (in the jargon, the "first generation" was instruments automating Sanger sequencing and the "second generation" the Roche 454, Illumina, and ABI SOLiD technologies). Ion Torrent has marketed an inexpensive instrument that yields reads in the 350-base range at relatively low cost. Both Roche 454 and Illumina have also marketed benchtop machines—the 454 Junior and Illumina MiSeq—that can yield sequence samples of about one-tenth the output of the larger instruments at reduced cost and increased convenience.

DNA Barcoding

Often it is not desirable to collect billions of bases of sequence information on a single sample, but rather it is more cost-effective and efficient to collect much less data per sample over many more samples. A popular approach to this is to engineer DNA barcodes into synthetic DNA primers used in preparation of sequencing libraries, and use separate primer sets to amplify each sample in a set. The amplification products can then be pooled together after library preparation, sequenced together, and separated out computationally after the run based on the barcode information in each sequence read (17, 18). Multiple strategies can be used to mark primers in this fashion. Barcode systems are now available for most of the major sequencing platforms.

Tag Sequencing

Several approaches are commonly used to acquire deep sequence data on microbiome populations. In one popular implementation, PCR is used to amplify conserved sequences present in bacteria or fungi, and then the collections of sequence tags are used to characterize a sample. The bacterial 16S rRNA gene contains highly conserved regions, which can be used as binding sites for PCR primers (19–22). An advantage to the use of 16S data is that well-curated databases are available containing 16S sequences together with phylogenetic annotation, and sophisticated pipelines are in place (QIIME, mothur) that can take in such data and output finished analysis (23, 24). For fungi, 18S rRNA can be used similarly as a tag, as well as the internal transcribed spacer region (25, 26).

A variety of methods have been worked out for comparing sets of communities with one another. Given a set of samples from, for example, healthy controls and immunocompromised subjects, one might want to ask whether there are general trends in the data that distinguish one from the other. Several methods have been developed for calculating pairwise distances between communities, so that all pairs can be calculated to form a matrix of distances between communities. Such matrices can then be used for statistical analysis of possible patterns in the data. For example, one can ask whether the mean distance between all pairs of samples of the same group is smaller than the mean distance for pairs of samples between groups. If yes, this is evidence for separate clustering, and allows simple statistical evaluation. The UniFrac method is one popular tool for generating distances in a phylogenetic framework (27–29) and is implemented in the QIIME pipeline (23). An example is shown in Fig. 1, illustrating the difference in microbial communities at different human body sites analyzed by UniFrac.

Shotgun Sequencing

Tag sequencing yields information on the organisms represented in a microbial population but does not report on the full complement of genes present. Bacteria of even the same species can vary by up to 30% of their genes (30), so naming a strain using tag sequence data provides only part of the picture. Thus, shotgun sequencing of total DNA followed by alignment to databases adds information not just on the organisms present but on the types of genes present in the community as well. The methods for analyzing shotgun metagenomic data are less well worked out than for tag sequencing data (31), and the data volumes can be very large, presenting challenges in data transfer and management that are not as severe with tag sequencing. However, methods are improving with each passing year. For example, MEGAN allows collection of aligned sequences to yield taxonomic attribution (32), MetaPhlAn uses a sequence tag approach over shotgun reads to annotate bacteria in an efficient fashion (33), and multiple databases allow assignment of genes detected to functional classes or pathways (34, 35).

Thus, although methods development is ongoing, methods for metagenomic research are in place and available to address many questions of interest in clinical immunology.

ARTIFACTS IN MICROBIOME RESEARCH

Essentially all the steps described for microbiome analysis above are imperfect. Carrying out a successful microbiome study involves understanding the limitations of the methods

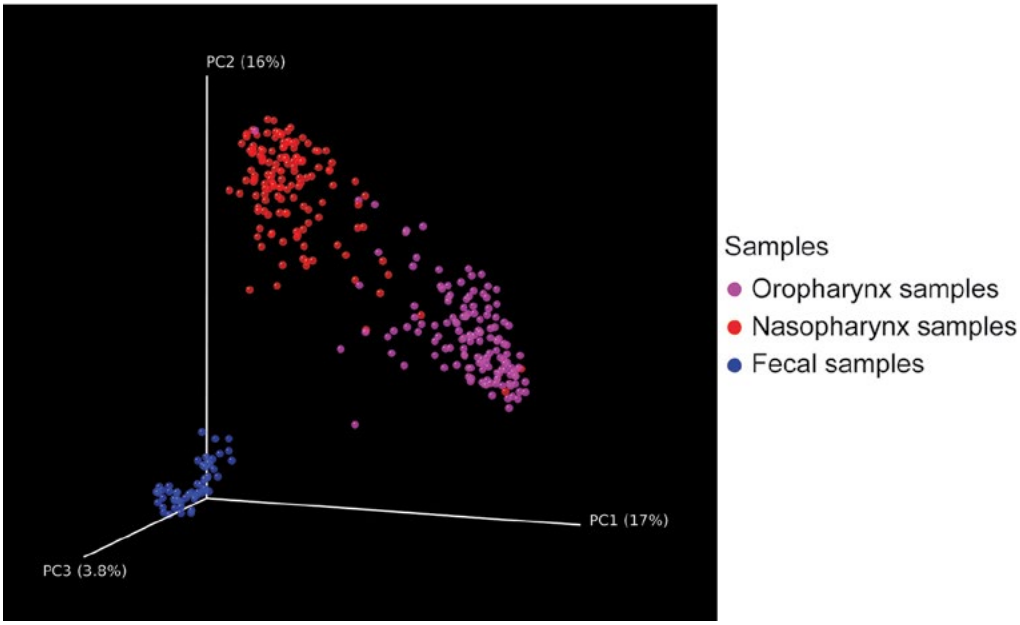

FIGURE 1 Clustering of bacterial communities by body site analyzed using UniFrac. Each dot represents one human microbiome sample, characterized by deep sequencing of 16S tags from the V1V2 region of the gene. Each sample was characterized using a few thousand sequence reads. PC indicates principal coordinates.

used and aligning the question posed with the strengths of methods and not the weaknesses. Some relevant reports have been published (4, 36, 37).

Biases in Sequence Tag Analysis

All of the 16S tag systems used to analyze bacteria are biased in the bacterial types they recover (4, 38, 39). This is unavoidable because the highly conserved sites in the 16S rRNA gene are not perfectly conserved, just well conserved, so that primers anneal to some target sequences better than others. Careful comparisons over defined communities can yield startlingly different results with different primer sets when relative abundance is queried, though differences are less when data are scored for presence and absence of relatively high-level taxonomic groups.

How much this matters depends entirely on the question posed. If the goal is to identify exactly the types and proportions of bacteria in a complex mixture, these biases are significant concerns. Tag sequence data provide an overview of much of the community, but further experimentation is needed to characterize abundance convincingly (e.g., quantitative PCR). However, if the goal is to compare two groups of samples—perhaps fecal samples from immunocompromised children to healthy controls—then the sequence sample returned in a typical 16S tag study may be fine for documenting a difference in communities such as separate clustering. As with any measurement in experimental science, it is always best to verify an important conclusion using multiple forms of measurement. For example, if a single bacterium is judged to be functionally important in distinguishing sample sets, then quantitative PCR could be used to verify the difference between groups.

Tag systems for analyzing microeukaryotes such as fungi present an even more extreme case. For such studies, researchers need to expect from the start that they are only looking at the slice of the fungal community accessible with the primers used. Careful studies are starting to appear comparing the fungi queried using different primer sets that provide a starting point for experimental design (25, 26).

Challenges with Low-Biomass Samples

Much of the work on the human microbiome has focused on the lower gastrointestinal tract, where bacteria are present in the range of 10^{11} per g of intestinal contents (1). Given such gigantic amounts of bacteria, one doesn't usually worry about other sources of bacterial DNA in a gut sample. However, the situation is much different for many other sample types. Bronchoalveolar lavage, skin scrapings, blood plasma, and multiple other sample types typically contain low levels of bacteria, so that admixture of environmental DNA from dust or contamination in commercial reagents can be a substantial fraction of the total.

Thus, it is absolutely critical to surround low-biomass samples with controls to assess the types and proportions of contaminating sequences. Never carry out such an experiment without working up DNA-free water through the full DNA purification procedure. Blank PCR reactions are another must. More-sophisticated controls include instrument washes and matched tissues from germ-free animals. Control samples are put through the DNA purification procedure side by side with the samples of interest and then sequenced with dedicated barcodes in the final deep sequencing run. A handful of reads can sometimes be obtained even from PCR reactions that appear blank after analysis by gel electrophoresis and staining with ethidium bromide, so it is important to sequence everything. In addition, it is valuable to use quantitative PCR to quantify the total number of 16S-complementary sequences per unit volume. Estimates of total 16S gene copies can then be compared between samples of interest and contamination controls to check whether the experimental samples indeed contain sequence counts above background.

These issues are particularly pronounced in studies of the fungal microbiome. Here the absolute amounts of fungal DNA in samples are commonly low, and environmental organisms are abundant. Achieving credibility for any study of the fungal microbiome requires reporting extensive contamination controls and a careful discussion of how these controls were incorporated in the interpretation. One approach to dissecting the contributions of different sources is the Bayesian SourceTracker software (40).

A further challenge comes in comparisons among samples with different starting numbers of 16S copies. Suppose that two sets of samples contain indistinguishable bacterial communities, but one set has a lower biomass. Now add the same number of contaminating environmental 16S DNA copies to each. The contaminating DNA comprises a larger proportion in the samples with fewer starting 16S DNA copies. A sensitive measure comparing communities can then falsely call the two sample sets as different when in reality they differed only in the amount of starting material.

Papers making extreme claims but lacking sufficient control of the above artifacts are common in the literature.

Cage Effects in Studies of Mouse Models

Another underappreciated artifact in microbiome studies using mouse models is the strength of cage effects. Mice are copraphagic, so all the mice in a cage quickly come to share a common set of gut microorganisms. Mice of the same treatment group or genotype in different cages can differ just because of cohousing. The effects can be so strong as to dominate over what would otherwise seem to be extreme treatments.

However, this is a solvable problem. The solution is to design the experiment so as to allow the cage effect to be treated explicitly as a variable in the final statistical analysis of the experiment. For two treatment groups, one can set up multiple cages for each group. It is okay to have relatively few mice per cage, but the number of cages needs to be sizeable. Then in the statistical analysis of sequence data, one can ask whether the microbial communities differ between groups given the measured effect of the cage variable.

Another approach involves longitudinal analysis, such as a drug treatment study, in which each mouse can serve as its own control. Thus the changes can be tabulated and compared between treatment groups. Such an analysis presupposes that differences in the starting communities due to cage effects do not influence the subsequent response to the treatment.

Cage effects are extremely strong for fungal populations. In one recent study (41), fungal populations were monitored longitudinally during an antibiotic intervention. Episodic increases in specific types of fungi were seen in all groups, including the untreated controls, and these waves of colonization differed between cages. Fungal colonization of mice has recently been reported to influence inflammatory bowel disease models (42), which are known to show different results in different mouse facilities, raising the possibility that fungal colonization and cage effects may represent an underappreciated confounding variable.

METAGENOMIC ANALYSIS OF VIRUSES

A number of compelling studies have examined the viruses of the human microbiome (43–51)—however, their analysis requires careful design. For example, it may be of interest to query shotgun sequence samples from total stool DNA to identify the virome present, but this presents major challenges. For one, genomes of all metazoans harbor integrated sequences from endogenous retroviruses and retrotransposons that are clearly related to exogenous retroviruses (12), obstructing clear assessment of this viral group. Additional gene families are known to be common between viruses and bacterial sequences, so that alignment of total shotgun sequence data to databases of viruses often falsely pulls out matches.

If feasible, one approach to studying viruses is to first purify viral particles—if samples are clean enough, one can be confident that each sequence analyzed likely came from a virus. A disadvantage of this approach is that any purification method likely recovers some viruses better than others, and some not at all, so only a portion of the viral population is queried.

This method is well suited for analysis of bacterial viruses. Global populations of bacterial viruses are thought to be gigantic—up to 10^7 particles per ml in rich seawater (43). These viruses are thus necessarily poorly represented in sequence databases, and so simply aligning newly acquired sequence to a database does a poor job in identifying bacterial viruses. In sequence surveys of highly purified natural viral communities, most of the reads look like nothing you have ever seen before, consistent with this picture.

As for bacteria and fungi, the method used is dictated by the question posed. For example, for hunting for new types of viruses in immunocompromised subjects, one can take database hits as candidates for validation by quantitative PCR and other methods. As long as downstream validation is part of the experimental plan, then metagenomic data can be simply treated as hypothesis generating, obviating many of the concerns above.

METAGENOMIC ANALYSIS TO INVESTIGATE DISEASE STATES

Despite the above challenges, the microbiome field has yielded much striking data, some of which bears on problems in clinical immunology. The Human Microbiome Project has completed draft sequences of thousands of bacteria, providing a rich resource for analysis of new sequences by alignment (52). Studies of immunocompromised states such as lung transplant (53, 54) or lentiviral infection (5) have shown characteristic changes in microbial community composition. These are likely to lead directly to improved methods for diagnosis of microbial colonization in immunocompromised patients. As the methods for sequence acquisition become less expensive, focus turns to collection of appropriate samples for analysis and development of analytical tools for interpreting data. Many groups are presently developing tools to allow molecular diagnostics based on deep sequencing data.

Another area of interest centers on understanding patterns in healthy and dysbiotic communities based on microbiome sequence data. One pattern characteristic of immunocompromised states is higher variance in composition. You could say that this parallels the famous Bumpus study of sparrow mortality in 1898 (http://fieldmuseum.org/explore/hermon-bumpus-and-house-sparrows), which may be the first application of multivariate mathematics to a problem in ecology. Bumpus studied sparrows that were knocked down by a violent storm. Some survived and others died. Bumpus took many anatomical measurements of each bird and asked how the birds that died differed from those that survived. Bumpus did find a pattern, but there was no single trait associated with mortality. Instead, the

birds that died tended to diverge more from the average "perfect" bird than did the survivors, but each fatality diverged in its own way. That is, the fatal cases were distinguished by higher variance, not by any single feature. A similar pattern is seen for microbial communities in immunocompromised subjects.

One example is provided by studies of lung transplant recipients. In bronchoalveolar lavage samples, the variance was higher for samples from lung transplant recipients than from healthy subjects. The lung transplant subjects also showed lower richness, which is the total number of species detected in the sample (53). All of this is consistent with outgrowth of specific organisms in each immunocompromised subject, but different organisms in each case. The drop in richness can be understood as a single microbial lineage proliferating and "shouldering out" other community members. Consistent with this picture, the total amount of 16S DNA was higher in lung transplant recipients than in healthy controls by PCR, and individual recipients showed outgrowths of *Pseudomonas*, *Staphylococcus*, *Achromobacter*, and other known species of concern. In one case, an organism not previously considered a lung resident, *Snethia*, was found to be predominant. This organism would not normally be tracked in transplant recipients, presenting an example of how the new sequencing methods can provide information that is unavailable with other commonly used diagnostic methods. Similar patterns of high variance are seen in metagenomic analysis of stool samples from pediatric subjects with primary immunodeficiencies (unpublished data).

The human microbiome has been implicated in multiple further aspects of human health and disease. Studies from Gordon and coworkers have emphasized that obesity can be associated with distinctive patterns of gut microbial colonization (5, 55–60). Strikingly, the obese phenotype in humans can be transferred to gnotobiotic (germ-free) mice by inoculation from obese but not lean individuals, suggesting that the gut microbiome plays a causal role in the obese phenotype. Going the other way, a recent study suggested that long-term diet dictates the composition of the gut microbiome (7), providing a potential mechanism connecting diet and the many health outcomes linked to dietary choices.

Another striking series of studies have recently linked metabolic products of the gut microbiome to heart disease (8, 9, 61). Hazen and coworkers began by analyzing metabolites associated with adverse cardiac outcome in a large cohort of subjects. Comparison of discovery and validation cohorts revealed phosphatidylcholine, choline, and trimethylamine oxide as metabolites linked to adverse outcome. Further studies added carnitine and trimethylamine to the pathway. Very extensive follow-up studies outlined a pathway involving the gut microbiome as a key step. Foods such as eggs and meat are rich sources of phosphatidylcholine and carnitine. The compounds are broken down to yield trimethylamine in a step dependent on the gut microbiome. Trimethylamine is then metabolized by liver oxidases to yield trimethylamine oxide, which is directly proatherogenic. The microbial genes for production of trimethylamine have recently been identified by Craciun and Balskus (62), opening up the possibility of modulating this pathway to minimize heart disease.

In summary, the new technology and new insights of microbiome research are tremendously potent, but with increased sensitivity comes new types of artifacts that are not to be underestimated. Nevertheless, microbiome analysis is becoming an important contributor to diagnostics and research in clinical immunology and many other fields.

REFERENCES

1. **Garrett WS, Gordon JI, Glimcher LH.** 2010. Homeostasis and inflammation in the intestine. *Cell* **140:**859–870.
2. **Song SJ, Lauber C, Costello EK, Lozupone CA, Humphrey G, Berg-Lyons D, Caporaso JG, Knights D, Clemente JC, Nakielny S, Gordon JI, Fierer N, Knight R.** 2013. Cohabiting family members share microbiota with one another and with their dogs. *eLife* **2:**e00458. doi:10.7554/eLife.00458.
3. **Faith JJ, Guruge JL, Charbonneau M, Subramanian S, Seedorf H, Goodman AL, Clemente JC, Knight R, Heath AC, Leibel RL, Rosenbaum M, Gordon JI.** 2013. The long-term stability of the human gut microbiota. *Science* **341:**1237439. doi:10.1126/science.1237439.
4. **Human Microbiome Project Consortium.** 2012. A framework for human microbiome research. *Nature* **486:**215–221.
5. **Ridaura VK, Faith JJ, Rey FE, Cheng J, Duncan AE, Kau AL, Griffin NW, Lombard V, Henrissat B, Bain JR, Muehlbauer MJ, Ilkayeva O, Semenkovich CF, Funai K, Hayashi DK, Lyle BJ, Martini MC, Ursell LK, Clemente JC, Van Treuren W, Walters WA, Knight R, Newgard CB, Heath AC, Gordon JI.** 2013. Gut microbiota from twins discordant for obesity modulate metabolism in mice. *Science* **341:**1241214. doi:10.1126/science.1241214.
6. **Arumugam M, Raes J, Pelletier E, Le Paslier D, Yamada T, Mende DR, Fernandes GR, Tap J, Bruls T, Batto JM, Bertalan M, Borruel N, Casellas F, Fernandez L, Gautier L, Hansen T, Hattori M, Hayashi T, Kleerebezem M, Kurokawa K, Leclerc M, Levenez F, Manichanh C, Nielsen HB, Nielsen T, Pons N, Poulain J, Qin J, Sicheritz-Ponten T, Tims S, Torrents D, Ugarte E, Zoetendal EG, Wang J, Guarner F, Pedersen O, de Vos WM, Brunak S, Doré J; MetaHIT Consortium, Antolín M, Artiguenave F, Blottiere HM, Almeida M, Brechot C, Cara C, Chervaux C, Cultrone A, Delorme C, Denariaz G, Dervyn R, Foerstner KU, Friss C, van de Guchte M, Guedon E, Haimet F, Huber W, van Hylckama-Vlieg J, Jamet A, Juste C, Kaci G, Knol J, Lakhdari O, Layec S, Le Roux K, Maguin E, Mérieux A, Melo Minardi R, M'rini C, Muller J, Oozeer R, Parkhill J, Renault P, Rescigno M, Sanchez N, Sunagawa S, Torrejon A, Turner K, Vandemeulebrouck G, Varela E, Winogradsky Y, Zeller G, Weissenbach J, Ehrlich SD, Bork P.** 2011. Enterotypes of the human gut microbiome. *Nature* **473:**174–180.
7. **Wu GD, Chen J, Hoffmann C, Bittinger K, Chen YY, Keilbaugh SA, Bewtra M, Knights D, Walters WA, Knight R, Sinha R, Gilroy E, Gupta K, Baldassano R, Nessel L, Li H, Bushman FD, Lewis JD.** 2011. Linking long-term dietary patterns with gut microbial enterotypes. *Science* **334:**105–108.
8. **Wang Z, Klipfell E, Bennett BJ, Koeth R, Levison BS, Dugar B, Feldstein AE, Britt EB, Fu X, Chung YM, Wu Y, Schauer P, Smith JD, Allayee H, Tang WH, DiDonato JA, Lusis AJ, Hazen SL.** 2011. Gut flora metabolism of phosphatidylcholine promotes cardiovascular disease. *Nature* **472:**57–63.
9. **Koeth RA, Wang Z, Levison BS, Buffa JA, Org E, Sheehy BT, Britt EB, Fu X, Wu Y, Li L, Smith JD, DiDonato JA, Chen J, Li H, Wu GD, Lewis JD, Warrier M, Brown JM, Krauss RM, Tang WH, Bushman FD, Lusis AJ, Hazen SL.** 2013. Intestinal microbiota metabolism of L-carnitine, a nutrient in red meat, promotes atherosclerosis. *Nat Med* **19:**576–585.
10. **Hu B, Elinav E, Huber S, Strowig T, Hao L, Hafemann A, Jin C, Wunderlich C, Wunderlich T, Eisenbarth SC, Flavell RA.** 2013. Microbiota-induced activation of epithelial IL-6 signaling links inflammasome-driven inflammation with transmissible cancer. *Proc Natl Acad Sci U S A* **110:**9862–9867.

11. **Qin J, Li Y, Cai Z, Li S, Zhu J, Zhang F, Liang S, Zhang W, Guan Y, Shen D, Peng Y, Zhang D, Jie Z, Wu W, Qin Y, Xue W, Li J, Han L, Lu D, Wu P, Dai Y, Sun X, Li Z, Tang A, Zhong S, Li X, Chen W, Xu R, Wang M, Feng Q, Gong M, Yu J, Zhang Y, Zhang M, Hansen T, Sanchez G, Raes J, Falony G, Okuda S, Almeida M, LeChatelier E, Renault P, Pons N, Batto JM, Zhang Z, Chen H, Yang R, Zheng W, Li S, Yang H, Wang J, Ehrlich SD, Nielsen R, Pedersen O, Kristiansen K, Wang J.** 2012. A metagenome-wide association study of gut microbiota in type 2 diabetes. *Nature* **490:**55–60.
12. **Bushman FD.** 2001. *Lateral DNA Transfer: Mechanisms and Consequences*. Cold Spring Harbor Laboratory Press, Cold Spring Harbor, NY.
13. **Wu GD, Lewis JD, Hoffmann C, Chen YY, Knight R, Bittinger K, Hwang J, Chen J, Berkowsky R, Nessel L, Li H, Bushman FD.** 2010. Sampling and pyrosequencing methods for characterizing bacterial communities in the human gut using 16S sequence tags. *BMC Microbiol* **10:**206. doi:10.1186/1471-2180-10-206.
14. **Margulies M, Egholm M, Altman WE, Attiya S, Bader JS, Bemben LA, Berka J, Braverman MS, Chen YJ, Chen Z, Dewell SB, Du L, Fierro JM, Gomes XV, Godwin BC, He W, Helgesen S, Ho CH, Irzyk GP, Jando SC, Alenquer ML, Jarvie TP, Jirage KB, Kim JB, Knight JR, Lanza JR, Leamon JH, Lefkowitz SM, Lei M, Li J, Lohman KL, Lu H, Makhijani VB, McDade KE, McKenna MP, Myers EW, Nickerson E, Nobile JR, Plant R, Puc BP, Ronan MT, Roth GT, Sarkis GJ, Simons JF, Simpson JW, Srinivasan M, Tartaro KR, Tomasz A, Vogt KA, Volkmer GA, Wang SH, Wang Y, Weiner MP, Yu P, Begley RF, Rothberg JM.** 2005. Genome sequencing in microfabricated high-density picolitre reactors. *Nature* **437:**376–380.
15. **Caporaso JG, Lauber CL, Walters WA, Berg-Lyons D, Huntley J, Fierer N, Owens SM, Betley J, Fraser L, Bauer M, Gormley N, Gilbert JA, Smith G, Knight R.** 2012. Ultra-high-throughput microbial community analysis on the Illumina HiSeq and MiSeq platforms. *ISME J* **6:**1621–1624.
16. **Eid J, Fehr A, Gray J, Luong K, Lyle J, Otto G, Peluso P, Rank D, Baybayan P, Bettman B, Bibillo A, Bjornson K, Chaudhuri B, Christians F, Cicero R, Clark S, Dalal R, Dewinter A, Dixon J, Foquet M, Gaertner A, Hardenbol P, Heiner C, Hester K, Holden D, Kearns G, Kong X, Kuse R, Lacroix Y, Lin S, Lundquist P, Ma C, Marks P, Maxham M, Murphy D, Park I, Pham T, Phillips M, Roy J, Sebra R, Shen G, Sorenson J, Tomaney A, Travers K, Trulson M, Vieceli J, Wegener J, Wu D, Yang A, Zaccarin D, Zhao P, Zhong F, Korlach J, Turner S.** 2009. Real-time DNA sequencing from single polymerase molecules. *Science* **323:**133–138.
17. **Hoffmann C, Minkah N, Leipzig J, Wang G, Arens MQ, Tebas P, Bushman FD.** 2007. DNA bar coding and pyrosequencing to identify rare HIV drug resistance mutations. *Nucleic Acids Res* **35:**e91. doi:10.1093/nar/gkm435.
18. **Binladen J, Gilbert MT, Bollback JP, Panitz F, Bendixen C, Nielsen R, Willerslev E.** 2007. The use of coded PCR primers enables high-throughput sequencing of multiple homolog amplification products by 454 parallel sequencing. *PLoS One* **2:**e197. doi:10.1371/journal.pone.0000197.
19. **Pace NR, Olsen GJ, Woese CR.** 1986. Ribosomal RNA phylogeny and the primary lines of evolutionary descent. *Cell* **45:**325–326.
20. **Sogin ML, Morrison HG, Huber JA, Mark Welch D, Huse SM, Neal PR, Arrieta JM, Herndl GJ.** 2006. Microbial diversity in the deep sea and the underexplored "rare biosphere." *Proc Natl Acad Sci U S A* **103:**12115–12120.
21. **Relman DA, Schmidt TM, Gajadhar A, Sogin M, Cross J, Yoder K, Sethabutr O, Echeverria P.** 1996. Molecular phylogenetic analysis of *Cyclospora*, the human intestinal pathogen, suggests that it is closely related to *Eimeria* species. *J Infect Dis* **173:**440–445.
22. **McKenna P, Hoffmann C, Minkah N, Aye PP, Lackner A, Liu Z, Lozupone CA, Hamady M, Knight R, Bushman FD.** 2008. The macaque gut microbiome in health, lentiviral infection, and chronic enterocolitis. *PLoS Pathog* **4:**e20. doi:10.1371/journal.ppat.0040020.
23. **Caporaso JG, Kuczynski J, Stombaugh J, Bittinger K, Bushman FD, Costello EK, Fierer N, Peña AG, Goodrich JK, Gordon JI, Huttley GA, Kelley ST, Knights D, Koenig JE, Ley RE, Lozupone CA, McDonald D, Muegge BD, Pirrung M, Reeder J, Sevinsky JR, Turnbaugh PJ, Walters WA, Widmann J, Yatsunenko T, Zaneveld J, Knight R.** 2010. QIIME allows analysis of high-throughput community sequencing data. *Nat Methods* **7:**335–336.
24. **Schloss PD, Westcott SL, Ryabin T, Hall JR, Hartmann M, Hollister EB, Lesniewski RA, Oakley BB, Parks DH, Robinson CJ, Sahl JW, Stres B, Thallinger GG, Van Horn DJ, Weber CF.** 2009. Introducing mothur: open-source, platform-independent, community-supported software for describing and comparing microbial communities. *Appl Environ Microbiol* **75:**7537–7541.
25. **Dollive S, Peterfreund GL, Sherrill-Mix S, Bittinger K, Sinha R, Hoffmann C, Nabel CS, Hill DA, Artis D, Bachman MA, Custers-Allen R, Grunberg S, Wu GD, Lewis JD, Bushman FD.** 2012. A tool kit for quantifying eukaryotic rRNA gene sequences from human microbiome samples. *Genome Biol* **13:**R60. doi:10.1186/gb-2012-13-7-r60.
26. **Schoch CL, Seifert KA, Huhndorf S, Robert V, Spouge JL, Levesque CA, Chen W, Fungal Barcoding Consortium, Fungal Barcoding Consortium Author List.** 2012. Nuclear ribosomal internal transcribed spacer (ITS) region as a universal DNA barcode marker for *Fungi*. *Proc Natl Acad Sci U S A* **109:**6241–6246.
27. **Lozupone C, Knight R.** 2005. UniFrac: a new phylogenetic method for comparing microbial communities. *Appl Environ Microbiol* **71:**8228–8235.
28. **Lozupone C, Hamady M, Knight R.** 2006. UniFrac—an online tool for comparing microbial community diversity in a phylogenetic context. *BMC Bioinformatics* **7:**371. doi:10.1186/1471-2105-7-371.
29. **Hamady M, Lozupone C, Knight R.** 2010. Fast UniFrac: facilitating high-throughput phylogenetic analyses of microbial communities including analysis of pyrosequencing and PhyloChip data. *ISME J* **4:**17–27.
30. **Rasko DA, Rosovitz MJ, Myers GS, Mongodin EF, Fricke WF, Gajer P, Crabtree J, Sebaihia M, Thomson NR, Chaudhuri R, Henderson IR, Sperandio V, Ravel J.** 2008. The pangenome structure of *Escherichia coli*: comparative genomic analysis of *E. coli* commensal and pathogenic isolates. *J Bacteriol* **190:**6881–6893.
31. **Liu B, Gibbons T, Ghodsi M, Treangen T, Pop M.** 2011. Accurate and fast estimation of taxonomic profiles from metagenomic shotgun sequences. *BMC Genomics* **12**(Suppl 2)**:**S4. doi:10.1186/1471-2164-12-S2-S4.
32. **Huson DH, Auch AF, Qi J, Schuster SC.** 2007. MEGAN analysis of metagenomic data. *Genome Res* **17:**377–386.
33. **Segata N, Waldron L, Ballarini A, Narasimhan V, Jousson O, Huttenhower C.** 2012. Metagenomic microbial community profiling using unique clade-specific marker genes. *Nat Methods* **9:**811–814.
34. **Natale DA, Galperin MY, Tatusov RL, Koonin EV.** 2000. Using the COG database to improve gene recognition in complete genomes. *Genetica* **108:**9–17.
35. **Kanehisa M, Goto S, Kawashima S, Okuno Y, Hattori M.** 2004. The KEGG resource for deciphering the genome. *Nucleic Acids Res* **32**(Database issue)**:**D277–D280.

36. **Navas-Molina JA, Peralta-Sánchez JM, González A, McMurdie PJ, Vázquez-Baeza Y, Xu Z, Ursell LK, Lauber C, Zhou H, Song SJ, Huntley J, Ackermann GL, Berg-Lyons D, Holmes S, Caporaso JG, Knight R.** 2013. Advancing our understanding of the human microbiome using QIIME. *Methods Enzymol* **531:**371–444.
37. **Charlson ES, Bittinger K, Haas AR, Fitzgerald AS, Frank I, Yadav A, Bushman FD, Collman RG.** 2011. Topographical continuity of bacterial populations in the healthy human respiratory tract. *Am J Respir Crit Care Med* **184:**957–963.
38. **Liu Z, Lozupone C, Hamady M, Bushman FD, Knight R.** 2007. Short pyrosequencing reads suffice for accurate microbial community analysis. *Nucleic Acids Res* **35:**e120. doi:10.1093/nar/gkm541.
39. **Schloss PD, Westcott SL.** 2011. Assessing and improving methods used in operational taxonomic unit-based approaches for 16S rRNA gene sequence analysis. *Appl Environ Microbiol* **77:**3219–3226.
40. **Knights D, Kuczynski J, Charlson ES, Zaneveld J, Mozer MC, Collman RG, Bushman FD, Knight R, Kelley ST.** 2011. Bayesian community-wide culture-independent microbial source tracking. *Nat Methods* **8:**761–763.
41. **Dollive S, Chen YY, Grunberg S, Bittinger K, Hoffmann C, Vandivier L, Cuff C, Lewis JD, Wu GD, Bushman FD.** 2013. Fungi of the murine gut: episodic variation and proliferation during antibiotic treatment. *PLoS One* **8:**e71806. doi:10.1371/journal.pone.0071806.
42. **Iliev ID, Funari VA, Taylor KD, Nguyen Q, Reyes CN, Strom SP, Brown J, Becker CA, Fleshner PR, Dubinsky M, Rotter JI, Wang HL, McGovern DP, Brown GD, Underhill DM.** 2012. Interactions between commensal fungi and the C-type lectin receptor Dectin-1 influence colitis. *Science* **336:**1314–1317.
43. **Rohwer F.** 2003. Global phage diversity. *Cell* **113:**141.
44. **Edwards RA, Rohwer F.** 2005. Viral metagenomics. *Nat Rev Microbiol* **3:**504–510.
45. **Zhang T, Breitbart M, Lee WH, Run JQ, Wei CL, Soh SW, Hibberd ML, Liu ET, Rohwer F, Ruan Y.** 2006. RNA viral community in human feces: prevalence of plant pathogenic viruses. *PLoS Biol* **4:**e3. doi:10.1371/journal.pbio.0040003.
46. **Reyes A, Haynes M, Hanson N, Angly FE, Heath AC, Rohwer F, Gordon JI.** 2010. Viruses in the faecal microbiota of monozygotic twins and their mothers. *Nature* **466:**334–338.
47. **Minot S, Sinha R, Chen J, Li H, Keilbaugh SA, Wu GD, Lewis JD, Bushman FD.** 2011. The human gut virome: inter-individual variation and dynamic response to diet. *Genome Res* **21:**1616–1625.
48. **Minot S, Bryson A, Chehoud C, Wu GD, Lewis JD, Bushman FD.** 2013. Rapid evolution of the human gut virome. *Proc Natl Acad Sci U S A* **110:**12450–12455.
49. **Minot S, Wu GD, Lewis JD, Bushman FD.** 2012. Conservation of gene cassettes among diverse viruses of the human gut. *PLoS One* **7:**e42342. doi:10.1371/journal.pone.0042342.
50. **Minot S, Grunberg S, Wu GD, Lewis JD, Bushman FD.** 2012. Hypervariable loci in the human gut virome. *Proc Natl Acad Sci U S A* **109:**3962–3966.
51. **Wylie KM, Mihindukulasuriya KA, Sodergren E, Weinstock GM, Storch GA.** 2012. Sequence analysis of the human virome in febrile and afebrile children. *PLoS One* **7:**e27735. doi:10.1371/journal.pone.0027735.
52. **Gevers D, Knight R, Petrosino JF, Huang K, McGuire AL, Birren BW, Nelson KE, White O, Methé BA, Huttenhower C.** 2012. The Human Microbiome Project: a community resource for the healthy human microbiome. *PLoS Biol* **10:**e1001377. doi:10.1371/journal.pbio.1001377.
53. **Charlson ES, Diamond JM, Bittinger K, Fitzgerald AS, Yadav A, Haas AR, Bushman FD, Collman RG.** 2012. Lung-enriched organisms and aberrant bacterial and fungal respiratory microbiota after lung transplant. *Am J Respir Crit Care Med* **186:**536–545.
54. **Charlson ES, Bittinger K, Chen J, Diamond JM, Li H, Collman RG, Bushman FD.** 2012. Assessing bacterial populations in the lung by replicate analysis of samples from the upper and lower respiratory tracts. *PLoS One* **7:**e42786. doi:10.1371/journal.pone.0042786.
55. **Ley RE, Bäckhed F, Turnbaugh P, Lozupone CA, Knight RD, Gordon JI.** 2005. Obesity alters gut microbial ecology. *Proc Natl Acad Sci U S A* **102:**11070–11075.
56. **Ley RE, Turnbaugh PJ, Klein S, Gordon JI.** 2006. Microbial ecology: human gut microbes associated with obesity. *Nature* **444:**1022–1023.
57. **Turnbaugh PJ, Ley RE, Mahowald MA, Magrini V, Mardis ER, Gordon JI.** 2006. An obesity-associated gut microbiome with increased capacity for energy harvest. *Nature* **444:**1027–1031.
58. **Turnbaugh PJ, Bäckhed F, Fulton L, Gordon JI.** 2008. Diet-induced obesity is linked to marked but reversible alterations in the mouse distal gut microbiome. *Cell Host Microbe* **3:**213–223.
59. **Turnbaugh PJ, Gordon JI.** 2009. The core gut microbiome, energy balance and obesity. *J Physiol* **587:**4153–4158.
60. **Henao-Mejia J, Elinav E, Jin C, Hao L, Mehal WZ, Strowig T, Thaiss CA, Kau AL, Eisenbarth SC, Jurczak MJ, Camporez JP, Shulman GI, Gordon JI, Hoffman HM, Flavell RA.** 2012. Inflammasome-mediated dysbiosis regulates progression of NAFLD and obesity. *Nature* **482:**179–185.
61. **Tang WH, Wang Z, Levison BS, Koeth RA, Britt EB, Fu X, Wu Y, Hazen SL.** 2013. Intestinal microbial metabolism of phosphatidylcholine and cardiovascular risk. *New Engl J Med* **368:**1575–1584.
62. **Craciun S, Balskus EP.** 2012. Microbial conversion of choline to trimethylamine requires a glycyl radical enzyme. *Proc Natl Acad Sci U S A* **109:**21307–21312.

Protein Analysis in the Clinical Immunology Laboratory

ROSHINI SARAH ABRAHAM AND DAVID R. BARNIDGE

4

THE ROLE OF PROTEIN ANALYSIS IN DIAGNOSTIC IMMUNOLOGY

The diagnostic immunology laboratory relies heavily on protein measurements, especially with the explosion of clinically relevant biomarker analysis. Of particular import are the tremendous advances that have been made in the technology for protein detection, and while not all of it has gained traction in the clinical immunology laboratory, this remains an area of huge growth. However, regulatory processes have not kept up with the burgeoning research in the area of protein analysis, and new diagnostic tests for protein analytes are approved for clinical testing at a glacial pace. Nonetheless, it is critical for the clinical immunologist to understand these advances and determine how they can best be utilized in the clinical laboratory. Besides keeping pace with the rapidly changing technology, the age-old fundamental principles of analytical validation of new tests, protein based or not, are still applicable. This chapter covers the basic principles of protein testing in the clinical laboratory and provides special emphasis on the role of mass spectrometry (MS) in diagnostic protein analysis.

PREANALYTICAL ISSUES IN PROTEIN ANALYSIS

Preanalytical parameters determine the validity of any diagnostic test result; therefore, the importance of considering preanalytical issues in clinical test development and validation cannot be overemphasized. The components of the preanalytical phase include both generic elements and those specific for protein analysis. Generic preanalytical measures include relevant test selection with appropriate analytical sensitivity and specificity to detect the biomarker (protein) of choice and the probability it will aid in diagnosing the disease or clinical condition (clinical sensitivity/specificity). Other factors to consider include preparation of patient and sample collection and handling (1). Each of these has to be individually assessed and validated so that the analysis is performed under predetermined conditions that will contribute to a reliable test result and interpretation.

Sources of Protein for Diagnostic Analysis

Diagnostically relevant proteins can be studied from a variety of sources, and sample collection depends on the protein of interest, which defines the optimal method for analysis. Most proteins measured in the immunology laboratory are soluble and present in serum or plasma, urine, or body fluids including ascites, cerebrospinal fluid (CSF), and peritoneal and bronchial fluid. However, other important sources of nonsoluble proteins include cells present either in fluid matrices (blood, urine, CSF, or other body fluids) or tissue matrices, obtained primarily from biopsy samples (2). Further, proteins can be studied *in vivo*, either for diagnostic or therapeutic purposes, either in the context of cells or soluble protein, using magnetic resonance and other imaging modalities that assess labeled proteins (3, 4). A notable example of *in vivo* protein analysis for determining diagnosis and monitoring response to treatment is the use of ^{123}I-labeled serum amyloid P component in systemic amyloidosis (5). Also, the use of labeled bisphosphonate bone tracers has been shown to be specific and sensitive in identifying transthyretin amyloid protein deposits in the heart (6).

Sample Collection and Its Impact on Protein Analysis

Many factors influence the measurement of proteins. These can be subdivided into four major categories: (i) physiological processes, (ii) collection processes, (iii) sample processing, and (iv) therapeutic intervention (2).

TYPES OF PROTEIN ANALYSIS

Diagnostic evaluation of proteins is dependent not only on the source and collection factors but also on how the result is used for interpretation or correlation with clinical and other findings. Therefore, protein analyses can be categorized into qualitative, semiquantitative, and quantitative measurements. Qualitative analyses are used largely in contexts in which the presence or absence of the protein of interest is sufficient for diagnostic utility, and there are typically large differences between positive and negative responses. Most qualitative protein tests use visual assessment to determine if the protein biomarker is present or absent. Other qualitative measurements include contexts of structural alteration of proteins necessitating some form of physical separation using chromatography, electrophoresis, or MS. The most common examples of this approach include monoclonal protein analysis by serum or urine standard electrophoresis

doi:10.1128/9781555818722.ch4

followed by immunofixation electrophoresis or assessment of α_1-antitrypsin variants by isoelectric focusing, which overcomes the imprecision of electrophoresis by determining protein migration based on its charge (isoelectric point) in a pH gradient (7).

Protein analyses can also be semiquantitative, whereby the absolute amount of the analyte in the sample is not provided but the relative proportion of the analyte of interest to other proteins in the mixture can be obtained. A common example of semiquantitative protein measurement is in the use of point-of-care dipsticks that measure urine protein. Newer dipsticks are available that can report albumin-to-creatinine or total protein-to-creatinine ratios, and though the analytical sensitivity is reasonable, there is significant variability in the specificity of these dipstick reagents. Therefore, the most definitive test for detecting proteinuria is the quantitative measurement of urine protein. Similarly, most diagnostic measurements of clinically relevant proteins require quantitative evaluation and comparison with age- and gender-matched reference values derived from healthy controls. Further, confounding factors in interpretation of many diagnostically relevant proteins include diurnal, seasonal, and exercise-related variability, and these elements have to be incorporated into clinical interpretation of results, besides being relevant in formulating reference values.

METHODS OF PROTEIN ANALYSIS

The above-discussed types of protein measurements can utilize a variety of methodologies, depending on whether it is relevant to quantify the amount of protein or the functional activity of the protein. Similarly, qualitative assays can use different methods for determining the presence or absence of protein or normal versus abnormal function without quantifying the magnitude of functional activity.

Methods for detecting protein function range from binding assays to enzyme activity assays measured by flow cytometry, immunoassays, or MS. Examples include NADPH oxidase activity as assessed by dihydrorhodamine flow cytometry (8–10) and C1 esterase inhibitor function as determined by an enzyme immunoassay using a labeled, activated target protein. This target protein facilitates complex formation between the "test" protein (enzyme inhibitor) and the target protein (enzyme substrate). Examples of these different methods are discussed below.

Immunoassays

There are many immunoassay formats used in the clinical immunology laboratory for the measurement of proteins or peptides. Most immunoassays offer quantitative analysis of proteins, although the degree of accuracy of quantitation may vary depending on the specific method. Immunoassays can be divided into those that use heterogeneous or homogeneous formats, with the former having either antibody or antigen immobilized on a solid substrate and a separate step and the latter having antigen-antibody complex formation taking place in the solution phase with no separation of bound and free ligand. Immunoassays were described extensively in the previous edition of this book (2); therefore, only a synopsis of key methodologies is provided herein.

RID

Radial immunodiffusion (RID) is a relatively old method that has been replaced in most laboratories. It is based on the classic precipitin reaction, in which antigen and antibodies react to form precipitates in liquid or semifluid gel media (11). Under conditions of antibody excess, the quantity of the precipitate is directly related to the quantity of antigen in the test sample. The major limitations include the duration of time required; the relative imprecision of the assay, with coefficients of variation often >10%; the relative insensitivity; and dependence on antigen quantity and structure.

Nephelometry

RID has been supplanted by nephelometry in most laboratories as the method of choice for measuring most proteins in body fluids, including immunoglobulins and intact or free light and heavy chains (12–14). Nephelometry is a method that relies on light scattering by soluble immune complexes in solution. The amount of light scatter produced by soluble immune complexes is directly proportional to the concentration of antigen. In contrast to the standard precipitin reaction, which requires that the concentrations of antigen and antibody be at equivalence, nephelometry often performs best with excess antibody. The two main types of nephelometric reactions include endpoint (fixed time) and rate (kinetic) nephelometry, which measure light scatter after equilibration of the antigen-antibody reaction and the peak rate of immune complex generation, respectively (12–14). The primary disadvantages of nephelometry include increased costs for instruments and reagents, although these can be offset by replacing manual methods with automation; variability in reagent antisera, especially to structurally altered proteins; and interfering substances that can alter light-scattering properties.

Electrophoresis

The migration of proteins on agarose electrophoresis is used most commonly for identification of monoclonal proteins in patients with monoclonal gammopathies (13, 15). In the serum protein electrophoresis depicted in Fig. 1, the stained protein bands representing albumin and α_1-, α_2-, and β-globulins can be easily visualized. While the most abundant protein bands, such as albumin, are clearly visualized with definition, immunoglobulins migrating in the γ region are often broad and diffuse. This lack of resolution in the γ region is due to the presence of many electrophoretically heterogeneous immunoglobulins that migrate in the same region. Serum protein electrophoresis can be used to qualitatively or semiquantitatively identify, by visual and densitometric analysis, the presence of monoclonal immunoglobulins, hypogammaglobulinemia, nephrotic syndrome, and polyclonal hypergammaglobulinemia. Serum electrophoresis is not a particularly sensitive method for the detection of hypogammaglobulinemia, and there should be additional confirmation with quantitation of immunoglobulins by nephelometry. Monoclonal proteins should be further assessed by immunofixation electrophoresis. Densitometric analysis of stained proteins after total serum electrophoresis is an acceptable method for following the response to therapy of diseases characterized by monoclonal proteins after an initial diagnosis.

Most proteins display a net charge in an electrical field, which allows for their electrophoretic separation. The size and shape of a protein molecule, the ionic strength of the buffer, the frictional resistance of the supporting medium, the applied current, the temperature of the reaction, and the duration of the applied current all influence the migration of proteins in a typical electrophoresis reaction (13, 16). As many as 12 discrete regions may be visualized with higher-resolution protein electrophoresis using agarose and controlled voltage and temperatures (Fig. 1).

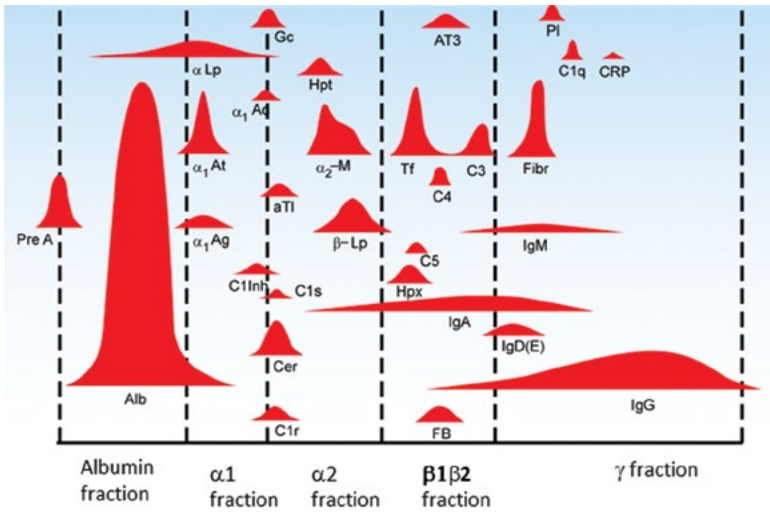

FIGURE 1 Agarose gel electrophoresis separation of plasma proteins based on their electrophoretic mobility. α1Ac, α1-antichymotrypsin; α1Ag, α1-acid glycoprotein; Alb, albumin, α1At, α1-antitrypsin; AT3, antithrombin III; C1Inh, C1 esterase inhibitor; Cer, ceruloplasmin; CRP, C-reactive protein; FB, factor B; Fibr, fibrinogen; Gc, Gc-globulin (vitamin D-binding protein); Hpt, haptoglobin; Hpx, hemopexin; α-Lp, α-lipoprotein; β-Lp, β-lipoprotein; α2-M, α1-macroglobulin; Pl, plasminogen; Pre A, prealbumin; Tf, transferrin. Reproduced from reference 11 with permission from Elsevier Ltd.

Besides serum analysis, other body fluids are evaluated in the clinical laboratory by electrophoresis. Urine samples are routinely tested in patients with serum monoclonal proteins to identify the monoclonal protein components, particularly light chains, and CSF can be tested for oligoclonal immunoglobulins that may be present in neurological disorders such as multiple sclerosis.

IFE

Immunofixation electrophoresis (IFE) is the most common method used for establishing the presence and isotype of a monoclonal immunoglobulin protein in serum and urine (13, 17). The use of a marker dye facilitates visual analysis of the monoclonal protein, and the location of the immunoprecipitate depends on the electrophoretic mobility of the specific monoclonal protein. Most clinical laboratories use IFE after screening samples by serum electrophoresis and/or quantitative immunoglobulin measurements. Although serum is the most common sample type, urine or CSF may also be examined to detect and/or characterize monoclonal proteins or their fragments. IFE has several advantages, including a shorter time to obtain results, increased sensitivity, better resolution, and greater ease of interpretation. However, the IFE method is not without its disadvantages, which include the enhanced quality, increased quantity, and greater cost of the antisera required. Optimal resolution necessitates that the exact amount of antisera be determined for each sample to avoid either excess dilution or excess antibody. In addition, because of the increased sensitivity of IFE, smaller bands are more frequently identified, which can confound the clinical interpretation.

ELISA

The enzyme-linked immunosorbent assay (ELISA) is probably the most widely used immunoassay (13, 18), and it is available in either competitive or noncompetitive formats. In the competitive format, unlabeled antigens compete with labeled antigens for limited antibody-binding sites. If the amount of unlabeled antigen increases, the amount of labeled antigen bound to antibody decreases, resulting in a decrease in detection signal if antibody-bound antigen is the readout or, conversely, increase in detection signal if labeled free antigen is the readout. In the noncompetitive format, antigens bind to an excess of labeled antibody, forming a complex, which increases with increase in antigen in the sample. ELISA is a highly sensitive method capable of measuring proteins in nanogram or picogram amounts, without the use of radioactive tags. While ELISA methods may be used to detect specific antibodies qualitatively or to make semiquantitative measurements of specific antibodies by use of a standard curve calibrated in arbitrary units, there are limitations on the accuracy and precision of semiquantitative tests performed by ELISA. Accurate and true quantitative applications of the basic ELISA method are less common.

More recently, detection of single protein molecules by ELISA has been reported using a novel modification of the standard ELISA technique (19). This method involves the use of a capture antibody immobilized to a matrix of thousands of microspheres. This assay format results in the measurement of individual target molecules, in contrast to the measurement of a collective signal generated in a conventional ELISA, and can be used to quantify low-abundance proteins. However, there are other bead-based, multiplex assays that have greater utility in the clinical laboratory, which are discussed in further detail in this chapter. Other protein detection methods include agglutination and immunofluorescence; these have been used for identification of pathogenic antibodies typically associated with autoimmune diseases.

Multiplex Methods for Protein Detection and Quantitation

The demand for simultaneous, quantitative measurement of several proteins of diagnostic interest has been growing, leading to a focus on multiplex technology (20–23). While

the benefits of multiplex methodology are apparent, analytical concerns include artifacts in quantitation due to matrix effects. Also, cross-reactivity between the capture and detecting reagents, which often are antibodies, can confound quantitation and data interpretation (24).

Among multiplex methods, protein arrays and bead-based technologies are most widely used at present, with rapidly evolving advances in both their chemistries and formats. There are five types of protein arrays most commonly used. These include planar glass or silicon chips; flow cytometric bead arrays; multiplex, microplate immunoassays; and nitrocellulose and three-dimensional microarrays (25); each has its advantages and disadvantages and specific applications. There are also antibody arrays available for protein analysis, which utilize either direct labeling, single-capture, or dual-antibody formats (Fig. 2) (25, 26). Alternatively, antigen or peptide capture arrays can be used with single readout antibodies (Fig. 3). The substrates for both of these microarrays and the signal readout are numerous. They include microplates, gels, slides, suspension arrays with colorimetry, fluorescence, radioactivity, chemiluminescence, enzyme-linked, nanoparticle, light scattering, and other signal-generation and -amplification procedures.

To improve the sensitivity (limit of detection) of these microarrays to detect extremely low concentrations of proteins, a robust signal-enhancement method called rolling circles amplification is used (27). This modification allows the limit of detection of a protein array assay to be increased into the picomolar and subpicomolar ranges, which represents a significant advance in the detection of proteins in biological samples. Studies with standard ELISA methods reveal comparable sensitivity between the two techniques. Alternatively, sensitivity can be enhanced by using bright fluorochromes for antibody detection, as well as optimizing surface chemistry and engineering antibodies to increase valency, or using intermediate detection agents that have multiple binding sites, such as streptavidin, or nanocrystals, such as quantum dots (Qdots) (27, 28). Multiplex methods for autoantibody detection are of particular relevance in the field of autoimmune diseases.

Considerations during selection and validation of a multiplex assay in the laboratory include evaluation of detection reagent and analyte cross-reactivity, stability of reagents, precision across different lots of multiplex kits, multianalyte interactions, the ability to achieve both the dynamic range and relevant sensitivity and specificity, and the impact of diverse matrices and biological states on the accuracy of the final result. The pros and cons of each array approach have to be carefully considered before selecting the appropriate format relevant to the goal of protein quantitation in a specific diagnostic context and the analytes being measured (Table 1). Multiplex cytokine analysis offers a good example of the benefits and disadvantages of multianalyte analysis. The most common biological sample for cytokine analysis is plasma or serum, although conceivably any body fluid matrix could be used. Multiplex cytokine assay formats include planar protein arrays or suspension arrays. Several cytokines can be simultaneously detected and quantified using either

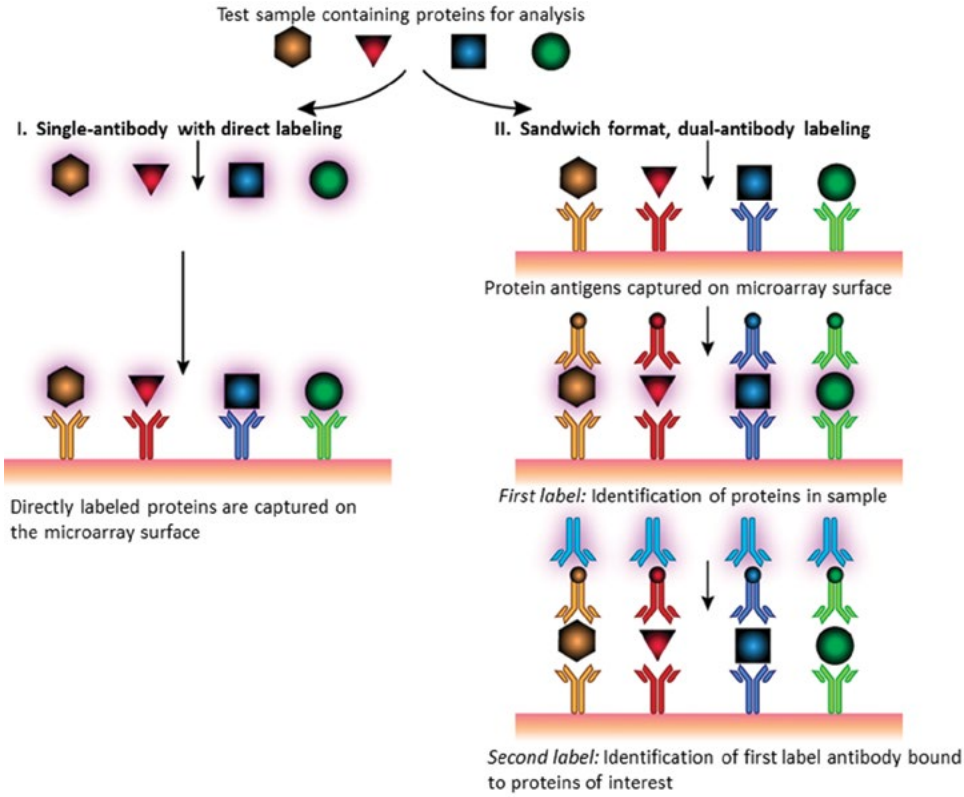

FIGURE 2 Representation of experimental formats for antibody microarrays. (I) Direct labeling of proteins and detection using a single antibody captured on the microarray. (II) Indirect assessment using a two-antibody system. The capture and the first detection antibody are matched, and the detector antibody is measured using a labeled second (readout) antibody.

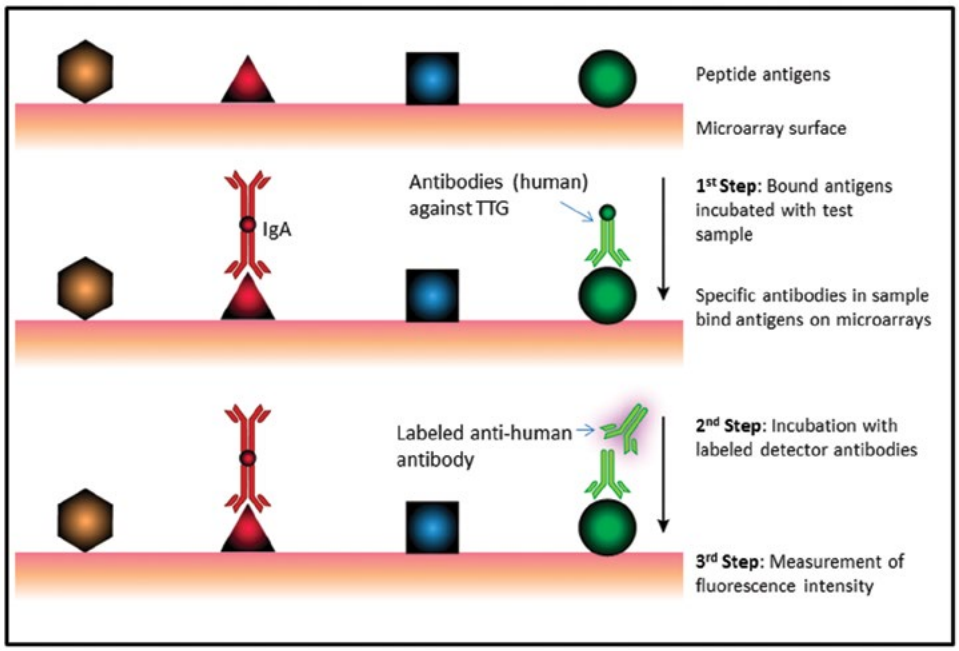

FIGURE 3 Representation of antigen microarray. Antigens are "caught" on the microarray through many different processes, which can be generalized as "printing." Antibodies against specific antigen are detected using a labeled second detector antibody. TTG, tissue transglutaminase.

the flow cytometry approach—Cytometric Bead Array (Becton Dickinson, San Jose, CA)—or the specialized instrument approach—the Luminex xMAP technology.

The accuracy of multiplex cytokine analysis methods has been compared to standard ELISA methods. Although overall correlations are relatively good, there is loss of such correlation for quantitative data (24). A study comparing three commercial multiplex cytokine assays revealed variability between kits from different manufacturers for various analytical parameters, such as accuracy, quantitation in different matrices, recovery, and reproducibility. This indicates that the introduction of a multiplex cytokine assay necessitates careful optimization and validation (29, 30). Besides various multiplex reagent kits, there are instrumentations that offer multiplex technology besides the flow cytometric and Luminex instruments described above. They include the Meso Scale Discovery, which uses a microplate format with electrochemiluminescence detection using labeled tags that emit light on electrochemical stimulation, and the Pierce Endogen SearchLight platform, which utilizes ELISA technology in a similar 96-well format. A study comparing multiplex cytokine analysis using these two platforms (31) revealed that while solid-phase multiplex assays can perform consistently within a platform, optimization and validation experiments should include recombinant cytokine spike recovery, linearity based on dilution analysis, stability

TABLE 1 Advantages and disadvantages of different protein arrays[a]

Types of protein arrays	Positive features	Negative features
Peptide (antigen capture)	Multiplex capability for several hundred analytes Requires a single detection antibody	Primarily useful for autoantibody detection and microbial serological diagnosis Extent of quantitation is variable Sensitivity is variable Specificity is variable
Single capture antibody	Multiplex capability for several hundred analytes Requires a single antibody for antigen capture	Sensitivity is low Specificity is low Analysis is semiquantitative and not absolute
Dual antibodies (capture and readout)	Absolute quantitation Sensitivity is high Specificity is high	Requires separate antibodies for antigen capture and detection Limited number of analytes that can be multiplexed in a single assay format

[a]Adapted from reference 25.

TABLE 2 Factors to consider in selecting multiplex assay platforms

Factor	Relative importance
Antibody cross-reactivity (other detecting reagents)	High
Accuracy of calibration curve	High
Source of antibodies used for capture and detection	High
Sample source (serum, plasma, body fluid)	High
Alternate assay reagents and effect on:	
Spike recovery	High
Accuracy	Low
Analytical measuring range	High
Nonspecific binding due to heterophile antibodies	Variable, depending on clinical context and sample
Consistency of detection of analyte	High

of samples, inter- and intraobserver variability, and consistent measurement of analytes of interest. In the clinical laboratory, the decision to choose an appropriate platform for multiplex cytokine analysis must take into account the various factors that contribute to variability in analyte measurement (Table 2).

The multiplex bead-based assays have a distinct advantage over ELISA in that they use direct fluorescent detection of the analyte, in contrast to an enzyme-mediated colorimetric detection; this provides greater sensitivity. Also, the capture reagents are prepared by covalent coupling of antibodies or antigens to beads, in contrast to passive adherence by adsorption in the ELISA method, which results in greater density of capture molecules and firmer adherence. Therefore, multiplex bead assays have become popular in the diagnostic setting, though they have not completely supplanted ELISA-based methods.

Cytokines are not the only analytes that can be measured by multiplex analysis. The function of anti-vaccine antibodies can be assessed using fluorescent flow cytometric beads conjugated with antigen. An example is the multiplex opsonophagocytic assay (OPA) that is used to detect functional antibody responses to capsular polysaccharides of *Streptococcus pneumoniae* (32) (Fig. 4 and 5). While most antibody detection formats offer multiplex quantitation of IgG antibodies to the 23 serotypes of the pneumococcal polysaccharides, functional antibody assessment using flow cytometry cannot be practically achieved for 23 serotypes due to the limitations related to time and complexity of analysis. Therefore, a clinical OPA can assess at the most six serotypes in a multiplex combination on a three-laser flow cytometer, which necessitates careful selection of serotypes for analysis, primarily based on their immunogenicity and their incorporation in either the protein conjugate or polysaccharide pneumococcal vaccine.

Flow Cytometry and Mass Cytometry for Protein Detection

This section is not meant to be a comprehensive treatise on the subject of flow cytometry but specifically discusses its use in relation to protein detection. Flow cytometry has been used in the clinical laboratory for a variety of applications, including diagnostic immunology for identifying cell

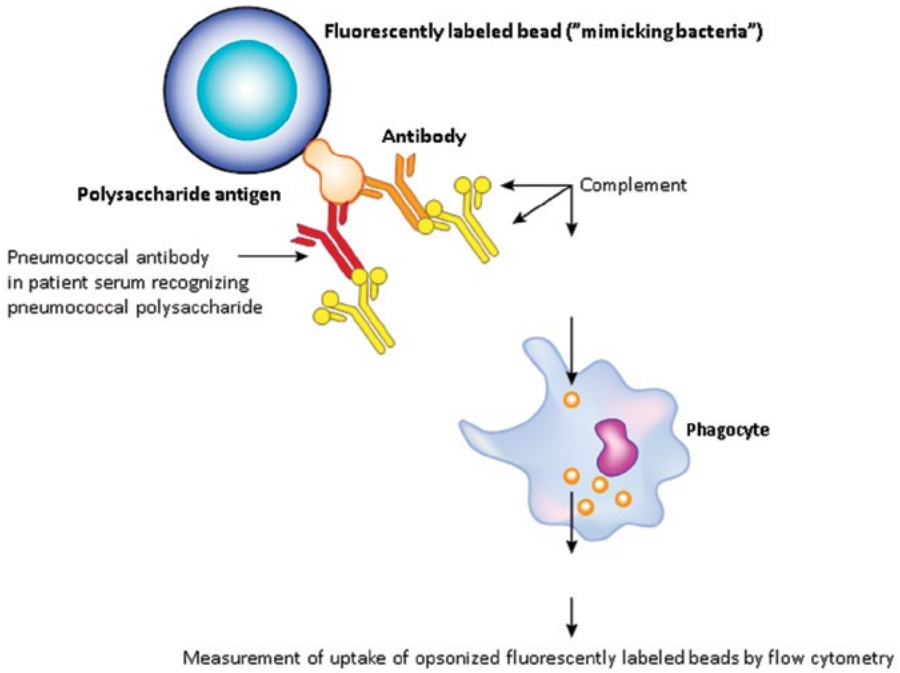

FIGURE 4 OPA for detection of functional antipneumococcal antibodies in serum after vaccination. The use of fluorescently labeled pneumococcal polysaccharide-coated beads permits flow cytometric assessment of the opsonic capability of antipneumococcal antibodies in serum, in the presence of exogenous complement, by measuring phagocytic uptake using a differentiated granulocyte cell line.

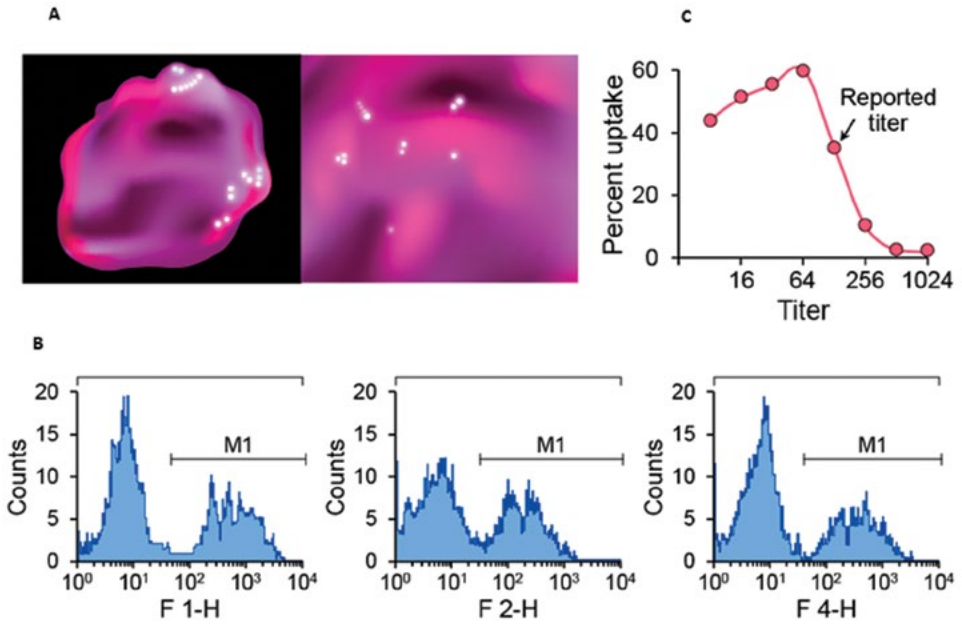

FIGURE 5 (A) Fluorescent microscopy showing differentiated granulocyte cell line with phagocytosed (opsonized) fluorescent beads coated with pneumococcal polysaccharide. (B) Flow cytometric analysis of fluorescent signal from phagocytosed beads. Each bead is coated with a unique polysaccharide, and a multiplex mixture of beads is used to measure functional antibodies produced for each specific pneumococcal serotype. (C) The reciprocal dilution that demonstrates 50% maximal uptake of labeled beads is calculated as the phagocytic titer.

populations of interest for both malignant and nonmalignant conditions. However, flow cytometry can also be used to look at the expression of particular cell surface receptors (proteins and glycoproteins) that are either constitutive or induced by cell activation. CD64, for instance, is expressed on monocytes. It is constitutive but also induced at high levels on neutrophils as a result of infection (Fig. 6A). Flow cytometry can also be used to perform intracellular protein analysis, including identification of proteins for a diagnostic purpose (present or absent). Illustrative examples are Bruton's tyrosine kinase (Btk) for the diagnosis of X-linked agammaglobulinemia (XLA) (Fig. 6B); functional alteration of proteins, including phosphorylation (Fig. 6C) (33); and cytokine production on cellular activation (see chapter 28). The distinct advantage of using flow cytometry for these applications is the ability to correlate the protein of interest with its cellular counterpart or association with specific function or expression under specific conditions. These relationships cannot be achieved in a comprehensive manner by static *in vitro* protein analysis. Flow cytometry has also been used to study protein-protein interactions *in situ* in live or intact cells using the fluorescence resonance energy transfer technique (34). While these approaches may sound somewhat futuristic in the clinical laboratory, phosphoprotein analysis and *ex vivo* measurement of cytokine-producing T cells is already part of the diagnostic armamentarium of specialized reference laboratories.

Similar to multiplex immunoassays, multiplex protein analysis by flow cytometry has made major advances. Fluorescence-based cytometry can quantify ~18 proteins at a rate of >10,000 cells/s. However, this can be exponentially increased using the new technology of mass cytometry, which combines flow cytometry and MS and can measure >36 proteins at a rate of 1,000 cells/s. This advanced methodology allows analysis of up to 45 simultaneous parameters without the use of fluorescent agents or interference from spectral overlap (35). Mass cytometry uses stable, nonradioactive isotopes of rare earth elements (lanthanides) as reporters. Mass cytometry is a modification of inductively coupled plasma MS for single-cell analysis. Similar to flow cytometry, cells are stained with antibodies labeled with metal isotopes. Cells can be stained with DNA intercalators, which provide information on DNA content and cell viability. In the specialized mass cytometer instrument, the stained cells are nebulized into single-cell droplets, and the charged atomic ions are subsequently introduced into the mass spectrometer. While there are distinct advantages of the mass cytometry technique, there are certain disadvantages compared with standard fluorescent polychromatic flow cytometry. The primary limitation is that the new method does not allow for cell sorting of viable cells for additional analysis. Also, the standard light-based measurements of forward and size scatter analysis for cell size and complexity, as well as assessment of cell proliferation (see chapter 28) and Ca^{2+} flux, among other analyses, cannot yet be studied by mass cytometry since metal-reporter equivalents are not available. Also, the sensitivity of lanthanide-labeled antibodies is lower than that of most fluorescent labels due to the chelating polymer used, and this could pose difficulty for analysis of cellular targets with low signal-to-noise ratios. Furthermore, the throughput of most commercial flow cytometers is much higher than that of the mass cytometer, which is limited to ~1,000 cells/s. At present, the best use of the mass cytometer is for the analysis of intracellular regulatory molecules (cytokines and phosphoproteins) for which autofluorescence can pose a confounder or in contexts of numerous simultaneous measurements (35). Complex immunophenotyping and rare-event analysis, on the other hand, may currently be best suited

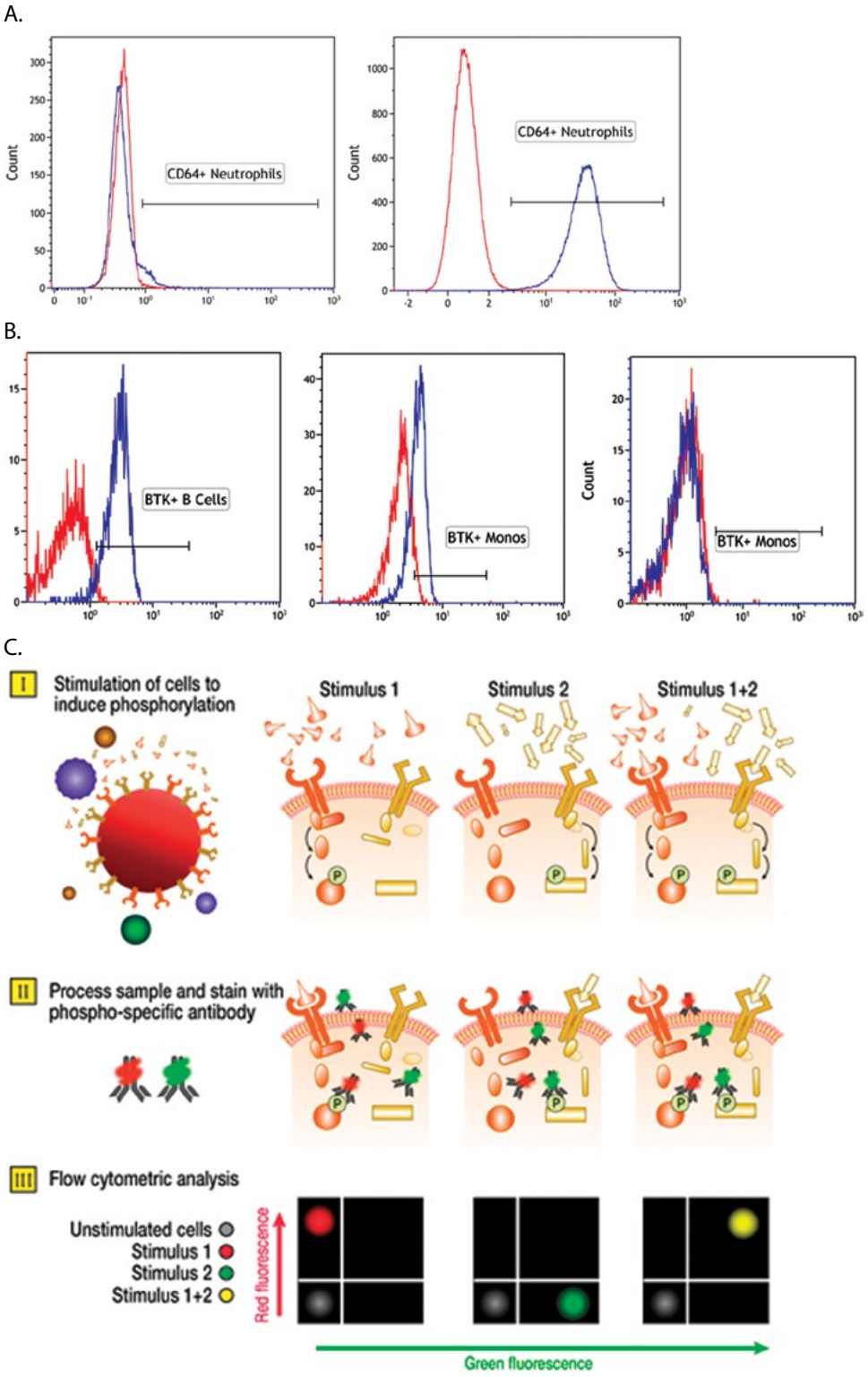

FIGURE 6 (A) Flow cytometric expression of CD64 on "resting" neutrophils (left panel), which is essentially absent because it is not a constitutive marker in this cellular subset. CD64 expression on neutrophils from a patient with bacterial sepsis (blue peak, right panel), as it is a marker expressed on neutrophil activation specifically in the context of infectious stimuli. (B) Flow cytometric analysis of an intracellular protein, Btk, in B cells from a healthy donor (left panel) and in monocytes (Monos) from a healthy donor (middle panel), and the absence of Btk protein in monocytes from a patient with XLA (right panel). Red peak, isotype control; blue peak, specific anti-human Btk antibody. (C) Flow cytometric analysis of modification (e.g., phosphorylation) of intracellular cell signaling proteins. Alterations in function of cell signaling pathways can be assessed after cell stimulation and activation. The assay format can be singleplex (stimulus 1 or stimulus 2 only) or multiplex (stimulus 1 and stimulus 2 in combination), assessing different cell signaling proteins simultaneously (i.e., single experiment). Panel C reproduced from reference 11 with permission from Elsevier Ltd.

for flow cytometry. However, since there is rapid evolution of instrumentation, reagents, and analytical software, these boundaries may blur with time and permit use of each technology interchangeably or for highly specific applications in the clinical laboratory.

QA AND QC ISSUES IN PROTEIN ANALYSIS

Every clinical laboratory must have a robust quality assurance (QA) and quality control (QC) program to ensure that diagnostic testing meets regulatory standards and is optimized for use in patient care. The QA program ensures that appropriate checks are present for the routine analytical process of testing but also for the elements related to analytical and clinical validation prior to introduction of a new test. These include preanalytical issues such as sample stability, anticoagulant, and interfering substances; analytical components including accuracy and precision, reportable range, and reference values; and postanalytical parameters of test reporting, interpretation, and test utilization. For appropriate use of clinical laboratory tests, there must be guidelines that define the clinical utility, strengths, and limitations of the assay. Additionally, implementation of a new test has to take into account appropriate training of lab personnel; documents detailing instrument evaluation and maintenance for robust performance; and strategies for handling poor-quality results, improperly handled specimens, and inaccurate data entry or reporting of test results. In the case of protein analysis, instrumentation and reagents are a critical aspect of test maintenance and performance in the laboratory. Therefore, protocols have to be developed to monitor both instruments and reagents, including regular instrument validation and lot-to-lot comparison of reagents, using predefined acceptance criteria for clinical use of a new lot of a reagent. Certain methodologies also can pose unique QA challenges, particularly multiplex assays (36). These have to be considered in detail before selecting the assay as well as in developing QA parameters for monitoring assay performance. QA programs also involve the use of QC materials, which can include calibrators, standards, and other well-characterized QC reagents available through national or international agencies. Different levels of QC assessment have to be performed for both instruments and assays. QC reagents for assays should include those that assess the analytical measuring range, e.g., low, medium, and high controls. The types of QCs used may vary depending on whether the assay is qualitative or quantitative. For the former, it may be sufficient to have materials that include those with negative and positive results, while for quantitative assays, a more graded QC assessment may be required, with measurement of the high and low end of the range, and possibly an intermediate level.

Another part of a clinical QA system is regular performance of proficiency testing (PT), which evaluates the entire process within the laboratory. This includes sample assessment for stability, interfering materials, analytical measurements, and postanalytical data reporting and interpretation. For some protein analytes, there are standardized PT materials available through regulatory agencies or professional societies (e.g., College of American Pathologists) in which multiple laboratories participate. For other more esoteric protein-based assays, especially those using flow cytometry or MS, standardized PT materials are not available. In these cases, laboratories must develop their own alternative assessment of proficiency (AAP), which is performed similarly to PT, at least twice a year, by the clinical lab staff. The AAP process can include split samples within the laboratory, shared samples between laboratories at different sites, or chart review for protein tests that are used as screening or diagnostic tests for a single clinical condition. In all cases, whether regular PT or AAP is performed, there must be appropriate documentation of PT and test results.

PROTEIN ANALYSIS: PROTEOMICS USING MS

Ionization Techniques

Mass spectrometers can now be found in many laboratories actively providing molecular mass data for proteins and peptides from a wide variety of biological matrices. Every mass spectrometer consists of three parts: an ion source, an analyzer, and a detector, all of which are linked to a vacuum system. Ions created in the source are separated in the analyzer region and then detected. The two most widely used ion sources for MS-based proteomics are electrospray ionization (ESI) (37) and matrix-assisted laser desorption ionization (MALDI) (38). These two ionization techniques have played a key role in the acceptance of mass spectrometers as practical protein chemistry lab tools. ESI and MALDI create intact molecular ions from high-molecular-mass proteins without destroying the polypeptide chain and are therefore referred to as "soft" ionization techniques. Once in the gas phase, protein ions can then be separated by their mass-to-charge ratio (m/z) in the analyzer region.

ESI

The ESI process transfers ions in solution to ions in the gas phase at atmospheric pressure. ESI sources continuously create ions as proteins and peptides arrive at the source through a solution running from a syringe pump or a liquid chromatograph to an electrically conductive capillary held at a high electric potential (3,000 to 6,000 V). A spray is created as the solution reaches the exit of the capillary (often referred to as a Taylor cone) due to the electrostatic field between the end of the capillary and the entrance to the mass spectrometer. The ions in the solution are transferred to the gas phase as spray droplets burst due to charge repulsion and are further reduced in size due to heated gas that evaporates the solvent surrounding the ions. When the ESI emitter is positively charged, proteins and peptides are positively charged via protonation, while a negatively charged ESI emitter results in negatively charged, deprotonated proteins and peptides. The mechanism of ESI creates multiple ions from the same protein, each with a different number of charges and therefore a different m/z value (39). For a molecule such as an immunoglobulin light chain with a molecular mass of 23,000 Da, a series of charges ranging from +10 to +25 is observed. Because of this, ESI spectra can be complex due to the fact that a single protein has multiple peaks. The molecular mass is determined after the multiply charged peaks are converted from the mass-to-charge (m/z) domain to the uncharged molecular mass (Da) domain, through the aid of a computer program (40). Figure 7 shows an ESI mass spectrum acquired on a quadrupole time-of-flight mass spectrometer (Q-TOF) showing the κ light chain of the therapeutic monoclonal antibody adalimumab after reduction with dithiothreitol. The mass spectrum at the top of the figure shows all the multiply charged ions from the monoclonal light chain of adalimumab, while the bottom figure shows a single peak after the multiply charged ions were converted to molecular mass. The average molecular mass observed was 23,412.19 Da, which matches closely with the known average molecular mass of 23,412.13 Da. The spectrum in Fig. 7 was acquired

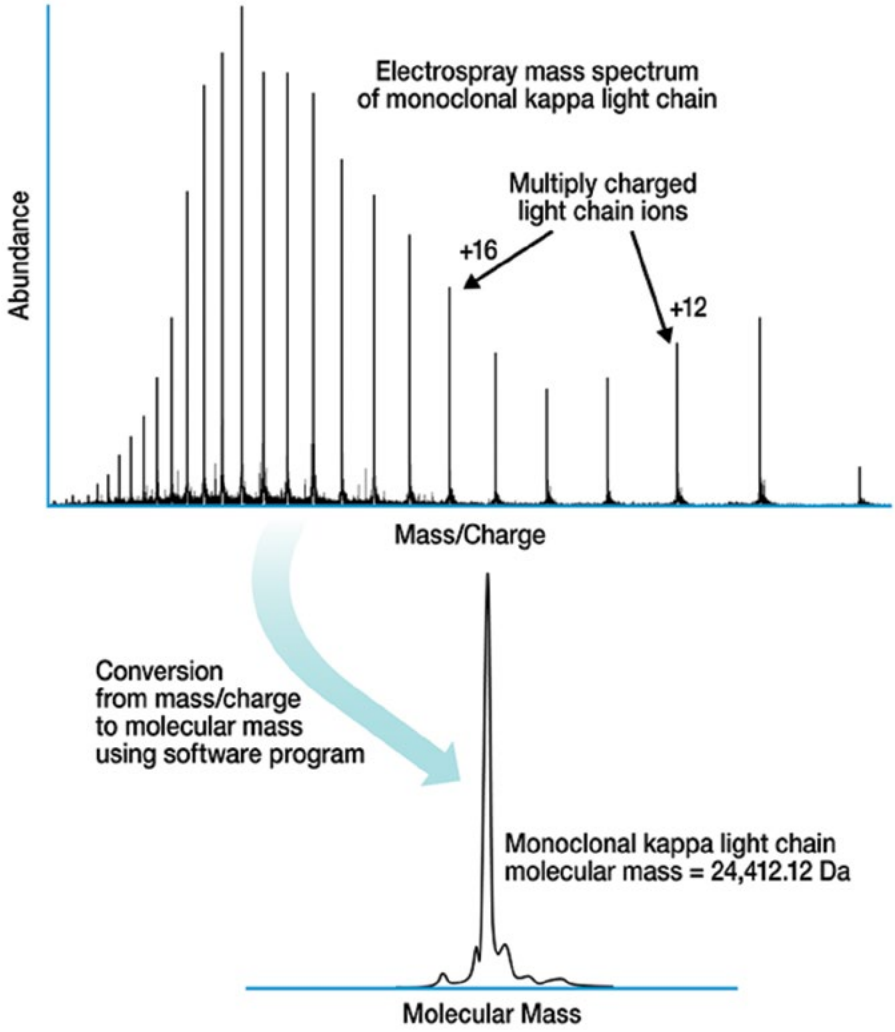

FIGURE 7 Mass spectrum of a monoclonal immunoglobulin light chain protein showing the multiply charged ions produced by ESI (top). Each peak represents the same light chain protein with a different number of protons attached, which changes each ion's mass/charge ratio (m/z). The molecular mass of the light chain is determined by converting each peak to the uncharged state through an algorithm performed by a computer program (bottom).

at a liquid chromatography (LC) flow rate of 25 μl/min with a 2-μl injection, but ESI can be performed at many different flow rates ranging from nanoliters per minute up to a milliliter per minute. Injection volumes for a sample can range from a few microliters to a few hundred microliters.

MALDI

MALDI, on the other hand, produces ions that have much lower charge states compared with ESI. For example, the predominant ions created for an immunoglobulin light chain are typically +1 and +2. MALDI typically creates ions under vacuum instead of atmospheric pressure using a saturated solution of an organic acid mixed with the analyte solution and then dried to form a crystalline matrix. The plate containing the dried spots is transferred into a vacuum via an airlock system. Then a laser is fired at the matrix to form ions. The organic acid matrix absorbs the light energy from the laser and rapidly heats, creating a plume where protons from the matrix are transferred to the analyte in positive-ion mode (41). Figure 8 shows a MALDI mass spectrum from the same sample shown in Fig. 7 of adalimumab monoclonal light chains after reduction with dithiothreitol collected on a TOF mass spectrometer. The difference in the number of charge states produced for the light chain of adalimumab by ESI versus MALDI is easy to see when the two spectra are compared. Because MALDI uses a laser to produce ions, it can be focused on a particular spot to produce an ion image from a tissue sample. MALDI MS imaging is a relatively new technique that is becoming more prevalent in clinical pathology laboratories (42). There are also new ionization techniques that combine dried samples and ESI, such as desorption ESI, that are gaining ground as tools for monitoring tissue samples in real time (43). Together, ESI and MALDI make up the vast majority of ion sources on instruments that analyze proteins and peptides for clinical assays.

Mass Analyzers

The triple-quadrupole mass spectrometer is the most common mass spectrometer encountered in clinical laboratories due to its ruggedness and reliability. The instruments

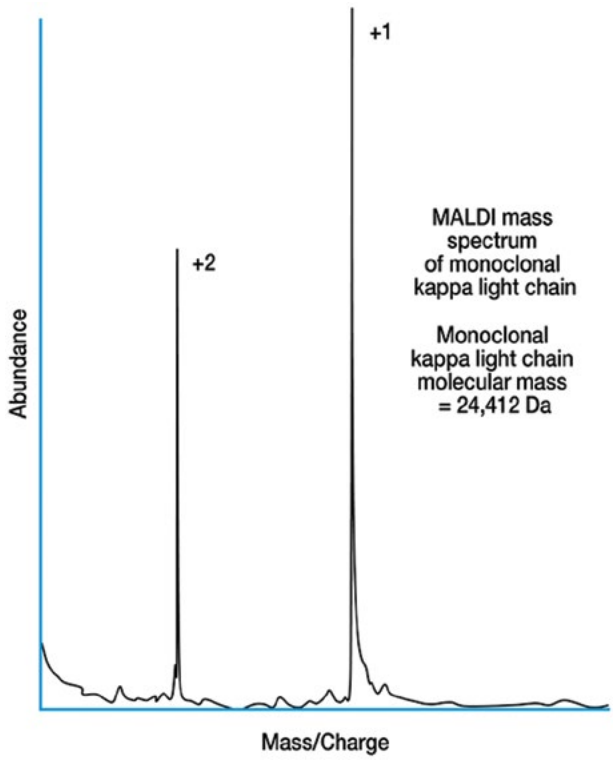

FIGURE 8 Mass spectrum of the same monoclonal immunoglobulin light chain protein shown in Fig. 7 ionized using MALDI. The spectrum clearly shows the prevalence of the +1 and +2 charge states as compared with the highly charged ions created by ESI. The molecular mass of the light chain with the +1 charge state is determined by subtracting the mass of a proton.

typically run at a resolution of 1,000 with mass measurement accuracy of ~40 ppm. The geometry of a quadrupole instrument is just as its name implies; it is made up of a set of four identical parallel rods (~20 cm in length and 1 cm in diameter). Rods that are opposite each other have the same polarity and the same DC voltage. An additional radio-frequency AC voltage is applied to all rods. As the polarity and the voltages are changed on the rod pairs, the electrical field oscillates and ions with the correct m/z remain stable and are transmitted through the quadrupole (44). Quadrupole instruments can be operated in scanning mode, which allows ions with different m/z to be transmitted through the detector, or they can be set to transmit only ions with a specific m/z. Triple-quadrupole mass spectrometers are used in the clinical laboratory due to the high level of sensitivity and specificity obtained using three different quadrupole analyzers in tandem. Ions entering a triple-quadrupole instrument first encounter a single quadrupole (Q1), followed by a collision cell (this is not a true quadrupole but is often referred to as Q2), followed by another single quadrupole (Q3). The first quadrupole is typically set to transmit a specific m/z, which is transferred to the collision cell, where neutral gas molecules (usually nitrogen) collide with the ions to form fragment ions. The fragment ions produced can be scanned in the third quadrupole, or the third quadrupole can be set to transmit a specific m/z that is unique to a fragment ion for the analyte. This series of events is called tandem MS, or MS/MS. When the first quadrupole is set to transmit a specific m/z to be fragmented in the collision cell and the third quadrupole is set to transmit a specific fragment ion m/z, the experiment is called selected reaction monitoring, or SRM (also referred to as multiple reaction monitoring, or MRM). This type of experiment is the mainstay of quantitative MS performed in clinical laboratories. Figure 9 shows a graphical representation of the SRM process.

Quadrupole ion trap mass spectrometers are another commonly used mass spectrometer in clinical laboratories. An ion trap is designed as either a three-dimensional ion trap where the ions oscillate in a circular fashion or a two-dimensional linear ion trap where the ions move back and forth. Both geometries use the same principles of modifying DC polarity and radio-frequency AC voltages to keep ions in a quadrupole trap. Instead of being transmitted down a linear path as in a triple-quadrupole mass spectrometer (45), ions are injected into the ion trap, excited, and then allowed to oscillate in the trap before being ejected and detected. The resolution of a quadrupole ion trap can be upwards of 4,000 with a mass measurement accuracy of ~40 ppm. The benefit of quadrupole ion traps is their scanning speed, which can be orders of magnitude faster than a quadrupole instrument. They are often used for structural analysis of peptides because they have the capacity to do MS/MS/MS. A specific peptide ion can be trapped and then fragmented multiple times all in the same experiment and at scanning rates much faster than with a triple-quadrupole instrument. Quadrupole ion traps also have the added benefit of being able to use different dissociation techniques to fragment ions, such as electron transfer dissociation (46).

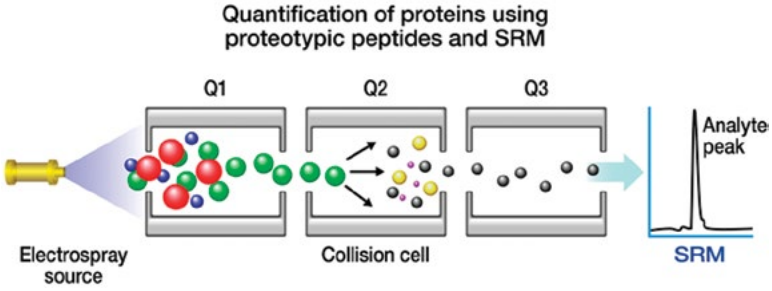

FIGURE 9 A graphical representation of the transmission through a triple-quadrupole mass spectrometer for a specific proteotypic peptide ion quantified using SRM. The intact peptide ion is created by ESI and is represented by the green balls. The peptide ion is selected in Q1 and fragmented in the collision cell (Q2), and then a proteotypic peptide-specific fragment ion is transmitted through Q3 on to the detector.

Such new methods can generate fragment ions containing posttranslational modifications that are not observed using other fragmentation techniques. One issue with ion traps is the space-charging effect, which can limit the linear dynamic range of the instrument and is not observed in triple-quadrupole mass spectrometers. Instrument manufacturers have employed techniques such as automatic gain control to limit the number of ions entering the trap, allowing new instruments to better manage space charging.

TOF mass spectrometers can also be found in the clinical laboratory and are well suited for measuring the molecular mass of large proteins (47). TOF instruments consist of a flight tube in which the *m/z* of an ion is determined by the time it takes to travel a set distance between a start position and the detector. This is called the flight time, and it is dependent on the ion's mass and the voltage on the pulser that forces the ions into the flight tube (48). There are two common types of TOF instruments, linear and reflectron. Linear TOF instruments measure the time it takes an ion to travel between two set points in a linear flight path from the ion source to the detector. A reflectron instrument contains a flight tube that includes a series of lenses that slow the ions and then force them to reverse direction on to the detector. The ions travel farther in a reflectron instrument and are more focused compared with a linear instrument, resulting in better resolution. There are differences in the resolution and mass measurement accuracy of ESI-TOF versus MALDI-TOF instruments due to the kinetic energy of the ions after they are created. In an ESI-TOF instrument, the ions enter the TOF region at a 90° angle, creating the orthogonal-TOF geometry. The steady stream of ions from the ESI source is pulsed into the flight tube in a tight beam, making their mass measurement highly accurate. MALDI-TOF instruments have the ions enter the flight tube after the laser pulse when the ions are dispersed throughout the ablated matrix plume. To compensate for the ion dispersion, delayed extraction is used to make a tighter ion beam before the ion packet is accelerated through the flight tube to the detector. Advances in the speed and data transfer rates of the electronics used in TOF instruments have made them faster and more reliable, enabling resolution of upwards of 30,000 with a mass measurement accuracy of 2 ppm for most high-end ESI-TOF instruments.

The newest generation of mass spectrometer is the Orbitrap, based on a new design developed by Makarov (49). The Orbitrap measures an ion's *m/z* by collecting the image current produced while the ions oscillate around an electrode assembly. The mass of each ion is found by converting the image current to *m/z* using the Fourier transform. The instrument is capable of attaining resolution of 240,000 with a mass measurement accuracy of <1 ppm. The high resolution is a function of the high precision and accuracy with which the frequency of the ions orbiting in the cell can be measured via the image current. The Orbitrap itself is <10 cm in length and is kept at very low pressure. The ions are injected into the Orbitrap (Fig. 10) using a C-trap that focuses the ions to a point within the cell where they begin their orbit around the center electrode. Orbitrap instruments were first introduced in research laboratories, but they are becoming more popular in clinical laboratories with the advent of new instruments that combine the robust attributes of quadrupole instruments with the Orbitrap.

Orbitrap and TOF mass spectrometers are often coupled with quadrupole mass spectrometers, resulting in a hybrid instrument. The reason for combining the two instruments stems from the fact that a quadrupole can function as an ion guide, in which all ions within a certain *m/z* range can be transmitted, or as an ion selector, in which only ions with a specific *m/z* are transmitted. The first generation of Orbitraps was hybrid instruments with a linear ion trap (LIT) in front of the Orbitrap, while the second generation combined a single quadrupole with the Orbitrap. Instruments with a LIT most often generate ion fragments in the LIT, while instruments with a quadrupole have a separate collision cell called a higher-energy collisional dissociation cell for generating fragment ions for structural analysis. In Q-TOF instruments, a quadrupole is coupled with a collision cell in the same manner as in a triple-quadrupole instrument and the third quadrupole is replaced by a TOF analyzer. Both Orbitrap and TOF hybrid instruments offer superior scanning speed, resolution, and mass measurement accuracy

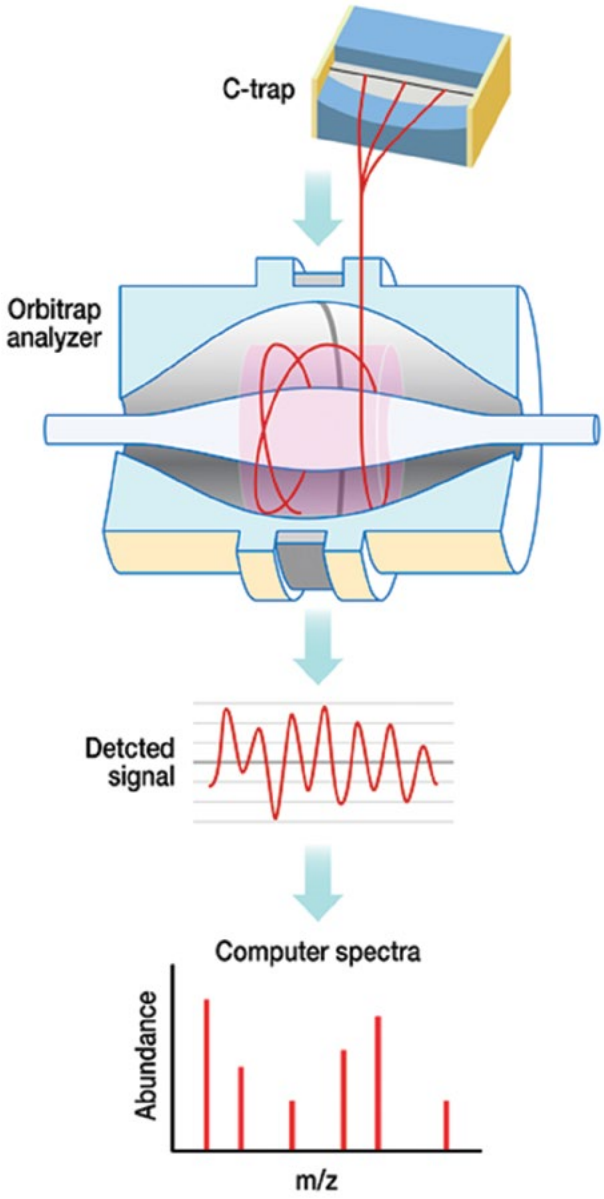

FIGURE 10 Diagram of an Orbitrap analyzer showing how ions are injected into the Orbitrap via the C-trap and then allowed to orbit the isolated electrodes. The induction current made by the ions is detected and then converted to *m/z* using the Fourier transform.

compared with triple-quadrupole and quadrupole ion trap mass spectrometers. While triple-quadrupole instruments with ESI sources have been the primary instrument for performing absolute quantification in the clinical laboratory, Orbitrap and Q-TOF mass spectrometers with ESI sources are being used more often for both qualitative and quantitative analysis. These hybrid instruments have a promising future in the clinical laboratory as they have the ability to provide high resolution and excellent mass measurement accuracy to address specific clinical questions related to unknown compounds and interferences.

LC Coupled with MS

High-performance LC has been used in clinical laboratories for decades, typically coupled with optical detectors such as UV-visible spectrophotometers. Because ESI is a flowing liquid-based ionization technique, it is perfectly suited to be coupled with LC (50). Manufacturers of mass spectrometers used in clinical laboratories now provide ESI sources that are robust and can easily handle running large volumes of samples using standard-flow LC methods. These ESI sources can be directly coupled to an LC with flow rates ranging from 10 to 1,000 μl/min and incorporate high temperature (up to 600°C) and heated gas to remove excess solvent to optimize the number of ions that enter the mass spectrometer (51). High-volume clinical laboratories often use multiplexed LC systems in which up to four columns running the same method take turns eluting into the ESI source in a "leapfrog" approach (52). These multiplexed systems may also incorporate two-dimensional LC, or LC/LC, in which columns are set in tandem to further purify the sample in a completely automated fashion. Between standard-flow and nanoflow LC systems are the micro LC systems that run at 10 to 50 μl/min. A micro LC uses less solvent and less sample and can be easily connected to a standard ESI source. Micro LC systems are not currently multiplexed, and the number of LC columns commercially available is limited compared with high-flow systems. In practice, one-dimensional LC is still the most commonly used LC setup in the clinical laboratory setting. Regardless of the LC flow rate, the majority of peptide and protein LC separations are done using reverse-phase LC columns with water and acetonitrile, or methanol, gradients containing formic acid for ion pairing when coupled with ESI (53).

Using MS to Analyze Peptides and Proteins

Mass spectrometers have played a central role in the identification, structural characterization, and quantification of proteins and peptides in research laboratories for decades. Since the early 1980s, MS has been used to quantify endogenous peptides of clinical importance, with many of the first studies focusing on neuropeptides (54, 55). Currently, clinical laboratories are beginning to use mass spectrometers for quantifying endogenous peptides such as insulin-like growth factor 1 and insulin (56–58), as well as endogenous peptide biomarkers (59). However, the majority of work is done using peptides obtained by digesting the sample with an enzyme before using MS.

MS/MS Analysis of Tryptic Peptides To Identify Proteins

Mass spectrometers routinely identify and quantify peptides from the proteolysis of protein mixtures. This is accomplished by what is often referred to as "bottom-up proteomics" (60). The term gets its name from the fact that an enzyme with known cleavage specificity, such as trypsin, is first used to digest proteins into peptides. The tryptic peptides are then analyzed by LC-MS/MS to obtain amino acid sequence information. The mass of the peptide combined with the amino acid sequence found by MS/MS is used to reconstruct each protein in the sample from the bottom up. The first bottom-up experiments in the early 1990s used the accurate mass of the tryptic peptide without the use of MS/MS amino acid sequence. The tryptic peptide masses observed were compared to the masses of the tryptic peptides expected from the protein database (61). This approach led to a high level of uncertainty due to large numbers of peptides with nearly the same intact mass but different amino acid sequences. Many of the first bottom-up experiments relied on SDS-PAGE to separate proteins followed by cutting out of the stained bands followed by in-gel digestion (61). Tryptic peptides were extracted from the gel and subjected to MS/MS to obtain peptide sequence information to compare to a protein database. The selection of the tryptic peptides to be sequenced by MS/MS was done manually at first, as was the protein database searching (62, 63).

By the turn of the millennium, advancements in automated peptide MS/MS acquisition combined with automated protein database search engines enabled Yates and coworkers to coin the term "shotgun proteomics." This refers to the broad swath of protein identifications that could be generated in one LC-MS/MS experiment (63, 64). At present, there are any number of mass spectrometers coupled with commercially available protein database search engines that can provide tens of thousands of MS/MS spectra, and thousands of protein identifications, from a single analysis, all performed in a matter of hours (65). A diagram of the shotgun proteomics process is shown in Fig. 11. While the majority of shotgun proteomics has been performed in a research setting, some clinical laboratories have adopted the approach to identify proteins present in biopsy samples, in which specific regions of the tissue are removed using laser capture dissection and then analyzed using shotgun proteomics (66, 67). The laser capture dissection-shotgun proteomics approach is essentially equivalent to immunohistochemistry using thousands of protein-specific antibodies. However, the mass spectrometer is a nonbiased detector, and it provides information on all the proteins present in the sample via tryptic peptide sequences. This results in more-sensitive and -specific results.

MS/MS Analysis of Proteolytic Peptides To Quantify Proteins Using SRM

Currently, the majority of MS-based clinical laboratory assays that quantify peptides quantify a protein-specific peptide created by digesting a sample with a protease. This approach was first described by Barr and coworkers (68) and has since been widely adopted by clinical laboratories to quantify a wide range of proteins (69–73). The peptide representing the protein to be quantified is commonly referred to as a proteotypic peptide (74). A proteotypic peptide represents the stoichiometric equivalent of the intact protein in the sample. This approach works when the sample is complex, such as serum, and the intact protein is present at a low concentration because the response by ESI is higher for peptides than for proteins.

The best proteotypic peptide to use for quantification can be found empirically by digesting a pure form of the protein if it is available. If purified protein is not available, then the best proteotypic peptides can be identified *in silico* using computer software (75). The software uses the known sequence of the protein and the enzyme that will be used to generate a list of the proteotypic peptides along with suggested collision energies. In addition, databases are being

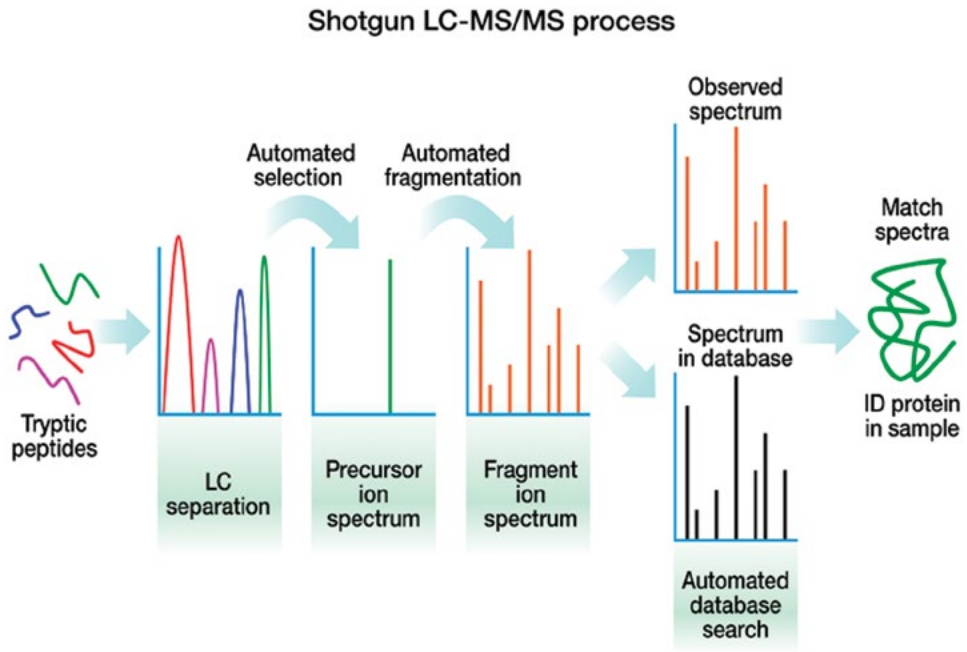

FIGURE 11 Stepwise depiction of a shotgun LC-MS/MS experiment. The figure shows how a tryptic peptide mixture is first separated by LC, ionized, and then scanned in the mass spectrometer. Tryptic peptides with sufficient signal are automatically selected for fragmentation, and the observed MS/MS data are automatically compared to a protein database. A list is provided of the best matches to tryptic peptides derived from proteins in the database.

created that give the proteotypic peptides that have been successful using publicly available data. There are numerous examples of assays being developed to quantify upwards of 50 proteins in serum and urine (76) using SRM on a triple-quadrupole mass spectrometer with an ESI source and a high-flow LC.

Research groups continue to push the number of proteins that can be quantified in a digest of plasma, serum, and urine by means of relative quantification. However, absolute quantification is the norm in clinical laboratories, which typically involves the use of a traceable protein standard. The ideal standard for protein quantification by SRM is a ^{13}C and ^{15}N stable isotope-labeled protein with the same amino acid sequence as the native protein. Stable isotope-labeled standards have the same solution chemistry as the native protein but have a different mass due to the added neutrons in the carbon and nitrogen nuclei. This allows the mass spectrometer to distinguish them from the native protein. Limited studies have been done using stable isotope-labeled protein standards because the proteins are made using recombinant expression systems (*Escherichia coli*, mammalian cell culture, etc.) and are not always easy to produce. Stable isotope-labeling reagents may also be cost-prohibitive. Examples of clinical studies using a stable isotope-labeled recombinant standard protein include the absolute quantification of urinary albumin (73), serum parathyroid hormone (72), and C-reactive protein (77). Alternatively, a stable isotope-labeled synthetic peptide with the same amino acid sequence as the proteotypic peptide can be produced at a reduced cost and can serve as an internal standard to monitor retention time and fragment ion ratios. Quantification is most often done using a standard curve and QC samples made using purified protein diluted in a similar matrix that is digested in the same way as the samples. Stable isotope-labeled peptide is added at the same concentration in every sample to serve as an internal standard. Peak areas from selected fragment ions are then used to calculate the concentration in unknown samples in the same manner as other LC-MS/MS assays quantifying small molecules.

MS/MS of Intact Proteins: Top-Down MS

The bottom-up LC-MS/MS approach to protein identification and quantification has a proven track record. However, there is the argument that information that could prove useful in clinical diagnostics is lost by cleaving the intact protein into peptides. Researchers continue to create new ways to identify proteins by LC-MS/MS without digesting them first. This approach is referred to as "top-down proteomics" and involves the fragmentation of intact proteins followed by piecing together the fragments in the same manner as protein database searching in shotgun proteomics (78, 79). There are a number of technical challenges that are faced when trying to identify a protein using fragment ions produced from the intact protein. The majority of top-down experiments use ESI to generate protein ions to be analyzed in the mass spectrometer. Because ESI generates multiple charge states for the intact protein, it also creates fragment ions with multiple charge states. Most tryptic peptides have +2, +3, or +4 charge states with fragment ions that primarily have a +1 charge state. In the case of proteins, there may be upwards of 20 different charge states for the same protein, and when a specific charge state is fragmented, it can generate hundreds of multiply charged fragment ions. Most top-down proteomics is done on instruments that have high resolution (>30,000) and high mass measurement accuracy (<2 ppm). This aids in the interpretation of the fragment ions using software specifically designed to identify a protein from the multiply charged intact protein ions and the large collection of multiply charged fragment ions (80). Another

challenge when doing top-down analysis of proteins is separating the proteins prior to ESI. LC is the method of choice; however, additional separation techniques such as preparative electrophoresis, in which proteins are first separated by their pI, have been reported (81). Clinical applications of top-down protein analysis include determining the mutation sites in transthyretin and hemoglobin from dried blood spots (82, 83). Top-down analysis is also being done on immunoglobulin light chains from patients with multiple myeloma, whereby the isotype of the light chain is determined by the singly charged fragment ions that originate from the constant region of the κ or λ light chain (84). Figure 12 shows an example of the top-down fragment ion spectrum acquired for a κ light chain. Although advances are being made in top-down protein analysis due to advances in high-resolution mass spectrometers with high mass measurement accuracy, the technique has yet to be used routinely in a clinical laboratory setting.

Intact Proteins—Phenotyping Proteins Using MS

MS has been used in the clinical laboratory to identify phenotypic changes in proteins by observing the shift in the molecular mass of the protein compared to the normal wild-type molecular mass. One of the first examples reported right after the discovery of ESI was the detection of mutations in hemoglobin (85). Since that time, many clinical groups have described using LC-ESI-MS to identify mutations in hemoglobin, and the assay is routinely performed in clinical labs because hemoglobin can be obtained easily in high concentrations from red blood cells (86). Another high-abundance protein that has been monitored for mutations using MS is transthyretin, as certain mutations are known to be associated with amyloid deposition (87). An online immunoaffinity-LC-ESI-MS assay was developed to purify transthyretin from serum to obtain an accurate molecular mass for transthyretin. Another protein phenotype assay developed for the clinical laboratory is an online

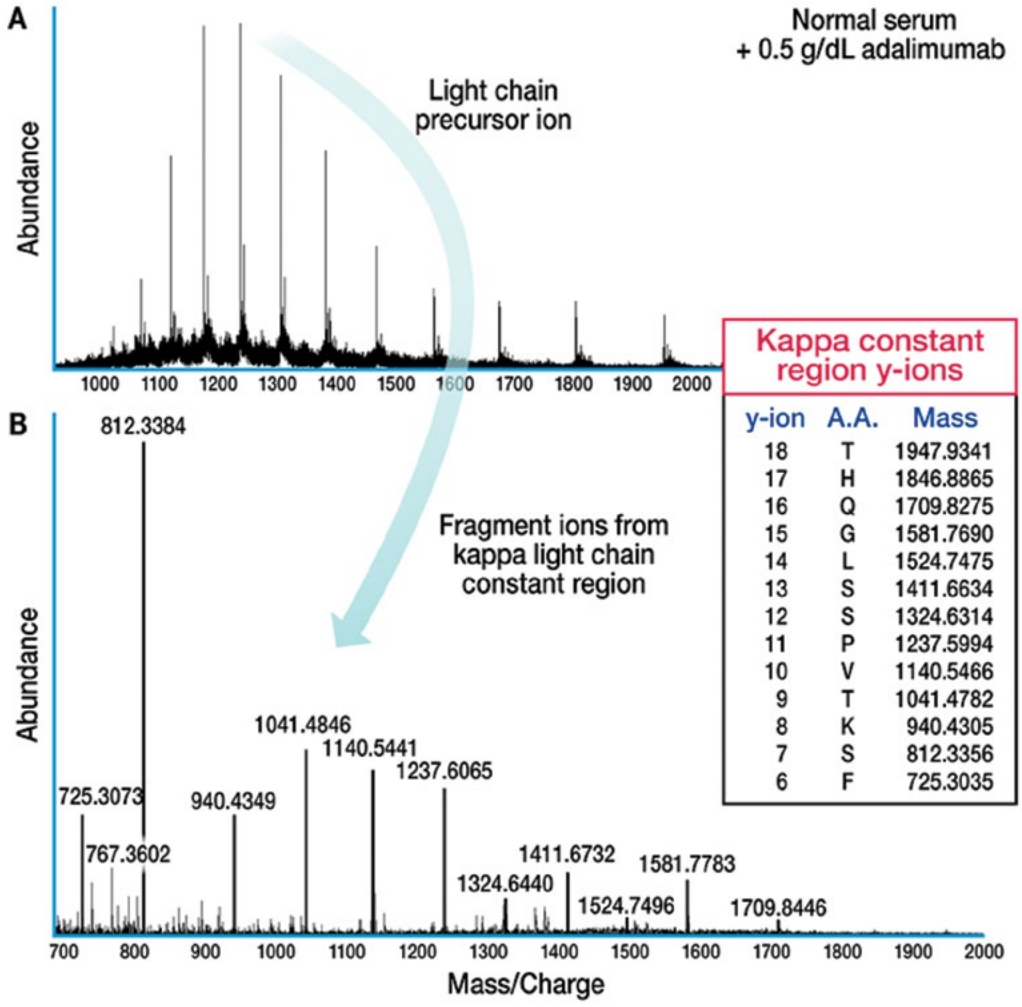

FIGURE 12 Top-down MS of adalimumab spiked into normal serum. The ion at m/z = 1,233 in the top spectrum matches the +19 charge state ion from the κ light chain of adalimumab and was selected for top-down MS. The arrow points to the fragment ion mass spectrum shown below. The labeled fragment ions match the expected masses for fragment ions from the C-terminal portion of the κ light chain, which contains the constant region. The calculated y ion masses for the κ light chain constant region-specific amino acid sequence are shown in the table.

immunoaffinity-LC-ESI-MS test for evaluating carbohydrate on transferrin (88). All of these examples use the mass spectrometer to provide an accurate molecular mass of the patient sample compared to a normal wild type. If the molecular mass of the patient sample does not match the normal sample, it indicates that a mutation is present. In the case of transferrin, a mass shift matching a change in carbohydrate structure indicates an alteration in metabolism.

Clinical Samples Analyzed by MS

The higher the concentration of the protein or peptide in a sample, the less sample preparation is needed prior to analysis. It is not surprising that proteins such as hemoglobin require minimal sample preparation due to the high concentration of the protein in red blood cells. When evaluating the preparation needed for proteins, one must also consider molecular mass and posttranslational modifications. As a general rule, the higher the mass, the less response, due to a number of physical factors in the ionization process whether using ESI or MALDI. If a protein has a mix of possible posttranslational modifications, this reduces the response for any one species. The three-dimensional structure of the protein also alters the ionization efficiency, and denaturation may be needed to obtain the best signal (89). If a protein or peptide needs to be purified prior to analysis, there are a number of methods that are often used to prepare clinical samples. One of the fastest and most inexpensive ways to isolate proteins is to use saturated ammonium sulfate to bring proteins out of solution. The pellet containing the sample can then be resolubilized, desalted, and then analyzed directly for intact proteins or digested for analysis of proteotypic peptides. The reverse holds true for small proteins and peptides, for which the supernatant from an ammonium sulfate protein precipitation can be analyzed instead of the pellet. Other methods of precipitating large proteins can also be used, such as adding organic solvent to create a protein pellet. There is also the option of using molecular weight cutoff filters to separate proteins and peptides. Various sizes are available and work due to centripetal force, preferentially forcing analytes of a specific size through a filter. Alternatively, solid-phase extraction can be used to capture peptides or proteins to remove low-molecular-weight compounds or to partition analytes with certain hydrophobicity, basicity, or acidity attributes.

Immunopurification can also be used to purify a protein or peptide prior to analysis using MS. When an immunocapture method is used, reagents used to remove the protein or peptide from the antibody need to be cleared from the sample before ionization. One of the more successful uses of immunocapture for clinical proteomics is stable isotope standards and capture by antipeptide antibodies (SISCAPA) (90). This method is based on capturing proteotypic peptides using antibodies raised against a specific proteotypic peptide. The technique dramatically lowers the level of detection for low-abundance proteins (91) and can be automated for high-throughput clinical laboratories. Ideally, a purification method should end with the final step having the analyte in a solvent matrix that will allow for the best separation when using LC-ESI-MS (92) or efficient ionization when doing MALDI MS (93). As a general rule, volatile buffers

TABLE 3 Key concepts in clinical MS

Test type	Common instrument format	Examples and references
Peptide quantitation	Standard-flow LC system coupled to an ESI source on a triple-quadrupole mass spectrometer. The LC system can be multiplexed for high throughput. Sample quantification is done by using a standard curve using a purified peptide standard.	Insulin-like growth factor and human growth hormone (97); see also reference 59
Protein quantification using a proteotypic peptide	Standard-flow LC system coupled to an ESI source on a triple-quadrupole mass spectrometer. The LC system can be multiplexed for high throughput. Sample quantification is done by using a standard curve using a protein standard. The sample is digested and a protein-specific proteotypic peptide is monitored by SRM. A stable isotope-labeled peptide or stable isotope-labeled intact protein may be used for quantification. Multiple proteins can be quantified at the same time. Proteotypic peptides can be enriched using immunoaffinity (SISCAPA).	Zinc-α_2 glycoprotein and prostate-specific antigen (70, 71); see also reference 98
Protein phenotyping—intact	Standard-flow LC system coupled to an ESI source coupled to a quadrupole, Q-TOF, or TOF mass spectrometer. MALDI can also be used. Protein can be immunopurified offline or online. The mutation is identified via a mass shift observed in the intact protein molecular mass.	References 87, 88, and 99
Protein phenotyping—mutation-specific peptides	Standard-flow LC system coupled to an ESI source coupled to a triple quadrupole, Q-TOF, or TOF mass spectrometer. MALDI can also be used. The LC system can be multiplexed for high throughput. The sample is digested and a mutation-specific peptide is monitored by SRM. Phenotype is determined using stable isotope-labeled peptides and mutation-positive samples.	References 85, 86, and 100
Proteomic profiling of tissue-derived samples	Nanoflow LC system coupled to an ESI source coupled to an Orbitrap mass spectrometer. The sample is extracted from a slide containing the tissue using laser capture dissection. The sample is digested and shotgun proteomics is performed with protein database searching. Phenotype is determined by the protein identifications from the database search.	References 67, 101, and 102

such as ammonium acetate and ammonium bicarbonate at concentrations of <50 mM are acceptable. Inorganic salts and acids can interfere with LC separation and ionization and should be avoided. Ionic detergents such as SDS are also problematic and should be removed or exchanged with a nonionic detergent. Two-dimensional LC systems can also be used to reduce matrix effects from the sample buffer by trapping proteins and peptides on a trap column, where they are held while the matrix is flushed to waste before eluting the sample onto the analytical column (94).

LC-ESI-MS assays, as with any other clinical assay, have their level of quantification based on the analyte concentration that is clinically relevant. In general, proteins or peptides at or above 1 μM in concentration are relatively easy to quantify by LC-ESI-MS. For SRM methods, much of the work is still trial and error. A digest is done on the sample and the expected proteotypic peptides are monitored. If a response is observed, then the specificities of the transitions are examined. The most effective way to determine specificity is to have a stable isotope-labeled peptide synthesized with the same amino acid sequence as the proteotypic peptide. If the LC retention time and fragment ion ratios of the stable isotope-labeled peptide match the native peptide, then specificity is established. This process becomes difficult to manage as the number of proteotypic peptides increases; however, it is becoming easier to manage due to advances in software and tryptic peptide databases that provide information on the proteotypic peptides that have already been observed by others to give the lowest level of detection (75, 95, 96). See Table 3 for a summary of the key concepts in clinical MS.

REFERENCES

1. **Livesey JH, Ellis MJ, Evans MJ.** 2008. Pre-analytical requirements. *Clin Biochem Rev* **29**(Suppl 1)**:**S11–S15.
2. **Remaley AT, Hortin GL.** 2006. Protein analysis for diagnostic applications, p 7–21. *In* Detrick B, Hamilton RG, Folds JD (ed), *Manual of Molecular and Clinical Laboratory Immunology,* 7th ed. ASM Press, Washington, DC.
3. **Ahrens ET, Bulte JW.** 2013. Tracking immune cells in vivo using magnetic resonance imaging. *Nat Rev Immunol* **13:**755–763.
4. **Hawkins PN.** 2002. Serum amyloid P component scintigraphy for diagnosis and monitoring amyloidosis. *Curr Opin Nephrol Hypertens* **11:**649–655.
5. **Sachchithanantham S, Wechalekar AD.** 2013. Imaging in systemic amyloidosis. *Br Med Bull* **107:**41–56.
6. **Perugini E, Guidalotti PL, Salvi F, Cooke RM, Pettinato C, Riva L, Leone O, Farsad M, Ciliberti P, Bacchi-Reggiani L, Fallani F, Branzi A, Rapezzi C.** 2005. Noninvasive etiologic diagnosis of cardiac amyloidosis using 99mTc-3,3-diphosphono-1,2-propanodicarboxylic acid scintigraphy. *J Am Coll Cardiol* **46:**1076–1084.
7. **Massi G, Fabiano A, Ragusa D, Auconi P.** 1979. Characterization of alpha-1-antitrypsin by isoelectric focusing on an ultrathin polyacrylamide gel layer. An economic high-resolution system for determining PiM subtypes. *Hum Genet* **53:**91–95.
8. **Mauch L, Lun A, O'Gorman MR, Harris JS, Schulze I, Zychlinsky A, Fuchs T, Oelschlägel U, Brenner S, Kutter D, Rösen-Wolff A, Roesler J.** 2007. Chronic granulomatous disease (CGD) and complete myeloperoxidase deficiency both yield strongly reduced dihydrorhodamine 123 test signals but can be easily discerned in routine testing for CGD. *Clin Chem* **53:**890–896.
9. **Vowells SJ, Fleisher TA, Sekhsaria S, Alling DW, Maguire TE, Malech HL.** 1996. Genotype-dependent variability in flow cytometric evaluation of reduced nicotinamide adenine dinucleotide phosphate oxidase function in patients with chronic granulomatous disease. *J Pediatr* **128:**104–107.
10. **Vowells SJ, Sekhsaria S, Malech HL, Shalit M, Fleisher TA.** 1995. Flow cytometric analysis of the granulocyte respiratory burst: a comparison study of fluorescent probes. *J Immunol Methods* **178:**89–97.
11. **Abraham RS, Barnidge DR, Lanza IR.** 2013. Assessment of proteins of the immune system, p 1145–1159. *In* Rich RR, Fleisher TA, Shearer WT, Schroeder HW Jr, Frew AJ, Weyand CM (ed), *Clinical Immunology: Principles and Practice,* 4th ed. Elsevier Saunders, Philadelphia, PA.
12. **Bradwell AR, Harding SJ, Fourrier NJ, Wallis GL, Drayson MT, Carr-Smith HD, Mead GP.** 2009. Assessment of monoclonal gammopathies by nephelometric measurement of individual immunoglobulin κ/λ ratios. *Clin Chem* **55:**1646–1655.
13. **Homburger HA, Singh R.** 2008. Assessment of proteins of the immune system, p 1419–1434. *In* Rich RR, Fleisher TA, Shearer WT, Schroeder HW Jr, Frew AJ, Weyand CM (ed), *Clinical Immunology: Principles and Practice,* 3rd ed. Mosby Saunders, Philadelphia, PA.
14. **Whicher JT, Price CP, Spencer K.** 1983. Immunonephelometric and immunoturbidimetric assays for proteins. *Crit Rev Clin Lab Sci* **18:**213–260.
15. **Keren DF.** 2003. *Protein Electrophoresis in Clinical Diagnosis*. Arnold, London, United Kingdom.
16. **Keren DF, Humphrey R.** 2006. Clinical indications and applications of serum and urine protein electrophoresis, p 75–87. *In* Detrick B, Hamilton RG, Folds JD (ed), *Manual of Molecular and Clinical Laboratory Immunology,* 7th ed. ASM Press, Washington, DC.
17. **Katzmann JA, Kyle RA.** 2006. Immunochemical characterization of immunoglobulins in serum, urine and cerebrospinal fluid, p 88–100. *In* Detrick B, Hamilton RG, Folds JD (ed), *Manual of Molecular and Clinical Laboratory Immunology,* 7th ed. ASM Press, Washington, DC.
18. **Lequin RM.** 2005. Enzyme immunoassay (EIA)/enzyme-linked immunosorbent assay (ELISA). *Clin Chem* **51:** 2415–2418.
19. **Rissin DM, Kan CW, Campbell TG, Howes SC, Fournier DR, Song L, Piech T, Patel PP, Chang L, Rivnak AJ, Ferrell EP, Randall JD, Provuncher GK, Walt DR, Duffy DC.** 2010. Single-molecule enzyme-linked immunosorbent assay detects serum proteins at subfemtomolar concentrations. *Nat Biotechnol* **28:**595–599.
20. **Earley MC, Vogt RF Jr, Shapiro HM, Mandy FF, Kellar KL, Bellisario R, Pass KA, Marti GE, Stewart CC, Hannon WH.** 2002. Report from a workshop on multianalyte microsphere assays. *Cytometry* **50:**239–242.
21. **Hsu HY, Joos TO, Koga H.** 2009. Multiplex microsphere-based flow cytometric platforms for protein analysis and their application in clinical proteomics—from assays to results. *Electrophoresis* **30:**4008–4019.
22. **Jun BH, Kang H, Lee YS, Jeong DH.** 2012. Fluorescence-based multiplex protein detection using optically encoded microbeads. *Molecules* **17:**2474–2490.
23. **Kettman JR, Davies T, Chandler D, Oliver KG, Fulton RJ.** 1998. Classification and properties of 64 multiplexed microsphere sets. *Cytometry* **33:**234–243.
24. **Elshal MF, McCoy JP.** 2006. Multiplex bead array assays: performance evaluation and comparison of sensitivity to ELISA. *Methods* **38:**317–323.
25. **Kingsmore SF.** 2006. Multiplexed protein measurement: technologies and applications of protein and antibody arrays. *Nat Rev Drug Discov* **5:**310–320.
26. **Ellington AA, Kullo IJ, Bailey KR, Klee GG.** 2010. Antibody-based protein multiplex platforms: technical and operational challenges. *Clin Chem* **56:**186–193.

27. **Wilson DS, Nock S.** 2003. Recent developments in protein microarray technology. *Angew Chem Int Ed Engl* **42:**494–500.
28. **Hultschig C, Kreutzberger J, Seitz H, Konthur Z, Büssow K, Lehrach H.** 2006. Recent advances of protein microarrays. *Curr Opin Chem Biol* **10:**4–10.
29. **Djoba Siawaya JF, Roberts T, Babb C, Black G, Golakai HJ, Stanley K, Bapela NB, Hoal E, Parida S, van Helden P, Walzl G.** 2008. An evaluation of commercial fluorescent bead-based luminex cytokine assays. *PloS One* **3:**e2535. doi:10.1371/journal.pone.0002535.
30. **Leng SX, McElhaney JE, Walston JD, Xie D, Fedarko NS, Kuchel GA.** 2008. ELISA and multiplex technologies for cytokine measurement in inflammation and aging research. *J Gerontol A Biol Sci Med Sci* **63:**879–884.
31. **Toedter G, Hayden K, Wagner C, Brodmerkel C.** 2008. Simultaneous detection of eight analytes in human serum by two commercially available platforms for multiplex cytokine analysis. *Clin Vaccine Immunol* **15:**42–48.
32. **Martinez JE, Clutterbuck EA, Li H, Romero-Steiner S, Carlone GM.** 2006. Evaluation of multiplex flow cytometric opsonophagocytic assays for determination of functional anticapsular antibodies to *Streptococcus pneumoniae*. *Clin Vaccine Immunol* **13:**459–466.
33. **Schulz KR, Danna EA, Krutzik PO, Nolan GP.** 2012. Single-cell phospho-protein analysis by flow cytometry. *Curr Protoc Immunol* 8.17.11–18.17.20.
34. **Vereb G, Nagy P, Szöllosi J.** 2011. Flow cytometric FRET analysis of protein interaction. *Methods Mol Biol* **699:**371–392.
35. **Bjornson ZB, Nolan GP, Fantl WJ.** 2013. Single-cell mass cytometry for analysis of immune system functional states. *Curr Opin Immunol* **25:**484–494.
36. **Kricka LJ, Master SR.** 2009. Quality control and protein microarrays. *Clin Chem* **55:**1053–1055.
37. **Fenn JB, Mann M, Meng CK, Wong SF, Whitehouse CM.** 1989. Electrospray ionization for mass spectrometry of large biomolecules. *Science* **246:**64–71.
38. **Karas M, Hillenkamp F.** 1988. Laser desorption ionization of proteins with molecular masses exceeding 10,000 daltons. *Anal Chem* **60:**2299–2301.
39. **Wilm M.** 2011. Principles of electrospray ionization. *Mol Cell Proteomics* **10:**M111.009407. doi:10.1074/mcp.M111.009407.
40. **Mann M, Meng CK, Fenn JB.** 1989. Interpreting mass-spectra of multiply charged ions. *Anal Chem* **61:** 1702–1708.
41. **Kafka AP, Kleffmann T, Rades T, McDowell A.** 2011. The application of MALDI TOF MS in biopharmaceutical research. *Int J Pharm* **417:**70–82.
42. **Norris JL, Caprioli RM.** 2013. Analysis of tissue specimens by matrix-assisted laser desorption/ionization imaging mass spectrometry in biological and clinical research. *Chem Rev* **113:**2309–2342.
43. **Pirro V, Eberlin LS, Oliveri P, Cooks RG.** 2012. Interactive hyperspectral approach for exploring and interpreting DESI-MS images of cancerous and normal tissue sections. *Analyst* **137:**2374–2380.
44. **Watson JT, Sparkman OD.** 2007. *Introduction to Mass Spectrometry: Instrumentation, Applications and Strategies for Data Interpretation*, 4th ed. John Wiley & Sons Ltd, Chichester, United Kingdom.
45. **Jonscher KR, Yates JR III.** 1997. The quadrupole ion trap mass spectrometer—a small solution to a big challenge. *Anal Biochem* **244:**1–15.
46. **Earley L, Anderson LC, Bai DL, Mullen C, Syka JE, English AM, Dunyach JJ, Stafford GC Jr, Shabanowitz J, Hunt DF, Compton PD.** 2013. Front-end electron transfer dissociation: a new ionization source. *Anal Chem* **85:**8385–8390.
47. **Ens W, Standing KG.** 2005. Hybrid quadrupole/time-of-flight mass spectrometers for analysis of biomolecules. *Methods Enzymol* **402:**49–78.
48. **Brown RS, Gilfrich NL.** 1992. Optimizing signal and mass resolution for matrix-assisted laser desorption utilizing a linear time-of-flight mass spectrometer. *Rapid Commun Mass Spectrom* **6:**697–701.
49. **Hu Q, Noll RJ, Li H, Makarov A, Hardman M, Graham Cooks R.** 2005. The Orbitrap: a new mass spectrometer. *J Mass Spectrom* **40:**430–443.
50. **Ikonomou MG, Blades AT, Kebarle P.** 1990. Investigations of the electrospray interface for liquid-chromatography mass-spectrometry. *Anal Chem* **62:**957–967.
51. **Covey T.** 1996. Analytical characteristics of the electrospray ionization process, p 21–59. *In* Snyder AP (ed), *Biochemical and Biotechnological Applications of Electrospray Ionization Mass Spectrometry*. American Chemical Society, Washington, DC.
52. **Jemal M, Ouyang Z, Powell ML.** 2000. Direct-injection LC-MS-MS method for high-throughput simultaneous quantitation of simvastatin and simvastatin acid in human plasma. *J Pharm Biomed Anal* **23:**323–340.
53. **Wang J, Aubry AF, Cornelius G, Caporuscio C, Sleczka B, Ranasinghe A, Wang-Iverson D, Olah T, Jemal M.** 2010. Importance of mobile phase and injection solvent selection during rapid method development and sample analysis in drug discovery bioanalysis illustrated using convenient multiplexed LC-MS/MS. *Anal Methods* **2:**375–381.
54. **Desiderio DM, Katakuse I.** 1983. Fast atom bombardment-collision activated dissociation-linked field scanning mass spectrometry of the neuropeptide substance P. *Anal Biochem* **129:**425–429.
55. **Desiderio DM, Katakuse I, Kai M.** 1983. Measurement of leucine enkephalin in caudate nucleus tissue with fast atom bombardment-collision activated dissociation-linked field scanning mass spectrometry. *Biomed Mass Spectrom* **10:**426–429.
56. **Bystrom CE, Sheng S, Clarke NJ.** 2011. Narrow mass extraction of time-of-flight data for quantitative analysis of proteins: determination of insulin-like growth factor-1. *Anal Chem* **83:**9005–9010.
57. **Chen Z, Caulfield MP, McPhaul MJ, Reitz RE, Taylor SW, Clarke NJ.** 2013. Quantitative insulin analysis using liquid chromatography–tandem mass spectrometry in a high-throughput clinical laboratory. *Clin Chem* **59:**1349–1356.
58. **Van Uytfanghe K, Rodríguez-Cabaleiro D, Stöckl D, Thienpont LM.** 2007. New liquid chromatography/electrospray ionisation tandem mass spectrometry measurement procedure for quantitative analysis of human insulin in serum. *Rapid Commun Mass Spectrom* **21:**819–821.
59. **Romanova EV, Dowd SE, Sweedler JV.** 2013. Quantitation of endogenous peptides using mass spectrometry based methods. *Curr Opin Chem Biol* **17:**801–808.
60. **Zhang Y, Fonslow BR, Shan B, Baek MC, Yates JR III.** 2013. Protein analysis by shotgun/bottom-up proteomics. *Chem Rev* **113:**2343–2394.
61. **Shevchenko A, Wilm M, Vorm O, Jensen ON, Podtelejnikov AV, Neubauer G, Shevchenko A, Mortensen P, Mann M.** 1996. A strategy for identifying gel-separated proteins in sequence databases by MS alone. *Biochem Soc Trans* **24:**893–896.
62. **Eng JK, McCormack AL, Yates JR.** 1994. An approach to correlate tandem mass spectral data of peptides with amino acid sequences in a protein database. *J Am Soc Mass Spectrom* **5:**976–989.
63. **Yates JR III, Eng JK, McCormack AL, Schieltz D.** 1995. Method to correlate tandem mass spectra of modified peptides to amino acid sequences in the protein database. *Anal Chem* **67:**1426–1436.

64. **Link AJ, Eng J, Schieltz DM, Carmack E, Mize GJ, Morris DR, Garvik BM, Yates JR III.** 1999. Direct analysis of protein complexes using mass spectrometry. *Nat Biotechnol* **17:**676–682.
65. **Jones KA, Kim PD, Patel BB, Kelsen SG, Braverman A, Swinton DJ, Gafken PR, Jones LA, Lane WS, Neveu JM, Leung HC, Shaffer SA, Leszyk JD, Stanley BA, Fox TE, Stanley A, Hall MJ, Hampel H, South CD, de la Chapelle A, Burt RW, Jones DA, Kopelovich L, Yeung AT.** 2013. Immunodepletion plasma proteomics by TripleTOF 5600 and Orbitrap Elite/LTQ-Orbitrap Velos/Q Exactive mass spectrometers. *J Proteome Res* **12:**4351–4365.
66. **de Groot CJ, Güzel C, Steegers-Theunissen RP, de Maat M, Derkx P, Roes EM, Heeren RM, Luider TM, Steegers EA.** 2007. Specific peptides identified by mass spectrometry in placental tissue from pregnancies complicated by early onset preeclampsia attained by laser capture dissection. *Proteomics Clin Appl* **1:**325–335.
67. **Vrana JA, Gamez JD, Madden BJ, Theis JD, Bergen HR 3rd, Dogan A.** 2009. Classification of amyloidosis by laser microdissection and mass spectrometry-based proteomic analysis in clinical biopsy specimens. *Blood* **114:**4957–4959.
68. **Barr JR, Maggio VL, Patterson DG Jr, Cooper GR, Henderson LO, Turner WE, Smith SJ, Hannon WH, Needham LL, Sampson EJ.** 1996. Isotope dilution–mass spectrometric quantification of specific proteins: model application with apolipoprotein A-I. *Clin Chem* **42:**1676–1682.
69. **Barnidge DR, Dratz EA, Martin T, Bonilla LE, Moran LB, Lindall A.** 2003. Absolute quantification of the G protein-coupled receptor rhodopsin by LC/MS/MS using proteolysis product peptides and synthetic peptide standards. *Anal Chem* **75:**445–451.
70. **Barnidge DR, Goodmanson MK, Klee GG, Muddiman DC.** 2004. Absolute quantification of the model biomarker prostate-specific antigen in serum by LC-MS/MS using protein cleavage and isotope dilution mass spectrometry. *J Proteome Res* **3:**644–652.
71. **Bondar OP, Barnidge DR, Klee EW, Davis BJ, Klee GG.** 2007. LC-MS/MS quantification of Zn-α2 glycoprotein: a potential serum biomarker for prostate cancer. *Clin Chem* **53:**673–678.
72. **Kumar V, Barnidge DR, Chen LS, Twentyman JM, Cradic KW, Grebe SK, Singh RJ.** 2010. Quantification of serum 1–84 parathyroid hormone in patients with hyperparathyroidism by immunocapture in situ digestion liquid chromatography–tandem mass spectrometry. *Clin Chem* **56:**306–313.
73. **Seegmiller JC, Barnidge DR, Burns BE, Larson TS, Lieske JC, Kumar R.** 2009. Quantification of urinary albumin by using protein cleavage and LC-MS/MS. *Clin Chem* **55:**1100–1107.
74. **Craig R, Cortens JP, Beavis RC.** 2005. The use of proteotypic peptide libraries for protein identification. *Rapid Commun Mass Spectrom* **19:**1844–1850.
75. **Bereman MS, MacLean B, Tomazela DM, Liebler DC, MacCoss MJ.** 2012. The development of selected reaction monitoring methods for targeted proteomics via empirical refinement. *Proteomics* **12:**1134–1141.
76. **Anderson L, Hunter CL.** 2006. Quantitative mass spectrometric multiple reaction monitoring assays for major plasma proteins. *Mol Cel Proteomics* **5:**573–588.
77. **Kilpatrick EL, Liao WL, Camara JE, Turko IV, Bunk DM.** 2012. Expression and characterization of ^{15}N-labeled human C-reactive protein in *Escherichia coli* and *Pichia pastoris* for use in isotope-dilution mass spectrometry. *Protein Expr Purif* **85:**94–99.
78. **Durbin KR, Tran JC, Zamdborg L, Sweet SM, Catherman AD, Lee JE, Li M, Kellie JF, Kelleher NL.** 2010. Intact mass detection, interpretation, and visualization to automate Top-Down proteomics on a large scale. *Proteomics* **10:**3589–3597.
79. **Tran JC, Zamdborg L, Ahlf DR, Lee JE, Catherman AD, Durbin KR, Tipton JD, Vellaichamy A, Kellie JF, Li M, Wu C, Sweet SM, Early BP, Siuti N, LeDuc RD, Compton PD, Thomas PM, Kelleher NL.** 2011. Mapping intact protein isoforms in discovery mode using top-down proteomics. *Nature* **480:**254–258.
80. **Taylor GK, Kim YB, Forbes AJ, Meng FY, McCarthy R, Kelleher NL.** 2003. Web and database software for identification of intact proteins using "top down" mass spectrometry. *Anal Chem* **75:**4081–4086.
81. **Kellie JF, Catherman AD, Durbin KR, Tran JC, Tipton JD, Norris JL, Witkowski CE II, Thomas PM, Kelleher NL.** 2012. Robust analysis of the yeast proteome under 50 kDa by molecular-mass-based fractionation and top-down mass spectrometry. *Anal Chem* **84:**209–215.
82. **Edwards RL, Griffiths P, Bunch J, Cooper HJ.** 2012. Top-down proteomics and direct surface sampling of neonatal dried blood spots: diagnosis of unknown hemoglobin variants. *J Am Soc Mass Spectrom* **23:**1921–1930.
83. **Théberge R, Infusini G, Tong W, McComb ME, Costello CE.** 2011. Top-down analysis of small plasma proteins using an LTQ-Orbitrap. Potential for mass spectrometry-based clinical assays for transthyretin and hemoglobin. *Int J Mass Spectrom* **300:**130–142.
84. **Barnidge DR1, Dasari S, Botz CM, Murray DH, Snyder MR, Katzmann JA, Dispenzieri A, Murray DL.** 2014. Using mass spectrometry to monitor monoclonal immunoglobulins in patients with a monoclonal gammopathy. *J. Proteome Res* **13:**1419–1427.
85. **Falick AM, Shackleton CH, Green BN, Witkowska HE.** 1990. Tandem mass spectrometry in the clinical analysis of variant hemoglobins. *Rapid Commun Mass Spectrom* **4:**396–400.
86. **Troxler H, Kleinert P, Schmugge M, Speer O.** 2012. Advances in hemoglobinopathy detection and identification. *Adv Clin Chem* **57:**1–28.
87. **Bergen HR III, Zeldenrust SR, Naylor S.** 2003. An on-line assay for clinical detection of amyloidogenic transthyretin variants directly from serum. *Amyloid* **10:**190–197.
88. **Lacey JM, Bergen HR, Magera MJ, Naylor S, O'Brien JF.** 2001. Rapid determination of transferrin isoforms by immunoaffinity liquid chromatography and electrospray mass spectrometry. *Clin Chem* **47:**513–518.
89. **Kuprowski MC, Boys BL, Konermann L.** 2007. Analysis of protein mixtures by electrospray mass spectrometry: effects of conformation and desolvation behavior on the signal intensities of hemoglobin subunits. *J Am Soc Mass Spectrom* **18:**1279–1285.
90. **Anderson NL, Anderson NG, Haines LR, Hardie DB, Olafson RW, Pearson TW.** 2004. Mass spectrometric quantitation of peptides and proteins using stable isotope standards and capture by anti-peptide antibodies (SISCAPA). *J Proteome Res* **3:**235–244.
91. **Anderson L, Hunter CL.** 2006. Quantitative mass spectrometric multiple reaction monitoring assays for major plasma proteins. *Mol Cell Proteomics* **5:**573–588.
92. **Taylor PJ.** 2004. Matrix effects: the Achilles heel of quantitative high-performance liquid chromatography–electrospray–tandem mass spectrometry. *Clin Biochem* **38:**328–334.
93. **Gusev AI, Wilkinson WR, Proctor A, Hercules DM.** 1995. Improvement of signal reproducibility and matrix/comatrix effects in MALDI analysis. *Anal Chem* **67:**1034–1041.
94. **Pascoe R, Foley JP, Gusev AI.** 2001. Reduction in matrix-related signal suppression effects in electrospray ionization

mass spectrometry using on-line two-dimensional liquid chromatography. *Anal Chem* **73:**6014–6023.

95. **Farrah T, Deutsch EW, Kreisberg R, Sun Z, Campbell DS, Mendoza L, Kusebauch U, Brusniak MY, Hüttenhain R, Schiess R, Selevsek N, Aebersold R, Moritz RL.** 2012. PASSEL: the PeptideAtlas SRMexperiment library. *Proteomics* **12:**1170–1175.
96. **Reiter L, Rinner O, Picotti P, Hüttenhain R, Beck M, Brusniak MY, Hengartner MO, Aebersold R.** 2011. mProphet: automated data processing and statistical validation for large-scale SRM experiments. *Nat Methods* **8:**430–435.
97. **Thevis M, Bredehöft M, Kohler M, Schänzer W.** 2010. Mass spectrometry-based analysis of IGF-1 and hGH. *Handb Exp Pharmacol* **195:**201–207.
98. **Shi TJ, Su D, Liu T, Tang K, Camp DG II, Qian WJ, Smith RD.** 2012. Advancing the sensitivity of selected reaction monitoring-based targeted quantitative proteomics. *Proteomics* **12:**1074–1092.
99. **Zanella-Cleon I, Joly P, Becchi M, Francina A.** 2009. Phenotype determination of hemoglobinopathies by mass spectrometry. *Clin Biochem* **42:**1807–1817.
100. **Chen Y, Snyder MR, Zhu Y, Tostrud LJ, Benson LM, Katzmann JA, Bergen HR III.** 2011. Simultaneous phenotyping and quantification of α-1-antitrypsin by liquid chromatography–tandem mass spectrometry. *Clin Chem* **57:**1161–1168.
101. **D'Souza A, Theis J, Quint P, Kyle R, Gertz M, Zeldenrust S, Vrana J, Dogan A, Dispenzieri A.** 2013. Exploring the amyloid proteome in immunoglobulin-derived lymph node amyloidosis using laser microdissection/tandem mass spectrometry. *Am J Hematol* **88:**577–580.
102. **Maleszewski JJ, Murray DL, Dispenzieri A, Grogan M, Pereira NL, Jenkins SM, Judge DP, Caturegli P, Vrana JA, Theis JD, Dogan A, Halushka MK.** 2013. Relationship between monoclonal gammopathy and cardiac amyloid type. *Cardiovasc Pathol* **22:**189–194.

Immunoglobulin Methods

section B

VOLUME EDITOR: ROBERT G. HAMILTON
SECTION EDITOR: DAVID F. KEREN

Introduction

DAVID F. KEREN

5

The section on immunoglobulin methods covers the basic genetic background for immunoglobulin production, measurement of immunoglobulins, identification of monoclonal protein products by serum protein electrophoresis and immunofixation, and detection of oligoclonal bands in cerebrospinal fluid. In addition, this section covers the characterization of cryoglobulins and cryofibrinogens and an overall strategy for using all the techniques in this section to detect, stratify risks of progression of, and monitor patients with monoclonal gammopathies.

Since the 7th edition of the *Manual of Molecular and Clinical Laboratory Immunology* (2006), there have been significant advances in the design and implementation of analytical tools to study immunoglobulins and interpret their results in a clinical context. The background for the molecular basis of immunoglobulin complexity and antigen specificity has evolved rapidly. Kipps, Ghia, and Rassenti (chapter 6) present a cogent discussion of the immunoglobulin heavy-chain and light-chain complexes together with a detailed explanation of the lack of uniform expression of each functional immunoglobulin heavy-chain variable gene. This is accompanied by a comprehensive overview of the molecular basis for immunoglobulin gene rearrangement and its relationship to the heterogeneity of the humoral immune response. This is illustrated using a detailed figure of the light- and heavy-chain gene complexes. They also describe how the detection of immunoglobulin gene rearrangements using PCR can aid in detecting clonal populations of B cells and how these highly sensitive methods may be deployed to investigate minimal residual disease.

Warren (chapter 7) reviews how IgG, IgA, IgM, immunoglobulin subclasses, serum free light chains, and even IgD and IgE are measured by nephelometric or immunoturbidimetric assay systems. Former gel diffusion and Laurell rocket techniques have fallen out of use. He makes note of their problem with the antigen excess effect and occasional nonlinearity in the serum free-light-chain test (1, 2). He highlights the recently FDA-approved heavy/light-chain assays. Using a nephelometric method similar to that used in quantifying serum free light chains, one may now separately measure IgG-kappa (IgGκ) from IgG-lambda (IgGλ), IgAκ from IgAλ, and IgMκ from IgMλ (3, 4).

This analysis may be especially useful in following the beta-region M proteins that are cloaked by transferrin and C3 bands.

Serum and urine protein electrophoreses are still the principal assays for the detection of monoclonal gammopathies and other immunoglobulin-based clinical abnormalities. In chapter 8, Keren and Humphrey review both the technical details and the clinical applications of serum and urine protein electrophoresis. Because of the expanded use of capillary electrophoresis since the previous edition, the chapter discusses both the classic gel and newer capillary electrophoresis patterns along with problems and pitfalls that may lead to false-positive or false-negative serum and urine findings. In addition, the chapter provides useful details for specimen processing, quality control, and quality assurance (5). The chapter illustrates the ability of capillary electrophoresis to detect polyclonal increases in IgG4 as part of IgG4-related systemic disease (6).

In cases where monoclonal gammopathies are detected or suspected, Sykes and Posey (chapter 9) present a thorough review of their characterization in serum and urine by immunofixation and immunosubtraction. Their presentation provides useful examples of both immunosubtraction (immunotyping) patterns, when capillary electrophoresis is used for the characterization, and immunofixation patterns, when gel techniques are employed. In addition, their chapter presents illustrative examples of isoelectric focusing with immunofixation in the evaluation of cerebrospinal fluid for the presence of oligoclonal bands.

Gorevic and Galanakis (chapter 10) discuss the state-of-the-art methodology in the detection and measurement of cryoglobulins. They also provide a thorough review of cryofibrinogenemia and pyroglobulins. This comprehensive chapter provides recent information on the importance of hepatitis C virus in both type II and type III cryoglobulins (7). Many practical suggestions are made about the importance of proper handling in the identification and characterization of these temperature-sensitive specimens (8). The section on cryofibrinogens has an up-to-date discussion of the effect of heparin and citrate anticoagulation on cryofibrinogen detection. Lastly, the authors discuss the peculiar phenomenon of pyroglobulins, which lack the clinical manifestations of cryoglobulins but can present confounding laboratory findings in heat-based assays such as those used to inactivate complement.

To coordinate the use of the above-mentioned techniques in the context of current clinical guidelines, Katzmann and Keren (chapter 11) first provide a handy

doi:10.1128/9781555818722.ch5

categorization of plasma cell proliferative disorders. This is followed by a diagnostic testing strategy that uses an efficient electrophoretic and nephelometric assay analysis. They recommend a basic diagnostic screening panel consisting of serum protein electrophoresis, immunofixation, and serum free-light-chain testing. However, the chapter provides caveats and illustrations of special cases to prevent missing low tumor burden conditions such as light-chain-type amyloidosis and light-chain deposition disease. They show how these measurements are useful in stratifying the risk of progression, in survival estimates, and in monitoring of monoclonal gammopathies. The authors discuss the use of immunosubtraction and the new heavy/light assays to monitor IgA and IgM monoclonal gammopathies that may be obscured by comigrating beta-region proteins.

REFERENCES

1. **Tate JR, Mollee P, Dimeski G, Carter AC, Gill D.** 2007. Analytical performance of serum free light-chain assay during monitoring of patients with monoclonal light-chain diseases. *Clin Chim Acta* **376:**30–36.
2. **Daval S, Tridon A, Mazeron N, Ristori JM, Evrard B.** 2007. Risk of antigen excess in serum free light chain measurements. *Clin Chem* **53:**1985–1986.
3. **Bradwell AR, Harding SJ, Fourier NJ, Wallis GL, Drayson MT, Carr-Smith HD, Mead GP.** 2009. Assessment of monoclonal gammopathies by nephelometric measurement of individual immunoglobulin kappa/lambda ratios. *Clin Chem* **55:**1646–1655.
4. **Katzmann JA, Rajkumar SV.** 2013. A window into immunoglobulin quantitation and plasma cell disease: antigen epitopes defined by the junction of immunoglobulin heavy and light chains. *Leukemia* **27:**1–2.
5. **Keren DF.** 2012. *Protein Electrophoresis in Clinical Diagnosis*. American Society for Clinical Pathology Press, Chicago, IL.
6. **Jacobs JFM, van der Molen RG, Keren DF.** 2014. Relatively restricted migration of polyclonal IgG4 may mimic a monoclonal gammopathy in IgG4-related disease. *Am J Clin Pathol* **142:**76–81.
7. **Russi S, Sansonno D, Mariggio MA, Vinella A, Pavone F, Lauletta G, Sansonno S, Dammacco F.** 2014. Assessment of hepatitis core protein in HCV-related mixed cryoglobulinemia. *Arthritis Res Ther* **18:**16.
8. **Warren JS.** 2013. Clinically unsuspected cryoglobulinemia. *Am J Clin Pathol* **139:**352–359.

Immunoglobulin Genes

THOMAS J. KIPPS, EMANUELA M. GHIA, AND LAURA Z. RASSENTI

6

IMMUNOGLOBULIN MOLECULES

Introduction

Immunoglobulins are a heterogeneous group of glycoproteins produced by B lymphocytes and plasma cells. A single person can synthesize 10 million to 100 million different immunoglobulin molecules, each having distinct antigen-binding specificities. This great diversity in the so-called humoral immune system allows us to generate antibodies specific for a variety of substances, including synthetic molecules not naturally present in our environment. Despite the diversity in the specificities of antibody molecules, the binding of an antibody to an antigen initiates a limited series of biologically important effector functions, such as complement activation and/or adherence of the immune complex to receptors on leukocytes (1). Resolution of the immunoglobulin structure has revealed how these molecules can have such great diversity in antigen-binding activities while maintaining conserved effector functions, such as complement activation.

Basic Immunoglobulin Structure

The basic unit of the immunoglobulin molecule is composed of two identical heavy chains and two identical light chains. These four polypeptides are held together by disulfide bonds and noncovalent interactions (2–5). The amino-terminal domains (110 to 120 amino acids) of the heavy and light chains are designated the variable regions, because their primary structures vary markedly among different immunoglobulin molecules (6). The carboxy-terminal domains, however, are referred to as constant regions, because their primary structures are the same among immunoglobulins of the same class or subclass. The amino acids in the light- and heavy-chain variable regions interact to form an antigen-binding site (2, 7). Each four-chain immunoglobulin basic unit has two identical binding sites. Stability for the immunoglobulin molecule is provided by the constant-region domains of the heavy and light chains. The specific effector functions of the different immunoglobulin classes are mediated by the heavy-chain constant regions (Table 1) (8).

There are two classes of immunoglobulin light chains, the κ and λ light chains, which differ in the amino acid sequences of the constant-region domains. The ratio of κ to λ chains in adult plasma is 2:1. The light-chain constant region's main purpose may be to allow for proper assembly and release of an intact immunoglobulin molecule. Soon after synthesis, the antibody light-chain constant region associates with the nascent immunoglobulin heavy chain, releasing the latter from the immunoglobulin-binding protein. In the absence of antibody light chain, the immunoglobulin-binding protein binds the first constant-region domain of the newly synthesized heavy chain, thereby retaining the heavy-chain polypeptide in the cell's endoplasmic reticulum (9).

Heavy-Chain Isotypes

Five major classes of immunoglobulin molecules—immunoglobulin G (IgG), IgA, IgM, IgD, and IgE—correspond to the five classes of heavy-chain isotypes (γ, α, μ, δ, and ε). The immunoglobulin molecule of each isotype can contain either a κ or a λ light chain but not both. The physical properties of each of these classes of immunoglobulin molecules are summarized in Table 1.

IgG

IgG is the most abundant of immunoglobulins found in adult plasma, accounting for approximately 80% of the total immunoglobulin. IgG is the predominant antibody produced during a secondary immune response. IgG molecules can penetrate extravascular spaces and cross the placental barrier to provide immunity to the fetus. These molecules have a four-chain 150-kDa immunoglobulin structure with a hinge region that can be attacked by proteolytic enzymes such as papain and pepsin, allowing for separation of the antigen-binding fragment(s), Fab or F(ab)2, from the crystallizable or constant fragment (Fc) of the antibody molecule. Receptors for the Fc (FcR) allow effector cells to recognize target cells coated with a specific antibody (10).

There are four subclasses of IgG: IgG1, IgG2, IgG3, and IgG4. Each subclass has a particular heavy-chain constant region and has different effector functions (8). The most abundant class is IgG1, which accounts for approximately 65% of the total IgG in the plasma. Of the IgG subclasses, IgG1 binds best to FcRI (CD64) and FcRII (CD32), with affinities (K_d) of 10^{-8} M and 5×10^{-7} M, respectively. IgG1 and IgG3 bind equally well to FcRIII (CD16), with a K_d of 2×10^{-6} M. FcRIII is the FcR expressed by natural killer cells (NK cells, or K cells) that mediate antibody-dependent cell-mediated cytotoxicity. Proteins of the IgG4 or IgG2 subclass bind poorly to FcRI (CD64) or FcRII (CD32) and do not bind to FcRIII (CD16) at all. The average half-life

doi:10.1128/9781555818722.ch6

TABLE 1 Physical properties of human immunoglobulins

Heavy-chain class (isotype)	Heavy-chain subclasses	No. of heavy-chain domains	Secretory form(s)	Molecular mass (Da)	Antigen-binding valency	Concn (mg/ml) in serum	% of total immunoglobulins
IgG (γ)	γ1, γ2, γ3, γ4	4	Monomer	150,000	2	8–16	80
IgA (α)	α1, α2	4	Monomer, dimer	160,000 (monomer)	2 (monomer)	1.4–4.0	13
				400,000 (secretory protein)	4 (secretory protein)		
IgM (μ)		5	Pentamer	900,000	10	0.5–2.0	6
IgD (δ)		4	Monomer	180,000	2	0–0.4	1
IgE (ε)		5	Monomer	190,000	2	17–450 ng/ml	0.002

of circulating IgG molecules is about 21 days. The response to a given antigen can result in a skewed IgG subclass response, and this is frequently a source of investigation as to correlates of protection or for the design of vaccines. Specific subclasses can be associated with individual disease processes. For example, in patients with pemphigus vulgaris, a mucocutaneous blistering disease, IgG4 antibodies to desmoglein 3 are pathogenic (11, 12).

IgA

The IgA molecules constitute 13% of the total plasma immunoglobulins. There are two major classes of IgA molecules, designated IgA1 and IgA2, with IgA1 being the more abundant (85% of total IgA in plasma). The half-life of IgA molecules is about 6 days.

IgA antibodies are synthesized during a secondary immune response and contribute to mucosal immunity (13–15). IgA antibodies are the primary antibodies in saliva, tears, breast milk, and the fluids of the gastrointestinal, respiratory, and urinary tracts (16). These secreted immunoglobulins consist of an IgA dimer bound to the joining (J)-chain polypeptide and a secretory protein with a molecular mass of 70 to 80 kDa. The J chain is required for proper hepatic transport of IgA (17). The secretory component is actually part of an FcR for dimeric IgA that is synthesized not by B cells but rather by epithelial cells of organs such as the intestine. This protein facilitates the transport of the IgA protein across the epithelial cell and may protect the secreted IgA molecule from proteolytic digestion by enzymes in the intestinal lumen. Since these molecules do not cross the placenta barrier and do not easily bind to cell surfaces, their main role may be to prevent foreign substances from binding to mucosal surfaces and entering the blood. Finally, it has been proposed that secretory IgA might also act as a potentiator of the immune response in intestinal tissue by means of uptake of antigen to dendritic cells (18).

IgM

The IgM immunoglobulins comprise about 6% of the immunoglobulins in adult plasma. These molecules have very high molecular weights (thus, they are called macroglobulins), and they are formed by the linking of five identical immunoglobulin units by disulfide bonds and a J chain. IgM is the predominant class found during a primary immune response. The IgM molecules do not cross the placenta and do not enter into extravascular spaces; however, they fix complement more efficiently than the monomeric IgG molecules. The half-life of IgM molecules in plasma is approximately 6 days. In addition, monomeric IgM is the main component of an antigen receptor expressed on B cells (B-cell receptor). The IgM monomer represents the ligand-binding part of the receptor. The component that is responsible for signal transduction consists of two glycoproteins, CD79a and CD79b. The cytoplasmic domains of CD79a and CD79b contain tyrosine motifs responsible for transduction of signal from the receptor (19).

IgD

The IgD molecules constitute only 1% of the plasma immunoglobulins, and they are expressed on B cells with IgM. These immunoglobulins do not cross the placenta and do not easily penetrate extravascular spaces. However, IgD molecules are found in relatively high concentrations in umbilical cord blood. IgD molecules are thought to function as B-cell membrane receptors for antigens and may help in the recruitment of B cells for specific antigen-driven responses (20). Similar to IgM, membrane-bound IgD is associated with CD79a and Cd79b for signaling. IgD is expressed on the membranes of B cells when they leave the marrow and populate secondary lymphoid organs. Most IgD-positive B cells also coexpress IgM, and both participate in B-cell receptor signaling through CD79a and CD79b. It has been proposed that membrane-bound IgD regulates B-cell fate at specific developmental stages through changes in activation status (21). B-cell stimulation and activation can result from the binding of specific bacterial proteins to the constant region of IgD. For example, circulating IgD can react with IgD-binding protein of *Moraxella catarrhalis*, independently of the variable regions of the antibody (22).

IgE

IgE has been called a reaginic antibody to denote its association with immediate hypersensitivity. IgE antibodies constitute a very small percentage of the total plasma immunoglobulins (0.002%). Although four human IgE isoforms can be produced by alternative splicing of the epsilon primary transcript (23), the isoforms appear to have similar functions. Plasma IgE levels may increase (5 to 20 times the baseline) in parasitic infections and children with atopic diseases. The Fc portion of the IgE molecule can bind with high affinity to receptors on the surfaces of basophils and mast cells. The cross-linking of IgE antibody by an allergen can induce the release of vasoactive amines, proteases, lipid-derived inflammatory mediators, and cytokines, such as tumor necrosis factor alpha, gamma interferon, or interleukins 1, 3, 4, 5, and 6. Studies indicate that the microenvironment of mucosal tissues in allergic disease favors class switching to IgE (24). Anti-IgE antibodies have been developed as therapy for allergy and asthma (25).

IMMUNOGLOBULIN GENE COMPLEXES

Immunoglobulin Heavy-Chain Gene Complex

Immunoglobulin Heavy-Chain Constant-Region Exons

The heavy-chain gene complex is located at band q32 on the long arm of chromosome 14 (26). This complex is composed of 38 to 46 functional heavy-chain variable-region genes (IGHV genes), over 80 nonfunctional IGHV pseudogenes, 23 functional diversity (IGHD) segments, 6 functional IGHJ minigenes, and exons encoding the constant regions for each of the immunoglobulin heavy-chain isotypes (27–29). The order (5′→3′) of the genes encoding each of the immunoglobulin heavy-chain isotypes is C_μ (M), C_δ (D), $C_\gamma 3$ (G3), $C_\gamma 1$ (G1), $C_\varepsilon 1$ (EP1, a nonfunctional pseudogene), $C_\alpha 1$ (A1), C_γ (GP, an open reading frame lacking the switch region), $C_\gamma 2$ (G2), $C_\gamma 4$ (G4), C_ε (E), and $C_\alpha 2$ (A2) (Fig. 1). The genes encoding the heavy-chain constant regions and each associated intronic switch region are as depicted in Fig. 1. These genes are labeled, and pseudogenes are also indicated in the figure.

Immunoglobulin Heavy-Chain Variable-Region Genes

The IGHV gene segments map within a region of approximately 1,100 kb that is telomeric to the IGHJ and constant-region genes (Fig. 1). Each IGHV gene can be assigned to one of seven IGHV gene subgroups. Each subgroup comprises IGHV genes, which share more than 80% nucleic acid sequence homology. Genes of the IGHV1, IGHV5, and IGHV7 subgroups have similarities in the primary structure, suggesting a common ancestral origin in evolution, whereas the IGHV2, IGHV4, and IGHV6 families share similarities that allow them to be classified into a different clan (30, 31). The IGHV3 genes constitute their own discrete clan.

The IGHV genes of each subgroup, except IGHV6, are interspersed throughout the immunoglobulin heavy-chain locus. By convention, the loci encoding each of the various IGHV genes are assigned a number corresponding to the IGHV gene subgroup followed by a hyphen and then the rank order distance from the heavy-chain D segments on chromosome 14 (Fig. 1). The immunoglobulin IGHV6 subgroup has only one functional IGHV gene. Since this is the first IGHV gene telomeric to the D segments, this gene is called IGHV6-1 (Fig. 1). There are an additional 50 loci that have been identified as functional IGHV genes (32) (Fig. 1). The largest subgroup is IGHV3, with 25 functional genes. The next largest are the IGHV1 and IGHV4 subgroups, each with 11 functional genes. The IGHV2, IGHV5, and IGHV7 subgroups each have one to four functional genes. Interspersed among the functional IGHV genes are several nonfunctional pseudogenes (Fig. 1).

The extent of identified genetic polymorphism varies between the different IGHV gene loci. Some immunoglobulin IGHV gene loci, e.g., IGHV6-1, IGHV5-51, or IGHV4-34, are highly conserved (33, 34). Indeed, the single-copy immunoglobulin IGHV6 gene, IGHV6-1, is conserved even among higher primates (35). Other loci have been used to identify genetic polymorphic variations. These allelic variations are of two different types. The first type of genetic polymorphism is the classic form, in which there are two or more alleles at a single locus, each differing from one another in one or more nucleotide bases. For example, IGHV3-30*18 (1.9III) and IGHV3-30*1 (hv3005) differ from each other at several nucleotide bases and share only 98.8% overall homology (98.3% coding sequence homology) but are alleles of locus IGHV3-30. The second type of allelic variation results from duplications, insertions, and/or deletions of whole segments of IGHV genes within the immunoglobulin heavy-chain gene complex. Duplication of an IGHV gene(s) results in some haplotypes having identical IGHV genes belonging to distinct loci, each possibly differing from their respective alleles by one or more nucleotide base substitutions. For example, there may be an insertion in and about the locus for IGHV3-30, in part consisting of another copy of this gene. As a result, alleles of IGHV3-30, e.g., IGHV3-30*18 (1.9III) and IGHV3-30*1 (hv3005), also may be alleles of locus IGHV3-30.5 in haplotypes containing this insertion. On the other hand, some haplotypes are missing gene loci altogether. For example, allele frequencies for IGHV3-30*1 (hv3005) and IGHV3-30*18 (1.9III) in the Caucasian population are 0.19 and 0.72, respectively (36). An additional haplotype(s) with an allele frequency of 0.08 lacks either IGHV3-30*18 (1.9III) or IGHV3-30*1 (hv3005) and thus apparently is a blank haplotype for this locus. Genetic disequilibrium also is noted for certain groups of IGHV genes on a given haplotype. For example, IGHV3-30-3*01 (56p1 or 3d216) is an insertion or deletion element that has been observed only with haplotypes carrying one or two copies of IGHV3-30*18 (1.9III).

The relative expression level of each functional IGHV gene is not uniform. Certain IGHV genes, e.g., IGHV3-23, IGHV4-34, or IGHV1-69, are overexpressed relative to their physical representation among other IGHV genes (36, 37). Each of nine IGHV3 genes (IGHV3-23, IGHV3-30, IGHV3-7, IGHV3-33, IGHV3-21, IGHV3-48, IGHV3-11, IGHV3-15, and IGHV3-30-3) accounts for 5 to 19% of the IGHV3 gene rearrangements, whereas the remaining functional IGHV3 genes contribute to less than 4% of the rearrangements. Some of the IGHV genes that encode a disproportionate share of the immunoglobulin expressed by normal adults also are polymorphic. For example, three deletion/insertion polymorphisms (Del I to Del III) with deletion allele frequencies ranging from 0.1 to 0.3 were identified. Del I is a polymorphism affecting three IGHV genes (IGHV1-8, IGH3-9, and IGHV2-10), of which two are functional. Greater than 10% of individuals in the human population may not have these gene segments in their genome, and ~44% may have only one copy of these gene segments (38). In Del II, a 50-kb insertion containing five IGHV genes (IGHV3-30-5, IGHV4-30-4, IGHV3-30-3, IGHV4-30-2, and IGHV4-30-1) was identified; this insertion has been observed in 45% of Caucasoids (39). Del III spans ~21 to 53 kb, involving four contiguous genes, among which only the functional gene IGHV4-39 has an identified null allele (40, 41). In addition, some persons have a deletion of the IGHV gene IGHV4-31, which otherwise may encode a significant proportion of the heavy-chain repertoire (36). The International Immunogenetics database (http://www.imgt.org/) provides an Internet listing of IGHV gene maps and alleles (42).

Immunoglobulin Light-Chain Gene Complexes

κ Light-Chain Complex

The κ light-chain gene complex is contained within band p11.2 on the short arm of chromosome 2 (Fig. 2). This gene complex consists of approximately 34 to 38 (4 genes may be functional or pseudogenes depending on the alleles) functional kappa light-chain variable-region genes (IGKV genes), 5 functional IGKJ genes, and 1 constant-region gene (Fig. 2) (43, 44).

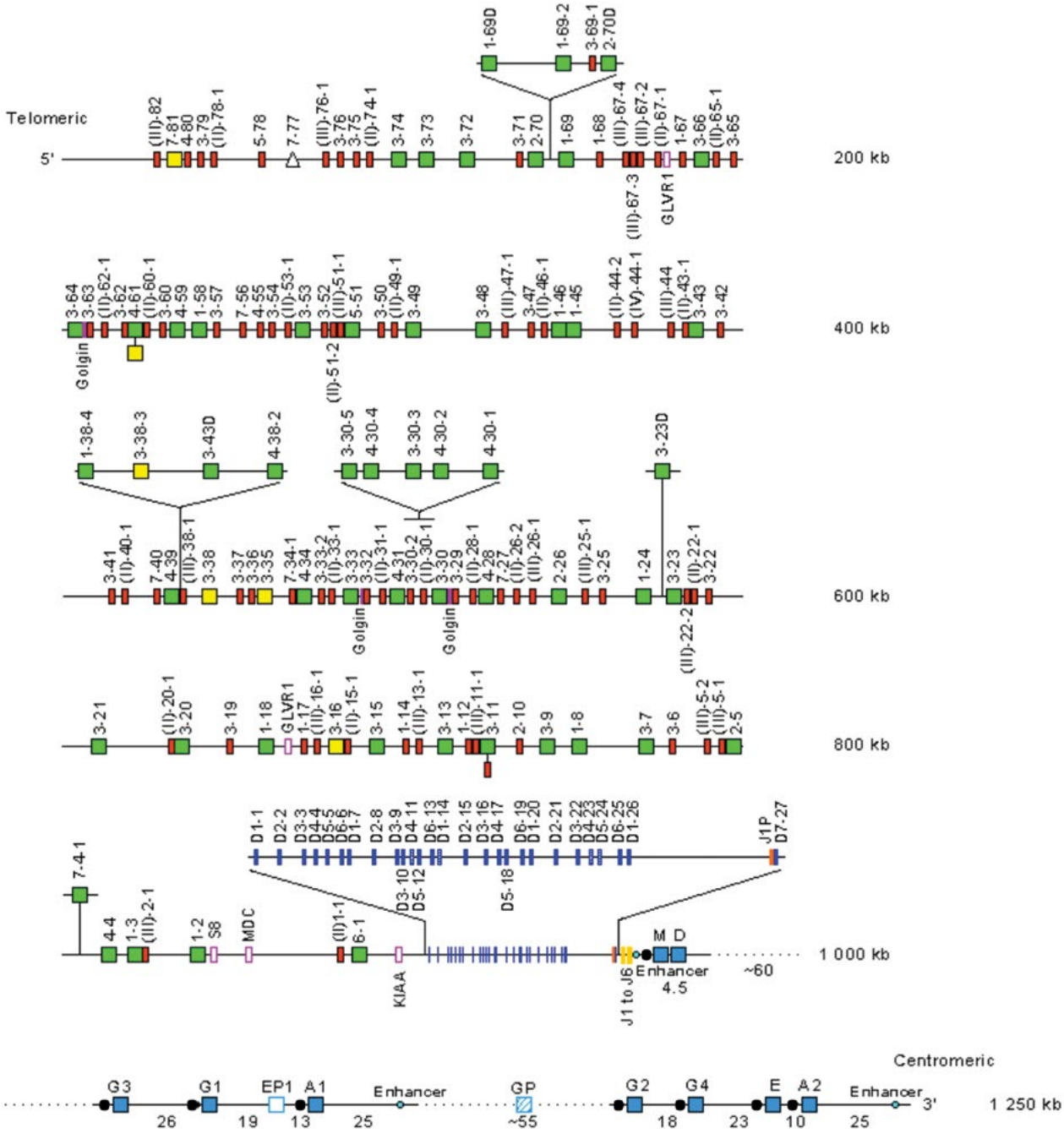

FIGURE 1 Immunoglobulin heavy-chain gene complex. The heavy-chain genes encoding the constant regions are represented by blue boxes. Switch regions are represented by a filled circle upstream of the IGHC genes. Enhancers are represented by light blue circles. Each IGHV, IGHD, and IGHJ gene is labeled on the right of each symbol. Functional IGHV, IGHD, and IGHJ genes are represented by green boxes, blue lines, and yellow lines, respectively. IGHV, IGJH, and IGHC pseudogenes are represented by red boxes, orange boxes, and blue open boxes, respectively. IGHV and IGHC open reading frames are represented by yellow boxes and blue dashed boxes, respectively. Unrelated pseudogenes are represented by purple open boxes. Colors are according to the international ImMunoGeneTics information system (IMGT) color menu for genes. Reproduced with the kind authorization of Marie-Paule Lefranc (IMGT [http://www.imgt.org]).

The IGKV genes in the κ light-chain gene complex are found in two regions: an IGKC-proximal region, designated the *p* region, and an IGKC-distal region, designated the d region. Each region spans approximately 500 kb. Approximately 800 kb separates the two regions (Fig. 2). The p region contains 40 IGKV gene segments, while the *d* region contains 36 gene segments (Fig. 2). The d region apparently arose through duplication of a large portion of the *p* region. Consequently, there are 33 pairs of IGKV genes that share 95 to 100% nucleic acid sequence homology,

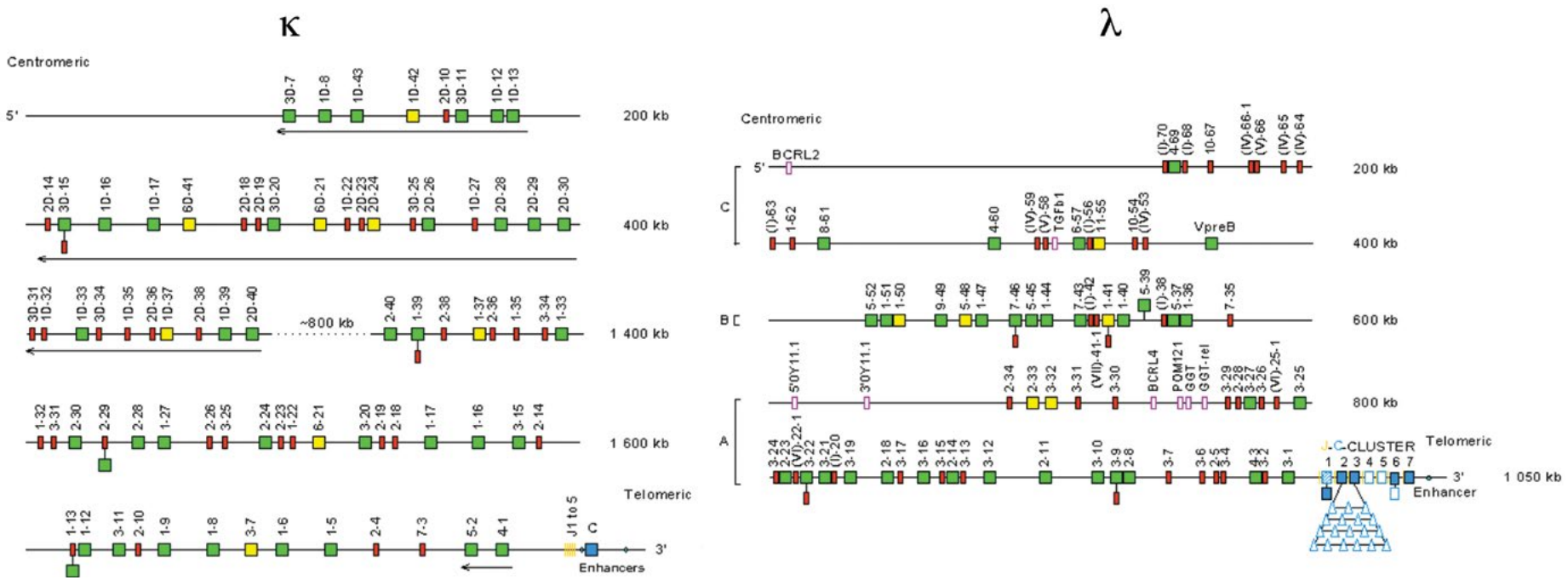

FIGURE 2 Immunoglobulin light-chain gene complexes. (Left) κ light-chain gene complex on chromosome 2p11-12. The blue box represents the functional IGLC gene. The IGKJ gene segments are indicated by yellow lines labeled "J1 to 5." The κ light-chain enhancers are represented by light blue circles. IGKV functional genes, pseudogenes, and open reading frame are indicated by green, red, and yellow boxes, respectively. The IGKV genes of the *p* region are designated by a number for the subgroup, followed by a hyphen and a number for the localization from 3′ to 5′ in the locus. The IGKV genes of the *d* region are designated by the same numbers as the corresponding genes in the *p* region, with the letter D added. Arrows show the IGKV genes whose orientation is opposite to that of the IGKJ gene segments. (Right) λ light-chain gene complex on chromosome 22q11.2. The blue boxes represent functional IGLJ and IGLC gene segments, whereas blue open boxes represent IGLJ and IGLC pseudogenes. IGLV functional genes, pseudogenes, and open reading frame are indicated by green, red, and yellow boxes, respectively. IGLV pseudogenes that could not be assigned to subgroups with functional genes are represented by red boxes and designated by a roman number in parentheses, corresponding to the clans, followed by a dash and a number for the localization from 3′ to 5′ in the locus. The IGLV genes are organized into three clusters, designated A, B, and C, which are indicated to the left of each cluster. Unrelated pseudogenes are represented by purple open boxes. The λ light-chain enhancer is represented by a light blue circle. Colors are according to the IMGT color menu for genes. Reproduced with the kind authorization of Marie-Paule Lefranc (IMGT, the international ImMunoGeneTics information system [http://www.imgt.org]).

accounting for 66 of the 76 IGKV genes in the κ light-chain complex (45, 46).

The IGKV genes in the κ light-chain gene complex can be categorized into three main subgroups (1 to 3) and several smaller subgroups (4, 5, 6, and 7), based on nucleotide sequence homology (47, 48). The largest subgroup is IGKV1, with 20 functional genes (Fig. 2). The next largest subgroups are IGKV2, with 10 functional genes, and IGKV3, with 7 functional genes. There are three open reading frame genes in the IGKV6 subgroup and one functional gene in each of the IGKV4 and IGKV5 subgroups. The IGKV7 subgroup has only one nonfunctional pseudogene.

Similar to the IGHV locus, there are several prominent alleles identified in the IGKV gene locus. The IGKV genes coding for segments IGKV1-13 (L4) and IGKV3D-15 (L16) each have several alleles, some having stop codons (49, 50). Moreover, the IGKV2D-29 (A2) gene also is polymorphic, with some alleles having defective promoters that preclude their expression into protein. Inheritance of defective IGKV2D-29 (A2) alleles has been associated with an increased risk for serious infection with type b *Haemophilus influenzae*, suggesting that the polymorphic variations in the germ line repertoire can influence the susceptibility to infectious disease (51).

As with the immunoglobulin IGHV genes, the expression of IGKV genes is not uniform. Eleven of the approximately 34 to 38 known functional IGKV genes encode most of the κ light-chain variable regions expressed in the normal adult repertoire (49). Moreover, of the 44 genes that are potentially functional, only 28 commonly encode κ light-chain variable regions (Fig. 2) (49, 50). This raises the possibility that some of the potentially functional IGKV genes have defects that preclude their ability to undergo light-chain gene rearrangement or to be expressed into protein. Alternatively, these genes may have an extremely low expression frequency.

λ Light-Chain Gene Complex

The λ light-chain gene complex is located at band q11.2 on the long arm of chromosome 22. These λ constant-region genes are telomeric to the λ variable-region genes (IGLV). Originally, the isotypes that they encoded were designated Mcg^+, Ke^- Oz^-, Ke^- Oz^+, and Ke^+ Oz^-, depending on their reactivity with Mcg, Kern, and Oz antisera that were raised against λ Bence Jones proteins of patients with multiple myeloma (52). These isotypes are now designated IGLC1, IGLC2, IGLC3, and IGLC7, respectively. In total, there are 7 to 11 IGLC genes telomeric to the IGLV genes, depending on the haplotype (53). Each IGLC gene is associated with its own IGLJ segment. The most prevalent haplotype contains four functional IGLC genes (IGLC1, IGLC2, IGLC3, and IGLC7, encoding the Mcg, Ke^- Oz^-, Ke^- Oz^+, and Ke^+ Oz^- isotypes, respectively) and three pseudogenes (IGLC4, IGLC5, and IGLC6) (Fig. 2) (54, 55).

There are approximately 29 to 33 functional IGLV genes and over 40 nonfunctional IGLV pseudogenes that are arranged into 10 subgroups (56–58). Each subgroup comprises IGLV genes sharing more than 75% nucleotide sequence homology (57, 59) (Fig. 2). Like that of the κ light-chain locus, the sequence organization suggests that large DNA duplications contributed to the generation of the germ line repertoire of IGLV gene segments (56). The IGLV genes are clustered into three large DNA segments located within 860 kb of the IGLJ and IGLC genes (56, 58, 60). The cluster most proximal to the IGLJ-IGLC exons, designated cluster A, comprises 16 functional IGLV genes, mostly belonging to the IGLV2 and IGLV3 gene subgroups, designated IGLV3-1 (3r, DPL23) through IGLV3-27 (V2-19) in Fig. 2. The next cluster, cluster B, contains 12 functional IGLV genes of the IGLV1, IGLV5, IGLV7, and IGLV9 gene subgroups, designated IGLV1-36 (1a, DPL1) through IGLV5-52 (5b). The third cluster, cluster C, contains five functional IGLV genes of the IGLV4, IGLV6, IGLV8, IGLV10, and IGLV11 gene subgroups, designated VpreB through IGLV4-69 (4b) (Fig. 2). As with the other immunoglobulin complexes, there are multiple nonfunctional pseudogenes interspersed between these functional IGLV genes in all three clusters.

As noted for the relative expression of individual IGHV and IGKV genes, the expression of individual IGLV genes appears to be nonrandom. IGLV genes of the IGLV1 and IGLV3 subgroups are used most frequently. These subgroups respectively encode approximately 44 or 40% of the λ light-chain immunoglobulins in normal adult sera (61). This proportionate representation apparently is not observed in B-cell plasmacytic disorders. Although the IGLV2 subgroup was identified on 3% of the λ light-chain immunoglobulins in normal adult sera, it accounted for 40% of the λ Bence Jones proteins and 60% of the λ macroglobulins from patients with Waldenström macroglobulinemia in one survey (61).

IMMUNOGLOBULIN GENE REARRANGEMENT

Immunoglobulin Gene Rearrangement and Expression in Ontogeny

As B cells develop, they generally first rearrange their immunoglobulin heavy-chain genes (62). One or more IGHD segments rearrange to become juxtaposed with a single IGHJ element. This generates an IGHD-IGHJ complex that then may rearrange with any one of approximately 38 to 46 functional IGHV genes.

Subsequently, gene rearrangements occur within the light-chain complexes. One of the 40 functional IGKV genes rearranges with any one of five IGKJ segments. Should these gene rearrangements fail to generate a functional IGKV-IGKJ exon, the Kde generally rearranges to a site in or immediately downstream of the IGKV-IGKJ exon, thus deleting the κ light-chain constant-region exon (63). Many of the IGKV genes in the *p* region are in the opposite orientation of the IGKJ segments, thus requiring that the V exons in this region undergo inversion during immunoglobulin gene rearrangement. The processes of *Ig* gene locus contraction and looping during V(D)J recombination are essential for creating a diverse antibody repertoire. Recently, a 650-bp sequence corresponding to DNase I hypersensitive sites HS1 and HS2 within the mouse IGKV-IGKJ intervening region was described. This sequence binds CCCTC-binding factor and specifies locus contraction and long-range IGKV gene usage. Its deletion results in a 7-fold increase in proximal IGKV gene usage along with an ~50% reduction in overall locus contraction (64). Subsequent to a failed κ light-chain gene rearrangement, one of the functional IGLV genes can rearrange with any one of the four or five functional IGLJ-IGLC exons to generate a gene that can encode a λ light chain (55).

The term progenitor B cells (or pro-B cells) is reserved for precursor B cells that have only rearranged IGHD and IGHJ elements, whereas precursor B cells that have completed immunoglobulin heavy-chain gene rearrangement and have a functional V_H-D-J_H complex are referred to as pre-B cells. The immunoglobulin light-chain loci of both pro-B cells and pre-B cells are generally in the germ line configuration.

Nevertheless, a small amount of immunoglobulin μ chain in association with "surrogate" light chains is expressed by pre-B cells. The surrogate light chain is made up of two noncovalently associated proteins called lambda-5 (λ_5) and VpreB, which together form a molecule having structural homology with conventional light chains (65). Thus, in the surrogate light chain, λ_5 replaces a light-chain constant region and VpreB the variable part although bearing an extra N-terminal protein sequence. Both are located on chromosome 22: the λ_5 gene is telomeric to the true light-chain locus, and the VpreB gene is located within the cluster of IGLV genes defined by breakpoints of chromosomal translocations found in a few leukemias and lymphomas (66). During the early stages of B-cell development, VpreB and λ_5 are covalently associated with the μ heavy chains to form a primitive immunoglobulin receptor referred to as pre-B-cell receptor (pre-BCR). Pre-B cells may be expressed on the surface membrane of such a receptor together with CD79a and CD79b (67). Monoclonal antibodies that recognize λ_5 or VpreB specifically bind to pre-B cells and can react with B-lineage acute lymphocytic leukemias (68).

Expression of the surrogate light chains plays a critical role in normal B-cell development. This is underscored by studies on transgenic mice that lack functional λ_5 genes (69). In these mice, B-cell development in the marrow is blocked at the pre-B-cell stage, thereby markedly reducing the numbers of functional mature B lymphocytes in the blood and lymphoid tissues (70). Similarly, humans that have inactivating mutations in the λ_5 genes on both alleles of chromosome 22 have agammaglobulinemia and markedly reduced numbers of B cells (71). When immunoglobulin μ chains form a complex with the "surrogate" λ light chains, the complementarity-determining region 3 (CDR3) of the "surrogate" λ light chain covers the CDR3 of the heavy chain in the pre-B-cell receptor, allowing the pre-B cell to avoid antigen-specific selection (72).

Even though the cell has two different sets of each of the immunoglobulin gene complexes that initially undergo seemingly independent immunoglobulin gene rearrangements, under normal conditions, immunoglobulin expression by each B lymphocyte or plasma cell is limited to only one immunoglobulin heavy-chain allele and one light-chain allele through a process called allelic exclusion. Allelic exclusion generally is observed in most B-cell tumors; however, rare cases of B-cell leukemia may lack allelic exclusion and express both immunoglobulin alleles (73).

Genetic Basis for Immunoglobulin Gene Rearrangement

Recombination signal sequences (RSSs) flanking each germ line V gene, D element, and J segment serve as the recognition site for the V(D)J recombinase and direct the site of DNA recombination. The RSSs consist of two conserved sequence elements of different lengths, one of 7 bp (the heptamer; consensus, 5′ CACAGTG 3′) and one of 9 bp (the A/T-rich nonamer; consensus, 5′ ACAAAAACC 3′), separated by either 12 bp or 23 bp of nominally conserved intervening DNA (12-RSS or 23-RSS, respectively) (74). V(D)J recombination is directed between distinct gene segments whose flanking RSSs contain different-length spacers (62, 75, 76). This is referred to as the 12/23 joining rule (77). Because all segments of a particular type (e.g., segments of IGKV genes) are flanked by one type of signal sequence and all the segments to which they should be joined (e.g., IGKJ segments) are flanked by the opposite type of signal sequence, the 12/23 rule ensures that the joining will be restricted to events that could be biologically productive. Although each spacer varies in sequence, the length of each spacer is conserved and corresponds to one or two turns of the DNA double helix. Each spacer serves to bring the heptamer and nonamer sequences to the same side of the DNA helix, where they both can be bound by a protein complex that catalyzes recombination.

This process of somatic DNA recombination is initiated when the recombination activating gene (RAG) endonuclease introduces DNA double-strand breaks (DSBs) at the border of two recombining gene segments and their flanking RSSs (78–80). DNA cleavage by RAG leads to four broken DNA ends that are repaired and joined through a process called nonhomologous DNA end joining (NHEJ) to form coding and signal joints (81, 82). Occasionally these DSBs can be repaired aberrantly, leading to the formation of chromosomal lesions such as translocations, deletions, or inversions (83, 84). If the breakpoints of these chromosomal lesions lie near potential oncogenes or tumor suppressor genes, they can lead to cellular transformation and lymphoid tumors. The mechanism of DNA rearrangement is similar for the heavy- and light-chain loci. However, only one joining event is needed to generate a light-chain gene, whereas two are needed to generate a complete heavy-chain gene. The most common mode of rearrangement involves the looping out and deletion of the DNA between two gene segments on the same chromosome; this occurs when the coding sequences of the two gene segments are in the same orientation in the DNA (85). The 12- and 23-mer-spaced RSSs are brought together by interactions between proteins that specifically recognize the length of the spacer between the heptamer and nonamer signals, thus accounting for the 12/23 joining rule (75, 76). The two DNA molecules then are broken and rejoined in a different configuration (86). By joining precisely in a head-to-head configuration, the ends of the heptamer sequences form a signal joint in a circular piece of extrachromosomal DNA that then is lost from the genome when the cell divides. However, the DNA that lies between the two gene segments is retained in an inverted orientation when a second mode of recombination occurs between two gene segments with opposite transcriptional orientations. Although this mode of recombination is less common, such rearrangements account for about one-half of all IGKV-to-IGKJ joins, as the transcriptional orientation of one-half of the human IGKV gene segments is opposite to that of the IGKJ gene segments.

RAG-1 and *RAG-2* are coexpressed normally only in developing lymphocytes that are undergoing receptor gene rearrangement. During B-cell development, the appearance of cytoplasmic immunoglobulin μ chains defines the pre-B cell. Pre-B cells, whose immunoglobulin μ chains can associate with the "surrogate" λ light chains, begin to express a pre-B-cell receptor. Its appearance turns off RAG1 and RAG2, preventing further immunoglobulin heavy-chain rearrangement (allelic exclusion). This is followed by four to six cycles of cell division (87). Late pre-B daughter cells reactivate RAG1 and RAG2 and begin to undergo light-chain rearrangement. Mice with either of these genes knocked out cannot undergo immunoglobulin or T-cell receptor gene rearrangements and consequently fail to produce mature B or T lymphocytes (88). A form of combined immune deficiency called Omenn syndrome in humans results from mutations that impair, but do not completely abolish, the function of *RAG-1* or *RAG-2* (89). It is interesting that patients with Omenn syndrome harbor point mutations in the RAG1 RING domain (see below) that reduces the efficiency of V(D)J recombination (90, 91).

After the RAG-1/RAG-2 endonuclease recognition of either the 12-mer-spaced or the 23-mer-spaced RSS, such

endonuclease introduces DSBs and remains bound to the DNA. The presence of mutations affecting the ability of the RAG proteins to bind and to maintain the broken ends in a stable postcleavage complex can lead to misrepair of the DSBs, thereby enhancing the risk for oncogenic chromosomal aberrations (92, 93). Involved in the processing and juxtaposition of these DSBs are several proteins, including the high-mobility-group proteins 1 and 2 (HMG1 and HMG2). HMG1 and HMG2 play an important role in the assembly of nucleoprotein complexes involved in DNA repair and transcription because they are widely expressed, abundant nuclear proteins that bind and bend DNA without sequence specificity (94). HMG1, facilitating the bending of the DNA, allows the components of one DSB-RAG complex to bind and to cleave the DNA at a different RSS, therefore, in accordance with the 12/23 joining rule, bringing together two disparate RSSs (75, 76).

The RAG complex introduces DSBs immediately adjacent to immune receptor gene segments, resulting in blunt phosphorylated signal ends and covalently sealed hairpinned coding termini that are joined by NHEJ (80). Coding and signal ends are joined at very different rates, rapid for coding ends while slower for signal ends (95). This is likely explained by the fact that the RAG complex remains tightly associated with signal ends after cleavage in a postcleavage complex, whereas coding ends are released from this postcleavage complex and need to be brought together again for repair (96). Seven NHEJ components are required for VDJ recombination: Artemis, Ku70, Ku80, DNA-dependent protein kinase (DNA-PK), XRCC4, XLF, and DNA ligase IV (Lig4) (97). Although all seven are required for efficient coding end joining, the dependence of signal end joining on these NHEJ factors is less absolute. The serine-threonine protein kinase (DNA-PK) is activated by DNA DSBs and is essential for the normal repair of DNA breaks induced by ionizing radiation, chemical agents, or VDJ recombination (98–100). DNA-PK-deficient mice can make only trivial amounts of immunoglobulin or T-cell receptors and are called severe combined immunodeficiency mice (101). Artemis-deficient mice have a "leaky" severe combined immunodeficiency phenotype and develop some T and B cells in later life (100). Artemis is not required for signal end joining but instead plays a specific role in opening the sealed hairpinned termini of cleaved coding ends (102). The dependence of signal end joining on DNA-PK is variable. Artemis's endonuclease activity requires physical interaction with DNA-PK as well as DNA-PK's enzymatic activity. Because Artemis is dispensable for signal end joining, it is reasonable to assume that signal end joining also might progress normally in the absence of DNA-PK (102). Indeed, signal end joining proceeds fairly efficiently in developing murine lymphocytes (10 to 50% of wild-type levels) and in some murine cell lines and one human cell line deficient in DNA-PK (103, 104). However, DNA-PK deficiency in other species (hamster, horse, dog) results in a more severe reduction in signal end joining (30- to 1,000-fold reduced) (105–107). Interestingly, mice deficient in Ku not only are deficient in T and B cells but also have small stature and other nonimmunologic defects, suggesting that the Ku proteins also play important roles in normal development (108, 109). Mice defects resulting from mutations in either Ku, XRCC4, Lig4, Artemis, or DNA-PK genes predispose to lymphoma (110, 111). The initial recognition and recruitment of repair proteins to DSBs is heavily dependent on phosphorylation events (e.g., kinase activity and autophosphorylation of DNA-PK), but the downstream repair events appear to be more dependent on E3-ubiquitin ligases (112).

Junctional diversity is generated in the sequences of the rearranged gene segments during the recombination process. Each coding joint originating from the hairpinned termini of gene segments is cleaved at random sites by an endonuclease. An overhanging flap is generated by the cleavage of a hairpin away from its apex and, if incorporated into the joint, results in the addition of palindromic nucleotides that contribute to junctional diversity. Further modifications on the opened hairpin ends by nucleases can remove a self-complementary overhang or cut further into the original coding sequence. In addition, the terminal deoxynucleotidyl transferase, a lymphocyte-specific enzyme, can add non-template-encoded nucleotides (113). Finally, nucleolytic activities that remove potential coding end nucleotides prior to the final ligation of the DNA breaks into one intact recombination joint can provide additional junctional diversity (86).

Lineage, stage, order, and feedback regulation of V(D)J recombination are mediated epigenetically by modulating the accessibility of particular loci or regions of loci to RAG (114). Numerous epigenetic accessibility markers, such as the histone H3 lysine 4 trimethylation, are enriched around IGHJ in early pro-B cells in association with germ line transcription (115). In addition, ubiquitination events can regulate recombination of immunoglobulin gene segments. The zinc finger region A of RAG1 includes an N-terminal RING domain that acts as an E3-ubiquitin ligase, which can ubiquitinate a panel of targets for various downstream events (77, 116–121) and can interact with other E2 enzymes to ubiquitinate substrates involved in V(D)J recombination, such as histone 3 (116, 117). Ubiquitination of RAG2 allows for rapid degradation of the protein upon entering S phase, thereby halting any potential off-target activities of RAG and limiting its capacity to induce V(D)J recombination during inappropriate phases of the cell cycle. DNA breaks during S phase are potentially harmful for cells, as such breaks can lead to deleterious translocations when misrepaired by homologous recombination. It is therefore crucial to limit V(D)J recombination activity within G_1 phase; this restriction appears to be controlled by RAG2 degradation (122–124).

Heavy-Chain Class Switching

A single B lymphocyte, during differentiation, can synthesize heavy chains with the same variable region coupled to different constant regions (125). As pre-B cells develop into mature B cells in early development, intact IgM monomers are inserted into the plasma membrane, followed by IgD molecules with the same antigen-binding specificity. The IgM and IgD constant-region genes generally are transcribed together. Alternative splicing permits simultaneous coproduction of IgM and IgD from a single species of RNA.

Later during development, these variable domains can associate with other isotypes (IgG, IgA, or IgE) through a controlled process called class switch recombination (CSR). CSR requires active transcription of the downstream constant-region exons encoding the switched immunoglobulin isotype. Such active transcription generally is triggered by stimulation of the B cell with antigen, mitogens, and/or ligation of CD40 via the ligand for CD40 (CD154), which is expressed by activated T cells. Patients with X-linked or autosomal recessive inheritance of mutations in CD154 or CD40, respectively, can have an immune deficiency syndrome (hyper-IgM syndrome type I), which is characterized by normal to high levels of IgM and extremely low levels of other immunoglobulin isotypes in serum (126, 127). Antigen-reactive T lymphocytes also provide interleukins that can influence whether the B cells continue to

express IgM or switch their immunoglobulin heavy-chain isotype to IgG, IgA, or IgE (125, 128).

Immunoglobulin CSR occurs in or near the switch region upstream of the gene and any one of the switch regions of the other heavy-chain isotype genes. Switch regions in Fig. 1 are represented by filled circles upstream of the IGHC genes. The μ switch region (Sμ) consists of approximately 150 repeats of the sequence $(GAGCT)_n(GGGGGT)$, where n is generally three but can be as many as seven. Other switch regions (S_γ, S_α, and S_ε) consist of similar sequences that contain repeats of the GAGCT and GGGGGT sequences. DNA recombination between S_μ and S_γ, S_α, or S_ε accompanied by the deletion of intervening DNA segments results in the apposition of the previously rearranged variable-region gene next to the new constant-region gene, thus switching the heavy-chain class. While VDJ recombination occurs mostly in the G_0 and/or G_1 stage of the cell cycle, CSR seems to require DNA replication (129).

Unlike VDJ recombination, CSR requires expression of activation-induced deaminase (AID), an enzyme expressed in activated B cells that also is required for somatic hypermutation (see "Generation of Antibody Diversity" below) (130–132). Inherited defects in AID can result in an immune deficiency syndrome called hyper-IgM syndrome type II, which is characterized by relatively high levels of IgM and negligible levels of other immunoglobulin isotypes in serum (133). Specific inactivation of the C-terminal AID domain, encoded by exon 5 (E5), allows very efficient deamination of the AID target regions but greatly impacts the efficiency and quality of subsequent DNA repair. Specifically eliminating E5 not only precludes CSR but also causes an atypical, enzymatic-activity-dependent, dominant-negative effect on CSR. This explains the autosomal dominant inheritance of AID variants with truncated E5 in patients with hyper-IgM syndrome type II and establishes that AID, through the E5 domain, provides a link between DNA damage and repair during CSR (134). The sites where CSR takes place in B cells activated in response to an antigen are germinal centers of the lymph nodes and spleen where AID is expressed (135).

Uracil-DNA glycosylase (UNG) is an enzyme that removes the uracils (dU) generated from the deamination of cytosines (dC) by AID. Inherited defects in this enzyme underlie an autosomal recessive form of the hyper-IgM immune deficiency syndrome, which is similar to that of patients with inherited defects in AID (6, 136). Apurinic/apyrimidinic endonuclease cleaves the abasic sites generated by UNG; the staggered nicks in the DNA are closely positioned and may result in DNA DSBs (137). Such DNA DSBs are end processed, repaired, and joined by mechanisms and proteins similar to those involved in NHEJ used for VDJ recombination. Since CSR occurs in the intron between the variable-region exon and the exon encoding the first constant-region domain, no mutations in the regions encoding the variable or constant regions of the newly generated immunoglobulin heavy chain are generated by this process (138).

GENERATION OF ANTIBODY DIVERSITY

The diversity among immunoglobulin variable regions can be generated by several mechanisms: (i) the germ line presence of multiple V, J, and D gene segments; (ii) the DNA segments randomly joining to produce a complete variable-region exon; (iii) uncorrected errors made during the recombination process; (iv) the heavy- and light-chain polypeptides pairing to produce a complete immunoglobulin monomer capable of binding an antigen; and (v) somatic mutations in the rearranged DNA segments themselves (62). The last of these occurs through a process called somatic hypermutation (SHM). This process occurs in antigen-activated B cells and cannot be triggered merely by mitogen-induced B-cell activation.

The SHM process primarily introduces single nucleotide exchanges into the rearranged immunoglobulin variable region, at a rate of 10^{-3} per base pair per generation. However, during discrete stages of B-cell differentiation and in particular during the secondary immune response to an antigen, expressed immunoglobulin variable genes can incur new mutations at rates as high as 10^{-3} base changes per base pair per generation over several cell divisions (139). Mutations generated by SHM are clustered in the region spanning from 300 bp 5′ of the rearranged variable-region exon to approximately 1 kb 3′ of the rearranged minigene J segment, frequently around hot spots defined by the primary DNA sequence, such as the sequence RGYW (R, purine [A or G]; Y, pyrimidine [C or T]; W, A or T) and its complement. Such sequences are hot spots for mutation that are conserved among species (140, 141).

SHM is dependent on the expression and activity of AID through a process that has some similarity to CSR (142). AID is responsible for initiating mutations at RGYW motifs. Mutations spread as a consequence of downstream events orchestrated by the mismatch repair and base excision repair pathways (143–147). In addition to having the hyper-IgM immune deficiency syndrome type II, patients with inherited defects in AID have B cells that lack the capacity to undergo SHM (131). As with CSR, SHM requires active transcription of the genes undergoing mutation. In the region encompassing the rearranged variable-region gene, AID most likely deaminates the dC, converting the dC into dU, which is converted into T after DNA replication, giving rise to CG-to-T or -A transitions. Alternatively, UNG may remove the dU, resulting in staggered nick cleavage of the DNA. Such abasic sites are subsequently cleaved by apurinic/apyrimidinic endonuclease. Low-fidelity DNA synthesis may repair these staggered nicks, resulting in frequent mutations. A complex called the mutasome, formed by DNA-cleaving enzymes and DNA repair enzymes (e.g., mismatch repair enzymes, base excision repair enzymes, proteins involved in NHEJ, etc.), also apparently binds the target DNA to reduce its tendency to incur complete DNA DSBs. Through this process, mostly transitional mutations are introduced at high frequencies into the expressed immunoglobulin V genes as well as other transcriptionally active genes within hot spots, which serve as substrates for AID, UNG, and the mutasome (140, 143, 148). Subsequently, "affinity maturation" of the antibodies expressed during the immune response to antigen takes place by selection of the B cell and its daughter cells that express mutated V genes encoding an immunoglobulin variable region with improved fitness for binding antigen (149). Such selection enhances the frequency of nonconservative base substitutions in the DNA sequences encoding the complementarity-determining regions that serve as the contact sites for antigen binding (150).

Immunoglobulin enhancers may account in part for the preferential somatic hypermutation of immunoglobulin genes. Combinations of immunoglobulin enhancers target somatic mutation to immunoglobulin genes by recruiting AID and/or by making the immunoglobulin genes better substrates for mutation (151). In addition, posttranslation AID ubiquitination has an important regulatory role during CSR and SHM (152, 153). Unlike RAG2, AID protein stability is not associated with phases of the cell cycle but rather with subcellular localization. In mouse B cells, nuclear AID is subjected to rapid turnover upon polyubiquitination (152).

DETECTION OF IMMUNOGLOBULIN GENE REARRANGEMENTS

Analysis for immunoglobulin gene rearrangements can detect clonal immunoglobulin gene rearrangements. Immunoglobulin gene rearrangement irreversibly alters the genomic DNA of the developing B cell and its descendant daughter cells. Because of the many possible distinct immunoglobulin gene rearrangements possible, a B cell's particular type of immunoglobulin gene rearrangement can serve as a clonal marker.

PCR Assays

Sensitive methods for detecting immunoglobulin gene rearrangements, such as PCR, can be used to examine for residual cells of a malignant B-cell clone following antitumor therapy. PCR, using sense strand oligonucleotide primers corresponding to an immunoglobulin V gene subgroup (Table 2) together with antisense strand oligonucleotide primers corresponding to the relevant J-region or constant-region exon, can amplify the rearranged V gene in genomic DNA or cDNA, respectively.

Because these gene segments are separated by large stretches of intervening DNA in germ line DNA, a PCR assay with genomic DNA and primers specific for a V gene subgroup and the J gene segment(s) will fail to amplify any immunoglobulin genes unless the genes have first undergone rearrangement. However, after immunoglobulin gene rearrangement, the variable-region gene leader sequence primers and J primers anneal to sites that are separated by fewer than 400 bp, making PCR straightforward (154). On the other hand, a PCR assay on genomic DNA with primers specific for a V gene subgroup and a constant-region exon does not amplify rearranged immunoglobulin genes because the distance between the J segment and the immunoglobulin constant-region exon is too large. Such primer pairs are better suited for amplifying cDNA derived from the immunoglobulin transcripts from which the intron separating the J region and the constant-region exon are deleted through RNA processing and splicing.

Genomic DNA is the most commonly used for PCR in clinical laboratories, as this does not require synthesis of cDNA from isolated RNA. However, care must be taken when using genomic DNA for PCR, which can amplify both the productively rearranged immunoglobulin gene and its unproductively rearranged allele. The use of downstream primers located in the constant region (isotype-specific primers) allows definition of the isotype and may be advantageous in the case of mutated sequences, since it is not targeted by the somatic hypermutation process (155).

Resolution of the junctional sequences in the rearranged immunoglobulin genes expressed by a tumor can provide a specific tumor marker. This marker can be used to examine for any tumor-derived immunoglobulin gene fragments amplified by PCR performed on genomic DNA of lymphoid tissue. Such methods are highly sensitive, allowing for detection of minimal residual disease of small numbers of lymphoid tumor cells that otherwise cause no detectable pathologic or immunophenotypic trace of residual disease after therapy.

TABLE 2 Sense and antisense strand oligonucleotide primers to amplify the rearranged V gene in genomic DNA or cDNA[a]

Gene	Primer sequence[b]
V_H genes	
V_H1/7	ATGGACTGGACCTGGAGVATCC
V_H2	CTCCACRCTCCTGCTGCTGAC
V_H3	GCTGGGTTTTCCTTGTTGC
V_H4	ATGAAACACCTGTGGTTCTTCCT
V_H5	ATGGGGTCAACCGCCATCCTYG
V_H6	CTGTCTCCTTCCTCATCTTCC
J_H	CTYACCTGARGAGACRGTGACC
C_μ	AACGGCCACGCTGCTCG
V_κ genes	
V_κ1/2	ATGAGGSTCCCYGCTCAGCTGCTGG
V_κ3	CTCTTCCTCCTGCTACTCTGGCTCCCAG
V_κ4	ATTTCTCGTTGCTCTGGATCTCTG
V_κ5	GACATCGTGATGACCCAG
V_κ6a	GAAATTGTGCTGACTCAG
V_κ6b	GATGTTGTGATGACACAG
C_κ	GTTTCTCGTAGTCTGCTTTGCTCA
V_λ genes	
V_λ1	GGTCCTGGGCCCAGTCTGTGCTG
V_λ2	GGTCCTGGGCCCAGTCTGCCCTG
V_λ3	GCTCTGTGACCTCCTATGAGCTG
V_λ4/5	GGTCTCTCTCSCAGCYTGTGCTG
V_λ6	GTTCTTGGGCCAATTTTATGCTG
V_λ7/8	TTCYCAGRCTGTGGTGACYCAG
V_λ9	CWGCCTGTGCTGACTCAG
V_λ10	CAGGCAGGGCTGACTCAG
C_λ	CACCAGTGTGGCCTTGTTGGCTTG

[a]Sense-strand oligonucleotide primers corresponding to the leader sequences of each of the major V gene subgroups and antisense strand oligonucleotide primers corresponding to the relevant J-region or constant-region exon.

[b]V, R, Y, S, and W represent degenerate bases (V is A or C or G; R is A or G; Y is C or T; S is C or G; and W is A or T).

REFERENCES

1. **Joiner KA, Fries LF, Frank MM.** 1987. Studies of antibody and complement function in host defense against bacterial infection. *Immunol Lett* **14:**197–202.
2. **Edelman GM.** 1991. Antibody structure and molecular immunology. *Scand J Immunol* **34:**1–22.
3. **Schroeder HW Jr, Cavacini L.** 2010. Structure and function of immunoglobulins. *J Allergy Clin Immunol* **125**(2 Suppl 2)**:**S41–S52.
4. **Torres RM, Imbonden JB, Schroeder HW Jr.** 2008. Antigen receptor genes, gene products, and co-receptors, p 53–77. *In* Rich RR, Fleisher TA, Shearer WT, Schroeder HW Jr, Frew AJ, Weyand CM (ed), *Clinical Immunology: Principles and Practice*, 3rd ed. Mosby Elsevier, London, United Kingdom.
5. **Virella G, Wang AC.** 1993. Immunoglobulin structure. *Immunol Ser* **58:**75–90.
6. **Kavli B, Andersen S, Otterlei M, Liabakk NB, Imai K, Fischer A, Durandy A, Krokan HE, Slupphaug G.** 2005. B cells from hyper-IgM patients carrying UNG mutations lack ability to remove uracil from ssDNA and have elevated genomic uracil. *J Exp Med* **201:**2011–2021.
7. **Harris LJ, Larson SB, Hasel KW, Day J, Greenwood A, McPherson A.** 1992. The three-dimensional structure of an intact monoclonal antibody for canine lymphoma. *Nature* **360:**369–372.
8. **Jefferis R, Lund J, Goodall M.** 1995. Recognition sites on human IgG for Fc gamma receptors: the role of glycosylation. *Immunol Lett* **44:**111–117.
9. **Lee YK, Brewer JW, Hellman R, Hendershot LM.** 1999. BiP and immunoglobulin light chain cooperate to control the folding of heavy chain and ensure the fidelity of immunoglobulin assembly. *Mol Biol Cell* **10:**2209–2219.

10. **Ravetch JV, Bolland S.** 2001. IgG Fc receptors. *Annu Rev Immunol* **19:**275–290.
11. **Parlowsky T, Welzel J, Amagai M, Zillikens D, Wygold T.** 2003. Neonatal pemphigus vulgaris: IgG4 autoantibodies to desmoglein 3 induce skin blisters in newborns. *J Am Acad Dermatol* **48:**623–625.
12. **Yeh SW, Cavacini LA, Bhol KC, Lin MS, Kumar M, Duval M, Posner MR, Ahmed AR.** 2006. Pathogenic human monoclonal antibody against desmoglein 3. *Clin Immunol* **120:**68–75.
13. **Corthesy B, Kraehenbuhl JP.** 1999. Antibody-mediated protection of mucosal surfaces. *Curr Top Microbiol Immunol* **236:**93–111.
14. **Lamm ME, Nedrud JG, Kaetzel CS, Mazanec MB.** 1995. IgA and mucosal defense. *APMIS* **103:**241–246.
15. **Mestecky J, Lue C, Russell MW.** 1991. Selective transport of IgA. Cellular and molecular aspects. *Gastroenterol Clin N Am* **20:**441–471.
16. **Woof JM, Mestecky J.** 2005. Mucosal immunoglobulins. *Immunol Rev* **206:**64–82.
17. **Niles MJ, Matsuuchi L, Koshland ME.** 1995. Polymer IgM assembly and secretion in lymphoid and nonlymphoid cell lines: evidence that J chain is required for pentamer IgM synthesis. *Proc Natl Acad Sci U S A* **92:**2884–2888.
18. **Corthesy B.** 2007. Roundtrip ticket for secretory IgA: role in mucosal homeostasis? *J Immunol* **178:**27–32.
19. **Brezski RJ, Monroe JG.** 2008. B-cell receptor. *Adv Exp Med Biol* **640:**12–21.
20. **Roes J, Rajewsky K.** 1993. Immunoglobulin D (IgD)-deficient mice reveal an auxiliary receptor function for IgD in antigen-mediated recruitment of B cells. *J Exp Med* **177:**45–55.
21. **Geisberger R, Lamers M, Achatz G.** 2006. The riddle of the dual expression of IgM and IgD. *Immunology* **118:**429–437.
22. **Riesbeck K, Nordstrom T.** 2006. Structure and immunological action of the human pathogen Moraxella catarrhalis IgD-binding protein. *Crit Rev Immunol* **26:**353–376.
23. **Lyczak JB, Zhang K, Saxon A, Morrison SL.** 1996. Expression of novel secreted isoforms of human immunoglobulin E proteins. *J Biol Chem* **271:**3428–3436.
24. **Gould HJ, Sutton BJ, Beavil AJ, Beavil RL, McCloskey N, Coker HA, Fear D, Smurthwaite L.** 2003. The biology of IGE and the basis of allergic disease. *Annu Rev Immunol* **21:**579–628.
25. **Chang TW, Wu PC, Hsu CL, Hung AF.** 2007. Anti-IgE antibodies for the treatment of IgE-mediated allergic diseases. *Adv Immunol* **93:**63–119.
26. **Kirsch IR, Morton CC, Nakahara K, Leder P.** 1982. Human immunoglobulin heavy chain genes map to a region of translocations in malignant B lymphocytes. *Science* **216:** 301–303.
27. **Kipps TJ.** 1997. Human B cell biology. *Int Rev Immunol* **15:**243–264.
28. **Matsuda F, Ishii K, Bourvagnet P, Kuma K, Hayashida H, Miyata T, Honjo T.** 1998. The complete nucleotide sequence of the human immunoglobulin heavy chain variable region locus. *J Exp Med* **188:**2151–2162.
29. **Ruiz M, Pallares N, Contet V, Barbi V, Lefranc MP.** 1999. The human immunoglobulin heavy diversity (IGHD) and joining (IGHJ) segments. *Exp Clin Immunogenet* **16:**173–184.
30. **Cook GP, Tomlinson IM.** 1995. The human immunoglobulin VH repertoire. *Immunol Today* **16:**237–242.
31. **Kirkham PM, Mortari F, Newton JA, Schroeder HW.** 1992. Immunoglobulin VH clan and family identity predicts variable domain structure and may influence antigen binding. *EMBO J* **11:**603–609.
32. **Tomlinson IM, Walter G, Marks JD, Llewelyn MB, Winter G.** 1992. The repertoire of human germline VH sequences reveals about fifty groups of VH segments with different hypervariable loops. *J Mol Biol* **227:**776–798.
33. **Pascual V, Capra JD.** 1991. Human immunoglobulin heavy-chain variable region genes: organization, polymorphism, and expression. *Adv Immunol* **49:**1–74.
34. **Sanz I, Kelly P, Williams C, Scholl S, Tucker P, Capra JD.** 1989. The smaller human VH gene families display remarkably little polymorphism. *EMBO J* **8:**3741–3748.
35. **Meek K, Eversole T, Capra JD.** 1991. Conservation of the most JH proximal Ig VH gene segment (VHVI) throughout primate evolution. *J Immunol* **146:**2434–2438.
36. **Milner EC, Hufnagle WO, Glas AM, Suzuki I, Alexander C.** 1995. Polymorphism and utilization of human VH genes. *Ann N Y Acad Sci* **764:**50–61.
37. **Sasso EH, Johnson T, Kipps TJ.** 1996. Expression of the immunoglobulin VH gene 51p1 is proportional to its germline gene copy number. *J Clin Invest* **97:**2074–2080.
38. **Pramanik S, Li H.** 2002. Direct detection of insertion/deletion polymorphisms in an autosomal region by analyzing high-density markers in individual spermatozoa. *Am J Hum Genet* **71:**1342–1352.
39. **Lefranc MP, Lefranc G.** 2001. *The Immunoglobulin Factsbook*. Academic Press, San Diego, CA.
40. **Cui X, Li H.** 2000. Human immunoglobulin VH4 sequences resolved by population-based analysis after enzymatic amplification and denaturing gradient gel electrophoresis. *Eur J Immunogenet* **27:**37–46.
41. **Chimge NO, Pramanik S, Hu G, Lin Y, Gao R, Shen L, Li H.** 2005. Determination of gene organization in the human IGHV region on single chromosomes. *Genes Immun* **6:**186–193.
42. **Ruiz M, Giudicelli V, Ginestoux C, Stoehr P, Robinson J, Bodmer J, Marsh SG, Bontrop R, Lemaitre M, Lefranc G, Chaume D, Lefranc MP.** 2000. IMGT, the international ImMunoGeneTics database. *Nucleic Acids Res* **28:**219–221.
43. **Kawasaki K, Minoshima S, Nakato E, Shibuya K, Shintani A, Asakawa S, Sasaki T, Klobeck HG, Combriato G, Zachau HG, Shimizu N.** 2001. Evolutionary dynamics of the human immunoglobulin kappa locus and the germline repertoire of the Vkappa genes. *Eur J Immunol* **31:**1017–1028.
44. **Tomlinson IM, Cook GP, Walter G, Carter NP, Riethman H, Buluwela L, Rabbitts TH, Winter G.** 1995. A complete map of the human immunoglobulin VH locus. *Ann N Y Acad Sci* **764:**43–46.
45. **Zachau HG.** 1993. The immunoglobulin kappa locus-or what has been learned from looking closely at one-tenth of a percent of the human genome. *Gene* **135:**167–173.
46. **Schable K, Thiebe R, Flugel A, Meindl A, Zachau HG.** 1994. The human immunoglobulin kappa locus: pseudogenes, unique and repetitive sequences. *Biol Chem Hoppe Seyler* **375:**189–199.
47. **Huber C, Huber E, Lautner-Rieske A, Schable KF, Zachau HG.** 1993. The human immunoglobulin kappa locus. Characterization of the partially duplicated L regions. *Eur J Immunol* **23:**2860–2867.
48. **Lautner-Rieske A, Huber C, Meindl A, Pargent W, Schable KF, Thiebe R, Zocher I, Zachau HG.** 1992. The human immunoglobulin kappa locus. Characterization of the duplicated A regions. *Eur J Immunol* **22:**1023–1029.
49. **Cox JP, Tomlinson IM, Winter G.** 1994. A directory of human germ-line V kappa segments reveals a strong bias in their usage. *Eur J Immunol* **24:**827–836.
50. **Klein R, Zachau HG.** 1995. Expression and hypermutation of human immunoglobulin kappa genes. *Ann N Y Acad Sci* **764:**74–83.
51. **Feeney AJ, Atkinson MJ, Cowan MJ, Escuro G, Lugo G.** 1996. A defective Vkappa A2 allele in Navajos which

may play a role in increased susceptibility to Haemophilus influenzae type b disease. *J Clin Invest* **97:**2277–2282.
52. **Hilschmann N.** 1987. The immunoglobulin receptor. *Behring Inst Mitt* **81:**98–99.
53. **Ghanem N, Dariavach P, Bensmana M, Chibani J, Lefranc G, Lefranc MP.** 1988. Polymorphism of immunoglobulin lambda constant region genes in populations from France, Lebanon and Tunisia. *Exp Clin Immunogenet* **5:**186–195.
54. **Dariavach P, Lefranc G, Lefranc MP.** 1987. Human immunoglobulin C lambda 6 gene encodes the Kern+Oz- lambda chain and C lambda 4 and C lambda 5 are pseudogenes. *Proc Natl Acad Sci U S A* **84:**9074–9078.
55. **Vasicek TJ, Leder P.** 1990. Structure and expression of the human immunoglobulin lambda genes. *J Exp Med* **172:**609–620.
56. **Kawasaki K, Minoshima S, Nakato E, Shibuya K, Shintani A, Schmeits JL, Wang J, Shimizu N.** 1997. One-megabase sequence analysis of the human immunoglobulin lambda gene locus. *Genome Res* **7:**250–261.
57. **Pallares N, Frippiat JP, Giudicelli V, Lefranc MP.** 1998. The human immunoglobulin lambda variable (IGLV) genes and joining (IGLJ) segments. *Exp Clin Immunogenet* **15:**8–18.
58. **Williams SC, Frippiat JP, Tomlinson IM, Ignatovich O, Lefranc MP, Winter G.** 1996. Sequence and evolution of the human germline V lambda repertoire. *J Mol Biol* **264:**220–232.
59. **Chuchana P, Blancher A, Brockly F, Alexandre D, Lefranc G, Lefranc MP.** 1990. Definition of the human immunoglobulin variable lambda (IGLV) gene subgroups. *Eur J Immunol* **20:**1317–1325.
60. **Frippiat JP, Williams SC, Tomlinson IM, Cook GP, Cherif D, Le Paslier D, Collins JE, Dunham I, Winter G, Lefranc MP.** 1995. Organization of the human immunoglobulin lambda light-chain locus on chromosome 22q11.2. *Hum Mol Genet* **4:**983–991.
61. **Abe M, Ozaki S, Wolfenbarger D, deBram-Hart M, Weiss DT, Solomon A.** 1994. Variable-region subgroup distribution among lambda-type immunoglobulins in normal human serum. *J Clin Lab Anal* **8:**4–9.
62. **Tonegawa S.** 1993. The Nobel Lectures in Immunology. The Nobel Prize for Physiology or Medicine, 1987. Somatic generation of immune diversity. *Scand J Immunol* **38:**303–319.
63. **Graninger WB, Goldman PL, Morton CC, O'Brien SJ, Korsmeyer SJ.** 1988. The kappa-deleting element. Germline and rearranged, duplicated and dispersed forms. *J Exp Med* **167:**488–501.
64. **Xiang Y, Park SK, Garrard WT.** 2013. Vkappa gene repertoire and locus contraction are specified by critical DNase I hypersensitive sites within the Vkappa-Jkappa intervening region. *J Immunol* **190:**1819–1826.
65. **Martensson IL, Ceredig R.** 2000. Review article: role of the surrogate light chain and the pre-B-cell receptor in mouse B-cell development. *Immunology* **101:**435–441.
66. **Melchers F, Karasuyama H, Haasner D, Bauer S, Kudo A, Sakaguchi N, Jameson B, Rolink A.** 1993. The surrogate light chain in B-cell development. *Immunol Today* **14:**60–68.
67. **Ten Boekel E, Yamagami T, Andersson J, Rolink A, Melchers F.** 1999. The formation and selection of cells expressing preB cell receptors and B cell receptors. *Curr Top Microbiol Immunol* **246:**3–9; discussion, **246:**10.
68. **Tsuganezawa K, Kiyokawa N, Matsuo Y, Kitamura F, Toyama-Sorimachi N, Kuida K, Fujimoto J, Karasuyama H.** 1998. Flow cytometric diagnosis of the cell lineage and developmental stage of acute lymphoblastic leukemia by novel monoclonal antibodies specific to human pre-B-cell receptor. *Blood* **92:**4317–4324.
69. **Kitamura D, Kudo A, Schaal S, Muller W, Melchers F, Rajewsky K.** 1992. A critical role of lambda 5 protein in B cell development. *Cell* **69:**823–831.
70. **Corcos D, Dunda O, Butor C, Cesbron JY, Lores P, Bucchini D, Jami J.** 1995. Pre-B-cell development in the absence of lambda 5 in transgenic mice expressing a heavy-chain disease protein. *Curr Biol* **5:**1140–1148.
71. **Minegishi Y, Coustan-Smith E, Wang YH, Cooper MD, Campana D, Conley ME.** 1998. Mutations in the human lambda5/14.1 gene result in B cell deficiency and agammaglobulinemia. *J Exp Med* **187:**71–77.
72. **Bankovich AJ, Raunser S, Juo ZS, Walz T, Davis MM, Garcia KC.** 2007. Structural insight into pre-B cell receptor function. *Science* **316:**291–294.
73. **Rassenti LZ, Kipps TJ.** 1997. Lack of allelic exclusion in B cell chronic lymphocytic leukemia. *J Exp Med* **185:**1435–1445.
74. **Lewis SM.** 1994. The mechanism of V(D)J joining: lessons from molecular, immunological, and comparative analyses. *Adv Immunol* **56:**27–150.
75. **Gellert M.** 1997. Recent advances in understanding V(D) J recombination. *Adv Immunol* **64:**39–64.
76. **Steen SB, Gomelsky L, Speidel SL, Roth DB.** 1997. Initiation of V(D)J recombination in vivo: role of recombination signal sequences in formation of single and paired double-strand breaks. *EMBO J* **16:**2656–2664.
77. **Schatz DG, Swanson PC.** 2011. V(D)J recombination: mechanisms of initiation. *Annu Rev Genet* **45:**167–202.
78. **Fugmann SD, Lee AI, Shockett PE, Villey IJ, Schatz DG.** 2000. The RAG proteins and V(D)J recombination: complexes, ends, and transposition. *Annu Rev Immunol* **18:**495–527.
79. **Oettinger MA.** 1999. V(D)J recombination: on the cutting edge. *Curr Opin Cell Biol* **11:**325–329.
80. **Gellert M.** 2002. V(D)J recombination: RAG proteins, repair factors, and regulation. *Annu Rev Biochem* **71:**101–132.
81. **Lieber MR.** 2010. The mechanism of double-strand DNA break repair by the nonhomologous DNA end-joining pathway. *Annu Rev Biochem* **79:**181–211.
82. **Rooney S, Chaudhuri J, Alt FW.** 2004. The role of the non-homologous end-joining pathway in lymphocyte development. *Immunol Rev* **200:**115–131.
83. **Gostissa M, Alt FW, Chiarle R.** 2011. Mechanisms that promote and suppress chromosomal translocations in lymphocytes. *Annu Rev Immunol* **29:**319–350.
84. **Nussenzweig A, Nussenzweig MC.** 2010. Origin of chromosomal translocations in lymphoid cancer. *Cell* **141:**27–38.
85. **Helmink BA, Sleckman BP.** 2012. The response to and repair of RAG-mediated DNA double-strand breaks. *Annu Rev Immunol* **30:**175–202.
86. **Grawunder U, West RB, Lieber MR.** 1998. Antigen receptor gene rearrangement. *Curr Opin Immunol* **10:**172–180.
87. **Matthias P, Rolink AG.** 2005. Transcriptional networks in developing and mature B cells. *Nat Rev Immunol* **5:**497–508.
88. **Shinkai Y, Rathbun G, Lam KP, Oltz EM, Stewart V, Mendelsohn M, Charron J, Datta M, Young F, Stall AM,** et al. 1992. RAG-2-deficient mice lack mature lymphocytes owing to inability to initiate V(D)J rearrangement. *Cell* **68:**855–867.
89. **Villa A, Santagata S, Bozzi F, Imberti L, Notarangelo LD.** 1999. Omenn syndrome: a disorder of Rag1 and Rag2 genes. *J Clin Immunol* **19:**87–97.
90. **Villa A, Sobacchi C, Notarangelo LD, Bozzi F, Abinun M, Abrahamsen TG, Arkwright PD, Baniyash M, Brooks EG, Conley ME, Cortes P, Duse M, Fasth A, Filipovich AM, Infante AJ, Jones A, Mazzolari E, Muller SM, Pasic S, Rechavi G, Sacco MG, Santagata S, Schroeder**

ML, Seger R, Strina D, Ugazio A, Valiaho J, Vihinen M, Vogler LB, Ochs H, Vezzoni P, Friedrich W, Schwarz K. 2001. V(D)J recombination defects in lymphocytes due to RAG mutations: severe immunodeficiency with a spectrum of clinical presentations. *Blood* **97:**81–88.

91. **Simkus C, Anand P, Bhattacharyya A, Jones JM.** 2007. Biochemical and folding defects in a RAG1 variant associated with Omenn syndrome. *J Immunol* **179:**8332–8340.
92. **Huye LE, Purugganan MM, Jiang MM, Roth DB.** 2002. Mutational analysis of all conserved basic amino acids in RAG-1 reveals catalytic, step arrest, and joining-deficient mutants in the V(D)J recombinase. *Mol Cell Biol* **22:**3460–3473.
93. **Tsai CL, Drejer AH, Schatz DG.** 2002. Evidence of a critical architectural function for the RAG proteins in end processing, protection, and joining in V(D)J recombination. *Genes Dev* **16:**1934–1949.
94. **Thomas JO, Travers AA.** 2001. HMG1 and 2, and related 'architectural' DNA-binding proteins. *Trends Biochem Sci* **26:**167–174.
95. **Schlissel MS.** 1998. Structure of nonhairpin coding-end DNA breaks in cells undergoing V(D)J recombination. *Mol Cell Biol* **18:**2029–2037.
96. **Jones JM, Gellert M.** 2001. Intermediates in V(D)J recombination: a stable RAG1/2 complex sequesters cleaved RSS ends. *Proc Natl Acad Sci U S A* **98:**12926–12931.
97. **Lieber MR.** 2008. The mechanism of human nonhomologous DNA end joining. *J Biol Chem* **283:**1–5.
98. **Goodarzi AA, Jeggo PA.** 2013. The repair and signaling responses to DNA double-strand breaks. *Adv Genet* **82:**1–45.
99. **Ma Y, Schwarz K, Lieber MR.** 2005. The Artemis:DNA-PKcs endonuclease cleaves DNA loops, flaps, and gaps. *DNA Repair* (Amsterdam) **4:**845–851.
100. **Taccioli GE, Amatucci AG, Beamish HJ, Gell D, Xiang XH, Torres Arzayus MI, Priestley A, Jackson SP, Marshak Rothstein A, Jeggo PA, Herrera VL.** 1998. Targeted disruption of the catalytic subunit of the DNA-PK gene in mice confers severe combined immunodeficiency and radiosensitivity. *Immunity* **9:**355–366.
101. **Khanna KK, Jackson SP.** 2001. DNA double-strand breaks: signaling, repair and the cancer connection. *Nat Genet* **27:**247–254.
102. **Ma Y, Pannicke U, Schwarz K, Lieber MR.** 2002. Hairpin opening and overhang processing by an Artemis/DNA-dependent protein kinase complex in nonhomologous end joining and V(D)J recombination. *Cell* **108:**781–794.
103. **Bogue MA, Jhappan C, Roth DB.** 1998. Analysis of variable (diversity) joining recombination in DNAdependent protein kinase (DNA-PK)-deficient mice reveals DNA-PK-independent pathways for both signal and coding joint formation. *Proc Natl Acad Sci U S A* **95:**15559–15564.
104. **Kulesza P, Lieber MR.** 1998. DNA-PK is essential only for coding joint formation in V(D)J recombination. *Nucleic Acids Res* **26:**3944–3948.
105. **Ding Q, Reddy YV, Wang W, Woods T, Douglas P, Ramsden DA, Lees-Miller SP, Meek K.** 2003. Autophosphorylation of the catalytic subunit of the DNA-dependent protein kinase is required for efficient end processing during DNA double-strand break repair. *Mol Cell Biol* **23:**5836–5848.
106. **Wiler R, Leber R, Moore BB, VanDyk LF, Perryman LE, Meek K.** 1995. Equine severe combined immunodeficiency: a defect in V(D)J recombination and DNA-dependent protein kinase activity. *Proc Natl Acad Sci U S A* **92:**11485–11489.
107. **Meek K, Kienker L, Dallas C, Wang W, Dark MJ, Venta PJ, Huie ML, Hirschhorn R, Bell T.** 2001. SCID in Jack Russell terriers: a new animal model of DNA-PKcs deficiency. *J Immunol* **167:**2142–2150.
108. **Gu Y, Sekiguchi J, Gao Y, Dikkes P, Frank K, Ferguson D, Hasty P, Chun J, Alt FW.** 2000. Defective embryonic neurogenesis in Ku-deficient but not DNA-dependent protein kinase catalytic subunit-deficient mice. *Proc Natl Acad Sci U S A* **97:**2668–2673.
109. **Ouyang H, Nussenzweig A, Kurimasa A, Soares VC, Li X, Cordon-Cardo C, Li W, Cheong N, Nussenzweig M, Iliakis G, Chen DJ, Li GC.** 1997. Ku70 is required for DNA repair but not for T cell antigen receptor gene recombination in vivo. *J Exp Med* **186:**921–929.
110. **Bassing CH, Suh H, Ferguson DO, Chua KF, Manis J, Eckersdorff M, Gleason M, Bronson R, Lee C, Alt FW.** 2003. Histone H2AX: a dosage-dependent suppressor of oncogenic translocations and tumors. *Cell* **114:**359–370.
111. **Celeste A, Difilippantonio S, Difilippantonio MJ, Fernandez-Capetillo O, Pilch DR, Sedelnikova OA, Eckhaus M, Ried T, Bonner WM, Nussenzweig A.** 2003. H2AX haploinsufficiency modifies genomic stability and tumor susceptibility. *Cell* **114:**371–383.
112. **Al-Hakim A, Escribano-Diaz C, Landry MC, O'Donnell L, Panier S, Szilard RK, Durocher D.** 2010. The ubiquitous role of ubiquitin in the DNA damage response. *DNA Repair* (Amsterdam) **9:**1229–1240.
113. **Komori T, Okada A, Stewart V, Alt FW.** 1993. Lack of N regions in antigen receptor variable region genes of TdT-deficient lymphocytes. *Science* **261:**1171–1175.
114. **Sleckman BP, Oltz EM.** 2012. Preparing targets for V(D)J recombinase: transcription paves the way. *J Immunol* **188:**7–9.
115. **Subrahmanyam R, Sen R.** 2012. Epigenetic features that regulate IgH locus recombination and expression. *Curr Top Microbiol Immunol* **356:**39–63.
116. **Grazini U, Zanardi F, Citterio E, Casola S, Goding CR, McBlane F.** 2010. The RING domain of RAG1 ubiquitylates histone H3: a novel activity in chromatin-mediated regulation of V(D)J joining. *Mol Cell* **37:**282–293.
117. **Jones JM, Bhattacharyya A, Simkus C, Vallieres B, Veenstra TD, Zhou M.** 2011. The RAG1 V(D)J recombinase/ubiquitin ligase promotes ubiquitylation of acetylated, phosphorylated histone 3.3. *Immunol Lett* **136:**156–162.
118. **Jones JM, Gellert M.** 2003. Autoubiquitylation of the V(D)J recombinase protein RAG1. *Proc Natl Acad Sci U S A* **100:**15446–15451.
119. **Kassmeier MD, Mondal K, Palmer VL, Raval P, Kumar S, Perry GA, Anderson DK, Ciborowski P, Jackson S, Xiong Y, Swanson PC.** 2012. VprBP binds full-length RAG1 and is required for B-cell development and V(D)J recombination fidelity. *EMBO J* **31:**945–958.
120. **Simkus C, Bhattacharyya A, Zhou M, Veenstra TD, Jones JM.** 2009. Correlation between recombinase activating gene 1 ubiquitin ligase activity and V(D)J recombination. *Immunology* **128:**206–217.
121. **Yurchenko V, Xue Z, Sadofsky M.** 2003. The RAG1 N-terminal domain is an E3 ubiquitin ligase. *Genes Dev* **17:**581–585.
122. **Jiang H, Chang FC, Ross AE, Lee J, Nakayama K, Desiderio S.** 2005. Ubiquitylation of RAG-2 by Skp2-SCF links destruction of the V(D)J recombinase to the cell cycle. *Mol Cell* **18:**699–709.
123. **Lee J, Desiderio S.** 1999. Cyclin A/CDK2 regulates V(D)J recombination by coordinating RAG-2 accumulation and DNA repair. *Immunity* **11:**771–781.
124. **Mizuta R, Mizuta M, Araki S, Kitamura D.** 2002. RAG2 is down-regulated by cytoplasmic sequestration and ubiquitin-dependent degradation. *J Biol Chem* **277:**41423–41427.
125. **Stavnezer J, Amemiya CT.** 2004. Evolution of isotype switching. *Semin Immunol* **16:**257–275.

126. **Durandy A, Revy P, Fischer A.** 2004. Human models of inherited immunoglobulin class switch recombination and somatic hypermutation defects (hyper-IgM syndromes). *Adv Immunol* **82:**295–330.
127. **Ferrari S, Plebani A.** 2002. Cross-talk between CD40 and CD40L: lessons from primary immune deficiencies. *Curr Opin Allergy Clin Immunol* **2:**489–494.
128. **Calame KL, Lin KI, Tunyaplin C.** 2003. Regulatory mechanisms that determine the development and function of plasma cells. *Annu Rev Immunol* **21:**205–230.
129. **Yamane A, Robbiani DF, Resch W, Bothmer A, Nakahashi H, Oliveira T, Rommel PC, Brown EJ, Nussenzweig A, Nussenzweig MC, Casellas R.** 2013. RPA accumulation during class switch recombination represents 5′-3′ DNA-end resection during the S-G2/M phase of the cell cycle. *Cell Rep* **3:**138–147.
130. **Honjo T, Kinoshita K, Muramatsu M.** 2002. Molecular mechanism of class switch recombination: linkage with somatic hypermutation. *Annu Rev Immunol* **20:**165–196.
131. **Muramatsu M, Kinoshita K, Fagarasan S, Yamada S, Shinkai Y, Honjo T.** 2000. Class switch recombination and hypermutation require activation-induced cytidine deaminase (AID), a potential RNA editing enzyme. *Cell* **102:**553–563.
132. **Muramatsu M, Nagaoka H, Shinkura R, Begum NA, Honjo T.** 2007. Discovery of activation-induced cytidine deaminase, the engraver of antibody memory. *Adv Immunol* **94:**1–36.
133. **Revy P, Muto T, Levy Y, Geissmann F, Plebani A, Sanal O, Catalan N, Forveille M, Dufourcq-Labelouse R, Gennery A, Tezcan I, Ersoy F, Kayserili H, Ugazio AG, Brousse N, Muramatsu M, Notarangelo LD, Kinoshita K, Honjo T, Fischer A, Durandy A.** 2000. Activation-induced cytidine deaminase (AID) deficiency causes the autosomal recessive form of the Hyper-IgM syndrome (HIGM2). *Cell* **102:**565–575.
134. **Zahn A, Eranki AK, Patenaude AM, Methot SP, Fifield H, Cortizas EM, Foster P, Imai K, Durandy A, Larijani M, Verdun RE, Di Noia JM.** 2014. Activation induced deaminase C-terminal domain links DNA breaks to end protection and repair during class switch recombination. *Proc Natl Acad Sci U S A* **111:**E988–E997.
135. **MacLennan IC.** 2005. Germinal centers still hold secrets. *Immunity* **22:**656–657.
136. **Imai K, Slupphaug G, Lee WI, Revy P, Nonoyama S, Catalan N, Yel L, Forveille M, Kavli B, Krokan HE, Ochs HD, Fischer A, Durandy A.** 2003. Human uracil-DNA glycosylase deficiency associated with profoundly impaired immunoglobulin class-switch recombination. *Nat Immunol* **4:**1023–1028.
137. **Chen X, Kinoshita K, Honjo T.** 2001. Variable deletion and duplication at recombination junction ends: implication for staggered double-strand cleavage in class-switch recombination. *Proc Natl Acad Sci U S A* **98:**13860–13865.
138. **Wang CL, Wabl M.** 2004. DNA acrobats of the Ig class switch. *J Immunol* **172:**5815–5821.
139. **Kaji T, Furukawa K, Ishige A, Toyokura I, Nomura M, Okada M, Takahashi Y, Shimoda M, Takemori T.** 2013. Both mutated and unmutated memory B cells accumulate mutations in the course of the secondary response and develop a new antibody repertoire optimally adapted to the secondary stimulus. *Int Immunol* **25:**683–695.
140. **Michael N, Martin TE, Nicolae D, Kim N, Padjen K, Zhan P, Nguyen H, Pinkert C, Storb U.** 2002. Effects of sequence and structure on the hypermutability of immunoglobulin genes. *Immunity* **16:**123–134.
141. **Rogozin IB, Sredneva NE, Kolchanov NA.** 1996. Somatic hypermutagenesis in immunoglobulin genes. III. Somatic mutations in the chicken light chain locus. *Biochim Biophys Acta* **1306:**171–178.
142. **Dudley DD, Chaudhuri J, Bassing CH, Alt FW.** 2005. Mechanism and control of V(D)J recombination versus class switch recombination: similarities and differences. *Adv Immunol* **86:**43–112.
143. **Di Noia JM, Neuberger MS.** 2007. Molecular mechanisms of antibody somatic hypermutation. *Annu Rev Biochem* **76:**1–22.
144. **Di Noia J, Neuberger MS.** 2002. Altering the pathway of immunoglobulin hypermutation by inhibiting uracil-DNA glycosylase. *Nature* **419:**43–48.
145. **Neuberger MS.** 2008. Antibody diversification by somatic mutation: from Burnet onwards. *Immunol Cell Biol* **86:**124–132.
146. **Peled JU, Kuang FL, Iglesias-Ussel MD, Roa S, Kalis SL, Goodman MF, Scharff MD.** 2008. The biochemistry of somatic hypermutation. *Annu Rev Immunol* **26:**481–511.
147. **Odegard VH, Schatz DG.** 2006. Targeting of somatic hypermutation. *Nat Rev Immunol* **6:**573–583.
148. **Storb U, Shen HM, Michael N, Kim N.** 2001. Somatic hypermutation of immunoglobulin and non-immunoglobulin genes. *Philos Trans R Soc Lond B Biol Sci* **356:**13–19.
149. **Ollila J, Vihinen M.** 2005. B cells. *Int J Biochem Cell Biol* **37:**518–523.
150. **Dorner T, Foster SJ, Brezinschek HP, Lipsky PE.** 1998. Analysis of the targeting of the hypermutational machinery and the impact of subsequent selection on the distribution of nucleotide changes in human VHDJH rearrangements. *Immunol Rev* **162:**161–171.
151. **Buerstedde JM, Alinikula J, Arakawa H, McDonald JJ, Schatz DG.** 2014. Targeting of somatic hypermutation by immunoglobulin enhancer and enhancer-like sequences. *PLoS Biol* **12:**e1001831.
152. **Aoufouchi S, Faili A, Zober C, D'Orlando O, Weller S, Weill JC, Reynaud CA.** 2008. Proteasomal degradation restricts the nuclear lifespan of AID. *J Exp Med* **205:**1357–1368.
153. **Delker RK, Zhou Y, Strikoudis A, Stebbins CE, Papavasiliou FN.** 2013. Solubility-based genetic screen identifies RING finger protein 126 as an E3 ligase for activation-induced cytidine deaminase. *Proc Natl Acad Sci U S A* **110:**1029–1034.
154. **Sonnenberg A, Marciniak JY, Rassenti L, Ghia EM, Skowronski EA, Manouchehri S, McCanna J, Widhopf GF II, Kipps TJ, Heller MJ.** 2014. Rapid electrokinetic isolation of cancer-related circulating cell-free DNA directly from blood. *Clin Chem* **60:**500–509.
155. **Langerak A.** 2009. From the patient to the sequence: selection of material, primers and PCR protol, clonality analysis, and sequencing protocol, p 23–31. *In* Ghia P, Rosenquist R, Davi F (ed), *Immunoglobulin Gene Analysis in Chronic Lymphocytic Leukemia*. Wolters Kluwer Health Italy Ltd., Milan, Italy.

Immunoglobulin Quantification and Viscosity Measurement

JEFFREY S. WARREN

7

Quantification of intact serum immunoglobulins has proven useful in the evaluation of patients with suspected immunodeficiency disorders, lymphocyte and plasma cell neoplastic diseases, allergic conditions, and some chronic inflammatory and autoimmune disorders. Since the advent of quantitative immunoglobulin assays nearly 50 years ago (1), increasingly robust analytical methods have been developed. The armamentarium of intact immunoglobulin assays was first substantively expanded by the development of immunoglobulin light-chain measurements in which the light chains are bound to heavy chains (intact immunoglobulins). The last decade has seen the development of both free (unbound) immunoglobulin light-chain assays and heavy/light-chain (HLC) or junctional epitope assays, the latter of which allows for individual measurements of IgGκ, IgGλ, IgAκ, IgAλ, IgMκ, and IgMλ (2, 3). Despite these advances in immunoglobulin and light-chain quantification methods, there remain technical complexities that can influence accuracy and, in turn, proper clinical application. Equally important, even with robust assays, is the need for thorough understanding of the clinical indications for, and limitations to, immunoglobulin and related measurements.

Viscosity is the internal friction of a fluid, caused by intermolecular attraction, leading to resistance of the fluid to flow (4). Viscosity measurements can be very complex (4). By extension, rigorous whole-blood, plasma, and serum measurements are also very complex. Fortunately, clinically useful measurements of viscosity are relatively straightforward. A variety of clinical conditions can affect the viscosity of blood (5). While abnormalities of the formed elements of blood (e.g., polycythemia, some hemoglobinopathies, and extreme leukocytosis) can result in clinically significant hyperviscosity, overwhelmingly the most common causes are either immunoglobulin concentration or abnormal immunoglobulin structure. There are several analytical methods for measurement of whole-blood, plasma, and serum viscosity. It is important to understand the uses and limitations of these measurements and how each is reported.

This chapter is divided into three sections. The first provides a brief review of immunoglobulin structure, important because of its direct relevance to quantitative immunoglobulin and related measurements. The second provides an overview of assay methods and highlights issues related to quality control, test validation, and quality assurance, as well as a brief discussion of the clinical application of immunoglobulin and related measurements. Developments since the 7th edition of this *Manual* include the advent of free-light-chain assays and heavy/light-chain or junctional epitope assays. The third section addresses fundamental technical aspects of clinically useful viscosity measurement and important interpretive considerations.

IMMUNOGLOBULIN STRUCTURE

Knowledge of immunoglobulin structure is important for understanding measurements of intact immunoglobulins and free light chains as well as in clinical viscometry. Basic antibody function (i.e., antigen binding) was recognized years before the elucidation of immunoglobulin structure (6). Early studies of antibody binding to highly purified carbohydrate antigens led to the deduction that antibody was composed of protein (6). The development of clinical electrophoresis led to the recognition that antibody migrated largely within the so-called gamma region of serum proteins, hence the names "gamma globulin" and "immunoglobulin" (Fig. 1) (7). In 1952, Colonel Ogden Bruton, a pediatrician, used serum protein electrophoresis (SPEP) to evaluate a boy suffering from recurrent bacterial infections (8). Recognition that the gamma fraction of protein was absent, coupled with the boy's favorable response to injections of gamma globulin from healthy donors, supported the conclusion that this serum fraction was important in host defense and led to the clinical definition of a specific immunodeficiency syndrome (Bruton's agammaglobulinemia). Recognition of *m*onoclonal immunoglobulin (also known as M-protein or "paraprotein") as the structurally uniform product of a clonal proliferation of neoplastic B lymphocytes or plasma cells was important in the recognition and understanding of such diseases as multiple myeloma and Waldenström's macroglobulinemia.

In contrast to serum alpha and beta globulins, which are composites of structurally homogeneous proteins (e.g., alpha-1 antiproteinase, transferrin, and complement protein 3), polyclonal immunoglobulins are structurally heterogeneous (9). This structural heterogeneity is accounted for at several levels. There are five major immunoglobulin classes (isotypes), each determined by heavy-chain type (see below) and each different in structure and function (Table 1). Subclasses within immunoglobulin G (IgG), IgA, and IgM (Table 2) also contribute to immunoglobulin heterogeneity, as do allotypic variations within both heavy- and light-chain

doi:10.1128/9781555818722.ch7

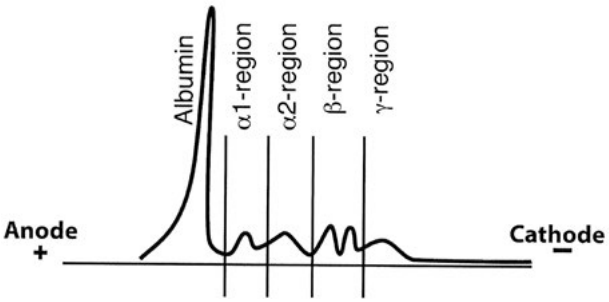

FIGURE 1 Serum protein electrophoresis: densitometric display of serum proteins separated by agarose gel electrophoresis using a pH 8.6 buffer. Capillary zone electrophoresis is liquid based; thus, no permanent gel is produced.

isotypes. Immunoglobulins are also subject to posttranslational modification. Overwhelmingly, however, the great heterogeneity of structure reflects the vast array of different amino acid sequences within the variable and hypervariable regions of immunoglobulin molecules. One of the pivotal scientific advances in the history of immunology was the elucidation of the molecular mechanisms responsible for the generation of antibody (immunoglobulin) diversity (chapter 6) (10). It is important to remember these different levels as contributors to the structural heterogeneity of immunoglobulins because they warrant consideration in both the quantification of polyclonal immunoglobulins by class (e.g., total IgG or IgM) and in the quantification of monoclonal immunoglobulins (e.g., in patients with multiple myeloma). The general structure of an intact immunoglobulin molecule includes two heavy chains (gamma, alpha, mu, delta, or epsilon), two light chains (kappa or lambda), and several bridging disulfide bonds (Fig. 2). Within each heavy and light chain are N-terminal variable and hypervariable (antigen-binding) domains and C-terminal constant domains. Antibody structure is best understood in the context of the genetic and molecular bases of structural and functional diversity (chapter 6).

Pioneering studies of antibody structure, carried out in the 1950s and 1960s, provided important insight into antibody function and resulted in the immunoglobulin subunit nomenclature still in use. In 1958, Porter (11) digested rabbit gamma globulin with the enzyme papain. Separation of the digestion products revealed two identical *a*ntigen-*b*inding *f*ragments (Fab) and one fragment that could be crystallized (Fc). Fab fragments had sedimentation coefficients of 3.5 S (Svedberg units). That the Fc fragment could be crystallized provided evidence that it was biochemically homogeneous. Digestion of purified antibody with pepsin yielded a different set of fragments. The largest, with a sedimentation coefficient of 5 S, had an antigen-binding valence of 2, hence its designation, $F(ab')_2$. Reduction of the disulfide bonds that hold an $F(ab')_2$ fragment intact resulted in the formation of two fragments that each resembled (but were not identical to) papain-generated Fab. In 1961, Edelman and Poulik reported that chemical reduction (of disulfide bonds in intact immunoglobulin molecules) leads to the formation of two "heavy" chains and two "light" chains (12).

As noted above, the structurally variable (and hypervariable) Fab domains of immunoglobulin molecules are responsible for antigen binding. In contrast, the Fc domain determines the biological function of a given immunoglobulin molecule. As summarized in Table 1, the biological functions of immunoglobulins are diverse, including such characteristics as complement fixation (e.g., IgG and IgM), placental transfer (IgG), and high-affinity cytophilic binding to mast cells (IgE) (13). IgM generally circulates as a pentamer that consists of five covalently linked IgM monomers with an antigen-binding valence of 10. Serum IgA occurs as a monomer that weighs nearly 160 Da with a valence of 2. In secretions, IgA commonly occurs as a multimer, usually a dimer.

Light chains (kappa and lambda) each possess an N-terminal 110-amino-acid variable (V) region and a C-terminal 107- to 110-amino-acid constant (C) domain. By analogy, heavy chains (gamma, alpha, mu, epsilon, and

TABLE 2 Characteristics of IgG subclasses

Property	IgG1	IgG2	IgG3	IgG4
Concn in serum (g/liter)	1.8–7.8	1.0–4.6	0.3–1.4	0.08–1.8
Half-life (days)	14–23	14–23	7–8	14–23
Complement fixation	Strong	Weak	Strong	None
Phagocyte binding (via Fc receptors)	Yes	No	Yes	No
Associated with allergies	No	No	No	Yes

TABLE 1 Characteristics of immunoglobulins[a]

Nomenclature	IgG	IgA	IgM	IgD	IgE
Heavy-chain class	Gamma	Alpha	Mu	Delta	Epsilon
Heavy-chain subclasses	1, 2, 3, 4	1, 2	1, 2		
Light-chain types	Kappa and lambda	Kappa and lambda	Kappa and lambda	Kappa and lambda	Kappa and lambda
Physical characteristics					
Molecular mass (Da)	143,000–160,000	159,000–447,000	900,000	177,000–185,000	187,000–200,000
Sedimentation coefficient (Svedberg units)	6.7–7.0	7.5–9.0	18–19	6.9–7.0	7.9–8.0
Functional characteristics					
Serum half-life (days)	7–23	5–6	5	2–8	1–5
Complement fixation	+	−	++	−	−
Placental transfer	+	−	−	−	−
Reaginic activity	±	−	−	−	++

[a] ±, borderline; +, present; ++, strong activity; −, no activity.

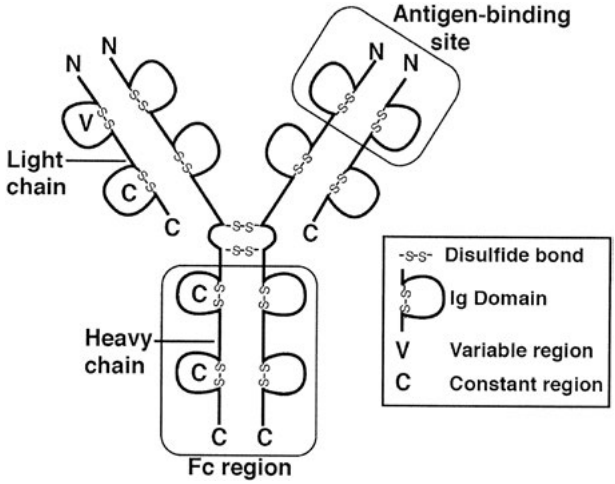

FIGURE 2 Schematic of an intact immunoglobulin G molecule. Antigen binding occurs between light and heavy chains in the N-terminal variable-hypervariable binding regions. IgG possesses an antigen-binding valence of 2. Monomeric immunoglobulin molecules, whether the heavy chains are gamma, alpha, mu, delta, or epsilon, possess the same general structure. Individual immunoglobulin molecules include either kappa *or* lambda light chains, *not both*.

delta) each possess a 110-amino-acid N-terminal variable region and, depending on the particular class, three or four 110-amino-acid constant-region domains. Individual variable- or constant-region domains are folded into globular motifs called "Ig domains." Ig domains are held in conformation by disulfide bonds (Fig. 2). Structurally apposed light- and heavy-chain variable regions form an antigen-binding domain. It is useful to think of the antigen-binding (Fab) region of an immunoglobulin molecule as a hand that grasps a uniquely shaped doorknob (antigen). Finally, as alluded to above, the genetic and molecular bases for immunoglobulin structure, antibody diversity, and immunoglobulin assembly and secretion have been studied intensively (chapter 6) (10, 13). Kappa light chains are encoded by chromosomal band 2p11, lambda light chains are encoded by 22q11, and the heavy chain is encoded by the loci on chromosome 14. A highly regulated series of DNA recombination, nucleic acid splicing, and subunit assembly steps is required to generate intact immunoglobulin molecules (10, 13). Immunoglobulins are produced only by B lymphocytes and plasma cells.

IMMUNOGLOBULIN CLASSES

IgG is the predominant class of serum immunoglobulins. More than 60% of circulating IgG is IgG1, with IgG2, IgG3, and IgG4, in that order, present in decreasing concentrations (Table 2) (13, 14). Except for IgG3, which has a serum half-life of 1 week, the IgG subclasses have half-lives of 2 to 3 weeks. IgG antibodies comprise the most important effector class of molecules in a secondary or anamnestic humoral immune response. Among large populations of B lymphocytes that express different cell surface IgG molecules, high-affinity antigen binding provides a selective advantage for subsequent clonal expansion (13). As a result, as a humoral immune response "matures" over time, increasing proportions of IgG antibodies exhibit higher degrees of antigen-binding affinity (affinity maturation). This is in part why repetitive exposures to a given antigen result in increasingly effective humoral immunity.

IgA is the most important immunoglobulin in the mucosal host defense system. Mucosal IgA exists chiefly as paired monomeric subunits linked by J ("joining") chains to form dimers (13). A 60-kDa peptide called the "secretory piece" is necessary for IgA to be secreted by various types of epithelial cells that line mucosal surfaces. IgA, like all immunoglobulins, is produced by B lymphocytes and plasma cells. Mucosal IgA is actively transported across mucosal epithelial layers (from the abluminal to the luminal surface). As noted in Table 1, IgA exists as IgA1 and IgA2 subclasses, the former present in higher concentration in serum and each having a half-life of 4 to 5 days.

Serum IgM circulates chiefly in the form of pentamers. Monomeric subunits include two mu heavy chains, which in turn each possess one more constant-region domain than most gamma heavy-chain species. As a result, pentameric IgM has a molecular mass of approximately 900 kDa (J chain plus 5 times nearly 180 kDa). IgM is the initial immunoglobulin class expressed on B cells during lymphocyte development and is the predominant immunoglobulin class in a primary humoral response (13).

IgD circulates in very low concentrations. Like IgM, B cell surface IgD is expressed early in lymphocyte development (13). Monomeric IgD consists of two heavy chains (each weighs approximately 60 kDa) and two identical kappa or lambda light chains. The biological role of serum IgD is not well understood, and clinical measurement of IgD has no value except for the rare patient with an IgD-secreting neoplasm (e.g., multiple myeloma) or the equally rare patient with a familial hyper-IgD fever syndrome.

The clinical utility of IgE measurements is discussed in greater detail in section M, which describes allergic diseases. Serum IgE molecules circulate as monomers that consist of two epsilon chains (each approximately 70 kDa) and two identical kappa or lambda light chains (14). Like mu heavy chains, epsilon heavy chains contain an additional constant-region domain. While IgE is normally present in low concentrations, elevated polyclonal IgE immunoglobulin is seen in a wide variety of allergic and autoimmune diseases. Antigen-specific IgE measurements are widely used in the evaluation and management of patients with specific atopic disorders (14). For instance, one may quantitatively measure IgE antipollen or IgE antipeanut antigen. These measurements require very sensitive analytical immunoassay systems that rely on detection of specific binding of IgE immunoglobulin molecules to their defined cognate antigens. Cytophilic IgE binds to mast cells and basophils via very-high-affinity Fcε receptors. Activation of such cells via divalent IgE-specific antigen binding results in the rapid release of vasoactive and chemotactic mediators that can cause localized swelling and/or a generalized, sometimes life-threatening reaction (anaphylaxis) (15). Measurement of total IgE and antigen-specific IgE antibodies is discussed in section M.

MEASUREMENT OF IMMUNOGLOBULINS

Currently, quantification of intact IgG, IgA, and IgM is almost exclusively performed by automated rate nephelometric or immunoturbidimetric assay systems (16). Application of nephelometry and immunoturbidimetry to immunoglobulin measurement represents a trend away from more labor-intensive, less sensitive, and slower manual methods such as radial immunodiffusion (RID) and the Laurell rocket technique (17, 18). Likewise, most serum-bound kappa and lambda light-chain measurements and total IgE measurements are also carried out using automated nephelometric

or immunoturbidimetric assay systems (16). More than 20% of clinical laboratories that participated in the 2004 College of American Pathologists (CAP) proficiency testing survey program used a RID method for IgG subclass measurements, and nearly all laboratories that measured total IgD employed a RID assay (17, 18). Currently, nearly all laboratories (that participate in the CAP proficiency testing program) utilize nephelometric or immunoturbidimetric assays (16). The exception is for total IgE, which is measured by nonisotopic immunoassay.

Nephelometric assays are based on rate reactions in which antigen, in this case an immunoglobulin such as IgG, is injected into a reaction chamber with an antigen-specific antibody (19). As antigen-antibody complexes form in suspension, they form a precipitin "cloud." ("Nephos" is derived from the Greek word for cloud.) Antigen-antibody complexes are detected with an intense light source. As immune complexes form, increasing numbers of photons are deflected at 30° to 90° angles. They are then quantified with a photomultiplier tube located on the inner side surface of the reaction chamber. As the antigen-antibody precipitin "cloud" grows in size and density, more photons are deflected and a greater signal is recorded. The rise in the number of light signal events (photons) as a function of time (in milliseconds) is determined by the concentrations of antigen and antibody. Modern rate nephelometers are sophisticated instruments that employ parallel duplicate assay chambers, thus ensuring precision; they exhibit high throughput and are programmed to run through a series of dilutions of antigen or antibody, thus allowing for the "finding of" a near-optimal precipitin-forming rate reaction. While rate nephelometers are robust, wildly aberrant results can occur as the result of extreme antigen excess (the high-dose "hook" effect) (20). This problem may be particularly pronounced when measuring an unusually high concentration of an analyte (outside the expected dynamic range of the assay) otherwise expected to have a relatively low concentration. Such antigen excess can escape detection via antigen excess checks (a series of repeated measurements with more-dilute antigen or antibody solutions). When measuring IgG subclasses, it is a useful quality check to sum the concentrations of all four subclasses to ascertain that their additive total approximates the separately measured total IgG concentration. Immunoturbidimetric assays are formatted similarly, but rather than relying upon the quantitation of deflected light, they rely on the interruption of light transmission (180°) through the suspension of immune complexes being formed by antigen and reagent antibody (21).

Nephelometric and immunoturbidimetric test systems have had a large economic impact on clinical laboratories because they are automated, can be used to measure many different analytes with a single platform, and allow rapid and high-volume throughput. As a result, employment of these methods yields a lower cost per test in laboratories that process significant volumes.

RID assays entail addition of reagent antibody to warm (50°C) agar while it is in the liquid state (1, 22). Liquefied antibody-containing agar is poured into a shallow, flat plastic dish or plate and allowed to cool to room temperature. The resulting semisolid agar has the consistency of cold Jell-O. Cylindrical vertical wells are then cut into the solidified agar. Standard dilutions of known concentrations of antigen, in this case, immunoglobulin such as a specific IgG subclass, are placed into multiple wells. Serum samples that contain patient IgG to be measured are placed in other wells. As the antigen (IgG subclass) diffuses in all directions from each well, a visible antigen-antibody precipitin line forms where antigen and antibody achieve equivalence. The concentration of the unknown analyte, in this case the serum IgG subclass, can be calculated by comparing the diameter of the precipitin ring to those precipitin rings of the standard curve generated by the serially diluted known concentrations of antigen added to different wells. Higher concentrations of antigen must diffuse further to reach concentrations low enough to form antigen-antibody complexes at equivalence. Typically, a 5 $\log_{10}$ dilution standard curve is employed (1, 22). The diameters measured from precipitin rings formed by patient samples can be interpolated from the set of standard curve diameters. RID offers the advantages that it is simple and requires very little equipment. The major disadvantages are that RID assays are manual, take 16 to 48 hours to run because of the diffusion time required, and often employ very expensive reagents. Technical artifacts attributable to lipids, monomeric IgM or IgA, or cross-reacting antibodies to animal proteins can lead to inaccurate results. When reagent antibody is monoclonal, as in many IgG subclass assays, the per-test cost can be extraordinarily high. One decade ago, when more than 20% of laboratories that participated in the CAP proficiency testing program used RID assays for IgG subclass measurement (17, 18), a single set of RID plates (enough to test nine patients) cost $400 (J. Warren, unpublished observation)! Inherent in RID immunoglobulin assays are higher coefficients of variation than those observed for nephelometric and immunoturbidimetric methods (greater than 10% versus less than or equal to 8%) (16–18). Because of high relative expense and long analytical times, the use of RID assays in clinical laboratories has decreased dramatically during the past 2 decades (16).

The Laurell rocket technique is very similar to RID, except that the diffusion phase of the assay is accelerated from hours to minutes by the application of an electrical field (23). While the endpoint is still the formation of a precipitin line (antigen-antibody complexes at equivalence in agar), the geometry is changed from a circle to that of a rocket-shaped arc, hence the designation "rocket." With the Laurell technique, the height of the precipitin rocket is proportional to the antigen concentration. As in the RID technique, a standard curve is constructed by running a series of different known concentrations of a standard antigen preparation. Again, immunoglobulin concentrations in patient samples are calculated based on interpolation from the standard curve. While Laurell rocket electrophoresis is faster than RID, the remaining shortcomings still hold, and use in clinical laboratories is very uncommon (16). Both RID and Laurell rocket assay systems may be most appropriate for very-low-volume laboratories, where a nephelometer may be too expensive.

MEASUREMENT OF FREE LIGHT CHAINS

In the past decade, an analytical approach to quantification of free (dissociated from heavy chain) immunoglobulin light chains in serum and/or urine has been developed, and the assay has been tested in a variety of clinical settings. Mature B lymphocytes and plasma cells typically produce approximately 40% excess of free light chains (13). Thus, early after the emergence of a single (disordered or neoplastic) clone, the "signal-to-noise" ratio of monoclonal light chains to "background" polyclonal light chains is low—making monoclonal populations difficult to detect. Identification of free monoclonal light chains in the sera of patients with multiple myeloma, other B cell disorders, and light-chain (amyloid light-chain [AL])-type amyloidosis is also limited, especially early in the course of the disease, because these proteins, by virtue of their low molecular mass (22 to 25

kDa), are filtered by glomeruli and subsequently reabsorbed by proximal renal tubular epithelial cells. Accordingly, SPEP may reveal no apparent abnormality. The diagnostic yield is increased by also testing urine for such Bence Jones proteins (monoclonal urinary free light chains). Again, low concentrations of Bence Jones protein may not be seen early in disease because proximal tubular reabsorption of such clonal proteins is relatively efficient until the quantities of protein increase and exceed the reabsorptive capacity of the tubular epithelium or until tubular damage (acquired Fanconi syndrome) occurs and there is increased excretion of Bence Jones protein. The advent of the nephelometric serum free-light-chain (sFLC) assay has increased the ability to detect monoclonal proteins (43) (see below).

In 2001, Bradwell et al. developed a sensitive immunoassay for the quantification of free immunoglobulin light chains in both urine and serum (2). Affinity-purified antibodies that react specifically with epitopes accessible only on *free* light chains (Fig. 3), but unable to reach the same epitopes sequestered in bound light chains, are linked to the surface of latex particles. These antibody-coated particles form aggregates when incubated with free light chains. Employment of such particles in automated nephelometric or immunoturbidimetric analyzers has resulted in a robust test system. Because free kappa and lambda (polyclonal) light chains are normally also present in serum and urine (and measured), the clinically useful assay for detection of monoclonality necessitates calculation of the ratio of free kappa to free lambda light chain. The occurrence of a significant clonal increase in either free kappa or free lambda light chains distorts this ratio. Thus, a very high or a very low ratio of kappa to lambda free light chains is reflective of a kappa monoclonal or lambda monoclonal process, respectively. Individual sFLC measurements, kappa *or* lambda, reflect the total circulating respective free-light-chain concentration.

Clinical studies since the widespread deployment of sFLC assays have led to a better understanding of when and how to utilize this test. Much of what has been learned was distilled into a set of practice guidelines published by the International Myeloma Working Group in 2009 (see below) and has since been reiterated, refined, and extended in more-recent studies (24–26).

The addition of sensitive and specific free-light-chain assays to the armamentarium of laboratory tests available for the diagnosis and management of patients suspected to have multiple myeloma, Waldenström's macroglobulinemia, B cell leukemias and lymphomas, and AL-type amyloidosis is an exciting prospect. As in other nephelometric and immunoturbidimetric immunoglobulin assays, sFLC measurements are prone to the high-dose "hook" effect (19, 20). This is of particular concern in measurements of serum free light chains in patients with B lymphocyte and plasma cell neoplasms because of the extreme variation in concentrations that can be seen in a single patient over time. There are several analytical limitations to sFLC assays. These include lot-to-lot variability and the fact that some sFLCs do not dilute in a linear fashion (27). It will be important for additional clinical studies to address the specific potential applications and limitations of these assays. Particular attention will need to be paid to comparisons between free-light-chain assays and *optimally* used "traditional" assays. For example, it will be appropriate to compare diagnostic sensitivities and specificities of free-chain-assays to those of serum *and* urine immunofixation assays, not merely serum *or* urine immunofixation assays. In addition, it will be important to assess the impact of sensitive free-light-chain assays on clinical outcomes in patients. Serum and urine free-light-chain assays are Food and Drug Administration cleared for use in the diagnosis and monitoring of patients with B cell and plasma cell neoplasms and collagen vascular diseases such as systemic lupus erythematosus (25).

Many important utilization and cost-effectiveness questions remain to be answered for these expensive tests. For instance, what are appropriate testing frequencies in the context of various disease processes and therapies? How should sFLC assays be utilized in the context of other laboratory testing? Any studies of cost-effectiveness of sFLC testing versus "traditional approaches" (SPEP, 24-hour Bence Jones protein quantification, etc.) should take into account not only the cost of "traditional" testing but also inconvenience (e.g., 24-hour urine collection) and technical limitations (e.g., quantification of urine Bence Jones protein and M-protein quantification by SPEP). Clearly, assessments of optimal utilization and cost-effectiveness encompass a broad set of questions and consideration of many factors.

JUNCTIONAL EPITOPE (HEAVY/LIGHT-CHAIN) ASSAYS

In 2009, Bradwell et al. described the development of an assay based on reagent antisera that specifically recognize and bind to unique epitopes displayed at the junction between

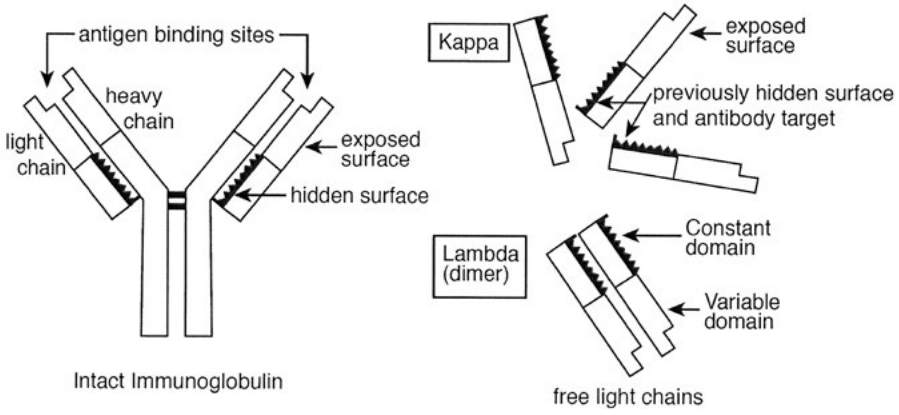

FIGURE 3 The serum free-light-chain (sFLC) assay is based on purified polyclonal antibodies that specifically bind epitopes that are accessible on free light chains but hidden (and inaccessible) in intact immunoglobulin molecules.

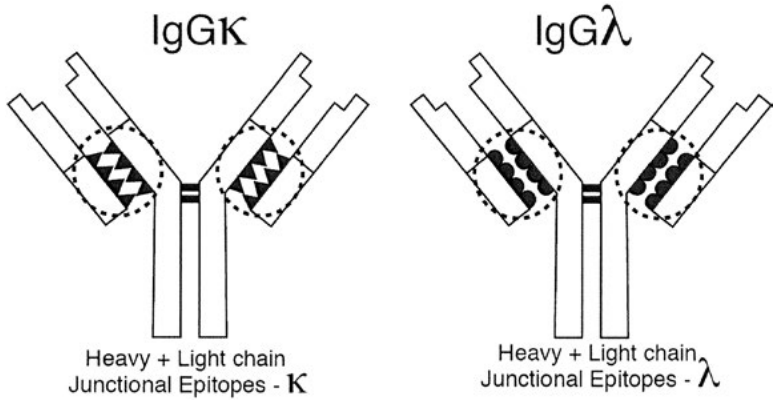

FIGURE 4 The heavy-light chain (HLC) assay, a junctional epitope assay, is based on purified polyclonal antibodies that specifically bind unique epitopes that occur where heavy and light chains are structurally apposed. Antibodies specifically bind IgGκ, IgGλ, IgAκ, IgAλ, IgMκ, and IgMλ (six reagents).

the heavy- and light-chain constant regions of IgGκ, IgGλ, IgAκ, IgAλ, IgMκ, and IgMλ molecules (six reagents), hence the name "junctional epitope" or so-called "*h*eavy/*l*ight" chain (HLC) assays (Fig. 4) (3). The quantitation of immunoglobulins by isotype-specific light chain type (e.g., IgGκ and IgGλ) may provide diagnostically useful information related to clonal proliferation, and HLC-pair ratios (e.g., IgGκ/IgGλ) coupled with individual heavy/light chain measurements (e.g., IgGκ *and* IgGλ) may be useful in disease monitoring (28). As noted with sFLC assays, demonstration of cost-effectiveness and impact on clinical outcomes in patients will be important considerations.

CLINICAL ASPECTS OF IMMUNOGLOBULIN MEASUREMENT

Serum immunoglobulin concentrations vary widely between children and adults (13, 29). Immunoglobulin G concentrations in a newborn are nearly equal to those observed in adults as a result of transplacental passage from the mother. (Maternal IgA and IgM do not pass into the fetal circulation.) Immunoglobulin G concentrations then decline to a nadir at approximately 6 months of age. After this nadir in the IgG concentration, it rises progressively until adult concentrations are reached during early adolescence. It is important to apply age-specific reference ranges when one interprets quantitative immunoglobulin measurements in prepubertal children. Likewise, it is important to recognize that there is some individual-to-individual variation in this pattern.

Many congenital and acquired immunodeficiency disorders are characterized by hypogammaglobulinemia (29). Depending upon the underlying etiology and accompanying abnormalities, humoral immunodeficiency syndromes are often accompanied by specific clinical manifestations. In general, patients with humoral immunoglobulin deficiencies are at risk for a variety of infections, including some caused by high-grade encapsulated bacteria such as *Streptococcus pneumoniae*, *Haemophilus influenzae*, etc. (29). A detailed discussion of humoral immunodeficiency syndromes is beyond the scope of this chapter, but many such disorders have been elucidated and are currently best classified based on identification of specific molecular defects. For example, children suspected of suffering from Bruton's (X-linked) agammaglobulinemia or a severe combined immunodeficiency and adults suffering from suspected common variable immunodeficiency all exhibit markedly subnormal concentrations of IgG, IgA, and IgM in serum. The most common congenital humoral immunodeficiency disorder is selective IgA deficiency, which ranges, depending on the ethnicity of the population, from 1 in 400 to 1 in 700 adults (29). Many patients with selective IgA deficiency are asymptomatic, but some suffer from recurrent mucosal infections and/or autoimmune phenomena. A subset of selective IgA deficiency patients exhibit concomitant IgG subclass deficiency. Aggressive treatment of patients with various neoplastic and autoimmune diseases has resulted in many individuals with acquired humoral immunodeficiencies. Like patients with congenital humoral immunodeficiency disorders, these individuals are at risk of high-grade bacterial and other infections. Likewise, multiple myeloma is frequently accompanied by both the presence of a monoclonal immunoglobulin spike (M-protein) and the suppression of polyclonal "background" gamma globulin (see below).

A vast array of chronic inflammatory and infectious diseases are accompanied by polyclonal increases in immunoglobulin concentration. In these settings, there is usually little to no value in specific quantitative measurements of IgG, IgA, or IgM. Serum protein electrophoresis, accompanied by densitometric measurement of the total gamma globulin concentration, usually suffices as a "first-tier" means to assess the humoral immune system.

A substantial majority of patients with multiple myeloma and essentially all patients with Waldenström's macroglobulinemia have monoclonal increases in immunoglobulins in serum, urine, or both (30). Serum protein electrophoresis and both serum and urine immunofixation electrophoresis (IFE) remain key assays used in the diagnosis and monitoring of disease progression/response to therapy in patients with multiple myeloma and related plasma cell/B lymphocyte proliferative diseases (30). Increasingly, clinical laboratories have shifted from agarose gel to capillary zone electrophoresis as the primary method for SPEP (31). Secreted monoclonal immunoglobulins (M-proteins) or immunoglobulin components (e.g., free light chains) are *de facto* tumor markers. Major limitations of SPEP and IFE in the evaluation of patients with myeloma and other plasma cell disorders have been lack of analytical sensitivity in oligosecretory lesions and the unwieldiness of 24-hour urine collections. "Traditional" SPEP and IFE studies are particularly insensitive in the evaluation of patients with AL amyloidosis (32).

Studies conducted since the development of the quantitative kappa and lambda sFLC assays have led to the creation of expert guidelines for the clinical applications of these tests (24). The combination of the sFLC assays, SPEP, and serum IFE is a highly sensitive screen for myeloma and related plasma/B cell proliferative diseases and, except in the case of suspected AL amyloidosis, negates the need for 24-hour urine studies (32–38). (Tissue biopsy is still required for definitive diagnosis of all of these entities.) Baseline sFLC measurements offer prognostic value in essentially all plasma cell disorders (including monoclonal gammopathy of undetermined significance [MGUS]) (39–42). The sFLC assay provides utility in quantitative monitoring of patients with "oligosecretory" plasma cell diseases including oligosecretory myeloma, nonsecretory myeloma (when there is an abnormal sFLC kappa or lambda concentration), and light-chain (AL) amyloidosis. (Elevations of sFLC are not observed in all patients with nonsecretory myeloma.) Several studies support the use of absolute sFLC measurements (i.e., free kappa and/or free lambda) in monitoring with AL amyloidosis, oligosecretory myeloma, nonsecretory myeloma (applicable cases), and solitary plasmacytoma (24). Currently, as emphasized by the 2009 International Myeloma Working Group guidelines, the data do not justify the use of serial sFLC measurements *rather than* serial measurements of *otherwise measurable* M-proteins by SPEP, serum IFE, and/or quantitative 24-hour urine Bence Jones protein quantification studies in patients with multiple myeloma (24).

Katzmann and Rajkumar recently summarized a series of studies that addressed the clinical utility of junctional epitope-HLC assays (28). First, Bradwell et al. (44) and Ludwig et al. (45) provided data that suggest that the diagnostic sensitivity of HLC-pair ratios (e.g., IgGκ/IgGλ) in multiple myeloma is similar to that of SPEP plus serum IFE. These investigators also observed that highly abnormal HLC-pair ratios were prognostic (44, 45). Finally, Katzmann et al. (46) used the junctional epitope assay to reveal that heavy/light-chain-pair suppression (e.g., suppression of IgGλ in patients with IgGκ MGUS) is an independent predictor of disease progression (MGUS to multiple myeloma). The last observation may refine risk assessment for MGUS patients beyond that available by simple estimation of serum M-protein concentration (30).

VISCOSITY MEASUREMENT

Viscosity is the intrinsic resistance of a fluid to flow. Abnormalities of the formed elements of blood (e.g., increased red blood cell mass, decreased red blood cell deformability, and changes in numbers and/or properties of white blood cells) and abnormalities of plasma proteins (e.g., increased immunoglobulin concentration) can cause hyperviscosity. While emerging technologies such as laser Doppler velocimetry and mass-detecting sensors can be used in clinical viscometry (47), most laboratories continue to employ either Ostwald, Wells-Brookfield, or falling-drop viscometers.

Ostwald viscometers are based on the relationship between fluid viscosity and the rate of flow through a fixed wall narrow-bore tube. The greater the viscosity of either anticoagulated whole blood, plasma, or serum, the lower the rate of flow. Typically, the flow rate of the sample of interest is compared to a standard (e.g., water). The Wells-Brookfield viscometer employs a stationary plate (sample cup) and a cone (needle) that is rotated within the cup by a motor run at a constant speed under standard temperature conditions (37°C). The fluid sample of interest is placed into the cup in which the cone rotates. (The fluid spreads between the apposed sample cup/plate and the rotating needle/cone.) The greater the viscosity of the fluid, the greater the torque generated. In turn, the torque is measured with a torque meter and translated into "viscosity." Falling-drop viscometry exploits the fact that particulates fall more slowly through a viscous fluid than through a less viscous fluid.

The viscosity of biological samples is typically reported in SI (International System of Units) unit centipoise (cP); normal plasma viscosity is approximately 1.35 to 1.85 cP. (Water exhibits a viscosity of 1.0 cP at 37°C). Whole-blood viscosity can also be expressed as "equivalent hematocrit of whole-blood viscosity," which is the viscosity equivalent to that exhibited by anticoagulated whole blood at the given hematocrit. Clinical interpretation of "equivalent hematocrit" requires an actual hematocrit measurement for comparison. For example, a patient with hyperviscosity due to a high concentration of a monoclonal paraprotein might exhibit a hematocrit equivalent of 55% and an actual hematocrit of 40%. In this case, the "excess" viscosity is attributable to the paraprotein. Conversely, a patient with polycythemia and hyperviscosity might exhibit a hematocrit equivalent of whole-blood viscosity of 55% and an actual hematocrit of 55%. In this case, the elevated viscosity is wholly attributable to the increase in red blood cell mass. Tables or figures that display the mathematical relationship between hematocrit and viscosity of whole blood are useful in clinical practice (4), particularly given the nonlinear relationship between hematocrit and whole-blood viscosity (see below).

CLINICAL ASPECTS OF VISCOSITY MEASUREMENT

The most common cause of hyperviscosity is the presence of a paraprotein. More than 80% of cases of hyperviscosity are due to an IgM paraprotein associated with Waldenström's macroglobulinemia. IgM molecules possess a high molecular mass (pentamers are approximately 900 kDa) as well as a shape that increases their intrinsic viscosity. IgA paraproteins, less commonly IgG paraproteins, and rarely, very high concentrations of polymerized or aggregated monoclonal light chains can also result in hyperviscosity (5). Increases in red blood cell mass (e.g., polycythemia), reduced deformability of red blood cells (e.g., hemoglobinopathies), and very high white blood cell counts (e.g., chronic lymphocytic leukemia) can also increase whole-blood viscosity. It is important to recognize that the arithmetic relationship between hematocrit and whole-blood viscosity is nonlinear (5). There is a steep upward inflection in viscosity near a hematocrit of 60%. As a result, a patient may be asymptomatic with a hematocrit of 55% and dramatically affected at 60%. As alluded to above, hyperviscosity attributable to a paraprotein increases both whole-blood *and* plasma (or serum) viscosity, while abnormalities of formed elements affect whole-blood viscosity *but not* plasma (or serum) viscosity.

Symptoms and signs of hyperviscosity are primarily rheologic but quite varied. They include fatigue, blurred vision, headache, tinnitus, decreased hearing, vertigo, paresthesias, segmental dilation of retinal veins, retinal hemorrhage, mucosal bleeding, nystagmus, ataxia, somnolence, stupor, and coma (5). Individual patients exhibit different thresholds and findings, but symptoms and signs of hyperviscosity "typically" occur when whole-blood viscosity exceeds 4 cP (2 to 3 times the normal level). For example, an individual with advanced atherosclerosis involving the cerebral vasculature might exhibit neurologic symptoms and signs of hyperviscosity with a plasma viscosity of 3 cP, while an otherwise healthy person (with patent and distensible vessels) might not become

symptomatic until plasma viscosity reaches 6 cP. Serum protein electrophoresis, IFE, a complete blood count with differential, and review of a peripheral blood smear nearly always elucidate the underlying cause of hyperviscosity. In the great majority of cases of clinically significant hyperviscosity, the underlying etiology has previously been established (e.g., Waldenström's macroglobulinemia and multiple myeloma).

REFERENCES

1. **Fahey J, McKelvey EM.** 1965. Quantitative determination of serum immunoglobulins in antibody-agar plates. *J Immunol* **94:**84–91.
2. **Bradwell RM, Carr-Smith HD, Mead GP, Tang LX, Showell PJ, Drayson MT, Drew R.** 2001. Highly sensitive automated immunoassay for immunoglobulin free light chains in serum and urine. *Clin Chem* **47:**673–680.
3. **Bradwell AR, Harding SJ, Fourier NJ, Wallis GL, Drayson MT, Carr-Smith HD, Mead GP.** 2009. Assessment of monoclonal gammopathies by nephelometric measurement of individual immunoglobulin kappa/lambda ratios. *Clin Chem* **55:**1646–1655.
4. **Brookfield Engineering Laboratories, Inc.** 2003. More solutions to sticky problems, p 1–17. Brookfield Engineering Laboratories, Inc., Middleboro, MA.
5. **Rajkumar SV, Kyle RA.** 2008. Plasma cell disorders, p 1426–1437. *In* Goldman L, Ausiello D (ed), *Cecil Medicine*, 23rd ed. Saunders Elsevier, Philadelphia, PA.
6. **Abbas AK, Janeway CA Jr.** 2000. Immunology: improving on nature in the twenty-first century. *Cell* **100:**129–138.
7. **Tiselius A.** 1932. A new apparatus for electrophoretic analysis of colloidal mixtures. *Trans Faraday Soc* **33:**524–531.
8. **Bruton OC.** 1952. Agammaglobulinemia. *Pediatrics* **9:**722–727.
9. **Kabat EA.** 1976. *Structural Concepts in Immunology and Immunochemistry*, 2nd ed. Holt, Rinehart, and Winston, New York, NY.
10. **Tonegawa S.** 1983. Somatic generation of antibody diversity. *Nature* **302:**575.
11. **Porter RR.** 1959. The hydrolysis of rabbit gamma globulin and antibodies with crystalline papain. *Biochem J* **73:**119–126.
12. **Edelman GM, Poulik MD.** 1961. Studies on structural units of the gamma globulins. *J Exp Med* **113:**867–884.
13. **Abbas AK, Lichtman AH, Pillai S.** 2012. *Cellular and Molecular Immunology*, 7th ed. Elsevier and Saunders, Philadelphia, PA.
14. **Shearer MH, Dark RD, Chodosh J, Kennedy RC.** 1999. Comparison and characterization of immunoglobulin G subclasses among primate species. *Clin Diagn Lab Immunol* **6:**953–958.
15. **Danilova N, Amemiya CT.** 2009. Going adaptive: the saga of antibodies. *Ann N Y Acad Sci* **1168:**130–155.
16. **College of American Pathologists.** 2012. *CAP Survey SE-B, 2012*. College of American Pathologists, Chicago, IL.
17. **College of American Pathologists.** 2004. *CAP Survey S2-B, 2004*. College of American Pathologists, Chicago, IL.
18. **College of American Pathologists.** 2004. *CAP Survey SE-B, 2004*. College of American Pathologists, Chicago, IL.
19. **Finely PR.** 1982. Nephelometry: principles and clinical laboratory applications. *Lab Manage* **20**(9)**:**34.
20. **Daval S, Tridon A, Mazeron N, Ristori JM, Evrard B.** 2007. Risk of antigen excess in serum free light chain measurements. *Clin Chem* **53:**1985–1986.
21. **Ashihara Y, Kasahara Y, Nakamura RM.** 2011. Immunoassays and immunochemistry, p 1426–1437. *In* McPherson RA, Pincus MR (ed), *Henry's Clinical Diagnosis and Management by Laboratory Methods*, 22nd ed. Saunders Elsevier, Philadelphia, PA.
22. **Mancini G, Carbonara AO, Heremans JF.** 1965. Immunochemical quantitation of antigens by single radial immunodiffusion. *Immunochemistry* **2:**235–254.
23. **Laurell, C.** 1975. The use of electroimmunoassay for determining specific proteins as a supplement to agarose gel electrophoresis. *J Clin Pathol Suppl* **6:**22–26.
24. **Dispenzieri A, Kyle R, Merlini G, Miguel JS, Ludwig H, Hajek R, Palumbo A, Jagannath S, Blade J, Lonial S, Dimopoulos M, Comenzo R, Einsele H, Barlogie B, Anderson K, Gertz M, Harousseau JL, Attal M, Tosi P, Sonneveld P, Boccadoro M, Morgan G, Richardson P, Sezer O, Mateos MV, Cavo M, Joshua D, Turesson I, Chen W, Shimizu K, Powles R, Rajkumar SV, Durie BG, International Myeloma Working Group.** 2009. International Myeloma Working Group guidelines for serum-free light chain analysis in multiple myeloma and related disorders. *Leukemia* **23:**215–224.
25. **Katzmann JA, Kyle RA, Benson J, Larson DR, Snyder MR, Lust JA, Rajkumar SV, Dispenzieri A.** 2009. Screening panels for detection of monoclonal gammopathies. *Clin Chem* **55:**1517–1522.
26. **Kumar S, Zhang L, Dispenzieri A, Van Wier S, Katzmann JA, Snyder M, Blood E, DeGoey R, Henderson K, Kyle RA, Bradwell AR, Greipp PR, Rajkumar SV, Fonseca R.** 2010. Relationship between elevated immunoglobulin free light chain and the presence of high translocations in multiple myeloma. *Leukemia* **24:**1498–1505.
27. **Tate JR, Mollee P, Dimeski G, Carter AC, Gill D.** 2007. Analytical performance of serum free light-chain assay during monitoring of patients with monoclonal light-chain diseases. *Clin Chim Acta* **376:**30–36.
28. **Katzmann JA, Rajkumar SV.** 2013. A window into immunoglobulin quantitation and plasma cell disease: antigen epitopes defined by the junction of immunoglobulin heavy and light chains. *Leukemia* **27:**1–2.
29. **Ochs HD, Smith CIE, Puck JM (ed).** 2013. *Primary Immunodeficiency Diseases: A Molecular and Genetic Approach*, 3rd ed. Oxford University Press, New York, NY.
30. **Kyle RA, Rajkumar SV.** 2009. Criteria for diagnosis, staging, risk stratification and response assessment of multiple myeloma. *Leukemia* **23:**3–9.
31. **Keren DF, Humphrey RL.** 2006. Clinical indications and applications of serum and urine protein electrophoresis, p 75–87. *In* Folds EC, Hamilton JD, Dietrich R (ed), *Manual of Clinical Immunology*, 7th ed. ASM Press, Washington, DC.
32. **Katzmann JA, Dispenzieri A, Kyle RA, Snyder MR, Plevak MF, Larson DR, Abraham RS, Lust JA, Melton LJ III, Rajkumar SV.** 2006. Elimination of the need for urine studies in the screening algorithm for monoclonal gammopathies by using serum immunofixation and free light chain assays. *Mayo Clin Proc* **81:**1575–1578.
33. **Kang SY, Suh JT, Lee HJ, Yoon HJ, Lee WI.** 2005. Clinical usefulness of free light chain concentration as a tumor marker in multiple myeloma. *Ann Hematol* **84:**588–593.
34. **Nowrousian MR, Brandhorst D, Sammet C, Kellert M, Daniels R, Schuett P, Poser M, Mueller S, Ebeling P, Welt A, Bradwell AR, Buttkereit U, Opalka B, Flasshove M, Moritz T, Seeber S.** 2005. Serum free light chain analysis and urine immunofixation electrophoresis in patients with multiple myeloma. *Clin Cancer Res* **11:**8706–8714.
35. **Bakshi NA, Gulbranson R, Garstka D, Bradwell AR, Keren DF.** 2005. Serum free light chain (FLC) measurement can aid capillary zone electrophoresis in detecting subtle FLC-producing M proteins. *Am J Clin Pathol* **124:**214–218.
36. **Abadie JM, Bankson DD.** 2006. Assessment of serum free light chain assays for plasma cell disorder screening in a veterans affairs population. *Ann Clin Lab Sci* **36:**157–162.

37. **Hill PG, Forsyth JM, Rai B, Mayne S.** 2006. Serum free light chains: an alternative to the urine Bence Jones proteins screening test for monoclonal gammopathies. *Clin Chem* **52:**1743–1748.
38. **Beetham R, Wassell J, Wallage MJ, Whiteway AJ, James JA.** 2007. Can serum free light chains replace urine electrophoresis in the detection of monoclonal gammopathies? *Ann Clin Biochem* **44:**516–522.
39. **Dingli D, Kyle RA, Rajkumar SV, Nowakowski GS, Larson DR, Bida JP, Gertz MA, Therneau TM, Melton LJ III, Dispenzieri A, Katzmann JA.** 2006. Immunoglobulin free light chains and solitary plasmacytoma of bone. *Blood* **108:**1979–1983.
40. **Dispenzieri A, Lacy MQ, Katzmann JA, Rajkumar SV, Abraham RS, Hayman SR, Kumar SK, Clark R, Kyle RA, Litzow MR, Inwards DJ, Ansell SM, Micallef IM, Porrata LF, Elliott MA, Johnston PB, Greipp PR, Witzig TE, Zeldenrust SR, Russell SJ, Gastineau D, Gertz MA.** 2006. Absolute values of immunoglobulin free light chains are prognostic in patients with primary systemic amyloidosis undergoing peripheral blood stem cell transplantation. *Blood* **107:**3378–3383.
41. **van Rhee F, Bolejack V, Hollmig K, Pineda-Roman M, Anaissie E, Epstein J, Shaughnessy JD Jr, Zangari M, Tricot G, Mohiuddin A, Alsayed Y, Woods G, Crowley J, Barlogie B.** 2007. High serum-free light chain levels and their rapid reduction in response to therapy define an aggressive multiple myeloma subtype with poor prognosis. *Blood* **110:**827–832.
42. **Kyle RA, Remstein ED, Therneau TM, Dispenzieri A, Kurtin PJ, Hodnefield JM, Larson DR, Plevak MF, Jelinek DF, Fonseca R, Melton LJ III, Rajkumar SV.** 2007. Clinical course and prognosis of smoldering (asymptomatic) multiple myeloma. *New Engl J Med* **356:**2582–2590.
43. **Le Bricon T, Bengoufa D, Benlakehal M, Bousquet B, Erlich D.** 2002. Urinary free light chain analysis by the Freelite immunoassay: a preliminary study in multiple myeloma. *Clin Biochem* **35:**565–567.
44. **Bradwell A, Harding S, Fourrier N, Mathiot C, Attal M, Moreau P, Harousseau JL, Avet-Loiseau H.** 2012. Prognostic utility of intact immunoglobulin Ig′κ /Ig′λ ratios in multiple myeloma patients. *Leukemia* **27:**202–207.
45. **Ludwig H, Milosavljevic D, Zojer N, Faint JM, Bradwell AR, Hübl W, Harding SJ.** 2012. Immunoglobulin heavy/light chain ratios improve paraprotein detection and monitoring, identify residual disease and correlate with survival in multiple myeloma patients. *Leukemia* **27:**213–219.
46. **Katzmann JA, Clark R, Kyle RA, Larson DR, Therneau TM, Melton LJ III, Benson JT, Colby CL, Dispenzieri A, Landgren O, Kumar S, Bradwell AR, Cerhan JR, Rajkumar SV.** 2012. Suppression of uninvolved immunoglobulins defined by heavy/light-chain pair suppression is a risk factor for progression of MGUS. *Leukemia* **27:**208–212.
47. **Shin S, Keum D-Y.** 2002. Measurement of blood viscosity using mass-sensing sensor. *Biosensors Bioelectronics* **17:**383–388.

Clinical Indications and Applications of Serum and Urine Protein Electrophoresis

DAVID F. KEREN AND RICHARD L. HUMPHREY

8

Protein electrophoresis is performed on serum (SPEP) and urine (UPEP) to detect and quantify monoclonal gammopathies (M proteins). In effect, serum and urine protein electrophoresis provides an immunochemical biopsy of the humoral immune system. However, other clinically relevant information is also available from examination of the proteins demonstrated from these studies. This chapter reviews basic principles of electrophoresis, the types of apparatus that are available, quality control and quality assurance procedures, costs, and illustrative patterns with recommended interpretations.

BACKGROUND ON PROTEIN STRUCTURE

Electrophoresis of serum and urine in the clinical laboratory takes advantage of the fact that each major protein has its own unique structure. Proteins are composed of amino acids, each of which contains a basic amino group ($-NH_2$), an acidic group ($-COOH$), and a portion that is specific to each amino acid, referred to as an R group (Fig. 1). The R groups may be acidic or basic, and they vary in size from a single hydrogen atom, to linear or branched hydrocarbon chains, or to a complex double ring structure. The complex structure and charge characteristics of these amino acids and the unique amino acid sequence of each protein determine the position that the protein migrates to on electrophoresis (1).

The primary structure of a protein results when amino acids connect to one another by linking the amino group of one amino acid to the carboxyl group of the next. During construction of this covalent peptide bond, a water molecule is released (Fig. 2). The resulting linear chain of amino acids is a polypeptide containing a free amino group at one end (N terminus) and a free carboxyl group at the other end (C terminus). Assembly takes place on the ribosome reading mRNA transcribed from DNA. The amino acid composition and linear structure of each protein are therefore determined by the information encoded in the individual's DNA.

As the polypeptide chain of amino acids takes form, a simple secondary structure is created by folding along one dimension and is held together primarily by hydrogen bonds. These may take the shape of random coils, an α helix, or a β-pleated sheet. A three-dimensional tertiary structure forms as a result of several types of attachment: hydrogen bonds, disulfide bonds, van der Waals forces, and hydrophobic bonds. In more complex molecules such as immunoglobulins, a quaternary structure forms when several polypeptide chains link together. For instance, consider the immunoglobulin M (IgM) molecule. Though classified as a single protein, it consists of 10 identical heavy chains, 10 identical light chains, and 1 joining chain. These protein chains combine to create a molecular mass of about 900 kDa. Finally, many proteins are glycosylated with carbohydrate groups that are covalently attached. These carbohydrate groups stabilize the protein's conformation (2). Following synthesis of the protein, post-translational modifications which convey heterogeneity to the protein may occur. These include phosphorylation, N-terminal acylation, side chain acylation, sulfation of tyrosine, C-terminal α-amidation of glycine, and γ-carboxylation of glutamic acid (1)

The charge on the protein molecule and, consequently, its migration on serum and urine protein electrophoresis are determined both by its constituent amino acids and by the pH of the buffer used for the electrophoresis. Each protein may be defined by its isoelectric point (pI), the pH at which its positive and negative charges are equal and hence migration does not occur in an electric field. At pH 8.6, which is used for agarose gel electrophoresis, the algebraic sum of the protein's positive and negative charges determines its migration through the gel. This allows the laboratory to separate the major serum proteins into unique bands and fractions that can be used to identify a wide variety of clinical conditions (Fig. 3).

PRINCIPLES OF PROTEIN ELECTROPHORESIS

The first studies on serum protein electrophoresis were performed entirely in a fluid-based system devised by Arne Tiselius, winner of the 1948 Nobel Prize in Chemistry. He called his method moving boundary electrophoresis (3, 4). In that regard, it is similar to the most recently available technique of capillary electrophoresis. In his system, Tiselius layered a mixture of proteins in the form of serum on a buffer in a U-shaped tube with electrodes at each end of the U. The migration of the proteins through the electrical field was detected by a sensitive Schlieren band optical system. With this technique, the major serum protein fractions of albumin and α, β, and gamma globulins were defined.

doi:10.1128/9781555818722.ch8

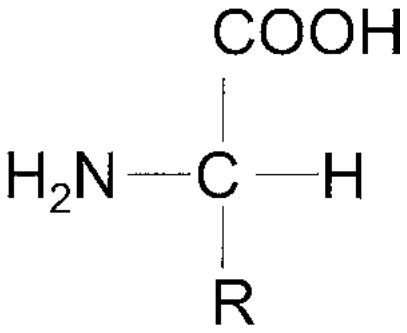

FIGURE 1 General structure of an amino acid. The R group determines the specific amino acid.

Zone Electrophoresis

In the late 1930s, filter paper was deployed as the first solid support medium to improve separation and allow direct visualization of the major protein fractions. The filter paper was placed between two reservoirs of buffer with electrodes at each end. The protein solution was carefully applied to the filter paper, and after electrophoresis, the major bands were visualized by use of a protein dye. However, the use of this support medium introduced new variables such as the texture of the medium, which provided resistance to protein migration, as well as charge effects due to endosmotic flow (5). The resistance would vary according to the filter paper brand and lot. Endosmotic flow changes reflected the fact that the support medium itself contained a net negative charge that could not migrate. As a consequence, the positive buffer ions would flow toward the cathode. The result was that weakly anionic proteins were pulled cathodally from the application point. The use of cellulose acetate and agarose began in the 1950s, and by the 1970s, they had vastly improved the resolution of protein electrophoresis. These clear support media allowed rapid electrophoresis, crisp separation of major protein fractions, and densitometric scanning to quantify the protein fractions (6).

The simplicity of separation in a fluid-based system has been revisited in the past decade with the development of capillary electrophoresis. In this procedure, instead of

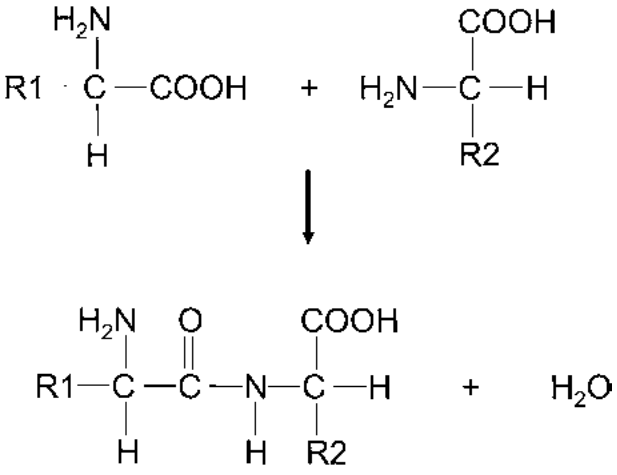

FIGURE 2 The peptide bond formation between two amino acids creates a dipeptide.

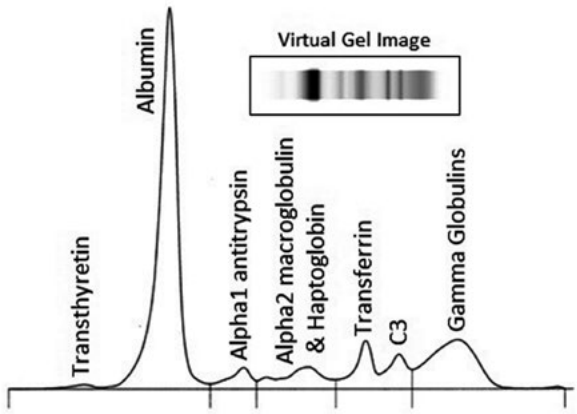

A/G 1.43
T.P.: 6.3

Fractions	%	Ref. %	g/dl	Ref. g/dl
Albumin	58.9	52.9 - 66.9	3.7	3.7 - 4.9
Alpha 1	3.7	3.0 - 5.8	0.2	0.2 - 0.4
Alpha 2	7.2	7.5 - 13.4	0.5	0.5 - 0.9
Beta	12.1	8.5 - 13.7	0.8	0.6 - 1.0
Gamma	18.1	8.8 - 19.2	1.1	0.6 - 1.4

FIGURE 3 The serum has sharp separation of major protein bands on the electropherogram (Sebia Capillarys). Ref., reference; T.P., total protein; A/G, albumin-to-globulin ratio.

a large, glass U-shaped tube, thin fused silica capillaries, about 25 μm in diameter, are the vessels through which the proteins pass. The narrow silica capillaries create a huge negatively charged surface area that results in a strong endosmotic flow toward the cathode. At strong alkaline pH (10.0), the proteins are pulled by the endosmotic flow past a UV detector which uses a 200- or 215-nm wavelength. It permits recording of the amount of each protein fraction on an electropherogram as a densitometric scan, and it is able to convert the values to a virtual gel image (Fig. 3) (7–13).

Unfortunately, while detection of peptide bond absorbance at 200 to 215 nm is efficient, it also detects other substances that absorb at those UV wavelengths. So far, the most frequent causes of false-positive deflections in the electropherogram have been radiocontrast dyes and, occasionally, antibiotics (8, 14–17). Radiocontrast dyes and some antibiotics can produce suspicious bands anywhere from the transthyretin (prealbumin) area through the γ region (Table 1).

One key feature in the evolution in electrophoresis systems has been the improvement in resolution. With the development of clear cellulose acetate gels in the 1950s, densitometric scans could distinguish five major protein fractions, with the bands in each fraction being relatively diffuse. Improvements have included an enclosed system that prevents evaporation of buffer. This helps to keep the ionic concentration of the buffer constant. Additional improvements have involved the addition of calcium lactate to buffer, the use of thin gels, and the use of cooling devices to control heat production. These improvements, applied to zone electrophoresis and capillary electrophoresis, have enhanced their ability to identify M proteins that are present in low concentrations and protein genetic variants, such as α_1 antitrypsin, that were difficult or impossible to visualize with previous techniques (Fig. 4).

TABLE 1 Location of radiocontrast and antibiotic spikes on capillary electrophoresis[a]

Location	Compound
Anodal to prealbumin	Ceftriaxone sodium
Prealbumin	Bilisegrol
Albumin (anodal edge)	Sulfamethoxazole
α_2 globulin	
Anodal	Gastrografin
	Urangiografin
Mid-region	Telebrix
	Xenetix
Cathodal	Iopamiro
	Omnitrast and Omnipaque
	Ultravist
β_2 globulin	
Anodal	Hexabrix
Mid-region	Optiray
	Iomeron

[a]Table from reference 1.

Guidelines for the diagnosis of monoclonal gammopathies recommend the use of electrophoretic systems that provide a crisp separation of the β_1 from β_2 region, and which are able to recognize M proteins as low as 0.05 g/dl in the γ region (18, 19). In the β region, measurement of M proteins is complicated by the presence of transferrin and C3. However, by taking advantage of so-called immunosubtraction techniques (see chapter 9) on capillary electrophoresis, one can determine the amount of the β region that is occupied by the M protein (see below).

With currently available semiautomated gel systems, the samples are placed in a well connected to special paper that wicks the sample to its sharp edge, which is applied directly to the surface of the gel. This application process can be interfered with by the presence of particulate matter in some urine samples or the precipitation of immunoglobulins in the serum of patients with cryoglobulinemia (8, 20). To prevent such problems, it is recommended to centrifuge the urine and ensure that the paper moistens all the way to the sharp edge. In addition, it is advisable to always compare the total protein value with the color intensity observed in the gel. This will aid in preventing false-negative results. Laboratories should establish their own reference ranges when adopting these techniques. While the different methods provide similar numbers, significant differences have been reported (Table 2) (16, 21).

QUALITY CONTROL AND QUALITY ASSURANCE

Specimen Requirements for Serum

For serum testing, the blood sample should be drawn into a Vacutainer tube without anticoagulant. After clotting, the serum is separated and stored at 4°C for up to 72 h. Although serum can be used after 72 h, C3 will deteriorate. Loss of C3 integrity will change the quantity of protein in the β_2 region of the electrophoresis. If the sample is to be held longer than 72 h before electrophoresis, freezing the sample at −20°C preserves the C3 for future analysis.

Proper sample collection is important because interferences can create special problems for interpretation. Hemolysis will provide a broadly migrating band in the α_2-β region, reflecting the presence of hemoglobin haptoglobin complexes. This may obscure or even mimic an M protein in this region. Lipemic samples may not disperse effectively

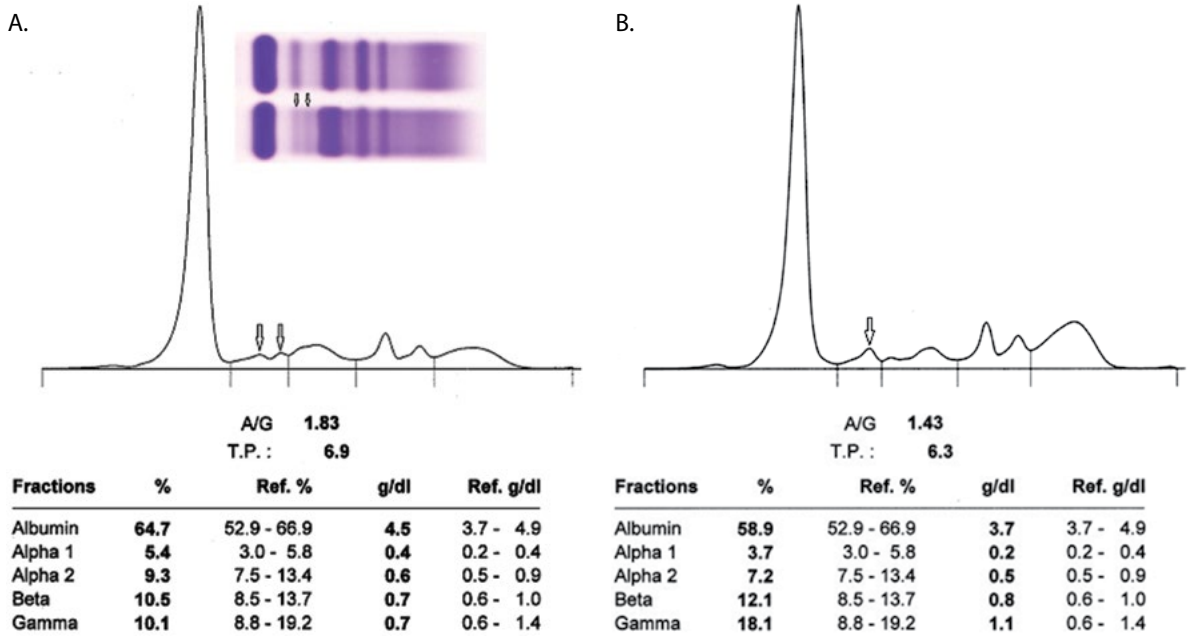

FIGURE 4 Heterozygous α_1 antitrypsin. The capillary zone electropherogram has two α_1 antitrypsin bands (arrows). Insert shows (top) a normal serum on a gel and (bottom) a heterozygous pattern with two α_1 antitrypsin bands. (B) The electropherogram pattern for a normal serum sample displays the single peak of the normal α_1 antitrypsin band (arrow). Ref., reference; T.P., total protein; A/G ratio, albumin-to-globulin ratio; L, low value.

TABLE 2 Comparison of serum protein intervals by agarose and capillary zone electrophoresis[a]

Group and fraction	Protein concn range (g/dl)	
	Agarose gel electrophoresis	Capillary electrophoresis
Men		
Albumin	4.19–5.36	4.17–5.23
α_1	0.13–0.27	0.26–0.45
α_2	0.38–0.70	0.34–0.64
β	0.65–1.14	0.58–0.95
γ	0.49–1.21	0.53–.32
Women		
Albumin	4.0–5.11	3.74–4.98
α_1	0.14–0.28	0.26–0.51
α_2	0.41–0.69	0.39–0.64
β	0.65–1.00	0.55–0.87
γ	0.49–1.21	0.53–1.32

[a]Data modified from those of Bossuyt et al. (16).

into a gel. Centrifugation followed by use of the clear layer below the lipid (the infranatant) may provide an adequate result if a better sample cannot be obtained.

Specimen Requirements for Urine

An early morning void collected into a container without preservative is adequate for screening for the presence of monoclonal free light chains (MFLC, or Bence Jones protein) (21). The urine should be stored at 4°C until electrophoresis. Prior to electrophoresis, the sample should be concentrated to optimize the detection of MFLC. The amount of concentrating necessary depends on the protein concentration of the urine. Usually, a 100-fold concentration is sufficient for urine samples with relatively small amounts of protein. One approach is to place the urine samples into a commercial ultrafiltration concentrating device and allow them to concentrate for a set period of time. One of our laboratories uses a concentration period of 4 h. Samples with small amounts of protein will concentrate more rapidly, up to 100 times, whereas urine specimens with high protein concentrations will concentrate to a lesser degree. If the patient is known to have an M protein in the serum and/or an MFLC in the urine, a 24-h urine sample should be collected in a container without preservative. Collection of the sample is key to obtaining accurate and reproducible information about the M protein. The first morning of the collection, the patient should be instructed to note the time when the collection is begun and to empty his or her bladder prior to the start. The next day, at the same time, finish the collection by including the final bit of urine in the 24-h collection. While this may seem excessively compulsive, if the first sample is included, it may be including urine which has been in the bladder for as long as 8 h (effectively making this a 32-h collection). The container should be refrigerated at 4°C between collections to minimize deterioration of proteins and growth of microorganisms. The 24-h collection is needed to quantify the amount of MFLC in the estimation of tumor burden and the response to therapy.

Internal Controls

Each protein electrophoresis analysis should have a control sample run on each gel. The percentage of the protein in each fraction should be recorded and compared day to day. Even with urine protein electrophoresis, serum controls are recommended because normal urine contains only trivial amounts of protein and would not serve as an adequate estimation of the migration of proteins on the gel. The controls should be evaluated for migration position of the major bands and for the amount of protein in each region. One convenient way to do this is by using a Levey-Jennings chart (Fig. 5). For systems such as capillary electrophoresis, which may have as many as 8 capillaries, each capillary should have such samples performed daily because the separation characteristics will differ slightly from one capillary to the next.

PROTEINS IDENTIFIED IN SERUM PROTEIN ELECTROPHORESIS

Using agarose or acetate electrophoresis, serum proteins were classified as the five major regions identified by electrophoresis: albumin, α_1, α_2, β, and γ. However, we now can recognize several specific major proteins by electrophoresis (Fig. 3). A tiny transthyretin (formerly named prealbumin) band may be seen on systems with superior resolution (Fig. 3). It is a 55-kDa protein that is used mainly to assess the nutritional status of patients with protein calorie malnutrition. The normal concentration in serum (20 to 40 mg/dl) is too small to be reliably evaluated by serum protein electrophoresis; therefore, measurements are usually performed by nephelometry. Rare genetic abnormalities of transthyretin are the most common cause of hereditary senile systemic amyloidosis and familial amyloidotic polyneuropathy (22).

Albumin is the main serum protein. It is a 69-kDa protein that is responsible for the osmotic effect of serum proteins and serves as a transport protein for a wide variety of molecules. An innocuous variant, bisalbuminemia, is occasionally seen. Analbuminemia is a rare condition where patients do surprisingly well. Occasionally, the latter patients require diuretics to control mild edema and some have had elevated cholesterol levels.

α_1 lipoprotein (high-density lipoprotein) is better evaluated by specific biochemical methods, but it may be seen on serum protein electrophoresis. On gel-based techniques, it usually accounts for the faint, diffusely staining broad band between the α_1 antitrypsin band and albumin. By capillary electrophoresis, it may migrate in the albumin or the α_1 region depending on the system used.

α_1 acid glycoprotein is a heavily glycosylated acute-phase reactant protein that migrates just anodal to α_1 antitrypsin. With its usual concentration of 50 to 150 mg/dl and heavy glycosylation, it is either barely visible or not seen on normal samples. However, with acute-phase reactions, it is seen on the anodal side of α_1 antitrypsin. Because the glycosylation interferes with protein staining, it is not seen well on gel-based methods. However, capillary electrophoresis methods show it as an anodal shoulder to the α_1 antitrypsin band. It may be especially prominent in patients with an acute-phase reaction.

α_1 antitrypsin is a 52-kDa protein that is a member of the serine protease inhibitors (serpins). It functions to inhibit a wide variety of proteases, including trypsin, and increases during an acute-phase reaction. This important protease inhibitor (PI) is usually present as PIMM, the normal homozygous type. However, there are several genetic variants. The Z and S variants are secreted in decreased amounts and are ineffective in inhibiting proteases. These variants in their homozygous form predispose the patient to emphysema and cirrhosis. The α_1 region must be carefully scrutinized to be certain that the α_1 antitrypsin band is present with

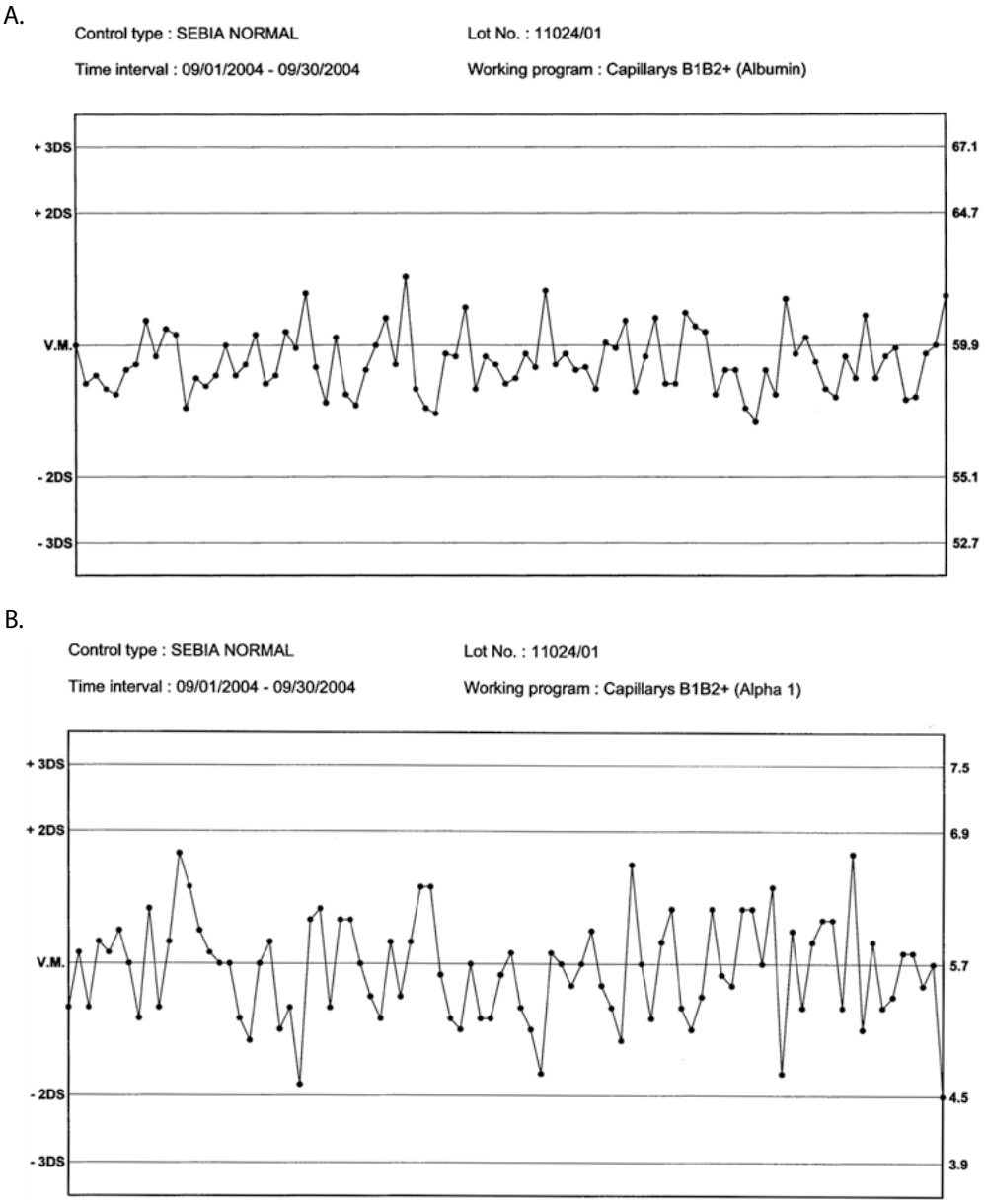

FIGURE 5 (A) This Levey-Jennings chart monitors the daily variation of albumin in the normal control sample performed on capillary zone electrophoresis for 3 months. No control sample is beyond 2SD (2 standard deviations) and no trend of high or low values is evident, indicating consistent precision. (B) This Levey-Jennings chart monitors the daily variation of the α_1 fraction in the normal control sample performed on capillary zone electrophoresis for 3 months. Wider swings of the daily value are present in the α_1 fraction than in albumin (panel A) due to the smaller percentage of proteins present in this fraction. Nonetheless, no sample is beyond 2SD and no trend of high or low values is evident on either chart, indicating consistent precision. V.M., median value.

appropriate migration. When heterozygotes are present, two discrete bands are seen (Fig. 4). When there is a homozygous PIZZ deficiency, the capillary electrophoresis electropherogram will show a flat α_1 region with the α_1 antitrypsin band missing. However, there is an underlying protein, orosomucoid (also known as α_1 acid glycoprotein), that may be present in sufficient amount to account for an α_1 fraction measurement in the lower end of the normal range (Fig. 6). In contrast, when a serum with a homozygous PIZZ deficiency is viewed on an agarose gel, the pattern indicates a virtual absence of protein staining in the α_1 region (Fig. 6). The disparity between these two techniques reflects the ability of capillary electrophoresis to measure orosomucoid more accurately than densitometry by agarose gels. This is because orosomucoid is a heavily glycosylated molecule that does not stain well with protein dyes and consequently is not seen on agarose gel electrophoresis. Since capillary electrophoresis uses peptide bond absorbance for detection, it is measured more accurately on capillary electrophoresis.

α_2 macroglobulin is a huge 720-kDa molecule that is a member of the thiol ester plasma proteins and functions as a protease inhibitor. Despite this, it is not an acute-phase

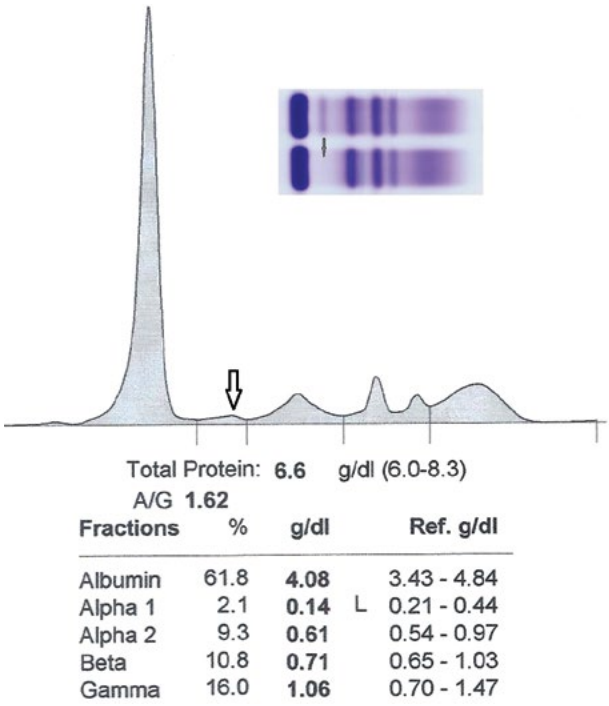

FIGURE 6 The capillary zone electropherogram pattern has a relatively flat α_1 fraction with a markedly blunted α_1 antitrypsin peak (arrow). This indicates the lack of the α_1 antitrypsin band which is consistent with the quantitative decrease of that fraction. However, the protein that remains in the α_1 fraction is orosomucoid (α_1 acid glycoprotein). This protein is measured by capillary zone electrophoresis, but not usually stained by protein dye on gel electrophoresis. Insert above shows two serum samples performed on gel electrophoresis. The top pattern shows a normal serum with a prominent α_1 antitrypsin band while the bottom pattern has a clear α_1 region because the α_1 antitrypsin band is not seen and the orosomucoid does not stain well with the protein dye. Ref., reference; T.P., total protein; A/G ratio, albumin-to-globulin ratio; L, low value.

protein. It is elevated in patients with nephrotic syndrome primarily due to its large size. Serum levels are moderately higher in cord blood.

Haptoglobin is the other major α_2 region protein. It binds free hemoglobin and exists in various forms. The 1-1 genotype, with a mass of 86 kDa, migrates slightly anodal to α_2 macroglobulin. The 2-1 genotype, with a mass of 86 to 300 kDa, completely overlaps α_2 macroglobulin, and the 2-2 genotype, with a mass of 170 to 900 kDa, is located slightly cathodal to α_2 macroglobulin. Because it binds free hemoglobin, haptoglobin is decreased in hemolysis but increases during an acute-phase reaction.

Transferrin, the major β_1 region molecule, is a 76.5-kDa protein that transports non-heme ferric iron. During acute-phase reactions, this protein decreases in concentration. In serum, it contains two complex carbohydrate chains, each with a sialic acid residue. Cerebrospinal fluid contains both this form of transferrin and one that lacks the sialic acid residues. The latter fraction of transferrin migrates in the β_2 region and has been used to distinguish leakage of cerebrospinal fluid from nasal or aural secretions.

β_1 lipoprotein (low-density lipoprotein) is more precisely evaluated by specific biochemical methods but may be seen in the β region on gel-based systems and in either the albumin or α_1 region on capillary electrophoresis methods. It is an enormous molecule measuring 2,750 kDa.

C3, the third component of complement and the only one readily visualized on serum protein electrophoresis, is the major β_2 region molecule. It consists of two chains, a 110-kDa α chain and a 75-kDa β chain. The level of C3 is elevated late during an acute-phase reaction. If the sample is not stored at 4°C, it quickly breaks down into smaller components.

Fibrinogen is a 340-kDa protein present in plasma but not in normal serum (Fig. 7). However, if the patient is anticoagulated, the sample is drawn into a tube containing an anticoagulant, or if the serum is separated before clotting is completed, the sample may have enough residual fibrinogen to give a band in the β-γ region that can be confused with an M protein.

C-reactive protein is a 135-kDa protein that migrates in the γ region. Its name derives from its ability to react with

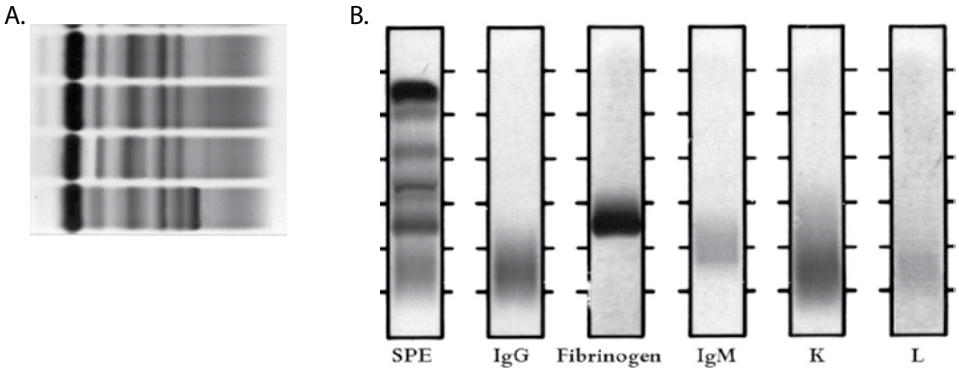

FIGURE 7 (A) Results of agarose gel electrophoresis for four samples are shown. The bottom sample has two unusual findings. The α_1 region shows two light staining bands that almost merge. This reflects the presence of an α_1 antitrypsin variant. In this case, it would be consistent with a faster-migrating variant (F) but needs to be confirmed by molecular studies. However, the second unusual feature is a densely staining band in the slow β region (β_2). This band could be an M protein; however, fibrinogen also migrates in this region. (B) IFE results for a sample similar to that shown in panel A are shown. Here the band reacts with anti-fibrinogen but not to anti-IgG, -IgM, -κ (K), or -λ (L) antisera.

the capsular polysaccharide of *Streptococcus pneumoniae*. It is an early indicator of an acute-phase reaction and is best measured by nephelometric techniques.

Immunoglobulins migrate mainly in the β and γ regions. IgG is the main serum immunoglobulin (700 to 1,600 mg/dl). It is a 160-kDa protein typically with a γ migration. It consists of four subclasses: IgG1, IgG2, IgG3, and IgG4. Because the body has many more B lymphocytes programmed to produce an IgG immunoglobulin after an appropriate antigen encounter, a neoplastic transforming event acting randomly on the available B cells will result in many more IgG M proteins than M proteins of the other major immunoglobulin classes (e.g., IgA or IgM). In multiple myeloma (MM), an IgG M protein usually produces a large γ region spike that is readily measured by densitometry on agarose gels or by a capillary electrophoresis electropherogram (Fig. 8). Polyclonal increases of IgG occur in chronic infections, liver disease, and some autoimmune diseases. These increases may be small or massive depending on the chronicity and severity of the condition. Typically, they are broad based, spanning the entire γ region and occasionally extending into the β-γ region (Fig. 9). However, a modest polyclonal increase in the IgG4 subclass gives a subtle, but noticeable, increase in the anodal portion of the γ region that, on occasion, may mimic an M protein (Fig. 10). Such polyclonal increases can be distinguished from M proteins by performing an immunofixation (IFE) or immunosubtraction (see chapter 9). IgG4-related systemic disease is a grouping of several conditions that share a diffuse lymphoplasmacytic infiltrate dominated by IgG4 plasma cells. The reports of this condition have included Mikulicz disease, autoimmune pancreatitis, sclerosing cholangitis, prostatitis, thyroiditis, and eosinophilic angiocentric fibrosis (23–25).

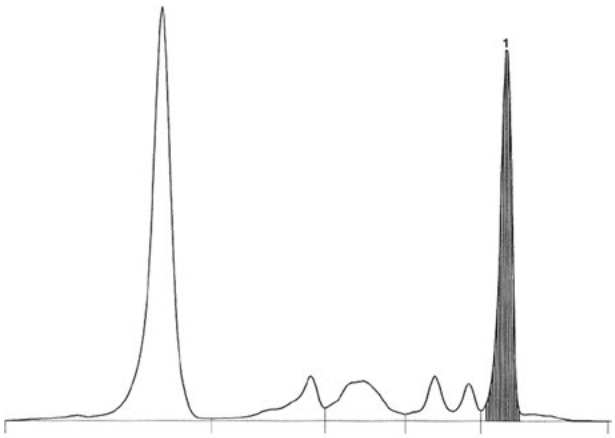

A/G Ratio : **0.98**
T.P. : **7.8**

Fractions	%	Ref. %	g/dl	Ref. g/dl
Albumin	**49.6**	50.9 - 65.5	**3.9**	3.6 - 4.9
Alpha 1	**7.4**	4.4 - 9.9	**0.6**	0.3 - 0.8
Alpha 2	**9.4**	6.3 - 13.1	**0.7**	0.5 - 1.1
Beta	**7.4**	8.6 - 14.2	**0.6**	0.6 - 1.1
Gamma	**26.2**	8.8 - 19.2	**2.0** H	0.6 - 1.5
1	**24.7**		**1.9**	

FIGURE 8 A capillary zone electropherogram is shown with a prominent M protein spike (shaded) and suppression of the normal gamma globulin. The spike measures 1.9 g/dl, and the total gamma globulin is 2.0 g/dl. Only 0.1 g/dl is accounted for by the gamma globulin not measured in the M protein spike. Ref., reference; T.P., total protein; A/G ratio, albumin-to-globulin ratio; H, high value.

IgM migrates in the β-γ region (40 to 230 mg/dl). It is a 900-kDa molecule that exists as a pentamer. It is the earliest immunoglobulin to respond to antigenic stimulation but does not appear to have a memory response. Uncommonly, an isolated polyclonal increase in IgM may produce a broad restriction in the anodal portion of the γ region.

IgA in the serum exists mainly as a 160-kDa monomer (70 to 400 mg/dl), but in mucosal secretions, it exists mainly as a dimer attached to secretory component (380 kDa). It is the second most common M protein involved in MM. A polyclonal increase in IgA results in a bridge between the β and γ regions. It can be quite prominent in some cases of cirrhosis, but more modest increases will occur in a wide variety of mucosal infections.

IgD is present mainly on the surface of lymphocytes, while in serum, only small quantities are found (0 to 8 mg/dl). IgD is the heavy chain type of 1 to 2% of MM cases. In such cases, it is often present in relatively small amounts, while the tumor secretes large amounts of MFLC.

IgE is present mainly on the surface of mast cells and basophils. Serum concentrations are measured only in patients with allergies, especially allergic bronchopulmonary aspergillosis, and in the extremely rare cases of IgE myeloma.

Free κ (25 kDa) and λ (50 kDa) light chains normally exist in the serum at concentrations too low to be visualized by serum protein electrophoresis. However, by using a sensitive nephelometric technique, they can be quantified in the serum (see chapter 7). Indeed, the ratio of free κ/free λ in serum can replace the necessity for urine in an initial screen for MM (26) (see chapter 11). However, follow-up for cases of light chain MM requires a measurement of the involved monoclonal light chain in a 24-h urine sample by protein electrophoresis with densitometric scanning and by IFE to establish κ or λ clonality.

PATTERN INTERPRETATION FOR SERUM

Although the main reason for performing serum protein electrophoresis is to detect and quantify M proteins, there are several other electrophoretic patterns that can be detected which may be of clinical use. Some of these findings were mentioned above with regard to each major protein; however, other important electrophoretic patterns are reviewed here.

Liver Disease Pattern

In patients with cirrhosis, synthesis of hepatocyte-derived proteins such as albumin, transferrin, and haptoglobin is decreased. As shown in the capillary electrophoresis electropherogram in Fig. 11, this usually forms a stepwise increase from the α_2 through the γ region. However, due to inflammation and rerouting of blood around the liver, other proteins may be increased. Typically, the serum demonstrates hypoalbuminemia. There may be anodal slurring of the albumin band if bilirubin is elevated. A decreased α_2 globulin may also occur with a prominent β-γ bridging due to a polyclonal increase in IgA and a broad increase in the γ region reflecting the polyclonal increase in IgG.

Protein Loss Patterns

With nephrotic syndrome, loss of protein occurs through damaged glomeruli. The serum shows hypoalbuminemia, low or low-normal α_1 globulin. On the electrophoretic pattern relative to albumin, there is a dramatically elevated

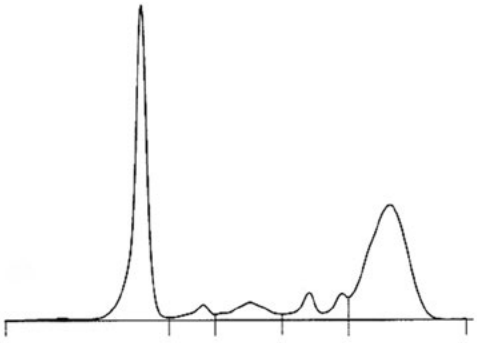

A/G 0.68
T.P. : 6.8

Fractions	%	Ref. %	g/dl		Ref. g/dl
Albumin	40.5	52.9 - 66.9	3.6	L	3.7 - 4.9
Alpha 1	2.8	3.0 - 5.8	0.2		0.2 - 0.4
Alpha 2	5.9	7.5 - 13.4	0.5		0.5 - 0.9
Beta	7.8	8.5 - 13.7	0.7		0.6 - 1.0
Gamma	43.0	8.8 - 19.2	3.8	H	0.6 - 1.4

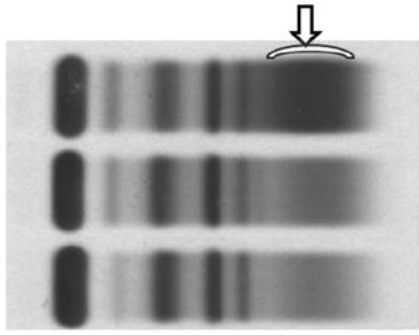

FIGURE 9 On the left, a capillary zone electropherogram demonstrates a slight decrease in albumin but a broad polyclonal increase in gamma globulins for a serum sample. On the right, three serum samples are shown on agarose gels. The top serum sample has a broad polyclonal increase in gamma globulins. The increased gamma globulins extend across the entire γ region. Ref., reference; T.P., total protein; A/G, albumin-to-globulin ratio; H, high value; L, low value.

α_2 globulin due to retention of its large molecules, such as α_2 macroglobulin and haptoglobin, in the serum. On gel electrophoresis, the β region may be increased due to an elevated β_1 lipoprotein. However, on capillary electrophoresis, the lipoproteins migrate more anodally, often in the albumin region. By either method, the gamma globulin is in the low-normal range or hypogammaglobulinemia range, depending on the severity of the disease (Fig. 12).

In protein-losing enteropathy such as celiac disease, damage to the gastrointestinal tract can produce findings in

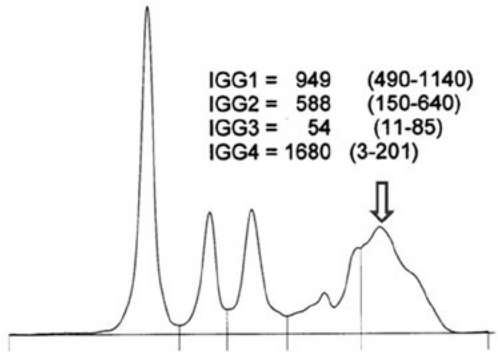

A/G 0.42
T.P. : 6.8

Fractions	%	Ref. %	g/dl		Ref. g/dl
Albumin	29.8	52.9 - 66.9	2.0	L	3.7 - 4.9
Alpha 1	11.9	3.0 - 5.8	0.8	H	0.2 - 0.4
Alpha 2	16.0	7.5 - 13.4	1.1	H	0.5 - 1.0
Beta	14.4	8.5 - 13.7	1.0		0.6 - 1.0
Gamma	27.9	8.8 - 19.2	1.9	H	0.6 - 1.4

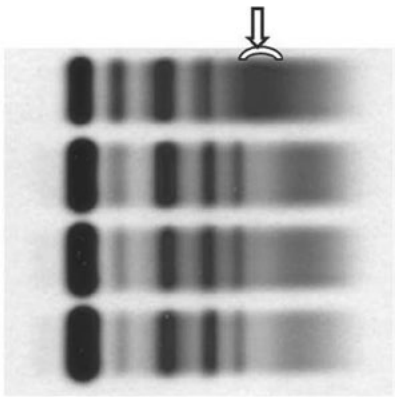

FIGURE 10 On the left, a capillary zone electropherogram is shown from a serum sample with an acute-phase reaction and a polyclonal increase in the IgG4 subclass. The acute-phase reaction is confirmed by the combination of low albumin (2.0 g/dl), increased α_1 and α_2 fractions, and a low transferrin (β_1) band. The γ region has relatively broad restriction, but it is limited to the anodal half of the γ region. This is a typical finding with a polyclonal increase in IgG4 subclass. As shown, the IgG4 subclass was increased 8-fold over the upper end of the normal range. On the right, four gel electrophoresis patterns are shown. The top one has a polyclonal increase in the IgG4 subclass. It shows a broad increase similar to that shown in Fig. 9, but this one extends from the slow β region to midway in the γ region. Polyclonal increases in the IgG4 subclass can be mistaken for monoclonal proteins unless an immunofixation electrophoresis is performed. Ref., reference; T.P., total protein; A/G, albumin-to-globulin ratio; H, high value; L, low value.

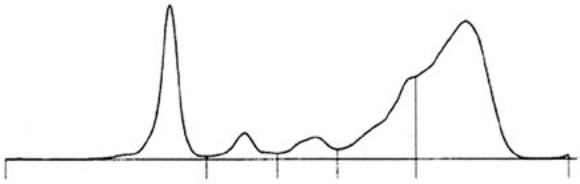

A/G 0.26
T.P.: 7.7

Fractions	%	Ref. %	g/dl	Ref. g/dl
Albumin	20.5	52.9 - 66.9	1.6 L	3.7 - 4.9
Alpha 1	4.5	3.0 - 5.8	0.3	0.2 - 0.4
Alpha 2	5.0	7.5 - 13.4	0.4 L	0.5 - 0.9
Beta	18.0	8.5 - 13.7	1.4 H	0.6 - 1.0
Gamma	52.0	8.8 - 19.2	4.0 H	0.6 - 1.4

FIGURE 11 This capillary zone electropherogram demonstrates a cirrhosis pattern. Ref., reference; T.P., total protein; A/G, albumin-to-globulin ratio; H, high value; L, low value.

serum similar to those of the nephrotic syndrome with hypoalbuminemia, hypogammaglobulinemia, and occasionally elevated α_2 macroglobulin.

Milder patterns of protein loss may result in only decreased albumin and gamma globulin. Because most serum protein electrophoresis analyses are performed for patients for whom an M protein is in the differential diagnosis, when we see these findings, we recommend performing a urine protein electrophoresis and IFE to rule out MFLC, which may damage the glomeruli due to conditions such as AL amyloid (light-chain-associated amyloid), light chain deposition disease, or myeloma kidney.

Acute-Phase Pattern

An acute-phase reaction is the result of recent damage that may occur due to processes including infections, trauma, and inflammation, or it may result from therapeutic measures such as surgery. In the serum, largely due to the effect of interleukin-6, there is a decrease in albumin and transferrin (β_1 globulin) with an increase in α_1 acid glycoprotein (orosomucoid), α_1 antitrypsin, and haptoglobin (Fig. 10). In the mid- to fast-γ region, depending on the electrophoresis system being used, the C-reactive protein band may be seen. Later in the course of the inflammation, C3 increases. This has also been referred to as a subacute inflammation pattern.

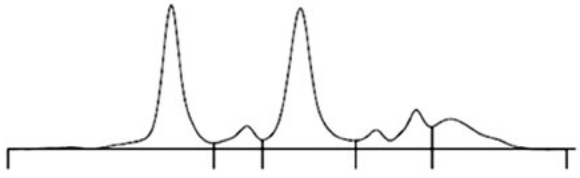

A/G 0.47
T.P.: 4.6

Fractions	%	Ref. %	g/dl	Ref. g/dl
Albumin	32.2	52.9 - 66.9	1.5 L	3.7 - 4.9
Alpha 1	5.5	3.0 - 5.8	0.3	0.2 - 0.4
Alpha 2	36.8	7.5 - 13.4	1.7 H	0.5 - 0.9
Beta	12.5	8.5 - 13.7	0.6	0.6 - 1.0
Gamma	13.0	8.8 - 19.2	0.6	0.6 - 1.4

FIGURE 12 This capillary zone electropherogram demonstrates a nephrotic pattern. The α_2 region is exaggerated by comparison with the dramatic decrease in albumin. Ref., reference; T.P., total protein; A/G, albumin-to-globulin ratio; H, high value; L, low value.

Hypogammaglobulinemia is never normal in an adult, even the elderly. When the total γ region value falls below the normal range of 2 standard deviations set in our laboratories, we note that hypogammaglobulinemia is present. This may be seen in a variety of conditions, including common variable immunodeficiency disease, chronic lymphocytic leukemia, well-differentiated lymphocytic lymphoma, light chain disease, and nonsecretory myeloma, or in patients who are receiving plasmapheresis or chemotherapy. About 10% of patients with isolated hypogammaglobulinemia defined in this manner will have an M protein that may be detected in serum and/or urine by IFE and/or by use of the serum free light chain test (27). Amyloid AL can sometimes be seen in cases of hypogammaglobulinemia. Measurement of the serum free light chains has been shown to help in detecting both cases of amyloid AL and cases of nonsecretory myeloma (see chapter 7) (28, 29).

Detection of M Proteins in Serum

Most M proteins belong to the IgG subclass and usually migrate in the γ region (Fig. 13, samples 6, 13, 14, 25, and 30). Since normal IgG migrates broadly throughout the slow β and γ regions, even a low concentration of M proteins measuring as little as 0.05 to 0.1 mg/dl can distort the pattern, especially in the presence of hypogammaglobulinemia. This is illustrated as the large β_2 region band in sample 24 of Fig. 13. Identification of the M protein requires immunologic demonstration that the M protein band is made up of only one heavy chain type and one light chain type. IFE and immunosubtraction electrophoresis are the two methods that are recommended for evaluating this condition.

M proteins, especially those of the IgA and IgM classes, are also commonly detected in the β region (Fig. 14). When there are M proteins in low concentrations, they can be more challenging to detect because of the presence of major proteins in that region, such as β_1 lipoprotein (on gel-based methods), transferrin, and C3 (Fig. 15). To detect

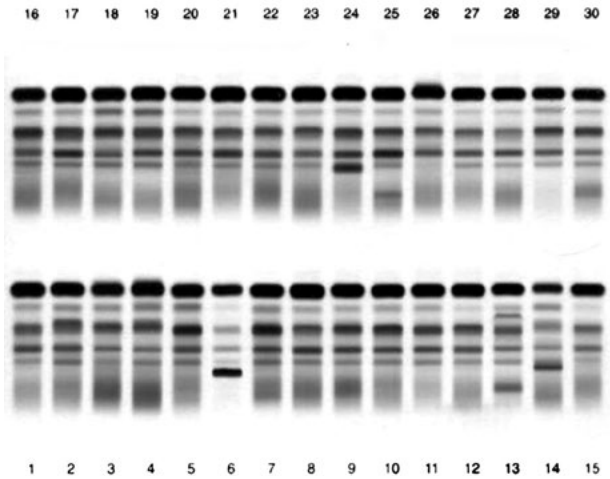

FIGURE 13 This agarose gel electrophoresis demonstrates 30 serum patterns. Samples 6, 13, 14, 25, and 30 demonstrate monoclonal restrictions in the γ region. Sample 24 shows an M protein overlying the usual C3 (β_2 region) band. When the usual β region bands appear fuzzy or enlarged, it often indicates the presence of an M protein. IFE is indicated.

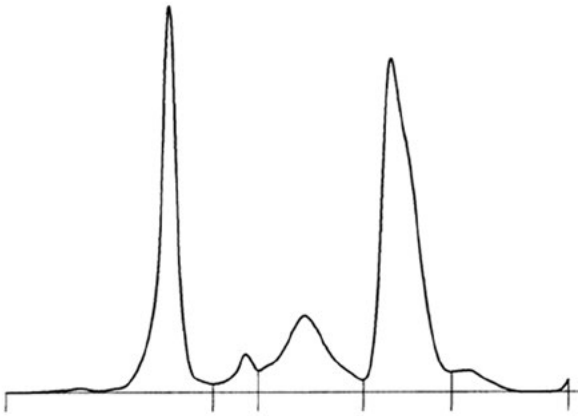

A/G 0.44
T.P.: 8.1

Fractions	%	Ref. %	g/dl	Ref. g/dl
Albumin	30.6	52.9 - 66.9	2.5 L	3.7 - 4.9
Alpha 1	3.5	3.0 - 5.8	0.3	0.2 - 0.4
Alpha 2	16.0	7.5 - 13.4	1.3 H	0.5 - 0.9
Beta	46.7	8.5 - 13.7	3.8 H	0.6 - 1.0
Gamma	3.2	8.8 - 19.2	0.3 L	0.6 - 1.4

FIGURE 14 This capillary zone electropherogram shows a prominent b region band due to the presence of an IgM M protein in this case of Waldenström's macroglobulinemia. Ref., reference; T.P., total protein; A/G, albumin-to-globulin ratio; H, high value; L, low value.

such low amounts of M proteins, a high-resolution electrophoresis system is needed. When elevations of proteins are seen in the β region on densitometry or the electropherogram, in the case of capillary zone electrophoresis, that is unexplained by β-γ bridging (an illustration of this is the cirrhosis pattern), IFE or immunosubtraction electrophoresis is indicated to rule out an M protein. Occasionally, M proteins will appear as a shoulder to one of the other bands or even migrate directly on top of the band, producing an aberrantly large C3 or transferrin band.

M proteins may rarely reside in the α_2 region. These are difficult to detect because of the higher concentration of the proteins that normally migrate there. This is one reason why a negative serum protein electrophoresis does not rule out the presence of a detectable serum M protein. When a negative serum protein electrophoresis is found in a patient with a strong suspicion of having an M protein, an IFE of the serum should be performed. Indeed, the recommendation of the International Myeloma Working Group is to perform serum protein electrophoresis, serum IFE, and serum free light chain analyses for individuals suspected of having MM (see chapter 11).

An aggressive approach is recommended to further evaluate suspicious bands on a serum protein electrophoresis that does not have further testing requested by reflexing them to a serum IFE. Katzmann et al. have provided guidance as to the yield of M proteins for different types of suspicious bands (see chapter 11) (Table 3) (30). An M spike is extremely specific, with all electrophoretic patterns given that designation identified as an M protein by IFE in their study. Fuzzy bands are the finding that has the highest yield of the other suspicious findings. A fuzzy band is when one has a broadened or distorted major band, most often C3 or transferrin (Fig. 13, specimen 24). The increased size of the band is often due to an M protein that either comigrates with it, thus broadening it, or migrates slightly cathodal or anodal to it, giving the band (Fig. 15).

Quantification of Serum M Proteins

When using electrophoresis systems with sharp resolution, the lower limit of visualization of M proteins has been estimated at about 0.02 to 0.04 g/dl if the M protein is in the γ region (31, 32). Detection of low-concentration M proteins can be clinically significant. While most such M proteins will fall into the category of monoclonal gammopathy of undetermined significance (MGUS), some will be seen in patients with light chain myeloma, IgD myeloma, IgE myeloma, amyloid (AL), and other B-cell lymphoproliferative processes such as chronic lymphocytic lymphoma or well-differentiated lymphocytic lymphoma. Furthermore, even in cases of MGUS with M proteins considered too low in concentration to measure, but which were confirmed by IFE, Murray et al. found that slightly less than 1% of these cases progressed to a malignant plasma cell or B-cell proliferative disorder (33).

Once an M protein has been detected and characterized immunologically, one should try to quantify it if it is not too low in concentration. As a guideline, the International Myeloma Working Group uses 1.0 g/dl as the minimal amount measured when monitoring a response to therapy. This does not mean one cannot measure smaller amounts. However, care should be taken to consider the underlying polyclonal immunoglobulins in the γ region and the interfering proteins in the β region.

For γ-migrating M proteins that are clearly distinguishable from other proteins and with minimal background normal immunoglobulins, we recommend measuring the M protein band itself by densitometry for gel-based systems or by use of the electropherogram for capillary electrophoresis. The demarcation for the M protein is placed at the

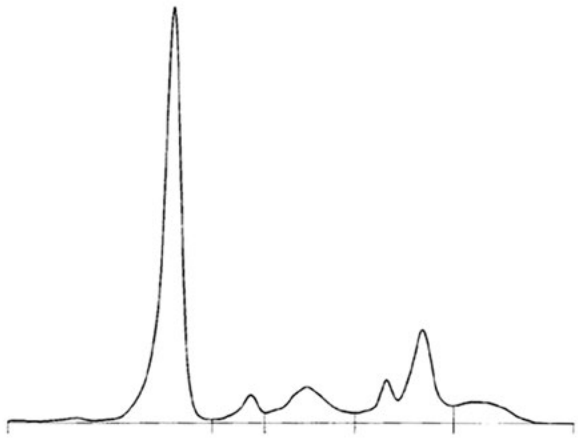

A/G Ratio: 1.32
T.P.: 6.8

Fractions	%	Ref. %	g/dl	Ref. g/dl
Albumin	56.9	52.9 - 66.9	3.9	3.7 - 4.9
Alpha 1	4.1	3.0 - 5.8	0.3	0.2 - 0.4
Alpha 2	11.0	7.5 - 13.4	0.7	0.5 - 0.9
Beta	21.1	8.5 - 13.7	1.4 H	0.6 - 1.0
Gamma	6.9	8.8 - 19.2	0.5 L	0.6 - 1.4

FIGURE 15 This capillary zone electropherogram shows an increase in the C3 band due to an IgA M protein overlying it. IFE is indicated. Ref., reference; T.P., total protein; A/G ratio, albumin-to-globulin ratio; H, high value; L, low value.

TABLE 3 Reflex testing for suspicious bands[a]

SPE[b] abnormality	Reflexed SPE cases (*n*)	IFE positive (*n* [% specificity])	MFLC by IFE (*n*)
M spike	169	169 (100)	
Fuzzy band	206	112 (54)	4
Questionable fuzzy band	263	47 (18)	0
Hypogammaglobulinemia (<0.55 g/dl)	85	10 (12)	5
Increased α_2 (≥1.4 g/dl)	48	2 (4)	0
Broad/extra α_2 band	9	0	0
Increased β (1.6–1.9 g/dl)	10	1 (10)	0
All abnormalities	790	341 (43)	9

[a]Table from reference 30.
[b]SPE, serum protein electrophoresis.

notch it forms with the normal immunoglobulins (Fig. 8). For M proteins that are not high in concentration and whose base is obscured by other proteins such as transferrin, C3, or normal gamma globulins, we do not quantify the M protein level (Fig. 16). If one can make this distinction, the quantitative measurement will usually be better for monitoring patients with M proteins than a measurement by nephelometry of the total immunoglobulin of that class. The M protein measurement excludes most of the polyclonal immunoglobulins, whereas the nephelometric measurement will include them. This obscures to some degree the changes in the M protein on subsequent measurements. The use of immunosubtraction electrophoresis in capillary electrophoresis has helped to make this distinction in the α and β regions (see chapter 11). In addition, a new nephelometric procedure that measures heavy-light chain combinations, i.e., IgG(κ) versus IgG(λ), may prove useful for such challenging cases (34–37).

PATTERN INTERPRETATION FOR URINE

On 100-fold-concentrated urine samples, albumin in small amounts may be seen on protein electrophoresis in a variety of conditions. Normally, one may detect up to 150 mg of albumin during 24 h. The amount may be increased following strenuous exercise and in patients with diabetes.

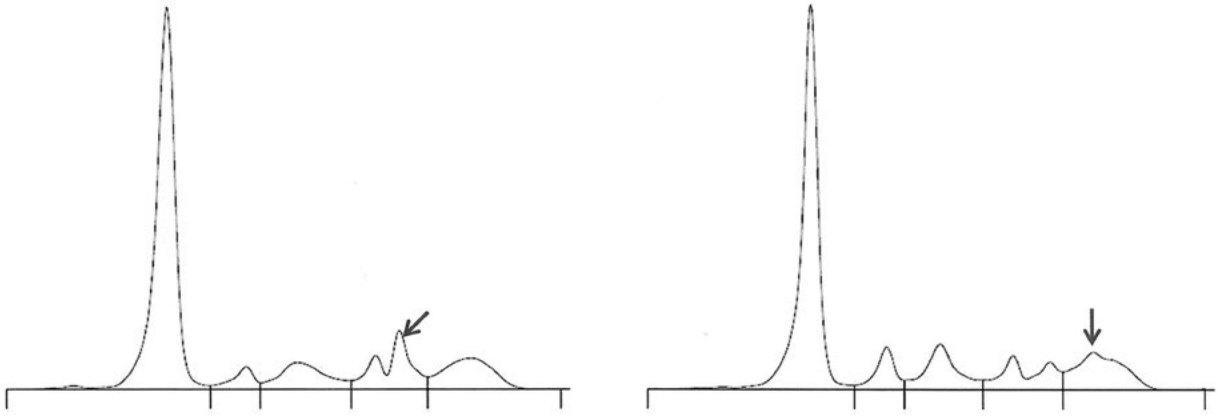

A/G 1.55
T.P.: 6.3

Fractions	%	Ref. %	g/dl	Ref. g/dl
Albumin	60.8	52.9 - 66.9	3.8	3.7 - 4.9
Alpha 1	3.9	3.0 - 5.8	0.2	0.2 - 0.4
Alpha 2	9.9	7.5 - 13.4	0.6	0.5 - 0.9
Beta	13.1	8.5 - 13.7	0.8	0.6 - 1.0
Gamma	12.3	8.8 - 19.2	0.8	0.6 - 1.4

A/G 1.28
T.P.: 5.6

Fractions	%	Ref. %	g/dl	Ref. g/dl
Albumin	56.1	52.9 - 66.9	3.1 L	3.7 - 4.9
Alpha 1	6.8	3.0 - 5.8	0.4	0.2 - 0.4
Alpha 2	11.6	7.5 - 13.4	0.6	0.5 - 0.9
Beta	10.7	8.5 - 13.7	0.6	0.6 - 1.0
Gamma	14.8	8.8 - 19.2	0.8	0.6 - 1.4

FIGURE 16 Two capillary zone electropherogram patterns are shown. On the left, the C3 band appears enlarged and distorted. In a normal serum sample, it is usually equal to or less than the transferrin (β_1) band. Here, it is not only larger but shifted anodally compared to a sample from another patient (on the right). It is difficult to determine how much of this area is due to the M protein. However, if one can immunosubtract this band, one may be able to improve such measurements (see chapters 9 and 11). The serum sample for which results are shown on the right also has a distinct, though small, M protein in the γ region. It should be characterized by IFE, but it is too small to measure due to the relatively large amount of underlying polyclonal immunoglobulins. Ref., reference; T.P., total protein; A/G, albumin-to-globulin ratio; L, low value.

Mild glomerular damage will demonstrate the moderately sized major serum proteins that normally do not pass effectively through the glomerular barrier (Fig. 17). As long as the tubular reabsorptive function is intact, little or no faintly staining protein will be seen in the α_2 and β regions. When the capacity for the tubules to reabsorb protein is exceeded, small bands will be seen in these regions along with the faintly staining γ region. With severe nonselective renal disease, a pattern that resembles that of serum protein electrophoresis including, to a lesser extent, the large molecules in the α_2 region is found.

If only the tubules are damaged, the large amount of small serum proteins that normally pass through the glomerulus will not be reabsorbed and will appear in the urine. Typically, one will find a small amount of albumin and numerous bands of various sizes in the α_1, α_2, β, and γ regions (Fig. 17). After the interpreter gets used to the usual bands of tubular proteinuria, if a band is found in a different location, an IFE should be performed to establish electrophoretic homogeneity and κ or λ specificity. This identifies the presence of MFLCs.

When a large excess of a relatively small molecule is present, such as in myoglobin, β-microglobulin, hemoglobin, and lysozyme, if the amount excreted is greater than the tubular reabsorptive capacity, an overflow proteinuria pattern is seen. This situation must be studied by IFE to rule out the possibility that the band represents an M protein.

Detection of M Proteins in the Urine

MFLC (Bence Jones proteins) typically occur as monomers (~25 kDa) and dimers (~50 kDa), both of which pass into the glomerular filtrate. Uncommonly, free κ chains may exist as tetramers and free λ chains may exist as hexamers which are too large to pass into the glomerular filtrate.

An early morning void is the best urine specimen for the initial detection of MFLC. However, for initial detection of MFLC, measurement of serum free light chains (FLC) by means of nephelometric techniques is as effective for detecting patients with light-chain MM. They obviate the need for a urine sample (see chapter 7). However, once MFLC have been demonstrated in patients with light-chain-only MM, the International Myeloma Working Group recommends that they should be monitored by measuring the MFLC peak on the densitometric scan of 24-h urine collections.

While the serum FLC measurements may eventually be used to monitor these patients, the lack of linearity and problems with antigen excess effects have thus far limited the technique. Nonetheless, in cases where there is too low of a concentration of light chain present in a 24-h urine collection, serum FLC measurements have proven useful, especially in cases of AL amyloidosis and oligosecretory MM (29).

MFLC and M proteins may migrate anywhere from the α through the γ region on urine protein electrophoresis. Once one becomes familiar with the common patterns of glomerular and tubular proteinuria discussed above, unusual bands will become more apparent. This is more difficult with tubular proteinuria and its many bands from small proteins not reabsorbed than with glomerular proteinuria.

For optimal detection of MFLC, we recommend performing IFE and urine protein electrophoresis on all samples. For the initial detection of MFLC, we review our files on the patient to see if there is a known M protein in the serum. This is especially important in the case of unusual conditions such as IgD or IgE myeloma.

Commonly, both the intact M protein and the MFLC can be found in the urine of a patient with MM. The urine

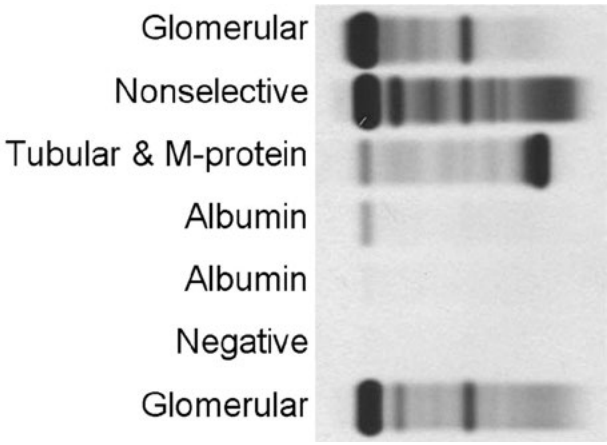

FIGURE 17 Several urine protein electrophoretic patterns are shown from concentrated urine samples. The arrow indicates the M protein in the third sample.

IFE is compared to the urine protein electrophoresis to determine which band is the MFLC. This band is measured by densitometry of the urine protein electrophoresis (Fig. 18). The concentration of the total protein in the urine is used with this measurement and the volume of the 24-h urine collection to determine the amount of MFLC per 24 h as follows: MFLC/24 h = (total protein concentration [mg/ml]) × (ml/24 h) × (% MFLC by densitometry).

The record of the urine protein electrophoresis and IFE is stored in a file with the serum protein electrophoresis, IFE or immunosubtraction (ISE), and serum FLC results.

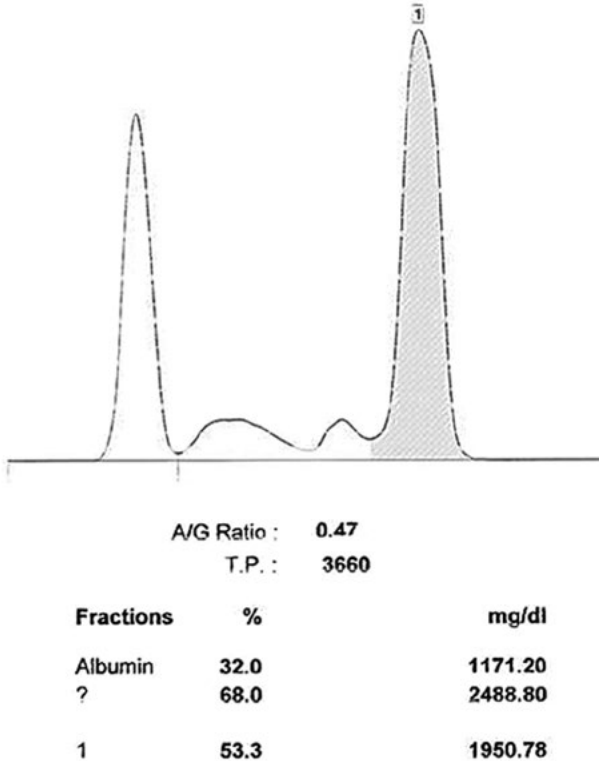

FIGURE 18 A densitometric scan of an agarose gel is shown from a urine sample with an MFLC measuring almost 2,000 mg/24 h. A/G ratio, albumin-to-globulin ratio; T.P., total protein.

This allows one to correlate the current results with previous results.

CLINICAL APPLICATIONS

Serum and urine protein electrophoresis are not general screening techniques. They are employed to detect M proteins in patients suspected of harboring plasma cell and B-lymphocyte proliferative disorders. For the initial detection of an M protein, serum protein electrophoresis, IFE, and serum FLC measurement are recommended to detect MM.

In occasional situations, such as suspicion of heavy-chain disease or AL amyloidosis in the face of negative serum and FLC studies, urine protein electrophoresis and urine IFE can provide useful information.

In addition to M proteins, however, performance of serum and urine protein electrophoresis often detects a wide variety of other abnormalities that can provide useful clinical information as described above. Therefore, attention to all regions of the electrophoretic pattern is needed, and such abnormalities should be included in the final report.

Avoiding False-Positive Results

Unexplained bands from the α through the γ regions may represent an M protein. However, before they are interpreted as being M proteins, this diagnosis should be secured by IFE or immunosubtraction (see chapter 9). In both capillary and gel-based electrophoresis, several proteins can produce bands that are not immunoglobulins but which may mimic an M protein. Fibrinogen, C-reactive protein, C3 variants, transferrin variants, hemoglobin-haptoglobin complexes, and markedly elevated β-lipoprotein can all be confused with an M protein band. Fibrinogen is commonly seen due to the presence of anticoagulants or an incompletely clotted specimen. It migrates in the slow β region on most gels, and because it is the only large band in that area that is not an immunoglobulin, it is easily ruled out by its position or by an IFE when in doubt (Fig. 7). Investigators quickly learn where fibrinogen and hemoglobin migrate on their gels. Other suspicious bands should be confirmed by IFE or immunosubtraction electrophoresis before being reported. When using capillary electrophoresis, interference from radiocontrast dyes and some antibiotics give deflections that may be misinterpreted as M proteins (Fig. 19). Some of these, such as sulfamethoxazole, produce a small deflection at the anodal end of albumin which should not be confused with an M protein (Table 1) (15, 17). Others, such as piperacillin-tazobactam (Tazocin; Wyeth), can produce a peak at the anodal end of the β region. One may remove these interfering substances by desalting or with activated charcoal (14, 38).

When performing IFE, the specificity of each new lot of reagent antiserum needs to be confirmed. The study of the antisera should include both serum and plasma. Even though plasma is not the specimen that is recommended for use, occasionally fibrinogen will be present for a number of reasons. These include the presence of anticoagulation therapy, inadequate time for the specimen to clot before the serum is removed from the clot, or drawing of the sample into a tube containing an anticoagulant. If the reagent antiserum against immunoglobulin contains reactivity for fibrinogen, a false-positive result may be recorded (39).

Correlation of Current with Previous Patient Results

Good quality assurance requires coordinating all available laboratory information on the patient. A record should be established for each patient the first time that an M protein is detected in the serum or urine. The record should contain the serum and urine protein electrophoresis and IFE or immunosubtraction electrophoresis gels and patterns along with key nephelometric studies, including serum FLC results and measurements of IgG, IgA, and IgM.

The patient's current specimen patterns should be compared with the first results obtained on the original M protein and also with the most recent previous sample. If the migration of the M protein matches that of the previous serum or urine sample, the amount of the M protein should be recorded on the report along with a statement as to whether it has increased, decreased, or remained unchanged since the previous sample. To have reproducible results, the International Myeloma Working Group requires M protein measurements of >1 g/dl to record a difference. It further defines a difference as a change of at least 25%. For urine MFLC measurements, they require at least 200 mg/24 h (40).

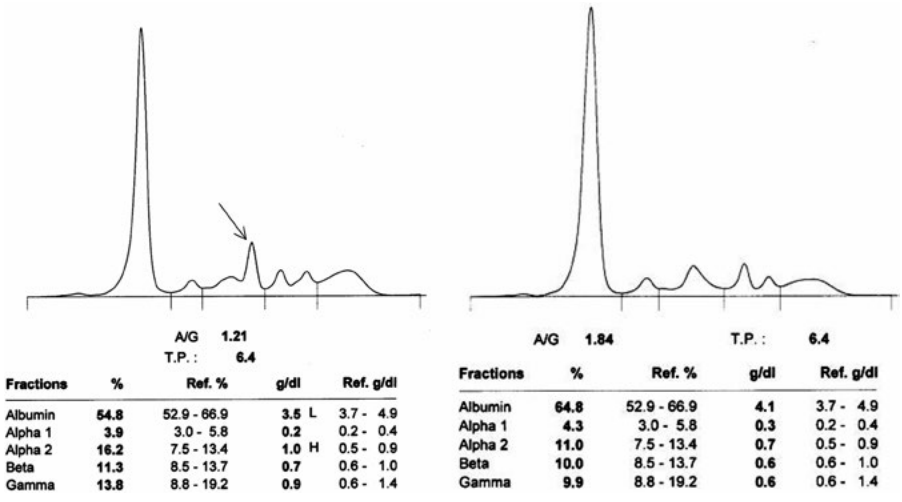

A/G 1.21
T.P.: 6.4

Fractions	%	Ref. %	g/dl		Ref. g/dl
Albumin	54.8	52.9 - 66.9	3.5	L	3.7 - 4.9
Alpha 1	3.9	3.0 - 5.8	0.2		0.2 - 0.4
Alpha 2	16.2	7.5 - 13.4	1.0	H	0.5 - 0.9
Beta	11.3	8.5 - 13.7	0.7		0.6 - 1.0
Gamma	13.8	8.8 - 19.2	0.9		0.6 - 1.4

A/G 1.84 T.P.: 6.4

Fractions	%	Ref. %	g/dl	Ref. g/dl
Albumin	64.8	52.9 - 66.9	4.1	3.7 - 4.9
Alpha 1	4.3	3.0 - 5.8	0.3	0.2 - 0.4
Alpha 2	11.0	7.5 - 13.4	0.7	0.5 - 0.9
Beta	10.0	8.5 - 13.7	0.6	0.6 - 1.0
Gamma	9.9	8.8 - 19.2	0.6	0.6 - 1.4

FIGURE 19 Two capillary zone electropherograms are shown. The one on the right is a control. The one on the left demonstrates the radiocontrast dye Omnipaque as a sharp band in the slow α_2 fraction (arrow). These samples require IFE or immunosubtraction electrophoresis to rule out a monoclonal protein. Ref., reference; T.P., total protein; A/G, albumin-to-globulin ratio; H, high value; L, low value.

With chemotherapy and/or stem cell transplantation, the original M protein usually declines and may disappear. This is accompanied by hypogammaglobulinemia, and occasionally, an oligoclonal response may be seen. Some oligoclonal bands may be as large as, or occasionally larger than, the M spike that can be seen with residual disease or a recurrence of the original M protein. However, as long as these oligoclonal bands do not have the same migration and isotype as the original M protein, they are not an indication of recurrence. Indeed, their presence may reflect recovery of normal immunoglobulin-producing clones and has been suggested as a favorable feature for event-free and overall survival by Alejandre et al. (41, 42).

The migration and the isotype identification of the M protein should be the same as that of the original M protein. If there is any change in migration, identification of the patient sample should be confirmed by IFE or ISE. If a new single M protein is identified, the clinician should be contacted to determine if the patient has had extensive chemotherapy and/or stem cell transplantation. Occasionally, one can find a very prominent band as part of an oligoclonal reaction. Usually, these will be transient. However, if there has been no significant change in the therapy, the appearance of a new M protein is highly unlikely. In that circumstance, it is recommended to repeat the SPEP on a freshly drawn sample to confirm that a likely patient identification error has occurred.

In the report, comment is also made about the remaining normal gamma globulins. Suppression of the gamma globulins is a negative prognostic indicator and, if severe enough, may predispose the patient to infections, possibly requiring gamma globulin replacement therapy (43).

Suppression of the normal immunoglobulins may be reported if the nephelometric measurements of the uninvolved immunoglobulin isotypes (IgA and IgM in the case of an IgG M protein) are below the normal range.

The International Myeloma Working Group recommends that if the intact M protein is present in the serum, its measurement should be used to monitor the response of the patient. However, about 20% of cases of MM only, or primarily, produce FLC. In that case, 24-h urine samples are indicated periodically (depending on the aggressiveness of the process and/or therapy) to monitor the tumor burden and to help estimate the degree of damage to the nephrons.

Patients with MGUS should have periodic urine and serum IFE depending on clinical judgment of the attending physician.

The availability of FLC testing in serum and urine has been shown to be useful both in the initial detection of MFLC and in monitoring patients with light chain disease (see chapter 7). The measurement of the FLC can replace the initial urine IFE for the detection of MFLC. Furthermore, serum FLC tests are useful to stratify the risk of progression to MM for individuals presenting with MGUS or smoldering MM.

The use of external quality assurance proficiency testing is essential to compare the results from one laboratory with those of others who are using the same system in the detection of M proteins and also to allow one to gauge the effectiveness of one manufacturer's electrophoretic system to correctly identify an abnormality versus the systems provided by other manufacturers.

Cost of Testing

Cost is mainly related to the number of samples assayed per day and selection of the most appropriate type of equipment used for the number of tests performed. In laboratories with relatively small volumes (2 to 4 serum samples per day), it may be worthwhile considering sending the test to a reference laboratory and using the resources of the laboratory for higher-volume testing or required stat testing. Laboratories with larger volumes (5 to 10 per day) may wish to use a manual assay and batch the testing once or twice per week. With a volume of about 20 per day, use of a semiautomated method decreases technologist time. At volumes of 40 or more per day, the bar-coded, automated capillary electrophoresis systems are highly efficient with excellent resolution.

REFERENCES

1. **Keren DF.** 2012. *Protein Electrophoresis in Clinical Diagnosis*, p 1–11. American Society for Clinical Pathology, Chicago, IL.
2. **Hortin GL.** 2012. Amino acids, peptides, and proteins, p 509–564. *In* Burtis CA, Ashwood ER, Bruns DE (ed), *Teitz Textbook of Clinical Chemistry and Molecular Diagnostics*. Elsevier-Saunders, St. Louis, MO.
3. **Tiselius A.** 1958. Electrophoresis, past, present and future. *Clin Chim Acta* **3:**1–9.
4. **Tiselius A.** 1932. A new apparatus for electrophoretic analysis of colloidal mixtures. *Trans Faraday Soc* **33:**524–531.
5. **Kunkel HG, Tiselius A.** 1951. Electrophoresis of proteins on filter paper. *J Gen Physiol* **35:**89–118.
6. **Kohn J.** 1957. A cellulose acetate supporting medium for zone electrophoresis. *Clin Chim Acta* **2:**297–304.
7. **Jolliff CR, Blessum CR.** 1997. Comparison of serum protein electrophoresis by agarose gel and capillary zone electrophoresis in a clinical setting. *Electrophoresis* **18:** 1781–1784.
8. **Bossuyt X.** 2004. Interferences in clinical capillary zone electrophoresis of serum proteins. *Electrophoresis* **25:**1485–1487.
9. **Luraschi P, Dea ED, Franzini C.** 2003. Capillary zone electrophoresis of serum proteins: effects of changed analytical conditions. *Clin Chem Lab Med* **41:**782–786.
10. **Keren DF.** 1998. Capillary zone electrophoresis in the evaluation of serum protein abnormalities. *Am J Clin Pathol* **110:**248–252.
11. **Katzmann JA, Clark R, Sanders E, Landers JP, Kyle RA.** 1998. Prospective study of serum protein capillary zone electrophoresis and immunotyping of monoclonal proteins by immunosubtraction. *Am J Clin Pathol* **110:**503–509.
12. **Lichtinghagen R, Pietsch D, Brand K.** 2010. Evaluation of an automated capillary electrophoresis system for serum protein electrophoresis with the determination of gender-specific reference values. *Clin Lab* **56:**119–126.
13. **Le Bricon T, Launay E, Houze P, Bengoufa D, Bousquet B, Gourmel B.** 2002. Determination of poorly separated monoclonal serum proteins by capillary zone electrophoresis. *J Chromatogr B Analyt Technol Biomed Life Sci* **775:**63–70.
14. **Arranz-Pena ML, Gonzalez-Sagrado M, Olmos-Linares AM, Fernandez-Garcia N, Martin-Gil FJ.** 2000. Interference of iodinated contrast media in serum capillary zone electrophoresis. *Clin Chem* **46:**736–737.
15. **Bossuyt X, Peetermans WE.** 2002. Effect of piperacillin-tazobactam on clinical capillary zone electrophoresis of serum proteins. *Clin Chem* **48:**204–205.
16. **Bossuyt X, Schiettekatte G, Bogaerts A, Blanckaert N.** 1998. Serum protein electrophoresis by CZE 2000 clinical capillary electrophoresis system. Clin Chem **44:**749–759.
17. **Bossuyt X, Verhaegen J, Marien G, Blanckaert N.** 2003. Effect of sulfamethoxazole on clinical capillary zone electrophoresis of serum proteins. *Clin Chem* **49:**340–341.
18. **Aguzzi F, Kohn J, Petrini C, Whicher JT.** 1986. Densitometry of serum protein electrophoretograms. *Clin Chem* **32:**2004–2005.
19. **Keren DF, Alexanian R, Goeken JA, Gorevic PD, Kyle RA, Tomar RH.** 1999. Guidelines for clinical and

laboratory evaluation patients with monoclonal gammopathies. *Arch Pathol Lab Med* **123:**106–107.
20. **Keren DF, Gulbranson R, Ebrom SJ.** 2004. False-negative urine protein electrophoresis by semi-automated gel electrophoresis. *Clin Chem* **50:**933–934.
21. **Brigden ML, Neal ED, McNeely MD, Hoag GN.** 1990. The optimum urine collections for the detection and monitoring of Bence Jones proteinuria. *Am J Clin Pathol* **93:**689–693.
22. **Benson MD.** 2001. Amyloidosis, p 5345–5378. *In* Scriver CR (ed), *The Metabolic Basis of Inherited Disease*. McGraw-Hill, Columbus, OH.
23. **Deshpande V, Khosroshahi A, Nielsen GP, Hamilos DL, Stone JH.** 2011. Eosinophilic angiocentric fibrosis is a form of IgG4-related systemic disease. *Am J Surg Pathol* **35:**701–706.
24. **Yamada K, Kawano M, Inoue R, Hamano R, Kakuchi Y, Fujii H, Matsumura M, Zen Y, Takahira M, Yachie A, Yamagishi M.** 2008. Clonal relationship between infiltrating immunoglobulin G4 (IgG4)-positive plasma cells in lacrimal glands and circulating IgG4-positive lymphocytes in Mikulicz's disease. *Clin Exp Immunol* **152:**432–439.
25. **Khosroshahi A, Stone JH.** 2011. A clinical overview of IgG4-related systemic disease. *Curr Opin Rheumatol* **23:** 57–66.
26. **Katzmann JA, Dispenzieri A, Kyle RA, Snyder MR, Plevak MF, Larson DR, Abraham RS, Lust JA, Melton LJ III, Rajkumar SV.** 2006. Elimination of the need for urine studies in the screening algorithm for monoclonal gammopathies by using serum immunofixation and free light chain assays. *Mayo Clin Proc* **81:**1575–1578.
27. **Lakshminarayanan R, Li Y, Janatpour K, Beckett L, Jialal I.** 2007. Detection by immunofixation of M proteins in hypogammaglobulinemic patients with normal serum protein electrophoresis results. *Am J Clin Pathol* **127:**746–751.
28. **Abraham RS, Katzmann JA, Clark RJ, Bradwell AR, Kyle RA, Gertz MA.** 2003. Quantitative analysis of serum free light chains. A new marker for the diagnostic evaluation of primary systemic amyloidosis. *Am J Clin Pathol* **119:**274–278.
29. **Drayson M, Tang LX, Drew R, Mead GP, Carr-Smith H, Bradwell AR.** 2001. Serum free light-chain measurements for identifying and monitoring patients with nonsecretory multiple myeloma. *Blood* **97:**2900–2902.
30. **Katzmann JA, Stankowski-Drengler TJ, Kyle RA, Karen SL, Snyder MR, Lust JA, Dispenzieri A.** 2010. Specificity of serum and urine protein electrophoresis for the diagnosis of monoclonal gammopathies. *Clin Chem* **56:**1899–1900.
31. **Bienvenu J, Graziani MS, Arpin F, Bernon H, Blessum C, Marchetti C, Righetti G, Somenzini M, Verga G, Aguzzi F.** 1998. Multicenter evaluation of the Paragon CZE 2000 capillary zone electrophoresis system for serum protein electrophoresis and monoclonal component typing. *Clin Chem* **44:**599–605.
32. **Smalley DL, Mayer RP, Bugg MF.** 2000. Capillary zone electrophoresis compared with agarose gel and immunofixation electrophoresis. *Am J Clin Pathol* **114:**487–488.
33. **Murray DL, Seningen JL, Dispenzieri A, Snyder MR, Kyle RA, Rajkumar SV, Katzmann JA.** 2012. Laboratory persistence and clinical progression of small monoclonal abnormalities. *Am J Clin Pathol* **138:**609–613.
34. **Bradwell AR, Harding SJ, Fourrier NJ, Wallis GL, Drayson MT, Carr-Smith HD, Mead GP.** 2009. Assessment of monoclonal gammopathies by nephelometric measurement of individual immunoglobulin kappa/lambda ratios. *Clin Chem* **55:**1646–1655.
35. **Ludwig H, Milosavljevic D, Zojer N, Faint JM, Bradwell AR, Hubl W, Harding SJ.** 2013. Immunoglobulin heavy/light chain ratios improve paraprotein detection and monitoring, identify residual disease and correlate with survival in multiple myeloma patients. *Leukemia* **27:**213–219.
36. **Katzmann JA, Clark R, Kyle RA, Larson DR, Therneau TM, Melton LJ III, Benson JT, Colby CL, Dispenzieri A, Landgren O, Kumar S, Bradwell AR, Cerhan JR, Rajkumar SV.** 2013. Suppression of uninvolved immunoglobulins defined by heavy/light chain pair suppression is a risk factor for progression of MGUS. *Leukemia* **27:**208–212.
37. **Bradwell A, Harding S, Fourrier N, Mathiot C, Attal M, Moreau P, Harousseau JL, Avet-Loiseau H.** 2013. Prognostic utility of intact immunoglobulin Ig′κ/Ig′λ ratios in multiple myeloma patients. *Leukemia* **27:**202–207.
38. **Blessum CR, Khatter N, Alter SC.** 1999. Technique to remove interference caused by radio-opaque agents in clinical capillary zone electrophoresis. *Clin Chem* **45:**1313.
39. **Register LJ, Keren DF.** 1989. Hazard of commercial antiserum cross-reactivity in monoclonal gammopathy evaluation. *Clin Chem* **35:**2016–2017.
40. **Durie BG, Harousseau JL, Miguel JS, Blade J, Barlogie B, Anderson K, Gertz M, Dimopoulos M, Westin J, Sonneveld P, Ludwig H, Gahrton G, Beksac M, Crowley J, Belch A, Boccadaro M, Cavo M, Turesson I, Joshua D, Vesole D, Kyle R, Alexanian R, Tricot G, Attal M, Merlini G, Powles R, Richardson P, Shimizu K, Tosi P, Morgan G, Rajkumar SV.** 2006. International uniform response criteria for multiple myeloma. *Leukemia* **20:** 1467–1473.
41. **Alejandre ME, Pavlovsky MA, Remaggi G, Corrado C, Fernandez I, Milone G, Pavlovsky A, Madalena L, Pandolfo M, Facio ML, Bresciani P, Pavlovsky S, Pizzolato MA.** 2012. Serum free light chains and oligoclonal bands in patients with multiple myeloma and autologous stem cell transplantation. *Clin Chem Lab Med* **50:**1093–1097.
42. **Alejandre ME, Madalena LB, Pavlovsky MA, Facio ML, Corrado C, Milone G, Bresciani PD, Fraind SA, Pavlovsky S, Pizzolato MA.** 2010. Oligoclonal bands and immunoglobulin isotype switch during monitoring of patients with multiple myeloma and autologous hematopoietic cell transplantation: a 16-year experience. *Clin Chem Lab Med* **48:**727–731.
43. **Walchner M, Wick M.** 1997. Elevation of $CD8^+$ $CD11b^+$ Leu-8^- T cells is associated with the humoral immunodeficiency in myeloma patients. *Clin Exp Immunol* **109:** 310–316.

Immunochemical Characterization of Immunoglobulins in Serum, Urine, and Cerebrospinal Fluid

ELIZABETH SYKES AND YVONNE POSEY

9

The characterization of immunoglobulins spans a spectrum of methods, including molecular analysis of gene usage and rearrangement, quantitation of immunoglobulin heavy chains as well as intact and free light chains, qualitative assessment and characterization of clonality, and identification of abnormalities that may be clinically significant, such as hyperviscosity syndrome, cryoglobulinemia, and amyloidosis (AL). This chapter focuses on qualitative methods for the assessment and characterization of clonality. The methods include agarose gel electrophoresis (AGE) with immunofixation, capillary electrophoresis (CE) with immunosubtraction (ISUB), and isoelectric focusing with immunoblotting or immunofixation. All three methods can be used to identify monoclonal, oligoclonal, and polyclonal immunoglobulin populations and to identify the heavy and/or light chains contained in the population. Immunofixation electrophoresis (IFE) and ISUB electrophoresis are diagnostic tools used for the identification of monoclonal gammopathies and, conversely, for the confirmation of polyclonal hypergammaglobulinemia. Isoelectric focusing with immunoblotting or immunofixation is a cerebrospinal fluid (CSF) diagnostic test for the identification of oligoclonal bands in multiple sclerosis (MS).

BACKGROUND

Intact immunoglobulins are products of clonal plasma cells that consist of two identical heavy chains (IgG, IgA, IgM, IgD, or IgE) and two identical light chains (kappa or lambda) (1). In order to ensure proper assembly, there is an approximately 40% excess of light-chain production; however, the free light chains are normally cleared and metabolized by the kidneys within hours of secretion (2, 3). In a normal immune response, each of the thousands of immunoglobulin idiotypes produced by plasma cell clones is present in a relatively small proportion. Because of the charge variability of the immunoglobulin molecules, they normally have a broad electrophoretic migration, described as polyclonal, on serum protein electrophoresis (PE). In contrast, a monoclonal gammopathy (paraprotein) represents a proliferation of a single plasma cell clone that produces an immunologically homogeneous protein commonly referred to as a monoclonal protein. It is essential that the laboratory distinguishes a monoclonal protein from a normal polyclonal distribution of immunoglobulins. Monoclonal proteins are often associated with a clonal process that is malignant or potentially malignant, whereas an increase in polyclonal immunoglobulins is due to an inflammatory or reactive process. Diagnoses associated with a serum monoclonal protein include monoclonal gammopathy of undetermined significance (MGUS), multiple myeloma (MM), Waldenström macroglobulinemia, smoldering MM, AL, lymphoproliferative diseases, and plasmacytoma (4). Table 1 lists the distribution of diseases from 31,479 monoclonal gammopathies diagnosed by the Mayo Clinic's practice from 1960 to 2003. MGUS is the most common finding; however, MM is regarded as the hallmark malignant diagnosis (5).

Monoclonal proteins usually consist of an intact immunoglobulin; however, a plasma cell clone may produce only a monoclonal free light chain or, rarely, a monoclonal heavy chain. Because of the excess production of free light chains by plasma cells, it is not uncommon to find a small amount of monoclonal free light chain in addition to the intact monoclonal protein in the serum. The excess monoclonal free light chain may also be detected in the patient's urine. In IgG myeloma, for example, approximately three-fourths of patients have an excess of monoclonal free light chains that are excreted and detectable in the urine (6).

LABORATORY INVESTIGATION

Routine laboratory testing used to determine whether serum contains polyclonal immunoglobulins or a monoclonal protein includes agarose gel or capillary PE, IFE, and capillary electrophoresis with ISUB. The term immunosubtraction was patented by Beckman, so other companies have had to devise different terms for the procedure. However, this chapter uses the term ISUB for further discussion of the technique. Depending on initial findings and the patient's clinical presentation, additional investigations may include serum free light chain quantitations, urine PE, and urine IFE. Katzmann reviewed the ability of different test combinations to identify a monoclonal protein (7); details of that study are reviewed in chapter 11.

Both IFE and ISUB rely on the principles of immunoprecipitation; this refers to the interaction of multivalent antigen and antibody molecules that result in a lattice formation or precipitate (8). If too much antigen or too much

doi:10.1128/9781555818722.ch9

TABLE 1 Distribution of plasma cell proliferative disorders at the Mayo Clinic from 1960 to 2003[a]

Disorder with monoclonal gammopathy	% of cases
Monoclonal gammopathy of undetermined significance	61
Multiple myeloma	17
Primary systemic amyloidosis	9
Lymphoproliferative disease	3
Smoldering myeloma	4
Solitary or extramedullary plasmacytoma	2
Macroglobulinemia	2
Other	2

[a]*n* = 31,479 (5).

antibody is present, the lattice formation does not occur and a precipitate does not form. Therefore, manufacturers of commonly used gel-based IFE (Helena Laboratories, Sebia, Grifols [maker of InterLab]) and ISUB (Sebia, Helena) techniques produce antiserum in a concentration such that a precipitate forms with the immunoglobulin concentrations found normally in human serum. However, laboratories must be aware of the potential for antigen excess or antibody excess, which can still exist and allow a monoclonal protein to be missed. Serum samples for these procedures should be collected and stored refrigerated until analyzed. Refrigerated samples are stable for at least 2 weeks and can be frozen indefinitely.

Immunofixation

IFE is the composite of PE and immunoprecipitation. Proteins are first separated by agarose gel electrophoresis, and then antiserum is applied to precipitate the proteins of interest. When first introduced, IFE was a manual procedure; however, although more automation has now been introduced, technologists' techniques often still play an important role in the completed gel. Depending on the manufacturer, IFE gels are available in different sizes and configurations. Regardless of size, most IFE gels comprise six lanes for each serum sample; the first lane is used as the reference lane, and the remaining five lanes are used to evaluate IgG, IgA, IgM, kappa, and lambda. Serum of a specified dilution is applied to the application point of each lane. When IFE was first introduced, laboratories measured serum immunoglobulin concentrations in order to determine the appropriate serum dilution and avoid the problem of antigen or antibody excess. However, manufacturers' instructions for serum dilutions are now usually based on the gamma globulin fraction or total immunoglobulin concentration. It is advisable to pay close attention to these dilution protocols in order to avoid the problems of antigen excess (serum may need to be diluted more) or antibody excess (serum should be diluted less or perhaps not at all).

After the proteins have been separated by electrophoresis, the reference lane is overlaid with an acid fixative, fixing all proteins to the gel. Specific antisera are then applied to each of the other lanes (IgG, IgA, IgM, kappa, lambda) and the gel is incubated, allowing immunoprecipitation to occur. The kappa and lambda antisera are directed toward total kappa and lambda light chains (i.e., bound and free). The subsequent washing step washes away all proteins other than those in the reference lane that have been fixed to the gel, and immunoglobulins precipitated by the specific antisera. After drying, a protein stain, usually acid violet, allows the interpreter to determine whether the immunoglobulins are in a diffuse/polyclonal distribution or whether a discrete band or monoclonal protein is present. The evaluation of IFE gels is a qualitative skill that takes experience for correct interpretation, and gels should always be examined directly by the interpreter. Figure 1B shows a normal IFE with polyclonal immunoglobulins, and Fig. 2B shows serum containing an IgG lambda monoclonal protein. In Fig. 2, the IgG and lambda bands line up with the monoclonal protein in the reference lane. Both Fig. 1 and 2 include the corresponding electropherogram.

It is important to be aware of the normal distribution of immunoglobulins on IFE. IgG is located throughout the whole of the gamma region, IgA migrates in the beta and beta-gamma regions, and IgM stays at or near the origin. Kappa and lambda staining usually corresponds to IgG, although when there is a significant polyclonal increase in IgA, the kappa and lambda staining extends more prominently into the beta region. The kappa and lambda lanes normally show identical staining distributions, but the kappa lane usually appears denser than the lambda lane, reflecting the increased concentration of total kappa compared to the concentration of total lambda light chains. By knowing the normal IFE pattern, an interpreter should easily recognize the occasional mishaps that can occur, such as application of a specific antiserum to the wrong lane or not applying antiserum or serum to a specific lane. The latter problem results in a lane without any staining at all and may be easily missed by the novice interpreter, especially if it involves the far-right lambda lane (Fig. 3). As an alternative to the

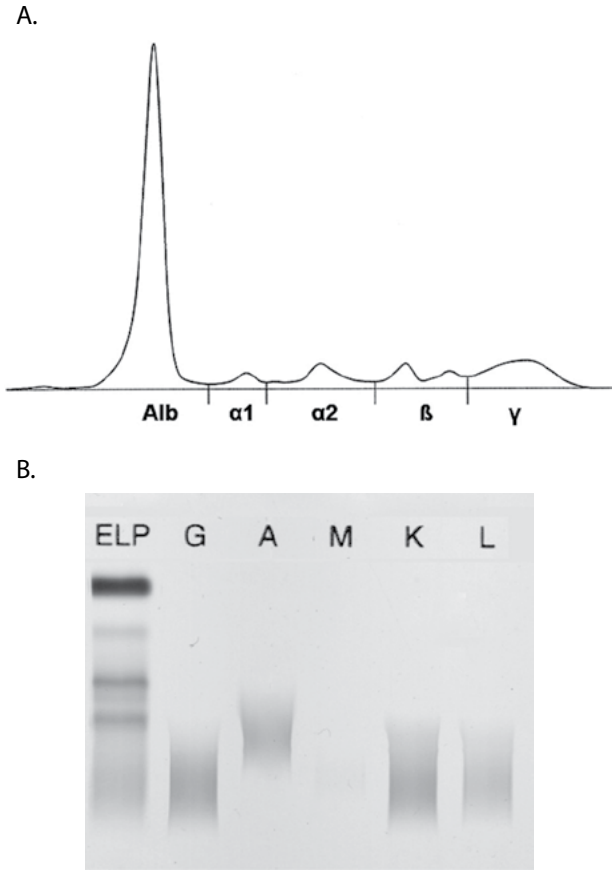

FIGURE 1 (A) Normal serum electropherogram; (B) normal serum immunofixation gel.

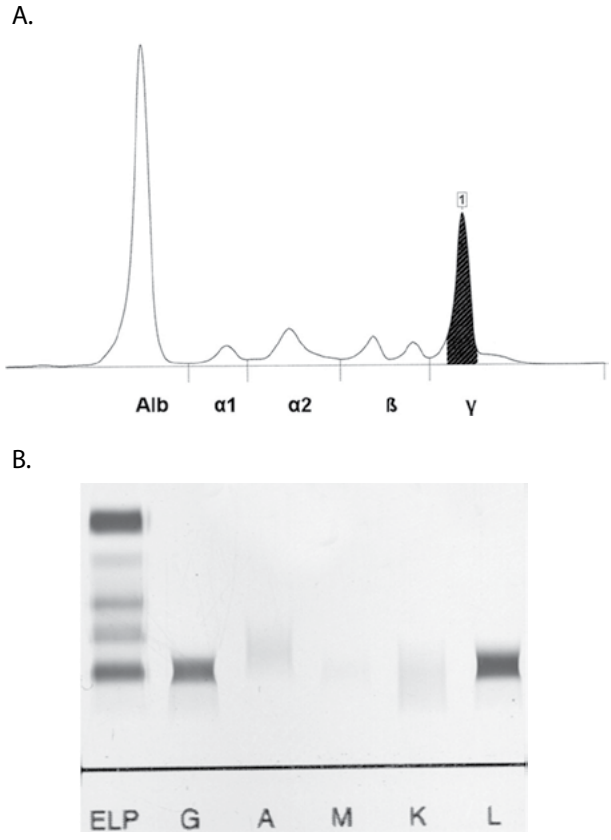

FIGURE 2 (A) Electropherogram with monoclonal protein in the gamma region; (B) immunofixation gel showing an IgG lambda monoclonal protein.

six-lane gel, manufacturers offer a pentavalent gel and antiserum. With this approach, a serum sample is applied only to a reference lane and one IFE lane. The reference lane is treated similarly to that of the six-lane IFE gel, but the IFE lane is overlaid with antiserum directed against a combination of IgG, IgA, IgM, kappa, and lambda. If a discrete band is noted in the IFE lane, a complete IFE must be performed to identify the monoclonal protein type. The immunofixation assay for urine studies is identical to the serum assay except that urine samples need to be concentrated to increase the detection sensitivity. Details of urine IFE will be described later in this chapter.

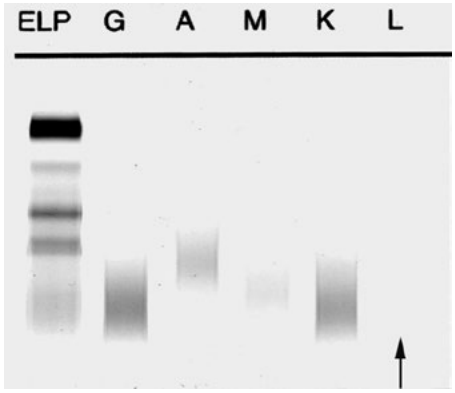

FIGURE 3 Serum immunofixation gel with no staining in the lambda lane due to lambda antiserum not being applied.

Immunosubtraction

Capillary electrophoresis is now used quite commonly to perform serum PE. It automates the electrophoretic procedure and allows for better positive-patient identification than some agarose gel approaches. Combining capillary electrophoresis with immunoprecipitation has resulted in the technique initially called immunosubtraction (ISUB). Because it is automated, ISUB is performed more rapidly than agarose gel IFE but is less sensitive for detection of small amounts of monoclonal protein (9–11). Beckman Coulter was the first company to introduce a commercial instrument for capillary electrophoresis; this was called capillary zone electrophoresis (CZE). However, Beckman no longer manufactures this particular electrophoretic instrument for routine clinical laboratory use, although they do manufacture other capillary electrophoresis systems, mainly for research purposes. CZE has now been replaced by other automated systems from Sebia and Helena. As indicated earlier, the term immunosubtraction was patented; therefore, Sebia uses "immunotyping" and Helena uses "immunodisplacement" for their specific techniques.

Manufacturers of the ISUB technique use prepackaged antisera against IgG, IgA, IgM, kappa, and lambda; these are placed on the instrument with the patient's serum sample. The process allows serum and each antiserum to mix and incubate. The exact contents of the antisera are proprietary, but they are thought to cause the precipitate of the patient's immunoglobulin and antiserum to be negatively charged and so they migrate anodally to albumin. After incubation, the pretreated samples undergo electrophoresis in the capillary columns. The resulting ISUB patterns are examined for polyclonal immunoglobulins or loss of a monoclonal peak, hence the term immunosubtraction. Figure 4 illustrates a normal serum ISUB pattern and Fig. 5 one with an IgG lambda monoclonal protein. In Fig. 4, the "subtraction" of IgG results in almost total removal of the gamma fraction except in the fast-gamma region, where IgA and IgM migrate. The anti-kappa and anti-lambda reagents decrease the gamma fraction by approximately two-thirds and one-third, respectively. The use of anti-IgA and -IgM decreases the background under the beta globulin and the beta-gamma

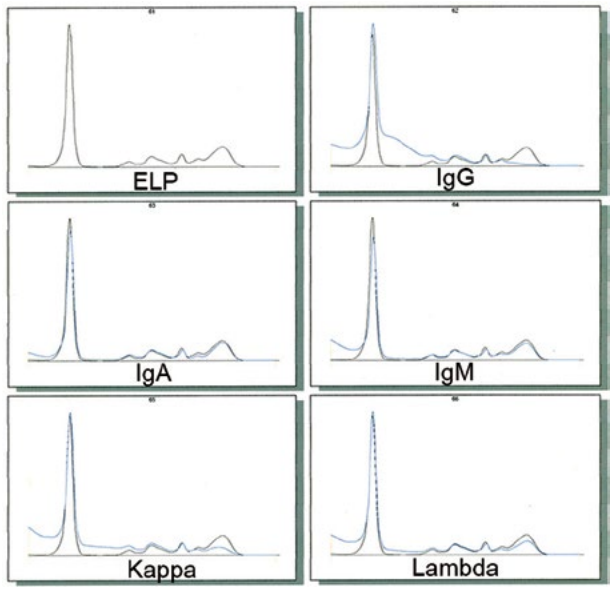

FIGURE 4 Normal serum immunosubtraction pattern.

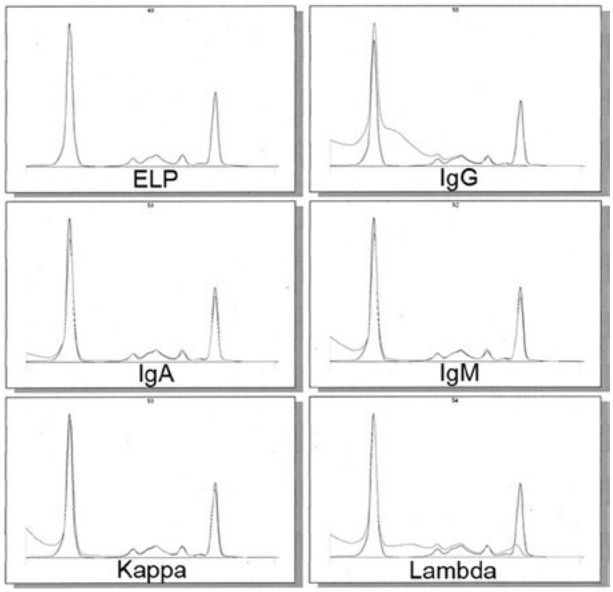

FIGURE 5 Serum immunosubtraction pattern with IgG lambda monoclonal protein.

globulin regions, respectively. In Fig. 5, the anti-IgG reagent removes the M spike as well as the polyclonal portion of the gamma fraction. The anti-lambda reagent removes the M spike as well as a portion of the polyclonal gamma fraction. Therefore, this is consistent with an IgG lambda monoclonal protein.

The main advantage of ISUB is that it is automated and so takes less technologist time and expertise to perform than current IFE gel procedures. However, as indicated earlier, ISUB is less sensitive at detecting small bands or small amounts of monoclonal protein because one needs to see the monoclonal antibody or peak on the reference electropherogram before one can say that it has been removed by ISUB (10, 11). In contrast, with the IFE procedure, other proteins have been washed away and a monoclonal protein is "amplified" because the protein stain stains a combination of the patient's immunoglobulin and the added antiserum. Therefore, as a screen to detect a small amount of monoclonal protein, IFE is preferred. Although many investigators have concentrated on the ability or inability of ISUB to detect small amounts of monoclonal protein, Schild et al. reported a case of a significant amount of IgM kappa monoclonal protein that was not detected by the Capillarys 2 (12). The authors concluded that the problem was caused by precipitation of the monoclonal by alkaline pH buffer and postulated that perhaps some of the reports of false-negative electrophoresis results may be related to pH-dependent precipitation. ISUB also has the current disadvantage of not being able to test for IgD or IgE monoclonal proteins or for other specific proteins. Whether the commercial companies will expand their ISUB capabilities is yet to be determined.

However, despite the disadvantages mentioned, ISUB does have some advantages compared to IFE. ISUB may more readily show which light and heavy chains are associated in serum containing two comigrating monoclonal proteins. This applies particularly to the situation where IgG, kappa, and lambda bands comigrate on IFE; these may represent IgG kappa and IgG lambda proteins or an intact IgG monoclonal protein plus a monoclonal free light chain. The ISUB procedure will clarify this type of IFE result. It can also be helpful in the identification of a small amount of monoclonal protein that migrates in a pattern of increased polyclonal immunoglobulins.

PATTERN INTERPRETATIONS AND CLINICAL DISORDERS

Polyclonal

Polyclonal increases in immunoglobulins occur in a variety of conditions, such as chronic infections, chronic inflammation, connective tissue disease, and chronic liver disease. Large increases may appear to have a restricted migration on PE, especially in capillary electrophoresis, and on occasion may be confused with a monoclonal gammopathy. However, use of IFE or ISUB should distinguish a polyclonal from a monoclonal gammopathy. Polyclonal increases in any of the immunoglobulins will appear as a darker, but diffuse, area of staining in the IFE heavy-chain lane(s) affected. There should also be a diffuse increase in staining for both corresponding kappa and lambda chains (Fig. 6). The ISUB pattern will be similar but more prominent than the normal ISUB polyclonal pattern described in the immunosubtraction section.

A marked polyclonal increase in the IgG4 subclass often results in an apparent band (agarose gel) or peak (capillary electrophoresis) in the beta-gamma region that may easily be misinterpreted as a monoclonal protein (8). However, IFE or ISUB should help clarify that there is a polyclonal distribution of IgG with both kappa and lambda light chains

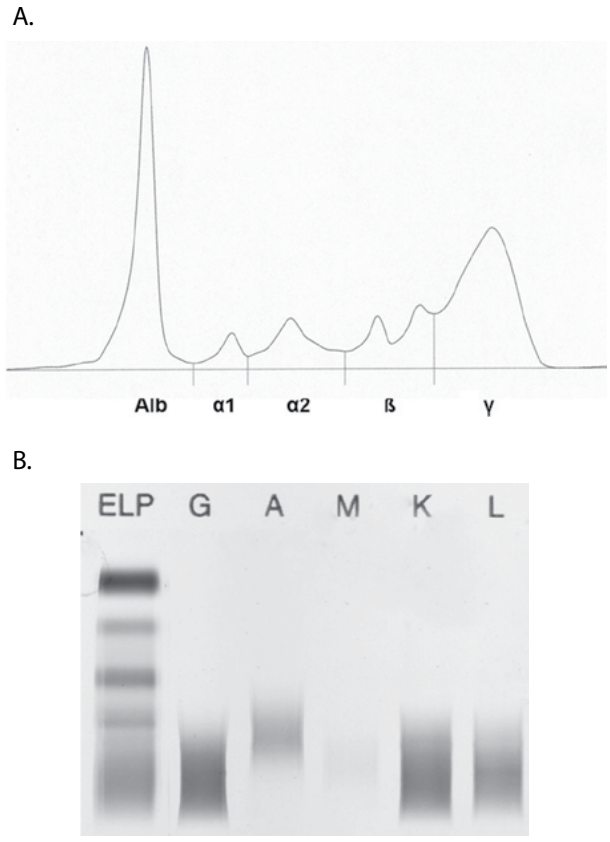

FIGURE 6 (A) Electropherogram with polyclonal increase in gamma globulins; (B) immunofixation gel with polyclonal increase in IgG (a "fuzzy" band is noted in the lambda lane).

increased (Fig. 7). Measurement of IgG subclasses will show a specific increase in the IgG4 subclass. A polyclonal increase in IgM may cause a similar localized staining (agarose gel) or a broad peak (capillary electrophoresis) in the beta-gamma region that can be initially misinterpreted as a broadly migrating monoclonal protein. In addition, with some of the smaller IFE gels, IgM migrates in a relatively short, localized region of the lane so that, on initial inspection, an increased IgM may suggest a monoclonal protein. Again, noting that both the kappa and lambda lanes also show an increase in staining corresponding to IgM will help clarify that this is a polyclonal increase. Interpretation of polyclonal increases in IgA is generally straightforward, occurring primarily in the beta region.

Because of the high protein content of sera with increased polyclonal immunoglobulins and the potential for rheumatoid factor to be present in these samples, sera may exhibit a point-of-application artifact on IFE. In addition, sera with polyclonal increases in immunoglobulins may exhibit several faint, fuzzy bands or restrictions in most or all of the IFE lanes. These may be interpreted as part of the polyclonal response to a particular stimulus; however, if they are sufficiently discrete, they can be referred to as oligoclonal bands. The bands (IFE) or small peaks (capillary electrophoresis) are assumed to represent increases in the production of specific immunoglobulins from a number of plasma cell clones.

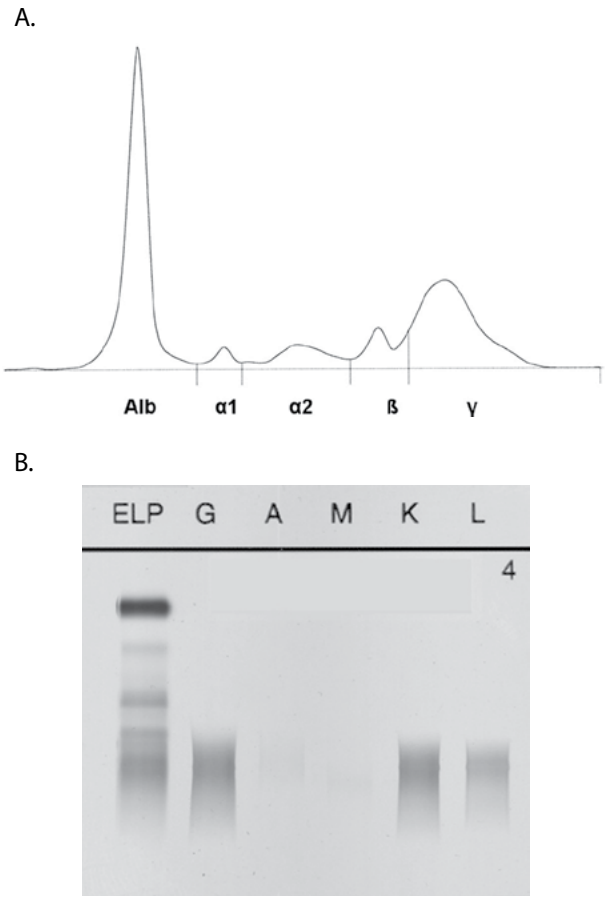

FIGURE 7 Polyclonal increase in an IgG4 subclass. (A) Electropherogram with a rounded peak in the beta-gamma region; (B) immunofixation gel showing an increase in staining in the beta-gamma region in the IgG and both kappa and lambda lanes.

Monoclonal Proteins

As described earlier in the chapter, monoclonal proteins are found under several conditions (Table 1). In addition, they are detected in the general population at a rate of approximately 3% (13, 14) in individuals above 70 years of age. Since IgG-producing plasma cells are present in the greatest numbers, it makes sense that IgG monoclonal proteins occur most frequently. A Mayo study showed that when all monoclonal proteins are considered, IgM monoclonals occur more frequently than IgA monoclonals. However, IgA predominates over IgM when only MM is considered (6); this is because most malignant IgM monoclonals are associated with Waldenström macroglobulinemia. IgD monoclonals are very uncommon and IgE monoclonals extremely rare. Waldenström macroglobulinemia (lymphoplasmacytic lymphoma) is associated with an IgM monoclonal that is readily detected by PE (7). In contrast, AL is usually associated with small amounts of a monoclonal free light chain, although in some patients no monoclonal protein is detected even by IFE.

Four percent of monoclonal proteins are biclonal or double gammopathies that result from two separate expanded clones of plasma cells (15). In order to use the term biclonal with confidence, one should have both a kappa and a lambda monoclonal protein. However, it is probably better either to simply describe the monoclonal protein types or to use the term "double gammopathy." If both bands are IgM, they likely represent monomeric and pentameric IgM (7S and 19S), and if they are identical IgA or IgG molecules, they are most likely monomers and dimers. For clinical purposes, the monoclonal protein quantitations are added together. An example of a sample containing both an IgG lambda and an IgA kappa monoclonal protein (two bands) is shown in Fig. 8; this also illustrates the problem of antigen excess. It is estimated that 0.09% of patients will have three monoclonal proteins.

Classically, a significant amount of monoclonal protein is seen as a relatively sharp spike on PE. In this situation, the monoclonal protein quantitation can be reported. However, some monoclonals have a broader distribution than others and can be confused with a polyclonal immunoglobulin pattern. In monoclonal protein cases, the IFE or ISUB pattern should show only kappa or lambda associated with the increased heavy-chain staining or peak. If only a small amount of monoclonal protein is present, it may be too small to fractionate; in this case, the report can indicate that there is

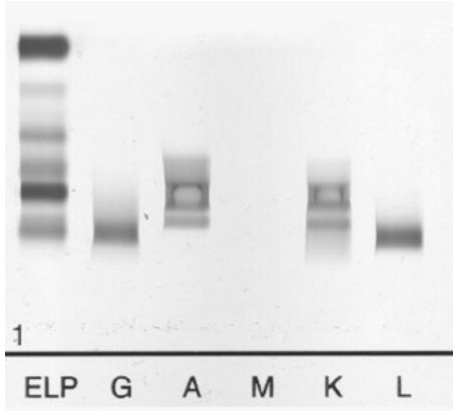

FIGURE 8 Serum immunofixation gel with a biclonal gammopathy (IgG lambda and IgA kappa). Antigen excess is also present in the IgA and kappa lanes.

a small amount of monoclonal protein within a polyclonal background or within the beta or alpha-2 globulin regions. Of course, in some cases, the monoclonal protein may be visible only by IFE.

Myeloma

Diagnostic criteria for MM are a clonal increase of bone marrow plasma cells of >10% or biopsy-proven plasmacytoma, together with any one or more of several myeloma-defining events that include evidence of end organ damage, serum free light chain ratio, focal lesions on MRI, or a clonal plasma cell count of >60%. A monoclonal quantitation is now only included in criteria for smoldering myeloma (16). Although the vast majority of MM patients have a significant amount of monoclonal protein at the time of diagnosis, nearly 3% have no detectable monoclonal heavy chain or light chain (17, 18). These nonsecretory MM patients have large numbers of plasma cells in their bone marrow. Most have clonal plasma cells with cytoplasmic kappa or lambda light chains, indicating a secretory defect. However, a small number of patients have no detectable cytoplasmic immunoglobulin in their plasma cells and are nonproducers. The most likely pattern on IFE or ISUB in nonsecretory MM is one of hypogammaglobulinemia. In cases of hypogammaglobulinemia, it is important to decrease the serum dilution, thus avoiding antibody excess and, potentially, missing a small amount of monoclonal protein.

Free Light Chain Diseases

Because free light chains are readily cleared from the plasma, patients with free light chain diseases often show only small or undetectable monoclonal proteins on serum PE. However, these diseases usually represent significant disorders that include light chain MM (light chain disease), AL, and light chain deposition disease. In a Mayo Clinic study, although monoclonal free light chains represented only 5% of all monoclonal gammopathies, light chain MM accounted for 20% of the MM cases (6). This overrepresentation of free light chains in multiple myeloma (20%) versus all monoclonal gammopathies (5%) emphasizes the importance of confirming small serum PE abnormalities by IFE or ISUB. It should be noted that free light chain monoclonal proteins are uncommon in MGUS.

Sera with monoclonal light chains will show a discrete kappa or lambda band (IFE) or peak (ISUB), but there will be no corresponding IgG, IgA, or IgM heavy chain (Fig. 9). Although IgD monoclonal proteins are uncommon and IgE monoclonal proteins are very rare, an apparent monoclonal free light chain result should be confirmed by retesting the sample with IgD and IgE antisera. This can be performed only by IFE in routine clinical laboratories because commercially available ISUB techniques do not currently provide reagents for IgD or IgE testing.

MGUS

Criteria for MGUS are bone marrow plasma cells of <10%, a monoclonal protein of <3 g/dl, and the absence of end organ damage that can be attributed to a plasma cell proliferative disorder (13). Progression to a significant plasma-lymphocytic disorder has been shown to occur if the monoclonal protein is ≥1.5 g/dl and there is a non-IgG isotype and an abnormal free light chain ratio (19).

Heavy Chain Disease

In heavy chain disease (HCD), monoclonal immunoglobulins are composed of truncated heavy chains that contain no light chain (20). These are often Fc regions with molecular masses ranging between 27 and 49 kDa. HCD disorders are named for the heavy chain involved: IgA (α HCD), IgG (γ HCD), and IgM (μ HCD). Because the heavy chain peptide is truncated, it may also be detected in urine. Each disorder has a different clinical presentation, and this should be taken into consideration at the time of interpretation. When PE is considered, the monoclonal band in γ HCD is often broad and not clearly localized; discrete bands have not been seen in α HCD, and hypogammaglobulinemia is often the only prominent feature of μ HCD.

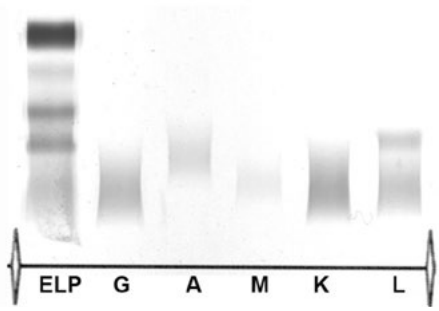

FIGURE 9 Serum immunofixation gel with a free lambda monoclonal protein.

In the past, identification of a monoclonal heavy chain was performed by immunoselection. This involved use of immunoelectrophoresis where anti-kappa and anti-lambda antisera were mixed into the agarose gel. Intact immunoglobulins precipitate at the application point, whereas free heavy chains electrophorese away from the origin. With the advent of IFE and ISUB, immunoselection is rarely used today. With IFE or ISUB, serum from a patient with HCD will show a heavy chain band or peak but no corresponding light chain abnormality (Fig. 10) (21). However, care should be taken with IFE, especially if α HCD is suspected. In some IgA myelomas, the corresponding monoclonal free light chain (frequently lambda) may not be clearly visible. This is thought to be due to the heavy chain covering the light chain determinant to which the antiserum is directed. The problem can usually be rectified by using a different manufacturer's antiserum or using a lesser dilution of the patient serum. In this situation, the possibility of antigen excess should also be considered.

Oligoclonal Banding

Oligoclonal banding refers to the presence of a few bands or peaks on PE, IFE, or ISUB. Each band or peak is caused by increased production of a specific immunoglobulin by a specific plasma cell clone in excess of the majority of other clones. The finding may be transient, may persist for months, and may change over time, with bands decreasing or disappearing, followed by the emergence of new bands. By IFE, it should be possible to line up heavy chain bands with either a kappa or a lambda band. On occasion, one band may be relatively prominent compared to the others; in such a case, it is appropriate to point this out and suggest repeat testing in 3 to 6 months to see whether the band regresses or, less likely, evolves into a monoclonal protein. Figure 11 illustrates an example of prominent oligoclonal banding by both ISUB and IFE.

Oligoclonal banding may be associated with a variety of conditions. When it occurs with a background of increased polyclonal immunoglobulins, the underlying condition is usually benign, e.g., chronic infections or autoimmune disorders. The sera of AIDS patients often exhibit prominent

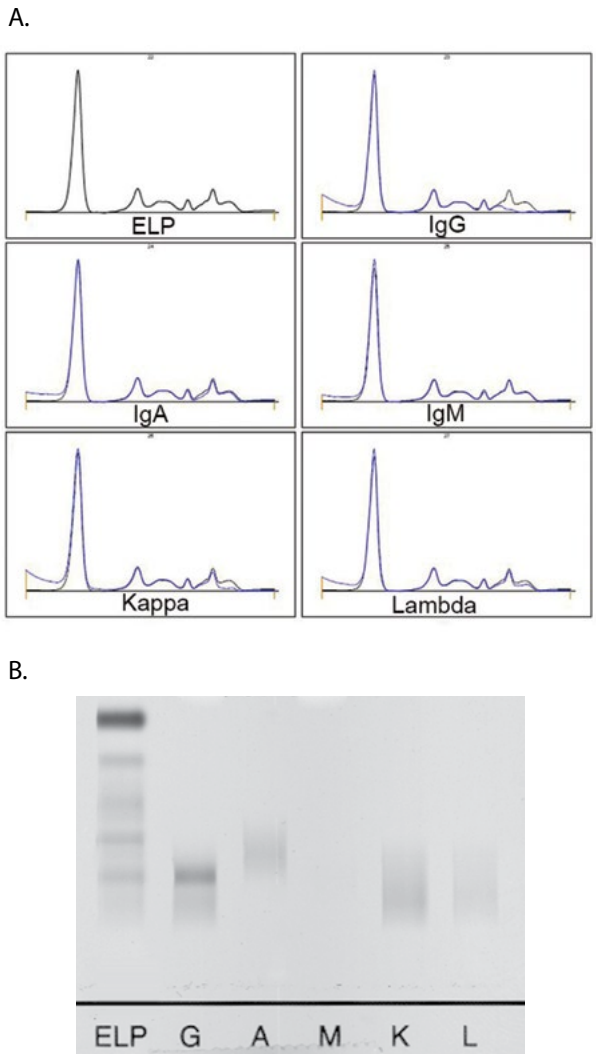

FIGURE 10 IgG heavy-chain disease. (A) Immunosubtraction showing removal of only IgG from the small gamma peak (no change is seen with kappa and lambda antisera); (B) immunofixation gel with only an IgG band.

oligoclonal banding; however, with the advent of better therapy, its prevalence in patients with HIV infection has decreased (22). When oligoclonal banding is seen with a background of decreased immunoglobulins, the possibility of a malignant condition should be considered. Examples include chronic lymphocytic leukemia and lymphoma. Patients who have undergone stem cell transplants or even cytotoxic therapy may also develop an oligoclonal banding pattern. If such a patient has a history of MM and one very prominent band or peak emerges in a pattern of oligoclonal banding, it is important to consider the type and location of the patient's original monoclonal protein.

Hypogammaglobulinemia

Hypogammaglobulinemia results in faintly staining lanes on IFE and relatively decreased gamma globulin fractions on ISUB. As noted previously, it is important to make sure antibody excess does not occur and that a monoclonal protein is not missed. In these cases, urine PE and IFE should be recommended.

Artifacts

Fibrinogen and hemoglobin-haptoglobin complexes can cause potentially confusing bands on PE, and radiographic contrast media (Fig. 12) can result in an extra peak using capillary electrophoresis (23, 24). The performance of either IFE or ISUB should provide evidence that no monoclonal protein is present in these cases. A very sharp band in each IFE lane at the application point indicates nonspecific staining that is due to protein not entering the agarose gel. This finding may represent immunoglobulin aggregates or cryoglobulins. The sample can be retested after treatment with a reducing agent such as 2-mercaptoethanol or dithiothreitol. If the application artifact persists, the patient should be investigated for cryoglobulinemia.

Very large amounts of monoclonal protein may give rise to the pattern of antigen excess (described where IFE is discussed), although this is not usually a problem with serum gels if the manufacturers' instructions are followed. Using IFE, the typical appearance of antigen excess (Fig. 8) is a band or block of staining with a "hole" in the middle; this absence of staining represents where there was an excess of the patient's immunoglobulin (antigen) such that the antigen-antibody complex was soluble and therefore washed away

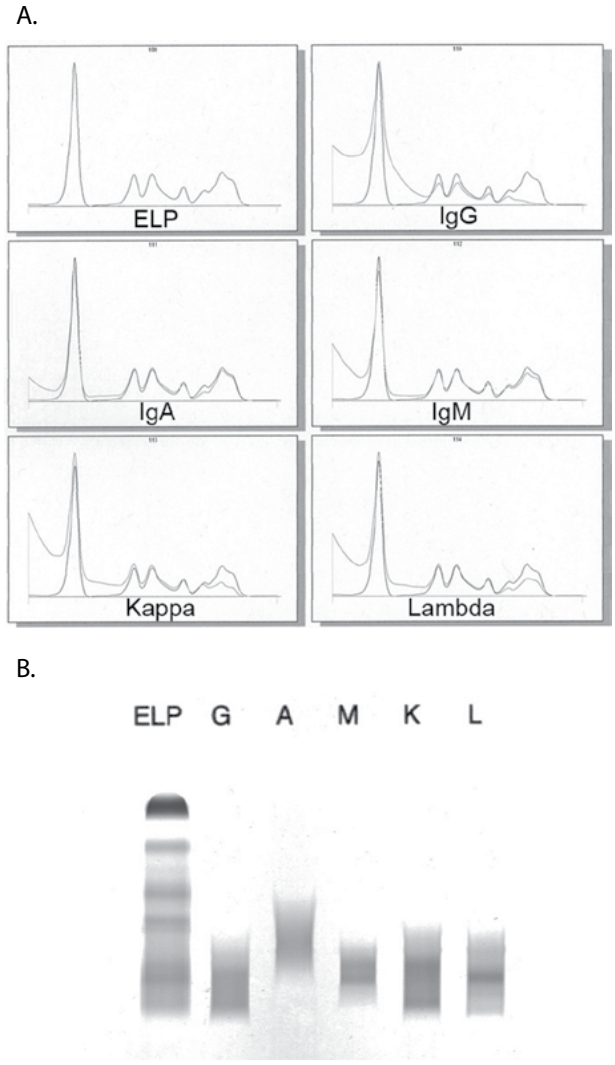

FIGURE 11 Prominent oligoclonal banding. (A) Immunosubtraction; (B) immunofixation gel.

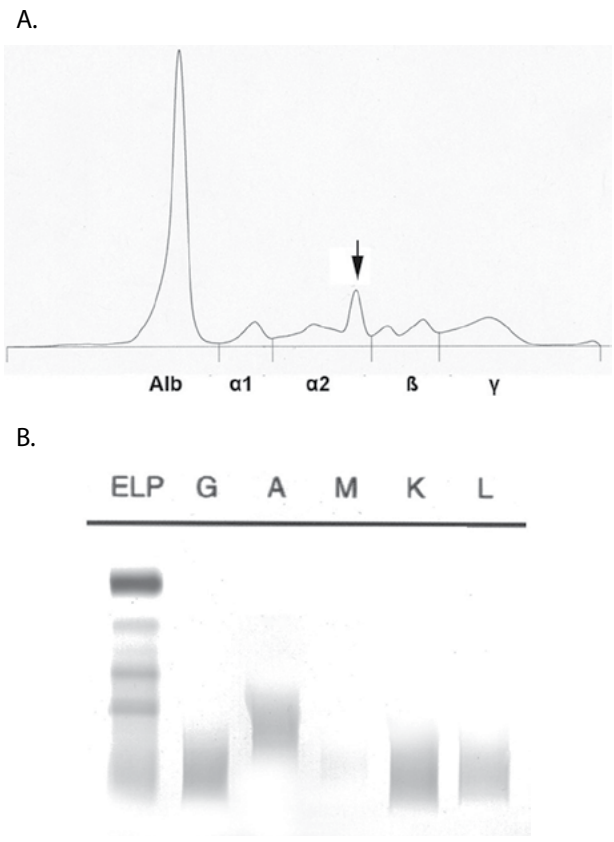

FIGURE 12 Contrast media artifact. (A) Electropherogram from capillary electrophoresis showing a peak (arrow) in the alpha-2/beta region; (B) immunofixation gel with no band corresponding to the contrast medium peak.

during the washing process. Large amounts of a monoclonal protein may also cause an IFE gel "shadow" artifact when it is not removed completely at the washing stage. Figure 13 illustrates this artifact in the case of a prominent IgG kappa monoclonal; here, a small band is detected in the IgA, IgM, and lambda lanes at the level of the monoclonal protein.

QUALITY CONTROL

New reagent lots should be tested against sera with known monoclonal proteins before being used for routine testing.

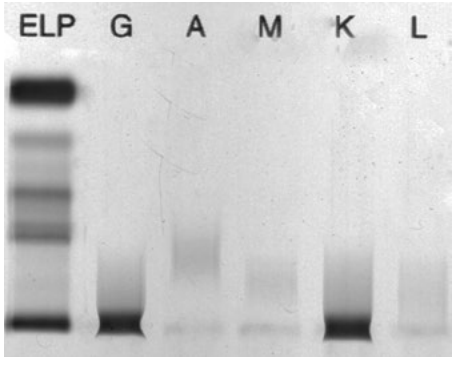

FIGURE 13 "Shadow" artifact on an immunofixation gel caused by incomplete washing of monoclonal protein from the gel (lanes IgA, IgM, and lambda).

In addition, antisera should be tested with a plasma sample to ensure that there is no cross-reactivity with fibrinogen. A sample containing a monoclonal protein of known immunotype should be tested each day. If a patient sample that has been previously immunotyped is part of the workload, that sample may serve as a daily control. The gels should be reviewed with respect to the sharpness of the bands and the correlation of the IFE bands with the monoclonal protein upon PE. IFE gels that are too faint or too dense should be retested with the appropriate dilution. In addition to the internal laboratory controls, external proficiency challenges are available for identification and characterization of monoclonal proteins. The College of American Pathologists' proficiency program supplies challenges, and its summary reports allow a laboratory to compare its performance with that of other laboratories as well as with those using other methods and reagents from different manufacturers.

URINE IMMUNOFIXATION

Monoclonal light chains without associated heavy chains are found in the sera of 5% of all patients with monoclonal gammopathies and 20% of patients with multiple myeloma (6). In monoclonal free light chain disorders, such as light chain multiple myeloma, AL, and light chain deposition disease, the serum concentration of the monoclonal free light chain is usually very low and the monoclonal protein is often not detected (7). However, because free light chains are freely filtered by the kidneys, monoclonal free light chains are far more likely to be found in the urine of patients with light chain disorders. In addition, about 75% of multiple myeloma patients with an intact monoclonal protein in their sera will have monoclonal free light chains in their urine (6). Because of this fact and because an increasing number of patients with smaller amounts of intact monoclonal protein in the serum (<1.5 g/dl) have been found with large amounts of clinically significant (>1 g/24 h) monoclonal free light chains in their urine (Fig. 14), we suggest that urine PE and IFE be performed on all patients with a measurable amount of serum monoclonal protein. Since urine monoclonal free light chains are uncommon in MGUS, urine PE and IFE can also be helpful in further defining this patient population. As indicated earlier, urine investigation is recommended for patients with hypogammaglobulinemia (gamma globulin fraction < 0.5 g/dl) who are older than 30 to 40 years.

It is important to note that routine urinalysis is not a reliable indicator of protein in urine containing immunoglobulin light chains. The dipstick test and some protein precipitation tests are biased toward detection of albumin; urine containing a significant amount of monoclonal protein may test negative for protein when a dipstick or protein precipitation method is used (8). In addition, the dye-binding methods used on many automated chemistry analyzers can have a variable ability to react with proteins of different charges. Despite this fact, dye-binding methods are widely used, and as long as the same assay is used consistently when an individual patient is followed, this is adequate for quantification of the patient's monoclonal protein (8). Methods used for the evaluation and detection of monoclonal proteins in urine are the same as those used for serum and include agarose gel PE, capillary electrophoresis (CE), and IFE. Because it is fairly common not to find an abnormality upon urine agarose gel PE or CE but still have a monoclonal free light chain in the urine, IFE is recommended as part of the screening and identification procedure. Our laboratory

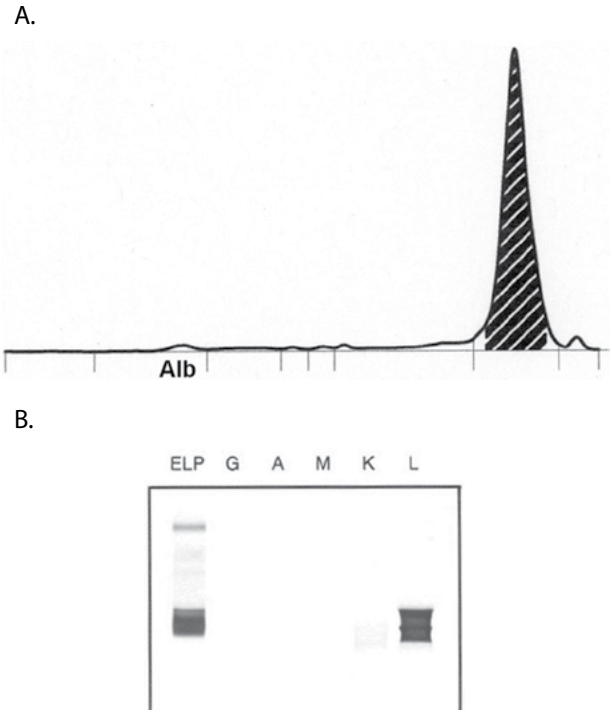

FIGURE 14 (A) Densitometric scan from a concentrated urine specimen showing a monoclonal protein (1,000 mg/24 h) in the gamma region on urine PE. The patient had 0.7 g/dl of IgG lambda monoclonal protein (including C3 complement) in the beta globulin region on serum PE/IFE. (B) Urine IFE performed on the specimen used in panel A demonstrates a free lambda monoclonal protein.

uses agarose gel PE and IFE with total kappa and lambda antisera as an initial screen; this is followed by a full immunofixation with antisera directed against IgG, IgA, and IgM heavy chains and total kappa and lambda light chains when a band is detected on the screening IFE.

Prior to the performance of electrophoresis, urine specimens need to be concentrated to increase monoclonal protein detection sensitivity. This is most often achieved through ultrafiltration. The final concentration of urine protein should be ideally between 1,000 and 8,000 mg/dl. We typically use a gravimetric ultrafiltration system augmented by placing the device on a rocker using the protocol outlined in Table 2. This allows for closer monitoring of the filtration process to achieve the desired concentration, but it is time-consuming and must be closely monitored to avoid under- and overconcentration of urine. Alternatively, we have used a procedure for concentrating protein on the gel by increasing the application time (Sebia method) or by increasing the number of applications (Helena method) of unconcentrated urine samples (if the urine protein is >100 mg/dl) or minimally concentrated urine samples (concentrated 10-fold if total protein is ≤100 mg/dl). Results with this approach were comparable to those obtained with our standard concentration procedure with respect to urine PE interpretation and monoclonal protein detection by IFE. The alternative procedures described allow for faster processing of the urine samples, but the disadvantage is that serum and urine samples cannot be conveniently run on the same gel. Other laboratories use centrifugal filtration systems, which are also faster, but monitoring to achieve the desired concentration can be difficult. If the urine is not concentrated enough, small but clinically significant monoclonal free light chains may not be detected. If the urine is overconcentrated, the sample may cause the gel or capillary to be overloaded and either obscure the monoclonal free light chains or cause the protein not to enter the gel or capillary at all. The limit of detection for monoclonal proteins in urine is 10 to 20 times higher than the detection limit for monoclonal proteins in the serum. The difference is a reflection of the lack of polyclonal background in many urine samples and the urine concentration step.

TABLE 2 Protocol for urine concentration used at Beaumont Laboratory

Total protein in urine (mg/dl)	Concn factor (multiple)
2–50	100 (maximal)
50–120	50
120–300	25
300–1,000	10
>1,000	10 to unconcentrated

A 24-h urine collection is recommended for monoclonal protein detection, quantification, and follow-up. However, for detection only, a first-void, early-morning urine specimen can be as sensitive but does not allow for quantification or follow-up of the monoclonal protein. Unpreserved urine samples collected over 24 h are the preferred specimens. They should be collected and stored refrigerated until analyzed. However, specimens are stable for 3 days at room temperature and also for 14 days refrigerated or frozen. Samples collected with a preservative should not be used. When monoclonal proteins are present on PE or CE in sufficient amounts, they can be quantified by densitometric scanning on PE or peak quantification on CE. Quantification of a monoclonal protein in urine should be based on a 24-h urine collection (mg/24 h) to effectively follow the patient's disease course. Quantification of a monoclonal protein based on urine protein concentration (mg/dl) can be misleading, as there can be wide fluctuations in urine concentrations collected at different times of day. Identification of monoclonal proteins in urine by ISUB has only recently been introduced; it works by the same principle as described for serum but is not widely used at the moment. Use of the free light chain immunoassay is not recommended (25).

On IFE, urine containing a relatively low protein concentration usually shows pale, diffuse staining in the kappa and lambda lanes corresponding to normal IgG migration. Kappa staining is slightly darker than in the lambda lane. In some cases, with urine protein concentrations that are very low, even if the urine has been maximally concentrated, it may not be possible to see any staining in the kappa and lambda lanes. As the urine protein concentration increases, it is common to see some polyclonal IgG and in some cases polyclonal IgA and IgM. With higher-resolution gels, such as the older Beckman IFE gels, it was common to see a few small bands (5 to 6) in both the kappa and lambda lanes, although the stain was generally darker in the kappa lane. The bands were equidistant and appeared like rungs of a ladder, hence the term "ladder pattern." We still see this occasionally on newer gels with lower resolution. The ladder pattern is caused by the relatively limited heterogeneity of normal polyclonal free light chains and should not be misinterpreted as monoclonal proteins. Identification of monoclonal proteins is generally straightforward using IFE. In addition to appearing as one kappa or lambda band on the IFE gel, some monoclonal free light chains may migrate as two discrete bands, representing monomers and dimers.

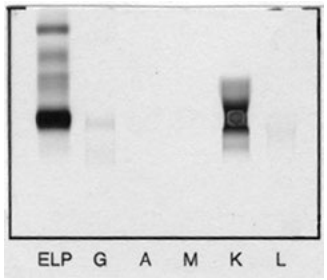

FIGURE 15 IFE of a concentrated urine specimen demonstrating a dominant free kappa and a smaller amount of IgG kappa monoclonal protein.

Occasionally, an intact immunoglobulin is also detected, although this is usually seen in patients with renal damage and significant glomerular or tubular proteinuria. Two relatively common findings in urine samples containing a large amount of monoclonal free light chains are those of antigen excess and the shadow artifact caused by the monoclonal protein not completely washing off the gel. Both these artifacts are described in the serum immunofixation section of this chapter. Bands on PE or peaks on CE, such as hemoglobin and beta-2 microglobulin, will be found not to consist of a monoclonal protein once the IFE is examined.

As discussed previously, most multiple myeloma patients with an intact immunoglobulin in the serum produce excess monoclonal free light chains. In these patients, the urine may reveal (i) monoclonal free kappa or lambda light chains, (ii) a monoclonal free kappa or lambda light chain and a smaller amount of intact monoclonal immunoglobulin (Fig. 15), and (iii) in the case of biclonal gammopathies, both monoclonal free kappa and free lambda light chains with or without intact monoclonal immunoglobulin(s) (Fig. 16). A small amount of monoclonal free light chain in the presence of nephrotic-range proteinuria due mainly to albumin is consistent with AL or light chain disposition disease (26). In 2 to 3% of patients with multiple myeloma, no monoclonal protein is detected by serum or urine immunofixation. Serum free kappa and free lambda light chain measurement by immunoassay has been found to be useful in these "nonsecretory" or "oligosecretory" cases. This assay may also provide a viable alternative to 24-h urine collections and follow-up of patients with light chain multiple myeloma (25).

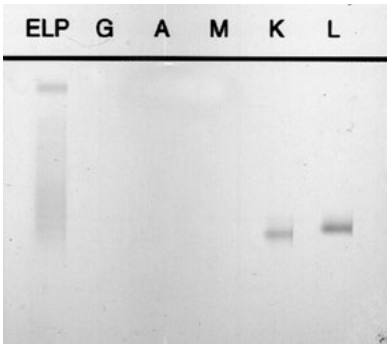

FIGURE 16 IFE of a concentrated urine specimen demonstrating a free kappa and a free lambda monoclonal protein in a patient with IgA kappa and IgA lambda monoclonal proteins detected on serum IFE.

If a monoclonal protein is found in the urine and a serum evaluation for monoclonal proteins has not been requested, then a serum evaluation should be recommended and vice versa. Quality control procedures for urine are similar to those described for serum except that the method used for urine concentration should be checked periodically to confirm that the total amount of protein expected is the amount recovered following concentration.

CEREBROSPINAL FLUID

The immunochemical characterization of immunoglobulins in the CSF is affected by the much smaller amount of proteins present in the CSF than in serum and the integrity of the blood-brain barrier. Adults typically have approximately 1/100th to 1/200th the amount of proteins in the CSF as there is in the serum. In evaluating patients for disorders associated with increased immunoglobulins in the CSF, an assessment as to whether the immunoglobulin increase is due to leakage of plasma proteins across a compromised blood-brain barrier or whether the increase is due to intrathecal production of immunoglobulins must be made. The pattern due to leakage of plasma proteins across the blood-brain barrier mimics that seen in serum whether it is polyclonal, oligoclonal, or monoclonal in nature. Because immunoglobulin-producing cells in the CSF tend to be more restricted in their heterogeneity than in serum, the pattern of immunoglobulin increase seen in disorders primarily affecting the central nervous system (CNS) tends to be oligoclonal. This is why it is important to evaluate any increase in immunoglobulins in the CSF with a corresponding serum collected at the same time.

The most common reason for evaluating immunoglobulins in the CSF is as an aid in the diagnosis of multiple sclerosis (MS). The CSF laboratory tests recommended by the National Multiple Sclerosis Society are the qualitative evaluation of oligoclonal banding and an increased CSF IgG index, both signs of increased intrathecal synthesis of immunoglobulins. In the past, high-resolution agarose gel electrophoresis (AGE) with protein staining was widely used to evaluate patients for oligoclonal banding in the CSF. Since 2003, based on a study by Fortini et al. (27), the National Multiple Sclerosis Society has recommended the use of isoelectric focusing with IgG immunoblotting over AGE for the evaluation of oligoclonal banding in CSF. Recent CAP surveys (2015) indicate that nearly 55% (77/141) of participants use isoelectric focusing as opposed to high-resolution AGE for detection of oligoclonal banding. Oligoclonal banding is detected in 60% of MS patients by high-resolution AGE and 90% of MS patients using isoelectric focusing with IgG immunoblotting with similar specificities (94% and 96%, respectively).

The finding of oligoclonal banding in other inflammatory diseases of the CNS, such as neurosyphilis, acute inflammatory polyradiculoneuropathy, Guillain-Barré syndrome, subacute sclerosing panencephalitis, viral encephalitis, CNS Lyme disease, transverse myelitis, and some fungal and parasitic encephalopathies, accounts for the decreased specificity (8). Therefore, the presence of oligoclonal banding for the diagnosis of MS must be interpreted in the appropriate clinical and radiological setting.

Laboratory Investigation

The Helena method uses isoelectric focusing on agarose gels with a pH gradient of 3 to 10. Five microliters of serum diluted 60-fold and 5 μl of CSF are applied to the gel. After electrophoresis, the separated proteins are transferred to a nitrocellulose membrane and blotted with an anti-IgG

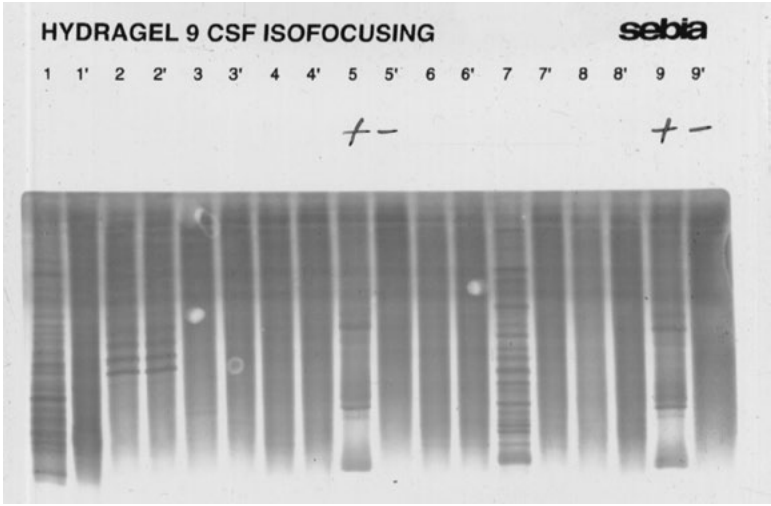

FIGURE 17 Seven paired CSF (lanes 1 to 4 and 6 to 8) and serum (lanes 1′ to 4′ and 6′ to 8′) specimens along with two positive CSF controls (lanes 5 and 9) and two negative CSF controls (lanes 5′ and 9′) were subjected to IEF for the detection of oligoclonal bands. The patient specimens in lanes 1 and 1′ and 7 and 7′ reveal oligoclonal bands consistent with MS. The pattern for the patient in lanes 2 and 2′ are consistent with the presence of a monoclonal protein (posttranslational changes account for the multiple monoclonal protein bands seen with IEF). The patterns in lanes 3 and 3′ have faint bands appearing in both the CSF and serum specimens; this is nondiagnostic. The patterns in lanes 4 and 4′ and 8 and 8′ are normal.

peroxidase conjugate for visualization. The IEF method developed by Sebia is similar except that visualization of bands is achieved by immunofixation. Oligoclonal bands are considered to be present if two or more bands are detected in the CSF but are not detected in the corresponding serum. Most patients with MS will have eight or more CSF-specific bands by this technique. Isoelectric focusing (Fig. 17) results in a greater number bands that are sharper, more distinct, and easier to interpret than those seen with agarose gel electrophoresis. Nondiagnostic patterns include (i) no bands present in paired CSF and serum samples, (ii) oligoclonal banding in the CSF, which is mirrored in the serum, (iii) a monoclonal band present in paired CSF and serum samples, or (iv) a single band seen in the CSF regardless of the serum pattern.

The IgG index, on the other hand, is based on a calculation using measured serum and CSF albumin and IgG. The equation is as follows:

$$\text{IgG index} = \frac{(\text{IgG})_{\text{CSF}}/(\text{IgG})_{\text{serum}}}{(\text{albumin})_{\text{CSF}}/(\text{albumin})_{\text{serum}}}$$

An IgG index of greater than or equal to 0.70 is considered to be consistent with MS. Ninety percent of MS patients have an elevated IgG index. Although neither test is specific for MS, the use of both the IgG index and oligoclonal banding increases the sensitivity to 90 to 95% (28).

As with all laboratory testing, quality control is essential. Every gel should contain a positive and negative CSF control sample with a known number of bands. The gel is acceptable if band resolution, separation, and staining allow identification of the appropriate number of bands. The number of bands detected in the controls should be none in the case of the negative control and within one band of the target for the positive control. All gels should be read independently by two readers. If the two readers do not agree on the test interpretation, then a third reader should be consulted. Proficiency testing should be performed by all members involved in the testing and interpretation of these gels on a periodic basis.

REFERENCES

1. **Schroeder HW, Cavacini L.** 2010. Structure and function of immunoglobulins. *J Allergy Clin Immunol* **125:**S41–S52.
2. **Solomon, A.** 1976. Bence Jones proteins and light chains of immunoglobulins. *N Engl J Med* **294:**17–23.
3. **Solomon, A.** 1985. Light chains of human immunoglobulins. *Methods Enzymol* **116:**101–121.
4. **Alexanian R, Weber D, Liu F.** 1999. Differential diagnosis of monoclonal gammopathies. *Arch Pathol Lab Med* **123:**108–113.
5. **Katzmann JA, Kyle RA.** 2006. Immunochemical characterization of immunoglobulins in serum, urine, and cerebrospinal fluid, p 89. *In* Detrick B, Hamilton RG, Folds JD (ed), *Manual of Molecular and Clinical Laboratory Immunology*, 7th ed. ASM Press, Washington, DC.
6. **Kyle RA, Gertz MA, Witzig TE, Lust JA, Lacy MQ, Dispenzieri A, Fonseca R, Rajkumar SV, Offord JR, Larson DR, Plevak ME, Therneau TM, Greipp PR.** 2003. Review of 1027 patients with newly-diagnosed multiple myeloma. *Mayo Clin Proc* **78:**21–33.
7. **Katzmann JA, Kyle RA, Benson J, Larson DR, Snyder MR, Lust JA, Rajkumar SV, Dispenzieri A.** 2009. Screening panels for detection of monoclonal gammopathies. *Clin Chem* **55:**1517–1522.
8. **Keren DF.** 2012. *Protein Electrophoresis in Clinical Diagnosis*. ASCP Press, Chicago, IL.
9. **Litwin CM, Anderson SK, Philipps G, Martins TB, Jaskowski TD, Hill HR.** 1999. Comparison of capillary zone and immunosubtraction with agarose gel and immunofixation electrophoresis for detecting and identifying monoclonal gammopathies. *Am J Clin Pathol* **112:**411–417.
10. **Yang Z, Harrison K, Park YA, Chaffin CH, Thigpen B, Easley PL, Smith JA, Robinson A, Lorenz RG, Hardy RW.** 2007. Performance of the Sebia Capillarys 2 for

detection and immunotyping of serum monoclonal paraproteins. *Am J Clin Pathol* **128:**293–299.
11. **Poisson J, Fedoriw Y, Henderson MPA, Hainsworth S, Tucker K, Uddin Z, McCudden CR.** 2012. Performance evaluation of the Helena V8 capillary electrophoresis system. *Clin Biochem* **45:**697–699.
12. **Schild C, Egger F, Kaelin-Lang A, Nuoffer JM.** 2011. Monoclonal gammopathy missed by capillary zone electrophoresis. *Clin Chem Lab Med* **49:**1217–1219.
13. **Therneau TM, Kyle RA, Melton J, Larson DR, Benson JT, Colby CL, Dispenzieri A, Kumar S, Katzmann JA, Cerhan JR, Rajkumar SV.** 2012. Incidence of monoclonal gammopathy of undetermined significance and estimation of duration before first clinical recognition. *Mayo Clin Proc* **87:**1071–1079.
14. **Kyle RA, Rajkumar SV.** 2005. Monoclonal gammopathy of undetermined significance. *Clin Lymphoma* **6:**102–114.
15. **Kyle RA, Robinson RA, Katzmann JA.** 1981. The clinical aspects of biclonal gammopathies. Review of 57 cases. *Am J Med* **71:**999–1008.
16. **Rajkumar SV, Dimopoulos MA, Palumbo A, Blade J, Merlini G, Mateos M-V, Kumar S, Hillengass J, Kastritis E, Richardson P, Landgren O, Paiva B, Dispenzieri A, Weiss B, LeLeu X, Zweegman S, Lonial S, Rosinol L, Zamagni E, Jagannath S, Sezer O, Kristinsson SY, Caers J, Usmani SZ, Lahuerta JJ, Johnsen HE, Beksac M, Cavo M, Goldschmidt H, Terpos E, Kyle RA, Anderson KC, Durie BGM, San Miguel JF.** 2014. International myeloma working group updated criteria for the diagnosis of myeloma. *Lancet Oncol* **15:**e538–548.
17. **Dreicer R, Alexanian R.** 1982. Nonsecretory multiple myeloma. *Am J Hematol* **13:**313–318.
18. **Rubio-Felix D, Giralt M, Giraldo MP, Martinez-Penuela JM, Oyarzabal F, Sala F, Raichs A.** 1987. Nonsecretory multiple myeloma. *Cancer* **59:**1847–1852.
19. **Rajkumar SV, Kyle RA, Buadi FK.** 2010. Advances in the diagnosis, risk stratification and management of monoclonal gammopathy of undetermined significance: implications for recategorizing disease entities in the presence of evolving scientific evidence. *Mayo Clin Proc* **85:** 945–948.
20. **Wahner-Roedler DL, Witzig TE, Loehrer LL, Kyle RA.** 2003. γ Heavy chain disease. Review of 23 cases. *Medicine* **82:**236–250.
21. **Luraschi P, Infusino I, Zorzoli I, Merlini G, Fundaro C, Franzini C.** 2005. Heavy chain disease can be detected by capillary zone electrophoresis. *Clin Chem* **51:**247–249.
22. **Konstaninopoulos PA, Dezube BJ, Pantanowitz L, Horowitz GL, Beckwith BA.** 2007. Protein electrophoresis and immunoglobulin analysis in HIV-infected patients. *Am J Clin Pathol* **128:**596–603.
23. **van der Watt G.** 2005. Pseudoparaproteinemia after iopamidol infusion for coronary angiography. *Clin Chem* **51:**273–274.
24. **Vermeersch P, Marien G, Bossuyt X.** 2006. Pseudoparaproteinemia related to iomeprol administration after angiocardiography: detection in the beta fraction by capillary zone electrophoresis. *Clin Chem* **52:**2312–2313.
25. **Dispenzieri A, Kyle R, Merlini G, Miguel JS, Ludwig H, Hajek R, Palumbo A, Jagannath S, Blade J, Lonial S, Dimopoulos M, Comenzo R, Einsele H, Barlogie B, Anderson K, Gertz M, Harousseau L, Attal M, Tosi P, Sonneveld P, Boccadoro M, Morgan G, Richardson P, Sezer O, Mateos MV, Cavo M, Joshua D, Turesson I, Chen W, Shimizu K, Powles R, Rajkumar SV, Durie BGM.** 2009. International myeloma working group guidelines for serum-free light chain analysis in multiple myeloma and related disorders. *Leukemia* **23:**215–224.
26. **Kyle RA, Gertz MA.** 1995. Primary systemic amyloidosis: clinical and laboratory features in 474 cases. *Semin Haematol* **32:**45–59.
27. **Fortini AS, Sanders EL, Weinshenker BG, Katzmann JA.** 2003. Cerebrospinal fluid oligoclonal bands in the diagnosis of multiple sclerosis. Isoelectric focusing with IgG immunoblotting compared with high-resolution agarose gel electrophoresis and cerebrospinal fluid IgG index. *Am J Clin Pathol* **120:**672–675.
28. **Lunding J, Midgard R, Vedeler CA.** 2000. Oligoclonal bands in cerebrospinal fluid: a comparative study of isoelectric focusing, agarose gel electrophoresis, and IgG index. *Acta Neurol Scand* **102:**322–325.

Cryoglobulins, Cryofibrinogenemia, and Pyroglobulins

PETER D. GOREVIC AND DENNIS GALANAKIS

10

CRYOGLOBULINS

Background

Cryoglobulinemia is one of a group of syndromes characterized by the induction of clinical and/or laboratory abnormalities by cold. Cryoglobulins are immunoglobulins (Igs) that precipitate out of solution below core body temperatures, either as a single isotype (simple cryoglobulins) or as immune complexes in which both antibody and antigen are Igs (mixed cryoglobulins). In some instances, cryoglobulinemia may coexist with other related but usually distinct forms of cold hypersensitivity, such as Raynaud's phenomenon, cold agglutinin activity, or cold-dependent activation of complement (CDAC) (1).

Simple cryoglobulins may be either an intact Ig or a cryoprecipitable Ig light chain (type I cryoglobulins) and are always clonal in terms of electrophoretic mobility or variable-region amino acid sequence. In mixed cryoglobulins, the antibody is almost always IgM (occasionally IgA), which may be monoclonal (type II) or polyclonal (type III) (2). The antigen in mixed cryoglobulins is usually polyclonal IgG, though in some instances, the IgG may be oligoclonal when analyzed as to subclass or as revealed by immunoblotting, immunofixation, or two-dimensional gel electrophoresis (3, 4). Mixed cryoglobulins are therefore cold-precipitable rheumatoid factors (RFs), with the serum often being positive when standard assays for IgM antiglobulin activity are used (5, 6). Many type II RFs have a predilection for the Cγ2-Cγ3 interface of the Fc portion of IgG and react with the binding site for staphylococcal protein A. Complexing of the two isotypes of Igs in mixed cryoglobulins is a prerequisite for *in vitro* cryoprecipitation. The binding affinity of the IgM RF and the stoichiometry of complexes formed by mixed cryoglobulins are significantly influenced by temperature (7). The relative frequency of the different types of cryoglobulins seen in a clinical immunology laboratory will vary significantly with the type of diseases referred for analysis and depending on how carefully sera are processed prior to study. The latter is particularly of concern in screening for type III cryoglobulins, which are generally present only at low levels and may require larger-than-normal volumes of serum for analysis (Table 1).

Concept

The decision to test a serum sample for cryoglobulins may be based on the knowledge that the patient has a specific known or suspected disease, be dictated by the evaluation of a particular clinical manifestation, or be carried out to clarify other abnormalities that have been uncovered in the course of a laboratory evaluation for another purpose. Type I cryoglobulinemia may be suspected in the presence of a known plasma cell dyscrasia (e.g., multiple myeloma, macroglobulinemia), immunochemical evidence of a monoclonal immunoglobulin (M-spike) or Ig light chain (Bence-Jones protein) in serum and/or urine, or clinical evidence of hyperviscosity, acrocyanosis, severe Raynaud's phenomenon, or ischemic vasculopathy. Type II cryoglobulinemia should be considered in B-cell neoplastic states that may be associated with RF and other autoimmune phenomena, in Sjögren's syndrome, and in chronic inflammatory liver diseases, particularly due to infection by hepatitis C virus (HCV) (1). Type III cryoglobulins have been associated with a wide variety of chronic infectious and autoimmune diseases, many of which are characterized by hyperimmunization and/or hyperglobulinemia. The presence of mixed cryoglobulins may be suggested by purpura or documented cutaneous vasculitis, clinical findings of or biopsy-proven glomerulonephritis, unexplained neuropathy or hepatitis, serum positive for RF, or markedly depressed C4 levels (1–3) (Table 2).

Other laboratory abnormalities may be consequences of the physicochemical properties of the cryoglobulins or reflect polyclonal B-cell activation or clonal B-cell proliferation often associated with these disorders. Since cryoprecipitation does not occur at core body temperatures and may begin within minutes of the cooling of serum, it is especially important to consider *ex vivo* artifacts in the interpretation of laboratory data in patients affected by these syndromes. The most important of these is the handling of the serum before separation (8), which can significantly affect quantitation, especially when the endpoint is to assess the effect of therapy by comparison of serial specimens. Others may be introduced in the handling of biopsy specimens, in measurements of serum viscosity (9), or by cooling of anticoagulated blood in processing for the Coulter counter (Table 3). The first clinical description of cryoglobulinemia in a patient with multiple myeloma in 1933 by Wintrobe (32) was based on the

doi:10.1128/9781555818722.ch10

TABLE 1 Classification of cryoglobulins[a]

Type	Frequency	% at a concn (mg/ml) of:		
		>1	1–5	>5
Simple (type I)	5–38	10	30	60
IgG, IgM, or IgA				
Ig light chain				
Mixed				
Monoclonal (type II)	14–72	20	40	40
Polyclonal (type III)	23–54	80	20	0

[a]From reference 2.

recognition of an apparently copious buffy coat fraction in an individual known to be cytopenic due to bone marrow replacement. In more recent experience, failure to recognize pseudoleukocytosis or pseudothrombocytosis due to a high-thermal-amplitude cryoglobulin during treatment with cytotoxic agents can significantly compromise care (10) (Fig. 1).

Procedures

Proper handling of blood samples is the single most important variable determining the success rate for identifying cryoglobulinemia and the most difficult to achieve. In the authors' experience, the best results have been obtained when the screen for cryoprecipitation is carried out by the individual in direct contact with the patient (i.e., the physician, house staff, or technician) and when proper attention is made to the importance of separating serum at 37°C from whole blood. Although less sensitive and specific than other tests for gammopathy or immune-complex disease, analysis of serum for cryoprecipitation has the advantage of simplicity, requiring minimal equipment, and is therefore very cost-efficient. It is also an excellent teaching instrument for students and other trainees, as all that is required is a "warm heart" (to keep the sample close to core body temperature and minimize *ex vivo* cryoprecipitation before separation), a refrigerator (in which to observe the sample overnight), and a source of warm running water (to prove that any precipitate that forms can be redissolved upon warming). Since cryoglobulins often come out of solution within 24 to 48 h, many sera can be efficiently screened within 1 to 2 days of collection, allowing the clinician to rapidly make further decisions regarding additional work-up.

Isolation, Quantitation, and Characterization of Cryoglobulins

1. Collect 10 to 20 ml of blood (2 red-top tubes) and keep them at 37°C for 30 to 60 min prior to separation. To ensure that cryoprecipitation does not occur *ex vivo*, the blood may be placed in a thermos kept at this temperature or put into a 37°C water bath prior to centrifugation (8). Patients previously found to have high levels of cryoglobulin may require lower volumes for serial studies, and those suspected of having type III cryoglobulins may require larger volumes for analysis. Occasionally, gel formation in the syringe or vacutainer tube may occur as the initial manifestation of cryoprecipitation (see also below). Serum is separated from the clot by centrifuging the specimen with warmth for 10 min at 2,500 rpm. Following separation, it should be carefully inspected for lipemia, which may complicate the visual inspection of the sample for cryoprecipitation over the several hours following collection. Serum thus collected antiseptically, or to which a drop of 0.1-g/liter sodium azide is added to prevent bacterial overgrowth, may be safely sent by overnight mail (even at room temperature) to a reference laboratory for detailed characterization.

2. Cryoglobulins are grossly apparent upon visual inspection down to the range of 50 to 100 μg/ml, depending on the volume of the serum sample submitted for analysis. Type I cryoglobulins are often apparent as flocculent, occasionally crystalline precipitates that are usually observed within 24 h of separation. Cryocrystalglobulins can be characterized as dense structured inclusions by light microscopy using Giemsa or hematoxylin and eosin stains, as extracellular material by electron microscopy using osmium and uranyl acetate stains, or as non-Congo red-binding birefringence visualized by polarizing microscopy. Type III cryoglobulins are usually gelatinous and may take up to a week to be fully apparent. Consequently, serum samples are observed at 4°C for 7 days after collection. This analysis may be facilitated by measurement of turbidity (e.g., using a jacketed spectrophotometer cuvette at 630 nm) at 15-min intervals, by cryoprecipitation from hypotonic media, or by flow cytometry for small diffracting particles (11). The kinetics of cryoprecipitation are variable, depending on the individual sample and the concentration of cryoglobulin present (12). This may reflect in part different mechanisms for cryoprecipitation, including lag periods overcome by nucleation events (2, 12). We have observed little variability when the kinetics of cryoprecipitation of serum, plasma, or isolated cryoglobulins have been compared by turbidimetric analysis (Fig. 2).

3. Positive sera are spun down in a refrigerated (4°C) centrifuge (Sorvall) at 3,000 rpm for 15 min and their supernatants removed for further analysis. The pellet is vortexed six times with 5 to 10 ml of ice-cold 0.15 M saline, each time with the precipitate spun for 15 min at 3,000 rpm; contaminating red blood cells may be lysed hypotonically. Finally, the sample is suspended in warm saline (1/10 to 1 volume of the initial serum) and incubated at 37°C for 1 h.

TABLE 2 Disease, clinical,[a] and laboratory associations

Type	Association(s) with:		
	Diseases[b]	Clinical syndromes	Laboratory manifestations
I	Macroglobulinemia, myeloma, idiopathic manifestations	Necrosis, Reynaud's syndrome, acrocyanosis	M-spike, increase in viscosity, cryocrystals
II	HCV infection, Sjögren's syndrome, CLL, lymphoma, macroglobulinemia	Purpura, neuropathy, keratoconjunctivitis	RF, nephritis, hepatitis, decrease in C4
III	Chronic infections, autoimmune disease	Vasculitis	RF, nephritis

[a]Reversible cyanosis of the helices of the ears and livedoid vasculitis are characteristics of IgG type I cryoglobulinemia, whereas purpura due to leukocytoclastic angiitis is characteristic of type II IgM(k)-IgG cryoglobulins.
[b]Idiopathic, no apparent underlying disease; CLL, chronic lymphocytic leukemia.

TABLE 3 Laboratory abnormalities in cryoglobulinemia

Findings and abnormality
Direct effects
Cryoprecipitation
Cryogel formation
Cryocrystalglobulins
Hyperviscosity
Present only with cooling
Accentuated by cooling
Immunochemical findings
Normal (frequent with type III)
Hyperglobulinemia
Diffuse elevation or M-spike on serum protein electrophoresis (SPEP)
Elevation of a specific isotype (IgG, IgA, or IgM) or subclass (type I)
Increased high (19S)- and low (7S)-molecular-weight IgM (type II)
Skewing of the normal (2/1) kappa/lambda ratio of Ig light chains (types I and II)
Hypoglobulinemia
Diffuse (occasionally with type II)
Noncryoglobulin isotypes (type I)
Clonal markers of B cells
Monoclonal gammopathy
Clonal populations of B cells revealed by surface Ig
Peripheral blood (heavy- and light-chain determinants)
Lymphoid aggregates in bone marrow (type II)
Evidence of Ig gene rearrangement
Antibody activity and immune-complex formation
19S IgM antiglobulins (RFs) (types II and III)
IgA (type II) or IgG (type I) RF
Elevated levels of circulating immune complexes, especially assays based on C1q binding activity
Antinuclear antibodies
Antiviral antibodies (Epstein-Barr virus, HBV, HCV)
Hypocomplementemia
Classical- or alternative-pathway activation as a manifestation of specific diseases (e.g., lupus)
In vivo/*ex vivo* activation by cryoprecipitates
Selective depression of C4
Cold-dependent activation independent of cryoprecipitation
Ex vivo artifacts (avoid by testing at 37°C)
Gelling of blood at the time of venipuncture
Increased erythrocyte sedimentation rate
Rouleaux formation of red blood cells
Pseudoleukocytosis
Pseudothrombocytosis
Pseudoerythrocytosis
Cytoplasmic inclusions in neutrophils and monocytes
Cryoprecipitation in biopsy material
Associated abnormalities
Proteinuria, hematuria, pyuria, casts
Abnormal liver function tests

Ideally, there should be complete dissolution of the precipitate with shaking. If this does not occur, the presence of fibrin or bacterial contamination should be considered; warm insoluble precipitate should be spun out at 37°C (3,000 rpm for 10 min) and the supernatant again cooled to 4°C and observed for cryoprecipitation.

4. The concentration of cryoglobulin can be determined as a cryocrit or as an absolute concentration of protein back-calculated for the initial volume of serum. Cryocrits are appropriate for serial measurements in individual patients (provided that the methodology is carefully reproduced between samples) and for the purposes of general comparison. Exact protein measurements are more accurate and can be compared to quantitation of specific Ig isotypes in serum, isolated cryoglobulins, and serum supernatant obtained following cryoprecipitation. To obtain a cryocrit, an aliquot of the initial warm serum is used to fill a disposable Wintrobe tube to the 10-mm mark. The tube is kept vertical at 4°C for the time period determined above for cryoprecipitation and then centrifuged cold at 2,000 rpm for 30 min; the percent total volume occupied by the pellet is then obtained by visual inspection. The total protein content of isolated cryoglobulin rigorously washed as described above is determined in our laboratory by the Bradford method using the bicinchoninic acid protein assay (Pierce). In some instances, repeated warming and cryoprecipitation lead to significant loss of material, and therefore quantitation is defined in terms of the initial isolation protocol for consistency.

5. Warmed dissolved cryoprecipitate is characterized by immunochemical analysis by agarose gel immunofixation electrophoresis (IFE). In addition to defining type I cryoglobulins, immunofixation may reveal the clonality of the IgM component or the oligoclonality of the IgG components of mixed cryoglobulins. Since the monoclonal components of type II cryoglobulins are almost invariably IgM(κ), the percent contribution of clonal IgM to total IgM present in a mixed cryoglobulin can be estimated by correlating the contribution of a clonal band to total immunoreactive IgM on a strip developed with anti-μ with the contribution of a band on a strip developed with anti-κ antiserum either by visual inspection or by densitometry (more-formal quantitation). Uncommon laboratory findings that may be predictive of occult and clinically significant cryoglobulinemia include a smeared M-spike in high-resolution agarose gel serum protein electrophoresis, precipitated protein at the point of serum application, >50% discrepancies between densitometric estimations of M-spike and its relevant serum Ig isotype, and smeared protein upon agarose gel IFE (13).

6. Other modalities which have been utilized include immunoblot analysis with anti-heavy- or -light-chain antisera of cryoglobulins separated under nondenaturing conditions on 4% polyacrylamide gels (which can also be used to demonstrate 7 S IgM in serum) or on composite agarose polyacrylamide gels. Immunoblotting combined with IFE can be performed on as little as 10 μg of material, can distinguish type II from type III mixed cryoglobulins, and may be particularly effective for the demonstration of the oligoclonality of each component of the complex. Another modality is two-dimensional gel electrophoresis, with the gel run under denaturing and reducing conditions in order to dissociate mixed cryoglobulins and separate Ig heavy and light chains by molecular weight and isoelectric focusing point. Two-dimensional polyacrylamide gel electrophoresis (PAGE) may be more sensitive than IFE for the demonstration of B-cell clonality in patients with cryoglobulinemia and has been combined with Fourier transform-ion cyclotron resonance mass spectrometry for the high-resolution analysis of cryoglobulin constituents (4, 14). A third modality is capillary zone electrophoresis, which has been adapted in some laboratories for the rapid characterization of cryoprecipitates. It may be particularly useful for type III cryoglobulins because of the sensitivity of the technique. Subtraction analysis of the gamma globulin curve before and after cryoprecipitation can be used as an alternative to protein and Ig determinations for quantitation (15).


A

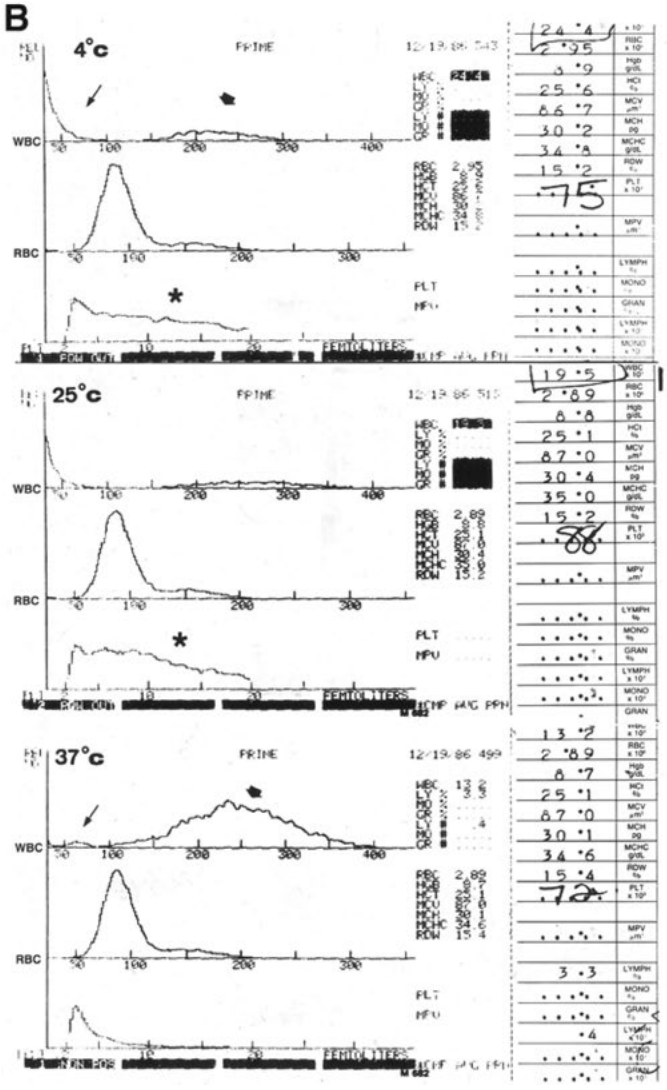
B
4°c
PRIME
25°c
PRIME
37°c
PRIME
WBC
RBC
PLT
MPV

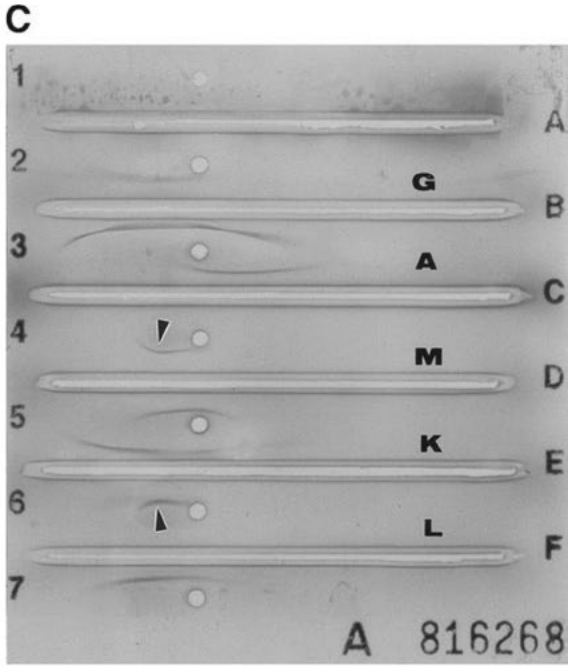
C
1
2
3
4
5
6
7
A
G
B
A
C
M
D
K
E
L
F
A 816268

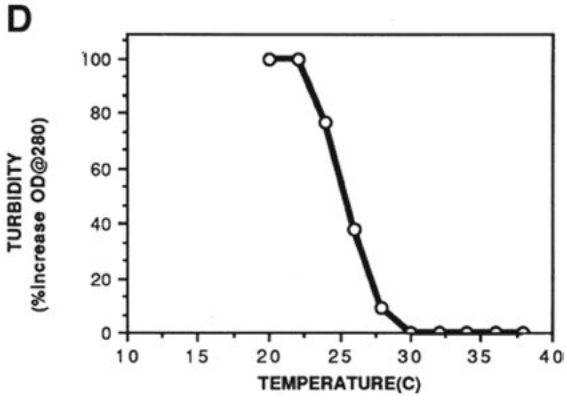
D
TURBIDITY
(%Increase OD@280)
100
80
60
40
20
0
10
15
20
25
30
35
40
TEMPERATURE(C)

7. The relative contributions of the different components of mixed cryoglobulins may be determined by nephelometry if sufficient material is available. This may be used to confirm the nature of mixed cryoglobulins and to show selective enhancement of specific antibody activity in cryoprecipitates compared to serum but is rarely of clinical significance. The power of this type of analysis has been significantly expanded in research studies through the use of capture enzyme-linked immunosorbent assays that employ both isotype- and idiotype-specific antibodies (16). Since most mixed cryoglobulins remain cryoprecipitable in the pH range 5.0 to 8.5, they can be dissociated under, e.g., acid conditions, and IgM can be separated from IgG and quantitated after ion-exchange chromatography, passage through specific immunoabsorbents (e.g., protein G columns), or size fractionation by high-pressure liquid chromatography or fast-protein liquid chromatography.

Assays for Specific Antibody Activities, Antigens, or Detection of Nucleic Acid

1. Mixed cryoglobulins contain IgM RF activity when tested by either standard assays or more-sensitive techniques (e.g., binding of radiolabeled aggregated IgG) (2). Unlike in rheumatoid arthritis, cryoglobulin RF activity, particularly in HCV-associated disease, is not associated with antibodies to cyclic citrullinated peptide. Although both cryo- and noncryoprecipitable RF activity can be detected, occasionally testing RF activity in serum may be invalid because it has been lost due to cryoprecipitation of a high-thermal-amplitude (i.e., one that rapidly cryoprecipitates above room temperature) mixed cryoglobulin (Fig. 1).

2. Individual case reports and small series have shown enrichment of a number of specific antibody activities, including binding to antigens such as IgG or HCV recombinant proteins, in cryoglobulins associated with specific disease states. Most of these antibodies (e.g., HCV antibodies [HCVAbs]) are associated with the IgG fraction of mixed cryoglobulins and can be quantitated by enzyme-linked immunosorbent assay, which should be normalized for total IgG quantitated in cryoglobulin relative to serum (16, 17). In some instances, we have found that a specific antibody activity was in fact not concentrated in the isolated cryoglobulin, as was the case for a patient with a type 1 IgG(κ) cryoglobulin without intrinsic HCVAb activity who developed HCV infection during the course of his illness.

3. The nature of mixed cryoglobulins as immune complexes in chronic infection by hepatitis B virus (HBV) and HCV is indicated by reports of selective enrichment of both antigens (e.g., HBV surface and HCV core antigens) and specific antibody activity in some isolated cryoprecipitates (16–18). Current experience is that 60 to 80% of type II cryoglobulins in patients with the syndrome of mixed cryoglobulinemia (purpura, arthralgias, renal disease) are associated with evidence of HCV infection, as assessed by anti-HCV antibody activity and/or amplification of specific nucleic acid using PCR following reverse transcription (RT). In our laboratory, HCVAb activity is assessed by recombinant immunoblot assay (RIBA) and the presence of HCV RNA determined initially by RT-PCR using nested primers framing conserved sequences in the 5′ untranslated region of the viral genome. RIBA for HCVAb measures primarily IgG antibody to HCV antigens. Controls include known positive and RF-positive HCVAb-negative sera; RT-PCR is also carried out with positive and negative samples, with care taken to control for carryover contamination. More accurate assessment of HCV copy number can be determined by commercially available quantitative assays, including those using competitive PCR (e.g., the Roche Amplicor system) or direct capture of viral RNA by complementary branched DNA (Chiron). Lower limits of detection for these assays are 600 and 615 IU/ml HCV RNA, respectively. Quantitative assays may be used to demonstrate selective enrichment of HCV RNA in cryoprecipitates (reported as being more frequent than enrichment of HCVAb), in some instances when serum supernatant is negative or below the level of detection of the particular assay, and to follow the clinical course and the effect of therapy with alpha interferon (IFN-α) (19). HCV genotype analysis is commercially available and may be used as one variable to anticipate the efficacy of therapy with IFN-α; however, its value for the evaluation of mixed cryoglobulinemia and other autoimmune manifestations of chronic infection is uncertain.

New HCV assays are likely to enhance the sensitivity and specificity of measurements of cryoglobulins associated with extrahepatic diseases associated with chronic infection. These include the quantitation of hepatitis core antigen (18) and real-time PCR assays for HCV RNA and the replicative intermediate (negative strand) (20). The former may be assayed by enzyme-linked immunosorbent assay (Chiron-Ortho Clinical Diagnostics) and has been found to be concentrated in isolated cryoprecipitates (18) and peripheral blood mononuclear cells; the latter may be a more sensitive marker for occult HCV infection in cryoglobulinemia (21) and a criterion for productive infection by virus in extrahepatic sites.

Complement Measurements in Cryoglobulinemia

Sera from type II mixed-cryoglobulinemia patients typically have low antigenic levels of the early components of complement, with relatively normal levels of C3 and factor B (6). Measurements are best made at 37°C in order to minimize artifacts introduced by *ex vivo* cryoprecipitation or activation by other complexes that may occur over time at 4°C. Serial studies have shown that hypocomplementemia

FIGURE 1 (A) Cryoglobulinemia was initially missed in a patient with cutaneous vasculitis documented by biopsy of a purpuric lesion on the right second digit (left). Because of deteriorating status, including renal failure, she was treated with high doses of steroids and then cytotoxic agents, with an apparently poor response in terms of an expected drop in white blood cell (WBC) counts. One weekend, while still in the intensive care unit, she was noted to have developed nasal purpura in the distribution of a cold-air oxygen mask (right). (B) The Coulter histograms obtained at 4°C, 25°C, and 37°C each display the leukocyte (top), erythrocyte (middle), and platelet (bottom) panels. The leukocyte panel shows small lymphocytes to the left (thin arrow) and larger polymorphonuclear leukocytes and monocytes to the right (thick arrow), with the ordinate displaying percentages of total cells; the platelet panels at 4°C and 25°C are unusual in having a long tail (*) after the expected narrow peak. Pseudoleukocytosis and pseudothrombocytosis are revealed at 37°C, which shows (i) all the leukocytes to be polymorphonuclear, with few lymphocytes, as expected in a patient on high-dose corticosteroids, and (ii) a narrow platelet peak. Both findings are reflected in the manual counts (right). Recognition of this artifact led to identification of a type II cryoglobulin with RF activity, with restricted IgM and kappa arcs by immunoelectrophoresis (C, arrowheads) and a high thermal amplitude of cryoprecipitation (D). OD@280, optical density at 280 nm.

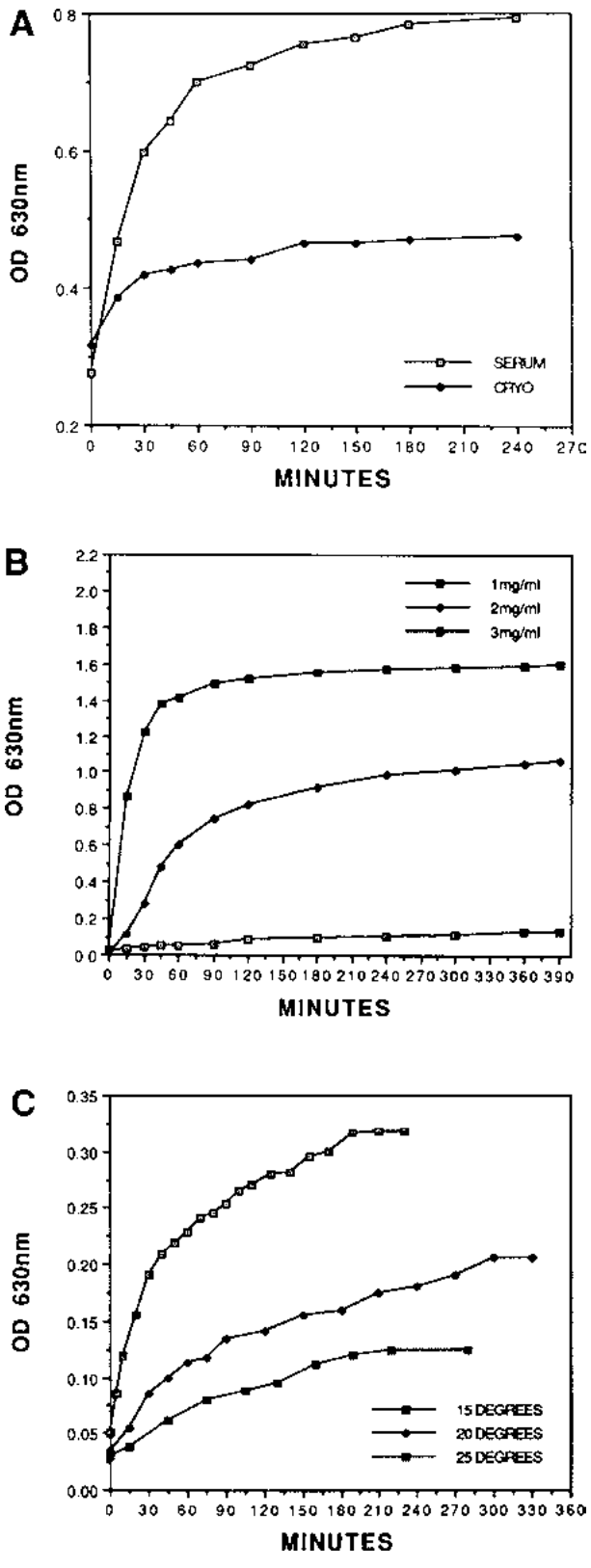

FIGURE 2 Kinetics of cryoprecipitation, assessed by turbimetric analysis, for a type II cryoglobulin, comparing serum and isolated cryoglobulin (A), different concentrations of isolated cryoglobulin (B), and different temperatures of cryoprecipitation (C). OD, optical density.

correlates only poorly with cryoglobulin levels. Most patients with type I cryoglobulinemia have normal complement levels, though occasional instances in which complement activation occurs and has been shown to be directly due to cryoprecipitate formation have been well described. In type III cryoglobulinemia, complement measurements may reflect abnormalities prevalent in the underlying disease (e.g., lupus erythematosus) or among the subset of patients predisposed to develop cryoglobulinemia (e.g., rheumatoid vasculitis, primary Sjögren's syndrome).

In sera manifesting CDAC, a similar profile of low CH_{50} and hemolytic C4 with normal hemolytic C5 to C9 is seen at 4°C, with normal values being obtained in EDTA-treated plasma and in serum kept at 37°C (the CH_{50} measures the total hemolytic activity of a test sample and is the reciprocal of the dilution of serum complement needed to lyse 50% of a standardized suspension of sheep erythrocytes coated with antierythrocyte antibody). Unlike in cryoglobulinemia, C1q and C4 antigenic levels are normal. CDAC may be a consequence of HCV antibody-monoclonal rheumatoid factor (mRF) complexes with differing stoichiometries, may be present in sera that do not contain detectable cryoprecipitates, and appears to correlate somewhat with liver damage and response to treatment with IFN-α (22). CDAC, RF, cryoglobulinemia, and elevated levels of IgM-containing immune complexes are all prevalent in HCV infection.

Conclusions

Although many clinical laboratories offer cryoglobulin determinations, rarely is testing rigorously carried out, and there is considerable interlaboratory variability (23). The most common sources of error are (i) false-negative results due to loss of cryoprecipitate during storage and (ii) false-positive results, usually due to residual fibrin in the sample, and failure to demonstrate redissolution of material with warming. In most instances, cryoglobulins are readily apparent by visual inspection of the specimen at 1 to 3 days. Many have thermal amplitudes characterized by 10^3- to 10^4-fold decreases in solubility occurring over a relatively restricted (<10°C) temperature range, which may be significantly influenced by the level of cryoprotein in the sample. Detailed characterization can be achieved using standard immunochemical techniques modified to be carried out above the temperature of cryoprecipitation.

CRYOFIBRINOGENEMIA

Background

The term "cryofibrinogenemia" denotes a circulating fraction of plasma that precipitates on incubation at refrigeration temperatures. The presence and/or increased levels of such a precipitate are associated with thromboembolic disease, chronic inflammation, malignancy, and occasionally connective tissue diseases, including cold-sensitive vasculitis (i.e., involving mostly exposed skin areas). A more accurate description of the origin of increased levels of plasma cryoprepreciptate might be hyperfibrinemia, since it reflects increased levels of soluble fibrin. In the presence of circulating fibrinogen, excess fibrin remains soluble by forming fibrinogen-fibrin complexes. Plasma cryoprecipitate typically redissolves at higher temperatures (e.g., 37°C). Its harvesting can be maximized by freezing plasma and thawing it at 4°C overnight, the standard procedure for manufacturing plasma cryoprecipitate for therapeutic infusion. It contains, in addition, major amounts of fibronectin, in and of itself a cryoprecipitable protein (Fig. 3). For precise quantitation,

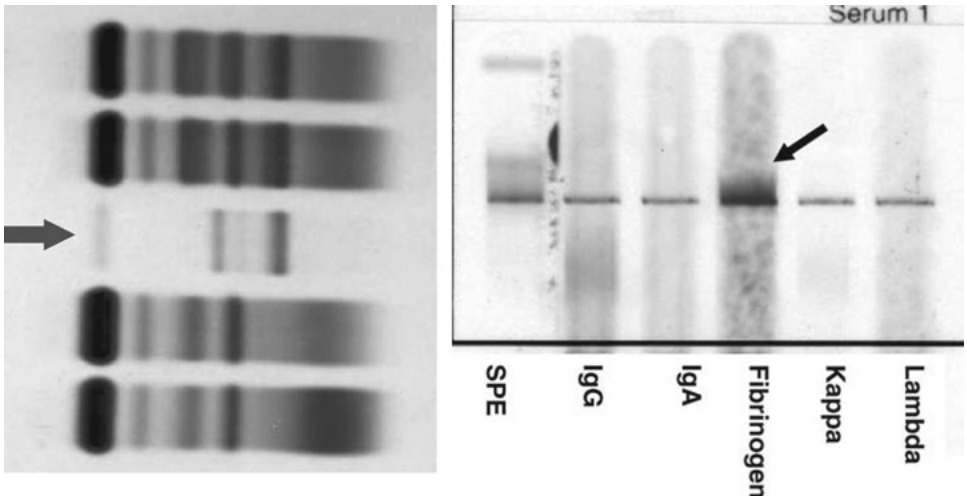

FIGURE 3 Isolated washed cryofibrinogen (arrows) visualized by agarose gel electrophoresis (left) and immunofixation (right). Gel electrophoresis reveals some residual albumin toward the anode, fibronectin in the beta region, an origin artifact, and fibrinogen, compared to serum samples in the upper and lower lanes. In the immunofixation on the right, an origin artifact is seen in all lanes due to precipitation on the cold gel. However, the antifibrinogen lane shows increased precipitate, thereby characterizing this as fibrinogen. SPE, serum protein electrophoresis. Courtesy of D. Keren, reproduced with permission.

the cryoprecipitate can be washed several or more times in cold buffer, such as phosphate-buffered saline, pH 6.4, redissolved at 37°C, and measured in a spectrophotometer at 280 nm. In summary, cryofibrinogenemia denotes circulating cold-precipitable complexes consisting of fibrin and fibrinogen which also contain fibronectin as the only other major constituent. Trace proteins, such as von Willebrand factor, factor VIII, and others, coprecipitate with these complexes. This precipitate may occur (i) when blood drawing is slow, allowing *ex vivo* thrombin generation that increases the level of soluble fibrin (24), (ii) in any disease in which increased levels of soluble fibrin occur (e.g., intravascular coagulation, sepsis, inflammation, cancer, thrombophilia), or (iii) in plasma obtained by use of plasmapheresis equipment, owing to prolonged extravascular exposure of blood.

Testing Considerations

The decision to test plasma for cryofibrinogenemia may be suggested by a variety of disorders. Some examples include purpura, particularly occurring on exposed skin associated with intolerance to cold temperatures, cold-induced urticaria, Raynaud's phenomenon, and evidence of thrombotic vasculopathy that cannot be explained by antiphospholipid autoantibodies or qualitative or quantitative clotting factor deficiencies. The test for cryofibrinogenemia may be part of a more general evaluation for causes of purpura, disseminated thrombohemorrhagic coagulopathy, other thromboembolic disorders, skin necrosis, chronic leg ulcers, or gangrene. Cryofibrinogenemia may be associated with neoplastic states and IgA nephropathy and is rarely familial; it has also been described in the absence of clear-cut underlying disease and in about 3% of random blood samples from hospitalized patients or asymptomatic healthy blood donors (25).

Examples of Cryofibrinogenemia

Case 1

A 14-year-old girl was evaluated for cold-sensitive vasculitic purpura, mainly of the extremities. The condition had become so severe that she required home tutoring throughout the year to avoid cold exposure. Her condition was followed by measuring her plasma "cryocrit," the column of insoluble material formed when citrated plasma was incubated at 4°C and centrifuged. This value rose markedly during exacerbations of her disease and decreased following each plasmapheresis treatment. Cryoprecipitate that formed when plasma was frozen and thawed at 4°C was also measured as another indicator of cryoprecipitable plasma protein. Relative to those of normal donors and to other patient plasma samples with similarly elevated fibrinogen levels, her cryoprecipitable protein was at least 3-fold higher during a quiescent period. Her isolated fibrinogen was functionally normal, as was that obtained from her parents. Her protease-free serum alone, or when it contained added fibrin-depleted fibrinogen isolated from her plasma or from that of a normal donor, did not form a cryoprecipitate.

Case 2

A 42-year-old man was referred for "cryogel" formation, occurring each time blood was drawn by venipuncture (Fig. 4). He was known to have chronic hepatitis due to HCV and had achieved only limited response to various regimens of IFN-α and ribavirin. Other significant clinical features were visual changes, purplish blotching notably involving the forehead, and erectile dysfunction. The initial coagulation profile disclosed a prolonged thrombin time and only partial correction when equal volumes of his plasma and normal donor plasma were mixed. Serial plasma dilutions yielded abnormally increasing thrombin times, consistent with the acquired dysfibrinogenemia of hepatic disorders. There was no family history of dysfibrinogenemia.

Repeated evaluations showed that drawn blood rapidly formed a gel-like material at 4°C that did not fully dissolve when rewarmed to 37°C; this gel did not contain significant Ig either by Ouchterlony analysis or SDS-PAGE. After removal, no further cryoprecipitation was observed; similarly, when plasma was clotted by the addition of thrombin at 37°C and the clot was synerized and removed after several

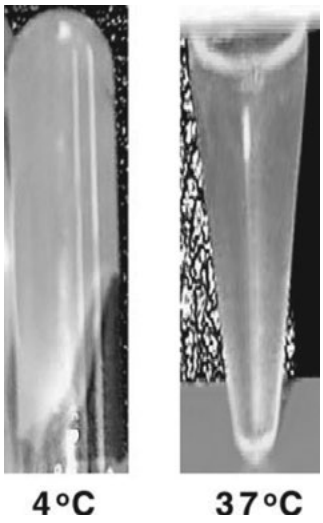

FIGURE 4 Reversible cryogel formation at 4°C (tube inverted) and 37°C (liquid).

hours, his serum formed no additional cryoprecipitate when left at 4°C. In contrast, citrated plasma cryoprecipitate obtained by conventional freeze-thawing was ~3-fold higher than that of normal controls.

All of the patient's symptoms improved following plasmapheresis but recurred progressively within 2 weeks or so, requiring repeat treatments. During the first few plasmapheresis, the intravenous line to the cell separator, as well as the plasma line to the disposal container, began to occlude with visible strands of clot; frequent flushing of lines with normal saline was only partially successful in overcoming this obstacle. The problem was solved by incorporating 6 to 10 U heparin/ml in the citrate anticoagulant solution used during the procedure. His plasma formed abnormally increased amounts of precipitate when left at 4°C overnight, whether obtained before plasmapheresis or after the procedure from the removed plasma. For testing, his serum was rendered protease free by addition of hirudin (20 U/ml), aprotinin (50 U/ml), and phenylmethylsulfonyl fluoride (100 mM); soluble fibrin was depleted by incubating fibrinogen solutions at 4°C, pH 6.4, and ionic strength 0.1 overnight, followed by removal of formed precipitates by centrifugation at 4°C. Such protease-free serum formed no cryoprecipitate with or without added fibrinogen that had been depleted of its soluble fibrin.

In subsequent weeks, the patient was placed on warfarin (Coumadin) and heparin was stopped; plasmapheresis was continued uneventfully over several months and eventually stopped without recurrence of symptoms.

Interpretation

In the first patient, pathologic fibrinemia was clearly related to the inflammatory vascular lesions and could be used as an index to follow the activity of the disease and its response to treatment. In the second patient, fibrinemia may have resulted from the delayed clearance of activated coagulant factors that is prevalent among patients with chronic liver disease. Paradoxically, dysfibrinogenemia may have contributed to the abnormal levels of circulating fibrin by allowing higher levels of soluble fibrinogen-fibrin complexes to accumulate, as fibrin monomers are normally soluble in high fibrinogen excess under physiologic conditions. Whether dysfibrinogenemia is congenital or acquired, such plasma often has a higher maximal capacity for soluble fibrin owing to defective coagulability or incoagulability of abnormal fibrinogen molecules.

Procedures

Choice of Anticoagulant

Various reports described use of either citrate or EDTA to collect blood for testing of cryofibrinogenemia. Paradoxically, EDTA is a potent inhibitor of fibrin polymerization in purified systems, demonstrable by decreased clot turbidity. In unpublished experiments by the author, clot turbidity was decreased to 1/8 that of the control. Similar previous observations led to a recommendation against EDTA use for such plasma tests. To address the differences between results from purified systems and those from EDTA-collected plasma, clotting of isolated fibrinogen was examined in the presence of 1% human albumin ($n = 3$) to simulate the plasma environment. Albumin incorporation consistently abolished the EDTA inhibition (Fig. 5). To assess this observation further, cryoprecipitates from nine randomly selected patient plasma samples from CBC (EDTA) tubes in the hematology laboratory were examined. These were obtained following plasma incubation at 4°C for several days and exhaustively washed by resuspending them in cold buffer, pH 6.4, and centrifuging them (4°C) to remove soluble proteins. SDS-PAGE analysis run under nonreducing conditions disclosed only fibrinogen/fibrin monomer bands in all cases. In a further experiment, plasma samples collected with citrate and EDTA from four normal donors were compared (Fig. 6). Their cryoprecipitates were harvested after freeze-thawing at 4°C overnight and exhaustively washed with cold buffer, pH 6.4. They were then dissolved in 6 M urea, pH 7.4, and the protein was measured spectrophotometrically (280 nm). The amounts of protein from plasma collected into EDTA ranged from 1.6 to 1.7 times that from its citrated counterpart. This established that EDTA is more sensitive than citrate when testing for cryofibrinogenemia.

Testing Procedures

1. To screen for cryofibrinogenemia, simultaneous plasma samples (normal and patient) are collected in EDTA at 37°C and allowed to stand at least overnight at 4°C. Blood should not be collected in heparin, unless care is taken to

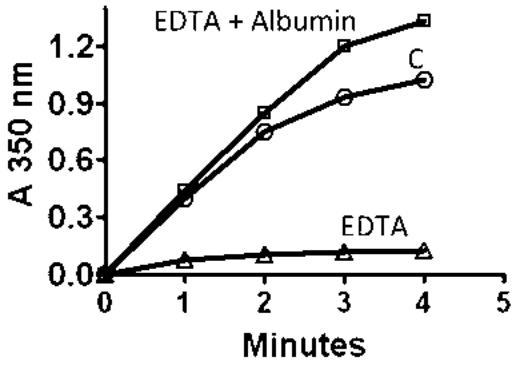

FIGURE 5 EDTA inhibition of fibrin polymerization abolished by albumin. Clotting was initiated by thrombin (final concentration, 0.2 U/ml) in a solution containing isolated (>96% pure) fibrinogen (1 μM in 0.15 NaCl, 0.01 M Tris-HCl, pH 7.4). Clots shown are the control (C), that containing EDTA (1 mM), and that containing EDTA plus human albumin (200 μM).

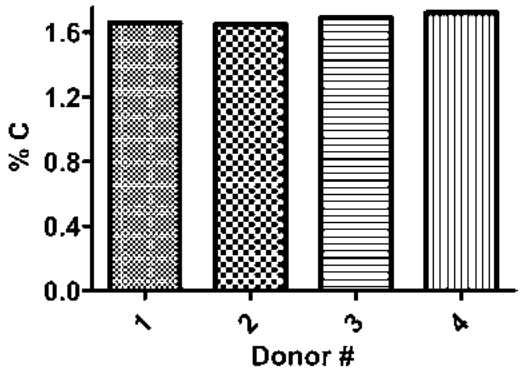

FIGURE 6 Higher cryoprecipitate contents in EDTA-collected than in citrate-collected plasma. Plasma from duplicate pairs of blood specimens from each of four normal donors was collected in tubes containing EDTA or citrate, frozen (−30°C) within an hour, and thawed overnight (4°C) to harvest cryoprecipitate. The cryoprecipitate was then washed and measured (280 nm) as detailed in the text. The protein content of cryoprecipitate from each donor is shown as a percentage of C, its citrate counterpart.

keep its concentration in collected blood at 3 U/ml or less. Significantly higher concentrations may induce increased incorporation of fibronectin in the cryoprecipitate (see item 6 below) and therefore yield false-positive results. To minimize *ex vivo* fibrin generation, blood should be collected rapidly in standard EDTA-containing vacuum or nonvacuum commercial tubes. The largest possible bore needle (e.g., 17 or 18 gauge) and a relatively short needle-to-tube plastic connector are ideal. Since cryoglobulins will also precipitate in plasma, the presence of a cryofibrinogen will be suggested by the absence of a comparable precipitate in a paired sample of serum (26).

2. Two alternative methods may be used to measure cryoprecipitable protein. One is to allow plasma collected in EDTA or citrate to remain undisturbed overnight or longer on ice or at 4°C, to centrifuge the plasma in a refrigerated centrifuge, and to measure the insoluble column as a percentage of total volume (cryocrit). This method, though imprecise, is useful when fibrinemia is pronounced. Another is to freeze the platelet-poor plasma sample shortly after its harvesting in a self-defrosting freezer (−8°C to 20°C) overnight (or for at least 6 h) and then thaw it at 4°C overnight. Centrifugation at cold temperatures yields insoluble material, which is harvested by discarding the supernatant. The cryoprecipitate can then be suspended in ice-cold, phosphate-buffered (pH 6.4 preferably) saline, in a 50- to 100-fold volume excess and recentrifuged to remove more noncryoprecipitable proteins. This washing should be repeated at least three times. More-exhaustive washing may progressively remove fibronectin as well. The final pellet is solubilized at 37°C or in 6 M urea; protein content is determined by diluting an aliquot in 6 M urea and measuring absorbance at 280 nm, which is compared to a control. To convert to milligrams of protein, an extinction coefficient (1%, 1 cm, 280 nm) of 14 or 15 (fibrinogen) can be used. Fibrinogen-fibrin remains as the major constituent protein, and washing tends to decrease the fibronectin content.

3. A third indicator of the fibrin content of plasma is the level of D dimers which can be measured by commercially available assay. Although the D dimer is a proteolytic fragment of the cross-linked clot, it also reflects soluble fibrin/fibrinogen polymers with cross-linked γ-γ chain contacts. That is to say, fibrinogen is an invariable component of soluble fibrin complexes whose solubility indicates that their intermolecular α-α chain contacts are not cross-linked by factor XIIIa, the thrombin-activated form of factor XIII. The D dimer, therefore, does not distinguish between soluble and insoluble fibrin/fibrinogen complexes. Elevated D dimer levels correlate with hypercoagulability and are widely used as indicators of pathologic thrombosis.

4. Fibrin-fibrinogen complexes in most, if not all, dysfibrinogenemic individuals can also be quantified by harvesting the cryoprecipitate obtained from frozen and thawed plasma as in item 2 above. This should also be washed in cold buffer as described above, prior to protein measurements. A unique feature of this cryoprecipitate is that it may contain mostly normal fibrinogen/fibrin (24, 27). That is to say, the overwhelming majority of dysfibrinogenemias occur in heterozygous individuals, and fibrinogen is a dimeric protein (27). Assuming random events during peptide synthesis, molecular assembly, and secretion, this means that the ratio of normal homodimers to hybrid dimers to abnormal homodimers is 1:2:1. Also, fibrin polymerization is typically impaired, so abnormal molecules may have a decreased capacity to polymerize, relative to their normal counterparts. As a result, fibrin-fibrinogen complexes are likely to consist of mostly normal molecules. An exception is abnormally formed fibrin-fibrinogen complexes owing to the specific structure defect. Such complexes will necessarily be incorporated into the cryoprecipitate, which has been observed by the author in one unpublished case. A different result may be encountered in very rare homozygous individuals with dysfibrinogenemia whose fibrinogen is incoagulable. In such instances, plasma may or may not form cryoprecipitate.

5. Commonly not appreciated is the increased *ex vivo* fibrinemia resulting from the use of blood cell separators in which the standard anticoagulant is citrate. By measuring cryoprecipitate content, the author observed up to five-times-higher levels in plasmapheresis plasma than in that from a blood donor whose plasma was harvested and frozen within 24 h or less. This is consistent with a similar effect produced by a very slow withdrawal of blood (24). If serum is harvested from such samples prematurely, it may subsequently form cryoprecipitates (i.e., at 4°C), which can be erroneously interpreted as "cryoglobulins." Its partial or complete failure to redissolve at 37°C may reflect cross-linked fibrin gel rather than cryoglobulin. This is easily demonstrable by failure of the precipitate to dissolve in 6 M urea or 2% acetic acid. A reasonable precaution is to allow whole blood to clot for at least 6 h at 37°C, remove the clot, and observe for another hour or so to ascertain that no further clot forms before harvesting serum to test for cryoglobulins. To confirm that no fibrinogen remains, one can perform a commercially available fibrinogen assay on the patient and a normal control serum.

6. If cryoglobulin analysis is performed on patients who are receiving heparin anticoagulation or on samples collected during plasmapheresis in which heparin has been administered, it is also important to be aware of the possibility of cryoprecipitation due to complexes between heparin and fibronectin (see above), which may increase cryoprecipitate formation; the relative contents of fibrinogen and fibronectin in isolated cryoprecipitates can be assessed by immunoblot analysis using monospecific antisera to these proteins (25). Although at *in vivo* therapeutic concentrations (i.e., <1 U of heparin/ml), this effect may be negligible, the heparin content of blood samples may range up to 5 U/ml or more, at which level it may contribute to cryoprecipitation. Moreover, either concentration range of heparin will

inhibit thrombin generation and thereby the formation of fibrin-fibrinogen complexes.

Summary and Conclusions

Cryofibrinogenemia usually results from elevated levels of fibrin-fibrinogen complexes in plasma, may reflect abnormally assembled complexes in dysfibrinogenemia, and on rare occasions result from complexes of fibrinogen and circulating antifibrinogen antibodies (28–30); in addition, fibronectin can form cold-insoluble complexes with Ig in various disease states (e.g., fibrillary glomerulonephritis) that may be associated with a granulomatous vasculitic component. Cryofibrinogenemia can be screened for by cryoprecipitating or freeze-thawing plasma collected in citrate or EDTA, notwithstanding the fact that the latter is more sensitive. Factors that minimize its *ex vivo* generation include thrombin inhibitors in the container anticoagulant and rapid withdrawal of blood to be tested. If heparin is used alone or incorporated in the anticoagulant to inhibit thrombin, its level should be <3 U/ml.

PYROGLOBULINEMIA

Background

Pyroglobulins are Igs that precipitate irreversibly as a gel when serum is heated to 56 to 60°C for 30 min; in contrast, heat precipitation of Bence-Jones proteins under similar conditions is reversible. Pyroglobulins are invariably single-component proteins and constitute <1% of monoclonal gammopathies overall and ~6% of Waldenström's macroglobulins.

Concept

Pyroglobulins of every Ig isotype (including IgD and IgE) have been reported in association with multiple myeloma, lymphoproliferative diseases, and plasma cell leukemia. Their occurrence has not been associated with specific clinical manifestations, though high levels of these proteins may also cause hyperviscosity or coagulopathies. A related phenomenon of heat-insoluble type 2 cryoglobulins has been described for patients with primary Sjögren's syndrome and as a cause of membranoproliferative glomerulonephritis (31).

Procedure

1. Pyroglobulins precipitate when warmed to 56°C and do not redissolve upon being heated to 100°C. They are usually apparent as an M-spike upon serum protein electrophoresis, which significantly decreases, or completely disappears, after pyroprecipitation. Serum immunofixation will thus define the specific M component forming the pyroglobulin, and this can be confirmed by SDS-PAGE of the isolated material.

2. As noted above, fibrinogen, fibrin, and their core proteins are also heat precipitable at these temperatures. Any remaining fibrinogen and/or fibrin due to dysfibrinogenemia (or an incompletely clotted blood sample) and their split products (typically containing the thermally sensitive D domain) will also form irreversible precipitates at 56°C. To control for this, serum can be treated with 2 IU or more of thrombin/ml and allowed to stand for 1 to 2 h at 37°C, and any clots formed can be removed by syneresis before the specimens are heated to 56°C.

3. Unlike with cryoglobulins, pyroglobulin formation is usually not significantly inhibited over the pH range 3 to 9 or by changing the ionic strength of the solution. Similarly, the effects of reducing (e.g., 2-mercaptoethanol) or dissociating (e.g., Triton X-100) agents on this phenomenon are varied. Occasionally, single patients have been described to have both cryo- and pyroglobulins.

Conclusion

Recognition of the laboratory phenomenon of pyroglobulinemia has importance as a potentially confounding factor for heat-based assays used to inactivate complement or to measure fibrinogen levels. Proper identification of a pyroglobulin as being a monoclonal component may in turn lead to the diagnosis of macroglobulinemia or plasma cell dyscrasia.

REFERENCES

1. **Ramos-Casals M, Stone JH, Cid MC, Bosch X.** 2012. The cryoglobulinemias. *Lancet* **379:**348–360.
2. **Grey HM, Kohler PF.** 1973. Cryoimmunoglobulins. *Semin Hematol* **10:**87–112.
3. **Brouet JC, Clauvel JP, Danon F, Klein M, Seligmann M.** 1974. Biologic and clinical significance of cryoglobulins. *Am J Med* **57:**775–788.
4. **Tissot J-D, Invernizzi F, Schifferli JA, Spertini F, Schneider P.** 1999. Two-dimensional electrophoretic analysis of cryoproteins: a report of 335 samples. *Electrophoresis* **20:**606–613.
5. **Derosa FG, Abel G, Agnello V.** 2009. Observations on cryoglobulin testing. *J Rheumatol* **36:**1953–1957.
6. **Gorevic PD.** 2012. Rheumatoid factor, complement and mixed cryoglobulinemia. *Clin Dev Immunol* **2012:**439018.
7. **Brandau DT, Trautman PA, Steadman BL, Lawson, EQ, Middaugh CR.** 1986. The temperature-dependent stoichiometry of mixed cryoimmunoglobulins. *J Biol Chem* **16:**16385–16391.
8. **Nahm MH, Chatham WW, Benjamin WH Jr.** 2012. Device for carrying blood samples at 37°C for cryoglobulin test. *Clin Vaccine Immunol* **19:**1555–1556.
9. **Della Rossa A, Tavoni A, Bombardieri S.** 2003. Hyperviscosity syndrome in cryoglobulinemia: clinical aspects and therapeutic considerations. *Semin Thromb Hemost* **29:**473–477.
10. **Fohlen-Walter A, Jacob C, Lecompte T, Lesesve J-F.** 2002. Laboratory identification of cryoglobulinemia from automated blood cell counts, fresh blood samples, and blood films. *Am J Clin Pathol* **117:**606–614.
11. **Muller RB, Vogt B, Winkler S, Munoz LE, Franz S, Kern P, Maihofner C, Sheriff A, Von Kempis J, Schett G, Hermann M.** 2012. Detection of low level cryoglobulins by flow cytometry. *Cytometry* **81A:**883–887.
12. **Lawson EQ, Brandau DT, Trautman PA, Aziz SE, Middaugh CR.** 1987. Kinetics of the precipitation of cryoimmunoglobulins. *Mol Immunol* **24:**897–905.
13. **Warren JS.** 2013. Clinically unsuspected cryoglobulinemia. *Am J Clin Pathol* **139:**352–359.
14. **Damoc E, Youhnovski N, Crettaz D, Tissot JD, Przybylski M.** 2003. High resolution proteome analysis of cryoglobulins using Fourier transform-ion cyclotron resonance mass spectrometry. *Proteomics* **3:**1425–1433.
15. **Shihabi, ZK.** 1996. Analysis and general classification of serum cryoglobulins by capillary zone electrophoresis. *Electrophoresis* **17:**1607–1612.
16. **Sansonno D, Iacobelli AR, Cornacchiulo V, Lauletta G, Distasi MA, Gatti P, Dammacco F.** 1996. Immunochemical and biomolecular studies of circulating immune complexes isolated from patients with acute and chronic hepatitis C virus infection. *Eur J Clin Invest* **26:**465–475.
17. **Schott P, Polzien F, Muller-Issberner A, Ramadori G, Hartmann H.** 1998. In vitro reactivity of cryoglobulin IgM and IgG in hepatitis C virus-associated mixed cryoglobulinemia. *J Hepatol* **28:**17–26.

18. **Russi S, Sansonno D, Mariggio MA, Vinella A, Pavone F, Lauletta G, Sansonno S, Dammacco F.** 2014. Assessment of hepatitis core protein in HCV-related mixed cryoglobulinemia. *Arthritis Res Ther* **18:**16.
19. **Naarendorp M, Kallemuchikkal U, Nuovo GJ, Gorevic PD.** 2001. Long-term efficacy of interferon-alpha for extrahepatic disease associated with hepatitis C virus infection. *J Rheumatol* **28:**2466–2473.
20. **Komurian-Pradel F, Perret M, Deiman B, Sodoyer M, Lotteau V, Paranhos-Baccala G, Andre P.** 2004. Strand specific quantitative real-time PCR to study replication of hepatitis C virus genome. *J Virol Methods* **116:** 103–106.
21. **Casato M, Lilli D, Donato G, Granata M, Conti V, Del Giudice G, Rivanera D, Scagnolari C, Antonelli G, Fiorilli M.** 2003. Occult hepatitis C virus infection in type II mixed cryoglobulinaemia. *J Viral Hepat* **10:**455–459.
22. **Wei G, Yano S, Kuroiwa T, Hiromura K, Maezawa A.** 1997. Hepatitis C virus (HCV)-induced IgG-IgM rheumatoid factor (RF) complex may be the main causal factor for cold-dependent activation of complement in patients with rheumatic disease. *Clin Exp Immunol* **107:**83–88.
23. **Vermeesch P, Gisbels K, Marien G, Lunn R, Egner W, White P, Bossuyt X.** 2008. A critical appraisal of current practice in the detection, analysis and reporting of cryoglobulins. *Clin Chem* **54:**39–43.
24. **Galanakis DK.** 1995. Plasma cryoprecipitation studies: major increase in fibrinogen yield by albumin enrichment of plasma. *Thromb Res* **78:**303–313.
25. **Amdo TD, Welker JA.** 2004. An approach to the diagnosis and treatment of cryofibrinogenemia. *Am J Med* **116:**332–337.
26. **Blain H, Cacoub P, Musset L, Costedoat-Chalumeau, N, Silberstein C, Chosidow O, Godeau P, Frances C, Piette JC.** 2000. Cryofibrinogenemia: a study of 49 patients. *Clin Exp Immunol* **120:**253–260.
27. **Galanakis DK, Neerman-Arbez M, Brennan S, Rafailovich M, Hyder L, Travlou A, Papadakis E, Manco-Johnson MJ, Henschen A, Scharrer I.** 2014. Thromboelastographic phenotypes of fibrinogen and its variants: clinical and nonclinical implications. *Thromb Res* **133:**1115–1123.
28. **Kierulf P, Godal HC.** 1983. Cryofibrinogen due to a naturally circulating monoclonal IgA anti-fibrinogen antibody. *Thromb Haemost* **50:**185.
29. **Euler HH, Zeuner RA, Beress R, Gutschmidt HJ, Christophers E, Schroeder JO.** 1996. Monoclonal cryoantifibrinogenemia. *Arthritis Rheum* **39:**1066–1069.
30. **Meh D, Siebenlist K, Galanakis DK, Bergstrom G, Mosesson MW.** 1995. The dimeric Aα chain composition of dysfibrinogenemic molecules with mutations at Aα16. *Thromb Res* **78:**531–539.
31. **Meng QH, Chibbar R, Pearson D, Kappel J, Krahn J.** 2007. Heat insoluble cryoglobulin in a patient with essential type 2 cryoglobulinemia and cryoglobulin occlusive membranoproliferative glomerulonephritis. *Clin Chim Acta* **406:**170–173.
32. **Wintrobe M, Buell M.** 1933. Hyperproteinemia associated with multiple myeloma. *Bull Johns Hopkins Hosp* **52:**156.

Strategy for Detecting and Following Monoclonal Gammopathies

JERRY A. KATZMANN AND DAVID F. KEREN

11

The preceding chapters in this section have dealt with several aspects of serum and urine protein analysis for immunoglobulins. Overwhelmingly, the single most important reason for performing these studies is to detect monoclonal gammopathies. This chapter briefly summarizes the various plasma cell proliferative diseases and then describes the use of the electrophoretic and nephelometric assays for the diagnosis, prognosis, and monitoring of monoclonal gammopathies. There are some general strategies for all laboratories as well as specific tests that are needed, depending on the disease presentation.

In plasma cell proliferative diseases, a monoclonal immunoglobulin (M protein) that can be used as a serologic "tumor" marker is usually secreted. Because of this secreted monoclonal immunoglobulin, these diseases are also referred to as monoclonal gammopathies. The secreted proteins can be used as a diagnostic tool for the identification of the clone of plasma cells as well as a quantitative marker to follow the course of the disease and response to therapy. Unlike many other tumor markers, M proteins are extremely diverse. Each M protein has a unique variable region sequence, and the molecules may run the gamut from pentameric IgM (~900,000 Da) to monomeric free light chains (FLCs) (~24,000 Da). In addition, although some plasma cell proliferative disorders present with M protein concentrations of grams per liter of serum, others have little or virtually no circulating M protein. The diversity of plasma cell proliferative diseases and of their secreted proteins and the concentrations of M proteins make M protein a challenging tumor marker. No single assay can effectively diagnose and monitor plasma cell proliferative diseases, and the laboratory needs to define strategies that encompass the spectrum of disease presentations. Protein electrophoresis (PEL), immunofixation electrophoresis (IFE), and immunosubtraction electrophoresis (ISE) of serum and urine have formed the hub of laboratory testing for detecting and monitoring monoclonal gammopathies (1–3). These electrophoretic assays provide analytic separation of immunoglobulins based on charge and size and allow the recognition and quantitation of M proteins distinct from the normal polyclonal immunoglobulins. In addition, quantitative immunoassays of immunoglobulins and FLCs (4) may be useful for diagnosis and/or monitoring disease.

CLASSIFICATION OF MONOCLONAL GAMMOPATHIES

Monoclonal gammopathies are disorders that include a diversity of plasma cell proliferative diseases. The diseases have different biological processes and may have different presentations, treatments, and outcomes. Once the laboratory has identified a monoclonal immunoglobulin, the clinician needs to make a specific diagnosis based on clinical presentation and perhaps bone marrow, imaging, or other tissue and blood studies. In Table 1 are listed the 39,929 monoclonal gammopathies that were detected in the Mayo Clinic practice between 1960 and 2008. The 18 diseases in Table 1 are listed by decreasing frequency of diagnosis. These disorders are often categorized as malignant, premalignant, and protein/low-tumor-burden diseases, as indicated in the table (5). The malignant disorders have large tumor burdens, which must be controlled or eradicated. The premalignant disorders have no clinical symptoms and need only be monitored for progression, and the protein/low-tumor-burden diseases may have low (or large) tumor burdens, but the secreted monoclonal proteins cause the disease processes. This classification of the various plasma cell proliferative diseases can be helpful in thinking about the biology of the diseases as well as the range of laboratory presentations.

Malignant Plasma Cell Proliferative Disorders

Multiple myeloma (MM) is the most common malignant plasma cell disease and is second to non-Hodgkin lymphoma as the most common hematologic malignancy (6). In the U.S. population, it is estimated that 22,350 new cases of MM were diagnosed in 2013. MM is a disease of older people, with the median age at diagnosis being 69 years, and it is rare in people younger than 40 (7, 8). The incidence is slightly higher in men and twice as high in blacks as in whites (9). The racial disparities as well as family studies suggest genetic factors, but environmental factors, such as exposure to agricultural and petroleum industry chemicals, have been shown to be risk factors as well (10). Myeloma cells reside in the bone marrow, often suppress other marrow elements, and may cause destructive bone lesions.

The presence of a large clone of bone marrow plasma cells (>10%) is not in itself sufficient for the diagnosis of MM. The diagnosis also requires symptoms that are due to

doi:10.1128/9781555818722.ch11

TABLE 1 Monoclonal gammopathies from the Mayo Clinic, 1960 to 2008

Disease	No. of cases	%	Classification		
			Malignant	Protein/low tumor burden	Premalignant
MGUS	23,179	58.0			×
Multiple myeloma	6,974	17.5	×		
Primary amyloid	3,781	9.5		×	
SMM	1,494	3.7			×
Lymphoproliferative disease	1,298	3.3	×		
Macroglobulinemia	940	2.4	×		
Plasmacytoma	774	1.9	×		
Bence Jones proteinuria	450	1.1			×
Cryoglobulinemia	379	0.9		×	
POEMS syndrome	217	0.5		×	
Light-chain deposition disease	113	0.3		×	
Plasma cell leukemia	90	0.2	×		
Cold agglutinin disease	74	0.2		×	
Acquired Fanconi syndrome	43	0.1		×	
Scleromyxedema	31	0.1		×	
BHPW	31	0.1		×	
Heavy-chain disease	31	0.1	×		
Capillary leak syndrome	29	0.1		×	
Total	39,929	100			

[a]MGUS, monoclonal gammopathy of undetermined significance; SMM, smoldering multiple myeloma; POEMS syndrome, syndrome with polyneuropathy, organomegaly, endocrinopathy, monoclonal protein, and skin changes; BHPW, benign hypergammaglobulinemia purpura of Waldenström's macroglobulinemia.

the plasma cell clone. In a series of 1,027 sequential patients, the symptoms at diagnosis were anemia (73%), bone pain (58%), elevated creatinine (48%), fatigue/weakness (32%), hypercalcemia (28%), and/or weight loss (24%) (7). The diagnosis of MM requires organ damage summarized by the acronym CRAB: increased serum calcium concentration, renal insufficiency, anemia, and lytic bone lesions. It is the manifestation of these clinical symptoms rather than pathology that distinguishes MM from the premalignant disorders of smoldering multiple myeloma (SMM) and monoclonal gammopathy of undetermined significance (MGUS) (11, 12).

The distribution of types of monoclonal immunoglobulins in a series of MM and MGUS patients is listed in Table 2. The immunoglobulin distributions are different between the two diseases. The most obvious difference is in the frequency of IgM. Most IgM disease that progresses to malignancy is classified as Waldenström's macroglobulinemia (WM). WM is a disease of clonal lymphoplasmacytic cells and is a clinicopathological entity distinct from MM. Another difference in the distributions of monoclonal proteins is that monoclonal FLCs and monoclonal IgD occur in MM at about 4-fold more than in MGUS. The laboratory detection of monoclonal FLCs or monoclonal IgD should always raise the suspicion of serious disease. Laboratorians who see samples that are mostly from MGUS patients and a few MM samples are almost always surprised by the relatively high frequency of light-chain multiple myeloma (LCMM) and nonsecretory multiple myeloma (NSMM) among MM patients.

The other malignant diseases listed in Table 1 include lymphoproliferative disease, plasmacytoma, plasma cell leukemia, and the heavy-chain diseases. A small percentage of B-cell lymphomas and leukemias will produce a monoclonal immunoglobulin usually found in low concentrations in serum. Plasmacytomas are solitary lesions that usually present with pain at the site of the lesion, which contains clonal plasma cells in the absence of any diffuse bone marrow involvement or CRAB symptoms. Plasmacytomas often have no or small amounts of secreted monoclonal protein and usually respond well to radiation. However, within 2 years, approximately 50% will recur as MM (13). Plasma cell leukemia is a rare and aggressive form of myeloma, with high numbers of circulating plasma cells. Interestingly, approximately 35% of plasma cell leukemia patients will have LCMM only and 10% will have NSMM (14). Heavy-chain diseases are exceedingly rare and are identified by the presence of a monoclonal heavy chain with no corresponding monoclonal light chain upon IFE (15). The heavy chain is often detected in significant concentrations in the urine, and urinary IFE is a useful confirmatory assay. Many heavy-chain disease patients have lost the ability to synthesize light chains, but some patients have mutations in the heavy chain that results in the inability to bind light chain. The latter patients may therefore present with an isolated monoclonal heavy chain detected by IFE plus monoclonal free light chain as detected by a significantly abnormal FLC kappa-to-lambda ratio (16).

TABLE 2 Distribution of monoclonal proteins in patients with multiple myeloma and monoclonal gammopathies of undetermined significance

Monoclonal immunoglobulin type or nature of disease	% of patients with[a]:	
	MM	MGUS
IgG	52	59
IgA	21	12
IgM	0.5	18
IgD	2	0.5
Biclonal	2	5
Light chain only	20	6
None detected	2.8	NA

[a]NA, not applicable.

Premalignant Plasma Cell Proliferative Disorders

Whereas small quantities of M proteins were once considered to be "benign monoclonal gammopathies," that term is no longer used. Conditions that were so categorized are now referred to as MGUS or SMM because they are precancerous lesions that can evolve to MM, WM, or other B-cell lymphoproliferative conditions. Both MGUS and SMM are monoclonal gammopathies that manifest no symptoms of MM or a related disease that can be attributed to the plasma cell clone or monoclonal protein. These laboratory disorders are therefore not diseases *per se*. They are called premalignant disorders because virtually all cases of MM are now considered to have been preceded by MGUS or SMM as many as 8 or more years earlier (17–19).

MGUS is an asymptomatic monoclonal gammopathy that is usually detected as an incidental finding when protein electrophoresis is done as part of laboratory studies for a wide range of symptoms (20). By definition, the monoclonal protein is <3 g/dl, and <10% of bone marrow (if tested) is monoclonal plasma cells. MGUS is a common disorder with a prevalence of 3% in the Caucasian population over the age of 50 (21). In the Mayo Clinic practice, MGUS represents 58% of all newly diagnosed monoclonal gammopathies (Table 1). Like MM, MGUS is a disorder of older people, occurs more frequently in men than in women, and is at least 2-fold more prevalent in Africans and African Americans than in Caucasians (22).

Long-term studies of the natural history of MGUS have indicated that MGUS patients have a 1%-per-year risk of progression, and the risk of progression remains at 1% per year regardless of the length of follow-up (23). MGUSs may be subdivided into three types based upon the M protein: non-IgM MGUS, IgM MGUS, and light-chain MGUS (24). Most cases fall into the category of non-IgM MGUS (usually IgG or IgA). These cases have an overall risk of 1% per year of progressing to SMM, MM, or light-chain amyloidosis (AL). Patients with IgM MGUS have a 1.5% risk of progressing mainly to WM but also to lymphoma or AL. Those with light-chain MGUS have an as-yet-undefined risk of progressing to light-chain MM and AL. A number of risk factors for progression have been identified in patients with IgG, IgA, and IgM MGUS. The risk factors include M-spike concentration, percent bone marrow plasma cells, heavy-chain isotype, urinary monoclonal protein, and FLC kappa-to-lambda ratio (23, 25, 26). Because few MGUS patients have their urine tested and even fewer have their bone marrow tested, the three serum factors of M-spike size, heavy-chain isotype, and FLC ratio have been combined into a risk stratification model for predicting MGUS progression. Low risk factors are an M-spike level of <1.5 g/dl, the presence of gamma heavy chain, and a normal FLC kappa-to-lambda ratio. In our study of patients in southeastern Minnesota, 42% of patients were low risk for all three factors and had a 0.1%-per-year risk instead of a 1%-per-year risk of progression (26). The risk for these patients is so low that laboratory monitoring is not needed.

SMM has also been known as asymptomatic myeloma, and until recently, individuals within this classification did not receive treatment. As with MGUS, it is distinguished from MM because there are no CRAB symptoms attributable to the plasma cell clone. SMM is distinguished from MGUS by having an M-spike level of >3 g/dl and/or >10% monoclonal bone marrow plasma cells (27). Whereas individuals with SMM superficially appear to be at some point between MGUS and MM, the kinetics of progression of SMM to MM suggests that SMM does not affect a uniform group of patients. In the first 5 years of follow-up, SMM patients progress at a rate of 10% per year and subsequently progress at approximately 1% per year (28, 29). SMM may affect a mixture of patients with early MM that have not yet manifested clinical symptoms and patients with MGUS. Factors that identify patients destined to progress within 2 to 3 years of diagnosis have been identified, and consensus is building to use these laboratory criteria to help define MM (30). High-risk SMM with >60% bone marrow plasma cells or an FLC ratio of >200 has a median time to progression of 7 months (31, 32). Mateos et al. recently evaluated treatment versus no treatment (the current standard of care) of 125 individuals at high risk for SMM. After a median of 40 months, they found that the treatment group had a significant prolongation of both the median time to progression and the 3-year survival rate and that the toxic effects of the therapy (lenalidomide plus dexamethasone) were mainly grade 2 or lower (33). Similar studies are ongoing at other centers. These patients break the pattern of MM being exclusively a clinical diagnosis. The distinctions of MGUS, SMM, and MM are made because the diseases have different biological processes. It should be recognized, however, that they have overlap. The critical distinction is when the decision is made to expose the patient to the risks that come with the treatment regimens for MM. As therapy moves to earlier forms of the disease, the significance of detecting and characterizing M proteins in asymptomatic patients attains greater relevance.

Protein (or Low-Tumor-Burden) Diseases

The protein diseases or low-tumor-burden diseases represent a group of monoclonal gammopathies in which there may not be a large clonal proliferation of plasma cells but in which the cell products cause pathology. In primary (light-chain) AL, the monoclonal free light chains deposit in organs as amyloid fibrils. Over many years of secretion of amyloidogenic light chains, amyloid fibrils slowly accumulate. At some point, the deposition of the amyloid may cause heart failure, nephrotic syndrome, hepatomegaly, or other organ dysfunction (34). The diagnosis of AL is dependent on demonstrating amyloid deposits in tissue and identifying monoclonal light chains as the predominant protein in the fibril. This is usually accompanied with evidence of a clonal proliferation of bone marrow plasma cells or a monoclonal protein in the serum or urine. The recognition of a monoclonal free light chain in the serum may be the first "red flag" to suggest AL. Although some patients with MM produce an amyloidogenic light chain, most AL patients have small clonal populations and small amounts

of secreted monoclonal light chain. A monoclonal serum protein can be detected in 75 to 90% of patients with AL, but an M-spike can be quantitated in only approximately 50% of them (35). The low serum and urine concentrations make early detection and hematologic monitoring very difficult and previously meant that organ function had to be used as an indirect monitoring method. The availability of quantitative serum FLC assays has made detection of FLCs more sensitive and allowed direct hematological monitoring of patients with AL amyloid (36, 37). Lambda light chain is found in 70% of patients with AL amyloid. In contrast, kappa light chain is the causative light chain in 90% of light-chain deposition disease (LCDD) patients. However, LCDD is a much rarer disorder than AL, and the light chains do not form amyloid fibrils. As with AL, the diagnosis is based on characteristic histopathologic features.

Because amyloid fibrils can slowly form in any number of tissues, the disease is often not diagnosed until very late in the disease process. The identification of a monoclonal light chain in the serum or urine is often the first clue to the diagnosis. When a biopsy specimen is obtained, stained with Congo red, and viewed under polarized light, the amyloid fibrils have an apple-green fluorescence. Because all types of amyloid give this result, it is important to identify the specific amyloidogenic protein. In AL amyloid for example, the amyloid fibrils are caused by immunoglobulin light-chain fragments, and therefore treatment needs to be directed against the plasma cell clone. This is important because MGUSs are so common in older individuals that an M protein in serum or urine may coexist with the rare (incidence about 1/100,000) familial forms of amyloidosis where the M protein is not related to the primary disease process. In familial AL, the most common amyloidogenic proteins are polymorphisms of transthyretin (also known as prealbumin). Transthyretin is synthesized in the liver, and the treatments are therefore unrelated to the bone marrow. The best method for identifying the type of protein in the amyloid tissue is the use of tissue microdissection combined with mass spectroscopy (38, 39). This proteomic method is rapidly replacing immunohistochemical staining, which has a low sensitivity and specificity. Because familial forms of amyloidosis are autosomal dominant conditions, their detection and appropriate characterization are important for genetic counseling.

Some patients with neuropathies harbor an M protein (usually IgM). About half of these patients have Waldenström's macroglobulinemia, with relatively large amounts of IgM in the serum. They usually present with symptoms of hyperviscosity. Another group of patients who suffer from motor or sensory peripheral neuropathies may have small amounts of M proteins in the serum that require immunofixation for detection. Some of these patients have POEMS syndrome (also called Crow-Fukase syndrome), an acronym for peripheral neuropathy, organomegaly, endocrine dysfunction, an M protein, and skin hyperpigmentation (40). Unlike with cases of MM or WM, cases of POEMS syndrome and individuals with peripheral neuropathies who have myelin-associated glycoprotein monoclonal antibodies require that immunofixation (IFE) be performed on serum for detection (41).

DIAGNOSTIC TESTING STRATEGY

The detection of M proteins relies predominantly on the ability to differentiate between monoclonal and polyclonal immunoglobulins. This has traditionally been done with electrophoretic assays (2). Agarose gel protein electrophoresis and capillary zone electrophoresis (CE) with resolution sufficient to clearly distinguish the beta 1 (transferrin) and beta 2 (C3) bands are relatively simple procedures that are used to detect monoclonal proteins based on their restricted migrations compared to those of polyclonal immunoglobulins (42, 43). Immunofixation electrophoresis in agarose and immunosubtraction electrophoresis in CE are used to identify and characterize the immunoglobulin heavy and/or light chains and therefore confirm the identity of the monoclonal protein. In the last few years, additional methods that complement the electrophoretic assays have been developed. Quantitation of serum kappa and lambda FLCs by nephelometric immunoassays supports some of the weaknesses of PEL and IFE (4, 44), and practice guidelines now include all three serum assays (45).

PEL separates proteins based on charge and size. Once the proteins have been separated by electrophoresis, they are precipitated in the gel and stained, the gel is washed and dried, and the distribution of the protein stain is digitized by scanning the gel and obtaining an electropherogram (Fig. 1). In normal serum, the gamma fraction has a broad Gaussian distribution due to the thousands of clones of plasma cells that secrete immunoglobulin into serum. The quantitation of the gamma fraction provides information about hypogammaglobulinemia or hypergammaglobulinemia, and the quantitation of the gamma fraction should be similar

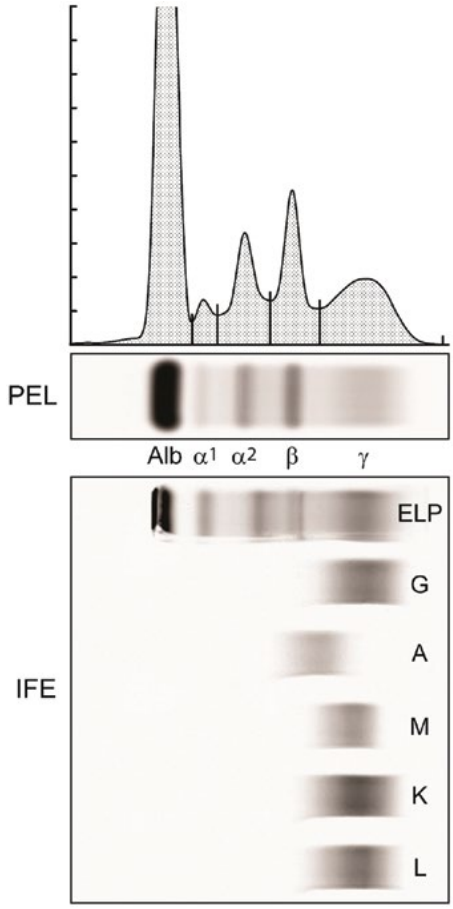

FIGURE 1 Normal serum protein electrophoresis (PEL) and immunofixation electrophoresis (IFE). The gel scan (electropherogram) is aligned above the PEL gel. Alb, albumin; ELP, electropherogram.

to IgG quantitation by immunonephelometric assays. In the serum of a patient with a monoclonal gammopathy, the monoclonal immunoglobulin is overrepresented and can be visualized as a restricted area of migration in the electrophoresis pattern (Fig. 2). All patients with a localized band or nonhomogeneous distribution upon serum PEL require IFE or ISE to confirm that the band is a monoclonal protein as well as to determine the heavy-chain class and/or light-chain type. A discrete band upon serum PEL is rarely a false-positive result. If the monoclonal protein migrates broadly or is at a low concentration, the PEL may appear to have a nonhomogeneous pattern. It is crucial to distinguish this from a restricted polyclonal response, and this can usually be done based on IFE.

In many patients, the use of serum PEL and IFE for the detection and quantitation of monoclonal proteins is very straightforward. There are, however, some types of monoclonal proteins that are more of a challenge. Patients with LCMM, for example, have lots of clonal plasma cells secreting monoclonal light chain, but the serum concentration may be low because the low-molecular-weight free light chain is quickly cleared into the urine. The PEL and IFE of serum and urine from a patient with LCMM are shown in Fig. 3. The serum PEL does not show an obvious M protein, although the IFE shows a discrete lambda band with no corresponding heavy-chain band. An additional IFE was performed with antisera to delta and epsilon chains and showed no reactivity suggesting IgD or IgE. Although this monoclonal lambda protein is detected in the serum by IFE, quantitation is not possible by serum PEL. The 24-h urine PEL, however, shows a large lambda M-spike that is easily detected and quantitated. When we envision serum from a patient with MM, we picture large serum M-spikes of intact immunoglobulin M protein; LCMM, however, represents 18 to 20% of patients with MM. It is because of patients like this that it is useful to test both serum and urine.

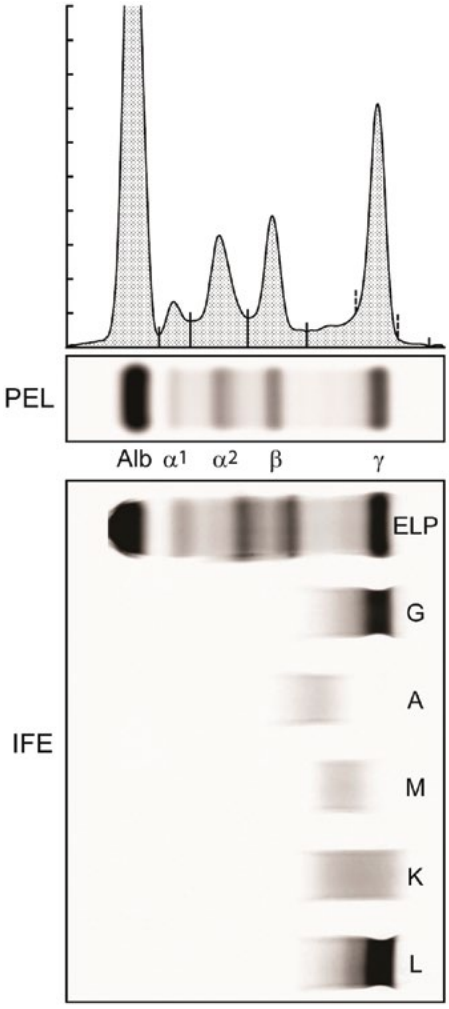

FIGURE 2 Monoclonal gammopathy serum protein electrophoresis (PEL) and immunofixation electrophoresis (IFE). The gel scan (electropherogram) is aligned above the PEL gel. The dashed lines on both sides of the M protein indicate the M-spike fraction.

Patients with nonmalignant low-tumor-burden diseases, such as AL, have serum and urine abnormalities that may be even more difficult for the laboratory to detect and quantitate. AL patients may have small numbers of bone marrow plasma cells and therefore small amounts of secreted monoclonal light chain. Examples of PEL and IFE of both serum and urine from an AL patient are illustrated in Fig. 4. Close examination reveals a faint monoclonal lambda band in the serum and urine. It is clear that if the concentration of the monoclonal lambda protein was slightly lower, we would not be able to see the abnormality. In addition, there is no way to quantitate and therefore monitor the abnormality. The introduction of quantitative serum FLC immunoassays has helped with the identification and quantitation of these monoclonal FLCs. Quantitative FLC assays use antisera directed against epitopes that are exposed only when the light chains are free (unbound to heavy chain) in solution. These cryptic sites are involved in the very tight noncovalent binding of light chains to heavy chains. The antisera have a 10,000-fold preference for FLCs over light chains contained within intact immunoglobulin molecules (4). That means that FLC immunoassays can be used to specifically quantitate FLCs even in the presence of large concentrations of polyclonal serum immunoglobulins. The approach is to quantitate the kappa FLCs and the lambda FLCs and use the ratio of kappa to lambda FLCs to detect unbalanced light-chain synthesis. This approach has proven surprisingly sensitive for detecting clonal free-light-chain diseases. Abnormal serum FLC ratios have been detected in 100% of patients with LCMM, 90% to 95% of AL patients, and 60% to 70% of patients with NSMM (46–48). In spite of the sensitivity of detection of FLC in free-light-chain diseases, abnormal serum FLC ratios have been detected in only 90 to 95% of patients with intact immunoglobulin MM and 40% of patients with MGUS (46). Although serum M proteins in these two patient groups have easily been detected by PEL and IFE, it is clear that not all monoclonal gammopathies secrete excess FLCs and that a combination of tests is needed to benefit from each test's strengths.

SCREENING PANELS FOR M PROTEIN DETECTION

There have been a number of studies identifying the best approach for detection of monoclonal proteins (49–54). The Mayo Clinic group performed a large study in which patients with an assortment of plasma cell proliferative diseases and who also had undergone serum PEL, IFE, and FLC tests were selected; urine PEL and IFE were also performed at the time of diagnosis. The cohort consisted of 1,851 patients with various monoclonal gammopathies (MM, WM, SMM, MGUS, plasmacytoma, POEMS syndrome, AL, and LCDD) (51). The data illustrated in Table 3 allow

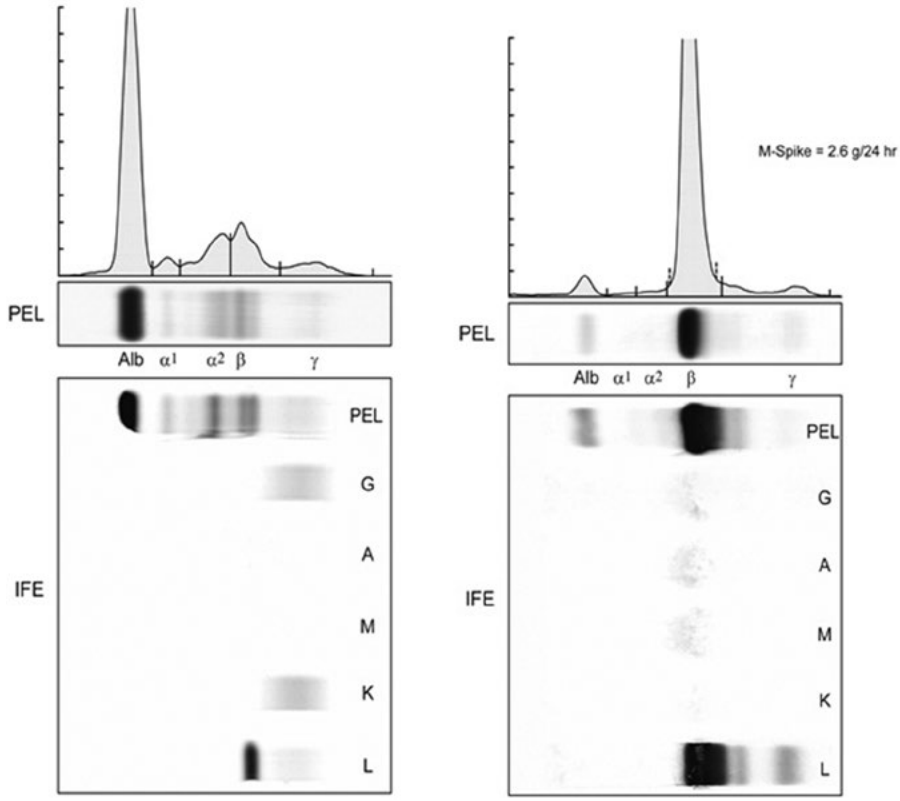

FIGURE 3 Light-chain multiple myeloma serum (left) and urine (right) tested by PEL and IFE.

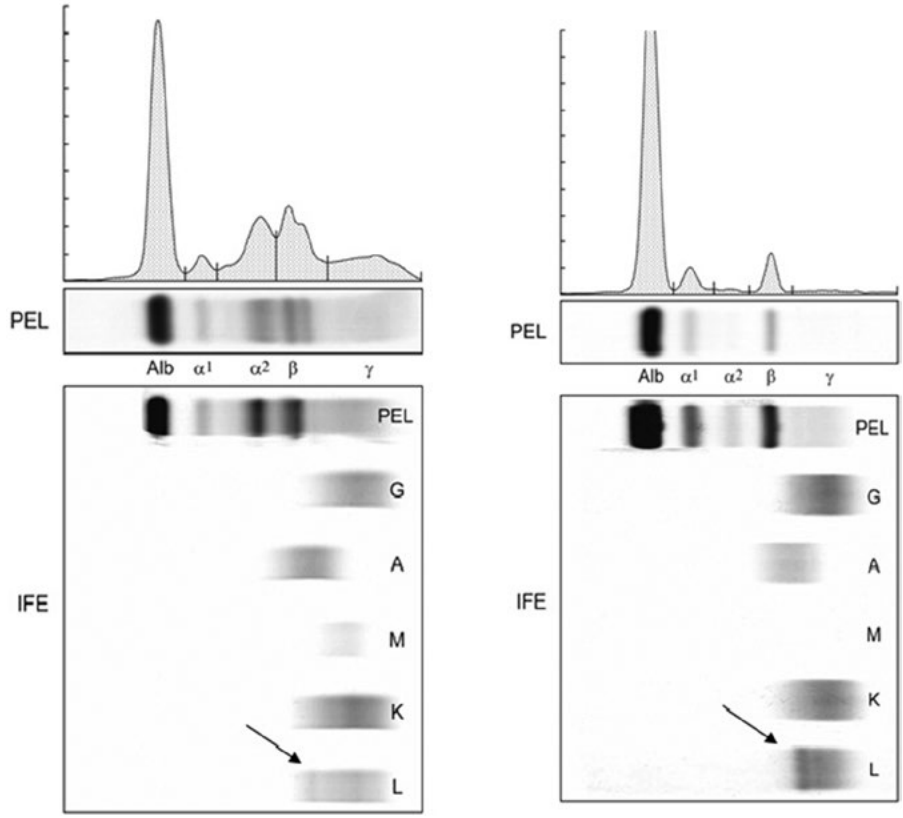

FIGURE 4 Primary amyloid tested by serum (left) and urine (right) PEL and IFE.

a retrospective determination of which patients would have had M proteins detected by the various tests singly or in combination. PEL, IFE, and FLC testing as single serum tests detected 79%, 87%, and 74% of the patients, respectively. A panel of all five assays detected 98.6% of the cases. Interestingly, if urine assays are removed from the diagnostic panel, there is no decrease in sensitivity for patients with MM, macroglobulinemia, plasmacytoma, extramedullary plasmacytoma, POEMS syndrome, or SMM. This and other studies have led the International Myeloma Working Group to recommend a screening panel of serum PEL, IFE, and FLC testing; panels that include urine are recommended if AL is suspected. In addition, once an M protein has been detected, analysis of urine may be required (45). This diagnostic panel of three serum assays simplifies the diagnostic algorithm and reduces costs for laboratories since only a single sample is transported and accessioned, and no preanalytic centrifugation or concentration of urine is needed. A simplified diagnostic panel of serum PEL and FLC testing is probably the bare-minimum screening panel that should be considered until we have more-sensitive detection systems.

STRATIFICATION OF RISK

The use of serum PEL, IFE, and FLC testing as a diagnostic panel also provides prognostic information for many plasma cell proliferative diseases. Survival in patients with MM is predicted by FLC testing, beta 2 microglobulin, and albumin (55); in AL, the FLC response to treatment predicts survival (36, 56), and in patients with plasmacytoma, the initial FLC result as well as the IFE results at 1 year predict relapse and survival (57). As mentioned earlier, the FLC ratio, PEL M-spike level, and IFE heavy-chain type predict progression to MGUS (26), and FLC testing and the percentage of bone marrow plasma cells predict the progression of SMM to MM (29, 32). The prediction of survival for patients with MM is important for stratifying clinical trials but has not yet broadly impacted treatment decisions. The predictions of progression to MGUS and SMM, however, play an important role in clinical practice. Recent demonstration of the efficacy of treatment in selected patients with high-risk SMM is changing the definition of MM. This allows SMM patients with FLC ratios of >200 to be treated before they return to the clinic with kidney failure and patients with >60% bone marrow plasma cells to potentially be spared anemia and bone lesions before the inevitable progression to symptomatic MM.

The effect of risk stratification for the low-risk MGUS patients is opposite to that for high-risk SMM. Progression rates of 0.1% per year for the low-risk MGUS patients mean that their physicians can reasonably tell them that they do not need continuous laboratory testing for progression to MM. This will save the patient time and money and will reduce anxiety about a malignant disease in their future. As electrophoretic methods have become more sensitive, we have detected monoclonal gammopathies at lower and lower concentrations, and the ability to define low-risk MGUS becomes increasingly important. We are detecting more of these smaller monoclonal proteins, and the laboratory is faced with a dilemma about reporting very small abnormalities. As indicated earlier, many very serious diseases may secrete low levels of monoclonal protein, but some apparent small monoclonal proteins may be part of a polyclonal immune response. The laboratory is therefore faced with trying to decide about reporting very low levels of monoclonal proteins and having clinicians reach monoclonal gammopathy overload. We have used the term IFE-MGUS to describe monoclonal proteins that are detectable by IFE but not readily by PEL. Fifteen to 20% of these IFE-MGUS abnormalities disappear with no treatment, but some eventually progress (12, 58). The use of FLC ratios and MGUS risk assessment may be useful tools to help us ignore some of the very small questionable abnormalities.

The addition of serum FLC testing to serum PEL and IFE is a good screening strategy and will detect almost all plasma cell proliferative disorders. The unknowns that remain for this three-assay diagnostic panel are as follows.

A. When should a urine sample be requested?
   1. If AL is part of the differential diagnosis, urine IFE may be needed if serum tests are normal.
   2. If heavy-chain disease is detected by serum IFE, urine IFE can be confirmatory.
   3. If a monoclonal protein is detected, 24-h urine studies are useful for documenting baseline renal function.

TABLE 3 Diagnostic sensitivities of monoclonal gammopathy screening panels with combinations of serum PEL, serum IFE, serum FLC, and/or urine IFE-PEL

Patient group	No. of patients	% of patients diagnosed by:					
		Serum PEL	Serum IFE	Serum FLC	All serum and urine tests	Serum PEL + IFE + FLC (no urine)	Serum PEL + FLC +
All	1,877	79.0	87.0	74.3	98.6	97.4	94.3
MM	467	87.6	94.4	98.6	100	100	100
WM	26	100	100	73.1	100	100	100
SMM	191	94.2	98.4	81.2	100	100	99.5
MGUS	524	81.9	92.8	42.4	100	97.1	88.7
Plasmacytoma	29	72.4	72.4	55.2	89.7	89.7	86.2
POEMS syndrome	31	74.2	96.8	9.7	96.8	96.8	74.2
Extramedullary plasmacytoma	10	10.0	10.0	10.0	20.0	10.0	10.0
AL	581	65.9	73.8	88.3	98.1	97.1	96.2
LCDD	18	55.6	55.6	77.8	83.3	77.8	77.8

B. When is a simplified screening panel of serum PEL and FLC testing sufficient?
   1. This two-assay panel efficiently detects MM and macroglobulinemia.
   2. If AL-, POEMS syndrome-, or MGUS-associated peripheral neuropathy is suspected, then serum IFE is needed.

MONITORING M PROTEINS

Once an M protein has been detected and a specific diagnosis has been determined, the quantitation of the M protein can be used as a marker of the plasma cell clone's response to therapy, stability, or progression. Just as there are multiple tests that may be required for diagnosing monoclonal gammopathies, there are multiple assays for measuring M proteins, and just as in diagnostic testing, the smaller the quantity of the M protein, the harder it is to quantify the abnormality. Quantitative tests include PEL for M-spike measurement and immunonephelometry for immunoglobulin quantitation, determination of FLC concentration, and heavy/light-chain measurements. If a serum M-spike (Fig. 2) and/or urine M-spike (Fig. 3) is present in a large enough concentration, it can easily be quantitated. The advantage of using the PEL M-spike when the abnormality is in the gamma fraction (as in Fig. 2) is that the fractionation of the M-spike separates the M protein from most of the polyclonal background. The International Myeloma Working Group defines serum M-spikes of >1 g/dl and urine M-spikes of >200 mg/24 h as being "measurable." "Measurable" means that the magnitude of the M-spike is large enough to be reliably quantified and is also large enough to document a decline in the M protein and, therefore, a hematological response. There are also disease presentations in which there is suppression of polyclonal immunoglobulin synthesis (Fig. 5). In cases where there is very little polyclonal immunoglobulin, the quantitation of immunoglobulin (IgG, IgA, or IgM) can also be used to monitor hematologic disease. Serum M-spike and immunoglobulin quantitations are not, however, always equivalent. In general, IgA monoclonal proteins have similar quantitations by immunonephelometry and M-spike testing, whereas monoclonal IgM protein concentrations are almost always higher by immunonephelometric quantitation than by PEL M-spike quantitation. It is important to realize that the two methods do not always correlate and that clinicians should not go back and forth between the methods. Many clinicians order both serum PEL and immunoglobulin quantitation as a quality check to see that both change in similar ways (59).

Not all patients can be monitored by levels of PEL M-spikes or quantitative immunoglobulins. Some patients have small concentrations of M protein (Fig. 6). In these cases, quantitation of the M protein will include substantial amounts of polyclonal immunoglobulins. The M-spike will be more enriched for the monoclonal protein than quantitative IgG, but the M protein will still be a minority of the M-spike. As this M-spike level gets smaller in response to therapy, the laboratory may still recognize the abnormality but has to make a judgment as to when to stop fractionating the M-spike. When the monoclonal protein appears to be less than one-quarter to one-third of the M-spike quantitation, we stop fractionating an M-spike and only report a "low concentration of monoclonal protein that we are unable to quantitate." That is not as satisfying as a quantitative result, but quantitation might be misleading as the polyclonal background changes.

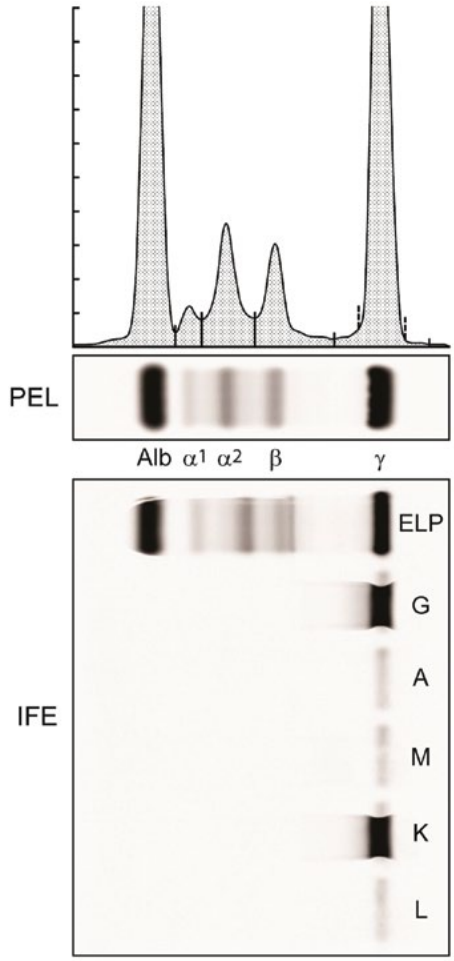

FIGURE 5 Large M protein with suppressed polyclonal immunoglobulins.

When small monoclonal IgA or IgM proteins migrate in the beta fraction instead of the gamma fraction, monitoring becomes more complex. In the case illustrated in Fig. 6, we might decide not to fractionate and quantitate, but we could still see the abnormality. If migration is in the beta fraction, we cannot visualize the protein because it is obscured by transferrin, C3, and other serum proteins. It is useful in these cases to use quantitative immunoglobulins to assist monitoring of IgA and IgM proteins. However, if one uses CE and ISE, which give good resolution of the beta 1 and beta 2 peaks, one may be able to isolate the abnormality or estimate the portion of the beta region that has been subtracted and provide a reliable value (Fig. 7) (60). Changes in the sizes of the beta fraction and the quantitative immunoglobulin or in the ISE-supported measurement should be concordant. New heavy/light-chain reagents that can separately quantify IgG kappa and IgG lambda, IgA kappa and IgA lambda, and IgM kappa and IgM lambda may be useful for these patients. The heavy/light, isotype-specific kappa-to-lambda ratio has been proposed as a potential monitoring method for M proteins migrating in the beta fraction. Even though the monoclonal protein is not visualized by PEL, an abnormal heavy/light kappa-to-lambda ratio indicates excess clonal synthesis analogous to the use of the FLC kappa-to-lambda ratio (61–63). The international guidelines do not address measurement of a low concentration monoclonal intact immunoglobulin.

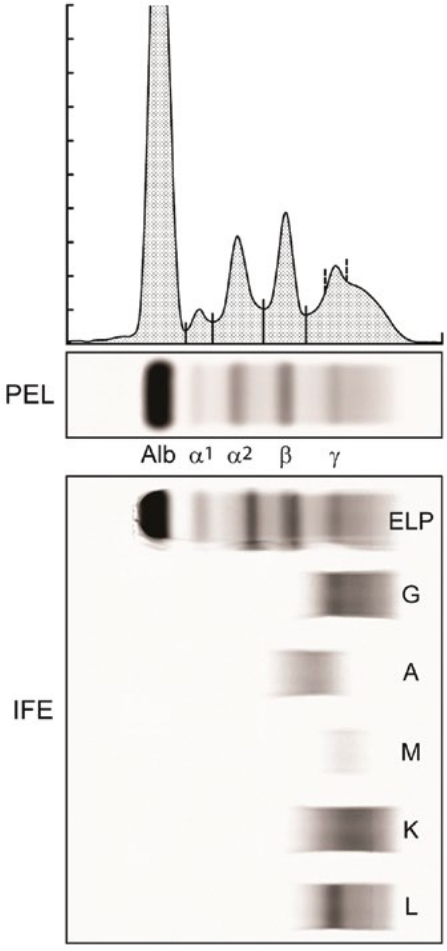

FIGURE 6 Small M protein within a background of polyclonal immunoglobulins.

The AL patient whose results are illustrated in Fig. 4 is an example of a case in which the lambda M protein cannot be quantified by serum or urine PEL M-spike, quantitative immunoglobulin, or heavy/light-chain assays. The FLC immunoassays, however, can be performed, and the lambda FLC concentration can be used to monitor this patient. The international guidelines for monitoring monoclonal gammopathies suggest that if the serum M-spike is less than 1 g/dl and the urine M-spike is less than 200 mg/24 h, only then should the FLC be considered for monitoring (45). The guidelines for FLC quantitation state that in order to monitor a "measurable" free light chain to document response to treatment, the FLC ratio should be abnormal and the concentration of the monoclonal FLC should be greater than 10 mg/dl (Table 4).

The international guidelines for "measurable" M proteins also define what changes are needed for partial, complete, and stringent responses when treating MM (Table 5) (64). A complete response is defined as a normal serum and urine IFE (as well as the absence of bone marrow plasma cells). A stringent complete response is a complete response plus a normal FLC kappa-to-lambda ratio. Partial responses are defined by the following decreases in measurable M proteins: a 50% decrease in the serum M-spike measurement, a 90% decrease in the urine M-spike measurement, and a 50% decrease in serum FLC concentration. In order to test

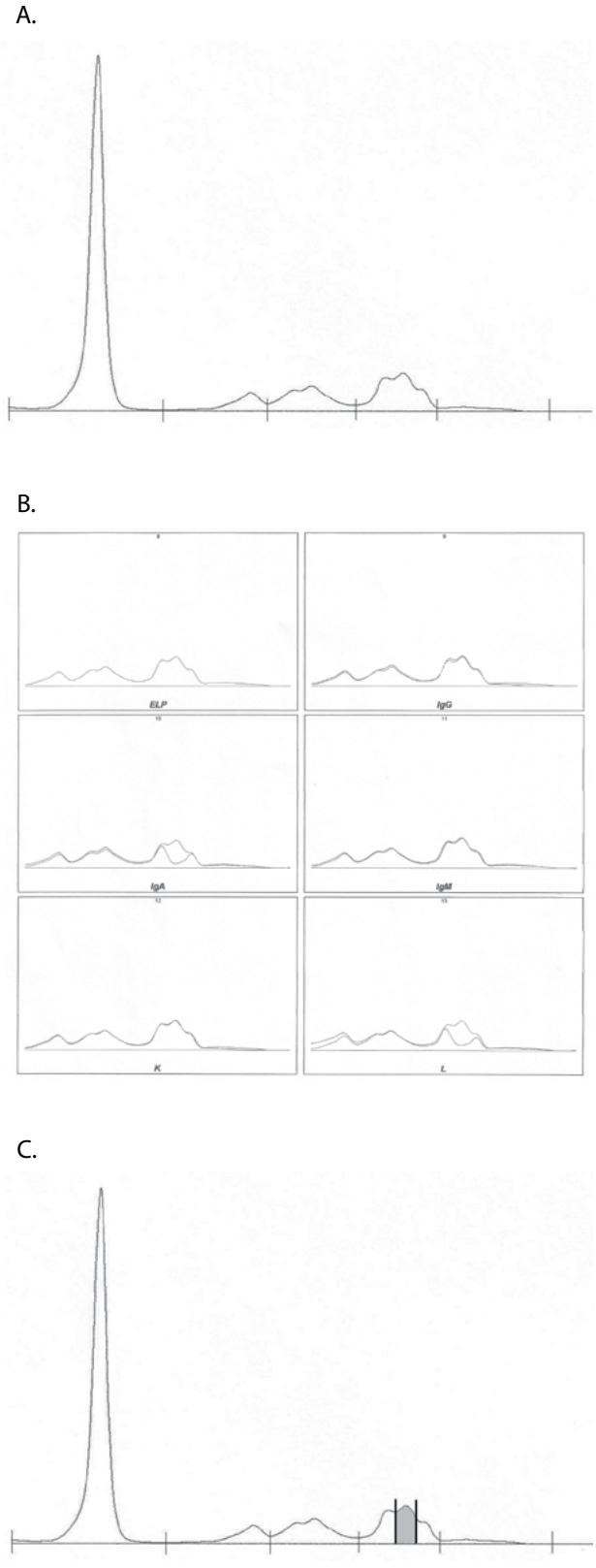

FIGURE 7 (A) Use of ISE to estimate the area of small beta-migrating M proteins. Capillary electropherogram with beta region restriction and hypogammaglobulinemia. (B) Immunosubtraction demonstrating that anti-IgA and anti-L subtract the M protein in the mid-beta region. (C) Use ISE data to demarcate and measure the M protein concentration.

TABLE 4 Response criteria for FLC determination[a]

Disease	FLC level and/or response or recommendation				
	Minimal measurable	Partial response	Complete response	Stringent complete response	Progression
AL without measurable serum or urine M protein	iFLC ≥ 10 mg/dl	50% reduction	Normal rFLC and bone marrow, complete response by IFE	ND	50% increase of iFLC to >10 mg/dl
MM without measurable serum or urine M protein	iFLC 10 mg/dl	50% reduction of dFLC	ND	Normal rFLC, complete response by IFE, and bone marrow	50% increase of dFLC
MM with measurable disease	Do not test FLC	Do not test FLC	Do not test FLC	Normal rFLC and bone marrow, complete response by IFE	Do not test FLC

[a]iFLC, involved free light chain; rFLC, ratio of free kappa/free lambda light chain; dFLC, difference between involved FLC types and uninvolved FLC types; ND, not determined. This table was modified from reference 66.

these partial-response guidelines, the Mayo group has studied the variability of long-term, sequential serum and urine samples in MM patients who have already reached stable, partial remissions (65). The study indicated that the biologic and disease-related variation in these stable patients was 8% for serum M-spike measurements, 12% for immunoglobulin quantitation, 28% for serum monoclonal FLC concentrations, and 36% for urine M-spike measurements. These variability data suggest that the serum FLC quantitation has variability that is more like that of the urine M-spike measurement. The concentrations of both serum FLC and urine M-spike depend on the synthesis and rapid clearance of the low-molecular-weight light chain. The serum M-spike depends on the synthesis and very slow clearance of intact immunoglobulin. The serum M-spike measurement has the lowest biological variability, and when possible, it is the parameter of choice for monitoring disease.

SUGGESTED ORDERING PATTERNS

Although plasma cell proliferative disorders are diverse, the suggested panel of serum PEL, IFE, and FLC provides relatively simple and sensitive diagnostic testing. However, a few suggestions that might encourage a more logical pattern of ordering based on initial presentation or monitoring needs are provided here. Order formats can provide several embedded clinical situations, allowing clinicians to request testing that is specific to their patient without needing to know details of the laboratory's armamentarium.

1. In an initial screen for MM, WM, or AL, perform a serum PEL-IFE-FLC three-assay screen. If the assay is negative, the clinician is sent a request to provide early-morning urine for urine IFE.
2. In an initial screen for POEMS syndrome or neuropathy (sensory or motor) suspected of being associated with an M protein, perform serum IFE only.
3. For follow-up for a known M protein in serum or urine, perform PEL only. If PEL is negative, resort to IFE.
4. For follow-up for abnormal serum FLC (includes oligosecretory MM and AL amyloid with no measurable urine light chains), perform serum FLC.
5. Confirm stringent complete remission by serum FLC.

SUMMARY

Depending on the particular monoclonal protein, the detection of M proteins may require serum PEL and IFE, urine PEL and IFE, and serum FLC quantitation. A diagnostic screening panel of serum PEL, IFE, and FLC has been recommended for detection of most plasma cell proliferative disorders. If AL is suspected, urine PEL and IFE should be included as well. The use of this diagnostic panel also guides laboratories and clinicians to the best approach to monitor disease.

TABLE 5 International Myeloma Working Group criteria for response to therapy

Response	IMWG criteria
Stringent complete response	Complete response, normal rFLC, and absence of clonal cells in bone marrow by immunohistochemistry or immunofluorescence
Complete response	Negative serum and urine IFE, disappearance of any soft tissue plasmacytomas, and ≤5% plasma cells in bone marrow
Very good partial response	Serum and urine M protein seen by IFE but not by electrophoresis or ≥90% reduction in serum M protein plus a urine M protein level of <100 mg/24 h
Partial response	≥50% reduction of serum M protein and reduction in 24-h urinary M protein by ≥90% or to <200 mg/24 h

REFERENCES

1. **Keren DF, Alexanian R, Goeken JA, Gorevic PD, Kyle RA, Tomar RH.** 1999. Guidelines for clinical and laboratory evaluation of patients with monoclonal gammopathies. *Arch Pathol Lab Med* **123:**106–107.
2. **Keren D.** 2012. *Protein Electrophoresis in Clinical Diagnosis*. ASCP Press, Chicago, IL.
3. **Kyle RA.** 1999. Sequence of testing for monoclonal gammopathies. *Arch Pathol Lab Med* **123:**114–118.
4. **Drew R.** 2001. Highly sensitive automated immunoassay for immunoglobulin free light chains in serum and urine. *Clin Chem* **47:**637–680.
5. **Katzmann JA.** 2009. Screening panels for monoclonal gammopathies: time to change. *Clin Biochem Rev* **30:**105–111.
6. **Siegel R, Naishadham D, Jemal A.** 2013. Cancer statistics, 2013. *CA Cancer J Clin* **63:**11–30.
7. **Kyle RA, Gertz MA, Witzig TE, Lust JA, Lacy MQ, Dispenzieri A, Fonseca R, Rajkumar SV, Offord JR, Larson DR, Plevak ME, Therneau TM, Greipp PR.** 2003. Review of 1027 patients with newly diagnosed multiple myeloma. *Mayo Clin Proc* **78:**21–33.
8. **Bladé J, Kyle RA.** 1998. Multiple myeloma in young patients: clinical presentation and treatment approach. *Leuk Lymphoma* **30:**493–501.
9. **Waxman AJ, Mink PJ, Devesa SS, Anderson WF, Weiss BM, Kristinsson SY, McGlynn KA, Landgren O.** 2010. Racial disparities in incidence and outcome in multiple myeloma: a population-based study. *Blood* **116:**5501–5506.
10. **Riedel DA, Pottern LM.** 1992. The epidemiology of multiple myeloma. *Hematol Oncol Clin North Am* **6:**225–247.
11. **Smith A, Wisloff F, Samson D.** 2005. UK Myeloma Forum, Nordic Myeloma Study Group, British Committee for Standards in Haematology. Guidelines on the diagnosis and management of multiple myeloma. *Br J Haematol* **132:**410–451.
12. **International Myeloma Working Group.** 2003. Criteria for the classification of monoclonal gammopathies, multiple myeloma and related disorders: a report of the International Myeloma Working Group. *Br J Haematol* **121:**749–757.
13. **Ozsahin M, Tsang RW, Poortmans P, Belkacémi Y, Bolla M, Dinçbas FO, Landmann C, Castelain B, Buijsen J, Curschmann J, Kadish SP, Kowalczyk A, Anacak Y, Hammer J, Nguyen TD, Studer G, Cooper R, Sengöz M, Scandolaro L, Zouhair A.** 2006. Outcomes and patterns of failure in solitary plasmacytoma: a multicenter Rare Cancer Network study of 258 patients. *Int J Radiat Oncol Biol Phys* **64:**210–217.
14. **Tiedemann RE, Gonzalez-Paz N, Kyle RA, Santana-Davila R, Price-Troska T, Van Wier SA, Chng WJ, Ketterling RP, Gertz MA, Henderson K, Greipp PR, Dispenzieri A, Lacy MQ, Rajkumar SV, Bergsagel PL, Stewart AK, Fonseca R.** 2008. Genetic aberrations and survival in plasma cell leukemia. *Leukemia* **22:**1044–1052.
15. **Wahner-Roedler DL, Kyle RA.** 2005. Heavy chain diseases. *Best Pract Res Clin Haematol* **18:**729–746.
16. **López-Anglada L, Puig N, Díez-Campelo M, Alonso-Ralero L, Barrena S, Aparicio MA, Gutiérrez NC, García-Sanz R.** 2010. Monoclonal free light chains can be found in heavy chain diseases. *Ann Clin Biochem* **47:**570–572.
17. **Landgren O, Kyle RA, Pfeiffer RM, Katzmann JA, Caporaso NE, Hayes RB, Dispenzieri A, Kumar S, Clark RJ, Baris D, Hoover R, Rajkumar SV.** 2009. Monoclonal gammopathy of undetermined significance (MGUS) consistently precedes multiple myeloma: a prospective study. *Blood* **113:**5412–5417.
18. **Tsai H, Caporaso NE, Kyle RA, Katzmann JA, Dispenzieri A, Hayes RB, Marti GE, Albitar M, Ghia P, Rajkumar SV, Landgren O.** 2009. Evidence of serum immunoglobulin abnormalities up to 9.8 years before diagnosis of chronic lymphocytic leukemia: a prospective study. *Blood* **114:**4928–4932.
19. **Weiss BM, Abadie J, Verma P, Howard RS, Kuehl WM.** 2009. A monoclonal gammopathy precedes multiple myeloma in most patients. *Blood* **113:**5418–5422.
20. **Kyle RA, Rajkumar SV.** 2006. Monoclonal gammopathy of undetermined significance. *Br J Haematol* **134:**573–589.
21. **Kyle RA, Therneau TM, Rajkumar SV, Larson DR, Plevak MF, Offord JR, Dispenzieri A, Katzmann JA, Melton LJ III.** 2006. Prevalence of monoclonal gammopathy of undetermined significance. *N Engl J Med* **354:**1362–1369.
22. **Wadhera RK, Rajkumar SV.** 2010. Prevalence of monoclonal gammopathy of undetermined significance: a systematic review. *Mayo Clin Proc* **85:**933–942.
23. **Kyle RA, Therneau TM, Rajkumar SV, Offord JR, Larson DR, Plevak MF, Melton LJ III.** 2002. A long-term study of prognosis in monoclonal gammopathy of undetermined significance. *N Engl J Med* **346:**564–569.
24. **Rajkumar SV.** 2012. Preventive strategies in monoclonal gammopathy of undetermined significance and smoldering multiple myeloma. *Am J Hematol* **87:**453–454.
25. **Cesana C, Klersy C, Barbarano L, Nosari AM, Crugnola M, Pungolino E, Gargantini L, Granata S, Valentini M, Morra E.** 2002. Prognostic factors for malignant transformation in monoclonal gammopathy of undetermined significance and smoldering multiple myeloma. *J Clin Oncol* **20:**1625–1634.
26. **Rajkumar SV, Kyle RA, Therneau TM, Melton LJ III, Bradwell AR, Clark RJ, Larson DL, Plevak MF, Dispenzieri A, Katzmann JA.** 2005. Serum free light chain ratio is an independent risk factor for progression in monoclonal gammopathy of undetermined significance (MGUS). *Blood* **106:**812–817.
27. **Kyle RA, Greipp PR.** 1980. Smoldering multiple myeloma. *N Engl J Med* **302:**1347–1379.
28. **Kyle RA, Remstein ED, Therneau TM, Dispenzieri A, Kurtin PJ, Hodnefield JM, Larson DR, Plevak MF, Jelinek DF, Fonseca R, Melton LJ III, Rajkumar SV.** 2007. Clinical course and prognosis of smoldering (asymptomatic) multiple myeloma. *N Engl J Med* **356:**2582–2590.
29. **Rosiñol L, Bladé J, Esteve J, Aymerich M, Rozman M, Montoto S, Giné E, Nadal E, Filella X, Queralt R, Carrió A, Montserrat E.** 2003. Smoldering multiple myeloma: natural history and recognition of an evolving type. *Br J Haematol* **123:**631–636.
30. **Rajkumar SV, Merlini G, San Miguel JF.** 2012. Haematological cancer: redefining myeloma. *Nat Rev Clin Oncol* **9:**494–496.
31. **Rajkumar SV, Larson DL, Kyle RA.** 2011. Diagnosis of smoldering multiple myeloma. *N Engl J Med* **365:**474–475.
32. **Larsen JT, Kumar SK, Dispenzieri A, Kyle RA, Katzmann JA, Rajkumar SV.** 2013. Serum free light chain ratio as a biomarker for high-risk smoldering multiple myeloma. *Leukemia* **27:**941–946.
33. **Mateos M, Hearnandez M, Giraldo P, de la Rubia J, de Arriba F, López Corral L, Rosiñol L, Paiva B, Palomera L, Bargay J, Oriol A, Prosper F, López J, Olavarría E, Quintana N, García JL, Bladé J, Lahuerta JJ, San Miguel JF.** 2013. Lenalidomide plus dexamethasone for high-risk smoldering multiple myeloma. *N Engl J Med* **369:**438–447.
34. **Gertz MA, Lacy MQ, Dispenzieri A, Hayman SR.** 2009. Immunoglobulin light-chain amyloidosis (primary amyloidosis), p 2439–2470. *In* Greer JP, Forester J, Rodgers GM, Paraskevus F, Glader B, Arber DA, Meares RT Jr (ed), *Wintrobe's Clinical Hematology*, 12th ed, vol 2. Wolters Kluwer Health/Lippincott Williams & Wilkins, Philadelphia, PA.
35. **Palladini G, Russo P, Bosoni T, Verga L, Sarais G, Lavatelli F, Nuvolone M, Obici L, Casarini S, Donadei S,**

Albertini R, Righetti G, Marini M, Graziani MS, Melzi D'Eril GV, Moratti R, Merlini G. 2009. Identification of amyloidogenic light chains requires the combination of serum-free light chain assay with immunofixation of serum and urine. *Clin Chem* **55:**499–504.

36. **Abraham R, Katzmann JA, Clark RJ, Bradwell AR, Kyle RA, Gertz MA.** 2003. Quantitative analysis of serum free light chains. A new marker for the diagnostic evaluation of primary systemic amyloidosis. *Am J Clin Pathol* **119:**274–278.
37. **Lachmann HJ, Gallimore R, Gillmore JD, Carr-Smith HD, Bradwell AR, Pepys MB, Hawkins PM.** 2003. Outcome in systemic AL amyloidosis in relation to changes in concentration of circulating free immunoglobulin light chains following chemotherapy. *Br J Haematol* **122:**78–84.
38. **Vrana JA, Gamez JD, Madden BJ, Theis JD, Bergen HR III, Dogan A.** 2009. Classification of amyloidosis by laser microdissection and mass spectrometry-based proteomic analysis in clinical biopsy specimens. *Blood* **114:**4957–4959.
39. **Brambilla F, Lavatelli F, Di Silvestre D, Valentini V, Rossi R, Palladini G, Obici L, Verga L, Mauri P, Merlini G.** 2012. Reliable typing of systemic amyloidoses through proteomic analysis of subcutaneous adipose tissue. *Blood* **119:**1844–1847.
40. **Dispenzieri A.** 2012. POEMS syndrome: update on diagnosis, risk-stratification, and management. *Am J Hematol* **87:**805–814.
41. **Latov N.** 1995. Pathogenesis and therapy of neuropathies associated with monoclonal gammopathies. *Ann Neurol* **37**(Suppl 1)**:**S32–S42.
42. **Katzmann JA, Clark R, Wiegert E, Sanders E, Oda RP, Kyle RA, Namyst-Goldberg C, Landers JP.** 1997. Identification of monoclonal proteins in serum: a quantitative comparison of acetate, agarose gel, and capillary electrophoresis. *Electrophoresis* **18:**1775–1780.
43. **Bienvenu J, Graziani MS, Arpin F, Bernon Blessum HC, Marchetti C, Righetti G, Somenzini M, Verga G, Aguzzi F.** 1998. Multicenter evaluation of the Paragon CZE 2000 capillary zone electrophoresis system for serum protein electrophoresis and monoclonal protein typing. *Clin Chem* **44:**599–605.
44. **Velthuis H, Knop I, Stam P, van den Broek M, Bos HK, Hol S, Teunissen E, Fischedick KS, Althaus H, Schmidt B, Wagner C, Melsert R.** 2011. N Latex FLC—new monoclonal high-performance assays for the determination of free light chain kappa and lambda. *Clin Chem Lab Med* **49:**1323–1332.
45. **Dispenzieri A, Kyle R, Merlini G, Miguel JS, Ludwig H, Hajek R, Palumbo A, Jagannath S, Blade J, Lonial S, Dimopoulos M, Comenzo R, Einsele H, Barlogie B, Anderson K, Gertz M, Harousseau JL, Attal M, Tosi P, Sonneveld P, Boccadoro M, Morgan G, Richardson P, Sezer O, Mateos MV, Cavo M, Joshua D, Turesson I, Chen W, Shimizu K, Powles R, Rajkumar SV, Durie BG, International Myeloma Working Group.** 2009. International Myeloma Working Group guidelines for serum-free light chain analysis in multiple myeloma and related disorders. *Leukemia* **23:**215–224.
46. **Katzmann JA, Abraham RS, Dispenzieri A, Lust JA, Kyle RA.** 2005. Diagnostic performance of quantitative kappa and lambda free light chain assays in clinical practice. *Clin Chem* **51:**878–881.
47. **Katzmann JA, Clark RJ, Abraham RS, Bryant S, Lymp FJ, Bradwell AR, Kyle RA.** 2002. Serum reference intervals and diagnostic ranges for free kappa and free lambda immunoglobulin light chains: relative sensitivity for detection of monoclonal light chains. *Clin Chem* **48:**1437–1444.
48. **Dispenzieri A, Zhang L, Katzmann JA, Snyder M, Blood E, Degoey R, Henderson K, Kyle RA, Oken MM, Bradwell AR, Greipp PR.** 2008. Appraisal of immunoglobulin free light chain as a marker of response. *Blood* **111:**4908–4915.
49. **Katzmann JA, Dispenzieri A, Kyle RA, Snyder MR, Plevak MF, Larson DR, Abraham RS, Lust JA, Melton JL, Rajkumar SV.** 2006. Elimination of the need for urine studies in the screening algorithms for monoclonal gammopathies by using serum immunofixation and free light chain assays. *Mayo Clin Proc* **81:**1575–1578.
50. **Piehler AP, Gulbrandsen N, Kierulf P, Urdal P.** 2008. Quantitation of serum free light chains in combination with protein electrophoresis and clinical information for diagnosing multiple myeloma in a general hospital population. *Clin Chem* **54:**1823–1830.
51. **Katzmann JA, Kyle RA, Benson J, Larson DR, Snyder MR, Lust JA, Rajkumar SV, Dispenzieri A.** 2009. Screening panels for detection of monoclonal gammopathies. *Clin Chem* **55:**1517–1522.
52. **Hill PG, Forsyth JM, Rai B, Mayne S.** 2006. Serum free light chains: an alternative test to urine Bence Jones proteins when screening for monoclonal gammopathies. *Clin Chem* **52:**1743–1748.
53. **Bakshi NA, Gulbranson R, Garstka D, Bradwell AR, Keren DF.** 2005. Serum free light chain (FLC) measurement can aid capillary zone electrophoresis in detecting subtle FLC-producing M-proteins. *Am J Clin Pathol* **124:**214–218.
54. **Nowrousian MR, Brandhorst D, Sammet C, Kellert M, Daniels R, Schiett P, Poser M, Mueller S, Ebeling P, Welt A, Bradwell AR, Buttkereit U, Opalka B, Flasshove M, Moritz T, Seeber S.** 2005. Serum free light chain analysis and urine immunofixation electrophoresis in patients with multiple myeloma. *Clin Cancer Res* **11:**8706–8714.
55. **Snozek CL, Katzmann JA, Kyle RA, Dispenzieri A, Larson DR, Therneau TM, Melton LJ III, Kumar S, Greipp PR, Clark RJ, Rajkumar SV.** 2008. Prognostic value of the serum free light chain ratio in newly diagnosed myeloma: proposed incorporation into the international staging system. *Leukemia* **22:**1933–1937.
56. **Dispenzieri A, Lacy MQ, Katzmann JA, Rajkumar SV, Abraham RS, Hayman SR, Kumar SK, Clark R, Kyle RA, Litzow MR, Inwards DJ, Ansell SM, Micallef IM, Porrata LF, Elliott MA, Johnston PB, Greipp PR, Witzig TE, Zeldenrust SR, Russell SJ, Gastineau D, Gertz MA.** 2006. Absolute values of immunoglobulin free light chains are prognostic in patients with primary systemic amyloidosis undergoing peripheral blood stem cell transplantation. *Blood* **107:**3378–3383.
57. **Dingli D, Kyle RA, Rajkumar SV, Nowakowski GS, Larson DR, Bida JP, Gertz MA, Therneau TM, Melton LJ III, Dispenzieri A, Katzmann JA.** 2006. Immunoglobulin free light chains and solitary plasmacytoma of bone. *Blood* **108:**1979–1983.
58. **Murray DL, Seningen JL, Dispenzieri A, Snyder MR, Kyle RA, Rajkumar SV, Katzmann JA.** 2012. Laboratory persistence and clinical progression of small monoclonal abnormalities. *Am J Clin Pathol* **138:**609–613.
59. **Murray DL, Rye E, Snyder MR, Katzmann JA.** 2009. Quantitation of serum monoclonal proteins: relationship between agarose gel electrophoresis and immunonephelometry. *Clin Chem* **55:**1523–1529.
60. **Keren DF.** 2012. *Laboratory Strategies for Diagnosing Monoclonal Gammopathies*, p 197– 211. ASCP Press, Chicago, IL.
61. **Bradwell AR, Harding SJ, Fourrier NJ, Wallis GLF, Drayson MT, Carr-Smith HD, Mead GP.** 2009. Assessment of monoclonal gammopathies by nephelometric measurement of individual immunoglobulin kappa/lambda ratios. *Clin Chem* **55:**1646–1655.
62. **Donato LJ, Zeldenrust SR, Murray DL, Katzmann JA.** 2011. A 71-year-old woman with multiple myeloma status after stem cell transplantation. *Clin Chem* **57:**1645–1648.

63. **Ludwig H, Milosavljevic D, Zojer N, Faint JM, Bradwell AR, Hubl W, Harding SJ.** 2013. Immunoglobulin heavy/light chain ratios improve paraprotein detection and monitoring, identify residual disease and correlate with survival in multiple myeloma patients. *Leukemia* **27:**213–219.
64. **Durie BGM, Harousseau J-L, Miguel JS, Blade J, Barlogie B, Anderson K, Gertz M, Dimopoulos M, Westin J, Sonneveld P, Ludwig H, Gahrton G, Beksac M, Crowley J, Belch A, Boccadaro M, Cavo M, Turesson I, Joshua D, Vesole D, Kyle R, Alexanian R, Tricot G, Attal M, Merlini G, Powles R, Richardson P, Shimizu K, Tosi P, Morgan G, Rajkumar SV, International Myeloma Working Group.** 2006. International uniform response criteria for multiple myeloma. *Leukemia* **20:**1467–1473.
65. **Katzmann JA, Snyder MR, Rajkumar SV, Kyle RA, Therneau TM, Benson JT, Dispenzieri A.** 2011. Long-term biological variation of serum protein electrophoresis M-spike, urine M-spike, and monoclonal serum free light chain quantification: implications for monitoring monoclonal gammopathies. *Clin Chem* **57:**1687–1692.
66. **International Myeloma Foundation.** 2011. *IMWG Guidelines for Serum Free Light Chain Analysis in Multiple Myeloma and Related Disorders*. International Myeloma Foundation, North Hollywood, CA. http://myeloma.org/pdfs/IMWG_Guidelines_for_Serum_Free_Light_Chain.pdf.

COMPLEMENT *section C*

VOLUME EDITOR: ROBERT G. HAMILTON
SECTION EDITOR: PATRICIA C. GICLAS

Introduction

PATRICIA C. GICLAS

12

The field of complementology has advanced remarkably in the past 2 decades, due to newly found connections between often subtle complement abnormalities and diverse diseases. This is reflected in the exponential growth of new publications and the development of novel therapeutics that were previously unavailable for treatment of patients with complement deficiencies or other abnormalities of the system (1). The interest in complement displayed by the pharmaceutical industry has been motivated not only by the desire to create therapeutics for patients with rare complement-mediated diseases but by the necessity to prevent undue adverse events caused by complement activation when new drugs or delivery systems are used *in vivo*. One of the first examples of this in humans was the development of an anaphylactoid response following the infusion of radiocontrast agents or exposure of blood to some of the early types of dialysis membranes that activated complement (2). Additional examples of complement activation by diverse compounds include liposomes, nanoparticles of various types, biologicals (mainly antibody based), and DNA- or RNA-based drugs such as phosphorothioate oligonucleotides (antisense) (3, 4). The term complement activation-related pseudoallergy, or CARPA, applies to some of these reactions (5).

Errors in the production of control proteins was beautifully demonstrated in the 1960s with the discovery of C1 inhibitor deficiency as the cause of hereditary angioedema (HAE) and the explanation of the two forms of deficiency: type I due to lack of production of the protein by the affected allele and type II caused by multiple polymorphisms in the gene sequence that result in production of dysfunctional protein (6, 7). Since the original classification, patients with hereditary forms of angioedema, but with normal C1 inhibitor, have continued to puzzle clinicians. Descriptions of the several forms of HAE have been published recently by international consensus groups. They include hereditary and acquired angioedema (HAE and AAE, respectively) with C1 inhibitor deficiency, idiopathic nonhistaminergic AAE, AAE related to angiotensin-converting enzyme, HAE with normal C1 inhibitor and factor XII mutation, and unknown HAE (8, 9, 10). Treatment is based on the administration of human plasma or purified or recombinant C1 inhibitor protein preparations to replace the missing inhibitor, or inhibitors of plasma kallikrein or a bradykinin receptor antagonist to prevent bradykinin production or activity. Older treatments still in use include epsilon aminocaproic acid (inhibitor of plasminogen) and its derivatives, and anabolic androgens that stimulate C1 inhibitor production (11).

A number of additional proteins involved in regulation of complement activity have been found to have dysfunctional forms. The availability of genetic analytical methods has made it possible to determine the exact defect responsible for a given deficiency as well as scan large portions of the genome. Interest in the inheritance of genetic factors that could be linked to age-related macular degeneration (AMD), a disease that causes debilitating loss of vision and eventual blindness in a large number of patients, led to the discovery of the involvement of complement in AMD pathology. The identification of a single nucleotide polymorphism in the gene for factor H that was associated with a high risk for AMD opened up a new approach to studies of complement in AMD (12, 13, 14). The discovery of the same polymorphisms in patients with certain rare kidney diseases, particularly those previously identified as forms of membranoproliferative glomerulonephritis, led to finding genes for proteins in control of the alternative pathway of complement that were also associated with risk. The treatment with monoclonal anti-C5 antibody has decreased the morbidity and mortality of these patients and offers a model for other therapeutic agents to control aberrant behavior by complement activity.

Another area of complement that has blossomed in the past 10 years is its connection through the lectin pathway to the primitive origins of innate immunity. Looking back through the ages, one can find complement-like activity in the early Cambrian era in ascidians and other creatures. They developed systems to trap invading microorganisms by a circulatory lectin system that first bound to the microbial surface sugars by way of pattern recognition and then initiated clotting of the hemolymph so that phagocytic cells in the circulation could ingest and destroy the potential pathogens. In the laboratory, scientists have taken advantage of this simple system from the horseshoe crab, using the lectin-binding, enzyme-activating ability to detect endotoxins in many compounds. As the acquired immune system evolved in vertebrates, the ability of C1q to recognize bound immunoglobulins gave complement the unique ability to identify a microbial target by means of lectin direct activation or classical pathway antibody-driven activation. As scientists, our ability to measure the latter event has been exploited in the laboratory in many different complement functional

doi:10.1128/9781555818722.ch12

assays, but the lectin pathway has not been widely explored as an adjunct to complement evaluation. A recent article by Atkinson and Frank discussed the ability of the lectin pathway to provide a bypass mechanism for generating C3 cleavage in serum deficient of C4 or C2, a mechanism that may explain the observation that patients lacking these proteins tend to have relatively mild disease (15). Chapter 14 in this section describes a new assay for analyzing the function of mannose-binding lectin that should be useful for further studies of this important system. More information about this system will be forthcoming in the near future.

REFERENCES

1. **Ricklin D, Lambris JD.** 2013. Progress and trends in complement therapeutics. *Adv Exp Med Biol* **735:**1–22.
2. **Craddock PR, Fehr J, Dalmasso AP, Brighan KL, Jacob HS.** 1977. Hemodialysis leukopenia. Pulmonary vascular leukostasis resulting from complement activation by dialyzer cellophane membranes. *J Clin Investig* **59:**879–888.
3. **Galbraith WM, Hobson WC, Giclas PC, Schechter PJ, Agrawal S.** 1994. Complement activation and hemodynamic changes following intravenous administration of phosphorothioate oligonucleotides in the monkey. *Antisense Res Dev* **4:**201–206.
4. **Henry SP, Jagels MA, Hugli TE, Manalili S, Geary RS, Giclas PC, et al.** 2014. Mechanism of alternative complement pathway dysregulation by a phosphorothioate oligonucleotide in monkey and human serum. *Nucleic Acid Ther* **24:**326–335.
5. **Szebeni J.** 2014. Complement activation-related pseudoallergy: a stress reaction in blood triggered by nanomedicines and biologicals. *Mol Immunol* **61:**163–173.
6. **Donaldson VH, Evans RR.** 1963. A biochemical abnormality in herediatry angioneurotic edema: absence of serum inhibitor of C′ 1-esterase. *Am J Med* **35:**37–44.
7. **Rosen FS, Alper CA, Pensky J, Klemperer MR, Donaldson VH.** 1971. Genetically determined heterogeneity of the C1 esterase inhibitor in patients with hereditary angioneurotic edema. *J Clin Investig* **50:**2143–2149.
8. **Bowen T, Cicardi M, Farkas H, Bork K, Longhurst HJ, Zuraw B, et al.** 2010. 2010 International consensus algorithm for the diagnosis, therapy and management of hereditary angioedema. *Allergy Asthma Clin Immunol* **6:**24.
9. **Zuraw BL, Bork K, Binkley KE, Banerji A, Christiansen SC, Castaldo A, et al.** 2012. Hereditary angioedema with normal C1 inhibitor function: consensus of an international expert panel. *Allergy Asthma Proc* **33**(Suppl 1)**:**S145–S156.
10. **Bork K, Wulff K, Meinke P, Wagner N, Hardt J, Witzke G.** 2011. A novel mutation in the coagulation factor 12 gene in subjects with hereditary angioedema and normal C1-inhibitor. *Clin Immunol* **141:**31–35.
11. **Cicardi M, Aberer W, Banerji A, Bas M, Bernstein JA, Bork K, et al.** 2014. Classification, diagnosis, and approach to treatment for angioedema: consensus report from the Hereditary Angioedema International Working Group. *Allergy* **69:**602–616.
12. **Edwards AO, Ritter R 3rd, Abel KJ, Manning A, Panhuysen C, Farrer LA.** 2005. Complement factor H polymorphism and age-related macular degeneration. *Science* **308:**421–424.
13. **Hageman GS, Anderson DH, Johnson LV, Hancox LS, Taiber AJ, Hardisty LI, et al.** 2005. A common haplotype in the complement regulatory gene factor H (HF1/CFH) predisposes individuals to age-related macular degeneration. *Proc Natl Acad Sci USA* **102:**7227–7232.
14. **Haines JL, Hauser MA, Schmidt S, Scott WK, Olson LM, Gallins P, et al.** 2005. Complement factor H variant increases the risk of age-related macular degeneration. *Science* **308:**419–421.
15. **Atkinson JP, Frank MM.** 2006. Bypassing complement: evolutionary lessons and future implications. *J Clin Investig* **116:**1215–1218.

The Classical Pathway of Complement

PATRICIA C. GICLAS

13

BACKGROUND

Complement evolved in parallel with coagulation as part of the primordial explosion of life in the Cambrian era. Remnants of this connection still exist in vertebrate animals as well as invertebrates. A classic example is the horseshoe crab, *Limulus polyphemus*, still sought after by scientists today to test substances for traces of bacterial lipopolysaccharide (endotoxin). The system used by the crabs had a molecule that recognized bacteria or other invaders that got into the hemolymph of the crab. An enzyme triggered by the first molecule induced local coagulation that served to trap the microbes so that they could be destroyed by phagocytes in the animal's circulation.

The complement system was discovered over 100 years ago by a group of scientists who detected its ability to kill bacteria that were injected into guinea pigs or exposed to fresh blood or serum *in vitro*. At that time, in the late 1800s to early 1900s, none of the components were known, and the phenomenon was described as an "activity" that was present in fresh serum but was destroyed by heat (1). We now understand how important the complement system is to innate and acquired immunity and its contribution to infection and the maintenance of health on many different fronts. The diversity of the complement system is displayed in its ability to rapidly react to a threat as part of innate immunity. As an illustration, the lectins, along with the classical complement pathway, are important components of the acquired immune response. They contribute to the alternative pathway's ability to amplify the power of complement activation.

Of the three pathways that initiate complement activation (Fig. 1), the classical pathway developed the ability to participate with evolving cellular and antibody responses of acquired immunity. It was this ability to complete, or "complement," the action of antibody-mediated defenses that gave the system its name. The following discussion will briefly describe the proteins and their interactions in the classical pathway and discuss some of the laboratory approaches to the diagnosis of patients with deficiencies in the classical pathway.

PROTEINS OF THE CP: C1q, C1r, C1s, C2, C4

Classical pathway (CP) activation is initiated when the C1 complex, comprising $C1q_1C1r_2C1s_2$+calcium, binds to an appropriate activator. C1q is a complex molecule that looks, on electron micrographs, like a bunch of six tulips. Using this analogy, the six stalks have protein sequences similar to collagen and are susceptible to collagenase. The six rigid stalks are each connected by flexible protein stems to the six "flowers" on their tips. It is the globular protein "flowers" that have binding specificity for immunoglobulins, apoptotic cell membranes, and several other surfaces.

The most common classical complement pathway activators are antibodies of the immunoglobulin M (IgM) or IgG class that are bound to antigen. The order of their binding affinity for C1q, in descending order, is as follows: IgM > IgG3 > IgG1 > IgG2. IgG4, IgA, and IgE antibodies do not activate C1. To start the classical complement pathway enzyme cascade, the C1q binds to at least two IgG antibodies, or one IgM antibody, by contacting the carbohydrate in the antibody's hinge region that was exposed when the antibody binds to its antigen. This causes a change in the C1q molecule so that the C1r and C1s proenzymes are released.

C1r rapidly converts to its active form and cleaves C1s. It is the latter molecule that was first identified as C1-esterase. The activity of these two enzymes is controlled in plasma by the serine protease inhibitor, C1-esterase inhibitor (C1-Inh) (2, 3).

The next two proteins to be activated in the CP are the two substrates of C1s: components C4 and C2. C4 is a major serum protein with some interesting properties. First, there are two forms of C4 in the circulation: C4A and C4B. These are named for their behavior as acidic or basic on separation by immunoelectrophoresis. The genes for C4A and C4B are on chromosome 6 within the class III region of the major histocompatibility complex, as are the genes for C2 and factor B of the alternative pathway. C4 molecules are synthesized primarily in the liver as a single chain. Posttranslational mature C4 has three chains (alpha, beta, and gamma) that are linked by disulfide bonds. The alpha chain is the site of an internal thioester bond that is critical for one of C4's primary functions: opsonization (4). C3 is the major opsonin of complement. It shares the thioester bond, which is a property that makes many of the reactions of complement possible (5).

The C3 convertase is generated from fragments of C4 and C2 after cleavage by C1s. First, the cleavage of C4 releases a small fragment, C4a, from the N-terminal end of the C4 alpha chain, causing the larger fragment, C4b, to reconfigure in a way that exposes the thioester bond and provides

doi:10.1128/9781555818722.ch13

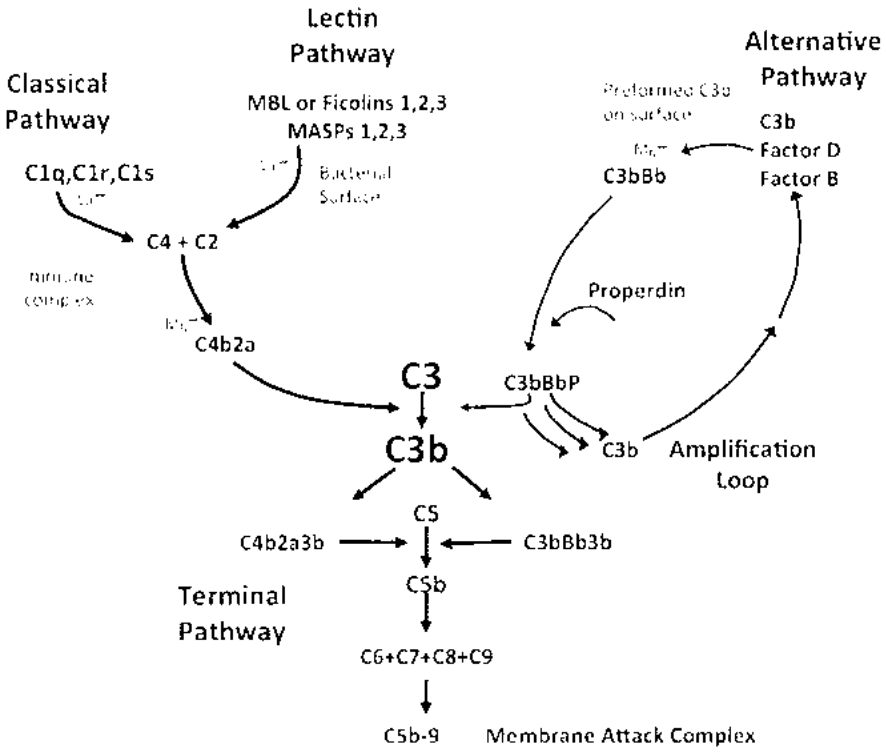

FIGURE 1 Schematic for the complement pathways of activation. The pathway initiators are shown at the top of each, with the components in sequence of their participation. Note the inclusion of the calcium- and magnesium-requiring steps as well as typical activators for each pathway. MBL, mannan-binding lectin.

a transient ability for C4b to bind covalently to nearby acceptor nucleophiles. The binding is in general nonspecific, but for C4b from the C4A haplotype, the preferred binding is to amino groups, while C4b from the C4B haplotype binds best to hydroxyl groups (6). The covalently bound C4b on cells, proteins, bacteria, virus particles, and other particulate matter acts as an anchor to which phagocytes, lymphocytes, and other scavenger cells with membrane C3/C4 receptors can bind, enhancing the efficiency with which these C4b-coated particles are cleared. The half-life of the thioester is only a few seconds, so the number of C4b fragments bound to the target is limited by the diffusion rate of the proteins. This time limitation also ensures that the C4b (or C3b) is deposited at the activation site in a cluster to which the phagocyte can achieve multiple attachments, thus increasing the avidity of the binding.

The surface-bound C4b also serves as the site of formation for the C3 convertase. C2 can bind loosely to the surface-bound C4b in a magnesium-dependent reaction, forming C4bC2, which is enzymatically inactive until the C1s cleaves the C2, releasing inactive C2b into the fluid phase and leaving C2a attached more stably to the C4b. C2a forms the catalytic unit of the C3 convertase, C4bC2a, while C4b acts as its cofactor. The reaction has a short time frame in which to occur. C4b deposits close to where it was formed when cleaved by C1s, and C2 has to bind to C4b while C1s is still near in order to be cleaved by it. C1-Inh is also in the vicinity and competes with the C2 for C1s. If the C1-Inh captures the C1s before it cleaves the C2, the loosely bound C4bC2 complex decays. The C4bC2a enzyme activity has a half-life of about 2 to 8 min before it decays. It is this inherent instability that acts as one of the major controls of the CP and contributes to the limitations on how much C3 conversion it can achieve (7).

CONTROL OF THE CP: C1-Inh, C4BP, CR1 (CD35), MCP (CD46), AND DAF (CD55)

The primary goal of control in complement is stopping the enzymatic activities before they do damage to host cell tissues, something of a balancing act. C1r and C1s are controlled by C1-Inh, a member of the Serpin family (*ser*ine *p*rotease *in*hibitor). The enzyme to be inhibited by Serpins cleaves a bait sequence on the inhibitor and is trapped by a subsequent tight bond with the enzyme. The complex of enzyme-inhibitor is cleared from the circulation, resulting in decreases in the local concentrations of both molecules. In hereditary angioedema patients, who already have low levels of C1-Inh, this additional decrease can trigger a reaction. C1-Inh is the only inhibitor for C1r and C1s, unlike the other enzymes that are susceptible to its action. These include the mannan-binding lectin-associated serine proteases (MASPs), factor XIIa, serum kallikrein, and other enzymes of the kinin-generating pathway that have additional inhibitors that can inactivate them.

There are two steps needed for inactivation of the C3 convertase. First, since C2a requires the cofactor C4b for activity, the C4bC2a complex must be dissociated. To accomplish this, C4BP (C4 binding protein) binds to a site on the C4b near where the C2a is bound and pushes C2a off the complex. C4b, being covalently bound to the surface, remains tied down, but C2a becomes inactive in the fluid phase. C4BP stays bound to the C4b and acts as a cofactor for factor I (FI). FI has trypsin-like activity that cleaves the

C4 alpha chain on both sides of the thioester bond, releasing the larger part of C4b as C4c. C4c contains about 80% of the C4 protein, and it is recognized by most of the polyclonal antisera used for measuring C4 in the circulation. If a large amount of C4 has been activated during an *in vivo* reaction, the C4c in the circulation adds to the mass of C4 measured and can give a value that is higher than the actual native C4 present. C4d, the small piece of the C4 alpha chain that contains the thioester bond, remains covalently bound to the original cell or other surface to which the C4b was bound. It remains attached by the thioester bond to the protein, immune complex, or whatever the C4b happened to bind to initially. Fluid-phase C4d can be detected in varying amounts in the circulation after classical pathway activation, but the C4d that is bound to erythrocytes or platelets is probably a better predictor of the amount of activation that has occurred (8, 9).

If the convertase has bound to host cell membranes, a similar reaction occurs except that host cell membranes are protected by membrane-bound complement control proteins: CD35 and CD46 have cofactor activity for FI and act in a similar fashion to C4BP to remove the C2a enzyme. Displaced C2a becomes rapidly inactive (C2ai), but unless the surface-bound C4b is inactivated, a new C2 could bind to it and start over. All except CD55 (decay-accelerating factor), which lacks cofactor activity for FI, completely inactivate C4b once the C2a has been removed from the enzyme complex. With the other control proteins, C2a is displaced into the fluid phase, where it remains inactive, and C4BP acts as a cofactor for FI cleavage to inactivate C4b. The first cleavage of C4b generates iC4b (inactive C4b), while further cleavage creates C4d and C4c. The small fragment C4d is at the location of the thioester bond and remains attached to the target. C4d is often found in stained tissue sections, since it is tightly bound to the surface. C4d on circulating cells, like erythrocytes and platelets, can be detected by flow cytometry, and it serves as a marker for the classical or lectin pathway activation (8, 9). Likewise, biopsy sections stained for C4d can indicate classical or lectin pathway activity. The large fragment C4c is not active. It represents about 80% of the protein mass of the original C4 and is recognized by most of the antibodies used for measuring C4 concentrations in clinical laboratories. C4a is converted to C4a-desArg by serum carboxypeptidase N. Unlike C3a and C5a with anaphylatoxin activity, C4a and C4a-desArg are both inactive.

SUMMARY OF THE CP AND BRIEF DESCRIPTION OF THE TERMINAL PATHWAY

- C1qrs binds to an immune complex containing IgM or IgG antibodies, or both, bound to antigens.
- The proenzymes C1r and C1s that were associated with C1q are released.
- C1r autoactivates and cleaves C1s, generating C1-esterase, the active form of C1s.
- C1s cleaves C4, generating surface-bound C4b (opsonin) and fluid-phase C4a (no known function).
- C2 binds to C4b and is cleaved by C1s to create fluid-phase C2b (no known function) and C4bC2a, the CP C3 convertase.
- C4bC2a cleaves C3, generating C3b (opsonin) and C3a (anaphylatoxin). Some of the C3b binds to the C4bC2a (through its thioester bond), generating C3bC4bC2a, the CP C5 convertase. The addition of the C3b to the C4bC2a provides a binding site for C5.
- C5 cleavage produces the potent anaphylatoxin C5a and the larger fragment C5b. C5b does not have a thioester bond like C4b and C3b, but it does have a short-lived hydrophobic region that can bind to C6, forming the nucleus for the membrane attack complex.
- C5b has an affinity for C6 and C7. The C5b67 complex binds to the lipid bilayer of nearby cell membranes, and the addition of C8 to this complex via the C8 beta chain causes insertion of the C8 alpha subunit of C8 into the membrane. The insertion of the C8 alpha chain starts the membrane perturbation that is accelerated when multiple C9 molecules then associate with the C5b678 on the membrane and polymerize to form the membrane attack complex C5b6789 (C5b-9). The resulting perturbation of the cell membrane induces osmotic lysis in susceptible cells. CD59 on host cell membranes inhibits C8 and C9 incorporation into the complex, and clusterin interacts with fluid-phase complexes and prevents lysis of "bystander" cells. The abbreviation sC5b-9 refers to the soluble form of the complex that is found in the circulation after activation of complement.

LABORATORY EVALUATION OF THE CP

The best approach to evaluating the CP is to start with measuring the function of the entire pathway: C1 to C9. In this test, the patient's serum is serially diluted (usually 3 to 5 dilutions) and mixed with a suspension of washed sheep erythrocytes (the target cells) that have been coated with antibodies (IgM or IgG) to antigens on the cell surface. This creates immune complexes that can bind C1q and start the activation process. The buffer used for this assay contains calcium and magnesium, both required by the CP. If the patient's complement is normal, the result will be lysis of the cells and the release of hemoglobin. The test tubes or microtiter plates are centrifuged to pellet the unlysed cells, and the amount of hemoglobin in the supernatant is measured on a spectrophotometer. The amount of lysis is calculated for each dilution for the specimen and reported as the reciprocal of the number (or percentage) of cells lysed for each dilution, compared to a buffer control as 0% and a distilled water control as 100%. The percentage of lysis is calculated for all of the dilutions run, and the point where dilution gives 50% lysis is reported as the CH50 (10, 11).

The functional activity of the intact pathway is best evaluated using the CH50 (above) or one of the many variants or equivalent assays that are available. The original hemolytic CH50 method is still useful for titrating the activity in sera, although the newer variations on the theme have faster turnaround times and can be used for high-throughput screens when large numbers of samples are to be run. It has been the experience in my laboratory that these methods are very good for screening the samples for possible defects or deficiencies. The CH50 hemolytic assay can be used as a backup method for confirming low results obtained by the other methods.

The alternative pathway assay that is the closest equivalent of the CH50 (complement 50% hemolysis) is the AH50 (alternative pathway 50% hemolysis). It is the same kind of test except that the cells used are rabbit erythrocytes that have a naturally charged surface that activates the alternative pathway. The buffer used for the AH50 contains EGTA, a chelator of calcium, to block any classical pathway activity, and magnesium needed for formation of the C3 convertase. The endpoint for this assay is similar to that of the CH50. Results are calculated from the 50%

TABLE 1 Interpretation of CH50 and AH50 test results

Location of defect	Result for:	
	CH50	AH50
Classical pathway	Low or 0	Normal
Terminal pathway	Low or 0	Low or 0
No defect	Normal	Normal
Alternative pathway	Normal	Low or 0

lysis. In addition to the CH50, the AH50 can be run on the same specimens to determine the status of the alternative pathway. Often, having both results saves time, the need for more tests, and expense. Interpretation of the two test results is straightforward (Table 1).

The individual proteins of the CP can be measured by standard immunoassays, including radial immunodiffusion using monospecific polyclonal antisera, enzyme-linked immunosorbent assay using monoclonal antibodies, and nephelometry for those components with relatively high serum concentrations.

C1r, C1s, and C2 are usually measured by radial immunodiffusion. C4 can easily be measured by nephelometry. A word of caution must be issued about C2, in particular. If the protein level is normal but the CH50 continues to be low, the function of C2 should be tested. There are several laboratories in the United States in which functional assays for individual complement proteins are available. With the advent of genetic screening, more polymorphisms are being found that affect the function of the components without altering the serum concentration. Like the situation with C1-Inh deficiency, it is often necessary to measure both the level and the function of the protein in question.

Looking back over the numbers of patients with complement deficiencies that were documented in my laboratory, there has been a trend toward increased disorders of function, particularly for C2 and C5 in the past 4 years. The number of samples that had normal levels of these proteins and low or no function has increased as a result of this. For C2, the answer is the discovery of more "silent" mutations that don't change the amount of protein produced but result in dysfunctional protein. Combined type I and type II C2 deficiencies have been found in several families in which the original finding was half normal protein but no function. For C5, I believe the trend is due to the increased use of eculizumab in treatment of paroxysmal nocturnal hemoglobinuria, atypical hemolytic-uremic syndrome, and other disorders of complement regulation. As more drugs are introduced in clinical practice, it will be a challenge to the complement analysts to separate the hereditary, acquired (including autoantibody induced), and medication-related deficiencies seen in the laboratory.

REFERENCES

1. **Nesargikar PN, Spiller B, Chavez R.** 2012. The complement system: history, pathways, cascade and inhibitors. *Eur J Microbiol Immunol* **2:**103–111.
2. **Donaldson VH, Evans RR.** 1963. A biochemical abnormality in hereditary angioneurotic edema: absence of serum inhibitor of C′ 1-esterase. *Am J Med* **35:**37–44.
3. **Ziccardi RJ.** 1983. The first component of human complement (C1): activation and control. *Springer Semin Immunopathol* **6:**213–230.
4. **Law SK, Dodds AW.** 1997. The internal thioester and the covalent binding properties of the complement proteins C3 and C4. *Protein Sci* **6:**263–274.
5. **Gadjeva M, Dodds AW, Taniguchi-Sidle A, Willis AC, Isenman DE, Law SK.** 1998. The covalent binding reaction of complement component C3. *J Immunol* **161:** 985–990.
6. **Isenman M.** 1984. The molecular basis for the difference in immune hemolysis activity of the Chido and Rodgers isotypes of human complement component C4. *J Immunol* **132:**3019–3027.
7. **Gigli I, Sorvillo J, Halbwachs-Mecarelli L.** 1985. Regulation and deregulation of the fluid-phase classical pathway C3 convertase. *J Immunol* **135:**440–444.
8. **Kao AH, Navratil JS, Ruffing MJ, Liu CC, Hawkins D, McKinnon KM, et al.** 2010. Erythrocyte C3d and C4d for monitoring disease activity in systemic lupus erythematosus. *Arthritis Rheum* **62:**837–844.
9. **Batal I, Liang K, Bastacky S, Kiss LP, McHale T, Wilson NL, et al.** 2012. Prospective assessment of C4d deposits on circulating cells and renal tissues in lupus nephritis: a pilot study. *Lupus* **21:**13–26.
10. **Giclas P.** 2006. Analysis of complement in the clinical laboratory, p 115–117. *In* Detrick B, Hamilton RG, Folds JD (ed), *Manual of Molecular and Clinical Laboratory Immunology,* 7th ed. ASM Press, Washington, DC.
11. **Harbeck RJ, Giclas PC.** 1991. *Diagnostic Immunology Laboratory Manual.* Raven Press, NY.

Analysis of Activity of Mannan-Binding Lectin, an Initiator of the Lectin Pathway of the Complement System

STEFFEN THIEL

14

The innate immune system has traditionally been described as the first line of the body's defense against invasive pathogens. Such a response then leads to an inflammatory response which may also include coagulation. Activation of the innate immune response is mediated by pattern recognition molecules, which may be membrane-bound (e.g., cell-associated Toll-like receptors, NOD-like receptors, and RIG-I-like receptors) or soluble proteins. Recognition of foreign or altered structures in the body by some of the soluble pattern recognition receptors may lead to activation of the complement system and thus trigger one of the innate antimicrobial defense mechanisms. Such complement-activating soluble pattern recognition molecules include the collectins (lectins, i.e., carbohydrate-binding proteins, that use a collagen helix for stabilization of the molecule), i.e., mannan-binding lectin (MBL, also known as mannose-binding lectin), collectin K1 (CL-K1), and collectin L1 (CL-L1), and the ficolins (proteins that contain a fibrinogen-like domain and use a collagen helix for stabilization of the molecule), i.e., H-ficolin, L-ficolin, and M-ficolin (1, 2).

MBL activates the complement system by binding to a defined carbohydrate pattern (1). The activation of complement by carbohydrate-binding proteins has been termed the lectin pathway of complement activation (Fig. 1). Two other complement pathways have been described previously and are discussed in other sections of this *Manual*; these are the classical and alternative pathways. In the classical pathway, the recognition molecule C1q recognizes a pattern of antibodies. The alternative pathway is initiated when a hydrolyzed form of C3 is cleaved, leading to deposition of the C3b fragment on a noninhibitory surface (Fig. 1), or whenever C3b is deposited on a surface without the ability to support inhibition of the complement system (3). Completion of any of the three complement pathways may eventually lead to death of the incoming microorganism by either lysis or phagocytosis (3). Activation of the complement system also leads to the initiation of other parts of the innate immune system, activation of humoral and cellular effectors, and identification and neutralization of the invasive pathogen (3).

It is of interest to estimate the level of MBL or the functional activity of MBL in human samples. Numerous reports have reported correlations between MBL deficiency or MBL pathway deficiency and various clinical conditions (4–8).

MBL is a large molecule that is found in blood as oligomers of a structural unit which itself contains three identical polypeptide chains. Each polypeptide chain contains one carbohydrate recognition domain (CRD) and one structural unit. Thus, the intact molecule contains 3 CRDs, and an oligomer of four (the predominant type) structural units contains 12 CRDs. Each CRD binds with low affinity, but the overall binding strength is high when multiple CRDs bind at the same time. MBL binds to microorganisms through the recognition of a pattern of certain sugars, e.g., mannose, glucose, L-fucose, and *N*-acetylglucosamine (1).

MBL is synthesized in the liver and the final product released into plasma, where it associates with the MBL-associated serine proteases (MASPs). These include MASP-1, MASP-2, and MASP-3, as well as two nonenzymatic proteins, MBL-associated protein of 19 kDa (MAp19) and MBL-associated protein of 44 kDa (MAp44) (1, 8). The MASPs are activated when MBL binds to a defined carbohydrate pattern. When MASP-2 becomes activated, it proteolytically cleaves complement components C4 and C2 (Fig. 1) and generates the C3 convertase C4bC2b. This leads to subsequent activation of the remainder of the complement system.

ASSAY OF MBL PATHWAY ACTIVITY

The following protocol describes how one can determine the ability of serum or plasma samples to mediate activation of complement factor C4 via the MBL pathway of complement. The method involves the detection of Eu^{3+}-labeled streptavidin in a time-resolved immunofluorometric assay (TRIFMA) (9). TRIFMAs are similar to enzyme-linked immunosorbent assays (ELISAs), with the only difference being the type of label used for the recorder molecule. Instead of the enzyme-linked antibodies or streptavidin routinely used in ELISAs, in TRIFMAs, Eu^{3+} attached to antibodies or streptavidin is used as a label. In ELISAs, a colorimetric reaction is detected, whereas in TRIFMAs, fluorescence is determined through time-resolved fluorometry. The TRIFMA format provides enhanced sensitivity, a broader dynamic range, and improved reproducibility over what can be achieved with an ELISA. An ELISA version of the assay has been described by Petersen et al. (10). The only difference with this assay is its use of enzyme-labeled streptavidin instead of europium-labeled streptavidin and the use of a colored substrate for the enzyme to produce a color reaction in the wells, which is then read by colorimetry.

doi:10.1128/9781555818722.ch14

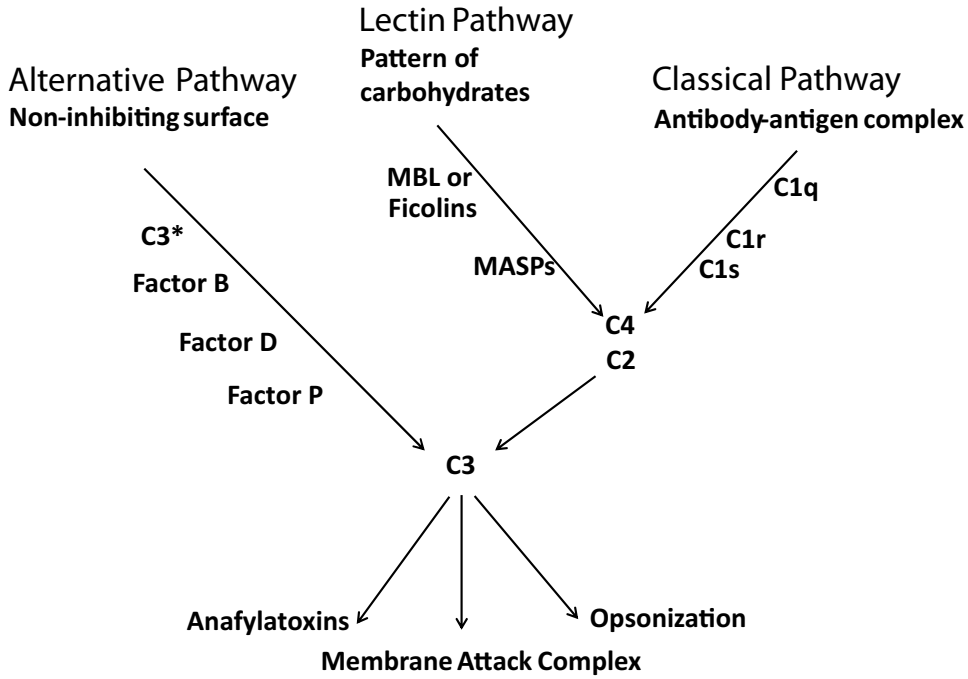

FIGURE 1 Complement activation pathways. The figure shows the events leading to the formation of enzyme complexes that cleave C3. The three pathways thus converge on C3. Thereafter, formation of the terminal membrane attack complex, opsonic factors (C3b), and chemotactic factors (e.g., C5a) may proceed. The classical pathway is activated by C1q in complex with C1s and C1r upon binding to antibody-antigen complexes. The lectin pathway is activated when MBL in complex with MASPs recognizes foreign carbohydrate patterns. As indicated in the figure, ficolins may activate complement via this pathway, but the assay described in this chapter is not influenced by these molecules, as they bind to a different set of ligands than those presented on the surface and used in the assay. The alternative pathway is constitutively activated by the formation of C3(H_2O)-factor B complexes and may be propagated on foreign surfaces by the other factors indicated. The assay described in this chapter measures the cleavage of C4 and the following deposition of C4b by MASP-2 bound to MBL.

A microtiter plate is coated with mannan, which is a preparation of carbohydrate structures from the surface of *Saccharomyces cerevisiae* and is used to bind MBL-MASP complexes from serum or plasma samples (Fig. 2). Any classical pathway activity that may occur due to the presence of anti-mannan antibodies in the sample can also result in C4 activation. This is inhibited by using a high-ionic-strength buffer that inhibits the binding of the C1q used in the assay. Since the activation of C4 by MASP-2 is inhibited by high-ionic-strength buffer, the assay requires a subsequent incubation with purified C4 in an isotonic buffer. After incubation with purified human C4 at 37°C, C4b deposition is detected with biotin-labeled antibodies against C4b and with europium-labeled streptavidin.

Preparation of Serum or Plasma

Whole blood from healthy individuals is drawn into serum Vacutainers and allowed to coagulate at room temperature for 1/2 h before centrifugation (2,000 × *g*, 10 min) and isolation of the serum. For the preparation of plasma, blood from healthy individuals is drawn into citrate-, EDTA-, or heparin-containing Vacutainers. The stabilized blood is centrifuged (2,000 × *g*, 10 min), and the plasma is removed. Serum and plasma aliquots are stored at −20°C until use or at −80°C for long-term storage. Both serum and plasma (with EDTA, citrate, or heparin) samples may be used, despite the presence of calcium in the dilution buffer (see below), since the high NaCl concentration in the dilution buffer inhibits coagulation. The high NaCl content also means that the assay is not influenced by possible variations of other serum factors, e.g., complement factor C4 or C1 inhibitor, which is a promiscuous serine protease inhibitor that also inhibits MASP-2 if present at physiological salt concentrations.

Materials, Reagents, and Equipment

Ninety-six-well microtiter plates (437958; FluoroNunc, Kamstrup, Denmark). When measuring europium in microtiter plate wells by time-resolved fluorometry, it is important that the plastic in the plates contains low levels of europium, as in FluoroNunc plates. The Maxisorb plates sold by Nunc and often used in ELISAs may contain substantial amounts of europium, which will give a high background in the assay.

Mannan (M7504; Sigma-Aldrich, St. Louis, MO)

Human serum albumin (HSA). HSA can be replaced with bovine serum albumin if this is more convenient. We use a stock solution of 200 mg/ml HSA that is normally used for infusion (10 96 97; CSL Behring, Marburg, Germany). Other sources of HSA may also be used.

Human complement C4 (A402; Quidel, San Diego, CA). If multiple assays are planned and cost is a problem, complement C4 can easily be purified from human plasma

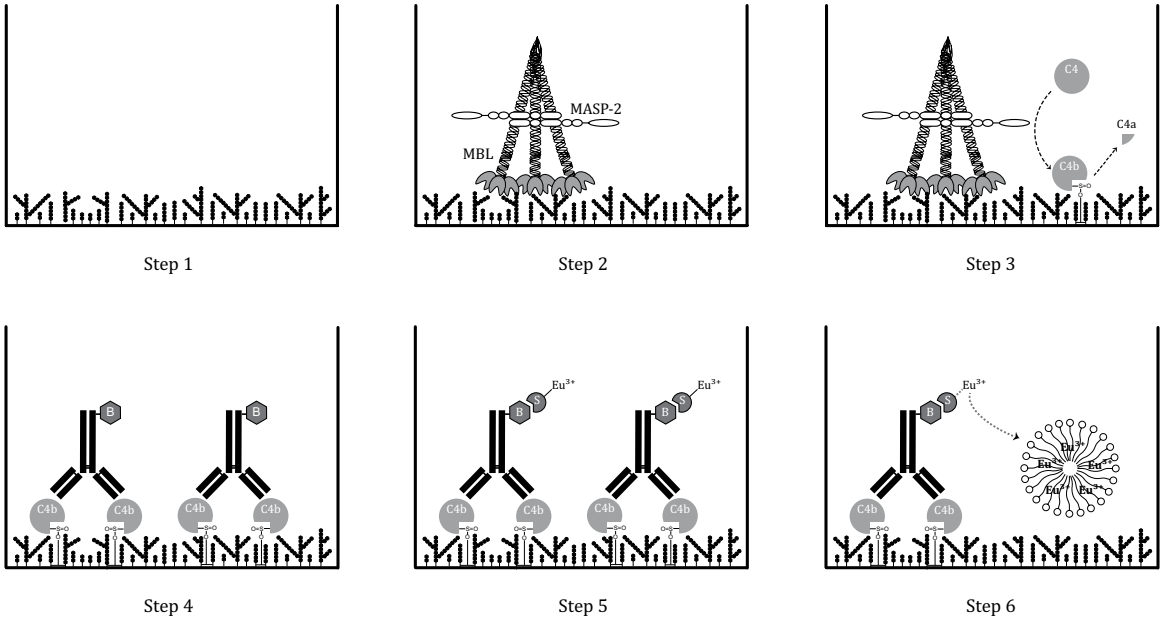

FIGURE 2 Assay of MBL pathway activity. Step 1, coating of the microtiter plate with mannan; step 2, MBL–MASP-2 complexes bind to immobilized mannan; step 3, incubation of C4, which is then cleaved, and deposition of C4b in the wells; step 4, anti-C4 antibody is bound to the deposited C4 fragment; step 5, binding of europium-labeled streptavidin to the biotinylated anti-C4 antibody; step 6, addition of enhancement solution to the wells, which is followed by reading of the plate by time-resolved fluorometry.

by conventional laboratory techniques, using a two-ion-exchange protocol that is described elsewhere (11).

Biotinylated anti-human C4 antibodies (e.g., rabbit anti-human C4 [lsqb]A0065; Dako, Glostrup, Denmark[rsqb]). If the investigator plans to produce this reagent, 1 mg of polyclonal anti-human C4c rabbit IgG (A0065; Dako, Glostrup, Denmark) is dialyzed against phosphate-buffered saline (see buffer composition below) for 2 h at room temperature. The dialysis tube is then transferred to phosphate-buffered saline, adjusted to pH 8.5 with 5% Na_2CO_3, and dialyzed for 3 h at room temperature. The dialysis tube is opened, and 167 μg fluorescein-5-ex *N*-hydroxysuccinimide ester (H1759; Sigma-Aldrich), which has been dissolved in dimethyl sulfoxide is added. The dialysis tube is closed and incubated for 4 h in the dark at room temperature with gentle rocking. The dialysis tube is then transferred to Tris-buffered saline overnight at room temperature and finally incubated twice for 2 h each in Tris-buffered saline–azide at room temperature.

Streptavidin-Eu^{3+} (1244-360; Perkin Elmer, Waltham, MA)

Time-resolved fluorometer, e.g., Victor X4 multilabel plate reader (Perkin Elmer), PHERAstar Plus instrument (BMG Labtech, Ortenberg, Germany), or similar equipment

Assay Solutions

1. NaN_3 is added to the following buffers as a bacteriostatic agent. If the buffers will not be stored for long periods, you can omit the addition of NaN_3 throughout the protocols. The sodium azide stock solution is 1.5 M NaN_3. Add 9.75 g NaN_3 to 100 ml water.
2. Coating buffer: 15 mM Na_2CO_3, 35 mM $NaHCO_3$, 15 mM NaN_3, pH 9.6. Add 500 ml water to a graduated cylinder. Weigh out 1.59 g Na_2CO_3 and 2.94 g $NaHCO_3$ and transfer them to the cylinder. Add 10 ml NaN_3 stock solution and add water to a volume of 900 ml. Mix and adjust the pH to 9.6 with HCl or NaOH. Bring the volume to 1 liter. Store at room temperature.
3. Blocking buffer: 1 mg/ml HSA in 10 mM Tris, 145 mM NaCl, 15 mM NaN_3, pH 7.4. Dissolve 1.21 g Tris and 8.47 g NaCl in 900 ml water. Add 10 ml NaN_3 stock solution and adjust the pH. Add 5 ml HSA (200 mg/ml) and bring the volume to 1 liter with water. Store at 4°C.
4. MBL binding buffer: 20 mM Tris, 1 M NaCl, 0.05% (vol/vol) Triton X-100, 10 mM $CaCl_2$, 15 mM NaN_3, 1 mg/ml HSA, pH 7.4. Dissolve 2.42 g Tris, 58.44 g NaCl, and 1.11 g $CaCl_2$ in 900 ml water. Add 10 ml NaN_3 stock solution and adjust the pH to 7.4. Add 0.5 ml Triton X-100 (9002-93-1; Sigma-Aldrich) and 5 ml HSA (200 mg/ml). Bring the volume to 1 liter and store at room temperature.
5. Washing buffer with calcium: 10 mM Tris, 145 mM NaCl, 5 mM $CaCl_2$, 15 mM NaN_3, 0.05% (vol/vol) Tween 20 (TW), 15 mM NaN_3, pH 7.4. Dissolve 1.21 g Tris, 8.47 g NaCl, and 0.55 g $CaCl_2$ in 900 ml water. Add 10 ml NaN_3 stock solution and 50 ml TW (8.17072; Merck, Darmstadt, Germany). Adjust the pH to 7.4 with HCl. Bring the volume to 1 liter and store at room temperature.
6. Washing buffer without calcium: As described above, but without the added $CaCl_2$.
7. C4 dilution buffer: 4 mM barbital, 145 mM NaCl, 2 mM $CaCl_2$, 1 mM $MgCl_2$, pH 7.4. Dissolve 0.37 g barbital (B0375; Sigma-Aldrich), 4.24 g NaCl, 0.11 g $CaCl_2$, and 0.05 g $MgCl_2$ in 400 ml water. Adjust the pH to 7.4 and bring the volume to 500 ml.
8. The 0.4 M EDTA, pH 7.4, solution is made by adding 76 g EDTA tetrasodium salt dihydrate (Sigma-Aldrich) to 500 ml water and adjusting the pH.

9. Europium dilution buffer: 10 mM Tris, 145 mM NaCl, 0.05% (vol/vol) TW, 15 mM NaN_3, 25 μM EDTA, pH 7.4. Dissolve 0.48 g Tris and 3.4 g NaCl in 350 ml water. Add 4 ml NaN_3 stock solution, 17.5 ml TW, and 25 μl of a 0.4 M EDTA solution. Add water to a final volume of 400 ml and store at room temperature.
10. The enhancement solution may be purchased from Perkin Elmer (catalog no. 1244-104). Alternatively, it can be prepared with the following reagents: 0.57% (vol/vol) acetic acid, 1% (wt/vol) polyethylene glycol 6000, 0.1% (vol/vol) Triton X-100, 15 μM 4,4,4 -trifluoro-1-(2-naphthyl)-1,3-butandion (β-NTA), 50 μM trioctylphosphine oxide (TOPO), pH 3.2. Add 5.7 ml of glacial acetic acid to 900 ml water and adjust the pH to 3.2 with potassium hydrogen phthalate (0.1 M in water). Dissolve 10 g polyethylene glycol 6000 in the solution and add 1 ml Triton X-100. Add 2 ml β-NTA–TOPO solution (see below) and dilute to a final volume of 1 liter with water. The enhancement solution should be stored at 4°C and kept in the dark.
11. The β-NTA–TOPO solution is composed of β-NTA (343633; Sigma-Aldrich) and TOPO (223301; Sigma-Aldrich) dissolved in methanol. For this solution, 0.03993 g β-NTA is dissolved in 10 ml methanol, and 0.19333 g TOPO is dissolved in 10 ml methanol. The two solutions are mixed and kept at −80°C.

It is important that MBL is a calcium-dependent lectin. Thus, all buffers for dilution and washing need to contain 5 mM $CaCl_2$. The exception is the europium dilution buffer, which contains 25 μM EDTA to ensure that free Eu^{3+} ions present in the Eu^{3+}-coupled streptavidin solution are chelated and thus prevented from adsorption onto the microtiter plate. The low micromolar EDTA concentration is not enough, however, to dissociate the Eu^{3+} ion from the streptavidin-coupled chelator or to elute MBL from the mannan-coated surface.

Assay Procedure

Perform all procedures at room temperature unless otherwise specified.

1. Coat a FluoroNunc 96-well plate with mannan at 100 μl/well, using 10 μg mannan/ml diluted in coating buffer, and incubate the plate at room temperature overnight in a moist chamber (Fig. 2, step 1). A plastic box with a lid and a wet paper towel inside may be used as a moist chamber.
2. Empty the wells and block all wells with 200 μl/well of blocking buffer. Incubate the plate for 1 h at room temperature. After incubation, wash the plate three times with washing buffer with $CaCl_2$. If plates are to be stored for later use, empty the wells, add 200 μl/well of washing buffer without $CaCl_2$, and store them at 4°C in a moist chamber.
3. Dilute test specimens in MBL binding buffer, add specimens to their appropriate wells at 100 μl/well, in duplicate, and incubate the plate in a moist chamber overnight at 4°C (Fig. 2, step 2). Wash the plate three times with washing buffer with $CaCl_2$. Usually, a 1:200 dilution is adequate if specimens with a high MBL content happen to be included in the assay. The sample may give a result higher than those observed on the standard curve, and if a more exact value is needed, such samples may be diluted up to 1,000-fold. For comparison of the activities in the samples, a standard curve must be included in the assay. We use a dilution series of a serum with a high MBL content (see "Calculation and Interpretation of Results" below), starting at a 1/10 dilution followed by 3-fold dilutions to 1/21,870. Also include wells with only the MBL binding buffer for background evaluation.
4. Add C4 to all wells (Fig. 2, step 3). Thaw C4 on ice and dilute it in C4 dilution buffer immediately before use. We advise that C4 be kept in aliquots with only enough protein for a single assay (i.e., to fill one microtiter plate), as C4 subjected to freeze-thaw cycles severely loses its activity. Add 0.5 μg/ml human C4 diluted in C4 dilution buffer at 100 μl/well and incubate the plate for 1.5 h at 37°C. This incubation time is important and should not be shortened or extended unless a less or more sensitive assay, respectively, is desired. Wash the plate three times with washing buffer with $CaCl_2$. Note that different preparations of purified C4 may differ in their activity. It is thus recommended to initially try the analysis with several concentrations (e.g., 1 μg/ml, 0.5 μg/ml, and 0.25 μg/ml) of C4 before testing precious specimens.
5. Detect deposited C4b fragments with 0.2 μg/ml biotinylated anti-human C4 antibody (Fig. 2, step 4). Dilute the biotinylated antibodies in washing buffer with $CaCl_2$ and use 100 μl/well; incubate the plate for 2 h at room temperature in a moist chamber. Wash the wells three times with washing buffer with $CaCl_2$.
6. Detect bound biotinylated anti-C4 with 1 μg/ml streptavidin-Eu^{3+} diluted in europium dilution buffer; incubate the plate for 1 h at room temperature in a moist chamber (Fig. 2, step 5). After incubation, wash the plate three times in washing buffer with $CaCl_2$.
7. Add 200 μl/well of enhancement solution to release the europium from the streptavidin and incorporate it into micelles (Fig. 2, step 6).
8. Shake the plate on a microplate shaker for 5 min before reading the result on a fluorometer supporting time-resolved fluorometry.

Calculation and Interpretation of Results

For comparisons of different sera in terms of MBL pathway activity, a standard curve is required (as mentioned above). The MBL pathway activity of the standard serum is given in arbitrary units (e.g., 1,000 mU/ml). The MBL pathway activities of test sera are interpolated from the standard curve and multiplied by the dilution factor 200. The final MBL pathway activities of the tested serum specimens are provided in milliunits per milliliter.

The data obtained from the reading of the assay should be plotted as depicted in Fig. 3. Plot the serum concentration on the *x* axis (log scale) and the results of time-resolved fluorometry (counts per second) on the y axis (log scale). For data analysis and plotting of the data, it is convenient to use a graphical software program, such as Prism, SigmaPlot, or Excel. The standard curve should be S-shaped, and the curve should contain at least three data points in the near-linear portion of the S-shaped curve (Fig. 3).

Internal controls should be run in each assay. We usually use plasma or serum samples with known high, medium, and low activities. The reproducibility of the assay can be evaluated based on the internal controls. The calculated interassay coefficient of variation should be <20% for the high and medium internal standards but slightly higher if

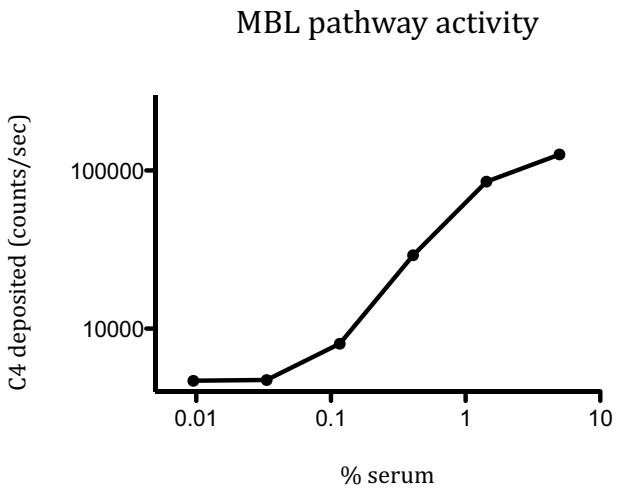

FIGURE 3 Appearance of a typical standard curve for the assay. The serum concentration is given on the *x* axis (log scale), and the signal is given on the *y* axis (log scale). In this figure, the highest serum concentration used is 1/20, followed by 3.5-fold dilutions. Other dilution schemes can also be used (e.g., 1/10 dilution followed by 3-fold dilutions).

the low internal standard is close to the lower end of the reference curve.

The time required to perform the assay as described above is 3 days. Preparing stocks of precoated plates with mannan can considerably shorten the process. The coated plates may be stored at 4°C for up to 2 months. We use overnight incubations for practical reasons, but the whole assay may easily be performed in 2 days, if desired, with precoated plates. Importantly, the incubation with C4 must be performed for the given time at 37°C.

Troubleshooting

If no fluorescence is seen, the possible errors could be as follows: (i) the enhancement buffer in the wells was discarded instead of left in the wells when the plate was measured in the fluorometer; (ii) the complement factor C4 was inactivated by incorrect storage (e.g., the freezer defrosted by itself or the C4 was thawed and frozen more than once); (iii) Ca^{2+} was omitted from the washing buffer, the sample buffer, or the C4 dilution buffer; or (iv) too much EDTA was present in the europium dilution buffer, i.e., 25 μM EDTA, not 25 μM EDTA, is to be used.

The MBL pathway activity closely follows the concentration of MBL in the sera tested. In rare cases, estimated to be 1 per 10,000 samples tested for a typical Caucasian population, a low MBL pathway activity in a serum with a normal MBL level may be found due to a deficiency of MASP-2 (7).

REFERENCES

1. **Thiel S.** 2007. Complement activating soluble pattern recognition molecules with collagen-like regions, mannan-binding lectin, ficolins and associated proteins. *Mol Immunol* **44:**3875–3888.
2. **Holmskov U, Thiel S, Jensenius JC.** 2003. Collectins and ficolins: humoral lectins of the innate immune defense. *Annu Rev Immunol* **21:**547–578.
3. **Ricklin D, Hajishengallis G, Yang K.** 2010. Complement: a key system for immune surveillance and homeostasis. *Nat Immunol* **11:**785–797.
4. **Thiel S, Frederiksen PD, Jensenius JC.** 2006. Clinical manifestations of mannan-binding lectin deficiency. *Mol Immunol* **43:**86–96.
5. **Heitzeneder S, Seidel M, Förster-Waldl E, Heitger A.** 2012. Mannan-binding lectin deficiency—good news, bad news, doesn't matter? *Clin Immunol* **143:**22–38.
6. **Møller-Kristensen M, Thiel S, Jensenius JC.** 2009. MBL polymorphisms and infectious diseases, p 303–332. *In* Vasta GR, Ahmed H (ed), *Animal Lectins: A Functional View*. CRC Press, Taylor and Francis Group, Boca Raton, FL.
7. **Stengaard-Pedersen K, Thiel S, Gadjeva M, Møller-Kristensen M, Sørensen R, Jensen LT, Sjøholm AG, Fugger L, Jensenius JC.** 2003. Inherited deficiency of mannan-binding lectin-associated serine protease 2. *N Engl J Med* **349:**554–560.
8. **Degn SE, Jensenius JC, Thiel S.** 2011. Disease-causing mutations in genes of the complement system. *Am J Hum Genet* **88:**689–705.
9. **Lovgren T, Hemmilä I, Halonen P.** 1985. Time-resolved fluorometry in immunoassay, p 203–217. *In* Collins WP (ed), *Alternative Immunoassays*. Wiley, New York, NY.
10. **Petersen SV, Thiel S, Jensen L, Steffensen R, Jensenius JC.** 2001. An assay for the mannan-binding lectin pathway of complement activation. *J Immunol Methods* **257:**107–116.
11. **Dodds AW.** 1993. Small-scale preparation of complement components C3 and C4. *Methods Enzymol* **223:**46–61.

The Nature of the Diseases That Arise from Improper Regulation of the Alternative Pathway of Complement

RICHARD J. H. SMITH

15

The complement system is the cornerstone of innate immunity. As one of the first lines of host defense, it plays a major role in microbial killing, immune complex handling, apoptotic cell clearance, tissue homeostasis, and modulation of adaptive immunity (1–3). Critical to these functions is the sequential triggering of a series of cascades that result in the generation of metastable protease complexes and culminate in the formation of membrane attack complex (MAC) (4). Improper regulation of these cascades is associated with the development of multiple different diseases. In this chapter, we focus on the clinical consequence of dysregulation of the alternative pathway (AP) of complement. We first provide a review of the AP and then illustrate the consequence of its dysregulation by describing two ultrarare diseases: atypical hemolytic uremic syndrome (aHUS) and C3 glomerulopathy (C3G).

ALTERNATIVE PATHWAY OF COMPLEMENT

In the broadest terms, activation of complement occurs in five sequential steps. The first step is its initiation by one of three independent pathways: the classical pathway (CP), the lectin pathway (LP), or the AP. The second step is the formation of C3 convertase, which exponentially amplifies the initial triggering pathway (step 3) and leads to the generation of C5 convertase (step 4). In step 5, C5 convertase triggers the terminal complement cascade, with generation of the MAC and the potent anaphylatoxin C5a (4) (Fig. 1).

For each pathway, the initiating triggers are different. For example, the CP is most commonly triggered by binding of C1 to the Fc region of antibodies in antibody-antigen complexes (either two molecules of IgG or one molecule of IgM is required), although binding of C1 to some structures, like lipopolysaccharides, on target microbes also can be a CP trigger. In this sense, the LP is very similar to the CP since the LP is typically triggered by the binding of mannose-binding lectin (MBL) to microbial surfaces that express mannose-containing polysaccharides called mannans (5).

Compared to both the CP and the LP, the AP is unique because it is constitutively active secondarily to the slow spontaneous hydrolysis of a labile thioester bond in the thioester domain (TED) of C3 (6). This process, known as "tick-over," leads to the formation of C3(H_2O), an active "C3b-like" C3 molecule that can associate with factors B and D. In so doing, a metastable serine protease, C3(H_2O)Bb, that can cleave nearby C3 to generate C3a and C3b is formed. The availability of C3b amplifies the generation of the C3 convertase (C3bBb) in a positive amplification loop. In addition, the proteolytic cleavage of C3 to C3b exposes the unstable thioester bond in the TED, which quickly reacts with available amine or hydroxyl groups to attach C3b covalently to target surfaces and fluid-phase proteins (7).

On microbes, this C3b tagging step is amplified, but in the host, there are multiple regulators of complement activation (RCAs) that tightly control this process. RCA proteins typically control complement by modulating the generation and breakdown of the C3 and C5 convertases. This type of control is extremely important because covalent attachment of C3b to targets is a random and inefficient process, with only about 10% of activated C3b attaching to intended targets (8). In fact, the majority of C3b thioesters react with water in the fluid phase, which neutralizes the thioester and limits the deposition of C3b on both host cells and microbial surfaces (9). Plasma proteins like C4, properdin, and immunoglobulin also serve as C3b "sinks" to neutralize the thioester (10–12).

RCA proteins regulate complement activation in the circulation (fluid phase) and on cell surfaces and extracellular membranes (surface phase) (5). Many RCAs are also involved in other activities, such as cell adhesion and extracellular matrix interactions. Important fluid-phase RCAs are complement factor H (CFH) and complement factor I (CFI), which downregulate the AP, C1 inhibitor (C1INH), which downregulates the CP and LP, and C4 binding protein (C4BP), which downregulates the CP. Fluid-phase regulators of the terminal complement pathway include clusterin and vitronectin (5). Relatively recently, complement factor H-related protein 1, a member of the complement factor H gene family, has been shown to downregulate C5 activation (13).

Many RCA proteins, including CFH, C4BP, CFH receptor 1 (CFHR1), clusterin, and vitronectin, can also attach to cell surfaces and biomembranes like the glomerular basement membrane in the kidney and Bruch's membrane in the retina (14–16). This attachment adds to these surfaces a protective layer known as the surface zone, which limits formation of active complement products (5). Further protection against unintended complement activity is provided by membrane-bound RCA proteins like CR1 (complement receptor 1, CD35), CD55 (decay-accelerating factor [DAF]), CD46 (membrane cofactor protein [MCP]), CD59,

doi:10.1128/9781555818722.ch15

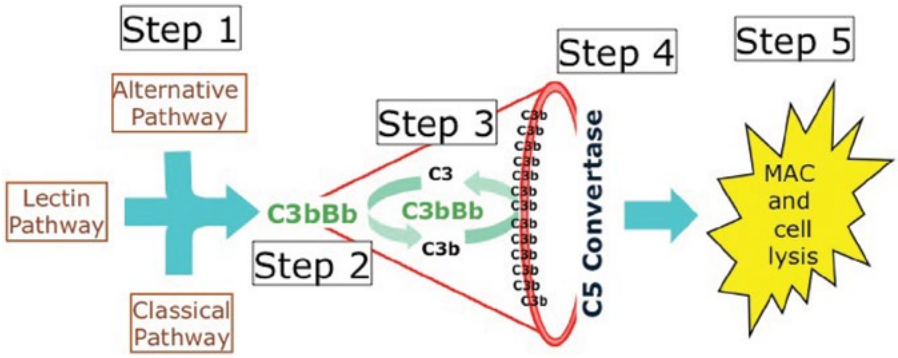

FIGURE 1 The complement system, an important arm of innate immunity, provides host defense and physiologic clearance of immune complexes and plays an adjuvant role in the immune response. Illustrated are the five steps in the complement cascade. Step 1 is the initiation of complement through one of three triggering pathways, the CP, LP, or AP. Step 2 is the formation of C3 convertase, C3bBb. Its amplification through a positive-feedback loop is step 3. The abundance of C3b leads to the generation of C5 convertase, C3bBbC3b, which is step 4. The final step is step 5, or the formation of the MAC. This step is initiated by the cleavage of C5 into C5a and C5b. Control of the amplification phase of complement is required to avoid complement-mediated host damage. This control is impaired in patients with aHUS and DDD. Eculizumab, an anticomplement drug, is a monoclonal antibody to C5. By binding to C5, it prevents C5 convertase-mediated cleavage of C5 to C5a and C5b. Because C5b is not formed, the MAC cannot be generated.

and the complement receptor of the immunoglobulin superfamily (CRIg, also known as VSIG4 [V-set and Ig domain-containing 4]) (17–24) (Fig. 2).

The cell specificities, levels of expression, and distributions of membrane-bound RCA proteins vary, which has important implications for complement-related diseases. In addition, an important distinction between fluid-phase and membrane-bound RCAs is that while the latter control all three initiating pathways by inactivating both C3 and C4 (CR1 and CD46, for example), in the fluid phase, RCAs

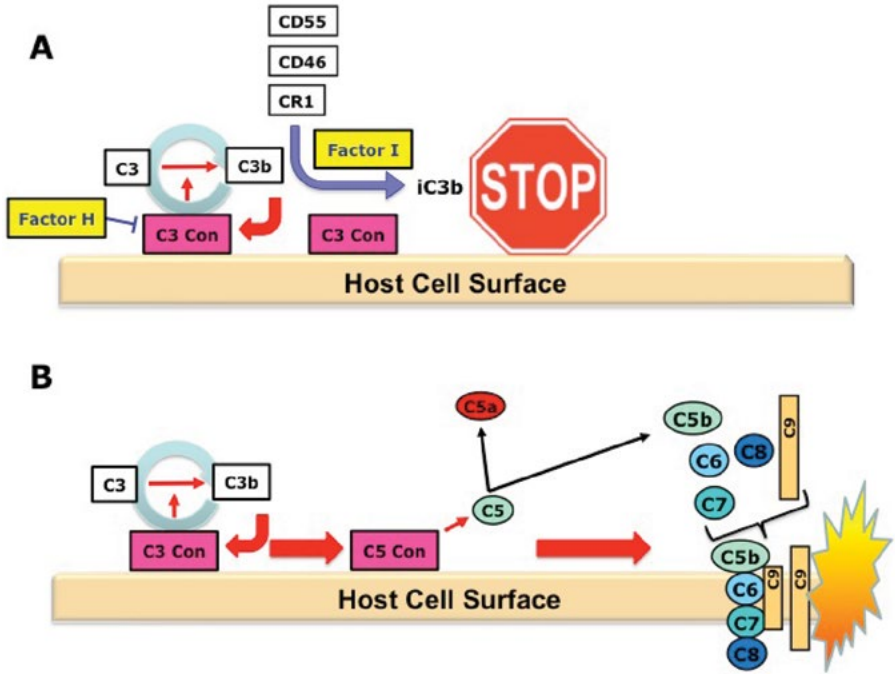

FIGURE 2 (A) Complement activity on host surfaces is prevented by RCA proteins in the "surface zone," which limits the formation of active complement products, and by membrane-bound RCA proteins, such as CR1, CD55, and CD46. CFH, an important RCA protein for fluid-phase control of the AP, also binds to surfaces to provide local control of complement activity. (B) In aHUS patients, host cell surface control of complement is abnormal. In some patients with aHUS, control is lost due to mutations in CFH, CFI, or CD46 that impair normal RCA protein function. In other patients, control is lost secondarily to the formation of autoantibodies to CFH that prevent CFH from binding to host cell surfaces. C3 and C5 Con, C3 and C5 convertase.

are pathway specific and control the AP, CP, or LP by acting exclusively on either C3 or C4 (5).

aHUS AND C3G

aHUS and C3G are prototypical examples of diseases that arise from improper regulation of the AP. aHUS is a type of thrombotic microangiopathy (TMA) in which the control of AP activity fails at the level of the glomerular and microvascular endothelial cell surface, with the clinical consequence being microangiopathic hemolytic anemia (MAHA), thrombocytopenia, and acute kidney failure (25). In C3G, in contrast, loss of AP control occurs in the fluid phase and C3 breakdown fragments deposit in the glomerulus. These fragments include inactive C3b, C3c, and C3dg and are detected by immunofluorescence (IF) using an antibody to C3c. Two broad subtypes of C3G are recognized: dense deposit disease (DDD) and C3 glomerulonephritis (C3GN) (26–28).

To understand the progress that has been made in our understanding of the pathophysiology of aHUS and C3G, it is essential to remember the following: (i) activation and regulation of the AP are focused on control of C3 cleavage to C3b, a change that is accompanied by a dramatic rearrangement of the domains of C3b; (ii) activation and regulation of the terminal complement pathway are focused on control of the C5 convertase and/or accessibility to C5; and (iii) C3 convertase operates upstream of C5 convertase, and therefore regulation of the latter will not impact the activity of the former, while the reverse is not true (preventing C3 convertase activity prevents the generation of C5 convertase).

Atypical Hemolytic Uremic Syndrome

HUS is a rare disease characterized by MAHA, thrombocytopenia, and acute renal failure. It is most frequently caused by infections of Shiga-like toxin-producing bacteria, such as *Escherichia coli* strains O157:H7, O111:H8, O103:H2, O123, and O26. In approximately 10% of HUS cases, however, there is no association with Shiga-like toxin (25). These cases are classified as aHUS and occur with an incidence of about 2 per million in the United States (29, 30). aHUS patients have a poorer prognosis than those with typical HUS, with acute-phase aHUS mortality being about 8% and with 50 to 80% of aHUS patients progressing to end-stage renal failure (25, 31, 32).

aHUS is often further subclassified as sporadic or familial. Familial aHUS is defined as the presence of aHUS in at least two members of the same family, with diagnoses at least 6 months apart. It accounts for less than 20% of all aHUS cases but nevertheless has provided important insights into our understanding of aHUS. From studies initially focused on familial aHUS, we now know that in both familial and sporadic aHUS, genetic and acquired abnormalities in the AP are present in up to 70% of patients. Gene mutations are most frequently found in complement genes, like *CFH*, *CFI*, *CFB*, *C3*, and *MCP*. The most frequently identified acquired abnormality is autoantibodies to factor H (FHAA). These are usually found in persons who are homozygous for deletion of two genes in the complement factor H gene family, *CFHR3* and *CFHR1*. Deletion of *CFHR3-CFHR1* is a common copy number variation in the general population, with one-third of European Americans carrying only one copy of these genes (33).

The consequence of genetic mutations in complement genes and factor H autoantibodies is the loss of AP control on endothelial cell surfaces, with endothelial damage secondary to the generation of C5 convertase and the MAC (Fig. 2). The recent development of eculizumab has proven life-saving for aHUS patients. Eculizumab is a monoclonal antibody that binds to C5, thereby making it resistant to C5 convertase-mediated cleavage into C5a and C5b. C5a is a potent proinflammatory peptide, so eculizumab has an anti-inflammatory effect, but because C5b is not generated, eculizumab prevents generation of the cytotoxic terminal complement complex C5b-9 (MAC) (34, 35).

Complement protein levels can be measured in aHUS patients; however, in about 60% of cases, all complement protein levels are normal (36). In these patients, if there is a complement-associated defect, it may be discovered by genetic analysis. Determining serum complement protein levels can, however, assist in the interpretation of genetic and functional data (Table 1). For example, low serum C3 with normal or decreased complement factor B (CFB) and normal C4 is consistent with AP-mediated complement activity. As a general rule, in aHUS patients, serum C4 levels are always in the normal range, while C3 levels are reduced in about 30% of patients. When C3 is reduced, the

TABLE 1 Interpretation of complement protein levels in aHUS[a]

Complement protein	Normal range (mg/liter) (−2 to +2 SD)	Measurement technique	Laboratory test	Interpretation
C3	660–1,250	Nephelometry	Basic	Severe complement consumption is indicated by very low levels of C3 and CFB in serum; however, usually only low levels of C3 are seen.
CFB	93–380	Nephelometry	Specialized	
CFH	330–680	ELISA	Specialized	CFH or CFI levels of <50% are consistent with quantitative deficiency.
CFI	40–80	ELISA	Specialized	
MCP	MFI	Flow cytometry analysis (FACS)[b] with anti-MCP PE-conjugated antibodies	Specialized	There is no MCP expression in patients with homozygous MCP deficiency. MFI in patients with a heterozygous deficiency is reduced by 50%.

[a]ELISA, enzyme-linked immunosorbent assay; MFI, mean fluorescence intensity; FACS, fluorescence-activated cell sorting; PE, phycoerythrin.
[b]Usually performed on granulocytes or peripheral blood mononuclear cells in EDTA-blood samples.

possibility of a C3 mutation should be considered. To date, 27 C3 mutations have been reported in 56 aHUS patients, with C3 reduced in 41 of 51 patients in whom serum C3 was measured. Serum levels of CFH and CFI can also clarify the mechanism of C3 consumption (36).

Although our understanding of aHUS has advanced significantly, familial aHUS has raised questions specifically regarding the high rate of incomplete penetrance. For example, about 50% of carriers of *CFH* and *MCP* aHUS-associated variants do not develop disease (37). The reason underlying this observation is unclear and means that at this point in time, disease penetrance cannot be predicted accurately, making genetic counseling imprecise. Efforts have therefore focused on identifying additional predisposing genetic variants and/or risk haplotypes in biological pathways that interact with the complement cascade to better understand factors relevant to disease onset in the face of environmental triggers, such as pregnancy, viral infection, cancer, organ transplantation, and the use of certain drugs.

In a recent study, targeted sequence capture and massively parallel sequencing of 85 genes in the complement and coagulation pathways in 36 European-American patients with sporadic aHUS identified 22 genetic variants previously associated with disease and an additional 20 variants predicted by multiple algorithms to be deleterious. As expected, nearly half of these 42 variants (19 or 45%) were in complement genes (*CFH*, *CD46*, *CFB*, *CFI*, and *C3*); however, *PLG*, a gene in the coagulation pathway, emerged as an important gene in the pathogenesis of aHUS (38).

This finding has refined our understanding of the pathogenesis of aHUS, with the key concept being a dysregulation loop driven by overactivation of complement or formation of thrombi in microvessels. Overactivation of complement causes endothelial cell lysis and leads to thrombus formation. Thrombi in microvessels cause mechanical damage to erythrocytes, with release of heme. Heme directly activates the AP and represses MCP and DAF expression on endothelial cells, making them more susceptible to complement damage and closing the loop. Dysregulation of complement and/or coagulation due to genetic abnormalities maintains the cycle (38) (Fig. 3).

It is hoped that these types of studies will continue to refine our understanding of aHUS and in so doing improve clinical care, make meaningful genetic counseling possible, and lead to the developmental of new therapeutic targets.

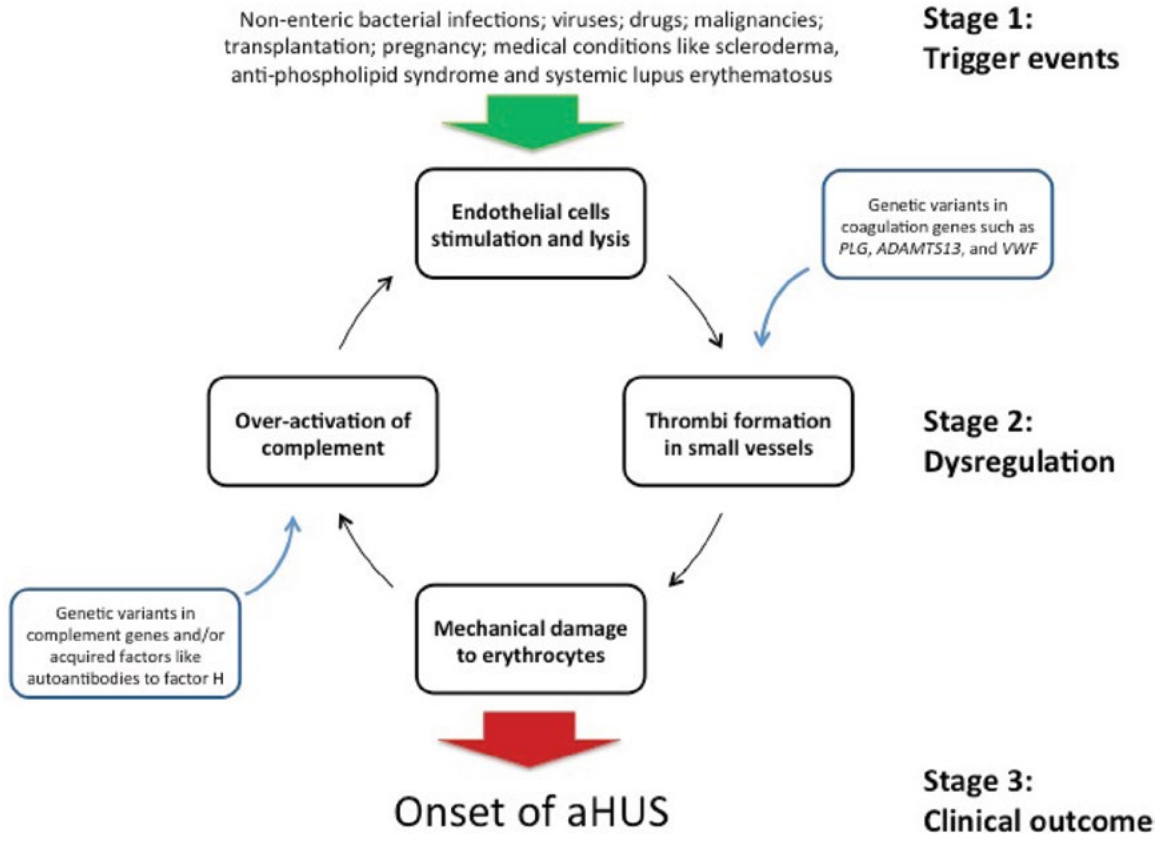

FIGURE 3 Environmental triggers of HUS include nonenteric bacterial infections, viruses, drugs, malignancies, transplantation, pregnancy, and medical conditions like scleroderma, antiphospholipid syndrome, and systemic lupus erythematosus. Following a trigger event, there is some degree of endothelial cell damage, with formation of microthrombi and activation of complement. Dysregulation can ensue if either the complement cascade, the coagulation pathway, or both are overactive. Overactivation of complement causes additional endothelial cell lysis and further clotting. Thrombi in microvessels in turn induce mechanical damage to erythrocytes, which then release heme. Heme directly activates the AP and also represses CD46 and CD55 expression on endothelial cells, which makes cells more susceptible to complement damage. The clinical consequence is aHUS.

TABLE 2 Biomarker assays for C3G

Assay	Measurement technique	Normal range	Company/reference
C3	Radial immunodiffusion	0.9 to 1.8 g/liter	The Binding Site
C3a	Direct sandwich ELISA	<122 μg/liter	Quidel Corp.
C3c	Direct sandwich ELISA	2.12 to 4.92 mg/liter	Palarasah et al. (45)
C3d	Direct sandwich ELISA	0.3 to 0.68 mg/liter	ProGen Biologics
Factor B	Indirect sandwich ELISA	155 to 250 mg/liter	Abcam
Ba	Direct sandwich ELISA	<0.9 mg/liter	Quidel Corp.
Bb	Direct sandwich ELISA	<2.5 mg/liter	Quidel Corp.
Properdin	Indirect sandwich ELISA	10 to 33 mg/liter	Hycult Biotech
C5	Indirect sandwich ELISA	55 to 125 mg/liter	Abcam
C5a	Direct sandwich ELISA	0 to 16 ng/liter	Quidel Corp.
C6	Indirect sandwich ELISA	63 to 145 mg/liter	Abcam
C7	Indirect sandwich ELISA	48 to 109 mg/liter	Abcam
C8	Indirect sandwich ELISA	24 to 121 mg/liter	Abcam
C9	Indirect sandwich ELISA	30 to 93 mg/liter	Abcam
sC5b-9	Direct sandwich ELISA	<0.3 mg/liter	Quidel Corp.

C3 Glomerulopathy

C3G designates a group of glomerular diseases characterized by an IF pattern of C3 dominance upon renal biopsy, with the descriptor "dominance" implying C3c IF intensity of at least 2 orders of magnitude greater than the intensity of any other immune reactant on a scale of 0 to 3 (including 0, trace, 1+, 2+, and 3+). The diagnosis of C3G carries with it the underlying assumption that these diseases are mechanistically related to an aberrant function of the AP, although this is not part of the formal definition (26–28).

Two major subgroups of C3G are recognized and are differentiated by differences in electron microscopy (EM) results. DDD is defined by the EM findings of extremely dense osmiophilic sausage-shaped discontinuous intramembranous glomerular basement membrane deposits; C3GN, in contrast, is defined by some combination of subepithelial, subendothelial, and/or less dense, discontinuous intramembranous and mesangial deposits not characteristic of DDD (28). Another term often associated with C3G is CFHR5 nephropathy, a subcategory of C3GN caused by a genetic rearrangement in *CFHR5* that leads to an abnormally long CFHR5 fusion protein (39, 40). A specific light microscopic pattern upon renal biopsy is not a part of the C3G disease definition.

C3G is driven by dysregulation of the C3 and C5 convertases, which can be substantially different from one patient

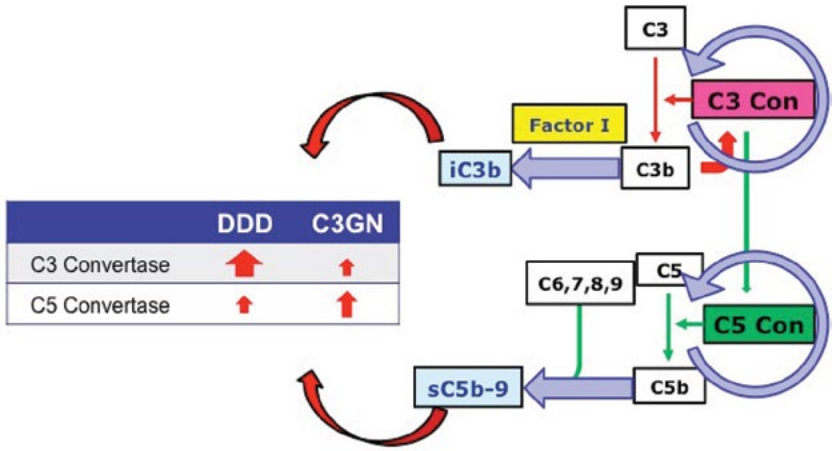

FIGURE 4 DDD and C3GN are driven by dysregulation of the C3 and C5 convertases, represented by the circular arrows. Biomarker profiling in these patients provides mechanistic insight into the degree of complement dysregulation. Serum C3 levels are significantly reduced in C3G patients compared to those in controls, with the reduction in C3 tending to be greater in patients with DDD. Although properdin is not shown in this illustration, it combines with and stabilizes C3 convertase, increasing its half-life about 10-fold. The addition of another C3b molecule to properdin-stabilized C3 convertase results in the formation of C5 convertase. C5 convertase cleaves C5 to form C5a and C5b, and in both C3GN and DDD patients, C5 levels are reduced compared to levels in normal controls. Because of the availability of eculizumab, the most important finding from a clinical perspective is the elevation in soluble C5b-9, a finding more often detected in patients with C3GN than in patients with DDD. The red arrows represent the relative degrees of convertase dysregulation in DDD and C3GN. iC3b, inactive C3b; sC5b-9, soluble C5b-9.

to the next (26, 27). For that reason, biomarker profiling in C3G patients provides detailed mechanistic insight into the underlying complement pathology and useful metrics to monitor in clinical management (Table 2). In both DDD and C3GN, serum C3 levels are significantly reduced compared to levels in controls, although the reduction in C3 tends to be greater in patients with DDD. In addition, and consistently with the continuous activation of the AP, there is a concomitant increase in C3d and a decrease in CFB, with an increase in its split products, Ba and Bb. Properdin levels are reduced in both patients with DDD and patients with C3GN, with the degree of reduction significantly greater in C3GN than in DDD patients.

Biomarker studies of C5 through C9 support a greater increase in terminal pathway activity and C5 convertase in C3GN patients than in DDD patients. In both C3GN and DDD patients, C5 is reduced compared to levels in normal controls, although only in C3GN is the level of its split product, C5a, elevated. In addition, and arguably the most important finding from a clinical perspective, soluble C5b-9 is elevated more often in C3GN than in DDD patients. This point is noteworthy because it predicts that some patients with C3G may benefit from treatment with eculizumab; however, because upstream dysregulation of the C3 convertase can still occur, eculizumab is more likely to lower the rate of disease progress than to be a curative therapy (26, 27, 41–44) (Fig. 4).

CONCLUSIONS

Dysregulation of the AP leads to a variety of diseases, two prototypical examples being aHUS and C3G. Although both of these diseases are ultrarare, detailed genetic and functional studies of the complement system have provided important mechanistic insights into the driving pathology. With aHUS, continued studies are required to understand the genetic complexity underlying issues such as reduced penetrance and whether long-term therapy with agents like eculizumab is universally required for all patients. With C3G, there is currently no effective disease-specific therapy, and as a consequence, treatment is focused on a variety of supportive measures. However, the availability of eculizumab supports efforts to identify C3G patients who may benefit from this drug by biomarker profiling of all patients carrying this diagnosis. In addition, as clinical trials for C3G evolve, biomarker changes must be monitored as primary efficacy endpoints of therapy and correlated with secondary clinical outcomes, such as changes in proteinuria or chronic kidney disease stage.

REFERENCES

1. **Volanakis JE.** 2002. The role of complement in innate and adaptive immunity. *Curr Top Microbiol Immunol* **266:**41–56.
2. **Walport MJ.** 2001. Complement. First of two parts. *N Engl J Med* **344:**1058–1066.
3. **Walport MJ.** 2001. Complement. Second of two parts. *N Engl J Med* **344:**1140–1144.
4. **Smith RJH, Harris CL, Pickering MC.** 2011. Dense deposit disease. *Mol Immunol* **48:**1604–1610.
5. **Zipfel PF, Skerka C.** 2009. Complement regulators and inhibitory proteins. *Nat Rev Immunol* **9:**729–740.
6. **Pangburn MK, Ferreira VP, Cortes C.** 2008. Discrimination between host and pathogens by the complement system. *Vaccine* **26**(Suppl 8)**:**I15–I21.
7. **Pangburn MK, Schreiber RD, Muller-Eberhard HJ.** 1981. Formation of the initial C3 convertase of the alternative complement pathway. Acquisition of C3b-like activities by spontaneous hydrolysis of the putative thioester in native C3. *J Exp Med* **154:**856–867.
8. **Mullereberhard HJ, Dalmasso AP, Calcott MA.** 1966. The reaction mechanism of beta-1C-globulin (C′3) in immune hemolysis. *J Exp Med* **123:**33–54.
9. **Law SK, Dodds AW.** 1997. The internal thioester and the covalent binding properties of the complement proteins C3 and C4. *Protein Sci* **6:**263–274.
10. **Kim YU, Carroll MC, Isenman DE, Nonaka M, Pramoonjago P, Takeda J, Inoue K, Kinoshita T.** 1992. Covalent binding of C3b to C4b within the classical complement pathway C5 convertase. Determination of amino acid residues involved in ester linkage formation. *J Biol Chem* **267:**4171–4176.
11. **Whiteman LY, Purkall DB, Ruddy S.** 1995. Covalent linkage of C3 to properdin during complement activation. *Eur J Immunol* **25:**1481–1484.
12. **van Dam AP, Hack CE.** 1987. Formation of C3-IgG complexes in serum by aggregated IgG and by non-immunoglobulin activators of complement. *Immunology* **61:**105–110.
13. **Fritsche LG, Lauer N, Hartmann A, Stippa S, Keilhauer CN, Oppermann M, Pandey MK, Köhl J, Zipfel PF, Weber BH, Skerka C.** 2010. An imbalance of human complement regulatory proteins CFHR1, CFHR3 and factor H influences risk for age-related macular degeneration (AMD). *Hum Mol Genet* **19:**4694–4704.
14. **Ferreira VP, Pangburn MK.** 2007. Factor H mediated cell surface protection from complement is critical for the survival of PNH erythrocytes. *Blood* **110:**2190–2192.
15. **Manuelian T, Hellwage J, Meri S, Caprioli J, Noris M, Heinen S, Jozsi M, Neumann HP, Remuzzi G, Zipfel PT.** 2003. Mutations in factor H reduce binding affinity to C3b and heparin and surface attachment to endothelial cells in hemolytic uremic syndrome. *J Clin Invest* **111:**1181–1190.
16. **Sanchez-Corral P, Gonzalez-Rubio C, Rodriguez de Cordoba S, Lopez-Trascasa M.** 2004. Functional analysis in serum from atypical hemolytic uremic syndrome patients reveals impaired protection of host cells associated with mutations in factor H. *Mol Immunol* **41:**81–84.
17. **He JQ, Wiesmann C, van Lookeren Campagne M.** 2008. A role of macrophage complement receptor CRIg in immune clearance and inflammation. *Mol Immunol* **45:**4041–4047.
18. **Isaak A, Prechl J, Gergely J, Erdei A.** 2006. The role of CR2 in autoimmunity. *Autoimmunity* **39:**357–366.
19. **Khera R, Das N.** 2009. Complement receptor 1: disease associations and therapeutic implications. *Mol Immunol* **46:**761–772.
20. **Kimberley FC, Sivasankar B, Morgan BP.** 2007. Alternative roles for CD59. *Mol Immunol* **44:**73–81.
21. **Roozendaal R, Carroll MC.** 2007. Complement receptors CD21 and CD35 in humoral immunity. *Immunol Rev* **219:**157–166.
22. **Seya T, Atkinson JP.** 1989. Functional properties of membrane cofactor protein of complement. *Biochem J* **264:**581–538.
23. **Spendlove I, Ramage JM, Bradley R, Harris C, Durrant LG.** 2006. Complement decay accelerating factor (DAF)/CD55 in cancer. *Cancer Immunol Immunother* **55:**987–995.
24. **Wiesmann C, Katschke KJ, Yin J, Helmy KY, Steffek M, Fairbrother WJ, McCallum SA, Embuscado L, DeForge L, Hass PE, van Lookeren Campagne M.** 2006. Structure of C3b in complex with CRIg gives insights into regulation of complement activation. *Nature* **444:**217–220.
25. **Noris M, Remuzzi G.** 2009. Atypical hemolytic-uremic syndrome. *N Engl J Med* **361:**1676–1687.
26. **Nester CM, Smith RJ.** 2013. Treatment options for C3 glomerulopathy. *Curr Opin Nephrol Hypertens* **22:**231–237.

27. **Nester CM, Smith RJ.** 2013. Diagnosis and treatment of C3 glomerulopathy. *Clin Nephrol* **80:**395–403.
28. **Pickering MC, D'Agati VD, Nester CM, Smith RJ, Haas M, Appel GB, Alpers CE, Bajema IM, Bedrosian C, Braun M, Doyle M, Fakhouri F, Fervenza FC, Fogo AB, Frémeaux-Bacchi V, Gale DP, Goicoechea de Jorge E, Griffin G, Harris CL, Holers VM, Johnson S, Lavin PJ, Medjeral-Thomas N, Morgan BP, Nast CC, Noel L-H, Peters DK, Rodríguez de Córdoba S, Servais A, Sethi S, Song W-C, Tamburini P, Thurman JM, Zavros M, Cook TH.** 2013. C3 glomerulopathy: consensus report. *Kidney Int* **84:**1079–1089.
29. **Loirat C, Fremeaux-Bacchi V.** 2011. Atypical hemolytic uremic syndrome. *Orphanet J Rare Dis* **6:**60.
30. **Zimmerhackl LB, Besbas N, Jungraithmay T, van de Kar N, Karch H, Karpman D, Landau D, Loirat C, Proesmans W, Prufer F, Rizzoni G, Taylor MC, European Study Group for Haemolytic Uraemic Syndromes and Related Disorders.** 2006. Epidemiology, clinical presentation, and pathophysiology of atypical and recurrent hemolytic uremic syndrome. *Semin Thromb Hemost* **32:**113–120.
31. **Noris M, Caprioli J, Bresin E, Mossali C, Pianetti G, Gamba S, Daina E, Fenili C, Castelletti F, Sorosina A, Piras R, Donadelli R, Maranta R, van der Meer I, Conway EM, Zipfel PF, Goodship TH, Remuzzi G.** 2010. Relative role of genetic complement abnormalities in sporadic and familial aHUS and their impact on clinical phenotype. *Clin J Am Soc Nephrol* **5:**1844–1859.
32. **Sellier-Leclerc AL, Fremeaux-Bacchi V, Dragon-Durey MA, Macher MA, Niaudet P, Guest G, Boudailliez B, Bouissou F, Deschenes G, Gie S, Tsimaratos M, Fischbach M, Morin D, Nivet H, Alberti C, Loirat C, French Society of Pediatric Nephrology.** 2007. Differential impact of complement mutations on clinical characteristics in atypical hemolytic uremic syndrome. *J Am Soc Nephrol* **18:**2392–2400.
33. **Bu F, Borsa N, Gianluigi A, Smith RJH.** 2012. Familial atypical hemolytic uremic syndrome: a review of its genetic and clinical aspects. *Clin Dev Immunol* **2012:**370426.
34. **Legendre CM, Licht C, Muus P, Greenbaum LA, Babu S, Bedrosian C, Bingham C, Cohen DJ, Delmas Y, Douglas K, Eitner F, Feldkamp T, Fouque D, Furman RR, Gaber O, Herthelius M, Hourmant M, Karpman D, Lebranchu Y, Mariat C, Menne J, Moulin B, Nürnberger J, Ogawa M, Remuzzi G, Richard T, Sberro-Soussan R, Severino B, Sheerin NS, Trivelli A, Zimmerhackl LB, Goodship T, Loirat C.** 2013. Terminal complement inhibitor eculizumab in atypical hemolytic-uremic syndrome. *N Engl J Med* **368:**2169–2181.
35. **Zimmerhackl LB, Hofer J, Cortina G, Mark W, Würzner R, Jungraithmayr TC, Khursigara G, Kliche KO, Radauer W.** 2010. Prophylactic eculizumab after renal transplantation in atypical hemolytic-uremic syndrome. *N Engl J Med* **362:**1746–1748.
36. **Roumenina LT, Loirat C, Dragon-Durey MA, Halbwachs-Mecarelli L, Sautes-Fridman C, Fremeaux-Bacchi V.** 2011. Alternative complement pathway assessment in patients with atypical HUS. *J Immunol Methods* **365:**8–26.
37. **Caprioli J, Noris M, Brioschi S, Pianetti G, Castelletti F, Bettinaglio P, Mele C, Bresin E, Cassis L, Gamba S, Porrati F, Bucchioni S, Monteferrante G, Fang CJ, Liszewski MK, Kavanagh D, Atkinson JP, Remuzzi G, International Registry of Recurrent and Familial HUS/TTP.** 2006. Genetics of HUS: the impact of MCP, CFH, and IF mutations on clinical presentation, response to treatment, and outcome. *Blood* **108:**1267–1279.
38. **Bu F, Maga T, Meyer NC, Wang K, Thomas CP, Nester CM, Smith RJH.** 2014. Comprehensive genetic analysis of complement-coagulation genes in atypical hemolytic uremic syndrome. *J Am Soc Nephrol* **25:**55–64.
39. **Gale DP, de Jorge EG, Cook HT, Martinez-Barricarte R, Hadjisavvas A, McLean AG, Pusey CD, Pierides A, Kyriacou K, Athanasiou Y, Voskarides K, Deltas C, Palmer A, Frémeaux-Bacchi V, de Cordoba SR, Maxwell PH, Pickering MC.** 2010. Identification of a mutation in complement factor H-related protein 5 in patients of Cypriot origin with glomerulonephritis. *Lancet* **376:**794–801.
40. **Athanasiou Y, Voskarides K, Gale DP, Damianou L, Patsias C, Zavros M, Maxwell PH, Cook HT, Demosthenous P, Hadjisavvas A, Kyriacou K, Zouvani I, Pierides A, Deltas C.** 2011. Familial C3 glomerulopathy associated with CFHR5 mutations: clinical characteristics of 91 patients in 16 pedigrees. *Clin J Am Soc Nephrol* **6:**1436–1446.
41. **McCaughan JA, O'Rourke DM, Courtney AE.** 2012. Recurrent dense deposit disease after renal transplantation: an emerging role for complementary therapies. *Am J Transplant* **12:**1046–1051.
42. **Daina E, Noris M, Remuzzi G.** 2012. Eculizumab in a patient with dense-deposit disease. *N Engl J Med.* **366:**1161–1163.
43. **Vivarelli M, Pasini A, Emma F.** 2012. Eculizumab for the treatment of dense-deposit disease. *N Engl J Med* **366:**1163–1165.
44. **Bomback AS, Smith RJ, Barile GR, Zhang Y, Heher EC, Herlitz L, Stokes MB, Markowitz GS, D'Agati VD, Canetta PA, Radhakrishnan J, Appel GB.** 2012. Eculizumab for dense deposit disease and C3 glomerulonephritis. *Clin J Am Soc Nephrol* **7:**748–756.
45. **Palarasah Y, Skjodt K, Brandt J, Teisner B, Koch C, Vitved L, Skjoedt MO.** 2010. Generation of a C3c specific monoclonal antibody and assessment of C3c as a putative inflammatory marker derived from complement factor C3. *J Immunol Methods* **362:**142–50.

Flow Cytometry *section D*

VOLUME EDITOR: JOHN L. SCHMITZ
SECTION EDITOR: MAURICE R. G. O'GORMAN

Introduction

MAURICE O'GORMAN

16

Since the last publication of the *Manual of Molecular and Clinical Laboratory Immunology* almost a decade ago, developments in computer technology, digital electronics, and laser and fluorochrome chemistry have led to the manufacture, adoption, and common availability of clinical flow cytometers with the capacity to routinely analyze 10 (or more) parameters simultaneously. This "polychromatic flow cytometry" capability requires significant expertise in all phases of clinical flow cytometry, from antibody panel design and sample preparation to cytometer setup and acquisition and, finally, the complex task of analyzing highly parametric data files. The first chapter of this section, from Philip McCoy's laboratory at the National Institutes of Health, Bethesda, MD, provides a comprehensive overview of the technology, sample preparation, quality control, and analytical challenges involved in the design and analysis of polychromatic flow cytometry. This chapter provides insight into the considerations required for the design and analysis of highly parametric flow cytometry assays and alerts the reader to the quality control and quality assurance practices necessary to ensure consistent and reliable polychromatic flow cytometry assays.

After the first chapter, each of the following seven chapters focuses on current clinical flow cytometry-based applications, and the section concludes with a final chapter from Holden Maecker on the future of flow cytometry. Chapter 18, from the laboratories of Robert Sutherland, Michael Keeney, and Andrea Illingworth, discusses in detail the key steps required for the sensitive and reproducible detection of both red and white blood cell clones known to be associated with paroxysmal nocturnal hemoglobinuria (PNH). Flow cytometric detection of cells lacking expression of glycosylphosphatidylinositol-anchored surface molecules has become established as the method of choice for diagnosing and monitoring PNH patients. Efforts aimed at increasing both the sensitivity and standardization of PNH testing have recently received considerable attention (1–3). The details of the latter efforts are provided in this chapter.

Chapter 19, on standardized enumeration of CD34-positive stem cells, also from the laboratories of Robert Sutherland and Michael Keeney (the original authors of the International Society of Hematotherapy and Graft Engineering [ISHAGE] guidelines), provides us with an update on the clinical context of CD34 measurements, with a detailed commentary on both the gating strategy and reagents required for accurate single-platform CD34 stem cell enumeration. The authors also present a strategy for further defining the immunophenotypes of specific CD34-positive subsets and discuss the merits of such an approach.

Following these two chapters, I discuss the role of flow cytometry in the evaluation and diagnosis of congenital immunodeficiency disease in chapter 20. The continued discovery of new genes associated with immune abnormalities (adding to the 200-plus already known genes) suggests that large-scale exome or genome sequencing might be the ideal diagnostic approach. Unfortunately, at present, long turnaround times and high costs mean that deep sequencing is not the ideal approach for the diagnosis of congenital immunodeficiency, as rapid diagnosis and treatment have been shown to be extremely important in the outcomes and costs of treating such patients. For these reasons, flow cytometry will continue to be an ideal modality for the screening, diagnosis, and monitoring of patients with primary immunodeficiencies. The chapter reviews the clinical context for flow cytometry assay applications and briefly reviews four novel functional assays which have been developed for the rapid and inexpensive screening of specific immune abnormalities associated with congenital immunodeficiency diseases.

The next four chapters cover the laboratory's role in the immunophenotypic assessment of hematologic neoplasia. Probably the most significant development in this area has been the clinical validation of minimal residual disease (MRD) measurements as a prognostic marker and a key indicator of therapeutic stratification of B cell malignancies. The first of these (chapter 21), from the laboratory of J. DiGiuseppe, provides an excellent overview of the utility of flow cytometry for the evaluation of acute lymphoblastic leukemia and lymphoblastic lymphoma. The information presented is an excellent review of original publications documenting the flow cytometry application strategies for the diagnosis of B and T cell leukemia, MRD testing, and the relationship between specific phenotypic patterns and genetic abnormalities. Included in this chapter are representative flow cytometric dot plots of normal and abnormal lymphoblastic leukemia immunophenotyping results as well as examples of MRD assessment.

In chapter 22, Brent Wood of the University of Washington addresses the application of flow cytometric immunophenotyping to the diagnosis, subclassification, and MRD assessment posttreatment of acute myeloid leukemia

doi:10.1128/9781555818722.ch16

(AML). Wood reminds us of the cardinal rule in the immunophenotypic assessment of hematolymphoid malignancies that "knowledge of immunophenotype of normal hematopoietic maturation is key to understanding changes induced by neoplastic transformation." Antigen expression patterns are presented, from the earliest pluripotent stem cell through commitment and maturation along the seven main myeloid lineages. The biology, epidemiology, and subclassifications of AML are followed by important methodological considerations for preparation, acquisition, analysis, and reporting by the laboratory. Clear tables covering relevant antigens useful in the assessment of AML as well as common signature immunophenotypic expression patterns associated with specific subcategories of AML are presented along with figures illustrating both normal and abnormal immunophenotypes in diagnostic and posttreatment specimens.

Immunophenotypic assessment of chronic lymphocytic leukemia (CLL) is presented in chapter 23 by Heba Degheidy (FDA), Mary Alice Stetler-Stevenson (NIH), and their colleagues. Recent studies reviewed in this chapter indicate that specific immunophenotyping patterns in early disease have prognostic implications and that the detection of residual abnormal cells is associated with both the response to treatment and the prognostication of the overall time of survival. Key recommendations for sensitive and reproducible measurements of specific immunophenotypes and ZAP-70 expression levels and for MRD detection based on standardized methods established by the European Research Initiative on CLL are discussed. Figures showing both normal and abnormal populations, ZAP-70 expression level measurements in both positive and negative cases, and gating strategies for MRD analysis in CLL are presented.

The final chapter, on immunophenotypic assessment of hematologic neoplasia, provides a detailed and comprehensive overview of the flow cytometric approach to plasma cell disorders, where the role of flow cytometry remains controversial and in need of standardization. Alberto Orfao's group at the University of Salamanca has extensive experience in the progressive application of flow cytometry analyses for the identification, quantitation, and categorization of specific plasma cell subtypes in the context of their relationship to risk stratification. An overview of the diagnostic classification of plasma cell disorders, risk of progression within each of the categories, and the need for sensitive MRD detection is followed by a discussion of the role of a standardized flow cytometric approach in the characterization of normal/reactive plasma cells versus aberrant plasma cell immunophenotypes in each of the plasma cell disorders. A discussion of a novel experimental stepwise approach that was used by the Euroflow consortium to develop and establish a two-tube, eight-color antibody panel for the assessment of plasma cell disorders is included. The applications of flow cytometry for diagnosis, classification, prognostic stratification, and MRD monitoring are also addressed in detail. The chapter concludes with a plea for the adoption of "highly standardized approaches" for the attainment of "reproducible and robust" results. Included in this chapter are tables outlining the current classification of plasma cell disorders, the International Myeloma Working Group's diagnostic criteria and treatment response categories for the major categories of plasma cell disorders, and a list of the most relevant plasma cell surface markers and their relevant clinical values. The figures illustrate plasma cell immunophenotyping in normal bone marrow, a patient with multiple myeloma, and a patient with detectable MRD, using a standardized immunophenotypic approach (Euroflow).

The concluding chapter of the clinical flow cytometry section, chapter 25 by Holden Maecker of Stanford University's Human Immune Monitoring Center, provides a glimpse of some of the potential future technologies and applications currently being adopted for research use. A major expansion of the practice of polychromatic flow cytometry (presented in the first chapter of the section) is being made possible by the development of time of flight-mass spectrometry instrumentation. Mass cytometry has expanded "flow" capabilities from the 10- to 20-parameter range to the analysis of >50 parameters on single cells in a single tube. With the number of installations of this new technology approaching 100 units and the commercial availability of new reagents, we are beginning to see results and applications that may have potential for clinical adoption. The other field reviewed by Maecker is the increased flow cytometric assessment of complex signaling pathways that are operative in specific leukocyte subsets undergoing specific normal and abnormal immune responses. Signaling pathways are being studied by measurement of the phosphorylated/dephosphorylated forms of specific signaling proteins activated following exposure to specific stimuli in health and disease. We are already seeing the adoption of this technology, commonly referred to as "phospho-flow," in highly specialized clinical flow cytometry laboratories (see chapter 20). The combination of mass cytometry with phospho-flow has the potential to allow for assessments of normal and abnormal signaling cascades within specific cell subsets that were not previously possible by any technology. This type of laboratory assessment will arguably be adopted for the provision of novel information in the rapidly developing fields of individualized medicine and targeted therapies.

Flow cytometry continues to evolve as an integral technology in the clinical laboratory, and it is anticipated that the chapters included in this section will provide clinical laboratories with sufficient information to adopt new tests, improve current ones, and potentially develop new applications for the assessment of their specific patient populations.

REFERENCES

1. **Fletcher M, Sutherland DR, Whitby L, Whitby A, Richards S, Acton A, Keeney M, Borowitz M, Illingworth A, Reilly JT, Barnett D.** 22 March 2014. Standardising leucocyte PNH clone detection: an international study. *Cytometry B Clin Cytom* doi:10.1002/cytob.21174.
2. **Davis BH, Keeney M, Brown R, Illingworth AJ, King MJ, Kumpel B, Meier ER, Sandler SG, Shaz BH, Sutherland DR.** 2014. *Red Blood Cell Diagnostic Testing Using Flow Cytometry; Approved Guideline, 2nd ed. Document H52-A2.* Clinical and Laboratory Standards Institute, Wayne, PA.
3. **Sutherland DR, Acton E, Keeney M, Davis BH, Illingworth A.** 2014. Use of CD157 in FLAER-based assays for high-sensitivity PNH neutrophil and PNH monocyte detection. *Cytometry B Clin Cytom* **86B:**44–55.

Polychromatic Flow Cytometry

ANGÉLIQUE BIANCOTTO AND J. PHILIP McCOY, JR.

17

For nearly half a century, flow cytometry has been a tool used by biologists to study features of individual cells in a rapid and unbiased manner. The measurement of cellular features has relied upon intrinsic properties of the cells which can be examined by laser-light scattering or by the addition of extrinsic fluorescent probes, such as dyes or fluorochrome-conjugated antibodies that can make cellular features quantifiable. The early flow cytometers relied on only one or two lasers, or a mercury arc bulb, for excitation light, and generally measured only one fluorescent parameter. In the late 1970s, Stohr (1) and Dean and Pinkel (2) described dual-laser excitation for flow cytometry, which permitted the simultaneous use of two spectrally distinct fluorochromes, signaling the genesis of polychromatic flow cytometry. At roughly the same time, Loken and colleagues proposed a method to overcome the difficulties caused by the spectral overlap of fluorochromes excited off a single laser—a method we now refer to as "compensation" (3). These developments laid the foundation for future high-polychromatic flow cytometry, as the bases for both multi-laser excitations as well as exciting multiple fluorochromes off each laser had now been described.

Technological advances in lasers and fluorochromes, while tremendously important to the evolution of modern flow cytometry, were, by themselves, not sufficient to mature this technology. While flow cytometers today are most often controlled by desktop computers, with data captured, stored, and analyzed on these same computers, it should be appreciated that desktop personal computers were not widely available for the early flow cytometers (the IBM PC was introduced in 1981 and the Apple I in 1976). Flow cytometers of the 1970s had extremely limited capacities for data capture, storage, and analysis, and it was not unusual for data to be recorded as Polaroid pictures or strip-chart recordings of the oscilloscope traces. As computers became commonplace in flow cytometry, the need for standards for data files and for increasingly sophisticated software became evident. The first file standards, appropriately called "Flow Cytometry Standard" files (*.fcs), were introduced in 1984 and are periodically updated and enhanced (4). These advances, in turn, led to two notable advancements crucial to the development of high-polychromatic flow cytometry: software compensation and "offline" (retrospective) data analysis. Hardware compensation, as described by Loken and colleagues, had limitations in the practical number of colors that could be compensated, due to the complexity of the compensation matrix as the number of colors increased. Software compensation is, in theory, limitless in the number of colors that could be compensated (5). Similarly, analyzing high-polychromatic data is often quite complex and time-consuming, constraints that are greatly offset by offline data analysis on powerful computers with robust software.

Parallel to these technological advancements were great strides in our understanding of the complexity of cellular phenotypes and their underlying functional properties, due in no small part to the development of antigen-specific monoclonal antibodies (mAbs) by Kohler and Milstein in 1975 (6). For example, while at one point in time, discerning T lymphocytes from B lymphocytes may have been considered sufficient to understand the immune subsets in a particular disease, we now appreciate the myriad subsets present within each of these lineages as exemplified by naive and mature subsets, or regulatory and effector subsets whose functions are characterized by the production of cytokines or the expression of particular chemokines or cytokine receptors. As the complexity of the biology was better understood, so our need increased for higher polychromatic flow cytometry to identify these cells.

Today, flow cytometry studies have been performed using as many as 18 fluorescent markers, and even higher-dimensional data have been acquired using nonfluorescence-based methods such as CyTOF mass cytometer (7) (DVS Sciences, Toronto, Ontario). Staying within the realm of fluorescence-based flow cytometry, new instrumentation using multispectral flow cytometry has been described, which is likely to increase the number of fluorochromes to be run simultaneously, making 25- or 30-color cytometry practical. Hand in hand with the development of advanced instrumentation capable of high-polychromatic cytometry is the significant advancement in fluorochromes and stains. Viability stains (those dyes used to assess whether a cell is dead or alive), once primarily limited to propidium iodide or 7-aminoactinomycin-D, are now available in a broad range of excitation and emission spectra. Examples of these include the family of Live-Dead (Life Technologies, Carlsbad, CA), Zombie (Biolegend, San Diego, CA), and Horizon (Becton Dickinson [BD], San Jose, CA) stains. Similarly, new fluorochromes have been developed that permit more extensive use of 407 nm (violet laser, such as quantum dots [QD], Life Technologies) and the

doi:10.1128/9781555818722.ch17

brilliant violet (BV) family of fluorochromes (Sirigen, BD, San Jose, CA). These can permit the simultaneous analysis of five or more distinct markers using the violet laser, a laser previously used only minimally in phenotypic analyses due to the lack of appropriate fluorochromes.

The final piece of the polychromatic flow cytometry puzzle is data analysis. As one moves from two- or three-color analysis to 15 colors or more, data analysis becomes almost exponentially more difficult, beginning with compensation and extending to thoroughly "mining" data for all possible information. Fluorescence compensation is made easier by compensation "wizards" that are components of most contemporary analysis programs for flow cytometry. These wizards set compensation values after the user enters data for cells or beads unstained and stained with each individual fluorochrome into the program. This alleviates what would otherwise be an overwhelming task to appropriately set manually determined compensation for high-polychromatic studies. However, even these compensation matrices should be checked to ensure against artifacts, such as those caused by aggregates of quantum dots. The challenge of thoroughly analyzing high-polychromatic data is more daunting. Properly compensated data can readily be analyzed in a predetermined, or guided, manner in which the pathway of gating is predetermined for the quantification of cell subsets with established phenotypes. By contrast, the "discovery" mode of analysis, in which all possible cellular phenotypes contained within a population are identified, is more complex and time-consuming in high-dimensional studies. Vast numbers of populations are mathematically possible (but perhaps not biologically) in polychromatic data, as the potential number of populations increases exponentially with the number of parameters studied. Assuming all populations existed as combinations of positive and negative staining (disregarding the possibility of dim and bright subsets), 10-color data could yield over 1,000 cell populations. Manual analysis of all of these putative populations would be extremely cumbersome, and therefore considerable effort is being made at developing automated approaches for in-depth analysis of high-polychromatic data.

The uses of flow cytometry are widely varied, but none are more important than the clinical applications. In the first decade of flow cytometry, attempts were made to apply studies of DNA content and cell cycling to clinical problems. These efforts met with mixed success. The discovery and later commercialization of mAbs provided the impetus for a broader array of assays of potential clinical utility to be developed. Foremost among these were enumeration of $CD4^+$ T cells in the context of HIV disease and immunophenotyping for the classification of leukemias and lymphomas. These assays established the clinical utility of flow cytometry and continue to be the most frequent clinical applications, as these tests are essential components in the clinical management of patients with these diseases. Flow cytometry is also particularly well suited for the detection of minimal residual disease in patients with hematologic neoplasms. Here, patients are screened for small numbers of residual cells from their disease with the potential to cause a relapse. Flow cytometry is capable of high-throughput analysis of thousands of cells per second in sensitive, polychromatic approaches for identifying leukemic cells present in frequencies as low as 1 per million normal leukocytes.

Clinical assays using flow cytometry encompass a wide array of applications, such as quantification of hematopoietic stem cells (usually identified using CD34 or CD133), diagnosis of paroxysmal nocturnal hemoglobinuria (based on cells that lack glycophosphatidylinositol-anchored proteins such as CD55 or CD59), detection of primary immunodeficiencies, studies of platelets, and leukocyte adhesion deficiencies (usually based on CD11b and CD18 expression), to name a few (8).

Research applications for flow cytometry are even more varied and include numerous scientific disciplines. For example, in marine biology, flow cytometry is widely used to study phytoplankton, algae, and aquatic bacteria in water samples. Other disciplines using various applications of flow cytometry include plant biology, pathology, animal husbandry, and molecular biology, but perhaps the most common uses are in immunology and hematology. Within these disciplines, flow cytometry is used not only for immunophenotyping studies, but also for uses such as the detection of intracellular cytokines, phosphorylation of signaling proteins, cellular proliferation and apoptosis, calcium fluxes, phagocytosis, membrane potential, antigen colocalization, and many others.

TECHNOLOGY

Instrumentation Overview

To appreciate flow cytometry instrumentation, it is necessary to understand the basics of how flow cytometry works. The typical flow cytometer relies on placing cells in a single-cell suspension, then moving the cells single file in a tightly focused stream past a light source (or multiple light sources) and detectors for scattered light as well as emitted fluorescence (Fig. 1). Downstream, the cells may be sorted or not, depending on the type of cytometer. If the cells are not sorted, they generally go to a biohazard waste and are discarded. As will be discussed below, prior to being placed in the flow cytometer, the cells are appropriately treated and stained for the cellular features one wishes to study. The tightly focused cells pass through one or more laser beams one at a time in rapid succession, in a sample core chamber, and the intersection of each laser and particle is called the point of interrogation. The lasers excite various fluorescent probes that have been used to stain the cells, and the light emitted from these stains is sent to an array of detectors (as well as forward- and side-scatter light from one of the lasers). Prior to reaching detectors, the light is separated into various predefined wavelengths using a succession of mirrors and filters in order to distinguish the emission of each of the stains from all others. The separated light then strikes the detectors, generating a signal that is amplified and digitized for subsequent analysis.

Beyond the basic method of operation just described, flow cytometers can vary greatly in their specific design. For example, cells may be focused into a tight stream either by the use of a sheath stream or by acoustic focusing without sheath. Light sources can range from mercury arc bulbs to as many as seven lasers of different powers and wavelengths. Detectors are most often photodiodes or photomultiplier tubes, although recently one model was developed that uses charge-coupled device (CCD) cameras as detectors. The number of detectors varies widely, ranging from four to 20 or more. A fairly standard, middle-of-the-road flow cytometer today would use sheath-based focusing, have three lasers, and be capable of measuring forward- and side-light scatter as well as eight fluorescent parameters.

Although most cytometers are designed in a manner consistent with the description given above, the specific configurations of commonly available cytometers can differ widely in specific areas such as the types, number, and power of lasers, the choice of optical filters, and the layout and number of detectors.

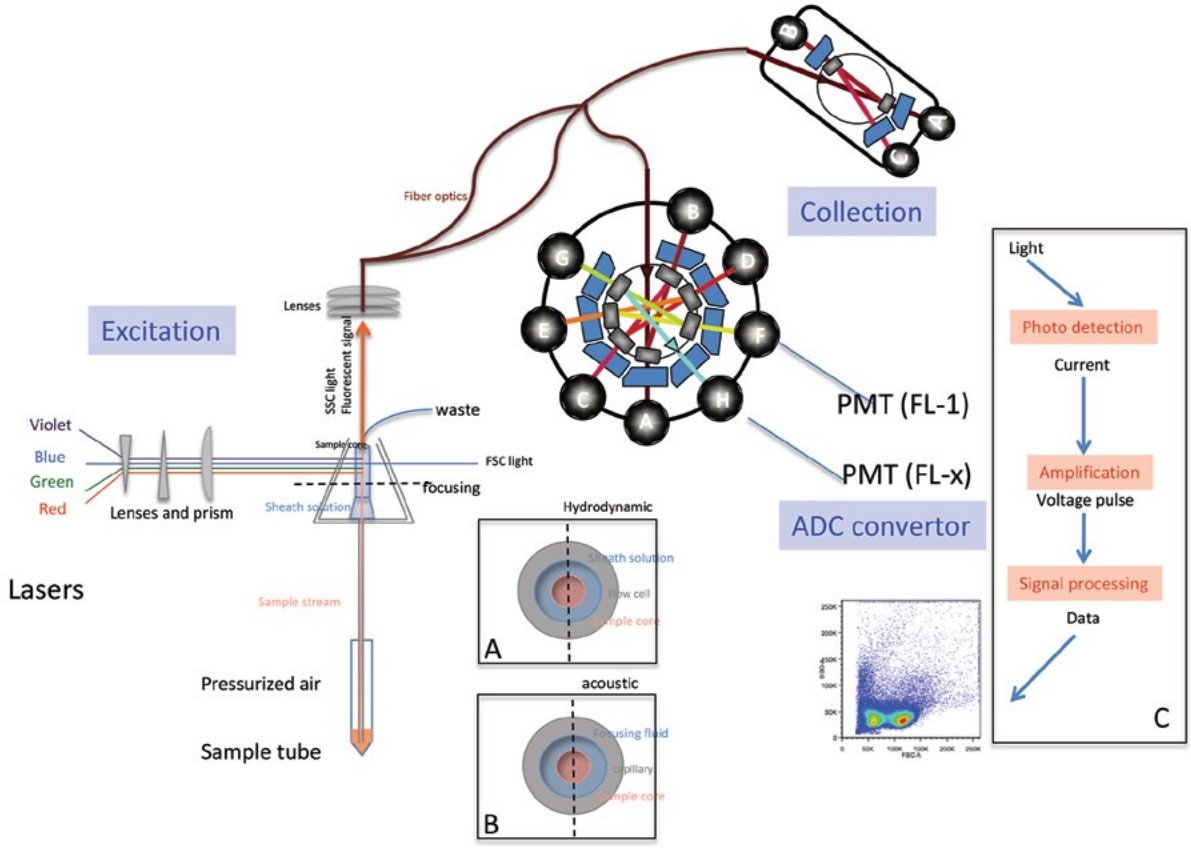

FIGURE 1 Schematics of the main components of a flow cytometer. A single-cell suspension goes through a tightly focused stream into the flow cell, where it encounters the different lasers. Insert A shows the position of different components of hydrodynamic focusing using a coaxial stream. Insert B shows the different components of acoustic focusing, where a capillary line of particles can be created using acoustic-radiation pressure. The signals emitted using the blue-laser excitation can measure physical characteristics of cells in addition to fluorescence measurements via transformation of fluorescence into voltage (see insert C). Each fluorescence channel measured is assigned to a PMT.

Fluidics

The role of fluidics is crucial to presenting the cells one at a time in a narrowly focused pattern to the laser beam. The fluidics system consists of a central channel in which the sample is injected, enclosed by an outer sheath that contains faster-flowing fluid (sheath fluid). As the sheath solution moves, it creates a massive drag effect on the narrowing central chamber. This alters the velocity of the fluid in the middle and the front becomes parabolic, creating a hydrodynamic focus (Fig. 1). Under optimal conditions (laminar flow) the fluid in the central chamber will not mix with the sheath fluid (see insert A in Fig. 1). After hydrodynamic focusing, each particle passes through one or more beams of laser light. The rate of the sample flow is regulated by a pressure regulator and may be continuously variable or fixed to defined settings (e.g., high, medium, and low), allowing speed-sample processing from perhaps 100 events per second to 20,000 events per second or more.

As an alternative to hydrodynamic focusing, other cytometers, such as the Attune cytometer, use acoustic focusing. This also results in the generation of a single-cell stream for passing the cells through to the laser beam, but without using sheath fluid. Cells are transported through a capillary system where an acoustic resonant device focuses them into a single tight line. The acoustic radiation is generated using a capillary coupled to a piezoelectric transducer (see insert B in Fig. 1) (9, 10).

Regardless of the type of focusing used, the single cells will encounter the laser beam in the sample core, where the point of contact between the particles and the laser is called the interrogation point.

Lasers

Most flow cytometers depend on lasers as a light source for excitation of fluorochromes as well as for light-scattering measurements. Light scattering provides information regarding cellular intrinsic properties such as granularity or size, while fluorescence emission (if the particle is labeled with a fluorochrome) provides information about cells' extended properties, such as the relative amount of a specific antigen present on the cell. As noted above, the mercury arc lamp is the most common alternative light source other than lasers in modern flow cytometry, although the increasingly low cost and minimal size of lasers are making the use of these lamps increasingly rare.

There are multiple types of lasers, and the choice of which laser to use on a particular cytometer is dependent on the needs, cost, size, and the performance of light-collecting detectors and optics (11–20).

Currently, there several types of lasers used in flow cytometry, with output wavelengths ranging from 300 to 700 nm. These include: water-cooled and air-cooled gas lasers (argon-ion, helium-neon [He-Ne], and helium-cadmium [He-Cd] lasers); diode lasers (in which laser light is generated by pumping electricity into a solid medium rather than a gas-plasma tube); diode-pumped solid-state (DPSS) lasers, which use a diode source to pump another crystalline material (frequently neodymium yttrium aluminum garnet, or ND-YAG); violet-diode lasers (VLD); and near-UV diode lasers (NUVLD). Indium-gallium nitride-laser diodes have been developed and extend the excitation range in the near-UV (370–385 nm).

Many flow cytometers are equipped with two or more lasers that permit the analysis of multiple fluorescent labels on each cell. In a system with multiple lasers, the lasers' spatial separation creates an issue that needs to be addressed, as a single cell intersects the multiple laser beams at different time intervals and therefore the fluorescence emissions from these different fluorochromes on the same cells arrive at their respective detectors at different time intervals. To assign the signals generated on different lasers to a particular cell, a function termed "laser delay" is used (Fig. 2). One laser, usually the blue (488 nm) laser, is used to obtain the forward- and side-scatter measurements and is considered the reference laser. Other lasers can be placed in a position so that a cell can pass through their beam either before or after the reference laser. Therefore, laser-delay setting can have either a positive or a negative value, depending on whether the cell passes through beams from the respective laser before or after the reference laser.

Once the lasers are chosen for a cytometer, their placement in relation to the reference blue laser needs to be adequate for optimal separation of the generated signals, as the time delay will be of importance when fluorescent signals are collected.

Optical Filters

The side-scatter light and fluorescence signals generated by the cells need to be directed to the appropriate detectors; for this purpose, various optical filters are used in a flow cytometer to direct the photons of the correct wavelength to the appropriate photo-multiplier tube (PMT). These filters block certain wavelengths from reaching the detector while permitting others (transmitting) to pass through. There are three major filter types: "long-pass" (LP) filters that allow passage of light above a defined wavelength while blocking lower-wavelength light; "short-pass" (SP) filters that allow passage of light below a defined wavelength and block higher wavelengths; and "band-pass" (BP) filters that transmit light

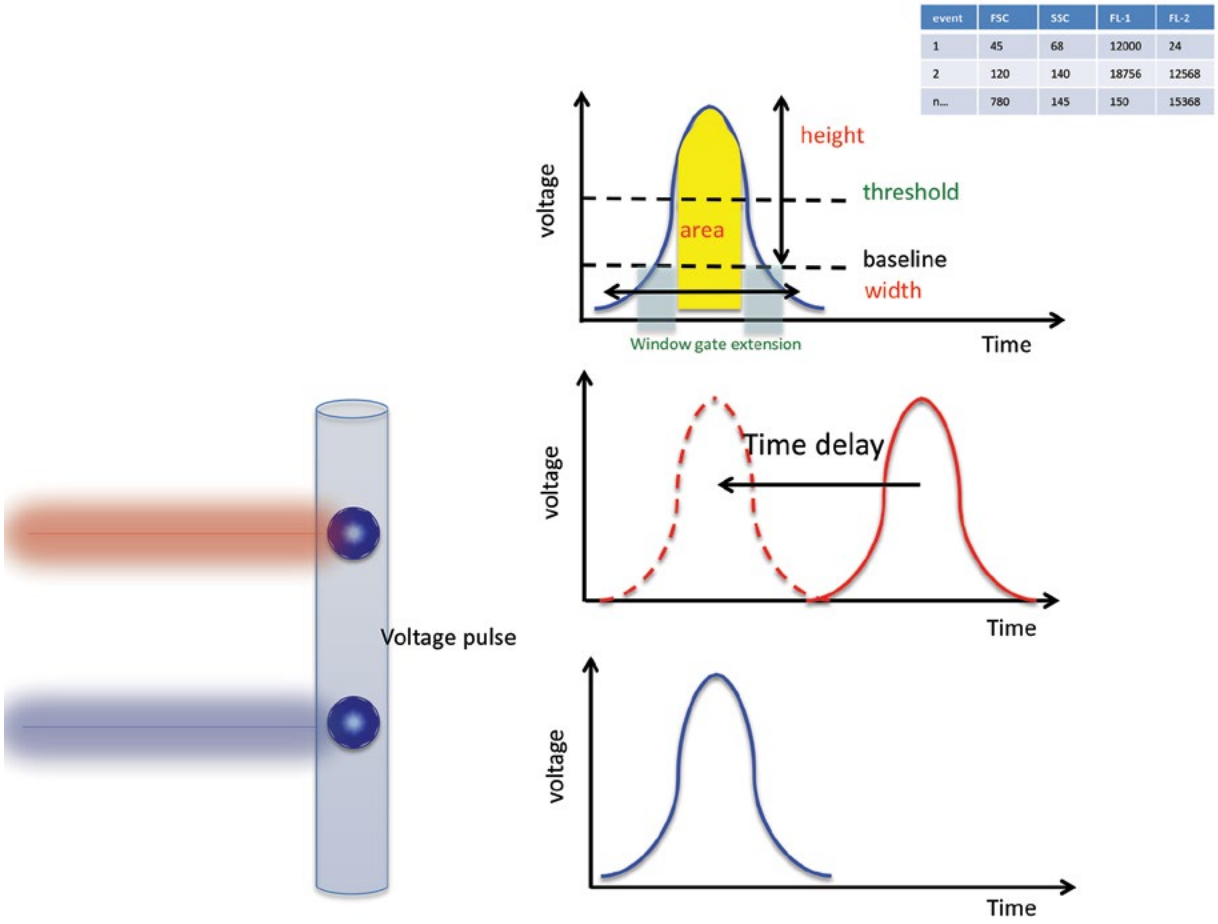

FIGURE 2 Schematics of the voltage pulse and time delay. Area, height, and width are the signals recorded for each single particle (text in red), and these measurements are influenced by the threshold and window-gate extension that are set up by the user (text in green). The voltage pulse generated by the red laser will need to be retrospectively assigned to the same particle-voltage pulse from the blue laser (time delay).

within a specified narrow range of wavelengths (termed a bandwidth) and are generally used immediately in front of a detector. Similar filters are positioned at a 45° angle to the light beam and are called dichroic filters/mirrors. In an LP dichroic filter, photons above a specific wavelength are transmitted straight ahead, while photons below the specific wavelength are reflected at a 90° angle.

For LP and SP filters, important performance parameters are the wavelength for 50% transmission (the cut-off for LP or the cut-on wavelength for SP), the peak transmission, and the slope at the cut-on or cut-off wavelength. For BP filters, important performance parameters are the peak wavelength of transmission, the percentage of light transmitted at the peak wavelength, and the bandwidth (measured as the separation of the 50%-transmission points).

Signal Processing and Configuration of Instrument Detectors

After excitation of the fluorochromes, the emitted light is filtered into specific wavelengths and then strikes a photodetector, which is a sensor capable of detecting photons. The photo-detector will generate a current whose associated voltage is proportional to the number of light photons striking the detector. Subsequently, this current goes through a series of amplifiers, which convert electrical current into a measurable electrical signal, the voltage pulse (see insert B in Fig. 1). Most amplifiers are analog-to-digital convertors (ADCs). The voltage pulse generated will be quantified by signal processors providing numerical values for area, height, and width (Fig. 2). The particle that will generate a signal is based on a threshold set up by the user.

The measurement from each detector is referred to as a "parameter": forward-scatter, side-scatter, or fluorescence. The configuration of an instrument is the assignment and location of each detector to each parameter.

Then, numerical data are processed by a computer system that will create list-mode files or FCS files and display data. The instrument configuration is the assignment of each detector to a given PMT.

Data Files and Analysis

When the cells or particles are interrogated by the lasers, signals are generated, amplified, digitized, and ultimately converted to a number that is proportional to the original light signals. This is stored in a computer in an .fcs format or list-mode file. Both list-mode and .fcs files are a list of sequential numerical values for each measured parameter of every individual cell. The data generated can be presented in single parameter (histogram) or double parameters (dot or contour plot).

Histograms are a direct graphical representation of the number of events occurring for the chosen parameters. The dot plot is a two-dimensional extension of the frequency histogram, where each cell is represented by *x*/*y* coordinates on *x*/*y* axes.

Other techniques can be employed to visualize three or more parameters in highly multiplexed parameter-analysis applications. Statistical analysis is performed by graphically applying regions of interest to data sets.

Flow Cytometer Standardization

Initial Performance Check

Prior to use, any flow cytometer should have its performance assessed for consistent, optimal measurement of fluorescent and light-scatter signals.

Quality assurance of the instrument's performance can be summarized in a three-step protocol including optimization, calibration, and standardization of laser components (laser power, laser delay), optical components (optical filter choices; dichroic-mirror reflection, dichroic-mirror transmission), and electronic components (PMT assignment, electronic noise, and window extension) (21, 22). Microspheres that contain dyes inside their core and have excellent photochemical and physical stability provide reliable reference signals for laser alignment, laser-beam focusing, and calibrating flow cytometers during the performance testing.

Laser Components

Flow cytometers depend on lasers as a source of excitation for all fluorochromes; alignment of lasers one to another is crucial for optimum fluorescence measurement. Microspheres are used to test laser alignment and to gauge the sensitivity and signal-to-noise ratios of detectors, laser power, and window extension (Fig. 3A). Laser-time-delay setup is crucial for accurate measurement of any type of sample.

Optical Components

The choice of optical filters that are used with each detector greatly influences the effective brightness of one fluorochrome versus another. Filter selection is a good news-bad news proposition: using a wider BP filter can increase the ability to detect a given fluorochrome, but may also increase the amount of spillover background contributed into that detector from other neighboring fluorochromes. Measurement of optical background (Br) should be assessed for each filter used in the instrument.

Electronic Components

Ideally, there is a linear relationship between voltage PMT and fluorescence intensity. To test the photoelectron efficiency, microspheres for a given PMT are run using different voltages, and plots of the variation of the voltage gain versus coefficient of variation (CV) of the mean fluorescence intensity are constructed. For each PMT, measurements are done in cascade using different voltages. Graphing the fluorescence intensity versus voltage will have an inflection point that shows minimum baseline voltage for optimal resolution between negative and positive measurements: this is detector efficiency (Qr) (11, 12, 17–19) (Fig. 3C). Microspheres are used with different graded levels of fluorescence, and their fluorescence measurements are used for the generation of calibration curves, establishing PMT settings, and evaluating sample fluorescence intensity (21, 23, 24). The most efficient PMT should be assigned to the detector that captures low-energy photons, in the longer wavelength, such as allophycocyanin (APC)-H7 or APC-Alexa 750 (21, 22, 25, 26).

It is convenient to visualize the instrument-performance checks over time to detect not only acute instrument failures, but also slow degradation of instrument performance. For this, the Levy-Jennings plot is most often used. This plot has time on one axis (which can vary to whatever length of time desired) and the quantitative measurements of one or more instrument-performance checks plotted on the *y*-axis (see Fig. 3D).

Daily Performance Check

To ensure accuracy and reliability of the fluorescence measurement, instrument performance needs to be calibrated daily.

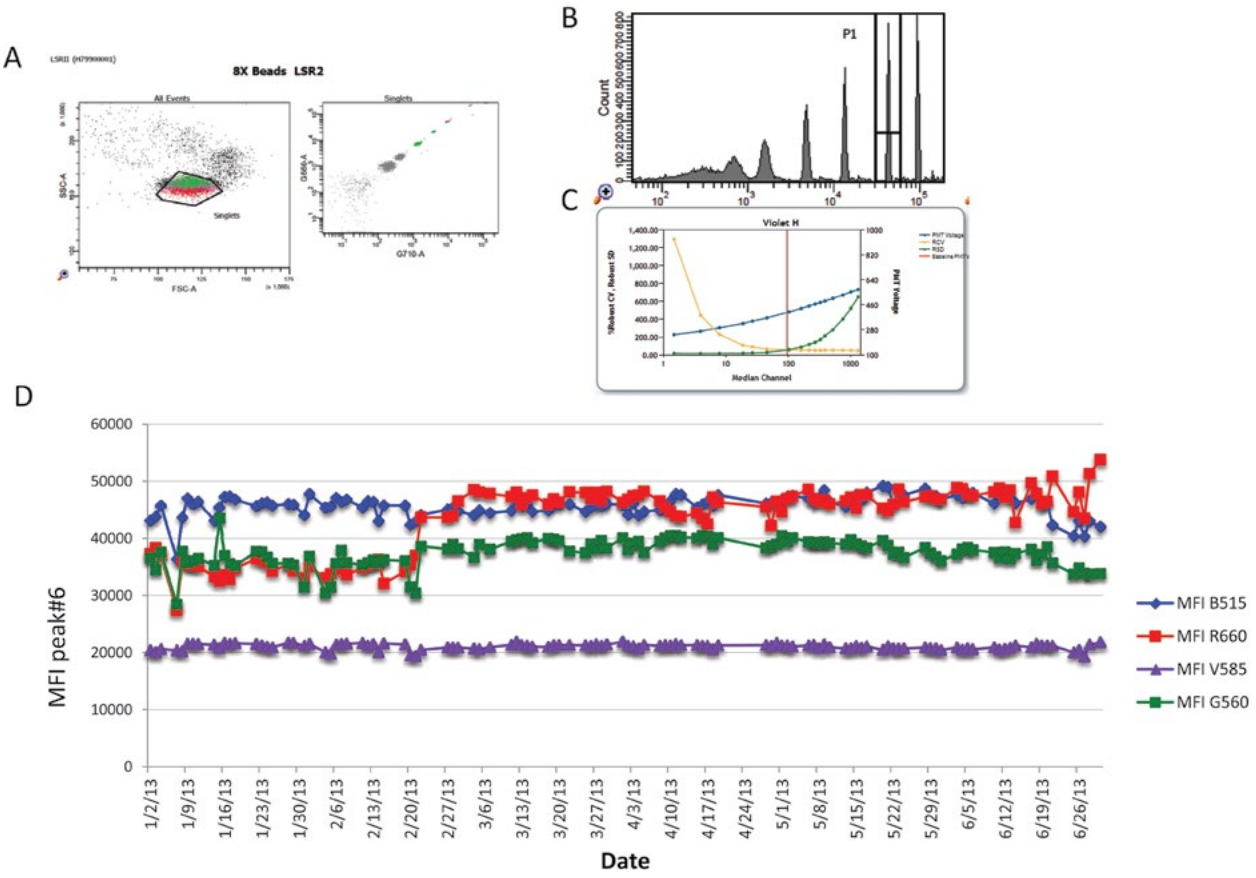

FIGURE 3 Example of dot plots generated by CST and QC Levy-Jennings. On a daily basis, eight peak beads are run on the cytometer after the CST performance check. (A) After doublet exclusion the fluorescence intensity is measured for each of the eight peaks in each detector. (B) Median fluorescence intensity of each PMT for each laser is generated by CST software (example of 1 Violet PMT V585). (C) Robust CV, robust SD of MFI of Violet PMT V585. Blue line represents the PMT voltage, the rCV is in yellow, rSD is in green, and the baseline PMT is the red line showing intersection of rCV with rSD. (D) Levy-Jennings plots, which display the performance characteristics of an instrument over time, are useful for assessing instrument variations. Here a Levy-Jennings plot of the MFI of bead standards at a constant voltage is shown for four PMTs across several months, with the performance of each detector shown in a different color.

Bead Setup and Tracking Features

Bead setup and tracking features are provided by the instrument manufacturer and include the beads and accompanying analysis software that uses algorithms to differentiate the fluorescence signals from each bead type based on size and fluorescence intensity in each detector for a specific instrument. The median fluorescence intensity (MFI) and percent robust CV (%rCV) are measured for each bead intensity in all fluorescence detectors (PMT). Linearity, detector efficiency (Qr), optical background (Br), electronic noise, and laser delays are all tracked. PMT voltages are then adjusted to maximize population resolution in each detector; PMT voltages should not vary more than 10 V from their baseline, and %rCV should be <6%. Levy-Jennings plots (PMT voltage over time) are used to facilitate monitoring of performance (Fig. 3D). One example of a manufacturer's performance check is the Cytometer Setting and Tracking (CST) beads from BD. CST beads are a set of fluorescent beads that can be used to assess the performance of the lasers and detectors, determine optimal values for laser delay, and determine optimal baseline voltages for every PMT.

In situations where automatic tracking features are not available or are not desired for a particular application, a similar generic approach can be used with third-party calibration beads. These beads are a mix of fluorescent beads with different intensities; for each bead, the %rCV of the MFI is measured and monitored. The acquisition of Spherotech beads (Spherotech, Lake Forest, IL) is performed at a constant voltage in which PMT values are fixed to arrive at a constants target channel (21, 23, 24, 27, 28).

SAMPLE PREPARATION

Sample Types and Requirements

Any single cell or particle suspension—which includes animal and plant cells, bacteria, yeast, dissociated tissue, peripheral blood leukocytes, bone marrow, cell lines, and cryopreserved cells—can be analyzed. Polystyrene beads can also be analyzed, and this is particularly useful if these are designed to capture soluble analyte for quantification (e.g., serum/plasma, cell culture supernatant, cell lysate, or other biological fluids).

To obtain single cells from tissues (e.g., tumor biopsies, lymph nodes), mechanical dissociation and/or enzymatic digestion is usually required. This is to break apart the cellular aggregates, to degrade extraneous material (such as collagen) from the tissue, and to facilitate optimal recovery of cells from the tissue. Conditions and enzyme requirements for digestion of each tissue of interest need to be determined empirically in order to keep the integrity of both the cells and antigens used for detection.

Certain cell types like monocytes, granulocytes, and adherent cell lines tend to be sticky and form aggregates. These aggregates can block the instrument's flow cell, and therefore samples containing these or other "sticky" cell types must be filtered to remove the aggregates or dispersed by some other method before being run on the flow cytometer.

Each type of sample needs to be carefully evaluated prior to preparation in order to ensure single-cell suspensions of intact cells for proper analysis (27–32).

Erythrocyte Lysis

In peripheral blood, erythrocytes outnumber white cells by 1,000 to 1. Due to their abundance and size, it is preferred to remove red blood cells from whole-blood samples if one only wishes to study leukocytes, as the presence of red cells will slow acquisition and create huge data files. It is not necessary to physically remove platelets and small debris, because these can be thresholded out during acquisition since a size threshold can be set empirically by the instrument operator. The effects of different erythrocyte-lysing methods commonly used in the analysis of human cells have been shown to influence recovery of certain cell types, such as blast enumeration, or consistency of CD4 and CD8 measurements (33–35).

Some of these methods allow for labeling of lymphocytes in whole blood, followed by erythrocyte lysis. Otherwise, using a solution of ammonium chloride (NH_4Cl), lysis can be performed prior to staining the lymphocyte subsets. The mechanism of lysis by this buffer is based on an osmotic shock of the red blood cells. Depending on the manufacturer, some of the ammonium chloride-based buffers include formaldehyde or diethylene glycol as fixatives.

For peripheral blood, the anticoagulant present in tubes into which the blood is collected (36–38), as well as the type of lysis reagent used for red blood cell removal, are among the factors that need to be evaluated prior to any experiment. It has been shown that a cytometric study of erythroid maturation requires a different method of specimen preparation than the red blood cell lysis methods commonly used to process blood and bone marrow. Commonly used lysing reagents leave only very early erythroid precursors (proerythroblasts) remaining in the sample (39).

Although the majority of clinical laboratories analyzing peripheral blood now use an ammonium chloride lysis method for whole blood prior to routine immunophenotyping, research laboratories wishing to measure lymphocyte functions or to cryopreserve samples for future analysis need to use lymphocytes obtained by Ficoll-Hypaque density-gradient separation (FDS).

Absolute Cell Counting

Absolute cell counting using flow cytometry is possible through the use of an internal microsphere-counting standard specific to the cellular sample. The microspheres can only be added to an erythrocyte-lysed sample, and these beads can be manually added to the sample (true-count beads) or the sample can be added to the beads lyophilized in a tube (true-count tube).

The concept to this counting approach is that a known number of cell counting beads are added to a known volume of cell sample. The beads are counted along with the cells but can be gated separately due to distinct light-scatter characteristics. During the acquisition, since the concentration of the beads is known, the number of cells per microliter is obtained by relating the number of cells counted to the total number of fluorescent-bead events. The rate of acquisition needs to be constant and not changed.

Some newer instruments, such as BD Accuri C6, contain a microprocessor-controlled peristaltic-pump system that accurately monitors the sample volume pulled per acquisition run, automatically calculating the cell counts per microliter for any gated population, without the need to index counting beads.

Density Gradients

Since the early 1970s, density gradients for the separation of mononuclear cells have become commonly used in numerous laboratories. These gradients are composed of a neutral, highly branched, high-mass, hydrophilic polysaccharide. The density gradient of Ficoll-Paque (1.077 g/ml) is optimized for the isolation of mononuclear cells from human blood. After the centrifugation step, Ficoll separates layers of blood, with lymphocytes and monocytes under a layer of plasma. Most importantly, this lymphocyte separation by density gradients leads to the separation of lymphocytes from granulocytes, the latter being cells of the innate immune system and which constitute the largest population of circulating white blood cells. However, the effects of granulocyte removal on immunophenotyping have not been thoroughly studied (Fig. 4).

Unfortunately, density-gradient techniques show only $60 \pm 20\%$ recovery of the lymphocytes present in the original blood sample, and the effects on specific subtypes of cells may be variable—thus the researcher should measure the effect of the Ficoll density gradient on each cell subtype of interest (40, 41). In density-gradient separation, adherence of cells to plastic test tubes and centrifugation and washing of the cells may contribute in part to cell loss and the degree of reproducibility of isolation. Selective loss of some T cells, NK cells, and other markers, such as chemokine receptors, occurs (40, 42). Density-gradient separation has also been reported to upregulate certain antigens such as CD54, CD62L, and CD11b (43) and to produce differences in the staining patterns of certain antigens (44–47).

Frozen Samples

In some instances it is impossible to stain and analyze fresh blood, and analysis of these samples is usually postponed by the use of cryopreservation. Cryopreservation is the use of low temperatures to preserve structurally intact living cells. Successful cryopreservation of cells requires that a standardized and reproducible protocol be followed, although each protocol may require optimization for a given cell type or line to achieve maximum viability upon thawing. The use of cryopreserved samples can introduce changes in antigen expression, and this needs to be carefully monitored (48–53).

Reagents

Fluorochromes

A fluorochrome is a chemical compound that absorbs light at one wavelength and re-emits light at higher wavelengths (spectrum). When a fluorochrome absorbs the light, its electrons become excited and move from a "resting state" to a maximal energy level called the "excited state." Subsequently, after energy is released as heat, the electrons fall to

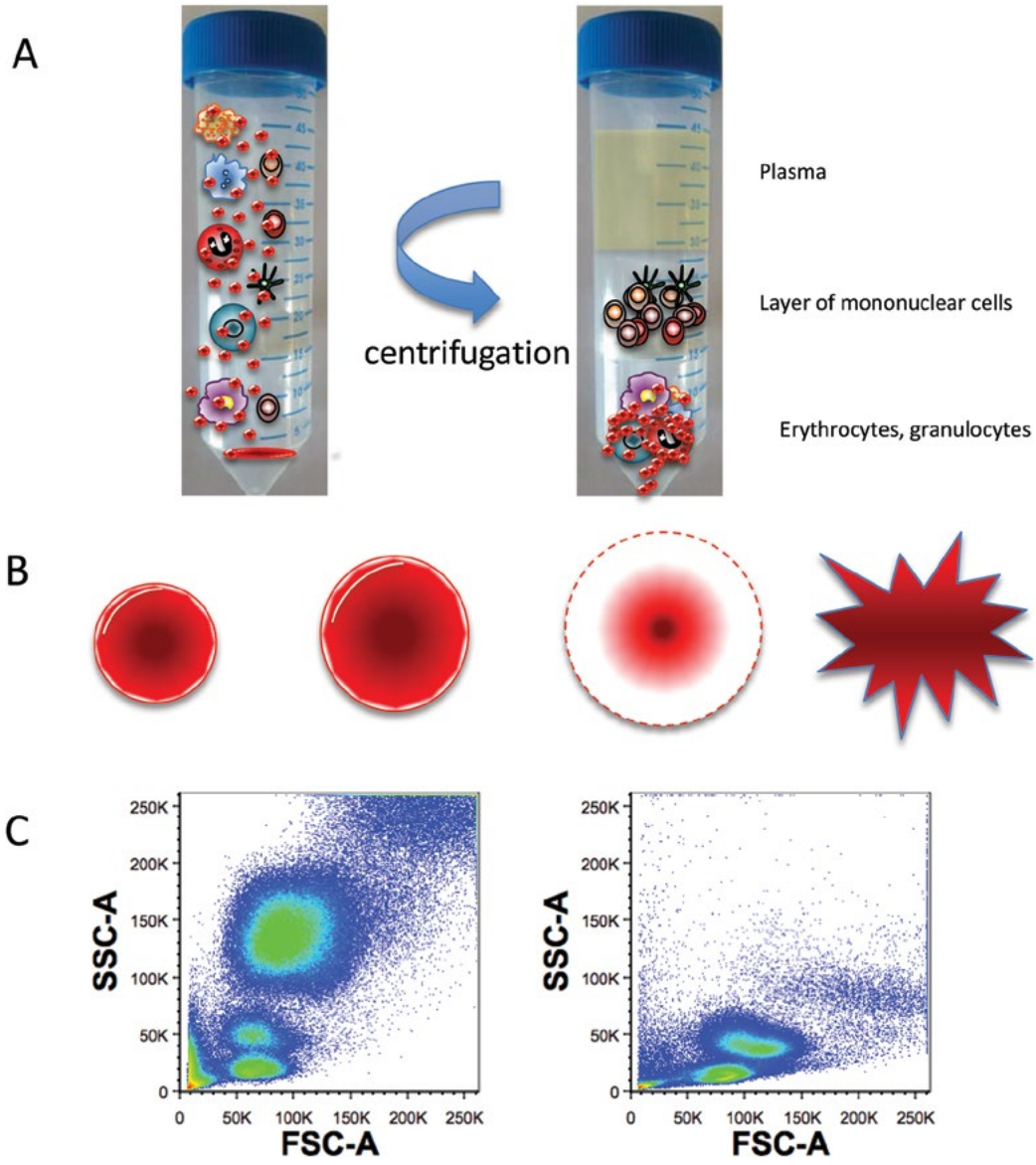

FIGURE 4 Illustration of Ficoll-Hypaque and whole blood as sample to stain. (A) Illustration of Ficoll-Hypaque. In noncoagulated blood after centrifugation in a Ficoll gradient, the plasma is on the top layer, followed by a layer of mononuclear cells, and then by a pellet of granulocytes and red blood cells at the bottom. (B) Illustration of red blood cell lysis. (C) A FSC versus SSC dot plot of the two types of samples: left, ammonium chloride-lysed sample; right, sample after a Ficoll gradient.

a lower, more stable, energy level called the "relaxed state." As electrons move back from the relaxed state to their resting state they release the remaining energy as fluorescence. The difference between the excitation wavelength and emission wavelength is called Stokes shift, and this wavelength value essentially determines how good a fluorochrome is for fluorescence studies. In addition to the Stokes shift, each fluorochrome is characterized by fluorescence quantum yield (ΦF). This is the ratio of photons absorbed to photons emitted through fluorescence, between the relaxed state and resting state.

For flow cytometry, most often fluorochromes are directly conjugated to mAbs specific for a cellular antigen. Direct conjugation of fluorochromes to antibodies permits one to be able to detect multiple antigens on the same cell at one time. A table of the common fluorochromes used in flow cytometry summarizes their excitation and emission range (Fig. 5).

As polychromatic flow cytometry uses several fluorochromes conjugated to several antibodies on one sample, the performance of each antibody-fluorochrome conjugate should be characterized individually and in combination with other conjugates.

The performance of an antibody-fluorochrome conjugate is measured by the mean fluorescence intensity (MFI) and stain index (SI) values (Fig. 6). MFI is the mean of the fluorescence intensity in the chosen fluorescence channel, and SI is the ratio of the difference between the positive signal and negative signal (D) and the width of the negative signal (W) ($SI = D/W$). Both MFI and SI should be obtained

Excitation color	Probe	Em (nm)	Function
355	Hydroxycoumarin	386	Reporter molecule
	Indo-1 bound to calcium	405	calcium flux
	Methoxycoumarin	410	Reporter molecule
	Cascade Blue	423	Reporter molecule
	DyLight 350	432	
	Aminocoumarin	445	Reporter molecule
	Alexa Fluor 350	445	phenotyping
	indo-1 unbound	490	calcium flux
	Lucifer yellow	528	Reporter molecule
	NBD	539	Reporter molecule
	Alexa Fluor 430	545	phenotyping
355 405	Qdot 565	565	phenotyping
	eFluor/Qdot/BV 605	605	phenotyping
	eFluor 625	625	phenotyping
	eFluor/BV 650	650	phenotyping
	Qdot 655	655	phenotyping
	BV711	711	phenotyping
	Qdot 800	800	phenotyping
405	Alexa Fluor 405	405	phenotyping
	DyLight 405	420	phenotyping
	BV421	421	phenotyping
	V450	448	phenotyping
	eFluor 450	450	phenotyping
	Pacific blue	455	phenotyping
	Amcyan	489	phenotyping
	V500	500	phenotyping
	krome orange	530	phenotyping
	Pacific orange	551	phenotyping
488	GFP	510	Reporter molecule
	DyLight 488	518	
	Fluo-3	530	Calcium flux
	Alexa Fluor 488	517	phenotyping
	FITC	519	phenotyping
	Alexa Fluor 555	565	phenotyping
	TRITC	572	phenotyping
488 532	R-Phycoerythrin (PE)	578	phenotyping
	PE-Texas Red	613	phenotyping
	PE-Cy5	670	phenotyping
	PerCP	675	phenotyping
	PerCP-Cy5.5	695	phenotyping
	PE-Cy5.5	695	phenotyping
	PerCP-eFluor710	710	phenotyping
	PE-Alexa Fluor 700	720	phenotyping
	PE-Cy7	767	phenotyping
532/560	YFP	534	Reporter molecule
	X-Rhodamine	576	menbrane potential
	DyLight 550	576	
	Lissamine Rhodamine B	590	menbrane potential
	Mitotracker	610	Mitochondrial menbrane tracker
	Texas Red	615	phenotyping
633	Allophycocyanin (APC)	660	phenotyping
	DyLight 633	658	
	Alexa Fluor 647	668	phenotyping
	APC-Cy5.5	695	phenotyping
	APC-Alexa Fluor 700	718	phenotyping
	Alexa Fluor 700	719	phenotyping
	APC-H7	765	phenotyping
	APC-Cy7	767	phenotyping
	APC-Alexa Fluor 750	779	phenotyping
	Alexa Fluor 750	779	phenotyping
	APC-eFluor780	780	phenotyping

Excitation color	Probe	Em (nm)
Nucleic acid		
335	Nuclear Yellow	495
343	Hoechst 33342	483
345	DAPI	455
345	Hoechst 33258	478
420	SYTO 40	441
420;480	Fura Red	660
423	Quinacrine Mustard	503
430	SYTO 41	454
431	SYTOX Blue	480
433	SYTO 42	460
434	ECFP	477
445	Chromomycin A3	575
445	Mithramycin	575
450	Chromomycin A3	570
455	SYTO 45	484
470	Acridine Yellow	550
484	SYTO 10	505
485	SYTO 9	498
490	SYTO 24	515
491	YOYO-1	509
488	EGFP	507
488	SYTO 13	509
488	SYTO 16	518
494	SYTO 21	517
499	SYTO 12	522
500	Acridine Orange	526
504	SYTOX Green	523
508	SYTO 11	524
547	SYTOX Orange	570
493	Ethidium Bromide	620
546	7-AAD	647
503	Acridine Orange	530/640
509	TOTO-1, TO-PRO-1	533
510	Thiazole Orange	530
514	EYFP	527
517	SYTO 14	549
518	Dihydroethidium (hydroethidine)	605
518	Hexidium Iodide	600
521	SYTO 25	556
536	Propidium Iodide (PI)	617
540	Pyronin Y	570
541	SYTO 82	560
541	TRITC	572
543	SYTO 83	559
557	DsRed-Express	579
563	DsRed2	582
567	SYTO 84	582
567	SYTO 85	583
599	SYTO 64	619
621	SYTO 17	634
622	SYTO 59	645
628	SYTO 61	645
642	TOTO-3, TO-PRO-3	661
649	SYTO 62	680
650	Cy5	670
652	SYTO 60	678
657	SYTO 63	673
675	Cy5.5	694
543;590	LDS 751	712;607
488;514;568	DRAQ5	655+

FIGURE 5 Summary tables of the most common fluorochromes used in flow cytometry. The left table shows fluorochromes and cytosolic dyes while the right table shows dyes to stain nucleic acids.

for each antibody-fluorochrome conjugate used in a staining combination.

Once each antibody-fluorochrome conjugate is characterized alone, the background fluorescence should be measured in the other detectors. Indeed, fluorescence background in a particular detector is influenced by several factors: cellular autofluorescence, nonspecific staining, electronic noise, and optical spillover from other fluorochromes. To the extent that these factors each contribute noise and/or signal, they increase the width of a negative population. As such, a good normalized functional measure of reagent brightness is SI (Fig. 6).

Antibodies: CD Designations, Etc.

The term "antigen" originally came from *anti*body *gen*erator and was coined in the early 1900s. An epitope is the molecular feature of an antigen capable of being bound by an antibody (a.k.a. antigenic determinant). An antigen will often have hundreds of epitopes. An antibody will bind specifically to an antigen; however, polyclonal

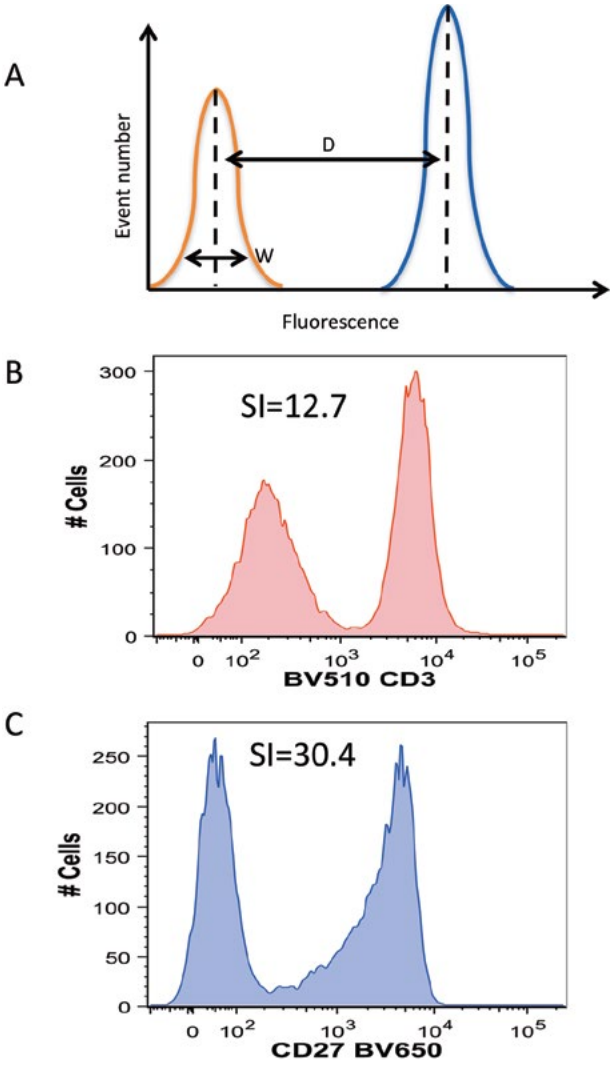

FIGURE 6 Illustration of the stain index. (A) Theoretical stain index (SI) representation. When testing different reagents, the effective brightness is measured using the stain index. SI = D/W, where D is the difference between the median fluorescence intensity of the positive and negative peaks of fluorescence, and W is the spread of the negative peak. (B) SI for CD3 BV510. (C) SI for CD27 BV650.

antibodies will recognize several epitopes of the same antigen while mAbs will recognize only one epitope. The latter are preferred for flow cytometry as they yield greater specificity. Cells can be characterized by their respective cell-surface antigens, and mAbs are made to recognize these cellular antigens. Since one cellular antigen could contain multiple epitopes and therefore be recognized by several different mAbs, a naming convention was needed for these reagents rather than simply calling these mAbs by their clone or trade names.

To address this issue, the 1st International Workshop and Conference on Human Leukocyte Differentiation Antigens (HLDA) was held in Paris in 1982 and organized by Human Cell Differentiation Molecules (HCDM), whose mission is to "characterize the function, structure and distribution of leucocyte surface molecules and other molecules of the immune system."

The cluster of differentiation (CD) nomenclature was proposed for the classification of the mAbs against epitopes on the surface molecules of leukocytes, usually transmembrane proteins. Indeed, the approach of the HLDA workshop was to code antibodies and to send them to multiple participating laboratories for blind analysis against multiple cell types. The data were collated and analyzed by the statistical procedure of "cluster analysis." This analytical method identified clusters of antibodies with very similar patterns of binding to leukocytes at various stages of differentiation, hence the "cluster of differentiation" (CD) nomenclature. The CD nomenclature allowed the scientific community to communicate results in a universal language. HLDA 10 is currently accepting antibodies submission, and the latest symposium was in December 2014 in Australia, with a particular emphasis on dendritic cells. Since its conception, the use of CD has expanded to many other cell types; for humans there are currently 363 CDs (54, 55).

In a recent study (56), based on a majority decision method, there are an estimated 5,539 human genes that code for membrane proteins, which corresponds to 26% of the human coding genes. Approximately 3,700 genes that coded for cell-surface transmembrane proteins (20% of all known genes) were identified (Table 1). Taking into account these numbers, as well as previous estimations on the number of plasma membrane proteins expressed by leukocytes (55, 57), it is very likely that the CD numbers will keep increasing (HCDM webpage, http://www.hcdm.org/) (58).

Many CD antigens are more than simply markers on the cell surface; they have functional roles and play an important role in immune reactions. They can act as receptors or ligands important to the cell, initiating a signal cascade and altering the behavior of the cell. Some CD antigens do not play a role in cell signaling but have other functions, such as cell adhesion. For example, CD4 is the coreceptor associated with the T-cell receptor (TcR) in T-helper cells and is important for T-cell activation; it is also expressed on monocytes and dendritic cells for other functions.

Viability Dyes

Exclusion of nonspecific binding of antibodies to dead cells is an essential component of any flow cytometry experiment. Multicolor flow cytometry often requires the measurement of low-frequency subtypes of cells, sometimes in cryopreserved samples. Dead cells in the sample may nonspecifically bind mAb-conjugates and cause significant artifacts; thus it is highly useful to exclude them during the analysis (29, 59–63). Fortunately, viability stains permit us to identify dead cells present in the sample and thus to be able to gate out the dead cells during analysis. Dead cells can compromise the integrity of the data and lead to misinterpretation of staining.

Several types of viability dyes are currently available, as follows.

Propidium iodide and 7-AAD cannot pass through intact cell membranes, but may freely enter cells with compromised cell membranes. Upon entering dead cells, propidium iodide will intercalate into double-stranded DNA or double-stranded RNA in a stoichiometric manner, while 7-AAD will intercalate only with double-stranded DNA. Because this intercalation is mediated by noncovalent forces, these dyes must remain present in the buffer used to resuspend cells for data acquisition so that dead cells will remain labeled.

Calcein dyes are nonfluorescent and membrane permeable. Upon entering the cells, the dyes are converted to membrane-impermeable, fluorescent compounds by

TABLE 1 List of the most abundant families of antigens and number of members with assigned CDs

Family name	No. of members	Members with CD	% of total
Ig superfamily	195	134	69
G-protein coupled receptor superfamily	147	22	15
C-type lectin family	49	23	47
Cytokine receptor family	44	28	64
Protein kinase superfamily	34	15	44
MHC family	30	6	20
Solute carrier family	29	3	10
TNF receptor superfamily	26	21	81
Integrin family	23	17	74
Tetraspanin family	20	9	45
Major facilitator superfamily	20	0	0
ABC transporters superfamily	18	2	11
TNF superfamily	17	11	65
Peptidase protein family	16	2	13
Transient receptor family	14	0	0
Cadherin family	13	3	23
Potassium channel family	13	0	0
Toll-like receptor family	12	9	75
Sialomucin family	12	9	75
Leucine-rich repeat family	11	5	45

intracellular esterases. Dead cells will not have active esterase activity, nor will they retain the fluorescent dyes. Thus, the calcein dyes allow viable cells to be fluorescently labeled for analysis in standard cell surface-staining protocols.

Fixable viability dyes (Live-Dead-Fixable [Life Technologies, Carlsbad, CA], Zombie [Biolegend, San Diego, CA], Horizon [BD] stains) can be used to irreversibly label dead cells prior to cryopreservation, fixation, and/or permeabilization procedures. Cells labeled with fixable viability dyes can be washed, fixed, permeabilized, and stained for intracellular antigens without any loss of staining intensity of the dead cells. Thus, fixable viability dyes are fully compatible with intracellular staining for molecules of interest such as cytokines (Table 2).

Procedures

Antibody Titration

Antibodies are often used together in mixtures often referred to as antibody cocktails. Each antibody is present in the cocktail at a concentration that is determined by titration. Antibodies have a range of concentrations in which they optimally bind to antigens. If too little is used, there will be an inaccurate amount of light produced by the fluorescence and, depending on the magnitude, a cell positive for the antibody may not be detected. However, if too much antibody is used, the true amount of the target antigen in the sample may be masked and the fluorescence of the negative cells may increase. The "saturating" concentration is the lowest concentration that gives nearly maximal fluorescence. The "separating" concentration represents the concentration that gives the best separation between the positive and negative peak of fluorescence.

During titration, serial dilutions of antibody are used to stain identical aliquots of cells, and the saturating concentration can be determined by the highest fluorescence intensity. The separating concentration can be determined by the difference between the two fluorescence intensities (Fig. 7C). For titration, each staining can be viewed on different axes (Fig. 7A) or on the same axes using concatenation (Fig. 7B).

Once the optimal separating concentration is determined, an appropriate staining buffer should be tested. The incorporation into a staining buffer of a reagent to block the binding of antibody Fc regions to cells is very common in fluorescent-activated cell sorter (FACS) staining buffer. Human Fc receptors (FcR) are expressed on a variety of cells, such as monocytes, granulocytes, B cells, and dendritic cells. Cells expressing these FcR can give false-positive staining due to the FcR-mediated immunoglobulin (Ig)-Fc binding (mainly due to species-specific recognition, as the antibodies for staining are often produced in mice). Blocking the FcR-involved unwanted staining without interfering with antibody-mediated specific staining of the cells is highly recommended; to this end, serum is added to the staining buffer. Serum can be human, mouse, goat, or fetal calf serum, or even bovine serum albumin. These are often used at a concentration of 0.5%. In addition, serum or Fc block can be used to increase the specificity of staining of extremely rare target cells, such as antigen-specific T or B cells, fetal cells in maternal blood, hematopoietic progenitor cells, or disseminated epithelial tumor cells. Note that this is not necessary for staining of whole blood because serum is present in high concentration during staining.

Other considerations in antibody cocktails are the variations due to pipetting errors when the cocktail mix is prepared, and product deterioration over time. The development of flow reagents stable at room temperature, including premixed cocktails, Lyoplates, and DuraClone, directly addresses these concerns.

Premixed Cocktails

Based on titration, directly conjugated antibodies are premixed to allow usage of the same mix for multispectral flow of all experiments or measurements of an entire clinical protocol.

Lyophilization of Cocktails

BD Lyoplate technology is a plate-based lyophilization process that uses a matrix to stabilize antibody cocktails. A proprietary matrix preserves the ability to stain, stimulate, and resolve cellular data by flow cytometry. Automated dispensing and lyophilization of the antibody ensures that consistent and reproducible staining reactions are possible for the duration of an entire immunophenotyping study over many months.

Dehydration of Cocktails

Beckman Coulter Duraclone technology uses drying in a specific solution to preserve the antibody cocktails.

TABLE 2 Summary of types of dyes used in flow cytometry

Laser	Wavelength (nm)	Nonpermeable dyes	Permeable dyes	Cell cycle nonpermeable	Cell cycle permeable	Cell division/proliferation nucleoside incorporation
UV	355	DAPI	Fixable Blue	Hoechst 33342	Hoechst 33342 DAPI	
Violet	407	SYTOX Blue	Fixable Violet Fixable Aquablue Zombie Aqua BD Fixable Viability stain 450	DyeCycle violet	SYTOX blue dye DyeCycle violet	click-iT Edu
Blue	488	SYTOX Green PI 7-AAD	Fixable Green Zombie Yellow	DyeCycle green	SYTOX green dye DyeCycle green PI 7-AAD	click-iT Edu Anti-Brdu CFSE Oregon green DiO Anti-Ki67
Green	532	SYTOX Orange PI 7-AAD	Fixable Red	DyeCycle orange	SYTOX orange dye PI 7-AAD	Anti-Brdu Dil Anti-Ki67
Red	633	SYTOX Red	Fixable Far Red Zombie NIR	DyeCycle red	SYTOX red dye	click-iT Edu Anti-Brdu DiD DDAO-SE Anti-Ki67

[a]Live-Dead (Life Technologies), Zombie (Biolegend), and Horizon (BD) stains are all trademarks.

Intracellular Antigen Detection

A large number of applications require intracellular staining, such as monitoring of cell proliferation, cell signaling, apoptosis, chromosome analysis, and production of cytokines. The permeabilization protocol needs to be optimized for each application, as the size, stability, and intracellular locations of the targets can be highly variable.

Intracellular staining brings with it two major technical problems: (i) compatibility of the permeabilization method with the staining of all markers in a particular tube, and (ii) the loss of cells associated with this procedure. These problems are addressed by empirical testing of fixation/permeabilization reagents for changing intensity of staining of surface markers compared to staining of fresh unfixed cells, while at the same time permitting optimal staining of the intracellular antigen. In terms of cell loss associated with the fixation/permeabilization and stain procedure, we have shown that roughly 40% of the loss is associated with staining procedures (29).

When surface and intracellular staining are to be performed in the same sample, it is advisable that the surface staining be performed first, since fixation/permeabilization treatments might decrease the availability of surface antigens, and to ensure that only the surface antigens (and not the same antigen also expressed intracellularly) are stained.

Antibodies should be prepared in permeabilization buffer to ensure penetration into the cells during the intracellular staining procedure. When gating on cell populations, the light-scatter profiles of the cells on the flow cytometer change considerably after permeabilization.

There are several methods of permeabilization available, but all of them have in common a fixation that will stabilize the proteins, and then disruption of membrane by detergent: formaldehyde followed by detergent, formaldehyde followed by methanol, methanol followed by detergent, acetone fixation, and permeabilization.

The detergents commonly used in cytometry protocol are: Triton X-100, NP-40 (0.1 to 1% in PBS), Tween 20, saponin, digitonin, and Leucoperm, which are mild membrane solubilizers. These will also partially dissolve the nuclear membrane and are therefore very suitable for nuclear antigen staining.

Detection of secreted proteins is difficult, as the protein will be released from the cell before detection or may degrade rapidly. Brefeldin A and other compounds are often used for Golgi-complex blocking (59). Cells are incubated with brefeldin A, which prevents protein being released from the Golgi complex. Any cells expressing the protein can then be detected intracellularly.

Panel Design, One Approach

To immunophenotype both the incredible breadth as well as fine detail of the immune system in a comprehensive approach, we proposed the use of multiple individual tubes together in a panel of highly polychromatic cocktails. A reasoned approach to construction of a comprehensive leukocyte immunophenotyping panel (CLIP) would be to structure a series of individual tubes that provide in-depth characterization of a specific cell type, but at the same time have a sufficient number of recurring markers among the tubes that a concatenation of the numerous phenotypes within a lineage can be assembled. The goal of our panel was to obtain in-depth immunophenotypic profiling of as many circulating human leukocyte populations as possible, in order to build an encyclopedic database. Historically, there have been relatively few leukocyte subsets examined in clinical studies or clinical research studies and for which reference ranges exist (64). One example of such a panel developed to obtain a synoptic snapshot of the cellular phenotypes in the immune system has been reported (29).

In order to select the reagents for a multicolor panel that would yield optimal detection and staining intensities, numerous antibody clones directed against a specific antigen and multiple antibody-fluorochrome combinations need to be tested (24, 29). The levels of the intensity of expression

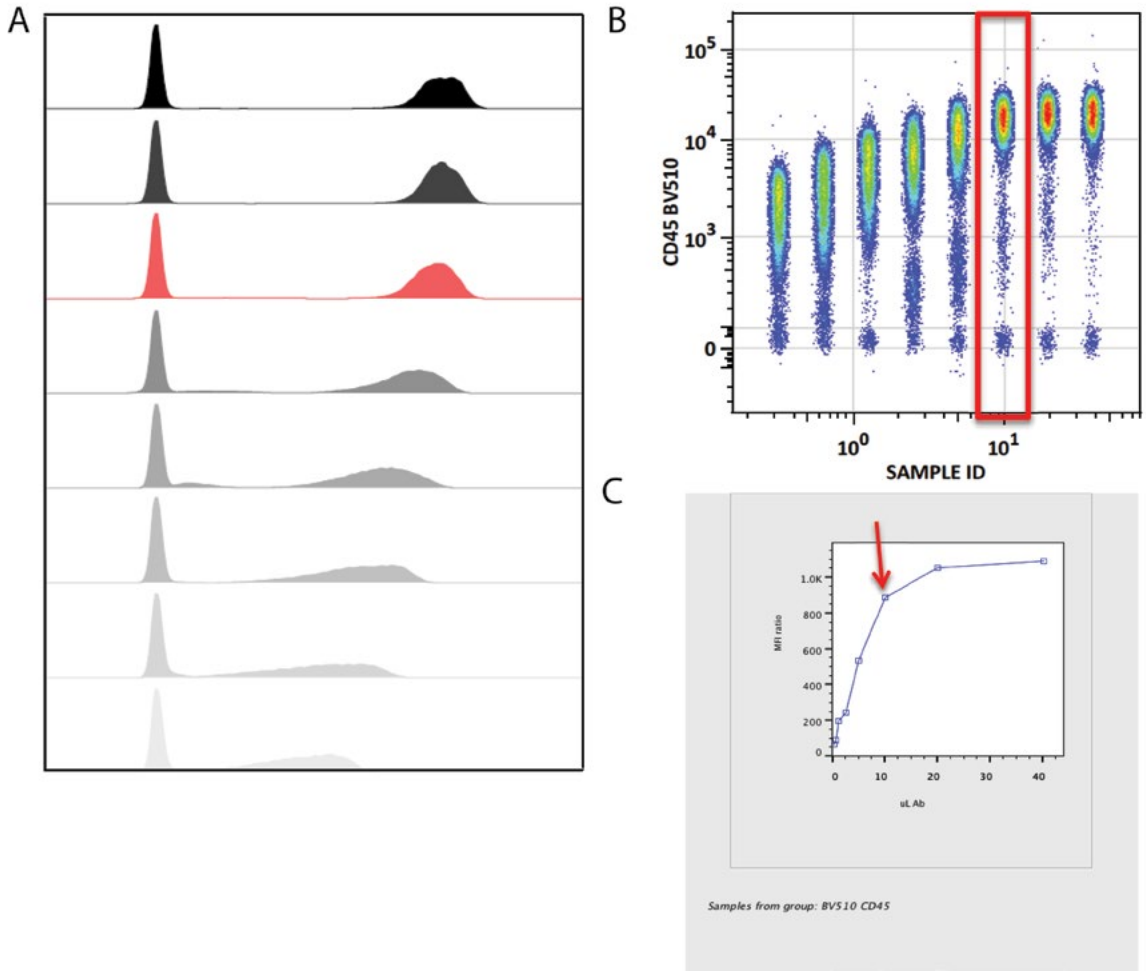

FIGURE 7 Illustration of titration of monoclonal antibody. An FCS file represented independently (A) or concatenated (B). (C) Determination of the separating concentration by graphing the ratio of the positive to negative peaks against the dilution. The histogram represented in red (A), or the dot plot highlighted by the red square (B) or red arrow (C), all mark the selected concentration for the given antibody.

for the selected markers should be established and then the optimal fluorochrome-antibody combinations may be selected based on their performance, i.e., discrimination of positive and negative populations, fluorescence intensity, percentages of positive cells, and ease of compensation. Generally, bright fluorochromes, such as phycoerythrin (PE) and APC, are preferentially chosen for weak antigens (or intracellular) where only low numbers of molecules are expressed per cell, or those that are expressed by only a very small fraction of cells, such as intracellular cytokines. Less bright fluorochromes are assigned to antigens that are expressed by a large proportion of cells and at a high molecular density, such as CD8.

Using the approach described above, we began to build our CLIP panel one 15-color tube at a time. This was done with the full understanding (i) that each tube represented only one small part of a comprehensive panel, (ii) that completely comprehensive analysis would not likely be achieved using the current approach, and (iii) that new markers and technologies would likely evolve to replace the current efforts.

CD45 is a transmembrane tyrosine phosphatase ubiquitously expressed by leukocytes and is important in modulating signals derived from integrin and cytokine receptors. The level of CD45 is expressed differentially throughout maturation, being lower on blasts and immature forms and highest on mature and lymphoid cells (39). Our approach was for each tube to have a specified purpose, but to have CD45 present in all tubes. Furthermore, within each lineage the tubes would have a number of recurring markers, both for quality-control purposes, but also in order for cross-tube concatenation of more detailed phenotypes. If viability, CD45, and CD3 are used for gating in each of the T-cell tubes, each of the T-cell tubes could yield 4,096 T-cell phenotypes (if one assumes all marker combinations could be expressed, and marker expression is defined only as positive or negative). Although not comprehensive for the entire immunome, the existing 14-tube CLIP panel could provide a breadth and depth of immunophenotyping not reported heretofore. To date, our panel consists of 14 15-color tubes (see complete list of the current tubes of the CLIP panel, along with the antibody clones and fluorochromes used, in Fig. 8).

Data Acquisition

During acquisition of the data, several factors can influence the quality of the data, as follows.

CHI CLIP panel

Excitation	Fluorochrome name	PMT name	T lineage				B lineage			NK lineage		Dendritic lineage	Mono lineage		Neutrophil lineage	
			T_1	T_2	T_3	T_4	B_1	B_2	B_3	NK_1	NK_2	DC_1	M_1	M_2	N_1	N_2
407 Excitation	V450	V450	CD4	CD4	CD4	CD4	Lambda	CD80	CD80	CD56	CD56	CD123	HLA-DR	CD31	CD62L	CD62L
	Aquablue	V545	Viability	Viability	Viability	Viability	Viability	Viability	Viability	Viability	Viability	Viability	Viability	Viability	Viability	Viability
	BV605	V605	CD8	CD8	CD8	CD8	CD10	CD27	CD27	CD8	CD8	CD27	CD163	CD163	CD279	CD3
	BV650	V655	CD27	CD27	CD27	CD27	CD19	CD19	CD19	CD30	NKp46	CD4	CD14	CD14	CD14	CD14
	BV785	V800	CD45	CD45	CD45	CD45	CD45	CD45	CD45	CD45	CD45	CD45	CD45	CD45	CD16	CD16
488 Excitation	FITC	B515	CD39	IL-23R	CD69	CD183	CD40	IgA	IgA (intra)	CD57	CD57	IFNa	CD77	CD235a	CD64	CD185
	PcPcy5.5	B710	CD38	CD196	IL-4	CD196	CD138	CD86	CD86	CD161	IFNg	TNFa	CD192	CD34	CD83	CD203c
532 Excitation	PE	G560	Foxp3	CD146	perforin	CD278	Kappa	CD21	IgE (intra)	CD337	Perforin	CD40	CD64	CD64	CD172b	CD303
	PE-TR	G610	CD45-RA	CD45-RO	CD45-RO	CD45-RA	CD38	CD38	CD38	CD94	CD25	HLA-DR	CD16	CD16	CD123	CD123
	PEcy5	G660	CD103	CD161	CD40L	CD40L	CD103	IgG	IgG (intra)	CD16	CD16	CD83	CD15	CD15	CD15	CD15
	PEcy5.5 /PE-A700	G710	HLA-DR	TNFa	TNFa	CD25	CD20	CD20	CD20	CD244	CD69	CD11c	CD4	CD4	HLA-DR	HLA-DR
	PEcy7	G780	CD25	IL-17A	IFNg	CD279	CD5	CD23	CD23	CD5	CD5	lineage *	CD13	CD13	CD13	CD13
633 Excitation	APC	R660	CD127	IL-22	IL-2	CD185	CD22	IgD	IgD (intra)	CD336	CD127	BDCA-2	CD36	CD36	CD11b	FCRe1
	Alexa700	R710	CD197	CD197	CD197	CD197	CD11c	IgM	IgM (intra)	CD158e1	CD158e1	CD33	CD33	CD33	CD33	CD33
	APCcy7	R780	CD3	CD3	CD3	CD3	CD25	CD10	CD10	CD3	CD3	CD86	CD206	HLA-DR	CD10	CD10

FIGURE 8 Tubes (staining) of CLIP panel organized by lineage. In black are markers present in all stainings of one lineage, and in blue are markers specific to one staining. *, Lineage mix = CD3+CD19+CD20+CD56+CD16+CD14.

Numbers of Cells To Acquire, Statistics of Event Numbers (67, 68)

The number of events acquired can affect the rigor of the statistics associated with immunophenotyping, and thus the confidence that one has in the accuracy of the distributions.

Consider the general case of enumerating a total of N events with a variance (var) and a standard deviation (SD):

$$\mathrm{CV} = \frac{\{\sqrt{[\mathrm{var}(R)] \times 100}\}}{R}$$

where R is positive cells and the proportion of positives is $P = R/N$.

A preparation of human peripheral blood mononuclear cells is labeled with an antibody to detect T cells. Flow cytometry then indicates that 10% of the cells present are positive for this marker. If three data sets (list-mode files) were collected for 1,000, 5,000, and 10,000 events, we would expect to observe 100, 500, and 1,000 positive cells with variances of 90, 450, and 900, respectively. Expressed as SDs, these would be 9.5, 21.2, and 30, and as CVs, 9.5, 4.2, and 3, respectively.

Good experimental practice within the biological field usually results in CVs on the order of 5%. Hence, the example above indicates that a list-mode file of 5,000 events will provide that level of confidence as expected from the argument relating to dogma: for a subpopulation of 10%, a total of 5,000 events would be adequate. It is obvious that the reliability of the frequency determinations is dependent on the number of events observed, a particularly crucial issue for rare-event detection. Consequently, for a desired level of reliability (CV), the number of rare events to be counted can be calculated from $R = (100/\mathrm{CV})^2$. To match typical experimental variations of 5%, approximately 400 rare events need to be observed, which at the defined limit of rare events (1 in 20), a list-mode file of 8,000 would be required.

In the CLIP panel, since one of the goals is to be able to mine the data at a later date for unknown populations, we wanted to be able to have rigorous statistics for cell populations as low as 0.1%. For this reason, between 1 million and 2 million cells were used for staining within each tube, and in the case of dendritic-cell staining, up to 5 million cells per tube were used if sufficient sample was available. Between 500,000 and 5 million events were collected per FCS file, depending on the number of cells available, in order to have sufficient events for statistical analysis of rare subsets defined by multiple markers.

If the staining requires intracellular marker staining, the number of cells initially placed into each tube must be proportionally higher than the number placed into tubes not requiring intracellular staining in order for equivalent large numbers of cells to be collected on the cytometer (30 to 50% higher).

Live-Gating Techniques

In stainings that use intracellular detection, we needed to use a fixable viability dye that would not leak out of the cells when permeabilized. We decided to use amine-reactive dyes, which differ from other viability markers because they react with free amines in the cytoplasm. Live cells exclude these dyes thanks to the integrity of their cell membrane, unlike dead cells, where the bound dye remains inside the cytoplasm. This reaction is irreversible, and the dye will remain bound to the amine even when the cells are permeabilized for intracellular staining (62). Like all antibodies used in the panel, amine-reactive dyes need to be titrated.

Doublet Exclusion

One important aspect of accurate analysis is the ability to exclude cell doublets. Coincident events (doublets and aggregates) occur when two (or more) cells or particles are in the beam at the same time and are seen by the system as a single, larger particle.

Cell doublet profiles appear differently in a graphical display according to their orientation and the parameters used (height, area, width). In a digital cytometer, a dot plot representation of FSC or SSC versus either height or width will help identify two cells passing through the beam together. Singlet cells will have FSC-A and FSC-H that are proportional to one another and thus appear as a diagonal when graphed against each other in a dot plot. Cells not falling along that diagonal are therefore doublets and should be excluded from further analysis.

QUALITY ASSURANCE AND QUALITY CONTROL

All assays of biological samples, whether clinical or research in nature, need to be performed in a reliable manner that assures one that if differences are observed between specimens, the differences are due to a biological reality and not a technical artifact. For flow cytometric assays, ensuring quality must encompass several levels, such as preanalytical variables including the anticoagulant used (if the specimen is peripheral blood), sample preparation methods and reagents, instrument performance and stability, and assay validation. Thus, protocols and procedures must be implemented at each level to ensure that data from flow cytometry assays are meaningful and reproducible. Many of these elements have been described in previous sections of this text, and therefore only the crucial components of assay validation will be discussed here.

Requirements for validation of an assay include:

- accuracy
- precision (repeatability/reproducibility)
- analytic sensitivity (detection limit)
- analytic specificity (interfering substances)
- sample types and stability
- reportable range
- reference intervals
- calibration and control materials

In addition to these measures, it is the feeling of these authors that in research flow cytometry, validation should also include methods to confirm that cell types identified by a specific combination of antigenic markers have been accurately and correctly classified. Most often, this confirmation would be made by sorting the cell types in question and demonstrating the function or genomic content associated with the presumed cell type.

Returning to the validation requirements listed above, accuracy refers to how close the measured value is to true value. For immunophenotyping studies, this may not be a simple determination, as there are no other methods that can identify and quantify cell types based on high-polychromatic immunophenotyping. A surrogate, but far from perfect, approach to determine accuracy could be quantification of beads by flow cytometry in which known amounts were placed into tubes.

Precision refers to the reproducibility of an assay—how similar repeated measurements of the same sample will be to each other. This is a far easier and arguably more important

aspect of immunophenotyping assays to determine. By repeatedly running one specimen multiple times, one can determine the optimal instrument precision. Intra-assay precision can be determined by staining multiple aliquots of one specimen at the same time and then running these specimens on the cytometer. This accounts for variability that might be introduced by pipetting, washing, centrifugation, and other factors not directly related to the cytometer. Inter-assay precision can be determined by staining aliquots of the same sample (cryopreserved or stabilized cells) at different times and then comparing the data. Compared to intra-assay precision, this looks at other potential confounding factors such as temperature fluctuations, technician variability, instrument fluctuations with time, and so forth. The additional requirements listed above cover additional elements of the assays, ranging from instrument performance to broader population studies. To be rigorously validated, assessments of flow cytometric assays should consider elements of all phases of the testing. For high-polychromatic immunophenotyping, the assurance of instrument stability and standardization, discussed previously, cannot be emphasized enough. Population studies, the study of a large number of different individuals using the same assay, can be used to create reference range values—values for which specified cellular subsets are found throughout a large population. These ranges reflect the heterogeneity in immune composition and responses found in different individuals. Most often, 95% or 99% confidence intervals are determined as the ranges in which one would expect to find the values from any healthy individual within the same population. Reference range values can be dependent upon ethnicity, race, gender, and age, as well as other variables. Furthermore, reference values can be influenced by the clones of antibodies used in the assays, fluorochromes, and other technical variables; thus it is preferable that each laboratory establish its own reference values. Reference values can be expressed as either percentages of leukocyte subsets or as absolute cell counts, or both.

An additional component of quality assurance is proficiency testing, a procedure to determine a laboratory's performance of specific assays in comparison to reference standards or a consensus of results from similar laboratories. Although not available for every panel a laboratory may run, programs are available that encompass a number of different immunophenotyping endeavors. Examples of proficiency testing programs include those run by the College of American Pathology (CAP) and the United Kingdom National External Quality Assessment Service (UK NEQAS), although many more exist for specific nations.

DATA ANALYSIS AND INTERPRETATION

The analysis and interpretation of polychromatic flow cytometry data is arguably the most difficult aspect of performing these assays. Flow cytometry data are most often collected as list-mode data files in the .fcs format, and therefore most software is designed primarily to analyze this file type, although these programs may also have the capability for other less common, and possibly proprietary, file types. Key features of the .fcs file type are the inclusion of keywords that can identify specific aspects of how the data were collected and the listing of all the data collected for every event in an event-by-event manner. Collecting data in this manner permits experiments to be compensated and analyzed repeatedly, if desired. These data are visually displayed as one- or two-dimensional graphs or frequency histograms. Data are compensated, as discussed previously, before being further analyzed. A very useful aspect of .fcs data files is that they can be subjected to gating, a process in which one can isolate a specific population of cells from others (e.g., lymphocytes in whole peripheral blood) in the same sample for further analysis. Gates can be combined using Boolean logic to further specify populations to be studied. Thresholds for determination of positive versus negative fluorescence staining can be established through the use of negative controls, fluorescence-minus-one (FMO) controls, or isotype controls, although the use of this last is controversial, as control isotypes are seldom matched for both concentration and fluorochrome-to-protein ratio. FMO controls consist of a sample in which all markers and fluorochromes are present except for the one for which a threshold of positive staining needs to be determined. These are particularly useful for markers where the positive staining does not result in a discrete population of positive cells, but rather the staining appears as a continuum of events extending from the negative population (as frequently observed in staining for intracellular cytokines or markers of cellular activation).

By segmenting data displays with the use of markers—or, in the case of two-dimensional plots, quadrants—statistical information can be obtained about specific cellular populations, such as what percentage of the parent gate these represent; what percentage of the total these represent; the mean, mode, and peak fluorescence intensity of these cells; and the spread (CV) of the cells. These statistics can elucidate differences found among samples due to reasons such as interindividual variations or effect of some type of treatment or intervention.

Historically, data analysis has been performed manually, perhaps aided by the use of layout templates or "batch" processing, in which multiple data files can be sequentially introduced into a standard analysis layout. For low-dimensional studies this is a feasible, albeit subjective, approach for thoroughly analyzing the cell populations represented by these data. The issue of subjectivity in manual analysis should not be taken lightly. As illustrated by Maecker et al. (27, 28), one of the main sources of variability in interlaboratory comparisons of flow cytometry data arises from manual gating. When analyzing high-polychromatic flow cytometry data, the weaknesses of manual gating become glaring: the sheer numbers of potential populations make these data nearly impossible to thoroughly manually analyze, and the subjective nature makes variability unacceptably high, particularly in rare populations. Therefore, it is most common for these files to be analyzed in a guided (directed) manner, in which only predetermined immunophenotypes are studied and the gating strategies to study these populations are determined at the time of designing the panel. This tremendously simplifies data analysis, but may leave some novel findings undiscovered. To address the issues associated with manual gating, considerable effort has been directed at devising algorithms capable of semi- or fully automated analysis of flow cytometry data. Historically, this has been a difficult task, as populations of cells characterized by dim, heterogeneous, and/or nondiscrete staining presented significant obstacles for accurate identification. This effort has been facilitated in many cases by the use of open-source software from Bioconductor and consortium efforts such as FlowCAP (69–73). These resources alleviate the need to "reinvent the wheel" for every effort at automation by providing basic tools useful in many of these approaches and by providing sample data for "challenges" to understand how well any given approach is working.

SUMMARY

Recently, manufacturers have begun to develop cytometers that diverge from traditional paradigms in various manners. One example is the Imagestream flow cytometer developed by Amnis-EMD Millipore. This cytometer is capable of capturing multicolor images of every cell that passes through the instrument, while at the same time collecting multicolor immunophenotyping data. This is achieved by replacing photomultiplier tubes for the collection of fluorescence data with CCD cameras and through the use of prisms to separate different wavelengths of fluorescent light and time-delay integration to achieve bright, sharp image resolution.

Another novel approach to fluorescence-based flow cytometry is multispectral flow cytometry as exemplified by the SP6800 Spectral Analyzer recently developed by Sony Biotechnology. This instrument has standard laser excitation and focusing using sheath fluid, and for a flow cell (point of cell-laser interrogation) uses a microfluidic chip. More importantly, it uses an array of 32 detectors to capture the entire spectrum of emitted fluorescent light (currently from 500 to 800 nm) (65, 74). The result of this is to improve the understanding of spectral overlap among the emitted fluorescence signals and to better establish spectral compensation values, particularly between fluorochromes with similar, but distinct, emission spectra. By doing this, it is theoretically possible to run and analyze more fluorochromes (and hence cellular markers) within the same bandwidth compared to cytometers constructed with a more traditional approach.

Finally, it is worth noting that flow cytometers are beginning to be developed that are not based on the detection of fluorescence. The leading example of this is the CyTOF developed by DVS, Inc. (66). This instrument replaced fluorescence with a mass spectroscopy-based time-of-flight measurement of heavy-metal isotope labels. Elimination of fluorescence removes the need for fluorescence compensation, thus facilitating easier high-dimensional immunophenotyping, as well as for the collection of data on more parameters. Although this approach has technical drawbacks in terms of yield and throughput, it is a milestone in moving away from the reliance on fluorescence-based assays and the accompanying technical limitations.

REFERENCES

1. **Stöhr M, Eipel H, Goerttler K, Vogt-Schaden M.** 1977. Extended application of flow microfluorometry by means of dual laser excitation. *Histochemistry* **51:**305–313.
2. **Dean PN, Pinkel D.** 1978. High resolution dual laser flow cytometry. *J Histochem Cytochem* **26:**622–627.
3. **Loken MR, Parks DR, Herzenberg LA.** 1977. Two-color immunofluorescence using a fluorescence-activated cell sorter. *J Histochem Cytochem* **25:**899–907.
4. **Murphy RF, Chused TM.** 1984. A proposal for a flow cytometric data file standard. *Cytometry* **5:**553–555.
5. **Bagwell CB, Adams EG.** 1993. Fluorescence spectral overlap compensation for any number of flow cytometry parameters. *Ann N Y Acad Sci* **677:**167–184.
6. **Köhler G, Milstein C.** 1975. Continuous cultures of fused cells secreting antibody of predefined specificity. *Nature* **256:**495–497.
7. **Bendall SC, Simonds EF, Qiu P, Amir el AD, Krutzik PO, Finck R, Bruggner RV, Melamed R, Trejo A, Ornatsky OI, Balderas RS, Plevritis SK, Sachs K, Pe'er D, Tanner SD, Nolan GP.** 2011. Single-cell mass cytometry of differential immune and drug responses across a human hematopoietic continuum. *Science* **332:**687–696.
8. **Samsel L, Dagur PK, Raghavachari N, Seamon C, Kato GJ, McCoy JP Jr.** 2013. Imaging flow cytometry for morphologic and phenotypic characterization of rare circulating endothelial cells. *Cytometry B Clin Cytom* **84:**379–389.
9. **Goddard G, Martin JC, Graves SW, Kaduchak G.** 2006. Ultrasonic particle-concentration for sheathless focusing of particles for analysis in a flow cytometer. *Cytometry A* **69:**66–74.
10. **Goddard GR, Sanders CK, Martin JC, Kaduchak G, Graves SW.** 2007. Analytical performance of an ultrasonic particle focusing flow cytometer. *Anal Chem* **79:**8740–8746.
11. **Kapoor V, Karpov V, Linton C, Subach FV, Verkhusha VV, Telford WG.** 2008. Solid state yellow and orange lasers for flow cytometry. *Cytometry A* **73:**570–577.
12. **Kapoor V, Subach FV, Kozlov VG, Grudinin A, Verkhusha VV, Telford WG.** 2007. New lasers for flow cytometry: filling the gaps. *Nat Methods* **4:**678–679.
13. **Shapiro HM.** 1986. Technical developments in flow cytometry. *Hum Pathol* **17:**649–651.
14. **Shapiro HM.** 1987. Laser noise and news. *Cytometry* **8:**248–250.
15. **Shapiro HM.** 2004. Lasers for flow cytometry. *Curr Protoc Cytom* **Chapter 1:**Unit 1.9.
16. **Shapiro HM.** 2004. The evolution of cytometers. *Cytometry A* **58:**13–20.
17. **Telford W, Kapoor V, Jackson J, Burgess W, Buller G, Hawley T, Hawley R.** 2006. Violet laser diodes in flow cytometry: An update. *Cytometry A* **69:**1153–1160.
18. **Telford WG.** 2011. Lasers in flow cytometry. *Methods Cell Biol* **102:**375–409.
19. **Telford WG, Babin SA, Khorev SV, Rowe SH.** 2009. Green fiber lasers: an alternative to traditional DPSS green lasers for flow cytometry. *Cytometry A* **75:**1031–1039.
20. **Telford WG, Hawley TS, Hawley RG.** 2003. Analysis of violet-excited fluorochromes by flow cytometry using a violet laser diode. *Cytometry A* **54:**48–55.
21. **Perfetto SP, Ambrozak D, Nguyen R, Chattopadhyay P, Roederer M.** 2006. Quality assurance for polychromatic flow cytometry. *Nat Protoc* **1:**1522–1530.
22. **Perfetto SP, Ambrozak D, Nguyen R, Chattopadhyay PK, Roederer M.** 2012. Quality assurance for polychromatic flow cytometry using a suite of calibration beads. *Nat Protoc* **7:**2067–2079.
23. **Maecker HT, Trotter J.** 2006. Flow cytometry controls, instrument setup, and the determination of positivity. *Cytometry A* **69:**1037–1042.
24. **Mahnke YD, Roederer M.** 2007. Optimizing a multicolor immunophenotyping assay. *Clin Lab Med* **27:**469–485, v.
25. **Harvath L.** 1988. Quality control in clinical flow cytometry. *Pathol Immunopathol Res* **7:**338–344.
26. **Le Meur N, Rossini A, Gasparetto M, Smith C, Brinkman RR, Gentleman R.** 2007. Data quality assessment of ungated flow cytometry data in high throughput experiments. *Cytometry A* **71:**393–403.
27. **Maecker HT, McCoy JP Jr, FOCIS Human Immunophenotyping Consortium, Amos M, Elliott J, Gaigalas A, Wang L, Aranda R, Banchereau J, Boshoff C, Braun J, Korin Y, Reed E, Cho J, Hafler D, Davis M, Fathman CG, Robinson W, Denny T, Weinhold K, Desai B, Diamond B, Gregersen P, Di Meglio P, Nestle FO, Peakman M, Villanova F, Ferbas J, Field E, Kantor A, Kawabata T, Komocsar W, Lotze M, Nepom J, Ochs H, O'Lone R, Phippard D, Plevy S, Rich S, Roederer M, Rotrosen D, Yeh JH.** 2010. A model for harmonizing flow cytometry in clinical trials. *Nat Immunol* **11:**975–978.
28. **Maecker HT, McCoy JP, Nussenblatt R.** 2012. Standardizing immunophenotyping for the Human Immunology Project. *Nat Rev Immunol* **12:**191–200.
29. **Biancotto A, Fuchs JC, Williams A, Dagur PK, McCoy JP Jr.** 2011. High dimensional flow cytometry for

comprehensive leukocyte immunophenotyping (CLIP) in translational research. *J Immunol Methods* **363:**245–261.
30. **Biancotto A, McCoy JP.** 2014. Studying the human immunome: The complexity of comprehensive leukocyte immunophenotyping. *Curr Top Microbiol Immunol* **377:**23–60.
31. **Valle A, Maugeri N, Manfredi AA, Battaglia M.** 2012. Standardization in flow cytometry: correct sample handling as a priority. *Nat Rev Immunol* **12:**864.
32. **Maecker HT, Moon J, Bhatia S, Ghanekar SA, Maino VC, Payne JK, Kuus-Reichel K, Chang JC, Summers A, Clay TM, Morse MA, Lyerly HK, DeLaRosa C, Ankerst DP, Disis ML.** 2005. Impact of cryopreservation on tetramer, cytokine flow cytometry, and ELISPOT. *BMC Immunol* **6:**17.
33. **Bossuyt X, Marti GE, Fleisher TA.** 1997. Comparative analysis of whole blood lysis methods for flow cytometry. *Cytometry* **30:**124–133.
34. **Einwallner E, Subasic A, Strasser A, Augustin D, Thalhammer R, Steiner I, Schwarzinger I.** 2013. Lysis matters: red cell lysis with FACS Lyse affects the flow cytometric enumeration of circulating leukemic blasts. *J Immunol Methods* **390:**127–132.
35. **Pelegrí C, Rodríguez-Palmero M, Morante MP, Comas J, Castell M, Franch A.** 1995. Comparison of four lymphocyte isolation methods applied to rodent T cell subpopulations and B cells. *J Immunol Methods* **187:**265–271.
36. **Kumar P, Satchidanandam V.** 2000. Ethyleneglycol-bis-(beta-aminoethylether)tetraacetate as a blood anticoagulant: preservation of antigen-presenting cell function and antigen-specific proliferative response of peripheral blood mononuclear cells from stored blood. *Clin Diagn Lab Immunol* **7:**578–583.
37. **Shalekoff S, Page-Shipp L, Tiemessen CT.** 1998. Effects of anticoagulants and temperature on expression of activation markers CD11b and HLA-DR on human leukocytes. *Clin Diagn Lab Immunol* **5:**695–702.
38. **Weinberg A, Betensky RA, Zhang L, Ray G.** 1998. Effect of shipment, storage, anticoagulant, and cell separation on lymphocyte proliferation assays for human immunodeficiency virus-infected patients. *Clin Diagn Lab Immunol* **5:**804–807.
39. **Wood B.** 2004. Multicolor immunophenotyping: human immune system hematopoiesis. *Methods Cell Biol* **75:**559–576.
40. **Tamul KR, O'Gorman MR, Donovan M, Schmitz JL, Folds JD.** 1994. Comparison of a lysed whole blood method to purified cell preparations for lymphocyte immunophenotyping: differences between healthy controls and HIV-positive specimens. *J Immunol Methods* **167:**237–243.
41. **Tamul KR, Schmitz JL, Kane K, Folds JD.** 1995. Comparison of the effects of Ficoll-Hypaque separation and whole blood lysis on results of immunophenotypic analysis of blood and bone marrow samples from patients with hematologic malignancies. *Clin Diagn Lab Immunol* **2:**337–342.
42. **Nieto JC, Cantó E, Zamora C, Ortiz MA, Juárez C, Vidal S.** 2012. Selective loss of chemokine receptor expression on leukocytes after cell isolation. *PLoS One* **7:**e31297. doi:10.1371/journal.pone.0031297
43. **Lin SJ, Chao HC, Yan DC, Huang YJ.** 2002. Expression of adhesion molecules on T lymphocytes in young children and infants—a comparative study using whole blood lysis or density gradient separation. *Clin Lab Haematol* **24:**353–359.
44. **Appay V, Reynard S, Voelter V, Romero P, Speiser DE, Leyvraz S.** 2006. Immuno-monitoring of CD8+ T cells in whole blood versus PBMC samples. *J Immunol Methods* **309:**192–199.
45. **Appay V, van Lier RA, Sallusto F, Roederer M.** 2008. Phenotype and function of human T lymphocyte subsets: consensus and issues. *Cytometry A* **73:**975–983.
46. **Hoffmeister B, Bunde T, Rudawsky IM, Volk HD, Kern F.** 2003. Detection of antigen-specific T cells by cytokine flow cytometry: The use of whole blood may underestimate frequencies. *Eur J Immunol* **33:**3484–3492.
47. **Renzi P, Ginns LC.** 1987. Analysis of T cell subsets in normal adults. Comparison of whole blood lysis technique to Ficoll-Hypaque separation by flow cytometry. *J Immunol Methods* **98:**53–56.
48. **Romeu MA, Mestre M, González L, Valls A, Verdaguer J, Corominas M, Bas J, Massip E, Buendia E.** 1992. Lymphocyte immunophenotyping by flow cytometry in normal adults. Comparison of fresh whole blood lysis technique, Ficoll-Paque separation and cryopreservation. *J Immunol Methods* **154:**7–10.
49. **Seale AC, de Jong BC, Zaidi I, Duvall M, Whittle H, Rowland-Jones S, Jaye A.** 2008. Effects of cryopreservation on CD4+ CD25+ T cells of HIV-1 infected individuals. *J Clin Lab Anal* **22:**153–158.
50. **Weinberg A, Louzao R, Mussi-Pinhata MM, Cruz ML, Pinto JA, Huff MF, de Castro AC, Sucupira MC, Denny TN.** 2007. Quality assurance program for peripheral blood mononuclear cell cryopreservation. *Clin Vaccine Immunol* **14:**1242–1244.
51. **Weinberg A, Song LY, Wilkening C, Sevin A, Blais B, Louzao R, Stein D, Defechereux P, Durand D, Riedel E, Raftery N, Jesser R, Brown B, Keller MF, Dickover R, McFarland E, Fenton T, Pediatric ACTG Cryopreservation Working Group.** 2009. Optimization and limitations of use of cryopreserved peripheral blood mononuclear cells for functional and phenotypic T-cell characterization. *Clin Vaccine Immunol* **16:**1176–1186.
52. **Weinberg A, Song LY, Wilkening CL, Fenton T, Hural J, Louzao R, Ferrari G, Etter PE, Berrong M, Canniff JD, Carter D, Defawe OD, Garcia A, Garrelts TL, Gelman R, Lambrecht LK, Pahwa S, Pilakka-Kanthikeel S, Shugarts DL, Tustin NB.** 2010. Optimization of storage and shipment of cryopreserved peripheral blood mononuclear cells from HIV-infected and uninfected individuals for ELISPOT assays. *J Immunol Methods* **363:**42–50.
53. **Weinberg A, Zhang L, Brown D, Erice A, Polsky B, Hirsch MS, Owens S, Lamb K.** 2000. Viability and functional activity of cryopreserved mononuclear cells. *Clin Diagn Lab Immunol* **7:**714–716.
54. **Zola H, Swart B, Banham A, Barry S, Beare A, Bensussan A, Boumsell L, D Buckley C, Bühring HJ, Clark G, Engel P, Fox D, Jin BQ, Macardle PJ, Malavasi F, Mason D, Stockinger H, Yang X.** 2007. CD molecules 2006—human cell differentiation molecules. *J Immunol Methods* **319:**1–5.
55. **Zola H, Swart B, Boumsell L, Mason DY, IUIS/WHO Subcommittee.** 2003. Human leucocyte differentiation antigen nomenclature: update on CD nomenclature. Report of IUIS/WHO Subcommittee. *J Immunol Methods* **275:**1–8.
56. **Fagerberg L, Jonasson K, von Heijne G, Uhlén M, Berglund L.** 2010. Prediction of the human membrane proteome. *Proteomics* **10:**1141–1149.
57. **Zola H, Swart BW.** 2003. Human leucocyte differentiation antigens. *Trends Immunol* **24:**353–354.
58. **Díaz-Ramos MC, Engel P, Bastos R.** 2011. Towards a comprehensive human cell-surface immunome database. *Immunol Lett* **134:**183–187.
59. **Maecker HT, Rinfret A, D'Souza P, Darden J, Roig E, Landry C, Hayes P, Birungi J, Anzala O, Garcia M, Harari A, Frank I, Baydo R, Baker M, Holbrook J, Ottinger J, Lamoreaux L, Epling CL, Sinclair E, Suni MA, Punt K, Calarota S, El-Bahi S, Alter G, Maila H, Kuta E, Cox J, Gray C, Altfeld M, Nougarede N, Boyer J, Tussey L, Tobery T, Bredt B, Roederer M, Koup R, Maino VC, Weinhold K, Pantaleo G, Gilmour J, Horton H, Sekaly**

RP. 2005. Standardization of cytokine flow cytometry assays. *BMC Immunol* **6:**13.
60. **Matteucci C, Grelli S, De Smaele E, Fontana C, Mastino A.** 1999. Identification of nuclei from apoptotic, necrotic, and viable lymphoid cells by using multiparameter flow cytometry. *Cytometry* **35:**145–153.
61. **O'Brien MC, Bolton WE.** 1995. Comparison of cell viability probes compatible with fixation and permeabilization for combined surface and intracellular staining in flow cytometry. *Cytometry* **19:**243–255.
62. **Perfetto SP, Chattopadhyay PK, Lamoreaux L, Nguyen R, Ambrozak D, Koup RA, Roderer M.** 2010. Amine-reactive dyes for dead cell discrimination in fixed samples. *Curr Protoc Cytom* **Chapter 9:**Unit 9.34.
63. **Schmid I, Ferbas J, Uittenbogaart CH, Giorgi JV.** 1999. Flow cytometric analysis of live cell proliferation and phenotype in populations with low viability. *Cytometry* **35:**64–74.
64. **McCoy JP Jr, Overton WR.** 1994. Quality control in flow cytometry for diagnostic pathology: II. A conspectus of reference ranges for lymphocyte immunophenotyping. *Cytometry* **18:**129–139.
65. **Piroozmand A, Hassan ZM.** 2010. Evaluation of natural killer cell activity in pre and post treated breast cancer patients. *J Cancer Res Ther* **6:**478–481.
66. **Sony Corporation.** 2012. Sony announces the development of the 'Spectral' cell analyzer, the industry's first cell analysis instrument capable of detecting full spectrum fluorescence to facilitate highly accurate analysis. 18 June 2012. Tokyo, Japan. http://www.sony.net/SonyInfo/News/Press/201206/12-082E/
67. **Davis BH, McLaren CE, Carcio AJ, Wong L, Hedley BD, Keeney M, Curtis A, Culp NB.** 2013. Determination of optimal replicate number for validation of imprecision using fluorescence cell-based assays: proposed practical method. *Cytometry B Clin Cytom* **84:**329–337.
68. **Hedley BD, Keeney M.** 2013. Technical issues: flow cytometry and rare event analysis. *Int J Lab Hematol* **35:**344–350.
69. **Aghaeepour N, Brinkman R.** 2014. Computational analysis of high-dimensional flow cytometric data for diagnosis and discovery. *Curr Top Microbiol Immunol* **377:**159–175.
70. **Aghaeepour N, Finak G, FlowCAP Consortium, DREAM Consortium, Hoos H, Mosmann TR, Brinkman R, Gottardo R, Scheuermann RH.** 2013. Critical assessment of automated flow cytometry data analysis techniques. *Nat Methods* **10:**228–238.
71. **Aghaeepour N, Jalali A, O'Neill K, Chattopadhyay PK, Roederer M, Hoos HH, Brinkman RR.** 2012. RchyOptimyx: cellular hierarchy optimization for flow cytometry. *Cytometry A* **81:**1022–1030.
72. **Craig FE, Brinkman RR, Ten Eyck S, Aghaeepour N.** 2014. Computational analysis optimizes the flow cytometric evaluation for lymphoma. *Cytometry B Clin Cytom* **86:**18–24.
73. **Zare H, Bashashati A, Kridel R, Aghaeepour N, Haffari G, Connors JM, Gascoyne RD, Gupta A, Brinkman RR, Weng AP.** 2012. Automated analysis of multidimensional flow cytometry data improves diagnostic accuracy between mantle cell lymphoma and small lymphocytic lymphoma. *Amer J Clin Pathol* **137:**75–85.
74. **Grimm KE, Barry TS, Chizhevsky V, Hii A, Weiss LM, Siddiqi N, Brynes RK, O'Malley DP.** 2012. Histopathological findings in 29 lymph node biopsies with increased IgG4 plasma cells. *Mod Pathol* **25:**480–491.

Online References

HCDM webpage
http://www.hcdm.org/
BD spectrum viewer
http://www.bdbiosciences.com/research/multicolor/spectrum_viewer/index.jsp
Ebioscience spectrum viewer
http://www.ebioscience.com/resources/fluorplan-spectra-viewer.htm
Chromocyte summary of flow training course
http://www.chromocyte.com/educate/Beginners-Guide-Training-Resources/Online-Training-Resources
BD buffer compatibility
http://www.cytobank.org/facselect/

High-Sensitivity Detection of Red and White Blood Cells in Paroxysmal Nocturnal Hemoglobinuria by Multiparameter Flow Cytometry

ANDREA ILLINGWORTH, MICHAEL KEENEY, AND
D. ROBERT SUTHERLAND

18

Paroxysmal nocturnal hemoglobinuria (PNH) is a rare, life-threatening acquired hematopoietic stem cell disorder resulting from the somatic mutation of the X-linked phosphatidylinositol-glycan complementation class A (PIG-A) gene (1–4). In normal individuals, this gene encodes an enzyme involved in the first stage of glycophosphatidylinositol (GPI) biosynthesis. In PNH, as a result of the mutation(s) in the PIG-A gene, there is a partial or absolute inability to make GPI-anchored proteins, including complement-defense structures such as CD55 and CD59 on red blood cells (RBCs) and white blood cells (WBCs) (5–8). Absence of CD59 in particular (9, 10) and CD55 on RBCs is largely responsible for intravascular hemolysis associated with clinical PNH (reviewed in reference 11).

CLINICAL FEATURES OF PNH

Clinical features of PNH include intravascular hemolysis (that leads to hemoglobinuria), bone marrow failure, and thrombosis, with the latter being a major cause of morbidity and mortality (12, 13). Prior to the advent of the complement C5 inhibitor eculizumab, 35% of PNH patients died within 5 years of diagnosis even with the best available treatment (12).

There is a well-documented relationship between aplastic anemia (AA) and PNH (12, 13), and with modern, high-sensitivity assays, up to 70% of AA patients have shown PNH clones (14–16). Some reports suggest that PNH+ AA patients respond to immunosuppressive therapy (IST) (17, 18), while other studies show that 10 to 25% of AA patients will exhibit a PNH clonal expansion and progress to clinical PNH (19).

Small populations of GPI-deficient PNH clones have been reported in patients with early-stage myelodysplastic syndrome (MDS), particularly the refractory cytopenias with unilineage dysplasia (RCUD) variant (13, 17). Preliminary analysis of data from a large study of patients with AA, MDS, and other bone marrow failure syndromes (EXPLORE) showed a significant number of MDS patients to have GPI-deficient cells. However, statistical reanalysis of those data generated solely with high-sensitivity methodologies from the same study found much lower incidences of true PNH clones in MDS (20).

WHO SHOULD BE TESTED FOR PNH?

PNH is a very rare disease with a prevalence of about 16 cases per million and only about 1.3 new cases diagnosed per million per year (Hill A, Platts PJ, Smith A, Richards, SJ, Cullen MJ, Hill, QA, Roman E, Hillmen P, unpublished observations). Nevertheless, the life-threatening and progressive nature of PNH warrants testing of appropriate patient populations at risk of PNH with early diagnosis essential for improved patient management and prognosis in PNH (21, 22). Such groups include:

1. Unexplained cytopenias (with evidence of increased levels of lactate dehydrogenase (LDH), low haptoglobin, or elevated reticulocyte count)
2. All AA patients and refractory-anemia MDS (with evidence of elevated LDH or low haptoglobin).
3. Unexplained thrombosis (despite anti-coagulation, in patients <50 years of age, in unusual sites, e.g., cerebral, hepatic portal, dermal vein), with evidence of elevated LDH, low haptoglobin or elevated reticulocyte count, or with other clinical manifestations of PNH (abdominal pain, chest pain, dyspnea, dysphagia, severe fatigue).
4. All patients with unexplained Coombs-negative hemolytic anemia, hemoglobinuria, and/or hematuria.

EARLY METHODS TO TEST FOR PNH

Because PNH was initially recognized as a type of hemolytic anemia, the earliest assays focused on RBCs. These included the Ham test (23) and the sugar-hemolysis test (24), both of which demonstrated the increased sensitivity of PNH RBC to complement-mediated hemolysis. The more specific complement lysis-sensitivity test showed that PNH cells lysed at lower concentrations than did normal cells (25). This test also led to the recognition (26) that some PNH patients have a population of cells with intermediate complement sensitivity (type II), which show an intermediate life span between normal RBCs (type I, 120 days) and the most sensitive PNH-type RBCs (type III, 10–15 days). These tests were laborious, difficult to standardize, and neither specific nor sensitive.

EVOLUTION OF FLOW CYTOMETRIC METHODS TO DETECT PNH

Since the early 1990s, flow cytometric detection of cells lacking expression of GPI-anchored surface molecules has become established as the method of choice for diagnosing

doi:10.1128/9781555818722.ch18

and monitoring PNH. Because of the historical role of RBCs in the diagnosis of PNH, early flow cytometric methods to detect PNH relied on detecting the loss of CD55 and CD59, two GPI-linked structures expressed on normal RBCs and WBCs (27, 28). Most laboratories used FDA-approved kits (Cellquant and Redquant, BioCytex, Marseille, France) or developed in-house assays that used CD55 and CD59. Typically, RBCs were identified and gated by forward vs side scatter in logarithmic mode (FS log vs SS log) and assessed using single-parameter histograms for CD55 and/or CD59 expression. Flow cytometric analysis of RBCs in nontransfused patients was used to enumerate the type III (complete GPI-antigen deficiency) and type II (partial GPI-antigen deficiency) PNH clones. Type I (normal GPI-antigen expression) represented remaining normal RBCs.

Flow cytometric analysis of WBCs used light scatter in linear mode (FS Lin versus SS Lin) to gate neutrophils in lysed whole-blood samples with similar assessment of CD55 and/or CD59 expression using single-parameter histograms.

ISSUES WITH EARLY FLOW METHODS

Although the ability to rapidly detect GPI-deficient cells by flow cytometry (27–29) has led to improved diagnosis, patient management, and prognosis in PNH and related disorders, simple CD55/CD59-based approaches were neither accurate nor sensitive below the 1 to 4% clone size, rendering them inadequate to detect small PNH clones present in most PNH+ AA and MDS cases (30). Furthermore, with respect to RBCs, simple "routine" assays that do not employ CD235a (anti-glycophorin a) to gate RBCs are susceptible to the effects of inaccurate pipetting and poor sample mixing (30) as well as identifying CD55/CD59-negative events that are not RBCs. Such errors can result in false-negative staining with CD55/CD59 antibodies and potentially lead to misdiagnosis.

Inaccurate results ("false positives" and "false negatives") can also be generated by suboptimal instrument setup, selection of poor antibody clones/conjugates that exhibit suboptimal signal-to-noise ratio, selection of poor conjugates of otherwise good clones, inadequate selection of lineage-specific gating antibodies/conjugates, and poor gating strategies. Finally, inexperience in interpretation of results, together with the use of nonstandardized, potentially misleading reporting forms, can all lead to misdiagnosis and dangerous clinical consequences.

With respect to the detection of GPI-deficient WBCs, an increasingly wide range of monoclonal antibodies have become available to detect GPI-anchored proteins (31), potentially obviating some of the shortcomings of simple CD55/CD59-based assays. Additionally, a variety of more sensitive approaches have more recently been developed for PNH WBC detection based on the fluorescent derivative of bacterial pro-aerolysin (FLAER) (30, 32–36). FLAER-based assays, whether alone or cocktailed with other antibodies, are still not universally deployed, however, and recent data from external quality assurance programs have highlighted the variable capabilities of laboratories to accurately detect WBC PNH clones in stabilized whole-blood samples (37).

Over the last few years, a humanized monoclonal antibody against the terminal complement protein C5 (38) (Eculizumab; Alexion, Cheshire, CT) has been approved for the treatment of patients with hemolytic PNH. This drug significantly reduces hemolysis, transfusion requirements, and thrombosis. It has improved the quality of life of PNH patients (39, 40) and has had a major impact on life expectancy of those with PNH (41–43). Therefore, accurate detection and monitoring of PNH clones have become increasingly important priorities for clinical flow laboratories performing PNH screening.

ROUTINE VERSUS HIGH-SENSITIVITY FLOW CYTOMETRY

To address these issues, the International Clinical Cytometry Society (ICCS) published guidelines for the diagnosis and monitoring of PNH and related disorders by flow cytometry (22). A variety of approaches for "routine" and "high-sensitivity" analyses (required in cases of MDS or AA) were outlined therein for both RBC and WBC lineages. However, standardized-operating protocols (SOPs) utilizing specific assay cocktails were not identified and defined analytic strategies were not detailed.

The development and validation of sensitive, standardized methodologies are essential to reliably detect GPI-deficient PNH phenotypes, especially for PNH clone sizes of less than 1%. Preliminary data from one large study of over 10,000 patients has shown that 40% of samples positive for the presence of PNH cells contain GPI-deficient cells at a level of 1% or less (Illingworth A, unpublished observations). Given that standardized, robust, high-sensitivity assays have now been developed (see below), we believe the dichotomy between routine and high-sensitivity assays (22) to be a false one and, from the technical perspective, irrelevant. The same high-sensitivity assays that are required to accurately detect very minor populations of GPI-deficient cells can also be used to detect PNH in patients with large clones; the only difference is in how the assays are deployed with respect to the numbers of cells acquired for accurate and precise determinations of GP-deficient cell numbers.

HIGH-SENSITIVITY ASSAYS FOR PNH RBCs AND WBCs

General Requirements

For high-sensitivity RBC analysis in particular, where a CD235a and CD59 combination is required, it has been problematic to identify conjugates that in combination do not cause major aggregation of red cells while still maintaining a good signal-to-noise ratio and the ability to adequately separate type II and type III PNH RBCs from normal (type I) cells (30). It is also the authors' experience that there is much variability between different antibody clones/conjugates among reagents used in the analysis of PNH in WBC lineages.

To successfully develop highly sensitive assays that are also robust and reliable, careful selection and titration of antibody clones/conjugates for lineage-specific gating (RBCs, neutrophils, and monocytes) and specific GPI-antigen detection within each cell lineage is required. The detection of rare PNH phenotypes in RBCs, neutrophils, and monocytes also requires proper assay-specific instrument setup (light-scatter voltages, photo-multiplier tube [PMT] voltages, and optimal fluorescence compensation) and rigorously maintained instrument fluidics and clean cell-washing reagents. Once established, the frequencies of PNH phenotypes in all three lineages in multiple normal samples must be determined. Additionally, the sensitivities of the assays have to be validated by titrating ("spiking") a PNH sample into a normal sample. The essential elements of high-sensitivity RBC, neutrophil, and monocyte assays were recently published in the *Practical Guidelines* (44 and supplementary data).

High-Sensitivity RBC Assay

In the development of a robust high-sensitivity RBC assay, a variety of CD235a and CD59 clones/conjugates were tested from several vendors in order to optimize and standardize a two-color flow assay for the detection of PNH RBCs (44 and supplementary data).

Antibody Clone/Conjugate Selection for High-Sensitivity PNH RBC Detection

RBC-Gating Antibodies

CD235a (glycophorin A) is currently the only gating reagent available that specifically identifies mature RBCs. Preliminary screening of CD235aFITC and CD235aPE conjugates of clone KC16 (Beckman Coulter) showed the phycoerythrin (PE) version to cause far more aggregation of RBCs (even after extensive titration) than its fluorescein isothiocyanate (FITC)-labeled counterpart (30). We subsequently screened a number of other CD235a antibody conjugates for this assay. Recommended conjugates are listed in Table 1.

GPI-Specific Antibodies

While loss of the GPI-linked CD55 and CD59 structures was traditionally used to detect PNH RBCs (27, 28), CD55 is inferior to CD59 (22) due to its dim expression and inability to delineate type II and type III PNH RBCs. For the *Practical Guidelines* (44) we thus focused on identifying CD59PE conjugates that offered the best separation of type I, type II, and type III RBCs. Several conjugates have been evaluated, and those recommended are listed in Table 1.

As CD235a antibodies in particular are known to cause significant RBC aggregation, all CD235a and CD59 antibody conjugates were individually titrated against RBCs from normal individuals to minimize this effect, while still providing adequate separation of type I, II, and III cells. It is important to note that all CD235a conjugates and the CD59PE conjugates of MEM43 and OV9A2 required considerable dilution below saturating levels to obviate this problem. Once optimally titrated, individual CD235a and CD59 conjugates were admixed in two-color combinations. Combinations of CD235aFITC (clone KC16 or 10F7MN)/CD59PE (clone MEM43 or OV9A2) proved to be the best combination for delineating normal type I RBCs as well as type II and type III PNH populations in all samples tested.

Instrument Setup Considerations: RBCs

For light scatter and PMT voltage setup, a normal blood sample was diluted 1:100 with clean phosphate-buffered saline (PBS). Forward-angle (FS) and side-angle (SS) light-scatter voltages were established in log:log format such that the cluster of unstained normal RBCs could be identified towards the middle of the bivariate histogram (see Fig. 1A, plot 1). When voltages are set in this manner, the presence of red-cell aggregates and other debris can be readily addressed. The discriminator/threshold should be set to exclude as much debris as possible while not excluding any of the RBC-target population.

For setting the FL-1 and FL-2 PMT voltages, all compensation is set to zero and the PMT voltages are established without the use of "baseline offset" for instruments so equipped. Gated RBCs from region R1 of plot 1 were displayed on an FL-1 versus FL-2 plot and the PMT voltages were adjusted so that the cells were comfortably on-scale (see Fig. 1A, plot 2). Two-color compensation adjustments were performed with samples individually stained with CD235aFITC (Fig. 1A upper-right plot) and CD59PE (Fig. 1A, lower-right plot). Instrument setup was verified by analyzing a fresh normal sample stained, as outlined below, with the optimized CD235aFITC/CD59PE antibody cocktail (Fig. 1B, plots 1–3).

TABLE 1 Recommended antibody conjugates for high-sensitivity detection of PNH RBCs

Target cells	Antibodies and conjugates	Purpose	Clone and (vendor)
RBC	CD235-FITC	Gating RBCs	KC16 (BC) 10F7MN (eBio) JC159 (DAKO)
	CD59-PE	GPI-linked for RBC	OV9A2 (eBio) MEM-43 (Invitrogen)

RBC Staining Protocol using CD235aFITC/CD59PE Cocktail

Anti-coagulated (EDTA is preferred, but heparin can also be used) peripheral-blood samples should be less than 48 hours old.

1. Prepare a 1:100 dilution of the sample with clean PBS.
2. Prepare antibody cocktail: Add 15 μl (1.5 μl/test) of CD235aFITC (clone KC16 Beckman Coulter) and 5 μl (0.5 μl/test) of CD59PE (clone MEM43 Invitrogen) to 180 μl PBS*
   Comment: Based on individual titrations of single lots of CD235aFITC and CD59PE, a cocktail of these reagents should be prepared. Examples are shown in Fig. 1.
3. Pipette 100 μl of diluted blood sample into a test tube using reverse-pipetting to avoid aerosol generation.
4. Pipette 20 μl of this diluted cocktail and add directly into the blood in the test tube with gentle mixing by up-and-down pipetting.
5. After careful removal of the pipette tip to avoid touching the sides of the tube, mix the sample by gently swirling the sample using a slow-speed vortex, again taking care not to generate aerosols.
6. Incubate the sample in the dark for 20 min at room temperature (incubation up to 60 min has been validated).
7. Wash twice with PBS by centrifugation, as is required to optimize separation of type I, II, and III RBCs.
8. Resuspend in 0.5 to 1.0 ml of PBS.
9. "Rack" the sample (drag across a hard plastic or metal test tube rack several times) to disrupt any RBC aggregates generated by the staining/washing procedure immediately before acquisition on the cytometer.
10. Acquire sample immediately, as delays longer than 15 min after the final washing step can show decreased CD235a staining and increased levels of reaggregation.
11. Acquire a minimum of 100,000 RBCs (gated on FS log vs SS log) in list mode for clinical test samples.
12. If two or more events were displayed in the type III PNH RBC region, data acquisition should be continued until 1 million events are acquired.

An example of the assay performed on a known PNH case is shown in Fig. 1C. With appropriate sample processing, the level of observed aggregates could be kept to 1.5% or less.

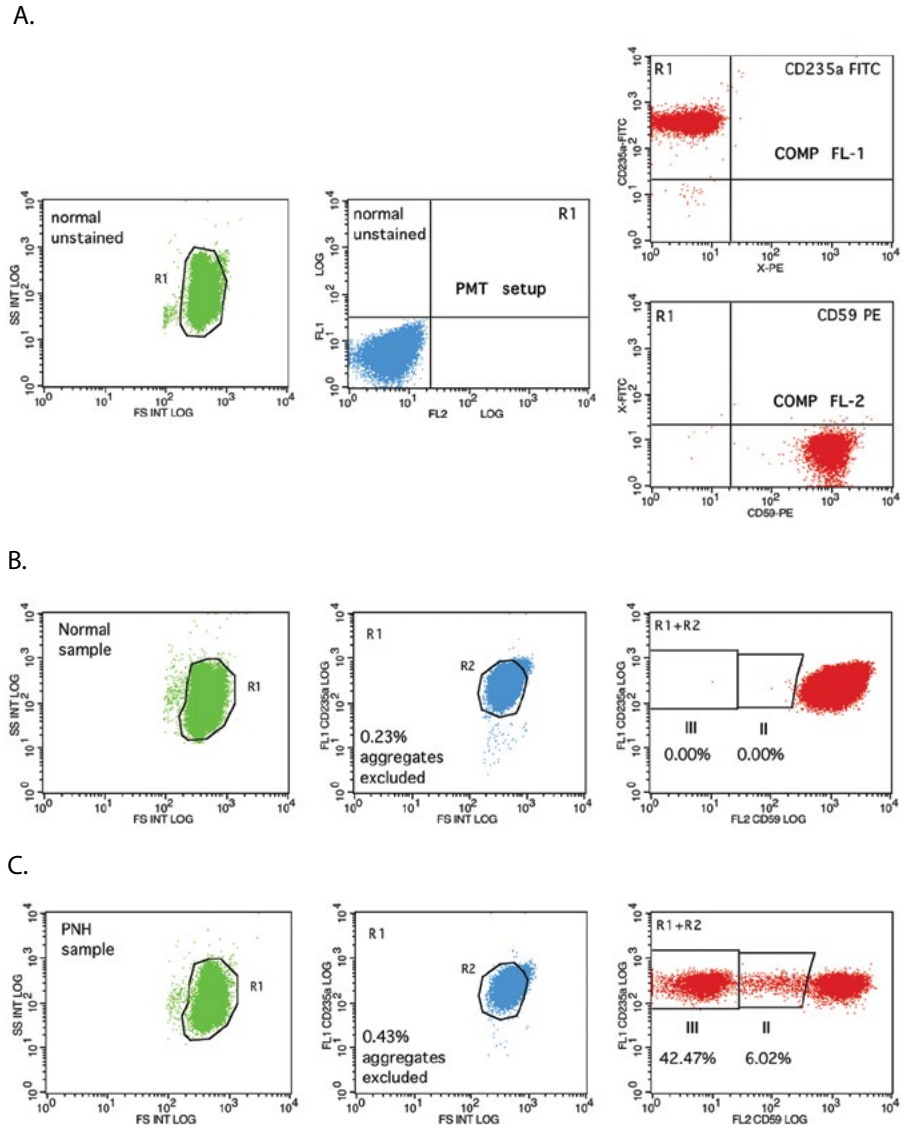

FIGURE 1 (A) Instrument setup for high-sensitivity RBC assay. Light-scatter voltages were established in logarithmic mode such that RBCs from a diluted normal PB sample clustered in the middle of the plot (left). Gated RBCs from region R1 were displayed on FL-1 versus FL-2 plot and PMT voltages were adjusted to get the unstained RBCs properly on-scale (middle). Samples were single stained with either CD235aFITC (top right) or CD59PE (bottom right) and compensation was adjusted to reduce spectral overlap. (B) Analysis of normal RBCs. Normal RBCs stained and acquired using the instrument settings established in panel A. RBCs gated in R1 (left) and displayed on CD235aFITC versus FS plot (middle). CD235a+ RBCs were gated in R2 and aggregated RBCs (see arrow; 0.23% of total) were excluded as shown. Cells from R1 and R2 were displayed on CD235aFITC versus CD59PE (right). A second sample stained only with CD235aFITC was analyzed to approximate the location of the type III gate (gate III). (C) Analysis of fresh PNH sample. A PNH sample was stained as described with the optimized RBC protocol as outlined in the Methods, and analyzed as described for the normal sample (panel B). Aggregated RBCs (0.43%) were excluded by gate R2. The sample contained 42.47% PNH type III cells and 6.02% PNH type II cells.

High-Sensitivity Four-Color WBC Assays

Antibody Clone/Conjugate Selection for Four-Color High-Sensitivity PNH WBC Detection

Gating Reagents for Neutrophils and Monocytes

In developing highly sensitive assays for neutrophils and monocytes, the ICCS Guidelines (22) stressed the need to use an antibody for gating each lineage as well as two GPI-specific markers for each lineage. While CD33 can be used to gate on both neutrophils and monocytes (30, 34), this reagent is not as effective as CD15 for delineating neutrophils or as effective as CD64 for delineating monocytes (44, 45), with MDS samples being particularly problematic (unpublished observations). Additionally, we have found occasional samples that failed to stain with CD33 conjugates regardless of which CD33 clone is used. Consequently,

TABLE 2 Recommended reagent conjugates for high-sensitivity detection of PNH WBCs: Beckman Coulter instruments

Target cells	Antibodies and conjugates	Purpose	Clone and (vendor)
WBC	FLAER-Alexa488	GPI-linked (all lineages)	NA (Cedarlane)
	CD24-PE	GPI-linked (neutrophils)	SN3 (eBio) ALB9 (BC)
	CD14-PE CD14APC-A700 (6-color)	GPI-linked (monocytes)	61D3 (eBio) RMO52 (BC)
	CD157-PE	GPI-linked (neutrophils and monocytes)	SY11B5 (eBio)
	CD15-PC5	Gating neutrophils	80H5 (BC)
	CD64-PC5 (4-color) CD64-ECD (5-color) CD64PC7 (6-color)	Gating monocytes	22 (BC)
	CD45-PC7 CD45-KO (6-color)	Debris exclusion and pattern recognition	J33 (BC)

conjugates of CD15 (for neutrophils) and CD64 (for monocytes) were selected for this purpose. Because of the variety of laser combinations available on legacy and newer-generation instruments, selection of specific clones/conjugates for gating neutrophils and monocytes must be done on an instrument-specific basis. Recommended gating reagents for neutrophils and monocytes for various instrument types are shown in Tables 2 and 3 for Beckman Coulter (BC) and Becton Dickinson (BD) instruments, respectively.

GPI-Specific Reagents for Neutrophils and Monocytes

Although CD55 and CD59 have been widely deployed to detect PNH since the development of the earliest flow-based assays (27, 28), recent studies using stabilized whole blood have shown that these reagents are not optimal for the detection of PNH neutrophils and monocytes (37). The ICCS Guidelines identified CD24, CD16, and CD66b along with FLAER as the most reliable reagents for PNH neutrophil detection. However, CD16 is polymorphic and is not expressed on eosinophils or immature neutrophils, rendering it less useful for the analysis of some MDS cases. With respect to CD66b, most conjugates of this reagent are incompatible with FLAER-based assays, and even PE-conjugated CD66b was found to be inferior to CD24 for delineating PNH neutrophils from their normal counterparts (46). Thus, we selected CD24 and FLAER as GPI-specific reagents for neutrophil assessment and CD14 and FLAER as GPI-specific reagents for monocyte assessment (44). For analysis on the FACSCalibur instrument (BD), CD15APC (clone HI98) and CD45PerCP (clone 2D1) (BD) were used together with FLAER and CD24PE.

In subsequent studies (47) performed to optimize four-color cocktails for both neutrophils and monocytes that could be used on BC and BD platforms, a large number of other clones/conjugates were extensively evaluated. The reagents found to be optimal for the four-color neutrophil and monocyte assays on BC and BD instruments are shown in Tables 2 and 3, respectively.

Instrument Setup Considerations: WBCs (Fig. 2 and 3)

For light-scatter voltage setup for WBC, 100 μl of a lysed and washed normal-blood sample was used. FS and SS light-scatter voltages were established in linear mode and the voltages were adjusted such that all major leukocyte subsets, including lymphocytes, were clearly visible above the FS threshold (see Fig. 2, plot 1, and Fig. 3, plot 1, for neutrophil and monocyte assays, respectively).

TABLE 3 Recommended reagent conjugates for high-sensitivity detection of PNH WBCs: Becton Dickinson instruments

Target cells	Antibodies and conjugates	Purpose	Clone and (vendor)
WBC	FLAER-Alexa488	GPI-linked (all lineages)	NA (Cedarlane)
	CD24-PE	GPI-linked (neutrophils)	SN3 (eBio) ML5 (BD)
	CD14-PE	GPI-linked (monocytes)	61D3 (eBio) MOP9 (BD)
	CD157-PE	GPI-linked (neutrophils and monocytes)	SY11B5 (eBio)
	CD15-APC (4-color)	Gating neutrophils	HI98 (BD)
	CD15-eFluor450 (5-color) or CD15-v450 or CD15-PerCP-eFluor710[a]	Gating neutrophils	MMA (eBio) MMA (BD) MMA (eBio)
	CD64APC	Gating monocytes	10.1 (BD) 10.1 (eBio)
	CD45-PerCP CD45-APC-H7[a]	Debris exclusion and pattern recognition	2D1 (BD)

[a]For two-laser Canto, use FLAER, CD157-PE, CD45APC-H7, CD64APC, CD15-PerCP-eFluor710.

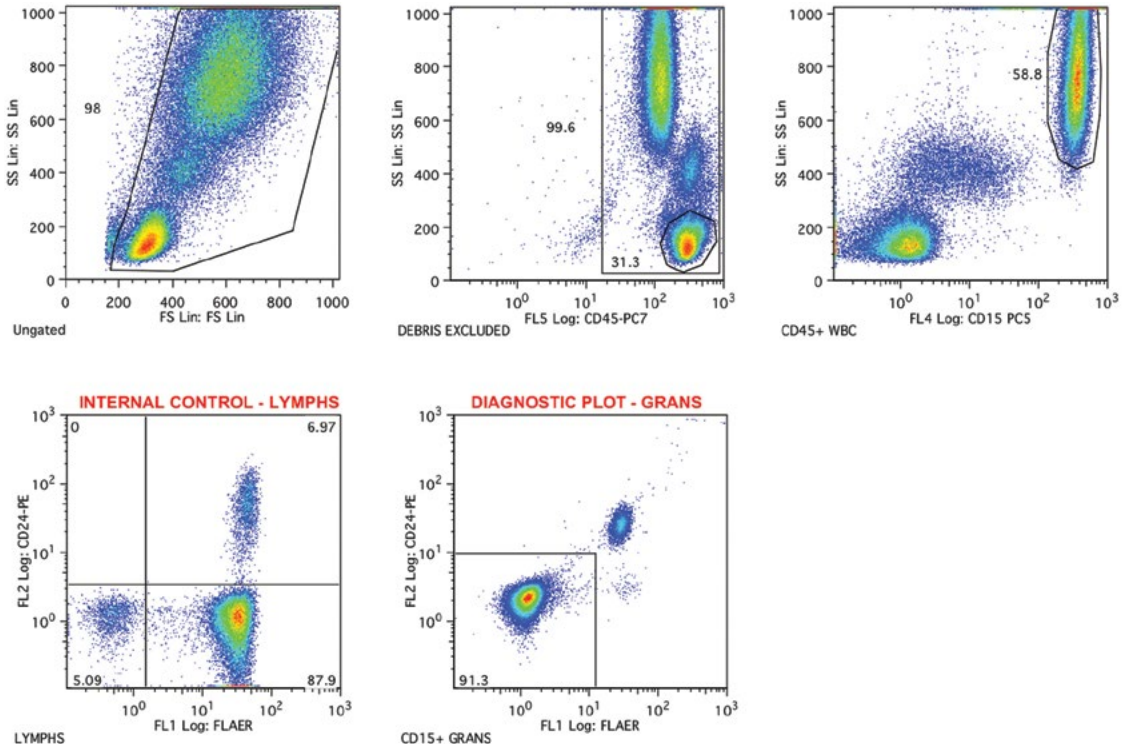

FIGURE 2 Example of high-sensitivity neutrophil assay. A sample from a long-term PNH patient was stained with FLAER, CD24PE, CD15PECy5, and CD45PECy7. Light-scatter voltages were established so that all nucleated cells were visible above the forward-scatter threshold (top left) and debris was excluded with a combination of light scatter and CD45 gating (top middle). CD45+ events were displayed on CD15 versus SS plot (top right) and neutrophils (bright CD15, high SS) were gated. Neutrophils displayed on a FLAER versus CD24 plot (bottom row, right) and PNH neutrophils (FLAER-negative, CD24-negative) were enumerated in the lower left quadrant. Normal neutrophils were enumerated in the upper right quadrant. Lymphocytes were gated by a combination of CD45/SS staining (top middle plot) and lack of CD15 expression (not shown) and assessed for PNH phenotypes in the lower-left quadrant. Normal T lymphocytes (FLAER+, CD24-negative) are visible in the lower right quadrant and normal B lymphocytes (FLAER+, CD24+) are visible on the upper right quadrant.

For BC instruments, setting the PMT voltages was performed with all compensation set to zero and the voltages were established with the baseline offset off. Because of the different emission spectra of Alexa488 and FITC, compensation was established using a FLAERAlexa488-stained sample in the FL-1 channel. Thus, the FL-1 PMT voltage was established using a PNH sample that contained some PNH lymphocytes. The sample was single-stained with FLAER-Alexa488, and the FL-1-PMT voltage was adjusted so that PNH lymphocytes were comfortably on scale. A second sample was stained with CD3PE, and the FL-2-PMT voltage was adjusted to ensure that non-T lymphocytes were also comfortably on scale. This procedure was repeated using CD3PECy5. The FL-5-PMT voltage was set using a sample stained with the pretitrated volume of CD45PECy7, and the PMT was set so that lymphocytes were positioned at the end of the 3rd decade of fluorescence of the 4-decade log scale of the FC500 cytometer. These voltages were used for the compensation process. Compensation adjustments on the FC500 were made using blood samples individually stained with either FLAER Alexa488 (FL-1), CD45PE (FL-2), CD45PECy5 (FL-4), or CD45PECy7 (FL-5). In the case of the CD45 conjugates, all individual reagents were pretitrated to so that lymphocytes were positioned at the end of the 3rd decade of fluorescence. Instrument settings were verified by analyzing a PNH sample and a normal sample stained with a FLAER, CD24PE, CD-15PECy5, and CD45PECy7 cocktail.

The methodology outlined above can also be used on a BC Navios instrument.

For BD FACSCalibur instrument set up, PMT settings were established for the FL-1 and FL-2 channel as described above for the FC500 platform. The FL-3 PMT was set with a sample stained with pretitrated volume of CD45PerCP and the voltage was adjusted to position the lymphocytes at the end of the 3rd decade of fluorescence. The FL-4 PMT was set as per FL-1 and FL-2 PMTs using a pretitrated volume of CD3APC. Compensation was performed with Calibrite beads and FACSComp software and verified with a PNH and a normal sample stained with a FLAER, CD24PE, CD-45PerCP, and CD15APC cocktail.

WBC Staining Procedure for Optimized Neutrophil and Monocyte Cocktails

All individual antibodies were verified for appropriate reactivity with target cells and titrated to optimize specific staining performance prior to being cocktailed for use in the high-sensitivity FLAER-based neutrophil and monocyte assays. The ICCS Guidelines recommended staining samples within the first 48 hours from sample draw (22) when white-cell viability is high.

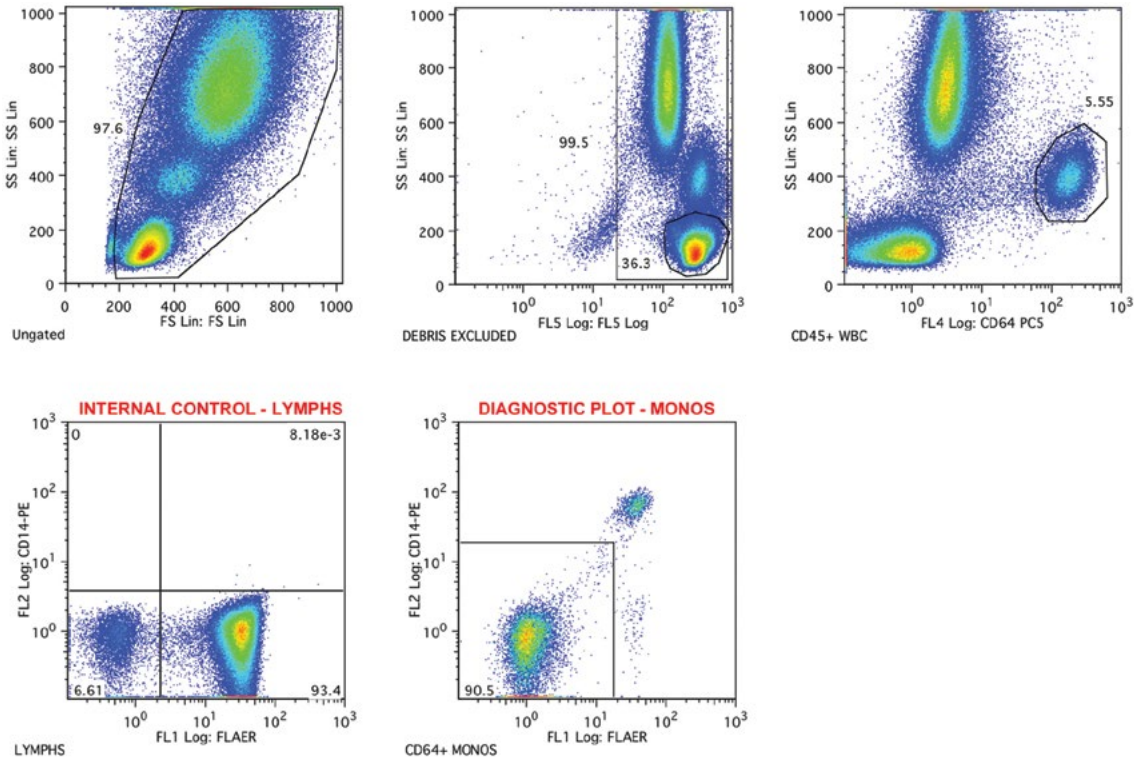

FIGURE 3 Example of high-sensitivity monocyte assay. A sample from a long-term PNH patient was stained with FLAER, CD14PE, CD64PECy5, and CD45PECy7 and analyzed in a manner similar to that shown for the neutrophil assay in Fig. 2. CD45+ events were displayed on CD64 versus SS plot (top right) and monocytes (bright CD64, intermediate SS) were gated. Monocytes were displayed on a FLAER versus CD14 plot (bottom row, right) and the PNH monocytes (FLAER-negative, CD14-negative) were enumerated in the lower left quadrant. Lymphocytes were gated by a combination of CD45/SS staining (top-middle plot) and lack of CD64 expression (not shown) and assessed for PNH phenotypes in the lower left quadrant. Normal lymphocytes (FLAER+, CD14-negative) are visible in the lower right quadrant.

1. Using reverse-pipetting, pipette 100 μl of fresh peripheral blood carefully into the bottom of a test tube without touching the side of the tube.
2. Add an appropriate volume of "neutrophil" (FLAER-Alexa488, CD24PE, CD15PECy5, and CD45PECy7) or "monocyte" (FLAERAlexa488, CD14PE, CD-64PECy5, and CD45PECy7) cocktail directly to the blood aliquot in the bottom of the tube and mix gently but thoroughly as described above for the RBC assay.
3. Incubate for 20 min in the dark.
4. Lyse the RBCs using an appropriate lysing agent. ImmunoPrep, Versalyse (BC), FACSLyse (BD), or ammonium chloride-based lysing agents are all acceptable; those containing fixatives may help retain cellular integrity better than those that do not.
5. After lysing, wash cells once with PBS.
6. Resuspend in 1 ml of PBS and acquire on the cytometer.
   Note: Samples should be acquired immediately, as delays can cause light-scatter changes, especially when fixative-free lysing agents are used.
7. Acquire a minimum of 50,000 neutrophils and 5,000 monocytes in list mode (neutrophil and monocyte assays, respectively) for clinical test samples.
8. If small numbers of GPI-deficient cells are observed, acquisition times should be increased until a statistically reliable number of "PNH phenotypes" are acquired (generally 50 to 100 PNH cells).

PRESENCE OF TYPE II POPULATIONS IN NEUTROPHILS AND MONOCYTES

The presence of RBCs with intermediate expression of CD59 (type II RBCs) has been reported extensively in the literature, describing RBCs with a partial protection from complement-mediated lysis, which have an intermediate life span between normal type I RBCs and type III PNH RBCs (complete absence of CD59). The presence of type II phenotypes in WBCs (neutrophils and monocytes) can also be seen in a subset of PNH patients since the advent of more modern, FLAER-based assays (Illingworth A, unpublished observations). The clinical significance of these type II populations in WBCs is uncertain at this time but, as for RBCs, it is important to include both type II and type III WBCs in a combined estimate of the total PNH-clone size. More recently, a greater range of GPI-specific reagents have been tested and optimized for use in combination with FLAER. CD14 (monocyte assay) and CD157 (neutrophils and monocyte assays) in particular can show a very pronounced separation between type II and type III WBCs when type II cells are present. The range of fluorescence intensities observed in samples containing type II cells can, in some cases, render very difficult the delineation of type II

PNH cells from normal type I cells. Two examples of samples containing both PNH type II and type III neutrophils and monocytes are shown in Fig. 4A and 4B.

High-Sensitivity Five-Color WBC Assays

Antibody Clone/Conjugate Selection for Five-Color High-Sensitivity PNH-WBC Detection

Other than CD24 and CD14 on neutrophils and monocytes, respectively, the expression of a variety of other GPI-linked structures on various blood cell lineages has been documented in peripheral blood (31, 47) and bone marrow (48). CD157 is another GPI-linked structure expressed on both neutrophils and monocytes that has been identified as a potentially useful reagent for the detection of GPI-deficient cells (31, 47, 48). However, until recently, CD157 was only available in FITC-conjugated form, ruling out its use in FLAER-Alexa488-based assays. The recent availability of a PE-conjugated version of CD157 (clone SY11B5, eBioscience) allowed direct comparison with CD24PE and with CD14PE in the 4-C neutrophil and 4-C monocyte protocols, respectively. It was subsequently shown that CD157PE was superior to CD24PE in the neutrophil assay and also compared favorably with CD14PE in the four-color monocyte assay. This study also showed that the four-color CD157 assays performed in an equivalent manner with similar sensitivities on PNH samples containing a wide range of clone sizes and exhibited similar low background rates on normal samples (46). Interestingly, the CD157-based assays tend to separate the type II neutrophils and type II monocytes from the type III neutrophils and type III monocytes more effectively compared to the CD24/CD14-based assays (see below).

Instrument Setup Considerations for Five-Color WBC Assay

The excellent performance of the CD157PE conjugate in both four-color neutrophil and monocyte assays raised the possibility that a single five-color combination of FLAER, CD157, CD64, CD15, and CD45 could be used to simultaneously evaluate GPI-deficient neutrophils and monocytes with a single tube for those with access to cytometers with five or more PMTs (46).

Beckman Coulter instruments

Light scatter and PMT voltages for the five-color assay on both FC500 and Navios cytometers were performed as above for the four-color assays except that the FL-3 PMT voltage was established using unstained B lymphocytes in a CD3ECD-stained sample. For compensation settings for the five-color assay, a sample stained with CD45ECD at pretitrated volumes was used. For FC500 and Navios platforms, the compensation matrix was verified with a PNH sample and a normal sample stained with a five-color cocktail comprising FLAER, CD157PE, CD64ECD, CD15PECy5, and CD45PECy7.

Becton Dickinson instruments

For FACSCanto II instruments with eight PMTs, light-scatter voltages were established using unstained cells. The PMT voltages for FLAER CD157PE, CD45PerCP, and CD64APC were established as described above. The PMT voltage for CD15eFluor450 (clone MMA, eBioscience) (or conjugate MMAv450, BD) was established using unstained lymphocytes in a CD15-stained normal blood sample. Compensation was performed with antibody-capture beads (UltraComp eBeads, eBioscience, or CompBeads, BD), except for FLAER, in which FLAER-stained lymphocytes were used. The compensation matrix was verified using a PNH sample and a normal sample stained with FLAER, CD157PE, CD45PerCp, CD64APC, and CD15eFluor 450 (Table 3). For FACSCanto instruments equipped with six PMTs and two lasers, a slightly modified reagent-conjugate cocktail is required (see Table 3) that utilizes FLAER, CD157PE, CD15PerCP-eFluor710 (clone MMA, eBioscience), CD64APC, and CD45APC-H7.

Staining Procedure for Five-Color High-Sensitivity Combined Neutrophil/Monocyte Assay

For analysis on BC instruments,samples were stained as above with a five-color cocktail comprising pretitrated volumes of FLAER, CD157PE, CD64ECD, CD15PECy5, and CD45PECy7. For analysis on a BD Canto II, a cocktail comprising FLAER, CD157PE, CD45PerCP, CD64APC, and CD15eFuor450 was used. All other sample-processing steps were performed as described above for the four-color neutrophil and monocyte assays. An example of a PNH sample stained with the five-color assay and analyzed on a BC Navios cytometer is shown in Fig. 5. Assays to validate the sensitivity (lower limits of detectability) and background rates of PNH phenotypes in 10 normal samples for the five-color assays were performed as described above for the four-color assays and were found to be essentially identical to the predicate four-color neutrophil and monocyte assays.

High-Sensitivity Six-Color WBC Assays

Antibody Clone/Conjugate Selection for Six-Color High-Sensitivity PNH WBC Detection

For laboratories equipped with cytometers with six or more PMTs, it is possible to design six-color assays for single-tube, simultaneous, high-sensitivity analysis of PNH neutrophils and PNH monocytes. Such reagent cocktails are composed of FLAER along with carefully selected and validated conjugates of CD15, CD64, CD24, CD14, and CD45. Instrument setup and compensation matrices are established along the lines outlined above for the five-color assays. An example of a six-color assay on a Navios cytometer is shown in Fig. 6 of a fresh PNH sample stained with FLAER, CD24PE, CD15PC5, CD64PC7, CD14APC-A700, and CD45KO. Assays to validate the sensitivity (lower limits of detectability) and background rates of PNH phenotypes in 10 normal samples for this six-color assay were performed as described above for the four-color assays and were found to be essentially identical to the predicate four-color neutrophil and monocytes assays (46).

QUALITY CONTROL AND ASSURANCE

Before deployment of high-sensitivity assays to detect GPI-deficient PNH cells in the clinical laboratory, it is important not only to optimize instrument and reagent performance, but to establish the sensitivity of the assay and establish the background level of PNH phenotypes in multiple normal samples (49, 50). In addition, ongoing quality control needs to be in place to ensure that established analytic specifications are controlled during patient testing.

Strategies for Ongoing Antibody-Conjugate Verification

For laboratories that perform testing for PNH only occasionally, it is recommended that staining cocktails for all deployed assays be checked on a normal sample at least once per month to ensure all antibody conjugates are staining in the expected manner (44, 49). It is also important to

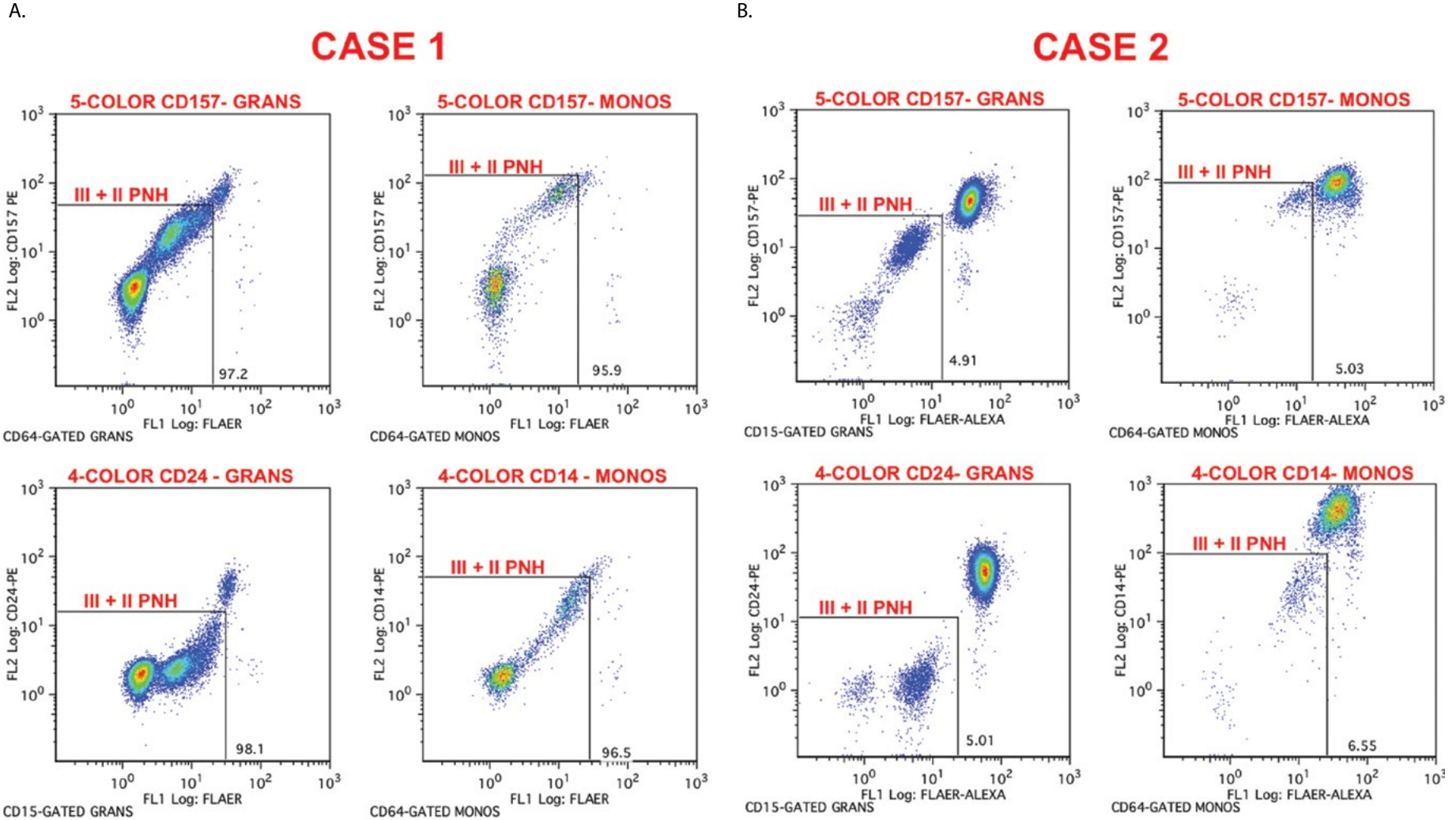

FIGURE 4 (A) Example of normal sample stained with high-sensitivity neutrophil assay. Normal sample stained and analyzed exactly as described in Fig. 2. Gated neutrophils displayed on FLAER versus CD24 plot (right) and zero PNH neutrophils were detected in the lower left quadrant. (B) Example of normal sample stained with the high-sensitivity monocyte assay. Normal sample stained and analyzed exactly as described in Fig. 3. Gated monocytes displayed on FLAER versus CD14 plot (right) and only 1 PNH monocyte phenotype was detected in the lower left quadrant.

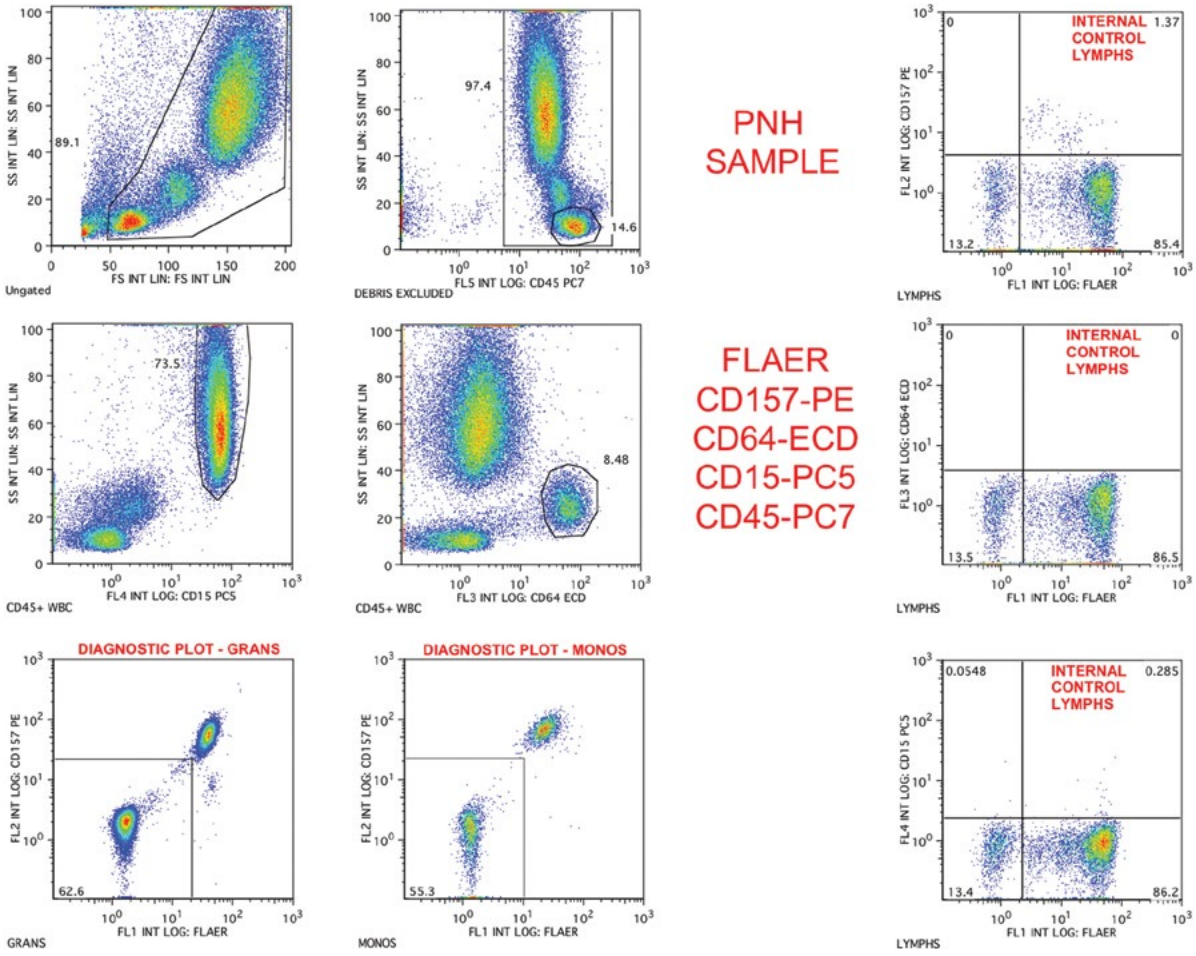

FIGURE 5 Five-color, single-tube, CD157-based assay for PNH neutrophil and monocytes. A fresh sample from a long-term PNH patient was stained with FLAER, CD157PE, CD64ECD, CD15PECy5, and CD45PECy7 and data were acquired on FC500. Debris was removed with light scatter (top row, left) and CD45 gating (top row, middle). Neutrophils (middle row, left) and monocytes (middle row, middle) were identified and gated based on CD15 and CD64 expression, respectively. Gated neutrophils (bottom row, left) and monocytes (bottom row, middle) were displayed on FLAER versus CD157 plots and PNH neutrophils and monocytes (FLAER-negative, CD157-negative) were identified. Gated lymphocytes (internal controls) were identified and sequentially gated based on CD45 and SS (top row middle) and lack of CD64 staining (not shown) and displayed on FLAER versus CD157 (top row, right) or FLAER versus CD64 (middle row, right) and FLAER versus CD15 (bottom row, right).

compare old lots of staining reagents with new lots, including cocktails (as recommended) to assure the performance of new reagent lots. Normal-blood samples are also adequate for this purpose.

For laboratories performing regular testing for PNH, it is not necessary to monitor assay performance in the aforementioned manner, as most samples that arrive for testing are normal with respect to PNH. Thus, normal RBCs serve as "internal controls" for instrument/reagent performance in the RBC assay. Similarly, performance of reagents used in four-color and five-color WBC assays can be closely monitored using internal controls. Lymphocytes provide excellent internal negative-control populations for all the critical reagents used in the four- and five-color WBC assays. For example, gating reagents CD15 and CD64 stain neutrophils and monocytes, respectively, while neither reagent should stain lymphocytes in the four-color assays. CD24 stains B lymphocytes (internal positive control) but not T cells (internal negative control) and CD14 stains normal monocytes (internal positive control) but not lymphocytes (internal negative control). Lymphocytes also serve as internal positive control for FLAER. Even for samples that contain effectively 100% PNH neutrophils and monocytes, lymphocytes can be observed to show that reagent performance is appropriate. While PNH lymphocytes can be found in patients who have had disease for some time, normal lymphocytes can always be detected that stain with FLAER, thus providing an internal positive staining control for this reagent. For the five-color WBC assay, CD157 stains both neutrophils and monocytes but does not stain lymphocytes.

Fluorescence-Minus Two Controls

Whichever WBC assays are employed, they should also be verified on a *bona fide* PNH sample when the opportunity arises. Sharing of such samples among laboratories is strongly recommended for this rare disease where feasible. If a PNH sample is unavailable, instrument settings can be checked by staining a "fluorescence-minus-two" (FM2)

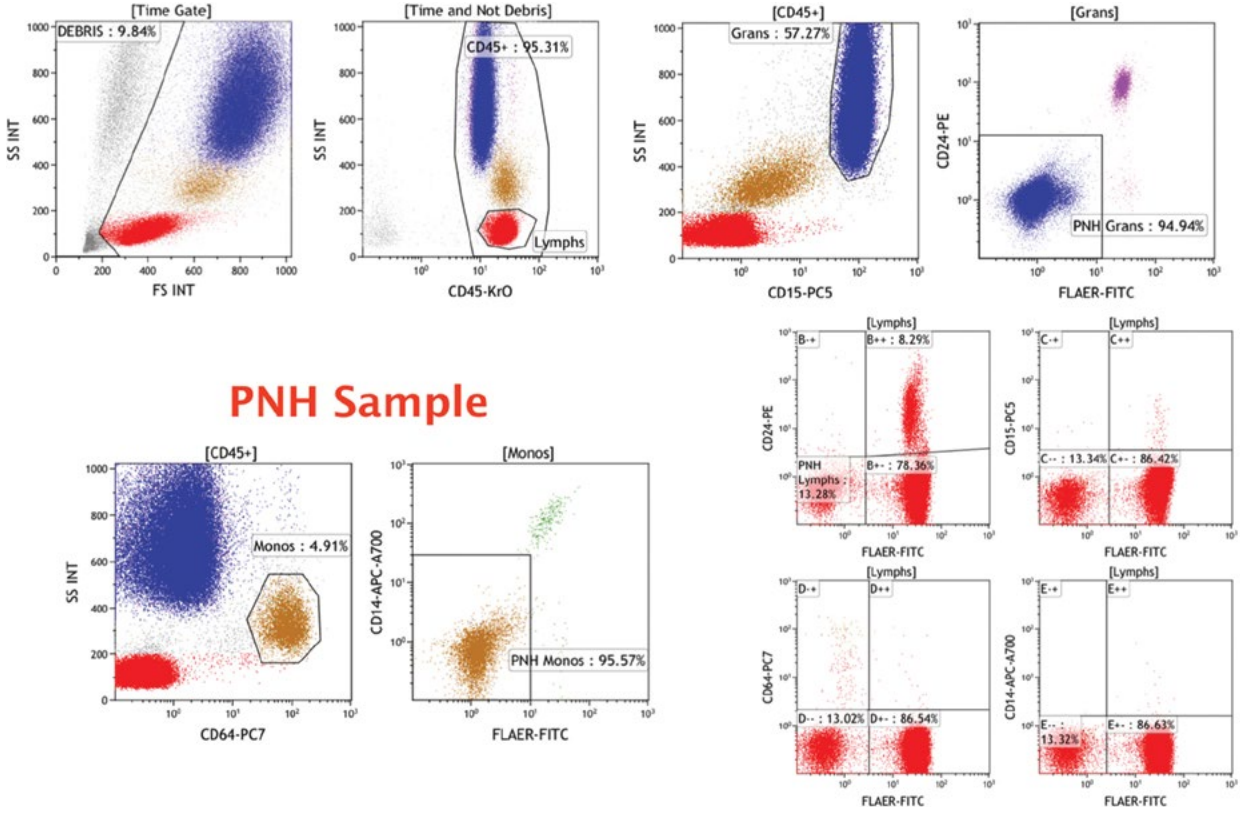

FIGURE 6 Six-color single-tube assay for PNH neutrophil and monocytes. Fresh PNH sample stained with FLAER, CD24PE, CD15PECy5, CD64PC7, CD14APC-A700, and CD45KO. Data acquired on Navios cytometer equipped with three lasers and 10 PMTs. Neutrophils were gated by sequential analysis of light scatter, CD45 gating, and CD15 expression (top row). Gated neutrophils were displayed on FLAER versus CD24PE plot (top right) to delineate PNH neutrophils (lower left quadrant) from normal neutrophils (upper right quadrant). Monocytes were sequentially gated by light scatter, CD45, and bright CD64 expression (bottom row, left). CD64-gated monocytes were displayed on adjacent FLAER versus CD14APC-A700 plot and PNH monocytes (lower left quadrant) were delineated from normal monocytes (upper right quadrant). Lymphocytes were gated by a combination of light scatter and CD45/SS staining and displayed on four bivariate dot plots (right lower and right bottom rows) displaying FLAER versus CD24, CD14, CD15, and CD64 to confirm optimal instrument setup/compensation and validate the performance of all antibody conjugate used in the assay.

sample in which only the gating antibodies CD45 and CD15 (neutrophil assay) or CD45 and CD64 (monocyte assay), or CD45, CD15, and CD64 (five-color assay), are used to stain a normal sample (in reference 44, see Fig. 9 and 10, respectively, of supplementary data). In FM2 stainings, all gated neutrophils, gated monocytes, and gated lymphocytes express a PNH phenotype since the GPI-specific reagents were not added. If these populations are not clearly visible and on-scale, PMT voltages and compensation matrices should be adjusted.

Ongoing Control of Assay Quality

Once the assay performance is established, the monitoring of internal cellular controls during patient-sample testing, as outlined above, is critically important. These internal-control cells verify not only antibody/reagent performance but can also indicate possible issues within the patient sample which may not be apparent in normal controls. Finally, rigorous monitoring of such internal cellular controls allows the cytometrist to monitor instrument performance, including PMT and compensation settings.

ASSAY VALIDATION

Using the standardized four-color neutrophil and monocyte assays described above on stabilized PNH whole-blood preparations, results have demonstrated very good interlaboratory performance characteristics among expert laboratories (51). Using fresh samples and the same standardized four-color assays, another recent study demonstrated good intra- and interlaboratory performance characteristics for both precision and reproducibility analyses and excellent correlation and agreement between centers for all target PNH clone sizes, even in laboratories with little prior experience performing PNH testing (52).

CONSIDERATIONS FOR VALIDATION OF HIGH-SENSITIVITY PNH ASSAYS

Verification of Instrument Set-Up and Antibody Performance

For instruments initially set up in the manner described above for RBCs ("High-Sensitivity RBC Assay"), the analysis of a normal sample will appear as shown in Fig. 1C.

For instruments initially set up as described above for four-color WBC assays ("High-Sensitivity Four-Color WBC Assays"), the analysis of a normal sample with the neutrophil and monocyte assays will appear as shown in Fig. 7A and 7B, respectively.

For those using the single-tube, five-color, CD157-based assay described above ("High-Sensitivity Five-Color WBC Assays"), the analysis of a normal sample will appear as shown in Fig. 6.

Determining Assay Sensitivity

Since very small numbers of PNH phenotypes can be detected in some cases of AA and MDS, it is important to know the sensitivity of the assays deployed in the clinical laboratory. Assay sensitivity is determined by two factors: the absolute lower limit of detectability of *bona fide* PNH cells, and the assay "background" on normal samples.

Lower Limit of Detectability of PNH RBCs

When the opportunity arises to test a *bona fide* PNH sample, it is recommended that a serial dilution or "spiking" experiment be performed in which the (1:100 prediluted) PNH blood is titrated into a similarly prediluted ABO blood type-matched normal-blood sample. Typically, a titration range of 1:10 through 1:10,000 is used (44). The spiked samples are stained in the normal manner, washed twice, racked, and acquired. Up to 1 million RBCs may need to be acquired on the more dilute samples to obtain the most statistically reliable results. Spiking experiments performed as above have established that as few as 20 type III PNH RBCs can be detected in a list mode file of 1 million RBCs with our assay (44).

Lower Limit of Detectability of PNH WBCs

A spiking experiment is used to establish the lower limit of detectability of PNH neutrophils and PNH monocytes in the same manner as that used for the high-sensitivity RBC assay, except undiluted blood samples are used. Spiked samples are stained in the normal manner with the four-, five-, or six-color reagent sets and washed twice, and the data are acquired on the cytometer. Data acquisition times of up to 15 min may be needed to obtain sufficient PNH phenotypes at the higher dilutions. Spiking experiments performed with the four-color neutrophil, four-color monocyte (44), and five-color combined assays (46), as well as the six-color combined assays, showed that the neutrophil assays could reliably detect as few as 10 PNH phenotypes per 100,000 neutrophils while the monocyte assays were slightly less sensitive due to the lower frequencies of monocytes in PB samples.

Verification of RBC and WBC Assay Backgrounds

Blood samples from normal individuals have been shown previously to contain very small numbers of neutrophils with PNH phenotypes (53). To establish background frequencies of PNH RBC, PNH neutrophil, and PNH monocyte phenotypes in normal-blood samples with our assays, 20 normal samples were screened with each assay in keeping with recently established International Guidelines (50, 54). For the RBC protocol, a range of two to six events falling in the type III RBC region per million RBCs was found (44) (see example shown in Fig. 1B). These data, together with the spiking experiments described above, establish the RBC assay sensitivity at better than 0.01%.

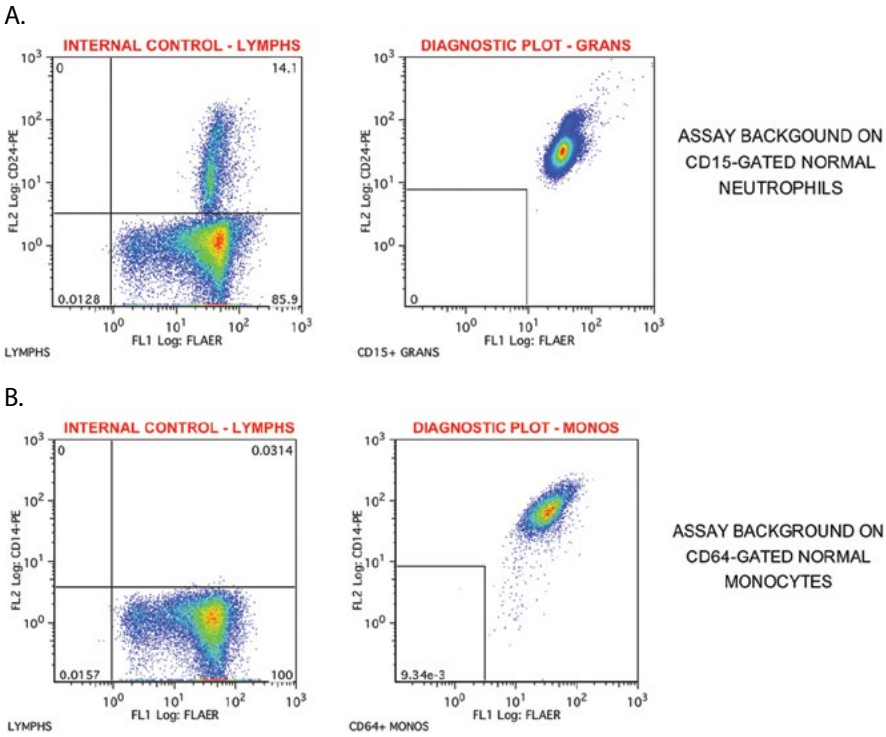

FIGURE 7 Examples of two samples containing type II neutrophils and monocytes. **(A)** Samples stained with five-color CD157-based assay (top row) or four-color neutrophil (bottom left plot) or four-color monocyte (bottom right plot) assays. CD157 separates PNH type II neutrophils from type III cells more effectively than CD24. When major populations of type II cells are present, as shown in case 1, this can lead to difficulty in delineating type I cells from PNH type II cells. This issue is also apparent in comparing CD157 (top right) and CD14 staining (bottom right) of monocytes.

For the four-, five-, and six-color neutrophil assays, frequencies of PNH phenotypes in normal samples were in the 0 to 6 per million range. Similar data were obtained from the four-, five-, and six-color monocyte assays. Thus the neutrophil and monocyte assays described here have sensitivities in the 0.01% and 0.04% ranges, respectively (44, 46).

With increasing deployment of the CD157-based five-color assays, we and others have detected rare non-PNH cases that failed to express (in total or in part) detectable CD157 in both neutrophil and monocyte lineages (Sutherland DR, unpublished observations). While the cause of this is currently under investigation, users of CD157-based assays should be aware of this issue. Given the built-in redundancy of the assays described herein, such cases were not misinterpreted as *bona fide* PNH, because FLAER expression on WBC lineages and CD59 expression on RBCs was entirely normal.

REFERENCES

1. **Dacie JV.** 1963. Paroxysmal nocturnal haemoglobinuria. *Proc R Soc Med* **56:**587–596.
2. **Oni SB, Osunkoya BO, Luzzatto L.** 1970. Paroxysmal nocturnal hemoglobinuria: evidence for monoclonal origin of abnormal red cells. *Blood* **36:**145–152.
3. **Miyata T, Takeda J, Iida Y, Yamada N, Inoue N, Takahashi M, Maeda K, Kitani T, Kinoshita T.** 1993. The cloning of PIG-A, a component in the early step of GPI-anchor biosynthesis. *Science* **259:**1318–1320.
4. **Takeda J, Miyata T, Kawagoe K, Iida Y, Endo Y, Fujita T, Takahashi M, Kitani T, Kinoshita T.** 1993. Deficiency of the GPI anchor caused by a somatic mutation of the PIG-A gene in paroxysmal nocturnal hemoglobinuria. *Cell* **73:**703–711.
5. **Nicholson-Weller A, March JP, Rosenfeld SI, Austen KF.** 1983. Affected erythrocytes of patients with paroxysmal nocturnal hemoglobinuria are deficient in the complement regulatory protein, decay acceleration factor. *Proc Natl Acad Sci USA* **80:**5066–5070.
6. **Holguin MH, Frederick LR, Bernshaw NJ, Wilcox LA, Parker CJ.** 1989. Isolation and characterization of a membrane protein from normal human erythrocytes that inhibits reactive lysis of the erythrocytes of paroxysmal nocturnal hemoglobinuria. *J Clin Invest* **84:**7–17.
7. **Rosse WF, Ware RE.** 1995. The molecular basis of paroxysmal nocturnal hemoglobinuria. *Blood* **86:**3277–3286.
8. **Nafa K, Bessler M, Castro-Malaspina H, Jhanwar S, Luzzatto L.** 1998. The spectrum of somatic mutations in the PIG-A gene in paroxysmal nocturnal hemoglobinuria includes large deletions and small duplications. *Blood Cells Mol Dis* **24:**370–384.
9. **Yamashina M, Ueda E, Kinoshita T, Takami T, Ojima A, Ono H, Tanaka H, Kondo N, Orii T, Okada N, Okada H, Inoue K, Kitani T.** 1990. Inherited complete deficiency of 20-kilodalton homologous restriction factor (CD59) as a cause of paroxysmal nocturnal hemoglobinuria. *N Engl J Med* **323:**1184–1189.
10. **Motoyama N, Okada N, Yamashina M, Okada H.** 1992. Paroxysmal nocturnal hemoglobinuria due to hereditary nucleotide deletion in the HRF20 (CD59) gene. *Eur J Immunol* **22:**2669–2673.
11. **Parker CJ.** 2002. Historical aspects of paroxysmal nocturnal haemoglobinuria: "defining the disease". *Br J Haematol* **117:**3–22.
12. **Hillmen P, Lewis SM, Bessler M, Luzzatto L, Dacie JV.** 1995. Natural history of paroxysmal nocturnal hemoglobinuria. *N Engl J Med* **333:**1253–1258.
13. **Parker CJ.** 2009. Bone marrow failure syndromes: paroxysmal nocturnal hemoglobinuria. *Hematol Oncol Clin North Am* **23:**333–346.
14. **Young NS.** 2009. Paroxysmal nocturnal hemoglobinuria and myelodysplastic syndromes: clonal expansion of PIG-A-mutant hematopoietic cells in bone marrow failure. *Haematologica* **94:**3–7.
15. **Scheinberg P, Marte M, Nunez O, Young NS.** 2010. Paroxysmal nocturnal hemoglobinuria clones in severe aplastic anemia patients treated with horse anti-thymocyte globulin plus cyclosporine. *Haematologica* **95:**1075–1080.
16. **Brodsky RA.** 2009. How I treat paroxysmal nocturnal hemoglobinuria. *Blood* **113:**6522–6527.
17. **Dunn DE, Tanawattanacharoen P, Boccuni P, Nagakura S, Green SW, Kirby MR, Kumar MS, Rosenfeld S, Young NS.** 1999. Paroxysmal nocturnal hemoglobinuria cells in patients with bone marrow failure syndromes. *Ann Intern Med* **131:**401–408.
18. **Sugimori C, Chuhjo T, Feng X, Yamazaki H, Takami A, Teramura M, Mizoguchi H, Omine M, Nakao S.** 2006. Minor population of CD55-CD59- blood cells predicts response to immunosuppressive therapy and prognosis in patients with aplastic anemia. *Blood* **107:**1308–1314.
19. **Tichelli A, Gratwohl A, Nissen C, Speck B.** 1994. Late clonal complications in severe aplastic anemia. *Leuk Lymphoma* **12:**167–175.
20. **Raza A, Ravandi F, Rastogi A, Bubis J, Lim SH, Weitz I, Castro-Malaspina H, Galili N, Jawde RA, Illingworth A.** 2013. A prospective multicenter study of paroxysmal nocturnal hemoglobinuria cells in patients with bone marrow failure. *Cytometry B Clin Cytom* **86:**175–182.
21. **Parker C, Omine M, Richards S, Nishimura J, Bessler M, Ware R, Hillment P, Luzzatto L, Young N, Kinoshita T, Rosse W, Socié G; International PNH Interest Group.** 2005. Diagnosis and management of paroxysmal nocturnal hemoglobinuria. *Blood* **106:**3699–3709.
22. **Borowitz MJ, Craig FE, Digiuseppe JA, Illingworth AJ, Rosse W, Sutherland DR, Witter CT, Richards SJ; Clinical Cytometry Society.** 2010. Guidelines for the diagnosis and monitoring of paroxysmal nocturnal hemoglobinuria and related disorders by flow cytometry. *Cytometry B Clin Cytom* **78:**211–230.
23. **Ham TH, Dingle JH.** 1939. Studies on the destruction of red blood cells. II. Chronic hemolytic anemia with paroxysmal nocturnal hemoglobinuria: certain immunological aspects of the hemolytic mechanism with special reference to serum complement. *J Clin Invest* **18:**657–672.
24. **Hartmann RC, Jenkins DE.** 1966. The "sugar-water" test for paroxysmal nocturnal hemoglobinuria. *N Engl J Med* **275:**155–157.
25. **Rosse WF, Dacie JV.** 1966. Immune lysis of normal human and paroxysmal nocturnal hemoglobinuria (PNH) red blood cells. II. The role of complement components in the increased sensitivity of PNH red cells to immune lysis. *J Clin Invest* **45:**749–757.
26. **Rosse WF, Hoffman S, Campbell M, Borowitz M, Moore JO, Parker CJ.** 1991. The erythrocytes in paroxysmal nocturnal haemoglobinuria of intermediate sensitivity to complement lysis. *Br J Haematol* **79:**99–107.
27. **van der Schoot CE, Huizinga TW, van 't Veer-Korthof ET, Wijmans R, Pinkster J, von dem Borne AE.** 1990. Deficiency of glycosyl-phosphatidylinositol-linked membrane glycoproteins of leukocytes in paroxysmal nocturnal hemoglobinuria, description of a new diagnostic cytofluorometric assay. *Blood* **76:**1853–1859.
28. **Hall SE, Rosse WF.** 1996. The use of monoclonal antibodies and flow cytometry in the diagnosis of paroxysmal nocturnal hemoglobinuria. *Blood* **87:**5332–5340.
29. **Richards SJ, Rawstron AC, Hillmen P.** 2000. Application of flow cytometry to the diagnosis of paroxysmal nocturnal hemoglobinuria. *Cytometry B Clin Cytom* **42:**223–233.
30. **Sutherland DR, Kuek N, Azcona-Olivera J, Anderson T, Acton E, Barth D, Keeney M.** 2009. Use of FLAER-based

WBC assay in the primary screening of PNH clones. *Am J Clin Pathol* **132:**564–572.
31. **Hernández-Campo PM, Almeida J, Sánchez ML, Malvezzi M, Orfao A.** 2006. Normal patterns of expression of glycosylphosphatidylinositol-anchored proteins on different subsets of peripheral blood cells: a frame of reference for the diagnosis of paroxysmal nocturnal hemoglobinuria. *Cytometry B Clin Cytom* **70:**71–81.
32. **Brodsky RA, Mukhina GL, Li S, Nelson KL, Chiurazzi PL, Buckley JT, Borowitz MJ.** 2000. Improved detection and characterization of paroxysmal nocturnal hemoglobinuria using fluorescent aerolysin. *Am J Clin Pathol* **114:**459–466.
33. **Peghini PE, Fehr J.** 2005. Clinical evaluation of an aerolysin-based screening test for paroxysmal nocturnal haemoglobinuria. *Cytometry B Clin Cytom* **67:**13–18.
34. **Sutherland DR, Kuek N, Davidson J, Chang H, Yeo E, Bamford S, Chin-Yee I, Keeney M.** 2007. Diagnosing PNH with FLAER and multiparameter flow cytometry. *Cytometry B Clin Cytom* **72:**167–177.
35. **Richards SJ, Barnett D.** 2007. The role of flow cytometry in the diagnosis of paroxysmal nocturnal hemoglobinuria in the clinical laboratory. *Clin Lab Med* **27:**577–590.
36. **Battiwalla M, Hepgur M, Pan D, McCarthy PL, Ahluwalia MS, Camacho SH, Starostik P, Wallace PK.** 2010. Multiparameter flow cytometry for the diagnosis and monitoring of small GPI-deficient cellular populations. *Cytometry B Clin Cytom* **78:**348–356.
37. **Richards SJ, Whitby L, Cullen MJ, Dickinson AJ, Granger V, Reilly JT, Hillmen P, Barnett D.** 2009. Development and evaluation of a stabilized whole-blood preparation as a process control material for screening of paroxysmal nocturnal hemoglobinuria by flow cytometry. *Cytometry B Clin Cytom* **76:**47–55.
38. **Rother RP, Rollins SA, Mojcik CF, Brodsky RA, Bell L.** 2007. Discovery and development of the complement inhibitor eculizumab for the treatment of paroxysmal nocturnal hemoglobinuria. *Nat Biotechnol* **25:**1256–1264.
39. **Hillmen P, Hall C, Marsh JC, Elebute M, Bombara MP, Petro BE, Cullen MJ, Richards SJ, Rollins SA, Mojcik CF, Rother RP**. 2004. Effect of eculizumab on hemolysis and transfusion requirements in patients with paroxysmal nocturnal hemoglobinuria. *N Engl J Med* **350:**552–559.
40. **Brodsky RA, Young NS, Antonioli E, Risitano AM, Schrezenmeier H, Schubert J, Gaya A, Coyle L, de Castro C, Fu CL, Maciejewski JP, Bessler M, Kroon HA, Rother RP, Hillmen P.** 2008. Multicenter phase 3 study of the complement inhibitor eculizumab for the treatment of patients with paroxysmal nocturnal hemoglobinuria. *Blood* **111:**1840–1847.
41. **Parker CJ.** 2012. Paroxysmal nocturnal hemoglobinuria. *Curr Opin Hematol* **19:**141–148.
42. **Kelly RJ, Hill A, Arnold LM, Brooksbank GL, Richards SJ, Cullen M, Mitchell LD, Cohen DR, Gregory WM, Hillmen P.** 2011. Long-term treatment with Eculizumab in paroxysmal nocturnal hemoglobinuria: sustained efficacy and improved survival. *Blood* **117:**6786–6792.
43. **Varela JC, Brodsky RA.** 2013. Paroxysmal nocturnal hemoglobinuria and the age of therapeutic complement inhibition. *Expert Rev Clin Immunol* **9:**1113–1124.
44. **Sutherland DR, Keeney M, Illingworth A.** 2012. Practical guidelines for the high-sensitivity detection and monitoring of paroxysmal nocturnal hemoglobinuria clones by flow cytometry. *Cytometry B Clin Cytom* **82:**195–208.
45. **Dalal BI, Khare NS.** 2013. Flow cytometric testing for paroxysmal nocturnal hemoglobinuria: CD64 is better for gating monocytes than CD33. *Cytometry Part B* **84:**33–36.
46. **Sutherland DR, Acton E, Keeney M, Davis BH, Illingworth A.** 2014. Use of CD157 in FLAER-based assays for high-sensitivity PNH granulocyte and PNH monocyte detection. *Cytometry B Clin Cytom* **86:**44–55.
47. **Hernández-Campo PM, Almeida J, Acevedo MJ, Sánchez ML, Alberca I, Vidriales B, Martínez E, Romero JR, Orfao A.** 2008. Detailed immunophenotypic characterization of different major and minor subsets of peripheral blood cells in patients with paroxysmal nocturnal hemoglobinuria. *Transfusion* **48:**1403–1414.
48. **Hernández-Campo PM, Almeida J, Matarraz S, de Santiago M, Sánchez ML, Orfao A.** 2007. Quantitative analysis of the expression of glycosylphosphatidylinositol-anchored proteins during the maturation of different hematopoietic cell compartments of normal bone marrow. *Cytometry B Clin Cytom* **72:**34–42.
49. **Davis BH, Keeney M, Brown R, Illingworth AJ, King MJ, Kumpel B, Meier ER, Sandler SG, Shaz BH, Sutherland DR.** 2014. *Red Blood Cell Diagnostic Testing Using Flow Cytometry; Approved Guideline*, Second Edition. Document H52-A2. Clinical and Laboratory Standards Institute, Wayne, PA.
50. **Davis BH, McLaren CE, Carcio AJ, Wong L, Hedley BD, Keeney M, Curtis A, Culp NB.** 2013. Determination of optimal replicate number for validation of imprecision using fluorescence cell-based assays: proposed practical method. *Cytometry B Clin Cytom* **84:**329–337.
51. **Fletcher M, Sutherland DR, Whitby L, Whitby A, Richards SJ, Acton E, Keeney M, Borowitz M, Illingworth A, Reilly JT, Barnett D.** 2014. Standardizing leucocyte PNH clone detection: an international study. *Cytometry B Clin Cytom* **86:**311–318.
52. **Marinov I, Kohoutová M, Tkáčová V, Lysák D, Holubová M, Stehlíková O, Železníková T, Žontar D, Illingworth A.** 2013. Intra- and interlaboratory variability of paroxysmal nocturnal hemoglobinuria testing by flow cytometry following the 2012 Practical Guidelines for high-sensitivity paroxysmal nocturnal hemoglobinuria testing. *Cytometry B Clin Cytom* **84:**229–236.
53. **Hu R, Mukhina GL, Piantadosi S, Barber JP, Jones RJ, Brodksy RA.** 2005. *PIG-A* mutations in normal hematopoiesis. *Blood* **105:**3848–3854.
54. **Sutherland DR, Illingworth A, Keeney M, Richards SJ.** 2015. High-sensitivity detection of PNH red blood cells, red cell precursors, and white blood cells. *Curr Protoc Cytom* **72:**6.37.1–6.37.29.

Standardized Flow Cytometry Assays for Enumerating CD34$^+$ Hematopoietic Stem Cells

D. ROBERT SUTHERLAND AND MICHAEL KEENEY

19

The pioneering studies of Thomas et al. in the late 1950s first established that a cellular component of syngeneic bone marrow was capable of regenerating multilineage hematopoiesis in cancer patients receiving supralethal doses of radiation (1, 2). For the next 20 or more years, the majority of autologous and allogeneic hematopoietic stem/progenitor cell transplants were performed utilizing bone marrow as a source of stem cells (reviewed in reference 3). Circulating stem cells were also detectable in steady-state peripheral blood but were extremely rare, as evidenced by their low plating efficiency relative to marrow leukocytes in early colony-forming cell assays (4). Although blood stem/progenitor cells could be collected from steady-state peripheral blood by leukapheresis, the number of procedures required to obtain sufficient cells for transplant initially precluded their widespread use (5). With the development of more sophisticated colony-forming cell assays, a variety of reports in the mid-1980s clearly demonstrated the feasibility of obtaining clinically useful numbers of peripheral blood stem/progenitor cells from cancer patients recovering from chemotherapy (6–8). The availability of a number of hematopoietic cytokines used either singly or in combination with other cytokines and/or chemotherapy (9) has facilitated the harvesting of peripheral blood stem cells (PBSC) to the point where it is a preferred alternative to marrow for autologous and, increasingly, allogeneic transplantation (reviewed in reference 10).

HEMATOPOIETIC STEM/PROGENITOR CELLS EXPRESS THE CD34 ANTIGEN

An important phenotypic characteristic of the stem/progenitor cells in marrow and peripheral blood responsible for multilineage engraftment in the transplant setting was initially established in the late 1980s with the development of two monoclonal antibodies: My10 (11) and B1.3C5 (12), which identified a small number (2 to 4%) of normal marrow leukocytes. This population contained the majority of colony-forming cells for myeloid and erythroid lineages and also contained a few cells exhibiting the phenotypic properties of primitive lymphoid cells. My10 and 3C5 identified similar molecular structures with molecular masses of about 110,000 (110 kDa) and were designated "CD34." Seminal studies using a CD34 antibody called 12.8 (13), which uniquely cross-reacted with a similar subset of baboon marrow cells, conclusively demonstrated that the CD34 antigen was also expressed on true hematopoietic stem cells that could reconstitute long-term multilineage hematopoiesis in lethally irradiated animals (14). Subsequent studies on humans (15) confirmed that CD34$^+$ cell transplants were safe, durable, and potentially therapeutically effective.

TRANSPLANTATION OF HEMATOPOIETIC STEM CELLS: MEASURING GRAFT ADEQUACY

When using bone marrow as a source of stem cells, a total nucleated cell count of 2.5×10^8 nucleated cells/kg patient weight will reliably permit hematopoietic reconstitution (16). However, the increased use of PBSC for autologous and allogeneic transplantation evolved in the absence of any consensus means to assess the engraftment potential of the stem cell product. In the past, the majority of centers performing PBSC transplants relied on the ability of harvested cells to form hematopoietic colony-forming units for granulocytes and macrophages (CFU-GM) in methylcellulose cultures to assess graft quality. Reinfusion of 10^5 CFU-GM/kg of body weight was usually sufficient for reconstitution of hematopoiesis following marrow ablative therapy. However, this assay takes at least 10 days to "read-out" and it cannot measure the most primitive stem cells in the graft that mediate long-term engraftment. Furthermore, due to technical differences in the way these assays were performed between different centers, it was difficult to perform meaningful comparisons on data obtained from different institutions. Thus, the minimum numbers of CFU-GM required to ensure durable and reproducible hematopoietic reconstitution were difficult to establish (17).

Clinically useful numbers of hematopoietic stem cells can also be found in umbilical cord blood (CB) (18, 19), and studies in animal models (20, 21) have indicated that CB represents a particularly rich source of hematopoietic stem/progenitor cells. Thereafter, a large number of CB banks were established worldwide that utilized a variety of methods of collection, processing (with or without T-cell depletion), and cryopreservation. In many cases, rapid, reliable, and standardized methods to measure the effects of such manipulations on the engraftment potential of the post-thawed CB product were not universally employed.

doi:10.1128/9781555818722.ch19

GRAFT ASSESSMENT BY CD34+ CELL ENUMERATION AND FLOW CYTOMETRY

Graft assessment by direct quantitation of $CD34^+$ cells using flow cytometry theoretically obviated the limitations of CFU assays, and the $CD34^+$ cell population encompasses the most primitive stem cells in addition to maturing, lineage-committed progenitors (22, 23). Furthermore, a standardized flow cytometry assay should generate data that are more directly comparable between different transplant centers. Multiparameter flow cytometry can address not just quantitative issues but can also allow a qualitative (i.e., $CD34^+$ cell subset) assessment of the PBSC product or of the level of T-lymphocyte contamination in a $CD34^+$ cell-selected product in the allotransplant setting. Thus, accurate enumeration of $CD34^+$ cells can provide crucial clinical information to the transplant physician. Currently, flow cytometry is the only methodology capable of rapidly measuring this most clinically useful surrogate marker of graft adequacy in all sources of hematopoietic stem cells.

CLINICAL ISSUES IN ENUMERATING STEM CELLS BY FLOW CYTOMETRY

Most transplant centers now determine graft adequacy based on the number of $CD34^+$ cells/kg of patient body weight. Early on, the absolute $CD34^+$ cell number was obtained by determining the percent $CD34^+$ cells by flow cytometry and multiplying it by the absolute leukocyte count as determined by an automated hematology analyzer (so-called two-platform methodology). Using such technology, the recommended minimum number of $CD34^+$ cells was 10^7/kg, although in the absence of a standardized assay to enumerate $CD34^+$ cells, a full consensus on the latter figure was difficult to establish (24, 25). In addition to determining the yield, the number of $CD34^+$ cells mobilized to the peripheral blood is also a predictor of the success of apheresis (26) and can be used to monitor the on-line yield of $CD34^+$ cells if necessary (27). Optimally timing the harvesting of $CD34^+$ cells may be particularly important in patients who have received extensive prior therapy and exhibit poor bone marrow function. For such "poor mobilizers," daily measurements of the $CD34^+$ cell concentration in the circulation to optimize early collection may have merit.

More recently, there has been a shift in interest from the minimum number of stem cells required, to attempts to maximize the $CD34^+$ cell dose, a factor that has been shown by several investigators to correlate inversely with time to engraftment of neutrophils and platelets (28). Furthermore, rapid reengraftment may correlate not only with total $CD34^+$ cell dose, but also with the presence or absence of certain specific subsets of $CD34^+$ cells (29). The clinical interest in subset analysis of rare populations of $CD34^+$ cells adds to the complexity of this assay and to demands on the clinical flow laboratory. Ultimately, the number of viable $CD34^+$ cells (or subsets thereof) actually reinfused to patients is the most clinically important variable determining graft success or failure. A systematic evaluation of viable stem cells from the time of collection to actual reinfusion would be ideal to the quality assurance of these products. We envision this process to involve measurements of peripheral blood $CD34^+$ cells in patients to optimally time apheresis, to evaluate the yield of viable cells postcollection, and to evaluate the number of viable $CD34^+$ cells postcryopreservation actually infused.

To be clinically relevant, any flow cytometric assay must meet the following criteria: (i) it must correlate with a clinically meaningful outcome such as time to multilineage engraftment; (ii) it must be applicable for the different stem cell products (i.e., peripheral blood, cord blood, and bone marrow); (iii) it must provide timely results (less than 2 hours) and must be reproducible between institutions; (iv) it should be sufficiently flexible to permit more sophisticated qualitative analysis of $CD34^+$ cell subsets using a multiparametric approach; (v) it should be able to determine the viability of the target (i.e., $CD34^+$) population; and (vi) it should be a single-platform assay (see below).

EARLY METHODS TO MEASURE CD34+ CELLS BY FLOW CYTOMETRY

Siena et al. (9) were the first to describe a flow cytometric method to measure percent $CD34^+$ cells. Initially, this method was based on mononuclear cell enrichment by density gradient centrifugation, followed by staining using indirect immunofluorescence techniques. The subsequent development of what became known as the Milan protocol (30) was due to the availability, around 1990, of CD34 antibodies which could be conjugated with fluorescein (FITC) without loss of binding activity. With the subsequent commercial availability of phycoerythrin (PE) conjugates of high-affinity CD34 antibodies, the accuracy and sensitivity of Milan-type protocols were slightly increased. The gating strategy utilized simple forward-angle (FSC) versus side-angle (SSC) light scatter to set a denominator. An isotype-matched control was used to set the positive analysis region for $CD34^+$ cells. In the CD34 antibody-stained sample, the number of events that stained brighter than the control and exhibited low to intermediate SSC were counted and used as the numerator in the calculation of percent $CD34^+$ cells. The total number of events counted was 50,000 or a minimum of 50 $CD34^+$ events.

Although a number of minor developments were subsequently incorporated to improve the Milan method, the inherent difficulties in enumerating *bona fide* $CD34^+$ cells in increasingly diverse sources of hematopoietic stem cells led to the development of more sophisticated methods utilizing multiparameter gating strategies. Bender et al. (31) developed a multiparameter assay in which an FITC-conjugated CD45 antibody which only stains nucleated white blood cells was used to generate a more stable denominator. Gated $CD45^+$ events were then analyzed in a manner similar to the Milan protocol, using an isotype control and CD34 staining versus SSC analysis to enumerate $CD34^+$ cells. Although early methods to enumerate $CD34^+$ cells were usually adequate for fresh peripheral blood and apheresis products in pristine condition, they were not sufficiently robust to be broadly applicable to the range of sample types that were increasingly being contemplated for use in the transplant settings (32, 33). Early assays were developed without taking into account the structural characteristics of the CD34 and CD45 molecules and the chemical composition of the epitopes detected by different monoclonal antibodies to these structures (see below). Not all conjugates of all CD34 antibodies were effective at detecting all glycoforms of the CD34 molecule (see below).

STATISTICAL ISSUES IN RARE-EVENT DETECTION

$CD34^+$ cell enumeration by flow cytometry is an example of rare-event analysis, and as such, Poisson statistics apply, where the standard deviation (SD) is equal to the square

root of the target events counted. Therefore, in order to ensure a coefficient variation (CV) of no higher than 10%, at least 100 $CD34^+$ cells need to be collected in the list-mode file. In other words, the lower the frequency of the target population, the larger the data file needs to be to satisfy Poisson statistics. Rare-event analysis also requires that the flow cytometer be rigorously cleaned and maintained, properly set up, and compensated for multiparameter analysis.

APPROPRIATE CONTROLS FOR RARE-EVENT DETECTION

Another key issue in rare-event detection is how to distinguish specific staining of such events from nonspecific staining of perhaps a greater number of events. Some isotype controls stain more events nonspecifically than are stained specifically in some samples, and modern $CD34^+$ cell enumeration methodologies have dispensed with their use entirely (34, 35). Instead, these methods have adopted a multiparameter approach utilizing Boolean gating strategies to distinguish specific from nonspecific staining. To further analyze subsets of already rare populations, modern strategies utilize the so-called "fluorescence-minus-one" (FMO) approach (36) in which all reagents are added to the control tube except for the key marker of interest. The control tube is analyzed for the same length of time and number of events as the test.

TECHNICAL ISSUES IN $CD34^+$ CELL ENUMERATION BY MULTIPARAMETER FLOW CYTOMETRY

CD34 Antigen: Structural Considerations and Choice of Fluorochromes

The CD34 antigen is a heavily glycosylated *O*-sialoglycoprotein (reviewed in references 37 and 38), the structural characteristics of which have important implications for the choice of an appropriate CD34 antibody clone for flow-based enumeration techniques (38, 39). Due to their dependence on terminal sialic acids, which are only found on the most fully glycosylated/processed forms of CD34, class I epitope-detecting CD34 antibodies generate the most aberrant data in clinical samples, whereas class II and class III reagents detect similar if not identical numbers of $CD34^+$ cells in a wide variety of normal and abnormal samples. Thus, for accurate enumeration of rare $CD34^+$ cells in hematopoietic samples, it is important to use a CD34 antibody that detects all glycosylation variants of the molecule, i.e., class II or class III antibodies (37–41).

It is generally advantageous to utilize an antibody conjugated to the brightest fluorochrome excitable, i.e., PE, by an argon laser-based flow cytometer. After parallel analysis of a large number of normal blood, cytokine-mobilized peripheral blood, cord blood, and normal marrow samples, as well as of $CD34^+$ cell lines that fail to express some class I CD34 epitopes, it is our experience that commercially made PE conjugates of the clones QBEnd10, 8G12, and 581 can be utilized with confidence (39–41). As described in detail elsewhere, if FITC conjugates of CD34 antibodies have to be used, only class III reagents such as HPCA2 and 581 can be recommended since these reagents detect similar if not identical numbers of $CD34^+$ cells in parallel analyses of clinical samples using the International Society of Hematotherapy and Graft Engineering (ISHAGE) protocol (see below) as their PE-conjugated versions (38, 39). In general, all potential conjugates that may be used should be rigorously evaluated alongside currently validated reagents before their introduction into the clinical laboratory. Overall, it is critically important to select an appropriate CD34 antibody clone that retains high specificity and avidity of binding after conjugation to the designated fluorochrome.

CD45 Antigen: Structural Considerations and Choice of Fluorochromes

Several protocols have been developed that use CD45 antibodies to gate total nucleated white blood cells, this number serving as the denominator in the calculation of percent $CD34^+$ cells. For such protocols, it is important that pan-CD45 antibodies that detect not just all isoforms, but all glycoforms, of this mucin-like molecule are used. In this respect, the clones J33, T29/33, and HLE-1 can be used with confidence (39–41). Note, however, that the peridinin chlorophyll protein (PerCP) conjugate of HLE-1, while usable on benchtop cytometers equipped with low-powered lasers, can be problematic if used on cell sorters equipped with higher-powered lasers. Of note, a very small fraction of $CD34^+$ cells that do not express CD45 comprises endothelial cells, which have been reported in increased numbers in the blood of patients with solid tumors (42). Although other pan-CD45 antibodies can be used for $CD34^+$ stem cell enumeration, the selected reagent should be carefully evaluated prior to routine use in clinical protocols, as at least one pan-CD45 clone (e.g., clone ALB12, Beckman-Coulter) has been shown to detect a glycosylation-dependent epitope (D. R. Sutherland, unpublished data).

$CD34^+$ CELL ENUMERATION USING SEQUENTIAL BOOLEAN GATING

Accurate enumeration of rare events such as $CD34^+$ cells in heterogeneous clinical samples by flow cytometry represents a serious challenge for both clinical and research laboratories. Cytometers measure events, whether they are white cells, red cells, platelets, dead cells, or debris. Therefore, to eliminate nonleukocytes and debris from the analysis and generate a much more stable denominator against which to measure $CD34^+$ cells, we used anti-CD45 as a counterstain as described previously (31). However, we also took advantage of the observations of Borowitz et al. (43) indicating that leukemic blast cells, which exhibit light scatter properties generally similar to those of lymphocytes, express lower levels of CD45 on their surfaces, thus providing a means of delineating lymphocytes from normal blast cells using this surface marker. Just as lymphocytes, monocytes, and granulocytes form discrete clusters on CD45 staining versus side-scatter analysis, so do $CD34^+$ cells. Thus, a sensitive and accurate multiparameter flow methodology was devised that utilizes the maximum information available of four parameters: CD34 and CD45 staining and forward- and side-angle light scatter. These four parameters were combined in a sequential or Boolean gating strategy that was usable on a variety of sources of hematopoietic stem cells (44). Thereafter, this basic protocol was incorporated into a set of clinical guidelines constructed for ISHAGE, now called the International Society for Cellular Therapy, to enumerate $CD34^+$ cells in peripheral blood and apheresis products (39).

The ISHAGE protocol is sensitive, being capable of detecting 10 to 20 $CD34^+$ cells per 100,000 $CD45^+$ nucleated white blood cells. The method is highly specific when appropriate pan-CD45 antibodies (that detect all isoforms and glycoforms) and CD34 conjugates (that detect all CD34 glycoforms) are used (see below). It is quick and can be performed on a variety of single- and dual-laser

flow cytometers, with only basic software being required for data analysis. The basic ISHAGE protocol can be used to enumerate $CD34^+$ cells in a variety of normal hematopoietic tissues, including marrow and cord blood, as well as in abnormal clinical samples from a variety of disease states. $CD34^+$ cells selected from both normal and abnormal marrow, cord blood, and peripheral blood samples can also be assessed for purity using this flexible method (45).

THE BASIC ISHAGE PROTOCOL AND GATING STRATEGY

The ISHAGE protocol and critical issues relating to the enumeration of $CD34^+$ cells have been published in detail elsewhere (39–41). Briefly, as shown in Fig. 1 on a 24-hour-old peripheral blood apheresis sample, the first gate (R1) is established from a plot of CD45 staining versus side scatter. As indicated above, this approach allows, during analysis of the list-mode data file, the exclusion of red cells, platelets, and other debris commonly found in hematopoietic samples, especially those prepared by lyse–no-wash methods. Sufficient events are acquired in region 1 (R1, histogram 1) such that at least 100 $CD34^+$ cells are displayed in the lymph-blast region, R4 (histogram 4). The acquired cells are then sequentially displayed on a plot of CD34 staining versus side scatter (histogram 2) and R2 is adjusted to include dim and bright $CD34^+$ events with low to intermediate side scatter. The events gated by both R1 and R2 are then displayed in turn on a plot of CD45 fluorescence versus side scatter (histogram 3), and true $CD34^+$ cells form a cluster characterized by low CD45 staining (relative to lymphocytes) and low to intermediate side scatter. It is this cluster that determines the size and location of gating R3. Excluded from this gated cluster (R3) are platelet aggregates, nonspecifically stained lymphocytes, monomyeloid cells, and debris. The cells gated within regions 1, 2, and 3 are then displayed on a light-scatter plot to confirm that the selected events fall into a generic lymph-blast region (R4). The optimal position of gate R4 is set using a duplicate plot 6 (containing a duplicate linked R4 gate) displaying lymphocytes gated from R5 on plot 1.

SINGLE-PLATFORM ABSOLUTE $CD34^+$ CELL COUNTING

While the original ISHAGE protocol was a dual-platform method requiring percent $CD34^+$ cells measured by flow cytometry and the absolute white blood cell count (from a hematology analyzer) to derive the absolute $CD34^+$ cell content of a sample, the use of dual-platform methods is prone to error, particularly if the sample is not in fresh condition, since platelet aggregates, dead cells, and other debris can compromise the accuracy of the absolute leukocyte count and the accuracy of the flow analysis. Furthermore, the variable presence of nucleated red blood cells in cord blood and other samples leads to an overestimate of the absolute $CD34^+$ cell count. By incorporating a known number of fluorescent counting beads in the flow cytometric analysis, an absolute $CD34^+$ cell count can be generated directly on a flow cytometer, thus eliminating the need for a nucleated cell count from a hematology analyzer (46). Assessment of the ratio between the number of beads and $CD34^+$ cells counted allows the direct calculation of the absolute $CD34^+$ cell count. This approach is used by Beckman-Coulter (Miami, FL) in their Stem-Kit assay, by Dako in their CD34 Count Kit, and by Becton Dickinson Biosciences (BD, San Jose, CA) in their single-platform variant of the ISHAGE protocol (SCE Kit) using TruCOUNT tubes (47). Regardless of which of these single-platform assays is used, accurate pipetting of samples (for sample dilution or aliquoting purposes) is required. For the single-platform ISHAGE protocol with Stem-Kit or CD34 Count Kit assays, careful resuspension and accurate pipetting of the beads are also critically important.

ISHAGE SINGLE PLATFORM INCLUDING VIABILITY ASSESSMENT

In the example shown in Fig. 1, from list-mode data acquired on a BD FACSCalibur cytometer, the basic ISHAGE method was modified to include a known number of Flowcount fluorospheres (Beckman-Coulter), and ammonium chloride lyse–no-wash sample processing was adopted. These modifications combine the accuracy and sensitivity provided by the sequential gating strategy of the original ISHAGE protocol with the capability to generate an absolute $CD34^+$ cell count directly from a flow cytometer (46). The number of $CD34^+$ cells are identified as above using gating regions R1 to R4 (gate 4 in gate statistics) and compared with the total number of singlet beads counted (concentration supplied by manufacturer) in the same list-mode file. In the example shown, total beads are gated in R6 of plot 5 and displayed on plot 7 (time versus forward scatter). Using Boolean gating logic (see Table 1 for details of logical gating setup on BD and Beckman cytometers), singlet beads are then gated in R7 (G7 in gate statistics). The calculation for generating an absolute $CD34^+$ cell count per microliter is: (number of $CD34^+$ cells $\times$ bead concentration $\times$ *DF*)/number of singlet beads, where the number of $CD34^+$ cells is determined from gate 4 (R1 through R4), the bead concentration is specified per lot, *DF* is the sample dilution factor, and the singlet bead count is determined from gate 7 (R6+R7).

The addition of the viability dye 7-amino-actinomycin D (7-AAD) to the single-platform ISHAGE method permits the determination of the absolute numbers of viable and nonviable $CD34^+$ cells from a sample (46). The ability to perform such sophisticated analysis has clinical utility in the accurate measurement of viable $CD34^+$ cells in packs that may have been manipulated (e.g., purged), potentially damaged by shipping to another site for analysis, or otherwise inappropriately stored prior to analysis. An example of how the 7-AAD is incorporated into the ISHAGE single-platform method is shown in Fig. 1, plot 8. Viable cells ($7\text{-}AAD^+$) are gated in R8 and only viable cells from R8 are displayed in plots 2, 3, 4, and 6. An absolute viable $CD34^+$ cell count of 157/μl is obtained.

When the $7\text{-}AAD^+$ (dead cells) are not excluded (by opening gate R8) as shown in Fig. 2, and the gating region R4 on plot 5 is adjusted to include all lymphocytes (live plus dead) from R5, a total absolute $CD34^+$ cell count of 286/μl is obtained.

Figures 1 and 2 were prepared using Cellquest Pro software (BD), and an expression editor is established to derive the absolute viable $CD34^+$ cell count from the above parameters. Other expression editors are designed to derive the other automatically calculated values shown in Fig. 1 and 2. Of these, the absolute viable $CD45^+$ cell count is very important as this value can be compared with the white blood cell count obtained from a hematology analyzer to confirm the accuracy of the single-platform flow methodology. As detailed above and elsewhere (39, 40, 46), for absolute counting of $CD34^+$ cells using bead-based methods, accurate pipetting of sample and beads (where appropriate)

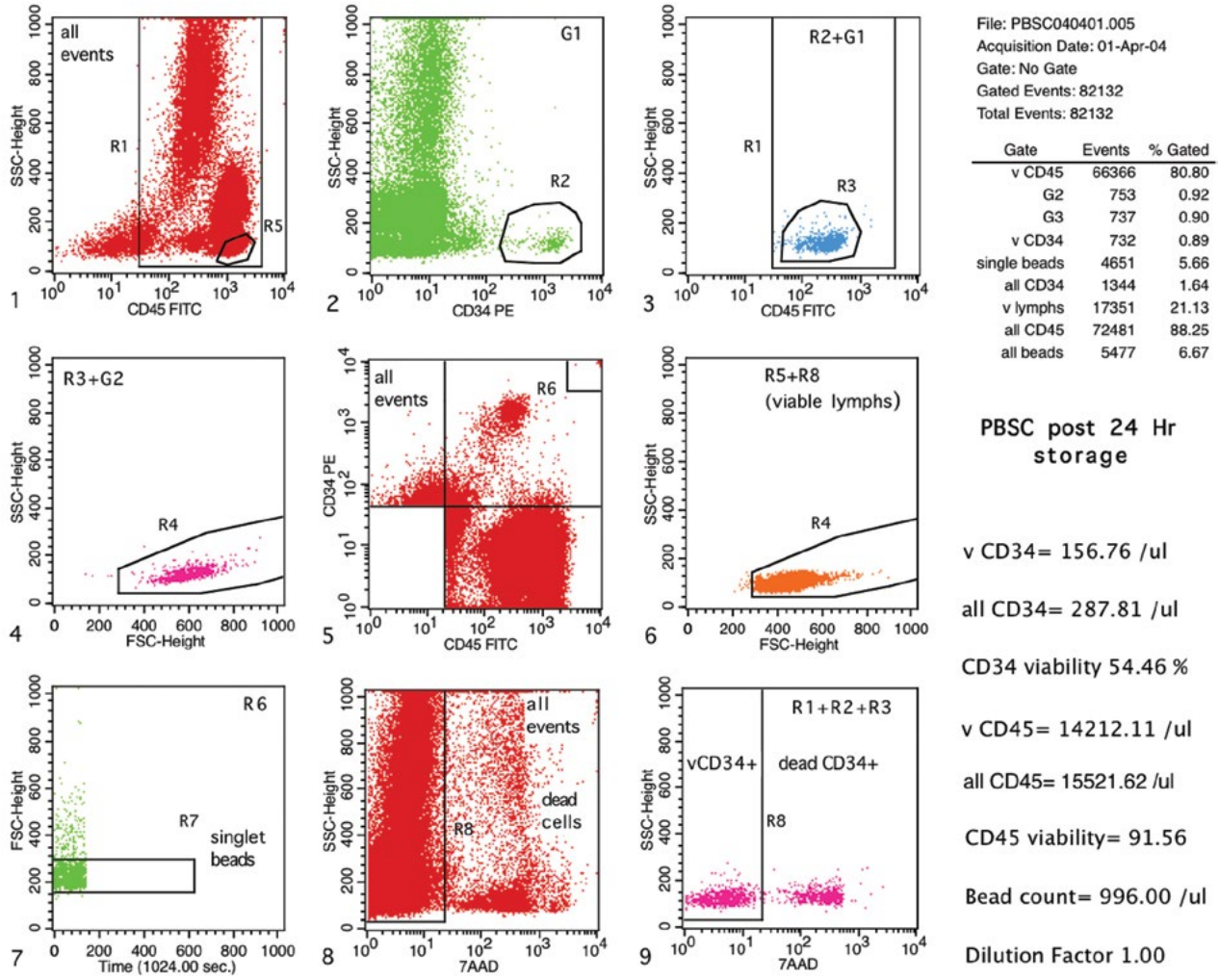

FIGURE 1 Enumeration of viable CD34$^+$ cells with the single-platform ISHAGE protocol (Stem-Kit) on a FACSCalibur cytometer equipped with CellQuest Pro, using 100 μl of a 24-hour-old PBSC sample diluted 1/10 with phosphate-buffered saline–1% bovine serum albumin and stained with CD34-FITC, CD45-PE, and 7-AAD (Stem-Kit) according to the manufacturer's instructions. After 25 min, the sample was lysed with 2 ml fresh NH_4Cl. After 10 min at room temperature, 100 μl of Flow-count beads was added and the sample was immediately analyzed on the FACSCalibur cytometer running Cellquest Pro 5.2, as described previously (44, 45, 50). Viable cells (7-AAD-) were gated in R8 of plots 8 and 9; only viable cells were analyzed by Boolean gating, as depicted in plots 2, 3, 4, and 6. The extra viability plot (plot 8) showing total CD34$^+$ cells (viable and nonviable) can be useful in samples containing large numbers of dead cells. This plot also confirms appropriate compensation between FL2 and FL3 PMTs, with the viable CD34$^+$ cells clearly visible and properly on-scale and dead cells excluded by R8. Viable lymphocytes (plot 6) are gated through R8 and R5 to set the lymph-blast region R4. As shown in the lower left quadrant of plot 5, the gate is set as a 'live' or 'not' gate prior to acquisition such that debris in this area resulting from the lyse–no-wash sample processing is excluded from the acquired list-mode file. Total beads are gated in R6 of plot 5 and singlet beads are identified in R7 of plot 7 (FSC versus time). A forward-scatter threshold or discriminator is set below the light scatter of the singlet beads so as to not exclude any beads from the data file (see plot 7). A total of 732 viable CD34$^+$ cells were counted in gate 4 (R8 and R1 through R4); 4,651 single beads were counted in gate 5 (R6 and R7), and the assayed bead concentration was 996/μl. Using expression editors, the sample contained 157 viable CD34$^+$ cells/μl and 14,212 viable CD45$^+$ cells/μl. CD34$^+$ cell viability was 54.46%.

is critically important to the reliability of the assay. In our standardized assay, 100 μl of sample and 100 μl of counting beads are used (44, 45).

The absolute viable CD34$^+$ value is multiplied by the apheresis pack volume (in liters) to convert this value to an absolute CD34$^+$ cell number $\times 10^6$ per apheresis pack. Note, plot 9 shows total CD34$^+$ cells (viable and nonviable) from gating regions R1+R2+R3 only and shows viable cells on-scale in about the first decade of fluorescence. This plot is useful when samples with poor viability are to be analyzed as it is easier to set R8 on plot 9 versus plot 8. Additionally, it shows that the fluorescence compensation between

TABLE 1 Logical gate setup for BD and Beckman instruments

Logical gate setup for Stem-Kit on BD FACSCalibur (Fig. 1 and 2):
Gate 1: (vCD45): R1 and R8
Gate 2: R2 and "vCD45"
Gate 3: R3 and G2
Gate 4: (vCD34): R4 and G3
Gate 5 (singlet beads): R6 and R7
Gate 6: (all CD34): R1 and R2 and R3
Gate 7: (v lymphs): R5 and R8
Gate 8: (all CD45): R1 and not R6
Gate 9: (all beads): R6
Logical gate setup for Stem-Kit on Beckman Coulter FC500 and Stem-CXP auto-software (Fig. 3):
Gate 1: (viable and $CD45^+$)
Gate 2: (viable and $CD45^+$ and $CD34^+$)
Gate 3: (viable and $CD45^+$ and $CD34^+$ and CD45 dim)
Gate 4: (viable and $CD45^+$ and $CD34^+$ and CD45 dim and $CD34^+$ HPC)
Gate 5: Beads
Gate 6: Viable and lymphs
Gate 7: Beads
Gate 8: Ungated
Gate 9: (all CD34): R1 and R2 and R3. *Manual acquisition/analysis only.
Logical gate setup for SCE Kit on BD FACSCanto II (Fig. 4):
Gate 1: (vCD45): not R7 and R1 and R8
Gate 2: R2 and "vCD45"
Gate 3: R3 and G2
Gate 4: (vCD34): R4 and G3
Gate 5: R6 (beads)
Gate 6: (all CD34): R1 and R2 and R3 and not R7
Gate 7: (v lymphs): R5 and R8
Gate 8: (all CD45): R1 and not R6 and not R7
Gate 9: R7 (debris)
Gate 10: R9 (alternate beads)
Logical gate setup for SCE Kit plus CD3 on BD FACSCalibur (Fig. 6):
Gates 1–6 and 8–10 as per Fig. 1
Gate 7: "vCD45" and R10

photomultiplier tube (PMT) 2 (CD34-PE) and PMT 3 (7-AAD) is optimally set with the viable $CD34^+$ cells properly on-scale in the first decade or so.

The essential components and fine technical details of the single-platform ISHAGE with viability protocol (46) are embodied in the "Basic Protocol" constructed for *Current Protocols in Cytometry* (CPC) (40) and its updated version (41). They are also embodied in the recommendations from the European Working Group on Clinical Cell Analysis (48), the Clinical Laboratory Standards Institute document H42-A2 (49), and the American Association of Blood Bankers (50), as well as in several national guidelines.

Like earlier versions of the ISHAGE protocols, the single-platform derivatives have been developed to work on both Beckman-Coulter and BD flow cytometers. However, there are minor technical differences in the way the assay is set up on the different instruments (detailed in references 39, 40, and 46). Briefly, there are two main differences. On BD instruments, the singlet counting beads are visualized using forward angle light scatter versus time (see plot 7 of Fig. 1 and 2). Since the beads are detected as smaller events than lymphocytes on BD instruments, the forward scatter threshold has to be lowered so as not to exclude the beads. As shown in plot 7 of Fig. 1 and 2, the lower limit of the singlet beads cluster appears around channel 160, whereas the viable lymphocytes shown in plot 5 are found above channel 280. On the Beckman-Coulter instruments, the beads appear above channel 800, so there is no need to adjust the forward angle light scatter discriminator from its normal setting, just below the smallest lymphocytes (50). However, it is our recent experience that certain stabilized samples, which are routinely distributed for quality assurance (QA) or proficiency testing purposes, exhibit reduced forward scatter properties. For the analysis of such samples, it is advisable to increase the forward scatter gain of the Coulter instruments to ensure that all $CD45^+$ leukocytes are included in the list-mode file. Although the counting beads can be detected on the Coulter instruments using the same parameters of forward scatter versus time, the presence of an extra FL-3 PMT (optimized to detect phycoerythrin-Texas red conjugates) allows the counting beads to be detected on an FL3 versus time plot (see Fig. 3, plot 7). By setting the singlet bead gating region as a CAL region and inputting the bead lot count, the software running the FC500 automatically calculates and prints the absolute viable $CD34^+$ and $CD45^+$ (LEUKS) cell counts. The 7-AAD is detected in the FL4 channel (Fig. 3, plot 8) (50).

COMMERCIAL KITS FOR $CD34^+$ CELL ENUMERATION BASED ON ISHAGE GUIDELINES

1. The Stem-Kit from Beckman-Coulter was the first commercial kit to utilize ISHAGE gating criteria to identify $CD34^+$ cells. The kit contains CD45-FITC/CD-34PE, 7-AAD, and Flow-count fluorospheres and is used as described above in Fig. 1–3. The kit also contains a CD45-FITC/CD34 isoclonic control

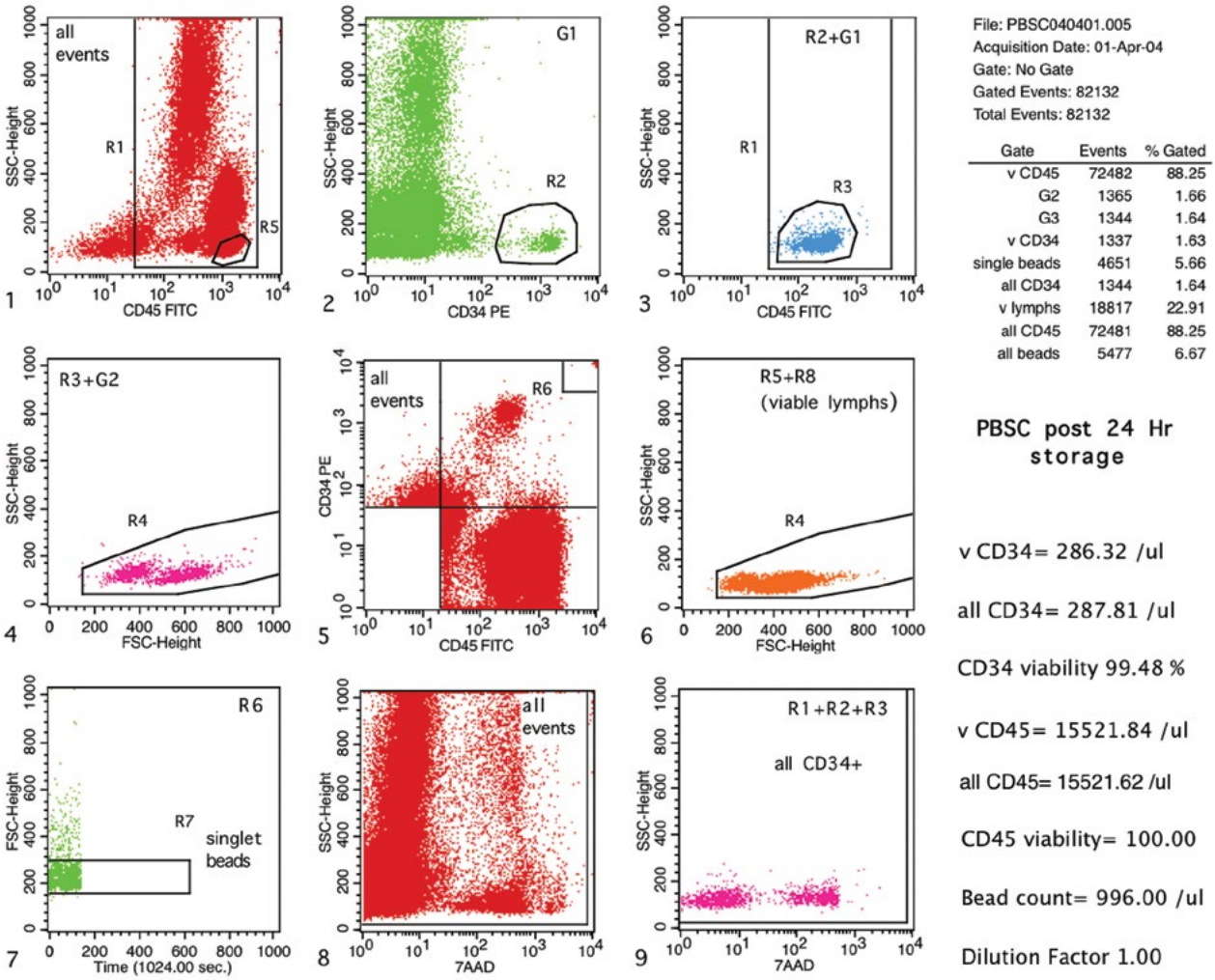

FIGURE 2 Importance of viability dye (7-AAD) inclusion in the analysis of non-fresh samples. Analysis of the same sample as in Fig. 1, except that viability discrimination with 7-AAD was NOT applied. When gating region R8 is expanded to include both viable and nonviable cells (plots 8 and 9) and region R4 is moved to include both live and dead lymphocytes (plot 6), both dead and live $CD34^+$ cells now cluster within the duplicate lymph-blast region R4 on plot 4. Both the absolute CD34 and CD45 counts are significantly increased versus the values obtained in Fig. 1. Note the extra population of both $CD34^+$ cells (plot 4) and lymphocytes (plot 6) with reduced forward-angle light scatter; these are the dead $CD34^+$ and dead lymphocytes, respectively. Sample contains 286 total (viable + nonviable) $CD34^+$ cells/μl.

to enumerate nonspecifically stained events. In this control, unconjugated CD34 antibody is present in large excess to block specific staining of PE-labeled CD34 present at the same concentration as the test. However, given the selectivity of the sequential gating strategy utilized in this protocol, we have not found that the isoclonic control makes a significant contribution to the accuracy and reliability of the assay (46) and, therefore, we consider this and other alternative negative antibody controls to be redundant (reviewed in references 34 and 35). Beckman-Coulter has developed a software package that automates instrument setup and compensation as well as automated data acquisition and analysis of samples prepared with the Stem-Kit. This software has been developed specifically for use on the Coulter Epics XL (Stem One) and, more recently, FC500 instruments (Stem CXP). Figure 3 shows an example of a sample analyzed with Stem CXP for viable $CD34^+$ cells in a fresh apheresis product. Almost identical values were obtained by manual gating (not shown). For samples in less pristine condition or that contain platelet aggregates, or for bone marrow samples or post-thawed samples, extreme care must be taken when using the Stem One and Stem CXP software, and manual analysis of the data file acquired with the autosoftware is often required. It is possible to use the Stem-Kit on Beckman-Coulter instruments using only manual software for both acquisition and analysis, and this is often preferred, especially for labs that regularly receive samples in less than pristine condition.

2. Dako (Denmark) has also produced the CD34 Count Kit, which contains CD45-FITC/CD34-PE, 7-AAD, an ammonium chloride-based lysing agent, and

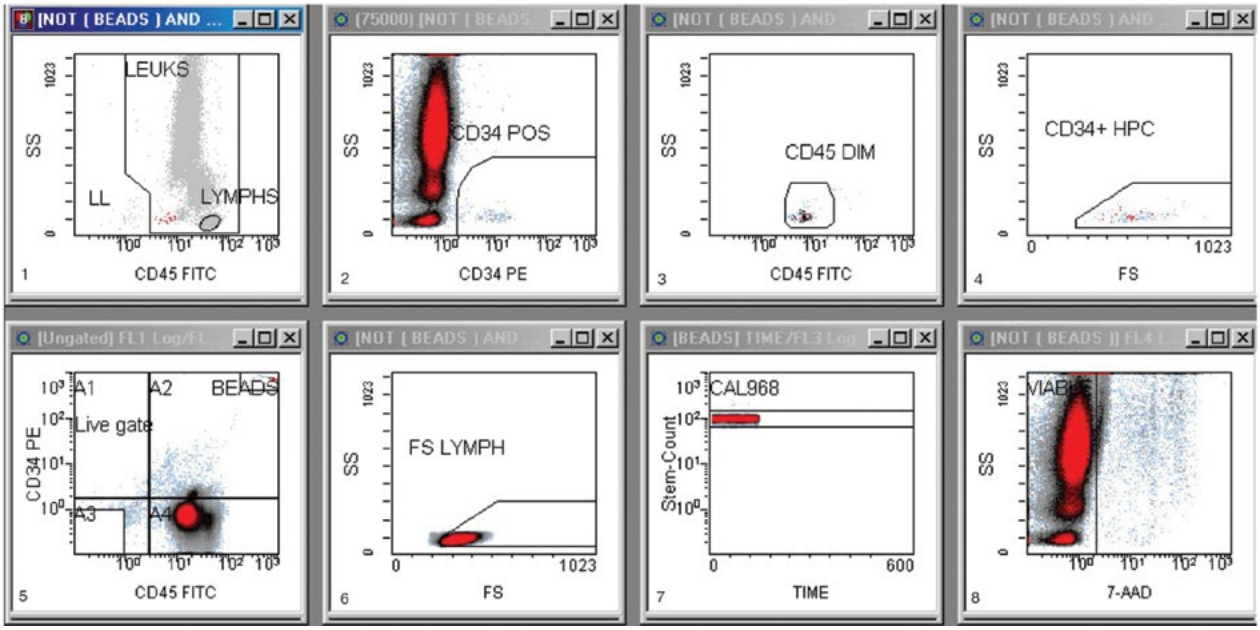

FIGURE 3 Enumeration of viable CD34+ cells with Stem-Kit and Automated STEM-CXP software analysis on a Beckman-Coulter FC500. Fresh apheresis sample diluted 1/10 with phosphate-buffered saline–1% bovine serum albumin. Plot 1: all CD45+ leukocytes, gated on 7-AAD negative (viable) events from histogram 8. Plots 2–4 are sequentially Boolean gated from plot 1. Plot 6 is gated on viable lymphocytes from plot 1 to allow the discriminator or threshold to be set on forward scatter. Total beads are gated as shown in plot 5 and Boolean gated on FL3 (stem count) versus time (plot 7) to enumerate singlets. A live gate in the bottom left corner of plot 5 is used to exclude debris from the list-mode file, as described for Fig. 1. The leukocyte count (CD45+, from plot 1) was 23.3 × 10^9/liter, and the absolute viable CD34 count was 23/μl (from plot 4). The overall CD45+ viability was 95.1% (from plot 8).

pipettable fluorescent counting beads for use alongside an ISHAGE gating protocol. The beads in this kit are too small to be used with a forward scatter threshold and the data are acquired using a threshold set on the FL-1 (CD45-FITC) channel. Additionally, like Flow-count beads, a Boolean gate is needed to gate the singlet beads.

3. As described by Brocklebank et al. (51), it is also possible to perform the ISHAGE protocol using TruCOUNT absolute counting tubes (BD) instead of a pipettable bead suspension such as used in the Stem-Kit and CD34 Count Kit. An advantage of this approach is that it eliminates the requirement to carefully suspend and accurately pipette the counting beads, as the TruCOUNT tubes contain a known number of freeze-dried beads. Becton Dickinson Biosciences has now developed the BD Stem Cell Enumeration Kit (SCE Kit) to closely follow ISHAGE gating criteria (47). Again, due to the small size of the beads, a threshold cannot be set on forward scatter, necessitating its setting on a fluorescence parameter (FL-1/CD45 FITC). However, accurate pipetting is still required if any predilution of the sample is required, as well as for the delivery of the sample into the TruCOUNT tube. Note that for TruCOUNT tubes, all beads (singlets and doublets) have to be counted (Fig. 4, plot 5, R6, or alternatively on plot 9, R9), so an extra Boolean gate is not required, in contrast to the singlet bead counts required for Stem-Kit and CD34 Count Kits. An example of the single-platform ISHAGE protocol performed on TruCOUNT tubes is shown in Fig. 4 (data acquired on Canto II instrument, then exported in FCS2 format for analysis in Cellquest Pro). Another modification that is required when using such small counting beads (TruCOUNT and CD34 Count) involves the setting of an exclusion or debris gate (R7 on plot 6). The reason for this is that very small debris and particles produced during the lyse–no-wash processing of the sample stain with the CD45-FITC reagent (plot 1), and these events can significantly increase the absolute CD45+ cell count in samples prepared this way. The debris-exclusion gate can be set as a 'not' gate or as a 'live' gate prior to data acquisition or later during analysis. In the example shown in Fig. 4 from a fresh PBSC sample, the debris-exclusion gate was applied after acquisition. However, if the gate is set prior to acquisition (which can significantly reduce the size of the list-mode file), care must be taken to ensure that no lymphocytes are excluded. In practice, the R7 gate can be set prior to acquisition in the 200 × 200 FSC/SSC setting and then optimized during analysis if required. Note, as per manual Stem-Kit analysis, plot 8 displays total CD34+ cells (viable and nonviable) from gating regions R1+R2+R3 and not R7 and shows viable cells on-scale in about the first decade of fluorescence. This plot is useful when samples with poor viability are to be analyzed, as it is easier to set R8 on this plot versus plot 7. Additionally, it shows that the fluorescence compensation between PMT 2 (CD34-PE) and PMT-3 (7-AAD) is optimally set. The absolute

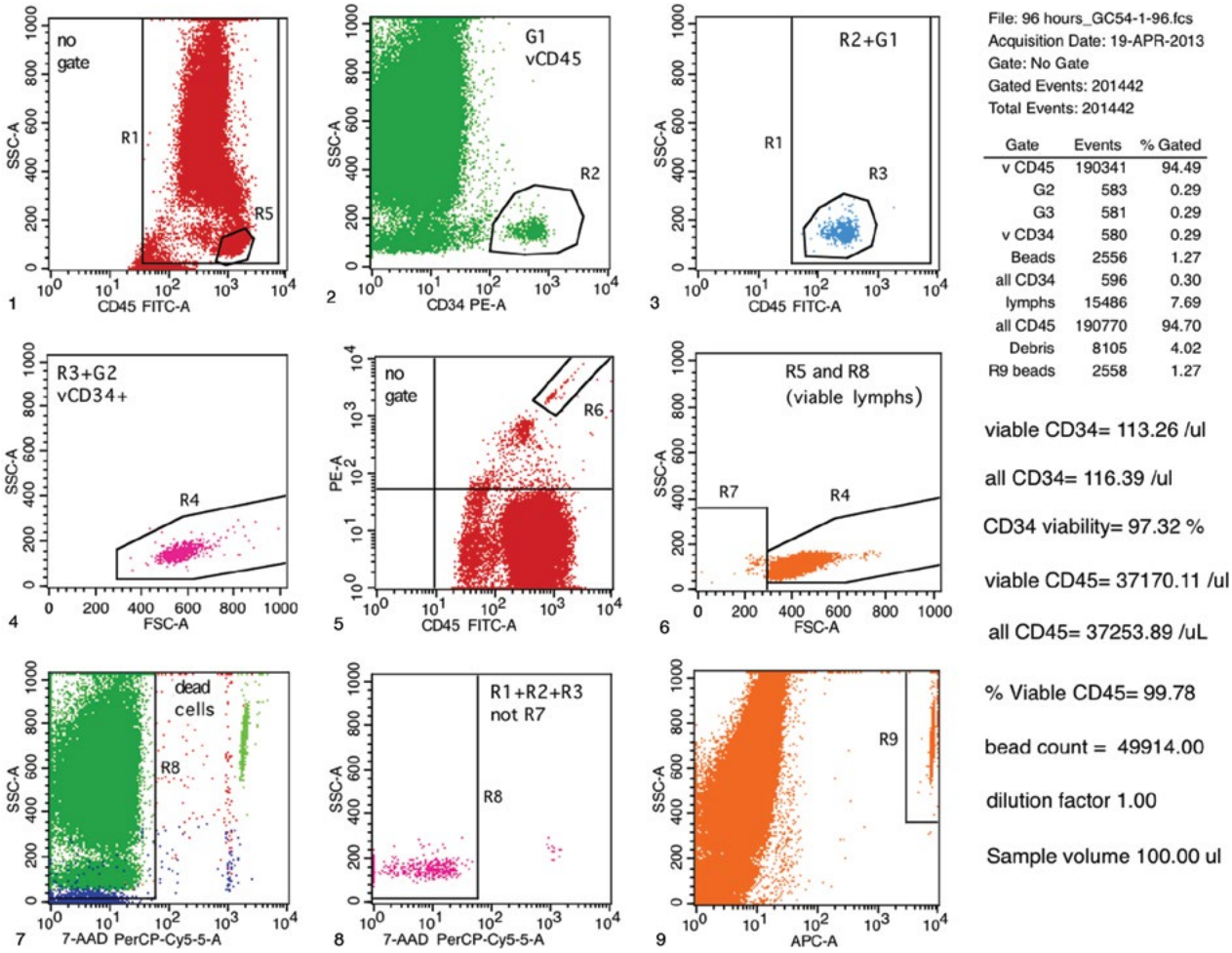

FIGURE 4 Absolute viable CD34$^+$ cell counting with the ISHAGE single-platform protocol using TruCOUNT tubes and BD FACSCanto II. We used 100 μl of a fresh PB sample stained with CD45-FITC, CD34-PE, and 7-AAD in a TruCOUNT tube (SCE Kit). A threshold was established on FL-1 (CD45-FITC, plot 1) because the size of the TruCOUNT beads precludes the use of an FSC threshold. A debris-exclusion gate (R7) is also necessary to remove fluorescent debris from the list-mode file (debris visualized in lower left of R1). This allows an accurate determination of absolute CD45$^+$ cells to be made. The total number of beads in the list-mode file is obtained from R6 of plot 5 (gate G5 = R6). An alternative means of enumerating the beads is shown in plot 9. This plot can be useful if aggregates of CD34$^+$ cells are present or if other debris contaminates R6 such that the beads cannot be accurately delineated, as can be the case in some CD34$^+$-selected samples or in samples containing large amounts of platelet aggregates. Other aspects of the analysis were performed as for Fig. 1. Canto II FCS3 data were exported as FCS2 files and analysis was performed using Cellquest Pro 6. Gate statistics were obtained from plot 1 (all events). The sample contained 113 viable CD34$^+$ cells/μl and 37,170 viable CD45$^+$ cells/μl.

viable CD34$^+$ cell numbers are automatically calculated using the expression editors in Cellquest Pro software according to the formula:

$$\text{absolute viable CD34}^+ = \frac{\text{vCD34} \times \text{bead lot count} \times DF}{\text{beads} \times \text{sample volume (μl)}}$$

One extra plot (plot 9) is shown in Fig. 4 to depict an alternative means of gating the beads collected during data acquisition. This allows the beads to separate better from debris, platelet aggregates, etc., which can occasionally contaminate the primary bead-gating region R6. We have found that for the analysis of purified CD34$^+$ cell fractions, where aggregates of CD34$^+$ cells can be present, separating beads from aggregates with R6 can be very difficult and R9 gating provides a more accurate way to delineate the beads (Sutherland, unpublished observations).

BENEFITS OF SINGLE-PLATFORM CD34$^+$ CELL ENUMERATION

By including an internal reference bead in the analysis, CD45 positivity is no longer used as a denominator in the calculation of absolute CD34$^+$ cells. The characteristic CD45 expression of CD34$^+$ cells is used solely as part of

the sequential gating strategy to accurately identify *bona fide* $CD34^+$ cells. It must be stressed that focused training is highly recommended for laboratory staff adopting single-platform flow methodologies. Notwithstanding the critical requirement for accurate pipetting in single-platform assays, addition of counting beads has the advantage of eliminating the potential introduction of errors in calculating the absolute $CD34^+$ cell count inherent in two-platform methodologies (40, 41). The flow cytometrist need not be concerned about the presence of nucleated red blood cells, platelet aggregates, and dead cells, which can be counted as leukocytes by some automated hematology analyzers. While the presence of significant numbers of nucleated red cells (which play no role in engraftment) in apheresis samples is quite rare, they are often abundant in CB collections and bone marrow aspirates, and single-platform analysis can significantly increase the accuracy of the absolute $CD34^+$ cell number in such cases.

NEGATIVE ANTIBODY CONTROLS

Many of the early methods of $CD34^+$ enumeration relied on the use of isotype controls to delineate specific from nonspecific staining (9, 25, 30, 31). However, for rare-event analysis such as $CD34^+$ cell enumeration, the use of isotype controls is not only redundant but can also lead to misleading results (32). Given the sequential gating strategy at the heart of the ISHAGE method, the use of isotype or isoclonic control antibodies to assess nonspecific binding of the specific antibody or to set the positive analysis region for $CD34^+$ cells would be inappropriate (32, 34, 35, 40, 41, 46). This approach has also been adopted by the European Working Group on Clinical Cell Analysis (48) and the Clinical and Laboratory Standards Institute (49).

LYSING AGENTS

While methods for sample preparation for flow cytometric enumeration of $CD34^+$ cells include both lyse–no-wash or lyse-and-wash steps, single-platform protocols can only be processed by lyse–no-wash methods. It is important to note that for some apheresis samples and post-thawed samples, red cell lysis is neither necessary (for fresh PBSC) nor recommended (for post-thawed samples), due to either the low concentration of red blood cells present (apheresis) or the lysis of the red cells inherent in the thawing procedure. As the measurement of viability is important in several sample types, lysing with simple ammonium chloride-based agents is necessary. However, samples lysed in ammonium chloride must be rapidly cooled on melting ice immediately after lysis (usually for 10 minutes). This will reduce apoptosis induced by prolonged exposure to ammonium chloride-based lysing agents. In any event, lysed samples must be acquired no later than 60 minutes post-lysis (40, 41, 46, 49, 50, 52).

QUALITY ASSURANCE OF $CD34^+$ CELL ENUMERATION

Quality control and quality assurance procedures are a necessary part of $CD34^+$ cell enumeration. Basic instrument setup and compensation are important, particularly as related to the use of 7-AAD as a viability dye. Clear attention must be paid to the CD34-PE and 7-AAD spectral overlap as under-compensation of this can lead to viable $CD34^+$ cells being classified as nonviable. Overcompensation, on the other hand, can lead to dead cells being included in the live-cell (7-AAD) region. Several manufacturers nowadays produce stabilized (fixed) whole blood control cells, which can be used as daily process controls. Their staining pattern with respect to CD34 and CD45 reagents can be used as an extra internal control to ensure that the FL1 and FL2 parameters of the cytometer are adequately set. However, as the cells in such preparations are fixed (i.e., dead), all cells take up the viability dye 7-AAD. In addition, the light-scatter properties of $CD34^+$ cells in stabilized controls are slightly different from those of fresh blood, and the degree to which this occurs varies between instrument manufacturers. Thus, it is important to take these issues into account as they have important implications for appropriate instrument setup for the analysis of stabilized samples. In general, it is important to ensure that the FSC gain and FSC threshold (if used) are appropriately set specifically for acquisition and analysis of such samples. Furthermore, if 7-AAD is used, the viability gating region R8 (BD instruments) must be opened fully so as not to exclude any cells. An example of the analysis of a stabilized whole-blood preparation with the SCE Kit on the FACSCanto II instrument is shown in Fig. 5.

Note that it is not recommended that acquisition of stabilized samples be performed using the automated version of Stem-CXP software on the Beckman-Coulter FC500 platform, as the viability gate is locked in an inappropriate position for the analysis of such samples.

Flow cytometric analysis of $CD34^+$ cells offers a potential means to quality assure all aspects of stem cell processing from mobilization to reinfusion. By analyzing list mode data by a variety of different gating strategies, Chang and Ma (53) demonstrated that gating strategies were a major contributing factor to result variability. For an individual sample, the use of different gating strategies could produce as much as a 2-fold variation in results. In their study, the gating strategy used in the ISHAGE protocol was the only method that gave reproducible results from all centers of within ±10% of the median $CD34^+$ cell value on both peripheral blood and PBSC collections. In a study undertaken by the European Working Group on Clinical Cell Analysis using the single-platform ISHAGE protocol, CVs of $<10\%$ were obtained by the majority of participating labs on a long-term stabilized blood sample with a target $CD34^+$ value of 170/μl (54). In a more recent study involving 36 participants from the Benelux countries, similar CVs were obtained. In contrast, the lowest between-laboratory CVs using dual-platform techniques were 16% (Benelux) and 21% (UK National External Quality Assessment Service) (55). Thus, the experience with $CD34^+$ cell counting confirms that the use of a common standardized protocol and targeted training, where needed, is able to significantly increase reproducibility and reduce variation between laboratories.

Data from the UK National External Quality Assessment Service for Leukocyte Immunophenotyping show that approximately 70% of users of this program are now claiming to use the ISHAGE gating strategy. Interestingly, a more in-depth survey found that up to 40% of the ISHAGE users were not deploying the method correctly. Further analysis between those groups that were correctly versus incorrectly applying the ISHAGE guidelines showed the latter group were 32% more likely to be flagged on a QA survey (56). As of 2010, 63% of those participating in the College of American Pathologists' CD34 external quality assurance program reported use of the ISHAGE gating strategy. In this North American program, interlaboratory CVs are routinely in the 10 to 15% range.

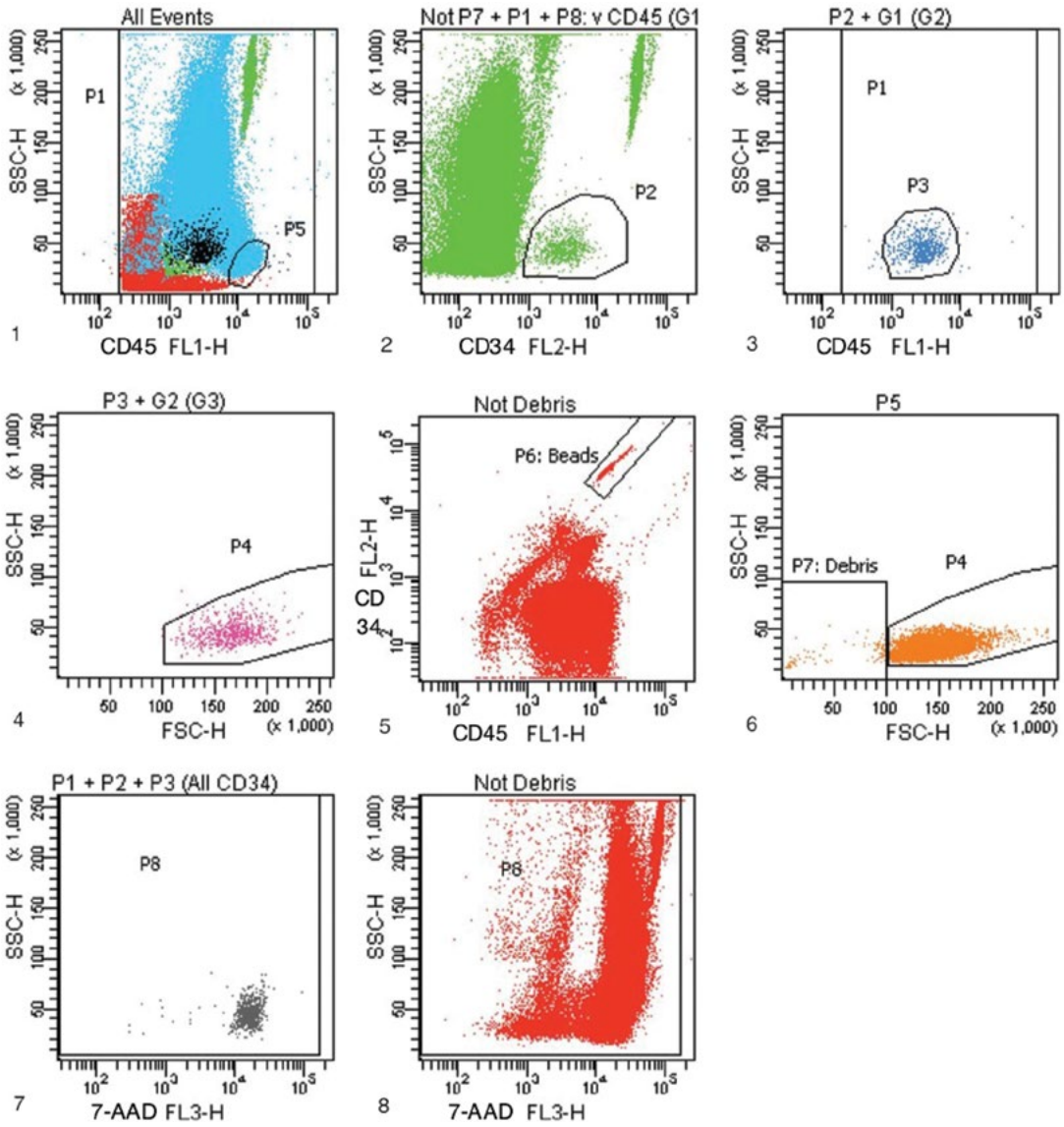

FIGURE 5 Absolute $CD34^+$ cell counting in stabilized PB sample with the ISHAGE single-platform protocol using TruCOUNT tubes and BD FACSCanto II. We used 100 μl of a stabilized whole-PB sample stained with CD45-FITC, CD34-PE, and 7-AAD in a TruCOUNT tube (SCE Kit). A threshold was established on FL-1 (CD45-FITC, plot 1) as was a debris-exclusion gate (R7) as described in Fig. 4. For analysis of stabilized (i.e., dead) samples, the viability gate P8 (plots 7 and 8) is fully opened so as to not exclude any cells (viable or nonviable) from analysis. The rest of the ISHAGE gating strategy is applied as shown in Fig. 4.

SIMULTANEOUS ENUMERATION OF $CD34^+$ AND $CD3^+$ CELLS IN THE ALLOGENEIC TRANSPLANT SETTING USING A MODIFIED SINGLE-PLATFORM ISHAGE PROTOCOL

An ability to accurately enumerate $CD3^+$ T cells at very low levels as well as $CD34^+$ and $CD45^+$ cells can be particularly useful in the allogeneic transplant setting, where reducing the number of $CD3^+$ cells in the graft has been shown to result in decreased severity of graft-versus-host disease. Phycoerythrin-cyanine 5 (PE-Cy5) or PerCP-conjugated CD3 antibody is added (in place of 7-AAD) as a third antibody conjugate. The CD3 conjugate is detected in the FL4 channel of a Beckman-Coulter XL or FC500 instrument and in the FL3 channel of the BD FACSCalibur cytometers. The modified assay can also be performed in the presence of counting beads, allowing the generation of absolute $CD3^+$ and $CD34^+$ cell counts from a single assay tube (44, 45). However, it may be important to retain the use of the viability dye in the assay, for example in situations where post-thawed cord blood units are to be used or if PBSC samples need to be shipped over large distances prior to infusion in the recipient, as is often the case. In this setting, the regular three-color with viability, single-platform ISHAGE protocol can be modified by the addition of CD3–PE-Cy7 (Beckman-Coulter instruments) or CD3-APC (BD Biosciences instruments). In Fig. 6, CD3-APC was added to the standardized TruCOUNT-based ISHAGE method on a BD FACSCalibur instrument. Viable $CD34^+$ cells were

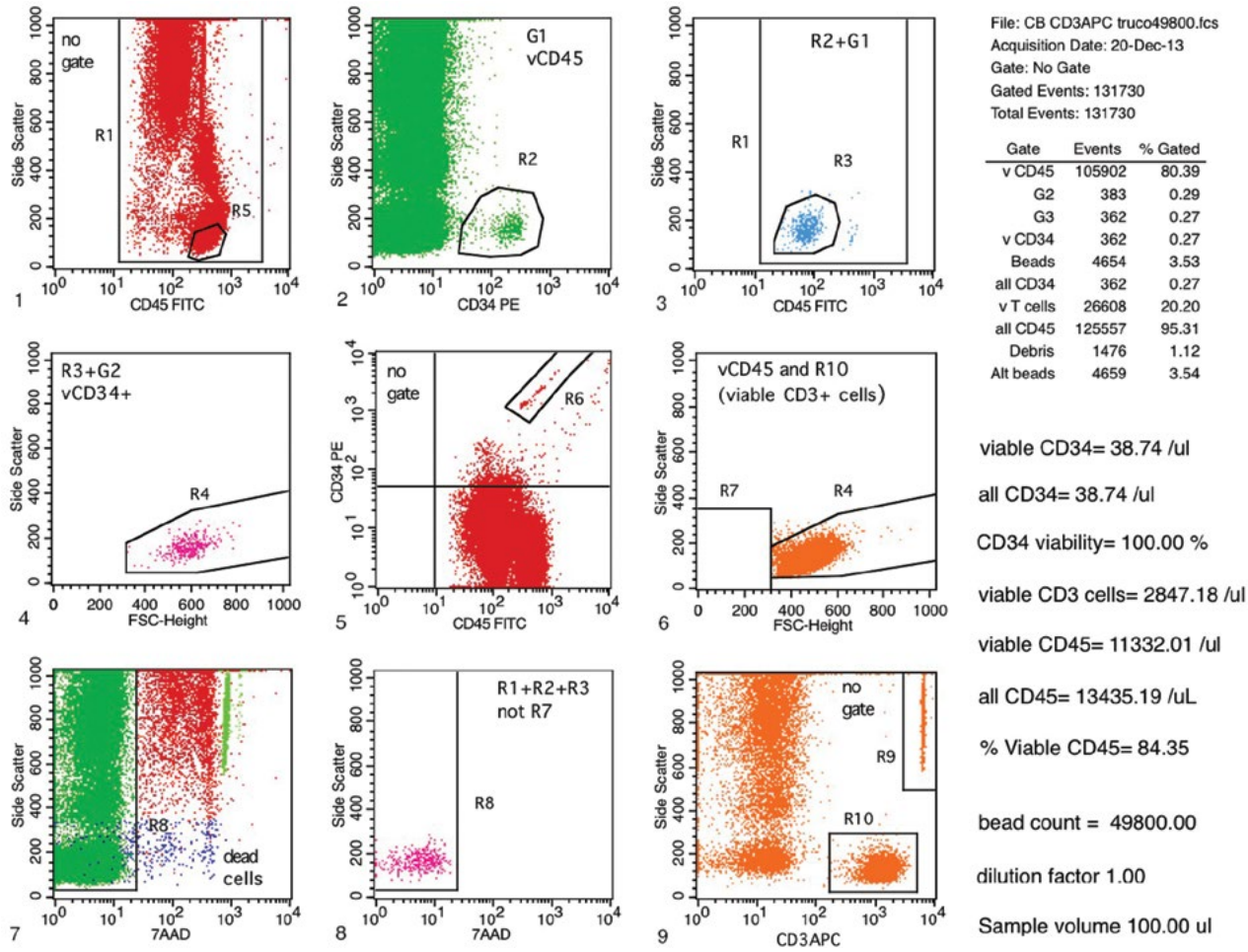

FIGURE 6 Simultaneous detection of absolute viable $CD34^+$ and $CD3^+$ cells using single-platform ISHAGE protocol in the allotransplant setting. PBSC sample for allotransplant stained with CD45-FITC, CD34-PE, 7-AAD, and CD3-APC. $CD34^+$ cells enumerated through Boolean gates R8 and R1 through R4 as in Fig. 4. $CD3^+$ cells enumerated through Boolean gates R10 (plot 9) and duplicate R4 (plot 6). TruCOUNT beads enumerated through gate R6 (plot 5) or alternatively with R9 (plot 9). Sample contained 39 viable $CD34^+$ cells/μl, 2,836 viable $CD3^+$ cells/μl, and 11,332 viable $CD45^+$ cells/μl.

enumerated exactly as described in Fig. 4 using gating regions R8 and R1 through R4 and not R7, while $CD3^+$ cells were enumerated from Boolean gates R10 (plot 9) and the duplicate region R4 (plot 6). The back-gated $CD3^+$ events are used to accurately set R4, rather than all lymphocytes from region R5 of plot 1 as shown in the three-color assay (Fig. 4). This template is also useful for enumerating residual $CD3^+$ cells and $CD34^+$ cells selected using $CD34^+$ cell immunomagnetic selection devices (57).

IMMUNOLOGICAL CHARACTERIZATION OF $CD34^+$ STEM CELLS

In vitro and *in vivo* models of hematopoiesis have shown that the cells responsible for sustained multilineage engraftment are contained in the most primitive subsets of $CD34^+$ cells. Such subsets of $CD34^+$ cells in bone marrow express very low levels of antigens associated with lineage commitment (lin–) (13) and are found in the CD34hi, $CD90^+$ (58, 59), $CD133^+$ (60), and CD38/CD71/HLA-DR^{dull}/negative fractions (61, 62). Several clinical trials using highly purified lin–$CD34^+CD90^+$ populations have shown rapid and sustained engraftment when as little as 8×10^5 selected lin–$CD34^+CD90^+$ cells/kg body weight were given to patients with breast cancer (63), non-Hodgkin's lymphoma (64), and multiple myeloma (65).

While this work showed that highly purified subsets of $CD34^+$ cells can be effective in certain circumstances, selection and high-speed sorting of $CD34^+$ subsets are expensive, technically demanding, and not suitable for routine deployment in the clinical setting. Since virtually all patients receiving the minimum dose of 2×10^6 to 2.5×10^6 $CD34^+$ cells/kg body weight engraft in a timely manner, it is unlikely that monitoring subsets in patients receiving at least the minimum target dose will provide any additional clinical information.

Furthermore, standardizing an assay to perform subset analysis is even more problematic since most antigens used to identify subsets of $CD34^+$ cells are not expressed on discrete, non-overlapping populations, but instead display a continuum of antigen density from negative to weakly positive. The approach we developed (detailed in references

40 and 41) makes use of the auto-fluorescence of the gated CD34$^+$ cells in an FMO approach (36) to define the lower FL intensity limit of the positive analysis region, following which the experimentally stained sample is to be analyzed (Fig. 7). Though this will not completely account for low-level nonspecific binding of the PE-conjugated antibody used to identify subsets of CD34$^+$ cells, it nevertheless greatly improves the ability to standardize the analysis of weakly stained subsets of CD34$^+$ cells (44, 45) on an individual instrument-specific basis.

In the example shown in Fig. 7, a fresh PBSC sample was stained with a combination of CD34-FITC and CD45–PE-Cy5. *Bona fide* CD34$^+$ cells were identified and gated as per ISHAGE protocol shown in Fig. 1 in R4 of plot 4 and displayed on a bivariate plot of CD34-FITC versus FL2 (Fig. 7, plot 1). Since no PE-conjugated antibody is present in this sample, the natural or auto-fluorescence in the PE (FL2) channel of the gated CD34$^+$ cells is used to establish the subset positive-gating region for the CD90 PE-stained sample shown in R5 of plot 2. The CD90$^+$ cells express the highest levels of CD34 and exhibit very uniform light-scatter characteristics (plot 3), in keeping with known characteristics of the most primitive CD34$^+$ cell subsets (58, 59).

All gating regions remain identical between the unstained (plot 1) and stained tubes (plot 2, CD90; plot 6, CD133; and plot 7, CD33). On a technical note, it is crucial to the reliability of the data generated that the flow cytometer be properly set up and compensated. As shown in plots 4 and 5, respectively, the fluorescence of lymphocytes from the unstained control (plot 3) and that of lymphocytes from the CD90 PE-stained sample (plot 4) are virtually identical with respect to their fluorescence in the FL2

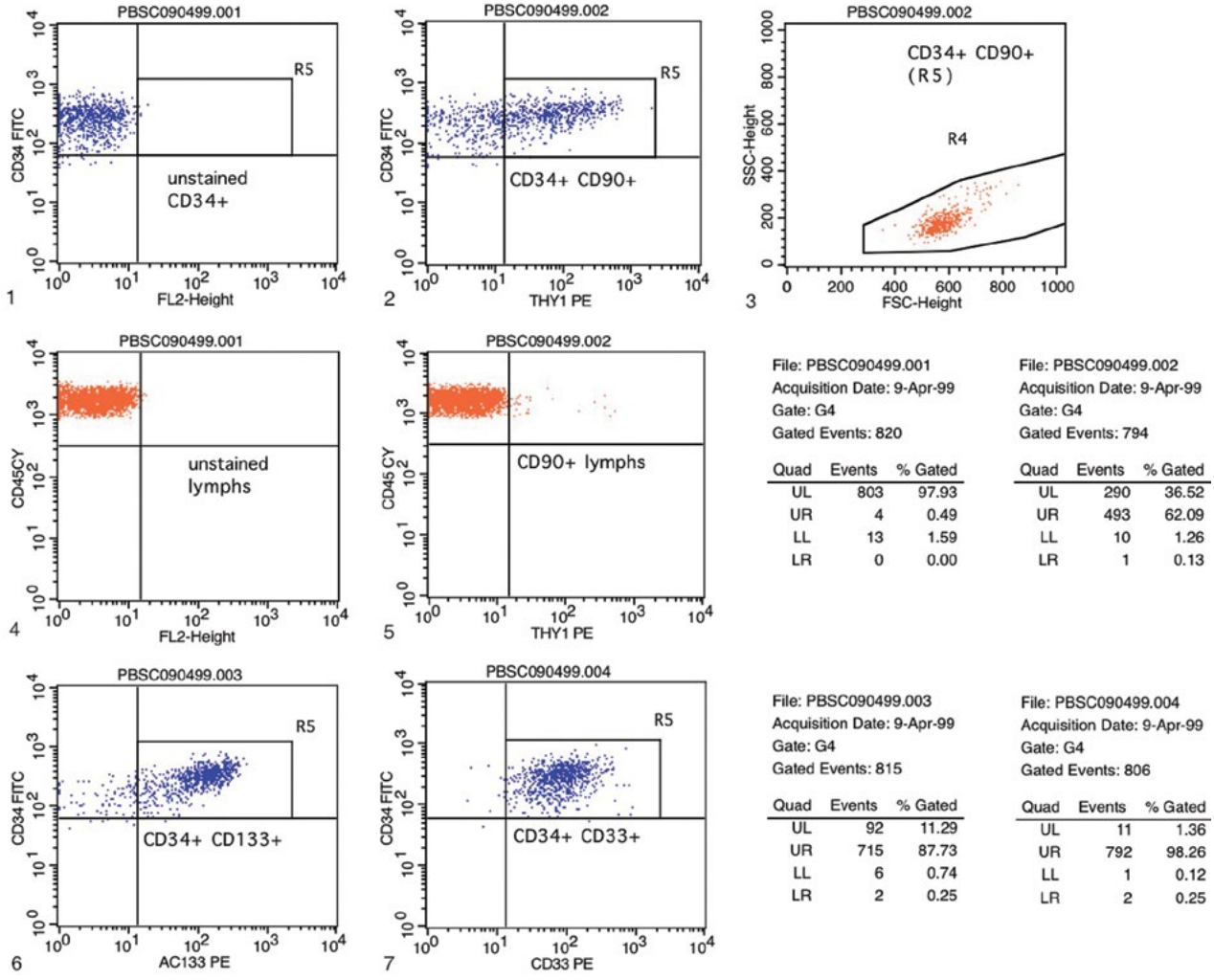

FIGURE 7 Identifying CD34$^+$ cell subsets using the CPC Support Protocol (44, 45). PBSC sample stained with CD34-FITC and CD45–PE-Cy5. CD34$^+$ cells (1.01% of the gated CD45$^+$ events) were identified as described in Fig. 1, plots 1–4, and displayed on CD34 versus FL2 to establish positive cell analysis region R5 (plot 1). Lymphocytes from the same list-mode file were also gated as described in Fig. 1 and displayed (plot 4) on a duplicate CD45 versus FL2 plot. Note the back-scattered lymphocytes (plot 4) have similar auto-fluorescence as gated CD34$^+$ cells (plot 1) and cluster parallel with horizontal axis, indicating optimized FL2/FL3 fluorescence compensation. Plots 2 and 5 show the staining of CD34$^+$ and lymphocytes, respectively, with CD90/Thy–1-PE. Plot 3 shows the light-scatter characteristics of the CD34$^+$ and CD90$^+$ cells. Plots 6 and 7 show the staining of the CD34$^+$ cells with CD133-PE and CD33-PE, respectively.

channel (apart from a small number of lymphocytes that have stained specifically with CD90, in keeping with known characteristics of a small subset of T cells). These plots not only demonstrate proper instrument setup and fluorescence compensation, but also show that the CD90 antibody used is optimally titrated and that, indeed, the staining of the subsets of interest is specific.

DOES ENUMERATING CD34+ SUBSETS HAVE CLINICAL UTILITY?

Whether enumerating specific CD34+ subsets has utility as a predictor of rapid re-engraftment remains somewhat controversial. Since several studies have shown that the rate of platelet engraftment is generally rapid in patients given at least 5×10^6 CD34+ cells per kg (28), it is unlikely that monitoring subsets in patients receiving this target dose (or greater) will provide any additionally useful clinical information. At the Toronto Hospital, we monitored CD34+ subsets on those patients in whom the target value of 5×10^6/kg CD34 cells was unlikely to be met. In this way, we hoped to enumerate specific subsets that correlated best with speed of engraftment. Subsets enumerated included CD90, CD133, CD38dim/−, CD33dim/−, and on some samples, CD109+ and CD117+. However, subsequent analysis showed that all patients transplanted with CD34+ cells in the 2×10^6 to 5×10^6/kg range engrafted platelets and neutrophils by days 12 to 14 (unpublished observations).

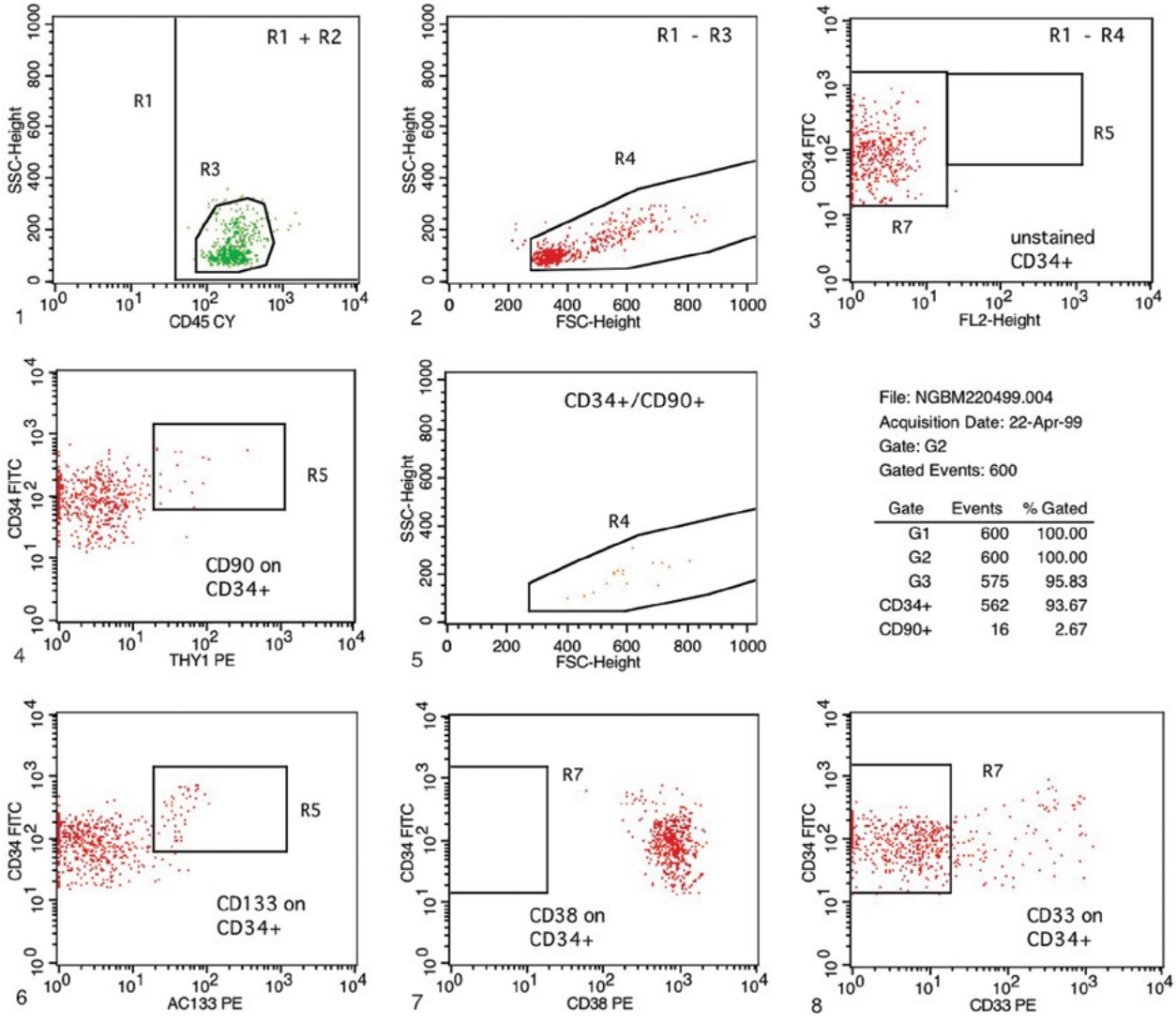

FIGURE 8 Identifying CD34+ cell subsets in the marrow of a poor mobilizer. CD34+ cells (2.00% of the total CD45+ events) were identified as shown in plots 1–4 of Fig. 1. Plots 1 and 2 show the equivalent of plots 3 and 4 from Fig. 1. The majority of CD34+ cells exhibit light-scatter characteristics of prelymphoid cells. An unstained control (no PE conjugate) of the gated CD34+ cells from R4 (plot 2) was used to establish gating regions R5 and R7 (plot 3). Plots 4, 6, 7, and 8 show the staining of gated CD34+ cells with CD90/Thy-1 (plot 4), CD133 (plot 6), CD38 (plot 7), and CD33 (plot 8). The light-scatter plot (plot 5) shows the light scatter of the CD34+/CD90+ cells. Most of the CD34+ cells exhibit staining and light-scatter characteristics of primitive B cell progenitors or hematogones. Very few CD34+ cells exhibit phenotype of primitive candidate engrafting cells ($CD34^{bright}$, CD90+, CD133+, $CD38^{dull/-}$).

In a study of patients with multiple myeloma undergoing PBSC treated with cyclophosphamide and a combination of methionyl human granulocyte colony-stimulating factor and methionyl human stem cell factor, the mobilization kinetics of $CD34^+$ subsets were monitored (66). Of 65 evaluable patients, 57 were considered not heavily pretreated and 96.5% obtained a target of $\geq 5 \times 10^6$ $CD34^+$ cells/kg in one collection. Subset analysis demonstrated the number of $CD38^-$, $CD33^-$, and $CD133^+$ subsets of $CD34^+$ cells peaked at day 11, while $CD34^+$, $CD90^+$ subsets peaked at day 10. The optimum day for leukapheresis was determined to be day 11. However, it must be noted that stem cell factor is not widely used nowadays to augment G-CSF mobilization due to safety concerns, and when it is employed, it has to be administered on an inpatient basis.

Given all of the above, it would appear that performing accurate enumeration of $CD34^+$ cells is perhaps more relevant to predicting platelet engraftment than is the qualitative composition of the $CD34^+$ cells, at least for patients receiving at least 2×10^6 to 2.5×10^6 $CD34^+$ cells/kg. In light of this analysis, it may be informative to analyze subsets only in patients whose collections are in the 1×10^6 to 3×10^6/kg range.

$CD34^+$ CELL SUBSETS IN BACKUP MARROW OF POOR MOBILIZERS

Other potential clinical applications for $CD34^+$ subset analysis might include evaluating poor mobilizers with inadequate or marginal CD34 collections, in addition to measuring qualitative differences in response to different cytokine regimens and quality assuring selected stem cell products during cell processing.

A number of studies have indicated that the use of back-up bone marrow cells does not improve engraftment in patients who failed to mobilize sufficient PBSC $CD34^+$ cells, perhaps suggesting that poor PBSC mobilization is reflective of poor marrow function (67). We analyzed the back-up marrows from a number of patients who had failed to mobilize an adequate number of PBSC $CD34^+$ cells. In the example shown in Fig. 8, $CD34^+$ cells were gated from a patient with poorly mobilized acute myeloid leukemia, and strikingly, as shown in plots 1 and 2 (the equivalent of plots 3 and 4 of Fig. 1), the majority of the $CD34^+$ cells identified exhibited the characteristics of pre-B cell or hematogones (i.e., low forward- and side-scatter signals). Subset gating regions R5 and R7 were established using the unstained sample (FMO control). When subset analysis was performed using CD90 (plot 4), CD133 (plot 6), CD38 (plot 7), and CD33 (plot 8), there was a demonstrable lack of $CD34^+$ cells exhibiting the composite phenotype of primitive candidate stem cells, with very few $CD34^+$ cells expressing the $CD34^{bright}/CD90^+/CD133^+/CD38^{dull}$ phenotype. Additionally, virtually all $CD34^+$ $CD33^{dull/-}$ cells exhibited the light scatter of lymphoid progenitors. Similar data were obtained from other poorly mobilizing patients (Sutherland, unpublished observations).

USE OF PLERIXAFOR IN PATIENTS WHO FAIL TO MOBILIZE WITH G-CSF

In 2008, the novel agent plerixafor, a CXCR4 chemokine receptor antagonist, was approved for use by the Food and Drug Administration in the United States. Plerixafor is indicated for first-line mobilization of hematopoietic stem cells into the peripheral blood for collection and subsequent autologous transplantation in patients with non-Hodgkin's lymphoma and multiple myeloma (reviewed in 68). The use of this mobilizing agent has greatly improved the ability to collect an engrafting dose of $CD34^+$ cells in patient groups known to be at risk of poor mobilization using G-CSF or its analogues alone. Several studies, including the initial phase III trials of plerixafor and G-CSF compared with G-CSF and placebo, have demonstrated that plerixafor can overcome some of the known risk factors for poor stem cell mobilization (69, 70). However, the extra cost involved in the use of plerixafor has, to date, somewhat limited its widespread use (68).

REFERENCES

1. **Thomas ED, Lochte Hl Jr, Lu JF, Ferrebee JW.** 1957. Intravenous infusion of bone marrow in patients receiving radiation and chemotherapy. *N Eng J Med* **257:**491–496.
2. **Thomas ED, Lochte Hl Jr, Cannon JH, Sahler OD, Ferrebee JW.** 1959. Supralethal whole-body irradiation and isologous marrow transplantation in man. *J Clin Invest* **38:**709–1716.
3. **Buckner CD.** 1999. Autologous bone marrow transplants to hematopoietic stem cell support with peripheral blood stem cells: a historical perspective. *J Hematother* **8:**233–236.
4. **McCredie KB, Hersh EM, Freireich EJ.** 1971. Cells capable of colony formation in the peripheral blood of man. *Science* **171:**293–294.
5. **Korbling M, Fleidner TM, Pflieger H.** 1980. Collection of large quantities of granulocyte macrophage progenitor cells (CFUc) in man by means of continuous-flow leukapheresis. *Scand J Haematol* **24:**22–28.
6. **Juttner CA, To LB, Haylock DN, Branford A, Kimber RJ.** 1985. Circulating autologous stem cells collected in very early remission from acute non-lymphoblastic leukemia produce prompt but incomplete hematopoietic reconstitution after high-dose melphalan or supralethal chemoradiotherapy. *Br J Haematol* **61:**739–745.
7. **Reiffers J, Bernard P, David B, Vezon H, Sarrat A, Marit G, Moulinier J, Broustet A.** 1986. Successful autologous transplantation with peripheral blood hemopoietic cells in a patient with acute leukemia. *Exp Hematol* **14:**312–315.
8. **Korbling M, Dorken B, Ho AD, Pezzuto A, Hunstein W, Fleidner TM.** 1986. Autologous transplantation of blood derived hemopoietic stem cells after myeloablative therapy in a patient with Burketts lymphoma. *Blood* **67:**529–532.
9. **Siena S, Bregni M, Brando B, Tarella C, Stern AC, Pieri A, Bonadonna G.** 1989. Circulation of $CD34^+$ hematopoietic stem cells in the peripheral blood of high-dose cyclophosphamide-treated patients: enhancement by intravenous recombinant human granulocyte-macrophage colony-stimulating factor. *Blood* **74:**1905–1914.
10. **To LB, Haylock DN, Simmons PJ, Juttner CA.** 1997. The biology and clinical uses of blood stem cells. *Blood* **89:**2233–2258.
11. **Civin C, Strauss LC, Brovall C. Fackler MJ, Schwartz JF, Shaper JH.** 1984. Antigenic analysis of hematopoiesis III. A hematopoietic progenitor cell surface antigen defined by a monoclonal antibody raised against KG1a cells. *J Immunol* **133:**157–165.
12. **Tindle RW, Nichols RAB, Chan L, Campana D, Catovsky D, Birnie GD.** 1985. A novel monoclonal antibody B1-3C5 recognizes myeloblasts and non-B non-T lymphoblasts in acute leukemias and CGL blast crises, and reacts with immature cells in normal bone marrow. *Leuk Res* **9:**1–9.
13. **Andrews RG, Singer JW, Bernstein ID.** 1986. Monoclonal antibody 12.8 recognizes a 115-Kd molecule present on both unipotent and multipotent colony-forming cells and their precursors. *Blood* **67:**842–845.
14. **Berenson RJ, Andrews RG, Bensinger WI, Kalamasz D, Knitter G, Buckner CD, Bernstein ID.** 1988. Antigen

CD34-positive marrow cells engraft lethally irradiated baboons. *J Clin Invest* **81:**951–955.
15. **Berenson RJ, Bensinger WI, Hill RS, Andrews RG, Garcia-Lopez J, Kalamaz DF, Still BJ, Spitzer G, Buckner D, Bernstein ID, Thomas ED.** 1991. Engraftment after infusion of CD34$^+$ marrow cells in patients with breast cancer or neuroblastoma. *Blood* **77:**1717–1722.
16. **Treleaven JG, Mehta J.** 1992. Bone marrow and peripheral blood stem cell harvesting. *J Hematother* **1:**215–223.
17. **Smith A, Keating A.** 1994. Peripheral blood progenitor cell transplantation: clinical, technical and economic considerations**.** *J Hematother* **3:**331–348.
18. **Wagner JE, Broxmeyer HE, Byrd RL Zehnbauer B, Schmeckpeper B, Shah N, Griffin C, Emanuel PD, Zuckerman S, Cooper S, Carow C, Bias W, Santos GW.** 1992. Transplantation of umbilical cord blood after myeloablative therapy: analysis of engraftment. *Blood* **79:**1874–1881.
19. **Cairo MS, Wagner JE.** 1997. Placental and/or umbilical cord blood: an alternative source of hematopoietic stem cells for transplantation. *Blood* **90:**4665–4678.
20. **Vormoor J, Lapidot T, Pflumio F, Risdon G, Patterson B, Broxmeyer HE, Dick JE.** 1994. Immature human cord blood progenitors engraft and proliferate to high levels in severe combined immunodeficient mice. *Blood* **83:**2489–2497.
21. **Wang JC, Doedens M, Dick JE.** 1997. Primitive human hematopoietic cells are enriched in cord blood compared with adult bone marrow or mobilized peripheral blood as measured by the quantitative *in vivo* SCID-repopulating cell assay. *Blood* **89:**3919–3924.
22. **Civin CI, Trischman T, Fackler MJ, Bernstein I, Buhring H, Campos L, Greaves MF, Kamoun M, Katz D, Lansdorp P, Look T, Seed B, Sutherland DR, Tindle R, Uchanska-Zeigler B.** 1989. Summary of CD34 cluster workshop section, p 818–825. *In* Knapp W, Dorken B, Gilks WR, Reiber EP, Schmidt RE, Stein H, von dem Borne AEGKr (ed), *Leukocyte Typing IV*. Oxford University Press, Oxford, United Kingdom.
23. **Greaves MF, Titley I, Colman SM, Buhring H-J, Campos L, Castoldi GL, Garrido F, Gaudernack G, Girard J-P, Ingles-Esteve J, Invernizi R, Knapp W, Lansdorp PM, Lanza F, Merle-Beral H, Parravicini C, Razak K, Ruiz-Cabello F, Springer TA, van der Schoot CE, and Sutherland DR.** 1995. Report on the CD34 cluster workshop, p 840–846. *In* Schlossman S, Boumsell L, Gilks W, Harlan JM, Kishimoto T, Morimoto C, Ritz J, Shaw S, Silverstein R, Springer T, Tedder TF, Todd RF (ed), *Leukocyte Typing V*. Oxford University Press, Oxford, United Kingdom.
24. **Tricot G, Jagannath S, Vesole DH, Nelson J, Tindle S, Miller L, Cheson B, Crowley J, Barlogie B.** 1995. Peripheral blood stem cell transplants for multiple myeloma: identification of favorable variables for rapid engraftment in 225 patients. *Blood* **85:**588–596.
25. **Bender JG, To LB, Williams S, Schwartzberg LS.** 1992. Defining a therapeutic dose of peripheral blood stem cells. *J Hematother* **1:**329–341.
26. **Chapple P, Prince HM, Quinn M, Bertoncello I, Juneja S, Wolf M, Januszewicz H, Brettell M, Gardyn J, Seymour C, Venter D.** 1998. Peripheral blood CD34$^+$ cell count reliably predicts autograft yield. *Bone Marrow Transplant* **22:**125–130.
27. **Luider J, Brown C, Selinger S, Quinlan D, Karlsson L, Ruether D, Stewart D, Klassen J, Russell JA.** 1997. Factors influencing yields of progenitor cells for allogeneic transplantation: optimization of G-CSF dose, day of collection, and duration of leukapheresis. *J Hematother* **6:**575–580.
28. **Weaver CH, Hazelton B, Birch R, Palmer P, Allen C, Schwartzberg L, West W.** 1995. An analysis of engraftment kinetics as a function of CD34 cell content of peripheral blood progenitor collections in 692 patients after the administration myeloablative chemotherapy. *Blood* **86:**3961–3969.
29. **Negrin RS, Atkinson K, Leemhuis T, Hanania E, Juttner C, Tierney D, Hu WW, Johnston LJ, Shizuru JA, Stockerl-Goldstein KE, Blume KG, Weissman IL, Bower S, Baynes R, Dansey R, Karanes C, Peters W, Klein J.** 2000. Transplantation of highly purified CD34$^+$Thy-1$^+$ hematopoietic stem cells in patients with metastatic breast cancer. *Biol Blood Marrow Transplant* **6:**262–271.
30. **Siena S, Bregni M, Brando B, Belli N, Ravagnani F, Gandola L, Stern AC, Lansdorp PM, Bonadonna G, Gianni AM.** 1991. Flow cytometry for clinical estimation of circulating hematopoietic progenitors for autologous transplantation in cancer patients. *Blood* **77:**400–409.
31. **Bender JG, Unverzagt K, Walker D.** 1994. Guidelines for determination of CD34$^+$ cells by flow cytometry: application to the harvesting and transplantation of peripheral blood stem cells, p 31–43. *In* Wunder E, Sovalat H, Henon PR, Serke S (ed), *Hematopoietic Stem Cells: The Mulhouse Manual*. AlphaMed Press, Dayton, OH.
32. **Sutherland DR, Anderson L, Keeney M, Nayar R, Chin-Yee I.** 1997. re: Towards a worldwide standard for CD34$^+$ enumeration? Response to Letter to the Editor. *J Hematother* **6:**85–89.
33. **Marti GE, Johnsen HE, Sutherland DR, Serke S.** 1998. A convergence of methods for a worldwide standard for CD34$^+$ cell enumeration. Letter to the Editor. *J Hematother* **7:**105–109.
34. **Keeney M, Chin-Yee I, Gratama JW, Sutherland DR.** 1998. Perspectives: Isotype controls in the analysis of lymphocytes and CD34$^+$ stem/progenitor cells by flow cytometry—time to let go! *Cytometry (Comm Clin Cytometry)* **34:**280–283.
35. **Hulspas R, O'Gorman MRG, Wood BL, Gratama JW, Sutherland DR.** 2009. Considerations for the control of background fluorescence in clinical flow cytometry. *Cytometry B* **76B:**355–364.
36. **Roederer M.** 2001. Spectral compensation for flow cytometry: visualization artifacts, limitations and caveats. *Cytometry* **45:**194–205.
37. **Sutherland DR, Keating A.** 1992. The CD34 antigen: structure, biology and potential clinical applications. *J Hematother* **1:**115–129.
38. **Lanza R, Healy L, Sutherland DR.** 2001. Structural and functional features of the CD34 antigen: an update. *J Biol Reg Homeos Ag* **15:**1–13.
39. **Sutherland DR, Anderson L, Keeney M, Nayar R, Chin-Yee I.** 1996. The ISHAGE guidelines for CD34$^+$ cell determination by flow cytometry. *J Hematother* **5:**213–226.
40. **Gratama JW, Keeney M, Sutherland DR.** 1999. Enumeration of CD34$^+$ hematopoietic stem and progenitor cells, p 6.4.1–6.4.22. *In* Robinson JP, Darzynkiewicz Z, Dean PN, Hibbs AR, Orfao A, Rabinovitch PS, Wheeless LL (ed), *Current Protocols in Cytometry*. John Wiley and Sons Inc, New York, NY.
41. **Sutherland DR, Keeney M, Gratama JW.** 2003. Enumeration of CD34$^+$ hematopoietic stem and progenitor cells, p 6.4.1–6.4.23. *In* Robinson JP, Darzynkiewicz Z, Dean PH, Dressler LG, Rabinovitch PS, Stewart CS, Tanke HJ, Wheeless LL (ed), *Current Protocols in Cytometry*. John Wiley and Sons Inc, New York, NY.
42. **Mancuso P, Burlini A, Pruneri G, Goldhirsch A, Martinelli G, Bertolini F.** 2001. Resting and activated endothelial cells are increased in the peripheral blood of cancer patients. *Blood* **97:**3658–3661.
43. **Borowitz MJ, Guenther KL, Schultz KE, Stelzer GT.** 1993. Immunophenotyping of acute leukemia by flow cytometry: use of CD45 and right-angle light scatter to gate

on leukemic blasts in three-color analysis. *Am J Clin Pathol* **100:**534–540.

44. **Sutherland DR, Keating A, Nayar R, Anania S, Stewart AK.** 1994. Sensitive detection and enumeration of $CD34^+$ cells in peripheral blood and cord blood by flow cytometry. *Exp Hematol* **22:**1003–1010.
45. **Sutherland DR, Yeo EL, Stewart AK, Nayar R, DiGiusto R, Hoffman R, Zanjani ED, Murray LJ.** 1996. Identification of $CD34^+$ subsets following glycoprotease selection: engraftment of $CD34^+$/Thy-1^+/Lin^-/stem cells in fetal sheep. *Exp Hematol* **24:**795–806.
46. **Keeney M, Chin-Yee I, Weir K, Popma J, Nayar R, Sutherland DR.** 1998. Single-platform flow cytometric absolute $CD34^+$ cell counts based on the ISHAGE Guidelines. *Cytometry (Comm Clin Cytom)* **34:**61–67.
47. **Sutherland DR, Nayyar R, Acton E, Giftakis A, Dean S, Mosiman V.** 2009. Comparison of two single-platform ISHAGE-based CD34 enumeration protocols on FACSCalibur and FACSCanto cytometers. *Cytotherapy* **11:**595–605.
48. **Gratama JW, Orfao A, Barnett D, Brando B, Huber A, Janossy G, Johnsen HE, Keeney M, Preijers F, Rothe G, Serke S, Sutherland DR, Van Der Schoot E, Schmitz G, Papa S.** 1998. Flow cytometric enumeration of $CD34^+$ hematopoietic progenitor cells. *Cytometry (Comm Clin Cytom)* **34:**128–142.
49. **Gratama JW, Kraan J, Keeney M, Mandy F, Sutherland DR, Wood BL.** 2007. Enumeration of immunologically defined cell populations by flow cytometry; approved guideline, 2nd ed. Document H42-A2 **27** No.16. Clinical and Laboratory Standards Institute, Wayne, PA.
50. **Sutherland DR, Keeney M.** 2009. Enumeration of $CD34^+$ cells by flow cytometry, p 538–554. *In* Aremen EM, Loper K (ed), *Cellular Therapy: Principles, Methods and Regulations. An American Association of Blood Bankers Cell Therapy Technical Manual.* American Association of Blood Bankers, Bethesda, MD.
51. **Brocklebank AM, Sparrow RL.** 2001. Enumeration of $CD34^+$ cells in cord blood: a variation on a single-platform flow cytometric method based on the ISHAGE gating strategy. *Cytometry* **46:**254–261.
52. **Keeney M, Chin-Yee I, Nayar R, Sutherland DR.** 1999. Effect of fixatives on $CD34^+$ cell enumeration. *J Hematother Stem Cell Res* **8:**327–329.
53. **Chang A, Ma DDF.** 1996. The influence of flow cytometric gating strategy on the standardization of $CD34^+$ cell quantitation: an Australian multicenter study. *J Hematother* **5:**605–616.
54. **Barnett D, Granger V, Kraan J, Whitby L, Reilly JT, Papa S, Gratama JW.** 2000. Reduction of intra- and interlaboratory variation in $CD34^+$ stem cell enumeration using stable test material, standard protocols and targeted training. CD34 Task Force of the European Working Group of Clinical Cell Analysis (EWGCCA). *Br J Haematol* **108:**784–792.
55. **Gratama JW, Kraan J, Keeney M, Sutherland DR, Granger V, Barnett D.** 2003. Validation of the single-platform ISHAGE method for $CD34^+$ hematopoietic stem and progenitor cell enumeration in an international multicenter study. *Cytotherapy* **5:**55–65.
56. **Whitby A, Whitby L, Fletcher M, Reilly JT, Sutherland DR, Keeney M, Barnett D.** 2012. ISHAGE Protocol: are we doing it correctly? *Cytometry B* **82B:**9–17.
57. **Walker I, Shehata N, Cantin C, Couture F, Dhedin N, Barty R, Foley R, Sutherland DR, Sigouin C, Schultz K, Mitchell D.** 2004. Canadian multicenter pilot trial of haploidentical donor transplantation. *Blood Cell Mol Dis* **33:**222–236.
58. **Baum CM, Weissman IL, Tsukamoto AS, Buckle AM, Peault B.** 1992. Isolation of a candidate human hematopoietic stem-cell population. *Proc Natl Acad Sci USA* **89:**2804–2808.
59. **Craig W, Kay R, Cutler RL, Lansdorp PM.** 1993. Expression of Thy-1 on human hematopoietic progenitor cells. *J Exp Med* **177:**1331–1242.
60. **Yin AH, Miraglia S, Zanjani ED, Almeida-Porada G, Ogawa M, Leary AG, Olweus J, Kearney J, Buck DW.** 1997. AC133, a novel marker for human hematopoietic stem and progenitor cells. *Blood* **90:**5002–5012.
61. **Sutherland H, Eaves C, Eaves A, Dragowska W, Landsdorp PM.** 1989. Characterization and partial purification of human marrow cells capable of initiating long-term hematopoiesis in vitro. *Blood* **74:**1563–1570.
62. **Terstappen LWMM, Huang S, Safford M, Lansdorp PM, Loken MR.** 1991. Sequential generations of hematopoietic colonies derived from single nonlineage-committed $CD34^+$ $CD38^-$ progenitor cells. *Blood* **77:**1218–1227.
63. **Negrin RS, Atkinson K, Leemhuis T, Hanania E, Juttner C, Tierney D, Hu WW, Johnston LJ, Shizuru JA, Stockerl-Goldstein KE, Blume KG, Weissman IL, Bower S, Baynes R, Dansey R, Karanes C, Peters W, Klein J.** 2000. Transplantation of highly purified $CD34^+$Thy-1^+ hematopoietic stem cells in patients with metastatic breast cancer. *Biol Blood Marrow Transplant* **6:**262–271.
64. **Vose JM, Bierman PJ, Lynch JC, Atkinson K, Juttner C, Hanania CE, Bociek G, Armitage JO.** 2001. Transplantation of highly purified $CD34^+$Thy-1^+ hematopoietic stem cells in patients with recurrent indolent non-Hodgkin's lymphoma. *Biol Blood Marrow Transplant* **7:**680–687.
65. **Michallet M, Philip T, Philip I, Godinot H, Sebban C, Salles G, Thiebaut A, Biron P, Lopez F, Mazars P, Roubi N, Leemhuis T, Hanania E, Reading C, Fine G, Atkinson K, Juttner C, Coiffier B, Fiere D, Archimbaud E.** 2000. Transplantation with selected autologous peripheral blood $CD34^+$Thy1^+ hematopoietic stem cells (HSCs) in multiple myeloma: impact of HSC dose on engraftment, safety, and immune reconstitution. *Exp Hematol* **28:**858–870.
66. **Chin-Yee IH, Keeney M, Stewart AK, Belch A, Bence-Buckler I, Couban S, Howson-Jan K, Rubinger M, Stewart D, Sutherland DR, Paragamian V, Bhatia M, Foley R.** 2002. Optimizing parameters for peripheral blood leukapheresis after r-metHuG-CSF (filgrastim) and r-metHuSCF (ancestim) in patients with multiple myeloma: a temporal analysis of $CD34^+$ absolute counts and subsets. *Bone Marrow Transplant* **30:**851–860.
67. **Watts MJ, Sullivan AM, Leverett D, Peniket AJ, Perry AR, Williams CD, Devereux S, Goldstone AH, Linch DC.** 1998. Back-up bone marrow is frequently ineffective in patients with poor peripheral-blood stem-cell mobilization. *J Clin Oncol* **16:**1554–1560.
68. **Shaughnessy P, Chao N, Shapiro J, Walters K, McCarty J, Abhyankar S, Shayani S, Helmons P, Leather H, Pazzalia A, Pickard S.** 2013. Pharmacoeconomics of hematopoietic stem cell mobilization: an overview of current evidence and gaps in the literature. *Biol Blood Marrow Transplant* **19:**1301–1309.
69. **Basak GW, Mikala G, Koristek Z, Jaksic O, Basic-Kinda S, Cegledi A, Reti M, Masszi T, Mayer J, Giebel S, Hübel K, Labar B, Wiktor-Jedrzejczak W.** 2011. Identification of prognostic factors for plerixafor-based hematopoietic stem cell mobilization. *Am J Hematol* **86:**550–553.
70. **Nademanee AP, DiPersio JF, Maziarz RT, Stadtmauer EA, Micallef IN, Stiff PJ, Hsu FJ, Bridger G, Bolwell BJ.** 2012. Plerixafor plus granulocyte colony-stimulating factor versus placebo plus granulocyte colony-stimulating factor for mobilization of $CD34^+$ hematopoietic stem cells in patients with multiple myeloma and low peripheral blood $CD34^+$ cell count: results of a subset analysis of a randomized trial. *Biol Blood Marrow Transplant* **18:**1564–1572.

Functional Flow Cytometry-Based Assays of Myeloid and Lymphoid Functions for the Diagnostic Screening of Primary Immunodeficiency Diseases

MAURICE R. G. O'GORMAN

20

Primary immunodeficiency diseases represent an extremely diverse group of disorders caused by mutations in genes that code for multiple components of both the innate and adaptive immune systems. These mutations adversely affect immune homeostasis ultimately leading to increased susceptibility to infections, autoinflammatory disorders, and other symptoms of immune dysregulation. Although there are now more than 200 diseases that have been officially classified (1), diagnosis of primary immunodeficiency remains challenging and is often delayed due to the extremely broad range of signs and symptoms, variations in the severity and range of symptoms at presentation, and the overlap of presenting clinical symptoms of immunodeficiency with the clinical signs and symptoms of common illnesses. The extremely broad and large number of genetic abnormalities that make up the primary immunodeficiency disorders would suggest that DNA sequencing of the exome or genome should be the ultimate diagnostic modality. A recently published article describes how such an approach (i.e., DNA sequencing of the whole exome) resulted in an increased ability to detect genes associated with both known and new immune disorders (2).

Although there are exemplary cases where deep sequencing has resulted in successful diagnoses of very complex cases, challenges to the broad and routine implementation of whole exome/whole genome sequencing as it stands today include the following: (i) the technology is still in its infancy and although the sequencing technology and genetic databases continue to improve in accuracy and automation, standardized phenotypic databases lag behind particularly in terms of standardization; (ii) the technology is expensive and reimbursement remains challenging; (iii) the turnaround times are very long ranging from several weeks to months; and (iv) there is a wide range of variability in the quality and quantity of interpretation of the extremely large amount of data generated. Because of these challenges and limitations, nongenomic laboratory testing technologies will continue to have a role in the diagnostic evaluation of patients suspected of primary immunodeficiency disease. Flow cytometry represents one such essential and powerful technology and will remain so for the foreseeable future.

Laboratory evaluation and the selection of appropriate testing for a patient suspected of a primary immune deficiency should be guided by the presenting signs and symptoms, physical exam, and a careful history. First line screening tests available in most laboratories include a complete blood count and differential, evaluation of serum complement with immunoglobulin levels, and basic flow cytometric evaluation of the proportions and absolute numbers of the major lymphocyte subsets (B, T, T-helper, T-cytotoxic, and NK cells). The results of these screening tests help to guide the next level of laboratory investigation. This chapter will present a few highly specialized functional flow cytometry based tests used in the diagnosis of specific primary immunodeficiency disorders.

Table 1 provides a list of some of the functional flow cytometry-based assays available from the diagnostic immunology laboratories of four different pediatric academic medical centers and the primary immunodeficiency disorders with which they have been associated (Seattle Children's, http://www.seattlechildrens.org/healthcare-professionals/access-services/diagnostic-services/laboratories/immunology-diagnostic-laboratory/; Cincinnati Children's, http://www.cincinnatichildrens.org/service/i/immune-deficiency/diagnostic-lab/; Lurie Children's in Chicago, https://www.luriechildrens.org/en-us/care-services/specialties-services/pathology-laboratory-medicine/specialties-laboratories/Pages/index.aspx; Milwaukee Children's, http://www.chw.org/medical-care/immune-deficiency/clinical-immunodiagnostic-research-laboratory). Individuals interested in the services of these laboratories should contact them directly to inquire about specimen requirements for specific tests.

FLOW CYTOMETRIC EVALUATION OF PHOSPHORYLATED KINASE SUBSTRATES TO EVALUATE ABNORMALITIES IN IMMUNE SIGNALING PATHWAYS

Cell signaling via cytokine, chemokine, and antigen receptors on the surface of cells of the immune system is controlled in part by the phosphorylation and dephosphorylation of an ordered series of kinase and phosphorylase targets along well defined pathways leading the transcription of specific target genes. Signaling via these surface molecules controls many functions of the immune response including proliferation, differentiation, cytotoxicity, cytokine secretion, antibody production, and apoptosis. The advent of reagents to detect specific phospho-epitopes within the cytoplasm and nucleus along with standardized methods of fixing and permeabilizing cells has led to a new line of functional "phospho-flow cytometry" based assays designed to assess signaling defects

doi:10.1128/9781555818722.ch20

TABLE 1 Functional flow cytometry-based assays which have been used as aids in the diagnosis of specific primary immunodeficiency diseases

- STAT1 phosphorylation in response to IFN-γ (screening test for IFN-γ receptor deficiency, in patients suspected of Mendelian Susceptibility to Mycobacterial Disease)
- STAT3 phosphorylation in response to IL-6 (hyper IgE syndrome screening)
- STAT4 phosphorylation in response to IFN-α and IL-12 (screening test for IL-12 receptor deficiency and Tyk2 deficiency)
- STAT5B phosphorylation in response to IL-2 (screening test for common gamma chain deficiency [X-linked SCID] and Janus kinase 3 deficiency)
- STAT5B phosphorylation in response to IL-7 (screening test for IL-7 receptor alpha deficiency)
- IκBα phosphorylation/degradation assay (screening for anhidrotic ectodermal dysplasia with immunodeficiency)
- Beta 2 leukocyte integrin upregulation on granulocytes (screening assay for LAD-1)
- *In vitro* assessment of CD40 ligand upregulation (screening assay for CD40 ligand deficiency [XHIM])
- Lymphocyte apoptosis, Fas-mediated (screening test for autoimmune lymphoproliferative syndrome)
- Apoptosis assays (screening test for autoimmune lymphoproliferative syndrome)
- Neutrophil oxidative burst assay (screening test for chronic granulomatous disease)
- NK cell function (screening for hemophagocytic lymphohistiocytosis (HLH))
- Cytotoxic T-cell degranulation (CD107a) assay (screening test for HLH)

in specific signaling pathways. For example, primary immunodeficiency diseases associated with mutations in signaling molecules (e.g., STAT1 and STAT3) or cytokine receptor genes (e.g., common gamma chain, gamma interferon [IFN-γ] receptors, and interleukin-7 [IL-7] and IL-12 receptors) can be screened by stimulating peripheral blood cells with specific agonists and comparing activation induced phosphorylation levels with baseline levels. Examples include the measurement of phosphorylated STAT5 following IL-2 stimulation to screen for abnormalities in the IL-2 signal transduction pathway associated with abnormalities in the common gamma chain, Janus kinase 3, or IL-7 receptor (Seattle Children's Website). Another example involves the measurement of STAT1 phosphorylation levels following IFN-γ stimulation to screen for abnormalities in the type 1 cytokine signal transduction pathway associated with chronic mucocutaneous candidiasis or recurrent atypical mycobacterial infections.

A relatively simple flow cytometric approach to assess abnormalities in STAT1 phosphorylation as the molecular etiology of disease in patients with chronic mucocutaneous candidiasis or patients suspected of Mendelian susceptibility to mycobacterial disease is presented.

INDUCTION AND MEASUREMENT OF STAT1 PHOSPHORYLATION LEVELS AS A SCREEN FOR TYPE 1 CYTOKINE SIGNALING ABNORMALITIES ASSOCIATED WITH PRIMARY IMMUNODEFICIENCY

Severe and recurring infections in family members with intracellular organisms including Bacille Calmette-Guerin (BCG) and nontuberculous mycobacteria (*Mycobacterium avium, Mycobacterium fortuitum, Mycobacterium chelonae*) led to the identification of mutations in genes involved in the type 1 cytokine signaling pathway (3, 4). This pathway involves IFN-γ receptors (IFN-γR1 and IFN-γR2), IL-12 (IL12p40), and IL-12 and IL-23 receptors (IL-12Rβ1). IL-12, secreted primarily by monocytes/macrophage, stimulates T cells and NK cells to synthesize and secrete INF-γ, which in turn activates macrophage and further stimulates cytolytic $CD4^+$ T cells and effector $CD8^+$ T cells, which then kill infected macrophage (5). Decreased IL-12 receptor expression and both increases and decreases in the level of expression of the IFN-γ receptors have been reported and can be detected by flow cytometry (3, 4, 6). In the dominant form of inheritance, mutations in the gene encoding the IFN-γ receptor leads to an increase in cell surface expression of the IFN-γ receptor due a deletion encompassing both the signaling and the recycling domains. The lack of specificity in associating surface receptor expression levels to specific genetic mutations has led to the development of surrogate functional flow cytometry assays based on the ability to detect phosphorylated STAT1 following *in vitro* stimulation with IFN-γ (3). Lack of STAT1 phosphorylation, as detected by flow cytometry following *in vitro* stimulation with IFN-γ, indicates either abnormal IFN-γ receptor molecules (IFN-γR1 or IFN-γR2) or abnormalities in STAT1 itself, whereas normal *in vitro* STAT1 phosphorylation levels in a patient with repeat atypical mycobacterial infections might suggest abnormalities in either the IL-12 gene or the IL12 receptor genes. Either result allows for the focused determination of the genes to be sequenced. The determination of the specific underlying genetic mutation is very important since (i) the prognosis is associated with the different forms of genetic lesions and (ii) the specific defect has implications for the design of optimal therapeutic interventions (7). Although the detection of intracellular phosphorylated STAT1 following *in vitro* stimulation with IFN-γ is relatively straightforward, development of a standardized, reproducible clinical procedure is relatively complex, is performed only in more specialized flow cytometry laboratories, and has been used primarily to help focus on the potential defect so that only a limited number of likely genes needs to be sequenced.

FLOW CYTOMETRIC DETERMINATION OF STAT1 GAIN-OF-FUNCTION ALLELES IN PATIENTS WITH CMCD

More recently, a modification of the STAT1 functional flow cytometry procedure was published that describes a relatively simple diagnostic approach to identify gain-of-function STAT1 mutations in patients with chronic mucocutaneous candidiasis (CMCD) (8). Patients with CMCD suffer from difficult-to-treat and recurrent infections with *Candida albicans* of the nails, skin, and mucous membranes. It has been reported that some patients with CMCD have mutations in the IL-17 pathway; however, this represents only a minority (8). More recently, gain-of-function mutations in STAT1 have been associated with a majority of patients with CMCD (9). Mizoguchi describes a modified flow cytometry

procedure for the measurement of STAT1 phosphorylation (8). Basically, peripheral blood mononuclear cells (PBMCs) are stimulated with IFN-γ in the presence of the tyrosine kinase inhibitor staurosporine, and the fluorescence intensity (mean fluorescence intensity) of STAT1 in CD14-labeled monocytes is assessed. The monocytes of patients with gain-of-function mutations in STAT1 exhibited significantly higher levels of phosphorylated STAT1 than the healthy controls both at baseline (unstimulated) and in the presence of staurosporine following IFN-γ stimulation. The abnormal decrease of phosphorylated STAT1 in patients with CMCD indicates that the dephosphorylation process is impaired. Although currently not commonly available, this assay may prove useful for screening patients with CMCD. Patients with abnormally high levels of phosphorylated STAT1 in the presence of staurosporine should be sequenced to confirm the abnormalities in the STAT1 gene.

CELL SURFACE ADHESION MARKER UPREGULATION AS A SCREEN FOR LAD-1

LAD-1, CD18 Deficiency

Leukocyte adhesion deficiency type-1 (LAD-1) is a rare inherited disorder of the innate immune system caused by an inability of immune cells to adhere to the endothelium and migrate to the site of infection. It is characterized clinically by defective wound healing, cold infections (i.e., no pus) with Gram-negative bacteria, delayed umbilical cord separation, gum disease (gingivitis and/or periodontitis), and very high peripheral blood white blood cell counts. These abnormalities are associated with mutations in the gene encoding the beta chain (CD18) of the β2-class of leukocyte integrins. The absence of the beta chain (CD18) results in its inability to complex with the alpha chains CD11a, CD11b, CD11c, and CD11d, resulting in the functional abnormality of four key cell surface receptors involved in the innate immune response (i.e., LFA-1 [CD18/CD11a], Mac1 [also known as complement receptor 3/CR3, CD18/CD11b], CR4 [CD18/CD11c], and CD18/CD11d [of which little is known]) (10).

Flow Cytometric Assessment of Cell Surface Adhesion Marker Upregulation as a Screen for LAD-1

A patient with a clinical history and laboratory findings (very high white blood cell count) consistent with LAD-1 presented to the emergency room and proved to have cell surface abnormalities consistent with LAD-1. With the patient's informed consent, our laboratory studied various stimuli (to measure both baseline and activated levels) and monoclonal antibody combinations to each of different beta-2 integrins in an effort to develop a whole blood flow cytometry-based diagnostic test (11). An efficient whole blood procedure was developed and remains in use in our laboratory. Briefly, an optimized concentration of phorbol myristate acetate is added to EDTA anti-coagulated whole blood for 15 minutes (stimulated sample) followed by the staining of the stimulated sample and a non-stimulated sample with anti-CD11b (CD11b-PE, BD Bioscience). A fluorochrome matched non-human antigen-specific monoclonal isotypic control is used to set the background level of fluorescence of the granulocyte cluster (by gating on forward versus right angle light scatter parameters). Note that the background fluorescence will be higher on the granulocytes than the level of fluorescence generally observed when gating on the lymphocyte cluster. The level of CD11b expressed on the surface of gated granulocytes is then measured (as the median fluorescent channel) on both resting (non-activated) and *in vitro* activated granulocytes (see gating and results of typical flow assay in Fig. 1). A normal range was established based on a group of 30 non-diseased control subjects and is used to evaluate the patient's results. Patients with LAD-1 can express CD11b significantly below normal on both resting and stimulated granulocytes. Performing *in vitro* stimulation is recommended, as occasionally patients with LAD-1 will have levels of CD11b on resting granulocytes that are consistent with normal; however, this level does not increase following stimulation. Patients with severe LAD-1 do not survive infancy and express no detectable CD18, CD11a, CD11b, or CD11c protein on the cell surface, whereas patients with the moderate form of LAD-1 express 1 to 10% of the level of normal and can survive into adulthood (12).

MEASUREMENT OF THE UPREGULATION OF CD40 LIGAND ON ACTIVATED T CELLS AS A SCREENING DIAGNOSTIC TEST FOR CD40 LIGAND DEFICIENCY (FORMALLY KNOWN AS XHIM)

The proliferation of B cells and their differentiation into plasma cells secreting IgG, IgA, and IgE (immunoglobulin gene class switching) requires a complex series of cellular interactions and molecular processing of the immunoglobulin genes. Immunoglobulin class switching and somatic mutation of the immunoglobulin genes are required for a functionally effective antibody response and normal humoral immunity. Patients with mutations in the genes involved in immunoglobulin gene class switching are unable to produce immunoglobulins other than IgM and suffer from infections very similar to those of patients with hypogammaglobulinemia. The CD40 ligand expressed on the surface of activated T-helper cells is essential for the proliferation, maturation, and differentiation of B cells to immunoglobulin class-switched plasma cells. Patients with mutations in the gene encoding CD40 ligand also suffer from opportunistic infections due to an abnormal T-cell response resulting from a failure of cross talk (co-stimulation) between activated T cells and B cells. These patients can also experience significant neutropenia (CD40 receptor is expressed on neutrophils) although the exact mechanism of neutropenia is not well understood. Our laboratory has developed a relatively rapid functional assay to assess the ability of T cells to upregulate the CD40 ligand. This assay has been successfully adopted to diagnose patients with CD40 ligand deficiency (X-linked hyper IgM syndrome or type 1 hyper IgM syndrome [XHIM]) as well as their X-linked carrier mothers (13).

MEASUREMENT OF CD40 LIGAND ON *IN VITRO*-ACTIVATED T-HELPER CELLS AND CD40 RECEPTOR ON B CELLS AS A SCREENING DIAGNOSTIC TEST FOR THE CD40 LIGAND DEFICIENCY

Following the discovery of the underlying cause of XHIM (i.e., mutations in the gene encoding the CD40 ligand) and the commercial availability of monoclonal antibody specific for CD40 ligand, our laboratory designed, developed, and validated a clinical flow cytometry procedure for the screening diagnosis of XHIM patients and carriers (11). Briefly, whole blood is stimulated with phorbol ester and a calcium ionophore for 4 hours, followed by the staining of

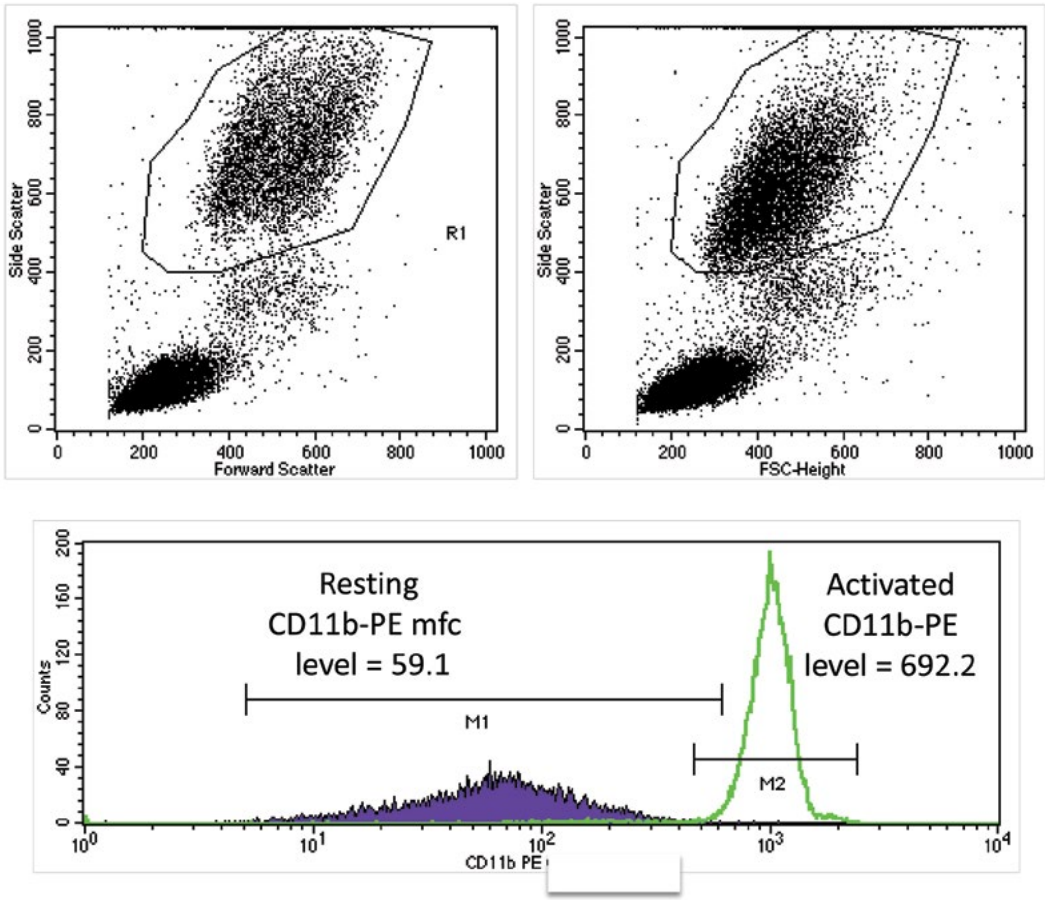

FIGURE 1 Flow cytometry-based LAD screening assay on a nondiseased healthy donor. Granulocytes are gated based on their innate forward and right angle light scatter properties. The level of CD11b-PE fluorescence on resting (purple) versus PMA-stimulated granulocytes is displayed. Note that in LAD-1 both the resting and activated levels of CD11b are considerably lower than normal. Normal ranges for the level of CD11b, expressed as the geometric mean fluorescence, were determined on 30 healthy nondiseased control patients. Normal CD11b was expressed as greater than the 5th percentile of normal.

lymphocytes with a panel of monoclonal antibodies including CD3, CD8, CD40 ligand (TRAP-10 clone conjugated with phycoerytherin, Pharmingen, San Diego, CA), and CD69 (as an *in vitro* stimulation control). Following the labeling procedure, the red blood cells are lysed, the cells are fixed, and the samples are acquired and analyzed on the flow cytometer using a novel gating strategy (see Fig. 2). During the development of this assay we observed the following *in vitro* induced immune alterations. Phorbol 12-myristate 13-acetate (PMA) induces the rapid modulation of the CD4 molecule off the cell surface. This requires a negative gating strategy (i.e., $CD3^{+}CD8^{-}$ cells). The process of PMA-induced CD40 ligand cell surface expression (transcription and translation) is calcium dependent. Therefore, EDTA anticoagulated blood is not recommended.

Abnormal CD40 ligand expression had been detected in all of our patients with mutations in the CD40 ligand gene until recently. Although a nonsense mutation in the gene was confirmed in one patient, the level of CD40 ligand detected was consistent with normal. Others have reported this observation in the past (14). This false-negative result led to a modification of the procedure to include the measurement of CD40 ligand expression levels using a directly fluoresceinated chimeric CD40 receptor reagent in addition to measuring CD40-ligand expression levels by the monoclonal antibody. To date, all patients with mutations in the CD40 ligand gene have had abnormal CD40 ligand protein expression in the modified assay. Most laboratories with a moderate amount of flow cytometry experience could perform this assay.

Mutations in the gene encoding the CD40 receptor (formerly classified as HIGM3) lead to a clinical phenotype virtually identical to the X-linked form of the hyper IgM syndrome. Abnormal expression of the CD40 receptor is detected by gating on B cells (CD19 or CD20) and measuring the percentage of CD40 positive events (normal range is defined as >90% of B cells expressing CD40 [unpublished data from our laboratory]). The latter form of autosomal recessive hyper IgM syndrome is very rare (15).

A FLOW CYTOMETRY-BASED OXIDATIVE BURST ASSAY AS A SCREEN FOR THE DIAGNOSIS OF CGD

Chronic Granulomatous Disease

Chronic granulomatous disease (CGD) is the most common of the phagocyte primary immunodeficiency disorders. The genetic abnormalities in CGD result in a severely reduced capability to generate superoxide and other reactive oxygen

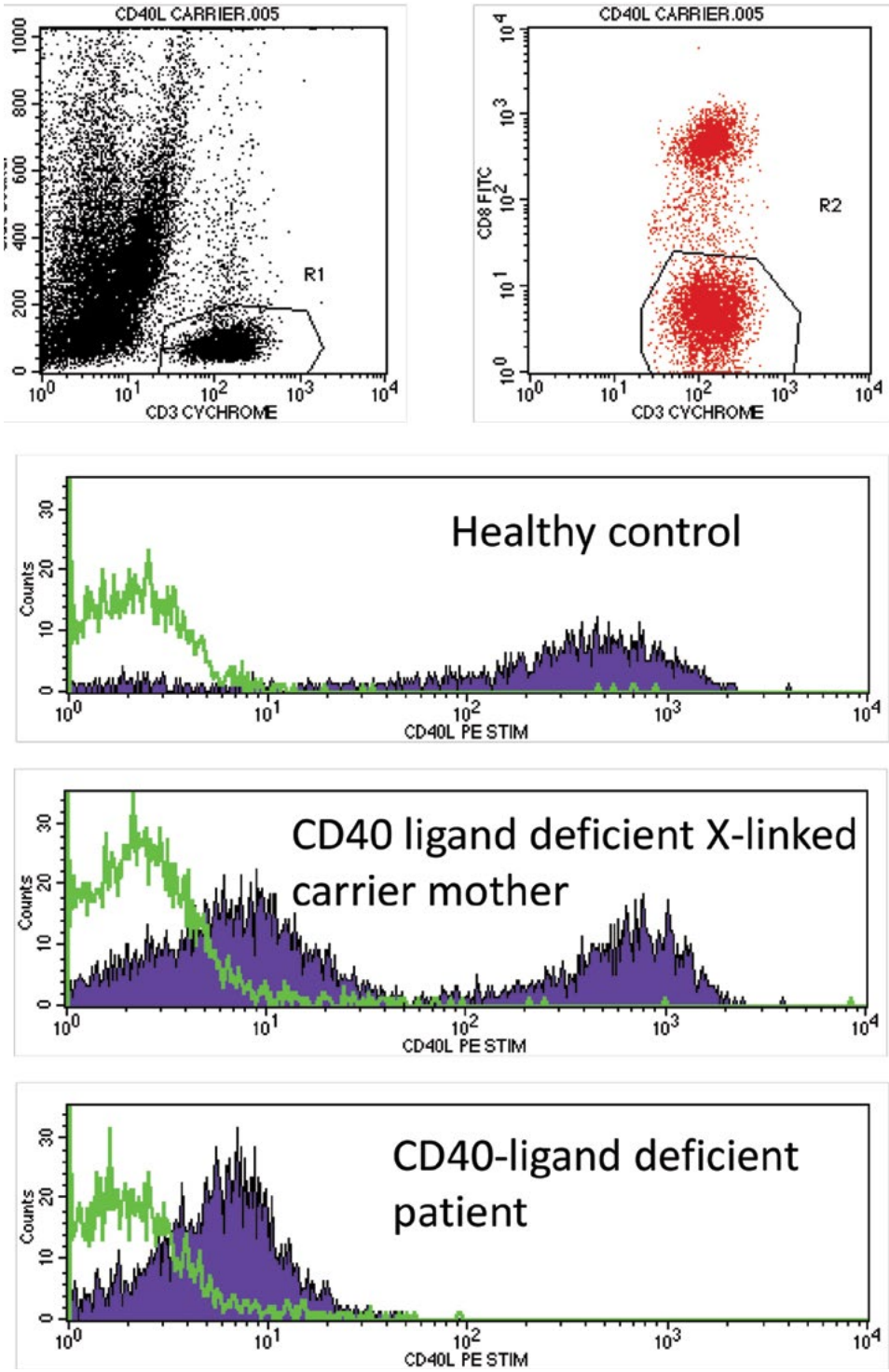

FIGURE 2 Gating algorithm and histogram display of CD40-ligand upregulation on *in vitro* activated CD4 positive T cells. (Upper left) Dot plot of right angle light scatter versus CD3 (T cells). A gate is drawn around the CD3 positive cluster (R1). The events within R1 are then displayed on a dot plot of CD3 (*x*-axis) vs. CD8 (*y*-axis). A gate is drawn around the CD3 positive events and the CD8 negative events which contain primarily CD4 positive T cells. The expression of CD40 ligand is then assessed on the $CD3^{+}CD8^{-}$ T cells. Each dot plot illustrates the level of CD40-ligand (purple) overlaid on an isotype control (green). Note the middle histogram displays the results from the CD40-ligand deficient patient's mother, who is an X-linked carrier. Note the two populations of T cells, one with a normal level and one with a level essentially overlapping the CD40 ligand level observed on the activated T cells of her son. These results are essentially diagnostic of the X-linked hyper IgM syndrome.

species, which in turn results in abnormal microbial killing within phagocytes. Abnormal phagocyte NADPH oxidase activity is caused by mutations in one of five known NADPH subunit genes, i.e., CYBB (gp91^{phox}), CYBA (p22 ^{phox}), NCF1 (p47 ^{phox}), NCF2 (p67 ^{phox}), and NCF4 (p40^{phox}). The most common form of CGD is caused by mutations in the X-linked gene, *gp91phox* (70% of CGD cases); the remainder of the cases occur as a result of mutations in the autosomally encoded genes: *p22phox* (the other component of membrane flavocytochrome b558), *p47phox*, and *p67phox* (16). Patients with mutations in any of these genes have a common phenotype, including susceptibility to recurrent bacterial and fungal infections as well as granuloma formation and other associated autoimmune complications. Most patients, if not diagnosed and treated, will succumb to the disease.

The Oxidative Burst Assay as a Screening Test for the Diagnosis of CGD

The principle of the flow cytometry-based oxidative burst assay is the detection of an increase in fluorescence from a nonfluorescent oxygen-sensitive dye following the induced exposure to reactive oxygen intermediates generated during an oxidative burst. Patients with CGD are unable generate an oxidative burst and are easily identified because they cannot oxidize the dye (i.e., dye will remain nonfluorescent). The first flow cytometry-based procedures utilized dichlorofluorescein diacetate (DCFH-DA), which was added to PBMCs following their isolation, washing, and counting. Our laboratory developed a simplified procedure using the uncharged nonfluorescent dye dihydrorhodamine 123 (DHR-123), added directly to whole blood. This modification simplified the procedure, allowing for the use of less blood and a much faster turnaround time than previously published methods (17, 18). The assay developed in our laboratory has become widely adopted internationally. Briefly, appropriately titered DHR-123 is added directly to diluted whole blood and incubated in a shaking water bath at 37°C for 15 minutes, followed by the addition of PMA for an additional 15 minutes at 37°C. After these incubations, the red blood cells are lysed (ammonium chloride-based solutions are preferred to prevent the dye from leaking out of the cells too quickly), the remaining cells are fixed in 1% paraformaldehyde, and samples are run immediately on the flow cytometer. Results are expressed as a ratio of the fluorescence in stimulated cells to the fluorescence observed in unstimulated cells, which is referred to as the normal oxidative index (NOI). It is recommended that laboratories performing this assay develop their own normal ranges. In the absence of confirmed CGD in a family member, abnormal results require follow-up genetic testing to confirm mutations in one of the known components of the phagocyte NADPH oxidase system. Generally patients with the autosomal form of CGD (p47phox) have significantly higher NOI than the patients with X-linked CGD (gp91phox) and the fluorescence levels can be more variable (increased CV) than those in both the X-linked CGD patients and healthy non-diseased controls (19). It is important to note that false-positive results (i.e., result is consistent with CGD) have been observed in patients with complete myeloperoxidase deficiency (20). It is recommended that MPO levels be assessed in all patients with a positive flow cytometry result (consistent with CGD).

The assay also successfully identifies patients who are carriers of the X-linked form of CGD. X-linked CGD carriers with less than 15% normal granulocytes can be readily identified in the flow cytometry based DHR123 assay, whereas such patients cannot be reliably diagnosed in the nitroblue tetrazolium CGD assay. Parents of CGD patients with the autosomal forms of the disease will have oxidative burst assay results that are consistent with normal (personal experience). The DHR-based flow cytometry oxidative burst assay is very sensitive. Vowells (19), using a similar flow-based DHR 123 procedure, was able to consistently detect 0.1% normal granulocytes when they were mixed with a CGD patient's cells. The gating and the results obtained from a normal control, an X-linked CGD patient, and the X-linked CGD patient's mother (an X-linked carrier) are presented as Fig. 3.

Measurement of Abnormal T Cell and NK Cell Cytotoxicity as an Aid in the Diagnosis of Patients Suspected of FHL Syndromes

Hemophagocytic lymphohistiocytosis (HLH) represents a life-threatening hyperinflammatory syndrome caused by the over-activation of T cells and macrophage. Primary or familial hemophagocytic lymphohistiocytosis (FHL) is fatal, and the only current treatment is bone marrow transplantation. Secondary HLH occurs in the setting of systemic autoimmunity, hematologic malignancy, and severe infection. Secondary HLH is clinically indistinguishable from FHL but has been successfully treated with immunosuppression. Both forms of the disease are triggered by infection and are very difficult to differentiate unless the underlying genetic etiology is identified. However, sequencing is expensive and can take several weeks, and not all genetic causes have been identified. An early test to differentiate primary versus secondary HLH would allow for the initiation of appropriate therapy early in the course of disease.

Killing by cytotoxic T cells and NK cells represents a significant immune function responsible for the elimination and control of virus-infected cells and transformed tumor cells. A surrogate of killing potential can be assessed by the stimulation and subsequent measurement of specific markers associated with the cytotoxic granule degranulation process expressed on the surface of NK cells and cytotoxic T cells (21). Flow cytometry-based degranulation assays have become available for the rapid diagnostic assessment of patients suspected of FHL syndromes. A recent prospective evaluation of a standardized functional assay of cytotoxic degranulation suggests this assay can provide a rapid and reliable method to help classify patients suspected of primary (FHL) versus secondary HLH (22).

MEASUREMENT OF CELL SURFACE CD107A AS A SURROGATE OF THE DEGRANULATION PROCESS INVOLVED IN T CELL AND NK CELL CYTOTOXICITY

CD107a is present in the lysosomes of NK cells and T cells along with perforin and is expressed on their cell surface following the engagement of the T cell receptor and activating receptors on NK cells. The induced expression of CD107a on the cell surface is thought to reflect exocytosis of lytic granules from these cells. Four European reference laboratories developed a standardized a procedure to measure the surface expression of CD107a on T cells and NK cells as a surrogate measure of cytotoxic degranulation and prospectively evaluated the ability of the assay to detect and differentiate primary (familial) from secondary HLH (20). The test is performed as follows. PBMCs are isolated from whole blood and rested either overnight in culture media with or without IL-2 (NK cell cytotoxicity) or in culture for 2 days with phytohemagglutinin (T cell cytotoxicity). Following the incubation period, the PBMCs (both resting

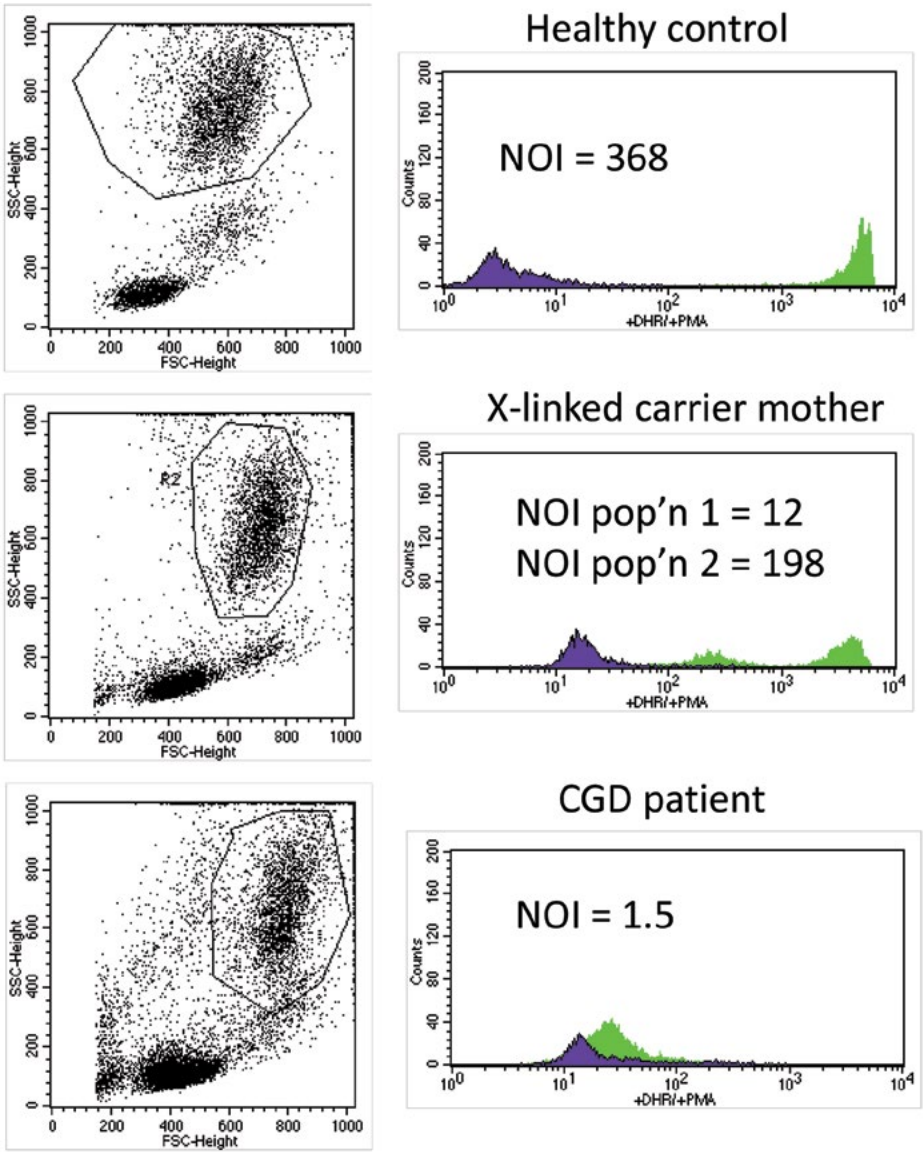

FIGURE 3 The flow cytometry oxidative burst assay for normal healthy control father (top), X-linked CGD carrier mother, and CGD patient. Granulocytes are gated on their innate forward and right angle light scatter properties (left column). The right-hand column presents histograms of the DHR (FL1/FITC) fluorescence levels of unstimulated whole blood granulocytes incubated with the dye (purple) overlaid on PMA-stimulated granulocytes that had been preincubated with DHR (green). Note the middle histogram results of the X-linked carrier mother with two populations of granulocytes, ne with a normal NOI (NOI = 198) and one with an abnormal NOI (NOI = 12). Normal NOI is >30 (developed in our laboratory by testing 35 normal healthy controls).

and activated) are cultured with and without K562 cells for 2 hours at 37°C and then stained for cell surface expression of CD107a and NK markers ($CD3^{-}CD56^{+}$). Cytotoxic T cell activity is assessed after 48 hours of incubation with phytohemagglutinin followed by staining with CD107a and cytotoxic T cell markers ($CD3^{+}CD8^{+}$).

Results are expressed as delta percent CD107a for NK cell cytotoxicity (difference in the percent positive between the NK cells cultured with versus NK cells cultured without NK-sensitive K562 target cells) or the delta mean fluorescent intensity of CD107a for activated T cells. The results of a prospective study of patients suspected of primary or secondary HLH indicated that the resting NK cell degranulation assay (not stimulated by IL-2 overnight) was 96% sensitive and 88% specific for reliably classifying patients as having primary HLH. Although the CTL assays performed equally well, the authors (20) suggest that CTL assays are optional and more useful for patients with very few NK cells. There are only a few institutions in the United States currently performing degranulation assays to help diagnose and classify HLH.

SUMMARY

Diagnosis of any of the more than 200 primary immunodeficiency diseases remains challenging due to the scope of genetic defects and variations in clinical presentations. The

ability to measure functional immune parameters *in vitro* has allowed for the development of flow cytometry procedures that aid in the diagnosis of specific primary immunodeficiency diseases, provide important adjunct information towards a diagnosis, or can serve to significantly limit the time, cost, and scope of the diagnostic odyssey. This chapter presents an overview of specific immunodeficiency diseases where relatively simple flow cytometry-based procedures have been developed to aid in their assessment.

REFERENCES

1. **Al-Herz W, Bousfiha A, Casanova JL, Chatila T, Conley ME, Cunningham-Rundles C, Etzioni A, Franco JL, Gaspar HB, Holland SM, Klein C, Nonoyama S, Ochs HD, Oksenhendler E, Picard C, Puck JM, Sullivan K, Tang ML.** 2014. Primary immunodeficiency diseases: an update on the classification from the international union of immunological societies expert committee for primary immunodeficiency. *Front Immunol* **5:**162. Erratum, *Front Immunol.* **5:**460, 2014.
2. **Nijman IJ, van Montfrans JM, Hoogstraat M, Boes ML, van de Corput L, Renner ED, van Zon P, van Lieshout S, Elferink MG, van der Burg M, Vermont CL, van der Zwaag B, Janson E, Cuppen E, Ploos van Amstel JK, van Gijn ME.** 2014. Targeted next-generation sequencing: a novel diagnostic tool for primary immunodeficiencies. *J Allergy Clin Immunol* **133:**529–534. PubMed
3. **Uzel G, Holland SM.** 2001. Chapter 37, p 37.1–37.18. *In* Rich RR, Fleisher TA, Shearer WT, Kotzin BL, Schroeder HW Jr (ed), *Clinical Immunology Principles and Practice*, 2nd ed. Mosby Int Ltd, St. Louis, MO.
4. **Ottenhoff TH, de Boer T, Verhagen CE, Verreck FA, van Dissel JT.** 2000. Human deficiencies in type 1 cytokine receptors reveal the essential role of type 1 cytokines in immunity to intracellular bacteria. *Microbes Infect* **2:**1559–1566. PubMed
5. **Ottenhoff TH, Mutis T.** 1995. Role of cytotoxic cells in the protective immunity against and immunopathology of intracellular infections. *Eur J Clin Invest* **25:**371–377. PubMed
6. **Jouanguy E1, Lamhamedi-Cherradi S, Lammas D, Dorman SE, Fondanèche MC, Dupuis S, Döffinger R, Altare F, Girdlestone J, Emile JF, Ducoulombier H, Edgar D, Clarke J, Oxelius VA, Brai M, Novelli V, Heyne K, Fischer A, Holland SM, Kumararatne DS, Schreiber RD, Casanova JL.** 1999. A human IFNGR1 small deletion hotspot associated with dominant susceptibility to mycobacterial infection. *Nat Genet* **21:**370–378.
7. **Ottenhoff TH, De Boer T, van Dissel JT, Verreck FA.** 2003. Human deficiencies in type-1 cytokine receptors reveal the essential role of type-1 cytokines in immunity to intracellular bacteria. *Adv Exp Med Biol* **531:**279–294. PubMed
8. **Mizoguchi Y, Tsumura M, Okada S, Hirata O, Minegishi S, Imai K, Hyakuna N, Muramatsu H, Kojima S, Ozaki Y, Imai T, Takeda S, Okazaki T, Ito T, Yasunaga S, Takihara Y, Bryant VL, Kong XF, Cypowyj S, Boisson-Dupuis S, Puel A, Casanova JL, Morio T, Kobayashi M.** 2014. Simple diagnosis of STAT1 gain-of-function alleles in patients with chronic mucocutaneous candidiasis. *J Leukocyte Biol* **95:**667–676.
9. **Liu L, et al.** 2011. Gain-of-function human STAT1 mutations impair IL-17 immunity and underlie chronic mucocutaneous candidiasis. *J Exp Med* **208:**1635–1648.
10. **MacPherson M, Lek HS, Morrison V, Fagerholm S.** 2013. Leukocyte beta2-integrins; genes and disease. *J Genet Syndr Gene Ther* **4:**154. doi:10.4172/2157-7412.1000154. http://www.omicsonline.org/leukocyte-beta2-integrins-genes-and-disease-2157-7412.1000154.php?aid=15565
11. **O'Gorman MR, McNally AC, Anderson DC, Myones BL.** 1993. A rapid whole blood lysis technique for the diagnosis of moderate or severe leukocyte adhesion deficiency (LAD). *Ann N Y Acad Sci* **677:**427–430. PubMed
12. **Dimanche-Boitrel MT, Le Deist F, Quillet A, Fischer A, Griscelli C, Lisowska-Grospierre B.** 1989. Effects of interferon-gamma (IFN-gamma) and tumor necrosis factor-alpha (TNF-alpha) on the expression of LFA-1 in the moderate phenotype of leukocyte adhesion deficiency (LAD). *J Clin Immunol* **9:**200–207. PubMed
13. **O'Gorman MR, Zaas D, Paniagua M, Corrochano V, Scholl PR, Pachman LM.** 1997. Development of a rapid whole blood flow cytometry procedure for the diagnosis of X-linked hyper-IgM syndrome patients and carriers. *Clin Immunol Immunopathol* **85:**172–181. PubMed
14. **Freyer DR, Gowans LK, Warzynski M, Lee WI.** 2004. Flow cytometric diagnosis of X-linked hyper-IgM syndrome: application of an accurate and convenient procedure. *J Pediatr Hematol Oncol* **26:**363–370. PubMed
15. **Ferrari S, Giliani S, Insalaco A, Al-Ghonaium A, Soresina AR, Loubser M, Avanzini MA, Marconi M, Badolato R, Ugazio AG, Levy Y, Catalan N, Durandy A, Tbakhi A, Notarangelo LD, Plebani A.** 2001. Mutations of CD40 gene cause an autosomal recessive form of immunodeficiency with hyper IgM. *Proc Natl Acad Sci USA* **98:**12614–12619.
16. **Segal BH, Leto TL, Gallin JI, Malech HL, Holland SM.** 2000. Genetic, biochemical, and clinical features of chronic granulomatous disease. *Medicine (Baltimore)* **79:**170–200. PubMed
17. **Rothe G, Oser A, Valet G.** 1988. Dihydrorhodamine 123: a new flow cytometric indicator for respiratory burst activity in neutrophil granulocytes. *Naturwissenschaften* **75:**354–355. PubMed
18. **O'Gorman MR, Corrochano V.** 1995. Rapid whole-blood flow cytometry assay for diagnosis of chronic granulomatous disease. *Clin Diagn Lab Immunol* **2:**227–232.
19. **Vowells SJ, Fleisher TA, Sekhsaria S, Alling DW, Maguire TE, Malech HL.** 1996. Genotype-dependent variability in flow cytometric evaluation of reduced nicotinamide adenine dinucleotide phosphate oxidase function in patients with chronic granulomatous disease. *J Pediatr* **128:**104–107. PubMed
20. **Mauch L, Lun A, O'Gorman MR, Harris JS, Schulze I, Zychlinsky A, Fuchs T, Oelschlägel U, Brenner S, Kutter D, Rösen-Wolff A, Roesler J.** 2007. Chronic granulomatous disease (CGD) and complete myeloperoxidase deficiency both yield strongly reduced dihydrorhodamine 123 test signals but can be easily discerned in routine testing for CGD. *Clin Chem* **53:**890–896. PubMed
21. **Alter G, Malenfant JM, Altfeld M.** 2004. CD107a as a functional marker for the identification of natural killer cell activity. *J Immunol Methods* **294:**15–22. PubMed
22. **Marcenaro S, Gallo F, Martini S, Santoro A, Griffiths GM, Aricó M, Moretta L, Pende D.** 2006. Analysis of natural killer-cell function in familial hemophagocytic lymphohistiocytosis (FHL): defective CD107a surface expression heralds Munc13-4 defect and discriminates between genetic subtypes of the disease. *Blood* **108:**2316–2323. PubMed

Acute Lymphoblastic Leukemia/Lymphoma: Diagnosis and Minimal Residual Disease Detection by Flow Cytometric Immunophenotyping

JOSEPH A. DiGIUSEPPE

21

Acute lymphoblastic leukemia (ALL) and lymphoblastic lymphoma are malignant neoplasms of progenitor cells committed to B-lineage or T-lineage lymphopoiesis, termed lymphoblasts (1). Distinction between lymphoblastic leukemia (predominantly bone marrow with or without peripheral blood involvement) and lymphoblastic lymphoma (predominantly mass-forming nodal and/or extranodal disease) is largely clinical; however, the presence of greater than 25% bone marrow blasts generally prompts the designation of "leukemia" in most protocols, regardless of the presence of a mass lesion (2, 3). In the most recent World Health Organization (WHO) classification (2–4), B lymphoblastic leukemia/lymphoma is further subclassified on the basis of recurrent genetic abnormalities, while T lymphoblastic leukemia/lymphoma, despite the existence of recurrent genetic abnormalities, is not further subclassified (Table 1).

On the basis of morphology alone, B and T lymphoblastic leukemia/lymphoma cannot be distinguished from one another; nor, in many instances, can either be distinguished from acute myeloid leukemia (AML). With an appropriate panel of monoclonal antibodies, though, immunophenotyping by flow cytometry enables accurate resolution among these diagnostic entities in a matter of hours, thereby permitting the institution of appropriate therapy in a timely fashion. In certain instances, flow cytometric immunophenotyping may also anticipate recurrent genetic abnormalities. Finally, flow cytometry has been used to identify rare leukemic cells in patients who have achieved remission by conventional clinical and pathologic criteria. The presence of such "minimal residual disease" (MRD) is strongly associated with risk of recurrence (5–7), and its early detection enables more precise risk stratification in the selection of postinduction therapy.

NORMAL COUNTERPARTS

Antigenic expression by neoplastic lymphoblasts resembles, albeit imperfectly, that of their normal counterparts. It is therefore helpful to understand the spectrum of antigenic changes that occurs during normal B-lymphopoiesis in the bone marrow and T-cell maturation in the thymus.

Although earlier stages in B-cell ontogeny have been detected in small numbers in normal human bone marrow (8, 9), as a practical matter, surface-membrane CD19 expression identifies a preponderance of bone marrow cells committed to B-lymphopoiesis. Immunophenotypic patterns of maturation among $CD19^+$ B-cell precursors (historically referred to as "hematogones") are characteristic (10–12) and are illustrated in Fig. 1. As maturation proceeds, expression of CD19, CD20, and CD45 increases, while that of terminal deoxynucleotidyl transferase (TdT) (not shown), CD10, CD34, and CD38 is lost (Fig. 1). Many of these changes are coordinated in a stepwise fashion such that early, intermediate, and late stages can be described (12). Polytypic surface-membrane immunoglobulin light chain expression is first detectable on intermediate- or late-stage precursors, after the loss of TdT and CD34, while mature B cells are $CD10^-$, with bright CD20 and CD45 (Fig. 1).

T-cell maturation in the thymus likewise proceeds through a series of immunophenotypic stages (11, 13). As with B-cell precursors in bone marrow, the earliest thymic T-cell precursors are TdT^+, $CD10^+$, $CD34^+$, and $CD45^{(dim)+}$ (Fig. 2). CD3 is expressed in the cytoplasm, but not on the cell membrane, in these $CD4^-/CD8^-$ ("double-negative") T cells, the least differentiated of which are termed early T-cell precursors (ETPs) (14). With maturation, there is progressive expression of CD4, which is subsequently accompanied by that of CD8 in so-called "double-positive" cortical thymocytes. Acquisition of CD4 and CD8 expression is accompanied by CD1a expression, an increase in CD45 density, and loss of TdT, CD10, and CD34. Loss of CD1a, acquisition of surface-membrane CD3, and loss of CD8 or CD4, respectively, yield mature $CD4^+$ or $CD8^+$ T cells.

DIAGNOSIS

As noted previously, flow cytometric immunophenotyping with an appropriate panel of monoclonal antibodies permits distinction of B- and T-lymphoblastic leukemia/lymphoma from each other and from AML. Although each clinical laboratory typically develops its own panel of antibodies, certain antigens are generally acknowledged as being most useful for the diagnosis of ALL/lymphoblastic lymphoma (reviewed in references 1–4, 15, and 16). More recent studies have identified additional antigens useful in the context of MRD detection (17–22). Table 2 lists the antibody combinations used in our laboratory. Not all of these are required in every case, though. Combinations 1, 2, and 8 through 10 would suffice to establish a diagnosis of B lymphoblastic

doi:10.1128/9781555818722.ch21

TABLE 1 World Health Organization classification of precursor lymphoid neoplasms (2–4)

B lymphoblastic leukemia/lymphoma, not otherwise specified
B lymphoblastic leukemia/lymphoma with recurrent genetic abnormalities
B lymphoblastic leukemia/lymphoma with t(9;22)(q34;q11.2); *BCR-ABL1*
B lymphoblastic leukemia/lymphoma with t(v;11q23); *MLL* rearranged
B lymphoblastic leukemia/lymphoma with t(12;21)(p13;q22); *TEL-AML1* (*ETV6-RUNX1*)
B lymphoblastic leukemia/lymphoma with hyperdiploidy
B lymphoblastic leukemia/lymphoma with hypodiploidy (Hypodiploid ALL)
B lymphoblastic leukemia/lymphoma with t(5;14)(q31;q32); *IL3-IGH*
B lymphoblastic leukemia/lymphoma with t(1;19)(q23;p13.3); *E2A-PBX1* (*TCF3-PBX1*)
T lymphoblastic leukemia/lymphoma

leukemia and to exclude mixed-phenotype acute leukemia, while combinations 1 and 6 through 10 would permit the diagnosis of T lymphoblastic leukemia and exclusion of mixed-phenotype acute leukemia. Antibody combinations used for the detection of MRD in B and T lymphoblastic leukemia are also indicated in Table 2.

Important methodologic and quality-control issues that are generally applicable to flow cytometric immunophenotyping have been discussed in detail separately (Biancotto and McCoy, chapter 17, this volume). However, a few specific practices are recommended to improve the quality of the immunophenotypic data acquired in acute leukemia: exclusion of cellular doublets and other coincident events, exclusion of debris and nonviable cells, and identification of an appropriate blast gate for the leukemia in question. When fluorochrome-conjugated antibodies bound to more than one cellular event are simultaneously excited by the laser, whether due to statistical coincidence or cellular aggregation, the resulting signals do not accurately reflect the phenotype of any single cellular population. These artifactual data can be excluded by gating on singlet events whose area, height, and width signals are highly correlated (23) (Fig. 3). Nonspecific binding of labeled antibodies and/or fluorochromes to cellular debris, platelets, and nonviable cells is another cause of spurious fluorescence signals. The latter can be reduced by gating on singlet events with the light scatter properties of viable cells (Fig. 3); however, care must be taken to ensure that the neoplastic cells are not inadvertently excluded. Finally, since lymphoblasts commonly express CD45 more weakly than their mature lymphoid counterparts (24), a blast gate comprising $CD45^{(dim)+}/SSC^{(low)}$ events frequently permits exclusion of mature lymphocytes and other cells that could contaminate a conventional mononuclear-cell gate (15) (Fig. 3).

A general principle in the design of antibody panels for lymphoblastic leukemia/lymphoma is that no single surface-membrane antigen is both sensitive and specific for B or T lymphoblastic leukemia. In the case of B lymphoblastic leukemia, CD19 and CD22 are the most commonly expressed lineage-related surface antigens and CD7 is essentially always expressed in T lymphoblastic leukemia. However, all three antigens may also be expressed in AML. Other surface antigens useful in the diagnosis of B lymphoblastic leukemia include CD10 (positive in the vast majority of cases), CD20 (relatively specific for B-cell lineage, but not sensitive), CD34 (positive in most cases), and HLA-DR (which is virtually always positive). In the case of T lymphoblastic leukemia, useful lineage-related surface

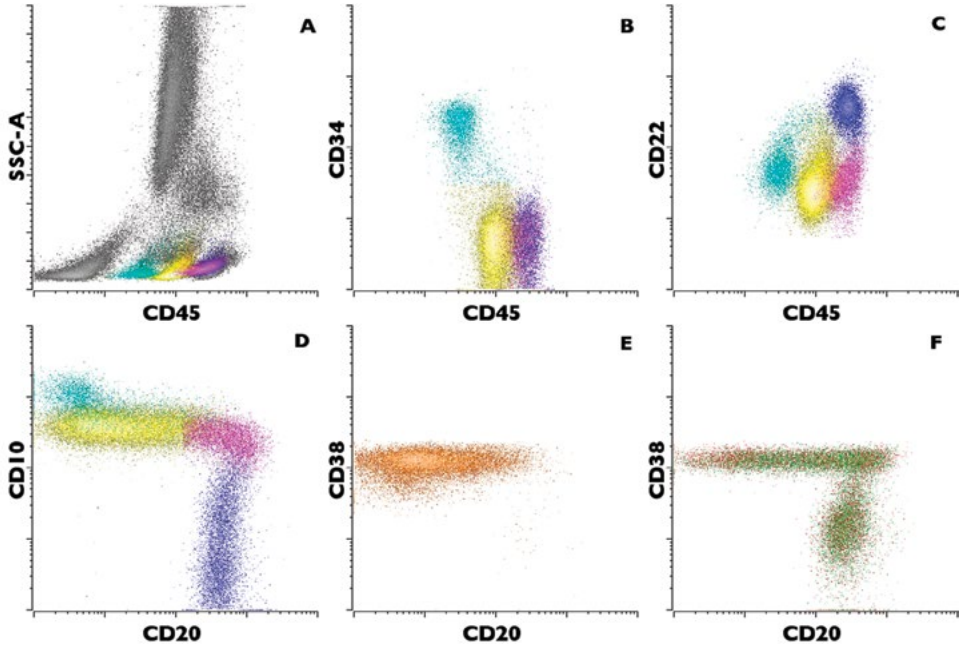

FIGURE 1 Immunophenotypic patterns of normal B-cell maturation in bone marrow. (A) Gated on all viable cells; B-cell maturational stages denoted by different colors. (B through D) Gated only on B cells; B-cell maturational stages denoted by different colors, from least mature (turquoise) to most mature (blue). (E and F) Acquisition of surface-membrane immunoglobulin light chain expression: (E) Gated on light chain-negative B cells (orange); (F) Gated on light chain-positive B cells: kappa (green), lambda (red).

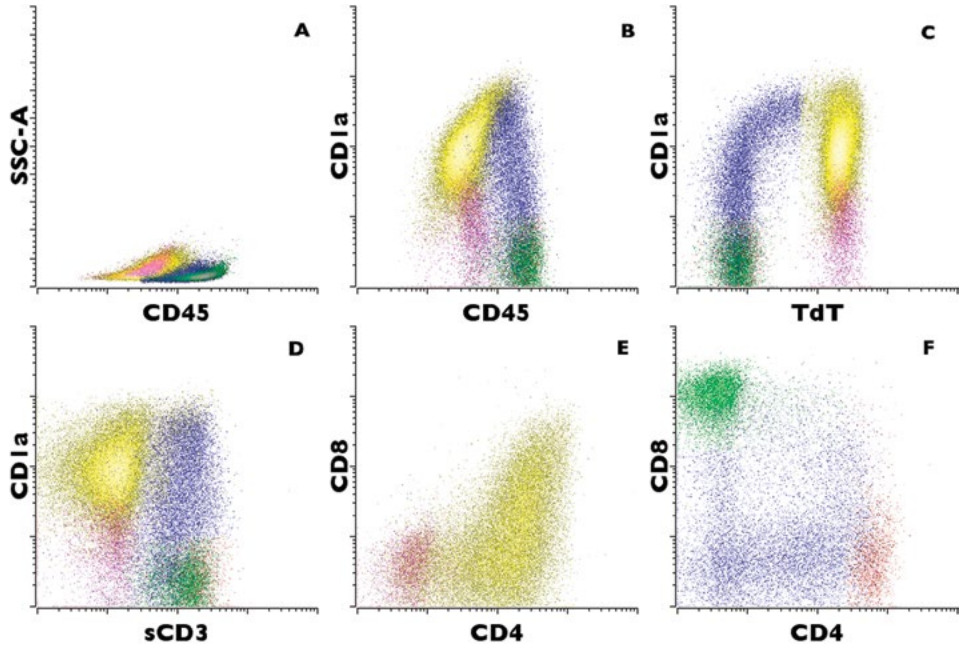

FIGURE 2 Immunophenotypic patterns of normal T-cell maturation in thymus. (A through D). Gated on all cytoplasmic $CD3^+$ T cells; T-cell maturational stages denoted by different colors, from least mature (violet) to most mature (red and green). (E) Gated on sCD3- T cells. (F) Gated on $sCD3^+$ T cells.

antigens include CD1a, CD2, CD3, CD4, CD5, and CD8. The most sensitive of these (CD2) is not specific, while the most specific (CD1a, CD3, and CD8) are seen in fewer than half of cases. CD10, CD34, and HLA-DR may also be expressed in T lymphoblastic leukemia but at a lower frequency than in B lymphoblastic leukemia.

Although no single surface antigen defines T-cell lineage, cytoplasmic expression of the epsilon chain of the T-cell receptor (cyCD3) is both sensitive and specific for T lymphoblastic leukemia (though activated adult natural killer cells apparently may also express cyCD3-ε; 25). A caveat to the use of cyCD3 to define T-cell lineage, however, is that polyclonal antibodies to CD3 commonly used for immunohistochemistry may also react with the zeta chain of the T-cell receptor, which is expressed in natural killer cells (26). In defining B-cell lineage, cytoplasmic CD22 expression is sensitive and relatively specific, though a cross-reacting protein has been reported in AML (27). In contrast, whereas cytoplasmic CD79a is often regarded as a specific pan–B-cell antigen, it is not uncommonly expressed in T lymphoblastic leukemia and in certain forms of AML. TdT is a nuclear antigen that is useful in distinguishing precursor neoplasms

TABLE 2 Sample antibody combinations and applications[a]

	FITC	PE	PerCP-Cy5.5	PE-Cy7	APC	APC-AF750	PB or BV421	V500	Application(s)
1	CD71	CD33	CD123	CD19	CD34	CD38	HLA-DR	CD45	Identify major normal marrow populations
2	Kappa	Lambda	CD20	CD19	CD10	CD38	CD5	CD45	Diagnosis (B lymphoblastic leukemia)
3	CD20	CD22	CD34	CD19	$CD13^+$ CD33	CD38	CD10	CD45	MRD (B lymphoblastic leukemia)
4	CD20	CD49f	CD34	CD19	CD58	CD38	CD10	CD45	MRD (B lymphoblastic leukemia)
5	CD24	CD304	CD34	CD19	CD86	CD38	CD10	CD45	MRD (B lymphoblastic leukemia)
6	CD16	CD56	CD5	CD3	CD7	CD8	CD4	CD45	Diagnosis and MRD (T lymphoblastic leukemia)
7	CD7	CD1a	CD3	CD2	CD5	CD8	CD4	CD45	Diagnosis and MRD (T lymphoblastic leukemia)
8	cyMPO	cyCD3	CD34	—	CD7	—	HLA-DR	CD45	Diagnosis (mixed phenotype acute leukemia, T/myeloid)
9	cyMPO	cyCD22	cyCD79a	CD19	CD34	—	HLA-DR	CD45	Diagnosis (mixed phenotype acute leukemia, B/myeloid)
10	nTdt	cyCD3	cyCD79a	CD19	CD34	—	HLA-DR	CD45	Diagnosis (B and T lymphoblastic leukemia)

[a]Column headings refer to the specific fluorophore to which each monoclonal antibody is conjugated; dashes indicate the absence of a specific fluorophore-conjugated antibody.

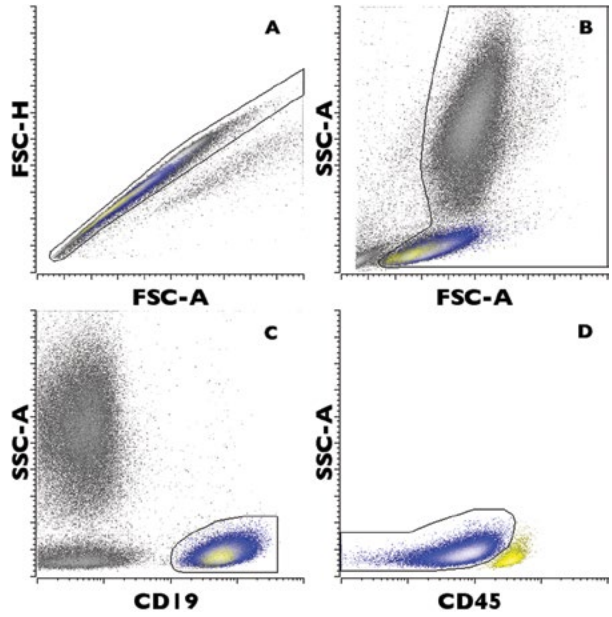

FIGURE 3 Typical gating strategy in B lymphoblastic leukemia. (A) All events displayed; a gate defining single events is illustrated. (B) All single events resulting from the gate shown in panel A are displayed; a gate defining viable cells is illustrated. (C) All viable single events are displayed; a gate defining all $CD19^+$ B cells is illustrated. (D) All viable, single $CD19^+$ B cells are displayed; blasts (blue) may be distinguished from mature B cells (yellow) by gating on CD45-negative to $CD45^{(dim)+}$ events.

from mature B- or T-cell non-Hodgkin lymphomas. TdT is positive in a preponderance of cases of B lymphoblastic leukemia and in somewhat fewer cases of T lymphoblastic leukemia. Since a significant minority of cases of AML also express TdT, though, this antigen cannot be used to distinguish lymphoblastic leukemia from AML.

The prototypic case of B lymphoblastic leukemia is $CD10^+$, $CD19^+$, $CD22^+$, and $CD34^+$, with absent, weak, or partial expression of CD20, dimmer CD45 than mature B cells, and absent immunoglobulin light chains (Fig. 4). Phenotypic variations are common, though. For instance, CD45 expression is highly variable, ranging from essentially absent to levels only slightly dimmer than those seen among mature lymphocytes (28). Monotypic immunoglobulin light chain expression is also a recognized phenotypic variant which is reported in a small minority of cases (29, 30). Expression of myeloid antigens (e.g., CD11b, CD13, CD15, CD33), which is generally weak and/or partial, represents a common phenotypic aberration in both B and T lymphoblastic leukemia and should not, in isolation, be regarded as evidence of mixed-phenotype acute leukemia (26).

Normal T-cell maturation has been used as a framework to distinguish several immunophenotypic patterns seen in T lymphoblastic leukemia/lymphoma (3, 15). Cases resembling pro-T and pre-T stages are negative for CD1a, surface CD3, CD4, and CD8; in fact, cytoplasmic CD3 and CD7 may be the only phenotypic features of T-lineage differentiation in such instances. Expression of CD1a and coexpression of CD4 and CD8 without surface CD3 typify the cortical thymic or "double-positive" phenotype (Fig. 5), while a more mature T-cell phenotype (i.e., CD1a/surface $CD3^+$ with either CD4 or CD8 expression) recapitulates the medullary T stage. Although T lymphoblastic leukemia/lymphoma seldom conforms precisely to these models in clinical practice (e.g., note the paucity of CD1a expression in the otherwise typical example of T lymphoblastic leukemia with a cortical thymic phenotype shown in Fig. 5), a specific immunophenotype corresponding with that of so-called early T-cell precursors (ETPs) appears to define a subset of cases with a distinct gene-expression profile and poor prognosis (31). ETP leukemia may be recognized phenotypically by an absence of CD1a and CD8 expression,

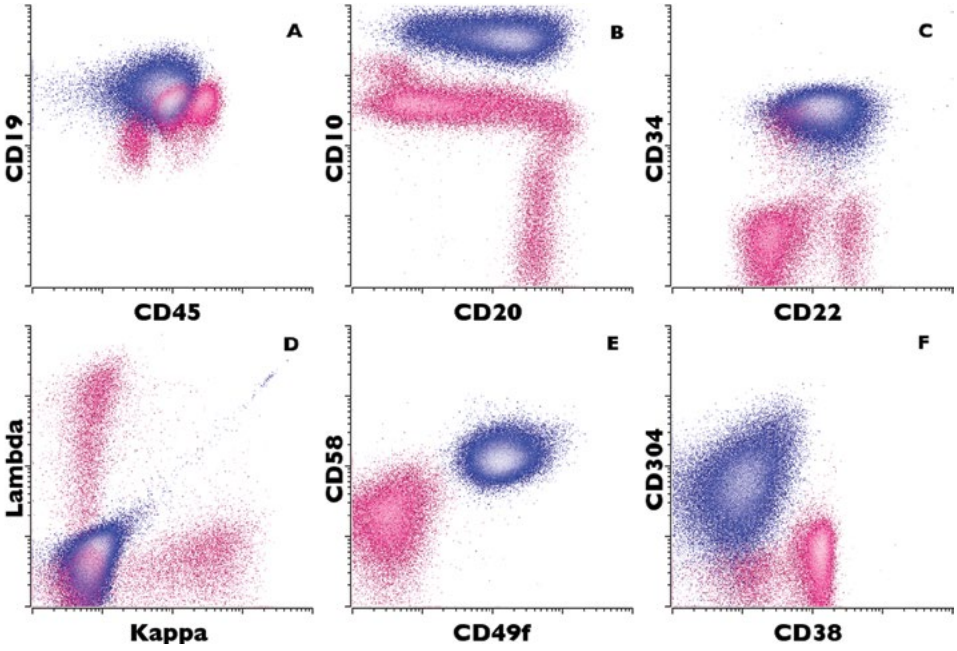

FIGURE 4 Example of B lymphoblastic leukemia. Phenotypic patterns of neoplastic B lymphoblasts (blue, gated as in Fig. 3) are compared with those of normal bone marrow B cells (pink).

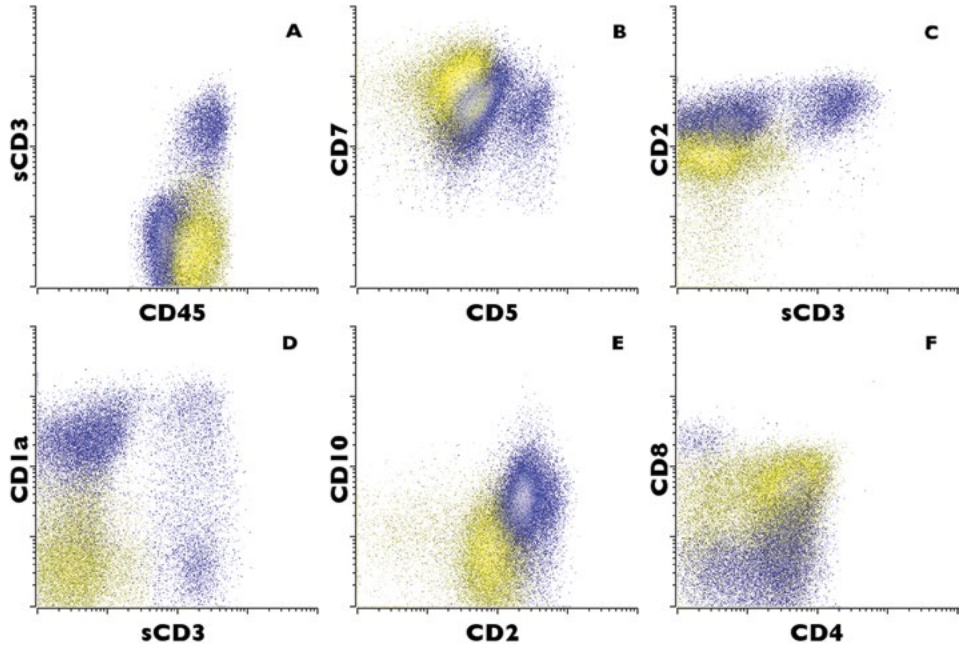

FIGURE 5 Example of T lymphoblastic leukemia. Phenotypic patterns of neoplastic T lymphoblasts (yellow) are compared with those of normal thymic T cells (blue).

with only weak, partial CD5 expression and expression of one or more of the following antigens: HLA-DR, CD11b, CD13, CD33, CD34, CD65, or CD117 (31) (Fig. 6). Since the mutational spectrum of ETP leukemia resembles that of myeloid leukemias, and its gene-expression profile is similar to those of both normal and myeloid leukemic hematopoietic stem cells, it has been speculated that the addition of myeloid-directed therapies might improve the poor prognosis of ETP leukemia (32).

Despite the application of an appropriate antibody panel, unequivocal lineage assignment (i.e., B-lymphoid, T-lymphoid, or myeloid) remains problematic in a small percentage of acute leukemias. Two general immunophenotypic patterns are seen in such cases, which have been

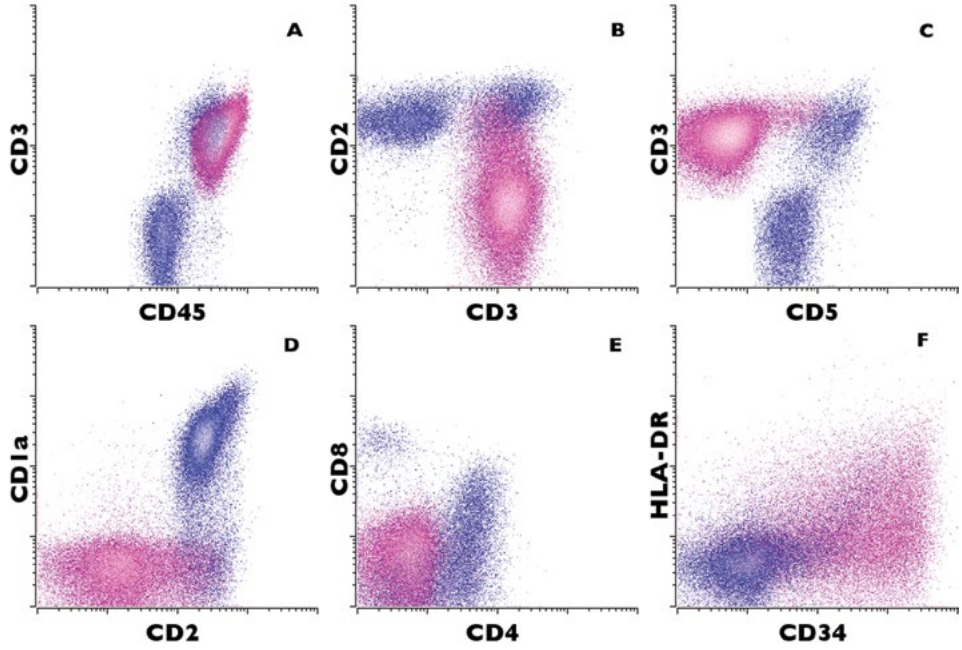

FIGURE 6 Example of early T-cell precursor (ETP) leukemia. In this example, the neoplastic T lymphoblasts (violet) are positive for surface-membrane CD3, with weak CD5 expression in significantly less than 75% of the blasts. CD1a and CD8 are negative, and at least 25% of the blasts express one or more myeloid or stem-cell marker (in this case, CD34). Normal thymic T cells are shown for comparison in blue.

designated "mixed-phenotype acute leukemia" (MPAL) in the most recent WHO classification (26). In the first of these patterns (formerly referred to as bilineal), two immunophenotypically distinct blast populations can be resolved, each with clear immunophenotypic evidence of differentiation along a different lineage (e.g., separate populations of B-lymphoblasts and myeloblasts). In the second pattern (formerly referred to as biphenotypic), a single population of blasts expresses antigens indicative of differentiation along more than one lineage. Since, as noted above, myeloid antigen expression is not unusual in B and T lymphoblastic leukemia, the WHO requirements for assigning more than one lineage to a single blast population are relatively strict: myeloperoxidase or two or more monocytic markers (from among CD11c, CD14, CD64, NSE, and lysozyme) for myeloid lineage; cytoplasmic or surface CD3 for T lineage; and CD19 plus strong expression of at least one (if CD19 is strong) or two (if CD19 is weak) from among CD10, cytoplasmic CD22, and cytoplasmic CD79a for B lineage (26). Notwithstanding the inconsistent definitions and treatments historically applied to MPAL, it appears that the prognosis of these leukemias is significantly worse than that of pediatric ALL (33, 34), though MPAL patients who fail an AML-type regimen may be successfully treated with an ALL-type regimen (33).

IMMUNOPHENOTYPIC-GENOTYPIC AND PROGNOSTIC CORRELATIONS

In certain instances, immunophenotypic features of the lymphoblasts may be associated with specific genetic abnormalities and/or prognosis (Table 3). For example, CD25 expression is significantly more frequent in cases of adult B lymphoblastic leukemia with *BCR-ABL1* than with *BCR-ABL1*-negative cases (35). Cases of B lymphoblastic leukemia with *MLL* rearrangement, and in particular those with *MLL-AF4*, are usually negative for CD10 and at least partially negative for CD24; many also express CD15 (36). B lymphoblastic leukemia with *TCF3-PBX1* is strongly associated with a composite immunophenotype characterized by homogeneous expression of CD9 and CD10, with at least partial absence of CD20 and complete absence of CD34 (37). By comparison, B lymphoblastic leukemia with *ETV6-RUNX1* does not display quite so stereotypic a composite immunophenotype; however, the expression of no more than partial CD9 and CD20 has a positive predictive value of nearly 50% for this translocation (38).

As noted previously, a subset of cases of T lymphoblastic leukemia displays an immunophenotypic profile reminiscent of that seen in normal ETPs. This composite immunophenotype (CD1a-negative, CD8-negative, with no more than weak, partial CD5 and one or more myeloid or stem-cell markers) (Table 3), which has been used to define ETP leukemia, predicts not only a specific gene-expression profile and mutational spectrum but also a poor prognosis (31, 32). Expression of CD13 is also an adverse prognostic factor in T lymphoblastic leukemia, independent of other conventional risk factors (39). Since the adverse prognostic effect of CD13 expression is limited to the subset of cases with a cortical/mature phenotype, it appears not to be attributable simply to its association with the ETP phenotype (39). In contrast, the apparently favorable prognostic effect of CD1a expression (40) could potentially be indirect, as CD1a expression is by definition limited to non-ETP leukemias. Finally, CD11b expression (20) and comparatively bright expression of CD20 (28) and CD45 (28, 41) are associated with poor prognosis in B lymphoblastic leukemia, independent of other risk factors; bright CD45 expression is also an independent adverse prognostic factor in T lymphoblastic leukemia (41).

MRD

With contemporary therapy, an overwhelming preponderance of children and a great majority of adults with ALL achieve disease remission, which is defined as the presence of fewer than 5% morphologic bone marrow blasts and restoration of normal hematopoiesis (42, 43). Nonetheless, an important principle in the curative therapy of patients with ALL is that treatment must continue for an extended period (typically for at least 2 years) in order to prevent an unacceptably high incidence of relapse (42, 43). These observations imply the persistence of residual leukemic blasts at submicroscopic levels in many patients who have attained remission. Indeed, it has been estimated that the total-body leukemic burden of patients with ALL in remission may be as high as 10^{10} (44). It has become clear that the precise quantification of such MRD is among the strongest prognostic factors in ALL and that flow cytometric immunophenotyping is well suited for MRD detection (reviewed in references 45 and 46).

In principle, the immunophenotypic detection of MRD relies on differences in antigen expression between leukemic cells and their normal counterparts. Phenotypic patterns of normal B- and T-lymphopoiesis have been well documented (10–13), and recent work has expanded the range of potentially informative antigens (17–22) such that at least 95% of cases of ALL (45, 46) and virtually all cases of B lymphoblastic leukemia (21) are now detectable by their abnormal immunophenotype (often referred to as a leukemia-associated immunophenotype). In early studies, the specific leukemia-associated immunophenotype documented at diagnosis was sought in posttreatment samples. It has since become apparent, though, that treatment induces phenotypic changes in

TABLE 3 Immunophenotypic-genotypic associations

Diagnostic entity	Phenotypic association(s)
B lymphoblastic leukemia with *BCR-ABL1*	$CD25^+$
B lymphoblastic leukemia with *MLL-AF4*	$CD10^-$, $CD15^+/^-$, $CD24^{-/partial+}$
B lymphoblastic leukemia with *TCF3-PBX1*	CD9 and $CD10^+$, $CD20^{-/partial+}$, $CD34^-$
B lymphoblastic leukemia with *ETV6-RUNX1*	CD9 and $CD20^{-/partial+}$
Early T-cell precursor (ETP) leukemia	CD1a and $CD8^-$, weak $CD5^+$ (<75% of blasts), >25% of blasts positive for one or more of the following: CD11b, CD13, CD33, CD34, CD65, CD117, HLA-DR

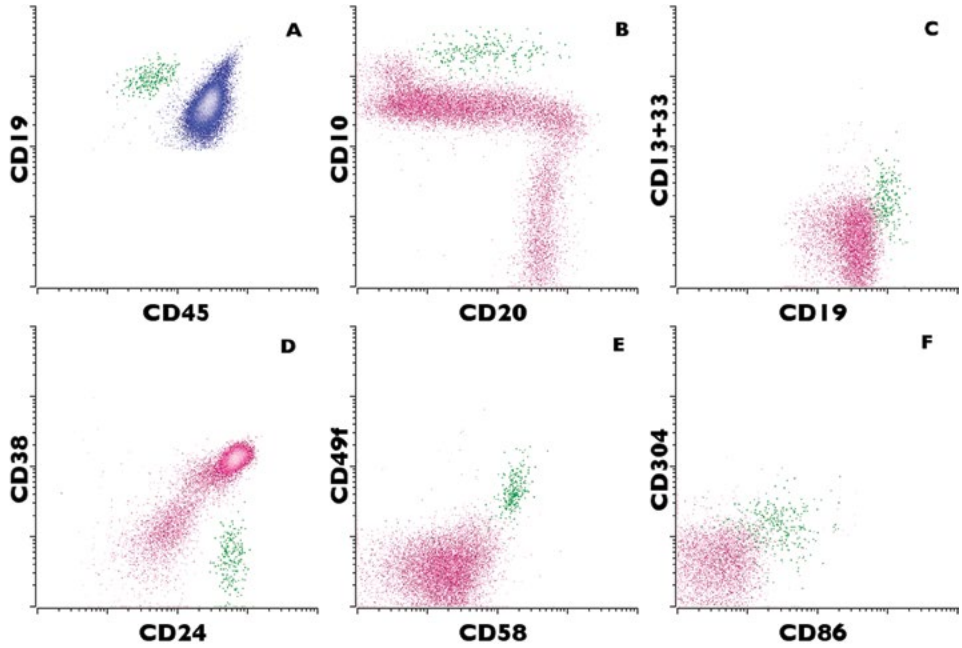

FIGURE 7 Detection of minimal residual disease in B lymphoblastic leukemia. (A) All viable, single $CD19^+$ bone marrow B cells are displayed; a small cluster of cells (0.04% of viable singlets) with comparatively dim CD45 expression (green) can be distinguished from a predominant population of normal B cells (blue). (B through F) Phenotypic features of the minimal residual disease (green, gated as in panel A) are compared with those of normal bone marrow B cells (pink). Compared with normal B-cell precursors, the residual neoplastic cells express abnormally bright CD10, CD19, CD49f, CD58, CD86, and CD304 and are further positive for CD13 and/or CD33. CD38 expression, moreover, is lost.

the leukemic blasts, termed immunophenotypic drift. These phenotypic changes generally reflect maturation of the blasts, an effect thought to be mediated by corticosteroids (47), and have been documented in both B lymphoblastic and T lymphoblastic leukemia (47, 48). As a practical matter, one must not simply evaluate posttreatment samples for the specific phenotype seen at diagnosis, but rather identify populations with a composite immunophenotype that differs from that of normal B- and T-cell precursors.

Although incorporation of several newly identified markers into MRD panels may yield a sensitivity of 0.001%, or 1 in 100,000 cells (21), a level previously attainable only by PCR-mediated amplification of antigen-receptor genes (49), most studies demonstrating the clinical significance of MRD in ALL have reported a sensitivity of 0.01% (1 in 10,000 cells). Visual recognition of a cluster of events in multiparametric space as a distinct cellular population depends both on the magnitude of antigenic deviation from normal and the extent to which antigen expression is homogeneous. However, in general, confident identification of MRD is difficult when fewer than 20 events comprise the putative cluster of cells. Since a sensitivity of 1 in 10,000 cells is required clinically, it is essential that no fewer than 200,000 viable cells be acquired. In our laboratory, as many as 1 million total events are acquired for each antibody combination; when fewer than 250,000 viable cells are collected in a given case, the report indicates that the sensitivity of the assay is compromised. It is also important to be mindful of spurious signals that could simulate a population of MRD. For instance, clinical flow cytometers may have carryover in the range of 0.1%, an order of magnitude higher than the expected analytic sensitivity of the assay. To mitigate the potential for carryover, tubes containing only saline may be placed between those containing antibody-labeled cells.

As noted above, many antigens are differentially expressed in leukemic lymphoblasts relative to normal lymphoid precursors. As a rule, though, these differences are quantitative rather than qualitative. Therefore, when a new antibody combination for MRD detection is implemented, it is essential to document the range of normal patterns of immunoreactivity using control samples from patients without leukemia, including samples from patients with active marrow regeneration following chemotherapy. The immunophenotypic properties of putative MRD populations may then be compared with these previously documented normal patterns to confirm or refute a diagnosis of MRD. The principal antibody combinations used for MRD detection in our laboratory are listed in Table 2 (3, 4, and 5 for B lymphoblastic leukemia; 6 and 7 for T lymphoblastic leukemia). Examples of MRD compared with normal patterns of antigen expression using these combinations are illustrated in Fig. 7 and 8.

SUMMARY

Flow cytometric immunophenotyping comprises an essential component in the diagnosis of ALL, enabling its reliable distinction from AML and acute leukemia of ambiguous lineage. In certain instances, the composite immunophenotype of the leukemic blasts may be associated with specific genetic abnormalities and/or prognosis. Finally, flow cytometry is well suited for the detection of MRD, one of the strongest prognostic factors in ALL.

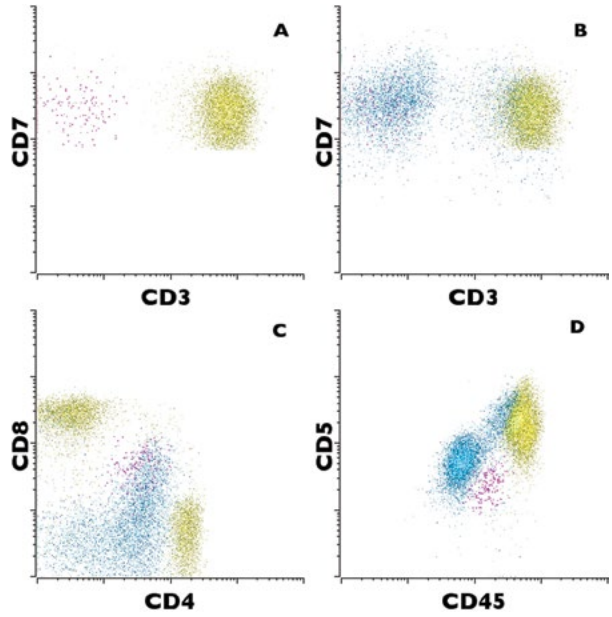

FIGURE 8 Detection of minimal residual disease in T lymphoblastic leukemia. (A) All viable, single bone marrow T cells are displayed; a small cluster of cells (0.2% of viable singlets) with loss of surface CD3 (violet) can be distinguished from a predominant population of normal $sCD3^+$ T cells (yellow). (B through D) The phenotypic features of the minimal residual disease are compared with those of normal thymic T cells (light blue) and the normal mature ($sCD3^+$) T cells contained in the bone marrow sample (yellow). With respect to absence of sCD3 (B) and weak coexpression of CD4 and CD8 (C), the neoplastic T cells resemble normal thymic T cells; however, T cells with a thymic immunophenotype are not detectable in normal bone marrow by flow cytometry. The combination of weak CD5 and intermediate CD45 seen in the minimal residual disease (D), though, differs from both normal thymic T cells and mature T cells. The residual leukemic cells were also partially positive for CD1a and CD10 (not shown).

REFERENCES

1. **Borowitz MJ, DiGiuseppe JA.** 2014. Acute lymphoblastic leukemia/lymphoblastic lymphoma, p 1019–1029. *In* Orazi A, Weiss LM, Foucar K, Knowles DM (ed), *Knowles' Neoplastic Hematopathology*, 3rd ed. Lippincott Williams & Wilkins, Philadelphia, PA.
2. **Borowitz MJ, Chan JKC.** 2008. B lymphoblastic leukaemia/lymphoma, not otherwise specified, p 168–170. *In* Swerdlow SH, Campo E, Harris NL, Jaffe ES, Pileri SA, Stein H, Thiele J, Vardiman JW (ed), *WHO Classification of Tumors of Haematopoietic and Lymphoid Tissues*, 4th ed. International Agency for Research on Cancer (IARC), Lyon, France.
3. **Borowitz MJ, Chan JKC.** 2008. T lymphoblastic leukaemia/lymphoma, not otherwise specified, p 176–178. *In* Swerdlow SH, Campo E, Harris NL, Jaffe ES, Pileri SA, Stein H, Thiele J, Vardiman JW (ed), *WHO Classification of Tumors of Haematopoietic and Lymphoid Tissues*, 4th ed. International Agency for Research on Cancer (IARC), Lyon, France.
4. **Borowitz MJ, Chan JKC.** 2008. B lymphoblastic leukaemia/lymphoma, with recurrent genetic abnormalities, p 171–175. *In* Swerdlow SH, Campo E, Harris NL, Jaffe ES, Pileri SA, Stein H, Thiele J, Vardiman JW (ed), *WHO Classification of Tumors of Haematopoietic and Lymphoid Tissues*, 4th ed. International Agency for Research on Cancer (IARC), Lyon, France.
5. **Coustan-Smith E, Sancho J, Behm FG, Hancock ML, Razzouk BI, Ribeiro RC, Rivera GK, Rubnitz JE, Sandlund JT, Pui CH, Campana D.** 2002. Prognostic importance of measuring early clearance of leukemic cells by flow cytometry in childhood acute lymphoblastic leukemia. *Blood* **100:**52–58.
6. **Dworzak MN, Fröschl G, Printz D, Mann G, Pötschger U, Mühlegger N, Fritsch G, Gadner H, Austrian Berlin-Frankfurt-Münster Study Group.** 2002. Prognostic significance and modalities of flow cytometric minimal residual disease detection in childhood acute lymphoblastic leukemia. *Blood* **99:**1952–1958.
7. **Borowitz MJ, Devidas M, Hunger SP, Bowman WP, Carroll AJ, Carroll WL, Linda S, Martin PL, Pullen DJ, Viswanatha D, Willman CL, Winick N, Camitta BM, Children's Oncology Group.** 2008. Clinical significance of minimal residual disease in childhood acute lymphoblastic leukemia and its relationship to other prognostic factors: a Children's Oncology Group study. *Blood* **111:**5477–5485.
8. **Dworzak MN, Fritsch G, Fröschl G, Printz D, Gadner H.** 1998. Four-color flow cytometric investigation of terminal deoxynucleotidyl transferase-positive lymphoid precursors in pediatric bone marrow: CD79a expression precedes CD19 in early B-cell ontogeny. *Blood* **92:**3203–3209.
9. **Israel E, Kapelushnik J, Yermiahu T, Levi I, Yaniv I, Shpilberg O, Shubinsky G.** 2005. Expression of CD24 on CD19- CD79a+ early B-cell progenitors in human bone marrow. *Cell Immunol* **236:**171–178.
10. **McKenna RW, Washington LT, Aquino DB, Picker LJ, Kroft SH.** 2001. Immunophenotypic analysis of hematogones (B-lymphocyte precursors) in 662 consecutive bone marrow specimens by 4-color flow cytometry. *Blood* **98:**2498–2507.
11. **Kroft SH.** 2004. Role of flow cytometry in pediatric hematopathology. *Am J Clin Pathol* **122**(Suppl 1)**:**S19–S32.
12. **Wood BL.** 2004. Multicolor immunophenotyping: human immune system hematopoiesis. *Methods Cell Biol* **75:**559–576.
13. **Li S, Juco J, Mann KP, Holden JT.** 2004. Flow cytometry in the differential diagnosis of lymphocyte-rich thymoma from precursor T-cell acute lymphoblastic leukemia/lymphoblastic lymphoma. *Am J Clin Pathol* **121:**268–274.
14. **Rothenberg EV, Moore JE, Yui MA.** 2008. Launching the T-cell-lineage developmental programme. *Nat Rev Immunol* **8:**9–21.
15. **DiGiuseppe JA.** 2007. Acute lymphoblastic leukemia: diagnosis and detection of minimal residual disease following therapy. *Clin Lab Med* **27:**533–549.
16. **DiGiuseppe JA, Mnayer L.** 2012. Acute leukemias, p 345–363. *In* Kottke-Marchant K, Davis B (ed), *Laboratory Hematology Practice*. Wiley-Blackwell, Hoboken, NJ.
17. **Hassanein NM, Alcancia F, Perkinson KR, Buckley PJ, Lagoo AS.** 2009. Distinct expression patterns of CD123 and CD34 on normal bone marrow B-cell precursors ("hematogones") and B lymphoblastic leukemia blasts. *Am J Clin Pathol* **132:**573–580.
18. **Muzzafar T, Medeiros LJ, Wang SA, Brahmandam A, Thomas DA, Jorgensen JL.** 2009. Aberrant underexpression of CD81 in precursor B-cell acute lymphoblastic leukemia: utility in detection of minimal residual disease by flow cytometry. *Am J Clin Pathol* **132:**692–698.
19. **DiGiuseppe JA, Fuller SG, Borowitz MJ.** 2009. Overexpression of CD49f in precursor B-cell acute lymphoblastic leukemia: potential usefulness in minimal residual disease detection. *Cytometry B Clin Cytom* **76B:**150–155.
20. **Rhein P, Mitlohner R, Basso G, Gaipa G, Dworzak MN, Kirschner-Schwabe R, Hagemeier C, Stanulla M, Schrappe M, Ludwig WD, Karawajew L, Ratei R.**

2010. CD11b is a therapy resistance and minimal residual disease-specific marker in precursor B-cell acute lymphoblastic leukemia. *Blood* **115:**3763–3771.

21. **Coustan-Smith E, Song G, Clark C, Key L, Liu P, Mehrpooya M, Stow P, Su X, Shurtleff S, Pui CH, Downing JR, Campana D.** 2011. New markers for minimal residual disease detection in acute lymphoblastic leukemia. *Blood* **117:**6267–6276.
22. **Solly F, Angelot F, Garand R, Ferrand C, Seillès E, Schillinger F, Decobecq A, Billot M, Larosa F, Plouvier E, Deconinck E, Legrand F, Saas P, Rohrlich PS, Garnache-Ottou F.** 2012. CD304 is preferentially expressed on a subset of B-lineage acute lymphoblastic leukemia and represents a novel marker for minimal residual disease detection by flow cytometry. *Cytometry A* **81A:**17–24.
23. **Wood B.** 2006. 9-color and 10-color flow cytometry in the clinical laboratory. *Arch Pathol Lab Med* **130:**680–690.
24. **Borowitz MJ, Guenther KL, Shults KE, Stelzer GT.** 1993. Immunophenotyping of acute leukemia by flow cytometric analysis. Use of CD45 and right-angle light scatter to gate on leukemic blasts in three-color analysis. *Am J Clin Pathol* **100:**534–540.
25. **Lanier LL, Chang C, Spits H, Phillips JH.** 1992. Expression of cytoplasmic CD3 epsilon proteins in activated human adult natural killer (NK) cells and CD3 gamma, delta, epsilon complexes in fetal NK cells. Implications for the relationship of NK and T lymphocytes. *J Immunol* **149:**1876–1880.
26. **Borowitz MJ, Bene M-C, Harris NL, Porwitt A, Matutes E.** 2008. Acute leukaemias of ambiguous lineage, p 150–155. *In* Swerdlow SH, Campo E, Harris NL, Jaffe ES, Pileri SA, Stein H, Thiele J, Vardiman JW (ed), *WHO Classification of Tumors of Haematopoietic and Lymphoid Tissues*, 4th ed. International Agency for Research on Cancer (IARC), Lyon, France.
27. **Boue DR, LeBien TW.** 1988. Expression and structure of CD22 in acute leukemia. *Blood* **71:**1480–1486.
28. **Borowitz MJ, Shuster J, Carroll AJ, Nash M, Look AT, Camitta B, Mahoney D, Lauer SJ, Pullen DJ.** 1997. Prognostic significance of fluorescence intensity of surface marker expression in childhood B-precursor acute lymphoblastic leukemia. A Pediatric Oncology Group Study. *Blood* **89:**3960–3966.
29. **Vasef MA, Brynes RK, Murata-Collins JL, Arber DA, Medeiros LJ.** 1998. Surface immunoglobulin light chain-positive acute lymphoblastic leukemia of FAB L1 or L2 type: a report of 6 cases in adults. *Am J Clin Pathol* **110:**143–149.
30. **Kansal R, Deeb G, Barcos M, Wetzler M, Brecher ML, Block AW, Stewart CC.** 2004. Precursor B lymphoblastic leukemia with surface light chain immunoglobulin restriction. A report of 15 patients. *Am J Clin Pathol* **121:**512–525.
31. **Coustan-Smith E, Mullighan CG, Onciu M, Behm FG, Raimondi SC, Pei D, Cheng C, Su X, Rubnitz JE, Basso G, Biondi A, Pui C-H, Downing JR, Campana D.** 2009. Early T-cell precursor leukaemia: a subtype of very high-risk acute lymphoblastic leukaemia. *Lancet Oncol* **10:**147–156.
32. **Zhang J, Ding L, Holmfeldt L, Wu G, Heatley SL, Payne-Turner D, Easton J, Chen X, Wang J, Rusch M, Lu C, Chen S-C, Wei L, Collins-Underwood JR, Ma J, Roberts KG, Pounds SB, Ulyanov A, Becksfort J, Gupta P, Huether R, Kriwacki RW, Parker M, McGoldrick DJ, Zhao D, Alford D, Espy S, Bobba KC, Song G, Pei D, Cheng C, Roberts S, Barbato MI, Campana D, Coustan-Smith E, Shurtleff SA, Raimondi SC, Kleppe M, Cools J, Shimano KA, Hermiston ML, Doulatov S, Eppert K, Laurenti E, Notta F, Dick JE, Basso G, Hunger SP, Loh ML, Devidas M, Wood B, Winter S, Dunsmore KP, Fulton RS, Fulton LL, Hong X, Harris CC, Dooling DJ, Ochoa K, Johnson KJ, Obenauer JC, Evans WE, Pui C-H, Naeve CW, Ley TJ, Mardis ER, Wilson RK, Downing JR, Mullighan CG.** 2012. The genetic basis of early T-cell precursor acute lymphoblastic leukaemia. *Nature* **481:**157–163.
33. **Rubnitz JE, Onciu M, Pounds S, Shurtleff S, Cao X, Raimondi SC, Behm FG, Campana D, Razzouk BI, Ribeiro RC, Downing JR, Pui C-H.** 2009. Acute mixed lineage leukemia in children: the experience of St Jude Children's Research Hospital. *Blood* **113:**5083–5089.
34. **Matutes E, Pickl WF, van't Veer M, Morilla R, Swansbury J, Strobl H, Attarbaschi A, Hopfinger G, Ashley S, Bene MC, Porwit A, Orfao A, Lemez P, Schabath R, Ludwig W-D.** 2011. Mixed-phenotype acute leukemia: clinical and laboratory features and outcome in 100 patients defined according to the WHO 2008 classification. *Blood* **117:**3163–3171.
35. **Paietta E, Racevskis J, Neuberg D, Rowe JM, Goldstone AH, Wiernik PH.** 1997. Expression of CD25 (interleukin-2 receptor alpha chain) in adult acute lymphoblastic leukemia predicts for the presence of BCR/ABL fusion transcripts: results of a preliminary laboratory analysis of ECOG/MRC Intergroup Study E2993. *Leukemia* **11:**1887–1890.
36. **Pui C-H, Frankel LS, Carroll AJ, Raimondi SC, Shuster JJ, Head DR, Crist WM, Land VJ, Pullen DJ, Steuber CP, Behm FG, Borowitz MJ.** 1991. Clinical characteristics and treatment outcome of childhood acute lymphoblastic leukemia with the t(4;ll)(q21;q23): a collaborative study of 40 cases. *Blood* **77:**440–447.
37. **Borowitz MJ, Hunger SP, Carroll AJ, Shuster JJ, Pullen DJ, Steuber CP, Cleary ML.** 1993. Predictability of the t(1;19)(q23; p13) from surface antigen phenotype: implications for screening cases of childhood acute lymphoblastic leukemia for molecular analysis: a Pediatric Oncology Group study. *Blood* **82:**1086–1091.
38. **Borowitz MJ, Rubnitz J, Nash M, Pullen DJ, Camitta B.** 1998. Surface antigen phenotype can predict TEL-AML1 rearrangement in childhood B-precursor ALL: a Pediatric Oncology Group study. *Leukemia* **12:**1764–1770.
39. **Van Vlierberghe P, Ambesi-Impiombato A, De Keersmaecker K, Hadler M, Paietta E, Tallman MS, Rowe JM, Forne C, Rue M, Ferrando AA.** 2013. Prognostic relevance of integrated genetic profiling in adult T-cell acute lymphoblastic leukemia. *Blood* **122:**74–82.
40. **Marks DI, Paietta EM, Moorman AV, Richards SM, Buck G, DeWald G, Ferrando A, Fielding AK, Goldstone AH, Ketterling RP, Litzow MR, Luger SM, McMillan AK, Mansour MR, Rowe JM, Tallman MS, Lazarus HM.** 2009. T-cell acute lymphoblastic leukemia in adults: clinical features, immunophenotype, cytogenetics, and outcome from the large randomized prospective trial (UKALL XII/ECOG 2993). *Blood* **114:**5136–5145.
41. **Cario G, Rhein P, Mitlöhner R, Zimmermann M, Bandapalli OR, Romey R, Moericke A, Ludwig W-D, Ratei R, Muckenthaler MU, Kulozik AE, Schrappe M, Stanulla M, Karawajew L.** 2014. High CD45 surface expression determines relapse risk in children with precursor B-cell and T-cell acute lymphoblastic leukemia treated according to the ALL-BFM 2000 protocol. *Haematol* **99:**103–110.
42. **Pui C-H, Evans WE.** 2006. Treatment of acute lymphoblastic leukemia. *N Engl J Med* **354:**166–178.
43. **Pui C-H, Robison LL, Look AT.** 2008. Acute lymphoblastic leukaemia. *Lancet* **371:**1030–1043.
44. **Pui C-H, Campana D.** 2000. New definition of remission in childhood acute lymphoblastic leukemia. *Leukemia* **14:**783–785.
45. **Campana D.** 2010. Minimal residual disease in acute lymphoblastic leukemia. *Hematology Am Soc Hematol Educ Program* **2010:**7–12.

46. **Gaipa G, Basso G, Biondi A, Campana D.** 2013. Detection of minimal residual disease in pediatric acute lymphoblastic leukemia. *Cytometry Part B* **84B:**359–369.
47. **Gaipa G, Basso G, Aliprandi S, Migliavacca M, Vallinoto C, Maglia O, Faini A, Veltroni M, Husak D, Schumich A, Ratei R, Biondi R, Dworzak MN, on behalf of the I-BFM-ALL-FCM-MRD-Study Group.** 2008. Prednisone induces immunophenotypic modulation of CD10 and CD34 in nonapoptotic B-cell precursor acute lymphoblastic leukemia cells. *Cytometry Part B* **74B:**150–155.
48. **Roshal M, Fromm JR, Winter S, Dunsmore K, Wood BL.** 2010. Immaturity associated antigens are lost during induction for T cell lymphoblastic leukemia: implications for minimal residual disease detection. *Cytometry Part B* **78B:**139–146.
49. **Stow P, Key L, Chen X, Pan Q, Neale GA, Coustan-Smith E, Mullighan CG, Zhou Y, Pui C-H, Campana D.** 2010. Clinical significance of low levels of minimal residual disease at the end of remission induction therapy in childhood acute lymphoblastic leukemia. *Blood* **115:**4657–4663.

Acute Myeloid Leukemia: Diagnosis and Minimal Residual Disease Detection by Flow Cytometry

BRENT WOOD AND LORI SOMA

22

Flow cytometry is an integral tool in both the diagnosis and posttherapy evaluation of acute myeloid leukemia (AML). The strength of the technology is its capacity for rapid, sequential single-cell analysis with simultaneous evaluation of multiple antigens, thus providing a comprehensive immunophenotype for discrete cellular subpopulations. As a result, it has become the methodology of choice for determining blast lineage and immunophenotype. Cytochemical or immunohistochemical evaluation, although useful and even required in some settings, has been surpassed by flow cytometry for the evaluation of blood and marrow in most instances (1, 2). Nevertheless, flow cytometric findings must be used in conjunction with morphology, molecular, and cytogenetic findings for the complete diagnosis and subclassification of AML. Evaluation of posttherapy samples for residual acute myeloid leukemia allows enumeration of blasts as low as 1% by morphology; however, distinguishing normal or regenerating progenitors from leukemic blasts rarely can be performed by morphologic examination alone. Flow cytometry not only allows a more sensitive assay, in some cases reaching a sensitivity of 0.01% (3–5), it is also able to identify aberrancies on the leukemic blast population that allow discrimination from normal or regenerating progenitors (2, 6, 7). These attributes make flow cytometry an ideal method for evaluating for minimal residual disease (MRD) in the posttherapy setting.

NORMAL MYELOID MATURATION AND ANTIGEN EXPRESSION

Knowledge of the immunophenotypic findings seen during normal hematopoietic maturation is critical to understanding the changes induced by neoplastic transformation and is the basis of all neoplastic immunophenotyping. The ability to distinguish leukemic blasts from normal progenitors, either for initial diagnosis or posttherapeutic monitoring, requires correlation of immunophenotypes from specific maturational stages of a particular lineage with the population of interest (Table 1) (8–10).

Hematopoietic maturation begins in the bone marrow with the hematopoietic stem cell, a cell having the properties of self-regeneration and multilineage differentiation potential. This stage of maturation is characterized by expression of high CD34, low to absent CD38 and CD133, low to intermediate levels of CD13 and HLA-DR, and relatively low levels of CD33, CD117, and CD123 (11–13). CD45 expression is low in comparison to mature lymphocytes, although it is higher than later CD34-positive myeloid progenitors. Hematopoietic stem cells also do not express markers of definitive lineage commitment, such as the myeloid antigens CD11b, CD14, CD15, CD16, or myeloperoxidase, the early B-cell antigens CD19 or CD10, or the elevated level of CD71 characteristic of early erythroid differentiation (Fig. 1) (2).

As the hematopoietic stem cell matures to early forms committed to the various lineages, the levels of CD34 and CD45 decrease slightly as CD38 increases to a relatively uniform intermediate level. This early CD34-positive progenitor devoid of lineage-specific antigenic expression is the prototype for what is often termed a "myeloid blast"; following this stage, the progenitors begin to express antigens characteristic of commitment to specific lineages. It is hypothesized that a common myeloid progenitor gives rise to the seven main myeloid lineages—erythroid, granulocytes, eosinophils, basophils, monocytes, megakaryocytes, and dendritic cells—but this is difficult to observe by routine immunophenotyping. However, it can readily be observed that the uniformly CD34-bright progenitors slightly increase expression of CD13, CD33, CD117, and HLA-DR as they move toward myelomonocytic differentiation, while early erythroid, B-cell and plasmacytoid dendritic cell lineages rapidly reduce their expression of CD13 and CD33 (2, 8, 14, 15). When observing immunophenotypic expression along myeloid lineages, it is important to note that the maturational patterns are a continuum with progressive gains and losses of antigens rather than static discrete populations characterized by the presence or absence of markers (Fig. 1).

As monocytic maturation arises from the early CD34-positive progenitor, the monoblasts/promonocytes express the highest levels of HLA-DR and CD33 seen on any hematopoietic population, with early expression of CD15 and CD64 at a moderate level and a rapid decrease of CD34 and CD117 (8, 9, 14, 15). At these early stages, CD13 expression is variably reduced from that seen on the bright CD34-positive progenitors; it then begins to increase in parallel with CD14, with both expressed at the highest level on mature monocytes.

Early erythroid progenitors express CD34 and show increasing levels of CD71 (transferrin receptor) with slightly later acquisition of CD36. Expression of CD117 is retained

doi:10.1128/9781555818722.ch22

TABLE 1 Antigens commonly evaluated in the diagnosis of acute myeloid leukemia

Designation	Associated lineage
CD4	Monocytic, T cells
CD5	Pan T cell, aberrant expression in some AML
CD7	Pan T cell, aberrant expression in some AML
CD11b	Myeloid, NK cells, some B and T cells
CD11c	Myeloid, NK cells, some T cells
CD13	Myeloid
CD14	Myelomonocytic
CD15	Myelomonocytic
CD16	Granulocytes, NK cells
CD19	B cells
CD33	Myeloid cells
CD34	Immature hematopoietic cell, stem cell
CD36	Monocytes, basophils, early erythroids, megakaryocytes
CD41	Glycoprotein IIb, platelets and megakaryocytes
CD42	Platelet glycoprotein, platelets and megakaryocytes
CD45	Leukocyte common antigen
CD56	NK cells, aberrant expression in some AML
CD61	Glycoprotein IIb/IIIa, platelets and megakaryocytes
CD64	Monocytes, activated granulocytes
CD71	Transferrin receptor, erythroid (CD71 bright) and cycling cells, not present on anucleate erythroid cells
CD117	Immature myelomonocytic and erythroid
CD123	Plasmacytoid dendritic cells, basophils, immature B cells
CD203c	Basophils
HLA-DR	Myeloid blasts, monocytes, B cells, activated T cells
Glycophorin A	Maturing erythroid (levels increase with erythroid maturation)
MPO	Myeloid (strongest on granulocytic) lineage
TDT	Lymphoid blast

by the pronormoblasts, which also express CD38 with loss of CD13, CD33, and CD34 (2, 15, 16). CD71 expression remains high throughout erythroid maturation and is lost upon extrusion of the nucleus to form the mature erythrocyte; however, the level of CD71 seen is dependent on processing with red cell lysing reagents, which often result in variably reduced levels of CD71. Glycophorin A (CD235a) is acquired slightly later than high CD71 but is maintained throughout maturation with expression on anucleate erythrocytes (10).

Discrete stages of megakaryocytic maturation are not as well identified by routine immunophenotyping. However, early megakaryocytic progenitors coexpress CD41 (glycoprotein IIb) and CD61 (glycoprotein IIIa), with expression of CD42 (glycoprotein 1b) acquired with maturation (17).

OVERVIEW OF AML

Biology and Epidemiology

AML is a myeloid stem cell neoplasm resulting in a clonal proliferation of bone marrow precursors having the expression of myeloid-associated antigens in the absence of lineage-defining lymphoid antigens (18). This includes apparent maturational arrest at variable progenitor stages up through the promyelocyte, promonocyte, or proerythroblast stages. AML is more frequently seen in adults, with a peak incidence in the 6th decade, although it can occur at any age. Risk factors associated with the development of AML include exposure to radiation, chemotherapy (particularly alkylating agents and topoisomerase II inhibitors), toxins (benzene, smoking), development of lower-grade myeloid stem cell disorders (myelodysplasia, chronic myeloproliferative neoplasms), and some congenital/inheritable factors (such as Fanconi anemia, Down syndrome, and familial *RUNX1* and *CEBPA* mutations) (19).

Classification

Historically, AML was classified based on the French-American-British (FAB) criteria, a cooperative effort to standardize the diagnosis and classification of acute leukemia. The FAB was first published in 1976 and required ≥30% myeloid blasts (or blast equivalents) in the bone marrow or peripheral blood by morphology (20). Cytochemical stains and morphologic features were used to define lineage at that time. Subsequently, the diagnostic criteria were revised in 2001 with the publication of the World Health Organization classification system for hematopoietic and lymphoid tumors (21). The morphologic blast percentage required for the diagnosis of AML was decreased to ≥20% in the bone marrow or blood, from the prior FAB criteria of ≥30%. Subclassification of AML in the 2001 and 2008 World Health Organization systems is based largely on recurrent genetic abnormalities, with less reliance on

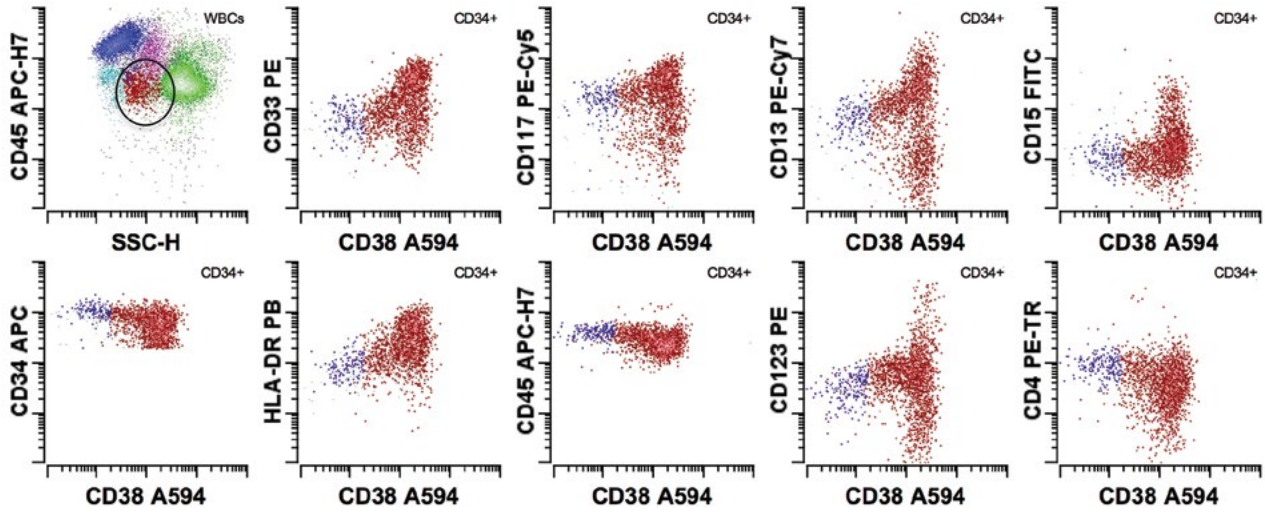

FIGURE 1 Example dot plots of normal, early stem cells (purple) and normal CD34-positive blasts (red). Upper left dot plot shows CD45 versus side scatter (blue: lymphocytes; pink: monocytes; green: maturing granulocytes; aqua: hematogones) with circled area defining the blast region. Remaining dot plots are selectively displaying CD34-positive progenitors only. Myeloid progenitors show increasing expression of CD13, CD33, CD117, and HLA-DR.

morphologic and immunophenotypic characteristics (18), although the latter continue to play a role for certain specific AML subtypes (see Table 2).

In the current era, flow cytometry and morphology are the mainstays in diagnosing AML, with molecular and cytogenetic findings providing further subclassification (1, 2, 18). Flow cytometry allows for: (i) identification and enumeration of an immature progenitor population; (ii) lineage assessment based on phenotypic expression; and (iii) assessment of aberrant antigen expression that can be used for subsequent posttherapeutic monitoring. Most AML demonstrates an immunophenotype similar to that seen on normal myeloid progenitors, often expressing CD13, CD33, CD34, CD117, and HLA-DR, with low CD45 expression (Fig. 2). However, the intensity of these antigens may be increased or decreased compared to a normal progenitor population, and they may be more homogeneous in expression, indicating a lack of the normal maturational spectrum that would be expected in a reactive/regenerative setting. Myeloid blasts in AML may also show abnormal asynchronous expression of mature myeloid antigens, such as CD11b, CD15, or CD64, as well as aberrant expression of lymphoid-associated antigens including CD2, CD5, CD7, CD19, or CD56 (2).

A complete description of AML subclassification using flow cytometry is beyond the scope of this chapter, and the reader is referred to a more comprehensive source (22). However, four subtypes of AML are worth specific mention because of their characteristic immunophenotypic findings:

TABLE 2 Immunophenotypic characteristics associated with certain AML subtypes

AML subclassification	Associated immunophenotypic nuance of blasts
AML with t(8;21)(q22;q22); *RUNX1-RUNX1T1*	High levels of CD34, expression of CD19 and TdT
APL with t(15;17)(q22;q12); *PML-RARA*	Lack of CD15, CD34, and HLA-DR; expression of high levels of CD33 and MPO; expression of CD2; increased right-angle light scatter
AML with t(6;9)(p23;q34); *DEK-NUP214*	TdT expression
AML with inv3(q21;q26.2) or t(3;3)(q21;q26.2); *RPN1-EVI1*	CD7 expression; subsets may express CD41/CD61
AML with FLT3/ITD	May lack CD34 and HLA-DR
AML with NPM1 mutation	May lack CD34 and express higher CD33
AML with monocytic or monoblastic differentiation	Bright CD33, CD64, and HLA-DR; often lacks CD34 and CD117; variable CD14
Acute erythroid leukemia	Bright CD71 and expression of CD235a (glycophorin-A); variable expression of CD117 but often lacks CD34; variably lacks CD13 and CD33
Acute megakaryoblastic leukemia	Expression of CD41 and CD61; often lacks CD13, CD33, CD34, and CD117

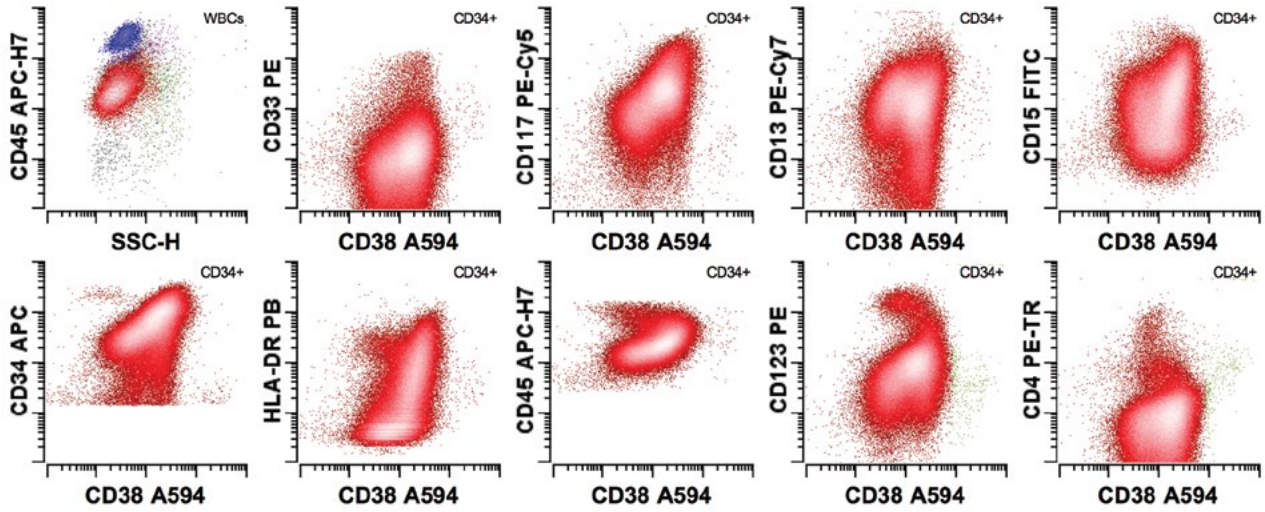

FIGURE 2 Example dot plots of acute myeloid leukemia (red). Upper left dot plot shows CD45 versus side scatter with blast population highlighted in red. Remaining dot plots are selectively displaying CD34-positive leukemic blasts only. Notice, compared to normal myeloid blasts in Fig. 1, these abnormal, leukemic blasts demonstrate lower side scatter, variably increased CD13, early/abnormal expression of CD15, decreased to absent CD33, variably increased CD34, variably decreased CD45, variably increased CD117, and variably decreased HLA-DR.

acute promyelocytic leukemia (APL), acute monocytic leukemia (AMoL), acute erythroid leukemia (AML-M6), and acute megakaryoblastic leukemia (AML-M7) (see Table 2).

AML with t(15;17) (APL) is an acute leukemia consisting of a marked expansion of promyelocytes (blast equivalents) without further granulocytic maturation (1, 2, 18). This is a particularly important subtype of AML to recognize due to the increased early death rate secondary to disseminated intravascular coagulation and its complications. However, this subtype is exquisitely sensitive to therapy with all-*trans* retinoic acid and arsenic trioxide, making it the AML with the highest overall disease-free survival rate if successfully supported through initial treatment (23, 24). Like normal promyelocytes, APL is characterized by variably high right-angle light scatter, high levels of myeloperoxidase, relative lack of HLA-DR, and low to intermediate CD64, and it most typically lacks CD34 and CD11b expression. However, unlike normal promyelocytes, APL typically demonstrates low to absent expression of CD15, abnormally increased CD33, and variable CD117. The microgranular variant of APL has a variant immunophenotype with somewhat lower right-angle light scatter, more frequent expression of CD34, and CD2 expression on a subset of cases.

AMoL (acute monocytic leukemia) shows an immunophenotype similar to promonocytes with intermediate to high right-angle light scatter and bright CD33, findings often seen in APL, but with a higher level of CD64, more frequent expression of HLA-DR, and low to absent myeloperoxidase (1, 2, 18). Monoblasts and promonocytes also generally lack CD14, CD34, and CD117, although they typically express a moderately high level of CD15, CD64, and HLA-DR. Additionally, monocytic leukemia will often show some degree of further monocytic maturation, including a subset of maturing/mature monocytes (with increased CD14 and CD45 expression) in addition to the immature promonocytic component. Aberrant CD56 expression is often seen on the monocytes (mature and immature) in AMoL.

Acute erythroid leukemia (AML-M6) consists of a proliferation of proerythoblasts either with or without a subset of abnormal myeloid progenitors (1, 2, 18). The proerythoblasts show decreased to absent CD45 expression, often with intermediate right-angle light scatter, often variably lack CD13, CD33 and CD34, but typically express some combination of CD36 and CD71 and may show expression of CD235a (glycophorin-A). Care must be taken in the assessment of CD71, as proliferating cells (including leukemic blasts) express CD71 (transferrin receptor); however, erythroid progenitors typically express CD71 at an exquisitely high level, with the caveat that this may be abnormally reduced in erythroleukemia. The progenitor antigen CD117 is typically expressed on erythroid progenitors.

Acute megakaryoblastic leukemia (AML-M7) is similar to AML-M6 in that the blasts often show decreased to absent CD45 expression, often with intermediate right-angle light scatter, and expression of CD36 and CD71 (1, 2, 18). Additionally, the blasts may lack CD34 as well as CD13, CD33, or CD117. However, by definition, the blasts must show expression of platelet-associated antigens such as CD41 and CD61 and must lack CD235a. When evaluating CD41/CD61 expression, care must be taken to exclude adherence of activated platelets to the cells of interest.

PREPARATION AND EVALUATION OF DIAGNOSTIC SAMPLES IN AML

Specimen Requirements and Processing

The diagnosis of AML is usually made on a bone marrow aspirate or peripheral blood sample; however, bone marrow biopsies or involved tissue samples may be evaluated. The samples should be obtained in a sterile manner. Bone marrow aspirate and peripheral blood should be collected in sodium heparin or EDTA anticoagulant, with sodium heparin providing more stability in samples that are more than 24 hours old. Bone marrow biopsies or tissue samples

should be placed in tissue culture media (25). If analysis is to occur within 24 to 48 hours, maintaining the sample at room temperature is appropriate (16 to 28°C). However, if a delay in evaluation beyond 48 hours is anticipated, refrigeration of the sample will delay sample degradation. Samples that are refrigerated should be brought back to room temperature prior to labeling. Prior to processing, sample cellularity should be assessed to ensure provision of the appropriate number of cells for analysis. This may require increasing the volume of low-cellularity samples or diluting highly cellular samples to maintain antibodies within an appropriate titer. In general, most antibodies are titered for use with 1 million cells, and this serves as a useful target for sample cellularity.

Antibodies are added to the aliquot of sample, preferably as a pretitered cocktail, and the mixture is incubated for 15 minutes at room temperature in the dark. After labeling, samples are processed with red blood cell lysing reagents, e.g., buffered ammonium chloride, followed by washing in order to obtain a single cell suspension of white blood cells with as little contamination by mature erythrocytes as possible, largely to allow efficient sample acquisition (26). Of note, if the sample is a bone marrow biopsy or tissue sample, it must initially undergo disaggregation to obtain a single cell suspension prior to further processing, usually by mechanical disaggregation with a scalpel, forceps, or mesh screen, although enzymatic digestion may also be used (27).

Reagent Panels

The reagent panels used for both AML diagnosis and MRD detection should ideally be similar and optimized to demonstrate both the early stages of myeloid progenitor maturation and common antigenic abnormalities seen in AML, e.g., expression of lymphoid-associated antigens (28). However, the diagnostic panel should be supplemented with lymphoid-associated antigens sufficient to definitively determine lineage. Some redundancy in reagents between aliquots is desirable to allow identification of similar populations between aliquots. There is currently poor standardization of reagent panels for AML diagnosis and MRD detection, but antigens that are commonly evaluated in the diagnosis of AML are listed in Table 1. We refer the reader to another source for a recommended AML (and AML MRD) panel (29). Although the simultaneous evaluation of three to four antigens has previously been standard, the use of six- to 10-color flow cytometers is becoming increasingly common (30). The use of increased numbers of simultaneous fluorochromes is less important for initial diagnosis where the blast population is easy to identify, but it can clarify maturational relationships and becomes more important to confidently identify small abnormal blast populations when evaluating for MRD (7).

Data Acquisition

In order to characterize all populations of interest, one must collect enough total events to allow evaluation of the least frequent population of interest in the sample. If the population of interest is present in high numbers, for instance at the time of AML diagnosis, evaluation of lower numbers of events will yield the information needed for correct identification/classification. However, if the population of interest is infrequent, for instance at the time of posttherapeutic monitoring, a larger number of events is needed for identification, characterization, and enumeration. Although the operator can make this decision in real time as the sample is being acquired, establishing a consistent number of events to acquire based on the diagnostic question is an approach better suited to a busy clinical laboratory. Acquisition of a specified number of total events allows one to consistently achieve the desired degree of sensitivity for a particular application.

Determination of the number of events to acquire is governed in large part by two factors: the number of events required to identify and enumerate a population, and the frequency of the population of interest, the latter being directly related to the desired analytical sensitivity of the assay. Although the identification of a population is possible with a very small number of events (<10) of the appropriate type, enumeration at this level is governed by Poisson counting statistics, and the precision can be estimated as:

$$\text{Coefficient of variation (CV)} = \sqrt{\frac{(n)}{n}}$$

where n is the number of events in the population. Consequently, with a target number of 100 events ($n = 100$), the CV is 10%, and this serves as a reasonable goal for most MRD assays. Increasing the number of events will decrease the CV and hence increase precision. When evaluating initial diagnostic samples, an analytical sensitivity of 0.1% (1 cell in 1,000) is an appropriate target to allow detection of unexpected, abnormal populations. Therefore, 100,000 total events should be acquired to provide 100 events in a population having a frequency of 0.1%. In contrast, for MRD applications, the clinically relevant target is currently 0.01%, in which case 1,000,000 events are required to achieve a similar level of reproducible enumeration. An additional consideration is carryover. Running a small amount of water through the cytometer, not only between patient samples but also between aliquots of the same sample, will reduce contamination that could produce artifactual small populations and be misinterpreted; this is particularly an issue for MRD analysis.

Data Analysis

Evaluation of immature populations is enhanced by specifically gating on the region where normal progenitors are expected to be present on a CD45 versus side-scatter dot plot, a gate often referred to as a "blast" gate. This method allows separation of the nucleated cells into six basic components: lymphocytes, monocytes, granulocytes, myeloid progenitors, lymphoid progenitors, and erythroid forms. Inclusion of CD45 in each aliquot/tube allows for consistency in progenitor or blast identification and is an approach almost universally used in clinical laboratories for acute leukemia diagnosis. This analytical approach allows more focused evaluation of progenitors by the exclusion of maturing forms from most lineages. However, gating in this way makes the assumption that neoplastic myeloid blasts share similar CD45 and right-angle light-scatter characteristics with their normal counterparts, which is not always the case. Therefore, one should not overly adhere to strict gating strategies but should examine regions outside of the blast gate and allow for variation in its location when warranted.

Reporting

In AML diagnosis, the blast percentage is very important. As stated previously, the current World Health Organization classification generally requires morphologic identification of $\geq$20% of blasts of marrow cellularity to be considered diagnostic of AML (18). However, when enumerating progenitors by flow cytometry, the denominator is potentially confounded by three competing factors: hemodilution,

reduced enumeration of erythroid precursors, and differences in the definition of blasts/progenitors between flow cytometry and morphology. Hemodilution is inevitable during marrow aspiration but is increasingly pronounced beyond 1 to 2 cc of marrow aspiration unless the needle is repositioned. The consequence of hemodilution is a relative increase in peripheral blood cells, which is particularly problematic in cases where relatively few progenitors are in the circulation, such as during MRD assessment. The net effect is a reduction in progenitor enumeration. In contrast, the use of erythrocyte lysing reagents compromises nucleated erythroid cells, resulting in a decrease in forward scatter that can cause underestimation of the total number of nucleated cells if either the acquisition threshold is too high so that they are not acquired or if viability gates are used and nucleated red cells are excluded from the denominator during analysis. It is often assumed that nucleated erythroid cells are lost with the use of red cell lysing reagents, but this is not the case if fixative-containing lysing reagents are used and wash steps are optimized for cell recovery. Due to this concern, the blast percentage has historically been reported as a percentage of white cells (CD45-positive events) by flow cytometry, but this practice needs to be reevaluated. Finally, cells that are considered blasts or blast equivalents by morphology consist of a variety of different immunophenotypic subsets by flow cytometry, so one must sum the appropriate immunophenotypic subsets if one is attempting to correlate with morphology. This problem may be particularly pronounced for progenitors that lack CD34 or CD117 expression, such as monocytic leukemia. Ultimately, the flow cytometric blast count must be correlated with a morphologic blast count for a definitive diagnosis of AML, particularly if the blast percentage by flow cytometry is not significantly above 20% and/or the sample is bone marrow. In peripheral blood samples where nucleated red blood cells are usually not present and hemodilution is not relevant, the flow cytometric progenitor count may more closely correlate with morphology.

In addition to reporting the percentage of myeloid progenitors, their immunophenotype should be reported (28). The immunophenotypic data should clearly identify the population being evaluated and how it was defined. Antigen expression should be reported in a way that relays relative intensity and whether the findings are normal or abnormal for a particular lineage of cells at a defined stage of maturation, something that is particularly important when assessing samples for subsequent MRD testing. The reporting of percentage positivity for each antibody tested is still common but is actively discouraged by consensus conferences as it does not convey either the relative intensity or pattern of expression, nor does it provide an indication of abnormality. Finally, the report should contain an interpretation of the results that attempts to integrate this complex immunophenotypic data with clinical findings to provide useful clinical information that can direct therapy.

POSTTHERAPY EVALUATION OF AML (MRD)

Evaluation for minimal residual disease after therapy is an important prognostic predictor in AML (7). The presence of minimal residual disease, even with levels <0.1%, is associated with adverse outcome (31).

Specimen Requirements, Processing, and Reagent Panels

The specimen requirements are similar between diagnostic and MRD AML testing. Although some have suggested that peripheral blood is an adequate sample for MRD analysis, the level of AML MRD detected is roughly 1 log lower in blood than in marrow, and current practice is to evaluate bone marrow aspirate samples (32, 33). The sample should be processed in the same way as a diagnostic AML sample, including the use of red cell lysis; however, it is important that sufficient cells are prepared to allow acquisition of the appropriate number of events for the desired degree of sensitivity (25, 26). For low-cellularity samples, this will require either concentration or evaluation of larger total amounts of sample.

Reagent panels for MRD testing need to be optimized to allow discrimination of normal progenitors from residual leukemic progenitors; this usually requires the use of backbone gating reagents that facilitate dissection of maturational subpopulations into relatively discrete stages where normal immunophenotypes are somewhat more homogeneous (6, 7). An important example is evaluation of the immunophenotype of hematopoietic stem cells ($CD34^{+}$, $CD38^{Low}$) via the use of CD34 and CD38 as gating reagents, as residual AML often persists as cells having this immature immunophenotype and can be overlooked if only total CD34-positive cells are evaluated (Fig. 3). Using an increased number of simultaneous fluorochromes facilitates this process. In addition, evaluation for AML MRD also allows for a more directed reagent panel to be utilized, in contrast to the assessment of more extensive lineage-associated antigens performed in a diagnostic setting for definitive lineage assignment.

More broadly, it is helpful if the same or similar panel of reagents is evaluated at both diagnosis and at MRD assessment, as this facilitates comparison between diagnostic and MRD samples and generally results in a single assay that can be well validated and its performance characteristics understood (we refer the reader elsewhere for a recommended AML MRD panel) (29). The creation of custom reagent combinations in an attempt to detect abnormalities noted at diagnosis is to be avoided as these represent unvalidated assays whose performance characteristics will not be well understood. In addition, limited or custom reagent combinations also presume constancy of immunophenotype posttherapy, which is known to not be the case in a significant subset of acute leukemia, including AML (7, 34–36).

Data Acquisition and Evaluation

Data acquisition and evaluation in AML MRD is essentially similar to that in AML at diagnosis, although a few important caveats should be noted. Unlike diagnostic samples where the population is usually present in sufficient numbers to confidently identify when acquiring 100,000 events, posttherapy or MRD analysis will hopefully be looking for populations that represent less than 1% of total cells. Therefore, a target for acquisition of 500,000 to 1,000,000 total events is desirable in order to allow reproducible identification and enumeration (see above). As a quality-control measure, when evaluating for small populations, identification of the population in more than a single reagent combination is helpful to confirm that the population is not a spurious or nonspecific finding, as well as to allow a more accurate estimate of population frequency. As mentioned previously, running water between each aliquot will decrease the risk of inter- and intrasample carryover, which could lead to a false-positive result and is of paramount importance when enumerating small populations.

The sensitivity of MRD testing is directly related to: i) the leukemic phenotype, ii) the presence of normal or

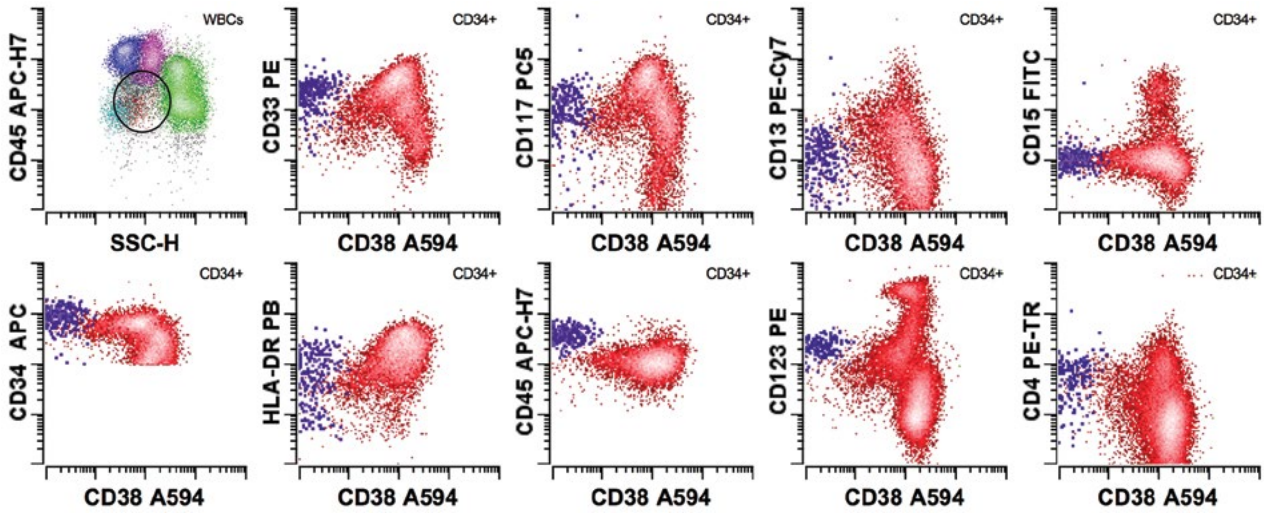

FIGURE 3 Example dot plots of minimal residual disease (MRD; purple population visualized on CD34 gating) with associated regenerating normal myeloid blasts (red). Upper left dot plot shows CD45 versus side scatter (blue, lymphocytes; pink, monocytes; green, maturing granulocytes; aqua, hematogones) with circled area defining the blast region. Remaining dot plots are selectively displaying emphasized, CD34-positive progenitors only. The MRD-positive population (purple) shows abnormal expression of CD4, decreased to absent CD13, uniform CD33, increased CD34, absent CD38, increased CD45, and subset CD56 (not shown) with normal expression of CD117 and HLA-DR and normal lack of CD15. Although the total CD34-positive population accounted for 2% of the white cells, the abnormal, MRD-positive population accounted for 0.03% of the white cells.

regenerating populations of similar immunophenotype, and iii) interpreter expertise. This assumes use of a sufficiently informative antibody combination and acquisition of an appropriate number of total events. It can be quite helpful to evaluate the diagnostic sample in the same laboratory performing evaluation for MRD, in order to understand the diagnostic immunophenotype using a procedure similar to that being used for MRD. However, it is important to recognize that changes in immunophenotype often occur as a result of therapy, and rigid reliance on stability of the original immunophenotype is unwise (2, 7, 14, 34–37). In particular, the use of predefined gates based on the diagnostic immunophenotype, as advocated by a strict leukemia-associated immunophenotypic approach, is to be avoided. Nevertheless, evaluating for an abnormal immunophenotype similar to the diagnostic sample is a useful starting point for evaluation when supplemented by evaluation for discrete abnormal populations having immunophenotypes that differ from normal or regenerating progenitors. Given the immunophenotypic heterogeneity of the myeloid blast population in AML, it is difficult to predict which component may be resistant to or undergo selection by therapy, further suggesting that reliance on single or presumed static immunophenotypic abnormalities is unwise. In some circumstances, the leukemic immunophenotype may be quite similar to normal progenitors, and differentiation between the two populations can be quite challenging with overlap of the populations. The use of increasing numbers of colors/fluorochromes allows evaluation of more antibodies in one tube, permitting more confident identification of small populations and improved separation from the normal myeloid progenitors by selective gating.

Lastly, the timing of MRD evaluation and the presence of regenerating populations are interrelated and can create difficulty in confident MRD assessment. Particularly problematic are marrows near day 21 after therapy when early regeneration is predominant, and posttherapy marrows when patients have been receiving granulocyte colony-stimulating factor therapy. With active marrow regeneration, the percentage of normal CD34-positive progenitors can be substantially increased, even exceeding 20% of cellularity in blood or marrow, and may exhibit mild immunophenotypic changes such as an increase in CD33, increased expression of CD7, and/or low level of CD5 (both generally variable on a small subset of the progenitors). With granulocyte colony-stimulating factor therapy, CD56 expression can be significantly increased on myelomonocytic progenitors and may extend even earlier to involve a subset of CD34-positive progenitors (14). CD56 expression is also constitutively seen on CD34-positive and myelomonocytic progenitors in Down syndrome and should not be mistaken for antigenic aberrancy (38).

Reporting

Reporting in AML MRD is similar to AML at diagnosis. Accurate enumeration of abnormal myeloid progenitors, currently as a percentage of white cells, is most important. Also important is a description of the immunophenotypic findings that identify the population as abnormal, i.e., that distinguish it from similar normal progenitors. As stated previously, it is critical that the immunophenotypic changes are interpreted in light of the patient's clinical setting (timing of therapy, growth factor therapy, transplant status) to reduce the risk of overinterpreting regenerative antigenic changes.

REFERENCES

1. **Craig FE, Foon KA.** 2008. Flow cytometric immunophenotyping for hematologic neoplasms. *Blood* **111:**3941–3967.
2. **Wood BL.** 2007. Myeloid malignancies: myelodysplastic syndromes, myeloproliferative disorders, and acute myeloid leukemia. *Clin Lab Med* **27:**551–575.

3. **Coustan-Smith E, Ribeiro RC, Rubnitz JE, Razzouk BI, Pui CH, Pounds S, Andreansky M, Behm FG, Raimondi SC, Shurtleff SA, Downing JR, Campana D.** 2003. Clinical significance of residual disease during treatment in childhood acute myeloid leukaemia. *Br J Haematol* **123:**243–252.
4. **San Miguel JF, Vidriales MB, Lopez-Berges C, Diaz-Mediavilla J, Gutierrez N, Canizo C, Ramos F, Calmuntia MJ, Perez JJ, Gonzalez M, Orfao A.** 2001. Early immunophenotypical evaluation of minimal residual disease in acute myeloid leukemia identifies different patient risk groups and may contribute to postinduction treatment stratification. *Blood* **98:**1746–1751.
5. **Venditti A, Buccisano F, Del Poeta G, Maurillo L, Tamburini A, Cox C, Battaglia A, Catalano G, Del Moro B, Cudillo L, Postorino M, Masi M, Amadori S.** 2000. Level of minimal residual disease after consolidation therapy predicts outcome in acute myeloid leukemia. *Blood* **96:**3948–3952.
6. **Al-Mawali A, Gillis D, Lewis I.** 2009. The role of multiparameter flow cytometry for detection of minimal residual disease in acute myeloid leukemia. *Am J Clin Pathol* **131:**16–26.
7. **Soma L, Wood BL.** 2013. Minimal residual disease testing in acute leukemia. *Int J Hematol Oncol* **216:**467–485.
8. **Arnoulet C, Bene MC, Durrieu F, Feuillard J, Fossat C, Husson B, Jouault H, Maynadie M, Lacombe F.** 2010. Four- and five-color flow cytometry analysis of leukocyte differentiation pathways in normal bone marrow: a reference document based on a systematic approach by the GTLLF and GEIL. *Cytometry B Clin Cytom* **78:**4–10.
9. **Gorczyca W, Sun ZY, Cronin W, Li X, Mau S, Tugulea S.** 2011. Immunophenotypic pattern of myeloid populations by flow cytometry analysis. *Methods Cell Biol* **103:**221–266.
10. **Wood B.** 2004. Multicolor immunophenotyping: human immune system hematopoiesis. *Methods Cell Biol* **75:**559–576.
11. **Garg S, Madkaikar M, Ghosh K.** 2013. Investigating cell surface markers on normal hematopoietic stem cells in three different niche conditions. *Int J Stem Cells* **6:**129–133.
12. **Manz MG, Miyamoto T, Akashi K, Weissman IL.** 2002. Prospective isolation of human clonogenic common myeloid progenitors. *Proc Natl Acad Sci USA* **99:**11872–11877.
13. **Ratajczak MZ.** 2008. Phenotypic and functional characterization of hematopoietic stem cells. *Curr Opin Hematol* **15:**293–300.
14. **Kussick SJ, Wood BL.** 2003. Using 4-color flow cytometry to identify abnormal myeloid populations. *Arch Pathol Lab Med* **127:**1140–1147.
15. **van Lochem EG, van der Velden VH, Wind HK, te Marvelde JG, Westerdaal NA, van Dongen JJ.** 2004. Immunophenotypic differentiation patterns of normal hematopoiesis in human bone marrow: reference patterns for age-related changes and disease-induced shifts. *Cytometry B Clin Cytom* **60:**1–13.
16. **Loken MR, Shah VO, Dattilio KL, Civin CI.** 1987. Flow cytometric analysis of human bone marrow**:** I. Normal erythroid development. *Blood* **69:**255–263.
17. **Tomer A, Harker LA, Burstein SA.** 1988. Flow cytometric analysis of normal human megakaryocytes. *Blood* **71:**1244–1252.
18. **Swerdlow SH, Campo E, Harris NL, Jaffe ES, Pileri SA, Stein H, Thiele J, Vardiman JW.** 2008. *World Health Organization Classification of Tumors of Hematopoietic and Lymphoid Tissues*. IARC Press, Lyon, France.
19. **Deschler B, Lubbert M.** 2006. Acute myeloid leukemia: epidemiology and etiology. *Cancer* **107:**2099–20107.
20. **Bennett JM, Catovsky D, Daniel MT, Flandrin G, Galton DA, Gralnick HR, Sultan C.** 1976. Proposals for the classification of the acute leukaemias. French-American-British (FAB) co-operative group. *Br J Haematol* **33:** 451–458.
21. **Jaffe ES, Harris NL, Stein H, Vardiman J.** 2001. *World Health Organization Classification of Tumors: Pathology and Genetics of Tumours of Hematopoietic and Lymphoid Tissues*. IARC Press, Lyon, France.
22. **Cherian S, Wood BL.** 2012. *Flow Cytometry in Evaluation of Hematopoietic Neoplasms: A Case-based Approach*. CAP Press, Northfield, IL.
23. **Lo-Coco F, Avvisati G, Vignetti M, Thiede C, Orlando SM, Iacobelli S, Ferrara F, Fazi P, Cicconi L, Di Bona E, Specchia G, Sica S, Divona M, Levis A, Fiedler W, Cerqui E, Breccia M, Fioritoni G, Salih HR, Cazzola M, Melillo L, Carella AM, Brandts CH, Morra E, von Lilienfeld-Toal M, Hertenstein B, Wattad M, Lubbert M, Hanel M, Schmitz N, Link H, Kropp MG, Rambaldi A, La Nasa G, Luppi M, Ciceri F, Finizio O, Venditti A, Fabbiano F, Dohner K, Sauer M, Ganser A, Amadori S, Mandelli F, Dohner H, Ehninger G, Schlenk RF, Platzbecker U; Gruppo Italiano Malattie Ematologiche dell'Adulto; German-Austrian Acute Myeloid Leukemia Study Group; Study Alliance Leukemia.** 2013. Retinoic acid and arsenic trioxide for acute promyelocytic leukemia. *N Engl J Med* **369:**111–121.
24. **Lallemand-Breitenbach V, de Thé H.** 2013. Retinoic acid plus arsenic trioxide, the ultimate panacea for acute promyelocytic leukemia? *Blood* **122:**2008–2010.
25. **Stelzer GT, Marti G, Hurley A, McCoy P, Jr, Lovett EJ, Schwartz A.** 1997. U.S.-Canadian consensus recommendations on the immunophenotypic analysis of hematologic neoplasia by flow cytometry: standardization and validation of laboratory procedures. *Cytometry* **30:**214–230.
26. **Carter PH, Resto-Ruiz S, Washington GC, Ethridge S, Palini A, Vogt R, Waxdal M, Fleisher T, Noguchi PD, Marti GE.** 1992. Flow cytometric analysis of whole blood lysis, three anticoagulants, and five cell preparations. *Cytometry* **13:**68–74.
27. **Braylan RC, Benson NA.** 1989. Flow cytometric analysis of lymphomas. *Arch Pathol Lab Med* **113:**627–633.
28. **Wood BL, Arroz M, Barnett D, DiGiuseppe J, Greig B, Kussick SJ, Oldaker T, Shenkin M, Stone E, Wallace P.** 2007. 2006 Bethesda International Consensus recommendations on the immunophenotypic analysis of hematolymphoid neoplasia by flow cytometry: optimal reagents and reporting for the flow cytometric diagnosis of hematopoietic neoplasia. *Cytometry B Clin Cytom* **72**(Suppl 1)**:**S14–22.
29. **Wood BL.** 2013. Flow cytometric monitoring of residual disease in acute leukemia. *Methods Mol Biol* **999:**123–136.
30. **Wood B.** 2006. 9-color and 10-color flow cytometry in the clinical laboratory. *Arch Pathol Lab Med* **130:**680–690.
31. **Walter RB, Buckley SA, Pagel JM, Wood BL, Storer BE, Sandmaier BM, Fang M, Gyurkocza B, Delaney C, Radich JP, Estey EH, Appelbaum FR.** 2013. Significance of minimal residual disease before myeloablative allogeneic hematopoietic cell transplantation for AML in first and second complete remission. *Blood* **122:**1813–1821.
32. **Campana D.** 2008. Status of minimal residual disease testing in childhood haematological malignancies. *Br J Haematol* **143:**481–489.
33. **Maurillo L, Buccisano F, Spagnoli A, Del Poeta G, Panetta P, Neri B, Del Principe MI, Mazzone C, Consalvo MI, Tamburini A, Ottaviani L, Fraboni D, Sarlo C, De Fabritiis P, Amadori S, Venditti A.** 2007. Monitoring of minimal residual disease in adult acute myeloid leukemia using peripheral blood as an alternative source to bone marrow. *Haematologica* **92:**605–611.
34. **Baer MR, Stewart CC, Dodge RK, Leget G, Sule N, Mrozek K, Schiffer CA, Powell BL, Kolitz JE, Moore JO,**

Stone RM, Davey FR, Carroll AJ, Larson RA, Bloomfield CD. 2001. High frequency of immunophenotype changes in acute myeloid leukemia at relapse: implications for residual disease detection (Cancer and Leukemia Group B Study 8361). *Blood* **97:**3574–3580.

35. **Langebrake C, Brinkmann I, Teigler-Schlegel A, Creutzig U, Griesinger F, Puhlmann U, Reinhardt D.** 2005. Immunophenotypic differences between diagnosis and relapse in childhood AML: implications for MRD monitoring. *Cytometry B Clin Cytom* **63:**1–9.
36. **Voskova D, Schoch C, Schnittger S, Hiddemann W, Haferlach T, Kern W.** 2004. Stability of leukemia-associated aberrant immunophenotypes in patients with acute myeloid leukemia between diagnosis and relapse: comparison with cytomorphologic, cytogenetic, and molecular genetic findings. *Cytometry B Clin Cytom* **62:**25–38.
37. **Kern W, Bacher U, Haferlach C, Schnittger S, Haferlach T.** 2010. The role of multiparameter flow cytometry for disease monitoring in AML. *Best Pract Res Clin Haematol* **23:**379–390.
38. **Karandikar NJ, Aquino DB, McKenna RW, Kroft SH.** 2001. Transient myeloproliferative disorder and acute myeloid leukemia in Down syndrome. An immunophenotypic analysis. *Am J Clin Pathol* **116:**204–210.

Chronic Lymphocytic Leukemia, the Prototypic Chronic Leukemia for Flow Cytometric Analysis

HEBA DEGHEIDY, DALIA A. A. SALEM, CONSTANCE M. YUAN, AND MARYALICE STETLER-STEVENSON

23

Chronic lymphocytic leukemia/small lymphocytic lymphoma (CLL/SLL) is a neoplasm of mature B lymphocytes involving peripheral blood (PB), bone marrow (BM), spleen, and lymph nodes (LN). CLL is the most common lymphoproliferative disorder in western countries and is primarily a disease of adults, often occurring during or after middle age. The diagnosis is established by blood counts, blood smears, and immunophenotyping by flow cytometry (FC) of circulating B lymphocytes (1). Although usually an indolent disease, some patients have a more rapid disease progression and require treatment earlier. Survival in patients varies from 1 year to 20 years with an 82% 5-year survival rate (2). FC demonstration of the typical CLL immunophenotype is vital for diagnosis. The differential diagnosis of CLL/SLL would primarily include monoclonal B-cell lymphocytosis (MBL) and mantle cell lymphoma (MCL), although B-prolymphocytic leukemia, marginal zone lymphoma, diffuse large B-cell lymphoma, and lymphoplasmacytic lymphoma can on occasion have some features of CLL/SLL (Table 1) (3).

CLL cells are small, mature round lymphocytes with scanty cytoplasm and a dense nucleus with clumped chromatin. Other larger, atypical, cleaved cells or prolymphocytes may be present but only up to 55% of the PB lymphocytes. Smudge cells (bare nuclei) are a characteristic morphologic feature (1). Diagnosis of CLL requires the presence of $\geq 5 \times 10^3$ circulating monoclonal B lymphocytes with a CLL immunophenotype/μl in the peripheral blood for at least 3 months. The diagnosis of CLL can be made with fewer circulating CLL lymphocytes in patients with cytopenias or disease-related symptoms. The term SLL designates nonleukemic cases where disease is primarily tissue based (4).

ROLE OF FC IN DIAGNOSIS OF CLL

FC immunophenotyping is pivotal in the diagnosis of CLL. CLL typically demonstrates a distinctive immunophenotype, expressing CD5, CD19, dim CD20, dim CD22, CD23, bright CD43, dim CD45, dim-to-negative CD79b, dim CD81, and dim monoclonal surface immunoglobulin (Ig), making it easy to differentiate this disease from normal B cells (Fig. 1) (5, 6). Typically, CD11c expression is dim or dim to negative and CD25 is expressed, but CD10, CD103, and CD123 as well as other T-cell and myeloid antigens are negative (1, 3, 7). MBL usually has an immunophenotype identical to that of CLL, but there are fewer than 5×10^3 circulating monoclonal B lymphocytes/μl (8). This is an important distinction, as MBL has a different prognosis, with the majority of patients failing to develop a hematolymphoid malignancy (9). CD200 is uniformly expressed in CLL while the majority of MCL are CD200 negative (10). Positivity for CD200 and CD23 in combination with dim CD20, CD22, CD45, CD79b, and CD81 as well as bright CD43 differentiates CLL from MCL. Infrequent immunophenotypic variations have been observed in CLL, such as lack of CD5 and CD23, increased intensity of CD11c, CD20, and CD79b, and aberrant expression of CD10 and T-cell (CD2 and CD7) and myeloid (CD13 and CD33) antigens (11–13). The expression of these aberrant antigens in CLL is seen as a single variation in a monoclonal B-cell population that otherwise has a typical CLL immunophenotype.

ROLE OF FC IN PROGNOSTICATION

In addition to its role in the diagnosis of CLL, FC can provide important prognostic information. Although clinical staging using the Rai and Binet prognostic scoring systems has been used to predict the behavior and address the biological diversity of this disease, neither of these is sufficient to predict aggressive disease in early stages of CLL. Ig variable heavy chain (IgVH) mutational status can be used to stratify the risk of progression in CLL (14). CLL patients can be divided into two subgroups based on the degree of somatic hypermutation of IgVH genes in the CLL cells, with CLL patients with somatic hypermutation exhibiting prolonged survival over those with the unmutated IgVH gene (15). Although a potent prognostic indicator, determination of Ig mutational status is labor-intensive, costly, and not widely available. For this reason, CD38 and ZAP-70 (zeta chain-associated protein kinase 70) have been heavily investigated because of their association with the lack of IgVH mutation.

CD38 expression in CLL was first noted to correlate with an aggressive clinical course and later was shown to correlate with IgVH mutational status (16–19). Unmutated cases displayed a higher percentage of $CD38^+$ cells than mutated cases, suggesting that CD38 may serve as a surrogate marker. The cutoff for the level of CD38 positivity for poor prognosis varies in the literature, with some investigators

doi:10.1128/9781555818722.ch23

reporting 30% CD38 positivity as an independent prognosticator (17, 18, 20) while others report that CD38 is discriminatory at lower levels (19). As there is typically a continuum of CD38 expression from moderate to negative, the percentage of CD38-positive cells is measured by gating on the CLL cells and using quadrant statistics to determine the percentage of CLL cells only that express CD38 above negative controls.

ZAP-70 is a member of the Syk–ZAP-70 protein tyrosine kinase family-linked T-cell receptor. FC detection of ZAP-70 in CLL was found to be the strongest surrogate biomarker for IgVH mutational status and is an independent prognosticator (21–23). Nevertheless, several technical issues have hindered the adoption of ZAP-70 testing for clinical use, including variations in anti-ZAP-70 antibody clone and fluorochrome conjugate, fixation and permeabilization procedures, appropriate and effective controls (either internal patient or external normal donor), gating strategies, and reporting methods, which currently lack standardization. ZAP-70 and CD38 provide complementary prognostic information. Patients who express both markers would have a poor prognosis, while those in whom both of these markers are negative would have good outcome.

Cytogenetic abnormalities can be detected in approximately 82% of CLL patients using interphase fluorescence in situ hybridization, several of which are well characterized and used to stratify CLL patients into three broadly recognized risk groups: (i) low-risk (del 13q14); (ii) intermediate risk group (normal cytogenetics or trisomy 12); and (iii) high-risk patients with del 17p or del 11q (24). FC quantification of the level of CD20 expression in CLL has been shown to be predictive of cytogenetic abnormalities with a significantly lower level of CD20 expression in $11q^-$ cases, while trisomy 12 cases had a significantly higher level of CD20 expression. In addition, elevated levels of CD20 expression correlated with an improved response to rituximab therapy (25).

In the past, CLL was considered an indolent disorder, receiving mainly palliative therapy. As more effective intensive and/or combination therapies were developed, long-standing clinical remissions were achieved in the majority of patients. Minimal residual disease (MRD), which is the detection of disease in the absence of cytologic and histologic evidence of disease, was studied in patients, and MRD levels during and after therapy were shown to be independent predictors of progression-free and overall survival in CLL (26–28). Since eradication of MRD is associated with prolonged survival and quantitation of MRD levels improves the prediction of outcome and may even be used to direct therapy, this assay has achieved clinical importance in monitoring CLL patients (26–28). Sensitive detection of MRD in CLL is currently possible through PCR-based or FC MRD testing. FC is generally more broadly available, faster, and less labor-intensive and requires less specialized equipment. CLL MRD detection using FC relies on the recognition of small numbers of cells with the unique immunophenotype of CLL.

SAMPLE PREPARATION FOR FC ANALYSIS: GENERAL

Appropriate samples for CLL FC include PB, BM, and LN biopsy or fine-needle aspiration (FNA). In general, proper collection, processing, analysis, and correlation with ancillary testing are all crucial to FC diagnostic evaluation of any hematolymphoid neoplasm (see reference 29 for additional technical details). Blood and BM specimens must be

TABLE 1 Immunophenotype of B-cell chronic lymphoproliferative disorders[a]

Diagnosis[b]	Result for[c]:											Comment
	CD19	CD20	CD22	CD5	CD23	CD10	CD11c	CD103	CD79b	CD25	sIg	
BL	+	+	+	–	–	+	–	–	+		+	IgM
FL	Dim+	+	+	–	+/–	+	–	–	+	–	+	BCL-2$^+$
CLL	+	Dim+	Dim+	+	+	–	Dim+/–	–	–/Dim+	+/–	Dim+	CD38, ZAP-70
MCL	+	+	+	+	–	–	–	–	+	+	+	Cyclin D1$^+$
DLBCL	+/–	+/–	+/–	+/–	+/–	+/–	–	–	+/–	+/–	+/–	CD30$^{+/-}$
HCL	+	Bright+	Bright+	–	–	–	Bright+	+	+	Bright+	+	CD123$^+$
HCLv	+	Bright+	Bright+	–	–	–	Bright+ to +/–	+/–	+	–	+	CD123$^{+/-}$
SMZL	+	+	+	–	–	–	+/–	–	+	–/+	+	CD123$^-$

[a]A homogeneous cluster of 20 neoplastic cells is sufficient for diagnosis of a B-cell lymphoproliferative disorder. The number of neoplastic cells sufficient for diagnosis of a T-cell lymphoproliferative disorder is highly variable and depends on the degree of abnormality of the immunophenotype (20 neoplastic cells is the minimum).

[b]BL, Burkitt lymphoma; FL, follicular lymphoma; CLL, chronic lymphocytic leukemia; MCL, mantle cell lymphoma; DLBCL, diffuse large-B-cell lymphoma; HCL, hairy cell leukemia; HCLv, hairy cell leukemia variant; SMZL, splenic marginal zone lymphoma.

[c]+, characteristically positive; –, characteristically negative; +/– , variable expression (positive in some cases and negative in others); Dim+, expressed at lower than normal levels; Bright+, expressed at brighter than normal levels.

TABLE 2 Immunophenotypes of T-cell chronic lymphoproliferative disorders[a]

Diagnosis[b]	Result for[c]:										Comments
	CD4	CD8	CD2	CD3	CD5	CD7	CD25	CD16	CD56	CD57	
MF	+	–	+	Dim+	+	–	+/–	–	–	–	$CD26^-$
ALCL	+/–	–	+/–	+/–	+/–	+/–	+/–	–	–	–	$CD30^+$, $ALK1^+$
AILT	+	–	+	+	+	+/–		–	–	–	$CD10^+$ (maybe partial)
ATL	+	–	+	Dim+	+	–	Bright+	–	–	–	$CD26^-$
ETTL	–	+/–		+	–	+			+/–	–	$CD103^+$, $CD30^{+/-}$
HSγδ	–	+/–	+	+	+/–	+/–	–	+/–	+/–	–	TCR-$γδ^+$
MCγδ	–	+/–	+	+	+/–	–	–	–	+/–	–	TCR-$γδ^+$

[a]A homogeneous cluster of 20 neoplastic cells is sufficient for diagnosis of a B-cell lymphoproliferative disorder. The number of neoplastic cells sufficient for diagnosis of a T-cell lymphoproliferative disorder is highly variable and depends on the degree of abnormality of the immunophenotype (20 neoplastic cells is the minimum).

[b]MF, mycosis fungoides; ALCL, anaplastic large-cell lymphoma; AILT, angioimmunoblastic T-cell lymphoma; ATL, adult T-cell leukemia/lymphoma; ETTL, enteropathy type T-cell lymphoma; HSγδ, hepatosplenic γδ T-cell lymphoma; MCγδ, mucocutaneous gd T-cell lymphomas.

[c]+, positive for antigen; –, negative for antigen; +/–, variable positivity; Dim+, expressed at lower than normal levels; Bright+, expressed at brighter than normal levels.

collected in an appropriate anticoagulant such as sodium heparin (preferable), EDTA, or ACD (acid citrate dextrose) (PB only, not appropriate for BM). PB samples are stable at room temperature for up to 72 h in sodium heparin and ACD but only up to 24 h in EDTA. BM samples are stable in sodium heparin for up to 24 h, while specimens placed in EDTA should be processed within 12 h. A LN biopsy specimen must be made into a cell suspension using mechanical tissue disaggregation (achieved by slicing, mincing, and teasing apart the tissue using commercial devices or manual tools). FNA samples usually do not require further disaggregation and can be directly stained. Adverse storage conditions before staining could damage the cells of interest, and overnight shipment of specimens (potentially exposing specimens to temperature extremes) has been shown to alter antigen expression (29–31). Viability should be assessed (especially in LN and FNA specimens) and samples with less than 75% viability rejected unless the sample is irreplaceable, in which case every effort must be made to obtain diagnostic information. Minimizing sample treatment before staining and timely sample processing greatly reduce the risk of losing cells of interest (especially in the case of CLL MRD) and maintain cell viability and integrity. However, the cells must be washed with warm or room temperature phosphate-buffered saline before staining for light chains to remove serum immunoglobulin and cytophilic antibody. Erythrocytes should be removed by lysis, not density gradient separation (29).

DIAGNOSIS OF CLL

CLL has a distinctive immunophenotype and can be diagnosed based upon FC testing in combination with complete blood count results. The antibody panel should always include a screening tube that allows identification of abnormal B, T, NK, granulocytic, and monocytic cells as well as the presence of blasts, even in patients with a confirmed diagnosis of CLL, as the patient might have a second neoplastic process (32). There are two general approaches, namely use of a minimal screening panel followed by a larger specific panel based upon preliminary results or use of a more extensive panel up front. The best approach in panel design depends on issues facing an individual laboratory, and these are discussed elsewhere (32). In the initial diagnosis of CLL and exclusion of other T- or B-cell lymphoproliferative disorders (Tables 1 and 2), we evaluate the following antigens up front: CD2, CD3, CD4, CD5, CD7, CD8, CD10, CD11c, CD19, CD20, CD22, CD23, CD25, CD38, CD43, CD45, CD56, CD57, CD79b, CD81, CD103, CD123, CD200, T-cell receptor γδ (TCR-γδ), surface kappa light chain (sIgκ), and lambda light chain. Since there is no screening tube, CD2, CD3, CD4, CD5, CD7, CD8, CD45, CD56, CD57, and TCR-γδ allow the identification of a T- or NK-cell lymphoproliferative process (Table 2). The Euroflow consensus panel utilizes a screening tube followed by a B-cell-specific panel which adds the additional antigens CD27, CD31, CD39, CD49d, CD62L, CD95, CD185, CD305, HLA-DR, and sIgM but does not evaluate CD25 and CD123 on B cells or CD2, CD7, and CD57 (T- and NK-cell processes are not evaluated after the initial screening tube) (33).

Diagnosis of CLL/SLL and exclusion of other B-cell lymphoproliferative disorders (Table 1) depends upon FC demonstration of the characteristic CLL immunophenotype. Analysis of FC data should first involve examination of all cells. B cells can then be further characterized in a lymphocyte gate based upon forward scatter (FSC) versus side scatter (SSC) (after validating, the gate includes T, B, and NK cells) augmented by a CD19 versus SSC gate. If

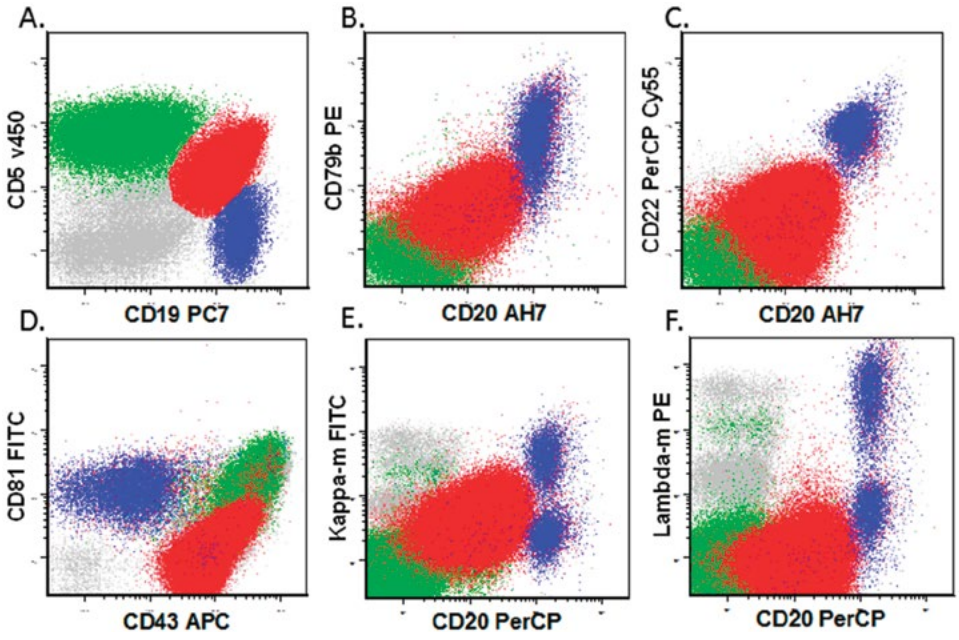

FIGURE 1 Peripheral blood specimen with CLL cells (red), patient's residual nonneoplastic B cells (blue), and T cells (green). (A) The red CLL cells are CD19 and CD5 positive. The blue nonneoplastic B cells are CD19 positive but CD5 negative. The normal T cells are CD5 positive but CD19 negative. (B) The nonneoplastic B cells (blue) show normal levels of CD20 and CD79b expression. The CLL cells (red) have dim CD20 and dim CD79b expression. (C) The nonneoplastic B cells have normal levels of CD20 and CD22, while the CLL cells are dim for both. (D) The nonneoplastic B cells have normal CD81 intensity and are dim to negative for CD43. The CLL cells are negative for CD81 and have bright CD43 expression. The normal T cells (green) provide an internal CD81 and CD43 positive control. (E, F) CD20 on the *x* axis helps to separate the B cells from non-B-cell elements and the CLL cells from the nonneoplastic B cells. The nonneoplastic B cells are polyclonal for kappa and lambda, while the CLL cells have dim kappa expression but are negative for lambda. PE, phycoerythrin; PerCP, peridinin chlorophyll protein; FITC, fluorescein isothiocyanate; APC, allophycocyanin v450, violet 450; PC7, phycoerythrin cyanin 7; AH7, allophycocyanin H7 (analog dye to APC-cyanin 7 dye).

CD45 gating is used, care must be taken to not gate out the dim CD45-positive cells. In nontreated CLL, CD19- and CD5-positive monoclonal (i.e., restricted to kappa or lambda light chain) B cells predominate and have dim expression of sIg, CD20, CD22, CD45, CD79b, and CD81 but moderate CD23 and bright CD43 (Fig. 1). In addition, they express CD200 but are negative for CD10, CD103, and CD123. Therefore, for interpretation of results, one must know the normal intensities of these antigens within the individual laboratory, since residual normal B cells can be rare in CLL and therefore not available for comparison. Comparison of CD43 and CD81 to expression on normal T cells can be helpful. Infrequently, an immunophenotype that is atypical for CLL is observed (lack of CD5 or CD23; aberrant CD10, T-cell, or myeloid antigens; normal expression of a B-cell antigen or sIg); however, some aspects of the typical CLL immunophenotype are usually present, giving a clue as to the correct diagnosis (11–13). Morphology, molecular studies, cytogenetics, and clinical history are helpful in such cases. In blood, the number of CD5-positive monoclonal B cells must be $\geq 5 \times 10^3/\mu l$ to meet the diagnostic criteria for CLL ($<5 \times 10^3/\mu l$ would be MBL), so correlation with complete blood count results is optimal.

Although CD19- and CD5-positive monoclonal B cells are also observed in MCL, there is moderate expression of CD20, CD22, CD45, and CD79b, while CD23 is dim or negative and CD200 is not expressed in MCL (10). Furthermore, detection of cyclin D1 also may be helpful in confirming MCL diagnosis. Some hairy cell leukemia cases may express CD5, but they express bright B-cell markers together with CD11c, CD103, and CD123 (34). CD5-positive follicular lymphoma has also been described, but again, the typical CLL immunophenotype is missing and CD10 expression is observed (35).

ZAP-70 ANALYSIS IN CLL

ZAP-70 is a labile protein that degrades over time, so specimens should be processed within 24 h of sample collection. Furthermore, rapid processing is necessary to maintain cell viability and reduce the risk of losing cells of interest. Washing the cells with 5% fetal bovine serum in phosphate-buffered saline is recommended, and lysis of red blood cells in bloody specimens is an essential step.

ZAP-70 Antibody Clone, Fluorochrome, and Methods of Permeabilization

The quality of FC ZAP-70 testing depends upon the combination of anti-ZAP-70 antibody clone (Fig. 2), fluorochrome conjugate, and method of fixation or permeabilization utilized. The ZAP-70 clone or conjugate should be selected based on its ability to highly discriminate between the levels of desired signal to the level of noise (signal-to-noise ratio). Validated permeabilization methods for ZAP-70 assessment include Triton (36), a saponin-based method (37), and the commercially available Fix & Perm (38). However, the

optimal fixation and permeabilization method may depend upon the antibody clone and fluorochrome conjugate utilized. The SBZAP-phycoerythrin (PE) clone had the highest known signal-to-noise ratio using a Triton-based method for permeabilization (36, 39, 40). Also, 1E7.2 AF488 was extensively used in a clinical laboratory and reported to have the best results using saponin as a method of permeabilization (37). It is recommended to test the specific ZAP-70 antibody clone or conjugate with permeabilization methods on normal donor cells before selecting the system to be utilized for ZAP-70 assessment.

Method of ZAP-70 Analysis and Reporting

Since the ZAP-70 protein is expressed at low levels, it is sometimes difficult to determine if CLL cells are negative or if there is dim expression. Several methods have been used to address this issue in ZAP-70 analysis, including the isotype method, determining the percent positive using the residual internal T-cell population (Fig. 2), using normal donor T cells as a reference point for the determination of percent positive (Fig. 2), and ratios using mean fluorescent intensity (MFI) (21, 23, 39, 41–44). The isotype method involves staining a specimen with an isotype control and with anti-ZAP-70 antibody. Positivity is defined as cells staining more intensely with the anti-ZAP-70 antibody than with isotype control with a cutoff value of 11% or higher ZAP-70 positivity (39, 41). Since normal T cells express ZAP-70, residual normal T cells can be used as an internal positive control to determine ZAP-70 positivity (21, 39). As residual normal T-cells may be low in number, others have used T-cell ZAP-70 positivity in a parallel normal donor specimen to determine the cutoff point for positivity (23, 39). A cutoff value of 20% has been utilized to determine percent positive using either the patient's residual normal T cells or normal donor T cells. Others have used a ratio of the MFI of ZAP-70 staining by the CLL cells and other populations, such as the ZAP-70 MFI in the patient's residual normal T cells/MFI in CLL cells (39, 42, 43), the MFI in normal donor T cells/MFI in CLL cells (39, 44), the MFI in the CLL cells/MFI in normal residual B cells (39, 42), and the MFI in the CLL cells/MFI in normal donor B cells (45). A cutoff value of <3.0 was considered positive for the ratiometric method using either patient or normal donor T cell MFI/MFI of CLL cells, and a value of >1.4 was considered positive using the ratio of MFI in CLL cells/MFI in B cells from either patients or normal donor. Shankey et al. developed the CLL-Z index for analysis of ZAP-70 in CLL (36). The CLL-Z index uses the MFI of ZAP-70 in the patient's CLL cells, residual normal B cells (negative for ZAP-70), and residual normal T cells.

$$\text{CLL-Z index} = \frac{(\text{CLL clone MFI} - \text{B-cell MFI})}{(\text{T-cell MFI} - \text{B-cell MFI})} \times 100$$

The CLL-Z index would need to be validated within an individual laboratory using the specific reagents. Shankey

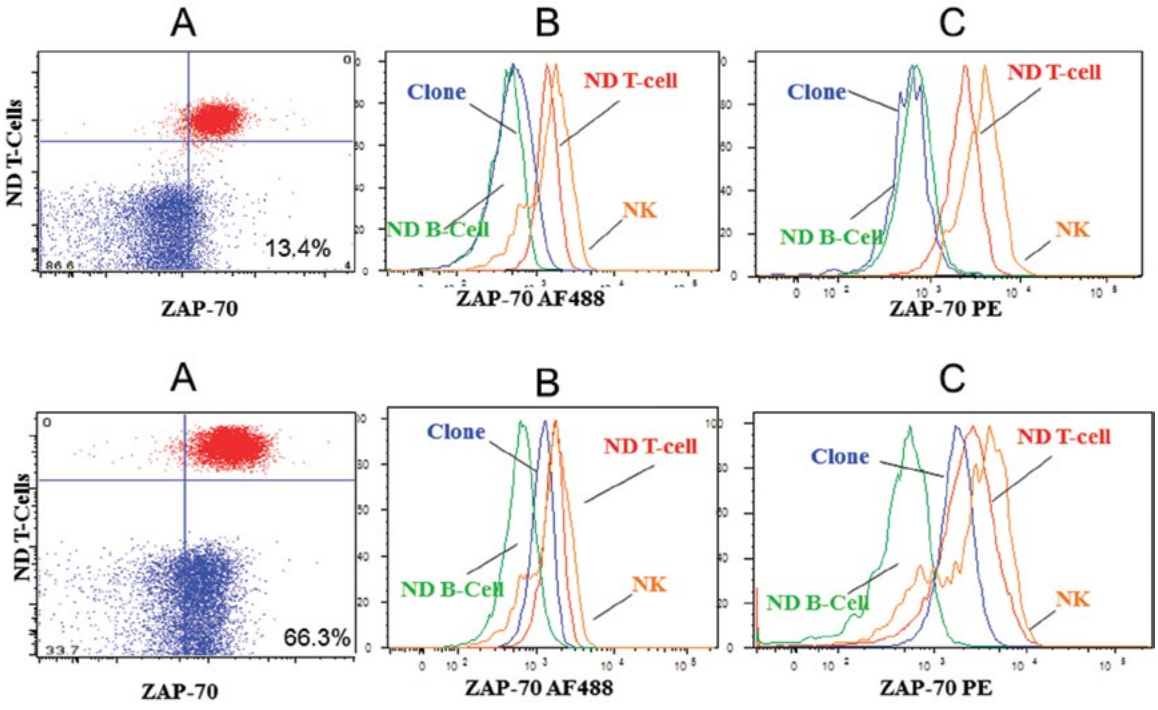

FIGURE 2 Flow cytometric analysis of ZAP-70 expression. The upper row is an example of a ZAP-70-negative case, while the lower row is an example of a ZAP-70-positive CLL case. Different methods of ZAP-70 reporting are shown. Panel A shows the percentile method, where the marker was placed so that the gated T cells ($CD3^+$, $CD19^-$) and natural killer (NK) cells ($CD16/56^+$, $CD19^-$) with a high level of ZAP-70 expression would appear in the upper right quadrant. Gated CLL cells ($CD19^+$, CD20 dim, $CD5^+$) were plotted using the same quadrant, and the percentage of CLL cells that showed ZAP-70 positivity (the lower right quadrant) was calculated using 20% as a cutoff value for positivity. Panels B and C show histograms demonstrating the overlay of normal donor (ND) B cells (green), CLL clonal cells (blue), ND T cells (red), and ND NK cells (orange) using ZAP-70 1E7.2 AF488 (B) and SBZAP PE (C). Note the high signal-to-noise ratio seen with the SBZAP PE clone compared to ZAP-70 1E7.2 AF488.

et al. reported values of 0.3 as negative, 6.0 as low positive, and 27.0 as high positive ZAP-70 expression in their laboratory (36).

Variability in ZAP-70 Testing

The reported level of ZAP-70 expression varies greatly depending not only on the antibody but also the method used to express the results. Studies have observed a difference in the percentage of CLL cells stained positive for ZAP-70 when different monoclonal antibodies were used, even when the same gating strategy was used on the same CLL population. Studies indicate that the ratiometric method results in a much lower interlaboratory variation than other reporting strategies and is recommended for multicenter studies (39, 46). The observed variation in ZAP-70 testing led to the concept that a scoring system combining four methods of analysis (including percent positive and ratiometric methods) and using two clones for assignment of ZAP-70 expression would improve the precision of testing (44). The rationale is that if one clone was unable to clearly assess ZAP-70 expression by four methods of analysis, the addition of a second clone might aid in this assessment. Even if ZAP-70 expression is positive by three or four methods of analysis, the confirmation by a second reagent enhances the analytic precision and improves its correlation with the two major primary prognostic CLL biomarkers: IgVH and cytogenetic abnormalities (44). It is important to note that using several methods of analysis, even with just one antibody, improves ZAP-70 expression assignment. The combined ZAP-70 score using two reagents permitted the assignment and resolution of equivocal cases that could not be solved using one reagent (44). A normalization step of adding B cells from a pool of normal donor peripheral blood mononuclear cells constitutes a second step toward improving test precision (23). More recently, the concept of combining normal donor cells and CLL patient samples in one tube was proposed in order to have an internal negative control (normal donor B cells) and positive control (normal donor T cells) (47). Using this combined sample, two anti-ZAP-70 clones that target different epitopes and simultaneous assessment of ZAP-70 expression by five methods of analysis allowed a

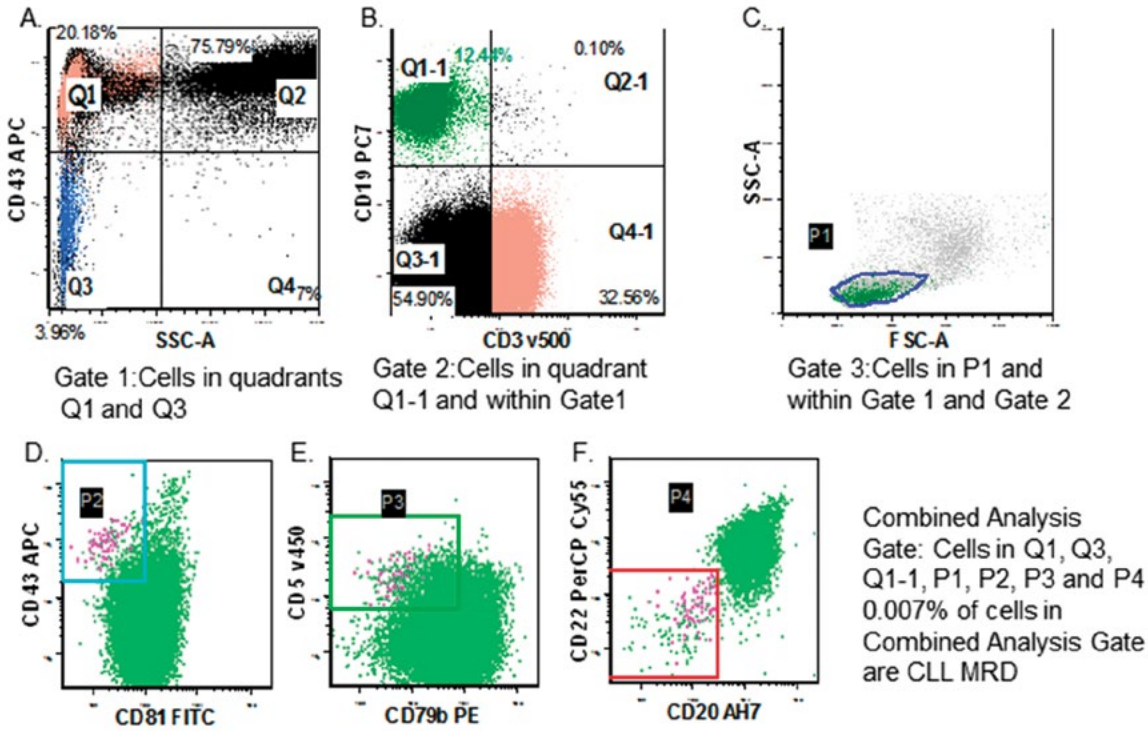

FIGURE 3 ERIC method of flow cytometric CLL MRD analysis. (A) All cells shown. A quadrant type of gate (gate 1) is set including the lymphocytes and monocytes in quadrant Q1 and quadrant Q3 (gate 1: $CD43^+$ and $CD43^-$, low SSC). (B) Cells from gate 1 shown. Gate 2 is restricted to the cells in gate 1 and the CD19-positive and CD3-negative cells in quadrant Q1-1 (gate 2: $CD19^+$, $CD3^-$, $CD43^+$, and $CD43^-$, low SSC). (C) Cells from gate 2 shown. Gate 3 is restricted to the cells in gate 2 and P1 (gate 3: $CD19^+$, $CD3^-$, $CD43^+$, and $CD43^-$, low SSC, FSC consistent with lymphocytes). (D) Cells in gate 3 shown. Gate P2 targets abnormal CD43-bright and CD81-dim-to-negative cells in gate 3 (gate 3: $CD19^+$, $CD3^-$, $CD43^+$, and $CD43^-$, low SSC, FSC consistent with lymphocytes). (E) Cells in gate 3 shown. Gate P3 targets abnormal CD79b-dim-to-negative and CD5-positive cells in gate 3 (gate 3: $CD19^+$, $CD3^-$, $CD43^+$, and $CD43^-$, low SSC, FSC consistent with lymphocytes). (F) Cells in gate 3 shown. Gate P4 targets abnormal CD20-dim and CD22-dim CD19-positive cells in gate 3 (gate 3: $CD19^+$, $CD3^-$, $CD43^+$, and $CD43^-$, low SSC, FSC consistent with lymphocytes). The final combined analysis gate for CLL MRD includes only cells in gates 1, 2, 3, P2, P3, and P4 which are CD19 positive, CD3 negative, CD43 bright positive, CD81 dim to negative, CD79b dim to negative, CD5 positive, CD20 dim positive, CD22 positive, with low SSC and FSC consistent with lymphocytes.

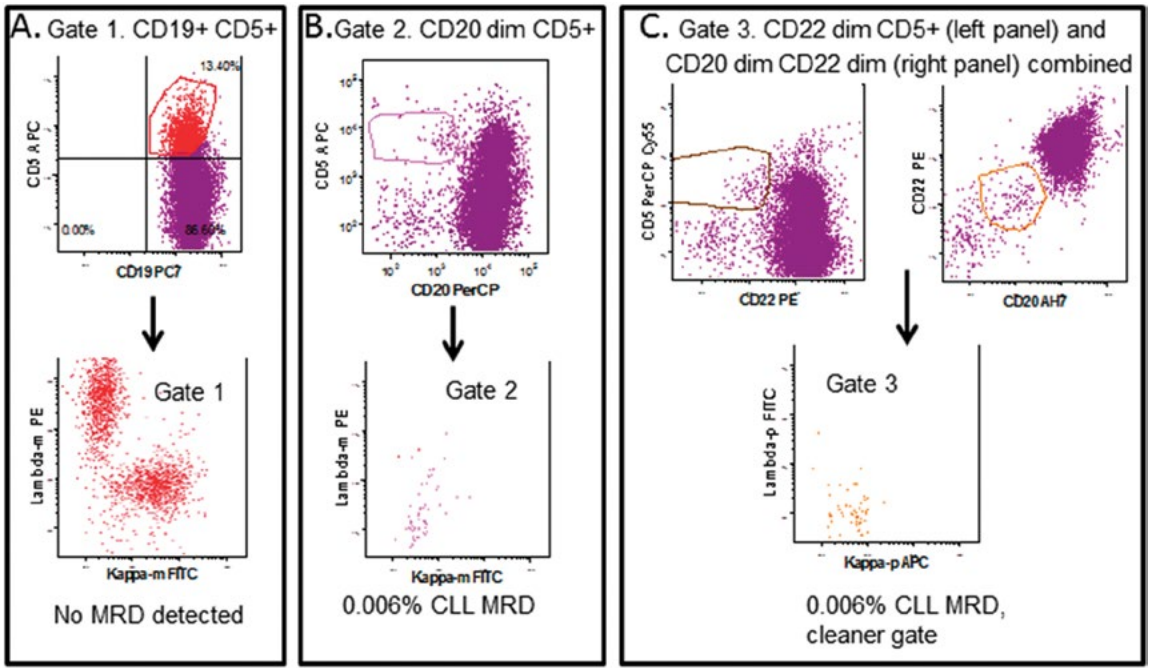

FIGURE 4 (A) CD19-positive lymphocytes (upper panel) and CD19- and CD5-positive cells (lower panel) are shown. In the upper panel, the CD19-positive and CD5-positive B cells are gated (in red), and in the lower panel, the lack of light chain restriction is demonstrated. No CLL MRD was detected. (B) CD19-positive lymphocytes (upper panel) and CD20-dim and CD5-positive cells (lower panel) are shown. In the upper panel, CD20-dim and CD5-positive B cells are gated (light purple), and in the lower panel, CLL MRD is demonstrated by light chain restriction. (C) CD19-positive lymphocytes (upper panel) and CD20-dim, CD22-dim, and CD5-positive cells (lower panel) are shown. In the upper panel, CD22-dim, CD5-positive, CD20-dim, and CD22-dim cells are gated (brown). In the lower panel, CLL MRD is demonstrated by light chain restriction and a cleaner analysis gate is achieved.

precise improved evaluation of ZAP-70 expression in one tube (47).

ZAP-70 and CD38 provide complementary prognostic information.

CLL MRD DETECTION

FC CLL MRD detection is performed in a manner similar to diagnosis of CLL with certain modifications. The simple historical approach incorporating analysis for CD19/CD5 coexpression coupled with clonality assessment using surface kappa/lambda expression is inadequate for CLL MRD studies. Several FC MRD CLL detection approaches have been previously described using different combinations of antibodies (5, 26, 48–51). Later, an international standardized approach was developed in 2007 and further expanded into the European Research Initiative in CLL (ERIC). This method is highly reproducible and has been validated in multicenter randomized clinical trials (5, 27, 50, 52, 53). The number of cells analyzed is critical for sensitive CLL detection. One million leukocytes is the lowest acceptable minimum number of cells to be acquired per tube, and a sensitivity of 0.001% can be attained with 1.8 million or higher acquisition (50, 51).

The ERIC approach to analysis involves a Boolean gating strategy in which CD19-positive B cells are evaluated and a series of analysis regions (called gates) created in areas where normal B-cell populations are not observed. This is utilized to detect very low numbers of abnormal B cells consistent with CLL (Fig. 3) (50). Simply looking at CD5- and CD19-positive B cells is not adequate (Fig. 4A). We have utilized methodology in which abnormal B-cell populations have been identified and kappa or lambda light chain restriction demonstrated (Fig. 4). This has been shown to be as effective as the ERIC method (54).

REFERENCES

1. **Muller-Hermelink HK, Montserrat ME, Catovsky D, Campo E, Harris NL, Stein H.** 2007. Chronic lymphocytic leukemia/small lymphocytic lymphoma, p 180–182. *In* Swerdlow SH, Campo E, Harris NL, Jaffe ES, Pileri SA, Stein H, Thiele J, Vardiman JW (ed), *WHO Classification of Tumors of Hematopoietic and Lymphoid Tissues*. IARC, Lyon, France.
2. **Binet JL, Auquier A, Dighiero G, Chastang C, Piguet H, Goasguen J, Vaugier G, Potron G, Colona P, Oberling F, Thomas M, Tchernia G, Jacquillat C, Boivin P, Lesty C, Duault MT, Monconduit M, Belabbes S, Gremy F.** 1981. A new prognostic classification of chronic lymphocytic leukemia derived from a multivariate survival analysis. *Cancer* **48:**198–205.
3. **Craig FE, Foon KA.** 2008. Flow cytometric immunophenotyping for hematologic neoplasms. *Blood* **111:**3941–3967.
4. **Hallek M, Cheson B, Catovsky D, Caligaris-Cappio F, Dighiero G, Dohner H, Hillmen P, Keating M, Montserrat E, Rai K, Kipps T.** 2008. Guidelines for the diagnosis and treatment of chronic lymphocytic leukemia: a report from the International Workshop on Chronic Lymphocytic

Leukemia updating the National Cancer Institute-Working Group 1996 guidelines. *Blood* **111:**5446–5456.
5. **Rawstron AC, Villamor N, Ritgen M, Böttcher S, Ghia P, Zehnder JL, Lozanski G, Colomer D, Moreno C, Geuna M, Evans PA, Natkunam Y, Coutre SE, Avery ED, Rassenti LZ, Kipps TJ, Caligaris-Cappio F, Kneba M, Byrd JC, Hallek MJ, Montserrat E, Hillmen P.** 2007. International standardized approach for flow cytometric residual disease monitoring in chronic lymphocytic leukaemia. *Leukemia* **21:**956–964.
6. **Moreau E, Matutes E, Ahern RP, Catovsky D.** 1997. Improvement of the chronic lymphocytic leukemia scoring system with the monoclonal antibody SN8 (CD79b). *Am J Clin Pathol* **108:**378–382.
7. **Venkataraman G, Aguhar C, Kreitman R, Yuan CM, Stetler-Stevenson M.** 2011. Characteristic CD103 and CD123 expression pattern defines hairy cell leukemia: utility of CD123 and CD103 in diagnosis of mature B-cell lymphoproliferative disorders. *Am J Clin Pathol* **136:**625–630.
8. **Marti G, Rawstron AC, Ghia P, Hillmen P, Houlston RS, Kay N, Schleinitz TA, Caporaso N, International Familial CLL Consortium.** 2005. Diagnostic criteria for monoclonal B-cell lymphocytosis. *Br J Haematol* **130:**325–332.
9. **Shanafelt TD, Ghia P, Lanasa MC, Landgren O, Rawstron AC.** 2010. Monoclonal B-cell lymphocytosis (MBL): biology, natural history and clinical management. *Leukemia* **24:**512–520.
10. **Alapat D, Coviello-Malle J, Owens R, Qu PP, Barlogie B, Shaughnessy JD, Lorsbach RB.** 2012. Diagnostic usefulness and prognostic impact of CD200 expression in lymphoid malignancies and plasma cell myeloma. *Am J Clin Pathol* **137:**93–100.
11. **Ahmad E, Steinberg SM, Goldin L, Hess CJ, Caporaso N, Kreitman RJ, Wiestner A, Wilson W, White T, Marti G, Stetler-Stevenson M.** 2008. Immunophenotypic features distinguishing familial chronic lymphocytic leukemia from sporadic chronic lymphocytic leukemia. *Cytometry B Clin Cytom* **74:**221–226.
12. **Kingma DW, Imus P, Xie XY, Jasper G, Sorbara L, Stewart C, Stetler-Stevenson M.** 2002. CD2 is expressed by a sub-population of normal B cells and is frequently present in mature B cell neoplasms. *Cytometry B Clin Cytom* **50:**243–248.
13. **Kampalath B, Barcos MP, Stewart C.** 2003. Phenotypic heterogeneity of B cells in patients with chronic lymphocytic leukemia/small lymphocytic lymphoma. *Am J Clin Pathol* **119:**824–832.
14. **Döhner H, Stilgenbauer S, Benner A, Leupolt E, Kröber A, Bullinger L, Döhner K, Bentz M, Lichter P.** 2000. Genomic aberrations and survival in chronic lymphocytic leukemia. *N Engl J Med* **343:**1910–1916.
15. **Hamblin TJ, Davis Z, Gardiner A, Oscier D, Stevenson F.** 1999. Unmutated Ig V(H) genes are associated with a more aggressive form of chronic lymphocytic leukemia. *Blood* **94:**1848–1854.
16. **Damle RN, Wasil T, Fais F, Ghiotto F, Valetto A, Allen SL, Buchbinder A, Budman D, Dittmar K, Kolitz J, Lichtman SM, Schulman P, Vinciguerra VP, Rai KR, Ferrarini M, Chiorazzi N.** 1999. Ig V gene mutation status and CD38 expression as novel prognostic indicators in chronic lymphocytic leukemia. *Blood* **94:**1840–1847.
17. **Del Poeta G, Maurillo L, Venditti A, Buccisano F, Epiceno A, Capelli G, Tamburini A, Suppo G, Battaglia A, Del Principe M, Del Moro B, Masi M, Amadori S.** 2001. Clinical significance of CD38 expression in chronic lymphocytic leukemia. *Blood* **98:**2633–2639.
18. **Ibrahim S, Keating M, Do KA, O'Brien S, Huh YO, Jilani I, Lerner S, Kantarjian HM, Albitar M.** 2001. CD38 expression as an important prognostic factor in B-cell chronic lymphocytic leukemia. *Blood* **98:**181–186.
19. **Durig J, Naschar M, Schmucker U, Renzing-Kohler K, Holter A, Huttmann T, Duhrsen U.** 2002. CD38 expression is an important prognostic marker in chronic lymphocytic leukaemia. *Leukemia* **16:**30–35.
20. **Hamblin TJ, Orchard JA, Ibbotson RE, Davis Z, Thomas PW, Stevenson FK, Oscier DG.** 2002. CD38 expression and immunoglobulin variable region mutations are independent prognostic variables in chronic lymphocytic leukemia but CD38 expression may vary during the course of the disease. *Blood* **99:**1023–1029.
21. **Crespo M, Bosch F, Villamor N, Bellosillo B, Colomer D, Rozman M, Marce S, Lopez-Guillermo A, Campo E, Montserrat E.** 2003. ZAP-70 expression as a surrogate for immunoglobulin-variable region mutations in chronic lymphocytic leukemia. *N Engl J Med* **348:**1764–1775.
22. **Wiestner A, Rosenwald A, Barry TS, Wright G, Davis RE, Henrickson SE, Zhao H, Ibbotson RE, Orchard JA, Davis Z, Stetler-Stevenson M, Raffeld M, Arthur DC, Marti GE, Wilson WH, Hamblin TJ, Oscier DG, Staudt LM.** 2003. ZAP-70 expression identifies a chronic lymphocytic leukemia subtype with unmutated immunoglobulin genes, inferior clinical outcome, and distinct gene expression profile. *Blood* **101:**4944–4951.
23. **Rassenti L, Huynh L, Toy TL, Chen L, Keating MJ, Gribben JG, Neuberg DS, Flinn IW, Rai KR, Byrd JC, Kay NE, Greaves A, Weiss A, Kipps TJ.** 2004. ZAP-70 compared with immunoglobulin heavy-chain gene mutation status as a predictor of disease progression in chronic lymphocytic leukemia. *N Engl J Med* **351:**893–901.
24. **Moreno C, Montserrat E.** 2008. New prognostic markers in chronic lymphocytic leukemia. *Blood Rev* **22:**211–219.
25. **Tam CS, Otero-Palacios J, Abruzzo LV, Jorgensen JL, Ferrajoli A, Wierda WG, Lerner S, O'Brien S, Keating MJ.** 2008. Chronic lymphocytic leukemia CD20 expression is dependent on the genetic subtype: a study of quantitative flow cytometry and fluorescent in-situ hybridization in 510 patients. *Br J Haematol* **141:**36–40.
26. **Rawstron AC, Kennedy B, Evans PA, Davies FE, Richards SJ, Haynes AP, Russell NH, Hale G, Morgan GJ, Jack AS, Hillmen P.** 2001. Quantitation of minimal disease levels in chronic lymphocytic leukemia using a sensitive flow cytometric assay improves the prediction of outcome and can be used to optimize therapy. *Blood* **98:**29–35.
27. **Moreton P, Kennedy B, Lucas G, Leach M, Rassam SM, Haynes A, Tighe J, Oscier D, Fegan C, Rawstron A, Hillmen P.** 2005. Eradication of minimal residual disease in B-cell chronic lymphocytic leukemia after alemtuzumab therapy is associated with prolonged survival. *J Clin Oncol* **23:**2971–2979.
28. **Schweighofer CD, Ritgen M, Eichhorst BF, Busch R, Abenhardt W, Kneba M, Hallek M, Wendtner CM.** 2009. Consolidation with alemtuzumab improves progression-free survival in patients with chronic lymphocytic leukaemia (CLL) in first remission: long-term follow-up of a randomized phase III trial of the German CLL Study Group (GCLLSG). *Br J Haematol* **144:**95–98.
29. **Stetler-Stevenson M, Ahmad E, Barnett D, Braylan RC, DiGiuseppe JA, Marti G, Menozzi D, Oldaker TA, Orfao A, Rabellino E, Stone EC, Walker C.** 2005. *Clinical Flow Cytometric Analysis of Neoplastic Hematolymphoid Cells. Approved Guideline*, 2nd ed. *CLSI Document H43-A2*. Clinical and Laboratory Standards Institute, Wayne, PA.
30. **Jasper GA, Arun I, Venzon D, Kreitman RJ, Wayne AS, Yuan CM, Marti GE, Stetler-Stevenson M.** 2011. Variables affecting the quantitation of CD22 in neoplastic B cells. *Cytometry B Clin Cytom* **80:**83–90.
31. **Wang L, Abbasi F, Jasper GA, Kreitman RJ, Liewehr DJ, Marti GE, Stetler-Stevenson M.** 2011. Variables in the quantification of CD4 in normals and hairy cell leukemia patients. *Cytom BClin Cytom* **80:**51–56.

32. **Wood BL, Arroz M, Barnett D, DiGiuseppe J, Greig B, Kussick SJ, Oldaker T, Shenkin M, Stone E, Wallace P.** 2007. 2006 Bethesda international consensus recommendations on the immunophenotypic analysis of hematolymphoid neoplasia by flow cytometry: optimal reagents and reporting for the flow cytometric diagnosis of hematopoietic neoplasia. *Cytometry B Clin Cytom* **72:**S14–S22.
33. **Van Dongen JJ, Lhermitte L, Böttcher S, Almeida J, van der Velden VH, Flores-Montero J, Rawstron A, Asnafi V, Lécrevisse Q, Lucio P, Mejstrikova E, Szczepński T, Kalina T, de Tute R, Brüggemann M, Sedek L, Cullen M, Langerak AW, Mendonça A, Macintyre E, Martin-Ayuso M, Hrusak O, Vidriales MB, Orfao A.** 2012. EuroFlow antibody panels for standardized n-dimensional flow cytometric immunophenotyping of normal, reactive and malignant leukocytes. *Leukemia* **26:**1908–1975.
34. **Shao H, Calvo KR, Grönborg M, Tembhare PR, Kreitman RJ, Stetler-Stevenson M, Yuan CM.** 2013. Distinguishing hairy cell leukemia variant from hairy cell leukemia: development and validation of diagnostic criteria. *Leuk Res* **37:**401–409.
35. **Barry TS, Jaffe ES, Kingma DW, Martin AW, Sorbara L, Raffeld M, Pittaluga S.** 2002. CD5+ follicular lymphoma: a clinicopathologic study of three cases. *Am J Clin Pathol* **118:**589–598.
36. **Shankey T, Scibelli P, Cobb J, Smith CM, Mills R, Bernal E, van der Heiden M, Keeney M, Popma J, Forman M.** 2006. An optimized whole blood method for flow cytometric measurement of ZAP-70 protein expression in chronic lymphocytic leukemia. *Cytometry B Clin Cytom* **70:**259–269.
37. **Rassenti LZ, Kipps TJ.** 2006. Clinical utility of assessing ZAP-70 and CD38 in chronic lymphocytic leukemia. *Cytometry B Clin Cytom* **70:**209–213.
38. **Sheikholeslami MR, Jilani I, Keating M, Uyeji J, Chen K, Kantarjian H, O'Brien S, Giles F, Albitar M.** 2006. Variations in the detection of ZAP-70 in chronic lymphocytic leukemia: comparison with IgVH mutation analysis. *Cytometry B Clin Cytom* **70:**270–275.
39. **Degheidy H, Venzon DJ, Farooqui MZH, Abbasi F, Arthur DC, Wilson WH, Wiestner A, Stetler-Stevenson M, Marti GE.** 2011. Methodological comparison of two anti-ZAP-70 antibodies. *Cytometry B Clin Cytom* **80:**300–308.
40. **Kern W, Dicker F, Schnittger S, Haferlach C, Haferlach T.** 2009. Correlation of flow cytometrically determined expression of ZAP-70 using the SBZAP antibody with IgVH mutation status and cytogenetics in 1,229 patients with chronic lymphocytic leukemia. *Cytometry B Clin Cytom* **76:**385–393.
41. **Orchard JA, Ibbotson RE, Davis Z, Wiestner A, Rosenwald A, Thomas PW, Hamblin TJ, Staudt LM, Oscier DG.** 2004. ZAP-70 expression and prognosis in chronic lymphocytic leukaemia. *Lancet* **363:**105–111.
42. **Bakke AC, Purtzer Z, Leis J, Huang J.** 2006. A robust ratio metric method for analysis of Zap-70 expression in chronic lymphocytic leukemia (CLL). *Cytometry B Clin Cytom* **70:**227–234.
43. **Rossi FM, Del Principe MI, Rossi D, Irno Consalvo M, Luciano F, Zucchetto A, Bulian P, Bomben R, Dal Bo M, Fangazio M, Benedetti D, Degan M, Gaidano G, Del Poeta G, Gattei V.** 2010. Prognostic impact of ZAP-70 expression in chronic lymphocytic leukemia: mean fluorescence intensity T/B ratio versus percentage of positive cells. *J Transl Med* **8:**23.
44. **Degheidy HA, Venzon DJ, Farooqui MZ, Abbasi F, Arthur DC, Wilson WH, Wiestner A, Stetler-Stevenson MA, Marti GE.** 2011. Improved ZAP-70 assay using two clones, multiple methods of analysis and clinical correlation. *Cytometry B Clin Cytom* **80:**309–317.
45. **Gachard N, Salviat A, Boutet C, Arnoulet C, Durrieu F, Lenormand B, Leprêtre S, Olschwang S, Jardin F, Lafage-Pochitaloff M, Penther D, Sainty D, Reminieras L, Feuillard J, Béné MC.** 2008. Multicenter study of ZAP-70 expression in patients with B-cell chronic lymphocytic leukemia using an optimized flow cytometry method. *Haematologica* **93:**215–223.
46. **Best OG, Ibbotson RE, Parker AE, Davis ZA, Orchard JA, Oscier DG.** 2006. ZAP-70 by flow cytometry: a comparison of different antibodies, anticoagulants, and methods of analysis. *Cytom BClin Cytom* **70:**235–241.
47. **Degheidy HA, Venzon DJ, Farooqui MZ, Abbasi F, Arthur DC, Wilson WH, Wiestner A, Stetler-Stevenson MA, Marti GE.** 2012. Combined normal donor and CLL: single tube ZAP-70 analysis. *Cytom BClin Cytom* **82:**67–77.
48. **Böttcher S, Ritgen M, Pott C, Bruggemann M, Raff T, Stilgenbauer S, Döhner H, Dreger P, Kneba M.** 2004. Comparative analysis of minimal residual disease detection using four-color flow cytometry, consensus IgH-PCR, and quantitative IgH PCR in CLL after allogeneic and autologous stem cell transplantation. *Leukemia* **18:**1637–1645.
49. **Moreno C, Villamor N, Colomer D, Esteve J, Giné E, Muntañola A, Campo E, Bosch F, Montserrat E.** 2006. Clinical significance of minimal residual disease, as assessed by different techniques, after stem cell transplantation for chronic lymphocytic leukemia. *Blood* **107:**4563–4569.
50. **Rawstron AC, Böttcher S, Letestu R, Villamor N, Fazi C, Kartsios H, de Tute RM, Shingles J, Ritgen M, Moreno C, Lin K, Pettitt AR, Kneba M, Montserrat E, Cymbalista F, Hallek M, Hillmen P, Ghia P.** 2013. Improving efficiency and sensitivity: European Research Initiative in CLL (ERIC) update on the international harmonised approach for flow cytometric residual disease monitoring in CLL. *Leukemia* **27:**142–149.
51. **Sartor MM, Gottlieb DJ.** 2013. A single tube 10-color flow cytometry assay optimizes detection of minimal residual disease in chronic lymphocytic leukemia. *Cytom BClin Cytom* **84:**96–103.
52. **Hillmen P, Cohen DR, Cocks K, Pettitt A, Sayala HA, Rawstron AC, Kennedy DB, Fegan C, Milligan DW, Radford J, Mercieca J, Dearden C, Ezekwisili R, Smith AF, Brown J, Booth GA, Varghese AM, Pocock C.** 2011. A randomized phase II trial of fludarabine, cyclophosphamide and mitoxantrone (FCM) with or without rituximab in previously treated chronic lymphocytic leukaemia. *Br J Haematol* **152:**570–578.
53. **Bottcher S, Hallek M, Ritgen M, Kneba M.** 2013. The role of minimal residual disease measurements in the therapy for CLL: is it ready for prime time? *Hematol Oncol Clin North Am* **27:**267–288.
54. **Santiago M, Salem DA, Addison MM, Yuan CM, Jasper GA, Stetler-Stevenson M.** 2013. Flow cytometric CLL MRD testing: impact of panel design and automated cell processing on sensitivity. *Cytom BClin Cytom* **84:**420–420.

Plasma Cell Disorders

JUAN FLORES-MONTERO, LUZALBA SANOJA, JOSÉ JUAN PÉREZ, FANNY POJERO, NOEMÍ PUIG, MARÍA BELÉN VIDRIALES, AND ALBERTO ORFAO

24

Clonal plasma cell disorders (PCDs) encompass a heterogeneous group of distinct entities characterized in common by a clonal expansion and accumulation of plasma cells (PCs) in the bone marrow (BM) and/or other tissues, which is associated in the vast majority of cases with the presence of their product(s) (monoclonal immunoglobulin [Ig], M component) at detectable amounts in serum or urine (1). Although the so-called diseases of immunoglobulin deposits (e.g., primary light chain [AL] amyloidosis) and lymphoplasmacytic lymphoma (e.g., Waldenström macroglobulinemia) also belong to this heterogeneous group of disorders, its most representative diagnostic subtypes include monoclonal gammopathy of undetermined significance (MGUS), solitary plasmacytoma, multiple myeloma (MM), plasma cell leukemia (PCL), and several subvariants of these entities (1, 2) (Table 1). The last four diagnostic categories of PCD are the main focus of this chapter.

Current diagnostic and classification criteria for PCD are largely based on the cytomorphological/histopathological demonstration of PC infiltration of BM (or other tissues such as the bone), the presence, subtype, and amount of the M component, and the occurrence of organ damage (e.g., the CRAB criteria, consisting of hypercalcemia, renal failure, anemia, and/or bone lesions) (Table 2). In contrast to what occurs in most other hematological malignancies, the clinical utility of flow cytometry immunophenotyping in the diagnosis and classification of PCDs remains frequently limited to a small subset of cases in which the PC nature of the tumor cell remains indefinite by other approaches. Despite this, the immunophenotypic features of the PCs infiltrating the BM and the pattern of involvement of the B lymphopoiesis in the BM by flow cytometry remain of major relevance for prognostic stratification of PCD patients and minimal residual disease (MRD) monitoring during and after therapy.

In this chapter, we review the clinical utility of multiparameter flow cytometry (MFC) immunophenotypic identification, quantification and characterization of PCs, and the discrimination between clonal and normal/reactive PC phenotypes in the diagnosis, prognostic stratification, and monitoring of patients with PCDs.

DIAGNOSTIC SUBGROUPS OF CLONAL PLASMA CELL DISORDERS

Important advances have been achieved in the last decades as regards the identification of distinct diagnostic categories of PCD such as MGUS, MM, solitary plasmacytoma, and their subvariants (Table 1). From all diagnostic subtypes of PCD, MGUS is by far the most frequent one, with a prevalence of ~5% among the general population of more than 70 years of age. At present, MGUS is defined by the presence of an M component of <30 g/liter, associated with low-level infiltration of BM by PCs (<10%) in the absence of end organ damage or signs of an underlying related lymphoma. Depending on the type of M component, three variants of MGUS are currently recognized: secretory IgM, secretory non-IgM, and light-chain MGUS; whereas all three may (rarely) evolve to systemic AL amyloidosis, the first most frequently transforms to Waldenström macroglobulinemia at a rate of 1.5% per year, and the last two typically evolve to MM at slightly lower rates (1% and 0.3% per year, respectively) (2–5). In contrast, the presence of a localized PC tumor is a rare disease condition that defines solitary plasmacytoma. From a diagnostic perspective, solitary plasmacytomas may occur in the absence or in the presence of minimal BM involvement by clonal PCs with a variable but greater rate of progression to MM than MGUS; e.g., at 3 years, 10% to 60% of cases evolve to MM (2, 6, 7). Finally, MM is defined by an M component greater than 30 g/liter and/or BM involvement by >10% PCs; the absence versus the presence of end organ damage (i.e., the CRAB criteria) distinguishes smoldering MM (SMM) from symptomatic MM (MM), except if there is massive BM involvement by PCs (>60%) which is a stand-alone criterion for MM, even in the absence of end organ damage (2). A summary of the different disease categories and their diagnostic criteria is included in Table 2. Similarly to MGUS, isolated plasmacytoma and MM are also more prevalent in the elderly, with a predominance in men over women and a higher incidence among the African-American population (1, 8). Thus, MM shows an age-adjusted incidence of 4 to 6 cases/100,000 inhabitants/year (twice as much among the African-American population as among the Caucasian and Asian populations), with a mean age at diagnosis of 70 years and a male-to-female ratio of 1.4:1 (1, 8). Finally, PCL is a rare and highly malignant PCD condition, which may occur *de novo* or through transformation of a previously diagnosed MM; from a clinical point of view, diagnosis of PCL requires the presence of a significant number (>20% or >2,000 PCs/μl) of circulating PCs in peripheral blood (PB) (Table 2).

doi:10.1128/9781555818722.ch24

TABLE 1 Current classification of clonal plasma cell disorders according to the WHO 2008 criteria refined by the IMWG in 2014[a]

MGUS
Non-IgM MGUS
IgM MGUS
Light-chain monoclonal MGUS
MM
Smoldering MM
Symptomatic MM
Plasma cell leukemia
Plasmacytoma
Solitary plasmacytoma
Solitary plasmacytoma with minimal marrow involvement
POEMS syndrome
Systemic AL amyloidosis

[a]WHO, World Health Organization; IMWG, International Myeloma Working Group; POEMS, polyneuropathy, organomegaly, endocrinopathy, monoclonal gammopathy, and skin changes. Data from references 1 and 2.

PROGRESSION OF MGUS, SOLITARY PLASMACYTOMA, AND SMM TO SYMPTOMATIC MM

Despite the clear-cut definition that currently exists for the distinct diagnostic subtypes of PCDs at present, MGUS, isolated plasmacytoma, SMM, symptomatic MM, and PCL are all viewed as a spectrum of the same disease; thus, the first three entities are considered to include premalignant disorder states of PCD (9), which may progress to symptomatic MM at variable rates. For example, SMM shows a yearly risk of transformation to MM of 10% (versus 1% for MGUS) during the first 5 years after diagnosis; thereafter, while the risk of progression of MGUS remains the same, the risk of SMM to progress decreases to 3% in the following 5 years and to 1% thereafter (2, 6, 8, 9); similarly, isolated plasmacytoma has been shown to progress to MM at various rates, depending on the absence versus the presence of low levels of clonal PCs in the BM and, among the latter, the specific location of the plasmacytoma (soft tissue versus bone), with an overall 3-year rate of progression of around 10%, 20%, and 60%, respectively (6, 7).

In this regard, it should be noted that until now, treatment of PCD patients has been typically restricted to the malignant conditions (e.g., symptomatic MM and PCL), while for premalignant states such as MGUS and SMM, it is recommended to wait and see, before deciding on the administration of active treatment. Despite this, recent studies suggest that early administration of therapy in high-risk SMM could be of significant clinical benefit (10). Therefore, identification of SMM patients (and potentially also of MGUS cases) at high risk of progression becomes of the utmost clinical relevance.

ROLE OF FLOW CYTOMETRY IMMUNOPHENOTYPING IN PCD

For decades now, the use of MFC immunophenotyping has been mandatory for the diagnosis and classification of most hematologic malignancies, particularly of acute leukemias and chronic lymphoproliferative disorders (11–14). In contrast, the diagnostic utility of MFC in PCD still remains controversial, and its usage varies widely among different clinical diagnostic laboratories (14, 15). In part, this is due to the initial lack of PC-specific markers and the lower percentages of PC detected in aspirated BM samples by MFC than by cytomorphology (16, 17), together with the disturbing levels of variability initially reported as regards the phenotypic characteristics of normal versus clonal PCs, due to a large extent to methodological differences and the lack of standardized flow cytometry procedures (18–22). In parallel, flow-cytometric assessment of MRD (flow-MRD) has become the preferred method for high-quality evaluation of complete remission (CR) and to monitor the effect of therapy in MM. From a practical point of view, usage of MFC immunophenotyping in PCDs requires accurate identification (and potentially also quantitation) of PCs in BM and other tissues, with the ability to discriminate between clonal and normal/reactive PC phenotypes, even when pathological PCs are present in very low numbers (21–29).

IMMUNOPHENOTYPIC IDENTIFICATION OF PLASMA CELLS

Mature PCs lack expression of most pan-B-cell-associated markers. For years, with the exception of cytoplasmic Ig (CyIg), no other PC-associated marker was identified (30, 31). Because of this, PCs were originally considered to be antigenically silent B cells. Later on (i.e., in the 1980s), CD38 emerged as a reliable and robust candidate PC-associated marker.

CD38 is a multifunctional ectoenzyme involved in cell adhesion, signal transduction, and calcium signaling (32), which is relatively broadly expressed across different hematopoietic cells and cell lineages, including the great majority of $CD34^+$ hematopoietic stem and precursor cells (20). Thus, CD38 is strongly upregulated on $CD34^+$ cells, where it can be seen at particularly high amounts in the B-cell committed precursors (33). Along the B-cell maturation pathway, CD38 expression is downregulated in the BM at the transitional/immature B-lymphocyte maturation stage, to become undetectable in naive B cells (34). Later on, B lymphocytes, which are activated by their antigen, reexpress and upregulate CD38 towards very high levels observed on germinal-center (GC) B cells (11, 34); further maturation of these $CD38^{hi}$ GC B lymphocytes into memory B cells leads to downregulation of CD38; in contrast, PC differentiation of GC B lymphocytes is associated with a further increase on CD38 positivity, leading to a uniquely strong expression of this marker ($CD38^{hi+}$) at levels significantly greater than those of GC B cells (34). In fact, normal PCs express CD38 at much higher levels than any other $CD38^+$ hematopoietic cell present in the PB and BM, e.g., monocytes, NK cells, activated T lymphocytes, or $CD34^+$ precursors and B-cell progenitors (e.g., hematogones) (20). Because of this, CD38 has long been considered one of the few (most) reliable markers and it is currently recommended for the identification of PCs by flow cytometry (15, 35).

Other markers that have been described to be either PC associated or PC specific include, for example, CD138, CD229, and CD319. Among them, CD138 (i.e., syndecan 1) (36) is the most well suited and preferred marker for the identification of BM PCs, in combination with CD38; importantly, CD138 is expressed at similar levels on both normal/reactive BM PCs and PCD PCs (15). In contrast to CD38, expression of CD138 within the hematopoietic system seems to be restricted to PCs and a small subset of lymphocytes, making it a rather specific PC marker (Fig. 1 and Table 3) (36). Nevertheless, downregulation of CD138 expression has been recurrently reported, particularly for aged samples (37) and on PCs from heparin- (in contrast to EDTA-) anticoagulated samples (because of potential binding of heparin to CD138 and possible epitope masking) (38).

TABLE 2 IMWG diagnostic criteria for the major categories of PCDs[a]

Disease category	% and site of infiltration	Type, amt of M component	PCD disease-caused end organ damage	Other criteria
MGUS				
Non-IgM MGUS	<10% BM cPCs	Serum non-IgM, <30 g/liter	No	
IgM MGUS	<10% BM LPC	Serum IgM, <30 g/liter	No	Absence of disease, constitutional symptoms, hyperviscosity, lymphadenopathies, or hepatosplenomegaly
Light-chain MGUS	<10% BM cPCs	Nondetectable by IF, <500 mg/24 h in urine	No	Abnormal FLC ratio <0.26 (if increased λ FLC) or >1.65 (if increased κ FLC) No amyloidosis
MM				
Smoldering MM	10–60% BM cPCs	Serum IgG or IgA, ≥30 g/liter or ≥500 mg/24 h in urine	No	Absence of MM-defining events or amyloidosis
Symptomatic MM	≥10% BM cPCs (or cPCs in bone or soft tissue by biopsy[d] + any MM-defining events)		Yes[b] Hypercalcemia: serum Ca >0.25 mmol/liter (>1 mg/dl), above the upper limit or >2.75 mmol/liter (>11 mg/dl) Renal failure: creatinine clearance <40 ml/min or serum creatinine >177 μmol/liter (>2 mg/dl) Anemia: >20 g/liter below the lower limit or Hb <100 g/liter Bone lesion(s) on skeletal X rays, CT, or PET-CT	Presence of biomarkers of malignancy[b] ≥60% BM cPC[d] Involved/uninvolved FLC ratio ≥100 (involved light chain ≥100 mg/liter) by Freelite assay[c] >1 focal (>5mm in size) lesion on MRI studies
Plasmacytoma				
Solitary plasmacytoma	Presence of cPCs in bone or soft tissue by biopsy Absence of BM cPCs		No	Otherwise normal skeletal survey and MRI (or CT), but for the presence of the solitary lesion
Solitary plasmacytoma with minimal BM involvement	Presence of cPCs in bone or soft tissue biopsy specimen, <10% BM cPCs		No	Otherwise normal skeletal survey and MRI (or CT), but for the presence of the solitary lesion
PCL	>20% PB PCs or $>2 \times 10^9$ PB PCs/liter			

[a]PCD, plasma cell disorders; IMWG, International Myeloma Working Group; Ig, immunoglobulin; BM, bone marrow; c, clonal; PCs, plasma cells; LPC, lymphoplasmacytic cells; CLPD, chronic lymphoproliferative disorders; IF, immunofixation; FLC, free light chain; CT, computed tomography; MRI, magnetic resonance imaging; PET-CT, 18F-fluorodeoxyglucose positron emission tomography with CT; PB, peripheral blood. Data from references 2 and 71.

[b]Myeloma-defining events.

[c]From Binding Site Group Ltd., Birmingham, United Kingdom.

[d]Clonality should be demonstrated by light-chain restriction by flow cytometry, immunohistochemistry, or immunofluorescence.

Based on all the above, a consensus has now existed for several years that combined use of CD38 and CD138 is mandatory for adequate identification of BM PCs, in both normal/reactive and PCD patient samples, in the diagnostic and MRD settings (15). In addition, for optimal exclusion of other non-PC events potentially contaminating the $CD38^{hi}$ $CD138^{+}$ PC gate, CD45 should also be stained simultaneously and used for PC gating purposes, in addition to right-angle light scatter (RALS) and forward-angle light scatter (FALS) (Fig. 1) (15, 35, 39).

Despite the above consensus regarding the most reliable combination of flow cytometric parameters for efficient PC identification, alternative markers may be required under specific circumstances, such as in MM patients undergoing new antibody-based targeted therapies (40). For example, the benefits of CD38 (daratumumab, SAR650984, and MOR 202) humanized antibody treatments are now being investigated in several clinical trials (41–45). Consequently, usage of CD38 as a PC identification marker in the context of MRD evaluation of patients treated with such novel antibody-based therapies is compromised and alternative markers/clones to the conventional CD38 (and also CD138) reagents have been investigated in the MRD settings. In this regard, CD229 and CD54, in addition to CD319, have emerged as potential candidate markers to replace CD38 and/or CD138 in MRD antibody combinations for the identification of PCs (Table 3) (46–49). However, further extensive testing, in large series of samples, of distinct clones and fluorochrome conjugates of CD54, CD229, and CD319 is still needed before they can be recommended in routine practice as valid alternative PC identification markers. In this regard, it might also be possible to replace currently used CD38 reagents with other CD38 antibody clones directed against different epitopes of the CD38 molecule from those targeted by the therapeutic humanized reagents, instead of changing CD38 with another PC-associated marker. Once again, further studies are still required to define which are (or might be) such alternative CD38 clones, since treatment with daratumumab, for example, appears to mask the binding of virtually all commercially available antibody clones evaluated so far (J. Flores-Montero, L. Sanoja, and A. Orfao, unpublished observations).

IMMUNOPHENOTYPIC CHARACTERISTICS OF NORMAL PLASMA CELLS

PCs represent the last stages of maturation of B lymphocytes into antibody-producing cells. Thus, PCs typically derive from antigen-activated B lymphocytes that have undergone a multistep maturation process that usually starts in secondary lymphoid tissues such as the lymph nodes, spleen, BM, and mucosa-associated lymphoid tissues (50). Recently produced PCs leave their tissue of origin and migrate to PB; from there, they reach and populate those tissues in which long-living PCs can be usually detected, such as the BM and the gastrointestinal mucosa, among other peripheral

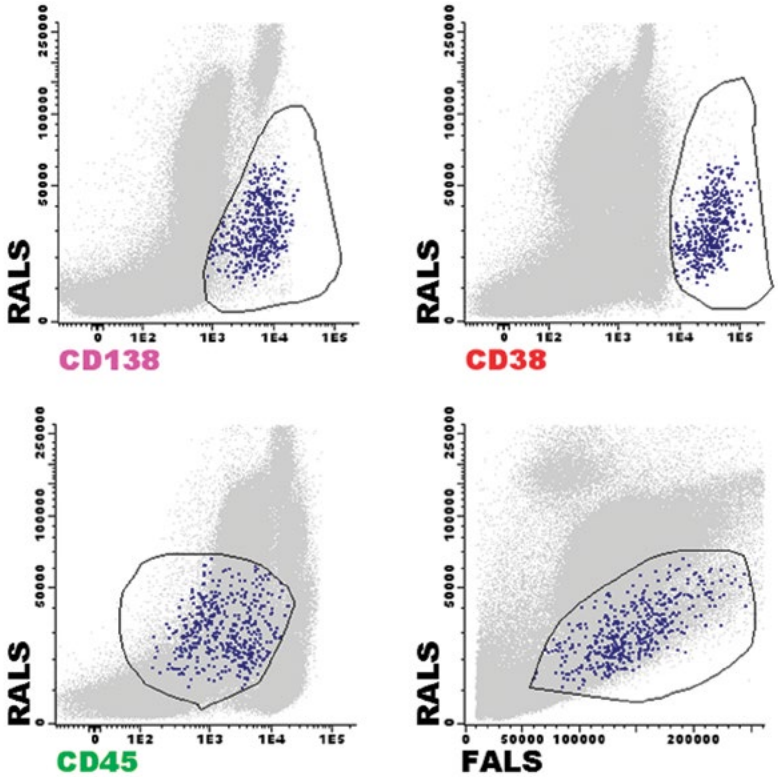

FIGURE 1 Normal bone marrow (BM) plasma cells (PCs) in an illustrating example of a consensus PC-gating strategy. Classic bivariate dot plots showing the minimal set of parameters recommended for accurate identification and gating of total BM PCs (dark blue dots). A combination of sequential gating, which must include CD138, CD38, and preferably CD45, together with light scatter properties, is recommended for accurate identification of PCs in BM samples. Once identified, PCs can be quantitated (0.12% of total nucleated cells in the illustrated example [gray dots]) and further characterized on phenotypic grounds. Abnormal PC populations may display lower levels of CD38 expression than normal BM PCs.

TABLE 3 List of the most relevant plasma cell (immunophenotypic) markers and their respective clinical values

Target	Normal BM PC expression pattern	MAP	% of MAP expression cases	Main recognized clinical utility
CD19	−/+ (% of $CD19^+ \approx 64\%$)	−	96	Phenotypic characterization of clonal versus normal PCs Differential diagnosis between PCDs versus B-CLPDs and IgM versus non-IgM MGUS Risk stratification in MM MRD detection
CD20	− (% of $CD20^+ \approx 4\%$)	dim^+	17–30	Phenotypic characterization of clonal versus normal PCs Differential diagnosis between PCDs versus B-CLPDs and IgM versus non-IgM MGUS Marginal utility for MRD detection versus other MRD markers
CD27	+ (% of $CD27^{dim}$, NR)	− or dim^+	40–68	Phenotypic characterization of normal versus clonal PCs MRD detection
CD28	− (% of $CD28^+ \approx 15\%$)	+	15–45	Phenotypic characterization of clonal versus normal PCs Risk stratification in MM MRD detection
CD33	− (% of $CD33^{dim} \approx 6\%$)	+	18	Phenotypic characterization of clonal versus normal PCs Marginal utility for MRD detection versus other MRD markers
CD38	Bright+	dim^+	80	Mandatory PC identification marker Phenotypic characterization of clonal versus normal PCs MRD detection Monoclonal antibody-based therapeutic target
CD45	−/+ (% of $CD45^+ \approx 6\%$)	−	73	Highly recommended PC identification marker Phenotypic characterization of clonal versus normal PCs Differential diagnosis between PCDs versus B-CLPDs and IgM versus non-IgM MGUS MRD detection
CD54	+	dim^+	60–80	Potentially useful PC identification marker Marginal utility for MRD detection versus other MRD markers
CD56	−/+ (% of $CD56^{dim} \approx 10\%$)	++	60–75	Phenotypic characterization or clonal versus normal PCs Differential diagnosis between PCD versus B-CLPD and IgM versus non-IgM MGUS MRD detection
CD81	+	− or dim^+	55	Phenotypic characterization of clonal versus normal PCs Risk stratification in MM MRD detection
CD117	−	+	30–32	Phenotypic characterization of clonal versus normal PCs Risk stratification in MM MRD detection
CD138	+	NR		Mandatory PC-specific identification marker Monoclonal antibody based therapeutic target
CD200	−/+ (% of $CD200^+ \approx 49\%$)	+/++	≥70	Phenotypic characterization of clonal versus normal PCs Marginal utility for MRD detection versus other MRD markers
CD229	+	NR		Potentially useful PC identification marker Potential monoclonal antibody-based therapeutic target
CD307	+	++	NR	Phenotypic characterization of clonal versus normal PCs Potentially useful for MRD detection
CD319	+	dim^+		Potentially useful PC identification marker Marginal utility for MRD detection versus other MRD markers Monoclonal antibody based therapeutic target
SmIg	−	+	<5	Differential diagnosis between PCDs versus B-CLPDs and IgM versus non-IgM MGUS Marginal utility for MRD detection versus other MRD markers

[a]BM, bone marrow; PC, plasma cell; MAP, myeloma-associated phenotype; PCD, plasma cell disorder; B-CLPD, B cell chronic lymphoproliferative disorder; MRD, minimal residual disease. NR, not reported. Immunophenotypic patterns are expressed as: −, negative; dim+, dim positive; +, positive; and ++, overexpressed as compared to normal.

locations (50, 51). Therefore, early-stage PCs (also termed plasmablasts) can be detected in secondary lymphoid tissues, as well as PB, while terminally differentiated PCs are more typically found in the BM (50, 51). Previous studies have shown that in fact, a continuous spectrum of immunophenotypic changes associated with a progressively higher degree of maturity can be observed, once PCs from several different tissues such as tonsils, PB, and BM are merged and phenotypically compared (34); however, whether the $CD38^{hi}$ PB PC compartment comprises both newly generated plasmablasts and PCs that recirculate from the BM still remains a matter of debate (51).

Overall, PB plasmablasts/PCs and the PCs that can be identified in BM show clear phenotypic differences between them (15, 24, 34, 51, 52). In contrast to BM PCs, circulating PB plasmablasts/PCs are all positive for both CD19 and CD45, and they completely lack CD56 expression; moreover, normal/reactive PB plasmablasts/PCs display slightly lower levels of CD38 than normal/reactive BM PCs, and they have variable and heterogeneous expression levels of both CD20 and CD138 (34, 52). Additionally, most PB plasmablasts/PCs (>70%) show surface membrane Ig^{lo} ($SmIg^{lo}$) expression of distinct Ig isotypes, at variable levels (51). Interestingly, such distinct and variable patterns of antigen expression observed both in the PB and the BM PC compartments are now considered to translate phenotypes of PCs at slightly different maturation stages. For example, $CD138^+$ PCs in PB typically show a more mature phenotype than the $CD138^-$ plasmablast/PC PB compartment: higher expression of CD38 and CyIg and lower levels of expression of CD45 and SmIg, in the absence of CD20 (51). In contrast, similar patterns of antigen expression have been reported for the $CD138^-$ and $CD138^+$ PB plasmablast/PC compartments regarding several adhesion molecules (e.g., ITGα4, ITGβ1, and ITGβ7) and chemokine receptors (e.g., CXCR4/CD184 and CCR10) (51). Interestingly however, both compartments show high Ki-67 staining (51), suggesting that these cells are still capable of undergoing proliferation, and therefore, they are still on the way to completing their maturation.

Despite what is described above for steady-state PB plasmablasts/PCs, it has been shown that newly generated PB plasmablasts/PCs after vaccination (e.g., after exposure to tetanus toxin) might show slight phenotypic differences, towards a more mature protein expression profile than that of steady-state PB plasmablasts/PCs; in this regard, such cells simultaneously show high CD38 and CD138 positivity, and they systematically lack CD20 (34). Altogether, these findings support the notion that CD138 expression on PB PCs is more likely related to post-GC maturation (51) and/or BM-driven migration (53), whereas it would not be a surrogate marker for PCs that recirculate from the BM into PB and back into the BM or other tissues; in such a case, CD138 cannot be seen as a marker that would discriminate between plasmablasts that have migrated to PB from secondary lymphoid tissues (e.g., lymph nodes) and BM recirculating PCs. Interestingly, once compared to more-mature BM PCs, PB plasmablasts/PCs also show clear positivity for CD229 together with a more heterogeneous pattern of expression of both CD54 and CD319 (49).

Similarly to what has been described above for the plasmablast/PC compartment circulating in PB, BM PCs also consist of several different, phenotypically well-defined subpopulations that display characteristic maturation-associated features (54, 55). As a whole, BM PCs typically lack expression of most pan-B-cell markers (e.g., CD20 and CD22) and SmIg; in contrast, they have heterogeneous expression of CD19, $CD45^{lo}$, and $CD56^{-/lo}$, together with higher levels of expression of both CD38 and CD138 than PB PCs (15, 24). Thus, most normal/reactive BM PCs express CD19, but around one-third of them are $CD19^-$; similarly, most $CD19^+$ and $CD19^-$ normal/reactive BM PC are $CD45^+$, $CD56^-$, and $CD81^+$, but small subsets of $CD45^-$, $CD81^-$, and $CD56^+$ normal/reactive PCs have also been detected whenever enough BM PCs are evaluated; these infrequent PC phenotypes can be specifically more prominent among the $CD19^-$ compartment of BM PC (Table 3) (29, 54, 55). Although the precise physiological significance of these small subsets of normal BM PCs still remains to be determined, recent results suggest that they might be associated with distinct maturational stages of BM PCs; in this regard, an increasing maturity of BM PCs would typically be associated with progressively lower cell numbers, for example, from the major $CD19^+$ $CD56^-$ subpopulation to the minor $CD19^-$ $CD56^-$ and $CD19^-$ $CD56^+$ subsets of PCs detectable in normal steady-state BM (56).

ABERRANT PLASMA CELL PHENOTYPES IN PCDs

Pathological PCs from PCDs such as MGUS, MM, PCL, and solitary plasmacytoma have long been shown to display phenotypes that deviate from those typically seen in normal PCs, particularly in normal and reactive BM PCs (18, 54, 57) (Fig. 2 and Table 3). In the past, markers that were frequently described to be aberrantly expressed on PCD PCs included CD19, CD56, CD45, CD38, CD27, and to a lesser extent also CD20, CD28, CD33, CD117, and SmIg (Table 3) (15, 21, 22, 24, 54, 58). More recently, other markers have been identified as aberrantly expressed on PCs from various percentages of MM and other PCD cases. Among the latter set of markers, CD81 (29), CD200 (59), CD54 (60), and CD307 (61) have emerged as (potentially) the most informative ones (Table 3). The frequencies at which individual markers have been reported to be aberrantly expressed on clonal PCs are listed in Table 3. However, it should be noted that such frequency may depend not only on the specific marker evaluated but also on the specific fluorochrome-conjugated antibody reagent used; sometimes even variable frequencies of altered patterns of antigen expression on pathological PCD PCs can be obtained with distinct antibody clones directed against the same marker, or when similar reagents from different commercial sources are used (21, 58). Altogether, this highlights the relevance of the specific reagents used in a panel, in addition to their CD codes, as regards the identification of a given phenotypic alteration (62). Briefly, typically described aberrant PCD-associated PC phenotypes include (i) underexpression of CD19, CD27, CD38, CD81, and/or CD45, (ii) overexpression of CD33, CD56, and/or CD28, and (iii) asynchronous expression of CD20 and/or CD117 (Table 3) (18, 19, 22, 23, 25, 63, 64). Despite this, it should be emphasized that such definitions of the PC-associated aberrant phenotypes are an oversimplification of the aberrant patterns of protein expression detected on PCD PCs versus normal/reactive PCs. Actually, very few truly aberrant PC markers exist, and evaluation of the utility of individual markers has always to be considered in the context of a multiparameter definition of aberrant phenotypes, where multiple individual markers synergistically contribute to an improved clear-cut distinction between normal/reactive and PCD PCs (65). For this purpose, the

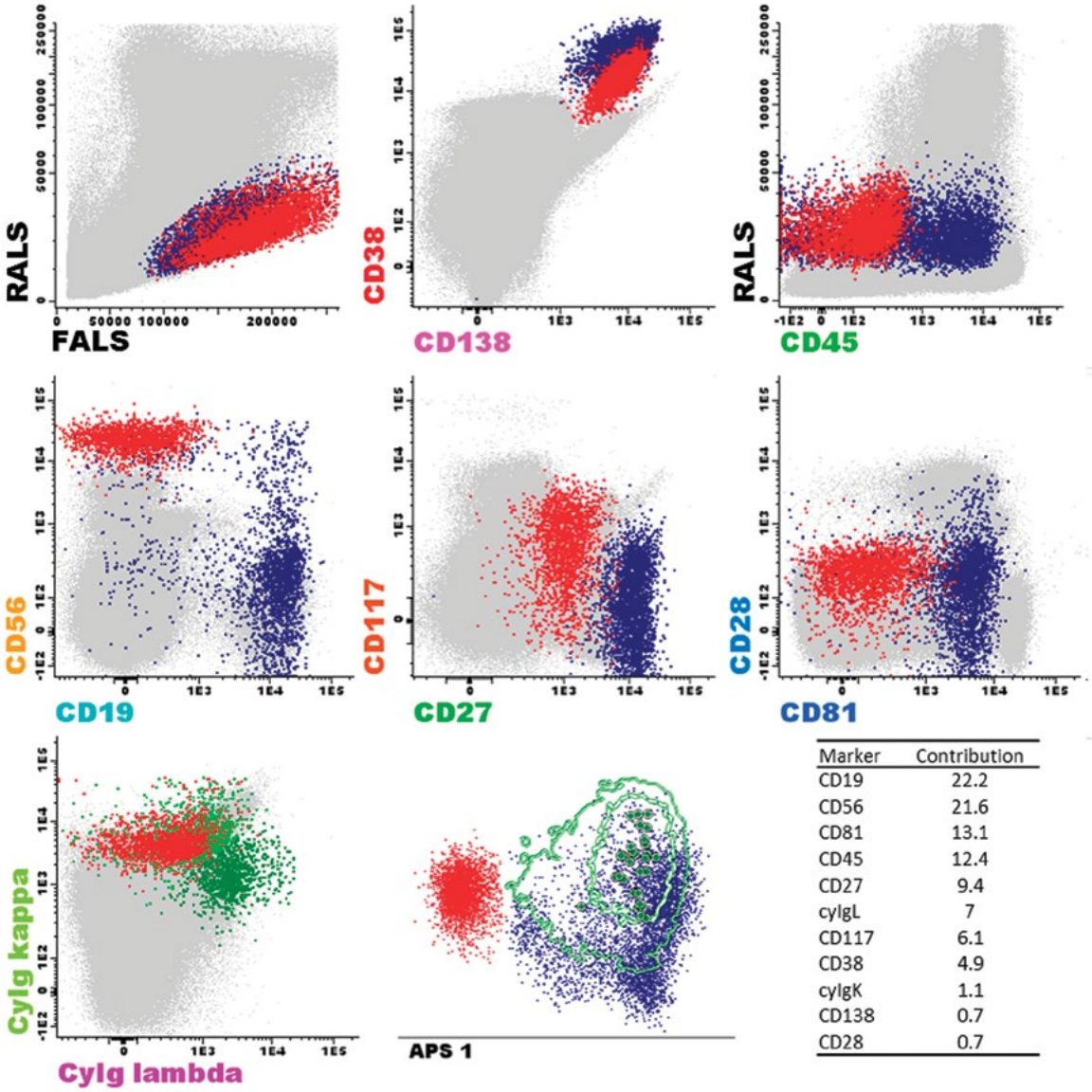

FIGURE 2 Illustrating example of a bone marrow (BM) sample from a multiple myeloma (MM) patient whose clonal plasma cells (PCs) aberrantly expressed several typical phenotypic markers, as may be seen through comparison against the immunophenotypic profile of normal PCs coexisting in the same BM sample. Classical bivariate dot plot representations illustrate the normal phenotypic characteristics of polyclonal PCs (dark blue dots) for surface membrane markers. The same dot plots also illustrate the aberrant phenotypic profiles expressed by the patient clonal PCs (red dots), i.e., $CD38^{dim}$, $CD45^{-}$, $CD19^{-}$, $CD56^{++}$, $CD117^{+}$, and $CD81^{-}$. In addition, the normal and myeloma PC populations were further discriminated by their cytoplasmic (Cy) expression of immunoglobulin (Ig) light chains, highlighting the polyclonal nature of normal PCs ($CyIg\kappa^{+}$ and $CyIg\lambda^{+}$ [ratio of 1:3], dark and light green events, respectively) versus the monotypic expression of CyIgk of clonal PCs (red dots). The middle bottom panel displays the automated population separator (APS) view of principal component 1 versus principal component 2 (*x* and *y* axes, respectively) specifically obtained for the two populations of BM PCs (normal versus myeloma PCs, red and blue dots, respectively) when compared to a set of normal/reactive PCs from 31 reference BM samples; circles represent the median fluorescence intensity of all fluorescence parameters stained, while dotted and continuous borders represent 1 and 2 standard deviations of the distribution obtained for the reference normal PC population; please note how normal PCs from the sample (blue dots) cluster within the reference population cloud, while phenotypically aberrant PCs (red dots) are clearly separated. The right panel in the row in the bottom shows the rank of individual markers and their contribution for the discrimination shown in the APS 1 plot for principal component 1. The overall PC populations correspond to 0.6% of all nucleated BM cells in the sample (gray dots). Normal PCs were 59.9%, while clonal PCs represented 40.1% of all BM PCs.

use of new graphical representations of flow cytometry data processed by multivariate analysis (e.g., principal component analysis or canonical analysis) facilitates the definition of the combined marker profiles that allow distinction from an interrogated population of PCD PCs and reference data for normal/reactive PCs (Fig. 2).

In fact, the majority of markers that have proven to be useful in detecting aberrant PC phenotypes are not strictly aberrant on their own. For example, although CD19 recurrently emerges among the most frequent aberrantly expressed (downregulated) markers in PCDs (15), there is a significant fraction of all normal/reactive BM PCs (around 30%) that are also negative for CD19 (Table 3) (39, 54). Similarly, CD56 has long been claimed to be aberrantly overexpressed in MGUS and MM PCs (15, 21); however, there is also a small subset (6 to 9%) of normal/reactive BM PCs that show unequivocal expression of CD56 at variable levels (Table 3) (39, 56). Similarly, other aberrant phenotypes defined by individual markers that are frequently observed in clonal PCs (e.g., $CD28^+$, $CD45^-$, $CD81^{-/lo}$, $CD27^{-/lo}$, or $CD200^+$) may also be detected in well-defined subpopulations of normal BM PCs (Table 3): the median frequency of normal PCs being $CD28^+$ is 15% (range, 0% to 59%), that of being $CD45^-$ is 22% (range, 0% to 69%), and that of being $CD200^+$ is 49% (range, 31% to 68%) (Flores-Montero et al., unpublished). In contrast, no $CD117^+$ PCs have been reported so far in normal/reactive BM (maximum sensitivity of $<10^{-4}$), while this marker is aberrantly expressed on clonal BM PC from around 30% of all symptomatic MM, 45% of SMM, and $>$ 70% of all MGUS cases (Table 3) (57).

MULTICOLOR PCD PANELS OF ANTIBODY REAGENTS

At present, a consensus exists that the identification of aberrant phenotypes in a significant fraction of all PCD cases requires a minimum combination of CD138 (for PC identification) and CD38 as well as CD45 (additional identification markers whose mean expression levels are frequently downregulated in clonal versus normal/reactive PCs), together with CD19 (negative in virtually every PCD case) and CD56 (expressed in around 60 to 75% of all PCD patients) (Table 3). The percentage of PCD cases in which a robust and sensitive discrimination between normal and clonal PCs may be achieved increases significantly when additional aberrant phenotypes are also investigated simultaneously. Such additional aberrant PC phenotypes include abnormally low expression levels of CD27 and CD81, plus overexpression of CD117. Based on these characteristics, accurate identification and enumeration of clonal versus normal/reactive PCs can be achieved in virtually every PCD patient (Fig. 2), as recently demonstrated by the EuroFlow Consortium (62). The only exception would be that of clonal PCs from secretory IgM-MGUS and Waldenström macroglobulinemia. In patients with the latter diseases, clonal BM PCs typically show an immature $CD45^+$ $CD19^+$ phenotype with variable levels of expression of CD20 and/or SmIgM, in the absence of the most characteristic aberrant patterns of protein expression observed in other PCD cases (e.g., absence of CD56 and CD117 expression and/or strong levels of expression of CD27 and CD81), similarly to what may be observed in other lymphoplasmacytic lymphomas (26, 65).

In order to define and establish the 8-color, 2-tube antibody combinations proposed for the diagnostic screening and classification of PCDs, the EuroFlow Consortium used for the first time an experimental stepwise comprehensive approach. Thus, the PCDs EuroFlow antibody panel was not based just on the experience and knowledge of experts and their consensus opinions (62). The process involved an initial selection phase for a list of potentially useful markers based on literature data and the experience of the groups involved (n = 14 markers); subsequently, careful selection of optimal antibody clones and high-quality conjugates led to a first configuration of the panel that was prospectively evaluated. Afterward, detailed analysis of the performance of the initial set of markers in such combinations against local panels led to the identification of the most informative combination of markers (CD138, CD38, CD45, CD19, CD56, CD81, CD27, CD117, CD28, β2-microglobulin, CyIgκ, and CyIgλ), using multivariate statistical comparisons. Further testing focused on identifying optimal fluorochrome positions and combinations of the selected markers; for this purpose, a total of seven rounds of evaluation, redesigning, and reevaluation were performed, until optimal configuration and performance were reached. Prospective evaluation of this marker combination based on the last configuration proposed by the EuroFlow Consortium for the diagnostic screening of PCDs showed occurrence of ≥1 aberrant phenotypic profiles in virtually all MM and MGUS cases evaluated who had abnormal/clonal PC populations (97%). In a small percentage of cases (3%), definitive definition of a clonal PC population might need the simultaneous assessment of PC clonality through detection of monotypic CyIg light-chain-restricted PC populations, as defined by the previously mentioned set of aberrant markers (62). Figure 2 presents an illustration of the performance of the proposed antibody panel in a diagnostic BM sample from an MM patient. Of note, the illustrated antibody combination also includes markers that allow efficient quality control of the BM sample analyzed through, e.g., the identification of normal residual BM cells such as mast cells ($CD117^{hi}$), myeloid precursors ($CD117^+$ $CD45^{lo}$ $CD38^+$) and hematogones ($CD19^+$ $CD45^{lo}$ $CD38^{hi}$ $FALS^{lo}$ $RALS^{lo}$ cells).

Despite all the careful evaluation steps performed as summarized above, further refinement of the specific fluorochrome-conjugated reagents and antibody clones employed in the above EuroFlow panel was required for MRD purposes. This was mainly due to usage of different sample preparation methods (e.g., bulk lysis procedures versus a single-tube fluorescence-activated cell sorter [FACS] lysing [BD Biosciences, San Jose, CA] approach) for MRD versus diagnostic BM samples, because of the requirement to interrogate many more BM cells and larger volumes of BM sample than in routine flow-MRD ($>5 \times 10^6$ BM cells). Thus, it can also be concluded that any change in the protocol involving the type of sample, the sample preparation method, and/or reagents might require full reevaluation (and potentially also redesigning) of a panel, in order to ensure its optimal performance as defined under those conditions under which it was initially evaluated and established.

FLOW CYTOMETRY QUANTITATION OF PCs IN BM ASPIRATED SAMPLES

The overall PC count in BM is a major diagnostic criterion for PCD. Currently, for diagnostic purposes, PC counts rely on conventional morphological assessments (1). In this regard, flow cytometry has never been considered a reliable surrogate approach for counting BM PCs, given the well-known discrepancy observed between the overall cytomorphological (or histopathological) and the MFC results, with a median bias of around 15% due to lower MFC than morphological PC counts (15–17, 66). Despite such

bias, the enumeration results of total BM PCs by the two techniques correlate well (66). Although there is no definitive explanation for such differences, several factors appear to be relevant. Thus, usage of second aspirates of the same BM for flow cytometry rather than first-pulled BM aspirated samples for cytomorphology (67), the high expression levels of adhesion molecules on PCs, and the selective loss of PCs during centrifugation all appear to contribute to the reported differences more than the potential existence of heterogeneous patterns of BM infiltration (14, 15, 66, 68). Of note, such differences most likely also affect other diagnostic techniques such as molecular/genetic methods (15).

In any case, in order to get sufficient representation of the PC population under study, an acquisition (in a single step) of at least 1×10^5 events from the whole (e.g., BM) sample cellularity is typically required in normal BM or in diagnostic BM samples for a sensitivity of at least 10^{-3} (detection of at least 1 cell in a total of 1,000 BM cells) (68). In turn, in the case of hypocellular BM samples, highly (hemo) diluted samples, or under MRD conditions, acquisition of significantly higher numbers of cells (e.g., $>5 \times 10^6$ cells in the MRD setting) is frequently needed in order to get a minimum population of 20 (preferably 30 to 50) PCs for their unequivocal identification, their reliable quantitation, and accurate characterization (15, 35).

CLINICAL UTILITY OF MFC IMMUNOPHENOTYPING OF PCDs

At present, it is well established that MFC immunophenotyping contributes to the diagnosis or to the classification, prognostic stratification, and monitoring of patients suspected of having a PCD or who have already been diagnosed with a PCD, respectively. Such clinical utility derives from the ability of MFC immunophenotyping to specifically identify and quantitate clonal/aberrant versus normal/reactive PC populations and to provide detailed characterization of their protein expression profiles.

In this section, we sequentially review the utility of MFC immunophenotyping of PCs for (i) the diagnostic screening and classification of PCD, (ii) its prognostic stratification, and (iii) monitoring of the effects of therapy in depleting tumor PCs and maintaining them under control at undetectable or very low levels (MRD monitoring).

MFC Immunophenotyping in the Diagnosis and Classification of PCD

For decades now, it has been well established that demonstration of the presence of phenotypically aberrant PCs with clonal features is an unequivocal sign of an underlying PCD, independently of where those aberrant PCs are located (e.g., BM, PB, lymph nodes, peripheral tissues, or distinct body fluids such as cerebrospinal fluid). Therefore, MFC immunophenotyping is considered a complementary tool in the diagnostic screening of patients suspected of having a PCD, and it may be applied to the study of virtually any type of sample. In this regard, it should be emphasized that at present, single 8-color stainings (see "Multicolor PCD Panels of Antibody Reagents" above), which ensure detection of aberrant/clonal PCs in virtually every PCD case, can be used, even when the pathologic PC population(s) is present at seemingly low levels (e.g., 0.1% of the whole diagnostic sample cellularity).

In turn, a more detailed characterization of the aberrant/clonal PC population identified may further contribute to the classification of PCDs. Thus, the presence of CyIgM-expressing PCs with an aberrantly immature BM PC phenotype ($SmIgM^{-/+}$ $CD20^{-/+}$ $CD19^+$ $CD45^+$) is typically observed in IgM-MGUS; whenever such a PC population is further accompanied by a $SmIgM^+$ clonal mature B-cell population, malignant transformation should be suspected and the diagnosis of Waldenström macroglobulinemia/lymphoplasmacytic lymphoma considered. Conversely, the presence of a population of non-IgM clonal PCs displaying aberrant phenotypes such as those described above in this chapter (e.g., $CD19^-$, $CD45^-$, $CD56^+$, $CD27^{-/lo}$, $CD81^{-/lo}$, and $CD200^+$ PCs) is characteristic of other PCD including non-IgM and light-chain MGUS, isolated plasmacytoma, SMM, MM, and/or PCL. In such cases, when the presence of clonal/aberrant PCs is restricted to a tissue other than BM or PB, diagnosis is fully compatible with solitary plasmacytoma. In solitary plasmacytoma patients, further sensitive analysis of the BM (and potentially also the PB) might contribute to subclassify the disease into solitary plasmacytoma with versus without BM involvement (Table 2). Of note, if only the BM is studied in such a case, the pattern of BM involvement associated with solitary plasmacytoma may fully mimic (and cannot be distinguished from) that of non-IgM and/or light-chain MGUS, in which a few clonal aberrant PCs typically coexist at various percentages (usually <95% of all BM PCs) with normal BM PCs (typically >5% of all BM PCs).

In contrast to solitary plasmacytoma and MGUS, SMM and particularly MM show greater levels of infiltration of BM by clonal aberrant PCs than by normal residual PCs. Thus, while in the majority of MGUS patients (>80%) the number of normal PCs exceeds 5% of the total BM PC compartment, this occurs only in a minority of MM cases (<15%) (5, 69). Consequently, identification of >5% normal PCs of all PCs in a BM sample is strongly associated with MGUS (or solitary plasmacytoma), whereas the opposite (<5% normal PCs among all BM PCs) is typically associated with MM; SMM shows an intermediate (mixed) profile, which more frequently overlaps with that observed in MM. A pattern similar to that of MM is also observed in PCL, usually in association with very high levels (>20%) of infiltration of PB. Of note, PB involvement by lower PC numbers is a hallmark of MM, whereas it is present in only a fraction (20 to 35%) of MGUS cases with conventional flow MRD-like approaches.

Regarding the specific immunophenotypic profile of aberrant PCs in (non-IgM or light-chain) MGUS versus SMM, MM, and PCL, it should be noted that no disease-specific PC phenotypes have been identified so far. However, for some aberrant phenotypes, different frequencies have been reported in the distinct diagnostic categories of PCDs. For example, the frequency of cases showing $CD117^+$ PCs progressively decreases from MGUS (70%) to SMM (45%) and MM (30%), while PCL typically shows a $CD56^-$ $CD117^-$ immunophenotype with stronger expression of CD45 than in SMM/MM and MGUS cases (21, 70, 71).

Based on all of the above, it may be concluded that the utility of MFC immunophenotyping for the diagnostic classification of PCD relies on a combination of the phenotypic features of the aberrant/clonal PC population, the precise tissue(s) involved, and the level of PC infiltration within the BM PC compartment.

Prognostic Stratification of PCD Patients

At present, the prognostic stratification of MGUS, isolated plasmacytoma, and SMM patients, including the identification of those cases that will more likely progress to symptomatic myeloma, remains a relevant clinical challenge that

has been only partially addressed. In addition, identification of biological and clinical subgroups of MM patients with significantly different outcomes and who could potentially benefit from distinct treatment modalities is also an active field of research.

As already stated above, the level of involvement of the BM PC compartment is significantly different in MGUS, SMM, and MM; despite this, within each disease category, it remains rather heterogeneous with, e.g., some MGUS cases showing an MM-like profile and vice versa. In fact, use of the same MFC diagnostic threshold as the one described above (i.e., <5% of normal PCs/total PCs) identifies a minor subgroup of MGUS and a significant proportion of SMM patients with higher risk of progression to MM, with respect to a majority of cases who show higher percentages of normal PCs in the BM (>5% of all BM PCs). From the prognostic point of view, these subgroups of MGUS and SMM patients also show significantly different rates of progression to symptomatic MM: 5-year progression rates of 25% versus 5% for MGUS and 64% versus 8% for SMM with >5% versus <5% normal PCs/total PCs, respectively (5); subsequently, high-risk SMM cases defined on the basis of the BM aberrant versus normal PC distribution and the presence of immune paresis have been shown to benefit from early therapy. In turn, the few symptomatic MM patients who show >5% normal PCs of all BM PCs display more favorable prognostic features and a better overall outcome; thus, they show (compared to other MM cases) lower levels of total BM PCs and M component, higher hemoglobin levels, a lower frequency of immune paresis, and a lower frequency of high-risk cytogenetic abnormalities, they more frequently achieve CR after a high-dose therapy with autologous stem cell transplantation (HDT/ASCT) treatment regimen, and they display longer progression-free survival (PFS) and overall survival (OS) rates (69).

In line with these observations in MM and despite the differences observed in the relative numbers of total BM PCs obtained by cytomorphology and by MFC, the overall percentage of PCs from the whole BM sample cellularity (as detected by MFC) has also been associated with patient outcome. In this regard, a study performed in a large cohort of MM patients evaluated at diagnosis showed that a threshold of 15% PCs from all nucleated BM cells in the sample discriminated two groups with a significantly different outcome: patients with <15% PCs showed a significantly longer PFS and OS than cases with >15% PCs (median PFS of 43 months in contrast to 36 months, and median OS of 97 months in contrast to 54 months, respectively) (66). Of note, the most informative MFC cutoff identified in this study was equivalent to a 30% PC threshold by cytomorphology; however, in contrast to MFC, cytomorphological PC BM counts did not emerge as an independent prognostic factor in the multivariate analysis (66).

In addition to the level of infiltration of the BM by clonal PCs, the prognostic impact of the immunophenotypic profile of abnormal PCs has also been extensively investigated (21). Thus, in a large cohort of uniformly treated MM patients, the patterns of expression of CD19, CD28, and CD117 were shown to provide prognostic information. In this study, positive staining of tumor PCs for CD19 and CD28 and absence of CD117 were associated with a significantly poorer outcome (shorter PFS and OS) (21, 70). Of note, when these markers were simultaneously considered, their prognostic value was enhanced; thus, based on the patterns of expression of both CD28 and CD117, 3 different risk groups, which were associated with significantly different outcomes, were defined: (i) CD28 and $CD117^+$ cases showed the longest PFS and OS; (ii) $CD28^+$ and $CD117^-$ samples had the shortest; (iii) and CD28/CD117 double-positive or double-negative samples constituted an intermediate risk group (21). More recently, $CD81^+$ expression in MM PCs has also been described as an independent adverse prognostic factor that negatively impacts PFS and OS, and at the same time it is associated with lower response rates after induction therapy. Of note, CD81 expression allowed discrimination between groups of patients with different prognostic risks both within MM patients with standard-risk and with high-risk cytogenetics (29). In turn, an association between lack of expression of CD200 on abnormal PCs and clinically aggressive disease has been recently reported (59).

In addition to the prognostic implications of the above-described PC numbers and phenotypes, MFC has recently proven to be of great clinical utility in the prognostic stratification of MM patients because of its ability to identify altered phenotypes on myeloid BM cell compartments, which fully overlap with those seen in myelodysplastic syndrome (MDS) patients (e.g., hypogranular neutrophils and $CD56^+$ monocytes). Such altered myeloid phenotypes have proven to be closely related with the presence of MDS-associated cytogenetic features and an age-independent poorer outcome. Further studies in large series of MM patients treated within randomized trials are needed to confirm the actual prognostic relevance of these MDS-associated phenotypes present in myeloid BM cell compartments of a significant percentage of all MM (and also MGUS) patients.

MRD Monitoring in MM

Major achievements have been reached in the last decades in the treatment of MM. Such advances have also fostered the development and implementation of standardized (and progressively more sensitive) MRD methods to evaluate responses to therapy. In addition to imaging techniques, which play a key role in detecting extramedullary disease, flow-MRD is currently considered the preferred method to evaluate BM MRD levels in MM (72–74). This is due to a large extent to the well-suited features of flow cytometry for monitoring MRD in MM patients' BM. Briefly, flow-MRD has the greatest applicability in MM since the presence of PC-associated aberrant phenotypes can be demonstrated in BM PCs from virtually every patient (62, 65); this implies that such aberrant phenotypes are also highly specific for disease persistence (reappearance) with an established sensitivity in routine clinical practice of at least $\geq 10^{-4}$ (i.e., detection of one tumor cell among ≥10,000 BM cells) (65). In addition, due to the increasing availability of clinical flow cytometers to the diagnostic hemato-oncology laboratories, the method has become (widely) available around the world, at acceptable costs. In turn, the spread of new digital flow cytometers with increasingly higher multicolor and software capabilities into clinical diagnostic laboratories also allows for the analysis of millions of cells in a few minutes, supporting fast diagnoses based on highly sensitive and robust flow-MRD in clinical routine (14).

Compared to flow-MRD, molecular techniques are recognized as more technically demanding (e.g., they require a diagnostic sample), and they are more time-consuming and less broadly applicable (<50% to 90% versus 100% for MFC), although they show a higher sensitivity than conventional flow-MRD (typically, 10^{-5} and 10^{-4} for molecular methods and MFC, respectively) (66, 73). In this regard, however, it should be noted that highly sensitive (and innovative) next-generation flow-MRD (NG-MRD) methods have been recently developed and led to a sensitivity beyond

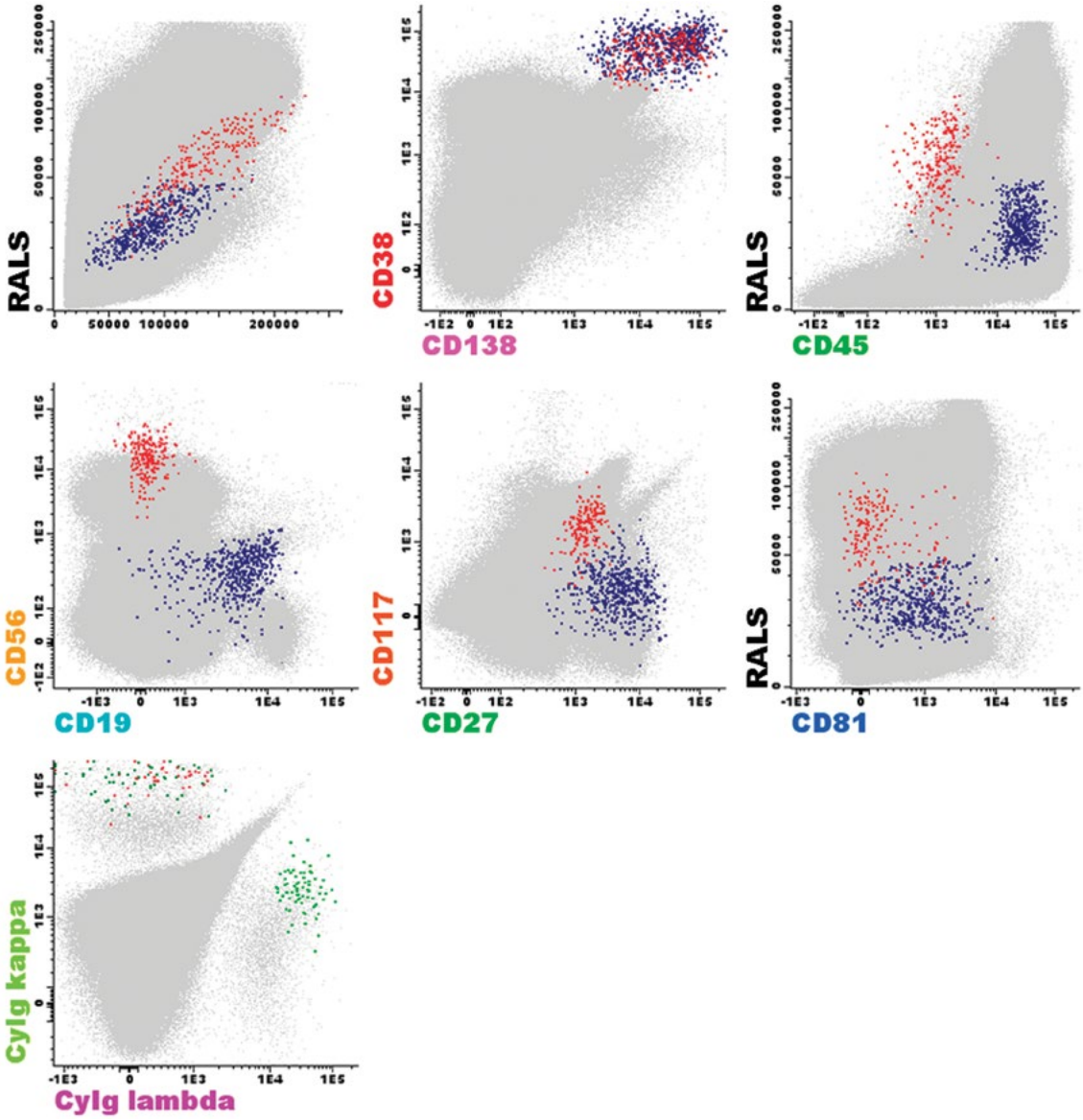

FIGURE 3 Highly sensitive minimal residual disease (MRD) detection in a bone marrow sample from a multiple myeloma (MM) patient. Bivariate dot plot representations of merged files from two different sample aliquots/tubes stained with the EuroFlow-International Myeloma Foundation MM MRD panel to illustrate the highly sensitive detection of aberrant/clonal myeloma plasma cells (PC; red events) coexisting with normal/polyclonal BM PCs (8×10^6 total BM events measured). Normal PCs display a characteristically normal phenotypic profile for surface membrane markers (dark blue dots). In turn, clonal PCs (red dots) from the same individual displayed a distinct pattern characterized by several myeloma-associated phenotypes (MAP; i.e., $CD45^-$, $CD19^-$, $CD56^{++}$, $CD117^+$, and $CD81^-$) in addition to higher forward and sideward scatter properties. Normal and abnormal PC populations could be further discriminated by their cytoplasmic (Cy) expression of immunoglobulin (Ig) light chains, highlighting the polyclonal nature of normal PCs ($CyIg\kappa^+$ and $CyIg\lambda^+$ [ratio of 0.8], dark and light green, respectively) versus monotypic expression of CyIgκ of clonal PCs. The overall BM PC population in this patient corresponded to 0.01% of all nucleated cells in the sample (gray dots); normal PCs were 0.008%, while clonal PCs represented 0.002% (227 dots) of all BM cells.

that of conventional flow-MRD approaches and even that of molecular techniques (between 10^{-5} and 10^{-6}), close to the sensitivity reached by next-generation sequencing approaches (65, 75). These NG-MRD methods (65, 75) have also addressed the need for standardization of conventional 4- to 8-color flow-MRD approaches, regarding antibody panels, sample preparation procedures, data acquisition and analysis, and interpretation of the results.

In the past, antibody combinations for flow-MRD were typically constructed as patient-specific immunophenotypic probes (25, 68). Nonetheless, the concept evolved to alternative approaches using fixed 4- to 6-color antibody panels that

TABLE 4 IMWG criteria for treatment response categories including those proposed for defining immunophenotypic and molecular CR[a,b]

Response category	Defining criteria
Progressive disease (PD)	Increase of <25% in any of the following: Serum M component (≥0.5 g/dl minimum absolute increase) or absolute level of ≥1 g/dl if the baseline value was ≥5 g/dl Urine M component (≥200 mg/24 h minimum absolute increase) Difference in involved and uninvolved FLC level (if M component is not measurable in serum or urine; >10 mg/dl minimum absolute increase) BM PCs (if serum or urine M component and FLC are not measurable; >10% minimum percentage increase) New bone lesion or plasmacytomas or increase in the size of preexisting ones Appearance of PCD-related hypercalcemia (>11.5 mg/dl)
Stable disease (SD)	Absence of CR, VGPR, PR, or PD criteria Lack of evidence of new or progressive bone lesions by imaging[c]
Partial response (PR)	Reduction of ≥50% of serum M component and ≥90% (or total <200 mg/24 h) in urine M component Reduction of ≥50% of involved and uninvolved FLC levels (if M component is not measurable) Reduction of ≥50% in BM PCs (baseline ≥30%; if neither M component nor FLC are measurable) Reduction of ≥50% in plasmacytoma size if present at diagnosis Absence of image evidence of new or progressive bone lesions[c]
Very good partial response (VGPR)	Negative M component by electrophoresis but detectable by IF Reduction of ≥90% in serum M component and urine M component <100 mg/24 h Absence of image evidence of new or progressive bone lesions[c]
Complete remission (CR)	<5% BM PCs Negative IF in serum and urine Nondetectable plasmacytomas Lack of evidence of any new or preexisting bone lesions by imaging[c]
Stringent complete remission (sCR)	CR status plus Normal FLC ratio Absence of BM cPCs by IHC or MFC (2–4 colors) Lack of evidence of new or progressive bone lesions by imaging[c]
Immunophenotypic CR	sCR plus Absence of phenotypically aberrant PCs by MFC in the BM[d]
Molecular CR	sCR plus Negative ASO-PCR in the BM (sensitivity of 10^{-5})

[a]Two consecutive evaluation studies are needed to establish the response categories. CR category if disease is measurable only by serum FLC is indicated by a normal FLC plus the other criteria listed. VGPR category if disease is measurable only by serum FLC is indicated by >90% reduction of the difference between involved and uninvolved FLC levels. BM evaluation in PD is required only if M-component and FLC levels are measurable. Data from reference 84.

[b]IMWG, International Myeloma Working Group; PCD, plasma cell disorders; BM, bone marrow; PC, plasma cell; IF, immunofixation; c, clonal; IHC, immunohistochemistry; MFC, multiparameter flow cytometry; FLC, free light chain; ASO-PCR, allele-specific oligonucleotide PCR.

[c]By X rays if performed; not strictly required.

[d]A minimum of 1×10^6 BM cells analyzed with >4-color flow cytometry.

cover those aberrant phenotypes common to most (>90%) MM cases, without the requirement for a diagnostic sample (27, 76, 77). In the meantime, consensus recommendations have been reached about the most informative markers that are essential for the identification and further characterization of BM PCs as carrying normal/reactive versus aberrant phenotypes (15). Despite this, so far, only a small number of MRD panels have been both technically and clinically validated (27, 76, 78–82). Detailed analysis of such panels shows that the transition from 4- to 6-color panels led to a more reliable identification of MRD at the 10^{-4} level; 8- to 10-color panels have also brought increased sensitivity whenever their usage is associated with the measurement of enough cells/tube (e.g., $>5 \times 10^6$ cells/tube) as proposed by the EuroFlow group (Fig. 3) (28, 82; J. Flores-Montero, B. Paiva, L. Sanoja-Flores, N. Puig, O. García, S. Böttcher, J. J. Pérez-Morán, M. B. Vidriales, M. V. Mateos, R. García-Sanz, C. Jimenez, M. Gonzalez, J. Martinez-López, M. C. del Cañizo, J. F. San Miguel, B. Durie, J. J. M. van Dongen, and A. Orfao, unpublished data). The specific way in which consensus MRD markers (e.g., CD38, CD138, CD45, CD19, CD56, CD27, CD81, and CD117 for identification of myeloma versus normal/reactive PCs, plus CyIgκ and CyIgλ for assessment of clonality within suspicious PC subsets identified with the

previous CD markers) are combined in a panel is a critical step in the success of flow-MRD (see above). In this regard, the use of highly sensitive fluorochromes is typically required for dimmer markers such as CD56, CD138, and CD117; in contrast, low-sensitivity fluorochromes are preferred for antigens highly expressed on PCs such as CD38; exactly the same principles that apply for MRD should be considered for diagnostic PCD panels, as well.

The clinical utility of flow-MRD in MM was first demonstrated in 2002 by both the Salamanca (Spain) and the Leeds (United Kingdom) groups (25, 83). They both showed that MRD detected by MFC was clinically relevant for the definition of patient groups with distinct PFS rates. The prognostic impact of MRD in MM has been further confirmed by the same groups and by other groups in more-recent treatment protocols for both ASCT-eligible and -noneligible MM patients (27, 65, 80–82). Thus, MRD detection by flow cytometry is currently considered one of the most relevant independent predictors of outcome in MM patients receiving HDT/ASCT (27, 81), independently of other prognostic factors such as tumor cytogenetics (27, 80, 81). Similarly, in the non-transplant-eligible patient group, detection of residual disease by flow-MRD has also been demonstrated to be a strong predictor for PFS, but differences in OS did not reach significance (76). In addition, a negative flow-MRD status after salvage therapy of relapsed MM patients was also shown to be associated with a significantly longer time to progression, specifically in the case of patients not included for allogenic stem cell transplant, while no differences were observed in the allogenic stem cell transplant group (79). Therefore, flow-MRD has been incorporated as a criterion for the definition of different levels of response to treatment categories (Table 4). Despite all this information, surrogate markers for a cure of MM are still needed, particularly as therapy improves and the rate of long-survivor MM patients is likely to increase in parallel.

CONCLUDING REMARKS

At present, the value and clinical relevance of MFC in the study of PCD patients are becoming increasingly recognized; thus, flow cytometry immunophenotyping has become an essential tool in the diagnostic work-up and the classification and monitoring of PCD patients. This is mostly due to the fact that MFC immunophenotyping allows accurate identification but also quantitation and detailed characterization of PCs in BM and other types of human samples, with clear-cut discrimination between (potentially) coexisting populations of normal/reactive PCs and clonal (phenotypically aberrant) PCs. Therefore, MFC identification, quantitation, and characterization of pathological (versus normal/reactive) PCs provide clinically relevant information that complements and completes optimal PCD patient evaluation by other standard approaches, both at diagnosis and during follow-up. In detail, MFC immunophenotyping contributes to the diagnostic screening of PCDs, its classification into the multiple different diagnostic subtypes of the disease and their variants, and prognostic stratification of preleukemic states such as MGUS and SMM; at the same time, MFC immunophenotyping also helps in defining the level of tumor PC depletion reached with therapy in MM and in monitoring MRD levels thereafter. Monitoring of flow-MRD levels also contributes to the prognostic stratification of MM patients after therapy, through the identification of patient groups at different risks of showing progressive disease. However, to take optimal advantage of MFC immunophenotyping in PCD, the use of highly standardized approaches, together with both technically and clinically validated panels in combination with new, innovative software tools, is critical for obtaining reproducible and robust results.

REFERENCES

1. **Swerdlow SH, Campo E, Harris NL, Jaffe ES, Pileri SA, Stein H, Thiele J, Vardiman JW.** 2008. *WHO Classification of Tumours of Haematopoietic and Lymphoid Tissues*, 4th ed. International Agency for Research on Cancer, Lyon, France.
2. **Rajkumar SV, Dimopoulos MA, Palumbo A, Blade J, Merlini G, Mateos MV, Kumar S, Hillengass J, Kastritis E, Richardson P, Landgren O, Paiva B, Dispenzieri A, Weiss B, LeLeu X, Zweegman S, Lonial S, Rosinol L, Zamagni E, Jagannath S, Sezer O, Kristinsson SY, Caers J, Usmani SZ, Lahuerta JJ, Johnsen HE, Beksac M, Cavo M, Goldschmidt H, Terpos E, Kyle RA, Anderson KC, Durie BG, Miguel JF.** 2014. International Myeloma Working Group updated criteria for the diagnosis of multiple myeloma. *Lancet Oncol* **15:**e538–e548.
3. **Turesson I, Kovalchik SA, Pfeiffer RM, Kristinsson SY, Goldin LR, Drayson MT, Landgren O.** 2014. Monoclonal gammopathy of undetermined significance and risk of lymphoid and myeloid malignancies: 728 cases followed up to 30 years in Sweden. *Blood* **123:**338–345.
4. **Dispenzieri A, Katzmann JA, Kyle RA, Larson DR, Melton LJ III, Colby CL, Therneau TM, Clark R, Kumar SK, Bradwell A, Fonseca R, Jelinek DF, Rajkumar SV.** 2010. Prevalence and risk of progression of light-chain monoclonal gammopathy of undetermined significance: a retrospective population-based cohort study. *Lancet* **375:** 1721–1728.
5. **Perez-Persona E, Vidriales MB, Mateo G, Garcia-Sanz R, Mateos MV, de Coca AG, Galende J, Martin-Nunez G, Alonso JM, de Las Heras N, Hernandez JM, Martin A, Lopez-Berges C, Orfao A, San Miguel JF.** 2007. New criteria to identify risk of progression in monoclonal gammopathy of uncertain significance and smoldering multiple myeloma based on multiparameter flow cytometry analysis of bone marrow plasma cells. *Blood* **110:**2586–2592.
6. **Rollig C, Knop S, Bornhauser M.** 2015. Multiple myeloma. *Lancet* **385:**21972208.
7. **Warsame R, Gertz MA, Lacy MQ, Kyle RA, Buadi F, Dingli D, Greipp PR, Hayman SR, Kumar SK, Lust JA, Russell SJ, Witzig TE, Mikhael J, Leung N, Zeldenrust SR, Rajkumar SV, Dispenzieri A.** 2012. Trends and outcomes of modern staging of solitary plasmacytoma of bone. *Am J Hematol* **87:**647–651.
8. **Rajkumar VS.** 2014. Multiple myeloma: 2014 update on diagnosis, risk-stratification, and management. *Am J Hematol* **89:**999–1009.
9. **Landgren O.** 2013. Monoclonal gammopathy of undetermined significance and smoldering multiple myeloma: biological insights and early treatment strategies. *Hematol Am Soc Hematol Educ Program* **2013:**478–487.
10. **Mateos MV, Hernandez MT, Giraldo P, de la Rubia J, de Arriba F, Lopez Corral L, Rosinol L, Paiva B, Palomera L, Bargay J, Oriol A, Prosper F, Lopez J, Olavarria E, Quintana N, Garcia JL, Blade J, Lahuerta JJ, San Miguel JF.** 2013. Lenalidomide plus dexamethasone for high-risk smoldering multiple myeloma. *N Engl J Med* **369:**438–447.
11. **Braylan RC.** 2004. Impact of flow cytometry on the diagnosis and characterization of lymphomas, chronic lymphoproliferative disorders and plasma cell neoplasias. *Cytometry A* **58:**57–61.
12. **Kaleem Z, Crawford E, Pathan MH, Jasper L, Covinsky MA, Johnson LR, White G.** 2003. Flow cytometric analysis of acute leukemias. Diagnostic utility and critical analysis of data. *Arch Pathol Lab Med* **127:**42–48.

13. **Vidriales MB, San-Miguel JF, Orfao A, Coustan-Smith E, Campana D.** 2003. Minimal residual disease monitoring by flow cytometry. *Best Pract Res Clin Haematol* **16:**599–612.
14. **Sewell WA, Smith SA.** 2011. Polychromatic flow cytometry in the clinical laboratory. *Pathology* **43:**580–591.
15. **Rawstron AC, Orfao A, Beksac M, Bezdickova L, Brooimans RA, Bumbea H, Dalva K, Fuhler G, Gratama J, Hose D, Kovarova L, Lioznov M, Mateo G, Morilla R, Mylin AK, Omede P, Pellat-Deceunynck C, Perez Andres M, Petrucci M, Ruggeri M, Rymkiewicz G, Schmitz A, Schreder M, Seynaeve C, Spacek M, de Tute RM, Van Valckenborgh E, Weston-Bell N, Owen RG, San Miguel JF, Sonneveld P, Johnsen HE.** 2008. Report of the European Myeloma Network on multiparametric flow cytometry in multiple myeloma and related disorders. *Haematologica* **93:**431–438.
16. **Nadav L, Katz BZ, Baron S, Yossipov L, Polliack A, Deutsch V, Geiger B, Naparstek E.** 2006. Diverse niches within multiple myeloma bone marrow aspirates affect plasma cell enumeration. *Br J Haematol* **133:**530–532.
17. **Smock KJ, Perkins SL, Bahler DW.** 2007. Quantitation of plasma cells in bone marrow aspirates by flow cytometric analysis compared with morphologic assessment. *Arch Pathol Lab Med* **131:**951–955.
18. **Harada H, Kawano MM, Huang N, Harada Y, Iwato K, Tanabe O, Tanaka H, Sakai A, Asaoku H, Kuramoto A.** 1993. Phenotypic difference of normal plasma cells from mature myeloma cells. *Blood* **81:**2658–2663.
19. **San Miguel JF, Gonzalez M, Gascon A, Moro MJ, Hernandez JM, Ortega F, Jimenez R, Guerras L, Romero M, Casanova F, Sanz A, Sanchez J, Portero JA, Orfao A.** 1991. Immunophenotypic heterogeneity of multiple myeloma: influence on the biology and clinical course of the disease. Castellano-Leones (Spain) Cooperative Group for the Study of Monoclonal Gammopathies. *Br J Haematol* **77:**185–190.
20. **Terstappen LW, Johnsen S, Segers-Nolten IM, Loken MR.** 1990. Identification and characterization of plasma cells in normal human bone marrow by high-resolution flow cytometry. *Blood* **76:**1739–1747.
21. **Mateo G, Montalban MA, Vidriales MB, Lahuerta JJ, Mateos MV, Gutierrez N, Rosinol L, Montejano L, Blade J, Martinez R, de la Rubia J, Diaz-Mediavilla J, Sureda A, Ribera JM, Ojanguren JM, de Arriba F, Palomera L, Terol MJ, Orfao A, San Miguel JF.** 2008. Prognostic value of immunophenotyping in multiple myeloma: a study by the PETHEMA/GEM cooperative study groups on patients uniformly treated with high-dose therapy. *J Clin Oncol* **26:**2737–2744.
22. **Mateo G, Castellanos M, Rasillo A, Gutierrez NC, Montalban MA, Martin ML, Hernandez JM, Lopez-Berges MC, Montejano L, Blade J, Mateos MV, Sureda A, de la Rubia J, Diaz-Mediavilla J, Pandiella A, Lahuerta JJ, Orfao A, San Miguel JF.** 2005. Genetic abnormalities and patterns of antigenic expression in multiple myeloma. *Clin Cancer Res* **11:**3661–3667.
23. **Ocqueteau M, Orfao A, Almeida J, Blade J, Gonzalez M, Garcia-Sanz R, Lopez-Berges C, Moro MJ, Hernandez J, Escribano L, Caballero D, Rozman M, San Miguel JF.** 1998. Immunophenotypic characterization of plasma cells from monoclonal gammopathy of undetermined significance patients. Implications for the differential diagnosis between MGUS and multiple myeloma. *Am J Pathol* **152:**1655–1665.
24. **Perez-Andres M, Santiago M, Almeida J, Mateo G, Porwit-MacDonald A, Bjorklund E, Valet G, Kraan J, Gratama JW, D'Hautcourt JL, Merle-Beral H, Lima M, Montalban MA, San Miguel JF, Orfao A.** 2004. Immunophenotypic approach to the identification and characterization of clonal plasma cells from patients with monoclonal gammopathies. *J Biol Regul Homeost Agents* **18:**392–398.
25. **San Miguel JF, Almeida J, Mateo G, Blade J, Lopez-Berges C, Caballero D, Hernandez J, Moro MJ, Fernandez-Calvo J, Diaz-Mediavilla J, Palomera L, Orfao A.** 2002. Immunophenotypic evaluation of the plasma cell compartment in multiple myeloma: a tool for comparing the efficacy of different treatment strategies and predicting outcome. *Blood* **99:**1853–1856.
26. **San Miguel JF, Vidriales MB, Ocio E, Mateo G, Sanchez-Guijo F, Sanchez ML, Escribano L, Barez A, Moro MJ, Hernandez J, Aguilera C, Cuello R, Garcia-Frade J, Lopez R, Portero J, Orfao A.** 2003. Immunophenotypic analysis of Waldenstrom's macroglobulinemia. *Semin Oncol* **30:**187–195.
27. **Rawstron AC, Child JA, de Tute RM, Davies FE, Gregory WM, Bell SE, Szubert AJ, Navarro-Coy N, Drayson MT, Feyler S, Ross FM, Cook G, Jackson GH, Morgan GJ, Owen RG.** 2013. Minimal residual disease assessed by multiparameter flow cytometry in multiple myeloma: impact on outcome in the Medical Research Council Myeloma IX Study. *J Clin Oncol* **31:**2540–2547.
28. **Robillard N, Bene MC, Moreau P, Wuilleme S.** 2013. A single-tube multiparameter seven-colour flow cytometry strategy for the detection of malignant plasma cells in multiple myeloma. *Blood Cancer J* **3:**e134.
29. **Paiva B, Gutierrez NC, Chen X, Vidriales MB, Montalban MA, Rosinol L, Oriol A, Martinez-Lopez J, Mateos MV, Lopez-Corral L, Diaz-Rodriguez E, Perez JJ, Fernandez-Redondo E, de Arriba F, Palomera L, Bengoechea E, Terol MJ, de Paz R, Martin A, Hernandez J, Orfao A, Lahuerta JJ, Blade J, Pandiella A, Miguel JF.** 2012. Clinical significance of CD81 expression by clonal plasma cells in high-risk smoldering and symptomatic multiple myeloma patients. *Leukemia* **26:**1862–1869.
30. **San Miguel JF, Caballero MD, Gonzalez M, Zola H, Lopez Borrasca A.** 1986. Immunological phenotype of neoplasms involving the B cell in the last step of differentiation. *Br J Haematol* **62:**75–83.
31. **Tazzari PL, Gobbi M, Dinota A, Bontadini A, Grassi G, Cerato C, Cavo M, Pileri S, Caligaris-Cappio F, Tura S.** 1987. Normal and neoplastic plasma cell membrane phenotype: studies with new monoclonal antibodies. *Clin Exp Immunol* **70:**192–200.
32. **Quarona V, Zaccarello G, Chillemi A, Brunetti E, Singh VK, Ferrero E, Funaro A, Horenstein AL, Malavasi F.** 2013. CD38 and CD157: a long journey from activation markers to multifunctional molecules. *Cytometry B Clin Cytom* **84:**207–217.
33. **Campana D, Suzuki T, Todisco E, Kitanaka A.** 2000. CD38 in hematopoiesis. *Chem Immunol* **75:**169–188.
34. **Perez-Andres M, Paiva B, Nieto WG, Caraux A, Schmitz A, Almeida J, Vogt RF Jr, Marti GE, Rawstron AC, Van Zelm MC, Van Dongen JJ, Johnsen HE, Klein B, Orfao A.** 2010. Human peripheral blood B-cell compartments: a crossroad in B-cell traffic. *Cytometry B Clin Cytom* **78:**S47–S60.
35. **Arroz M, Came N, Lin P, Chen W, Yuan C, Lagoo A, Monreal M, de Tute R, Vergilio JA, Rawstron AC, Paiva B.** 2015. Consensus guidelines on plasma cell myeloma minimal residual disease analysis and reporting. *Cytometry B Clin Cytom* doi:10.1002/cyto.b.21228.
36. **Wijdenes J, Vooijs WC, Clement C, Post J, Morard F, Vita N, Laurent P, Sun RX, Klein B, Dore JM.** 1996. A plasmocyte selective monoclonal antibody (B-B4) recognizes syndecan-1. *Br J Haematol* **94:**318–323.
37. **Jourdan M, Ferlin M, Legouffe E, Horvathova M, Liautard J, Rossi JF, Wijdenes J, Brochier J, Klein B.** 1998. The myeloma cell antigen syndecan-1 is lost by apoptotic myeloma cells. *Br J Haematol* **100:**637–646.
38. **Yang Y, Borset M, Langford JK, Sanderson RD.** 2003. Heparan sulfate regulates targeting of syndecan-1 to a functional domain on the cell surface. *J Biol Chem* **278:**12888–12893.

39. **Liu D, Lin P, Hu Y, Zhou Y, Tang G, Powers L, Medeiros LJ, Jorgensen JL, Wang SA.** 2012. Immunophenotypic heterogeneity of normal plasma cells: comparison with minimal residual plasma cell myeloma. *J Clin Pathol* **65:**823–829.
40. **Sherbenou DW, Behrens CR, Su Y, Wolf JL, Martin TG III, Liu B.** 2015. The development of potential antibody-based therapies for myeloma. *Blood Rev* **29:**81–91.
41. **Khagi Y, Mark TM.** 2014. Potential role of daratumumab in the treatment of multiple myeloma. *OncoTargets Ther* **7:**1095–1100.
42. **Ocio EM, Richardson PG, Rajkumar SV, Palumbo A, Mateos MV, Orlowski R, Kumar S, Usmani S, Roodman D, Niesvizky R, Einsele H, Anderson KC, Dimopoulos MA, Avet-Loiseau H, Mellqvist UH, Turesson I, Merlini G, Schots R, McCarthy P, Bergsagel L, Chim CS, Lahuerta JJ, Shah J, Reiman A, Mikhael J, Zweegman S, Lonial S, Comenzo R, Chng WJ, Moreau P, Sonneveld P, Ludwig H, Durie BG, Miguel JF.** 2014. New drugs and novel mechanisms of action in multiple myeloma in 2013: a report from the International Myeloma Working Group (IMWG). *Leukemia* **28:**525–542.
43. **Deckert J, Wetzel MC, Bartle LM, Skaletskaya A, Goldmacher VS, Vallee F, Zhou-Liu Q, Ferrari P, Pouzieux S, Lahoute C, Dumontet C, Plesa A, Chiron M, Lejeune P, Chittenden T, Park PU, Blanc V.** 2014. SAR650984, a novel humanized CD38-targeting antibody, demonstrates potent antitumor activity in models of multiple myeloma and other CD38+ hematologic malignancies. *Clin Cancer Res* **20:**4574–4583.
44. **Zonder JA, Mohrbacher AF, Singhal S, van Rhee F, Bensinger WI, Ding H, Fry J, Afar DE, Singhal AK.** 2012. A phase 1, multicenter, open-label, dose escalation study of elotuzumab in patients with advanced multiple myeloma. *Blood* **120:**552–559.
45. **Lonial S, Vij R, Harousseau JL, Facon T, Moreau P, Mazumder A, Kaufman JL, Leleu X, Tsao LC, Westland C, Singhal AK, Jagannath S.** 2012. Elotuzumab in combination with lenalidomide and low-dose dexamethasone in relapsed or refractory multiple myeloma. *J Clin Oncol* **30:**1953–1959.
46. **Atanackovic D, Panse J, Hildebrandt Y, Jadczak A, Kobold S, Cao Y, Templin J, Meyer S, Reinhard H, Bartels K, Lajmi N, Zander AR, Marx AH, Bokemeyer C, Kroger N.** 2011. Surface molecule CD229 as a novel target for the diagnosis and treatment of multiple myeloma. *Haematologica* **96:**1512–1520.
47. **Veillette A, Guo H.** 2013. CS1, a SLAM family receptor involved in immune regulation, is a therapeutic target in multiple myeloma. *Crit Rev Oncol Hematol* **88:**168–177.
48. **Noborio-Hatano K, Kikuchi J, Takatoku M, Shimizu R, Wada T, Ueda M, Nobuyoshi M, Oh I, Sato K, Suzuki T, Ozaki K, Mori M, Nagai T, Muroi K, Kano Y, Furukawa Y, Ozawa K.** 2009. Bortezomib overcomes cell-adhesion-mediated drug resistance through downregulation of VLA-4 expression in multiple myeloma. *Oncogene* **28:**231–242.
49. **Pojero F, Flores-Montero J, Sanoja L, Perez JJ, Puig N, Paiva B, Bottcher S, van Dongen JJM, Orfao A.** 2015. Utility of CD54, CD229, and CD319 for the identification of plasma cells in patients with clonal plasma cell diseases. *Cytometry B Clin Cytom* doi:10.1002/cyto.b.21269.
50. **Radbruch A, Muehlinghaus G, Luger EO, Inamine A, Smith KG, Dorner T, Hiepe F.** 2006. Competence and competition: the challenge of becoming a long-lived plasma cell. *Nat Rev Immunol* **6:**741–750.
51. **Caraux A, Klein B, Paiva B, Bret C, Schmitz A, Fuhler GM, Bos NA, Johnsen HE, Orfao A, Perez-Andres M.** 2010. Circulating human B and plasma cells. Age-associated changes in counts and detailed characterization of circulating normal CD138- and CD138+ plasma cells. *Haematologica* **95:**1016–1020.
52. **Mei HE, Yoshida T, Sime W, Hiepe F, Thiele K, Manz RA, Radbruch A, Dorner T.** 2009. Blood-borne human plasma cells in steady state are derived from mucosal immune responses. *Blood* **113:**2461–2469.
53. **Belnoue E, Pihlgren M, McGaha TL, Tougne C, Rochat AF, Bossen C, Schneider P, Huard B, Lambert PH, Siegrist CA.** 2008. APRIL is critical for plasmablast survival in the bone marrow and poorly expressed by early-life bone marrow stromal cells. *Blood* **111:**2755–2764.
54. **Robillard N, Wuilleme S, Moreau P, Bene MC.** 2014. Immunophenotype of normal and myelomatous plasma-cell subsets. *Front Immunol* **5:**137.
55. **Cannizzo E, Bellio E, Sohani AR, Hasserjian RP, Ferry JA, Dorn ME, Sadowski C, Bucci JJ, Carulli G, Preffer F.** 2010. Multiparameter immunophenotyping by flow cytometry in multiple myeloma: the diagnostic utility of defining ranges of normal antigenic expression in comparison to histology. *Cytometry B Clin Cytom* **78:** 231–238.
56. **Schmidt-Hieber M, Paiva B, Perez-Andres M, Gutierrez ML, Dybkaer K, Rasillo A, Tabernero MD, Lopez A, Kryukov F, Carrasco P, Sanchez ML, Rosiñol L, Lopez JM, Oriol A, de Arriba F, Palomera L, Bengoechea E, Lahuerta JJ, Blade J, Schmitz A, Johnsen HE, San Miguel JF, Orfao A.** 2013. CD56+ Clonal plasma cells in multiple myeloma are associated with unique disease characteristics and have a counterpart of CD56+ normal plasma cells with increased maturity. *Blood* **122:**751.
57. **Ocqueteau M, Orfao A, Garcia-Sanz R, Almeida J, Gonzalez M, San Miguel JF.** 1996. Expression of the CD117 antigen (c-Kit) on normal and myelomatous plasma cells. *Br J Haematol* **95:**489–493.
58. **Lin P, Owens R, Tricot G, Wilson CS.** 2004. Flow cytometric immunophenotypic analysis of 306 cases of multiple myeloma. *Am J Clin Pathol* **121:**482–488.
59. **Alapat D, Coviello-Malle J, Owens R, Qu P, Barlogie B, Shaughnessy JD, Lorsbach RB.** 2012. Diagnostic usefulness and prognostic impact of CD200 expression in lymphoid malignancies and plasma cell myeloma. *Am J Clin Pathol* **137:**93–100.
60. **Iqbal MS, Otsuyama K, Shamsasenjan K, Asaoku H, Mahmoud MS, Gondo T, Kawano MM.** 2009. Constitutively lower expressions of CD54 on primary myeloma cells and their different localizations in bone marrow. *Eur J Haematol* **83:**302–312.
61. **Ise T, Nagata S, Kreitman RJ, Wilson WH, Wayne AS, Stetler-Stevenson M, Bishop MR, Scheinberg DA, Rassenti L, Kipps TJ, Kyle RA, Jelinek DF, Pastan I.** 2007. Elevation of soluble CD307 (IRTA2/FcRH5) protein in the blood and expression on malignant cells of patients with multiple myeloma, chronic lymphocytic leukemia, and mantle cell lymphoma. *Leukemia* **21:**169–174.
62. **van Dongen JJ, Lhermitte L, Bottcher S, Almeida J, van der Velden VH, Flores-Montero J, Rawstron A, Asnafi V, Lecrevisse Q, Lucio P, Mejstrikova E, Szczepanski T, Kalina T, de Tute R, Bruggemann M, Sedek L, Cullen M, Langerak AW, Mendonca A, Macintyre E, Martin-Ayuso M, Hrusak O, Vidriales MB, Orfao A.** 2012. EuroFlow antibody panels for standardized n-dimensional flow cytometric immunophenotyping of normal, reactive and malignant leukocytes. *Leukemia* **26:**1908–1975.
63. **Pellat-Deceunynck C, Bataille R, Robillard N, Harousseau JL, Rapp MJ, Juge-Morineau N, Wijdenes J, Amiot M.** 1994. Expression of CD28 and CD40 in human myeloma cells: a comparative study with normal plasma cells. *Blood* **84:**2597–2603.
64. **Moreau P, Robillard N, Jego G, Pellat C, Le Gouill S, Thoumi S, Avet-Loiseau H, Harousseau JL, Bataille R.** 2006. Lack of CD27 in myeloma delineates different presentation and outcome. *Br J Haematol* **132:**168–170.

65. **Paiva B, van Dongen JJ, Orfao A.** 2015. New criteria for response assessment: role of minimal residual disease in multiple myeloma. *Blood* **125:**3059–3068.
66. **Paiva B, Vidriales MB, Perez JJ, Mateo G, Montalban MA, Mateos MV, Blade J, Lahuerta JJ, Orfao A, San Miguel JF.** 2009. Multiparameter flow cytometry quantification of bone marrow plasma cells at diagnosis provides more prognostic information than morphological assessment in myeloma patients. *Haematologica* **94:**1599–1602.
67. **Manasanch EE, Salem DA, Yuan CM, Tageja N, Bhutani M, Kwok M, Kazandjian D, Carter G, Steinberg SM, Zuchlinski D, Mulquin M, Calvo K, Maric I, Roschewski M, Korde N, Braylan R, Landgren O, Stetler-Stevenson M.** 2015. Flow cytometric sensitivity and characteristics of plasma cells in patients with multiple myeloma or its precursor disease: influence of biopsy site and anticoagulation method. *Leuk Lymphoma* **56:**1416–1424.
68. **Paiva B, Almeida J, Perez-Andres M, Mateo G, Lopez A, Rasillo A, Vidriales MB, Lopez-Berges MC, Miguel JF, Orfao A.** 2010. Utility of flow cytometry immunophenotyping in multiple myeloma and other clonal plasma cell-related disorders. *Cytometry B Clin Cytom* **78:**239–252.
69. **Paiva B, Vidriales MB, Mateo G, Perez JJ, Montalban MA, Sureda A, Montejano L, Gutierrez NC, Garcia de Coca A, de las Heras N, Mateos MV, Lopez-Berges MC, Garcia-Boyero R, Galende J, Hernandez J, Palomera L, Carrera D, Martinez R, de la Rubia J, Martin A, Gonzalez Y, Blade J, Lahuerta JJ, Orfao A, San-Miguel JF.** 2009. The persistence of immunophenotypically normal residual bone marrow plasma cells at diagnosis identifies a good prognostic subgroup of symptomatic multiple myeloma patients. *Blood* **114:**4369–4372.
70. **Schmidt-Hieber M, Perez-Andres M, Paiva B, Flores-Montero J, Perez JJ, Gutierrez NC, Vidriales MB, Matarraz S, San Miguel JF, Orfao A.** 2011. CD117 expression in gammopathies is associated with an altered maturation of the myeloid and lymphoid hematopoietic cell compartments and favorable disease features. *Haematologica* **96:**328–332.
71. **Fernandez de Larrea C, Kyle RA, Durie BG, Ludwig H, Usmani S, Vesole DH, Hajek R, San Miguel JF, Sezer O, Sonneveld P, Kumar SK, Mahindra A, Comenzo R, Palumbo A, Mazumber A, Anderson KC, Richardson PG, Badros AZ, Caers J, Cavo M, LeLeu X, Dimopoulos MA, Chim CS, Schots R, Noeul A, Fantl D, Mellqvist UH, Landgren O, Chanan-Khan A, Moreau P, Fonseca R, Merlini G, Lahuerta JJ, Blade J, Orlowski RZ, Shah JJ.** 2013. Plasma cell leukemia: consensus statement on diagnostic requirements, response criteria and treatment recommendations by the International Myeloma Working Group. *Leukemia* **27:**780–791.
72. **Davies FE, Rawstron AC, Owen RG, Morgan GJ.** 2002. Minimal residual disease monitoring in multiple myeloma. *Best Pract Res Clin Haematol* **15:**197–222.
73. **Puig N, Sarasquete ME, Balanzategui A, Martinez J, Paiva B, Garcia H, Fumero S, Jimenez C, Alcoceba M, Chillon MC, Sebastian E, Marin L, Montalban MA, Mateos MV, Oriol A, Palomera L, de la Rubia J, Vidriales MB, Blade J, Lahuerta JJ, Gonzalez M, Miguel JF, Garcia-Sanz R.** 2014. Critical evaluation of ASO RQ-PCR for minimal residual disease evaluation in multiple myeloma. A comparative analysis with flow cytometry. *Leukemia* **28:**391–397.
74. **Gupta R, Bhaskar A, Kumar L, Sharma A, Jain P.** 2009. Flow cytometric immunophenotyping and minimal residual disease analysis in multiple myeloma. *Am J Clin Pathol* **132:**728–732.
75. **van Dongen JJ, van der Velden VH, Bruggemann M, Orfao A.** 2015. Minimal residual disease diagnostics in acute lymphoblastic leukemia: need for sensitive, fast, and standardized technologies. *Blood* **125:**3996–4009.
76. **Paiva B, Martinez-Lopez J, Vidriales MB, Mateos MV, Montalban MA, Fernandez-Redondo E, Alonso L, Oriol A, Teruel AI, de Paz R, Larana JG, Bengoechea E, Martin A, Mediavilla JD, Palomera L, de Arriba F, Blade J, Orfao A, Lahuerta JJ, San Miguel JF.** 2011. Comparison of immunofixation, serum free light chain, and immunophenotyping for response evaluation and prognostication in multiple myeloma. *J Clin Oncol* **29:**1627–1633.
77. **Mathis S, Chapuis N, Borgeot J, Maynadie M, Fontenay M, Bene MC, Guy J, Bardet V.** 2015. Comparison of cross-platform flow cytometry minimal residual disease evaluation in multiple myeloma using a common antibody combination and analysis strategy. *Cytometry B Clin Cytom* **88:**101–109.
78. **Landgren O, Gormley N, Turley D, Owen RG, Rawstron A, Paiva B, Barnett D, Arroz M, Wallace P, Durie B, Yuan C, Dogan A, Stetler-Stevenson M, Marti GE.** 2014. Flow cytometry detection of minimal residual disease in multiple myeloma: Lessons learned at FDA-NCI roundtable symposium. *Am J Hematol* **89:**1159–1160.
79. **Paiva B, Chandia M, Puig N, Vidriales MB, Perez JJ, Lopez-Corral L, Ocio EM, Garcia-Sanz R, Gutierrez NC, Jimenez-Ubieto A, Lahuerta JJ, Mateos MV, San Miguel JF.** 2015. The prognostic value of multiparameter flow cytometry minimal residual disease assessment in relapse multiple myeloma. *Haematologica* **100:**e53–e55.
80. **Paiva B, Gutierrez NC, Rosinol L, Vidriales MB, Montalban MA, Martinez-Lopez J, Mateos MV, Cibeira MT, Cordon L, Oriol A, Terol MJ, Echeveste MA, de Paz R, de Arriba F, Palomera L, de la Rubia J, Diaz-Mediavilla J, Sureda A, Gorosquieta A, Alegre A, Martin A, Hernandez MT, Lahuerta JJ, Blade J, San Miguel JF.** 2012. High-risk cytogenetics and persistent minimal residual disease by multiparameter flow cytometry predict unsustained complete response after autologous stem cell transplantation in multiple myeloma. *Blood* **119:**687–691.
81. **Paiva B, Vidriales MB, Cervero J, Mateo G, Perez JJ, Montalban MA, Sureda A, Montejano L, Gutierrez NC, Garcia de Coca A, de Las Heras N, Mateos MV, Lopez-Berges MC, Garcia-Boyero R, Galende J, Hernandez J, Palomera L, Carrera D, Martinez R, de la Rubia J, Martin A, Blade J, Lahuerta JJ, Orfao A, San Miguel JF.** 2008. Multiparameter flow cytometric remission is the most relevant prognostic factor for multiple myeloma patients who undergo autologous stem cell transplantation. *Blood* **112:**4017–4023.
82. **Roussel M, Lauwers-Cances V, Robillard N, Hulin C, Leleu X, Benboubker L, Marit G, Moreau P, Pegourie B, Caillot D, Fruchart C, Stoppa AM, Gentil C, Wuilleme S, Huynh A, Hebraud B, Corre J, Chretien ML, Facon T, Avet-Loiseau H, Attal M.** 2014. Front-line transplantation program with lenalidomide, bortezomib, and dexamethasone combination as induction and consolidation followed by lenalidomide maintenance in patients with multiple myeloma: a phase II study by the Intergroupe Francophone du Myelome. *J Clin Oncol* **32:**2712–2717.
83. **Rawstron AC, Davies FE, DasGupta R, Ashcroft AJ, Patmore R, Drayson MT, Owen RG, Jack AS, Child JA, Morgan GJ.** 2002. Flow cytometric disease monitoring in multiple myeloma: the relationship between normal and neoplastic plasma cells predicts outcome after transplantation. *Blood* **100:**3095–3100.
84. **Rajkumar SV, Harousseau JL, Durie B, Anderson KC, Dimopoulos M, Kyle R, Blade J, Richardson P, Orlowski R, Siegel D, Jagannath S, Facon T, Avet-Loiseau H, Lonial S, Palumbo A, Zonder J, Ludwig H, Vesole D, Sezer O, Munshi NC, San Miguel J.** 2011. Consensus recommendations for the uniform reporting of clinical trials: report of the International Myeloma Workshop Consensus Panel 1. *Blood* **117:**4691–4695.

Future Cytometric Technologies and Applications

HOLDEN T. MAECKER

25

The past several years have seen a rapid evolution of flow cytometry technology, moving toward more parameters with the development of instruments containing smaller and less expensive lasers and with the discovery of new dyes that extend the range of emissions that can be detected by those lasers. This is exemplified by the emergence of violet diode lasers (1) and associated quantum dot nanocrystals (2) and brilliant violet dyes (3) that are excited by violet (and most recently by UV) lasers. These developments make flow cytometry in the range of 15 or so parameters more practical than ever.

In the last few years, a competing flow cytometry platform, termed mass cytometry, has also emerged (4–6). This technology uses heavy metal ion labeling in place of fluorophores, with detection by time-of-flight mass spectrometry (Fig. 1). A commercial instrument (CyTOF; DVS Sciences) has been developed for this purpose. The benefits of this technology are twofold. First, the number of parallel parameters that can be measured is increased tremendously (currently to about 40 but potentially 50 or more) (7). Second, the spillover common to fluorescence-based detection is all but eliminated, making compensation between detector channels unnecessary (Fig. 2). The combined impact of these two benefits is enormous. Forty-parameter panels can now be designed with much fewer problems than would be encountered with 10- to 15-parameter panels on fluorescence-based instruments. To be sure, there are still caveats (8), including sensitivity considerations for very low abundance targets; a small amount of signal contamination due to oxidation, isotopic impurities, sample contaminants, and detector infidelity; and a considerable cell loss in the instrument. However, these issues are often a reasonable trade-off for the exponentially increased information content that can now be derived from a single cell sample.

One can ask whether 40-plus parameters are needed in flow cytometry, especially in the clinical realm. However, recent publications using mass cytometry have already uncovered tremendous diversity of phenotypes and functions within hematopoietic cells, which can only be appreciated by the parallel application of many probes to dissect the various subpopulations (9–11). Furthermore, there are clinical cytometric applications, such as leukemia and lymphoma analysis, that currently require several multicolor staining cocktails for precise diagnosis (12). These could certainly be simplified, and even extended, by the use of highly multiparametric mass cytometry.

As alluded to above, it is not only the cell surface phenotyping markers that are of interest in analyzing immune cells. There are also a myriad of intracellular markers, many of which correspond to phosphorylated signaling states (13) or cytokines (14) that can be induced by short-term *in vitro* stimulation. The availability of flow cytometry-compatible antibodies to these markers, and the development of protocols to analyze them, has been another area of advancement in recent years. The number of research laboratories now routinely performing such functional cytometric assays is at an all-time high. Thus, the marriage of highly multiparametric flow or mass cytometry with functional readouts such as phosphoepitopes, is creating a new era of cellular immunology, with an unprecedented level of information content. The mining of this information will undoubtedly provide new biomarkers for the diagnosis and prognosis of disease and immunological monitoring of diseases and therapeutic interventions. This chapter will describe the underlying technologies in some detail, with emphasis on how they may eventually affect clinical flow cytometry.

MASS CYTOMETRY

The use of time-of-flight mass spectrometry to perform multiparameter analysis of single cells was first described by Tanner et al. (4). The implications of this technology for immune cell analysis were truly demonstrated in the Nolan laboratory, beginning with the seminal publication by Bendall et al. (9) and continuing with a series of publications thereafter (15–20). However, other groups are joining this revolution (10, 11, 21), and the number of installed instruments should reach 100 by the time of this publication.

Logistic Considerations

Along with the benefits of highly multiparametric, compensation-free experiments, come a number of logistical and technical caveats. On the logistical front, the instrumentation is expensive and requires physical adaptations of facility ventilation and power. There is a considerable usage of ultrahigh-purity argon, and the machine requires regular tuning and maintenance, including periodic replacement of the detector.

doi:10.1128/9781555818722.ch25

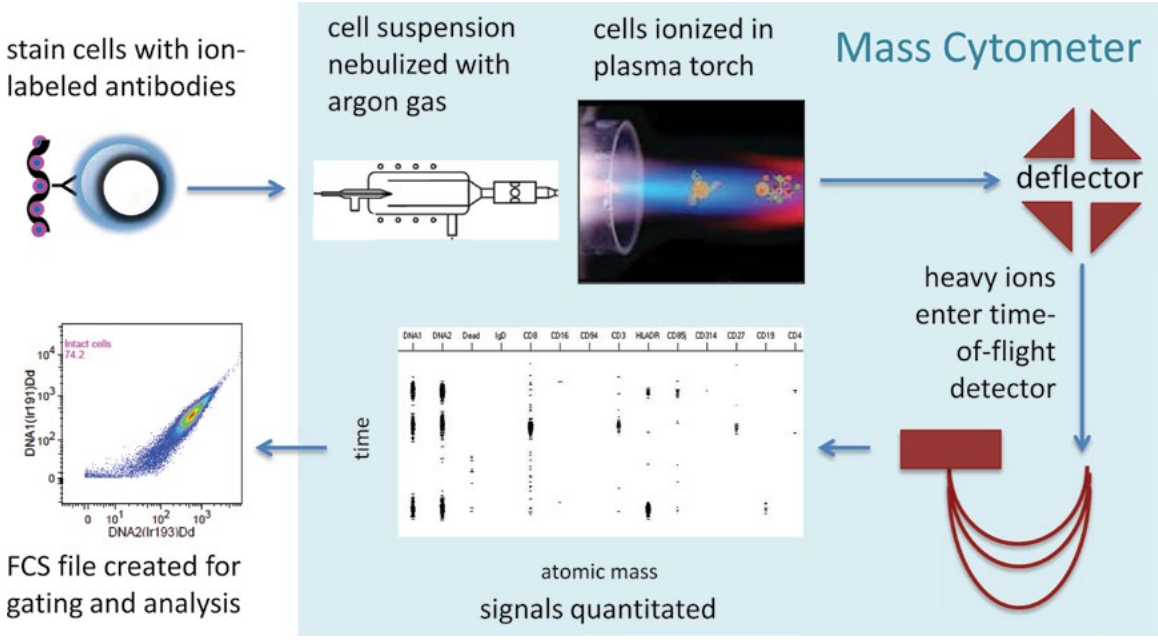

FIGURE 1 Mass cytometry workflow overview. A cell suspension is first stained with antibodies labeled with heavy metal ions, via covalently coupled chelator molecules. The stained cell suspension is then nebulized and directed into a plasma torch in the mass cytometer, using a stream of argon gas. The extremely hot plasma breaks cellular components into elemental ions, and the heavier ions are focused into a time-of-flight detector. The signals from this detector are recorded over time, and pulses corresponding to cell events are quantitated. The data for each cell event is transcribed into a Flow Cytometry Standard (FCS) file, such that it can be gated and analyzed with traditional flow cytometry software.

Acquisition Speed

Technically, there are caveats to the performance of mass cytometry experiments as well. Perhaps most significantly, the speed of acquisition is currently limited to <1,000 events/s (7), although practically, we find the optimum for heterogeneous cell populations to be even lower (300 to 500 events/s). This is to avoid too many coincident events (doublets), which are not easily removed from the analysis and which, if retained, could lead to spurious results. Because mass detection is done from a diffused ion cloud, rather than an intact cell, there are fundamental limitations to the detection speed of this platform, although one could hope for improvements in the form of optimally timed introduction of cells to the machine.

One way to improve doublet discrimination is through sample barcoding, which has been adapted from fluorescence to mass cytometry (16). By labeling a number of related samples (e.g., different stimulation conditions from the same donor), each with a unique combination of mass labels, the samples can be combined, stained, and analyzed as a single composite sample. In addition to equalizing the staining condition of the barcoded samples and conserving the amount

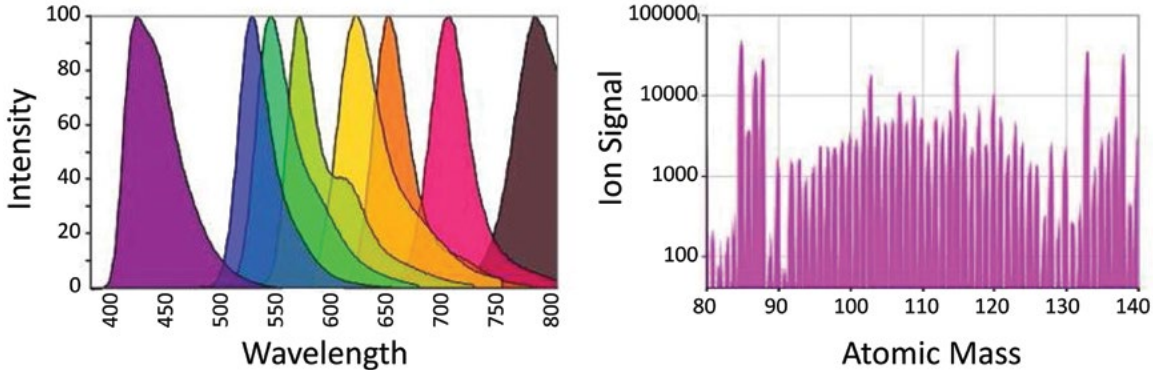

FIGURE 2 Comparison of fluorescence emission spectra (left) and mass spectrometry (right). The latter allows for the detection of many more discrete labels, with very little spillover between detector channels.

of antibody used, barcoding has two additional side benefits. One is that cross-contamination of the barcoded samples is largely avoided, allowing for less between-sample cleaning. A second is that, when deconvolving the composite sample, doublets of two different barcodes are eliminated. If 10 barcodes are combined to make a composite sample, this theoretically should eliminate 9/10 of the cell doublets (as doublets of the same barcode would still remain).

While barcoding can have an impact on doublet discrimination, it has little effect on the overall speed limitations of the CyTOF. To partly alleviate this issue, preenrichment of rare populations can be done, e.g., with magnetic beads. This strategy has effectively been used for analysis of major histocompatibility complex-peptide tetramer binding by mass cytometry (10, 21). In one of these studies, tetramers labeled with multiple metal ions have been used to increase the number of tetramers that can be studied with a limited number of mass channels as well as to increase the specificity of identifying tetramer-positive events (21). An analogous method was previously described for fluorescence-based tetramers (22).

Cell Loss

Another limitation of CyTOF comes from the instrument fluidics, which consist of nebulized droplets focused by an argon makeup gas. This system results in about two-thirds of the introduced cells being lost before entering the plasma torch. To be fair, cells are conserved relative to fluorescence flow cytometry by the ability to condense multitube panels into a single tube with 40 or so markers. However, this level of cell loss is a consideration for very small samples, for which losing the majority of cells may simply not be tolerable.

Sensitivity

There are also limitations to the sensitivity of mass cytometry as currently implemented. Bendall et al. have compared the sensitivity of mass and fluorescence cytometry (7) and make two important points. First, there is no mass channel with equal resolution sensitivity to the brightest available fluorophores. However, this can be partially overcome by the use of multiple markers to define cell populations. Second, while there is a range of sensitivity according to atomic mass, it is considerably less than the sensitivity difference between the brightest and dimmest commercial fluorophores. Thus, one is left with a platform that can analyze many parameters in combination but that is not always sensitive enough for reliable single-channel resolution of populations displaying the least-abundant cellular markers.

Spillover and Contamination

Finally, there is the issue of signal contamination. The notion that there is no spillover in mass cytometry is not formally correct. Spillover between mass channels can come from a variety of sources. One is isotopic impurity; while the vast majority of isotopes sold for mass cytometry are highly pure, there are some that contain a few percentages of contaminating ions of known, and different, atomic mass (AM). Another source of spillover is detector infidelity, which results most frequently in a small signal in the next-highest AM channel (so-called M+1 spillover). This has purportedly been improved with the second generation of the CyTOF instrument. A third source of spillover is oxidation, whereby incomplete plasma ionization results in oxidation products, which are seen in the M+16 channel. This is controlled, albeit to a variable degree, by optimal tuning of the makeup gas flow rate (23). It is also most pronounced in the lower atomic mass range, with insignificant oxidation above AM 170. Observed spillovers across the mass range of the CyTOF, using antibody conjugate-labeled capture beads, are shown in Fig. 3. In addition to these sources of spillover, there can also be frank contamination of the sample with extraneous heavy metals, which can derive from sources such as the plasticware, buffers, or carryover from previously run samples.

Because of the presence of minor spillover in at least some mass cytometry experiments, panel design still requires certain considerations, though not to the same degree as highly multiparametric fluorescence flow cytometry. Guidelines for panel design have been recently published by our group (8).

Data Analysis

It seems unfair to list as a limitation the overwhelming amount of data generated by mass cytometry, since this is inherently an advantage. Yet, making sense of such complex data does provide a challenge. Fortunately, there are already several visualization approaches that have proven helpful for displaying and interpreting these data sets. The first and most widely used is SPADE (15), which is a clustering algorithm that organizes the found clusters by their relatedness in a dendrogram that can then be compared between samples. An example is shown in Fig. 4.

A similar visualization approach, but one which displays the relatedness of individual cells, rather than clusters, is viSNE (20). Both SPADE and viSNE have been shown to be capable of identifying and tracking rare cell populations, including hematopoietic stem cells and minimal residual leukemia cells, respectively.

Heat maps and principal component analysis (PCA) have also been used to display and analyze mass cytometry data (10). These both allow for display of individual cells, although heat maps become overwhelming with high numbers and complexity of cells. PCA is very useful for showing differences between cell populations but does not immediately show the parameters responsible for the differences. These can, however, be inferred from examination of the factors contributing to weighting of the PCA components.

PHOSPHO-FLOW

The use of antibodies to quantitate phosphorylated forms of signaling proteins is often termed "phospho-flow." It is a technology also pioneered in the Nolan lab (24), several years before the rise of mass cytometry. Like other functional assays, such as intracellular cytokine staining, phospho-flow has the advantage of not only enumerating cell lineages and cell surface phenotypes but also simultaneously quantitating their responsiveness to various kinds of stimuli. This can yield more robust differentiation of normal and disease states than is possible by examination of resting cells alone (24, 25). Phospho-flow has been applied in particular to the study of lymphomas (24, 25) and systemic lupus erythematosus (26) as well as normal immune cell subset differentiation (27). It has also been shown to be useful for *in vitro* drug screening (28).

Technical Considerations

Functional assays such as phospho-flow are more complex than phenotypic assays in that they involve a biological activation step as well as fixation, permeabilization, and intracellular staining. All of these steps can increase variability compared to an assay that requires only cell surface phenotyping. Methodological reviews have been published (13),

Detector median dual counts

Bead Label	Pr 141	Pr 142	Nd 143	Nd 144	Nd 145	Nd 146	Sm 147	Nd 148	Sm 149	Nd 150	Eu 151	Sm 152	Eu 153	Sm 154	Gd 155	Gd 156	Gd 157	Gd 158	Tb 159	Gd 160	Dy 161	Dy 162	Dy 164	Ho 165	Er 166	Er 167	Er 168	Tm 169	Er 170	Yb 171	Yb 172	Yb 173	Yb 174	Lu 175	Yb 176	Hf 177	Hf 178	Hf 179	Hf 180	Ta 181	W 182	W 183	W 184	Re 185	W 186	Re 187	Os 188	Os 189	Os 190	Ir 191	Os 192	Ir 193
Pr141	115	-0.2	-0.5	-0.5	-0.5	-0.5	-0.5	-0.5	-0.5	-0.5	-0.5	-0.5	-0.5	-0.5	-0.5	-0.5	-0.5	1.6	-0.5	-0.5	-0.5	-0.5	-0.5	-0.5	-0.5	-0.5	-0.5	-0.5	-0.5	-0.5	-0.5	-0.5	-0.5	-0.5	-0.5	-0.5	-0.5	-0.5	-0.5	-0.5	-0.5	-0.5	-0.5	-0.5	-0.5	-0.5	-0.5	-0.5	-0.5	-0.5	-0.5	-0.5
Pr142	-0.5	226	0.9	-0.4	-0.5	-0.4	-0.5	-0.5	-0.5	-0.5	-0.5	-0.5	-0.5	-0.4	-0.5	-0.5	-0.5	6.6	-0.4	-0.5	-0.5	-0.5	-0.5	-0.5	-0.5	-0.5	-0.5	-0.5	-0.5	-0.5	-0.5	-0.5	-0.5	-0.5	-0.5	-0.5	-0.5	-0.5	-0.5	-0.5	-0.5	-0.5	-0.5	-0.5	-0.5	-0.5	-0.5	-0.5	-0.5	-0.5	-0.5	-0.5
Nd143	-0.5	-0.4	107	1.1	-0.4	-0.5	-0.5	-0.5	-0.5	-0.5	-0.5	-0.5	-0.5	-0.5	-0.5	-0.5	-0.5	-0.5	2.5	-0.5	-0.5	-0.5	-0.5	-0.5	-0.5	-0.5	-0.5	-0.5	-0.5	-0.5	-0.5	-0.5	-0.5	-0.5	-0.5	-0.5	-0.5	-0.5	-0.5	-0.5	-0.5	-0.5	-0.5	-0.5	-0.5	-0.5	-0.5	-0.5	-0.5	-0.5	-0.5	-0.5
Nd144	-0.5	-0.5	-0.4	111	-0.1	-0.4	-0.5	-0.5	-0.5	-0.5	-0.5	-0.5	-0.5	-0.5	-0.5	-0.5	-0.5	-0.5	-0.5	2.4	-0.5	-0.5	-0.5	-0.6	-0.5	-0.5	-0.5	-0.5	-0.5	-0.5	-0.5	-0.5	-0.5	-0.5	-0.5	-0.5	-0.5	-0.5	-0.5	-0.5	-0.5	-0.5	-0.5	-0.5	-0.5	-0.5	-0.5	-0.5	-0.5	-0.5	-0.5	-0.5
Nd145	-0.5	-0.5	-0.5	-0.3	137	2.3	-0.5	-0.5	-0.5	-0.5	-0.5	-0.5	-0.5	-0.5	-0.5	-0.5	-0.5	-0.5	-0.5	-0.5	2.0	-0.4	-0.5	-0.5	-0.5	-0.5	-0.5	-0.5	-0.5	-0.5	-0.5	-0.5	-0.5	-0.5	-0.5	-0.5	-0.5	-0.5	-0.5	-0.5	-0.5	-0.5	-0.5	-0.5	-0.5	-0.5	-0.5	-0.5	-0.5	-0.5	-0.5	-0.5
Nd146	-0.5	-0.4	-0.4	-0.4	-0.3	102	1.1	-0.3	-0.5	-0.4	-0.5	-0.5	-0.5	-0.5	-0.5	-0.5	-0.5	-0.5	-0.5	-0.5	-0.5	8.3	-0.5	-0.4	-0.5	-0.5	-0.5	-0.5	-0.5	-0.5	-0.5	-0.5	-0.5	-0.5	-0.5	-0.5	-0.5	-0.5	-0.5	-0.5	-0.5	-0.5	-0.5	-0.5	-0.5	-0.5	-0.5	-0.5	-0.5	-0.5	-0.5	-0.5
Sm147	-0.5	-0.5	-0.5	-0.5	-0.5	-0.4	215	5.3	-0.1	-0.4	-0.5	-0.3	-0.5	-0.4	-0.5	-0.5	-0.5	-0.5	-0.5	-0.5	-0.5	-0.5	-0.5	-0.5	-0.4	-0.5	-0.5	-0.5	-0.5	-0.5	-0.5	-0.5	-0.5	-0.5	-0.5	-0.5	-0.5	-0.5	-0.5	-0.5	-0.5	-0.5	-0.5	-0.5	-0.5	-0.5	-0.5	-0.5	-0.5	-0.5	-0.5	-0.5
Nd148	-0.5	-0.5	-0.5	-0.4	-0.5	-0.4	-0.5	126	-0.2	-0.4	-0.5	-0.5	-0.5	-0.5	-0.5	-0.5	-0.5	-0.5	-0.5	-0.5	-0.5	-0.5	1.3	-0.5	-0.5	-0.5	-0.5	-0.5	-0.5	-0.5	-0.5	-0.5	-0.5	-0.5	-0.5	-0.5	-0.5	-0.5	-0.5	-0.5	-0.5	-0.5	-0.5	-0.5	-0.5	-0.5	-0.5	-0.5	-0.5	-0.5	-0.5	-0.5
Sm149	-0.5	-0.5	-0.5	-0.5	-0.5	-0.5	-0.4	-0.2	139	2.1	-0.4	-0.3	-0.5	-0.4	-0.5	-0.5	-0.5	-0.5	-0.5	-0.5	-0.5	-0.5	-0.5	-0.2	-0.5	-0.5	-0.5	-0.5	-0.5	-0.5	-0.5	-0.5	2.9	-0.5	-0.5	-0.5	-0.5	-0.5	-0.5	-0.5	-0.5	-0.5	-0.5	-0.5	-0.5	-0.5	-0.5	-0.5	-0.5	-0.5	-0.5	-0.5
Nd150	-0.5	-0.4	-0.5	-0.4	-0.5	-0.4	-0.5	-0.4	-0.4	162	0.3	-0.4	-0.5	-0.5	-0.5	-0.5	-0.5	-0.5	-0.5	-0.5	-0.5	-0.5	-0.5	-0.5	2.0	-0.5	-0.5	-0.5	-0.5	-0.5	-0.5	-0.5	-0.5	-0.5	-0.5	-0.5	-0.5	-0.5	-0.5	-0.5	-0.5	-0.5	-0.5	-0.5	-0.5	-0.5	-0.5	-0.5	-0.5	-0.5	-0.5	-0.5
Eu151	-0.5	-0.5	-0.5	-0.5	-0.5	-0.5	-0.5	-0.5	-0.5	-0.4	354	1.7	0.3	-0.5	-0.5	-0.5	-0.5	-0.5	-0.5	-0.5	-0.5	-0.5	-0.5	-0.5	-0.5	-0.5	-0.5	-0.5	-0.5	-0.5	-0.5	-0.5	-0.5	-0.5	-0.5	-0.5	-0.5	-0.5	-0.5	-0.5	-0.5	-0.5	-0.5	-0.5	-0.5	-0.5	-0.5	-0.5	-0.5	-0.5	-0.5	-0.5
Sm152	-0.5	-0.5	-0.5	-0.5	-0.5	-0.5	-0.5	-0.5	-0.5	-0.4	-0.4	176	0.5	-0.3	-0.5	-0.5	-0.5	-0.5	-0.5	-0.5	-0.5	-0.5	-0.5	-0.5	-0.5	-0.5	-0.3	-0.5	-0.5	-0.5	-0.5	-0.5	-0.5	-0.5	-0.5	-0.5	-0.5	-0.5	-0.5	-0.5	-0.5	-0.5	-0.5	-0.5	-0.5	-0.5	-0.5	-0.5	-0.5	-0.5	-0.5	-0.5
Eu153	-0.5	-0.5	-0.5	-0.5	-0.5	-0.5	-0.5	-0.5	-0.5	-0.5	-0.4	-0.4	339	1.0	-0.4	-0.5	-0.5	-0.5	-0.5	-0.5	-0.5	-0.5	-0.5	-0.5	-0.5	-0.5	-0.5	-0.5	-0.5	-0.5	-0.5	-0.5	-0.5	-0.5	-0.5	-0.5	-0.5	-0.5	-0.5	-0.5	-0.5	-0.5	-0.5	-0.5	-0.5	-0.5	-0.5	-0.5	-0.5	-0.5	-0.5	-0.5
Sm154	-0.5	-0.5	-0.5	-0.5	-0.5	-0.5	-0.5	-0.5	-0.5	-0.4	-0.5	1.3	-0.3	654	2.0	-0.4	-0.5	-0.5	-0.5	-0.5	-0.5	-0.5	-0.5	-0.5	-0.5	-0.5	-0.5	-0.5	-0.5	1.6	-0.5	-0.5	-0.5	-0.4	-0.5	-0.5	-0.5	-0.5	-0.5	-0.5	-0.5	-0.5	-0.5	-0.5	-0.5	-0.5	-0.5	-0.5	-0.5	-0.5	-0.5	-0.5
Gd155	-0.5	-0.5	-0.5	-0.5	-0.5	-0.5	-0.5	-0.5	-0.5	-0.5	-0.5	-0.5	-0.5	-0.4	185	6.3	-0.3	-0.4	-0.5	-0.4	-0.5	-0.5	-0.5	-0.5	-0.5	-0.5	-0.5	-0.5	-0.5	-0.5	-0.2	-0.5	-0.5	-0.5	-0.5	-0.5	-0.5	-0.5	-0.5	-0.5	-0.5	-0.5	-0.5	-0.5	-0.5	-0.5	-0.5	-0.5	-0.5	-0.5	-0.5	-0.5
Gd156	-0.5	-0.5	-0.5	-0.5	-0.5	-0.5	-0.5	-0.5	-0.5	-0.5	-0.5	-0.5	-0.5	-0.4	1.1	387	8.7	0.7	-0.5	-0.4	-0.5	-0.5	-0.5	-0.5	-0.5	-0.5	-0.5	-0.5	-0.5	-0.5	-0.5	2.5	-0.4	-0.5	-0.4	-0.5	-0.5	-0.5	-0.5	-0.5	-0.5	-0.5	-0.5	-0.5	-0.5	-0.5	-0.5	-0.5	-0.5	-0.5	-0.5	-0.5
Gd157	-0.5	-0.5	-0.5	-0.5	-0.5	-0.5	-0.5	-0.5	-0.5	-0.5	-0.5	-0.5	-0.5	-0.5	-0.2	11.9	5500	4.2	-0.5	-0.5	-0.5	-0.5	-0.5	-0.5	-0.5	-0.5	-0.5	-0.5	-0.5	-0.5	-0.5	-0.5	-0.3	-0.5	-0.5	-0.5	-0.5	-0.5	-0.5	-0.5	-0.5	-0.5	-0.5	-0.5	-0.5	-0.5	-0.5	-0.5	-0.5	-0.5	-0.5	-0.5
Gd158	-0.5	-0.5	-0.5	-0.5	-0.5	-0.5	-0.5	-0.5	-0.5	-0.5	-0.5	-0.5	-0.5	-0.5	-0.3	0.1	12.0	1177	14.1	4.0	-0.5	-0.5	-0.5	-0.5	-0.5	-0.5	-0.5	-0.5	-0.5	-0.5	-0.5	-0.5	-0.5	-0.5	-0.5	-0.5	-0.5	-0.5	-0.5	-0.5	-0.5	-0.5	-0.5	-0.5	-0.5	-0.5	-0.5	-0.5	-0.5	-0.5	-0.5	-0.5
Tb159	-0.5	-0.5	-0.5	-0.5	-0.5	-0.5	-0.5	-0.5	-0.5	-0.5	-0.5	-0.5	-0.5	-0.5	-0.5	-0.5	-0.5	-0.3	1377	3.8	-0.4	-0.5	-0.5	-0.5	-0.5	-0.5	-0.5	-0.5	-0.5	-0.5	-0.5	-0.5	-0.5	-0.5	-0.5	-0.5	-0.5	-0.5	-0.5	-0.5	-0.5	-0.5	-0.5	-0.5	-0.5	-0.5	-0.5	-0.5	-0.5	-0.5	-0.5	-0.5
Gd160	-0.5	-0.5	-0.5	-0.5	-0.5	-0.5	-0.5	-0.5	-0.5	-0.5	-0.5	-0.5	-0.5	-0.5	-0.3	-0.1	-0.2	2.3	-0.4	2831	0.8	-0.5	-0.5	-0.5	-0.5	-0.5	-0.5	-0.5	-0.5	-0.5	-0.5	-0.5	-0.5	-0.5	-0.5	-0.5	-0.5	-0.5	-0.5	-0.5	-0.5	-0.5	-0.5	-0.5	-0.5	-0.5	-0.5	-0.5	-0.5	-0.5	-0.5	-0.5
Dy161	-0.5	-0.5	-0.5	-0.5	-0.5	-0.5	-0.5	-0.5	-0.5	-0.5	-0.5	-0.5	-0.5	-0.5	-0.5	-0.5	-0.5	-0.5	-0.5	-0.4	137	4.2	-0.4	-0.5	-0.5	-0.5	-0.5	-0.5	-0.5	-0.5	-0.5	-0.5	-0.5	-0.5	-0.5	-0.4	-0.5	-0.5	-0.5	-0.5	-0.5	-0.5	-0.5	-0.5	-0.5	-0.5	-0.5	-0.5	-0.5	-0.5	-0.5	-0.5
Dy162	-0.5	-0.5	-0.5	-0.5	-0.5	-0.5	-0.5	-0.5	-0.5	-0.5	-0.5	-0.5	-0.5	-0.5	-0.5	-0.5	-0.5	-0.5	-0.5	-0.4	5.2	917	0.3	-0.5	-0.5	-0.5	-0.5	-0.5	-0.5	-0.5	-0.5	-0.5	-0.5	-0.5	-0.5	-0.5	0.4	-0.5	-0.5	-0.5	-0.5	-0.5	-0.5	-0.5	-0.5	-0.5	-0.5	-0.5	-0.5	-0.5	-0.5	-0.5
Dy164	-0.5	-0.5	-0.4	-0.5	-0.5	-0.5	-0.5	-0.5	-0.5	-0.5	-0.5	-0.5	-0.5	-0.5	-0.5	-0.5	-0.5	-0.5	-0.5	-0.4	-0.2	0.5	1406	3.5	-0.3	-0.5	-0.5	-0.5	-0.4	-0.5	-0.5	-0.5	-0.5	-0.5	-0.5	-0.5	-0.5	-0.5	-0.5	9.1	-0.4	-0.4	-0.5	-0.5	-0.5	-0.5	-0.5	-0.5	-0.5	-0.5	-0.5	-0.5
Ho165	-0.5	-0.5	-0.5	-0.5	-0.5	-0.5	-0.5	-0.5	-0.5	-0.5	-0.5	-0.5	-0.5	-0.5	-0.5	-0.5	-0.5	-0.5	-0.5	-0.5	-0.5	-0.5	-0.3	371	2.3	-0.3	-0.5	-0.5	-0.5	-0.5	-0.5	-0.5	-0.5	-0.5	-0.5	-0.5	-0.5	-0.5	-0.5	-0.5	1.7	-0.5	-0.5	-0.5	-0.5	-0.5	-0.5	-0.5	-0.5	-0.5	-0.5	-0.5
Er166	-0.5	-0.5	-0.5	-0.5	-0.5	-0.5	-0.5	-0.5	-0.5	-0.5	-0.5	-0.5	-0.5	-0.5	-0.5	-0.5	-0.5	-0.5	-0.5	-0.5	-0.5	-0.5	-0.4	-0.3	417	4.5	-0.1	-0.5	-0.4	-0.5	-0.5	-0.5	-0.5	-0.5	-0.5	-0.5	-0.5	-0.5	-0.5	-0.5	-0.5	2.5	-0.4	-0.5	-0.5	-0.5	-0.5	-0.5	-0.5	-0.5	-0.5	-0.5
Er167	-0.5	-0.5	-0.5	-0.5	-0.5	-0.5	-0.5	-0.5	-0.5	-0.5	-0.5	-0.5	-0.5	-0.5	-0.5	-0.5	-0.5	-0.5	-0.5	-0.5	-0.5	-0.5	-0.5	-0.5	0.0	188	3.9	-0.3	-0.4	-0.5	-0.5	-0.5	-0.5	-0.5	-0.5	-0.5	-0.5	-0.5	-0.5	-0.5	-0.5	-0.5	0.4	-0.5	-0.5	-0.5	-0.5	-0.5	-0.5	-0.5	-0.5	-0.5
Er168	-0.5	-0.5	-0.5	-0.5	-0.5	-0.5	-0.5	-0.5	-0.4	-0.5	-0.5	-0.5	-0.5	-0.5	-0.5	-0.5	-0.5	-0.5	-0.5	-0.5	-0.5	-0.5	-0.5	-0.4	-0.1	4.1	756	4.3	-0.1	-0.5	-0.5	-0.5	-0.5	-0.5	-0.5	-0.5	-0.5	-0.5	-0.5	-0.5	-0.5	-0.5	-0.5	6.8	-0.4	-0.5	-0.5	-0.5	-0.5	-0.5	-0.5	-0.5
Tm169	-0.5	-0.5	-0.5	-0.5	-0.5	-0.5	-0.5	-0.5	-0.5	-0.5	-0.5	-0.5	-0.5	-0.5	-0.5	-0.5	-0.5	-0.5	-0.5	-0.5	-0.5	-0.5	-0.5	-0.5	-0.5	-0.5	-0.4	763	1.1	-0.5	-0.5	-0.5	-0.5	-0.5	-0.5	-0.5	-0.5	-0.5	-0.5	-0.5	-0.5	-0.5	-0.5	-0.5	-0.5	-0.4	-0.5	-0.5	-0.5	-0.5	-0.5	-0.5
Er170	-0.5	-0.5	-0.5	-0.5	-0.5	-0.5	-0.5	-0.5	-0.5	-0.5	-0.5	-0.5	-0.5	-0.5	-0.5	-0.5	-0.5	-0.5	-0.5	-0.5	-0.5	-0.5	-0.5	-0.5	-0.1	-0.2	0.9	-0.3	354	3.0	-0.3	-0.5	-0.5	-0.5	-0.5	-0.5	-0.5	-0.5	-0.5	-0.5	-0.5	-0.5	-0.5	-0.5	-0.5	-0.5	3.3	-0.5	-0.5	-0.5	-0.5	-0.5
Yb171	-0.5	-0.5	-0.5	-0.5	-0.5	-0.5	-0.5	-0.5	-0.5	-0.5	-0.5	-0.5	-0.5	-0.5	-0.5	-0.5	-0.5	-0.5	-0.5	-0.5	-0.5	-0.5	-0.5	-0.5	-0.5	-0.5	-0.5	-0.5	-0.4	128	2.9	-0.4	-0.4	-0.5	-0.5	-0.5	-0.5	-0.5	-0.5	-0.5	-0.5	-0.5	-0.5	-0.5	-0.5	-0.5	-0.5	-0.5	-0.5	-0.5	-0.5	-0.5
Yb172	-0.5	-0.5	-0.5	-0.5	-0.5	-0.5	-0.5	-0.5	-0.5	-0.5	-0.5	-0.5	-0.5	-0.5	-0.5	-0.5	-0.5	-0.5	-0.5	-0.5	-0.5	-0.5	-0.5	-0.5	-0.5	-0.5	-0.5	-0.5	-0.5	-0.2	46.8	7.3	-0.1	-0.5	-0.5	-0.5	-0.5	-0.5	-0.5	-0.5	-0.5	-0.5	-0.5	-0.5	-0.5	-0.5	-0.5	-0.5	-0.5	-0.5	-0.5	-0.5
Yb173	-0.5	-0.5	-0.5	-0.5	-0.4	-0.5	-0.5	-0.5	-0.5	-0.5	-0.5	-0.5	-0.5	-0.5	-0.5	-0.5	-0.5	-0.5	-0.5	-0.5	-0.5	-0.5	-0.5	-0.5	-0.5	-0.5	-0.5	-0.5	-0.5	-0.3	7.1	564	20.9	-0.2	-0.4	-0.5	-0.5	-0.5	-0.5	-0.5	-0.5	-0.5	-0.5	-0.5	-0.5	-0.5	-0.5	-0.5	-0.5	-0.5	-0.5	-0.5
Yb174	-0.5	-0.5	-0.5	-0.5	-0.5	-0.5	-0.5	-0.5	-0.5	-0.5	-0.5	-0.5	-0.5	-0.5	-0.5	-0.5	-0.5	-0.5	-0.5	-0.5	-0.5	-0.5	-0.5	-0.5	-0.5	-0.5	-0.5	-0.5	-0.4	-0.4	-0.2	2.7	1272	5.3	-0.1	-0.5	-0.5	-0.5	-0.5	-0.5	-0.5	-0.5	-0.5	-0.5	-0.5	-0.5	-0.5	-0.5	-0.4	-0.5	-0.5	-0.5
Lu175	-0.5	-0.5	-0.5	-0.5	-0.5	-0.5	-0.5	-0.5	-0.5	-0.5	-0.5	-0.5	-0.5	-0.5	-0.5	-0.5	-0.5	-0.5	-0.5	-0.5	-0.5	-0.5	-0.5	-0.5	-0.5	-0.5	-0.5	-0.5	-0.5	-0.5	-0.5	-0.5	-0.4	240	4.6	-0.3	-0.5	-0.5	-0.5	-0.5	-0.5	-0.5	-0.5	-0.5	-0.5	-0.5	-0.5	-0.5	-0.5	0.7	-0.5	-0.5
Yb176	-0.5	-0.5	-0.5	-0.5	-0.5	-0.5	-0.5	-0.5	-0.5	-0.5	-0.5	-0.5	-0.5	-0.5	-0.5	-0.4	-0.5	-0.5	-0.5	-0.5	-0.5	-0.5	-0.5	-0.5	-0.5	-0.5	-0.5	-0.5	-0.5	-0.5	-0.5	-0.5	-0.4	1.2	-0.3	200	2.4	-0.3	-0.5	-0.5	-0.5	-0.5	-0.5	-0.5	-0.5	-0.5	-0.5	-0.5	-0.5	-0.5	-0.5	-0.5

FIGURE 3 Spillover across the mass window of the CyTOF. Antibody capture beads were labeled with antibody conjugates for each of the indicated metals and collected on the CyTOF in cell mode. The relative percentage of signal in each detector channel is as shown. Note the major signals outside of the primary channel tend to occur in M+1 and (for certain isotopes) M+16 channels. The former is largely due to detector infidelity, while the latter is due to oxidation, a partially preventable consequence of incomplete plasma ionization. Occasional signals are seen in other channels, and these are generally a result of specific isotopic impurities. Data courtesy of Michael Leipold, Stanford University.

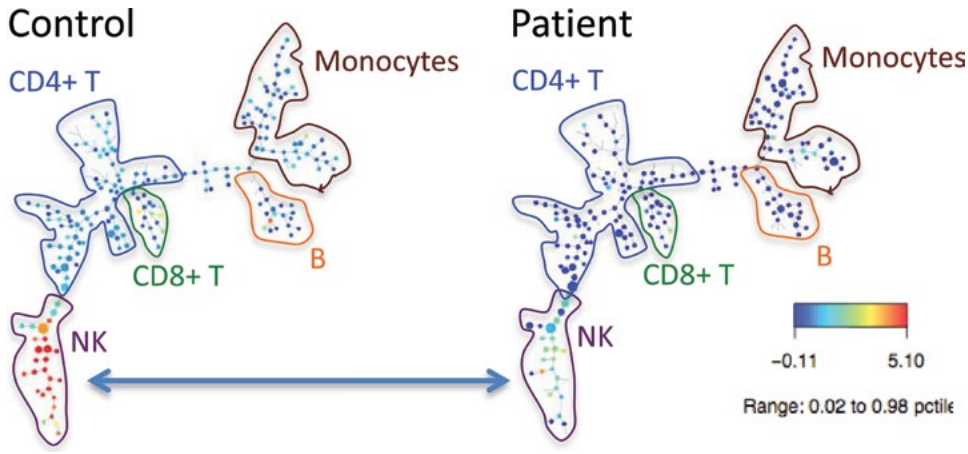

FIGURE 4 Example of SPADE analysis. Peripheral blood mononuclear cells from a healthy donor and a cancer patient were stained for surface and intracellular markers and analyzed by CyTOF. Clustering was performed in SPADE (15) using major cell surface lineage markers. The major cell lineages were annotated by examination of the staining patterns of these markers. The distribution of other markers can then be visualized, as shown here for granzyme B. Note the lack of granzyme B expression in the cancer patient relative to the control. pctile, percentile. Data courtesy of Serena Chang and Holbrook Kohrt, Stanford University.

so a complete discussion will not be attempted here. Rather, selected key considerations will be presented.

Optimization of a phospho-flow assay requires selection of stimulus concentration, timing of stimulation, selection of appropriate antibodies, titration of antibodies, selection of fixation and permeabilization buffers, and choice of staining conditions (especially pre- versus postpermeabilization staining).

Stimuli

Stimuli can include cytokines, antibodies to B-cell and T-cell receptors, and Toll-like receptor agonists, among others. These stimulations are sometimes measured in the presence or absence of a drug (28) to measure *in vitro* pharmacodynamics at a single-cell level. While most signaling events are measured in a time scale of minutes, we have seen phospho-flow assays that perform optimally with as little as 2 to 4 min of stimulation (e.g., pPLCγ2), while others are readily detectable even after 2 h (e.g., pS6). Most stimuli, such as cytokines, are usually used at saturating concentrations, but in some cases, dose-response effects may be of interest and titered doses can be used.

Antibodies

Commercially available phosphospecific antibodies, when marketed for use in flow cytometry, generally perform acceptably, but there can be clone-specific and vendor-specific differences. While many antibodies are sold pretitered, some are not, and performance of a titration curve is advisable in any case.

Fixation and Permeabilization

There are multiple fixation and permeabilization buffers on the market, since not all phosphospecific antibodies perform equally well with a single buffer system. In general, detection of intranuclear targets, such as pSTAT molecules, requires harsher permeabilization (usually methanol). Detection of cytoplasmic targets (pErk and pAkt, etc.) is compatible (and sometimes even optimal) with gentler, detergent-based permeabilization (e.g., saponin).

Staining of Cell Surface Epitopes

A conundrum in phospho-flow protocols is whether to stain for cell surface epitopes before or after permeabilization. In fact, there are a very limited number of antibody clones to cell surface markers that perform well on methanol-permeabilized cells, and even saponin permeabilization compromises most cell surface epitopes. Yet staining prior to permeabilization has two caveats: it still must be performed postfixation (to preserve the phosphorylation state of the cells), and protein fluorophores can be destroyed by alcohol-based permeabilization buffers. The latter issue is avoided fairly easily by using small-molecule fluorophores for cell surface staining. The former issue, however, means that some cell surface epitopes will be poorly detected in phospho-flow and should be relegated to live cell-staining assays only. Even antibodies to some relatively bright major lineage markers, like CD14 and CD16, can suffer tremendously when used on fixed epitopes. In these cases, choice of an optimal clone and careful titration are necessary. There is also online information from manufacturers to help in this regard (e.g., http://www.bdbiosciences.com/documents/antibodies_human_cellsurface_marker.pdf#search=phospho-flow).

Data Analysis

In general, phospho-flow experiments are analyzed by sequential gating to deconvolve barcoded populations (if applicable) and to identify the cell subsets of interest. This is followed by quantitation of the phosphospecific antibody-staining intensities in each of these cell populations. These intensities have been summarized as either the median or 90th percentile fluorescence; the latter statistic has the advantage of being more sensitive to detecting shifts in fluorescence involving only a minor subset of the cells. From these fluorescence values, relative change (stimulated/unstimulated) can be calculated and displayed in a heat map. Software such as Cytobank and SPADE can automatically calculate and display relative change heat maps (Fig. 5).

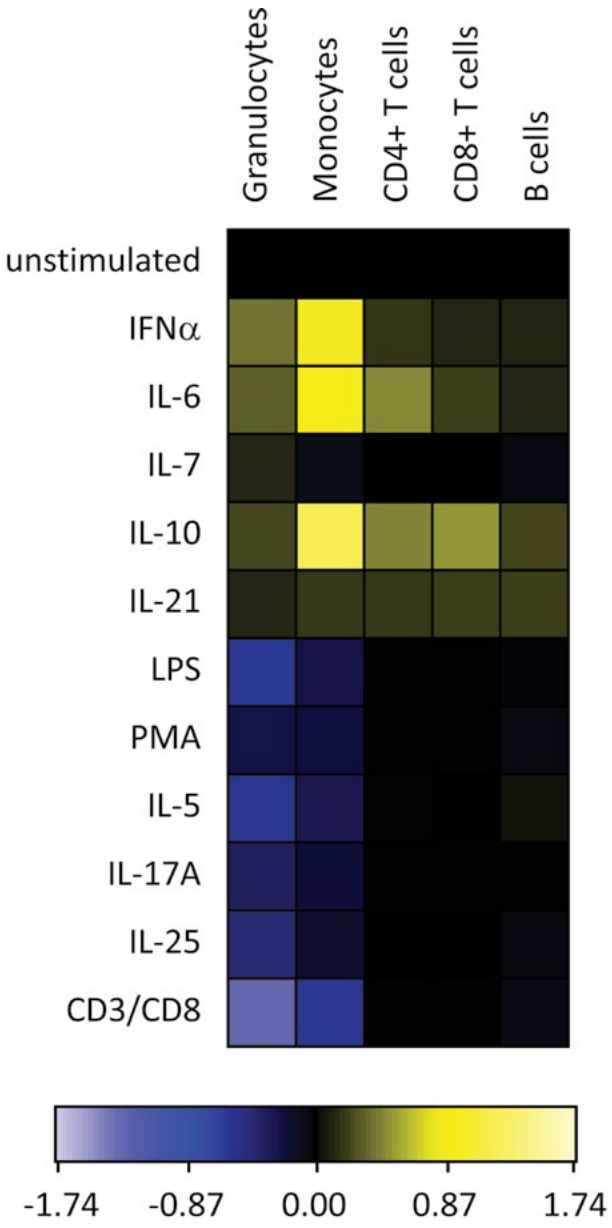

FIGURE 5 Example of heat map calculation in Cytobank. Upon analysis of phospho-CyTOF data, readout of phosphorylation signal changes in each sample can be displayed as a heat map. Here we see pSTAT5 induction in five major cell lineages (columns) with 12 different stimulation conditions (rows), for a healthy control peripheral blood mononuclear cell sample. For CyTOF data, an arcsinh transformation of the median intensity signal was performed in the software and the arcsinh ratio relative to the unstimulated sample was displayed using the color scale indicated. Relative change using medians or percentile statistics, along with other data transformations, are also available in the software. IFN, interferon; IL, interleukin; LPS, lipopolysaccharide; PMA, phorbol myristate acetate. Data courtesy of Rosemary Fernandez, Stanford University.

Combining Mass Cytometry and Phospho-Flow

The first application of mass cytometry to in-depth analysis of the immune system actually combined cell surface phenotyping and phosphoepitope analysis (9). However, in our experience, this has been the most difficult assay to optimize on the CyTOF platform. This is mainly because of the issue, mentioned above, that most antibodies to cell surface determinants show compromised staining of fixed epitopes. Since a major point of using mass cytometry for this application is to do a detailed phenotyping in combination with signaling analysis, there is a desire to use antibodies to cell surface markers beyond the most robust major lineage markers, and these are often the most difficult to resolve after fixation. Combined with this, the fact that CyTOF sensitivity is less than that of the best fluorophores in the fluorescence world means that very low abundance proteins (including some of the phosphoepitope targets) are very difficult to detect. Nevertheless, we have successfully created a panel that allows dissection of approximately 32 cell subsets (from Tregs to plasmablasts to pDCs) while simultaneously interrogating 8 different phosphorylated signaling intermediates (Table 1). When used with a panel of 8 standard stimuli, this results in a matrix of 2,048 potential readouts per sample. We are now using this panel with immune cells from a variety of diseases.

Such detailed fingerprinting of not only cell phenotypes but their underlying signaling capabilities will doubtless be useful for diagnosis, prognosis, and elucidation of disease mechanisms, provided it can be adequately standardized. We are already using a customized robotic liquid-handling system to help reduce staining and cell handling variability. A side benefit of this system is the ability to use less antibody, due to reproducibly lower residual volumes after washing and aspiration, with the robot than with manual handling.

CLINICAL APPLICATIONS

Will technologies as complex and demanding as mass cytometry and phospho-flow make it into the realm of clinical flow cytometry? I believe this is just a matter of time and of the right disease application. There are certainly many assays that do not require 40 parameters and for which simpler platforms will suffice. In general, mass cytometry should probably remain a research tool, with its ability to broadly probe the immune system, liberated from specific hypotheses. When biomarkers of clinical interest are identified, they can be transferred for clinical practice to a simpler (and less expensive) platform such as fluorescence flow cytometry or other methods.

However, a case can be made that some clinical applications are ready-made for mass cytometry. A seemingly obvious one is leukemia and lymphoma diagnosis. Here, the use of multiple fluorescence panels, often performed in succession based on the outcome of an initial screening cocktail, could be obviated by a single-tube mass cytometry staining. On the one hand, this would waste reagents, as it would use "all antibodies, all the time." But labor is usually far more costly in the clinical lab than reagents, and a single-tube staining would certainly save time. With one cocktail for complete diagnosis, this approach would be sample-sparing as well. Finally, given the already established importance of signaling for prognosis of B-cell lymphomas (25), the addition of phosphorylation analysis could increase the value of flow cytometry to clinical diagnosis of these tumors. Perhaps this could tip the scales towards raising flow cytometry from a second-line diagnostic for most leukemias and lymphomas to become the technology of choice.

As for the phospho-CyTOF assays, these might be thought of as yielding a "fingerprint" of the immune system at a cellular level. Whether we eventually derive relevant metrics of disease from these fingerprints, and whether the assays then make it into clinical practice (using CyTOF or

TABLE 1 Phospho-CyTOF panel optimized in the author's laboratory[a]

Metal label	Specificity	Clone (manufacturer)	Source
102–110Pd	Barcoding (opt)		
115In	Live/dead		
142Nd	CD19	HIB19	DVS
145Nd	CD4	RPA-T4	DVS
147Sm	CD20	H1 (BD)	In-house
149Sm	CD7	CD7-687 (BioLegend)	In-house
150Nd	CD3	UCHT1 (BD)	In-house
151Eu	CD123	9F5	DVS
152Sm	CD27	0323 (BioLegend)	In-house
153Eu	CD45RA	H100	DVS
154Sm	CD45 (opt)	HI30	DVS
156Gd	pp38	D3F9	DVS
157Gd	CD24	ML5 (BioLegend)	In-house
158Gd	pSTAT3	4/P-Stat3	DVS
159Tb	CD11c	Bu15	DVS
160Gd	CD14	M5E2	DVS
161Dy	IgD	IA6-2 (BioLegend)	In-house
162Dy	pErk1/2	20A (BD)	In-house
163Dy	IkBtot	L35A5 (CST)	In-house
164Dy	CD25	M-A251 (BD)	In-house
165Ho	pS6	N7-548 (BD)	In-house
166Er	CD16	B73.1 (BD)	In-house
167Er	CD38	HIT-2	DVS
168Er	CD8	SK1	DVS
169Tm	pSTAT1	4a (BD)	In-house
170Er	CD3	UCHT1	DVS
171Yb	CD66 (opt)	CD66a-B1.1	DVS
172Yb	pSTAT5	47/Stat5(pY694) (BD)	In-house
173Yb	pPLCg2	K86-68937 (BD)	In-house
174Yb	HLA-DR	L243	DVS
175Lu	CD56	HCD56 (BioLegend)	In-house
176Yb	CD127	A019D5	DVS

[a]Opt., optional; IgD, immunoglobulin D; CST, Cell Signaling Technologies; DVS, DVS Sciences (now Fluidigm).

a simpler platform), can only be speculated at present. But laboratories that provide research level assays for human studies might wish to learn the technologies of phospho-flow and CyTOF, as it's only with the accumulation of relevant human data that we have a chance of turning the speculation into reality.

I thank Michael Leipold, Serena Chang, Holbrook Kohrt, and Rosemary Fernandez for providing example data for figures.

This work was supported in part by grants 5U19AI05722909, 5U19AI09001904, and S10RR027582 from the NIAID, NIH.

REFERENCES

1. **Telford W, Kapoor V, Jackson J, Burgess W, Buller G, Hawley T, Hawley R.** 2006. Violet laser diodes in flow cytometry: an update. *Cytometry A* **69:**1153–1160.
2. **Chattopadhyay PK, Price DA, Harper TF, Betts MR, Yu J, Gostick E, Perfetto SP, Goepfert P, Koup RA, De Rosa SC, Bruchez MP, Roederer M.** 2006. Quantum dot semiconductor nanocrystals for immunophenotyping by polychromatic flow cytometry. *Nat Med* **12:**972–977.
3. **Chattopadhyay PK, Gaylord B, Palmer A, Jiang N, Raven MA, Lewis G, Reuter MA, Nur-ur Rahman AK, Price DA, Betts MR, Roederer M.** 2012. Brilliant violet fluorophores: a new class of ultrabright fluorescent compounds for immunofluorescence experiments. *Cytometry A* **81:**456–466.
4. **Tanner SD, Bandura DR, Ornatsky O, Baranov VI, Nitz M, Winnik MA.** 2008. Flow cytometer with mass spectrometer detection for massively multiplexed single-cell biomarker assay. *Pure Appl Chem* **80:**2627–2641.
5. **Bandura DR, Baranov VI, Ornatsky OI, Antonov A, Kinach R, Lou X, Pavlov S, Vorobiev S, Dick JE, Tanner SD.** 2009. Mass cytometry: technique for real time single cell multitarget immunoassay based on inductively coupled plasma time-of-flight mass spectrometry. *Anal Chem* **81:**6813–6822.
6. **Ornatsky O, Bandura D, Baranov V, Nitz M, Winnik MA, Tanner S.** 2010. Highly multiparametric analysis by mass cytometry. *J Immunol Methods* **361:**1–20.
7. **Bendall SC, Nolan GP, Roederer M, Chattopadhyay PK.** 2012. A deep profiler's guide to cytometry. *Trends Immunol* **33:**323–332.
8. **Leipold MD, Newell EW, Maecker HT.** 2015. Multiparameter phenotyping of human PBMCs using mass cytometry. *Methods Mol Biol* **1343:**81–95.
9. **Bendall SC, Simonds EF, Qiu P, Amir EAD, Krutzik PO, Finck R, Bruggner RV, Melamed R, Trejo A, Ornatsky OI, Balderas RS, Plevritis SK, Sachs K, Pe'er D, Tanner SD, Nolan GP.** 2011. Single-cell mass cytometry of differential immune and drug responses across a human hematopoietic continuum. *Science* **332:**687–696.
10. **Newell EW, Sigal N, Bendall SC, Nolan GP, Davis MM.** 2012. Cytometry by time-of-flight shows combinatorial cytokine expression and virus-specific cell niches within a continuum of CD8+ T cell phenotypes. *Immunity* **36:**142–152.
11. **Horowitz A, Strauss-Albee DM, Leipold M, Kubo J, Nemat-Gorgani N, Dogan OC, Dekker CL, Mackey S, Maecker H, Swan GE, Davis MM, Norman PJ, Guethlein LA, Desai M, Parham P, Blish CA.** 2013. Genetic and environmental determinants of human NK cell diversity revealed by mass cytometry. *Sci Transl Med* **5:**208ra145.
12. **van Dongen JJM, Lhermitte L, Böttcher S, Almeida J, van der Velden VHJ, Flores-Montero J, Rawstron A, Asnafi V, Lécrevisse Q, Lucio P, Mejstrikova E, Szczepański T, Kalina T, de Tute R, Brüggemann M, Sedek L, Cullen M, Langerak AW, Mendonça A, Macintyre E, Martin-Ayuso M, Hrusak O, Vidriales MB, Orfao A.** 2012. EuroFlow antibody panels for standardized n-dimensional flow cytometric immunophenotyping of normal, reactive and malignant leukocytes. *Leukemia* **26:**1908–1975.
13. **Perez OD, Mitchell D, Campos R, Gao GJ, Li L, Nolan GP.** 2005. Multiparameter analysis of intracellular phosphoepitopes in immunophenotyped cell populations by flow cytometry. *Curr Protoc Cytom* **6:**6.20.
14. **Lovelace P, Maecker HT.** 2011. Multiparameter intracellular cytokine staining. *Methods Mol Biol* **699:**165–178.
15. **Qiu P, Simonds EF, Bendall SC, Gibbs KD, Bruggner RV, Linderman MD, Sachs K, Nolan GP, Plevritis SK.** 2011. Extracting a cellular hierarchy from high-dimensional cytometry data with SPADE. *Nat Biotechnol* **29:**886–891.
16. **Bodenmiller B, Zunder ER, Finck R, Chen TJ, Savig ES, Bruggner RV, Simonds EF, Bendall SC, Sachs K, Krutzik PO, Nolan GP.** 2012. Multiplexed mass cytometry profiling of cellular states perturbed by small-molecule regulators. *Nat Biotechnol* **30:**858–867.

17. **Behbehani GK, Bendall SC, Clutter MR, Fantl WJ, Nolan GP.** 2012. Single-cell mass cytometry adapted to measurements of the cell cycle. *Cytometry A* **81:**552–566.
18. **Fienberg HG, Simonds EF, Fantl WJ, Nolan GP, Bodenmiller B.** 2012. A platinum-based covalent viability reagent for single-cell mass cytometry. *Cytometry A* **81:**467–475.
19. **Finck R, Simonds EF, Jager A, Krishnaswamy S, Sachs K, Fantl W, Pe'er D, Nolan GP, Bendall SC.** 2013. Normalization of mass cytometry data with bead standards. *Cytometry A* **83:**483–494.
20. **Amir EAD, Davis KL, Tadmor MD, Simonds EF, Levine JH, Bendall SC, Shenfeld DK, Krishnaswamy S, Nolan GP, Pe'er D.** 2013. viSNE enables visualization of high dimensional single-cell data and reveals phenotypic heterogeneity of leukemia. *Nat Biotechnol* **31:**545–552.
21. **Newell EW, Sigal N, Nair N, Kidd BA, Greenberg HB, Davis MM.** 2013. Combinatorial tetramer staining and mass cytometry analysis facilitate T-cell epitope mapping and characterization. *Nat Biotechnol* **31:**623–629.
22. **Newell EW, Klein LO, Yu W, Davis MM.** 2009. Simultaneous detection of many T-cell specificities using combinatorial tetramer staining. *Nat Methods* **6:**497–499.
23. **Leipold MD, Maecker HT.** 2012. Mass cytometry: protocol for daily tuning and running cell samples on a CyTOF mass cytometer. *J Vis Exp* **69:**e4398.
24. **Irish JM, Hovland R, Krutzik PO, Perez OD, Bruserud Ø, Gjertsen BT, Nolan GP.** 2004. Single cell profiling of potentiated phospho-protein networks in cancer cells. *Cell* **118:**217–228.
25. **Irish JM, Myklebust JH, Alizadeh AA, Houot R, Sharman JP, Czerwinski DK, Nolan GP, Levy R.** 2010. B-cell signaling networks reveal a negative prognostic human lymphoma cell subset that emerges during tumor progression. *Proc Natl Acad Sci USA* **107:**12747–12754.
26. **Hale MB, Krutzik PO, Samra SS, Crane JM, Nolan GP.** 2009. Stage dependent aberrant regulation of cytokine-STAT signaling in murine systemic lupus erythematosus. *PLoS One* **4:**e6756.
27. **Irish JM, Czerwinski DK, Nolan GP, Levy R.** 2006. Kinetics of B cell receptor signaling in human B cell subsets mapped by phosphospecific flow cytometry. *J Immunol* **177:**1581–1589.
28. **Krutzik PO, Crane JM, Clutter MR, Nolan GP.** 2007. High-content single-cell drug screening with phosphospecific flow cytometry. *Nat Chem Biol* **4:**132–142.

Functional Cellular Assays

section E

VOLUME EDITOR: BARBARA DETRICK
SECTION EDITOR: STEVEN D. DOUGLAS

Introduction

STEVEN D. DOUGLAS

26

A number of remarkable and seminal advances in basic immunology, molecular biology, cellular physiology, and molecular diagnosis have led to the development of new and unique assays. These techniques, in many instances, have been applied to both research and clinical laboratories. They afford unique sensitivity and specificity for a panoply of diagnostic laboratory procedures. This section of the *Manual* focuses on the laboratory-based assays related to functional cellular assays and their application to clinical diagnoses (Fig. 1). The chapters in this section include major aspects of these assays.

Adriana Weinberg presents a state-of-the-science approach to cryopreservation of peripheral blood mononuclear cells. This methodology offers several major advantages for *in vitro* studies, including assaying multiple samples in single runs (thus avoiding interassay variability), cost reduction through efficient utilization of labor and reagents, and meaningful comparisons for longitudinal studies.

Roshini Sarah Abraham has addressed, in detail, the methodology for the approach to studying lymphocyte activation. In this comprehensive chapter, she has provided the major approaches used in the diagnostic immunology laboratory, namely immune-phenotyping of cell surfaces or intercellular activation markers following a variety of stimuli and functional assays. These approaches include direct assessment of cell proliferation, downstream effects of lymphocyte activation, and lymphocyte cytotoxicity. These assays permit a determination of the activation status and immune competence of T cells as well as their interactions with other cells, including B cells, NK cells, and dendritic cells. Abraham has shown the interrelationships for the assessment of T cell antigen recognition, activation, expansion, proliferation, and postactivation functions related to effector and memory T cells. In addition, this chapter provides a basis for identification of natural killer cells and their subsets.

Moon H. Nahm and Robert L. Burton have described a series of methods for determining functional assays for B cells and antibodies. In this chapter, the types of B cells and their characterization are discussed. In addition, the functions of the humoral response related to the class of antibody and the differentiation states of B cells are analyzed. These include cell surface expression, the relationship of immunoglobulin class switching, and functional assays for B cell antibody defects. Approaches toward understanding B cell development as well as impairment of B cells in primary and secondary immune deficiencies are briefly considered. Functional titers for measuring serum antibodies are discussed, including those related to typical vaccine components of tetanus, diphtheria, pneumococcus, and *Haemophilus influenzae*. A series of assays, including whole-blood lymphocyte proliferation as well as those that utilize bactericidal function for antibodies and opsonophagocytosis assays, are considered. These B cell system analyses also require determination of the protein, to include immunoglobulin function, and they measure phagocytic killing of the various organisms. The chapter provides a wide array of approaches for determining functional assays for B cell function. In addition, a companion chapter is found in section K of this *Manual*, describing the approach toward severe combined immune deficiency newborn screening, by James Verbsky and John Routes. These authors review methods for determination of T cell receptor excision circles to screen for T cell lymphopenia, as well as various forms of severe combined immune deficiency (see chapter 74).

A methodology for the determination of antigen-specific T cells, by enzyme-linked immunosorbent spot (ELISPOT) assay, is described in chapter 30 by Barbara Shacklett and Douglas Nixon. In this chapter, the ELISPOT technology, as well as intracellular staining and tetramer staining, is discussed. The simplest of these, ELISPOT, offers some advantages over intracellular cytokine staining and major histocompatibility complex (MHC) class I tetramer staining. The ELISPOT assay has been modified to detect cytokine-secreting cells using nitrocellulose membranes and cytokine-specific monoclonal antibodies. ELISPOT detects both CD8 and CD4 T cell responses to antigens from a broad range of infectious agents, vaccine preparations, tumor antigens, and autoantigens. This technology is useful toward the comprehensive mapping of the T cell epitope.

The chapter by Theresa Whiteside is a detailed consideration of regulatory T cell (T-reg) assays. Whiteside provides a segue, determining the frequency and functions of the T-reg cells in relation to clinical disease. T-regs are a minor subset of CD4 cells, which can be phenotyped using flow-based phenotyping and their standardization, namely CD3, CD4, CD25, and Fox P3. In addition, negative expression of CD127 is relevant. Further, a variety of suppressor assays have had significant utility in determining the profile of regulatory T cells. These assays have been summarized in comprehensive tables of the characteristics of both N T-reg and

doi:10.1128/9781555818722.ch26

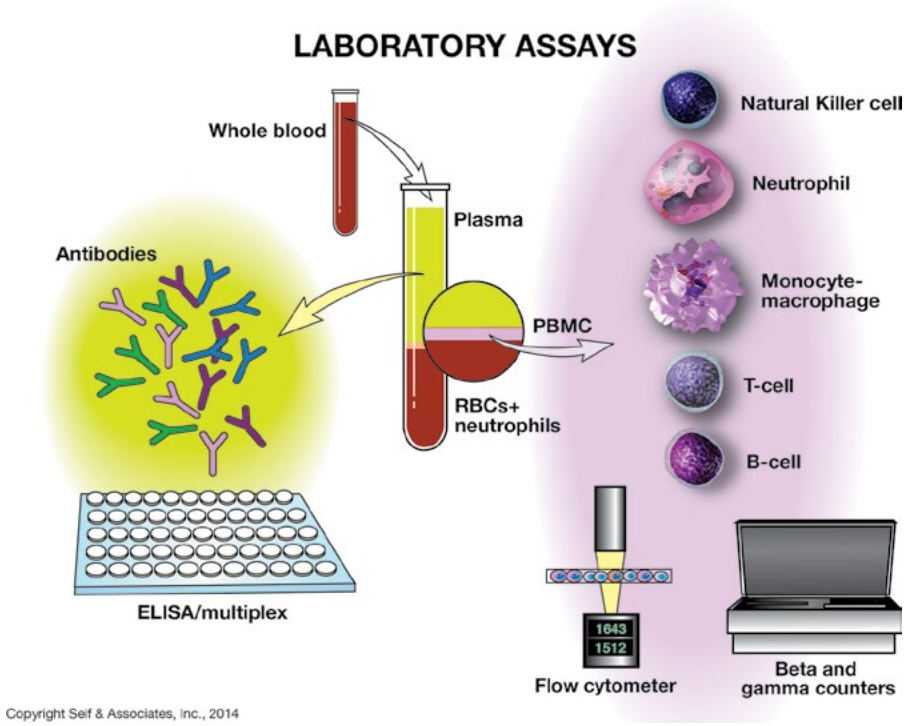

FIGURE 1 Laboratory-based assays related to functional cellular assays and their application to clinical diagnoses.

I T-reg cells and CD4 conventional T cells (see Table 1 in chapter 31). In addition, Whiteside has provided a summary of the functional assays for human N T-reg and I T-reg.

Samuel Chiang and Yenan Bryceson present a detailed chapter for the determination of NK cells, using multiparameter flow cytometry and assays for flow-cytometric measurements of NK phenotype and development. In addition, this chapter discusses the determination of functional responses of NK cells using a variety of target cells. Detailed procedures are provided for studies of the NK phenotype, using state-of-the-art-methodology.

Debra Long Priel and Douglas Kuhns report on the functional assays for the diagnosis of chronic granulomatous disease. Assays using activation of the NOX2 complex by phagocytic cells by flow cytometry are described in detail. In addition, the techniques for isolation and characterization of polymorphonuclear neutrophils are provided. Priel and Kuhns also provide molecular methodology for this diagnosis through immunoblot analysis of the phox subunits of NOX2. Their discussion is augmented by referring to a chapter in section K by Steven Holland (chapter 78), which discusses the overall clinical approach to neutropenia and neutrophil defects.

Related chapters in the sections on flow cytometry and immune deficiency closely interface with this section on functional cellular assays. A schematic overall diagram is provided to introduce the section of functional cellular assays (Fig. 1).

Cryopreservation of Peripheral Blood Mononuclear Cells

ADRIANA WEINBERG

27

The utility of cryopreserved peripheral blood mononuclear cells (PBMC) in clinical and diagnostic immunology is widely recognized. The use of cryopreserved PBMC offers multiple advantages for *in vitro* studies. The ability to batch specimens permits significant cost reductions through efficient utilization of labor and reagents and permits testing of multiple samples in a single run, thus avoiding interassay variability and providing more meaningful comparisons in longitudinal studies.

Immunologic assays on cryopreserved PBMC provide important endpoints for studies of natural history of disorders that may affect the immune system and clinical trials of therapeutic interventions and vaccines (1).

Transportation of frozen PBMC to laboratories for highly specialized tests has certain advantages over shipping fresh blood. Certain populations of blood cells have a limited life span outside the human body, whereas cryopreserved PBMC are stable for prolonged periods when adequately stored or shipped in liquid nitrogen tanks (2–4).

Tests developed after the collection of clinical samples can be applied to cryopreserved PBMC. This allows for utilization of archived samples obtained from well-characterized study subjects to answer new scientific questions and avoids costly and unnecessary repetition of clinical studies (3).

Finally, cryopreserved PBMC are used to treat congenital or iatrogenic immune defects. For example, *ex vivo* generation of anti-cytomegalovirus, anti-Epstein-Barr virus, or anti-adenovirus cytotoxic T lymphocytes (CTL) can be used to protect stem cell transplant recipients against these infections (5).

The utility of cryopreserved cells depends on the viability and function retention of PBMC after freezing and thawing (6–10). To achieve optimal results in this respect, technical aspects are critical, but the intrinsic fragility of PBMC subpopulations can also play a role (11–16). Training and monitoring of personnel in clinical sites that perform the cryopreservation have taken the forefront effort in recent years, leading to the development of successful models (17–24).

TECHNICAL ASPECTS OF PBMC CRYOPRESERVATION

The goal of the cryopreservation is to freeze and thaw the PBMC without compromising the cell viability. Cryoprotective agents are essential in order to avoid water crystals and cell burst with freezing. Both glycerol and dimethyl sulfoxide (DMSO) can provide this function, but only DMSO has been extensively studied for cryopreservation of PBMC. Other critical steps of the cryopreservation procedure include inhibiting cell metabolism while in the presence of DMSO, rate-controlled freezing to avoid cell dehydration, rapid thawing, and resuspension in serum-containing medium, which protects the cells against osmotic trauma.

To maintain the viability and functionality of cryopreserved PBMC, it is critical that blood be processed within 8 hours of collection. Ficoll-Hypaque-separated PBMC are washed at 4°C, counted, and resuspended in cold fetal calf serum containing 10% DMSO at 10^7 PBMC/ml. The cell suspension is aliquoted into cryovials kept on ice, which are then inserted into a Nalgene "Mr. Frosty" freezing apparatus, BioCision CoolCell alcohol-free freezing containers, or a Cryomed freezing chamber. The cells are gradually cooled at a rate of −1°C/min during the first 24 h down to −70 or −80°C and kept at this temperature for a short time until shipped to the testing laboratory or repository center on dry ice or in liquid nitrogen (LN_2) Dewar tanks. It is important to note that although the cell viability does not change over up to 12 weeks of storage at −70 to −80°C, the functionality decreases after the first week. To preserve both viability and functionality for prolonged times, PBMC need to be transferred and stored in LN_2 tanks or −150°C freezers. At these ultralow temperatures, cryopreserved PBMC typically maintain their viability and functionality for decades. However, after storage at ultralow temperatures, cells need to be shipped in LN_2 Dewar tanks to fully preserve their functional characteristics (10). Dry ice shipment of PBMC that have been kept at ultralow temperatures is not advised because it is associated with a loss of functionality (2, 7).

Multiple clinical trials and vaccine networks developed programs to ensure that processing of PBMC is adequate for immunological assays. These quality control programs have been highly instrumental in providing adequate PBMC for immunological endpoints (17, 19, 21, 22).

For thawing, cryovials are incubated with agitation in a 37°C water bath until almost all the cryovial content has become fluid. The cell suspension is then transferred to a 15-ml polypropylene conical tube, and warm RPMI containing 10% fetal calf or human AB serum is slowly added, at a rate of approximately 1 ml/min for the first 5 min, followed by

doi:10.1128/9781555818722.ch27

rapid addition of another 5 to 10 ml of medium. Benzonase (Novagen) or other DNases can be added to the thawing medium to avoid excessive clumping. While the use of these products may improve PBMC recovery, it does not affect viability or function. Thawed cells are washed 2 or 3 times by centrifugation, counted, and assessed for viability before being used in immunologic assays (6).

FUNCTIONAL ASSAYS USING CRYOPRESERVED PBMC

Lymphoproliferative Assays

Lymphoproliferative responses measure mainly CD4-dependent immune responses. Severely impaired CD4 responses confer broad immunodeficiency. More subtle CD4 deficits impair defenses against certain pathogens, such as viruses, mycobacteria, yeast, and certain protozoa, that are highly dependent on cell-mediated immunity.

Several studies compared responder cell frequency (RCF) and lymphocyte proliferation assays (LPA), traditionally used to assess CD4 responses, in cryopreserved versus fresh PBMC collected from immunocompromised patients or normal hosts (6, 8). These investigations showed that antigen- and mitogen-induced proliferation of fresh and frozen cells were highly correlated, despite the loss of responders or decrease in stimulation indices in cryopreserved cells compared with fresh cells (Fig 1). In Fig. 1, which shows a plot correlating CMV-specific responders in fresh and frozen PBMC, the majority of the data points fall below the line of equivalency, illustrating the loss of responders in cryopreserved preparations.

The viability of cryopreserved PBMC significantly affects the results of proliferative assays (6, 7, 9). Data from studies of normal hosts and HIV-infected patients, illustrated in Fig. 2, show that a viability of ≥70% of cryopreserved PBMC is necessary to reproduce the LPA results obtained with fresh cells. In contrast, LPA responses of PBMC with a viability of <70% increase or decrease with the viability of the cell preparation, introducing a variable that is extraneous to the immunity of the host. In addition, the cell recovery of cryopreserved PBMC and the CD4 cell numbers of the donor do not affect the results of lymphoproliferative responses in cryopreserved PBMC by comparison with fresh cells.

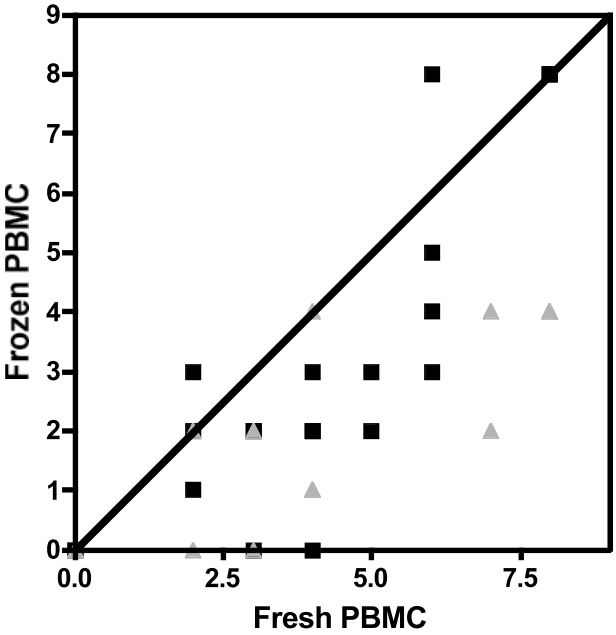

FIGURE 1 CMV-specific RCF in cryopreserved versus fresh PBMC from HIV-infected patients and uninfected controls. Data were derived from samples from HIV-infected patients (HIV+, triangles) and uninfected controls (HIV−, squares). The diagonal represents the slope of equivalence between fresh- and frozen-cell assays.

Cytotoxic Assays

Defenses against viral infections and malignancies rely predominantly on cytotoxic immune responses. Several studies in bone marrow transplant patients have shown that protective immunity against cytomegalovirus coincides with the return of specific CTL (5). Exogenous generation and transfusion of specific CTL can protect immunocompromised hosts against several viral infections and malignancies (5).

The CTL activity of cryopreserved PBMC is comparable with that obtained with fresh cell assays. The use of cryopreserved PBMC allows for better scheduling of these complex assays that involve effector and target preparation.

Natural killer cell (NK) activity, in contrast to CTL, is more labile in response to freezing and thawing. Several investigators, but not all, have found significant changes of NK-mediated lysis following cryopreservation (13). Because of these conflictive data, the use of cryopreserved PBMC for NK assays is recommended only after carefully controlled experiments validate this procedure locally.

Cytokine-Based Assays

Cell-mediated responses are modulated by cytokines released by mononuclear phagocytes, NK cells, and T lymphocytes. These cytokines, which regulate many cell surface recognition molecules and affect the recruitment of inflammatory cells into an area of infection, are likely to play a pivotal role in the expression of cell-mediated immunity. PBMC make a range of cytokines in tissue culture following mitogen and antigen stimulation, which have been used to characterize their functional status.

Inducible cytokine assays measure the amount of cytokine released by stimulated PBMC in the culture supernatant. Studies in HIV-infected patients and uninfected controls show that gammainterferon (IFN-γ) production is essentially the same in fresh and cryopreserved PBMC (Fig. 3) (8). There are conflicting data on interleukin 2 (IL-2) levels in frozen versus fresh cell cultures, and more studies are necessary to clarify this subject (16). However, the rank correlation between either IFN-γ or IL-2 released by cryopreserved compared with fresh cells is highly significant, indicating that inducible cytokine assays on cryopreserved cells are suitable for comparative analyses of the immune response, such as longitudinal observations.

Single-cell intracellular cytokine assays use flow cytometry to enumerate antigen- or mitogen-stimulated PBMC that synthesize cytokines. The single-cell intracellular cytokine assays provide a sensitive and specific indication of the cell-mediated response. Furthermore, the single-cell assay can analyze the phenotype of the cytokine-producing cells, thus further characterizing the immune response. The findings with viable frozen PBMC in these assays are highly correlated with those obtained with fresh PBMC (6, 12, 14). However, a key measure to ensure accurate results is to gate on viable cells only, because dead cells tend to nonspecifically bind

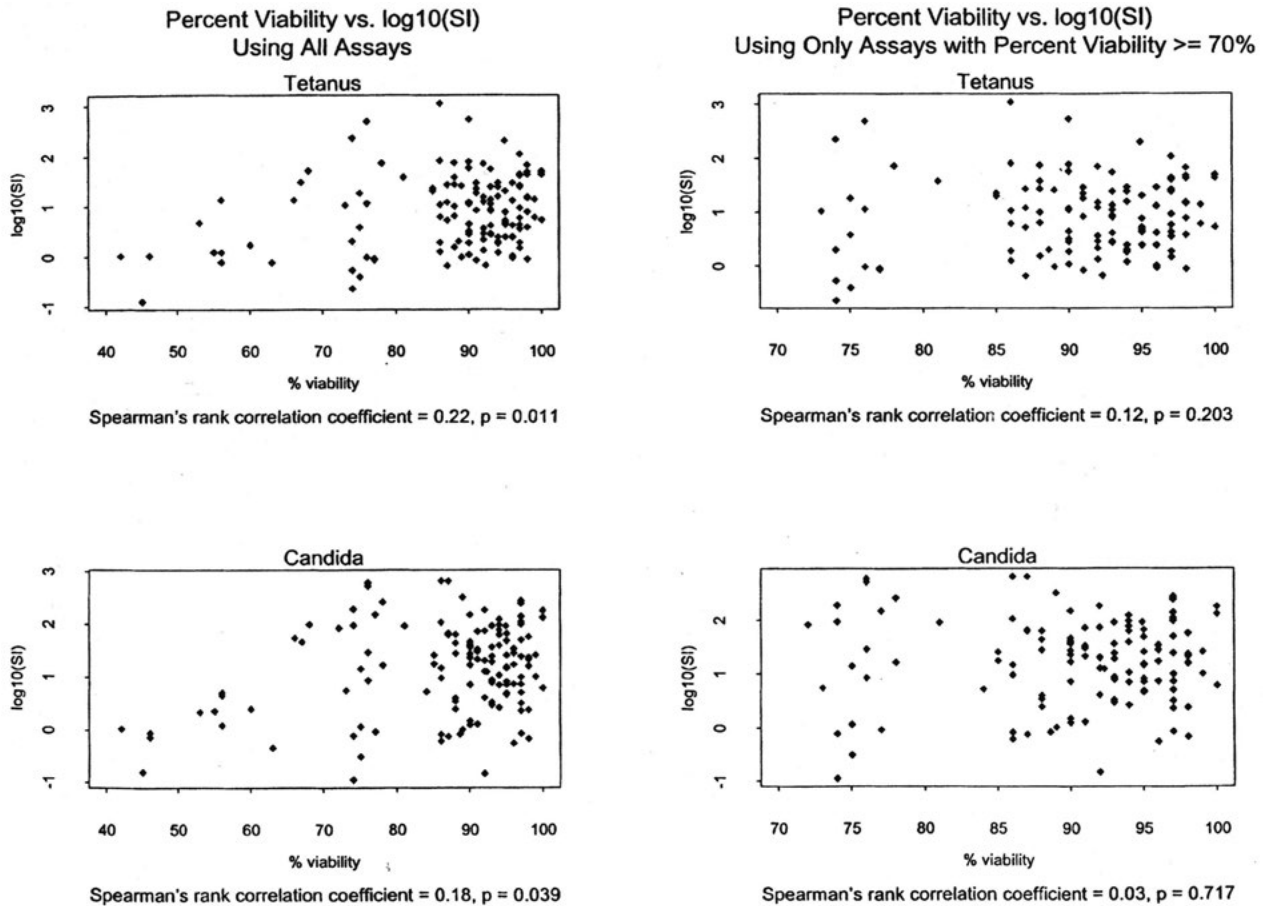

FIGURE 2 Effect of viability on cryopreserved PBMC LPA results. Data were derived from samples from HIV-infected patients. The panels on the left show that when analyzing all samples, the LPA results significantly increase with higher viability. A breakpoint in the distribution pattern can be observed at a viability of 70%. The panels on the right show that when analyzing only samples with a viability of ≥70%, the LPA results are independent of the PBMC viability. SI, stimulation index.

fluorochrome-conjugated antibodies (25). Flow-cytometric assays on cryopreserved PBMC can be reproduced across laboratories, such that quality control programs of intracellular cytokines regularly use cryopreserved PBMC.

The enzyme-linked immunosorbent spot (ELISPOT) assay is yet another format for quantifying cytokine-producing cells. This assay detects captured cytokines diffusing from single antigen- or mitogen-stimulated cells. The assay is extremely sensitive and versatile. It can be performed using fractionated PBMC, such as purified CD8 or CD4 cells. The ELISPOT assay has traditionally measured IFN-γ-producing responder cells but has been adapted to detect other cytokines, including IL-2, IL-17, granzyme B, tumor necrosis factor alpha, and others. ELISPOT is commonly performed on cryopreserved PBMC because the results are comparable with those obtained with fresh cells and there are considerable cost savings when assays are done in batches. Similar to other functional assays, reliable and reproducible T-cell ELISPOT results require a PBMC viability of ≥70% (7). In addition, optimal results are obtained when PBMC are rested overnight before setting up ELISPOT assays.

SURFACE MARKERS ON CRYOPRESERVED PBMC

Immunophenotyping by Flow Cytometry

Enumeration of PBMC subsets by flow cytometry provides important information on the immune capacity of the host. As such, flow cytometry-based immune phenotyping is a standard procedure in the evaluation of immunodeficiency disorders. The distribution of major surface markers, such as CD3, CD4, CD8, CD19, and CD14, is essentially unchanged by cryopreservation. The percentage of cells in fresh and cryopreserved PBMC typically shows statistically significant correlations, despite the fact that fresh-cell assays are typically performed on whole blood, whereas frozen-cell assays use PBMC separated by Ficoll-Hypaque. The percentage of cells bearing certain immune phenotypic markers (CD4, CD8, etc.) was stable over many decades of frozen PBMC storage in the Multicenter AIDS Cohort Study. As with LPA, cell recovery does not influence the distribution of T cell phenotypes on cryopreserved PBMC. However, gating on viable cells only is critical. Results of cryopreserved PBMC phenotyping are stable across a wide range of

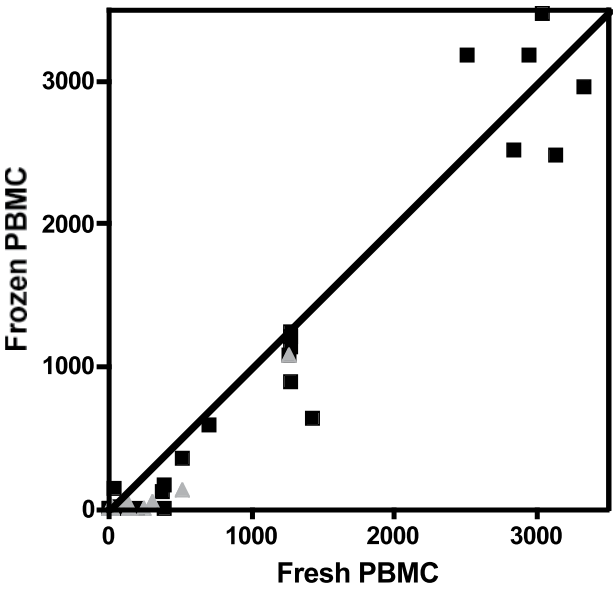

FIGURE 3 CMV-specific IFN-γ in cryopreserved versus fresh PBMC from HIV-infected patients (triangles) and controls (squares). Data were derived from samples from HIV-infected patients and uninfected controls. The diagonal represents the slope of equivalence between fresh- and frozen-cell assays.

baseline CD4 cell numbers, demonstrating the robustness of this complex procedure.

Cell membrane markers used for immunophenotyping, such as CD21, CD22, CD28, CD38, HLA DR, CD95 (Fig. 4A), and CD45RA and RO are well preserved during the freezing and thawing processes. In contrast, CD62L, which is commonly used for the identification of naive T cell populations, is present in a significantly lower amount on the surface of cryopreserved PBMC than on fresh ones (Fig. 4B). Hence, it is desirable to avoid the use of anti-CD62L monoclonal antibodies for advanced immunophenotyping of cryopreserved PBMC. CXCR5 is another marker that may be cleaved during the process of PBMC separation and, therefore, shows lower representation in cryopreserved PBMC than in whole-blood fresh-cell assays.

TCR Vβ Repertoire

Definition of the T cell receptor repertoire (TCR) has become increasingly prevalent in studies of the maturation and senescence of the immune system. These assays can provide valuable information about immune deficiency stages and immune restoration. Flow cytometry- and PCR-based methods are used for TCR characterization. The two techniques seem to yield similar results when performed on fresh and cryopreserved PBMC.

B-Cell Functional Assays

Cryopreserved PBMC are significantly less sensitive than fresh cells for detection of plasmablasts both by flow cytometry using phenotypic markers and by ELISPOT assay using functional properties. Hence, it is safe to conclude that plasmablasts survive poorly the process of cryopreservation. In contrast, memory B cells can be readily detected in cryopreserved preparations. Both flow cytometry assays based on the detection of antigen-specific B-cell receptors and ELISPOT assays that measure immunoglobulin production against specific antigens have been successfully performed using cryopreserved PBMC. A viability threshold has not been established for B-cell assays, but based on

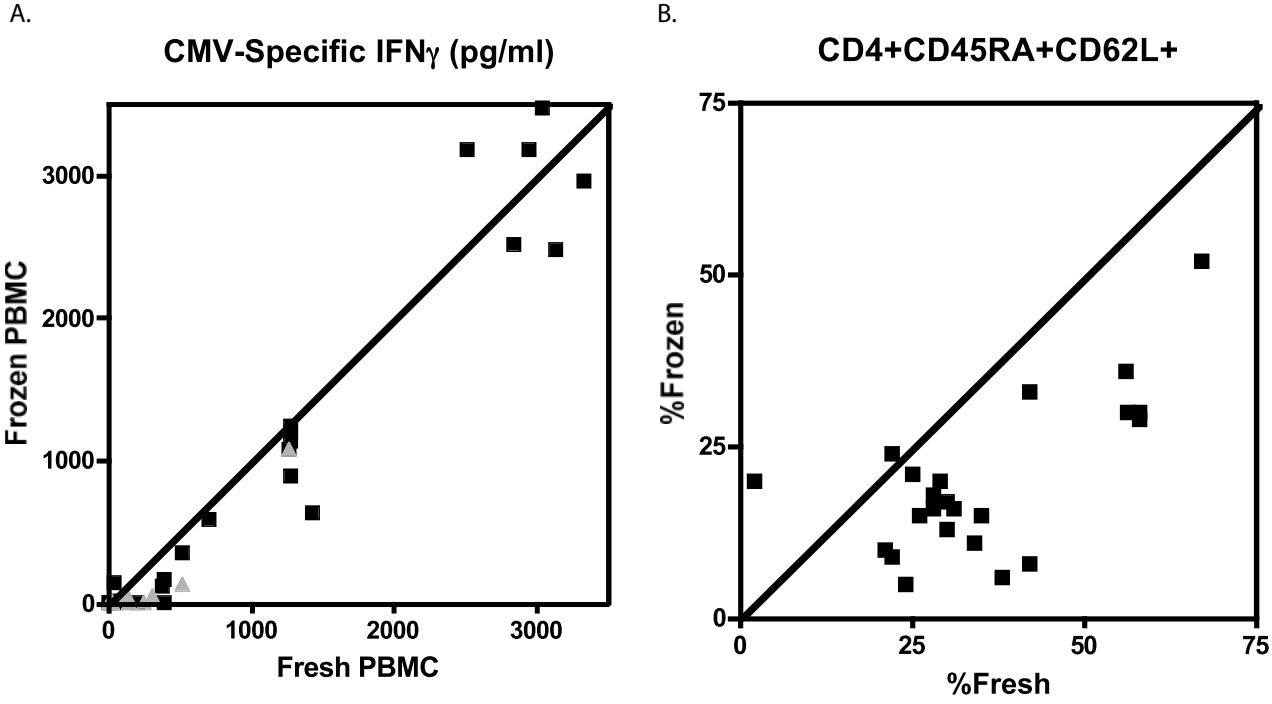

FIGURE 4 Effect of cryopreservation on flow cytometric immunophenotyping. Data were derived from samples from HIV-infected subjects (triangles) and controls (squares). The diagonal represents the slope of equivalence between fresh- and frozen-cell assays. (A) Example of a cell surface marker that is well preserved during cryopreservation (CD95). (B) Loss of CD62L during cryopreservation.

the cumulative experience with other functional assays, it is reasonable to assume that PBMC with high viability provide the most reliable results. It is important to note, however, that after *in vitro* nonspecific stimulation that aims at stimulating immunoglobulin production, many PBMC become apoptotic, compromising the overall viability of the stimulated cells. The implications of this effect are not known, but it may be prudent to take into account only the viable cells when setting up the immunoglobulin detection assays.

mRNA Quantification Assays

The mRNA quantification assay is a very powerful technique that has been increasingly utilized to study innate and adaptive immunity. Although ideally cells should be cryopreserved in special buffers such as Trizol to maximize the yield of mRNA, cryopreserved PBMC can be used for next-generation sequencing or microarray assays. After RNA extraction, the quantity and quality of the nucleic acids can be evaluated to determine the adequacy of the sample for mRNA studies.

Anne Sevin (deceased) performed the statistical analysis of the data presented in Fig. 2 and prepared these illustrations.

REFERENCES

1. **Autran B, Carcelain G, Li TS, Blanc C, Mathez D, Tubiana R, Katlama C, Debre P, Leibowitch J.** 1997. Positive effects of combined antiretroviral therapy on CD4+ T cell homeostasis and function in advanced HIV disease. *Science* **277:**112–116.
2. **Bull M, Lee D, Stucky J, Chiu YL, Rubin A, Horton H, McElrath MJ.** 2007. Defining blood processing parameters for optimal detection of cryopreserved antigen-specific responses for HIV vaccine trials. *J Immunol Methods* **322:**57–69.
3. **Kleeberger CA, Lyles RH, Margolick JB, Rinaldo CR, Phair JP, Giorgi JV.** 1999. Viability and recovery of peripheral blood mononuclear cells cryopreserved for up to 12 years in multicenter study. *Clin Diagn Lab Immunol* **6:**14–19.
4. **Weinberg A, Betensky R, Zhang L, Ray G.** 1998. Effect of shipment, storage, anticoagulant and cell separation on lymphoproliferative responses in HIV-infected patients. *Clin Diagn Lab Immunol* **5:**804–807.
5. **Gerdemann U, Katari UL, Papadopoulou A, Keirnan JM, Craddock JA, Liu H, Martinez CA, Kennedy-Nasser A, Leung KS, Gottschalk SM, Krance RA, Brenner MK, Rooney CM, Heslop HE, Leen AM.** 2013. Safety and clinical efficacy of rapidly-generated trivirus-directed T cells as treatment for adenovirus, EBV, and CMV infections after allogeneic hematopoietic stem cell transplant. *Mol Ther* **21:**2113–2121.
6. **Weinberg A, Song LY, Wilkening C, Sevin A, Blais B, Louzao R, Stein D, Defechereux P, Durand D, Riedel E, Raftery N, Jesser R, Brown B, Keller MF, Dickover R, McFarland E, Fenton T, Pediatric ACTG Cryopreservation Group.** 2009. Optimization and limitations of use of cryopreserved peripheral blood mononuclear cells for functional and phenotypic T cell characterization. *Clin Vaccine Immunol* **16:**1176–1186.
7. **Weinberg A, Song LY, Wilkening CL, Fenton T, Hural J, Louzao R, Ferrari G, Etter PE, Berrong M, Canniff JD, Carter D, Defawe OD, Garcia A, Gerrelts TL, Gelman R Lambrecht LK, Pahwa S, Pilakka-Kanthikeel S, Shugarts DL, Tustin NB.** 2010. Optimization of storage and shipment of cryopreserved peripheral blood mononuclear cells from HIV-infected and uninfected individuals for ELISPOT assays. *J Immunol Methods* **363:**42–50.
8. **Weinberg A, Wohl DA, Brown DG, Pott GB, Zhang L, Ray MG, van der Horst C.** 2000. Effect of cryopreservation on measurement of cytomegalovirus-specific cellular immune responses in HIV-infected patients. *J Acquir Immune Defic Syndr* **25:**109–114.
9. **Weinberg A, Zhang L, Brown D, Erice A, Polsky B, Hirsch MS, Owens S, Lamb K, ACTG Team 360.** 2000. Viability and functional activity of cryopreserved mononuclear cells. *Clin Diagn Lab Immunol* **7:**714–716.
10. **Smith JG, Joseph HR, Green T, Field JA, Wooters M, Kaufhold RM, Antonello J, Caulfield MJ.** 2007. Establishing acceptance criteria for cell-mediated-immunity assays using frozen peripheral blood mononuclear cells stored under optimal and suboptimal conditions. *Clin Vaccine Immunol* **14:**527–537.
11. **Hviid L, Albeck G, Hansen B, Theander TG, Talbot A.** 1993. A new portable device for automatic controlled-gradient cryopreservation of blood mononuclear cells. *J Immunol Methods* **157:**135–142.
12. **Maecker HT, Moon J, Bhatia S, Ghanekar SA, Maino VC, Payne JK, Kuus-Reichel K, Chang JC, Summers A, Clay TM, Morse MA, Lyerly HK, DeLaRosa C, Ankerst DP, Disis ML.** 2005. Impact of cryopreservation on tetramer, cytokine flow cytometry, and ELISPOT. *BMC Immunol* **6:**17.
13. **Mata MM, Mahmood F, Sowell RT, Baum LL.** 2014. Effects of cryopreservation on effector cells for antibody dependent cell-mediated cytotoxicity (ADCC) and natural killer (NK) cell activity in (51)Cr-release and CD107a assays. *J Immunol Methods* **406:**1–9.
14. **Reimann KA, Chernoff M, Wilkening C, Nickerson C, Landay A, ACTG Immunology Advanced Technology Laboratories.** 2000. Preservation of lymphocyte immunophenotype and proliferative responses in cryopreserved peripheral blood mononuclear cells from HIV-1-infected donors: implications for multicenter clinical trials. *Clin Diagn Lab Immunol* **7:**352–359.
15. **Sleasman JW, Leon BH, Aleixo LF, Rojas M, Goodenow MM.** 1997. Immunomagnetic selection of purified monocyte and lymphocyte populations from peripheral blood mononuclear cells following cryopreservation. *Clin Diagn Lab Immunol* **4:**653–658.
16. **Ventakaraman M.** 1992. Cryopreservation-induced enhancement of interleukin-2 production in human peripheral blood mononuclear cells. *Cryobiology* **29:**165–174.
17. **Aziz N, Margolick JB, Detels R, Rinaldo CR, Phair J, Jamieson BD, Butch AW.** 2013. Value of a quality assessment program in optimizing cryopreservation of peripheral blood mononuclear cells in a multicenter study. *Clin Vaccine Immunol* **20:**590–595.
18. **Boaz MJ, Hayes P, Tarragona T, Seamons L, Cooper A, Birungi J, Kitandwe P, Semaganda A, Kaleebu P, Stevens G, Anzala O, Farah B, Ogola S, Indangasi J, Mhlanga P, Van Eeden M, Thakar M, Pujari A, Mishra S, Goonetilleke N, Moore S, Mahmoud A, Sathyamoorthy P, Mahalingam J, Narayanan PR, Ramanathan VD, Cox JH, Dally L, Gill DK, Gilmour J.** 2009. Concordant proficiency in measurement of T-cell immunity in human immunodeficiency virus vaccine clinical trials by peripheral blood mononuclear cell and enzyme-linked immunospot assays in laboratories from three continents. *Clin Vaccine Immunol* **16:**147–155.
19. **Ducar C, Smith D, Pinzon C, Stirewalt M, Cooper C, McElrath MJ, Hural J.** 2014. Benefits of a comprehensive quality program for cryopreserved PBMC covering 28 clinical trials sites utilizing an integrated, analytical web-based portal. *J Immunol Methods* **409:**9–20.
20. **Sambor A, Garcia A, Berrong M, Pickeral J, Brown S, Rountree W, Sanchez A, Pollara J, Frahm N, Keinonen S, Kijak GH, Roederer M, Levine G, D'Souza MP, Jaimes**

M, Koup R, Denny T, Cox J, Ferrari G. 2014. Establishment and maintenance of a PBMC repository for functional cellular studies in support of clinical vaccine trials. *J Immunol Methods* **409:**107–116.

21. **Sanchez AM, Rountree W, Berrong M, Garcia A, Schuetz A, Cox J, Frahm N, Manak M, Sarzotti-Kelsoe M, D'Souza MP, Denny T, Ferrari G.** 2014. The External Quality Assurance Oversight Laboratory (EQAPOL) proficiency program for IFN-gamma enzyme-linked immunospot (IFN-gamma ELISpot) assay. *J Immunol Methods* **409:**31–43.
22. **Sarzotti-Kelsoe M, Needham LK, Rountree W, Bainbridge J, Gray CM, Fiscus SA, Ferrari G, Stevens WS, Stager SL, Binz W, Louzao R, Long KO, Mokgotho P, Moodley N, Mackay M, Kerkau M, McMillion T, Kirchherr J, Soderberg KA, Haynes BF, Denny TN.** 2014. The Center for HIV/AIDS Vaccine Immunology (CHAVI) multi-site quality assurance program for cryopreserved human peripheral blood mononuclear cells. *J Immunol Methods* **409:**21–30.
23. **Staats JS, Enzor JH, Sanchez AM, Rountree W, Chan C, Jaimes M, Chan RC, Gaur A, Denny TN, Weinhold KJ.** 2014. Toward development of a comprehensive external quality assurance program for polyfunctional intracellular cytokine staining assays. *J Immunol Methods* **409:**44–53.
24. **Weinberg A, Louzao R, Mussi-Pinhata MM, Cruz ML, Pinto JA, Huff MF, de Castro AC, Sucupira MC, Denny TW.** 2007. Quality assurance program for peripheral blood mononuclear cell cryopreservation. *Clin Vaccine Immunol* **14:**1242–1244.
25. **Horton H, Thomas EP, Stucky JA, Frank I, Moodie Z, Huang Y, Chiu YL, McElrath MJ, De Rosa SC.** 2007. Optimization and validation of an 8-color intracellular cytokine staining (ICS) assay to quantify antigen-specific T cells induced by vaccination. *J Immunol Methods* **323:**39–54.

Lymphocyte Activation

ROSHINI SARAH ABRAHAM

28

Measurement of lymphocyte activation is a key diagnostic component in the work-up of several immunological diseases: either primary in nature or altered as a result of immune-modifying therapies or other diseases that are not genetic immune deficiencies. There are many ways to measure lymphocyte activation, but the two main approaches in the diagnostic immunology laboratory include immunophenotyping (measurement of cell surface or intracellular activation markers after lymphocyte stimulation) and functional assays (where there is direct assessment of a certain function, e.g., proliferation after lymphocyte activation or cytotoxicity). Among the lymphocyte subsets that are typically assessed for activation status as a measure of immune competence, T cells are the most common, though in some contexts it is also appropriate to evaluate B cell and NK cell activation or function. This chapter focuses primarily on discussing assays and methods related to measurement of T cell activation and function.

T CELL ACTIVATION AND FUNCTION

Naive T cells recognize antigens and become activated in peripheral lymphoid organs (1). This process results in expansion of the antigen-specific T cell pool and differentiation of cells into effector and memory T cells. Activation of effector T cells takes place in secondary lymphoid organs or the periphery (nonlymphoid tissue) through antigen recognition in the local milieu, resulting in propagation of their effector functions. T cells typically require antigen-presenting cells (APCs) for activation, especially for initiation of antigen-specific responses. APCs provide both the cognate signal (a peptide in the context of major histocompatibility complex [MHC] class I or class II molecules) and "secondary" (costimulatory) signals (2). The requirement for naive T cell activation is more stringent than that for effector T cells; hence, antigen presentation to naive T cells is usually accomplished only by "professional" APCs, such as dendritic cells and macrophages. Antigen-experienced effector T cells have a lower threshold for activation and therefore can "recognize" antigens from a larger pool of APCs. Certain global T cell stimulants, such as mitogens and superantigens, do not require the classical process of antigen presentation for T cell activation (3). Once T cells are activated through their T cell receptor (TCR), they serially express activation markers that include chemokine and cytokine receptors, adhesion molecules, costimulatory molecules, and MHC class II proteins (4). There is also a difference in CD4 T cell expression when T cells are stimulated with phytohemagglutinin (PHA) *in vitro* over time, for a maximum of 72 h, while CD8 expression remains unchanged. However, stimulation with phorbol myristate acetate (PMA) and ionomycin results in a complete loss of CD4 expression on T cells within 24 h, while CD8 expression on T cells remains unchanged even at 72 h of stimulation.

The two most commonly used markers of immediate early activation of T cells are CD69 and CD40L (CD154). Both of these cell surface markers can be measured by flow cytometry (5). CD69 is a signaling membrane glycoprotein involved in inducing T cell proliferation. CD69 is expressed at very low levels on resting CD4 and CD8 T cells (<5 to 10% of T cells in a peripheral blood mononuclear cell [PBMC] preparation); however, it is rapidly upregulated (within 1 h) by TCR stimulation or by use of T cell activating agents, such as phorbol esters (PMA), which stimulate T cells via a protein kinase C-dependent pathway (6, 7). Expression of CD69 peaks within 16 to 24 h and then declines, and it is close to undetectable 72 h after removal of the stimulus. However, the kinetics of CD69 expression can vary depending on the stimulant used. There is no expression of CD69 at 2 h and 4 h with PHA stimulation; however, on both CD4 and CD8 T cells, CD69 is induced at 24 h and expressed through 72 h poststimulation. On the other hand, CD69 expression is induced early, at 2 h, with PMA-ionomycin stimulation and is maintained until 72 h, though the number of cells expressing CD69 in the CD4 T cell compartment decreases over time. The inability to upregulate CD69 following TCR activation may be associated with impaired T cell function. CD40L (CD154) is another cell surface costimulatory protein that is expressed on activated T cells. CD40L binds its receptor, CD40, on APCs and activates several signaling pathways, including mitogen-activated protein kinase, NK-κB, and STAT3 pathways. CD40L expression is induced within 1 to 2 h after TCR stimulation (through the activity of NFAT and AP-1), peaks at approximately 6 h poststimulation, and declines by 16 to 24 h. Just as with CD69, the kinetics of CD40L expression on CD4 T cells is different with PHA versus PMA-ionomycin stimulation, and expression on CD8 T cells is extremely weak. CD40L expression is biphasic, and the addition of anti-CD28 costimulation or exogenous

doi:10.1128/9781555818722.ch28

interleukin-2 (IL-2) along with TCR stimulation leads to sustained expression of CD40L for several days. Expression of CD40L on resting CD4 and CD8 T cells is very low (<1% PBMCs), and this is substantially increased on CD4 T cells upon T cell activation. The inability to upregulate CD40L on T cell activation could be multifactorial but ultimately leads to T cell dysfunction and impairment of downstream T cell activity. Further, the function of the CD40L molecule can be assessed by flow cytometry by evaluating its ability to bind to a soluble receptor (CD40-muIg), and this function is often used in the diagnosis of CD40L deficiency, which is associated with X-linked hyper-IgM syndrome (8). There are other T cell activation markers that are often measured in the clinical laboratory, including CD95 (Fas), CD25 (IL-2Rα), and MHC class II (HLA DR) (3).

Direct Measurement of T Cell Activation by Using Functional Assays

Measurement of T Cell Proliferation by Using [^{3}H] Thymidine

The method of determining impaired T cell function by culturing human PBMCs *in vitro* with mitogenic plant lectins (mitogens), such as PHA and pokeweed mitogen (PWM), has been part of the diagnostic immunology repertoire for many years. A widely used method for assessing lymphocyte proliferation hitherto has been the measurement of [^{3}H] thymidine incorporated into the DNA of proliferating cells. The disadvantages of the [^{3}H]thymidine method of lymphocyte proliferation are as follows: (i) the technique is cumbersome due to the use of radioactivity, (ii) it does not allow discrimination of responding cell populations in response to stimulation, and (iii) it does not provide any information on the contribution of activation-induced cell death to the interpretation of the final result. Further, decreased lymphocyte proliferation could be due to several factors, including an overall diminution of T cell proliferation, a decrease in proliferation of only a subset of T cells, or an apparent decrease in total lymphocyte proliferation due to T cell lymphopenia and an underrepresentation of T cells in the PBMC pool. None of these can be discriminated by the thymidine uptake assay, but they can be assessed by flow cytometry, which uses antibodies to identify specific responder cell populations (Fig. 1A). Cell viability can also be measured within the same assay, without requiring additional cell manipulation or sample volume (Fig. 1B), using both annexin V and 7-aminoactinomycin D (7-AAD). Measurement of cell viability by flow cytometry is more accurate than using dye-exclusion methods, such as trypan blue staining, since the latter is unable to differentiate between apoptotic cells and viable cells and therefore can overestimate the number of viable cells.

Flow Cytometric Measurement of T Cell Proliferation

The flow cytometric methods for measuring cell proliferation include the use of fluorescent dyes to identify proliferating cells. One of the more commonly used dyes, carboxyfluorescein diacetate succinimidyl ester (CFSE), must be used carefully for measuring lymphocyte proliferation *in vitro*, since it can be toxic to cells and nonoptimal labeling conditions can affect the measurement of cell proliferation and the interpretation of results (9, 10). CFSE is a fluorescent, cell membrane-permeating dye similar in physical properties to the commonly used fluorochrome fluorescein isothiocyanate (FITC). Alternatives to CFSE include related compounds, such as cell trace violet and the cell proliferation dye eFluor 670, which have excitation and emission spectra that are different from those of CFSE. These dyes can be used for tracking of lymphocyte proliferation status *in vivo* in animal models and can also permit measurement of up to 11 cell divisions (11). Another alternative to CFSE and its related dyes is the use of a thymidine analog, 5-ethynyl-2′-deoxyuridine (Edu), which can combine with a fluorescent azide in a copper-catalyzed cycloaddition reaction (referred to as "click" chemistry) and permits flow cytometric evaluation of lymphocyte proliferative responses by assessment of its incorporation into cellular DNA (12–14). Edu labeling has been shown to be a fast and sensitive method for measuring cell proliferation and also facilitates identification of dividing cells. Edu is relatively more photo-stable than CFSE and is added to cells after completion of the stimulation period, and its measurement is comparable to the thymidine method in that gain of signal is the endpoint. It is relevant that while CFSE, as previously mentioned, can be toxic to cells at certain concentrations (37 nM to 10 μM) due to an increase in cell death, it also modulates the expression of activation markers, resulting in decreases in CD69, HLA DR, and CD25 (15). Also, it has been reported that there is an increase in the number of false-positive results with CFSE and that this method is therefore unsuitable for measuring lymphocyte proliferation in patients with severe cellular immunodeficiencies (15). The Edu assay has not shown such limitations and has been used to evaluate lymphocyte proliferation in a spectrum of patients, including those with severe combined immunodeficiencies. In fact, this assay has been particularly useful for discriminating between functional T cells and nonfunctional T cells in the context of severe T cell lymphopenia, which cannot be achieved with the standard thymidine assay. All the proliferation data shown in this chapter were obtained by this Edu-based measurement of T cell proliferation.

Ki-67 Assay

Another approach to measuring cell proliferation involves the use of an intracellular (nuclear) protein involved in regulation of cell division, i.e., Ki-67 (16). Ki-67 is frequently used in the field of tumor biology to measure the proliferative capacity of tumor cells (17), since this protein is expressed at all active phases of cell division but not during DNA repair or cell quiescence. More recently, the use of Ki-67 to measure antigen-specific T cell proliferation after vaccination has gained traction (16, 18–20). Ki-67 expression in T cells has been shown to be a specific and quantitative indicator of proliferation and provides results comparable to those obtained with other methods (Fig. 2), and though it is not widely used in the diagnostic immunology laboratory at present, it is likely to gain entry in due course as flow cytometry replaces the thymidine method for assessing lymphocyte proliferative responses.

Cytokine Production

In addition to cellular proliferation as a readout for T cell function, the production of cytokines by activated T cells is another important component for evaluating T cell functional activity. T cells typically are not monofunctional, producing a single cytokine on activation, but rather are multi- or polyfunctional, and their cytokines are produced in a sequential manner rather than simultaneously, though a population of stimulated T cells will have individual T cells producing different cytokines in a temporally regulated manner (21–23). These cytokines can be measured by intracellular flow cytometry after T cell activation with mitogens for both CD4 and CD8 T cell subsets. Typically, the cytokines produced include IL-2, gamma interferon (IFN-γ) and tumor necrosis factor alpha (TNF-α). Figures 3A and B

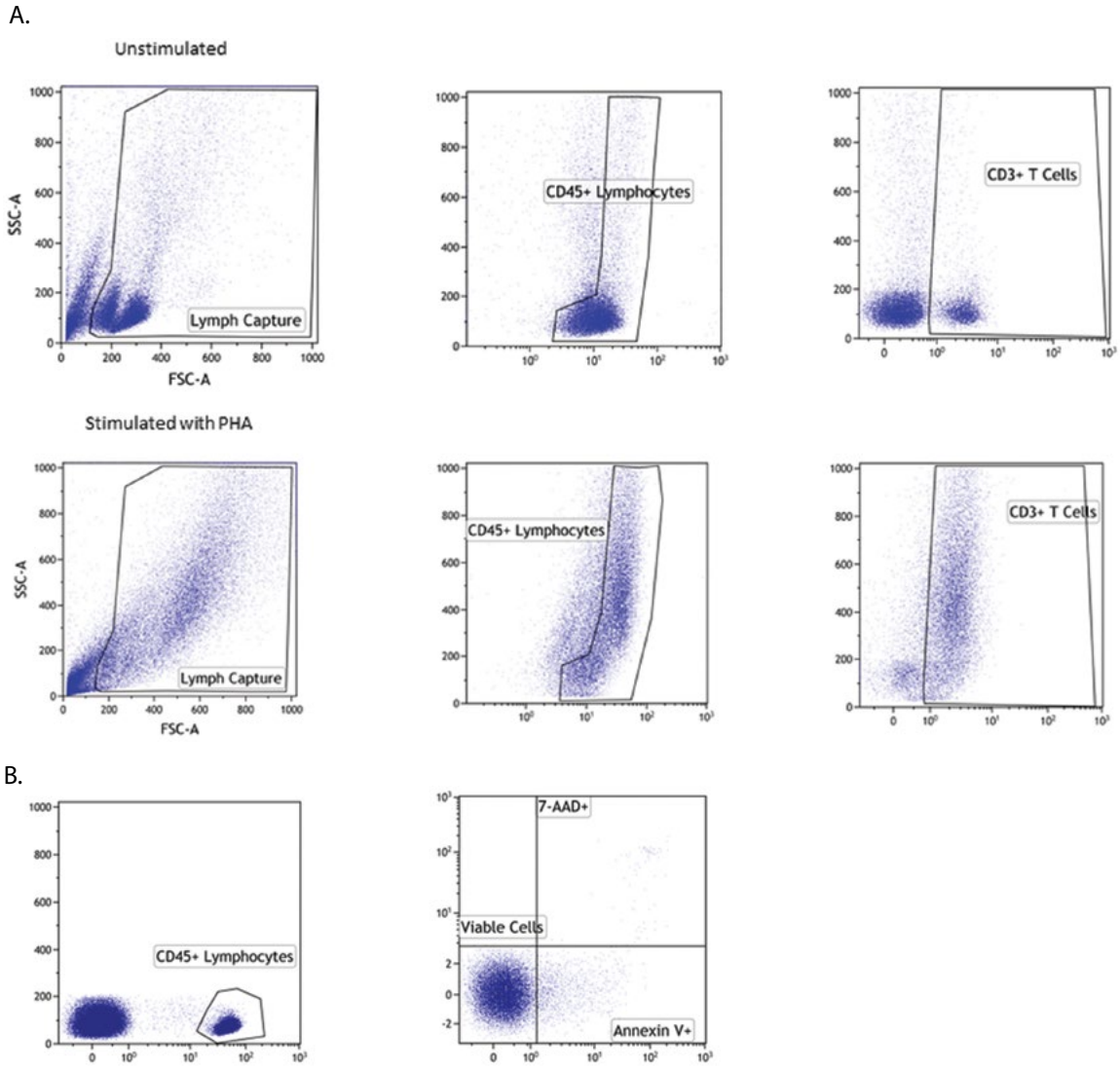

FIGURE 1 (A) Flow cytometric measurement of cellular proliferation with Edu. The flow cytometry results show a detailed assessment of proliferating lymphocytes after stimulation with PHA. Proliferating cells are apparent in comparing the unstimulated (upper panels) to stimulated (lower panels) samples, and the use of specific antibodies (CD45, total lymphocytes; and CD3, total T cells) allows further characterization. (B) Assessment of cell viability for lymphocyte proliferation assays. The CD45 marker is used to identify lymphocytes. Viable, apoptotic, and dead cells are identified in the original sample used for cell proliferation, prior to initiation of cell culture, by using a combination of two fluorescent dyes: annexin V and 7-AAD. Viable cells are negative for both markers, while dead cells are positive for both annexin V and 7-AAD. Only apoptotic cells are positive for annexin V alone.

demonstrate the production of multiple cytokines by CD4 and CD8 T cells, respectively, after PMA-ionomycin stimulation of cells from a healthy donor and a patient.

Mitogens and Antigens Used To Drive Proliferation

Mitogens are very potent stimulators of T cell activation and proliferation, independent of their antigenic specificity. It has been suggested that mitogens can induce T cell proliferative responses even if the cells are incapable of responding adequately to antigenic (physiologic) stimuli. Therefore, abnormal T cell responses to mitogens are considered a diagnostically less sensitive but more specific test of aberrant T cell function (24). Lectin mitogens have been shown to bind the TCR, which is glycosylated through its carbohydrate moiety, thereby activating quiescent T cells (25). Mitogenic stimulation has been shown to increase the intracellular calcium (Ca^{2+}) level in T cells, which is absolutely essential for T cell proliferation. While PHA is a strong T cell mitogen (Fig. 4A), PWM is a weak T cell mitogen, but it also induces B cell activation and proliferation (Fig. 4B). While mitogens such as PHA activate T cells by binding to cell membrane glycoproteins, including the TCR-CD3 complex, there are a number of mitogenic or comitogenic antibodies, including those directed against the CD3 coreceptor, that can stimulate T cell proliferation (26). Typically, anti-CD3 antibodies provide an initial activation signal but do not induce significant proliferation (Fig. 5A and B) (27), and the addition of a costimulatory

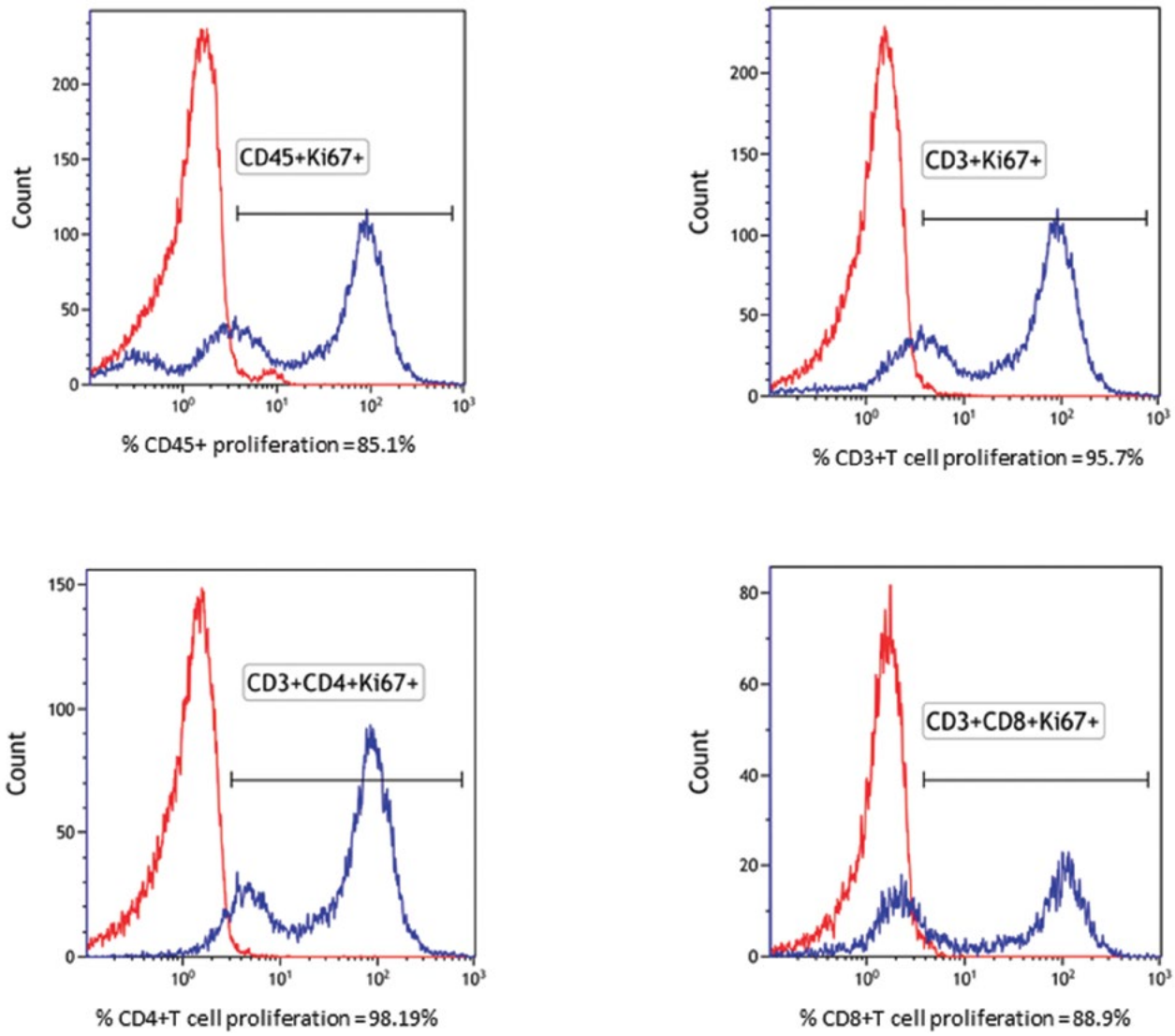

FIGURE 2 Ki-67-based cell proliferation. There are several markers available for flow cytometric measurement of cellular proliferation, including CFSE, Edu, and Ki-67. Ki-67 is a nuclear marker that assesses cell proliferation, and the use of specific antibodies in conjunction with this marker permits identification of proliferating subsets of T cells.

antibody (anti-CD28) provides the stimulus for robust proliferation (28) (Fig. 5A and B). An exogenous T cell growth factor, such as IL-2, may also be used as an alternative to anti-CD28 costimulation, and for patients with suspected IL-2 receptor-associated signaling defects, it may be more helpful than the use of anti-CD28 (Fig. 5A and B). IL-2, an autocrine cytokine, has been demonstrated to be critical for T cell proliferation and regulation of T cell growth (29–31). IL-2 stimulates T cell proliferation by binding to a heterotrimeric receptor complex consisting of 3 chains—α, β, and γ (IL-2Rα, IL-2Rβ, and IL-2Rγ)—on the surfaces of T cells. Triggering of the TCR leads to synthesis of IL-2 in certain T cell subsets and to induction of high-affinity IL-2Rs on antigen- or mitogen-activated T cells, and the binding of IL-2 to IL-2R ultimately leads to T cell proliferation. The use of exogenous IL-2 in association with anti-CD3 allows discrimination of whether T cells which cannot proliferate in response to other mitogenic signals can respond to a potent growth factor, such as IL-2. Stimulation of T cells with soluble antibodies to anti-CD3 (and the associated TCR complex) causes mobilization of cytoplasmic calcium and translocation of protein kinase C from the cytoplasm to the cell membrane. This stimulation also causes induction of phosphatidylinositol metabolism and subsequent IL-2 production for proliferation. T cell activation induced by anti-CD3 antibody requires prolonged stimulation of protein kinase C, which apparently can be achieved by the concomitant use of the anti-CD28 antibody for costimulation, without addition of other mitogenic stimuli, such as PMA. PMA can stimulate T cells by direct activation of protein kinase C (32).

Antigens such as *Candida* and tetanus toxoid (TT) have been used widely to measure antigen-specific recall (anamnestic) T cell responses for assessing cellular immunity. In fact, these methods may be more revealing about cellular immune compromise than assessing the response of

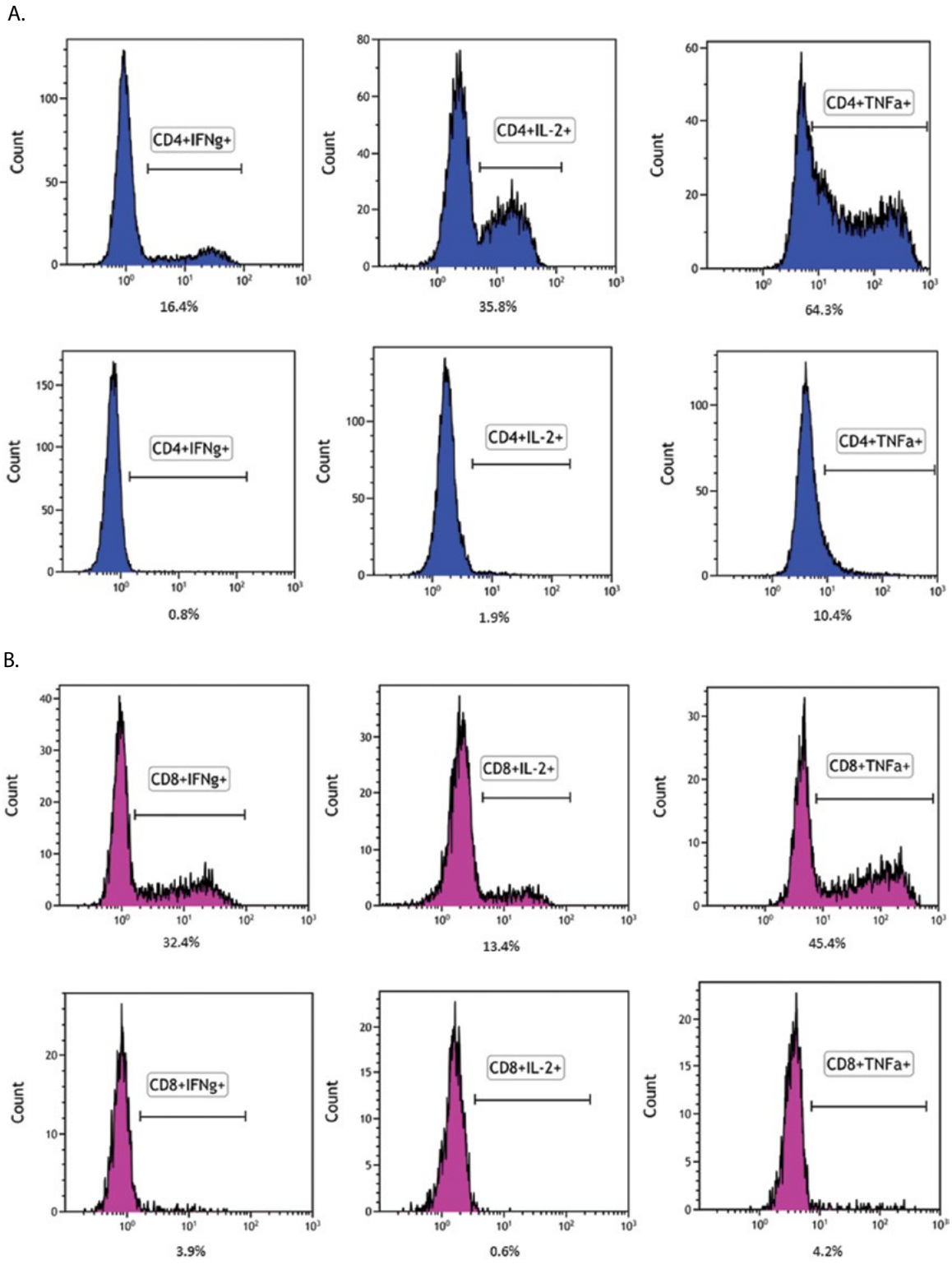

FIGURE 3 Activated T cells produce various cytokines in a temporally regulated manner. The important cytokines produced during the temporal course of T cell activation and differentiation include IL-2, IFN-γ, and TNF-α. (A) Polyfunctional T cell analysis of $CD4^+$ T cells. The cytokines are measured by intracellular flow cytometry analysis of $CD4^+$ T cells. The top panels show normal production of these cytokines in activated $CD4^+$ T cells from a healthy donor after cell stimulation *in vitro* with PHA. The bottom panels show the absence of cytokine production after stimulation of $CD4^+$ T cells from a patient with compromised cellular function. (B) Polyfunctional T cell analysis of $CD8^+$ T cells. The cytokines are measured by intracellular flow cytometry analysis of $CD8^+$ T cells. The top panels show normal production of these cytokines in activated $CD8^+$ T cells from a healthy donor after cell stimulation *in vitro* with PHA. The bottom panels show the absence of cytokine production after stimulation of $CD8^+$ T cells from a patient with compromised cellular function.

A.

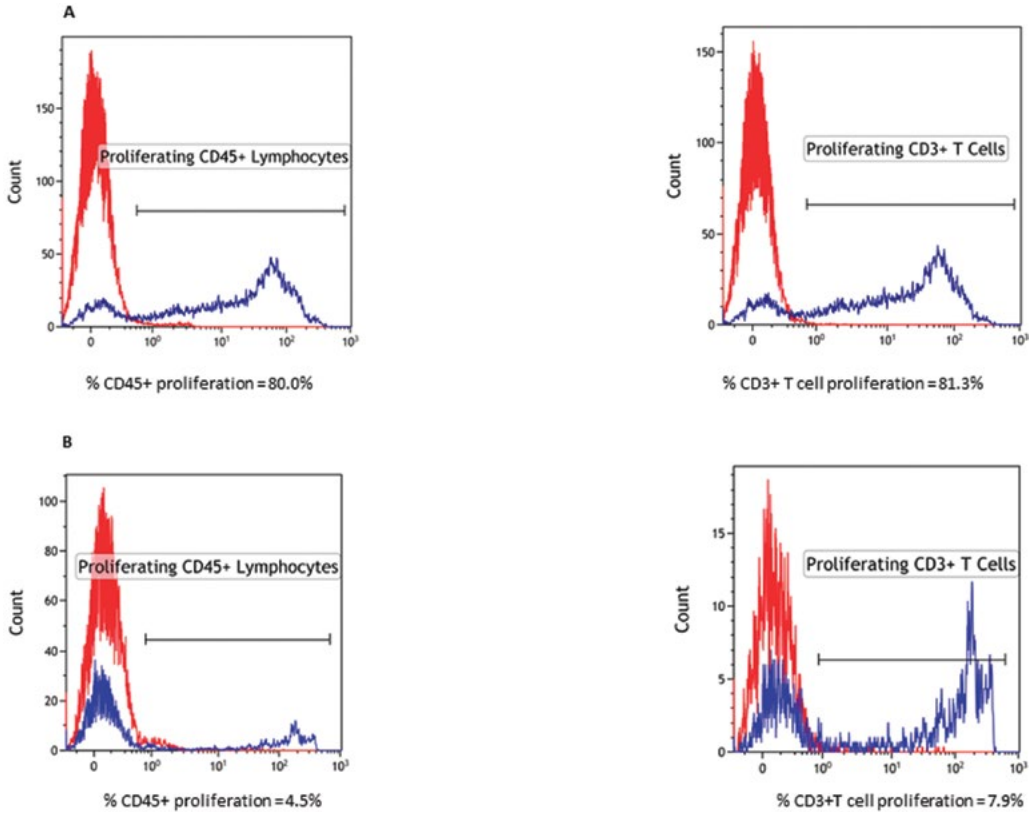
A
Proliferating CD45+ Lymphocytes
Count
% CD45+ proliferation = 80.0%
Proliferating CD3+ T Cells
Count
% CD3+ T cell proliferation = 81.3%
B
Proliferating CD45+ Lymphocytes
Count
% CD45+ proliferation = 4.5%
Proliferating CD3+ T Cells
Count
% CD3+T cell proliferation = 7.9%

B.

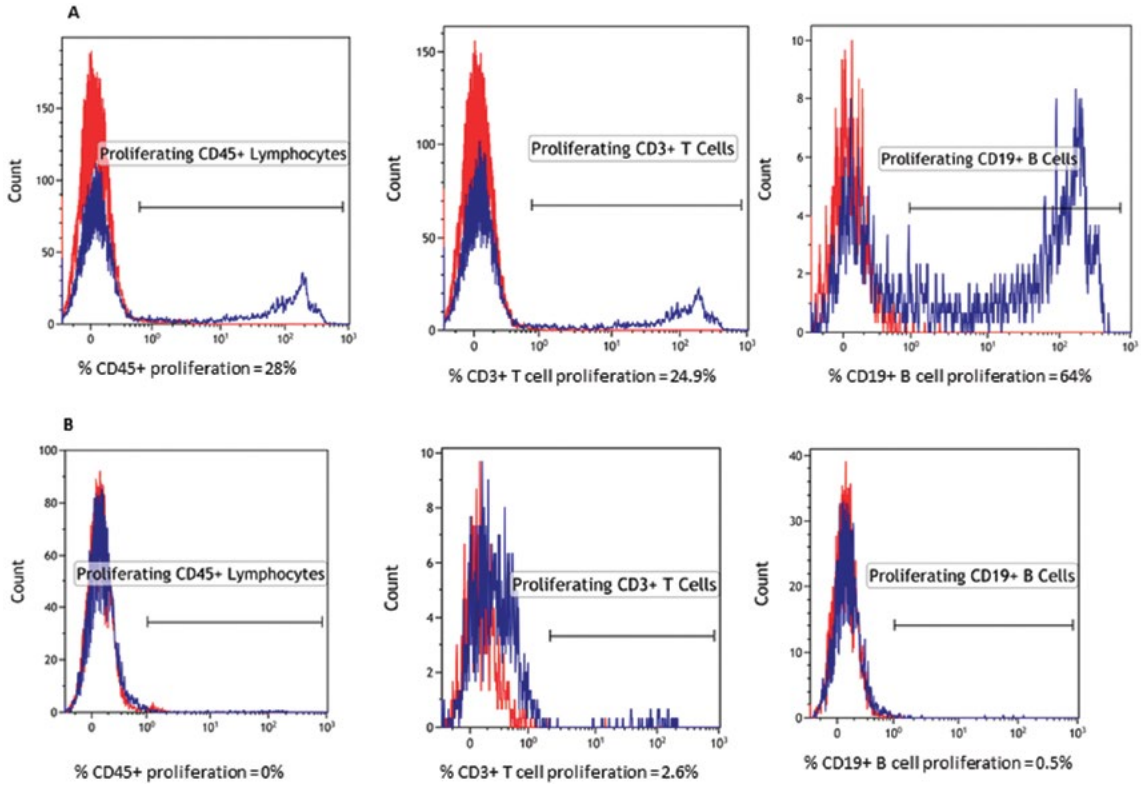
A
Proliferating CD45+ Lymphocytes
Count
% CD45+ proliferation = 28%
Proliferating CD3+ T Cells
Count
% CD3+ T cell proliferation = 24.9%
Proliferating CD19+ B Cells
Count
% CD19+ B cell proliferation = 64%
B
Proliferating CD45+ Lymphocytes
Count
% CD45+ proliferation = 0%
Proliferating CD3+ T Cells
Count
% CD3+ T cell proliferation = 2.6%
Proliferating CD19+ B Cells
Count
% CD19+ B cell proliferation = 0.5%

lymphocytes to mitogens, because the latter can induce T cell proliferative responses even if the T cells are incapable of responding adequately to antigenic (physiologic) stimuli. Therefore, abnormal T cell responses to antigens are considered a diagnostically more sensitive but less specific test of aberrant T cell function (24). Antigens used in recall assays measure the ability of T cells bearing specific TCRs to respond to such antigens when they are processed and presented by APCs. The antigens used for assessment of the cellular immune response are selected to represent antigens seen by a majority of the population, either through natural exposure (*Candida*) or as a result of vaccination (TT).

Cytotoxicity Assays

Functional assays of cytotoxic T cells include measurement of degranulation (exposure of cytotoxic granule membrane proteins on the cell surface after T cell activation) and direct assessment of cytotoxicity (33–35). Measurement of cellular degranulation is an assay that is currently available in some clinical immunology laboratories and involves flow cytometric analysis of CD107a and CD107b, which are cytotoxic granule membrane proteins that are expressed on the cell surface during degranulation following T cell activation (36) or in NK cells, the difference being that cytotoxic granules are organized in CD8 T cells only following antigen exposure and activation and are not present in naive CD8 T cells. NK cells constitutively possess cellular granules capable of participating in cytotoxic function. Cellular degranulation is a feature of antigen-experienced cells (37); however, contrary to popular conception, it does not always serve as a surrogate marker of cellular cytotoxic function, since the ability to mediate cytotoxicity depends on cytotoxic granule protein content rather than the actual degranulation process. At least half of the patients with perforin (*PRF1*) deficiency associated with familial hemophagocytic lymphohistiocytosis type 2 in one study (38) had normal degranulation but abnormal cytotoxic function due to the absence of a key cytotoxic protein, perforin. Degranulation is not only a function of cytotoxic T cells but also part of the mechanism of cytotoxic activity of NK cells. Degranulation is often used in the diagnostic setting for assessment of patients with suspected hemophagocytic lymphohistiocytosis, particularly the familial forms (38). Detailed procedures for measuring T cell cytotoxicity and NK cell cytotoxicity can be found in chapters 32 and 79, by Chiang and Bryceson and by Risma and Marsh, respectively.

ASSESSMENT OF Treg FUNCTION

While assays for measuring T and NK cell activation and function are relatively widespread in the diagnostic immunology realm, there is a growing recognition of the need for assays to evaluate and measure human regulatory T cell (Treg) function *in vitro* to facilitate diagnostic work-up in the appropriate clinical contexts (autoimmunity, primary immunodeficiencies, transplantation, and cancer), as well as adoptive immunotherapy approaches. Human Tregs, conventionally identified as $CD4^+$ $CD25^{high}$ $CD127^{low}$ $FOXP3^+$, are critical to maintaining the balance essential for immunological tolerance and normal immune function (39, 40). Tregs have a suppressive effect on T cell activation and proliferation by effector cells, and this feature can be exploited in the development of *in vitro* diagnostic tests to measure Treg function (41, 42). A rapid diagnostic test for Treg function involves Treg-mediated inhibition of the T cell activation markers CD69 and CD40L (CD154) on activated T cells stimulated with immobilized anti-CD3 and anti-CD28 for 7 h of coculture (42). There are several other protocols available for measuring Treg function (43, 44) that are amenable to adaptation for the clinical laboratory. Tregs suppress effector T cell activity in a cytokine-dependent manner both *in vivo* and *in vitro* (45–48). Treg suppression assays require purification or sorting of Tregs to coculture with effector cells, and this can be achieved via flow cytometry-based cell sorting (BD Biosciences, San Jose, CA) or magnetic bead sorting (Stem Cell Technologies, Vancouver, Canada; Miltenyi Biotec Ltd., Surrey, United Kingdom). While there are some varied reports in the literature as to whether bead-isolated Tregs have a suppressive function (41, 49), advances in magnetic bead sorting indicate that it is a viable process for deriving purified populations of Tregs for use in *in vitro* assays. A detailed procedure for Treg assays can be found in chapter 31 by Whiteside.

SUMMARY

The preceding sections provide ample evidence that lymphocyte activation is a complex process and a key component to maintaining normal immune function. The clinical relevance of studying and measuring lymphocyte activation is particularly noteworthy in the context of primary immunodeficiencies, caused by monogenic defects that affect various components and functions of the immune system. There are several genetic defects identified in recent years that affect T and/or NK cell function, including DOCK8, MAGT1, p85α, IL-17RA, IL-17F, and STAT3 deficiencies (50), and this is not a comprehensive list of such defects. Also, measurement of lymphocyte activation is relevant to solid organ transplantation, recovery of immune function in hematopoietic cell transplantation, and assessment of immune competence in patients on biological or pharmacological immunosuppressive therapies. This chapter provides a primer on the concepts and practical approaches to assessing T and NK cell function in the clinical immunology laboratory.

METHODOLOGY FOR MEASURING LYMPHOCYTE ACTIVATION IN THE LABORATORY

Note that the following methods are not laboratory standard operating procedures or complete protocols. They are meant only to provide broad guidelines on how various lymphocyte activation assays are performed. Please consult an actual standard operating procedure or protocol for specific details on setting up and validating these assays for the clinical laboratory.

FIGURE 4 (A) Flow cytometry analysis of T cell proliferation in response to PHA. PHA is a commonly used mitogen for global assessment of T cell function. The top panels show normal proliferative responses to PHA for a healthy individual, and the bottom panels show decreased T cell proliferation for a patient with T cell dysfunction. (B) Flow cytometry analysis of cell proliferation in response to PWM. PWM is a relatively weak T cell mitogen compared to PHA. However, PWM also induces B cell proliferation; hence, it is still used in the clinical laboratory. The top panels show normal proliferative responses to PWM for a healthy individual, and the bottom panels show decreased proliferation in both T and B cells for a patient with immunodeficiency.

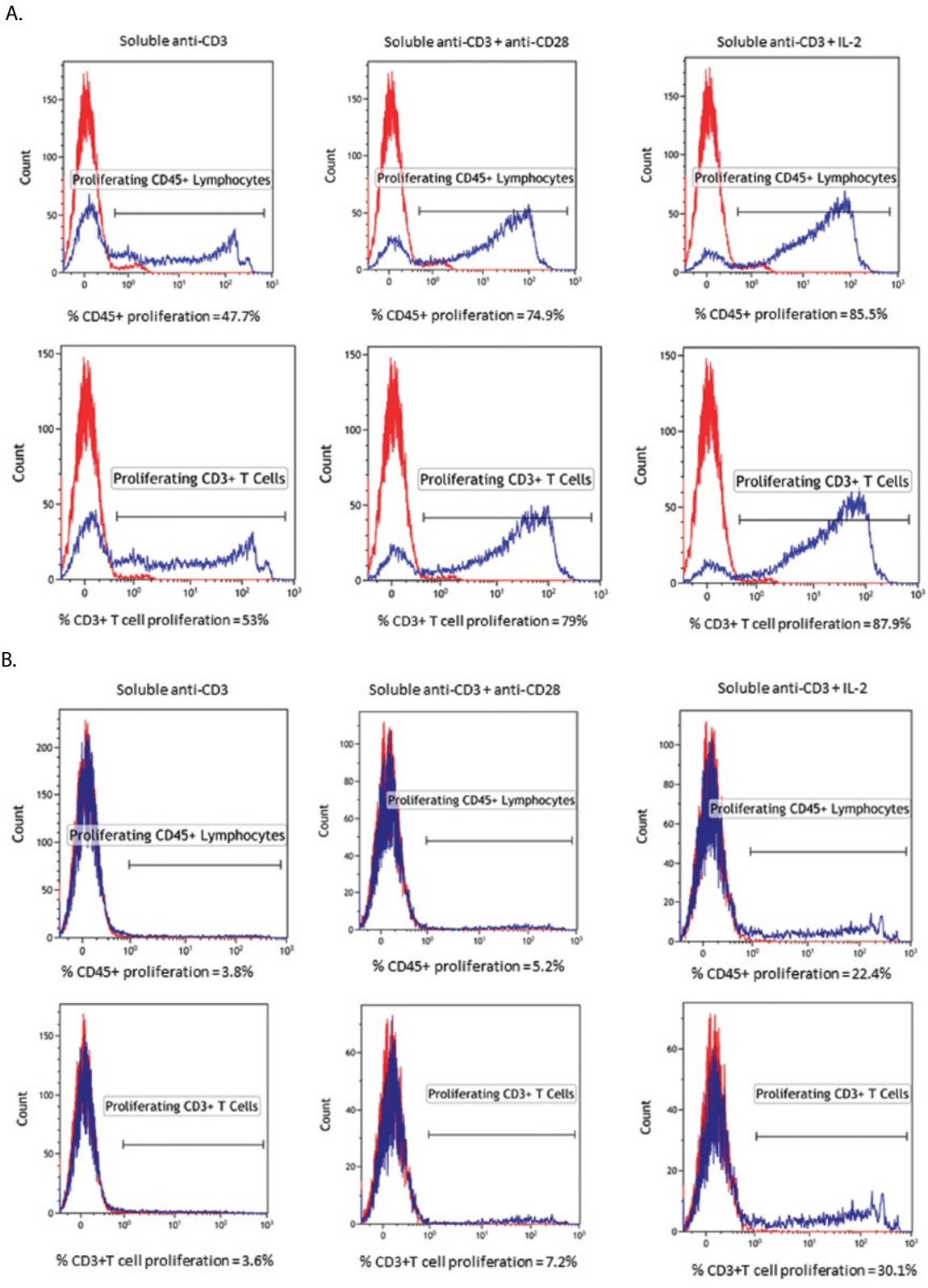

FIGURE 5 (A) Flow cytometry analysis of T cell proliferation in response to anti-CD3 stimulants for a healthy donor. Anti-CD3 antibody is often used to assess T cell functional competence, particularly in contexts where a detailed evaluation of T cell proliferative responses is essential. Soluble anti-CD3 alone delivers a weak mitogenic signal, although the addition of anti-CD28 or exogenous IL-2 to soluble anti-CD3 improves the proliferative response, as shown here. (B) Flow cytometry analysis of T cell proliferation in response to anti-CD3 stimulants in a patient with immunodeficiency. Soluble anti-CD3 alone delivers a weak signal, and addition of anti-CD28 does not show incremental proliferation. However, addition of exogenous IL-2 to soluble anti-CD3 modestly improves the proliferative response, though it remains outside the normal values for age.

Lymphocyte Proliferation Assay Using Edu-Based Flow Cytometry (Fig. 1)

1. PBMCs are isolated from sodium heparin-blood from patient or healthy donor samples by using a manual or automated method.
2. Cells are resuspended in medium with 5% human AB serum to a final concentration of 0.5×10^6 cells per well in a 48-well flat-bottom plate for mitogens alone. Cells are resuspended in medium with 5% human AB serum to a final concentration of 1.0×10^6 cells per well in a 48-well flat-bottom plate for antigens and the anti-CD3 panel.
3. Cells are incubated with various concentrations of PHA (0.5 to 20 μg/ml), PWM (0.5 to 20 μg/ml), *Candida*, TT (1 to 20 μg/ml), soluble anti-CD3 alone, anti-CD28 (5 to 25 ng/ml), or soluble anti-CD3 with IL-2 (5 to 25 ng/ml with 40 standardized units of IL-2/ml) for 3 days at 37°C in a 5% CO_2 incubator.
4. On day 3 of culture with mitogens or anti-CD3 panel stimulants (72 h of stimulation), the cells are pulsed for 18 to 24 h with 10 μM Edu (final concentration) in the presence of copper to obtain a covalent bond with the fluorescent azide AlexaFluor488. For antigens, cells are cultured for 6 days before pulsing for 18 to 24 h.
5. Following pulsing, the cells are harvested and analyzed by flow cytometry for viable, apoptotic, and dead lymphocytes by using a combination of anti-human CD45 antibody (identification of lymphocytes along with the side scatter parameter), annexin V (apoptotic cells), and 7-AAD (dead cells are positive for both annexin V and 7-AAD, while viable cells are negative for both markers). Cell proliferation is assessed by staining the cultured cells for CD45 (lymphocytes), CD3 (T cells), and CD19 (B cells only for PWM proliferation) along with CD69 (T cell activation marker). The percentage of proliferating cells in each category (total lymphocytes [$CD45^+$], $CD3^+$ T cells, and $CD19^+$ B cells) is determined by identifying the proportion of Edu-positive cells relative to the total parent population. The delta percentage is derived by subtracting the proliferation in the background (medium control) wells from that in the stimulated wells.
6. The flow cytometric analysis can be performed on any 6-, 8-, or 10-color digital flow cytometer (BD FACS Canto A or Canto II or Beckman Coulter Gallios).
7. The flow cytometric assay typically collects 20,000 events in the lymphocyte or $CD3^+$ T cell category, though the assay shows linearity and precision for a range of 200 to 20,000 events.
8. Standard flow cytometry practices must be followed to ensure instrument and assay performance.
9. Ki-67 proliferation can be measured in a manner similar to that described above, with the following differences. Following stimulation with PHA, similar to that described above, the cells are washed with 1% bovine serum albumin (BSA) and then stained for cell surface antigens for 15 min at room temperature with the following antibodies: CD45RA–phycoerythrin (PE)–Cy7 (optional), CD45RO–FITC (optional), CD3-allophycocyanin-AF750, CD4-PE (optional), and CD8-PB (optional). Following incubation, 1 ml FACS Lyse solution (BD Biosciences, San Jose, CA) is added to each tube for 15 min, and the sample is subsequently washed with 2 ml stain buffer (BD Biosciences) and resuspended in 500 μl of Fix/Perm buffer for 30 min (BD Biosciences). An additional wash is performed with 2 ml Fix/Perm wash buffer (BD Biosciences). The cells are stained with Ki-67–allophycocyanin for 30 min at room temperature and then washed again with 2 ml Fix/Perm wash buffer and resuspended in 500 μl of 1% paraformaldehyde.

Assessment of Cell Surface Markers on T Cells after Activation with Mitogenic Stimuli (Fig. 4)

1. PBMCs are isolated from sodium heparin-blood from patient or healthy donor samples by using a manual or automated method.
2. Cells are incubated in 48-well plates in 5% human AB serum-enriched medium to a final cell concentration of 0.5×10^6 cells/ml.
3. Cells are stimulated with either PHA (final concentration of 5 μg/ml) or PMA plus ionomycin (125 ng/ml and 5 μg/ml, respectively).
4. Cells are cultured for either 2, 4, 24, 48, or 72 h at 37°C in a 5% CO_2 incubator. At each time point, cells are harvested and washed with 1% BSA-containing phosphate-buffered saline for 5 min at $500 \times g$ and then resuspended in 100 μl of 1% BSA.
5. The following antibody cocktail is added: CD45-KO, CD3-PE-Cy7, CD69-allophycocyanin, CD40L-PE, CD25-allophycocyanin-Cy7, CD4-peridinin chlorophyll protein, CD8-PB, and HLA DR-FITC. Cells are incubated with the antibodies for 15 min at room temperature, followed by a wash with 1% BSA–phosphate-buffered saline for 5 min at $500 \times g$. The cells are resuspended in 1% paraformaldehyde.
6. Samples are analyzed on a 10-color Beckman Coulter Gallios flow cytometer collecting 20,000 $CD45^+$lymphocytes, and analysis is performed using Kaluza v.1.2 software (Beckman Coulter).

Measurement of Polyfunctional T Cells after Stimulation with Mitogens (Intracellular Cytokine Production by CD4 and CD8 T Cells after Activation) (Fig. 3)

1. Each patient sample is prepared in a set of three tubes: unstimulated, stimulated with PMA-ionomycin, and stimulated with PHA.
2. Stimulants and other reagents are prepared to the final concentrations indicated below in RPMI medium.
   - PMA, 25 ng/ml
   - Ionomycin, 20 μg/ml
   - PHA, 20 μg/ml
   - Brefeldin A (BFA)/Golgi Stop, 1:5 for BFA and 1:15 for Golgi Stop (add 2 μl/ml of BFA and 0.7 μl/ml for Golgi Stop)
3. BFA and Golgi Stop are added to each tube.
4. PMA-ionomycin or PHA is added as appropriate to the relevant tubes.
5. To each of the tubes, 1 ml sodium heparin-blood is added and mixed gently.
6. The tubes are incubated at 37°C in 5% CO_2 for 3 h.
7. The samples are then removed from the incubator and brought back to room temperature.
8. The following antibodies are added to appropriately labeled tubes for flow staining: CD45-KO, CD3-allophycocyanin-AF750, CD4-allophycocyanin, CD8-PB, and CD14-FITC.
9. To each tube, 100 μl blood is added and incubated at room temperature in the dark for 20 min.

10. One milliliter of 1 × lysis buffer is added to each tube, vortexed immediately, and incubated at room temperature in the dark for an additional 10 min.
11. To each sample, 2 ml stain buffer is added, and cells are washed, fixed, and permeabilized using Fix/Perm solution.
12. Following this, cells are mixed and incubated for 20 min in the dark at room temperature.
13. Cells are washed in Perm/Wash buffer and stained with the following antibodies by mixing and incubating for 20 min in the dark at room temperature: IFN-γ–PE, TNF-α–PE7, and IL-2–peridinin chlorophyll protein–Cy5.5.
14. Cells are washed in Perm/Wash buffer and resuspended in 1% paraformaldehyde.
15. Flow cytometry analysis is performed on a Beckman Coulter Gallios instrument, and data analysis is performed using Kaluza v.1.2 software (Beckman Coulter, Miami, FL).

All figures were generated in my Cellular and Molecular Immunology Laboratory, Department of Laboratory Medicine and Pathology, Mayo Clinic, Rochester, MN. from flow cytometry analyses using healthy donor or patient samples.

REFERENCES

1. **Smith-Garvin JE, Koretzky GA, Jordan MS.** 2009. T cell activation. *Annu Rev Immunol* **27:**591–619.
2. **Watts C.** 1997. Capture and processing of exogenous antigens for presentation on MHC molecules. *Annu Rev Immunol* **15:**821–850.
3. **Biselli R, Matricardi PM, D'Amelio R, Fattorossi A.** 1992. Multiparametric flow cytometric analysis of the kinetics of surface molecule expression after polyclonal activation of human peripheral blood T lymphocytes. *Scand J Immunol* **35:**439–447.
4. **Shipkova M, Wieland E.** 2012. Surface markers of lymphocyte activation and markers of cell proliferation. *Clin Chim Acta* **413:**1338–1349.
5. **Caruso A, Licenziati S, Corulli M, Canaris AD, De Francesco MA, Fiorentini S, Peroni L, Fallacara F, Dima F, Balsari A, Turano A.** 1997. Flow cytometric analysis of activation markers on stimulated T cells and their correlation with cell proliferation. *Cytometry* **27:**71–76.
6. **Lim LC, Fiordalisi MN, Mantell JL, Schmitz JL, Folds JD.** 1998. A whole-blood assay for qualitative and semiquantitative measurements of CD69 surface expression on CD4 and CD8 T lymphocytes using flow cytometry. *Clin Diagn Lab Immunol* **5:**392–398.
7. **Simms PE, Ellis TM.** 1996. Utility of flow cytometric detection of CD69 expression as a rapid method for determining poly- and oligoclonal lymphocyte activation. *Clin Diagn Lab Immunol* **3:**301–304.
8. **Davies EG, Thrasher AJ.** 2010. Update on the hyper immunoglobulin M syndromes. *Br J Haematol* **149:**167–180.
9. **Hawkins ED, Hommel M, Turner ML, Battye FL, Markham JF, Hodgkin PD.** 2007. Measuring lymphocyte proliferation, survival and differentiation using CFSE time-series data. *Nat Protoc* **2:**2057–2067.
10. **Quah BJ, Warren HS, Parish CR.** 2007. Monitoring lymphocyte proliferation in vitro and in vivo with the intracellular fluorescent dye carboxyfluorescein diacetate succinimidyl ester. *Nat Protoc* **2:**2049–2056.
11. **Quah BJ, Parish CR.** 2012. New and improved methods for measuring lymphocyte proliferation in vitro and in vivo using CFSE-like fluorescent dyes. *J Immunol Methods* **379:**1–14.
12. **Salic A, Mitchison TJ.** 2008. A chemical method for fast and sensitive detection of DNA synthesis in vivo. *Proc Natl Acad Sci USA* **105:**2415–2420.
13. **Yu Y, Arora A, Min W, Roifman CM, Grunebaum E.** 2009. EdU incorporation is an alternative non-radioactive assay to [(3)H]thymidine uptake for in vitro measurement of mice T-cell proliferations. *J Immunol Methods* **350:**29–35.
14. **Zeng C, Pan F, Jones LA, Lim MM, Griffin EA, Sheline YI, Mintun MA, Holtzman DM, Mach RH.** 2010. Evaluation of 5-ethynyl-2′-deoxyuridine staining as a sensitive and reliable method for studying cell proliferation in the adult nervous system. *Brain Res* **1319:**21–32.
15. **Last'ovicka J, Budinsky V, Spisek R, Bartunkova J.** 2009. Assessment of lymphocyte proliferation: CFSE kills dividing cells and modulates expression of activation markers. *Cell Immunol* **256:**79–85.
16. **Soares A, Govender L, Hughes J, Mavakla W, de Kock M, Barnard C, Pienaar B, Janse van Rensburg E, Jacobs G, Khomba G, Stone L, Abel B, Scriba TJ, Hanekom WA.** 2010. Novel application of Ki67 to quantify antigen-specific in vitro lymphoproliferation. *J Immunol Methods* **362:**43–50.
17. **Scholzen T, Gerdes J.** 2000. The Ki-67 protein: from the known and the unknown. *J Cell Physiol* **182:**311–322.
18. **Cellerai C, Harari A, Vallelian F, Boyman O, Pantaleo G.** 2007. Functional and phenotypic characterization of tetanus toxoid-specific human CD4+ T cells following reimmunization. *Eur J Immunol* **37:**1129–1138.
19. **Miller JD, van der Most RG, Akondy RS, Glidewell JT, Albott S, Masopust D, Murali-Krishna K, Mahar PL, Edupuganti S, Lalor S, Germon S, Del Rio C, Mulligan MJ, Staprans SI, Altman JD, Feinberg MB, Ahmed R.** 2008. Human effector and memory CD8+ T cell responses to smallpox and yellow fever vaccines. *Immunity* **28:**710–722.
20. **Stubbe M, Vanderheyde N, Goldman M, Marchant A.** 2006. Antigen-specific central memory CD4+ T lymphocytes produce multiple cytokines and proliferate in vivo in humans. *J Immunol* **177:**8185–8190.
21. **Haining WN.** 2012. Travels in time: assessing the functional complexity of T cells. *Proc Natl Acad Sci USA* **109:**1359–1360.
22. **Han Q, Bagheri N, Bradshaw EM, Hafler DA, Lauffenburger DA, Love JC.** 2012. Polyfunctional responses by human T cells result from sequential release of cytokines. *Proc Natl Acad Sci USA* **109:**1607–1612.
23. **Newell EW, Sigal N, Bendall SC, Nolan GP, Davis MM.** 2012. Cytometry by time-of-flight shows combinatorial cytokine expression and virus-specific cell niches within a continuum of CD8+ T cell phenotypes. *Immunity* **36:**142–152.
24. **Stone KD, Feldman HA, Huisman C, Howlett C, Jabara HH, Bonilla FA.** 2009. Analysis of in vitro lymphocyte proliferation as a screening tool for cellular immunodeficiency. *Clin Immunol* **131:**41–49.
25. **Chilson OP, Boylston AW, Crumpton MJ.** 1984. Phaseolus vulgaris phytohaemagglutinin (PHA) binds to the human T lymphocyte antigen receptor. *EMBO J* **3:**3239–3245.
26. **Ledbetter JA, Gentry LE, June CH, Rabinovitch PS, Purchio AF.** 1987. Stimulation of T cells through the CD3/T-cell receptor complex: role of cytoplasmic calcium, protein kinase C translocation, and phosphorylation of pp60c-src in the activation pathway. *Mol Cell Biol* **7:**650–656.
27. **Lamers CH, van de Griend RJ, Braakman E, Ronteltap CP, Bénard J, Stoter G, Gratama JW, Bolhuis RL.** 1992. Optimization of culture conditions for activation and large-scale expansion of human T lymphocytes for bispecific antibody-directed cellular immunotherapy. *Int J Cancer* **51:**973–979.

28. **Trickett A, Kwan YL.** 2003. T cell stimulation and expansion using anti-CD3/CD28 beads. *J Immunol Methods* **275:**251–255.
29. **Cornish GH, Sinclair LV, Cantrell DA.** 2006. Differential regulation of T-cell growth by IL-2 and IL-15. *Blood* **108:**600–608.
30. **Kaempfer R.** 1994. Regulation of the human interleukin-2/interleukin-2 receptor system: a role for immunosuppression. *Proc Soc Exp Biol Med* **206:**176–180.
31. **Lifson J, Raubitschek A, Benike C, Koths K, Ammann A, Sondel P, Engleman E.** 1986. Purified interleukin-2 induces proliferation of fresh human lymphocytes in the absence of exogenous stimuli. *J Biol Response Mod* **5:**61–72.
32. **Kay JE.** 1991. Mechanisms of T lymphocyte activation. *Immunol Lett* **29:**51–54.
33. **Barber DL, Wherry EJ, Ahmed R.** 2003. Cutting edge: rapid in vivo killing by memory CD8 T cells. *J Immunol* **171:**27–31.
34. **Liu L, Chahroudi A, Silvestri G, Wernett ME, Kaiser WJ, Safrit JT, Komoriya A, Altman JD, Packard BZ, Feinberg MB.** 2002. Visualization and quantification of T cell-mediated cytotoxicity using cell-permeable fluorogenic caspase substrates. *Nat Med* **8:**185–189.
35. **Liu L, Packard BZ, Brown MJ, Komoriya A, Feinberg MB.** 2004. Assessment of lymphocyte-mediated cytotoxicity using flow cytometry. *Methods Mol Biol* **263:**125–140.
36. **Betts MR, Brenchley JM, Price DA, De Rosa SC, Douek DC, Roederer M, Koup RA.** 2003. Sensitive and viable identification of antigen-specific CD8+ T cells by a flow cytometric assay for degranulation. *J Immunol Methods* **281:**65–78.
37. **Wolint P, Betts MR, Koup RA, Oxenius A.** 2004. Immediate cytotoxicity but not degranulation distinguishes effector and memory subsets of CD8+ T cells. *J Exp Med* **199:**925–936.
38. **Bryceson YT, Pende D, Maul-Pavicic A, Gilmour KC, Ufheil H, Vraetz T, Chiang SC, Marcenaro S, Meazza R, Bondzio I, Walshe D, Janka G, Lehmberg K, Beutel K, zur Stadt U, Binder N, Arico M, Moretta L, Henter JI, Ehl S.** 2012. A prospective evaluation of degranulation assays in the rapid diagnosis of familial hemophagocytic syndromes. *Blood* **119:**2754–2763.
39. **Liu W, Putnam AL, Xu-Yu Z, Szot GL, Lee MR, Zhu S, Gottlieb PA, Kapranov P, Gingeras TR, Fazekas de St Groth B, Clayberger C, Soper DM, Ziegler SF, Bluestone JA.** 2006. CD127 expression inversely correlates with FoxP3 and suppressive function of human CD4+ T reg cells. *J Exp Med* **203:**1701–1711.
40. **Sakaguchi S.** 2004. Naturally arising CD4+ regulatory T cells for immunologic self-tolerance and negative control of immune responses. *Annu Rev Immunol* **22:**531–562.
41. **Baecher-Allan C, Wolf E, Hafler DA.** 2005. Functional analysis of highly defined, FACS-isolated populations of human regulatory CD4+ CD25+ T cells. *Clin Immunol* **115:**10–18.
42. **Canavan JB, Afzali B, Scottà C, Fazekasova H, Edozie FC, Macdonald TT, Hernandez-Fuentes MP, Lombardi G, Lord GM.** 2012. A rapid diagnostic test for human regulatory T-cell function to enable regulatory T-cell therapy. *Blood* **119:**e57–e66.
43. **Boks MA, Zwaginga JJ, van Ham SM, ten Brinke A.** 2010. An optimized CFSE-based T-cell suppression assay to evaluate the suppressive capacity of regulatory T-cells induced by human tolerogenic dendritic cells. *Scand J Immunol* **72:**158–168.
44. **Collison LW, Vignali DA.** 2011. In vitro Treg suppression assays. *Methods Mol Biol* **707:**21–37.
45. **Asseman C, Mauze S, Leach MW, Coffman RL, Powrie F.** 1999. An essential role for interleukin 10 in the function of regulatory T cells that inhibit intestinal inflammation. *J Exp Med* **190:**995–1004.
46. **Collison LW, Pillai MR, Chaturvedi V, Vignali DA.** 2009. Regulatory T cell suppression is potentiated by target T cells in a cell contact, IL-35- and IL-10-dependent manner. *J Immunol* **182:**6121–6128.
47. **Kingsley CI, Karim M, Bushell AR, Wood KJ.** 2002. CD25+CD4+ regulatory T cells prevent graft rejection: CTLA-4- and IL-10-dependent immunoregulation of alloresponses. *J Immunol* **168:**1080–1086.
48. **Szymczak-Workman AL, Workman CJ, Vignali DA.** 2009. Cutting edge: regulatory T cells do not require stimulation through their TCR to suppress. *J Immunol* **182:**5188–5192.
49. **Elkord E, Hopcraft L, Burt D, Stern PL.** 2006. Bead-isolated human CD4+CD25+ T regulatory cells are anergic and significantly suppress proliferation of CD4+CD25− T responder cells. *Clin Immunol* **120:**232–233.
50. **Milner JD, Holland SM.** 2013. The cup runneth over: lessons from the ever-expanding pool of primary immunodeficiency diseases. *Nat Rev Immunol* **13:**635–648.

Functional Assays for B Cells and Antibodies

MOON H. NAHM AND ROBERT L. BURTON

29

The primary cells of the adaptive immune system are T cells, B cells, and natural killer cells. These lymphocytes assist the host in eliminating both intracellular pathogens (T cells and NK cells) and extracellular pathogens (B cells) through B cell-T cell interactions, as well as interactions with other cells and molecules of the innate immune system. B cells recognize foreign antigen by the B-cell receptor (BCR), a membrane-bound immunoglobulin generated through a complex genetic recombination process (1). The BCR recognizes conformational protein antigens as well as nonprotein antigens. Two types of B cells have been described based on expression of cell surface molecules and function. B1 ($CD5^+$) B cells are thought to be a more "natural" type of B cell which respond to T-cell-independent forms of antigen (i.e., bacterial polysaccharides) (2, 3). B2 B cells respond to T-cell-dependent antigens, such as the classic protein antigens tetanus and diphtheria toxoids. Both classes of B cells respond to BCR binding of antigen by proliferation, differentiation into antibody-secreting plasma cells, and formation of memory B cells.

The function of the humoral immune response differs depending on the class of antibody produced and the differentiation state of the B cell. Naive B cells express CD19, CD20, and surface IgM and IgD (Table 1). After BCR stimulation, B cells become memory cells or plasma cells, which express unique antigens. In addition, immunoglobulin class switching occurs and IgG, IgA, or IgE is produced. Each of these immunoglobulin classes has distinct functions. IgM can bind pathogens and activate complement. IgG can directly neutralize bacterial toxins, block adhesion of pathogens, and also activate complement. IgA can also neutralize toxins and block adhesion of pathogens, but it functions primarily at mucosal sites, while IgE plays a role in the immune response to parasites. After BCR stimulation, the immunoglobulin produced by B cells also increases its affinity for antigen, therefore improving the functionality of the humoral response.

Primary defects in the humoral components of the immune response are often manifested early in life. Certain types of infection, or frequent or incompletely cleared infections, are signs of possible B cell/antibody defects (Table 2). Primary immunodeficiencies are covered in greater detail in chapters 75 and 76. A more immediate concern to most physicians is the increasing incidence of secondary immune deficiencies due to infections such as HIV (covered in chapter 72), cancer (multiple myeloma), chronic renal failure, autoimmune processes, or posttransplantation immunosuppression.

In some patients, the absence of B-cell function is simply due to a lack of B cells. In many cases, patients may have B cells, but their function is abnormal because the B cells are either tolerized or anergic. There is also a need to measure functionality of antibodies since not all antibodies are protective. Very young children, elderly adults, and HIV-positive individuals may be more prone to producing ineffective antibodies. These ineffective antibodies may express inappropriate isotypes or V regions, resulting in low-avidity antibodies or the inability to activate complement.

APPROACHES FOR ASSESSING B CELL FUNCTION

A complete blood count (CBC) is often the first test performed in the evaluation of the humoral immune response. However, the CBC is clearly not a good indicator of underlying disease, as often the total lymphocyte count in humoral immunodeficiencies is normal or only slightly decreased. Therefore, the next step in the evaluation of a possible humoral immunodeficiency is the measurement of antibody production.

In Vivo B-Cell Function

Immunoglobulins

The most direct measure of *in vivo* B-cell function is immunoglobulin secretion by plasma cells. Serum immunoglobulin concentrations (routinely IgG, IgA, and IgM) are most commonly measured by automated nephelometry or turbidimetry (described in detail in chapter 7). The normal ranges for serum immunoglobulins vary depending on both the age and gender of the individual (4). A significant seasonal variation in serum IgA levels has also been described (5). In addition to the measurement of total serum immunoglobulin concentrations, levels of subclasses of IgG and IgA can also be determined by automated nephelometry. Patients have been reported to have deficiencies of one or more subclasses of IgG even though they have normal levels of total serum IgG. However, the true biological significance of IgG subclass deficiencies remains controversial (6, 7). Conversely, the incidence of bacterial infections is increased in some individuals

doi:10.1128/9781555818722.ch29

TABLE 1 B-cell markers used in flow cytometry

Marker	B-cell population
CD19	Early B cells to B-cell blasts
CD20	Pre-B cells to B-cell blasts
CD23	Activated B cells
CD27	Memory B cells
CD5	B1 B cells
Surface IgM	Immature, mature, and memory B cells
Surface IgD	Mature and memory B cells
Surface IgG, IgA, and IgE	Isotype-switched memory B cells
CD138 (syndecan 1)	Plasma cells

with normal IgG subclass concentrations, such as IgG2 in patients with Wiskott–Aldrich syndrome who cannot produce antibodies to many bacterial polysaccharides (8).

The presence of antibodies against common antigens is indicative of an intact humoral immune system in patients. The levels of anti-A or anti-B isohemagglutinin IgM antibodies are often determined for this purpose. The presence of these antibodies against blood-group antigens depends on both the age of the patient and the patient's blood group (i.e., no blood-group antibodies are found in the serum of blood type AB individuals). As IgM is produced by the newborn, this type of testing can be performed earlier than testing for vaccine-induced immunoglobulins. A titer of 8 or above is considered normal (9).

It is more clinically significant to measure serum antibody levels to typical vaccine components, such as tetanus, diphtheria, pneumococcus, or *Haemophilus influenzae* type b. If immunoglobulin titers against common vaccine antigens are low, then specific antigen challenge should be performed. Serum samples are obtained before and 2 to 4 weeks after vaccination. These paired sera are then tested simultaneously and a patient is generally considered to mount an adequate response if a 4-fold or greater rise in specific titer is seen. This type of challenge can be performed with neoprotein antigens such as bacteriophage ϕX174 or keyhole limpet hemocyanin, but clinically available vaccines such as pneumococcal vaccines are often used (10–12).

To quantify antibody levels against pneumococcal capsular polysaccharides (PSs), an enzyme-linked immunosorbent assay (ELISA) has been developed and well characterized (reviewed in reference 13). The current WHO consensus protocol (described in more detail in the Methodologies section "Pneumococcal ELISA" below), which includes absorption with cell wall polysaccharides (C-PS) and capsular PS from serotype 22F, has been used extensively in licensure studies for pneumococcal conjugate vaccines. Inclusion of 22F PS for absorption increased the assay specificity, especially when testing samples from children for vaccine serotypes. One limitation of this method is that it is used to quantify the IgG response only. There is mounting evidence of a significant IgM response to pneumococcal conjugate vaccine (14, 15). Thus, inclusion of IgM antibody levels against vaccine antigens may be needed for a complete evaluation of response to pneumococcal vaccines.

TABLE 2 Associations with humoral or B-lymphocyte deficiencies

Infectious agents
Streptococcus pneumoniae
Streptococcus pyogenes
Haemophilus influenzae
Ureaplasma urealyticum
Giardia lambia
Clinical conditions
Recurrent otitis
Recurrent pharyngitis
Recurrent sinusitis
Recurrent bronchitis
Recurrent conjunctivitis

In order to determine the overall response to pneumococcal vaccination, antibody levels to multiple serotypes must be determined. Thus, many reference laboratories that analyze clinical samples have developed multiplexed immunoassays for pneumococcal antibodies, most based on the technology described by Pickering et al. (16). A recent comparison study found significant differences in antibody levels from different laboratories using multiplexed assays, although the study concluded that the clinical classification of patients as "protected" or "nonprotected" was comparable between the laboratories (17), with additional commentary (18). Thus, absolute antibody levels may be not be suitable as a determinant of an adequate immunological response to vaccine, but fold increase may still be useful provided pre- and post-vaccine levels are determined by the same laboratory.

Peripheral Blood B Cells

The actual number of B cells in the peripheral blood cannot be determined by the CBC. B cells can, however, be identified through the use of flow cytometry (refer to chapters 18 and 20). In this technique, cells are characterized by their expression of cell surface markers, and the percentage and absolute cell number of B cells expressing certain immunophenotypes is compared to age-matched reference intervals (19). The most classic B-cell surface markers are CD19 and CD20 (Table 1). CD19 is a critical signal transduction molecule that regulates B lymphocyte development, differentiation, and activation. It is expressed on B cells from the earliest recognizable B lineage (early Ig gene rearrangements) to B-cell blasts. However, the expression is lost upon plasma cell maturation. CD20 is expressed on B cells from the pre-B stage to the B-cell lymphoblast stage but is not found on early B-cell progenitors or plasma cells. In general, $CD19^+CD20^+$ cells are between 5 and 10% of the total peripheral blood lymphocyte pool. Upon antigen activation, a number of cell surface markers are detected on B cells (Table 1). The presence or absence of these markers can be useful in the evaluation of B cell deficiencies in patients. One such example is the absence of $CD27^+IgD^-IgM^-$ mature class-switched memory B cells in X-linked hyper-IgM syndrome and a sub-population of patients with common variable immunodeficiency (20–22). It has also been shown that flow cytometry can identify antigen-specific B cells through BRC binding of labeled specific antigen (23).

In Vitro B-Cell Function

Flow cytometric analysis of B-cell populations is only useful for identifying defects in the actual numbers of B cells. In order to identify functional abnormalities, additional studies must be undertaken. The classic evaluation of B-cell function is through the isolation of peripheral blood lymphocytes from the patient and culturing them with agents known to activate normal B cells. This assay is known as the lymphocyte proliferation assay (LPA) (24, 25). In the LPA, either whole blood or purified peripheral blood mononuclear cells (PBMC) are cultured with a variety of stimulants

to determine the B-cell response. The cells are cultured with the stimulants for 3 to 7 days, and the effects of this activation can be measured by cellular proliferation and/or antibody secretion. The agents that specifically activate B cells are listed in Table 3. B cells can also be exposed to protein antigens such as tetanus toxoid, and the specific antibody (and isotype) secreted into the media can be characterized. As the amount of antibody secreted is low, these levels cannot be detected by nephelometry—ELISA (see chapter 35) or enzyme-linked immunosorbent spot assay (ELISPOT, see chapter 30) must be used instead. As LPAs are not available in most clinical immunology laboratories, this testing must often be performed on patient samples that are shipped to a specialized testing facility. This sample transport introduces a significant concern regarding sample integrity, as the testing requires live, functional B cells for accuracy. Many laboratories performing LPAs consequently require a normal sample to be shipped with the patient sample, to control for such transport issues. A complete LPA protocol can be found in the Methodologies section below.

Cellular Proliferation

The ability of B cells to proliferate in response to stimulation in the LPA is usually presented as the stimulation index (SI). Currently the proliferative response is measured by the incorporation of tritiated thymidine ([^{3}H]thymidine) into DNA of replicating cells. Therefore the SI is expressed as the counts per minute (cpm) of the stimulated wells divided by the cpm of the control wells (wells with B cells, but no stimulus). A second method of reporting is the net cpm, which is the cpm of the stimulated wells minus the cpm of the control wells. An alternative method for the measurement of proliferation in the LPA is the analysis of the cell cycle by flow cytometry (26). In this readout of proliferation, stimulated and control cells are permeabilized and stained with propidium iodide, and the number of cells in the S phase of the cell cycle are counted. Normal ranges for proliferation in the LPA have been difficult to establish due to a high degree of variability in assay culture conditions in different laboratories. Therefore the LPA is best utilized as a qualitative indicator of lymphocyte function, rather than as a quantitative assay.

Secretion of Soluble Mediators

In addition to proliferation, stimulation of B cells in the LPA induces B cells to produce and secrete immunoglobulins. Measurement of mitogen or antigen-induced immunoglobulin secretion will assess whether the immunoglobulin class or isotype of interest is produced in the amounts expected by age or disease state. The total culture levels of immunoglobulins are assayed by ELISA (see chapter 35). The amount of immunoglobulins produced may also be assayed at the single-cell level by enzyme-linked immunosorbent spot assay, but this assay is most useful for determining antigen-specific B-cell frequency, which is not determined by proliferation or total immunoglobulin assays.

TABLE 3 *In vitro* activators of B cell proliferation and immunoglobulin production

Activator[a]	Target	Dose	Source[c]	Reference
SAC	BCR	0.004%	Calbiochem	50
Anti-IgM	BCR	10 μg/ml	BioRad	50
PWM	See below[b]	1–10 μg/ml	Sigma	51
Tetanus Toxoid	BCR	1–20 μg/ml	Pfizer	51

[a]SAC, *Staphylococcus aureus* Cowan I; PWM, pokeweed mitogen.
[b]PWM requires T cells to be present for its mitogenic effect on B cells. Therefore, it is not a specific assay of B-cell function.
[c]Multiple sources exist for some products.

APPROACHES FOR ASSESSING ANTIBODY FUNCTION

Antibodies provide protection to the host in a variety of ways. They can neutralize toxins (e.g., tetanus toxin, diphtheria toxin), neutralize viruses (e.g., influenza A), prevent the adhesion of bacteria to the host cells (e.g., *Escherichia coli*), kill bacteria in the presence of complement (e.g., *Haemophilus influenza* type b), and opsonize bacteria for phagocytes (e.g., *Streptococcus pneumoniae*) (27–31). Antibodies can also opsonize host cells for lysis, primarily by NK cells, in a process known as antibody-dependent cell-mediated cytotoxicity (reviewed in reference 32). Consequently, a variety of assays have been developed to measure antibody function. While antibody function assays can be performed in experimental animals, *in vivo* assays are impractical and, thus, *in vitro* assays are widely used. Two such assays, *in vitro* bactericidal assays and *in vitro* opsonization assays, are described in detail below. Also, an antibody-dependent cell-mediated cytotoxicity assay kit has recently become available (www.promega.com).

Bactericidal Assays

In serum bactericidal assays (SBAs), test serum is mixed with bacteria and complement. If present, antibodies in the test serum bind to the bacteria and activate the complement cascade resulting in formation of the membrane attack complex and ultimately death of the bacteria. The number of surviving bacteria can be determined by plating a sample of reaction mixture on an agar plate. By testing the bactericidal activity of the serum samples at multiple dilutions, a titer can be determined, with titer defined as the highest dilution of serum that kills ≥50% of the target bacteria. This mechanism is primarily relevant in the study of antibodies to Gram-negative bacteria, although there have been examples seen in Gram-positive bacteria (33).

SBAs were extensively used in the development of meningococcal vaccines (34). Studies with meningococcal antibodies have shown that the source of the complement used in the SBA can influence the results. For example, when used as a complement source, rabbit serum produces higher bactericidal titers than human serum in SBAs for antibodies to meningococcus (35, 36). This discrepancy has been associated with the fact that meningococci bind to human factor H but not to rabbit factor H (37).

A major technical problem associated with the use of the bactericidal assay is enumeration of surviving bacteria. The classical approach is to plate a sample on an agar plate and manually count the bacterial colonies. However, manual colony counting is too tedious, especially for a large number of samples. Thus, a significant effort has been made to automate the counting of bacterial colonies. Additionally, other investigators have explored the use of dyes that either develop color or become fluorescent in proportion to the number of live bacteria (38–40). Quantifying the survival of bacteria is relevant for opsonophagocytic killing assays as well (see below).

Opsonophagocytosis Assays (OPAs)

Opsonophagocytosis is the primary protective mechanism of antibodies against Gram- positive bacteria. Various methods have been developed to measure the opsonizing capacity

of antibodies *in vitro*, including the "killing-type" OPA and the "uptake-type" OPA developed for *Streptococcus pneumoniae*. The classical approach is to perform the killing-type OPA where target bacteria are opsonized (coated) with antibodies and complement (41). The opsonized bacteria are subsequently internalized and killed by phagocytes, and the number of surviving bacteria is then determined. As with the bactericidal assays mentioned previously, if multiple dilutions of serum are tested, a titer can be calculated for each serum sample.

In an attempt to increase automation, an alternate approach, the uptake-type OPA, was developed. In this assay, target bacteria are fluorescently labeled, and the uptake of bacteria by phagocytes is measured with a flow cytometer by monitoring the increase in fluorescence of the granulocytes (42, 43). Fluorescent bacteria can be prepared by chemical tagging with a fluorochrome or by inserting a gene for a fluorescent protein. Because the assay is complex, it is primarily used for phagocytosis research.

Since the development and licensure of pneumococcal vaccines involve testing a large number of samples for multiple (7 to 23) serotypes that are included in the vaccines, there is a need for functional assays to study antibodies against multiple serotypes simultaneously. Such multiplexed assays would reduce not only the amount of work and expensive reagents, but would also reduce the volume of serum needed for testing. This reduction in serum volume is important when studying children, especially with the increasing valency of pneumococcal conjugate vaccines. Consequently, multiplexed killing-type OPAs were developed using antibiotic-resistant target bacteria (31, 44–46). As an example, this methodology may use one serotype susceptible to optochin but resistant to streptomycin and use a second serotype that is susceptible to streptomycin but resistant to optochin. If these two serotypes are tested together, the number of surviving bacteria of each strain can be determined by using agar plates containing either antibiotic. This strategy is simple to use and has been successfully implemented for up to seven target bacteria (44).

The increased use of functional assays has shown the importance of standardization. Early versions of the killing-type OPA utilized peripheral blood granulocytes as phagocytes. However, peripheral-blood granulocytes can differ depending on the donor's genetic traits (e.g., Fc receptor allelism) or health status. Thus, the use of a cell line, such as HL-60, was promoted. It should be noted that even the source of the cell line must be standardized because samples of the same cell line from different sources appear to have different biological properties (47). Using differentiated HL-60 cells as phagocytes, the CDC previously coordinated a collaborative study demonstrating that functional assays can be standardized if various aspects of the assays (e.g., protocol and reagents) are carefully controlled (48). Since it is not feasible to have a common lot of OPA reagents for all users, there is an ongoing study to examine the possibility of standardizing data from different laboratories (that use different protocols and different lots of critical reagents) by inclusion of a reference serum pool (such as pneumococcal reference serum, lot 007sp, from the U.S. FDA). Results of this study are expected in 2016.

METHODOLOGIES

Pneumococcal ELISA

A detailed consensus protocol for the WHO pneumococcal ELISA can be found at www.vaccine.uab.edu. It is important to note that many reagents used in the assay (microtiter plates, capsular PS used for coating plates, and secondary antibody) must be screened. Additionally, the optimal concentrations of the capsular PS and secondary antibody must be determined for each reagent lot, including microtiter plates.

When coating plates with PS, it is critical to use highly purified water for the coating buffer. Any contaminants found in the coating buffer (LPS, fungal components, etc.) may adhere to the microtiter plate and will be detected if antibodies to these contaminants are present in the test serum.

Finally, it is important to closely adhere to the incubation times and temperatures. For example, we have found that incubating plates coated with PS from serotype 3 at room temperature for 18 hours produces inconsistent results (unpublished data). Thus, we incubate plates coated with type 3 PS for 2 hours at room temperature.

In Vitro Whole-Blood Lymphocyte Proliferation Assay

Materials and Reagents

Unless specified, any supplier should suffice.

RPMI 1640 ("RPMI")
L-Glutamine
Human AB serum (heat-inactivated at 56°C for 1 hour)
Penicillin and streptomycin solution (P/S)
Mitogens/activators (see Table 3)
Tritiated thymidine ([^{3}H]thymidine) sterile, aqueous solution
96-well round-bottom tissue culture plates with lids (sterile)
Scintillation fluid
Pipette tips (sterile)
Ficoll-Hypaque (density 1.077 g/liter)
Phosphate-buffered saline (PBS, sterile)
Centrifuge tubes (15 ml)
Pipettes (sterile)

Procedure

1. Obtain fresh heparinized venous blood sample. The sample should be held at room temperature prior to analysis and should be analyzed within 24 hours of draw. A normal healthy control should be drawn at the same time as the patient sample and treated in a similar manner.
2. Dilute blood 1:2 with sterile PBS and transfer 10 ml to 15-ml sterile conical centrifuge tubes.
3. Underlay the Ficoll-Hypaque solution, using 3 ml Ficoll-Hypaque per 10 ml blood/PBS mixture.
4. Centrifuge 20 minutes at 400 × *g* in a refrigerated centrifuge at 18 to 20°C, with no brake.
5. Harvest the PBMC from the interface using a sterile pipette and wash three times in PBS (200 × *g*, 10 minutes, 18 to 20°C).
6. Resuspend PBMC in RPMI with 10% AB serum, P/S, and L-glutamine at 1×10^6 live cells/ml (viability can be ascertained by trypan blue exclusion). Use PBMC within 1 hour.
7. Add 100 μl of each antigen/mitogen concentration being tested to wells of a 96-well tissue culture (round-bottom) plate. These need to be tested in triplicate.
8. Add 100 μl of the diluted PBMCs to each well.
9. Replace the plate lids and incubate plates at 37°C with 5% CO_2.

10. To determine cell proliferation by tritiated thymidine incorporation, on the morning of day 3, each well is pulsed with 0.5 μCi of tritiated thymidine in 20 μl RPMI (no serum). After 6 hours the cells are harvested on glass fiber filters using a cell harvester. The filters are placed into scintillation fluid and counted on a beta scintillation counter. Triplicates are averaged and the stimulation index is reported.
11. To assay for total antibody production, the plates are incubated for 7 days at 37°C with 5% CO_2. Remove the culture supernatant and use for ELISA determination (see chapter 35).

Serum Bactericidal Assay for Functional Antibodies against *Haemophilus influenzae* Type b

This procedure was adapted from Dr. Romero-Steiner's protocol used by the U.S. CDC (30).

Materials and Reagents

Unless specified, any supplier should suffice.

96-well, round-bottom microtiter plates

Cryovials

Chocolate II agar plates (Becton Dickinson)

Fildes enrichment (Becton Dickinson) (Note 1)

Brain heart infusion (BHI) broth

1× Hanks' balanced salt solution (HBSS) with Ca^{2+} and Mg^{+} (Invitrogen)

Target bacteria (*H. influenzae* type b, strain Eagan or GB3292)

Baby rabbit complement (Pel-Freez Biologicals)

CBER standard serum (lot 1983, a serum standard from U.S. FDA with 70 μg of antibody/ml).

Intravenous immunoglobulin (any commercial preparation, for quality control purposes)

Glass vials (50 ml)

Glycerol

Prepared solutions

Dilution Buffer

Add 1 ml of Fildes enrichment to 49 ml of 1× HBSS with Ca^{2+} and Mg^{2+}

Procedure for Preparing Bacteria

1. Inoculate bacteria onto a chocolate II agar plate and incubate the plate overnight (~16 hours) at 37°C in a 5% CO_2 incubator.
2. Transfer about 10 isolated bacterial colonies to 20 ml of BHI broth with 2% Fildes enrichment (49) in a 50-ml glass vial and incubate at 37°C and 5% CO_2 until the optical density at 600 nm becomes 0.4 to 0.5 (Note 2).
3. Add 3 ml of sterile glycerol to the bacterial culture (20 ml). Mix well. Dispense 0.5 ml into each cryovial.
4. Quickly freeze all cryovials (except one) at −70°C. Once frozen, store the vials at −70°C until use. The nonfrozen vial will be used in step 5.
5. Determine the bacterial recovery from frozen vials (it should be greater than 80%).
   a. Thaw a vial of frozen bacterial aliquot (step 4); vial should be frozen at least 2 hours.
   b. Dilute both the nonfrozen and thawed bacteria (step 4) 10^{-6}, 10^{-7}, and 10^{-8} in dilution buffer.
   c. Plate 100 μl from each dilution on a chocolate II agar plate.
   d. Incubate the plates overnight at 37°C in a candle jar.
   e. Count the colonies.
   f. Determine the ratio of the number of thawed bacteria to the number of nonfrozen bacteria. If the ratio is <0.8, the working stocks should be discarded and new stocks prepared.
6. Determine the dilution necessary to get ~1000 CFU per 20 μl.
   a. Prepare 6 tubes with 0.9 ml of dilution buffer
   b. Rapidly thaw an aliquot of bacteria.
   c. Add 100 μl of thawed bacteria to dilution buffer in tube #1.
   d. Perform 10-fold serial dilutions by transferring 100 μl from tube #1 to #2. Continue through tube #6.
   e. Plate 10 μl from each tube, in triplicate, onto a chocolate II agar plate.
   f. Incubate the plates overnight at 37°C in a candle jar.
   g. Count the colonies and determine the average of the triplicates.
   h. Determine the bacterial density and calculate the dilution factor required to yield 1000 CFU per 20 μl.

Assay Procedure (see Note 4)

1. Prepare 2-fold serial dilutions (8 to 10 dilutions) of antisera (heat-inactivated at 56°C for 30 minutes) with dilution buffer.
2. Add 10 μl of diluted antiserum to duplicate wells of a microtiter plate.
3. Thaw an aliquot of bacteria.
4. Dilute the thawed bacteria in dilution buffer to prepare a solution containing ~1000 CFU/20 μl.
5. Add 20 μl of the diluted bacterial suspension to all wells.
6. Incubate at 37°C for 15 min in a 5% CO_2 incubator.
7. Add 25 μl of baby rabbit complement (Note 3).
8. Add 25 μl of dilution buffer.
9. Incubate the plates at 37°C for 60 min in a 5% CO_2 incubator.
10. Plate 5 μl of the reaction mixture onto chocolate II agar plates.
11. Incubate the plates at 37°C in 5% CO_2 for 16 h.
12. Count the number of surviving bacteria.
13. Determine the serum dilution that kills ≥50% of the bacteria.

Assay Notes

Note 1. Fildes enrichment is a peptic digest of sheep blood. It is rich in hemin and NAD. Although 5% supplement is usually used (44), we found that 2% supplement is sufficient for bactericidal assays.

Note 2. Bacteria will be in the exponential phase of growth. It takes about 2 to 3 hours. The broth acquires an amber color.

Note 3. Complement lots should be qualified prior to use in the assay. Both active and heat-inactivated baby rabbit complement are used to show that no non-specific killing occurs during the 1-hour incubation period.

Note 4. Serum growth controls (all reagents except complement source) should be included when the serum source is unknown or it is suspected to contain antibiotics (or other inhibitory substances).

Multiplexed Opsonophagocytic Killing Assay (MOPA4) for Functional Antibodies against *Streptococcus pneumoniae*

This procedure was adapted from the procedure described by Burton and Nahm (31). A detailed protocol can be found at www.vaccine.uab.edu.

Materials and Reagents

Unless specified, any supplier should suffice.

Tissue culture flask, vent cap (150 cm^2)

Microtiter plate (round bottom, tissue culture treated) (no. 3799; CoStar)

Square petri dish (12 cm by 12 cm by 1.5 cm) (no. 688102; Greiner Bio-One)

N,*N*-Dimethylformamide (DMF)

2,3,5,-Triphenyltetrazolium chloride (TTC) (no. T-8877; Sigma)

Streptomycin sulfate (no. S-6501; Sigma)

Optochin (ethylhydrocupreine HCl) (no. E-9876; Sigma)

Spectinomycin dihydrochloride pentahydrate (no. S-9007; Sigma)

Trimethoprim (no. T-7883; Sigma)

Todd-Hewitt broth (no. 249240; Becton Dickinson)

Yeast extract (no. 212750; Becton Dickinson)

Bacto Agar (no. 214010; Becton Dickinson)

10× HBSS (without Ca^{2+}, Mg^{2+}, or phenol red) (no. 14185-052; Invitrogen)

10× HBSS (with Ca^{2+} and Mg^{2+}, without phenol red) (no. 14065-056; Invitrogen)

RPMI-1640 ("RPMI")

GlutaMax-1 (100× solution) (no. 35050-061; Invitrogen)

Bovine serum (Fetalclone 1, for HL-60 cell maintenance) (no. SH30080.03; HyClone)

Premium fetal bovine serum (FBS, for preparation of assay buffer [OBB]) (no. 11150; Atlanta Biologicals)

Baby rabbit complement (BRC) (no. 31061; Pel-Freez Biologicals)

HL-60 cell line (no. CCL240; ATCC)

Blood agar plates

Glycerol

Gelatin

Dimethyl sulfoxide (DMSO)

Target bacteria (see Table 4)

Prepared Solutions

Streptomycin stock solution

Prepare a 300 mg/ml stock solution in water. Sterile filter and prepare 1 ml aliquots. Store at −20°C. See Note 5.

Optochin stock solution

Prepare an 8 mg/ml stock solution in water. Sterile filter and prepare 1 ml aliquots. Store at −20°C. See Note 5.

Trimethoprim stock solution

Prepare a 25 mg/ml stock solution in DMSO. Prepare 1 ml aliquots and store at −20°C. See Note 5.

Spectinomycin stock solution

Prepare a 300 mg/ml stock solution in DMSO. Prepare 1 ml aliquots and store at −20°C. See Note 5.

Glycerol stock (~80%)

Mix 20 ml of water and 100 g glycerol. Autoclave and store at room temperature (RT).

TABLE 4 Pneumococcal target strains for the MOPA[a]

Strain name	Serotype	Selective antibiotic
SPEC1	1	Spectinomycin
STREP2	2	Streptomycin
OREP3	3	Optochin
OREP4	4	Optochin
STREP5	5	Streptomycin
TREP6A	6A	Trimethoprim
SPEC6B	6B	Spectinomycin
SPEC6C	6C	Spectinomycin
SPEC6D	6D	Spectinomycin
OREP7F	7F	Optochin
STREP8	8	Streptomycin
SPEC9N	9N	Spectinomycin
EMC9V	9V	Streptomycin
OREP10A	10A	Optochin
TREP11A	11A	Trimethoprim
TREP12F	12F	Trimethoprim
STREP14	14	Streptomycin
TREP15B	15B	Trimethoprim
OREP17F	17F	Optochin
OREP18C	18C	Optochin
TREP19A	19A	Trimethoprim
SPEC19F	19F	Spectinomycin
SPEC20B	20B	Spectinomycin
TREP22F	22F	Trimethoprim
EMC23F	23F	Trimethoprim
STREP33F	33F	Streptomycin

[a]Any four target strains can be tested simultaneously, provided each strain has a unique antibiotic resistance (for example, SPEC1 and SPEC6B cannot be tested together). Also, members of the same serogroup should not be tested together (for example, TREP6A and SPEC6B should be tested separately).

Gelatin stock solution (1%)

Add 1 g of gelatin to 100 ml of water. Autoclave and store at RT.

TTC stock solution

Prepare a 25 mg/ml solution in water. Sterile filter and store at 4°C, protected from light, for up to 2 months.

Todd-Hewitt yeast broth (THY broth)

Add 30 g of Todd-Hewitt broth and 5 g of yeast extract to 1 liter of water. Sterile filter, and store at 4°C for up to 1 month.

Todd-Hewitt-yeast agar plate (THYA plate)

Add 30 g of Todd-Hewitt broth, 5 g of yeast extract, and 15 g of Bacto agar to 1 liter of water. Autoclave and allow to cool (to about 56°C). Add 25 ml to each square petri dish, and allow the plates to cool to RT. Store at 4°C in a humidified chamber for up to one month.

Overlay agar

Add 30 g of Todd-Hewitt broth, 5 g of yeast extract, and 7.5 g of Bacto agar to 1 liter of water. Autoclave and allow to cool (to about 56°C). Keep in 56°C water bath until needed (up to 12 hours).

Opsonization assay buffer B (OBB)

In a sterile tube, combine 40 ml water, 5 ml 10× HBSS (with Mg^{2+} and Ca^{2+}), 5 ml gelatin (1% stock

solution), and 2.6 ml premium FBS (previously inactivated at 56°C for 30 minutes). Keep at RT until needed (up to 12 hours).

Procedures

Initiation of HL-60 Cultures

1. Quickly thaw master stock vial and transfer contents to sterile tube containing 10 ml of RPMI with 20% Fetal Clone I and 1% glutamine.
2. Centrifuge at ~350 × *g* for 5 minutes.
3. Remove supernatant, and suspend pellet in 70 ml of RPMI with 20% Fetal Clone I and 1% glutamine. Transfer to T-150 flask and place flask into tissue culture incubator (37°C, 5% CO_2, See Note 1).
4. After 3 to 4 days, add 50 ml of fresh media (RPMI with 20% Fetal Clone I and 1% glutamine).
5. Every 3 to 4 days, remove 60 ml of cells and discard. Add 60 ml of fresh media (RPMI with 20% Fetal Clone I and 1% glutamine).
6. After cells have been in culture for 2 weeks, begin feeding with RPMI with 10% Fetal Clone I and 1% glutamine (every 3 to 4 days, remove 60 ml of cells, discard, and add 60 ml of fresh media [RPMI with 10% Fetal Clone I and 1% glutamine]).
7. After cells have been in culture for 3 to 4 weeks, the cell concentration needs to be adjusted. This is best done on a Wednesday or Friday. If done on Wednesday, count cells and adjust concentration to ~8×10^5 cells/ml in old culture supernatant. Aliquot 40 ml of cells to each T-150 flask and add 80 ml of fresh media (RPMI with 10% Fetal Clone I and 1% glutamine). If done on Friday, count cells and adjust concentration to ~8×10^5 cells/ml in old culture supernatant. Aliquot 20 ml of cells to each T-150 flask and add 60 ml of fresh media (RPMI with 10% Fetal Clone I and 1% glutamine).
8. Begin routine propagation schedule below.

Routine HL-60 Propagation

1. On Mondays, add 40 of fresh media (RPMI with 10% Fetal Clone I and 1% glutamine) to each T-150 flask.
2. On Wednesdays, remove 80 ml of cells from each flask. The removed cells can be pooled and differentiated (see below) or discarded. Add 80 ml of fresh media (RPMI with 10% Fetal Clone I and 1% glutamine) to each flask.
3. On Fridays, remove all but 20 ml from each flask (i.e., remove ~100 ml). The removed cells can be pooled and differentiated (see below) or discarded. Add 60 ml of fresh media (RPMI with 10% Fetal Clone I and 1% glutamine) to each flask.

HL-60 Cell Differentiation

1. Centrifuge the HL-60 cells at ~350 × *g* for 5 to 10 min at RT.
2. Remove supernatant, and suspend the cell pellet in differentiating medium (RPMI with 10% Fetal Clone I, 1% glutamine, and 0.8% [v/v] DMF).
3. Adjust the cell concentration to ~4×10^5 cells/ml with differentiating medium, and add 100 ml of cells to each T-150 flask.
4. Incubate the flasks (lying flat) in a tissue culture incubator (37°C, 5% CO_2) for 5 to 6 days. Do not feed the culture during this period.

Preparing Target Bacteria Working Stocks

1. Inoculate bacteria on a blood agar plate and incubate overnight in an incubator (37°C, 5% CO_2, Note 3).
2. Pneumococci yield alpha-hemolytic colonies that can be identified by a green halo surrounding the colony. Transfer 20 to 30 isolated colonies to a sterile tube containing 50 ml of THY broth. Incubate the tube for 3 to 8 hours in a 37°C water bath until the top of the culture broth (i.e., do not mix) has an optical density at 600 nm of ~0.6 to 0.9.
3. Harvest the top 10 ml of the broth from the tube and transfer to a sterile tube.
4. Add 5 ml of glycerol (80% stock solution) and 10 ml of fresh THY broth. Mix well, and prepare 0.5 ml aliquots in cryovials. Store the vials frozen at −70°C until used (up to ~18 months).
5. Determine the dilution necessary to get about 100 CFU/10 µl, see Note 2.

MOPA4

1. Incubate the serum samples to be tested at 56°C for 30 min to inactivate the endogenous complement. Also, a small volume (0.1 ml) of heat-inactivated BRC will be needed for the assay.
2. Dry the THYA plates (eight THYA plates will be needed for every assay plate) by removing the lids and placing the plates in a laminar-flow hood for 30 to 60 minutes (see Note 4). After plates are dry, replace lids to prevent overdrying, and keep at RT until needed.
3. Prepare overlay agar (~200 ml will be needed for every assay plate), OBB (1 tube as prepared above is sufficient for 4–5 assay plates), 50 ml of 1× HBSS (without Ca^{2+}, Mg^{2+}, or phenol red), and 50 ml of 1× HBSS (with Ca^{2+} and Mg^{2+}, without phenol red).
4. Prepare the microtiter assay plates (see Fig. 1 for assay plate layout):
   a. For plate 1, add 20 µl of OBB to rows A through G, columns 1 through 12. Also, add 20 µl of OBB to row H, columns 1 and 2 only. For all other assay plates, add 20 µl of OBB to rows A through G, columns 1 through 12.
   b. For plate 1, add 30 µl of heat-inactivated serum samples (in duplicate) to row H, columns 3 through 12, according to the plate layout. For all other assay plates, add 30 µl of heat-inactivated serum samples (in duplicate) to row H, columns 1 through 12. Serum samples added to row H are undiluted. Serum samples yielding a high titer may have to be retested at a higher starting dilution.
   c. Perform 3-fold serial dilutions by transferring 10 µl from H to G, mixing, and transferring 10 µl from G to F, etc. After transferring 10 µl from B to A, mix the contents of A, and discard 10 µl. Repeat for all assay plates.
5. Prepare the target bacteria.
   a. Rapidly thaw a frozen aliquot of each of the four target bacterial strains.
   b. Wash each of the target strains with 1 ml of OBB by centrifugation.
   c. After the final centrifugation, remove the OBB and suspend the pellet in 0.5 ml of OBB.
   d. To 10 ml of OBB, add the desired volume of each of the four target strains according to the dilution factors calculated earlier (Note 2) in OBB.
6. Add 10 µl of the diluted bacterial mixture to each well, including all control wells.

Assay Plate 1

Column Number

Row Letter	1	2	3 & 4	5 & 6	7 & 8	9 & 10	11 & 12
A	Bac + HI BRC + HL60	Bac + BRC + HL60	1/8748	1/8748	1/8748	1/8748	1/8748
B	Bac + HI BRC + HL60	Bac + BRC + HL60	1/2916	1/2916	1/2916	1/2916	1/2916
C	Bac + HI BRC + HL60	Bac + BRC + HL60	1/972	1/972	1/972	1/972	1/972
D	Bac + HI BRC + HL60	Bac + BRC + HL60	1/324	1/324	1/324	1/324	1/324
E	Bac + HI BRC + HL60	Bac + BRC + HL60	1/108	1/108	1/108	1/108	1/108
F	Bac + HI BRC + HL60	Bac + BRC + HL60	1/36	1/36	1/36	1/36	1/36
G	Bac + HI BRC + HL60	Bac + BRC + HL60	1/12	1/12	1/12	1/12	1/12
H	Bac + HI BRC + HL60	Bac + BRC + HL60	1/4	1/4	1/4	1/4	1/4
	Control A	Control B	Sample 1	Sample 2	Sample 3	Sample 4	Sample 5

Sample Dilution

Additional Assay Plates

Column Number

Row Letter	1 & 2	3 & 4	5 & 6	7 & 8	9 & 10	11 & 12
A	1/8748	1/8748	1/8748	1/8748	1/8748	1/8748
B	1/2916	1/2916	1/2916	1/2916	1/2916	1/2916
C	1/972	1/972	1/972	1/972	1/972	1/972
D	1/324	1/324	1/324	1/324	1/324	1/324
E	1/108	1/108	1/108	1/108	1/108	1/108
F	1/36	1/36	1/36	1/36	1/36	1/36
G	1/12	1/12	1/12	1/12	1/12	1/12
H	1/4	1/4	1/4	1/4	1/4	1/4
	Sample 6	Sample 7	Sample 8	Sample 9	Sample 10	Sample 11

Sample Dilution

FIGURE 1 Assay plate layout.

7. Incubate the microtiter plates at room temperature for 30 min with shaking (700 rpm).
8. During this time, remove the BRC from the freezer to thaw.
9. Also, during this incubation, prepare the differentiated HL-60 cells:
   a. Transfer the DMF-differentiated HL-60 cells from the culture flasks to 50 mL centrifuge tubes.
   b. Centrifuge the HL-60 cells at 350 × *g* for 5 min at RT.
   c. Remove the supernatant and wash the cells with 50 ml of 1× HBSS (without Ca^{2+} and Mg^{2+}) by centrifugation as above.
   d. Remove the supernatant and wash the cells with 50 ml of 1× HBSS (with Ca^{2+} and Mg^{2+}) by centrifugation as above.
   e. Remove the supernatant, and suspend the cells at 1×10^7 cells/ml in OBB. Keep the cells at room temperature until needed.
10. Following the 30-minute incubation above, prepare a 1:4 mixture of heat-activated BRC and HL-60 cells by mixing 100 μl of heat-inactivated BRC and 400 μl of HL-60 cell suspension. Add 50 μl of this mixture to plate 1, column 1, rows A through H.
11. Prepare a 1:4 mixture of active BRC and HL-60 cells (~5 ml of mixture will be needed for each assay plate). Add 50 μl of this mixture to all rows of plate 1, columns 2 through 12. Also, add 50 μl of this mixture to all wells of remaining assay plates.
12. Incubate the microtiter plates on a shaker (700 rpm) for 45 minutes at 37°C, 5% CO_2.
13. After the incubation period, place the microtiter plates on ice for 15 to 20 minutes (to stop the phagocytic process).
14. Using a 12-channel pipettor, spot 10 μl from the wells of row H onto each of four replicate THYA plates. After spotting the 10 microliters onto the plate, immediately tilt the plate to allow the spot to form a small strip of fluid (~1.5 to 2 cm long). Repeat the spotting procedure for rows G, F, and E onto the same set of four THYA plates. Rows D, C, B, and A are spotted onto a second set of four THYA plates. Continue this procedure for the remaining assay plates.
15. Leave the plates at RT for 10 to 20 minutes to let the excess fluid seep into the agar.
16. Aliquot the desired volume of overlay agar (cooled to 56°C) to four glass bottles. Add TTC to each bottle to a final concentration of 25 mg/liter.
17. To one bottle, add optochin to a final concentration of 8 mg/liter. Add 25 ml of this overlay to the first replicate of the THYA plates spotted above.
18. To one bottle, add spectinomycin to a final concentration of 300 mg/liter. Add 25 ml of this overlay to the second replicate of the THYA plates spotted above.
19. To one bottle, add streptomycin to a final concentration of 300 mg/liter. Add 25 ml of this overlay to the third replicate of the THYA plates spotted above.

20. To one bottle, add trimethoprim to a final concentration of 25 mg/liter. Add 25 ml of this overlay to the fourth replicate of the THYA plates spotted above.
21. After the overlay has solidified (~10 min), place the plates, upside down, in an incubator (37°C, 5% CO_2) and incubate overnight. Colonies that grow on the THYA plates with the optochin overlay are bacteria of the optochin-resistant serotype; those that grow on the THYA plates containing streptomycin are bacteria of the streptomycin-resistant serotype, etc.
22. Count colonies and calculate the opsonization titer of each serum. The opsonization titer is the final dilution of serum that results in a ≥50% reduction in the number of colonies when compared to the Control-B (no serum control) wells. If an undiluted serum sample kills 55% of the bacteria in dilution 1, but the next dilution (3-fold) kills 15% of the bacteria, then the opsonization titer is 4 (e.g., 20/80 = 1:4 dilution; where 20 is the volume of serum in microliters and 80 is the total volume of the reaction in microliters).

Assay Notes

Note 1. It is important to maintain the CO_2 concentration at ~5% as HL-60 cells are sensitive to subtle pH changes that can occur when the CO_2 concentration changes. It is recommended the percent CO_2 be checked regularly with an outside reference (such as a FYRITE gas analyzer produced by Bacharach, Pittsburgh, PA).

Note 2. BRC and/or HL-60 cells can influence the number of CFU. Therefore, the optimal dilution of each strain must be determined in assay conditions (without test serum). This can be easily accomplished by testing multiple bacterial dilutions using the MOPA procedure. The desired colony number in Control B is 100 to 150 CFU/spot.

Note 3. To maintain the integrity of the pneumococcal bacterial stock cultures, remove the stock vial(s) containing bacteria from the freezer, quickly remove a fleck of ice from the stock vial, and immediately streak onto a blood agar plate. Replace the stock vial into the freezer promptly.

Note 4. Drying the THYA plates for the correct amount of time is very important. Usually 30 to 60 minutes is sufficient, although drying times vary depending on the humidity in the air. Underdrying the plates results in an excess number of colonies around the perimeter of the spot. This can affect the counting of the colonies. Overdrying the plates can cause the spots to run together when the plates are tilted.

Note 5. We have found differences in potency between different lots of antibiotics. Therefore, the potency of each batch must be determined using all targets of interest.

REFERENCES

1. **Kindt TJ, Goldsby RA, Osborne BA, Kuby J.** 2007. *Immunology*, 6th ed. WH Freeman, New York, NY.
2. **Martin F, Kearney JF.** 2001. B1 cells: similarities and differences with other B cell subsets. *Curr Opin Immunol* **13:**195–201.
3. **McHeyzer-Williams MG**. 2003. B cells as effectors. *Curr Opin Immunol* **15:**354–61.
4. **Buckley RH, Dees SC, O'Fallon WM.** 1968. Serum immunoglobulins. I. Levels in normal children and in uncomplicated childhood allergy. *Pediatrics* **41:**600–611.
5. **Weber-Mzell D, Kotanko P, Hauer AC, Goriup U, Haas J, Lanner N, Erwa W, Ahmaida IA, Haitchi-Petnehazy S, Stenzel M, Lanzer G, Deutsch J.** 2004. Gender, age and seasonal effects on IgA deficiency: a study of 7293 Caucasians. *Eur J Clin Investig* **34:**224–228.
6. **Buckley RH.** 2002. Immunoglobulin G subclass deficiency: fact or fancy? *Curr Allergy Asthma Rep* **2:**356–360.
7. **Maguire GA, Kumararatne DS, Joyce HJ.** 2002. Are there any clinical indications for measuring IgG subclasses? *Ann Clin Biochem* **39:**374–377.
8. **Nahm MH, Blaese RM, Crain MJ, Briles DE.** 1986. Patients with Wiskott-Aldrich syndrome have normal IgG2 levels. *J Immunol* **137:**3484–3487.
9. **Carneiro-Sampaio MM, Grumach AS, Manissadjian A.** 1991. Laboratory screening for the diagnosis of children with primary immunodeficiencies. *J Investig Allergol Clin Immunol* **1:**195–200.
10. **Balmer P, North J, Baxter D, Stanford E, Melegaro A, Kaczmarski EB, Miller E, Borrow R.** 2003. Measurement and interpretation of pneumococcal IgG levels for clinical management. *Clin Exp Immunol* **133:**364–369.
11. **Fleisher TA, Oliveira JB.** 2004. Functional and molecular evaluation of lymphocytes. *J Allergy Clin Immunol* **114:**227–234; quiz 35.
12. **Noroski LM, Shearer WT.** 1998. Screening for primary immunodeficiencies in the clinical immunology laboratory. *Clin Immunol Immunopathol* **86:**237–245.
13. **Wernette CM, Frasch CE, Madore D, Carlone G, Goldblatt D, Plikaytis B, Benjamin W, Quataert SA, Hildreth S, Sikkema DJ, Kayhty H, Jonsdottir J, Nahm MH.** 2003. Enzyme-linked immunosorbent assay for quantitation of human antibodies to pneumococcal polysaccharides. *Clin Diagn Lab Immunol* **10:**514–519.
14. **Park S, Nahm MH.** 2011. Older adults have a low capacity to opsonize pneumococci due to low IgM antibody response to pneumococcal vaccinations. *Infect Immun* **79:**314–320.
15. **Simell B, Nurkka A, Ekstrom N, Givon-Lavi N, Kayhty H, Dagan R.** 2012. Serum IgM antibodies contribute to high levels of opsonophagocytic activities in toddlers immunized with a single dose of the 9-valent pneumococcal conjugate vaccine. *Clin Vaccine Immunol* **19:**1618–1623.
16. **Pickering JW, Martins TB, Greer RW, Schroder MC, Astill ME, Litwin CM, Hildreth SW, Hill HR.** 2002. A multiplexed fluorescent microsphere immunoassay for antibodies to pneumococcal capsular polysaccharides. *Am J Clin Pathol* **117:**589–596.
17. **Zhang X, Simmerman K, Yen-Lieberman B, Daly TM.** 2013. Impact of analytical variability on clinical interpretation of multiplex pneumococcal serology assays. *Clin Vaccine Immunol* **20:**957–961.
18. **Hill HR, Pickering JW.** 2013. Reference laboratory agreement on multianalyte pneumococcal antibody results: an absolute must! *Clin Vaccine Immunol* **20:**955–956.
19. **Shearer WT, Rosenblatt HM, Gelman RS, Oyomopito R, Plaeger S, Stiehm ER, Wara DW, Douglas SD, Luzuriaga K, McFarland EJ, Yogev R, Rathore MH, Levy W, Graham BL, Spector SA.** 2003. Lymphocyte subsets in healthy children from birth through 18 years of age: the Pediatric AIDS Clinical Trials Group P1009 study. *J Allergy Clin Immunol* **112:**973–980.
20. **Agematsu K, Futatani T, Hokibara S, Kobayashi N, Takamoto M, Tsukada S, Suzuki H, Koyasu S, Miyawaki T, Sugane K, Komiyama A, Ochs HD.** 2002. Absence of memory B cells in patients with common variable immunodeficiency. *Clin Immunol* **103:**34–42.
21. **Piqueras B, Lavenu-Bombled C, Galicier L, Bergeron-van der Cruyssen F, Mouthon L, Chevret S, Debré P, Schmitt C, Oksenhendler E.** 2003. Common variable immunodeficiency patient classification based on impaired B

cell memory differentiation correlates with clinical aspects. *J Clin Immunol* **23:**385–400.
22. **Warnatz K, Denz A, Drager R, Braun M, Groth C, Wolff-Vorbeck G, Eibel H, Schlesier M, Peter HH.** 2002. Severe deficiency of switched memory B cells ($CD27^+IgM^-IgD^-$) in subgroups of patients with common variable immunodeficiency: a new approach to classify a heterogeneous disease. *Blood* **99:**1544–1551.
23. **Thiel A, Scheffold A, Radbruch A.** 2004. Antigen-specific cytometry—new tools arrived! *Clin Immunol* **111:**155–161.
24. **Folds JD, Schmitz JL.** 2003. Clinical and laboratory assessment of immunity. *J Allergy Clin Immunol* **111:**S702–S711.
25. **Scott MG, Nahm MH.** 1984. Mitogen-induced human IgG subclass expression. *J Immunol* **133:**2454–2460.
26. **Aguilar P, Renoult E, Jarrosson L, Kolopp-Sarda MN, Mathieu CP, Faure GC, Kessler M, Bene MC, Kohler C, Kennel De March A.** 2003. Anti-HBs cellular immune response in kidney recipients before and 4 months after transplantation. *Clin Diagn Lab Immunol* **10:**1117–1122.
27. **Sonobe MH, Trezena AG, Guilhen FB, Takano VL, Fratelli F, Sakauchi D, Morais JF, Prado SMA, Higashi HG.** 2007. Determination of low tetanus or diphtheria antitoxin titers in sera by a toxin neutralization assay and a modified toxin-binding inhibition test. *Braz J Med Biol Res* **40:**69–76.
28. **Stab V, Nitsche S, Niezold T, Storcksdieck Genannt Bonsmann M, Wiechers A, Tippler B, Hannaman D, Ehrhardt C, Überla K, Grunwald T, Tenbusch M.** 2013. Protective efficacy and immunogenicity of a combinatory DNA vaccine against influenza A virus and the respiratory syncytial virus. *PLoS One* **8:**e72217. doi:10.1371/journal.pone.0072217.
29. **Langermann S, Palaszynski S, Barnhart M, Auguste G, Pinkner JS, Burlein J, Barren P, Koenig S, Leath S, Jones CH, Hultgren SJ.** 1997. Prevention of mucosal *Escherichia coli* infection by FimH-adhesin-based systemic vaccination. *Science* **276:**607–611.
30. **Romero-Steiner S, Spear W, Brown N, Holder P, Hennessy T, Gomez De Leon P, Carlone GM.** 2004. Measurement of serum bactericidal activity specific for *Haemophilus influenzae* type b by using a chromogenic and fluorescent metabolic indicator. *Clin Diagn Lab Immunol* **11:**89–93.
31. **Burton RL, Nahm MH.** 2006. Development and validation of a fourfold multiplexed opsonization assay (MOPA4) for pneumococcal antibodies. *Clin Vaccine Immunol* **13:**1004–1009.
32. **Seidel UJ, Schlegel P, Lang P.** 2013. Natural killer cell mediated antibody-dependent cellular cytotoxicity in tumor immunotherapy with therapeutic antibodies. *Frontiers Immunol* **4:**76.
33. **Fusco PC, Perry JW, Liang SM, Blake MS, Michon F, Tai JY.** 1997. Bactericidal activity elicited by the beta C protein of group B streptococci contrasted with capsular polysaccharides. *Adv Exp Med Biol* **418:**841–845.
34. **Vermont C, van den Dobbelsteen G.** 2002. *Neisseria meningitidis* serogroup B: laboratory correlates of protection. *FEMS Immunol Med Microbiol* **34:**89–96.
35. **Zollinger WD, Mandrell RE.** 1983. Importance of complement source in bactericidal activity of human antibody and murine monoclonal antibody to meningococcal group B polysaccharide. *Infect Immun* **40:**257–264.
36. **Santos GF, Deck RR, Donnelly J, Blackwelder W, Granoff DM.** 2001. Importance of complement source in measuring meningococcal bactericidal titers. *Clin Diagn Lab Immunol* **8:**616–623.
37. **Granoff DM, Welsch JA, Ram S.** 2009. Binding of complement factor H (fH) to *Neisseria meningitidis* is specific for human fH and inhibits complement activation by rat and rabbit sera. *Infect Immun* **77:**764–769.
38. **Lin JS, Park MK, Nahm MH.** 2001. Chromogenic assay measuring opsonophagocytic killing capacities of antipneumococcal antisera. *Clin Diagn Lab Immunol* **8:**528–533.
39. **Mountzouros KT, Howell AP.** 2000. Detection of complement-mediated antibody-dependent bactericidal activity in a fluorescence-based serum bactericidal assay for group B *Neisseria meningitidis*. *J Clin Microbiol* **38:**2878–2884.
40. **Rodriguez T, Lastre M, Cedre B, del Campo J, Bracho G, Zayas C, Taboada C, Diaz M, Sierra G, Perez O.** 2002. Standardization of *Neisseria meningitidis* serogroup B colorimetric serum bactericidal assay. *Clin Diagn Lab Immunol* **9:**109–114.
41. **Romero-Steiner S, Libutti D, Pais LB, Dykes J, Anderson P, Whitin JC, Keyserling HL, Carlone GM.** 1997. Standardization of an opsonophagocytic assay for the measurement of functional antibody activity against *Streptococcus pneumoniae* using differentiated HL-60 cells. *Clin Diagn Lab Immunol* **4:**415–422.
42. **Jansen WT, Vakevainen-Anttila M, Kayhty H, Nahm M, Bakker N, Verhoef J, Snippe H, Verheul AF.** 2001. Comparison of a classical phagocytosis assay and a flow cytometry assay for assessment of the phagocytic capacity of sera from adults vaccinated with a pneumococcal conjugate vaccine. *Clin Diagn Lab Immunol* **8:**245–250.
43. **Martinez JE, Romero-Steiner S, Pilishvili T, Barnard S, Schinsky J, Goldblatt D, Carlone GM.** 1999. A flow cytometric opsonophagocytic assay for measurement of functional antibodies elicited after vaccination with the 23-valent pneumococcal polysaccharide vaccine. *Clin Diagn Lab Immunol* **6:**581–586.
44. **Bogaert D, Sluijter M, De Groot R, Hermans PW.** 2004. Multiplex opsonophagocytosis assay (MOPA): a useful tool for the monitoring of the 7-valent pneumococcal conjugate vaccine. *Vaccine* **22:**4014–4020.
45. **Kim KH, Yu J, Nahm MH.** 2003. Efficiency of a pneumococcal opsonophagocytic killing assay improved by multiplexing and by coloring colonies. *Clin Diagn Lab Immunol* **10:**616–621.
46. **Nahm MH, Briles DE, Yu X.** 2000. Development of a multi-specificity opsonophagocytic killing assay. *Vaccine* **18:**2768–2771.
47. **Fleck RA, Romero-Steiner S, Nahm MH.** 2005. Use of HL-60 cell line to measure opsonic capacity of pneumococcal antibodies. *Clin Diagn Lab Immunol* **12:**19–27.
48. **Romero-Steiner S, Frasch C, Concepcion N, Goldblatt D, Kayhty H, Vakevainen M, C. Laferriere, Wauters D, Nahm MH, Schinsky MF, Plikaytis BD, Carlone GM.** 2003. Multilaboratory evaluation of a viability assay for measurement of opsonophagocytic antibodies specific to the capsular polysaccharides of *Streptococcus pneumoniae*. *Clin Diagn Lab Immunol* **10:**1019–1024.
49. **Bergeron MG, Simard P, Provencher P.** 1987. Influence of growth medium and supplement on growth of *Haemophilus influenzae* and on antibacterial activity of several antibiotics. *J Clin Microbiol* **25:**650–655.
50. **Butch AW, Macke KA, Scott MG, Inkster M, Nahm MH.** 1989. Mitogen-induced human IgG subclass expression. II. IgG1 and IgG3 subclasses are preferentially stimulated by a combination of *Staphylococcus aureus* Cowan I and pokeweed mitogen. *Hum Immunol* **24:**207–218.
51. **James SP.** 2004. Measurement of basic immunological characteristics of human mononuclear cells, p 7.10.1–7.10.6. *In* Coligan JE, Kruisgeek AM, Margulies DH, Shevach EM, Strober W (ed), *Current Protocols in Immunology*. John Wiley & Sons, New York, NY.

Methods for Detection of Antigen-Specific T Cells by Enzyme-Linked Immunospot Assay (ELISPOT)

BARBARA L. SHACKLETT AND DOUGLAS F. NIXON

30

$CD3^+CD8^+$TcR αβ thymus-derived T cells form the major effector cell component of the immune response against intracellular pathogens. Naive $CD8^+$ T cells encounter antigen, expand, and divide, and effector cells mediate a range of functions. These include major histocompatibility complex (MHC) class I restricted killing of infected host cells, noncytolytic suppression, and release of soluble cytokines and chemokines. After the acute infection is contained the number of active effector cells declines, but antigen-specific memory $CD8^+$ T cells persist, ready to expand rapidly upon antigen re-exposure. Most $CD8^+$ antigen-specific T cells recognize viral antigen as a peptide presented by an MHC class I molecule. The T-cell receptor of the antigen-specific $CD8^+$ cell interacts with the MHC class I antigenic peptide complex on the surface of the antigen-presenting cell (1).

Antigen-specific $CD8^+$ T cells can be detected by identification of a specific T cell receptor which will interact with a unique MHC-class I peptide complex, or functionally, through effector activities after stimulation with specific antigen. The traditional method for the detection of antigen-specific $CD8^+$ T cells has been the ^{51}Cr release assay. This assay detects the ability of an effector cell population to lyse a target cell population labeled with the gamma emitter ^{51}Cr. Over the past 2 decades, other approaches have been developed to study antigen-specific $CD8^+$ T-cell responses. These include intracellular cytokine staining (2, 3), MHC class I tetramer staining (4), and enzyme-linked immunospot, abbreviated as ELISPOT. These newer assays present numerous advantages including ease of use, rapidity, and sensitivity (5, 6). The simplest and most cost-effective of these methods is the ELISPOT assay. This assay detects the secretion of cytokine after specific stimulation, usually a specific peptide or recombinant vaccinia virus with a foreign gene insert. The sensitivity of the assay has been estimated as 50 or fewer antigen-specific T-cells per 1×10^6 lymphocytes, at least 1 $\log_{10}$ more sensitive than traditional limiting dilution analysis or bulk ^{51}Cr release assay (7).

The ELISPOT assay was first described in 1983 as an alternative to the plaque-forming assay for the detection of antibody-secreting cells (ASC) (8). In the initial report, spleen cells from immunized mice were incubated in antigen-coated, 96-well polystyrene plates. After removal of the cells, bound antibodies were detected by an immunoenzyme procedure. In areas of the plate where antibody production had occurred, the substrate was deposited in circular zones (spots), which could then be enumerated (8). It was not long before the ELISPOT assay was modified for the detection of cytokine-secreting T-cells, using nitrocellulose membranes and cytokine-specific monoclonal antibodies (9). ELISPOT is now used to detect both $CD8^+$ and $CD4^+$ T-cell responses to antigens from a broad range of infectious agents and vaccine preparations (10–16), as well as tumor antigens (14, 17) and autoantigens (18). ELISPOT has also become the method of choice for comprehensive mapping of T-cell epitopes (19–22).

ENZYME-LINKED IMMUNOSPOT ASSAY (ELISPOT) PROTOCOL

The protocol given below is for the detection and enumeration of gamma interferon (IFN-γ)-secreting T cells from individuals infected with HIV-1, after specific stimulation of PBMC with recombinant vaccinia viruses expressing HIV-1 gene products (23). This assay may be adapted for use with synthetic peptides, including overlapping peptide pools, as described in detail elsewhere (19, 20, 24). Studies comparing the recombinant vaccinia-based ELISPOT to the peptide-based method suggest that these two variants provide similar results (25, 26).

Day 1: Coating of ELISPOT Plates

1. Mix 25 μl anti-IFNγ mAb clone 1-D1K (1 mg/ml; Catalog #3420-3-1000, Mabtech AB, Nacka Strand, Sweden) with 5 ml sodium bicarbonate buffer, pH 9.6 (2.93 g $NaHCO_3$, 1.59 g Na_2CO_3, 0.2% NaN_3 in a volume of 1 liter H_2O, sterile filtered). (Note that some laboratories use standard phosphate-buffered saline [PBS] as a coating buffer.)
2. Add 50 μl of the above primary antibody solution to each well of a sterile MultiScreen 96-well filtration plate (#MAHA S4510; Millipore, Billerica, MA), ensuring that the bottom of each well is entirely covered; refrigerate at 4°C overnight.
   Note: Coated plates must be left in the refrigerator for a minimum of 5 hours, or can remain at 4°C for up to 5 days before proceeding to the next step. Care should be taken to limit evaporation from peripheral wells, for example by wrapping plates with plastic film.

doi:10.1128/9781555818722.ch30

Day 2: Addition of Cells and Stimulating Antigen

3. Invert the plate to discard unbound primary antibody and pat down firmly onto paper towels to remove excess liquid from wells. Using a multichannel pipettor, add 200 μl PBS to each well. Avoid touching the bottom of wells with pipette tips. Invert the plate to discard liquid, and again pat down firmly onto paper towels. Repeat the above washing step with PBS three more times. (Note: plates may also be washed using a hand-held squirt bottle.)
4. Mix 5 ml heat-inactivated pooled human AB serum (PHS) with 45 ml RPMI 1640 medium and sterile filter. Add 50 μl of the above blocking solution to each well and incubate plate at 37°C, 5% CO_2 for 1 hour.
5. While plate is incubating in blocking solution, prepare cells for adding to plate. Either fresh or frozen PBMC can be used. Usually 1×10^5 to 2×10^5 cells are required per well, and each condition is assayed in triplicate. As an example, an assay in which responses to the HIV antigens Env, Gag, Pol, and Nef are being measured will require 4×3 wells in addition to triplicate background and one positive control well (four additional wells). If the optimal 2×10^5 cells are added per well, 3.2×10^6 cells are required. Frozen cells may be thawed, or fresh PBMC may be isolated from whole blood, followed by washing 3× in RPMI 1640 supplemented with 15% FCS, and resuspending cells in 5% PHS solution (same as blocking solution in step 4) at a concentration of 1×10^5 to 2×10^5 cells per 100 μl.
6. After the 1-hour incubation in step 4, add 100 μl cell suspension to each well. It is not necessary to remove the blocking solution.
7. If using recombinant vaccinia virus (rVV) to stimulate cells, add rVV to appropriate wells at a multiplicity of infection (MOI) of 2. Note: For consistency it is recommended that all rVV be diluted to the same concentration; a versatile concentration is 2×10^8 rVV/ml. If using peptide to stimulate cells, add peptide such that the final concentration of the peptide in each well (150 μl total volume) is 10 μg/ml. For a positive control, add phytohemagglutinin (PHA) to the well such that the final concentration of PHA is 10 μg/ml. Incubate plate at 37°C, 5% CO_2 for 1 hour. (If not using vaccinia viruses, incubate overnight at 37°C, 5% CO_2, then proceed to step 9.)
8. If using vaccinia viruses, add 30 μl filtered fetal calf serum to each well. Return plate to incubator at 37°C, 5% CO_2 and incubate overnight (14–20 hours).

Day 3: Assay Development

9. Aspirate the contents of each well, being careful not to touch membrane at the bottom of the well. Add 200 μl 0.05% Tween solution to each well (250 μl Tween 20, 500 ml PBS). Invert plate to discard washing solution and pat firmly on paper towels to remove excess liquid from wells. Repeat wash three more times.
10. Mix 5 μl biotin-conjugated anti-IFNγ mAb clone 7-B6-1 (1 mg/ml Mabtech #3420-6) with 5 ml PBS. Add 50 μl of the above secondary antibody solution to each well and incubate plate at 37°C, 5% CO_2 for 2 hours.
11. At least 20 minutes before the end of the 2-hour incubation, prepare the avidin-peroxidase complex solution (Vectastain ABC kit; Vector Laboratories Elite PK-6100 Standard, Burlingame, CA). Add 1 drop each solution A and B to 5 ml 0.1% Tween solution (the washing solution used in step 12). This complex must be prepared at least 20 minutes prior to use.
12. Invert plate to discard unbound secondary antibody and pat firmly on paper towels to remove excess liquid from wells. Add 200 μl 0.1% Tween solution to each well (500 μl Tween 20, 500 ml PBS). Discard wash solution as above and repeat wash three more times.
13. Add 50μl of this ABC solution (prepared in step 11) to each well and incubate at room temperature on a flat surface for 1 hour.
14. Wash wells 4× as in step 12.
15. Add 50 μl stable diaminobenzidine (DAB) (#750118; Life Technologies, Carlsbad, CA) to each well. Incubate at room temperature for 5 minutes on a flat surface.
16. Invert plate to discard DAB into waste receptacle. Rinse wells thoroughly with tap water 3×. Remove the plastic underdrain, wipe the back of plates gently with absorbent paper towels, and allow the plate to air dry. Count spots under an inverted microscope or with the aid of an automated reader (such as AID ELISPOT Reader Classic ELR07; Autoimmun Diagnostika GmbH, Strassberg, Germany, and San Diego, CA).
17. Analyze ELISPOT data by subtracting the average spot-forming cells (SFC) in triplicate background wells (stimulated by media alone) from the average SFC in test wells. Convert the result to spot-forming cells per 10^6 cells by multiplying by 5 (in the case of 2×10^5 cells/well) or 10 (in the case of 1×10^5 cells/well).

METHODS OF ENHANCING ELISPOT SENSITIVITY

In an effort to increase the sensitivity of ELISPOT, several groups have developed modifications of the standard protocol involving the addition of exogenous cytokines, costimulatory antibodies, or antigen-presenting cells. A partial listing of these methods is given in Table 1; for additional details the original references should be consulted.

Positive Controls

Considerable methodological variation exists among laboratories; however, in recent years there has been an effort to standardize laboratory procedures in view of large-scale clinical trials (7, 17, 24, 27–31).

As a positive control for cytokine release, many laboratories rely on polyclonal stimuli (PHA or staphylococcal enterotoxin B [SEB]). However, these reagents may give rise to a nearly confluent lawn of spots. Currier and colleagues developed a control peptide pool consisting of 23 peptides derived from influenza virus, cytomegalovirus (CMV), and Epstein-Barr virus (EBV), corresponding to known CD8 epitopes restricted by a variety of MHC class I alleles (32). This pool, known as "CEF" (CMV-EBV-Flu), is recognized by approximately 85% of the general population and is available through the NIH AIDS Reagent Program, Germantown, MD, or commercially through JPT Peptide Technologies, Berlin, Germany.

The quality of ELISPOT results may be affected by cell viability, cell concentration, addition of antigen-presenting cells, source of stimulating antigen, length of stimulating peptides, DMSO content of peptide preparations, infectivity of vaccinia stocks, operator variability, reader variability,

TABLE 1 Methods of enhancing ELISPOT sensitivity

Method	Comments	Reference(s)
Costimulatory antibodies	May increase background	Ott et al. (41)
Monocyte-derived dendritic cells	Mature DC are more efficient than immature DC	Larsson et al. (42)
B cells	May increase background	Altfeld et al. (43)
IL-2, -7, and/or -15	May increase background	Calarota et al., Chitnis et al., Kim et al., Jennes et al. (15, 44–46)
MHC class I/II transfected K562 cells	Reduces background; requires specialized reagents	Britten et al. (47)

and numerous other factors. These issues are addressed in detail by several reports, as shown in Table 2.

Interpreting ELISPOT Data: Establishing Background Levels and Identifying Positive Responses

Statistical methods for evaluating ELISPOT results and determining the appropriate positive cutoff have varied considerably between laboratories. Although many research laboratories continue to rely on empirical approaches, several recent reviews have addressed the need to standardize ELISPOT data analysis for Phase I and II clinical trials. A summary of analytical methods reported in the literature is given in Table 3.

Research and Clinical Applications of the ELISPOT Assay

Since the first reports describing the T-cell ELISPOT assay more than 20 years ago, ELISPOT has been used to detect T-cell responses to antigens from a variety of infectious agents, including bacteria, viruses, and protozoa (10–16). During this time, advances in cellular immunology have revealed a surprising level of functional heterogeneity and developmental plasticity among mammalian T-cell subsets (33–35). These advances have led to a new awareness of the complex roles played by $CD4^+$ and $CD8^+$ T-cells during an adaptive immune response. While many vaccine studies continue to focus on a limited repertoire of cytokines, notably IFN-γ and interleukin-2 (IL-2), commercial reagents now permit the detection of a broad range of factors. These include IL-1β, IL-2, IL-4, IL-5, IL-6, IL-9, IL-10, IL-12, IL-13, IL-17, IL-23, IL-31, IFN-γ, granulocyte macrophage colony-stimulating factor (GM-CSF), tumor necrosis factor alpha (TNF-α), TGF-β, RANTES/CCL-5, CXCL8/IL-8, MIG/CXCL9, IP-10/CXCL10, Granzyme B, Perforin, and FAS ligand/TNFSF6. Multi-color ELISPOT (36) and "fluorospot" (37) protocols have been developed, permitting the simultaneous detection of two to three secreted factors using specialized ELISPOT readers.

As ELISPOT technology has become more accessible, there has been increasing awareness of the potential sources of intra- and interassay variability. The necessity of harmonizing protocols for adoption by network-based clinical trials has led to a series of coordinated efforts to standardize assay validation (7, 27, 28). Several recent validation studies have been conducted by large, multi-laboratory consortia, including the Cancer Vaccine Consortium (CVC/SVI), the Clinical Trials in Organ Transplant (CTOT) Consortium, and the NIH-funded ELISPOT Collaborative Study Group (38–40). As ELISPOT protocols continue to

TABLE 2 Parameters influencing ELISPOT assay variability

Parameter	Comments	Reference(s)
Background	Assays with background >120 SFC/10^6 considered invalid	Mwau et al. (27)
Cell number (PBMC)	Optimal number is 2×10^5/well	Russell et al. (7)
Cryopreservation	Average recovery 60%; viability 90%	Russell et al. (7)
	Positive responses remain detectable	Russell et al. (7)
	Magnitude of responses diminished	Mwau et al. (27)
	Controlled stepwise freezing is optimal	Mwau et al. (27)
Detection threshold	50 SFC/10^6 PBMC (0.005%)	Russell et al. (7)
ELISPOT reader	Automated readers superior to manual counting	Herr et al., Janetzki et al. (29, 48)
Incubation time	16–20 hours	Russell et al. (7)
Peptide preparations	DMSO <1%	Mwau et al., Russell et al. (7, 27)
	Optimal length: 15-mers	Russell et al. (7)
	Effect of concentration: 2 μg/ml adequate	Russell et al. (7)
	5–10 μg/ml maximal; 20 μg/ml inhibitory	
	Peptides should be filtered	Karlsson et al. (49)
Vaccinia viruses	Titer on susceptible cell line	Larsson et al., Sun et al. (23, 25)
	Routinely verify expression of foreign protein by Western blot	

TABLE 3 Methods of analyzing ELISPOT data

Data analysis method	Reference
Empirical approaches	
Positive response: ≥3× mean of negative control wells and >50 SFC/10^6 PBMC	Addo et al. (20)
Positive response: >2× mean of background wells and >20 SFC/10^6 PBMC	Currier et al. (32)
Positive response: ≥5 more SFC/well than negative controls and >2× mean of negative control wells	Ewer et al. (16)
Positive response: >2× average of background wells and >50 SFC/10^6 PBMC	Mwau et al. (27)
Positive response: >4× mean background; > mean background + 3 standard deviations of negative control; >55 SFC/10^6 PBMC	Streeck et al. (24)
Statistical approaches	
Unpaired T-test to determine whether SFC are significantly greater in test wells than controls	Herr et al. (48)
Exact binomial test to determine whether SFC are significantly greater in test wells than controls	Russell et al. (7)
Compares several statistical methods; recommends a permutation-based criterion using a resampling adjustment for multiple comparisons.	Hudgens et al. (28)
Uses within-plate differences between negative control and test wells; defines positivity threshold based on their statistical distribution over each plate.	Alexander et al. (50)

improve and research applications continue to proliferate, the trend towards increased standardization and validation is likely to continue to accelerate in the future.

REFERENCES

1. **Murphy K.** 2012. T cell-mediated immunity, p 335–352. *In* Murphy K (ed), *Janeway's Immunology*, 8th ed. Garland Science, New York, NY.
2. **Picker LJ, Singh MK, Zdraveski Z, Treer JR, Waldrop SL, Bergstresser PR, Maino VC.** 1995. Direct demonstration of cytokine synthesis heterogeneity among human memory/effector T cells by flow cytometry. *Blood* **86:**1408–1419.
3. **Lamoreaux L, Roederer M, and Koup R.** 2006. Intracellular cytokine optimization and standard operating procedure. *Nature Protocols* **1:**1507–1516.
4. **Altman JD, Moss PA, Goulder PJ, Barouch DH, McHeyzer-Williams MG, Bell JI, McMichael AJ, Davis MM.** 1996. Phenotypic analysis of antigen-specific T lymphocytes. *Science* **274:**94–96.
5. **Doherty PC.** 1998. The new numerology of immunity mediated by virus-specific $CD8^+$ T cells. *Curr Opin Microbiol* **1:**419–422.
6. **McMichael AJ, O'Callaghan CA.** 1998. A new look at T cells. *J Exp Med* **187:**1367–1371.
7. **Russell ND, Hudgens MG, Ha R, Havenar-Daughton C, McElrath MJ.** 2003. Moving to human immunodeficiency virus type 1 vaccine efficacy trials: defining T cell responses as potential correlates of immunity. *J Infect Dis* **187:**226–242.
8. **Czerkinsky CC, Nilsson LA, Nygren H, Ouchterlony O, Tarkowski A.** 1983. A solid-phase enzyme-linked immunospot (ELISPOT) assay for enumeration of specific antibody-secreting cells. *J Immunol Methods* **65:**109–121.
9. **Czerkinsky C, Andersson G, Ekre HP, Nilsson LA, Klareskog L, Ouchterlony O.** 1988. Reverse ELISPOT assay for clonal analysis of cytokine production. I. Enumeration of gamma-interferon-secreting cells. *J Immunol Methods* **110:**29–36.
10. **Weiskopf D, Angelo MA, de Azeredo EL, Sidney J, Greenbaum JA, Fernando AN, Broadwater A, Kolla RV, De Silva AD, de Silva AM, Mattia KA, Doranz BJ, Grey HM, Shresta S, Peters B, Sette A.** 2013. Comprehensive analysis of dengue virus-specific responses supports an HLA-linked protective role for $CD8^+$ T cells. *Proc Natl Acad Sci USA* **110:**E2046–2053.
11. **Ledgerwood JE, Hu Z, Gordon IJ, Yamshchikov G, Enama ME, Plummer S, Bailer R, Pearce MB, Tumpey TM, Koup RA, Mascola JR, Nabel GJ, Graham BS.** 2012. Influenza virus h5 DNA vaccination is immunogenic by intramuscular and intradermal routes in humans. *Clin Vaccine Immunol* **19:**1792–1797.
12. **Lindestam Arlehamn CS, Gerasimova A, Mele F, Henderson R, Swann J, Greenbaum JA, Kim Y, Sidney J, James EA, Taplitz R, McKinney DM, Kwok WW, Grey H, Sallusto F, Peters B, Sette A.** 2013. Memory T cells in latent *Mycobacterium tuberculosis* infection are directed against three antigenic islands and largely contained in a $CXCR3^+CCR6^+$ Th1 subset. *PLoS Pathog* **9:**e1003130.
13. **Danta M, Semmo N, Fabris P, Brown D, Pybus OG, Sabin CA, Bhagani S, Emery VC, Dusheiko GM, Klenerman P.** 2008. Impact of HIV on host-virus interactions during early hepatitis C virus infection. *J Infect Dis* **197:**1558–1566.
14. **Ferraro B, Talbott KT, Balakrishnan A, Cisper N, Morrow MP, Hutnick NA, Myles DJ, Shedlock DJ, Obeng-Adjei N, Yan J, Kayatani AK, Richie N, Cabrera W, Shiver R, Khan AS, Brown AS, Yang M, Wille-Reece U, Birkett AJ, Sardesai NY, Weiner DB.** 2013. Inducing humoral and cellular responses to multiple sporozoite and liver-stage malaria antigens using exogenous plasmid DNA. *Infect Immun* **81:**3709–3720.
15. **Kim KH, Greenfield W, Shotts E, Nakagawa M.** 2007. Detection of human papillomavirus type 16-specific T lymphocytes by a recombinant vaccinia virus-based enzyme-linked immunospot assay. *Clin Vaccine Immunol* **14:**362–368.
16. **Ewer K, Deeks J, Alvarez L, Bryant G, Waller S, Andersen P, Monk P, Lalvani A.** 2003. Comparison of T-cell-based assay with tuberculin skin test for diagnosis of *Mycobacterium tuberculosis* infection in a school tuberculosis outbreak. *Lancet* **361:**1168–1173.
17. **Asai T, Storkus WJ, Whiteside TL.** 2000. Evaluation of the modified ELISPOT assay for gamma interferon production in cancer patients receiving antitumor vaccines. *Clin Diagn Lab Immunol* **7:**145–154.
18. **Maier R, Miller S, Kurrer M, Krebs P, de Giuli R, Kremer M, Scandella E, Ludewig B.** 2005. Quantification and characterization of myosin peptide-specific $CD4^+$

T cells in autoimmune myocarditis. *J Immunol Methods* **304:**117–125.

19. **Anthony DD, Lehmann PV.** 2003. T-cell epitope mapping using the ELISPOT approach. *Methods* **29:**260–269.
20. **Addo MM, Yu XG, Rathod A, Cohen D, Eldridge RL, Strick D, Johnston MN, Corcoran C, Wurcel AG, Fitzpatrick CA, Feeney ME, Rodriguez WR, Basgoz N, Draenert R, Stone DR, Brander C, Goulder PJ, Rosenberg ES, Altfeld M, Walker BD.** 2003. Comprehensive epitope analysis of human immunodeficiency virus type 1 (HIV-1)-specific T-cell responses directed against the entire expressed HIV-1 genome demonstrate broadly directed responses, but no correlation to viral load. *J Virol* **77:**2081–2092.
21. **de Souza MS, Ratto-Kim S, Chuenarom W, Schuetz A, Chantakulkij S, Nuntapinit B, Valencia-Micolta A, Thelian D, Nitayaphan S, Pitisuttithum P, Paris RM, Kaewkungwal J, Michael NL, Rerks-Ngarm S, Mathieson B, Marovich M, Currier JR, Kim JH.** 2012. The Thai phase III trial (RV144) vaccine regimen induces T cell responses that preferentially target epitopes within the V2 region of HIV-1 envelope. *J Immunol* **188:**5166–5176.
22. **Long HM, Leese AM, Chagoury OL, Connerty SR, Quarcoopome J, Quinn LL, Shannon-Lowe C, Rickinson AB.** 2011. Cytotoxic $CD4^+$T cell responses to EBV contrast with CD8 responses in breadth of lytic cycle antigen choice and in lytic cycle recognition. *J Immunol* **187:**92–101.
23. **Larsson M, Jin X, Ramratnam B, Ogg GS, Engelmayer J, Demoitie MA, McMichael AJ, Cox WI, Steinman RM, Nixon D, Bhardwaj N.** 1999. A recombinant vaccinia virus based ELISPOT assay detects high frequencies of Pol-specific CD8 T cells in HIV-1-positive individuals. *AIDS* **13:**767–777.
24. **Streeck H, Frahm N, Walker BD.** 2009. The role of IFN-gamma Elispot assay in HIV vaccine research. *Nat Protoc* **4:**461–469.
25. **Sun Y, Iglesias E, Samri A, Kamkamidze G, Decoville T, Carcelain G, Autran B.** 2003. A systematic comparison of methods to measure HIV-1 specific CD8 T cells. *J Immunol Methods* **272:**23–34.
26. **Xu J, Lori F, Lisziewicz J.** 2003. Vaccinia assay for the rapid detection of functional HIV-specific $CD8^+$ cytotoxic T lymphocytes. *J Immunol Methods* **276:**45–57.
27. **Mwau M, McMichael AJ, Hanke T.** 2002. Design and validation of an enzyme-linked immunospot assay for use in clinical trials of candidate HIV vaccines. *AIDS Res Hum Retroviruses* **18:**611–618.
28. **Hudgens MG, Self SG, Chiu YL, Russell ND, Horton H, McElrath MJ.** 2004. Statistical considerations for the design and analysis of the ELISpot assay in HIV-1 vaccine trials. *J Immunol Methods* **288:**19–34.
29. **Janetzki S, Schaed S, Blachere NE, Ben-Porat L, Houghton AN, Panageas KS.** 2004. Evaluation of Elispot assays: influence of method and operator on variability of results. *J Immunol Methods* **291:**175–183.
30. **Cox JH, Ferrari G, Janetzki S.** 2006. Measurement of cytokine release at the single cell level using the ELISPOT assay. *Methods* **38:**274–282.
31. **Janetzki S, Cox JH, Oden N, Ferrari G.** 2005. Standardization and validation issues of the ELISPOT assay. *Methods Mol Biol* **302:**51–86.
32. **Currier JR, Kuta EG, Turk E, Earhart LB, Loomis-Price L, Janetzki S, Ferrari G, Birx DL, Cox JH.** 2002. A panel of MHC class I restricted viral peptides for use as a quality control for vaccine trial ELISPOT assays. *J Immunol Methods* **260:**157–172.
33. **Murphy KM, Stockinger B.** 2010. Effector T cell plasticity: flexibility in the face of changing circumstances. *Nat Immunol* **11:**674–680.
34. **Mucida D, Husain MM, Muroi S, van Wijk F, Shinnakasu R, Naoe Y, Reis BS, Huang Y, Lambolez F, Docherty M, Attinger A, Shui JW, Kim G, Lena CJ, Sakaguchi S, Miyamoto C, Wang P, Atarashi K, Park Y, Nakayama T, Honda K, Ellmeier W, Kronenberg M, Taniuchi I, Cheroutre H.** 2013. Transcriptional reprogramming of mature $CD4(^+)$ helper T cells generates distinct MHC class II-restricted cytotoxic T lymphocytes. *Nat Immunol* **14:**281–289.
35. **Akondy RS, Monson ND, Miller JD, Edupuganti S, Teuwen D, Wu H, Quyyumi F, Garg S, Altman JD, Del Rio C, Keyserling HL, Ploss A, Rice CM, Orenstein WA, Mulligan MJ, Ahmed R.** 2009. The yellow fever virus vaccine induces a broad and polyfunctional human memory $CD8^+$ T cell response. *J Immunol* **183:**7919–7930.
36. **Boulet S, Ndongala ML, Bernard NF.** 2010. Dual-color ELISPOT assay for the simultaneous detection of IL-2 and/or IFN-gamma secreting T cells. *Cold Spring Harb Protoc* **2010:**pdb prot5369.
37. **Ahlborg N, Axelsson B.** 2012. Dual- and triple-color fluorospot. *Methods Mol Biol* **792:**77–85.
38. **Janetzki S, Panageas KS, Ben-Porat L, Boyer J, Britten CM, Clay TM, Kalos M, Maecker HT, Romero P, Yuan J, Kast WM, Hoos A.** 2008. Results and harmonization guidelines from two large-scale international Elispot proficiency panels conducted by the Cancer Vaccine Consortium (CVC/SVI). *Cancer Immunol Immunother* **57:**303–315.
39. **Ashoor I, Najafian N, Korin Y, Reed EF, Mohanakumar T, Ikle D, Heeger PS, Lin M.** 2013. Standardization and cross validation of alloreactive IFNgamma ELISPOT assays within the clinical trials in organ transplantation consortium. *Am J Transplant* **13:**1871–1879.
40. **Cox JH, Ferrari G, Kalams SA, Lopaczynski W, Oden N, D'Souza PM.** 2005. Results of an ELISPOT proficiency panel conducted in 11 laboratories participating in international human immunodeficiency virus type 1 vaccine trials. *AIDS Res Hum Retrovir* **21:**68–81.
41. **Ott PA, Berner BR, Herzog BA, Guerkov R, Yonkers NL, Durinovic-Bello I, Tary-Lehmann M, Lehmann PV, Anthony DD.** 2004. CD28 costimulation enhances the sensitivity of the ELISPOT assay for detection of antigen-specific memory effector CD4 and CD8 cell populations in human diseases. *J Immunol Methods* **285:**223–235.
42. **Larsson M, Wilkens DT, Fonteneau JF, Beadle TJ, Merritt MJ, Kost RG, Haslett PA, Cu-Uvin S, Bhardwaj N, Nixon DF, Shacklett BL.** 2002. Amplification of low-frequency antiviral CD8 T cell responses using autologous dendritic cells. *AIDS* **16:**171–180.
43. **Altfeld MA, Trocha A, Eldridge RL, Rosenberg ES, Phillips MN, Addo MM, Sekaly RP, Kalams SA, Burchett SA, McIntosh K, Walker BD, Goulder PJ.** 2000. Identification of dominant optimal HLA-B60- and HLA-B61-restricted cytotoxic T-lymphocyte (CTL) epitopes: rapid characterization of CTL responses by enzyme-linked immunospot assay. *J Virol* **74:**8541–8549.
44. **Jennes W, Kestens L, Nixon D, Shacklett B.** 2002. Enhanced ELISPOT detection of antigen-specific T cell responses from cryopreserved specimens with addition of both IL-7 and IL-15—the Amplispot assay. *J Immunol Methods* **270:**99.
45. **Calarota SA, Otero M, Hermanstayne K, Lewis M, Rosati M, Felber BK, Pavlakis GN, Boyer JD, Weiner DB.** 2003. Use of interleukin 15 to enhance interferon-gamma production by antigen-specific stimulated lymphocytes from rhesus macaques. *J Immunol Methods* **279:**55–67.
46. **Chitnis V, Pahwa R, Pahwa S.** 2003. Determinants of HIV-specific CD8 T-cell responses in HIV-infected pediatric patients and enhancement of HIV-gag-specific responses with exogenous IL-15. *Clin Immunol* **107:**36–45.

47. **Britten CM, Meyer RG, Kreer T, Drexler I, Wolfel T, Herr W.** 2002. The use of HLA-A*0201-transfected K562 as standard antigen-presenting cells for CD8(+) T lymphocytes in IFN-gamma ELISPOT assays. *J Immunol Methods* **259:**95–110.
48. **Herr W, Linn B, Leister N, Wandel E, Meyer zum Buschenfelde KH, Wolfel T.** 1997. The use of computer-assisted video image analysis for the quantification of $CD8^+$ T lymphocytes producing tumor necrosis factor alpha spots in response to peptide antigens. *J Immunol Methods* **203:**141–152.
49. **Karlsson RK, Jennes W, Page-Shafer K, Nixon DF, Shacklett BL.** 2004. Poorly soluble peptides can mimic authentic ELISPOT responses. *J Immunol Methods* **285:**89–92.
50. **Alexander N, Fox A, Lien VT, Dong T, Lee LY, Hang Nle K, Mai le Q, Horby P.** 2013. Defining ELISpot cut-offs from unreplicated test and control wells. *J Immunol Methods* **392:**57–62.

Regulatory T Cell (Treg) Assays: Repertoire, Functions, and Clinical Importance of Human Treg

THERESA L. WHITESIDE

31

Regulatory T cells (Treg) are a small subset (<5%) of circulating $CD4^+$ T cells. Due to their ability to suppress functions of other lymphocytes, Treg are responsible for maintaining immune responses in balance. This system of immune checks and balances exists to protect us from autoimmune diseases, prevent tissue damage resulting from intense inflammatory responses induced by infectious or non-infectious injuries and to contain chronic inflammatory reactions that might promote tumor development (1). Treg seem to be capable of fulfilling all these functions, largely due to their plasticity, which allows them to readily adjust to conditions in the local microenvironment (2). Viewed in this context, Treg can be considered as a protective mechanism designed to limit inflammatory tissue damage, but also as a potentially dangerous suppressor of immune responses that benefit the host. For example, in chronic viral infections such as HIV-1 infections, Treg could either suppress excessive immune activation, thus benefiting the host, or limit antiviral immunity needed by the host to contain the infection. Today, the role of Treg in HIV-1 remains highly controversial (3). In cancer, Treg are emerging both as contributors to cancer progression, because of their ability to block anti-tumor immune responses, and also as inhibitors of cancer progression via their ability to suppress cancer-promoting inflammation (4). It is unclear whether the anti-inflammatory activity of Treg or their suppression of antitumor immunity contributes to disease outcome, and the mechanisms responsible for regulation of Treg functions remain unknown. Factors that govern Treg behavior *in situ* are being intensely investigated in various human diseases. An excess of Treg (e.g., in some cancers) or their numerical or functional deficiency (e.g., in autoimmune diseases) is associated with clinical symptoms and may predict outcome. For these reasons, measurements of Treg frequency and function in the circulation, and especially in tissues, are of great importance.

Human Treg, as opposed to murine Treg, are difficult to study. This is in part because Treg are a minor subset of $CD4^+$ T cells, but mainly because no marker specific for human Treg has been defined so far. FOXP3, a transcription factor, is a reliable biomarker of murine Treg; however, in humans, FOXP3 may be transiently expressed in activated conventional $CD4^+$ T cells, may be absent in some inducible Treg, and may be found in tumor cells (4, 5). For these reasons, it is not considered to be "specific" for human Treg. Thus, the only reliable identification of human Treg depends on their functional ability to suppress activities of other lymphocytes. While initially, Treg were considered to be a distinct subset of functionally defined suppressor cells, more recent data point to the existence of distinct Treg subsets responsible for specifically targeted regulatory activities (4). This functional heterogeneity of human Treg as well as their phenotypic plasticity have created considerable confusion in the field, and the definition of Treg subsets remains controversial, as reflected by recent attempts to update their nomenclature (6).

CURRENT NOMENCLATURE OF Treg

The recently adapted nomenclature for Treg renames natural (n)Treg to "thymic-derived (t)Treg," while the former inducible (i)Treg are now referred to as "peripheral (p)Treg" to reflect their differentiation in the periphery as opposed to the thymus. *In vitro*-induced Treg, which simulate pTreg, are now called Tr1 cells (6). This revised nomenclature correctly emphasizes the distinct origin of various Treg subsets. It also acknowledges the fact that pTreg can and, in fact do, differentiate in the periphery from the conventional $CD4^+$ Treg under conditions of antigenic stimulation and an appropriate cytokine milieu (7). In this chapter, I have selected to use the older terminology of iTreg rather than pTreg because, in my view, it better defines the inducible versus naturally acquired character of the Treg subsets detectable in the human peripheral circulation.

PHENOTYPING OF HUMAN Treg

There is currently no agreement as to the best phenotypic assay for human Treg. A 2013 international canvas resulted in a list of 21 markers used for flow-based phenotyping of Treg. Of these, only 4 (CD3, CD4, CD25, and FOXP3) were used by 95 to 100% of the canvas participants. Negative expression of CD127 was used by 77%, and of CD45RA by only 27%, of participants. These six markers were considered the "backbone" markers. All other markers, including CTLA-4, CD39, CCR7, HELIOS, or CD69, were considered "optional."

It has been suggested that, in the absence of a well-defined and stable marker for all human Treg, it might be useful to consider a combination of markers that could help define distinct Treg subsets, allowing, for example, for discrimination of circulating Treg from those preferentially recruited to lymph nodes or to other tissue sites. Indeed, a

doi:10.1128/9781555818722.ch31

TABLE 1 Phenotypic characteristics of human nTreg, iTreg, and CD4+T conventional[a]

Markers	nTreg	iTreg	$CD4^+$conv	Comment
CD3	+	+	+	
CD4	+	+	+	
CD25	High	±	Int/low	Activation marker
CD122/CD132	±	++	±	
FOXP3*	+	±	±	Transient expression in activated T cells
SATIB1	−	±	±	Transcription factor regulated by FOXP3 negative Treg marker
CD45RA	+	−	+ or −	iTreg are $CD45RO^+$
CTLA-4	+	+	+	Upregulated on Treg
CD127	−	−	+	Used for negative selection of Treg
HELIOS[b]*	+	−[b]	±	Transient expression in activated T cells
ICOS#	±	+	+	iTreg in melanoma TIL upregulate its expression
NRP1#	±	+	±	Restricted expression
CD39#	+	++	−	Ectonucleotidase; hydrolyzes eATP to 5AMP; upregulated on Treg in TIL
CD73*#	+	±[c]	±[d]	Ectonucleotidase; when coexpressed with CD39 on cell surface in activated Treg, it hydrolyzes 5′ AMP to adenosine
CD26[e]	−	±	+	Peptidase linked to ADA1; used as a negative Treg marker
GITR#	+	+	+	
CD134	±	++	±	Upregulated on Treg
CD137#	+	++	±	Upregulated on iTreg in TIL
PD-1#	±	++	±	As above
PD-L1#	±	++	±	As above
TIM-3#	+	++	?	As above
LAG-3#	+	++	+	As above
CCR-4#	+	++	±	As above
CCR6#	+	++	±	As above
CCR7#	+	++	±	As above
GARP/LAP[f]#	+	++	−	Upregulated on the surface of circulating Treg in cancer
TGF-β*#	+	++	−	
IL-10*#	+	+	−	
GrB/perforin#	±	++	−	
COX-2#	−	+	−	
Ki67*#	±	+	±	Treg proliferate *in vivo*

[a]The list is not comprehensive and includes most commonly studied Treg markers. The iTreg column includes data for *ex vivo*-evaluated cells and/or for *in vitro*-generated cells. For a more in-depth commentary on expression of the listed markers on nTreg and iTreg, see reference 9. Symbols: * indicates intracytoplasmic/intranuclear expression; # indicates that expression levels are variable and dependent on the state of Treg activation. Table reproduced with permission from reference 9.

[b]Expression of HELIOS in nTreg versus iTreg has been debated and its usefulness for discriminating between nTreg and iTreg is not entirely clear.

[c]CD73 is abundantly present in the cytoplasm of Treg but appears to be readily downregulated (probably enzymatically cleaved) from their cell surface; it is seen on the cell surface in highly variable proportions of iTreg and only <1% of nTreg.

[d]CD73 is expressed on the cell surface of a small subset (8 to 18%) of $CD4^+CD73^+$ T cells in the peripheral blood of normal donors.

[e]ADA1 is an enzyme (adenosine deaminase 1).

[f]GARP (glycoprotein A repetitions predominant) or garpin and LAP (latency-associated peptide) are TGF-β^- associated membrane-bound molecules.

combination of $CD4^+FOXP3^+CD25^{high}CD39^+$ Treg characterizes a subset of Treg capable of suppressing functions of autologous Teff cells, and the presence of CCR4, CCR6, or CCR7 chemokine receptors might suggest the ability of these cells to migrate to tissues in response to their respective ligands (8). Also, marker combinations could better discriminate activated Treg from their precursors or serve to distinguish iTreg from nTreg. Table 1 provides a list of phenotypic markers that are being used alone or in various combinations with other markers for flow cytometry assessments of Treg frequency and the functional attributes that can be evaluated by the use of flow cytometry. The list (reproduced with permission from reference 9) is not comprehensive, but it includes markers that have been most commonly used to study human Treg.

An alternative approach to a study of human Treg may be to focus on a Treg subset that is known to be biologically important and selectively defined by expression of a stable surface marker. For example, the subset of Treg and iTreg expressing CD39, an ectoenzyme that catalyzes hydrolysis of exogenous ATP to ADP and then to 5′ AMP is of considerable interest because $CD39^+$ Treg have been shown to produce extracellular adenosine (ADO), which exerts potent immunosuppressive activity (10). CD39 is present on the surface of Treg but not other $CD4^+$ T cells, and it defines a functionally active Treg subset that appears to be expanded in disease (9). This subset of Treg was first described in the seminal papers by Borsellino et al. and Deaglio et al. (11, 12). Our own studies have contributed to defining the role of $CD39^+$ Treg in cancer and HIV (9, 13) and have suggested that the adenosinergic pathway is one of the major components of tumor-induced or HIV-I-induced immune suppression.

Suppressor Assays for Human Treg

In view of the lack of Treg-specific markers in humans and the phenotypic profile combining multiple markers (Table 1), Treg suppressive activity remains the only reliable means of their identification regardless of the phenotypic subtype. Conventionally, inhibition of responder T-cell proliferation or of T-cell activation has been considered a useful functional assay for Treg (9). More recently, Ki67, the universal proliferation marker, proved to be useful as a functional Treg marker but only *in vivo* and only in mice, whereas Treg were shown to proliferate vigorously and express Ki67 (14).

Human Treg proliferate poorly *in vitro*. Table 2 lists *in vitro* suppressor assays commonly used to evaluate functions of human Treg. In addition, expression of certain phenotypic markers by Treg could be taken as evidence of their suppressor function. For example, markers such as CD39 and CD73 ectonucleotidases, expressed on the Treg subset that produces immunosuppressive adenosine (10), have readily measurable enzymatic activity and can be used to differentiate iTreg from nTreg (15). Expression of other markers such as the latency-associated peptide (LAP) and/or glycoprotein A repetitions predominant (GARP) on iTreg suggests the involvement of the TGF-β pathway in iTreg-mediated suppression (9). Intracellular expression of granzyme B and/or perforin granules in Treg, as well as surface expression of FasL in activated Treg (9), has been associated with suppressive functions of these cells; although none of these markers are specific for Treg, their flow cytometry-based detection in combination with the constellation of phenotypic Treg markers, such as $CD25^{high}$ and FOXP3, for example, are quite useful. They allow for estimations of Treg suppressor function without isolation of Treg from body fluids. The process of Treg isolation by immune capture on antibody-coated beads is complex, and it is dependent either on negative selection (e.g., the absence of CD127 or CD26 expression on Treg) or on positive selection (e.g., a high expression level of CD25 or the presence of CD39 on Treg) to differentiate these cells from conventional $CD4^+$ T cells. The recovery of purified Treg by this process in numbers sufficient for the performance of the conventional carboxyfluorescein succinimidyl ester (CFSE)-based suppressor assays (Table 2) represents a frequently encountered difficulty (9). Often, either the number or the purity of isolated Treg is insufficient for reliable performance or adequate interpretation of suppressor assays. For these reasons, flow cytometry-based assays incorporating the detection and measurements of levels of expression of biologically active markers in human Treg without cell isolation are useful. They allow for correlations of the Treg phenotype with Treg suppressor functions in selected tissue locations such as the tumor microenvironment or an inflammatory site of interest. For example, studying by flow cytometry expression levels of the checkpoint inhibitory molecules such as CTLA-4, PD-1, LAG-3, or TIM-3 on Treg found in tumor-infiltrating lymphocytes (TIL), we have observed increased surface expression of these molecules on Treg *in situ* (16). The implication of this finding

TABLE 2 Functional assays for human nTreg and iTreg[a]

Assay type	Suppressor cell (Ts)	Responder cell (Tr)	Measurement
Multiparameter flow cytometry	*Ex vivo*-activated T cells (6–12 h)	–	Intracellular expression of 1–5 cytokines
As above	nTreg or iTreg	–	GARP/LAP expression
As above	nTreg or iTreg	CD4+T conv *ex vivo* activated, 7–20 h	Downregulation of CD69 or CD154 expression on Tr
Supernatants	nTreg or iTreg ± activation	–	Adenosine, PGE2, TGF-β, IL-10 production
Cocultures[b]	nTreg or iTreg	CFSE-labeled CD4+T conv	Proliferation inhibition
FOXP3 demethylation (MS-QPCR)	nTreg	–	Detects T-reg specific demethylation region (TSDR)

[a]Table reproduced with permission from reference 9. Abbreviations: CFSE, carboxyfluorescein; MS-QPCR, mass spectrometry-quantitative PCR. Other abbreviations as listed in Table 1.
[b]Cocultures of suppressor with responder cells require assays set up at different Ts/TR ratios.

is that Treg-mediated suppression of antitumor immune responses *in situ* involves signaling via these regulatory molecules (16). These flow cytometry-based assessments make it possible to simultaneously estimate the frequency of human Treg and of their functional attributes *in situ*.

CORRELATIONS OF Treg MEASURES WITH DISEASE

Although considerable progress in understanding the role of Treg in human health and disease has been made, reports correlating the Treg frequency, and especially their suppressive activity, with disease progression are not always consistent or reliable. For example, elimination or downregulation of Treg activity has long been considered to be a desirable strategy in cancer immunotherapy, and various agents, including cyclophosphamide, daclizumab (anti-CD25 Ab), and denileukin diftitox (ONTAC), or tyrosine kinase inhibitors such as sunitinib, have been utilized in preclinical and clinical studies to deplete Treg (reviewed in reference 9). However, it has not been possible to convincingly correlate Treg depletion by these agents with clinical benefits in patients with cancer (17). This is likely to be a reflection of Treg diversity as much as of difficulties associated with reliable assessments of this small, phenotypically and functionally heterogenous lymphocyte subset. Nevertheless, the excessive accumulations of Treg (e.g., at tumor sites in some human cancers) and, conversely, the reduction/depletion of Treg in autoimmune diseases have been linked to cancer progression or to improvement of clinical manifestations, respectively (9). Furthermore, newer data on the effects of immune therapies on the Treg suggest that modulating the frequency and/or regulatory functions of these cells may be beneficial to patients (9). Therefore, accurate measurements of the changes in Treg before, during, and after therapy are critically important, and the development of reliable, readily applicable monitoring tools for Treg subsets in the peripheral circulation and tissues of patients remains a priority.

SUMMARY

Treg play an important role in homeostasis of antitumor, antiviral, and autoreactive immunity. For this reason, Treg remain an attractive target for immunotherapy. Measurements of their frequency and functions in health or disease and the understanding of mechanisms Treg utilize for mediating immune suppression are critical for the development of therapeutic strategies for autoimmune diseases, cancer, and chronic viral infections such as HIV-1. Treg may be beneficial to the host by containing excessive immune activation such as occurs in HIV-1 or in cancers associated with chronic local inflammation. They could also serve as biomarkers for disease progression/regression if more solid correlations between their presence/activity and disease outcome or response to therapy are established in the future. For either of these reasons, assessments of Treg in the circulation and tissues are an essential component of comprehensive immune monitoring of patients with dysfunctions of the immune system.

This work is in part supported by NIH grant R0-1 CA168628 to TLW.

REFERENCES

1. **Mougiakakos D, Choudhury A, Lladser A, Kiessling R, Johansson CC.** 2010. Regulatory T cells in cancer. *Adv Cancer Res*. **107:**57–117.
2. **Addey C, White M, Dou L, Coe D, Dyson J, Chai JG.** 2011. Functional plasticity of antigen-specific regulatory T cells in context of tumor. *J Immunol*. **186:**4557–4564.
3. **Angin M, Sharma S, King M, Murooka TT, Ghebremichael M, Mempel TR, Walker BD, Bhasin MK, Addo MM.** 2014. HIV-1 infection impairs regulatory T cell suppressive capacity on a per-cell basis. *J Infect Dis* **210:**899–903.
4. **Whiteside TL.** 2012. What are regulatory T cells (Treg) regulating in cancer and why? *Semin Cancer Biol* **22:**327–334.
5. **deLeeuw RJ, Kost SE, Kakal JA, Nelson BH.** 2012. The prognostic value of FOXP3$^+$ tumor-infiltrating lymphocytes in cancer: a critical review of the literature. *Clin Cancer Res* **18:**3022–3029.
6. **Abbas AK, Benoist C, Bluestone JA, Campbell DJ, Ghosh S, Hori S, Jiang S, Kuchroo VK, Mathis D, Roncarolo MG, Rudensky A, Sakaguchi S, Shevach EM, Vignali DA, Ziegler SF.** 2013. Regulatory T cells: recommendations to simplify the nomenclature. *Nat Immunol* **14:**307–308.
7. **Bergmann C, Strauss L, Zeidler R, Lang S, Whiteside TL.** 2007. Expansion of human T regulatory type 1 cells in the microenvironment of cyclooxygenase 2 overexpressing head and neck squamous cell carcinoma. *Cancer Res* **67:**8865–8873.
8. **Schuler PJ, Schilling B, Harasymczuk M, Hoffmann T, Johnson J, Lang S, Whiteside TL.** 2012. Phenotypic and functional characteristics of ATP-hydrolysing CD4$^+$CD39$^+$FOXP3$^+$ and CD4$^+$CD39$^+$FOXP3^{neg} T cell subsets in patients with cancer. *Eur J Immunol* **42:**1876–1885.
9. **Whiteside TL.** 2014. Induced regulatory T cells in inhibitory microenvironments created by cancer. *Expert Opin Biol Ther* **14:**1411–1425.
10. **Whiteside TL, Schuler P, Schilling B.** 2012. Induced and natural regulatory T cells in human cancer. *Expert Opin Biol Ther* **12:**1383–1397.
11. **Borsellino G, Kleinewietfeld M, Di Mitri D, Sternjak A, Diamantini A, Giometto R, Höpner S, Centonze D, Bernardi G, Dell'Acqua ML, Rossini PM, Battistini L, Rötzschke O, Falk K.** 2007. Expression of ectonucleotidase CD39 by FoxP3$^+$ Treg cells: hydrolysis of extracellular ATP and immune suppression. *Blood* **110:**1225–1232.
12. **Deaglio S, Dwyer KM, Gao W, Friedman D, Usheva A, Erat A, Chen JF, Enjyoji K, Linden J, Oukka M, Kuchroo VK, Strom TB, Robson SC.** 2007. Adenosine generation catalyzed by CD39 and CD73 expressed on regulatory T cells mediates immune suppression. *J Exp Med* **204:**1257–1265.
13. **Schuler PJ, Macatangay BJ, Saze Z, Jackson EK, Riddler SA, Buchanan WG, Hilldorfer BB, Mellors JW, Whiteside TL, Rinaldo CR.** 2013. CD4$^+$CD73$^+$ T cells are associated with lower T cell activation and C reactive protein levels and are depleted in HIV-1 infection regardless of viral suppression. *AIDS* **27:**1545–1555.
14. **Vukmanovic-Stejic M, Zhang Y, Cook JE, Fletcher JM, McQuaid A, Masters JE, Rustin MH, Taams LS, Beverley PC, Macallan DC, Akbar AN.** 2006. Human CD4$^+$ CD25hi FOXP3$^+$ regulatory T cells are derived by rapid turnover of memory populations in vivo. *J Clin Invest* **116:**2423–2433.
15. **Mandapathil M, Hilldorfer B, Szczepanski MJ, Czystowska M, Szajnik M, Ren J, Lang S, Jackson EK, Gorelik E, Whiteside TL.** 2010. Generation and accumulation of immunosuppressive adenosine by human CD4+CD25high-FOXP3+ regulatory T cells. *J Biol Chem* **285:**7176–7186.
16. **Jie HB, Gildener-Leapman N, Li J, Srivastava RM, Gibson SP, Whiteside TL, Ferris RL.** 2013. Intratumoral regulatory T cells upregulate immunosuppressive molecules in head and neck cancer patients. *Br J Cancer* **109:**2629–2635.
17. **Elkord E, Alcantar-Orozco EM, Dovedi SJ.** 2010. T regulatory cells in cancer: recent advances and therapeutic potential. *Expert Opin Biol Ther* **10:**1573–1586.

Measurement of NK Cell Phenotype and Activity in Humans

SAMUEL C. C. CHIANG AND YENAN T. BRYCESON

32

Natural killer (NK) cells are a subset of innate lymphocytes initially identified for their ability to specifically kill virally infected and transformed cells without prior antigen sensitization. NK cells efficiently kill target cells through directed release of perforin-containing secretory lysosomes, a feature shared with cytotoxic T lymphocytes (CTLs) (1). Despite similarities in effector mechanisms, the strategies employed by NK cells and CTLs for target cell recognition are distinct yet complementary with respect to immune defense. Whereas CTLs express recombined, clonally distributed antigen receptors that dictate their activation and are selected for recognition of cells presenting nonself peptides in the context of major histocompatibility (MHC) class I molecules, NK cells rely on dynamic integration of signals from various germ line-encoded receptors for target cell discrimination. NK cells express numerous inhibitory receptors to detect normal expression of MHC class I and can selectively kill target cells that downregulate these molecules (2). NK cell activation by target cells with low MHC class I levels does not occur by default, but rather is mediated through engagement of different activating receptors (3). Representing an effector arm of humoral immunity, NK cells express the low-affinity Fc receptor CD16, which facilitates antibody-dependent cellular cytotoxicity (4). Moreover, supporting first-line defense against virally infected or stressed cells, a multiplicity of activating receptors that participate in natural cytotoxicity have been identified. In general, engagement of each such receptor alone is not sufficient to induce NK cell cytotoxicity. However, certain combinations of receptor signals can synergistically activate NK cell effector functions (5). Reflecting the expression of several activating receptors on NK cells that bind ligands exclusively expressed on hematopoietic cells, the ability of NK cells to kill autologous, activated immune cells is increasingly appreciated as an important immunoregulatory mechanism to control and shape adaptive immune responses (6). Upon activation, NK cells not only release granules but also abundantly produce chemokines and cytokines (7).

In humans, NK cells are commonly defined as $CD3^-$ $CD56^+$ cells and typically constitute 5 to 15% of peripheral blood lymphocytes (8). NK cells are also abundant in certain tissues such as the liver and uterus. During pregnancy, NK cells are attributed an important role in vascularization of the placenta (9). Increasingly, various NK cell subsets with differing functional properties are being described (10). A major distinction has been made between $CD3^-$ $CD56^{bright}$ and $CD3^-CD56^{dim}$ NK cells, in which the former is considered a precursor of the latter (11). $CD3^-CD56^{bright}$ NK cells all express NKG2A, an inhibitory receptor for HLA-E, as well as CD62L, a selectin that mediates homing to secondary lymphoid tissues, and produce abundant gamma interferon (IFN-γ) in response to combinations of exogenous cytokines including interleukin-2 (IL-2), IL-15, IL-12, and IL-18. Comparatively, $CD3^-CD56^{dim}$ NK cells are more cytotoxic and produce higher levels of tumor necrosis factor (TNF) and IFN-γ upon target cell recognition relative to $CD3^-CD56^{bright}$ NK cells (7). $CD3^-CD56^{dim}$ NK cells can also be divided into subsets based on variegated expression of inhibitory NKG2A and KIR receptors for HLA. Generally, levels of KIR increase while NKG2A and CD62L decrease upon differentiation. Compared with adaptive lymphocyte subsets, NK cells are generally considered to be relatively short-lived. However, upon infection with certain viruses such as cytomegalovirus, longer-lived NK cell subsets have been characterized in mice (12, 13). The nature and requirements for differentiation of similar, adaptive NK cells in humans is a topic of current research.

In humans, a few isolated primary NK cell deficiencies have been characterized (14, 15). Heterozygous mutations in *GATA2* may present as isolated NK cell deficiency, which has been designated classical NK cell deficiency (CNKD) 1 (16). GATA2 is a transcription factor implicated in development of multiple hematopoietic lineages. Remarkably, *GATA2* haploinsufficiency is associated with selective deficiency in monocytes, B cells, and NK cells and clinically associated with severe papilloma and herpesvirus infections as well as development of myelodysplastic syndromes that may progress to acute myeloid leukemia (17–20). Furthermore, autosomal recessive missense mutations in *MCM4*, encoding a protein involved in DNA replication, have been associated with NK cell deficiency and termed CNKD2 (21). MCM4 deficiency is associated with an absence of $CD56^{dim}$ NK cells and severe viral infections as well as adrenal insufficiency. Furthermore, a rare autosomal missense mutation in *FCGR3A*, leading to an L66H amino acid substitution in the extracellular domain of CD16, has been associated with severe herpesvirus infections in three unrelated families and so far represents the only described isolated functional NK cell deficiency (FNKD1) (14). Surprisingly, patients with CD16 L66H mutations displayed decreased natural

doi:10.1128/9781555818722.ch32

cytotoxicity but normal antibody-dependent cellular cytotoxicity, which might be attributed to abrogated biochemical interactions between CD16 and CD2 receptors (22).

Several primary immunodeficiencies have revealed genes required for development of NK cells as well as other lymphocyte subsets, for example, SCID caused by mutations in *ADA*, *AK2*, *IL2RG*, and *JAK3* (14, 15). In addition, patients with autosomal recessive *STAT5B* mutations manifest with a growth hormone insensitivity syndrome that is immunologically associated with low T-cell numbers and NK cell deficiency (23). Furthermore, autosomal recessive mutations in multiple genes required for NK cell- and CTL-mediated cytotoxicity have been associated with disease (1). Clinically, congenital impairments in lymphocyte cytotoxic function are associated with hyperinflammatory syndromes such as hemophagocytic lymphohistiocytosis (HLH) (24). Autosomal recessive mutations in *PRF1*, encoding perforin, abrogate lymphocyte cytotoxicity (25). In patients with *PRF1* mutations, typically perforin expression is absent while degranulation is normal (26). In other patients presenting with HLH, degranulation is defective, a feature that has been linked to autosomal recessive mutations in *UNC13D*, *STXBP2*, *STX11*, *RAB27A*, and *LYST* (mutations in the two latter genes also cause hypopigmentation) (26). Finally, autosomal recessive mutations in *ORAI1* and *STIM1*, required for store-operated Ca^{2+} entry, are associated with combined immunodeficiency and result in defective NK cell degranulation and cytokine production (27). Other genes have been associated with reduced NK cell numbers or impaired NK cell function. For a more comprehensive review of genes that have been associated with abnormalities in NK cell development and function, see reference 14.

In clinical diagnostic settings, cellular assays can offer rapid answers and, in some cases, identify defects that may not be revealed by conventional genetic screening approaches (28). Thus, cellular assays complement genetic screening approaches. Strategies to identify patients with primary defects in lymphocyte cytotoxicity based on laboratory assays have been developed and rely to a large extent on evaluation of NK cell cytotoxic activity (24, 26). Assays quantifying ^{51}Cr release from radioactively labeled K562 cells, an erythroleukemia-derived target cell line devoid of MHC class I expression, have represented a gold standard with respect to clinical evaluation of NK cell activity (29). Although widely used, ^{51}Cr release assays in particular and cytotoxicity assays in general have some limitations. First, the protocols used to study NK cell cytotoxicity are labor-intensive, usually involve radioactivity, and are thus not widely available. Second, the cytotoxicity assays using bulk peripheral blood mononuclear cells (PBMCs) do not discriminate between individuals with a reduced frequency rather than reduced function of NK cells. Thus, defects in NK cell development versus function are not revealed. Third, with respect to functional NK cell defects, cytotoxicity assays do not differentiate between defects in expression of granule constituents or granule release. Thus, with the advent of multiparameter flow cytometry, current procedures for the diagnosis of primary defects in lymphocyte cytotoxicity rather rely on flow cytometric assays, which may offer more-robust means of assessing NK cell activity and indicate defects in NK cell development or function (26). It should be noted that assays measuring NK cell cytotoxicity are not obsolete. NK cell cytotoxicity relies on a multifactorial process, while NK cell degranulation does not necessarily equate to target cell cytotoxicity (5, 30). In practical terms, however, the assessment of NK cell granule constituents, combined with quantification of the degranulative capacity of NK cells, typically provides a good estimate of NK cell cytotoxic activity.

Here we provide detailed protocols for the flow cytometric measurements of NK cell frequency, phenotype, and function. An NK cell phenotypic assay, including intracellular assessment of the expression levels of the lytic granule constituents perforin, granzyme A, granzyme B, and CD107a, is detailed. In addition, a functional assay for quantification of the ability of NK cells to degranulate (estimated by assessment of CD107a surface expression), produce the chemokine macrophage inflammatory protein 1β (MIP-1β) and the cytokine TNF, as well as upregulate the activation marker CD69 is also detailed. The assays are of value for the diagnosis of diseases associated with congenital defects in NK cell development and function. Moreover, they may also be useful for gaining further understanding of how NK cells are regulated by different physiological conditions and how their function correlates with the pathophysiology of other, more common diseases.

PROCEDURES

Sample Requirements

NK cells from peripheral blood or suspensions of cells isolated from body fluids or tissues can be used for assessment of NK cell phenotype and function. The flow cytometric assays do not require any specific isolation of NK cells. However, the outlined assays are optimized for cells subjected to density gradient centrifugations for purification of PBMCs according to standard procedures. When evaluating PBMC preparations, a minimum of 2×10^6 PBMCs are needed from each subject (translating to ~2×10^5 NK cells). Besides samples collected in sodium or lithium heparin vials, the outlined assays can be reproduced with cells collected in citrate vials, whereas samples collected in EDTA vials display diminished functional responses. Unless subjects are severely lymphopenic, 3 ml of heparinized venous blood should provide sufficient cells for the outlined assays. Importantly, quantification of NK cells in peripheral blood is recommended in order to determine necessary volumes for cell isolation and aid diagnostics in patients with suspected deficiencies in NK cell development. Absolute numbers of $CD3^-CD56^+$ NK cells in peripheral blood can be determined by flow cytometry using commercial kits that include fluorospheres. When analyzing the phenotype and function of NK cells from other fluids or tissues, it is important to make sure sufficient NK cells are present in the samples to allow flow cytometric analyses.

Ideally, when examining peripheral blood NK cell phenotype and function, blood should be drawn in the morning to avoid diurnal variation and be processed as soon after phlebotomy as possible. Blood samples that require transport to a reference laboratory should be shipped at ambient (~25°C) temperature and be processed within 24 h of collection. For analyses of cells from other fluids or tissues, it is equally important to process and isolate cells in a timely manner.

For assessment of the function of freshly isolated NK cells, at least 8 h of incubation in medium in a 37°C humidified incubator is recommended. Whereas assessment of NK cell cytotoxicity is best performed with fresh, not cryopreserved, samples, flow cytometric assessment of NK cell phenotype and function is less sensitive to cryopreservation. Thus, in studies comparing NK cell phenotype and function in cohorts of samples collected at different times, cryopreservation and subsequent collective analyses of samples may reduce interassay variability. In diagnostic settings in which

assays are run on a routine basis, good quality control procedures are imperative.

Materials and Reagents

Effector cells: PBMCs or NK cells separated from heparinized body fluids or tissue

Target cells: K562 cells (ATCC CCL-243) and P815 cells (ATCC TIB-64)

Complete medium (RPMI 1640 supplemented with 10% heat-inactivated fetal bovine serum and 2 mM L-glutamine)

Extracellular staining solution (phosphate-buffered saline supplemented with 2% fetal bovine serum and 2 mM EDTA)

Fixation solution, formaldehyde based (e.g., BD Biosciences' Cytofix/Cytoperm)

Permeabilization solution, saponin based (e.g., working concentration of BD Biosciences' Perm/Wash buffer)

Titrated, fluorochrome-conjugated antibodies to CD3 (clone S4.1), CD14 (clone M5E2), CD16 (clone 3G8), CD19 (clone HIB19), CD56 (clone NCAM16.2), CD69 (clone TP1.55.3), CD107a (clone H4A3), perforin (clone δG9), granzyme A (clone CB9), granzyme B (clone GB11), MIP-1β (clone D21-1351), and TNF (clone MAb11)

Dead cell marker (DCM) for flow cytometry (e.g., Molecular Probes' LIVE/DEAD Fixable Dead Cell Stain Kits)

Brefeldin A-containing solution (e.g., BD Biosciences' GolgiPlug diluted in complete medium as per manufacturer's recommendations)

15-ml conical polypropylene tubes

96-well V-bottom plates and plate covers

Equipment and Instrumentation

Multichannel micropipettor capable of delivering 100 μl

Centrifuge for 15-ml tubes and 96-well plates

Flow cytometer capable of measuring at least eight parameters (a BD Fortessa [BD Biosciences] instrument with four lasers was used in the design of the sample panels)

Experimental Procedure

Assessment of Lytic Granule Content

Experimental Protocol 1

1. For effector cell suspensions from each subject/sample, determine the number of viable cells by trypan blue exclusion or by other viability assay. Transfer the cells to 15-ml conical polypropylene tubes, centrifuge at 300 × *g* for 10 min, and resuspend the cells in complete medium (For PBMCs, the recommendation is 4×10^5 PBMCs, resuspended at 2.0×10^6 live cells/ml, approximately equivalent to a total of 4×10^4 NK cells.
2. Aliquot 150 μl of effector cell suspensions from each subject into single wells on consecutive rows of a V-bottom 96-well plate.
3. Centrifuge the plate at 300 × *g* for 4 min. Flick off supernatant.
4. Prepare a surface stain master mix consisting of ice-cold extracellular staining solution supplemented with fluorochrome-conjugated antibodies to CD3, CD14, CD16, CD19, and CD56, as well as DCM. Refer to Table 1 for a suggested staining panel. Optimal concentrations of antibodies for flow cytometric analysis should be titrated beforehand.

TABLE 1 Suggested antibody panels

Laser	Fluorochrome[a]	Antibody	Master mix
Protocol 1: Phenotypic assay			
Blue	FITC	IgG/Perforin	**Internal**
Red	APC	IgG/Granzyme B	**Internal**
Red	APC-AF700	CD3	External
Violet	Pacific Blue		
	Violet 500	DCM, CD14, CD19	External
	Brilliant Violet 711	CD16	External
Yellow-green	PE	IgG/Granzyme B	**Internal**
	ECD	IgG/CD107a	**Internal**
	PE-Cy7	CD56	External
Protocol 2: Functional assay			
Blue	FITC	CD107a	External
Red	APC	TNF	**Internal**
Red	APC-Cy7	CD3	External
Violet	Pacific Blue	(CD57)	(Optional External Master Mix)
	Violet 500	DCM, CD14, CD19	External
	Qdot 705	(CD8)	(Optional External Master Mix)
Yellow-green	PE	MIP-1β	**Internal**
	ECD	CD69	**Internal**
	PE-Cy7	CD56	External

[a]Abbreviations: APC, allophycocyanin; Cy, cyanine; ECD, electron-coupled dye; FITC, fluorescein isothiocyanate; PE, phycoerythrin.

5. Resuspend cells in 50 μl of ice-cold surface stain master mix and incubate at 4°C for 20 min in the dark.
6. Top up each well with ice-cold staining solution. Centrifuge the plate at 300 × *g* for 4 min. Flick off supernatant.
7. Resuspend the cells in 100 μl of fixation solution and fix the cells at room temperature for 10 min in the dark.
8. Resuspend the cells by gentle pipetting and transfer 50 μl of cell suspension to the adjacent well. Thus, there should be two wells of cells from each subject divided into two columns.
9. Top up wells with staining solution and centrifuge the plate at 300 × *g* for 4 min. Flick off supernatant.
10. Prepare master mixes for intracellular staining as follows:
    a. Prepare intracellular staining master mix A of ice-cold permeabilization solution supplemented with fluorochrome-conjugated antibodies to perforin, granzyme A, granzyme B, and CD107a.
    b. Prepare intracellular staining master mix B of ice-cold permeabilization solution supplemented with fluorochrome-conjugated isotype control antibodies at equal concentrations to the antibodies used in the intracellular staining master mix A.
11. Resuspend cells in the first row with 50 μl of ice-cold intracellular stain master mix A and cells in the second row with 50 μl of ice-cold intracellular stain master mix B. Incubate the plate at 4°C for 30 min in the dark.
12. Top up each well with staining solution. Centrifuge the plate at 400 × *g* for 4 min. Flick off supernatant.
13. Resuspend cells in 200 μl of ice-cold staining solution. Acquire data on a calibrated flow cytometer.

Analysis of Flow Cytometric Data

1. Perform proper compensation for all parameters measured.
2. First analyze the isotype control sample from a healthy control. Consecutively gate as outlined (Fig. 1):
    a. Lymphocytes on a forward-scatter height versus side-scatter height plot.
    b. Single cells on a forward-scatter height versus forward-scatter area plot.
    c. Viable (DCM^-), $CD14^-$, and $CD19^-$ cells on a histogram plot.
    d. $CD3^-CD56^{dim}$ NK cells on a CD3 versus CD56 plot.
3. Calculate the median fluorescence intensity (MFI) of isotype controls.
4. Copy the outlined gating strategy to samples stained with antibodies to granule constituents. Subtract the MFI values of isotype control stainings from those of the granule constituents.
5. Compare the MFI levels for the various granule constituents among subjects.

Assessment of NK Cell Function

Experimental Protocol 2

1. Preparation of effector cells:
    a. For effector cell suspensions from each subject/sample, determine the number of viable cells by trypan blue exclusion or by other viability assay. Transfer the cells to 15-ml conical polypropylene tubes, centrifuge at 300 × *g* for 10 min, and resuspend the cells in complete medium (For PBMCs, the recommendation is 2×10^5 PBMCs, resuspended at 2.0×10^6 live cells/ml, approximately equivalent to a total of 2×10^4 NK cells.).
    b. Aliquot 100 μl of effector cell suspensions into 4 wells of a 96-well plate, with consecutive rows for each subject.
    c. Centrifuge the plate at 300 × *g* for 4 min. Flick off supernatant.
    d. Resuspend cells in 100 μl of complete media containing brefeldin A (e.g., use 1:500 final dilution of GolgiPlug).
2. Preparation of target cells:
    a. Culture K562 and P815 cell lines in complete media. Maintain and use cell lines in logarithmic growth phase.
    b. Determine target cell viability by trypan blue exclusion or by other viability assay. For each subject/sample, 2×10^5 K562 cells and 4×10^5 P815 cells are needed. Transfer the K562 cells to one 15-ml conical polypropylene tube and the P815 cells to two 15-ml conical polypropylene tubes. Centrifuge

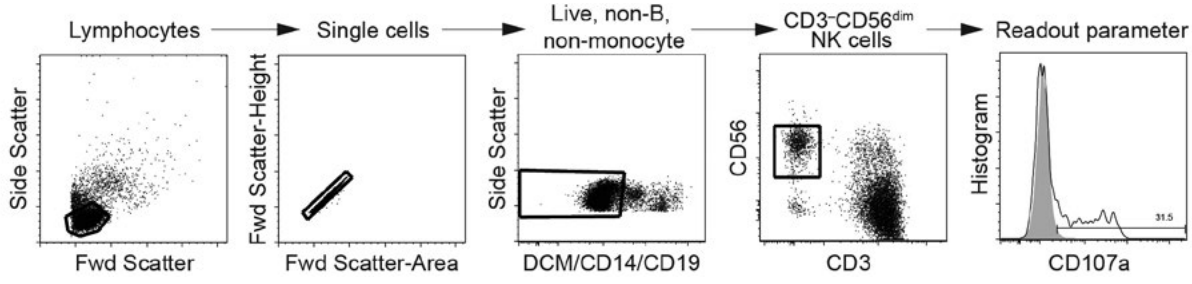

FIGURE 1 Gating strategy for flow cytometric analysis of NK cells. The strategy for consecutive gating of $CD3^-CD56^{dim}$ NK cells is depicted. First, lymphocytes are gated on forward-scatter versus side-scatter characteristics. Second, single cells are gated on forward-scatter height versus forward-scatter area characteristics. Third, a histogram representing a dump channel with staining for dead cells, $CD14^+$ monocytes, and $CD19^+$ B cells. Viable, nonmonocyte, non-B cells are gated. Fourth, $CD3^-CD56^{dim}$ NK cells are gated on a CD3 versus CD56 plot. Finally, phenotypic or functional readouts can be assessed in histograms.

the cells at 300 × *g* for 10 min and resuspend cell pellets at 2×10^6 cells/ml in complete medium.
   c. To one of the tubes of P815 cells, add unconjugated anti-CD16 antibody to a final concentration of 1 μg/ml. Vortex to mix.
3. To the plates with effector cells, add 100 μl of complete medium to each well with effector cells in the first column (acting as unstimulated controls), 100 μl of K562 cells to each well in the second column, 100 μl of P815 cells to each well in the third column, and 100 μl of P815 cells supplemented with anti-CD16 antibody to each well in the fourth column. Every well should hereafter have a total volume of 200 μl.
4. Resuspend all wells and incubate the plate in a humidified incubator for 3 h at 37°C.
5. Centrifuge the plate at 300 × *g* for 4 min. Flick off supernatant.
6. Prepare a surface stain master mix consisting of ice-cold extracellular staining solution supplemented with fluorochrome-conjugated antibodies to CD3, CD14, CD19, CD56, and CD107a, as well as DCM. Refer to Table 1 for a suggested staining panel. Optimal concentrations of antibodies for flow cytometric analysis should be titrated beforehand.
7. Resuspend cells in 50 μl of ice-cold surface stain master mix and incubate at 4°C for 20 min in the dark.
8. Top up each well with staining solution. Centrifuge the plate at 300 × *g* for 4 min. Flick off supernatant.
9. Resuspend the cells in 50 μl of fixation solution and fix the cells at room temperature for 10 min in the dark.
10. Top up each well with staining solution. Centrifuge the plate at 400 × *g* for 4 min. Flick off supernatant.
11. Resuspend cells with 50 μl of ice-cold intracellular stain master mix and incubate the plate at 4°C for 30 min in the dark. Add in the appropriate fluorochrome-conjugated antibodies to CD69, MIP-1β, and TNF.
12. Top up each well with staining solution. Centrifuge the plate at 400 × *g* for 4 min. Flick off supernatant.
13. Resuspend cells in 200 μl of ice-cold staining solution. Acquire data on a calibrated flow cytometer.

Analysis of Flow Cytometric Data

1. Perform proper compensation for all parameters measured.
2. First analyze the unstimulated sample from a healthy control. Consecutively gate as outlined (Fig. 1):
   a. Lymphocytes on a forward-scatter height versus side-scatter height plot.
   b. Single cells on a forward-scatter height versus forward-scatter area plot.
   c. Viable (DCM^-), $CD14^-$, and $CD19^-$ cells on a histogram plot.
   d. $CD3^-CD56^{dim}$ NK cells on a CD3 versus CD56 plot.
3. Gate for percentage of NK cells expressing CD107a, CD69, MIP-1β, and TNF. Typically at a resting stage, there should be <1% positive-staining cells for CD107a and TNF, whereas the percentages of cells positive for CD69 and MIP-1β may be higher.
4. Copy the outlined gating strategy to samples stimulated with various target cells.
5. Examine the percentage of positive cells for readouts of activation in unstimulated samples and calculate the induced responses by subtracting values for unstimulated samples from those for samples with various target cells. Background percentages of CD107a, CD69, MIP-1β, and TNF from the stimulated samples should also be examined. Compare the results of the various markers in patients and healthy controls.

Controls

The NK cell assay should include several different types of controls, as follows:

Instrument controls: Fluorescent bead controls for calibration of instrument sensitivity and generation of compensation matrices.

Intra-assay controls: Replicates of PBMCs from a single healthy donor are tested with different plate layouts to control for inherent variability in pipetting as well as variability potentially caused by varying positioning on plate.

Interassay controls: Cryopreserved, thawed, and pretested PBMCs from different selected healthy donors, ideally with high and low levels of NK cell functional responses, are tested every time the assay is performed. Thus, these samples are included in assays over weeks and months, providing a measure of the assay's reproducibility.

Transport controls: When assessing patient samples that are shipped to a reference laboratory, samples from healthy donors from the patient sample origin should always be included, in addition to healthy donors recruited locally at the reference laboratory, to control for deterioration of NK cell activity during transport due to long transportation times or suboptimal handling.

Biological variability controls: At various time intervals, fresh PBMCs from the same healthy donors are repeatedly obtained and used to chart the biological variability in NK cell numbers, phenotype, and functional responses over time.

Quality Control and Assurance

Assay reproducibility needs to be established and monitored in each individual laboratory. Criteria for acceptable NK cell assays are defined on the basis of intra- and interassay variability. A quality control program needs to be in effect, accepting or rejecting NK cell assay results based on strict criteria. The following components should be included in a quality control program:

A formulated standard operating procedure (SOP) and strict definition of acceptable assay results based on continuous monitoring of fresh as well as standard, cryopreserved cells.

Strict adherence to the SOP and written documentation of any changes that may be introduced.

Regular maintenance and quality control of the flow cytometer.

Titration and control of new batches of antibodies to ensure optimal stainings.

Routine thawing of new target cells from a large batch of cryopreserved cells with low passage number.

Continued maintenance and frequent (at least every 6 months) cumulative analyses of the control cell performances to confirm the reproducibility of the assay.

Pitfalls and Troubleshooting

Phenotypic assays with intracellular staining as well as functional assays require considerable effort to reproducibly

perform and reliably interpret. Many sources of variability exist. Antibodies should be carefully titrated and tested. New target cells should be thawed every 2 to 3 months to ensure reproducibility in stimulations. Target cells can be avoided entirely, with stimulation based on antibodies to activating receptors alone. However, we find that NK cell functional assays are less consistent when target cells are omitted. To control interassay variability, inclusion of cryopreserved controls in repeated assays is useful to ensure consistent assay performance and enable comparisons across assays. We recommend using samples from three donors with high, intermediate, and low NK cell responses.

With respect to assessing multiple readouts of NK cell activation, each readout displays distinct kinetics. CD107a surface expression, acting as a readout of cytotoxic lymphocyte degranulation, occurs rapidly following engagement of activating receptors (30). Production of the chemokine MIP-1β and induction of CD69 expression can be measured at later time points, followed by TNF and IFN-γ production (7). If longer time points are necessary to reliably quantify expression of cytokines, addition of monensin to the assay may be useful to prevent reinternalization of CD107a and underestimation of NK cell degranulation (31).

Specimen handling is a major concern, particularly when samples require shipment and the time and conditions from phlebotomy to cell isolation cannot be controlled. In such settings, transport controls are imperative for interpretation of results. Notably, samples that have endured long or poor transport conditions can display reduced responses to K562 cells, whereas Fc receptor engagement may still mediate strong activation (32).

In some samples, including those from patients with infections or hyperinflammatory conditions, NK cell frequencies may be reduced. The outlined assays require a minimal number of NK cells for reliable assessment of phenotype and function. Interpretation of phenotypic and functional results is recommended only if data on a minimum of 100 NK cells are acquired. With respect to possible defects in cytotoxic lymphocyte degranulation, NK cell assays may be complemented with assays for the evaluation of cytotoxic effector T-cell degranulation (33). For examining T-cell degranulation, PBMCs are incubated for 3 h with P815 cells supplemented with a final concentration of 2.5 μg/ml of fluorescent conjugated anti-CD3 antibody (clone S4.1). The analysis strategy is similar to that described in the method above, but degranulation is evaluated in the $CD3^+CD8^+$ $CD57^{bright}$ population rather than $CD3^-CD56^{dim}$ NK cells. To this end, the inclusion of CD8 (clone 3B5) and CD57 (HCD57) surface staining is required in protocol 2, step 10. The same applies for T-cell granule staining in protocol 1, step 6.

Interpretation

With respect to NK cell development, NK cell numbers and frequencies vary considerably among individuals. Among a population of 200 healthy adult volunteers, we quantified $CD3^-CD56^+$ NK cell numbers in peripheral blood to 208 ± 110 cells/μl (mean ± standard deviation; range, 30 to 565 cells/μl), with a frequency of 11.0% ± 5.8% (mean ± standard deviation; range, 1.5 to 31.3%) among peripheral blood lymphocytes, consistent with other reports from smaller cohorts (34, 35). On average, the numbers of NK cells in peripheral blood are somewhat higher in children, particularly in infancy (34, 35). Specific guidelines for the diagnosis of NK cell deficiency have not been established. For CNKD1 with mutations in *GATA2*, patients have been reported to display a $CD3^-CD56^{bright}$ NK cell population

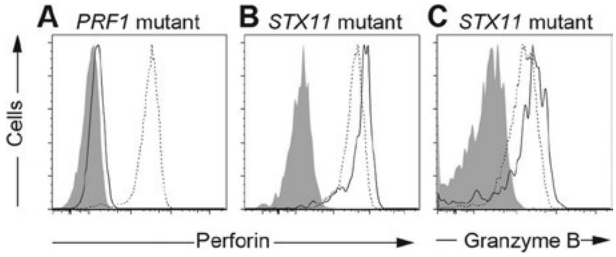

FIGURE 2 Lytic granule expression in $CD3^-CD56^{dim}$ NK cells from patients and healthy controls. PBMCs were stained and assessed according to protocol 1. Histograms depict expression of perforin (A, B) or granzyme B (C) in a patient with biallelic *PRF1* mutations (solid line) relative to a healthy control (dashed line) (A) or a patient with biallelic *STX11* mutations (solid line) relative to a healthy control (dashed line) (B, C).

that is <0.5% of the total $CD3^-CD56^+$ peripheral blood NK cells (16). For CNKD2 with mutations in *MCM4*, patients have been reported to display $CD3^-CD56^+$ NK cell numbers in peripheral blood of <200 cells/μl and frequencies of <4% among lymphocytes, with an absence of $CD3^-CD56^{dim}$ NK cells (21). When primary deficiencies in NK cell development are suspected, genetic tests are recommended to confirm a possible diagnosis.

A prerequisite for lymphocyte cytotoxicity is the intracellular expression of lytic granule constituents. Low or absent perforin expression is usually observed in patients with biallelic mutations in *PRF1* (as exemplified in Fig. 2A), which typically present with familial HLH or hematologic malignancies. Of note, individuals may display increased expression of perforin and granzymes (Fig. 2B), which is a feature of familial HLH patients and other patients with hyperinflammatory disease activity (36, 37).

With respect to functional responses, simultaneously probing several readouts of NK cell activation is useful for determining the overall responsiveness of cells and identifying possible defects in signaling pathways and effector functions. Healthy individuals normally display between 10 and 30% $CD107a^+$ degranulating $CD3^-CD56^{dim}$ NK cells following K562 stimulation, with stronger responses following engagement of CD16 (26, 33). Notably, upon stimulation with K562 cells, $CD3^-CD56^{dim}$ NK cell degranulation of <5% offers a 96% sensitivity and 88% specificity for the identification of patients with mutations in genes required for cytotoxic lymphocyte degranulation (26). Patients with primary defects in lymphocyte degranulation often also manifest constitutively high CD69 expression but poor induction of TNF upon stimulation with target cells (Fig. 3). Notably, more-general defects in lymphocyte activation, such as those caused by mutations in *ORAI1* and *STIM1*, required for store-operated Ca^{2+} entry, significantly reduce NK cell degranulation and cytokine production but only partially impair induction of MIP-1β (27).

In certain cases in which resting NK cell degranulation is absent and familial HLH is suspected, there is a noticeable recovery of function after activation with IL-2 (36, 38), which can direct genetic analyses and may be explained by redundancies among soluble *N*-ethylmaleimide-sensitive factor attachment protein receptors (SNARE proteins) for lytic granule exocytosis (26, 39). To determine possible gain

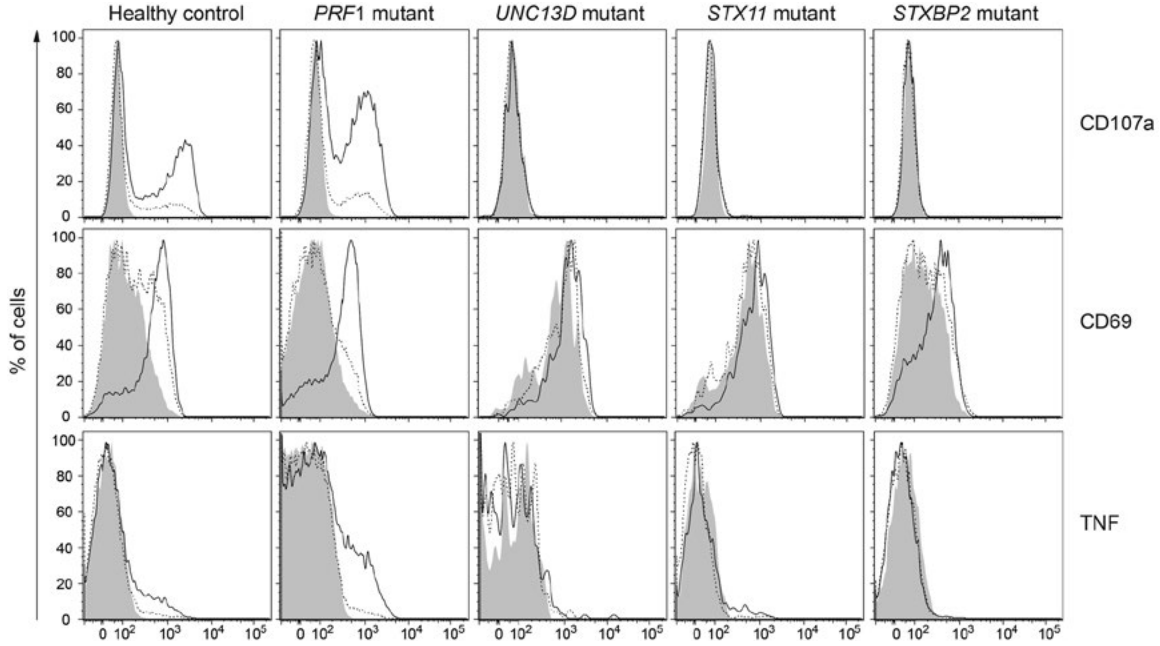

FIGURE 3 Functional responses by $CD3^{-}CD56^{dim}$ NK cells from patients and healthy controls. PBMCs were mixed with target cells and assessed according to protocol 2. Histograms depict expression of CD107a, CD69, and TNF, as indicated, on NK cells from a healthy control or patients with biallelic mutations in *PRF1*, *UNC13D*, *STX11*, or *STXBP2*. Expression in unstimulated cells (filled histograms), cells incubated with K562 cells (dashed lines), or P815 cells with added anti-CD16 mAb (solid lines) is depicted.

of degranulation upon NK cell activation, protocol 2 is repeated on PBMCs preactivated for 36 to 48 h in complete media containing 500 IU/ml of IL-2.

An explanation of selective defects in NK cell activation following incubation with K562 cells may be mutations in *FCGR3A* consistent with FNKD1. Remarkably, the CD16 L66H variant destroys an epitope recognized by the anti-CD16 mAb B73.1, whereas recognition of the anti-CD16 mAb 3G8 is unperturbed. However, loss of the anti-CD16 mAb B73.1 epitope does not necessarily imply FNKD1 (40). Thus, genetic analyses are necessary to confirm a diagnosis of FNKD1.

Table 2 summarizes the primary immunodeficiencies that may be detected with the outlined assays. Additional primary immunodeficiencies affecting NK cell development and function may be considered (14).

TABLE 2 Genes associated with strong defects in NK cell development or function[a]

Gene	Syndrome	Inheritance	Protein	Peripheral blood NK cells	Cytotoxicity defect	Partial albinism	Cellular diagnostic evaluation[b]
GATA2	CNKD1	AD	GATA2	Low ($CD56^{dim}$)	Yes	No	NK cell phenotype
MCM4	CNKD2	AR		Low ($CD56^{bright}$)	Yes	No	NK cell phenotype
ADA	SCID	AR	Adenosine deaminase	$B^{-}T^{-}NK^{-}$	Likely	No	
IL2RG	SCID	XL	IL-2 receptor γ chain	$B^{+}T^{-}NK^{-}$	Likely	No	
JAK3	SCID	AR	JAK3	$B^{+}T^{-}NK^{-}$	Likely	No	
STAT5B		AR	STAT5b	$B^{+}T^{low}NK^{-}$	Likely	No	
CD16	FNKD1	AR	CD16	Present	Natural cytotoxicity	No	Absent activity toward K562 cells

(Continued on next page)

TABLE 2 *(Continued)*

Gene	Syndrome	Inheritance	Protein	Peripheral blood NK cells	Cytotoxicity defect	Partial albinism	Cellular diagnostic evaluation[b]
PRF1	FHL2	AR	Perforin	Present	Yes	No	Absent intracellular perforin expression
UNC13D	FHL3	AR	Munc13-4	Present	Yes	No	Defective degranulation
STX11	FHL4	AR	Syntaxin-11	Present	Yes	No	Defective degranulation
STXBP2	FHL5	AR	Munc18-2	Present	Yes	No	Defective degranulation
RAB27A	GS2	AR	RAB27A	Present	Yes	Yes	Defective degranulation
LYST	CHS1	AR	LYST	Present	Yes	Yes	Defective degranulation
ORAI1	CID	AR	ORAI1	Present	Yes	No	Defective target cell activation
STIM1	CID	AR	STIM1	Present	Yes	No	Defective target cell activation

[a]Abbreviations: AD, autosomal dominant; AR, autosomal recessive; CHS, Chediak-Higashi syndrome; CID, combined immunodeficiency; FHL, familial hemophagocytic lymphohistiocytosis; GS, Griscelli syndrome; XL, X linked.
[b]Cellular phenotypic assays may fail to diagnose disease caused by coding mutations that impair protein function without affecting protein expression.

CONCLUSIONS

Herein we have detailed two flow cytometric assays that require small amounts of cells, facilitating analysis in many settings, including samples from infants or from small tissue samples. The assay measuring NK cell maturation and granule content can be useful for ascertaining normal NK cell development and detecting patients with primary immunodeficiencies with defective NK cell development. Moreover, evaluation of intracellular granule contents may reveal patients with primary immunodeficiency caused by biallelic *PRF1* mutations or indicate a hyperinflammatory state. The second assay, quantifying NK cell responses, can reveal primary immunodeficiency patients with defects in lytic granule exocytosis or general NK cell activation. The assays can easily be modified to probe function downstream of specific NK cell receptors or more generally assess lymphocyte function. They may also be modified to incorporate evaluation of target cell killing by flow cytometry. Not only are these assays useful for the diagnosis of primary immunodeficiency syndromes, they can also contribute to improving our understanding of NK cell function in various settings including tumor surveillance, organ development, and immune homeostasis.

REFERENCES

1. **de Saint Basile G, Ménasché G, Fischer A.** 2010. Molecular mechanisms of biogenesis and exocytosis of cytotoxic granules. *Nat Rev Immunol* **10:**568–579.
2. **Long EO.** 2008. Negative signaling by inhibitory receptors: the NK cell paradigm. *Immunol Rev* **224:**70–84.
3. **Bryceson YT, Chiang SC, Darmanin S, Fauriat C, Schlums H, Theorell J, Wood SM.** 2011. Molecular mechanisms of natural killer cell activation. *J Innate Immun* **3:**216–226.
4. **Perussia B.** 1998. Fc receptors on natural killer cells. *Curr Top Microbiol Immunol* **230:**63–88.
5. **Bryceson YT, Ljunggren HG, Long EO.** 2009. Minimal requirement for induction of natural cytotoxicity and intersection of activation signals by inhibitory receptors. *Blood* **114:**2657–2666.
6. **Welsh RM, Waggoner SN.** 2013. NK cells controlling virus-specific T cells: rheostats for acute vs. persistent infections. *Virology* **435:**37–45.
7. **Fauriat C, Long EO, Ljunggren HG, Bryceson YT.** 2010. Regulation of human NK cell cytokine and chemokine production by target cell recognition. *Blood* **115:**2167–2176.
8. **Caligiuri MA.** 2008. Human natural killer cells. *Blood* **112:**461–469.
9. **Moffett-King A.** 2002. Natural killer cells and pregnancy. *Nat Rev Immunol* **2:**656–663.
10. **Cichocki F, Miller JS, Anderson SK, Bryceson YT.** 2013. Epigenetic regulation of NK cell differentiation and effector functions. *Front Immunol* **4:**55. doi:10.3389/fimmu.2013.00055.
11. **Romagnani C, Juelke K, Falco M, Morandi B, D'Agostino A, Costa R, Ratto G, Forte G, Carrega P, Lui G, Conte R, Strowig T, Moretta A, Münz C, Thiel A, Moretta L, Ferlazzo G.** 2007. $CD56^{bright}CD16^{-}$ killer Ig-like receptor^{-} NK cells display longer telomeres and acquire features of $CD56^{dim}$ NK cells upon activation. *J Immunol* **178:**4947–4955.
12. **Sun JC, Lanier LL.** 2011. NK cell development, homeostasis and function: parallels with $CD8^{+}$ T cells. *Nat Rev Immunol* **11:**645–657.
13. **Narni-Mancinelli E, Vivier E, Kerdiles YM.** 2011. The 'T-cell-ness' of NK cells: unexpected similarities between NK cells and T cells. *Int Immunol* **23:**427–431.
14. **Orange JS.** 2013. Natural killer cell deficiency. *J Allergy Clin Immunol* **132:**515–525; quiz 526.

15. **Jouanguy E, Gineau L, Cottineau J, Béziat V, Vivier E, Casanova JL.** 2013. Inborn errors of the development of human natural killer cells. *Curr Opin Allergy Clin Immunol* **13:**589–595.
16. **Mace EM, Hsu AP, Monaco-Shawver L, Makedonas G, Rosen JB, Dropulic L, Cohen JI, Frenkel EP, Bagwell JC, Sullivan JL, Biron CA, Spalding C, Zerbe CS, Uzel G, Holland SM, Orange JS.** 2013. Mutations in *GATA2* cause human NK cell deficiency with specific loss of the $CD56^{bright}$ subset. *Blood* **121:**2669–2677.
17. **Hsu AP, Sampaio EP, Khan J, Calvo KR, Lemieux JE, Patel SY, Frucht DM, Vinh DC, Auth, RD, Freeman AF, Olivier KN, Uzel G, Zerbe CS, Spalding C, Pittaluga S, Raffeld M, Kuhns DB, Ding L, Paulson ML, Marciano BE, Gea-Banacloche JC, Orange JS, Cuellar-Rodriguez J, Hickstein DD, Holland SM.** 2011. Mutations in *GATA2* are associated with the autosomal dominant and sporadic monocytopenia and mycobacterial infection (MonoMAC) syndrome. *Blood* **118:**2653–2655.
18. **Dickinson RE, Griffin H, Bigley V, Reynard LN, Hussain R, Haniffa M, Lakey JH, Rahman T, Wang XN, McGovern N, Pagan S, Cookson S, McDonald D, Chua I, Wallis J, Cant A, Wright M, Keavney B, Chinnery PF, Loughlin J, Hambleton S, Santibanez-Koref M, Collin M.** 2011. Exome sequencing identifies GATA-2 mutation as the cause of dendritic cell, monocyte, B and NK lymphoid deficiency. *Blood* **118:**2656–2658.
19. **Hahn CN, Chong CE, Carmichael CL, Wilkins EJ, Brautigan PJ, Li XC, Babic M, Lin M, Carmagnac A, Lee YK, Kok CH, Gagliardi L, Friend KL, Ekert PG, Butcher CM, Brown AL, Lewis ID, To LB, Timms AE, Storek J, Moore S, Altree M, Escher R, Bardy PG, Suthers GK, D'Andrea RJ, Horwitz MS, Scott HS.** 2011. Heritable *GATA2* mutations associated with familial myelodysplastic syndrome and acute myeloid leukemia. *Nat Genet* **43:**1012–1017.
20. **Ostergaard P, Simpson MA, Connell FC, Steward CG, Brice G, Woollard WJ, Dafou D, Kilo T, Smithson S, Lunt P, Murday VA, Hodgson S, Keenan R, Pilz DT, Martinez-Corral I, Makinen T, Mortimer PS, Jeffery S, Trembath RC, Mansour S.** 2011. Mutations in *GATA2* cause primary lymphedema associated with a predisposition to acute myeloid leukemia (Emberger syndrome). *Nat Genet* **43:**929–931.
21. **Gineau L, Cognet C, Kara N, Lach FP, Dunne J, Veturi U, Picard C, Trouillet C, Eidenschenk C, Aoufouchi S, Alcaïs A, Smith O, Geissmann F, Feighery C, Abel L, Smogorzewska A, Stillman B, Vivier E, Casanova JL, Jouanguy E.** 2012. Partial MCM4 deficiency in patients with growth retardation, adrenal insufficiency, and natural killer cell deficiency. *J Clin Invest* **122:**821–832.
22. **Grier JT, Forbes LR, Monaco-Shawver L, Oshinsky J, Atkinson TP, Moody C, Pandey R, Campbell KS, Orange JS.** 2012. Human immunodeficiency-causing mutation defines CD16 in spontaneous NK cell cytotoxicity. *J Clin Invest* **122:**3769–3780.
23. **Bernasconi A, Marino R, Ribas A, Rossi J, Ciaccio M, Oleastro M, Ornani A, Paz R, Rivarola MA, Zelazko M, Belgorosky A.** 2006. Characterization of immunodeficiency in a patient with growth hormone insensitivity secondary to a novel *STAT5b* gene mutation. *Pediatrics* **118:**e1584–e1592.
24. **Henter JI, Horne A, Aricó M, Egeler RM, Filipovich AH, Imashuku S, Ladisch S, McClain K, Webb D, Winiarski J, Janka G.** 2007. HLH-2004: diagnostic and therapeutic guidelines for hemophagocytic lymphohistiocytosis. *Pediatr Blood Cancer* **48:**124–131.
25. **Stepp SE, Dufourcq-Lagelouse R, Le Deist F, Bhawan S, Certain S, Mathew PA, Henter JI, Bennett M, Fischer A, de Saint Basile G, Kumar V.** 1999. Perforin gene defects in familial hemophagocytic lymphohistiocytosis. *Science* **286:**1957–1959.
26. **Bryceson YT, Pende D, Maul-Pavicic A, Gilmour KC, Ufheil H, Vraetz T, Chiang SC, Marcenaro S, Meazza R, Bondzio I, Walshe D, Janka G, Lehmberg K, Beutel K, zur Stadt U, Binder N, Arico M, Moretta L, Henter JI, Ehl S.** 2012. A prospective evaluation of degranulation assays in the rapid diagnosis of familial hemophagocytic syndromes. *Blood* **119:**2754–2763.
27. **Maul-Pavicic A, Chiang SC, Rensing-Ehl A, Jessen B, Fauriat C, Wood SM, Sjöqvist S, Hufnagel M, Schulze I, Bass T, Schamel WW, Fuchs S, Pircher H, McCarl CA, Mikoshiba K, Schwarz K, Feske S, Bryceson YT, Ehl S.** 2011. ORAI1-mediated calcium influx is required for human cytotoxic lymphocyte degranulation and target cell lysis. *Proc Natl Acad Sci U S A* **108:**3324–3329.
28. **Meeths M, Chiang SC, Wood SM, Entesarian M, Schlums H, Bang B, Nordenskjöld E, Björklund C, Jakovljevic G, Jazbec J, Hasle H, Holmqvist BM, Rajic L, Pfeifer S, Rosthøj S, Sabel M, Salmi TT, Stokland T, Winiarski J, Ljunggren HG, Fadeel B, Nordenskjöld M, Henter JI, Bryceson YT.** 2011. Familial hemophagocytic lymphohistiocytosis type 3 (FHL3) caused by deep intronic mutation and inversion in *UNC13D*. *Blood* **118:**5783–5793.
29. **Whiteside TL.** 2006. Measurement of NK cell activity in humans, p 296–300. *In* Detrick B, Hamilton RG, Folds JD (ed), *Manual of Molecular and Clinical Laboratory Immunology*, 7th ed. ASM Press, Washington DC.
30. **Bryceson YT, March ME, Barber DF, Ljunggren HG, Long EO.** 2005. Cytolytic granule polarization and degranulation controlled by different receptors in resting NK cells. *J Exp Med* **202:**1001–1012.
31. **Alter G, Malenfant JM, Altfeld M.** 2004. CD107a as a functional marker for the identification of natural killer cell activity. *J Immunol Methods* **294:**15–22.
32. **Entesarian M, Chiang SC, Schlums H, Meeths M, Chan MY, Mya SN, Soh SY, Nordenskjöld M, Henter JI, Bryceson YT.** 2013. Novel deep intronic and missense *UNC13D* mutations in familial haemophagocytic lymphohistiocytosis type 3. *Br J Haematol* **162:**415–418.
33. **Chiang SC, Theorell J, Entesarian M, Meeths M, Mastafa M, Al-Herz W, Frisk P, Gilmour KC, Ifversen M, Langenskiöld C, Machaczka M, Naqvi A, Payne J, Perez-Martinez A, Sabel M, Unal E, Unal S, Winiarski J, Nordenskjöld M, Ljunggren HG, Henter JI, Bryceson YT.** 2013. Comparison of primary human cytotoxic T-cell and natural killer cell responses reveal similar molecular requirements for lytic granule exocytosis but differences in cytokine production. *Blood* **121:**1345–1356.
34. **Comans-Bitter WM, de Groot R, van den Beemd R, Neijens HJ, Hop WC, Groeneveld K, Hooijkaas H, van Dongen JJ.** 1997. Immunophenotyping of blood lymphocytes in childhood. Reference values for lymphocyte subpopulations. *J Pediatr* **130:**388–393.
35. **Huenecke S, Behl M, Fadler C, Zimmermann SY, Bochennek K, Tramsen L, Esser R, Klarmann D, Kamper M, Sattler A, von Laer D, Klingebiel T, Lehrnbecher T, Koehl U.** 2008. Age-matched lymphocyte subpopulation reference values in childhood and adolescence: application of exponential regression analysis. *Eur J Haematol* **80:**532–539.
36. **Bryceson YT, Rudd E, Zheng C, Edner J, Ma D, Wood SM, Bechensteen AG, Boelens JJ, Celkan T, Farah RA, Hultenby K, Winiarski J, Roche PA, Nordenskjöld M, Henter JI, Long EO, Ljunggren HG.** 2007. Defective cytotoxic lymphocyte degranulation in syntaxin-11 deficient familial hemophagocytic lymphohistiocytosis 4 (FHL4) patients. *Blood* **110:**1906–1915.
37. **Mellor-Heineke S, Villanueva J, Jordan MB, Marsh R, Zhang K, Bleesing JJ, Filipovich AH, Risma KA.**

2013. Elevated granzyme B in cytotoxic lymphocytes is a signature of immune activation in hemophagocytic lymphohistiocytosis. *Front Immunol* **4:**72. doi:10.3389/fimmu.2013.00072.

38. **Meeths M, Entesarian M, Al-Herz W, Chiang SC, Wood SM, Al-Ateeqi W, Almazan F, Boelens JJ, Hasle H, Ifversen M, Lund B, van den Berg JM, Gustafsson B, Hjelmqvist H, Nordenskjöld M, Bryceson YT, Henter JI.** 2010. Spectrum of clinical presentations in familial hemophagocytic lymphohistiocytosis type 5 patients with mutations in *STXBP2*. *Blood* **116:**2635–2643.
39. **Hackmann Y, Graham SC, Ehl S, Höning S, Lehmberg K, Aricò M, Owen DJ, Griffiths GM.** 2013. Syntaxin binding mechanism and disease-causing mutations in Munc18-2. *Proc Natl Acad Sci U S A* **110:**E4482–4491. doi:10.1073/pnas.1313474110.
40. **Lenart M, Trzyna E, Rutkowska M, Bukowska-Strakova K, Szaflarska A, Pituch-Noworolska A, Szczepanik A, Zembala M, Siedlar M.** 2010. The loss of the CD16 B73.1/Leu11c epitope occurring in some primary immunodeficiency diseases is not associated with the FcγRIIIa-48L/R/H polymorphism. *Int J Mol Med* **26:**435–442.

Functional Assays for the Diagnosis of Chronic Granulomatous Disease

DEBRA LONG PRIEL AND DOUGLAS B. KUHNS

33

Chronic granulomatous disease (CGD) is a rare genetic disease (~1 in 200,000 in the U.S.) first described in the 1950s (1). It is characterized by a failure of phagocytes (polymorphonuclear neutrophils [PMN], monocytes, macrophages, and eosinophils) to generate superoxide ($O_2^{\cdot-}$) and other related reactive oxygen species (ROS), leading to recurrent infections, granulomatous complications, and premature death. Generation of $O_2^{\cdot-}$ requires the assembly and activation of a multicomponent enzyme, NADPH oxidase (NOX2) or phagocyte oxidase (phox), a complex consisting of numerous cytosolic proteins, including $p47^{phox}$ (2), $p67^{phox}$ (2), and $p40^{phox}$ (3), and two membrane proteins, $p22^{phox}$ and $gp91^{phox}$, that constitute cytochrome b_{558} (4, 5). NOX2 catalyzes the reduction of molecular O_2 to $O_2^{\cdot-}$ using NADPH generated by the oxidation of glucose through the pentose-phosphate pathway. $O_2^{\cdot-}$ is converted to H_2O_2 either spontaneously or enzymatically. H_2O_2 and $O_2^{\cdot-}$ can react to form the highly reactive hydroxyl radical, OH·. The molecular defect in CGD results from mutations in any one of 5 protein subunits of NOX2, that include $gp91^{phox}$ (~70% of patients), $p47^{phox}$ (~25%), $p22^{phox}$ (<5%), $p67^{phox}$ (<5%), and $p40^{phox}$ (one case identified). Because the molecular defect in CGD is the inability to generate ROS, most of the assays used in the diagnosis of CGD that are described below are based on assessments of ROS production using different probes and different detection platforms. The last two assays—flow cytometric analysis of NOX2 expression and immunoblot analysis of phox subunits—focus on identifying the specific protein defect and defining the target for genetic sequencing.

ANALYSIS OF PMN H_2O_2 PRODUCTION BY FLOW CYTOMETRY OF DIHYDRORHODAMINE 123 STAINING

Principle

Activation of the NOX2 complex of phagocytic cells results in the generation of $O_2^{\cdot-}$ as well as other ROS. The products of NOX2 activation can be measured in individual cells by flow cytometry using dihydrorhodamine 123 (DHR) (6), a weakly fluorescent probe that greatly increases its fluorescence upon oxidation to rhodamine in the presence of H_2O_2. Leukocytes are loaded with DHR by passive diffusion, and then stimulated with phorbol 12-myristate 13-acetate (PMA) for 15 min at 37°C. Using the NOX2-derived H_2O_2, endogenous cellular peroxidases (e.g., myeloperoxidase in PMN) convert DHR to rhodamine. Catalase is added to the medium to prevent cell-to-cell diffusion of H_2O_2.

PMN can be easily segregated from other leukocyte populations by flow cytometry using forward light scattering (FS) and right-angle light scattering (SS). However, stimulation of PMN with PMA results in a relocalization of the PMN population within the FS × SS plot, with a shift to the left and overall reduction in the variance of the forward light scattering (compare the Basal FS × SS plot with the PMA FS × SS plot in Fig. 1). Moreover, the distribution of PMN within the FS × SS region is not symmetric; the DHR^+ PMN, indicated in red, cluster along the lower left region of the gated population (note the back-gated FS × SS dot plot from an X-linked carrier in Fig. 1C).

The major advantages of the flow cytometric analysis of DHR assay are its sensitivity, signal-to-noise ratio, and ease of counting a large number of cells. Moreover, it has been shown that the DHR assay yields reliable results on EDTA- or heparin-treated blood samples that have been stored overnight.

Reagents

Lysis buffer

100 ml sterile distilled water

0.83 g ammonium chloride

0.2 ml of 0.5 M EDTA, pH 8.0 (51234, Lonza, Walkersville, MD)

0.2 g potassium bicarbonate

Add 0.83 g ammonium chloride, 0.2 ml EDTA, and 0.2 g potassium bicarbonate to water and sterilize through a 0.2-μm filter.

Flow buffer

0.5 g albumin (from human serum, fraction V, A9511, Sigma-Aldrich, St. Louis, MO)

500 ml Hanks' balanced salt solution without Ca^{2+}, Mg^{2+}, or phenol red (HBSS, 10-547F, Lonza)

1 ml of 0.5 M EDTA, pH 8.0 (51234, Lonza)

Mix reagents well and sterilize through a 0.2-μm filter.

doi:10.1128/9781555818722.ch33

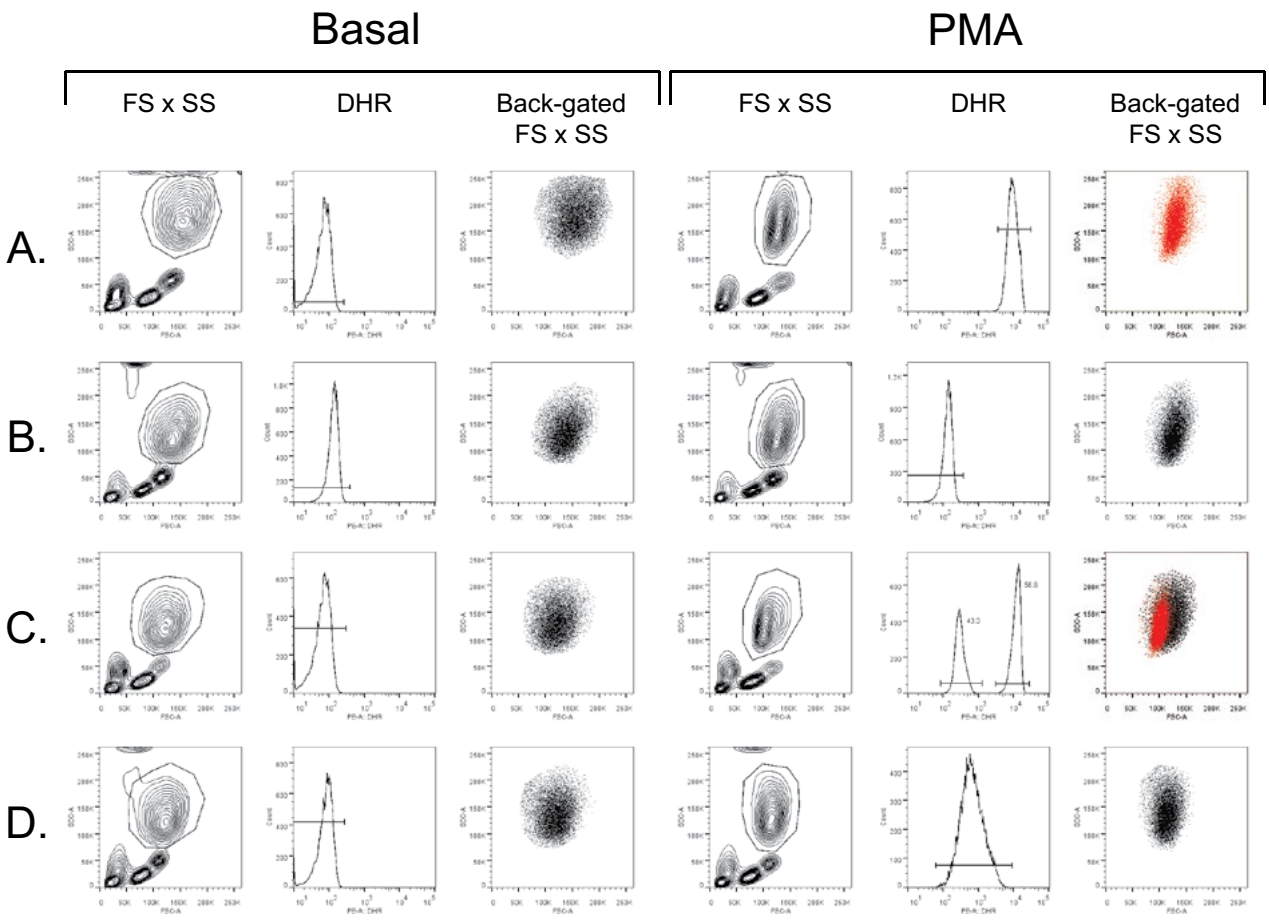

FIGURE 1 Analysis of H_2O_2 production by dihydrorhodamine-123 staining. PMN populations of buffer-treated (Basal) and PMA-treated (PMA) samples were gated using FS × SS shown in the contour plots on the left panel for each condition. The middle panel for each condition represents the DHR histogram which is presented on a log scale. The right panel for each condition represents a dot plot of the back-gated region of the DHR histogram to identify the nature of the population analyzed. Stimulation with PMA induces a shift in the FS × SS pattern of the PMN population in all subjects tested: a normal subject (A), a patient with $gp91^{phox}$ CGD (B), an X-linked carrier of CGD (C), and a patient with $p47^{phox}$ CGD (D). DHR^+ cells are indicated in red in back-gated FS × SS dot plots.

Catalase (10 mg/ml)

100 mg catalase (C-40, Sigma-Aldrich)

10 ml phosphate-buffered saline (PBS, 17-512F, Lonza)

Dissolve 10 mg catalase in 10 ml PBS. Store at −85°C in 100-μl aliquots.

Dihydrorhodamine 123 (DHR, 25 mM)

10 mg DHR (D-632, Molecular Probes, Life Technology, Grand Island, NY)

1.156 ml dimethyl sulfoxide (DMSO, D2650, Sigma-Aldrich)

Prepare solution by dissolving 10 mg DHR in 1.156 ml DMSO. Store at −85°C in 25-μl aliquots wrapped with foil to protect from light.

PMA (phorbol 12-myristate 13-acetate, 2 μg/ml)

PMA (P8139, Sigma-Aldrich)

DMSO

Prepare a stock solution of PMA (2 mg/ml) by dissolving 5.0 mg PMA in 2.5 ml DMSO. Store at −85°C in 100-μl aliquots. Dilute stock PMA solution to a 2-μg/ml working concentration in flow buffer.

Procedure

1. Collect patient blood samples in K_2EDTA blood-collection tubes (36661; Becton Dickinson, Franklin Lakes, NJ). A blood sample from a normal subject is also needed to serve as a control to validate the assay.
2. Warm the lysis buffer in a 37°C water bath.
3. Add 12 ml warm lysis buffer to a 15-ml polypropylene conical centrifuge tube.
4. Add 1.2 ml whole blood to the 12 ml lysis buffer. Cap the tube and invert several times to mix the blood.
5. Incubate at 37°C for 5 min.
6. Spin at 600 × *g* for 5 min, aspirate supernatant fluid, and wash the cells by adding 12 ml of flow-HBSS buffer, then repeat spin.
7. Aspirate the supernatant. If there is evidence of red blood cells in the leukocyte pellet (which can interfere with the DHR analysis), repeat steps 6 and 7.
8. Resuspend the cells in flow buffer to a cell concentration of 2×10^6 cells/ml.

9. Transfer 400 μl of cells to two 12 × 75 mm polypropylene tubes labeled "Basal" and "PMA-stimulated."
10. Add 2 μl of 25 mM DHR to each tube.
11. Add 2.5 μl of 10 mg/ml catalase to each tube and mix by vortexing.
12. Incubate at 37°C in a shaking water bath for 5 min.
13. Add 100 μl PMA to the "PMA-stimulated" tube. Add 100 μl flow buffer to the "Basal" tube.
14. Incubate at 37°C in a shaking water bath for 15 min.
15. Analyze the samples on a flow cytometer within 25 min of adding DHR to the tubes, using FS × SS to gate on the PMN population (Fig. 1). Collect at least 5,000 events within the PMN gate. When the number of DHR^+ cells is expected to be <1%, the number of events collected in the PMN gate should be increased to 200,000 to obtain an accurate determination of a minor population.

Results and Normal Range

Treatment of PMN from a normal subject with PMA results in a 2-log shift in the mean fluorescence intensity (MFI) in more than 90% of the PMN (Fig. 1A). In our laboratory, the expected MFI for PMN with buffer alone is 90 ± 34 arbitrary units (AU) (mean ± standard deviation); after stimulation with PMA, the expected MFI for PMN is 11,367 ± 2,719 AU. In general, PMN from patients with CGD exhibit less than a 1-log shift in fluorescence after stimulation with PMA (Fig. 1B). PMN from a female X-linked carrier of CGD exhibit two populations, an abnormal DHR^- population expressing the mutant allele and a brightly stained DHR^+ population expressing the normal allele (Fig. 1C). PMN from patients with $p47^{phox}$ CGD (Fig. 1D) and some CGD patients with missense mutations in $gp91^{phox}$, $p22^{phox}$, or $p67^{phox}$ can exhibit significant increases (up to a log) in the MFI, but still much less than observed in PMN from a normal subject.

Interpretation and Limitations

The DHR assay is probably the most commonly used assay to establish a diagnosis of CGD. However, subjects with myeloperoxidase deficiency (7), found in 1 per 2,000 individuals, as well as several other disease states (8) can give a false-negative DHR response, depending on the extent of their deficiency. Therefore, a negative DHR should be confirmed with a negative nitroblue tetrazolium (NBT) test and/or abnormal $O_2^{-\cdot}$ generation using superoxide dismutase-inhibitable ferricytochrome *c* reduction. Analysis of $O_2^{-\cdot}$ production by cytochrome *c* reduction in PMN from a patient with myeloperoxidase deficiency will yield normal/supranormal production of $O_2^{-\cdot}$. The myeloperoxidase deficiency can be confirmed by either histochemical staining or quantitation of myeloperoxidase by enzyme-linked immunosorbent assay (ELISA).

CGD patients with mutations in the PU.1 binding domain of the promoter region of *CYBB* may express DHR^+ eosinophils, while PMN are DHR^- (9). In addition, in two CGD patients, we have noted small populations (2% and 7%) of DHR^+ PMN that may result from genetic reversion. It is often necessary to increase the number of events in the PMN gate to accurately assess these minor populations of cells.

Blood samples older than 24 h can be analyzed by the DHR assay, but the results may become difficult to interpret because of decreased viability. Nonviable PMN in the analysis region are interpreted as DHR^- cells. Hence, a normal subject can be misread as an X-linked CGD carrier. For the same reason, overnight samples should not be used to definitively rule out X-linked heterozygosity, since a highly lyonized CGD carrier (>90% DHR^+) could yield a DHR similar to an aged sample from a normal subject. In these cases, sequence analysis of *CYBB* is needed to substantiate the final diagnosis.

ISOLATION AND CHARACTERIZATION OF PMN

Principle

For some assays, PMN must be purified from erythrocytes and other leukocytes to obtain an accurate estimation of ROS production. PMN isolation protocols use differences in the cell density as the primary basis for cell separation. The relative densities of blood cells are as follows: erythrocytes > PMN and eosinophils > monocytes, lymphocytes, and basophils > platelets. Ficoll-Paque has a density (1.077 g/ml) that falls between that of PMN and that of the mononuclear cells. To isolate PMN, whole blood is diluted with saline and underlayered with Ficoll-Paque. After centrifugation for 30 min at 500 × *g*, the less-dense monocytes, lymphocytes, basophils, and platelets remain at the upper interface of the Ficoll-Paque, while the denser erythrocytes and PMN pass through the Ficoll-Paque and pellet at the bottom. The plasma, mononuclear cells, and Ficoll-Paque are aspirated carefully without disturbing the erythrocyte/PMN interface. The erythrocyte/PMN pellet is resuspended with saline and mixed with 3% dextran. Dextran promotes the formation of rouleaux by the erythrocytes, causing them to sediment rapidly at 1 × *g*. The PMN-enriched supernatant fluid is harvested from the bulk of the erythrocytes. Contaminating erythrocytes are removed by a brief (30 s) hypotonic lysis. The isotonicity is quickly restored with an equal volume of re-equilibration buffer. A second hypotonic lysis removes many of the residual erythrocyte ghosts.

Alternatively, a PMN-isolation protocol that uses a discontinuous gradient of plasma/Percoll minimizes exposure of PMN to trace contamination by bacterial lipopolysaccharide (LPS) and reduces PMN priming (10).

In our laboratory, isolated PMN are routinely frozen in pellets containing 5 × 10^6 PMN. For immunoblot studies, PMN resuspended in HBSS (1 × 10^6 cells/ml) are pretreated for 20 min with the cell-permeant, irreversible serine-protease inhibitor diisopropylfluorophosphate (DFP, 5 mM). This treatment prevents proteolytic cleavage of PMN proteins after detergent solubilization of protease-rich granules in PMN prior to electrophoresis. The cells are then spun at 400 × g for 10 min and the supernatant fluid is removed prior to freezing. These frozen PMN, though not viable, can be used as a source of PMN proteins for immunoblot analysis and DNA for genetic analysis.

Reagents

Ficoll-Paque Premium (17-5442-02, GE Healthcare, Piscataway, NJ)

3% Dextran

15 g dextran (200,000–300,000 MW, 101514, MP Biomedicals, Solon, OH)

500 ml 1× PBS (17-512F, Lonza, Walkersville, MD)

Add 15 g dextran to 500 ml PBS. Mix well and sterilize through a 0.2-μm filter.

Hypotonic Lysis Buffer

13.6 ml 10× PBS (17-515F, Lonza)

600 ml sterile, distilled H_2O (17-724F, Lonza)

Add 13.6 ml 10× PBS to 600 ml sterile, distilled H_2O.

PBS Re-Equilibration Buffer

108.1 ml 10× PBS

500 ml sterile distilled H_2O

Add 108.1 ml 10× PBS to 500 ml sterile distilled H_2O.

HBSS without Mg^{2+}, Ca^{2+}, or Phenol Red

Procedure

1. Collect patient blood in sodium-heparin (5–10 U/ml whole blood, final concentration) or acid-citrate-dextrose (ACD-A) blood-collection tubes (BD Vacutainer 367874 or 364606, Becton Dickinson).
2. Dispense 15 ml HBSS to a 50-ml conical centrifuge tube.
3. Transfer 15 to 20 ml heparinized blood to tube.
4. Carefully underlay blood mixture with 12 ml Ficoll-Paque Premium.
5. Spin for 30 min at 500 × *g*, with brake off.
6. Aspirate mononuclear cells, remaining plasma, and Ficoll-Paque Premium from the tube, leaving the PMN and erythrocyte-rich pellet.
7. Dilute with HBSS for a final volume of 20 ml.
8. Add 20 ml of 3% dextran. Invert the tube several times to mix. Allow erythrocytes to sediment at 1 × *g* for 20 min at room temperature.
9. Transfer the PMN-rich supernatant fluid to a new tube. Dilute with HBSS.
10. Spin at 300 × *g* for 10 min. Remove the supernatant fluid.
11. Lyse the remaining erythrocytes with 10 ml hypotonic lysis buffer, followed by the quick addition (within 30 s) of 10 ml PBS re-equilibration buffer to restore the isotonicity. Dilute further with 20 ml HBSS.
12. Spin at 300 × *g* for 10 min, aspirate the supernatant fluid, wash, and repeat process twice. Repeat lysis if there is significant erythrocyte contamination.
13. Resuspend PMN in HBSS. Count the cells using an automated cell counter.

Results and Normal Range

In general, 1×10^6 to 2×10^6 PMN can be isolated per ml of whole blood from a normal subject, with a purity and viability of >95%.

Interpretation and Limitations

The most common cell contaminants of the PMN preparation are eosinophils; however, some lymphocytes and monocytes may also be present. Some PMN studies require a purity higher than >95%. Further purification of the PMN preparation with anti-CD16 magnetic immunobeads (130-045-701; Miltenyi Biotec Inc., Auburn, CA) eliminates contaminating eosinophils and results in a PMN preparation that is >99%.

PMN from patients with specific granule deficiency have decreased density because of their lack of specific granules and fail to penetrate the Ficoll-Paque density cushion, instead colocalizing with the peripheral blood mononuclear cells atop the density cushion.

HISTOCHEMICAL STAINING OF PMN WITH NBT

Principle

The NBT test is a qualitative histochemical assay used to detect the production of ROS by oxidation-reduction reactions in phagocytes. NBT, yellow in solution, is an electron acceptor and is reduced in the presence of $O_2^{\cdot-}$ to formazan, an insoluble blue-black precipitate. Either whole blood or isolated PMN are added to the NBT solution in a chamber slide and stimulated with PMA for 15 to 30 min at 37°C. The PMN are allowed to adhere to the slide. The slide is air dried, counterstained with 0.6% safranin, and examined using a 100× objective of a microscope. The NBT test yields a visual record of ROS generation by individual cells. Under basal conditions, PMN from a normal subject do not generate ROS and cannot convert NBT to formazan; the cytosol and nucleus of the PMN appear pink because of the safranin counterstain (Fig. 2A). Treatment of PMN from a normal subject with PMA results in the production of ROS and the appearance of blue-black formazan deposits in the cytosol of the PMN (Fig, 2B). Treatment of PMN from a CGD patient with PMA does not induce ROS production (Fig. 2C), leading to an appearance similar to normal PMN under basal conditions. As observed with the DHR assay, treatment of PMN from a female X-linked carrier of CGD will exhibit both NBT^+ and NBT^- PMN because of random inactivation of the X chromosome (Fig. 2D).

Reagents

HBSS with Ca^{2+} and Mg^{2+} with 10 mM HEPES (HBSS/HEPES), pH 7.35–7.40

500 ml HBSS with Ca^{2+} and Mg^{2+} (10-527F, Lonza)

5.0 ml of 1.0 M HEPES buffer (15630-080, Life Technologies)

Add 5.0 ml 1.0 M HEPES to 500 ml HBSS. Adjust the pH within the range of 7.35 to 7.40. Prepare on day of use.

HBSS/HEPES with 1% Bovine Serum Albumin

1 g bovine serum albumin (BSA, A-2153, Sigma Aldrich)

100 ml HBSS/HEPES

Add 1 g BSA to 100 ml HBSS/HEPES. Mix well and sterilize through a 0.2-μm filter. Store at 4°C.

NBT (0.2%, N5514, Sigma-Aldrich)

1 tablet (10 mg) NBT

5.0 ml HBSS/HEPES

Add 1 NBT tablet to 5.0 ml HBSS/HEPES. Mix well and sterilize through a 0.2-μm filter. Prepare fresh on day of use.

PMA (20 μg/ml)

Prepare a working solution of PMA (20 μg/ml) by adding 10 μl stock PMA (2 mg/ml) to 990 μl 50% DMSO.

Safranin O (0.6%, 65092B-95; Harleco, EMD Millipore, Gibbstown, NJ)

Procedure

1. Transfer 0.1 ml isolated PMN (1×10^7 cells/ml) into a labeled conical tube.
2. Add 0.4 ml of 1% BSA in HBSS/HEPES.
3. Add 0.5 ml of 0.2% NBT solution.
4. Add 5 μl of 20 μg/ml PMA and mix well.

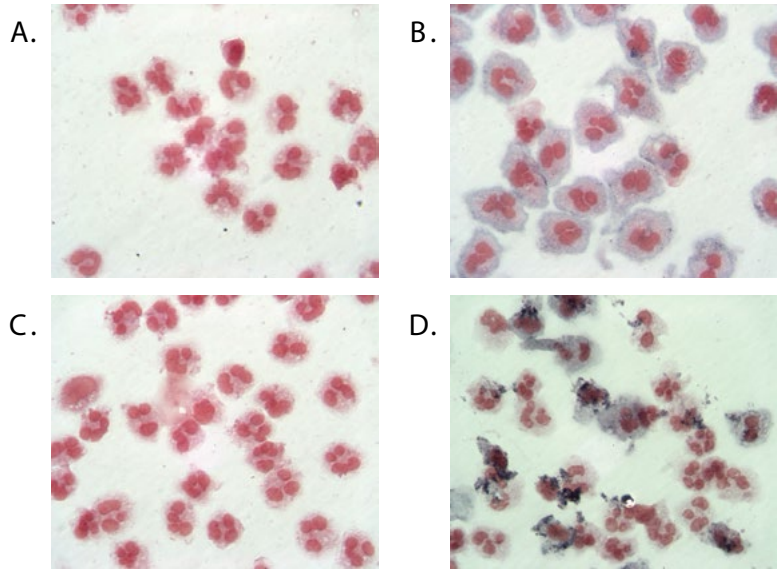

FIGURE 2 Histochemical staining of PMN with NBT. (A) PMN from a normal subject under basal condition exhibit only the safranin counterstain of the cytosol and nucleus. (B) PMN from a normal subject stimulated with PMA exhibit blue-black formazan deposits in the cytosol and the safranin counterstain in the nucleus. (C) PMN from a patient with gp91^{phox} CGD stimulated with PMA fail to generate ROS and exhibit only the safranin counterstain of the cytosol and nucleus. (D) PMN from an X-linked carrier of CGD stimulated with PMA exhibit both an NBT^- population and an NBT^+ population of PMN. In this case, the X-linked carrier was 52% NBT^+.

5. Transfer 500 μl (in duplicate) to a well of a chamber slide (177445, Nunc Lab-Tek; Thermo Fisher Scientific, Inc., Waltham, MA).
6. Incubate the slide for 15 min at 37°C.
7. Wash the slide with HBSS/HEPES.
8. Fix the slide with methanol.
9. Counterstain with 0.6% safranin for 5 min.
10. Allow the slide to dry before viewing the cells on the microscope.
11. Enumerate the % NBT^+ cells by counting 200 PMN, differentiating between NBT^+ and NBT^-.

Results and Normal Range

Treatment of PMN from a normal subject with PMA in the presence of NBT results in the formation of blue-black formazan in the cytosol and a pink counterstained nucleus in 98 to 100% of the cells (Fig. 2B).

Interpretation and Limitations

PMN that fail to reduce NBT include those that have little or no oxidase activity. This can include patients with CGD or glucose-6-phosphate dehydrogenase deficiency. In general, an NBT test on PMN from a patient with CGD exhibits only the safranin-counterstained nucleus with no formazan precipitate in the cytosol (Fig. 2C). Very few, if any, cells are NBT^+, although some patients with p47^{phox} CGD can stain weakly. Hence, the ability to reduce NBT does not exclude the diagnosis of CGD.

The NBT test can also be used to diagnose X-linked carriers of CGD (Fig. 2D) but cannot differentiate autosomal carriers from normal subjects. Because of inactivation of one of the X chromosomes, an NBT test on PMN from a carrier of CGD reveals two populations of PMN: PMN that are functioning correctly and able to generate ROS contain blue-black precipitate in the cytosol from the reduction of NBT to insoluble formazan, whereas PMN that do not generate ROS contain only pink-counterstained cytosol. The NBT test has a wide distribution in X-linked carriers of CGD, from as little as 5% NBT^+ to as much as 95% NBT^+.

The drawback of the NBT test is the time required to view sufficient individual cells and the subjectivity of the technician interpreting the response in each cell.

QUANTITATIVE ANALYSIS OF $O_2^{\cdot-}$ GENERATION USING SOD-INHIBITABLE FERRICYTOCHROME *c* REDUCTION

Principle

The release of ROS such as $O_2^{\cdot-}$ and H_2O_2 is an important component of the bactericidal machinery of PMN. The production of $O_2^{\cdot-}$ can be detected using the reduction of cytochrome *c*. $O_2^{\cdot-}$ causes a one-to-one stoichiometric reduction of ferricytochrome *c* to ferrocytochrome *c*, with a resultant increase in the absorption spectrum at 549.5 nM. Superoxide dismutase (SOD) is added to an identical tube to act as a blank by removing the substrate, thereby validating $O_2^{\cdot-}$ production. Resultant supernatants are analyzed by spectrophotometry using an analytical wavelength of 549.5 nm for peak absorbance and background wavelengths of 541 nm and 556 nm. The amount of $O_2^{\cdot-}$ generated is calculated from the optical density (OD) of reduced cytochrome *c* to nanomoles of $O_2^{\cdot-}$ released using the micromolar extinction coefficient of 0.0211. However, since cytochrome *c* is not permeable to the cells, the detection of $O_2^{\cdot-}$ is limited to that released into the extracellular milieu. An estimate of normal $O_2^{\cdot-}$ generated in 60 min can be obtained by reducing the number of PMN in the assay to 2×10^5 cells. PMN isolated from most patients with CGD fail to generate significant $O_2^{\cdot-}$ in response to PMA in 60 min. However,

some patients with autosomal forms of CGD have low but detectable $O_2^{-\cdot}$ production in 60 min. PMN isolated from X-linked heterozygous carriers of CGD can yield a full spectrum of $O_2^{-\cdot}$ production. Since the data represent the average $O_2^{-\cdot}$ generation of both functional and dysfunctional cells, a highly lyonized X-linked carrier with few DHR^+ or NBT^+ cells can exhibit less total $O_2^{-\cdot}$ generation than a CGD patient with some residual NOX2 activity. These data suggest that it is more immunologically advantageous to express a small population of PMN with normal NOX2 activity than the entire population of PMN with reduced NOX2 activity. Although the detection of $O_2^{-\cdot}$ by reduction of cytochrome *c* is useful in the diagnosis of patients with CGD, it cannot be used in the diagnosis of carriers because of the wide spectrum of responses that result from the degree of X-chromosome lyonization.

Recent studies have shown that $O_2^{-\cdot}$ determinations on PMN isolated from whole blood stored overnight are sufficiently reliable to diagnose CGD. By 48 h of storage, however, there are marked reductions in the PMA response and the data are no longer valid. Hence, analyses can be performed on blood samples shipped by overnight express. A normal control blood sample should accompany the sample to ensure proper shipment conditions and handling.

Reagents

HBSS/HEPES

Cytochrome *c* (200 μM)

26 mg cytochrome *c* (C7752, Sigma-Aldrich)
10 ml HBSS/HEPES

Dissolve 26 mg cytochrome *c* in 10 ml HBSS/HEPES.

Catalase (10 mg/ml)

SOD (10 mg/ml)

20 mg SOD (S2515, Sigma-Aldrich)
2.0 ml PBS without Ca^{2+} and Mg^{2+}

Dissolve 20 mg SOD in 2.0 ml PBS. Store at −85°C in 100-μl aliquots.

PMA (20 μg/ml)

Procedure

1. Add 200 μl catalase to 10 ml cytochrome *c* solution.
2. Resuspend PMN at 2×10^6 cells/ml in HBSS with Ca^{2+} and Mg^{2+}.
3. Label 6 × 1-ml polypropylene microtubes (#1 through 6) and prepare tubes as described in Table 1. It is important that PMN be added last.
4. After addition of PMN, immediately place tubes on an end-over-end rotator (12 rpm) in a 37°C incubator and incubate for either 10 min or 60 min (note: in a 60-min incubation, PMN from normal subjects, or carriers of CGD with DHR^+ PMN >20%, should be diluted 1:5 for tubes #4 through 6).
5. At the end of the incubation, immediately place tubes on ice and spin at 500 × *g* for 15 min at 4°C.
6. Transfer supernatants to cuvettes and read on spectrophotometer, using an analytical wavelength of 549.5 nm and background isosbestic (equivalent absorbance for both oxidized and reduced cytochrome *c*) wavelengths of 541 nm and 556 nm. The background wavelengths represent the intersections of the spectral scans of oxidized and reduced (determined after the addition of a few grains of dithionite) cytochrome c.
7. The net absorbance of each sample is determined using the following formula:

$$OD_{549.5\ nm} - \{[(OD_{556.0\ nm} - OD_{541.0\ nm}) \times (8.5/15)] + OD_{541.0\ nm}\}$$

8. The basal production of $O_2^{-\cdot}$ generated (nanomoles/10^6 cells) is calculated by subtracting the net absorbance of the SOD-containing sample (tube #3) from the mean of net absorbance of tubes #1 and 2 and dividing the difference by 0.0211, the micromolar extinction coefficient for reduced cytochrome *c*. Repeat the calculations for tubes #4 through 6. For 60-min samples with reduced cell numbers (20%), multiply by 5 to normalize to 10^6 cells.

TABLE 1 Experimental design for quantitative analysis of $O_2^{-\cdot}$ generation using superoxide dismutase-inhibitable ferricytochrome c reduction[a]

Conditions	Tube no.	Vol (μl)			
		Cytochrome *c*/ catalase soln	SOD	PMA	PMN
Resting	1,2	500	—	—	500
Resting-SOD	3	500	10	—	500
PMA	4,5	500	—	5	500
PMA-SOD	6	500	10	5	500

[a]SOD, superoxide dismutase; PMA, phorbol 12-myristate 13-acetate

Results and Normal Range

PMN isolated from normal subjects produce 0.41 ± 0.32 nmol/10^6 PMN/10 min and 2.15 ± 1.60 nmol/10^6 PMN/60 min under basal conditions. Treatment of normal PMN with PMA results in 43.53 ± 12.61 nmol/10^6 PMN/10 min and 235.38 ± 55.69 nmol/10^6 PMN/60 min.

Interpretation and Limitations

Since cytochrome *c* is not cell-permeant, the data obtained using this assay represent only a portion of the total ROS production, i.e., that $O_2^{-\cdot}$ released from the cell and detected in the extracellular milieu. In addition, $O_2^{-\cdot}$ generation using ferricytochrome *c* reduction reflects the average response of all the cells in the population. For example, a CGD patient with 100% of cells functioning at 10% cannot be distinguished from an X-linked CGD carrier with 10% of cells functioning at 100% capacity. Hence, detection of $O_2^{-\cdot}$ generation by ferricytochrome *c* reduction alone is insufficient to diagnose X-linked carriers, and it should be used in conjunction with the DHR or NBT assay.

The $O_2^{-\cdot}$ generated by PMN isolated from CGD patients ranges from 0.50 to as much as 60 nmol/10^6 cell/60 min. Although NOX2 function is impaired in all patients with CGD, there is variability (0.1 to 27% of normal) in residual ROS production by patient PMN. Analysis of this residual ROS production allowed discrimination of CGD into subgroups with different rates of mortality (11). The production of ROS has become an important tool to perform risk assessment in patients with CGD. Patients with the lowest ROS generation (<1% of normal generation) have lower predicted survival than patients with higher ROS generation (3 to 10% of normal).

ANALYSIS OF PMN ROS GENERATION BY LUMINOL-ENHANCED CHEMILUMINESCENCE

Principle

While the analysis of $O_2^{\cdot-}$ generation using ferricytochrome *c* reduction is a reasonable approach to quantitate extracellular ROS production, it does not provide an estimate of intracellular ROS production. An estimate of both intracellular and extracellular ROS production can be determined using ROS-mediated, luminol-enhanced chemiluminescence. It should be noted that the kinetics of PMA-induced chemiluminescence are different from the kinetics of PMA-induced $O_2^{\cdot-}$ generation using ferricytochrome *c* reduction.

Reagents

HBSS/HEPES

Luminol (50 mM)

35.44 mg luminol (A8511, Sigma-Aldrich)

4.0 ml DMSO

Add 35.4 mg luminol to 4.0 ml DMSO. Store at −85°C in 50-μl aliquots wrapped with foil to protect from light. On the day of analysis, prepare a working solution of 400 μM.

PMA (400 ng/ml)

Prepare a 400 ng/ml working concentration of PMA by adding 20 μl PMA (20 μg/ml) to 980 μl HBSS/HEPES buffer.

Procedure

1. Isolate PMN from whole blood as described previously. Resuspend PMN in HBSS/HEPES at 1×10^6 cells/ml.
2. Transfer 10^5 PMN/100 μl in triplicate for each condition to a 96-well, white analysis microplate (655207; Greiner Bio-One, Monroe, NC).
3. Add 50 μl luminol to each well of the microplate containing PMN. Incubate for 10 min at 37°C.
4. Transfer 50 μl buffer or PMA to the proscribed wells of the analysis microplate using an 8-channel pipettor. Immediately place the plate into a luminometer, thermally regulated at 37°C.
5. Measure the luminescence of each well every 2 min for up to 120 min, shaking the plate at medium speed prior to each reading.

Results and Normal Range

Luminol-enhanced chemiluminescence is a measure of both intracellular and extracellular ROS production, specifically $O_2^{\cdot-}$ production. Addition of SOD causes significant reduction in both the peak height and area under the curve after stimulation with PMA, whereas addition of catalase has much less impact. The luminescence signal is in photons/second and is expressed as relative light units (RLU). The kinetics of the response varies with the activator used. Stimulation of PMN from a normal subject leads to a rapid peak of luminescence with a prolonged decay that persists for almost 2 h (Fig. 3). PMN from a patient with gp91^{phox} CGD exhibits little detectable luminescence. PMN from an gp91^{phox} X-linked carrier CGD exhibits an intermediate signal that is consistent with the percentage of DHR$^+$ cells within the population. PMN from a patient with p47^{phox} CGD, as observed with other assays of ROS production, exhibit low but detectable luminescence, particularly at longer incubation times. Comparing the responses from different subjects is typically performed by comparing the area under the curves.

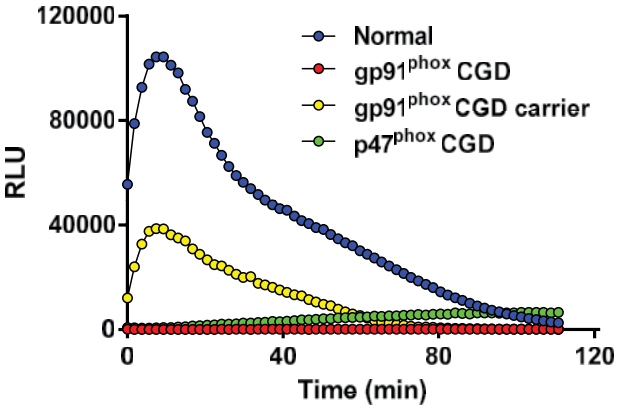

FIGURE 3 Analysis of PMN ROS generation by luminol-enhanced chemiluminescence. PMN (1×10^5 cells/200 μl HBSS/HEPES with 100 μM luminol) were incubated for 120 min in the presence of PMA (100 ng/ml). Luminescence of each well was determined every 2 min. The data from each subject were performed in triplicate. Blue circles represent the mean response of normal subjects ($n = 20$); yellow circles, an X-linked carrier of gp91^{phox} CGD; green circles, a patient with p47^{phox} CGD; red circles, a patient with gp91^{phox} CGD.

The primary advantage of the luminol-enhanced chemiluminescence is the increased sensitivity with reduced cell numbers. In addition, PMN from several different subjects can be stimulated with several different stimuli on the same plate.

Interpretation and Limitations

Similar to detection of $O_2^{\cdot-}$ generation by ferricytochrome *c* reduction, luminol-enhanced chemiluminescence reflects the average response of all the cells in the population; alone is insufficient to diagnose X-linked carriers; and should be used in conjunction with the DHR or NBT assay. In addition, luminol-enhanced chemiluminescence is not directly quantifiable. Instead, comparison of responses of cells from normal subjects and patients is usually based on a comparison of the area under the curves for each subject.

ANALYSIS OF gp91^{phox} SURFACE EXPRESSION BY FLOW CYTOMETRY

Principle

The NADPH oxidase is a multicomponent enzyme that transfers electrons from NADPH to O_2 to generate superoxide anion radical ($O_2^{\cdot-}$), a key part of the phagocytic or PMN respiratory burst response. Flavocytochrome b_{558} is the catalytic component of the phagocyte NADPH oxidase and consists of a transmembrane heterodimer composed of a large glycoprotein, gp91^{phox}, and a smaller protein, p22^{phox}. The expression of flavocytochrome b_{558} on the cell surface antigens can be determined by flow cytometric analysis of PMN stained with fluorescently labeled monoclonal antibody 7D5, which recognizes a specific extracellular epitope (12, 13). PMN stained with nonspecific isotype antibodies are used to determine the nonspecific background staining. To determine the expression of circulating PMN and avoid artifacts induced by PMN isolation, an aliquot of whole

blood can be stained with the appropriate antibody prior to lysis of the erythrocytes. During flow cytometric analysis, the PMN are generally easy to identify using FS × SS gating.

Reagents

Fluorescein Isothiocyanate (FITC)-Labeled Anti-Flavocytochrome *b*558 Monoclonal Antibody 7D5 (500 μg/ml, D162-4; MBL International Corporation, Woburn, MA)

Mouse IgG_1 FITC Isotype Control (50 μg/ml, 349041, BD Biosciences)

OptiLyse C, No-Wash Lysing Solution (A11895, Beckman Coulter, Indianapolis, IN)

PBS with 2% BSA

2 g BSA (A-9543, Sigma-Aldrich)

PBS

Dissolve 2 g BSA in 100 ml PBS. Mix well and sterilize through a 0.2-μm filter.

Procedure

1. Label 12 × 75 mm polypropylene tubes with the designations "IgG_1" or "7D5" and add either 20 μl IgG_1 isotype or 4 μl monoclonal antibody 7D5 to designated tubes.
2. Add 100 μl whole blood to each tube and vortex.
3. Cover samples with foil and incubate at 4°C for 30 min.
4. Add 500 μl Optilyse C to each tube and vortex immediately. Cover tubes with foil and incubate at 4°C for 30 min.
5. Add 2.0 ml PBS with 2% BSA to each tube.
6. Spin tubes at 400 × *g* for 5 min, decant and repeat wash.

Resuspend PMN in 0.2 ml of PBS with 2% BSA and analyze by flow cytometry.

Results and Normal Range

The expression of Ab 7D5 on PMN from normal subjects is typically 830 ± 442 compared to the IgG_1 isotype (95.1 ± 25.4). Activation of isolated PMN with formyl-methionyl-leucyl phenylalanine (fMLF) or LPS can lead to mobilization of latent $gp91^{phox}$ stored in specific granules.

Interpretation and Limitation

PMN from CGD patients with either defects in $p22^{phox}$ or $gp91^{phox}$ generally exhibit abnormal expression of Ab 7D5. However, often patients with missense mutations in $gp91^{phox}$ in the nucleotide-binding domains can exhibit normal expression of $gp91^{phox}$.

IMMUNOBLOT ANALYSIS OF phox SUBUNITS OF NOX2

Principle

NOX2 consists of two membrane components, $p22^{phox}$ and $gp91^{phox}$; three cytosolic components, $p47^{phox}$, $p67^{phox}$, and $p40^{phox}$; and several GTP-binding proteins. The severity of CGD may be related to the specific protein defect. Determination of the specific protein defect in CGD by immunoblot analysis also provides direction for determination of the specific genetic defect as well as enabling appropriate genetic counseling for the extended family. A validated normal control is included on each gel for band identification and intensity comparisons. A typical phox protein immunoblot of a PMN lysate from a normal subject is presented in Fig. 4, lane 1. Patients with mutations in $gp91^{phox}$ can exhibit different protein expression. Some CGD patients with missense mutations in $gp91^{phox}$ can express detectable mutant protein (Fig. 4, lanes 2 and 3). Because $p22^{phox}$ and $gp91^{phox}$ exist as a membrane complex, increased $gp91^{phox}$ protein expression is accompanied by a proportionately higher expression of $p22^{phox}$. CGD patients with nonsense mutations in $gp91^{phox}$ exhibit undetectable expression of $gp91^{phox}$; however, there is low but detectable expression of $p22^{phox}$ (Fig. 4, lane 4). In our laboratory, we typically include a PMN lysate from known $gp91^{phox}$ CGD on each blot to ensure adequate development of $p22^{phox}$. CGD patients with mutations in $p22^{phox}$ are immunoblot-negative for both $p22^{phox}$ and $gp91^{phox}$ (Fig. 4, lane 5). CGD patients with mutations in $p47^{phox}$ CGD exhibit no detectable protein expression (Fig. 4, lane 6). Similarly, CGD patients with mutations in $p67^{phox}$ CGD generally exhibit undetectable protein expression (Fig. 4, lane 7); however, we have analyzed one patient with a missense mutation in $p67^{phox}$ who exhibits detectable protein expression.

PMN isolated from overnight samples can be used to diagnose $p47^{phox}$ deficiency because of the stability of the protein. However, detection of defects in other phox protein in overnight samples can be more problematic because of proteolysis of $p67^{phox}$ and the $gp91^{phox}$:$p22^{phox}$ complex.

Reagents

3-(*N*-Morpholino)propanesulfonic acid (MOPS)–sodium dodecyl sulfate (SDS) running buffer (2.0 liters, 1×)

100 ml NuPAGE MOPS-SDS running buffer (20X, NP0001; Novex Life Technologies)

1,900 ml distilled H_2O

Add 100 ml 20× running buffer to 1,900 ml H_2O.

Antioxidant Solution (NP0005, Novex Life Technologies)

Protease-Inhibitor Solution (10×)

1 Complete Mini Protease-Inhibitor tablet (68196820; Boehringer Mannheim, Gaithersburg, MD)

1 ml distilled H_2O

Dissolve one Complete Mini Protease-Inhibitor tablet in 1 ml H_2O.

Sample Buffer (1×)

250 μl 4× sample buffer (NP0003, Novex Life Technologies)

100 μl 10× protease inhibitor solution

650 μl distilled H_2O

Add 250 μl 4× sample buffer and 100 μl 10× protease inhibitor solution to 650 μl dH_2O.

Reducing Agent (NP0004, Novex Life Technologies)

SeeBlue Plus2 Prestained Standards (LC5625, Novex Life Technologies)

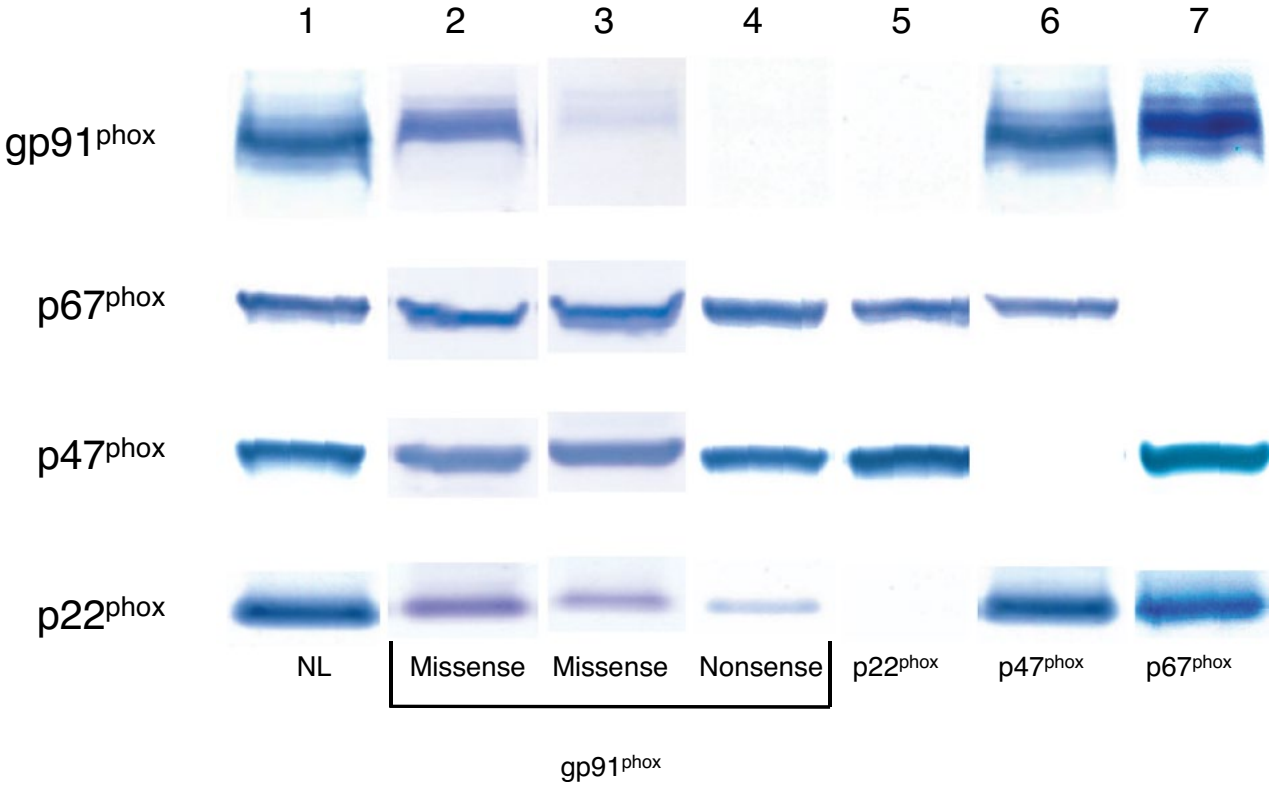

FIGURE 4 Immunoblot analysis of phox subunits of NOX2. DFP-treated PMN (5×10^6 cells) were sonicated in 100 μl of sample buffer. For each subject, an aliquot (20 μl or 1×10^6 cell equivalents) of PMN lysate was loaded into a well of the precast BisTris SDS-PAGE gel. In this composite figure, the bands corresponding to each phox subunit from each subject have been aligned. Lane 1 represents PMN from a normal subject and defines the position and the expression of each phox subunit. Lanes 2 and 3 represent CGD patients with missense mutations in $gp91^{phox}$ and illustrate the proportional expression observed with $gp91^{phox}$ and $p22^{phox}$. Lane 4 represents a CGD patient with a nonsense mutation in $gp91^{phox}$ with undetectable expression of $gp91^{phox}$ but faint expression of $p22^{phox}$. Lane 5 represents a CGD patient with $p22^{phox}$ deficiency with undetectable expression of both $p22^{phox}$ and $gp91^{phox}$. Lane 6 represents a CGD patient with undetectable $p47^{phox}$. Lane 7 represents a CGD patient with undetectable expression of $p67^{phox}$.

NuPAGE Novex Bis-Tris Gels

NuPAGE Novex 10% Bis-Tris Gel 1.0 mm, 10 well (NP0301, Novex Life Technologies) for detection of $p47^{phox}$ and $p67^{phox}$ and NuPAGE Novex 4 to 12% Bis-Tris Gel 1.0 mm, 10 well (NP0321, Novex Life Technologies) for detection of $p22^{phox}$ and $gp91^{phox}$.

Tris-Buffered Saline (TBS)

80 ml 1.0 M Tris, pH 7.4 (16-014F, Lonza)
116.8 g NaCl (S9625, Sigma-Aldrich)
3,920 ml H_2O

Add 80 ml 1.0 M Tris and 116.8 g NaCl to 3.920 ml H_2O.

TBS/0.5% Tween

1.0 liter TBS
5 ml Tween 20 (P1379, Sigma-Aldrich)

Add 5 ml Tween 20 to 1.0 liter TBS.

Transfer Buffer (3.0 liters, 1×)

150 ml NuPAGE Transfer buffer (20×, NP0006, Novex Life Technologies)
3.0 ml antioxidant solution (NP0005, Novex Life Technologies)
300 ml methanol
2,547 ml distilled H_2O

Add 150 ml 20× transfer buffer, 3.0 ml antioxidant solution, and 300 ml methanol to 2,547 ml H_2O.

Immobilon-P Transfer Membrane (IPVH 00010; EMD Millipore, Billerica, MA)

Sodium Azide (1.0 M)

0.65 g sodium azide
10 ml H_2O

Add 0.65 g sodium azide to 10 ml of H_2O.

Membrane-Blocking Solution

10 g nonfat dry milk
100 μl Tween 20
200 ml TBS
200 μl 1.0 M sodium azide

Add 10 g dry milk and 100 μl Tween 20 to 200 ml TBS. Add 200 μl 1.0 M sodium azide as a preservative.

Primary Goat Antibodies against $p22^{phox}$, $p47^{phox}$, $p67^{phox}$, and $gp91^{phox}$
Obtained from Harry Malech and Tom Leto (National Institute of Allergy and Infectious Diseases, National Institutes of Health).

50 μl antibody
50 μl 1.0 M sodium azide
2.5 g nonfat dry milk
25 μl Tween 20
50 ml TBS

Add 50 μl of the desired antibody to solution containing 50 ml TBS with 2.5 g nonfat milk and 25 μl Tween 20. Add 50 μl 1.0 M sodium azide as a preservative (shelf life: 6 months).

Goat IgG, Whole Molecule, Peroxidase-Labeled (A5420, Sigma-Aldrich)
20.0 μl peroxidase anti-goat IgG
10 g nonfat milk
100 μl Tween 20
200 ml TBS

Dilute peroxidase-labeled anti-goat IgG antibody (1:10,000) by adding 20.0 μl anti-goat IgG to a solution containing 200 ml TBS, 10 g nonfat milk, and 100 μl Tween 20.

TMB One Component Horseradish Peroxidase (HRP) Membrane Substrate (TMBM-0100-01; SurModics IVD, Eden Prairie, MN)
Warm to room temperature before use.

Procedure

1. Add 90 μl 1× sample buffer and 10 μl reducing agent to DFP-treated PMN pellet (5×10^6 cells/pellet). Sonicate the PMN pellet for 80 short (<1-s) pulses at low setting to prevent sample loss. Cool on ice and repeat sonication for an additional 80 pulses.
2. Spin at 10,600 × *g* for 5 min.
3. Repeat sonication for 40 pulses at low setting, if necessary.
4. Place gel in electrophoresis apparatus according to manufacturer's instruction.
5. Fill the upper chamber with 1× running buffer (600 ml) + antioxidant (1.5 ml) and check for leakage. Fill the lower chamber with ~350 ml of buffer (without antioxidant). Add sufficient buffer until each chamber is full.
6. Load 10 μl of the SeeBlue Plus2 prestained molecular weight standards in lane 1 of each gel—two 10% gels for detection of $p47^{phox}$ and $p67^{phox}$ and two 4–12% gels for detection of $p22^{phox}$ and $gp91^{phox}$.
7. Load 20 μl of a normal PMN lysate in lane 2 and load 20 μl of PMN lysate from each patient in lanes 3 through 10 of all four gels.
8. Run the gels at 4°C using constant voltage (125 V) until the dye front reaches the bottom of the gel.
9. Turn off the power supply and disconnect the gel apparatus from the power supply.
10. Remove the precast gel(s) from the gel chamber and remove the gels from the cassette according to the manufacturer's instruction.
11. Transfer the gels to the Immobilon-P membrane according to the instructions supplied with blotting apparatus.

    To ensure adequate protein transfer to the membrane, check the gels for residual prestained standards. Using a pen, mark the membrane at the leading edge of each of the prestained molecular weight standards.
12. Place the membrane in the membrane-blocking solution and incubate for at least 6 h at 4°C with gentle rocking.
13. Remove the membrane from the blocking solution and wash the membrane 3× for 5 min with TBS/0.5% Tween 20.
14. Add the appropriate primary antibody solution to blot and incubate overnight at 4°C with gentle rocking.
15. Remove the membrane from the primary antibody solutions, reserving the primary antibody.
16. Wash the membrane 3× for 5 min with TBS/0.5% Tween 20.
17. Add the secondary antibody solution to the membrane and incubate with gentle rocking for 2 h at room temperature.
18. Wash the membrane 3× for 5 min with TBS/0.5% Tween 20.
19. Add the membrane peroxidase substrate to the membrane.
20. Carefully monitor development of the membrane to ensure adequate staining, particularly for detection of $p22^{phox}$. A faint $p22^{phox}$ band is generally observed in patients with $gp91^{phox}$ -deficient CGD.
21. To stop the development, quickly wash the membrane twice with distilled H_2O.

Results and Normal Range

For each immunoblot analysis, a PMN lysate from at least one normal subject should be included on each gel for comparison. The expression of each phox protein can be determined by densitometric scanning. Alternatively, the expression of each protein can be assigned a value based on a semiquantitative scale, comparing the expression of each protein to the expression observed in a normal subject, e.g., "0," lack or absence of expression; "1," trace expression; "2," intermediate expression; and "3," normal expression. The primary goal of the immunoblot analysis is the identification of the protein defect in patients with CGD, targeting the gene for sequence analysis.

Interpretation and Limitations

The membrane components $gp91^{phox}$ and $p22^{phox}$ are expressed as a complex. Absence of $gp91^{phox}$ results in faint expression of $p22^{phox}$. However, absence of $p22^{phox}$ results in absence of bands for both $p22^{phox}$ and $gp91^{phox}$. Missense mutations in $gp91^{phox}$ often result in decreased expression of $gp91^{phox}$ as well as a parallel decrease in expression of $p22^{phox}$. Reduced or absent expression of $p47^{phox}$ or $p67^{phox}$ has little or no impact on the expression of the other phox proteins.

CONCLUSION

Although the DHR assay is probably the single most used assay for diagnosis of CGD, other assays used can complement the findings of the DHR. Since there are conditions which can give a false-negative DHR response (as in myeloperoxidase deficiency), the $O_2^{\cdot-}$ dependent ferricytochrome *c* reduction assay can confirm the DHR finding. Similarly, X-linked carriers of CGD can exhibit a very low value in the $O_2^{\cdot-}$ dependent ferricytochrome *c* reduction assay. However, the DHR may indicate that the patient has very few DHR^+ cells. Hence, a final diagnosis of CGD or carrier of CGD

should not be based on a single assay, but rather it should be based on several assays with results that agree among them.

This project has been funded in whole or in part with federal funds from the National Cancer Institute, National Institutes of Health, under Contract No. HHSN261200800001E. The content of this publication does not necessarily reflect the views or policies of the Department of Health and Human Services, nor does mention of trade names, commercial products, or organizations imply endorsement by the U.S. Government.

REFERENCES

1. **Berendes H, Bridges RA, Good RA.** 1957. A fatal granulomatous of childhood: The clinical study of a new syndrome. *Minn Med* **40:**309–312.
2. **Volpp BD, Nauseef WM, Clark RA.** 1988. Two cytosolic neutrophil oxidase components absent in autosomal chronic granulomatous disease. *Science* **242:**1295–1297.
3. **Matute JD, Arias AA, Wright NA, Wrobel I, Waterhouse CC, Li XJ, Marchal CC, Stull ND, Lewis DB, Steele M, Kellner JD, Yu W, Meroueh SO, Nauseef WM, Dinauer MC.** 2009. A new genetic subgroup of chronic granulomatous disease with autosomal recessive mutations in $p40^{phox}$ and selective defects in neutrophil NADPH oxidase activity. *Blood* **114:**3309–3315.
4. **Parkos CA, Dinauer MC, Walker LE, Allen RA, Jesaitis AJ, Orkin SH.** 1988. Primary structure and unique expression of the 22-kilodalton light chain of human neutrophil cytochrome b. *Proc Natl Acad Sci USA* **85:**3319–3323.
5. **Segal AW, Cross AR, Garcia RC, Borregaard N, Valerius NH, Soothill JF, Jones OT.** 1983. Absence of cytochrome b_{245} in chronic granulomatous disease. A multicenter European evaluation of its incidence and relevance. *N Engl J Med* **308:**245–251.
6. **Emmendörffer A, Hecht M, Lohmann-Matthes ML, Roesler J.** 1990. A fast and easy method to determine the production of reactive oxygen intermediates by human and murine phagocytes using dihydrorhodamine 123. *J Immunol Methods* **131:**269–275.
7. **Mauch L, Lun A, O'Gorman MR, Harris JS, Schulze I, Zychlinsky A, Fuchs T, Oelshschägel U, Brenner S, Kutter D, Rösen-Wolff A, Roesler J.** 2007. Chronic granulomatous disease (CGD) and complete myeloperoxidase deficiency both yield strongly reduced dihydrorhodamine 123 test signals but can be easily discerned in routine testing for CGD. *Clin Chem* **53:**890–896.
8. **Ferguson PJ, Lokuta MA, El-Shanti HI, Muhle L, Bing X, Huttenlocher A.** 2008. Neutrophil dysfunction in a family with a SAPHO syndrome-like phenotype. *Arthritis Rheum* **58:**3264–3269.
9. **Weening RS, De Boer M, Kuijpers TW, Neefjes VME, Hack WW, Roos D.** 2000. Point mutations in the promoter region of the CYBB gene leading to mild chronic granulomatous disease. *Clin Exp Immunol* **122:**410–417.
10. **Haslett C, Guthrie LA, Kopaniak MM, Johnston RB Jr, Henson PM.** 1985. Modulation of multiple neutrophil functions by preparative methods or trace concentrations of bacterial lipopolysaccharide. *Am J Pathol* **119:**101–110.
11. **Kuhns DB, Alvord WG, Heller T, Feld JJ, Pike KM, Marciano BE, Uzel G, DeRavin SS, Long Priel DA, Soule BP, Zarember KA, Malech HL, Holland SM, Gallin JI.** 2010. Residual NADPH oxidase and survival in chronic granulomatous disease. *N Engl J Med* **363:**2600–2610.
12. **Nakamura M, Murakami M, Koga T, Tanaka Y, Minakami S.** 1987. Monoclonal antibody 7D5 raised to cytochrome b_{558} of human neutrophils: immunocytochemical detection of the antigen in peripheral phagocytes of normal subjects, patients with chronic granulomatous disease, and their carrier mothers. *Blood* **69:**1404–1408.
13. **Yamauchi A, Yu L, Pötgens AJ, Kuribayashi F, Nunoi H, Kanegasaki S, Roos D, Malech HL, Dinauer MC, Nakamura M.** 2001. Location of the epitope for 7D5, a monoclonal antibody raised against human flavocytochrome b_{558}, to the extracellular peptide portion of primate $gp91^{phox}$. *Microbiol Immunol* **45:**249–257.

Cytokines and Chemokines

section F

VOLUME EDITOR: BARBARA DETRICK
SECTION EDITOR: JOHN J. HOOKS

Introduction

JOHN J. HOOKS

34

Nearly 60 years ago, the first cytokine was described. Today, >300 cytokines, chemokines, and adhesion molecules have been identified. We have witnessed an explosion in knowledge about cytokine biology. This can be highlighted by reviewing the interferon (IFN) molecules as an example. IFN was first identified in 1957 as a potent antiviral molecule. We now know that there are four major types of IFNs (alpha, beta, gamma, and lambda). Although IFN was first identified as an antiviral protein, IFNs are now recognized as critical immunoregulatory proteins capable of altering various cellular processes, including cell growth, differentiation, gene transcription, and translation. The advent of innate immunity and Toll-like receptors revealed the intimate role of IFNs in innate immune responses. The presence of IFN-α is a critical component of the autoimmune disease systemic lupus erythematosus. Advances in biotechnology and molecular biology have generated highly specific reagents with clinical relevance. In fact, the IFNs have been approved by the Food and Drug Administration for the treatment of infections, malignancies, autoimmunity, and immunodeficiency. IFN-α treatment is efficacious for hepatitis C infection, IFN-β for multiple sclerosis, and IFN-γ for chronic granulomatous disease. The examples outlined for the IFNs can be replayed throughout the cytokine kingdom.

The key element throughout this section is the measurement of cytokines. We need to know what to measure, how to measure, and the utility of this measurement. The five chapters in this section provide us with this knowledge and much more.

Chapter 35, by Duffy and Remick, provides a critical review of reasons and ways to measure cytokines. They identify ways to monitor the proteins, beginning with the standard enzyme-linked immunosorbent assay, and then present insight into multiplex assays. It is of interest to note that they include a cost comparison of these assay systems. Molecular methods to measure cytokine mRNA are then presented, with an analysis of *in situ* hybridization and PCR assays. The authors keenly note that cytokines are critical from birth (gestation) to death (apoptosis).

Chapter 36, written by Maecker, expands on cytokine measurement with a focus on flow cytometry. This assay method allows for the measurement of these proteins on a single-cell basis. In fact, multiparameter flow cytometry provides the investigator with a detailed characterization of the cytokine-producing cells.

The next chapter, prepared by Islam, Medoff, and Luster, is a detailed description of the chemokine and chemokine receptor system. This critical topic highlights the concept that the movement of leukocytes toward a site of antigen challenge, infection, or tissue damage is a central component in establishing inflammation. These chemokine experts offer an overview of basic principles of chemokines and chemokine receptors and their role in several disease states. Finally, they identify ways to measure chemokines and the clinical applications for this analysis.

The final two chapters are new additions for the section in the 8th edition of the *Manual* that deliver insight into advances in cytokine biology. Vashisht and Niewold provide us with a concise description of the newer diagnostic and clinical applications of cytokines. They stress the concept that cytokine measurements are helpful in the diagnosis and prognosis of autoimmune diseases and discuss how cytokine patterns provide insights into the causes of diseases. In particular, they highlight the role of IFN-α in systemic lupus erythematosus and interleukin-1 in juvenile idiopathic arthritis. They also discuss the key concept of cytokine inhibitors and recombinant cytokines in the treatment of human disease.

Chapter 39, by Browne, identifies the key role of anticytokine autoantibodies in human diseases. This is a rapidly expanding field of study that cuts across several medical disciplines. The reason for this diversity lies in the various cytokine pathways inhibited and the resulting diverse manifestations of disease. Browne highlights examples, such as antierythropoietin autoantibodies and pure red cell aplasia, anti-IFN-γ autoantibodies and severe opportunistic infection, and anti-granulocyte-macrophage colony-stimulating factor autoantibodies and pulmonary alveolar proteinosis. The author characterizes methods of measurement and notes that diagnosis can directly influence clinical management because therapy can focus on the autoantibody.

The primary function of this section is to identify ways to monitor cytokines and chemokines in a laboratory setting. Beyond this mission, the authors of this section have also provided us with a greater understanding of the role of cytokines, chemokines, and their receptors in human diseases. Moreover, they provide insight into how this knowledge can lead to the development of novel therapeutic approaches to combat these diseases.

doi:10.1128/9781555818722.ch34

Multiplex Cytokine Assays

ELIZABETH R. DUFFY AND DANIEL G. REMICK

35

Cytokines are low-molecular-weight proteins representing important components of inflammatory and immune reactions (1). In response to multiple stimuli (2), cytokines are rapidly induced and secreted into the extracellular milieu. However, in some situations, cytokines are constitutively present. Cytokines exert numerous biological activities which are critical for host defense, physiologic responses to stress, and immune surveillance. Cytokines, along with complement, are considered to be part of the innate immune system. The world of cytokine biology has exploded in the past decades. It can be said without hyperbole that cytokines are critical from birth (gestation) (3) to death (apoptosis) (4).

Given the wide range of activities induced by cytokines, there is great interest in accurate measurement of these critical mediators. It is important to know if the cytokines are present during a particular disease process since they may potentially serve as a target for therapy (5). Conversely, there may be value in documenting that cytokines are depressed during a disease state such that the appropriate therapy is administration of exogenous cytokines, e.g., granulocyte colony-stimulating factor. Clear evidence of the interest in measuring cytokines is demonstrated by the numerous companies which prepare and market kits for quantifying levels of cytokines.

Since there are numerous cytokines, a final biological outcome may not be dependent upon a single cytokine. Indeed, it has been reported that the ratio of cytokines to cytokine inhibitors provides the best predictor for progression of disease (6, 7). The best insights into the disease state will probably be achieved when multiple parameters are analyzed and assessed. As in making a clinical diagnosis, as much information as possible is needed in order to arrive at the correct determination for the precise disease process.

As a result of these issues, multiplex cytokine assays have been developed which will allow measurement of several cytokines simultaneously. While some of these assays were described several years ago, they have mushroomed in the commercial sector. As will be discussed further below, flow cytometric bead array assays are now marketed by numerous vendors. The technology has developed to the point that papers are now being written which directly compare the different kits from different vendors (8, 9).

While this chapter will examine measurement of cytokines, it should be borne in mind that the technology is not limited to measuring only these inflammatory mediators. Indeed, virtually any molecule that exhibits a specific interaction with another molecule may be measured by either a traditional enzyme-linked immunosorbent assay (ELISA) or a multiplex assay. Whether the interaction is a ligand-receptor interaction, a nucleic acid-protein interaction (10), or the traditional antibody-antigen interaction, the multiplex technology may be adapted to allow measurement (11). The principal consideration is the specificity of the interaction, such that the results are specific for measuring the analyte in question.

This chapter will explore both traditional ELISAs and the newer multiplexed assays. The methods, technology, instrumentation, and data analysis will be examined. Pitfalls that may arise with the assay will be explored to provide a better understanding of the limitations of the technique in question. We will also briefly describe the principles of nucleic acid detection by *in situ* hybridization and PCR.

TRADITIONAL ELISA

The traditional ELISA serves as an appropriate starting point. This is done because most of the newer assays are still based on the same antibody-antigen interaction that is most easily understood through examination of a single ELISA for a single cytokine. Virtually all ELISAs are based on the concept that a specific antibody will recognize a specific antigen. This concept dates back to the pioneering work of Yalow and Berson, who discovered that an antibody could recognize insulin (12). This single finding revolutionized the process for the detection and quantification of specific analytes.

Most commercially available ELISAs are based on a sandwich, or two-antibody, technique. A simpler method is the direct ELISA. For this assay, the antigen is bound directly to the surface of the microtiter well in the plate (Fig. 1). An antibody which specifically detects the cytokine in question is then added. For purposes of illustration, the cytokine interleukin 6 (IL-6) will be used in the schematic figures. There are multiple methods for detecting the antibody bound to the antigen. The antibody may be directly conjugated to an enzyme such as horseradish peroxidase, and the enzymatic reaction will occur within the well of the microtiter plate, as illustrated in Fig. 1. Alternatively, the antibody may be detected by a second antibody.

doi:10.1128/9781555818722.ch35

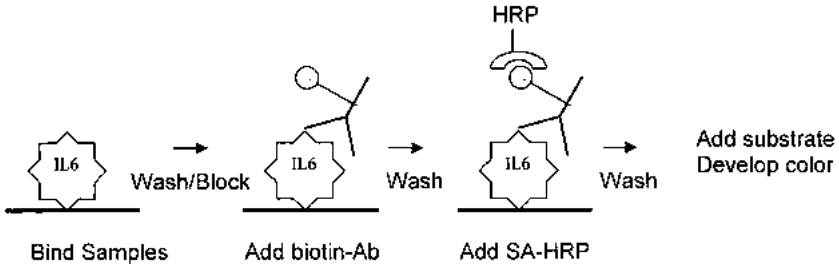

FIGURE 1 Direct ELISA. In the direct ELISA, the analyte is first bound to the bottom of the microtiter well. In this example, the analyte is IL-6. Unbound IL-6 is washed away, and excess protein binding sites are blocked in order to reduce background. In the next step, biotin-labeled antibody directed against IL-6 is added; the small circle represents the biotin moiety directly attached to the antibody. After washing, streptavidin (SA) conjugated to horseradish peroxidase (HRP) is added and a final wash is performed. Following addition of a colorimetric substrate, the color develops. The intensity of the color development is directly proportional to the amount of IL-6 in the first step.

For example, the first antibody may be a mouse monoclonal antibody which recognizes human IL-6. The second antibody may then be a goat anti-mouse antibody which has been labeled with horseradish peroxidase. An alternative method for detecting the primary antibody is to attach a biotin moiety to the antibody. Streptavidin conjugated to horseradish peroxidase is applied next, since the streptavidin will bind to the biotinylated antibody bound to IL-6. For all of these assays, the enzyme conjugated to the detection moiety produces the color. The process follows a fairly simple equation in which more antigen present results in more antibody binding, which results in greater concentrations of the enzyme, which results in stronger color development.

A slight modification is used for the sandwich ELISA. First, an antibody is bound to the surface of the microtiter well (Fig. 2). This antibody has specificity for the cytokine which will be detected, in this case IL-6. The sample is then applied to the well, and the IL-6 binds to the antibody. During washing, all the proteins which are not IL-6 should be washed away. The only entity remaining in the well should be the IL-6 bound to the antibody. Subsequent development steps are similar to those for the direct ELISA described above. Typically, the sandwich ELISA is more sensitive than the direct ELISA.

There are several critical elements in developing a sensitive and specific ELISA. These same critical elements apply to multiplexing assays, but again the concepts are more easily understood when a single cytokine is considered. First and foremost, the primary factor driving the sensitivity and specificity is the quality of the antibodies (13, 14). There is simply no substitute for having high-quality antibodies for the assay. As a specific example, antibodies are available which detect the precursor form of IL-1β but not the mature, processed form (15, 16). This may result in gross underestimation of the total amount of IL-1β present in cell lysates, because the antibodies selected for detection may not be appropriate. In many situations, the antibodies have already been matched for the development of a sandwich ELISA. With a few simple techniques, it is possible to buy these antibodies and establish ELISAs for the detection of cytokines (17). In this regard, the commercial vendors are excellent sources of good-quality reagents.

Another important aspect is the selection of the proper blocking reagent. Blocking reagents are added to the wells to prevent nonspecific binding. After the antigen (direct ELISA, Fig. 1) or the antibody (sandwich ELISA, Fig. 2) has been applied to the plate, it is important that nonspecific binding sites on the plate are blocked. Frequently, it is

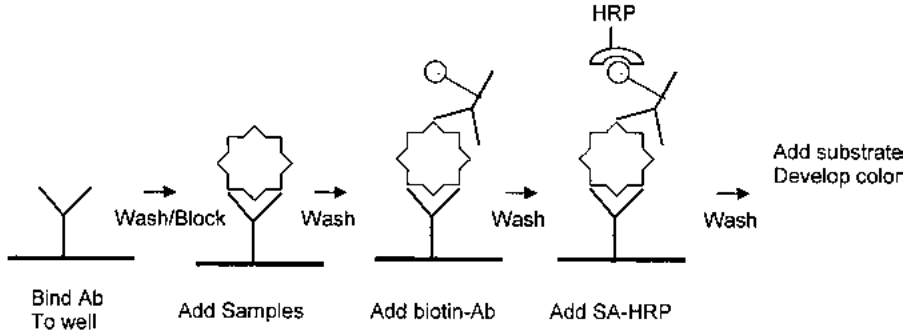

FIGURE 2 Indirect or sandwich ELISA. This ELISA shares many features with the assay described in the legend to Fig. 1. The major difference is in the first step, in which an antibody (Ab) directed against the analyte is bound to the bottom of the microtiter well. This antibody is termed the capture or coating antibody. Following addition of the analyte, the biotin-labeled detection antibody (biotin-Ab) is applied, followed by horseradish peroxidase (HRP)-conjugated streptavidin (SA-HRP). Color development proceeds, and the intensity of the color is directly related to the amount of the analyte. This is termed a sandwich ELISA because the analyte is sandwiched between two antibodies.

not possible to predict the optimal blocking reagent, and testing needs to be done in order to determine which reagent will work the best. The "matrix" of the sample may also affect the best blocking reagent. For example, in tissue culture supernatants, the protein content is extremely low compared to that in organ homogenates or plasma. A blocking reagent such as bovine serum albumin which works quite well for tissue culture supernatants may be suboptimal for measuring cytokines in human plasma. Testing different blocking reagents, which are available from the commercial vendors, will generally produce a low background.

Different enzymes may be conjugated to the detection moiety, whether it is an antibody or streptavidin. Horseradish peroxidase is the most commonly used enzyme, but alkaline phosphatase may also be used.

A number of substrates may be used in the assay; the substrate will depend upon the enzyme used for detection. The color development reagents are available from a number of commercial vendors, and they may be purchased already prepared. It is also possible to buy the individual reagents necessary for the substrate preparation and assemble one's own color detection components. This results in significant cost savings compared to purchasing already prepared material and usually results in similar sensitivity and specificity (17). Several authors have reported that the use of chemiluminescent reagents results in greater sensitivity (18–21). However, if careful attention to detail is used in the development of a colorimetric ELISA, better sensitivity than the chemiluminescent assay can be achieved, as well as significant cost savings (22).

Once the assay has been completed, it is necessary to calculate the results. Typically, the readout from an ELISA reader is the absorbance measured at a specific wavelength. If a fluorescent or chemiluminescent detection reagent has been used, then relative light units are the output. Regardless of the output, the actual concentrations of the cytokine in the sample are determined by comparison to a standard curve. There are several commercial software programs available which will perform these calculations. These programs may come bundled with the plate reader, or one may purchase separate, stand-alone software. Examples of data analysis are presented later in this chapter.

This has been a brief overview of the traditional ELISA, an assay that is run in hundreds of labs thousands of times every week. This assay is robust and relatively straightforward and has exquisite sensitivity and specificity. Given the tremendous utility of measuring a single cytokine, a natural extension is to measure multiple cytokines. Each of the steps in a traditional ELISA have been detailed (23).

SEQUENTIAL ELISA

The sequential ELISA is an easy method for measuring multiple cytokines in a single sample. In most biological samples, multiple cytokines are present simultaneously. The antibody directed against the cytokine which is present on the plate should react only with its specific cytokine. When the sample containing multiple cytokines is added to the microtiter well, only the cytokine recognized by the antibody will remain bound on the plate (Fig. 3). Therefore, when the sample is removed, all of the other cytokines will be taken away and will be available for detection by another ELISA. Thus, it is possible to measure the cytokines in sequence, which allows use of the sample to detect multiple cytokines. A basic description of this technique has been published previously (24). Others have also reported on the ability of sequential ELISAs to detect several cytokines simultaneously (25, 26).

The sequential ELISA still has several pitfalls. First, the sample volume necessary is still greater than that used in most multiplex assays. Second, the amount of time required to measure each one of the cytokines is not reduced in the sequential ELISA, so there is no cost savings with regards to time. Third, if there is potential cross-reactivity of the antibodies, then measurement of the first cytokine will result in an overestimate of the amount of that cytokine present, and measurement of the next cytokine in the sequence will result in an underestimate of the amount of that cytokine

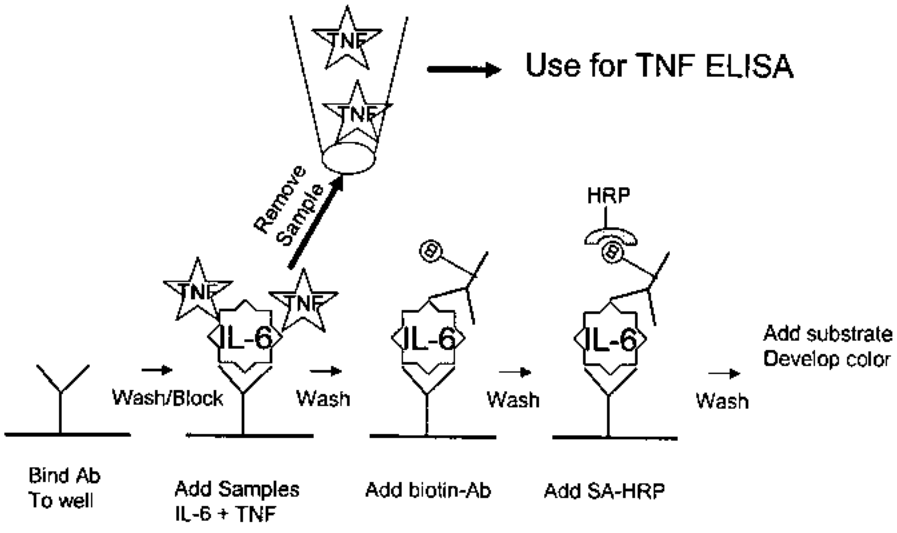

FIGURE 3 Sequential ELISA. A sample containing a mixture of cytokines is applied to an IL-6 ELISA. IL-6 binds to the anti-IL-6 antibody attached to the bottom of the well. When the sample is removed, cytokines which are not IL-6, such as tumor necrosis factor (TNF), may be used in a subsequent ELISA. Ab, antibody; B, biotin moiety; biotin-Ab, biotin-labeled antibody; HRP, horseradish peroxidase; SA-HRP, horseradish peroxidase-conjugated streptavidin.

present. Despite these caveats, the sequential ELISA is a method that is available to anyone presently running traditional ELISAs.

MICROARRAYS

Glass Slides

Glass slides have been used extensively for gene chip analysis. For traditional gene chips, portions of nucleic acid are spotted onto the slide. Each bit of nucleic acid codes for a specific gene (27), similar to what is described in the section on *in situ* hybridization. A similar format is used for the protein microarrays; however, instead of placing nucleic acid sequences onto slides and performing DNA hybridization, a compound which will interact with a specific protein is placed onto the slide. Typically, this means that an antibody directed against cytokines is placed on the individual slide.

The antibodies used for the protein microarrays are usually those which have already been demonstrated to be effectively employed in an ELISA format. These antibodies usually have been screened to determine that they have appropriate sensitivity. Additionally, when the antibodies are purchased from commercial vendors, they have frequently been tested against multiple different cytokines to ensure appropriate specificity. A careful examination of the antibody description supplied by the company will allow one to determine if cross-reactivity may represent a potential problem.

For protein microarrays, the capture antibody is placed onto the slide. The surface of the glass slide may be altered to enhance the binding of the antibody. Alternatively, a matrix may be applied to the surface to enhance the antibody binding. A number of different coatings are available for this purpose, although one of the simpler solutions is to affix nitrocellulose membranes to the surface of the slide. Nitrocellulose has a high protein binding affinity and will avidly capture the antibody (28). However, appropriate blocking reagents must be used in order to prevent a high background resulting from nonspecific binding of other proteins. Several different blocking reagents are available, but there is frequently a trade-off with these reagents. The trade-off arises because although one blocking reagent may be optimal for one antibody pair, a different blocking reagent is optimal for another antibody pair. In other words, the best blocking reagent for detecting tumor necrosis factor may be bovine

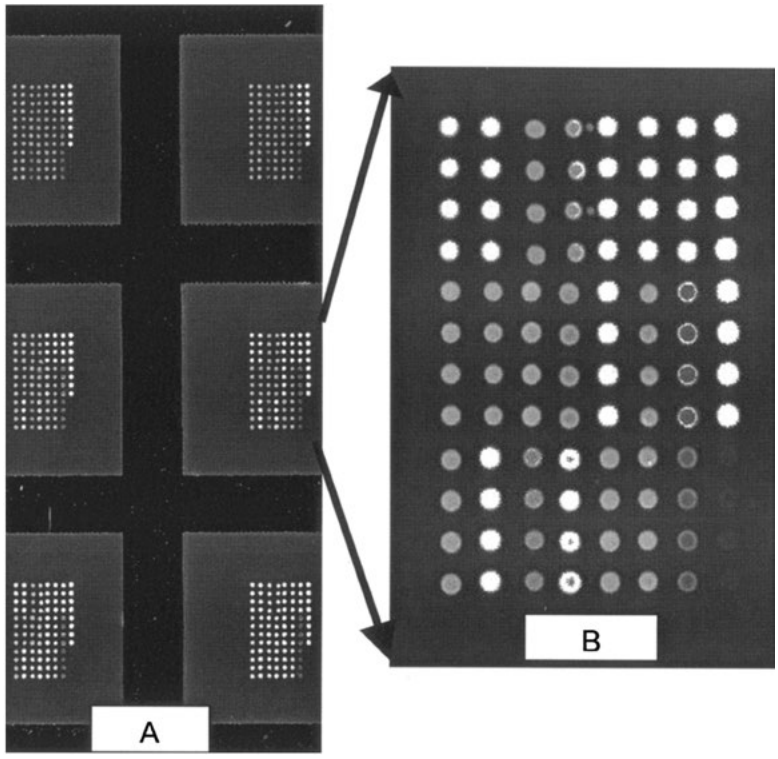

FIGURE 4 Example of a microarray. Panel A shows six individual nitrocellulose pads arranged on a glass slide. Each pad has been spotted in an 8-by-12 format. The black area between the pads is the place where a silicon gasket was adhered to the surface to allow each of the wells to function individually, similar to the way in which an individual well in a 96-well plate is independent from its neighbors. The antibodies have been spotted in an identical manner onto each of the nitrocellulose pads. Panel B is an enlarged picture of one of the individual pads and highlights the detail of the spots. The antibodies have been spotted in quadruplicate. Each individual spot has a diameter of 150 μm, and the distance between the spots is 300 μm. The total volume delivered to each spot was 350 to 367 pl. In the far right column of spots, those in the top eight positions are extremely bright and the lower four have virtually no signal. This line of eight plus four spots may be used for alignment of the image from the protein chip. The intensity of the individual spots may be quantified and used to determine the cytokine concentration in the sample. This image shows excellent reproducibility of the quadruple spots.

serum albumin, and the best blocking reagent for the antibodies detecting IL-6 may be casein. As in the traditional ELISA, a significant amount of trial and error is necessary in order to arrive at the appropriate combination of reagents.

Once the slide has been blocked, the detection antibodies are added. Because the assay is in a multiplex format, all of the detecting antibodies are added at once in a cocktail of cytokine detection antibodies. Usually these antibodies have a biotin moiety attached to them in order to improve the sensitivity of the signal. Each of the individual antibodies needs to be appropriately titered in order to achieve a strong signal with low background. It is also important to keep the antibodies at the correct concentrations in order to prevent cross-reactivity. If an antibody is present in too high a concentration, it is possible that there will be a loss of specificity.

Many of the slide microarray formats detect the antibodies through the use of fluorescent tags. These fluorescent reagents are directly attached to streptavidin, which binds to the biotin attached to the detection antibody. The slide is then read in a glass slide reader by using the same equipment used for the gene chip array work. Similar software is also employed in order to properly align the individual spots and quantitate the intensity of the signal. An example of a spotted microarray is shown in Fig. 4, which was directly obtained from the image obtained from a glass slide reader.

The fluorescent tags commonly used to determine the intensity of the spots are the cyanine (Cy) dyes. These dyes are extremely stable and emit with a bright intensity. Two principal dyes are used: Cy3, which has an emission maximum at 563 nm, and Cy5, which has an emission maximum at 662 nm. These dyes may be used together since the spectra essentially do not overlap.

When the cytokines are detected in the multiplex format, antibody specificity becomes an even more critical issue. Even slight cross-reactivity between individual antibodies may result in false-positive signals. Rigorous testing must be performed in order to document that the antibodies detect only that against which they are directed. This testing may be accomplished in the multiplex format by running the entire assay and detecting the presence of a cocktail of cytokines. In this cocktail of cytokines, one of the cytokines will be left out. In the multiplex assay which detects 18 different cytokines, 19 different cocktails will need to be prepared. One of these will have all of the cytokines present, and the fluorescence intensity for each individual cytokine will be determined. The remaining 18 cocktails will each have one of the cytokines intentionally left out. When these cocktails are run on the microarray, the intensity should be virtually nonexistent for the cytokines which are missing. Figure 5 represents an example of this type of study for examining cross-reactivity. In this example, the cocktail was prepared with 17 different cytokines, although the microarray was designed to detect 18 cytokines. The missing cytokine for this assay was IL-12. As can be observed, no signal was detected from any of the spots that were arrayed with the antibodies detecting IL-12. This demonstrates that this assay has the appropriate level of specificity. Similar results were obtained in the other studies in which the individual cytokines were deleted.

After the intensity of the individual spots has been quantified, data analysis becomes the next critical issue. In order to efficiently manage the information, the software needs to generate a mathematical model of the standard curve. The concentrations of the cytokines in the unknown samples are then calculated by referring back to the model of the standard curve.

Multiple mathematical models may be used to generate the appropriate fit for the standard curve. The same set of data may be analyzed by different iterations of the standard curve. For example, the data may be analyzed by plotting the number of relative light units (i.e., fluorescence intensity) versus the concentration of the cytokine. A simple linear expression may then be used to draw a straight line

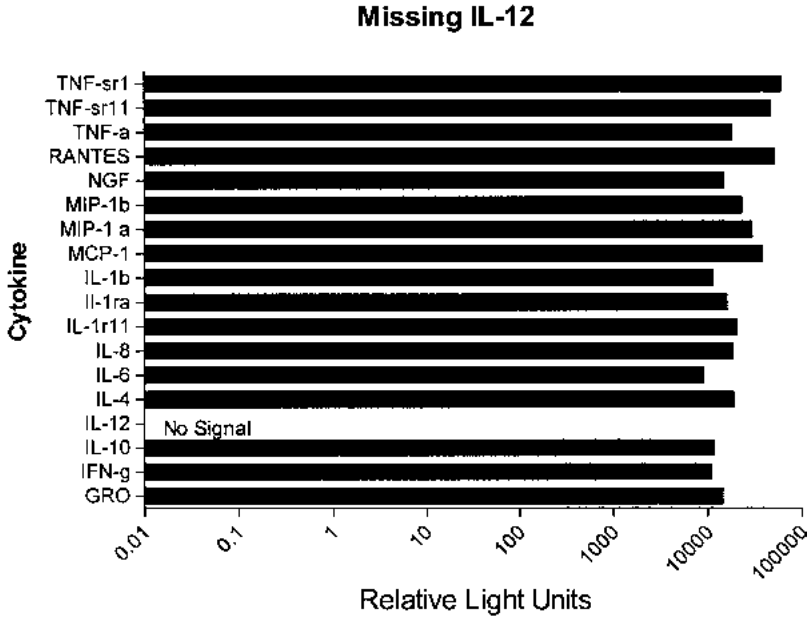

FIGURE 5 Specificity of the microarray. For this microarray, 18 different cytokines were tested. A cocktail containing recombinant cytokines was prepared, but IL-12 was not added to the cocktail. There is a strong signal from all the other cytokines, but no fluorescence was observed on the array for IL-12. This demonstrates the specificity for the array.

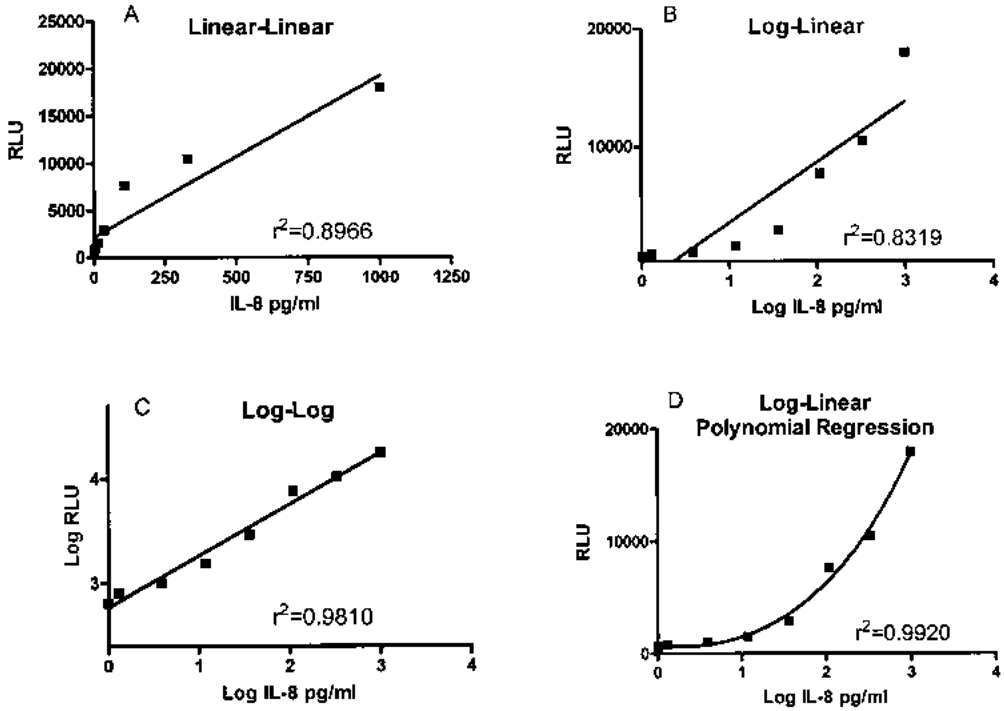

FIGURE 6 Mathematical modeling of the standard curve. Data from a microarray standard curve were used to generate a mathematical model for calculations for unknown samples. In panel A, the number of relative light units (RLU) and the concentration of the cytokine (IL-8) were plotted on a linear-linear scale. The correlation coefficient (r^2) was not very precise. In panel B, the concentration of the IL-8 was plotted on a log scale and the number of RLU was plotted on a linear scale. This resulted in even worse correlation. In panel C, both the number of RLU and the IL-8 concentration were plotted on a log scale and a very good linear regression could be fitted. However, the optimal modeling of the curve was obtained when the number of RLU was plotted on a linear scale, the IL-8 concentration was plotted on a log scale, and a fourth-order polynomial regression line was used. The results for all four panels were obtained using the same data from the IL-8 standard curve, but similar results are observed with most other cytokines.

through the points. Alternatively, the data may be graphed on a log-log scale, and again, a straight line may be fitted to the points. Software is available which automates and reduces the time necessary for data analysis (Fig. 6).

Examples of a standard curve prepared from the multiplex assay for the cytokine IL-8 are shown in Fig. 7. The exact same standard curve was subjected to different mathematical models to determine the one which would yield the optimum performance. As can be observed, plotting the information on a log-linear scale and using polynomial regression result in the highest correlation between the standard curve and the actual data.

Another level of data analysis is needed when substantial amounts of information are collected: analysis of the biological significance of the findings. In contrast to gene chip data, where only the relative abundances of different genes are determined, the actual levels of the cytokines have been measured. The levels may be important, because previous publications have indicated that the levels of some cytokines are associated with worse prognosis. For example, plasma IL-6 concentrations predict outcome in mouse models of infection (29, 30).

There are circumstances in which the standard curve is not appropriate due to a technical error, but where all of the samples have been run appropriately. It is possible to back calculate the concentrations of these samples using a different standard curve (31, 32). Using this approach, it is not necessary to rerun all of the samples, which may be important if there are limited volumes.

A modification of the slide-based microarray method has been developed which allows amplification of the signal (33). The same sandwich-type ELISA is used, but the detection antibody contains a small fragment of a DNA primer. A circular piece of DNA hybridizes to the primer conjugated to the antibody, and the circular piece of DNA is used for the amplification step. Amplification occurs when DNA polymerase is incubated with the sample in the presence of labeled nucleotides. As the DNA polymerase works on the circular piece of nucleic acid, an elongated string of labeled nucleic acid is generated. With this method, researchers were able to measure up to 75 cytokines. However, because of antibody cross-reactivity, it was necessary to separate the samples into two separate reaction mixtures. This helps to illustrate the point, raised previously, that the major limitation for many of these methods is specificity of the antibodies.

There is another variation that is used with the glass slides, a method that compares normal to abnormal samples but does not quantify the amount of protein present. For this type of assay, samples are obtained from healthy sources and also from those in altered states. Altered-state sources may be patients who have disease, or may be tissue or stimulated cells. All of the proteins from one sample are labeled with one color; for example, the normal samples may be

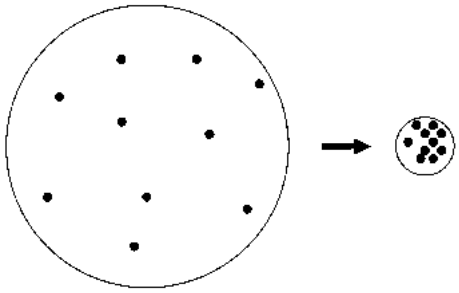

FIGURE 7 Increase in signal intensity with smaller spot size. On the left, each black dot represents the analyte bound to an antibody, which spreads across the entire well. On the right, the same number of antibodies are bound to the analyte, but they now occupy a smaller space, with a resulting increase in signal intensity.

labeled in green. All of the diseased or altered-state samples are labeled with a second color, such as red. The proteins from the normal and the diseased or altered-state samples are then mixed together. In this situation, there is a mixture of red and green molecules in the same tube.

As a specific example, one could take tissue culture supernatants from endotoxin-stimulated macrophages to represent the altered state and label these in red. Among these proteins would be IL-6. Tissue culture supernatant from unstimulated cells would represent the control state and in this situation would be labeled in green. Both of these protein samples would compete for binding to the antibodies which had been placed on the slide. In this example, there would be a large amount of IL-6 labeled red because the stimulated cells would secrete a large amount of IL-6. Normal, unstimulated cells would have very low concentrations of IL-6, and there would be virtually no IL-6 labeled green. When the samples were placed on the slide, the IL-6-specific antibodies would be occupied mostly by red IL-6. Looking at the ratio between the red and green proteins would reveal the relative increase or decrease in the disease or altered state. For this example, the results would predict that lipopolysaccharide upregulates IL-6. This approach has been used successfully in several experiments and has been used specifically to demonstrate that certain proteins become upregulated following radiation treatment (34). A pitfall to this technique is that the number of samples is typically limited to 16.

Special Equipment Required

Spotter. A high-quality spotter is required in order to prepare the microarrays. It is possible to obtain acceptable results using the same type of equipment used to prepare slides for gene chip studies. However, for spotting of proteins, noncontact printing generally results in better quality arrays. Commercial companies presently produce prespotted slides with the capture antibodies already spotted onto the slides. Custom arrays may also be prepared by commercial vendors.

Detection equipment. The glass slide may be read in a glass slide reader, or there are commercial services that will read the slides.

PLATE-BASED MICRO-ELISAS

None of the previously described techniques using traditional ELISA plates measure multiple cytokines at once. The breakthrough in technology comes about when several cytokines may be detected simultaneously from a small sample volume. The first report demonstrating the feasibility of this approach was published in 1999 (35). This publication documented the ability to detect up to eight different analytes simultaneously in a single well. The analytes that the researchers detected were immunoglobulins derived from different species, such as rabbit, guinea pig, and human. The detection was achieved by placing very small amounts of these immunoglobulins in the bottom of a 96-well glass-bottom plate. The amount of immunoglobulin that was placed on the bottom of a well was approximately 200 pl. This is in contrast to a typical ELISA, in which the bottom of the entire well is coated with a single antibody directed against a single cytokine, with a volume of approximately 100 µl. Therefore, the amount of antibody used for detection is 500,000 times smaller in the microarray assay than in the traditional ELISA. As will be discussed in greater detail below, the use of a smaller volume of antibody does not result in lower signal intensity.

An individual spot of the immunoglobulin was designated as an element, and six-by-six arrays of these elements were printed onto the bottom of each well. Four identical arrays could be printed, resulting in the deposition of up to 144 elements. Precise control of the locations of the individual elements is necessary so that the locations can be appropriately mapped to the later images.

Each one of the immunoglobulins affixed to the glass bottoms of the wells was then detected with the appropriate biotinylated secondary antibody. For this assay, alkaline phosphatase was used as the detection enzyme. This enzyme results in color development in the region of the spot. A charge-coupled device (CCD) camera was used to record the image. Typically, special modifications to the CCD camera are made, including the addition of specialized hardware and cooling to improve the optical image. Additionally, a black Teflon mask is usually applied around the individual wells to prevent scatter of the light from one well to the next.

Once the image has been captured, the intensity of the individual spot is mapped back to its precise location. Since each element detects a single cytokine, the intensity of an element is directly proportional to the concentration of the cytokine. Similar to the method in traditional ELISA, a standard curve is prepared with a separate set of wells. The intensity of the color, or the number of relative light units if fluorescence or chemiluminescence has been utilized, is compared back to the standard curve to determine the concentration of the analyte in question.

Although the technique described in this initial publication was used only to measure immunoglobulins, which are present in high concentrations and relatively easy to detect, the next innovation was the simultaneous measurement of multiple discrete molecules within the same well (35). This served as a launching point for the development of other assays.

Shortly after this report was published, another study used a 96-well plate to detect three separate molecules simultaneously (36). In this study, prostate-specific antigen, prostate-specific antigen bound to 1-antitrypsin, and IL-6 were measured at the same time. The report carefully compared the results of the protein microarray with the results obtained from a traditional ELISA. The results were surprisingly consistent, especially when one considers that the researchers included serum samples from patients. However, the sensitivity of the individual determinations was not exceptional.

Another report published in the same year from a commercial vendor showed that this technology could be used

to detect multiple human cytokines (37). In this study, the sensitivity was very close to that observed in a traditional ELISA. This initial study had three-by-three arrays of the monoclonal antibodies detecting seven different cytokines. More recent iterations of this technology have detected far more cytokines.

As one can imagine, when one is working with extremely small sample volumes the printing of the arrays is a critical issue. The deposition of the small sample volumes must be uniform, and the alignment must be extremely precise (38). There are several manufacturers of spotters used to accurately place the proteins. In many situations, spotters that have been used for the preparation of DNA microarrays may be successfully used for protein applications. These are typically contact type printers, where a quill tip is dipped into the protein solution and the solution is dotted onto the substrate. While these work quite well for nucleic acid microarrays, better results are typically obtained with noncontact printers. In one extremely novel and low-cost approach, a standard ink jet printer was used for depositing the antibodies (39).

The substrate onto which the antibodies are spotted is also important. Nucleic acids spot quite well onto glass slides, but antibodies are not optimally placed onto glass. The surface of the glass slide may be derivatized in order to improve binding of the antibodies (38). Alternatively, the antibodies may be spotted onto other substrates such as nitrocellulose that have a high protein-binding capacity. Other membranes are also suitable. For 96-well plates, traditional ELISA plates may be used since these have already been developed and tested for binding of antibodies. A potential disadvantage is that it may be difficult to spot onto the bottom of the 96-well plate.

Since only a small amount of antibody is spotted and the spot is extremely small, the immediate concern is that the signal intensity would be extremely weak. In fact, the signal intensity may be greater with the smaller amounts of antibody. In a traditional ELISA, the antibodies spread across the bottom of the entire plate. Once the analyte binds to the antibody, the signals also spread across the entire plate. In contrast, with the microarrays, the antibodies are usually at higher concentrations. This is shown schematically in Fig. 7. In this figure, each of the black dots represents an antibody to IL-6 that has been coupled with IL-6 and subsequently detected. If the same amount of one analyte (IL-6) is bound to the same number of antibodies but the antibodies are now more closely spaced, the resulting signal intensity will be higher.

Special Equipment Required

Spotting device. Accurately placing each of the individual spots into the well of the microtiter plate requires a high-quality spotting device. This device must be capable of accurately and reproducibly placing the capture antibody in a precise location. Additionally, because of the depth of the microtiter plate, the robotic arm doing the plating must have pipette tips able to clear the tops of the wells. This problem does not occur with the glass slide-based arrays, yet the number of samples that can be done on the plate versus the slide does make up for the extra time required during the spotting process. Noncontact printers provide the most uniform arrays when working with proteins. This is a rapidly changing market, and the investigator should carefully research the spotters available on the market before purchase.

Detection equipment. Microarray assays are run using a colorimetric reagent, and a CCD camera is used to record the image. This is a high-quality camera which is specially modified in order to reduce background and provide a greater range of sensitivity and specificity. Other methods have been used using near-infrared dyes coupled to the secondary antibodies and then scanned on a special scanner that can detect near-infrared.

MEMBRANE-BOUND ANTIBODY ARRAYS

A series of recent papers have been published which describe technology capable of detecting multiple cytokines in a relatively simple format (40–43). The authors have manually arrayed antibodies to several cytokines on a membrane. Simplicity of design represents an attractive feature of this methodology. In the initial study, several important steps were evaluated to arrive at the optimal conditions for the assay. Some of the parameters that were studied include the concentrations of antibodies and the best membranes for use.

For this type of assay, there are multiple antibodies directed against specific cytokines bound to a membrane. Each antibody is spotted onto the membrane in a different location, and the location is determined by the map. Diluted samples are placed onto the membrane, which is then incubated for 1 h. Following washing, a cocktail of detection antibodies is placed onto the membrane. After washing again, the detection reagent is added and the spots representing the individual cytokines are detected by chemiluminescence. X-ray film or a phosphorimager may be used to determine the intensity of the individual spots. These arrays may be used for screening in a semiquantitative manner or for actual quantification.

Advantages to this technology are that it is easily performed in virtually any laboratory. The incubation may be done in a simple six-well tissue culture dish, and the cytokines are arrayed on a membrane about the size of a postage stamp.

An important disadvantage to this technology is reduced sensitivity. Published results have shown that the sensitivity of the membranes is at least 2 logs lower than that of the traditional ELISA for several cytokines (44).

Special Equipment Required

X-ray film processor or phosphorimager. X-ray film may be used to capture the relative intensities of the individual spots, or this step may be done more quantitatively using the phosphorimager. Most institutions have an X-ray film processor available from molecular biology experiments in which older style Northern blots were developed, so it may not be accurate to consider this as special equipment.

CAPILLARY ELECTROPHORESIS

A recent paper has described a novel method for rapidly detecting cytokines. In a special apparatus, antibodies directed to specific analytes were placed in the injection ports, where they were permanently bound (45). The samples containing the cytokines were then added, and all the bound proteins were labeled with Alexa Fluor 633. Electrophoresis was performed by lowering the pH, which dissociated the labeled cytokine from the antibody. The retention time determined the cytokine, and the intensity of the label correlated with the concentration. The entire process was very rapid and

could be completed in just a few minutes. Additionally, the sample volume required for the assay was only a few microliters. By using this technology, six cytokines could be quantitated in less than 2 min. However, the chemistry of coupling the antibodies and performing the electrophoresis and detection presently are beyond the capabilities of most laboratories.

BEAD ARRAY ASSAYS

Bead array assays have become standard for cytokine measurement. They have become sufficiently routine that papers are now being written comparing multiplex bead assays to traditional ELISAs (46). The first papers hinting at the capabilities of using a flow cytometer to measure cytokines were published more than 20 years ago (47, 48). There are several commercial vendors marketing the bead array assays. The assays may generally be divided into two groups, and the differences between these two types of assays will be described in greater detail below. The bead array assays may be used to measure proteins such as cytokines and immunoglobulins. Additionally, they have been used extensively for the development of assays for examining polymorphisms in genetic material (49, 50). HLA typing has been revolutionized by the adaptation of this technology (51). Bead array assays for the measurement of cytokines are all based on the standard antibody-cytokine interactions already described. They are represented schematically in Fig. 8. The first and most important step in the bead array assay is finding a specific antibody that may be conjugated to the bead. The quality of the antibody drives the sensitivity and specificity of the assay, as with virtually all immunoassays. The steps are similar to the basic steps shown in Fig. 2 for a sandwich ELISA. As the first step, the capture antibody is conjugated to the bead. This bead mixture is then incubated with the samples containing the cytokines. After the cytokines are bound to the capture antibody, a biotinylated detection antibody is added, followed by streptavidin which is coupled to a fluorescent probe. The entire mixture is then run on a flow cytometer. Although this is a simple description of the overall assay, several features allow the assay to be performed rapidly and in a multiplexed manner.

The beads are an important part of the overall assay since they are the component that allows the samples to be run in a multiplexed manner (52). There are variations on the way the individual beads are detected. In the first version, a single fluorescent molecule is incorporated into the beads (53). The beads are distinguished by the various amounts of fluorescent probe inside the beads. Careful manufacturing allows the individual groups of beads to be distinguished from one another. For this example, the antibodies to IL-6 would be conjugated to bead set 1, and the antibodies to tumor necrosis factor would be conjugated to bead set 2. When these beads are mixed together, the fluorescence intensity of the fluorochrome inside each bead indicates whether one is analyzing tumor necrosis factor or IL-6. Multiple sets of beads may be distinguished with this method.

Another method for discriminating among the individual bead sets involves mixing two different fluorescent dyes in various mixtures. The individual groups of beads are then differentiated based on two-color analysis. The groups of beads may be clumped according to the relative intensities of the two separate fluorochromes. Similar to the method for the assay previously described, one group of beads is conjugated to antibodies to tumor necrosis factor, and a separate group of beads is conjugated to antibodies to IL-6. Up to 100 different discrete sets of beads may be differentiated on the basis of the various concentrations of the two fluorescent dyes. There are several commercial vendors who manufacture the beads conjugated to the antibodies. An example of an assay run using the Luminex platform is shown in Fig. 9.

We have described how the individual beads are grouped, but how does the quantification of the cytokines occur? Quantification takes place through measurement of the intensity of the fluorescent tag attached to streptavidin. As in the traditional ELISA, the intensity of the signal is directly related to the amount of detection antibody that is attached to the cytokine. A standard curve with several concentrations of cytokines is prepared and run in the assay. Figure 10 shows an example of the standard curve with mouse IL-1β. The steps that are involved with the precise measurement of the cytokine include, first, the detection of the groups of the beads. The intensity of the streptavidin fluorescent tag for each group of beads is then assayed and compared to the standard curve in order to determine the concentrations of the cytokines within the sample. In Fig. 9, there are 22 individual groups of beads that may be assayed, which indicates that there are 22 individual groups or individual cytokines that may be measured in this multiplexed assay.

There are several advantages to the bead array assays. First, it is possible to perform the assays without washing the beads, limiting many of the time-consuming and tedious steps in a traditional ELISA (52, 54). It is possible to do these assays without washing because the fluorescence intensity of only the molecules bound to the beads is measured, not the intensity of everything in the solution. In a traditional ELISA, the fluorescence intensity or color is measured in the well. Unless unbound antibodies are washed away, the background will be extremely high. In the bead array assay,

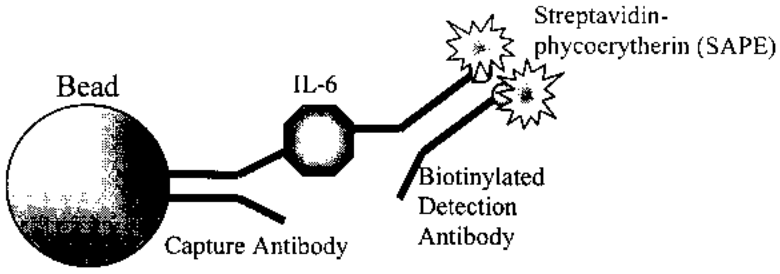

FIGURE 8 Schematic representation of the principle of a flow cytometric bead-based assay. The capture antibody specific for the analyte, in this example IL-6, is attached to a bead. The IL-6 binds to this antibody, which is then followed by a detection antibody which is biotinylated. Streptavidin conjugated to phycoerythrin is then added, and the entire complex is analyzed with the flow cytometer.

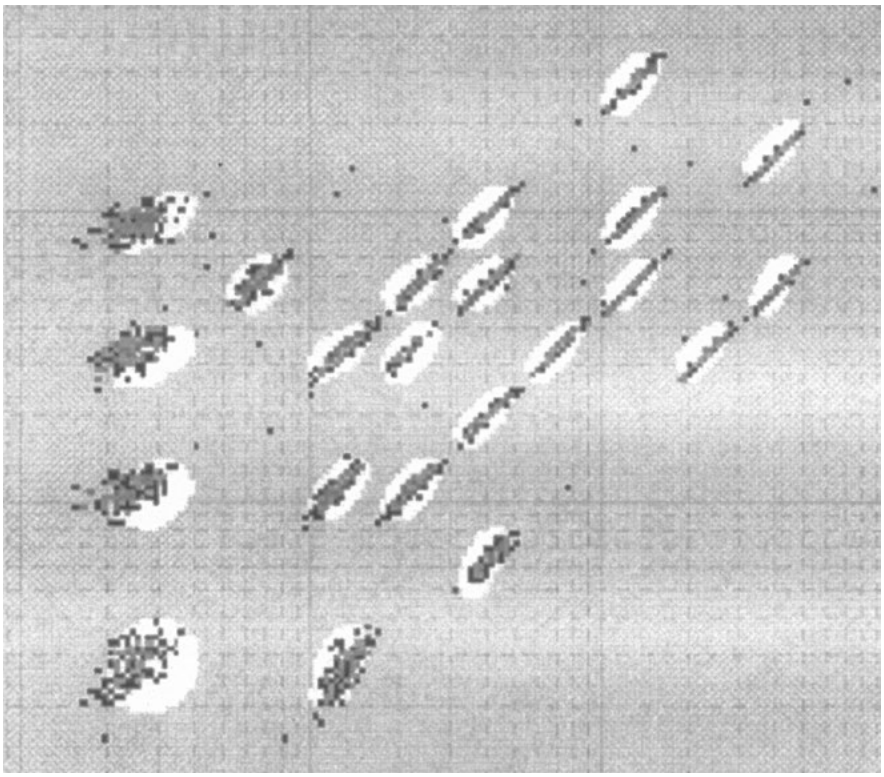

FIGURE 9 Example of the readout from a bead-based flow cytometry assay. In this example, the individual beads have different concentrations of two fluorescent dyes. The groups of beads are detected on the basis of the fluorescence intensities. The individual dots represent individual beads, and the darker-colored dots are doublets. The clear areas around collections of beads indicate those areas used for analysis. In this example, 22 individual cytokines have been detected. The intensity of the fluorescence of each individual bead is captured in a third fluorescent channel and compared to the standard curve in order to determine the concentration of the cytokine.

the flow cytometer will analyze the group of beads to determine the specific fluorescence intensity and not the overall fluorescence intensity.

A second significant advantage is that up to 100 discrete groups of beads may be analyzed; thus, up to 100 different cytokines may be measured in a multiplexed assay. The major limitation is obtaining an antibody with sufficient specificity in order to prevent cross-reactivity.

Many of the steps for the bead array assays may be automated, which is a third distinct advantage of this methodology. Automated sampling of each of the discrete wells used for an individual sample may be done, allowing walk-away ease of use. Finally, the volume of sample required to measure multiple cytokines is extremely small. This is an advantage of any of the multiplexed assays, which generally require smaller sample volumes than the traditional ELISA. Even use of the sequential ELISA requires a larger sample volume than that typically used in a bead array assay.

At the present time, there are at least 75 different identified cytokines that may be measured by using this platform. The cytokines include those of human, rat, and mouse. Additionally, this technology may be used for allergy testing, tissue typing, detection of cardiac markers and cancer markers, and diagnosis of infectious diseases. The bead array assays have been successfully used to measure cytokines in human plasma (55), though appropriate caution must be used when working with plasma or serum samples (56). Additionally, there may be false positives using human samples if rheumatoid factor is present (57).

Special Equipment Required

Preparation of Beads

While it is possible to conjugate the antibodies to the purchased beads, in reality this is technically difficult to do. Fortunately, there are several vendors in the marketplace at the present time. This is encouraging news for investigators, since it is not likely that all of the vendors would terminate manufacturing of beads at the same time. Inevitably as the market matures, there will be fewer vendors, but the strong should survive such that those companies with excellent technical assistance, range of reagents, and ease of use will continue to sell products. The fact that several companies are marketing their products for the bead array assays also indicates that business analysts have determined that there is a robust market available for their wares. Again, this increases enthusiasm among investigators since the technology is more likely to persist. Additionally, the technology has been used to detect more than just cytokines. As a result, the flow cytometry apparatus is more widely available since it can be used for multiple applications. Vendors are also beginning to produce kits that allow antibody conjugation to beads, so that investigators can make their own reagents; this can both reduce cost and allow for a very custom array.

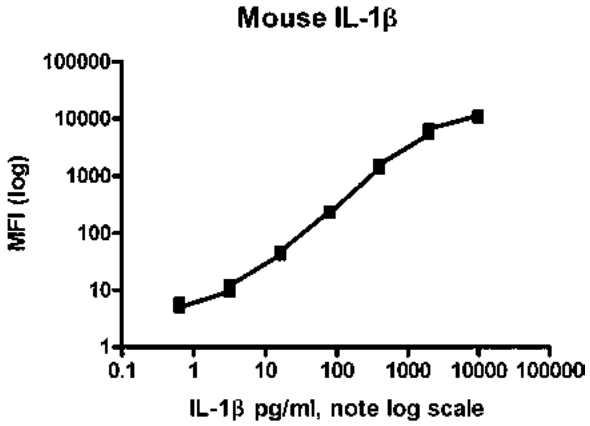

FIGURE 10 Example of a standard curve generated from the bead-based flow cytometry assay. In this example, a standard curve using recombinant mouse IL-1β is displayed. MFI, mean fluorescence intensity.

By working with the vendors, it is possible to have custom-prepared sets of beads. The companies are pleased to conjugate specific antibodies to the beads and then multiplex the reagents into kits for the customer. Provided that there is an appropriate antibody available, there is really no limitation on what is available.

Flow Cytometry

For some of the commercial kits, it is not necessary to have a special, dedicated instrument. Any standard flow cytometer may be used for measuring cytokines provided that the appropriate software has been employed. Since many institutions already have flow cytometers which have been used for routine cell work, there is no real additional expense for running the assays.

COST COMPARISON

A true comparison of different multiplexed formats requires a delineation of the costs involved. A cost comparison was made using a bead array assay compared to a conventional ELISA performed in the sequential format. For the ELISA, the cost remains essentially the same for each cytokine that is measured. However, in the bead array the cost decreases with the number of cytokines that are measured. This savings comes about as the cost of the kits decreases as the number of cytokines multiplexed increases. The cost analysis is carefully delineated in Table 1. The analysis was carefully constructed to include the time of a skilled technician as well as the cost of reagents. When the ELISA is performed, the major component of the cost is the salary of the person who actually performs the assay. The cost analysis was based on a single technician being able to process five plates of samples per day. Five plates of samples would amount to measuring approximately 200 samples for a single cytokine per day. The calculated cost of the beads was based on using only a single well of the 96-well plate for each sample. Many investigators would use two individual wells to measure a sample, and the cost would proportionally increase. As can be observed in Table 1, the total cost for measuring a single cytokine by ELISA is about $11, whereas the same sample run in a multiplexed assay would cost about $59. These cost estimates will vary depending on the ability to obtain competitive pricing from the antibody vendors.

TABLE 1 Cost analysis for cytokine measurements[a]

Parameter	Assay	
	ELISA	Bead array
No. of cytokines	1	17
Vol (μl)	50	50
Cost per sample (U.S. dollars)	1.95	59
Cost per cytokine (U.S. dollars)	1.95	1.87–3.31
Lower limit of detection	1–10	1–10
Range (logs)	3	3
Expandability	Not expandable	Expandable

[a]The cost of measuring cytokines by traditional ELISA, used in the sequential format, is directly compared to the cost of doing a bead array assay. Included in these costs are the necessary reagents, including buffers, antibodies, and kits purchased from the manufacturer. Also included is the time of a technician, assuming that the technician could test up to five full plates (about 200 samples) per day. The cost of this time is also included in cost analysis for the bead assays.

However, the cost decreases as the number of cytokines that are measured increases. This is delineated in Table 2, demonstrating that there is a sliding scale for the cost of measuring cytokines in a single sample. When approximately 17 cytokines are measured, it is less expensive to use the bead array assay than to perform multiple ELISAs. Again, it must be borne in mind that the cost of doing the ELISA principally involves the time of a technician, and that has been included in the cost calculation.

There is one significant cost which has not been included in these analyses, that of the capital equipment necessary to perform some of these assays. Specifically, these analyses did not include the cost of a plate reader or a flow cytometer. Typically, these large pieces of equipment are purchased through capital funds and may be considered a fixed cost for the assays. In other words, if one cytokine is measured there is still the cost of buying a flow cytometer, and this cost is the same if one runs 100,000 cytokines.

Issues concerning the sample volumes necessary to run the individual assays also become important. These are especially critical when dealing with rodents such as mice from which only a small volume of plasma may be obtained (58). Since only a single sample is required to run the multiplexed assay, the bead array assays or the spotted arrays consume significantly less sample volume than even a sequential ELISA. The amounts of sample necessary to run several different cytokines are listed in Table 3.

While this cost analysis was performed for measuring cytokines in a bead array assay, similar comments may be made regarding an alternative multiplexed format such as the spotted arrays on glass slides or spotted arrays in a 96-well plate. Additionally, analysis of issues such as the purchase

TABLE 2 Sliding-scale cost of measuring cytokines[a]

No. of cytokines	Cost (U.S. dollars) for:	
	ELISA	Bead array assay
4	7.80	13.25
6	11.70	19.28
14	27.30	27.95
17	33.15	31.79

[a]As the number of cytokines measured in a multiplexed assay increases, the cost decreases. The cost per cytokine per assay remains relatively fixed in the ELISA format, but as more antibodies are multiplexed to different sets of beads, the bead array assay decreases in cost. At about 17 cytokines, the bead array assay becomes more cost-effective than the ELISA.

TABLE 3 Sample volumes required for performing assays[a]

No. of cytokines	Vol (μl) needed for:	
	ELISA	Bead array
1	50	25
6	75	25
20	145	25

[a]As the number of cytokines measured increases, the sample volume necessary for the ELISA increases while that for the bead array assays remains static. The calculation of the sample volumes for the ELISA assumes that the assay is being performed in sequential manner.

of capital equipment and the amount of a technician's time necessary to perform the assays would probably give similar results. Specifically, as more cytokines are measured, the cost per cytokine would go down for the multiplexed assay and would remain the same, of course, for the sequential ELISA. Additionally, the sample volume would remain static for a spotted microarray.

MOLECULAR METHODS FOR MEASURING CYTOKINES

The standard molecular approach to measuring cytokines quantifies the amount of mRNA coding for the cytokine protein. There are many methods for measuring mRNA, including some which are primarily of historical interest such as Northern blots. In current practice, most cytokine mRNA is detected by either *in situ* hybridization or PCR.

In Situ Hybridization

In situ hybridization detects the cytokine mRNA typically on a tissue section fixed to a glass slide. The advantage of this method is that it allows one to determine exactly which cell is making the cytokine, which may be of biological relevance. For example, it may be important to know whether the endothelial cells or the epithelial cells are producing cytokine mRNA in the lung. For this methodology, a piece of labeled nucleic acid is incubated with a tissue section. The sequence of nucleotides in the nucleic acid should be specific for the mRNA that one wishes to detect. If one wants to determine whether mRNA for TNF is present, the nucleic acid sequence would be specific for the mRNA coding for TNF. Any cells that were expressing mRNA for TNF would show positive staining.

In situ hybridization is built on the basic concept that a defined sequence of nucleotides will hybridize or bind to complementary nucleic acid. This follows the typical tenets of molecular biology with base pairs joining to each other. The piece of nucleic acid is specifically designed using appropriate software so that it will only bind to mRNA coding for the cytokine in question. This piece of nucleic acid should only bind to TNF, and not to IL-6 or other cytokines. The nucleic acid sequence is labeled such that it may be detected after it is firmly bound or hybridized to the mRNA. The label may be either an enzyme, such as horseradish peroxidase, or biotin. If the nucleic acid is labeled with biotin, then streptavidin conjugated to horseradish peroxidase or another enzyme is used for detection. Substrates are added to the slide, and positive cells are typically stained brown if they contain the appropriate mRNA.

The sequence of nucleotides that will be used as detection probes may be either DNA or RNA. The most important element is that the nucleic acid has specificity for the mRNA. DNA:RNA binding interactions are usually stronger than RNA:RNA interactions, which allows more stringent washes to clear away any unbound nucleic acid probe.

PCR

PCR is the most commonly used method for the detection of cytokine mRNAs. This technology was developed based on the discovery of a DNA polymerase which remained active even after exposure to high temperatures (59). The Nobel Prize was awarded for the discovery of this enzyme, highlighting the contribution to science. There are several steps that need to be performed carefully and in the correct order to produce a positive result. The first step is the extraction of the mRNA from the sample. This sample may be cells isolated from blood, cells from a tissue culture flask, or a sample isolated from a paraffin block used to make glass slides. Extraction of the mRNA must be done carefully since this nucleic acid is highly labile and easily degraded. The second step is to create a DNA strand complementary to the mRNA, the cDNA. This is done using the enzyme reverse transcriptase, which will bind to double-stranded nucleic acid and create a reverse transcript. Two approaches may be used to create the cDNA. One approach is to generate cDNA for any mRNA present in the sample by using a poly(T) nucleic acid which will bind to any mRNA containing a poly(A) tail. The second approach is to use a small sequence of nucleic acid which binds specifically to the mRNA that will be amplified. Creating cDNAs from all the mRNA has the advantage of creating a pool of cDNAs that may then be amplified, if there is an interest in detecting several cytokines. Using a probe specific for the cytokine that will be detected increases the specificity of the reaction.

Once the cDNA has been created, PCR will substantially amplify the final product. To understand how this amplification occurs, one must know the steps involved. Two nucleic acid primers are created specific for the cytokine you wish to detect, called the forward and reverse primers. The PCR goes through a series of reactions or cycles. In the first cycle, the double-stranded nucleic acid is denatured into two separate single strands by raising the temperature. These single strands are then incubated with both primers, which will bind to their individual strands when the temperature is lowered. Once the primers have annealed, the DNA polymerase will adhere to the double-stranded DNA (created by the primer binding to the denatured DNA) and proceed to create a new piece of nucleic acid which is complementary to the original piece. The second cycle then starts again, by denaturing the newly created double-stranded DNA.

There are several considerations in this relatively simple sequence of events. First, the DNA polymerase must remain active when the temperature is raised to allow the DNA to denature. The discovery of the thermostable DNA polymerase was the significant achievement that allowed this to occur. Second, all of the necessary components are in a single tube so that raising and lowering the temperature is all that is required for the reaction cycles to take place. There is no need to open the tube to add additional reagents. Third, each cycle amplifies the products from the previous reaction. This allows a geometric increase in the number of amplified sequences ($1 \rightarrow 2 \rightarrow 4 \rightarrow 8 \rightarrow 16$, etc.), which provides unparalleled sensitivity. PCR has been used to detect virtually any nucleic acid, in addition to cytokines. For example, it may be used to detect cytokine mRNA (60) in addition to pathogens (61).

CONCLUSIONS

Multiplex assays for measuring cytokines are rapidly becoming standard across the world. A clear indicator of the enthusiasm for these assays may be found in the large number of companies which are presently producing and manufacturing multiplex cytokine kits. There are several platforms that are available for measuring the cytokines, and the market is not yet sufficiently mature to conclusively address which of these offers the best speed, sensitivity, and specificity, and the lowest cost. Molecular techniques are also used to detect cytokine mRNAs.

This work has been supported in part by NIH grants GM 97320 and T32 GM86308.

REFERENCES

1. **Remick DG, Friedland JS.** 1997. *Cytokines in Health and Disease*, 2nd ed. Marcel Dekker, Inc, New York, NY.
2. **Jin C, Flavell RA.** 2013. Innate sensors of pathogen and stress: linking inflammation to obesity. *J Allergy Clin Immunol* **132:**287–294.
3. **Chaouat G, Ledee-Bataille N, Dubanchet S, Zourbas S, Sandra O, Martal J.** 2004. TH1/TH2 paradigm in pregnancy: paradigm lost? Cytokines in pregnancy/early abortion: reexamining the TH1/TH2 paradigm. *Int Arch Allergy Immunol* **134:**93–119.
4. **Martinon F, Tschopp J.** 2004. Inflammatory caspases: linking an intracellular innate immune system to autoinflammatory diseases. *Cell* **117:**561–574.
5. **Mease PJ, Fleischmann R, Deodhar AA, Wollenhaupt J, Khraishi M, Kielar D, Woltering F, Stach C, Hoepken B, Arledge T, van der Heijde D.** 2014. Effect of certolizumab pegol on signs and symptoms in patients with psoriatic arthritis: 24-week results of a Phase 3 double-blind randomised placebo-controlled study (RAPID-PsA). *Ann Rheum Dis* **73:**48–55.
6. **Akalin H, Akdis AC, Mistik R, Helvaci S, Kilicturgay K.** 1994. Cerebrospinal fluid interleukin-1 beta/interleukin-1 receptor antagonist balance and tumor necrosis factor-alpha concentrations in tuberculous, viral and acute bacterial meningitis. *Scand J Infect Dis* **26:**667–674.
7. **Atwell DM, Grichnik KP, Newman MF, Reves JG, McBride WT.** 1998. Balance of proinflammatory and antiinflammatory cytokines at thoracic cancer operation. *Ann Thorac Surg* **66:**1145–1150.
8. **Khan SS, Smith MS, Reda D, Suffredini AF, McCoy JP Jr.** 2004. Multiplex bead array assays for detection of soluble cytokines: comparisons of sensitivity and quantitative values among kits from multiple manufacturers. *Cytometry B Clin Cytom* **61:**35–39.
9. **Kohler K, Seitz H.** 2012. Validation processes of protein biomarkers in serum—a cross platform comparison. *Sensors (Basel)* **12:**12710–12728.
10. **Brody EN, Willis MC, Smith JD, Jayasena S, Zichi D, Gold L.** 1999. The use of aptamers in large arrays for molecular diagnostics. *Mol Diagn* **4:**381–388.
11. **Zhu H, Snyder M.** 2003. Protein chip technology. *Curr Opin Chem Biol* **7:**55–63.
12. **Yalow RS, Berson SA.** 1959. Assay of plasma insulin in human subjects by immunological methods. *Nature* **184**(Suppl 21)**:**1648–1649.
13. **Nielsen UB, Geierstanger BH.** 2004. Multiplexed sandwich assays in microarray format. *J Immunol Methods* **290:**107–120.
14. **Vignali DA.** 2000. Multiplexed particle-based flow cytometric assays. *J Immunol Methods* **243:**243–255.
15. **Herzyk DJ, Berger AE, Allen JN, Wewers MD.** 1992. Sandwich ELISA formats designed to detect 17 kDa IL-1 beta significantly underestimate 35 kDa IL-1 beta. *J Immunol Methods* **148:**243–254.
16. **Herzyk DJ, Wewers MD.** 1993. ELISA detection of IL-1 beta in human sera needs independent confirmation. False positives in hospitalized patients. *Am Rev Respir Dis* **147:**139–142.
17. **Nemzek JA, Siddiqui J, Remick DG.** 2001. Development and optimization of cytokine ELISAs using commercial antibody pairs. *J Immunol Methods* **255:**149–157.
18. **Lewkowich IP, Campbell JD, HayGlass KT.** 2001. Comparison of chemiluminescent assays and colorimetric ELISAs for quantification of murine IL-12, human IL-4 and murine IL-4: chemiluminescent substrates provide markedly enhanced sensitivity. *J Immunol Methods* **247:**111–118.
19. **Obenauer-Kutner LJ, Jacobs SJ, Kolz K, Tobias LM, Bordens RW.** 1997. A highly sensitive electrochemiluminescence immunoassay for interferon alfa-2b in human serum. *J Immunol Methods* **206:**25–33.
20. **Petrovas C, Daskas SM, Lianidou ES.** 1999. Determination of tumor necrosis factor-alpha (TNF-alpha) in serum by a highly sensitive enzyme amplified lanthanide luminescence immunoassay. *Clin Biochem* **32:**241–247.
21. **Rongen HA, van der Horst HM, van Oosterhout AJ, Bult A, van Bennekom WP.** 1996. Application of xanthine oxidase-catalyzed luminol chemiluminescence in a mouse interleukin-5 immunoassay. *J Immunol Methods* **197:**161–169.
22. **Siddiqui J, Remick DG.** 2003. Improved sensitivity of colorimetric compared to chemiluminescence ELISAs for cytokine assays. *J Immunoassay Immunochem* **24:**273–283.
23. **Chiswick EL, Duffy E, Japp B, Remick D.** 2012. Detection and quantification of cytokines and other biomarkers. *Methods Mol Biol* **844:**15–30.
24. **O'Connor KA, Holguin A, Hansen MK, Maier SF, Watkins LR.** 2004. A method for measuring multiple cytokines from small samples. *Brain Behav Immun* **18:**274–280.
25. **Osuchowski MF, Remick DG.** 2006. The repetitive use of samples to measure multiple cytokines: the sequential ELISA. *Methods* **38:**304–311.
26. **Osuchowski MF, Siddiqui J, Copeland S, Remick DG.** 2005. Sequential ELISA to profile multiple cytokines from small volumes. *J Immunol Methods* **302:**172–181.
27. **Olson JA Jr.** 2004. Application of microarray profiling to clinical trials in cancer. *Surgery* **136:**519–523.
28. **Tonkinson JL, Stillman BA.** 2002. Nitrocellulose: a tried and true polymer finds utility as a post-genomic substrate. *Front Biosci* **7:**c1–c12.
29. **Remick DG, Bolgos GR, Siddiqui J, Shin J, Nemzek JA.** 2002. Six at six: interleukin-6 measured 6 h after the initiation of sepsis predicts mortality over 3 days. *Shock* **17:**463–467.
30. **Turnbull IR, Javadi P, Buchman TG, Hotchkiss RS, Karl IE, Coopersmith CM.** 2004. Antibiotics improve survival in sepsis independent of injury severity but do not change mortality in mice with markedly elevated interleukin 6 levels. *Shock* **21:**121–125.
31. **Natarajan S, Remick DG.** 2008. The ELISA Standard Save: calculation of sample concentrations in assays with a failed standard curve. *J Immunol Methods* **336:**242–245.
32. **Natarajan S, Remick DG.** 2013. ELISA rescue protocol: recovery of sample concentrations from an assay with an unsuccessful standard curve. *Methods* **61:**69–72.
33. **Schweitzer B, Roberts S, Grimwade B, Shao W, Wang M, Fu Q, Shu Q, Laroche I, Zhou T, Tchernev VT, Christiansen J, Valleca M, Kingsmore SF.** 2002. Multiplexed protein profiling on microarrays by rolling-circle amplification. *Nature Biotechnol* **20:**359–365.
34. **Sreekumar A, Nyati MK, Varambally S, Barrette TR, Ghosh D, Lawrence TS, Chinnaiyan AM.** 2001. Profiling

of cancer cells using protein microarrays: discovery of novel radiation-regulated proteins. *Cancer Res* **61:**7585–7593.
35. **Mendoza LG, McQuary P, Mongan A, Gangadharan R, Brignac S, Eggers M.** 1999. High-throughput microarray-based enzyme-linked immunosorbent assay (ELISA). *Biotechniques* **27:**778–780, 782–776, 788.
36. **Wiese R, Belosludtsev Y, Powdrill T, Thompson P, Hogan M.** 2001. Simultaneous multianalyte ELISA performed on a microarray platform. *Clin Chem* **47:**1451–1457.
37. **Moody MD, Van Arsdell SW, Murphy KP, Orencole SF, Burns C.** 2001. Array-based ELISAs for high-throughput analysis of human cytokines. *Biotechniques* **31:**186–190, 192–184.
38. **Huang RP.** 2003. Protein arrays, an excellent tool in biomedical research. *Front Biosci* **8:**d559–d576.
39. **Roda A, Guardigli M, Russo C, Pasini P, Baraldini M.** 2000. Protein microdeposition using a conventional ink-jet printer. *Biotechniques* **28:**492–496.
40. **Huang RP.** 2001. Detection of multiple proteins in an antibody-based protein microarray system. *J Immunol Methods* **255:**1–13.
41. **Huang RP.** 2001. Simultaneous detection of multiple proteins with an array-based enzyme-linked immunosorbent assay (ELISA) and enhanced chemiluminescence (ECL). *Clin Chem Lab Med* **39:**209–214.
42. **Huang RP, Huang R, Fan Y, Lin Y.** 2001. Simultaneous detection of multiple cytokines from conditioned media and patient's sera by an antibody-based protein array system. *Anal Biochem* **294:**55–62.
43. **Lin Y, Huang R, Santanam N, Liu YG, Parthasarathy S, Huang RP.** 2002. Profiling of human cytokines in healthy individuals with vitamin E supplementation by antibody array. *Cancer Lett* **187:**17–24.
44. **Copeland S, Siddiqui J, Remick D.** 2004. Direct comparison of traditional ELISAs and membrane protein arrays for detection and quantification of human cytokines. *J Immunol Methods* **284:**99–106.
45. **Phillips TM.** 2004. Rapid analysis of inflammatory cytokines in cerebrospinal fluid using chip-based immunoaffinity electrophoresis. *Electrophoresis* **25:**1652–1659.
46. **Dossus L, Becker S, Achaintre D, Kaaks R, Rinaldi S.** 2009. Validity of multiplex-based assays for cytokine measurements in serum and plasma from "non-diseased" subjects: comparison with ELISA. *J Immunol Methods* **350:**125–132.
47. **Frengen J, Schmid R, Kierulf B, Nustad K, Paus E, Berge A, Lindmo T.** 1993. Homogeneous immunofluorometric assays of alpha-fetoprotein with macroporous, monosized particles and flow cytometry. *Clin Chem* **39:**2174–2181.
48. **McHugh TM.** 1994. Flow microsphere immunoassay for the quantitative and simultaneous detection of multiple soluble analytes. *Methods Cell Biol* **42:**575–595.
49. **Iannone MA, Taylor JD, Chen J, Li MS, Rivers P, Slentz-Kesler KA, Weiner MP.** 2000. Multiplexed single nucleotide polymorphism genotyping by oligonucleotide ligation and flow cytometry. *Cytometry* **39:**131–140.
50. **Iannone MA, Taylor JD, Chen J, Li MS, Ye F, Weiner MP.** 2003. Microsphere-based single nucleotide polymorphism genotyping. *Methods Mol Biol* **226:**123–134.
51. **Pei R, Lee J, Chen T, Rojo S, Terasaki PI.** 1999. Flow cytometric detection of HLA antibodies using a spectrum of microbeads. *Hum Immunol* **60:**1293–1302.
52. **Kellar KL, Douglass JP.** 2003. Multiplexed microsphere-based flow cytometric immunoassays for human cytokines. *J Immunol Methods* **279:**277–285.
53. **Morgan E, Varro R, Sepulveda H, Ember JA, Apgar J, Wilson J, Lowe L, Chen R, Shivraj L, Agadir A, Campos R, Ernst D, Gaur A.** 2004. Cytometric bead array: a multiplexed assay platform with applications in various areas of biology. *Clin Immunol* **110:**252–266.
54. **Swartzman EE, Miraglia SJ, Mellentin-Michelotti J, Evangelista L, Yuan PM.** 1999. A homogeneous and multiplexed immunoassay for high-throughput screening using fluorometric microvolume assay technology. *Anal Biochem* **271:**143–151.
55. **Prabhakar U, Eirikis E, Davis HM.** 2002. Simultaneous quantification of proinflammatory cytokines in human plasma using the LabMAP assay. *J Immunol Methods* **260:**207–218.
56. **Prabhakar U, Eirikis E, Reddy M, Silvestro E, Spitz S, Pendley C II, Davis HM, Miller BE.** 2004. Validation and comparative analysis of a multiplexed assay for the simultaneous quantitative measurement of Th1/Th2 cytokines in human serum and human peripheral blood mononuclear cell culture supernatants. *J Immunol Methods* **291:**27–38.
57. **Churchman SM, Geiler J, Parmar R, Horner EA, Church LD, Emery P, Buch MH, McDermott MF, Ponchel F.** 2012. Multiplexing immunoassays for cytokine detection in the serum of patients with rheumatoid arthritis: lack of sensitivity and interference by rheumatoid factor. *Clin Exp Rheumatol* **30:**534–542.
58. **Weixelbaumer KM, Raeven P, Redl H, van Griensven M, Bahrami S, Osuchowski MF.** 2010. Repetitive low-volume blood sampling method as a feasible monitoring tool in a mouse model of sepsis. *Shock* **34:**420–426.
59. **Saiki RK, Gelfand DH, Stoffel S, Scharf SJ, Higuchi R, Horn GT, Mullis KB, Erlich HA.** 1988. Primer-directed enzymatic amplification of DNA with a thermostable DNA polymerase. *Science* **239:**487–491.
60. **Chen Y, Dong L, Weng D, Liu F, Song L, Li C, Tang W, Chen J.** 2013. 1,3-β-glucan affects the balance of Th1/Th2 cytokines by promoting secretion of anti-inflammatory cytokines in vitro. *Mol Med Rep* **8:**708–712.
61. **Pusterla N, Madigan JE, Leutenegger CM.** 2006. Real-time polymerase chain reaction: a novel molecular diagnostic tool for equine infectious diseases. *J Vet Intern Med* **20:**3–12.

Cytokine Measurement by Flow Cytometry

HOLDEN T. MAECKER

36

In the years since intracellular cytokine staining (ICS) was first developed (1), this method has become a standard way to analyze the functions of immune cells by flow cytometry. It has been used with specific antigen stimulation (2, 3) to read out T cell populations responsive to vaccines (4–6), pathogens (7, 8), cancer (9–11), or allergens (12), in both human and animal models. The technique has been combined with MHC-peptide multimer staining (11, 13), including combinatorial tetramer staining that allows the interrogation of many epitope specificities at once (14, 15). Combined assays with tetramers can be done by first staining with tetramer(s), then stimulating with a nonspecific agent such as PMA+ionomycin, which bypasses the tetramer-occupied T cell receptors. ICS has also increasingly been used with detection of CD154 (16, 17) or CD107a (18) induction, as markers of activation and degranulation, respectively. When used with cell surface and other intracellular phenotyping markers, such multiparameter ICS assays are a tool of choice for functional characterization of T cells and other cytokine-producing cell populations. ICS has also successfully been converted to the mass cytometry platform (19) allowing the use of many more simultaneous markers without significant spillover between readouts.

Alternatives for assessing cytokines at the cellular level include enzyme-linked immunospot (ELISPOT) (20) and cytokine capture technology (21). While ELISPOT assays provide a relatively low-cost and high-throughput method for quantitating cytokine-producing cells, they do not offer the additional dimensions of cellular phenotyping possible with flow cytometry. They have been adapted in recent years to the detection of multiple cytokines, most effectively done with a fluorescence readout (so-called fluorospot assays [22, 23]). Conversely, the cytokine capture assay allows for multiparameter flow cytometry analysis and even sorting of live cells (21). It has not been widely used, however, beyond the experimental situations in which live cell sorting for downstream assays is employed. A comparison of the various types of antigen-specific T cell assays and their features is shown in Table 1.

SPECIMEN TYPES

In order to assess the population of antigen- or mitogen-responsive cells by ICS or cytokine capture assays, short-term *in vitro* stimulation is used. This can be done either in whole blood (3) or isolated peripheral blood mononuclear cells (PBMC) (2) or other sources of mononuclear cells. Addition of exogenous antigen-presenting cells (APC) is not required, though purified autologous APC such as dendritic cells can be used when stimulating APC-depleted or deficient cell samples. For whole blood, heparin is the preferred anticoagulant, as EDTA or acid citrate dextrose (ACD) will block the cytokine stimulation pathways. For PBMC, the anticoagulant is not critical, as the cells are washed free of it prior to stimulation.

STIMULATION VESSELS

Either tubes or multiwell plates can be used for stimulation (24). At least 200 μl of whole blood is advised for detection of antigen-specific responses, or at least 5×10^5 PBMC, per sample. Up to 2×10^6 cells can be accommodated in a 96-well plate, for typical stimulation periods of 6 to 8 h. Round- or V-bottom plates are preferred, both for promoting cell-cell contact and for best performance when pelleting and washing the cells poststimulation.

RESTING PRIOR TO STIMULATION

Particularly with cryopreserved and thawed PBMC, resting of the cells at 37°C prior to stimulation is helpful, increasing both the number of responsive cells and the cytokine staining intensity per cell (24). Resting for at least 2 h, and up to 24 h, is advised.

COSTIMULATION

With the use of whole-protein antigens, stimulation in the presence of costimulatory antibodies, such as anti-CD28 and anti-CD49d, has been shown to increase the frequency of responsive T cells (25). This effect is less dramatic when using peptide stimulation, particularly optimal-length peptides (e.g., 9-amino-acid residues for CD8+ T cell responses) at saturating concentrations (around 1 μg/ml). Costimulatory antibodies can also increase the background of cytokine-producing cells in the unstimulated condition (for some donors), so their use should be carefully considered and tested in the system of interest.

doi:10.1128/9781555818722.ch36

TABLE 1 Comparison of antigen-specific T cell assay features

Cell recovery	Cytokine readout only	Cytokines + phenotypes	
		Without epitope specificity	With multiple epitope specificities
No live cell recovery	ELISPOT	ICS (protein or peptide pool stimulation)	ICS with tetramers (PMA+ionomycin stimulation)
Live cell recovery		Cytokine capture assay (protein or peptide pool stimulation)	Cytokine capture assay with tetramers (PMA+ionomycin stimulation)

STIMULATION ANTIGENS

Either peptides or protein antigens can be used for stimulation, and most assays rely on endogenous host antigen-presenting cells (APC). There is no need to preload a population of autologous APC unless one wishes to study such a system. While intact proteins can be processed and the resulting major histocompatibility complex (MHC) class II-restricted peptides can be presented to CD4+ T cells, exogenous proteins are inefficiently presented via MHC class I for stimulation of CD8+ T cells (26). Therefore, a common strategy has been to use mixtures of overlapping peptides, spanning a protein sequence, to stimulate both CD4+ and CD8+ T cell responses (27). The use of 15-amino-acid peptides with 11-amino-acid overlap has been most popular and provides a reasonable balance of cost and efficiency for both CD4+ and CD8+ T cell stimulation (27, 28). While mixtures of several hundred peptides can be used in this fashion, there is some evidence for gradual reduction of responses when using more than 100 peptides per mix (29).

SECRETION INHIBITORS

For ICS, the *in vitro* stimulation must be accompanied by addition of a secretion inhibitor, usually brefeldin A or monensin. The choice of optimal secretion inhibitor(s) depends on the readouts of interest. Most proinflammatory cytokines are best retained intracellularly using brefeldin A (30, 31), while monensin is best for detection of IL-10 and TGFβ (our unpublished data). Monensin is also useful for the detection of CD107 (18) and CD154 (17), because it prevents the acidification of internalized vesicles that recycle these molecules. In these assays, the CD107 and/or CD154 antibody conjugate(s) are usually added during the stimulation, so that even target proteins that are transiently expressed can be stained and the fluorochrome is not degraded upon internalization. Monensin and brefeldin A can be combined (e.g., 5 μg/ml each) for applications where both proinflammatory cytokines and CD107/CD154 are targeted.

STIMULATION KINETICS

The optimal time course of *in vitro* stimulation will depend upon the stimulating antigen(s) and the targeted cytokines and/or activation markers. When antigen processing is required, a 2-h incubation prior to addition of secretion inhibitors is helpful; when using peptides or mitogens that do not require antigen processing, the secretion inhibitor can be added simultaneously with the stimulus. Six- to 8-h stimulation is sufficient for detecting most cytokines (32), although interleukin-10 (IL-10) production does not peak until 12 to 24 h. Additional incubation time, with secretion inhibitor present, is not detrimental until it becomes toxic to the cells; a maximum of 12 h in 10 μg/ml of brefeldin A is advised (32). For CD107 and CD154 detection, incubation times of not more than 5 to 6 h are optimal (17, 33).

These kinetics obviously place some constraints on the readouts that can be feasibly combined without loss of signal. For example, combining IL-10 detection with CD107 or CD154 would be unadvised, since their kinetics are so different. However, combination of CD107/CD154 with proinflammatory cytokines is easily accomplished, using a 6-h stimulation time in a combination of brefeldin A and monensin (5 μg/ml each). Similarly, combination of proinflammatory cytokine and IL-10 detection is possible using a stimulation time of around 12 h, with brefeldin A and monensin present for most if not all of this time.

If needed, stimulations can be automated using a programmable heat block, incubator, or water bath. The device is set for the desired incubation period at 37°C, followed by cooling and holding of samples at 4 to 18°C until further processing. Temperatures of 15 to 18°C are preferred for whole blood to avoid excessive platelet activation; 4°C is fine for PBMC (our unpublished data). Ideally, a CO_2 incubator should be used, but we have also obtained good results using *N*-2-hydroxyethylpiperazine-*N*′-2-ethanesulfonic acid (HEPES)-buffered media in a non-CO_2-enriched environment.

CELL PROCESSING

Important variables in the processing of stimulated cells include the choice of fixation and permeabilization buffers, centrifugation speeds, and choice of staining antibodies and conditions.

Commercial systems for fixation and permeabilization are available and are usually based on formaldehyde-based fixation and permeabilization with either saponin or other detergents. Of note, saponin-based permeabilization is reversible, so the detergent needs to be maintained during the intracellular staining steps and washes. There are some trends towards better performance of certain systems with certain cytokines, e.g., a saponin-based system such as Cytofix/Cytoperm (BD Biosciences, San Diego, CA) is superior for detection of IL-10 and transforming growth factor-beta (TGF-β) (34). However, for most cytokines and other targets, the differences are small. An exception is staining for transcription factors, such as FoxP3, for which specialized (harsher) permeabilization systems should be used. In these cases, it is safest to use the permeabilization system of the vendor producing the transcription factor antibody.

Initial centrifugation of live cells should be done at relatively low speed (250 to 300 × *g*) to preserve cell integrity.

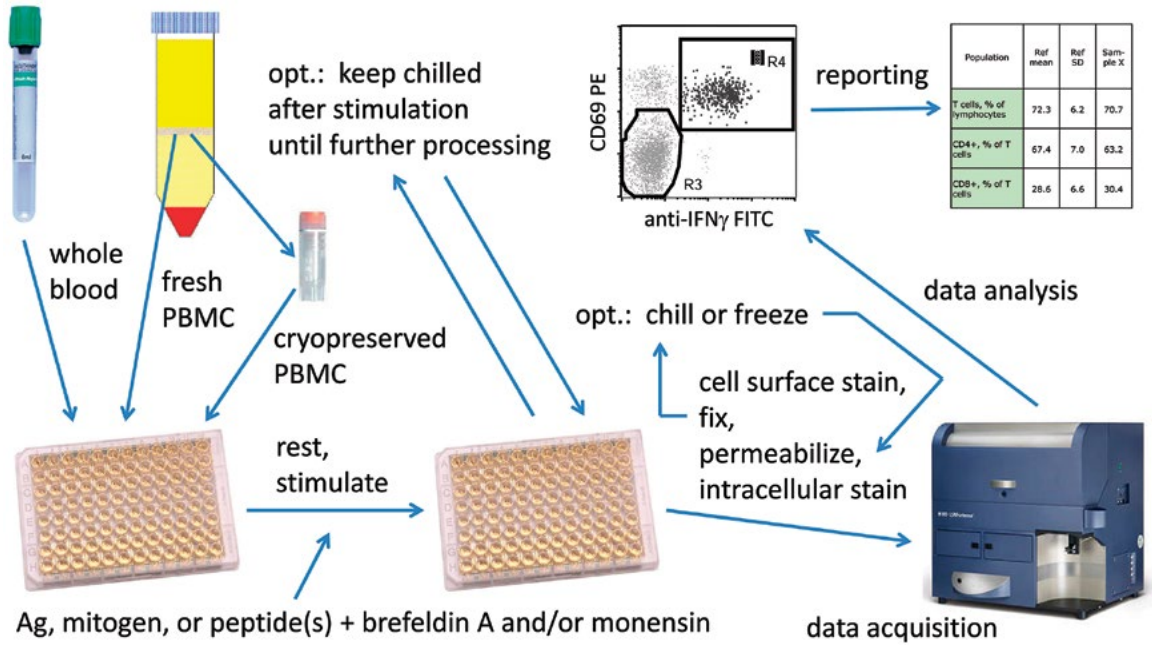

FIGURE 1 Workflow of ICS assays. Steps in the ICS assay, with variations and optional stopping points as shown.

However, fixed cells are much more buoyant, and centrifugation should be harder (at least 500 × *g*) to avoid loss of cells during washing. When using multiwell plates, a fixed-length vacuum manifold is helpful for aspiration of supernatants after washing, for both speed and consistency of residual volumes. Efficient washing, particularly after the intracellular staining step, is critical to reduce nonspecific staining.

Considerations for multicolor antibody panels have been published (35, 36) and will not be repeated here. Suggestions for 8- to 10-color panels combining intracellular cytokines and T-cell markers are also available (29, 34). One specific consideration is the staining of CD3, CD4, and/or CD8 before or after fixation/permeabilization. These antigens are specifically internalized during stimulation with antigen or T cell mitogens. Thus, while antibodies will have generally higher binding to live versus fixed epitopes, the ability to stain already internalized antigen may improve the ability to detect activated T cells in ICS assays, particularly with strong stimuli, such as phorbol-myristate-acetate (PMA)+ionomycin, or high concentrations of optimal-length peptides (27).

DATA ANALYSIS

Recently, a proficiency panel was conducted to test the reproducibility of gating intracellular cytokine data across laboratories (37). The results showed that differential gating strategies were rampant and greatly affected the results. Previous studies have also highlighted the importance of standardized gating to achieve reproducible results with ICS (38, 39). An important variable is the inclusion of cells that are dim in CD3, CD4, and CD8, since these are often activated cells (see previous paragraph). Also important is the relative placement of the cytokine-positive gate, to minimize background in unstimulated samples while maximizing the detection of rare positive events. Placement of the lymphocyte gate, inclusion/exclusion of CD4+CD8+ T cell populations, gate uniformity, and adjustment of biexponential scaling are also important (37).

In order to draw conclusions about whether ICS results are significantly above background, it is important to collect enough events. Statistical significance of results can be determined using a power calculation (see reference 40), which takes into account the number of relevant cells (e.g., CD4+ or CD8+ T cells) in both the unstimulated and test samples, as well as the proportion of positive events in each. As a practical benchmark, one can distinguish a response of 0.1% from an unstimulated background of 0.03%, with 99% power and $P < 0.005$, by collecting a minimum of 45,000 relevant (CD4+ or CD8+) cells.

It is helpful for large studies to apply batch analysis routines, which can be combined with automated cluster finding if desired. Such options are available within traditional flow cytometry software packages, as well as through R packages such as Bioconductor (http://www.bioconductor.org) and new algorithms such as those tested in the FlowCAP workshops (41). It is important to stress, however, that close manual oversight of these processes is still important, to avoid spurious results.

DETAILED PROTOCOLS AND ADDITIONAL INFORMATION

A detailed ICS protocol, which also discusses many of the above technical variables, has been published relatively recently (34). Concise general protocols for activation and cell surface and intracellular staining, with notes on key variables, are also available on the Web (http://maeckerlab.typepad.com/maeckerlab_weblog/maeckerlab_protocols_and_tools). Figure 1 shows the general workflow of ICS assays, with potential variables and stopping points that can be employed. Finally, information on validation of ICS assays has also been published (29, 42).

This work was supported in part by grants 5U19AI05722909 and 5U19AI09001904 from the NIAID, NIH.

REFERENCES

1. **Prussin C, Metcalfe DD.** 1995. Detection of intracytoplasmic cytokine using flow cytometry and directly conjugated anti-cytokine antibodies. *J Immunol Methods* **188:**117–128.
2. **Picker LJ, Singh MK, Zdraveski Z, Treer JR, Waldrop SL, Bergstresser PR, Maino VC.** 1995. Direct demonstration of cytokine synthesis heterogeneity among human memory/effector T cells by flow cytometry. *Blood* **86:**1408–1419.
3. **Suni MA, Picker LJ, Maino VC.** 1998. Detection of antigen-specific T cell cytokine expression in whole blood by flow cytometry. *J Immunol Methods* **212:**89–98.
4. **Horton H, Havenar-Daughton C, Lee D, Moore E, Cao J, McNevin J, Andrus T, Zhu H, Rubin A, Zhu T, Celum C, McElrath MJ.** 2006. Induction of human immunodeficiency virus type 1 (HIV-1)-specific T-cell responses in HIV vaccine trial participants who subsequently acquire HIV-1 infection. *J Virol* **80:**9779–9788.
5. **De Rosa SC, Lu FX, Yu J, Perfetto SP, Falloon J, Moser S, Evans TG, Koup R, Miller CJ, Roederer M.** 2004. Vaccination in humans generates broad T cell cytokine responses. *J Immunol* **173:**5372–5380.
6. **Bos R, van Duikeren S, van Hall T, Lauwen MM, Parrington M, Berinstein NL, McNeil B, Melief CJ, Verbeek JS, van der Burg SH, Offringa R.** 2007. Characterization of antigen-specific immune responses induced by canarypox virus vaccines. *J Immunol* **179:**6115–6122.
7. **Streitz M, Fuhrmann S, Thomas D, Cheek E, Nomura L, Maecker H, Martus P, Aghaeepour N, Brinkman RR, Volk HD, Kern F.** 2012. The phenotypic distribution and functional profile of tuberculin-specific CD4 T-cells characterizes different stages of TB infection. *Cytometry B Clin Cytom* **82B:**360–368.
8. **Betts MR, Price DA, Brenchley JM, Loré K, Guenaga FJ, Smed-Sorensen A, Ambrozak DR, Migueles SA, Connors M, Roederer M, Douek DC, Koup RA.** 2004. The functional profile of primary human antiviral CD8+ T cell effector activity is dictated by cognate peptide concentration. *J Immunol* **172:**6407–6417.
9. **Inokuma M, dela Rosa C, Schmitt C, Haaland P, Siebert J, Petry D, Tang M, Suni MA, Ghanekar SA, Gladding D, Dunne JF, Maino VC, Disis ML, Maecker HT.** 2007. Functional T cell responses to tumor antigens in breast cancer patients have a distinct phenotype and cytokine signature. *J Immunol* **179:**2627–2633.
10. **Maecker HT, Auffermann-Gretzinger S, Nomura LE, Liso A, Czerwinski DK, Levy R.** 2001. Detection of CD4 T-cell responses to a tumor vaccine by cytokine flow cytometry. *Clin Cancer Res* **7**(3 Suppl)**:**902s–908s.
11. **Lee PP, Yee C, Savage PA, Fong L, Brockstedt D, Weber JS, Johnson D, Swetter S, Thompson J, Greenberg PD, Roederer M, Davis MM.** 1999. Characterization of circulating T cells specific for tumor-associated antigens in melanoma patients. *Nat Med* **5:**677–685.
12. **DeLong JH, Simpson KH, Wambre E, James EA, Robinson D, Kwok WW.** 2011. Ara h 1-reactive T cells in individuals with peanut allergy. *J Allergy Clin Immunol* **127:**1211–1213.
13. **He XS, Rehermann B, Boisvert J, Mumm J, Maecker HT, Roederer M, Wright TL, Maino VC, Davis MM, Greenberg HB.** 2001. Direct functional analysis of epitope-specific CD8+ T cells in peripheral blood. *Viral Immunol* **14:**59–69.
14. **Newell EW, Klein LO, Yu W, Davis MM.** 2009. Simultaneous detection of many T-cell specificities using combinatorial tetramer staining. *Nature Methods* **6:**497–499.
15. **Newell EW, Sigal N, Nair N, Kidd BA, Greenberg HB, Davis MM.** 2013. Combinatorial tetramer staining and mass cytometry analysis facilitate T-cell epitope mapping and characterization. *Nature Biotechnol* **31:**623–629.
16. **Frentsch M, Arbach O, Kirchhoff D, Moewes B, Worm M, Rothe M, Scheffold A, Thiel A.** 2005. Direct access to CD4+ T cells specific for defined antigens according to CD154 expression. *Nat Med* **11:**1118–1124.
17. **Chattopadhyay PK, Yu J, Roederer M.** 2005. A live-cell assay to detect antigen-specific CD4+ T cells with diverse cytokine profiles. *Nat Med* **11:**1113–1117.
18. **Betts MR, Brenchley JM, Price DA, De Rosa SC, Douek DC, Roederer M, Koup RA.** 2003. Sensitive and viable identification of antigen-specific CD8+ T cells by a flow cytometric assay for degranulation. *J Immunol Methods* **281:**65–78.
19. **Newell EW, Sigal N, Bendall SC, Nolan GP, Davis MM.** 2012. Cytometry by time-of-flight shows combinatorial cytokine expression and virus-specific cell niches within a continuum of CD8+ T cell phenotypes. *Immunity* **36:**142–152.
20. **Czerkinsky C, Andersson G, Ekre HP, Nilsson LA, Klareskog L, Ouchterlony O.** 1988. Reverse ELISPOT assay for clonal analysis of cytokine production. I. Enumeration of gamma-interferon-secreting cells. *J Immunol Methods* **110:**29–36.
21. **Brosterhus H, Brings S, Leyendeckers H, Manz RA, Miltenyi S, Radbruch A, Assenmacher M, Schmitz J.** 1999. Enrichment and detection of live antigen-specific CD4(+) and CD8(+) T cells based on cytokine secretion. *Eur J Immunol* **29:**4053–4059.
22. **Gazagne A, Claret E, Wijdenes J, Yssel H, Bousquet F, Levy E, Vielh P, Scotte F, Goupil TL, Fridman WH, Tartour E.** 2003. A Fluorospot assay to detect single T lymphocytes simultaneously producing multiple cytokines. *J Immunol Methods* **283:**91–98.
23. **Ahlborg N, Axelsson B.** 2012. Dual- and triple-color fluorospot. *Methods Mol Biol* **792:**77–85.
24. **Suni MA, Dunn HS, Orr PL, Laat R de, Sinclair E, Ghanekar SA, Bredt BM, Dunne JF, Maino VC, Maecker HT.** 2003. Performance of plate-based cytokine flow cytometry with automated data analysis. *BMC Immunol* **4:**9.
25. **Waldrop SL, Davis KA, Maino VC, Picker LJ.** 1998. Normal human CD4+ memory T cells display broad heterogeneity in their activation threshold for cytokine synthesis. *J Immunol* **161:**5284–5295.
26. **Maecker HT, Ghanekar SA, Suni MA, He XS, Picker LJ, Maino VC.** 2001. Factors affecting the efficiency of CD8+ T cell cross-priming with exogenous antigens. *J Immunol* **166:**7268–7275.
27. **Maecker HT, Dunn HS, Suni MA, Khatamzas E, Pitcher CJ, Bunde T, Persaud N, Trigona W, Fu TM, Sinclair E, Bredt BM, McCune JM, Maino VC, Kern F, Picker LJ.** 2001. Use of overlapping peptide mixtures as antigens for cytokine flow cytometry. *J Immunol Methods* **255:**27–40.
28. **Draenert R, Altfeld M, Brander C, Basgoz N, Corcoran C, Wurcel AG, Stone DR, Kalams SA, Trocha A, Addo MM, Goulder PJ, Walker BD.** 2003. Comparison of overlapping peptide sets for detection of antiviral CD8 and CD4 T cell responses. *J Immunol Methods* **275:**19–29.
29. **Horton H, Thomas EP, Stucky JA, Frank I, Moodie Z, Huang Y, Chiu YL, McElrath MJ, De Rosa SC.** 2007. Optimization and validation of an 8-color intracellular cytokine staining (ICS) assay to quantify antigen-specific T cells induced by vaccination. *J Immunol Methods* **323:**39–54.
30. **Nylander S, Kalies I.** 1999. Brefeldin A, but not monensin, completely blocks CD69 expression on mouse lymphocytes: efficacy of inhibitors of protein secretion in protocols for intracellular cytokine staining by flow cytometry. *J Immunol Methods* **224:**69–76.

31. **Bueno C, Almeida J, Alguero MC, Sánchez ML, Vaquero JM, Laso FJ, San Miguel JF, Escribano L, Orfao A.** 2001. Flow cytometric analysis of cytokine production by normal human peripheral blood dendritic cells and monocytes: comparative analysis of different stimuli, secretion-blocking agents and incubation periods. *Cytometry* **46:**33–40.
32. **Nomura LE, Walker JM, Maecker HT.** 2000. Optimization of whole blood antigen-specific cytokine assays for CD4(+) T cells. *Cytometry* **40:**60–68.
33. **Betts MR, Koup RA.** 2004. Detection of T-cell degranulation: CD107a and b. *Methods Cell Biol* **75:**497–512.
34. **Lovelace P, Maecker HT.** 2010. Multiparameter intracellular cytokine staining, p 165–178. *In* Hawley TS, Hawley RG (ed), *Flow Cytometry Protocols*. Humana Press, Totowa, NJ.
35. **Maecker HT.** 2009. Multiparameter flow cytometry monitoring of T cell responses. *Methods Mol Biol* **485:**375–391.
36. **Maecker HT, Frey T, Nomura LE, Trotter J.** 2004. Selecting fluorochrome conjugates for maximum sensitivity. *Cytometry* **62A:**169–173.
37. **McNeil LK, Price L, Britten CM, Jaimes M, Maecker H, Odunsi K, Matsuzaki J, Staats JS, Thorpe J, Yuan J, Janetzki S.** 2013. A harmonized approach to intracellular cytokine staining gating: results from an international multiconsortia proficiency panel conducted by the Cancer Immunotherapy Consortium (CIC/CRI). *Cytometry* A **83:**728–738.
38. **Maecker HT, Rinfret A, D'Souza P, Darden J, Roig E, Landry C, Hayes P, Birungi J, Anzala O, Garcia M, Harari A, Frank I, Baydo R, Baker M, Holbrook J, Ottinger J, Lamoreaux L, Epling CL, Sinclair E, Suni MA, Punt K, Calarota S, El-Bahi S, Alter G, Maila H, Kuta E, Cox J, Gray C, Altfeld M, Nougarede N, Boyer J, Tussey L, Tobery T, Bredt B, Roederer M, Koup R, Maino VC, Weinhold K, Pantaleo G, Gilmour J, Horton H, Sekaly RP.** 2005. Standardization of cytokine flow cytometry assays. *BMC Immunol* **6:**13.
39. **Jaimes MC, Maecker HT, Yan M, Maino VC, Hanley MB, Greer A, Darden JM, D'Souza MP.** 2010. Quality assurance of intracellular cytokine staining assays: analysis of multiple rounds of proficiency testing. *J Immunol Methods* **363:**143–157.
40. **Maecker HT.** 2005. The role of immune monitoring in evaluating cancer immunotherapy, p 59–72. *In* Disis ML (ed), *Cancer Drug Discovery and Development: Immunotherapy of Cancer*. Humana Press, Totowa, NJ.
41. **Aghaeepour N, Finak G, FlowCAP Consortium, DREAM Consortium, Hoos H, Mosmann TR, Brinkman R, Gottardo R, Scheuermann RH.** 2013. Critical assessment of automated flow cytometry data analysis techniques. *Nat Methods* **10:**228–238.
42. **Maecker HT, Hassler J, Payne JK, Summers A, Comatas K, Ghanayem M, Morse MA, Clay TM, Lyerly HK, Bhatia S, Ghanekar SA, Maino VC, Delarosa C, Disis ML.** 2008. Precision and linearity targets for validation of an IFNgamma ELISPOT, cytokine flow cytometry, and tetramer assay using CMV peptides. *BMC Immunol* **9:**9. doi:10.1186/1471-2172-9-9

Chemokine and Chemokine Receptor Analysis

SABINA A. ISLAM, BENJAMIN D. MEDOFF, AND ANDREW D. LUSTER

37

The active movement of leukocytes towards a site of antigen challenge, infection, or tissue damage represents a central aspect of the establishment of both inflammatory and immune responses (1–4). The movement of cells towards a chemical gradient of a particular stimulus or chemotactic factor is called chemotaxis. Chemotactic factors that induce the directional movement of leukocytes include the chemokines, a super family of proteins 8 to 10 kDa in size that signal chemotaxis through seven transmembrane G protein-coupled cell surface receptors (GPCRs) (1, 2). In this chapter, the methodological approaches to studying the role of chemokines and chemokine receptors in the physiology of immune and inflammatory responses are described. Although assays of chemokines or chemokine receptors have yet to be used for widespread clinical applications, this chapter briefly reviews the role of these proteins in the pathophysiology of several inflammatory diseases and illustrates potential clinical settings in which measuring these proteins or studying their functional activity may be of useful.

CHEMOKINE AND CHEMOKINE RECEPTORS: BASIC PRINCIPLES

Chemokines

Comprehensive analyses of the human and mouse genomes have identified more than 50 chemokines that share 20 to 70% homology in amino acid sequence identity (1, 2) (Table 1). Chemokines share the common function of attracting leukocytes to sites of an inflammatory or immune response. A standardized nomenclature in which chemokines were given numerical names, like the interleukins and the chemokine receptors, was proposed more than a decade ago and is now widely used (2). In this nomenclature, CC chemokines are named CCL*n*, for CC chemokine ligand since they have two adjacent cysteines near the N terminus, where *n* is the number that corresponds to the gene symbol number given to each chemokine when they were called SCY "n" for small secreted cytokine, followed by a number. Likewise, the CXC chemokines are named CXCL*n*, for CXC chemokine ligands, since the two N-terminal cysteines are separated by one amino acid represented in this name with an "X."

As mentioned, chemokine families are defined on the basis of the spacing of the first two cysteine amino acids in the mature protein. Based on this, four families of chemokines exist. In α or CXC chemokines, the cysteine residues are separated by a single amino acid. A further subdivision of CXC chemokines relates to the presence or absence of the sequence glutamic acid-lysine-arginine (ELR) near the N terminus of the protein. In general, ELR CXC chemokines chemoattract neutrophils, whereas non-ELR-containing CXC chemokines attract lymphocytes. In β or CC chemokines, the cysteine residues are adjacent to each other. The first and third cysteine are missing in the (X) C family of chemokines, which includes the chemokine XCL1. CX3CL1 is a single member of the CXXXC chemokine family, with three intervening amino acids between the proximal two cysteine residues. CX3CL1 and CXCL16 are also unique in that they exist in both soluble and membrane-anchored forms; the membrane-anchored form is expressed as a cell surface glycoprotein, with the "chemokine domain" sitting on top of a mucin-like stalk, and has both transmembrane and cytoplasmic domains.

Chemokine Receptors

All chemokines signal via seven transmembrane-spanning GPCRs (1), which are named by a numbering system based on the type of chemokine to which they bind (CC, CXC, CX3C, C) (Tables 1 and 2). GPCRs are a highly versatile group of proteins that have evolved to sense subtle changes in concentration gradients and are involved in signal transduction for vision, olfaction, hormone reception, and neurotransmission in addition to directional cell movement (1). As signal transducers of chemotaxis, the GPCRs appear to be highly conserved in evolution, being present on amoebae and slime molds, and are involved in the signaling of chemotaxis in these simple eukaryotes.

GPCRs consist of an extracellular N terminus, an intracellular C terminus, and seven transmembrane-spanning regions (1). Chemokine binding to the extracellular portion of the receptor results in intracytoplasmic signaling, which is mediated in part through heterotrimeric G proteins of the $G\alpha_i$ subclass. Chemokines may present to chemokine receptors in both the liquid and solid phases (5). Chemokine receptor binding occurs between both the chemokine in solution and the chemokine bound to matrix and cell surface glycosaminoglycans (1). The binding of chemokine to receptor results in a complex signaling cascade that may result in directed cell movement, cell activation, differentiation, and/or cell proliferation (1–4). The activation of chemokine

doi:10.1128/9781555818722.ch37

TABLE 1 Chemokines

Chemokine	Other names	Receptor	Key/main immune function
CXCL1	GROα, MGSA, mouse KC	CXCR2	
CXCL2	GROβ, MIP-2α, mouse MIP2	CXCR2	Neutrophil trafficking
CXCL3	GROγ, MIP-2β	CXCR2	
CXCL4	PF4	?	Procoagulant
CXCL5	ENA-78, mouse LIX	CXCR2	
CXCL6	GCP-2	CXCR1, CXCR2	Neutrophil trafficking
CXCL7	NAP-2	CXCR2	
CXCL8	IL-8 (no mouse)	CXCR1, CXCR2	
CXCL9	Mig	CXCR3	
CXCL10	IP-10	CXCR3	Th1 response; Th1, CD8, NK trafficking
CXCL11	I-TAC	CXCR3	
CXCL12	SDF-1	CXCR4	Bone marrow homing
CXCL13	BLC, BCA-1	CXCR5	B-cell and Tfh positioning LN
CXCL14	BRAK	?	Macrophage skin homing (human)
CXCL15	Lungkine (mouse only)	?	?
CXCL16		CXCR6	NKT and iLC migration and survival
CCL1	I-309, mouse TCA3	CCR8	Th2 cell and Treg trafficking
CCL2	MCP-1, mouse JE	CCR2	Inflammatory monocyte trafficking
CCL3	MIP-1α	CCR1, CCR5	Macrophage and NK cell migration; T-cell–DC interactions
CCL4	MIP-1β	CCR5	
CCL5	RANTES	CCR1, CCR3, CCR5	
CCL6	C-10, MRP-1 (mouse only)	Unknown	?
CCL7	MCP-3, mouse Fic or MARC	CCR2, CCR3	Monocyte mobilization
CCL8	MCP-2	CCR1, CCR2, CCR3, CCR5 (human); CCR8 (mouse)	Th2 response; skin-homing mouse
CCL9/10	MIP-1γ, MRP-2 (mouse only)	Unknown	?
CCL11	Eotaxin-1	CCR3	Eosinophil and basophil migration
CCL12	MCP-5 (mouse only)	CCR2	Inflammatory monocyte trafficking
CCL13	MCP-4	CCR2, CCR3, CCR5	Th2 responses
CCL14	HCC-1	CCR1	?
CCL15	Leukotactin-1, HCC-2, MIP-5	CCR1, CCR3	?
CCL16	HCC-4, NCC-4, LEC	CCR1, CCR2, CCR5	?
CCL17	TARC	CCR4	Th2 responses, Th2 cell migration, Treg, lung and skin homing
CCL18	PARC, DC-CK1	CCR8	Th2 response; marker AAM, skin homing
CCL19	ELC, MIP-3β	CCR7	T-cell and DC homing to LN
CCL20	MIP-3α, LARC	CCR6	Th17 responses; B and DC homing to gut-associated lymphoid tissue
CCL21	SLC, 6CKine	CCR6, CCR7	T-cell and DC homing to LN
CCL22	MDC	CCR4	Th2 response, Th2 cell migration, Treg migration
CCL23	MPIF-1, MIP-3	Unknown	?
CCL24	Eotaxin-2, MPIF-2	CCR3	Eosinophil and basophil migration
CCL25	TECK	CCR9	T-cell homing to gut; thymocyte migration
CCL26	Eotaxin-3	CCR3, CX3CR1	Eosinophil and basophil migration
CCL27	CTAK	CCR10	T-cell homing to skin
CCL28	MEC	CCR3, CCR10	T-cell and IgA plasma cell homing to mucosa
XCL1	Lymphotactin, SCM-1α	XCR1	Cross-presentation by CD8+ DCs
XCL2	SCM-1β	XCR1	
CX3CL1	Fractalkine	CX3CR1	NK, monocyte, and T-cell migration

TABLE 2 Chemokine receptors[a]

Receptor	Immune cell expression	Key immune function
G protein-coupled receptors		
CXCR1	N > Mo, NK, MC, Ba, CD8 T_{EFF}	Neutrophil trafficking
CXCR2	N > Mo, NK, MC, Ba, CD8 T	B-cell lymphopoiesis Neutrophil egress from bone marrow Neutrophil trafficking
CXCR3	Th1, CD8 T_{CM} and T_{EM}, NK, NKT, pDC, B, Treg, T_{FH}	Th1-type adaptive immunity
CXCR4	Most (if not all) leukocytes	Hematopoiesis Organogenesis Bone marrow homing
CXCR5	B, T_{FH}, T_{FR}, CD8 T_{EM}	B-cell and T-cell trafficking in lymphoid tissue to B-cell zone/follicles
CXCR6	Th1, Th17, γδ T, iLC, NKT, NK, PC	Innate lymphoid cell function Adaptive immunity
CCR1	Mo, MΦ, N, Th1, Ba, DC	Innate immunity Adaptive immunity
CCR2	Mo, MΦ, Th1, iDC, Ba, NK	Monocyte trafficking Th1-type adaptive immunity
CCR3	Eo > Ba, MC	Th2-type adaptive immunity Eosinophil distribution and trafficking
CCR4	Th2, skin- and lung-homing T, Treg, > Th17, CD8 T, Mo, B, iDC	Homing of T cells to skin and lung Th2-type immune response
CCR5	Mo, MΦ, Th1, NK, Treg, CD8 T, DC, N	Type 1 adaptive immunity
CCR6	Th17 > iDC, γδ T, NKT, NK, Treg, T_{FH}	iDC trafficking; GALT development Th17 adaptive immune responses
CCR7	T_N, T_{CM}, T_{RCM}, mDC, B	mDC and B-cell and T-cell trafficking in lymphoid tissue to T cell zone Egress of DC and T cells from tissue
CCR8	Th2, Treg, skin T_{RM}, γδ T, Mo, MΦ	Immune surveillance in skin Type 2 adaptive immunity thymopoiesis
CCR9	Gut homing T, thymocytes, B, DC, pDC	Homing of T-cells to gut GALT development and function thymopoiesis
CCR10	Skin-homing T, IgA-plasmablasts	Humoral immunity at mucosal sites Immune surveillance in skin
XCR1	Cross-presenting CD8+ DC, thymic DC	Ag cross-presentation by $CD8^+$ DCs
CX3CR1	Resident Mo, MΦ, MG, Th1, CD8 T_{EM}, NK, γδ T, DC	Patrolling monocytes in innate immunity Microglial cell and NK cell migration Type 1 adaptive immunity
Atypical (nonsignaling) receptors		
ACKR1 (DARC; Duffy)	RBC, LEC	Chemokine transcytosis Chemokine scavenging
ACKR2 (D6)	LEC, DC, B	Chemokine scavenging
ACKR3 (CXCR7)	Stromal cells, B	Shaping chemokine gradients for CXCR4
ACKR4 (CCRL1; CCX-CKR)	Thymic epithelium	Chemokine scavenging

[a]This table was adapted from reference 1. Abbreviations: B, B-cell; Ba, basophil; Eo, eosinophils; GALT, gut-associated lymphoid tissue; iDC, immature DC; LEC, lymphatic endothelium; MΦ, macrophage; MG, microglia; Mo, monocyte; N, neutrophil; pDC, plasmacytoid DC; PC, plasma cell; RBC, red blood cell; T_{CM}, central memory T cell; T_{EFF}, effector T cell; T_{FH}, follicular helper T cell; T_{FR}, follicular regulatory T cell; T_N, naive T cell; T_{RCM}, recirculating memory T cell.

receptors is usually accompanied by a transient rise in intracellular calcium. The G protein is itself coupled to a number of downstream intracytoplasmic signal transduction pathways, including those involving protein kinase C, tyrosine kinases, and PI-3 kinase (1–4) (Fig. 1). The direct link between these signal transduction pathways and the activation of the cytoskeletal machinery involved in cell motility has become better understood in recent years. Rho proteins, which are known to mediate actin-dependent processes, are thought to be involved in linking chemokine receptor activation to activation of the cytoskeletal machinery (6, 7). It is now understood that the synaptotagmin family of proteins, which are known to regulate calcium-dependent lysosomal vesicle transport and fusion, link chemokine-induced elevated intracellular calcium to activation of the cytoskeletal machinery and directed cell migration (8).

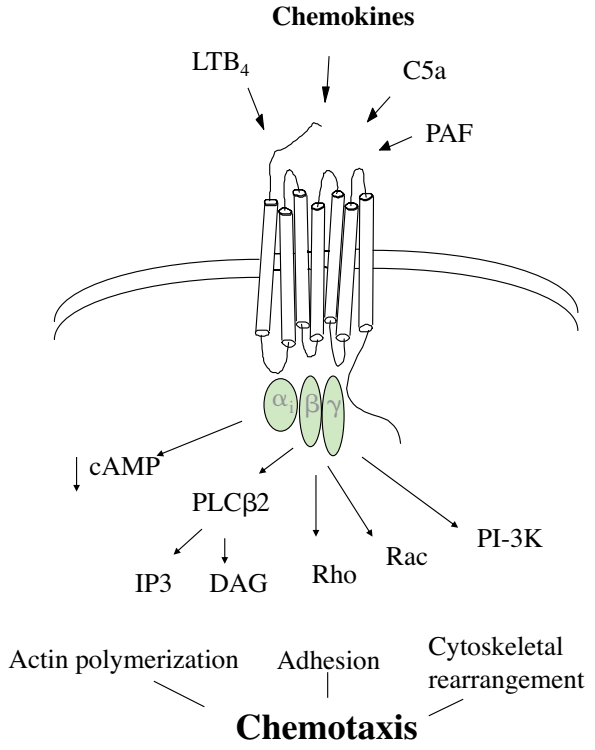

FIGURE 1 Chemokine receptor signal transduction. Chemokine receptors are a subfamily of G protein-coupled seven transmembrane-spanning cell surface receptors. They are coupled to heterotrimeric G proteins of the Gi subclass, which are distinguished by their pertussis toxin sensitivity. Chemokine receptor activation leads to the stimulation of multiple signal transduction pathways, including the activation of phosphatidylinositol 3-kinase (PI3K) and phospholipase C (PLC), leading to generation of inositol triphosphates, intracellular calcium release, and protein kinase C (PKC) activation. Chemokine signaling also induces the upregulation of integrin affinity and the activation of Rho, leading to cytoskeletal reorganization. Agonist-stimulated receptors also activate G protein receptor kinases, which leads to receptor phosphorylation, arrestin binding, G protein uncoupling (desensitization), and clathrin-mediated receptor endocytosis (internalization).

ROLE OF CHEMOKINES AND CHEMOKINE RECEPTORS IN DISEASE

The attraction of leukocytes to sites of inflammation and infection is an essential component of the host response to disease. Chemokines and chemokine receptors have been shown to be an integral part of this process and have been implicated in the pathophysiology of many infectious diseases and inflammatory disorders (1–4). Although chemokines are clearly important for the ability of the host to control infections, they can also be detrimental in certain inflammatory diseases, such as asthma, atherosclerosis, and rheumatoid arthritis (RA), and transplant rejection, in which inflammatory cells are recruited to tissue sites of inflammation and produce tissue damage (1, 9–12). For example, inflammation is a critical component of atherosclerosis, and the expression of multiple chemokines has been shown to be upregulated in human atherosclerotic lesions (10, 13). Prominent leukocyte recruitment occurs in almost every stage of lesion development, and the recruited monocytes and T lymphocytes are thought to play a key role in the pathogenesis of atherosclerotic plaque; thus, the molecular signals that attract these cells into the lesions are likely important for their formation (10, 14, 15). Mouse models of atherosclerosis have implicated the CC chemokine receptors (CCR) CCR2 and CCR5 as well as the CX3C chemokine receptor CX3CR1, which are important for monocyte trafficking and mobilization in the formation of atherosclerotic lesions, and highlight the importance of monocytes in the pathogenesis of atherosclerotic inflammation (16–18).

In contrast, the underlying pathology of RA is notable for very prominent infiltration of the synovial tissue of the joints by neutrophils in addition to mononuclear leukocytes, which presumably helps propagate the inflammation and joint destruction. Neutrophil (CXCL8, CXCL5, CXCL1), monocyte (i.e., CCL3, CCL5, CCL2), and T-cell (i.e., CXCL10, CXCL9, CCL3, CCL5, CCL17)-attracting chemokines are expressed by fibroblasts and macrophages in the synovium of RA patients (12, 19). Consistent with this chemokine expression, synovial fluid T cells recovered from patients with active RA express high levels of the chemokine receptors CCR5 and CXCR3 (20). Confirming the importance of neutrophils in the pathogenesis of RA, in a serum-transfer mouse model of RA, inflamed synovial tissue cells produced different neutrophil-active CCR1 and CXCR2 ligand chemokines, which are absolutely required for the induction of arthritis in this model (21). Initially, CCR1 ligands and, later, CXCR2 ligands in the joint amplify the recruitment of neutrophils which, by releasing multiple mediators such as LTB_4, IL-1β, and CXCL2, orchestrate inflammation in the joint. This mouse model of arthritis also highlights an important principle of chemokine-mediated inflammation *in vivo*, in that the generation of full-blown arthritis requires that this sequential cascade must run its course; otherwise, inflammation is dampened.

As another example, asthma is a disease characterized by chronic inflammation of the airways; studies in animal models and humans suggest that allergen inhalation initiates a cascade of events that leads to the recruitment of eosinophils, neutrophils, lymphocytes, and mast cells into the airways (22–24). Chemokines have been implicated as important mediators of this cellular recruitment and are likely crucial for the development of allergic inflammation in the airways (23, 24). Data from bronchoalveolar lavage (BAL) and lung biopsy studies have demonstrated the upregulation of the chemokines CCL11, CCL24, CCL7, CCL13, CCL5, CCL17, CCL22, and CXCL10 in patients with asthma attacks or after an allergen challenge (24, 25). Some of these chemokines recruit eosinophils and others affect T-cell trafficking. Analogous to RA, animal models of asthma, however, suggest that no single chemokine controls all aspects of cell trafficking into the airway; rather, multiple chemokines likely work in a sequential and redundant manner to orchestrate the inflammation (24).

Chemokines also have been implicated in the organ transplant setting. Although a transplant is often life-saving therapy for the large number of patients with end-stage kidney, liver, heart, or lung disease, it ushers in a new set of problems and diseases for the organ recipient. These include increased risk of infection, organ ischemia-reperfusion injury, acute rejection, and chronic organ dysfunction from chronic rejection. These processes involve recruitment of leukocytes into the transplanted organs, with neutrophil recruitment dominating infections and ischemia-reperfusion injury and lymphocytes and monocyte recruitment involved in rejection. Infections of organs, organ ischemia-reperfusion injury, acute rejection, and chronic rejection

lead to increased expression of multiple chemokines. These chemokines are surprisingly similar in all organs after transplantation, although organ-specific differences do exist (26, 27). In studies looking at chemokine expression following human organ transplantation, the expression of CXCL8/IL-8 has been associated with ischemia-reperfusion injury (28), while CCL5, CCL2, CCL3, CCL4, CXCL9, CXCL10, and CXCL11 have been associated with acute rejection (26, 28–32). In chronic rejection of lungs, CXCL8, CCL5, CXCL9, CXCL10, CXCL11, and CCL2 are upregulated and may be predictive of the development of this complication (29, 33).

In conclusion, as illustrated above, different leukocyte subsets bear signature combinations of chemokine receptors (Table 2), and the chemokine-chemokine receptor axis likely promotes pathologic accumulation of specific leukocyte subsets, which in turn facilitate different types of inflammation in affected tissues (34). In such disorders, it has been suggested that the chemokine-chemokine receptor axis could be used as a diagnostic tool for characterizing the type of inflammation and the functional phenotype of the leukocytes that provoke the inflammation; this information could then be used to develop targeted therapeutics for controlling inflammation (1, 35). Tailored therapeutics directed against the chemokine-chemokine receptor axis in diseases such as asthma, RA, and transplant rejection may provide a means of avoiding the adverse side effects of the broad immunesuppressive therapies that are currently used to treat these diseases in clinical practice.

Clinical Applications for Analyzing Chemokine Expression in Disease

In the past decade, validated assays for measuring chemokine mRNA and protein have become widely available. In particular, more than a few commercial kits routinely allow for the simultaneous multiplexed measurement of many inflammatory cytokine and chemokine proteins from small amounts of sample. Assays that measure chemokines in serum and affected tissue could provide a noninvasive and relatively inexpensive adjunct diagnostic tool for diagnosis as well as phenotypic classification and provide a means of quantifying disease severity for the purposes of stratification, prognostication, and treatment. These assays may thus be useful in guiding the initiation of therapy and aid in monitoring the subsequent response to therapy. For instance, a clinical setting in which such a strategy might be usefully employed is in the management of refractory asthma. Currently, clinicians monitor the effectiveness of therapy in people with asthma based on symptom reporting and crude measures of lung function. Acute exacerbations of asthma are life-threatening complications of this disorder that often occur rapidly. In addition, it is hypothesized that long-term low-grade inflammation, which can be missed with routine monitoring, may lead to scarring of the airways and permanent changes in lung function. Importantly, it is now appreciated that human asthma is a heterogeneous disease, and therapeutic strategies directed at a single allergic inflammation-promoting cytokine may be successful only in subpopulations of patients with asthma in whom the therapy is matched to the underlying pathophysiology (36, 37). Unfortunately, available technology does not allow us to easily measure the degree of asthmatic airway inflammation and thus predict a patient's risk for an exacerbation or airway scarring/remodeling. Nor does it allow for the characterization of the type of inflammation driving the particular subtype of asthmatic airway inflammation to predict the most effective targeted therapy. Chemokine expression in the lung or blood could be used as a reliable noninvasive marker of inflammation in the airways and thus would be of great value in the management of asthma. The technology to measure chemokine levels in exhaled breath condensates is available and has been used in limited studies for measurements in children with asthma (38). In addition, expectorated sputum or serum has been used in assays to measure chemokine levels and predict exacerbations in patients (39). Finally, allergic asthma can often be confused with related disorders such as emphysema, bronchiolitis, and eosinophilic bronchitis. These disorders have different forms of airway inflammation and thus may have a different profile of chemokines expressed. Thus, it may be possible to use the chemokine or chemokine receptor profiles of samples from the lung or serum to accurately diagnose a patient with airway inflammation. The use of measurements of markers of inflammation such as chemokines could have a large impact in the diagnosis and management of asthmatics.

Another disease in which monitoring chemokines in serum or affected tissue may have implications for disease prognosis and management is RA, as suggested by some recent supportive data. In a nested case-control study, a Scandinavian study monitored 30 chemokines and cytokines by multiplex analysis in banked blood samples of 69 individuals prior to the onset of symptoms of joint disease and subsequent to the diagnosis of RA (12). After anticyclic citrullinated peptide (anti-CCP) antibodies, the most important elevated factors that differentiated asymptomatic patients who went on to develop RA from control subjects included the chemokines CCL11, CCL2, CXCL10, and CCL3 and the cytokines IL-13, IL-10, IL-9, and IL-1Ra. The factors that best discriminated between patients after the onset of RA and control subjects included anti-CCP antibodies, the chemokines CCL4, CXCL9, and CCL11, and the cytokines IL-6, IL-10, and G-CSF. A second study measured chemokines and cytokines in synovial fluid by multiplex analysis and found that the chemokines CCL11, CXCL11, CCL8, CXCL9, CCL5, CCL17, and CXCL8 were elevated in synovial fluid from RA compared with those in osteoarthritis (19). The finding of CCL11, a chemokine associated with eosinophil migration and allergic inflammation, in both of these studies, and elevated serum Th2 cytokines in the first study, is surprising and provides potential new insights for investigation to understand the pathophysiology of RA. Finally, monitoring serum chemokines and cytokines in association with anti-CCP antibodies may provide better sensitivity and specificity in at-risk asymptomatic individuals than anti-CCP antibodies alone in predicting the risk of developing RA, to possibly aid in preventing disease progression.

In solid organ transplant, frequent episodes of acute rejection and untreated low-grade rejection are thought to lead to chronic organ dysfunction, which is the major limiting factor in long-term graft survival. Thus, the ability to better detect these processes could have a major impact in the management of posttransplant patients. The expression of specific chemokines during episodes of acute rejection or in low-grade chronic rejection may be a biomarker of inflammation and could allow better detection of these processes. In the renal transplant setting, the finding that chemokines were important mediators of allograft injury in animal studies (40) prompted investigators to develop assays to monitor chemokines in the urine of human kidney transplant recipients. These studies led to the finding that urine CXCL9, CXCL10, and CXCL11 mRNA are elevated in patients with acute rejection, acute tubular injury, or BK

virus nephropathy compared with individuals with chronic rejection or stable renal function and healthy individuals, suggesting their potential utility as biomarkers (32, 41). Urine chemokine measurements may also have a role in predicting late graft failure, as urine CCL2 levels 6 months posttransplant were associated with the development of interstitial fibrosis, tubular atrophy, and graft dysfunction at 24 months (42). Thus, measuring urinary chemokine biomarkers could be a cost-effective noninvasive graft-sparing alternative to allograft biopsy that may limit long-term allograft injury, particularly in high-risk patients. Ongoing prospective multicenter validations of these assays and clinical trials, to test whether urinary chemokine levels can guide immunosuppressant withdrawal in low-risk patients and direct specific therapeutic strategies to limit graft injury for better individualized treatment strategies, will help to determine better the clinical utility of urinary chemokines as biomarkers. In conclusion, the ability to measure chemokine levels in serum or sputum suggests that noninvasive, reliable, cost-effective chemokine biomarkers may also have a useful role in the setting of other organ transplants to assess the risk of graft injury to prolong graft survival.

METHODOLOGICAL APPROACHES

Overview

Since inflammatory and immune cell localization appears to be central to the pathogenesis of a wide variety of diseases, numerous avenues for studying the role of chemokines and chemokine receptors have emerged. These techniques follow a logical progression from the characterization of the inflammatory or immune cell infiltrate through the measurement of chemokine and chemokine receptor distribution in diseased tissues, the establishment of *in vitro* models of chemotaxis, and *in vivo* dissection of the role of chemokines in animal models of the disease process. This series of approaches has enabled the definition of the role of chemokine and chemokine receptor-driven immune and inflammatory cell localization in a variety of diseases.

Analysis of the Cellular Infiltrate and Chemokine/Chemokine Receptor Milieu

The first step toward understanding whether localization of immune or inflammatory cells influences a disease process is to define the cellular composition of the infiltrate seen in sites in the body that are affected by the disease. This may be best done by one of two methods: immunohistochemistry of tissue sections or staining of cellular preparations obtained from disaggregated pathological specimens. There are a large number of monoclonal antibodies that enable the definition of subpopulations of immune and inflammatory cells and the characterization and quantitation of chemokine and chemokine receptor expression (43, 44). Monoclonal antibodies that are reactive to specific antigens expressed on T cells, B cells, monocytes, macrophages, dendritic cells, neutrophils, eosinophils, and basophils/mast cells can be utilized to detect these cells or specific subsets of these cells in frozen sections using immunohistochemical techniques. The immunoperoxidase technique using the avidin-biotin complex has enhanced sensitivity, and stained slides can be mounted and stored permanently. In addition, sections can be counterstained with hematoxylin and eosin, for example, to provide additional morphologic information. Serial sectioning allows the assessment of three-dimensional (3D) relationships between subsets of immune and inflammatory cells in tissue specimens. Appropriate isotype controls should be run with experimental immunostaining to establish levels of background nonspecific staining.

Fluorescent conjugated monoclonal antibodies targeting specific cell surface molecules can be similarly used to establish the cellular makeup of a tissue infiltrate (43). Tissue samples can be physically disaggregated and then passed through a sterile sieve. Mononuclear cell preparations can then be stained with monoclonal antibodies and the immunophenotype of cell populations can be determined by fluorescence-activated cell sorting–based flow cytometry. As many as 18 different fluorochromes can be used, depending on the number of available lasers, to define cell subpopulations. Again, appropriate isotype antibody controls should be used to establish background and nonspecific staining.

Another aspect of the analysis of cellular infiltrates is the determination of levels of chemokine or chemokine receptor expression. A combination of methods can be used, including RNA *in situ* hybridization, immunohistochemistry, quantitative reverse transcriptase PCR (QPCR), ELISA or protein multiplexing technology, and flow cytometry. Monoclonal antibodies directed against a number of chemokines suitable for use in staining tissue sections, ELISA, or protein multiplexing have been defined and validated over the past decade. These antibodies can be used as a basis for measuring chemokine protein concentrations from tissue lysates and fluid collections. A number of different chemokines can be detected by sandwich ELISAs, which are commercially available as kits. Initially, microtiter plates are coated with the capture antibody and nonspecific protein binding is adsorbed with goat serum or bovine serum albumin. Chemokine-containing samples are then added to the wells of the plate and this is followed by exposure to a second enzyme-conjugated antibody. A caveat, when using ELISAs for the measurement of proteins in serum and tissue such as synovial fluid from individuals with autoimmune disorders, is the presence of heterophilic human anti-animal antibodies such as anti-mouse antibodies, which can cause false-positive and false-negative results (19). Use of appropriate blocking reagents and diluents can obviate these technical issues (19).

Multiplex microwell protein array kits are now widely available and can also be manufactured to detect custom combinations of proteins. Similarly, these chemokine-specific monoclonal antibodies are also available conjugated to a fluorochrome or to fluorescent bead arrays, which allows them to be used to assess intracellular chemokine levels in permeablized cells or to assess the levels of multiple chemokines simultaneously in various biologic samples using flow cytometry technology. Monoclonal antibodies specific for individual chemokine receptors are also commercially available and are used to determine the expression of chemokine receptors on individual cells *in situ* or those isolated from inflammatory tissue or fluid via immunohistochemistry or flow cytometry.

Analysis of Chemotactic Responses: *In Vitro* Assays

Having defined the chemokine and chemokine receptor expression in the diseased tissue, one can examine the chemotactic responses of the specific leukocyte subpopulations to chemokines. A variety of transmigration assays exist which exploit the ability of migratory cells to polarize and migrate in response to a chemotactic gradient. The *in vivo* correlate of *in vitro* transmigration is thought to be the migration of cells towards sites of tissue injury, pathogen invasion, and/or immune challenge. Cells to be used in the transmigration assays can be derived from a number of sources, including the diseased tissue itself or purified subpopulations of inflammatory and immune cells isolated from the peripheral blood.

Boyden Chamber

The Boyden chamber, designed in 1962, represents the original system by which the chemotactic responses of cells can be quantitated (45). The assembly consists of two chambers, an upper and a lower, separated by a polycarbonate filter of standard pore sizes. Disposable Boyden chambers containing polycarbonate membranes with defined pore sizes for different cell types are commercially available. Membranes with a pore size of 3 μm for neutrophils; 5 μm for lymphocytes, monocytes, and eosinophils; and 8 μm for fibroblasts, endothelial cells, and tumor cells are used to assay migration. The chemokine, dissolved in medium containing a low percentage of serum or 0.5% bovine serum albumin, is loaded into the lower chamber. A fixed number of indicator cells in suspension at cell concentrations of 10^6 to 10^7/ml are loaded in an identical medium into the upper chamber. The unit is then sealed and incubated at 37°C for 30 min to 1 h for granulocytes, 1 to 2 h for monocytes, and 2 to 4 h for lymphocytes.

Transmigration is then assessed in a number of ways. The polycarbonate membrane is carefully removed from the assembly, and the cells that are adherent to the underside of the filter are stained with Giemsa and quantitated. Alternatively, the cells that have transmigrated into the lower chamber are counted using a hemocytometer and the proportion of migrating cells is determined. If the migration index is low and cells are adherent to the bottom chamber, an inverted light microscope may be used to count multiple fields within the chamber after the experiment or after fixation with 10% buffered formalin. Ultimately, a so-called checkerboard analysis of chemotaxis can be performed in which every combination of chemokine concentration in the lower chamber is combined with every tested concentration of chemokine in the upper chamber. Chemotaxis is defined as cell movement toward increasing chemokine concentration. Chemokinesis refers to random or nondirectional cell movement in response to a stimulus. In the checkerboard analysis, chemotaxis is measured when there is a greater concentration of chemokine in the lower chamber, and chemokinesis is measured when the concentration of chemokine is equivalent on both sides of the membrane (Fig. 2). Chemotactic index is calculated by normalizing the number of cells that migrate at a concentration of chemokine to the number of cells that migrate in response to medium alone.

Automated quantitation of transmigration can also be achieved by loading cells to be tested with a vital fluorescent dye such as 5-chloromethylfluorescein diacetate (CMFDA), acridine orange, or Calcein AM and then using a fluorescent plate reader to quantitate the number of cells in the lower chamber (46). Alternatively, migrated cells can be lysed and labeled with a DNA-binding dye such as Cyquant and quantitated with a fluorescent plate reader. A further modification of the fluorescent plate reader includes the ability to read the kinetic changes of transmigration into the lower chamber over time.

Transwell Assays

More recently, transmigration assays have been performed in a transwell system (47). In this assembly, each lower chamber is associated with an independently removable upper chamber containing the polycarbonate membrane of fixed pore size. A checkerboard analysis of chemotaxis can be similarly performed in the transwell system. The Boyden chamber appears to be markedly better for analyzing granulocyte movement with a polycarbonate membrane of 3 μm pore size, whereas transwells containing membranes with a 5-μm or 8-μm pore size have proven useful for quantitating mononuclear cell migration. Several modifications of transmigration have been designed. These include the assessment of transmigration through a layer of cells grown on the transwell membrane. Transmigration of lymphocytes, eosinophils, or monocytes through an endothelial cell layer has been assessed by this means. Transmigration systems allow further phenotypic characterization of responding cell subpopulations from a complex mixture of input cells. Using flow cytometry, cells that transmigrate can be phenotypically compared with those that do not.

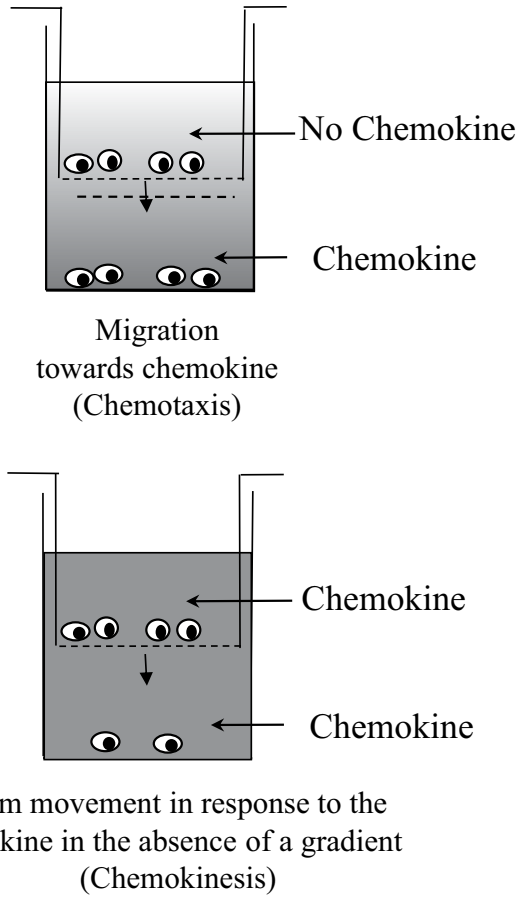

FIGURE 2 Transmigration assay system. Positive, negative, and absent gradients of a chemokine are established in order to assess chemotaxis (movement towards a chemokine) and chemokinesis (random movement of cells in response to a chemokine in the absence of a gradient). Cells are plated into the upper chamber of the transwell system or Boyden chamber and the proportion of migrating cells determined by accurate counting of cells that migrate to the lower chamber. The upper and lower chambers are separated by a polycarbonate membrane of standard pore size (3 μm to 8 μm), depending on the migrating cell type.

Direct Visualization

Additional modifications of the Boyden chamber have been made, including the use of an image analyzer to quantitate the number of labeled cells that migrate in response to a chemokinetic agent (48). Transmigration with a Boyden chamber or transwell assay can also be confirmed using time-lapse video microscopy with a direct-viewing approach in which cells migrate on a horizontal surface (Fig. 3) (49). The active movement of cells is viewed with a video camera

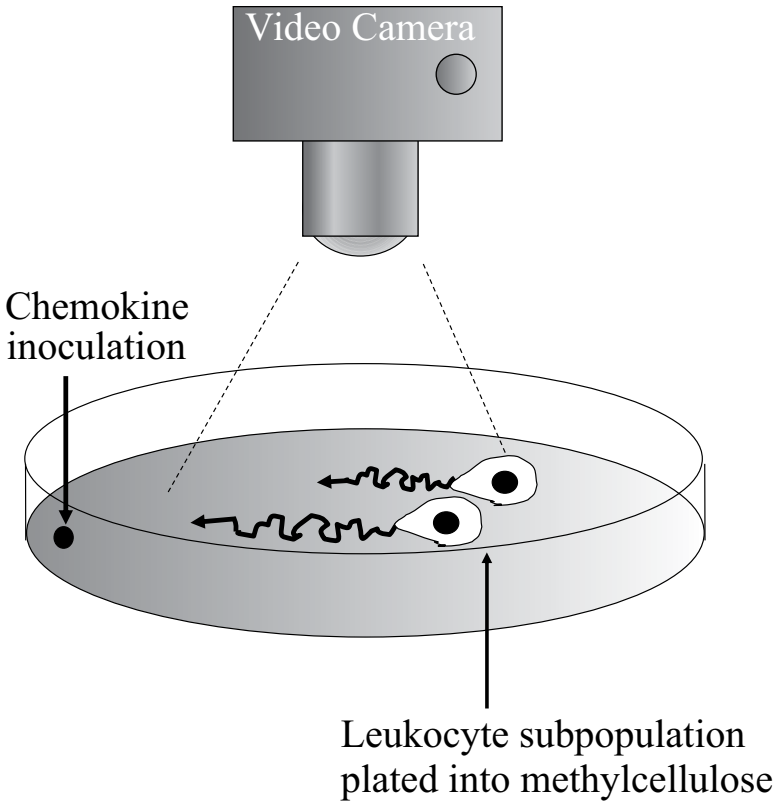

FIGURE 3 Digitized time-lapse photography of cells moving in the presence of a gradient of chemokine. Positive and negative gradients of a chemokine can be established in methylcellulose, as previously described (49). Cells are plated into methylcellulose and a gradient is established by inoculating the methylcellulose at a fixed point with the chemokine. Cells are then visualized migrating in response to the gradient using time-lapse video microscopy.

as they respond to gradients of a chemokinetic agent. A continuous gradient of chemokine or a point source of chemokine can be used to manipulate the directional movement of cells. Cell movement can also be tracked using digital video and images analyzed for cell polarization and speed of movement towards a chemokine source, using leukocytes or other organisms such as *Dictyostelium* (50, 51). These modalities allow the measurement of many parameters such as cell morphology, area, and location during chemotaxis. Automated chemotaxis and cell morphology assays in a 96-unit direct-viewing plate in a high-throughput format can also now be achieved (52). In recent years, the EZ-Taxiscan has become commercially available (53, 54). The EZ-Taxiscan is a horizontal viewable chemotaxis chamber in which a microchannel connects a compartment containing ligand and another compartment containing cells. A stable chemoattractant concentration gradient is formed and maintained through the channel without the flow of medium. The migration of cells in the chambers can be traced with time-lapse intervals using a charge-coupled device camera.

Adhesion Assays

The migratory response of immune cells *in vivo* involves a rapid adhesive event in which the circulating cell is stimulated to adhere firmly to the endothelial surface over which it flows and rolls; this event is necessary for a cell to undergo diapedesis into an immune organ or an inflammatory site (1–4). This event is triggered by chemokines and involves the upregulation of integrin affinity on leukocytes. This aspect of cell migration can be studied *in vitro* in a static adhesion assay or dynamically using a flow chamber to visualize the adhesion of leukocytes to endothelial cell monolayers. In these latter systems, endothelial cell layers are established on cover slips, and fluorescently labeled leukocytes are passed over these monolayers at controlled flow rates; the number of cells rolling or sticking to the endothelial layer is determined using image analysis and digitized time-lapse video microscopy. *In vivo* flow systems have been designed that use intravital microscopy (IVM) to visualize and quantitate the adhesion and transmigration of fluorescently labeled leukocytes in the vasculature of living animals (55).

Assays To Measure Integrin Conformation Change

In the steady state, leukocytes express integrins, which are in an inactive conformation that does not mediate adhesion. Chemokines activate integrin function by inducing a change in integrin conformation that increases the affinity and/or avidity of the integrin for its ligand, which leads to inside-out integrin activation. This chemokine-mediated conformational change that transiently results in high-affinity integrins can be measured with monoclonal antibody (MAb)-based flow cytometry assays (56). Chemokine-induced integrin conformational changes in activated integrins result in exposure of previously masked epitopes, which can be detected with monoclonal antibodies that detect high-affinity integrins. Detection of high-affinity β2 integrins can be achieved using the antibody MAb24 (57). Binding of this antibody occurs only at 37°C. Leukocytes are stimulated with chemokines in

the presence of MAb24, rapidly cooled on ice to terminate any additional MAb24 binding, and fixed with paraformaldehyde (58). Likewise, a high-affinity β1 integrin can be detected by flow cytometry after stimulation with chemokine with the HUTS-21 MAb (59).

Analysis of Signal Transduction Associated with Active Cell Movement

The signal transduction events activated by ligand binding controlling leukocyte migration are not entirely defined and involve many different signaling pathways. A dramatic polarization of the cell occurs in response to a chemotactic gradient which is the result of asymmetric signal transduction and the establishment of intracellular molecular gradients. While all of the molecular details remain to be elucidated, certain signaling molecules appear to play important roles in chemokine-induced cell movement. Chemokine receptors are coupled to the Gi subfamily of G proteins and pertussis toxin (PTX), which ADP-ribosylates and irreversibly inactivates the Gα subunits of the αi class and inhibits the majority of chemokine-induced effects on leukocytes, including chemotaxis, calcium flux, and integrin activation (1). Other signaling events activated by the majority of chemokine receptors include the activation of phospholipase C (PLC), leading to generation of inositol triphosphates, intracellular calcium release, and protein kinase C (PKC) activation. Inhibition of chemokine-induced chemotaxis by wortmannin implicates phosphatidylinositol 3-kinase (PI3K) in chemokine receptor signal transduction. Mouse strains engineered with a null mutation of the p110 subunit of PI3Kγ have defects in chemokine-induced neutrophil and macrophage migration, confirming the importance of this enzyme in directed leukocyte movement (60). PMA activation of integrins implicates PKC as a potential mediator by which chemokines activate integrins. Chemokine signaling also leads to guanine nucleotide exchange on Rho, indicating the activation of Rho (7). Rac and Rho are small GTP-binding proteins involved in controlling cell locomotion through regulation of actin cytoskeletal rearrangement, leading to membrane ruffling and pseudopod formation.

The first and most immediate indication of a signal being transduced in relation to chemokine-induced signaling is a measurable rise in intracellular calcium concentration. The calcium flux is transient and may be detected using several methods (61). Cells are examined within cuvette-based techniques that assess calcium flux in populations of cells and flow cytometry-based systems, which assess individual cell calcium flux responses to chemokine. Emission ratio dyes such as Indo-1 and Fura-2 are commonly used for flow cytometry-based and cuvette-based methods, respectively. Cells to be tested, including monocytes and lymphocytes, are loaded with ionic calcium-binding dyes. Cells are then exposed to sequential pulses of chemokine, and the change in intracytoplasmic fluorescence is monitored. Control substances include ionomycin, which selectively causes a large calcium flux because it serves as a calcium ion channel in the membrane. EDTA can be used to deplete all calcium from the medium and hence eradicate any cell-related calcium flux. Modifications have been made in order to determine the calcium flux in single cells. Adherent cells on a single slide can be visualized, and loading of calcium dyes and intracytoplasmic changes in calcium concentrations can be monitored directly under a fluorescent microscope with an associated image analyzer. The GTPγS exchange assay can also be used in both cell membranes and permeabilized peripheral blood lymphocytes to assess the first step of G protein-coupled receptor activation (62).

Activation of additional signal transduction pathways can be measured in cells in response to activation by chemokines (1). Adenylate cyclase assays, phosphoinositide turnover, protein kinase activation, and assays of protein tyrosine kinase activity have all been used to measure chemokine receptor activation.

Although the precise mechanistic link between chemokine receptor activation and the activation of the cytoskeletal machinery, which induces cellular migration, remains unknown, the polymerization of filamentous F-actin has been used as a measure of chemokine-induced functional signaling (63). Intracellular F-actin polymerization can be quantitated using FITC-labeled phalloidin and flow cytometry (63). This technique has been especially useful for assaying small numbers of responding cells. Polymerized F-actin can also be visualized in cells by using confocal microscopy in conjunction with a fluorescently labeled MAb directed against F-actin. These studies have revealed that signal transduction occurring after exposure to a chemokinetic gradient results in the polarization of the cell's cytoskeletal elements and polymerization of activated actin at the leading edge of a cell's newly formed pseudopodia. The Arp2/3 complex has recently been shown to colocalize with and nucleate sites of actin polymerization. An engineered GFP-Arp2/3 fusion protein has been used to visualize sites of actin polymerization in the advancing pseudopods of migrating cells by using phase contrast fluorescent time-lapse photography (64). A time-lapse fluorescent microscope with a digital spot camera can be used to visualize the polarization of actin polymerization and pseudopod formation in cells transduced with the GFP-Arp2/3 construct and exposed to gradients of chemokines.

In Vivo Analysis of Chemotactic Responses

In Vivo Recruitment Assays

Several systems have been developed to assess leukocyte infiltration into specific anatomical sites *in vivo*. Chemokines can be injected intradermally, subcutaneously, or intratracheally or into the intraperitoneal space, and leukocyte infiltration can thus be quantified (65). Recruitment of endogenous leukocytes or adoptively transferred leukocytes can be assessed in this manner. Leukocytes can be labeled *ex vivo* with radiolabels such as indium-111 or with fluorescent dyes such as green fluorescent protein (GFP) or CMFDA (5-chloromethylfluorescein diacetate-green). In addition, MAbs exist that can recognize adoptively transferred antigen-specific T cells or congenic allelic markers. A transgenic mouse has been engineered in which the vast majority of T cells express a T-cell receptor (TCR) which binds ovalbumin (OVA) (66). This specific TCR chain can itself be detected using an MAb (66). T cells reactive to a specific antigen can be quantitated, and the localization of adoptively transferred OVA-specific T cells in specific anatomic sites can be detected by immunostaining for OVA-specific TCR.

In vivo Imaging

More recent technology, known as molecular imaging, allows scientists to assay several different aspects of chemokine biology in intact organisms. It is now possible to evaluate, with imaging, the distribution of injected chemokines as well as to track the movement of cells in response to chemokines or inflammation (67). This is a rapidly developing field that uses techniques of molecular and cell biology, advanced imaging technology, and highly specific probes

that serve as sources for the imaging signal. Specifically, whole-body imaging of animals or humans after injection of radiolabeled chemokines or bioluminescent cells allows localization of the labeled material to specific organs and areas of the body. Whole-body imaging of radioactive material or light generated deep within the body is now feasible in laboratory animals and, potentially, in humans, representing an exciting new tool for studying chemokine biology.

Multiphoton IVM

For almost 2 decades, intravital microscopy (IVM) enabled the two-dimensional imaging of leukocyte adhesion to endothelial cells, as well as leukocyte migration and extravasation from blood into tissue *in vivo* and in models of organ systems *in vitro* through bright-field transillumination and epifluorescence videomicroscopy (55). The advent of two-photon microscopy (2-PM) for *in vivo* live-cell imaging a decade ago revolutionized IVM because it provided an unprecedented live 3D window into leukocyte migration, cellular interactions, and the dynamics of innate and adaptive immune responses in lymphoid and peripheral tissues (Fig. 4) (68–71). Conventional single-photon fluorescence microscopy uses excitation wavelengths within the visible spectrum; 2-PM uses very brief laser pulses of excitation wavelengths in the infrared spectrum to generate optical sections of fluorescent signals hundreds of micrometers below the surface of solid tissues.

In 2-PM microscopy, a single fluorochrome molecule has to be hit nearly simultaneously by two infrared photons that are double the wavelength but half the energy of visible light (68–71). Infrared excitation light is scattered less because of its longer wavelength and, as such, has a

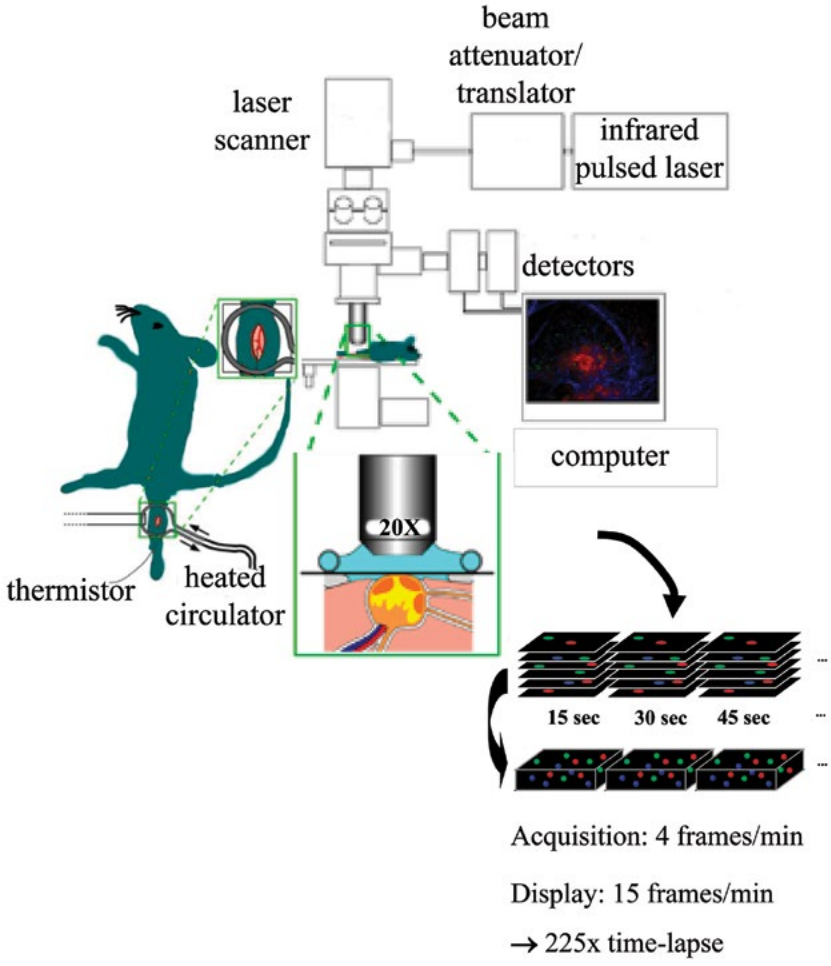

FIGURE 4 *In vivo* analysis of cell motility by multiphoton IVM in popliteal lymph node. The basic multiphoton microscope system consists of an infrared laser to deliver two-photon excitation; a laser intensity adjuster to decrease the laser power; a beam translation optical system to convey the laser beam to the back aperture of the objective; a laser scan head to raster scan the field of view with the microscope objective by rapid synchronized movement of dichroic steering mirrors; a low-magnification high-numerical-aperture water immersion objective; and external nondescanned detectors to concurrently acquire multiple fluorescent channels. The popliteal lymph node is visualized by making a skin incision in the knee, which is immersed in saline and sealed with a cover slip and vacuum grease after percutaneous clamps are used to prevent tissue movement. A thermistor is used to monitor temperature close to the lymph nodes, and the temperature is adjusted with a heating coil. Fluorescence is induced only in the focal plane; vertical image stacks are repetitively acquired that are then transformed into 3D images. Figure adapted from Mempel et al. (73).

higher penetration depth. Ultrashort laser pulses elicit the near-simultaneous excitation of two infrared photons with identical fluorochrome molecules; this occurs only within a very small volume of the focal point of the optical system. Consequently, as light scatter and fluorochrome bleaching outside of the focal plane are eliminated, tissue photodamage is minimized and fluorescent properties of the specimen are conserved to allow continuous imaging of the same area of tissue for several hours. In contrast to single-photon excitation microscopy, multiphoton microscopy also allows several fluorescent dyes or proteins with distinct emission and excitation characteristics to be visualized concurrently with two-photon excitation. Thus, the behavior and movement of different cell subsets labeled with different fluorescent dyes or proteins can be captured in deep tissue simultaneously with the rapid acquisition of 3D image stacks. The combination of MPM technology with IVM (MP-IVM) enables the investigation of the dynamic nature of cell behavior and migration deep within living tissue through time-lapse movies of 3D tissue reconstructions (Fig. 4) (68).

The utility of MP-IVM can be harnessed only if cells and tissue structures are fluorescently labeled (69, 70). In this respect, blood vessels can be labeled as structural landmarks with fluorescent high-molecular-weight dextran or with fluorescent semiconductor nanocrystals (quantum dots), which leak less into the interstitium than dextran (69, 70). *In vivo* labeling of nonhematopoietic cells with fluorescently conjugated antibodies is also possible (72). *Ex vivo* labeling of leukocytes with cell-permeable vital fluorescent dyes like CMAC (blue), CFSE (green), CMTMR (orange), CMPTX (red), or SNARF (far red) and adoptively transferring them into syngeneic recipients allow tracking until the dyes are diluted out in dividing cell populations. Besides these dyes, infrared fluorescent dyes have recently been developed that will allow imaging of deeper tissues (69).

Fluorescent cells from reporter mice that express the GFP-derived proteins eGFP, eCFP, and eYFP, and dsRed-derived proteins tdTomato and mCherry can also be used because they are less susceptible to phototoxicity at high laser intensities. Cells from these mice can be adoptively transferred or used to generate mosaic mice with mixed-radiation bone marrow chimeras. Mice with lineage-specific expression of fluorescent proteins have also been created. These mouse strains can be used to evaluate radiation-resistant cells that are difficult to isolate and adoptively transfer. Alternatively, inducible lineage-specific fluorescent reporter gene expression can be used to obtain information about functional proteins. This has been used to label cells based on the expression of transcription factors Blimp1 and Foxp3; the production of cytokines such as IL-2, IL-4, IFNγ, IL-17, and IL-10; and the production of chemokines such as CXCL12, CCL17, CXCL9, and CXCL10 as well as chemokine receptors such as CX3CR1 and CXCR6 (69, 70). Increasingly, fluorescent reporter expression of targeted genes in transgenic mice, partnered with advances in multiphoton imaging, are tools that are becoming more widely used and are enabling scientists to understand the *in vivo* dynamics and cellular interactions of immune cells at a molecular level.

Animal Models To Assess the Role of Chemokines and Chemokine Receptors in Development and Disease

The above-mentioned techniques provide data that suggest how chemokines and their receptors may play a role in immune/inflammatory cell function in health and disease. Genetically modified mice in which the gene for a specific chemokine or chemokine receptor has been deleted or is overexpressed in a tissue-specific manner have been used to study both physiological and pathological processes. The effect of neutralization of a specific chemokine or chemokine receptor by specific antibodies on disease processes has also been utilized. These animal models currently provide the cornerstone for determining functional roles of chemokines and chemokine receptors *in vivo* (1–4).

The role of chemokines and their receptors *in vivo* is complex. In an attempt to correlate *in vitro* determinations of chemokine activities and chemokine receptor expression with *in vivo* physiology and pathology, gene-targeted mice have been created by selective homologous recombination, which fails to express a chemokine or chemokine receptor (1–4). The phenotype of the so-called "knockout" is then compared under physiological and pathological conditions. The generation of knockout mice involves the introduction of a mutant gene into embryonic stem cells *in vitro* and the selection for homologous recombination at the desired locus, which results in the deletion of a specific gene. Animals are then produced that are homozygous for the deleted gene. Embryonic, fetal, and neonatal development is then examined in these mice with a targeted disruption of both wild-type alleles in order to determine whether the gene deletion affects embryogenesis, hematopoiesis, or immunologic abnormalities such as thymic development. In the adult mouse, inflammatory and immune responses can be examined. Knockout mice for over 10 of the chemokines and for all of the chemokine receptors have been developed (1, 2). So far, only the deletions of the CXCL12 and CXCR4 genes have been shown to be embryonically lethal and are associated with severe neurological, cardiological, and hematological abnormalities (1, 2). In contrast, fetal development is not affected in other chemokine and chemokine receptor knockouts such as CCL11, CCL2, and CCR2 (1, 2).

Many important roles for chemokines and their receptors have been elucidated in experiments using knockouts and inhibitory antibodies. Different aspects of the host response to infectious pathogens have been shown to be dependent on neutrophil-active chemokines and their receptors, such as CXCL1 and CXCR2; monocyte-active chemokines and their receptors, such as CCL2 and CCR2; T-cell active chemokines and their receptors, such as CXCL10; and natural killer cell-active chemokines such as CCL3 (1–4, 34). Likewise, individual chemokine receptor knockouts have revealed an important role for this family of molecules in inflammatory and autoimmune diseases and allograft transplantation. For example, attenuated immunopathology has been noted in CCL2 knockout and CCR2 knockout mice in models of atherosclerosis and glomerulonephritis (1). Decreased inflammatory responses and increased allograft survival have been noted in CCR1 and CXCR3 (1). CCR1 and CXCR2 are absolutely required for arthritis in a serum transfer model of RA (21). CCR4 and CCR8 have been found to be essential in different models of allergic inflammation (1). These *in vivo* experiments have revealed the significant role of individual chemokine and chemokine receptors in the immune and inflammatory response that could not be appreciated by *in vitro* assays that implicated apparent functional redundancy.

CONCLUSIONS

The Boyden chamber stood for more than 20 years as the singular system for quantitating leukocyte migration in response to chemokinetic agents. However, in the past 20 years, and since the discovery of the chemokine and chemokine receptor

superfamilies, there has been a considerable expansion in the number of methodological approaches available to scientists for quantitation and analysis of cell migration. These techniques vary widely, from phase contrast fluorescent digital video microscopy to examine individual cell movement in response to chemokines, to the use of knockout or fluorescent reporter mice with multiphoton IVM to delineate the effects of specific chemokines and chemokine receptors *in vivo*. These diverse methodological approaches have revealed an intricate world of immune and inflammatory cell localization that appears critical to the pathophysiology of a wide variety of disease processes ranging from allergic lung inflammation, through atherosclerosis, to the way in which the immune system handles infectious agents such as *Toxoplasma gondii*.

During the next 10 years, we should expect to see a further expansion in the methodological approaches to studying the roles of chemokines and chemokine receptors, which should itself lead to a greater understanding of human diseases and the development of novel therapeutic approaches in order to combat them.

REFERENCES

1. **Bachelerie F, Ben-Baruch A, Burkhardt AM, Combadiere C, Farber JM, Graham GJ, Horuk R, Sparre-Ulrich AH, Locati M, Luster AD, Mantovani A, Matsushima K, Murphy PM, Nibbs R, Nomiyama H, Power CA, Proudfoot AE, Rosenkilde MM, Rot A, Sozzani S, Thelen M, Yoshie O, Zlotnik A.** 2014. International Union of Pharmacology. LXXXIX. Update on the extended family of chemokine receptors and introducing a new nomenclature for atypical chemokine receptors. *Pharmacol Rev* **66:**1–79. PubMed
2. **Zlotnik A, Yoshie O.** 2012. The chemokine superfamily revisited. *Immunity* **36:**705–716. PubMed
3. **Sadik CD, Luster AD.** 2012. Lipid-cytokine-chemokine cascades orchestrate leukocyte recruitment in inflammation. *J Leukoc Biol* **91:**207–215. PubMed
4. **Förster R, Sozzani S.** 2013. Emerging aspects of leukocyte migration. *Eur J Immunol* **43:**1404–1406. PubMed
5. **Rot A.** 1993. Neutrophil attractant/activation protein-1 (interleukin-8) induces *in vitro* neutrophil migration by haptotactic mechanism. *Eur J Immunol* **23:**303–306. PubMed
6. **del Pozo MA, Vicente-Manzanares M, Tejedor R, Serrador JM, Sánchez-Madrid F.** 1999. Rho GTPases control migration and polarization of adhesion molecules and cytoskeletal ERM components in T lymphocytes. *Eur J Immunol* **29:**3609–3620. PubMed
7. **Laudanna C, Campbell JJ, Butcher EC.** 1996. Role of Rho in chemoattractant-activated leukocyte adhesion through integrins. *Science* **271:**981–983. PubMed
8. **Colvin RA, Means TK, Diefenbach TJ, Moita LF, Friday RP, Sever S, Campanella GS, Abrazinski T, Manice LA, Moita C, Andrews NW, Wu D, Hacohen N, Luster AD.** 2010. Synaptotagmin-mediated vesicle fusion regulates cell migration. *Nat Immunol* **11:**495–502. PubMed
9. **Cravedi P, Heeger PS.** 2012. Immunologic monitoring in transplantation revisited. *Curr Opin Organ Transplant* **17:**26–32. PubMed
10. **Koenen RR, Weber C.** 2011. Chemokines: established and novel targets in atherosclerosis. *EMBO Mol Med* **3:**713–725. PubMed
11. **Sadik CD, Kim ND, Luster AD.** 2011. Neutrophils cascading their way to inflammation. *Trends Immunol* **32:**452–460. PubMed
12. **Kokkonen H, Söderström I, Rocklöv J, Hallmans G, Lejon K, Rantapää Dahlqvist S.** 2010. Up-regulation of cytokines and chemokines predates the onset of rheumatoid arthritis. *Arthritis Rheum* **62:**383–391. PubMed
13. **Libby P, Ridker PM.** 2004. Inflammation and atherosclerosis: role of C-reactive protein in risk assessment. *Am J Med* **116**(Suppl 6A)**:**9S–16S. PubMed
14. **Gerszten RE, Mach F, Sauty A, Rosenzweig A, Luster AD.** 2000. Chemokines, leukocytes, and atherosclerosis. *J Lab Clin Med* **136:**87–92. PubMed
15. **Mach F, Sauty A, Iarossi AS, Sukhova GK, Neote K, Libby P, Luster AD.** 1999. Differential expression of three T lymphocyte-activating CXC chemokines by human atheroma-associated cells. *J Clin Invest* **104:**1041–1050. PubMed
16. **Swirski FK, Libby P, Aikawa E, Alcaide P, Luscinskas FW, Weissleder R, Pittet MJ.** 2007. Ly-6Chi monocytes dominate hypercholesterolemia-associated monocytosis and give rise to macrophages in atheromata. *J Clin Invest* **117:**195–205. PubMed
17. **Quinones MP, Martinez HG, Jimenez F, Estrada CA, Dudley M, Willmon O, Kulkarni H, Reddick RL, Fernandes G, Kuziel WA, Ahuja SK, Ahuja SS.** 2007. CC chemokine receptor 5 influences late-stage atherosclerosis. *Atherosclerosis* **195:**e92–e103. PubMed
18. **Combadière C, Potteaux S, Rodero M, Simon T, Pezard A, Esposito B, Merval R, Proudfoot A, Tedgui A, Mallat Z.** 2008. Combined inhibition of CCL2, CX3CR1, and CCR5 abrogates Ly6C(hi) and Ly6C(lo) monocytosis and almost abolishes atherosclerosis in hypercholesterolemic mice. *Circulation* **117:**1649–1657. PubMed
19. **Hampel U, Sesselmann S, Iserovich P, Sel S, Paulsen F, Sack R.** 2013. Chemokine and cytokine levels in osteoarthritis and rheumatoid arthritis synovial fluid. *J Immunol Methods* **396:**134–139. PubMed
20. **Loetscher M, Loetscher P, Brass N, Meese E, Moser B.** 1998. Lymphocyte-specific chemokine receptor CXCR3: regulation, chemokine binding and gene localization. *Eur J Immunol* **28:**3696–3705. PubMed
21. **Chou RC, Kim ND, Sadik CD, Seung E, Lan Y, Byrne MH, Haribabu B, Iwakura Y, Luster AD.** 2010. Lipid-cytokine-chemokine cascade drives neutrophil recruitment in a murine model of inflammatory arthritis. *Immunity* **33:**266–278. PubMed
22. **Busse WW, Lemanske RF Jr.** 2001. Asthma. *N Engl J Med* **344:**350–362. PubMed
23. **Islam SA, Luster AD.** 2012. T cell homing to epithelial barriers in allergic disease. *Nat Med* **18:**705–715. PubMed
24. **Medoff BD, Thomas SY, Luster AD.** 2008. T cell trafficking in allergic asthma: the ins and outs. *Annu Rev Immunol* **26:**205–232. PubMed
25. **Thomas SY, Banerji A, Medoff BD, Lilly CM, Luster AD.** 2007. Multiple chemokine receptors, including CCR6 and CXCR3, regulate antigen-induced T cell homing to the human asthmatic airway. *J Immunol* **179:**1901–1912. PubMed
26. **DeVries ME, Hosiawa KA, Cameron CM, Bosinger SE, Persad D, Kelvin AA, Coombs JC, Wang H, Zhong R, Cameron MJ, Kelvin DJ.** 2003. The role of chemokines and chemokine receptors in alloantigen-independent and alloantigen-dependent transplantation injury. *Semin Immunol* **15:**33–48. PubMed
27. **Abdi R, Means TK, Ito T, Smith RN, Najafian N, Jurewicz M, Tchipachvili V, Charo I, Auchincloss H Jr, Sayegh MH, Luster AD.** 2004. Differential role of CCR2 in islet and heart allograft rejection: tissue specificity of chemokine/chemokine receptor function *in vivo*. *J Immunol* **172:**767–775. PubMed
28. **De Perrot M, Sekine Y, Fischer S, Waddell TK, McRae K, Liu M, Wigle DA, Keshavjee S.** 2002. Interleukin-8 release during early reperfusion predicts graft function in human lung transplantation. *Am J Respir Crit Care Med* **165:**211–215. PubMed
29. **Belperio JA, Keane MP, Burdick MD, Lynch JP III, Xue YY, Li K, Ross DJ, Strieter RM.** 2002. Critical role for CXCR3 chemokine biology in the pathogenesis of

bronchiolitis obliterans syndrome. *J Immunol* **169:**1037–1049. PubMed

30. **de Perrot M, Young K, Imai Y, Liu M, Waddell TK, Fischer S, Zhang L, Keshavjee S.** 2003. Recipient T cells mediate reperfusion injury after lung transplantation in the rat. *J Immunol* **171:**4995–5002. PubMed
31. **Zhao DX, Hu Y, Miller GG, Luster AD, Mitchell RN, Libby P.** 2002. Differential expression of the IFN-gamma-inducible CXCR3-binding chemokines, IFN-inducible protein 10, monokine induced by IFN, and IFN-inducible T cell alpha chemoattractant in human cardiac allografts: association with cardiac allograft vasculopathy and acute rejection. *J Immunol* **169:**1556–1560. PubMed
32. **Jackson JA, Kim EJ, Begley B, Cheeseman J, Harden T, Perez SD, Thomas S, Warshaw B, Kirk AD.** 2011. Urinary chemokines CXCL9 and CXCL10 are noninvasive markers of renal allograft rejection and BK viral infection. *Am J Transplant* **11:**2228–2234.
33. **Reynaud-Gaubert M, Marin V, Thirion X, Farnarier C, Thomas P, Badier M, Bongrand P, Giudicelli R, Fuentes P.** 2002. Upregulation of chemokines in bronchoalveolar lavage fluid as a predictive marker of post-transplant airway obliteration. *J Heart Lung Transplant* **21:**721–730. PubMed
34. **Bromley SK, Mempel TR, Luster AD.** 2008. Orchestrating the orchestrators: chemokines in control of T cell traffic. *Nat Immunol* **9:**970–980. PubMed
35. **Griffith JW, Luster AD.** 2013. Targeting cells in motion: migrating toward improved therapies. *Eur J Immunol* **43:**1430–1435. PubMed
36. **Corren J, Lemanske RF, Hanania NA, Korenblat PE, Parsey MV, Arron JR, Harris JM, Scheerens H, Wu LC, Su Z, Mosesova S, Eisner MD, Bohen SP, Matthews JG.** 2011. Lebrikizumab treatment in adults with asthma. *N Engl J Med* **365:**1088–1098. PubMed
37. **Kraft M.** 2011. Asthma phenotypes and interleukin-13—moving closer to personalized medicine. *N Engl J Med* **365:**1141–1144. PubMed
38. **Leung TF, Wong GW, Ko FW, Lam CW, Fok TF.** 2004. Increased macrophage-derived chemokine in exhaled breath condensate and plasma from children with asthma. *Clin Exp Allergy* **34:**786–791. PubMed
39. **Kurashima K, Mukaida N, Fujimura M, Schröder JM, Matsuda T, Matsushima K.** 1996. Increase of chemokine levels in sputum precedes exacerbation of acute asthma attacks. *J Leukoc Biol* **59:**313–316. PubMed
40. **Schnickel GT, Bastani S, Hsieh GR, Shefizadeh A, Bhatia R, Fishbein MC, Belperio J, Ardehali A.** 2008. Combined CXCR3/CCR5 blockade attenuates acute and chronic rejection. *J Immunol* **180:**4714–4721. PubMed
41. **Fischereder M, Schroppel B.** 2009. The role of chemokines in acute renal allograft rejection and chronic allograft injury. *Front Biosci (Landmark Ed)* **14:**1807–1814. PubMed
42. **Ho J, Rush DN, Gibson IW, Karpinski M, Storsley L, Bestland J, Stefura W, HayGlass KT, Nickerson PW.** 2010. Early urinary CCL2 is associated with the later development of interstitial fibrosis and tubular atrophy in renal allografts. *Transplantation* **90:**394–400. PubMed
43. **Ponath P, Kassam N, Qin S.** 2000. Monoclonal antibodies to chemokine receptors, p 231–242. *In* Proudfoot AE, Wells TN, Power CA (ed), *Methods in Molecular Biology: Chemokine Protocols*. Humana Press Inc, Totowa, NJ.
44. **Waldmann TA.** 1991. Monoclonal antibodies in diagnosis and therapy. *Science* **252:**1657–1662. PubMed
45. **Boyden S.** 1962. The chemotactic effect of mixtures of antibody and antigen on polymorphonuclear leucocytes. *J Exp Med* **115:**453–466. PubMed
46. **Moshfegh A, Halldén G, Lundahl J.** 1999. Methods for simultaneous quantitative analysis of eosinophil and neutrophil adhesion and transmigration. *Scand J Immunol* **50:**262–269. PubMed
47. **Bleul CC, Fuhlbrigge RC, Casasnovas JM, Aiuti A, Springer TA.** 1996. A highly efficacious lymphocyte chemoattractant, stromal cell-derived factor 1 (SDF-1). *J Exp Med* **184:**1101–1109. PubMed
48. **Richards KL, McCullough J.** 1984. A modified microchamber method for chemotaxis and chemokinesis. *Immunol Commun* **13:**49–62. PubMed
49. **Poznansky MC, Olszak IT, Foxall R, Evans RH, Luster AD, Scadden DT.** 2000. Active movement of T cells away from a chemokine. *Nat Med* **6:**543–548. PubMed
50. **Parent CA, Blacklock BJ, Froehlich WM, Murphy DB, Devreotes PN.** 1998. G protein signaling events are activated at the leading edge of chemotactic cells. *Cell* **95:**81–91. PubMed
51. **van Es S, Wessels D, Soll DR, Borleis J, Devreotes PN.** 2001. Tortoise, a novel mitochondrial protein, is required for directional responses of *Dictyostelium* in chemotactic gradients. *J Cell Biol* **152:**621–632. PubMed
52. **Meyvantsson I, Vu E, Lamers C, Echeverria D, Worzella T, Echeverria V, Skoien A, Hayes S.** 2011. Image-based analysis of primary human neutrophil chemotaxis in an automated direct-viewing assay. *J Immunol Methods* **374:**70–77. PubMed
53. **Ishii M, Kikuta J, Shimazu Y, Meier-Schellersheim M, Germain RN.** 2010. Chemorepulsion by blood S1P regulates osteoclast precursor mobilization and bone remodeling in vivo. *J Exp Med* **207:**2793–2798. PubMed
54. **Nitta N, Tsuchiya T, Yamauchi A, Tamatani T, Kanegasaki S.** 2007. Quantitative analysis of eosinophil chemotaxis tracked using a novel optical device—TAXIScan. *J Immunol Methods* **320:**155–163. PubMed
55. **Sumen C, Mempel TR, Mazo IB, von Andrian UH.** 2004. Intravital microscopy: visualizing immunity in context. *Immunity* **21:**315–329. PubMed
56. **Schürpf T, Springer TA.** 2011. Regulation of integrin affinity on cell surfaces. *EMBO J* **30:**4712–4727. PubMed
57. **Dransfield I, Cabañas C, Craig A, Hogg N.** 1992. Divalent cation regulation of the function of the leukocyte integrin LFA-1. *J Cell Biol* **116:**219–226. PubMed
58. **Weber KS, Klickstein LB, Weber C.** 1999. Specific activation of leukocyte beta2 integrins lymphocyte function-associated antigen-1 and Mac-1 by chemokines mediated by distinct pathways via the alpha subunit cytoplasmic domains. *Mol Biol Cell* **10:**861–873.
59. **Chan JR, Hyduk SJ, Cybulsky MI.** 2001. Chemoattractants induce a rapid and transient upregulation of monocyte alpha4 integrin affinity for vascular cell adhesion molecule 1 which mediates arrest: an early step in the process of emigration. *J Exp Med* **193:**1149–1158. PubMed
60. **Hirsch E, Katanaev VL, Garlanda C, Azzolino O, Pirola L, Silengo L, Sozzani S, Mantovani A, Altruda F, Wymann MP.** 2000. Central role for G protein-coupled phosphoinositide 3-kinase gamma in inflammation. *Science* **287:**1049–1053. PubMed
61. **Buser R, Proudfoot AE.** 2000. Calcium mobilization, p 143–148. *In* Proudfoot AE, Wells TN, Power CA (ed), *Methods in Molecular Biology: Chemokine Protocols*. Humana Press Inc, Totowa, NJ.
62. **Gonsiorek W, Zavodny P, Hipkin RW.** 2003. The study of CXCR3 and CCR7 pharmacology using [^{35}S]GTPgammaS exchange assays in cell membranes and permeabilized peripheral blood lymphocytes. *J Immunol Methods* **273:**15–27. PubMed
63. **Rivière C, Subra F, Cohen-Solal K, Cordette-Lagarde V, Letestu R, Auclair C, Vainchenker W, Louache F.** 1999. Phenotypic and functional evidence for the expression of CXCR4 receptor during megakaryocytopoiesis. *Blood* **93:**1511–1523. PubMed
64. **Weiner OD, Servant G, Welch MD, Mitchison TJ, Sedat JW, Bourne HR.** 1999. Spatial control of actin

polymerization during neutrophil chemotaxis. *Nat Cell Biol* **1:**75–81. PubMed
65. **Campanella GS, Medoff BD, Manice LA, Colvin RA, Luster AD.** 2008. Development of a novel chemokine-mediated in vivo T cell recruitment assay. *J Immunol Methods* **331:**127–139. PubMed
66. **Carbone FR, Sterry SJ, Butler J, Rodda S, Moore MW.** 1992. T cell receptor alpha-chain pairing determines the specificity of residue 262 within the Kb-restricted, ovalbumin257-264 determinant. *Int Immunol* **4:**861–867. PubMed
67. **Weissleder R, Mahmood U.** 2001. Molecular imaging. *Radiology* **219:**316–333. PubMed
68. **Germain RN, Robey EA, Cahalan MD.** 2012. A decade of imaging cellular motility and interaction dynamics in the immune system. *Science* **336:**1676–1681. PubMed
69. **Niesner RA, Hauser AE.** 2011. Recent advances in dynamic intravital multi-photon microscopy. *Cytometry A* **79:**789–798.
70. **Phan TG, Bullen A.** 2010. Practical intravital two-photon microscopy for immunological research: faster, brighter, deeper. *Immunol Cell Biol* **88:**438–444. PubMed
71. **Pittet MJ, Weissleder R.** 2011. Intravital imaging. *Cell* **147:**983–991. PubMed
72. **Phan TG, Grigorova I, Okada T, Cyster JG.** 2007. Subcapsular encounter and complement-dependent transport of immune complexes by lymph node B cells. *Nat Immunol* **8:**992–1000. PubMed
73. **Mempel TR, Scimone ML, Mora JR, von Andrian UH.** 2004. *In vivo* imaging of leukocyte trafficking in blood vessels and tissues. *Curr Opin Immunol* **16:**406–417. PubMed

Cytokines: Diagnostic and Clinical Applications

PRIYANKA VASHISHT AND TIMOTHY B. NIEWOLD

38

Many cytokines can be measured in the circulation via antibody-based detection protocols such as enzyme-linked immunosorbent assays and multianalyte bead systems. These measurement systems are robust and adaptable to many different analytes, and thus the large-scale measurement of cytokines in the circulation in human populations and disease states is possible. The measurement of cytokines in the circulation may provide a unique window into the immune response and the biology of human immune-related diseases. Cytokines represent messages sent between cells of the immune system, and thus confer a great deal information about ongoing immune processes. It is attractive to think that by intercepting these messages, we may be able to gain valuable insights regarding human disease diagnosis, prognosis, and potential therapeutic avenues. In this chapter, we review some of the ways in which cytokines are applied to clinical medicine. While cytokines can also be detected in tissue, this requires a biopsy, and for the purpose of this chapter we focus our discussion on circulating cytokines.

In the realm of diagnosis, we discuss how cytokine profiles may be applied to the diagnosis of autoimmune disease. While most of these efforts are still in the research arena, this is a promising area that may be implemented in the diagnostic algorithms in the near future. We also discuss the role of cytokines in the etiology of immune-related diseases. This is a broad area, and we focus on a few illustrative stories. For example, in some settings, genetic background can lead to the alteration of cytokine profiles or signaling, which subsequently leads to the development of disease. Another example demonstrates the use of modern gene expression profiling techniques to implicate cytokine pathways in human disease, which can enable novel therapeutic strategies. Circulating cytokines may also provide prognostic information. In autoimmune disease, differences in cytokine profile may indicate differences in disease severity and clinical manifestations between different patients. In this way, the measurement of cytokines in circulation may predict disease outcome. Additionally, baseline cytokine profiles may be useful in predicting therapeutic outcomes, indicating which patients may be appropriate for a particular therapy.

Cytokines and cytokine inhibitors have also been used in the treatment of human diseases. In the last section of this chapter, we summarize some of the major uses of recombinant human cytokines as well as cytokine inhibitors in the treatment of human disease. For example, in rheumatoid arthritis (RA), a number of cytokine inhibitors have been approved by the Food and Drug Administration (FDA) for treatment. Therapeutic algorithms in inflammatory bowel disease also include the use of cytokine inhibitors. In other cases, recombinant human cytokines have been used as therapeutics in human disease. In chronic viral hepatitis C, alpha interferon (IFN-α) has been used as a therapeutic with great success, augmenting the subject's own viral immunity. Additionally, IFN-β has been used with great success in the treatment of multiple sclerosis. It is not possible to summarize all possible ways in which the measurement of circulating cytokines may prove useful in human disease, but in this chapter we provide some illustrative examples that span multiple fields of clinical medicine.

DIAGNOSIS

Profiles of circulating cytokines may be useful in the diagnosis of autoimmune conditions. Autoimmune conditions are caused by primary disturbances in the immune system, characterized by immune system activation and the loss of self/nonself discrimination, resulting in chronic inflammation in characteristic tissue sites that differ among diseases. The use of cytokines to aid in the diagnosis of autoimmune diseases aims to leverage the information that can be gained by measuring immune system response modifiers and the between-cell communications in the circulation. We will discuss two examples in which work examining circulating cytokines may be applicable to diagnosis in autoimmune disease: RA and systemic lupus erythematosus (SLE).

In RA, a number of studies have examined profiles of circulating cytokines. Cytokines that are elevated include tumor necrosis factor alpha (TNF-α), interleukin-6 (IL-6), IFN-γ, and others (1). Interestingly, studies have also assessed cytokine profiles in samples taken from individuals before they developed RA (2). This study design leverages existing blood banks that have a sample stored from a date prior to the time that an individual developed RA. In these samples that predate the clinical onset of disease, an increasing prevalence of elevations in a number of inflammatory cytokines can be observed, which intensifies as the subject approaches the date of diagnosis (2). This would suggest that elevations in circulating cytokines and activation of the immune system predate disease by many years. While this information is not yet used clinically, it is possible that

doi:10.1128/9781555818722.ch38

circulating cytokines could be useful in early diagnosis or in the prediction of disease. While this is not currently possible, it seems that the feasibility of this approach could be enhanced by including other data such as family history, genetic markers, and environmental risk factors.

Cytokines may not be sufficient for the complete diagnosis of autoimmune conditions, but they are an important parameter. One approach has been to incorporate cytokines in the circulation along with autoantibodies and other disease manifestations and attempt to make a multimodal biomarker composite score (3). These are currently being developed, and one is now available for practicing physicians for RA. It will be interesting to see how these evolve over time, as our knowledge of the pathogenesis of disease is still incomplete and it is likely that additional marker sets will be developed in the future. For example, despite brisk progress in genetics, much of the genetic variation underlying autoimmune diseases remains to be discovered. Additionally, most autoimmune diseases demonstrate both clinical and biological heterogeneity—differences between patients who are diagnosed with the same condition. While clinicians have long appreciated this idea, new studies are identifying some of the biological and immune system parameters that underlie this clinical heterogeneity (4); incorporating these features into diagnostic algorithms would be useful and improve our diagnostic capacity.

In SLE, elevated cytokines include IFN-α, TNF-α, as well as IL-6, and interestingly, IL-2 cytokine levels are low (5). With regard to the elevation of IFN-α, this is one of the most impressive abnormalities when examining peripheral blood gene expression profiles. The remarkable elevation of IFN-α-induced transcripts in the peripheral blood has led to use of the term "interferon signature" to describe this finding. The coordinate upregulation of such a large number of IFN-induced transcripts strongly supports that IFN-α is present in the circulation and signaling through the receptors on the cells. Not all patients with lupus exhibit the IFN signature, but it is a major discriminator between cases and controls in those cases that have the signature. This is not yet being used as a diagnostic test but holds promise for future diagnostics.

ETIOLOGY: GENETICS AND GENOMICS OF HUMAN CYTOKINE RESPONSES

IFN-α in SLE

IFN-α is an antiviral cytokine in the type I IFN family. It is classically induced following activation of viral pattern recognition receptors like endosomal Toll-like receptors (TLRs) and cytosolic nucleic acid sensors (6). IFN-α signaling causes a spectrum of effects upon the immune system, including upregulation of the major histocompatibility complex molecules and activation of antigen-presenting cells (6). IFN-α is in a critical position bridging the innate and adaptive immune responses and thereby could be instrumental in setting thresholds for autoimmunity (7). There are many reports in the literature to support the involvement of IFN-α as a primary pathogenic factor in the human autoimmune syndrome SLE (7). Major lines of evidence that support a primary role of IFN-α in the pathogenesis of human lupus are as follows.

1. Serum IFN-α levels are high in human SLE.
2. Therapeutic IFN-α can induce SLE in humans.
3. High serum IFN-α is a heritable risk factor for SLE.
4. SLE-associated autoantibodies are strongly associated with serum IFN-α in SLE patients.
5. SLE-associated genetic variations in the IFN-α pathway are gain-of-function.
6. Novel genetic loci are associated with IFN-α and autoantibodies in SLE.

Serum IFN-α Levels Are High in Human SLE

As early as the 1970s, many investigators detected elevated levels of type I IFNs in SLE patient sera (8, 9). Subsequent gene expression microarray studies in peripheral blood cells revealed that overexpression of type I IFN-induced genes is a common pattern in SLE (10, 11). Because large-scale measurement using either microarray or real-time PCR of freshly isolated circulating blood cells was limiting, and enzyme-linked immunosorbent assay has been characterized by poor sensitivity and specificity in human sera, a method of assessing serum IFN-α was developed using human cell lines (12, 13). WISH cells were chosen based on their known sensitivity to type I IFNs and their use in the initial viral inhibition assays employed to detect type I IFNs. In this assay:

1. The WISH cells are incubated with serum for 6 h, and then the cells are lysed.
2. Total mRNA is purified from the cells, and then this mRNA is converted to cDNA.
3. Three classical IFN-induced genes are quantified using real-time PCR (*IFIT1*, *MX1*, and *PKR*) (13), and expression of these genes is compared to housekeeping gene expression in the same sample.
4. The level of induction of IFN-induced gene expression caused by the patient sera is then normalized to the mean and standard deviation of the induction of the same genes by healthy donor sera in WISH cells. This step accounts for the fact that different transcripts are induced to different degrees after stimulation with the same amount of IFN-α. If gene expression values are summed directly, then the most highly induced transcripts tend to dominate the overall score.
5. After the genes are normalized in this way, the various levels of induction are summed, and a standardized IFN-induced gene score is generated.

Standard curves can be run with known amounts of IFN-α, and if desired, the IFN-induced gene score could be converted back to a picograms-per-milliliter measurement. One important benefit of this assay is that frozen serum banks can be studied, and the need for live or fresh cells is obviated. Additionally, the WISH cell line is clonal and stable, and the response to a given amount of IFN is reliable from experiment to experiment. Patient cells are more heterogeneous, likely due to differences in genetic background between people and differences in cellular activation states and the proportional composition of the various immune cells in either whole blood or mononuclear cell fractions. This heterogeneity can be interesting but also likely makes the interpretation of the IFN signature more complicated and less direct as a measurement of IFN in the circulation. WISH cell assays for circulating type I IFN activity are correlated with microarray IFN signatures run on the same sample, but as expected, the correlation is not perfect, likely due to the issues raised above. The WISH cells are epithelial-type cells, and while they express the type I IFN receptor, they do not express many other immune receptors such as TLRs, etc., and cycloheximide does not reduce the amount of IFN detected, suggesting that autocrine and paracrine IFN-related signaling is not contributing to the WISH cell output.

Therapeutic IFN-α Can Induce SLE in Humans

There are a number of published reports describing IFN-α-induced SLE in patients receiving recombinant human IFN-α to treat malignancy and chronic viral infection (14, 15). These patients show the highly specific and characteristic manifestations typical of idiopathic SLE. When IFN-α was withdrawn, many of these cases improved or resolved, supporting the idea that the IFN-α was causal (15). This human experience provides a proof of principle that IFN-α can break tolerance (16) and that this IFN-α-induced tolerance break in some individuals results in the very specific autoimmune phenotype of SLE. Importantly, not all patients who receive exogenous IFN-α develop SLE, which indicates that signaling through this pathway is polymorphic in nature and is dependent on other host factors.

High Serum IFN-α Is a Heritable Risk Factor for SLE

Abnormally high levels of IFN-α are present in healthy first-degree relatives of SLE patients as compared with healthy unrelated subjects (13), suggesting that high serum IFN-α is an inherited risk factor for SLE. A number of genetic variants have now been associated with increased IFN-α in SLE (17, 18), which further supports the concept of heritability. The familial nature of the high-IFN-α trait is common across SLE patients of all ancestral backgrounds, suggesting that high serum IFN-α is a common shared pathway to SLE susceptibility.

SLE-Associated Autoantibodies Are Strongly Associated With Serum IFN-α in SLE Patients

SLE patients produce autoantibodies that bind to double-stranded DNA or small RNA-binding proteins such as Ro, La, Sm, and RNP. Immune complexes formed by these autoantibodies can activate normal antiviral immunity through the endosomal TLRs and generate IFN-α. *In vitro* experiments have supported this idea, showing that SLE-associated immune complexes can induce IFN-α production in human peripheral blood mononuclear cell (PBMC) and dendritic cell cultures (19). In SLE patients, autoantibody profiles provide the strongest correlation with serum IFN-α as compared with other clinical features (13, 20), supporting the idea that the *in vitro* model is relevant in humans *in vivo*. A two-hit model may apply, in which the formation of SLE-associated autoantibodies exacerbates an underlying genetic tendency toward greater IFN-α production or greater IFN-α sensitivity, resulting in clinical development of lupus.

SLE-Associated Genetic Variations in the IFN-α Pathway Are Gain-of-Function

A number of the genetic polymorphisms that contribute to susceptibility to SLE are found in the genes that function in the IFN-α pathway. These polymorphisms have been linked to greater IFN-α activity or greater sensitivity to IFN, and hence are gain-of-function in nature. For example, genetic variations in both interferon regulatory factor 5 (IRF5) and IRF7 have been associated with lupus (21). These transcription factors work downstream of the endosomal TLRs and can induce the transcription of IFN-α. Interestingly, these genetic variations are linked to higher IFN-α levels only in those SLE patients who have specific autoantibodies (22). This suggests an induced model, in which the chronic stimulation of the TLR system by autoantibody immune complexes results in dysregulation of circulating IFN in the presence of these gain-of-function variants in IRF5 and IRF7 (23). Other gene polymorphisms reported include polymorphisms in STAT4 (24), IRF8 (25), IFIH1 (IFN induced with helicase C domain 1) (26), and PTPN22 (protein tyrosine phosphatase N22) (17), among others. See Fig. 1 for an illustration of these genes positioned in their proposed cellular pathways. Additionally, through genetic mapping of high IFN levels in SLE, a number of novel loci have been discovered that have an impact on IFN levels in SLE (18). This further supports the idea that IFN levels are influenced by genetics and that activation of this pathway is heterogeneous among SLE patients. In conclusion, multiple lines of evidence support the involvement of IFN-α in the primary pathogenesis of human SLE. There is intriguing genetic evidence that signaling through this pathway is highly polymorphic in humans, and this may explain the heterogeneity in response to exogenous IFN-α. This same heterogeneity in IFN-α signaling seems to underlie idiopathic SLE as well.

IL-1 in Juvenile Idiopathic Arthritis

Systemic-onset juvenile idiopathic arthritis (SoJIA) contributes to ~10% of cases of arthritis with onset in childhood (27). This disease is characterized by prolonged and severe clinical manifestations, severity of joint involvement, and lack of response to TNF blockade (27, 28). Due to frequent poor outcomes and long-term disability, this disease represents a serious challenge to pediatric rheumatologists. Patients frequently need prolonged courses of steroids and/or methotrexate to control their disease. Anti-TNF therapy works in some types of juvenile idiopathic arthritis; however, most SoJIA patients do not respond.

The exact molecular pathogenesis of SoJIA remains an enigma, but treatment has been significantly advanced by the use of IL-1 inhibitors. A seminal gene expression study by Pascual et al. (29) supported the idea that IL-1 is a major mediator of the inflammatory cascade that underlies SoJIA and that an IL-1 receptor antagonist (IL-1Ra) would be effective as a treatment for this disease. The key results that indicate the role of IL-1 in SoJIA are as follows. The incubation of healthy PBMCs with SoJIA serum upregulated transcription of innate immunity genes, including several members of the IL-1 cytokine/cytokine receptor family, specifically IL-1a and IL-1b as well as their receptors, IL-1R1 and IL-1R2 (29). Additionally, SoJIA sera induced healthy PBMCs to produce multifold-increased levels of IL-1b, and sera from febrile patients were more efficient in inducing the secretion in comparison with afebrile sera. High levels of IL-1b were also produced by activated SoJIA PBMCs. Dramatic responses have been observed with the use of IL-1 antagonism in this disease, including resolution of fever and systemic symptoms, even in highly refractory cases not responding to conventional treatment (29, 30). Parallel improvements in inflammatory markers and blood counts are typically observed. To summarize, the central role of IL-1 in SoJIA is supported by gene expression studies in the disease and illustrated by the remarkable clinical response of patients to IL-1Ra.

TREATMENT: CYTOKINE INHIBITORS AND RECOMBINANT CYTOKINES AS THERAPY

Treatment with Cytokine Inhibitors

RA

Joint inflammation results from an imbalance in the cytokine cascade. The clinical management of RA has been revolutionized by the introduction of "biological agents," including monoclonal antibodies (MAbs), fusion proteins, and Fab (fragment antigen-binding) portions of MAbs (Table 1). The

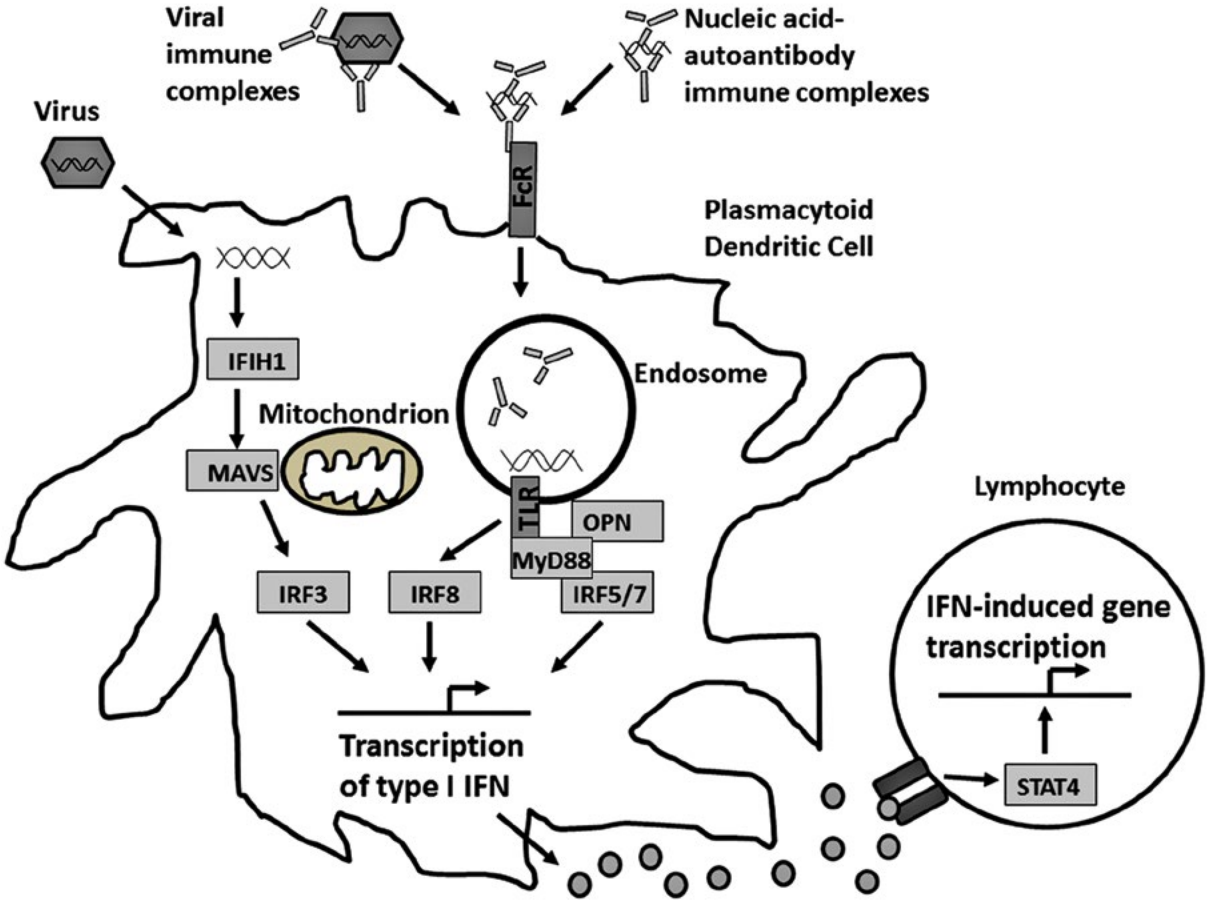

FIGURE 1 Diagram illustrating the proposed cascade of IFN production in SLE, with SLE risk genes demonstrated in boxes within the cells. Viruses and immune complexes made from SLE-associated autoantibodies can stimulate both the TLR and cytosolic nucleic acid recognition systems. Multiple SLE risk genes are found in these pathways, resulting in augmented type I IFN production in plasmacytoid dendritic cells. IFN is recognized by other cells in the immune system via the type I IFN receptor, and some SLE risk genes such as STAT4 are associated with greater IFN-induced gene expression. MAVS, mitochondrial antiviral signaling protein; MyD88, myeloid differentiation primary response gene 88; OPN, osteopontin.

biological therapeutics approved for use in RA target the proinflammatory cytokines TNF-α, IL-1, and IL-6, which are key players in the pathogenesis of RA (31). We will focus our discussion on each of these three mechanisms of action. Of note, there are two additional biologic agents that target the B-cell-specific antigen CD20 and T-cell antigen CD28, respectively, and these will not be dealt with in detail as their mechanisms are not direct cytokine inhibition.

TNF-α Inhibition

Beginning in the late 1990s, TNF-α-inhibiting drugs have received regulatory approval for use in RA. Currently available drugs include MAbs directed at TNF-α (either chimeric mouse-human or fully human antibodies), antibody fragments that target TNF-α, and soluble decoy receptors that can bind TNF-α but do not result in any signaling, effectively neutralizing the biological effect of TNF-α. TNF-α inhibitors have been used in combination with methotrexate or alone in the treatment of RA.

Mechanism of action. MAbs that target TNF-α bind to both soluble and membrane-bound TNF-α with high affinity, forming stable nondissociating immune complexes. This binding neutralizes the biological activity of TNF-α by inhibiting its binding to receptor. The TNF-α receptor decoy can bind to both soluble TNF-α and soluble TNF-β (lymphotoxin-α). Blocking TNF-α inhibits the release of proinflammatory cytokines (IL-1, IL-6, IL-8, and granulocyte-macrophage colony-stimulating factor) and acute-phase reactants. This alteration of cytokine profiles in the disease results in inhibition of the activation of eosinophils and neutrophils, as well as inhibition of leukocyte migration (32). Through the binding of MAbs to membrane-bound TNF-α, cells expressing TNF-α can be lysed in the presence of complement.

Adverse events. Several side effects have been noted in patients taking anti-TNF-α agents. The chances of tuberculosis (TB) are increased in patients receiving TNF-α inhibitors, and therefore testing for latent TB is recommended prior to initiating therapy. If latent TB is suspected, then treatment of latent TB infection is recommended before starting TNF-α inhibition (33). It seems likely that TNF-α inhibition may destabilize old granulomas containing latent

TABLE 1 Anticytokine therapy in RA

Name of biologic (commercial name)	Approval year (FDA)	Class	Type	Target
Infliximab (Remicade)	1998	Chimeric MAb	IgG1	TNF-α
Etanercept (Enbrel)	1998	Human dimeric fusion protein	Fusion protein	TNF-α
Adalimumab (Humira)	2002	Human MAb	IgG1	TNF-α
Certolizumab pegol (Cimzia)	2008	Humanized Fab fragment	Pegylated Fab	TNF-α
Golimumab (Simponi)	2009	Human MAb	IgG1	TNF-α
Tocilizumab (RoActemra)	2009	Humanized MAb	IgG1	IL-6R
Anakinra (Kineret)	2001	Human IL-1ra	Receptor antagonist	IL-1

TB, allowing the infection to become active. Worsening of chronic hepatitis B infection is also a concern, and testing for hepatitis B is recommended prior to beginning therapy. Other common adverse events are headache, vertigo, viral infection, flushing, upper and lower respiratory tract infection, dyspnea, sinusitis, nausea, infusion-related reactions, diarrhea, dyspepsia, urticaria, abdominal pain, and elevated liver enzymes. Because rates of bacterial infection are increased, careful observation of patients is important for the early awareness of development of signs and symptoms of infection during and after therapy. The production of antibodies directed at the therapeutic protein has been observed in patients with RA (34), and it seems possible that some of these antibodies are able to neutralize the efficacy of the drug, although in many cases no decrease in efficacy is observed. Additionally, new onset or increase in titer of antinuclear autoantibodies, similar to those detected in SLE and connective tissue diseases, has been reported in patients taking anti-TNF-α agents (35). Additionally, some patients have developed a multiple sclerosis-like syndrome that typically improves when the drug is stopped. A risk of lymphoma had been suggested in early data sets and resulted in a package label warning, although many recent studies have not supported the association between TNF-α inhibition in RA and the development of lymphoma (36).

Clinical efficacy. A number of large double-blind, randomized trials have been conducted examining the use of TNF-α inhibitors in RA patients. Some have examined the addition of a TNF-α inhibitor to standard therapy with methotrexate, and others have included study arms examining use of the anti-TNF-α agent alone (37–39). These trials have demonstrated that anti-TNF-α therapies can reduce signs and symptoms of active RA, inhibit radiographic progression of structural damage, and improve physical function. These studies have included thousands of patients in both early and later stages of disease (35).

IL-6 Inhibition

A MAb targeting the IL-6 receptor (IL-6R) was approved by the FDA in 2010 for the treatment of RA patients with moderate to severe active RA who do not respond to one or more conventional RA drugs such as methotrexate or TNF antagonist therapies. This humanized anti-IL-6R antibody is engineered by grafting the complementarity-determining regions of a mouse anti-human IL-6R antibody into human IgG1κ to create a humanized MAb with specificity to human IL-6R.

Mechanism of action. The anti-IL-6 therapy binds to the IL-6 binding site of human IL-6R and competitively inhibits IL-6 signaling, neutralizing the action of IL-6. Tocilizumab binds specifically to both soluble and membrane-bound IL-6Rs and has been shown to inhibit soluble and membrane-bound IL-6R-mediated signaling. IL-6 is a pleiotropic proinflammatory cytokine that has widespread effects on acute-phase reactants and hematopoietic lineages, such as induction of Ig production in B cells, T-cell proliferation, and differentiation into cytotoxic T cells (40).

Adverse events. As with all immunosuppressive treatments for RA, careful observation of patients is important for the early awareness of signs and symptoms of infection during and after therapy. Common adverse reactions may include lung infection (pneumonia), abnormal liver function tests, conjunctivitis, headache, hypertension, and serious hypersensitivity reactions. Regular monitoring of liver enzymes, blood counts, and serum lipids is required with IL-6 signaling blockade. In particular, both neutropenia and thrombocytopenia have been observed with IL-6 signaling blockade.

Clinical efficacy. Several multicenter, double-blind, placebo-controlled, phase 3 trials were conducted to evaluate the efficacy of IL-6 signaling blockade. These studies have documented significant improvement in standardized disease outcome measures in thousands of RA patients (41). These studies compared patients taking standard therapy with methotrexate to those receiving both methotrexate and IL-6 signaling blockade, and demonstrated a nonredundant effect of IL-6 blockade in addition to standard therapy on RA disease features, similar to that seen with the anti-TNF-α agents outlined above.

IL-1 Inhibition

A recombinant human IL-1Ra was approved by the FDA in November 2001 for use in RA patients who have failed one or more traditional RA drugs. It is the first selective blocker of IL-1, a cytokine that plays an important role in RA pathogenesis. This molecule is a recombinant,

nonglycosylated form of the human IL-1Ra, which is produced in *Escherichia coli* expression systems. Anakinra differs from native human IL-1Ra in that it has the addition of a single methionine residue at its amino terminus (31).

Mechanism of action. The recombinant IL-1Ra molecule blocks the biologic activity of IL-1a and IL-1b by competitively inhibiting their binding to the IL-1R. IL-1 is an inflammatory mediator that binds to the IL-1R and triggers the inflammatory response. The presence of IL-1 in the synovial tissue of the affected joints induces production of osteoclasts that further exacerbate the inflammation. Anakinra neutralizes responses elicited by IL-1 *in vitro*, including the induction of nitric oxide and prostaglandin E_2 and/or collagenase production by synovial cells, chondrocytes, and fibroblasts.

Adverse events. The most common and frequently reported side effect is injection-site reaction, which is usually mild, characterized by erythema, ecchymosis, inflammation, and pain, and lasts for 15 days to 1 month. Other frequent side effects may include bacterial infection such as cellulitis, bone and joint infections, and pneumonia, similar to those reported with other biological agents used in RA. Patients are also prone to develop neutropenia, which can increase the infection risk (31).

Clinical efficacy. Double-blind clinical trials have been performed using recombinant IL-1Ra to treat patients with RA. These studies have suggested some clinical efficacy of IL-1 antagonism, generally concluding modest efficacy and relative safety (42). Because many consider the other approved therapies in RA to have greater efficacy, the use of IL-1 antagonists in RA has been somewhat limited, but as noted in the section above, they have been highly effective in a particular form of juvenile-onset RA.

Inflammatory Bowel Disease

Inflammatory bowel disease is a group of chronic disorders of the gastrointestinal tract comprising Crohn's disease (CD) and ulcerative colitis (UC). Their etiologies are unknown, but they are characterized by an imbalanced production of proinflammatory mediators, e.g., TNF-α, as well as increased recruitment of leukocytes to the site of inflammation. Increased understanding of the role of the inflammatory pathways in inflammatory bowel disease has led to new therapies, including the TNF-α inhibitors outlined above. TNF inhibitors have been shown to be effective in treating moderate to severe CD and UC (43).

Several double-blind, placebo-controlled trials have demonstrated that TNF inhibitors are efficacious in moderate to severe CD, as both first- and second-line therapy, and in maintenance of response and remission (44, 45). TNF inhibitors also allowed tapering of glucocorticoid therapy and mucosal healing in CD patients (44, 45).

Similar results have been observed in UC, with randomized, controlled trials demonstrating benefit from TNF inhibitors (46, 47) in inducing and maintaining clinical remission. Interestingly, the TNF decoy receptor has not been effective in CD and UC, suggesting that there is some mechanistic difference in the way these drugs work between RA and inflammatory bowel disease. One main difference is the ability of the MAbs and antibody fragments to bind membrane-bound TNF-α and possibly induce cell death or otherwise alter cellular signaling via membrane-bound TNF-α, while the decoy receptor binds to soluble TNF-α.

Treatment with Recombinant Cytokines

Chronic Viral Hepatitis C Treated with IFN-α

Recombinant human IFN-α has been a major therapeutic option in the treatment of chronic viral hepatitis C. While some newer antiviral therapies are currently revolutionizing treatment of hepatitis C, combination regimens that include recombinant human IFN-α are still common (48). The rationale for IFN-α in the treatment of hepatitis C is directly related to its properties as an antiviral protein, which are summarized above in the section on SLE. The common side effects are largely related to the action of the drug on the immune system, including flu-like symptoms on the day of injection, injection-site reactions, and in some cases features of autoimmune disease such as antinuclear antibodies and SLE (15).

Multiple Sclerosis Treated with IFN-β

Multiple sclerosis has been treated effectively with recombinant human IFN-β (49). This is somewhat surprising at first glance, given that multiple sclerosis is an autoimmune disease and the related cytokine IFN-α has been associated with the development of autoimmune disease, as noted above. While we do not know the exact reasons why different highly related members of the same cytokine family can induce or treat different autoimmune diseases, there are interesting theories currently. Circulating levels of IFN are low in multiple sclerosis, the opposite of SLE, and it is possible that the decrease in IFN levels present in multiple sclerosis is pathogenic in the disease (50). This would suggest that either too much or too little type I IFN may predispose to autoimmune disease. It is likely that this story will become more complex as more is understood about IFNs in autoimmunity. Side effects of IFN-β are similar to those of IFN-α, although interestingly, reports of new-onset connective tissue disease seem to be uncommon in multiple sclerosis patients treated with IFN-β.

REFERENCES

1. **Astry B, Harberts E, Moudgil KD.** 2011. A cytokine-centric view of the pathogenesis and treatment of autoimmune arthritis. *J Interferon Cytokine Res* **31:**927–940.
2. **Deane KD, O'Donnell CI, Hueber W, Majka DS, Lazar AA, Derber LA, Gilliland WR, Edison JD, Norris JM, Robinson WH, Holers VM.** 2010. The number of elevated cytokines and chemokines in preclinical seropositive rheumatoid arthritis predicts time to diagnosis in an age-dependent manner. *Arthritis Rheum* **62:**3161–3172.
3. **Curtis JR, van der Helm-van Mil AH, Knevel R, Huizinga TW, Haney DJ, Shen Y, Ramanujan S, Cavet G, Centola M, Hesterberg LK, Chernoff D, Ford K, Shadick NA, Hamburger M, Fleischmann R, Keystone E, Weinblatt ME.** 2012. Validation of a novel multibiomarker test to assess rheumatoid arthritis disease activity. *Arthritis Care Res (Hoboken)* **64:**1794–1803.
4. **Ko K, Koldobskaya Y, Rosenzweig E, Niewold TB.** 2013. Activation of the interferon pathway is dependent upon autoantibodies in African-American SLE patients, but not in European-American SLE patients. *Front Immunol* **4:**309. doi:10.3389/fimmu.2013.00309.
5. **Lourenço EV, La Cava A.** 2009. Cytokines in systemic lupus erythematosus. *Curr Mol Med* **9:**242–254.
6. **Pestka S, Krause CD, Walter MR.** 2004. Interferons, interferon-like cytokines, and their receptors. *Immunol Rev* **202:**8–32.
7. **Niewold TB.** 2011. Interferon alpha as a primary pathogenic factor in human lupus. *J Interferon Cytokine Res* **31:**887–892.

8. **Hooks JJ, Moutsopoulos HM, Geis SA, Stahl NI, Decker JL, Notkins AL.** 1979. Immune interferon in the circulation of patients with autoimmune disease. *N Engl J Med* **301:**5–8.
9. **Ytterberg SR, Schnitzer TJ.** 1982. Serum interferon levels in patients with systemic lupus erythematosus. *Arthritis Rheum* **25:**401–406.
10. **Baechler EC, Batliwalla FM, Karypis G, Gaffney PM, Ortmann WA, Espe KJ, Shark KB, Grande WJ, Hughes KM, Kapur V, Gregersen PK, Behrens TW.** 2002. Interferon-inducible gene expression signature in peripheral blood cells of patients with severe lupus. *Proc Natl Acad Sci U S A* **100:**2610–2615.
11. **Bennett L, Palucka AK, Arce E, Cantrell V, Borvak J, Banchereau J, Pascual V.** 2003. Interferon and granulopoiesis signatures in systemic lupus erythematosus blood. *J Exp Med* **197:**711–723.
12. **Hua J, Kirou K, Lee C, Crow MK.** 2006. Functional assay of type I interferon in systemic lupus erythematosus plasma and association with anti-RNA binding protein autoantibodies. *Arthritis Rheum* **54:**1906–1916.
13. **Niewold TB, Hua J, Lehman TJ, Harley JB, Crow MK.** 2007. High serum IFN-α activity is a heritable risk factor for systemic lupus erythematosus. *Genes Immun* **8:**492–502.
14. **Ioannou Y, Isenberg DA.** 2000. Current evidence for the induction of autoimmune rheumatic manifestations by cytokine therapy. *Arthritis Rheum* **43:**1431–1442.
15. **Niewold TB, Swedler WI.** 2005. Systemic lupus erythematosus arising during interferon-alpha therapy for cryoglobulinemic vasculitis associated with hepatitis C. *Clin Rheumatol* **24:**178–181.
16. **Niewold TB.** 2008. Interferon alpha-induced lupus: proof of principle. *J Clin Rheumatol* **14:**131–132.
17. **Kariuki SN, Crow MK, Niewold TB.** 2008. The PTPN22 C1858T polymorphism is associated with skewing of cytokine profiles toward high interferon-α activity and low tumor necrosis factor α levels in patients with lupus. *Arthritis Rheum* **58:**2818–2823.
18. **Kariuki SN, Franek BS, Kumar AA, Arrington J, Mikolaitis RA, Utset TO, Jolly M, Crow MK, Skol AD, Niewold TB.** 2010. Trait-stratified genome-wide association study identifies novel and diverse genetic associations with serologic and cytokine phenotypes in systemic lupus erythematosus. *Arthritis Res Ther* **12:**R151. doi:10.1186/ar3101.
19. **Lövgren T, Eloranta ML, Båve U, Alm GV, Rönnblom L.** 2004. Induction of interferon-α production in plasmacytoid dendritic cells by immune complexes containing nucleic acid released by necrotic or late apoptotic cells and lupus IgG. *Arthritis Rheum* **50:**1861–1872.
20. **Weckerle CE, Franek BS, Kelly JA, Kumabe M, Mikolaitis RA, Green SL, Utset TO, Jolly M, James JA, Harley JB, Niewold TB.** 2011. Network analysis of associations between serum interferon-α activity, autoantibodies, and clinical features in systemic lupus erythematosus. *Arthritis Rheum* **63:**1044–1053.
21. **Graham RR, Kozyrev SV, Baechler EC, Reddy MV, Plenge RM, Bauer JW, Ortmann WA, Koeuth T, González Escribano MF, Argentine and Spanish Collaborative Groups, Pons-Estel B, Petri M, Daly M, Gregersen PK, Martín J, Altshuler D, Behrens TW, Alarcón-Riquelme ME.** 2006. A common haplotype of interferon regulatory factor 5 (IRF5) regulates splicing and expression and is associated with increased risk of systemic lupus erythematosus. *Nature Genet* **38:**550–555.
22. **Niewold TB, Kelly JA, Flesch MH, Espinoza LR, Harley JB, Crow MK.** 2008. Association of the IRF5 risk haplotype with high serum interferon-α activity in systemic lupus erythematosus patients. *Arthritis Rheum* **58:**2481–2487.
23. **Salloum R, Niewold TB.** 2011. Interferon regulatory factors in human lupus pathogenesis. *Transl Res* **157:**326–331.
24. **Kariuki SN, Kirou KA, MacDermott EJ, Barillas-Arias L, Crow MK, Niewold TB.** 2009. Cutting edge: autoimmune disease risk variant of STAT4 confers increased sensitivity to IFN-α in lupus patients in vivo. *J Immunol* **182:**34–38.
25. **Chrabot BS, Kariuki SN, Zervou MI, Feng X, Arrington J, Jolly M, Boumpas DT, Reder AT, Goulielmos GN, Niewold TB.** 2013. Genetic variation near IRF8 is associated with serologic and cytokine profiles in systemic lupus erythematosus and multiple sclerosis. *Genes Immun* **14:**471–478.
26. **Robinson T, Kariuki SN, Franek BS, Kumabe M, Kumar AA, Badaracco M, Mikolaitis RA, Guerrero G, Utset TO, Drevlow BE, Zaacks LS, Grober JS, Cohen LM, Kirou KA, Crow MK, Jolly M, Niewold TB.** 2011. Autoimmune disease risk variant of IFIH1 is associated with increased sensitivity to IFN-α and serologic autoimmunity in lupus patients. *J Immunol* **187:**1298–1303.
27. **Bowyer SL, Roettcher PA, Higgins GC, Adams B, Myers LK, Wallace C, Rennebohm R, Moore TL, Pepmueller PH, Spencer C, Wagner-Weiner L, Rabinovich E, Passo M, Lovell DJ, McCurdy D, Zemel L, Schikler KN, Szer I, Kurtin P, Lindsley C.** 2003. Health status of patients with juvenile rheumatoid arthritis at 1 and 5 years after diagnosis. *J Rheumatol* **30:**394–400.
28. **Wallace CA, Levinson JE.** 1991. Juvenile rheumatoid arthritis: outcome and treatment for the 1990s. *Rheum Dis Clin North Am* **17:**891–905.
29. **Pascual V, Allantaz F, Arce E, Punaro M, Banchereau J.** 2005. Role of interleukin-1 (IL-1) in the pathogenesis of systemic onset juvenile idiopathic arthritis and clinical response to IL-1 blockade. *J Exp Med* **201:**1479–1486.
30. **Verbsky JW, White AJ.** 2004. Effective use of the recombinant interleukin 1 receptor antagonist anakinra in therapy resistant systemic onset juvenile rheumatoid arthritis. *J Rheumatol* **31:**2071–2075.
31. **Malviya G, Salemi S, Laganà B, Diamanti AP, D'Amelio R, Signore A.** 2013. Biological therapies for rheumatoid arthritis: progress to date. *BioDrugs* **27:**329–345.
32. **Scallon BJ, Moore MA, Trinh H, Knight DM, Ghrayeb J.** 1995. Chimeric anti-TNF-α monoclonal antibody cA2 binds recombinant transmembrane TNF-α and activates immune effector functions. *Cytokine* **7:**251–259.
33. **Gardam MA, Keystone EC, Menzies R, Manners S, Skamene E, Long R, Vinh DC.** 2003. Anti-tumour necrosis factor agents and tuberculosis risk: mechanisms of action and clinical management. *Lancet Infect Dis* **3:**148–155.
34. **Rau R.** 2002. Adalimumab (a fully human anti-tumour necrosis factor α monoclonal antibody) in the treatment of active rheumatoid arthritis: the initial results of five trials. *Ann Rheum Dis* **61**(Suppl 2)**:**ii70–ii73.
35. **Genovese MC, Bathon JM, Martin RW, Fleischmann RM, Tesser JR, Schiff MH, Keystone EC, Wasko MC, Moreland LW, Weaver AL, Markenson J, Cannon GW, Spencer-Green G, Finck BK.** 2002. Etanercept versus methotrexate in patients with early rheumatoid arthritis: two-year radiographic and clinical outcomes. *Arthritis Rheum* **46:**1443–1450.
36. **Kaiser R.** 2008. Incidence of lymphoma in patients with rheumatoid arthritis: a systematic review of the literature. *Clin Lymphoma Myeloma* **8:**87–93.
37. **Lipsky PE, van der Heijde DM, St Clair EW, Furst DE, Breedveld FC, Kalden JR, Smolen JS, Weisman M, Emery P, Feldmann M, Harriman GR, Maini RN, Anti-Tumor Necrosis Factor Trial in Rheumatoid Arthritis with Concomitant Therapy Study Group.** 2000. Infliximab and methotrexate in the treatment of rheumatoid arthritis. *N Engl J Med* **343:**1594–1602.

38. **Breedveld FC, Weisman MH, Kavanaugh AF, Cohen SB, Pavelka K, van Vollenhoven R, Sharp J, Perez JL, Spencer-Green GT.** 2006. The PREMIER study: a multicenter, randomized, double-blind clinical trial of combination therapy with adalimumab plus methotrexate versus methotrexate alone or adalimumab alone in patients with early, aggressive rheumatoid arthritis who had not had previous methotrexate treatment. *Arthritis Rheum* **54:**26–37.
39. **van der Heijde D, Klareskog L, Rodriguez-Valverde V, Codreanu C, Bolosiu H, Melo-Gomes J, Tornero-Molina J, Wajdula J, Pedersen R, Fatenejad S, TEMPO Study Investigators.** 2006. Comparison of etanercept and methotrexate, alone and combined, in the treatment of rheumatoid arthritis: two-year clinical and radiographic results from the TEMPO study, a double-blind, randomized trial. *Arthritis Rheum* **54:**1063–1074.
40. **Kishimoto T.** 20045. Interleukin-6: from basic science to medicine—40 years in immunology. *Annu Rev Immunol* **23:**1–21.
41. **Nishimoto N, Hashimoto J, Miyasaka N, Yamamoto K, Kawai S, Takeuchi T, Murata N, van der Heijde D, Kishimoto T.** 2007. Study of active controlled monotherapy used for rheumatoid arthritis, an IL-6 inhibitor (SAMURAI): evidence of clinical and radiographic benefit from an x ray reader-blinded randomised controlled trial of tocilizumab. *Ann Rheum Dis* **66:**1162–1167.
42. **Mertens M, Singh JA.** 2009. Anakinra for rheumatoid arthritis: a systematic review. *J Rheumatol* **36:**1118–1125.
43. **Pedersen J, Coskun M, Soendergaard C, Salem M, Nielsen OH.** 2014. Inflammatory pathways of importance for management of inflammatory bowel disease. *World J Gastroenterol* **20:**64–77.
44. **Hanauer SB, Feagan BG, Lichtenstein GR, Mayer LF, Schreiber S, Colombel JF, Rachmilewitz D, Wolf DC, Olson A, Bao W, Rutgeerts P, Accent I Study Group.** 2002. Maintenance infliximab for Crohn's disease: the ACCENT I randomised trial. *Lancet* **359:**1541–1549.
45. **Targan SR, Hanauer SB, van Deventer SJ, Mayer L, Present DH, Braakman T, DeWoody KL, Schaible TF, Rutgeerts PJ, Crohn's Disease cA2 Study Group.** 1997. A short-term study of chimeric monoclonal antibody cA2 to tumor necrosis factor α for Crohn's disease. *N Engl J Med* **337:**1029–1035.
46. **Rutgeerts P, Sandborn WJ, Feagan BG, Reinisch W, Olson A, Johanns J, Travers S, Rachmilewitz D, Hanauer SB, Lichtenstein GR, de Villiers WJ, Present D, Sands BE, Colombel JF.** 2005. Infliximab for induction and maintenance therapy for ulcerative colitis. *N Engl J Med* **353:**2462–2476.
47. **Reinisch W, Sandborn WJ, Hommes DW, D'Haens G, Hanauer S, Schreiber S, Panaccione R, Fedorak RN, Tighe MB, Huang B, Kampman W, Lazar A, Thakkar R.** 2011. Adalimumab for induction of clinical remission in moderately to severely active ulcerative colitis: results of a randomised controlled trial. *Gut* **60:**780–787.
48. **Aronsohn A, Jensen D.** 2014. Interferon-combination strategies for the treatment of chronic hepatitis C. *Semin Liver Dis* **34:**30–36.
49. **Javed A, Reder AT.** 2006. Therapeutic role of beta-interferons in multiple sclerosis. *Pharmacol Ther* **110:**35–56.
50. **Feng X, Reder NP, Yanamandala M, Hill A, Franek BS, Niewold TB, Reder AT, Javed A.** 2012. Type I interferon signature is high in lupus and neuromyelitis optica but low in multiple sclerosis. *J Neurol Sci* **313:**48–53.

Detection of Anticytokine Autoantibodies and Clinical Applications

SARAH K. BROWNE

39

Anticytokine autoantibodies are an emerging mechanism of disease pathogenesis that have been shown to elicit a broad range of clinical phenotypes. Some anticytokine autoantibodies can lead to immune susceptibility, with examples including nontuberculous mycobacteria, salmonellae, or fungi due to autoantibodies against gamma interferon (IFN-γ) (1); staphylococcal infection due to anti-interleukin-6 (IL-6) autoantibodies (2); *Burkholderia gladioli* infection due to anti-IL-12p70 autoantibodies (3); chronic mucocutaneous candidiasis due to anti-IL-17 and anti-IL-22 autoantibodies (4, 5); and cryptococcal meningitis (6) or *Nocardia* infection due to anti-granulocyte-macrophage colony-stimulating factor (GM-CSF) autoantibodies (7). Other diseases in which immunodeficiency is not the primary presentation include the severe lung disease pulmonary alveolar proteinosis (PAP) caused by anti-GM-CSF autoantibodies; pure red cell aplasia (8); pure red-cell aplasia due to antierythropoietin autoantibodies (9); and severe osteoporosis associated with antiosteoprotegerin autoantibodies (10). For other anticytokine autoantibodies, such as anti-IFN-α autoantibodies detected in thymoma or autoimmune polyendocrinopathy-candidiasis-ectodermal dystrophy (APECED) syndrome, their biological effect is not immediately apparent (11). Diagnosis has important implications for management because therapies can be used to directly target the underlying mechanism, i.e., a neutralizing antibody, and not just their ultimate clinical consequences, with approaches such as B-cell depletion (12–14) or receptor agonists (15).

The diagnosis of anticytokine autoantibody syndromes must be specifically considered and carefully sought, particularly in the context of idiopathic disease in previously healthy adults, because clues to their presence may not be readily apparent on routine laboratory testing. PAP remained idiopathic for 40 years (16) before anti-GM-CSF autoantibodies were recognized as causal in ~90% of cases (17, 18). Understandably, it was not immediately apparent how a focal lung disease would result from blocking hematopoietic growth factors. In fact, it was the observation that GM-CSF cytokine-null (19) and receptor-null (20) mice both developed lung pathology strongly reminiscent of human PAP that gave clues as to the mechanism. The story continues to evolve: while even the initial report described opportunistic infection in the context of PAP (16), it has only recently been appreciated that anti-GM-CSF autoantibodies could lead to infection in the absence of PAP altogether (6, 7). It remains unknown how tightly autoantibody titers correlate with disease activity or response to therapy, but the ability to quantitate antibody levels over time may have implications for monitoring and managing disease beyond initial diagnosis.

Once an autoantibody is identified, evaluation for biological activity is paramount, given that anticytokine autoantibodies have been identified extensively in health and disease but without clear pathogenic consequences (21). Analogous to this phenomenon is the observation that only a small subset of patients who have antiphospholipid autoantibodies actually carry an increased risk of thrombosis (22). In addition to demonstrating that the autoantibody is both present and neutralizing, there should also be a biological rationale that supports a direct pathogenic role. The fact that many of the currently appreciated anticytokine autoantibody syndromes share phenotypic similarities with genetic defects in the same pathway supports the hypothesis that the autoantibody is producing a clinical "phenocopy" of the corresponding genetic deficiency. For example, anti-IFN-γ autoantibodies and mutations to the IFN-γ receptor both result in disseminated mycobacterial infection (Table 1). Assessing the functional activity of the autoantibody and considering what a deficiency in that pathway might induce can help determine if the underlying mechanism of disease has been identified or, conversely, if an alternative diagnosis must still be sought.

DETECTION STRATEGIES

Many approaches have been used to evaluate for the presence and activity of anticytokine autoantibodies, often conducted in independent laboratories on a research basis. The techniques themselves as well as the interpretation of these data (including normal ranges) remain largely unstandardized. Further, the relative values produced by each technique are difficult, if not impossible, to compare. Each technique has unique features such as cost, requirement for specialized technology, types of reagents, and amount of plasma needed. These relative attributes may have more or less import depending on the diagnostic circumstances.

Enzyme-Linked Immunosorbent Assay

In an enzyme-linked immunosorbent assay (ELISA), the cytokine of interest is bound to the surface of a 96-well plate

doi:10.1128/9781555818722.ch39

TABLE 1 Anticytokine autoantibody-associated syndromes[a]

Cytokine target	Clinical manifestations	Laboratory and radiologic manifestations	Functional assays	Infections	Biological rationale
GM-CSF	PAP; insidious and progressive respiratory failure (8); newly described cases of isolated cryptococcal meningitis and CNS nocardiosis in HIV-uninfected individuals (6, 7)	BAL fluid contains large foamy macrophages or monocyte-like macrophages (41, 42) and elevated levels of surfactant proteins; characteristic CT of chest demonstrates ground-glass opacities with thickening of intralobular septae, "crazy paving." PFTs demonstrate restrictive and diffusion defects.	Anti-GM-CSF autoantibodies inhibit pSTAT5 production (6), PU.1 expression (43), and MIP-1α protein production (6).	Pulmonary and extrapulmonary infections with *Nocardia* (44–54), *Aspergillus* (55), and *Proteus* (54, 56) spp.; histoplasmosis (57); and cryptococcosis (6, 16)	Mutations in GM-CSF receptor α or β subunits lead to early-onset (often neonatal) and severe PAP (8). GM-CSF receptor-null (20) and cytokine-null (19) mice develop PAP.
IFN-γ	Chronic infections with intracellular pathogens, particularly lymphadenitis, skin, soft tissue, and bone infections; can be multiple organisms simultaneously or sequentially; reactive dermatoses; constitutional symptoms common	Elevated erythrocyte sedimentation rate, CRP, and β_2-microglobulin; anemia; hypergammaglobulinemia. CT imaging may demonstrate abscess formation or osteomyelitis.	Anti-IFN-γ autoantibodies inhibit pSTAT1 production (1, 29), IFN-γ-inducible gene expression (32), and IL-12p70 and TNF-α protein production (1, 29).	Nontuberculous mycobacteria, tuberculosis, nontyphoidal *Salmonella*, *Histoplasma*, *Penicillium*, *Cryptococcus*, *Burkholderia pseudomallei*, and varicella-zoster virus	Mutations in *IFNgR1*, *IFNgR2*, *STAT1*, *IL-12Rβ1*, *IL-12Rβ2*, and *IL-12p40*, all directly within the *IFN-γ–IL-12* axis, lead to similar infections (58).
IL-17A, IL-17F, and IL-22	Recurrent candidal infections of mucosal surfaces, nails, and skin; infection may become resistant to antifungals.	None	Anti-IL-17 autoantibodies inhibit IL-17-induced IL-6 (4).	*Candida* spp.	Mutations in *IL-17RA*, *IL-17F* (59), and other genetic diseases with impairment in Th17 cells (59) lead to mucocutaneous candidiasis.
IL-6	Recurrent staphylococcal skin infections	Undetectable CRP	Anti-IL-6 autoantibodies prevent IL-6-induced CRP mRNA (2, 60).	*Staphylococcus aureus* (two cases) and empyema with *Streptococcus intermedius* and *Escherichia coli* (one case)	Mutations in *STAT3*, immediately downstream of the IL-6 receptor, cause Job's syndrome, which predisposes to *S. aureus* skin infections (61).
OPG	Severe, high-turnover osteoporosis (10) with pathologic fractures	Elevated alkaline phosphatase level	Anti-OPG autoantibodies prevent OPG inhibition of RANKL-induced NF-κB.	NA	Mutation in *TNFRSF11B*, the gene encoding OPG, results in childhood hyperphosphatemia, rapid bone turnover, and pathologic fractures (62).
EPO	Pure red cell aplasia	Low hemoglobin and hematocrit levels with absence of erythroid cells on bone marrow biopsy and absence of circulating erythrocytes; low or inappropriately normal endogenous EPO levels (9, 33)	Serum prevents formation of erythroid colonies from erythroid progenitor cells.	NA	NA

[a]Abbreviations: ABC, adenosine triphosphate-binding cassette; BAL, bronchoalveolar lavage; CNS, central nervous system; CT, computed tomography; EPO, erythropoietin; IRF, interferon regulatory factor; MIP, macrophage inflammatory protein; NA, not applicable; NEMO, NF-κB essential modulator; OPG, osteoprotegerin; PFT, pulmonary function test; RANKL, receptor activator of NF-κB ligand; SP, surfactant protein; TNF, tumor necrosis factor.

(Fig. 1A) (23) and patient plasma or serum is applied to the well containing the protein. The plate is washed, and if an autoantibody is present that recognizes the cytokine, it remains bound to the plate while the remaining material, including all nonspecific antibody, is removed. A secondary anti-human IgG detection antibody linked to an enzyme is added, which binds the IgG remaining on the plate. After washing, a substrate for the enzyme is added that changes color. Thus, only if detection antibody is present will the well change color, with an intensity that is a function of how much antibody is bound to the plate. This can be compared to a standard curve in which known amounts of an anticytokine antibody are added to the plate to determine the relationship between quantity and enzyme-related color shift.

A variation on the direct ELISA uses a plate that quantifies a given cytokine rather than the autoantibody. In this case, a known concentration of cytokine is mixed with patient plasma and the amount of cytokine detected by ELISA is less than the input amount if a neutralizing antibody is present in the plasma. This method is indirect, because it assumes but does not prove that the neutralizing "factor" is an antibody. However, because the factor blocks detection of the cytokine, it provides some additional evidence not only that the (presumed) autoantibody is present but also that it may indeed have neutralizing activity *in vivo*.

The benefits are that these assays are relatively inexpensive assays that do not require sophisticated technology and thus can be performed in most laboratories, including resource-limited settings. The disadvantages are the risk of high, nonspecific signal background and poor resolution between different concentrations, making them less quantitative than other approaches.

Luminex

Luminex is essentially a liquid-phase ELISA whereby the cytokine is coupled to a bead in suspension rather than to the surface of a plate (Fig. 1B). In this system, the beads themselves fluoresce, each at a different wavelength, so that they can be distinguished from each other when combined in the same well. Each unique set of beads can be coupled to a different cytokine so that multiple autoantibodies can be measured simultaneously with minimal plasma requirements. The beads are mixed with plasma, and after washing, a fluorescently labeled anti-human IgG binds any autoantibody that recognizes a particular cytokine-coupled bead. When run on a Luminex instrument, the bead fluorescence indicates what cytokine the autoantibody recognizes and the magnitude of fluorescence from the detection antibody quantifies the amount of each autoantibody that is present.

The Luminex technology requires a specific instrument for running this assay as well as availability of purified recombinant cytokines. However, if the instrument is available, the test is rapid, inexpensive, sensitive, specific, and reproducible (24). The ability to test for multiple cytokines in one assay minimizes plasma requirements to less than a microliter per test and allows for high-throughput screening of dozens of targets simultaneously.

Luciferase Immunoprecipitation Systems

In this technique, the cytokine is made to fluoresce by inserting the gene for the cytokine of interest into an expression vector next to the *Renilla* luciferase gene (Fig. 1C). A mammalian cell line is transfected with the expression vector, leading the cells to generate large amounts of the fluorescing cytokine (25, 26). The crude extracts from this cell line containing fluorescent protein are incubated with patient plasma, and subsequently the IgG from the plasma is captured with protein A/G-Sepharose beads (Fig. 1C). Whereas in the ELISA and Luminex assays only the specific autoantibody binds the surface, in this case total IgG is captured, but only that which binds the fluorescent protein is detected. The values are measured in arbitrary light units and are a function of autoantibody titer.

This is a sensitive and specific technique for which virtually any fusion protein can be synthesized, hence alleviating the need for purified recombinant proteins. Because the protein is expressed in a mammalian cell line, both conformation and posttranslational modifications should remain largely intact, which can improve epitope recognition.

Radioimmunoassays

Radioimmunoassays are similar to luciferase immunoprecipitation systems in that the cytokine "bait" is the labeled moiety that is incubated with serum (Fig. 1C). Either recombinant protein is synthesized with incorporation of radioactive [^{35}S]methionine into the protein (27), or recombinant protein is coupled to radioactive iodine (^{125}I) (28). A fixed amount of radioactivity (protein), measured in counts per minute, is combined with plasma (27). Total IgG is captured on protein A/G-Sepharose beads, and the degree of radioactivity compared with a negative control is a function of how much specific antibody is present that is binding the radioactive "bait." The main limitation of this assay is the need to work with radioactive reagents.

Immunoblotting

In immunoblotting, also known as Western blotting, denatured recombinant cytokine is run by agarose gel electophoresis and migrates based on its intrinsic size and charge (29) (Fig. 1D). The protein is transferred from the gel to a membrane (typically polyvinylidene difluoride or nitrocellulose) that is subsequently "blotted" using diluted plasma. As in ELISA, the detection antibody detects human IgG and is enzyme bound. If there is an autoantibody to the cytokine, the detection antibody remains bound to the autoantibody-cytokine complex after washing of the membrane. Addition of substrate causes light emission that can be used to develop light-sensitive film, revealing a band. The amount of light produced is a function of how much autoantibody there is, as indicated by the width and darkness of the band produced on the film.

The benefits of this assay are that it can be performed in most labs given that the technology is commonly used for many applications and has been available for decades. However, it is less sensitive than other approaches, more technically cumbersome, and requires more plasma compared with other diagnostic strategies. Furthermore, because it is usually performed with denatured protein, conformational epitopes may be lost.

Protein Array

Recently, investigators have used a protein array to screen for anticytokine autoantibodies (30). The concept is similar to ELISA, Luminex, and immunoblotting in that plasma is incubated with known protein that has been attached to a surface and the amount of antibody in the plasma binding the cytokine is quantified with a secondary antibody that recognizes human IgG. It is similar to microarray except that cytokines and not RNA are printed on a nitrocellulose-surface glass slide. The slide is incubated with plasma and subsequently quantified with a fluorescently labeled anti-human IgG that detects any human antibody that binds a cytokine present on the slide. Microarray software analyzes the degree of binding to each target, and heat maps can be

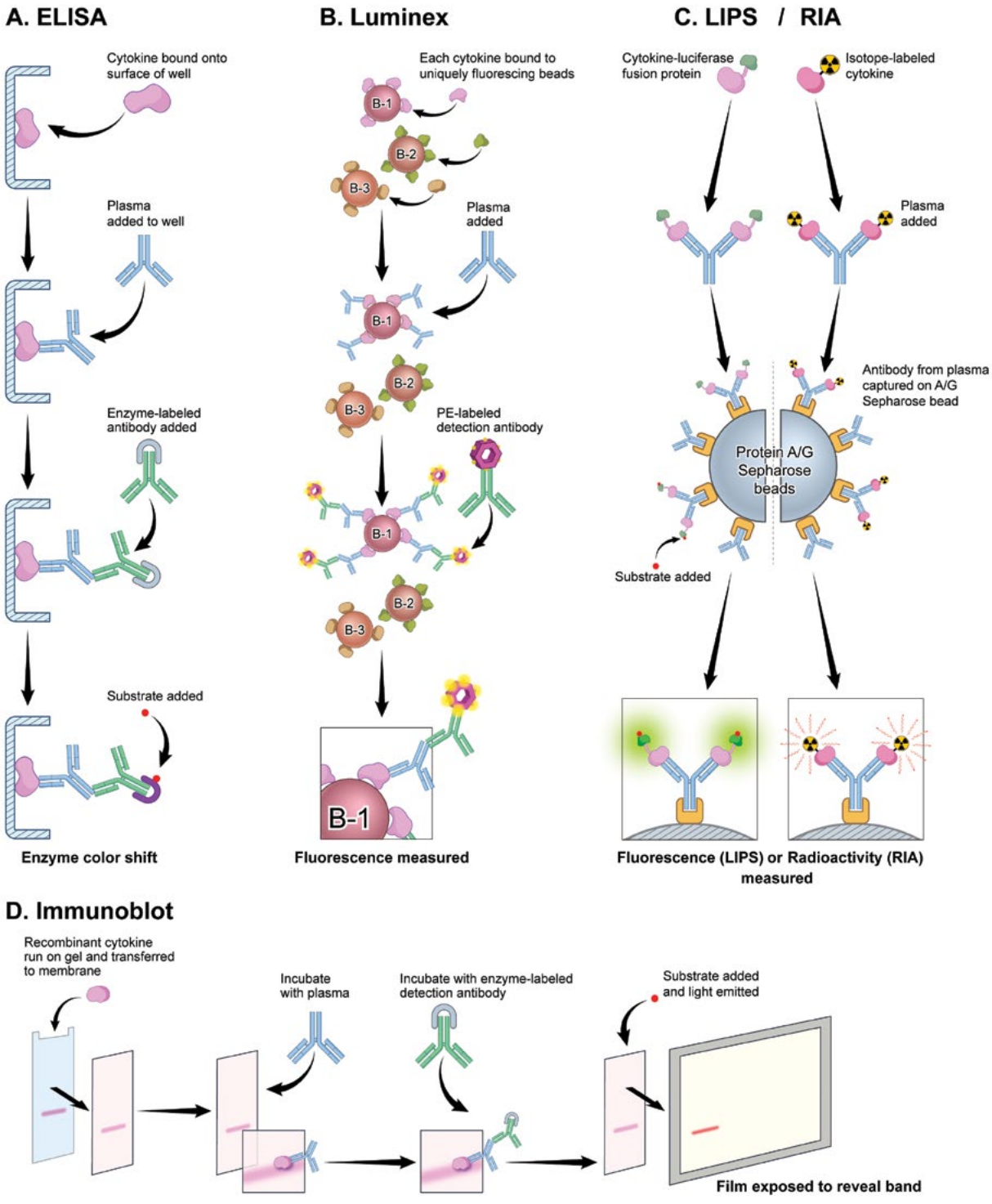

FIGURE 1 Summary of anticytokine autoantibody detection assays. LIPS, luciferase immunoprecipitation system; PE, phycoerythrin; RIA, radioimmunoassay.

generated that show relative binding to each of dozens to potentially hundreds of targets. This assay requires technical expertise regarding microarray platforms and data analysis. It has the capacity to simultaneously screen for the largest number of proteins. One patient can be screened per array, so this approach may be better for discovering novel autoantibodies or searching for patterns in autoantibody profiles within certain diseases rather than diagnosing specific anticytokine autoantibodies, for which a narrower panel may be sufficient and more cost-effective.

FUNCTIONAL ASSAYS

Upon identification of an anticytokine autoantibody, biological activity should be assessed. This is an important aspect of evaluating autoantibodies to cytokines, particularly when the phenotype is not clear-cut, as many anticytokine autoantibodies have been identified in both health and disease (31) without apparent physiological consequences. In general, when autoantibodies are causal, they are high-titer and neutralizing and have a clear clinical phenotype. This does not necessarily mean lower-titer or nonneutralizing autoantibodies do not have significant biological relevance; it may just be more difficult to detect or prove, and the effects may be physiologic rather than pathogenic. Nonneutralizing autoantibodies might alternatively represent an epiphenomenon devoid of immunomodulatory effects. A variety of assays have been used to evaluate the functionality of anticytokine autoantibodies with the common goal being to determine if the autoantibody prevents the ability of the cytokine to induce its normal inflammatory response (Table 1). Ideally, the patient cells are washed of autologous plasma and also evaluated for their ability to both elaborate and respond to cytokines appropriately, hence excluding cell-intrinsic defects.

The general strategy for functional assays is to use primary human cells (or cell lines) that are known to express a receptor for the cytokine of interest. The cells are stimulated with the cytokine in the presence of subject or control plasma. Finally, techniques such as flow cytometry, quantitative real-time PCR, microarray, immunoblotting, or cytokine detection assays evaluate if the normal cells respond appropriately to the cytokine in the presence of plasma. Each of these assays detects the downstream effects of the cytokine, such as activation/phosphorylation of signaling molecules, cytokine-induced RNA expression, or cytokine-induced protein production. For example, intracellular phosphorylation of STAT1 occurs when normal monocytes are stimulated with IFN-γ. Thus, monocytes can be stimulated with IFN-γ in the presence of subject plasma and the amount of phosphorylated STAT1 (pSTAT1) produced can be quantified by flow cytometry or immunoblotting. If the plasma contains an autoantibody that blocks IFN-γ, then the cells will appear as if they have not been stimulated; i.e., no additional pSTAT1 will be detected. Similarly, these neutralizing autoantibodies have been shown to prevent IFN-γ-induced RNA expression (13, 32) and protein production (29). Functional assays have been developed for many of the anticytokine autoantibodies reported in association with disease. Examples include GM-CSF-induced pSTAT5 production, PU.1 gene expression, or macrophage inflammatory protein 1α production in monocytes or alveolar macrophages; IL-6-induced pSTAT3, as well as IL-6-induced C-reactive protein (CRP) mRNA and protein expression (2); IL-12-induced IFN-γ; IL-17A-induced IL-6; osteoprotegerin (4) inhibition of RANKL-induced NF-κB (10) (Table 1); and erythropoietin-induced erythroid colony formation (33). In each of these cases, plasma from patients with biologically active autoantibodies prevents the cytokine from exerting normal effects on a specific cell population. These assays are essential in the assessment of anticytokine autoantibodies because many of these autoantibodies have been reported in healthy controls or outside of their specific disease associations.

ISOTYPE AND SUBCLASS ANALYSIS

So far, all the reported syndromes associated with anticytokine autoantibodies have been reported as IgG. Assays such as Luminex and ELISA can assess isotype and subclass by varying the detection antibody to detect total IgG, specific IgG subclasses, or different isotypes altogether. It has been demonstrated that in PAP, anti-GM-CSF autoantibodies tend to be IgG1 and IgG2 (34), whereas in immunodeficiency due to anti-IFN-γ autoantibodies, they tend to be IgG3 or IgG4 (1), possibly suggesting syndrome-specific mechanisms underlying autoantibody production. In PAP, it has also been suggested that the IgG κ/λ ratios predict disease severity (35). In pemphigus vulgaris, a blistering skin condition caused by anti-desmoglein 3 autoantibodies, it was shown that anti-desmoglein 3 IgG4 titers track with disease activity, whereas anti-desmoglein 3 IgG1 levels are seen in quiescent disease or unaffected relatives. Thus, in the future, evaluation and monitoring of the IgG subclass of certain autoantibodies might have clinically important implications for prognosis and disease activity (36, 37).

TITER

The titer of a specific anticytokine autoantibody may play a role in disease activity. This has not been thoroughly studied in any of these conditions, and reports vary across diseases in the instances in which it has been evaluated. Studies have demonstrated efficacy of inhaled GM-CSF for patients with PAP despite no predictable change in autoantibody levels relative to disease activity (38, 39). In contrast, we have found that the titer of anti-IFN-γ autoantibodies does appear to track closely with disease activity and may even predict relapse (13; unpublished data). Research is needed to evaluate the relationship between titer and disease activity as this could eventually be used to guide preemptive therapy or heightened surveillance for relapse.

OTHER DIAGNOSTIC CONSIDERATIONS

Although titer may vary dramatically between patients, antibody levels for a given patient tend to remain relatively stable over time (39). Given the potential for interassay variability within one technique and the difficulty in translating results between assays, it can be helpful to store banked samples for a patient. Over time, autoantibody levels can be tested in parallel to eliminate differences in assays and tracked for a given patient with regard to disease activity and clinical interventions. Ideally, the samples should be stored in aliquots to avoid repeated freeze-thaw cycles.

SUMMARY

Although anticytokine autoantibodies have been recognized for decades, appreciation for their direct role in disease pathogenesis is more recent and rapidly evolving. If we look to known autoantibody-mediated syndromes, other idiopathic diseases may someday find their origins in a neutralizing autoantibody. They may extend beyond cytokines to other soluble factors (as seen in diabetes associated with anti-insulin autoantibodies), receptors (as seen in myasthenia gravis and anti-acetylcholine receptor autoantibodies), or other extracellular elements (as seen in pemphigus vulgaris associated with autoantibodies against the basement membrane protein desmoglein 3). While many autoantibodies are inhibitory, some may be stimulatory, akin to anti-thyroid receptor autoantibodies in Graves' disease or recombinant anti-IL-2 autoantibodies (40). Despite broad disparities in clinical phenotype, the principles and diagnostic strategies (along with their pitfalls) for autoantibody-mediated conditions overlap. Because anticytokine autoantibodies, like other autoantibodies, may

be found in the absence of overt clinical consequences, it is helpful to evaluate the functionality of the antibody and establish a biological rationale that links the autoantibody and the clinical phenotype. Understanding the natural history and pathogenesis of anticytokine autoantibody-associated syndromes will inform the management of these unique diseases. Ultimately, these syndromes may help define critical pathways of immune homeostasis and dysregulation, autoimmunity, and immunodeficiency.

This work was supported by the Division of Intramural Research, National Institute of Allergy and Infectious Diseases, National Institutes of Health (Bethesda, MD).

REFERENCES

1. **Browne SK, Burbelo PD, Chetchotisakd P, Suputtamongkol Y, Kiertiburanakul S, Shaw PA, Kirk JL, Jutivorakool K, Zaman R, Ding L, Hsu AP, Patel SY, Olivier KN, Lulitanond V, Mootsikapun P, Anunnatsiri S, Angkasekwinai N, Sathapatayavongs B, Hsueh PR, Shieh CC, Brown MR, Thongnoppakhun W, Claypool R, Sampaio EP, Thepthai C, Waywa D, Dacombe C, Reizes Y, Zelazny AM, Saleeb P, Rosen LB, Mo A, Iadarola M, Holland SM.** 2012. Adult-onset immunodeficiency in Thailand and Taiwan. *N Engl J Med* **367:**725–734. PubMed
2. **Puel A, Picard C, Lorrot M, Pons C, Chrabieh M, Lorenzo L, Mamani-Matsuda M, Jouanguy E, Gendrel D, Casanova JL.** 2008. Recurrent staphylococcal cellulitis and subcutaneous abscesses in a child with autoantibodies against IL-6. *J Immunol* **180:**647–654. PubMed
3. **Sim BT, Browne SK, Vigliani M, Zachary D, Rosen L, Holland SM, Opal SM.** 2013. Recurrent Burkholderia gladioli suppurative lymphadenitis associated with neutralizing anti-IL-12p70 autoantibodies. *J Clin Immunol* **33:**1057–1061. PubMed
4. **Puel A, Döffinger R, Natividad A, Chrabieh M, Barcenas-Morales G, Picard C, Cobat A, Ouachée-Chardin M, Toulon A, Bustamante J, Al-Muhsen S, Al-Owain M, Arkwright PD, Costigan C, McConnell V, Cant AJ, Abinun M, Polak M, Bougnères PF, Kumararatne D, Marodi L, Nahum A, Roifman C, Blanche S, Fischer A, Bodemer C, Abel L, Lilic D, Casanova JL.** 2010. Autoantibodies against IL-17A, IL-17F, and IL-22 in patients with chronic mucocutaneous candidiasis and autoimmune polyendocrine syndrome type I. *J Exp Med* **207:**291–297. PubMed
5. **Kisand K, Bøe Wolff AS, Podkrajsek KT, Tserel L, Link M, Kisand KV, Ersvaer E, Perheentupa J, Erichsen MM, Bratanic N, Meloni A, Cetani F, Perniola R, Ergun-Longmire B, Maclaren N, Krohn KJ, Pura M, Schalke B, Ströbel P, Leite MI, Battelino T, Husebye ES, Peterson P, Willcox N, Meager A.** 2010. Chronic mucocutaneous candidiasis in APECED or thymoma patients correlates with autoimmunity to Th17-associated cytokines. *J Exp Med* **207:**299–308.
6. **Rosen LB, Freeman AF, Yang LM, Jutivorakool K, Olivier KN, Angkasekwinai N, Suputtamongkol Y, Bennett JE, Pyrgos V, Williamson PR, Ding L, Holland SM, Browne SK.** 2013. Anti-GM-CSF autoantibodies in patients with cryptococcal meningitis. *J Immunol* **190:**3959–3966.
7. **Rosen LB, Pereira NR, Figueirdo C, Fiske LC, Ressner RA, Hong JC, Gregg KS, Henry TL, Pak KJ, Baumgarten KL, Seoane L, Garcia-Diaz J, Olivier KN, Zelazny AM, Holland SM, Browne SK.** 2015. Nocardia-induced GM-CSF is neutralized by autoantibodies in disseminated/extrapulmonary nocardiosis NEW. *Clin Infect Dis* **60:**1017–1025. PubMed
8. **Carey B, Trapnell BC.** 2010. The molecular basis of pulmonary alveolar proteinosis. *Clin Immunol* **135:**223–235.
9. **Casadevall N, Dupuy E, Molho-Sabatier P, Tobelem G, Varet B, Mayeux P.** 1996. Autoantibodies against erythropoietin in a patient with pure red-cell aplasia. *N Engl J Med* **334:**630–633. PubMed
10. **Riches PL, McRorie E, Fraser WD, Determann C, van't Hof R, Ralston SH.** 2009. Osteoporosis associated with neutralizing autoantibodies against osteoprotegerin. *N Engl J Med* **361:**1459–1465. PubMed
11. **Browne SK.** 2014. Anticytokine autoantibody-associated immunodeficiency. *Annu Rev Immunol* **32:**635–657.
12. **Borie R, Debray MP, Laine C, Aubier M, Crestani B.** 2009. Rituximab therapy in autoimmune pulmonary alveolar proteinosis. *Eur Respir J* **33:**1503–1506. PubMed
13. **Browne SK, Zaman R, Sampaio EP, Jutivorakool K, Rosen LB, Ding L, Pancholi MJ, Yang LM, Priel DL, Uzel G, Freeman AF, Hayes CE, Baxter R, Cohen SH, Holland SM.** 2012. Anti-CD20 (rituximab) therapy for anti-IFN-γ autoantibody-associated nontuberculous mycobacterial infection. *Blood* **119:**3933–3939.
14. **Kavuru MS, Malur A, Marshall I, Barna BP, Meziane M, Huizar I, Dalrymple H, Karnekar R, Thomassen MJ.** 2011. An open-label trial of rituximab therapy in pulmonary alveolar proteinosis. *Eur Respir J* **38:**1361–1367. PubMed
15. **Macdougall IC, Rossert J, Casadevall N, Stead RB, Duliege AM, Froissart M, Eckardt KU.** 2009. A peptide-based erythropoietin-receptor agonist for pure red-cell aplasia. *N Engl J Med* **361:**1848–1855. PubMed
16. **Rosen SH, Castleman B, Liebow AA.** 1958. Pulmonary alveolar proteinosis. *N Engl J Med* **258:**1123–1142. PubMed
17. **Kitamura T, Tanaka N, Watanabe J, Uchida, Kanegasaki S, Yamada Y, Nakata K.** 1999. Idiopathic pulmonary alveolar proteinosis as an autoimmune disease with neutralizing antibody against granulocyte/macrophage colony-stimulating factor. *J Exp Med* **190:**875–880. PubMed
18. **Tanaka N, Watanabe J, Kitamura T, Yamada Y, Kanegasaki S, Nakata K.** 1999. Lungs of patients with idiopathic pulmonary alveolar proteinosis express a factor which neutralizes granulocyte-macrophage colony stimulating factor. *FEBS Lett* **442:**246–250. PubMed
19. **Dranoff G, et al.** 1994. Involvement of granulocyte-macrophage colony-stimulating factor in pulmonary homeostasis. *Science* **264:**713–716. PubMed
20. **Robb L, Drinkwater CC, Metcalf D, Li R, Köntgen F, Nicola NA, Begley CG.** 1995. Hematopoietic and lung abnormalities in mice with a null mutation of the common beta subunit of the receptors for granulocyte-macrophage colony-stimulating factor and interleukins 3 and 5. *Proc Natl Acad Sci USA* **92:**9565–9569. PubMed
21. **Watanabe M, Uchida K, Nakagaki K, Trapnell BC, Nakata K.** 2010. High avidity cytokine autoantibodies in health and disease: pathogenesis and mechanisms. *Cytokine Growth Factor Rev* **21:**263–273. PubMed
22. **de Laat HB, Derksen RH, Urbanus RT, Roest M, de Groot PG.** 2004. beta2-glycoprotein I-dependent lupus anticoagulant highly correlates with thrombosis in the antiphospholipid syndrome. *Blood* **104:**3598–3602. PubMed
23. **Höflich C, Sabat R, Rosseau S, Temmesfeld B, Slevogt H, Döcke WD, Grütz G, Meisel C, Halle E, Göbel UB, Volk HD, Suttorp N.** 2004. Naturally occurring anti-IFN-gamma autoantibody and severe infections with Mycobacterium cheloneae and Burkholderia cocovenenans. *Blood* **103:**673–675. PubMed
24. **Ding L, Mo A, Jutivorakool K, Pancholi M, Holland SM, Browne SK.** 2012. Determination of human anticytokine autoantibody profiles using a particle-based approach. *J Clin Immunol* **32:**238–245. PubMed
25. **Burbelo PD, Browne SK, Sampaio EP, Giaccone G, Zaman R, Kristosturyan E, Rajan A, Ding L, Ching KH,**

Berman A, Oliveira JB, Hsu AP, Klimavicz CM, Iadarola MJ, Holland SM. 2010. Anti-cytokine autoantibodies are associated with opportunistic infection in patients with thymic neoplasia. *Blood* **116:**4848–4858. PubMed

26. **Burbelo PD, Ching KH, Klimavicz CM, Iadarola MJ.** 2009. Antibody profiling by luciferase immunoprecipitation systems (LIPS). *J Vis Exp* **32:**1549. doi:10.3791/1549 PubMed
27. **Oftedal BE, Wolff AS, Bratland E, Kämpe O, Perheentupa J, Myhre AG, Meager A, Purushothaman R, Ten S, Husebye ES.** 2008. Radioimmunoassay for autoantibodies against interferon omega; its use in the diagnosis of autoimmune polyendocrine syndrome type I. *Clin Immunol* **129:**163–169. PubMed
28. **de Lemos Rieper C, Galle P, Svenson M, Pedersen BK, Hansen MB.** 2009. Preparation and validation of radio iodinated recombinant human IL-10 for the measurement of natural human antibodies against IL-10. *J Immunol Methods* **350:**46–53. PubMed
29. **Patel SY, Ding L, Brown MR, Lantz L, Gay T, Cohen S, Martyak LA, Kubak B, Holland SM.** 2005. Anti-IFN-gamma autoantibodies in disseminated nontuberculous mycobacterial infections. *J Immunol* **175:**4769–4776. PubMed
30. **Price JV, Haddon DJ, Kemmer D, Delepine G, Mandelbaum G, Jarrell JA, Gupta R, Balboni I, Chakravarty EF, Sokolove J, Shum AK, Anderson MS, Cheng MH, Robinson WH, Browne SK, Holland SM, Baechler EC, Utz PJ. 2013**. Protein microarray analysis reveals BAFF-binding autoantibodies in systemic lupus erythematosus. *J Clin Invest* **123:**5135–5145. PubMed
31. **Watanabe M, Uchida K, Nakagaki K, Kanazawa H, Trapnell BC, Hoshino Y, Kagamu H, Yoshizawa H, Keicho N, Goto H, Nakata K.** 2007. Anti-cytokine autoantibodies are ubiquitous in healthy individuals. *FEBS Lett* **581:**2017–2021. PubMed
32. **Kampmann B, Hemingway C, Stephens A, Davidson R, Goodsall A, Anderson S, Nicol M, Schölvinck E, Relman D, Waddell S, Langford P, Sheehan B, Semple L, Wilkinson KA, Wilkinson RJ, Ress S, Hibberd M, Levin M.** 2005. Acquired predisposition to mycobacterial disease due to autoantibodies to IFN-gamma. *J Clin Invest* **115:**2480–2488. PubMed
33. **Casadevall N, Nataf J, Viron B, Kolta A, Kiladjian JJ, Martin-Dupont P, Michaud P, Papo T, Ugo V, Teyssandier I, Varet B, Mayeux P.** 2002. Pure red-cell aplasia and antierythropoietin antibodies in patients treated with recombinant erythropoietin. *N Engl J Med* **346:**469–475. PubMed
34. **Kitamura T, Uchida K, Tanaka N, Tsuchiya T, Watanabe J, Yamada Y, Hanaoka K, Seymour JF, Schoch OD, Doyle I, Inoue Y, Sakatani M, Kudoh S, Azuma A, Nukiwa T, Tomita T, Katagiri M, Fujita A, Kurashima A, Kanegasaki S, Nakata K.** 2000. Serological diagnosis of idiopathic pulmonary alveolar proteinosis. *Am J Respir Crit Care Med* **162:**658–662. PubMed
35. **Nei T, Urano S, Itoh Y, Kitamura N, Hashimoto A, Tanaka T, Motoi N, Kaneko C, Tazawa R, Nakagaki K, Arai T, Inoue Y, Nakata K.** 2013. Light chain (κ/λ) ratio of GM-CSF autoantibodies is associated with disease severity in autoimmune pulmonary alveolar proteinosis. *Clin Immunol* **149:**357–364. PubMed
36. **Bhol K, Mohimen A, Ahmed AR.** 1994. Correlation of subclasses of IgG with disease activity in pemphigus vulgaris. *Dermatology* **189**(Suppl 1)**:**85–89. PubMed
37. **Bhol K, Natarajan K, Nagarwalla N, Mohimen A, Aoki V, Ahmed AR.** 1995. Correlation of peptide specificity and IgG subclass with pathogenic and nonpathogenic autoantibodies in pemphigus vulgaris: a model for autoimmunity. *Proc Natl Acad Sci USA* **92:**5239–5243. PubMed
38. **Tazawa R, Inoue Y, Arai T, Takada T, Kasahara Y, Hojo M, Ohkouchi S, Tsuchihashi Y, Yokoba M, Eda R, Nakayama H, Ishii H, Nei T, Morimoto K, Nasuhara Y, Ebina M, Akira M, Ichiwata T, Tatsumi K, Yamaguchi E, Nakata K.** 2013. Duration of benefit in patients with autoimmune pulmonary alveolar proteinosis after inhaled granulocyte-macrophage colony-stimulating factor therapy. *Chest* **145:**729–737.
39. **Tazawa R, Trapnell BC, Inoue Y, Arai T, Takada T, Nasuhara Y, Hizawa N, Kasahara Y, Tatsumi K, Hojo M, Ishii H, Yokoba M, Tanaka N, Yamaguchi E, Eda R, Tsuchihashi Y, Morimoto K, Akira M, Terada M, Otsuka J, Ebina M, Kaneko C, Nukiwa T, Krischer JP, Akazawa K, Nakata K.** 2010. Inhaled granulocyte/macrophage-colony stimulating factor as therapy for pulmonary alveolar proteinosis. *Am J Respir Crit Care Med* **181:**1345–1354. PubMed
40. **Courtney LP, Phelps JL, Karavodin LM.** 1994. An anti-IL-2 antibody increases serum half-life and improves anti-tumor efficacy of human recombinant interleukin-2. *Immunopharmacology* **28:**223–232. PubMed
41. **Iyonaga K, Suga M, Yamamoto T, Ichiyasu H, Miyakawa H, Ando M.** 1999. Elevated bronchoalveolar concentrations of MCP-1 in patients with pulmonary alveolar proteinosis. *Eur Respir J* **14:**383–389. PubMed
42. **Schoch OD, Schanz U, Koller M, Nakata K, Seymour JF, Russi EW, Boehler A.** 2002. BAL findings in a patient with pulmonary alveolar proteinosis successfully treated with GM-CSF. *Thorax* **57:**277–280. PubMed
43. **Shibata Y, Berclaz PY, Chroneos ZC, Yoshida M, Whitsett JA, Trapnell BC.** 2001. GM-CSF regulates alveolar macrophage differentiation and innate immunity in the lung through PU.1. *Immunity* **15:**557–567. PubMed
44. **Andersen BR, Ecklund RE, Kellow WF.** 1960. Pulmonary alveolar proteinosis with systemic nocardiosis. A case report. *JAMA* **174:**28–31. PubMed
45. **Andriole VT, Ballas M, Wilson GL.** 1964. The association of nocardiosis and pulmonary alveolar proteinosis: a case study. *Ann Intern Med* **60:**266–275. PubMed
46. **Burbank B, Morrione TG, Cutler SS.** 1960. Pulmonary alveolar proteinosis and nocardiosis. *Am J Med* **28:**1002–1007. PubMed
47. **Carlsen ET, Hill RB Jr, Rowlands DT Jr.** 1964. Nocardiosis and Pulmonary Alveolar Proteinosis. *Ann Intern Med* **60:**275–281. PubMed
48. **Clague HW, Harth M, Hellyer D, Morgan WK.** 1982. Septic arthritis due to Nocardia asteroides in association with pulmonary alveolar proteinosis. *J Rheumatol* **9:**469–472. PubMed
49. **Fried J, Hinthorn D, Ralstin J, Gerjarusak P, Liu C.** 1988. Cure of brain abscess caused by Nocardia asteroides resistant to multiple antibiotics. *South Med J* **81:**412–413. PubMed
50. **Oerlemans WG, Jansen EN, Prevo RL, Eijsvogel MM.** 1998. Primary cerebellar nocardiosis and alveolar proteinosis. *Acta Neurol Scand* **97:**138–141. PubMed
51. **Raich RA, Casey F, Hall WH.** 1961. Pulmonary and cutaneous nocardiosis. The significance of the laboratory isolation of Nocardia. *Am Rev Respir Dis* **83:**505–509. PubMed
52. **Taleghani-Far M, Barber JB, Sampson C, Harden KA.** 1964. Cerebral Nocardiosis and Alveolar Proteinosis. *Am Rev Respir Dis* **89:**561–565. PubMed
53. **Walker DA, McMahon SM.** 1986. Pulmonary alveolar proteinosis complicated by cerebral abscess: report of a case. *J Am Osteopath Assoc* **86:**447–450. PubMed
54. **Wongthim S, Charoenlap P, Udompanich V, Punthumchinda K, Suwanagool P.** 1991. Pulmonary nocardiosis in Chulalongkorn Hospital. *J Med Assoc Thai* **74:**271–277. PubMed
55. **Björkholm B, Elgefors B.** 1986. Cerebellar aspergilloma. *Scand J Infect Dis* **18:**375–378. PubMed

56. **Jones CC.** 1960. Pulmonary alveolar proteinosis with unusual complicating infections; a report of two cases. *Am J Med* **29:**713–722. PubMed
57. **Hartung M, Salfelder K.** 1975. Pulmonary alveolar proteinosis and histoplasmosis: report of three cases. *Virchows Arch A Pathol Anat Histol* **368:**281–287. PubMed
58. **Al-Muhsen S, Casanova JL.** 2008. The genetic heterogeneity of mendelian susceptibility to mycobacterial diseases. *J Allergy Clin Immunol* **122:**1043–1051, quiz 1052–1053. PubMed
59. **Puel A, Cypowyj S, Bustamante J, Wright JF, Liu L, Lim HK, Migaud M, Israel L, Chrabieh M, Audry M, Gumbleton M, Toulon A, Bodemer C, El-Baghdadi J, Whitters M, Paradis T, Brooks J, Collins M, Wolfman NM, Al-Muhsen S, Galicchio M, Abel L, Picard C, Casanova JL.** 2011. Chronic mucocutaneous candidiasis in humans with inborn errors of interleukin-17 immunity. *Science* **332:**65–68. PubMed
60. **Nanki T, Onoue I, Nagasaka K, Takayasu A, Ebisawa M, Hosoya T, Shirai T, Sugihara T, Hirata S, Kubota T, Harigai M, Miyasaka N.** 2013. Suppression of elevations in serum C reactive protein levels by anti-IL-6 autoantibodies in two patients with severe bacterial infections. *Ann Rheum Dis* **72:**1100–1102. PubMed
61. **Holland SM, DeLeo FR, Elloumi HZ, Hsu AP, Uzel G, Brodsky N, Freeman AF, Demidowich A, Davis J, Turner ML, Anderson VL, Darnell DN, Welch PA, Kuhns DB, Frucht DM, Malech HL, Gallin JI, Kobayashi SD, Whitney AR, Voyich JM, Musser JM, Woellner C, Schäffer AA, Puck JM, Grimbacher B.** 2007. STAT3 mutations in the hyper-IgE syndrome. *N Engl J Med* **357:**1608–1619. PubMed
62. **Cundy T, Hegde M, Naot D, Chong B, King A, Wallace R, Mulley J, Love DR, Seidel J, Fawkner M, Banovic T, Callon KE, Grey AB, Reid IR, Middleton-Hardie CA, Cornish J.** 2002. A mutation in the gene TNFRSF11B encoding osteoprotegerin causes an idiopathic hyperphosphatasia phenotype. *Hum Mol Genet* **11:**2119–2127. PubMed

Immunohistology and Immunopathology

section G

VOLUME EDITOR: ROBERT G. HAMILTON
SECTION EDITOR: R. NEAL SMITH

Introduction

ROBERT G. HAMILTON

40

Immunohistochemistry techniques are integral to the practice of anatomic pathology. In contrast to the 7th edition of this *Manual*, in which a separate chapter discusses the principles and advances of immunohistochemistry, these techniques have been directly incorporated in two chapters along with figures illustrating the detection of antibodies involved in renal and cardiac diseases. In the first chapter, Collins et al. provide a brief history of immunofluorescence. Methods for the handling, freezing, and storage of tissue specimens, typically obtained by biopsy, are discussed. While most immunofluorescence studies are performed with unfixed frozen tissue, tissue fixation and tissue sectioning are detailed. Direct immunofluorescence is illustrated for the detection of immunoglobulin G (IgG), IgA, IgM, C3, C1q, fibrinogen, and kappa and lambda light chain deposition in renal tissue. A brief discussion of dual fluorescence and microscope instrumentation is followed by an overview of interpretation. In the second chapter, Collins and Smith discuss Western blot analysis for the detection of antibodies specific for glomerular basement membrane and phospholipase A2 receptors. Special requirements are highlighted for antigen presentation, enzymatic digestion of glomeruli, and transfer onto nitrocellulose paper. Section G provides an overview of immunohistology and immunopathology measurements in present-day clinical practice.

doi:10.1128/9781555818722.ch40

Immunofluorescence Methods in the Diagnosis of Renal and Cardiac Diseases

A. BERNARD COLLINS, JAMES R. STONE, AND R. NEAL SMITH

41

Immunofluorescence is a well-established technique for the detection of antigens in tissue sections or cell suspensions (1, 2). The technique was developed in 1941 by Albert Coons to demonstrate the presence of pneumococcal antigens in tissue (3). Since then, immunofluorescence has become a crucial tool in the diagnosis and determination of prognoses of immunologically mediated disease (4). Direct immunofluorescence (defined as the application of specific antibodies to detect specific antigens in tissue) is a sensitive and well-established technique for the detection of tissue-bound immunoglobulins, their subclasses, complement components (C3, C1q, and C4d), amyloidogenic proteins, and fibrin-fibrinogen. In the kidney, many forms of primary glomerulonephritis are characterized by deposition of immunoreactants in distinctive diagnostic patterns. The primary renal targets are the glomerulus, the proximal tubules, and the interstitium. In the heart or open fat pad biopsy specimens, direct immunofluorescence is useful to speciate the type of amyloid identified on specimens with positive Congo red staining in paraffin-embedded tissue (5). The diagnosis of antibody-mediated rejections in heart and kidney allografts is facilitated by the detection of C4d (6–8). This chapter will also emphasize the common immunofluorescence techniques used for diagnosis and interpretation with kidney and skin biopsy specimens.

TISSUES FOR IMMUNOFLUORESCENCE

Tissue submitted for immunofluorescence studies is usually obtained by biopsy, nephrectomy, or heart explantation. For biopsy specimens, a hand lens or dissecting microscope is useful to determine if the tissue is adequate and not just fibrofatty tissue. For needle renal biopsy specimens, a 1-mm portion is cut from each end of the two cores and placed immediately in Karnovsky's fixative for electron microscopy studies. One core is frozen for direct immunofluorescence studies, and the second core is placed into 10% buffered formalin for light microscopic studies. Renal or cardiac tissue at autopsy is usually suitable for immunofluorescence. In the case of endomyocardial biopsy specimens, multiple separate fragments are received. One should be frozen, one should be placed in Karnovsky's fixative, and the remaining fragments should be fixed in formalin. Ultrastructural review of cardiac tissue is useful to confirm the presence of amyloid, especially if the immunofluorescence pattern is negative, if storage disorders are noted in the differential, or if the immunofluorescence analysis identifies immunoglobulin/complement deposition, which is Congo red negative. Open fat pad biopsy specimens are useful for the detection of amyloid. A section of the fat pad biopsy specimen should be frozen for amyloid subtyping. If the Congo red is positive on the formalin-fixed and paraffin-embedded tissue, the type of amyloid (usually kappa versus lambda) can be determined. Fine-needle aspiration of fat pad biopsy specimens for Congo red is not optimal because Congo red staining can often be indeterminate due to artifact. Renal or cardiac tissue at autopsy is usually suitable for immunofluorescence. Amyloid that cannot be subtyped can be speciated by proteomic analysis (9).

TISSUE HANDLING AND FREEZING PROCEDURE

Tissue for immunofluorescence studies should be obtained fresh and kept moist until it is rapidly frozen or snap-frozen. Freezing should be performed within 20 to 30 min if possible. However, the tissue can be kept on a saline-moistened piece of gauze or filter paper in a closed vial or small petri dish. For longer delay times (due to transport) or as an alternative to freezing, the specimen can be put into Michel's immunofluorescence transport medium. The medium is composed of an 85% saturated solution of ammonium sulfate, the protease inhibitor *N*-ethylmaleimide, and magnesium sulfate, in citrate buffer, pH 7.25 (available commercially from Zeus Scientific, Inc., Raritan, NJ). The solution is stable at room temperature but must be kept in a tightly capped container to prevent absorption of CO_2 and acidification. The ammonium sulfate reversibly denatures all proteins in the biopsy specimen. Specimens stored in the transport medium are stable for at least 2 to 4 weeks at room temperature. Specimens in transport media often show increased background. When the specimen is received in the laboratory, the ammonium sulfate is removed by placing the tissue into the wash solution (three 10-min washes; Zeus Scientific, Inc.).

Tissue is frozen by immersing properly oriented tissue into a small amount of OCT compound, a water-soluble resin (Miles Laboratories, Inc., Naperville, IL), on a precooled metal chuck in a cryostat and applying the heat extractor until the OCT is opaque and the tissue frozen. Tissue is then ready for sectioning in less than 3 min.

doi:10.1128/9781555818722.ch41

Many of the difficulties in immunofluorescence studies are related to tissue-handling techniques, suboptimal freezing procedures, drying, or inappropriate frozen storage conditions. If tissue is allowed to freeze too slowly, ice crystal formation can occur, causing structural disruption.

STORAGE CONDITIONS FOR FROZEN SPECIMENS

Frozen specimens should be stored frozen at −70°C in a small plastic bag with as little air as possible. At −70°C, it is possible to store tissue blocks for long periods, often for years, and still obtain adequate results. Tissue can be stored at −20°C, but at this temperature, the duration of satisfactory preservation usually does not exceed several months. Frozen tissue deteriorates during storage, usually from ice crystal formation or desiccation.

FIXATION

Most diagnostic studies using direct immunofluorescence techniques are performed with unfixed frozen tissue sections, since many antigens can be altered or destroyed by fixation. However, demonstration of the presence of some cytoplasmic antigens, such as viral antigens, for diagnostic purposes may require fixation. The optimal fixation conditions must be empirically determined for each antigen of interest. Fixation may also cause the physical redistribution of some antigens. For example, in anti-neutrophil cytoplasmic antibody assays, alcohol fixation of the neutrophil slide preparation causes the myeloperoxidase contained in the primary azurophilic granules in the cytoplasm of neutrophils to redistribute to a perinuclear or nuclear location.

FROZEN-TISSUE SECTIONING

Frozen sections for direct immunofluorescence should be cut in a cryostat at a thickness of 2 to 4 mm. The frozen blocks of tissue should be equilibrated in the cryostat at −25 to −20°C before frozen sectioning. The tissue sections are picked up on single-end SuperFrost/Plus glass slides (Fisher Scientific, Pittsburgh, PA) to facilitate labeling and decrease the chance that tissue will be lost by wiping it off the wrong side. The tissue attaches because the slides are at a higher temperature than the tissue and are positively charged, reducing the likelihood of washing off the tissue. Furthermore, the Plus slide pretreatment eliminates the time-consuming need for coating slides with tissue adhesive solutions (albumin, poly-L-lysine, or 3-aminopropyltriethoxysilane). If necessary to determine if the tissue is adequate, an initial frozen tissue section can be stained using a 1% toluidine blue solution. If the specimen is small, a circle is marked around the tissue with a diamond or aqueous insoluble pencil because it can be difficult to find the tissue on the slide after coverslips are placed on the tissue sections.

Three sections are placed on each slide and either air dried and stained immediately or stored frozen at −20°C in a slide box covered with aluminum foil or plastic wrap. Storing slides overnight allows more effective organization of technical time.

DIRECT IMMUNOFLUORESCENCE

Principle

In the direct immunofluorescence technique, frozen tissue sections are incubated at room temperature in a moist chamber using well-characterized fluorochrome-conjugated antibodies. After incubation, the unbound labeled antibody is washed from the tissue sections, the slides are placed on coverslips, and the bound, labeled antibody is detected by examination and interpretation using a fluorescence microscope. For large workloads, automated stainers enhance technical uniformity and efficiency.

Staining Procedure

Kidney specimens are routinely stained with a panel of immunoglobulin G (IgG) fractions of fluorescein-labeled monospecific antisera to IgG, IgA, IgM, C3, C1q, fibrin-fibrinogen, kappa and lambda light chains, and, in the case of renal biopsy specimens, albumin as a negative control. For genetic renal diseases of the glomerular basement membrane, antibodies to the alpha 1, 3, and 5 chains of type IV collagen can be used to distinguish thin basement membrane disease from an Alport's type of hereditary nephritis. If amyloid is suspected for cardiac specimens or non-light-chain amyloid for renal specimens, antibodies to IgA, IgG, IgM, fibrin-fibrinogen, kappa, lambda, amyloid A, apolipoprotein A1, transthyretin, and β2-microglobulin are used.

1. Prior to staining, cryostat sections (2 to 5 μm) are air dried for 30 min at room temperature to maximize adherence. Afterward, slides are washed for 5 min in 0.01 M sodium phosphate-buffered saline (PBS)–0.15 M NaC1 (pH 7.3) to remove unbound serum proteins which contribute to background staining. The slides are loaded into a staining rack of a Tissue-Tek II (Miles Laboratories) slide-staining unit, which is placed on a clinical rotator adjusted to give gentle stirring.
2. After washing, one slide at a time is removed, the excess PBS is blotted from around the tissue section, and 50 to 100 μl of appropriately diluted fluorescein conjugate is applied to the tissue section while it is still moist. A drop of conjugate should be added just above the tissue section, and to ensure that the conjugate covers the entire specimen, the slide should be gently tipped to one side and then the other. The slides are then incubated for 30 min at room temperature in a moist, level chamber or in petri dishes containing a moistened piece of filter paper. It is essential that tissue remain moistened after being hydrated to avoid problems with background staining.
3. After incubation, the slides are tipped to one side to allow the excess conjugate to run off and the slides are washed as in step 1 in PBS four times for 5 to 10 min each time to remove unbound fluorochrome-labeled conjugate from the section.
4. The excess PBS is blotted from around the specimen, and the moistened tissue is placed on a coverslip with mounting medium. Aqua-Mount (Lerner Labs, Pittsburgh, PA) is used as a mounting medium.
5. The slides are examined using a fluorescence microscope with epi-illumination equipment, which consists of barrier and excitation filters contained in a dichroic mirror package, to allow the visualization of fluorescein.

The above steps are adequate for small laboratories with small workloads. Automated stainers are a better choice because of their technical uniformity and efficiency.

C4d Staining of Renal Allografts

In addition to being stained with the routine direct immunofluorescence panel, allograft kidney or allograft cardiac biopsy specimens are stained for C4d as a marker of

antibody-mediated rejection by using a three-step immunofluorescence technique (6). Diffuse staining of C4d in peritubular renal capillaries or cardiac capillaries has been shown to be associated with circulating antibodies to donor HLA class I and class II antigens in alloantibody-mediated rejections (7–9).

TWO-COLOR IMMUNOFLUORESCENCE

Two-color immunofluorescence can be used to colocalize immunoglobulin deposits with a known antigen. This is a most useful technique used clinically to show that the membranous deposits of IgG4 colocalize with the phospholipase A2 receptor (PLA2R), the antigen of idiopathic/primary membranous nephropathy (10). In this technique, a single slide is air dried for 30 min at room temperature, preblocked first with avidin and then D-biotin, and then incubated sequentially first with anti-human IgG4 fluorescein isothiocyanate (FITC)-labeled (green) subclass antibody, then rabbit anti-PLA2R antibody, biotinylated goat anti-rabbit IgG(H+L), and finally, Cy3 streptavidin. Between each incubation step, the slides are washed in PBS 3 times for 2 to 3 min. Colocalization is identified as yellow when examined under fluorescence microscope using dual excitation filters for FITC and Cy3. Alternatively, separate green and red pictures can be photographed and merged using a camera or, alternatively, software (11).

MOUNTING MEDIUM

A polyvinyl alcohol-glycerol-PBS solution is a common mounting medium. It immobilizes the coverslip by forming a semisolid gel when it sets and allows storage for several weeks at 4°C without significant loss of fluorochrome intensity. Polyvinyl alcohol (Monsanto, St. Louis, MO) is a water-soluble resin available commercially under the name of Aqua-Mount (Lerner Laboratories). For most purposes, the pH of mounting medium should be neutral. However, the pH of mounting medium can be adjusted to achieve more intense fluorescence or to emphasize one color over another, which is particularly helpful in performing double staining. The green fluorescence of fluorescein is quenched at lower pHs, which accents the visualization of the red fluorescence of rhodamine; at high alkaline pHs, both fluorochromes fluoresce yellow. If slides are mounted in Aqua-Mount and stored without light exposure at 4°C or frozen, the fluorescence can be preserved for at least 4 to 8 weeks and longer if the staining is intense.

Rapid fading of fluorescence after excitation is a serious limitation of immunofluorescence preparations, since it restricts reexamination of slides for further evaluation. To ensure that sufficient sections are available for interpretation and reevaluation, several can be placed on the same slide or staining can be done in duplicate. Photography can also be used to document results.

The fading of immunofluorescence slides is related to a combination of factors, including photochemical reactions, fluorochrome oxidation, and the physical and chemical properties of the FITC conjugate. As mentioned previously, it may be necessary to mount the specimens with a medium containing compounds to reduce fluorescence burnout, such as Permafluor (Shandon Lipshaw). Alternatively, newer green fluorochromes are commercially available that are resistant to fading.

QUALITY CONTROL AND ANTIBODY SPECIFICITY

Fluorescein-conjugated antibodies are available from commercial sources. The conjugate should be diluted according to the manufacturer's recommendations. Optimal dilutions of the fluorochrome conjugates are determined empirically using known positive and negative control specimens. The range of working dilutions for direct immunofluorescence studies using fluorochrome-labeled conjugates is usually 1:5 to 1:40 (or about 50 to 150 mg of protein/ml). The range of working dilutions for direct immunofluorescence is usually lower than that for indirect immunofluorescence because of the amplification effect. The appropriate dilution should be determined empirically.

Specificity is an important prerequisite for labeled antibodies used in immunofluorescence studies. Many commercial suppliers sell monospecific fluorochrome-labeled reagents that produce satisfactory results. Relative monospecificity is achieved by absorption, usually non-human immunoglobulins. However, confirmation of specificity and sensitivity is the core responsibility of the user. Commercial suppliers of antibodies usually provide information about the specificity and sensitivity of the fluorochrome-labeled antisera. However, if specificity is defined from Ouchterlony immunodiffusion studies or immunoelectrophoresis, results may be insufficiently sensitive to detect minor contaminating antibodies.

The best method for determining the specificities of labeled antibodies used in diagnostic immunofluorescence studies is to assess their reactivities with known positive and negative tissue controls. For example, a renal biopsy specimen from a patient with membranous glomerulonephritis that has previously been shown to contain only IgG but not IgA is very helpful in defining the specificity of a new lot of labeled anti-human IgA. When in doubt, specificity can be established by blocking or absorption studies. To block staining, the tissue is incubated with unlabeled specific antibody prior to being incubated with the specific fluorochrome-labeled antibody. Although this sometimes results in diminished fluorescence, complete prevention of staining is rarely seen. If specificity is in question, alternative techniques may be required to confirm specificity. Useful positive controls for immunoglobulins can include touch preparations and frozen tissue sections of tonsil or small intestine. Another useful approach is to compare old lots of antisera to new ones with respect to their abilities to detect a known antigen in archival positive cases.

Polyclonal antibody preparations may contain extraneous antibodies, such as antinuclear antibodies, because the antigenic preparation used for immunization can be contaminated with nuclear fragments. Unwanted antibodies can be removed by incubation of the antiserum with appropriate insoluble preparations, such as tissue homogenates or washed red blood cells. It is necessary to use insoluble antigens, since soluble complexes cannot be removed effectively by centrifugation and may bind to the tissue. One method of insolubilizing proteins is to conjugate cross-reactive antigens to CNBr-activated Sepharose beads (Pharmacia, Uppsala, Sweden). These methods should be unnecessary because most commercial sources of antibodies have already absorbed undesirable specificities from the antibodies.

Analytical specificity is more easily ascertained than analytical sensitivity. It is quite possible that a paraprotein or amyloidogenic light chain might have sequence abnormalities that cause loss of epitopes detected by conventionally anti-heavy or -light chain antibodies. So with new lots of antibodies, in addition to specificity studies on samples with readily detectable deposits or amyloid, analytical sensitivity studies should also be done on samples with marginal reactivity. Assessing analytical sensitivity is also problematic for C4d deposition. Both two-step

and three-step indirect immunofluorescence techniques are used to improve sensitivity. Testing a new lot of C4d antibody initially on a known acute antibody-mediated rejection specimen or on a membranous or lupus glomerulonephritis specimen is usually satisfactory and adequate. However, the intensity of C4d staining can vary from faint and segmental to diffuse and intense on both renal and cardiac allograft specimens (6, 8, 12, 13). However, for optimal laboratory quality, testing on a variety of samples is optimal to ensure adequate sensitivity. Because C4d staining correlates with anti-donor alloantibody, multiple samples from patients with known alloantibodies should be tested to adjust the sensitivity of the C4d assay to capture as many of the alloantibody-positive samples as possible while minimizing excess background staining. This is important for cardiac samples. In negative allograft renal biopsy specimens (no peritubular capillary staining), glomeruli invariably show a weak-to-moderate smooth linear staining, which is helpful to assess the strength of staining and the reliability of a negative result. In cardiac allografts, no such internal positive control exists, so the adequacy of the positive control is important.

FLUORESCENCE MICROSCOPES

Fluorescence microscopy depends on the principle that fluorochromes have electrons that are readily excited to unstable higher energy states by absorbing photons of light of specific energies. They then release stored energy as light but at a lower energy level and a longer wavelength.

This loss of energy is emitted as fluorescent light. An excitation filter is chosen to provide incident photons of optical energy at the correct wavelength, and a barrier filter is chosen to block most of the photons of excitation energy and allow only those with lower energies (the fluorescent or emitted photons) to pass through. For example, fluorescein is maximally excited at around 490 nm and has a peak emission at around 510 to 517 nm. FITC interference and excitation filters take advantage of the strong absorption of fluorescein at 490 nm, and when combined with a barrier filter, they block energy with a wavelength of less than 500 nm. This combination of filters results in an apple green color with fluorescein-labeled antibodies.

Tissues or cells stained with fluorescein conjugates can be examined with fluorescence microscopes equipped with appropriate excitation and barrier filters. The most commonly used system is that of epi-illumination, composed of a vertical illuminator and dichroic mirrors. The dichroic mirrors serve as both excitation and barrier filters, since they allow the passage of excitation energy in one direction and emission energy in the other. One limitation of epi-illumination is that the intensity of light at lower magnifications is considerably less than with a dark-field condenser. Another problem is that fluorescence signals of structures above or below the plane of focus result in a background glow or halo effect. This can interfere with interpretation and is frequently more of a concern with cell suspension preparations than with tissue sections. Reduction of these out-of-focus signals can be accomplished by using laser confocal microscopy, usually not necessary for diagnostic applications but more useful for research purposes. Despite these disadvantages, there are several advantages of epi-illumination: (i) no oil is needed; (ii) the intensity of illumination is constant, once the objective is focused so that the brightnesses of staining of different specimens can be more reliably compared; and (iii) viewing can be combined with standard-phase microscopy, which is important for cell suspension studies and for definition of morphological detail in tissue sections, and examination in double-staining studies is easier because of interchangeable FITC and rhodamine dichroic filter systems.

The light source for most fluorescence microscopes is a high-pressure mercury lamp. Illumination is very important, since the brightness of fluorescence depends on the light source, the efficiency of the fluorochrome in converting incident light into fluorescent light, and the concentration of the fluorochrome in the specimen.

EXAMINATION OF SLIDES AND EVALUATION AND RECORDING OF STAINING RESULTS

Preferably, slides should be examined on the day of staining, and a detailed record of the results should be kept on worksheets. Positive and negative controls should be run with each biopsy specimen until one gains confidence in the specificity of staining with a given fluorochrome-labeled reagent. Unexpected findings should always be confirmed before results are reported.

The fluorescence staining of kidney specimens should be described according to location, extent, pattern, and intensity in the glomerular basement membrane (GBM), mesangium, arterioles, tubules, capillaries, interstitium, and casts. For cardiac specimens, descriptions of the staining should include myocytes, capillaries, arterioles, and interstitium.

PHOTOGRAPHY

Photography is the only permanent record one has of the immunofluorescence findings. Laboratories now use digital cameras interfaced with a computer to capture fluorescence images for documentation of results. For routine digital photography, an automated exposure is satisfactory. However, for issues of clonality of light chains, amyloid, or collagen stains, fixed-exposure comparisons are better. This is because automated exposures will intensify weaker staining with longer exposures, thereby making the resultant images appear more similar. It is better to start with a short exposure that just outlines the tissue with faint fluorescence on the most negative reactant and then use that exposure for the other positive or more-positive reactants.

The appendix shows illustrative examples of how immunofluorescence is used on frozen tissues for the identification of immune complexes and speciation of types of amyloid.

Figure 1 shows examples of positive capillary staining for C4d in patients with anti-HLA alloantibodies and acute antibody-mediated rejections of the heart (Fig. 1, left panel) and kidney (Fig. 1, right panel). Figure 1, left panel, shows a cardiac allograft with diffuse capillary staining for C4d. Figure 1, right panel, shows a renal allograft with diffuse peritubular capillary staining for C4d.

Figure 2 shows an example of how immunofluorescence is used to identify cardiac kappa light chain amyloidosis. Figure 2, left panel, shows excess amyloid stain for kappa light chain. Figure 2, right panel, shows negative staining for lambda light chain. Other reactants are also negative.

Figure 3 identifies cardiac lambda light chain amyloidosis. Figure 3, left panel, shows excessive anti-lambda light chain staining of the amyloid deposits. Figure 3, middle panel, shows negative kappa light chain staining. Figure 3, right panel, shows a weak blush of transthyretin staining, which is negative and is background staining when compared to a positive control for transthyretin amyloid (see Fig. 5, right panel). Some reactants, most commonly transthyretin and IgG, show weak background staining within

amyloids. Only a single dominant stain can be called positive. Otherwise, the assay is indeterminate.

Figure 4 shows IgM kappa pseudothrombi (large intraglomerular capillary subendothelial deposits) in a patient with hepatitis C-related cryoglobulinemia. Figure 4, left panel, identifies IgM pseudothrombi within glomerular capillary loops. Figure 4, right panel, identifies kappa light chain staining of the pseudothrombi.

The image shown in Fig. 5 allows diagnosis of the cardiac amyloid as transthyretin, and in this case, it can be called cardiac or senile systemic amyloidosis due to amyloid deposition containing native transthyretin. Figure 5, left panel, shows a negative anti-IgG with background staining. Figure 5, right panel, shows intense positive anti-transthyretin staining.

Figure 6 shows characteristic granular mesangial IgA staining diagnostic of IgA nephropathy. C3, kappa, and lambda staining are similar. IgG can be do-dominant with IgA or less intense. C1q is usually sparse.

Figures 7A and 7B show fluorescent images characteristic of proliferative lupus nephritis, classes III and IV. Figure 7A, left panel, shows strong granular IgG within the GBM and mesangium; kappa and lambda light chain staining are similar. Figure 7A, middle panel, shows segmental granular IgM in the GBM with wire loops (intense coalescing deposits within the GBM). Figure 7A, right panel, shows segmental granular IgA within the GBM with a wire loop. Figure 7B, left panel, shows strong granular C3 within the GBM and mesangium. Figure 7B, middle panel, shows granular C1q within the GBM and mesangium. Figure 7B, right panel, shows granular IgG in the tubular basement membranes with tissue antinuclear antibody (ANA). Granular IgG in the tubular basement membranes (green granular staining within green rings, which are tubules) and tissue ANA (intense green ovals in cells, which are nuclei) are very commonly seen in active lupus glomerulonephritis.

Figure 8 shows colocalization of membranous deposits, which contain IgG (often IgG4 dominant) and the antigen PLA2R of podocytes in idiopathic/primary membranous nephropathy. Figure 8, left panel, shows finely granular IgG4 within the GBM (green, FITC). Figure 8, middle panel, shows finely granular anti-PLA2R staining within the GBM and staining of the podocytes (both red, Cy3). Figure 8, right panel, shows colocalization of the granular IgG4 deposits with the PLA2R antigen (yellow). Colocalization can be done with appropriate filters or by overlaying the green and red images using image software.

REFERENCES

1. **Collins AB, Bhan AK, Dienstag JL, Colvin RB, Haupert GT Jr, Mushahwar IK, McCluskey RT.** 1983. Hepatitis B immune complex glomerulonephritis: simultaneous glomerular deposition of hepatitis B surface and e antigens. *Clin Immunol Immunopathol* **26:**137–153. PubMed
2. **Walker PD, Cavallo T, Bonsib SM, Ad Hoc Committee on Renal Biopsy Guidelines of the Renal Pathology Society.** 2004. Practice guidelines for the renal biopsy. *Mod Pathol* **17:**1555–1563. PubMed
3. **Coons AH, Creech HJ, Jones RN, Berliner E.** 1942. The demonstration of pneumococcal antigen in tissues by the use of immunofluorescent antibody. *J Immunol* **45:**159–170.
4. **McCluskey RT, Collins AB, Niles JL.** 1995. Kidney, p 109–122. *In* Colvin RB, Bhan AK, McCluskey RT (ed), *Diagnostic Immunopathology*. Raven, New York, NY.
5. **Collins AB, Smith RN, Stone JR.** 2009. Classification of amyloid deposits in diagnostic cardiac specimens by immunofluorescence. *Cardiovasc Pathol* **18:**205–216. PubMed
6. **Collins AB, Schneeberger EE, Pascual MA, Saidman SL, Williams WW, Tolkoff-Rubin N, Cosimi AB, Colvin RB.** 1999. Complement activation in acute humoral renal allograft rejection: diagnostic significance of C4d deposits in peritubular capillaries. *J Am Soc Nephrol* **10:**2208–2214. PubMed
7. **Mauiyyedi S, Colvin RB.** 2002. Humoral rejection in kidney transplantation: new concepts in diagnosis and treatment. *Curr Opin Nephrol Hypertens* **11:**609–618. PubMed
8. **Mauiyyedi S, Pelle PD, Saidman S, Collins AB, Pascual M, Tolkoff-Rubin NE, Williams WW, Cosimi AA, Schneeberger EE, Colvin RB.** 2001. Chronic humoral rejection: identification of antibody-mediated chronic renal allograft rejection by C4d deposits in peritubular capillaries. *J Am Soc Nephrol* **12:**574–582. PubMed
9. **Sethi S, Theis JD, Vrana JA, Fervenza FC, Sethi A, Qian Q, Quint P, Leung N, Dogan A, Nasr SH.** 2013. Laser microdissection and proteomic analysis of amyloidosis, cryoglobulinemic GN, fibrillary GN, and immunotactoid glomerulopathy. *Clin J Am Soc Nephrol* **8:**915–921. PubMed
10. **Larsen CP, Messias NC, Silva FG, Messias E, Walker PD.** 2013. Determination of primary versus secondary membranous glomerulopathy utilizing phospholipase A2 receptor staining in renal biopsies. *Mod Pathol* **26:**709–715. PubMed
11. **Collins AB, Farkash EA, Beck LH, Smith RN, Colvin RB.** 2013. Detection of PLA2R in glomerular deposits in membranous nephropathy cases seronegative for anti-PLA2R, abstr FR-OR008. American Society of Nephrology, Washington, D.C.
12. **Haas M, Sis B, Racusen LC, Solez K, Glotz D, Colvin RB, Castro MC, David DS, David-Neto E, Bagnasco SM, Cendales LC, Cornell LD, Demetris AJ, Drachenberg CB, Farver CF, Farris AB III, Gibson IW, Kraus E, Liapis H, Loupy A, Nickeleit V, Randhawa P, Rodriguez ER, Rush D, Smith RN, Tan CD, Wallace WD, Mengel M, Banff Meeting Report Writing Committee.** 2014. Banff 2013 meeting report: inclusion of c4d-negative antibody-mediated rejection and antibody-associated arterial lesions. *Am J Transplant* **14:**272–283. PubMed
13. **Smith RN, Brousaides N, Grazette L, Saidman S, Semigran M, Disalvo T, Madsen J, Dec GW, Perez-Atayde AR, Collins AB.** 2005. C4d deposition in cardiac allografts correlates with alloantibody. *J Heart Lung Transplant* **24:**1202–1210. PubMed

APPENDIX

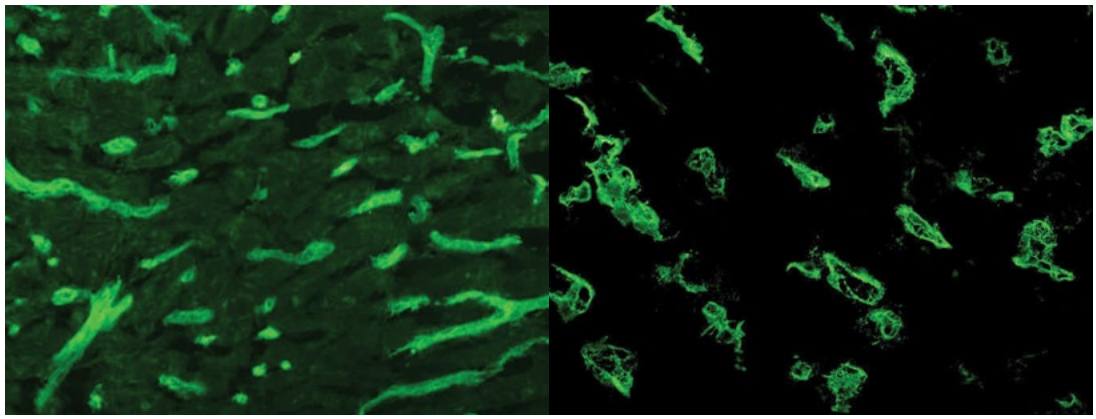

FIGURE 1 Acute alloantibody-mediated rejections. (Left) Cardiac allograft with diffuse capillary staining for C4d. (Right) Acute alloantibody-mediated rejection of a renal allograft with diffuse peritubular capillary staining for C4d.

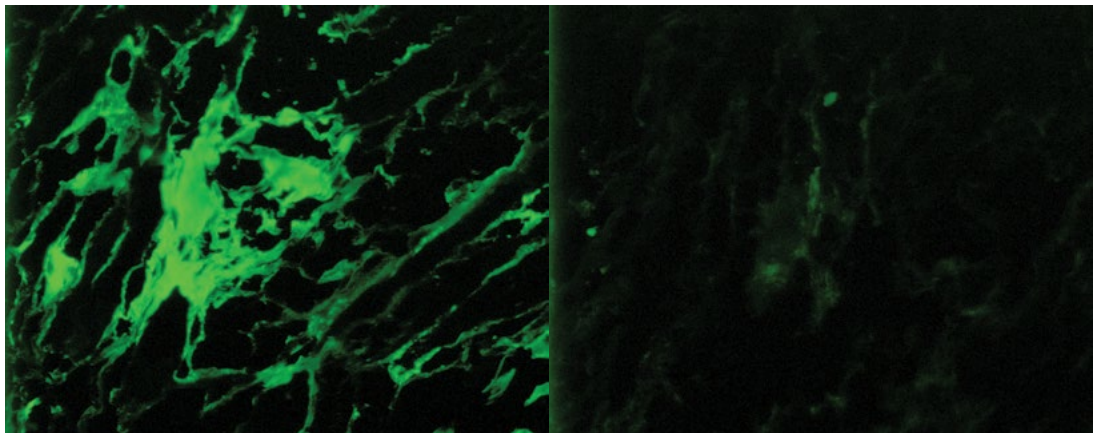

FIGURE 2 Cardiac kappa light chain amyloidosis. (Left) Positive anti-kappa light chain, 200 ms. (Right) Negative anti-lambda light chain, 200 ms.

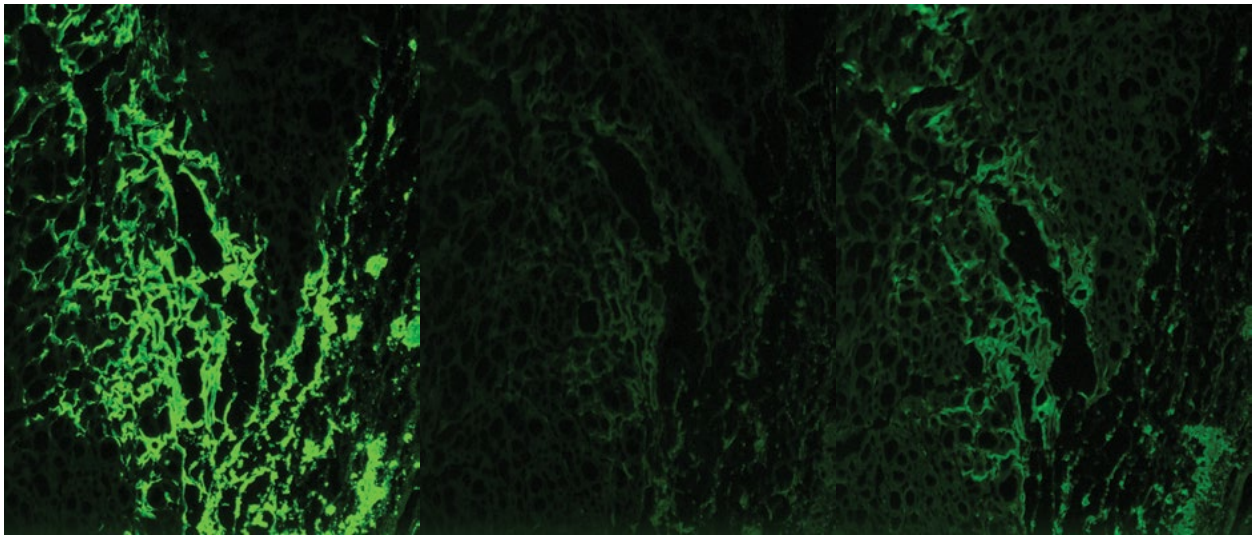

FIGURE 3 Cardiac lambda light chain amyloidosis. (Left) Positive anti-lambda light chain, 500 ms. (Middle) Negative kappa light chain, 500 ms. (Right) Negative transthyretin light chain with background staining, 500 ms.

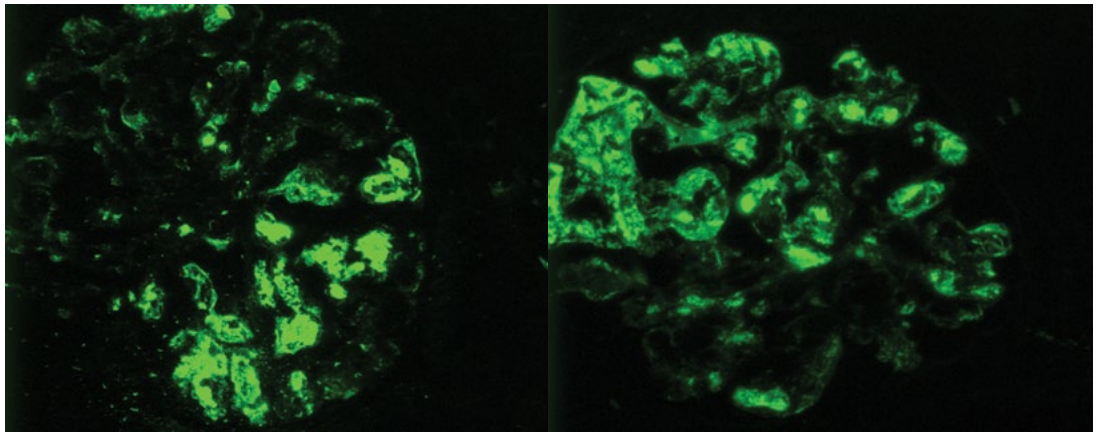

FIGURE 4 Kidney, cryoglobulinemic glomerulonephritis, and hepatitis C-related IgM (left) and kappa (right) pseudothrombi.

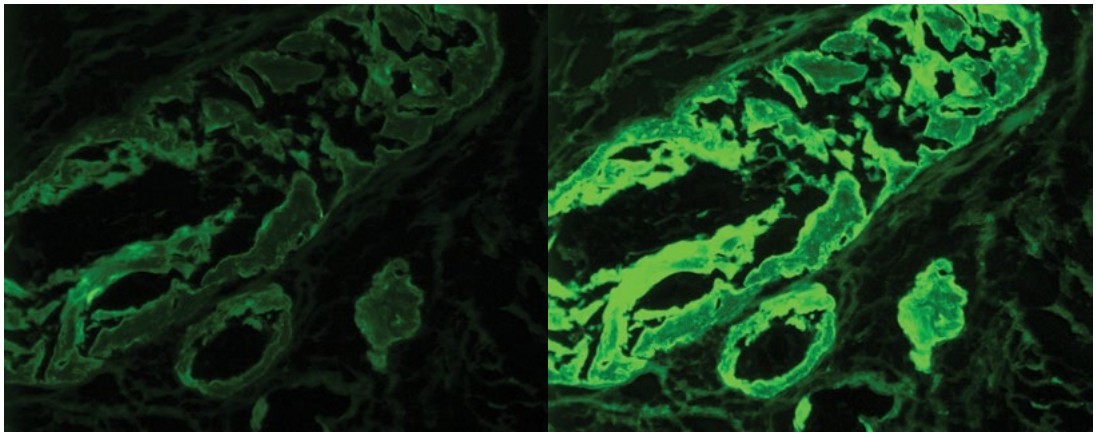

FIGURE 5 Caridac senile systemic amyloidosis (native transthyretin). (Left) Negative anti-IgG with background staining, 200 ms. (Right) Positive anti-transthyretin, 200 ms.

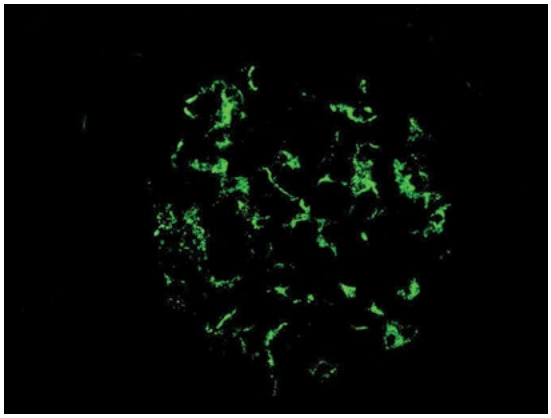

FIGURE 6 IgA nephropathy: mesangial IgA deposits.

A.

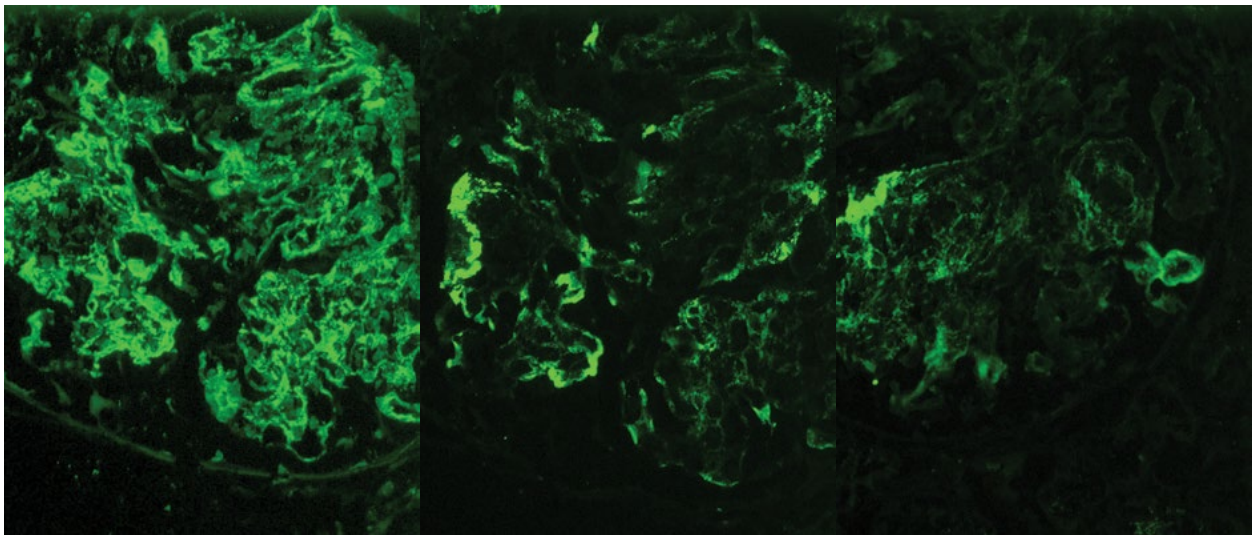

B.

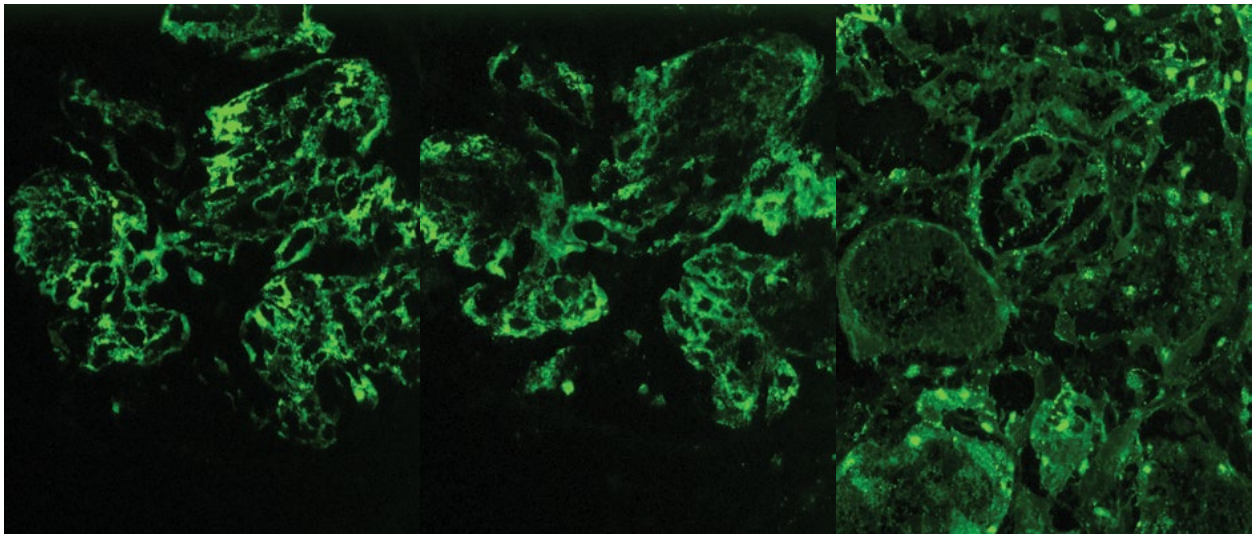

FIGURE 7 Lupus nephritis: granular IgG within the GBM and mesangium. (Panel A, left) Kappa and lambda similar; (middle) segmental granular IgM in the GBM with wire loops; (right) segmental granular IgA within the GBM with wire loop. (Panel B, left) Granular C3 within the GBM and mesangium; (middle) granular C1q within the GBM and mesangium; (right) granular IgG in the tubular basement membranes, tissue ANA.

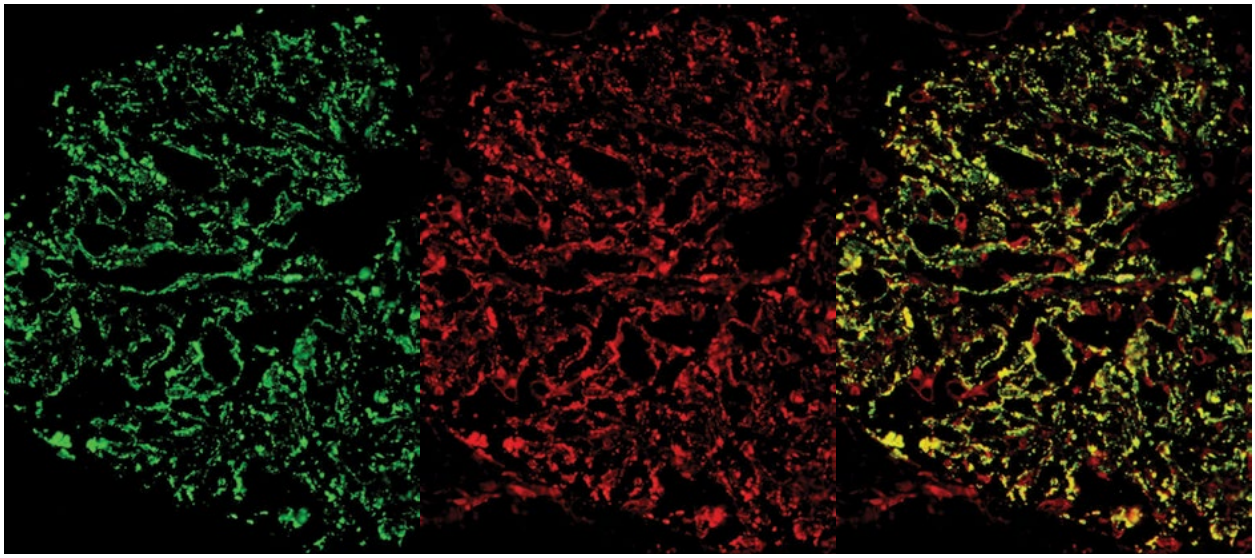

FIGURE 8 Idiopathic/primary membranous nephropathy. (Left) Granular IgG4 within the GBM (green). (Middle) Granular PLA2R within the GBM and staining of the podocytes (red). (Right) Colocalization of the granular IgG4 with the PLA2R antigen (yellow).

Western Blot Analysis for the Detection of Anti-Glomerular Basement Membrane Antibodies and Anti-Phospholipase A2 Receptor Antibodies

A. BERNARD COLLINS AND R. NEAL SMITH

42

Anti-basement membrane antibodies and diffuse alveolar hemorrhage (Goodpasture's syndrome) receives its eponym from Ernest Goodpasture. While studying the influenza pandemic after World War I, Goodpasture studied an 18-year-old male, who died of pulmonary hemorrhage, and diagnosed his pathological findings as systemic vasculitis (1). Although the disease that Goodpasture described is probably different from the disease that now carries his eponym (2), Goodpasture's disease is now well recognized as one of the causes of pulmonary hemorrhage and/or acute renal failure. Immunofluorescence later identified that some cases of pulmonary hemorrhage and renal failure were associated with the linear deposition of immunoglobulins deposited along the pulmonary and glomerular basement membranes (GBM) (3–5). The term Goodpasture's is now generally reserved for the diseases of pulmonary hemorrhage and renal failure with anti-basement membrane antibodies (6, 7).

Animals immunized to basement membranes first established the immunological basis of this disease (8–10), and human anti-basement membrane antibodies passively transfer the disease to monkeys (11). Additional confirmation occurred when Alport's patients lost their allografts to anti-GBM nephritis (12–15). The disease is complement dependent (7, 16). Animal models of pulmonary and glomerular anti-basement membrane disease strongly support the pathogenic nature of these autoantibodies (17–20). The autoantibodies are immunoglobulin G (IgG), predominantly IgG1 (21), and complement fixing (16). Plasmapheresis removes autoantibodies and complement and mitigates the disease (6, 22, 23). Recurrence of antibodies can cause relapse (24, 25). Why some patients develop only pulmonary or renal disease is unknown.

The antigenic sites identified by autoantibodies in anti-basement membrane disease are within the type IV basement membrane collagen (26–28), specifically and most commonly the antigenic target is the non-collagenous globular domain (NC1) of the alpha 3 chain of type IV collagen (29–31). The antigen in the alveolar basement membrane is thought to be the same as that of the GBM (32, 33). Fine specificity analysis identifies two binding sites for pathological autoantibodies within the NC1 domain that are normally sequestered within the alpha 3 chain (34, 35). Autoantibodies against these two epitopes correlate with disease severity as compared to autoantibodies against other basement membrane antigens (36–38). Patients with anti-basement membrane disease have two normal alpha 3 collagen genes (COL4A3) (39). Studies of the molecular architecture of basement membrane identify that the quaternary structure of the alpha 345 NC1 hexamer must be perturbed to expose the cryptic autoantigenic epitopes within the alpha 345 NC1 hexamer. These epitopes elicit autoantibodies because anti-GBM autoantibodies are nonreactive to the native intact hexamer (40). In contrast, in posttransplantation anti-GBM nephritis in Alport's, these anti-GBM antibodies bind to intact hexamers (40). This seminal study also showed that titers to the alpha 3 NC1 correlated with disease activity, as did the presence of alpha 5 NC1 autoantibodies, likely developing through epitope spreading.

There is a strong association of class II genes and human anti-basement membrane disease, which is consistent with genetic immune response gene control within the major histocompatibility complex (39, 41–43). Similar findings are found in mice (44). Additional non-major histocompatibility complex genetic variation in disease susceptibility is found in mice (18, 45). The mere presence of anti-basement membrane antibodies does not necessarily lead to disease. In spite of the normal clonal selection against B cells with reactivity to alpha 3(IV) NC1 epitopes (46), some human immunodeficiency virus patients, possibly due to B-cell dysregulation, have anti-basement membrane antibodies without Goodpasture's disease (47, 48). Anti-alpha 3(IV) NC1 antibodies are found in normal sera (49) with much lower titers and avidity than in sera from patients with Goodpasture's. In addition, the subclass distribution was different, with IgG1 present in the sera of a patient with disease compared to IgG2 in normal sera, suggesting the importance of complement. T-cell tolerance may be broken by T-cell priming to bacterial antigens which cross-react on alpha 3(IV) NC1 epitopes (epitope mimicry) (50). Variation in host natural killer T cells, transforming growth factor β, Fc receptor, and kallikrein esterase activity may exacerbate or mitigate disease activity (18, 51, 52). Because the alpha 3(IV) NC1 pathogenic epitopes are sequestered within the normal hexamer, pathogenic antibodies may still be excluded from binding (40, 53). In a mouse model of anti-basement membrane disease, mice resistant to anti-basement membrane disease became susceptible with injections of interleukin-2 or gamma interferon (54),

doi:10.1128/9781555818722.ch42

suggesting that inflammation or other pulmonary injury can promote disease by making the pathogenic epitopes available for antibody binding. This is an intriguing hypothesis because many reports of anti-basement membrane disease were temporarily associated with viral infection, smoking, or inhalation injury (55–62). An additional complexity in the pathophysiology of anti-basement membrane disease is that 20 to 30% of patients with anti-alpha 3(IV) NC1 autoantibodies also have anti-neutrophil cytoplasmic antibodies (ANCA) to myeloperoxidase or proteinase 3 (44, 63–67). A detailed serological analysis suggested that double-positive patients had fewer antibodies to the two pathogenic epitopes of alpha 3(IV) NC1 than patients with only anti-basement membrane antibodies. This suggests that some double-positive patients should have a disease pattern more closely resembling ANCA disease. However, some double-positive patients have fulminant disease, more closely resembling anti-basement membrane disease, so it is impossible to distinguish which autoimmune process is more pathogenic. It is possible that the ANCA disease in anti-GBM susceptible patients causes sufficient basement membrane injury to unmask the cryptic alpha 3(IV) NC1 epitopes and allow T-cell epitope spreading, permitting an anti-alpha 3(IV) NC1 antibody response (35–37).

Pathologically, there is diffuse alveolar hemorrhage and/or crescentic glomerulonephritis. By immunofluorescence, there is strong linear staining for IgG, which exceeds albumin (anti-GBM immunofluorescence). The staining must be linear and not granular. The presence of granular IgG GBM staining indicates the presence of immune complexes, which would most likely exclude anti-GBM disease in most cases. Confirmation of anti-basement membrane disease requires a positive Western blot, the most sensitive assay for anti-basement membrane disease, confirming bands at 28 and 48 to 50 kDa (67). Monitoring of anti-alpha 3(IV) NC1 titers guides therapy and can identify early relapse (68). Determination of anti-GBM antibodies by Western blotting is the most critically important test in the differentiation of acute pulmonary hemorrhage because negative enzyme immunoassays may miss low titers, which are readily detected as positive by Western blotting.

WESTERN BLOT ANALYSIS

Our laboratory uses a sensitive and specific assay developed for the detection of circulating anti-GBM antibodies using Western blot analysis. This assay is advantageous because the exact molecular weight of the antigen recognized by the autoantibody is determined and compared to the reactivity of a known Goodpasture serum to the α3(IV) chain. The antigenic preparation used is a collagenase digest of isolated human GBM prepared by the enzymatic digestion of the GBM, which releases the NC1 domains of the type IV collagen, including the α3(IV) NC1, the Goodpasture antigen. Separation of the soluble proteins by polyacrylamide gel electrophoresis (PAGE), followed by transfer to nitrocellulose paper for immunoblotting, allows discrimination between antibody reacting to the Goodpasture antigen and those reacting with other components of the GBM.

ANTIGEN PREPARATION FOR ANTI-GBM ANTIBODIES

GBM is prepared from normal human kidneys obtained at autopsy or from nephrectomy specimens. Use of autopsy specimens is limited to no more than 10 to 12 h after death, and in the case of surgical specimens, only the normal portion at least 1 to 2 cm distal from any tumor is taken. The kidneys are then stored frozen at −70°C for glomerular isolation.

The tissue is thawed in 0.01 M phosphate-buffered saline (PBS), pH 7.2, containing 10 mM phenylmethylsulfonyl fluoride as a protease inhibitor. All subsequent isolation steps are carried out in the presence of phenylmethylsulfonyl fluoride. The cortical portion of the kidneys is cut away from the medulla and placed in ice-cold PBS. Glomeruli are isolated from the cortical tissue using differential sieving. The glomeruli are washed two or three times with PBS. After the final wash with PBS, the glomeruli are washed twice with distilled water to rupture the cell membranes. To further remove cellular material, the glomeruli are sonicated by pulsation using a W200 P Sonifier cell disrupter (Heat Systems-Ultrasonics, Inc., Plainview, NY) equipped with a microtip at a 40% duty cycle. After the initial sonication, the preparation is examined using phase microscopy and the sonication step is repeated until only refractile GBM remains. The GBM is dialyzed against distilled water overnight at 4°C, lyophilized, and stored in a desiccator at 4°C.

ENZYMATIC DIGESTION OF GLOMERULI

The GBM is digested using chromatographically purified collagenase type VII prepared from *Clostridium histolyticum* (Sigma, St. Louis, MO). The collagenase preparation is substantially free of nonspecific protease, clostripain, and tryptic activities. Ten milligrams of lyophilized GBM is suspended in 2 ml of 0.1 M Tris-HCl (pH 7.5) in a 15-ml centrifuge tube with 5 mM $CaCl_2$ added to facilitate digestion. The mixture is sonicated for 30 min in a Bransonic 220 water bath sonicator (Branson Co., Shelton, CT). Collagenase type VII (1,000 U/mg of GBM) is added, and the GBM is digested at 37°C in a shaking water bath for 48 h. The pH is monitored at 30, 60, and 120 min and adjusted to 7.5 if necessary using 1 N Tris-HCl or 1 N Trizma base. After digestion, 1 ml of 0.1 M Tris-HCl, pH 7.5, containing 2 mM EDTA is added to chelate free Ca^{2+} and thus quench the reaction. The particulate solution is centrifuged at 1,500 × *g* for 30 min at 4°C. The clear supernatant is recovered and assayed for protein concentration. The solubilized antigen is then stored frozen at −70°C in 50-μl aliquots.

In initial studies, the GBM was subjected to various durations of enzymatic digestion, from 24 to 96 h, to maximize the degradation of the collagenous portions of the membrane. Protein determinations by the Lowry method were performed, and the results obtained showed that approximately 50 to 60% (wt/wt) of the membrane was solubilized in the first 24 h. The solubilization occurred less rapidly after that but continued for up to 72 to 96 h.

PAGE AND TRANSFER TO NITROCELLULOSE PAPER

An aliquot of the soluble antigen preparation obtained from the collagenase digestion of the GBM is thawed, and 200 μg is added to each precast gel (Jule, Inc., Milford, CT) and then separated by sodium dodecyl sulfate-PAGE in 12% unreduced gels using a Mighty Small II gel apparatus (Hoefer Scientific, San Francisco, CA) at a constant current of 40 mA for 1 h. Included as a marker is a low-molecular-weight standard (Bio-Rad, Richmond, CA). After PAGE, the separated proteins are transferred to nitrocellulose paper (GE Healthcare Amersham Hybond-ECL Fisher Scientific, Agawam, MA) using a TE series Transphor electrophoresis unit (Hoefer Scientific) and a PS 500X direct current power

supply. The transfer electrophoresis is carried out using a constant current of 200 mA for 1 h with a circulating water cooling system. To verify and visualize the separated transferred proteins, the nitrocellulose paper is cut from one side of the paper to include the molecular weight standard and the soluble GBM antigen digest and placed into 0.1% India ink on a slow rotator for 30 to 60 min, followed by a PBS wash. The remainder of the nitrocellulose paper is stored dry between two pieces of Whatman filter paper at room temperature. Storing paper in this manner allows sera to be tested quickly and efficiently. Paper can be stored dry for up to 2 months.

WESTERN BLOTTING

An appropriate piece of the dried nitrocellulose paper is cut for the number of serum samples to be tested and placed into 5% skim milk buffer for 1 h, with agitation, for blocking. After blocking, the nitrocellulose paper is cut into 3- to 4-mm-wide strips and placed into the wells of a Mighty Small incubation tray (Hoefer Scientific). The strips are incubated in 1 ml of test serum diluted 1:10 in 0.5% skim milk buffer for a minimum of 1 h. After incubation, the excess serum is aspirated and the strips are washed three times for 5 min each time with 0.5% skim milk buffer. They are then incubated with 1 ml of biotin-conjugated goat anti-human IgG (heavy and light chains; Vector Labs, Burlingame, CA) at 1:250 for 1 h, with agitation. After incubation, excess conjugate is aspirated and the strips are washed with 0.5% skim milk buffer. To detect bound labeled antibody, the strips are incubated in 1 ml of avidin biotin complex (Vector Labs) for 60 min, the excess reagent is aspirated, and the nitrocellulose strips are washed in the 0.5% skim milk buffer as described above. The last incubation is with 3-amino-9-ethyl carbazole (1 ml per well), a chromogen for horseradish peroxidase. Finally, the strips are washed in distilled water for 5 to 10 min and blotted dry between two pieces of Whatman filter paper, so the strips can be examined for reactivity to the α3(IV) NC1 (the Goodpasture antigen) or reactivities to other NC1 domains of type IV collagen. The total time for performance of the test is 4 to 5 h.

Figure 1 shows a positive and negative Western blot for anti-GBM antibodies.

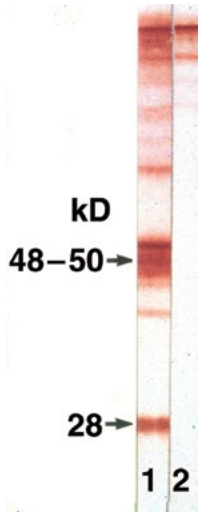

FIGURE 1 Lane 1 shows a Western blot of known positive anti-GBM (1:20) identifying the required bands of 28 and 48 to 50 kDa. Lane 2 shows a negative serum sample. Note the higher-molecular-mass bands in both the positive and negative sera.

ELISA FOR α3(IV) NC1

Western blot analysis is a sensitive and specific assay for detecting anti-GBM antibodies, but for monitoring disease activity, quantitation is required. A satisfactory monitoring commercial enzyme-linked immunosorbent assay (ELISA) kit (Scimedx Corp., Denville, NJ) uses microtiter strips coated with the monomer of the α3(IV) NC1 subunit. The value, in ELISA units (EU), for each unknown serum is determined from a standard curve constructed from analysis of known positive sera containing assigned values of 5, 20, 80, and 320 EU/ml. A positive serum and a negative serum are also included in each determination. The level of antibody is expressed as EU per milliliter. A value equal to or greater than 15 EU/ml is considered positive. A value equal to 5.1 to 14.9 EU/ml is considered equivocal, and a value equal to or less than 5 EU/ml is considered negative. Differences in sensitivity and specificity were observed when the results of ELISA and Western blot analysis were compared using the same serum. The differences in results were evident for treated patients, particularly when plasmapheresis was part of the treatment regimen. However, the ELISA is clearly less sensitive than Western blotting. Often after treatment, the ELISA will become negative, while the Western blot analysis remains positive. False positives are also a problem in this ELISA; we have obtained positive ELISA results with sera from nine patients with no evidence of anti-GBM disease by biopsy or Western blot analysis. Therefore, the most sensitive and specific current method for detecting circulating anti-GBM antibodies is Western blot analysis. In our laboratory, positive anti-GBM antibody results obtained by ELISA are never reported without confirmation by Western blot analysis. It is also important to note that the antibody titer obtained in the ELISA for different patients cannot be used as a measure of the disease severity, since the antibodies may have different affinities and biological activities. The test is most useful for monitoring an individual patient, comparing subsequent samples with the initial sample.

ANTIGEN PREPARATION FOR ANTI-PHOSPHOLIPASE A2 RECEPTOR ANTIBODIES

The antigen preparation for the detection of anti-phospholipase A2 receptor antibodies is identical to the methods of Beck et al. (69) in their supplementary appendix. Cortical sections are snap-frozen and stored at −70°C from deceased human kidneys not used for transplantation. Cortical sections are pressed through a gradient of sieves (Fisher Scientific) with cold PBS to enrich for glomeruli. Pellets of glomeruli with an equal volume of 100 mM Tris, pH 8.1, 1 mM $MgCl_2$ are freeze-thawed at −80°C. An equal volume (twice the glomerular pellet volume) of radioimmunoprecipitation assay buffer (50 mM Tris-HCl, pH 7.4, 150 mM NaCl, 1% NP-40, 0.5% sodium deoxycholate, 0.1% sodium dodecyl sulfate; Boston BioProducts, Ashland, MA) is added with 1× protease inhibitor cocktail set I (Calbiochem/EMD Chemicals, Inc., San Diego, CA), and the glomeruli are manually Dounce homogenized while on ice. Glomerular proteins are extracted on ice for 40 min, with intermittent vortexing. Radioimmunoprecipitation assay-insoluble debris is removed by a 10-min centrifugation at 14,000 rpm at 4°C. Due to the presence of contaminating human IgG in this preparation, the human glomerular extract was incubated for 4 h (or overnight) at 4°C with

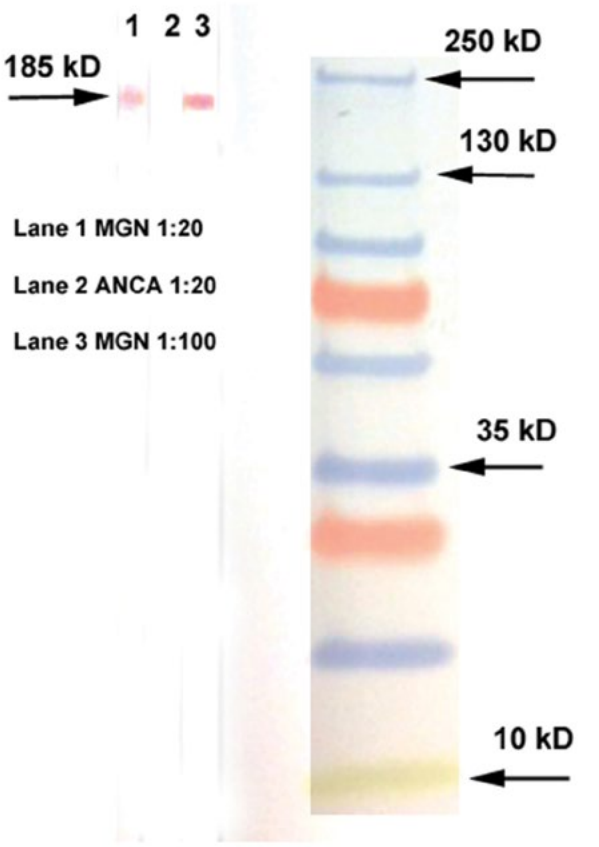

FIGURE 2 Example of a Western blot for anti-phospholipase A2 receptor antibodies. Lanes 1 and 3 show positive serum samples at 1:20 (lane 1) and 1:100 (lane 3) dilutions from a patient with primary/idiopathic membranous nephropathy (MGN) of the anti-phospholipase A2 receptor type. Lane 2 shows a negative control at 1:20 dilution from an ANCA-positive patient. On the right are molecular mass markers.

immobilized Protein G Plus (Thermo Fisher) and the beads discarded. Human glomerular extract was tested by Western blotting with anti-human IgG to ensure that all detectable IgG had been removed.

WESTERN BLOT FOR ANTI-PHOSPHOLIPASE A2 RECEPTOR ANTIBODIES

The Western blot procedure for anti-phospholipase A2 receptor antibodies is the same as described above for anti-GBM antibodies, except that electrophoresis is performed with 7.5% nonreducing gels and transfer is done using Immobilon polyvinylidene difluoride paper (Millipore Corp, San Diego, CA). See Fig. 2.

REFERENCES

1. **Goodpasture EW.** 1919. The significance of certain pulmonary lesions in relation to the etiology of influenza. *Am J Med Sci* **158:**863–870. PubMed
2. **Stanton MC, Tange JD.** 1958. Goodpasture's syndrome (pulmonary haemorrhage associated with glomerulonephritis). *Australas Ann Med* **7:**132–144. PubMed
3. **Scheer R, Grossman M.** 1964. Immune aspects of the glomerulonephritis associated with pulmonary hemmorhage. *Ann Intern Med* **60:**1009–1021.
4. **Duncan DA, Drummond KN, Michael AF, Vernier RL.** 1965. Pulmonary hemorrhage and glomerulonephritis. Report of six cases and study of the renal lesion by the fluorescent antibody technique and electron microscopy. *Ann Intern Med* **62:**920–938. PubMed
5. **Sturgill BC, Westervelt FB.** 1965. Immunofluorescence studies in a case of Goodpasture's syndrome. *JAMA* **194:**914–916. PubMed
6. **Simpson IJ, Doak PB, Williams LC, Blacklock HA, Hill RS, Teague CA, Herdson PB, Wilson CB.** 1982. Plasma exchange in Goodpasture's syndrome. *Am J Nephrol* **2:**301–311. PubMed
7. **Wilson CB, Dixon FJ.** 1973. Anti-glomerular basement membrane antibody-induced glomerulonephritis. *Kidney Int* **3:**74–89. PubMed
8. **Germuth FG Jr, Choi IJ, Taylor JJ, Rodriguez E.** 1972. Antibasement membrane disease. I. The glomerular lesions of Goodpasture's disease and experimental disease in sheep. *Johns Hopkins Med J* **131:**367–384. PubMed
9. **Ohnuki T.** 1975. Crescentic glomerulonephritis induced in the goat by immunization with homologous or heterologous glomerular basement membrane antigen. *Acta Pathol Jpn* **25:**319–331. PubMed
10. **Steblay RW.** 1962. Glomerulonephritis induced in sheep by injections of heterologous glomerular basement membrane and Freund's complete adjuvant. *J Exp Med* **116:**253–272. PubMed
11. **Lerner RA, Glassock RJ, Dixon FJ.** 1967. The role of anti-glomerular basement membrane antibody in the pathogenesis of human glomerulonephritis. *J Exp Med* **126:**989–1004. PubMed
12. **Goldman M, Depierreux M, De Pauw L, Vereerstraeten P, Kinnaert P, Noël LH, Grünfeld JP, Toussaint C.** 1990. Failure of two subsequent renal grafts by anti-GBM glomerulonephritis in Alport's syndrome: case report and review of the literature. *Transpl Int* **3:**82–85. PubMed
13. **Oliver TB, Gouldesbrough DR, Swainson CP.** 1991. Acute crescentic glomerulonephritis associated with anti-glomerular basement membrane antibody in Alport's syndrome after second transplantation. *Nephrol Dial Transplant* **6:**893–895. PubMed
14. **Shah MK, Hugghins SY.** 2002. Characteristics and outcomes of patients with Goodpasture's syndrome. *South Med J* **95:**1411–1418. PubMed
15. **Teruel JL, Liaño F, Mampaso F, Moreno J, Serrano A, Quereda C, Ortuño J.** 1987. Allograft antiglomerular basement membrane glomerulonephritis in a patient with Alport's syndrome. *Nephron* **46:**43–44. PubMed
16. **Mercola KE, Hagadorn JE.** 1973. Complement-dependent acute immunologic lung injury in an experimental model resembling Goodpasture's syndrome. *Exp Mol Pathol* **19:**230–240. PubMed
17. **Abbate M, Kalluri R, Corna D, Yamaguchi N, McCluskey RT, Hudson BG, Andres G, Zoja C, Remuzzi G.** 1998. Experimental Goodpasture's syndrome in Wistar-Kyoto rats immunized with alpha3 chain of type IV collagen. *Kidney Int* **54:**1550–1561. PubMed
18. **Nakamura A, Yuasa T, Ujike A, Ono M, Nukiwa T, Ravetch JV, Takai T.** 2000. Fcgamma receptor IIB-deficient mice develop Goodpasture's syndrome upon immunization with type IV collagen: a novel murine model for autoimmune glomerular basement membrane disease. *J Exp Med* **191:**899–906. PubMed
19. **Reynolds J, Moss J, Duda MA, Smith J, Karkar AM, Macherla V, Shore I, Evans DJ, Woodrow DF, Pusey CD.** 2003. The evolution of crescentic nephritis and alveolar haemorrhage following induction of autoimmunity to glomerular basement membrane in an experimental model of Goodpasture's disease. *J Pathol* **200:**118–129. PubMed

20. **Sado Y, Boutaud A, Kagawa M, Naito I, Ninomiya Y, Hudson BG.** 1998. Induction of anti-GBM nephritis in rats by recombinant alpha 3(IV)NC1 and alpha 4(IV) NC1 of type IV collagen. *Kidney Int* **53:**664–671. PubMed
21. **Segelmark M, Butkowski R, Wieslander J.** 1990. Antigen restriction and IgG subclasses among anti-GBM autoantibodies. *Nephrol Dial Transplant* **5:**991–996. PubMed
22. **Johnson JP, Whitman W, Briggs WA, Wilson CB.** 1978. Plasmapheresis and immunosuppressive agents in antibasement membrane antibody-induced Goodpasture's syndrome. *Am J Med* **64:**354–359. PubMed
23. **Levy JB, Turner AN, Rees AJ, Pusey CD.** 2001. Long-term outcome of anti-glomerular basement membrane antibody disease treated with plasma exchange and immunosuppression. *Ann Intern Med* **134:**1033–1042. PubMed
24. **Dahlberg PJ, Kurtz SB, Donadio JV, Holley KE, Velosa JA, Williams DE, Wilson CB.** 1978. Recurrent Goodpasture's syndrome. *Mayo Clin Proc* **53:**533–537. PubMed
25. **Keller F, Nekarda H.** 1985. Fatal relapse in Goodpasture's syndrome 3 years after plasma exchange. *Respiration* **48:**62–66. PubMed
26. **Butkowski RJ, Wieslander J, Wisdom BJ, Barr JF, Noelken ME, Hudson BG.** 1985. Properties of the globular domain of type IV collagen and its relationship to the Goodpasture antigen. *J Biol Chem* **260:**3739–3747. PubMed
27. **Wieslander J, Langeveld J, Butkowski R, Jodlowski M, Noelken M, Hudson BG.** 1985. Physical and immunochemical studies of the globular domain of type IV collagen. Cryptic properties of the Goodpasture antigen. *J Biol Chem* **260:**8564–8570. PubMed
28. **Yaar M, Foidart JM, Brown KS, Rennard SI, Martin GR, Liotta L.** 1982. The Goodpasture-like syndrome in mice induced by intravenous injections of anti-type IV collagen and anti-laminin antibody. *Am J Pathol* **107:**79–91. PubMed
29. **Neilson EG, Kalluri R, Sun MJ, Gunwar S, Danoff T, Mariyama M, Myers JC, Reeders ST, Hudson BG.** 1993. Specificity of Goodpasture autoantibodies for the recombinant noncollagenous domains of human type IV collagen. *J Biol Chem* **268:**8402–8405. PubMed
30. **Saus J, Wieslander J, Langeveld JP, Quinones S, Hudson BG.** 1988. Identification of the Goodpasture antigen as the alpha 3(IV) chain of collagen IV. *J Biol Chem* **263:**13374–13380. PubMed
31. **Turner N, Mason PJ, Brown R, Fox M, Povey S, Rees A, Pusey CD.** 1992. Molecular cloning of the human Goodpasture antigen demonstrates it to be the alpha 3 chain of type IV collagen. *J Clin Investig* **89:**592–601. PubMed
32. **Gunwar S, Bejarano PA, Kalluri R, Langeveld JP, Wisdom BJ Jr, Noelken ME, Hudson BG.** 1991. Alveolar basement membrane: molecular properties of the noncollagenous domain (hexamer) of collagen IV and its reactivity with Goodpasture autoantibodies. *Am J Respir Cell Mol Biol* **5:**107–112. PubMed
33. **Yoshioka K, Iseki T, Okada M, Morimoto Y, Eryu N, Maki S.** 1988. Identification of Goodpasture antigens in human alveolar basement membrane. *Clin Exp Immunol* **74:**419–424. PubMed
34. **Chen L, Hellmark T, Wieslander J, Bolton WK.** 2003. Immunodominant epitopes of alpha3(IV)NC1 induce autoimmune glomerulonephritis in rats. *Kidney Int* **64:**2108–2120. PubMed
35. **Kalluri R, Wilson CB, Weber M, Gunwar S, Chonko AM, Neilson EG, Hudson BG.** 1995. Identification of the alpha 3 chain of type IV collagen as the common autoantigen in antibasement membrane disease and Goodpasture syndrome. *J Am Soc Nephrol* **6:**1178–1185. PubMed
36. **Yang R, Hellmark T, Zhao J, Cui Z, Segelmark M, Zhao MH, Wang HY.** 2007. Antigen and epitope specificity of anti-glomerular basement membrane antibodies in patients with Goodpasture disease with or without anti-neutrophil cytoplasmic antibodies. *J Am Soc Nephrol* **18:**1338–1343. PubMed
37. **Yang R, Hellmark T, Zhao J, Cui Z, Segelmark M, Zhao MH, Wang HY.** 2009. Levels of epitope-specific autoantibodies correlate with renal damage in anti-GBM disease. *Nephrol Dial Transplant* **24:**1838–1844. PubMed
38. **Zhao J, Cui Z, Yang R, Jia XY, Zhang Y, Zhao MH.** 2009. Anti-glomerular basement membrane autoantibodies against different target antigens are associated with disease severity. *Kidney Int* **76:**1108–1115. PubMed
39. **Persson U, Hertz JM, Carlsson M, Hellmark T, Juncker I, Wieslander J, Segelmark M.** 2004. Patients with Goodpasture's disease have two normal COL4A3 alleles encoding the NC1 domain of the type IV collagen alpha 3 chain. *Nephrol Dial Transplant* **19:**2030–2035. PubMed
40. **Pedchenko V, Bondar O, Fogo AB, Vanacore R, Voziyan P, Kitching AR, Wieslander J, Kashtan C, Borza DB, Neilson EG, Wilson CB, Hudson BG.** 2010. Molecular architecture of the Goodpasture autoantigen in anti-GBM nephritis. *N Engl J Med* **363:**343–354. PubMed
41. **Rees AJ, Peters DK, Amos N, Welsh KI, Batchelor JR.** 1984. The influence of HLA-linked genes on the severity of anti-GBM antibody-mediated nephritis. *Kidney Int* **26:**445–450. PubMed
42. **Rees AJ, Peters DK, Compston DA, Batchelor JR.** 1978. Strong association between HLA-DRW2 and antibody-mediated Goodpasture's syndrome. *Lancet* **i:**966–968. PubMed
43. **Perl SI, Pussell BA, Charlesworth JA, Macdonald GJ, Wolnizer M.** 1981. Goodpasture's (anti-GBM) disease and HLA-DRw2. *N Engl J Med* **305:**463–464. PubMed
44. **Kalluri R, Danoff TM, Okada H, Neilson EG.** 1997. Susceptibility to anti-glomerular basement membrane disease and Goodpasture syndrome is linked to MHC class II genes and the emergence of T cell-mediated immunity in mice. *J Clin Investig* **100:**2263–2275. PubMed
45. **Hopfer H, Maron R, Butzmann U, Helmchen U, Weiner HL, Kalluri R.** 2003. The importance of cell-mediated immunity in the course and severity of autoimmune anti-glomerular basement membrane disease in mice. *FASEB J* **17:**860–868. PubMed
46. **Zhang Y, Su SC, Hecox DB, Brady GF, Mackin KM, Clark AG, Foster MH.** 2008. Central tolerance regulates B cells reactive with Goodpasture antigen alpha3(IV)NC1 collagen. *J Immunol* **181:**6092–6100. PubMed
47. **Calderon EJ, Wichmann I, Varela JM, Respaldiza N, Regordan C, Fernandez-Alonso J, Medrano FJ, Cano S, Cuello JA, Nuñez-Roldan A.** 1997. Presence of glomerular basement membrane (GBM) antibodies in HIV-patients with Pneumocystis carinii pneumonia. *Clin Exp Immunol* **107:**448–450. PubMed
48. **Szczech LA, Anderson A, Ramers C, Engeman J, Ellis M, Butterly D, Howell DN.** 2006. The uncertain significance of anti-glomerular basement membrane antibody among HIV-infected persons with kidney disease. *Am J Kidney Dis* **48:**e55–e59. PubMed
49. **Cui Z, Wang HY, Zhao MH.** 2006. Natural autoantibodies against glomerular basement membrane exist in normal human sera. *Kidney Int* **69:**894–899. PubMed
50. **Arends J, Wu J, Borillo J, Troung L, Zhou C, Vigneswaran N, Lou YH.** 2006. T cell epitope mimicry in antiglomerular basement membrane disease. *J Immunol* **176:**1252–1258. PubMed
51. **Mesnard L, Keller AC, Michel ML, Vandermeersch S, Rafat C, Letavernier E, Tillet Y, Rondeau E, Leite-de-Moraes MC.** 2009. Invariant natural killer T cells and TGF-beta attenuate anti-GBM glomerulonephritis. *J Am Soc Nephrol* **20:**1282–1292. PubMed

52. **Liu K, Li QZ, Delgado-Vega AM, Abelson AK, Sánchez E, Kelly JA, Li L, Liu Y, Zhou J, Yan M, Ye Q, Liu S, Xie C, Zhou XJ, Chung SA, Pons-Estel B, Witte T, de Ramón E, Bae SC, Barizzone N, Sebastiani GD, Merrill JT, Gregersen PK, Gilkeson GG, Kimberly RP, Vyse TJ, Kim I, D'Alfonso S, Martin J, Harley JB, Criswell LA, Wakeland EK, Alarcón-Riquelme ME, Mohan C, Profile Study Group, Italian Collaborative Group, German Collaborative Group, Spanish Collaborative Group, Argentinian Collaborative Group, SLEGEN Consortium.** 2009. Kallikrein genes are associated with lupus and glomerular basement membrane-specific antibody-induced nephritis in mice and humans. *J Clin Investig* **119:**911–923. PubMed
53. **Kalluri R, Sun MJ, Hudson BG, Neilson EG.** 1996. The Goodpasture autoantigen. Structural delineation of two immunologically privileged epitopes on alpha3(IV) chain of type IV collagen. *J Biol Chem* **271:**9062–9068. PubMed
54. **Queluz TT, Andres G.** 1990. Pathogenesis of an experimental model of Goodpasture's haemorrhagic pneumonitis. *Nephrol Dial Transplant* **5**(Suppl 1)**:**3–5. PubMed
55. **Bombassei GJ, Kaplan AA.** 1992. The association between hydrocarbon exposure and anti-glomerular basement membrane antibody-mediated disease (Goodpasture's syndrome). *Am J Ind Med* **21:**141–153. PubMed
56. **García-Rostan y Pérez GM, García Bragado F, Puras Gil AM.** 1997. Pulmonary hemorrhage and antiglomerular basement membrane antibody-mediated glomerulonephritis after exposure to smoked cocaine (crack): a case report and review of the literature. *Pathol Int* **47:**692–697. PubMed
57. **Yamamoto T, Wilson CB.** 1987. Binding of anti-basement membrane antibody to alveolar basement membrane after intratracheal gasoline instillation in rabbits. *Am J Pathol* **126:**497–505. PubMed
58. **Bernis P, Hamels J, Quoidbach A, Mahieu P, Bouvy P.** 1985. Remission of Goodpasture's syndrome after withdrawal of an unusual toxic. *Clin Nephrol* **23:**312–317. PubMed
59. **Beirne GJ, Brennan JT.** 1972. Glomerulonephritis associated with hydrocarbon solvents: mediated by antiglomerular basement membrane antibody. *Arch Environ Health* **25:**365–369. PubMed
60. **Beirne GJ, Octaviano GN, Kopp WL, Burns RO.** 1968. Immunohistology of the lung in Goodpasture's syndrome. *Ann Intern Med* **69:**1207–1212. PubMed
61. **Jones JG, Minty BD, Lawler P, Hulands G, Crawley JC, Veall N.** 1980. Increased alveolar epithelial permeability in cigarette smokers. *Lancet* **i:**66–68. PubMed
62. **Keogh AM, Ibels LS, Allen DH, Isbister JP, Kennedy MC.** 1984. Exacerbation of Goodpasture's syndrome after inadvertent exposure to hydrocarbon fumes. *Br Med J (Clin Res Ed)* **288:**188. PubMed
63. **Clyne S, Frederick C, Arndt F, Lewis J, Fogo AB.** 2009. Concurrent and discrete clinicopathological presentations of Wegener granulomatosis and anti-glomerular basement membrane disease. *Am J Kidney Dis* **54:**1116–1120. PubMed
64. **Lindic J, Vizjak A, Ferluga D, Kovac D, Ales A, Kveder R, Ponikvar R, Bren A.** 2009. Clinical outcome of patients with coexistent antineutrophil cytoplasmic antibodies and antibodies against glomerular basement membrane. *Ther Apher Dial* **13:**278–281. PubMed
65. **Denton M, Magee C, Niles J.** 2002. Rapidly progressive glomerulonephritis. *Ann Intern Med* **137:**W1. PubMed
66. **Arimura Y, Minoshima S, Kamiya Y, Nakabayashi K, Kitamoto K, Nagasawa T.** 1992. A case of Goodpasture's syndrome associated with anti-myeloperoxidase antibodies. *Intern Med* **31:**239–243. PubMed
67. **Hellmark T, Niles JL, Collins AB, McCluskey RT, Brunmark C.** 1997. Comparison of anti-GBM antibodies in sera with or without ANCA. *J Am Soc Nephrol* **8:**376–385. PubMed
68. **Jaskowski TD, Martins TB, Litwin CM, Hill HR.** 2002. Comparison of four enzyme immunoassays for the detection of immunoglobulin G antibody against glomerular basement membrane. *J Clin Lab Anal* **16:**143–145. PubMed
69. **Beck LH Jr, Bonegio RG, Lambeau G, Beck DM, Powell DW, Cummins TD, Klein JB, Salant DJ.** 2009. M-type phospholipase A2 receptor as target antigen in idiopathic membranous nephropathy. *N Engl J Med* **361:**11–21. PubMed

Infectious Diseases Caused by Bacteria, Mycoplasmas, Chlamydiae, and Rickettsiae

section H

VOLUME EDITOR: JOHN L. SCHMITZ
SECTION EDITOR: CHRISTINE LITWIN

Introduction

CHRISTINE M. LITWIN

43

This section contains chapters describing methods for the immunologic diagnosis of acute, chronic, or latent infections and nonsuppurative sequelae caused by bacteria, rickettsiae, mycoplasmas, bartonellae, and borreliae. The majority of the methods described in these chapters measure antibodies. In situations where it is difficult to culture the infectious agent, antibody detection is one of the only effective ways to identify the infecting organism. The described methods cover a wide range of antibody assays, including hemagglutination, indirect fluorescence, complement fixation, and enzyme-linked immunosorbent assays.

The newer cellular immune response assays for *Mycobacterium tuberculosis* (e.g., skin testing and gamma interferon release assays) are described. These assays are used for the detection of latent disease, as opposed to the case for assays for other organisms, in which antibody serology is used for the assessment of active or recent infection.

Also described in this section are antigen detection assays which use organism-specific polyclonal or monoclonal antibodies as capture and/or indicator reagents. Such assays include assays of urinary lipoarabinomannan for the detection of active tuberculosis and assays of *Helicobacter pylori* antigens in stool.

Molecular methods for diagnosing infectious diseases are presented in chapters where appropriate, since these methods are often performed in combination with serologic testing in clinical immunology laboratories.

Notable changes to section H from the previous edition of this *Manual* include moving the assessment of vaccine efficacy to the more relevant section E, which addresses functional cellular assays. Syphilis serology is now covered in a separate chapter from that for Lyme disease, borrelliosis, and leptospirosis. In addition, a new chapter has been added which addresses tests for diagnosing infections with *Francisella tularensis*, *Brucella* species, and *Bartonella* species.

doi:10.1128/9781555818722.ch43

Diagnostic Methods for Group A Streptococcal Infections

CHRISTINE M. LITWIN, SHELDON E. LITWIN, AND HARRY R. HILL

44

Group A streptococcus, also known as *Streptococcus pyogenes*, is an important bacterial pathogen that is the most frequent bacterial cause of acute pharyngitis. It also causes a multitude of other cutaneous and systemic infections, including impetigo, scarlet fever, necrotizing fasciitis, and streptococcal toxic shock syndrome. The pathogen has a unique tendency to initiate autoimmunity after acute infection, resulting in the nonsuppurative sequelae acute rheumatic fever (ARF) and poststreptococcal acute glomerulonephritis (AGN). The heart disease resulting from ARF has been responsible for substantial morbidity and mortality in all parts of the world.

Group A streptococci are Gram-positive, nonmotile, non-spore-forming, catalase-negative, and facultatively anaerobic bacteria belonging to the genus *Streptococcus*. The initial classification of streptococci dates back to 1903, from the description by Schötmuller of the blood agar method of differentiating hemolytic from nonhemolytic streptococci. Further classification by patterns of hemolysis was made in 1919 by Brown, who introduced the terms alpha, beta, and gamma hemolysis. In 1933, the beta-hemolytic streptococci were classified by Lancefield into distinct serogroups (20 in all; groups A to H and K to V) based on immunologic and biochemical characteristics (1). Most strains found to be pathogenic to humans were found to belong to serogroup A (*S. pyogenes*). Lancefield further established the important role of the M protein of streptococcus as a virulence factor. The ability to differentiate serotypes of the M protein of group A streptococcus (and later *emm* types) has allowed epidemiologic associations of ARF and AGN with certain M serotypes. Over 100 different M proteins have been identified in the group A streptococci, but there are specific M types that are identified most often with ARF, pharyngitis-associated AGN, and pyoderma-associated AGN in the United States (Table 1).

Sizeable epidemics of scarlet fever have been reported since the 12th and 13th centuries, in association with consumption of nonpasteurized milk, in surgery wards, obstetric wards, schools, and day care centers, and among families. Transmission of group A streptococci is usually by the oral route, from aerosolized droplets or from ingestion of contaminated milk or other foods. The incidences of group A streptococcus infections, ARF, and rheumatic heart disease decreased over the course of the 20th century in many parts of the world. The decline in infection rate was particularly steep during the 1960s and 1970s. One notable outbreak, however, occurred in 1968, when a sudden and abrupt epidemic of group A streptococcal pharyngitis developed in over 1,000 cadets at the U.S. Air Force Academy in Colorado during a 7-day period. An epidemiologic investigation implicated hard-boiled eggs in tuna salad as the source of the outbreak (2). Careful observation and follow-up of the cadets did not identify any nonsuppurative sequelae.

A resurgence of ARF occurred in the United States in the mid-1980s, in multiple regions. In early 1985, an epidemic of ARF occurred in Salt Lake City, UT, and the surrounding intermountain area (3, 4). During the years 1985 through 1992, patients who sought medical treatment for ARF at Primary Children's Medical Center in Salt Lake City, UT, came predominantly from middle class families (84%), with carditis as the major manifestation (68%) (5). The resurgence continued, and by 2000, more than 500 cases had been diagnosed. The striking and sudden reappearance of ARF in Salt Lake City was likely due to the rheumatogenicity of the prevalent group A streptococci in the area at that time. A study of the isolates from these patients demonstrated that specific strains of a mucoid group A streptococcus, primarily M protein type 18, were associated with the two periods with the highest incidences of rheumatic fever in Salt Lake City, i.e., 1985–1986 and 12 years later, 1997–1998. During these outbreaks, there was a statistically significant association between the percentage of mucoid strains and the number of cases of ARF (6–8). At around the same time, small clusters of epidemics, ranging from 15 to 40 cases each, were also reported in Kansas City, MO, Dallas, TX, Columbus and Akron, OH, Nashville and Memphis, TN, Morgantown and Charleston, WV, Pittsburgh, PA, and New York City, NY (9). And for the first time since the 1960s, outbreaks were again occurring in navy and army training camps (10). This unexplained resurgence ultimately resulted in a heightened public health concern for the accurate diagnosis of group A streptococcal infections, thus allowing prevention of ARF and, ultimately, rheumatic heart disease.

ARF is a delayed, nonsuppurative sequela of a group A streptococcal upper respiratory infection, usually pharyngitis. ARF occurs in 0.1 to 2.5% of individuals after untreated group A pharyngitis. Table 2 describes the acute manifestations of acute group A streptococcal infection versus ARF. ARF is an inflammatory disease with lesions primarily

doi:10.1128/9781555818722.ch44

TABLE 1 M serotypes associated with nonsuppurative sequelae[a]

ARF	M serotype	
	Pharyngitis-associated AGN	Pyoderma-associated AGN
1	1	2
3	4	49
5	12	55
6	25	57
14	49[b]	59
18	55[b]	60
19		61
24		

[a]ARF, acute rheumatic fever; AGN, acute glomerulonephritis.
[b]M types 49 and 55 have occasionally caused pharyngitis-associated AGN.

involving the joints, heart, central nervous system, and subcutaneous tissues. The classic form of ARF is acute, febrile, and predominantly self-limited. Studies of ARF have shown that the disease occurs only after an immunologically significant streptococcal infection, with elevated serum levels of antistreptococcal antibodies almost always documenting a recent streptococcal infection (11, 12). An unexplained but intriguing aspect of ARF is that cutaneous infections do not initiate ARF but, rather, poststreptococcal AGN. ARF may require the lymphoid tissue of the pharyngeal site for initiation of the disease, or the pyoderma strains that cause AGN may not be rheumatogenic.

The signs and symptoms of ARF can occur singly or with multiple symptoms. The most important signs and symptoms are termed the major manifestations and include carditis, polyarthritis, chorea, subcutaneous nodules, and erythema marginatum. Additional findings that are often present in ARF but are nonspecific are called the minor manifestations, and these include fever, arthralgia, heart block, and elevated levels of acute-phase reactants in the blood.

The latent period between pharyngitis and the onset of ARF is 19 days, on average. Arthritis is usually the first manifestation, although this may be preceded by abdominal pain (13). Overall, the arthritis occurs in about 75% of initial attacks with ARF. Carditis, if it appears, also does so early in the course of disease, approximately 20 days after the pharyngitis, with a frequency of about 50% of ARF patients (14). Carditis is the one manifestation of ARF that can cause long-term residual morbidity or mortality. Chorea occurs in 15% of cases, and subcutaneous nodules and erythema marginatum occur in fewer than 10% of cases (15).

Poststreptococcal AGN is a delayed nonsuppurative sequela of either pharyngeal or cutaneous infection with certain nephritogenic group A streptococcal strains. It is characterized by diffuse proliferative glomerular lesions and by clinical manifestations of renal disease, such as edema, hypertension, hematuria, and proteinuria (16). Patients may also complain of lethargy, weakness, anorexia, headache, and dull back pain. Fever is not a usual feature. About 5 to 10% of patients develop severe hypertension complicated by encephalopathy, ranging from headache and vomiting to confusion and convulsions. Conversely, many cases of AGN can be quite mild.

The long-term sequela of ARF is rheumatic heart disease. The prognosis of ARF is usually related to the severity of cardiac involvement during the acute phase of the disease. In a large comprehensive study performed in the United Kingdom and the United States, only 6% of patients with no carditis or with questionable carditis were found to have heart murmurs 10 years later. Heart disease was present at the 10-year follow-up in 30% of patients initially found to have only apical systolic murmurs, 40% of those with basal diastolic murmurs, and 68% of those who initially suffered from congestive heart failure and/or pericarditis (17). While ARF is usually associated with mitral valve regurgitation, recurrent bouts of ARF with carditis are the main cause of later development of mitral valve stenosis.

Laboratory findings of poststreptococcal AGN include an elevated erythrocyte sedimentation rate, mild normocytic normochromic anemia, slight hypoproteinemia, and elevations of the BUN and serum creatinine concentrations. Hypercholesterolemia and hyperlipemia may also be present. Total hemolytic complement and C3 complement levels are reduced in a majority of patients. As discussed later, anti-streptolysin O (ASO) responses are weak in pyoderma-associated (cutaneous infection) AGN, and it is frequently necessary to perform an anti-DNase B measurement to provide evidence of poststreptococcal sequelae.

This chapter focuses primarily on different laboratory methods for diagnosing acute group A infections and the nonsuppurative sequelae ARF and AGN. The different laboratory methods discussed include the "gold standard" (culture and identification), rapid antigen detection, molecular detection, and serological tests to measure the human response to group A streptococcal antigens for the diagnosis of nonsuppurative sequelae.

CULTURE AND IDENTIFICATION

Detailed throat culture procedures have been published by the American Heart Association (18). Culture of the throat or wound remains the gold standard for establishing

TABLE 2 Clinical manifestations of group A streptococcal infection and ARF

Acute group A streptococcal infection	ARF[a]	
	Major	Minor
Beefy, swollen, red uvula	Carditis	Arthralgias and fever
Fever	Polyarthritis	Elevated acute-phase reactants (erythrocyte sedimentation rate or C-reactive protein)
Headache	Chorea	Prolonged PR interval
Nausea, vomiting, and abdominal pain	Erythema marginatum	
Pain with swallowing	Subcutaneous nodules	

[a]Two major manifestations or one major and two minor manifestations must be present for diagnosis.

the presence of group A streptococci. Sheep blood agar is preferred because unambiguous patterns of hemolysis are observed with this medium. Group A colonies grown in 5% sheep blood agar at 35°C to 37°C overnight are typically surrounded by a clear zone of hemolysis (beta-hemolytic). Plates that are initially negative should be kept and reexamined after another 24 h. There have been some discussions in the literature with regard to variations of this culture procedure. Some publications suggest that the addition of trimethoprim-sulfamethoxazole to the blood agar helps to suppress the competing normal pharyngeal biota. There has also been debate over the optimal atmosphere for incubation—aerobic, aerobic in the presence of 5 to 10% CO_2, or anaerobic. A presumptive identification can be made by demonstrating a zone of growth inhibition around bacitracin disks (0.04 IU) placed on the surface of the blood agar. Serologic grouping and identification may be performed using commercially available kits.

Definitive identification is made by cell wall carbohydrate grouping. This involves extraction of the carbohydrate by use of hydrochloric acid or formamide followed by incubating the streptococcal antigen with group-specific antisera. Rapid grouping methods that involve latex agglutination (LA) (Streptex; Wellcome Diagnostics) have generally replaced traditional grouping techniques in the modern laboratory. Because no group A streptococci resistant to penicillin or cephalosporin have yet to be detected, antibiotic testing for resistance to these drugs is unnecessary. The same holds true for macrolides in the United States.

M Protein Serotyping

The classification of group A streptococcal strains by M protein serotyping is used primarily for epidemiological studies, basic laboratory research, and, potentially, vaccine development. The identification of M types is performed using type-specific antisera. Over 80 different M types of strains have been characterized using this method. The M protein antigen is extracted from streptococci by using a hot hydrochloric acid method and then incubated with type-specific antisera (19). M type identification uses a precipitation reaction between the M protein and the corresponding type-specific antiserum.

A protein antigen very closely associated with the M protein molecule of group A streptococci is the serum opacity factor. Streptococcal serum opacity factor is a type-specific strain marker produced by certain serotypes of group A streptococci. In 1946, Lancefield described the serologic classification of group A streptococci based on their surface T antigens. Four of the 20 T antigens have been revealed to be pili. Both T-antigen serotyping and opacity factor type determination are alternative methods that can be used to characterize group A streptococcal strains (20).

Molecular Approaches to Characterization of Group A Streptococci

emm Typing

Prior to molecular approaches to strain typing, many group A streptococcal strains were nontypeable because of a lack of expression of the M protein or a lack of reactivity with the antisera or, most often, because they expressed previously unidentified M proteins. The introduction of *emm* gene sequence typing permitted M type determination of nearly all strains of group A streptococci by any laboratory with DNA sequencing capability. The molecular technique of *emm* typing consists of sequencing the 5′ end of the group A streptococcal *emm* gene (which encodes the M protein) by rapid PCR analyses using nucleotide primer pairs. The molecular procedure is detailed at the CDC website (http://www.cdc.gov/streplab/protocol-emm-type.html). In large-scale epidemiologic investigations of group A streptococcus isolates, restriction digests of *emm* amplicons can be electrophoresed and the resulting restriction patterns compared. Strains with common patterns can be grouped and sequencing performed on representatives from the group. There are now 124 recognized M genotypes based on this technique (21).

PFGE

Pulsed-field gel electrophoresis (PFGE) has been employed widely for epidemiologic typing of many species of bacteria. When PFGE is used for group A streptococcal epidemiological studies, the DNA is typically treated with the restriction enzyme SmaI. The DNA fragments are then separated by pulsed electrical fields on agarose gels to obtain restriction enzyme patterns. The restriction patterns of the different isolates are compared to identify relatedness or clonality. PFGE typing of group A streptococcus, however, does not have a standardized nomenclature (22).

RAPID STREPTOCOCCAL ANTIGEN AND MOLECULAR DETECTION TESTS

One of the major disadvantages of throat culture is the delay in obtaining a diagnostic result. To overcome this delay, commercial rapid antigen detection tests (RADTs) were developed in the 1980s for the immediate identification of group A streptococcus from the throat. These RADTs allow for expedited diagnosis and management shortly after seeing patients in the clinic or emergency department. The tests involve an acid extraction step to solubilize the cell wall carbohydrate, followed by an antigen-antibody immunologic reaction. The early RADTs used the principle of LA, which is a relatively insensitive technique with unclear endpoints. Newer tests based on enzyme immunoassay have increased the sensitivity and have much more clearly defined endpoints. Some tests, such as the QuickVue In-Line Strep A test (Quidel, San Diego, CA), have been given a Clinical Laboratory Improvement Amendments (CLIA)-waived status. An alternative antigen detection technique that has been developed is optical immunoassay, which has been reported to be as sensitive as culture. The overall sensitivity and specificity of the newer optical immunoassay methods are 84% and 93%, respectively (23).

Molecular RADTs

The most recent advances in antigen detection use molecular biologic techniques. One commercial method uses a nucleic acid hybridization test based on a chemiluminescent single-stranded DNA probe that detects specific rRNA sequences unique to group A streptococci (Group A Streptococcus Direct test; Gen-Probe, Inc., San Diego, CA). A study comparing the DNA test with conventional culture showed sensitivity and specificity values of 86 and 95%, respectively (24). Another available method is a test that combines rapid PCR and real-time detection of amplified DNA (LightCycler Strep-A assay; Roche Applied Science, Indianapolis, IN). Compared to routine culture, the LightCycler PCR showed 93 and 98% sensitivity and specificity, respectively (25). The recently FDA-approved *illumi*gene group A streptococcus DNA amplification assay (Meridian Bioscience Inc., Cincinnati, OH) uses loop-mediated isothermal amplification technology in a process by which designed primers allow specific isothermal amplification of DNA. A recent study applied this approach to test 796

deidentified remnant throat swabs, using a routine culture method as the gold standard. The loop-mediated isothermal amplification technology demonstrated sensitivity and specificity values of 100% (95% confidence interval, 95% to 100%) and 94.2% (95% confidence interval, 92% to 95%), respectively (26).

Recommendations on Use of RADTs from National Advisory Groups

A number of advisory groups have made recommendations regarding the use of RADTs for the diagnosis of group A pharyngitis. The Committee on Infectious Diseases of the American Academy of Pediatrics recommends that when a patient suspected of having group A streptococcus pharyngitis has a negative RADT, a culture should be performed to confirm the results of the RADT (27). A positive test, however, does not require confirmation with a culture because of the high specificity of the RADT. Rapid antigen detection tests using DNA probes or PCR may be more sensitive than the earlier RADTs, and some experts think that these newer tests may be sufficiently sensitive to be used without culture backup.

The Infectious Diseases Society of America also states that positive RADT results do not require culture confirmation (28). For children and adolescents, a negative result should be confirmed with a culture unless the physician has determined in his/her practice that the RADT performs comparably to culture. However, the Infectious Diseases Society of America suggests that because adults have a lower incidence of group A streptococcal pharyngitis than children and are at a low risk of acquiring ARF, negative RADT results do not need to be confirmed with cultures. Providers should keep in mind that the risk of streptococcal pharyngitis may be higher in certain adults, such as teachers, whose occupation brings them into close association with children, or parents of young school-aged children.

Pathogenesis of ARF and AGN

A number of theories have been proposed regarding the mechanism by which group A streptococcus induces rheumatic fever, including a serum sickness-like reaction caused by antigen-antibody complexes, toxic effects of streptococcal products, such as streptolysin O or S, and an autoimmune response induced by molecular mimicry (29). The most currently accepted theory on the pathogenesis of ARF is that of molecular mimicry, or the sharing of a number of epitopes between streptococcal bacterial antigens and the tissues of the human host. Much of the interest in this theory has been supported by the identification of antibodies in the sera of patients with ARF that react with the human heart. For example, epitopes of the M proteins have been found to share epitopes with articular cartilage, synovium, cardiac myosin, and sarcolemmal membrane proteins (12, 29). Cross-reactions have also been described between group A polysaccharide and a structural glycoprotein isolated from human heart valves (30). Children with Sydenham's chorea have been found to have circulating antibodies that react both with neurons of the caudate and subthalamic nuclei and with group A streptococcal cell membranes (31). In conclusion, there is much cumulative evidence that indicates that the production of streptococcal antibodies cross-reactive to various human tissues provides a plausible autoimmune explanation for many of the individual manifestations of ARF.

Antibody Responses to Group A Streptococcus

In response to infection with group A streptococci, the host mounts specific antibody responses to both extracellular and cellular antigenic components of the organism (Table 3). The extracellular antigens streptolysin O and DNase B are classified as nonspecific markers of group A infection yet are the most useful biomarkers used clinically for the diagnosis of a previous streptococcal infection. The cellular components of the streptococcus elicit antibody responses specific for streptococcus infections. In general, these types of antibodies are not used for clinical assessment of poststreptococcal sequelae but rather are used in clinical research related to acute rheumatic heart disease.

Figure 1 depicts the overall structure of the cell envelope of group A streptococci and the locations of the streptococcal components. The structure can be divided into four parts: the cell surface, capsule, cell wall, and cytoplasmic membrane. The cell surface of group A streptococcus contains the fimbrial portion of the M protein, lipoteichoic acids, and fibronectin-binding proteins. The capsule is largely composed of hyaluronic acid and is similar in structure to human connective tissue. The cell wall contains the group A carbohydrate as well as peptidoglycan. The cytoplasmic membrane is composed of highly complex lipoproteins and contains antigens similar in structure to human cardiac, skeletal, and smooth muscle, heart valve fibroblasts, and neuronal tissues (12).

TABLE 3 Host immune response to group A streptococcal infection

Streptococcal serological test	Antigen
Test for extracellular streptococcal antigen response	
Tests for nonspecific immunogenic antigens (extracellular antigens)	
Anti-streptolysin O (ASO)	Streptolysin O
Anti-DNase B	DNase B
Anti-streptokinase[a]	Streptokinase
Anti-streptococcal hyaluronidase[a]	Hyaluronidase
Anti-NADase[a]	NADase
Tests for specific immunogenic antigens (cellular components)	
Anti-streptococcal C5a peptidase[a] (anti-SCPA)	Streptococcal C5a peptidase (group A)
M protein antibody[a]	Type-specific M protein
Anti-A-carbohydrate[a]	Group A carbohydrate

[a]Not commercially available but used in research laboratories.

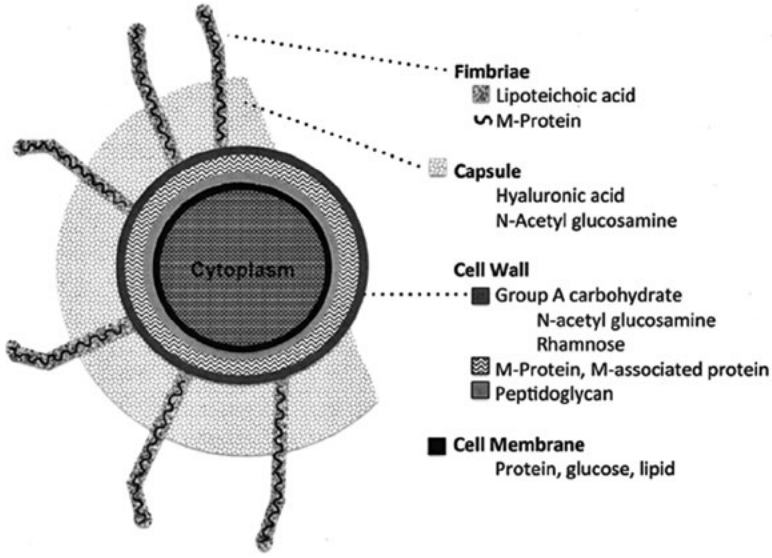

FIGURE 1 Schematic diagram of cellular and extracellular antigens of group A streptococci.

DETECTION OF ANTIBODIES TO EXTRACELLULAR ANTIGENS

Streptozyme Screening Test

The Streptozyme test (Wampole Laboratories, Cranbury, NJ) is a screening test for the detection of antibodies to several of the extracellular antigens, including NADase, DNase, hyaluronidase, streptokinase, and streptolysin. The test is rapid and simple to perform but is much less reliable than the ASO and anti-DNase B tests, which are the preferred tests. Sheep red blood cells are coated with the antigens. The reagent is mixed with a 1:100 dilution of patient serum. The methodology is hemagglutination, with agglutination of the red blood cells representing a positive result. Positive samples are titrated to the endpoint. Values of [mt]100 streptozyme units are considered positive.

Golubjatnikov et al. found both false-positive and false-negative results when the Streptozyme test was compared to the ASO and anti-DNase B assays. The Streptozyme test fails to detect up to 25% of elevated anti-DNase B titers (32). Therefore, if the test is to be used at all, it should be used in conjunction with the ASO and anti-DNase B tests when the sequelae of group A streptococcal infection are suspected.

ASO Test

Group A streptococcus produces two extracellular hemolysins: streptolysin S and streptolysin O. Only streptolysin O is antigenic and induces naturally occurring antibodies. It is a member of a family of pore-forming cytolysins that hemolyze erythrocytes and lyse polymorphonuclear leukocytes. The antibody against streptolysin O, ASO, has been well characterized. Identification of ASO is one of the main tests in use for the serodiagnosis of a previous streptococcal infection. The ASO antibody is thought to be composed of IgG, IgA, and IgM isotypes (33). Usually ASO is measured concurrently with anti-DNase B.

The ASO test provides serological evidence of preceding group A streptococcal infections and is used primarily for patients suspected of having rheumatic fever or AGN. Finding ASO antibodies following skin infections is uncommon. Therefore, anti-DNase B antibodies should also be measured to support the diagnosis in these cases. ASO titers are not used for the diagnosis of acute group A streptococcal infections. Culture or rapid antigen detection is a more appropriate test in these circumstances.

More than 80% of patients with ARF following streptococcus pharyngitis will develop a positive ASO titer of [mt]200 Todd units/ml if the serum sample is obtained within 2 months of onset. The antibody response rises 7 to 10 days after infection and reaches a peak about 3 to 6 weeks later. Antibody levels decline after about 6 to 8 weeks in uncomplicated cases, but they can remain elevated for indefinite periods in some individuals. The ASO antibody, however, has not been shown to have a protective role against repeat infections. Antibiotic therapy may decrease the antibody response.

A few limitations of the ASO test should be mentioned. About 20% of infected individuals do not respond to infection by having elevated ASO titers (34). A negative ASO titer should prompt testing for other antibodies, such as anti-DNase B (detectable for 6 to 9 months following infection), if such tests were not already ordered in tandem. False-positive ASO titers can be due to increased levels of serum beta-lipoprotein produced in liver disease and by "contamination" of serum by *Bacillus cereus* and *Pseudomonas* species. Group C and G streptococcal infections may result in elevated ASO titers, since these groups also produce streptolysin O. False-negative results or low titers may occur if the serum sample has undergone multiple freeze-thaw cycles.

The classic method of measurement of ASO is based on neutralization of the hemolytic activity of streptolysin O by ASO antibodies. The classic protocol is detailed in the 7th edition of this *Manual* (35) and is summarized here. Dilutions of serum from the patient are added to streptolysin O reagent. After a brief incubation at room temperature, a 5% red blood cell suspension is added. If the patient serum contains ASO antibodies and neutralizes the streptolysin O reagent, there will be no hemolysis. If there is hemolysis, no ASO antibodies are present. The reciprocal of the highest dilution of serum without hemolysis is expressed as Todd

units or international units (depending on whether the streptolysin reagent used is the Todd standard or the World Health Organization international standard, respectively).

LA is a much simpler procedure that has also been used for the measurement of ASO antibodies and requires no special equipment or expertise. With LA, latex particles coated with streptolysin O can react with ASO antibodies in the serum. Agglutination occurs when the level of antibody in serum is higher than 200 IU/ml. Compared to the standard neutralization test, the LA procedure shows a sensitivity of 91% and a specificity of 86% (36).

Nephelometry has replaced the classic hemolytic method for streptococcal antibody determination in most clinical and reference laboratories. Nephelometry has been shown to be more sensitive than the standard hemolytic inhibition assay, is simpler to perform on automated nephelometric instruments, and can detect antibody within the range of 25 to 28,800 IU/ml (37). The sensitivities and specificities of single antibody titers with standard ASO and anti-DNase B methods range from 70.5 to 72.7% and 86.4 to 93.2%, respectively (38). A study of 114 patients with or without evidence of streptococcal infection was performed using the Beckman Coulter IMMAGE rate nephelometry system. This analysis showed an increased sensitivity (88%) and a decreased specificity (68%) (39). Combining the nephelometric ASO assay with the anti-DNase B assay increased the sensitivity of diagnosis to 96%, with a specificity of 63%.

The nephelometric ASO test measures the rate of increase in light scattered from particles suspended in solution as a result of complexes formed during an antigen-antibody reaction of ASO in the serum sample with particle-bound streptolysin O (antigen) provided as the reagent. Following calibration, the signal is converted to international units by the analyzer (37). Results are reported in ASO international units (per milliliter). Each laboratory establishes its own reference levels based on the patient population. In general, for babies and children aged 0 to 1 year, the normal reference range is <200 IU/ml; for children of 2 to 12 years, the range is <240 IU/ml; and for patients aged 13 years and older, the range is <330 IU/ml (40). Measurements of acute- and convalescent-phase sera taken 2 weeks apart are recommended to detect a significant rise in antibody titer.

Nephelometric Method

Specimens

Serum samples are recommended. Plasma samples can be used.

Equipment

Nephelometer

Centrifuge capable of 90,000 × *g*

Reagents

Standard kit components: ASO cartridge containing ASO antigen (purified recombinant protein attached to polystyrene particles) and evaporation caps

Calibrators and at least two levels of control material

Wash solution, buffer, and diluent provided by the nephelometer manufacturer

Quality Control and Calibration

Perform calibration with calibrators provided by the nephelometer manufacturer. It is recommended that at least two levels of control material, normal and abnormal, be analyzed daily. Controls should also be run with each new calibration, with a new lot of reagent or buffer, and after maintenance. Calibrations are automatically checked by the nephelometer and will produce a calibration report. Using the reagents made specifically for the instrument, the instrument performs a single-point calibration.

Procedure

Most clinical instruments designed for nephelometric assays are highly automated. Series of sixfold dilutions of calibrator and test samples are performed automatically. Using a preprogrammed curve-fitting program, light-scattering signals are converted to concentrations. The instrument automatically checks for antigen excess and out-of-range specimens and gives instructions for dilutions and reassays.

Interpretation

Results of the ASO test are reported in international units per milliliter. The test is designed to detect concentrations of this analyte by using an initial 1:6 sample dilution. The initial analytical range is 25 to 800 IU/ml and can be extended to 25 to 28,800 IU/ml with dilution. The upper limit of normal is defined as the highest titer that is exceeded by only 20% of a population. Expected values are typically lower than 100 IU/ml. A twofold increase in the ASO value for serial analysis of samples obtained 1 to 2 weeks apart is supportive of a prior streptococcal infection. A single ASO analysis may not be meaningful due to the variability of ASO values within the healthy population.

Limitations

1. False-positive results may be associated with liver disease or bacterial contamination of specimens.
2. Streptococcal infections already treated with antibiotics may not produce increased values.
3. Abnormally high ASO results should not be used as a single diagnostic indicator but should be correlated with other clinical findings. Serial measurements at 1- to 2-week intervals are recommended.

Interferences

Quantitation of ASO in lipemic specimens may produce inaccurate results. Grossly lipemic specimens should be delipidated by ultracentrifugation prior to determination of ASO concentrations. Bilirubin (5 to 30 mg/dl), lipid (50 to 400 mg/dl), and hemoglobin (200 to 1,000 mg/dl) will not interfere with test results. Dust particles or other particulate matter in the reaction solution may result in extraneous light-scattering signals.

Anti-DNase B Test

DNase B is the most immunogenic of the four DNases (A, B, C, and D) produced by group A streptococci following infection (34). DNase B antibody concentrations usually begin to rise within 1 to 2 weeks of the initial pharyngitis or skin infection. DNase B antibodies usually peak 6 to 8 weeks after initial infection, in contrast to ASO, which tends to peak 3 to 6 weeks after initial infection. DNase B antibodies also remain in the serum longer (2 to 3 months) than ASO (6 to 8 weeks). Thus, the anti-DNase B test is a more reliable test for establishing a diagnosis for patients with suspected Sydenham's chorea, in whom symptoms may not be observed for several months.

DNase B is usually used along with the ASO titer to diagnose ARF or AGN following group A streptococcal infections. Unlike in the ASO test, infections of the skin will produce a strong response in the anti-DNase B test, and

this test is more reliable for providing evidence of a recent streptococcal infection in patients with sequelae following pyoderma (41). Anti-DNase B antibodies should also be measured in patients with suspected sequelae following pharyngeal infection when ASO titers are negative. Failure to demonstrate positive antistreptococcal antibody titers by using either the ASO or anti-DNase B test makes the diagnosis of ARF or AGN unlikely. The exception is in the case of a patient with isolated symptoms of chorea. In this particular circumstance, antibody titers may have decreased to the normal range because of the long latent period between the acute streptococcal infection and the onset of chorea. Also, if the diagnosis of carditis has been delayed significantly, antibody titers may have dropped into the normal reference range.

Similar to the classic ASO test, the classic methyl green anti-DNase B test is also a neutralization test. Antibodies in the patient's serum will neutralize the enzyme DNase B, preventing it from depolymerizing DNA. The classic protocol is detailed in the literature (42) and summarized briefly here. Dilutions of patient serum are incubated at 37°C with DNase B to allow the antibodies, if present, to neutralize the enzyme. The substrate is then added to each tube. After an overnight incubation at 37°C, the tubes are observed for color formation. Methyl green is green when complexed with DNA. When DNase B hydrolyzes DNA, the methyl green is unbound from the hydrolyzed DNA and becomes colorless. The reciprocal of the highest dilution of serum that shows definite inhibition of enzyme activity represents the antibody titer for that serum. The test should be performed on acute- and convalescent-phase sera, with a fourfold rise considered evidence of a recent group A streptococcal infection. Normal reference ranges for the classic methyl green dye test quoted in the literature are titers of <120 for preschoolers and <1,360 for older children.

As with ASO titers, nephelometry has largely replaced the classic methyl green dye anti-DNase B test in most clinical and reference laboratories. Nephelometry has been shown to be more sensitive than the reference test and is simpler to perform on automated nephelometric instruments (39). In the same study of patients described above, the Beckman Coulter IMMAGE system demonstrated 84% sensitivity for anti-DNase B. This improves upon the 70.5 to 72.7% sensitivity often seen with standard methods. The specificity of measuring anti-DNase B levels in that study was 49%. The low specificity was attributed to the small number of positively diagnosed cases in the study. Therefore, to increase the sensitivity and specificity, it is recommended that both ASO and DNase B antibodies be measured. An abnormally high anti-DNase B test result should not be used as a single diagnostic indicator. It is important to use serial analysis of samples taken 1 to 2 weeks apart to detect rising values in anti-DNase B levels as evidence of streptococcal disease.

The method for measuring anti-DNase B levels is the same as that described above for ASO, except that particle-bound DNase B is added to patient serum to form immune complexes. The rate of light scatter as the complexes are formed is extrapolated from values from the classic method and reported in units per milliliter. As for ASO titers measured by nephelometry, each laboratory establishes its own reference levels based on the patient population. In general, for babies and children aged 0 to 6 years, the normal reference range is <250 U/ml; for children aged 7 to 17 years, the range is <310 U/ml; and for adults 18 years and older, the range is <260 U/ml. The limitations and interferences are the same as those of the ASO nephelometric test.

RESEARCH USE ONLY TESTS

Anti-DNase B and ASO are the most useful biomarkers used clinically for the diagnosis of a previous streptococcal infection. Measurements of antibodies to other streptococcal cellular components are used for research purposes, or they were used in the past for the diagnosis of streptococcal disease and are now used only for research purposes. These antibody tests are summarized in Table 4 and are briefly discussed below.

Anti-Hyaluronidase Test

The pattern of human antibody responses to hyaluronidase is very similar to that for ASO. The number of patients who develop antibodies to the hyaluronidase following a group A streptococcal infection is somewhat smaller than the number of patients who develop ASO antibodies (34). Before the introduction of anti-DNase B testing, the anti-hyaluronidase test was the most widely used streptococcal antibody test other than the ASO test. However, because of difficulty in standardization, wide differences in titers reported between healthy and rheumatic fever patients, and a number of technical difficulties encountered with the test, the anti-hyaluronidase test is no longer commercially available and is now usually performed only in research laboratories (43).

TABLE 4 Research Use Only tests for detection of antibodies to extracellular antigens

Test	Overall characteristic
Anti-hyaluronidase test	Follows same pattern as that for ASO antibodies, but with a lower incidence
Anti-streptokinase test	Follows same pattern as that for ASO antibodies, but with a lower incidence
Anti-NADase test	Tends to produce higher titers following AGN initiated by pharyngitis and inconsistent titers for AGN initiated by pyoderma
Anti-SCPA test	Highly immunogenic in children after pharyngitis, antibody remains through adulthood
Anti-A-carbohydrate test	Higher antibody responses in patients with rheumatic carditis and rheumatic mitral valve disease
Anti-M-protein test	Antibodies take months to appear after acute streptococcal infection

Anti-Streptokinase Test

The rise in anti-streptokinase titer following a streptococcal infection follows the same general pattern as that for the ASO titer (34). Several studies indicate that the antibody response occurs less frequently, which may be explained by differences in production of streptokinase by different infecting strains. A quantitative method for assaying anti-streptokinase levels, involving a neutralization test, was developed by Kaplan in 1946. Because of the low reproducibility of the test and the relative infrequency of the antibody response in ARF patients, the test is available only in research laboratories.

Anti-NADase Test

NAD-hydrolyzing enzyme (NADase; previously known as DPNase) is an extracellular enzyme and toxin produced not only by group A hemolytic streptococci but also by group C and group G strains of streptococci. There is significant strain variation in regard to the production of NADase by group A streptococcus, with serotype M12 and other nephritogenic strains expressing more protein. The NADase enzyme of group A streptococcus elicits inconsistent antibody responses following AGN previously initiated by pyoderma, but it tends to produce high antibody titers following AGN initiated by pharyngitis (44). The NADase test is based on the ability of antibodies in the sera to neutralize the NADase enzyme. The test is now usually performed only in research laboratories.

DETECTION OF ANTIBODIES TO CELLULAR ANTIGENS

Anti-C5a Peptidase Antibodies (Anti-SCPA)

Streptococcal C5a peptidase (SCPA) is a highly specific surface endopeptidase that cleaves C5a. C5a is important for leukocyte activation and chemotaxis. Cleavage of C5a therefore inhibits chemotaxis of phagocytes, preventing clearance of the streptococci and allowing colonization, invasion, and infection. SCPA is highly immunogenic in children after recent pharyngitis. Shet et al. (45) examined acute- and convalescent-phase sera from 202 children with group A pharyngitis and found parallel anti-ASO and anti-DNase B antibody responses in both acute- and convalescent-phase samples. The antibodies in response to SCPA following infection remain through adulthood. O'Connor et al. (46) developed an enzyme-linked immunosorbent assay (ELISA) to detect human IgG and IgA antibodies against SCPA. The ELISA, however, is used only in research laboratories.

Anti-A-Carbohydrate Test

The group A carbohydrate is the basis for the Lancefield classification of the 20 serologic groups of streptococci. Although it is not a virulence factor, it does elicit antibodies after infection. Antibody levels usually peak 1 to 3 weeks after the initial pharyngitis and may remain for a prolonged period in patients with rheumatic heart disease. Todome et al. (47) developed an ELISA for anti-A-carbohydrate antibodies to study 45 patients with rheumatic fever and found significantly higher antibody responses in patients with rheumatic fever. Appleton et al. (48) similarly found an association between the persistence of group A carbohydrate antibodies and the presence of rheumatic carditis and rheumatic mitral valve disease. The anti-A-carbohydrate test is only available at a few research laboratories.

Anti-M-Protein Antibodies

The M proteins are the basis for the Lancefield classification of over 100 group A serotypes. M protein antibodies appear very slowly, over several months. Both IgA and IgG antibodies against M proteins are produced in response to infection. IgA M protein antibodies have been found to inhibit streptococcal adherence to pharyngeal cells. IgG M protein antibodies, in turn, prevent internalization of the streptococci into epithelial cells. These antibodies have opsonic properties and have been shown to protect against group A streptococcal infection (49). Tests to detect M protein antibodies are available only in research laboratories and are used mainly for vaccine research.

CONCLUSIONS

Group A streptococcus is an important bacterial pathogen that is the most frequent bacterial cause of acute pharyngitis. The organism has the ability to initiate autoimmunity after acute infection, resulting in the nonsuppurative sequelae ARF and AGN. Several diagnostic tests are available for the diagnosis of acute group A streptococcal infection. Although culture and identification remain the gold standard for diagnosing acute group A streptococcal infections, rapid antigen detection methods are now used in most clinical settings due to their efficiency, ease of use, and immediate results. Streptococcal culture is still recommended as a backup for negative rapid antigen test results for children. Streptococcal antibody tests (i.e., ASO and anti-DNase B tests) should not be used for the diagnosis of an acute group A streptococcal infection but rather to provide evidence of prior infection in the past 2 to 12 weeks. Newer molecular antigen detection methods may be sufficiently sensitive to not need a backup culture, especially for adults.

Both the ASO and anti-DNase B antibody tests provide evidence of a preceding group A streptococcal infection and support the diagnosis of sequelae to group A streptococcal infection in combination with clinical findings. ASO antibodies are not useful in cases of AGN following a pyodermal infection, since ASO antibodies are not often found in these cases. Unlike in the ASO test, infections of the skin will produce a strong response in the anti-DNase B test. Therefore, anti-DNase B testing is more reliable in clinical circumstances where poststreptococcal sequelae of skin infection are suspected. Anti-DNase B antibodies should also be measured in patients with suspected sequelae following pharyngeal infection when ASO titers are negative. The anti-DNase B test is a more reliable test for establishing a diagnosis for patients with suspected Sydenham's chorea, since antibody titers remain for longer periods. Failure to demonstrate positive antistreptococcal antibody titers by using either the ASO or anti-DNase B test makes the diagnosis of ARF or AGN unlikely, unless a late diagnosis of chorea or carditis has been made.

Tests for anti-hyaluronidase, anti-streptokinase, and anti-NADase antibodies are no longer being offered commercially for the diagnosis of preceding group A streptococcal infections. They are now used only for research purposes. Tests for antibodies against the cellular antigens C5a peptidase, group A carbohydrate, and M proteins are actively used in research.

REFERENCES

1. **Lancefield RC.** 1933. A serological differentiation of human and other groups of hemolytic streptococci. *J Exp Med* **57:**571–595.

2. **Hill HR, Zimmerman RA, Reid GVK, Wilson E, Kilton RM.** 1969. Food-borne epidemic of streptococcal pharyngitis at the United States Air Force Academy. *N Engl J Med* **280:**917–921.
3. **Veasy LG, Wiedmeier SE, Orsmond GS, Ruttenberg HD, Boucek MM, Roth SJ, Tait VF, Thompson JA, Daly JA, Kaplan EL, Hill HR.** 1987. Resurgence of acute rheumatic fever in the intermountain area of the United States. *N Engl J Med* **316:**421–427.
4. **Kaplan EL, Hill HR.** 1987. Return of rheumatic fever: consequences, implications, and needs. *J Pediatr* **111:**244–246.
5. **Veasy LG, Tani LY, Hill HR.** 1994. Persistence of acute rheumatic fever in the intermountain area of the United States. *J Pediatr* **124:**9–16.
6. **Veasy LG, Tani LY, Daly JA, Korgenski K, Miner L, Bale J, Kaplan EL, Hill HR.** 2004. Temporal association of the appearance of mucoid strains of *Streptococcus pyogenes* with a continuing high incidence of rheumatic fever in Utah. *Pediatrics* **113:**e168–e172.
7. **Miner LJ, Petheram SJ, Daly JA, Korgenski EK, Selin KS, Firth SD, Veasy LG, Hill HR, Bale JF Jr, Post-Streptococcal Syndrome Study Team.** 2004. Molecular characterization of *Streptococcus pyogenes* isolates collected during periods of increased acute rheumatic fever activity in Utah. *Pediatr Infect Dis J* **23:**56–61.
8. **Stockmann C, Ampofo K, Hersh AL, Blaschk AJ, Kendall BA, Korgenski K, Daly J, Hill HR, Byington CL, Pavia AT.** 2012. Evolving epidemiologic characteristics of invasive group A streptococcal disease in Utah, 2002–2010. *Clin Infect Dis* **55:**479–487.
9. **Wallace MR, Garst PD, Papadimos TJ, Oldfield EC, III.** 1989. The return of acute rheumatic fever in young adults. *JAMA* **262**:2557–2561.
10. **Centers for Disease Control (CDC).** 1988. Acute rheumatic fever among Army trainees—Fort Leonard Wood, Missouri, 1987–1988. *MMWR Morb Mortal Wkly Rep* **37:**519–522.
11. **Veasy LG, Hill HR.** 1997. Immunologic and clinical correlations in rheumatic fever and rheumatic heart disease. *Pediatr Infect Dis J* **16:**400–407.
12. **Martins TB, Hoffman JL, Augustine NH, Phansalkar AR, Fischetti VA, Zabriskie JB, Cleary PP, Musser JM, Veasy LG, Hill HR.** 2008. Comprehensive analysis of antibody responses to streptococcal and tissue antigens in patients with acute rheumatic fever. *Int Immunol* **20:**445–452.
13. **Alsaeid K, Majeed HA.** 1998. Acute rheumatic fever: diagnosis and treatment. *Pediatr Ann* **27:**295–300.
14. **Ravisha MS, Tullu MS, Kamat JR.** 2003. Rheumatic fever and rheumatic heart disease: clinical profile of 550 cases in India. *Arch Med Res* **34:**382–387.
15. **Ahn SY, Ingulli E.** 2008. Acute poststreptococcal glomerulonephritis: an update. *Curr Opin Pediatr* **20:**157–162.
16. **Stollerman GH.** 1991. Rheumatogenic streptococci and autoimmunity. *Clin Immunol Immunopathol* **61:**131–142.
17. **United Kingdom and United States Joint Report on Rheumatic Heart Disease.** 1955. The treatment of acute rheumatic fever in children. A cooperative clinical trial of ACTH, cortisone and aspirin. *Circulation* **11**:343–377.
18. **Rheumatic Fever Committee, American Heart Association.** 1972. *Throat Cultures for Rational Treatment of Sore Throat*. American Heart Association, New York, NY.
19. **Johnson DR, Kaplan EL, Sramek J, Bicova R, Havlicek J, Havlickova H, Motlova J, Kriz P.** 1996. *Laboratory Diagnosis of Group A Streptococcal Infections*. World Health Organization, Geneva, Switzerland.
20. **Johnson D, Kaplan E.** 1993. A review of the correlation of T-agglutination patterns and M-protein typing and opacity factor production in the identification of group A streptococci. *J Med Microbiol* **38:**311–315.
21. **Facklam RF, Martin DR, Lovgren M, Johnson DR, Efstratiou A, Thompson TA, Gowan S, Kriz P, Tyrrell GJ, Kaplan E, Beall B.** 2002. Extension of the Lancefield classification for group A streptococci by addition of 22 new M protein gene sequence types from clinical isolates: emm103 to emm124. *Clin Infect Dis* **34:**28–38.
22. **Johnson DR, Wotton JT, Shet A, Kaplan EL.** 2002. A comparison of group A streptococci from invasive and uncomplicated infections: are virulent clones responsible for serious streptococcal infections? *J Infect Dis* **185:** 1586–1595.
23. **Gerber MA, Shulman ST.** 2004. Rapid diagnosis of pharyngitis caused by group A streptococci. *Clin Microbiol Rev* **17:**571–580.
24. **Steed LL, Korgenski EK, Daly JA.** 1993. Rapid detection of *Streptococcus pyogenes* in pediatric patient specimens by DNA probe. *J Clin Microbiol* **11:**2996–3000.
25. **Uhl JR, Adamson SC, Vetter EA, Schleck CD, Harmsen WS, Iverson LK, Santrach PJ, Henry NK, Cockerill FR.** 2003. Comparison of LightCycler PCR, rapid antigen immunoassay, and culture for detection of group A streptococci from throat swabs. *J Clin Microbiol* **41:** 242–249.
26. **Anderson NW, Buchan BW, Mayne D, Mortensen JE, Mackey TA, Ledeboer NA.** 2013. Multicenter clinical evaluation of the *illumi*gene group A streptococcus DNA amplification assay for detection of group A streptococcus from pharyngeal swabs. *J Clin Microbiol* **51:**1474–1477.
27. **Committee on Infectious Diseases.** 2012. Group A streptococcal infections, p 686–688. *In* Pickering LK (ed), *Red Book: 2012. Report of the Committee on Infectious Diseases*. American Academy of Pediatrics, Elk Grove Village, IL.
28. **Bisno AL, Peter GS, Kaplan EL.** 2002. Diagnosis of strep throat in adults: are clinical criteria really good enough? *Clin Infect Dis* **15:**126–129.
29. **Baird RW, Bronze MS, Kraus W, Hill HR, Veasey LG, Dale JB.** 1991. Epitopes of group A streptococcal M protein shared with antigens of articular cartilage and synovium. *J Immunol* **146:**3132–3137.
30. **Goldstein I, Rebeyrotte P, Parlebas J, Halpern B.** 1968. Isolation from heart valves of glycopeptides which share immunological properties with *Streptococcus haemolyticus* group A polysaccharides. *Nature* **219:**866–868.
31. **Husby G, Van de Rijn I, Zabriskie JB, Abdin ZH, Williams RC, Jr.** 1976. Antibodies reacting with cytoplasm of subthalamic and caudate nuclei neurons in chorea and acute rheumatic fever. *J Exp Med* **144:**1094–1110.
32. **Golubjatnikov R, Koehler JE, Buccowich J.** 1977. Comparative study of antistreptolysin O, antideoxyribonuclease B and multi-enzyme tests in streptococcal infections. *Health Lab Sci* **14:**284–290.
33. **Barbosa SF, Nakamura PM, Hoshino-Shimizu S.** 1996. Detection of antibody isotypes to streptolysin O by dot ELISA. *Braz J Med Biol Res* **29:**763–767.
34. **Wannamaker L, Ayoub E.** 1960. Antibody titers in acute rheumatic fever. *Circulation* **21:**598–614.
35. **Shet A, Kaplan E.** 2006. Diagnostic methods for group A streptococcal infections, p 428–433. *In* Detrick B, Hamilton RG, Folds JD (ed), *Manual of Molecular and Clinical Laboratory Immunology*, 7th ed. ASM Press, Washington, DC.
36. **Gerber MA, Caparas LS, Randolph MF.** 1990. Evaluation of a new latex agglutination test for detection of streptolysin O antibodies. *J Clin Microbiol* **28:**413–415.
37. **Pacifico L, Mancuso G, Properzi E.** 1995. Comparison of nephelometric and hemolytic techniques for determination of antistreptolysin O antibodies. *Am J Clin Pathol* **103:**396–399.
38. **Blythe CC, Robertson PW.** 2006. Anti-streptococcal antibodies in the diagnosis of acute and post-streptococcal

disease: streptokinase versus streptolysin O and deoxyribonuclease B. *Pathology* **38:**152–156.
39. **Freyaldenhoven BS, Moos G, Hinzmann RD, Lütticken R.** 2004. Evaluation of recombinant antigens for the measurement of antibodies to streptolysin O and streptococcal DNase B on the Beckman Coulter IMMAGE system and comparison with a method employing conventional antigens. *Clin Lab* **50:**667–673.
40. **Beckman Coulter Synchron Systems.** April 2013. ASO—antistreptolysin O: chemistry information sheet. https://www.beckmancoulter.com/wsrportal/techdocs?docname=/cis/A18459/%25%25/EN_ASO-.pdf. Accessed 18 November 2015.
41. **Kaplan E, Anthony B, Chapman S, Ayoub E, Wannamaker L.** 1970. The influence of the site of infection on the immune response to group A streptococci. *J Clin Invest* **49:**1405–1414.
42. **Klein GC, Baker CN, Addison BV, Moody MD.** 1969. Micro test for streptococcal antideoxyribonuclease B. *Appl Microbiol* **18:**204–206.
43. **Murphy RA.** 1972. Improved antihyaluronidase test applicable to the microtitration technique. *Appl Microbiol* **23:**1170–1171.
44. **Bulletin of the World Health Organization.** 1978. Recent advances in rheumatic fever control and future prospects: a WHO memorandum. *Bull World Health Organ* **56:**887–912.
45. **Shet A, Kaplan EL, Johnson DR, Cleary PP.** 2003. Immune response to group A streptococcal C5a peptidase in children: implications for vaccine development. *J Infect Dis* **188:**809–817.
46. **O'Connor SP, Darip D, Fraley K, Nelson CM, Kaplan EL, Cleary PP.** 1991. The human antibody response to streptococcal C5a peptidase. *J Infect Dis* **163:**109–116.
47. **Todome Y, Ohkuni H, Yokomuro K, Kumura Y, Hamada S, Johnston KH, Zabriskie JB.** 1988. Enzyme-linked immunosorbent assay of antibody to group A streptococcus-specific C carbohydrate with trypsin-pronase-treated whole cells as antigen. *J Clin Microbiol* **26:**464–470.
48. **Appleton RS, Victorica BE, Tamer D, Ayoub EM.** 1985. Specificity of persistence of antibody to the streptococcal group A carbohydrate in rheumatic valvular heart disease. *J Lab Clin Med* **105:**114–119.
49. **Lancefield RC.** 1959. Persistence of type specific antibodies in man following infection with group A streptococci. *J Exp Med* **110:**271–292.

Diagnosis of *Helicobacter pylori* Infection and Assessment of Eradication

BRUCE E. DUNN AND SUHAS H. PHADNIS

45

CLINICAL PRESENTATION AND OUTCOMES OF INFECTION WITH *HELICOBACTER PYLORI*

Helicobacter pylori is a Gram-negative, microaerophilic spiral bacterium which is recognized as the primary cause of chronic gastritis in humans. Untreated *H. pylori* infection precedes and is required for the development of most cases of gastric and duodenal ulcers (1, 2). Further, *H. pylori* infection substantially increases the risk of development of gastric cancer in some populations. Following the discovery and identification of *H. pylori* as a significant human pathogen, it is now recognized as probably the most common bacterial infection of humankind, infecting approximately 50% of the world's population. Specific antibiotics combined with proton pump inhibitors are now routinely used to treat and eliminate previously chronic gastroduodenal diseases. For their novel work in helping us to understand the critical role played by *H. pylori* in peptic ulcer disease, Robin Warren and Barry Marshall were awarded the Nobel Prize in Physiology or Medicine in 2005.

H. pylori infection occurs in all human populations; the observed incidence of infection ranges from about 30% in developed countries to more than 90% in some developing countries. In general, *H. pylori* infection occurs in childhood in developing countries, and unless specifically treated, the infection persists throughout the lifespan of the individual (1, 2). In developed countries, a higher rate of infection is generally observed in older individuals. It has been suggested that improvements in hygiene in developed countries since the 1950s have resulted in a reduction of *H. pylori* infection rates within younger populations. Chronic infection with *H. pylori* is now recognized as a significant risk factor for gastric carcinoma and gastric mucosa-associated lymphoid tissue (MALT) lymphoma. The prevalence of *H. pylori* infection, gastritis, and gastric carcinoma increases with age and is associated with low socioeconomic status (1, 2).

The mode of transmission of *H. pylori* is unclear, although both the fecal-oral and oral-oral routes are likely. There is evidence suggesting that transmission occurs between members of the same family. A definitive natural reservoir of *H. pylori* external to the human body has not been identified. Species closely related to *H. pylori* in the *Helicobacter* genus are known to colonize several mammalian species.

There are a variety of clinical circumstances in which testing for the presence of *H. pylori* infection should be considered. Guidelines published in 2007 by the American College of Gastroenterology (3) include the following. (i) Testing for *H. pylori* should be done only if the clinician plans to offer treatment for positive results. (ii) Testing is indicated for patients with gastric MALT lymphoma, active peptic ulcer disease, or a past history of documented peptic ulcer. (iii) Testing and treating (if results are positive) are a proven management strategy for patients under the age of 55 with uninvestigated dyspepsia and no concerning features for cancer, such as bleeding, anemia, early satiety, unexplained weight loss, progressive dysphagia, odynophagia, recurrent vomiting, family history of gastrointestinal cancer, or previous esophagogastric malignancy. The test-and-treat strategy avoids the cost and inconvenience of endoscopy for patients for whom the risk of gastric cancer is low. (iv) Deciding which test to use in which clinical situation depends in large part on whether the patient requires evaluation with upper endoscopy. The sensitivity, specificity, and costs of the individual tests to be used must also be considered (3). The American College of Gastroenterology guidelines also recommend confirmation of eradication in the following settings: (i) individuals with an *H. pylori*-associated ulcer, (ii) those with persistent dyspeptic symptoms despite the test-and-treat strategy, (iii) individuals with *H. pylori*-associated MALT lymphoma, and (iv) those having undergone resection of the stomach for early gastric cancer (3).

It should be noted that *H. pylori* is linked in the literature with a variety of extragastric diseases, with little or no causative effect, including neurological disorders, cardiovascular diseases, dermatologic diseases, and allergic disorders (4). However, there is some evidence to support eradication of *H. pylori* in patients with unexplained idiopathic thrombotic purpura, iron deficiency anemia, and vitamin B_{12} deficiency (4).

GENETIC HETEROGENEITY OF *H. PYLORI* STRAINS

Advances in molecular genetic methods have allowed the elucidation of the complete genome sequences of several *H. pylori* strains. In addition, DNA sequencing of a number of defined regions, along with other genetic techniques, has shown a high degree of heterogeneity among *H. pylori* strains, perhaps due to frequent genetic exchange between strains. With the notable exception of the CagA and VacA

doi:10.1128/9781555818722.ch45

status of the infecting strain, little is known about the impact of strain heterogeneity on serologic detection methods.

The CagA protein, which is highly immunogenic, is one of the most widely studied virulence factors of *H. pylori*. The *cag*A gene is one of the genes in the *cag* pathogenicity island (5). The severity of *H. pylori*-related disease is correlated with the presence of the *cag* pathogenicity island. The CagA protein is injected into gastric epithelial cells by a type IV secretion mechanism; once in these cells, it becomes tyrosine phosphorylated and mediates changes in the host cell signal transduction pathways and actin skeleton reorganization (5). Another important virulence factor, vacuolating cytotoxin (VacA), is so named because it causes vacuolization of cultured eukaryotic cells. The *vac*A gene encodes a 140-kDa toxin precursor and is present in all strains. However, its expression is transcriptionally regulated; therefore, only about 50% of all strains express the toxin. Epidemiological studies have shown an increased risk of developing gastric or peptic ulcers and/or gastric carcinoma in patients infected with *cag*A- and *vac*A-positive strains (6). More recently, researchers have focused on a variety of additional virulence factors, including the *ice*A, *bab*A, *oip*A, and *sab*A genes. In addition, an array of pro- and anti-inflammatory cytokine polymorphisms in the host are known to affect the infectious outcome (7). Despite marked progress in defining host and bacterial genotypes and their associations with gastroduodenal pathology, a definitive model describing pathogenesis is only beginning to emerge.

METHODS FOR DETECTION OF *H. PYLORI*

Multiple techniques have been developed for the diagnosis of *H. pylori* infection (8, 9). Due to the significant potential and actual clinical impact of *H. pylori* infection, the number of commercial tests available to diagnose infection has proliferated significantly over the past decade. In this chapter, the tests are discussed generically rather than listed specifically. These methods can be categorized into two broad categories. The first category includes invasive assays (which generally require the availability of gastric tissue obtained by endoscopic biopsy for histological examination), culture, molecular assays (such as PCR), and urease tests. Within the past several years, a minimally invasive string test has also become available. The second category involves noninvasive assays, which detect either an immunologic response (e.g., specific antibodies directed against *H. pylori*) in blood, urine, or saliva, metabolic products of *H. pylori* urease activity (urea breath test), or bacterial antigens or nucleic acid present in stool. The most common diagnostic tests for the detection of *H. pylori* infection are summarized in Table 1. Molecular methods not only permit highly sensitive detection of *H. pylori* but also allow detailed characterization of the infecting strain by detecting virulence-associated genes and/or antimicrobial-resistance genes. However, molecular techniques are generally available only in research laboratories. Local validation of diagnostic tests is important since factors such as the local prevalence of *H. pylori* infection, in addition to characteristics of the tests themselves, influence the predictive value of the tests.

Invasive Tests

Histologic examination of gastric tissue permits evaluation of the type and degree of inflammation and direct observation of bacteria, if present. The bacteria can be identified based on their characteristic spiral morphology and supramucosal location. *H. pylori* can sometimes be difficult to detect on hematoxylin-and-eosin-stained slides. Thus, special stains, such as the Warthin-Starry stain, in which darkly stained spiral bacteria appear prominent on a lightly colored background, are frequently employed, despite the technical demands and higher cost involved. Other staining methods, such as Giemsa staining, fluorescence *in situ* hybridization, and immunohistochemical staining, provide additional information, such as the direct detection of clarithromycin resistance (10). Histologic examination is required whenever conditions such as gastric cancer or MALT lymphoma are suspected.

Microbiological culture of *H. pylori* is the most specific diagnostic method, but the sensitivity of culture is usually significantly lower than that of other methods. There are several reasons for this low sensitivity. The patchy distribution of *H. pylori* organisms in gastric mucosa can lead to endoscopic sampling error, resulting in false-negative cultures. In addition, the isolation of *H. pylori* is technically demanding and requires proper specimen handling and transport, use of specialized media, and microaerophilic growth conditions. Isolation of the organism is highly recommended, however, whenever antimicrobial susceptibility testing of *H. pylori* is desired, such as when patients fail to respond to bacterial-eradication therapy.

An important characteristic of *H. pylori* that forms the basis of several diagnostic tests (the biopsy urease test and urea breath test) is the ability of the bacterium to produce large amounts of the enzyme urease. Urease catalyzes the hydrolysis of urea to ammonia and carbon dioxide. This reaction causes an increase in the pH of the surrounding medium, which can be detected by a pH indicator dye. Thus, the presence of urease activity, and hence of *H. pylori*, is heralded by a color change in the indicator. Commercial biopsy urease tests which provide a gel medium in which to incubate gastric biopsy specimens in the presence of urea and a pH indicator to detect the presence of preformed urease and hence of *H. pylori* are available; an example is the CLOtest. Results are available within 2 to 24 h, depending on the test and conditions used. Compared with histologic and culture methods, biopsy urease tests are the endoscopic method of choice for rapid diagnosis of *H. pylori* infection on the basis of low cost and excellent sensitivity and specificity. Because of the desire to know the patient's *H. pylori* status prior to discharge from the endoscopy suite, rapid urease tests in which biopsies are sandwiched between a reagent strip with a pH indicator and a pad containing urea have been developed. These tests' sensitivities and specificities at 1 h are slightly lower than those observed for agar gel tests at 24 h (11).

Once the biopsy specimen is obtained, the bacteria present can be detected or analyzed by molecular assays without the need for bacterial culture. PCR-based molecular assays have been developed to detect *H. pylori*-specific DNA from gastric biopsy specimens and from paraffin-embedded tissues. Additionally, genotyping of *H. pylori* strains for virulence factors such as *cag*A and *vac*A is possible using such specimens. However, PCR-based assays remain relatively labor-intensive and expensive and are generally not available in routine clinical laboratories.

As an alternative to endoscopic detection of *H. pylori*, a minimally invasive string test has become available (12). In this test, the patient swallows a capsule attached to a string. Subsequently, the string is removed and the upper 30 cm of the string is cut and discarded to reduce contamination with oral microbial microbiota. The material collected is then used to culture *H. pylori* on selective plates or to perform PCR testing to allow identification and characterization of *H. pylori* strains. Culture of *H. pylori* or detection of its presence

TABLE 1 Overview of diagnostic tests for detection of *H. pylori*

Test(s)	Requirement for endoscopy	Advantage(s)	Disadvantage(s)	Approximate sensitivity, specificity (%)
Histology	Yes	Allows evaluation of the type and degree of inflammation; required to determine whether malignancy is present	Results may vary, depending on pathologist experience; multiple biopsies are recommended	>75, >95
Culture	Yes	Allows strain characterization, including identification of antibiotic-resistant isolates and virulence factors	Results vary depending on gastric sampling and laboratory experience; considerable risk of false-negative results	>75, 100
Biopsy urease test (agar gel)	Yes	Rapid and inexpensive; endoscopic method of choice	May be falsely negative immediately after antibiotic treatment or during treatment with omeprazole	>90, >95
Rapid urease test	Yes	Results available within 1 h	As above; sensitivity and specificity are reduced compared to those of a biopsy urease test	~90, ~90
String test	No	Minimally invasive; alternative to endoscopy	Less sensitive than endoscopy	~80, 100
Urea breath tests using ^{14}C- or ^{13}C-labeled urea	No	Noninvasive; sealed breath samples can be sent to reference laboratories; the [^{13}C]urea breath test is preferred for children and when multiple tests are required; useful to assess eradication of *H. pylori*	[^{14}C]urea breath test involves low-level radiation exposure; [^{13}C]urea breath test requires specialized equipment (mass spectrometer)	>95, >95
Stool antigen	No	Noninvasive; monoclonal antibody-based tests give best results; useful to assess eradication of *H. pylori*	May be less sensitive in detecting eradication than urea breath test	>90, >95
Serology	No	Noninvasive; inexpensive and available commercially; suitable for population prevalence studies	Prolonged delays (mos) before antibody levels decrease after eradication	>95, >90
Urine antibody	No	Noninvasive; easy to obtain especially in children	Not available universally	>85, >90
Salivary antibody	No	Noninvasive; results are easy to obtain, especially for children	Not available universally	>80, >80
Molecular tests	Depends on specimen	Allow sensitive detection of *H. pylori* and specific virulence and antibiotic resistance markers	Not well standardized or available in routine clinical laboratories	Variable

by PCR using the string test has a sensitivity of about 80% or 91% compared to that of culture or PCR, respectively, of gastric biopsy specimens. The method is suitable for use in remote areas in which endoscopy is not available.

Noninvasive Tests

Urea breath testing involves oral administration of urea that has been labeled with either the ^{13}C or ^{14}C carbon isotope. In infected individuals, urea is metabolized to ammonia and carbon dioxide; the latter is excreted in the breath as labeled carbon dioxide. The amount of labeled carbon dioxide which is excreted can then be quantified. The [^{14}C]urea breath test involves low levels of radiation exposure but has the advantage that it can be performed in a relatively large number of laboratories equipped to detect such radioactivity. In contrast, the [^{13}C]urea breath test uses a nonradioactive isotope of urea, which requires a mass spectrometer to detect $^{13}CO_2$ in the breath sample (13). The [^{13}C]urea breath test is preferred when repeated testing of an individual is required. The [^{13}C]urea breath test has been validated for children as well. Urea breath testing is an excellent noninvasive method by which to evaluate successful eradication of *H. pylori*, since it reflects active bacterial metabolism and responds rapidly to changes in *H. pylori* infection status. Many referral centers now accept urea breath samples for analysis of $^{13}CO_2$ at moderate expense. The urea breath test has been considered to be the gold standard among noninvasive tests for the detection of active infection by *H. pylori* (8).

H. pylori colonizing the gastroduodenal regions tend to slough specific antigens into the stool, thus forming the basis of another method of detection: the stool antigen test. Rapid advances in the commercial development of *H. pylori* stool antigen test kits using polyclonal or monoclonal antibodies directed against specific antigens have made these tests affordable, with a sensitivity and specificity comparable to those of urea breath testing (9). As the next-most-common test after urea breath testing, stool antigen tests are recommended for noninvasive diagnosis of *H. pylori* before and after eradication therapy. In general, stool antigen tests using monoclonal antibody directed against *H. pylori* antigens are more sensitive than are tests using polyclonal antibodies. The high sensitivity (~95%) of monoclonal stool antigen tests is comparable to that observed using invasive testing procedures (14, 15). While polyclonal antibody-based stool testing is slightly less sensitive, a commercial polyclonal antibody-based stool antigen test showed a sensitivity of 84 to 94% and a specificity of 90 to 100% in a comparison with urea breath testing (14). In general, these stool antigen tests are performed within a clinical laboratory; hence, results may be delayed somewhat. Rapid stool antigen tests which can be performed at the point of care are now available. The reported sensitivities and specificities for initial diagnosis were 93 to 95% and 87 to 89%, respectively (14, 15).

Serologic Assays

Infection with *H. pylori* results in a systemic immune response characterized by circulating specific immunoglobulins (immunoglobulin G [IgG], IgA, and, acutely, IgM) (16). Spontaneous eradication of *H. pylori* infection rarely occurs. Thus, the presence of *H. pylori*-specific antibodies is indirect evidence of active infection. Serology was the first noninvasive test that became available after the successful cultivation of *H. pylori*. Since that time, serologic assays have proven particularly useful in studies of *H. pylori* prevalence in diverse populations around the world.

Enzyme-linked immunosorbent assay (ELISA) methodology is considered the optimal approach to serologic testing for *H. pylori* antibodies because such tests are noninvasive, simple to perform, rapid, and cost-effective compared to endoscopic biopsy. Further, serologic testing allows "global" sampling of gastric mucosal infection, whereas biopsy-based assays allow only localized sampling of the gastric mucosa. The choice of antigen is critical for the success of the ELISA. In general, four types of antigen have been used for detection of *H. pylori*-specific antibodies (17). These preparations include crude antigens, such as whole cells and whole-cell sonicates, cell fractions, such as glycine extracts and heat-stable antigens, component-enriched antigenic fractions, such as urease and the 120-kDa protein associated with vacuolating cytotoxic activity, and specific recombinant antigens, such as CagA. The sensitivities and specificities of several of the enriched antigen preparations typically exceed 95%. While analysis of whole-cell preparations of *H. pylori* by sodium dodecyl sulfate-polyacrylamide gel electrophoresis reveals a large number of polypeptides, generally no more than about 25 protein antigens are recognized by immunoblotting using sera from infected individuals. There is significant heterogeneity in the specificities of these antibodies. As shown by a variety of techniques, very few, if any, antigens are recognized by all positive sera. Among the most commonly recognized antigens are the 62- and 30-kDa subunits of urease and the 58-kDa homolog of the Cpn60 family of heat shock proteins (HspB). Considering the genetic heterogeneity of *H. pylori* strains, it is generally thought that use of pooled extracts from multiple and genetically diverse strains as antigen preparations for detection of antibody will improve diagnostic performance. A significant fraction of individuals infected with *H. pylori* also produce serum and local antibodies directed against the 120-kDa CagA protein and the 89-kDa VacA protein. Antibodies directed against CagA and/or VacA protein antigen have a strong association with the severity of gastritis and with gastric cancer (18).

Use of Specific Antigens in ELISA

H. pylori is a diverse bacterial species, with different clusters found in different parts of the world. Some authors have emphasized the need to use local strains as the source of antigen rather than foreign strains to obtain the best test results. This may be especially true in Asia (17).

Some serologic assays against specific virulence factors of *H. pylori* have been developed. The most important factor in using immunological methods for identifying VacA-specific antibodies by ELISA is the antigen preparation used to detect circulating antibodies. VacA proteins are quite diverse among *H. pylori* strains and are broadly classified as of the s1/m1 or s2/m2 type. While commercial kits are available for the detection of VacA antibodies by using immunoblot assays, most ELISAs have been developed with purified or enriched VacA protein fractions; this is a time-consuming and expensive approach (19). The availability of recombinant VacA protein will help to make the VacA ELISA more widely available.

Commercial assays which use recombinant CagA protein to detect CagA-specific IgG are now available (see http://www.antibodyresource.com for cytokine-associated gene A antibodies). These assays also use anti-human IgG monoclonal antibody enzyme conjugate to detect the presence of specific IgG. At least one assay has been automated to operate in a high-speed walk-away analyzer for 96-well ELISAs. Generally speaking, the use of ELISAs for the detection of antibodies to specific antigens is limited to research laboratories.

The possibility of false-negative serologic test results for *H. pylori* has to be considered for any individual with

an impaired immune response, e.g., the elderly, dialysis patients, immunosuppressed individuals, and organ recipients. In addition, chronic nonsteroidal anti-inflammatory drug treatment may suppress infection and decrease the sensitivity of serologic tests. False-negative results may also occur during the first few weeks of infection if methods which detect only IgG or IgA are used.

Value of Analysis of Specific Immunoglobulin Classes

In general, measurement of *H. pylori*-specific IgM levels has not proven useful in clinical laboratories because the time of infection is rarely known and patients' symptoms at the time of infection, if any, are nonspecific. A number of studies have evaluated the relative value of detecting *H. pylori*-specific IgG and IgA. Detection of *H. pylori*-specific IgA alone is generally less sensitive than detection of specific IgG antibodies alone. Testing for the presence of *H. pylori*-specific IgA in addition to IgG may increase test sensitivity slightly. However, the specificity of *H. pylori*-specific IgA appears to be at least equal to that of *H. pylori*-specific IgG (8, 9). Individuals who have IgA but not IgG antibodies against *H. pylori* are uncommon. As a result, most commercial serologic tests are based on the detection of *H. pylori*-specific IgG only.

H. pylori-Specific Antibodies in Body Fluids Other Than Serum

In an attempt to eliminate the need for venipuncture, diagnostic tests for the detection of IgG antibodies in the saliva and urine of adults and children have been developed (reviewed in reference 20). The sensitivity of detection of *H. pylori* antibodies in saliva generally ranges from 80 to 85%, while specificity generally ranges from 70 to 80%. The sensitivities of detection of *H. pylori* antibodies in urine generally range from 90 to 95%, with specificities of 90 to 95%. The ease of obtaining specimens is an obvious advantage of using urine as a source of IgG antibodies against *H. pylori* infection, especially with children (21, 22).

Immunoblot Analysis

Immunoblot analysis of whole-cell lysates of *H. pylori* permits a detailed analysis of antibody profiles and is useful for identifying immunologic responses to specific antigens. However, beyond research studies, immunoblot technology is of limited utility for several reasons. First, antibodies in some patients infected by specific strains of *H. pylori* may not recognize antigens if a single strain of *H. pylori* is used in the immunoblot assay. Second, the resolution of the immunoblot is limited, permitting only about 25 distinctive bands to be detected. It may be difficult to distinguish between antigens with similar molecular sizes. Finally, since immunoblot assays are labor-intensive and semiquantitative, this type of assay is not suitable for automation or for screening large collections of sera. One new commercial immunoblot method showed high sensitivity (99%) and specificity (98%) compared with those of three other methods (23). However, when CagA antibodies were determined by this assay, false-positive reactions were detected in patients infected with CagA-negative strains and in individuals not infected with *H. pylori* (23, 24). In general, immunoblot analysis is a research technique not available in routine clinical laboratories.

Rapid Serologic Tests

Over the past several years, a number of rapid near-patient tests have been marketed to detect antibodies to *H. pylori* in untreated individuals. These rapid tests are generally based on latex agglutination or flowthrough membrane-based enzyme immunoassays. Serum, plasma, or whole blood can be tested. Most of these tests detect IgG antibodies. While some studies have shown acceptable sensitivity and specificity, many qualitative rapid antibody tests have been clearly inferior to quantitative ELISAs. The use of rapid tests has not been recommended in Europe (2). The present authors recommend that if near-patient testing for *H. pylori* is to be instituted, the results of such tests must be correlated with results of serologic tests from the local reference laboratory on a select group of well-characterized patients before the test is accepted for widespread clinical use. These near-patient tests are generally more expensive than laboratory-based tests and have not been used widely.

Molecular Methods

Over the past decade and a half, a variety of DNA-based molecular techniques to detect *H. pylori*, determine susceptibility to clarithromycin, and serve as tools for strain typing have been developed. A major limitation of PCR-based detection methods for *H. pylori* is the inability to distinguish between living and dead organisms. Thus, PCR-based detection of *H. pylori* results in higher sensitivity than with other methods of detection. While molecular methods have been applied to the detection of *H. pylori*, such methods are not generally suitable for use in ordinary clinical settings.

PCR is as sensitive as culture in detecting *H. pylori* in gastric biopsy specimens. PCR has the advantage of allowing the detection of virulence factors such as *cagA*, *vacA* alleles, and other genetic factors. Real-time PCR has been used to estimate the gastric mucosal density of *H. pylori* (25). Chisholm et al. developed a multiplex PCR technique to detect *vacA* alleles in a single step (26). The latter authors reported perfect correlation with the genotypes determined directly in gastric biopsy specimens and in the *H. pylori* isolates cultured from the specimens. "Fingerprinting" of *H. pylori* strains can be performed on gastric biopsy specimens directly using PCR-restriction fragment length polymorphism analysis without having to culture bacteria. Real-time PCR using TaqMan technology has been applied to determine the bacterial load of *H. pylori* in the gastric mucosa. A good correlation was obtained with results obtained using the urea breath test (25). PCR has also been used to detect the presence of *H. pylori* in gastric samples collected using the string test.

Molecular methods to detect the resistance of *H. pylori* to clarithromycin by using cultured isolates or gastric biopsy specimens directly have been developed. Clarithromycin resistance is due to single point mutations in the peptidyltransferase region of the 23S rRNA gene (27); hence, detection of such mutations is well suited to PCR analysis. More recently, real-time PCR protocols which allow the detection of clarithromycin resistance-associated point mutations on the 23S rRNA have been developed (28).

PCR tests have been developed to detect *H. pylori* in human stool specimens (29). There are a number of potential limitations to the PCR method for detection of *H. pylori* in stool specimens. First, false-negative results may occur due to the presence of PCR inhibitors or to genetic variability. Second, false-positive results may occur as a result of contamination or nonspecific amplification of human genomic DNA. Finally, PCR detection of *H. pylori* has not yet been standardized and is not generally available in routine clinical laboratories. However, when appropriate steps are taken to purify DNA in fecal specimens by using various biochemical,

immunological, and physical steps prior to PCR amplification, the sensitivity and specificity of stool-based PCR for detection of *H. pylori* can approach 100% in the appropriate research setting (29). One-step PCR protocols using radiolabeled primers, an efficient extraction protocol, and 80 cycles of amplification to genotype *vacA* and detect *cagA* in stool specimens of *H. pylori*-infected individuals have been developed. PCR tests to detect *H. pylori* in stool specimens are used almost exclusively in research settings.

GENERAL APPROACH TO SEROLOGIC TESTING

Clinical Indications

As noted above, an accurate diagnosis of the presence of *H. pylori* infection should precede antimicrobial therapy. Routine serologic follow-up of patients after treatment for *H. pylori* infection is not recommended, since no clear guidelines to quantify the reduction of antibody level or the time period required to observe such a reduction or to correlate it with bacterial eradication have been established outside research settings.

Specimens

Generally, serum can be collected using standard phlebotomy techniques. There are no dietary restrictions prior to collection of the serum sample. Typically, no more than 10 μl of serum is needed to perform a single test.

Procedure

A variety of ELISA kits are available from manufacturers in North America and Europe. A general outline of methods involved in detecting *H. pylori*-specific IgG antibodies by ELISA is provided below. All procedures described in the package insert must be followed exactly as described for the particular test kit being used. In typical commercial ELISA kits, antigen is attached to the surfaces of microtiter plate wells, diluted serum is added to individual wells, and the *H. pylori*-specific IgG antibody, if present, binds to the antigen. All unbound antibody is washed away, and enzyme-conjugated anti-human IgG is added. The enzyme conjugate binds to the antibody complex. Excess enzyme conjugate is then washed away, and substrate is added. Bound enzyme conjugate begins a hydrolytic reaction. After a specified period, the enzyme reaction is stopped. The results are read by a spectrophotometer, which gives an indirect measurement of the amount of *H. pylori*-specific IgG antibody present in the serum.

Results and Interpretation

Typically, ELISA kits have a predetermined cutoff for absorbance values considered to be positive or negative. There is usually a range of absorbance values between which the reading is considered equivocal. It is recommended by many manufacturers that specimens giving equivocal results be retested. If the retest result is also equivocal, the report should be reported as "equivocal" and the sample should be retested by an alternate method or with a new serum specimen drawn after an interval of at least four weeks.

Commercial ELISAs are designed for use in the qualitative detection of *H. pylori*-specific IgG antibodies in human serum. Such tests typically assess the serologic status by using a single serum specimen per individual and are intended to be used as an aid in the diagnosis of *H. pylori* infection in individuals with gastrointestinal symptoms. Virtually all individuals infected with *H. pylori* possess IgG antibodies. Because infection with *H. pylori* is so prevalent and because it may be asymptomatic, many individuals apparently free of gastrointestinal symptoms exhibit *H. pylori*-specific antibodies. The prevalence of *H. pylori* antibodies increases with age. *H. pylori* antibodies are found in men and women at approximately equal rates. Blacks, Hispanics, and persons born outside the United States tend to show higher rates of infection with *H. pylori*.

Technical Limitations

Typically, icteric, lipemic, hemolyzed, or heat-inactivated serum may cause erroneous results; such samples should be avoided if possible. A positive test result indicates that the individual has antibodies to *H. pylori*. Such a result does not indicate that any existing symptoms are necessarily due to *H. pylori* infection. In the absence of prior therapy to eradicate *H. pylori* infection, the positive test result very probably indicates active infection with *H. pylori*. However, in the absence of an adequate patient history, a single positive serologic test result does not differentiate between active and past infection. A negative serologic test result indicates that the individual does not have detectable levels of antibody to *H. pylori*. If a sample is drawn too early during *H. pylori* infection, IgG antibodies may not be present.

Limitations of Serologic Assays in Monitoring Eradication

There are two basic limitations to the clinical utility of serology in monitoring the eradication of *H. pylori* infection. First, baseline and follow-up sera must be analyzed at the same time to minimize assay variability. Significant variability may result from assaying sera at different times or using different lots of reagent. Therefore, pretreatment sera must be saved to be analyzed along with posttherapy samples. This limitation requires that pretreatment specimens be saved for up to 12 months. The second limitation is that serology must be monitored for at least 3 months (and for 6 to 9 months in many cases) before a significant decrease in antibody concentration is observed. Depending on the clinical circumstances, this may represent an unacceptable delay. The percent decrease in the concentration of *H. pylori*-specific IgG which indicates eradication of infection in an individual patient has not been clearly established.

When serologic analysis is used in the evaluation of treatment success under controlled conditions, the absolute concentrations of *H. pylori*-specific IgG antibodies in the serum are less important than are the changes in concentrations from the pretreatment level. For example, over 60% of individuals from whom *H. pylori* was eradicated continued to have seropositive IgG levels (index value, >1.0) at 6, 9, and 12 months despite demonstrating a 20% reduction in antibody concentration (8). Thus, a single serum specimen from such an individual appears to reflect active infection with *H. pylori* in the absence of an adequate clinical history. In addition, specific antibodies may persist for years even after eradication of *H. pylori*. Some antigens, in particular the 120-kDa CagA protein, induce very persistent antibodies.

In summary, ELISAs for the detection of *H. pylori*-specific antibodies are sensitive, specific, and cost-effective for untreated individuals. The major limitation of such tests is the lack of a rapid, clear serologic response to the eradication of bacterial infection.

Assessment of Eradication of *H. pylori*

Because of the patchy nature of *H. pylori* infection, invasive methods are not optimal to assess bacterial eradication, since therapy may reduce the burden of *H. pylori* infection

but not completely eradicate the organism; biopsies may therefore provide false-negative results. PCR methods may give false-positive results by detecting residual nucleic acid from dead or dying bacteria. Serologic methods are not suitable for assessment of eradication since antibody levels can remain elevated for months to years even after successful eradication. The best methods for assessment of eradication of *H. pylori* are those which are capable of detecting active infection, such as the urea breath test and stool antigen test (30).

Pediatric iron deficiency has been recognized as an extragastric manifestation of *H. pylori* infection in otherwise asymptomatic *H. pylori* gastritis (4). In 2012, the FDA approved [^{13}C]urea breath testing in children under the age of 18 (http://www.fda.gov/NewsEvents/Newsroom/PressAnnouncements/ucm293278.htm). In the pediatric population, the stool antigen test and the [^{13}C]urea breath test are the methods of choice for diagnosis and "tests for cure" of *H. pylori*. These tests, in addition to endoscopy and histology, are now accepted standards of care in the United States (31). Diagnosis of *H. pylori* infection in children has been reviewed recently (19, 32).

The two noninvasive methods generally recommended for assessment of eradication of *H. pylori* are the urea breath test and the stool antigen test. Urea breath testing performed at least 4 weeks after treatment has been promoted as the test of choice to confirm bacterial eradication (2, 30). Both the [^{13}C]urea and [^{14}C]urea breath tests have been approved by the FDA for use in adults, while the [^{13}C]urea breath test was recently approved for children below 18 years of age. Stool antigen testing is a more widely available alternative, but it should not be performed sooner than 4 to 6 weeks after completion of treatment because of both false-positive and false-negative results in this time period (14, 15). However, the unpleasantness of the stool collection procedure may limit acceptance of this assay by patients. Posteradication, it has been reported that in populations with low *H. pylori* prevalence, the performance of the urea breath test is superior to that of the stool antigen test (2, 14).

It should be kept in mind that in individuals who fail eradication therapy, a gastric biopsy with culture may be necessary to determine the susceptibility of the infecting *H. pylori* strain(s).

As noted above, serologic tests are generally not useful to confirm eradication due to the significant time required for anti-*H. pylori* antibodies to decrease after therapy and due to the fact that the percent reduction in antibody titer signifying bacterial eradication has not been established.

Finally, it should be noted that while a low rate of reinfection with *H. pylori* has been noted in developed countries, a much higher rate of reinfection is observed in the developing world. Thus, caution is required to distinguish between failed eradication and reinfection by *H. pylori* in individual patients in developing countries (33).

REFERENCES

1. **Makola D, Peura DA, Crowe SE.** 2007. *Helicobacter pylori* infection and related gastrointestinal diseases. *J Clin Gastroenterol* **41:**548–558.
2. **Malfertheiner P, Megraud F, O'Morain CA, Atherton J, Axon AT, Bazzoli F, Gensini GF, Gisbert JP, Graham DY, Rokkas T, El-Omar EM, Kuipers EJ, European Helicobacter Study Group.** 2012. Management of *Helicobacter pylori* infection—the Maastricht IV/Florence Consensus Report. *Gut* **61:**646–664.
3. **Chey WD, Wong BC, Practice Parameters Committee of the American College of Gastroenterology.** 2007. American College of Gastroenterology guideline on the management of *Helicobacter pylori* infection. *Am J Gastroenterol* **102:**1808–1825.
4. **Malfertheiner P, Selgard M.** 2010. *Helicobacter pylori* infection and current clinical areas of contention. *Curr Opin Gastroenterol* **26:**618–623.
5. **Segal ED, Cha J, Lo J, Falkow S, Tompkins LS.** 1999. Altered states: involvement of phosphorylated CagA in the induction of host cellular growth changes by *Helicobacter pylori*. *Proc Natl Acad Sci U S A* **96:**14559–14564.
6. **Sokic-Milutinovi T, Wex T, Todorovic V, Milosavljevic T, Malfertheiner P.** 2004. Anti-CagA and anti-VacA antibodies in *Helicobacter pylori*-infected patients with and without peptic ulcer disease in Serbia and Montenegro. *Scand J Gastroenterol* **3:**222–226.
7. **Wu M, Chow L, Lin J, Chiou S.** 2008. Proteomic identification of biomarkers related to *Helicobacter pylori*-associated gastroduodenal disease: challenges and opportunities. *J Gastroenterol Hepatol* **23:**1657–1661.
8. **McNulty CAM, Lehours P, Megraud F.** 2011. Diagnosis of *Helicobacter pylori* infection. *Helicobacter* **16:**10–18.
9. **Tonkic A, Tonkic M, Lehours P, Megraud F.** 2012. Epidemiology and diagnosis of *Helicobacter pylori* infection. *Helicobacter* **17:**1–8.
10. **Camorlinga-Ponce M, Romo C, Gonzalez-Valencia G, Munoz O, Torres J.** 2004. Topographical localization of cagA positive and cagA negative *Helicobacter pylori* strains in the mucosa: an *in situ* hybridization study. *J Clin Pathol* **57:**822–828.
11. **Nishikawa K, Sugiyama T, Kato M, Ishizuka J, Kagaya H, Hokari K, Asaka M.** 2000. A prospective evaluation of new rapid urease tests before and after eradication treatment of *Helicobacter pylori*, in comparison with histology, culture and ^{13}C-urea breath test. *Gastrointest Endosc* **51:**164–168.
12. **Windsor HM, Abioye-Kutey EA, Marshall BJ.** 2005. Methodology and transport medium for collection of *Helicobacter pylori* on a string test in remote location. *Helicobacter* **10:**630–634.
13. **Graham DY, Opekun AR, Hammoud F, Yamaoka Y, Reddy R, Osato MS, El-Zimaity HM.** 2003. Studies regarding the mechanism of false negative urea breath tests with proton pump inhibitors. *Am J Gastroenterol* **98:**1005–1009.
14. **Veijola L, Myllyluoma E, Korpela R, Rautelin H.** 2005. Stool antigen tests in the diagnosis of *Helicobacter pylori* infection before and after eradication therapy. *World J Gastroenterol* **11:**7340–7344.
15. **Wu DC, Wu IC, Wang SW, Lu CY, Ke HL, Yuan SS, Wang YY, Chang WH, Wang TE, Bair MJ, Ku FC.** 2006. Comparison of stool enzyme immunoassay and immunochromatographic method for detecting *Helicobacter pylori* antigens before and after eradication. *Diagn Microbiol Infect Dis* **56:**373–378.
16. **Bergy B, Marchildon P, Peacock J, Megraud F.** 2003. What is the role of serology in assessing *Helicobacter pylori* eradication? *Aliment Pharmacol Ther* **18:**635–639.
17. **Hoang TT, Wheeldon TU, Bengtsson C, Phung DC, Sorberg M, Granstrom M.** 2004. Enzyme-linked immunosorbent assay for *Helicobacter pylori* needs adjustment for the population investigated. *J Clin Microbiol* **42:**627–630.
18. **Krah A, Miehlke S, Pleissner KP, Zimny-Arndt U, Kirsch C, Lehn N, Meyer TF, Jungblut PR, Aebischer T.** 2004. Identification of candidate antigens for serologic detection of *Helicobacter pylori*-infected patients with gastric carcinoma. *Int J Cancer* **108:**456–463.
19. **Perez-Perez GI, Peek RM, Atherton JC, Blaser MJ, Cover TL.** 1999. Detection of anti-VacA antibody response in

serum and gastric juice samples using types 1/ma and s2/m2 *Helicobacter pylori* VacA antigens. *Clin Diagn Lab Immunol* **6:**489–493.
20. **Megraud F, Lehours P.** 2007. *Helicobacter pylori* detection and antimicrobial susceptibility testing. *Clin Microbiol Rev* **20:**280–322.
21. **Leal YA, Flores LL, Garcia-Cortes LB, Cedillo-Rivera R, Torres J.** 2008. Antibody-based detection tests for the diagnosis of *Helicobacter pylori* infection in children: a meta-analysis. *PLoS One* **3:**e3751.
22. **Shimizu T, Yarita Y, Haruna H, Kaneko K, Yamashiro Y, Gupta R, Anazawa A, Suzuki K.** 2003. Urine-based enzyme-linked immunosorbent assay for the detection of *Helicobacter pylori* antibodies in children. *J Paediatr Child Health* **39:**606–610.
23. **Monteiro L, Bergey B, Gras N, Megraud F.** 2002. Evaluation of the performance of the Helico Blot 2.1 as a tool to investigate the virulence properties of *Helicobacter pylori*. *Clin Microbiol Infect* **8:**676–679.
24. **Park CY, Cho YK, Kodama T, El-Zimaity HM, Osato MS, Graham DY, Yamaoka Y.** 2002. New serological assay for detection of putative *Helicobacter pylori* virulence factors. *J Clin Microbiol* **40:**4753–4756.
25. **Kobayashi D, Eishi Y, Ohkusa T, Ishige T, Suzuki T, Minami J, Yamada T, Takizawa T, Koike M.** 2002. Gastric mucosal density of *Helicobacter pylori* estimated by real-time PCR compared with results of urea breath test and histological grading. *J Med Microbiol* **51:**305–311.
26. **Chisholm SA, Teare EL, Patel B, Owen RJ.** 2002. Determination of *Helicobacter pylori* VacA allelic types by single-step multiplex PCR. *Lett Appl Microbiol* **35:**42–46.
27. **Hao Q, Li Y, Zhang ZJ, Liu Y, Gao H.** 2004. New mutation points in 23S rRNA gene associated with *Helicobacter pylori* resistance to clarithromycin in northeast China. *World J Gastroenterol* **10:**1075–1077.
28. **Oleastro M, Menard A, Santos A, Lamouliatte H, Monteiro L, Barthelemy P, Megraud F.** 2003. Real-time PCR assay for rapid and accurate detection of point mutations conferring resistance to clarithromycin in *Helicobacter pylori*. *J Clin Microbiol* **41:**397–402.
29. **Kabir S.** 2004. Detection of *Helicobacter pylori* DNA in feces and saliva by polymerase chain reaction: a review. *Helicobacter* **9:**115–123.
30. **Selgrad M, Malfertheiner P.** 2011. Treatment of *Helicobacter pylori*. *Curr Opin Gastroenterol* **27:**565–570.
31. **Crone J, Gold BD.** 2004. *Helicobacter pylori* infection in pediatrics. *Helicobacter* **9**(Suppl 1)**:**49–56.
32. **Leal YA, Flores LL, Fuentes-Panana EM, Cedillo-Rivera R, Torres J.** 2011. ^{13}C-urea breath test for the diagnosis of Helicobacter pylori infection in children: a systematic review and meta-analysis. *Helicobacter* **16:** 327–337.
33. **Moya DA, Crissinger KD.** 2012. *Helicobacter pylori* persistence in children: distinguishing inadequate treatment, resistant organisms, and reinfection. *Curr Gastroenterol Rep* **14:**236–242.

Laboratory Diagnosis of Syphilis

JOHN L. SCHMITZ

46

BACKGROUND

The laboratory diagnosis of syphilis has relied, in large part, upon serologic methods for over 100 years (1). The causative organism, *Treponema pallidum*, is not amenable to *in vitro* culture, and antigen detection and nucleic acid amplification techniques have not become routinely used. While many of the serologic methods in use now have been in use for decades, their application, specifically the standard testing algorithm, is changing. In order to understand the interpretation of alternative testing algorithms, a thorough understanding of test characteristics is necessary. This chapter will review serologic tests for syphilis and their interpretation when they are applied to adults with and without HIV infection and to children.

EPIDEMIOLOGY

From 2005 through 2013, the rates of primary and secondary syphilis increased to 5.3 cases per 100,000 population (2). The largest increases were noted in men who have sex with men in the 25- to 29-year-old age group. The rate of primary and secondary syphilis in women was 0.9 per 100,000 in both 2005 and 2013. A slight increase in rates was noted between 2005 and 2009, followed by a decline to the 2013 level. In the United States, the rate of congenital syphilis was 7.8 cases per 100,000 live births in 2012. The rate reflects a decline in incidence over several years corresponding to the decline in incidence of primary and secondary syphilis in women. Globally, the WHO estimates 10.6 million new cases of syphilis annually in adults (48), while congenital syphilis is estimated to occur in 1 million pregnancies per year globally (3). The burden of infection is particularly heavy in resource-limited areas. This fact has stimulated the development of rapid, point-of-care diagnostics that can be used for large-scale testing with a limited traditional laboratory infrastructure.

MICROBIOLOGY

Four related spirochetes are agents of human treponemal disease. They are long (10 to 15 μm), slender (0.1 to 0.2 μm) corkscrew-shaped organisms that have not been cultivated *in vitro*. Because of their size, they cannot be visualized by standard bright-field microscopy. Dark-field microscopy is necessary for visualization from infected lesions. *T. pallidum* subsp. *pallidum*, the cause of venereal syphilis, is a human bacterial pathogen with no natural reservoir. The other pathogenic treponemes (4) that cause human infection include *T. pallidum* subsp. *endemicum* (bejel), *T. pallidum* subsp. *pertenue* (yaws), and *T. carateum* (pinta). These organisms are closely related genetically and exhibit serologic cross-reactivity.

NATURAL HISTORY OF ACQUIRED AND CONGENITAL SYPHILIS

In the natural history of acquired and congenital syphilis (5), the transmission of *T. pallidum* has occurred via contact with infectious primary or secondary lesions, blood transfusion (6), or transplantation (7). Vertical transmission can lead to the development of congenital syphilis. The incubation period of venereal syphilis is 10 to 90 days, after which the signs and symptoms of syphilis appear. Primary syphilis includes development of a chancre at the site of inoculation that may be associated with regional lymphadenopathy. Lesions contain viable treponemes that can be detected with dark-field microscopy. Spirochetes disseminate during this stage, leading to manifestations of secondary syphilis in approximately 25% of untreated patients weeks to months after primary disease.

The manifestations of secondary syphilis include skin lesions that may involve the palms and soles, fever, malaise, headache, lymphadenopathy, alopecia, hepatitis, gastrointestinal symptoms, and renal, musculoskeletal, neurologic, and ocular findings. Upon resolution of these symptoms, patients enter the latent phase of syphilis. Latent infection of less than 1 year in duration is classified as early latent, while duration of greater than 1 year is termed late latent syphilis. Eventually, up to 40% of individuals develop late (tertiary) syphilis. The manifestations of late syphilis include neurosyphilis and cardiovascular and gummatous syphilis.

Genital ulcer diseases have been suggested to increase the rate of acquisition of HIV infection (8). Some evidence that syphilis may influence HIV load exists as well (9). Clinical manifestations of syphilis appear typical for the most part in HIV-infected individuals, although some cases of more rapid progression and disease severity have been reported. The diagnosis of syphilis in HIV-infected patients is likewise usually typical, with occasional exceptions (10).

doi:10.1128/9781555818722.ch46

Manifestations of congenital syphilis are varied and can occur in fetuses, newborns, and children without treatment (11). Spontaneous abortion (stillbirth) may occur. Infants born with congenital infection may be asymptomatic at birth or present with various manifestations resulting from widespread dissemination of *T. pallidum* organisms. Early congenital syphilis (affecting those <2 years old) most commonly presents with hepatomegaly, nasal drainage, rash, lymphadenopathy, skeletal abnormalities, cerebrospinal fluid (CSF) abnormalities, or hematologic findings. Late latent congenital syphilis (>2 years of age) develops in 40% of untreated children and may manifest with facial abnormalities or with ocular, otic, oral, skin, neurologic, skeletal, or renal disease.

INDICATIONS FOR SYPHILIS TESTING

Individuals presenting with signs/symptoms of primary, secondary, or tertiary syphilis as well as persons with sexual exposure to an individual with any stage of syphilis infection should have serologic testing for syphilis (12). Sexually active men who have sex with men should be tested at least annually. Testing is also recommended for pregnant women at their first prenatal visit, in the third trimester, and at delivery if the patient is at high risk for syphilis. Infants born to mothers with reactive serologic tests for syphilis should also receive testing. The effectiveness of therapy should be assessed with nontreponemal testing 6 and 12 months after treatment.

LABORATORY DIAGNOSTIC METHODS

Direct Detection

Direct detection of *T. pallidum* in clinical samples relies upon microscopic examination. Dark-field microscopy is used to detect motile spirochetes in serous fluid from primary or secondary lesions, mucous patches, or lymph node aspirates that contain sufficient numbers of viable spirochetes (13). This technique is useful for diagnosis in primary, secondary, and early congenital infection.

Dark-field examination requires a properly calibrated microscope and skilled personnel. In addition, these resources must be physically close to the patient because slides must be examined immediately after preparation to ensure that viable organisms with characteristic morphology and motility are retained for proper interpretation. Serous fluid or aspirates are collected and placed on a glass slide that is coverslipped and immediately examined for appropriate morphology and motility. Results are reported as dark-field microscopy positive, dark-field microscopy negative, or dark-field microscopy unsatisfactory. The sensitivity of dark-field microscopy is approximately 80% (14). Examination of lesions from the oral cavity is not recommended due to the presence of *Treponema denticola*, a component of the oral flora. Additionally, antibiotic therapy or application of topical antibiotics may result in false-negative results. Likewise, the examination of healing lesions may also yield negative results.

The direct fluorescent antibody test for *Treponema pallidum* (15) is an alternative method for detection of *T. pallidum* in lesions. It utilizes the same sample types as used for dark-field examination. In addition, this approach can be used for oral and rectal samples due to its ability to specifically identify pathogenic species of *T. pallidum* in the presence of endogenous spirochetes. There is also a version of the direct fluorescent antibody test for *T. pallidum* that has been adapted for use in tissue sections (16).

PCR-based methods for the detection of *T. pallidum* DNA have been developed. They are of potential usefulness during early primary infection when seroconversion has not occurred and/or dark-field microscopy is unavailable. They may also be of use in the diagnosis of neurosyphilis due to the limitations of CSF antibody testing and in congenital syphilis due to the confounding of serologic testing by maternal antibody and limited experience with *T. pallidum*-specific IgM testing. The most commonly reported application of PCR-based detection of *T. pallidum* has been observed in samples derived from skin lesions and CSF. A recent meta-analysis (17) indicated that the highest likelihood ratios were found in studies using swabs from primary- or secondary-syphilis cases. For congenital syphilis, the highest likelihood ratios were found in CSF and blood from neonates. While of potential utility, PCR is not routinely available for the diagnosis of syphilis. It is available in some commercial reference laboratories (Focus Diagnostics).

SEROLOGY

Nontreponemal Tests

Because of the inability to culture *T. pallidum* and the limitations of available direct detection methods, serologic testing is the mainstay of syphilis diagnostics. Serologic testing employs two categories of assays differentiated by the antigen preparation used. The nontreponemal antibody tests employ a combination of cardiolipin, cholesterol, and lecithin as the antigen preparation, as opposed to antigens derived from *T. pallidum* itself. All of the nontreponemal methods are based on a flocculation reaction that develops upon reaction of IgG and/or IgM antibodies in serum with the nontreponemal antigen. These antibodies are produced to lipoidal materials released from damaged host cells or from treponemes (18). There are four standard nontreponemal antibody tests (Table 1). These tests differ in the ways in which flocculation is detected, the levels of stability of prepared antigens, and the sample types used. Procedural details are available for all four methods (19). The RPR card test (ASI [Arlington Scientific, Inc.]) is summarized here as an example.

A. Pipet 50 μl of serum into one circle of the testing card and spread it with a plastic stirrer.
B. Add 1 drop of well-shaken antigen suspension onto each circle.
C. Rotate cards for 8 min at 100 rpm under a humidifying cover.
D. Immediately visualize the test results under a high-intensity lamp.
E. Interpret as follows.
   1. A slight but definite clumping ranging to marked and intense clumping indicates reactivity.

TABLE 1 Nontreponemal serologic tests for syphilis

Test[a]	Antigen storage temp (°C)	Sample type(s)	Readout
VDRL	2–8	Serum[b], CSF	Microscopic
USR	2–8	Serum	Microscopic
RPR	2–8	Serum, plasma	Macroscopic
TRUST	2–30	Serum, plasma	Macroscopic

[a]VDRL, Veneral Disease Research Laboratory; USR, unheated serum reagin test; RPR, rapid plasma reagin; TRUST, toluidine red unheated serum test.
[b]Serum must be heated to 56°C for 30 min prior to testing.

2. A slight roughness or no clumping indicates nonreactivity.
3. All tests with a reactive or nonreactive rough RPR card test result should be tested by the quantitative procedure.

F. For the quantitative test, prepare a serial dilution of sample (undiluted and diluted 1:2, 1:4, 1:8, and 1:16 with 0.9% saline) directly on the RPR card. Dilutions of >1:16 should be made with a 1:50 dilution of nonreactive serum in place of 0.9% saline.
G. Add 1 drop of antigen suspension to each circle.
H. Rotate the card for 8 min at 100 rpm under a humidifying cover.
I. Read the results as instructed above. The endpoint titer is reported as the highest dilution giving a reactive result.

Interpretation of Nontreponemal Tests

The nontreponemal tests offer the advantages of simplicity and low cost. In addition, they provide a semiquantitative result (titer) that can be used to monitor the response to therapy. Positive results in these tests usually reflect active infection. Resolution of infection is associated with a decline in titer. The four nontreponemal tests have similar sensitivities that vary by disease stage, ranging from 78 to 86% in primary infections, 100% in secondary infections, 95 to 98% in latent infections, and 71 to 73% in late latent syphilis infections (20). Falsely negative results are more likely encountered during early primary infection and late latent syphilis. Especially during secondary-stage infections, these tests can be susceptible to the prozone effect (21–23). High levels of nontreponemal antibodies (antibody excess) can cause apparently nonreactive results. Dilution of samples suspected of exhibiting a prozone is necessary to detect reactivity. As discussed in the following paragraphs, a treponemal test may be better suited to assess infection status during late latent syphilis because of the decrease in sensitivity of nontreponemal tests. Nontreponemal tests can be used and interpreted in a similar fashion in HIV-infected individuals. However, unusually low and high results have been encountered (12).

The CSF Venereal Disease Research Laboratory (VDRL) assay is the only test considered standard for CSF analysis. Its performance should be limited to patients with reactive serologic tests for syphilis (24), and it should be accompanied by a CSF cell count and protein determination. It is considered specific for neurosyphilis; however, its sensitivity is not optimal. A CSF cell count of >5 cells/μl and a protein level of >40 mg/dl in a seropositive individual are consistent with neurosyphilis in the absence of a reactive CSF VDRL assay.

The diagnosis of congenital syphilis requires clinical and serologic evaluation of the mother and child (25). Serologic testing of neonates should be performed on serum (not cord blood). The use of the serologic tests in infants at risk of or suspected of having congenital syphilis is confounded by maternal antibody. While some infants have been found to have nontreponemal titers 4-fold greater than the maternal titer (considered highly probable for congenital infection), this finding is not common (26). Follow-up testing with nontreponemal tests should demonstrate a decline in titer to nonreactivity by 6 months in untreated infants without infection.

Success of treatment can and should be monitored with quantitative nontreponemal titers collected 6 and 12 months after therapy (12). Effective therapy is associated in most cases with a 4-fold decline in titer and eventual seroreversion. However, the time to seroreversion may be influenced by the stage of infection during which therapy is started. Twenty percent, or more, of treated individuals may not serorevert and remain serofast (27, 28). Treponemal antibodies typically do not serorevert with therapy. Successful treatment of neurosyphilis results in a decline in nontreponemal titers in the CSF, in addition to in blood.

Nontreponemal tests have limitations. False-positive tests can be encountered in a variety of infections and autoimmune and malignant diseases, as well as during pregnancy and with advancing age (20). Although the four tests use the same basic antigen preparation, slight variations in the antigen can lead to differing degrees of reactivity. As such, these tests should not be used interchangeably when an individual is monitored longitudinally for therapeutic response. The same test should be used in these instances. Due to the potential for false-positive reactions with these nonspecific tests, reactive results should be confirmed by performing a test using *T. pallidum*-specific antigens, i.e., a treponemal antibody test.

Treponemal Antibody Tests

In contrast to the nontreponemal tests, treponemal antibody tests use *T. pallidum* organisms or antigens to detect the presence of antibodies (20). These tests have typically been used as confirmatory assays for samples with reactive nontreponemal test results. Because of their increased sensitivities compared to those of nontreponemal tests in late latent syphilis, they may be used as the first-line test in suspect patients. A variety of test methods have been used for the detection of treponemal antibodies (20). The most common assays currently employed (Table 2) include the fluorescent treponemal antibody absorption (FTA-ABS) test, the *T. pallidum* passive particle agglutination (TP-PA) test, enzyme immunoassay (EIA), and chemiluminescent immunoassay (CLIA).

The FTA-ABS (29, 30) test is an indirect fluorescent antibody test that employs glass slides with whole *T. pallidum* organisms fixed to the surface. Sera are first diluted in sorbent, an extract from *Treponema phagedenis*, to reduce false-positive reactions. Absorbed patient serum is applied to the wells and incubated. After the wells are washed, fluorescein isothiocyanate-conjugated anti-human immunoglobulin is added. If IgM and/or IgG antibodies are bound to the organisms on the slides, the fluorescein isothiocyanate conjugate will bind. Unbound anti-immunoglobulin is washed away, and the slides are then coverslipped and viewed with a fluorescence microscope. The presence of apple green treponemes is a positive test indicating the presence of *T. pallidum*-specific antibody. Results are reported as reactive, minimally reactive, or nonreactive or with atypical fluorescence observed. A version of this test that detects *T. pallidum*-specific IgM antibodies has been reported (31); however, it is not in common use.

EIAs (32, 33) are also available for the detection of *T. pallidum*-specific antibody. A number of assays using various antigens and enzyme-labeled anti-IgG or anti-immunoglobulin are available (33, 34). In addition, IgM-specific EIA is available in some laboratories and may be of use in the diagnosis of congenital or early infectious syphilis (26, 35). EIAs are amenable to automation and have replaced nontreponemal tests as screening assays (reverse syphilis testing algorithm) in many large laboratories with high testing volumes. Their sensitivities and specificities are comparable to those of standard treponemal assays (33). CLIAs, like EIAs are also increasingly used in reverse testing algorithms. These assays are available on random-access instruments which perform a variety of immunoassays simultaneously in a high-throughput fashion (36).

TABLE 2 Common treponemal antibody tests[a]

Test[b]	Sample type(s)	Equipment	Readout
MHA-TP	Serum	Minimal	Agglutination
TP-PA test	Serum, plasma	Minimal	Agglutination
FTA-ABS test	Serum, CSF	Fluorescence microscope	IFA
EIA	Serum	EIA reader, EIA washer	Indirect EIA[c]
CLIA	Serum	Automated analyzer	Chemiluminescence

[a]All reagents were stored at 2 to 8°C.
[b]MHA-TP, microhemagglutination test for *T. pallidum*; TP-PA, *T. pallidum* particle agglutination; FTA-ABS, fluorescent treponemal antibody absorption; EIA, enzyme immunoassay; CLIA, chemiluminescent immunoassay; IFA, indirect fluorescent antibody test.
[c]For *T. pallidum*-specific IgM detection, IgM-capture assays are preferred.

The TP-PA test (37, 38) is a modification of the microhemagglutination test for *T. pallidum* (39) that substitutes gelatin particles for red cells as the carrier of *T. pallidum* antigen. A gelatin particle suspension coated with *T. pallidum* antigen is incubated with patient serum. If *T. pallidum* antibody is present, the particles agglutinate and form a mat in the bottom of the well of the microtiter tray. If no antibody is present, the gelatin particles form a button in the bottom of the well. The test requires no expensive equipment and is simple to perform. This test has sensitivity and specificity similar to those of the other treponemal antibody tests. A procedural outline for the Serodia TP-PA (Fujirebio Diagnostics, Inc.) test is provided as an example.

A. Reconstitute lyophilized sensitized (*T. pallidum* antigen) or nonsensitized (control) gelatin particles.
B. Place 4 drops (100 μl) of sample diluent in well 1 and 1 drop (25 μl) in wells 2 through 4 of a U-bottom microtiter plate.
C. Add 25 μl of patient specimen (serum or plasma) or reactive or nonreactive control sera into the first wells of four rows.
D. Mix the contents of well 1 and transfer 25 μl into well 2. Mix the contents of well 2 and transfer 25 μl into well 3. Mix the contents of well 3 and transfer 25 μl into well 4. Mix the contents of well 4 and discard 25 μl of solution from that well.
E. Add 25 μl of unsensitized particles to well 3 and 25 μl of sensitized particles to well 4.
F. Mix the contents of the wells, cover the plate, and incubate it at room temperature for 2 h. The incubation can be extended to overnight.
G. Place the plate onto a flat surface, preferably with a white background, and observe the pattern of agglutination in each well. A plate viewer may be used to enhance the visual interpretation.
    1. A nonreactive result occurs when gelatin particles form a button or a ring with a small hole in the center at the center of the well.
    2. An inconclusive result occurs when gelatin particles from a ring with a hole in the center.
    3. A reactive result occurs when a large ring with a rough outer margin is visible and peripheral agglutination is surrounded by a small red circle (1+), the bottom of the well is covered with agglutinated particles surrounded by a red circle (2+), or a smooth mat of cells covers the entire bottom of the well with or without a faint ring (3+).

A specimen that is nonreactive with unsensitized particles and reactive with sensitized particles is interpreted as reactive in this test. If a serum specimen demonstrates a positive reaction with both the sensitized and unsensitized particles, it can be retested by an absorption procedure. Specimens that are nonreactive with unsensitized particles but have an inconclusive reaction with sensitized particles are classified as having inconclusive results. The assay should be rerun or a new sample obtained for testing. Samples that are nonreactive with sensitized particles are classified as nonreactive.

Interpretation of Treponemal Tests

A reactive treponemal test is consistent with current or past infection. The sensitivities of the tests are similar to those of nontreponemal tests in primary infection (76 to 84%), secondary infection (100%), and latent infection (97 to 100%). They perform better in patients with late latent syphilis, however, as most people maintain treponemal antibodies for many years. Whether infections are cleared naturally or with antibiotics, people usually remain reactive (20). The use of the FTA-ABS test on CSF has been found to be more sensitive but less specific than the CSF VDRL test. As such, it has been considered to rule out neurosyphilis if it is negative. One must be particularly cognizant of the potential for false-positive reactivity if the CSF sample is contaminated with blood (40).

Although these tests use *T. pallidum* antigen, false-positive results can be encountered in healthy individuals (41) and in those with a variety of diseases (20). Recognized causes of false-positive results include infections with related spirochetes, systemic lupus erythematosus and other autoimmune diseases, and aging.

Rapid Point-of-Care Tests

A number of rapid tests for syphilis have been developed (42) in response to the need to provide testing in resource-limited settings where traditional serologic tests for syphilis may not be feasible or optimal for routine use. Point-of-care tests provide a fast, simple means to diagnose syphilis in both clinical and nonclinical settings, addressing the need to increase testing in these areas (43). These tests are commonly formatted as an immunochromatographic assay using treponemal antigens. One test has received CLIA-waived status, the Syphilis Health Check (Diagnostics Direct). A recent survey of 15 published studies calculated a median sensitivity of 86% and a specificity of 99% for rapid tests, which is comparable to those of nontreponemal screening (44).

QUALITY CONTROL AND ASSURANCE

Specific, detailed quality control practices are provided in the manual of tests for syphilis (19). Positive and negative

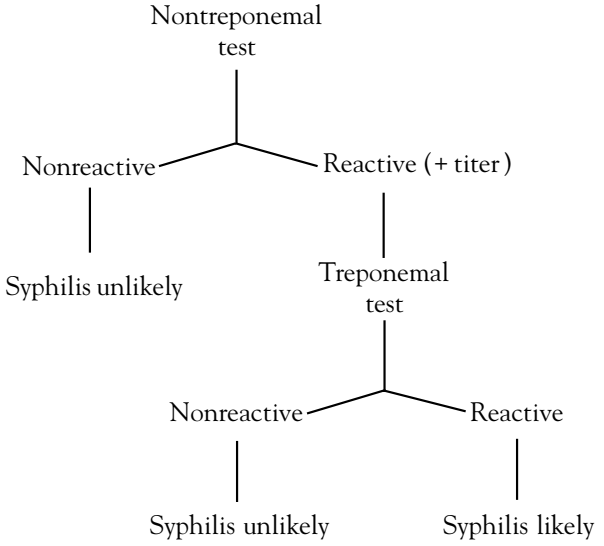

FIGURE 1 Traditional algorithm.

controls are available and run each day that the tests are performed. Detailed daily monitoring of equipment (e.g., needles and rotators for nontreponemal tests) is required to ensure consistency of results. External proficiency testing for syphilis serologic testing is available from several vendors, including the College of American Pathologists. Samples are provided for nontreponemal and treponemal testing of serum and VDRL testing of CSF. Proficiency testing for direct detection methods is not available, and laboratories must implement systems to assess proficiency for accreditation purposes.

TESTING ALGORITHMS

The classic approach for serologic diagnosis of infectious syphilis in adults is the standard algorithm (Fig. 1). In this approach, sera are first tested for the presence of nontreponemal antibody. If reactive in undiluted sera, the samples are serially diluted to determine the endpoint titer. Reactive results may indicate active infection. However, due to the potential for false-positive reactions with nontreponemal tests, reactive samples are confirmed with a treponemal antibody test. Treponemal tests are performed in a qualitative fashion, and titrations are not performed. A reactive treponemal result confirms syphilis infection. The limitations of this approach are its insufficient sensitivity in very early and late latent syphilis. In cases in which late latent syphilis is suspected after a nonreactive nontreponemal test, initial testing by treponemal methods is warranted.

Recently, an alternative to the standard algorithm has been employed. The reverse sequence testing algorithm (Fig. 2) is an alternative approach that employs a treponemal test, usually an EIA or CLIA, as the screening assay. If positive, a nontreponemal antibody test, such as RPR, is performed, and if the sample is reactive**,** a titer is obtained. In the case of a nonreactive nontreponemal test result, an alternative treponemal test (e.g., FTA-ABS or TP-PA test) is recommended to determine if the screening EIA or CLIA was falsely positive. It should be kept in mind that highly sensitive CLIA assays may detect lower levels of antibody than standard treponemal tests (FTA-ABS and TP-PA tests), which might lead to discordant results not due to a false-positive result.

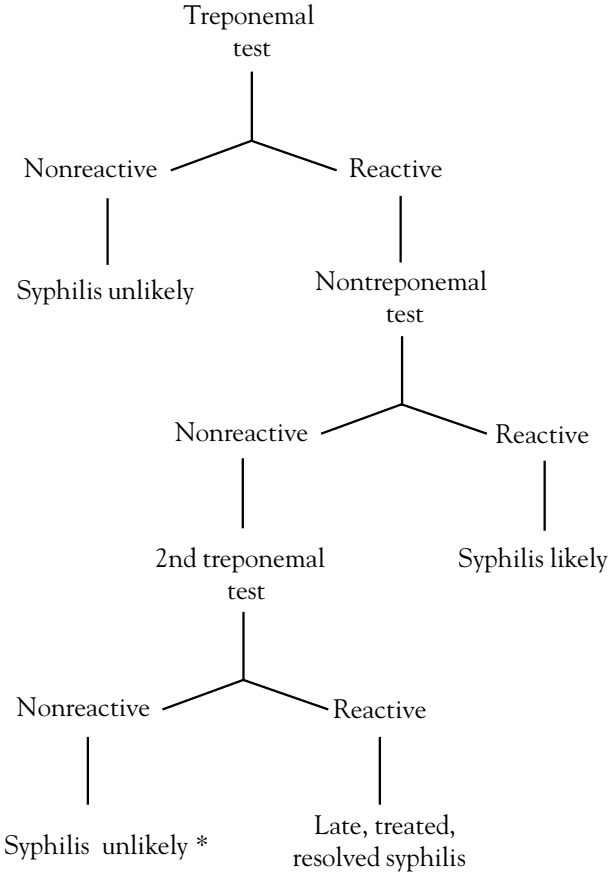

FIGURE 2 Reverse algorithm. *, may indicate a false-positive screening test result; however, a very sensitive screening test, such as CLIA, might be positive when the standard treponemal test is nonreactive.

The false-positivity rates of the screening EIAs or CLIAs vary based on the prevalence of syphilis in the population being tested (45). This approach has been developed in part to accommodate large test runs, rapid turnaround times, and objective analyses, as favored by commercial reference laboratories. In addition, it can effectively detect very early or late latent syphilis that may be missed with the standard algorithm (46, 47). However, sera that are confirmed treponemal-test reactive but nontreponemal-test nonreactive may present a more challenging interpretation. They may arise from cases of untreated late latent syphilis or syphilis treated in the past.

REFERENCES

1. **Wassermann AANCB.** 1906. Eine serodiagnostische Reaktion bei Syphilis. *Dtsch Med Wochenschr* **32:**745–746.
2. **Patton ME, Su JR, Nelson R, Weinstock H.** 2014. Primary and secondary syphilis—United States, 2005–2013. *MMWR Morb Mortal Wkly Rep* **63:**402–406.
3. **Walker DG, Walker GJ.** 2004. Prevention of congenital syphilis—time for action. *Bull World Health Organ* **82:**401.
4. **Marangoni A, Sambri V, Cavrini F, Frabetti A, Storni E, Accardo S, Servidio D, Foschi F, Montebugnoli L, Prati C, Cevenini R.** 2005. *Treponema denticola* infection is not a cause of false positive *Treponema pallidum* serology. *New Microbiol* **28:**215–221.

5. **Hook EW III, Marra CM.** 1992. Acquired syphilis in adults. *N Engl J Med* **326:**1060–1069.
6. **Zou S, Stramer SL, Dodd RY.** 2012. Donor testing and risk: current prevalence, incidence, and residual risk of transfusion-transmissible agents in US allogeneic donations. *Transfus Med Rev* **26:**119–128.
7. **Tariciotti L, Das I, Dori L, Perera MT, Bramhall SR.** 2012. Asymptomatic transmission of *Treponema pallidum* (syphilis) through deceased donor liver transplantation. *Transpl Infect Dis* **14:**321–325.
8. **Greenblatt RM, Lukehart SA, Plummer FA, Quinn TC, Critchlow CW, Ashley RL, D'Costa LJ, Ndinya-Achola JO, Corey L, Ronald AR, Holmes KK.** 1988. Genital ulceration as a risk factor for human immunodeficiency virus infection. *AIDS* **2:**47–50.
9. **Palacios R, Jimenez-Onate F, Aguilar M, Galindo MJ, Rivas P, Ocampo A, Berenguer J, Arranz JA, Rios MJ, Knobel H, Moreno F, Ena J, Santos J.** 2007. Impact of syphilis infection on HIV viral load and CD4 cell counts in HIV-infected patients. *J Acquir Immune Defic Syndr* **44:**356–359.
10. **Zellan J, Augenbraun M.** 2004. Syphilis in the HIV-infected patient: an update on epidemiology, diagnosis, and management. *Curr HIV/AIDS Rep* **1:**142–147.
11. **Woods CR.** 2005. Syphilis in children: congenital and acquired. *Semin Pediatr Infect Dis* **16:**245–257.
12. **Workowski KA, Berman S.** 2010. Sexually transmitted diseases treatment guidelines, 2010. *MMWR Recomm Rep* **59:**1–110.
13. **Kennedy EJ, Creighton ET.** 1998. Dark field microscopy for the detection and identification of *Treponema pallidum*, p 118–134. *In* Larsen SA, Pope V, Johnson RE, Kennedy EJ (ed), *A Manual of Tests for Syphilis*, 9th ed. American Public Health Association, Washington, DC.
14. **Romanowski B, Forsey E, Prasad E, Lukehart S, Tam M, Hook EW III.** 1987. Detection of *Treponema pallidum* by a fluorescent monoclonal antibody test. *Sex Transm Dis* **14:**156–159.
15. **George RW, Hunter EF, Fears MB.** 1998. Direct fluorescent antibody test for *Treponema pallidum* (DFA-TP), p 135–146. *In* Larsen SA, Pope V, Johnson RE, Kennedy EJ (ed), *A Manual of Tests for Syphilis*, 9th ed. American Public Health Association, Washington, DC.
16. **George RW, Hunter EF, Fears MB.** 1998. Direct fluorescent antibody tissue test for *Treponema pallidum* (DFAT-TP), p 147–156. *In* Larsen SA, Pope V, Johnson RE, Kennedy EJ (ed), *A Manual of Tests for Syphilis*, 9th ed. American Public Health Association, Washington, DC.
17. **Gayet-Ageron A, Lautenschlager S, Ninet B, Perneger TV, Combescure C.** 2013. Sensitivity, specificity and likelihood ratios of PCR in the diagnosis of syphilis: a systematic review and meta-analysis. *Sex Transm Infect* **89:**251–256.
18. **Belisle JT, Brandt ME, Radolf JD, Norgard MV.** 1994. Fatty acids of *Treponema pallidum* and *Borrelia burgdorferi* lipoproteins. *J Bacteriol* **176:**2151–2157.
19. **Larsen SA, Pope V, Johnson RE, Kennedy EJ (ed).** 1998. *A Manual of Tests for Syphilis*, 9th ed. American Public Health Association, Washington, DC.
20. **Larsen SA, Steiner BM, Rudolph AH.** 1995. Laboratory diagnosis and interpretation of tests for syphilis. *Clin Microbiol Rev* **8:**1–21.
21. **Liu LL, Lin LR, Tong ML, Zhang HL, Huang SJ, Chen YY, Guo XJ, Xi Y, Liu L, Chen FY, Zhang YF, Zhang Q, Yang TC.** 2014. Incidence and risk factors for the prozone phenomenon in serologic testing for syphilis in a large cohort. *Clin Infect Dis* **59:**384–389.
22. **Post JJ, Khor C, Furner V, Smith DE, Whybin LR, Robertson PW.** 2012. Case report and evaluation of the frequency of the prozone phenomenon in syphilis serology—an infrequent but important laboratory phenomenon. *Sex Health* **9:**488–490.
23. **el-Zaatari MM, Martens MG, Anderson GD.** 1994. Incidence of the prozone phenomenon in syphilis serology. *Obstet Gynecol* **84:**609–612.
24. **Albright RE Jr, Christenson RH, Emlet JL, Graham CB III, Estevez EG, Wilson ML, Reller LB, Schneider KA.** 1991. Issues in cerebrospinal fluid management. CSF Venereal Disease Research Laboratory testing. *Am J Clin Pathol* **95:**397–401.
25. **Workowski KA, Bolan GA.** 2015. Sexually transmitted diseases treatment guidelines, 2015. *MMWR Recomm Rep* **64:**1–137.
26. **Schmitz JL, Gertis KS, Mauney C, Stamm LV, Folds JD.** 1994. Laboratory diagnosis of congenital syphilis by immunoglobulin M (IgM) and IgA immunoblotting. *Clin Diagn Lab Immunol* **1:**32–37.
27. **Sena AC, Wolff M, Martin DH, Behets F, Van Damme K, Leone P, Langley C, McNeil L, Hook EW.** 2011. Predictors of serological cure and serofast state after treatment in HIV-negative persons with early syphilis. *Clin Infect Dis* **53:**1092–1099.
28. **Tong ML, Lin LR, Liu GL, Zhang HL, Zeng YL, Zheng WH, Liu LL, Yang TC.** 2013. Factors associated with serological cure and the serofast state of HIV-negative patients with primary, secondary, latent, and tertiary syphilis. *PLoS One* **8:**e70102.
29. **Hunter EF, Deacon WE, Meyer PE.** 1964. An improved FTA test for syphilis, the absorption procedure (FTA-ABS). *Public Health Rep* **79:**410–412.
30. **George RW, Hunter EF, Fears MB.** 1998. Fluorescent treponemal antibody-absorption (FTA-ABS) test, p 223–245. *In* Larsen SA, Pope V, Johnson RE, Kennedy EJ (ed), *A Manual of Tests for Syphilis*, 9th ed. American Public Health Association, Washington, DC.
31. **Ozanne G, d'Halewyn MA, Larsen SA.** 1993. Comparison of the fluorescent treponemal antibody absorption (FTA-ABS) test with the FTA-ABS double staining test for detection of antitreponemal immunoglobulin M in the 19S fraction of human serum. *J Clin Microbiol* **31:**102–106.
32. **Nayar R, Campos JM.** 1993. Evaluation of the DCL Syphilis-G enzyme immunoassay test kit for the serologic diagnosis of syphilis. *Am J Clin Pathol* **99:**282–285.
33. **Cole MJ, Perry KR, Parry JV.** 2007. Comparative evaluation of 15 serological assays for the detection of syphilis infection. *Eur J Clin Microbiol Infect Dis* **26:**705–713.
34. **Sena AC, White BL, Sparling PF.** 2010. Novel *Treponema pallidum* serologic tests: a paradigm shift in syphilis screening for the 21st century. *Clin Infect Dis* **51:**700–708.
35. **Lefevre JC, Bertrand, Andreo M, Gauthier G, Groupe Etude et Prevention des Maladies Transmissibles, Sexuellement.** 1989. Evaluation of an IgM antibody capture enzyme immunoassay Captia Syphilis-M in treated and untreated syphilis. *J Chemother* **1:**898–899.
36. **Knight CS, Crum MA, Hardy RW.** 2007. Evaluation of the LIAISON chemiluminescence immunoassay for diagnosis of syphilis. *Clin Vaccine Immunol* **14:**710–713.
37. **Castro RR, Prieto ES, Santo I, Azevedo J, Exposto FL.** 2001. Evaluation of the passive particle agglutination test in the serodiagnosis and follow-up of syphilis. *Am J Clin Pathol* **116:**581–585.
38. **Pope V, Fears MB.** 1998. Serodia *Treponema pallidum* passive particle agglutination (TP-PA) test, p 365–378. *In* Larsen SA, Pope V, Johnson RE, Kennedy EJ (ed), *A Manual of Tests for Syphilis*, 9th ed. American Public Health Association, Washington, DC.
39. **Rathlev T.** 1967. Haemagglutination test utilizing pathogenic *Treponema pallidum* for the sero-diagnosis of syphilis. *Br J Vener Dis* **43:**181–185.

40. **Davis LE, Sperry S.** 1979. The CSF-FTA test and the significance of blood contamination. *Ann Neurol* **6:**68–69.
41. **Goldman JN, Lantz MA.** 1971. FTA-ABS and VDRL slide test reactivity in a population of nuns. *JAMA* **217:**53–55.
42. **Kay NS, Peeling RW, Mabey DC.** 2014. State of the art syphilis diagnostics: rapid point-of-care tests. *Expert Rev Anti Infect Ther* **12:**63–73.
43. **Low N, Broutet N, Adu-Sarkodie Y, Barton P, Hossain M, Hawkes S.** 2006. Global control of sexually transmitted infections. *Lancet* **368:**2001–2016.
44. **Tucker JD, Bu J, Brown LB, Yin YP, Chen XS, Cohen MS.** 2010. Accelerating worldwide syphilis screening through rapid testing: a systematic review. *Lancet Infect Dis* **10:**381–386.
45. **Centers for Disease Control and Prevention.** 2011. Discordant results from reverse sequence syphilis screening—five laboratories, United States, 2006–2010. *MMWR Morb Mortal Wkly Rep* **60:**133–137.
46. **Binnicker MJ, Jespersen DJ, Rollins LO.** 2012. Direct comparison of the traditional and reverse syphilis screening algorithms in a population with a low prevalence of syphilis. *J Clin Microbiol* **50:**148–150.
47. **Gratrix J, Plitt S, Lee BE, Ferron L, Anderson B, Verity B, Prasad E, Bunyan R, Zahariadis G, Singh AE.** 2012. Impact of reverse sequence syphilis screening on new diagnoses of late latent syphilis in Edmonton, Canada. *Sex Transm Dis* **39:**528–530.
48. **World Health Organization.** 2008. *Global Incidence and Prevalence of Selected Curable Sexually Transmitted Infections—2008*. World Health Organization, Geneva, Switzerland. http://apps.who.int/iris/bitstream/10665/75181/1/9789241503839_eng.pdf?ua=1

Lyme Disease, Relapsing Fever, and Leptospirosis

GUIQING WANG AND MARIA E. AGUERO-ROSENFELD

47

Lyme disease, relapsing fever, and leptospirosis are infections caused by spirochetes, a phylogenetically ancient and distinct group of microorganisms among the prokaryotes.

The taxonomy of the spirochetes has undergone significant revisions during the past decade. While all spirochetes remain in a single order, *Spirochaetales*, in the class *Spirochaetia* of the phylum *Spirochaetes* phy. nov., the order *Spirochaetales* has been reclassified into four families in the second edition of *Bergey's Manual of Systematic Bacteriology: Spirochaetaceae* (family I), *Brachyspiraceae* (family II), *Brevinemataceae* (family III), and *Leptospiraceae* (family IV) (1). The family *Spirochaetaceae* consists of four genera: *Spirochaeta* (genus I), *Borrelia* (genus II), *Cristispira* (genus III), and *Treponema* (genus IV). Family *Brachyspiraceae* contains a single genus, *Brachyspira*. Family *Brevinemataceae* fam. nov. has recently been validated with one genus, *Brevinema*. Family *Leptospiraceae* encompasses three genera: *Leptospira*, *Leptonema*, and *Turneriella* (1).

Three genera of spirochetes, *Borrelia*, *Leptospira*, and *Treponema*, are pathogenic to humans and are associated with Lyme disease and relapsing fever, leptospirosis, and syphilis, respectively. This chapter focuses on the laboratory diagnosis of Lyme disease, relapsing fever, and leptospirosis. The diagnosis of syphilis is presented in chapter 46 of this *Manual*.

LYME DISEASE

Taxonomy of Lyme *Borrelia*

The genus *Borrelia* comprises more than 40 species of arthropod vector-borne spirochetes that can be classified into two major groups. The first group of spirochetes contains 19 *Borrelia* species that have been validated or proposed since 1984 (2–4). The term "*Borrelia burgdorferi sensu lato*" has been collectively used to refer to all *Borrelia* species and isolates in this group. *Borrelia* species in the first group are transmitted by the hard *Ixodes* ticks and are associated with Lyme disease, or Lyme borreliosis (3). The second group of spirochetes includes 25 validated or proposed *Borrelia* species transmitted by soft ticks *Argasidae* with a few exceptions (i.e., louse-borne *B. recurrentis* and hard-tick-borne *Borrelia miyamotoi* and *Borrelia lonestari*). *Borrelia* species in the second major group are associated with human relapsing fever (RF). The term "relapsing fever *Borrelia*" has been used to refer to all *Borrelia* species and isolates in this group (5). In this chapter, we use the terms "Lyme *Borrelia*" to refer to *B. burgdorferi sensu lato* and "RF *Borrelia*" to refer to relapsing-fever-related *Borrelia* species.

Table 1 summarizes the characteristics of selected *Borrelia* species associated with human Lyme disease and relapsing fever. A complete list of current *Borrelia* species and their differential characteristics can be found in the recently published *Bergey's Manual of Systematic Bacteriology* (5).

Fourteen validated *Borrelia* species belong to the Lyme *Borrelia* group. They are *B. burgdorferi sensu stricto*, *Borrelia garinii*, *Borrelia afzelii*, *Borrelia japonica*, *Borrelia valaisiana*, *Borrelia lusitaniae*, *Borrelia tanukii*, *Borrelia turdi*, *Borrelia sinica*, *Borrelia spielmanii*, *Borrelia americana*, *Borrelia carolinensis*, *Borrelia bivariensis*, and *Borrelia kurtenbachii*. Among these, only *B. burgdorferi sensu stricto*, *B. garinii*, *Borrelia bivariensis*, and *B. afzelii* are well known to cause human diseases. Rare cases associated with infections of *B. valaisiana*, *B. lusitaniae*, and *B. spielmanii* have been reported; the pathogenicity of these species in humans remains to be elucidated.

Five additional *Borrelia* species in the Lyme *Borrelia* group have been proposed, but their taxonomic status has not been validly published due to the lack of sufficient data. These are *Borrelia andersonii*, *Borrelia bissettii*, *Borrelia californiensis*, *Borrelia yangtze*, and *Borrelia finlandensis*.

Epidemiology and Disease Spectrum

Lyme disease is widely distributed in the northern hemisphere among patients residing in North America, Europe, and Asia. It is the most common vector-borne disease in North America and Europe. Between 1992 and 2011, a total of 439,738 cases of Lyme disease, with an average of approximately 20,000 cases each year, were reported to the Centers for Disease Control and Prevention (CDC) in the U.S. Over 30,000 confirmed and probable cases are reported annually in recent years, while it is estimated that the number of annual cases may be more than 300,000, if including those unreported patients (6). Most reported Lyme disease cases in the U.S. are from the northeastern and midwestern states. In 2012, 95% of Lyme disease cases were reported from 13 states: Connecticut, Delaware, Maine, Maryland, Massachusetts, Minnesota, New Hampshire, New Jersey, New York, Pennsylvania, Vermont, Virginia, and Wisconsin (7).

Areas of endemic Lyme disease in Europe include the British Isles, Scandinavia, western Europe and states of

doi:10.1128/9781555818722.ch47

TABLE 1 Characteristics of selected *Borrelia* species associated with Lyme disease and relapsing fever[a]

Taxon	Vector	Host	Distribution	Disease
Borrelia burgdorferi sensu lato				
B. afzelii	*Ixodes ricinus*, *Ixodes persulcatus*	Rodents	Europe, Asia	Lyme borreliosis
B. bavariensis	*Ixodes ricinus*, *Ixodes persulcatus*	Birds, rodents	Europe, Asia	Lyme borreliosis
B. bissettii	*Ixodes pacificus*, *Ixodes spinipalpis*, *Ixodes scapularis*	Rodents, birds	U.S., Europe?	Probably Lyme borreliosis
B. burgdorferi sensu stricto	*Ixodes scapularis*, *Ixodes pacificus*, *Ixodes ricinus*	Rodents, birds	U.S., Europe	Lyme borreliosis
B. garinii	*Ixodes ricinus*, *Ixodes persulcatus*	Birds, rodents	Europe, Asia	Lyme borreliosis
B. lusitaniae	*Ixodes ricinus*	Rodents, lizards	Central Europe	Probably Lyme borreliosis
B. spielmanii	*Ixodes ricinus*	Rodents	Europe	Probably Lyme borreliosis
B. valaisiana	*Ixodes ricinus*, *Ixodes nipponensis*, *Ixodes columnae*	Rodents, birds	Europe, Asia	Probably Lyme borreliosis
Relapsing fever borreliae				
B. baltazardii	Unknown	Unknown	Iran	Tick-borne relapsing fever
B. caucasica	*Ornithodoros verrucosus*	Rodents, humans	Caucasus	Tick-borne relapsing fever
B. coriaceae	*Ornithodoros coriaceus*	Probably deer	Western U.S.	Probably epizootic bovine abortion
B. crocidurae	*Ornithodoros sonrai*	Rodents, humans	Africa, Near East, Central Asia	Tick-borne relapsing fever
B. duttonii	*Ornithodoros moubata*	Man	Africa	Tick-borne relapsing fever
B. graingeri	*Ornithodoros graingeri*	Rodents, humans	East Africa	Tick-borne relapsing fever
B. hermsii	*Ornithodoros hermsi*	Rodents, humans	Western U.S. and Canada	Tick-borne relapsing fever
B. hispanica	*Ornithodoros erraticus*	Rodents, humans	Spain, Portugal, Morocco, Algeria, Tunisia	Tick-borne relapsing fever
B. lonestari	*Amblyomma americanum*	Rodents, birds?	Southeastern U.S.	Lyme-like illness? (Southern tick-associated rash illness)
B. latyschewii	*Ornithodoros tartakov-*	Rodents, reptiles, humans	Iran, Central Asia	Tick-borne relapsing fever
B. mazzottii	*Ornithodoros talaje*	Rodents, armadillos, monkeys, humans	Mexico and Guatemala	Tick-borne relapsing fever
B. miyamotoi	*Ixodes persulcatus*, *Ixodes scapularis*, *Ixodes ricinus*	Rodents	Japan, U.S., Sweden	Tick-borne borreliosis
B. parkeri	*Ornithodoros parkeri*	Rodents, humans	Western U.S.	Tick-borne relapsing fever
B. persica	*Ornithodoros tholozani*	Rodents, bats, humans	Middle East, Central Asia	Tick-borne relapsing fever
B. recurrentis	*Pediculus humanus*, subsp. *humanus*	Man	South America, Europe, Africa, Asia	Louse-borne relapsing fever
B. turicatae	*Ornithodoros turicatae*	Rodents, humans	U.S. and Mexico	Tick-borne relapsing fever
B. venezuelensis	*Ornithodoros rudis*	Rodents, humans	Central and South America	Tick-borne relapsing fever

[a]Adapted from reference 5.

the former USSR, from the Baltic States east through Russia to the Pacific Coast. It is estimated that more than 50,000 Lyme disease cases occur annually in the European countries (8). Lyme disease is also well documented in far-eastern Russia, Japan, and China.

B. burgdorferi is transmitted among reservoirs and hosts by ticks of the family *Ixodidae*, mainly ticks in the *Ixodes ricinus* complex. *Ixodes scapularis* and *I. pacificus* in the U.S. and *I. ricinus* and *I. persulcatus* in Eurasia are the principal vectors of the spirochaetes. The prevalence rate of *B. burgdorferi* in *I. scapularis* collected from endemic areas of the U.S. varies from 12% to almost 100% (9), and in *I. ricinus* in Europe from 0 to 58% (10). Coinfection with *B. burgdorferi* and other tick-borne pathogens such as *Babesia* sp. and *Anaplasma* sp. has been reported.

Clinical manifestations of human Lyme disease depend upon the stage of the infection and may affect dermatological, neurological, cardiac, and musculoskeletal systems (Table 2). Stage 1 consists of early infection (localized erythema migrans, EM), followed by stage 2 (disseminated infection) within days or weeks. Stage 3 (late infection) may develop months or years after the disease onset.

The clinical manifestations of Lyme disease also vary depending on the *Borrelia* species causing the disease. Although all species cause EM as the early manifestation, *B. burgdorferi sensu stricto* more frequently causes arthritis, and *B. afzelii* causes acrodermatitis chronica atrophicans (ACA) as late manifestations. By contrast, *B. garinii* is more frequently associated with early neurological manifestations (radiculoneuritis) (3).

EM is the clinical hallmark of early Lyme disease. It is recognized in about 60 to 80% of the patients with objective clinical evidence of *B. burgdorferi* infection (11). The rash typically begins at the site of the tick bite as an expanding red macule (erythema), sometimes with central clearing. At this stage, patients may be either asymptomatic or present with flu-like symptoms, such as headache, myalgia, arthralgias, and fever.

TABLE 2 Clinical manifestations of Lyme disease and specimen types for laboratory diagnosis

Clinical manifestation	Specimen for culture or PCR	Specimen for serologic testing
Stage I (early or localized infection): EM	Skin biopsy	Serum
	Plasma (10 to 20 ml for culture)	
Stage II (early or disseminated infection)		
Multiple EM	Skin biopsy	Serum
	Plasma (10 to 20 ml for culture)	
Lyme carditis		Serum
Neuroborreliosis	CSF	Serum and CSF
Stage III (late infection)		
Lyme arthritis	Synovial fluid or tissue	Serum
ACA	Skin biopsy	Serum
Neuroborreliosis	CSF	Serum and CSF

Dissemination of *B. burgdorferi* to the nervous system, joints, heart or other skin areas, and occasionally to other organs may give rise to a wide spectrum of manifestations in the involved systems. Usually, patients at this stage experience one or more of the following syndromes: multiple EM lesions, Lyme carditis, arthritis, and early neuroborreliosis including meningoradiculoneuritis (Bannwarth's syndrome), meningitis, meningoencephalitis, and/or facial palsy.

Late Lyme disease may develop among some untreated patients months to years after the onset of the disease. The major manifestations of late Lyme disease include Lyme arthritis, chronic neuroborreliosis and ACA. Post-Lyme disease syndrome, characterized by persistent arthralgia or neurocognitive or fatigue syndrome, has been reported in a small percentage of patients. There is currently no evidence that such persistent subjective symptoms are caused by active *B. burgdorferi* infection.

The diagnosis of Lyme disease can easily be made in an endemic area when the characteristic skin lesions, i.e., EM, borrelial lymphocytoma at typical sites (nipple or ear lobe) or ACA, are present. These last two clinical manifestations are most frequently seen in Europe. A history of a recent tick bite may be supportive, but only 30 to 54% of the culture-confirmed EM patients could recall a tick bite (12). In patients with EM, laboratory testing is neither necessary nor recommended (13). Diagnosis of Lyme disease on the basis of the presence of manifestations other than EM is challenging. Thus, laboratory confirmation is necessary for the diagnosis of Lyme disease in these patients.

Laboratory Diagnosis

Laboratory approaches for diagnosis of Lyme disease include direct detection of the spirochete or nucleic acid by culture and PCR, and indirect measurement of Lyme *Borrelia*-specific antibodies in suspected patients by various immunologic test methods. Because of limited utility of direct detection of *B. burgdorferi* in clinical specimens by culture and PCR assay, serology is currently the mainstay of laboratory testing to support the clinical diagnosis of Lyme disease, especially in patients with atypical EM and late Lyme disease. Elevated specific antibody to *B. burgdorferi* titers can usually be demonstrated.

Immunologic Test Methods

The U.S. FDA has approved over 70 commercial assays for serodiagnosis of Lyme disease since the late 1980s. It is estimated that 2.8 million to 3.4 million serologic tests for Lyme disease, with a cost of more than $100 million, are performed annually in the U.S. (13). Similarly, the overall expected cost for Lyme disease serologic testing and treatment is approximately 51 million Euros in Germany alone (14).

Lyme *Borrelia* Antigens of Importance in Immunodiagnosis

Protein profile analysis shows that the whole-cell lysates of the Lyme *Borrelia* comprise more than 50 visible protein bands in silver- or Coomassie blue-stained polyacrylamide gels. The *Borrelia* antigens of importance in serodiagnosis of early Lyme disease include flagellin (41 kDa), outer surface lipoprotein C (OspC, 21 to 25 kDa), Borrelia membrane protein A (P39 or BmpA, ~39 kDa), and Vmp-like protein (VlsE, 25 kDa). Patients with early Lyme disease usually develop antibodies against these antigens. Thus, IgM antibodies to these antigens are of most diagnostic importance in early Lyme disease.

Flagellin is an important structural and functional protein of *Borrelia* spp. It is a highly immunogenic and cross-reactive antigen. Strong IgG and IgM responses to this protein are developed within a few days after infection with the Lyme *Borrelia*. Many currently available immunoassays consist of purified flagella alone or have it as an antigenic mixture. Although highly immunogenic, this antigen is highly cross-reactive with antigens in other bacteria, particularly when denatured, as in immunoblots. Certain flagellin epitopes are also cross-reactive with antigens found in mammalian tissues such as neural tissues, synovium, and myocardial muscle. P39 is another conserved outer-surface lipoprotein among Lyme *Borrelia* that is highly immunogenic. IgG antibody against P39 is detectable in 15 to 64% of Lyme disease patients, depending on the clinical stage at which the sample is taken (15).

The Lyme *Borrelia* has a large number of surface-exposed lipoproteins, encoded by genes located on plasmids (16). Two of these lipoproteins, OspC and VlsE, are differentially expressed in different environmental conditions that the organism encounters. By contrast to OspA, which is expressed while *B. burgdorferi* is located in the midgut of the unfed tick, the expression of OspC is upregulated in the presence of blood components and at higher temperatures (35 to 37°C versus 25°C), i.e., after the tick obtains a blood meal from the susceptible mammal. The VlsE is a surface-exposed lipoprotein in Lyme *Borrelia* with functional similarity to the variable membrane proteins (Vmps) in RF borreliae. Although VlsE undergoes extensive antigenic variation *in vivo*, antibodies against an invariable region of the VlsE (IR6) are detectable in patients with acute EM and late stages of clinical disease and have been used for serodiagnosis of Lyme disease.

As disease progresses, antibodies to a larger number of borrelial antigens will develop, as will occur in any infectious disease. Therefore, patients with late manifestations of Lyme disease have antibodies to a larger number of antigens, such as to the 93-, 66-, 58-, 30-, 28-, and 18-kDa antigens. Untreated patients presenting with later manifestations of the disease are expected to present with a higher amount of antibodies reacting to a larger number of *B. burgdorferi* antigens. Lack of antibodies in a patient presenting with late manifestations of Lyme disease will make the diagnosis unlikely.

IFA for Antibody Detection

IFA uses cultured organisms fixed onto glass slides. Serum specimens are diluted in preparations that may include an absorbent such as material derived from Reiter treponema or egg yolk sac to remove nonspecific antibodies. After addition of fluorescein isothiocyanate-labeled anti-human IgG or IgM, the presence of antibodies is detected by fluorescence microscopy. Specimens testing reactive at screening dilutions are serially diluted. In general, antibody titers of $\geq$64 and $\geq$256 are considered as positive on the IFA with and without prior absorption, respectively (17). Limitations of this assay include the need for fluorescence microscopy and for well-trained personnel and the subjectivity in reading and interpreting fluorescence microscopy. Although IFAs are still commercially available, they have been largely replaced by enzyme immunoassays such as enzyme-linked immunosorbent technology (ELISA or EIA), and Western immunoblot.

Enzyme Immunoassays for Antibody Detection

The most common methods for detection of antibodies to *B. burgdorferi* are ELISA (13). Most of these assays use the whole-cell lysate of *B. burgdorferi* strain B31 as the source of antigen. Other strains of *B. burgdorferi* have been used in assays developed in the United States, and various Lyme *Borrelia* (*B. burgdorferi*, *B. garinii* and *B. afzelii*) species have been employed in in-house or commercial assays available in Europe. The antigen for whole-cell lysate-based assays is typically a complex mixture containing multiple immunogenic proteins, lipoproteins and carbohydrates. ELISA assays that detect IgM and IgG antibodies to *B. burgdorferi* routinely include a low-positive control used to assess the reactivity of patient samples. Patient reactivity (optical density, OD) is divided by the low-positive control and an index is calculated. Frequently, sera with an index of $<$0.8 are considered negative (nonreactive); those with an index of $>$0.8 to $<$1.09 are considered equivocal, and those with an index of $>$1.09 are considered positive.

Using sonicated whole-cell preparations of low-passage *B. burgdorferi sensu lato*, the sensitivity of ELISA is in general less than 50% in acute-phase sera of patients with EM of a duration of $<$1 week. Sensitivity increases over time after the first week in untreated patients with EM. Sensitivity is also high in patients with EM presenting with constitutional signs and symptoms or in those who have multiple EMs. Sensitivity is very high in patients with objective evidence of extracutaneous involvement (e.g., carditis or neuroborreliosis). ELISA is almost invariably positive in sera of patients with late disease such as arthritis.

The Lyme ELISA has advantages over other immunoassays, including ease of testing, objective generation of numerical values that correlate in relative terms with the quantity of antibodies present, and the capability of automation. One of the limitations of ELISA for detection of *B. burgdorferi sensu lato* antibodies is lack of standardization. Variations exist between assays in terms of antigenic composition and in the detection of specific immunoglobulin classes, particularly in the detection of IgM antibodies. Such variations may occur among different commercial kits as well as between lots of the same kit. Another limitation of the Lyme ELISA is the lack of specificity due to the use of whole-cell antigen preparations. The specificity of ELISA for detection of *B. burgdorferi* antibodies varies from 72 to 97% (13, 18).

Western Immunoblot for Antibody Detection

Whether *B. burgdorferi sensu lato* antigens elicit IgM versus IgG antibodies depends on the duration of infection and the manifestation of Lyme disease. The use of immunoblot assay allows the determination of which Lyme *Borrelia* antigens are immunoreactive at different stages of Lyme disease. In early Lyme disease, the most common IgM and IgG antibodies are directed to OspC and the flagellar antigens (41 kDa), while variable rates of IgM and IgG response to P39, VlsE, and other antigens (i.e., P93, P66, P45, P35, P30, and P18) may also be detected by immunoblot.

The number of antigens recognized in the IgM immunoblot and the intensity of the immune response as determined by band intensity are greater in sera of patients with EM and constitutional signs and symptoms, those with multiple EMs, or those with EM of a duration of more than 2 weeks at presentation, compared to asymptomatic patients with a solitary EM of a duration of less than 2 weeks. Interpretive criteria have been suggested for a standardized immunoblot for the three species of *B. burgdorferi sensu lato* that cause human disease in Europe (19).

In general, immunoblot has comparable or slightly higher sensitivity than ELISA for detection of early Lyme disease. The specificity of immunoblot is greater than that of ELISA, as interpretation of immunoblot relies on the

presence of specific immunoreactive bands. The major limitations of the immunoblot assay include the visual scoring and subjective interpretation of band intensity that may lead to false-positive readings, the higher cost, and the variability of antibody responses in patients with the same clinical manifestations of Lyme disease. Of particular concern is the scoring of weak bands on the IgM immunoblots, which leads to an erroneous positive interpretation. For these reasons, immunoblots perform better as supplemental tests of a sensitive EIA and should not be used as single-step testing.

Two-Tier Serologic Testing Algorithm

The use of earlier assays lacking the significant *B. burgdorferi* antigens, plus the indiscriminate use of serologic assays in populations with low prevalence for Lyme disease, has contributed to the belief that serology is not helpful in this disease. In 1994, the U.S. Association of State and Territorial Public Health Laboratory Directors and the CDC recommended a two-step approach in which samples are examined first by a sensitive test, such as ELISA or IFA. Samples testing reactive (equivocal and positive) by first-step assays are tested by separate IgG and IgM immunoblots. Samples showing reactivity to 2 of 3 significant bands, 41-, 39-, or 23-kDa (OspC) are considered positive by the IgM criteria. Samples showing 5 of 10 significant bands: 93, 66, 58, 45, 41, 39, 30, 28, 23 (OspC), and 18 kDa in IgG blots are considered positive by the IgG criteria (20). This two-step approach is also widely used by laboratories in Europe. Furthermore, the recommendations stated that the IgM immunoblot criteria should be used in patients with disease of <1 month duration, and IgG criteria could be used at any stage of the disease.

Evaluation of the two-tier testing in well-characterized populations of patients with different stages of Lyme disease has found that this approach offers a sensitivity of about 40% during the acute phase of EM and increases to over 60% during convalescence. Antibody development occurs regardless of antimicrobial treatment in a majority of patients. The sensitivity of the two-step approach is about 90% in patients presenting with early dissemination with neurological symptoms, particularly when the IgM immunoblot criteria is used and is close to 100% in those with late manifestations such as arthritis (21–23) (Table 3).

Limitations of the two-step test are that the first- and second-step assays are not independent, since both include antigenic mixtures of *B. burgdorferi*, in addition to the difficulty in interpreting immunoblot results and their high cost. Recently, several studies have addressed whether a one-step test, such as ELISAs using the VlsE C6 peptide as antigen, or an alternative two-tiered test that consists of a whole-cell sonicate EIA followed by a VlsE C6 EIA (22, 24), are of sufficient sensitivity and specificity to replace the widely used two-step approach. Given the variability of immunodominant antigens observed among different pathogenic Lyme *Borrelia* species and subtypes, particularly in Europe, and its slightly lower specificity, the one-step EIA strategy is not recommended for serodiagnosis of Lyme disease (18, 22). Compared to the standard two-step approach using EIA and immunoblot, recent studies demonstrated comparable sensitivity and specificity but lower cost by a new two-EIA test strategy (18, 22). These data are based on studies from a few laboratories in a limited number of patients. More studies are needed to determine the applicability of this two-EIA approach to replace the current standard two-step tests for serodiagnosis of patients with various manifestations of Lyme disease in both the U.S. and Europe.

Use of Recombinant or Peptide Antigens in Serology of Lyme Disease

Several antigens have been purified and recombinants have been developed and evaluated as a source of antigens in immunoassays. Among those are recombinant OspC, internal fragments of 41 kDa (41-i), P39 (BmpA), P66, P93, DbpA (decorin-binding protein A), BBK32, and others. The performance of these recombinant and peptide antigens for detection of IgM, IgG, or polyvalent antibodies in patients with various stages of Lyme disease has been reviewed elsewhere (21).

Peptide antigens that have been found to hold great promise include the pepC10 that contains the conserved C-terminal 10 amino acids of OspC. Although less variable than the parent OspC, this peptide also binds IgM antibodies present in sera of patients with early disease. Evaluations of the performance of this peptide antigen have shown it to be sensitive and specific. An ELISA test based on another peptide, OspC1, a highly conserved 20-amino-acid peptide epitope, showed comparable sensitivity but higher specificity than a pepC10-based method (25).

Another peptide antigen that has attracted great attention is the VlsE C6. This is a synthetic peptide reproducing the highly conserved invariable region 6 of the VlsE antigen. The C6 peptide-based ELISA and Western immunoblot assays with the addition of a VlsE band (26) have been reported to be comparable or more sensitive for laboratory diagnosis of patients with early and late Lyme disease. ELISA assays that use recombinant antigen or peptides or a combination have been approved by the FDA as first-step assays. Recent FDA-cleared first-step assays include the use of recombinant VlsE and synthetic pepC10 in a bead format (AtheNA Multi-Lyte system, Zeus Scientific, Inc.) and VlsE in a chemiluminescence assay (LIASON, DiaSorin S.p.A.).

TABLE 3 Comparative sensitivity of different immunologic methods to detect antibodies to *B. burgdorferi* in Lyme disease patients from the United States[a]

Test	% Reactivity in patients with:			
	EM, acute phase	EM, convalescent phase	Neurological involvement	Arthritis
Whole-cell EIA[b]	33–52	76–94	79–100	Nearly 100
VlsE C6 EIA[b]	34–43	59–92	67–100	67–100
Two-EIA[b]	37	89	100	100
Standard two-tier testing[c]	27–40	29–78	87–100	97–100

[a]Adapted from references 21–23.
[b]EIA, enzyme immunoassay; two-EIA, whole-cell EIA followed by VlsE C6 EIA (22).
[c]Two-tier algorithm including a screening EIA and a confirmatory immunoblot as recommended by the CDC (20).

Other Immunologic Methods

Other immunologic methods for serodiagnosis of Lyme diseases include the measurement of functional borreliacidal antibodies, antibodies bound to circulating immune complexes, and host cellular immune response by T-lymphocyte and mononuclear cell proliferation assays. These assays have seldom been used as diagnostic tests due to their cumbersome nature and concerns about specificity and standardization.

Clinical Applications and Limitations of Serologic Tests

Current serological tests may be limited by the delay in development of an antibody response, cross-reactivity with other organisms, high background seroprevalence in asymptomatic persons residing in endemic areas, difficulty in distinguishing past from present infections, and lack of standardization. In addition, antigenic heterogeneity of *B. burgdorferi sensu lato* may influence the sensitivity and specificity of serological tests for Lyme disease, especially in Europe where three pathogenic species of *B. burgdorferi sensu lato* and at least eight OspA serotypes are well documented.

European investigators have long used assays including recombinant antigens derived from *B. garinii* and *B. afzelii*, the predominant *Borrelia* species causing disease in Europe. The antigenic variability is of greater magnitude in Lyme disease-causing organisms in different geographic regions of Europe than in the United States. Attempts have been made to standardize serologic testing in Europe.

It is noteworthy that serological tests for *B. burgdorferi* antibodies should be used only to support a clinical diagnosis of Lyme disease and not as the primary basis for making a diagnosis or for treatment decisions. The positive predictive value (the ability to diagnose disease) of a test depends on both the sensitivity and specificity of the assay and the prevalence of the disease in the population in which the test is being applied.

In addition, some technical issues need to be addressed in the laboratory performing the Lyme serologic tests. For example, evaluation of newly introduced first-tier assays and lots with well-characterized samples before their use in the laboratory is strongly recommended. Variations in reactivity using different lots from the same manufacturer as well as from different assays are not uncommon. Inclusion of well-characterized specimens testing weakly reactive or with borderline reactivities are also recommended.

For immunoblot tests, the most important limitation of these assays is the subjective interpretation. The most frequent error is the over-reading of the IgM immunoblots. These antibodies may remain detectable for long periods after successful treatment of early disease and may be present in low concentration in immunoblots. Scoring of faint bands leads to misinterpretation of IgM immunoblots. Inclusion of weak controls against which a band is read as well as scoring of bands using densitometry may be of help in solving this problem. IgM blots during acute disease characteristically show strong reactivity to the OspC and very frequently to the 41- and/or the 39-kDa antigens (Fig. 1).

IgG blots fulfilling the CDC criteria are found in sera of patients with disease of more than 1-month duration. Problems in fulfilling blot criteria may be found in sera of patients with early disseminated neurological disease who usually fulfill IgM criteria but may not yet have a positive IgG blot.

Direct Detection of *B. burgdorferi*

Microbiological confirmation of the presence of *B. burgdorferi* in clinical specimens provides definitive evidence of *B. burgdorferi* infections in patients with suspected Lyme disease. *B. burgdorferi* in clinical samples can be detected by microscopic examination of intact spirochetes, antigen test, *in vitro* cultivation of *B. burgdorferi*, and polymerase chain reaction analysis of *B. burgdorferi* nucleic acids. Of these, direct microscopic examination and antigen test are rarely used in clinical laboratories due to their low sensitivity and specificity. Direct detection of spirochetes in tissue specimens by histochemical staining is not reliable, because spirochetes cannot be distinguished easily from elastic tissue or procollagen fibers.

B. burgdorferi can be cultured *in vitro* in liquid Barbour Stoenner Kelly medium under microaerophilic conditions. The optimum growth temperature for *B. burgdorferi* is 30 to 34°C. *B. burgdorferi* has been cultured in up to 80% of skin biopsy samples of patients with EM. The organism has also been cultured on whole blood, serum, or plasma in up to 40% of samples collected from patients with early Lyme disease (27). Better yield of blood culture in early disease has been achieved by culturing blood volumes similar to those used in routine bacterial blood cultures. Recently, a new method of culturing spirochetes from the serum of U.S. patients with Lyme disease was reported to have exceptionally high clinical sensitivity (94%) and specificity (100%). Assessment of the culture results revealed potential false positivity due to laboratory contamination of patient samples (28). *B. burgdorferi* has been infrequently isolated from other samples, such as cerebrospinal fluid (CSF).

Molecular Diagnosis of *B. burgdorferi* Infection

Polymerase chain reaction detection of *B. burgdorferi* DNA represents an alternative approach for diagnosis of Lyme disease (reviewed in references 21 and 29). The diagnostic value of PCR may vary depending on the clinical diseases and PCR method being used. Currently, PCR-based molecular tests are employed in research settings. Such uses have involved (i) detection of nucleic acids of tick-borne pathogens in *Ixodes* ticks, (ii) culture confirmation of *B. burgdorferi*, and (iii) direct detection on skin or synovial tissues.

PCR has been used to detect the DNA of *B. burgdorferi* in skin biopsy, blood, urine, CSF, and synovial fluid specimens with variable diagnostic value. The sensitivity of PCR for detection of *B. burgdorferi* DNA in skin lesions is usually high with a median percent positivity of 69% for patients with EM and 76% for patients with ACA (21). In general, the sensitivity of PCR for detection of *B. burgdorferi* DNA in blood, plasma, or serum samples from patients with Lyme disease is low (<20%) due to the lack of spirochetemia or to transient or low-level spirochetemia. In a U.S. retrospective study, only 6 of 5,703 (0.1%) blood and 14 of 15,939 (0.09%) CSF specimens examined by a real-time PCR assay in the Mayo Clinic Laboratory were positive (30). PCR has also been successful on joint fluid or tissues from patients with untreated Lyme arthritis. PCR has a median sensitivity of 78% and is more sensitive than culture for detection of *B. burgdorferi* in synovial fluid specimens (21).

Limitations of Direct-Detection Methods

Due to the lack of commercially available and adequately validated assays, a reliable and standardized PCR protocol is needed to address the current challenges of persistent misconceptions, misunderstanding, and misdiagnosis of Lyme disease (31). Due to the above reasons, use of PCR in clinical settings—particularly on blood, CSF, or other body fluids, with the exception of synovial—should be discouraged.

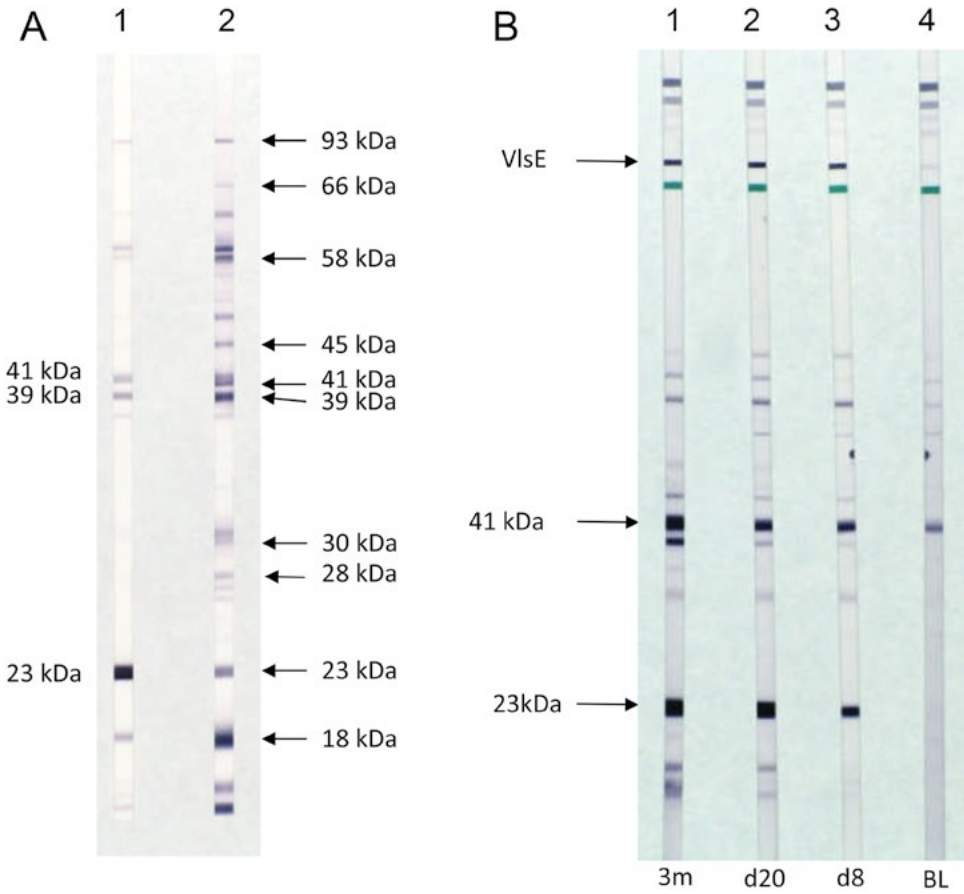

FIGURE 1 (A) Examples of positive Lyme IgM (lane 1) and IgG (lane 2) Western blots (MarDx Inc). The IgM and IgG bands in the CDC interpretive criteria are indicated. (B) VlsE–IgG Western blots (Viralab Inc, not currently FDA-approved in the U.S.) (26). Sequential sera from a culture-confirmed EM patient are shown in lanes 1 to 4. Serum samples were collected at Baseline (BL, lane 4), 8 days (d8, lane 3), 20 days (d20, lane 2) and 3 months (3m, lane 1) post onset of illness.

Test Interpretation and Practical Considerations

Diagnosis of EM is clinical and is based on the presence of an erythematous skin lesion at the site of the tick bite. Such lesion should be of a minimum of 5-cm diameter. For patients with atypical EM and noncutaneous manifestations or late Lyme disease, laboratory evidence of *B. burgdorferi* infection is required for confirmation of a diagnosis. Table 4 shows a comparison of the different diagnostic modalities used to confirm the diagnosis of Lyme disease.

The use of diagnostic methods aiming at the direct detection of *B. burgdorferi* in clinical samples such as culture or PCR is currently restricted to research laboratories in academic centers. PCR is also available through commercial laboratories, and its use should be restricted to joint fluids or joint tissues. A positive PCR result in a synovial-fluid specimen of a patient with exposure to an area where Lyme disease is endemic and who also has a positive *B. burgdorferi sensu lato* ELISA and IgG immunoblot is strongly supportive of a diagnosis of Lyme arthritis. Untreated patients with Lyme arthritis, as well as patients during the first days to weeks of therapy, may exhibit a positive PCR result in synovial fluid.

Positive PCR results for *B. burgdorferi sensu lato* nucleic acids obtained in samples from patients with possible extracutaneous manifestations of Lyme disease in the absence of serological evidence of *B. burgdorferi sensu lato* infection, however, should be interpreted with caution. In those situations, PCRs are often false positive. One of the limitations of nucleic acid-amplification methods is the generation of false-positive results due to contamination. Adherence to rigorous quality control steps is of utmost importance.

Serology is the most useful laboratory test that is widely available to support a clinical diagnosis of Lyme disease. The current recommended approach includes the use of two-tier testing. Interpretation of serology in Lyme disease requires an understanding of the use and limitations of the currently available tests for *B. burgdorferi sensu lato* antibodies, as follows.

(i) These tests detect antibodies reacting with *B. burgdorferi sensu lato* and can support the clinical suspicion of Lyme disease, but in and of themselves they do not diagnose Lyme disease.

(ii) Antibodies may not be detectable at the time the patient presents with signs and symptoms of early Lyme disease with EM, and their presence correlates directly with the duration of disease prior to seeking medical attention as well as with the presence of symptoms or objective signs of dissemination (for example, multiple EMs or cranial nerve palsies). For patients with early Lyme disease who have EM, the diagnosis is established on clinical grounds if the skin

TABLE 4 Comparison of different modalities for laboratory diagnosis of Lyme disease

Test method	Sensitivity (%)[a]
Culture	
Skin biopsy (EM, ACA)	60–80
Blood	10–40
PCR	
Skin biopsy (EM, ACA)	60–80
Blood and CSF	10–30
Synovial fluid	50–70
Two-tier serology	
EM, acute phase	30–40
EM, convalescent phase	80
Neuroborreliosis	80–90
Lyme arthritis	90–100

[a]Adapted from reference 21.

lesion is characteristic. In situations where the skin lesion is atypical or absent, tests to detect *B. burgdorferi sensu lato* antibodies may be necessary, as follows.

(a) When antibodies are not detectable or not diagnostic in the acute-phase serum specimen, a convalescent-phase specimen should be collected 2 to 4 weeks later and tested for *B. burgdorferi sensu lato* antibodies.

(b) In patients treated with antimicrobials, testing of the convalescent-phase sample within 1 month of onset of symptoms will maximize sensitivity, since the criteria for test positivity at this time point include IgM immunoblot seroconversion, whereas after 1 month IgG seroconversion is required for seropositivity.

(iii) Testing for *B. burgdorferi sensu lato* antibodies should include the two-tier approach as currently recommended. In those specimens testing positive or equivocal by first-tier assays, second-tier immunoblot is used to improve specificity. Immunoblot assay should not be used with sera testing negative by the first tier, as this would reduce specificity compared to the two-tier testing strategy.

(iv) *B. burgdorferi sensu lato* antibodies, both IgG and IgM, may persist for many years after successful treatment of Lyme disease. Thus, persistent seropositivity is not, *per se*, an indication of treatment failure. Persistence of antibodies to *B. burgdorferi sensu lato* in sera of individuals residing in areas where Lyme disease is endemic and who have been treated for Lyme disease, or who have resolved an asymptomatic infection, may limit the utility of future serologic testing as a diagnostic tool when such persons present with a new clinical event. In these circumstances, a change in reactivity between acute- and convalescent-phase specimens may be of assistance, although this has never been systematically evaluated. An increase in antibody concentration as determined by optical density in EIA, or by IFA titers, in first-tier assays, or by an increase in intensity or appearance of new immunoreactive bands by immunoblot might suggest a new or recent *B. burgdorferi sensu lato* infection. Physicians caring for these patients should store an aliquot of an acute-phase serum specimen to be submitted along with the convalescent-phase sample for testing in parallel for *B. burgdorferi sensu lato* antibodies.

(v) Patients with late manifestations of Lyme disease usually have a high concentration of antibodies by first-step tests and have numerous immunoreactive bands in IgG blots, often far surpassing the number of bands required in the IgG immunoblot interpretation criteria. A lack of seropositivity in patients suspected of having late Lyme disease practically excludes this diagnosis.

(vi) Laboratories performing *B. burgdorferi sensu lato* serology should use assays of proven performance as determined by the summary of surveys run by the College of American Pathologists or local or state proficiency programs.

(vii) Laboratorians should make an attempt to avoid scoring weak bands leading to false-positive readings in immunoblot, particularly IgM immunoblot. This can be avoided by strict adherence to comparison of band intensity to those of cutoff-intensity-control materials.

(viii) The use of laboratory tests or interpretation strategies that have not been appropriately validated is of great concern and is strongly discouraged. Currently there are commercial laboratories offering *B. burgdorferi sensu lato* urine antigen tests, immunofluorescent staining for cell wall-deficient forms of *B. burgdorferi sensu lato*, and lymphocyte transformation tests. In addition, some laboratories are performing PCR for *B. burgdorferi sensu lato* DNA on inappropriate samples, such as blood and urine, or are interpreting immunoblot by using criteria that have not been validated.

(ix) The use of *B. burgdorferi sensu lato* antibody testing should be restricted to patients with a 0.2 to 0.8 pretest probability of having Lyme disease, as recommended by the American College of Physicians (13). The use of these tests in unselected populations with a low pretest probability of the disease is more likely to yield false-positive than true-positive results. Testing is not recommended for patients presenting with classic EM, since treatment without testing is more cost effective, and *B. burgdorferi sensu lato* antibody assays have low sensitivity at this stage. Since the specificity of *B. burgdorferi sensu lato* antibody testing is not 100% and since 2.8 to 3.4 million tests are estimated to be done annually in the U.S., for every 1% reduction in test specificity there will be approximately 28,000 to 34,000 false-positive results per year, dwarfing the true-positive incidence of about 33,000 cases/year.

RELAPSING FEVER

Taxonomy

Currently there are 23 validated species in the RF *Borrelia* group (5). All but two of the 23 RF *Borrelia* species, *Borrelia coriaceae* and *Borrelia miyamotoi*, were described before the delineation of *B. burgdorferi* in 1984. The "new" RF *Borrelia* species isolated from patient blood samples and *Ornithodoros erraticus* ticks in Spain in the mid-1990s was recently confirmed to be *Borrelia hispanica* based on multilocus sequence data analysis (32). Recent genomic sequence analysis raises the possibility that *B. recurrentis*, *B. duttonii*, and *B. microti* may belong to a single species (33).

A few novel RF *Borrelia*-related species have been described, including *Borrelia lonestari* from hard tick *Amblyomma americanum* in North America, *Borrelia mvumii* from *Ornithodoros* ticks and patients in Tanzania, and *Borrelia microti* from *O. erraticus* in Iran.

Epidemiology and Disease Spectrum

Relapsing fever has been reported in continents of both the northern and southern hemispheres. It was once the cause of worldwide epidemic disease, especially for louse-borne relapsing fever (LBRF). Although the incidence of LBRF has decreased significantly during the last century, largely

due to improved living standards, there have been recent reports of LBRF in homeless people from France and there still exist areas of endemicity in Ethiopia and Sudan (34). Some authors have cautioned that relapsing fever is underreported and not considered in the differential diagnosis of febrile illnesses, particularly that tick-borne relapsing fever (TBRF) *Borrelia* can infect a variety of hosts, establishing a vast reservoir (34). Relapsing fever is now mostly a sporadic disease in most regions of the Old and New World, including the western U.S., southern British Columbia in Canada, the plateau regions of Mexico, Central and South America, the Mediterranean, Central Asia, and throughout much of Africa (35). In the U.S., human TBRF is typically distributed in a few states no further east than Montana, Colorado, New Mexico, and Texas.

Human relapsing fever is caused by at least 15 *Borrelia* species and is transmitted by the soft tick *Ornithodoros*, with the exception of LBRF, which has only humans as reservoirs and is transmitted only by the human-specific body louse *Pediculus humanus*. TBRF cases associated with infection of *B. miyamotoi*-like spirochete and transmitted by *Ixodes* ticks have recently been reported in Russia and the northeastern U.S.

In the U.S., human TBRF is mainly caused by infections of *B. hermsii* and *B. turicatae*, which are transmitted by soft ticks *O. hermsi* and *O. turicata*, respectively. TBRF in Eurasia is attributed mainly to *B. persica*, although other *Borrelia* species have also been described. *O. tholozani* is the most important tick vector for TBRF in Eurasia and can be found in India and Kashmir, the southern countries of the former USSR, Iran, Iraq, Syria, Jordan, Turkey, Israel, Egypt, and Cyprus. *B. hispanica* is responsible for the majority of cases in the Mediterranean regions where *O. erraticus* is predominant.

The overall clinical manifestations of louse LBRF and TBRF are similar, although not identical. Characteristically, both types of relapsing fever have recurring episodes of fever and nonspecific symptoms, i.e., severe headache, myalgias, arthralgias, and lethargy. The primary febrile episode normally has an acute onset with high fever that subsides in 3 to 6 days. After 7 to 9 days, fever and symptoms recur, although the duration and the intensity of the symptoms progressively decrease with each relapse. LBRF is usually associated with a single relapse, whereas multiple relapses can been seen in TBRF. The most common clinical signs of relapsing fever may include altered sensorium, conjunctival suffusion, petechiae, and diffuse abdominal tenderness with hepatomegaly and splenomegaly (35, 36).

Direct Microscopic Examination of Spirochete in Blood

Relapsing fever has traditionally been diagnosed by the demonstration of spirochetes in the blood of patients during febrile episodes. During the febrile illness, RF borreliae multiply in the bloodstream and are often present at levels in excess of 10^5 organisms/μL of blood. Among febrile patients, spirochetes can be found in approximately 70% of cases when blood smears are examined in Giemsa- or Wright's-stained thin and thick films by light microscopy, or by use of dark-field or phase-contrast microscopy of wet preparations (36). The sensitivity of microscopic methods can be improved by the use of acridine orange-stained blood smears with a fluorescence microscope or by examination of buffy coat smears.

The use of a centrifugation-based enrichment method, followed by Giemsa staining, allows detection of less than 10 spirochetes/ml in blood (37). If validated, this simple method can be an interesting alternative in a rural relapsing fever-endemic area.

Molecular Detection and Genotyping of Relapsing Fever Borreliae

PCR-based molecular techniques have shown promise for improved clinical diagnosis and epidemiologic assessment of relapsing fever (38). Elbir et al. reported that a multiplex real-time PCR assay targeting the 16S rRNA, *glpQ*, *recN*, and *recC* not only detected but also speciated the four closely related RF borreliae: *B. crocidurae*, *B. duttonii*, *B. recurrentis*, and *B. hispanica*, found in Africa (38).

Serologic Test Methods

Serological methods are not widely in use for laboratory diagnosis and management of patients with RF. Serologic tests include IFA, ELISA, and Western immunoblot. The currently available serological approaches that use whole-cell spirochete lysates as antigen sources may fail to discriminate between different *Borrelia* species, resulting in probable misidentification of patients as cases of Lyme disease. Also, seroconversion is rarely demonstrated during the first febrile episode, and prompt antibiotic therapy may abrogate the antibody response. Therefore, while positive results in any of these assays may strongly support the clinical diagnosis of relapsing fever, negative results are inconclusive.

Recent data suggest that relapsing fever may be distinguished from Lyme disease based on the presence of antibodies against an immunoreactive 39-kDa surface protein, glycerophosphodiester phosphodiesterase (GlpQ) (39) or a 57-kDa *Borrelia* immunogenic protein A (BipA) (40). Further evaluation and standardization of assays utilizing this antigen may justify its greater use. Despite the utility of laboratory diagnostic tests, the importance of a detailed case history and clinical presentation in the diagnosis of relapsing-fever borreliosis cannot be overemphasized.

Culture of Relapsing Fever Borreliae

Like *B. burgdorferi*, a variety of RF borreliae, including *B. hermsii*, *B. parkeri*, *B. turicatae*, *B. duttonii*, and *B. recurrentis*, can be cultivated *in vitro* in Barbour-Stoenner-Kelly medium. The sensitivity of culture is not yet sufficient for diagnosis and now is infrequently used compared to that in Lyme disease.

Alternatively, intraperitoneal injection of patient blood into mice or rats usually produces large numbers of spirochetes in the animals' blood within 3 to 5 days for TBRF borreliae. This provides another means for the isolation and presumptive identification of RF *Borrelia*.

Clinical Indications and Test Interpretation

Relapsing fever has usually an acute onset of high fever with systemic symptoms. During the course of illness, fever is remittent and often accompanied by tachycardia and tachypnea. Laboratory confirmation is recommended for patients with suspected LBRF or TBRF, based on the patient's clinical syndrome, tick bite history, and local epidemiological data.

The definitive diagnosis of relapsing fever is established by demonstrating the presence of borreliae in the peripheral blood of infected patients. The most direct and simple method is by microscopy. During acute febrile phases, spirochetemia often reaches 10^6 to 10^8 spirochetes/ml, and motile spirochetes can be visualized by dark-field microscopy

from wet preparations. In patients with low spirochetemia, concentration of the spirochetes by buffy coat or other approaches will increase the yield of positivity.

Like Lyme disease, culture is not a practical approach for laboratory diagnosis of relapsing fever. Real-time PCR assays are promising tools in detecting and genotyping the infecting spirochetes in patients in early stages of relapsing fever if available. Serologic tests are not routinely employed in the laboratory for the confirmation of relapsing fever. Immunoassay using recombinant GlpQ antigen is worthy of further exploration.

LEPTOSPIROSIS

Taxonomy

The genus *Leptospira* belongs to the family *Leptospiraceae* within the order *Spirochaetales* and class *Spirochaetes*. Historically, *Leptospira* was the only genus in the family *Leptospiraceae*. It was divided into two species: *L. interrogans*, comprising all pathogenic strains, and *L. biflexa*, containing the free-living, saprophytic strains from the environment. Within each species, strains are further differentiated by serovars on the basis of their reactivity with representative agglutination antibodies. Since a large number of serovars (>250) were described for pathogenic leptospires, antigenically related serovars were grouped into serogroups for convenience in serologic testing.

During the past 2 decades, the classification of spirochetes in the family *Leptospiraceae* has undergone significant changes. Many new species have been defined based on their genetic characteristics and relatedness. The family *Leptospiraceae* has now three genera. The genus *Leptospira* consists of at least 15 species with variable pathogenicity to humans, while single, nonpathogenic species belonging to the genera *Leptonema* and *Turneriella* have been defined (1).

Currently, there are 15 validated species and four additional genospecies with tentative species names in the genus *Leptospira* (Table 5). Based on 16S rRNA gene sequences, these *Leptospira* species are grouped into pathogenic, saprophytic species and intermediate species with uncertain pathogenicity. However, some species may contain both pathogenic and nonpathogenic serovars and strains, and one serovar may be found in more than one species. Therefore, it has been suggested that *Leptospira* strains should be characterized by both serologic and DNA-based techniques, and accurate differentiation of *Leptospira* species must rely on molecular characterization comparing 16S rRNA sequences or DNA-DNA reassociation analysis (41).

TABLE 5 *Leptospira* species and selected pathogenic serovars

Species	Selected pathogenic serovars
Pathogenic species	
L. interrogans	Icterohaemorrhagiae, Copenhageni, Canicola, Pomona, Australis, Autumnalis, Pyrogenes, Bratislava, Lai
L. alexanderi	Manhao 3
L. borgpetersenii	Ballum, Hardjo, Javanica
L. kirschneri	Bim, Bulgarica, Grippotyphosa, Cynopteri
L. meyeri	Sofia
L. noguchii	Panama, Pomona
L. santarosai	Bataviae
L. weilii	Celledoni, Sarmin
Leptospira genomospecies 1	Sichuan
B. Saprophytic species	
L. biflexa	
L. wolbachii	
Leptospira genomospecies 3	
Leptospira genomospecies 4	
Leptospira genomospecies 5	
C. Indeterminate	
L. broomii	
L. fainei	Hurtsbridge
L. inadai	
L. licerasiae	
L. wolffii	

Epidemiology and Disease Spectrum

Leptospirosis is a globally important zoonotic disease and an important public health problem in developing countries. Human infections are endemic in most regions, with the peak incidence occurring during the rainy season in tropical regions and during late summer to early fall in temperate regions.

The World Health Organization estimates the incidence of leptospirosis is 0.1 to 1.0 per 100,000 population per year in regions with a temperate climate, and >10 cases per 100,000 population in humid tropical regions. As a neglected infectious disease, the incidence of leptospirosis is probably largely underestimated, because of its asymptomatic nature in most cases and the limited diagnostic capacity in the regions where it has the highest prevalence. The most recent epidemics in Nicaragua (2007), Sri Lanka (2008), and the Philippines (2009) each affected thousands of patients and caused hundreds of deaths (42). In the United States, the highest incidence is found in Hawaii, with an annual incidence of approximately 128 cases/100,000 based on active surveillance in 1992.

Leptospirosis is maintained in nature by chronic renal infection of carrier animals. The most important reservoirs are rodents and other small mammals. Infected animals may excrete leptospires in their urine intermittently or continuously throughout life. Human infection often occurs through direct or indirect contact with urine or tissues of infected animals due to occupational exposure (i.e., veterinarians, workers in milking sheds on dairy farms, abattoir works, butchers, hunters, and animal handlers) or recreational or accidental contact.

Human leptospirosis is associated with a very broad spectrum of severity, ranging from subclinical, self-limited mild systemic illness to severe, potentially fatal illness accompanied by renal failure and liver failure. Approximately 90% of infected individuals have a subclinical presentation of mild severity. The clinical presentation in symptomatic patients usually has two distinct stages: an initial septicemic phase

followed by an immune phase in which the severe symptoms occur.

The acute septicemic phase of illness lasts 5 to 7 days in the majority of cases and presents with a febrile illness of sudden onset, fever (38 to 40°C), headache, chills, myalgias, abdominal pain, and conjunctivitis without purulent discharge. The immune phase of illness generally lasts 4 to 30 days with clinical symptoms such as jaundice, renal failure, cardiac arrhythmias, pulmonary symptoms, aseptic meningitis, conjunctivitis with or without hemorrhage, photophobia, eye pain, muscle tenderness, lymphadenopathy, and hepatosplenomegaly. Weil's disease, characterized by impaired hepatic and renal function, is the most distinctive form of severe leptospirosis.

Due to its nonspecific clinical presentations and potentially severe disease outcome, an early diagnosis of leptospirosis is essential for patient management because antibiotic treatment is most effective when initiated early in the course of the disease.

Serologic Diagnosis

Microscopic Agglutination Test

The microscopic agglutination test (MAT) detects both IgM and IgG classes of agglutinating antibodies against the surface antigens of *Leptospira*. MAT is considered the standard reference assay for laboratory diagnosis of leptospirosis.

Serum sample is the preferred specimen for serologic testing. The antibodies can be detected approximately 1 week after onset of symptoms and reach peak titers usually within 4 weeks. The titers following acute infection may be extremely high and may take months, or even years, to fall to low levels. Therefore, a pair of sera should be drawn at least 1 week apart and tested to confirm a diagnosis of leptospirosis if available.

Test Method

The MAT is an agglutination test, in which patients' sera are reacted with live or killed antigen suspension representing different serogroups or serovars of *Leptospira*. After incubation, the serum-antigen mixtures are examined by darkfield microscopy for agglutination and the titers are determined.

The MAT uses a panel of serovars (antigen) relevant to a testing region. The most commonly used serovars in the panel include Alexi, Australis, Autumnalis, Ballum, Bataviae, Borincana, Bratislava, Canicola, Celledoni, Copenhageni or Icterohaemorrhagiae, Cynopteri, Djasiman, Georgia, Grippotyphosa, Javanica, Mankarso, Pomona, Pyrogenes, Tarassovi, and Wolffi. The MAT is generally done using live spirochetes, but formalin-killed *Leptospira* may also be used. If the latter are used, titers are lower and the reactivity is somewhat less specific.

Also, a collection of antisera, corresponding to each serovar with a titer of ≥3,200, is needed as homologous controls for each antigen used in the assay. Antisera are available commercially or from the National Veterinary Services Laboratories, Ames, Iowa. A detailed protocol for performing the MAT can be found in the 7th edition of this *Manual* (43).

Interpretation and Limitations

The MAT results are reported as the reciprocal of the serum dilution that tested reactive for each antigen; a titer of ≥100 is considered positive.

The MAT can be used for confirmation and presumptive diagnosis of human leptospirosis cases, especially for febrile patients with nonspecific symptoms in endemic areas. It can also be used with human and animal sera in epidemiologic studies or outbreaks to determine the potential source of infection.

A 4-fold or greater increase in MAT titer to one or more serovars between paired serum specimens run in parallel, regardless of the interval between samples, confirms a diagnosis of leptospirosis. If only a single serum sample is available for testing, a titer of at least 800 in the presence of compatible symptoms is generally considered diagnostic in areas of endemic infection. In regions where leptospirosis is not endemic, the threshold titer for a presumptive diagnosis may be correspondingly lower. Currently, the U.S. Centers for Disease Control and Prevention uses a titer of ≥200 in a patient with clinically compatible illness as evidence for recent or current infection to indicate a probable case for epidemiological surveillance.

The diagnostic and epidemiological applications of the MAT are limited by its relatively low sensitivity when acute serum samples are tested. Up to 10% of patients may have delayed seroconversion or fail to seroconvert within 30 days of the clinical onset. Also, cross-reactive antibodies may be associated with syphilis, relapsing fever, Lyme disease, viral hepatitis, human immunodeficiency virus (HIV) infection, legionellosis, and autoimmune diseases.

In addition, antibodies in serum may cross-react between different serovars, especially in acute-phase samples; this is attributed to IgM antibodies. Most MAT assays use only 12 to 19 of the more than 250 known serovars. Thus, the MAT should not be used to infer the identity of the infecting serovar.

Rapid IgM Antibody Screening Tests

Due to the complexity of performance and interpretation, the use of MAT is now limited to regional and national reference laboratories. A rapid screening test for serum samples from suspected leptospirosis plays an important role in immediate case detection and clinical management. Several rapid screening tests are currently available. They are primarily IgM detection assays. Use of these assays as screening tests offers the potential to enhance the diagnostic capacity of many laboratories, particularly in developing countries, where most cases of leptospirosis occur.

Test Methods

Rapid IgM detection assays are available in several formats, including conventional IgM antibody-capture microplate ELISA (IgM ELISA) assay and some rapid diagnostic tests (RDTs).

The IgM ELISA assay is a useful screening tool for testing few or large numbers of specimens. It is commercially available or it can be prepared in house. Most IgM ELISA assays use whole-cell-derived antigens. It has been reported that the selection of antigens representing local serovars and the use of antigen prepared from intermediate species, such as *L. fainei*, may increase the assay sensitivity (44). The commercially available *Leptospira* IgM ELISA kit (PANBIO Inc, Columbia, MD) contains antigen-coated plates (12 8-well strips), wash buffer concentrate, serum diluent, horseradish peroxidase-conjugated anti-human IgM, tetramethyl benzidine substrate, stop solution, positive control serum, cutoff calibrator serum, and negative control serum. It is a solid-phase assay in which IgM present in serum binds to leptospiral antigen attached to the polystyrene surface of the microwell. Peroxidase-conjugated anti-human IgM reacts with the antigen-bound antibody. The detection system is a colorless substrate, tetramethyl benzidine substrate plus

hydrogen peroxide, which is hydrolyzed by the enzyme, and the chromogen changes to a blue color. The color intensity is directly related to the concentration of anti-*Leptospira* IgM antibodies in the test sample.

A variety of RDTs have been described and evaluated for screening of suspected cases of leptospirosis. These RDTs are based either on the immunochromatographic lateral flow technology (i.e., LeptoTek Lateral Flow, Organon Teknika BV, Boxtel, The Netherlands; Leptocheck-WB, Zephyr Biomedicals, Verna Goa, India) or on latex agglutination (i.e., LeptoTek Dri Dot, bioMérieux BV, Boxtel, The Netherlands). The dot ELISA dipstick (INDX Dip-S-Ticks; PANBIO Inc, Columbia, MD) uses a genus-specific antigen (*L. biflexa* serovar Patoc) dispensed as discrete dots on a solid membrane. Diluted patient serum reacts with the antigens on the assay strip, and alkaline phosphatase-conjugated anti-human immunoglobulin reacts with the bound antibodies from the patient's serum.

Interpretation and Limitations

The rapid IgM ELISA and RDTs can be quantitative or qualitative. The cutoff for positive may be test-kit and assay-specific and may need to be adjusted, verified, or established by the testing laboratory based on the prevalence of testing population.

A recent meta-analysis of IgM ELISAs reported an overall sensitivity and specificity of 80% and 94%, respectively (45). These IgM detection assays are intended for use in the diagnosis of acute infection. The presence of IgM antibody is considered suggestive of a recent or acute *Leptospira* infection. However, IgM may persist for months or years following recovery in some cases. Most rapid IgM assays should be used for screening tests, and confirmation of results with MAT and alternative tests is strongly recommended. The assay detects antibodies earlier than do the agglutination assays (indirect hemagglutination assay and MAT) and is ideal for use when only a few specimens are tested at a time.

Because IgM antibodies are not detectable until days 5 to 7 days after symptom onset, the sensitivity of these assays is low for patients in the early acute phase of illness. Cross-reactions in this assay have been observed with sera positive for autoimmune diseases, cytomegalovirus, HIV, group C *Neisseria meningitidis*, and viral hepatitis.

Culture of *Leptospira* in Body Fluids and Tissues

Leptospira can be detected by culture from blood, CSF, and peritoneal dialysate fluids during the first 10 days of illness, and from urine samples from the beginning of the second week of symptomatic illness. In some severe cases, the organisms can be detected in almost all tissues and organs and in urine for several weeks. For culture, the specimens should be collected as soon as possible while the patient is febrile and before the initiation of antibiotic treatment. Whole blood and deposit from spun plasma specimens are the preferred types of blood for culture.

The medium for cultivation of *Leptospira* is the semisolid Ellinghausen-McCullough-Johnson-Harris (EMJH) medium or Fletcher medium (Difco EMJH or Difco Fletcher medium; BD Diagnostic Systems, Sparks, MD). A modified solid medium (LVW agar) has also been described for rapid isolation and susceptibility testing of *Leptospira* spp. (46). Cultures in EMJH medium are incubated in sealed bottles at 28 to 30°C and examined weekly by dark-field microscopy. In one prospective cohort study in Thailand, the median time to culture positivity for the primary culture was 21 days, ranging from 7 to 84 days, indicating that the cultures should be maintained for at least 3 months before a negative result can be reported (47).

A positive culture provides the definitive diagnosis for leptospirosis in patients with compatible clinical syndromes. The overall yield of culture is only approximately 10% for patients with suspected leptospirosis (48).

Molecular Methods for Diagnosis and Subtyping

Because of the difficulty in culture and serologic identification of *Leptospira*, the development of accurate molecular tests for direct detection of leptospiral nucleic acid in clinical specimens has been a major advance in enabling early diagnosis of leptospirosis.

The most widely applicable molecular method is real-time PCR. 16S rRNA (*rrs*) is the most commonly used target for PCR assays (48). In a recent study, Agampodi et al. reported that the diagnostic sensitivity of a quantitative real-time PCR assay was 18.4% and 51.0% for whole blood and serum specimens, respectively (49). The bacterial load in serum and blood ranged from 10^2 to 10^6 organisms/ml, with a median leptospiral load of 8,616, 11,007, 36,100, and 15,882 organisms/ml for uncomplicated, renal failure, myocarditis, and multi-organ failure patients, respectively (49).

Two recent studies demonstrated that real-time PCR assays, using primers and probes targeting a gene encoding surface lipoprotein LipL32, have comparable sensitivity but higher specificity to *rrs*-based assays (50, 51). These LipL32-based PCR assays can potentially be a reliable, sensitive, and rapid test for the detection of *Leptospira* in acute patients.

Of the numerous molecular methods evaluated for subtyping, pulsed-field gel electrophoresis is the recommended method for strain typing and subtyping.

Clinical Indications and Test Interpretation

Culture and the microscopic agglutination test are gold-standard methods for leptospirosis diagnosis; however, they are not useful for early diagnosis. Current whole-cell-based rapid serological tests have low sensitivity for early phase leptospirosis and may have low specificity in highly endemic areas. PCR is demonstrably useful for early diagnosis, but it is unavailable in most developing countries. Thus, diagnostic methods that not only have higher sensitivity and accuracy for early phase leptospirosis but that are also widely applicable in developing countries remain to be developed. The availability of genome sequences and genetic tools of *Leptospira* spp. will accelerate our understanding of *Leptospira* pathogenesis and provide insights into the development of more efficient and accurate diagnostic tests for acute-phase leptospirosis.

REFERENCES

1. **Krieg NR, Staley JT, Brown DR, Hedlund BP, Paster BJ, Ward NL, Ludwig W, Whitman WB.** 2011. The *Bacteroidetes*, *Spirochaetes*, *Tenericutes* (*Mollicutes*), *Acidobacteria*, *Fibrobacteres*, *Fusobacteria*, *Dictyoglomi*, *Gemmatimonadetes*, *Lentisphaerae*, *Verrucomicrobia*, *Chlamydiae*, and *cetes*. *In Bergey's Manual of Systematic Bacteriology*, 2nd ed, vol 4. Springer, New York, NY.
2. **Johnson RC.** 1984. *Borrelia burgdorferi* sp. nov.: etiological agent of Lyme disease. *Int J Syst Bacteriol* **34:**496–497.
3. **Wang G, Van Dam AP, Schwartz I, Dankert J.** 1999. Molecular typing of *Borrelia burgdorferi sensu lato:* taxonomic, epidemiological, and clinical implications. *Clin Microbiol Rev* **12:**633–653.
4. **Stanek G, Reiter M.** 2011. The expanding Lyme *Borrelia* complex—clinical significance of genomic species? *Clin Microbiol Infect* **17:**487–493.

5. **Wang G, Schwartz I.** 2011. Genus *Borrelia*, p 484–531. *In* Krieg NR, Staley JT, Brown DR, Hedlund BP, Paster BJ, Ward NL, Ludwig W, Whitman WB (ed), *Bergey's Manual Of Systematic Bacteriology*, vol 4: *The Bacteroidetes*, *Spirochaetes*, *Tenericutes (Mollicutes)*, *Acidobacteria*, *Fibrobacteres*, *Fusobacteria*, *Dictyoglomi*, *Gemmatimonadetes*, *Lentisphaerae*, *Verrucomicrobia*, *Chlamydiae*, and *Planctomycetes*, 2nd ed. Springer, New York, NY.
6. **Kuehn BM.** 2013. CDC Estimates 300,000 US cases of Lyme disease annually. *JAMA* **310:**1110.
7. **Centers For Disease Control And Prevention.** 2012. Summary of notifiable diseases—United States, 2010. *MMWR* **59:**1–116.
8. **O'Connell S, Granstrom M, Gray JS, Stanek G.** 1998. Epidemiology of European Lyme borreliosis. *Zentralbl Bakteriol* **287:**229–240.
9. **Anderson JF.** 1989. Epizootiology of *Borrelia* in *Ixodes* tick vectors and reservoir hosts. *Rev Infect Dis* **11**(Suppl 6)**:**S1451–S1459.
10. **Hubalek Z, Halouzka J.** 1998. Prevalence rates of *Borrelia burgdorferi sensu lato* in host-seeking *Ixodes ricinus* ticks in Europe. *Parasitol Res* **84:**167–172.
11. **Steere AC.** 2001. Lyme disease. *N Engl J Med* **345:**115–125.
12. **Strle F, Nadelman RB, Cimperman J, Nowakowski J, Picken RN, Schwartz I, Maraspin V, Aguero-Rosenfeld ME, Varde S, Lotric-Furlan S, Wormser GP.** 1999. Comparison of culture-confirmed erythema migrans caused by *Borrelia burgdorferi sensu stricto* in New York State and by *Borrelia afzelii* in Slovenia. *Ann Intern Med* **130:**32–36.
13. **Tugwell P, Dennis DT, Weinstein A, Wells G, Shea B, Nichol G, Hayward R, Lightfoot R, Baker P, Steere AC.** 1997. Laboratory evaluation in the diagnosis of Lyme disease. *Ann Intern Med* **127:**1109–1123.
14. **Muller I, Freitag MH, Poggensee G, Scharnetzky E, Straube E, Schoerner C, Hlobil H, Hagedorn HJ, Stanek G, Schubert-Unkmeir A, Norris DE, Gensichen J, Hunfeld KP.** 2012. Evaluating frequency, diagnostic quality, and cost of Lyme borreliosis testing in Germany: a retrospective model analysis. *Clin Develop Immunol* **2012:**595427.
15. **Aguero-Rosenfeld ME, Nowakowski J, Bittker S, Cooper D, Nadelman RB, Wormser GP.** 1996. Evolution of the serologic response to *Borrelia burgdorferi* in treated patients with culture-confirmed erythema migrans. *J Clin Microbiol* **34:**1–9.
16. **Fraser CM, Casjens S, Huang WM, Sutton GG, Clayton R, Lathigra R, White O, Ketchum KA, Dodson R, Hickey EK, Gwinn M, Dougherty B, Tomb JF, Fleischmann RD, Richardson D, Peterson J, Kerlavage AR, Quackenbush J, Salzberg S, Hanson M, Van Vugt R, Palmer N, Adams MD, Gocayne J, Venter JC.** 1997. Genomic sequence of a Lyme disease spirochaete, *Borrelia burgdorferi*. *Nature* **390:**580–586.
17. **Schriefer ME.** 2011. *Borrelia*, p 924–940. *In* Versalovic J, Carroll KC, Funke G, Jorgensen JH, Landry RL, Warnock DW (ed), *Mannual of Clinical Microbiology*, 10th ed. ASM Press, Washington, DC.
18. **Wormser GP, Levin A, Soman S, Adenikinju O, Longo MV, Branda JA.** 2013. Comparative cost effectiveness of two-tiered testing strategies for the serodiagnosis of Lyme disease with non-cutaneous manifestations. *J Clin Microbiol* **51:**4045–4049.
19. **Hauser U, Lehnert G, Wilske B.** 1999. Validity of interpretation criteria for standardized Western blots (immunoblots) for serodiagnosis of Lyme borreliosis based on sera collected throughout Europe. *J Clin Microbiol* **37:**2241–2247.
20. **Centers for Disease Control and Prevention.** 1995. Recommendations for test performance and interpretation from the Second National Conference on Serologic Diagnosis of Lyme Disease. *MMWR* **44:**590–591.
21. **Aguero-Rosenfeld ME, Wang G, Schwartz I, Wormser GP.** 2005. Diagnosis of Lyme borreliosis. *Clin Microbiol Rev* **18:**484–509.
22. **Branda JA, Linskey K, Kim YA, Steere AC, Ferraro MJ.** 2011. Two-tiered antibody testing for Lyme disease with use of 2 enzyme immunoassays, a whole-cell sonicate enzyme immunoassay followed by a VlsE C6 peptide enzyme immunoassay. *Clin Infect Dis* **53:**541–547.
23. **Bacon RM, Biggerstaff BJ, Schriefer ME, Gilmore RD Jr, Philipp MT, Steere AC, Wormser GP, Marques AR, Johnson BJ.** 2003. Serodiagnosis of Lyme disease by kinetic enzyme-linked immunosorbent assay using recombinant VlsE1 or peptide antigens of *Borrelia burgdorferi* compared with 2-tiered testing using whole-cell lysates. *J Infec Dis* **187:**1187–1199.
24. **Wormser GP, Schriefer M, Aguero-Rosenfeld ME, Levin A, Steere AC, Nadelman RB, Nowakowski J, Marques A, Johnson BJ, Dumler JS.** 2013. Single-tier testing with the C6 peptide ELISA kit compared with two-tier testing for Lyme disease. *Diagn Microbiol Infect Dis* **75:**9–15.
25. **Arnaboldi PM, Seedarnee R, Sambir M, Callister SM, Imparato JA, Dattwyler RJ.** 2013. Outer surface protein C peptide derived from *Borrelia burgdorferi sensu stricto* as a target for serodiagnosis of early Lyme disease. *Clin Vaccine Immunol* **20:**474–481.
26. **Branda JA, Aguero-Rosenfeld ME, Ferraro MJ, Johnson BJ, Wormser GP, Steere AC.** 2010. 2-tiered antibody testing for early and late Lyme disease using only an immunoglobulin G blot with the addition of a VlsE band as the second-tier test. *Clin Infect Dis* **50:**20–26.
27. **Wormser GP, Bittker S, Cooper D, Nowakowski J, Nadelman RB, Pavia C.** 2001. Yield of large-volume blood cultures in patients with early Lyme disease. *J Infec Dis* **184:**1070–1072.
28. **Johnson BJ, Pilgard MA, Russell TM.** 2014. Assessment of new culture method to detect *Borrelia* species in serum of Lyme disease patients. *J Clin Microbiol* **52:**721–724.
29. **Schmidt BL.** 1997. PCR in laboratory diagnosis of human *Borrelia burgdorferi* infections. *Clin Microbiol Rev* **10:**185–201.
30. **Babady NE, Sloan LM, Vetter EA, Patel R, Binnicker MJ.** 2008. Percent positive rate of Lyme real-time polymerase chain reaction in blood, cerebrospinal fluid, synovial fluid, and tissue. *Diagn Microbiol Infect Dis* **62:**464–466.
31. **Halperin JJ, Baker P, Wormser GP.** 2013. Common misconceptions about Lyme disease. *Am J Med* **126:**264.
32. **Toledo A, Anda P, Escudero R, Larsson C, Bergstrom S, Benach JL.** 2010. Phylogenetic analysis of a virulent *Borrelia* species isolated from patients with relapsing fever. *J Clin Microbiol* **48:**2484–2489.
33. **Lescot M, Audic S, Robert C, Nguyen TT, Blanc G, Cutler SJ, Wincker P, Couloux A, Claverie JM, Raoult D, Drancourt M.** 2008. The genome of *Borrelia recurrentis*, the agent of deadly louse-borne relapsing fever, is a degraded subset of tick-borne *Borrelia duttonii*. *Plos Genet* **4:**E1000185.
34. **Cutler SJ.** 2006. Possibilities for relapsing fever reemergence. *Emerg Infect Dis* **12:**369–374.
35. **Dworkin MS, Schwan TG, Anderson DE Jr, Borchardt SM.** 2008. Tick-borne relapsing fever. *Infect Dis Clin North Am* **22:**449–468.
36. **Rhee KY, Johnson WD Jr.** 2010. Borrelia species (relapsing fever), p 3067–3069. *In* Mandell GLB, Dolin JE (ed), *Principles and Practice of Infectious Diseases*, 7th ed. Churchill Livingstone, Philadelphia, PA.
37. **Larsson C, Bergstrom S.** 2008. A novel and simple method for laboratory diagnosis of relapsing fever borreliosis. *Open Microbiol J* **2:**10–12.
38. **Elbir H, Henry M, Diatta G, Mediannikov O, Sokhna C, Tall A, Socolovschi C, Cutler SJ, Bilcha KD, Ali J, Campelo D, Barker SC, Raoult D, Drancourt M.** 2013.

Multiplex real-time PCR diagnostic of relapsing fevers in Africa. *Plos Negl Trop Dis* **7:**E2042.

39. **Porcella SF, Raffel SJ, Schrumpf ME, Schriefer ME, Dennis DT, Schwan TG.** 2000. Serodiagnosis of louse-borne relapsing fever with glycerophosphodiester phosphodiesterase (GlpQ) from *Borrelia recurrentis*. *J Clin Microbiol* **38:**3561–3571.
40. **Lopez JE, Schrumpf ME, Nagarajan V, Raffel SJ, Mccoy BN, Schwan TG.** 2010. A novel surface antigen of relapsing fever spirochetes can discriminate between relapsing fever and Lyme borreliosis. *Clin Vaccine Immunol* **17:**564–571.
41. **Levett PN.** 2001. Leptospirosis. *Clin Microbiol Rev* **14:** 296–326.
42. **Hartskeerl RA, Collares-Pereira M, Ellis WA.** 2011. Emergence, control and re-emerging leptospirosis: dynamics of infection in the changing world. *Clin Microbiol Infect* **17:**494–501.
43. **Pope V, Ari MD, Schriefer ME, Levett PN.** 2006. Immunologic methods for diagnosis of spirochetal diseases, p 477–492. *In* Detrick B, Hamilton RG, Folds JD (ed), *Manual of Molecular and Clinical Laboratory Immunology*, 7th ed. ASM Press, Washington, DC.
44. **Bourhy P, Vray M, Picardeau M.** 2013. Evaluation of an in-house ELISA using the intermediate species *Leptospira fainei* for diagnosis of leptospirosis. *J Med Microbiol* **62:**822–827.
45. **Signorini ML, Lottersberger J, Tarabla HD, Vanasco NB.** 2013. Enzyme-linked immunosorbent assay to diagnose human leptospirosis: a meta-analysis of the published literature. *Epidemiol Infect* **141:**22–32.
46. **Wuthiekanun V, Amornchai P, Paris DH, Langla S, Thaipadunpanit J, Chierakul W, Smythe LD, White NJ, Day NP, Limmathurotsakul D, Peacock SJ.** 2013. Rapid isolation and susceptibility testing of *Leptospira* spp. using a new solid medium, LVW agar. *Antimicrob Agents Chemother* **57:**297–302.
47. **Wuthiekanun V, Chierakul W, Limmathurotsakul D, Smythe LD, Symonds ML, Dohnt MF, Slack AT, Limpaiboon R, Suputtamongkol Y, White NJ, Day NP, Peacock SJ.** 2007. Optimization of culture of *Leptospira* from humans with leptospirosis. *J Clin Microbiol* **45:**1363–1365.
48. **Limmathurotsakul D, Turner EL, Wuthiekanun V, Thaipadungpanit J, Suputtamongkol Y, Chierakul W, Smythe LD, Day NP, Cooper B, Peacock SJ.** 2012. Fool's gold: why imperfect reference tests are undermining the evaluation of novel diagnostics: a reevaluation of 5 diagnostic tests for leptospirosis. *Clin Infect Dis* **55:**322–331.
49. **Agampodi SB, Matthias MA, Moreno AC, Vinetz JM.** 2012. Utility of quantitative polymerase chain reaction in leptospirosis diagnosis: association of level of leptospiremia and clinical manifestations in Sri Lanka. *Clin Infect Dis* **54:**1249–55.
50. **Cermakova Z, Kucerova P, Pliskova L, Kubickova P.** 2013. Real-time PCR method for the detection of the gene encoding surface lipoprotein lipL32 of pathogenic *Leptospira*: use in the laboratory diagnosis of the acute form of leptospirosis. *Scand J Infect Dis* **45:**593–599.
51. **Villumsen S, Pedersen R, Borre MB, Ahrens P, Jensen JS, Krogfelt KA.** 2012. Novel TaqMan PCR for detection of *Leptospira* species in urine and blood: pit-falls of *in silico* validation. *J Microbiol Methods* **91:**184–190.

Immunological Tests in Tuberculosis

CHRISTINE M. LITWIN

48

EPIDEMIOLOGY

Tuberculosis (TB) is one of the most common serious bacterial infections and remains a major challenge to global health. One-third of the human population has been infected with *Mycobacterium tuberculosis*. Globally, drug-resistant tuberculosis is emerging as a new epidemic, with approximately 0.5 million new multidrug-resistant cases annually. TB is second only to HIV as a worldwide cause of death from an infectious disease, and HIV infection, in turn, is a major risk factor for TB.

In 2011, there were an estimated 8.7 million new cases of TB (13% coinfected with HIV) and 1.4 million people died from the disease. These figures include almost 1 million deaths among HIV-negative individuals and 430,000 among people who were HIV positive. Unfortunately, the impairment of immunity caused by HIV infection implies that traditional immunological tests may be of limited value in the diagnosis of coexistent TB. The value of TB immunological testing in HIV-positive individuals is discussed for each of the available assays.

MODE OF SPREAD, RISK OF INFECTION, AND RISK OF PROGRESSION TO ACTIVE DISEASE

Most infections with *M. tuberculosis* are due to inhalation of bacteria-laden droplet nuclei transmitted by close contact with heavily infected individuals. After exposure to *M. tuberculosis*, approximately 30% of persons develop active infection (1). The remainder of infected persons harbor tubercle bacilli, which are either slowly replicating or killed in granulomas, and are without clinical symptoms. However, if cell-mediated immunity becomes impaired, residual living organisms may no longer be held in check and lead to the development of active TB. Latent TB infection (LTBI) is therefore defined as a clinical condition in which an individual has been infected with *M. tuberculosis*, but has no clinical manifestation of disease and negative cultures for the organism. In general, about 3 to 4% of infected individuals progress to active TB after the first year of exposure, and an additional 5% carry a lifetime risk of progressing to active disease (2).

DIAGNOSIS

Culture of the tubercle bacillus remains the gold standard for the diagnosis of active TB. Yet, at least one-third of patients with TB do not have a positive culture because of the inherent difficulty to grow *Mycobacterium* spp. Nucleic-amplification assays offer another technique for the direct detection of *M. tuberculosis* in clinical specimens. Significant progress has been made in the area of molecular diagnostics of TB infections. In July 2013, the FDA approved the Xpert MTB/RIF assay, which, in addition to having the ability to detect *M. tuberculosis* in clinical specimens, can also simultaneously determine if the *M. tuberculosis* strains contain genetic markers that makes them resistant to rifampin. For the diagnosis of LTBI, a delayed-hypersensitivity reaction to tuberculin or a blood test based on gamma interferon (IFN-γ) production by effectors and memory immune responses directed against *M. tuberculosis* antigens can be used. Currently, there are two commercially available FDA-approved IFN-γ release assays.

IMMUNOLOGY

TB requires a cellular immune response for control of infection. Antibodies are produced during active disease, but play no role in host defense. During infection, the different immune cells (e.g., macrophages, T cells) involved in the immune response directed against *M. tuberculosis* act to contain the infection (3). *M. tuberculosis* infection triggers a complex immune response that usually leads to the establishment of long-lasting memory T cells specifically directed against *M. tuberculosis* antigens. CD4 T cells that specifically recognize *M. tuberculosis* antigens produce IFN-γ essential for the activation of *M tuberculosis*-infected macrophages which, upon activation, can inhibit growth of the bacillus (4). IFN-γ release assays have been shown to predominantly measure the presence of *M. tuberculosis*-specific effector-memory T cells, the presence of which are considered indicative of previous *in vivo* exposure to the bacilli.

SCREENING TESTS FOR LATENT TB INFECTION

Tuberculin Testing

The tuberculin skin test (TST) has been used as a screening test for latent *M. tuberculosis* infection for more than a century. The test relies on the principles of delayed hypersensitivity to recruit memory T cells to the TST site. The

doi:10.1128/9781555818722.ch48

TST was first described by Koch in 1890 and developed by Mantoux in 1907. The first reagent used in skin testing, old tuberculin, was prepared by autoclaving and filtering autolyzed 8-week-old liquid cultures of *M. tuberculosis*. This protein extract was termed purified protein derivative (PPD). A large single lot of PPD produced by Seibert in 1939 (PPD-S) has become the international standard. Subsequent preparations have equivalent biological reactivity. The concentration has been determined such that 0.1 ml will be biologically equivalent to 0.1 μg of PPD-S (5 tuberculin units).

Tuberculin testing is performed by intradermal injection of PPD (0.1 ml) on the volar surface of the forearm with a beveled 26- or 27-gauge needle with the bevel facing upward (Mantoux test). The skin becomes raised and blanched with a 6 to 10 mm wheal if the injection has been properly placed intradermally. Deeper injections may result in false negatives due to wash out by vascular flow. The skin reaction is read at 48 to 72 h. The appropriate measurement is the diameter of induration, not the area of erythema. The diameter of induration should be read transversely across the forearm. The edge of induration can be established using a ballpoint pen.

Interpretation of the Tuberculin Test

Based on the sensitivity and specificity of the TST, three cutoff levels have been recommended for positive reactions: 5 mm, 10 mm, and 15 mm, depending on the clinical situation (Table 1). The 5-mm cutoff is used for high-risk patients such as those exposed to TB-infected persons or immunocompromised patients. The 10-mm cutoff is used for other types of high-risk patients. The 15-mm cutoff is used for patients with no risk factors.

The sensitivity of the TST ranges from 75 to 90% with 10 mm of induration, and nearly all patients with greater than 15 mm of induration are infected with *M. tuberculosis*. False-positive reactions may be caused by prior Bacilli-Calmette Guérin (BCG) vaccination or by cross-reactions caused by nontuberculous mycobacteria (NTM) (5). Technical failure due to improper injection of the PPD in the subcutaneous tissue rather than intradermally may cause a false-negative reaction. False-negative reactions occur in at least 20% of patients with active TB. Most of these false-negatives are due to the general illness and malnutrition that can reduce delayed hypersensitivity. These patients will become PPD positive 2 to 3 weeks after effective treatment of TB is initiated. Vaccination with live virus (measles, smallpox), viral infections (HIV), reticuloendothelial disease, and corticosteroid therapy may also cause false-negative reactions. During HIV infection, delayed hypersensitivity and tuberculin reactivity decreases as the CD4 cell count decreases. Testing for cutaneous anergy with antigens such as *Candida* or tetanus toxoid to control for this decrease in delayed hypersensitivity is not recommended because of the lack of reproducibility and standardization. Responsiveness to control antigens but not PPD will not necessarily exclude tuberculous infection. Immunosuppression due to stress, age, and various infectious diseases are other common causes of anergy.

Booster Effect

Tuberculin can restimulate remote hypersensitivity that has deteriorated over many years. The booster effect (a positive TST after a negative one) develops over several days after a first injection and may be persistent. This may cause interpretation problems, especially if a negative result is followed by a positive test approximately 10 weeks after a negative TST. For this reason, the "two-step method" is recommended at the time of initial testing for persons who may be tested periodically on a routine basis (e.g., health care workers). Nonreactors are retested 1 to 3 weeks after the initial test. If the second test result is positive, this indicates boosting rather than a recent tuberculin conversion due to a recent exposure. The individual should be considered infected and evaluated accordingly. However, booster reactions cannot always be distinguished from false-positive reactions due to past exposure to atypical mycobacteria.

TABLE 1 Definition of a positive tuberculin test

Diam of induration (mm)	Clinical situation
>5	Recent contacts of TB-case patients
	Human immunodeficiency virus (HIV)-infected persons
	Persons with fibrotic changes on chest radiograph consistent with prior TB
	Patients with organ transplants or otherwise immunosuppressed (e.g., receiving the equivalent of ≥15 mg/day of prednisone for 1 month or more)
>10	Recent immigrants (i.e., within the last 5 years) from countries with a high prevalence of TB
	Residents and employees of high-risk congregate settings: prisons and jails, nursing homes and long-term care facilities, hospitals, residential facilities for patients with AIDS, homeless shelters
	Injection-drug users
	Persons with the following clinical conditions that place them at high risk: silicosis, diabetes mellitus, chronic renal failure, some hematologic disorders (e.g., leukemias and lymphomas), other specific malignancies (e.g., carcinoma of the head, neck, or lung) weight loss of ≥10% of ideal body weight, gastrectomy, jejunoileal bypass
	Children <5 years of age
	Infants, children, and adolescents exposed to adults at high risk for developing active TB
>15	Patients with no known risk factor for tuberculosis

IFN-γ Release Assays

In the past 10 years, IFN-γ release assays have been developed for the identification of an immune response to *M. tuberculosis*-specific antigens and are approved by the U.S. FDA and recommended by the U.S. Centers for Disease Control and Prevention (CDC) as an aid for the detection of LTBI. A major scientific advance has been the identification of the region of difference 1 (RD1) of *M. tuberculosis*, which is absent from all strains of BCG, thus reducing the potential for cross-reactivity with BCG. Sequence data show that RD1 was deleted upon attenuation of *Mycobacterium bovis* for development of BCG. Several antigenic proteins of *M. tuberculosis* encoded by genes located in RD1 have potential for specific diagnosis of TB. The best-studied RD1 proteins are culture-filtered protein 10 (CFP-10) and early-secreted antigenic-target 6-kDa protein (ESAT-6). These two proteins have been utilized as specific antigens in the IFN-γ release assays.

Currently, there are two commercially available FDA-approved IFN-γ release assays: the QuantiFERON-TB Gold In-Tube assay (QFT-GIT) (Cellestis Ltd, Australia) and T-SPOT.*TB* assay (T-SPOT.*TB*) (Oxford Immunotec, UK). The characteristics of the two different assays are summarized in Table 2.

QuantiFERON-TB Gold In-Tube Assay

The QFT-GIT is performed by drawing 1.0 ml of blood into each of three specialized blood collection tubes: the nil control tube, the mitogen control tube (containing phytohemagglutinin, a T-cell-activating mitogen), and a TB antigen tube. The TB antigen tube contains three highly specific *M. tuberculosis* antigens: ESAT-6, CFP-10, and TB7.7. In contrast to the PPD, the antigens in the QFT-GIT are absent in most NTM and BCG strains except for *M. marinum*, *M. kansasii*, and *M. szulgai*. *M. flavescens*, *M. gastrii*, *M. xenopi*, and *M. gordonae* may also be associated with false-positive reactions with either the QFT-GIT or the T-SPOT.*TB*.

Within 16 h of collection, the tubes are incubated for 16 to 24 h at 37°C. The incubation is needed to allow memory CD4 T-cells to respond to the TB antigen. The plasma is harvested after centrifugation to separate the plasma and the red cells to assess the concentration of IFN-γ by an enzyme-linked immunosorbent assay (ELISA).

Method for Quantiferon-TB Gold In-Tube Assay

Specimen. QuantiFERON-TB GIT uses the following collection tubes:

Nil control (gray cap with white ring)
TB antigen (red cap with white ring)
Mitogen control (purple cap with white ring)

Collection. For each subject, collect 1 ml of blood by venipuncture directly into each of the QuantiFERON-TB GIT blood collection tubes. The black mark on the side of the tubes indicates the 1-ml fill volume.

Antigens have been dried onto the inner wall of the blood-collection tubes, so it is essential that the contents of the tubes be thoroughly mixed with the blood after blood draw.

Incubation.

1. Incubate the tubes upright at 37°C for 16 to 24 h.
2. After incubation of the tubes at 37°C, harvesting of plasma is facilitated by centrifuging tubes for 15 min at 2,000 to 3,000 relative centrifugal force (RCF).
3. Plasma samples can be loaded directly from blood-collection tubes into the ELISA plate.
4. Alternatively, plasma samples can be stored prior to ELISA, either in the centrifuged tubes or collected into plasma-storage containers.

Reagents. Included within the QuantiFERON-TB GIT kit:

Microplate strips coated with murine anti-human IFN-γ monoclonal (2 × 96-well plates)
Human IFN-γ standard, lyophilized (contains recombinant human IFN-γ, 8 IU/ml when reconstituted, bovine casein, 0.01% wt/vol thimerosal) (1 × vial)

TABLE 2 Methodological characteristics of T-SPOT and QFT-GIT assays

Characteristic	T-SPOT-*TB*	QFT-GIT
Format	ELISPOT	ELISA
Assay time	PBMC isolation & setup: 0.5 h	Incubation at 37°C: 16–24 h
	Incubation at 37°C: 16–20 h	Testing: 3.5 h
	Testing: 6 h	
	Drying time: 4–16 h	
Specimen	Peripheral blood mononuclear cells	Whole blood
Instrumentation	Microplate washer	Microplate washer and reader
	Hemocytometer or hematology analyzer	Centrifuges
	Stereomicroscope or plate imager	
	Centrifuges	
TB antigens	ESAT-6, CFP-10	ESAT-6, CFP-10, TB7.7
Positive control (mitogen)	Phytohemagglutinin	Phytohemagglutinin
Units	Spot-forming units (SFU)	IU/ml IFN-γ
Equivocal zone	5–7 SFU	None
Positive result	≥8 SFU	≥0.35 IU/ml, and >25% of nil
Indeterminate	>10 SFU in Nil, or <20 SFU Mitogen	>8 IU/ml nil and/or <0.5 IU/ml

Green diluent (contains bovine casein, normal mouse serum, 0.01% wt/vol thimerosal) (1 × 30 ml)

Conjugate 100× concentrate, lyophilized (murine anti-human IFN-γ horseradish peroxidase [HRP], contains 0.01% wt/vol thimerosal when reconstituted) (1 × 0.3 ml)

Wash buffer 20× concentrate (pH 7.2, contains 0.01% wt/vol thimerosal) (1 × 100 ml)

Enzyme-substrate solution (contains H_2O_2, 3,3′,5,5′ tetramethylbenzidine) (1 × 30 ml)

Enzyme-stopping solution (contains 0.5M H_2SO_4) (1 × 15 ml)

Store kit refrigerated at 2 to 8°C.

Equipment and supplies.

Biohazard cabinet class II

Mechanical pipetting device

Sterile graduated 5- or 10-ml pipettes (1 pipette/patient)

37°C humidified incubator (5% CO_2 optional)

1 ml microtubes with caps in 96-well format racks for plasma storage (20 patients/rack)

QuantiFERON microplate shaker capable of speeds between 50 and 1,000 revolutions per min (RPM)

Calibrated variable-volume pipettes capable of delivering 10 to 1,000 μl with disposable tips

Multichannel pipette capable of delivering 50 μl and 100 μl with disposable tips

Centrifuge capable of centrifuging the blood tubes at least to 3,000 RCF (*g*)

Variable-speed vortex

Timer

Measuring cylinder, 1 or 2 liters

Deionized or distilled water (enzyme immunoassay [EIA] quality), 2 liters

Microplate washer (optional)

Microplate reader fitted with 450- and 620-nm (or 650-nm) filters

Protective clothing for handling potentially infectious material

Reservoirs (polypropylene)

Procedure.

1. All plasma samples and reagents, except for conjugate 100× concentrate, must be brought to room temperature (22 ± 5°C) before use.
2. ELISA PLATE. Remove strips that are not required from the frame, reseal in the foil pouch, and return to the refrigerator for storage until required. Allow at least two strips for the QuantiFERON-TB Gold IT standards and sufficient strips for the number of subjects being tested.
3. HUMAN IFN-γ STANDARD. Reconstitute the human IFN-γ kit standard with the volume of deionized or distilled water as indicated on the label of the standard vial, ensuring complete resolubilization. Mix gently to minimize frothing. Reconstitution of the standard to the correct volume will produce a solution with a concentration of 8.0 IU/ml.
   a. Use the reconstituted kit standard to produce a dilution series of eight IFN-γ concentrations.
   b. 300 μl of the kit standard to a tube labeled as Standard 1.
   c. 150 μl of green diluent to 7 tubes (labeled Standard 2–Standard 8).
   d. Perform serial dilutions by transferring 150 μl of each standard to the next tube. Mix each tube thoroughly before the next transfer.
   e. The undiluted kit standard serves as the highest concentration (Standard 1).
   f. Green diluent serves as the zero standard (Standard 8).
4. CONJUGATE (contains 0.01% wt/vol thimerosal). Reconstitute freeze-dried conjugate 100× concentrate with 0.3 ml of deionized or distilled water.
5. Add 50 μl of freshly prepared working-strength conjugate to each ELISA well.
6. Add 50 μl of test plasma samples to appropriate wells. Finally, add 50 μl each of the Standards 1 to 8. The standards should be assayed in at least duplicate.
7. Mix the conjugate and plasma samples/standards thoroughly using a microplate shaker for 1 min at 500 to 1,000 RPM.
8. Cover each plate and incubate at room temperature (22 ± 5°C) for 120 ± 5 min.
   a. Plates should not be exposed to direct sunlight during incubation.
   b. Deviation from specified temperature range can lead to erroneous results.
9. WASH BUFFER. Each plate (12 × 8-well strips) requires 1 liter of working-strength wash buffer. Dilute 1 part wash buffer 20× concentrate with 19 parts deionized or distilled water and mix thoroughly.
10. Wash wells with 400 μl of working-strength wash buffer. Perform wash steps at least six times.
11. Add 100 μl of enzyme-substrate solution to each well and mix for 1 min at 500 to 1,000 RPM using a microplate shaker.
12. Cover each plate with a lid and incubate at room temperature (22 ± 5°C) for precisely 30 min.
13. After 30 min, add 50 μl of enzyme-stopping solution to each well and mix by gentle agitation.

Read the absorbance of each well within 5 min of terminating the reaction using a 450-nm filter, with either a 620-nm or 650-nm reference filter. Absorbance values are used to calculate results.

Calculations. The QuantiFERON-TB GIT analysis software (version 2.13 or later) that is used to generate standard curves for IFN-γ and to calculate results for the patient values is available from Cellestis. The software performs quality control of the assay, generates a standard curve, and provides a test result from calculations performed on each plasma test based on the method of interpretation.

Interpretation Criteria QFT-GIT

The positive-control mitogen assesses the performance of the test by measuring the ability of T cells to produce IFN-γ. A low-mitogen result may indicate low T-cell counts or immunosuppression, or may also indicate improper handling of the specimen. A mitogen result less than 0.5 IU/ml will result in an indeterminate result.

The negative-control nil tube assesses the background IFN-γ levels in the patient. High-background IFN-γ can be seen in patients with recent viral illness or recent live-virus vaccination (i.e., measles, polio). High-background nil levels above 8 IU/ml will result in an indeterminate result.

The nil-tube IFN-γ value is subtracted from the TB-antigen IFN-γ value and mitogen IFN-γ value to determine their absolute numbers. A positive result consistent with previous exposure to *M. tuberculosis* is an absolute TB-antigen value of ≥0.35 IU/ml that is also greater than 25% of the nil value.

Preanalytical Sources of Variability and Quality Control Issues, QFT-GIT

During the sample-collection process, there are several possible sources of error or variability of the IFN-γ quantitative result. If any of the three blood draw tubes (nil, antigen, mitogen) are underfilled or overfilled from the recommended 1.0 ml, an incorrect measurement of the IFN-γ level will occur, changing the IFN-γ quantitative result and possibly the qualitative interpretation. Additionally, if there is incomplete mixing of the TB-antigen or mitogen tubes following the blood draw, there is a potential for a false-negative result in the antigen tube or an indeterminate result due to a low mitogen-tube response. Delays in incubation or processing also negatively impact the IFN-γ result.

Quality-control issues have been discovered with the QFT-GIT in two separate incidents. In November 2011, the Stanford Hospital and Clinics clinical microbiology laboratory noted a sharp increase in positivity rate in their QFT-GIT (6). They had previously instituted a daily surveillance program since 2010 for tracking positive rates. On investigation of the increase in positivity rate, all TB-antigen tubes giving false results were traced to a single lot number. Efforts undertaken by the laboratory and the manufacturer could not discover the root cause of the problem. The FDA was contacted and subsequently that particular lot number was recalled from all laboratories in the U.S.

The second incident involving quality control with the QFT-GIT was reported by the Veterans Affairs Palo Alto Health Care System (6). A sharp increase in the indeterminate rate was discovered on review of patient results. The source of error was traced to the transportation route of the blood draw tubes through the Panama Canal; it was discovered that there was heat damage to the mitogen peptides in the tubes, subsequently resulting in low mitogen results.

These isolated problems in reagent quality of the QFT-GIT highlight the need to institute a surveillance system to monitor and detect sudden changes in positivity and indeterminate rates, and also the need to conduct parallel testing of new lots with old lots to ensure quality control is maintained.

Reproducibility, Conversions, and Reversions: Proposal of an Equivocal Range for the QFT-GIT

The QFT-GIT does not have an FDA-approved equivocal range. Studies examining the reproducibility of the QFT-GIT have observed reversions and conversions of the QFT-GIT with frequencies ranging from 12% to 50% (7–9). Conversions and reversions are thought to be secondary either to biological factors such as within-subject fluctuations, laboratory artifact, or test-related error (10, 11). There has been no consensus for how to interpret the accuracy of the test in situations where there are conversions and reversions. Because of this variability, a gray zone has been suggested for persons with fluctuating results (12, 13). Most of the reversions and conversions in the studies occurred with IFN-γ levels between 0.35 and 0.69 IU/ml. Thanassi et al. (14) used receiver-operating-characteristic (ROC) analysis on serial QFT-IT results in 575 U.S. health care workers to find the separation point between those who test repeatedly positive and those who revert. Their recommendation was to retest low-risk individuals with initial QFT results <1.11 IU/ml.

Most reversions of QFT-GITs from positive to negative come to attention when the positive result is suspected to be a false positive and the clinician repeats the test. Reversions, however, may also occur spontaneously or after therapy. Reversions after therapy are thought to represent immune clearing of the infection. Studies have shown a decrease in quantitative results of IFN-γ responses with the treatment of LTBI. Studies, however, have not confirmed that LTBI treatment increases the reversion rate of IGRAs from positive to negative (15).

T-SPOT. *TB* Assay

For the T-SPOT.*TB* assay, 8 ml of whole blood is required and the assay must be performed within 8 h of blood collection. Alternatively, the manufacturer provides a reagent (T-Cell Xtend) which extends processing time to 32 h after blood collection. The T-cell-containing peripheral blood mononuclear cell (PBMC) fraction is separated from whole blood, counted, and inoculated into four separate microtiter plate wells (250,000 cells/well) provided in the T-SPOT.*TB* assay kit. The microtiter wells are precoated with antibodies against IFN-γ. Specific TB antigens (ESAT-6 and CFP-10) and mitogen (PHA) are also added.

Microtiter-plate wells are incubated 16 to 20 h at 37°C with 5% CO_2. During incubation, IFN-γ is released from activated T-cells and captured by monoclonal antibodies. The number of IFN-γ-secreting T-cells (represented as spot-forming units [SFU]) are detected by ELISPOT assay, an enzyme-linked immunospot assay that labels the IFN-γ-secreting T-cells as dark spots on the plate wells. After incubation, the wells are washed and a secondary conjugated IFN-γ antibody is added and incubated for 1 h. After another wash, substrate is added, which produces spots where the IFN-γ was secreted by the activated T-cells. The spots are counted using a magnifying glass or stereomicroscope.

Method for T-SPOT.*TB* Test

Specimen.

1. When using the T-SPOT.*TB* test without the use of T-Cell Xtend reagent, blood samples should be processed within 8 h of collection.
2. Samples may be collected into either sodium citrate or sodium heparin Vacutainer-CPT tubes with PBMCs separated in the tube.
3. Alternatively, blood samples may be collected into lithium-heparin tubes, with PBMCs being subsequently separated using standard separation techniques such as Ficoll-Paque or alternative methods to purify the PBMC fraction.
4. Blood-collection tubes containing the anticoagulant ethylenediaminetetraacetic acid (EDTA) should not be used.
5. If using Ficoll-Paque Plus, dilute the blood with an equal volume of RPMI-1640 medium (1 part blood to 1 part RPMI).
6. Layer carefully the diluted blood onto Ficoll-Paque Plus (2 to 3 parts diluted blood to 1 part Ficoll-Paque) and centrifuge at 1,000 RCF (*g*) for 22 min at room temperature (18 to 25°C).
7. When using the T-SPOT.*TB* test with T-Cell Xtend reagent, blood samples should be collected into lithium-heparin tubes. The T-Cell Xtend reagent

should be added prior to PBMC separation using standard separation techniques. Whole-blood samples should be stored at room temperature (18 to 25°C) between 0 and 32 h postvenipuncture with the use of T-Cell Xtend reagent.

8. Collect the white, cloudy band of PBMCs using a pipette and transfer to a 15-ml conical centrifuge tube. Bring the volume to 10 ml with prewarmed cell culture medium.
9. Centrifuge at 600 RCF (*g*) for 7 min. Pour off the supernatant and resuspend the pellet in 1 ml medium.
10. Bring the volume to 10 ml with fresh medium and centrifuge at 350 RCF (*g*) for 7 min.
11. Pour off the supernatant and resuspend the pellet in 0.7 ml cell-culture medium.

Reagents. Included within the T-SPOT.*TB* Kit:

1 microtiter plate: 96 wells, supplied as 12 × 8-well strips in a frame, coated with a mouse monoclonal antibody to IFN-γ.

2 vials (0.8 ml each) Panel A: contains ESAT-6 antigens.

2 vials (0.8 ml each) Panel B: contains CFP-10 antigens.

2 vials (0.8 ml each) positive control: contains phytohemagglutinin (PHA).

1 vial (50 μl) 200× concentrated conjugate reagent: mouse monoclonal antibody to the cytokine IFN-γ conjugated to alkaline phosphatase.

1 bottle (25 ml) substrate solution: BCIP/NBT plus solution.

Equipment and supplies.

8-well strip plate frame.

Biohazard cabinet class II.

Blood-collection tubes, such as Vacutainer CPT or heparinized tubes.

T-Cell Xtend reagent: whole-blood samples stored at room temperature (18 to 25°C) between 0 and 32 h postvenipuncture; can be processed with the use of T-Cell Xtend reagent.

Ficoll (if not using CPT tubes).

A centrifuge for preparation of PBMCs (capable of at least 1,800 RCF (*g*) and able to maintain the samples at room temperature (18 to 25°C) if using density centrifugation methods to separate the PBMCs).

Equipment and reagents to enable counting of PBMCs, either manually using trypan blue (or other appropriate stain) and a hemocytometer on a microscope or automatically using a suitable hematology analyzer.

A humidified incubator capable of 37 ± 1°C with a 5% CO_2 supply.

An automatic microtiter plate washer or an 8-channel or stepper pipette to manually wash plates.

Adjustable pipettes to cover a range of volumes from 1 to 1,000 μl (such as four Gilson pipettes capable of delivering volumes of 1–10 μl, 2–20 μl, 20–200 μl, and 100–1,000 μl) and sterile pipette tips.

Sterile phosphate-buffered saline (PBS) solution such as GIBCO 1× D-PBS (Invitrogen; catalogue no. 14040-133).

Distilled or deionized water.

A means of visualizing the wells or capturing a digital image of the well, such as a stereomicroscope, magnifying glass, or plate imager to allow counting of spots.

Sterile cell culture medium such as GIBCO AIM-V. Cell culture media should be prewarmed to 37°C before use with the T-SPOT.*TB* test.

Reagent preparation.

1. The vials of *M. tuberculosis* ESAT-6 antigens, *M. tuberculosis* CFP-10 antigens, and the positive control are supplied ready to use.
2. Prepare a 1:200 dilution working conjugate-reagent solution.
3. The substrate solution is supplied ready to use.

Cell counting and dilution. The T-SPOT.*TB* test requires 250,000 ± 50,000 PBMCs per well. A total of four wells are required for each patient sample; thus 1×10^6 PBMCs is required per patient. The number of *M. tuberculosis* T cells in the specimen is normalized to a fixed number of PBMCs.

1. Perform a PBMC count. Cells can be counted by a variety of methods, including manual counting using trypan blue (or other appropriate stain) and a hemocytometer, or using an automated hematology analyzer.
2. Calculate the concentration of PBMCs present in the stock cell suspension.

Plate setup and incubation.

1. The T-SPOT.*TB* test requires four wells to be used for each patient sample. An ESAT-6, CFP-10, nil control, and positive control well should be run for each individual patient sample. No standard curves are required.
2. Remove the precoated 8-well strips from the packaging, clip into a plate frame, and allow to equilibrate to room temperature. Remove the required number of strips only, reseal any remaining unused strips and the desiccant pouch in the outer foil packaging, and return to storage at 2 to 8°C.
3. Add 50 μl of AIM-V cell culture for nil, positive control, and CFP-10 or ESAT-6 to one of the four wells for each patient sample.
4. To each of the four wells to be used for a patient sample, add 100 μl of the patient's final cell suspension (containing 250,000 cells). Use a new tip for each individual patient's cells to avoid cross-contamination between wells.
5. Incubate the plate with the lid on in a humidified incubator at 37°C with 5% CO_2 for 16 to 20 h.

Spot development and counting.

1. Remove the plate from the incubator and discard the cell-culture medium.
2. Add 200 μl PBS solution to each well.
3. Discard the PBS solution. Repeat the well washing an additional 3 times with PBS.
4. Dilute concentrated conjugate reagent 200× in PBS.
5. Add 50 μl conjugate-reagent solution to each well and incubate at 2 to 8°C for 1 h.
6. Discard the conjugate and perform four PBS washes.
7. Add 50 μl substrate solution to each well and incubate at room temperature for 7 min.
8. Wash the plate thoroughly with distilled water to stop the reaction.

9. Allow the plate to dry. Allow 4 h drying time at 37°C or at least 16 h at room temperature.
10. Count and record the number of distinct, dark-blue spots on the membrane of each well.

Interpretation Criteria: T-SPOT.*TB* Test

As with the QFT-GIT, the positive-control mitogen assesses the performance of the test by measuring the ability of T-cells to produce IFN-γ and should be at least ≥8 SFU for the test to be valid. A low mitogen result may indicate low T-cell counts, immunosuppression, or improper handling of the specimen.

The negative-control nil tube assesses the background IFN-γ levels in the patient. High background IFN-γ levels of >10 SFU will result in an indeterminate result and can be seen in patients with recent viral illness or recent live-virus vaccination. When a patient's sample shows indeterminate results or borderline results (5 to 7 SFU), it is recommended that new blood samples be drawn and retested. If after retesting the results remain indeterminate and a technical error is ruled out, T-cell anergy may be a possible explanation. A positive result consistent with previous exposure to *M. tuberculosis* is a TB antigen value of ≥8 SFU.

Interpretation of Quantitative IGRA (QFT-GIT or T-SPOT.*TB*) Results

According to CDC recommendations, "both the qualitative results and the quantitative assay measurements for IGRAs should be reported" (16). However, in the absence of interpretive guidelines, the practice of reporting quantitative results can lead to false assumptions and misinterpretation. It is not clear whether higher IFN-γ levels correlate with greater risk of progression to active TB. There are two recommendations that should be followed with regard to the interpretation of quantitative IGRA results. First, there is not enough evidence at this time to use quantitative results for the purpose of therapeutic monitoring or to predict the risk of progression to active disease. Quantitative results, however, are useful for predicting the likelihood for reversion or conversion of test results when the IFN-γ response is in the gray zone (i.e., between 0.35 and 1.11 IU/ml; see discussion above).

Advantages and Disadvantages of IGRAs

IGRAs detect the presence of persistent cellular immune responses toward *M. tuberculosis* specific antigens ESAT-6, CFP-10, and TB7.7 (additionally for QFT-GIT), which are known to be absent in most NTM as well as in BCG strains. Therefore, there will be fewer false-positive reactions in patients previously vaccinated with BCG and those patients previously infected with NTM. There are, however, a number of NTM that are known or reported to cause a positive IGRA; these include *M. flavescens, M. marinum*, *M. kansasii*, *M. szulgai*, *M. xenopi*, and *M. gordonae*. It is important to note that these same patients may also have a positive PPD, though usually ≤10 mm. Since IGRAs detect the presence of *M. tuberculosis*-specific effector-memory T-cells, it cannot distinguish between latent or active disease. Clinical manifestations, culture, sputum microscopy, and chest X ray may be needed to confirm the diagnosis of active TB infection. As discussed earlier, the higher specificity of the antigens used in IGRAs may decrease the number of false-positive test results when investigating LTBI and, therefore, prevent further medical evaluations and treatment. Individuals being tested for LTBI need only present once to the testing facility for blood draw, increasing the likelihood that a diagnosis will be made. The *in vitro* assays have a rapid turnaround time and are standardized to decrease interperson variability when interpreting the results.

There are several disadvantages of performing IGRA testing that should be pointed out. IGRA testing requires drawing blood from individuals, which may be especially problematic in children. The QFT-GIT requires 3 ml of blood, whereas the T-SPOT.*TB* requires 8 ml. The testing needs to be conducted within a specific time period. The QFT-GIT needs to be incubated at 37°C by the blood-draw laboratory within 16 h after blood draw, spun down after 16 to 24 h of incubation, then sent (refrigerated) to a reference laboratory. With the T-SPOT.*TB*, the blood draw needs to be received by the reference lab and the T-cells need to be isolated within 8 h of the blood draw and processed. These tests are more technically demanding and have higher laboratory resource needs. Highly trained personnel are required along with access to reagents and laboratory instrumentation.

Direct and Indirect Costs of IGRAs versus TST

Two types of costs for IGRAs should be considered: direct costs and indirect costs. In a cost-effectiveness study of LTBI contact screening in the United Kingdom by Pooran et al. (17), QFT-GIT testing cost 54 EUR ($69 U.S. dollars), T-SPOT.*TB* cost €66 ($85 US), and TST cost €19.30 ($24 US). The main conclusion of the study was that although the direct costs of IGRAs are overall more than for the TST, a dual strategy of reflex-testing positive TSTs to an IGRA for confirmation was the most cost-effective strategy.

In a study by Shah et al. (18), in a low TB-prevalence setting in the U.S., the QFT-GIT cost $44 per test. They found in testing for LTBI that the dual strategy was, again, the most cost-saving algorithm. Numerous other studies have shown that IGRAs are more cost-saving than TST for certain groups such as close contacts, those infected with HIV, and foreign-born, regardless of time in the country. In conclusion, IGRAs lead to fewer false-positive results, and consequently to fewer chest X rays, fewer prescriptions of prophylaxis, and fewer clinic visits, leading overall to a more cost-effective diagnostic test either as a single test or dual-strategy test. Cost effectiveness values will increase in areas with a lower prevalence of LTBI.

Sensitivity and Specificity of IGRAs in the Diagnosis of LTBI

The ability to judge the accuracy of the TST and IGRAs has been complicated by the lack of a gold standard for LTBI. Sensitivity has been estimated by using culture-confirmed cases. Using culture as a gold standard is problematic since active disease and latent infection are two distinct disease conditions with very different clinical outcomes. More accurate estimates based on progression of LTBI to active TB are now being used. There are wide variations in sensitivity estimates for the QFT-GIT, T-SPOT.*TB*, and TST depending on the type of population studied and the type of study. When meta-analyses are conducted on a large number of studies, overall, the T-SPOT.*TB* tends to be more sensitive than QFT-GIT, whereas the QFT-GIT tends to be more specific. In an extensive review of a number of studies comparing the TST and IGRAs in patients with culture-confirmed TB, the overall sensitivities for T-SPOT.*TB*, QFT-GIT, and TST were 90%, 83%, and 89%, respectively (16) (Table 3). In the same study, the collective specificities for T-SPOT.*TB*, QFT-GIT, and TST were 88%, 99%, and 85%, respectively. Yet, in a number of studies involving patients who progressed to active

TB after exposure to active TB, the sensitivities have been widely variable, ranging from 40 to 100% (13). These results emphasize the caveat that a negative IGRA does not necessarily rule out the diagnosis of LTBI. IGRAs, especially the QFT-GIT, have a distinct advantage over TST in diagnosing LTBI in BCG-vaccinated populations, as the IGRAs do not give false positives in BCG-vaccinated patients. In a systematic review and meta-analysis by Pai et al. (19), the specificity of QFT-GIT in BCG-nonvaccinated and BCG-vaccinated populations was 99% and 96%, respectively (Table 3). The specificity for T-SPOT.*TB* and TST in non-BCG-vaccinated populations was 100% and 97%, respectively. In contrast, the specificity for T-SPOT.*TB* and TST in BCG-vaccinated populations was only 84.7% and 59%, respectively (Table 3). Therefore, in a low-risk, BCG-vaccinated patient with a positive TST and negative IGRA, it is reasonable to assume that the TST result is a false positive.

In the case of a patient with a negative TST and positive IGRA, if the individual is considered to be high risk, then the negative TST should not preclude further studies. Longitudinal studies suggest that the TST is more sensitive than the IGRA in high-risk populations (20). IGRAs, however, may be more sensitive than TST in detecting recent exposure.

Is There a Role of IGRAs in the Diagnosis of Active TB?

Active TB infection is diagnosed by evaluating the patient's medical history, physical exam, and chest X ray and by identifying *M. tuberculosis* by microbiologic techniques such as sputum-smear microscopy and/or culture, or by molecular techniques such as nucleic acid amplification. IGRAs have not been developed for the diagnosis of active TB. IGRAs were primarily developed to detect the cell-mediated immune response toward a set of recombinant *M. tuberculosis* antigens. Therefore, these tests cannot differentiate between active and latent TB infection.

However, in certain clinical circumstances—such as in patients with extrapulmonary TB, in patients who test negative for acid-fast bacilli in sputum and/or are negative on culture, in TB diagnosis in children, or in the differential diagnosis of NTM—IGRAs may provide useful supplementary information. Overwhelming active TB infection may, however, suppress the cellular immune response and cause a negative IGRA result.

In a meta-analysis assessing the accuracy of QFT-GIT, T-SPOT.*TB*, or TST in patients with a clinical suspicion of active TB disease, both culture-confirmed and nonconfirmed cases, the pooled sensitivities of the QFT-GIT, T-SPOT.*TB*, and TST were 80% (95% confidence interval [CI] 75–84%), 81% (95% CI 78–84%), and 65% (95% CI 61–68%), respectively (21). In the same meta-analysis, the specificity of IGRAs in the diagnosis of TB specificity was assessed in control groups who were considered to have a low risk of being infected with *M. tuberculosis*. The pooled specificities of the QFT-GIT, T-SPOT.*TB*, and TST were 79% (95% CI 75–82%), 56% (95% CI 56–62%), and 59% (75% CI 72–78%), respectively (21). Quantitative results from IGRAs have not been shown to have a predictive value for progression to active disease. Therefore, quantitative results should not be used for risk assessment for patients with a concern for active TB disease.

IGRAs in Immunocompromised Persons and HIV-Infected Patients

Immunocompromised patients, such as those who are receiving immunosuppressive drugs or individuals with HIV, represent a group of patients who are at a high risk of reactivating latent TB infection. Screening for LTBI is highly recommended for these groups of individuals. However, there are only a limited number of studies available on the accuracy of IGRAs in these high-risk groups. There are no U.S. data on the predictive value of IGRAs in HIV-infected patients, and poor concordance has been reported between TSTs and IGRAs in this population (22). Current CDC guidelines recommend treatment of LTBI in HIV-infected patients with either a positive TST or IGRA. Immunocompromised patients have been shown to have reduced IGRA responses compared to immunocompetent patients, with immunocompromised patients exhibiting a higher percentage of indeterminate results. It is recommended that IGRAs be performed as early as possible in the course of HIV infection, before a decline in CD4 T-cell counts occurs.

The positive-control mitogen tube will measure the ability of the patient's CD4 T-cells to produce IFN-γ. This function will be impaired with CD4 T-cell counts below 100/ml. False-negative or indeterminate IGRA results are commonly seen in HIV-infected individuals with advanced HIV infection and low CD4 T-cell counts. Studies have suggested that the T-SPOT.*TB* test may have less indeterminate results since a standardized number of cells per assay is used for lower CD4 T-cell counts, whereas the QFT-GIT test uses a standardized volume of blood per assay (23).

False-positive QFT-TB results have also been reported in HIV-infected patients. A study by Gray et al. in 2012 (24) observed that 80.5% of U.S.-born HIV-infected patients at low risk for TB exposure reverted to negative from positive in serial testing. Seventy-six percent of the reversions occurred in patients with an IFN-γ level of <1.0 IU/ml, which is consistent with the reversion rate observed in a number of previous studies of low-risk individuals with low-positive IGRA results (see discussion in previous section).

TABLE 3 Sensitivities and specificities of QFT-GIT, T-SPOT, and TST assays

Assay	Overall for LTBI (%)[a]		Non-BCG-vaccinated for LTBI[b] (%)	BCG-vaccinated for LTBI[b] (%)	Suspected active TB[c] (%)	
	Sensitivity	Specificity	Specificity	Specificity	Sensitivity	Specificity
QFT-GIT	83	99	99	96	80	79
T-SPOT.*TB*	90	88	100	84.7	81	56
TST	89	85	97	59	65	59

[a]Reference 16: meta-analysis of the overall accuracy of all three assays.
[b]Reference 19: specificity of all three assays in non-BCG- and BCG-vaccinated populations for LTBI.
[c]Reference 21: meta-analysis assessing the accuracy of all three assays in suspected active TB disease.

However, 24.2% of the HIV-positive patients who reverted to negative had IFN-γ IU/ml levels that were >1.0 IU/ml on initial testing. The authors of the study concluded that the positive predictive value of IGRAs is quite low when testing a large number of HIV-infected patients at low risk for TB. This study thus provided supportive evidence for the high rate of poor concordance between IGRAs and TSTs in HIV patients in the U.S. in general (22). They promoted the strategy of retesting positive IGRAs in HIV-infected patients with no TB exposure risks.

IGRAs in Children

A very limited number of studies exist describing the utility of QFT-GIT and T-SPOT.*TB* testing in children, especially for those aged <5 years. For this reason, and because rates of progression from latent infection to active disease are higher in infants and young children, extreme caution is warranted when using IGRAs in children aged <5 years. Lewinsohn et al. (25) observed that indeterminate rates for IGRAs were much more frequent in immunocompromised children and in young children <5 years of age. The authors also concluded that children ≥5 years of age can be tested with IGRAs for LTBI and that IGRAs may be used as an adjunct to other tests for active TB.

Although the majority of indeterminate results in children are thought to be due to a low mitogen response, the reasons for low mitogen responses in young children are not clear. The mitogen might not work well in young children as a result of a lack of immunologic maturity. Children ≥5 years are less likely to develop active TB or to have severe forms of the disease. Therefore, less caution might be required when implementing IGRA testing in these older children.

The sensitivity of IGRAs in children is expected to be comparable to TST. In one study of 28 children with culture-confirmed active TB who were aged 4 months to 7 years, estimates of sensitivity for TST, QFT-GIT, and T-SPOT.*TB* were comparable at 100%, 93%, and 93%, respectively ($P = 0.15$) (26). However, in a recent study performed in Africa by Machingaidze et al. (27), there was no clear evidence that IGRAs should replace TST for detecting LTBI in children. These investigators concluded that it may be best to use both tests in screening for LTBI. Sensitivity of the IGRA for TB disease was no different from TST, and a significantly reduced IGRA sensitivity was found in high-burden TB settings compared with low-burden TB settings. The specificity of IGRAs in children, however, should be expected to be high. In one study, QFT-GIT and T-SPOT.*TB* showed high specificity for *M. tuberculosis* infection even among children whose TST specificity was reduced to 22% because of NTM infections (26).

SEROLOGIC TESTS FOR ACTIVE TB INFECTION

The first attempt to diagnose active TB by serology was in 1898 by Arloing (28), who reported that sera from TB patients could agglutinate tubercle bacilli. Since the introduction of the ELISA methodology, there has been a considerable amount of interest in the development of serologic tests for the detection of active TB infection, particularly with regard to patients who are unable to produce adequate sputum, are sputum-smear negative, or are suspected of having extrapulmonary TB. Although the role of antibody-mediated immunity in the protection against *M. tuberculosis* is unclear, active *M. tuberculosis* infection often elicits the production of antibodies to several antigens that may be used as markers of active TB infection. Most researchers in the field agree that accurate serological tests for the diagnosis of active TB will require using multiple TB antigens (29, 30). Any single *M. tuberculosis* antigen is probably not sensitive enough to be used to cover the multiple-antibody profiles of active-TB patients. A number of companies have developed and marketed commercial tests for the serological detection of antibodies, mostly of the IgG class, typically using the ELISA technique.

Sensitivity and Specificity of Commercial TB Serological Tests

Commercially available TB serological tests have varied widely in accuracy, with reported sensitivities and specificities that range from 10% to 90% and 47% to 100%, respectively, depending on antigens used, number of subjects, study design, and geographic site (31).

Although recent studies have identified important problems in TB serodiagnostics, they have also identified several promising candidate antigens (32–35). Important methodological problems have been identified that are inherent with ELISA testing in general, including false-positive results due to autoimmune disease and false-negatives due to immunosenescence or immune deficiency (36). Despite their limitations, TB serologic tests could eventually have adjunctive value in smear-negative pulmonary and extrapulmonary cases. Testing for IgG antibodies to *M. tuberculosis* multiepitope recombinant antigens is offered only in a few reference laboratories and ELISA kits are available commercially.

URINE ANTIGEN TESTING FOR THE DIAGNOSIS OF ACTIVE TB INFECTION

M. tuberculosis urinary-antigen detection has been viewed as a possible future adjunctive test for the diagnosis of active TB infection, since it has the potential to overcome the limitations inherent with immune-based assays. The most studied *M. tuberculosis* urinary diagnostic assay detects the cell wall lipopolysaccharide lipoarabinomannan (LAM).

Simple lateral-flow versions of the LAM assay have been produced as point-of-care tests. The first clinical evaluation of the Determine TB-LAM (Alere, Waltham, MA) was conducted among HIV-infected patients in South Africa. The overall sensitivity was low (28.2%) but was highest in those with the lowest CD4 count (<50 cells/ml), with a sensitivity of 66.7% (37). In a second study from South Africa, two groups of patients were recruited: HIV-infected patients suspected of having TB and a control group of HIV-infected patients with a non-TB diagnosis (37). Sensitivity was 45% when compared to a gold standard that additionally incorporated clinical-radiological diagnoses with a positive response to TB treatment. Sensitivity increased to 71% when the results were combined with those of sputum-smear microscopy. Specificity, however, was poor, 66% when using a very faint positive band as a positive, but improved to 96% when a darker positive band was used. Cross-reactivity studies with the LAM ELISA system showed low-level cross-reactivity with *M. avium*, *M. kansasii*, and *M. fortuitum*.

In summary, the high specificity and moderate sensitivity of a urinary antigen LAM may be useful in the diagnosis of active TB in HIV-infected patients, especially those with advanced immunodeficiency. Further studies will be needed to evaluate the clinical indications and usefulness of the assay as an adjunctive TB diagnostic.

REFERENCES

1. **Grzybowski S, Barnett GD, Styblo K.** 1975. Contacts of cases of active pulmonary tuberculosis. *Bull Int Union Tuberc* **50:**90–106.
2. **Horsburgh CR Jr.** 2004. Priorities for the treatment of latent tuberculosis infection in the United States. *N Eng J Med* **350:**2060–2067.
3. **Tufariello JM, Chan J, Flynn JL.** 2003. Latent tuberculosis: mechanisms of host and bacillus that contribute to persistent infection. *Lancet Infect Dis* **3:**578–590.
4. **Nathan CF, Murray HW, Wiebe ME, Rubin BY.** 1983. Identification of interferon-gamma as the lymphokine that activates human macrophage oxidative metabolism and antimicrobial activity. *J Exp Med* **158:**670–689.
5. **ATS/CDC Statement Committee on Latent Tuberculosis Infection Membership List.** 2000. Targeted tuberculin testing and treatment of latent tuberculosis infection. American Thoracic Society. *MMWR Morb Mortal Wkly Rep* **49**(RR06)**:**1–54.
6. **Slater M, Parsonnet J, Banaei N.** 2012. Investigation of false-positive results given by the QuantiFERON-TB Gold In-Tube assay. *J Clin Microbiol* **50:**3105–3107.
7. **Detjen AK, Loebenberg L, Grewal HM, Stanley K, Gutschmidt A, Kruger C, Du Plessis N, Kidd M, Beyers N, Walzl G, Hesseling AC.** 2009. Short-term reproducibility of a commercial interferon gamma release assay. *Clin Vaccine Immunol* **16:**1170–1175.
8. **Pai M, Joshi R, Dogra S, Zwerling AA, Gajalakshmi D, Goswami K, Reddy MV, Kalantri A, Hill PC, Menzies D, Hopewell PC.** 2009. T-cell assay conversions and reversions among household contacts of tuberculosis patients in rural India. *Int J Tuberc Lung Dis* **13:**84–92.
9. **Ewer K, Millington KA, Deeks JJ, Alvarez L, Bryant G, Lalvani A.** 2006. Dynamic antigen-specific T-cell responses after point-source exposure to *Mycobacterium tuberculosis*. *Am J Respir Crit Care Med* **174:**831–839.
10. **van Zyl-Smit RN, Pai M, Peprah K, Meldau R, Kieck J, Juritz J, Badri M, Zumla A, Sechi LA, Bateman ED, Dheda K.** 2009. Within-subject variability and boosting of T-cell interferon-gamma responses after tuberculin skin testing. *Am J Respir Crit Care Med* **180:**49–58.
11. **Perry S, Sanchez L, Yang S, Agarwal Z, Hurst P, Parsonnet J.** 2008. Reproducibility of QuantiFERON-TB gold in-tube assay. *Clin Vaccine Immunol* **15:**425–432.
12. **Pai M, Joshi R, Dogra S, Mendiratta DK, Narang P, Kalantri S, Reingold AL, Colford JM Jr, Riley LW, Menzies D.** 2006. Serial testing of health care workers for tuberculosis using interferon-gamma assay. *Am J Respir Crit Care Med* **174:**349–355.
13. **Herrera V, Perry S, Parsonnet J, Banaei N.** 2011. Clinical application and limitations of interferon-gamma release assays for the diagnosis of latent tuberculosis infection. *Clin Infect Dis* **52:**1031–1037.
14. **Thanassi W, Noda A, Hernandez B, Newell J, Terpeluk P, Marder D, Yesavage JA.** 2012. Delineating a retesting zone using receiver operating characteristic analysis on serial QuantiFERON tuberculosis test results in US healthcare workers. *Pulm Med* **2012:**291294.
15. **Lee SH, Lew WJ, Kim HJ, Lee HK, Lee YM, Cho CH, Lee EJ, Lee DY, Ryu SW, Oh SY, Kim SO, Shim TS.** 2010. Serial interferon-gamma release assays after rifampicin prophylaxis in a tuberculosis outbreak. *Respir Med* **104:**448–453.
16. **Mazurek GH, Jereb J, Vernon A, LoBue P, Goldberg S, Castro K; IGRA Expert Committee; Centers for Disease Control and Prevention (CDC).** 2010. Updated guidelines for using Interferon Gamma Release Assays to detect *Mycobacterium tuberculosis* infection—United States, 2010. *MMWR Recomm Rep* **59:**1–25.
17. **Pooran A, Booth H, Miller RF, Scott G, Badri M, Huggett JF, Rook G, Zumla A, Dheda K.** 2010. Different screening strategies (single or dual) for the diagnosis of suspected latent tuberculosis: a cost effectiveness analysis. *BMC Pulm Med* **10:**7.
18. **Shah M, Miele K, Choi H, DiPietro D, Martins-Evora M, Marsiglia V, Dorman S.** 2012. QuantiFERON-TB gold in-tube implementation for latent tuberculosis diagnosis in a public health clinic: a cost-effectiveness analysis. *BMC Infect Dis* **12:**360.
19. **Pai M, Zwerling A, Menzies D.** 2008. Systematic review: T-cell-based assays for the diagnosis of latent tuberculosis infection: an update. *Ann Intern Med* **149:**177–184.
20. **Dheda K, van Zyl Smit R, Badri M, Pai M.** 2009. T-cell interferon-gamma release assays for the rapid immunodiagnosis of tuberculosis: clinical utility in high-burden vs. low-burden settings. *Curr Opin Pulm Med* **15:**188–200.
21. **Sester M, Sotgiu G, Lange C, Giehl C, Girardi E, Migliori GB, Bossink A, Dheda K, Diel R, Dominguez J, Lipman M, Nemeth J, Ravn P, Winkler S, Huitric E, Sandgren A, Manissero D.** 2011. Interferon-γ release assays for the diagnosis of active tuberculosis: a systematic review and meta-analysis. *Eur Respir J* **37:**100–111.
22. **Cattamanchi A, Ssewenyana I, Davis JL, Huang L, Worodria W, den Boon S, Yoo S, Andama A, Hopewell PC, Cao H.** 2010. Role of interferon-gamma release assays in the diagnosis of pulmonary tuberculosis in patients with advanced HIV infection. *BMC Infect Dis* **10:**75.
23. **Rangaka MX, Wilkinson KA, Seldon R, Van Cutsem G, Meintjes GA, Morroni C, Mouton P, Diwakar L, Connell TG, Maartens G, Wilkinson RJ.** 2007. Effect of HIV-1 infection on T-cell-based and skin test detection of tuberculosis infection. *Am J Respir Crit Care Med* **175:**514–520.
24. **Gray J, Reves R, Johnson S, Belknap R.** 2012. Identification of false-positive QuantiFERON-TB Gold In-Tube assays by repeat testing in HIV-infected patients at low risk for tuberculosis. *Clin Infect Dis* **54:**e20–23.
25. **Lewinsohn DA, Lobato MN, Jereb JA.** 2010. Interferon-gamma release assays: new diagnostic tests for *Mycobacterium tuberculosis* infection, and their use in children. *Curr Opin Pediatr* **22:**71–76.
26. **Detjen AK, Keil T, Roll S, Hauer B, Mauch H, Wahn U, Magdorf K.** 2007. Interferon-gamma release assays improve the diagnosis of tuberculosis and nontuberculous mycobacterial disease in children in a country with a low incidence of tuberculosis. *Clin Infect Dis* **45:**322–328.
27. **Machingaidze S, Wiysonge CS, Gonzalez-Angulo Y, Hatherill M, Moyo S, Hanekom W, Mahomed H.** 2011. The utility of an interferon gamma release assay for diagnosis of latent tuberculosis infection and disease in children: A systematic review and meta-analysis. *Pediatr Infect Dis J* **30:**694–700.
28. **Arloing S.** 1898. Agglutination de bacille de la tuberculose vrate. *C R Acad Sci* **126:**1398–1400.
29. **Abebe F, Holm-Hansen C, Wiker HG, Bjune G.** 2007. Progress in serodiagnosis of *Mycobacterium tuberculosis* infection. *Scand J Immunol* **66:**176–191.
30. **Garg SK, Tiwari RP, Tiwari D, Singh R, Malhotra D, Ramnani VK, Prasad GB, Chandra R, Fraziano M, Colizzi V, Bisen PS.** 2003. Diagnosis of tuberculosis: available technologies, limitations, and possibilities. *J Clin Lab Anal* **17:**155–163.
31. **Steingart KR, Henry M, Laal S, Hopewell PC, Ramsay A, Menzies D, Cunningham J, Weldingh K, Pai M.** 2007. Commercial serological antibody detection tests for the diagnosis of pulmonary tuberculosis: a systematic review. *PLoS Med* **4:**e202. doi:10.1371/journal.pmed.0040202
32. **Samanich K, Belisle JT, Laal S.** 2001. Homogeneity of antibody responses in tuberculosis patients. *Infect Immun* **69:**4600–4609.

33. **Sartain MJ, Slayden RA, Singh KK, Laal S, Belisle JT.** 2006. Disease state differentiation and identification of tuberculosis biomarkers via native antigen array profiling. *Mol Cell Proteomics* **5:**2102–2113.
34. **Hendrickson RC, Douglass JF, Reynolds LD, McNeill PD, Carter D, Reed SG, Houghton RL.** 2000. Mass spectrometric identification of mtb81, a novel serological marker for tuberculosis. *J Clin Microbiol* **38:**2354–2361.
35. **Houghton RL, Lodes MJ, Dillon DC, Reynolds LD, Day CH, McNeill PD, Hendrickson RC, Skeiky YA, Sampaio DP, Badaro R, Lyashchenko KP, Reed SG.** 2002. Use of multiepitope polyproteins in serodiagnosis of active tuberculosis. *Clin Diagn Lab Immunol* **9:**883–891.
36. **Welch RJ, Lawless KM, Litwin CM.** 2012. Antituberculosis IgG antibodies as a marker of active *Mycobacterium tuberculosis* disease. *Clin Vaccine Immunol* **19:**522–526.
37. **Lawn SD.** 2012. Point-of-care detection of lipoarabinomannan (LAM) in urine for diagnosis of HIV-associated tuberculosis: a state of the art review. *BMC Infect Dis* **12:**103.

Mycoplasma: Immunologic and Molecular Diagnostic Methods

KEN B. WAITES, MARY B. BROWN, AND JERRY W. SIMECKA

49

Mycoplasmas and ureaplasmas are members of a unique group of organisms (class *Mollicutes*) that are characterized by their small genomes, lack of cell walls, sterols in cell membranes, and complex nutritional requirements. The role of *Mycoplasma* and *Ureaplasma* species in human diseases was largely underappreciated until recent years. As a result, most diagnostic laboratories ignored them. Because of their complex nutritional requirements as well as their adaptation to the host during infection, these fastidious organisms can be difficult and time-consuming to culture from patient samples. However, there are improved methods for detection, including PCR detection assays, serologic assays, and commercially available growth media, but these are still limited compared with the products for other organisms.

Several organisms in the class *Mollicutes* are associated with human disease. The best-known *Mycoplasma* disease in humans is *Mycoplasma pneumoniae* respiratory disease, and it remains a leading cause of respiratory illness worldwide. Some members of the *Mollicutes* are also significant causes of urogenital tract disease; these include *Mycoplasma genitalium*, *Ureaplasma* species, and *Mycoplasma hominis*. A number of other mycoplasma species occur in humans, which in some instances, may also contribute to disease. Thus, mycoplasmas are emerging as primary etiologic agents in a number of human diseases. Additional evidence supports their role in exacerbation of other diseases. As diagnostic approaches become better established and more frequently used by clinical laboratories, the impact of this unique group of infectious agents in humans is likely to become better appreciated.

The purpose of this chapter is to discuss the advantages and disadvantages of current molecular and serological diagnostic techniques for mycoplasmal and ureaplasmal infections. Established approaches to the detection of *M. pneumoniae*, *Ureaplasma* spp., *M. genitalium*, and *M. hominis* infections are discussed. In addition to immunologic and molecular-based methods for detection of these organisms, several molecular-based methods have been applied to typing clinical isolates for epidemiological purposes. Such procedures are not yet suitable or necessary for diagnostic purposes in a clinical setting. It is beyond the scope of this chapter to include descriptions of molecular typing systems, as this information has been summarized in other publications (1).

M. PNEUMONIAE

M. pneumoniae occurs endemically and epidemically in persons of all age groups. The most frequent clinical syndrome is tracheobronchitis, often accompanied by upper respiratory tract symptoms. Typical symptoms can persist for weeks to months and include hoarseness, fever, cough, sore throat, headache, chills, coryza, and general malaise (2). *M. pneumoniae* may occur in up to 20% of adults requiring hospitalization for community-acquired pneumonias in the United States and probably an even greater proportion of those not requiring hospitalization. The incubation period is 1 to 3 weeks, and spread throughout households often occurs. *M. pneumoniae* can persist in the respiratory tract for several months after initial infection and sometimes for years in hypogammaglobulinemic persons (2). Some people may experience extrapulmonary complications, including skin rashes, pericarditis, hemolytic anemia, arthritis, meningoencephalitis, and peripheral neuropathy (2).

Serology

Historically, serology was the most common laboratory means of diagnosis of *M. pneumoniae* respiratory tract infections. It has the advantages of not requiring viable microorganisms, of allowing easy acquisition of small amounts of serum for storage and testing, and of having the availability of many different commercially available assays in various formats. *M. pneumoniae* has both lipid and protein antigens, which elicit antibody responses in clinical infections that can usually be detected after about 1 week of illness, peaking at 3 to 6 weeks, followed by a gradual decline, allowing the use of several different serologic assays based on different antigens and technologies. Although serology is a historically common and useful approach to the diagnosis of *Mycoplasma* infection, its use alone has several potential disadvantages.

One disadvantage of serology is that both acute- and convalescent-phase sera collected 3 to 4 weeks apart need to be tested for IgM and IgG levels for the most accurate diagnosis of recent or current *M. pneumoniae* infection, especially in adults older than 40 years, in whom an IgM response may be minimal or absent, presumably because of reinfection (2). Infants younger than 6 months of age may also lack IgM production following acute *M. pneumoniae* infection. A 4-fold or greater rise in antibody titer indicates

doi:10.1128/9781555818722.ch49

a current or recent infection. The duration of the IgM response can be variable; it usually peaks after about 3 weeks and then gradually declines. However, IgM antibodies can last for several weeks to months in some cases, further complicating the interpretation of serologic data in diagnosis of acute M. *pneumoniae* infection and making it risky to base a diagnosis on the analysis of a single serum specimen. M. *pneumoniae* is primarily a pathogen of mucosal surfaces, and therefore IgA antibodies are produced early in infection. Serum IgA levels decrease quickly, since the half-life of IgA in serum is short. Thus, IgA may theoretically be more reliable and useful for diagnosis of acute infection than IgM. However, our experience is that IgA measured in sera from children and adults with pneumonia proven to be caused by M. *pneumoniae* by culture and/or PCR assay does not detect any more seropositive specimens than can be identified by a positive IgM. A Japanese study also did not find a significant advantage of IgA in detection of acute M. *pneumoniae* infection in children (3).

One of the first serologic indicators used in diagnosis of M. *pneumoniae* infection is the presence of cold agglutinins, which does not rely on *Mycoplasma*-specific antibody responses. Cold agglutinins are IgM antibodies that agglutinate human erythrocytes at 4°C. They occur in association with M. *pneumoniae* infection in about 50% of cases within a few days, and their levels remain elevated for about 6 weeks. One hypothesis is that cold agglutinins result from cross-reactive autoantibodies against the I antigen of human erythrocytes. Another is that they develop directly as a result of antigenic alteration of erythrocytes caused by M. *pneumoniae* infection.

Performance of a qualitative "bedside cold-agglutinin test" involves placing 1 ml of anticoagulated blood in a cup of crushed ice for several minutes and then visually examining it for agglutination. On warming, the agglutination will resolve, but repeating the cooling procedure can reproduce it. A positive test for a patient in whom mycoplasmal infection is strongly suspected may have some clinical value. A more precise test is to determine the cold-agglutinin titer by reacting 0.1 ml of doubling dilutions of patient sera with 0.1 ml of a 1% suspension of washed human type O erythrocytes in a microtiter plate and determining the highest dilution at which agglutination occurs after 30 min of incubation at 4°C. Titers of 64 to 128 or a 4-fold or greater rise in titer suggest a recent M. *pneumoniae* infection, and the magnitude of the cold-agglutinin response may correlate directly with the severity of pulmonary disease. Detection of cold agglutinins is generally not recommended for the diagnosis of M. *pneumoniae* infection since cold agglutinins are associated with a wide variety of conditions, such as viral infections and collagen vascular diseases, and, more importantly, M. *pneumoniae*-specific serologic assays are now widely available.

Complement fixation (CF) was the major diagnostic technique used to measure M. *pneumoniae*-specific serum antibodies for many years. Seroconversion, defined as a 4-fold change in titer, measured in paired sera collected 3 to 4 weeks apart and assayed simultaneously, provides the greatest diagnostic accuracy. However, CF measures mainly the early IgM response and is unable to differentiate the other antibody classes. In addition, CF has limited sensitivity and specificity because the glycolipid antigen mixture used is not specific for M. *pneumoniae* and may be found in other microorganisms, as well as human tissues and even plants. Cross-reactions with other organisms, most notably M. *genitalium*, are well recognized, and false-positive results due to cross-reactive autoantibodies induced by acute inflammation from other unrelated causes may occur. To help overcome the problem with cross-reactivity, confirmation of positive CF results using Western blotting can be done, but this adds to the time and cost. Commercial assays for detection of M. *pneumoniae* antibodies by Western immunoblotting are available in Europe but not yet in the United States.

Most clinical laboratories have replaced CF with techniques of greater sensitivity and specificity. Numerous assay formats have been developed over the past several years and sold as commercial kits. Commercial kits are often evaluated using CF as the reference method. However, considering its lack of antibody class distinction and its cross-reactivity with other microorganisms, CF is not really suitable as a reference standard. Many of these tests, however, have not been fully evaluated and compared. In addition, the extent to which newer commercial serologic assays for M. *pneumoniae* will cross-react with M. *genitalium* or other mycoplasmas was not established with certainty, but this seems less likely to be a problem than with CF.

In-depth discussions of various types of commercial M. *pneumoniae* antibody assays and comparative evaluations of several products are available in other publications (2, 4–8). Table 1 summarizes the most popular types of serologic assays used to detect M. *pneumoniae* infection that have been developed commercially. These are indirect immunofluorescence, particle agglutination, and enzyme immunoassay (EIA).

Experience with EIAs dates back to the 1970s, and these assays are now the most widely used techniques for measuring antibodies against M. *pneumoniae*. A review of Food and Drug Administration-approved diagnostic tests reveals at least a dozen different M. *pneumoniae* EIAs marketed in the United States over the past several years, all of which are described as having either moderate or high complexity according to Clinical Laboratory Improvement Amendment (CLIA) classification. EIAs are more sensitive for detecting acute infection than is culture and can be comparable in sensitivity to PCR, provided that sufficient time has elapsed since infection for antibody to develop, if paired sera are tested, and if the patient has a functional immune system. Although most EIAs are sold as 96-well microtiter plate formats, some can be obtained as breakaway microwell strips, which allow smaller numbers of sera to be tested economically.

Two EIAs are packaged as qualitative membrane-based procedures for the detection of single test specimens. These are truly rapid EIAs (taking 10 minutes or less) and are simple to perform. The Meridian Immuno*Card* (Meridian Bioscience, Inc., Cincinnati, OH) is an IgM-only assay that is simple to read and is especially useful for testing pediatric samples. The Remel EIA (Thermo Fisher Scientific, Inc., Waltham, MA) is another membrane-based assay that detects IgM and IgG simultaneously. As discussed above, there are limitations in interpreting the results of IgM-only assays when a single acute-phase specimen is tested due to the potential for delayed or absent IgM response in many persons. This is more of a reflection on the erratic humoral immune response against M. *pneumoniae* than on the performance of a specific assay type. Multiple investigations, involving adults as well as children, have shown that the Immuno*Card* sensitivity for detection of acute M. *pneumoniae* infection is well below 50%, but it improves considerably if convalescent sera are tested (5, 7, 9). Similar poor sensitivity has been documented for other IgM assays when testing is limited to the acute phase when a positive PCR assay was used to define infection (5). Likewise, a single IgG measurement has no diagnostic meaning for an acute infection and is useful

TABLE 1 Major commercial serologic test formats for *M. pneumoniae* in the United States

Assay format[a]	Antibodies measured	Equipment required	Comments and limitations
EIA	IgM, IgG, or IgA separately	Spectrophotometer/ EIA reader	EIAs are typically performed using a microtiter plate format in which antigens are adsorbed onto the polystyrene surface. Dilutions of test serum are added to the wells and incubated. Antibodies bound to the solid-phase antigen are visualized by using enzyme-labeled conjugates directed against the primary antibody and substrate read in a spectrophotometer. The amount of conjugate reacting is proportional to the levels of antibody present. EIAs have the advantages of requiring very small serum volumes (<100 μl), are adaptable to testing larger or small numbers of specimens, and can be made isotype specific.
Membrane EIA	IgM or IgG separately	None	Membrane EIAs are rapid, qualitative, point-of-care procedures designed for testing single-serum specimens. A permeable membrane or filter paper is impregnated with antigen to which serum is added. This step is followed by addition of anti-human IgG or IgM enzyme conjugate. Development of color after enzyme substrate is added constitutes a positive test. Lipemic or hemolyzed serum samples will interfere with results.
PA	IgG or IgM separately or simultaneously	None	PA tests utilize latex or gelatin as carrier particles coated with antigen that are incubated with test serum. If specific antibodies are present, the particles agglutinate, resulting in a visible reaction. PA products may provide qualitative results that can be visualized on a card or quantitative data read in a microtiter plate format. PA assays do not offer any advantages over other techniques such as EIAs or IFAs, except possibly their ease and simplicity of performance.
IFA	IgG or IgM separately	Fluorescence microscope	Antigen is fixed to glass slides. Specific antibody is detected in dilutions of test serum after staining with anti-human IgM or IgG fluorochrome conjugate. Results can be affected by the presence of rheumatoid factor and high *M. pneumoniae*-specific IgG antibody levels. Additional procedures to validate IgM results are needed in these settings. IFA provides quantitative data, but interpretation is very subjective.

[a]PA, particle agglutination; IFA, indirect immunofluorescence.

only in prevalence studies since the time of seroconversion cannot be determined. Although acute- and convalescent-phase sera should be tested quantitatively for both IgG and IgM for greatest diagnostic accuracy, the practical value of the qualitative single point-of-care tests offered by both kits is lost if paired specimens are required. Thus, these single point-of-care tests can be useful in some settings if the potential limitations are considered in the diagnosis. Csango et al. (10) concluded in their evaluation of 4 commercial EIAs sold in Europe that a substantial proportion of healthy adult blood donors were serologically positive for IgA, IgM, and/or IgG, suggesting the likelihood that these tests result in overdiagnosis of acute *M. pneumoniae* infections. Despite limitations on the analysis of a single serum specimen, many commercial kits provide interpretive criteria for single measurements of IgM or IgG. Such information should be interpreted with great caution. It is clear that there are potential problems with all of the commercial antibody tests used to detect the immune response to acute *M. pneumoniae* infection that have been evaluated in independent studies. For tests that have not undergone such comparisons, nothing is known about their diagnostic accuracies beyond what the manufacturer states in package inserts.

Molecular Biology-Based Techniques

The attention focused on nucleic acid amplification techniques (NAATs) such as PCR has largely eclipsed earlier interest in nonamplified antigen detection or DNA hybridization systems. Numerous studies since the late 1980s using simulated clinical specimens, animal models, and clinical trials have validated the ability of the PCR assay to detect *M. pneumoniae*, often in conjunction with serology and/or culture. The same types of clinical specimens that can undergo culture, such as throat swabs, nasopharyngeal swabs, sputum, and other sterile tissues or body fluids, can also be tested by the PCR assay. Additional advantages of PCR assays are that they can be used to detect mycoplasmas in tissue that has already been processed for histologic examination or in cultures that are contaminated. Furthermore, PCR assays generally require only one specimen, can be completed in 1 day, may give positive results earlier in infection than serology does, and do not require viable organisms.

Most PCR-based techniques are somewhat similar and do not differ in principle from PCR assays used for detection of other microorganisms. Although most approaches focus on amplifying sequences of genomic DNA, RNA-based amplification has also been used. Specific advantages of

RNA-based amplification techniques are the high sensitivity that can be achieved due to the large number of rRNA copies per mycoplasmal cell and the fact that its detection is more indicative of viable mycoplasmas in a clinical sample. NAATs for *M. pneumoniae* that are used in diagnostic laboratories have usually been developed in-house and have not been subjected to rigorous comparisons with culture, serology, or other NAATs. During the past few years, most newly described assays have utilized real-time detection as opposed to conventional gel-based PCR techniques. Numerous advantages exist for this newer technology, including greater sensitivity, lower risk of contamination-related false positives, shorter turnaround time, and the ability to provide quantitative results. Gene targets for PCR assays for detection of *M. pneumoniae* in clinical specimens have included 16S rRNA, *P1*, *tuf*, *parE*, *dnak*, *pdh*A, ATPase operon, CARDS toxin gene (*mpn372*), the non-coding repetitive element *repMp1*, and intracellular protease gene. Various detection systems have also been described (Table 2), and multiple types of instrumentation have been used. Both conventional and real-time nucleic acid sequence based amplification (NASBA) have also been used to detect *M. pneumoniae* RNA. There have been very few side-by-side comparisons to determine whether one assay format or gene target is better than another. Many of the evaluations that have been done compared PCR with culture and/or serology as a reference method and, predictably, yielded disparate results in some cases.

Over the past several years, various commercialized kits have become available in Europe for the detection of *M. pneumoniae* alone or in combination with other respiratory tract bacteria or viruses, either in mono or in multiplex formats. Two molecular-based NAATs are now FDA-approved for use in the United States. One of these is the illumigene Mycoplasma Assay (Meridian Bioscience, Inc., Cincinnati, OH). This loop-mediated isothermal amplification assay (LAMP) enables detection of *M. pneumoniae* in as many as 10 clinical specimens that can be tested simultaneously within 1 hour after extracted DNA is set up in the incubator/reader. This instrumentation, which does not require a thermocycler, can easily be incorporated into clinical microbiology laboratories that do not have extensive molecular diagnostic facilities. The second NAAT sold commercially in the United States is the multiplex Biofire Diagnostics FilmArray RP (BioFire Diagnostics, Salt Lake City, UT; recently merged with bioMérieux, Marcy l'Etoile, France). This kit detects nucleic acids in nasopharyngeal swabs for 20 respiratory tract pathogens, including *M. pneumoniae*, processing one sample at a time with results in about an hour. The BioFire Diagnostics FilmArray performance was shown to be comparable to real-time PCR for detection of *M. pneumoniae* in one study (11). This assay is also available in Europe. Additional technical information, primer sequences, and tabulations of various nucleic acid amplification assays according to respiratory specimen tested and further discussion of commercial NAATs are available in other recent publications on these topics (1, 12–15).

Comparison of various NAATs, mainly PCR assays, with culture has yielded varied results. In view of the enhanced analytical sensitivity of the PCR assay over culture, a positive PCR result together with negative culture can be easily explained. However, in a situation of a negative PCR assay with a positive culture, the presence of inhibitors or some other technical problem with the PCR assay must be considered. Interestingly, PCR inhibition may be more likely to occur with nasopharyngeal aspirates than with throat swabs, and sputum may be more likely to be PCR-positive than nasopharyngeal specimens, throat swabs, or throat washes. However, from a practical standpoint in sampling young children and many adults with fairly mild illness, sputum is not produced in *M. pneumoniae* infections, so nasopharyngeal or oropharyngeal samples may be the only specimen types available. Sometimes dilution of samples overcomes inhibition of PCR due to a reduction in inhibitors during the reaction, but this is at the cost of diminished sensitivity because the nucleic acid is diluted along with any inhibitors. Several commercial reagents with automated procedures for nucleic acid purification are effective in removing most inhibitors of amplification in PCR assays, and these appear to work as well as nonproprietary methods. Thus, the type of sample and its preparation can influence the ability to detect *Mycoplasma* infection using the PCR assay.

PCR results may not always correspond with serologic results. For example, elderly adults with pneumonia might have age-related impairment in immunity, resulting in low serologic responses after *M. pneumoniae* infection. The

TABLE 2 Examples of *M. pneumoniae* nucleic acid amplification assays

Gene target	Assay type	Detection format	Mono or multiplex	Reference
P1	PCR	Real-time	Monoplex	38
P1	LAMP[a]	Turbidimeter	Monoplex	39
P1	PCR	Scorpion probe	Monoplex	40
P1	PCR	Hybridization	Multiplex	41
repMp1 in P1	PCR	Real-time	Monoplex	42
CARDS toxin	PCR	Real-time	Monoplex	43
ATPase	PCR	Real-time	Monoplex	43
tuf	Broad-range PCR	Real-time	Monoplex	44
16S rRNA	PCR	Real-time	Multiplex	45
16S rRNA	PCR	Molecular beacons	Monoplex	46
16S rRNA	PCR	Real-time	Monoplex	47
16S rRNA	NASBA[b]	Real-time	Monoplex	48
Not specified	PCR	Resequencing microarray	Multiplex	49

[a]LAMP, loop-mediated isothermal amplification.
[b]NASBA, nucleic acid sequence based amplification.

same situation may occur with very young infants. A positive PCR test together with a negative serologic test could also mean that the specimen was collected too soon in the course of the illness to allow sufficient time for antibody to develop. Analysis of paired acute and convalescent sera might help resolve this situation. PCR results may also become negative within days following antibiotic treatment, whereas serologic results should remain positive for a longer time. It is not known with certainty whether there is a specific threshold quantity of *M. pneumoniae* in respiratory tract tissues that can differentiate colonization versus infection. Therefore, relying solely on a positive result by PCR may overestimate the clinical importance of *M. pneumoniae* as a pathogen if the population sampled has a high carriage rate, which sometimes occurs in children, or at a time when there is an epidemic ongoing in a given community and exposure rates would be elevated and because of the propensity of this organism to cocirculate with other bacterial and viral pathogens. Concern for spread of clinically significant macrolide-resistant *M. pneumoniae* has become a major issue because of its high prevalence in Asia and growing presence in the United States and Europe. Various real-time PCR assays to detect 23S rRNA mutations associated with macrolide resistance have been described and can be incorporated into a diagnostic scheme so that clinicians can be told whether an infection might be suitably treated with a macrolide antibiotic at the same time a positive PCR result for *M. pneumoniae* is provided (1, 13).

Published studies describing multicenter comparisons of various NAATs for *M. pneumoniae* detection (16, 17) reported significant variations in test performance among participating laboratories, making a strong case for an organized proficiency test program, which has been pilot-tested in Europe. Proficiency testing panels for NAATs for various pathogens, including *M. pneumoniae*, are also available through the College of American Pathology.

Recommended Diagnostic Approach

Clinical manifestations, radiographic presentation, and general laboratory tests are not sufficiently specific to allow the differentiation of *M. pneumoniae* infection from infections caused by other common microorganisms, and more specific laboratory methods are needed to confirm the diagnosis. This situation is complicated further by the fact that mycoplasmal respiratory infections often coexist with infections caused by several other respiratory pathogens. Most *M. pneumoniae* infections are relatively mild and amenable to management on an outpatient basis, so physicians may rely on clinical suspicion and provide empiric treatment. However, a microbiological diagnosis should be sought if illness is sufficient to warrant hospitalization, if there is unsatisfactory clinical response to initial antimicrobial therapy, if there are underlying comorbid conditions or immunosuppression that would make severe and disseminated disease more likely, or if significant extrapulmonary symptoms are present.

The ideal diagnostic strategy, especially in children, can take advantage of both serology for IgM and PCR, since culture is laborious, time-consuming, insensitive, and expensive and because serology or PCR alone can be problematic for reasons discussed above. If a single serological test is to be performed, the rapid EIAs mentioned earlier may be the most logical alternatives. The additional expense of performing two tests has to be considered along with the very limited availability of PCR assays in the United States.

M. GENITALIUM

M. genitalium is a very fastidious, slow-growing mycoplasma first identified in 1981 from the urethras of men with urethritis. Its role in human disease is now becoming more apparent, mainly as a result of epidemiological studies that have used PCR to detect infections. Despite the increased awareness of the pathogenic potential of *M. genitalium*, there are relatively few clinical isolates of the microbe because of its extremely fastidious nature. This mycoplasma is known to play a role in cervicitis and pelvic inflammatory disease in women and in urethritis in men.

Serology

A microimmunofluorescence assay for *M. genitalium* can detect antibody responses in men with nongonococcal urethritis and women with salpingitis (18). This method is rapid, reproducible, and quite sensitive and specific, with less cross-reactivity with *M. pneumoniae* than is seen with other methods. EIA protocols using lipid-associated membrane protein antigens were applied to population studies, and the results were confirmed by Western blotting (19). These antigens have limited cross-reactivity with *M. pneumoniae*, and the EIA platform is more amenable to large-scale testing than is Western blot analysis. However, these assays are not available outside of specialized research laboratories and therefore cannot be recommended for diagnostic purposes.

Molecular Biology-Based Techniques

Perhaps more than for any other mycoplasma, molecular biology-based techniques have played the critical and indeed defining role in diagnosis of *M. genitalium* infections. *M. genitalium* is notoriously difficult to culture, perhaps in part because of its ability to persist in the intracellular environment but also because of its fastidious growth requirements and extremely slow generation time (18 h). The anatomical sites that are sampled, preparation of DNA template material, and PCR approaches are basically similar to those used for other mycoplasmas. *M. pneumoniae* and *M. genitalium* are structurally and antigenically related, with 98% homology in their respective 16S rRNA, thus challenging development of specific diagnostic assays that can differentiate them, even though *M. pneumoniae* is much less likely to be found in the urogenital tract. Quantitative, rapid, real-time PCR assays for *M. genitalium* have utilized targets such as the MgPa operon, 16S rRNA, the 115-kDa gene, and *gap* encoding glyceraldehyde-3-phosphate dehydrogenase (20–24). Use of *gap* as a gene target overcomes some of the limitations identified for 16S rRNA and MgPa (1, 13). Since PCR-based assays are the primary means of *M. genitalium* diagnosis, it is essential that whichever type of procedure is employed should be stringently controlled and carefully monitored. There is a strong association between serology and PCR for *M. genitalium*, but the analytic sensitivity of a single PCR assay for *M. genitalium* will certainly vary according to the technique and gene targets that are used. Additional techniques such as transcription-mediated amplification (TMA) have been developed for detection of *M. genitalium*. Multiplex PCR-based systems for detection of *M. genitalium*, along with *Chlamydia trachomatis*, *Neisseria gonorrhoeae*, and other urogenital mycoplasmas and ureaplasmas, are sold as kits in several European countries by multiple companies using various formats and instrument platforms. PCR assays have also been developed that can detect mutations mediating antimicrobial resistance in *M. genitalium* (1).

Recommended Diagnostic Approach

The lack of readily available molecular diagnostic testing for M. *genitalium* in clinical laboratories and the unavailability of culture or serology as alternatives has had the expected result that clinicians in the United States rarely request microbiological confirmation of infections suspected to be due to this organism. Some reference and specialty laboratories offer their own in-house PCR assays for this mycoplasma, but none of these assays are validated. Few comparative studies of different assay formats and gene targets have been performed, and no organized proficiency testing program is available. Given the rapid development of molecular-based tests for M. *pneumoniae* over the past few years in Europe and the introduction of two FDA-cleared tests, it seems possible that commercially available rapid diagnostic tests for M. *genitalium* may soon come to the United States as they have in Europe. Since M. *genitalium* is less commonly detected in the lower urogenital tract in the absence of clinical infection than is *Mycoplasma hominis* or *Ureaplasma* spp., when it is detected by PCR in the lower urogenital tract of a symptomatic individual, it should be considered clinically significant.

M. HOMINIS

Like *Ureaplasma* species and M. *genitalium*, M. *hominis* is associated with urogenital infections. However, unlike *Ureaplasma* species, detection of M. *hominis* in the vagina is of clinical significance since this microbe is a component of the suite of bacteria associated with bacterial vaginosis. M. *hominis* is also more closely linked to systemic diseases, including pyelonephritis, postpartum endometritis, arthritis, pericarditis, peritonitis, and wound infections in adults, as well as meningitis, bacteremia, and pneumonia in infants. Like *Ureaplasma* species, M. *hominis*, although somewhat slower growing, is relatively easy to cultivate and can be isolated using commercial SP4 agar and broth or 10B broth and A8 agar. Classic "fried-egg" colonies can be observed within 3 to 7 days.

Serology

As with the other urogenital mycoplasmas, no commercial serological assays are available in the United States. An EIA is based on lipid-associated membrane antigens and is more broadly cross-reactive among different M. *hominis* strains than are assays using cell lysates as antigens. Confirmation by immunoblot analysis is also appropriate. Seroepidemiology to determine exposure to M. *hominis* within a population can be done with a single serum sample. However, for diagnostic purposes, paired acute- and convalescent-phase sera are likely to be more informative. As is the case for ureaplasmas, clinical experience using serology for diagnosis of M. *hominis* infections is scant.

Molecular Biology-Based Techniques

The molecular biology-based techniques and considerations are essentially the same as for the other mycoplasmal species. Both multiplex PCR and real-time PCR assays have been developed, some of which are commercially sold in Europe but not in the United States at this time. PCR assays for M. *hominis* have mainly utilized 16S rRNA or 16S-23S intergenic spacer regions as gene targets (25, 26). Since heterogeneity may occur in the 16S rRNA gene of M. *hominis*, other targets, including *fstY*, *yidC*, *tuf*, and *rpoB*, have been developed (1, 13, 27–30). Microtiter plate hybridization assays used with M. *genitalium* and *Ureaplasma* spp. have also been employed for M. *hominis* (26, 31).

Recommended Diagnostic Approach

Since no serologic or molecular assays are available commercially in the United States, most clinical laboratories still depend on culture using specific procedures designed to recover these organisms. M. *hominis* is the easiest of the pathogenic human mycoplasma species to grow in culture using the appropriate methods. Use of Columbia blood agar or automated blood culture systems is discouraged because the number of false-negative results would be significant, and culture results would therefore be unreliable. Since M. *hominis* is a common inhabitant of the female cervix and male urethra, a positive PCR assay or culture may not be meaningful in the absence of clinical manifestations commonly associated with infections with this organism. However, an organism load exceeding 10^4 colony-forming units (CFU)/ml may be clinically significant. In addition, a positive culture or PCR from an extragenital site should be considered clinically significant.

U. UREALYTICUM AND *U. PARVUM*

Ureaplasma spp. are implicated in a number of human urogenital infections. *Ureaplasma* was proven to cause nongonococcal urethritis in experimental infection studies of humans. However, demonstrating their role in disease is complicated due to the high carriage rate of the microbe in the lower genital tract of asymptomatic persons. Colonization of the placenta and/or amniotic fluid with *Ureaplasma* spp. is also associated with histologic chorioamnionitis and premature birth. Importantly, colonization of developing fetuses *in utero* or preterm neonates is linked to the development of chronic lung disease and is associated with necrotizing enterocolitis, and the organisms can also cause neonatal bacteremia and meningitis.

Originally, human ureaplasmas were thought to consist of a single species with two biovars composed of 14 serotypes. *Ureaplasma* is now recognized as two species: *Ureaplasma parvum* (formerly biovar 1; serovars 1, 3, 6, and 14) and *Ureaplasma urealyticum* (formerly biovar 2; serovars 2, 4, 5, and 7 to 13). Although some serovars are more fastidious than others, most ureaplasmas are relatively easy to culture and develop classic colonies on A7 or A8 agar within 2 to 3 days, making culture the most common means for diagnosis used by clinical laboratories.

Serology

Although several EIA protocols have been published, no commercial product is available in the United States. The EIA does not differentiate between *U. parvum* and *U. urealyticum*, and other approaches, such as monoclonal antibody capture assays, microimmunofluorescence, growth inhibition, and metabolic inhibition, were used to detect serovar differences. As with M. *pneumoniae*, seroconversion, a 4-fold rise in titer, or change in subclass-specific response may be useful for epidemiological studies. However, serology has never been used to any significant degree for the diagnosis of ureaplasmal infections in a clinical setting, and assays have never been standardized.

Molecular Biology-Based Techniques

The same principles, limitations, and considerations that were discussed for M. *pneumoniae* also apply to the detection of *Ureaplasma* species. The most commonly tested samples from adults include urine, urethral swabs, semen, prostatic fluid, vaginal swabs, endocervical swabs, placental or endometrial tissues, amniotic fluid, and synovial

fluid. Synovial fluid has a particular problem in that some samples appear to be inhibitory for PCR assays, and therefore, false-negative results can occur. Due to high carriage rates, vaginal swabs are of limited clinical significance for *Ureaplasma*. In contrast, urethral swabs from males are more informative than are those from females due to lower carriage rates. In addition, first-void urine is a frequent sample used for PCR, but again there is the inherent caveat that first-void urine may reflect transient contamination rather than a clinically significant finding. Thus, the type of samples and carriage rates will impact interpretation of the results obtained.

The newest molecular biology-based tools using real-time PCR permit the identification of the individual species, although this is not essential for diagnostic purposes (1, 13). Ureaplasma-specific primers have been developed to target several different genes in real-time PCR assays; the most commonly used are the urease, multiple-band antigen (*mba*), and 16S rRNA genes, but other systems have been described based on the *U. UREALYTICUM*063 gene, which encodes a conserved hypothetical protein that is identical in all 4 serovars of *U. parvum* and *U. UREALYTICUM*R10_0680 that is conserved in all 10 serovars of *U. urealyticum* (13, 32) (Table 3). One approach incorporates hybridization with specific labeled probes to standard PCR reactants in a microtiter plate format (26, 31, 33). This system has the advantage of using a single primer pair to amplify the 16S rRNA target from the major genital mycoplasmal species, as well as the two ureaplasmal species, followed by a probe specific to each of the species. Multiplex PCR assays have been developed for several sexually transmitted microbes, including *U. urealyticum* and *U. parvum*, as well as *M. hominis*, *M. genitalium*, *Chlamydia trachomatis*, *Neisseria gonorrhoeae*, and *Trichomonas vaginalis* (1). Some are now sold commercially in Europe, but not in the United States. Multiplex PCR can also be used in combination with other techniques, including reverse line hybridization blotting (mPCR/RLB) and microarrays. The mPCR/RLB technique integrates multiplex PCR using biotin-labeled primer pairs or biotin-dNTPs to generate labeled PCR products that hybridize with highly specific, membrane-bound, amine-labeled oligonucleotide probes by reverse line blot hybridization. To visualize the hybridized PCR products, the membrane is incubated with peroxidase-labeled streptavidin and chemiluminescent detection liquid. Chemiluminescence results can be detected by a light-sensitive film or a lumino-imager. The mPCR/RLB technique has been used to develop assays that detect numerous respiratory pathogens, including *M. pneumoniae* and a variety of urogenital pathogens, including *Ureaplasma* spp., *M. genitalium*, and *M. hominis* (34–36). The microarray used for the detection of *Ureaplasma* spp. is based on immobilizing probes on a glass surface that hybridize to their complementary biotin labeled-DNA targets produced by a previous PCR procedure. The microarray is then incubated with gold-conjugated streptavidin. The interaction of biotin and streptavidin leads to silver precipitation visualized on the microarray. *In situ* hybridization (ISH) is a non-PCR-based molecular technique that has been specifically utilized for detection of ureaplasmas in lung tissue samples (37). Thus, there are a wide variety of molecular-based approaches that are developed to detect ureaplasmas in samples.

Recommended Diagnostic Approach

Since none of the serologic or PCR assays are available commercially in the United States, most diagnostic laboratories

TABLE 3 Examples of real-time PCR-based assays and gene targets for detection of urogenital mycoplasmas

Species	Gene target/ region	Analytical sensitivity (no. of genome copies or CFU/reaction)	References
U. urealyticum and *U. parvum*	16S rRNA	10 copies	50
U. parvum	Urease	5 copies	51
U. parvum	UU063	0.6 CFU	32
U. parvum	Urease	10 copies	52
U. parvum	Urease	1 CFU	53
U. urealyticum	Urease	10 copies	52
U. urealyticum	Urease	5 copies	51
U. urealyticum	Urease	3 CFU	53
U. urealyticum	UUR10_0680	0.8 CFU	32
M. genitalium	*gap*	5 copies	23
M. genitalium	16S rRNA	10 copies	54
M. genitalium	16S rRNA	1 copy	20
M. genitalium	16S rRNA	10 copies	55
M. genitalium	MgPa	<5 copies	22
M. hominis	16S rRNA	10 copies	56
M. hominis	*gap*	10 copies	28
M. hominis	*yidC*	7 copies	27
M. hominis	*fstY*	10 copies	29
M. hominis	*tuf*	100 copies	30

depend on the use of culture for detection of ureaplasmas in clinical specimens, because results can usually be provided within 2 to 3 days. The 10B broth and A8 agar used for culture are available commercially from various vendors. Even though PCR is clearly more sensitive than culture from an analytical perspective, it is considerably more expensive and much less practical for laboratories that may receive specimens on an occasional basis and particularly if they do not have molecular diagnostic facilities. A positive ureaplasma culture or PCR from the urethra or urine of men or women with symptoms consistent with urethritis, from prostatic fluid, or from an extragenital site in adults should be considered clinically significant. Similarly, if organisms are detected in samples from the lower respiratory tract in neonates with lung disease or from normally sterile sites such as the bloodstream or cerebrospinal fluid, these results should be considered clinically significant. *U. urealyticum* may be more pathogenic than *U. parvum* in some conditions, such as male urethritis, so it may be useful to identify the species present in these cases. However, no such associations have been consistently shown for other conditions.

REFERENCES

1. **Waites KB, Xiao L, Paralanov V, Viscardi RM, Glass JI.** 2013. *Mycoplasma* and *Ureaplasma*, p 229–281. *In* de Filippis I, McKee ML (ed), *Molecular Typing in Bacterial Infections*. Springer Science, New York, NY.
2. **Waites KB, Talkington DF.** 2004. *Mycoplasma pneumoniae* and its role as a human pathogen. *Clin Microbiol Rev* **17:**697–728.
3. **Narita M.** 2005. [Evaluation of ELISA kits for detection of *Mycoplasma pneumoniae*-specific IgG, IgA, IgM antibodies on the diagnosis of *Mycoplasma pneumoniae* infection in children]. *Kansenshogaku Zasshi* **79:**457–463.
4. **Loens K, Goossens H, Ieven M.** 2010. Acute respiratory infection due to *Mycoplasma pneumoniae*: current status of diagnostic methods. *Eur J Clin Microbiol Infect Dis* **29:**1055–1069.
5. **Beersma MF, Dirven K, van Dam AP, Templeton KE, Claas EC, Goossens H.** 2005. Evaluation of 12 commercial tests and the complement fixation test for *Mycoplasma pneumoniae*-specific immunoglobulin G (IgG) and IgM antibodies, with PCR used as the "gold standard." *J Clin Microbiol* **43:**2277–2285.
6. **Busson L, Van den Wijngaert S, Dahma H, Decolvenaer M, Di Cesare L, Martin A, Vasseur L, Vandenberg O.** 2013. Evaluation of 10 serological assays for diagnosing *Mycoplasma pneumoniae* infection. *Diagn Microbiol Infect Dis* **76:**133–137.
7. **Talkington DF, Shott S, Fallon MT, Schwartz SB, Thacker WL.** 2004. Analysis of eight commercial enzyme immunoassay tests for detection of antibodies to *Mycoplasma pneumoniae* in human serum. *Clin Diagn Lab Immunol* **11:**862–867.
8. **Petitjean J, Vabret A, Gouarin S, Freymuth F.** 2002. [Evaluation of four commercial immunoglobulin G (IgG)- and IgM-specific enzyme immunoassays for diagnosis of *Mycoplasma pneumoniae* infections]. *Pathol Biol (Paris)* **50:**530–537.
9. **Ozaki T, Nishimura N, Ahn J, Watanabe N, Muto T, Saito A, Koyama N, Nakane K, Funahashi K.** 2007. Utility of a rapid diagnosis kit for *Mycoplasma pneumoniae* pneumonia in children, and the antimicrobial susceptibility of the isolates. *J Infect Chemother* **13:**204–207.
10. **Csango PA, Pedersen JE, Hess RD.** 2004. Comparison of four *Mycoplasma pneumoniae* IgM-, IgG- and IgA-specific enzyme immunoassays in blood donors and patients. *Clin Microbiol Infect* **10:**1094–1098.
11. **Pierce VM, Elkan M, Leet M, McGowan KL, Hodinka RL.** 2012. Comparison of the Idaho Technology FilmArray system to real-time PCR for detection of respiratory pathogens in children. *J Clin Microbiol* **50:**364–371.
12. **Loens K, van Loon AM, Coenjaerts F, van Aarle Y, Goossens H, Wallace P, Claas E J, Ieven M.** 2012. Performance of different mono- and multiplex nucleic acid amplification tests on a multipathogen external quality assessment panel. *J Clin Microbiol* **50:**977–987.
13. **Waites KB, Xiao L, Paralanov V, Viscardi RM, Glass JI.** 2012. Molecular methods for the detection of *Mycoplasma* and *Ureaplasma* infections in humans: a paper from the 2011 William Beaumont Hospital Symposium on molecular pathology. *J Mol Diagn* **14:**437–450.
14. **Touati A, Benard A, Hassen AB, Bebear CM, Pereyre S.** 2009. Evaluation of five commercial real-time PCR assays for detection of *Mycoplasma pneumoniae* in respiratory tract specimens. *J Clin Microbiol* **47:**2269–2271.
15. **Dumke R, Jacobs E.** 2009. Comparison of commercial and in-house real-time PCR assays used for detection of *Mycoplasma pneumoniae*. *J Clin Microbiol* **47:**441–444.
16. **Ursi D, Ieven M, Noordhoek GT, Ritzler M, Zandleven H, Altwegg M.** 2003. An interlaboratory comparison for the detection of *Mycoplasma pneumoniae* in respiratory samples by the polymerase chain reaction. *J Microbiol Methods* **53:**289–294.
17. **Loens K, Beck T, Ursi D, Pattyn S, Goossens H, Ieven M.** 2006. Two quality control exercises involving nucleic acid amplification methods for detection of *Mycoplasma pneumoniae* and *Chlamydophila pneumoniae* and carried out 2 years apart (in 2002 and 2004). *J Clin Microbiol* **44:**899–908.
18. **Furr PM, Taylor-Robinson D.** 1984. Microimmunofluorescence technique for detection of antibody to *Mycoplasma genitalium*. *J Clin Pathol* **37:**1072–1074.
19. **Baseman JB, Cagle M, Korte JE, Herrera C, Rasmussen WG, Baseman JG, Shain R, Piper JM.** 2004. Diagnostic assessment of *Mycoplasma genitalium* in culture-positive women. *J Clin Microbiol* **42:**203–211.
20. **Jurstrand M, Jensen JS, Fredlund H, Falk L, Molling P.** 2005. Detection of *Mycoplasma genitalium* in urogenital specimens by real-time PCR and by conventional PCR assay. *J Med Microbiol* **54:**23–29.
21. **Deguchi T, Yoshida T, Yokoi S, Ito M, Tamaki M, Ishiko H, Maeda S.** 2002. Longitudinal quantitative detection by real-time PCR of *Mycoplasma genitalium* in first-pass urine of men with recurrent nongonococcal urethritis. *J Clin Microbiol* **40:**3854–3856.
22. **Jensen JS, Bjornelius E, Dohn B, Lidbrink P.** 2004. Use of TaqMan 5′ nuclease real-time PCR for quantitative detection of *Mycoplasma genitalium* DNA in males with and without urethritis who were attendees at a sexually transmitted disease clinic. *J Clin Microbiol* **42:**683–692.
23. **Svenstrup HF, Jensen JS, Bjornelius E, Lidbrink P, Birkelund S, Christiansen G.** 2005. Development of a quantitative real-time PCR assay for detection of *Mycoplasma genitalium*. *J Clin Microbiol* **43:**3121–3128.
24. **Dupin N, Bijaoui G, Schwarzinger M, Ernault P, Gerhardt P, Jdid R, Hilab S, Pantoja C, Buffet M, Escande JP, Costa J M.** 2003. Detection and quantification of *Mycoplasma genitalium* in male patients with urethritis. *Clin Infect Dis* **37:**602–605.
25. **Grau O, Kovacic R, Griffais R, Launay V, Montagnier L.** 1994. Development of PCR-based assays for the detection of two human mollicute species, *Mycoplasma penetrans* and *M. hominis*. *Mol Cell Probes* **8:**139–147.
26. **Yoshida T, Maeda S, Deguchi T, Miyazawa T, Ishiko H.** 2003. Rapid detection of *Mycoplasma genitalium*, *Mycoplasma hominis*, *Ureaplasma parvum*, and *Ureaplasma urealyticum* organisms in genitourinary samples by PCR-microtiter plate hybridization assay. *J Clin Microbiol* **41:**1850–1855.

27. **Ferandon C, Peuchant O, Janis C, Benard A, Renaudin H, Pereyre S, Bebear C.** 2011. Development of a real-time PCR targeting the yidC gene for the detection of Mycoplasma hominis and comparison with quantitative culture. *Clin Microbiol Infect* **17:**155–159.
28. **Baczynska A, Svenstrup HF, Fedder J, Birkelund S, Christiansen G.** 2004. Development of real-time PCR for detection of *Mycoplasma hominis*. *BMC Microbiol* **4:**35.
29. **Menard JP, Fenollar F, Henry M, Bretelle F, Raoult D.** 2008. Molecular quantification of *Gardnerella vaginalis* and *Atopobium vaginae* loads to predict bacterial vaginosis. *Clin Infect Dis* **47:**33–43.
30. **Cunningham SA, Mandrekar JN, Rosenblatt JE, Patel R.** 2013. Rapid PCR detection of *Mycoplasma hominis*, *Ureaplasma urealyticum*, and *Ureaplasma parvum*. *Int J Bacteriol* **2013:**7.
31. **Maeda S, Deguchi T, Ishiko H, Matsumoto T, Naito S, Kumon H, Tsukamoto T, Onodera S, Kamidono S.** 2004. Detection of *Mycoplasma genitalium*, *Mycoplasma hominis*, *Ureaplasma parvum* (biovar 1) and *Ureaplasma urealyticum* (biovar 2) in patients with non-gonococcal urethritis using polymerase chain reaction-microtiter plate hybridization. *Int J Urol* **11:**750–754.
32. **Xiao L, Glass JI, Paralanov V, Yooseph S, Cassell GH, Duffy LB, Waites KB.** 2010. Detection and characterization of human *Ureaplasma* species and serovars by real-time PCR. *J Clin Microbiol* **48:**2715–2723.
33. **Povlsen K, Jensen JS, Lind I.** 1998. Detection of *Ureaplasma urealyticum* by PCR and biovar determination by liquid hybridization. *J Clin Microbiol* **36:**3211–3216.
34. **McKechnie ML, Hillman R, Couldwell D, Kong F, Freedman E, Wang H, Gilbert GL.** 2009. Simultaneous identification of 14 genital microorganisms in urine by use of a multiplex PCR-based reverse line blot assay. *J Clin Microbiol* **47:**1871–1877.
35. **Wang Y, Kong F, Gilbert GL, Brown M, Gao W, Yu S, Yang Y.** 2008. Use of a multiplex PCR-based reverse line blot (mPCR/RLB) hybridisation assay for the rapid identification of bacterial pathogens. *Clin Microbiol Infect* **14:**155–160.
36. **Wang H, Kong F, Jelfs P, James G, Gilbert GL.** 2004. Simultaneous detection and identification of common cell culture contaminant and pathogenic mollicutes strains by reverse line blot hybridization. *Appl Environ Microbiol* **70:**1483–1486.
37. **Benstein BD, Crouse DT, Shanklin DR, Ourth DD.** 2003. Ureaplasma in lung. 1. Localization by in situ hybridization in a mouse model. *Exp Mol Pathol* **75:**165–170.
38. **Pitcher D, Chalker VJ, Sheppard C, George RC, Harrison TG.** 2006. Real-time detection of *Mycoplasma pneumoniae* in respiratory samples with an internal processing control. *J Med Microbiol* **55:**149–155.
39. **Saito R, Misawa Y, Moriya K, Koike K, Ubukata K, Okamura N.** 2005. Development and evaluation of a loop-mediated isothermal amplification assay for rapid detection of *Mycoplasma pneumoniae*. *J Med Microbiol* **54:**1037–1041.
40. **Di Marco E, Cangemi G, Filippetti M, Melioli G, Biassoni R.** 2007. Development and clinical validation of a real-time PCR using a uni-molecular Scorpion-based probe for the detection of *Mycoplasma pneumoniae* in clinical isolates. *New Microbiol* **30:**415–421.
41. **Ginevra C, Barranger C, Ros A, Mory O, Stephan JL, Freymuth F, Joannes M, Pozzetto B, Grattard F.** 2005. Development and evaluation of Chlamylege, a new commercial test allowing simultaneous detection and identification of *Legionella*, *Chlamydophila pneumoniae*, and *Mycoplasma pneumoniae* in clinical respiratory specimens by multiplex PCR. *J Clin Microbiol* **43:**3247–3254.
42. **Dumke R, Schurwanz N, Lenz M, Schuppler M, Luck C, Jacobs E.** 2007. Sensitive detection of *Mycoplasma pneumoniae* in human respiratory tract samples by optimized real-time PCR approach. *J Clin Microbiol* **45:**2726–2730.
43. **Winchell JM, Thurman KA, Mitchell SL, Thacker W, Fields BS.** 2008. Evaluation of three real-time PCR assays for the detection of *Mycoplasma pneumoniae* in an outbreak investigation. *J Clin Microbiol*. **46:**3116–3118.
44. **Stormer M, Vollmer T, Henrich B, Kleesiek K, Dreier J.** 2009. Broad-range real-time PCR assay for the rapid identification of cell-line contaminants and clinically important mollicute species. *Int J Med Microbiol* **299:**291–300.
45. **Khanna M, Fan J, Pehler-Harrington K, Waters C, Douglass P, Stallock J, Kehl S, Henrickson KJ.** 2005. The pneumoplex assays, a multiplex PCR-enzyme hybridization assay that allows simultaneous detection of five organisms, *Mycoplasma pneumoniae*, *Chlamydia* (*Chlamydophila*) *pneumoniae*, *Legionella pneumophila*, *Legionella micdade*i, and *Bordetella pertussis*, and its real-time counterpart. *J Clin Microbiol* **43:**565–571.
46. **Morozumi M, Nakayama E, Iwata S, Aoki Y, Hasegawa K, Kobayashi R, Chiba N, Tajima T, Ubukata K.** 2006. Simultaneous detection of pathogens in clinical samples from patients with community-acquired pneumonia by real-time PCR with pathogen-specific molecular beacon probes. *J Clin Microbiol* **44:**1440–1446.
47. **Raggam RB, Leitner E, Berg J, Muhlbauer G, Marth E, Kessler HH.** 2005. Single-run, parallel detection of DNA from three pneumonia-producing bacteria by real-time polymerase chain reaction. *J Mol Diagn* **7:**133–138.
48. **Loens K, Ieven M, Ursi D, Beck T, Overdijk M, Sillekens P, Goossens H.** 2003. Detection of *Mycoplasma pneumoniae* by real-time nucleic acid sequence-based amplification. *J Clin Microbiol* **41:**4448–4450.
49. **Lin B, Blaney KM, Malanoski AP, Ligler AG, Schnur JM, Metzgar D, Russell KL, Stenger DA.** 2007. Using a resequencing microarray as a multiple respiratory pathogen detection assay. *J Clin Microbiol* **45:**443–452.
50. **Yoshida T, Deguchi T, Meda S, Kubota Y, Tamaki M, Yokoi S, Yasuda M, Ishiko H.** 2007. Quantitative detection of *Ureaplasma parvum* (biovar 1) and *Ureaplasma urealyticum* (biovar 2) in urine specimens from men with and without urethritis by real-time polymerase chain reaction. *Sex Transm Dis* **34:**416–419.
51. **Mallard K, Schopfer K, Bodmer T.** 2005. Development of real-time PCR for the differential detection and quantification of *Ureaplasma urealyticum* and *Ureaplasma parvum*. *J Microbiol Methods* **60:**13–19.
52. **Cao X, Wang Y, Hu X, Qing H, Wang H.** 2007. Real-time TaqMan polymerase chain reaction assays for quantitative detection and differentiation of *Ureaplasma urealyticum* and *Ureaplasma parvum*. *Diagn Microbiol Infect Dis* **57:**373–378.
53. **Vancutsem E, Soetens O, Breugelmans M, Foulon W, Naessens A.** 2011. Modified real-time PCR for detecting, differentiating, and quantifying *Ureaplasma urealyticum* and *Ureaplasma parvum*. *J Mol Diagn* **13:**206–212.
54. **Yoshida T, Deguchi T, Ito M, Maeda S, Tamaki M, Ishiko H.** 2002. Quantitative detection of *Mycoplasma genitalium* from first-pass urine of men with urethritis and asymptomatic men by real-time PCR. *J Clin Microbiol* **40:**1451–1455.
55. **Yoshida T, Maeda S, Deguchi T, Ishiko H.** 2002. Phylogeny-based rapid identification of mycoplasmas and ureaplasmas from urethritis patients. *J Clin Microbiol* **40:**105–110.
56. **Pascual A, Jaton K, Ninet B, Bille, Greub G.** 2010. New diagnostic real-time PCR for specific detection of *Mycoplasma hominis* DNA. *Int J Bacteriol* **2010:**4.

Chlamydia and *Chlamydophila* Infections

ROSEMARY SHE

50

Chlamydiaceae is a unique family of bacteria which consists of small Gram-negative coccobacilli that are obligate intracytoplasmic organisms, typically causing infection in warm-blooded animals (1). The genus name *Chlamydia* first appeared in the literature in 1945 but was not fully recognized until 1956 (1, 2). The family had only one genus until 1999 when the genus *Chlamydophila* was added. However, the name *Chlamydophila* has not become widely adopted in the medical community, and *Chlamydophila* spp. are still commonly referred to as *Chlamydia* spp.

The diverse species of *Chlamydia* and *Chlamydophila* are unified by their characteristic two-stage developmental cycle, alternating between the elementary body and the reticulate body. The small (~ 0.3 μm), extracellular, and metabolically inactive elementary body infects eukaryotic cells. After being internalized, it develops within an inclusion body into the metabolically active reticulate body, which then undergoes multiple rounds of binary fission. The reticulate body is larger (~1 μm) and has a cell membrane resembling that of other Gram-negative bacteria. Within the host membrane-bound inclusion, it differentiates into elementary bodies, lysing the host cell and releasing infective organisms to repeat the cycle (3). Organisms in the *Chlamydiaceae* are reliant on the host cell for energy or ATP (4). Organisms in the *Chlamydiaceae* family cause several important and pervasive human diseases. *Chlamydia trachomatis* causes venereal and ocular disease and *Chlamydophila pneumoniae* causes respiratory infections. Rarely, *Chlamydophila psittaci* causes zoonotic infection in bird handlers.

C. TRACHOMATIS

Organism Description

The 20 genotypes and serovars of *C. trachomatis* are differentiated by their major outer membrane protein (MOMP). Serovars A to K are the most common and infect epithelial cells of the human genital tract and eye. L1, L2, L2a, and L3 serovars cause lymphogranuloma venereum (LGV) and infect mononuclear cells (5).

Clinical Disease

Chlamydia trachomatis is the cause of the most common reportable sexually transmitted infection in the United States (6). Serovars D to K have a predilection for the genital tract, where they can infect both the lower and upper genital tracts. The disease tends to be mild or asymptomatic in both males and females, but particularly in females. For this reason, annual screening is recommended in all sexually active females 25 years of age or younger, as well as in older women with risk factors such as new or multiple sexual partners. In males, the organism can cause urethritis and epididymitis (7). There are no recommendations for routine screening in males except in sexually active men who have sex with men (MSM) (8). In females, as the organism is capable of establishing chronic infection, it can further lead to complications such as chronic pelvic pain, pelvic inflammatory disease, tubal scarring, and ectopic pregnancy. In the MSM population, *C. trachomatis* is a major cause of proctitis and less commonly a cause of pharyngeal infection. *C. trachomatis* may also cause neonatal conjunctivitis and infant pneumonia (8).

Serovars A, B, Ba, and C cause trachoma, a leading cause of blindness worldwide that has recently been subject to intense eradication efforts. Infections frequently begin as a keratoconjunctivitis in children who then develop pathological scarring and blindness as adults. Recurrent infections are thought to sustain the inflammatory response (9).

LGV is more prevalent in developing countries but there has been a recent surge in rectal LGV among MSM in Western Europe and the United States (10). In the genital tract, the disease is characterized by formation of buboes and ulcers. LGV may also involve the rectum in those practicing anal sex. Untreated, the disease may result in scarring with subsequent lymphatic obstruction and elephantiasis of the genital region, rectal fistulas, or rectal stricture formation (5).

Laboratory Diagnosis

Recommended Laboratory Tests

For screening and diagnosis of genital tract infection caused by *C. trachomatis*, the Centers for Disease Control and Prevention (CDC) recommends nucleic acid amplification testing (NAAT). Vaginal and endocervical swabs and urine are acceptable for female patients. Urine or a urethral swab is collected for male patients. Urine specimens should be a first-catch 10 to 30 ml collection (8). Detailed screening recommendations are available elsewhere (8). Test of cure, such as may be done 3 to 4 weeks after initiation of therapy, is specifically not recommended by the CDC except in

doi:10.1128/9781555818722.ch50

pregnancy. The concern is that nucleic acid from nonviable organisms may be present and detectable by NAATs despite effective therapy, leading to false positive results. On the other hand, persistence of low-level infection may be difficult to detect and result in false-negative results. It is, however, recommended that retesting of newly infected patients be done 3 months after treatment. This follow-up testing is mainly to assess for reinfection, which increases the risk of complications (8).

For sexual abuse cases, legally acceptable testing will depend on the locality. Because of its superior specificity, chlamydial culture has long been considered the only acceptable test, until recently. Although not FDA-cleared for testing in children, NAAT has gained wider acceptance for testing in cases of suspected sexual abuse. When culture is not available and positive NAAT results can be confirmed by an alternate target, NAAT may be acceptable. Studies have been done on vaginal and urinary specimens from girls, but no recommendations are made for boys. It is important for laboratories to retain and not prematurely discard specimens tested for medicolegal reasons in the case that further testing is needed (8).

Specimen Collection

Swabs of the suspected site of infection are taken to collect cellular specimens. Besides genitourinary sources, eye, rectal, and throat swabs may be tested depending on the patient history. In LGV, an aspirate or biopsy of an affected lymph node may be examined or tested by culture or NAAT (if validated by the laboratory). In neonates, nasopharyngeal collection may be appropriate if respiratory *C. trachomatis* infection is suspected from vertical transmission.

Collection devices and transport media for *C. trachomatis* NAAT are test-specific and available from the manufacturer. Some kits are conveniently FDA-cleared for use on liquid-based Pap specimen media (i.e., BD SurePath or ThinPrep Autocyte) if aliquoted before cytology testing. For culture or antigen detection methods, specimens should be transported in sucrose-containing media such as 2-sucrose phosphate (2SP), M4, or universal transport media. In terms of timing of specimen collection for serologic testing, most patients develop detectable IgM and IgG response within 2 to 3 weeks (11).

Culture

Tissue culture for *C. trachomatis* is done with cells such as McCoy, Buffalo green monkey, or HeLa 229. The addition of 1% cycloheximide to the isolation media helps to optimize recovery; it is thought that cycloheximide inhibits host cell metabolism, thereby increasing availability of ATP for chlamydial organisms that may be present (12). Centrifugation yields 100- to 1000-fold more organisms with culture (4). The typical protocol is to centrifuge inoculated shell vials at 1,000 to 3,000 × *g* for 1 hour at 30 to 35°C (12). Blind passage of cells increases yield by 5 to 10% but must be balanced with increased labor, expense, and turnaround time (13). Blind stains should be done after 48 to 72 hours of incubation. Fluorescent antibodies, not Giemsa or other nonspecific stains, should be used (Fig. 1). Laboratories may choose to start with less expensive, genus-specific antibodies, and if positive, confirm with species-specific MOMP monoclonal antibodies (8).

Because of its poor sensitivity compared to NAAT, culture is not widely used or performed. The delay associated with specimen transport to an off-site laboratory can decrease recovery of these fastidious organisms (14). It is still of value in instances of medicolegal testing, when there is suspected failure of therapy requiring an isolate for susceptibility testing, or when non-genitourinary specimen types are not validated by the laboratory for NAAT (8).

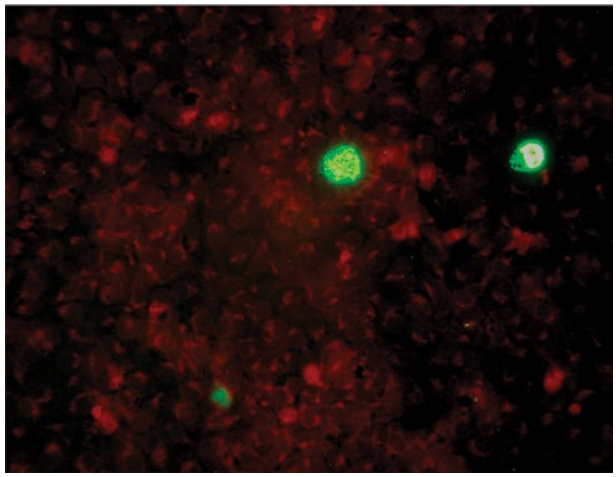

FIGURE 1 Example of culture positive for *Chlamydia trachomatis*, as confirmed by fluorescently labeled monoclonal antibody to chlamydial group antigens using reagents from Diagnostic Hybrids (Athens, OH).

Direct Antigen Detection

Older methods of direct antigen detection for *C. trachomatis* such as enzyme immunoassay and Giemsa staining are insensitive and not recommended for routine clinical testing (15). The classic intracytoplasmic inclusions of *Chlamydia* may occasionally be appreciated on histologic or cytologic specimens, but are not a reliable finding. Examination of lymph node tissue for LGV reveals somewhat nonspecific pathology, although in the appropriate clinical context it can suggest the correct diagnosis (16).

Direct fluorescent antibody testing for *C. trachomatis* involves detection of elementary bodies in smears of patient cells. It has limited utility but is an option when NAAT has not been validated and a rapid test would be helpful, e.g., for ocular sources. Although highly specific, its sensitivity is only 50 to 70% compared to that of NAAT (17).

Nonamplified nucleic acid detection methods used more widely in the past (i.e., Gen-Probe [Hologic] PACE 2 and Digene Hybrid Capture 2) also lack sensitivity compared to NAAT (18). The PACE 2 assay's only advantages are that it is inexpensive and FDA-cleared for use on conjunctival specimens.

Serology

Serologic diagnosis is challenged by cross-reactivity of antibodies between species of *Chlamydia* and *Chlamydophila*. It should not be used as the primary diagnostic modality for *C. trachomatis* infection. Antibody response may be delayed up to 1 month after infection, and elevated titers may be seen in the case of either current or past infection. If used, serologic testing for *C. trachomatis* is best done using paired specimens, e.g., collected in the acute and convalescent phases of illness. It may sometimes be useful in patients previously treated with antibiotics or patients with upper genital tract infection, in whom detection of the organism may be difficult (19). Serologic testing can also support the clinical presentation in the diagnosis of LGV (5, 8). Because LGV is an invasive infection, high titers, i.e., > 1:128, are usually

observed, but do not necessarily distinguish LGV from invasive infections caused by other serovars (5). Studies suggest that an elevated IgA titer may be useful in detecting anorectal LGV (20). Infants with suspected chlamydial pneumonitis may also benefit from serologic testing with an assessment for an IgM response (21).

Microimmunofluorescence (MIF) antibody testing is considered the gold standard for detection of chlamydial antibodies, although complement fixation and enzyme immunoassay (EIA) methods are also described. In MIF, formalin-fixed elementary bodies are spotted onto a glass slide for incubation with patient sera. This method is highly manual and technically complex and subjective. Subjectivity in interpreting endpoint titers and lack of interlaboratory agreement are some of the issues to consider (22). Most available serologic tests do not distinguish antibodies to LGV serovars from A to K serovars, but specialized testing for LGV serovars can be done at reference laboratories or research centers. Because elevated titers against *C. trachomatis* may result from cross-reactivity with related species, it is advisable to obtain titers against a panel of chlamydial species, e.g., *C. pneumoniae*, *C. psittaci*, and *C. trachomatis*, to ensure that the highest titer is to *C. trachomatis*. Interpretation of chlamydial antibody panels must be made carefully, taking into account the high incidence of both *C. trachomatis* and *C. pneumoniae* infection (23).

IgM antibodies by MIF testing appear to be less heterologous than IgG antibodies, but false positive titers may result from presence of rheumatoid factor or with Epstein Barr virus infection (24). Notably, a rise in IgM is observed after primary but not repeat exposure to *C. trachomatis*; therefore, single-point serology for *C. trachomatis* is difficult to interpret and rarely useful in sexually active individuals (25).

Molecular Testing

The standard of care for *C. trachomatis* screening and diagnosis from genital, pharyngeal, and rectal sources is NAAT (8). Numerous FDA-cleared methods are available and can suit different laboratory test volumes and workflow considerations (Table 1). The different methods include PCR, strand displacement amplification, and transcription-mediated amplification. Performance characteristics of these tests are roughly equivalent (26, 27). For testing in females, urine may be less sensitive than vaginal or endocervical swabs (28). The available assays can also target *Neisseria gonorrhoeae* in the same kit or platform. Although NAAT is recommended for diagnosis of rectal and pharyngeal infection, as of yet there has been no FDA clearance of such specimen sources (8). Performance will depend on laboratory validation of these sources according to Clinical Laboratory Improvement Amendments standards. The FDA-cleared NAATs are not approved for use in children, but NAAT has been shown to perform reliably in girls undergoing evaluation for sexual abuse, detecting all culture-positive cases and being able to be confirmed by secondary target testing. Recommendations are not made for boys (29). NAAT tests for *C. trachomatis* are designed to detect all serovars, but specific identification of LGV serovars requires specialized molecular tests available at some public health laboratories and the CDC.

The sensitivity of NAAT testing for *C. trachomatis* is indisputably superior to other available methods. The specificity approaches that of culture, but it is important that laboratories follow strict practices to minimize the possibility of contamination of the testing environment. Many of the FDA-cleared systems are considered closed environments, but laboratories should still monitor surfaces for contamination. Internal or amplification controls are either included or an available option among most FDA-cleared assays. Repeat or alternate target testing was once recommended to confirm positive results in low-prevalence areas. But because of evidence demonstrating a lack of overall benefit of this approach, it is no longer advocated for most circumstances (30).

Several NAATs target the cryptic DNA plasmid of *C. trachomatis* as this target is present in 7 to 10 copies per cell. Plasmid-deficient strains are rare as the plasmid appears to play a significant role in the virulence of the organism (31). It is noted that in 2006, a strain with a plasmid harboring a 377-base-pair deletion emerged in Sweden, with limited spread within Europe (32). Because of the deletion, the variant strain could not be detected by the Abbott m2000 PCR or the Roche AMPLICOR assays (33). Most current NAAT systems are designed to detect this variant.

C. PNEUMONIAE

Organism Description

Chlamydia strain TWAR was renamed *Chlamydia pneumoniae* in 1989, then 10 years later was reclassified into a new genus as *Chlamydophila pneumoniae* based on nucleic acid sequence analysis (34). It is distinct from *C. trachomatis* in several ways, such as having a characteristically pear-shaped instead of round elementary body. The organism is globally distributed and there is only one known serovar (22, 35).

Clinical Disease

C. pneumoniae is a common pathogen with a high population seroprevalence and is well described to cause atypical pneumonia, asthma exacerbation, tracheobronchitis, pharyngitis, laryngitis, and sinusitis (36). The prevalence among patients with community-acquired pneumonia is reported to be 6 to 22% (22). It is also known to cause sporadic outbreaks of respiratory tract infection (37). Prolonged duration of relatively mild respiratory symptoms is characteristic and may help differentiate it from other agents of respiratory tract infection (35, 38). *C. pneumoniae* commonly coinfects the respiratory tract with other pathogens, raising questions regarding its pathogenic role (39). Because it is believed to be capable of causing latent infection, it has been implicated in diverse extrapulmonary disease processes. *C. pneumoniae* has been associated with multiple sclerosis, Alzheimer's disease, and atherosclerosis, among other illnesses, although its exact role is still debated (40).

Laboratory Diagnosis

It is important to distinguish *C. pneumoniae* from other respiratory tract pathogens as treatment can differ. *C. pneumoniae* is an obligate intracellular organism best treated with a macrolide or tetracycline and not with beta-lactam drugs. Unfortunately, laboratory diagnosis in the outpatient setting, where most *C. pneumoniae* infections present, is infrequently undertaken due to poor availability of onsite testing. Diagnostic methods include culture, PCR, and serology, but *C. pneumoniae* suffers from a lack of a true gold standard for laboratory diagnosis. Culture requires extended incubation times and has a poor rate of recovery. PCR and serology are considered more reliable tests though performance is nonstandardized and laboratory dependent (22). Recent advances in technology may make molecular testing more readily available in the future.

TABLE 1 Select nucleic acid-amplified methods (FDA-cleared) for detection of *Chlamydia trachomatis* from clinical specimens

Kit name and manufacturer	Method	Gene target	FDA-cleared sources	Comments
APTIMA Combo 2, APTIMA CT; Gen-Probe (San Diego, CA)	Transcription-mediated amplification	23s rRNA	Male and female urine Endocervical, vaginal (clinician- or patient-collected), and male urethral swabs	Kit for alternate target testing available No internal control included PreservCyt solution, liquid Pap specimens also FDA cleared
GeneXpert CT/NG; Cepheid (Sunnyvale, CA)	PCR	Chromosomal DNA	Male and female urine Endocervical swab Patient-collected vaginal swab (in a clinical setting)	Clinical Laboratory Improvement Amendments – moderate complexity
ProbeTec ET (BD, Franklin Lakes, NJ)	Strand displacement amplification	Cryptic plasmid DNA	Male and female urine Endocervical and male urethral swabs Patient-collected vaginal swab (in a clinical setting)	SurePath and PreservCyt solution Liquid-based Pap media also FDA cleared
COBAS AMPLICOR CT/NG Test; Roche (Indianapolis, IN)	PCR	Cryptic plasmid DNA	Male and female urine Endocervical and male urethral swabs	PreservCyt solution Liquid Pap specimens also FDA cleared Does not detect Swedish variant with 377-bp deletion in cryptic plasmid DNA
RealTime CT/NG; Abbott Diagnostics (Santa Clara, CA)	PCR	Cryptic plasmid DNA	Male and female urine Endocervical, vaginal (clinician- or patient-collected), and male urethral swabs	Dual cryptic plasmid targets

Specimen Collection

C. pneumoniae has been isolated from a variety of body sites but the optimal specimen type has not been thoroughly examined. It is currently presumed that for respiratory tract infections, a variety of specimen types are acceptable, including sputum, nasopharyngeal swab, throat swab, tracheal specimens, and bronchoalveolar samples. One study found that nasopharyngeal swabs yielded more positive results for *C. pneumoniae* by PCR than throat, throat wash, or sputum samples, but could not rule out nasopharyngeal colonization unrelated to lower respiratory tract infection (39). It is best to use swabs with a Dacron tip and to avoid wooden shafts. For culture, specimens should be kept at 4°C and only frozen at –70°C if culture cannot be set up within 24 h (35, 41, 42). All specimens should be transported in 2SP, M4, or universal transport media. For NAAT assays, it is best to collect specimens as early in the course of disease as possible because sensitivity has been shown to decrease after the first week of illness (43). If collecting samples for serologic testing, it is important to note that IgM antibodies may not appear until 2 to 3 weeks after illness onset (11, 43). Paired IgG samples are required for diagnosis of acute infection, one taken during acute phase and one taken 6 to 8 weeks later (11).

Culture

Culture has been shown to be insensitive compared to serology or PCR for diagnosis of *C. pneumoniae* infection (39). Furthermore, it is a specialized test requiring tissue culture, and thus it is mainly limited to reference laboratories. Organisms lose infectivity during prolonged storage, which may explain why recovery in culture is inconsistent, especially in the reference laboratory setting (44). HEp-2 cells appear to be the most effective at cultivating *C. pneumoniae*, although use of other cells, such as HL or McCoy cells, has also been described (45). Centrifugation of specimen onto tissue culture monolayers enhances organism recovery (46). Organisms grow slowly and cultures may take up to one week. Passage of cells during the course of culture and blind stain using fluorescently labeled antibodies are recommended as these procedures enhance detection and identification (47). The CDC recommends at least two passages to optimize culture sensitivity (41).

Serology

Serologic assays for *C. pneumoniae*, which include MIF, complement fixation, and EIA, are criticized for their lack of standardization and their inability to provide a timely diagnosis (22, 48). The reader is referred to the 7th edition of this manual for more detailed information on the performance of serologic methods. MIF can be accomplished by using in-house laboratory preparations of chlamydial elementary bodies or by using commercial kits (e.g., from Labsystems [Vantaa, Finland], Savyon Diagnostics [Ashdod, Israel], etc.). Agreement between the various MIF tests is dependent on differences in antigen preparation, bacterial strains used, and interpretation of the stain (48). Nonetheless, MIF is considered the gold standard and is the serologic method recommended by the CDC (Fig. 2) (41). The *C. pneumoniae* MOMP is not species specific, and as already mentioned, there is substantial cross-reactivity between *Chlamydiaceae* antibodies (35). Therefore, as with *C.*

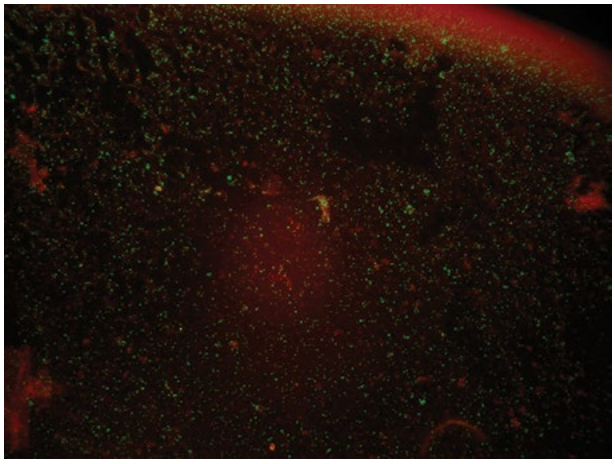

FIGURE 2 Example of a positive microimmunofluorescence (MIF) serologic reaction for *C. pneumoniae*. Bright green fluorescent dot-like staining highlights the elementary bodies which have reacted with the patient serum (100× magnification). Photo courtesy of Marc R Couturier.

trachomatis antibody testing, it is best to interpret antibody titers to *C. pneumoniae* in the context of antibody titers to other species of this family.

EIA or enzyme-linked immunosorbent assay (ELISA)-based methods are objective and less labor-intensive than MIF and thus may be a good alternative, although performance characteristics are kit dependent (43). Several kits, such as the Labsystems *C. pneumoniae* IgG EIA, the Medac sandwich ELISA (Medac, Wedel, Germany), and the Biopharm Elegance EIA (R-Biopharm, Darmstadt, Germany), have shown good correlation with MIF (49). False-negative results for some assays, including the SeroCP ELISA (Savyonn Diagnostics), Medac sandwich ELISA, and LabSystems EIA, have been noted in specimens with low IgG titers by MIF (50). False-positive results have also been documented, with one study showing cross-reactivity of the LabSystems EIA for *C. pneumoniae* IgG when high titers of *C. trachomatis* antibodies were present (51). In outbreak situations, a recombinant EIA (Medac) and the LabSystems EIA were found to be highly sensitive and specific when compared to MIF (52). While IgM by EIA or ELISA has been shown to aid in identifying cases during *C. pneumoniae* outbreaks, they are also less specific than IgG antibodies, with ~8% of asymptomatic healthy persons having positive results (50, 53).

Paired IgG serology results are recommended for a more reliable diagnosis of acute infection (41). A 4-fold or greater change in titer is considered diagnostic of recent *C. pneumoniae* infection. Given that paired samples should be drawn 6 to 8 weeks apart and that single-point serology is not recommended, an accurate serologic diagnosis of acute *C. pneumoniae* infection is retrospective. Admittedly, the prevailing clinical practice is to request single-point serology for the sake of convenience and a timely result. Clinicians should be advised that even high single-point titers (e.g., IgG ≥1:512 or IgM ≥1:16) are commonly seen in healthy, asymptomatic individuals (54).

When elevated, IgM antibodies for *C. pneumoniae* are considered indicative of acute infection. The utility of IgM is hampered by the fact that it may not be elevated early in the disease course or with reinfection. Rheumatoid factor has been shown to produce false-positive IgM results (11). During repeat infection, IgM may be low titer or absent, whereas IgG titers usually greatly increase within 1 to 2 weeks of reinfection (35).

Molecular Testing

Numerous laboratory-developed NAATs for *C. pneumoniae* have been described in the literature (39, 54). Early in disease onset, PCR has been shown to be highly sensitive and superior to culture and possibly more predictive of infection than serology in the outbreak setting (39). Nonetheless, in peer-reviewed studies there is great discrepancy in test results between NAAT, serology, and culture. Performance of NAATs as a whole is difficult to assess due to the lack of standardization and difficulty in defining a gold standard for *C. pneumoniae* infection. Interestingly, the positivity rate by PCR has not been as high as serology in multiple studies (22, 44). This may be related to sporadic occurrence of disease, timing of specimen collection, and lack of specificity of serologic testing, among other variables. Caution should be taken with interpreting NAAT results as *C. pneumoniae* is known to asymptomatically colonize the respiratory tract and can be shed for up to 8 weeks after infection (54).

Real-time PCR testing may be performed using commercially available analyte-specific reagents either in single-target format or multiplexed for simultaneous detection of other atypical bacterial pathogens of the respiratory tract. Reagents include those from Focus Diagnostics (Cypress, CA), ELiTech Molecular Diagnostics (Princeton, NJ), ARGENE (bioMérieux) (Durham, NC), Seegene (Seoul, Korea), and others. Recently, the FilmArray Respiratory Panel (BioFire Diagnostics Inc, Salt Lake City, UT) became the first FDA-cleared PCR assay with *C. pneumoniae* as one of the analytes on this sample-to-answer multiplexed assay. More convenient, affordable, and accurate test options for *C. pneumoniae* are still needed in the outpatient setting.

C. PSITTACI

Organism Description

The agent causing psittacosis was described as early as 1930 and eventually placed in the genus *Chlamydia* in 1966 (55). In 1999 it was reclassified as *Chlamydophila psittaci*. The species name is derived from the Greek for parrot, or psittakos. *C. psittaci* consists of eight serovars (34).

Clinical Disease

C. psittaci infects individuals who come in close contact with birds or bird secretions, such as pet shop keepers, poultry handlers, bird owners, and veterinarians. Infectious agents are found in the nasal discharge, feces, or tissues of the infected bird. In human cases, transmission is most common from infected birds of the parrot family but has also occurred with poultry and free-ranging birds (56). An average of 16 cases per year were reported to the CDC in the United States between 2000 and 2009 (57). This zoonotic illness known as psittacosis consists of influenza-like symptoms which uncommonly result in severe pneumonia. It is thought that many milder presentations go unrecognized or misdiagnosed (56).

Laboratory Diagnosis

Laboratory tests for diagnosis of psittacosis are performed only by a handful of reference laboratories. While numerous studies on diagnostic testing have been performed in birds, few have examined optimal test modalities in humans. Serologic testing and culture are used most commonly. As

with the other chlamydial species, MIF is considered to be the most reliable. A 4-fold increase in IgG between paired serum samples drawn 2 to 4 weeks apart, or an IgM titer elevated at least to 1:32, supports diagnosis. Because cross-reactivity is observed with other chlamydial species (23), it is best to obtain titers to *C. pneumoniae* and *C. trachomatis* concomitantly to be able to interpret results. The IgG titer to *C. psittaci* should also be highly elevated (≥1:128) to support the diagnosis (56).

C. psittaci may also be cultivated from respiratory or peripheral blood specimens (56). Centrifugation of the specimen onto the cell monolayer and treatment of cells with cycloheximide are shown to improve organism recovery (58). HeLa, McCoy, and mouse L cells have been used successfully (58, 59). Because of its low incidence, reference laboratories do not generally offer NAAT testing for *C. psittaci*. Testing may be performed by the CDC.

OTHER ZOONOTIC CHLAMYDIAL INFECTIONS

Besides *C. psittaci*, several other chlamydial species have been reported to cause rare, sporadic infections in people who come into contact with an infected animal. *C. psittaci* has, in fact, been separated into five species: *C. psittaci*, *C. pecorum*, *C. felis*, *C. abortus*, and *C. caviae*. *Chlamydophila felis*, which causes conjunctivitis and respiratory tract infection in cats, has been suggested to rarely cause human disease according to various case reports (60). *Chlamydophila abortus* infection causes abortion in sheep and other ruminants and has been reported to cause systemic infection and miscarriage in pregnant women (61). Testing for these zoonotic Chlamydiaceae is limited and done only in specialized reference laboratories.

REFERENCES

1. **Breed RS, Murray EGD, Smith NR.** 1957. *Bergey's Manual of Determinative Bacteriology*, 7th ed. Williams & Wilkins Co, Baltimore, MD.
2. **Jones H, Rake G, Stearns B.** 1945. Studies on lymphogranuloma venereum. III. The action of the sulfonamides on the agent of lymphogranuloma venereum. *J Infect Dis* **76:**55–69.
3. **Abdelrahman YM, Belland RJ.** 2005. The chlamydial developmental cycle. *FEMS Microbiol Rev* **29:**949–959.
4. **Moulder JW.** 1991. Interaction of chlamydiae and host cells in vitro. *Microbiol Rev* **55:**143–190.
5. **Mabey D, Peeling RW.** 2002. Lymphogranuloma venereum. *Sex Transm Infect* **78:**90–92.
6. **Centers for Disease Control and Prevention.** 2012. Notice to readers: final 2012 reports of nationally notifiable infectious diseases. *MMWR* **62:**669–682.
7. **Johnson RE, Newhall WJ, Papp JR, Knapp JS, Black CM, Gift TL, Steece R, Markowitz LE, Devine OJ, Walsh CM, Wang S, Gunter DC, Irwin KL, DeLisle S, Berman SM.** 2002. Screening tests to detect *Chlamydia trachomatis* and *Neisseria gonorrhoeae* infections—2002. *MMWR Recomm Rep* **51:**1–38.
8. **Workowski KA, Berman S.** 2010. Sexually transmitted diseases treatment guidelines, 2010. *MMWR Recomm Rep* **59:**1–110.
9. **Taylor HR.** 2009. Doyne lecture: trachoma, is it history? *Eye* (Lond) **23:**2007–2022.
10. **Nieuwenhuis RF, Ossewaarde JM, Gotz HM, Dees J, Thio HB, Thomeer MG, den Hollander JC, Neumann MH, van der Meijden WI.** 2004. Resurgence of lymphogranuloma venereum in western Europe: an outbreak of *Chlamydia trachomatis* serovar l2 proctitis in The Netherlands among men who have sex with men. *Clin Infect Dis* **39:**996–1003.
11. **Wang S.** 2000. The microimmunofluorescence test for *Chlamydia pneumoniae* infection: technique and interpretation. *J Infect Dis* **181:**S421–S425.
12. **Corsaro D, Greub G.** 2006. Pathogenic potential of novel Chlamydiae and diagnostic approaches to infections due to these obligate intracellular bacteria. *Clin Microbiol Rev* **19:**283–297.
13. **Jones RB, Katz BP, van der Pol B, Caine VA, Batteiger BE, Newhall WJ.** 1986. Effect of blind passage and multiple sampling on recovery of *Chlamydia trachomatis* from urogenital specimens. *J Clin Microbiol* **24:**1029–1033.
14. **Mahony JB, Chernesky MA.** 1985. Effect of swab type and storage temperature on the isolation of *Chlamydia trachomatis* from clinical specimens. *J Clin Microbiol* **22:**865–867.
15. **Van Dyck E, Ieven M, Pattyn S, Van Damme L, Laga M.** 2001. Detection of *Chlamydia trachomatis* and *Neisseria gonorrhoeae* by enzyme immunoassay, culture, and three nucleic acid amplification tests. *J Clin Microbiol* **39:**1751–1756.
16. **Ioachim HL, Medeiros LJ.** 2009. *Ioachim's Lymph Node Pathology*, 4th ed, p 119–122. Lippincott Williams & Wilkins, Philadelphia, PA.
17. **Schachter J.** 1997. DFA, EIA, PCR, LCR and other technologies: what tests should be used for diagnosis of chlamydia infections? *Immunol Invest* **26:**157–161.
18. **Black CM, Marrazzo J, Johnson RE, Hook EW, 3rd, Jones RB, Green TA, Schachter J, Stamm WE, Bolan G, St Louis ME, Martin DH.** 2002. Head-to-head multicenter comparison of DNA probe and nucleic acid amplification tests for *Chlamydia trachomatis* infection in women performed with an improved reference standard. *J Clin Microbiol* **40:**3757–3763.
19. **Chernesky M, Luinstra K, Sellors J, Schachter J, Moncada J, Caul O, Paul I, Mikaelian L, Toye B, Paavonen J, Mahony J.** 1998. Can serology diagnose upper genital tract *Chlamydia trachomatis* infections? Studies on women with pelvic pain, with or without chlamydial plasmid DNA in endometrial biopsy tissue. *Sex Transm Dis* **25:**14–19.
20. **de Vries HJ, Smelov V, Ouburg S, Pleijster J, Geskus RB, Speksnijder AG, Fennema JS, Morre SA.** 2010. Anal lymphogranuloma venereum infection screening with IgA anti-*Chlamydia trachomatis*-specific major outer membrane protein serology. *Sex Transm Dis* **37:**789–795.
21. **Black CM.** 1997. Current methods of laboratory diagnosis of *Chlamydia trachomatis* infections. *Clin Microbiol Rev* **10:**160–184.
22. **Kumar S, Hammerschlag MR.** 2007. Acute respiratory infection due to *Chlamydia pneumoniae*: current status of diagnostic methods. *Clin Infect Dis* **44:**568–576.
23. **She RC, Welch R, Wilson AR, Davis D, Litwin CM.** 2011. Correlation of *Chlamydia* and *Chlamydophila* spp. IgG and IgM antibodies by microimmunofluorescence with antigen detection methods. *J Clin Lab Anal* **25:**305–308.
24. **Mahony JB, Chernesky MA, Bromberg K, Schachter J.** 1986. Accuracy of immunoglobulin M immunoassay for diagnosis of chlamydial infections in infants and adults. *J Clin Microbiol* **24:**731–735.
25. **Moss TR, Darougar S, Woodland RM, Nathan M, Dines RJ, Cathrine V.** 1993. Antibodies to *Chlamydia* species in patients attending a genitourinary clinic and the impact of antibodies to *C. pneumoniae* and *C. psittaci* on the sensitivity and the specificity of *C. trachomatis* serology tests. *Sex Transm Dis* **20:**61–65.
26. **Van der Pol B, Liesenfeld O, Williams JA, Taylor SN, Lillis RA, Body BA, Nye M, Eisenhut C, Hook EW 3rd.** 2012. Performance of the cobas CT/NG test compared to the Aptima AC2 and Viper CTQ/GCQ assays for detection of *Chlamydia trachomatis* and *Neisseria gonorrhoeae*. *J Clin Microbiol* **50:**2244–2249.

27. **Van der Pol B, Quinn TC, Gaydos CA, Crotchfelt K, Schachter J, Moncada J, Jungkind D, Martin DH, Turner B, Peyton C, Jones RB.** 2000. Multicenter evaluation of the AMPLICOR and automated COBAS AMPLICOR CT/NG tests for detection of *Chlamydia trachomatis*. *J Clin Microbiol* **38:**1105–1112.
28. **Van der Pol B, Ferrero DV, Buck-Barrington L, Hook E, 3rd, Lenderman C, Quinn T, Gaydos CA, Lovchik J, Schachter J, Moncada J, Hall G, Tuohy MJ, Jones RB.** 2001. Multicenter evaluation of the BDProbeTec ET system for detection of *Chlamydia trachomatis* and *Neisseria gonorrhoeae* in urine specimens, female endocervical swabs, and male urethral swabs. *J Clin Microbiol*. **39:**1008–1016.
29. **Hammerschlag MR, Guillen CD.** 2010. Medical and legal implications of testing for sexually transmitted infections in children. *Clin Microbiol Rev* **23:**493–506.
30. **Association of Public Health Laboratories & Centers for Disease Control and Prevention.** 2009. Laboratory Diagnostic Testing for *Chlamydia trachomatis* and *Neisseria gonorrhoeae*. *Expert Consultation Meeting Summary Report*. 13–15 January 2009. Centers for Disease Control and Prevention, Atlanta, GA. http://www.aphl.org/aphlprograms/infectious/std/documents/ctgclabguidelinesmeetingreport.pdf
31. **Song L, Carlson JH, Whitmire WM, Kari L, Virtaneva K, Sturdevant DE, Watkins H, Zhou B, Sturdevant GL, Porcella SF, McClarty G, Caldwell HD.** 2013. *Chlamydia trachomatis* plasmid-encoded Pgp4 is a transcriptional regulator of virulence-associated genes. *Infect Immun* **81:**636–644.
32. **Savage EJ, Ison CA, van de Laar MJ.** 2007. Results of a Europe-wide investigation to assess the presence of a new variant of *Chlamydia trachomatis*. *Euro Surveill* **12:**E3–E4.
33. **Ripa T, Nilsson P.** 2006. A variant of *Chlamydia trachomatis* with deletion in cryptic plasmid: implications for use of PCR diagnostic tests. *Euro Surveill* **11:**E061109–E061102.
34. **Everett KD, Bush RM, Andersen AA.** 1999. Emended description of the order Chlamydiales, proposal of *Parachlamydiaceae* fam. nov. and *Simkaniaceae* fam. nov., each containing one monotypic genus, revised taxonomy of the family *Chlamydiaceae*, including a new genus and five new species, and standards for the identification of organisms. *Int J Syst Bacteriol* **49:**415–440.
35. **Kuo CC, Jackson LA, Campbell LA, Grayston JT.** 1995. *Chlamydia pneumoniae* (TWAR). *Clin Microbiol Rev* **8:**451–461.
36. **Thom DH, Grayston JT, Wang SP, Kuo CC, Altman J.** 1990. *Chlamydia pneumoniae* strain TWAR, *Mycoplasma pneumoniae*, and viral infections in acute respiratory disease in a university student health clinic population. *Am J Epidemiol* **132:**248–256.
37. **Conklin L, Adjemian J, Loo J, Mandal S, Davis C, Parks S, Parsons T, McDonough B, Partida J, Thurman K, Diaz MH, Benitez A, Pondo T, Whitney CG, Winchell JM, Kendig N, Van Beneden C.** 2013. Investigation of a *Chlamydia pneumoniae* outbreak in a federal correctional facility in Texas. *Clin Infect Dis* **57:**639–647.
38. **File TM Jr., Plouffe JF Jr., Breiman RF, Skelton SK.** 1999. Clinical characteristics of *Chlamydia pneumoniae* infection as the sole cause of community-acquired pneumonia. *Clin Infect Dis* **29:**426–428.
39. **Verkooyen RP, Willemse D, Hiep-van Casteren SC, Joulandan SA, Snijder RJ, Van den Bosch JM, Van Helden HP, Peeters MF, Verbrugh HA.** 1998. Evaluation of PCR, culture, and serology for diagnosis of *Chlamydia pneumoniae* respiratory infections. *J Clin Microbiol* **36:**2301–2307.
40. **Tufano A, Di Capua M, Coppola A, Conca P, Cimino E, Cerbone AM, Di Minno G.** 2012. The infectious burden in atherothrombosis. *Semin Thromb Hemost* **38:**515–523.
41. **Dowell SF, Peeling RW, Boman J, Carlone GM, Fields BS, Guarner J, Hammerschlag MR, Jackson LA, Kuo CC, Maass M, Messmer TO, Talkington DF, Tondella ML, Zaki SR.** 2001. Standardizing *Chlamydia pneumoniae* assays: recommendations from the Centers for Disease Control and Prevention (USA) and the Laboratory Centre for Disease Control (Canada). *Clin Infect Dis* **33:**492–503.
42. **Maass M, Dalhoff K.** 1995. Transport and storage conditions for cultural recovery of *Chlamydia pneumoniae*. *J Clin Microbiol* **33:**1793–1796.
43. **Hvidsten D, Halvorsen DS, Berdal BP, Gutteberg TJ.** 2009. *Chlamydophila pneumoniae* diagnostics: importance of methodology in relation to timing of sampling. *Clin Microbiol Infect* **15:**42–49.
44. **She RC, Thurber A, Hymas WC, Stevenson J, Langer J, Litwin CM, Petti CA.** 2010. Limited utility of culture for *Mycoplasma pneumoniae* and *Chlamydophila pneumoniae* for diagnosis of respiratory tract infections. *J Clin Microbiol* **48:**3380–3382.
45. **Maass M, Harig U.** 1995. Evaluation of culture conditions used for isolation of *Chlamydia pneumoniae*. *Am J Clin Pathol* **103:**141–148.
46. **Tjhie JH, Roosendaal R, MacLaren DM, Vandenbroucke-Grauls CM.** 1997. Improvement of growth of *Chlamydia pneumoniae* on HEp-2 cells by pretreatment with polyethylene glycol in combination with additional centrifugation and extension of culture time. *J Clin Microbiol* **35:**1883–1884.
47. **Kuo CC, Grayston JT.** 1990. A sensitive cell line, HL cells, for isolation and propagation of *Chlamydia pneumoniae* strain TWAR. *J Infect Dis* **162:**755–758.
48. **Peeling RW, Wang SP, Grayston JT, Blasi F, Boman J, Clad A, Freidank H, Gaydos CA, Gnarpe J, Hagiwara T, Jones RB, Orfila J, Persson K, Puolakkainen M, Saikku P, Schachter J.** 2000. *Chlamydia pneumoniae* serology: interlaboratory variation in microimmunofluorescence assay results. *J Infect Dis* **181:**S426–S429.
49. **Hoymans VY, Bosmans JM, Van Renterghem L, Mak R, Ursi D, Wuyts F, Vrints CJ, Ieven M.** 2003. Importance of methodology in determination of *Chlamydia pneumoniae* seropositivity in healthy subjects and in patients with coronary atherosclerosis. *J Clin Microbiol* **41:**4049–4053.
50. **Hermann C, Graf K, Groh A, Straube E, Hartung T.** 2002. Comparison of eleven commercial tests for *Chlamydia pneumoniae*-specific immunoglobulin G in asymptomatic healthy individuals. *J Clin Microbiol* **40:**1603–1609.
51. **Gnarpe J, Naas J, Lundback A.** 2000. Comparison of a new commercial EIA kit and the microimmunofluorescence technique for the determination of IgG and IgA antibodies to *Chlamydia pneumoniae*. *APMIS* **108:**819–824.
52. **Persson K, Boman J.** 2000. Comparison of five serologic tests for diagnosis of acute infections by *Chlamydia pneumoniae*. *Clin Diagn Lab Immunol* **7:**739–744.
53. **Miyashita N, Obase Y, Fukuda M, Shoji H, Mouri K, Yagi S, Yoshida K, Ouchi K, Oka M.** 2006. Evaluation of serological tests detecting *Chlamydophila pneumoniae*-specific immunoglobulin M antibody. *Intern Med* **45:** 1127–1131.
54. **Hyman CL, Roblin PM, Gaydos CA, Quinn TC, Schachter J, Hammerschlag MR.** 1995. Prevalence of asymptomatic nasopharyngeal carriage of *Chlamydia pneumoniae* in subjectively healthy adults: assessment by polymerase chain reaction-enzyme immunoassay and culture. *Clin Infect Dis* **20:**1174–1178.
55. **Page LA.** 1966. Revision of the family *Chlamydiaceae* Rake (Rickettsiales): unification of the psittacosis-lymphogranuloma venereum-trachoma group of organisms in the genus *Chlamydia* Jones, Rake and Stearns, 1945. *Int J Syst Bacteriol* **16:**223–252.
56. **Smith KA, Campbell CT, Murphy J, Stobierski MG, Tengelsen LA.** 2011. Compendium of measures to control *Chlamydophila psittaci* infection among humans (psittacosis) and pet birds (avian chlamydiosis), 2010 National

Association of State Public Health Veterinarians (NASPHV). *J Exotic Pet Med* **20:**32–45.
57. **Centers for Disease Control and Prevention.** 2012. Summary of notifiable diseases—United States, 2010. *MMWR* **59:**1–111.
58. **Spears P, Storz J.** 1979. *Chlamydia psittaci*: growth characteristics and enumeration of serotypes 1 and 2 in cultured cells. *J Infect Dis* **140:**959–967.
59. **Pearson JE, Gustafson GA, Senne DA, Peterson LA.** 1989. Isolation and identification of *Chlamydia psittaci* from pet birds. *J Am Vet Med Assoc* **195:**1564–1567.
60. **Eidson M.** 2002. Psittacosis/avian chlamydiosis. *J Am Vet Med Assoc* **221:**1710–1712.
61. **Rohde G, Straube E, Essig A, Reinhold P, Sachse K.** 2010. Chlamydial zoonoses. *Dtsch Arztebl Int* **107:** 174–180.

The *Rickettsiaceae*, *Anaplasmataceae*, and *Coxiellaceae*

LUCAS S. BLANTON AND DAVID H. WALKER

51

Organisms belonging to the families *Rickettsiaceae*, *Anaplasmataceae*, and *Coxiellaceae* are a diverse group of intracellular bacteria that cause a variety of infections in humans. As in the case of the *Rickettsiaceae* and *Anaplasmataceae*, hematophagous arthropod vectors play a role in maintaining the agents in nature and transmit the agents to cause disease. *Coxiella burnetii*, the sole pathogen of the family *Coxiellaceae*, is a zoonosis spread to humans by the inhalation of contaminated aerosols. In the last 2 decades, there has been an emergence of new rickettsial and ehrlichial species as well as new syndromes attributed to species previously deemed nonpathogenic. The growing list of pathogens and syndromic illnesses adds a layer of complexity to their recognition. Additionally, the clinical manifestations of infections caused by these agents are protean and nonspecific. For these reasons, establishing an accurate and timely diagnosis is often difficult. Therefore, knowledge of available laboratory tests, their interpretation, and their shortcomings is crucial for the management of infections caused by these bacteria.

TAXONOMY

The order *Rickettsiales* consists of two families – *Rickettsiaceae* and *Anaplasmataceae* (Fig. 1). Members of both families are small obligately intracellular Gram-negative bacteria. The family *Rickettsiaceae* contains the genera *Rickettsia* and *Orientia*, both coccobacilli. Historically named *Rickettsia tsutsugamushi*, phenotypic and genotypic differences prompted the creation of the genus *Orientia* in 1995 (1). Rickettsiae implicated in human disease are divided into two main groups, the spotted fever group (SFG) and the typhus group (TG). The distinction between these groups is based on antigenic differences of the lipopolysaccharides, the presence of outer membrane protein A in the SFG, and phylogenetic relationships. Although the TG consists of two species, *R. prowazekii* and *R. typhi*, the SFG consists of over 20 named species and species candidates. The recent designation of a third group, the transitional group, classifies species that have variable serologic cross-reactivity and phylogenic placement between the SFG and TG. Members of the transitional group consist of *R. felis*, *R. australis*, and *R. akari* (2). *Orientia tsutsugamushi* is an antigenically diverse species with over 70 different strains. Although the genus has been traditionally recognized as consisting of only one species, a newly isolated strain has been proposed to be different enough to warrant classification as a separate species, *O. chuto* (3). The family *Anaplasmataceae* consists of five genera, *Ehrlichia*, *Anaplasma*, *Neorickettsia*, *Neoehrlichia*, and *Wolbachia* (4). These organisms are pleomorphic cocci that form inclusion-like clusters in host cell vacuoles. Whereas *Ehrlichia*, *Anaplasma*, *Neorickettsia*, and *Neoehrlichia* cause diseases in humans, *Wolbachia* is an endosymbiont of arthropods and filarial nematodes (5). *Coxiella burnetii* is the agent responsible for Q fever. As a small pleomorphic Gram-negative coccobacillus, it was once classified in the order *Rickettsiales*, but it is now classified in the order *Legionellales* (*Gammaproteobacteria*) (6).

EPIDEMIOLOGY

Rickettsiae have a worldwide distribution (Table 1). Those in the SFG cause disease in geographic locations that correspond to the ecological niches of their tick vectors. Although SFG rickettsioses have a variety of names, some of which are geographic, they do not necessarily reflect their full distribution. For example, Rocky Mountain spotted fever (RMSF), caused by *R. rickettsii*, is more prevalent in the southeastern and south-central regions of the United States than it is in the Rocky Mountain region. The organism also causes disease throughout the Americas with cases reported in Mexico, Costa Rica, Panama, Colombia, Brazil, and Argentina (7). *R. conorii* is a prevalent SFG organism with a distribution that includes the Mediterranean basin, Africa, and Asia. It is transmitted by the ubiquitous brown dog tick, *Rhipicephalus sanguineus*. Consequently, infection caused by *R. conorii* is known by several names: Mediterranean spotted fever (MSF), Marseilles fever, Kenya tick typhus, Israeli tick typhus, Astrakhan spotted fever, and Indian tick typhus. *Rickettsia slovaca* causes disease in Europe (8). Other SFG rickettsiae worth noting include *R. africae* and *R. parkeri*, which cause a relatively mild disease in sub-Saharan Africa and the Americas, respectively (9, 10).

Typhus-group organisms include *R. prowazekii* and *R. typhi*. *R. prowazekii* causes typhus, which is also known as epidemic typhus. The human body louse, *Pediculus humanus corporis*, is the vector responsible for transmission of *R. prowazekii* between infected humans. Lice become infected by feeding on rickettsemic patients prior to finding a new host. The new host becomes infected by either scratching *Rickettsia*-laden louse feces into the louse-bite site or by

doi:10.1128/9781555818722.ch51

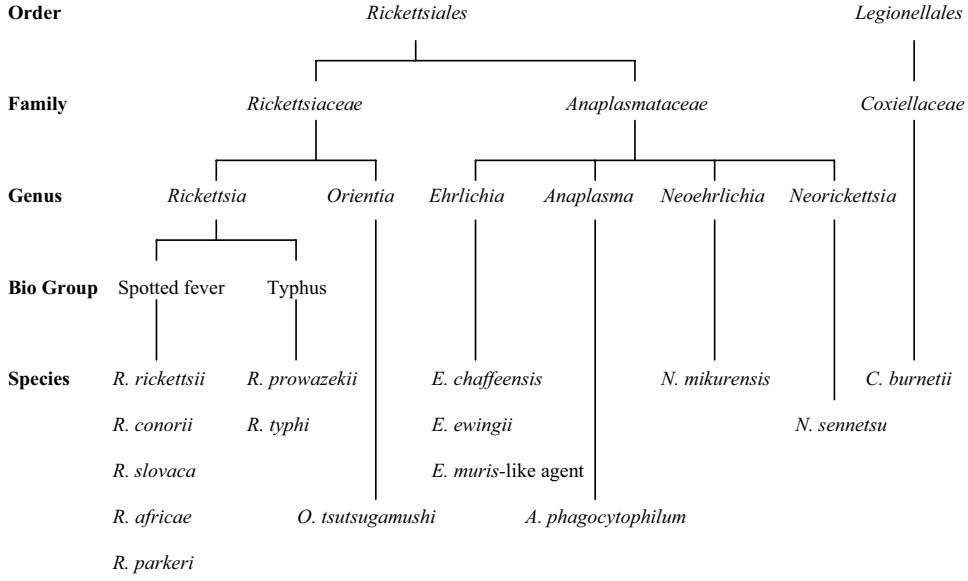

FIGURE 1 Taxonomy of representative human pathogens in the order *Rickettsiales* with the addition of *Coxiella*, formerly in the order *Rickettsiales*.

inoculating the organism into mucous membranes. After recovery, *R. prowazekii* may remain in a latent state and result in recrudescent infection later in life. This reactivation syndrome is known as Brill-Zinsser disease, and if reactivation occurs under conditions that promote louse infestation (e.g., extreme cold, poverty, war, overcrowding, poor hygiene), epidemics may occur. Louse-borne typhus is now an uncommon infection, but it still has a natural endemicity in the Peruvian Andes and has caused recent outbreaks in Burundi and Rwanda (11). A sylvatic cycle for the transmission of *R. prowazekii* exists in eastern North America, where *Glaucomys volans*, the southern flying squirrel, acts as an extrahuman reservoir for *R. prowazekii*. Infection is rare and occurs when humans are exposed to the feces of flying squirrel ectoparasites (12).

In contrast to infection caused by *R. prowazekii*, *R. typhi* infection occurs throughout the world and is especially prevalent in tropical and subtropical seaboard regions. Rats (*Rattus* sp.) are the primary reservoir, and their fleas (*Xenopsylla cheopis*) serve as vectors. This cycle is often responsible for disease in urban environments where rats thrive. In the United States, most cases occur in southern California and south Texas where a suburban cycle for transmission involves opossums and cat fleas (*Ctenocephalides felis*) as reservoirs and vectors, respectively (13).

O. tsutsugamushi is the causative agent of scrub typhus. The disease is endemic within the triangle-shaped region bound by northern Australia, Afghanistan, and the Primorje region of eastern Russia. Larval trombiculid mites (chiggers) maintain *O. tsutsugamushi* transovarially and transmit disease to humans while feeding. Rats are important in the maintenance of the chigger population. Transmission most frequently occurs in rural and suburban areas (14).

E. chaffeensis is the cause of human monocytotropic ehrlichiosis (HME). It is primarily transmitted by *Amblyomma americanum* ticks and occurs predominantly in the south-central and southeastern United States where these ticks are most prevalent. The organism is transtadially transmitted from one tick stage to another, but it is not transovarially maintained. Persistently infected white-tailed deer play a key role in maintaining the bacterium in nature by acting as a reservoir for acquisition of the infection by uninfected ticks. HME is likely vastly underdiagnosed (7). Other ehrlichiae of human importance include *Ehrlichia ewingii* and the recently described *E. muris*-like agent. *E. ewingii* is also transmitted by *A. americanum*. Most cases have been recognized in immunocompromised hosts (15). The *E. muris*-like agent has been recognized only in Wisconsin and Minnesota, with case descriptions suggesting an HME-like illness (16).

Similar to the aforementioned ehrlichioses, *Anaplasma phagocytophilum* is a tick-transmitted bacterium of the family *Anaplasmataceae*. This agent causes human granulocytotropic anaplasmosis (HGA). *Ixodes scapularis* is the vector responsible for transmission to humans. Infection occurs in the northeastern and upper midwestern United States and less often in California, in parallel to Lyme disease, which shares the same vector. HGA also occurs in northern Europe and Asia, where it is transmitted by other *Ixodes* species ticks (7).

Other members of the family *Anaplasmataceae* of human importance include *Neorickettsia sennetsu*, *Neoehrlichia mikurensis*, and *Wolbachia* sp. *N. sennetsu* causes a mononucleosis-like illness. It is believed to be acquired from the ingestion of infected uncooked fish in Japan, Malaysia, and Laos (17). *N. mikurensis* can cause severe and occasionally prolonged illness in immunocompromised persons or mild illness after exposure to *Ixodes ricinus* ticks in Europe or *I. persulcatus* and *Haemaphysalis concinna* ticks in Asia (18–23). Although the filarial endosymbiont *Wolbachia* does not directly cause human infection, the organism influences the pathogenesis of infections caused by their filarial hosts in human disease (5).

Coxiella burnetii is responsible for Q fever, a zoonosis transmitted to humans by the inhalation of contaminated aerosols. With the exception of New Zealand, *C. burnetii* causes disease throughout the world. The organism has been found in ticks and in a wide variety of animals where it is maintained (24). Cattle, sheep, and goats are important animal reservoirs (25). During the pregnancy of infected animals, the organism reactivates and increases in number within placental tissue. At the time of parturition, the

TABLE 1 Summary of representative human pathogens

Species	Disease	Distribution	Transmission	Target cells	Cellular location	LPS	C + G content (%)
R. rickettsii	RMSF	Americas	Tick bite	Endothelium	Cytosol	Yes	32.5
R. conorii	MSF	Europe, Asia, North Africa	Tick bite	Endothelium	Cytosol	Yes	32.4
R. slovaca	Tick-borne lymphadenopathy	Europe	Tick bite	Endothelium	Cytosol	Yes	32.5
R. africae	African tick bite fever	Sub-Saharan Africa	Tick bite	Endothelium	Cytosol	Yes	32.4
R. parkeri	Unnamed	Americas	Tick bite	Endothelium	Cytosol	Yes	32.4
R. prowazekii	Epidemic typhus	Africa, South America	Infected louse feces	Endothelium	Cytosol	Yes	29
	Sylvatic typhus	United States	Contact with flying squirrels				
R. typhi	Murine typhus	Worldwide	Infected flea feces	Endothelium	Cytosol	Yes	28.9
O. tsutsugamushi	Scrub typhus	Asia	Chigger bite	Endothelium	Cytosol	No	30.5
E. chaffeensis	HME	United States	*A. americanum*	Mononuclear phagocytes	Early endosome	No	30.1
E. ewingii	HGE	United States	*A. americanum*	Granulocytes	Nonlysosomal compartment	No	
E. muris-like agent	HME	United States	*Ixodes* ticks	—[a]	Uncharacterized cytoplasmic vacuole	—[a]	—[a]
A. phagocytophilum	HGA	United States, Europe, Asia	*Ixodes* ticks	Granulocytes	Nonlysosomal compartment	No	41.6
N. sennetsu	Sennetsu ehrlichiosis	Japan and Malaysia	Metacercaria in fish	Mononuclear phagocytes	Early endosome	No	41.4
N. mikurensis	Unnamed	Asia, Europe, and Africa	Tick bite	Granulocytes	Uncharacterized cytoplasmic vacuole	—[a]	—[a]
C. burnetii	Q fever	Worldwide	Inhalation of infected aerosols	Mononuclear phagocytes	Phagolysosome	Yes	42.3–42.7

[a]Currently unknown.

organism is shed and aerosolized (26). Therefore, those handling livestock are at higher risk for exposure (25).

PATHOBIOLOGY

Upon inoculation of *Rickettsia* sp., rickettsial surface proteins such as Omp B, Sca1, and Sca2 act as adhesins to promote attachment and induce entry into endothelial cells, their principal target cell. The SFG has an additional surface protein, OmpA, which also facilitates the host cell entry process. Within the cell, rickettsiae have transport mechanisms to take advantage of the host cell cytosol to provide necessary energy and nutrients (e.g., adenosine triphosphate, amino acids, and phosphorylated sugars). The SFG organisms are able to polymerize the host cell's actin filaments to mediate propulsion through the cytosol and invasion of neighboring cells. Organisms of the typhus group do not exhibit actin-based motility, but cause their host cell to burst, resulting in spread to other cells. The endothelial tropism of rickettsiae leads to the inflammation and vascular hyperpermeability that are responsible for the clinicopathologic features of rickettsioses (27).

The clinical spectrum of rickettsial infections varies from severe to mild, depending on the infecting pathogen. Of the SFG rickettsiae, *R. rickettsii* is the most pathogenic (untreated case-fatality rate of RMSF is 23%) while *R. africae*, the agent responsible for African tick bite fever (ATBF), has never been implicated in a human death (7). Typical manifestations of SFG rickettsial infection include fever, headache, myalgias, and rash. The rash of RMSF occurs in up to 90% of patients, is typically macular or maculopapular, and begins peripherally (wrists and ankles) before spreading proximally (28). Rash is also a frequent finding in MSF, and an eschar (a cutaneous lesion with a black necrotic center) is found in up to 72% of patients at the tick bite site (29). Infections with *R. africae*, *R. parkeri*, and *R. slovaca* are also associated with an eschar but cause milder illnesses compared to RMSF and MSF (8–10). In addition to an eschar usually occurring on the scalp, *R. slovaca* causes lymphadenopathy of the draining cervical lymph nodes, but seldom causes fever and rash.

Typhus-group rickettsioses have similar clinical manifestations as those caused by SFG rickettsiae. Both epidemic and murine typhus cause an undifferentiated febrile illness. The rash is typically macular or maculopapular and is first noted on the trunk prior to spreading to the extremities. Although clinical suspicion for a TG rickettsiosis is often prompted by the presence of rash, the sign may be subtle and difficult to detect in those with darkly pigmented skin. In those afflicted with epidemic typhus during a large outbreak in Burundi, rash was detected in only 20 to 40% (11). Rash is detected in 54% of those with murine typhus (30). Since outbreaks of louse-borne epidemic typhus often occur in the setting of great stress (e.g., wars, famine, and migration), the case-fatality rate may be quite high. The untreated case-fatality rate in the worst conditions of malnutrition is as high as 50% (11). In contrast, flying squirrel-associated typhus and murine typhus are generally less severe (12, 30).

O. tsutsugamushi infection follows the bite of a trombiculid mite, which releases *O. tsutsugamushi* from its salivary glands as it feeds on tissue fluids from the dermis. The organism enters cells by induced phagocytosis. The initial targets are likely dendritic cells, which phagocytose the pathogen and carry it to draining lymph nodes prior to its hematogenous spread. The primary target cells of *O. tsutsugamushi* are vascular endothelial cells and macrophages (31). As with infections caused by the aforementioned *Rickettsia* spp., scrub typhus is largely characterized by nonspecific symptoms (e.g., fever, headache, myalgia) that are often indistinguishable from symptoms caused by other endemic diseases, e.g., malaria, dengue fever, and leptospirosis. The finding of an eschar at the usually unrecognized mite bite site separates scrub typhus from these other infections. Patients often have tender draining lymph nodes proximal to the eschars. Severe manifestations such as pneumonia, prerenal azotemia, and meningoencephalitis may occur (14).

After inoculation by a feeding infected tick, ehrlichiae and *Anaplasma phagocytophilum* spread to the bone marrow and spleen where they infect their respective hematopoietic target cells. *E. chaffeensis* primarily infects monocytes and *A. phagocytophilum* infects neutrophils. These organisms reside in cytoplasmic vacuoles where they manipulate the host cell to promote their survival and evade host defenses, e.g., through the inhibition of phagosome-lysosome fusion. Clinical illness is a consequence of the host's immune system more than a result of direct cellular damage by the bacteria. For the most part, HME and HGA are clinically indistinguishable from infections caused by other species discussed in this chapter. Symptoms include fever, chills, headache, myalgia, and malaise. Physical examination is usually unremarkable, and unlike SFG and TG rickettsial infections, rash is an infrequent finding (up to 36% in those with HME). Laboratory abnormalities (leukopenia, thrombocytopenia, and hepatic-transaminase elevation) may suggest infection with these agents in the appropriate epidemiologic scenario. Although many patients experience mild illness, severe manifestations (septic shock, respiratory insufficiency, acute kidney injury, and, in HME, meningoencephalitis) may occur (32, 33).

C. burnetii-infected ruminants typically do not manifest illness. At the time of parturition, the heavily infected placenta sheds the organism (34). Viable bacteria can be found for weeks in the environment. After inhalation, the organism proliferates in the lungs followed by bloodstream invasion and eventual dissemination to other organs (35). *C. burnetii* undergoes phase variation in the laboratory. The phase I state is the form found in nature and reacts slightly with early sera and strongly with sera of chronically infected hosts. Phase II avirulent organisms occur after serial passage in embryonated chicken eggs or cell culture owing to deletion of genes for the synthesis of complete lipopolysaccharide. A stable form gives the organism the ability to survive in harsh environments (36).

The most frequent form of acute Q fever in humans is a self-limited nonspecific illness characterized by fever, chills, fatigue, and headache. In some areas, the relatively high percentage of seropositive individuals without previous history of severe febrile illness and outbreak investigation predicts that 60% of infections are asymptomatic. Pneumonia is often a feature of Q fever and may manifest as a spectrum of mild to severe manifestations. Incidentally discovered pulmonary infiltrates found on chest radiography are the most frequent pulmonary finding. Others may have symptoms of cough and pleuritic chest pain that mimic other causes of viral or atypical bacterial pneumonia. Rarely, severe progressive pneumonia leads to respiratory failure. Hepatitis is another manifestation of Q fever. It usually presents with hepatic transaminases elevated up to 3-fold the upper limit of normal in the setting of fever or pneumonia. A liver biopsy reveals granulomatous hepatic inflammation. An important manifestation of Q fever occurring as a chronic infection is endocarditis, which often afflicts those with preexisting valvular abnormalities. Associated signs and

symptoms include digital clubbing, pruritic rash, and hepatosplenomegaly (24).

LABORATORY DIAGNOSIS

As obligately intracellular organisms, laboratory isolation of the bacteria described in this chapter requires technical expertise and specialized facilities that are not readily available to most physicians and diagnostic clinical laboratories. Because of the ability of small inocula to cause illness when aerosolized, *Rickettsia* sp., *O. tsutsugamushi*, and *C. burnetii* require isolation to be carried out in a biosafety level-3 laboratory. Isolation of *Ehrlichia* and *Anaplasma* can be undertaken in a biosafety level-2 laboratory. Culture of these organisms may also require a significant amount of time for growth to occur when compared to more typical bacteria. This situation limits isolation as a method for diagnosis in acute infections (24, 36, 37). For these reasons, serologic methods are the mainstay of diagnosis for all infections described in this chapter. Unfortunately, serology can only confirm a diagnosis retrospectively, and results of such studies should not preclude prompt empiric therapy if such an infection is suspected. In the past several years, molecular methods such as PCR-based assays have become more refined and continue to show promise as a method for the diagnosis of infections caused by these organisms during the acute stage of illness. In the following sections, the current serologic and molecular methods of diagnosis are presented. Additionally, promising new techniques are discussed.

Immunodiagnosis

Rickettsia and *Orientia*

The gold-standard serodiagnostic method for diagnosis of RMSF is the indirect immunofluorescence assay (IFA). This method uses a fluorescein-labeled conjugate to detect serum antibodies bound to antigen (*R. rickettsii*-infected cells) fixed on a slide. The performance of IFA has greatly surpassed that of older methods, e.g., Weil-Felix, latex agglutination, and complement fixation (38). The test is available commercially and is also available through state health laboratories. Antigens used by various laboratories may differ in quality. Consequently, each laboratory should have its own cutoff titer, which it has validated as diagnostic for the population tested. As with infections caused by all the pathogens discussed in this chapter, the patient antibody response lags behind clinical illness. As a patient's illness progresses, a detectable antibody response follows. The sensitivity of IFA two weeks after the onset of illness is 94 to 100% (39). The timing of the IgM and IgG responses is similar in patients with RMSF. Antibodies of both isotypes increase simultaneously during the second week of illness (40). Since the appearance of IgM does not occur sooner, and IgM antibodies cross-react with nonrickettsial antigens more often than the IgG isotype, testing for IgM does not offer greater sensitivity or specificity during early illness. IFA testing for IgM is also affected by rheumatoid factor, necessitating the use of rheumatoid factor absorbent. Because IFA predictably fails to detect antibodies during the acute phase of illness, paired sera should be obtained during acute illness and after convalescence. Seroconversion or a 4-fold rise from acute-to convalescent-phase samples confirms the diagnosis (39).

Another commercially available and quite sensitive test for RMSF is the enzyme-linked immunosorbent assay (ELISA). The ELISA is sensitive, and its automation lends itself well to high-throughput applications. The subjective nature of reading IFA slides and requirement for a proficient microscopist is also avoided by using the ELISA technique (40). Because of the qualitative nature of ELISA, this assay is unable to quantify antibody titers. ELISA is therefore unable to monitor the change in antibody response over time. Like IFA, results depend on the particular laboratory, quality of the antigen, and threshold levels determined to yield a result considered reactive (39).

Other SFG rickettsioses can be diagnosed serologically as described above. Species belonging to this group induce antibodies that cross-react with antigens of other SFG members. Serum antibody titers are usually higher or the same when reacted with homologous antigens as compared to heterologous antigens. Therefore, it is helpful to use antigen prepared from *Rickettsia* species endemic to the area of interest. The micromethod format of the IFA is an efficient method to test for seroreactive antibodies to several different rickettsial antigens. This method may be useful in areas where several rickettsial species coexist and cause human diseases. The micro-IFA can detect antibodies to up to nine antigens within a single well containing multiple antigen dots (35).

The serodiagnosis of typhus-group rickettsioses is similar to that of RMSF and other SFG rickettsioses. IFA is the serologic method of choice (41). Antibodies may not be present during early illness, but almost all patients will have developed antibodies detected by IFA 2 weeks after the onset illness (30). Seroconversion or a 4-fold rise in antibody titer from the acute phase of illness to convalescence confirms the diagnosis of a typhus-group infection. As in the case with the SFG, the serologic response to infection with one species of the typhus group induces cross-reactive antibodies to the other species. Although a patient's clinical history and difference in IFA titers using both *R. prowazekii* and *R. typhi* antigens can offer clues to the offending agent, standard serologic methods may not establish a definitive species-specific diagnosis. *R. felis*, a flea-borne organism with features that resemble both the SFG and typhus groups, induces an antibody response that is variably cross-reactive with members of the typhus group and SFG organisms. Because *R. prowazekii* and *R. typhi* tend to burst cells during their propagation in cells, IFA slides using these organisms as antigen may show the presence of many extracellular organisms. Fluorescence of these small extracellular forms creates what has been described as a fine gold dust-like appearance, which is often mistaken for background fluorescence. IFA slides for the typhus group have been therefore considered as being more difficult to read than those of the SFG or *O. tsutsugamushi* (42).

The conventional methods of serodiagnosis are unable to distinguish a species-specific cause for a rickettsiosis. Whereas knowledge of the epidemiological situation in which the infection was acquired may be a helpful clue in typhus group infections, the diversity of the SFG renders it very difficult to determine a species-specific cause based on clinical and epidemiological assumptions. Although molecular methods or cultivation of the pathogen are the methods of choice for determining the exact etiologic agent implicated in an infection, a cross-absorption study can help determine a species-specific cause. Cross-absorption is performed by separately mixing the serum in question with the different bacterial antigens involved in the cross-reaction. This results in the disappearance of homologous and heterologous antibodies by Western blotting when absorption is carried out with the agent responsible for the disease. The disappearance of homologous antibodies by Western blotting occurs only when absorption is carried out with the

agent responsible for the cross-reaction. This technique is time-consuming. Although relatively straightforward for the distinction of two agents, cross-absorption becomes quite cumbersome when multiple rickettsial agents are in question and impossible when the actual agent is not included in the absorptions and reactions or has yet to be discovered (43).

Immunohistochemical staining of rickettsiae within formalin-fixed paraffin-embedded tissues is useful to demonstrate the presence of the offending agent prior to the patient's developing reactive antibodies (44). Prior to molecular methods, immunohistochemistry (IHC) was the only approach with the ability to reliably yield a diagnosis during acute illness. The technique can be performed on autopsy specimens including those from the skin, liver, spleen, lung, heart, kidney, and brain. In patients with RMSF, skin biopsy of the rash has a reported sensitivity and specificity of 70% and 100%, respectively (45). This technique can be used to detect other members of the SFG as well as those of the typhus group (46, 47). Of the SFG species causing eschars, such as *R. conorii*, *R. africae*, and *R. parkeri*, IHC can demonstrate the organism within eschar-biopsy specimens. The chance of demonstrating rickettsiae within tissues is greatest prior to or within 24 hours of antimicrobial administration (39).

The serodiagnostic methods of choice for the diagnosis of infection caused by *O. tsutsugamushi* (scrub typhus) include the indirect immunofluorescent and the immunoperoxidase assays. IFA has a high sensitivity and specificity, but as with the aforementioned rickettsioses, specific antibodies to *O. tsutsugamushi* are often absent during early illness (48). The use of the immunoperoxidase assay (IPA) yields comparable titers to those by IFA but holds a cost advantage, as it does not require a fluorescence microscope to view prepared slides (49, 50). Both the IFA and IPA are more sensitive than the Weil-Felix test (the first serologic test for the diagnosis of scrub typhus) and are much more specific (50). Over 70 strains of *O. tsutsugamushi* exist, and there is variable cross-reactivity among these strains. Therefore, prototype strains of *O. tsutsugamushi* (Karp, Kato, and Gilliam) are used in addition to local strains during the preparation of antigen for these assays. A definitive diagnosis can be established by demonstrating a 4-fold rise in antibody titer between acute and convalescent samples. Caution should be taken when using a single unpaired sample, as there is no consensus with regard to titer cutoff values to suggest recent infection. Each laboratory should base its cutoff titers on the local prevalence and titer of scrub typhus antibodies. In highly endemic areas, a titer as high as 1:400 may be appropriate (51). The reading of IFA and IPA slides and determination of endpoint titers are somewhat subjective. It appears that there is more inter-operator variability between microscopists with less experience than those with extensive experience (42).

Ehrlichia and *Anaplasma*

Serology remains the mainstay for the diagnosis of both ehrlichiosis and anaplasmosis. The IFA using *E. chaffeensis*-and *A. phagocytophilum*-infected cells is the method of choice for the serodiagnosis of HME and HGA, respectively. Slides incubated with sera reactive with the respective antigen will reveal morulae (characteristic mulberry-like microcolonies of bacteria) in the cytoplasm of cultured cells. Those living in areas where these diseases are endemic may have baseline serologic reactivity due to previous exposure to these or other antigenically related pathogens (52). It is therefore necessary to observe a 4-fold rise in titer by testing both acute-and convalescent-phase serum samples. In patients with HME, relatively few patients (22 to 44%) will demonstrate a reciprocal titer of at least 1:80 when tested in the first week of illness. After the first week of illness, the geometric mean titer rises sharply so that 68% of patient sera tested will yield a diagnostic titer. By week 4 or more of illness, all patients with HME should have seroconverted. The geometric mean titer peaks at 1:1280 in week 6 (53). Those with HGA have a slow early antibody response similar to those with HME; antibodies against *A. phagocytophilum* are detected in only 24 to 44% of patients in the acute stage of infection (54, 55). All patients with HGA will have seroconverted by the fourth week of illness (55).

Immunohistochemical analysis is an effective technique for the visualization of morulae within infected tissues. Whereas serodiagnosis requires the collection of convalescent sera to retrospectively confirm or refute a diagnosis, IHC can provide more timely results. The bone marrow, liver, lung, spleen, lymph nodes, kidneys, and adrenal gland have yielded positive results when collected at autopsy (56). Many of these tissues, such as the bone marrow, can be easily sampled during the course of a patient's workup and visually yield the presence of the organism. This technique uses formalin-fixed paraffin-embedded tissue incubated with biotinylated anti-*E. chaffeensis* antibodies followed by incubation with avidin-alkaline phosphatase (57).

Coxiella

As with infections caused by the aforementioned bacteria, acute Q fever is usually confirmed via serologic means. It is important to understand the host's immunoglobulin responses to the phase I and phase II antigens when interpreting serologic assays. In acute infection, IgM and IgG antibodies to phase II antigen appear prior to antibodies to phase I antigen. There is also a greater magnitude of antibody response to phase II antigen early after infection. Although the magnitude of IgM as measured in reciprocal titers to both phase I and II antigens decreases over time, these IgM antibodies may persist for several months (58) and even up to 2 years (59). IgG antibodies decrease over time but persist for life. In chronic Q fever, IgG-antibody titers to phase I antigens are quite high (60).

Several serologic methods for the detection of anti-*Coxiella* antibodies have been described. Techniques include microagglutination (61), complement fixation (62), microimmunofluorescence (63), and the ELISA (64). All of these methods are effective for the diagnosis of acute Q fever (65). The ELISA offers automation and the advantage of removing the subjectivity and inter-observer variation associated with IFA, but the sensitivity is not as high (66). The preferred and most frequently used serodiagnostic method in the United States is the indirect immunofluorescence assay, which is commercially available (67).

A 4-fold rise in phase II IgG titers by IFA from sera obtained during acute and convalescent stages of illness (separated by 3 to 6 weeks) confirms the diagnosis of acute Q fever, as almost all patients will have seroconverted by week 3 of illness (67). A single IgM titer to phase II antigen is not useful as a stand-alone test as the sensitivity in early disease is low and cross-reaction with other pathogens limits its specificity (68, 69). Early diagnosis and treatment of those with acute Q fever does not seem to prevent the IgG-antibody response (70). Paired samples should be sent to the same laboratory, and if possible, the acute-phase specimen should be frozen and sent with the convalescent specimen for simultaneous processing. This is to eliminate interlaboratory, interassay, and antigen variation (67).

Chronic Q fever can be diagnosed when the associated clinical picture is paired with the characteristic antibody profile. During chronic infection, IgG antibodies to phase I antigen are used to help confirm the diagnosis. The modified Duke Criteria, a diagnostic schema that includes clinical, microbiologic, and echocardiographic data for the diagnosis of endocarditis, includes a single phase I IgG-antibody titer of >1:800 or a single positive blood culture for C. *burnetii* as a major criterion. This, in combination with a second major criterion (echocardiographic evidence of endocarditis) or three minor criteria (predisposing heart condition, fever, vascular phenomena, immunologic phenomena), confirms a clinical diagnosis of Q fever endocarditis (71). Although the 1:800 cutoff value has been reported to be sensitive (100%) with a high positive predictive value (98%) (72), use of higher cutoffs such as 1:1,024 have been proposed based on follow-up studies of patients from large outbreaks in Europe (60, 73, 74). The Centers for Disease Control and Prevention recommend that the diagnosis of chronic Q fever can be demonstrated using a single phase I IgG titer of 1:1,024 in the setting of an identifiable chronic infection (endovascular infection, granulomatous hepatitis, chronic septic arthritis, osteomyelitis, or chronic pulmonary infection) (67).

Current serodiagnostic methods for Q fever are well established, but, as with most serologic tests, have limitations. The identification of novel seroreactive protein biomarkers is an attractive strategy for the development of safe and efficient diagnostic assays. Potential markers have been identified by immunoproteomic and microarray approaches (75, 76). The recombinant proteins corresponding to these immunoreactive antigens may aid in the development of new serologic tests. An enzyme-linked immunospot assay to measure C. *burnetii*-specific T-cell responses has been developed and shows promise as a useful diagnostic tool to identify an immunologic profile consistent with chronic Q fever (77).

Molecular Diagnosis

Rickettsia and *Orientia*

The use of PCR to amplify rickettsial DNA offers a rapid method to diagnose rickettsioses during acute infection. Prior to molecular methods, IHC was the only means of confirming a diagnosis early in disease. Conventional, nested, and real-time PCR techniques have been developed to amplify portions of various rickettsial genes. These methods can be used to detect rickettsial DNA within blood or tissue samples. Due to the intracellular endothelial tropism of organisms in the genus *Rickettsia*, few bacteria are found in the circulating bloodstream. This limits the sensitivity of PCR when performed on whole blood, except in late-stage or fatal cases (78, 79). The ability of PCR to detect organisms within biopsied tissue, such as the skin, makes these samples of much higher diagnostic yield when a rickettsiosis is suspected. Eschar biopsy specimens are also a good source for the detection of rickettsial DNA (35). The swabbing of eschars has also shown promise in the detection of rickettsial DNA. This technique uses a sterile saline-dipped swab rubbed onto the base of an unroofed eschar as a DNA-collection method. The swab is then placed in a tube with a small amount of saline for storage prior to processing (80). As in the case of culture and IHC methods, the sensitivity of PCR-based diagnosis decreases after the administration of effective antibiotics (39).

Screening for the presence or absence of rickettsial DNA within a sample can be achieved initially by using genus-specific primers designed to amplify conserved portions of genes encoding citrate synthase, OmpB, or the 17-kDa-antigen gene (78, 81, 82). Real-time PCR assays using primers and probes to detect these genes offer much greater sensitivity (83). If a sample screen detects target DNA, further analysis using primers to amplify OmpA, common to the SFG, can help delineate a SFG from typhus group infection.

For most clinical purposes, determination of a species-specific cause is not necessary after a rickettsial diagnosis is established, as treatment of these infections is identical. When identification of an infecting rickettsial agent is sought, the nucleotide-sequence analysis of PCR amplicons can reveal the exact causative agent. Since many primer sets amplify relatively conserved portions of genes encoding OmpA, OmpB, citrate synthase, and the 17-kDa antigen, it may be necessary to analyze portions of sequences from a gene fragment with sufficient diversity to identify the infecting species. An inexpensive alternative method to sequencing is restriction-fragment-length polymorphism (RFLP) analysis, which can be performed using products amplified from the aforementioned genes. The differentiation of rickettsiae can be achieved by using the endonuclease AluI for citrate synthase (82, 84) and the 17-kDa antigen gene PCR products (85). Digestion of an *ompB* PCR product using RsaI enables differentiation of several SFG rickettsiae (84). Finally, a primer set to amplify a portion of the *ompA* gene digested with a combination of endonucleases (RsaI, PstI, AluI, XbaI, and AvaII) can help identify most of the recognized SFG rickettsiae (86, 87).

O. *tsutsugamushi* DNA may be detected by PCR of whole blood, buffy coat, eschars, and other tissues to aid in the diagnosis of scrub typhus. Primers to amplify portions of a variety of genes have been described: the 56 kDa protein gene, 47 kDa protein gene, *groEL*, and 16S rRNA gene. Methods using conventional, nested, and real-time PCR techniques have been described. A nested PCR reaction to amplify a portion of the gene encoding the 56-kDa protein from eschars was 86% sensitive and 100% specific for the diagnosis of scrub typhus when compared to IFA as the gold standard test (88). Real-time PCR assays show promise of a high sensitivity as predicted from their ability to detect low copy numbers of O. *tsutsugamushi* in a variety of samples (89, 90).

Considering the nonspecific clinical presentations of rickettsioses and scrub typhus, they are undoubtedly mistaken for other prevalent febrile illnesses throughout the world. The development of inexpensive, reliable, and multiplexed point-of-care tests for the diagnosis of acute infections is a great need. Although attempts at PCR-based methods in resource-limited settings is troubled by cost and need for specialized equipment (91), reports of loop-mediated isothermal PCR assays show promise by offering an inexpensive and less technically demanding method for the amplification of pathogen DNA. Assays targeting the *ompB* and *groEL* genes of *Rickettsia* species and O. *tsutsugamushi*, respectively, have been described (92, 93).

Ehrlichia and *Anaplasma*

The presence of *Ehrlichia* within the bloodstream of those with acute infection makes PCR a useful tool during the early phases of these illnesses. In one study, PCR amplification of each of three targets (16S rRNA gene, the variable-length PCR target gene, and the *groEL* operon) was able to detect ehrlichial DNA in all cases of acute culture-proven HME (94). Techniques using conventional, nested, and real-time PCR and PCR with reverse-line blot hybridization have all been developed for the detection of *Ehrlichia* species (95–97). Quantitative real-time PCR offers the opportunity to detect

as few as one gene copy per reaction. The use of species-specific probes, rather than QuantiNova SYBR Green PCR (QIAGEN, Germantown, MD), has been demonstrated to increase species specificity (95). The pathogen can be detected from whole blood, buffy coat, cerebrospinal fluid, and tissue samples (56, 98, 99). PCR has demonstrated serum to contain ehrlichial DNA (97), but the yield of serum in those with HME is likely much lower than the aforementioned sources. The use of multiplexed assays may be of particular interest in regions where several pathogens coexist. A quantitative multiplexed real-time PCR assay using primers for the *Ehrlichia*-specific disulfide bond formation gene (*dsb*) has been developed to detect DNA of both *E. chaffeensis* and *E. ewingii* in human blood (100).

As in the case of ehrlichiosis, those with HGA have organisms circulating in the peripheral blood (within neutrophils) that are readily detected by PCR (101, 102). Utility of PCR is greatest during early illness. The likelihood of diagnostic PCR results diminish as the patient develops antibodies and clears the organism (103). The *A. phagocytophilum p44* gene is reported to be much more sensitive than targeting the 16S rRNA gene due to the presence of a large number of *p44* paralogs in the genome (104). A loop-mediated isothermal amplification assay targeting the *msp2* gene has been developed in hopes of offering molecular diagnostics to rural areas (105). In addition to use as a diagnostic tool, molecular methods have identified new pathogens causing human disease. Melt-curve analysis of a real-time PCR assay targeting the *groEL* heat shock protein operon found melt curves outside the typical range for *E. chaffeensis*, *E. ewingii*, and *A. phagocytophilum* in several patients with a syndrome resembling HGA and HMA. Further analysis revealed a novel organism, *Ehrlichia muris*-like agent, to be the pathogenic cause (16).

Coxiella

The molecular identification of *Coxiella* is performed with both conventional and real-time PCR methods. A variety of gene targets have been studied in these assays. Sensitivity and specificity may differ depending on the assay. It appears that real-time PCR assays targeting an insertion sequence with multiple genomic copies (IS1111) are quite sensitive (106). In the diagnosis of acute Q fever, an assay that detects the IS1111 target has been touted to have a sensitivity of 98% in those tested prior to the IgM phase II antibody response. With the progressive appearance of IgM and IgG antibodies, the ability to detect *Coxiella* DNA is lost (107). Since those with chronic Q fever may experience recurrent bacteremia, blood or serum should be sent for PCR when the diagnosis is suspected. PCR may also be performed on tissue from excised heart valves or other tissues taken from the site of infection (67). A loop-mediated isothermal-amplification assay has been developed, which may serve as a platform to offer a simple and cost-effective approach to support the molecular diagnosis of Q fever in resource-limited settings. Matrix-assisted laser desorption-time of flight (MALDI-TOF) mass spectrometry is a highly reproducible method that shows promise in the molecular diagnosis of Q fever by detecting protein markers consistent with a *C. burnetii* fingerprint (108).

INTERPRETATION

The protean manifestations of the diseases described in this chapter make a definitive clinical diagnosis difficult without the use of confirmatory laboratory testing. However, several important caveats need to be considered when interpreting the aforementioned serologic and molecular diagnostic assays. The unifying principle of utmost importance is to consider the results of these tests in the context of a clinically compatible syndrome. For reasons discussed below, positive test results obtained from those without a current or preceding compatible syndrome may be difficult to interpret accurately.

Because many of these infections go unnoticed and undiagnosed, there may be a substantial number of individuals residing in endemic areas with baseline antibodies to these agents. For example, up to 11% of healthy blood donors in Westchester County, New York, have been demonstrated to have antibodies reactive to *A. phagocytophilum* by IFA (52). A serosurvey of representative individuals throughout the United States found a seroprevalence of 3.1% to *C. burnetii* (109). This underscores the importance of demonstrating seroconversion or a 4-fold rise in titers in sera obtained during acute illness and convalescence. Unlike other organisms described in this chapter, *C. burnetii* may cause chronic forms of infection. The appropriate phase I IgG-cutoff value to support the diagnosis of chronic Q fever has been disputed and depends largely on local prevalence rates (60, 73, 74). All these points highlight the need to correlate serology with clinical findings.

Cross-reactivity of serum antibodies is also a concern when interpreting serologic data. The diversity of the genus *Rickettsia* exemplifies this. An infection with a SFG organism will induce an antibody response that will react to heterologous SFG antigens (35). Therefore, in the context of a serologic assay, infection with *R. parkeri* may appear no different than an infection with *R. rickettsii*. The prevalence of nonpathogenic or mildly pathogenic rickettsiae within ticks biting humans may contribute to confusing serologic results. The SFG species, *R. amblyommii*, is highly prevalent within the tick *Amblyomma americanum*, an aggressive and nondiscriminant feeder that frequently bites humans. Exposure to *R. amblyommii* and the resultant cross-reactivity of antibodies to *R. rickettsii* have likely contributed to the skyrocketing reported incidence of RMSF in the United States (7). Although cross-reactivity between SFG and TG rickettsiae may be present, the extent is less than that of species within the same group (35). It is also possible for sera to cross-react with other bacteria, such as *Legionella* and *Proteus* species (110). Serologic cross-reactivity not only exists among members of the genus *Rickettsia*, but also exists among strains of *O. tsutsugamushi* and among species in the genus *Ehrlichia*.

Finally, establishing a serologic diagnosis is retrospective. As mentioned above, the patient's antibody response generally lags behind the symptoms of early illness. It may take 2 or more weeks for detectable antibodies to appear. Many of these infections cannot be differentiated from one another clinically in their early stage, and since some of these infections, such as RMSF, have a high case-fatality rate, treatment should not be withheld while awaiting confirmatory serologic results. Even if clinicoepidemiologic data suggest exposure to an organism of mild virulence (as in the traveler to sub-Saharan Africa with suspected African tick bite fever), early appropriate treatment can quickly alleviate fever and other systemic symptoms.

PCR-based techniques have the potential to yield useful results during an acute illness. The ability of PCR to detect the presence of bacterial nucleic acids is highly dependent on the host-target cells. For example, rickettsiae, which primarily infect the vascular endothelium, do not cause sufficient rickettsemia to allow consistent PCR amplification of rickettsial DNA from whole blood. In contrast, the monocyte and neutrophil targets of *E. chaffeensis* and

A. phagocytophilum, respectively, allow relatively easy detection in whole blood or buffy coat preparations (39). Because of the variable sensitivities of these assays, the presence of PCR inhibitors in blood samples, and the effect of bacterial clearance in those treated early with antibiotics, negative PCR results do not definitively rule out infection or preclude the use of empiric antimicrobial treatment. Although PCR-based assays offer the ability to detect only a few organisms, these exquisitely sensitive techniques can generate false-positive results due to amplicon carryover from previous reactions. In laboratories processing many clinical samples without strict separation of processing, amplification, and analysis steps, PCR contamination can render results invalid. Melt-curve analysis of real-time PCR assays may allow the differentiation between true amplification of the target gene and non-specific DNA amplification.

REFERENCES

1. **Tamura A, Ohashi N, Urakami H, Miyamura S.** 1995. Classification of *Rickettsia tsutsugamushi* in a new genus, *Orientia* gen. nov., as *Orientia tsutsugamushi* comb. nov. *Int J Syst Bacteriol* **45:**589–591.
2. **Gillespie JJ, Williams K, Shukla M, Snyder EE, Nordberg EK, Ceraul SM, Dharmanolla C, Rainey D, Soneja J, Shallom JM, Vishnubhat ND, Wattam R, Purkayastha A, Czar M, Crasta O, Setubal JC, Azad AF, Sobral BS.** 2008. *Rickettsia* phylogenomics: unwinding the intricacies of obligate intracellular life. *PLoS One* **3:**e2018. doi:10.1371/journal.pone.0002018
3. **Izzard L, Fuller A, Blacksell SD, Paris DH, Richards AL, Aukkanit N, Nguyen C, Jiang J, Fenwick S, Day NP, Graves S, Stenos J.** 2010. Isolation of a novel *Orientia* species (*O. chuto* sp. nov.) from a patient infected in Dubai. *J Clin Microbiol* **48:**4404–4409.
4. **Dumler JS, Barbet AF, Bekker CP, Dasch GA, Palmer GH, Ray SC, Rikihisa Y, Rurangirwa FR.** 2001. Reorganization of genera in the families *Rickettsiaceae* and *Anaplasmataceae* in the order *Rickettsiales*: unification of some species of *Ehrlichia* with *Anaplasma*, *Cowdria* with *Ehrlichia* and *Ehrlichia* with *Neorickettsia*, descriptions of six new species combinations and designation of *Ehrlichia equi* and 'HGE agent' as subjective synonyms of *Ehrlichia phagocytophila*. *Int J Syst Evol Microbiol* **51:**2145–2165.
5. **LePage D, Bordenstein SR.** 2013. *Wolbachia*: can we save lives with a great pandemic? *Trends Parasitol* **29:**385–393.
6. **Weisburg WG, Dobson ME, Samuel JE, Dasch GA, Mallavia LP, Baca O, Mandelco L, Sechrest JE, Weiss E, Woese CR.** 1989. Phylogenetic diversity of the *Rickettsiae*. *J Bacteriol* **171:**4202–4206.
7. **Walker DH, Paddock CD, Dumler JS.** 2008. Emerging and re-emerging tick-transmitted rickettsial and ehrlichial infections. *Med Clin North Am* **92:**1345–1361, x.
8. **Raoult D, Lakos A, Fenollar F, Beytout J, Brouqui P, Fournier PE.** 2002. Spotless rickettsiosis caused by *Rickettsia slovaca* and associated with *Dermacentor* ticks. *Clin Infect Dis* **34:**1331–1336.
9. **Raoult D, Fournier PE, Fenollar F, Jensenius M, Prioe T, de Pina JJ, Caruso G, Jones N, Laferl H, Rosenblatt JE, Marrie TJ.** 2001. *Rickettsia africae*, a tick-borne pathogen in travelers to sub-Saharan Africa. *N Engl J Med* **344:**1504–1510.
10. **Paddock CD, Finley RW, Wright CS, Robinson HN, Schrodt BJ, Lane CC, Ekenna O, Blass MA, Tamminga CL, Ohl CA, McLellan SL, Goddard J, Holman RC, Openshaw JJ, Sumner JW, Zaki SR, Eremeeva ME.** 2008. *Rickettsia parkeri* rickettsiosis and its clinical distinction from Rocky Mountain spotted fever. *Clin Infect Dis* **47:**1188–1196.
11. **Bechah Y, Capo C, Mege JL, Raoult D.** 2008. Epidemic typhus. *Lancet Infect Dis* **8:**417–426.
12. **Reynolds MG, Krebs JS, Comer JA, Sumner JW, Rushton TC, Lopez CE, Nicholson WL, Rooney JA, Lance-Parker SE, McQuiston JH, Paddock CD, Childs JE.** 2003. Flying squirrel-associated typhus, United States. *Emerg Infect Dis* **9:**1341–1343.
13. **Traub R, Wisseman CL.** 1978. The ecology of murine typhus-a critical review. *Trop Dis Bull* **75:**237–317.
14. **Paris DH, Shelite TR, Day NP, Walker DH.** 2013. Unresolved problems related to scrub typhus: A seriously neglected life-threatening disease. *Am J Trop Med Hyg* **89:**301–307.
15. **Paddock CD, Folk SM, Shore GM, Machado LJ, Huycke MM, Slater LN, Liddell AM, Buller RS, Storch GA, Monson TP, Rimland D, Sumner JW, Singleton J, Bloch KC, Tang YW, Standaert SM, Childs JE.** 2001. Infections with *Ehrlichia chaffeensis* and *Ehrlichia ewingii* in persons coinfected with human immunodeficiency virus. *Clin Infect Dis* **33:**1586–1594.
16. **Pritt BS, Sloan LM, Johnson DK, Munderloh UG, Paskewitz SM, McElroy KM, McFadden JD, Binnicker MJ, Neitzel DF, Liu G, Nicholson WL, Nelson CM, Franson JJ, Martin SA, Cunningham SA, Steward CR, Bogumill K, Bjorgaard ME, Davis JP, McQuiston JH, Warshauer DM, Wilhelm MP, Patel R, Trivedi VA, Eremeeva ME.** 2011. Emergence of a new pathogenic *Ehrlichia* species, Wisconsin and Minnesota, 2009. *N Engl J Med* **365:**422–429.
17. **Newton PN, Rolain JM, Rasachak B, Mayxay M, Vathanatham K, Seng P, Phetsouvanh R, Thammavong T, Zahidi J, Suputtamongkol Y, Syhavong B, Raoult D.** 2009. *Sennetsu neorickettsiosis*: A probable fish-borne cause of fever rediscovered in Laos. *Am J Trop Med Hyg* **81:**190–194.
18. **Kawahara M, Rikihisa Y, Isogai E, Takahashi M, Misumi H, Suto C, Shibata S, Zhang C, Tsuji.** 2004. Ultrastructure and phylogenetic analysis of '*Candidatus* Neuehrlichia mikurensis' in the family *Anaplasmataceae*, isolated from wild rats and found in *Ixodus ovatus* ticks. *Int J Syst Evol Microbiol* **54**:1837–1843.
19. **Welinder-Olsson C, Kjellin E, Vaht K, Jacobsson S, Wenerås C.** 2010. First case of human "*Candidatus* Neoehrlichia mikurensis" infection in a febrile patient with chronic lymphocytic leukemia. *J Clin Microbiol* **48**:1956–1959.
20. **Fehr JS, Bloemberg GV, Ritter C, Hombach M, Luscher TF, Weber R, Keller PM.** 2010. Septicemia caused by tick-borne bacterial pathogen *Candidatus* Neoehrlichia mikurensis. *Emerg Infect Dis* **16**:1127–1129.
21. **von Loewenich FD, Geissdörfer W, Disqué C, Matten J, Schett G, Sakka SG, Bogdan C.** 2010. Detection of "*Candidatus* Neuehrlichia mikurensis" in two patients with severe febrile illnesses: evidence for a European sequence variant. *J Clin Microbiol* **48:**2630–2635.
22. **Pekova S, Vydra J, Kabickova H, Frankova S, Haugvicova R, Mazal O, Cmejla R, Hardekopf DW, Jancuskova T, Kozak T.** 2011. *Candidatus* Neuroehrlichia mikurensis infection identified in 2 hematooncologic patients: benefit of molecular techniques for rare pathogen detection. *Diagn Microbiol Infect Dis* **69:**266–270.
23. **Li H, Jiang JF, Liu W, Zheng YC, Huo QB, Tang T, Zuo SY, Liu K, Jiang BG, Yang H, Cao WC.** 2012. Human infection with *Candidatus* Neoehrlichia mikurensis, China. *Emerg Infect Dis* **18:**1636–1639.
24. **Maurin M, Raoult D.** 1999. Q fever. *Clin Microbiol Rev* **12:**518–553.
25. **McQuiston JH, Childs JE.** 2002. Q fever in humans and animals in the United States. *Vector Borne Zoonotic Dis* **2:**179–191.
26. **Benenson AS, Tigertt WD.** 1956. Studies on Q fever in man. *Trans Assoc Am Physicians* **69:**98–104.

27. **Uchiyama T.** 2012. Tropism and pathogenicity of rickettsiae. *Front Microbiol* **3:**230.
28. **Helmick CG, Bernard KW, D'Angelo LJ.** 1984. Rocky Mountain spotted fever: clinical, laboratory, and epidemiological features of 262 cases. *J Infect Dis* **150:**480–488.
29. **Oteo JA, Portillo A.** 2012. Tick-borne rickettsioses in Europe. *Ticks Tick Borne Dis* **3:**271–278.
30. **Dumler JS, Taylor JP, Walker DH.** 1991. Clinical and laboratory features of murine typhus in south Texas, 1980 through 1987. *JAMA* **266:**1365–1370.
31. **Moron CG, Popov VL, Feng HM, Wear D, Walker DH.** 2001. Identification of the target cells of *Orientia tsutsugamushi* in human cases of scrub typhus. *Mod Pathol* **14:**752–759.
32. **Olano JP, Walker DH.** 2002. Human ehrlichioses. *Med Clin North Am* **86:**375–392.
33. **Bakken JS, Krueth J, Wilson-Nordskog C, Tilden RL, Asanovich K, Dumler JS.** 1996. Clinical and laboratory characteristics of human granulocytic ehrlichiosis. *JAMA* **275:**199–205.
34. **Welsh HH, Lennette EH, Abinanti FR, Winn JF.** 1958. Air-borne transmission of Q fever: The role of parturition in the generation of infective aerosols. *Ann N Y Acad Sci* **70:**528–540.
35. **La Scola B, Raoult D.** 1997. Laboratory diagnosis of rickettsioses: current approaches to diagnosis of old and new rickettsial diseases. *J Clin Microbiol* **35:**2715–2727.
36. **McCaul TF, Williams JC.** 1981. Developmental cycle of *Coxiella burnetii*: structure and morphogenesis of vegetative and sporogenic differentiations. *J Bacteriol* **147:**1063–1076.
37. **Standaert SM, Yu T, Scott MA, Childs JE, Paddock CD, Nicholson WL, Singleton J Jr, Blaser MJ.** 2000. Primary isolation of *Ehrlichia chaffeensis* from patients with febrile illnesses: clinical and molecular characteristics. *J Infect Dis* **181:**1082–1088.
38. **Kaplan JE, Schonberger LB.** 1986. The sensitivity of various serologic tests in the diagnosis of Rocky Mountain spotted fever. *Am J Trop Med Hyg* **35:**840–844.
39. **Chapman AS, Bakken JS, Folk SM, Paddock CD, Bloch KC, Krusell A, Sexton DJ, Buckingham SC, Marshall GS, Storch GA, Dasch GA, McQuiston JH, Swerdlow DL, Dumler SJ, Nicholson WL, Walker DH, Eremeeva ME, Ohl CA; Tickborne Rickettsial Diseases Working Group; CDC.** 2006. Diagnosis and management of tick-borne rickettsial diseases: Rocky Mountain spotted fever, ehrlichioses, and anaplasmosis—United States: a practical guide for physicians and other health-care and public health professionals. *MMWR Recomm Rep* **55:**1–27.
40. **Clements ML, Dumler JS, Fiset P, Wisseman CL Jr, Snyder MJ, Levine MM.** 1983. Serodiagnosis of Rocky Mountain spotted fever: comparison of IgM and IgG enzyme-linked immunosorbent assays and indirect fluorescent antibody test. *J Infect Dis* **148:**876–880.
41. **Eremeeva ME, Balayeva NM, Raoult D.** 1994. Serological response of patients suffering from primary and recrudescent typhus: comparison of complement fixation reaction, Weil-Felix test, microimmunofluorescence, and immunoblotting. *Clin Diagn Lab Immunol* **1:**318–324.
42. **Phetsouvanh R, Thojaikong T, Phoumin P, Sibounheuang B, Phommasone K, Chansamouth V, Lee SJ, Newton PN, Blacksell SD.** 2013. Inter-and intra-operator variability in the reading of indirect immunofluorescence assays for the serological diagnosis of scrub typhus and murine typhus. *Am J Trop Med Hyg* **88:**932–936.
43. **La Scola B, Rydkina L, Ndihokubwayo JB, Vene S, Raoult D.** 2000. Serological differentiation of murine typhus and epidemic typhus using cross-adsorption and Western blotting. *Clin Diagn Lab Immunol* **7:**612–616.
44. **Walker DH, Cain BG, Olmstead PM.** 1978. Laboratory diagnosis of Rocky Mountain spotted fever by immunofluorescent demonstration of *Rickettsia* in Cutaneous lesions. *Am J Clin Pathol* **69:**619–623.
45. **Walker DH.** 1995. Rocky Mountain spotted fever: A seasonal alert. *Clin Infect Dis* **20:**1111–1117.
46. **Walker DH, Feng HM, Ladner S, Billings AN, Zaki SR, Wear DJ, Hightower B.** 1997. Immunohistochemical diagnosis of typhus rickettsioses using an anti-lipopolysaccharide monoclonal antibody. *Mod Pathol* **10:**1038–1042.
47. **Walker DH, Parks FM, Betz TG, Taylor JP, Muehlberger JW.** 1989. Histopathology and immunohistologic demonstration of the distribution of *Rickettsia typhi* in fatal murine typhus. *Am J Clin Pathol* **91:**720–724.
48. **Bozeman FM, Elisberg BL.** 1963. Serological diagnosis of scrub typhus by indirect immunofluorescence. *Proc Soc Exp Biol Med* **112:**568–573.
49. **Yamamoto S, Minamishima Y.** 1982. Serodiagnosis of tsutsugamushi fever (scrub typhus) by the indirect immunoperoxidase technique. *J Clin Microbiol* **15:**1128–1132.
50. **Kelly DJ, Wong PW, Gan E, Lewis GE Jr.** 1988. Comparative evaluation of the indirect immunoperoxidase test for the serodiagnosis of rickettsial disease. *Am J Trop Med Hyg* **38:**400–406.
51. **Blacksell SD, Bryant NJ, Paris DH, Doust JA, Sakoda Y, Day NP.** 2007. Scrub typhus serologic testing with the indirect immunofluorescence method as a diagnostic gold standard: A lack of consensus leads to a lot of confusion. *Clin Infect Dis* **44:**391–401.
52. **Aguero-Rosenfeld ME, Donnarumma L, Zentmaier L, Jacob J, Frey M, Noto R, Carbonaro CA, Wormser GP.** 2002. Seroprevalence of antibodies that react with *Anaplasma phagocytophila*, the agent of human granulocytic ehrlichiosis, in different populations in Westchester County, New York. *J Clin Microbiol* **40:**2612–2615.
53. **Dawson JE, Fishbein DB, Eng TR, Redus MA, Green NR.** 1990. Diagnosis of human ehrlichiosis with the indirect fluorescent antibody test: kinetics and specificity. *J Infect Dis* **162:**91–95.
54. **Walls JJ, Aguero-Rosenfeld M, Bakken JS, Goodman JL, Hossain D, Johnson RC, Dumler JS.** 1999. Inter-and intralaboratory comparison of *Ehrlichia equi* and human granulocytic ehrlichiosis (HGE) agent strains for serodiagnosis of HGE by the immunofluorescent-antibody test. *J Clin Microbiol* **37:**2968–2973.
55. **Bakken JS, Haller I, Riddell D, Walls JJ, Dumler JS.** 2002. The serological response of patients infected with the agent of human granulocytic ehrlichiosis. *Clin Infect Dis* **34:**22–27.
56. **Dawson JE, Paddock CD, Warner CK, Greer PW, Bartlett JH, Ewing SA, Munderloh UG, Zaki SR.** 2001. Tissue diagnosis of *Ehrlichia chaffeensis* in patients with fatal ehrlichiosis by use of immunohistochemistry, in situ hybridization, and polymerase chain reaction. *Am J Trop Med Hyg* **65:**603–609.
57. **Dumler JS, Dawson JE, Walker DH.** 1993. Human ehrlichiosis: hematopathology and immunohistologic detection of *Ehrlichia chaffeensis*. *Hum Pathol* **24:**391–396.
58. **Dupuis G, Péter O, Peacock M, Burgdorfer W, Haller E.** 1985. Immunoglobulin responses in acute Q fever. *J Clin Microbiol* **22:**484–487.
59. **Worswick D, Marmion BP.** 1985. Antibody responses in acute and chronic Q fever and in subjects vaccinated against Q fever. *J Med Microbiol* **19:**281–296.
60. **Kampschreur LM, Oosterheert JJ, Koop AM, Wegdam-Blans MC, Delsing CE, Bleeker-Rovers CP, De Jager-Leclercq MG, Groot CA, Sprong T, Nabuurs-Franssen MH, Renders NH, van Kasteren ME, Soethoudt Y, Blank SN, Pronk MJ, Groenwold RH, Hoepelman AI, Wever PC.** 2012. Microbiological challenges in the diagnosis of chronic Q fever. *Clin Vaccine Immunol* **19:**787–790.

61. **Fiset P, Ormsbee RA, Silberman R, Peacock M, Spielman SH.** 1969. A microagglutination technique for detection and measurement of rickettsial antibodies. *Acta Virol* **13:**60–66.
62. **Murphy AM, Field PR.** 1970. The persistence of complement-fixing antibodies to Q-fever (*Coxiella burneti*) after infection. *Med J Aust* **1:**1148–1150.
63. **Field PR, Hunt JG, Murphy AM.** 1983. Detection and persistence of specific IgM antibody to *Coxiella burnetii* by enzyme-linked immunosorbent assay: A comparison with immunofluorescence and complement fixation tests. *J Infect Dis* **148:**477–487.
64. **Péter O, Dupuis G, Bee D, Lüthy R, Nicolet J, Burgdorfer W.** 1988. Enzyme-linked immunosorbent assay for diagnosis of chronic Q fever. *J Clin Microbiol* **26:**1978–1982.
65. **Wegdam-Blans MC, Wielders CC, Meekelenkamp J, Korbeeck JM, Herremans T, Tjhie HT, Bijlmer HA, Koopmans MP, Schneeberger PM.** 2012. Evaluation of commonly used serological tests for detection of *Coxiella burnetii* antibodies in well-defined acute and follow-up sera. *Clin Vaccine Immunol* **19:**1110–1115.
66. **Kantsø B, Svendsen CB, Jørgensen CS, Krogfelt KA.** 2012. Comparison of two commercially available ELISA antibody test kits for detection of human antibodies against *Coxiella burnetii*. *Scand J Infect Dis* **44:**489–494.
67. **Anderson A, Bijlmer H, Fournier PE, Graves S, Hartzell J, Kersh GJ, Limonard G, Marrie TJ, Massung RF, McQuiston JH, Nicholson WL, Paddock CD, Sexton DJ.** 2013. Diagnosis and management of Q fever—United States, 2013: recommendations from CDC and the Q Fever Working Group. *MMWR Recomm Rep* **62:**1–30.
68. **La Scola B, Raoult D.** 1996. Serological cross-reactions between *Bartonella quintana*, *Bartonella henselae*, and *Coxiella burnetii*. *J Clin Microbiol* **34:**2270–2274.
69. **Raven CF, Hautvast JL, Herremans T, Leenders AC, Schneeberger PM.** 2012. Solitary IgM phase II response has a limited predictive value in the diagnosis of acute Q fever. *Epidemiol Infect* **140:**1950–1954.
70. **Wielders CC, Kampschreur LM, Schneeberger PM, Jager MM, Hoepelman AI, Leenders AC, Hermans MH, Wever PC.** 2012. Early diagnosis and treatment of patients with symptomatic acute Q fever do not prohibit IgG antibody responses to *Coxiella burnetii*. *Clin Vaccine Immunol* **19:**1661–1666.
71. **Li JS, Sexton DJ, Mick N, Nettles R, Fowler VG Jr, Ryan T, Bashore T, Corey GR.** 2000. Proposed modifications to the Duke criteria for the diagnosis of infective endocarditis. *Clin Infect Dis* **30:**633–638.
72. **Dupont HT, Thirion X, Raoult D.** 1994. Q fever serology: cutoff determination for microimmunofluorescence. *Clin Diagn Lab Immunol* **1:**189–196.
73. **Healy B, van Woerden H, Raoult D, Graves S, Pitman J, Lloyd G, Brown N, Llewelyn M.** 2011. Chronic Q fever: different serological results in three countries—results of a follow-up study 6 years after a point source outbreak. *Clin Infect Dis* **52:**1013–1019.
74. **Wegdam-Blans MC, Kampschreur LM, Delsing CE, Bleeker-Rovers CP, Sprong T, van Kasteren ME, Notermans DW, Renders NH, Bijlmer HA, Lestrade PJ, Koopmans MP, Nabuurs-Franssen MH, Oosterheert JJ.** 2012. Chronic Q fever: review of the literature and a proposal of new diagnostic criteria. *J Infect* **64:**247–259.
75. **Beare PA, Chen C, Bouman T, Pablo J, Unal B, Cockrell DC, Brown WC, Barbian KD, Porcella SF, Samuel JE, Felgner PL, Heinzen RA.** 2008. Candidate antigens for Q fever serodiagnosis revealed by immunoscreening of a *Coxiella burnetii* protein microarray. *Clin Vaccine Immunol* **15:**1771–1779.
76. **Xiong X, Wang X, Wen B, Graves S, Stenos J.** 2012. Potential serodiagnostic markers for Q fever identified in *Coxiella burnetii* by immunoproteomic and protein microarray approaches. *BMC Microbiol* **12:**35.
77. **Limonard GJ, Thijsen SF, Bossink AW, Asscheman A, Bouwman JJ.** 2012. Developing a new clinical tool for diagnosing chronic Q fever: The *Coxiella* ELISPOT. *FEMS Immunol Med Microbiol* **64:**57–60.
78. **Tzianabos T, Anderson BE, McDade JE.** 1989. Detection of *Rickettsia rickettsii* DNA in clinical specimens by using polymerase chain reaction technology. *J Clin Microbiol* **27:**2866–2868.
79. **Sexton DJ, Kanj SS, Wilson K, Corey GR, Hegarty BC, Levy MG, Breitschwerdt EB.** 1994. The use of a polymerase chain reaction as a diagnostic test for Rocky Mountain spotted fever. *Am J Trop Med Hyg* **50:**59–63.
80. **Mouffok N, Socolovschi C, Benabdellah A, Renvoise A, Parola P, Raoult D.** 2011. Diagnosis of rickettsioses from eschar swab samples, Algeria. *Emerg Infect Dis* **17:**1968–1969.
81. **Roux V, Raoult D.** 2000. Phylogenetic analysis of members of the genus *Rickettsia* using the gene encoding the outer-membrane protein rOmpB (ompB). *Int J Syst Evol Microbiol* **50:**1449–1455.
82. **Regnery RL, Spruill CL, Plikaytis BD.** 1991. Genotypic identification of rickettsiae and estimation of intraspecies sequence divergence for portions of two rickettsial genes. *J Bacteriol* **173:**1576–1589.
83. **Kato CY, Chung IH, Robinson LK, Austin AL, Dasch GA, Massung RF.** 2013. Assessment of real-time PCR assay for detection of *Rickettsia* spp. and *Rickettsia rickettsii* in banked clinical samples. *J Clin Microbiol* **51:**314–317.
84. **Eremeeva M, Yu X, Raoult D.** 1994. Differentiation among spotted fever group rickettsiae species by analysis of restriction fragment length polymorphism of PCR-amplified DNA. *J Clin Microbiol* **32:**803–810.
85. **Boostrom A, Beier MS, Macaluso JA, Macaluso KR, Sprenger D, Hayes J, Radulovic S, Azad AF.** 2002. Geographic association of *Rickettsia felis*-infected opossums with human murine typhus, Texas. *Emerg Infect Dis* **8:**549–554.
86. **Roux V, Fournier PE, Raoult D.** 1996. Differentiation of spotted fever group rickettsiae by sequencing and analysis of restriction fragment length polymorphism of PCR-amplified DNA of the gene encoding the protein rOmpA. *J Clin Microbiol* **34:**2058–2065.
87. **Peniche-Lara G, Zavala-Velazquez J, Dzul-Rosado K, Walker DH, Zavala-Castro J.** 2013. Simple method to differentiate among *Rickettsia* species. *J Mol Microbiol Biotechnol* **23:**203–208.
88. **Kim DM, Kim HL, Park CY, Yang TY, Lee JH, Yang JT, Shim SK, Lee SH.** 2006. Clinical usefulness of eschar polymerase chain reaction for the diagnosis of scrub typhus: A prospective study. *Clin Infect Dis* **43:**1296–1300.
89. **Paris DH, Aukkanit N, Jenjaroen K, Blacksell SD, Day NP.** 2009. A highly sensitive quantitative real-time PCR assay based on the *groEL* gene of contemporary Thai strains of *Orientia tsutsugamushi*. *Clin Microbiol Infect* **15:**488–495.
90. **Jiang J, Chan TC, Temenak JJ, Dasch GA, Ching WM, Richards AL.** 2004. Development of a quantitative real-time polymerase chain reaction assay specific for *Orientia tsutsugamushi*. *Am J Trop Med Hyg* **70:**351–356.
91. **Sokhna C, Mediannikov O, Fenollar F, Bassene H, Diatta G, Tall A, Trape JF, Drancourt M, Raoult D.** 2013. Point-of-care laboratory of pathogen diagnosis in rural Senegal. *PLoS Negl Trop Dis* **7:**e1999. doi:10.1371/journal.pntd.0001999
92. **Paris DH, Blacksell SD, Newton PN, Day NP.** 2008. Simple, rapid and sensitive detection of *Orientia tsutsugamushi* by loop-isothermal DNA amplification. *Trans R Soc Trop Med Hyg* **102:**1239–1246.
93. **Pan L, Zhang L, Wang G, Liu Q.** 2012. Rapid, simple, and sensitive detection of the *ompB* gene of spotted fever

group rickettsiae by loop-mediated isothermal amplification. *BMC Infect Dis* **12:**254.

94. **Childs JE, Sumner JW, Nicholson WL, Massung RF, Standaert SM, Paddock CD.** 1999. Outcome of diagnostic tests using samples from patients with culture-proven human monocytic ehrlichiosis: implications for surveillance. *J Clin Microbiol* **37:**2997–3000.
95. **Loftis AD, Massung RF, Levin ML.** 2003. Quantitative real-time PCR assay for detection of *Ehrlichia chaffeensis*. *J Clin Microbiol* **41:**3870–3872.
96. **Schouls LM, Van De Pol I, Rijpkema SG, Schot CS.** 1999. Detection and identification of *Ehrlichia*, *Borrelia burgdorferi sensu lato*, and *Bartonella* species in Dutch *Ixodes ricinus* ticks. *J Clin Microbiol* **37:**2215–2222.
97. **Massung RF, Slater K, Owens JH, Nicholson WL, Mather TN, Solberg VB, Olson JG.** 1998. Nested PCR assay for detection of granulocytic ehrlichiae. *J Clin Microbiol* **36:**1090–1095.
98. **Paddock CD, Sumner JW, Shore GM, Bartley DC, Elie RC, McQuade JG, Martin CR, Goldsmith CS, Childs JE.** 1997. Isolation and characterization of *Ehrlichia chaffeensis* strains from patients with fatal ehrlichiosis. *J Clin Microbiol* **35:**2496–2502.
99. **Dunn BE, Monson TP, Dumler JS, Morris CC, Westbrook AB, Duncan JL, Dawson JE, Sims KG, Anderson BE.** 1992. Identification of *Ehrlichia chaffeensis* morulae in cerebrospinal fluid mononuclear cells. *J Clin Microbiol* **30:**2207–2210.
100. **Doyle CK, Labruna MB, Breitschwerdt EB, Tang YW, Corstvet RE, Hegarty BC, Bloch KC, Li P, Walker DH, McBride JW.** 2005. Detection of medically important *Ehrlichia* by quantitative multicolor TaqMan real-time polymerase chain reaction of the dsb gene. *J Mol Diagn* **7:**504–510.
101. **Horowitz HW, Aguero-Rosenfeld ME, McKenna DF, Holmgren D, Hsieh TC, Varde SA, Dumler SJ, Wu JM, Schwartz I, Rikihisa Y, Wormser GP.** 1998. Clinical and laboratory spectrum of culture-proven human granulocytic ehrlichiosis: comparison with culture-negative cases. *Clin Infect Dis* **27:**1314–1317.
102. **Edelman DC, Dumler JS.** 1996. Evaluation of an improved PCR diagnostic assay for human granulocytic ehrlichiosis. *Mol Diagn* **1:**41–49.
103. **Schotthoefer AM, Meece JK, Ivacic LC, Bertz PD, Zhang K, Weiler T, Uphoff TS, Fritsche TR.** 2013. Comparison of a real-time PCR method with serology and blood smear analysis for diagnosis of human anaplasmosis: importance of infection time course for optimal test utilization. *J Clin Microbiol* **51:**2147–2153.
104. **Wang X, Rikihisa Y, Lai TH, Kumagai Y, Zhi N, Reed SM.** 2004. Rapid sequential changeover of expressed *p44* genes during the acute phase of *Anaplasma phagocytophilum* infection in horses. *Infect Immun* **72:**6852–6859.
105. **Pan L, Zhang L, Wang G, Liu Q, Yu Y, Wang S, Yu H, He J.** 2011. Rapid, simple, and sensitive detection of *Anaplasma phagocytophilum* by loop-mediated isothermal amplification of the *msp2* gene. *J Clin Microbiol* **49:**4117–4120.
106. **Tilburg JJ, Melchers WJ, Pettersson AM, Rossen JW, Hermans MH, van Hannen EJ, Nabuurs-Franssen MH, de Vries MC, Horrevorts AM, Klaassen CH.** 2010. Interlaboratory evaluation of different extraction and real-time PCR methods for detection of *Coxiella burnetii* DNA in serum. *J Clin Microbiol* **48:**3923–3927.
107. **Schneeberger PM, Hermans MH, van Hannen EJ, Schellekens JJ, Leenders AC, Wever PC.** 2010. Real-time PCR with serum samples is indispensable for early diagnosis of acute Q fever. *Clin Vaccine Immunol* **17:**286–290.
108. **Shaw EI, Moura H, Woolfitt AR, Ospina M, Thompson HA, Barr JR.** 2004. Identification of biomarkers of whole *Coxiella burnetii* phase I by MALDI-TOF mass spectrometry. *Anal Chem* **76:**4017–4022.
109. **Anderson AD, Kruszon-Moran D, Loftis AD, McQuillan G, Nicholson WL, Priestley RA, Candee AJ, Patterson NE, Massung RF.** 2009. Seroprevalence of Q fever in the United States, 2003–2004. *Am J Trop Med Hyg* **81:**691–694.
110. **Raoult D, Dasch GA.** 1995. Immunoblot cross-reactions among *Rickettsia*, *Proteus* spp. and *Legionella* spp. in patients with Mediterranean spotted fever. *FEMS Immunol Med Microbiol* **11:**13–18.

The *Bartonellaceae*, *Brucellaceae*, and *Francisellaceae*

CHRISTINE M. LITWIN, BURT ANDERSON,
RENEE TSOLIS, AND AMY RASLEY

52

The three families of bacteria described in this chapter share several common characteristics despite the phylogenetic distance between the group that includes *Bartonella* and *Brucella*, from the *Alphaproteobacteria*, and the more distantly related *Francisella* in the *Gammaproteobacteria* class. All three genera are zoonotic bacteria with species capable of infecting both animals and humans and are fastidious with special growth requirements; many species among these three genera cause emerging infections in humans. The diversity of natural animal reservoirs for members of the genera *Bartonella* and *Brucella* are just now becoming fully defined and appreciated and are likely all around us. *Brucella* spp. and *Francisella* spp. are well-established as agents that warrant special attention and focus because of their potential for misuse and intentional release in acts of bioterrorism or biowarfare. This chapter briefly summarizes our knowledge of the taxonomy, epidemiology, and pathobiology of these zoonotic bacteria and describes the immunologic and molecular tools for the laboratory diagnosis of infections caused by these microbes.

TAXONOMY

Bartonella

The genera *Bartonella* and *Brucella* are classified within the order *Rhizobiales*, with *Bartonella* belonging to the family *Bartonellaceae* and *Brucella* to the family *Brucellaceae* (Fig. 1). There are currently 31 validated *Bartonella* species, 11 of which have been associated with human disease. Most reported cases of human infection involve *B. bacilliformis*, *B. henselae*, or *B. quintana*. However, *B. clarridgeiae*, *B. elizabethae*, *B. vinsonii* subsp. *berkhoffii*, *B. vinsonii* subsp. *arupensis*, *B. koehlerae*, *B. alsatica*, *B. rochalimae*, and *B. grahamii* have all been associated with infections in humans.

Brucella

Brucella species have traditionally been grouped according to their ability to transmit naturally within their zoonotic reservoir hosts. Six "classical" *Brucella* species, *B. abortus* (cattle), *B melitensis* (sheep and goats), *B. suis* (swine and some wildlife species), *B. canis* (dogs), *B. ovis* (sheep), and *B. neotomae* (desert wood rat) have been described, of which the first four are able to cause zoonotic infections in humans. Recently, new *Brucella* species have been isolated from marine mammals (*B. pinnepedialis* and *B. ceti)*, from voles (*B. microti*), and from a breast implant wound (*B. inopinata*) (1, 2). While a proposal to consider all of the *Brucella* species as subspecies of *B. melitensis* has been adopted by some databases such as the National Center for Biotechnology Information, the individual species names are considered by many to provide valuable biological information and continue to be used in the literature (3).

Francisella

Francisella tularensis is a small, highly pleomorphic, Gram-negative coccobacillus and the etiologic agent of tularemia. First isolated in 1911 in Tulare County, CA, the organism was ultimately assigned to a new genus named *Francisella*, in honor of Dr. Edward Francis, who detailed the human disease decades after the organism was first described (4). Over the past century, the taxonomy of *F. tularensis* has remained complicated and ever changing due to the expanding diversity of the genus *Francisella*. *Francisella* is the sole genus in the family *Francisellaceae*, falling within the class *Gammaproteobacteria*. *Francisella* contains two established species, *F. tularensis* and *F. philomiragia*, and several newly proposed species. *F. novicida* was recently reclassified as a subspecies within *F. tularensis* rather than a species (5). Currently, *F. tularensis* contains four recognized subspecies: *F. tularensis* subsp. *tularensis*, *F. tularensis* subsp. *holarctica*, *F. tularensis* subsp. *novicida*, and *F. tularensis* subsp. *mediasiatica* (Fig. 1) (6).

EPIDEMIOLOGY

Bartonella

Cats, and in particular kittens, serve as the natural host for *B. henselae*, the main causative agent for cat scratch disease (CSD). CSD can result from a cat scratch or bite. The cat flea, *Ctenocephalides felis*, plays a critical role in the horizontal cat-to-cat transmission of *B. henselae*. Zangwill et al. found that patients with CSD were more likely to have at least one kitten that was infested with fleas, to own a kitten 12 months or younger, and to have been scratched or bitten by a kitten (7). Rare cases of CSD occur after exposure to dogs, presumably from flea bites.

CSD has a worldwide distribution and is generally a disease of children and young adults, with 80% of cases occurring in children. It infrequently causes serious illness, with the severity and presentation of disease usually related to immune status.

doi:10.1128/9781555818722.ch52

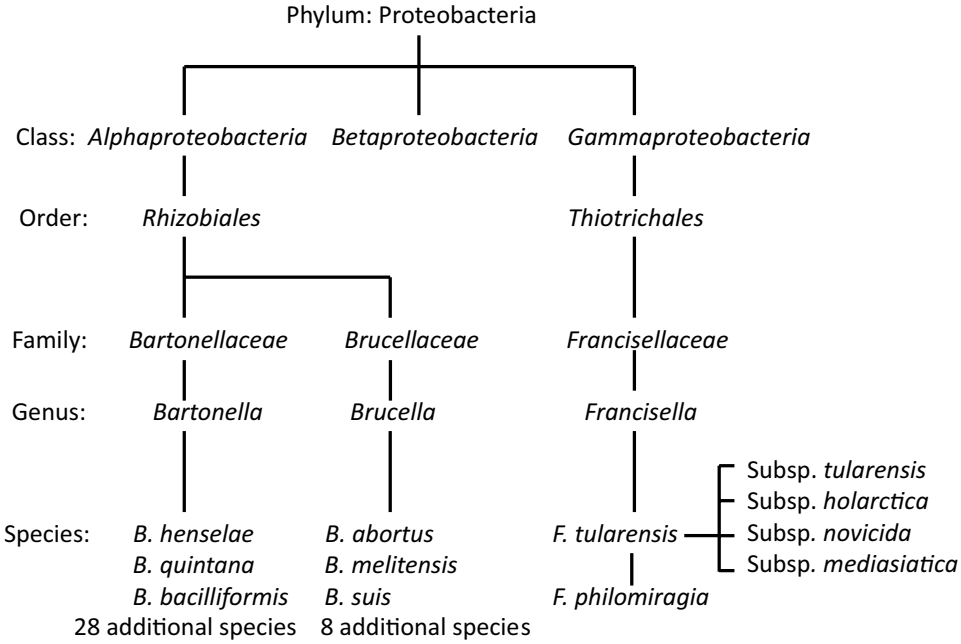

FIGURE 1 Taxonomy of the major human pathogens in the families *Bartonellaceae*, *Brucellaceae*, and *Francisellaceae*. Additional *Bartonella* spp. and *Brucella* spp. not shown here have also been associated with human disease but are not listed due to space constraints. Members of the *Bartonella* and *Brucella* genera are *Alphaproteobacteria*, while members of the genus *Francisella* are *Gammaproteobacteria*.

However, there have been accounts of severe disease such as endocarditis, persistent bacteremia, and bacillary angiomatosis reported in immune-competent individuals. On the other hand, CSD-like symptoms can also occur in immunocompromised patients and have been described in patients who have undergone solid organ transplantation. Contact with cats and previous valvular disease serve as the major risk factors for *B. henselae* endocarditis. HIV-infected patients with bacillary angiomatosis and bacillary peliosis caused by *B. henselae* also usually have an epidemiologic link to cat exposure.

During World War I, *B. quintana* infection became a major source of morbidity and mortality among soldiers and was commonly known as trench fever. Lice generally have been considered to be the major vector for *B. quintana* in classic trench fever. Three lice species, *Pediculus humanus* var. *capitis* (head louse), *P. humanus* var. *corporis* (body louse), and *P. humanus* var. *pubis* (pubic louse), can potentially transmit *B. quintana*. The body louse is felt to be the predominant vector. After World War II, reports of *B. quintana* infections were rare until infections with HIV were described. Both *B. henselae* and *B. quintana* can cause bacillary angiomatosis, especially in HIV patients. Homelessness, alcoholism, and body lice are now the major risk factors associated with contemporary *B. quintana* trench fever infections, bacteremia, and endocarditis (8).

Bartonellosis (or Carrion's disease) caused by *B. bacilliformis* is usually confined to limited areas of South America within the Andes, with the sand fly (*Lutzomyia verrucarum*) as the presumed vector in Peru. Occasional cases among travelers to other countries in South America such as Ecuador and Colombia suggests that other additional vectors may be involved in the transmission of *B. bacilliformis*.

Brucella

Brucellosis is a zoonotic infection with worldwide distribution. In the United States, brucellosis is mainly associated with travel to areas of endemicity such as the Middle East, the Balkan peninsula, Central Asia, and countries of Latin America, especially Mexico and Peru (9). However, in these areas, brucellosis is encountered frequently and is a significant cause of morbidity and disability, with an estimated 500,000 new cases annually.

The majority of brucellosis cases result from consumption of unpasteurized dairy products, especially goat's milk and cheese. In individuals with occupational exposure to *Brucella*-infected animals, infection may occur via mucosal or respiratory routes or via breaks in the skin. *Brucella* spp. can form highly infectious aerosols during manipulation of cultures in the laboratory, and for this reason, brucellosis is one of the most frequently reported laboratory-acquired infections (10).

Francisella

Tularemia is a zoonotic disease transmissible by inoculation, ingestion, or inhalation of *F. tularensis* (6). Clinical disease is caused largely by *F. tularensis* subsp. *tularensis* (type A strains), endemic in North America, and *F. tularensis* subsp. *holarctica* (type B strains), endemic in the terrestrial ecozones comprising the holarctic regions (6). The association of type A strains with lagomorphs and type B strains with rodents and aquatic environments is well described (6). Geographically, the distribution of type A and type B strains appears largely similar in the United States.

CLINICAL MANIFESTATIONS

Bartonella

The clinical syndromes associated with *Bartonella* species are varied and include CSD, cutaneous bacillary angiomatosis (BA), extracutaneous infection such as bacillary peliosis, fever with bacteremia, trench fever, and endocarditis (11).

CSD typically presents as a subacute regional lymphadenitis with an associated inoculation site due to a cat scratch or bite. With the originally described trench fever, symptoms are usually described as an abrupt-onset high fever, severe frontal or retro-orbital headache, rash, conjunctivitis, and bone and muscle tenderness, particularly involving the shins. In urban trench fever, the symptoms described above are present more variably and are less prevalent than in the initial description of the disease.

Disseminated infections by *B. henselae* or *B. quintana* have been reported in both immunocompetent and immunocompromised patients but are far more common in the latter group. In HIV-infected patients with BA, multiple cutaneous and interstitial subcutaneous nodules that contain bacteria are present. These nodular lesions have a unique histopathology characterized by proliferation of endothelial cells and angiogenesis, similar to that observed in the verruga peruana resulting from infection with *B. bacilliformis*.

B. bacilliformis causes Oroya fever and verruga peruana. The bacteremia of Oroya fever begins 3 to 12 weeks after a bite from an infected sand fly. The illness may range from mild to very severe. In severe cases, fever, chills, headache, sweating, aches, dyspnea, mental status changes, and seizure may occur. Verruga peruana occurs after organisms invade capillary endothelial cells and produce hemangioma-like nodules in the skin and mucous membranes. Verruga peruana can appear 2 to 8 weeks after the patient has apparently recovered from Oroya fever, although most patients do not have a previous history of febrile illness.

Brucella

Brucellosis is a febrile illness characterized by an acute or gradual onset of symptoms, including night sweats, fatigue, weight loss, lack of appetite, headache, and joint and muscle pain. In addition to constitutional symptoms, enlargement of the spleen, liver, or lymph nodes is present in a subset of patients; these result from localization of bacteria to the mononuclear phagocyte system. Focal complications of brucellosis are most frequent in the large, weight-bearing joints and in the spine; however, any organ may be affected. Brucellosis is difficult to diagnose, especially in areas where it is not endemic such as North America. The rare occurrence and nonspecific presentation of brucellosis in these areas often result in a failure of clinicians to consider brucellosis as a possible diagnosis.

Three species of *Brucella* have a high zoonotic potential: *B. melitensis*, *B. abortus*, and *B. suis*. *B. melitensis*, which has goats and sheep as its zoonotic reservoirs, is by far the most common cause of human infection and is most frequently acquired via consumption of unpasteurized goat's milk and cheese. *B. abortus* naturally infects cattle, and while some reports of foodborne infection exist, these appear to be less common than those caused by *B. melitensis*. Occupational infections with *B. abortus*, *B. melitensis*, and *B. suis* have been reported in veterinarians, farmers, abbatoir workers, and laboratorians. Human infection with a fourth species, *B. canis*, is infrequently reported and results from transmission from infected dogs (12).

Francisella

Six clinical forms of tularemia, caused mainly by *F. tularensis* subsp. *tularensis* and subsp. *holarctica*, have been described to date in which the type and severity of disease depend on the infecting strain, dose, and route of infection (13). Although disease caused by *F. tularensis* type A strains can be severely debilitating and even fatal, diagnoses of disease caused by less virulent strains remains problematic due to the nondescript nature of the symptoms.

Infection through the skin, following the bite of an infected vector or through direct contact with infected animals, results in ulceroglandular and glandular tularemia. Ulceroglandular tularemia is the most common clinical presentation. Nondescript flulike symptoms can occur abruptly following a relatively short incubation period (3 to 6 days). In the case of ulceroglandular disease, a localized ulcer develops at the site of infection. Subsequent bacterial dissemination from the inoculation site results in enlarged draining lymph nodes resembling the classic bubo associated with bubonic plague. Systemic dissemination can occur, yet this form of disease is rarely fatal. The clinical presentation of glandular tularemia is very similar, but the formation of an ulcer at the inoculation site does not occur (13). Oculoglandular tularemia is a rare presentation of disease in which the conjunctiva is the initial site of infection, usually as a result of inadvertent transfer of the bacteria present on an individual's fingertips to the eye.

Oral exposure can result in oropharyngeal or gastrointestinal tularemia, often via ingestion of infected foods or drinking water. Sore throat and enlarged tonsils and cervical lymph nodes often accompany oropharyngeal disease, while gastrointestinal tularemia is characterized by abdominal pain and mild diarrhea. If the infectious dose is high, an acute, potentially life-threatening disease marked by extensive ulceration of the bowel may ensue.

Typhoidal tularemia is a systemic form of disease, although the route of infection is unknown. Clinical presentation includes septicemia without lymphadenopathy or formation of an ulcer; mortality rates of 30 to 60% have been reported.

Inhalation of *F. tularensis* subsp. *tularensis* or subsp. *holarctica* can result in pneumonic tularemia, which can also develop as a secondary complication of ulceroglandular disease. Clinical presentation of pneumonic disease can vary widely and may or may not include ulcers, dry cough, and chest pain or be accompanied by pneumonia. Inhalational pneumonic disease is considered the most acute form of tularemia, with a reported case-fatality rate of approximately 40%. Naturally occurring cases of inhalation tularemia have been associated with agriculture and/or landscaping activities that promote the generation of infectious aerosols.

LABORATORY DIAGNOSIS

Bartonella

Microbiologic Culture

Since most *Bartonella* isolates require a 2-to 6-week incubation for primary isolation, routine bacterial culture methods usually do not allow *Bartonella* spp. to be detected. Specialized procedures are needed for the isolation of *Bartonella* from tissue and blood. Isolation and culture of *Bartonella* spp. are covered in detail in the 11th edition of the *Manual of Clinical Microbiology*.

Serology

Indirect Fluorescent Antibody Assay

Serology is used frequently for diagnosing infections with *Bartonella* spp., since culture is usually not feasible. The indirect fluorescent antibody (IFA) (14) assay is the most routinely used method for the detection of *B. henselae* and *B. quintana* antibodies. Originally developed by Regnery et al. (15), IFA uses a Vero cell cocultivated antigen to reduce the autoadherent nature of the bacterium.

Interpretation of test results. A positive IgM titer of ≥16 is indicative of acute infection. The use of IgM serology can be somewhat limited since the window of IgM production is often very early and minimal. Often, patients present to clinicians with symptoms (e.g., lymphadenopathy in CSD) and are tested long after IgM titers have reverted to negative (16).

A positive IgG titer of >1:64 is suggestive of recent infection. Stronger evidence of recent infection is a 4-fold or greater rise in IgG titer in acute-and convalescent-phase serum samples drawn at least 2 weeks apart. Serial measurements of antibody titers is highly recommended since antibody titers may remain high above controls for a year or more after infection. Initial titers of ≥1:64–256 are generally considered seropositive for *Bartonella* spp. infection. However, very high titers of ≥800 suggest a clinical diagnosis of *Bartonella* endocarditis.

Although there is widespread use of the IFA methodology, the assays often demonstrate wide variations in sensitivities and specificities in different in-house preparations and commercially manufactured IFAs. Numerous cross-reactivity issues have also been found with the IFA. Sensitivities for the IgM IFA assay vary between 54–98% and 69–96% for the IgG assay, according to numerous publications (17). Overall, the sensitivity of the IFA does not appear to be optimal, especially with the IgG assays.

Enzyme-Linked Immunosorbent Assay

Enzyme-linked immunosorbent assay (ELISA) is used by a few commercial laboratories for the detection of *B. henselae* antibodies (18, 19). Many in-house ELISA assays use *B. henselae* sonicated (whole-cell) proteins or outer membrane proteins fractionated by *N*-lauroyl-sarcosine (insoluble or soluble) (18). IgM ELISAs have been reported to also show wide variations in accuracy, with sensitivities and specificities ranging between 53–75% and 91–100%, respectively. IgG ELISAs tend to show sensitivities and specificities ranging from 28–77% to 91–94%, respectively (17).

A recombinant *B. henselae* 17-kDa antigen first described by Anderson et al. (20) has been developed into a commercial IgG ELISA with a reported sensitivity and specificity of 71.1% and 93.0%, respectively (21). An IgM-capture ELISA-based assay has also been developed using this antigen, with sensitivity and specificity values of 100% and 97.1%, respectively, based on comparisons with *B. henselae* IgM IFA IgM-negative and positive samples (19). IFA, indirect hemagglutination, and ELISA tests are available for the detection of antibodies to *B. bacilliformis*. Cutoffs for determining a positive, negative, or equivocal ELISA result vary with the manufacturer.

Interpretation of test results. Immunologic cross-reactivity as a result of conserved epitope recognition across species occurs frequently for many bacterial serological assays, including the *Bartonella* antibody assays. The first serological cross-reactivity between a *Bartonella* species and a heterologous pathogen was first reported in 1976 by Cooper et al. (22) when *C. burnetii* (Q fever) antibody-positive sera were discovered to cross-react and cause false-positive reactions with the hemagglutination test used in the diagnosis of trench fever (*B. quintana*).

Since that first publication, numerous cross-reactions have been cited with other bacterial and viral agents, including *Afipia felis*, *Anaplasma phagocytophila*, *Brucella* spp., *Chlamydophila pneumoniae*, *Chlamydia psittaci*, *C. trachomatis*, cytomegalovirus, Epstein-Barr virus, *Ehrlichia canis*, *Orientia tsutsugamushi*, *Rickettsia conorii*, *Rickettsia prowazekii*, *Rickettsia rickettsii*, and *Rickettsia typhi* (22–24). Studies using serologic assays other than the IFA, including ELISA, Western blot, immunoperoxidase staining, immunohistochemistry, and the passive hemagglutination test, have all described significant cross-reactivities, especially between *B. henselae* and *B. quintana* in patients with confirmed or suspected CSD or bacillary angiomatosis (22–24). Due to this high degree of cross-reactivity, most reference labs include both *B. quintana* and *B. henselae* in their antigenic panel of serologic assays. The degree of antibody reaction to either species in the IFA can then allow inference about which species might be responsible for a particular infection. The titer of the infecting organism is typically higher than the titer of the noninfecting organism. This is more important when the species can cause overlapping infections such as fever with bacteremia, endocarditis, or bacillary angiomatosis but is less important with CSD.

Other Immunological Methods

CSD typically produces primary inoculation papules followed a number of weeks later by lymphadenopathy, whereas bacillary angiomatosis produces cutaneous or subcutaneous angiomatous lesions. Microscopic evaluation of infected tissue using more specific immunohistochemistry, along with the Warthin-Starry (silver impregnation) stain, has been used to give a pathologic diagnosis of *Bartonella* spp. infection, especially in cases of CSD, bacillary angiomatosis, and endocarditis (25). Warthin-Starry stains have historically been the preferred method for the detection of *Bartonella* species. The use of this stain for diagnostic purposes is technically challenging due to the high background of silver precipitate in the tissue, which may result in false-positive diagnoses.

Lymph node removal or biopsy may be performed to determine the cause of lymphadenopathy or angiomatous lesion. The histologic findings of CSD (i.e., lymphadenopathy) may be nonspecific and the findings may be dependent on the stage of the disease. Nonspecific reactive follicular hyperplasia is usually seen early in disease. Later in disease, the lymph nodes develop stellate suppurative granulomas with acellular necrotic centers with a surrounding zone of histiocytes and an outer zone of plasma cells and lymphocytes. Immunoreactive bacteria are usually identified within the areas of necrosis in the suppurative granulomas. The typical angiomatous lesions of bacillary angiomatosis produce characteristic lobular proliferations of blood vessels histologically distinct from the granulomatous lymph node lesions of CSD. The immunoreactive bacteria are identified within the proliferative endothelial cells in the blood vessels. In patients with *Bartonella* endocarditis, clusters of bacteria are usually seen in an extracellular location in the fibrin deposits, mainly in the valvular vegetation.

As a rule, the immunohistochemical assay is performed on formalin-fixed, paraffin-embedded sections of embedded lymph nodes or biopsy tissue that are routinely sectioned to 5-mm-thick slices. A commercially available monoclonal antibody specific for *B. henselae* (clone H2A10; Biocare Medical, Concord, CA) is available. For the H2A10 clone, cross-reactivity tests were performed with *B. quintana*, *B. elizabethae*, *B. grahamii*, *B. taylorii*, *B. doshiae*, and *B. vinsonii* strains. Reactivity was obtained only with *B. henselae*.

A polyclonal rabbit antibody that does not differentiate between *B. henselae* and *B. quintana* can be used to detect CSD, bacillary angiomatosis, and peliosis hepatis. In a study by Caponetti et al. (25) on patients with suspected CSD, immunohistochemical analysis was positive in 25% of cases and PCR was positive in 38% of 22 patients with

lymphadenopathy and histopathological findings compatible with CSD. Overall, the diagnostic sensitivity of immunohistochemical analysis is low for the detection of *B. henselae* in tissue. PCR is slightly more sensitive than immunohistochemical analysis and should be performed on all cases negative by immunohistochemical analysis. Warthin-Starry seems to be the most sensitive test, but it is the least specific for *Bartonella* because of issues with background staining.

Molecular Diagnosis

PCR has played an important role in the association of *Bartonella* spp. with new disease syndromes. In fact, the initial association of *Bartonella* (then *Rochalimaea*) with bacillary angiomatosis resulted from the amplification and subsequent sequencing of 16S rRNA genes from the lesions of patients with bacillary angiomatosis (26). A similar approach, when applied to preparations of CSD skin test antigens, identified only the *B. henselae* 16S rRNA gene sequence, which provided compelling evidence that the delayed hypersensitivity reaction, used for many years to diagnose CSD, was elicited by a *B. henselae* antigen (27).

Currently, most applications of PCR in the clinical microbiology laboratory fall primarily into two areas. The first is the identification and strain typing of *Bartonella* isolates, a powerful tool for research microbiologists but somewhat impractical and time-consuming in the clinical laboratory since it relies on growth of the *Bartonella* isolates. The second is the detection of *Bartonella* DNA directly in clinical specimens. Recently, a strategy was described that combined enrichment culture in liquid media of bartonellae from clinical specimens, followed by PCR for detection and identification (28). PCR identification from clinical specimens is currently available only in a few select reference laboratories.

Initial approaches for PCR of *Bartonella* used primers to amplify all or part of the 16S rRNA gene coupled with sequencing (26, 29). However, the utility of the 16S RNA gene as a means of species identification is limited, as it is highly conserved among *Bartonella* spp. (30). Many other target genes have been used for PCR detection of *Bartonella*, including specific primers for serine protease (*htrA*) (31, 32); NADH dehydrogenase gamma subunit (*nuoG*) (33); RNA polymerase beta subunit (*rpoB*) (33); heme-binding protein A/Pap31 (*hbpA/pap31*) (34); the intergenic region between the 16S and 23S rRNA genes (35); and tmRNA (*ssrA*) (36). Newer approaches utilizing real-time PCR have been described which shorten the time to obtain results. Liberto et al. used real-time PCR to detect the *Bartonella bqtR* transcriptional regulator gene in blood specimens and demonstrated differential melting curves to specifically distinguish *B. henselae* from *B. quintana* (37). Diaz et al. utilized real-time PCR of the *ssrA* gene coupled with sequencing to differentiate among *Bartonella* species DNA amplified from blood specimens collected from wild and domestic animals (36). More recently, a two-step approach using real-time PCR of the *gltA* gene and pyrosequencing was applied to clinical specimens to detect and differentiate *Bartonella* species (38). However, currently, there is no consensus on the optimal approach to detect *Bartonella* DNA or RNA in clinical specimens, and a wide range of methods is employed by both commercial and reference laboratories.

Brucella

Microbiologic Culture

Definitive diagnosis of human brucellosis requires the isolation of *Brucella* spp. from clinical specimens such as blood, bone marrow, or joint aspirates. The success in obtaining positive blood cultures from patients varies, depending on the stage of the disease and the culture methods. In patients presenting acutely with brucellosis, between 40 and 90% of patients are culture positive, while in patients presenting with focal, chronic or recurrent infection, this decreases to 5 to 20% (39). Culture from bone marrow and lysis centrifugation have been shown to improve culture yields in patients with brucellosis. Methods for isolation and culture of *Brucella* spp. are detailed in chapter 47 of the *Manual of Clinical Microbiology*, 11th ed. (40), and a detailed comparison of yields from different culture methods can be found in reference 39.

Serology

Serum Agglutination Test (SAT)

Because of the long incubation time for primary culture, difficulty in reliable isolation of *Brucella* spp. from clinical specimens, and biohazards associated with culturing *Brucella* in the laboratory, serological assays are important tools for the rapid diagnosis of brucellosis. The humoral response to *Brucella* infection is dominated by antibodies specific for the O-polysaccharide moiety of lipopolysaccharide (LPS). During the early stage of primary infection, IgM predominates, while later during the course of infection, IgG and IgA can be detected (41). Early during the course of infection, serologic results may be negative, and if the patient's clinical presentation and history are consistent with brucellosis, it is important to perform a repeat serology test after 2 weeks (42). A shortcoming of all serological tests is the lack of standardization of the antigen preparations, and this can influence the sensitivity and specificity of these assays. Further, agglutination tests tend to lack sensitivity in patients with chronic or complicated brucellosis (39–43). For suspected infections with *B. canis* or with the veterinary vaccine RB51, which do not make the LPS O-antigen, serologic testing is not available.

The serum agglutination test (SAT), which detects IgM, IgA, and IgG responses to *Brucella* infection, is considered to be the definitive test because of its sensitivity and specificity. The test is performed by incubating a fixed volume and concentration of an inactivated *Brucella* cell suspension with doubling serial dilutions of serum for 24 h. The highest dilution with more than 50% of the suspension agglutinated is the titer.

Interpretation of test results. In areas of nonendemicity, an agglutination titer of ≥1:160, or a 4-fold rise in titers between acute-and convalescent-phase samples, is considered to be positive in symptomatic patients. In areas of endemicity, repeated exposure to *Brucella* or previous infection may lead to persistently elevated agglutination titers in the absence of an active infection, which must be considered when interpreting serology results. In the United States, because of the low number of suspected cases and the need for standardized assay conditions, the SAT is performed primarily by reference laboratories. A variation on this test, the microagglutination test (MAT), uses a microtiter format.

Rose Bengal Test

A second agglutination test, the Rose Bengal test, is a rapid slide agglutination test that utilizes a stained suspension of *B. abortus* buffered to a pH of 3.65 to inhibit nonspecific agglutinins (44). Rose Bengal is an inexpensive, simple, and sensitive test that can be performed rapidly in resource-limited settings.

Interpretation of test results. While studies with smaller numbers of samples have found the Rose Bengal test to have lower sensitivity than the SAT, a recent large-scale comparative study found that use of the Rose Bengal test with serum dilutions yielded a sensitivity and specificity similar to those of the SAT (45). While the Rose Bengal test performs well under optimal conditions, the varying sensitivity and specificity reported in the literature for this test has led to a recommendation by the World Health Organization that the results of the Rose Bengal test be confirmed by a second test method (46).

ELISA

Several commercial vendors offer ELISA kits for detection of *Brucella*-specific IgG and IgM, and in-house assays have been developed using *Brucella* antigen as well. ELISA has been reported to perform well in an area of endemicity (47). Further, it can be performed within a few hours and was shown to be superior to agglutination assays in diagnosis of chronic brucellosis (43). In an area of nonendemicity, IgM ELISA was reported to yield some false-positive results (48, 49). As a result, confirmation of positive ELISA results with serial sampling and a second test method, such as SAT, has been recommended (48).

Other Antibody Detection Assays

The Coombs test is used as a follow up to a negative SAT to detect incomplete, blocking, or non-agglutinating antibodies (50). In this test, the cell suspensions from the negative SAT are centrifuged. The resulting cell pellets are washed and incubated with anti-human IgG, then incubated to detect agglutination. The Coombs test is useful for complicated and chronic cases, in which it was shown to yield titers from 16-to 256-fold higher than the SAT (51). A second assay for the detection of nonagglutinating antibodies is the Brucellacapt (Vircell, Santa Fe, Spain), a commercially available immunocapture test for total anti-*Brucella* antibodies (52). This assay is simple to perform but was found to be inferior to the Coombs test for following small changes in antibody titer in chronically infected patients (53).

Interpretation of test results. Serologic tests continue to play an important role in diagnosis of brucellosis in the clinical laboratory. These assays are well suited for use in areas of endemicity because of their low cost and low degree of technical complexity. However, for each area, the appropriate cutoff for positive serology should be determined based on the regional prevalence of positive-serology *Brucella* spp. in the healthy population.

The interpretation of serologic test results for brucellosis requires consideration of the clinical presentation and the patient's detailed history, including possibility of zoonotic or occupational exposure to the agent. For patients with confirmed brucellosis, serological tests are used to monitor treatment progress. Declining antibody titers with antibiotic treatment are indicative of a good prognosis, while a rebound in titers suggests possible relapse or reinfection (43).

It should be emphasized that a single negative serology result is insufficient to rule out brucellosis. Since some patients may be seronegative at disease onset, paired serum samples taken at presentation and 2 weeks later should be compared and/or a second serologic test should be performed. *B. canis* and some of the newly described *Brucella* species differ in their LPS composition from the other zoonotic species and can therefore be missed using serologic assays based on LPS-containing antigen preparations from *B. abortus* or *B. melitensis* (54). A second instance in which serologic tests may fail to detect infection is occupational exposure to the veterinary vaccine strain RB51, which does not harbor the serodominant LPS O-antigen. In this case, high-risk exposures may warrant postexposure antibiotic prophylaxis (55).

In areas of endemicity, repeated exposure to *Brucella* spp., or past infection, may cause persistently high IgG titers in the absence of active infection. Since serology is based primarily on antibody responses to LPS, infections with bacteria that share epitopes on their LPS, including *Escherichia coli* O157, *Yersinia enterocolitica* O9, *Vibrio cholerae*, *Salmonella enterica* serotype Urbana, and *Francisella tularensis*, could elicit positive responses in the serological tests for brucellosis (56). However, in this case, the patient would not be expected to have the 4-fold increase in anti-*Brucella* titer between acute-and convalescent-phase sera that is required for a definitive diagnosis (43). In the United States, brucellosis is a reportable disease, and *Brucella* spp. are among the organisms that have been developed as bioweapons; therefore, a confirmed case of brucellosis in an individual with no history of exposure could prompt concerns of bioterrorism as well as a costly epidemiologic investigation by public health authorities (48). For this reason, a diagnosis based on serology in the absence of a positive culture result should utilize two independent test results and be prompted by a compatible clinical presentation and patient history.

Molecular Diagnosis

PCR has been shown to be a rapid and highly sensitive way to detect *Brucella* spp. DNA in serum and tissue samples (57). Multiple targets for PCR assays have been evaluated and have been shown to have differing levels of sensitivity. The 16S-23S rRNA spacer region, present in three copies in the genomes of *B. abortus*, *B. suis*, and *B. melitensis*, has shown promise as a diagnostic target; however, standardization is necessary. *Brucella* spp. DNA has been detected in circulation weeks to months after successful antibiotic treatment and resolution of symptoms, so a positive PCR result may not always be indicative of an active infection with *Brucella* spp. (58). PCR tests for the diagnosis of *Brucella* infection are offered only in a few reference laboratories and are not available commercially.

Francisella

Microbiologic Culture

Tularemia can be diagnosed by culturing the isolate from relevant clinical samples, by antigenic and molecular detection methodologies, and by serological analyses. *F. tularensis* is a notoriously fastidious organism that is difficult to culture, requires advanced containment laboratories, and is potentially hazardous to laboratory personnel, underscoring the challenges of recovery and culture of an isolate directly from clinical specimens. Isolation and culture of *Bartonella* spp. is covered in detail in the 11th edition of the *Manual of Clinical Microbiology*.

Serology

Serology relies on the presence of anti-*F. tularensis* antibodies and has been used historically for definitive diagnosis of tularemia, yet cross-reactivity has been observed (59). As such, most cases of tularemia are diagnosed qualitatively based on clinical presentation of symptoms compatible with tularemia coupled with semiquantitative serology.

Tube Agglutination and Microagglutination

During the course of infection, peak antibody responses typically occur during the end of the second week after

disease onset, at which point titers begin to decline slowly upon recovery from disease, although these antibody responses can be long-lived, having been shown to persist for years. Two agglutination methodologies, tube agglutination and microagglutination (MA), demonstrate marked sensitivity and specificity (59).

Interpretation of test results. When an individual presents clinically with symptoms compatible with tularemia, *F. tularensis* antibody titers of ≥160 during the acute phase of the disease support a presumptive tularemia diagnosis. Definitive tularemia diagnosis relies on a 4-fold rise in *F. tularensis* antibody titers between acute- and convalescent-phase sera, usually 2 to 4 weeks. While cross-reactivity has been reported at low titers with serum from patients with brucellosis or yersiniosis, the specificity of serology for tularemia is high. However, a titer ≥160 may also reflect past infection and may not be indicative of active disease (59), underscoring the importance of considering clinical symptoms in combination with serology for disease diagnosis.

ELISA

In addition to agglutination assays, a variety of ELISAs have been described, most of which use *F. tularensis*-derived LPS as antigen. ELISA detection methodologies have also been shown to achieve high degrees of sensitivity and specificity and also allow for the differentiation of antibody isotypes (60). More important, ELISA cannot distinguish past *F. tularensis* infections from current infections. A competitive ELISA (cELISA) assay was recently developed, based on the ability of serum antibodies to inhibit the binding of monoclonal antibodies (MAbs) directed against *F. tularensis* lipopolysaccharide antigens, and was reported to exhibit superior levels of sensitivity and specificity for serodiagnosis of human disease compared with the standard MA method (61).

More recently, a strategy termed *in vivo* microbial antigen discovery (InMAD) was reported for the identification of *F. tularensis* antigens that are shed into serum in mice during infection. While preliminary, such a strategy could ultimately lead to a more rapid diagnosis of *F. tularensis*, thereby facilitating timely, effective treatment of disease (62). In addition, recent efforts—comparing both commercially available and noncommercial immunochromatographic assay (ICA) (63) for tularemia diagnostics with the traditional, gold-standard MA assay—demonstrated that ICA achieved similar levels of sensitivity and specificity as MA, and the commercial ICA exhibited no cross-reactivity when screened against human immune and nonimmune sera. The ease of use of ICA indicates that this method could be more broadly adapted for tularemia diagnostics.

Immunological Methods

Immunofluorescence analysis has been broadly applied to detect *F. tularensis* in wild animal carcasses and laboratory necropsy specimens, but it has not been widely applied for the diagnosis of human tularemia due, in large part, to the lack of specialized reagents and media, the qualitative nature of the technique, and the inherently weak staining of *F. tularensis* using standard reagents.

The direct fluorescence antibody (DFA) assay, based on the use of fluorescein isothiocyanate (FITC)-labeled anti-whole cell *F. tularensis*, is a rapid and specific test used routinely for the identification of *F. tularensis* (type A and type B) by the Centers for Disease Control and Prevention. It should be noted that the DFA has sensitivity limitations, and in rare cases of infection caused by *F. philomiragia* or *F. tularensis* subsp. *novicida*, DFA results were negative (64, 65).

Molecular Methods

The development of molecular-based assays remains paramount both for the detection of *F. tularensis* and for the diagnosis of disease. Over the years, myriad PCR-based methodologies have emerged for tularemia diagnostics, and subsequent iterations of these assays have led to improved limits of detection and more rapid sample processing (66–68). PCR has been increasingly utilized to diagnose human disease, as culture of *F. tularensis* directly from human samples, long considered the gold standard for definitive diagnosis, remains challenging for the reasons mentioned above. The development of PCR assays for tularemia diagnostics have largely focused on targeting genes encoding the outer membrane lipoproteins Tul4 and FopA, as well as the *isfut2* insertion sequence element (69). Sequencing methodologies have recently been employed for the rapid identification of suspected isolates of *Francisella* species in clinical or environmental samples (70).

We would like to thank Christopher Polage for helpful discussions during the preparation of this section.

REFERENCES

1. **Wattam AR, Foster JT, Mane SP, Beckstrom-Sternberg SM, Beckstrom-Sternberg JM, Dickerman AW, Keim P, Pearson T, Shukla M, Ward DV, Williams KP, Sobral BW, Tsolis RM, Whatmore AM, O'Callaghan D.** 2014. Comparative phylogenomics and evolution of the brucellae: a path to virulence. *J Bacteriol* **196:**920–930.
2. **Whatmore AM.** 2009. Current understanding of the genetic diversity of *Brucella*, an expanding genus of zoonotic pathogens. *Infect Genet Evol* **9:**1168–1184.
3. **Ficht T.** 2010. Brucella taxonomy and evolution. *Future Microbiol* **5:**859–866.
4. **McCoy GW, Chapin CW.** 1912. Further observations on a plague-like disease of rodents with a preliminary note on the causative agent, *Bacterium tularense*. *J Infect Dis* **10:**61–72.
5. **Busse HJ, Huber B, Anda P, Escudero R, Scholz HC, Seibold E, Splettstoesser WD, Kämpfer P.** 2010. Objections to the transfer of *Francisella novicida* to the subspecies rank of *Francisella tularensis*: response to Johansson et al. *Int J Syst Evol Microbiol* **60:**1718–1720.
6. **Foley JE, Nieto NC.** 2010. Tularemia. *Vet Microbiol* **140:**332–338.
7. **Zangwill KM, Hamilton DH, Perkins BA, Regnery RL, Plikaytis BD, Hadler JL, Cartter ML, Wenger JD.** 1993. Cat scratch disease in Connecticut. Epidemiology, risk factors, and evaluation of a new diagnostic test. *N Engl J Med* **329:**8–13.
8. **Raoult D, Fournier PE, Drancourt M, Marrie TJ, Etienne J, Cosserat J, Cacoub P, Poinsignon Y, Leclercq P, Sefton AM.** 1996. Diagnosis of 22 new cases of Bartonella endocarditis. *Ann Intern Med* **125:**646–652.
9. **Bechtol D, Carpenter LR, Mosites E, Smalley D, Dunn JR.** 2011. *Brucella melitensis* infection following military duty in Iraq. *Zoonoses Public Health* **58:**489–492.
10. **Harding AL, Byers KB.** 2006. Epidemiology of laboratory-associated infections, p 53–77. *In* Fleming DO, Hunt DL (ed), *Biological Safety: Principles and Practices*, 4th ed. ASM Press, Washington, DC.
11. **Anderson BE, Neuman MA.** 1997. *Bartonella spp.* as emerging human pathogens. *Clin Microbiol Rev* **10:**203–219.
12. **Lucero NE, Corazza R, Almuzara MN, Reynes E, Escobar GI, Boeri E, Ayala SM.** 2010. Human *Brucella canis* outbreak linked to infection in dogs. *Epidemiol Infect* **138:**280–285.
13. **Tarnvik A, Berglund L.** 2003. Tularaemia. *Eur Respir J* **21:**361–373.

14. **Bergmans AM, Peeters MF, Schellekens JF, Vos MC, Sabbe LJ, Ossewaarde JM, Verbakel H, Hooft HJ, Schouls LM.** 1997. Pitfalls and fallacies of cat scratch disease serology: evaluation of *Bartonella henselae*-based indirect fluorescence assay and enzyme-linked immunoassay. *J Clin Microbiol* **35:**1931–1937.
15. **Regnery RL, Olson JG, Perkins BA, Bibb W.** 1992. Serological response to "*Rochalimaea henselae*" antigen in suspected cat-scratch disease. *Lancet* **339:**1443–1445.
16. **Conrad DA.** 2001. Treatment of cat-scratch disease. *Curr Opin Pediatr* **13:**56–59.
17. **Vermeulen MJ, Verbakel H, Notermans DW, Reimerink JH, Peeters MF.** 2010. Evaluation of sensitivity, specificity and cross-reactivity in Bartonella henselae serology. *J Med Microbiol* **59:**743–745.
18. **Tsuruoka K, Tsuneoka H, Kawano M, Yanagihara M, Nojima J, Tanaka T, Yamamoto M, Ichihara K.** 2012. Evaluation of IgG ELISA using *N*-lauroyl-sarcosine-soluble proteins of *Bartonella henselae* for highly specific serodiagnosis of cat scratch disease. *Diagn Microbiol Infect Dis* **74:**230–235.
19. **Hoey JG, Valois-Cruz F, Goldenberg H, Voskoboynik Y, Pfiffner J, Tilton RC, Mordechai E, Adelson ME.** 2009. Development of an immunoglobulin M capture-based enzyme-linked immunosorbent assay for diagnosis of acute infections with *Bartonella henselae*. *Clin Vaccine Immunol* **16:**282–284.
20. **Anderson B, Lu E, Jones D, Regnery R.** 1995. Characterization of a 17-kilodalton antigen of *Bartonella henselae* reactive with sera from patients with cat scratch disease. *J Clin Microbiol* **33:**2358–2365.
21. **Loa CC, Mordechai E, Tilton RC, Adelson ME.** 2006. Production of recombinant *Bartonella henselae* 17-kDa protein for antibody-capture enzyme-linked immunosorbent assay. *Diagn Microbiol Infect Dis* **55:**1–7.
22. **Cooper MD, Hollingdale MR, Vinson JW, Costa J.** 1976. A passive hemagglutination test for diagnosis of trench fever due to *Rochalimaea quintana*. *J Infect Dis* **134:**605–609.
23. **Pappalardo BL, Correa MT, York CC, Peat CY, Breitschwerdt EB.** 1997. Epidemiologic evaluation of the risk factors associated with exposure and seroreactivity to *Bartonella vinsonii* in dogs. *Am J Vet Res* **58:**467–471.
24. **Litwin CM, Johnson JM, Martins TB.** 2004. The *Bartonella henselae sucB* gene encodes a dihydrolipoamide succinyltransferase protein reactive with sera from patients with cat-scratch disease. *J Med Microbiol* **53:**1221–1227.
25. **Caponetti GC, Pantanowitz L, Marconi S, Havens JM, Lamps LW, Otis CN.** 2009. Evaluation of immunohistochemistry in identifying *Bartonella henselae* in cat-scratch disease. *Am J Clin Path* **131:**250–256.
26. **Relman DA, Loutit JS, Schmidt TM, Falkow S, Tompkins LS.** 1990. The agent of bacillary angiomatosis. An approach to the identification of uncultured pathogens. *N Engl J Med* **323:**1573–1580.
27. **Anderson B, Kelly C, Threlkel R, Edwards K.** 1993. Detection of *Rochalimaea henselae* in cat-scratch disease skin test antigens. *J Infect Dis* **168:**1034–1036.
28. **Duncan AW, Maggi RG, Breitschwerdt EB.** 2007. A combined approach for the enhanced detection and isolation of *Bartonella* species in dog blood samples: pre-enrichment liquid culture followed by PCR and subculture onto agar plates. *J Microbiol Methods* **69:**273–281.
29. **Dauga C, Miras I, Grimont PA.** 1996. Identification of *Bartonella henselae* and *B. quintana* 16s rDNA sequences by branch-, genus- and species-specific amplification. *J Med Microbiol* **45:**192–199.
30. **Kosoy M, Hayman DT, Chan KS.** 2012. *Bartonella* bacteria in nature: where does population variability end and a species start? *Infect Genet Evol* **12:**894–904.
31. **Anderson B, Sims K, Regnery R, Robinson L, Schmidt MJ, Goral S, Hager C, Edwards K.** 1994. Detection of *Rochalimaea henselae* DNA in specimens from cat scratch disease patients by PCR. *J Clin Microbiol* **32:**942–948.
32. **Colborn JM, Kosoy MY, Motin VL, Telepnev MV, Valbuena G, Myint KS, Fofanov Y, Putonti C, Feng C, Peruski L.** 2010. Improved detection of *Bartonella* DNA in mammalian hosts and arthropod vectors by real-time PCR using the NADH dehydrogenase gamma subunit (*nuo*G). *J Clin Microbiol* **48:**4630–4633.
33. **Renesto P, Gautheret D, Drancourt M, Raoult D.** 2000. Determination of the *rpoB* gene sequences of *Bartonella henselae* and *Bartonella quintana* for phylogenic analysis. *Res Microbiol* **151:**831–836.
34. **Rolain JM, Franc M, Davoust B, Raoult D.** 2003. Molecular detection of *Bartonella quintana*, *B. koehlerae*, *B. henselae*, *B. clarridgeiae*, *Rickettsia felis*, and *Wolbachia pipientis* in cat fleas, France. *Emerg Infect Dis* **9:**338–342.
35. **Birtles RJ, Hazel S, Bown K, Raoult D, Begon M, Bennett M.** 2000. Subtyping of uncultured bartonellae using sequence comparison of 16 S/23 S rRNA intergenic spacer regions amplified directly from infected blood. *Mol Cell Probes* **14:**79–87.
36. **Diaz MH, Bai Y, Malania L, Winchell JM, Kosoy MY.** 2012. Development of a novel genus-specific real-time PCR assay for detection and differentiation of *Bartonella* species and genotypes *J Clin Microbiol* **50:**1645–1649.
37. **Liberto MC, Lamberti AG, Marascio N, Matera G, Quirino A, Quirino A, Barreca GS, Baudi F, Focà A.** 2011. Molecular identification of *Bartonella quintana infection* using species-specific real-time PCR targeting transcriptional regulatory protein (*bqtR*) gene. *Mol Cell Probes* **25:**238–242.
38. **Buss SN, Gebhardt LL, Musser KA.** 2012. Real-time PCR and pyrosequencing for differentiation of medically relevant *Bartonella* species. *J Microbiol Methods* **91:**252–256.
39. **Al Dahouk S, Nockler K.** 2011. Implications of laboratory diagnosis on brucellosis therapy. *Expert Rev Anti Infect Ther* **9:**833–845.
40. **Araj GF.** 2011. *Brucella*, p 863–872. *In* Jorgensen JH, Pfaller MA (ed.), *Manual of Clinical Microbiology*, 11th ed. ASM Press, Washington, DC.
41. **Serre A.** 1989. Immunology and pathophysiology of human brucellosis, p 85–95. *In* Young EJ, Corbel MJ (ed), *Brucellosis: Clinical and Laboratory Aspects*. CDC Press, Boca Raton, FL.
42. **Centers for Disease Control and Prevention.** 1997. Case definitions for infectious conditions under public health surveillance. *MMWR Recomm Rep* **46:**1–55.
43. **Araj GF.** 2010. Update on laboratory diagnosis of human brucellosis. *Int J Antimicrob Agents* **36:**S12–17.
44. **Rose JE, Roepke MH.** 1957. An acidified antigen for detection of nonspecific reactions in the plate-agglutination test for bovine brucellosis. *Am J Vet Res* **18:**550–555.
45. **Diaz R, Casanova A, Ariza J, Moriyon I.** 2011. The Rose Bengal Test in human brucellosis: a neglected test for the diagnosis of a neglected disease. *PLoS Negl Trop Dis* **5:**e950.
46. **Corbel MJ.** 2006. Brucellosis in humans and animals. Food and Agriculture Organization of the United Nations, World Organisation for Animal Health, and World Health Organization. http://www.who.int/csr/resources/publications/Brucellosis.pdf. (Accessed October 17, 2015).
47. **Araj GF, Kattar MM, Fattouh LG, Bajakian KO, Kobeissi SA.** 2005. Evaluation of the PANBIO Brucella immunoglobulin G (IgG) and IgM enzyme-linked immunosorbent assays for diagnosis of human brucellosis. *Clin Diagn Lab Immunol* **12:**1334–1335.
48. **Centers for Disease Control and Prevention.** 2008. Public health consequences of a false-positive laboratory test result for Brucella—Florida, Georgia, and Michigan, 2005. *MMWR Morb Mortal Wkly Rep* **57:**603–605.

49. **Welch RJ, Litwin CM.** 2010. A comparison of Brucella IgG and IgM ELISA assays with agglutination methodology. *J Clin Lab Anal* **24:**160–162.
50. **Coombs RR, Mourant AE, Race RR.** 1945. A new test for the detection of weak and incomplete Rh agglutinins. *Br J Exp Pathol* **26:**255–266.
51. **Díaz R, Moriyon I.** 1989. Laboratory techniques in the diagnosis of human brucellosis, p 76–79. *In* Young EJ, Corbel MJ (ed), *Brucellosis: Clinical and Laboratory Aspects*. CRC Press, Boca Raton, FL.
52. **Orduna A, Almaraz A, Prado A, Gutierrez MP, Garcia-Pascual A, Dueñas A, Cuervo M, Abad R, Hernández B, Lorenzo B, Bratos MA, Torres AR.** 2000. Evaluation of an immunocapture-agglutination test (Brucellacapt) for serodiagnosis of human brucellosis. *J Clin Microbiol* **38:**4000–4005.
53. **Casanova A, Ariza J, Rubio M, Masuet C, Diaz R.** 2009. BrucellaCapt versus classical tests in the serological diagnosis and management of human brucellosis. *Clin Vaccine Immunol* **16:**844–851.
54. **Zygmunt MS, Jacques I, Bernardet N, Cloeckaert A.** 2012. Lipopolysaccharide heterogeneity in the atypical group of novel emerging Brucella species. *Clin Vaccine Immunol* **19:**1370–1373.
55. **Centers for Disease Control and Prevention.** 2012. Brucellosis: Serology. www.cdc.gov/brucellosis/clinicians/serology.html. (Accessed October 17, 2015.)
56. **Morse EV, Ristic M, Robertstad GW, Schneider DW.** 1953. Cross-agglutination reactions among *Brucella*, *Vibrio*, and other microorganisms. *Am J Vet Res* **14:**324–327.
57. **Tomaso H, Kattar M, Eickhoff M, Wernery U, Al Dahouk S, Straube E, Neubauer H, Scholz HC.** 2010. Comparison of commercial DNA preparation kits for the detection of Brucellae in tissue using quantitative real-time PCR. *BMC Infect Dis* **10:**100.
58. **Maas KS, Mendez M, Zavaleta M, Manrique J, Franco MP, Mulder M, Bonifacio N, Castañeda ML, Chacaltana J, Yagui E, Gilman RH, Guillen A, Blazes DL, Espinosa B, Hall E, Abdoel TH, Smits HL.** 2007. Evaluation of brucellosis by PCR and persistence after treatment in patients returning to the hospital for follow-up. *Am J Trop Med Hyg* **76:**698–702.
59. **Sato T, Fujita H, Ohara Y, Homma M.** 1990. Microagglutination test for early and specific serodiagnosis of tularemia. *J Clin Microbiol* **28:**2372–2374.
60. **Carlsson HE, Lindberg AA, Lindberg G, Hederstedt B, Karlsson KA, Agell BO.** 1979. Enzyme-linked immunosorbent assay for immunological diagnosis of human tularemia. *J Clin Microbiol* **10:**615–621.
61. **Sharma N, Hotta A, Yamamoto Y, Fujita O, Uda A, Fujita O, Uda A, Morikawa S, Yamada A, Tanabayashi K.** 2013. Detection of *Francisella tularensis*-specific antibodies in patients with tularemia by a novel competitive enzyme-linked immunosorbent assay. *Clin Vaccine Immunol* **20:**9–16.
62. **Nuti DE, Crump RB, Dwi Handayani F, Chantratita N, Peacock SJ, Bowen R, Felgner PL, Davies DH, Wu T, Lyons CR, Brett PJ, Burtnick MN, Kozel TR, AuCoin DP.** 2011. Identification of circulating bacterial antigens by in vivo microbial antigen discovery. *MBio* **16:**2.
63. **Kilic S, Celebi B, Yesilyurt M.** 2012. Evaluation of a commercial immunochromatographic assay for the serologic diagnosis of tularemia. *Diagn Microbiol Infect Dis* **74:**1–5.
64. **Brett M, Doppalapudi A, Respicio-Kingry LB, Myers D, Husband B, Pollard K, Mead P, Petersen JM, Whitener CJ.** 2012. *Francisella novicida* bacteremia after a near-drowning accident. *J Clin Microbiol* **50:**2826–2829.
65. **Kugeler KJ, Mead PS, McGowan KL, Burnham JM, Hogarty MD, Ruchelli E, Pollard K, Husband B, Conley C, Rivera T, Kelesidis T, Lee WM, Mabey W, Winchell JM, Stang HL, Staples JE, Chalcraft LJ, Petersen JM.** 2008. Isolation and characterization of a novel *Francisella* sp. from human cerebrospinal fluid and blood. *J Clin Microbiol* **46:**2428–2431.
66. **Lamps LW, Havens JM, Sjostedt A, Page DL, Scott MA.** 2004. Histologic and molecular diagnosis of tularemia: a potential bioterrorism agent endemic to North America. *Mod Pathol* **17:**489–495.
67. **Molins CR, Carlson JK, Coombs J, Petersen JM.** 2009. Identification of *Francisella tularensis* subsp. *tularensis* A1 and A2 infections by real-time polymerase chain reaction. *Diagn Microbiol Infect Dis* **64:**6–12.
68. **Junhui Z, Ruifu Y, Jianchun L, Songle Z, Meiling C, Fengxiang C, Hong C.** 1996. Detection of *Francisella tularensis* by the polymerase chain reaction. *J Med Microbiol* **45:**477–482.
69. **Kantardjiev T, Padeshki P, Ivanov IN.** 2007. Diagnostic approaches for oculoglandular tularemia: advantages of PCR. *Br J Ophthalmol* **91:**1206–1208.
70. **Kuroda M, Sekizuka T, Shinya F, Takeuchi F, Kanno T, Sata T, Asano S.** 2012. Detection of a possible bioterrorism agent, *Francisella* sp., in a clinical specimen by use of next-generation direct DNA sequencing. *J Clin Microbiol* **50:**1810–1812.

Mycotic and Parasitic Diseases

section I

VOLUME EDITOR: ROBERT G. HAMILTON
SECTION EDITOR: THOMAS B. NUTMAN

Introduction

THOMAS B. NUTMAN

53

Combining the sections on parasitic and fungal infections into one unit stems not so much from the similarity between parasites and fungi but rather from their not being part of the infectious diseases mainstream. From a phylogenetic perspective, parasites (even the single-cell protozoa) differ from the fungi by a considerable evolutionary distance; interestingly, based on phylogenetic analyses, the differences between protozoan parasites and fungi are less significant than the differences between protozoa and helminth parasites.

Parasitic diseases are historically defined as infectious illnesses caused by unicellular protozoa or multicellular helminths distinct from viral, bacterial, or fungal etiologic agents. They are the special health care problem of tropical and subtropical countries, where their marked prevalence imposes major medical and economic burdens. These infections afflict billions of people worldwide and are responsible for millions of deaths every year. The importance of parasitic illness has received recent additional emphasis by the emergence of *Toxoplasma*, *Leishmania*, *Cryptosporidium*, and *Strongyloides* as pathogens in patients who are immunosuppressed.

Both protozoan and helminth pathogens have characteristically complex life cycles, often with two or more developmental stages present in the host during infection. Because each stage of parasite development may be antigenically distinct, protozoan or helminth infections are often characterized by a series of discrete immune responses that evolve at different times during the course of disease. Immune responses directed against a single stage may be circumvented by parasite differentiation. Each stage of parasite development may also entail a change in tissue trophism, introducing a compartmental feature to the immune responses. This temporal evolution of antigenic complexity and tissue trophism is unique to parasite immunology and further distinguishes this field from that of viral, fungal, or bacterial immunology.

Nevertheless, the immunology and molecular biology of fungal and parasitic infections converge at several levels. First, based on parasite and yeast genomics, many of the diagnostic antigens used for both parasitic and fungal infections are more specific now than heretofore. Moreover, since the diagnosis of mycotic infections cannot always be definitively addressed by culture or histology, the diagnosis of most parasitic infections has relied most commonly on the identification of the organism in appropriately collected specimens. At present, diagnoses of both mycotic and parasitic infections are most often based on immunologic and molecular methods of diagnosis.

Indeed, antigen detection immunoassays have been extraordinarily useful in diagnosing infections caused by *Aspergillus*, *Candida*, *Cryptococcus*, *Histoplasma*, and *Paracoccidioides* among the fungi and in parasitic infections caused by *Entamoeba*, *Giardia*, *Cryptosporidium*, *Wuchereria*, and *Plasmodium*. Many of these antigen detection systems have moved into the commercial arena and are available for use. In contrast, PCR-based assays, although definitive in many instances, are not in widespread use, but a number of multiplex platforms are becoming available for clinical microbiology laboratories, albeit at a significant cost.

Continued efforts to improve the predictive value (both positive and negative) of immunologically and molecularly based assays will remain the major goal of those interested in the diagnosis of both mycotic and parasitic infections. Although heralded as the new diagnostic gold standard, molecularly based assays are not yet in the mainstream. Notwithstanding the cost of molecular assays and issues related to quality control, the time required for sample preparation, PCR itself, and detection of the product suggests that other methods for diagnosis of fungal and parasitic infections are on the horizon, with the most hope placed on rapid antigen detection systems or nonisothermal DNA amplification.

doi:10.1128/9781555818722.ch53

Immunological and Molecular Approaches for the Diagnosis of Parasitic Infections

PATRICIA P. WILKINS AND THOMAS B. NUTMAN

54

Definitive diagnosis of parasitic infections is made by identification of parasites in properly collected specimens or in affected tissues. Microscopy for observation and identification of parasites is the laboratory method of choice for the diagnosis of some important parasitic infections, namely, malaria, babesiosis, and enteric parasitic infections. There are, however, important parasitic diseases that cannot be diagnosed by microscopic examination of clinical specimens. In infections such as angiostrongyliasis, schistosomiasis, paragonimiasis, and strongyloidiasis, parasites may be detected in stool or other specimens, but due to the limitations of intermittent shedding or sampling, direct observation of parasites is not sensitive or reliable. So, for these infections and others caused by parasites that are localized and sequestered in tissues, such as baylisascariasis, cysticercosis, echinococcosis, toxocariasis, toxoplasmosis, or trichinellosis, detection of specific antibodies is almost always required to confirm clinical suspicion.

Most parasitic infections induce a vigorous humoral immune response, so the presence of parasite-specific antibodies can be a valuable indicator of infection, especially if the patient has no prior history of exposure. The presence of specific antibodies, however, does not necessarily indicate current infection in a patient who resides or has recently lived in an area of endemicity. In general, detection of antibodies to parasitic antigens indicates infection at some indeterminate time and not necessarily acute or current infection. Parasite-specific antibodies may persist for as little as 6 months after infection or treatment or for many years, depending on the infecting parasite.

The humoral immune response usually precedes clinical manifestations for most parasitic infections; therefore, IgG is being produced by the time serological testing is considered, making collection of acute-phase serum specimens and the ordering of assays to detect parasite-specific IgM-based assays unnecessary. Detection of IgA and IgE alone is not informative, so tests for parasite-specific IgG are the primary tests that should be ordered. The notable exception to this is detection of *Toxoplasma*-specific IgM and IgA as indicators of acute neonatal toxoplasmosis. In some cases, detection of parasite-specific IgG4 has proven useful and more specific than detection of parasite-specific IgG (1–4). IgG4 detection has been shown to be particularly useful for the diagnosis of filarial infections (5). In many cases, if infection with a parasite is suspected and blood film, stool, or urine examinations are either not indicated or negative, then a serology test for parasite-specific Ig/IgG antibodies should be requested. If the test for parasite-specific IgG is negative, a positive IgM, IgA, or IgE result is generally a false-positive reaction and should be interpreted with caution.

Serological testing for parasitic diseases is limited to a few commercial laboratories in the United States (Table 1), with confirmatory testing available at the Centers for Disease Control and Prevention (CDC). Commercial laboratories and the CDC utilize a combination of test types: commercial kits that are approved or cleared by the U.S. Food and Drug Administration (FDA) for *in vitro* diagnostic use, commercial kits that are manufactured for research use only, and laboratory-developed tests. Federal regulations require that laboratories conduct rigorous evaluations when commercial kits designated for research use and laboratory-developed tests are adopted for clinical diagnosis. The levels of reliability of commercially manufactured kits vary widely, so suspicious results, both positive and negative, should be repeated or confirmed. Standardized proficiency testing surveys for serology tests for parasitic diseases are limited (Table 2). The participant summaries include information about the performance of specific kits, if applicable. This information can be used to inform specific test selection. Proficiency must be demonstrated by alternative assessments using split-sample testing of patient-derived material if commercially prepared challenges are not available.

Parameters for development and evaluation of tests used for clinical diagnosis are mandated by CLIA regulations and can be found in guidance documents published by the CLSI, CAP, and FDA. Optimally, determinations of test sensitivity, specificity, and precision should be made using specimens collected from patients with definitive diagnoses. Unfortunately, a definitive diagnosis is often not possible for parasitic infections caused by tissue-dwelling parasites, such as those causing toxoplasmosis, toxocariasis, or trichinellosis. Specimens from well-defined clinical cases may be used for evaluations of tests for these diseases. Panels should be prepared from specimens that represent the spectrum of clinical illness and should reflect the diagnostic dilemmas encountered in clinical practice. For example, immunodiagnosis is needed prior to surgery if echinococcosis is suspected. Accordingly, tests for *Echinococcus*-specific antibody should be evaluated using some specimens that were collected prior to surgery. Patients who have undergone

doi:10.1128/9781555818722.ch54

TABLE 1 Serological testing for parasitic infections available in commercial laboratories[a]

Organism (disease)	Serological test(s) used at[b]:						
	CDC	ARUP	Focus	LabCorp	Mayo	PDC	Quest
Angiostrongylus cantonensis						EIA	
Ascaris		IgE[c]		IgE[c]	IgE[c]	EIA	
Babesia microti	IFA	IFA	IFA	IFA	IFA (Focus)		IFA
Babesia duncani	IFA		IFA				IFA (Focus)
Baylisascaris	IB						
Taenia solium (cysticercosis)	IB	EIA, IB	EIA, IB	EIA	EIA, IB (Focus)	EIA, IB	EIA, IB (Focus)
Echinococcus granulosus	IB	EIA	EIA, IB	EIA	EIA, IB (Focus)	EIA	IgE, EIA, IB (Focus)
Entamoeba histolytica (amebiasis)	EIA	EIA	EIA	EIA	EIA	EIA	
Fasciola						EIA	
Filaria	EIA	EIA	EIA		EIA (Focus)	EIA	EIA (Focus)
Giardia		IFA	IFA				IFA (Focus)
Hookworm						EIA	
Leishmania	IFA, EIA		IFA		IC	EIA	IFA (Focus)
Plasmodium (malaria)	IFA	EIA			IFA (PDC)	IFA	
Paragonimus	IB					EIA	
Schistosoma	EIA, IB	EIA	EIA	IgE[c]	FMI (Focus)	EIA	FMI (Focus)
Strongyloides	EIA	EIA	EIA		EIA (ARUP)	EIA	EIA (Focus)
Toxocara	EIA	EIA	EIA		EIA (Focus)	EIA	EIA (Focus)
Toxoplasma	EIA	EIA, ICMA	EIA, avidity	EIA, ICMA	EIA, dye test (PAMF), ELFA (PAMF)	EIA	EIA, dye test, avidity, AC/HS
Trichinella	EIA	EIA	EIA	EIA	EIA	EIA	EIA (Focus)
Trypanosoma cruzi	IFA, EIA, IB	IA	EIA	EIA	EIA	IA	

[a]Test offerings were gathered from review of the following laboratory Web pages (last accessed 1 September 2013): ARUP Laboratories (ARUP; http://www.aruplab.com); Focus Diagnostics (Focus; http://www.focusdx.com); Laboratory Corporation of America (LabCorp; http://www.labcorp.com); Mayo Medical Laboratories (Mayo; http://www.mayomedicallaboratories.com/); Parasitic Disease Consultants (PDC; http://www.parasitic.com); Quest Diagnostics, Nichols Institute of Valencia (Quest; http://www.questdiagnostics.com/); and PAMF, Palo Alto Medical Foundation, Palo Alto, CA (http://www.pamf.org/). A laboratory name in parentheses in the table indicates that the test is referred to that laboratory.

[b]Abbreviations: AC/HS, the test for differential agglutination of acetone (AC)-fixed tachyzoites versus that of formalin (HS)-fixed tachyzoites; IFA, indirect fluorescent antibody; EIA, enzyme immunoassay; IB, immunoblotting; FMI, fluorescent microsphere immunoassay; IC, immunochromatographic strip assay ; ELFA, enzyme-linked fluorescence assay; ICMA, immunochemiluminometric assay; dye test, Sabin-Feldman dye test; Diff Aggl, differential agglutination.

[c]IgE testing refers to allergen testing and is listed for completeness; clinical utility has not been demonstrated.

surgery for echinococcal liver cysts will almost always have detectable antibodies immediately after surgery; these same patients may have been seronegative prior to surgery. A test for echinococcosis that has been evaluated with specimens collected only postsurgery will have close to 100% sensitivity, but a test will have a lower sensitivity if it is evaluated with specimens collected before surgery. An understanding of test performance in the presurgery setting is important and, when available, provides a valuable basis for result interpretation to the clinician.

The antigen is generally the assay component which has the most influence on test sensitivity and specificity. Consideration of the specific parasite life cycle stage is critical when selecting antigens for immunodiagnosis. Ideally, antigens derived from the specific parasite stage seen in human infection are preferred over antigens that are present in all stages or only in intermediate hosts. For instance, diagnostic assays for schistosomiasis that utilize worm antigens theoretically detect infections earlier than those that utilize egg antigens (6). Other factors that affect test performance include the purity of the antigen and the solid phase used in the assay.

For decades, immunodiagnostic assays for parasitic infections were based on detection of antibodies to native parasite antigens present in crude parasite extracts. Over time, crude parasite materials have become more difficult to obtain as fewer laboratories maintain animal models of infection. Fortunately, the availability of recombinant antigens for the diagnosis of parasitic infections has increased. Recombinant-antigen-based assays have several advantages over existing technologies. In general, recombinant-protein-based assays are more specific because the cross-reacting molecules in the crude mixture are not present, but because recombinant-protein-based assays generally rely on one or just a few antigens, these methods may be less sensitive, since the full-scope extent of the humoral immune response

TABLE 2 CAP challenges for proficiency testing for parasitic infections[a]

Analyte	CAP panel code(s)	Challenge panel name	Grading method
Anti-*Toxoplasma* antibodies	VR3	Infectious disease serology	80% participant consensus
Anti-*Trypanosoma cruzi* antibodies	VM4	Viral markers	80% participant consensus
Anti-*Babesia* antibodies	TTD	Tick-transmitted diseases	80% participant consensus
Blood parasites for parasite identification in a parasite screen, namely, *Plasmodium*, *Babesia*, *Trypanosoma*, and microfilariae	BP	Blood parasite	80% participant consensus
Giardia for parasite identification in a parasite screen (parasitology, immunoassay), *Cryptosporidium* (immunoassay)	P, P3, P4, P5	Parasitology	80% participant consensus
Malaria antigen	RMAL	Rapid malaria detection	Educational challenge, not formally evaluated
Helminths	WID	Worm identification	Educational challenge, not formally evaluated

[a]Based on the 2014 CAP surveys.

is not measured. The use of recombinant proteins eliminates the need for crude parasite materials. Therefore, the development of recombinant-protein-based assays for diagnosing parasitic infections should be less expensive to manufacture and consequently may make reliable methods more available to reference, commercial, and hospital laboratories.

In addition to antibody detection assays, antigen detection assays are commonly used to confirm the diagnosis of parasitic infections. This is especially true for enteric protozoal infections, as detection of parasite antigens is indicative of current infection and testing can be completed in a short amount of time by most technicians. Many antigen detection systems are commercially available for the intestinal parasites *Cryptosporidium parvum*, *Entamoeba histolytica*, *Giardia lamblia*, and *Trichomonas vaginalis*. Antigen detection tests are also increasingly considered for the diagnosis of malaria. These tests will be discussed in detail below.

Detection of parasite nucleic acids by PCR is now available for diagnosing many parasitic infections. In general, parasite DNA can be detected in the same specimen type used for direct parasite detection; however, some fixatives typically used for parasitological examination, especially formalin, interfere with the DNA amplification process, making some fixed specimens unsuitable for PCR analyses. For a more comprehensive presentation of available molecular methods, we refer readers to a recently published text on molecular methods for parasitic disease diagnosis (7).

Although immunodiagnosis and antigen and nucleic acid detection methods are important laboratory tools used to establish a diagnosis for many parasitic infections, definitive diagnosis is made by visualization and identification of the parasite. For detailed procedures and information about the morphological identification of parasites of clinical importance, see the CDC website DPDx, http://dpd.cdc.gov/dpdx/, and other texts dedicated to classical parasitology (8, 9).

Finally, this review chapter will focus on the most frequently used methods for detection of parasite-specific antibodies that are currently used for the diagnosis of parasitic diseases in the United States. Experimental antibody detection tests may be discussed if they add insight into test selection or result interpretation. For some diseases, testing is not available in the United States. Although the CDC can recommend international laboratories where testing may be available, their results generally cannot be reported by referring laboratories, since international laboratories are not CLIA approved. Results from international laboratories may be treated as results from research tests. The terms "sensitivity" and "specificity," as used here, refer to diagnostic sensitivity and diagnostic specificity, or the ability of the test to detect diseased cases and truly negative cases, respectively.

SPECIMEN REQUIREMENTS

Specimens for Antibody Detection

Serum and plasma are acceptable specimens for virtually all serological tests that are used for parasitic-disease diagnosis. For toxocariasis and toxoplasmosis, aqueous and vitreous eye fluids may be tested when accompanied by a serum specimen. For central nervous system infections, such as cysticercosis or toxoplasmosis, cerebrospinal fluid (CSF) accompanied by a serum specimen may be tested. In general, acute- and convalescent-phase specimens are not required; valid results generally can be obtained by testing only one specimen because many parasitic infections have progressed past the acute stage when initially considered. Sera may be stored for up to a week with refrigeration prior to shipment but should be frozen if storage for a longer period is anticipated. Specimens for serological testing may be shipped at room temperature.

Specimens for Antigen Detection

Fresh or preserved stool samples are acceptable for most antigen detection testing for enteric protozoa, but refer to the specific manufacturer's recommendations in the package insert, as exceptions do exist. Venous blood collected in EDTA and fingerstick blood samples are acceptable specimens for testing using rapid malaria diagnostic tests. Generally, fresh specimens are preferred for molecular testing; however, stools fixed in polyvinyl alcohol (PVA) may be acceptable. Formalin-fixed specimens are not acceptable for molecular testing. Refer to the testing laboratory's specific shipping requirements before shipping specimens for antigen and molecular testing.

AFRICAN TRYPANOSOMIASIS

African sleeping sickness or human African trypanosomiasis (HAT), caused by *Trypanosoma brucei gambiense*, is diagnosed using a 3-step laboratory algorithm: screening, diagnostic confirmation, and staging (10). Detection of specific antibodies is the best method for screening; diagnostic confirmation and staging require examination of CSF for trypanosomes. The card agglutination test for trypanosomiasis (CATT/*T. b. gambiense*) is the most reliable test available for initial serological screening (11–13). The CATT utilizes whole, fixed, Coomassie blue-stained trypanosomes that react with serum IgG or IgM antibodies to form a visible precipitate. False-positive results can occur in patients with malaria and other parasitic diseases, including transient infection with nonhuman trypanosomes. Rare false-negative results have been reported and may be the result of infection with trypanosomes that lack the surface antigen (LiTat 1.3) used in the CATT assay. Positive CATT results must be confirmed by microscopic detection of trypanosomes in lymph node aspirates, blood, or CSF. If trypanosomes are present and HAT is confirmed, classification of HAT into the first (hemolymphatic) or second (meningoencephalitic) stage of the disease is recommended before treatment (14).

The CATT is available through the World Health Organization, Geneva, Switzerland, or the National Reference Centre for Parasitology (NRCP) in Montreal, Canada (https://www.mcgill.ca/tropmed/services/national-reference-centre-parasitology/immunodiagnostic-service).

AMEBIASIS CAUSED BY *ENTAMOEBA HISTOLYTICA*

Several protozoan species in the genus *Entamoeba* infect humans, but not all are pathogenic. *Entamoeba histolytica* is associated with both intestinal and extraintestinal infections. Antibody detection is most useful in patients with extraintestinal disease, i.e., amebic liver abscess, when organisms are not generally found upon stool examination. Antigen detection and PCR may be useful adjuncts to microscopic diagnosis especially for differentiating between pathogenic and nonpathogenic *Entamoeba* infections (15).

The serological tests for diagnosing amebiasis detect antibodies to antigens present in crude soluble extracts of axenically cultured organisms. Enzyme immunoassays (EIA) are most frequently used, but indirect hemagglutination assays (IHA) are also available in some laboratories. Various EIA kits are manufactured commercially, making serology available in most specialty laboratories and at larger research hospitals. EIA kits detect antibodies specific for *E. histolytica* in approximately 95% of patients with extraintestinal amebiasis, 70% of patients with active intestinal infections, and 10% of asymptomatic patients with intestinal *E. histolytica* infections. If antibodies are not detectable in patients with an acute presentation of suspected amebic liver abscess, a second specimen should be drawn 7 to 10 days later. If the second specimen does not show seroconversion, other agents should be considered. Detectable *E. histolytica*-specific antibodies may persist for years after successful treatment, so the presence of antibodies does not necessarily indicate acute or current infection. The specificity of the EIA that utilize culture-derived parasites is 95% or higher. Detection of *E. histolytica*-specific IgM antibodies has been reported but is not reliable; the sensitivity of the IgM tests is only about 65% in patients with invasive disease. Several commercial EIA kits for antibody detection are available in the United States.

Immunodetection of *E. histolytica* antigens in fecal specimens may be used to distinguish the morphologically identical pathogenic *E. histolytica* and nonpathogenic *Entamoeba dispar*. Several FDA-cleared kits for antigen detection of the *E. histolytica*/*E. dispar* group are available in the United States (Table 3). These assays detect the galactose-inhibitable adherence protein, which is necessary for pathogenesis, and have excellent sensitivity and specificity. Assays that detect the *E. histolytica*-specific antigen require a fresh or frozen stool sample instead of a fixed sample; stool has to be collected specifically for this test.

Differentiation of *E. histolytica* and *E. dispar* DNA can also be made by PCR. This assay is available in some commercial laboratories, in state public health laboratories, and from the CDC. Contact information for specific state health laboratories is available at the Association of Public Health Laboratories website, http://www.aphl.org.

AMEBIASIS CAUSED BY FREE-LIVING AMEBAE

Granulomatous Amebic Encephalitis

Granulomatous amebic encephalitis (GAE) caused by *Acanthamoeba* spp. and *Balamuthia mandrillaris* is best diagnosed by immunoperoxidase or immunofluorescent staining of parasites in tissue sections. Electron microscopy and observation of parasites in wet preparations of CSF have also been used successfully, although *Acanthamoeba* or *Balamuthia* is rarely found in CSF (16). Methods to detect *Balamuthia*-specific antibodies have been reported, but their usefulness in clinical diagnosis is unproven (16, 17).

Primary Amebic Meningoencephalitis

Primary amebic meningoencephalitis (PAM) is a rare and devastating infection of the brain caused by a single free-living ameba species, *Naegleria fowleri*. Because of the rapid progression of PAM, immediate diagnosis is required; immunodiagnosis is not useful. Like GAE, PAM is diagnosed by observation of parasites in CSF and biopsy specimens.

PCR methods that can differentiate all three free-living amebae discussed here have been developed and used successfully to diagnosis GAE or PAM (18).

ANGIOSTRONGYLIASIS

Immunodiagnostic tests for the detection of antibodies to *Angiostrongylus cantonensis*, which may cause eosinophilic meningitis, or *Angiostrongylus costaricensis*, the causative agent of abdominal angiostrongyliasis, are not commercially available (19). Serological testing is currently offered in a few laboratories worldwide; contact the Division of Parasitic Diseases & Malaria, CDC, at dpdx@cdc.gov for information on the availability of diagnostic testing.

TABLE 3 FDA-cleared tests for detection of parasite antigens[a]

Organism(s) and kit name	Manufacturer	Assay type[b]
Cryptosporidium, *Giardia*, and *Entamoeba histolytica*		
Triage Micro parasite panel	Alere	ICT
Cryptosporidium and *Giardia*		
Cryptosporidium/*Giardia* direct fluorescent antigen assay	IVD Research	DFA assay
Merifluor *Cryptosporidium*/*Giardia*	Meridian Biosciences	DFA assay
Immuno *Card* STAT! *Crypto*/*Giardia*	Meridian Biosciences	ICT
ProSpecT *Giardia*/*Cryptosporidium*	Thermo Scientific	EIA
Xpect *Giardia*/*Cryptosporidium* lateral-flow assay	Thermo Scientific	ICT
Giardia/*Cryptosporidium* Chek	TechLab	EIA
Giardia/*Cryptosporidium* Quik Chek	TechLab	ICT
Cryptosporidium		
ProSpecT *Cryptosporidium*	Thermo Scientific	EIA
Xpect *Cryptosporidium*	Thermo Scientific	ICT
Cryptosporidium II	TechLab	EIA
Giardia		
ProSpecT *Giardia* EZ	Thermo Scientific	EIA
ProSpecT *Giardia*	Thermo Scientific	EIA
Xpect *Giardia*	Thermo Scientific	ICT
Giardia II	TechLab	EIA
Entamoeba histolytica		
ProSpecT *Entamoeba histolytica*	Thermo Scientific	EIA
E. histolytica II	TechLab	EIA
Plasmodium		
BinaxNOW malaria	Alere	ICT
Trichomonas vaginalis		
OSOM *Trichomonas*	Sekisui	ICT

[a]Based on data from the FDA website (http://www.accessdata.fda.gov/scripts/cdrh/devicesatfda/) and the following manufacturers' websites: Alere (http://www.alere.com); Gold Standard Diagnostics (GSD; http://www.gsdx.us/); InBios (http://www.inbios.com/); IVD Research, Inc. (http://www.ivdresearch.com); Meridian Bioscience, Inc. (http://www.meridianbioscience.com); Thermo Scientific (http://www.thermoscientific.com/); Sekisui Diagnostics (http://www.sekisuidiagnotics.com); and TechLab, Inc. (http://www.techlab.com).

[b]DFA, direct fluorescent antibody; ICT, immunochromatographic card test; EIA, enzyme immunoassay.

A recently developed PCR test for *A. cantonensis* can be performed at the CDC for cases of acute eosinophilic meningoencephalitis. Clinical sensitivity is yet to be defined, but a positive result can be interpreted with confidence, whereas a negative result does not rule out angiostrongyliasis (20).

BABESIOSIS

Natural transmission of *Babesia microti* occurs primarily in the coastal areas of the northeastern United States and in Minnesota and Wisconsin. Rare human infections with *Babesia duncani* in California, Washington, Missouri, and Kentucky have occurred (includes strains formerly known as *Babesia* WA-1, WA-2, CA-5, and CA-6), *Babesia* CA-1, CA-3, and CA-4, and *Babesia divergens*-like organisms, which are antigenically distinct from *B. microti* (21). Because *Ixodes scapularis*, the primary tick vector of *B. microti* in the United States, also transmits the causative agents of Lyme disease and ehrlichiosis, dual and triple infections of *B. microti*, *Borrelia burgdorferi*, and *Ehrlichia* may occur (22, 23). Tick vectors for the other human *Babesia* species in the United States have not been described.

Diagnosis of *Babesia* infection should be made after microscopic review of thick and thin Giemsa-stained blood smears. Antibody detection tests are useful, however, for identifying infected individuals with very low levels of parasitemia (such as asymptomatic blood donors in transfusion-associated babesiosis), for posttherapy diagnosis after parasitemia is no longer detectable, and for discrimination between *Plasmodium falciparum* and *B. microti* infection in cases that cannot be differentiated by blood film examination.

The indirect fluorescent antibody (IFA) test using *B. microti* parasites as the antigen detects antibodies in 88 to 96% of patients with *B. microti* infection (24). IFA antigen slides are prepared using washed, parasitized erythrocytes produced in hamsters. Patients' antibody levels generally rise to ≥1:1,024 during the first weeks of illness and decline gradually over 6 months to levels of 1:16 to 1:256, but antibodies may remain detectable at low levels for a year or more. Antibodies produced in response to other tick-borne infections do not cross-react. Cross-reactions may occur in sera from patients with malaria.

Babesia microti, *B. duncani*, and *B. divergens* are antigenically distinct, and minimal cross-reactivity is seen with heterologous *Babesia* antigens; generally, antibody levels are highest with the homologous *Babesia* antigen. Therefore, a negative *B. microti* antibody result for a patient exposed on the West Coast may be uninformative and testing using a

B. duncani-specific test should be considered. There is a high level of background reactivity in the *B. duncani* IFA assay (25) that is not well understood, and this has led to false-positive results in the *B. duncani* IFA assay for patients who are not infected with this species. Positive *B. duncani* IFA results for patients with no history of exposure to ticks on the West Coast and no history of transfusion should be considered with caution and confirmed at the CDC. IFA assays for *B. microti* and *B. duncani* are available at the CDC and from commercial laboratories, and *B. microti* and *B. duncani* IFA antigen slides are also available commercially. IFA assays for infections caused by the *B. divergens*-like parasites are available at the CDC, after consultation.

B. microti PCR assays are available in several commercial laboratories and at the CDC. PCR is at least as sensitive as microscopy, but the persistence of *Babesia* DNA is variable, ranging from 3 weeks posttherapy to 3 or more months in untreated patients. Antibody detection is the initial test of choice for the detection of *B. microti* infection in asymptomatic infected blood donors or in patients posttherapy, because it is more sensitive than microscopy or nucleic acid detection in these situations. If *Babesia* organisms are observed and serology tests are negative, blood specimens should be collected in EDTA for species determinations made by DNA sequence analysis at the CDC (21).

BAYLISASCARIASIS

Baylisascariasis is a severe infection requiring immediate diagnosis. Histological sectioning of infected tissues is informative if parasites can be observed in the tissue sections, but organisms may not be present in the sections obtained, so negative results do not rule out infection. Immunodiagnostic methods have been the most reliable method for laboratory diagnosis. Antibodies can be detected in serum or CSF using an immunoblot assay that detects antibodies to a recombinant protein, repeated antigen 1 (rRAG1) (26). The rRAG1 immunoblot does not detect cross-reacting *Toxocara* antibodies and therefore represents an important improvement in testing over previously used EIA (27).

Because of the small number of cases reported to date, specimens are not available in sufficient quantity for robust calculations of sensitivity for any of the immunodiagnostic methods described for baylisascariasis. Serological testing for baylisascariasis using rRAG1-based immunoblotting is available at the CDC or the National Reference Center for Parasitology in Montreal, Canada.

CHAGAS' DISEASE

Infections with *Trypanosoma cruzi* may occur throughout Central and South America. During the acute stage of illness, blood film examination generally reveals the presence of trypomastigotes. During the chronic stage of infection, parasites are rare or absent from the circulation and immunodiagnosis is the method of choice for determining whether the patient is infected. Although differentiating between acute and chronic infection is very important in determining the necessity for therapy, serology cannot be used to make this distinction. A positive antibody response indicates only infection at some unknown time and not specifically acute infection.

When Chagas' disease is suspected in patients with HIV/AIDS, it is important to differentiate chagasic brain lesions from those caused by *Toxoplasma*. Serological tests as well as direct examination of CSF for parasites and PCR should be performed. Negative serology results can rule out Chagas' disease in these patients, especially in patients with no history of intravenous drug use (28). In contrast, serological tests may be negative for patients who are immunosuppressed due to organ transplantation (29, 30).

A variety of serological tests for the diagnosis of Chagas' disease are used throughout Latin America, where the greatest experience exists. Diagnosis usually requires positive results from at least two different serological methods (31). A laboratory algorithm that uses EIA methods for screening, followed by confirmatory testing if screening tests generate positive results, has been proposed. Serological methods include IHA, IFA assays, complement fixation, EIA, immunoblotting, and radioimmunoprecipitation (32–38). These assays detect antibodies that react with parasite antigens found in crude trypanosome extracts or in the excretory-secretory (ES) products of cultured parasites or recombinant proteins (39). An immunoblot which detects antibodies that react with the ES antigens of a trypomastigote fraction, TESA blotting, has been proposed as a reliable confirmatory test (40, 41).

The IFA assay, an EIA, and TESA blotting are employed at the CDC. IFA antigen slides are prepared from a suspension of epimastigotes, and crude soluble antigens of epimastigotes are used in EIA. Although the IFA assay is sensitive, cross-reactivity occurs with sera from patients with leishmaniasis. The sensitivities (93 to 98%) and specificities (99%, excluding patients with leishmaniasis) of EIA that use crude antigens are similar to those of the IFA assay. EIA kits utilize a variety of antigens, either crude parasite lysate, recombinant proteins, or a combination of both. The sensitivities and specificities of the EIA kits vary widely (39). Two FDA-cleared kits are available in the United States for clinical diagnosis (Table 4). In the United States, the radioimmunoprecipitation assay has been used as a confirmatory test for blood donor screening (36). It is important to recognize that a test that is FDA cleared for blood donor screening does not imply clearance or approval for *in vitro* diagnostic use.

Molecular detection of *T. cruzi* DNA is most useful for cases of transfusion or transplant transmission or for congenital Chagas' disease. Laboratory exposures can also be monitored using PCR. At the CDC, molecular detection of *T. cruzi* DNA is performed using a combination of three real-time PCR assays (42). Acceptable specimen types are EDTA blood (minimum of 2.2 ml), heart biopsy tissue (in saline or paraffin embedded), and, in cases of suspected cerebral involvement, CSF. Using PCR to detect *T. cruzi* DNA in EDTA blood is appropriate only when the parasitemia is expected to be high, such as in the acute phase of the infection or if reactivation of chronic Chagas' disease due to immunosuppression is suspected.

In the United States, specific laboratory testing to confirm Chagas' disease may be required before release of drugs that are available only under an investigational new drug (IND) application.

CRYPTOSPORIDIOSIS

Microscopic identification of *Cryptosporidium* parasites and detection of antigen in stool specimens are the current diagnostic tests of choice. Antigen detection methods provide sensitivity that is equal to or greater than microscopy. Table 3 lists 11 commercial products (two direct fluorescent antibody [DFA] tests, four EIA, and five rapid tests) that are FDA cleared (approved) for diagnosis of cryptosporidial infections. Seven of the kits are combined tests for *Cryptosporidium* and *Giardia*, and one test detects *Cryptosporidium*,

TABLE 4 Commercially available FDA-cleared kits for detection of parasite specific antibodies[a]

Organism and company, test	IgG kit(s)	IgM kit(s)
Echinococcus granulosus		
Euroimmun	EIA	
Leishmania		NA
InBios, Kalazar Detect	ICT	NA
Toxoplasma gondii		
Beckman	Access	Access
bioMérieux	Vidas, IgG avidity	Vidas
Bio-Rad	BioPlex, EIA	BioPlex, EIA
Diamedix	EIA, IFA	EIA
DiaSorin	Liaison	Liaison
GenBio	EIA, IFA	EIA, IFA
GSD	EIA	EIA
Ortho Clinical Diagnostics	Vitros	Vitros
Siemens	Advia, Immulite	Advia, Immulite
Trinity Biotech	EIA	EIA
Trypanosoma cruzi (Chagas' disease)		
Hemagen	EIA	NA
Wiener Laboratories	EIA	NA

[a]Based on data from the FDA website (http://www.accessdata.fda.gov/scripts/cdrh/devicesatfda/) and the following manufacturers' websites: Alere (http://www.alere.com), Beckman Coulter (http://www.beckmancoulter.com), bioMérieux (http://www.biomerieux-diagnotics.com), Bio-Rad (http://www.bio-rad.com), Diamedix (http://www.diamedix.com), DiaSorin (http://www.diasorin.com), Euroimmun US (http://www.euroimmun.us/fda-released/elisa), Gold Standard Diagnostics (GSD, http://www.gsdx.us/), GenBio (http://www.genbio.com), Hemagen (http://www.hemagen.com), Ortho (http://www.orthoclinical.com), Siemens (http://usa.healthcare.siemens.com/laboratory-diagnostics), Trinity Biotech (http://www.trinitybiotech.com), and Wiener (http://www.wiener-lab.com). NA, not applicable.

[b]Access, Vidas, Advia, Liaison, and Vitros are automated laboratory systems.

Giardia, and *E. histolytica*. The most sensitive (99%) and specific (100%) method is the DFA test, which identifies oocysts in concentrated or unconcentrated fecal samples by using a fluorescein isothiocyanate-labeled monoclonal antibody (43). A combined DFA test for the simultaneous detection of cryptosporidial oocysts and *Giardia* cysts is available; however, this method did not perform better than routine microscopy in a recent study (44).

Four commercial EIAs are available in the microplate format for the detection of cryptosporidial antigen in fresh or frozen stool samples and also in stool specimens preserved in formalin, merthiolate-iodine-formalin, or sodium acetate-acetic acid-formalin fixatives. Concentrated or PVA-treated samples are unsuitable for testing with antigen detection EIA kits. The kits are reportedly superior to microscopy (especially acid-fast staining), and their results show good correlation with those of the monoclonal antibody-based DFA test. In head-to-head studies comparing multiple kits in clinical settings, sensitivities ranged from 70% to 100%; specificities are typically high, 99% to 100% (43, 45–47). Laboratories which use these EIA kits need to be aware of potential problems with anecdotal reports of false-positive results and take steps to monitor a kit's performance (48).

Four rapid immunochromatographic assays are available for detection of *Cryptosporidium* antigens alone or in combination with *Giardia* or *Giardia* and *E. histolytica* (Table 3). These tests are easy to use and provide results for more than one organism in a single reaction device. Initial evaluations indicate sensitivity and specificity comparable to those of microplate assays (or EIA) (43).

PCR tests are available in commercial laboratories and at the CDC for detection of *Cryptosporidium* DNA in stool specimens (49). These tests are highly sensitive and specific but require either fresh stool specimens or stools collected in PVA. Formalin-fixed stools are not acceptable for molecular studies.

Tests for the detection of *Cryptosporidium*-specific antibodies are not currently recommended due to a lack of sensitivity and specificity. Serological tests have been reported for *Cryptosporidium*, but their use should be limited to epidemiological studies.

CYCLOSPORIASIS

Cyclosporiasis in humans is caused by *Cyclospora cayetanensis*. Currently, the most practical diagnostic method of diagnosis is identification of oocysts in stool specimens. The sediment from concentrated stool specimens can be examined microscopically with different techniques: wet mounts (by conventional light microscopy, which can be enhanced by UV fluorescence microscopy or differential interference contrast) or stained smears, using modified acid-fast stain or a modified safranin stain. If cyclosporiasis is suspected, these special tests should be ordered specifically, as classical ova and parasite examination may not detect *Cyclospora*. Tests for antibody detection for cyclosporiasis have not been developed to date. Sensitive and specific PCR tests are available and can be used to detect parasite DNA in stool specimens (50). Molecular tests require either fresh stool specimens or stools collected in PVA. Formalin-fixed stools are not acceptable for molecular studies.

CYSTICERCOSIS (LARVAL *TAENIA SOLIUM*)

Diagnosis of neurocysticercosis (NCC), caused by the larval stages of *Taenia solium*, is established using a combination of imaging and serological results. Today, the CDC enzyme-linked immunoelectrotransfer blot (CDC-EITB) assay and EIA are the antibody detection test formats most frequently used for the diagnosis of NCC.

The CDC-EITB assay, which utilizes partially purified *T. solium* antigens, is the immunodiagnostic test of choice for confirming a presumptive clinical and radiologic diagnosis of neurocysticercosis (51). Briefly, the CDC-EITB assay is an immunoblot test that detects antibodies to one or more of seven lentil lectin-bound glycoproteins (LLGP) present in an extract of *T. solium* cysts. It has a sensitivity superior to that of any other test yet evaluated.

In the original description of the assay, serum specimens from 97% of 108 confirmed parasitological cases of cysticercosis had detectable antibodies (52). No serum samples from 376 patients with other microbial infections contained antibodies that reacted with any of the *T. solium*-specific antigens. After several decades of use, the most important factors identified as determining positive immunoblot reactions are the numbers and stage of development of cysticerci. Cumulative clinical experience has confirmed that in patients with multiple (more than two) lesions, the test has a sensitivity of more than 95% (51). However, seropositivity in biopsy-confirmed patients with single, enhancing parenchymal cysts was <50%; in clinically defined patients with a single cyst but who were not biopsied, sensitivity was 70%. Seropositivity in the sera and CSF of patients with multiple but only

calcified cysts was 82% and 77%, respectively. Seropositivity in the sera and CSF of patients with intraventricular neurocysticercosis was 93% (single cyst) and 95% (two or more cysts). In all patients, regardless of their clinical presentation, the immunoblot assay is 10% more sensitive with serum than with CSF specimens: consequently, there is no need to obtain CSF solely for use in the immunoblot assay.

The specificity of the CDC-EITB assay using LLGP is remarkable (virtually 100%), with only rare anecdotal reports of false-positive results documented (53, 54). However, in one study, only 2 of 13 patients with antibodies to only the gp50 protein were associated with a clinical diagnosis of neurocysticercosis; seven cases had other final diagnoses (55). Therefore, in patients for whom the suspicion of neurocysticercosis is low, reactivity to the gp50 protein alone should be interpreted with caution.

Other EITB tests, or immunoblot methods, have been described (56) and are manufactured and offered by commercial laboratories (Table 1). These other EITB methods do not necessarily utilize the LLGP antigen extract used in the CDC-EITB assay, so interpretation of results from these other tests should be made carefully, recognizing that the performance attributes of the CDC-EITB assay may not apply to other immunoblot-based methods (57).

EIA methods continue to be used extensively for clinical diagnosis, mainly because of their technical simplicity. In general, EIA methods are reliable if CSF, not serum, is tested. Many EIA have high rates of false positivity (with specificities ranging from 81% to 97%) and false negativity (with sensitivities ranging from 62% to 93%) compared to the CDC-EITB assay (58–61); results should be confirmed using the CDC-EITB assay if they are deemed inconsistent with the clinical picture (62).

Serology is not useful for evaluating the outcomes and prognoses in patients treated with anthelmintics (63). However, recent studies showed that antigen detection may be useful in cases for monitoring NCC patients with live parasites. Antigen was detected more frequently in CSF than in serum, so CSF is the preferred specimen type for NCC antigen testing (64–66). Antigen testing is available at the CDC for management of specific cases after consultation.

It is important to note that the presence of *T. solium* ova or tapeworm segments in stool specimens does not diagnose NCC but rather taeniasis (infection with the adult tapeworm stage of the parasite). Identification and treatment of taeniasis are important public health measures that can prevent NCC. Follow-up with family members associated with cases of NCC reported to the Los Angeles County Health Department from 1988 to 1991 demonstrated at least one active tapeworm carrier among family contacts of 22% of locally acquired cases and 5% of imported cases (67).

ECHINOCOCCOSIS

Immunodiagnostic tests can be very helpful in the diagnosis of echinococcal disease, and they should be used before surgery (68, 69). However, the clinician must have some knowledge of the characteristics of the available tests and the factors associated with false results. False-positive reactions may occur in persons with other helminthic infections, cancer, and chronic immune disorders. Negative test results do not rule out echinococcosis because approximately 10% of patients with cysts are seronegative (70). The presence of detectable antibodies is dependent on the physical location, structural integrity, and viability of the larval cyst. Cysts in the liver are more likely to elicit an antibody response than cysts in the lungs, and, regardless of localization, antibody detection tests are least sensitive in patients with intact hyaline cysts. Cysts in the lungs, brain, and spleen are associated with decreased or nondetectable antibody levels, whereas those in bone appear to elicit a detectable immune response. Fissuration or rupture of a cyst is followed by an abrupt stimulation of antibody production. A patient with senescent, calcified, or dead cysts is generally found to be seronegative.

Detection of *Echinococcus*-specific IgG4 antibodies has been shown to be more sensitive than detection of total IgG and has been associated with progression of cystic echinococcosis (71, 72). Specific IgG4 is not specifically measured by any of the kits available today, but next-generation assays may exploit detection of IgG4.

Molecular tools are used primarily for isolate or strain identification for epidemiological purposes and not for clinical diagnosis.

Cystic Echinococcal Disease (*Echinococcus granulosus*)

EIA and immunoblotting are sensitive tests for detecting antibodies in the sera of patients with cystic echinococcal disease; sensitivity rates vary from 60 to 90%, depending on the characteristics of the cases. Crude hydatid cyst fluid is generally employed as the antigen. At present, the best available serologic diagnosis is obtained by using combinations of tests. EIA are used to screen all specimens; a positive reaction is confirmed by immunoblotting. Although these confirmatory assays give false-positive reactions with sera from 5 to 25% of persons with neurocysticercosis, the clinical and epidemiological presentation of neurocysticercosis patients should be rarely confused with that of cystic echinococcosis.

Antibody responses have also been monitored as a way of evaluating the results of treatment, but with mixed results. Following successful radical surgery, antibody levels decline and sometimes disappear; antibodies rise again if secondary hydatid cysts develop. Antibody levels do not consistently decline following chemotherapy. Consequently, the usefulness of serology to monitor the course of disease is limited; imaging techniques provide a more accurate assessment of the patient's condition.

Alveolar Echinococcal Disease (*Echinococcus multilocularis*)

Immunodiagnostic tests utilizing specific *E. multilocularis* antigens are available, but tests developed for the detection of *E. granulosus* antibodies can also be used, although *E. granulosus*-based immunoblot assays detect only 50% of *E. multilocularis* cases. EIA that use affinity-purified or recombinant forms of several *E. multilocularis* antigens, Em2, Em10, or Em18, are available in Europe and can detect specific antibodies in more than 95% of alveolar cases (73–76). Em18 is highly specific, so if positive results are obtained, a diagnosis of alveolar echinococcosis can be made. Tests for *E. multilocularis* infection are not presently available in the United States but may be in the immediate future. As in cystic echinococcosis, antibody detection tests are more useful for postoperative follow-up than for monitoring the effectiveness of chemotherapy.

FASCIOLIASIS

The acute manifestations of human fascioliasis may precede the appearance of eggs in the stool by several weeks; immunodiagnostic tests may be useful for early indication of *Fasciola* infection as well as for confirmation of chronic fascioliasis when egg production is low or sporadic and for

ruling out "pseudofascioliasis" associated with ingestion of parasite eggs in sheep or calf liver.

The current test of choice for immunodiagnosis of human *Fasciola hepatica* infection is an EIA that uses ES antigens combined with confirmation of positive results by immunoblotting (77, 78). Antibodies specific to *Fasciola* may be detectable within 2 to 4 weeks after infection, which is 5 to 7 weeks before eggs appear in stool. The sensitivity of the Falcon assay screening test (FAST) system enzyme-linked immunosorbent assay (FAST-ELISA) was reported to be 95%, while the sensitivity of immunoblotting using 12-, 17-, and 63-kDa antigens appeared to be 100%. Cross-reactivity may occur in the FAST-ELISA with serum specimens of patients with schistosomiasis. Antibody levels decrease to normal 6 to 12 months after chemotherapeutic cure and can be used to predict the success of therapy. More recently, an EIA that measures antibodies to a recombinant cathepsin L-protease has been developed (78). This assay reports greater than 99% sensitivity and 99% specificity and is available in the NRCP in Canada.

In the United States, specific laboratory testing to confirm fascioliasis may be required before release of drugs that are available only under an IND application. Testing for fascioliasis is available at the NRCP in Montreal, Canada.

FILARIAL INFECTIONS

Among the eight filarial species that commonly infect humans, the four most likely to be pathogenic are three blood-borne filariae—*Brugia malayi, Wuchereria bancrofti*, and *Loa loa*—and the skin-dwelling parasite *Onchocerca volvulus*. For each of these infections and the other filariae (*Mansonella perstans*, *Mansonella ozzardi*, *Mansonella streptocerca*, and *Brugia timori*) demonstration of the parasite or parasite DNA by PCR (microfilariae in the blood or skin or adult parasites in tissue samples) remains the gold standard for definitive diagnosis. Nevertheless, diagnosis can be elusive not only because occult infections (low parasite burdens) occur but also because microfilariae (for most *Brugia* and *Wuchereria* organisms at least) are nocturnally periodic.

Lymphatic Filariasis (*Wuchereria bancrofti* and *Brugia* spp.)

A definitive diagnosis of lymphatic filariasis can be made only by detection of *Wuchereria bancrofti* and *Brugia* species parasites and hence can be difficult. Adult worms localized in lymphatic vessels or lymph nodes are largely inaccessible. Microfilariae can be found in blood, in hydrocele fluid, or (occasionally) in other body fluids. Such fluids can be examined microscopically, either directly or—for greater sensitivity—after concentration of the parasites by the passage of fluid through a polycarbonate cylindrical pore filter (pore size, 3 μm) or by the centrifugation of fluid fixed in 2% formalin (Knott's concentration technique). The timing of blood collection is critical and should be based on the periodicity of the microfilariae in the region of endemicity involved. Many infected individuals do not have microfilaremia, and definitive diagnoses in such cases can be difficult. Assays for circulating antigens of *W. bancrofti* permit the diagnosis of microfilaremic and cryptic (amicrofilaremic) infection. Two tests are commercially available: one is an ELISA and the other a rapid-format immunochromatographic card test. Both assays have sensitivities that range from 96 to 100% and specificities that approach 100% (79, 80). There are currently no tests for circulating antigens in Brugian filariasis.

PCR-based assays for DNA of *W. bancrofti* and *B. malayi* in blood have been developed (81). A number of studies indicate that this diagnostic method has a sensitivity equivalent to or greater than those of parasitologic methods, detecting patent infection in almost all infected subjects.

Immunologically based diagnostics which measure IgG responses against crude extracts of *Brugia* or *Dirofilaria* worms have traditionally suffered from poor specificity. Extensive cross-reactivity is found in the sera of individuals infected with closely related helminth parasites and even certain protozoal parasites. Further, it is difficult to differentiate previous infection or exposure to the parasite (aborted infection) from current active infection; most residents of regions where filariasis is endemic are IgG antibody positive. Nevertheless, such serologic assays for IgG antibody have a definite place in diagnosis, as a negative assay result effectively excludes past or present infection. The prominent role of antifilarial antibodies of the IgG4 subclass in filarial infection has led to the development of serodiagnostic assays based on antibodies of this subclass. Antifilarial IgG4 assays have improved specificity (82), but positive assays may still be seen in uninfected individuals living in areas of endemicity and in those infected with other filarial species (e.g., *O. volvulus*, *L. loa*, and *Mansonella* spp.). More recently, a *Wuchereria bancrofti*-specific recombinant antigen (named Wb123) has been identified and used in both IgG4- and IgG-based immunoassays (ELISA, Luciferase immunoprecipitation assays, Luminex) for more-specific screening applications, with the understanding that, again, these antibody-based assays cannot distinguish between current and previous infections (83–85).

In cases of suspected lymphatic filariasis, examination of the scrotum or the female breast using high-frequency ultrasound in conjunction with Doppler techniques may result in the identification of motile adult worms within dilated lymphatics. Worms may be visualized in the lymphatics of the spermatic cord in up to 80% of men infected with *W. bancrofti*.

Confirmation of serological results obtained at commercial laboratories is usually required for release of therapeutics (e.g., diethylcarbamazine) administered under an IND application.

Onchocerciasis

Definitive diagnosis of onchocerciasis depends on the detection of an adult worm in an excised nodule or, more commonly, of microfilariae in a skin snip or in the anterior chamber of the eye using a slit lamp. Skin snips are obtained with a corneal-scleral punch, which collects a blood-free skin biopsy sample extending to just below the epidermis, or by lifting of the skin with the tip of a needle and excision of a small (1- to 3-mm) piece with a sterile scalpel blade. The biopsy tissue is incubated in tissue culture medium or in saline on a glass slide or flat-bottomed microtiter plate. After incubation for 2 to 4 h (or occasionally overnight in light infections), microfilariae emergent from the skin can be visualized by low-power microscopy.

Because detection of parasites in the skin is invasive and insensitive, immunodiagnostic assays have been sought. IgG antifilarial antibody assays, while positive in individuals with onchocerciasis, suffer from the same lack of specificity and positive predictive value seen in the blood-borne filarial infections. The combined use of three groups of recombinant antigens provided sensitivities and specificities that approach 100% for the serological assessment of onchocerciasis (86, 87). Although no recombinant antigen test is available commercially, an experimental rapid card test that detects IgG4 antibodies in serum or whole blood to the Ov-16 recombinant antigen has been shown to have

>90% sensitivity and specificity (88, 89) and should be available commercially in mid- to late 2014. Antigen detection methods for use on serum/plasma or urine specimens are theoretically feasible, but prototypes have lacked both specificity and sensitivity.

Assays using PCR to detect onchocercal DNA in skin snips are now in use in filariasis research laboratories and are highly sensitive and specific (90, 91).

Loiasis

Definitive diagnosis of loiasis requires the detection of microfilariae in the peripheral blood or the isolation of the adult worm from the eye or from a subcutaneous biopsy specimen from a site of swelling developing after treatment. PCR-based assays for the detection of *L. loa* DNA in blood are now available in filariasis research laboratories (and a few clinical microbiology departments) and are highly sensitive and specific.

Antifilarial IgG and IgG4 may be useful in confirming the diagnosis of loiasis in visitors to areas of endemicity who have suggestive clinical symptoms or unexplained eosinophilia; however, currently available methods using crude antigen extracts from *Brugia* or *Dirofilaria* species do not differentiate between *L. loa* and other filarial pathogens. The utility of such testing in populations living where the disease is endemic is limited by the presence of antifilarial antibodies in up to 95% of individuals in some regions. A *Loa*-specific recombinant antibody (Ll-SXP-1) has been tested; IgG4 antibody-based assays have been found to be >95% specific, but with limited (50%) sensitivity (92). When used with a luciferase immunoprecipitation system format, the Ll-SXP-1 test has been shown to provide a high degree of both sensitivity and specificity (93).

Confirmation of serological results obtained at commercial laboratories is usually required for release of therapeutics (e.g., diethylcarbamazine) administered under an IND application.

GIARDIASIS

Giardia lamblia is the most common human intestinal protozoal pathogen in the United States and is an important cause of diarrhea in children and adults. Outbreaks of disease are common within day care centers as a result of person-to-person contact and may also occur in communities as a result of drinking water contaminated by infected-human or -animal feces. Infected persons often excrete cysts intermittently, so multiple stools collected over at least several days must sometimes be examined to detect the parasite. Tests for antibody detection of *Giardia* infection are available at commercial laboratories but are not currently recommended because of a lack of sensitivity and specificity. Highly sensitive and specific PCR tests are available and can be used to detect parasite DNA in stool specimens (94). Molecular tests require either fresh stool specimens or stools collected in PVA. Formalin-fixed stools are not acceptable for molecular studies.

Table 3 lists 12 FDA-cleared (approved) kits for diagnosis of giardiasis (two DFA tests, five EIA, and five rapid tests). DFA assays that employ fluorescein isothiocyanate-labeled monoclonal antibody for detection of *Giardia* cysts may be purchased in a combined kit for the simultaneous detection of *Giardia* cysts and *Cryptosporidium* oocysts. Both the sensitivity and the specificity of these kits were 100% compared to those of microscopy. They may be used for quantitation of cysts and oocysts and thus may be useful for epidemiologic and control studies.

Five commercial EIA are available in the microplate format for the detection of *Giardia* antigen in fresh or frozen stool samples and also in stool specimens preserved in formalin, merthiolate-iodine-formalin, or sodium acetate-acetic acid-formalin fixatives. Concentrated or PVA samples are not suitable for testing with EIA kits. EIA kit sensitivity rates were recently reported as ranging from 94 to 100%, while all specificity rates were 100% (63, 95).

Five rapid immunochromatographic assays are available for the detection of *Giardia* alone or in combination with *Cryptosporidium* or *Cryptosporidium* and *E. histolytica*. These offer the advantage of short test times and multiple results in one reaction device. Initial evaluations indicate a sensitivity and specificity comparable to those of previously available tests.

GNATHOSTOMIASIS

Immunodiagnostic tests for the detection of antibodies to *Gnathostoma* are not available in the United States. If gnathostomiasis is suspected, contact the CDC at dpdx@cdc.gov for information on the availability of diagnostic testing.

LEISHMANIASIS

Diagnostic testing for leishmaniasis should include examination of bone marrow aspirates and tissue impression smears and culture for parasite isolation followed by isoenzyme analysis or molecular tests for species determination. If visceral leishmaniasis is suspected, antibody detection tests can be a useful adjunct to clinical findings. In contrast, the sensitivity of antibody tests for cutaneous leishmaniasis is poor, as most infections do not induce a detectable circulating antibody response to the parasite; serological testing in not recommended for cases of cutaneous leishmaniasis.

The IFA tests and EIA are used for the detection of antibodies to *Leishmania* (96). IFA slide antigens are prepared from cultured epimastigotes of various *Leishmania* species, while EIA antigens are usually crude solubilized epimastigotes. These procedures can differentiate leishmaniasis from other clinically similar conditions but cannot determine the species of *Leishmania*. Cross-reactions also occur in patients with antibodies to *T. cruzi* (Chagas' disease). Antibody detection tests can be a useful because test sensitivity is >95%. A recombinant protein, K39, has been used in rapid immunochromatographic card tests and EIA formats to detect *Leishmania*-specific antibodies with success in immunocompetent patients (97); however, the sensitivity is greatly reduced (~20%) in HIV-infected patients (98). More recently, another recombinant protein, rK28, has been evaluated in a limited study and has been shown to perform better than K39 in both EIA and a rapid diagnostic test (RDT) format (99).

Recently, molecular methods have been developed for discrimination of *Leishmania* species (100). This method is based on PCR amplification followed by DNA sequencing analysis of the *Leishmania* ITS2 fragment. The method was shown to be highly concordant with culture/isoenzyme analysis, and results can be obtained within days, compared to the weeks required for culture.

In the United States, specific laboratory testing to confirm leishmaniasis may be required before release of drugs that are available only under an IND application.

MALARIA

Diagnosis of malaria is based on microscopic review of thick and thin Giemsa-stained blood smears. Serological tests for

malaria antibodies are not recommended for diagnosing malaria except in a few specific instances: (i) testing a febrile patient suspected of having malaria who is repeatedly blood smear negative, (ii) diagnosing cases of suspected tropical splenomegaly syndrome, and (iii) screening blood donors involved in cases of transfusion-induced malaria. IFA tests and EIA are available in commercial laboratories in the United States (Table 1).

IFA tests for malarial antibody detection are 97% sensitive and 99% specific, but the presence of antibodies indicates that infection occurred at some time in the past and does not necessarily indicate current infection (101). Antibodies may persist for years, especially in cases from areas where malaria is endemic. Interestingly, antibody titers decreased significantly after treatment (within 6 months) in troops after their return from Vietnam, suggesting that antibodies may not be long lived in naive hosts (102). Although multiple IFA tests are frequently performed using IFA slides prepared from *Plasmodium falciparum*, *Plasmodium vivax*, or *Plasmodium malariae* parasites, determination of the infecting *Plasmodium* species should not be inferred from IFA titers.

There are many RDTs for the detection of *Plasmodium* antigens in blood or serum available outside the United States. One RDT has been cleared by the FDA for *in vitro* diagnostic use in the United States (Table 4). The BinaxNOW malaria test detects the histidine-rich protein 2 (HRP-2) of *P. falciparum* and lactate dehydrogenase, a pan-malarial parasite antigen. Carefully review the package insert for test interpretation. Recently, some *P. falciparum* isolates from Peru and nearby countries that lack the HRP-2 protein and thus produce false-negative results in the BinaxNOW malaria RDT were identified (103). Microscopic examination of Giemsa-stained blood films should be performed for all cases regardless of RDT results to determine the species of *Plasmodium* identified and to quantify the parasitemia as well as to rule out false-negative results from infections with HRP-2-negative strains. More information about the BinaxNOW malaria RDT is available at http://www.cdc.gov/malaria/diagnosis_treatment/rdt.html.

PCR is a sensitive method for diagnosing malaria (104) and is available in commercial laboratories, some state public health laboratories, and at the CDC. If malaria is suspected, submit blood smears for morphological examination and EDTA blood for PCR. The blood smears should be examined first for the presence of parasites. If malarial parasites are observed and the species is determined, the diagnosis is complete. However, if parasites are not observed or if parasites are observed but the infecting species cannot be determined morphologically, PCR can then be performed. PCR should also be ordered if cerebral malaria is suspected, as it is more sensitive than blood film examination for the diagnosis of cerebral malaria. *Plasmodium* DNA generally becomes nondetectable within a week of antimalarial chemotherapy.

For more information about malaria and its diagnosis, visit http://www.cdc.gov/malaria.

PARAGONIMIASIS

Pulmonary paragonimiasis is the most common presentation of patients infected with *Paragonimus* spp., although extrapulmonary (cerebral, abdominal) paragonimiasis may occur. Detection of eggs in the sputum or feces of patients with paragonimiasis is often difficult; therefore, serodiagnosis may be helpful in confirming infections and for monitoring the results of individual chemotherapy.

Both EIA and immunoblot tests are used for immunodiagnosis of paragonimiasis. The immunoblot assay for antibody detection performed with a crude antigen extract of *Paragonimus westermani* has been in use at the CDC since 1988 (105). Positive antibody reactions, based on demonstration of reactivity with an 8-kDa antigen, were obtained with serum samples of 96% of patients with parasitologically confirmed *P. westermani* infection. Specificity was ≥99%; of 210 serum specimens from patients with other parasitic and nonparasitic infections, only 1 serum sample from a patient with *Schistosoma haematobium* reacted. Antigens present in *P. westermani* extracts may also be useful for the diagnosis of infections with other *Paragonimus* species, such as *P. kellicotti*, but species-specific tests may be more sensitive (106, 107). Serological methods for clinical diagnosis are available only at the CDC at this time.

SCHISTOSOMIASIS

Antibody detection can be useful to indicate schistosome infection in patients who have traveled in areas of schistosomiasis endemicity if schistosome eggs cannot be demonstrated in fecal or urine specimens. The test sensitivities and specificities of the many tests reported for the serologic diagnosis of schistosomiasis vary widely and are influenced by both the type of antigen preparation used (crude, purified, adult worm, egg, cercarial) and the test format.

At the CDC, a combination of tests with purified adult worm antigens are used for antibody detection (108, 109). All serum specimens are initially tested by FAST-ELISA using *Schistosoma mansoni* adult microsomal antigen (MAMA). A positive reaction indicates infection with *Schistosoma* species. The sensitivity of the FAST-ELISA is 99% for *S. mansoni* infection, 95% for *Schistosoma haematobium* infection, and >50% for *Schistosoma japonicum* infection. The specificity of this assay for detecting schistosome infection is 99%. Because test sensitivity with the MAMA is reduced for species other than *S. mansoni*, immunoblots of the species appropriate to the patient's travel history are also tested to ensure antibody detection of *S. haematobium* and *S. japonicum* infections. Infections caused by *Schistosoma mekongi* can be detected using *S. japonicum* immunoblotting (110), and *Schistosoma intercalatum* can be diagnosed using *S. haematobium* blotting. The number of serum specimens from confirmed cases of *S. mekongi* and *S. intercalatum* is limited, so sensitivity cannot be calculated. Immunoblots with adult worm microsomal antigens are species specific, and so a positive antibody reaction indicates the infecting species. The presence of antibody is indicative only of schistosome infection at some time and cannot be correlated with clinical status, worm burden, egg production, or prognosis.

Immunodiagnostic tests offered in commercial laboratories utilize *S. mansoni* antigens. It is important to note that these assays may have limited sensitivity to detect infections caused by other schistosome species.

Detection of schistosome antigens in serum and urine has been suggested as an indicator of cure after chemotherapy. These techniques are being used in control programs in Africa, but antigen detection tests for clinical use are not yet available in the United States (111). Similarly, quantitative stool or urine exams can be performed, but their limits of detection are usually not adequate to monitor cure.

STRONGYLOIDIASIS

Immunodiagnostic tests for strongyloidiasis are indicated when the infection is suspected and the organism cannot be demonstrated by duodenal aspiration, string tests, or repeated examinations of stool. Antibody detection tests

should use antigens derived from *Strongyloides stercoralis* filariform larvae for the highest sensitivity and specificity. A variety of different EIA are currently available, and many have reported sensitivities in the range of 90 to 95% (112–116). Although some *Strongyloides* EIA perform well, with good sensitivity and specificity, other tests may be unreliable, neither sensitive nor specific. Cross-reactions in patients with most filarial infections and some other nematode infections may occur (117). Several limitations are recognized: approximately 5 to 10% of individuals infected with *Strongyloides* are seronegative, and a single antibody test result cannot be used to differentiate between past and current infection. A positive test warrants continuing efforts to establish a parasitological diagnosis followed by anthelmintic treatment. Suspicious results, positive or negative, which are not consistent with clinical presentation, should be confirmed in a reference laboratory.

The sensitivity for detecting *Strongyloides*-specific antibodies in immunocompromised patients is variable depending on the type or cause of immunosuppression. Reactivity in patients with HIV/AIDS or human T cell leukemia virus type 1 (HTLV-1) infection or hematological malignancies may be reduced (118, 119). Immunocompromised persons with disseminated strongyloidiasis usually have detectable IgG antibodies despite immunosuppression (120). Transplant recipients may be seronegative.

Serologic monitoring may be useful in the follow-up of treated immunocompetent patients; antibody levels decrease markedly within 6 months after successful chemotherapy, but the decrease is less dramatic in patients from areas of endemicity or in those who have been infected for years (121, 122).

The use of a recombinant protein, NIE, shows promise for improving the serodiagnosis of strongyloidiasis. In one evaluation, in immunocompetent persons, the assay demonstrated 97% sensitivity and 100% specificity; seropositivity was not associated with *Ascaris* or hookworm coinfections (116).

TOXOCARIASIS (LARVA MIGRANS)

Antibody detection tests are the best means of confirmation of a clinical diagnosis of visceral larva migrans (visceral toxocariasis), ocular larva migrans (ocular toxocariasis), and covert toxocariasis, the most common clinical syndromes associated with *Toxocara* infections (123, 124). The currently recommended serologic test for toxocariasis is an EIA that utilizes larval-stage antigens extracted from embryonated eggs or released *in vitro* by cultured infective larvae (125). *Toxocara canis* excretory-secretory antigens are preferable to larval extracts because they are convenient to produce and because an absorption-purification step is not required to obtain maximum specificity. *T. canis* excretory-secretory antigens prepared from *T. canis* larvae also detect antibodies produced during *Toxocara cati* infections (126).

Evaluation of the true sensitivity and specificity of serologic tests for toxocariasis in human populations is not possible because very few patients who have been definitively diagnosed exist. This inherent problem results in underestimations of sensitivity and specificity. Evaluation of the *Toxocara* EIA in groups of patients with presumptive diagnoses of visceral larva migrans or ocular larva migrans (OLM) indicated sensitivities of 78 and 73%, respectively, at an antibody titer of ≥1:32. When the cutoff titer for OLM cases was lowered to 1:8, sensitivity was increased to 90%. Further confirmation of the specificity of the serologic diagnosis of OLM can be obtained by testing aqueous or vitreous humor samples for antibodies. Specificity has been reported to be >90% at an antibody level of ≥1:32.

When interpreting the serologic findings, clinicians must be aware that a detectable antibody level may not necessarily indicate current clinical *Toxocara* infection. In addition, in most human populations, a number of those tested have positive EIA antibody levels that apparently reflect the prevalence of asymptomatic toxocariasis. In a recent study, approximately 14% of the U.S. population was determined to be seropositive, with the percentage varying according to age, race, and socioeconomic status (127).

TOXOPLASMOSIS

Numerous immunodiagnostic tests are available at commercial laboratories for toxoplasmosis diagnosis and are used to distinguish acute versus chronic toxoplasmosis. Commercial laboratories offer testing for *Toxoplasma*-specific IgG and IgM using kits that are FDA cleared or approved (Table 4). Additional tests, such as the Sabin-Feldman dye test, the test for differential agglutination of acetone (AC)-fixed versus formalin (HS)-fixed tachyzoites (AC/HS test), and an IgG avidity test, as well as tests for *Toxoplasma*-specific IgA and IgE, are used to try to establish the time of infection. The College of American Pathologists offers *Toxoplasma* antibody proficiency testing as part of the Infectious Disease Serology survey (Table 2). The participant summary includes information about the performance of the different kits that can be used to inform specific test selection. Commercial kit comparison studies indicated that most kits perform comparably in detecting *Toxoplasma*-specific IgG antibodies but vary markedly in detecting *Toxoplasma*-specific IgM antibodies (128). To help evaluate the accuracy of commercial *Toxoplasma* antibody test kits, the CDC created a *Toxoplasma* serum panel, the CDC 1998 *Toxoplasma* human serum panel, that contains known positive and negative sera. The FDA now requires that any new commercial test kit intended to measure *Toxoplasma* antibodies performs adequately based on results obtained using this panel (129), which is available from the CDC.

The Clinical and Laboratory Standards Institute has published a guideline entitled *Clinical Use and Interpretation of Serologic Tests for* Toxoplasma gondii to assist clinical microbiologists and physicians in interpreting serological tests for toxoplasmosis (130). EIA or IFA tests for IgG and IgM antibodies are the tests most commonly ordered. Patients should be initially tested for the presence of *Toxoplasma*-specific IgG antibodies to determine their immune status. A positive IgG titer indicates infection with the organism at some time. If more precise knowledge of the time of infection is necessary, then an IgG-positive person should have an IgM test performed by an IgM capture EIA. A negative IgM test essentially rules out infection in recent months. A positive IgM titer combined with a positive IgG titer may be suggestive of recent infection. However, *Toxoplasma*-specific IgM antibodies may be detected by EIA for as long as 18 months after acute acquired infection.

If a patient is tested initially for both *Toxoplasma*-specific IgM and IgG antibodies, the results will sometimes be positive for IgM but negative for IgG. A positive IgM result with a negative IgG result in the same specimen should be viewed with great suspicion. A follow-up serum specimen then should be collected 2 weeks after the first and tested together with the first specimen if possible. If the first specimen was drawn very early after infection, the patient should have highly positive IgG and IgM antibodies in the second sample. If the IgG is negative and the IgM is positive in

both specimens, the IgM result should be considered to be a false-positive result and the patient can be considered to be uninfected.

If the patient is pregnant, an IgG avidity test should then be performed. A high-avidity result in the first 12 to 16 weeks of pregnancy (with time dependent upon the commercial test kit) essentially rules out an infection acquired during gestation. A low-IgG-avidity result should not be interpreted as indicating recent infection, because some individuals have persistent low-IgG-avidity antibodies for many months after infection. Suspected recent infection of a pregnant woman should be confirmed prior to intervention by having samples tested at a toxoplasmosis reference laboratory, such as the Toxoplasmosis Serology Laboratory, Palo Alto Medical Foundation, Palo Alto, CA (http://www.pamf.org). Newborn infants suspected of having congenital toxoplasmosis should be tested by both an IgM- and an IgA-capture EIA. Detection of *Toxoplasma*-specific IgA antibodies is more sensitive than IgM detection in congenital infections.

Toxoplasma-specific IgG antibody levels in HIV-AIDS patients often are low to moderate, but occasionally no specific IgG antibodies can be detected. Because toxoplasmosis in HIV-AIDS patients and in patients with other immunodepressed disease states typically represents activation of a previously latent infection, tests for IgM antibodies are generally negative.

Detection of *T. gondii* DNA by PCR is useful for diagnosing congenital, ocular, and central nervous system toxoplasmosis and reactivation disease. PCR performed on amniotic fluid is especially useful to establish early diagnosis of congenital toxoplasmosis (131, 132).

TRICHINELLOSIS

The immunodiagnostic test for trichinellosis that is currently used in the United States is an EIA that detects antibodies specific to *Trichinella spiralis* ES products produced by cultured larvae (133). The TSL-1 group of larval secretory antigens is conserved in all species/isolates of *Trichinella* and thus can be used to detect infection in animals or people infected with any of the species of *Trichinella* currently recognized. Positive antibody reactions are detectable at some time during infection in serum samples of 80 to 100% of patients with clinically symptomatic trichinellosis. *Trichinella*-specific antibodies typically are detectable between 3 and 5 weeks after infection but may take as long as 60 days postinfection to develop (134, 135). As a result, serology may not be useful for diagnosing acute cases. Multiple serum specimens should be drawn several weeks apart to demonstrate seroconversion in patients whose initial specimen was negative. Positive serology results are ultimately seen in 80 to 100% of patients with clinically symptomatic trichinellosis. The antibody response is affected by the infecting dose of larvae: the higher the infecting dose, the sooner specific antibodies will develop. IgG, IgM, and IgE antibodies are detectable in many patients; however, tests based on IgG antibodies are most sensitive. Antibody levels peak in the second or third month postinfection and then decline slowly for several years. Antibody tests that utilize *T. spiralis* ES antigens can be used to detect human cases of trichinellosis caused by other *Trichinella* species (136, 137).

TRICHOMONIASIS

Trichomoniasis, an infection caused by *Trichomonas vaginalis*, is a common sexually transmitted disease. Diagnosis is made by detection of trophozoites in vaginal secretions or urethral specimens by wet-mount microscopic examination, culture, or detection of parasite antigens or nucleic acid. The sensitivities of the assays compared to that of culture were reported as 60% for wet mounts, 86% for DFA tests, 80% for the Affirm VP test, 78.5% for the OSOM rapid test, and 78% for the XenoStrip rapid test (138, 139). The DFA test, the nucleic acid probe test, and two rapid antigen detection tests are available commercially (Table 4). Antibody detection methods are not used for clinical diagnosis. PCR methods are also available to detect parasite-specific nucleic acids.

REFERENCES

1. **Ottesen EA, Skvaril F, Tripathy SP, Poindexter RW, Hussain R.** 1985. Prominence of IgG4 in the IgG antibody response to human filariasis. *J Immunol* **134:**2707–2712. PubMed
2. **Maher K, El Ridi R, Elhoda AN, El-Ghannam M, Shaheen H, Shaker Z, Hassanein HI.** 1999. Parasite-specific antibody profile in human fascioliasis: application for immunodiagnosis of infection. *Am J Trop Med Hyg* **61:**738–742. PubMed
3. **Santra A, Bhattacharya T, Chowdhury A, Ghosh A, Ghosh N, Chatterjee BP, Mazumder DN.** 2001. Serodiagnosis of ascariasis with specific IgG4 antibody and its use in an epidemiological study. *Trans R Soc Trop Med Hyg* **95:**289–292. PubMed
4. **Norsyahida A, Riazi M, Sadjjadi SM, Muhammad Hafiznur Y, Low HC, Zeehaida M, Noordin R.** 2013. Laboratory detection of strongyloidiasis: IgG-, IgG4- and IgE-ELISAs and cross-reactivity with lymphatic filariasis. *Parasite Immunol* **35:**174–179. PubMed
5. **Weil GJ, Curtis KC, Fischer PU, Won KY, Lammie PJ, Joseph H, Melrose WD, Brattig NW.** 2011. A multicenter evaluation of a new antibody test kit for lymphatic filariasis employing recombinant *Brugia malayi* antigen Bm-14. *Acta Trop* **120**(Suppl 1)**:**S19–S22. PubMed
6. **Jaureguiberry S, Paris L, Caumes E.** 2010. Acute schistosomiasis, a diagnostic and therapeutic challenge. *Clin Microbiol Infect* **16:**225–231.
7. **Liu D.** 2012. *Molecular Detection of Human Parasitic Pathogens*, 1st ed. CRC Press, Boca Raton, FL.
8. **Orihel TC, Ash LR.** 2007. *Atlas of Human Parasitology*, 5th ed. American Society of Clinical Pathology Press, Chicago, IL.
9. **Orhiel TC, Ash LR.** 1995. *Parasites in Human Tissues*, 1st ed. ASCP Press, Chicago, IL.
10. **Jamonneau V, Solano P, Garcia A, Lejon V, Djé N, Miezan TW, N'Guessan P, Cuny G, Büscher P.** 2003. Stage determination and therapeutic decision in human African trypanosomiasis: value of polymerase chain reaction and immunoglobulin M quantification on the cerebrospinal fluid of sleeping sickness patients in Côte d'Ivoire. *Trop Med Int Health* **8:**589–594. PubMed
11. **Magnus E, Vervoort T, Van Meirvenne N.** 1978. A card-agglutination test with stained trypanosomes (C.A.T.T.) for the serological diagnosis of *T. b. gambiense* trypanosomiasis. *Ann Soc Belg Med Trop* **58:**169–176. PubMed
12. **Chappuis F, Stivanello E, Adams K, Kidane S, Pittet A, Bovier PA.** 2004. Card agglutination test for trypanosomiasis (CATT) end-dilution titer and cerebrospinal fluid cell count as predictors of human African trypanosomiasis (*Trypanosoma brucei gambiense*) among serologically suspected individuals in southern Sudan. *Am J Trop Med Hyg* **71:**313–317. PubMed
13. **Chappuis F, Loutan L, Simarro P, Lejon V, Büscher P.** 2005. Options for field diagnosis of human African trypanosomiasis. *Clin Microbiol Rev* **18:**133–146. PubMed
14. **Lejon V, Bentivoglio M, Franco JR.** 2013. Human African trypanosomiasis. *Handb Clin Neurol* **114:**169–181. PubMed

15. **Tanyuksel M, Petri WA Jr.** 2003. Laboratory diagnosis of amebiasis. *Clin Microbiol Rev* **16:**713–729. PubMed
16. **Visvesvara GS, Moura H, Schuster FL.** 2007. Pathogenic and opportunistic free-living amoebae: *Acanthamoeba* spp., *Balamuthia mandrillaris*, *Naegleria fowleri*, and *Sappinia diploidea*. *FEMS Immunol Med Microbiol* **50:**1–26. PubMed
17. **Schuster FL, Yagi S, Wilkins PP, Gavali S, Visvesvara GS, Glaser CA.** 2008. *Balamuthia mandrillaris*, agent of amebic encephalitis: detection of serum antibodies and antigenic similarity of isolates by enzyme immunoassay. *J Eukaryot Microbiol* **55:**313–320. PubMed
18. **Qvarnstrom Y, da Silva AJ, Schuster FL, Gelman BB, Visvesvara GS.** 2009. Molecular confirmation of *Sappinia pedata* as a causative agent of amoebic encephalitis. *J Infect Dis* **199:**1139–1142. PubMed
19. **Wilkins PP, Qvarnstrom Y, Whelen AC, Saucier C, da Silva AJ, Eamsobhana P.** 2013. The current status of laboratory diagnosis of *Angiostrongylus cantonensis* infections in humans using serologic and molecular methods. *Hawaii J Med Public Health* **72**(Suppl 2)**:**55–57. PubMed
20. **Qvarnstrom Y, da Silva AC, Teem JL, Hollingsworth R, Bishop H, Graeff-Teixeira C, da Silva AJ.** 2010. Improved molecular detection of *Angiostrongylus cantonensis* in mollusks and other environmental samples with a species-specific internal transcribed spacer 1-based TaqMan assay. *Appl Environ Microbiol* **76:**5287–5289. PubMed
21. **Herwaldt BL, de Bruyn G, Pieniazek NJ, Homer M, Lofy KH, Slemenda SB, Fritsche TR, Persing DH, Limaye AP.** 2004. *Babesia divergens*-like infection, Washington State. *Emerg Infect Dis* **10:**622–629. PubMed
22. **Magnarelli LA, Dumler JS, Anderson JF, Johnson RC, Fikrig E.** 1995. Coexistence of antibodies to tick-borne pathogens of babesiosis, ehrlichiosis, and Lyme borreliosis in human sera. *J Clin Microbiol* **33:**3054–3057. PubMed
23. **Mitchell PD, Reed KD, Hofkes JM.** 1996. Immunoserologic evidence of coinfection with *Borrelia burgdorferi*, *Babesia microti*, and human granulocytic *Ehrlichia* species in residents of Wisconsin and Minnesota. *J Clin Microbiol* **34:**724–727. PubMed
24. **Krause PJ.** 2003. Babesiosis diagnosis and treatment. *Vector Borne Zoonotic Dis* **3:**45–51. PubMed
25. **Prince HE, Lapé-Nixon M, Patel H, Yeh C.** 2010. Comparison of the *Babesia duncani* (WA1) IgG detection rates among clinical sera submitted to a reference laboratory for WA1 IgG testing and blood donor specimens from diverse geographic areas of the United States. *Clin Vaccine Immunol* **17:**1729–1733. PubMed
26. **Rascoe LN, Santamaria C, Handali S, Dangoudoubiyam S, Kazacos KR, Wilkins PP, Ndao M.** 2013. Interlaboratory optimization and evaluation of a serological assay for diagnosis of human baylisascariasis. *Clin Vaccine Immunol* **20:**1758–1763. PubMed
27. **Dangoudoubiyam S, Vemulapalli R, Ndao M, Kazacos KR.** 2011. Recombinant antigen-based enzyme-linked immunosorbent assay for diagnosis of *Baylisascaris procyonis* larva migrans. *Clin Vaccine Immunol* **18:**1650–1655. PubMed
28. **Córdova E, Maiolo E, Corti M, Orduña T.** 2010. Neurological manifestations of Chagas' disease. *Neurol Res* **32:**238–244. PubMed
29. **Lazo J, Meneses AC, Rocha A, Ferreira MS, Marquez JO, Chapadeiro E, Lopes ER.** 1998. Chagasic meningoencephalitis in the immunodeficient. *Arq Neuropsiquiatr* **56:**93–97. PubMed
30. **Riarte A, Luna C, Sabatiello R, Sinagra A, Schiavelli R, De Rissio A, Maiolo E, Garcìa MM, Jacob N, Pattin M, Lauricella M, Segura EL, Vázquez M.** 1999. Chagas' disease in patients with kidney transplants: 7 years of experience 1989–1996. *Clin Infect Dis* **29:**561–567. PubMed
31. **Bern C, Montgomery SP, Herwaldt BL, Rassi A Jr, Marin-Neto JA, Dantas RO, Maguire JH, Acquatella H, Morillo C, Kirchhoff LV, Gilman RH, Reyes PA, Salvatella R, Moore AC.** 2007. Evaluation and treatment of Chagas disease in the United States: a systematic review. *JAMA* **298:**2171–2181. PubMed
32. **Kirchhoff LV, Gam AA, Gusmao RA, Goldsmith RS, Rezende JM, Rassi A.** 1987. Increased specificity of serodiagnosis of Chagas' disease by detection of antibody to the 72- and 90-kilodalton glycoproteins of *Trypanosoma cruzi*. *J Infect Dis* **155:**561–564. PubMed
33. **Chandler FW, Watts JC.** 1988. Immunofluorescence as an adjunct to the histopathologic diagnosis of Chagas' disease. *J Clin Microbiol* **26:**567–569. PubMed
34. **Gomes YM.** 1997. PCR and sero-diagnosis of chronic Chagas' disease. Biotechnological advances. *Appl Biochem Biotechnol* **66:**107–119. PubMed
35. **Chatel G, Gulletta M, Matteelli A, Marangoni A, Signorini L, Oladeji O, Caligaris S.** 1999. Short report: diagnosis of tick-borne relapsing fever by the quantitative buffy coat fluorescence method. *Am J Trop Med Hyg* **60:**738–739. PubMed
36. **Leiby DA, Wendel S, Takaoka DT, Fachini RM, Oliveira LC, Tibbals MA.** 2000. Serologic testing for *Trypanosoma cruzi*: comparison of radioimmunoprecipitation assay with commercially available indirect immunofluorescence assay, indirect hemagglutination assay, and enzyme-linked immunosorbent assay kits. *J Clin Microbiol* **38:**639–642. PubMed
37. **Malan AK, Avelar E, Litwin SE, Hill HR, Litwin CM.** 2006. Serological diagnosis of *Trypanosoma cruzi*: evaluation of three enzyme immunoassays and an indirect immunofluorescent assay. *J Med Microbiol* **55:**171–178. PubMed
38. **Diaz JH.** 2008. Recognizing and reducing the risks of Chagas disease (American trypanosomiasis) in travelers. *J Travel Med* **15:**184–195. PubMed
39. **Umezawa ES, Luquetti AO, Levitus G, Ponce C, Ponce E, Henriquez D, Revollo S, Espinoza B, Sousa O, Khan B, da Silveira JF.** 2004. Serodiagnosis of chronic and acute Chagas' disease with *Trypanosoma cruzi* recombinant proteins: results of a collaborative study in six Latin American countries. *J Clin Microbiol* **42:**449–452. PubMed
40. **Umezawa ES, Nascimento MS, Kesper N Jr, Coura JR, Borges-Pereira J, Junqueira AC, Camargo ME.** 1996. Immunoblot assay using excreted-secreted antigens of *Trypanosoma cruzi* in serodiagnosis of congenital, acute, and chronic Chagas' disease. *J Clin Microbiol* **34:**2143–2147. PubMed
41. **Furuchó CR, Umezawa ES, Almeida I, Freitas VL, Bezerra R, Nunes EV, Sanches MC, Guastini CM, Teixeira AR, Shikanai-Yasuda MA.** 2008. Inconclusive results in conventional serological screening for Chagas' disease in blood banks: evaluation of cellular and humoral response. *Trop Med Int Health* **13:**1527–1533. PubMed
42. **Qvarnstrom Y, Schijman AG, Veron V, Aznar C, Steurer F, da Silva AJ.** 2012. Sensitive and specific detection of *Trypanosoma cruzi* DNA in clinical specimens using a multi-target real-time PCR approach. *PLoS Negl Trop Dis* **6:**e1689.
43. **Johnston SP, Ballard MM, Beach MJ, Causer L, Wilkins PP.** 2003. Evaluation of three commercial assays for detection of *Giardia* and *Cryptosporidium* organisms in fecal specimens. *J Clin Microbiol* **41:**623–626. PubMed
44. **Manser M, Granlund M, Edwards H, Saez A, Petersen E, Evengard B, Chiodini P.** 2014. Detection of *Cryptosporidium* and *Giardia* in clinical laboratories in Europe—a comparative study. *Clin Microbiol Infect* **20:**O65–O71.
45. **Garcia LS, Shimizu RY.** 1997. Evaluation of nine immunoassay kits (enzyme immunoassay and direct fluorescence) for detection of *Giardia lamblia* and *Cryptosporidium parvum* in human fecal specimens. *J Clin Microbiol* **35:**1526–1529. PubMed

46. **Kehl KS, Cicirello H, Havens PL.** 1995. Comparison of four different methods for detection of *Cryptosporidium* species. *J Clin Microbiol* **33:**416–418. PubMed
47. **Zimmerman SK, Needham CA.** 1995. Comparison of conventional stool concentration and preserved-smear methods with Merifluor *Cryptosporidium/Giardia* direct immunofluorescence assay and ProSpecT *Giardia* EZ microplate assay for detection of *Giardia lamblia*. *J Clin Microbiol* **33:**1942–1943. PubMed
48. **Cronquist A, Beach M, Johnston S, DaSilva A, Centers for Disease Control and Prevention (CDC).** 2004. Manufacturer's recall of rapid cartridge assay kits on the basis of false-positive *Cryptosporidium* antigen tests—Colorado, 2004. *MMWR Morb Mortal Wkly Rep* **53:**198–199. PubMed
49. **Hadfield SJ, Robinson G, Elwin K, Chalmers RM.** 2011. Detection and differentiation of *Cryptosporidium* spp. in human clinical samples by use of real-time PCR. *J Clin Microbiol* **49:**918–924. PubMed
50. **Pieniazek NJ, Slemenda SB, da Silva AJ, Alfano EM, Arrowood MJ.** 1996. PCR confirmation of infection with *Cyclospora cayetanensis*. *Emerg Infect Dis* **2:**357–359. PubMed
51. **Rodriguez S, Wilkins P, Dorny P.** 2012. Immunological and molecular diagnosis of cysticercosis. *Pathog Glob Health* **106:**286–298. PubMed
52. **Tsang VC, Brand JA, Boyer AE.** 1989. An enzyme-linked immunoelectrotransfer blot assay and glycoprotein antigens for diagnosing human cysticercosis (*Taenia solium*). *J Infect Dis* **159:**50–59. PubMed
53. **Ong S, Talan DA, Moran GJ, Mower W, Newdow M, Tsang VC, Pinner RW, EMERGEncy ID NET Study Group.** 2002. Neurocysticercosis in radiographically imaged seizure patients in U.S. emergency departments. *Emerg Infect Dis* **8:**608–613. PubMed
54. **Kojic EM, White AC Jr.** 2003. A positive enzyme-linked immunoelectrotransfer blot assay result for a patient without evidence of cysticercosis. *Clin Infect Dis* **36:**e7–e9. PubMed
55. **Furrows SJ, McCroddan J, Bligh WJ, Chiodini P.** 2006. Lack of specificity of a single positive 50-kDa band in the electroimmunotransfer blot (EITB) assay for cysticercosis. *Clin Microbiol Infect* **12:**459–462.
56. **Gottstein B, Tsang VC, Schantz PM.** 1986. Demonstration of species-specific and cross-reactive components of *Taenia solium* metacestode antigens. *Am J Trop Med Hyg* **35:**308–313. PubMed
57. **Blocher J, Schmutzhard E, Wilkins PP, Gupton PN, Schaffert M, Auer H, Gotwald T, Matuja W, Winkler AS.** 2011. A cross-sectional study of people with epilepsy and neurocysticercosis in Tanzania: clinical characteristics and diagnostic approaches. *PLoS Negl Trop Dis* **5:**e1185. PubMed
58. **Feldman M, Plancarte A, Sandoval M, Wilson M, Flisser A.** 1990. Comparison of two assays (EIA and EITB) and two samples (saliva and serum) for the diagnosis of neurocysticercosis. *Trans R Soc Trop Med Hyg* **84:**559–562. PubMed
59. **Diaz JF, Verastegui M, Gilman RH, Tsang VC, Pilche JB, Gallo C, Garcia HH, Torres P, Montenegro T, Miranda E, The Cysticercosis Working Group in Peru (CWG).** 1992. Immunodiagnosis of human cysticercosis (*Taenia solium*): a field comparison of an antibody-enzyme-linked immunosorbent assay (ELISA), an antigen-ELISA, and an enzyme-linked immunoelectrotransfer blot (EITB) assay in Peru. *Am J Trop Med Hyg* **46:**610–615. PubMed
60. **Sloan L, Schneider S, Rosenblatt J.** 1995. Evaluation of enzyme-linked immunoassay for serological diagnosis of cysticercosis. *J Clin Microbiol* **33:**3124–3128. PubMed
61. **Wilkins PP, Wilson M, Allan J, Tsang V.** 2002. *Taenia solium* cysticercosis: immunodiagnosis of neurocysticercosis and taeniasis, p 329–341. *In* Singh G, Prabhkar S (ed), Taenia solium C*ysticercosis*, vol 1. CABI Publishing, Oxon, UK.
62. **White AC Jr.** 2000. Neurocysticercosis: updates on epidemiology, pathogenesis, diagnosis, and management. *Annu Rev Med* **51:**187–206. PubMed
63. **Garcia HH, Gilman RH, Catacora M, Verastegui M, Gonzalez AE, Tsang VC, Cysticercosis Working Group in Peru.** 1997. Serologic evolution of neurocysticercosis patients after antiparasitic therapy. *J Infect Dis* **175:**486–489. PubMed
64. **Rodriguez S, Dorny P, Tsang VC, Pretell EJ, Brandt J, Lescano AG, Gonzalez AE, Gilman RH, Garcia HH, Cysticercosis Working Group in Peru.** 2009. Detection of *Taenia solium* antigens and anti-*T. solium* antibodies in paired serum and cerebrospinal fluid samples from patients with intraparenchymal or extraparenchymal neurocysticercosis. *J Infect Dis* **199:**1345–1352. PubMed
65. **Shey-Njila O, Zoli PA, Awah-Ndukum J, Nguekam, Assana E, Byambas P, Dorny P, Brandt J, Geerts S.** 2003. Porcine cysticercosis in village pigs of North-West Cameroon. *J Helminthol* **77:**351–354. PubMed
66. **Zea-Vera A, Cordova EG, Rodriguez S, Gonzales I, Pretell EJ, Castillo Y, Castro-Suarez S, Gabriël S, Tsang VC, Dorny P, Garcia HH, Cysticercosis Working Group in Peru.** 2013. Parasite antigen in serum predicts the presence of viable brain parasites in patients with apparently calcified cysticercosis only. *Clin Infect Dis* **57:**e154–e159. PubMed
67. **Sorvillo FJ, Waterman SH, Richards FO, Schantz PM.** 1992. Cysticercosis surveillance: locally acquired and travel-related infections and detection of intestinal tapeworm carriers in Los Angeles County. *Am J Trop Med Hyg* **47:**365–371. PubMed
68. **McManus DP, Zhang W, Li J, Bartley PB.** 2003. Echinococcosis. *Lancet* **362:**1295–1304. PubMed
69. **Siles-Lucas MM, Gottstein BB.** 2001. Molecular tools for the diagnosis of cystic and alveolar echinococcosis. *Trop Med Int Health* **6:**463–475. PubMed
70. **Maddison SE, Slemenda SB, Schantz PM, Fried JA, Wilson M, Tsang VC.** 1989. A specific diagnostic antigen of *Echinococcus granulosus* with an apparent molecular weight of 8 kDA. *Am J Trop Med Hyg* **40:**377–383. PubMed
71. **Shambesh MK, Craig PS, Wen H, Rogan MT, Paolillo E.** 1997. IgG1 and IgG4 serum antibody responses in asymptomatic and clinically expressed cystic echinococcosis patients. *Acta Trop* **64:**53–63. PubMed
72. **Daeki AO, Craig PS, Shambesh MK.** 2000. IgG-subclass antibody responses and the natural history of hepatic cystic echinococcosis in asymptomatic patients. *Ann Trop Med Parasitol* **94:**319–328. PubMed
73. **Gottstein B.** 1985. Purification and characterization of a specific antigen from *Echinococcus multilocularis*. *Parasite Immunol* **7:**201–212. PubMed
74. **Helbig M, Frosch P, Kern P, Frosch M.** 1993. Serological differentiation between cystic and alveolar echinococcosis by use of recombinant larval antigens. *J Clin Microbiol* **31:**3211–3215. PubMed
75. **Ito A, Ma L, Schantz PM, Gottstein B, Liu YH, Chai JJ, Abdel-Hafez SK, Altintas N, Joshi DD, Lightowlers MW, Pawlowski ZS.** 1999. Differential serodiagnosis for cystic and alveolar echinococcosis using fractions of *Echinococcus granulosus* cyst fluid (antigen B) and *E. multilocularis* protoscolex (EM18). *Am J Trop Med Hyg* **60:**188–192. PubMed
76. **Ito A, Sako Y, Yamasaki H, Mamuti W, Nakaya K, Nakao M, Ishikawa Y.** 2003. Development of Em18-immunoblot and Em18-ELISA for specific diagnosis of alveolar echinococcosis. *Acta Trop* **85:**173–182. PubMed
77. **Hillyer GV.** 1993. Serological diagnosis of *Fasciola hepatica*. *Parasitol Dia* **17:**130–136.

78. **Gonzales Santana B, Dalton JP, Vasquez Camargo F, Parkinson M, Ndao M.** 2013. The diagnosis of human fascioliasis by enzyme-linked immunosorbent assay (ELISA) using recombinant cathepsin L protease. *PLoS Negl Trop Dis* **7:**e2414. PubMed
79. **Chanteau S, Moulia-Pelat JP, Glaziou P, Nguyen NL, Luquiaud P, Plichart C, Martin PM, Cartel JL.** 1994. Og4C3 circulating antigen: a marker of infection and adult worm burden in *Wuchereria bancrofti* filariasis. *J Infect Dis* **170:**247–250. PubMed
80. **Weil GJ, Lammie PJ, Weiss N.** 1997. The ICT filariasis test: a rapid-format antigen test for diagnosis of bancroftian filariasis. *Parasitol Today* **13:**401–404. PubMed
81. **Zhong M, McCarthy J, Bierwert L, Lizotte-Waniewski M, Chanteau S, Nutman TB, Ottesen EA, Williams SA.** 1996. A polymerase chain reaction assay for detection of the parasite *Wuchereria bancrofti* in human blood samples. *Am J Trop Med Hyg* **54:**357–363. PubMed
82. **Lal RB, Ottesen EA.** 1988. Enhanced diagnostic specificity in human filariasis by IgG4 antibody assessment. *J Infect Dis* **158:**1034–1037. PubMed
83. **Hamlin KL, Moss DM, Priest JW, Roberts J, Kubofcik J, Gass K, Streit TG, Nutman TB, Eberhard ML, Lammie PJ.** 2012. Longitudinal monitoring of the development of antifilarial antibodies and acquisition of *Wuchereria bancrofti* in a highly endemic area of Haiti. *PLoS Negl Trop Dis* **6:**e1941.
84. **Kubofcik J, Fink DL, Nutman TB.** 2012. Identification of Wb123 as an early and specific marker of *Wuchereria bancrofti* infection. *PLoS Negl Trop Dis* **6:**e1930.
85. **Steel C, Golden A, Kubofcik J, LaRue N, de Los Santos T, Domingo GJ, Nutman TB.** 2013. Rapid *Wuchereria bancrofti*-specific antigen Wb123-based IgG4 immunoassays as tools for surveillance following mass drug administration programs on lymphatic filariasis. *Clin Vaccine Immunol* **20:**1155–1161. PubMed
86. **Ramachandran CP.** 1993. Improved immunodiagnostic tests to monitor onchocerciasis control programmes—a multicenter effort. *Parasitol Today* **9:**77–79. PubMed
87. **Burbelo PD, Leahy HP, Iadarola MJ, Nutman TB.** 2009. A four-antigen mixture for rapid assessment of *Onchocerca volvulus* infection. *PLoS Negl Trop Dis* **3:**e438. PubMed
88. **Weil GJ, Steel C, Liftis F, Li BW, Mearns G, Lobos E, Nutman TB.** 2000. A rapid-format antibody card test for diagnosis of onchocerciasis. *J Infect Dis* **182:**1796–1799. PubMed
89. **Golden A, Steel C, Yokobe L, Jackson E, Barney R, Kubofcik J, Peck R, Unnasch TR, Nutman TB, de los Santos T, Domingo GJ.** 2013. Extended result reading window in lateral flow tests detecting exposure to *Onchocerca volvulus*: a new technology to improve epidemiological surveillance tools. *PLoS One* **8:**e69231. PubMed
90. **Boatin BA, Toé L, Alley ES, Nagelkerke NJ, Borsboom G, Habbema JD.** 2002. Detection of *Onchocerca volvulus* infection in low prevalence areas: a comparison of three diagnostic methods. *Parasitology* **125:**545–552. PubMed
91. **Lakwo TL, Garms R, Rubaale T, Katabarwa M, Walsh F, Habomugisha P, Oguttu D, Unnasch T, Namanya H, Tukesiga E, Katamanywa J, Bamuhiiga J, Byamukama E, Agunyo S, Richards F.** 2013. The disappearance of onchocerciasis from the Itwara focus, western Uganda after elimination of the vector *Simulium neavei* and 19 years of annual ivermectin treatments. *Acta Trop* **126:**218–221. PubMed
92. **Klion AD, Vijaykumar A, Oei T, Martin B, Nutman TB.** 2003. Serum immunoglobulin G4 antibodies to the recombinant antigen, Ll-SXP-1, are highly specific for *Loa loa* infection. *J Infect Dis* **187:**128–133. PubMed
93. **Burbelo PD, Ramanathan R, Klion AD, Iadarola MJ, Nutman TB.** 2008. Rapid, novel, specific, high-throughput assay for diagnosis of *Loa loa* infection. *J Clin Microbiol* **46:**2298–2304. PubMed
94. **Asher AJ, Waldron LS, Power ML.** 2012. Evaluation of a PCR protocol for sensitive detection of *Giardia* intestinalis in human faeces. *Parasitol Res* **110:**853–858. PubMed
95. **Aldeen WE, Carroll K, Robison A, Morrison M, Hale D.** 1998. Comparison of nine commercially available enzyme-linked immunosorbent assays for detection of *Giardia lamblia* in fecal specimens. *J Clin Microbiol* **36:** 1338–1340. PubMed
96. **Sundar S, Rai M.** 2002. Laboratory diagnosis of visceral leishmaniasis. *Clin Diagn Lab Immunol* **9:**951–958. PubMed
97. **Sundar S, Reed SG, Singh VP, Kumar PC, Murray HW.** 1998. Rapid accurate field diagnosis of Indian visceral leishmaniasis. *Lancet* **351:**563–565. PubMed
98. **Medrano FJ, Cañavate C, Leal M, Rey C, Lissen E, Alvar J.** 1998. The role of serology in the diagnosis and prognosis of visceral leishmaniasis in patients coinfected with human immunodeficiency virus type-1. *Am J Trop Med Hyg* **59:**155–162. PubMed
99. **Pattabhi S, Whittle J, Mohamath R, El-Safi S, Moulton GG, Guderian JA, Colombara D, Abdoon AO, Mukhtar MM, Mondal D, Esfandiari J, Kumar S, Chun P, Reed SG, Bhatia A.** 2010. Design, development and evaluation of rK28-based point-of-care tests for improving rapid diagnosis of visceral leishmaniasis. *PLoS Negl Trop Dis* **4:**4. PubMed
100. **de Almeida ME, Steurer FJ, Koru O, Herwaldt BL, Pieniazek NJ, da Silva AJ.** 2011. Identification of *Leishmania* spp. by molecular amplification and DNA sequencing analysis of a fragment of rRNA internal transcribed spacer 2. *J Clin Microbiol* **49:**3143–3149. PubMed
101. **Sulzer AJ, Wilson M, Hall EC.** 1969. Indirect fluorescent-antibody tests for parasitic diseases. V. An evaluation of a thick-smear antigen in the IFA test for malaria antibodies. *Am J Trop Med Hyg* **18:**199–205. PubMed
102. **Wilson M, Sulzer AJ, Rogers WA Jr, Fried JA, Mathews HM.** 1971. Comparison of the indirect-fluorescent antibody and indirect-hemagglutination tests for malarial antibody. *Am J Trop Med Hyg* **20:**6–9. PubMed
103. **Koita OA, Doumbo OK, Ouattara A, Tall LK, Konaré A, Diakité M, Diallo M, Sagara I, Masinde GL, Doumbo SN, Dolo A, Tounkara A, Traoré I, Krogstad DJ.** 2012. False-negative rapid diagnostic tests for malaria and deletion of the histidine-rich repeat region of the *hrp2* gene. *Am J Trop Med Hyg* **86:**194–198. PubMed
104. **Snounou G, Viriyakosol S, Zhu XP, Jarra W, Pinheiro L, do Rosario VE, Thaithong S, Brown KN.** 1993. High sensitivity of detection of human malaria parasites by the use of nested polymerase chain reaction. *Mol Biochem Parasitol* **61:**315–320. PubMed
105. **Slemenda SB, Maddison SE, Jong EC, Moore DD.** 1988. Diagnosis of paragonimiasis by immunoblot. *Am J Trop Med Hyg* **39:**469–471. PubMed
106. **Procop GW.** 2009. North American paragonimiasis (caused by *Paragonimus kellicotti*) in the context of global paragonimiasis. *Clin Microbiol Rev* **22:**415–446. PubMed
107. **Fischer PU, Curtis KC, Folk SM, Wilkins PP, Marcos LA, Weil GJ.** 2013. Serological diagnosis of North American paragonimiasis by Western blot using *Paragonimus kellicotti* adult worm antigen. *Am J Trop Med Hyg* **88:**1035–1040. PubMed
108. **Al-Sherbiny MM, Osman AM, Hancock K, Deelder AM, Tsang VCW.** 1999. Application of immunodiagnostic assays: detection of antibodies and circulating antigens in human schistosomiasis and correlation with clinical findings. *Am J Trop Med Hyg* **60:**960–966. PubMed
109. **Tsang VCW, Wilkins PP.** 1997. Immunodiagnosis of schistosomiasis. *Immunol Invest* **26:**175–188. PubMed
110. **Leshem E, Meltzer E, Marva E, Schwartz E.** 2009. Travel-related schistosomiasis acquired in Laos. *Emerg Infect Dis* **15:**1823–1826. PubMed

111. **Coulibaly JT, N'Gbesso YK, Knopp S, N'Guessan NA, Silué KD, van Dam GJ, N'Goran EK, Utzinger J.** 2013. Accuracy of urine circulating cathodic antigen test for the diagnosis of *Schistosoma mansoni* in preschool-aged children before and after treatment. *PLoS Negl Trop Dis* **7:**e2109. PubMed
112. **Conway DJ, Lindo JF, Robinson RD, Bundy DA, Bianco AE.** 1994. *Strongyloides stercoralis*: characterization of immunodiagnostic larval antigens. *Exp Parasitol* **79:**99–105. PubMed
113. **Gam AA, Neva FA, Krotoski WA.** 1987. Comparative sensitivity and specificity of ELISA and IHA for serodiagnosis of strongyloidiasis with larval antigens. *Am J Trop Med Hyg* **37:**157–161. PubMed
114. **Badaró R, Carvalho EM, Santos RB, Gam AA, Genta RM.** 1987. Parasite-specific humoral responses in different clinical forms of strongyloidiasis. *Trans R Soc Trop Med Hyg* **81:**149–150. PubMed
115. **Genta RM.** 1988. Predictive value of an enzyme-linked immunosorbent assay (ELISA) for the serodiagnosis of strongyloidiasis. *Am J Clin Pathol* **89:**391–394. PubMed
116. **Krolewiecki AJ, Ramanathan R, Fink V, McAuliffe I, Cajal SP, Won K, Juarez M, Di Paolo A, Tapia L, Acosta N, Lee R, Lammie P, Abraham D, Nutman TB.** 2010. Improved diagnosis of *Strongyloides stercoralis* using recombinant antigen-based serologies in a community-wide study in northern Argentina. *Clin Vaccine Immunol* **17:**1624–1630. PubMed
117. **Siddiqui AA, Berk SL.** 2001. Diagnosis of *Strongyloides stercoralis* infection. *Clin Infect Dis* **33:**1040–1047. PubMed
118. **Porto AF, Oliveira Filho J, Neva FA, Orge G, Alcântara L, Gam A, Carvalho EM.** 2001. Influence of human T-cell lymphocytotropic virus type 1 infection on serologic and skin tests for strongyloidiasis. *Am J Trop Med Hyg* **65:**610–613. PubMed
119. **Schaffel R, Nucci M, Carvalho E, Braga M, Almeida L, Portugal R, Pulcheri W.** 2001. The value of an immunoenzymatic test (enzyme-linked immunosorbent assay) for the diagnosis of strongyloidiasis in patients immunosuppressed by hematologic malignancies. *Am J Trop Med Hyg* **65:**346–350. PubMed
120. **Keiser PB, Nutman TB.** 2004. *Strongyloides stercoralis* in the immunocompromised population. *Clin Microbiol Rev* **17:**208–217. PubMed
121. **Loutfy MR, Wilson M, Keystone JS, Kain KC.** 2002. Serology and eosinophil count in the diagnosis and management of strongyloidiasis in a non-endemic area. *Am J Trop Med Hyg* **66:**749–752. PubMed
122. **Gann PH, Neva FA, Gam AA.** 1994. A randomized trial of single- and two-dose ivermectin versus thiabendazole for treatment of strongyloidiasis. *J Infect Dis* **169:**1076–1079. PubMed
123. **Smith JV.** 1993. Antibody reactivity in human toxocariasis, p 91–109. *In* Lewis JW, Maizels RM (ed), *Toxocara and Toxocariasis: Clinical, Epidemiological, and Molecular Perspectives*. Institute of Biology and the British Society for Parasitology, London, United Kingdom.
124. **Despommier D.** 2003. Toxocariasis: clinical aspects, epidemiology, medical ecology, and molecular aspects. *Clin Microbiol Rev* **16:**265–272. PubMed
125. **de Savigny DH, Voller A, Woodruff AW.** 1979. Toxocariasis: serological diagnosis by enzyme immunoassay. *J Clin Pathol* **32:**284–288. PubMed
126. **Hogarth-Scott RS.** 1966. Visceral larva migrans—an immunofluorescent examination of rabbit and human sera for antibodies to the ES antigens of the second stage larvae of *Toxocara canis*, *Toxocara cati* and *Toxascaris leonina* (Nematoda). *Immunology* **10:**217–223. PubMed
127. **Won KY, Kruszon-Moran D, Schantz PM, Jones JL.** 2008. National seroprevalence and risk factors for zoonotic *Toxocara* spp. infection. *Am J Trop Med Hyg* **79:**552–557. PubMed
128. **Wilson M, Jones JL, McAuley JM.** 2003. *Toxoplasma*, p 1970–1980. *In* Murray PR, Baron EJ, Pfaller MA, Jorgensen JH, Yolken RH (ed), *Manual of Clinical Microbiology*, 8th ed. American Society for Microbiology, Washington, DC.
129. **Lopez A, Dietz VJ, Wilson M, Navin TR, Jones JL.** 2000. Preventing congenital toxoplasmosis. *MMWR Recomm Rep* **49:**59–68.
130. **NCCLS.** 2004. *Clinical Use and Interpretation of Serologic Tests for* Toxoplasma gondii. *Approved Guideline*. NCCLS, Wayne, PA.
131. **Bastien P.** 2002. Molecular diagnosis of toxoplasmosis. *Trans R Soc Trop Med Hyg* **96**(Suppl 1)**:**S205–S215. PubMed
132. **Switaj K, Master A, Skrzypczak M, Zaborowski P.** 2005. Recent trends in molecular diagnostics for *Toxoplasma gondii* infections. *Clin Microbiol Infect* **11:**170–176.
133. **Murrell KD, Bruschi F.** 1994. Clinical trichinellosis. *Prog Clin Parasitol* **4:**117–150. PubMed
134. **Bruschi F, Tassi C, Pozio E.** 1990. Parasite-specific antibody response in *Trichinella* sp. 3 human infection: a one year follow-up. *Am J Trop Med Hyg* **43:**186–193. PubMed
135. **Pozio E, Varese P, Morales MA, Croppo GP, Pelliccia D, Bruschi F.** 1993. Comparison of human trichinellosis caused by *Trichinella spiralis* and by *Trichinella britovi*. *Am J Trop Med Hyg* **48:**568–575. PubMed
136. **Jongwutiwes S, Chantachum N, Kraivichian P, Siriyasatien P, Putaporntip C, Tamburrini A, La Rosa G, Sreesunpasirikul C, Yingyourd P, Pozio E.** 1998. First outbreak of human trichinellosis caused by *Trichinella pseudospiralis*. *Clin Infect Dis* **26:**111–115. PubMed
137. **Hall RL, Lindsay A, Hammond C, Montgomery SP, Wilkins PP, da Silva AJ, McAuliffe I, de Almeida M, Bishop H, Mathison B, Sun B, Largusa R, Jones JL.** 2012. Outbreak of human trichinellosis in northern California caused by *Trichinella murrelli*. *Am J Trop Med Hyg* **87:**297–302. PubMed
138. **Schwebke JR, Burgess D.** 2004. Trichomoniasis. *Clin Microbiol Rev* **17:**794–803. PubMed
139. **Huppert JS, Batteiger BE, Braslins P, Feldman JA, Hobbs MM, Sankey HZ, Sena AC, Wendel KA.** 2005. Use of an immunochromatographic assay for rapid detection of *Trichomonas vaginalis* in vaginal specimens. *J Clin Microbiol* **43:**684–687. PubMed

Serological and Molecular Diagnosis of Fungal Infections*

MARK D. LINDSLEY

55

Analysis of the signs and symptoms of disease, in conjunction with an evaluation of available epidemiologic information and the results of modern imaging procedures, can often provide a presumptive clinical diagnosis of a fungal infection. However, the clinical presentation of many mycotic diseases is nonspecific, and a presumptive diagnosis must therefore be confirmed by appropriate laboratory tests. A definitive diagnosis of fungal disease is usually based upon the isolation of the etiologic agent in culture and/or microscopic demonstration of the organism in histopathologic or other clinical specimens. Unfortunately, these laboratory methods are insensitive and often unsuccessful, despite repeated sampling efforts. In the absence of positive microscopy or culture, immunologic and molecular tests offer alternative laboratory procedures to aid in the diagnosis of a mycotic disease. Advances in molecular diagnostic methods and the commercial introduction of new antigen and antibody detection tests hold promise for an earlier and more specific diagnosis than previously possible. Antibody detection tests are often helpful for the diagnosis of fungal infections. For example, when acute- and convalescent-phase serum specimens are tested, seroconversion from negative to positive or a 4-fold rise in antibody titer is considered to be diagnostic.

Despite recent advances in the production of purified antigens using biochemical and recombinant techniques, many antigens used in antibody detection tests possess cross-reactive epitopes that are shared among different fungal genera or which cross-react with entirely different classes of microorganisms. To rule out possible false-positive results, several serologic tests must be performed with a battery of antigens (including those from antigenically related genera).

Likewise, mycotic infection is not definitively excluded by negative antibody results, which may be a result of obtaining the specimen before the antibody response can be detected. In this instance, an examination of serial serum specimens to detect temporal changes in titer may be helpful. Furthermore, no or low antibody production may be the result of an altered immune response in some immunocompromised individuals.

Patients who are immunosuppressed are very susceptible to many fungal infections in which false-negative antibody assay results are common. Non-antibody-dependent diagnostic assays, such as detection of fungal antigens, are not dependent on a functioning immune system and may therefore allow diagnosis early in the infectious episode, before an antibody response occurs. Fungal antigens such as β-1-3-D-glucan, galactomannan, and glucuronoxylomannan, the capsular polysaccharide antigen of *Cryptococcus*, are very stable and have long half-lives in a patient's specimen. Assays for the detection of these antigens are often very sensitive.

Nucleic acid-based tests also offer the promise of increased sensitivity and specificity compared to conventional diagnostic tests in both immunocompromised and immunocompetent patients. Nucleic acids, once extracted from clinical materials, can be amplified using PCR or other DNA or RNA amplification technologies. An advantage of molecular diagnostic tests is the capacity to identify the infecting organism to the species level and to detect mixed as well as single-organism infections. However, whereas amplification technologies may provide greater test sensitivity and specificity for the above reasons, these advantages are counterbalanced by the concomitant increased risk of sample contamination resulting in false positivity and a loss of specificity. Moreover, the extraction of fungal DNA or RNA from clinical materials is not a straightforward or standardized process at present. The rigid fungal cell wall can be difficult to penetrate and may result in a reduced DNA yield. In these instances, isolation of extracellular DNA may be helpful; however, the presence of DNases in the specimen may affect the assay sensitivity. Also, procedures used to remove inhibitors of the PCR assay may cause loss of target DNA, thereby reducing test sensitivity. Many DNA-based tests have been developed in single laboratories and are quite successful; confirmation of the usefulness of these technologies awaits multicenter clinical evaluations.

It is important to note that the performance of the different methods discussed is not mutually exclusive. Combinations of methods often provide an increase in diagnostic sensitivity. When available, a combination of antibody and antigen assays can result in enhanced sensitivity. Likewise, the use of DNA and antigen assays may improve diagnostic sensitivity.

This chapter is divided into two sections. The first section provides the methods used for the diagnosis of fungal infections. The second section describes the most

*This chapter contains information presented by Mark D. Lindsley, David W. Warnock, and Christine J. Morrison in chapter 66 of the 7th edition of this *Manual*.

doi:10.1128/9781555818722.ch55

TABLE 1 Commercially available antibody detection tests for fungal diseases

Disease and test[a]	Specimen	Antigen	Interpretation	Sensitivity	Specificity	Source(s)[b]
Aspergillosis						
CF	Serum	Culture filtrate from *A. fumigatus*	Titer of ≥1:8 is strong evidence for *Aspergillus* infection; seroconversion or ≥4-fold increase in titer between acute- and convalescent-phase sera confirms diagnosis	Aspergilloma: 79% ABPA: 46% Invasive pulmonary or disseminated: 20%	95–100%	IMMY
EIA	Serum	Purified recombinant *Aspergillus* proteins	<5 AU[c], negative; 5–<10 AU, intermediate; ≥10 AU, positive	CAP: 90.2–94.1% ABPA: 92.3%	Colonized but not infected: 54.3–84.0% No pulmonary disease: 99.5–100%	Bio-Rad
ID	Serum	Culture filtrate from *Aspergillus* spp.[d]	≥1 line of identity indicates aspergilloma, ABPA, or IA; ≥3 lines of identity is strong evidence for aspergilloma	ABPA: 50–61% Aspergilloma: 80–93%	97–100%	Gibson, IMMY, Meridian, Microgen
Blastomycosis						
CF	Serum	Purified A antigen	Titer of ≥1:8 is presumptive evidence of infection; titer of ≥1:32 is strong presumptive evidence of recent infection; seroconversion or ≥4-fold increase in titer between acute- and convalescent-phase sera confirms diagnosis	Disseminated: 50% Localized: 33%	97–100%	IMMY
EIA	Serum	Proprietary mixture of purified yeast-phase antigens	EIA units: <1.0, negative; 1.0–<1.5, indeterminate; ≥1.5, positive	83.3–100%	100%	IMMY
ID	Serum	Purified A antigen	Presence of A band suggests recent infection	Disseminated: 85% Localized: 33%	100%	Gibson, IMMY, Meridian
Candidiasis						
EIA	Serum	Purified mannan from *C. albicans*	<5 AU, negative; 5–<10 AU, intermediate; ≥10 AU, positive; >20 AU, dilute serum 1:4 and retest	*C. albicans*: 71–88% Other *Candida* spp.: 25–77%	63–94%	Bio-Rad Candida Ab
	Serum, plasma	Purified mannan from *C. albicans*	<5 AU, negative; 5–<10 AU, intermediate; ≥10 AU, positive; >80 AU, dilute serum 1:10 and retest	62.5%	65.0%	Bio-Rad Candida Ab Plus
ID	Serum	Culture filtrate and cell lysate of yeast-phase *C. albicans*	≥1 line of identity is positive for the presence of antibody; seroconversion or increase in number of lines suggests systemic infection; the greater the number of lines, the more severe the infection in immunocompetent patients	58–94%	94–98%	IMMY, Gibson
IFA	Serum	Germ tubes of *C. albicans*	Titer of ≥1:640 suggests invasive candidiasis	78–85%	85–100%	Vircell
Coccidioidomycosis						
CF	Serum, CSF	Culture filtrate (coccidioidin)	Titer of ≥1:2 is positive for acute pulmonary disease; titer of ≥1:16 suggests disseminated disease	Acute pulmonary: 75% Disseminated: 98%	80–95%	IMMY, Meridian

EIA	Serum, CSF	Mixture of purified TP and CF antigens to detect IgM or IgG, respectively	Absorbance values: <0.150, negative; 0.150–<0.200, indeterminate; ≥0.200, positive	IgM only: 74% IgG only: 92% IgM and IgG: 97%	IgM only: 96% IgG only: 97% IgM and IgG: 94%	Meridian
	Serum	TP antigen-coated wells (IgM), CF antigen-coated wells (IgG)	For both CF and TP antigens (EIA units): <1.0, negative; 1.0–<1.5, indeterminate; ≥1.5, positive	92.5%	Normal population: 98.3% Other fungal infections: 95.2%	IMMY
IDCF	Serum, CSF	Culture filtrate (coccidioidin)	Band of identity with reference serum indicates active infection	77%	100%	IMMY, Meridian, Gibson
IDTP	Serum	Heat-treated culture filtrate (coccidioidin, 60°C, 30 min)	Band of identity with reference serum indicates active infection	75–91%	—[e]	IMMY, Meridian
LA	Serum	Heat-treated coccidioidin-coated latex particles	≥2+ agglutination is positive for the presence of antibody; must confirm with ID and/or CF	65–70%	93%	IMMY, Meridian
Histoplasmosis						
CF	Serum, CSF	Mycelial culture filtrate (histoplasmin)	Titer of ≥1:8 is presumptive evidence for infection; titer of ≥1:32 is strongly presumptive for infection	21%	81–99%	IMMY, Meridian
	Serum, CSF	Yeast cell suspension	Titer of ≥1:8 is presumptive evidence for infection; titer of ≥1:32 is strongly presumptive for infection	82%	81–88%	
ID	Serum, CSF	Mycelial culture filtrate (histoplasmin)	M band indicates acute or chronic histoplasmosis (observed in 75% of patients); H and M bands indicate acute histoplasmosis (observed in 20% of patients); positivity for H and/or M band indicates *Histoplasma* meningitis	65–100%	89–100%	IMMY, Meridian, Gibson
EIA	Serum	Inactivated *Histoplasma* antigen	EIA units: <0.9, negative; ≥0.9–≤1.10, equivocal; >1.0, positive	58.0–82.4%	88.0–93.3%	Focus Diagnostics
LA	Serum	Mycelial culture filtrate (histoplasmin)	Titer of ≥1:16 is presumptive evidence of active or very recent infection	Acute: 97–100% Chronic: 46–96%	97% 97%	IMMY
Paracoccidioidomycosis						
ID	Serum, CSF	Mycelial culture filtrate (contains gp43 and other antigens)	Band of identity with reference serum indicates active infection	94%	95–99%	IMMY
		Ag7		84%	99%	
Sporotrichosis						
LA	Serum	*Sporothrix* antigen	Titer of ≥1:8 is presumptive evidence of sporotrichosis	Disseminated: 100% Articular: 86–100% Pulmonary: 73–87% Cutaneous: 56–93%	100%	IMMY

[a]For abbreviations, see the text.
[b]Vendor contact information is given at the end of the chapter.
[c]Arbitrary units compared to a standard curve.
[d]Detection of precipitins to *A. fumigatus*, *A. flavus*, *A. nidulans*, *A. niger*, or *A. terreus* was performed separately.
[e]Insufficient data.

TABLE 2 Commercially available antigen detection tests for fungal diseases

Disease and antigen test[a]	Specimen	Antigen detected	Interpretation	Sensitivity	Specificity	Source(s)[b]
Aspergillosis						
EIA MAb (EBA-2)[c]	Serum (boiled)	Galactomannan	EIA index: ≥0.5 units, positive; detection limit, 1 ng/ml	60–100%	78–99%	Bio-Rad
Candidiasis						
EIA MAb (EBCA-1)	Serum (boiled)	α-(1,2)-Oligomannosides	<0.25 ng/ml, negative; ≥0.25 to <0.5 ng/ml, intermediate; ≥0.5 ng/ml, positive	Overall, 52%; *C. albicans*, 53–60%; other *Candida* spp., 20–70%	85–100%	Bio-Rad Candida Ag
Mab (EBCA-1)	Serum, plasma		<62.5 pg/ml, negative; ≥62.5 to <125 pg/ml, intermediate; ≥125 pg/ml, positive	69.6%	93.5%	Bio-Rad Candida Ag Plus
LA PAb	Serum (not boiled)	Uncharacterized heat-labile *C. albicans* antigen	Titer of ≥1:4 suggests invasive candidiasis	Titer of 1:4, 48–81%; titer of 1:8, 2–59%; titer of 1:16, 59%	Titer of 1:4, 80–97%; titer of 1:8, 93–95%; titer of 1:16, 98%	Ramco
Cryptococcosis						
EIA PAb	Serum, CSF	Capsular polysaccharide antigen	Visual: definite yellow color, positive Spectrophotometric: <0.100 OD, negative; ≥0.100–<0.150 OD, intermediate; ≥0.150 OD, positive Detection limit: 0.63 ng/ml	96–100%	93–99%	Meridian
MAb	Serum, CSF	Capsular polysaccharide antigen	≤0.265, negative; >0.265, positive Detection limit: serum, 5.3 ng/ml; CSF, 1.7 ng/ml	100%	99.8%	IMMY
LA PAb	Pronase-treated serum; CSF (boiled)	Capsular polysaccharide antigen	≥2+ agglutination is positive; titrate positive sera; titer of ≥1:8 is strongly suggestive evidence for infection	93–100%	93–98%	IMMY, Meridian
LFA MAb	Serum, CSF	Capsular polysaccharide antigen	Positive, control and test band visible; negative, only control band visible	98–100%	94–100%	IMMY
LA MAb (E1)	Urine; pronase-treated serum, CSF, BAL fluid	Glucuronoxylomannan	Any agglutination indicates positivity; titrate positive sera; detection limit, 50 ng/ml	Overall, 92%; urine, 93%; serum, 85%; CSF, 100%; BAL fluid, 100%	Overall, 98%; urine, 97%; serum, 100%; CSF, 100%; BAL fluid, 100%	Bio-Rad
Panfungal[d]						
Modified *Limulus* amebocyte assay	Serum	(1,3)-β-D-Glucan	Negative, <60 pg/ml; indeterminate, 60–79 pg/ml; positive, ≥80 pg/ml	100%	90%	Associates of Cape Cod

[a]For abbreviations, see the text.
[b]Vendor contact information is given at the end of the chapter.
[c]Clone name in parentheses.
[d]Detects species of *Candida*, *Aspergillus*, *Pneumocystis*, *Fusarium*, and *Trichosporon asahii* but not *Zygomycetes* or *Cryptococcus* spp.

extensively evaluated or routinely used tests for the serodiagnosis of mycotic infections. Commercially available antibody and antigen detection tests are listed in Tables 1 and 2; vendor contact information is provided at the end of the chapter. Specific details regarding the clinical indications for test application and the mechanics of test performance are presented in the body of the text. Experimental antigen and antibody detection tests and molecular biological tests are reviewed briefly in the text.

Abbreviations. ABPA, allergic bronchopulmonary aspergillosis; AC, anticomplementary; AU, arbitrary units; BAL, bronchoalveolar lavage; BDG, (1,3)-β-D-glucan; CAGTA, *Candida albicans* germ tube-specific antibodies; CF, complement fixation; CH_{50}, amount of complement required for 50% hemolysis; CNPA, chronic necrotizing pulmonary aspergillosis; CSF, cerebrospinal fluid; EIA, enzyme immunoassay (fluid or solid phase); ELISA, enzyme-linked immunosorbent assay; FDA, Food and Drug Administration; GM, galactomannan; HIV, human immunodeficiency virus; HSCT, hematopoietic stem cell transplant; IA, invasive aspergillosis; ID, immunodiffusion in an agarose gel; IDCF, immunodiffusion variation to detect antibody to the CF F antigen in patients with coccidioidomycosis; IDTP, immunodiffusion variation to detect antibody to the tube precipitin antigen in coccidioidomycosis; IFA, immunofluorescent antibody; Ig, immunoglobulin; ITS, internal transcribed spacer region of the rRNA gene; LA, latex agglutination; LFA, lateral flow assay; MAb, monoclonal antibody; OD, optical density; PAb, polyclonal antibody; PCP, *Pneumocystis* pneumonia; QC, quality control; RBCs, red blood cells; SOT, solid-organ transplant; SRBCs, sheep erythrocytes; TP, tube precipitin; VBD, veronal-buffered diluent; WB, Western blotting.

METHODS USED FOR THE DIAGNOSIS OF FUNGAL INFECTIONS

Immunodiffusion

Theory

The ID assay is a solid-phase assay based on the liquid tube agglutination assay in which, when solubilized antigen and antibody are combined at equimolar concentrations, a "latticework" complex is formed, producing a visible precipitate denoting a positive result. The ID assay is performed by placing antigen and antibody in opposing wells formed in an agar matrix. The reagents diffuse into the agar matrix, and when equimolar concentrations are achieved, the latticework is formed and a visible precipitin line, or band, is visualized as the positive result. A seven-well format is used in the performance of this procedure (Fig. 1).

Sample Requirements

Serum or CSF may be used in the ID test. Because the reported sensitivity of the ID test is low early in infection, patients with negative serum reactions during the acute phase of infection should have additional sera drawn 3 to 4 weeks later to detect the development of precipitin bands that would indicate seroconversion and recent infection. Concomitant evaluation of patient specimens by using the CF test is also recommended.

Materials

Plexiglas matrix (3-mm-diam wells) with 17 patterns of seven wells each

Plastic petri dish, 15 by 100 mm

Agar medium (see below for formulation)

Spatula, 1-mm tip (flattened)

Organism-specific reference antigen

Aspergillus: genus-specific antigen

Species-specific antigens: *A. fumigatus*, *A. niger*, *A. flavus*, *A. terreus*

Histoplasma: histoplasmin

Blastomyces: *Blastomyces* A antigen

Coccidioides: *Coccidioides* IDCF antigen (F antigen), *Coccidioides* IDTP antigen

Paracoccidioides: yeast antigen

Organism-specific reference antisera

Humidified chamber

Light box with indirect backlighting

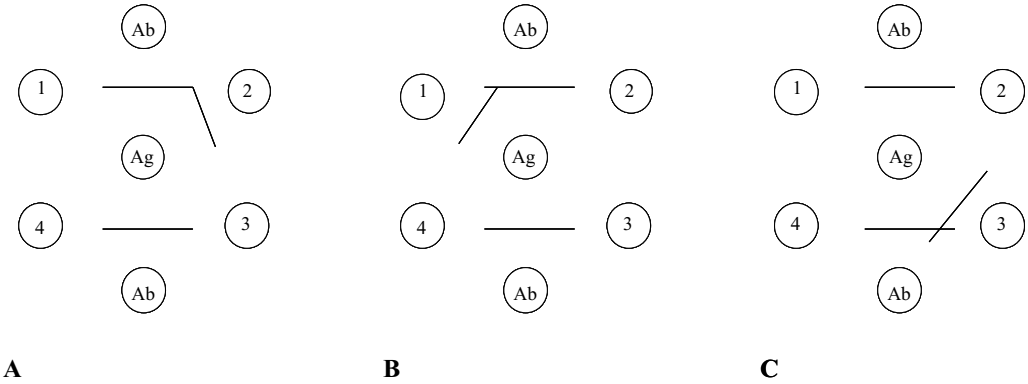

FIGURE 1 Examples of ID results observed when a seven-well agar gel pattern is used. (A) Band of identity (patient 2); (B) band of partial identity (patient 1); (C) band of nonidentity (patient 3). Ag, reference antigen; Ab, reference antiserum; 1 to 4, patient test sera. A standard reference band is shown midway between the antiserum-containing wells and the central antigen-containing wells in all three panels.

Agar Medium: *Aspergillus* Formulation

Stock barbital buffer (pH 8.6), 0.05 M, made up to 500 ml.

Sodium diethylbarbiturate	5.16 g
Diethylbarbituric acid	0.92 g
Sodium acetate	2.05 g

Store at 4°C. Buffer is stable for 2 months. Discard if bacterial growth develops.

Phenolized medium.

Noble agar (or equivalent)	1.00 g
Phenol, liquefied	0.25 ml
Stock barbital buffer (above)	25.0 ml
Distilled water	to 100 ml

Heat until the agar is completely dissolved.

Agar Medium: Dimorphic Pathogen Formulation

Phenolized medium.

Sodium chloride	0.9 g
Noble agar (or equivalent)	1.0 g
Sodium citrate ($Na_3C_6H_5O_7 \cdot 2H_2O$)	0.4 g
Phenol, liquefied	0.25 ml
Glycine	7.5 g
Distilled water	to 100 ml

Autoclave the mixture at a pressure of 15 lb/in^2 for 10 min. The final pH of the medium should be 6.3 to 6.4.

Larger volumes of agar can be produced and divided into aliquots in smaller containers for later use. Store at 4°C. Aliquots can be reliquefied in a boiling water bath or microwave set at low power.

Procedure

Making Agar ID Plates

1. Using a pipette, place 6.5 ml of molten (60 to 75°C) agar into a petri dish (15 by 100 mm) and allow to solidify for at least 2 h.
2. Overlay the first agar layer with 3.5 ml of molten (85 to 90°C) agar and immediately place the Plexiglas matrix on top of the liquid agar.
3. Plates may be used 30 min after the agar has solidified or may be stored for up to 1 week at 4°C in a humidified chamber.

Preparing and Inoculating ID Plates

1. Number each seven-well pattern on the bottom of the dish (not on the template).
2. Place plates on a dark background to facilitate well filling.
3. Carefully remove the excess agar from the upper section of the template wells with the pointed end of the spatula.
4. Place the reference serum in the top and bottom wells of each pattern and place the patient's test sera in the four lateral wells (Fig. 1). Note, wells should be filled with the proper reagent, but overfilling and accidental mixing of well reagents should be avoided.
5. At this step, with assays for antibodies against *Aspergillus*, *Blastomyces* A antigen, or *Coccidioides* IDTP antigen, the plate should be covered and incubated at room temperature for 30 min before going on to step 6. For all other assays, preincubation is not necessary and you can proceed directly to step 6.
6. Place the reference antigen in the center well of each pattern. All wells must be examined for air bubbles.
7. If bubbles are observed, they should be broken by being gently pierced with toothpicks. Separate toothpicks should be employed for each different antigen and antibody solution.
8. Place closed plates on a level surface in a humidified chamber and incubate them at 25°C for 48 h.

Reading of ID Plates

1. Remove the Plexiglas matrix by gently pressing the sides of the petri dish. Place Plexiglas matrix in a 10% solution of bleach for 15 min, and then wash and rinse.
2. Gently wash the agar surface with water and finish by adding enough water to sufficiently cover the agar surface.
3. Cover the petri dish and incubate it for 10 to 30 min, allowing the ID band to intensify.
4. Read ID reactions using a light box with indirect lighting and record visible reactions.
5. Very carefully, remove the upper layer of agar overlay by gently sweeping the surface with a cotton swab.
6. Wash the remaining agar with water to remove excess agar from the upper layer.
7. Cover the agar with a minimal volume of water.
8. Examine the plate for lines of identity between test and reference wells.

Interpretation

1. Visible ID bands must be present between the antigen and reference antisera for each seven-well pattern inoculated.
2. The lack of ID bands between the antigen and reference antisera invalidates the results of the sera for that pattern, and the test must be repeated.
3. Four results may be observed for the ID reactions with patient sera (Fig. 1).
   a. No band present: negative reaction. Note, this reaction can occur in the event of antibody excess. If the index of suspicion for infection is great, serum dilutions should be performed.
   b. Band of identity: patient serum precipitates an antigen with identical specificities.
   c. Band of partial identity: patient serum precipitates an antigen that possesses common but not identical antigen determinants.
   d. Band of nonidentity: patient serum precipitates an antigen with no antigenic determinant in common; precipitation occurs with a component of the antigen preparation that is different from that with which the specific reference antisera reacts.
4. A band of identity is considered a positive reaction. Bands of partial and nonidentity are bands of unknown significance.
5. Patient serum must react with the homologous reference antigen to form a line of identity with the reference band to be considered positive.

Notes for the Performance of the ID Assay

1. Some antigenic extracts (particularly *Aspergillus)* contain C substance, and this can react with C-reactive protein in the serum of some patients with inflammatory disease.

The resulting complex forms a precipitate, which may be erroneously interpreted as the presence of anti-*Aspergillus* antibodies. This false-positive reaction is easily eliminated if the test plates are soaked in 5% sodium citrate for 45 min before being read. In addition, C substance generally produces lines of nonidentity with reference antisera.

2. When using in-house-prepared antigen and/or reference antisera, the reagents must be titrated to determine the optimum concentration for use in the assay. For example, to determine the optimum concentration of antigen, serial dilutions of antigen are sequentially placed in the 6 wells surrounding the center well. The center well receives the reference antisera at the previously determined optimum concentration. Read the ID reactions after incubation for 48 h at room temperature. The optimum concentration is that which places the ID band equidistant between the antigen and antibody well.

3. The sensitivity of the ID assay is sometimes compromised due to the presence of antibody below the level of detection of the assay. Concentration of serum 4- to 8-fold increases the concentration of antibody in the serum and subsequently the sensitivity of the assay. Concentration can be performed through evaporation using a Savant SpeedVac (Thermo Scientific; Waltham, MA) or an Amicon/Centricon centrifugal filter device (EMD Millipore; Billerica, MA).

Commercial ID Test Procedures

Kits and/or individual reagents for the ID assay are available for purchase from several vendors, as listed in Table 1.

Materials

Reagents purchased commercially necessary to perform this assay are as follows:

1. Precast agar medium available using different formulations
   a. Agarose
   b. Cleargel (IMMY); note, Cleargel plates are not to be used with rabbit antiserum
   c. Well sizes can vary between vendors which require a variable amount of reagents and patient serum to perform the assay
2. Organism-specific reference antigen
3. Organism-specific reference antisera (purchase twice the volume of antisera as antigen, since two wells are used for the reference antisera to one of antigen per 7-well pattern) (Fig. 1)
4. Humidified chamber
5. Light box with indirect backlighting

Procedure

Performance of the ID procedure using commercial reagents should follow the procedure as described in the vendor's package insert. Briefly, the inoculation of the ID plates and reading of the ID reactions are identical to those listed above. Inoculated agar plates are placed in a humidified chamber. Positive results are reported after 24 h of incubation, and negative results are reported after 72 h of incubation.

Interpretation

Refer to the manufacturer's package insert for the interpretation of the results using commercial reagents.

Notes for Performance of Commercial ID Assays

1. Commercial antigens and antibodies should be used with the agar plates provided by the vendor.

2. An advantage with precast agar medium is, unlike the method described above, there is no Plexiglas template that obscures the view of precipitin band formation. Therefore, the ID bands can be visualized regularly; positive reactions can be determined after 24 h and negative results can be monitored throughout the entire 72 h of incubation.

Complement Fixation Assay

Theory

Complement is a series of lytic proteins that binds to antibody/antigen complexes and ultimately causes the lysis of cells by embedding into and disrupting the cell membrane. The CF assay takes advantage of the complement binding or "fixing" to antibody/antigen complexes. Antigen specific for the disease in question is combined with the patient serum along with a known quantity of complement. Specific antibody in the patient serum, if present, binds to the antigen. Complement binds to the antibody/antigen complex, reducing the amount of active complement in the mixture; the greater amount of antibody present, the greater the number of antibody/antigen complexes formed and the greater the reduction of active complement. In patients with no antibody present in their serum (seronegative patients) antibody/antigen complexes are not formed, and subsequently, there is no reduction of active complement in the mixture.

The amount of active complement present in the mixture is measured using antibody-coated RBCs as an indicator system. The greater percentage of RBCs lysed, the greater amount of active complement present in the mixture. Total lysis of the RBCs indicates the lack of antibody present in the patient serum. No lysis of the RBCs indicates a large amount of antibody present in the patient serum. Methods and assay interpretation are detailed below.

The advantage of the CF test is that it provides a quantitative measurement of the amount of antibody present in the test specimen. To assess disease progression or treatment efficacy, the titer for a given early (acute-phase) specimen can then be compared to the titer of a later (convalescent-phase) specimen as measured by the respective increase or decrease in antibody titer. For accurate comparisons, serially acquired specimens must be tested in parallel during the same assay.

The disadvantages of the CF test are as follows: (i) it is a relatively complex, labor-intensive assay that should be performed by only highly trained technical staff; (ii) accuracy depends on constant, complex QC standardization or titration of test reagents (hemolysin, complement, SRBCs) each time a new lot of reagent is obtained; and (iii) specimens may possess AC activity (i.e., patient serum fixes or destroys complement in the absence of any added antigen), making test results in these wells uninterpretable.

If infection by one of the dimorphic pathogens is suspected, it is important to include antigens for each of the dimorphic pathogens when performing CF because cross-reactivity can occur at low antibody titers. Furthermore, overlap of the areas of endemicity for *Histoplasma*, *Blastomyces*, and *Coccidioides* and the ease of travel between zones of endemicity may confound the diagnosis. *Paracoccidioides* antigen should also be included when there is a history of travel to Central or South America.

Because of the complexity of the procedure, only an abbreviated description of the CF test is outlined below. Readers are directed to a more detailed protocol (1) or a modified version, available from Immuno-Mycologics for use with their reagents. No commercial kits are available

for the CF test, but antigens, antisera, and other reagents can be purchased individually from the commercial sources listed in Table 1.

Sample Requirements

Serum, peritoneal fluid, or CSF may be used in the CF test. Serum is most often tested in cases of suspected acute fungal infections. CSF may be used to detect localized antibody production if meningitis is suspected. Other body fluids are examined in cases of suspected disseminated disease. Acute-phase sera should be obtained after the onset of symptoms, and convalescent-phase sera should be collected 3 to 4 weeks later and tested in parallel to identify changes in titer compared to the titer obtained for the acute-phase sera. To remove any red or white blood cells, CSF should be centrifuged before being tested. Sera and CSF are heated at 56°C for 30 min immediately prior to use to inactivate endogenous complement activity.

Serum and CSF can be stored at 4°C for 72 h or stored for longer periods in frozen aliquots at −20°C or colder in a nondefrosting freezer. Repeated freezing and thawing of the samples, which can reduce reactivity, should be avoided.

Unacceptable Specimens

1. Plasma. Blood collected with any anticoagulant is an unacceptable specimen for the CF assay.

2. Excessively pigmented specimens. As the results of the CF assay are measured by the hemolysis of red blood cells, excessively hemolyzed specimens can interfere with test interpretation. Slightly pigmented specimens may be used because the color will be diluted out during sample processing and titer determination which will not interfere with test interpretation.

3. Excessively lipemic specimens. Lipids should be removed with a 0.45- to 0.8-μm-pore-size filter attached to a syringe (Millipore Corp.).

Materials

Antigens and reference antisera may be purchased from Immuno-Mycologics, Inc., or from Meridian Diagnostics, Inc. Other key materials, listed below, may be purchased from vendors that sell biological products (e.g., Lonza, Walkersville, MD; Rockland Immunochemicals, Inc., Gilbertsville, PA; TCS Biosciences Ltd., Buckingham, United Kingdom; and Colorado Serum Company, Denver, CO).

Equipment

pH meter
Centrifuge with microtiter plate carriers
Incubator (37°C)
Glass serologic tubes (15 by 125 mm and 12 by 75 mm)
Pipettes (1, 5, and 10 ml)
Water baths (37 and 56°C)
Refrigerator
Microtiter equipment
25- to 50-μl multichannel pipetter
U-bottom polystyrene microtiter plates
Reading mirror (concave)

Procedure

Reagent Preparation and Standardization

1. Gelatin solution. Make a 0.05% (wt/vol) solution of gelatin in deionized H_2O and heat to 100°C. Allow it to cool to room temperature, and use it to dilute 5× VBD to 1×. The shelf life of the 0.5% gelatin water solution is 7 days at 4°C.

2. VBD. VBD is prepared and stored as a 5× stock solution. The working 1× VBD solution is prepared by diluting the 5× stock solution of VBD to 1× with 0.05% gelatin-water solution. The 1× VBD is used throughout the test procedure as a reagent diluent. The pH of the 1× VBD must be between 7.3 and 7.4; if it is not, prepare new 1× VBD from the 5× stock. Do not adjust the pH of the 1× VBD. If the pH of the 1× VBD is continually out of range, obtain new 5× buffer. Keep the 1× VBD on ice during the assay. The shelf life of 1× VBD is 24 h at 4°C.

3. SRBCs, supplied in Alsever's solution. SRBCs must be washed three times with 1× VBD by gentle centrifugation on the day the CF test is to be performed (final working concentration, 2.8% [vol/vol] in 1× VBD). If red pigment remains after three consecutive washes, the SRBCs are too old and too fragile for use. A fresh lot of SRBCs should be obtained (SRBCs should be between 5 and 28 days old at the time of use). The shelf life of the stock SRBCs in Alsever's solution is 1 month, whereas the shelf life of washed and diluted SRBCs in 1× VBD is 24 h.

4. Hemolysin. Hemolysin (complement-fixing, anti-SRBC antibody) is used to "sensitize" (i.e., coat with antibody) the SRBCs, allowing them to be lysed in the presence of complement. To determine the optimal concentration of hemolysin for the sensitization of SRBCs, serially dilute hemolysin in 1× VBD in 15- by 125-mm glass tubes (1:1,500, 1:2,000, 1:2,500, 1:3,000, 1:4,000, and 1:8,000) and titrate it against multiple dilutions of guinea pig complement (1:300, 1:350, and 1:400 [see item 5 below]). After adding SRBCs and incubating them in a water bath at 37°C for 1 h, centrifuge tubes and determine the percent hemolysis in each tube by comparison to a standard curve (color standards) constructed from differing proportions of hemoglobin and 0.28% SRBCs (percent lysis = 0, 10, 20, 30, 40, 50, 60, 70, 80, 90, and 100). Plot the percent hemolysis against the hemolysin dilution, and identify the second dilution on the plateau of the graph. This hemolysin dilution is optimum to sensitize SRBCs for complement titration, antigen titration, and serum tests. Hemolysin must be titrated each time a new lot of SRBCs or hemolysin is obtained. The shelf life of the stock hemolysin (a 1:100 dilution of hemolysin in VBD containing 0.2% phenol) at 2 to 8°C is up to 1 year.

5. Guinea pig complement. Reconstitute guinea pig complement into single-use glass vials, and freeze at −70°C until ready to use. Storage in plastic vials will cause a reduction of complement activity over time. The complement must be subjected to titer determination before each use.

Titration of guinea pig complement. (Note: during this procedure, the stock complement, VBD, and further complement dilutions must be kept on ice, unless otherwise instructed. Tubes and flasks should be made of glass and kept on ice while performing the procedure.)

a. Remove an aliquot of complement from the −70°C freezer and thaw on ice.
b. Keep complement and subsequent dilutions on ice, unless otherwise instructed.
c. Serially dilute complement with VBD (1:200, 1:250, 1:300, 1:350, and 1:400) in 12- by 75-mm glass test tubes and add 0.20, 0.25, 0.30, and 0.40 ml of each complement dilution to 0.60, 0.55, 0.50, and 0.40 ml of VBD, respectively.

d. Then add 0.20 ml of sensitized SRBCs (see below) to the tubes, shake the mixture, and incubate the tubes in a 37°C water bath for 30 min (shake again after 15 min and return the tubes to water bath).
e. Remove the tubes, and centrifuge the cells. Determine the percent hemolysis compared to the color standards.
f. Calculate the ratio of lysed to unlysed cells (lysis ratio = lysed/[100 − lysed], i.e., 10/[100 − 10] = 0.111).
g. Using log-log graph paper, plot the volume of complement added to the tubes (0.20, 0.25, 0.30, and 0.40) against the lysis ratio. For valid analysis, the lysis ratio values of the two lower complement concentrations (0.2 and 0.25) must be less than 1, and the lysis ratio values of the two higher complement concentrations (0.30 and 0.40) must be greater than 1.
h. With a ruler, join the two points plotted for the two lowest volumes of complement and do the same for the two highest volumes. Draw a line connecting the midpoint of one line to the midpoint of the other line.
i. From the point where this line intersects the vertical line at 1 on the *x* axis, draw a horizontal line to the *y* axis on the left. This is the volume, in milliliters, that contains 1 CH_{50} unit. Multiply this value by 5 to obtain the equivalent of 5 CH_{50} units.

6. Sensitized SRBCs. While gently swirling the flask, slowly add an equal volume of SRBCs to an equal volume of the optimum concentration of hemolysin (determined as described in item 4 above). Incubate the mixture for 15 min in a 37°C water bath before use.

CF Test

1. All reagents (hemolysin, complement, SRBCs, and VBD) must be optimally standardized as described above before the test is used with patient samples or the positive control.

2. Using cold VBD, prepare a 1:8 dilution of the following samples in plastic screw-cap tubes: patient sample, positive control, and negative control. Samples may also be diluted 1:2 instead of 1:8 or may be diluted more than 1:8 during repeat testing to detect lower or higher antibody titers, respectively.

3. Heat the diluted sera for 30 min in a 56°C water bath, and cool to room temperature.

4. Label the microtiter plates as shown in Fig. 2.

5. Pipette 25 μl of cold VBD into the wells of rows B to H of columns 1 to 12 of the patient plate(s) (Fig. 2A) and columns 1 to 9 of the control plate (Fig. 2B).

6. Add 50 μl of heat-inactivated patient sera to wells 1 to 6 of row A for patient 1 and wells 7 to 12 of row A for patient 2. Add 50 μl of control sera to the appropriate wells in row A of the control plate that correspond to the appropriate antigen.

7. Using a multichannel pipette, serially pass 25 μl of serum sequentially from row A through row H and mix. Remove 25 μl from the wells in row H and discard (25 μl of serially diluted sera should remain in all wells).

8. Dilute fungal antigens to the appropriate concentration as determined by the antigen titration assay performed for that lot of antigen. Add 25 μl of diluted antigen to wells A through H of the appropriate columns as follows:

a. *Histoplasma* mycelial antigen (histoplasmin) to columns 2 and 8 on patient plate(s) and column 2 of the control plate.
b. *Histoplasma* yeast antigen to columns 3 and 9 on patient plate(s) and column 3 of the control plate.
c. *Blastomyces* A antigen to columns 4 and 10 on patient plate(s) and column 5 on the control plate.
d. *Coccidioides* culture filtrate antigen (coccidioidin) to columns 5 and 11 on the patient plate(s) and column 7 on the control plate.
e. *Paracoccidioides* antigen in columns 6 and 12 on the patient plate(s) and column 9 on the control plate.

9. Add 25 μl of cold VBD to columns 1 and 7 on the patient plate(s) and columns 1, 4, 6, and 8 on the control plate to control for serum activity in the CF test.

10. Thaw guinea pig complement on ice, and dilute with cold VBD in a glass container to the concentration determined by the complement titration assay. Allow to stand on ice for at least 20 min, but use within 2 h.

11. Add 50 μl of diluted complement to all patient specimen wells and columns 1 to 9 of the control plate.

12. A complement "back titration" is performed with each assay to determine the accuracy of the complement titration/dilution. On the control plate, add 50 μl of cold VBD to rows A to F in columns 11 and 12.

a. Add 100 μl of diluted complement to wells A to F of column 10. Serially transfer 50 μl of diluted complement from wells A to F of column 10 to wells A to F of column 11 and then to wells A to F of column 12. After gently mixing the content of the wells of column 12, remove 50 μl of diluted complement and discard.
b. Add 50 μl of cold VBD to wells 10 to 12 in row A. In wells 10 to 12 of rows B to F, add 25 μl of cold VBD.
c. Add 25 μl of diluted antigen from step 8 to the appropriate wells in rows B to F of columns 10 to 12.

13. Finally, add 100 μl of cold VBD to wells 11 and 12 of row H. Each well should now contain a total volume of 100 μl.

14. Mix the contents of the wells for 5 to 10 s on a vibrating microtiter plate shaker.

15. Place plates at 2 to 8°C for 15 to 18 h. Cover the plates to prevent evaporation (an unused plate can serve this function; plates can be placed in stacks of five to eight plates).

16. Place VBD and SRBCs on ice and store at 2 to 8°C for use in the following steps.

17. As the incubation period in step 15 concludes, sensitize SRBCs are sensitized as described above; add 25 μl of sensitized SRBCs to all wells of the patient and control plates.

18. Mix the contents of the wells for 5 to 10 s on a vibrating microtiter plate shaker.

19. Cover the plates, and incubate them at 37°C for 30 min. Stack the plates no more than two high.

20. Centrifuge the plates for 5 min at 400 to 450 × *g*.

21. Read the plates for percent hemolysis compared to the color standard.

Reading and Interpretation of CF Reactions

1. Control sera must display the titer recommended by the manufacturer (or the typical titer for laboratory-derived control sera) ± 1 dilution. If not, the sera must be repeated for the particular antigen.

2. The complement back titration controls should display 95 to 100% lysis in column 10, 90 to 100% lysis in column 11, 30 to 50% lysis in the VBD control well (A of

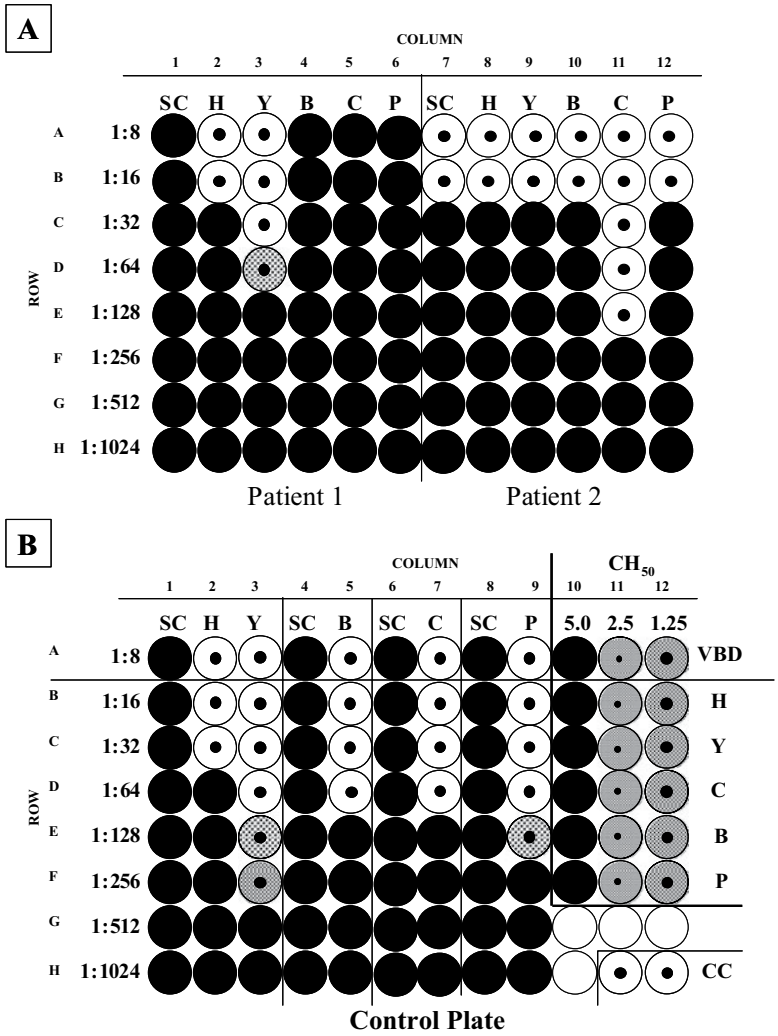

FIGURE 2 Diagram displaying organization of the microtiter plates and results for the CF assay. Solid circles, 100% lysis; shaded circles, 30 to 90% lysis; open circles, 0% lysis. SC, serum control wells receiving buffer in place of antigen; H, column receiving *Histoplasma* mycelial histoplasmin antigen; Y, column receiving *Histoplasma* yeast antigen; B, column receiving *Blastomyces* antigen; C, column receiving *Coccidioides* coccidioidin antigen; P, column receiving *Paracoccidioides* yeast antigen; CC, cell control; CH_{50}, amount of complement required for 50% lysis of SRBC. (A) Patient plate. Patient 1 demonstrates serum that is positive for *Histoplasma* antibodies with a 1:16 titer against mycelial histoplasmin antigen and a 1:64 titer against *Histoplasma* yeast antigen. Patient 2 displays serum that contains an AC titer of 1:16. However, because antibodies to coccidioidin are present at a titer that is >2 dilutions beyond the AC titer, the patient CF result is AC 1:16, *Coccidioides* 1:128. (B) Control plate. Columns 1 to 9 depict the reactivity of the control sera to specific fungal antigens. Columns 10 to 12, rows A to F, depict the results of the back titration of complement in CH_{50} units (5, 2.5, or 1.25) in the presence of fungal antigens or the VBD buffer control. Columns 11 and 12, row H, depict the cell control wells that receive SRBC only.

column 12), and 0 to 50% lysis in the antigen control wells (B to F of column 12). The cell control wells (H 11 to 12) should display no lysis (0%).

3. Wells with patient or control serum that display ≤30% lysis are considered positive. The dilution at which the last well of serially diluted serum displays ≤30% lysis is the antibody titer for that sample. Serum control wells should display >70% lysis.

4. Serum that displays ≤70% lysis in a serum control well is considered AC at that serum dilution, and results cannot be interpreted for that dilution (Fig. 2A, patient 2). AC activity often disappears as the serum is serially diluted. A patient's serum may contain an antibody titer that is greater than that of the AC activity. In this case, a titer of the fungal antigen can be interpreted and reported (i.e., a patient serum with AC activity that ends at a serum dilution of 1:8 and with a positive antibody to *Coccidioides* antigen observed at a 1:64 dilution can be reported as AC at 1:8 and positive for antibody to *Coccidioides* at 1:64). Parallel testing of serum using the ID assay can help to resolve antibody detection in serum that contains AC activity, as ID results are not affected by AC. However, ID tests may not be as sensitive as the CF test. Also, all of the QC measures described in the text under "Reagent Preparation and Standardization" above must be followed for optimal operation of the test.

Latex Agglutination

Theory

The LA test is a qualitative slide agglutination assay using latex particles to detect antibodies or antigen of interest. Antigen-coated latex particles measure antibody levels, and antibody-coated particles measure the presence of antigen in the specimen. Like the ID assay, the LA test depends on the formation of latticework structures to agglutinate the latex particles, resulting in visible clumping. Results are graded according to the level of agglutination (1+ to 4+ agglutination) observed for a particular dilution of serum. If a patient specimen contains an excessive quantity of antigen or antibody, a false negative, or prozone effect, may occur. In these instances, dilution of the patient specimen may reveal the positive reaction.

Commercial Methods—Antibody Detection

The assay is rapid and simple to perform, and no special equipment is needed. Commercial sources are listed in Table 1. The LA test yields results in a matter of minutes and may be used with sera giving AC activity in the CF test.

Sample Requirements

Blood should be collected into tubes that contain no anticoagulant, since anticoagulant can interfere with test performance. Specimens can be held at 2 to 8°C for up to 72 h before being tested but must be placed at −20°C or colder for long-term storage. Specimens should not be stored in frost-free freezers because repeated freezing and thawing can affect test results. Serum must be heat inactivated at 56°C for 30 min before being tested.

Performance of the LA assay procedure using commercial reagents should follow the procedure as described in the vendor's package insert. Briefly, serum and latex particles are placed on a reaction card provided by the manufacturer, mixed using a separate applicator stick for each serum to avoid cross contamination of samples, and placed on a rotary shaker or rotated by hand for the recommended time and speed. The reaction card is immediately examined macroscopically for signs of agglutination.

Agglutination is graded as follows: negative, a homogeneous suspension of particles with no visible clumping; 1+, fine granulation against a milky background; 2+, small but definite clumps against a slightly cloudy background; 3+, large and small clumps against a clear background; 4+, large clumps against a clear or very clear background. An agglutination grade of 2+ or greater is considered positive.

Avoid freezing of the latex particle suspension, since this can result in granularity, leading to false-positive results. Materials should not be allowed to dry on the slide.

Commercial Methods—Antigen Detection

The LA test for antigen detection is a noncompetitive direct-binding slide agglutination test to detect fungal antigens in clinical samples by employing latex particles adsorbed with an antigen-specific detection antibody (monoclonal or polyclonal). Specimens can be screened using a single dilution; positive samples are subsequently diluted serially to obtain an end point titer (2–4).

Sample Requirements

1. Various vendors provide kits for antigen detection for latex agglutination. Follow the requirements listed in the kit's package insert, as they vary as to the specimens for which they are approved. For cryptococcosis, most tests are approved for serum and CSF; some are also approved for BAL fluid. Plasma may not be used.

2. For serum, most kits recommend pretreatment with pronase before testing to disrupt antigen/antibody complexes. Pronase must be inactivated with pronase inhibitor or by boiling prior to use.

3. For CSF, heat in a boiling-water bath for 5 to 10 min as directed by the manufacturer. Pronase treatment of CSF is generally not recommended but was reported to increase LA titers by 2 to 3 dilutions in 14 (20%) of 70 CSF specimens tested (5).

4. BAL fluids should be treated with pronase prior to assay.

Performance of the LA assay procedure for antigen detection using commercial reagents should follow the procedure as described in the vendor's package insert. The procedure for antigen detection is the same as for antibody detection described above except that specimens are heat inactivated and/or pronase treated to remove immune complexes prior to use. An agglutination grade of 2+ or greater is considered positive. However, a 1+ reaction may be the result of a prozone effect as a result of excess antigen present in the specimen. If suspected, the assay should be repeated after serially diluting the specimen.

If desired, samples with a positive result upon initial screening can be diluted for end point titer determinations using serial 2-fold dilutions up to 1:1,024; greater dilutions may be required if testing determines that the specimen is still positive at the 1:1,024 dilution.

Enzyme Immunoassay

Theory

The EIA is a sensitive, solid-phase immunoassay that is used for the detection of either antibody or antigen. For antibody detection, a specific antigen, coated on the surface of a plastic microtitration well, binds or immobilizes specific antibody present in the patient's serum. The addition of an enzyme-labeled anti-human antibody results in the formation of an antigen/antibody/enzyme-labeled antibody complex. After the addition of the enzyme's substrate, a positive reaction is indicated by a color change measured spectrophotometrically.

Antigen is detected by coating the microtiter wells with a polyclonal or monoclonal antibody to the specific antigen. Antigen in the patient specimen is immobilized by the coating antibody and is detected by the addition of an enzyme-labeled antibody specific for the antigen. As with the antibody assay, the presence of enzyme is demonstrated by the addition of the appropriate substrate. While this method is very sensitive, often more sensitive than other methods, the specificity is variable depending on the specificity of the reagents employed in the assay. While several enzyme/substrate combinations can be used, horseradish peroxidase-tetramethylbenzidine is most frequently used.

EIA for Detection of Antifungal Antibody

EIAs available commercially for the detection of antifungal antibodies in patient specimens are detailed in Table 1. The kit contains all necessary reagents and microtiter plates precoated with antigen. Microtiter plates are composed of eight-well strips so that the entire plate does not have to be used at one time. Unused microwells must be placed back inside the foil ziplock pouch provided and sealed immediately to protect them from moisture.

A detailed stepwise procedure can be found in the package insert included with each kit. Briefly, all reagents should be brought to room temperature prior to performing the

assay. Diluted specimens are added to the antigen-coated microtiter plate, followed stepwise with a peroxidase-conjugated anti-human antibody and substrate solution. Each step is followed by an incubation and washing of the microwells using a plate washer. Plates are read spectrophotometrically at 450 nm or at 450/630 nm, if a dual-wavelength plate reader is available.

To reduce assay background, it is essential that excess wash buffer is removed after each wash by forcefully inverting the microtiter plate onto a paper towel until no more moisture is seen on the paper towel. Care must be taken that the microtiter well strips do not come loose from the microtiter well frame.

EIA for Detection of Fungal Antigen

Assays available commercially for the detection of fungal antigens in patient specimens are listed in Table 2. Such assays include the Platelia assays for *Aspergillus* GM antigen and for *Candida* antigen (BioRad) and a variety of tests for cryptococcal antigen. As with the antibody assay above, detailed stepwise procedures can be found in the package insert included with each kit. The methods are essentially the same as that for the EIA for antibody detection. The major difference between the two assays is that the wells of the microtiter plate are coated with antigen-specific antibody instead of antigen.

Lateral Flow Assay

Theory

The LFA is a rapid, low-complexity, immunochromatographic assay in which diluted serum/CSF travels by capillary action along a filter test strip to a sector containing immunogold-conjugated antibody. If antigen is present, antibody/antigen complexes form, continue to travel down the test strip, and are finally trapped by a line of immobilized anti-antigen antibodies. A red/purple line appears, resulting from the accumulation of immunogold particles and signifying a positive reaction. LFA results are available in 10 min.

Sample Requirements

Acceptable specimens are nonhemolyzed serum and aseptically collected CSF. Store specimens at 2 to 8°C for up to 72 h. For longer periods, store below −20°C. Do not repeatedly thaw and refreeze. If shipping is required, specimens should be maintained at 2 to 8°C or below −20°C.

Materials

The LFA kit contains all reagents necessary to perform the test. The kit is stored at room temperature (22 to 25°C).

Details of the procedure can be found in the kit package insert. Briefly, the patient specimen and specimen diluent are combined in a reaction tube, followed by placement of the LFA strip into the tube. After a 10-min incubation, the results are observed.

Interpretation

1. Positive: a line of any intensity visible on the LFA strip at the test position, plus a strong positive line at the control position.
2. Negative: a strong positive line at the control position on the LFA strip with no visible line at the test position.
3. Invalid test: no line present at the strip control position. The results are invalid and the test should be repeated.

Panfungal Detection Using 1,3-β-D-Glucan Assay

Theory

BDG is a component of the cell wall of all fungi except the Mucormycetes, and only low levels of BDG are released from *C. neoformans* (6). BDG activates factor G, a coagulation enzyme found in horseshoe crab amoebocyte lysates. Once activated by BDG, the enzyme cleaves a chromogenic substrate (*t*-butyloxycarbonyl-Leu-Gly-Arg-*p*-nitroanilide) included in the test, releasing *p*-nitroanilide. The free *p*-nitroanilide can then be quantitated with respect to a glucan standard. Two methods have been employed to measure the reaction, a colorimetric method and a turbidimetric method.

Two species of horseshoe crab, the North American horseshoe crab (*Limulus polyphemus*) and the Asian horseshoe crab (*Tachypleus tridentatus*) have been used in the production of BDG assays. The FDA-approved Fungitell assay (Associates of Cape Cod, East Falmouth, MA) uses the amoebocyte lysate from *Limulus polyphemus* and employs the colorimetric method. Alternative colorimetric (Fungitec G Test MK [Seikagaku Kogyo Co., Ltd., Tokyo, Japan] and BGSTAR β-glucan test [Maruhua, Tokyo, Japan]) (7) and turbidimetric (Wako-WB003; Wako Pure Chemical Industries, Ltd., Osaka, Japan) (8) forms of amoebocyte lysate assays are available in Japan (9).

Materials Required

The kit provides all necessary reagents

Pipette tips, must be glucan free

13- by 100-mm borosilicate glass test tubes, must be glucan free

Certified glucan-free tips and tubes can be purchased from the kit manufacturer

Spectrophotometer, capable of maintaining a temperature of 37°C and capable of dual-wavelength monitoring at 405 and 490 nm with a dynamic range up to at least 2.0 absorbance units

Computer with appropriate kinetic assay software

Specimen Requirements

Sterile serum samples should be placed in a container that is free of interfering levels of BDG and stored at 2 to 8°C before assay or frozen at <-20°C. False-positive results have been observed in specimens from patients undergoing hemodialysis when certain cellulose dialysis membranes are used (10, 11). Treatment with fractionated blood products such as serum albumin and immunoglobulins (12) have also resulted in false-positive results. Likewise, care must be taken with subjects or specimens exposed to glucan-containing gauze. Surgical gauzes and sponges can leech high levels of BDG that may contribute to a contamination-based transient positive result, as has been observed in postsurgical patients (13). In these cases, sera should be drawn 3 to 4 days after final exposure (hemodialysis or surgical exposure to BDG-containing sponges and gauze).

Procedure

Note, the outside wells of the microtiter well plate are not used in this assay. When first performing the assay, it is recommended to test patient sera and glucan standards in triplicate. As the use of the assay becomes more familiar and results more consistent, the assay can be performed in duplicate. During the procedure, avoid the use of gauze or other glucan-containing material which may contaminate

the specimen or assay. Use suitable protective clothing and powder-free gloves when handling patient specimens.

The Fungitell assay is quantitative, which measures the reaction from the patient specimen compared to the reaction of serially diluted glucan standard (measuring 31.25 to 500 pg/ml). For a detailed description of the procedure, refer to the package insert that is provided with the assay kit. Briefly, the patient specimen is initially treated with an alkaline reagent (equal volumes of 0.25 M KOH and 1.2 M KCl), converting triple-helix glucans that may be present in the serum into more-reactive single-stranded glucans (14, 15). This reagent also prevents false-positive and false-negative results by inactivating serine proteases and serine-protease inhibitors (16). The patient specimen is combined with the alkaline reagent in the microwell and incubated for 10 min in the spectrophotometer, preheated to 37°C. At the end of the incubation period, the standards and negative controls are added to appropriate wells of the microtiter plate and the Fungitell reagent (a BDG-specific LAL) is added to all reagent-containing wells. The microtiter plate is placed into the spectrophotometer (37°C) and shaken for 5 to 10 s with the lid on, and the plate is read at 405 to 490 nm, with the lid removed, for 40 min at 37°C. The spectrophotometer is set to collect data using the kinetic data point, reading the result as frequently as allowed by the software and instrument over the 40-min period of the test, and plotted using "linear/linear" or equivalent.

Interpretation

Negative, <60 pg/ml

Indeterminate, 60 to 79 pg/ml

Positive, ≥80 pg/ml

The accuracy of the assay is up to 500 pg/ml. For accurate results, specimens for which results are greater than 500 pg/ml must be diluted and retested. Results are multiplied by the dilution factor for the final result.

SERODIAGNOSIS OF FUNGAL INFECTIONS

Aspergillosis

Clinical Indications and Diagnostic Rationale

Patients with ABPA, pulmonary aspergilloma (fungus ball), or CNPA and immunocompetent patients with obscure pulmonary or sinus infections should be tested for *Aspergillus* antibodies. ABPA should be considered in patients with asthma, transient pulmonary infiltrates, and peripheral eosinophilia. Pulmonary aspergilloma occurs when *A. fumigatus* or other *Aspergillus* species colonize preexisting cavities of tuberculosis, sarcoidosis, or bronchiectasis. Assays to detect antibodies to *Aspergillus* species should be applied in such cases (see below; Table 1). Antibody testing has been suggested by some to play a role in the diagnosis of IA in nonneutropenic, high-risk SOT recipients. The sensitivity of such testing may be low, however, requiring repeated testing to detect the antibody response.

The commercial antigen detection test for IA (Platelia; Bio-Rad) detects circulating cell wall GM from medically important *Aspergillus* species (see below; Table 2) (17). The GM EIA may be used as a screening tool for high-risk patient populations such as allogeneic HSCT recipients. The European Organization for Research and Treatment of Cancer/Mycoses Study Group (EORTC/MSG) consensus group now includes a positive GM result as one of the factors in the definition of probable and possible fungal infections (18).

The website www.aspergillus.org.uk offers a listing of *Aspergillus* diagnostic tests approved for use in the United States and in Europe.

Antibody Assays for the Diagnosis of Aspergillosis

Serologic results can be helpful for the diagnosis of aspergillosis, but results from these assays should be used in conjunction with other diagnostic procedures including culture, histopathologic examination of biopsied tissues, and radiologic evidence of infection.

Immunodiffusion

The ID test is effective and specific for diagnosing aspergillosis in immunocompetent persons, and individual reagents can be purchased from several different sources (Table 1). Precipitins can be found in over 90% of patients with aspergillomas and in 70% of patients with ABPA or CNPA (19). Only serum samples that produce a line or lines of identity with reference serum from a patient with a proven case of human aspergillosis are considered positive in the ID test. Although one or two precipitins may occur when serum from patients with any clinical form of aspergillosis is used, the presence of three or more bands is usually associated with either aspergilloma or CNPA. Pulmonary fungus balls can also be produced by *Pseudallescheria boydii* and by other fungi; noninfectious conditions or other abnormalities may also be misinterpreted as aspergillomas on chest radiographs. In such cases, the *Aspergillus* ID test is usually negative. However, the ID test may also be negative in some patients with aspergillosis who are receiving long-term antifungal or corticosteroid therapy.

Complement Fixation

Reagents for the detection of anti-*Aspergillus fumigatus* antibodies by CF are available commercially (Table 1). While the specificity of the assay is very good, the sensitivity has been reported to be low for tests using cell homogenate antigens and to be variable (20 to 79%) for tests employing culture filtrate antigens (20). Few laboratories now use the CF test for the diagnosis of aspergillosis.

Enzyme Immunoassay

A commercial EIA (Platelia Aspergillus IgG; Bio-Rad, Redman, WA) for the diagnosis of aspergillosis using purified recombinant antigens has recently become available for the detection of antibodies in serum or plasma. In immunocompetent patients (329 sera) diagnosed with noninvasive aspergillosis, including ABPA (164 sera) and chronic pulmonary aspergillosis (16 sera), the sensitivity of the assay was 92.3% and 90.2 to 94.1%, respectively (21). The specificity was measured using sera from control patients suspected of having noninvasive aspergillosis but where aspergillosis was ruled out (114 sera) and was found to be 67.2 to 84.0%. Sera (n = 222) from noninfected persons displayed a specificity of 99.5 to 100%. Further reports will be needed to determine the usefulness of this assay.

Antigen Assays for the Diagnosis of Aspergillosis

Enzyme Immunoassay

A commercial monoclonal sandwich EIA to detect circulating serum GM antigen is effective in diagnosing IA in the immunocompromised host (Platelia *Aspergillus* EIA; Bio-Rad, Inc.), and it detects the disease approximately 1 week before clinical signs of infection. This assay uses a rat MAb, EB-A2, as both the capture and detector antibody for the (1,5)-β-D-galactofuranose residues of GM, an outer

cell wall component found in the most clinically important species of *Aspergillus*. The detection limit of this assay is 1 ng of GM per ml (Table 2) (22, 23).

Serum specimens may be collected at regular intervals before suspicion of infection and collected serially during the infectious episode. A 300-μl volume of patient serum is consumed each time the test is performed. Because the test may need to be repeated more than once and because some sample loss occurs during immune complex removal (precipitation of serum proteins during boiling in the presence of neutral disodium EDTA), at least 1 ml of patient serum is required for testing. The FDA has recently approved the use of BAL specimens in the GM assay. BAL fluids from lung transplant patients with proven or probable cases of IA demonstrate a sensitivity of 81.8% (24). Specificities in lung transplant patients not colonized with *Aspergillus* were 95.8 and 96.6% when using cutoffs of 0.5 and 1.0, respectively.

Results are expressed as an index (i.e., the ratio of the OD of the test sample to the OD of the mean cutoff control serum provided in the kit). An index of ≥0.5 is considered a positive result, and an index of <0.5 is considered a negative result. Positive results obtained with the Platelia *Aspergillus* EIA should be interpreted in conjunction with other diagnostic procedures including culture, histopathologic examination of biopsied tissues, and radiologic evidence of infection. For all positive samples, it is recommended that a second aliquot of the same sample be retested and a new sample collected from the same patient be tested in a follow-up procedure. In the absence of positive culture or histopathology, if tests for serum GM are repeatedly positive in patients at risk for IA, such results may be interpreted as a probable *Aspergillus* infection. On the other hand, negative test results do not rule out a diagnosis of IA. Even in cases of culture-proven or histopathologically proven IA, not every serum sample from each patient is expected to be positive.

Neonatal or pediatric serum samples have been reported to give a higher rate of false-positive results, and this may be related to the finding that the EB-A2 MAb used in the test reacts with components found in infant milk formulas and with the lipoteichoic acid of a common neonatal gut commensal, *Bifidobacterium bifidum*. False-positive test results may also occur in patients receiving piperacillin-tazobactam and amoxicillin-clavulanic acid antibiotics, since these agents also react with the EB-A2 MAb in vitro. Positive test results in such individuals should be interpreted with caution and confirmed by other diagnostic means. Other fungal genera, including species of *Histoplasma*, *Penicillium*, *Alternaria*, and *Paecilomyces*, have demonstrated reactivity with the EB-A2 MAb used in the Platelia *Aspergillus* test and could cause false-positive test results. Other possible reasons for false-positive results have been suggested, including reactions with cyclophosphamide and/or adsorption of dietary GM through a damaged intestinal wall.

Reduced detection of GM may occur in patients with chronic granulomatous disease or hyper IgE (or Job's) syndrome or in those with IA who are receiving antifungal therapy (25). Sera from such patients giving negative results should be retested. False-negative results have also been attributed to limited invasion of blood vessels by the organism or to especially high antibody titers in the host.

Lateral Flow Assay

Recently, an *Aspergillus* LFA was developed using MAb JF5, which is specific for a protein epitope on a glycoprotein antigen (26). In a guinea pig model of IA, the LFA was shown to be more sensitive and specific than the GM and BDG assays (27). In hematology patients with IA (28), LFA was more sensitive and specific than GM: 81.8 versus 77.3% and 98.0 versus 91.5%, respectively. The authors found that PCR was more sensitive (95.5%) but less specific (96.6%) than LFA. The combination of PCR and LFA provided the best sensitivity (100%) and specificity (100%). There is no commercial source for this assay, and it is still considered experimental.

1,3-β-D-Glucan

Several reviews regarding the diagnosis of invasive aspergillosis using nonculture methods, including the detection of BDG, have recently been published (29–31). Sensitivity and specificity for the diagnosis of IA are approximately 70 to 71% and 82 to 87%, respectively (29, 30), and 77 and 85%, respectively, for invasive fungal infections in general (32). Combining BDG detection with the GM assay further enhances the diagnostic capabilities of both assays to 80 to 88% sensitivity and 98 to 100% specificity (29, 33, 34).

Immunohistochemistry

Aspergillosis may also be diagnosed histopathologically by observing in biopsy tissue the typical dichotomous, branched, septate hyphae after Grocott's methenamine silver or periodic acid-Schiff staining (35). However, other filamentous fungal agents may appear similar morphologically to *Aspergillus*. A murine MAb, WF-AF-1, directed against a cell wall fraction of *A. fumigatus*, is commercially available (AbD Serotec, Raleigh, NC) for the immunohistochemical diagnosis of major *Aspergillus* species in tissues (36). After the tissue is deparaffinized and antigen cross-linking is disrupted, the tissue is stained using a standard immunohistochemistry method (36). The primary mouse MAb is placed on the slide followed by a secondary, anti-mouse antibody conjugated with a fluorescent or enzymatic label. If a fluorescent label is used, the slide is now ready to be examined using a fluorescence microscope with the appropriate filters specific for the fluorescent label. If an enzymatic label is used, the slide is next treated with a substrate solution specific for the enzyme label. The substrate reacts with the enzyme, forming a colored precipitate which is deposited on the tissue in places where the antibody is located, and can be detected using a bright field microscope.

Blastomycosis

Clinical Indications and Diagnostic Rationale

Blastomyces dermatitidis is a thermally dimorphic fungus that has a range of endemicity from the upper Midwestern states of the United States extending east and northeast through the St. Lawrence River Valley. While recent outbreaks suggest that exposure may occur in more urban environments, and with less active outdoor exposure (37, 38), the classic mode of infection is inhalation of conidia of disturbed moist soil, most frequently in relation to watershed areas and nearby waterways (39, 40). Infections may resolve spontaneously or slowly progress as a slow indolent process. Dissemination to multiple organs including bone, skin, and genitourinary system may occur. Antibody detection tests for blastomycosis should be performed with sera from patients showing signs of suspected acute pulmonary blastomycosis, especially if they reside in or have recently traveled to geographic areas where blastomycosis is endemic (40). Symptoms of acute pulmonary blastomycosis include a nonspecific respiratory infection characterized by fever, chills, productive cough, myalgia, arthralgia, pleuritic chest pain, and weight loss. Antibody detection tests should also be performed with sera from patients presenting with symptoms of chronic pulmonary blastomycosis, which are similar

to those of tuberculosis and include productive cough, hemoptysis, night sweats, malaise, weight loss, and low-grade fever. Antibody detection can be helpful when lesions are present on the skin, a common site of dissemination, and for monitoring CSF specimens from patients with suspected blastomycotic meningitis.

Immunocompromised patients are predisposed to severe forms of the disease, which can relapse and are often associated with a high mortality rate. Up to 40% of AIDS patients with blastomycosis have central nervous system disease that manifests as either meningitis or brain lesions. Others have presented with a septic shock-like syndrome. Experimental antigen detection tests, should they prove to be sensitive and specific, would be helpful for the diagnosis of disseminated blastomycosis in immunocompromised patient populations whose antibody responses may be limited or variable.

Antibody Assays for the Diagnosis of Blastomycosis

Substantial improvement in the serodiagnosis of blastomycosis can be attributed to the use of a purified surface antigen of *Blastomyces dermatitidis* called the "A antigen" by one group of investigators (41) and WI-1 by another group (42); both are released from the yeast form of *B. dermatitidis* by autolysis and are recovered from culture filtrates. Immunologically, the A antigen and WI-1 are related in that antibodies directed against the WI-1 antigen recognize the A antigen and vice versa. The A antigen has a molecular mass of 135 kDa and is glycosylated, whereas the WI-1 antigen is a 120-kDa protein that is not glycosylated.

ID test kits and reagents to conduct the ID and CF tests are commercially available (Table 1) for the detection of anti-*B. dermatitidis* antibodies. The A antigen is now incorporated into most commercially available kits and is also supplied as a reagent for in-house ID and CF testing.

Immunodiffusion

A positive reaction in an ID test using the purified A antigen is specific and diagnostic for blastomycosis. However, a negative ID test does not rule out a diagnosis of blastomycosis, since this test has been reported to be negative in 10% of patients with disseminated infection and over 60% of patients with localized disease.

Complement Fixation

Initial CF assays for the diagnosis of blastomycosis used a crude yeast antigen which resulted in unsatisfactory sensitivity and specificity. With the incorporation of purified A antigen into the CF assay, the specificity improved markedly from initial reports of 30 to 87% (43–45) to 97 to 100% (43, 45). However, the sensitivity still remains unsatisfactory for the diagnosis of disseminated infection (50%) or localized infection (33%) (43). Although the CF test is still in use, its sensitivity is poor and much reduced compared to the ID test, and it is therefore not discussed in further detail here.

Interpretation. The ID test performed using a *B. dermatitidis* yeast-form culture filtrate containing the A antigen is highly specific for blastomycosis. A positive reaction denotes a recent or current infection with *B. dermatitidis*. Positive reactions can therefore be the basis for immediate treatment of the patient without parallel testing for coccidioidomycosis or histoplasmosis. Negative test results, however, do not exclude a diagnosis of blastomycosis because the sensitivity of the ID test has been reported to range from 33% for localized infection to 88% for disseminated disease. In the absence of a positive A precipitin band or in cases where the CF test is positive for blastomycosis but the ID test is negative, patients should be examined extensively for evidence of infection with other endemic fungi as well as with *B. dermatitidis* (especially because the areas of endemicity for blastomycosis and histoplasmosis overlap and cross-reactivity can occur).

In patients where a high suspicion for blastomycosis exists, testing of an additional serum drawn 3 to 4 weeks after initial sampling may be necessary to detect the development of an A precipitin band indicating seroconversion and recent infection. In addition, sera should be drawn at 3-week intervals and examined by CF and ID tests with *B. dermatitidis*, *Coccidioides immitis*, and *Histoplasma capsulatum* antigens. Such testing may detect increases in CF titers to a causative organism other than *B. dermatitidis* or the development of precipitin bands diagnostic for blastomycosis, histoplasmosis, or coccidioidomycosis. In established cases of blastomycosis, the disappearance of the precipitin line is evidence for a favorable prognosis. The serologic response, however, is often not as rapid as the clinical response.

Enzyme Immunoassay

A commercial EIA (*Blastomyces* antibody enzyme immunoassay; IMMY) using a proprietary mixture of fungal yeast-phase antigens has recently been developed. The manufacturer reports a sensitivity of 83.3% compared to positive CF titers at ≥1:8 and 100% at ≥1:16. Sensitivity and specificity are 100% compared to ID. This assay looks very promising given the less than desirable results of the ID and CF assays. Independent evaluation of this assay has not been reported at this time.

Antigen Assay for the Diagnosis of Blastomycosis

Enzyme Immunoassay

A double-antibody sandwich EIA employing rabbit polyclonal antibodies to detect an uncharacterized antigen from *B. dermatitidis* in urine, serum, CSF, BAL fluid, and other body fluids is available only through a commercial reference laboratory (MiraVista Labs, Indianapolis, IN). Test sensitivity was reported to be 89 and 100%, respectively, for the detection of urinary antigen in the disseminated and pulmonary forms of blastomycosis (46). Little or no cross-reactivity was observed when specimens obtained from healthy volunteers or from patients with aspergillosis, candidiasis, coccidioidomycosis, or cryptococcosis were used, but significant cross-reactivity occurred when specimens from patients with disseminated histoplasmosis (96%), paracoccidioidomycosis (100%), or penicilliosis marneffei (70%) were used (46). Because the areas of endemicity for blastomycosis and histoplasmosis overlap, additional tests are required to obtain a specific diagnosis. The assay has recently been converted to a quantitative assay in which the result from the patient specimen is evaluated against a standard curve derived from serial dilutions of *B. dermatitidis* galactomannan isolated from the pooled urine of blastomycosis patients (47). The sensitivity of the assay on average is 89.9% but ranged from 88.2% in patients with only extrapulmonary involvement to 92.3% in patients with isolated pulmonary involvement. However, the assay continues to cross-react with 95.6% of samples from histoplasmosis patients. Patients with paracoccidioidomycosis and penicilliosis marneffei were not evaluated with the updated version. Individual case reports have shown that the assay appears to correlate well with confirmed cases of blastomycosis.

The use of the *Blastomyces* antigen test in outbreak investigations has displayed only a low success rate for the diagnosis of blastomycosis (37). The lack of sensitivity in this

case may reflect the delay in patient presentation until after the antigen in urine is cleared.

Candidiasis

Clinical Indications and Diagnostic Rationale

Candida albicans and other *Candida* species are part of the normal microbiological flora of humans, often found on the skin and in the respiratory and gastrointestinal tracts. Disease ranges from superficial cutaneous/mucocutaneous infections to severe disseminated infections. Tests for *Candida* antibodies have been extensively evaluated but remain of uncertain usefulness in the diagnosis of invasive forms of candidiasis. The clinical utility of these tests has been hampered by false-positive results in patients who are colonized with *Candida* species or who have superficial infections as well as by false-negative results in immunocompromised patients, who produce small or variable quantities of antibodies. Those most at risk for these infections include neutropenic cancer patients, HSCT and SOT recipients receiving immunosuppressive agents, and patients receiving critical care, particularly those in adult surgical and neonatal intensive care units. On the other hand, in immunocompetent patients, seroconversion from antibody negative to antibody positive may be diagnostically helpful. A decision to treat a patient with antifungal drugs must not be based on serologic data alone, however, but rather should be made after consideration of all available clinical and laboratory data.

Antibody Assays for the Diagnosis of Candidiasis

Immunodiffusion

ID tests to detect antibodies to *Candida* species have been applied using sera from patients with acute disseminated candidiasis, chronic hepatosplenic candidiasis, or localized deep-organ candidiasis (e.g., endocarditis). Patient serum containing antibodies that react with homogenate antigens of *C. albicans* in the ID test may produce one or several lines of identity. Systemic candidiasis should be suspected when serial serum specimens demonstrate seroconversion (i.e., when negative antibody test results become positive) or show temporal increases in the number of precipitins. ID kits are commercially available (Table 1).

The ID test for antibodies has good specificity (94 to 98%) but has variable sensitivity, ranging from >90% for confirmed cases of invasive candidiasis in immunocompetent hosts to much lower in more localized or superficial infections (Table 1).

Interpretation. Sera from candidiasis patients, which react with homogenate antigens of *C. albicans* in the ID test, may produce between one and seven precipitin bands. Seroconversion from negative to positive or an increase in the number of positive bands may be a strong indication for the diagnosis of systemic candidiasis. Negative results do not rule out the diagnosis of candidiasis. The serum may have been obtained too early, before the generation of antibodies. Serial specimens can be obtained every 2 to 3 weeks to observe seroconversion.

Enzyme Immunoassay

An EIA to detect antibodies to circulating mannoprotein, a major cell wall component of *Candida* species, is commercially available in some countries but not in the United States (Platelia *Candida* Antibody; Bio-Rad). The assay uses a four-point calibrator range (2.5 to 20.0 AU) that is created through user-developed dilutions. Clinical evaluations of the test with sera from patients with invasive candidiasis demonstrated that the test specificity ranged from 63 to 94% but the test sensitivity ranged from 25 to 88%, depending on the identity of the infecting *Candida* species (the lowest sensitivity occurred for detecting *C. parapsilosis* infections, and the highest occurred for detecting *C. albicans* infections) (Table 1).

An updated version of the antibody EIA was recently developed (Platelia Candida Ab Plus; Bio-Rad), allowing measurement of antibody levels in either serum or plasma. Prediluted assay calibrator reagents are provided which form a five-point curve with a broader range (0 to 80 AU/ml). Sensitivity and specificity for the diagnosis of candidiasis are maximized when combining the results of the antimannan antibody assay with the *Candida* mannan antigen assay (see below).

The production and use of recombinant proteins as antigens has recently displayed promise for the serodiagnosis of candidiasis. A panel of four recombinant *Candida* antigens was evaluated in an EIA format for the detection of anti-*Candida* antibodies in serum of systemic candidiasis patients (48, 49). A combination of these assays displayed a sensitivity of 96.6% and specificity of 95.6% (37). It has been suggested that the use of a panel of recombinant *Candida* antigens improves utility in the diagnosis of candidiasis, as antibody titers to individual antigens vary during infection (49). EIAs using recombinant enolase and fructose-bisphosphate aldolase (50) for the diagnosis of candidemia were 72 and 95% and 87 and 93% sensitive and specific, respectively. Combining the results of both assays resulted in a sensitivity and specificity of 90 and 91%, respectively. There are no commercial sources for assays using recombinant antigens for the serodiagnosis of candidiasis, and they are still considered experimental.

IFA Assay

An IFA assay to detect antibodies to *C. albicans* is available commercially (Table 1). The assay detects antibodies to the germ tubes of *C. albicans* cells (CAGTA) and has a sensitivity and specificity of 76 to 94% and 95 to 100%, respectively (51). In a study of nonneutropenic intensive care unit patients, mortality rates were significantly lower in patients that developed CAGTA (52). A significantly larger number of patients with invasive candidiasis displayed CAGTA antibodies compared to uninfected or colonized patients. Combining the results of CAGTA and BDG resulted in a sensitivity of 87% and a specificity of 94 to 100% (50, 53, 54).

Antigen Assays for the Diagnosis of Candidiasis

Antibody detection tests have limited sensitivity for the diagnosis of invasive candidiasis in immunocompromised patients because antibody production may be limited due to the suppressed immune response. Furthermore, antibody that is present may be bound to antigen present in the sera. Therefore, antigen detection assays have been developed to aid in diagnosis in these cases. Among these are tests to detect heat-labile antigens by reverse passive LA (Cand-Tec test; Ramco Laboratories, Inc., Stafford, TX) and heat-stable *Candida* cell wall mannan by EIA (Platelia *Candida* Ag EIA; Bio-Rad Laboratories, Inc.).

Latex Agglutination

The Cand-Tec test has been commercially available for many years. The nature of the antigen is unknown, but its susceptibility to heat (56°C), pronase, 2-mercaptoethanol, and sodium periodate treatment suggests that it may be a

glycoprotein. Test sensitivity varied widely among studies (2 to 59%), whereas test specificity ranged from 93 to 95%, using a threshold titer of ≥1:8. A threshold titer of ≥1:4 resulted in a somewhat increased sensitivity (41 to 81%) and a specificity of 80 to 97% (55–57) (Table 2).

Enzyme Immunoassay

The Platelia *Candida* Ag (Bio-Rad Laboratories) (Table 2) is a commercial double-antibody sandwich EIA antigenemia detection test that can be conducted as either a quantitative (results are compared to a standard curve) or a qualitative (results are expressed as an index relative to the calibrator serum) test. This assay uses a rat MAb, EB-CA1, as both the capture and detector antibody for α-(1,2)-linked oligomannosides, outer cell wall components of most clinically important species of *Candida* (58). The assay is not available in the United States. The quantitative assay uses a four-point calibration curve (0.25 to 2.0 ng/ml) from which the patient antigen concentration is calculated. The Platelia *Candida* Ag EIA has an overall sensitivity of 52% and a specificity of 85 to 95%.

An updated version of the *Candida* antigen EIA has recently become available (Platelia Candida Ag Plus; Bio-Rad) which measures antigen levels in both serum and plasma. Prediluted assay calibrator reagents are provided and form a five-point curve with a broader range (0 to 500 pg/ml). The Platelia *Candida* Ag Plus EIA has an overall sensitivity of 62% and a specificity of 98 to 99%. The reduced sensitivity is due to the extremely low sensitivity of the assay in detecting infections due to *C. parapsilosis*, *C. krusei*, and *C. guilliermondii* (59). Sensitivity and specificity for the diagnosis of candidiasis is maximized when combining the results of the anti-mannan antibody assay with the *Candida* mannan antigen assay.

Sample requirements. Serum and/or plasma (i.e., EDTA, heparin, or citrate anticoagulants) specimens should be collected serially during the infectious episode. If the test is to be used as a screening tool in high-risk patient populations, such as SOT recipients and critical care patients, sera may also be collected at regular intervals before any symptoms develop. Mannan is found in the serum in low nanogram-per-milliliter concentrations and is rapidly cleared from the circulation, necessitating frequent sampling of patients during periods of high risk. Therefore, the use of multiple serum specimens, collected at least twice per week, increases test sensitivity.

Strict compliance with the prescribed 100°C temperature for the boiling water bath is essential for success of the test. A negative control serum (no mannan), a calibrator serum (containing 2.0 ng of mannan per ml and the concentration from which to prepare a standard curve for the quantitative assay or from which to dilute to 0.5 ng for the qualitative assay), and a positive control serum (containing between 0.5 and 1.5 ng of mannan) are included in each kit. Results are expressed in nanograms per milliliter extrapolated from the standard curve (quantitative assay) or as an index (semiquantitative assay; i.e., the ratio of the OD of the test sample to the OD of the mean calibrator serum provided in the kit). In both test modes, OD values for the calibrator, for the four points comprising the standard curve (quantitative mode), and for the positive and negative controls must be within their designated ranges.

Interpretation. Serum samples with a mannan concentration of less than 0.25 ng/ml are considered negative, serum samples with a mannan concentration of between 0.25 and 0.5 ng/ml are considered intermediate, and serum samples with a mannan concentration greater than or equal to 0.5 ng/ml are considered positive. Range points used to plot the standard curve do not allow precise determination of mannan concentrations above 2.5 ng/ml, and strongly positive sera should be diluted 1:5 (vol/vol) with negative serum and retested. Positive results obtained with the Platelia *Candida* Ag test should be interpreted in conjunction with other diagnostic procedures including culture, histopathology of biopsied tissues, and radiographic evidence of infection. Negative test results do not rule out a diagnosis of invasive candidiasis. Even in cases of culture or histopathologically proven candidiasis, not every serum sample from each patient is expected to be positive.

The EB-CA1 MAb is specific for an α-linked mannopentose common to all *Candida* species (60), but test sensitivity varies depending upon the *Candida* species being detected. For example, in a retrospective study conducted on 106 patients (366 sera) residing in various hospital wards (surgery, hematology, intensive care, burns, and others) and from whom *Candida* species were isolated from the blood or other sterile body sites, the overall sensitivity of the EIA was 52%. For infections with specific *Candida* species, however, sensitivities were 70% for *C. tropicalis*; 50 to 58% for *C. kefyr*, *C. albicans*, and *C. glabrata*; 38% for *C. parapsilosis*; and only 20% for *C. krusei*. The moderate sensitivity exhibited by the test does not provide an optimum negative predictive value for diagnosing invasive candidiasis. However, because the overall specificity of the EIA is so high (98%), a positive result obtained with samples from patients at risk suggests infection.

1,3-β-D-Glucan Assay

BDG has been evaluated for utility in the diagnosis and prognosis of patients with candidiasis. In a study of patients in a surgical intensive care unit, the sensitivity of BDG to detect invasive candidiasis on the day of diagnosis was 87% with specificity of 73% (61). In 3 patients, however, the BDG became positive 4 to 8 days prior to diagnosis. BDG may be more useful in determining the prognosis of the infection. Serial samples from invasive candidiasis patients showed a decline in BDG levels in successfully treated patients compared to those with treatment failure that resulted in increased levels of BDG (62, 63).

Coccidioidomycosis

Clinical Indications and Diagnostic Rationale

Coccidioides species are thermally dimorphic fungi that are endemic to the desert southwestern United States, northern Mexico, and parts of Central and South America. While infections in many cases are asymptomatic, symptomatic infection is known as Valley fever, a severe pulmonary disease in immunocompetent persons and sometimes fatal, disseminated infection in immunocompromised individuals. *Coccidioides* is found in dry desert soil and when disturbed by manmade or natural forces, the coccidioidal arthroconidia are aerated and infection is initiated upon inhalation of the arthroconidia. Serologic tests should be considered whenever patients display signs and symptoms of coccidioidomycosis and have lived in or traveled to areas where *C. immitis* (California) or *C. posadasii* (Arizona, New Mexico, Utah, Texas, Mexico, and Central and South America) are endemic. Coccidioidin, a liquid culture filtrate of *Coccidioides immitis*, is the antigen upon which the serologic assays are based. The antigen is prepared from cultures grown in synthetic asparagine-glycerol salt medium (64). Serologic assays do not distinguish between the two species of *Coccidioides*.

Tests to detect anti-*C. immitis* antibodies are of proven usefulness for the diagnosis and management of coccidioidomycosis. One of the original serologic methods for the diagnosis of this disease was the TP test which detects IgM antibodies reactive against a heat-stable, carbohydrate-containing component in coccidioidin. However, this assay is rarely used today. Current serologic test formats include ID (IDTP and IDCF), LA, CF and EIA. The IDTP and LA assays measure predominantly IgM, IDCF and CF predominantly measure IgG, and the EIA measures both IgG and IgM.

The CF and TP assays were the original, liquid-phase assays that used unheated coccidioidin (containing F antigen) and heated (60°C, 30 min) coccidioidin. Through the heating process, the predominant F antigen is inactivated, revealing the heat-stable TP antigen. These assays were subsequently converted to solid-phase ID assays: IDCF and IDTP.

Antibody Assays for the Diagnosis of Coccidioidomycosis

Immunodiffusion

The ID test format can be used to simultaneously detect IgM (IDTP) and IgG (IDCF) antibodies. Both the IDTP and the IDCF tests are performed using separate seven-well ID patterns. Positive control IDTP and IDCF sera are placed in independent wells and are tested against patient sera using optimally diluted heated (for IDTP) or unheated (for IDCF) coccidioidin. Lines of identity between patient sera and positive reference sera, corresponding to reactive IgM (for IDTP) and IgG (for IDCF) antibodies, can then be observed for positive cases of early or late disease, respectively (65). Serum demonstrating AC activity, making CF test results difficult to interpret, can be successfully used in the ID test. In addition, the ID test is more specific than CF and may help resolve CF cross-reactivity issues often encountered among the endemic mycoses during CF testing. Commercial sources for ID kits and reagents for use in ID tests are listed in Table 1.

Sample requirements. Serum from symptomatic patients may give negative or indeterminate test results early in infection. Additional serum from such patients should be obtained 3 to 4 weeks later, and the tests should be repeated. CSF should be obtained and tested in parallel with serum specimens from patients presenting with signs and symptoms of meningitis. The sensitivity of the IDTP and IDCF tests can be increased by 4- to 8-fold concentration of serum prior to testing. Serum can be concentrated by evaporation *in vacuo* (Speed-Vac; Thermo Fisher Scientific, Waltham, MA) or by the use of centrifugal ultrafiltration devices (Centricon; Millipore, Billerica, MA). Concentration of test serum may be especially helpful to improve IDTP detection of low levels of IgM antibodies present early in infection or to improve IDCF detection of IgG antibodies in specimens from patients with chronic disease.

Interpretation. *IDTP.* Observation of a band of identity in the IDTP assay indicates that the patient is in the early stages of coccidioidomycosis. Of patients with coccidioidomycosis, 75% develop a detectable IDTP antibody response as early as 1 week after the onset of symptoms and 91% are positive within 3 weeks. Negative test results, however, do not exclude a diagnosis of coccidioidomycosis. In the absence of a positive precipitin band, or in cases where the CF test is positive but the IDTP test is negative, patients should be examined extensively for evidence of infection with another endemic fungus as well as with *C. immitis*. In addition, sera should be drawn at 3-week intervals and examined using CF and ID tests with *B. dermatitidis*, *C. immitis*, and *H. capsulatum* antigens to detect increases in CF titer specific for infection with one of the endemic fungi or to detect the development of precipitin bands diagnostic for blastomycosis, histoplasmosis, or coccidioidomycosis. IDTP antibodies may not be detected in immunosuppressed patients with disseminated coccidioidomycosis (66). False-positive IDTP reactions have been reported to occur in 15% of sera obtained from cystic fibrosis patients in the absence of a positive culture for *C. immitis* (67). A positive IDTP test can also rarely indicate the presence of chronic pulmonary cavities. Although infrequent, a positive result using CSF in the IDTP test indicates the presence of acute meningitis. IDTP-reactive antibodies may also occur in cases of disseminated coccidioidomycosis; 347 (48%) of 722 patients with disseminated infections demonstrated reactivity to this antigen, and in some cases, patient sera were reactive for up to several years (68). Persistence of IDTP-reactive antibodies (along with positive CF titers) may therefore be an indication of disease severity.

Interpretation. *ICDF.* Observation of a band of identity in the IDCF assay is presumptive evidence that the patient had recent or chronic coccidioidomycosis. IDCF-reactive antibodies can usually be detected within 2 to 6 weeks after the onset of symptoms. Occasionally, a band of nonidentity may be observed very close to the ID well containing the patient's serum. This band may represent the presence of reactive IgM antibodies; in such cases, the IDTP test should be performed.

Although the IDCF test is generally not performed as a quantitative test, it can be used in this manner after serial dilution of patient serum to obtain an end point titer. Titers obtained by using the quantitative IDCF test are not identical to titers obtained from the CF test, but the observed trends are comparable (titers of each will rise or fall in parallel). Results using specimens collected longitudinally may show differences in the intensity of bands or in banding patterns which have prognostic value. On the other hand, IDCF-reactive antibodies may not be detected in immunosuppressed patients with disseminated coccidioidomycosis (66).

Latex Agglutination

The LA test is a simple and rapid method, using particles adsorbed with heated coccidioidin, to measure early antibody production corresponding to that detected by the TP or IDTP tests. The LA test is a qualitative slide agglutination assay in which antibodies to *C. immitis* present in patient specimens bind to the antigen-coated latex particles and are graded according to the level of agglutination observed for a particular dilution of serum. The assay measures predominantly IgM antibodies and therefore is used to diagnose early coccidioidomycosis. Commercial sources are listed in Table 1.

Interpretation. Agglutination of 2+ or greater is considered a positive test result, indicating early or primary coccidioidomycosis. The LA test is more sensitive than the IDTP test but is less specific; 5 to 10% false-positive rates have been reported (69, 70). Therefore, a positive LA result with undiluted serum or CSF must be confirmed by ID and/or CF testing (65). This false-positivity rate is greater if sera have been diluted before testing. Therefore, the LA test cannot be used as a quantitative test and results which are positive by this method must be confirmed by the IDTP test. The

LA test, however, may yield a positive result earlier than the IDTP test. False-negative LA results may occur in specimens from immunocompromised patients. Also, 10 to 30% of individuals with culturally or serologically (CF or ID) positive results may demonstrate a negative or 1+ reaction in the LA test, limiting the test's negative predictive value. Such test negativity is thought to be related to the rapid rise and fall of IgM levels early in infection.

Complement Fixation

The CF assay, using unheated coccidioidin antigen, detects antibodies predominantly of the IgG subtype. Sera from approximately 98% of patients with disseminated infection are positive in the CF test within 2 to 6 weeks after the onset of illness. The CF-reactive antibodies typically disappear within 6 months after onset but can persist in disseminated or chronic infection. An advantage to the use of the CF test for the diagnosis of coccidioidomycosis is that it is a sensitive assay which provides quantitative results. Testing serial specimens to detect rising or falling antibody titers can reveal the progression or regression of illness (65, 71) and the response to antifungal therapy. The major disadvantage of the CF assay is that it is a laborious and time-consuming test that requires experienced personnel for optimum performance. No commercial CF test kit is available, but reagents for in-house use can be obtained from the vendors listed in Table 1.

Sample requirements. The CF test may be performed with serum and CSF. Pleural, peritoneal, and joint fluids (in conjunction with serum) may also be tested when the corresponding anatomical sites are thought to be involved. Concentration of sera before performance of the CF test can be useful in the detection of chronic cases of coccidioidomycosis which might otherwise be missed.

Interpretation. A CF titer to coccidioidin at any dilution should be considered presumptive evidence for *C. immitis* infection. Sera giving titers of 1:2 to 1:8 in the CF test that are also positive in the IDCF test reflect currently active or recent infection. CF titers of >1:16 generally indicate extrapulmonary dissemination, whereas titers of 1:2 or 1:4 usually indicate early, residual, or meningeal coccidioidomycosis. However, titers of 1:2 and 1:4 have also been obtained when sera from patients without coccidioidomycosis were used. The parallel use of the IDCF test and the CF test can therefore help confirm or refute the significance of low titers. Negative serologic test results do not exclude a diagnosis of coccidioidomycosis. Patients with clinical presentations consistent with coccidioidomycosis whose sera give negative or low CF titers should be retested at 3- to 4-week intervals; all sera should then be tested in parallel to detect any increases in titer or to detect seroconversion. Approximately 5% of all CSF specimens from patients with coccidioidal meningitis are negative in the CF test. Sera from patients with chronic cavitary coccidioidomycosis may also frequently be negative.

Enzyme Immunoassay

The Premier *Coccidioides* EIA (Meridian Diagnostics, Inc.) is a qualitative test to determine the presence of anti-*Coccidioides* IgG and IgM antibodies in serum or CSF by using microtiter plates coated with a mixture of purified CF and TP antigens. Antibodies in serum or CSF are detected colorimetrically after addition of peroxidase-labeled, class-specific, anti-human IgM or IgG. The assay detects IgG and IgM antibodies separately, but maximum test sensitivity is achieved by using results from the detection of both IgG and IgM antibodies (Table 1). It is recommended that any positive result in the EIA be confirmed by the ID assay.

Interpretation. Absorbance values of ≥0.200 are considered positive, and values of <0.150 are considered negative. Specimens with absorbance values between 0.150 and 0.199 are defined as indeterminate, and testing must be repeated. A new specimen should be obtained from any patient whose original specimen gives repeatedly indeterminate results. Because the test uses a mixture of TP and CF antigens to coat microtiter plate wells, it does not distinguish between antibodies reactive to one antigen or the other. The kit may be used to detect reactive antibodies of a single class (IgG or IgM); however, optimum test sensitivity is obtained by using results for both Ig classes. Attempts to operate the Premier *Coccidioides* EIA as a quantitative test have not given results that correlate precisely with titers obtained by the conventional CF test. Nonetheless, the EIA has been used as a qualitative test in a series of evaluations and has been demonstrated to have an estimated sensitivity of 95 to 100%, a specificity of 96 to 99%, and positive and negative predictive values of >95% (72–74). There have been some reports questioning the specificity of the IgM result, particularly in cases that are IgG negative. While the manufacturer reports a 4 to 6% false-positivity rate in IgM-only positive patients, others report 18% and as high as 82% false-positivity rates (75–77). It has been suggested that IgM-positive results from patients with a high suspicion of infection are less likely to be false positives (76, 78). Therefore, positive EIA test results should be confirmed by IDTP and IDCF assays. The standard CF test should be employed in cases where there is concern about possible extrapulmonary dissemination (79).

Enzyme Immunoassay

Another commercial EIA for the antibody diagnosis of coccidioidomycosis has recently become available (Omega *Coccidioides* antibody EIA; IMMY) which uses a mixture of recombinant and native antigens. In contrast to the previous EIA, this kit provides 196 wells (2 plates). The wells from one plate are coated with CF antigen and the others with TP antigen. In comparison to complement fixation, the assay is 92.5% sensitive and 98.7% specific in a "normal" population. The specificity was 78.6%, with 16.7% indeterminate and 4.8% (2/42) false positive, using sera from patients with other fungal infections. These results were reported by the manufacturer. Studies to determine the efficacy of this assay by independent laboratories have not yet been reported.

Interpretation. Results are reported in EIA units which are calculated by dividing the absorbance reading from the patient serum by the absorbance reading from an internal calibrator control provided by the manufacturer. Results of <1.0 are considered negative and ≥1.5 are considered positive. Results of ≥1 to <1.5 are indeterminate.

Antigen Assays for the Diagnosis of Coccidioidomycosis

Enzyme Immunoassay

A commercial antigen assay for the detection of *Coccidioides* antigens in urine (*Coccidioides* antibody EIA) is offered as a fee-for-service assay at a commercial reference laboratory (MiraVista Laboratories, Indianapolis, IN). The assay has been shown to be 70.8% sensitive (80). Polyclonal capture antibodies for this assay were produced by injecting

rabbits with a mixture of purified *Coccidioides* galactomannan and formalin-killed mold. The specificity of the assay was 99.4% when compared to healthy individuals and patients with nonfungal infections. There was a 10.7% cross-reaction with other endemic molds.

Cryptococcosis

Clinical Indications and Diagnostic Rationale

Cryptococcus neoformans and *C. gattii* are yeasts that are ubiquitous in nature. While infection can occur in immunocompetent persons (81), cryptococcosis is most often associated with HIV infection or other immunocompromising disorders. Antibody assays are generally not considered helpful in the diagnosis of cryptococcosis, as most individuals have been exposed and have seroconverted early in life (82). However, serologic tests to detect *C. neoformans*/*C. gattii* antigens are an indispensable tool for the rapid diagnosis of pulmonary, meningeal, or disseminated forms of cryptococcosis and should be considered for immunosuppressed patients with signs and symptoms of a subacute meningitis or meningoencephalitis. In HIV-infected persons, headache and fever are common, but overt neurological symptoms and signs are unusual. In HIV-negative persons, headache may be common, but fever is often minimal or absent until late in the course of the infection. A subset of HIV-negative persons infected with *C. gattii* preferentially develop pulmonary disease instead of neurologic disease.

Antigen assays for the diagnosis of cryptococcosis have been developed using a variety of formats including LA, EIA, and most recently, the LFA. The *Cryptococcus* LA test to detect capsular polysaccharide in CSF and serum of patients infected with *C. neoformans*/*C. gattii* is one of the most reliable diagnostic tests in immunomycology. The EIA provides more objective end points with equivalent sensitivity and is more amenable to large numbers of specimens. A new assay based on lateral flow technology has been developed for the detection of capsular antigen. All three assays are designed to detect antigen in serum and CSF and are commercially available (Table 2). The selection of the method to use is dependent upon the laboratory's specimen load and equipment available. The LA and LFA are less amenable to large specimen loads.

Antigen Assays for the Diagnosis of Cryptococcosis

Latex Agglutination

The LA test is a noncompetitive direct-binding slide agglutination test to detect *C. neoformans*/*C. gattii* antigens in clinical samples. Latex particles adsorbed to anti-*C. neoformans* antibodies are employed and can be used to screen specimens for positivity, and positive samples can subsequently be diluted serially to obtain an end point titer (2–4). There are multiple commercial sources for LA tests to detect cryptococcal antigen, including those which adsorb latex particles with PAbs (Latex-Cryptococcus antigen test [Immuno-Mycologics, Inc.], CALAS [Meridian Diagnostics]) or with mouse anti-glucuronoxylomannan MAb (Pastorex Crypto Plus; Bio-Rad Laboratories) (Table 2). Results and end point titers vary among LA tests from different manufacturers, and reagents are not interchangeable. Generally, tests detect both *C. neoformans* and *C. gattii* infections. Similar sensitivities were reported for the MAb-based LA test compared to the two PAb-based LA tests using sera obtained from patients with culture-confirmed cryptococcosis (4). Unlike the PAb-based tests, the MAb-based LA test is recommended for use with BAL fluid and urine specimens as well as with serum and CSF (4).

Before running the assay, sera should undergo a pronase treatment step and CSF specimens should be boiled for 5 to 10 min to remove interfering substances which may cause false reactions in the LA assay. False-negative reactions may occur as the result of immune complex formation resulting from patient antibody masking the antigen epitopes recognized by the antibody-coated latex particles. On the other hand, the presence of rheumatoid factor in serum can result in a false-positive reaction. Rheumatoid factor, an anti-IgG autoantibody, can cause false agglutination by cross-linking the IgG antibody-coated latex particles.

Also, specimens containing a high concentration of cryptococcal antigen may show false-negative reactivity due to prozone effect, where excessive antigen inhibits the agglutination reaction, displaying weak or no agglutination. In cases where negative or weak reactions are observed but cryptococcosis is strongly suspected, the specimen should be retested after dilution (1:10 and 1:100) in glycine-buffered saline. Rarely, false-negative results may occur when sera from patients infected with poorly encapsulated strains of *C. neoformans* are tested. Such strains produce insufficient amounts of polysaccharide antigen to be detected and give false-negative results.

Latex particles should not be frozen, since this can result in granularity, leading to false-positive results; excessive hand rotation during observation may also lead to misinterpretation of results. False-positive reactions have also been reported to occur as the result of inadequate removal of detergent from the surface of reusable glass ring slides used for the LA test. Detergent can be removed by soaking slides in 10% bleach followed by thorough washing with distilled water. Rare false-positive results may be caused by the presence of contaminating hydroxyethyl starch, by nonspecific reactivity found in the serum of HIV-infected patients, and by cross-reactions with serum from patients infected with *Capnocytophaga canimorsus* or *Trichosporon asahii*.

Periodically, the sensitivity of the latex particles coated with anti-cryptococcal globulin should be tested by titration against purified capsular polysaccharide antigen included in the kit. Pronase provided in the kit must be stored frozen in aliquots after initial reconstitution to eliminate exposure to repeated freezing and thawing and subsequent loss of enzyme activity. Also, at least once per month, an aliquot of frozen pronase should be examined for proteolytic activity by testing, in parallel, goat anti-rabbit globulin (PAb-based systems) or goat anti-mouse globulin (MAb-based systems) that have and have not been pronase treated before use. The untreated pronase control must demonstrate agglutination of 2+ or greater, and the pronase-treated control must demonstrate agglutination of less than 1+ in the reaction.

Interpretation. The LA test to detect *C. neoformans* antigen has both diagnostic and prognostic value. A positive LA reaction at a titer of 1:4 or less using CSF, serum, or urine from an untreated patient is suggestive of cryptococcal infection, whereas titers of 1:8 or greater usually indicate active cryptococcosis (strong presumptive evidence). Antigen is detected in the CSF of over 90% of patients with untreated meningeal cryptococcosis. On the other hand, a negative serum antigen test result does not exclude a diagnosis of cryptococcosis, particularly if only a single specimen has been tested and the patient continues to have symptoms consistent with cryptococcal infection.

In HIV-negative patients, the antigen titer is usually proportional to the extent of infection. Whereas increasing titers reflect progressive infection and a poor prognosis, declining

titers generally indicate a favorable response to chemotherapy and progressive recovery; failure of the titer to fall during therapy suggests inadequate treatment. High initial titers of antigen (1:1,024 or greater) in the serum or CSF prior to treatment indicate a poor prognosis, and high titers at the end of treatment often predict later relapse. In contrast, HIV-positive patients may manifest elevated titers that decline very slowly even in the face of clinical improvement, whereas an unchanged or increased titer in the CSF of these patients is often associated with clinical and mycological failure to respond to treatment. Positive CSF antigen tests, despite no recovery of viable cryptococci from the CSF, may indicate persistent release of capsular antigen from dead as well as from living cells or may indicate slow elimination of capsular antigen from the CSF rather than ongoing infection.

Enzyme Immunoassay

The Premier Cryptococcal Antigen test (Meridian Diagnostics, Inc.) is a double-antibody sandwich EIA for the detection of cryptococcal polysaccharide antigen in patient serum and CSF. Rabbit polyclonal anti-*C. neoformans* antibodies, adsorbed onto the surface of microtiter plate wells, are used to capture cryptococcal polysaccharide antigen found in the serum and CSF of patients with cryptococcosis. Peroxidase-labeled detector MAbs are applied, and plates are read visually or spectrophotometrically after the addition of peroxide and a colorimetric substrate. Its sensitivity has been reported to be equivalent to or somewhat better than that of the LA test produced by the same manufacturer, and it does not require serum to be heat inactivated or pretreated with pronase to remove immune complexes or rheumatoid factor, nor does it require that CSF be boiled before testing (2–4). The EIA is not subject to prozone effects and has also been reported to detect cryptococcal antigen earlier, and at lower concentrations, than does the LA test (2). LA titers and EIA titers are not equivalent but generally follow the same trend (i.e., both titers increase and decrease in parallel).

Sample requirements. Serum and CSF samples may be tested, but urine may not be tested. Sample preparation of CSF and serum for the EIA consists only of centrifugation to remove any cells or other particulate matter. Pretreatment of specimens is not recommended by the manufacturer. However, samples that have previously been pronase or heat treated (56°C for 15 min) may be used in the screening assay but should not be tested in the semiquantitative test mode, since such treatment may alter EIA titration results. Therefore, it is recommended that all serial specimens from a given patient be pronase or heat treated in the same manner and that all samples be assayed in parallel when monitoring patients for disease changes or response to drug therapy; earlier specimens collected as part of these series should be aliquoted and frozen if stored for longer than 72 h at 2 to 8°C.

Procedure. A detailed stepwise protocol can be found in the package insert included with each kit. The EIA can be performed in one of two modes: (i) as a screening assay examining a patient specimen at a single concentration and designed solely for the differentiation of positive from negative specimens, and (ii) as a semiquantitative assay where the patient specimen is serially diluted (starting at 1:2) to obtain an end point titer. An analysis of a series of specimens collected longitudinally can be used to monitor relative changes in antigen levels in serum and CSF for the evaluation of patient progress and to monitor the efficacy of drug therapy. Specimens from the same patient should be assayed in parallel, in the same run, for accurate comparisons between time points.

Interpretation. For the screening assay, results can be recorded either visually or spectrophotometrically. For visual reading: negative, colorless well; positive, definite yellow color in well. For spectrophotometric reading with a single wavelength (OD_{450}): negative, <0.100; indeterminate, ≥ 0.100 and <0.150; positive, ≥ 0.150. For spectrophotometric reading with a dual wavelength ($OD_{450/630}$): negative, <0.070; indeterminate, ≥ 0.070 and <0.100; positive, ≥ 0.100. Tests giving indeterminate results should be repeated; if the results are still indeterminate, a second specimen should be obtained and tested. Extremely strong reactions may produce a purple precipitate, but these samples are considered positive.

If the 1:2 dilution of the specimen yields an OD of <0.100 when using the semiquantitative method, the assay should be repeated using an undiluted sample. A negative result does not preclude a diagnosis of cryptococcosis, especially if only a single specimen has been tested and if the patient shows symptoms consistent with the disease. The sensitivity of the EIA was reported to be 93% for serum and 100% for CSF (3), whereas the specificity of the EIA was reported to be 97% (83).

A new commercial EIA is available for the detection of cryptococcal antigen (ALPHA cryptococcal antigen enzyme immunoassay; IMMY) and has recently been approved by the FDA. The manufacturer-reported positive and negative agreements for serum were 98.5% and 97.7% and those for CSF were 93.5% and 99.2%, respectively, compared with the Premier EIA. In an evaluation with 118 sera and 15 fungal culture filtrates, the specificity was 96.1%; *Paracoccidioides* culture filtrates were positive 67% of the time. An independent comparison of the ALPHA cryptococcal antigen enzyme immunoassay to other cryptococcal antigen assays (84) reported a 100% sensitivity and a 99.8% specificity when compared to the consensus result of the other assays. Limitations of this study were the low number of positive patients evaluated and that specimens from patients with other fungal infections were not examined.

Lateral Flow Assay

The latest methodology for use in fungal serology is the LFA (IMMY). Cryptococcal antigen LFA is a rapid, low-complexity assay with results available in 10 min. Compared to EIA, the sensitivity and specificity are 96 to 100% and 96 to 100%, respectively (85, 86). Similar sensitivity and specificity values were also seen when LFA was compared to LA and culture (87). The limit of sensitivity of the cryptococcal LFA is 1 ng/ml for serotypes A and B and 4 to 16 ng/ml for serotypes C and D (88). The use of cryptococcal antigen LFA shows tremendous promise. The assay is inexpensive and does not require significant laboratory infrastructure or refrigeration. Currently, the incidence of infection is greatest in the more underdeveloped areas of Africa and Southeast Asia. Needing no cold chain for shipment to the end user, the LFA can be provided to the most remote areas of these continents. The potential to detect antigen prior to onset of symptoms may reduce morbidity and mortality through the initiation of earlier treatment (89, 90).

Histoplasmosis

Clinical Indications and Diagnostic Rationale

Histoplasma capsulatum is a thermally dimorphic fungus that is endemic to the Mississippi and Ohio River valleys of the

United States and parts of Central and South America. *Histoplasma* is found particularly in soil that has been enriched with bird or bat guano. Therefore bat-infested caves and highly frequented bird roosts are locations with high endemicity of infection. In the absence of culture or microscopic evidence of infection, the primary methods used to diagnose histoplasmosis are the ID, CF, and LA antibody detection tests and EIA to detect *H. capsulatum* antigen. Antibodies in primary pulmonary infections are generally demonstrable within 4 weeks after exposure to the fungus or, frequently, when symptoms appear. Serologic tests for histoplasmosis should be applied to clinical specimens (serum, peritoneal fluid, CSF, or urine) from patients with respiratory illness, hepatosplenomegaly, signs of extrapulmonary systemic infection, or meningeal involvement. The patient's residence, travel, and occupational history is useful as a guide to the application of these tests.

Antibody Assays for the Diagnosis of Histoplasmosis

Immunodiffusion

The ID procedure detects *H. capsulatum* precipitins directed against the immunodominant H and M glycoprotein antigens present in histoplasmin (91, 92). In the immunodiffusion reaction, the M band is found closer to the antigen well and the H band is found closer to the antiserum well. The ID test is a useful screening procedure or adjunct to the CF test for the serologic diagnosis of histoplasmosis. In contrast to the CF test, the ID test is generally performed as a qualitative rather than a quantitative test. The ID assay is generally more specific but less sensitive than the CF test, so that when both assays are employed, the overall sensitivity and specificity to detect histoplasmosis are quite good (85%). Because of this enhanced specificity, the ID test provides a more accurate diagnosis than the CF test, particularly in samples that display CF cross-reactivity to other fungal diseases. The ID test may also help to resolve the diagnosis in cases where the CF results are made uninterpretable by AC activity in the test sample.

Interpretation. In the ID test, the M band is demonstrated with serum from patients with acute or chronic pulmonary histoplasmosis and is frequently the first to appear in patients with acute disease (4 to 8 weeks after exposure). A positive M band is considered presumptive evidence of *H. capsulatum* infection and may be attributed to active or previous disease. Antibodies to the H antigen are specific for active disease but occur in fewer than 20% of cases; they usually disappear within the first 6 months of infection and are seldom, if ever, found in the absence of M precipitins. The demonstration of both the M and H precipitin bands in serum is highly suggestive of active histoplasmosis. Seroconversion from no bands to the presence of an M or H band is strong evidence for recent infection. The detection of M and H precipitins in CSF specimens indicates meningeal histoplasmosis (93). Precipitins can frequently be detected in the CSF of patients with meningeal histoplasmosis before *H. capsulatum* is detected by culture and when cultures are sterile.

Complement Fixation

The CF test is very sensitive, but the current incorporation of unpurified antigens reduces test specificity. Cross-reactions may occur with sera from patients with blastomycosis, coccidioidomycosis, and other mycoses. Sera from patients with leishmaniasis may cross-react in the CF test with *H. capsulatum* yeast-form antigens. It is generally recommended that both the ID and CF tests be performed to obtain maximum sensitivity and specificity. Use of the histoplasmosis ID and CF tests in parallel, with histoplasmin as the antigen, results in an overall sensitivity of approximately 85%. The CF and ID tests are also useful in diagnosing meningitis caused by *H. capsulatum* (93).

CF tests can be valuable in the diagnosis of acute, chronic, disseminated, and meningeal histoplasmosis. The CF microtitration procedure (1) yields information of both diagnostic and prognostic value. Over 90% of patients with culture-proven histoplasmosis demonstrate a positive CF test if serum is collected and tested at 2- to 3-week intervals during infection. For the serodiagnosis of histoplasmosis, the CF assay incorporates two different antigen preparations: "histoplasmin," a soluble filtrate of mycelial-phase broth cultures (containing the H and M antigens), and *Histoplasma* yeast antigen, a suspension of merthiolate-killed, whole yeast-form cells. Histoplasmin is produced by harvesting and filtering the supernatant from *H. capsulatum* cultures grown at 25°C for approximately 4 to 5 weeks in Smith's synthetic asparagine broth on a gyratory shaker at 150 rpm (94). The optimal dilution for each antigen is determined by a block titration. These antigens may also be purchased commercially (Table 1). The CF assay is more sensitive (82% versus 21%) but less specific (88% versus 99%) when yeast cells rather than mycelial antigens are used. Antibodies to yeast cells are usually the first to appear and the last to disappear after resolution of infection. However, antibodies produced during infection with other fungi such as *Coccidioides* or *B. dermatitidis*, and with bacterial infections such as tuberculosis, may react with the yeast antigen and give false-positive results (95). Antibodies to the yeast antigen usually appear within 4 weeks after exposure, whereas antibodies to the mycelial antigen occur later and have titers which are considerably lower. In contrast, histoplasmin titers are usually higher when serum from patients with chronic histoplasmosis is used.

Interpretation. CF test results can be difficult to interpret because cross-reactions or nonspecific reactions with the yeast or histoplasmin antigens are often encountered. In such instances, titers usually range between 1:8 and 1:32 and occur mainly against yeast-form antigen. Many serum samples from culture-proven cases of histoplasmosis, however, give titers in the same range. Consequently, titers of 1:8 and greater with either antigen are generally considered presumptive evidence of histoplasmosis. Titers above 1:32 or rising titers offer strong presumptive evidence of infection. The probability of infection increases in proportion to the CF titer.

On the other hand, one cannot rely solely on CF titers above 1:32 as a means of diagnosis because false-positive reactions of similar magnitude may occur in patients with other endemic mycoses. For example, the first serologic response noted in a patient with histoplasmosis may be obtained only with *B. dermatitidis* antigen. Some patients with histoplasmosis may demonstrate antibodies against the antigens of *H. capsulatum*, *B. dermatitidis*, and *C. immitis* or may demonstrate antibodies to only some of these antigens or to none. Furthermore, a lack of immunologic response does not exclude histoplasmosis, particularly when only one specimen has been tested and when the clinical picture strongly suggests a pulmonary mycosis. For example, in cases of disseminated or terminal histoplasmosis, humoral antibody responses may or may not be positive. In contrast, the CF test is usually positive when CSF specimens obtained from patients with chronic meningitis are used; titers in such cases may range from 1:8 to 1:128.

Increases or decreases in titer of 4-fold or greater are significant indicators of disease progression or remission, respectively. However, culture, clinical, and other laboratory data should also be considered in assessing the patient's prognosis or making treatment decisions. Occasionally, in some patients, positive titers decline slowly and persist long after the patient has been cured. The significance of persistently elevated or fluctuating CF titers is unclear, as is the effect of antifungal treatment on antibody clearance.

Latex Agglutination

The histoplasmosis LA test is a rapid, semiquantitative test that uses latex particles sensitized with histoplasmin for the detection of agglutinating antibodies against *H. capsulatum*. This assay measures predominantly the IgM subclass of antibodies and therefore is most useful in the early diagnosis of acute histoplasmosis. A positive LA test result can be obtained as early as 2 to 3 weeks after exposure and has been reported to have an overall sensitivity (including both acute and chronic forms of the disease) of 62% and a specificity of 97% (96). Antibody to *H. capsulatum* present in the patient's specimen binds to the antigen-coated latex particles, resulting in visible clumping. Results are graded according to the level of agglutination observed for a particular dilution of serum. The assay is rapid and simple to perform, and no special equipment is needed. Histoplasmin-sensitized latex particles are available commercially prepared (Table 2).

The histoplasmosis LA test is satisfactory for the detection of acute primary infections but may yield negative results for sera from persons with chronic histoplasmosis (96). It is particularly valuable in the detection of early disease. Because of the transitory nature of the agglutinins, the LA test cannot be considered a replacement for the CF test.

Interpretation. The LA test yields results in a matter of minutes and may be used with sera giving AC activity in the CF test. Although the LA test may be negative with sera from persons with chronic histoplasmosis or from immunosuppressed individuals, it is an excellent presumptive test aiding in the early diagnosis of acute histoplasmosis. A titer of 1:16 or greater is presumptive evidence of infection, and a titer of 1:32 or greater is considered strong presumptive evidence for active or very recent infection. Although a positive LA test result can be demonstrated as early as 2 to 3 weeks after infection by *H. capsulatum*, false-positive results can occur with other systemic mycoses. It is therefore recommended that results be confirmed by using ID or other laboratory tests. Low-titer results from single specimens should especially be interpreted with caution. In such cases, the test should be performed with another specimen collected 4 to 6 weeks later.

Enzyme Immunoassay

Attempts to replace the CF test with an EIA format have been frustrated because of cross-reactive carbohydrate moieties found on the immunodominant H and M antigens (97, 98). Periodate treatment of the M antigen before use in an immunoblot format, however, was reported to remove most of the cross-reactivity and increase the test specificity to 91% (98, 99). Recently, an ELISA for the early diagnosis of histoplasmosis was described in which purified native histoplasmin was compared to its deglycosylated counterpart (100). Deglycosylation resulted in an increase in test specificity from 93 to 96%; more surprisingly, the test sensitivity also increased from 57 to 92% (98–100). The sensitivity of the assay was 100% for patients with acute histoplasmosis and mediastinal histoplasmosis. However, sensitivity was reduced in other forms of histoplasmosis: 90% in chronic disease, 89% for disseminated disease, and 86% in disseminated disease in HIV-infected patients (101). An EIA for histoplasmosis antibodies using "inactivated" histoplasmin antigen to coat microtiter wells is commercially available (Histoplasma DxSelect; Focus Diagnostics). According to the manufacturer, when compared to CF titers of $\geq$1:8, the assay has 82.4% sensitivity and 88% specificity. When compared to CF titers of $\geq$1:32, specificity is improved to 93.3%; however, sensitivity was reduced to 58%. There are currently no independent reports evaluating the performance of this commercial assay.

Antigen Assays for the Diagnosis of Histoplasmosis

Enzyme Immunoassay

EIA for detecting *Histoplasma* antigen in urine and serum is useful for diagnosing disseminated histoplasmosis, particularly in AIDS patients (102). Antigen detection is less effective in diagnosing histoplasmosis in immunocompetent patients with self-limited disease or in cases of chronic pulmonary disease (103). Although less sensitive for the diagnosis of primary disease than disseminated disease, the test can be useful for diagnosis in the early stages of acute pulmonary disease (first 3 to 4 weeks after onset), permitting appropriate therapy to be initiated sooner.

An EIA to *Histoplasma* antigen uses polyclonal rabbit antisera against formalin-killed yeast forms of *H. capsulatum* as both the capture and detector antibody (103). This test is performed as a fee-for-service reference test (MiraVista Diagnostics, Indianapolis, IN, www.miravistalabs.com). The antigen detected is poorly defined but is believed to be a galactomannan based on its stability to heat (100°C for 30 min) and its reduced reactivity after passage through a concanavalin A affinity column (99, 104). Antigen can be detected very early in disease (during the first 2 weeks after the onset of symptoms), and then its level rapidly declines in self-limited disease. It can be detected for longer periods in cases of disseminated disease. The MiraVista assay has undergone various revisions of specimen and assay performance since it was first designed. Acceptable specimens include urine, serum, plasma, CSF, and BAL fluid. CSF and serum are initially pretreated with EDTA to dissociate antigen/antibody complexes. Results are reported quantitatively through comparison to a standard curve made from antigen serially diluted from 19.0 to 0.4 ng/ml (105). Significant EIA cross-reactivity has been reported for the other endemic mycoses, particularly blastomycosis, paracoccidioidomycosis, and penicilliosis marneffei.

The use of the antigen assay, however, may not be the most sensitive assay with all patient populations. A multicenter study (106) compared the efficacy of detecting antigen in urine to conventional antibody detection for the diagnosis of histoplasmosis. The antigen assay was more sensitive for the diagnosis of disseminated infection in immunocompromised patients (69 to 84% [antibody] versus 92 to 94% [antigen]). However, in immunocompetent patients with disseminated or localized pulmonary infections, antibody diagnosis was more sensitive (86 to 100% [antibody] versus 39 to 80% [antigen]). Therefore, diagnostic sensitivity and specificity of these assays are dependent upon the particular population that is being tested. Therefore, test results must be interpreted in light of the clinical presentation and the patient's history of travel to or residence in areas of endemicity in conjunction with other laboratory results, including those for antibody detection and for culture.

Recently, another commercial antigen assay has been developed and is available for purchase (*Histoplasma* antigen enzyme immunoassay; IMMY). This assay uses rabbit polyclonal antibodies for antigen detection and was stated by the manufacturer to have a sensitivity and specificity of 80.9% and 98.7%, respectively. However, an independent report showed much lower values (62% and 79%, respectively) (107). A new version of this assay uses monoclonal antibodies for antigen detection and provides a much better sensitivity and specificity (90.5% and 96.3%, respectively) (107, 108).

Paracoccidioidomycosis

Clinical Indications and Diagnostic Rationale

Paracoccidioides brasiliensis is a dimorphic fungus whose endemic range is found in parts of Central and South America. Infection is found most frequently in persons 30 years or older and most commonly in men. Primary infection occurs in the lungs as observed through abnormal chest X rays but is often asymptomatic. Secondary manifestation can be observed in the mucous membranes, reticuloendothelial system, skin, adrenals, and other organs. Serologic tests for paracoccidioidomycosis should be performed on specimens from patients with symptoms of chronic disease or who present with ulcerative lesions of the mucosa (oral, nasal, or intestinal) or the skin. A history of travel to or residence in Latin America in conjunction with typical clinical signs should raise suspicion for paracoccidioidomycosis. Serologic tests are useful for the rapid presumptive diagnosis of paracoccidioidomycosis, particularly for diagnosing cases of disseminated disease and for monitoring the response to treatment.

Antibody Assays for the Diagnosis of Paracoccidioidomycosis

Immunodiffusion

The ID test is simple to perform and is among the most specific procedures available (reported sensitivities, 84 to 94%; reported specificity, 99%). The ID test employing concentrated yeast-form culture filtrate antigens and reference sera is 100% specific and has a sensitivity of 94% when sera from patients with paracoccidioidomycosis are tested. The major diagnostic precipitin is a 43-kDa glycoprotein referred to as gp43 (also known as E_2 or A) and is found in 95 to 98% of patients with paracoccidioidomycosis (109, 110). Commercial mycelium-phase *P. brasiliensis* culture filtrate antigens, containing gp43 and other antigens are available from IMMY (Table 1).

Interpretation. The ID test is valuable for the diagnosis of acute or chronic pulmonary infection and disseminated paracoccidioidomycosis. The greatest number of precipitin bands has occurred when sera from patients with lung involvement or disseminated disease have been used; up to three precipitin bands have been observed (111). A major diagnostic precipitin is consistently found in the sera of patients with paracoccidioidomycosis, which reacts with a soluble, specific *P. brasiliensis* antigen. Band 1, which appears closest to the antigen-containing well, is thought to contain gp43 on the basis of immunochemical analysis. The precipitin that reacts with the gp43 antigen has been observed to occur in 95 to 99% of sera from patients with active paracoccidioidomycosis and can be found in patient serum for longer periods following infection than the other two major serum precipitins; the latter disappear during a favorable response to treatment. The positive predictive value of a positive ID test result is 100%.

Complement Fixation

CF tests that use unpurified antigens have a similar sensitivity to the ID (87%) but are less specific (68%) (112). Therefore, the ID test should be performed in conjunction with the CF test. The CF test detects antibodies in 80 to 96% of patients with paracoccidioidomycosis. CF antibodies are diagnostic, but CF test results with *P. brasiliensis* yeast-form culture filtrate antigens are not always specific, and cross-reactions may occur when sera from patients with other endemic mycoses, particularly histoplasmosis, are used. These cross-reactions are infrequent and occur mainly at titers of 1:8 or below. Nonetheless, concomitant use of the CF and ID tests allows a correct serodiagnosis of paracoccidioidomycosis in over 98% of cases. No commercial reagents for CF are available.

Culture filtrate antigens of *P. brasiliensis*, referred to as paracoccidioidin, are prepared by growing *P. brasiliensis* in a tryptic soy broth-dialysate medium supplemented with glucose, ammonium sulfate, and vitamins (113). Yeast-form shake cultures of three stock isolates of *P. brasiliensis* are grown singly at 35°C in this medium for up to 4 weeks. Consult references 112 and 114 for isolate selection. The culture filtrate from each isolate is dialyzed, concentrated 10-fold, and mixed in equal volumes with those from the other isolates. The optimal dilution for each antigen pool is determined by titration with low- and high-titer CF-positive sera from human paracoccidioidomycosis cases or by the use of ID tests with precipitin-positive sera. References 111 and 114 give details of the kinetics of *P. brasiliensis* antigen production during growth and discuss alternative growth media.

Interpretation. CF titers of ≥1:8 are considered presumptive evidence of paracoccidioidomycosis. However, 85 to 95% of patients with active disease have titers of ≥1:32. Low CF titers are usually associated with localized disease or involvement of the mononuclear phagocyte system, whereas high titers are found in patients with pulmonary lesions or multifocal disease. Sera from young children with disseminated paracoccidioidomycosis are an exception and ordinarily show low or negative CF reactivity. Serial CF determinations are prognostic in that a decreasing titer generally indicates effective therapy, whereas relapses are accompanied by increasing titers. High and fluctuating titers suggest a poor prognosis. Low levels of CF antibodies may persist long after the patient is cured.

Experimentally, other approaches have also been explored for the detection of antibodies to *Paracoccidioides*. A WB method (115) used to detect antibodies against gp43 in patient sera showed an increase in sensitivity when compared to ID (80% versus 95.5%). However, specificity was better with ID. Another approach evaluated the use of latex agglutination assay for the diagnosis of paracoccidioidomycosis (116). Using serum, the LA assay was 73% sensitive and 79% specific. However, when the serum was first pretreated with a citrate buffer for dissociation of immune complexes, sensitivity and specificity of the assay improved to 90% and 90%, respectively (116).

Penicilliosis Marneffei

Clinical Indications and Diagnostic Rationale

Penicillium marneffei is a thermally dimorphic fungus endemic only to portions of Southeast Asia. Disseminated infection with *P. marneffei* is observed almost exclusively in

immunocompromised patients who either live in or have traveled through Southeast Asia. Recent taxonomic evaluation has determined that *P. marneffei* is closely aligned with the genus *Talaromyces* and renaming this mould to *Talaromyces marneffei* has been proposed (117). However, as *P. marneffei* is still most frequently used in the literature, the name *P. marneffei* will continued to be used in this section to avoid any confusion.

Diagnosis of *P. marneffei* infections relies mainly on culture and/or histopathologic identification. Serologic tests for the diagnosis of *P. marneffei* infections should be considered for use with patients who have lived in or traveled to Southeast Asia and who display symptoms of intermittent fever, marked weight loss, nonproductive cough, and debilitation. About 60 to 70% of patients present with multiple papular lesions, some of which show a central necrotic umbilication resembling molluscum contagiosum. Other presenting signs include hepatosplenomegaly, generalized lymphadenopathy, anemia, and thrombocytopenia. These symptoms may be confused with those of other fungal infections such as histoplasmosis or cryptococcosis as well as with those of tuberculosis. No commercial serology assays are currently available in the United States.

A major antigenic protein of *P. marneffei*, Mp1p, has recently been cloned and expressed in the yeast *Pichia pastoris* (118). Rabbit polyclonal antibodies and mouse monoclonal antibodies were subsequently produced against the recombinant protein for the development of antigen capture assays using either the MAb or PAb as capture antibodies and the MAb as the detector antibody. An antibody EIA was also produced using the recombinant antigen to coat the microwells for a microtiter plate. Evaluation of each assay was performed with sera from confirmed penicilliosis marneffei cases and control sera. Sensitivity and specificity of the antigen detection assays were 55% and 99% compared to 75% and 99% using the PAb and the MAb as capture antibodies, respectively. While the antibody assay was equally as specific (98%), the sensitivity was only 30%. A combination of antigen and antibody assays improved the diagnostic sensitivity to 85% with the MAb antigen assay and 100% with the PAb antigen assay, with a 98% specificity for both.

Pneumocystosis

Clinical Indications and Diagnostic Rationale

The cause of pneumocystis disease in humans has recently been reclassified as *Pneumocystis jirovecii* (119). Until 1988, these organisms were widely thought to be protozoa, but comparative DNA sequence analysis demonstrated that *Pneumocystis* strains were phylogenetically more closely related to the fungi (120). The route of transmission of *P. jirovecii* is not understood, but seroprevalence studies have suggested that exposure occurs in early childhood. It was hypothesized that the strains acquired during first exposure persisted in the lungs in a dormant state throughout life and became active on subsequent immunosuppression of the host (119, 121). However, this hypothesis has recently been challenged, and it has been suggested that *P. jirovecii* organisms are frequently acquired and cleared by the immune system in immunocompetent hosts and do not persist (122).

Pneumonia caused by *P. jirovecii* (PCP) is rare in immunocompetent adults but is a leading cause of illness and death in individuals with impaired immunity including malnourished or premature children, persons with AIDS, SOT recipients, and patients receiving long-term corticosteroid therapy. It is often described as interstitial plasma cell pneumonia; histopathologic studies of patients' lungs typically show alveolar interstitial thickening and the presence of a frothy eosinophilic exudate in the lumina. The clinical presentation in children is characterized by cyanosis, mild cough without fever, and, in severe disease, intercostal retractions. In contrast, adults with PCP frequently present with dyspnea, nonproductive cough, chest tightness, night sweats, and an inability to breathe deeply. Tachypnea and low-grade fever often occur, but hemoptysis is rarely present. Adults with CD4 counts below 200 per μl are at increased risk for PCP, and persons with AIDS have a more insidious progression than those who are immunosuppressed but HIV negative. Extrapulmonary pneumocystosis has been reported in 1 to 3% of postmortem examinations of patients known to have pulmonary infections (123, 124) and most often involves the lymph nodes (44%) and the spleen, bone marrow, and liver (33%). Infection at multiple extrapulmonary sites is associated with a rapidly fatal outcome (123, 124).

The laboratory diagnosis of pneumocystosis depends largely on the use of Gomori methenamine silver, calcofluor white, Gram-Weigert, toluidine blue-O, or fluorescent antibody staining of lung biopsy specimens, induced sputum, or BAL fluid specimens to detect the cyst form of the organism and the use of Giemsa stain to detect the trophozoite form or clusters of cysts containing intracystic bodies. Specific anti-*Pneumocystis* MAbs have been developed that can detect not only the cyst form of the organism but also the significantly more abundant trophozoite form (125, 126). The sensitivity of the MAbs with either induced sputum or BAL fluid specimens has been reported to be similar to or somewhat greater than that of conventional staining methods.

Indirect and direct immunofluorescent assays employing MAbs have most commonly been used for the detection of *P. jirovecii* in induced sputum and in BAL fluid samples; however, less frequently, these reagents have also been used for tissue diagnosis (127–129). MAbs directed against *Pneumocystis* for use in direct or indirect staining procedures are available commercially from Axis-Shield Diagnostics (Dundee, United Kingdom), Bio-Rad Laboratories, Inc., Chemicon International, Inc. (Temecula, CA), and Meridian Diagnostics. Other immunologic methods including counterimmunoelectrophoresis, ELISA, WB, and LA tests have also been developed experimentally and are discussed in more detail below. Finally, the increased sensitivity of molecular biology-based diagnostic methods may allow a minimally invasive procedure, such as oral washings (130), to be sufficient for diagnostic purposes.

The serologic diagnosis of pneumocystosis has proven to be difficult because most humans become seropositive for *Pneumocystis* antibodies at an early age and are exposed to the organism multiple times throughout life. Therefore, the detection of serum antibodies may not correlate with true infection. In addition, conflicting results have been obtained, primarily because different test methods have been used (LA, WB, ELISA, and indirect immunofluorescence), a variety of antigen sources have been employed (rat versus human), and the antigens used have been purified to different degrees (column purified or recombinant).

Other tests include the detection of antigens ranging from 35 to 45 kDa, as well as a 95-kDa major surface glycoprotein antigen, in BAL fluids (131). WB analysis demonstrated that the 35- to 45-kDa antigen was found in 88% of the BAL fluids tested, whereas the 95-kDa antigen was detected in only 49% of specimens. Recent analysis of sera from HIV-infected patients show that those infected with PCP contain much higher antibody titers to a recombinant protein that is part of the major surface glycoprotein (Msg), particularly MsgC, when compared to HIV-infected

patients without PCP (132). It has also been demonstrated that health care workers who care for HIV-infected PCP-positive patients are also more likely to have antibodies to MsgC (133, 134).

A recent meta-analysis of 12 studies analyzed the usefulness of BDG in the diagnosis of *Pneumocystis* infection which included the use of any of the commercially available BDG assays. The study concluded that BDG in PCP patients was 96% sensitive and 84% specific (135). Another particularly useful study showed that a decrease in BDG levels following treatment strongly correlated with a favorable outcome (136).

Sporotrichosis

Clinical Indications and Diagnostic Rationale

Sporothrix schenckii organisms, while found worldwide, are found in the soil and plants of tropical and subtropical regions of North, Central, and South America. The disease sporotrichosis is a subdermal infection that begins after a skin injury where the fungal conidia are implanted resulting in ulcerated, verrucous, or erythematous nodules which may spread locally through the lymphatics. Rarely, a pneumonitis can occur if conidia are inhaled. Dissemination may occur in both immunocompetent and immunosuppressed individuals.

Serologic tests for sporotrichosis may be applied to sera from patients with skin lesions, subcutaneous nodules, bone and joint lesions, lymphadenopathy, or pulmonary disease and to CSF from patients with undiagnosed chronic meningitis. The disease should be suspected in individuals whose work brings them into contact with soil, plants, timber, plant materials, or sphagnum moss. Cutaneous sporotrichosis is more common in adults than in children, and extracutaneous disease is found more often in men older than 30 years. Although not common, disseminated infection is more likely to occur in immunosuppressed than immunocompetent individuals.

Serologic tests are sometimes helpful for the diagnosis of the extracutaneous or systemic forms of sporotrichosis. A slide agglutination test to detect anti-*Sporothrix schenckii* antibodies has been demonstrated to be the most useful method. This test has been reported to have sensitivities of 100, 86, 73, and 56% for disseminated, articular, pulmonary, and cutaneous disease, respectively, and a specificity of 100% (137). Antibodies are most probably directed toward a peptido-L-rhamno-D-mannan, localized in the outer layer of the *S. schenckii* cell wall. Comparable sensitivity for the detection of *S. schenckii* antibodies has not been reported for an ID test format.

Antibody Assays for the Diagnosis Of Sporotrichosis

Latex Agglutination

The LA test is a semiquantitative slide agglutination assay in which *S. schenckii* antigen-coated latex particles are used to detect antibody to *S. schenckii*. The assay is rapid and simple to perform and requires no special equipment. A commercial kit is available from IMMY (Table 1).

Interpretation. LA titers of 1:8 or greater are considered presumptive evidence of sporotrichosis. False-positive reactions have, however, been noted at titers of 1:8 when sera from patients with nonfungal infections were used. Sera from patients with localized cutaneous, lymphocutaneous, or extracutaneous sporotrichosis may display titers ranging from 1:8 to 1:512. An increasing titer or a sustained high titer indicates pulmonary sporotrichosis. The test has limited prognostic value, since antibody levels may show little change during and after convalescence. Slide latex agglutinin titers of >1:8 with CSF are considered presumptive evidence of meningeal sporotrichosis.

Mucormycosis

Clinical Indications and Diagnostic Rationale

The primary agents of mucormycosis in the order Mucorales include species of *Lichtheimia*, *Apophysomyces*, *Cunninghamella*, *Mucor*, *Rhizopus*, *Rhizomucor*, and *Saksenaea*, and those in the order Entomophthorales include *Conidiobolus* and *Basidiobolus* (104, 138). The major risk factors for mucormycosis are neutropenia, uncontrolled diabetes mellitus, other forms of metabolic acidosis, and burns. Other contributing factors include corticosteroid use and treatment with deferoxamine. Although ID tests have been successfully used to detect antibodies in patients with active mucormycosis (97, 139), these methods have not been extensively evaluated.

Immunohistochemistry

In tissue, these organisms are difficult to differentiate and appear as sparsely septate, irregularly branched, broad, ribbon-like hyphae (138, 140). A murine MAb, WSSA-RA-1 (141), directed against somatic antigens of *Rhizopus arrhizus* (*oryzae*), has been reported to react specifically with *Lichtheimia corymbifer* (*Absidia corymbifera*), *R. arrhizus* (*oryzae*), and *Rhizomucor pusillus* when applied as an immunoperoxidase histopathology stain; this reagent is commercially available (AbD Serotec; Raleigh, NC). The method used for staining is the same as that for *Aspergillus* and can be found in the section above.

MOLECULAR METHODS FOR FUNGAL DETECTION

DNA-based methods have been used extensively to identify fungi from biological specimens in culture. However, DNA-based identification methods for isolate identification are outside the scope of this chapter; for the description of molecular methods used for identification of fungal cultures, the readers are referred to CLSI document MM18-A (142).

Methods for direct detection and diagnostics of fungal DNA in biological specimens remain experimental and can be divided into two major groups based on the method that is used for DNA detection and identification, such as (i) PCR amplification using universal fungal primers followed by DNA sequencing and (ii) real-time PCR amplification using species-specific molecular probes.

Panfungal PCR with universal fungal primers is most frequently used for diagnostics when the exact agent of infection is unknown. For this procedure, total DNA is extracted from the biological samples and amplified using panfungal primers specific to portions of the rRNA gene locus, such as ITS1, ITS2, and/or portions of the 28 rRNA gene (143). The PCR products are then visualized, purified, and sequenced. The fungus is identified by comparing the DNA sequence with those in the GenBank or other fungal databases (MycoBank, www.mycobank.org; Fusarium-ID, http://isolate.fusariumdb.org). The advantage of this approach is that it can be used to amplify and detect pathogens for which molecular probes have not been developed. For example, recently this method was used to detect and identify DNA of *Exserohilum rostratum* in fluids and tissues from an outbreak of fungal meningitis

and other infections associated with contaminated steroids (144). This approach is also frequently used for detection/identification of fungi in formalin-fixed paraffin-embedded tissues (145, 146).

Real-time PCR with species-specific molecular probes can be used for detection/identification when the agent of infection is already known or strongly suspected. The advantage of real-time PCR is that this method is more sensitive than conventional PCR. However, the disadvantage is that molecular probes used for identification are targeted toward specific species and would miss other pathogens that might be causing infection. In addition, because real-time PCR does not include a DNA sequencing step, extensive testing is required to ensure the specificity of the probes. Converse to the panfungal PCR method described above, probes and PCR primers for real-time PCR are often designed to amplify unique regions of DNA. Some of the studies where real-time PCR has been used for detection of fungal infections include *Aspergillus fumigatus* in sera of patients with suspected invasive aspergillosis (147, 148), *Pneumocystis jirovecii* in respiratory samples of non-AIDS patients (149, 150), *Candida* sp. DNA in blood of neonatal patients (151–153), and *Coccidioides* sp. in respiratory specimens of suspected cases of Valley fever (154, 155).

Regardless of the method that is used for the detection of fungal DNA, one of the most challenging aspects of molecular detection is obtaining sufficient amounts of fungal DNA from the patients' specimens. This procedure is complicated by (i) the presence of thick cell walls that need to be disrupted to release fungal DNA from cells prior to extraction and (ii) excess human DNA that competes with fungal DNA when using extraction columns. To release fungal DNA from hyphae, cell walls can be mechanically disrupted by bead beating (147, 148), sonication, or shaking or enzymatically digested using protease (156) or lyticase (145). Once the fungal cell walls are fragmented, a variety of DNA purification methods can be used. Some studies have compared such methods (148). As an alternative, free circulating fungal DNA can be concentrated and purified using methods developed for extraction of viral DNA from body fluids, such as the QIAamp UltraSens virus kit (Qiagen). Furthermore, when fungal DNA is extracted from formalin-fixed paraffin-embedded tissue scrolls, removal of paraffin and rehydration of specimens need to be performed (145, 146).

SUPPLIERS

Accurate Chemical Scientific Corp. (www.accuratechemical.com)
AbD Serotec (http://www.abdserotec.com/)
Associates of Cape Cod (www.acciusa.com)
Axis-Shield, Plc. (www.axis-shield.com)
Bio-Rad Laboratories, Inc. (www.bio-rad.com)
Chemicon Antibodies (www.millipore.com)
Gibson Bioscience, Inc. (http://www.gibsonbioscience.com/)
Immuno-Mycologics (IMMY) (www.immy.com)
Meridian Bioscience, Inc. (www.meridianbioscience.com)
Microgen Bioproducts, Ltd. (www.microgenbioproducts.com)
Ramco Laboratories, Inc. (www.ramcolab.com)
Remel Laboratories, Inc. (www.remelinc.com)
Vircell, S.L. (www.vircell.com)
Lonza (www.lonza.com)
Rockland Immunochemicals, Inc. (www.rockland-inc.com)
TCS Biosciences Ltd. (www.tcsbiosciences.co.uk)
Colorado Serum Company (www.colorado-serum.com)

The findings and conclusions in this report are those of the author and do not necessarily represent the official position of the Centers for Disease Control and Prevention. Use of trade names and commercial sources is for identification only and does not imply endorsement by the Centers for Disease Control and Prevention.

REFERENCES

1. **Palmer DF, Kaufman L, Kaplan W, Cavalaro JJ.** 1977. *Serodiagnosis of Mycotic Diseases*. Charles C Thomas, Springfield, IL.
2. **Gade W, Hinnefeld SW, Babcock LS, Gilligan P, Kelly W, Wait K, Greer D, Pinilla M, Kaplan RL.** 1991. Comparison of the PREMIER cryptococcal antigen enzyme immunoassay and the latex agglutination assay for detection of cryptococcal antigens. *J Clin Microbiol* **29:**1616–1619.
3. **Tanner DC, Weinstein MP, Fedorciw B, Joho KL, Thorpe JJ, Reller L.** 1994. Comparison of commercial kits for detection of cryptococcal antigen. *J Clin Microbiol* **32:**1680–1684. PubMed
4. **Temstet A, Roux P, Poirot JL, Ronin O, Dromer F.** 1992. Evaluation of a monoclonal antibody-based latex agglutination test for diagnosis of cryptococcosis: comparison with two tests using polyclonal antibodies. *J Clin Microbiol* **30:**2544–2550. PubMed
5. **Gray LD, Roberts GD.** 1988. Experience with the use of pronase to eliminate interference factors in the latex agglutination test for cryptococcal antigen. *J Clin Microbiol* **26:**2450–2451. PubMed
6. **Obayashi T, et al.** 1995. Plasma (1→3)-beta-D-glucan measurement in diagnosis of invasive deep mycosis and fungal febrile episodes. *Lancet* **345:**17–20. PubMed
7. **Takesue Y, Kakehashi M, Ohge H, Imamura Y, Murakami Y, Sasaki M, Morifuji M, Yokoyama Y, Kouyama M, Yokoyama T, Sueda T.** 2004. Combined assessment of beta-D-glucan and degree of candida colonization before starting empiric therapy for candidiasis in surgical patients. *World J Surg* **28:**625–630. PubMed
8. **Kawazu M, Kanda Y, Nannya Y, Aoki K, Kurokawa M, Chiba S, Motokura T, Hirai H, Ogawa S.** 2004. Prospective comparison of the diagnostic potential of real-time PCR, double-sandwich enzyme-linked immunosorbent assay for galactomannan, and a (1→3)-beta-D-glucan test in weekly screening for invasive aspergillosis in patients with hematological disorders. *J Clin Microbiol* **42:**2733–2741. PubMed
9. **Wright WF, Overman SB, Ribes JA.** 2011. (1→3)-β-D-Glucan assay: a review of its laboratory and clinical application. *Lab Med* **42:**679–685.
10. **Kanda H, Kubo K, Hamasaki K, Kanda Y, Nakao A, Kitamura T, Fujita T, Yamamoto K, Mimura T.** 2001. Influence of various hemodialysis membranes on the plasma (1→3)-beta-D-glucan level. *Kidney Int* **60:**319–323. PubMed
11. **Kato A, Takita T, Furuhashi M, Takahashi T, Maruyama Y, Hishida A.** 2001. Elevation of blood (1→3)-beta-D-glucan concentrations in hemodialysis patients. *Nephron* **89:**15–19. PubMed
12. **Ogawa M, Hori H, Niiguchi S, Azuma E, Komada Y.** 2004. False-positive plasma (1→3)-beta-D-glucan test following immunoglobulin product replacement in an adult bone marrow recipient. *Int J Hematol* **80:**97–98. PubMed
13. **Kanamori H, Kanemitsu K, Miyasaka T, Ameku K, Endo S, Aoyagi T, Inden K, Hatta M, Yamamoto N, Kunishima H, Yano H, Kaku K, Hirakata Y, Kaku M.** 2009. Measurement of (1→3)-beta-D-glucan derived from different gauze types. *Tohoku J Exp Med* **217:**117–121. PubMed

14. **Aketagawa J, Tanaka S, Tamura H, Shibata Y, Saitô H.** 1993. Activation of limulus coagulation factor G by several (1→3)-beta-D-glucans: comparison of the potency of glucans with identical degree of polymerization but different conformations. *J Biochem* **113:**683–686. PubMed
15. **Saitô H, Yoshioka Y, Uehara N, Aketagawa J, Tanaka S, Shibata Y.** 1991. Relationship between conformation and biological response for (1→3)-beta-D-glucans in the activation of coagulation factor G from limulus amebocyte lysate and host-mediated antitumor activity. Demonstration of single-helix conformation as a stimulant. *Carbohydr Res* **217:**181–190. PubMed
16. **Tamura H, Arimoto Y, Tanaka S, Yoshida M, Obayashi T, Kawai T.** 1994. Automated kinetic assay for endotoxin and (1→3)-beta-D-glucan in human blood. *Clin Chim Acta* **226:**109–112. PubMed
17. **Marr KA, Balajee SA, McLaughlin L, Tabouret M, Bentsen C, Walsh TJ.** 2004. Detection of galactomannan antigenemia by enzyme immunoassay for the diagnosis of invasive aspergillosis: variables that affect performance. *J Infect Dis* **190:**641–649. PubMed
18. **De Pauw B, Walsh TJ, Donnelly JP, Stevens DA, Edwards JE, Calandra T, Pappas PG, Maertens J, Lortholary O, Kauffman CA, Denning DW, Patterson TF, Maschmeyer G, Bille J, Dismukes WE, Herbrecht R, Hope WW, Kibbler CC, Kullberg BJ, Marr KA, Muñoz P, Odds FC, Perfect JR, Restrepo A, Ruhnke M, Segal BH, Sobel JD, Sorrell TC, Viscoli C, Wingard JR, Zaoutis T, Bennett JE, European Organization for Research and Treatment of Cancer/Invasive Fungal Infections Cooperative Group, National Institute of Allergy and Infectious Diseases Mycoses Study Group (EORTC/MSG) Consensus Group.** 2008. Revised definitions of invasive fungal disease from the European Organization for Research and Treatment of Cancer/Invasive Fungal Infections Cooperative Group and the National Institute of Allergy and Infectious Diseases Mycoses Study Group (EORTC/MSG) Consensus Group. *Clin Infect Dis* **46:**1813–1821. PubMed
19. **Coleman RM, Kaufman L.** 1972. Use of the immunodiffusion test in the serodiagnosis of aspergillosis. *Appl Microbiol* **23:**301–308. PubMed
20. **Bardana EJ Jr, Gerber JD, Craig S, Cianciulli FD.** 1975. The general and specific humoral immune response to pulmonary aspergillosis. *Am Rev Respir Dis* **112:**799–805. PubMed
21. **Guitard J, Sendid B, Thorez S, Gits M, Hennequin C.** 2012. Evaluation of a recombinant antigen-based enzyme immunoassay for the diagnosis of noninvasive aspergillosis. *J Clin Microbiol* **50:**762–765. PubMed
22. **Rohrlich P, Sarfati J, Mariani P, Duval M, Carol A, Saint-Martin C, Bingen E, Latge JP, Vilmer E.** 1996. Prospective sandwich enzyme-linked immunosorbent assay for serum galactomannan: early predictive value and clinical use in invasive aspergillosis. *Pediatr Infect Dis J* **15:**232–237. PubMed
23. **Verweij PE, Stynen D, Rijs AJ, de Pauw BE, Hoogkamp-Korstanje JA, Meis JF.** 1995. Sandwich enzyme-linked immunosorbent assay compared with Pastorex latex agglutination test for diagnosing invasive aspergillosis in immunocompromised patients. *J Clin Microbiol* **33:** 1912–1914. PubMed
24. **Husain S, Clancy CJ, Nguyen MH, Swartzentruber S, Leather H, LeMonte AM, Durkin MM, Knox KS, Hage CA, Bentsen C, Singh N, Wingard JR, Wheat LJ.** 2008. Performance characteristics of the platelia Aspergillus enzyme immunoassay for detection of Aspergillus galactomannan antigen in bronchoalveolar lavage fluid. *Clin Vaccine Immunol* **15:**1760–1763. PubMed
25. **Verweij PE, Weemaes CM, Curfs JH, Bretagne S, Meis JF.** 2000. Failure to detect circulating *Aspergillus* markers in a patient with chronic granulomatous disease and invasive aspergillosis. *J Clin Microbiol* **38:**3900–3901. PubMed
26. **Thornton CR.** 2008. Development of an immunochromatographic lateral-flow device for rapid serodiagnosis of invasive aspergillosis. *Clin Vaccine Immunol* **15:**1095–1105. PubMed
27. **Wiederhold NP, Najvar LK, Bocanegra R, Kirkpatrick WR, Patterson TF, Thornton CR.** 2013. Interlaboratory and interstudy reproducibility of a novel lateral-flow device and influence of antifungal therapy on detection of invasive pulmonary aspergillosis. *J Clin Microbiol* **51:**459–465. PubMed
28. **White PL, Parr C, Thornton C, Barnes RA.** 2013. Evaluation of real-time PCR, galactomannan enzyme-linked immunosorbent assay (ELISA), and a novel lateral-flow device for diagnosis of invasive aspergillosis. *J Clin Microbiol* **51:**1510–1516. PubMed
29. **Karthaus M, Buchheidt D.** 2013. Invasive aspergillosis: new insights into disease, diagnostic and treatment. *Curr Pharm Des* **19:**3569–3594. PubMed
30. **Lackner M, Lass-Flörl C.** 2013. Up-date on diagnostic strategies of invasive aspergillosis. *Curr Pharm Des* **19:**3595–3614. PubMed
31. **Marty FM, Koo S.** 2009. Role of (1→3)-beta-D-glucan in the diagnosis of invasive aspergillosis. *Med Mycol* **47**(Suppl 1)**:**S233–S240. PubMed
32. **Karageorgopoulos DE, Vouloumanou EK, Ntziora F, Michalopoulos A, Rafailidis PI, Falagas ME.** 2011. β-D-glucan assay for the diagnosis of invasive fungal infections: a meta-analysis. *Clin Infect Dis* **52:**750–770. PubMed
33. **Gao X, Chen L, Hu G, Mei H.** 2010. Invasive pulmonary aspergillosis in acute exacerbation of chronic obstructive pulmonary disease and the diagnostic value of combined serological tests. *Ann Saudi Med* **30:**193–197. PubMed
34. **Pazos C, Pontón J, Del Palacio A.** 2005. Contribution of (1→3)-beta-D-glucan chromogenic assay to diagnosis and therapeutic monitoring of invasive aspergillosis in neutropenic adult patients: a comparison with serial screening for circulating galactomannan. *J Clin Microbiol* **43:**299–305. PubMed
35. **Guarner J, Brandt ME.** 2011. Histopathologic diagnosis of fungal infections in the 21st century. *Clin Microbiol Rev* **24:**247–280. PubMed
36. **Jensen HE, Halbaek B, Lind P, Krogh HV, Frandsen PL.** 1996. Development of murine monoclonal antibodies for the immunohistochemical diagnosis of systemic bovine aspergillosis. *J Vet Diagn Investig* **8:**68–75. PubMed
37. **Pfister JR, Archer JR, Hersil S, Boers T, Reed KD, Meece JK, Anderson JL, Burgess JW, Sullivan TD, Klein BS, Wheat LJ, Davis JP.** 2011. Non-rural point source blastomycosis outbreak near a yard waste collection site. *Clin Med Res* **9:**57–65. PubMed
38. **Roy M, Benedict K, Deak E, Kirby MA, McNiel JT, Sickler CJ, Eckardt E, Marx RK, Heffernan RT, Meece JK, Klein BS, Archer JR, Theurer J, Davis JP, Park BJ.** 2013. A large community outbreak of blastomycosis in Wisconsin with geographic and ethnic clustering. *Clin Infect Dis* **57:**655–662. PubMed
39. **Saccente M, Woods GL.** 2010. Clinical and laboratory update on blastomycosis. *Clin Microbiol Rev* **23:**367–381. PubMed
40. **Smith JA, Kauffman CA.** 2010. Blastomycosis. *Proc Am Thorac Soc* **7:**173–180. PubMed
41. **Hurst SF, Kaufman L.** 1992. Western immunoblot analysis and serologic characterization of *Blastomyces dermatitidis* yeast form extracellular antigens. *J Clin Microbiol* **30:**3043–3049. PubMed
42. **Klein BS, Jones JM.** 1994. Purification and characterization of the major antigen WI-1 from *Blastomyces dermatitidis* yeasts and immunological comparison with A antigen. *Infect Immun* **62:**3890–3900. PubMed

43. **Klein BS, Kuritsky JN, Chappell WA, Kaufman L, Green J, Davies SF, Williams JE, Sarosi GA.** 1986. Comparison of the enzyme immunoassay, immunodiffusion, and complement fixation tests in detecting antibody in human serum to the A antigen of *Blastomyces dermatitidis*. *Am Rev Respir Dis* **133:**144–148. PubMed
44. **Lambert RS, George RB.** 1987. Evaluation of enzyme immunoassay as a rapid screening test for histoplasmosis and blastomycosis. *Am Rev Respir Dis* **136:**316–319. PubMed
45. **Turner S, Kaufman L.** 1986. Immunodiagnosis of blastomycosis. *Semin Respir Infect* **1:**22–28. PubMed
46. **Durkin M, Witt J, Lemonte A, Wheat B, Connolly P.** 2004. Antigen assay with the potential to aid in diagnosis of blastomycosis. *J Clin Microbiol* **42:**4873–4875. PubMed
47. **Connolly P, Hage CA, Bariola JR, Bensadoun E, Rodgers M, Bradsher RW Jr, Wheat LJ.** 2012. Blastomyces dermatitidis antigen detection by quantitative enzyme immunoassay. *Clin Vaccine Immunol* **19:**53–56. PubMed
48. **Clancy CJ, Nguyen ML, Cheng S, Huang H, Fan G, Jaber RA, Wingard JR, Cline C, Nguyen MH.** 2008. Immunoglobulin G responses to a panel of *Candida albicans* antigens as accurate and early markers for the presence of systemic candidiasis. *J Clin Microbiol* **46:**1647–1654. PubMed
49. **Lain A, Elguezabal N, Amutio E, Fernandez de Larrinoa I, Moragues MD, Ponton J.** 2008. Use of recombinant antigens for the diagnosis of invasive candidiasis. *Clin Dev Immunol* **2008:**721950. doi:721910.721155/722008/721950.
50. **Li FQ, Ma CF, Shi LN, Lu JF, Wang Y, Huang M, Kong QQ.** 2013. Diagnostic value of immunoglobulin G antibodies against Candida enolase and fructose-bisphosphate aldolase for candidemia. *BMC Infect Dis* **13:**253. PubMed
51. **Moragues MD, Ortiz N, Iruretagoyena JR, García-Ruiz JC, Amutio E, Rojas A, Mendoza J, Quindós G, Pontón-San Emeterio J.** 2004. Evaluación de una nueva técnica comercializada (*Candida albicans* IFA IgG) para el diagnóstico de la candidiasis invasiva. *Enferm Infecc Microbiol Clin* **22:**83–88. PubMed
52. **Zaragoza R, Peman J, Quindos G, Iruretagoyena JR, Cuetara MS, Ramirez P, Gomez MD, Camarena JJ, Viudes A, Ponton J, Candida albicans Germ Tube Antibody Detection in Critically Ill Patients.** 2009. Clinical significance of the detection of Candida albicans germ tube-specific antibodies in critically ill patients. *Clin Microbiol Infect* **15:**592–595.
53. **León C, Ruiz-Santana S, Saavedra P, Castro C, Ubeda A, Loza A, Martín-Mazuelos E, Blanco A, Jerez V, Ballús J, Alvarez-Rocha L, Utande-Vázquez A, Fariñas O.** 2012. Value of β-D-glucan and Candida albicans germ tube antibody for discriminating between Candida colonization and invasive candidiasis in patients with severe abdominal conditions. *Intensive Care Med* **38:**1315–1325. PubMed
54. **Pemán J, Zaragoza R.** 2012. Combined use of nonculture-based lab techniques in the diagnosis and management of critically ill patients with invasive fungal infections. *Expert Rev Anti Infect Ther* **10:**1321–1330. PubMed
55. **Bär W, Hecker H.** 2002. Diagnosis of systemic *Candida* infections in patients of the intensive care unit. Significance of serum antigens and antibodies. *Mycoses* **45:**22–28. PubMed
56. **Merz WG, Evans GL, Shadomy S, Anderson S, Kaufman L, Kozinn PJ, Mackenzie DW, Protzman WP, Remington JS.** 1977. Laboratory evaluation of serological tests for systemic candidiasis: a cooperative study. *J Clin Microbiol* **5:**596–603. PubMed
57. **Misaki H, Iwasaki H, Ueda T.** 2003. A comparison of the specificity and sensitivity of two *Candida* antigen assay systems for the diagnosis of deep candidiasis in patients with hematologic diseases. *Med Sci Monit* **9:**MT1–MT7. PubMed
58. **Sendid B, Tabouret M, Poirot JL, Mathieu D, Fruit J, Poulain D.** 1999. New enzyme immunoassays for sensitive detection of circulating *Candida albicans* mannan and antimannan antibodies: useful combined test for diagnosis of systemic candidiasis. *J Clin Microbiol* **37:**1510–1517. PubMed
59. **Held J, Kohlberger I, Rappold E, Busse Grawitz A, Häcker G.** 2013. Comparison of (1→3)-β-D-glucan, mannan/anti-mannan antibodies, and Cand-Tec *Candida* antigen as serum biomarkers for candidemia. *J Clin Microbiol* **51:**1158–1164. PubMed
60. **Suzuki S.** 1997. Immunochemical study on mannans of genus *Candida*. I. Structural investigation of antigenic factors 1, 4, 5, 6, 8, 9, 11, 13, 13b and 34. *Curr Top Med Mycol* **8:**57–70. PubMed
61. **Mohr JF, Sims C, Paetznick V, Rodriguez J, Finkelman MA, Rex JH, Ostrosky-Zeichner L.** 2011. Prospective survey of (1→3)-beta-D-glucan and its relationship to invasive candidiasis in the surgical intensive care unit setting. *J Clin Microbiol* **49:**58–61. PubMed
62. **Jaijakul S, Vazquez JA, Swanson RN, Ostrosky-Zeichner L.** 2012. (1,3)-β-D-glucan as a prognostic marker of treatment response in invasive candidiasis. *Clin Infect Dis* **55:**521–526. PubMed
63. **Sims CR, Jaijakul S, Mohr J, Rodriguez J, Finkelman M, Ostrosky-Zeichner L.** 2012. Correlation of clinical outcomes with β-glucan levels in patients with invasive candidiasis. *J Clin Microbiol* **50:**2104–2106. PubMed
64. **Kaufman L, Reiss E.** 1992. Serodiagnosis of fungal diseases, p 506–528. *In* Rose NR, de Macario EV, Fahey JL, Friedman H, Penn GM (ed), *Manual of Clinical Laboratory Immunology*, 4th ed. American Society for Microbiology, Washington, DC.
65. **Pappagianis D, Zimmer BL.** 1990. Serology of coccidioidomycosis. *Clin Microbiol Rev* **3:**247–268. PubMed
66. **Abrams DI, Robia M, Blumenfeld W, Simonson J, Cohen MB, Hadley WK.** 1984. Disseminated coccidioidomycosis in AIDS. *N Engl J Med* **310:**986–987. PubMed
67. **Dosanjh A, Theodore J, Pappagianis D.** 1998. Probable false positive coccidioidal serologic results in patients with cystic fibrosis. *Pediatr Transplant* **2:**313–317. PubMed
68. **Smith CE, Saito MT, Simons SA.** 1956. Pattern of 39,500 serologic tests in coccidioidomycosis. *J Am Med Assoc* **160:**546–552. PubMed
69. **Huppert M, Peterson ET, Sun SH, Chitjian PA, Derrevere WJ.** 1968. Evaluation of a latex particle agglutination test for coccidioidomycosis. *Am J Clin Pathol* **49:**96–102. PubMed
70. **Drutz DJ, Catanzaro A.** 1978. Coccidioidomycosis. Part I. *Am Rev Respir Dis* **117:**559–585. PubMed
71. **Cox RA, Magee DM.** 1998. Protective immunity in coccidioidomycosis. *Res Immunol* **149:**417–428, 506–417.
72. **Kaufman L, Sekhon AS, Moledina N, Jalbert M, Pappagianis D.** 1995. Comparative evaluation of commercial Premier EIA and microimmunodiffusion and complement fixation tests for *Coccidioides immitis* antibodies. *J Clin Microbiol* **33:**618–619. PubMed
73. **Martins TB, Jaskowski TD, Mouritsen CL, Hill HR.** 1995. Comparison of commercially available enzyme immunoassay with traditional serological tests for detection of antibodies to *Coccidioides immitis*. *J Clin Microbiol* **33:**940–943. PubMed
74. **Zartarian M, Peterson EM, de la Maza LM.** 1997. Detection of antibodies to *Coccidioides immitis* by enzyme immunoassay. *Am J Clin Pathol* **107:**148–153. PubMed
75. **Blair JE, Currier JT.** 2008. Significance of isolated positive IgM serologic results by enzyme immunoassay for coccidioidomycosis. *Mycopathologia* **166:**77–82. PubMed
76. **Crum NF, Lederman ER, Stafford CM, Parrish JS, Wallace MR.** 2004. Coccidioidomycosis: a descriptive survey

of a reemerging disease. Clinical characteristics and current controversies. *Medicine* (Baltimore) **83:**149–175. PubMed

77. **Kuberski T, Herrig J, Pappagianis D.** 2010. False-positive IgM serology in coccidioidomycosis. *J Clin Microbiol* **48:**2047–2049. PubMed
78. **Blair JE, Mendoza N, Force S, Chang Y-H, Grys TE.** 2013. Clinical specificity of the enzyme immunoassay test for coccidioidomycosis varies according to the reason for its performance. *Clin Vaccine Immunol* **20:**95–98. PubMed
79. **Johnson SM, Zimmermann CR, Pappagianis D.** 1996. Use of a recombinant *Coccidioides immitis* complement fixation antigen-chitinase in conventional serological assays. *J Clin Microbiol* **34:**3160–3164. PubMed
80. **Durkin M, Connolly P, Kuberski T, Myers R, Kubak BM, Bruckner D, Pegues D, Wheat LJ.** 2008. Diagnosis of coccidioidomycosis with use of the Coccidioides antigen enzyme immunoassay. *Clin Infect Dis* **47:**e69–e73. PubMed
81. **Harris JR, Lockhart SR, Debess E, Marsden-Haug N, Goldoft M, Wohrle R, Lee S, Smelser C, Park B, Chiller T.** 2011. Cryptococcus gattii in the United States: clinical aspects of infection with an emerging pathogen. *Clin Infect Dis* **53:**1188–1195. PubMed
82. **Goldman DL, Khine H, Abadi J, Lindenberg DJ, Pirofski LA, Niang R, Casadevall A.** 2001. Serologic evidence for Cryptococcus neoformans infection in early childhood. *Pediatrics* **107:**E66. PubMed
83. **Sekhon AS, Garg AK, Kaufman L, Kobayashi GS, Hamir Z, Jalbert M, Moledina N.** 1993. Evaluation of a commercial enzyme immunoassay for the detection of cryptococcal antigen. *Mycoses* **36:**31–34. PubMed
84. **Binnicker MJ, Jespersen DJ, Bestrom JE, Rollins LO.** 2012. Comparison of four assays for the detection of cryptococcal antigen. *Clin Vaccine Immunol* **19:**1988–1990. PubMed
85. **Jarvis JN, Percival A, Bauman S, Pelfrey J, Meintjes G, Williams GN, Longley N, Harrison TS, Kozel TR.** 2011. Evaluation of a novel point-of-care cryptococcal antigen test on serum, plasma, and urine from patients with HIV-associated cryptococcal meningitis. *Clin Infect Dis* **53:**1019–1023. PubMed
86. **Lindsley MD, Mekha N, Baggett HC, Surinthong Y, Autthateinchai R, Sawatwong P, Harris JR, Park BJ, Chiller T, Balajee SA, Poonwan N.** 2011. Evaluation of a newly developed lateral flow immunoassay for the diagnosis of cryptococcosis. *Clin Infect Dis* **53:**321–325. PubMed
87. **Klausner JD, Vijayan T, Chiller T.** 2013. Sensitivity and specificity of a new cryptococcal antigen lateral flow assay in serum and cerebrospinal fluid. *MLO Med Lab Obs* **45:**16–20. PubMed
88. **Gates-Hollingsworth MA, Kozel TR.** 2013. Serotype sensitivity of a lateral flow immunoassay for cryptococcal antigen. *Clin Vaccine Immunol* **20:**634–635. PubMed
89. **Harris JR, Lindsley MD, Henchaichon S, Poonwan N, Naorat S, Prapasiri P, Chantra S, Ruamcharoen F, Chang LS, Chittaganpitch M, Mehta N, Peruski L, Maloney SA, Park BJ, Baggett HC.** 2012. High prevalence of cryptococcal infection among HIV-infected patients hospitalized with pneumonia in Thailand. *Clin Infect Dis* **54:**e43–e50. PubMed
90. **Meya DB, Manabe YC, Castelnuovo B, Cook BA, Elbireer AM, Kambugu A, Kamya MR, Bohjanen PR, Boulware DR.** 2010. Cost-effectiveness of serum cryptococcal antigen screening to prevent deaths among HIV-infected persons with a CD4+ cell count < or = 100 cells/microL who start HIV therapy in resource-limited settings. *Clin Infect Dis* **51:**448–455. PubMed
91. **Heiner DC.** 1958. Diagnosis of histoplasmosis using precipitin reactions in agar gel. *Pediatrics* **22:**616–627. PubMed
92. **Wiggins GL, Schubert JH.** 1965. Relationship of histoplasmin agar-gel bands and complement-fixation titers in histoplasmosis. *J Bacteriol* **89:**589–596. PubMed
93. **Negroni R, Robles AM, Arechavala AL, Iovannitti C, Helou S, Kaufman L.** 1995. Chronic meningoencephalitis due to *Histoplasma capsulatum*. Usefulness of serodiagnostic procedures in diagnosis. *Serodiagn Immunother Infect Dis* **7:**84–89.
94. **Kwon-Chung J, Bennett JE.** 1994. *Medical Mycology*. Lea and Febiger, Melvern, PA.
95. **Wheat J, French ML, Kamel S, Tewari RP.** 1986. Evaluation of cross-reactions in *Histoplasma capsulatum* serologic tests. *J Clin Microbiol* **23:**493–499. PubMed
96. **Hill GB, Campbell CC.** 1962. Commercially available histoplasmin sensitized latex particles in an agglutination test for histoplasmosis. *Mycopathologia* **18:**160–176. PubMed
97. **Kaufman L, Kovacs JA, Reiss E.** 1997. Clinical immunomycology, p 585–604. *In* Rose NR, de Macario EC, Folds JD, Lane HC, Nakamura RM (ed), *Manual of Clinical Laboratory Immunology*, 5th ed. ASM Press, Washington, DC.
98. **Zancopé-Oliveira RM, Bragg SL, Reiss E, Peralta JM.** 1994. Immunochemical analysis of the H and M glycoproteins from *Histoplasma capsulatum*. *Clin Diagn Lab Immunol* **1:**563–568. PubMed
99. **Hamilton AJ.** 1998. Serodiagnosis of histoplasmosis, paracoccidioidomycosis and penicilliosis marneffei; current status and future trends. *Med Mycol* **36:**351–364. PubMed
100. **Guimarães AJ, Pizzini CV, De Matos Guedes HL, Albuquerque PC, Peralta JM, Hamilton AJ, Zancopé-Oliveira RM.** 2004. ELISA for early diagnosis of histoplasmosis. *J Med Microbiol* **53:**509–514. PubMed
101. **Guimarães AJ, Pizzini CV, De Abreu Almeida M, Peralta JM, Nosanchuk JD, Zancopé-Oliveira RM.** 2010. Evaluation of an enzyme-linked immunosorbent assay using purified, deglycosylated histoplasmin for different clinical manifestations of histoplasmosis. *Microbiol Res* (Pavia) **2:**7–14. PubMed
102. **Wheat LJ, Connolly-Stringfield P, Blair R, Connolly K, Garringer T, Katz BP, Gupta M.** 1992. Effect of successful treatment with amphotericin B on *Histoplasma capsulatum* variety *capsulatum* polysaccharide antigen levels in patients with AIDS and histoplasmosis. *Am J Med* **92:**153–160. PubMed
103. **Wheat LJ, Garringer T, Brizendine E, Connolly P.** 2002. Diagnosis of histoplasmosis by antigen detection based upon experience at the histoplasmosis reference laboratory. *Diagn Microbiol Infect Dis* **43:**29–37. PubMed
104. **Richardson RD, Warnock DW.** 1997. *Fungal Infection: Diagnosis and Management*, 2nd ed. Blackwell Science, Malden, MA.
105. **Connolly PA, Durkin MM, Lemonte AM, Hackett EJ, Wheat LJ.** 2007. Detection of histoplasma antigen by a quantitative enzyme immunoassay. *Clin Vaccine Immunol* **14:**1587–1591. PubMed
106. **Hage CA, Ribes JA, Wengenack NL, Baddour LM, Assi M, McKinsey DS, Hammoud K, Alapat D, Babady NE, Parker M, Fuller D, Noor A, Davis TE, Rodgers M, Connolly PA, El Haddad B, Wheat LJ.** 2011. A multicenter evaluation of tests for diagnosis of histoplasmosis. *Clin Infect Dis* **53:**448–454. PubMed
107. **Zhang X, Gibson B Jr, Daly TM.** 2013. Evaluation of commercially available reagents for diagnosis of histoplasmosis infection in immunocompromised patients. *J Clin Microbiol* **51:**4095–4101. PubMed
108. **Theel ES, Jespersen DJ, Harring J, Mandrekar J, Binnicker MJ.** 2013. Evaluation of an enzyme immunoassay for detection of *Histoplasma capsulatum* antigen from urine specimens. *J Clin Microbiol* **51:**3555–3559. PubMed

109. **Brummer E, Castaneda E, Restrepo A.** 1993. Paracoccidioidomycosis: an update. *Clin Microbiol Rev* **6:**89–117. PubMed
110. **Puccia R, Schenkman S, Gorin PA, Travassos LR.** 1986. Exocellular components of *Paracoccidioides brasiliensis*: identification of a specific antigen. *Infect Immun* **53:**199–206. PubMed
111. **Camargo ZP, Unterkircher C, Travassos LR.** 1989. Identification of antigenic polypeptides of *Paracoccidioides brasiliensis* by immunoblotting. *J Med Vet Mycol* **27:**407–412. PubMed
112. **Bueno JP, Mendes-Giannini MJ, Del Negro GM, Assis CM, Takiguti CK, Shikanai-Yasuda MA.** 1997. IgG, IgM and IgA antibody response for the diagnosis and follow-up of paracoccidioidomycosis: comparison of counterimmunoelectrophoresis and complement fixation. *J Med Vet Mycol* **35:**213–217. PubMed
113. **Restrepo-Moreno A, Schneidau JD Jr.** 1967. Nature of the skin-reactive principle in culture filtrates prepared from *Paracoccidioides brasiliensis*. *J Bacteriol* **93:**1741–1748. PubMed
114. **De Camargo Z, Unterkircher C, Campoy SP, Travassos LR.** 1988. Production of *Paracoccidioides brasiliensis* exoantigens for immunodiffusion tests. *J Clin Microbiol* **26:**2147–2151. PubMed
115. **Perenha-Viana MC, Gonzales IA, Brockelt SR, Machado LN, Svidzinski TI.** 2012. Serological diagnosis of paracoccidioidomycosis through a Western blot technique. *Clin Vaccine Immunol* **19:**616–619. PubMed
116. **Silveira-Gomes F, Marques-da-Silva SH.** 2012. Effects of pretreating serum samples on the performance of a latex agglutination test for serodiagnosis of paracoccidioidomycosis. *Clin Vaccine Immunol* **19:**386–390. PubMed
117. **Samson RA, Yilmaz N, Houbraken J, Spierenburg H, Seifert KA, Peterson SW, Varga J, Frisvad JC.** 2011. Phylogeny and nomenclature of the genus Talaromyces and taxa accommodated in Penicillium subgenus Biverticillium. *Stud Mycol* **70:**159–183. PubMed
118. **Wang YF, Cai JP, Wang YD, Dong H, Hao W, Jiang LX, Long J, Chan C, Woo PC, Lau SK, Yuen KY, Che XY.** 2011. Immunoassays based on Penicillium marneffei Mp1p derived from Pichia pastoris expression system for diagnosis of penicilliosis. *PLoS One* **6:**e28796. PubMed
119. **Stringer JR, Beard CB, Miller RF, Wakefield AE.** 2002. A new name (*Pneumocystis jiroveci*) for *Pneumocystis* from humans. *Emerg Infect Dis* **8:**891–896. PubMed
120. **Edman JC, Kovacs JA, Masur H, Santi DV, Elwood HJ, Sogin ML.** 1988. Ribosomal RNA sequence shows *Pneumocystis carinii* to be a member of the fungi. *Nature* **334:**519–522. PubMed
121. **Stringer JR, Cushion MT, Wakefield AE.** 2001. New nomenclature for the genus *Pneumocystis*. *J Eukaryot Microbiol* **48**(Suppl)**:**184S–189S. PubMed
122. **Wakefield AE, Lindley AR, Ambrose HE, Denis CM, Miller RF.** 2003. Limited asymptomatic carriage of *Pneumocystis jiroveci* in human immunodeficiency virus-infected patients. *J Infect Dis* **187:**901–908. PubMed
123. **Ng VL, Yajko DM, Hadley WK.** 1997. Extrapulmonary pneumocystosis. *Clin Microbiol Rev* **10:**401–418. PubMed
124. **Telzak EE, Armstrong D.** 1994. Extrapulmonary infection and other unusual manifestations of *Pneumocystis carinii*, p 361–380. *In* Walzer PD (ed), *Pneumocystis carinii Pneumonia*, 2nd ed. Marcel Dekker, Inc, New York, NY.
125. **Gill VJ, Evans G, Stock F, Parrillo JE, Masur H, Kovacs JA.** 1987. Detection of *Pneumocystis carinii* by fluorescent-antibody stain using a combination of three monoclonal antibodies. *J Clin Microbiol* **25:**1837–1840. PubMed
126. **Kovacs JA, Gill V, Swan JC, Ognibene F, Shelhamer J, Parrillo JE, Masur H.** 1986. Prospective evaluation of a monoclonal antibody in diagnosis of *Pneumocystis carinii* pneumonia. *Lancet* **ii:**1–3. PubMed
127. **Amin MB, Mezger E, Zarbo RJ.** 1992. Detection of *Pneumocystis carinii*. Comparative study of monoclonal antibody and silver staining. *Am J Clin Pathol* **98:**13–18. PubMed
128. **Kobayashi M, Moriki T, Uemura Y, Takehara N, Kubonishi I, Taguchi H, Miyoshi I.** 1992. Immunohistochemical detection of *Pneumocystis carinii* in transbronchial lung biopsy specimens: antigen difference between human and rat Pneumocystis carinii. *Jpn J Clin Oncol* **22:**387–392. PubMed
129. **Radio SJ, Hansen S, Goldsmith J, Linder J.** 1990. Immunohistochemistry of *Pneumocystis carinii* infection. *Mod Pathol* **3:**462–469. PubMed
130. **Helweg-Larsen J, Jensen JS, Benfield T, Svendsen UG, Lundgren JD, Lundgren B.** 1998. Diagnostic use of PCR for detection of *Pneumocystis carinii* in oral wash samples. *J Clin Microbiol* **36:**2068–2072. PubMed
131. **Smulian AG, Linke MJ, Cushion MT, Baughman RP, Frame PT, Dohn MN, White ML, Walzer PD.** 1994. Analysis of *Pneumocystis carinii* organism burden, viability and antigens in bronchoalveolar lavage fluid in AIDS patients with pneumocystosis: correlation with disease severity. *AIDS* **8:**1555–1562. PubMed
132. **Daly KR, Koch J, Levin L, Walzer PD.** 2004. Enzyme-linked immunosorbent assay and serologic responses to Pneumocystis jiroveci. *Emerg Infect Dis* **10:**848–854. PubMed
133. **Fong S, Daly KR, Tipirneni R, Jarlsberg LG, Djawe K, Koch JV, Swartzman A, Roth B, Walzer PD, Huang L.** 2013. Antibody responses against Pneumocystis jirovecii in health care workers over time. *Emerg Infect Dis* **19:**1612–1619. PubMed
134. **Tipirneni R, Daly KR, Jarlsberg LG, Koch JV, Swartzman A, Roth BM, Walzer PD, Huang L.** 2009. Healthcare worker occupation and immune response to Pneumocystis jirovecii. *Emerg Infect Dis* **15:**1590–1597. PubMed
135. **Onishi A, Sugiyama D, Kogata Y, Saegusa J, Sugimoto T, Kawano S, Morinobu A, Nishimura K, Kumagai S.** 2012. Diagnostic accuracy of serum 1,3-β-D-glucan for *Pneumocystis jiroveci* pneumonia, invasive candidiasis, and invasive aspergillosis: systematic review and meta-analysis. *J Clin Microbiol* **50:**7–15. PubMed
136. **Held J, Wagner D.** 2011. β-d-Glucan kinetics for the assessment of treatment response in Pneumocystis jirovecii pneumonia. *Clin Microbiol Infect* **17:**1118–1122. PubMed
137. **Roberts GD, Larsh HW.** 1971. The serologic diagnosis of extracutaneous sporotrichosis. *Am J Clin Pathol* **56:**597–600. PubMed
138. **Walsh TJ, Chanock SJ.** 1998. Diagnosis of invasive fungal infections: advances in nonculture systems. *Curr Clin Top Infect Dis* **18:**101–153. PubMed
139. **Kaufman L, Turner LF, McLaughlin DW.** 1989. Indirect enzyme-linked immunosorbent assay for zygomycosis. *J Clin Microbiol* **27:**1979–1982. PubMed
140. **Chandler FW, Kaplan W, Ajello L.** 1980. *Color Atlas and Text of the Histopathology of Mycotic Diseases*. Year Book, Chicago, IL.
141. **Jensen HE, Aalbaek B, Lind P, Krogh HV.** 1996. Immunohistochemical diagnosis of systemic bovine zygomycosis by murine monoclonal antibodies. *Vet Pathol* **33:**176–183. PubMed
142. **Clinical and Laboratory Standards Institute.** 2008. *Interpretive Criteria for Identification of Bacteria and Fungi by DNA Target Sequencing; Approved Guideline. CLSI document MM18-A*. Clinical and Laboratory Standards Institute, Wayne, PA.

143. **White TJ, Bruns T, Lee S, Taylor J.** 1990. Amplification and direct sequencing of fungal ribosomal RNA genes for phylogenetics, p 315–322. *In* Innis MA, Gelfand DH, Sninsky JJ, White TJ (ed), *PCR Protocols. A Guide to Methods and Applications*. Academic Press, San Diego, CA.
144. **Gade L, Scheel CM, Pham CD, Lindsley MD, Iqbal N, Cleveland AA, Whitney AM, Lockhart SR, Brandt ME, Litvintseva AP.** 2013. Detection of fungal DNA in human body fluids and tissues during a multistate outbreak of fungal meningitis and other infections. *Eukaryot Cell* **12:**677–683. PubMed
145. **Muñoz-Cadavid C, Rudd S, Zaki SR, Patel M, Moser SA, Brandt ME, Gómez BL.** 2010. Improving molecular detection of fungal DNA in formalin-fixed paraffin-embedded tissues: comparison of five tissue DNA extraction methods using panfungal PCR. *J Clin Microbiol* **48:**2147–2153. PubMed
146. **Arunmozhi Balajee S, Hurst SF, Chang LS, Miles M, Beeler E, Hale C, Kasuga T, Benedict K, Chiller T, Lindsley MD.** 2013. Multilocus sequence typing of Histoplasma capsulatum in formalin-fixed paraffin-embedded tissues from cats living in non-endemic regions reveals a new phylogenetic clade. *Med Mycol* **51:**345–351. PubMed
147. **Springer J, Morton CO, Perry M, Heinz WJ, Paholcsek M, Alzheimer M, Rogers TR, Barnes RA, Einsele H, Loeffler J, White PL.** 2013. Multicenter comparison of serum and whole-blood specimens for detection of Aspergillus DNA in high-risk hematological patients. *J Clin Microbiol* **51:**1445–1450. PubMed
148. **White PL, Bretagne S, Klingspor L, Melchers WJ, McCulloch E, Schulz B, Finnstrom N, Mengoli C, Barnes RA, Donnelly JP, Loeffler J, European Aspergillus PCR Initiative.** 2010. Aspergillus PCR: one step closer to standardization. *J Clin Microbiol* **48:**1231–1240. PubMed
149. **Hauser PM, Bille J, Lass-Flörl C, Geltner C, Feldmesser M, Levi M, Patel H, Muggia V, Alexander B, Hughes M, Follett SA, Cui X, Leung F, Morgan G, Moody A, Perlin DS, Denning DW.** 2011. Multicenter, prospective clinical evaluation of respiratory samples from subjects at risk for *Pneumocystis jirovecii* infection by use of a commercial real-time PCR assay. *J Clin Microbiol* **49:**1872–1878. PubMed
150. **Monroy-Vaca EX, Armas YD, Illnait-Zaragozi MT, Torano G, Diaz R, Vega D, Alvarez-Lam I, Calderon EJ, Stensvold CR.** 2014. Prevalence and genotype distribution of *Pneumocystis jirovecii* in Cuban infants and toddlers with whooping cough. *J Clin Microbiol* **52:**45–51. PubMed
151. **Schell WA, Benton JL, Smith PB, Poore M, Rouse JL, Boles DJ, Johnson MD, Alexander BD, Pamula VK, Eckhardt AE, Pollack MG, Benjamin DK Jr, Perfect JR, Mitchell TG.** 2012. Evaluation of a digital microfluidic real-time PCR platform to detect DNA of Candida albicans in blood. *Eur J Clin Microbiol Infect Dis* **31:**2237–2245. PubMed
152. **Trovato L, Betta P, Romeo MG, Oliveri S.** 2012. Detection of fungal DNA in lysis-centrifugation blood culture for the diagnosis of invasive candidiasis in neonatal patients. *Clin Microbiol Infect* **18:**E63–E65. PubMed
153. **Venkatesh M, Flores A, Luna RA, Versalovic J.** 2010. Molecular microbiological methods in the diagnosis of neonatal sepsis. *Expert Rev Anti Infect Ther* **8:**1037–1048. PubMed
154. **Binnicker MJ, Buckwalter SP, Eisberner JJ, Stewart RA, McCullough AE, Wohlfiel SL, Wengenack NL.** 2007. Detection of *Coccidioides* species in clinical specimens by real-time PCR. *J Clin Microbiol* **45:**173–178. PubMed
155. **Vucicevic D, Blair JE, Binnicker MJ, McCullough AE, Kusne S, Vikram HR, Parish JM, Wengenack NL.** 2010. The utility of Coccidioides polymerase chain reaction testing in the clinical setting. *Mycopathologia* **170:**345–351. PubMed
156. **Mandhaniya S, Iqbal S, Sharawat SK, Xess I, Bakhshi S.** 2012. Diagnosis of invasive fungal infections using real-time PCR assay in paediatric acute leukaemia induction. *Mycoses* **55:**372–379. PubMed

Viral Diseases

section J

VOLUME EDITOR: JOHN L. SCHMITZ
SECTION EDITORS: RICHARD L. HODINKA AND JOHN L. SCHMITZ

Introduction

JOHN SCHMITZ

56

It is probably not unreasonable to say that the clinical virology laboratory has experienced the greatest amount of change of any clinical pathology laboratory since the last edition of this *Manual*. The traditional virology laboratory, as found in many larger hospital-based facilities, often no longer exists, having been replaced by molecular diagnostics. Accordingly, the first chapter in this section now covers rapid and molecular diagnostic methods as well as the traditional diagnostic procedures that still pertain. Rarely are culture or antigen detection methods still in regular use. Likewise, the ability to detect low copy numbers of viral nucleic acids, as well as the ability to accurately quantify the amount of virus present based on nucleic acid amplification, has limited the practical application of serologic methods to immune status testing, with a few well-known exceptions. There are many obvious benefits associated with the adoption of molecular diagnostics for viral infections, such as an increase in the diagnostic sensitivity. In addition, these technologies allow for the rapid deployment of tests for newly described viral pathogens. Quantitative methods facilitate diagnosis and allow prognostic application and facilitate patient management. This is not to say that serologic methods have been stagnant. There has been increasing adoption of avidity-based testing for chronic viral infections to facilitate the differentiation of primary infection from reactivation.

As viral diagnostic methods have evolved, so has this section of the 8th edition of this *Manual*. Several important revisions have been made, the most significant of which concerns HIV. Rather than an entire section, a single chapter on HIV diagnosis now details the application of the recently adopted new HIV diagnostic algorithms and no longer addresses viral load testing or genotyping.

Further changes include the combination of three chapters from the 7th edition into one authoritative discussion of respiratory viruses. The measles and mumps and rubella chapters likewise have been merged because they stress a common theme; since these three childhood viruses are easily managed by vaccination, serology remains important to identify unvaccinated or nonimmune individuals. Finally, the remaining chapters in this section offer the current state of the art concerning herpes simplex virus; varicella-zoster virus; Epstein-Barr virus and cytomegalovirus; human herpesviruses 6, 7, and 8; parvovirus B19; viral hepatitis; viral agents of gastroenteritis; arboviruses; hantavirus; rabies virus; human T-cell lymphotropic virus types 1 and 2; and prions.

doi:10.1128/9781555818722.ch56

Immunologic and Molecular Methods for Viral Diagnosis

MARIE LOUISE LANDRY AND YI-WEI TANG

57

Tremendous strides have been made in viral diagnosis in the past decade. Many infections are now treatable and, for optimum effect, antivirals must be started early. For hospitalized patients, rapid and accurate viral diagnosis is essential not only for patient management, but for infection control and prevention of nosocomial transmission. The impact of seasonal and pandemic influenza on morbidity and mortality of all ages has received increasing attention in both the medical literature and the popular press. Emerging, highly virulent viruses such as severe acute respiratory syndrome (SARS) coronavirus (CoV), Middle East respiratory syndrome CoV, and avian influenza H5N1 and H7N9 have also heightened concerns. Lastly, immunosuppressed and other vulnerable populations at risk for serious or life-threatening viral infections continue to increase. In response to these needs, there has been an explosion in viral diagnostic test development.

Tests are now available that can provide results within minutes of sample collection for some viruses and within hours for others, thus significantly shortening the time to diagnosis over conventional culture and serologic methods. In the past, on-site availability of viral diagnosis was limited by the need for cell culture facilities and expertise. Now, with simple-to-use, FDA-cleared immunologic and molecular tests, viral diagnosis has become more widely available and has entered the mainstream of diagnostic testing.

This chapter will present a practical approach to the rapid diagnosis of acute viral infections, focusing on the advantages and limitations of common methods and, importantly, the availability of new molecular methods. Routine serology and conventional cell culture techniques will not be covered, but details can be found in other texts (1).

VIRAL DIAGNOSTIC METHODS

The methods used for diagnosis of acute viral infection can be generally grouped according to the following strategies: (i) direct detection of viral proteins or particles in clinical specimens; (ii) biochemical amplification of nucleic acid in clinical samples; (iii) biologic amplification of infectious virus in culture followed by early detection of viral antigens in the infected cells; and (iv) detection of an IgM antibody response to viral infection. The test of choice may vary with the virus and the circumstance (Table 1).

Immunoassays historically have provided the most rapid results, with the most common antigen detection tests consisting of only one step, no reagent additions, and 10 to 20 min of incubation. Rapid cell culture methods, with incubation times of only 1 to 2 days followed by monoclonal antibody (MAb) staining, provide efficient detection of multiple viruses. Nucleic acid amplification techniques (NAATs) have been significantly shortened by more rapid thermocycling and real-time detection strategies. Some provide "on-demand" or "random-access" testing.

Whereas conventional culture and electron microscopy can detect the unexpected, immunologic and molecular methods detect only the specific agent(s) sought. However, multiplex strategies can now detect multiple viruses associated with a particular syndrome in a single reaction and more quickly, and thus have led to replacement of culture methods in many situations.

IMMUNOLOGIC METHODS

Direct Detection of Viral Antigens in Clinical Specimens

With direct antigen detection methods, the target is not amplified; thus, these tests are inherently less sensitive than culture or NAATs. Nevertheless, immunoassays are still widely used for influenza, respiratory syncytial virus (RSV), and rotavirus antigens, due to ease of use, cost, ability to accommodate single to multiple samples, rapid time to result, point-of-care (POC) capability including use in resource-poor or remote areas, and potential impact on patient management (Table 2). However, during the 2009 H1N1 influenza pandemic, the suboptimal sensitivity of rapid influenza diagnostic tests (RIDT) received a great deal of attention (2). This has led to a renewed focus on improving sensitivity of simple antigen assays. As molecular methods become more user-friendly and less expensive, antigen immunoassays must become more sensitive if they are to remain relevant.

Immunofluorescence

Immunofluorescence (IF) is by far the most demanding antigen detection technique and requires careful attention to detail throughout. When done well, it is an excellent test. When done poorly, it is neither sensitive nor specific. First, cells are applied to slides by touch prep, by pipette, or by cytocentrifugation. After fixation in acetone, methanol, or

doi:10.1128/9781555818722.ch57

TABLE 1 Application of various methods for rapid diagnosis of acute or primary viral infections[a]

Commonly encountered virus	Immunologic				Comments
	Viral antigen	Rapid culture	IgM	Molecular: NAAT	
Adenovirus	+	++	NA	+++	DFA suboptimal for adenovirus; rapid antigen assays available for enteric adenovirus in stool; rapid culture may require longer incubation than 2 days for optimal sensitivity; NAAT can be falsely negative or falsely low due to genome diversity
Arboviruses[b]	NA	NA	+++	++	Serology is primary diagnostic method for encephalitis-associated arboviruses; NAAT is commercially available only for WNV and dengue
Coronavirus	NA	NA	NA	+++	NAAT for common respiratory CoV is available as part of some commercial multiplex respiratory virus panels
Cytomegalovirus	++	++	+/−	+++	CMV pp65 antigenemia can be used to monitor viral load; rapid culture useful for congenital CMV urine or saliva, BAL, and tissue biopsy samples; quantitative NAAT most common method for viral load; while IgM can be useful in diagnosis of primary infection in normal hosts, it lacks specificity
Enterovirus and parechovirus	NA	++/−	NA	+++	NAAT preferred for CNS enterovirus infection; separate NAAT required for parechovirus detection
Epstein-Barr virus	NA	NA	+++	+++	Serology is test of choice for routine diagnosis; NAAT useful for virus-related tumors; quantitative NAAT useful for monitoring viral load in blood of transplant recipients; ISH can be used on tumor biopsies
Hepatitis A virus	NA	NA	+++	NA	Serology is the standard diagnostic test; false-positive IgM common in low-prevalence areas
Hepatitis B virus	+++	NA	+++	+++	Detection of specific viral antigens and antibodies allows for diagnosis and for monitoring the course of infection; NAAT used to monitor therapy and determine genotype
Hepatitis C virus	NA	NA	NA	+++	Serology is used for diagnosis; qualitative NAAT used to confirm active infection; quantitative NAAT used to monitor response to therapy; genotyping helps determine duration of therapy
Herpes simplex virus	++	++	Not reliable	+++	IFA used for rapid detection in skin/mucous membrane lesions or tissue specimens; NAAT is test of choice for CNS infection and used for other sample types as well; serology, including HSV-2-specific serology, used to determine prior infection
Herpesvirus 6	NA	NA	+	+++	NAAT test of choice for diagnosis; MAbs available to differentiate virus isolates and for IHC; serology can document primary infection in children
Human immunodeficiency virus	++	NA	++	+++	Serology is primary diagnostic method; rapid antibody testing becoming more widely available; proviral DNA and plasma RNA tests used to diagnose neonatal infection; quantitative RNA tests used to guide therapy and monitor response
Human metapneumovirus	++	++	NA	+++	NAAT is the test of choice for diagnosis; DFA and shell vial culture rapid and fairly sensitive; conventional culture difficult
Human T-cell lymphotropic virus	NA	NA	NA	+++	Serology is primary diagnostic method; NAAT useful for virus identification in HTLV Western blot-positive but untypeable specimens
Influenza virus	+/++	++	NA	+++	Rapid antigen tests widely used but suboptimal in sensitivity and specificity; DFA and rapid culture more sensitive; NAAT most sensitive and increasingly available; serology useful for epidemiological studies or retrospective diagnosis

(Continued on next page)

TABLE 1 Application of various methods for rapid diagnosis of acute or primary viral infections[a] *(Continued)*

Commonly encountered virus	Immunologic				Comments
	Viral antigen	Rapid culture	IgM	Molecular: NAAT	
Measles virus[b]	NA	NA	+++	+++	Serology most useful for diagnosis and determination of immunity; isolation only useful if attempted early (prodromal period to 4 days post-rash); NAAT done at CDC
Mumps virus[b]	NA	++	++	+++	Serology used most commonly for diagnosis and determination of immunity; NAAT done at CDC
Norovirus	NA	NA	NA	+++	NAAT challenging due to strain variability; reagents for antigen detection not commercially available
Parainfluenza virus	NA/++	++	NA	+++	IFA most common rapid detection method; NAAT more sensitive than isolation but not widely available, except as part of multiplex panel
Papillomavirus	NA	NA	NA	+++	NAAT test of choice for detection and genotype differentiation. Cytopathology useful for diagnosis; serologic diagnosis of exposure not available
Parvovirus	NA	NA	++	+++	Serology used to diagnose acute B19; NAAT test of choice for amniotic fluid or fetal tissue and for individuals who cannot mount an antibody response or who present early, before antibody has developed; NAAT can be used to detect human bocavirus
Polyomavirus	Kidney or brain tissue	NA	NA	+++	NAAT test of choice, but genetic variability can lead to falsely low or negative results; JCV DNA detection in CSF used for presumptive diagnosis of PML; BKV DNA quantification in plasma/urine used for pre-emptive diagnosis of PVAN; IHC and EM useful for biopsy tissues
Respiratory syncytial virus	+/++	++	NA	+++	Rapid antigen tests, such as DFA, more sensitive than culture; NAAT most sensitive, especially in adults
Rhinovirus	NA	NA	NA	+++	NAAT much more sensitive than culture; cross-reaction with enteroviruses can occur
Rotavirus	++	NA	NA	+++	Direct antigen detection useful for diagnosis; NAAT testing now commercially available as part of panels
Rubella virus[b]	NA	NA	+++	+++	Serology used for diagnosis of acute infection and immunity; NAAT most sensitive, but not commercially available; isolation useful for postnatal rubella if attempted early (prodromal period to 4 days post-rash); in CRS, virus can be isolated for weeks to months after birth
Varicella-zoster virus	++	+	Not reliable	+++	DFA and NAAT are most commonly used tests; rapid culture less sensitive than DFA; conventional culture insensitive; serology most useful for determination of immunity

[a]Key: +++, most sensitive and rapid; ++, moderately sensitive; +, least sensitive; −, not sensitive; NA, not available for routine clinical use in hospital or commercial laboratories. Pathology and tissue stains not included. Abbreviations: BAL, bronchoalveolar lavage; BKV, BK virus; CNS, central nervous system; CRS, congenital rubella syndrome; EM, electron microscopy; HTLV, human T-cell lymphotropic virus; IFA, immunofluorescent assay; IHC, immunohistochemistry; ISH, *in situ* hybridization; JCV, JC virus; PML, progressive multifocal leukoencephalopathy; PVAN, polyomavirus-associated nephropathy; WNV, West Nile virus.

[b]Additional specialized tests available at CDC and possibly other public health laboratories.

formalin, the cells are overlaid with antibodies labeled with fluorophores. After incubation and washing to remove unreacted antibodies, slides are examined under a fluorescence microscope. Free virus cannot be detected by IF microscopy; rather, viral proteins that accumulate during viral replication are visualized in infected target cells. IF is commonly performed on cell smears from skin lesions and nasopharyngeal (NP) aspirates or swabs, and has also been successfully applied to peripheral blood leukocytes (PBL). Advantages of IF include the opportunity to assess the quality of the sample (i.e., presence of an adequate number of target cells for a valid result), to discern specific from nonspecific staining patterns, to detect a single infected cell, and, in contrast to other immunoassays, to test one sample for multiple viral pathogens in a single cell spot. It can be applied to single or multiple samples, and per-test reagent costs are generally less than for other methods. Time to result is typically 1 to 2 hours.

Clinical utility of IF has been enhanced by reducing total time to as little as 25 min (D^3 FastPoint, Diagnostic Hybrids), by using cytocentrifugation to enhance slide quality (3), and by combining antibodies with different fluorochrome labels

TABLE 2 Uses and limitations of immunologic detection methods for viral antigens[a]

Method	Common clinical applications	Time required	Uses	Limitations
Direct antigen detection				
Immunofluorescence	RSV, influenza A and B, parainfluenza 1–3, adenovirus, HMPV in respiratory cells; VZV and HSV in skin-lesion smears; CMV in leukocytes	0.5–2 h	Can evaluate quality of sample, characteristic staining pattern and morphology; can detect a single positive cell, multiple pathogens in single sample, or quantitate CMV load in leukocytes; can test single or multiple samples; can run test multiple times a day; more sensitive than other antigen tests	Requires significant expertise and training; endpoints subjective; needs good sample with adequate cells; requires fluorescent microscope with good-quality objectives; cytocentrifuge desirable
Microwell, tube, or bead EIA	Rotavirus, HBV, fourth-generation HIV test	2–4 h	Suitable for large test volumes, batch testing; breakaway strips for smaller sample size; cheaper per test reagent costs; objective endpoints, computerized data analysis, automated format	Sensitivity varies with virus and kit used; neutralization test needed to detect nonspecific reactions; multiple controls processed with each run; EIA reader and washer, multichannel pipette required
Membrane EIA	RSV, influenza	15–30 min	Simple format, minimal training required; can test single or multiple samples, and run test multiple times a day; no major equipment	Relatively expensive per test reagent cost; nonspecific reactions difficult to detect; single agent detected
Latex agglutination	Rotavirus, enteric adenovirus	30 min	Simple format, no major equipment; suitable for single-sample testing	Subjective; weak positives difficult to read; nonspecific reactions; not as sensitive as EIA
Lateral flow immunoassay	Influenza, RSV, fourth-generation HIV test	10–20 min	Simple format, add sample, no reagent additions; no major equipment required; suitable for single-sample testing; many CLIA-waived tests for POC or resource-poor areas	Subjective unless reader used; weak positives difficult to read; some transport media may give spurious results
Rapid culture[b]				
Shell vial centrifugation culture	CMV, VZV, HSV, RSV, influenza A and B, parainfluenza 1–3, adenovirus, HMPV, enterovirus	16–48 h	Centrifugation enhances infectivity; characteristic staining pattern enhances specificity; can detect a single positive cell; can detect multiple viruses in one culture by combining two cell cultures in one shell vial and staining with pool of antibodies; detects replicating and not latent virus	Cell culture toxicity and contamination can reduce sensitivity; requires infectious virus; labor-intensive; need expertise in cell culture and IF; tissue culture facilities, centrifuge, fluorescent microscope required
Immune response				
IgM antibody	Parvovirus B19, EBV, arboviruses including West Nile virus, HBV, HAV, rubella, measles, mumps, CMV, HIV	1–4 h	Valuable when virus detection methods not available and/or disease is immune mediated and IgM antibodies detectable at clinical presentation; economical screening test	Compromised hosts and neonates may not have detectable antibodies; heterologous antibody rises can occur; appearance of IgM can be delayed until week 2 of illness; rheumatoid factor and IgG may interfere

[a]All rapid methods except electron microscopy are limited to the detection of suspected viruses; direct antigen tests do not amplify the target, thus are less sensitive than culture and NAATs.

[b]Limited to viruses that grow in commonly available cell cultures.

in one reagent to simultaneously detect and differentiate multiple viruses in the same cell spot (4). The dual fluorophore approach has been used to simultaneously test for herpes simplex virus (HSV) and varicella-zoster virus (VZV) in skin lesion samples, and influenza A and RSV in respiratory epithelial cells (SimulFluor Millipore). For a more comprehensive respiratory virus screen, a pool of MAbs to seven or eight common viruses (RSV; influenza A and B; parainfluenza types 1, 2, and 3; adenovirus; and human metapneumovirus [HMPV]) can be used without compromising test sensitivity. With D3 Ultra DFA (Diagnostic Hybrids), either the RSV or influenza A MAb is labeled with a yellow-gold fluorophore, and the remaining MAbs are labeled with green fluorescein. If the screen is positive with a green fluorescein-labeled MAb, additional slides must be stained with dual or single reagents to determine the infecting pathogen.

The essential prerequisites for accurate IF testing are an experienced and well-trained microscopist, sensitive and specific reagents, a fluorescence microscope with high-quality objectives, and a sufficient and steady flow of samples to develop and maintain expertise. IF works best in settings that allow re-collection of inadequate specimens. Established criteria for interpretation must be strictly followed, and results should be validated initially and intermittently thereafter by culture or other methods. IF staining can be more sensitive than culture for detection of RSV in NP aspirates, VZV in skin lesions, and cytomegalovirus (CMV) in blood leukocytes, but is variable for other viruses or sample types, ranging from 60% to 95% compared to culture (5, 6). IF is a labor-intensive, manual method, highly operator dependent, and not amenable to automation or high-volume testing. Most reagents now use the faster direct fluorescence staining method (i.e., the primary antiviral antibody is labeled) and are referred to as direct immunofluorescence assays (DFA).

Reasonable sensitivity, speed, and multiplex capability make DFA an attractive alternative to culture, particularly for respiratory viruses in pediatric patients. DFA has also been shown to reduce antibiotic use and lead to reduced hospitalization costs (7, 8). However, NAAT tests, such as BioFire FilmArray with 1-hour time to result, detect more pathogens, provide more sensitive results, and require less expertise than DFA. Although DFA is less expensive than NAAT, its use has decreased (9).

EIA

Enzyme immunoassay (EIA) employs an enzyme label and a colorimetric substrate and is the main test format in clinical laboratories for the detection of antibodies. In indirect EIA for antigen detection, antiviral antibody is immobilized on a solid support, sample is added, and viral antigen, if present, binds to the antibody. A second enzyme-labeled antibody is added, followed by addition of a substrate that usually generates a colorimetric signal. The reaction can be detected visually or with a spectrophotometer. Whereas IF microscopy can only visualize viral antigens produced in infected cells, EIA detects both cell-associated and cell-free antigens in clinical samples. Therefore, EIA can be used for noncellular samples, such as serum and stool. However, with EIA one cannot assess the quality of the sample and cannot distinguish nonspecific reactions unless a neutralization or blocking antibody test is done. EIA using microtiter plates is well suited to automated, high-volume batched-sample testing, with results analyzed by computer. Samples may be held until a sufficient number are available for testing and assay times are 2 to 4 hours. Alternatively, rapid membrane EIA in single sample cassettes with 15- to 30-min assay times can be performed multiple times a day as needed.

EIA for detection of viral antigens has been most successful when high titers are present in clinical samples and is most useful for viruses that do not grow in routine cell cultures, such as rotavirus, hepatitis B virus (HBV), and HIV (10, 11). Membrane EIA was widely used for influenza and RSV, especially in pediatric patients, until replaced with lateral flow assays. EIA has been less successful for other pathogens, such as HMPV. Although readily implemented in laboratories without virology experience, EIAs may not be commercially available for the desired pathogen or in the preferred format.

CLIA

In the chemiluminescence immunoassay (CLIA), a chemiluminescent label combined with a trigger reagent produces light. Random access instruments using CLIA are beginning to replace batch testing of blood samples by EIA. Testing can be performed "on demand" throughout operating hours, as samples arrive in the laboratory. Time to result is generally 1 hour. Compared to EIA, CLIA is more sensitive, has a lower background, and has a greater dynamic range.

An important advance in the diagnosis of acute HIV infections is the fourth-generation HIV screening test that combines IgM and IgG detection with detection of HIV-1 p24 antigen. Once antibody develops, p24 is bound in immune complexes, but prior to the appearance of antibody, p24 antigen is a sensitive marker for acute HIV infection. Currently one fourth-generation HIV EIA (Bio-Rad Genetic Systems), one CLIA (Abbott Architect), and one lateral flow immunoassay (Alere) are FDA cleared in the United States, although numerous fourth-generation HIV tests have long been used in Europe (11).

Latex Agglutination

The advantages of latex agglutination assays include simplicity, speed, and lack of expensive equipment. Antiviral antibody bound to latex beads is mixed with sample. If antigen is present, the beads clump or agglutinate, which can be seen by eye. When the specimens contain large amounts of viral antigen, agglutination assays can be used with acceptable results. This would include rotavirus and enteric adenovirus in stools of infants with gastroenteritis (12). When antigen is present in great excess, however, a prozone reaction can occur, leading to a false-negative result. This can be detected by repeating the test at a higher sample dilution. Limitations are lack of sensitivity, subjective interpretation of results, and difficulty reading borderline samples.

LFIA

In a lateral flow immunoassay (LFIA) for antigen detection, a sample is applied to a device or a strip and antigen, if present, binds to labeled antiviral antibodies. Antigen-antibody complexes move along the test strip by capillary action until bound by capture antibodies at the distal end of the strip, giving rise to a visible band. Whereas EIA involves a series of reagent additions, incubations, wash steps to remove unreacted materials, addition of substrate, and stop reagent, LFIA requires addition of sample only and provides results in 10 to 20 min that are comparable to EIA. Almost all rapid influenza and RSV tests are currently LFIA. These tests can be used at the point of care and have been shown to affect management (13). Both membrane EIA and lateral flow assays must be read within 5 to 10 min of assay completion for valid results. It should be noted that kit performance can be adversely affected by the transport media used. Media with gelatin such as M4 RT (Remel), especially when cold, can impair flow and lead to spurious results (false positives and false negatives). Like EIA, LFIA requires high viral load in

the sample for a positive result and thus performs best in infants and young children. Rapid influenza diagnostic tests (RIDT), predominantly LFIA, received increased scrutiny during the 2009 influenza pandemic and their inadequate sensitivity was widely recognized. Furthermore, detection of circulating influenza strains varies year to year, affecting kit performance.

To improve sensitivity, several rapid influenza and RSV LFIA tests utilize a fluorescence label, instead of the standard colloidal gold, and a small reader. Two readers (3M by Focus Diagnostics and Sofia by Quidel) are walkaway, provide a printout, and can be interfaced to the laboratory information system (LIS) (2, 14–16). One reader (Veritor, Becton Dickinson) is less expensive but is not walkaway (17). RIDT false positives are a significant problem when influenza prevalence is low. Due to the public health implications of influenza and advantages of having a simple POC test, the Centers for Disease Control and Prevention (CDC) has begun to monitor performance with currently circulating strains and has encouraged manufacturers to prioritize improved performance. Research into improving labels and enhancing sensitivity are a priority (18). For an update on use of RIDT, consult the CDC website at http://www.cdc.gov/flu/professionals/diagnosis/.

POC tests combining viral antigen with IgM and IgG antibody detection have been recently developed for HIV (Determine, Alere) and for dengue viruses (19).

Rapid Detection of Viruses in Culture by Immunologic Methods

Conventional virus isolation typically requires inoculation of multiple cell lines in roller tubes, followed by daily microscopic examination of cell monolayers for virus-induced cytopathic effects (CPE), which can take days to weeks to appear. The expertise required and the delay in virus detection limit the impact of conventional culture on patient therapy and management.

Rapid Culture

In contrast, rapid cultures involve centrifugation of samples onto cell monolayers in shell vials or multiwall plates, then fixation of cells after 16 to 48 hours of incubation, followed by staining with virus-specific MAbs to detect viral proteins in infected cells. Rapid culture for CMV utilizes one cell line, usually a human fibroblast, and staining with a MAb to CMV immediate-early antigen (20).

To detect a spectrum of viruses in conventional culture requires inoculation of multiple cell lines. To simplify the process for rapid cultures, two to three cell lines have been combined into one vial, and after sample inoculation and incubation for 1 to 2 days and up to 5 days, the cell monolayer is stained with a pool of antibodies to potential viral pathogens (21, 22). There are a variety of mixed cell cultures to choose from (Diagnostic Hybrids), depending on whether herpesviruses, respiratory viruses, or enteroviruses are sought (Table 3). The training time for personnel to become competent at interpreting IF staining in shell vial cultures is much shorter than required for conventional CPE or DFA of clinical samples.

Detection of Antibody Response to Virus Infections

In general, rapid diagnosis of acute viral infections in a timeframe to impact patient management relies on detection of the virus itself. Antibody develops in response to viral replication and therefore appears later. Nevertheless, in some virus infections, antibody detection remains the initial test of choice for several reasons.

IgM

IgM detection is primarily useful when viral detection methods are not readily available or are too slow to give clinically useful results, or when patients present coincident with the appearance of IgM. Examples include arboviruses and rubella, measles, and mumps viruses. In most infections, IgM antibodies can usually be detected within 5 to 7 days of clinical symptoms, but may require up to 2 weeks.

Third- and fourth-generation HIV tests that detect both IgM and IgG provide an earlier diagnosis than provided by first- and second-generation tests, which detected only IgG (11). Likewise, some hepatitis C virus (HCV) antibody tests detect both IgM and IgG and reduce the seronegative window after initial infection.

For some virus infections, the clinical symptoms prompting medical attention are immune mediated; therefore, IgM is usually detectable when the patient first presents. Examples include hepatitis A virus (HAV), HBV, parvovirus B19, and Epstein-Barr virus (EBV). Antibodies to several distinct viral antigens provide useful information regarding the stage of HBV and EBV infections.

Limitations of IgM testing include variability in test methods, weak or undetectable antibody responses in immunocompromised patients or neonates, heterologous IgM responses, interference by IgM-class rheumatoid factor (RF), competition between IgG and IgM antibodies leading to false positives and false negatives, failure to detect IgM due to timing of sample collection, persistence of IgM in some chronic viral infections, and frequent absence of IgM in reinfections or reactivations. For CMV, IgM antibody

TABLE 3 Mixed-cell cultures available commercially[a]

Culture type	Cell culture composition	Viruses targeted by staining[b]	Other potentially recoverable viruses
R-mix	Mink lung (Mv1Lu) and A549	RSV; influenza A and B; parainfluenza 1, 2, and 3; adenovirus (antibody pool); HMPV (separate antibody)	HSV, VZV, CMV, enterovirus
R-mix Too	MDCK and A549	Same as R-mix, except not susceptible to SARS CoV	HSV, VZV, enterovirus
H&V Mix	African green monkey kidney (strain CV-1) and MCR-5 cells	HSV-1 and 2, VZV	CMV, mumps, measles, RSV, rotavirus, SV40, rhinovirus, adenovirus, enterovirus
Super E-mix	BGMK-hDAF and A549	Enterovirus	HSV, VZV, adenovirus

[a]Diagnostic Hybrids, a Quidel Company. Table modified from reference 2. Abbreviations: A549, human lung carcinoma; BGMK, Buffalo green monkey kidney; BHK, baby hamster kidney; MDCK, Madin-Darby canine kidney; MRC-5, human diploid fibroblasts; SV40, simian virus 40.

[b]IF staining is at 1 and 2 days for mixed cells except Super E-mix, for which staining at 2 and 5 days is recommended.

increases with age in seropositive individuals, presumably due to subclinical reactivation. Cross-reactions between anti-parvovirus, rubella, and measles IgM are a particular problem if one is investigating a rash in pregnancy.

Methods to remove RF or interfering IgG prior to testing have been developed. While the best approach has been use of the IgM-class capture-assay format to improve specificity (23), background subtraction may still be necessary (24). Nevertheless, false-positive IgM results are common and can lead to inappropriate care. Although a positive IgM result may be the first indication of the viral pathogen, IgM tests are not definitive, but require confirmation by detection of virus or seroconversion of IgG or, for arboviruses, the more specific plaque-reduction neutralization test. The relative intensity of IgM and IgG reactivity (i.e., high IgM and low or negative IgG), followed by a rise in IgG over time, increases the likelihood of a true result. False-positive IgMs are a particular problem when the disease prevalence is low, as is commonly seen with HAV IgM in the U.S. population. The use of synthetic peptides to replace virion antigen-based immunoassays may reduce, but not eliminate, interference by RF, nonspecific reactions, and cross-reactivity.

MOLECULAR METHODS

Recent advances in nucleic acid amplification, detection, sample processing, and extraction techniques have enabled increased adoption of molecular tests for the diagnosis and monitoring of viral infections (2, 25–27). Molecular viral testing offers several advantages, including rapid detection of outbreaks and newly emerging strains or genotypes, identification of resistant viral pathogens, and the ability to correlate viral load with disease severity, all of which contribute to timely therapeutic decisions and early infection-control interventions. For discussion, molecular techniques can be divided into four main categories based on the numbers of targets detected and the diagnostic purpose. Table 4 provides an overview and comparison of commercial molecular *in vitro* diagnostic devices (IVD) that have been cleared by the U.S. FDA for detection, quantification, and genotyping of viral pathogens in clinical virology. Details and updates concerning these devices are available from the FDA website (http://www.fda.gov/MedicalDevices/ProductsandMedicalProcedures/InVitroDiagnostics/ucm330711.htm#microbial). In addition to IVDs, laboratory-developed tests (LDT) and commercial analyte-specific reagents (ASR) are used in laboratories with molecular expertise that are capable of validating and troubleshooting these tests for clinical use.

Monoplex Assays

Conventional PCR includes three steps: sample extraction, target nucleic acid amplification, and amplicon detection. Real-time amplification methods greatly accelerated the transition to NAATs in clinical laboratories and have become the main platform for detection and identification of viral pathogens. In real-time PCR, nucleic acid amplification and amplicon detection occur simultaneously in a closed tube, thus shortening time to result and reducing cross contamination.

Numerous LDTs using molecular technologies have been in the forefront of the effort to implement rapid and sensitive detection methods. One of the first molecular assays used successfully for clinical diagnosis was PCR for detection of HSV in cerebrospinal fluid (CSF) (28). PCR quickly became the test of choice when studies demonstrated that CSF PCR was equivalent to culture of brain tissue for diagnosis of HSV encephalitis and meningitis (28, 29). Interestingly, after almost a quarter of a century, probably due to market size, there were no FDA-cleared commercial HSV assays designated for CSF specimens until Simplexa HSV 1 & 2 was approved in 2014. In contrast, quite a few commercial NAATs are now available for detection and identification of HSV in skin and mucosal lesions (30). Among them, MultiCode-RTx HSV 1 & 2 (Luminex Corp), PROBETEC HSV (Becton Dickinson), and IsoAmp HSV (Quidel) are FDA-cleared IVD (30).

TABLE 4 FDA-cleared molecular methods for detection, quantification, and genotyping of viral pathogens[a]

Testing method	Viruses covered	TAT	Applications	Limitations
Monoplex	Adenovirus, CMV, dengue viruses, enterovirus, HCV, HSV, HMPV, HPV, influenza, and WNV	0.5–4 hours	Virus detection and infection diagnosis	"One stone for one bird"; limited test capacity; cannot be used as a test-of-cure
Multiplex[b]	Respiratory panel: adenovirus, bocavirus, coronavirus (4 species), influenza A and B, HMPV, parainfluenza 1, 2, 3, and 4, RSV, enterovirus, and rhinovirus Gastroenteritis panel: rotavirus, norovirus	1–8 hours	"One stone for many birds"; enhance diagnostic yields; reveal mixed infections	Slightly decreased sensitivities; cross-reaction can occur
Quantification	CMV, HIV, HBV, HCV	4-8 hours	Viral load determination; predict disease; monitor therapeutic response	Not ideal for diagnosis or confirmation; lack of inter-lab standardization
Genotyping	HCV, HPV, HIV, influenza	6–48 hours	Predict antiviral resistance; direct therapeutic regimens and prognosis; foresee means of spread of infection	Unknown and emerging mutations; indirect clinical correlation

[a]In addition to FDA-cleared IVD kits, commercial analyte-specific reagents are available for many viruses. Abbreviations: TAT, test turnaround time; WNV, West Nile virus.

[b]In addition to viral pathogens, these multiplex panels may cover nonviral pathogens; see companies' product inserts for details.

Studies have shown the superior sensitivity of real-time PCR-based assays compared to other assays for the detection of respiratory viruses (2, 27). Recent FDA approval of a number of commercial molecular assays for influenza virus testing has prompted many laboratories to discontinue culture or RIDT (2). Devices that have received FDA clearance include Human Influenza Virus Real-time RT-PCR Detection and Characterization Panel (CDC, Atlanta, GA), Xpert Flu (Cepheid, Sunnyvale, CA), Simplexa Flu A/B & RSV test (Focus Diagnostics, Cypress, CA), Liat Influenza A/B Assay (IQuum, Marlborough, MA), Autus Influenza A/B RG RT-PCR Kit (Qiagen, Inc., Germantown, MD), and Influenza A+B Assay (Quidel Corporation, San Diego, CA) (31). It merits mention that influenza-diagnostic test performance can be adversely affected by viral genetic and antigenic changes and should be re-assessed annually. Variability in sensitivity and specificity of the same test in different settings highlights the need for each laboratory to ensure optimal procedures and work with clinicians to improve sample quality (32).

Recently, the FDA has accelerated its clearance pace for a variety of viral pathogens (33). In addition to HSV and influenza, the FDA has cleared real-time PCR-based devices for adenovirus, CMV, dengue virus, enterovirus, HBV, HCV, HIV, HMPV, RSV, human papillomavirus, (HPV), and West Nile virus (33).

The monoplex assay will likely be the main platform for urgent, random-access, low-throughput assays such as POC testing that can be performed at home, in the workplace, at pharmacies and physician's offices, outpatient clinics, emergency rooms, or at the bedside of patients. POC test development has been driven by the need to make rapid, evidence-based, clinical, and therapeutic decisions at or near the site of patient care (30). While currently there are no FDA-approved molecular assays that can be used in a POC setting, considerable effort has been expended in developing POC devices including Xpert (Cepheid), Liat (IQuum), illumigene (Meridian Biosciences, Madison, WI), and iNAT (Alere Scarborough, Scarborough, ME).

Multiplex Assays

Multiplex design enables simultaneous detection and identification of multiple viral agents in a single reaction. Relative simplicity, powerful multiplexing capabilities, and high-throughput detection make multiplex assays most attractive for screening and detection of a panel of respiratory viruses. These methods are able to identify multiple pathogens more rapidly and with greater sensitivity than culture. This is particularly important in immunocompromised hosts. In addition, multiplex assays provide potent tools to detect mixed infections. Multiplex assays with relatively high throughput will likely become the main platform for batched specimens.

Multiplex reverse-transcriptase (RT)-PCR-based detection of respiratory viral pathogens has become part of the routine diagnostic algorithm in clinical laboratories over the past 5 years (25, 34) and several systems are commercially available. Some are rapid but low-throughput, whereas others use slower, conventional PCR assays, but with higher throughput. Examples include the FilmArray Respiratory Panel from BioFire Inc., the Infiniti Respiratory Viral Panel from AutoGenomics, Inc., the Jaguar system from HandyLab, Inc., the Multi-Code-PLx respiratory virus panel from EraGen Biosciences, the NGEN Respiratory Virus ASR from Nanogen, the ResPlex II assay from Qiagen, the Seeplex respiratory virus detection assay from Seegene, Inc., the eSensor Respiratory Virus Panel from GenMark Diagnostics, Verigene Respiratory Virus Nucleic Acid Test from Nanosphere, and the xTAG Respiratory Viral Panel from Luminex Molecular Diagnostics (25, 31, 34–36). Among them, the BioFire FilmArray Respiratory Panel, the GenMark eSensor Respiratory Virus Panel, the Nanosphere Verigene Respiratory Virus Nucleic Acid Test, and the Luminex xTAG Respiratory Viral Panel have been cleared by FDA.

With the success of multiplexing molecular detection in the respiratory arena, one would anticipate that highly multiplexed molecular assays will soon become a reality for detection of gastroenteritis pathogens (37). Indeed, progress has been made in the past few years on this front and there are a few multiplex RT-PCR-based commercial assays available for multi-target detection and identification in a single sample for gastroenteritis. Seegene's Seeplex Diarrhea ACE Detection detects diarrhea-causing viruses and/or bacteria directly from stool and rectal swab (38). A FilmArray GI Panel has been developed by BioFire to detect a panel of pathogens including adenovirus genotypes 40/41, human astrovirus, norovirus GI/GII, rotavirus A, and sapovirus. The xTAG Gastrointestinal Pathogen Panel (Luminex) using the xMAP Technology platform detects and identifies 11 pathogens including adenovirus 40/41, rotavirus A, and norovirus GI/GII and has become available as an IVD recently in the U.S. (39). The overall assay turnaround time is approximately 5 hours with bead-based detection on either the Luminex 100/200 or MAGPIX instruments.

Opening of postamplification tubes and subsequent pipetting steps in some test systems that use conventional PCR increase the risk for intra- and inter-run contamination. Careful attention should be paid to contamination control measures including the re-establishment of dedicated post-amplification laboratory space, which had become unnecessary in the real-time PCR era. Simultaneous testing for all possible pathogens is an efficient means to obtain a conclusive result and improves etiologic diagnosis (35, 36, 40). Assaying for all potential pathogens may also yield crucial information regarding coinfections or secondary infections (41). However, one study from the Netherlands indicated that implementation of multiple molecular assays for the etiologic diagnosis of lower respiratory tract infections increased the diagnostic yield considerably, yet did not reduce antibiotic use or costs (42). Thus, the clinical relevance and cost-effectiveness of simultaneous multi-pathogen detection and identification strategies merit further investigation.

Quantitative Assays

One of the first applications of NAAT in virology included quantitative detection of HIV, followed by assays to detect HBV and HCV. Over time, these assays have progressed from conventional to real-time methods with increased automation and have been extensively evaluated and shown to be essential to monitor and guide patient management. Calibration can be performed using a calibrator within each reaction or by comparing the quantitative results versus those generated using a stored calibration curve. The precision and linear range of viral loads can be measured precisely across the observed concentration range in plasma or serum collected from infected persons.

HIV infection results in lifelong viral persistence. In chronically infected patients, the HIV-1 RNA viral load in the plasma together with CD4 T cell numbers are the two routine laboratory markers used to guide antiretroviral therapy (ART) initiation, monitor treatment effectiveness, determine clinical progression, and modify treatment regimens. An HIV-1 RNA level below the detection limit is indicative of excellent adherence by patients and ART efficacy (43). Commercially available devices, including COBAS AmpliPrep/TaqMan HIV-1 (Roche), VERSANT

HIV-1 RNA (Siemens), NucliSens HIV-1 RNA QT (bioMerieux), and RealTime m2000 HIV-1 (Abbott Molecular), have been cleared by the FDA.

Abbott Molecular, Roche, and/or Siemens provide FDA-cleared devices for HCV and/or HBV viral load determination in plasma or serum (26, 44). Development of a World Health Organization (WHO) standard has resulted in the use of international units (IU) per milliliter and has improved agreement between assays (45). With the exception of the branched-DNA quantitative assay, the analytical sensitivity of these assays approaches limits of detection as low as 12 IU/ml (44). The highly sensitive quantitative data are used to help determine the rate of sustained virologic response (46).

Real-time PCR-based assays are commonly used for diagnosis and monitoring of CMV viral load in hematopoietic stem cell and solid organ transplant recipients (47, 48). Subsequent to CMV, quantitative viral load testing has been extended to monitoring other viruses in various transplant groups, including EBV, BK virus, and adenoviruses (49). However, the biggest challenge associated with the use of these mostly LDT quantitative assays is the inability to compare viral load results obtained across laboratories due to differences in genomic target (single versus multi-copy genes), extraction methods (manual versus automated), and detection platforms and the lack of international standards and calibrators (50). These limitations have made the establishment of quantitative thresholds for treatment difficult to establish (51, 52). However, the variability in viral loads measured across methods might be solved for some viruses with the recent introduction of the first WHO international standards for CMV (51) and EBV (52), as well as the availability of the first FDA-approved commercial real-time quantitative assay from Roche for monitoring of CMV viral loads (53).

Genotyping Assays

Genotyping is defined broadly here as assays that provide sequence or genotype, track disease outbreaks, provide strain resistance data and/or treatment prognosis, and determine the method or source and means of spread of infection. A variety of commercial tests, based on PCR coupled with sequencing, matrix probe hybridization, or electrospray ionization/mass spectrometry (ESI-MS), are available for genotype determination (43, 54, 55).

HIV-1 drug resistance tests—which include genotyping assays to detect known resistance-associated nucleotide mutations in the viral genome—and phenotype assays to detect viral replication in the presence of antiretroviral drugs have become routine in the management of patients receiving ART. Genotypic drug resistance testing has been recommended by the International AIDS Society-USA panel as an important tool to guide changes in therapy, the overall direction of therapy, and more recently, the initiation of therapy. There are currently two FDA-approved commercial drug resistance assays: (i) the TruGene HIV-1 Genotyping Kit and OpenGene DNA Sequencing System (Siemens Healthcare Diagnostics, Tarrytown, NY), and (ii) the ViroSeq HIV-1 Genotyping System (Abbott Molecular, Des Plaines, IL) (55). Both systems generate reverse transcriptase and protease gene sequences following RT-PCR amplification. TruGene HIV-1 was recently discontinued by Siemens but will be made available through RTT Molecular Dx (Buford, GA). LDT-PCR assays coupled with sequencing have been used to detect antiviral drug resistance-related mutations such as those in CMV (UL97 mutations) (56) and influenza viruses (neuraminidase gene) (57).

HCV genotyping is widely used to determine therapy duration in conjunction with baseline viremia and viral load kinetics during treatment. A wide variety of technical platforms are available, including PCR followed by strip-based reverse hybridization, PCR followed by Sanger sequencing, and real-time PCR (58). All of these assays use the 5′ untranslated region (UTR) as their primary target, which has difficulty reliably differentiating between genotypes 1 and 6, as well as between subtypes, such as 1a and 1b. To remedy this, a second target region (core or NS5b) has been added to some of the 5′ UTR-based assays (59). Two complications impact current genotyping assays. First, multiple genotypes have been detected in intravenous drug users, and current population-based sequencing assays may miss minor genotype populations (60). The other complication is the presence of recombinant HCV isolates; current assays likely do not detect recombinants (61). Next-generation sequencing is predicted to provide more accurate HCV genotyping in these complicated settings (62). Currently, the Abbott RealTime HCV Genotype II, which differentiates genotypes 1, 1a, 1b, 2, 3, 4, and 5, is FDA-cleared to aid in determining the appropriate approach to treatment (63).

Recently, HPV vaccines have demonstrated effectiveness in preventing type-specific persistent infection and disease. To monitor the impact of vaccine implementation strategies, determine type-specific persistence, and evaluate the clinical significance of coinfection with multiple genotypes, type-specific results are desirable (64). Most established HPV typing assays are based on consensus PCR to amplify the relatively conserved L1 gene region with hybridization, restriction enzyme digestion, or sequencing of the amplicon to determine type(s) (65). Recently, several solid or liquid microarray-based techniques have been reported for simultaneous detection and typing of HPV (54). Currently, there are four FDA-approved tests for detection of HPV in endocervical specimens. Among them, the Cervista HPV 16/18 (Hologic, Inc.) and the Cobas HPV Test (Roche) are the two FDA-cleared devices providing limited HPV genotyping information (33, 65). Microarrays have also been used to characterize and type other viral pathogens, including rotavirus, norovirus, astrovirus, and HBV (66–68). The PLEX-ID Flu Assay (Abbott Molecular Inc., Des Plaines, IL), which incorporates multilocus PCR and ESI-MS, has been recently cleared by FDA to detect and differentiate influenza A 2009 H1N1, seasonal H1N1, H3N2, and influenza B in nasopharyngeal swab specimens (37).

TEST SELECTION, VALIDATION, AND MONITORING

Selecting which tests to offer in the laboratory has become more challenging as each diagnostic method has advantages and limitations (Table 1). An assessment and understanding of clinical needs, including communication with clinicians, is essential. In what settings would intervention, either therapeutic or preventive, be benefited by a laboratory diagnosis? Is targeted diagnosis of one or two agents acceptable, or is a test that detects multiple pathogens needed? Turnaround time, anticipated test volume, personnel expertise, fit with laboratory workflow, cost, equipment needed, number of tests available on the platform, etc. should be carefully considered. In smaller hospital laboratories, testing may be limited, whereas in laboratories serving large tertiary care hospitals, multiple methodologies are commonly available and algorithms for test use should be in place.

Once a test is selected, it is important to establish how the test functions in the setting into which it will be introduced, and not to rely on manufacturer's claims in the package insert or publications from other institutions. If the test does not function as anticipated, the reasons should be investigated (e.g., poor sample collection, transport media used, improper test procedure, different patient population, lack of technical expertise, etc.) and corrective action should be taken or a more suitable method employed. Each test offered should be monitored and periodically re-evaluated to assess its performance and to determine whether it continues to serve the needs of patients and physicians. For DFA and in-house amplification methods in particular, the pitfalls are many and careful monitoring of results is critical. Genetic and antigenic variability and genetic change can be a problem with any virus, but particularly with influenza viruses. Commercial kits provide many advantages, but primer and probe sequences are proprietary and can become outdated over time. Users should be aware that molecular tests can miss high-positive samples due to primer or probe mismatches. In critical situations when the molecular diagnosis is questioned, retesting with a different molecular assay may be warranted. Monitoring clinical correlation for test results and seeking feedback from clinicians are best practices that should be ongoing.

SUMMARY AND CONCLUSIONS

The choices for rapid viral diagnosis continue to increase. A variety of test formats are available, from walk-away automated systems to single-specimen immunoassays read visually. The number and types of techniques chosen will vary with the individual viruses, laboratory expertise, and clinical needs, and will continue to change as both test methods and antiviral therapy evolve. Laboratories must establish and monitor the performance of each test in their hands and their patient population. To provide clinically relevant, cost-effective, and accurate information for patient management, it is important to work with clinicians to establish priorities, improve sample collection, and seek clinical correlation and feedback.

Efforts to improve the sensitivity of simple immunoassays are underway. NAATs continue to evolve at a dazzling rate, with increasing automation, high-volume throughput, random access capability, faster time to result, and highly multiplexed test capability. With increasing demand, manufacturers are now motivated to seek FDA approval for their products, which in turn has increased adoption of NAAT in clinical laboratories.

NAATs are now the standard against which other methods are judged. Yet NAAT reagent costs are higher than other methods and equipment can be costly. To facilitate implementation, some facilities restrict more expensive NAATs to the patient groups that will benefit most from a viral diagnosis. Although we can detect more viruses more quickly, the significance of a positive result may sometimes be unclear in the individual patient. Outcomes research is urgently needed to provide guidance to both laboratories and clinicians on the cost-effective use of viral diagnostic tests to improve outcomes in diverse patient groups and clinical settings.

REFERENCES

1. **Leland DS, Landry ML.** 2010. Virus isolation, p 98–112. *In* Jerome KR (ed), *Laboratory Diagnosis of Viral Infections*, 4th ed. Informa Press, New York, NY.
2. **Ginocchio CC, Zhang F, Manji R, Arora S, Bornfreund M, Falk L, Lotlikar M, Kowerska M, Becker G, Korologos D, de Geronimo M, Crawford JM.** 2009. Evaluation of multiple test methods for the detection of the novel 2009 influenza A (H1N1) during the New York City outbreak. *J Clin Virol* **45:**191–195. PubMed
3. **Landry ML, Ferguson D, Wlochowski J.** 1997. Detection of herpes simplex virus in clinical specimens by cytospin-enhanced direct immunofluorescence. *J Clin Microbiol* **35:**302–304. PubMed
4. **Landry ML, Ferguson D.** 2000. SimulFluor respiratory screen for rapid detection of multiple respiratory viruses in clinical specimens by immunofluorescence staining. *J Clin Microbiol* **38:**708–711. PubMed
5. **Gerna G, Revello MG, Percivalle E, Morini F.** 1992. Comparison of different immunostaining techniques and monoclonal antibodies to the lower matrix phosphoprotein (pp65) for optimal quantitation of human cytomegalovirus antigenemia. *J Clin Microbiol* **30:**1232–1237. PubMed
6. **Landry ML, Ferguson D.** 1993. Comparison of quantitative cytomegalovirus antigenemia assay with culture methods and correlation with clinical disease. *J Clin Microbiol* **31:**2851–2856. PubMed
7. **Barenfanger J, Drake C, Leon N, Mueller T, Troutt T.** 2000. Clinical and financial benefits of rapid detection of respiratory viruses: An outcomes study. *J Clin Microbiol* **38:**2824–2828. PubMed
8. **Byington CL, Castillo H, Gerber K, Daly JA, Brimley LA, Adams S, Christenson JC, Pavia AT.** 2002. The effect of rapid respiratory viral diagnostic testing on antibiotic use in a children's hospital. *Arch Pediatr Adolesc Med* **156:**1230–1234. PubMed
9. **Couturier MR, Barney T, Alger G, Hymas WC, Stevenson JB, Hillyard D, Daly JA.** 2013. Evaluation of the FilmArray® Respiratory Panel for clinical use in a large children's hospital. *J Clin Lab Anal* **27:**148–154. PubMed
10. **Gautam R, Lyde F, Esona MD, Quaye O, Bowen MD.** 2013. Comparison of Premier™ Rotaclone®, ProSpecT™, and RIDASCREEN® rotavirus enzyme immunoassay kits for detection of rotavirus antigen in stool specimens. *J Clin Virol* **58:**292–294. PubMed
11. **Mitchell EO, Stewart G, Bajzik O, Ferret M, Bentsen C, Shriver MK.** 2013. Performance comparison of the 4th generation Bio-Rad Laboratories GS HIV Combo Ag/Ab EIA on the EVOLIS™ automated system versus Abbott ARCHITECT HIV Ag/Ab Combo, Ortho Anti-HIV 1+2 EIA on Vitros ECi and Siemens HIV-1/O/2 enhanced on Advia Centaur. *J Clin Virol* **58**(Suppl 1)**:**e79–e84. PubMed
12. **Dusetty P, Velázquez FR, Gutiérrez-Escolano AL, Ludert JE.** 2013. Evaluation of the second generation of a commercial latex agglutination test for the detection of rotavirus antigens in fecal samples. *J Clin Virol* **57:**88–90. PubMed
13. **Bonner AB, Monroe KW, Talley LI, Klasner AE, Kimberlin DW.** 2003. Impact of the rapid diagnosis of influenza on physician decision-making and patient management in the pediatric emergency department: results of a randomized, prospective, controlled trial. *Pediatrics* **112:**363–367. PubMed
14. **Dale SE, Mayer C, Mayer MC, Menegus MA.** 2008. Analytical and clinical sensitivity of the 3M rapid detection influenza A+B assay. *J Clin Microbiol* **46:**3804–3807. PubMed
15. **Lee CK, Cho CH, Woo MK, Nyeck AE, Lim CS, Kim WJ.** 2012. Evaluation of Sofia fluorescent immunoassay analyzer for influenza A/B virus. *J Clin Virol* **55:**239–243. PubMed
16. **Rath B, Tief F, Obermeier P, Tuerk E, Karsch K, Muehlhans S, Adamou E, Duwe S, Schweiger B.** 2012. Early detection of influenza A and B infection in infants and children using conventional and fluorescence-based rapid testing. *J Clin Virol* **55:**329–333. PubMed
17. **Peters TR, Blakeney E, Vannoy L, Poehling KA.** 2013. Evaluation of the limit of detection of the BD Veritor™

system flu A+B test and two rapid influenza detection tests for influenza virus. *Diagn Microbiol Infect Dis* **75:**200–202. PubMed

18. **Linares EM, Kubota LT, Michaelis J, Thalhammer S.** 2012. Enhancement of the detection limit for lateral flow immunoassays: evaluation and comparison of bioconjugates. *J Immunol Methods* **375:**264–270. PubMed
19. **Blacksell SD, Jarman RG, Bailey MS, Tanganuchitcharnchai A, Jenjaroen K, Gibbons RV, Paris DH, Premaratna R, de Silva HJ, Lalloo DG, Day NP.** 2011. Evaluation of six commercial point-of-care tests for diagnosis of acute dengue infections: The need for combining NS1 antigen and IgM/IgG antibody detection to achieve acceptable levels of accuracy. *Clin Vaccine Immunol* **18:**2095–2101. PubMed
20. **Gleaves CA, Smith TF, Shuster EA, Pearson GR.** 1984. Rapid detection of cytomegalovirus in MRC-5 cells inoculated with urine specimens by using low-speed centrifugation and monoclonal antibody to an early antigen. *J Clin Microbiol* **19:**917–919. PubMed
21. **Fong CK, Lee MK, Griffith BP.** 2000. Evaluation of R-Mix FreshCells in shell vials for detection of respiratory viruses. *J Clin Microbiol* **38:**4660–4662. PubMed
22. **Buck GE, Wiesemann M, Stewart L.** 2002. Comparison of mixed cell culture containing genetically engineered BGMK and CaCo-2 cells (Super E-Mix) with RT-PCR and conventional cell culture for the diagnosis of enterovirus meningitis. *J Clin Virol* **25**(Suppl 1)**:**S13–S18. PubMed
23. **Besselaar TG, Blackburn NK, Aldridge N.** 1989. Comparison of an antibody-capture IgM enzyme-linked immunosorbent assay with IgM-indirect immunofluorescence for the diagnosis of acute Sindbis and West Nile infections. *J Virol Methods* **25:**337–345. PubMed
24. **Rawlins ML, Swenson EM, Hill HR, Litwin CM.** 2007. Evaluation of an enzyme immunoassay for detection of immunoglobulin M antibodies to West Nile virus and the importance of background subtraction in detecting nonspecific reactivity. *Clin Vaccine Immunol* **14:**665–668. PubMed
25. **Yan Y, Zhang S, Tang YW.** 2011. Molecular assays for the detection and characterization of respiratory viruses. *Semin Respir Crit Care Med* **32:**512–526. PubMed
26. **Caliendo AM, Valsamakis A, Bremer JW, Ferreira-Gonzalez A, Granger S, Sabatini L, Tsongalis GJ, Wang YF, Yen-Lieberman B, Young S, Lurain NS.** 2011. Multilaboratory evaluation of real-time PCR tests for hepatitis B virus DNA quantification. *J Clin Microbiol* **49:**2854–2858. PubMed
27. **Mahony JB.** 2008. Detection of respiratory viruses by molecular methods. *Clin Microbiol Rev* **21:**716–747. PubMed
28. **Rowley AH, Whitley RJ, Lakeman FD, Wolinsky SM.** 1990. Rapid detection of herpes-simplex-virus DNA in cerebrospinal fluid of patients with herpes simplex encephalitis. *Lancet* **335:**440–441. PubMed
29. **Tang YW, Mitchell PS, Espy MJ, Smith TF, Persing DH.** 1999. Molecular diagnosis of herpes simplex virus infections in the central nervous system. *J Clin Microbiol* **37:**2127–2136. PubMed
30. **Lemieux B, Li Y, Kong H, Tang YW.** 2012. Near instrument-free, simple molecular device for rapid detection of herpes simplex viruses. *Expert Rev Mol Diagn* **12:**437–443. PubMed
31. **Buller RS.** 2013. Molecular detection of respiratory viruses. *Clin Lab Med* **33:**439–460. PubMed
32. **Landry ML.** 2011. Diagnostic tests for influenza infection. *Curr Opin Pediatr* **23:**91–97. PubMed
33. **Emmadi R, Boonyaratanakornkit JB, Selvarangan R, Shyamala V, Zimmer BL, Williams L, Bryant B, Schutzbank T, Schoonmaker MM, Amos Wilson JA, Hall L, Pancholi P, Bernard K.** 2011. Molecular methods and platforms for infectious diseases testing a review of FDA-approved and cleared assays. *J Mol Diagn* **13:**583–604. PubMed
34. **Caliendo AM.** 2011. Multiplex PCR and emerging technologies for the detection of respiratory pathogens. *Clin Infect Dis* **52**(Suppl 4)**:**S326–S330. PubMed
35. **Li H, McCormac MA, Estes RW, Sefers SE, Dare RK, Chappell JD, Erdman DD, Wright PF, Tang YW.** 2007. Simultaneous detection and high-throughput identification of a panel of RNA viruses causing respiratory tract infections. *J Clin Microbiol* **45:**2105–2109. PubMed
36. **Mahony J, Chong S, Merante F, Yaghoubian S, Sinha T, Lisle C, Janeczko R.** 2007. Development of a respiratory virus panel test for detection of twenty human respiratory viruses by use of multiplex PCR and a fluid microbead-based assay. *J Clin Microbiol* **45:**2965–2970. PubMed
37. **Dunbar SA, Zhang H, Tang YW.** 2013. Advanced techniques for detection and identification of microbial agents of gastroenteritis. *Clin Lab Med* **33:**527–552. PubMed
38. **Higgins RR, Beniprashad M, Cardona M, Masney S, Low DE, Gubbay JB.** 2011. Evaluation and verification of the Seeplex Diarrhea-V ACE assay for simultaneous detection of adenovirus, rotavirus, and norovirus genogroups I and II in clinical stool specimens. *J Clin Microbiol* **49:**3154–3162. PubMed
39. **Navidad JF, Griswold DJ, Gradus MS, Bhattacharyya S.** 2013. Evaluation of Luminex xTAG gastrointestinal pathogen analyte-specific reagents for high-throughput, simultaneous detection of bacteria, viruses, and parasites of clinical and public health importance. *J Clin Microbiol* **51:**3018–3024. PubMed
40. **Schulert GS, Lu Z, Wingo T, Tang YW, Saville BR, Hain PD.** 2013. Role of a respiratory viral panel in the clinical management of pediatric inpatients. *Pediatr Infect Dis J* **32:**467–472. PubMed
41. **Brunstein JD, Cline CL, McKinney S, Thomas E.** 2008. Evidence from multiplex molecular assays for complex multipathogen interactions in acute respiratory infections. *J Clin Microbiol* **46:**97–102. PubMed
42. **Oosterheert JJ, van Loon AM, Schuurman R, Hoepelman AI, Hak E, Thijsen S, Nossent G, Schneider MM, Hustinx WM, Bonten MJ.** 2005. Impact of rapid detection of viral and atypical bacterial pathogens by real-time polymerase chain reaction for patients with lower respiratory tract infection. *Clin Infect Dis* **41:**1438–1444. PubMed
43. **Tang YW, Lowery KS, Valsamakis A, Schaefer VC, Chappell JD, White-Abell J, Quinn CD, Li H, Washington CA, Cromwell J, Giamanco CM, Forman M, Holden J, Rothman RE, Parker ML, Ortenberg EV, Zhang L, Lin YL, Gaydos CA.** 2013. Clinical accuracy of a PLEX-ID flu device for simultaneous detection and identification of influenza viruses A and B. *J Clin Microbiol* **51:**40–45. PubMed
44. **Vermehren J, Kau A, Gärtner BC, Göbel R, Zeuzem S, Sarrazin C.** 2008. Differences between two real-time PCR-based hepatitis C virus (HCV) assays (RealTime HCV and Cobas AmpliPrep/Cobas TaqMan) and one signal amplification assay (Versant HCV RNA 3.0) for RNA detection and quantification. *J Clin Microbiol* **46:**3880–3891. PubMed
45. **Madej RM, Davis J, Holden MJ, Kwang S, Labourier E, Schneider GJ.** 2010. International standards and reference materials for quantitative molecular infectious disease testing. *J Mol Diagn* **12:**133–143. PubMed
46. **Kanda T, Yokosuka O, Omata M.** 2013. Treatment of hepatitis C virus infection in the future. *Clin Transl Med* **2:**9. PubMed
47. **Li H, Dummer JS, Estes WR, Meng S, Wright PF, Tang YW.** 2003. Measurement of human cytomegalovirus loads by quantitative real-time PCR for monitoring clinical intervention in transplant recipients. *J Clin Microbiol* **41:**187–191. PubMed

48. **Razonable RR, Paya CV, Smith TF.** 2002. Role of the laboratory in diagnosis and management of cytomegalovirus infection in hematopoietic stem cell and solid-organ transplant recipients. *J Clin Microbiol* **40:**746–752. PubMed
49. **Espy MJ, Uhl JR, Sloan LM, Buckwalter SP, Jones MF, Vetter EA, Yao JD, Wengenack NL, Rosenblatt JE, Cockerill FR III, Smith TF.** 2006. Real-time PCR in clinical microbiology: applications for routine laboratory testing. *Clin Microbiol Rev* **19:**165–256. PubMed
50. **Caliendo AM, Shahbazian MD, Schaper C, Ingersoll J, Abdul-Ali D, Boonyaratanakornkit J, Pang XL, Fox J, Preiksaitis J, Schönbrunner ER.** 2009. A commutable cytomegalovirus calibrator is required to improve the agreement of viral load values between laboratories. *Clin Chem* **55:**1701–1710. PubMed
51. **Pang XL, Fox JD, Fenton JM, Miller GG, Caliendo AM, Preiksaitis JK; American Society of Transplantation Infectious Diseases Community of Practice; Canadian Society of Transplantation.** 2009. Interlaboratory comparison of cytomegalovirus viral load assays. *Am J Transplant* **9:**258–268. PubMed
52. **Preiksaitis JK, Pang XL, Fox JD, Fenton JM, Caliendo AM, Miller GG; American Society of Transplantation Infectious Diseases Community of Practice.** 2009. Interlaboratory comparison of epstein-barr virus viral load assays. *Am J Transplant* **9:**269–279. PubMed
53. **Boaretti M, Sorrentino A, Zantedeschi C, Forni A, Boschiero L, Fontana R.** 2013. Quantification of cytomegalovirus DNA by a fully automated real-time PCR for early diagnosis and monitoring of active viral infection in solid organ transplant recipients. *J Clin Virol* **56:**124–128. PubMed
54. **Miller MB, Tang YW.** 2009. Basic concepts of microarrays and potential applications in clinical microbiology. *Clin Microbiol Rev* **22:**611–633. PubMed
55. **Stürmer M, Berger A, Preiser W.** 2004. HIV-1 genotyping: comparison of two commercially available assays. *Expert Rev Mol Diagn* **4:**281–291. PubMed
56. **Drew WL.** 2010. Cytomegalovirus resistance testing: pitfalls and problems for the clinician. *Clin Infect Dis* **50:**733–736. PubMed
57. **Moscona A.** 2009. Global transmission of oseltamivir-resistant influenza. *N Engl J Med* **360:**953–956. PubMed
58. **Weck K.** 2005. Molecular methods of hepatitis C genotyping. *Expert Rev Mol Diagn* **5:**507–520. PubMed
59. **Jacka B, Lamoury F, Simmonds P, Dore GJ, Grebely J, Applegate T.** 2013. Sequencing of the hepatitis C virus: A systematic review. *PLoS One* **8:**e67073. doi:10.1371/journal.pone.0067073 PubMed
60. **Pham ST, Bull RA, Bennett JM, Rawlinson WD, Dore GJ, Lloyd AR, White PA.** 2010. Frequent multiple hepatitis C virus infections among injection drug users in a prison setting. *Hepatology* **52:**1564–1572. PubMed
61. **González-Candelas F, López-Labrador FX, Bracho MA.** 2011. Recombination in hepatitis C virus. *Viruses* **3:**2006–2024. PubMed
62. **Dietz J, Schelhorn SE, Fitting D, Mihm U, Susser S, Welker MW, Füller C, Däumer M, Teuber G, Wedemeyer H, Berg T, Lengauer T, Zeuzem S, Herrmann E, Sarrazin C.** 2013. Deep sequencing reveals mutagenic effects of ribavirin during monotherapy of hepatitis C virus genotype 1-infected patients. *J Virol* **87:**6172–6181. PubMed
63. **Shinol RC, Gale HB, Kan VL.** 2012. Performance of the Abbott RealTime HCV Genotype II RUO assay. *J Clin Microbiol* **50:**3099–3101. PubMed
64. **Huh W, Einstein MH, Herzog TJ, Franco EL.** 2010. What is the role of HPV typing in the United States now and in the next five years in a vaccinated population? *Gynecol Oncol* **117:**481–485. PubMed
65. **Eide ML, Debaque H.** 2012. HPV detection methods and genotyping techniques in screening for cervical cancer. *Ann Pathol* **32:**e15–23, 401–409.
66. **Honma S, Chizhikov V, Santos N, Tatsumi M, Timenetsky Mdo C, Linhares AC, Mascarenhas JD, Ushijima H, Armah GE, Gentsch JR, Hoshino Y.** 2007. Development and validation of DNA microarray for genotyping group A rotavirus VP4 (P[4], P[6], P[8], P[9], and P[14]) and VP7 (G1 to G6, G8 to G10, and G12) genes. *J Clin Microbiol* **45:**2641–2648. PubMed
67. **Pas SD, Tran N, de Man RA, Burghoorn-Maas C, Vernet G, Niesters HG.** 2008. Comparison of reverse hybridization, microarray, and sequence analysis for genotyping hepatitis B virus. *J Clin Microbiol* **46:**1268–1273. PubMed
68. **Jääskeläinen AJ, Maunula L.** 2006. Applicability of microarray technique for the detection of noro- and astroviruses. *J Virol Methods* **136:**210–216. PubMed

Herpes Simplex Virus

D. SCOTT SCHMID

58

Human infections with herpes simplex virus type 1 (HSV-1) and type 2 (HSV-2) are common throughout the world. HSV infection can cause a variety of illnesses depending on the anatomic site infected, whether it is a primary or recurrent infection, and the immune status of the person infected. Persons at risk for serious or prolonged active HSV infection are those with eczema, severe burns, or immunosuppressive conditions, such as organ transplant patients or HIV-infected persons. Primary infection occurs in individuals who have not previously been infected with either HSV-1 or HSV-2. Primary infections may be subclinical or mild enough to be unrecognized in a majority of cases, whereas clinically apparent infections comprise a wide array of presentations, ranging from mild pharyngitis or cutaneous infections to severe generalized disease and, on rare occasions, death (1). HSV-1 has a greater propensity to cause oral infections and is typically acquired during childhood. The most frequent manifestation of primary HSV-1 infection in children is gingivostomatitis. Primary HSV-1 infection in adolescents and adults usually manifests as pharyngitis or tonsillitis. Conjunctivitis, keratitis, vesicular eruptions of the skin, herpes whitlow, and encephalitis occur much less frequently. While the most common manifestation of sexually acquired HSV-2 is genital disease, both HSV-2 and HSV-1 can cause genital infection. HSV is the most common cause of genital ulcer disease in developed countries. In recent years, HSV-1 has been more frequently implicated as the etiologic agent (1). Complications of HSV-2 infection include aseptic meningitis and other neurological complications, extragenital lesions, and disseminated infection. Neonatal herpes is caused by mother-to-child transmission of HSV-1 or HSV-2 *in utero*, during the birth process, or during the neonatal period. Infants infected during delivery or postpartum present in one of three ways: (i) disease localized to the skin, eyes, or mouth; (ii) central nervous system disease with or without skin, eye, or mouth disease; or (iii) disseminated infection. HSV-1 seroprevalence in the United States declined about 7% from 1999 to 2004 and from 2005 to 2010, with roughly 60% of persons being HSV-1 seropositive among 40- to 49-year-olds (2). HSV-2 seroprevalence in the United States increased by more than 50% between the mid-1970s and the mid-1990s but then began to decline; in 2005 to 2010, the estimated seroprevalence was 25% in 40- to 49-year-olds (2).

As with all human herpesviruses, HSV-1 and HSV-2 establish a lifelong latent infection following primary infection, in this instance by colonizing sensory neurons of either the trigeminal or the lumbosacral ganglia (1, 3). Reactivation from either site may result in subclinical or clinical disease, both with viral shedding. Recurrent infection in the form of fever blisters or, rarely, ocular herpes occurs in up to 40% of HSV-1-seropositive people (1, 3). Genital eruptions may recur in one-third to two-thirds of individuals infected with HSV-2 (1, 3); reactivation is less frequent with genital HSV-1 than with genital HSV-2 infection. Recurrent infections are frequently subclinical and, as such, may result in unrecognized virus transmission, including neonatal infection (4, 5). A previous oral HSV-1 infection does not protect a person against a genital HSV-2 infection; however, persons with prior HSV-1 infection who are subsequently infected with HSV-2 frequently experience a less severe clinical course (1).

CLINICAL INDICATIONS

A presumptive clinical diagnosis of HSV infection can frequently be made from the appearance of cutaneous or mucosal lesions alone; however, given the large differential diagnoses for genital ulcer disease, laboratory confirmation of the infection should always be sought. The serologic results obtained after waiting to collect and test an appropriately timed convalescent-phase serum sample offer little guidance for therapy in the clinical management of most patients. The definitive diagnostic method is HSV type-specific PCR (1, 6), which has largely supplanted other methods, e.g., viral culture, direct fluorescent-antibody assay (DFA), and the Tzanck smear. HSV PCR has been shown to be substantially more sensitive than virus culture (2- to 4-fold more sensitive) in a head-to-head comparison (7). Culture is valuable primarily because it provides a viable isolate for further study, but this is unlikely to be a paramount consideration in most clinical settings. Some patients suspected of having HSV encephalitis may have negative PCR results, in which case parallel testing of serum and cerebrospinal fluid (CSF) for HSV antibody should be considered (8–10). A CSF-to-serum HSV antibody index of >2 (10) or an antibody titer in CSF that exceeds 6% of the titer in serum strongly suggests intrathecal production of HSV-specific antibody and recent central nervous system infection. Tests for HSV antibody may also be helpful in the diagnosis of HSV infection in immunosuppressed patients

doi:10.1128/9781555818722.ch58

with prolonged fever of unknown etiology and infants with undiagnosed congenital disease.

Procedures for the determination of type-specific antibody to HSV are most useful in epidemiologic, clinicopathologic, and natural history studies (1, 2, 6, 11, 12). Serologic confirmation of HSV-2 infection may alert physicians to the need for prophylactic treatment of severely immunosuppressed patients and guide physicians in their discussions of acyclovir therapy, the risk of recurrence, and ways to decrease the risk of HSV transmission with contacts. An accurate diagnosis for persons with mild or unrecognized clinical manifestations also aids in infection control and in issues associated with pregnancy (5, 13). The prenatal detection of specific HSV antibodies indicates which women may be at risk of transmitting HSV-1 or HSV-2 to their infants at delivery, although the presence of IgG antibody does not inform when active HSV shedding occurs in the genital tract. Conversely, a negative result indicates that a woman may be at risk of acquiring HSV-1 or HSV-2 during pregnancy, particularly if her partner is positive (5, 13). Finally, HSV-1 and HSV-2 PCR testing should be considered part of the rule-out diagnosis for suspected cases of bioterrorism-related smallpox (14, 15).

SPECIMEN COLLECTION

Clinical specimens for HSV-1 or HSV-2 culture can be obtained by swabbing skin lesions that have been unroofed. Polyester swabs with synthetic applicator sticks should be used, as cotton swabs with wooden sticks may complicate nucleic acid extraction and PCR testing. Culture may also be successfully performed with specimens of aspirated vesicular fluid or CSF. Direct detection methods require swabbing the base of unroofed lesions to ensure that infected epithelial cells are collected. In patients with disseminated HSV, peripheral blood mononuclear cells may be useful as specimens for either culture or PCR. For PCR or electron microscopy (EM) detection, scabs from crusted-over lesions are excellent specimens, but they are not useful for virus culture or direct detection methods. Specimens for PCR may be stored under dry conditions for extended periods at ambient temperature without substantial loss in specimen quality. In contrast, swabs collected for direct detection methods should be immersed in a small volume of isotonic transport medium and, ideally, tested within 24 h of collection. Virus isolation in cell culture is far more likely to succeed if specimens are inoculated immediately after collection.

VIRUS ISOLATION

Collected specimens are quite labile and must be transported to the laboratory and processed without delay. It is advisable to use several different HSV-susceptible cell lines, such as HEp-2, Vero-E6, and RD, to maximize the chance for successful culture. Inoculated cells should be checked daily for 7 days (incubated at 37°C, 5% CO_2) for the appearance of cytopathic effect. Positive wells should be used to reinoculate conventional tissue culture for additional conformational testing.

ELECTRON MICROSCOPY

EM is not commonly used as a method for diagnosing HSV infection, since individual species of the herpesvirus family are indistinguishable on the basis of virion morphology. It is chiefly used today by specialized pathology laboratories as an initial screening tool to narrow probable etiology. Suitable specimens for EM include dried smears of material from lesions (which can be resolubilized and placed on a copper grid), vesicular fluid, and scabs that have been ground in water. The chief limitations of this method are its relative insensitivity (the sensitivity is low compared with those of methods other than virus isolation) and the nonspecific result produced. EM is capable of identifying an agent as a member of the herpesvirus family on the basis of its distinctive morphology, but individual species cannot be discriminated on the basis of morphology. The method can be rendered specific by using type-specific monoclonal antibodies coupled to electron-dense particles.

PCR METHODS

Serological methods are not useful for detecting current HSV infection or viral shedding, and culture is relatively insensitive even when performed under optimal conditions. HSV-specific PCR has now been clearly established as the method of choice for the direct detection of active HSV infection (1, 16), whether due to primary infection, reactivation, or reinfection. HSV PCR of CSF has also largely supplanted brain biopsy as the method of choice for diagnosing herpes encephalitis (17), although as previously mentioned, HSV PCR-negative results can often be resolved by measuring HSV-specific intrathecal antibody synthesis. A variety of different methods have been described, including single-agent methods (17, 18), multiplex methods (16, 19), and real-time PCR (7). In studies directly contrasting the performance of PCR with that of culture, direct fluorescent-antibody assay, and other techniques, PCR is invariably more sensitive and at least comparably specific. The most frequently used target genes for type-specific PCR are the glycoprotein D (gD) and gB genes, although reported methods have also targeted the thymidine kinase, gG, UL42, DNA polymerase, and ICP27 genes. The highly conserved DNA polymerase gene has been used most frequently for consensus PCR methods that amplify all recognized human herpesviruses. As commercial PCR formats for clinical diagnosis have become more widely available, the use of PCR in clinical settings for routine diagnosis has become increasingly common. It is the most sensitive and specific method available for the detection of HSV in a wide variety of specimens. Since atypical HSV-1 and HSV-2 disease was, as with varicella, historically misdiagnosed as smallpox prior to eradication, HSV PCR is also recommended as part of a testing panel to exclude smallpox used as a bioterrorist weapon. It must also be kept in mind, however, that not all PCR methods are created equal. Direct comparisons of various formats have sometimes revealed substantial differences in the performance standards. In addition, care should be taken to ensure that substances potentially inhibitory to PCRs are eliminated during DNA purification.

DIRECT DETECTION METHODS

Tzanck (Giemsa) Smear

The Tzanck smear technique is not in common use currently, having been replaced by more sensitive and specific type-specific HSV PCR protocols. Smears of material from mucocutaneous lesions can be dried on glass microscopic slides, stained with Giemsa reagent, and examined for the presence of cellular anomalies (syncytia, cytoplasmic ballooning, intranuclear inclusions). These anomalies are observed in all alphaherpesvirus infections and as such do not provide a specific diagnosis.

Direct Fluorescent-Antibody Assay

For the DFA, the same type of clinical specimen as for the Tzanck smear is used, except that the test sample is suspended in transport medium. Cellular matter is then pelleted by centrifugation, and the pellet is washed and resuspended in a small volume. The cell suspension is spotted onto glass slides, thoroughly air dried, fixed in ice-cold isopropyl alcohol, and stained with fluorescent antibodies specific for HSV-1 or HSV-2. If monoclonal antibody reagents are used in the protocol, it is preferable to use more than one type-specific antibody for each agent, since an individual epitope may be missing due to mutations in some circulating strains. Variations of this method include the use of shell vial monolayers that are first inoculated with specimen and then examined with HSV-specific fluorescent-antibody reagents.

There is also a commercially available enzyme-linked virus-inducible system that takes advantage of a genetically engineered reporter cell line. The cell line includes a hybrid gene that is induced by the HSV UL39 gene product to express bacterial galactosidase. Cells infected with HSV undergo a colorimetric change with the addition of the substrate. Type specificity is determined by use of fluorescent antibodies. As with conventional DFA, this method is considerably less sensitive than HSV-specific PCR.

SERODIAGNOSTIC TESTS

Enzyme immunoassays (EIA), immunoblotting, the indirect fluorescence assay, and the neutralization assay have had the widest application for serodiagnosis and serosurveys. Radioimmunoassays (3) are rarely used because current EIA and immunoblotting procedures fulfill the same purpose and avoid the problem of using and disposing of radioisotopes.

Type-Specific Antibody Tests

The extensive cross-reactivity between HSV-1 and HSV-2 prevents accurate delineation of type-specific antibody with standard antigen preparations (1, 3, 4, 20). Early efforts to devise type-specific serologic assays met with limited success, and none of these formats is currently regarded as reliable. The discovery of a type-specific protein, gG, and the crafting of assays using gG1 and gG2 have largely resolved the problem of discriminating antibodies to HSV-1 and HSV-2 (20, 21). This approach concomitantly solved the problem of cross-reactivity to the other human alphaherpesvirus, varicella-zoster virus (VZV), since no gG protein is encoded in the VZV genome. A variety of protocols based on the use of gG have been developed over the years, including Western blotting (22, 23), monoclonal antibody blocking EIA (24), indirect IgG enzyme-linked immunosorbent assay (ELISA) (25), and capture ELISA (26). A number of comparisons of the performances of commercial type-specific EIA have been conducted, and several excellent commercial gG type-specific assays are now available. There are still some marketed methods that rely on techniques like antigen cross-absorption, but these methods do not reliably discriminate HSV-1 and HSV-2 antibody (27). Excellent reviews of the history of the development of type-specific and gG-based assays have been published by Bergström and Trybala (20) and Ashley (28). gC of HSV-1 was initially believed to be type specific but was later found to have epitopes that cross-react with HSV-2 antibodies (3, 23). Subsequently, gG1 and gG2 were discovered and shown to be type-specific targets for the human immune response by an immunodot EIA (24), immunoblot assays (1, 3, 12), and EIA (5, 25). The availability of these type-specific recombinant or purified proteins from commercial sources (29–31) has now made possible large-scale testing of human sera in a variety of type-specific formats. HSV-2-specific monoclonal antibodies have also been used to directly bind gG2 to microtitration plates and detect HSV-2 antibodies by EIA (6). Although the immune response to gGl and gG2 is not immunodominant, sufficient antibodies to these proteins are made within a month postinfection (29) that gG assays can usually determine the HSV-1/-2 infection history of a patient.

Immunoblotting

The immune response to HSV can be finely dissected by the immunoblot assay as developed by Ashley and colleagues (3, 29). Briefly, the proteins of HSV-1 and HSV-2 recovered from lysed infected cells are separated by sodium dodecyl sulfate-polyacrylamide gel electrophoresis (SDS-PAGE), transferred to a nitrocellulose substrate, and reacted with human sera. Bound antibody is detected with a peroxidase-conjugated anti-human IgG and a substrate with an insoluble colored product. In each test, one HSV-2 nitrocellulose strip is incubated with a monoclonal antibody that identifies the 92-kDa band of gG2 as a positive control. Sera with predominant reactivity on the HSV-1 strip and no reaction with the gG2 band on the HSV-2 strip have only HSV-1 antibodies. Sera with predominant reactivity on the HSV-2 strip, including the gG2 band, have HSV-2 antibodies. Sera with both profiles reveal an infection history by both viruses. Sera with atypical or equivocal results, without a clear 92-kDa gG2 band on the HSV-2 strip, are adsorbed separately with HSV-1 and HSV-2 antigens, and each aliquot is retested with both HSV strips. The immunoblot assay described by Ashley (28) is a highly sensitive and specific assay for HSV type-specific antibodies. Control sera with known reactivity for HSV-1 and HSV-2 are required. Since immunoblot assays include multiple HSV proteins that detect a range of both type-specific and type-common antibodies, they remain the standard by which other type-specific assays are evaluated (20, 21).

A modification of this approach using baculovirus-expressed gG1 and gG2 has also been described (25). Abundant quantities of HSV gG1 and gG2 have been produced in insect cells by use of a baculovirus expression system (12, 32). Insect cells infected with recombinant baculovirus expressing gG1 or gG2 are harvested and disrupted under conditions that release the proteins. The partially purified proteins are separated by SDS-PAGE, transferred to nitrocellulose, and incubated with test and control sera. This method has been extensively compared with other HSV antigen-specific methods and has high specificity and sensitivity (12, 32).

Immunodot EIA

Lee et al. (11) purified gG1 and gG2 antigens with immunoaffinity columns prepared with HSV type-specific murine monoclonal antibodies for an immunodot EIA performed on nitrocellulose disks in 96-well microtitration plates that required very little antigen. The assays are developed using an enzyme immunoaffinity colorimetric reaction. This is a high-throughput technique that has been instrumental in determining population-based seroprevalence rates for HSV-2 in the United States (2).

Commercially Available Type-Specific Assays

A number of commercially available gG2-based EIA have been evaluated against serum samples from persons with culture-confirmed HSV-1 and/or HSV-2 infection (8, 27, 30) or by using gG-based Western blotting as a gold standard (33, 34). With some variation, nearly all of these methods

performed with acceptably high specificity and sensitivity compared with those of the gold standards of HSV culture and gG-based Western blotting. Some caution is advised in the interpretation of slightly positive results (possible false-positive results), and such samples should be further evaluated with a confirmatory test. At least two rapid point-of-care tests for the detection of HSV-2 antibody are also commercially available; both have been evaluated against immunoblot assays and were shown to perform with excellent sensitivity (29, 35). The sensitivity and specificity of the tests in comparison with the immunoblot results were in the 90 to 95% range. Timing in the collection of sera is important because it was shown that the median time for the point-of-care kit HSV-2 test and the immunoblot assay to become positive after the onset of symptoms was 13 days, and only 80% of the samples were positive at the end of 4 weeks. Almost all of these methods that use HSV gG have shown good agreement when evaluated with specimens from cross-sectional studies (21). A study in which samples were collected serially over a 2-year period from Thai military recruits found that the serologic status of some individuals determined by gG assays changed from positive to negative over time (12). The inaccuracy was found in four separate assays, and the variation was not confined to the same specimens with each assay. In some cases, the loss of positivity may be associated with weakly positive specimens. It is suggested that testing of cohort specimens from population-based studies in addition to clinical ones should be part of any assay evaluation scheme (12). Commercial gG-based methods have also been developed based on technologies other than standard ELISA, including flow cytometry and lateral-flow, gG peptide-based, and luciferase immunoprecipitation.

Neutralization Assay

Several neutralization methods have been described but have not been adopted for routine clinical use and have been used only sporadically in studies of HSV epidemiology (36–39).

IgG Avidity

Methods for measuring the avidity of the IgG response to HSV-2 have been reported in the literature and, as with neutralization, have not been extensively used to characterize responses on a population level in the literature (40, 41). It has been proposed that the method would serve a useful routine diagnostic role in the assessment of relative risk for neonatal HSV infection (40, 42).

ELISpot Assay

ELISpot methods for detecting gamma interferon (43) and tumor necrosis factor beta (44) have been developed to evaluate the HSV-specific T cell response. While these methods have been used to generate useful information about the T cell response to HSV, they are probably too cumbersome in their current form to be adopted for routine clinical use.

Interpretation

Infection with either type of HSV gives rise to humoral and cell-mediated immune responses that, while capable of neutralizing HSV and destroying virus-infected cells, do not eliminate latent infection or prevent recurrent disease. Humans produce antibody to the structural components of the virus, namely, the envelope, capsid, and internal proteins, as well as soluble virally encoded proteins not included in the virion. A majority of persons are HSV-1 seropositive by 29 years of age (1). Consequently, evidence of antibody against HSV-1 or HSV-2 in a single serum sample by any serologic test, with the exceptions of an IgM-specific antibody assay (25, 45) and the avidity assay described below (46), provides no information about the time of onset of infection or reactivation. Serologic diagnosis of active infection with either virus type depends on demonstration of a significant increase in antibody titer. The two HSV types share many epitopes that give rise to extensively homologous antigens (1, 3, 4), and a major portion of the antibody produced in response to a primary infection is cross-reactive to these shared epitopes. Virus culture or type-specific serologic tests, many of which are now commercially available (29–31), must be performed to determine whether an individual has been infected with HSV-1, HSV-2, or both. Primary infection with either HSV type is documented by testing for seroconversion in paired serum samples (consisting of an acute-phase serum sample collected as close as possible to the onset of illness and a convalescent-phase serum sample collected 10 days to 3 weeks later) by any of the type-specific serologic tests. Evidence for primary infection can also be documented using an IgG avidity assay. An HSV IgG avidity assay was found to distinguish primary HSV infections from nonprimary HSV infections for as long as 100 days after the onset of infection (46). Detection of HSV-specific IgM in the absence of other evidence is proof of recent exposure (primary infection, reactivation, or reexposure) but does not demonstrate a primary infection (45).

The immune response to recurrent infection or reinfection with either HSV type is much more complicated and depends on the number, frequency, and type of previous infections as well as the severity of the subsequent infection. After primary HSV infection, antibody levels may decline and then be boosted by subsequent recurrences or infection with the heterologous type. Patients who experience severe recurrences, particularly those associated with systemic or neurologic symptoms, may have a significant rise in antibody levels. On the other hand, most adults with recurrent localized HSV-1 or HSV-2 lesions show stable, typically high titers (1, 3) in the neutralization test, complement fixation test, and many EIA (45). Initial infection with HSV-2 in persons previously infected with HSV-1 (or vice versa) usually causes a significant rise in the level of antibodies to both the shared HSV antigens and the specific antigens of the infecting type. The only human herpesvirus that shows significant cross-reactivity with HSV-1 and HSV-2 is VZV. Paired serum samples from patients with recent VZV infection who have preexisting HSV antibody may sometimes show a rise in the level of antibodies to HSV-1 and HSV-2 in nonspecific tests (6). A similar rise in the level of antibody to VZV may occur in patients with recent HSV infection who have prior antibody to VZV. This concern has been eliminated with the adoption of type-specific serologic methods that use gG as the antigen source, since VZV does not encode a gG protein.

The findings and conclusions in this report are those of the author and do not necessarily represent the official views of the Centers for Disease Control and Prevention.

REFERENCES

1. **Roizman B, Knipe DM, Whitley RJ.** 2013. Herpes simplex virus, p 1823–1896. *In* Knipe DM, Howley PM (ed), *Fields Virology*, 6th ed. Lippincott, Williams and Wilkins, Philadelphia, PA.
2. **Bradley H, Markowitz LE, Gibson T, McQuillan GM.** 2014. Seroprevalence of herpes simplex virus types 1 and 2—United States, 1999-2010. *J Infect Dis* **209:**325–333. PubMed

3. **Ashley RL, Corey L.** 1989. Herpes simplex virus, p 265–317. *In* Schmidt NJ, Emmons RW (ed), *Diagnostic Procedures for Viral, Rickettsial and Chlamydial Infections*, 6th ed. American Public Health Association, Washington, DC.
4. **Bernstein MT, Stewart JA.** 1971. Method for typing antisera to *Herpesvirus hominis* by indirect hemagglutination inhibition. *Appl Microbiol* **21:**680–684. PubMed
5. **Kulhanjian JA, Soroush V, Au DS, Bronzan RN, Yasukawa LL, Weylman LE, Arvin AM, Prober CG.** 1992. Identification of women at unsuspected risk of primary infection with herpes simplex virus type 2 during pregnancy. *N Engl J Med* **326:**916–920. PubMed
6. **Arvin AM, Prober CG.** 1999. Herpes simplex viruses, p 878–887. *In* Murphy PR, Baron EJ, Faller MA, Tenover EC, Yolken RH (ed), *Manual of Clinical Microbiology*, 7th ed. American Society for Microbiology, Washington, DC.
7. **Wald A, Huang ML, Carrell D, Selke S, Corey L.** 2003. Polymerase chain reaction for detection of herpes simplex virus (HSV) DNA on mucosal surfaces: comparison with HSV isolation in cell culture. *J Infect Dis* **188:**1345–1351. PubMed
8. **Cremer NE, Cossen CK, Hanson CV, Shell GR.** 1982. Evaluation and reporting of enzyme immunoassay determinations of antibody to herpes simplex virus in sera and cerebrospinal fluid. *J Clin Microbiol* **15:**815–823. PubMed
9. **Denes E, Labach C, Durox H, Adoukonou T, Weinbreck P, Magy L, Ranger-Rogez S.** 2010. Intrathecal synthesis of specific antibodies as a marker of herpes simplex encephalitis in patients with negative PCR. *Swiss Med Wkly* **140:**w13107. PubMed
10. **Monteyne P, Albert F, Weissbrich B, Zardini E, Ciardi M, Cleator GM, Sindic CJ, European Union Concerted Action on Virus Meningitis and Encephalitis.** 1997. The detection of intrathecal synthesis of anti-herpes simplex IgG antibodies: comparison between an antigen-mediated immunoblotting technique and antibody index calculations. *J Med Virol* **53:**324–331. PubMed
11. **Lee FK, Pereira L, Griffin C, Reid E, Nahmias A.** 1986. A novel glycoprotein for detection of herpes simplex virus type 1-specific antibodies. *J Virol Methods* **14:**111–118. PubMed
12. **Schmid DS, Brown DR, Nisenbaum R, Burke RL, Alexander D, Ashley R, Pellett PE, Reeves WC.** 1999. Limits in reliability of glycoprotein G-based type-specific serologic assays for herpes simplex virus types 1 and 2. *J Clin Microbiol* **37:**376–379. PubMed
13. **Brown ZA, Selke S, Zeh J, Kopelman J, Maslow A, Ashley RL, Watts DH, Berry S, Herd M, Corey L.** 1997. The acquisition of herpes simplex virus during pregnancy. *N Engl J Med* **337:**509–515. PubMed
14. **Hutchins SS, Sulemana I, Heilpern KL, Schaffner W, Wax G, Lerner EB, Watson B, Baltimore R, Waltenburg RA, Aronsky D, Coffin S, Ng G, Craig AS, Behrman A, Meek J, Sherman E, Chavez SS, Harpaz R, Schmid S.** 2008. Performance of an algorithm for assessing smallpox risk among patients with rashes that may be confused with smallpox. *Clin Infect Dis* **46**(Suppl 3)**:**S195–S203. PubMed
15. **Hanrahan JA, Jakubowycz M, Davis BR.** 2003. A smallpox false alarm. *N Engl J Med* **348:**467–468, discussion 467–468. PubMed
16. **Markoulatos P, Georgopoulou A, Kotsovassilis C, Karabogia-Karaphillides P, Spyrou N.** 2000. Detection and typing of HSV-1, HSV-2, and VZV by a multiplex polymerase chain reaction. *J Clin Lab Anal* **14:**214–219. PubMed
17. **O'Sullivan CE, Aksamit AJ, Harrington JR, Harmsen WS, Mitchell PS, Patel R.** 2003. Clinical spectrum and laboratory characteristics associated with detection of herpes simplex virus DNA in cerebrospinal fluid. *Mayo Clin Proc* **78:**1347–1352. PubMed
18. **Athmanathan S, Reddy SB, Nutheti R, Rao GN.** 2002. Comparison of an immortalized human corneal epithelial cell line with Vero cells in the isolation of Herpes simplex virus-1 for the laboratory diagnosis of Herpes simplex keratitis. *BMC Ophthalmol* **2:**3. PubMed
19. **Nicoll S, Brass A, Cubie HA.** 2001. Detection of herpes viruses in clinical samples using real-time PCR. *J Virol Methods* **96:**25–31. PubMed
20. **Bergström T, Trybala E.** 1996. Antigenic differences between HSV-1 and HSV-2 glycoproteins and their importance for type-specific serology. *Intervirology* **39:**176–184. PubMed
21. **Ashley RL.** 1998. Type-specific antibodies to HSV-1 and -2: review of methodology. *Herpes* **5:**33–38.
22. **Ashley RL, Militoni J, Lee F, Nahmias A, Corey L.** 1988. Comparison of Western blot (immunoblot) and glycoprotein G-specific immunodot enzyme assay for detecting antibodies to herpes simplex virus types 1 and 2 in human sera. *J Clin Microbiol* **26:**662–667. PubMed
23. **Lee FK, Coleman RM, Pereira L, Bailey PD, Tatsuno M, Nahmias AJ.** 1985. Detection of herpes simplex virus type 2-specific antibody with glycoprotein G. *J Clin Microbiol* **22:**641–644. PubMed
24. **Slomka MJ, Ashley RL, Cowan FM, Cross A, Brown DW.** 1995. Monoclonal antibody blocking tests for the detection of HSV-1- and HSV-2-specific humoral responses: comparison with western blot assay. *J Virol Methods* **55:**27–35. PubMed
25. **Ho DWT, Field PR, Sjögren-Jansson E, Jeansson S, Cunningham AL.** 1992. Indirect ELISA for the detection of HSV-2 specific IgG and IgM antibodies with glycoprotein G (gG-2). *J Virol Methods* **36:**249–264. PubMed
26. **Hashido M, Lee FK, Inouye S, Kawana T.** 1997. Detection of herpes simplex virus type-specific antibodies by an enzyme-linked immunosorbent assay based on glycoprotein G. *J Med Virol* **53:**319–323. PubMed
27. **Morrow RA, Friedrich D, Krantz E, Wald A.** 2004. Development and use of a type-specific antibody avidity test based on herpes simplex virus type 2 glycoprotein G. *Sex Transm Dis* **31:**508–515. PubMed
28. **Ashley RL.** 2001. Sorting out the new HSV type specific antibody tests. *Sex Transm Infect* **77:**232–237. PubMed
29. **Ashley RL, Eagleton M, Pfeiffer N.** 1999. Ability of a rapid serology test to detect seroconversion to herpes simplex virus type 2 glycoprotein G soon after infection. *J Clin Microbiol* **37:**1632–1633. PubMed
30. **Eis-Hübinger AM, Däumer M, Matz B, Schneweis KE.** 1999. Evaluation of three glycoprotein G2-based enzyme immunoassays for detection of antibodies to herpes simplex virus type 2 in human sera. *J Clin Microbiol* **37:**1242–1246. PubMed
31. **Groen J, Van Dijk G, Niesters HGM, Van Der Meijden WI, Osterhaus ADME.** 1998. Comparison of two enzyme-linked immunosorbent assays and one rapid immunoblot assay for detection of herpes simplex virus type 2-specific antibodies in serum. *J Clin Microbiol* **36:**845–847. PubMed
32. **Sánchez-Martínez D, Schmid DS, Whittington W, Brown D, Reeves WC, Chatterjee S, Whitley RJ, Pellett PE.** 1991. Evaluation of a test based on baculovirus-expressed glycoprotein G for detection of herpes simplex virus type-specific antibodies. *J Infect Dis* **164:**1196–1199. PubMed
33. **Ngo TD, Laeyendecker O, La H, Hogrefe W, Morrow RA, Quinn TC.** 2008. Use of commercial enzyme immunoassays to detect antibodies to the herpes simplex virus type 2 glycoprotein G in a low-risk population in Hanoi, Vietnam. *Clin Vaccine Immunol* **15:**382–384. PubMed
34. **Turner KR, Wong EH, Kent CK, Klausner JD.** 2002. Serologic herpes testing in the real world: validation of new type-specific serologic herpes simplex virus tests in a public health laboratory. *Sex Transm Dis* **29:**422–425. PubMed

35. **Shevlin E, Morrow RA.** 2014. Comparative performance of the Uni-Gold™ HSV-2 Rapid: a point-of-care HSV-2 diagnostic test in unselected sera from a reference laboratory. *J Clin Virol* **61:**378–381. PubMed
36. **Ashley RL, Dalessio J, Dragavon J, Koutsky LA, Lee FK, Nahmias AJ, Stevens CE, Holmes KK, Corey L.** 1993. Underestimation of HSV-2 seroprevalence in a high-risk population by microneutralization assay. *Sex Transm Dis* **20:**230–235. PubMed
37. **Ashley RL, Dalessio J, Sekulovich RE.** 1997. A novel method to assay herpes simplex virus neutralizing antibodies using BHKICP6LacZ-5 (ELVIS) cells. *Viral Immunol* **10:**213–220. PubMed
38. **Mbopi-Kéou FX, Bélec L, Dalessio J, Legoff J, Grésenguet G, Mayaud P, Brown DW, Morrow RA.** 2003. Cervicovaginal neutralizing antibodies to herpes simplex virus (HSV) in women seropositive for HSV Types 1 and 2. *Clin Diagn Lab Immunol* **10:**388–393. PubMed
39. **Whitbeck JC, Muggeridge MI, Rux AH, Hou W, Krummenacher C, Lou H, van Geelen A, Eisenberg RJ, Cohen GH.** 1999. The major neutralizing antigenic site on herpes simplex virus glycoprotein D overlaps a receptor-binding domain. *J Virol* **73:**9879–9890. PubMed
40. **Herrera-Ortiz A, Conde-Glez CJ, Vergara-Ortega DN, García-Cisneros S, Olamendi-Portugal ML, Sánchez-Alemán MA.** 2013. Avidity of antibodies against HSV-2 and risk to neonatal transmission among Mexican pregnant women. *Infect Dis Obstet Gynecol* **2013:**140142. PubMed
41. **Morrow RA, Friedrich D.** 2003. Inaccuracy of certain commercial enzyme immunoassays in diagnosing genital infections with herpes simplex virus types 1 or 2. *Am J Clin Pathol* **120:**839–844. PubMed
42. **Lindsay MK.** 2006. HSV neutralizing antibodies further refinement in preventing neonatal Herpes infection. *Am J Obstet Gynecol* **195:**4–6. PubMed
43. **Posavad CM, Magaret AS, Zhao L, Mueller DE, Wald A, Corey L.** 2011. Development of an interferon-gamma ELISPOT assay to detect human T cell responses to HSV-2. *Vaccine* **29:**7058–7066. PubMed
44. **Schmid DS, Thieme ML, Gary HE Jr, Reeves WC.** 1997. Characterization of T cell responses to herpes simplex virus type 1 (HSV-1) and herpes simplex virus type 2 (HSV-2) using a TNF-β ELISpot cytokine assay. *Arch Virol* **142:**1659–1671. PubMed
45. **Hashido M, Kawana T.** 1997. Herpes simplex virus-specific IgM, IgA and IgG subclass antibody responses in primary and nonprimary genital herpes patients. *Microbiol Immunol* **41:**415–420. PubMed
46. **Hashido M, Inouye S, Kawana T.** 1997. Differentiation of primary from nonprimary genital herpes infections by a herpes simplex virus-specific immunoglobulin G avidity assay. *J Clin Microbiol* **35:**1766–1768. PubMed

Varicella-Zoster Virus

D. SCOTT SCHMID

59

Varicella-zoster virus (VZV) is a readily contagious alphaherpesvirus that commonly causes two distinct exanthematous illnesses. Primary infection with VZV causes varicella, known colloquially as chicken pox, which is characterized by a generalized vesicular rash typically accompanied by fever and other nonspecific symptoms. VZV establishes a lifelong latent infection in the dorsal root ganglia during the first infection, and it can reactivate decades later to cause zoster, also called shingles, a dermatomally distributed and often painful vesicular rash (1, 2). A number of zoster patients present with postherpetic neuralgia, characterized by severe pain that may persist for long periods after the rash has resolved. Some rare complications of zoster include encephalitis, conjunctivitis, keratitis and other eye disorders, Ramsey-Hunt syndrome, neurogenic bladder, and transverse myelitis.

Most varicella cases are mild in nature and resolve without serious sequelae. Varicella may be complicated by bacterial infections, pneumonia, encephalitis, cerebellar ataxia, hepatitis, thrombocytopenia, and nephritis. Studies have shown that patients with recent varicella have a 40-fold greater risk of developing severe group A streptococcal disease. Populations at increased risk for serious VZV disease include immunocompromised adults and children, VZV-seronegative adults, pregnant women, and newborn infants (2). Prior to the introduction of the varicella vaccine, complications of varicella infections resulted in approximately 100 deaths and 10,000 hospitalizations each year in the United States (1–3).

A live, attenuated varicella vaccine was approved for use in the United States in 1995 and is recommended for routine immunization of children and for susceptible adolescents and adults (4). National coverage for the vaccine in the United States is now greater than 90% for children, and a proportionate reduction in varicella incidence has been observed, with evidence of herd immunity (5, 6). A mild rash can occasionally occur in the first 2 to 6 weeks after vaccination, and breakthrough infections by wild-type VZV strains sometimes occur in vaccinated patients, usually causing less severe disease than a typical primary infection. The vaccine virus establishes latency and can reactivate to cause herpes zoster, albeit less frequently than the wild-type virus. The observation of varicella outbreaks among children in highly vaccinated populations (7–10) led to the recommendation of a second dose of varicella vaccine for children, to be administered at 4 to 6 years of age (4). A more potent preparation of Oka vaccine (zoster vaccine) was shown in a large clinical trial to reduce the risk of herpes zoster by 50% and that of severe zoster and postherpetic neuralgia by more than 60% (3). The zoster vaccine was recommended for routine immunization of adults of ≥60 years of age in 2008 (11).

When varicella was commonplace in the United States, laboratory testing to verify varicella or zoster was generally unnecessary, since both varicella and zoster could readily be diagnosed by a clinician. The dramatically reduced incidence of varicella, together with the increasingly common occurrence of modified disease and zoster among vaccinated persons, has made laboratory confirmation of VZV infection and discrimination of the vaccine strain from the wild-type virus increasingly important. Serology has limited usefulness for the confirmation of acute infection, and among various direct virus detection methods, VZV PCR has emerged as the most reliable method for confirming VZV infection. VZV PCR methods designed to both detect the virus and distinguish the vaccine strain (Oka) from wild-type viruses in vaccinated persons have been developed but are currently available only in a few government, academic, and corporate laboratories. Screening of persons at high risk of varicella for susceptibility is important and can be accomplished using most available serologic methods, even those that are insufficiently sensitive to consistently detect vaccine seroconversion. This is particularly true for adults (e.g., for health care workers), in whom varicella tends to be more severe than it is in children. Persons who have been immunized with varicella vaccine are presumed to be protected; documentation of vaccine seroconversion is not recommended, since most methods are unable to reliably detect it. In many cases of VZV neurologic disease, VZV DNA is undetectable in the cerebrospinal fluid. In those instances, detection of synthesis of intrathecal immunoglobulin can be used to confirm the etiology. Routine varicella immunization has led to a >90% reduction of the incidence of varicella, and young physicians are less likely to encounter cases of varicella; this is further complicated by the increased likelihood of encountering disease that does not meet the conventional case definition for varicella. Consequently, effective monitoring of the changing epidemiology of this virus will depend critically on reliable diagnostic testing. Furthermore, laboratory services are essential for the identification of

doi:10.1128/9781555818722.ch59

susceptible health care workers or other individuals at high risk for exposure to varicella or zoster. Varicella vaccine is recommended for all susceptible adults; those at elevated risk for VZV exposure should receive special consideration for vaccination (4, 12).

In the aftermath of several instances of deliberate release of anthrax as a bioterrorism agent, there was heightened concern about a deliberate release of smallpox. Since varicella was the disease most commonly mistaken for smallpox during the eradication program, a recommendation was made that VZV PCR testing should be performed as part of the rule-out diagnosis for suspected cases of bioterrorism-related smallpox (13, 14).

GENETIC STABILITY OF VZV

A variety of techniques, including complete genomic sequencing, have revealed that the VZV genome is highly conserved. Only about 0.1% of the nucleotides vary among individual strains of VZV, and the sequence diversity is distributed randomly throughout the genome. Thus far, nine distinct circulating VZV clades have been identified from clinical VZV isolates around the globe, three of which are provisional pending more complete genetic information (15–17; my unpublished observation). Notably, VZV clades have been shown in several publications to have distinctive geographic distributions, perhaps driven by a combination of climate and immigration patterns (18–20). Clades 1 and 3 dominate in North America, Europe, and Australia, with smaller numbers of clade 4 viruses in the same regions; clade 2 dominates in Asia; and clade 5 dominates in Africa. The attenuated vaccine strain (Oka) is derived from a Japanese clade 2 strain that has only 42 base-pair differences from the parental strain. Vaccine preparations are now known to contain a mixture of strains, and only four of the vaccine markers—all of which are located in open reading frame 62 (ORF62)—are relatively fixed in all vaccine strains (21). The mutations responsible for vaccine attenuation have not yet been determined, however. Limited as it is, the genetic variability can affect the performance of serological assays, particularly those involving the use of VZV-specific monoclonal antibodies (MAbs).

METHODS

Specimen Collection

Laboratory diagnosis of VZV infection requires the identification of the virus or one of its products in skin lesions, tissues, or fluids from the patient. In the absence of suitable specimens for direct detection, VZV infection can be confirmed with serum or plasma by evidence of seroconversion or by a fourfold or greater increase in IgG titer between acute- and convalescent-phase sera. Primary VZV infection in an unvaccinated person can also be confirmed by detection of low-avidity VZV IgG in a single serum sample, which is dependent on the production of sufficient levels of VZV IgG by the patient. Direct detection techniques are preferable and include isolation of the virus in tissue culture, direct immunofluorescence staining of cells obtained from lesions, and detection of the virus genome by techniques based on PCR. Among these techniques, PCR-based detection methods are easily the most sensitive. Suitable clinical samples for VZV testing include smears or swabs of vesicular fluid, skin scrapings, crusts, cerebrospinal fluid, and various tissues obtained by biopsy or at autopsy. Vesicular lesions may be sampled by unroofing a vesicle with a sterile needle and then vigorously swabbing the base of the lesion with a sterile swab, applying enough pressure to collect epithelial cells without causing bleeding. Collection of infected epithelial cells from the base of the lesion is important because the majority of VZV virions are cell associated. It is best to use swabs made from synthetic materials, as it may be difficult to elute virus from cotton swabs, porous wooden sticks may absorb the extraction buffer, and substances in wood may inhibit PCR. To avoid contamination, each swab must be placed directly into a separate tube and labeled. Vesicular fluid can also be collected onto a glass slide and air dried (again, taking care that specimens are placed in separate containers to avoid contamination). For virus isolation, vesicular fluid may be collected in sealed capillary tubes; however, VZV is extremely sensitive to heat and desiccation, making isolation difficult under the best of circumstances. Ideally, vesicular fluid should be inoculated into cell culture immediately upon harvesting. Samples may be frozen at −80°C for several days prior to culture, but this procedure results in a significant loss of infectivity. Crusts are also outstanding specimens for PCR detection of VZV DNA; they may be collected in sterile tubes or plastic bags. Refrigeration is preferred for smears to be examined for viral antigen, but air-dried specimens for PCR can be kept at ambient temperature indefinitely.

Virus Isolation

VZV can be isolated from vesicular fluids of patients with zoster or varicella following the onset of rash as long as new vesicles erupt, but culture of VZV from respiratory secretions or biopsy specimens is rarely successful. Crusts do not contain infectious virus. Various tissue cell lines can be used to culture VZV from vesicular fluid, including human fetal diploid lung or kidney cells, human embryonic lung fibroblasts (MRCS or WI38), human melanoma (MeWo) cells, and human lung fibroblasts. Primary embryonic guinea pig cells will support VZV propagation but are generally less productive than human cells. Sufficient cell culture medium must be used to maintain the culture for 10 to 14 days without change. Several studies have shown that even under optimal conditions, virus isolation is significantly less sensitive than direct immunodetection or PCR for the detection of VZV. VZV produces a distinctive specific cytopathic effect (CPE) in cell monolayers. In human lung fibroblasts, the CPE is characterized by discrete football-shaped foci of different sizes and consists of rounded and swollen cells. The CPE most often appears between 4 and 7 days into culture but may manifest as early as day 3 or as late as day 14 after inoculation. If VZV-specific CPE has not appeared after a week to 14 days, it may be useful to passage the inoculated cultures. CPE may develop even if the amount of vesicular fluid in the capillary tube is barely discernible to the naked eye, if the specimens are obtained within the first 2 days of rash. Confirmation of VZV-specific CPE may be obtained, if necessary, by staining with a fluorescein-labeled specific antibody.

Preliminary identification of VZV can be made on the basis of the characteristic CPE, which is usually more focalized and progresses significantly more slowly than the CPE from herpes simplex virus (HSV). However, the definitive identification of VZV requires additional testing with immunological assays or PCR. Specific identification of a VZV isolate can be made by demonstrating its ability to interact with reference sera from patients who have had a clinically diagnosed case of varicella or with a VZV-specific MAb. Human sera used for identification of VZV should be free of antibodies against other human herpesviruses that may

cross-react with VZV proteins due to structural homology (e.g., HSV-1 and HSV-2). VZV-specific MAbs are commercially available and are the preferred reagents, since they significantly increase the sensitivity and specificity of detection compared with those for human serum or polyclonal serum produced in animals. Specific VZV identification can be accomplished by direct or indirect immunofluorescence staining of infected cells. Due in part to the fragility of VZV, viral culture is substantially less sensitive than PCR. In one study, only 44% of samples from PCR-confirmed cases were successfully cultured (22).

Direct Examination of Material from Skin Lesions

Scrapings of vesicular lesions obtained with a scalpel blade or the beveled edge of a microscope slide can be examined for giant cells or intranuclear inclusions by staining with Giemsa reagent (Tzanck smear). Staining for examination for inclusions must be performed properly, using specific methods for this purpose, or specimens may yield false-negative results. It should be recognized that the presence of intranuclear inclusions or multinucleated giant cells is not specific for VZV; similar changes are seen with HSV. Thus, the method is limited to identifying the presence of an alphaherpesvirus. The method is also not as sensitive as PCR (22). Direct fluorescent-antibody staining appears to have good sensitivity and specificity, although its performance is also substantially inferior to that of PCR (23). Staining of the scrapings with conjugated anti-VZV MAbs can enable specific identification. A number of MAbs are available for this purpose, although more than one MAb reagent should be used, since false-negative results have been obtained due to VZV strains lacking the specific target epitope. Specimens must be collected with care; scraping of unroofed lesions must be sufficiently vigorous to ensure the collection of infected cells, but the specimen should contain as little blood as possible, since this can produce false-negative results. Crusts cannot be used for direct detection methods.

Electron Microscopy

Vesicular fluids, crusts that have been ground in water, or skin lesion sections can be examined by electron microscopy (EM). Good results can be obtained with air-dried smears of fluids prepared on glass microscope slides, which can be resolubilized and transferred to a grid. This method is useful only for the identification of herpesviruses as a family; it does not facilitate the identification of VZV. The finding of a virus with a morphology characteristic of herpesviruses identifies the etiological agent as a member of the *Herpesviridae* and serves to distinguish it from orthopoxviruses and other agents. Specificity can be accomplished through the use of a specific antibody conjugated to an electron-dense material, such as colloidal gold. EM is somewhat insensitive, as it is capable of reliably detecting virions only at relatively high concentrations. It has been estimated that more than a quarter of direct-fluorescent-antibody-positive specimens may give negative results by EM. EM was also shown to be considerably less sensitive than PCR in a head-to-head comparison (24). The availability of PCR methods with superior performance and no requirement for costly equipment has greatly reduced reliance on EM as a diagnostic tool for this purpose. EM is now employed most frequently as a preliminary screening tool for case patients with diseases of unknown etiology.

PCR

PCR is the most accurate and sensitive method for VZV detection and differentiation. In addition, virus isolation and culture are time-consuming, and viral DNA is much more stable than infectious virus. Accordingly, quite apart from its superior performance specifications, PCR is the much preferred method for confirming the presence of VZV in a specimen. PCR is particularly useful for confirming mild VZV disease in vaccine recipients or patients in the late stages of varicella, when crusted lesions contain no viable virus. Amplification and analysis of targeted VZV DNA regions form the method of choice for discriminating vaccine from wild-type VZV isolates. For routine laboratory diagnostic purposes, the best materials to use are vesicular fluids or swab samples collected with capillaries or swabs, scrapings dried onto glass slides, or crusts from lesions. For disseminated disease, VZV DNA can be detected in various tissues, including the lungs, liver, kidneys, skin and adrenal glands, trigeminal ganglia, and dorsal root ganglia. The viral genome can also sometimes be detected in peripheral mononuclear cells, cerebrospinal fluids, bronchoalveolar lavage fluids, breast milk, oropharyngeal swabs, throat swabs, peripheral blood mononuclear cells, and nasal secretions. In some specific situations, VZV DNA can be found in other tissues, such as the synovial fluid of patients with arthritis; intraocular fluids, corneal scrapings, and tear films of patients with retinal necrosis; temporal bone sections from patients who had herpes zoster oticus; and amniotic fluid, fetal tissues, and the placenta during neonatal varicella. There has also been some success at detecting VZV DNA in environmental samples, which is a potentially useful tool for evaluating outbreaks whose index case has already resolved (25, 26). The VZV PCR protocols available commercially or through testing laboratories are generally designed for DNA detection only, but several laboratories have designed PCR strategies for both VZV DNA detection and vaccine and wild-type strain discrimination. These include methods that rely on restriction fragment length polymorphism (27), real-time fluorescence resonance energy transfer (28), and TaqMan real-time PCR (26, 29, 30). All of these methods share a strategy for detecting one or more single nucleotide polymorphisms that are (i) unique to the Oka vaccine or (ii) unique to the clade 2 subvariant from which the Oka vaccine was derived. Reliance on single nucleotide polymorphisms in the latter category is no longer sufficient by itself, since wild-type clade 2 viruses with the parental Oka profile have now been isolated in the United States (31). Currently available commercial VZV PCR methods perform with excellent sensitivity and specificity if only the detection of VZV DNA is desired.

Serologic Testing

Serologic testing is useful primarily for determining susceptibility to VZV in outbreak settings or as a screening tool for persons at high risk of exposure or severe disease. As a diagnostic tool, in cases where suitable specimens for direct detection by PCR are unavailable, IgG testing of acute- and convalescent-phase sera can be used to confirm seroconversion to VZV or to provide evidence for suspected breakthrough infection. Acute-phase serum should be obtained as soon as possible after the onset of illness, and the convalescent-phase serum should be obtained 4 to 6 weeks after onset. A variety of methods are available to determine whether there are significant rises in the level of VZV-specific serum immunoglobulin; however, all must be performed in an endpoint dilution format. Assay formats used for simple determination of VZV serostatus include enzyme-linked immunosorbent assay (ELISA), assay of fluorescent antibody to membrane antigen (FAMA assay), latex bead agglutination assay, and lateral flow assay. Each of these test formats has limitations, which are discussed in greater detail

below. Measurements of IgM antibody in individuals with known recent exposure to VZV are inconsistent, and the detection of IgM may reflect primary infection, reinfection, or reactivation. IgM testing cannot be used to confirm a primary infection.

Commercial Serologic Tests

A number of commercial products for the detection of VZV antibodies have been marketed in recent years. These include ELISA, latex bead agglutination, and flowthrough membrane-based enzyme immunoassay (EIA) methods. Serum, plasma, or in some instances whole blood can be tested. In general, these assays are designed to detect IgG antibodies. A number of these methods have been compared against various gold standard methods and can vary considerably in their performance specifications (32–34; unpublished data). None of them is as reliable as either glycoprotein-based ELISA (gpELISA) or FAMA tests, particularly for detecting seroconversion in VZV-vaccinated persons. One study revealed that the latex bead agglutination test can be prone to false-positive results (35). Most commercial methods are sufficiently reliable to identify unvaccinated health care workers and other persons at high risk for exposure to VZV. As with HSV, the use of VZV serologic methods to detect VZV-specific intrathecal antibody synthesis can be used to confirm the etiology of neurological illness, for which viral DNA is detectable in only about a third of cases (36–38).

FAMA Assay

The FAMA assay is one of the most sensitive assays for the detection of VZV antibodies when it is performed in an experienced laboratory. It has been recognized for some time as one of several tests sufficiently sensitive and specific to reliably detect VZV antibodies in vaccinated individuals. In part, the enhanced sensitivity of this assay may be attributable to the preservation of the natural three-dimensional configuration of VZV glycoproteins expressed on the surfaces of infected cells. Chemical fixation of infected cells inevitably results in modifications of surface antigen structures, and this generally leads to a decrease in assay sensitivity. The FAMA assay can be used in various formats to detect any of the major classes of specific immunoglobulin. While this method can be quite powerful, accurate interpretation of results is somewhat subjective, and extensive experience is needed to perform the method reliably. An adaptation of the FAMA assay to an objective flow cytometric readout resulted in a slightly diminished sensitivity and specificity of the method (39). The FAMA assay is not available commercially.

gpELISA

Merck and Company developed a highly sensitive and specific ELISA method predicated on the use of a purified, concentrated solution of VZV glycoproteins. It is another method that, like the FAMA assay, reliably detects seroconversion in response to VZV vaccination, and it was used for the large efficacy trial of the Varivax Oka vaccine. The method is not currently available commercially and has been performed routinely only by a few laboratories that have obtained supplies of the purified glycoproteins from Merck and Company through material transfer agreements. Direct comparison between the FAMA assay and gpELISA reveals that they have comparable levels of performance, and the ELISA method has the advantage of being easily performed (my unpublished data). A commercially available purified VZV glycoprotein preparation (Virusys Corporation, Tarrytown, MD) was recently shown to perform indistinguishably from the Merck antigens, provided that a custom-ordered normal tissue control antigen is used to subtract background reactivity (my unpublished observation). Hopefully this development will lead to a commercially available VZV gpELISA in the near future.

TRFIA

A time-resolved fluorescence immunoassay (TRFIA) was developed in England and was shown in a pilot study to have performance specifications comparable to those of gpELISA (32). A subsequent study provided additional support for the performance specifications of the method (33). The method has the advantage of performing comparably to gpELISA without relying on highly purified and concentrated glycoprotein antigen preparations. Rather, crude lysate from VZV-infected cells is used as an antigen source. One drawback is that it requires the use of a fluorometric reader, which may be too costly compared with conventional spectrophotometers. As with gpELISA and the FAMA assay, TRFIA is not currently commercially available and has not been reviewed or approved by the FDA.

NT Tests

The presence of neutralizing antibodies in serum can be detected by using a neutralization (NT) assay based on reductions of plaque formation by titrated VZV preparations pretreated with serum (40). VZV is aggressively cell associated in tissue culture, making the production of cell-free virus preparations with reliable titers problematic. The Oka vaccine is relatively cell-free and can be used as a virus reagent for these protocols, although it is important to determine an accurate titer before use. NT assays for VZV will likely prove helpful for evaluating the duration of protective immunity among vaccine recipients. They may also be useful for identifying the primary neutralization targets for VZV. There are no clear recommendations or standardized data for the evaluation of neutralizing antibody for VZV. A high-throughput NT method using a semiautomated protocol is in development at the CDC and is currently being validated.

Antibody Avidity

Evaluations of antibody avidity are straightforward to perform and can provide useful insights into the relative maturity of immunoglobulin responses to VZV (41). As such, they provide the only reliable laboratory test for primary VZV infection, other than measuring seroconversion in acute- and convalescent-phase sera. A recent study indicated that 14% of adult health care workers who received a two-dose regimen of varicella vaccine were still producing low-avidity IgG, and half of the recipients with no detectable IgG seroconverted upon receiving a third dose, with the production of low-avidity antibody (41). This suggests that a substantial fraction of adults may either respond to varicella vaccine with suboptimal T cell engagement or fail to establish B cell memory. Determination of antibody avidity is based on the separation of low- and high-avidity antibodies by using chemicals that disrupt hydrogen bonding in immunoassays (EIA) or immunofluorescence assays. Chemicals used for this purpose include guanidine hydrochloride, diethylamine, isothiocyanate, and urea. Calculations of the avidity results have been approached in several ways historically. Most commonly, avidity is expressed as the percent ratio of antibody titers or EIA absorbance values, with and without dissociation. Avidity results based on endpoint titration, with and without denaturant, are considered to be the "gold standard" for avidity determination. An IgG

avidity method has been developed at the CDC and is now being validated for inclusion under the Clinical Laboratory Improvement Amendments (CLIA).

INTERPRETATION

PCR-based methods are more sensitive and informative than the other methods, since they are agent specific and also can be designed to discriminate the vaccine strain from wild-type isolates. Moreover, real-time single-tube methods and more rapid DNA extraction have greatly reduced the turnaround time required to obtain a result. Serologic testing is not a preferred method for confirming an acute infection, as paired acute- and convalescent-phase sera are required and greatly delay test results. In addition, significant rises in titer between acute-phase and convalescent-phase sera are not always observed. For determination of susceptibility, a properly standardized and specific method is essential. Serologic assay specificity trumps sensitivity as a consideration if the goal is to determine susceptibility to varicella in persons at high risk of VZV exposure. Passively acquired antibody may also yield false-positive test results, and immunocompromised patients may have lower levels of antibody that may be difficult to detect in some immune patients if the test used is too insensitive.

OTHER CONSIDERATIONS

Serologic Testing

There have been several reports of inappropriate management of patients due to false-positive reactions (35, 42). While this is the greatest concern in settings where susceptible adults are at high risk of VZV exposure, it is also clear that the majority of VZV serologic assays currently available fail to consistently detect seroconversion in response to vaccination. In some public health organizations, this has led to unnecessary multiple vaccinations of the same individual. The use of serology to confirm seroconversion in response to vaccination is not recommended; rather, persons who have received the recommended two-dose regimen are presumed to be immune. Suitable normal tissue control antigens in an ELISA are essential to reduce the risk of false-positive test results, although such controls are generally not included in commercially available assays. New methods are commonly validated by comparing their performances with that of an established method that is itself inevitably inaccurate, since no method is perfect. Ideally, a set of well-defined samples (e.g., pre- and postvaccination sera from toddlers) should be evaluated by receiver operating characteristic analysis rather than being compared to another method, however well the "gold standard" assay is thought to perform. Samples for VZV test validation that are seronegative with a high degree of confidence are difficult to obtain. Sera from seronegative susceptible individuals with no reported history of varicella can be used to standardize an assay, although vaccine recipients increasingly fail to develop detectable antibody titers as determined by some methods and might inadvertently be selected. The establishment of optimal cutoff values for seropositivity will ideally employ a combination of evaluation criteria (e.g., receiver operating characteristic analysis of sensitivity and specificity, reproducibility with the same operator, and reproducibility between operators). VZV IgM test results are difficult to interpret. IgM antibody capture assays are preferred because they avoid the obfuscating effect of rheumatoid factor and are the most effective means for eliminating all of the IgG in serum specimens. IgM kits that rely on absorbents to remove IgG are commercially available, but they may not succeed in removing all of the IgG from a specimen. In addition, extensive studies of sera from persons with documented recent exposures to VZV indicate that VZV IgM antibodies are inconsistently detectable even in persons with PCR-documented infections. Finally, since naïve B lymphocytes are constantly replenished, IgM is inevitably produced on every exposure to antigen. As such, IgM assays are not able to establish primary infection and cannot distinguish infection from VZV reinfection or reactivation.

The findings and conclusions in this chapter are those of the author and do not necessarily represent the official views of the Centers for Disease Control and Prevention. The use of product names in this chapter does not imply their endorsement by the U.S. Department of Health and Human Services.

REFERENCES

1. **Arao Y, Schmid DS, Pellett PE, Inoue N.** 1999. Herpesviruses beyond HSV-1 and -2. *Clin Microbiol Newsl* **21:**153–160.
2. **Arvin AM, Gilden D.** 2013. Varicella-zoster virus, p 2015–2057. *In* Knipe DM, Howley PM, Cohen JI, Griffin DE, Lamb RA, Martin MA, Racaniello VR, Roizman B (ed), *Fields Virology*, 6th ed. Lippincott Williams & Wilkins, Philadelphia, PA.
3. **Oxman MN, Levin MJ, Johnson GR, Schmader KE, Straus SE, Gelb LD, Arbeit RD, Simberkoff MS, Gershon AA, Davis LE, Weinberg A, Boardman KD, Williams HM, Zhang JH, Peduzzi PN, Beisel CE, Morrison VA, Guatelli JC, Brooks PA, Kauffman CA, Pachucki CT, Neuzil KM, Betts RF, Wright PF, Griffin MR, Brunell P, Soto NE, Marques AR, Keay SK, Goodman RP, Cotton DJ, Gnann JW Jr, Loutit J, Holodniy M, Keitel WA, Crawford GE, Yeh SS, Lobo Z, Toney JF, Greenberg RN, Keller PM, Harbecke R, Hayward AR, Irwin MR, Kyriakides TC, Chan CY, Chan IS, Wang WW, Annunziato PW, Silber JL, Shingles Prevention Study Group.** 2005. A vaccine to prevent herpes zoster and postherpetic neuralgia in older adults. *N Engl J Med* **352:**2271–2284. PubMed
4. **Marin M, Güris D, Chaves SS, Schmid S, Seward JF, Advisory Committee on Immunization Practices, Centers for Disease Control and Prevention (CDC).** 2007. Prevention of varicella: recommendations of the Advisory Committee on Immunization Practices (ACIP). *MMWR Recomm Rep* **56**(RR-4)**:**1–40. PubMed
5. **Bialek SR, Perella D, Zhang J, Mascola L, Viner K, Jackson C, Lopez AS, Watson B, Civen R.** 2013. Impact of a routine two-dose varicella vaccination program on varicella epidemiology. *Pediatrics* **132:**e1134–e1140. PubMed
6. **Marin M, Watson TL, Chaves SS, Civen R, Watson BM, Zhang JX, Perella D, Mascola L, Seward JF.** 2008. Varicella among adults: data from an active surveillance project, 1995–2005. *J Infect Dis* **197**(Suppl 2)**:**S94–S100. PubMed
7. **Centers for Disease Control and Prevention (CDC).** 2004. Outbreak of varicella among vaccinated children—Michigan, 2003. *MMWR Morb Mortal Wkly Rep* **53:**389–392. PubMed
8. **Lopez AS, Guris D, Zimmerman L, Gladden L, Moore T, Haselow DT, Loparev VN, Schmid DS, Jumaan AO, Snow SL.** 2006. One dose of varicella vaccine does not prevent school outbreaks: is it time for a second dose? *Pediatrics* **117:**e1070–e1077. PubMed
9. **Parker AA, Reynolds MA, Leung J, Anderson M, Rey A, Ortega-Sanchez IR, Schmid DS, Guris D, Gensheimer KF.** 2008. Challenges to implementing second-dose varicella vaccination during an outbreak in the absence of a

routine 2-dose vaccination requirement—Maine, 2006. *J Infect Dis* **197**(Suppl 2)**:**S101–S107. PubMed
10. **Tugwell BD, Lee LE, Gillette H, Lorber EM, Hedberg K, Cieslak PR.** 2004. Chickenpox outbreak in a highly vaccinated school population. *Pediatrics* **113:**455–459. PubMed
11. **Harpaz R, Ortega-Sanchez IR, Seward JF, Advisory Committee on Immunization Practices (ACIP) Centers for Disease Control and Prevention (CDC).** 2008. Prevention of herpes zoster: recommendations of the Advisory Committee on Immunization Practices (ACIP). *MMWR Recomm Rep* **57**(RR-5)**:**1–30. PubMed
12. **Galil K, Mootrey GP, Seward J, Wharton M.** 1999. Prevention of varicella. Update recommendations of the Advisory Committee on Immunization Practices. *MMWR Recomm Rep* **48**(RR-6)**:**1–5. PubMed
13. **Seward JF, Galil K, Damon I, Norton SA, Rotz L, Schmid S, Harpaz R, Cono J, Marin M, Hutchins S, Chaves SS, McCauley MM.** 2004. Development and experience with an algorithm to evaluate suspected smallpox cases in the United States, 2002–2004. *Clin Infect Dis* **39:**1477–1483. PubMed
14. **Hutchins SS, Sulemana I, Heilpern KL, Schaffner W, Wax G, Lerner EB, Watson B, Baltimore R, Waltenburg RA, Aronsky D, Coffin S, Ng G, Craig AS, Behrman A, Meek J, Sherman E, Chavez SS, Harpaz R, Schmid S.** 2008. Performance of an algorithm for assessing smallpox risk among patients with rashes that may be confused with smallpox. *Clin Infect Dis* **46**(Suppl 3)**:**S195–S203. PubMed
15. **Breuer J, Grose C, Norberg P, Tipples G, Schmid DS.** 2010. A proposal for a common nomenclature for viral clades that form the species varicella-zoster virus: summary of VZV Nomenclature Meeting 2008, Barts and the London School of Medicine and Dentistry, 24–25 July 2008. *J Gen Virol* **91:**821–828. PubMed
16. **Loparev VN, Rubtcova EN, Bostik V, Govil D, Birch CJ, Druce JD, Schmid DS, Croxson MC.** 2007. Identification of five major and two minor genotypes of varicella-zoster virus strains: a practical two-amplicon approach used to genotype clinical isolates in Australia and New Zealand. *J Virol* **81:**12758–12765. PubMed
17. **Zell R, Taudien S, Pfaff F, Wutzler P, Platzer M, Sauerbrei A.** 2012. Sequencing of 21 varicella-zoster virus genomes reveals two novel genotypes and evidence of recombination. *J Virol* **86:**1608–1622. PubMed
18. **Barrett-Muir W, Scott FT, Aaby P, John J, Matondo P, Chaudhry QL, Siqueira M, Poulsen A, Yaminishi K, Breuer J.** 2003. Genetic variation of varicella-zoster virus: evidence for geographical separation of strains. *J Med Virol* **70**(Suppl 1)**:**S42–S47. PubMed
19. **Loparev VN, Gonzalez A, Deleon-Carnes M, Tipples G, Fickenscher H, Torfason EG, Schmid DS.** 2004. Global identification of three major genotypes of varicella-zoster virus: longitudinal clustering and strategies for genotyping. *J Virol* **78:**8349–8358. PubMed
20. **Schmidt-Chanasit J, Sauerbrei A.** 2011. Evolution and world-wide distribution of varicella-zoster virus clades. *Infect Genet Evol* **11:**1–10. PubMed
21. **Quinlivan M, Breuer J, Schmid DS.** 2011. Molecular studies of the Oka varicella vaccine. *Expert Rev Vaccines* **10:**1321–1336. PubMed
22. **Nahass GT, Goldstein BA, Zhu WY, Serfling U, Penneys NS, Leonardi CL.** 1992. Comparison of Tzanck smear, viral culture, and DNA diagnostic methods in detection of herpes simplex and varicella-zoster infection. *JAMA* **268:**2541–2544. PubMed
23. **Bezold GD, Lange ME, Gail H, Peter RU.** 2001. Detection of cutaneous varicella zoster virus infections by immunofluorescence versus PCR. *Eur J Dermatol* **11:**108–111.
24. **Jain S, Wyatt D, McCaughey C, O'Neill HJ, Coyle PV.** 2001. Nested multiplex polymerase chain reaction for the diagnosis of cutaneous herpes simplex and herpes zoster infections and a comparison with electron microscopy. *J Med Virol* **63:**52–56. PubMed
25. **Leung J, Kudish K, Wang C, Moore L, Gacek P, Radford K, Lopez A, Sosa L, Schmid DS, Cartter M, Bialek S.** 2010. A 2009 varicella outbreak in a Connecticut residential facility for adults with intellectual disability. *J Infect Dis* **202:**1486–1491. PubMed
26. **Lopez AS, Burnett-Hartman A, Nambiar R, Ritz L, Owens P, Loparev VN, Guris D, Schmid DS.** 2008. Transmission of a newly characterized strain of varicella-zoster virus from a patient with herpes zoster in a long-term-care facility, West Virginia, 2004. *J Infect Dis* **197:**646–653. PubMed
27. **LaRussa P, Lungu O, Hardy I, Gershon A, Steinberg SP, Silverstein S.** 1992. Restriction fragment length polymorphism of polymerase chain reaction products from vaccine and wild-type varicella-zoster virus isolates. *J Virol* **66:**1016–1020. PubMed
28. **Loparev VN, McCaustland K, Holloway BP, Krause PR, Takayama M, Schmid DS.** 2000. Rapid genotyping of varicella-zoster virus vaccine and wild-type strains with fluorophore-labeled hybridization probes. *J Clin Microbiol* **38:**4315–4319. PubMed
29. **Harbecke R, Oxman MN, Arnold BA, Ip C, Johnson GR, Levin MJ, Gelb LD, Schmader KE, Straus SE, Wang H, Wright PF, Pachucki CT, Gershon AA, Arbeit RD, Davis LE, Simberkoff MS, Weinberg A, Williams HM, Cheney C, Petrukhin L, Abraham KG, Shaw A, Manoff S, Antonello JM, Green T, Wang Y, Tan C, Keller PM, Shingles Prevention Study Group.** 2009. A real-time PCR assay to identify and discriminate among wild-type and vaccine strains of varicella-zoster virus and herpes simplex virus in clinical specimens, and comparison with the clinical diagnoses. *J Med Virol* **81:**1310–1322. PubMed
30. **Parker SP, Quinlivan M, Taha Y, Breuer J.** 2006. Genotyping of varicella-zoster virus and the discrimination of Oka vaccine strains by TaqMan real-time PCR. *J Clin Microbiol* **44:**3911–3914. PubMed
31. **Pahud BA, Glaser CA, Dekker CL, Arvin AM, Schmid DS.** 2011. Varicella zoster disease of the central nervous system: epidemiological, clinical, and laboratory features 10 years after the introduction of the varicella vaccine. *J Infect Dis* **203:**316–323. PubMed
32. **Maple PAC, Gray J, Breuer J, Kafatos G, Parker S, Brown D.** 2006. Performance of a time-resolved fluorescence immunoassay for measuring varicella-zoster virus immunoglobulin G levels in adults and comparison with commercial enzyme immunoassays and Merck glycoprotein enzyme immunoassay. *Clin Vaccine Immunol* **13:**214–218. PubMed
33. **Maple PAC, Rathod P, Smit E, Gray J, Brown D, Boxall EH.** 2009. Comparison of the performance of the LIAISON VZV-IgG and VIDAS automated enzyme linked fluorescent immunoassays with reference to a VZV-IgG time-resolved fluorescence immunoassay and implications of choice of cut-off for LIAISON assay. *J Clin Virol* **44:**9–14. PubMed
34. **Sauerbrei A, Schäfler A, Hofmann J, Schacke M, Gruhn B, Wutzler P.** 2012. Evaluation of three commercial varicella-zoster virus IgG enzyme-linked immunosorbent assays in comparison to the fluorescent-antibody-to-membrane-antigen test. *Clin Vaccine Immunol* **19:**1261–1268. PubMed
35. **Behrman A, Schmid DS, Crivaro A, Watson B.** 2003. A cluster of primary varicella cases among healthcare workers with false-positive varicella zoster virus titers. *Infect Control Hosp Epidemiol* **24:**202–206. PubMed
36. **Nandhagopal R, Khmeleva N, Jayakrishnan B, White T, Al Azri F, George J, Heintzman A, Al Zeedy K, Rorke-Adams L, Guijar AR, Schmid DS, Al-Asmi A, Nagel MA, Jacob PC, Gilden D.** 2014. Varicella zoster virus

pneumonitis and brain stem encephalitis without skin rash in an immunocompetent adult. *Open Forum Infect Dis* **1:**ofu064.

37. **Haug A, Mahalingam R, Cohrs RJ, Schmid DS, Corboy JR, Gilden D.** 2010. Recurrent polymorphonuclear pleocytosis with increased red blood cells caused by varicella zoster virus infection of the central nervous system: case report and review of the literature. *J Neurol Sci* **292:**85–88. PubMed
38. **Gilden D, Nagel MA, Cohrs RJ, Mahalingam R.** 2013. The variegate neurological manifestations of varicella zoster virus infection. *Curr Neurol Neurosci Rep* **13:**374.
39. **Lafer MM, Weckx LY, de Moraes-Pinto MI, Garretson A, Steinberg SP, Gershon AA, LaRussa PS.** 2011. Comparative study of the standard fluorescent antibody to membrane antigen (FAMA) assay and a flow cytometry-adapted FAMA assay to assess immunity to varicella-zoster virus. *Clin Vaccine Immunol* **18:**1194–1197. PubMed
40. **Asada H, Nagayama K, Okazaki A, Mori Y, Okuno Y, Takao Y, Miyazaki Y, Onishi F, Okeda M, Yano S, Kumihashi H, Gomi Y, Maeda K, Ishikawa T, Iso H, Yamanishi K, Shozu Herpes Zoster (SHEZ) Study Group.** 2013. An inverse correlation of VZV skin-test reaction, but not antibody, with severity of herpes zoster skin symptoms and zoster-associated pain. *J Dermatol Sci* **69:**243–249. PubMed
41. **Behrman A, Lopez AS, Chaves SS, Watson BM, Schmid DS.** 2013. Varicella immunity in vaccinated healthcare workers. *J Clin Virol* **57:**109–114. PubMed
42. **Martin KA, Junker AK, Thomas EE, Van Allen MI, Friedman JM.** 1994. Occurrence of chickenpox during pregnancy in women seropositive for varicella-zoster virus. *J Infect Dis* **170:**991–995. PubMed

Epstein-Barr Virus and Cytomegalovirus

HENRY H. BALFOUR, JR., KRISTIN A. HOGQUIST, AND
PRIYA S. VERGHESE

60

Epstein-Barr virus (EBV; also known as human herpesvirus 4 [HHV-4]) and cytomegalovirus (CMV; also known as HHV-5) logically belong in the same chapter. Both of these human herpesviruses are major pathogens for the immunocompromised host, and both are capable of causing disease during primary infection, reactivation, or superinfection. They, along with BK polyomavirus, are the feared viral triumvirate that complicates hematopoietic cell transplantation (HCT) or solid organ transplantation. This chapter emphasizes recognition of EBV and CMV diseases and focuses on the clinical relevance of laboratory findings.

EBV

Background and Biology

EBV was discovered in 1964 by Epstein et al., who visualized it by electron microscopy of suspension cultures of African Burkitt's lymphoma cells (1). Four years later, EBV was conclusively linked to infectious mononucleosis, which is its most common clinical manifestation (2).

EBV, whose systematic name is HHV-4, is one of the eight human herpesviruses recognized to date. The EBV virion has a double-stranded linear DNA genome of approximately 170 kb surrounded by a protein capsid. Mature virions vary in size from 120 to 180 nm in diameter. A protein tegument lies between the capsid and the lipid envelope, which carries embedded glycoproteins that are important for cell tropism, host range, and receptor recognition. The EBV genome of about 85 genes has been described in detail (3).

EBV is classified as type 1 or type 2 (also referred to as type A or type B), based on sequence variation in the EBV nuclear antigen (EBNA) genes EBNA-2, -3A, -3B, and -3C (4). The pathogenic potentials of the two types are not clearly differentiated. EBV type 1 predominates in most areas of the globe. Genetic diversity exists at other gene loci, especially in the latent membrane protein 1 gene (5). However, the link between strain variation, disease, and geographic distribution is unclear (6).

EBV invades and maintains itself in the host through interactions between infected B lymphocytes and infected oropharyngeal epithelial cells (7). EBV infects B cells by binding of its viral gp350 protein to CD21 (8, 9). EBV gp42 then interacts with B cell HLA class II molecules and triggers fusion with the host membrane. To infect oral epithelial cells, which lack CD21, the EBV transmembrane glycoprotein BMRF-2 interacts with β1 integrins (10), and the EBV envelope glycoproteins gH/gL trigger fusion by interacting with integrin αvβ6 or αvβ8 (11). Endocytosis of the virus by vesicles and fusion of the virus with the vesicle membrane release the nucleocapsid into the cytoplasm. Once the viral nucleocapsid is dissolved, the genome is transported to the nucleus, where it is replicated by DNA polymerases. Viral DNA polymerase accomplishes linear viral replication, which occurs during the lytic phase of the viral life cycle. There are three temporal classes of viral lytic gene products (immediate early [IE], early [E], and late [L]), as reviewed by Tsurumi et al. (12). BZLF1 and BRLF1 are some of the IE products that further act as transactivators of the viral lytic program. Activation of lytic replication or reactivation from latency is key to transmission. The early products (e.g., BNLF2a) have a wide array of functions, including replication, metabolism, and blockade of antigen processing, while late products tend to be structural proteins, such as the viral capsid antigens and gene products used for immune evasion (e.g., BCRF1). An important consequence of EBV infection in B cells is to activate their growth program and trigger differentiation into memory B cells via the germinal center reaction. Infected memory B cells are released into the peripheral circulation, resulting in detectable levels of virus in the blood. The number of infected B cells decreases over time after the onset of symptoms of primary infection, but these cells are never entirely eliminated.

Latency is the state of persistent viral infection without active viral proliferation. EBV establishes latency in the memory B cell compartment, and possibly also in epithelial cells. It is generally thought that EBV genomes in latently infected B cells exist as episomes (13), although it is possible that they also exist as integrated DNA (14). Memory B cells do not express EBV proteins during latency and hence cannot be recognized by the host's immune system (15).

Reactivation of EBV is thought to occur when B cell receptor stimulation by antigens not related to EBV induces memory B cells to differentiate into plasma cells, which are capable of initiating active viral replication (16). Viral progeny can then infect new B cells and epithelial cells, rendering the host infectious to other persons.

Humans are the only natural hosts for EBV. Primary infection occurs in the oral compartment in adolescents and

doi:10.1128/9781555818722.ch60

young adults, who most often acquire the virus from deep kissing (17). We presume that primary infection in young children is also acquired by the oral route, but this has not been documented conclusively.

Besides oral transmission, EBV has been acquired from blood transfusions (18) or from transplanted hematopoietic cells (19) or solid organs (20), and such infections can be life-threatening, especially among recipients who were EBV naive before transplantation (21). Several reports of intrauterine transmission of EBV have been published, but none has been substantiated by appropriate viral laboratory data.

The overall prevalence of EBV antibody, indicative of past infection, varies widely by geographic location (22–24). Primary EBV infection occurs at a younger age among persons from lower versus higher socioeconomic backgrounds (25) and among non-Hispanic whites versus non-Hispanic blacks or Mexican Americans (26). Acquisition of EBV by young children indicates that it can be transmitted without deep kissing. However, this does not rule out saliva as the source of EBV, because young children commonly share objects that they put in their mouths.

Healthy people continue to shed EBV for many months after their acute infection and are potentially capable of transmitting it (27, 28). Because such virus "donors" are asymptomatic and hence not considered as sources of infection, they often go unrecognized. For the most part, shedding becomes intermittent rather than continuous several months after the primary infection. Hadinoto et al. reported that EBV is shed continuously in the saliva at relatively stable levels over short periods (hours or days), but quantities vary as much as 4 to 5 $\log_{10}$ copies over months or years (7). This suggests that a person's likelihood of transmitting EBV fluctuates over time.

Indications for Laboratory Tests and Their Interpretation

Table 1 outlines recommended tests for the diagnosis and management of various states of EBV infection, which are discussed in some detail below.

Documentation of Past EBV Infection

Documentation of past infection is most commonly done to determine the dose and duration of antiviral prophylaxis after solid organ transplantation or HCT. EBV-naive recipients usually receive a longer course of posttransplant prophylaxis than recipients who have previously experienced an EBV infection. As shown in Table 1, the best single test for documenting a past EBV infection is detection of IgG antibodies against the viral capsid antigen (VCA) of EBV. There are various platforms for this test, with the most widely used being an enzyme immunoassay (EIA). Indirect immunofluorescence assay (IFA) used to be the criterion standard method until assays suitable for high throughput, such as EIAs, were perfected (29). Detecting IgG antibodies against EBNA-1 can distinguish past from subacute infection, because EBNA-1 IgG antibodies generally do not develop until 3 months or longer after primary infection. However, they are not as sensitive as VCA IgG antibodies for documenting a previous EBV infection. Among subjects who experienced primary EBV infections while being monitored prospectively, 82/82 (100%) developed VCA IgG antibodies, whereas 67/74 (91%) subjects became EBNA-1 IgG positive (17; unpublished data). Patterns of EBV-specific antibody responses associated with various stages of infection are shown in Table 2.

Description of Primary EBV Infection and Diagnostic Approaches

Primary EBV infections, especially those in children under the age of 10 years, often go undiagnosed, either because they are entirely asymptomatic or because they do not present as the typical infectious mononucleosis syndrome. A clinical dilemma for making the correct diagnosis in children is that point-of-care laboratory tests, which are essentially all heterophile antibody assays, may be falsely negative (30, 31). Hence, even infections in children suspected of having EBV infection might not be confirmed. Primary EBV infection may not be recognized in adolescents and young adults, either, but 90% of these patients report some symptoms, especially sore throat, if seen shortly after the onset of infection (17), and the infection can be diagnosed with appropriate laboratory tests.

Infectious mononucleosis was named in 1920 by Sprunt and Evans, who used the term to describe a syndrome that resembled an acute infectious disease accompanied by atypical large peripheral blood lymphocytes in the peripheral blood (32). We now understand that these atypical lymphocytes, also called Downey cells, are activated CD8 T lymphocytes that are responding to EBV-infected B cells. Interestingly, EBV, the major cause of infectious mononucleosis, was not identified until 44 years after infectious mononucleosis was recognized as a distinct disease (1).

It is important to emphasize that the diagnosis of infectious mononucleosis cannot be made on clinical grounds alone. The illness most often begins insidiously, with vague malaise followed several days later by fever, sore throat, swollen cervical lymph nodes, and fatigue. Some patients experience an abrupt influenza-like onset, with fever, chills, body aches, and sore throat. Hepatitis, documented by abnormal liver function tests, is seen in 80% of cases and thus should be considered part of the acute disease rather than a complication. Liver involvement is subclinical in 90 to 95% of patients, but the remainder develop jaundice, and a few of them complain of tenderness in the right upper quadrant of the abdomen that is likely due to hepatic swelling with pressure on the liver capsule. Eyelid edema, which gives the patient a slit-eyed appearance and may be accompanied by facial puffiness, is a valuable clinical finding that is unique to primary EBV infection (33). Unfortunately, eyelid edema is present in only 10% of cases (34).

The median duration of infectious mononucleosis is 10 days (17), which is much longer than those of most acute viral illnesses. Recovery is gradual, and it may take months for the patient to feel entirely well (35). Fatigue interferes with productivity and quality of life and is usually the last symptom to resolve.

The severity of primary EBV infection increases with age, and adults older than 40 years of age are especially prone to serious illness (36, 37). They have more prolonged fever and more serious hepatic involvement but less noticeable lymphadenopathy than younger patients.

A flare-up of symptoms before the acute illness ends occurs occasionally (38). However, recurrences or "second cases" of infectious mononucleosis, documented by laboratory evidence of active EBV infection after recovery from the acute illness, are very uncommon. Hoagland reported no recurrences in his series of 200 patients, most of whom were hospitalized during their acute illness, according to military policy (39). We have had just one laboratory-documented recurrence among 132 subjects who acquired infectious mononucleosis between the ages of 16 and 26 years (Balfour, Jr., unpublished data).

TABLE 1 Recommended laboratory tests for diagnosis and management of EBV infections[a]

Indication	Recommended test	Alternative test	Comment(s)
Documentation of past infection	VCA IgG antibody test	EBNA-1 IgG antibody test	A small percentage of patients (~3%) never develop EBNA-1 antibody.
Detection of primary EBV infection (acute)	Heterophile antibody test	VCA IgM antibody test	Heterophile antibody testing may be negative in children of <4 years of age and may not become positive in older children and adults until 10 days after onset of symptoms.
Detection of primary EBV infection (subacute)	Tests for VCA IgM and IgG antibodies		This is usually considered to be 3 weeks to 3 months after primary infection.
Monitoring posttransplant EBV infections	Blood viral load measurement		The matrix tested in most centers is whole blood, but some prefer plasma. Serial testing at the same center is important.
Diagnosis of PTLD	ISH of biopsy material for detection of EBER	Blood viral load measurement	The PTLD risk has been shown to increase significantly with the peak whole-blood viral load.
Diagnosis of oral hairy leukoplakia	Diagnosis usually based on clinical findings without lab tests	ISH of lesion swab or biopsy specimen for detection of EBV DNA	EBV is actively produced under these conditions and usually responds to antiviral agents, such as acyclovir or ganciclovir.
Diagnosis of EBV central nervous system infection	PCR of cerebrospinal fluid		A positive result, regardless of quantity, should initiate a thorough neurologic evaluation, including imaging.
Diagnosis of EBV-associated cancers	ISH of biopsy material for detection of EBER		EBV-associated cancers include nasopharyngeal carcinoma, Hodgkin's lymphoma, endemic Burkitt's lymphoma, gastric carcinoma, and leiomyosarcoma.
Diagnosis of EBV-associated lymphoproliferative diseases in nonimmunocompromised hosts[b]	Determination of antibody profile of primary EBV strain and phenotype of infected cell type	Clonality analysis	CAEBV is the most common form.

[a]Abbreviations: CAEBV, chronic active EBV; EBER, EBV-encoded RNA; EBNA, EBV nuclear antigen; ISH, *in situ* hybridization; PTLD, posttransplant lymphoproliferative disorder; VCA, viral capsid antigen.
[b]These include CAEBV, hematophagocytic lymphohistiocytosis, severe mosquito bite allergy, and hydroa vacciniforme.

Complications of primary EBV infection may be due to tissue-invasive viral disease or to immune-mediated damage. Many complications have been associated with infectious mononucleosis, but nearly all of them are uncommon or rare (40, 41). Complications reported in ≥1% of cases are airway obstruction, meningoencephalitis, hemolytic anemia, thrombocytopenia, and maculopapular rash (34). Splenic rupture is a rare but serious complication that excludes athletes from contact sports for various lengths of time.

The correlations between time of primary infection, disease expression, immune responses, and viral loads are shown in Fig. 1. EBV infects the host approximately 42 days before the onset of overt symptoms. The first laboratory indicator of primary infection is oral viral shedding, which can occur as early as 2 weeks before the onset of symptoms. This is not a good test for diagnosis of acute primary EBV infection, because essentially all persons ever infected by EBV shed virus intermittently from the oral compartment. The next indicators of primary infection arise almost simultaneously. They are development of VCA IgM antibodies, development of heterophile antibodies, and viremia. These may be detected as early as 7 days before symptoms develop. Viremia, found in approximately 75% of patients, is short-lived in most cases but may persist for up to 6 months in unusual instances (17, 28).

A heterophile antibody test is the practical choice for the diagnosis of acute infectious mononucleosis (Table 1),

TABLE 2 EBV infection category according to patterns of EBV-specific antibody tests[a]

Infection category	Presence of antibody		
	VCA IgM	VCA IgG	EBNA-1 IgG
Common patterns			
Never infected (naive)	−	−	−
Acute primary infection	++	−	−
Subacute primary infection	++	+	−
Convalescent-phase primary infection	±	++	±
Past infection (>6 months old)	−	+++	+++
Unusual patterns			
Past infection (>6 months old)	−	+++	−
Past infection (>6 months old)	−	−	++

[a]Symbols for presence and semiquantitation of antibody response: −, no antibody response; ±, equivocal result; +, low positive response; ++, moderate positive response; +++, strong positive response.

because of its simplicity and relatively low cost (42). Heterophile antibody tests use various mammalian erythrocytes to detect IgM class antibodies that are present during the generalized immune upregulation that characterizes acute primary EBV infection. Paul and Bunnell discovered heterophile antibodies in 1932 (43), which they defined as "having the capacity to react to certain antigens, which are quite different from, and phylogenetically unrelated to the one instrumental in producing the antibody response [in this case EBV]."

Heterophile antibody tests do have drawbacks. As mentioned above, children 4 years of age or younger may not develop heterophile antibodies during primary EBV infection (31). Thus, the heterophile antibody test may be falsely negative for young children. Second, heterophile antibodies are nonspecific and may be present in infections not caused by EBV or in malignancies or autoimmune diseases (44, 45). Finally, these antibodies may persist for a year or more and therefore are not always diagnostic of an acute EBV infection (46).

If the clinical impression is primary EBV infection but heterophile antibodies are absent, we recommend testing for the following three EBV-specific antibodies: anti-VCA IgM, anti-VCA IgG, and anti-EBNA-1 IgG. The category of EBV infection can then be assigned as naive (never infected), acute (1 to 3 weeks old), convalescent (4 weeks to 6 months old), or past (>6 months old), as shown in Table 2. The criterion standard for measuring these antibodies used to be IFAs, but assays with a higher throughput that are less labor-intensive, such as EIAs, have essentially supplanted them (29).

Examination of a peripheral blood smear may be helpful, especially when antibody results are inconclusive. In acute primary EBV infection, large atypical lymphocytes (also known as Downey cells) may constitute 10% or more of the total lymphocyte population (47). We now understand that these are $CD8^+$ cytotoxic lymphocytes, most of which are probably reacting against EBV-infected B cells (48).

IgG antibody against VCA is first detected at different times during the course of primary EBV infection, depending on the target antigen used in the test. If the target antigen is EBV p18, which is the antigen reagent in the Diamedix EIA, the antibody response starts about 10 days after the onset of illness. If it is p23, the VCA IgG antibody response may be seen as early as the first few days of illness. The EBNA-1 antibody response develops slowly and normally is not detected until at least a month after the onset of symptoms (17). Because of its late appearance, the presence

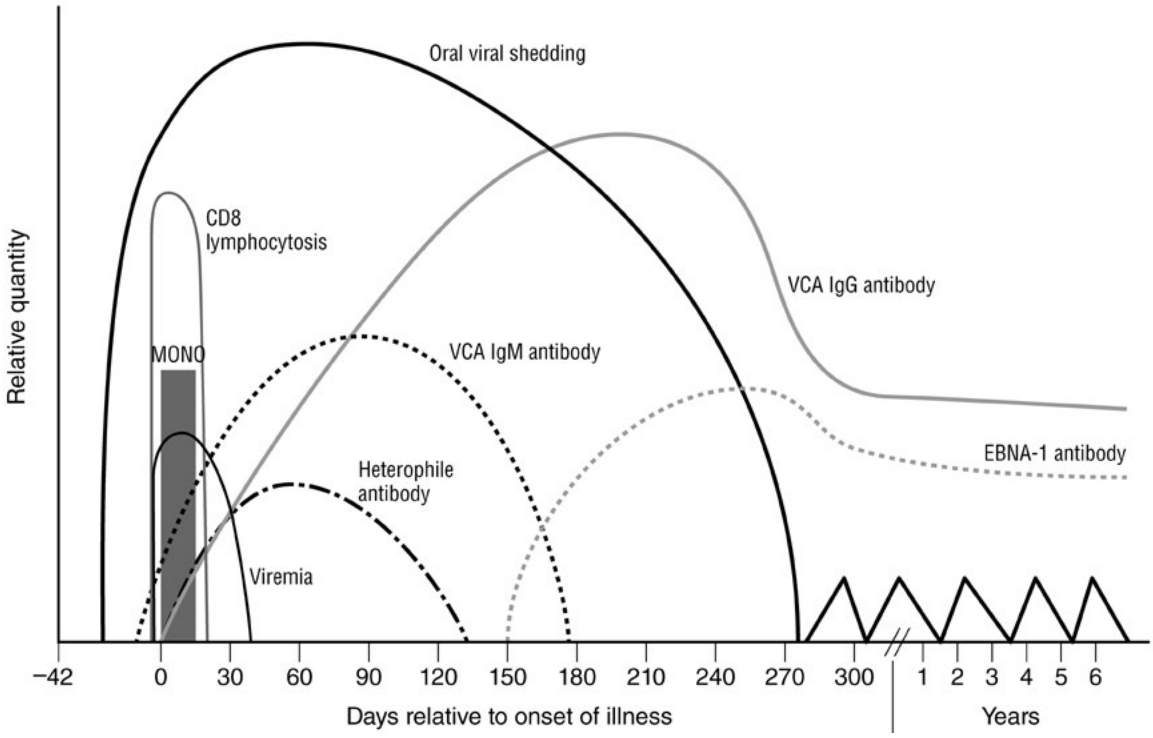

FIGURE 1 Correlations between time of primary infection, disease expression, immune responses, and viral loads.

of EBNA-1 antibody is useful for distinguishing past from recent or subacute infections. Also, EBNA-1 antibody indices are significantly elevated in patients with multiple sclerosis compared with matched controls (49).

Monitoring Infections in the Immunocompromised Host

EBV infections in immunocompromised patients are best evaluated in the laboratory by serial measurements of the blood viral load (Table 1) (50, 51). Most assays employ a DNA template, and the matrix tested is usually blood, so EBV blood viral loads are also referred to as EBV DNAemia. While there are options in terms of platforms, volumes, probes, and targets, a multicenter comparison of different real-time PCR assays suggested that if samples are tested at one center on the same platform, real-time PCR is a precise technique for measuring viral load. However, substantial quantitative differences were found when samples were tested in different laboratories (52). A WHO quantitative calibration standard is now available, which should improve interlaboratory variability (53).

At a number of institutions, viral loads of >4,000 copies/ml of whole blood (54, 55) or steadily rising levels often prompt a reduction of immunosuppression and initiation of specific treatment for solid organ transplant recipients. The threshold triggering an intervention is lower for hematopoietic cell transplants (usually ~1,000 copies/ml). The best matrix to use for monitoring EBV infections has been a subject of debate. Some centers consider EBV in plasma to be more indicative of active infection (56), but the majority favor whole blood (57, 58). Copy numbers in plasma are usually 10- to 100-fold lower than those in concomitant whole-blood samples. The diagnosis of posttransplant lymphoproliferative disorder (PTLD) requires a tissue diagnosis, but some centers consider rising blood viral loads, especially those exceeding 100,000 copies/ml, to be consistent with PTLD (Table 1) and treat patients accordingly (59).

An unusual manifestation of EBV infection, oral hairy leukoplakia (OHL), is seen mainly in patients with HIV/AIDS but occasionally occurs in individuals not infected with HIV. OHL lesions are characterized as white, nonremovable plaques most commonly seen on the lateral borders of the tongue. These can usually be diagnosed clinically and do not require laboratory confirmation. In atypical instances, *in situ* hybridization (ISH) to detect EBV DNA in incisional biopsy tissue or lesion swabs may be used to make the diagnosis (60). Because OHL plaques are the result of active EBV replication, they often regress during antiviral therapy (61).

Central Nervous System Infections

Cerebrospinal fluid testing by PCR is the method of choice to diagnose EBV infection of the central nervous system (Table 1). A positive result, regardless of quantity, should initiate a thorough neurologic evaluation, including imaging.

EBV-Associated Cancers

EBV is best identified by examination of biopsy or surgical samples of cancer tissue by using immunohistochemical (IHC) approaches (Table 1). ISH to detect EBV-encoded RNA transcripts (EBERs) is the criterion standard for detecting EBV in tissue (62). PCR is the technique of choice for detecting and quantifying EBV in body fluids and can also be used to quantify the virus in tissue samples (63). Diagnosis and monitoring of therapy of nasopharyngeal carcinoma by noninvasive sampling techniques, such as quantification of EBV DNA in bronchial brushings, are under investigation (64, 65).

EBV-Associated T or NK Cell Lymphoproliferative Diseases

A subset of patients do not recover from primary EBV infection because they develop clonal proliferation of EBV-infected T or NK cells. The majority of these individuals are Japanese, with a median age of onset of 8 years (66). These patients have no prior evidence of immune dysfunction; therefore, this group of diseases has been referred to as EBV-associated lymphoproliferative diseases in nonimmunocompromised hosts. There are four clinical categories: chronic active EBV, hematophagocytic lymphohistiocytosis, severe mosquito bite allergy, and hydroa vacciniforme. These conditions are life-threatening, with an overall mortality of 40 to 50%. The diagnosis is based on documentation of a primary EBV infection followed by determination of the phenotype of the infected cells by immunobead separation or ISH followed by flow cytometry. Viral clonality may also be assessed by Southern blot analysis using an EBV terminal repeat probe. Most patients' EBV-infected cells are monoclonal.

Laboratory Methods

Methods in Clinical Use

Methods are presented in order of relative clinical value for both methods in clinical use and research methods with potential clinical application.

Detection of Heterophile Antibody

There are numerous commercial kits that detect heterophile antibodies (also referred to as monospot tests). Our laboratory employs the Acceava Mono test, which is an immunoassay using a qualitative membrane strip for the detection of heterophile antibodies in anticoagulated whole blood, plasma, or serum. The membrane strip is coated with a bovine erythrocyte antigen extract at the test line on each strip. Diluent and a specimen sample are added in the proper dilution to a small tube, and the strip is placed into the solution, which migrates up the membrane strip. A colored line appears in the test strip if heterophile antibodies are present. No colored line in the test strip area indicates a lack of heterophile antibodies. Each strip contains a control to show that proper volumes and wicking of the sample are present.

Detection of EBV-Specific Antibodies (VCA IgG, VCA IgM, and EBNA-1 IgG) by EIA

A number of commercial assays are available for detection of EBV-specific antibodies. We use the semiquantitative Diamedix platform, which has proven to be quite reliable. We have published three studies in which the EBV-specific antibody responses correlated closely with clinical findings for primary EBV infection and EBV loads (17, 28, 67). Serum is the preferred matrix, but plasma is acceptable. For the detection of EBV VCA IgG, VCA IgM, and EBNA-1 IgG antibodies, recombinant VCA antigen or recombinant EBNA-1 antigen is bound to plastic microwells. A cutoff calibrator, negative and positive controls, and diluted patient serum samples are pipetted into the microwells for incubation. A diluent is supplied for the IgG or IgM antibodies and is not lot specific. The specimen and diluent are used at a 1:21 ratio for IgG testing and a 1:101 ratio for IgM testing. If EBV antibodies are present in the sample, they will bind to the antigen coating the wells, forming an antigen-antibody

complex. Other antibodies that may be in the specimen are eliminated through aspiration or "flicking" of the sample in the wells and then washing of the wells with a prepared wash solution. A kit-specific conjugate (horseradish peroxidase-labeled anti-human IgG or IgM) is added to the wells to bind to the antigen-antibody complex. Unbound conjugate is removed through aspiration or "flicking" and washing. A substrate solution of 3,3′,5,5′-tetramethylbenzidine is then added to the well for incubation. The substrate is converted to the end product by a bound enzyme. The reaction is stopped with 1 N H_2SO_4. The absorbance at 450 nm of the end product is measured by using a spectrophotometer (with reference band reading at 630 nm). The amount of color produced is relative to the quantity of antibody in the specimen.

Some laboratories prefer an antibody capture assay, especially for detection of VCA IgM antibodies. The major advantage of this method is enhanced specificity. The procedure involves coating wells with an anti-human IgM antibody that "captures" the patient's antibody. VCA antigen and an anti-EBV antibody conjugate are then added, followed by a color substrate to visualize the bound enzyme.

Detection of EBV DNA by PCR

Detection and quantification of EBV DNA by PCR currently form the criterion standard for monitoring EBV infections and disease posttransplantation. DNA is extracted from the sample through a series of washes with buffers of various salt concentrations. Membranes are ruptured using protease enzymes, and DNA is removed from cellular and extracellular debris during DNA extraction by using columns that loosely bind DNA. The DNA is washed off in a final step with a salt solution. Both in-house and commercial assays are in use, and a number of EBV DNA targets have been designed, including BNRF-1, BALF-5, and EBNA-1. We employ an in-house TaqMan assay with an amplicon that is a 71-bp segment of the EBNA-1 gene. TaqMan technology for the determination of viral load uses fluorescently labeled probes that lie between specific primers. Each probe is labeled on its 5′ end with a reporter dye that allows for product detection during amplification and is labeled on its 3′ end with tetramethylrhodamine or another quencher dye to reduce the unbound fluorescence signal and prevent the probe from acting as a primer. Probes attach to their complementary DNA sequence targets, and when the PCR proceeds, the fluorescence signal is released at a rate relative to the quantity of EBV DNA in the sample. Most assays are run for 40 to 45 thermocycles. The cycle threshold is reached sooner when the sample contains large amounts of EBV DNA and later when smaller quantities are present. The controls that we use include serial dilutions of Namalwa cells (these contain two copies of EBV DNA per cell), no template, and six quantitative amplicon standards calibrated to contain 10^2, 10^3, 10^4, 10^5, 10^6, and 10^7 copies of EBV/ml. Patient samples are run as a pair, with one well containing an internal control to ensure that the sample does not inhibit detection of DNA. The best matrix to use for monitoring chronic EBV infections is still in question. As discussed above, whole blood is preferred by many centers, whereas some test plasma.

In Situ Hybridization

ISH is an IHC technique to detect and localize a target sequence in samples that have been treated to fix the target in place and to facilitate access of the probe to the area of interest. ISH is the method of choice to diagnose tissue-invasive EBV disease. The assay is quite sensitive if probes designed to bind to EBV-encoded RNAs (EBER-1 and EBER-2) are employed, because latently infected B lymphocytes contain ~10^6 copies of EBERs/cell, which aggregate in the nucleus. Commercial reagents are available from several manufacturers. Controls should include EBER-positive and -negative specimens.

Detection of EBV EA IgG Antibody

Antibody against EBV early antigen (EA) can be detected in serum or plasma by use of an EIA, IFA, or immunoblotting. Henle et al. identified two distinct patterns of immunofluorescence staining, diffuse and restricted, using sera from patients with infectious mononucleosis, Burkitt's lymphoma, and nasopharyngeal carcinoma (68). The more common diffuse pattern antigen (EA-D) is encoded by the BMRF-1 gene and is characterized by nuclear and cytoplasmic staining. The restricted pattern antigen (EA-R), encoded by the BHRF-1 gene, consists of cytoplasmic aggregates of various sizes without nuclear staining. Both patterns can be seen in the same cell. In early infectious mononucleosis, the predominant pattern was EA-D, but later on, EA-D and EA-R became nearly equal. Nasopharyngeal carcinoma patients dominantly showed the EA-D pattern, whereas sera from Burkitt's lymphoma patients most frequently contained EA-R. The clinical utility of EA testing is questionable today. It is not sensitive for diagnosing acute infectious mononucleosis because only 60 to 80% of patients are positive (29). It is not specific for reactivation of EBV because healthy blood donors have been found to be positive for serum EA IgG antibodies (69).

Detection of EBV IgA Antibody

The EBV IgA antibodies purported to have clinical application are VCA IgA and EA IgA. They have practical value only for diagnosis and management of patients with nasopharyngeal carcinoma (70). The sensitivity and specificity of VCA IgA antibody detection appear to be superior to those of EA IgA detection for the diagnosis of nasopharyngeal carcinoma (71). VCA IgA antibody has been proposed as a marker of reactivation. However, it is not specific, as VCA IgA antibodies have been reported for 74% of primary EBV infections and have also been seen in 13% of healthy subjects (72).

Research Methods with Potential Clinical Application

Immunoblotting

Immunoblotting can include immediate early, early, and late EBV antigens on one test strip, which may permit evaluation of the relative stage of EBV infection by use of a single serum or plasma sample (73). Our virology research laboratory uses the Mikrogen line blot immunoassay system, which provides a choice of reagents for detection of IgA, IgG, and IgM class antibodies and IgG antibody avidity. Briefly, highly purified recombinant EBV antigens are fixed onto nitrocellulose membrane strips. The test strips are incubated with the diluted sample, and specific antibodies attach to the EBV antigens on the test strip. Unbound antibodies are then flushed away by a wash procedure. In the second step, the strips are incubated with anti-human immunoglobulin antibodies (IgG, IgA, and/or IgM), which are coupled to horseradish peroxidase. Unbound conjugate antibodies are then flushed away by a wash procedure. Specifically bound antibodies are detected by a staining reaction

catalyzed by the peroxidase. If an antigen-antibody reaction has taken place, a dark band will appear on the strip at the corresponding point. Each test strip contains three control bands. The reaction control band, at the upper end of the test strip, must show a reaction for every serum/plasma sample. Next on the strip is the conjugate control (IgG, IgA, or IgM), which is used for verification of the antibody class detected. If, for example, the test strip is used for the detection of IgG antibodies, the conjugate control IgG must show a clearly defined band. Finally, there is a cutoff control. The intensity of the antigen-antibody bands produced by the test sample must exceed that of the cutoff control in order to be called positive.

EBV Culture

The classic way to isolate EBV is to incubate body fluid or tissue samples with fresh umbilical cord B cells. The cells are observed for 6 weeks for evidence of transformation, which includes persistent proliferation, mitotic figures, large vacuoles, granular morphology, and cell aggregation. There is little value in performing this labor-intensive assay that takes weeks to give results, because molecular techniques, especially nucleic acid detection, are available and are much more sensitive than viral culture for identification and quantification of EBV.

Neutralization Assays

Neutralization assays are important for evaluation of antibody responses to candidate EBV vaccines. These used to rely on viral culture in human lymphocytes, with comparison of endpoint dilutions of infectivity or transformation. A streamlined neutralization assay was recently described in detail by Sashihara et al. (74). They elegantly showed that antibody titers against EBV gp350 correlated tightly with neutralization of infectivity. The neutralization assay is based on coincubating Raji cells (a Burkitt's lymphoma cell line) with B95-8 cells (cotton top tamarin lymphocytes transformed by EBV from an infectious mononucleosis subject) that contain green fluorescent protein. The green fluorescent protein-positive Raji cells indicate infection and are enumerated by flow cytometry after a 3-day incubation period. The ability of antibody to inhibit Raji cell infection can be quantitated by serial dilution of the plasma or serum specimen.

Assays of EBV-Specific T Lymphocytes

The two most popular methods to identify and study EBV-specific T lymphocytes are HLA-peptide tetramer (75) and gamma interferon (IFN-γ) enzyme-linked immunosorbent spot (ELISPOT) (76) assays. An extensive list of $CD4^+$ and $CD8^+$ T cell epitopes derived from EBV proteins has been identified (77) and facilitates the use of these assays. Measuring virus-stimulated IFN-γ production, typically by ELISPOT assay, is a very sensitive and specific means to detect virus-specific T cells and is used widely to study EBV-specific $CD4^+$ and $CD8^+$ T cells. By using mixtures of peptides from different viral proteins and different HLA alleles (78, 79) or by using EBV-infected lymphoblastoid cell lines from patients' own B cells (80), ELISPOT assays can be quite comprehensive and do not require knowledge of the HLA type of the individual. Nonetheless, not all virus-specific T cells produce IFN-γ, and if T cells become exhausted due to overstimulation, they may fail to produce IFN-γ (79, 81). This is particularly problematic for detection of EBV during acute infection. Identification of virus-specific T cells by use of HLA-peptide tetramers avoids this issue.

During acute infection, large numbers of tetramer-binding (EBV-specific) $CD8^+$ T cells are observed in the peripheral blood (77, 80, 82), as well as $CD4^+$ T cells, to a lesser extent (83). However, since our knowledge of EBV epitopes and the alleles that present them is not exhaustive, neither ELISPOT assays nor tetramers can identify all of the EBV-specific T cells in an individual. Nonetheless, the pattern of expansion and contraction of tetramer-binding T cells over time after primary infection is generally similar to that of total $CD8^+$ T cells in peripheral blood (17). Some studies have estimated the total number of pathogen-specific T cells during infection by assessment of cell surface activation markers, such as CD38 and HLA-DR, assuming that these activated T cells are pathogen specific (84). However, our study clearly showed that "bystander" $CD8^+$ T cells (those specific for other viruses) become activated during acute EBV infection as well (48). Although it remains challenging to precisely determine the fraction of T cells that are specific for EBV, it is clear that the $CD8^+$ T lymphocytosis observed during acute EBV infection is unusually large and that this effect is not as pronounced for $CD4^+$ T cells.

Finally, HLA-peptide tetramers can be combined with flow cytometric analysis of cytokine production, cell cycle markers, cytolytic proteins, activation/memory/exhaustion markers, and survival proteins. These types of studies have provided great insight into the kinetics and character of the T cell responses to different EBV epitopes (77) but are not yet being employed to distinguish pathogenic versus protective responses in the clinical setting.

Detection of Encapsidated versus Naked EBV DNA

Whether circulating cell-free DNA is encapsidated in virions or exists as fragments of naked DNA may be important for managing patients with EBV-related malignancies. It is thought that fragments of naked EBV DNA are released from tumor cells undergoing apoptosis, whereas encapsidated EBV DNA reflects lysis of cells undergoing active EBV replication (13). If most of the DNA is encapsidated, signaling ongoing viral replication, then antiviral therapy might be effective. On the other hand, naked DNA may be a measure of tumor cell burden, and its disappearance after a transient increase following radiation or chemotherapy could be a positive prognostic factor signifying destruction of cancer cells.

Ryan et al. developed a test to distinguish encapsidated from naked EBV DNA (85). Their assay is based on the observation that viral capsids protect EBV DNA from degradation by DNase I. The assay measures the EBV load by real-time TaqMan PCR before and after exposure to DNase I. A marked reduction in viral copy number after DNase I treatment indicates that the sample contains mostly or all naked EBV DNA.

Clonality Analysis

During lytic replication, EBV forms linear intermediates of different sizes produced by random cleavage between the variable-number terminal repeats in the viral genome. If malignant transformation occurs, the same fused terminal repeat pattern is inherited by all progeny of the original malignant cell. Clonality analysis involves digestion of EBV DNA with a restriction endonuclease, such as BamHI, that does not cut the genome within the terminal repeats. The fragments containing the terminal repeats are detected by Southern blotting using specific probes. If the EBV-infected

cell population is monoclonal, the fragments have a single size and appear as a single band when visualized by staining or autoradiography. Multiple bands indicate oligoclonality or polyclonality, which implies a less aggressive disease.

CMV

Background and Biology

CMV has a very distinct cytopathology that was first described by the German pathologist Hugo Ribbert at a medical meeting in Bonn in 1881 (86). Similar cells with eccentrically placed nuclei containing a central nuclear body surrounded by a clear halo were identified in the lungs, kidneys, and liver of an 8-month-old stillborn fetus (87). The first indication that these cells with intranuclear inclusions were related to viruses rather than to protozoa, as previously believed, occurred in 1925, when similar cells were discovered in a man with herpes zoster and herpes genitalis (88, 89).

In 1950, Wyatt et al. reviewed the published data on conditions associated with this unique cytopathology, added six cases of their own, and concluded that "the etiologic agent of the disease is a specific virus [and] the morphology and cytology of the inclusion-bearing cells is pathognomonic of the disease" (90). In addition, renal tubules were identified as a uniform site of involvement, and thus a cytological preparation from the urinary sediment of a suspected case patient became the first successful diagnostic test for what was now being called "cytomegalic inclusion disease" (91). In 1953, electron microscopy revealed 199-nm particles in the clear halo around the intranuclear inclusion, consistent with a viral etiology (92). After Enders et al. discovered how to grow human cells in culture (93), for which they received the Nobel Prize in 1954, CMV was isolated in cell culture by independent laboratories (94–96). The virus was then available for the laboratory studies that provided the data presented below.

CMV, whose systematic name is HHV-5, is one of the eight human herpesviruses recognized to date. CMV is a prototypic member of the betaherpesvirus subfamily, and its DNA genome is approximately 230 kb long, the largest among known human viruses, and consists of unique long (UL) and unique short (US) segments, each of which is flanked by inverted repeats (RL and RS). Most of the approximately 200 genes encode proteins, but some express only noncoding RNAs, including approximately 14 microRNAs. The central portion of the UL region contains clusters of core genes that have homologs in other herpesviruses, such as genes encoding DNA polymerase, glycoprotein B (gB), and glycoprotein H (gH), whereas the remainder of the genome contains genes primarily found only in betaherpesviruses or unique to human CMV. By convention, CMV genes are named by their position within the genome, although some also have additional descriptive names. For example, UL54 (the 54th gene in the UL region, according to the original report of the CMV strain AD169 sequence) is the DNA polymerase gene (97).

Following initial infection, a complex set of nonspecific and humoral host responses attempt to limit CMV replication, but the virus has lived in its human host for a very long time and has evolved successful evasion strategies. The interaction between CMV and the host immune system is complex, since the virus itself can cause suppression or enhancement of host immune responses and can infect the lymphoid system. Nonspecific host defense mechanisms include NK cells and IFNs. In humans and murine models, NK cell deficiency has been linked to severe CMV disease (98), and NK cells have been shown to lyse cells infected with CMV (99). At least seven genes are able to modulate, and in many cases inhibit, NK cell function (100). The production of IFN-α and -β is an important part of the defense against murine CMV in the early stages of infection. In humans, too, CMV infection prompts cellular membrane sensors, such as the lymphotoxin beta receptor, to initiate the production of antiviral cytokines such as IFN. However, virion factors, such as pp65 (ppUL83) and viral proteins made soon after infection, repress this response by interfering with steps in the activation of IFN regulatory factor 3 and NF-κB. CMV then exerts a multipronged attack on downstream IFN signaling. CMV has multiple genes involved in blocking the function of IFN-induced effectors (101).

Adaptive T cell responses are critical for keeping the virus inactive. Restoration of $CD8^+$ and $CD4^+$ T cells is a strong correlate of control of the virus after transplantation (102, 103). Adoptive transfer of CMV-specific T cells protects against clinical reactivation (104).

In antibody-positive humans, a strikingly large proportion (10% or more) of circulating T lymphocytes target CMV, and the proportion of CMV-specific T cells tends to increase with age, which supports the hypothesis that CMV contributes to immune system exhaustion and dysfunction associated with aging (105). However, our understanding of these inflammatory memory CD8 T cells is incomplete, and they alternatively may serve an essential protective role (106). Antibodies in CMV-infected individuals have been useful for establishing immune status. Although it has long been thought that only antibodies to gB or gH neutralize the virus, other viral genes, including UL128, UL130, and UL131A, also mediate entry into endothelial and epithelial cells.

Like other herpesviruses, once the primary infection is brought under control by the host immune response, CMV persists in a state of cellular latency in which infected cells are not producing any infectious virus or are replicating it at a very low level, below the threshold of current detection methods. The latent virus retains the complete genome, with the potential to start producing virus at any time. The site of CMV latency has been thought to possibly be circulating leukocytes. During kidney transplantation, donors are thought to transmit CMV via the organ, which is undoubtedly contaminated with leukocytes. However, since CMV has a propensity to reactivate within the transplanted organ, perhaps parenchymal cells harbor latent virus.

CMV replication and the host immune system are in a delicate balance, such that even relatively minor perturbations, such as pregnancy or admission to an intensive care unit, allow CMV reactivation, often without overt CMV disease (107). Moreover, subtle effects of subclinical reactivation or quiescent CMV infection might contribute to chronic immune system dysfunction and predispose individuals to other illnesses, including infections by other microbes (108).

Clinical Relevance

CMV is a ubiquitous virus, and infections are usually asymptomatic and acquired relatively early in life. The high frequency of CMV antibody in the general population without previous overt disease suggests that CMV infection is fairly frequent. Transmission occurs during direct contact with body fluids. Once a person is infected, the virus establishes lifelong latency, with periodic reactivations usually resulting in asymptomatic shedding of virus. Unfortunately, CMV infection is not always asymptomatic. CMV is the most common cause of congenital infections that result in

sensorineural hearing loss and psychomotor retardation, with a 5 to 10% mortality rate (109). The birth prevalence of congenital CMV is 0.64%, with 11% of these infants being symptomatic (110). Symptoms can include jaundice, hepatosplenomegaly, hydrops, thrombocytopenia, anemia, microcephaly, seizures, and chorioretinitis. Even asymptomatic infants remain at risk for later symptoms, such as sensorineural hearing loss (109). CMV may also be a cause of antenatal stillbirth (111). In immunocompetent adults, CMV can cause a self-limiting mononucleosis syndrome, and in immunocompromised patients, it can present with mild to severe organ involvement that may be fatal. Moreover, even subclinical CMV viremia has been associated with deterioration in kidney function in kidney transplant recipients (112, 113) and, more recently, was cited as a risk factor for cardiovascular disease in transplant recipients (114). Breakthrough infections occur despite routine viral prophylaxis with valganciclovir for 3 to 12 months posttransplantation in all transplant recipients (115).

Laboratory Methods

Methods in Clinical Use

Since CMV disease can have nonspecific clinical manifestations, laboratory confirmation is essential for diagnosis. A summary of the laboratory tests for diagnosis and management of CMV infections is provided in Table 3.

Nucleic Acid Amplification Tests

The sensitivity of PCR technology to detect minute amounts of viral nucleic acid in clinical samples has made this the preferred method of CMV diagnosis, particularly after solid organ transplantation or HCT, when timely diagnosis is of the essence. Nucleic acid amplification tests (NATs) can detect CMV nucleic acid in a variety of samples, including blood, cerebrospinal fluid, respiratory samples, and aqueous or vitreous humor fluid, but the matrices most often tested are whole blood and plasma. Since the vast majority of CMV NATs are developed and validated by

TABLE 3 Laboratory tests for diagnosis and management of CMV infections

Test	Indication	Comment(s)
NAT against DNA	Detects active or latent CMV infection	Detects latent DNA, making it a good qualitative test but less useful clinically, since it is sensitive but not specific
NAT against RNA	Detects active CMV infection	RNA intermediates are mainly produced during active replication, so the test is specific for acute CMV but has reduced sensitivity, since RNA is easily degradable.
qNAT	Useful for diagnosis, risk assessment, and therapeutic guide for active CMV infection	The test is sensitive and specific and is the most clinically utilized and useful test for detection of CMV infection or disease.
Non-PCR amplification	Detects active CMV infection	Based on signal amplification and is therefore less sensitive and less utilized clinically
Histopathology	Diagnosis of tissue-invasive or compartmentalized disease	While very specific for disease, it requires an invasive procedure or biopsy for specimen retrieval. In addition, atypical features may overlap the features of other viral diseases.
ISH/IHC	Diagnosis of tissue-invasive or compartmentalized disease	More sensitive and specific than histopathology but still requires an invasive procedure or biopsy for specimen retrieval
Viral culture	Useful for samples not suitable for molecular testing	Although very specific, it has a reduced sensitivity, long turnaround time, and laborious method.
pp65 antigen testing	Diagnoses active CMV infection	This is a rapid test, but it utilizes a laborious method with subjective interpretation. In addition, there is an increased risk of false-negative results in cases of severe leukopenia.
Antibody testing	Useful for risk stratification of transplant patients for CMV disease, detects past infection	Denotes past or recent infection but is not useful for initiating or monitoring the response to therapy
IgG avidity assay	Detects recent primary infection	Not commercially available in the United States

each performing laboratory, results are not interchangeable given the different limits of detection, assay characteristics, and levels of precision and accuracy. The U.S. FDA recently approved a CMV NAT called the CAP/CTM CMV test (Roche) for viral load monitoring in patients receiving antiviral therapy for CMV disease.

In most CMV NATs, the target nucleic acid is CMV DNA, which accounts for their high sensitivity, since DNA is very stable over time. However, since latent viral DNA is also detected by this test, its specificity is reduced. This concern led to the development of a CMV NAT to detect RNA, since RNA intermediates are produced mainly during active replication. But since RNA molecules are readily degraded, the sensitivity of the test is lowered.

CMV NAT can be developed as a qualitative test, but this is less useful than quantitative testing, whose results are reported as absolute values per volume of specimen. Quantitative NAT (qNAT) allows for CMV disease risk assessment, since higher initial and peak viral loads or a rapid rise in viral load is associated with a higher risk of CMV disease development (116, 117) and more severe CMV disease. qNAT also guides the initiation and duration of preemptive therapy for prevention of CMV disease and allows rapid and sensitive diagnosis of CMV disease so that prompt therapy can be initiated. The effectiveness of antiviral therapy for CMV disease, treatment duration, risk of relapse, and risk of antiviral resistance can be assessed by qNAT.

Non-PCR amplification methods based on signal amplification rather than direct detection of CMV DNA or RNA are less sensitive and therefore less utilized clinically.

Histopathology

While histopathology remains the reference standard for the diagnosis of tissue-invasive CMV disease, it requires an invasive procedure/biopsy to obtain tissue samples. Therefore, many clinicians rely on a NAT coupled with compatible clinical signs and symptoms to make a diagnosis of CMV disease. However, in the case of compartmentalized or localized CMV disease, blood testing may be negative for CMV. Histopathology is critical in such cases. Testing for allograft biopsy pathology is also useful if transplant rejection is a diagnostic consideration for patients with CMV viremia. Histopathologic features of CMV infection are classic and include cellular and nuclear enlargement with amphophilic to basophilic cytoplasmic inclusions. But since there are sometimes atypical features that may overlap the presentation of other viruses, ISH or IHC testing is a useful confirmatory test. ISH testing uses CMV-specific DNA probes that bind to viral DNA in the cellular material, while IHC testing uses a monoclonal/polyclonal antibody against early CMV antigen. This increases the sensitivity and specificity of histopathology as a diagnostic test for CMV disease.

Viral Culture

Viral culture is highly specific and can be done using a conventional plaque assay or the more rapid shell vial centrifugation culture system. Isolation of CMV from most clinical samples is highly predictive of CMV disease. The exception is recovery of CMV from the urine, saliva, or stool samples of antibody-positive recipients, in which case the shedding is usually of no clinical consequence. The utility of CMV culture is limited by its low sensitivity, labor-intensiveness, and long turnaround time. The shell vial centrifugation method has a shorter turnaround time because the cultured cells are stained with monoclonal antibodies to detect immediate early antigen production during CMV replication, allowing diagnosis in as little as 2 days. Viral culture is useful mainly when samples are not suitable for molecular testing. Viral culture used to be required for phenotypic drug resistance testing, but molecular genotypic assays are now the methods of choice.

Antigen Testing

The CMV antigenemia assay uses monoclonal antibodies to detect CMV lower matrix phosphoprotein pp65 antigen, a structural late protein expressed in CMV-infected leukocytes during early CMV replication. The result is reported as the number of positive cells per total number of cells counted and generally signifies active CMV infection. This test is rapid and is easier to perform and more sensitive than viral culture, and it can detect CMV infection earlier than viral culture. The degree of pp65 antigenemia can be used to pre-emptively treat patients to prevent CMV disease, since it is correlated with the risk of subsequent CMV disease, although this is not absolute. The number of pp65-positive leukocytes usually declines during successful antiviral therapy, and persistence may indicate suboptimal dosing or drug resistance.

Despite all these potential uses, it is labor-intensive and manual, unlike CMV NATs, and blood must be processed rapidly to optimize sensitivity. In addition, the interpretation of the test is subjective, making interlaboratory standardization difficult. Since the test relies on a sufficient number of polymorphonuclear leukocytes, false-negative results may occur in patients with severe leukopenia. Therefore, the CMV NATs by PCR described above are considered by most to be more sensitive and can detect CMV much earlier than the pp65 antigenemia test.

Antibody Tests

Serologic tests that detect CMV IgM and IgG antibodies are widely available from commercial laboratories. Enzyme-linked immunosorbent assay is the most commonly used antibody method, but various fluorescence, indirect hemagglutination, and latex agglutination tests are also available. These tests are performed to detect current active CMV infection or past infection in immunosuppressed persons at risk for reactivation of CMV infection.

In the field of transplantation, knowledge of donor and recipient antibody statuses allows stratification of the risk for CMV disease. The highest-risk antibody category is donor positive and recipient negative (D+R−), moderate-risk categories are D+R+ and D−R+, and the lowest-risk category is D−R− (118). Recommended viral prophylactic regimens often vary depending on the risk category. In addition, lack of antibody development by 6 months may be useful for identifying patients at risk for late-onset CMV disease (119, 120). Antibody testing may also be performed to detect CMV infection in newborns.

The presence of antibodies to CMV indicates a current or past infection but does not determine when the primary infection occurred. However, if tests performed on paired acute- and convalescent-phase sera show a 4-fold rise in CMV IgG antibody and CMV IgM antibody is present, or if CMV is cultured from a urine or oral sample, then an active CMV infection is probable.

The detection of CMV IgM antibody by itself is not diagnostic of primary CMV infection because both CMV reactivation and exogenous reinfection may elicit a CMV IgM antibody response.

IgG avidity assays, which measure antibody maturity, can detect recent primary CMV infection. During primary

infection, the body produces low-avidity IgG, followed 2 to 4 months later by high-avidity IgG. Therefore, finding low-avidity antibodies suggests that the patient has had a recent primary CMV infection.

Research Methods with Potential Clinical Application

Delayed recovery of CMV-specific T cells predicts the risk of progressive CMV infections in transplants (121), and therefore it is of great interest to develop methods to quantify and characterize such cells. Like the case for EBV, the most widely used research methods to do this utilize HLA-peptide tetramers and functional assays that measure IFN production or degranulation (122). Many CD4 and CD8 T cell epitopes have been identified for CMV, which facilitates these approaches. CMV-specific T cells in healthy seropositive individuals exhibit a "late differentiation" phenotype ($CD45RA^+$ $CD27^-$) and lower overall frequencies of naive T cells (123). This phenotype is not observed following infection with other herpesviruses, such as herpes simplex virus (124) or EBV (48), suggesting that CMV is unique in eliciting memory T cells with this phenotype. Interestingly, this phenotype was associated with control of viral reactivation, and in patients with uncontrolled reactivations, this phenotype did not develop (125). In contrast, chronic viral replication can impair T cell responses through exhaustion via programmed death 1 (PD-1) (126). Increased expression of PD-1 was observed on CMV-specific CD8 T cells with active CMV replication (127), and antibody-mediated blockade restored function (128, 129). Expression of PD-1 and cytotoxic T lymphocyte-associated antigen 4 on CMV-specific CD4 T cells was also recently demonstrated to be a specific phenotype associated with CMV viremia in transplant recipients (130).

For measurements of functional responses, T cells are typically stimulated with viral antigens, and cytokines such as IFN-γ, tumor necrosis factor alpha, and interleukin-2 are measured using the enzyme-linked immunosorbent assay-based QuantiFERON-CMV assay, an ELISPOT assay, or flow cytometric intracellular staining (131, 132). Quantitative decreases of specific immunity are associated with symptomatic CMV infection (132–134), and a failure to reconstitute CMV-specific immunity soon after the onset of CMV viremia is associated with higher peak viral loads (135). Also, by examining cytokine production and degranulation in CMV-specific T cells, Krol and colleagues observed that IFN-γ and interleukin-2 double-producing CD8 T cells were present in patients who controlled CMV reactivation, whereas CD8 T cells that produced IFN-γ alone were present in noncontrollers (136).

For all these reasons, phenotypic and functional analyses of CMV-specific T cells are promising approaches to predict CMV reactivation episodes (137), and several studies have begun to report on the comparative precision and reproducibility of the different assays (135, 137–141). It is very likely that in the future, such assays will serve as a guide to treating patients at risk of developing progressive CMV disease.

REFERENCES

1. **Epstein MA, Achong BG, Barr YM.** 1964. Virus particles in cultured lymphoblasts from Burkitt's lymphoma. *Lancet* **i:**702–703. PubMed
2. **Henle G, Henle W, Diehl V.** 1968. Relation of Burkitt's tumor-associated herpes-type virus to infectious mononucleosis. *Proc Natl Acad Sci USA* **59:**94–101. PubMed
3. **Farrell PJ.** 2005. Epstein-Barr virus genome, p 263–287. *In* Robertson ES (ed), *Epstein-Barr Virus*. Caister Academic Press, Norfolk, England.
4. **Sample J, Young L, Martin B, Chatman T, Kieff E, Rickinson A, Kieff E.** 1990. Epstein-Barr virus types 1 and 2 differ in their EBNA-3A, EBNA-3B, and EBNA-3C genes. *J Virol* **64:**4084–4092. PubMed
5. **Chang CM, Yu KJ, Mbulaiteye SM, Hildesheim A, Bhatia K.** 2009. The extent of genetic diversity of Epstein-Barr virus and its geographic and disease patterns: a need for reappraisal. *Virus Res* **143:**209–221. PubMed
6. **Puchhammer-Stöckl E, Görzer I.** 2006. Cytomegalovirus and Epstein-Barr virus subtypes—the search for clinical significance. *J Clin Virol* **36:**239–248. PubMed
7. **Hadinoto V, Shapiro M, Sun CC, Thorley-Lawson DA.** 2009. The dynamics of EBV shedding implicate a central role for epithelial cells in amplifying viral output. *PLoS Pathog* **5:**e1000496. PubMed
8. **Nemerow GR, Wolfert R, McNaughton ME, Cooper NR.** 1985. Identification and characterization of the Epstein-Barr virus receptor on human B lymphocytes and its relationship to the C3d complement receptor (CR2). *J Virol* **55:**347–351. PubMed
9. **Speck P, Haan KM, Longnecker R.** 2000. Epstein-Barr virus entry into cells. *Virology* **277:**1–5. PubMed
10. **Xiao J, Palefsky JM, Herrera R, Berline J, Tugizov SM.** 2009. EBV BMRF-2 facilitates cell-to-cell spread of virus within polarized oral epithelial cells. *Virology* **388:**335–343. PubMed
11. **Chesnokova LS, Nishimura SL, Hutt-Fletcher LM.** 2009. Fusion of epithelial cells by Epstein-Barr virus proteins is triggered by binding of viral glycoproteins gHgL to integrins alphavbeta6 or alphavbeta8. *Proc Natl Acad Sci USA* **106:**20464–20469. PubMed
12. **Tsurumi T, Fujita M, Kudoh A.** 2005. Latent and lytic Epstein-Barr virus replication strategies. *Rev Med Virol* **15:**3–15. PubMed
13. **Ambinder RF, Lin L.** 2005. Mononucleosis in the laboratory. *J Infect Dis* **192:**1503–1504. PubMed
14. **Henderson A, Ripley S, Heller M, Kieff E.** 1983. Chromosome site for Epstein-Barr virus DNA in a Burkitt tumor cell line and in lymphocytes growth-transformed in vitro. *Proc Natl Acad Sci USA* **80:**1987–1991. PubMed
15. **Thorley-Lawson DA, Gross A.** 2004. Persistence of the Epstein-Barr virus and the origins of associated lymphomas. *N Engl J Med* **350:**1328–1337. PubMed
16. **Laichalk LL, Thorley-Lawson DA.** 2005. Terminal differentiation into plasma cells initiates the replicative cycle of Epstein-Barr virus in vivo. *J Virol* **79:**1296–1307. PubMed
17. **Balfour HH Jr, Odumade OA, Schmeling DO, Mullan BD, Ed JA, Knight JA, Vezina HE, Thomas W, Hogquist KA.** 2013. Behavioral, virologic, and immunologic factors associated with acquisition and severity of primary Epstein-Barr virus infection in university students. *J Infect Dis* **207:**80–88. PubMed
18. **Gerber P, Walsh JH, Rosenblum EN, Purcell RH.** 1969. Association of EB-virus infection with the post-perfusion syndrome. *Lancet* **i:**593–595. PubMed
19. **Alfieri C, Tanner J, Carpentier L, Perpête C, Savoie A, Paradis K, Delage G, Joncas J.** 1996. Epstein-Barr virus transmission from a blood donor to an organ transplant recipient with recovery of the same virus strain from the recipient's blood and oropharynx. *Blood* **87:**812–817. PubMed
20. **Hanto DW, Frizzera G, Purtilo DT, Sakamoto K, Sullivan JL, Saemundsen AK, Klein G, Simmons RL, Najarian JS.** 1981. Clinical spectrum of lymphoproliferative disorders in renal transplant recipients and evidence for the role of Epstein-Barr virus. *Cancer Res* **41:**4253–4261. PubMed

21. **Paya CV, Fung JJ, Nalesnik MA, Kieff E, Green M, Gores G, Habermann TM, Wiesner PH, Swinnen JL, Woodle ES, Bromberg JS.** 1999. Epstein-Barr virus-induced post-transplant lymphoproliferative disorders. ASTS/ASTP EBV-PTLD Task Force and The Mayo Clinic Organized International Consensus Development Meeting. *Transplantation* **68:**1517–1525.
22. **Chang RS, Char DF, Jones JH, Halstead SB.** 1979. Incidence of infectious mononucleosis at the Universities of California and Hawaii. *J Infect Dis* **140:**479–486. PubMed
23. **Dan R, Chang RS.** 1990. A prospective study of primary Epstein-Barr virus infections among university students in Hong Kong. *Am J Trop Med Hyg* **42:**380–385. PubMed
24. **de-Thé G, Day NE, Geser A, Lavoué MF, Ho JH, Simons MJ, Sohier R, Tukei P, Vonka V, Zavadova H.** 1975. Sero-epidemiology of the Epstein-Barr virus: preliminary analysis of an international study—a review. *IARC Sci Publ* **1975:**3–16. PubMed
25. **Lehane DE.** 1970. A seroepidemiologic study of infectious mononucleosis. The development of EB virus antibody in a military population. *JAMA* **212:**2240–2242. PubMed
26. **Balfour HH Jr, Sifakis F, Sliman JA, Knight JA, Schmeling DO, Thomas W.** 2013. Age-specific prevalence of Epstein-Barr virus infection among individuals aged 6–19 years in the United States and factors affecting its acquisition. *J Infect Dis* **208:**1286–1293. PubMed
27. **Fafi-Kremer S, Morand P, Brion JP, Pavese P, Baccard M, Germi R, Genoulaz O, Nicod S, Jolivet M, Ruigrok RW, Stahl JP, Seigneurin JM.** 2005. Long-term shedding of infectious Epstein-Barr virus after infectious mononucleosis. *J Infect Dis* **191:**985–989. PubMed
28. **Balfour HH Jr, Holman CJ, Hokanson KM, Lelonek MM, Giesbrecht JE, White DR, Schmeling DO, Webb CH, Cavert W, Wang DH, Brundage RC.** 2005. A prospective clinical study of Epstein-Barr virus and host interactions during acute infectious mononucleosis. *J Infect Dis* **192:**1505–1512. PubMed
29. **Hess RD.** 2004. Routine Epstein-Barr virus diagnostics from the laboratory perspective: still challenging after 35 years. *J Clin Microbiol* **42:**3381–3387. PubMed
30. **Ginsburg CM, Henle W, Henle G, Horwitz CA.** 1977. Infectious mononucleosis in children. Evaluation of Epstein-Barr virus-specific serological data. *JAMA* **237:**781–785. PubMed
31. **Horwitz CA, Henle W, Henle G, Goldfarb M, Kubic P, Gehrz RC, Balfour HH Jr, Fleisher GR, Krivit W.** 1981. Clinical and laboratory evaluation of infants and children with Epstein-Barr virus-induced infectious mononucleosis: report of 32 patients (aged 10–48 months). *Blood* **57:**933–938. PubMed
32. **Sprunt TP, Evans FA.** 1920. Mononuclear leucocytosis in reaction to acute infections ("infectious mononucleosis"). *Johns Hopkins Hosp Bull* **31:**410–417.
33. **Hoagland RJ.** 1952. Infectious mononucleosis. *Am J Med* **13:**158–171. PubMed
34. **Odumade OA, Hogquist KA, Balfour HH Jr.** 2011. Progress and problems in understanding and managing primary Epstein-Barr virus infections. *Clin Microbiol Rev* **24:**193–209. PubMed
35. **Rea TD, Russo JE, Katon W, Ashley RL, Buchwald DS.** 2001. Prospective study of the natural history of infectious mononucleosis caused by Epstein-Barr virus. *J Am Board Fam Pract* **14:**234–242. PubMed
36. **Auwaerter PG.** 1999. Infectious mononucleosis in middle age. *JAMA* **281:**454–459. PubMed
37. **Horwitz CA, Henle W, Henle G, Schapiro R, Borken S, Bundtzen R.** 1983. Infectious mononucleosis in patients aged 40 to 72 years: report of 27 cases, including 3 without heterophil-antibody responses. *Medicine* (Baltimore) **62:**256–262. PubMed
38. **McKinlay CA.** 1935. Infectious mononucleosis. Part I. Clinical aspects. *JAMA* **105:**761–764.
39. **Hoagland RJ.** 1960. The clinical manifestations of infectious mononucleosis: a report of two hundred cases. *Am J Med Sci* **240:**55–63. PubMed
40. **Jenson HB.** 2000. Acute complications of Epstein-Barr virus infectious mononucleosis. *Curr Opin Pediatr* **12:**263–268. PubMed
41. **Robinson RG.** 1988. Abdominal complications of infectious mononucleosis. *J Am Board Fam Pract* **1:**207–210. PubMed
42. **Bell AT, Fortune B, Sheeler R.** 2006. Clinical inquiries. What test is the best for diagnosing infectious mononucleosis? *J Fam Pract* **55:**799–802. PubMed
43. **Paul JR, Bunnell WW.** 1932. The presence of heterophile antibodies in infectious mononucleosis. *Am J Med Sci* **183:**90–103. PubMed
44. **Fisher BA, Bhalara S.** 2004. False-positive result provided by rapid heterophile antibody test in a case of acute infection with hepatitis E virus. *J Clin Microbiol* **42:**4411. PubMed
45. **Horwitz CA, Henle W, Henle G, Penn G, Hoffman N, Ward PC.** 1979. Persistent falsely positive rapid tests for infectious mononucleosis. Report of five cases with four—six-year follow-up data. *Am J Clin Pathol* **72:**807–811. PubMed
46. **Blake JM, Edwards JM, Fletcher W, McSwiggan DA, Pereira MS.** 1976. Measurement of heterophil antibody and antibodies to EB viral capsid antigen IgG and IgM in suspected cases of infectious mononucleosis. *J Clin Pathol* **29:**841–847. PubMed
47. **Downey H, McKinlay CA.** 1923. Acute lymphadenosis compared with acute lymphatic leukemia. *Arch Intern Med* **32:**82–112.
48. **Odumade OA, Knight JA, Schmeling DO, Masopust D, Balfour HH Jr, Hogquist KA.** 2012. Primary Epstein-Barr virus infection does not erode preexisting $CD8^+$ T cell memory in humans. *J Exp Med* **209:**471–478. PubMed
49. **Munger KL, Levin LI, O'Reilly EJ, Falk KI, Ascherio A.** 2011. Anti-Epstein-Barr virus antibodies as serological markers of multiple sclerosis: a prospective study among United States military personnel. *Mult Scler* **17:**1185–1193. PubMed
50. **Baldanti F, Grossi P, Furione M, Simoncini L, Sarasini A, Comoli P, Maccario R, Fiocchi R, Gerna G.** 2000. High levels of Epstein-Barr virus DNA in blood of solid-organ transplant recipients and their value in predicting post-transplant lymphoproliferative disorders. *J Clin Microbiol* **38:**613–619. PubMed
51. **Meerbach A, Wutzler P, Häfer R, Zintl F, Gruhn B.** 2008. Monitoring of Epstein-Barr virus load after hematopoietic stem cell transplantation for early intervention in post-transplant lymphoproliferative disease. *J Med Virol* **80:**441–454. PubMed
52. **Hayden RT, Hokanson KM, Pounds SB, Bankowski MJ, Belzer SW, Carr J, Diorio D, Forman MS, Joshi Y, Hillyard D, Hodinka RL, Nikiforova MN, Romain CA, Stevenson J, Valsamakis A, Balfour HH Jr, U S EBV Working Group.** 2008. Multicenter comparison of different real-time PCR assays for quantitative detection of Epstein-Barr virus. *J Clin Microbiol* **46:**157–163. PubMed
53. **WHO International Laboratory Standards and Control.** 2014. 1st WHO International Standard for Epstein-Barr Virus (EBV) for Nucleic Acid Amplification Techniques. NIBSC code 09/260. http://www.nibsc.org/documents/ifu/09-260.pdf.
54. **van Esser JW, van der Holt B, Meijer E, Niesters HG, Trenschel R, Thijsen SF, van Loon AM, Frassoni F, Bacigalupo A, Schaefer UW, Osterhaus AD, Gratama JW, Löwenberg B, Verdonck LF, Cornelissen JJ.** 2001. Epstein-Barr virus (EBV) reactivation is a frequent event

after allogeneic stem cell transplantation (SCT) and quantitatively predicts EBV-lymphoproliferative disease following T-cell-depleted SCT. *Blood* **98:**972–978. PubMed

55. **Wadowsky RM, Laus S, Green M, Webber SA, Rowe D.** 2003. Measurement of Epstein-Barr virus DNA loads in whole blood and plasma by TaqMan PCR and in peripheral blood lymphocytes by competitive PCR. *J Clin Microbiol* **41:**5245–5249. PubMed
56. **Wagner HJ, Wessel M, Jabs W, Smets F, Fischer L, Offner G, Bucsky P.** 2001. Patients at risk for development of posttransplant lymphoproliferative disorder: plasma versus peripheral blood mononuclear cells as material for quantification of Epstein-Barr viral load by using real-time quantitative polymerase chain reaction. *Transplantation* **72:**1012–1019. PubMed
57. **Rowe DT, Webber S, Schauer EM, Reyes J, Green M.** 2001. Epstein-Barr virus load monitoring: its role in the prevention and management of post-transplant lymphoproliferative disease. *Transpl Infect Dis* **3:**79–87. PubMed
58. **Stevens SJ, Pronk I, Middeldorp JM.** 2001. Toward standardization of Epstein-Barr virus DNA load monitoring: unfractionated whole blood as preferred clinical specimen. *J Clin Microbiol* **39:**1211–1216. PubMed
59. **Holman CJ, Karger AB, Mullan BD, Brundage RC, Balfour HH Jr.** 2012. Quantitative Epstein-Barr virus shedding and its correlation with the risk of posttransplant lymphoproliferative disorder. *Clin Transplant* **26:**741–747. PubMed
60. **De Souza YG, Freese UK, Greenspan D, Greenspan JS.** 1990. Diagnosis of Epstein-Barr virus infection in hairy leukoplakia by using nucleic acid hybridization and noninvasive techniques. *J Clin Microbiol* **28:**2775–2778. PubMed
61. **Resnick L, Herbst JS, Ablashi DV, Atherton S, Frank B, Rosen L, Horwitz SN.** 1988. Regression of oral hairy leukoplakia after orally administered acyclovir therapy. *JAMA* **259:**384–388. PubMed
62. **Gulley ML.** 2001. Molecular diagnosis of Epstein-Barr virus-related diseases. *J Mol Diagn* **3:**1–10. PubMed
63. **Gulley ML, Tang W.** 2010. Using Epstein-Barr viral load assays to diagnose, monitor, and prevent posttransplant lymphoproliferative disorder. *Clin Microbiol Rev* **23:**350–366. PubMed
64. **Adham M, Kurniawan AN, Muhtadi AI, Roezin A, Hermani B, Gondhowiardjo S, Tan IB, Middeldorp JM.** 2012. Nasopharyngeal carcinoma in Indonesia: epidemiology, incidence, signs, and symptoms at presentation. *Chin J Cancer* **31:**185–196. PubMed
65. **Stevens SJ, Verkuijlen SA, Hariwiyanto B, Harijadi, Paramita DK, Fachiroh J, Adham M, Tan IB, Haryana SM, Middeldorp JM.** 2006. Noninvasive diagnosis of nasopharyngeal carcinoma: nasopharyngeal brushings reveal high Epstein-Barr virus DNA load and carcinoma-specific viral BARF1 mRNA. *Int J Cancer* **119:**608–614. PubMed
66. **Kimura H, Ito Y, Kawabe S, Gotoh K, Takahashi Y, Kojima S, Naoe T, Esaki S, Kikuta A, Sawada A, Kawa K, Ohshima K, Nakamura S.** 2012. EBV-associated T/NK-cell lymphoproliferative diseases in nonimmunocompromised hosts: prospective analysis of 108 cases. *Blood* **119:**673–686. PubMed
67. **Balfour HH Jr, Hokanson KM, Schacherer RM, Fietzer CM, Schmeling DO, Holman CJ, Vezina HE, Brundage RC.** 2007. A virologic pilot study of valacyclovir in infectious mononucleosis. *J Clin Virol* **39:**16–21. PubMed
68. **Henle G, Henle W, Klein G.** 1971. Demonstration of two distinct components in the early antigen complex of Epstein-Barr virus-infected cells. *Int J Cancer* **8:**272–282. PubMed
69. **Wohlrabe P, Färber I, Wutzler P, Uhlig R.** 1989. Antibodies to Epstein-Barr virus-induced early antigens in blood donors. *Acta Virol* **33:**344–348. PubMed
70. **Li S, Deng Y, Li X, Chen QP, Liao XC, Qin X.** 2010. Diagnostic value of Epstein-Barr virus capsid antigen-IgA in nasopharyngeal carcinoma: a meta-analysis. *Chin Med J* **123:**1201–1205. PubMed
71. **Tsang RK, Vlantis AC, Ho RW, Tam JS, To KF, van Hasselt CA.** 2004. Sensitivity and specificity of Epstein-Barr virus IgA titer in the diagnosis of nasopharyngeal carcinoma: a three-year institutional review. *Head Neck* **26:**598–602. PubMed
72. **Nikoskelainen J, Neel EU, Stevens DA.** 1979. Epstein-Barr virus-specific serum immunoglobulin A as an acute-phase antibody in infectious mononucleosis. *J Clin Microbiol* **10:**75–79. PubMed
73. **Bauer G.** 2001. Simplicity through complexity: immunoblot with recombinant antigens as the new gold standard in Epstein-Barr virus serology. *Clin Lab* **47:**223–230. PubMed
74. **Sashihara J, Burbelo PD, Savoldo B, Pierson TC, Cohen JI.** 2009. Human antibody titers to Epstein-Barr Virus (EBV) gp350 correlate with neutralization of infectivity better than antibody titers to EBV gp42 using a rapid flow cytometry-based EBV neutralization assay. *Virology* **391:**249–256. PubMed
75. **Sims S, Willberg C, Klenerman P.** 2010. MHC-peptide tetramers for the analysis of antigen-specific T cells. *Expert Rev Vaccines* **9:**765–774. PubMed
76. **Letsch A, Scheibenbogen C.** 2003. Quantification and characterization of specific T-cells by antigen-specific cytokine production using ELISPOT assay or intracellular cytokine staining. *Methods* **31:**143–149. PubMed
77. **Hislop AD, Taylor GS, Sauce D, Rickinson AB.** 2007. Cellular responses to viral infection in humans: lessons from Epstein-Barr virus. *Annu Rev Immunol* **25:**587–617. PubMed
78. **Yang J, Lemas VM, Flinn IW, Krone C, Ambinder RF.** 2000. Application of the ELISPOT assay to the characterization of CD8(+) responses to Epstein-Barr virus antigens. *Blood* **95:**241–248. PubMed
79. **Vogl BA, Fagin U, Nerbas L, Schlenke P, Lamprecht P, Jabs WJ.** 2012. Longitudinal analysis of frequency and reactivity of Epstein-Barr virus-specific T lymphocytes and their association with intermittent viral reactivation. *J Med Virol* **84:**119–131. PubMed
80. **Pender MP, Csurhes PA, Pfluger CM, Burrows SR.** 2012. CD8+ T cells far predominate over CD4+ T cells in healthy immune response to Epstein-Barr virus infected lymphoblastoid cell lines. *Blood* **120:**5085–5087. PubMed
81. **Macedo C, Webber SA, Donnenberg AD, Popescu I, Hua Y, Green M, Rowe D, Smith L, Brooks MM, Metes D.** 2011. EBV-specific CD8+ T cells from asymptomatic pediatric thoracic transplant patients carrying chronic high EBV loads display contrasting features: activated phenotype and exhausted function. *J Immunol* **186:**5854–5862. PubMed
82. **Callan MF, Tan L, Annels N, Ogg GS, Wilson JD, O'Callaghan CA, Steven N, McMichael AJ, Rickinson AB.** 1998. Direct visualization of antigen-specific CD8+ T cells during the primary immune response to Epstein-Barr virus in vivo. *J Exp Med* **187:**1395–1402. PubMed
83. **Long HM, Chagoury OL, Leese AM, Ryan GB, James E, Morton LT, Abbott RJ, Sabbah S, Kwok W, Rickinson AB.** 2013. MHC II tetramers visualize human CD4+ T cell responses to Epstein-Barr virus infection and demonstrate atypical kinetics of the nuclear antigen EBNA1 response. *J Exp Med* **210:**933–949. PubMed
84. **Miller JD, van der Most RG, Akondy RS, Glidewell JT, Albott S, Masopust D, Murali-Krishna K, Mahar PL, Edupuganti S, Lalor S, Germon S, Del Rio C, Mulligan MJ, Staprans SI, Altman JD, Feinberg MB, Ahmed R.** 2008. Human effector and memory CD8+ T cell responses to smallpox and yellow fever vaccines. *Immunity* **28:**710–722. PubMed

85. **Ryan JL, Fan H, Swinnen LJ, Schichman SA, Raab-Traub N, Covington M, Elmore S, Gulley ML.** 2004. Epstein-Barr Virus (EBV) DNA in plasma is not encapsidated in patients with EBV-related malignancies. *Diagn Mol Pathol* **13:**61–68. PubMed
86. **Ribbert H.** 1904. Ueber protozoenartige Zellen in der Niere eines syphilitischen Neugeborenen und in der Parotis von Kindern. *Zentralbl Allg Pathol* **15:**945–948.
87. **Jesionek A, Kiolemenoglou B.** 1904. Ueber einen Befund von protozoenartigen Gebilden in den Organen eines hereditar-luetischen Foetus. *Munch Med Wochenschr* **51:**1905–1907.
88. **Vonglahn WC, Pappenheimer AM.** 1925. Intranuclear inclusions in visceral disease. *Am J Pathol* **1:**445–466.3. PubMed
89. **Lipschuetz B.** 1921. Untersuchungen ueber die Aetiologie der Krankheiten der Herpes genitalis. *Arch Dermatol Syph* **136:**428–482.
90. **Wyatt JP, Saxton J, Lee RS, Pinkerton H.** 1950. Generalized cytomegalic inclusion disease. *J Pediatr* **36:**271–294. PubMed
91. **Fetterman GH.** 1952. A new laboratory aid in the clinical diagnosis of inclusion disease of infancy. *Am J Clin Pathol* **22:**424–425. PubMed
92. **Minder WH.** 1953. Die Atiologie der Cytomegalia infantium. *Schweiz Med Wochenschr* **83:**1180–1182. PubMed
93. **Enders JF, Weller TH, Robbins FC.** 1949. Cultivation of the Lansing strain of poliomyelitis virus in cultures of various human embryonic tissues. *Science* **109:**85–87. PubMed
94. **Smith MG.** 1956. Propagation in tissue cultures of a cytopathogenic virus from human salivary gland virus (SGV) disease. *Proc Soc Exp Biol Med* **92:**424–430. PubMed
95. **Rowe WP, Hartley JW, Waterman S, Turner HC, Huebner RJ.** 1956. Cytopathogenic agent resembling human salivary gland virus recovered from tissue cultures of human adenoids. *Proc Soc Exp Biol Med* **92:**418–424. PubMed
96. **Craig JM, Macauley JC, Weller TH, Wirth P.** 1957. Isolation of intranuclear inclusion producing agents from infants with illnesses resembling cytomegalic inclusion disease. *Proc Soc Exp Biol Med* **94:**4–12. PubMed
97. **Sylwester AW, Mitchell BL, Edgar JB, Taormina C, Pelte C, Ruchti F, Sleath PR, Grabstein KH, Hosken NA, Kern F, Nelson JA, Picker LJ.** 2005. Broadly targeted human cytomegalovirus-specific CD4+ and CD8+ T cells dominate the memory compartments of exposed subjects. *J Exp Med* **202:**673–685. PubMed
98. **Bancroft GJ, Shellam GR, Chalmer JE.** 1981. Genetic influences on the augmentation of natural killer (NK) cells during murine cytomegalovirus infection: correlation with patterns of resistance. *J Immunol* **126:**988–994. PubMed
99. **Starr SE, Garrabrant T.** 1981. Natural killing of cytomegalovirus-infected fibroblasts by human mononuclear leucocytes. *Clin Exp Immunol* **46:**484–492. PubMed
100. **Wilkinson GW, Tomasec P, Stanton RJ, Armstrong M, Prod'homme V, Aicheler R, McSharry BP, Rickards CR, Cochrane D, Llewellyn-Lacey S, Wang EC, Griffin CA, Davison AJ.** 2008. Modulation of natural killer cells by human cytomegalovirus. *J Clin Virol* **41:**206–212. PubMed
101. **Marshall EE, Geballe AP.** 2009. Multifaceted evasion of the interferon response by cytomegalovirus. *J Interferon Cytokine Res* **29:**609–619. PubMed
102. **Bunde T, Kirchner A, Hoffmeister B, Habedank D, Hetzer R, Cherepnev G, Proesch S, Reinke P, Volk HD, Lehmkuhl H, Kern F.** 2005. Protection from cytomegalovirus after transplantation is correlated with immediate early 1-specific CD8 T cells. *J Exp Med* **201:**1031–1036. PubMed
103. **Gerna G, Lilleri D, Fornara C, Comolli G, Lozza L, Campana C, Pellegrini C, Meloni F, Rampino T.** 2006. Monitoring of human cytomegalovirus-specific CD4 and CD8 T-cell immunity in patients receiving solid organ transplantation. *Am J Transplant* **6:**2356–2364. PubMed
104. **Gerdemann U, Katari UL, Papadopoulou A, Keirnan JM, Craddock JA, Liu H, Martinez CA, Kennedy-Nasser A, Leung KS, Gottschalk SM, Krance RA, Brenner MK, Rooney CM, Heslop HE, Leen AM.** 2013. Safety and clinical efficacy of rapidly-generated trivirus-directed T cells as treatment for adenovirus, EBV, and CMV infections after allogeneic hematopoietic stem cell transplant. *Mol Ther* **21:**2113–2121. PubMed
105. **Moss P.** 2010. The emerging role of cytomegalovirus in driving immune senescence: a novel therapeutic opportunity for improving health in the elderly. *Curr Opin Immunol* **22:**529–534. PubMed
106. **Derhovanessian E, Maier AB, Hähnel K, Zelba H, de Craen AJ, Roelofs H, Slagboom EP, Westendorp RG, Pawelec G.** 2013. Lower proportion of naive peripheral CD8+ T cells and an unopposed pro-inflammatory response to human cytomegalovirus proteins in vitro are associated with longer survival in very elderly people. *Age* (Dordr) **35:**1387–1399. PubMed
107. **Limaye AP, Boeckh M.** 2010. CMV in critically ill patients: pathogen or bystander? *Rev Med Virol* **20:**372–379. PubMed
108. **Fishman JA, Emery V, Freeman R, Pascual M, Rostaing L, Schlitt HJ, Sgarabotto D, Torre-Cisneros J, Uknis ME.** 2007. Cytomegalovirus in transplantation—challenging the status quo. *Clin Transplant* **21:**149–158. PubMed
109. **Dollard SC, Grosse SD, Ross DS.** 2007. New estimates of the prevalence of neurological and sensory sequelae and mortality associated with congenital cytomegalovirus infection. *Rev Med Virol* **17:**355–363. PubMed
110. **Kenneson A, Cannon MJ.** 2007. Review and meta-analysis of the epidemiology of congenital cytomegalovirus (CMV) infection. *Rev Med Virol* **17:**253–276. PubMed
111. **Iwasenko JM, Howard J, Arbuckle S, Graf N, Hall B, Craig ME, Rawlinson WD.** 2011. Human cytomegalovirus infection is detected frequently in stillbirths and is associated with fetal thrombotic vasculopathy. *J Infect Dis* **203:**1526–1533. PubMed
112. **Smith JM, Corey L, Bittner R, Finn LS, Healey PJ, Davis CL, McDonald RA.** 2010. Subclinical viremia increases risk for chronic allograft injury in pediatric renal transplantation. *J Am Soc Nephrol* **21:**1579–1586. PubMed
113. **Li L, Chaudhuri A, Weintraub LA, Hsieh F, Shah S, Alexander S, Salvatierra O Jr, Sarwal MM.** 2007. Subclinical cytomegalovirus and Epstein-Barr virus viremia are associated with adverse outcomes in pediatric renal transplantation. *Pediatr Transplant* **11:**187–195. PubMed
114. **Courivaud C, Bamoulid J, Chalopin JM, Gaiffe E, Tiberghien P, Saas P, Ducloux D.** 2013. Cytomegalovirus exposure and cardiovascular disease in kidney transplant recipients. *J Infect Dis* **207:**1569–1575. PubMed
115. **Scott GM, Naing Z, Pavlovic J, Iwasenko JM, Angus P, Jones R, Rawlinson WD.** 2011. Viral factors influencing the outcome of human cytomegalovirus infection in liver transplant recipients. *J Clin Virol* **51:**229–233. PubMed
116. **Emery VC, Sabin CA, Cope AV, Gor D, Hassan-Walker AF, Griffiths PD.** 2000. Application of viral-load kinetics to identify patients who develop cytomegalovirus disease after transplantation. *Lancet* **355:**2032–2036. PubMed

117. **Razonable RR, Hayden RT.** 2013. Clinical utility of viral load in management of cytomegalovirus infection after solid organ transplantation. *Clin Microbiol Rev* **26:**703–727. PubMed
118. **Kaden J, Zenker S, Eichler C, Groth J, May G, Strobelt V, Oesterwitz H, Scholz D, Lippert J, Adamczyk G.** 1991. Risk of CMV infection and illness after kidney transplantation. *Allerg Immunol* (Leipz) **37:**47–58. PubMed
119. **Humar A, Mazzulli T, Moussa G, Razonable RR, Paya CV, Pescovitz MD, Covington E, Alecock E, Valganciclovir Solid Organ Transplant Study Group.** 2005. Clinical utility of cytomegalovirus (CMV) serology testing in high-risk CMV D+/R[minus] transplant recipients. *Am J Transplant* **5:**1065–1070. PubMed
120. **Paya CV, Smith TF, Ludwig J, Hermans PE.** 1989. Rapid shell vial culture and tissue histology compared with serology for the rapid diagnosis of cytomegalovirus infection in liver transplantation. *Mayo Clin Proc* **64:**670–675. PubMed
121. **Gratama JW, Boeckh M, Nakamura R, Cornelissen JJ, Brooimans RA, Zaia JA, Forman SJ, Gaal K, Bray KR, Gasior GH, Boyce CS, Sullivan LA, Southwick PC.** 2010. Immune monitoring with iTAg MHC tetramers for prediction of recurrent or persistent cytomegalovirus infection or disease in allogeneic hematopoietic stem cell transplant recipients: a prospective multicenter study. *Blood* **116:**1655–1662. PubMed
122. **Egli A, Humar A, Kumar D.** 2012. State-of-the-art monitoring of cytomegalovirus-specific cell-mediated immunity after organ transplant: a primer for the clinician. *Clin Infect Dis* **55:**1678–1689. PubMed
123. **Almanzar G, Schwaiger S, Jenewein B, Keller M, Herndler-Brandstetter D, Würzner R, Schönitzer D, Grubeck-Loebenstein B.** 2005. Long-term cytomegalovirus infection leads to significant changes in the composition of the $CD8^+$ T-cell repertoire, which may be the basis for an imbalance in the cytokine production profile in elderly persons. *J Virol* **79:**3675–3683. PubMed
124. **Derhovanessian E, Maier AB, Hähnel K, Beck R, de Craen AJ, Slagboom EP, Westendorp RG, Pawelec G.** 2011. Infection with cytomegalovirus but not herpes simplex virus induces the accumulation of late-differentiated CD4+ and CD8+ T-cells in humans. *J Gen Virol* **92:**2746–2756. PubMed
125. **Moins-Teisserenc H, Busson M, Scieux C, Bajzik V, Cayuela JM, Clave E, de Latour RP, Agbalika F, Ribaud P, Robin M, Rocha V, Gluckman E, Charron D, Socié G, Toubert A.** 2008. Patterns of cytomegalovirus reactivation are associated with distinct evolutive profiles of immune reconstitution after allogeneic hematopoietic stem cell transplantation. *J Infect Dis* **198:**818–826. PubMed
126. **Wherry EJ.** 2011. T cell exhaustion. *Nat Immunol* **12:**492–499. PubMed
127. **La Rosa C, Krishnan A, Longmate J, Martinez J, Manchanda P, Lacey SF, Limaye AP, Diamond DJ.** 2008. Programmed death-1 expression in liver transplant recipients as a prognostic indicator of cytomegalovirus disease. *J Infect Dis* **197:**25–33. PubMed
128. **Sester U, Presser D, Dirks J, Gärtner BC, Köhler H, Sester M.** 2008. PD-1 expression and IL-2 loss of cytomegalovirus-specific T cells correlates with viremia and reversible functional anergy. *Am J Transplant* **8:**1486–1497. PubMed
129. **Dirks J, Egli A, Sester U, Sester M, Hirsch HH.** 2013. Blockade of programmed death receptor-1 signaling restores expression of mostly proinflammatory cytokines in anergic cytomegalovirus-specific T cells. *Transpl Infect Dis* **15:**79–89. PubMed
130. **Dirks J, Tas H, Schmidt T, Kirsch S, Gartner BC, Sester U, Sester M.** 2013. PD-1 analysis on CD28([minus]) CD27([minus]) CD4 T cells allows stimulation-independent assessment of CMV viremic episodes in transplant recipients. *Am J Transplant* **13:**3132–3141.
131. **Kotton CN, Kumar D, Caliendo AM, Asberg A, Chou S, Danziger-Isakov L, Humar A, Transplantation Society International CMV Consensus Group.** 2013. Updated international consensus guidelines on the management of cytomegalovirus in solid-organ transplantation. *Transplantation* **96:**333–360. PubMed
132. **Sester M, Sester U, Gärtner B, Heine G, Girndt M, Mueller-Lantzsch N, Meyerhans A, Köhler H.** 2001. Levels of virus-specific CD4 T cells correlate with cytomegalovirus control and predict virus-induced disease after renal transplantation. *Transplantation* **71:**1287–1294. PubMed
133. **Walker S, Fazou C, Crough T, Holdsworth R, Kiely P, Veale M, Bell S, Gailbraith A, McNeil K, Jones S, Khanna R.** 2007. Ex vivo monitoring of human cytomegalovirus-specific CD8+ T-cell responses using QuantiFERON-CMV. *Transpl Infect Dis* **9:**165–170. PubMed
134. **Westall G, Kotsimbos T, Brooks A.** 2006. CMV-specific CD8 T-cell dynamics in the blood and the lung allograft reflect viral reactivation following lung transplantation. *Am J Transplant* **6:**577–584. PubMed
135. **Tey SK, Kennedy GA, Cromer D, Davenport MP, Walker S, Jones LI, Crough T, Durrant ST, Morton JA, Butler JP, Misra AK, Hill GR, Khanna R.** 2013. Clinical assessment of anti-viral CD8+ T cell immune monitoring using QuantiFERON-CMV® assay to identify high risk allogeneic hematopoietic stem cell transplant patients with CMV infection complications. *PLoS One* **8:**e74744. PubMed
136. **Król L, Stuchlý J, Hubáček P, Keslová P, Sedláček P, Starý J, Hrušák O, Kalina T.** 2011. Signature profiles of CMV-specific T-cells in patients with CMV reactivation after hematopoietic SCT. *Bone Marrow Transplant* **46:**1089–1098. PubMed
137. **Egli A, Humar A, Kumar D.** 2012. State-of-the-art monitoring of cytomegalovirus-specific cell-mediated immunity after organ transplant: a primer for the clinician. *Clin Infect Dis* **55:**1678–1689. PubMed
138. **Ravkov EV, Pavlov IY, Hanson KE, Delgado JC.** 2012. Validation of cytomegalovirus immune competence assays for the characterization of CD8(+) T cell responses posttransplant. *Clin Dev Immunol* **2012:**451059. PubMed
139. **Maecker HT, Hassler J, Payne JK, Summers A, Comatas K, Ghanayem M, Morse MA, Clay TM, Lyerly HK, Bhatia S, Ghanekar SA, Maino VC, Delarosa C, Disis ML.** 2008. Precision and linearity targets for validation of an IFNgamma ELISPOT, cytokine flow cytometry, and tetramer assay using CMV peptides. *BMC Immunol* **9:**9. PubMed
140. **Borchers S, Bremm M, Lehrnbecher T, Dammann E, Pabst B, Wölk B, Esser R, Yildiz M, Eder M, Stadler M, Bader P, Martin H, Jarisch A, Schneider G, Klingebiel T, Ganser A, Weissinger EM, Koehl U.** 2012. Sequential anti-cytomegalovirus response monitoring may allow prediction of cytomegalovirus reactivation after allogeneic stem cell transplantation. *PLoS One* **7:**e50248. PubMed
141. **Abu-Khader A, Krause S.** 2013. Rapid monitoring of immune reconstitution after allogeneic stem cell transplantation—a comparison of different assays for the detection of cytomegalovirus-specific T cells. *Eur J Haematol* **91:**534–545. PubMed

Human Herpesviruses 6, 7, and 8

RICHARD L. HODINKA

61

Herpesviruses 6, 7, and 8 are the most recently described members of the human herpesvirus family. Like other herpesviruses, they have the ability to establish a latent or persistent infection following primary infection, and reactivation may occur in healthy and immunocompromised people in response to different stimuli. A variety of methods are available or under development for the laboratory diagnosis of each virus, including viral isolation in cell culture, demonstration of viral antigens or nucleic acids in body fluids or tissues, and serology for detection of virus-specific antibodies. This chapter focuses on the immunologic and molecular diagnosis and monitoring of infections with human herpesvirus 6 (HHV-6), HHV-7, and HHV-8, and provides information on the unique features of the epidemiology and biological and clinical characteristics of these viruses.

HHV-6

Introduction

HHV-6 is a lymphotropic virus which was discovered in 1986 in cultures of lymphocytes from patients with lymphoproliferative disorders and AIDS. Since that time, much has been learned about the biology, epidemiology, clinical features, and diagnosis of HHV-6, and a number of comprehensive reviews have been published (see references 1 to 6 for examples of reviews).

HHV-6 is similar in morphology to other known human herpesviruses but is genetically and serologically distinct (Table 1). The completed virion has a diameter of 160 to 200 nm and consists of an internal core containing double-stranded DNA of approximately 160 to 170 kb and an icosahedral nucleocapsid surrounded by a tegument and a protein-spiked envelope. The virus has a primary cell tropism for mature $CD4^+$ T lymphocytes but also infects $CD8^+$ T cells, natural killer (NK) cells, monocytes, macrophages, megakaryocytes, epithelial cells, endothelial cells, fibroblasts, and neural cells. CD46 has been identified as part of the cellular receptor for infection; this marker is expressed on the surfaces of many human cell types, leading to the broad cellular tropism of HHV-6. Viral replication occurs in the nucleus of the host cell, and the viral envelope is acquired during maturation within cytoplasmic vacuoles before budding of the completed virus from the host cell membrane.

The DNA genome of HHV-6 differs from that of other human herpesviruses by both restriction mapping and nucleic acid hybridization and is unique in that it has a significantly lower guanine-plus-cytosine content at 43 to 44%. Regions of sequence homology between HHV-6 and cytomegalovirus (CMV) have been identified, and HHV-6 is now classified with CMV among the betaherpesviruses. Together with HHV-7, it is a member of the genus *Roseolovirus*. Genetic polymorphism among different isolates of HHV-6 exists, and evidence suggests that HHV-6 isolates form two distinct but very closely related groups (variants A and B) that differ in molecular, biological, and clinical properties. Most isolates of HHV-6 from patients with symptomatic primary infections have been of variant B. Variant A has been isolated or detected only rarely in children with primary HHV-6 infection, with the exception of African children with febrile illnesses. Both variants have been isolated from immunocompromised individuals, including AIDS patients, transplant recipients, and patients with leukemia; dual infections with both variants also have been described. Variant A is seen more frequently in patients with human immunodeficiency virus (HIV) infection, and it may be more neurotropic than variant B. Otherwise, an etiologic role for variant A in causing disease has not been clearly identified. Recently, HHV-6A and HHV-6B have been formally classified as distinct virus species by the International Committee on Virus Taxonomy.

The HHV-6 genome has a coding capacity of approximately 100 to 120 proteins, and a number of polypeptides ranging in size from 30 to 220 kDa, including six or seven glycoproteins, have been identified. A 101-kDa nucleocapsid protein was found to be highly reactive with human sera by Western immunoblotting and appears to be a specific marker for HHV-6 infection. A set of five monoclonal antibodies has been developed and used to identify nine proteins designated gp105 and gp82; gp116, gp64, and gp54; gp102; p41 and p110; and p135.

A unique feature of the DNA genome of HHV-6 is that it can integrate into the subtelemeric region of host cell chromosomes in approximately 1% of the human population (see references 7 and 8 for reviews). This chromosomally integrated form of HHV-6 DNA is passed from parent to child through the germline, and both HHV-6A and HHV-6B can integrate into the chromosomes. Because the viral genome can be found in every human somatic and germ cell in the body, individuals with chromosomally integrated HHV-6 will have very high levels of HHV-6 DNA in blood and tissues.

doi:10.1128/9781555818722.ch61

TABLE 1 Biological characteristics of HHV-6, HHV-7, and HHV-8

Characteristics	HHV-6	HHV-7	HHV-8
Family *Herpesviridae*			
Subfamily	*Betaherpesvirinae*	*Betaherpesvirinae*	*Gammaherpesvirinae*
Genus	*Roseolovirus*	*Roseolovirus*	*Rhadinovirus*
Properties			
Genome (linear double-stranded DNA)	~159 kb; encodes 110–120 proteins	~145 kb; encodes at least 70 proteins	~165 kb; 97 genes identified
DNA relatedness (% homology)	CMV (66%)	HHV-6 (50-60%)	Herpes saimiri (51%), EBV (39%)
Species/strains	Species HHV-6A, HHV-6B	Unknown	HHV-8 strains A, B, and C
Cell tropism *in vitro*	$CD4^+$ T lymphocytes, NK cells, macrophages, $CD8^+$ T cells, megakaryocytes, neural and epithelial cells	$CD4^+$T lymphocytes	$CD19^+$ B lymphocytes, spindle cells, endothelial cells
Virus interactions	EBV, CMV, HIV, parvovirus B19, human papillomaviruses	HHV-6, CMV, HIV	EBV, HIV

The clinical consequences of this are not fully understood, and chromosomal integration is often mistaken for active infection and unnecessarily treated with antiviral drugs.

Similar to cases of CMV and Epstein-Barr virus (EBV) infection, infections with HHV-6 are common and often mild or inapparent; however, HHV-6 is now recognized as the causative agent of roseola (roseola infantum, exanthem subitum, sixth disease) in children aged 6 months to 3 years (see reference 9 for a review). The disease presents with an onset of high fever (39 to 40°C) for 3 to 5 days that resolves abruptly and is followed by the appearance of an erythematous, blanching, maculopapular, nonpruritic rash beginning on the neck or trunk and spreading to the face and other areas of the body. The rash usually lasts for 1 to 3 days, and there are no subsequent desquamation or pigment changes. Recovery is usually rapid and without complications. Interestingly, most cases of acute primary HHV-6 infection in young children do not result in an illness recognizable as roseola. Studies have revealed that acute viremic HHV-6 infection accounts for 14% of febrile children younger than 2 years seen in an emergency room, most of whom have a nonspecific febrile illness without a rash. Other clinical manifestations of primary infection include rash without fever, fever of >40°C, intussusception, bulging of the anterior fontanelle, lymphadenopathy, hepatitis, an infectious mononucleosis-like syndrome, inflamed tympanic membranes, myocarditis, aseptic meningitis, meningoencephalitis, and encephalitis (see references 10 to 14 for reviews). Febrile seizures are a common complication of roseola; approximately one-third of all febrile seizures in childhood have been attributed to HHV-6 infection. Primary infection in adults is rare but may result in prolonged lymphadenopathy, hepatitis, encephalitis of variable severity, or an illness resembling infectious mononucleosis. Reactivated infection in healthy persons is asymptomatic. It remains to be fully established whether HHV-6 causes or contributes to disease in immunocompromised hosts, although reactivation of clinical importance in recipients of hematopoietic stem cell and solid-organ transplantation has been associated with isolated fever, hepatitis, leukopenia, delayed engraftment, neurologic dysfunction, skin rashes resembling graft-versus-host disease, bone marrow suppression, and interstitial pneumonitis (see references 15 to 20 for reviews). Also, reactivation of HHV-6 has been associated with the pathogenesis of drug-induced hypersensitivity syndrome or drug rash with eosinophilia and systemic symptoms syndrome. Evidence suggests that HHV-6 infection may contribute to disease progression with HIV type 1 (HIV-1) and may interact with other viruses, such as CMV, EBV, parvovirus B19, and human papillomaviruses, to affect their behavior and exacerbate disease. HHV-6 has also been associated with a number of other diseases in patients in whom elevated titers of HHV-6 antibody have been detected and from whom replicating virus was isolated and/or viral antigens or DNA was found. The role of the virus in most of these clinical settings, however, remains unproven and controversial.

HHV-6 is a ubiquitous virus, and humans are the only known natural host (Table 2). The mode of transmission of the virus is poorly understood but presumably requires direct, personal contact. Virus has been identified in saliva, peripheral blood mononuclear cells (PBMC), cervical and vaginal secretions, urine, and various tissues, including skin, lymph nodes, liver, spleen, heart, lungs, kidneys, and brain. HHV-6B, but not HHV-6A, actively replicates in the salivary glands of children and adults, making oral secretions the most likely source of transmission for this species. Intrauterine or perinatal transmission has been suggested. Congenital infections with HHV-6 have been described to occur in 1% of births; infected infants are asymptomatic at birth, in contrast to the acute febrile illnesses observed with primary postnatal infection (3). In this study, species A was responsible for one-third of the congenital infections, whereas species B was observed in all postnatal infections. The incidence of antibody to HHV-6 is high throughout the world, although variation in seroprevalence based on age and the serologic method employed has been reported. Newborn infants have titers of antibody to HHV-6 that are comparable to those in adults, suggesting passive transfer of transplacental maternal antibodies. With the loss of maternal antibody, the seroprevalence to HHV-6 decreases significantly by 4 to 6 months of age but subsequently rises to 90% at the end of

TABLE 2 Epidemiologic and clinical characteristics of HHV-6, HHV-7, and HHV-8

Characteristics	HHV-6	HHV-7	HHV-8
Epidemiology			
Distribution	Worldwide	Worldwide	Worldwide
Natural host	Human	Human	Human
Transmission	Oral secretions (HHV-6B only); possible blood and urine; intrauterine and perinatal transmission	Oral secretions; possibly blood and urine	Predominantly sexual contact; possibly oral secretions and blood; transplanted allograft
Seroprevalence	90% or greater	80–90%	0–25% in healthy American and European blood donors; higher in some African and Mediterranean populations; 75–95% of KS patients
Population affected	Infants (0–3 yr), organ transplant recipients	Infants (1–5 yr)	Homosexual or bisexual HIV^+ males or their sexual partners; Mediterranean males; Africans; organ transplant recipients
Incubation period	9–10 days	Unknown	Unknown
Attributable clinical illnesses	Exanthem subitum, infantile febrile illnesses without rash, rash without fever, febrile seizures, infectious mononucleosis-like illness in adults, posttransplantation and central nervous system diseases, hepatitis, drug-induced hypersensitivity syndrome/ drug rash with eosinophilia and systemic symptoms, malignancies	Exanthem subitum, infantile febrile illnesses without rash, febrile seizures, other neurologic events in children, pityriasis rosea (?)	KS, multicentric Castleman disease, primary effusion lymphoma, herpesvirus inflammatory cytokine syndrome

the first year of life. By 3 years of age, almost 100% of individuals have antibody to HHV-6; immunity is maintained throughout childhood, adolescence, and early adulthood but may decline after 40 years of age and then rise to high titers following increased rates of reactivation in elderly persons. With the exception of HHV-7, no significant serologic cross-reactivity between different herpesviruses and HHV-6 has been detected.

Immunology of HHV-6 Infection

The host response to HHV-6 infection is thought to involve both humoral and cell-mediated immunity. Children with exanthem subitum develop an immunoglobulin M (IgM) response on day 4 of illness, and the response peaks between 7 and 14 days and declines over a period of 1 to 2 months. In addition, IgM antibodies to HHV-6 can persist for extended periods after a primary infection and can reappear in reactivated infections. IgG appears on day 7 of illness, peaks at approximately 4 weeks, and persists for long periods.

The role of cell-mediated immunity in HHV-6 infections is less well defined. However, the virus appears to have the ability to modulate or alter the expression of a number of cytokines and immune activation molecules. Increased levels of alpha interferon (IFN-α) have been found during the febrile phase of exanthem subitum, while an increase in NK cell activity has been observed during the exanthem period. *In vitro* infection of PBMC with HHV-6 decreases the expression of interleukin 2 (IL-2) and cell proliferation, upregulates NK cell cytotoxicity, and induces the synthesis of the soluble cytokines IFN-γ, IL-1β, tumor necrosis factor alpha, and IL-15. The virus can downregulate CD3, CD46, and CXCR4 expression and upregulate the chemokine receptor CCR7 in infected T cells and can stimulate IL-10 and IL-12 expression in monocytes and macrophages. Also, HHV-6 infection of transformed T-cell lines *in vitro* results in an enhanced susceptibility to apoptosis. The significance of these immunomodulating properties to the interaction of infected T cells with other components of the immune system and to the pathogenesis of the virus is unclear. Macrophages are infected with HHV-6 following primary infection and may serve as a reservoir for reactivation of the virus.

Clinical Indications

Although a diagnosis of exanthem subitum in a child can be made on the basis of clinical presentation alone, laboratory confirmation is needed to detect atypical and more severe manifestations of HHV-6 infection and to more clearly define the role of HHV-6 in other childhood illnesses and in diseases of adults and immunocompromised persons (see references 21 and 22 for reviews). Various diagnostic methods can be used, including viral isolation in cell culture, demonstration of viral antigens or nucleic acids in body fluids or tissues, and serology for detection of virus-specific antibodies (Table 3).

Immunologic Diagnosis

Antigen Detection

Immunohistochemistry

Monoclonal antibodies suitable for the direct detection of HHV-6 antigens by immunofluorescence have been developed and employed with tissue samples (1). Some are

TABLE 3 Diagnostic methods for HHV-6, HHV-7, and HHV-8

Method	HHV-6	HHV-7	HHV-8
Virus culture	PBMC grown in primary culture or cocultured with CBC or donor PBMC; culture in continuous T-cell lines (HSB-2, MOLT-3, Sup-T1, J-Jhan, MT-4, ET62); spin amplification shell vial assay	PBMC grown in primary culture or cocultured with CBC or donor PBMC; culture in continuous T-cell line (Sup-T1)	Not available; $CD19^+$ B cells, BB19 papillomavirus-transformed endothelial cells, and adenovirus-transformed human kidney epithelial cell line 293 have been used to attempt culture without success
Antigen detection	Immunohistochemistry (IHC), EIA	IHC	IHC
Antibody detection	IgG and IgM by IFA, ACIF, EIA, NT test, and immunoblotting; IgG antibody avidity assay	IgG and IgM by IFA, EIA, NT, and immunoblotting	IgG by IFA using latent or lytic cells; IgG by EIA using whole-virus lysates and recombinant proteins; immunoblotting using latent and lytic recombinant proteins
Nucleic acid detection	Qualitative and quantitative real-time PCR from whole blood, PBMC, plasma, serum, and CSF; multiplex assays with other herpesviruses; reverse transcriptase PCR for mRNA transcripts	Qualitative and quantitative real-time PCR from whole blood, PBMC, plasma and serum; multiplex assays with other herpesviruses	Qualitative and quantitative real-time PCR; tissues, whole blood, PBMC, plasma, serum; urine, saliva, bone marrow, semen

available commercially and react with HHV-6A and/or HHV-6B, although discrimination of the two species is not necessary for clinical purposes. HHV-6 antigen has been demonstrated in biopsy material from allografts of kidney transplant patients, lung tissue from bone marrow transplant recipients with interstitial pneumonitis, cervical lymph nodes of patients with histiocytic necrotizing lymphadenitis and lymphoma, oligodendrocytes from patients with multiple sclerosis, abortive villous tissues from spontaneous abortions, patients with AIDS, and the salivary and bronchial glands of latently infected individuals. Productive infection of tissues with HHV-6 can be detected by using monoclonal antibodies reactive against the structural protein p101 of species B and the structural protein gp82 of species A. More recently, an HHV-6 antigenemia assay similar to that described for detecting CMV has been developed to monitor active HHV-6 infection in liver and allogeneic stem cell transplant recipients (23, 24). This immunohistochemical method involves the cytocentrifugation of purified PBMC onto microscope slides followed by the detection of HHV-6-specific early and structural antigens by monoclonal antibodies and indirect immunoperoxidase staining. The significance of the results from immunohistochemical testing is still unclear, and the results must be further validated and correlated with clinical findings and data obtained from other laboratory tests.

EIA

A commercial antigen capture enzyme immunoassay (EIA) has been developed for the detection of HHV-6 antigens directly from clinical specimens (25). The assay is based on the gp116-gp64-gp54 antigen and is specific for HHV-6 species A and B. The EIA has a sensitivity similar to that of viral culture from plasma obtained from children with exanthem subitum. Additional studies are needed to determine the utility of this EIA for rapid diagnosis of HHV-6 infection and for monitoring of HHV-6 activity in the immunocompromised host. The EIA has the advantages of being relatively simple and inexpensive to perform relative to culture or nucleic acid detection methods.

Viral Identification in Conventional Cell Culture

HHV-6 can be isolated from PBMC grown in primary culture or by cocultivation of these cells with stimulated cord blood cells (CBC) or donor PBMC (26) and has been considered the reference method for the diagnosis of active infection. Saliva and other body fluids and tissues can be cocultured with activated donor cells for isolation of the virus as well. The optimal time for collection of specimens from children with roseola is during the febrile phase, before the development of rash. Infected PBMC show a specific cytopathic effect, with intracytoplasmic and intranuclear inclusion bodies appearing within 7 to 10 days. The cytopathic effect on primary isolation can be subtle and difficult to recognize, and virus production from infected cells should be confirmed by detection of viral antigens, *in situ* hybridization, or electron microscopy. Viral antigens can be detected by indirect immunofluorescence assay (IFA), anticomplement immunofluorescence (ACIF), or EIA with commercially available reagents or kits. IFA staining reveals a characteristic granular nuclear and cytoplasmic fluorescence in infected cells. The sensitivity and specificity of immunologic reagents for confirmation of viral growth have not been extensively studied, and it is recommended that appropriate antigen and antibody controls be used when attempting to identify infected cells. HHV-6 infects a number of established continuous T-cell lines, most notably HSB-2, MOLT-3, Sup-T1, J-Jhan, MT-4, and ET62, which are used mainly to grow virus following primary isolation. The two species can be differentiated in culture by their growth in different cell lines; species B strains of HHV-6 do not replicate in HSB-2 cells, and species A strains do not replicate in MOLT-3 cells. The described culture methods are insensitive, slow, and labor-intensive and require a high level of technical expertise. Their routine use in clinical laboratories is quite limited and they are primarily performed for research purposes.

Spin Amplification Shell Vial Assay

The human diploid lung fibroblast line MRC-5 has been reported to support primary virus isolation and has been used

in a centrifugation-assisted shell vial amplification assay for the detection of the immediate-early antigen of HHV-6 from PBMC of patients (27). Panspecific polyclonal and monoclonal antibodies to the immediate-early antigen of species A and B of HHV-6 and monoclonal antibodies specific to either species A or B are commercially available; they stain the nucleus of infected MRC-5 cells as early as 12 h after infection and give maximum staining within 48 to 72 h of infection. In the assay, PBMC are obtained from heparinized whole blood by Ficoll-Hypaque density gradient centrifugation, washed once with Hanks' balanced salt solution, and resuspended in 1 ml of RPMI 1640 medium supplemented with 10% fetal bovine serum, 20 mM HEPES, and 2 μg of Polybrene per ml. MRC-5 cells are grown to confluency on 12-mm-diameter round coverslips in 1-dram (3.7-ml) vials and inoculated with 0.5 ml of specimen to each of two vials. After inoculation, the vials are centrifuged at 800 × *g* for 45 min at 25°C, and then 1.5 ml of RPMI 1640 medium is added as described above. The cultures are incubated at 37°C for 48 to 72 h, fixed in cold (−20°C) acetone for 10 min, and stained by IFA. Uninfected and HHV-6-infected monolayers are included as negative and positive controls, respectively. The monolayers are counterstained with Evans blue. Coverslips are scanned at magnifications of ×200 to ×250 with a fluorescence microscope, and specific staining is confirmed at ×400 to ×630. Staining of immediate-early antigen occurs in the nucleus of an infected fibroblast and appears as a speckled or an even matte green fluorescence. The spin amplification shell vial assay has the important features of being more rapid and less labor-intensive than conventional culture, but the sensitivity and specificity of this assay are not well defined.

In general, positive culture results are most useful to diagnose primary infection but can be difficult to interpret for immunocompromised hosts and during reactivation of the virus, when the presence of the virus may be unrelated to the clinical presentation. As with conventional cell culture, spin amplification cultures have limited utility and are not routinely used in most clinical laboratories.

Antibody Detection

A number of tests have been developed for the serodiagnosis of HHV-6 infection, of which IFA, ACIF, EIA, and the neutralization (NT) test have been most commonly employed (see references 1 and 26 for reviews). The method that is chosen depends on the volume of specimens, turnaround time, cost, equipment needs, ease of performance, reagent availability, and levels of assay sensitivity and specificity. Some commercial reagents and kits are available from a limited number of manufacturers. Overall, variation in the rates of seropositivity for HHV-6 appears to be related to the assay systems and the need for standardization of methods and reagents. The use of different cutoff values and serum dilutions and the method of preparing antigen substrates for individual assays can have a marked effect on the percentage of serum specimens that are determined to be positive for antibody to HHV-6. Overall, higher rates of seropositivity are observed when either NT or EIA is used than when the less sensitive method of IFA is used.

Collection and Storage of Specimens

Serum is the specimen of choice for most serologic assays, although plasma can normally be used as well. A total of 1 to 2 ml of serum should be collected from clotted blood. The serum should be refrigerated at 4°C shortly after collection and during transport to the laboratory. If an extended delay in transport or testing of a specimen is anticipated, the specimen should be frozen to at least –20°C. Freeze-thawing of specimens that have been frozen should be avoided. A single serum specimen is required to determine the immune status of an individual or to detect IgM-specific antibody. Paired serum specimens, collected 2 to 3 weeks apart, are required for the diagnosis of a current or recent HHV-6 infection when specimens for IgG antibody are examined. The acute-phase serum should be obtained as soon as possible after the onset of illness. The most useful results are obtained by submitting acute- and convalescent-phase sera together to be tested simultaneously.

Methods

IFA

The IFA is the most widely used method for detecting antibodies to HHV-6. Initially, IFAs were found to be both insensitive and nonspecific, in part because of the use of infected CBC as a source of antigen but also because of variations in the criteria used for positive results. With the preparation of HHV-6 antigen in continuous T-cell lines, such as HSB-2, MOLT-4, and J-Jhan, and following improvements in the definition of seropositivity, IFAs have become increasingly more sensitive and reliable.

In the IFA, HHV-6-infected cells are spotted onto wells of Teflon-coated slides, allowed to air dry completely, and then fixed in cold (–20°C) acetone for 10 min. Fixed slides can be used immediately or stored at 4°C for short periods or at –20 to –70°C for extended times. Serial dilutions of patient and positive and negative control sera are added to individual wells, and the slides are incubated at 37°C for 30 min in a humidified chamber. The slides are then washed two or three times in phosphate-buffered saline (PBS), and an appropriate dilution of fluorescein-labeled anti-human IgG or IgM is added to each well. The slides are again incubated at 37°C for 30 min in a humidified chamber, washed two or three times in PBS, counterstained with Evans blue, and air dried. Coverslips are mounted in buffered glycerol (pH 8.0), and the slides are examined at magnifications of ×200 to ×400 under a fluorescence microscope. The presence of HHV-6 antibodies in the serum is determined by the observation of positive fluorescence within infected cells. Antigen substrate slides can be purchased commercially, and some manufacturers provide kits that contain all the necessary reagents for staining, including diluted conjugated antibody, wash buffer, mounting fluid, control sera, and substrate slides. When testing for HHV-6-specific IgM antibodies, serum samples should be appropriately treated before the test, to decrease the incidence of false-positive results due to interfering rheumatoid factor or false-negative results caused by high levels of specific IgG antibodies blocking the binding of IgM to HHV-6 antigen.

ACIF

The ACIF test is an immunofluorescence assay that has been developed to reduce the nonspecific fluorescence observed when CBC are used in the IFA. It also has the added advantage of enhancing the fluorescent signal from positive cells. As with IFA, HHV-6-infected cells are spotted onto wells of Teflon-coated slides, allowed to air dry completely, and then fixed in cold (–20°C) acetone for 10 min. Sera are heat inactivated at 56°C for 30 min, and serial dilutions are added to individual wells. The slides are incubated at 37°C for 30 min in a humidified chamber and then washed two or three times in PBS. HHV-6-specific antibody bound to the infected cells is detected by incubating the slides with a source of complement at 37°C for 30 min in a humidified

chamber, washing the slides in PBS, and then incubating the slides with fluorescein-conjugated anticomplement antibodies for a final 30 min at 37°C. The slides are washed, counterstained, air dried, mounted in buffered glycerol (pH 8.0), and examined at magnifications of ×200 to ×400 under a fluorescence microscope. The presence of nuclear and cytoplasmic fluorescence within infected cells indicates positivity for antibodies to HHV-6.

EIA

EIAs for the determination of HHV-6 antibodies have been developed. HHV-6-infected and uninfected HSB-2 cells are harvested by centrifugation and disrupted by one of several methods, such as sonication in glycine buffer (pH 9.5) for 30 s, solubilization in Tris-Triton X-100 buffer, or cycles of freezing and thawing. Polystyrene 96-well microtiter plates are then coated with optimal dilutions of antigen by overnight adsorption of the antigen at 4°C. Coated plates can be stored at –20°C for extended periods. Prior to use, the plates are washed three times in PBS-0.05% Tween 20 and the wells are blocked for 30 min with PBS containing 1% bovine serum albumin. Diluted patient serum and controls are added to antigen wells of infected and uninfected cells, and the plates are incubated for 1 h at 37°C. The plates are then washed three times with PBS-Tween 20, and bound antibody is detected by reaction with an enzyme-conjugated anti-human IgG or IgM antibody at 37°C for 1 h. After washing is performed as described above, a substrate is added, and the plates are incubated for 30 to 45 min at room temperature. Following color development, the reaction is stopped and the absorbance of each well is read with a spectrophotometer. The results are calculated by subtracting the absorbance in wells containing uninfected cell antigen from the absorbance in wells containing infected cell antigen. The main advantages of the EIA are that it is rapid and more sensitive than the IFA and the results can be evaluated in an objective manner. In addition, the EIA is applicable to large numbers of specimens, and the potential for automation is excellent. Kits that detect HHV-6 IgG and IgM antibodies are now commercially available, although the performance characteristics of these reagents have not been fully elucidated. A μ-capture EIA has been developed to enhance the specificity for the detection of HHV-6-specific IgM antibody in human sera (28).

NT Assay

Neutralizing antibodies to HHV-6 are determined in the NT assay by mixing serial two-fold dilutions of patient sera in microtiter plates with an equal volume of cell-free virus containing $10^{2.5}$ 50% tissue culture infective doses per 0.1 ml. After 1 h of incubation at 37°C, 2×10^5 HSB-2 or MOLT-4 cells or CBC are added to each well, and the cultures are maintained for 7 days at 37°C. The antibody titer is determined as the reciprocal of the highest dilution of serum that completely prohibits the observation of viral cytopathic effect or the detection of antigen by IFA. The NT assay has a sensitivity and a specificity that are comparable to those of EIA, but the method is cumbersome, labor-intensive, and less suited to a routine diagnostic laboratory.

Antibody Avidity Assay

An indirect immunofluorescence antibody avidity test has been used to distinguish primary from past infections with HHV-6 (29). Since the binding of an antibody increases with time after exposure to an antigen, a primary antibody response to HHV-6 infection would be of much lower avidity than an antibody response that had occurred in the more distant past or following viral reactivation. By using urea to disrupt hydrogen bonds following binding of HHV-6-specific IgG antibody to antigens in the immunofluorescence assay, low-avidity antibody-antigen reactions are preferentially dissociated and differentiated from high-avidity antibody-antigen reactions. This test has been successfully used to diagnose primary HHV-6 infection in children with rashes and to distinguish primary from secondary antibody responses in solid-organ transplant recipients.

Other Serologic Tests

Western immunoblots and radioimmunoprecipitation are other serologic assays that are used to measure antibody to HHV-6. These assays have been used mainly in research settings to identify and analyze the role of specific proteins in the immune response to HHV-6. More recently, a microwell-adapted immunoblot system using recombinant antigens has been developed to distinguish specific antibody responses to HHV-6A and HHV-B (30).

Molecular Diagnosis

The diagnosis of HHV-6 infection is increasingly being made by the amplification of viral DNA by molecular methods (see references 31 and 32 for reviews), and PCR is now considered the reference method used by most clinical laboratories worldwide. Many in-house and some commercial qualitative assays have been developed and have been shown to be sensitive and specific for the diagnosis of HHV-6 infection. Multiplex conventional and real-time PCR assays for the simultaneous detection and differentiation of HHV-6 species A and B and HHV-7 also have been described (33, 34), although it is not clinically necessary to discriminate between the two species of HHV-6. Amplification has been performed with a number of different primer pairs, including those from the immediate-early antigen 1 and 2, large tegument protein (U31), DNA polymerase, U22, U65-U66, and U67 regions of the HHV-6 genome. PCR has been used successfully to qualitatively detect HHV-6 DNA in a variety of clinical specimens from solid-organ and hematopoietic stem cell transplant recipients; children with roseola, acute febrile illnesses, encephalitis, and other clinical manifestations of primary HHV-6 infection; AIDS patients; and individuals with less common forms of HHV-6 infection. However, qualitative PCR for HHV-6 diagnosis cannot reliably distinguish between active disease and asymptomatic infection or latency, and HHV-6 DNA can often be detected in saliva and, to a lesser extent, in blood of healthy individuals. Measuring the level of HHV-6 DNA appears to be necessary to predict and diagnose HHV-6 disease, particularly in immunocompromised individuals such as transplant recipients with illnesses that may be associated with reactivation of the virus or that are possibly caused by another pathogen. Consequently, conventional and real-time quantitative PCR assays have been developed (35–39) and used to monitor the levels of HHV-6 DNA in a variety of different body fluids and tissues of both healthy subjects and selected patient populations. Similar to the diagnostic paradigm for CMV, these assays may be useful to associate HHV-6 infection with disease, to predict and monitor disease progression, to assess the efficacy of antiviral drugs, and to facilitate our understanding of the natural history and pathogenesis of this virus. Currently, there is a definite need for traceable and commutable international reference HHV-6 DNA standards for institutional comparison of results, since significant variability in HHV-6 quantification has been observed between laboratories (40). As with CMV, viremia is considered to be the best predictor of disease, and quantitative measures of HHV-6 DNA in PBMC,

plasma, serum, or whole blood have proven useful for the continued surveillance and management of transplant recipients. When testing transplant recipients, it is more important to monitor the relative changes in DNA levels from serial blood specimens collected over time, since absolute HHV-6 DNA levels or breakpoints for symptomatic disease have not been determined. It may also be important to monitor both plasma and PBMC fractions of blood or to use whole blood, since it has been reported that both HHV-6 species A and B are detected in plasma but only species B can be found in PBMC of patients after bone marrow transplantation (41). In general, whole blood is considered to be the most practical specimen of choice for the detection of HHV-6 viremia by PCR (42). Plasma has been shown not to be as sensitive as whole blood or PBMC for detecting HHV-6 and may not be as useful to distinguish between active viral replication and chromosomal integration since HHV-6 DNA in plasma may reflect the presence of infected blood cells rather than circulating virus particles indicative of active infection (43, 44).

Reverse transcriptase PCR assays for the detection and quantification of specific HHV-6 mRNA transcripts that are expressed only during active infection have been used as a substitute for quantitative measures of DNA in blood to assist in identifying patients at greatest risk for developing symptomatic infection (45, 46). These assays have targeted immediate-early, early, and late gene transcripts and may prove to be more specific and applicable to correlate detection with active disease. In a recent study, reverse transcriptase PCR was shown to accurately distinguish between primary HHV-6 infection, chromosomal integration of HHV-6, and latent HHV-6 infection. Alternatively, qualitative detection of HHV-6 in cell-free specimens such as serum or plasma can be diagnostically useful in supporting a causal relationship between active HHV-6 infection and disease (47).

Antiviral Susceptibility Testing

Resistance of HHV-6 to ganciclovir is extremely rare, but has been reported in a patient with AIDS and in recipients of solid organ and hematopoietic stem cell transplantation (48). Mutations in the U69 and/or U38 genes confer resistance to ganciclovir. Both culture-based phenotypic assays and PCR-based molecular genotypic assays have been described to measure the susceptibility of HHV-6 to antiviral drugs, although neither system is currently available for use in a clinical setting.

Interpretation of Results

The ubiquitous distribution of HHV-6 throughout the world, its latency in a variety of cell types, and the integration of the complete HHV-6 genome into the human genome complicates the interpretation of laboratory studies, and a combination of methods may be required to confirm the relationship of HHV-6 infection with various diseases. Also, most diagnostic methods for HHV-6 are not fully developed; the sensitivity, specificity, and positive and negative predictive values of each assay have not been systematically evaluated in controlled, prospective studies; and reagents have only more recently been made available to diagnostic laboratories through commercial sources.

In general, conventional and spin amplification culture-based assays for growth of HHV-6 from specimens have limited utility and little to no impact on clinical decision making due to their overall lack of sensitivity and technical difficulties in performing these assays. Serologic testing is most useful for diagnosing primary infections with HHV-6 in children with acute illnesses and for studies of the epidemiology, clinical pathology, and natural history of the virus. For interpretation of serologic tests, a history of seroconversion from a negative to a positive IgG antibody response to HHV-6 between acute- and convalescent-phase sera or the presence of IgM or low-avidity IgG in a single serum sample during a primary infection helps establish HHV-6 as the causative agent. If a serum sample from early in an illness contains HHV-6 antibodies and a four-fold or greater rise in titer is demonstrated in a second specimen taken several weeks later, a diagnosis of recent infection due to reactivation or reinfection can be made. If acute- and convalescent-phase sera are both positive for HHV-6 antibody but the antibody titer is unchanged, the result is interpreted as HHV-6 infection at some time in the past. Screening a single serum specimen for IgG antibody to HHV-6 can also provide evidence of previous exposure to the virus and assists in identifying individuals at risk for HHV-6 infection.

The use of serologic techniques to establish the presence of active HHV-6 infection can be problematic; the detection of HHV-6-specific IgG or IgM antibodies may not always indicate primary infection, and in the setting of reactivation or latent infection, conventional serologic studies have limited value in establishing an association with disease. Increased titers of IgG to HHV-6 may occur during infections with other herpesviruses, such as CMV, EBV, or HHV-7, and the relative importance of each virus in producing disease may be difficult to determine. Variations in the detection of HHV-6-specific antibodies have been observed and may be related to the methods and reagents used. The use of insensitive assays may inappropriately indicate that HHV-6 infection has been excluded or that a positive seroconversion had occurred when, in fact, this may represent an inability to detect low levels of antibody during reactivation. Assays should also be extensively evaluated for specificity to detect potential cross-reactivity with other herpesviruses. Results of serologic tests for IgM antibody should be interpreted with caution; IgM antibody can appear in both primary and reactivated HHV-6 infections and can persist for extended periods after a primary infection. Also, some children may not develop detectable IgM responses during primary infection. A recognized technical problem with HHV-6 IgM assays is the occurrence of false-positive and false-negative reactions due to high levels of competing rheumatoid factor and HHV-6-specific IgG.

In the immunocompromised host, the use of direct detection methods to diagnose HHV-6 disease is most beneficial for patient care. To implicate HHV-6 as the cause of an illness, laboratory confirmation of active disease in an appropriate clinical setting is required. However, the proper selection of methods for the diagnosis and monitoring of HHV-6 disease is a challenge. Differentiation between primary, latent, or reactivated infection or chromosomally integrated HHV-6 can be difficult and may require that more than one assay be used. Quantitative measures of HHV-6 DNA may provide a rapid diagnosis of active disease, identify patients at risk of developing disease, assess the progression of disease, and possibly direct the initiation of antiviral therapy in most patients, while detection and quantification of specific HHV-6 mRNA transcripts may also be necessary to differentiate active disease in individuals suspected of having chromosomally integrated HHV-6. Of note, in the small percentage of individuals who have chromosomally integrated HHV-6, viral loads are persistently high in specimens such as whole blood, plasma, PBMC, saliva, urine, and hair follicles and other tissues in the absence of viral replication, and viral loads of $>1 \times 10^6$ copies/ml in whole blood or 1×10^4 copies/ml in plasma are strongly suggestive of chromosomally integrated HHV-6 DNA rather than active infection (7, 8).

However, these values are not absolute, and overlapping viral loads have been observed in children during primary infections and in immunocompromised patients with symptomatic reactivated infections. Such levels are normally transient and will decline with time in the latter populations, while serial testing of patients with chromosomally integrated HHV-6 DNA will show persistently high HHV-6 viral loads. Also of concern is the fact that in patients with chromosomally integrated HHV-6 DNA who have acute neurologic presentations and a cerebrospinal fluid (CSF) pleocytosis due to other pathogens, a CSF PCR for HHV-6 DNA may be incidentally positive and not be a true reflection of central nervous system disease with this virus. Recently, a droplet digital PCR assay has been developed which appears to accurately identify chromosomally integrated HHV-6 DNA in cellular patient specimens by determining the ratio of HHV-6 to cellular DNA; a ratio of 1:1 of virus to human genomes confirms the diagnosis (49). Lastly, testing of hair follicles or nails by real-time PCR can also be used to confirm the presence of chromosomally integrated HHV-6 since only individuals with HHV-6 DNA integrated into the host chromosome have detectable HHV-6 DNA in these tissues (50, 51). However, receipt and processing of these types of specimens in a clinical laboratory is unusual.

The lack of well-defined, commercially available reagents and standardized methods and controls has made the interpretation of laboratory results for HHV-6 more difficult. Whenever possible, serologic diagnoses of HHV-6 infection should be confirmed by virus isolation or suitable direct detection methods. To implicate HHV-6 as the cause of certain diseases, it may also be necessary to use methods that measure active virus replication, since the qualitative detection of virus or viral DNA may simply indicate the presence of the virus in a latent state. A more accurate assessment of the involvement of HHV-6 in a given disease may be provided by the detection of cell-free viral DNA in serum or plasma by PCR, by qualitative or quantitative amplification of specific HHV-6 mRNA transcripts, by detection of viral antigen expression in tissues or PBMC by immunohistochemistry or *in situ* hybridization, or by quantitative assessment of the viral load by DNA PCR.

HHV-7

Introduction

HHV-7 was first isolated in 1989 from PBMC of a healthy individual (52) and belongs to the genus *Roseolovirus* (Table 1). In contrast to HHV-6, little is known about the prevalence, biology, and pathogenesis of this virus. HHV-7 is morphologically identical to other herpesviruses but, like HHV-6, is characterized by having a tropism for $CD4^+$ T lymphocytes, by causing infection early in life, and by being ubiquitous, with a seroprevalence rate of more than 85% in U.S. and European populations (see references 5, 11, 21, and 53 for reviews). Lower rates of seropositivity in Japan have been reported. After primary infection, HHV-7 can persist in the host in a latent state and reactivation can occur. Primary infection in children is thought to occur somewhat later in life than primary infection by HHV-6, usually after 24 months of age and by 5 years of age, although higher rates of seropositivity have been reported at a younger age (54). Salivary glands appear to be a main site of viral replication for HHV-7 as the virus is frequently and consistently isolated from the saliva of infected individuals, and transmission is likely to occur from contact with respiratory secretions. HHV-7 has also been detected in breast milk, PBMCs of most healthy adults, cervical secretions, bone marrow, cerebrospinal fluid, and bronchoalveolar lavage fluid. Seroconversion to HHV-7 antibody positivity is a separate and distinct event from production of antibody to HHV-6. The virus can be grown in PBMC or CBC and shows a characteristic cytopathic effect of membrane blebbing and large, refractile multinucleated giant cells indistinguishable from the cytopathic effect of HHV-6. A single continuous T-cell line (Sup-T1) can support the growth of HHV-7 with variable success. In general, HHV-7 has a narrower cell tropism and its growth in culture is more cell associated, less cytopathic, and slower than HHV-6. The virus is closely related to HHV-6 but has been shown to be genetically and immunologically distinct. Unlike for HHV-6, genetic variants have not been described for HHV-7. The linear, double-stranded DNA of HHV-7 is approximately 145 kb and has no homology to that of EBV, herpes simplex virus, or varicella-zoster virus and has limited homology to that of CMV. Therefore, HHV-7 has been classified as a member of the subfamily of betaherpesviruses with HHV-6 and CMV. Virus particles of HHV-7 measure 170 nm and contain an icosahedral nucleocapsid surrounded by a tegument and an envelope containing virus-encoded glycoproteins. Western immunoblot analyses of viral proteins reveal different patterns for HHV-6- and HHV-7-infected cells, although monoclonal antibodies to HHV-6 can cross-react with HHV-7-infected cells. The HHV-7 genome has the capacity to code for 84 different proteins and a number of viral proteins have been identified, ranging in size from 30 to 136 kDa.

The clinical spectrum of disease caused by HHV-7 is poorly understood. Most infections are asymptomatic, but HHV-7 has been associated with up to 10% of roseola cases and, as with HHV-6, primary infection is thought to be responsible for febrile seizures and other neurologic events in children (Table 2) (see reference 55 for a review). The virus also has been isolated from patients with a chronic viral syndrome and occasionally in children with a nonspecific febrile syndrome without rash. No viruses other than HHV-7 were isolated in these cases, and a seroconversion to HHV-7 but not HHV-6 positivity was documented. There is some evidence to suggest that HHV-7 also may play an etiologic role in pityriasis rosea. Little is known about disease caused by HHV-7 in immunocompromised patients, although reactivation of the virus in bone marrow and solid-organ transplant recipients is common (see reference 16 for a review). The glycoprotein CD4 is a critical component of the receptor on the surface of T lymphocytes for HHV-7; it has been shown that a selective and progressive downregulation of the expression of CD4 in HHV-7-infected T cells leads to a marked reciprocal interference of HIV infection, although the clinical significance of this interaction is unknown. Infection of PBMC with HHV-7 enhances NK cell cytotoxicity by induction of IL-15. HHV-7 also may interact with other herpesviruses, leading to the reactivation of HHV-6 and CMV. Reactivation of HHV-7 has been reported to be a cofactor for the progression of CMV disease in renal transplant patients infected with CMV, and isolated cases of encephalitis, meningitis, myelitis, and optical neuritis have been reported following stem cell transplantation.

Immunologic and Molecular Diagnosis

The methods for laboratory diagnosis of HHV-7 are essentially identical to those for diagnosis of HHV-6 (Table 3) and currently include the direct examination of clinical specimens for viral antigens by immunohistochemistry (56) or viral nucleic acids by *in situ* hybridization and PCR (35,

57), virus identification in cell culture (52), and detection of antibodies against the virus (54). An HHV-7 antigenemia assay similar to that described above for HHV-6 has been developed for the detection of HHV-7 early and late antigens in PBMC isolated from recipients of liver and allogeneic stem cell transplants (23). The serodiagnosis of HHV-7 infection can be made by IFA, EIA, and Western immunoblot assays, using HHV-7-infected cells as an antigen source. Seroconversion to HHV-7 antibody positivity, as determined by IFA, is independent of that to HHV-6 antibody positivity and is diagnostic for primary infection. An antibody response to HHV-7 is induced only by HHV-7 infection, since neither seroconversion nor a significant rise in the titer of antibody to HHV-7 can be detected following primary infection with HHV-6. Conversely, seroconversion to HHV-7 antibody positivity can cause a simultaneous rise in the titer of antibody to HHV-6. This is thought to be due to the ability of HHV-7 to induce a response of memory B cells against HHV-6 cross-reactive antigens or to be due to reactivation of HHV-6 during infection with HHV-7. HHV-6 antibodies are not protective against HHV-7 infection, since seroconversion to HHV-7 antibody positivity can occur in the presence of high titers of antibody to HHV-6. The presence of antigenic cross-reactivity between HHV-6 and HHV-7 should be considered when performing serologic assays; it may be necessary to preadsorb patient sera to infected cells for specific determination of titers of antibody to each virus. Antibody assays based on an 89-kDa protein or glycoprotein B of HHV-7 also have been developed and do not appear to cross react with antibodies to HHV-6. More recently, an HHV-7 antibody avidity assay has been developed and validated and used in conjunction with the HHV-6 avidity test described above to detect and distinguish primary from past infections with either HHV-6 or HHV-7. In addition, dual primary HHV-6 and HHV-7 infections have been confirmed by using these assays.

Both conventional and real-time PCR assays have been described for the detection of HHV-7 DNA from clinical specimens. As with HHV-6, qualitative PCR assays are not able to differentiate active disease from asymptomatic infection or latency, and HHV-7 DNA is frequently found in saliva and PBMC of healthy individuals. To this end, PCR assays for quantitating HHV-7 DNA from whole blood and mononuclear and polymorphonuclear cells in infected individuals have been developed and are being evaluated for the ability to correlate the viral load of HHV-7 with clinical disease and response to antiviral therapy, and to facilitate studies of the epidemiology of the virus (35, 42, 58, 59).

The interpretation of laboratory results for HHV-7 is similar to that described for HHV-6 and is confounded by a paucity of commercially available reagents and, as with HHV-6, by the ubiquitous nature of this virus. In addition, caution is needed in interpreting the results of serologic studies because of the cross-reactivity of HHV-7 with HHV-6 and because of the ability of HHV-7 to reactivate other members of the herpesvirus family. With serologic evidence of dual infection, it may be difficult to determine the relative importance of each virus in causing disease. Virologic methods, including viral culture, rapid direct detection of antigens and/or nucleic acids, and serology, must be combined with a clinical assessment of the patient to provide a reliable determination of HHV-7 infection and to establish a clear relationship between infection and human disease. It may also be necessary to monitor viral load or other measures of active virus replication to help in our understanding of the natural history and pathogenesis of this virus.

HHV-8

Introduction

Using the molecular technique of representational difference analysis, HHV-8, also termed Kaposi's sarcoma (KS)-associated herpesvirus, was first identified by Chang et al. (5) in 1994 in more than 90% of KS tissues obtained from patients with AIDS. Subsequently, HHV-8 has been detected in patients with all forms of KS from all parts of the world, including AIDS-related or epidemic KS and classic KS in older men of Mediterranean and Eastern European origin, HIV-1-negative African endemic KS of adults and children, and KS in persons with iatrogenic immunosuppression, most often organ transplant recipients (see references 60 to 65 for reviews). HHV-8 also has been detected in other lymphoproliferative disorders such as AIDS-related primary effusion lymphomas (formerly called body cavity-based lymphomas) and multicentric Castleman disease and in KS-associated herpesvirus inflammatory cytokine syndrome (66, 67). In addition, HHV-8 has been implicated in the pathogenesis of other diseases, including multiple myeloma, sarcoidosis, angiosarcoma, non-KS skin lesions (including squamous and basal cell carcinomas) of immunocompromised patients, and multiple sclerosis. However, numerous follow-up studies using PCR-based and serologic assays have failed to corroborate the original findings, making it unlikely that HHV-8 is associated with these latter disorders. Little is known about primary HHV-8 infection in healthy individuals, and the diseases associated with this virus are thought to be more probably due to viral reactivation. Primary infection in immunocompetent children may be associated with fever and a maculopapular rash and severe clinical manifestations, including marked fever, splenomegaly, pancytopenia, lymphoid hyperplasia and occasionally rapid-onset-KS among immunocompromised solid organ transplant recipients and HIV-infected individuals.

The biology, epidemiology, and pathogenesis of this virus are still not fully understood, but significant advances have been made over the years (see references 60, 61, and 68 to 70 for reviews). HHV-8 is classified as a gammaherpesvirus in the genus *Rhadinovirus* and has sequence homology to the simian virus herpesvirus saimiri and EBV (Table 1). These viruses establish persistent, latent infection and are associated with immortalization and transformation of cells and play an important role in the development of malignancies. The replicative form of the HHV-8 genome is approximately 165 kb in length, and 97 genes have been identified. Several genes have homology to human genes, such as those encoding cyclin D (a cell cycle inducer), various cytokines, and Bcl-2 (a blocker of apoptosis). Expression of these genes may help explain the association of HHV-8 with cell transformation and the development of tumors. Viral replication may be affected by interaction with other viruses such as HIV-1 and EBV, since body cavity lymphoma cells are frequently coinfected with EBV and tumors associated with HHV-8 are often seen in persons infected with HIV-1. It also has been demonstrated that HIV-1 can increase HHV-8 replication in a body cavity lymphoma cell line. Genetic diversity exists among viral isolates of HHV-8, resulting in the identification of strains A, B, and C; strain A has been found mainly in patients with AIDS-associated or classical KS, while strains B and C are seen more often among African patients. The virus has a broad cell tropism and can infect $CD19^+$ B lymphocytes, the flat endothelial cells lining vascular spaces, macrophages, and the perivascular spindle cells of KS lesions. Its distribution is worldwide, although it is not ubiquitous in most populations and

there is considerable variation in its prevalence, which is related to the geographic and demographic distribution of KS (Table 2). The precise modes of transmission are unknown. Based on the epidemiology of HHV-8, however, it is thought to be transmitted through sexual contact, predominantly among homosexual and bisexual HIV-1-positive males or their sexual partners. Likely sources of infection for sexual transmission are semen and possibly female genital secretions; HHV-8 DNA has been found in the semen of male AIDS patients and in cervicovaginal specimens from HHV-8-seropositive women. Although HHV-8 DNA has yet to be found in feces, sexual practices involving oral-anal contact may be a risk factor for homosexual transmission. HHV-8 also has been detected in oral secretions and PBMC of HIV-1-infected males and in the blood of an apparently healthy blood donor following multiple donations. Widespread horizontal transmission from oral secretions may be responsible for the high rate of HHV-8 infection in areas where KS is hyperendemic. However, the transmission of HHV-8 by blood or the respiratory route in populations at low risk for KS is likely to be uncommon. Transmission through organ transplantation has been documented and is of concern for this patient population.

Immunologic and Molecular Diagnosis

The laboratory diagnosis of HHV-8 infection is possible using molecular methods such as PCR or using serologic assays (Table 3) (see reference 71 for a review), although the clinical need for testing has not been defined. These methods have been used mainly to study the epidemiology of HHV-8 and to investigate the relationship between HHV-8 and the pathogenesis of various diseases. Assays are currently available only in research laboratories, and there are few commercial sources of reagents.

PCR is the primary method used for the direct detection of HHV-8 from tissues, from body fluids such as serum, plasma, urine, saliva, bone marrow, and semen, and in PBMC from infected individuals. The most widely used primers are those originally described by Chang et al. (72) and are specific for the highly conserved 233-bp region of the KS330Bam fragment (open reading frame [ORF] 26). Other useful primer sets have been evaluated and include those that amplify gene sequences of ORFs 8, 25, 37, 65, 72, 73, 75, K5, and K6. Quantitative conventional (73) and real-time (74–78) PCR assays have been developed to measure the HHV-8 viral load in PBMC, plasma, or tissues of individuals with AIDS-associated KS, classical KS, AIDS-related primary effusion lymphomas, and multicentric Castleman disease and organ transplant recipients. These assays may be useful to determine the exact mode(s) of transmission of the virus, to assist in the diagnosis of KS and other diseases associated with HHV-8 infection, to identify those individuals at highest risk of disease, to predict the progression to and development of KS, and to assess the efficacy of different therapeutic regimens. It has been shown that individuals with HHV-8-related diseases have more HHV-8 DNA in either plasma or PBMC than do persons without disease, but the level of HHV-8 DNA in plasma is significantly higher than that in PBMC. Quantitation of HHV-8 in plasma, therefore, may be more accurate for evaluating the risk of HHV-8 disease progression and the efficacy of therapy.

Attempts to culture HHV-8 have met with great difficulty, and current methods are labor-intensive and impractical for diagnostic use. Nevertheless, $CD19^+$ B cells, the human papillomavirus-transformed endothelial cell line BB19, and the adenovirus-transformed human kidney epithelial cell line 293 have been used to grow virus from KS spindle cells, fluids from body cavity lymphomas, and filtered cell culture fluids from $CD19^+$ cells positive for HHV-8. However, continual replication in these cell lines has not been successful. Monoclonal antibodies specific to HHV-8 have been described and are currently being used to localize HHV-8 in infected cells and tissue by immunocytochemistry and flow cytometry. These antibodies are not widely available for diagnostic use.

Serologic testing for HHV-8 can be done by a variety of formats, including IFA, EIA, and immunoblot assays. Similar to serologic tests for EBV, these assays have been designed to detect antibody responses to HHV-8-specific antigens expressed during latency or lytic infection. Antigens currently used in HHV-8 serologic assays include purified viral particles, whole cells, or isolated nuclei prepared from HHV-8-infected cell lines derived from body cavity-based lymphomas, whole-cell lysates, recombinant viral proteins, and synthetic peptides.

IFAs for measuring HHV-8-specific antibody responses from patient sera are usually done with HHV-8-infected whole cells fixed onto slides as the substrate. The cell lines BC-1 and HBL-6, which are latently infected with HHV-8 and coinfected with EBV, were originally used to develop some of the first IFAs for the detection of HHV-8 antibodies against nonstructural latent antigens of the virus, particularly the latency-associated nuclear antigen (LANA). Antibody cross-reactivity is of primary concern with assays that use cells infected with both HHV-8 and EBV; cell lines such as BCP-1 and BCBL-1, which are infected with HHV-8 alone, are now being used in most whole-cell IFAs to minimize cross-reactions with antibodies to other herpesviruses. For measurement of antibodies to lytic antigens by IFA, HHV-8-infected cell lines are treated with phorbol esters or sodium butyrate. This results in the chemical induction of a lytic cycle of viral replication and the expression of lytic antigens that usually correspond to structural viral proteins. When using IFA, the presence of stippled immunofluorescence in the nuclei of uninduced cells is representative of an antibody response to LANA, while antibodies against HHV-8 lytic antigens are measured by observing fluorescence as diffuse cytoplasmic staining, spots in the nucleus, or localized to the membrane of the induced cells. A monoclonal antibody-enhanced IFA (mIFA) has been described and uses a mouse monoclonal antibody and induced or uninduced BCBL-1 cells for detecting antibodies to latent and lytic HHV-8 antigens. Although IFAs can be used to detect a range of antibody responses to various latent and lytic proteins of HHV-8, the procedures are labor-intensive and subjective, requiring considerable experience and critical evaluation to ensure reliable results. Extensive quality control is also needed to monitor the appropriate expression of lytic antigens in induced cells and to prepare the substrate slides.

EIAs have been developed that use whole viral lysates as antigens for detecting HHV-8 antibodies. The whole-virus EIA is designed to detect IgG antibodies to nonstructural and most structural HHV-8 antigens; it uses a viral lysate prepared from sucrose gradient-purified whole virions obtained from the cell line KS-1. More recently, recombinant proteins of the lytic viral capsid antigen from ORF 65 or peptides corresponding to a fragment of the minor capsid protein from ORF 26 have been used in the development of HHV-8 serologic EIAs.

Immunogenic latent (encoded by ORF 73 [LANA]) and lytic (encoded by ORFs 65, K8.1, K8.1A, and K8.1B, and ORF 26) proteins have also been recombinantly expressed and used in immunoblot assays (79). Reactions to LANA on immunoblot assays are seen as a high-molecular-mass

doublet of 226 and 234 kDa. The ORFs corresponding to K8.1 encode HHV-8-specific envelope glycoproteins of 35 to 40 kDa. As a whole, the performance characteristics of these immunoblot assays have not been fully established.

With most of the available serologic assays, HHV-8-specific antibodies have been detected in the majority of individuals with KS, AIDS-related primary effusion lymphomas, or multicentric Castleman disease. Among persons infected with HIV-1, the seroprevalence for HHV-8 is highest in HIV-1-infected homosexual males, indeterminate in intravenous drug users and persons infected through heterosexual contact, and lowest in hemophiliacs, women, and children. It also has been shown that seroconversion to HHV-8 antibody positivity precedes the progression to KS and predicts the subsequent appearance of KS lesions in HIV-1-infected individuals. In the general population, the highest seroprevalence rates for HHV-8 are seen in sub-Saharan Africa and Mediterranean countries, while rates in northern European, North American, and Southeast Asian countries are relatively low.

In several studies done to compare the various HHV-8 antibody assays (79–81), good assay correlation was obtained when testing sera from individuals with KS. The most significant discrepancies between assays were observed when determining the seroprevalence of HHV-8 in high-risk groups without KS or in groups at minimal risk for HHV-8 infection, such as blood donors. While the different methods showed similar antibody trends within the various epidemiological and population groups, they did not always agree. Considerable variation in sensitivity and specificity was observed from one assay to another when testing individual serum specimens within defined panels of sera from different populations. This appears to be related to the choice of assays, the use of different serum dilutions and cutoff values, the selection and preparation of antigen(s) used, and the lack of standardized methods and reagents. In general, the mIFA using lytic antigens identifies the highest number of individuals with HHV-8-specific antibodies, while assays based on latent antigens or individual HHV-8 proteins and peptides are less sensitive. The specificity of the lytic mIFA has been questioned because this assay detects HHV-8 antibodies in a much higher percentage of healthy blood donors and the results have not been corroborated by other assays. However, it is still unknown whether the lytic mIFA is just more sensitive or truly detects cross-reactive antibodies. In general, nonspecific reactions have been found to occur when IFAs are performed with sera at dilutions of <1:40, particularly if the cells used as an antigen source were chemically induced. Dilutions as high as 1:100 or 1:160 have been recommended to avoid such reactions, but such dilutions also may lead to false-negative results. Single-antigen assays do not appear to detect all antibody responses to infection with HHV-8, but use of these tests has demonstrated that individuals may differ in their abilities to recognize different HHV-8 proteins and that different antibody profiles can develop during the course of HHV-8 infection (81). It is clear that no one assay is completely sensitive and specific, and that combinations of several assays or combinations of several antigens in a single assay may be required to accurately determine the seropositivity to HHV-8, particularly in the general population (81). Zhu et al. (79) have shown that IFA antibody positivity to both latent and lytic antigens followed by confirmation with an immunoblot assay using a panel of latent and lytic immunogenic recombinant antigens provides a reliable, sensitive, and specific measure of HHV-8 antibodies. More recently, a luciferase immunoprecipitation assay has been developed that can measure profiles of antibody responses against multiple latent and lytic HHV-8 antigens (82). Significant differences in antibody levels were observed between patients with KS, multicentric Castleman disease, and primary effusion lymphoma when using this assay, possibly reflecting altered protein expression and/or differences in immune recognition among these diseases.

Until serologic assays are extensively evaluated and better standardized, their utility for diagnosing HHV-8 infection and for determining the immune status of an individual is limited and the interpretation of results is difficult. As with HHV-6 and HHV-7, it may be necessary to correlate serologic results with direct antigen and/or nucleic acid detection and to quantify the HHV-8 viral load to reliably detect infection and to establish a clear relationship between infection and human disease.

REFERENCES

1. **Braun DK, Dominguez G, Pellett PE.** 1997. Human herpesvirus 6. *Clin Microbiol Rev* **10:**521–567. PubMed
2. **Dockrell DH.** 2003. Human herpesvirus 6: molecular biology and clinical features. *J Med Microbiol* **52:**5–18. PubMed
3. **Hall CB, Caserta MT, Schnabel KC, Boettrich C, McDermott MP, Lofthus GK, Carnahan JA, Dewhurst S.** 2004. Congenital infections with human herpesvirus 6 (HHV6) and human herpesvirus 7 (HHV7). *J Pediatr* **145:**472–477. PubMed
4. **Flamand L, Komaroff AL, Arbuckle JH, Medveczky PG, Ablashi DV.** 2010. Review, part 1: human herpesvirus-6-basic biology, diagnostic testing, and antiviral efficacy. *J Med Virol* **82:**1560–1568. PubMed
5. **Caselli E, Di Luca D.** 2007. Molecular biology and clinical associations of Roseoloviruses human herpesvirus 6 and human herpesvirus 7. *New Microbiol* **30:**173–187. PubMed
6. **Krug LT, Pellett PE.** 2014. Roseolovirus molecular biology: recent advances. *Curr Opin Virol* **9:**170–177. PubMed
7. **Pellett PE, Ablashi DV, Ambros PF, Agut H, Caserta MT, Descamps V, Flamand L, Gautheret-Dejean A, Hall CB, Kamble RT, Kuehl U, Lassner D, Lautenschlager I, Loomis KS, Luppi M, Lusso P, Medveczky PG, Montoya JG, Mori Y, Ogata M, Pritchett JC, Rogez S, Seto E, Ward KN, Yoshikawa T, Razonable RR.** 2012. Chromosomally integrated human herpesvirus 6: questions and answers. *Rev Med Virol* **22:**144–155. PubMed
8. **Lee S-O, Brown RA, Razonable RR.** 2012. Chromosomally integrated human herpesvirus-6 in transplant recipients. *Transpl Infect Dis* **14:**346–354. PubMed
9. **Stone RC, Micali GA, Schwartz RA.** 2014. Roseola infantum and its causal human herpesviruses. *Int J Dermatol* **53:**397–403. PubMed
10. **Agut H.** 2011. Deciphering the clinical impact of acute human herpesvirus 6 (HHV-6) infections. *J Clin Virol* **52:**164–171. PubMed
11. **Ward KN.** 2005. Human herpesviruses-6 and -7 infections. *Curr Opin Infect Dis* **18:**247–252. PubMed
12. **Ablashi DV, Devin CL, Yoshikawa T, Lautenschlager I, Luppi M, Kühl U, Komaroff AL.** 2010. Review Part 3: human herpesvirus-6 in multiple non-neurological diseases. *J Med Virol* **82:**1903–1910. PubMed
13. **Yao K, Crawford JR, Komaroff AL, Ablashi DV, Jacobson S.** 2010. Review part 2: human herpesvirus-6 in central nervous system diseases. *J Med Virol* **82:**1669–1678. PubMed
14. **Ward KN.** 2014. Child and adult forms of human herpesvirus 6 encephalitis: looking back, looking forward. *Curr Opin Neurol* **27:**349–355. PubMed
15. **Clark DA, Griffiths PD.** 2003. Human herpesvirus 6: relevance of infection in the immunocompromised host. *Br J Haematol* **120:**384–395. PubMed
16. **Dockrell DH, Paya CV.** 2001. Human herpesvirus-6 and -7 in transplantation. *Rev Med Virol* **11:**23–36. PubMed

17. **Zerr DM.** 2012. Human herpesvirus 6 (HHV-6) disease in the setting of transplantation. *Curr Opin Infect Dis* **25:**438–444. PubMed
18. **Lautenschlager I, Razonable RR.** 2012. Human herpesvirus-6 infections in kidney, liver, lung, and heart transplantation: review. *Transpl Int* **25:**493–502. review. PubMed
19. **Razonable RR.** 2010. Infections due to human herpesvirus 6 in solid organ transplant recipients. *Curr Opin Organ Transplant* **15:**671–675. PubMed
20. **Razonable RR.** 2013. Human herpesviruses 6, 7 and 8 in solid organ transplant recipients. *Am J Transplant* **13(Suppl 3):**67–77, quiz 77–78. PubMed
21. **Ward KN.** 2005. The natural history and laboratory diagnosis of human herpesviruses-6 and -7 infections in the immunocompetent. *J Clin Virol* **32:**183–193. PubMed
22. **Agut H, Bonnafous P, Gautheret-Dejean A.** 2015. Laboratory and clinical aspects of human herpesvirus 6 infections. *Clin Microbiol Rev* **28:**313–335. PubMed
23. **Lautenschlager I, Lappalainen M, Linnavuori K, Suni J, Höckerstedt K.** 2002. CMV infection is usually associated with concurrent HHV-6 and HHV-7 antigenemia in liver transplant patients. *J Clin Virol* **25(Suppl 2):**S57–S61. PubMed
24. **Volin L, Lautenschlager I, Juvonen E, Nihtinen A, Anttila VJ, Ruutu T.** 2004. Human herpesvirus 6 antigenaemia in allogeneic stem cell transplant recipients: impact on clinical course and association with other betaherpesviruses. *Br J Haematol* **126:**690–696. PubMed
25. **Marsh S, Kaplan M, Asano Y, Hoekzema D, Komaroff AL, Whitman JE Jr, Ablashi DV.** 1996. Development and application of HHV-6 antigen capture assay for the detection of HHV-6 infections. *J Virol Methods* **61:**103–112. PubMed
26. **Krueger GRF, Ablashi DV, Josephs SF, Salahuddin SZ, Lembke U, Ramon A, Bertram G.** 1991. Clinical indications and diagnostic techniques of human herpesvirus-6 (HHV-6) infection. *In Vivo* **5:**287–295. PubMed
27. **Singh N, Carrigan DR.** 1996. Human herpesvirus-6 in transplantation: an emerging pathogen. *Ann Intern Med* **124:**1065–1071. PubMed
28. **Nielsen L, Vestergaard BF.** 2002. A μ-capture immunoassay for detection of human herpes virus-6 (HHV-6) IgM antibodies in human serum. *J Clin Virol* **25:**145–154. PubMed
29. **Ward KN, Turner DJ, Parada XC, Thiruchelvam AD.** 2001. Use of immunoglobulin G antibody avidity for differentiation of primary human herpesvirus 6 and 7 infections. *J Clin Microbiol* **39:**959–963. PubMed
30. **Thäder-Voigt A, Jacobs E, Lehmann W, Bandt D.** 2011. Development of a microwell adapted immunoblot system with recombinant antigens for distinguishing human herpesvirus (HHV)6A and HHV6B and detection of human cytomegalovirus. *Clin Chem Lab Med* **49:**1891–1898. PubMed
31. **Hill JA, Sedlak RH, Jerome KR.** 2014. Past, present, and future perspectives on the diagnosis of Roseolovirus infections. *Curr Opin Virol* **9:**84–90. PubMed
32. **Kainth MK, Caserta MT.** 2011. Molecular diagnostic tests for human herpesvirus 6. *Pediatr Infect Dis J* **30:**604–605. PubMed
33. **Kidd IM, Clark DA, Bremner JAG, Pillay D, Griffiths PD, Emery VC.** 1998. A multiplex PCR assay for the simultaneous detection of human herpesvirus 6 and human herpesvirus 7, with typing of HHV-6 by enzyme cleavage of PCR products. *J Virol Methods* **70:**29–36. PubMed
34. **Safronetz D, Humar A, Tipples GA.** 2003. Differentiation and quantitation of human herpesviruses 6A, 6B and 7 by real-time PCR. *J Virol Methods* **112:**99–105. PubMed
35. **Secchiero P, Zella D, Crowley RW, Gallo RC, Lusso P.** 1995. Quantitative PCR for human herpesviruses 6 and 7. *J Clin Microbiol* **33:**2124–2130. PubMed
36. **Gautheret-Dejean A, Manichanh C, Thien-Ah-Koon F, Fillet A-M, Mangeney N, Vidaud M, Dhedin N, Vernant JP, Agut H.** 2002. Development of a real-time polymerase chain reaction assay for the diagnosis of human herpesvirus-6 infection and application to bone marrow transplant patients. *J Virol Methods* **100:**27–35. PubMed
37. **Flamand L, Gravel A, Boutolleau D, Alvarez-Lafuente R, Jacobson S, Malnati MS, Kohn D, Tang Y-W, Yoshikawa T, Ablashi D.** 2008. Multicenter comparison of PCR assays for detection of human herpesvirus 6 DNA in serum. *J Clin Microbiol* **46:**2700–2706. PubMed
38. **Karlsson T, Mannonen L, Loginov R, Lappalainen M, Höckerstedt K, Lautenschlager I.** 2012. Development of a new quantitative real-time HHV-6-PCR and monitoring of HHV-6 DNAaemia after liver transplantation. *J Virol Methods* **181:**25–36. PubMed
39. **Cassina G, Russo D, De Battista D, Broccolo F, Lusso P, Malnati MS.** 2013. Calibrated real-time polymerase chain reaction for specific quantitation of HHV-6A and HHV-6B in clinical samples. *J Virol Methods* **189:**172–179. PubMed
40. **de Pagter PJ, Schuurman R, de Vos NM, Mackay W, van Loon AM.** 2010. Multicenter external quality assessment of molecular methods for detection of human herpesvirus 6. *J Clin Microbiol* **48:**2536–2540. PubMed
41. **Nitsche A, Müller CW, Radonic A, Landt O, Ellerbrok H, Pauli G, Siegert W.** 2001. Human herpesvirus 6A DNA Is detected frequently in plasma but rarely in peripheral blood leukocytes of patients after bone marrow transplantation. *J Infect Dis* **183:**130–133. PubMed
42. **Géraudie B, Charrier M, Bonnafous P, Heurté D, Desmonet M, Bartoletti M-A, Penasse C, Agut H, Gautheret-Dejean A.** 2012. Quantitation of human herpesvirus-6A, -6B and -7 DNAs in whole blood, mononuclear and polymorphonuclear cell fractions from healthy blood donors. *J Clin Virol* **53:**151–155. PubMed
43. **Caserta MT, Hall CB, Schnabel K, Lofthus G, Marino A, Shelley L, Yoo C, Carnahan J, Anderson L, Wang H.** 2010. Diagnostic assays for active infection with human herpesvirus 6 (HHV-6). *J Clin Virol* **48:**55–57. PubMed
44. **Achour A, Boutolleau D, Slim A, Agut H, Gautheret-Dejean A.** 2007. Human herpesvirus-6 (HHV-6) DNA in plasma reflects the presence of infected blood cells rather than circulating viral particles. *J Clin Virol* **38:**280–285. PubMed
45. **Van den Bosch G, Locatelli G, Geerts L, Fagà G, Ieven M, Goossens H, Bottiger D, Oberg B, Lusso P, Berneman ZN.** 2001. Development of reverse transcriptase PCR assays for detection of active human herpesvirus 6 infection. *J Clin Microbiol* **39:**2308–2310. PubMed
46. **Bressollette-Bodin C, Nguyen TVH, Illiaquer M, Besse B, Peltier C, Chevallier P, Imbert-Marcille B-M.** 2014. Quantification of two viral transcripts by real time PCR to investigate human herpesvirus type 6 active infection. *J Clin Virol* **59:**94–99. PubMed
47. **Secchiero P, Carrigan DR, Asano Y, Benedetti L, Crowley RW, Komaroff AL, Gallo RC, Lusso P.** 1995. Detection of human herpesvirus 6 in plasma of children with primary infection and immunosuppressed patients by polymerase chain reaction. *J Infect Dis* **171:**273–280. PubMed
48. **Piret J, Boivin G.** 2014. Antiviral drug resistance in herpesviruses other than cytomegalovirus. *Rev Med Virol* **24:**186–218. PubMed
49. **Sedlak RH, Cook L, Huang M-L, Magaret A, Zerr DM, Boeckh M, Jerome KR.** 2014. Identification of chromosomally integrated human herpesvirus 6 by droplet digital PCR. *Clin Chem* **60:**765–772. PubMed
50. **Ward KN, Leong HN, Nacheva EP, Howard J, Atkinson CE, Davies NW, Griffiths PD, Clark DA.** 2006. Human herpesvirus 6 chromosomal integration in

immunocompetent patients results in high levels of viral DNA in blood, sera, and hair follicles. *J Clin Microbiol* **44:**1571–1574.
51. **Hubacek P, Virgili A, Ward KN, Pohlreich D, Keslova P, Goldova B, Markova M, Zajac M, Cinek O, Nacheva EP, Sedlacek P, Cetkovsky P.** 2009. HHV-6 DNA throughout the tissues of two stem cell transplant patients with chromosomally integrated HHV-6 and fatal CMV pneumonitis. *Br J Haematol* **145:**394–398. PubMed
52. **Frenkel N, Schirmer EC, Wyatt LS, Katsafanas G, Roffman E, Danovich RM, June CH.** 1990. Isolation of a new herpesvirus from human $CD4^+$ T cells. *Proc Natl Acad Sci USA* **87:**748–752. PubMed
53. **Ablashi DV, Berneman ZN, Kramarsky B, Whitman J Jr, Asano Y, Pearson GR.** 1995. Human herpesvirus-7 (HHV-7): current status. *Clin Diagn Virol* **4:**1–13. PubMed
54. **Clark DA, Freeland ML, Mackie LK, Jarrett RF, Onions DE.** 1993. Prevalence of antibody to human herpesvirus 7 by age. *J Infect Dis* **168:**251–252. PubMed
55. **Leach CT.** 2000. Human herpesvirus-6 and -7 infections in children: agents of roseola and other syndromes. *Curr Opin Pediatr* **12:**269–274. PubMed
56. **Kempf W, Müller B, Maurer R, Adams V, Campadelli Fiume G.** 2000. Increased expression of human herpesvirus 7 in lymphoid organs of AIDS patients. *J Clin Virol* **16:**193–201. PubMed
57. **Berneman ZN, Ablashi DV, Li G, Eger-Fletcher M, Reitz MS Jr, Hung CL, Brus I, Komaroff AL, Gallo RC.** 1992. Human herpesvirus 7 is a T-lymphotropic virus and is related to, but significantly different from, human herpesvirus 6 and human cytomegalovirus. *Proc Natl Acad Sci USA* **89:**10552–10556. PubMed
58. **Fernandez C, Boutolleau D, Manichanh C, Mangeney N, Agut H, Gautheret-Dejean A.** 2002. Quantitation of HHV-7 genome by real-time polymerase chain reaction assay using MGB probe technology. *J Virol Methods* **106:**11–16. PubMed
59. **Zerr DM, Huang ML, Corey L, Erickson M, Parker HL, Frenkel LM.** 2000. Sensitive method for detection of human herpesviruses 6 and 7 in saliva collected in field studies. *J Clin Microbiol* **38:**1981–1983. PubMed
60. **Ablashi DV, Chatlynne LG, Whitman JE Jr, Cesarman E.** 2002. Spectrum of Kaposi's sarcoma-associated herpesvirus, or human herpesvirus 8, diseases. *Clin Microbiol Rev* **15:**439–464. PubMed
61. **Sarid R, Olsen SJ, Moore PS.** 1999. Kaposi's sarcoma-associated herpesvirus: epidemiology, virology, and molecular biology. *Adv Virus Res* **52:**139–232. PubMed
62. **Dittmer DP, Damania B.** 2013. Kaposi sarcoma associated herpesvirus pathogenesis (KSHV)—an update. *Curr Opin Virol* **3:**238–244. PubMed
63. **Gramolelli S, Schulz TF.** 2015. The role of Kaposi sarcoma-associated herpesvirus in the pathogenesis of Kaposi sarcoma. *J Pathol* **235:**368–380. PubMed
64. **Dow DE, Cunningham CK, Buchanan AM.** 2014. A review of human herpesvirus 8, the Kaposi's sarcoma-associated herpesvirus, in the pediatric population. *J Pediatric Infect Dis Soc* **3:**66–76. PubMed
65. **Edelman DC.** 2005. Human herpesvirus 8—a novel human pathogen. *Virol J* **2:**78. doi:10.1186/1743-422X-2-78 PubMed
66. **Kaplan LD.** 2013. Human herpesvirus-8: kaposi sarcoma, multicentric Castleman disease, and primary effusion lymphoma. *Hematology (Am Soc Hematol Educ Program)* **2013:**103–108. PubMed
67. **Ammari ZA, Mollberg NM, Abdelhady K, Mansueto MD, Massad MG.** 2013. Diagnosis and management of primary effusion lymphoma in the immunocompetent and immunocompromised hosts. *Thorac Cardiovasc Surg* **61:**343–349. PubMed
68. **Gantt S, Casper C.** 2011. Human herpesvirus 8-associated neoplasms: the roles of viral replication and antiviral treatment. *Curr Opin Infect Dis* **24:**295–301. PubMed
69. **Cousins E, Nicholas J.** 2014. Molecular biology of human herpesvirus 8: novel functions and virus-host interactions implicated in viral pathogenesis and replication. *Recent Results Cancer Res* **193:**227–268. PubMed
70. **Campbell DM, Rappocciolo G, Jenkins FJ, Rinaldo CR.** 2014. Dendritic cells: key players in human herpesvirus 8 infection and pathogenesis. *Front Microbiol* **5:**452. PubMed
71. **Tedeschi R, Dillner J, De Paoli P.** 2002. Laboratory diagnosis of human herpesvirus 8 infection in humans. *Eur J Clin Microbiol Infect Dis* **21:**831–844. PubMed
72. **Chang Y, Cesarman E, Pessin MS, Lee F, Culpepper J, Knowles DM, Moore PS.** 1994. Identification of herpesvirus-like DNA sequences in AIDS-associated Kaposi's sarcoma. *Science* **266:**1865–1869. PubMed
73. **Curreli F, Robles MA, Friedman-Kien AE, Flore O.** 2003. Detection and quantitation of Kaposi's sarcoma-associated herpesvirus (KSHV) by a single competitive-quantitative polymerase chain reaction. *J Virol Methods* **107:**261–267. PubMed
74. **Lallemand F, Desire N, Rozenbaum W, Nicolas JC, Marechal V.** 2000. Quantitative analysis of human herpesvirus 8 viral load using a real-time PCR assay. *J Clin Microbiol* **38:**1404–1408. PubMed
75. **Stamey FR, Patel MM, Holloway BP, Pellett PE.** 2001. Quantitative, fluorogenic probe PCR assay for detection of human herpesvirus 8 DNA in clinical specimens. *J Clin Microbiol* **39:**3537–3540. PubMed
76. **Simonelli C, Tedeschi R, Gloghini A, Talamini R, Bortolin MT, Berretta M, Spina M, Morassut S, Vaccher E, De Paoli P, Carbone A, Tirelli U.** 2009. Plasma HHV-8 viral load in HHV-8-related lymphoproliferative disorders associated with HIV infection. *J Med Virol* **81:**888–896. PubMed
77. **Oksenhendler E, Carcelain G, Aoki Y, Boulanger E, Maillard A, Clauvel J-P, Agbalika F.** 2000. High levels of human herpesvirus 8 viral load, human interleukin-6, interleukin-10, and C reactive protein correlate with exacerbation of multicentric castleman disease in HIV-infected patients. *Blood* **96:**2069–2073. PubMed
78. **Sayer R, Paul J, Tuke PW, Hargreaves S, Noursadeghi M, Tedder RS, Grant P, Edwards SG, Miller RF.** 2011. Can plasma HHV8 viral load be used to differentiate multicentric Castleman disease from Kaposi sarcoma? *Int J STD AIDS* **22:**585–589. PubMed
79. **Zhu L, Wang R, Sweat A, Goldstein E, Horvat R, Chandran B.** 1999. Comparison of human sera reactivities in immunoblots with recombinant human herpesvirus (HHV)-8 proteins associated with the latent (ORF73) and lytic (ORFs 65, K8.1A, and K8.1B) replicative cycles and in immunofluorescence assays with HHV-8-infected BCBL-1 cells. *Virology* **256:**381–392. PubMed
80. **Rabkin CS, Schulz TF, Whitby D, Lennette ET, Magpantay LI, Chatlynne L, Biggar RJ, HHV-8 Interlaboratory Collaborative Group.** 1998. Interassay correlation of human herpesvirus 8 serologic tests. HHV-8 Interlaboratory Collaborative Group. *J Infect Dis* **178:**304–309. PubMed
81. **Spira TJ, Lam L, Dollard SC, Meng Y-X, Pau CP, Black JB, Burns D, Cooper B, Hamid M, Huong J, Kite-Powell K, Pellett PE.** 2000. Comparison of serologic assays and PCR for diagnosis of human herpesvirus 8 infection. *J Clin Microbiol* **38:**2174–2180. PubMed
82. **Burbelo PD, Issa AT, Ching KH, Wyvill KM, Little RF, Iadarola MJ, Kovacs JA, Yarchoan R.** 2010. Distinct profiles of antibodies to Kaposi sarcoma-associated herpesvirus antigens in patients with Kaposi sarcoma, multicentric Castleman disease, and primary effusion lymphoma. *J Infect Dis* **201:**1919–1922. PubMed

Parvovirus B19

STANLEY J. NAIDES

62

Autonomous parvoviruses capable of helper-virus-independent replication have been isolated from many animal species. The human serum parvovirus B19 was accidentally discovered in 1975 in healthy donor blood used in the development of hepatitis B virus surface antigen diagnostic tests. To date, three B19-type genotypes have been described: types 1 (B19), 2 (A6/K71), and 3 (V9). Disease variation has not been reported amongst the three genotypes (1–3). Bocavirus, another parvovirus, has been associated with pulmonary infection (4). PARV4 has been identified in a parenteral drug abuser, but human disease causation has not been confirmed (5, 6). Recently, a proposal was submitted to the International Committee on Taxonomy of Viruses to reclassify B19 as primate erythroparvovirus type 1. The most frequent clinical presentation of B19 infection is erythema infectiosum, or fifth disease, a common childhood exanthem. Application of sensitive molecular biological and immunological methods to viral diagnosis has allowed recognition of the ever-expanding spectrum of clinical presentation (7).

BIOLOGICAL, CLINICAL, AND EPIDEMIOLOGICAL FEATURES

Physicobiochemical Characteristics

B19 and its variants are currently members of the *Erythrovirus* genus, subfamily *Parvovirinae*, family *Parvoviridae*; the genus contains members of the family that infect mammalian hosts and are autonomous in their ability to replicate in host erythroid precursors. Parvovirus B19 is one of the smallest (18 to 26 nm in diameter) DNA viruses known to infect humans. It forms nonenveloped icosahedral virions. The single-stranded genome contains approximately 5,600 nucleotides (8) and has double-stranded palindromic hairpin termini. B19 encapsidates a single copy of genome. Progeny virus populations are represented by equal numbers of virions containing positive- or negative-sense DNA.

B19 employs a simple coding strategy. A single strong promoter at map unit 6 initiates transcription for both a left-handed nonstructural protein region and a right-handed structural protein region (9). The nonstructural protein, NS1, is approximately 74,000 Da and is encoded between nucleotides 435 and 2448. NS1 is a helicase that provides the "nickase" activity for reduction of replicative DNA forms to progeny virus DNA that can be packaged into the virion and may also play a role in the assembly of viral DNA into mature capsids during viral replication. NS1 causes apoptosis in replication-permissive erythroid precursor cells as well as in nonpermissive cells, e.g., hepatocytes (10, 11).

Both structural proteins, VP1 and VP2, are encoded in the same open reading frame by nucleotides at positions 2444 to 4786 and 3125 to 4786 and are 84,000 and 58,000 Da, respectively. VP2 transcription is initiated at an alternate start site at nucleotide 3125 (12). Small proteins measuring 7.5 kDa and 11 kDa, respectively, are encoded in the capsid region, but their function has not been well defined.

Pathogenesis and Pathology

Experiments on healthy volunteers provided a detailed picture of the natural history of B19 infection in the normal host (13). When B19 viremic plasma was inoculated into the nostrils of previously seronegative individuals, B19 was first detected in recipient serum by day 6 postinoculation. Viremia lasted up to 7 days, with the peak occurring on days 8 and 9 postinoculation. During this period, B19 DNA appeared in nasal and oropharyngeal secretions but virus was not detected in urine or stool. Approximately 11 days postinoculation, high-titer anti-B19 immunoglobulin M (IgM) antibody developed, followed by the appearance of anti-B19 IgG antibody. Volunteers with a significant level of preexistent anti-B19 antibody did not show any evidence of viremia or anti-B19 IgM response. During the viremic phase, some of the subjects had a flulike illness with malaise, myalgia, and transient fever. Coincident with the onset of viremia, reticulocytosis was absent and remained so for up to 10 days. Viremia was cleared with the onset of the anti-B19 IgM antibody response, which was associated with the second phase of clinical illness, characterized by rash, arthralgia, and arthritis (13). The cell receptors for B19 have been reported to be the neutral glycosphingolipid globoside, which is widely distributed in various cell types (14–16). α_5 β_1-Integrins and Ku80 may serve as coreceptors (17, 18). Endothelial cell uptake may occur by anti-B19 IgG-bound C1q via C1q receptor on endothelial cells (19). Cell injury occurs by NS1-mediated host cell DNA damage and resulting apoptosis and downstream events (10, 20–24).

During natural infection, the incubation period may vary from 6 to 18 days, with a maximum of 28 days. By the time most patients present, usually with rash, polyarthralgia,

doi:10.1128/9781555818722.ch62

and/or polyarthritis, an anti-B19 IgM response has begun and the patients are not infectious. An exception is the patient with aplastic crisis, who typically presents during the viremic phase. Usually, anti-B19 IgM is present for up to 2 to 3 months postinfection, after which its level may wane. Specific IgG response to B19 is long-lived. Approximately 50% of the adult population has anti-B19 IgG antibodies (25).

Clinical Manifestations

The clinical spectrum of parvovirus B19 infection may be classified by common (Table 1) and uncommon (Table 2) presentations.

Nearly half of infected children and adults have subclinical or asymptomatic infection. Erythema infectiosum, or fifth disease of childhood, is the best-known manifestation of B19 infection. Children aged 4 to 7 years are typically infected as they enter school, but children as young as 1 year of age and adolescents may present with fifth disease. Prodromal symptoms are often mild. The majority of the children have the hallmark rash characterized by bright red "slapped cheeks." The rash may also appear on the torso and extremities. It may recur after sun exposure, hot bath, or physical activity. Usually the exanthem is a lacy, reticular, "fish net," or blotchy macular or maculopapular eruption, but occasionally it is vesicular or hemorrhagic. Other symptoms usually are mild and include sore throat, headache, fever, cough, anorexia, vomiting, diarrhea, and arthralgia. Children presenting with rash usually have serum anti-B19 IgM antibody present at presentation. Uncommon dermatological manifestations include vesiculopustular eruption, purpura with or without thrombocytopenia, and a "socks-and-gloves" erythema. Erythema infectiosum may also be encountered in adults in whom the rash tends to be more subtle and the bright red slapped-cheeks symptom is often absent; the flu-like symptoms may be more severe in adults.

Approximately 10% of children with erythema infectiosum have associated arthritis and arthralgia. In adults, the polyarthralgia and joint swelling tend to be more prominent (26–28). The arthropathy typically appears as an acute, moderately severe, symmetric, peripheral polyarthritis. The joints most frequently affected include the metacarpophalangeal joints, proximal interphalangeal joints, wrists, knees, and ankles. The duration of these symptoms is usually brief (approximately 10 days), but one-third of patients continue to have persistent joint symptoms 2 to 3 months after onset of the disease. About half of patients who have chronic parvovirus arthropathy meet the criteria of the American Rheumatism Association for a diagnosis of rheumatoid arthritis (27). Patients may have transient expression of autoantibodies, usually in low to moderate titer, including rheumatoid factor, anti-DNA, antilymphocyte, antinuclear, anticardiolipin, and antiphospholipid antibodies (28, 29). Unlike rheumatoid arthritis, there is no major histocompatibility HLA DR4 predisposition to B19 arthropathy (30, 31). The pathogenesis of B19 arthropathy has not been fully elucidated. In patients with chronic B19 arthropathy, B19 DNA may be found in bone marrow aspirates and in synovial biopsy specimens, suggesting B19 viral persistence in apparently immunocompetent individuals (32–34). B19 DNA has been detected in the normal synovium of young adults by using sensitive PCR techniques (33, 34). One group reported B19 DNA and capsid protein in rheumatoid synovium (35). Coculture of B19-positive rheumatoid synovium with normal cells increased tumor necrosis factor alpha production, a finding typical of rheumatoid arthritis; the group suggested that B19 may be a causative agent of rheumatoid arthritis, a provocative suggestion that remains to be confirmed (35). Others observed that inoculation of normal synovial fibroblasts with B19 virus induces a cartilage matrix invasive phenotype more typical of rheumatoid arthritis synoviocytes (36). Transgenic mice expressing B19 nonstructural protein, NS1, are prone to developing polyarthritis (37).

Fetal parvovirus B19 infection presents as fetal or congenital anemia, hydrops fetalis, spontaneous abortion, or stillbirth. In some cases, fetal infection is asymptomatic and self-limited. During B19 infection *in utero*, virus infects fetal erythroid progenitor cells, causing maturation arrest and severe anemia. The resulting hypoxia causes high-output cardiac failure with fluid accumulation in body cavities and generalized edema of the fetus. B19 may also infect the fetal liver, spleen, kidneys, heart, lungs, thymus, adrenal glands, skeletal muscle, eyes, and placental tissue (7, 10, 38).

Individuals with inherited or acquired conditions causing a decrease in reticulocyte production or shortened erythrocyte survival may develop aplastic crisis during an acute B19 infection. These predisposing conditions include iron deficiency; congenital dyserythropoietic anemia; α- and β-thalassemias; hereditary spherocytosis, stomatocytosis, or elliptocytosis; deficiencies in the production of erythrocyte enzymes such as glucose-6-phosphate dehydrogenase, pyruvate kinase, pyrimidine-5′-nucleotidase; sickle cell disease;

TABLE 1 Common clinical presentations of parvovirus B19 infection

Asymptomatic infection
Aplastic crisis
Erythema infectiosum (fifth disease)
Hydrops fetalis
Arthropathy, acute and/or chronic
Chronic or recurrent bone marrow suppression in immunocompromised individuals

TABLE 2 Less common clinical presentations of parvovirus B19 infection

Skin
Vesiculopustular eruption
Henoch-Schönlein purpura
Thrombotic thrombocytopenic purpura
Socks-and-gloves syndrome
Hematological
Anemia
Thrombocytopenia
Leukopenia
Benign acute lymphadenopathy
Hemophagocytic syndrome
Cardiovascular
Polyarteritis nodosa
Wegener's granulomatosis
Myocarditis
Liver
Hepatocellular enzyme elevations
Hepatitis
Non-A, non-B, non-C, non-E, non-G fulminant liver failure
Nervous system
Paresthesias
Meningitis
Sensorineural hearing loss

chronic autoimmune hemolytic anemia; antibody-mediated autoimmune hemolytic anemia; paroxysmal nocturnal hemoglobinuria; virus-associated hemophagocytosis; and blood loss. In healthy individuals, B19 causes transiently decreased reticulocyte production, but this is not usually clinically evident (39, 40).

Chronic or recurrent bone marrow suppression with anemia, thrombocytopenia, and/or leukopenia has been found in patients with immune compromise including Nezelof's syndrome; those who had undergone prior chemotherapy for lymphoproliferative disorders including acute lymphocytic leukemia, chronic myeloid leukemia, Burkitt's lymphoma, acute lymphoblastic lymphoma, myelodysplastic syndrome, astrocytoma, and Wilms' tumor; those with human immunodeficiency virus infection and AIDS; and those who were receiving immunosuppressive therapy for bone marrow or organ transplantation. In immunocompetent hosts, anti-B19 IgM and acute-phase IgG antibody recognize antigenic determinants on VP2 and may last for 2 months or more. Convalescent-phase anti-B19 IgG antibody recognizes determinants on VP1 (40). VP1 differs from VP2 by containing unique N-terminal determinants absent from the shorter VP2 (12). Patients with congenital or acquired immunodeficiencies fail to produce convalescent-phase IgG antibodies to VP1, and their serum is unable to neutralize B19 *in vitro* (40). These individuals have less intensive viremia than that experienced during acute infection or aplastic crisis, but viremia may be recurrent or chronic and associated with recurrent or chronic suppression of one or more bone marrow-derived lineages, causing anemia, leukopenia and/or thrombocytopenia. Since IgG seroprevalence in the adult population is approximately 50%, neutralizing activity to B19 is present in commercially available pooled immunoglobulin. Administration of commercial immunoglobulin with anti-B19 activity to patients with immunodeficiency who have chronic B19 infection and cytopenias is effective in clearing B19 infection and allowing bone marrow recovery (41).

Several uncommon presentations of B19 infection have been described, including idiopathic thrombocytopenia purpura, transient erythroblastopenia of childhood, Diamond-Blackfan anemia, encephalitis, aseptic meningitis, brachial plexus neuropathy, paresthesias, neuralgic amyotrophy, and motor weakness. Unusual rheumatologic presentations attributed to B19 infection include systematic vasculitis, Henoch-Schönlein purpura, Kawasaki's disease, polyarteritis nodosa, adult Still's disease, fibromyalgia, and systemic lupus erythematosus. Parvovirus B19 has also been associated with hepatitis, acute fulminant liver failure, myocarditis, mononucleosis-like syndrome, Koplik's spots, and pneumonia (7, 10, 39, 41–44).

Epidemiology

Parvovirus B19, genotype 1, has a worldwide distribution. Genotypes 2 and 3 tend to be found in Europe and Africa (1–3). B19 infection occurs in all age groups throughout the year in epidemics or as sporadic cases. The peak incidence is seasonal, occurring predominantly in late winter and early spring. Serological studies show that B19 has usually infected 2 to 15% of children under the age of 5 years, 15 to 60% of school-age children (5 to 19 years old), and 30 to 60% of adults. The highest rates of natural infection (50 to 60%) were observed during outbreaks of erythema infectiosum or B19-induced aplastic crisis (45, 46).

Natural transmission of B19 occurs mostly via respiratory secretions or vertically from mother to fetus. Recently, transmission via transfusion of blood and blood products was reported. The frequency of contamination of blood obtained from single donors usually ranges from 1 in 30,000 to 1 in 50,000 donations. However, the frequency of contamination of pooled clotting-factor concentrates can be much higher (47).

LABORATORY DIAGNOSIS

Cell Culture

A major limitation in studies of B19 has been the absence of appropriate cell lines permissive for the virus. Attempts to detect B19 virus in standard cell cultures have not been successful. Several investigators use cell cultures of erythroid origin for B19 propagation. B19 infection of primary cell cultures of erythroid precursors derived from human fetal liver and bone marrow or of human megakaryocytic leukemic cell lines has been successful. However, cultivation of B19 in these cell cultures is not routine, and the viral yield tends to be low. Attempts to use animals, including anthropoid primates, for modeling B19 infection have been unsuccessful.

Electron Microscopy

Standard electron microscopy methods of negative staining allow the examination of a liquid sample dried on an electron microscopy grid that had been previously coated with a thin layer of plastic, followed by staining with phosphotungstic acid or uranyl acetate. Electron-dense material accumulates around viral particles, giving a bas relief appearance or negative-contrast image (Fig. 1).

Specific viral identification may be confirmed by immunoaggregation with polyclonal or monoclonal anti-B19 antibodies (immunoelectron microscopy [IEM]), or by immunogold labeling. However, successful IEM requires the absence of excess endogenous anti-B19 antibody in the sample. In serum samples, "bare" virions are present only in the very early stages of infection before specific antibody develops. IEM may be useful when used with nonserum body fluids or tissues in which anti-B19 antibody is not present in high titer. After incubation of the sample with specific antiserum or anti-B19 monoclonal antibody, centrifugation, and negative staining, the aggregated virions can be seen by electron microscopic examination.

Combined pseudoreplica-immunochemical staining may be more useful, even in the presence of endogenous anti-B19 antibody, since even a few antigenic sites may be adequate to allow the labeling of B19 by specific anti-B19 monoclonal antibodies. Virus can be detected in various body fluids by this method (38). In the pseudoreplica technique, a sample is absorbed into an agarose block, leaving viral particles on the surface. The agarose is then overlaid with a plastic film, which, after hardening, is floated off the agarose, inverted, applied to a support grid, and negatively stained. Combined pseudoreplica-immunochemical staining uses second-stage gold-conjugated labeling antibodies to detect first-stage anti-B19 monoclonal antibody before negative staining. Examination of viral particles with specific colloidal-gold-conjugated antibodies permits species identification. Otherwise, it may be difficult to discriminate B19 virions from other nonenveloped icosahedral viruses of a similar size, such as enteroviruses, on the basis of morphology alone. B19 may be present as "full" particles with the contrast stain excluded, or stain may enter the capsid, giving the appearance of an "empty" shell (Fig. 1). Although these methods have high specificity, they require special equipment and experienced examiners and are labor-intensive, rendering them suboptimal for routine diagnosis (38).

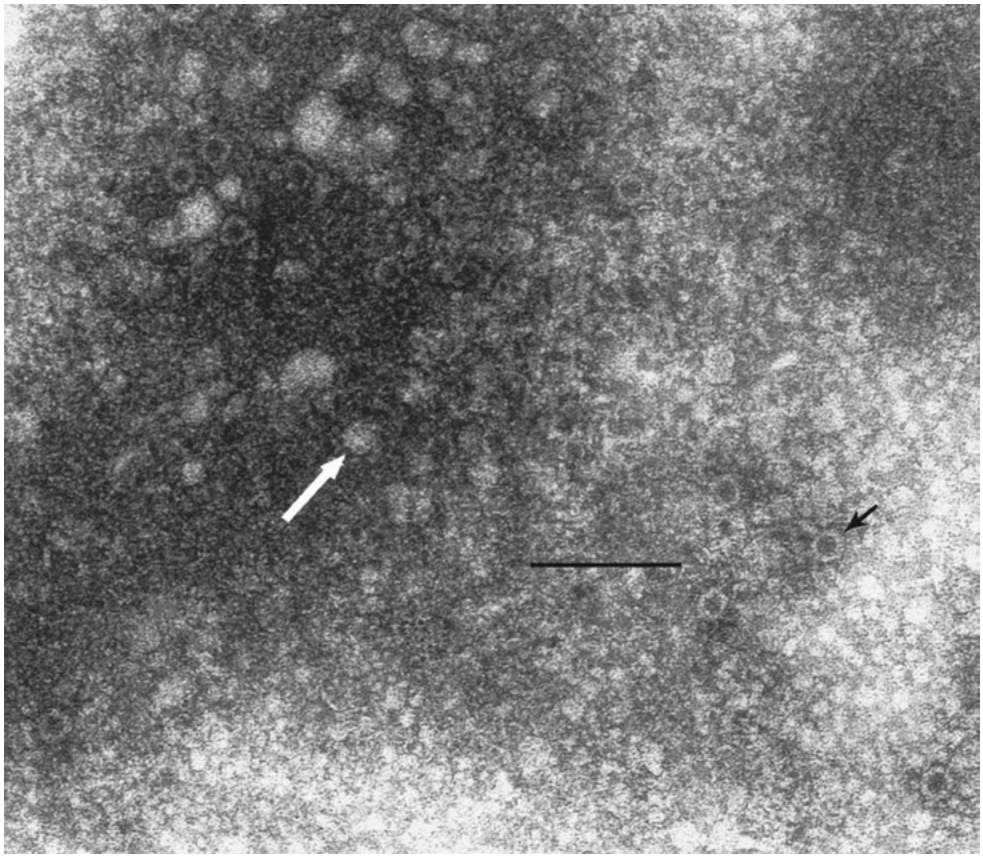

FIGURE 1 Electron micrograph of serum from a patient with sickle cell disease and aplastic crisis, showing full (white arrow) and empty (black arrow) nonenveloped, icosahedral viral particles measuring ~23 nm in diameter, visualized by negative staining with uranyl acetate. Bar, 100 nm (original magnification, ×196,000). Reprinted from reference 26 with permission of the publisher.

Immunoassays

Immunofluorescence assay, radioimmunoassay (RIA), and enzyme-linked immunosorbent assay (ELISA) have been used to detect both B19 antigen and specific anti-B19 antibody. The indirect immunofluorescence assay was successfully applied to the cellular localization of B19 antigen in tissue and cell culture samples but has not found wide clinical application. Several RIA and ELISA systems were developed for detecting B19 antigen and anti-B19 IgM and IgG antibody. Prior to laboratory cloning and production of recombinant capsid proteins, native virus from viremic patients served as an antigen source (Fig. 2A) (48, 49). Briefly, for antibody capture RIA or ELISA to detect anti-B19 IgM or anti-B19 IgG, microtiter plates (solid phase) are incubated overnight to coat the wells with anti-human IgM (μ-chain specific) or anti-human IgG (γ-chain specific) antibody, respectively. After the plates have been washed with phosphate-buffered saline containing a low concentration of nonionic detergent to prevent nonspecific aggregation, the serum to be tested for antibody is added. After incubation and washing with buffer, a high-titer B19 viremic serum without endogenous anti-B19-specific antibodies is added as an antigen source; an antigen-negative control serum may be added to parallel wells to detect nonspecific reagent cross-reactivity. Detection of such cross-reactivity may be necessary to avoid false-positive results for patients presenting with autoantibodies such as rheumatoid factor (27). After overnight incubation and washing with buffer, murine monoclonal antibody with anti-B19 activity is added. After nonadherent anti-B19 murine monoclonal antibody is washed off, anti-mouse class-specific antibody labeled with ^{125}I (RIA) or peroxidase (ELISA) is added. After incubation and washing, radioactivity is counted or color developer is added in the presence of hydrogen peroxide, and the reaction is stopped with 2 M H_2SO_4.

If the RIA or ELISA is used for detection of antigen, a defined serum with high-titer anti-B19 IgM is added instead of patient serum. After incubation and washing, the serum to be tested for virus is added instead of known viremic serum. In the antigen capture assay, parallel wells with an anti-B19 IgM negative control capture serum and parallel wells with appropriate virus negative control sample (e.g., normal serum, body fluid, and cell lysate) must be added to detect nonspecific reagent cross-reactivity. In both the antibody capture and antigen capture assays, test wells must be compared to background wells for a given sample (27).

Identification of a stock of high-titer viremic serum without endogenous anti-B19 antibody for use as antigen in immunoassays (Fig. 2A and B) requires significant effort. B19 virus in a panel of candidate antigen sources may be detected by screening antigen capture RIA or ELISA (Fig. 2C) and confirmed by molecular detection of B19 DNA. Screening may be performed for sera candidates by PCR methods, and positive samples may be tested in an antibody capture assay to eliminate those with endogenous anti-B19 antibody.

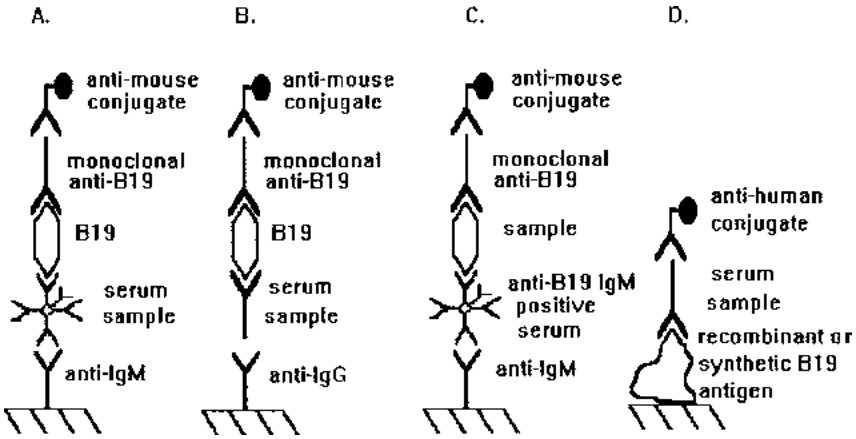

FIGURE 2 ELISA-based tests showing antibody capture ELISA for anti-B19 IgM antibody (A), antibody capture ELISA for anti-B19 IgG antibody (B), antigen capture ELISA for B19 virus (C), and recombinant or synthetic B19 antigen-based ELISA for detection of B19 antibody (D).

To overcome the problem of limited access to antigen for diagnostic testing, a number of commercially available antibody capture ELISA assays were developed using recombinant VP2 (Fig. 2D). VP2 protein expressed in Chinese hamster ovary cells, bacteria, or baculovirus expression systems spontaneously self-assembles into empty capsids (10, 50–54).

Antibodies to genotypes 1 and 3 may be detected equally well by using ELISAs targeting B19 or V9, respectively (47).

Methods for Detection of B19 Nucleic Acid

B19 DNA may be detected by hybridization with cDNA probes, riboprobes (synthetic RNA), or synthetic oligonucleotide probes. Hybridization may be performed directly on tissue or cells by *in situ* hybridization allowing localization of viral DNA. Disrupted virus-containing sample or extracted DNA may be blotted onto a nitrocellulose or nylon membrane before being hybridized with B19-specific probe. Numerous modifications of this basic approach have been used to detect B19 in body fluids, blood products, tissue, and cell culture extracts. Nonradioactive labels for probes may be used for safety and long shelf life. B19 DNA has been detected in serum by using a digoxigenin-labeled RNA probe to hybridize with target DNA, followed by capture of the hybrid onto a solid phase (microtiter wells) previously coated with a second anti-B19 oligonucleotide probe to an unhybridized portion of the B19 target DNA; an alkaline phosphatase-conjugated antidigoxigenin antibody and chemiluminescent substrate allow the detection of B19 DNA on a scintillation counter.

PCR-based technologies offer exquisite sensitivity and the ability to detect B19 DNA in different types of clinical specimens. Various oligonucleotide primers directed against sequences in both the nonstructural and viral capsid protein genes have been used (55–58). PCR is more sensitive than traditional dot blot hybridization; the use of an internal radiolabeled probe to detect amplification product by Southern analysis is still more sensitive than dot blot hybridization. Many investigators have now reported the use of PCR to detect B19 in fetal and adult tissues, body fluids, blood products, and cell cultures. However, PCR detection of B19 DNA in clinical samples is not problem free. The most common problem is the presence in clinical samples of inhibitors of *Taq* polymerase (56). Different approaches to avoid this problem have been used, including controlled heating of the sample, detergent extraction of DNA, and the use of a second round of amplification with nested primers. In antigen capture or immunoadherence PCR, virus is adhered to PCR tubes precoated with anti-B19 monoclonal antibody, and after incubation and washing, the PCR mixture (containing primers, deoxynucleoside triphosphates, and *Taq* polymerase) is added, virions are disrupted by heating, and viral DNA is amplified. This approach avoids nonspecific inhibition and provides high sensitivity and specificity (34, 38). While PCR primers and conditions may be optimized to preferentially amplify genotypes 2 and 3, B19-specific assays detect most isolates of genotypes 2 (A6/K71) or 3 (V9) (58).

Interpretation

Molecular testing for B19 DNA in serum is helpful during the viremic phase in acute infection. Viremia is accompanied by constitutional symptoms of fever, chills, and malaise, but once arthralgia, arthritis and/or rash appears in immunocompetent individuals, standard PCR methods are typically negative. However, immunocompromised patients may have chronic viremia or intermittent viremia for years. A positive PCR test confirms a B19 infection in any setting, but in acute infection viremia is typically 10^{11} virions or more per mL (39). In chronic infection in immunocompromised patients, viremia may be as low as 10^3 virions per mL (59). Initial PCR screening methods had analytical sensitivity of as little as 5 virions per mL (60).

When immunocompetent individuals present with arthralgia, arthritis and/or rash, they typically have B19 IgM. B19 IgG is often present, but if not present initially, it usually appears within a few days. Sensitivity for B19 IgM detection at this time using commercially available kits is essentially 100%. Specificity ranged between 94.2 and 98.5% in patients with other acute infections or autoimmune diseases (61).

DISEASE PREVENTION AND THERAPY

Parvovirus B19 infection is widespread in the community. It is therefore difficult to prevent exposure and to control the spread of infection. Community and household contacts are frequently asymptomatic. Hospital exposures may occur. However, isolation of viremic patients may decrease the level of exposure (46).

Specific antiviral therapy has not been identified. In general, patient management is symptomatic and supportive.

Patients with acute aplastic crisis may require blood transfusion. Adults with chronic B19 arthropathy are managed with nonsteroidal antiinflammatory drugs (27). Fetal transfusion *in utero* may be required to support the fetus during B19 infection complicated by severe anemia; fetuses transfused *in utero* and surviving the aplastic crisis have been born without apparent long-term sequelae (38). Immunocompromised patients who lack neutralizing anti-B19 antibodies and who present with manifestations of persistent B19 infection benefit from commercial intravenous immunoglobulin (41). Intramuscular immunoglobulin for prophylaxis following B19 exposure has not been adequately evaluated (55). Specific antiviral chemotherapy for parvovirus B19 has not been demonstrated.

REFERENCES

1. **Candotti D, Etiz N, Parsyan A, Allain JP.** 2004. Identification and characterization of persistent human erythrovirus infection in blood donor samples. *J Virol* **78:**12169–12178. PubMed
2. **Hokynar K, Norja P, Laitinen H, Palomäki P, Garbarg-Chenon A, Ranki A, Hedman K, Söderlund-Venermo M.** 2004. Detection and differentiation of human parvovirus variants by commercial quantitative real-time PCR tests. *J Clin Microbiol* **42:**2013–2019. PubMed
3. **Nguyen QT, Wong S, Heegaard ED, Brown KE.** 2002. Identification and characterization of a second novel human erythrovirus variant, A6. *Virology* **301:**374–380. PubMed
4. **Martin ET , Kuypers J, McRoberts JP, Englund JA, Zerr DM.** 2015. Human bocavirus-1 primary infection and shedding in infants. *J Infect Dis* **212:**516–524. PubMed
5. **Matthews PC, Malik A, Simmons R, Sharp C, Simmonds P, Klenerman P.** 2014. PARV4: an emerging tetraparvovirus. *PLoS Pathog* **10:**e1004036. PubMed
6. **Benjamin LA, Lewthwaite P, Vasanthapuram R, Zhao G, Sharp C, Simmonds P, Wang D, Solomon T.** 2011. Human parvovirus 4 as potential cause of encephalitis in children, India. *Emerg Infect Dis* **17:**1484–1487.
7. **Naides SJ.** 1999. Infection with Parvovirus B19. *Curr Infect Dis Rep* **1:**273–278. PubMed
8. **Shade RO, Blundell MC, Cotmore SF, Tattersall P, Astell CR.** 1986. Nucleotide sequence and genome organization of human parvovirus B19 isolated from the serum of a child during aplastic crisis. *J Virol* **58:**921–936. PubMed
9. **Blundell MC, Beard C, Astell CR.** 1987. In vitro identification of a B19 parvovirus promoter. *Virology* **157:**534–538. PubMed
10. **Naides SJ.** 2000. Parvoviruses, p 487–500. *In* Specter S, Hodinka RL, Young SA (ed), *Clinical Virology Manual*. ASM Press, Washington, DC.
11. **Poole BD, Karetnyi YV, Naides SJ.** 2004. Parvovirus B19-induced apoptosis of hepatocytes. *J Virol* **78:**7775–7783. PubMed
12. **Brunstein J, Söderlund-Venermo M, Hedman K.** 2000. Identification of a novel RNA splicing pattern as a basis of restricted cell tropism of erythrovirus B19. *Virology* **274:**284–291. PubMed
13. **Anderson MJ, Higgins PG, Davis LR, Willman JS, Jones SE, Kidd IM, Pattison JR, Tyrrell DA.** 1985. Experimental parvoviral infection in humans. *J Infect Dis* **152:**257–265. PubMed
14. **Cooling LL, Zhang DS, Naides SJ, Koerner TA.** 2003. Glycosphingolipid expression in acute nonlymphocytic leukemia: common expression of shiga toxin and parvovirus B19 receptors on early myeloblasts. *Blood* **101:**711–721. PubMed
15. **Cooling LLW, Koerner TA, Naides SJ.** 1995. Multiple glycosphingolipids determine the tissue tropism of parvovirus B19. *J Infect Dis* **172:**1198–1205. PubMed
16. **Cooling LLW, Zhang DS, Naides SJ, Koerner TAW.** 2003. Glycosphingolipid expression in acute nonlymphocytic leukemia: common expression of shiga toxin and parvovirus B19 receptors on early myeloblasts. *Blood* **101:**711–721. PubMed
17. **Weigel-Kelley KA, Yoder MC, Srivastava A.** 2003. Alpha5beta1 integrin as a cellular coreceptor for human parvovirus B19: requirement of functional activation of beta1 integrin for viral entry. *Blood* **102:**3927–3933. PubMed
18. **Munakata Y, Saito-Ito T, Kumura-Ishii K, Huang J, Kodera T, Ishii T, Hirabayashi Y, Koyanagi Y, Sasaki T.** 2005. Ku80 autoantigen as a cellular coreceptor for human parvovirus B19 infection. *Blood* **106:**3449–3456. PubMed
19. **von Kietzell K, Pozzuto T, Heilbronn R, Grössl T, Fechner H, Weger S.** 2014. Antibody-mediated enhancement of parvovirus B19 uptake into endothelial cells mediated by a receptor for complement factor C1q. *J Virol* **88:**8102–8115. PubMed
20. **Moffatt S, Yaegashi N, Tada K, Tanaka N, Sugamura K.** 1998. Human parvovirus B19 nonstructural (NS1) protein induces apoptosis in erythroid lineage cells. *J Virol* **72:**3018–3028. PubMed
21. **Kivovich V, Gilbert L, Vuento M, Naides SJ.** 2010. Parvovirus B19 genotype specific amino acid substitution in NS1 reduces the protein's cytotoxicity in culture. *Int J Med Sci* **7:**110–119. PubMed
22. **Kivovich V, Gilbert L, Vuento M, Naides SJ.** 2012. The putative metal coordination motif in the endonuclease domain of human Parvovirus B19 NS1 is critical for NS1 induced S phase arrest and DNA damage. *Int J Biol Sci* **8:**79–92. PubMed
23. **Poole BD, Kivovich V, Gilbert L, Naides SJ.** 2011. Parvovirus B19 nonstructural protein-induced damage of cellular DNA and resultant apoptosis. *Int J Med Sci* **8:**88–96. PubMed
24. **Thammasri K, Rauhamäki S, Wang L, Filippou A, Kivovich V, Marjomäki V, Naides SJ, Gilbert L.** 2013. Human parvovirus B19 induced apoptotic bodies contain altered self-antigens that are phagocytosed by antigen presenting cells. *PLoS One* **8:**e67179. PubMed
25. **Eis-Hübinger AM, Oldenburg J, Brackmann HH, Matz B, Schneweis KE.** 1996. The prevalence of antibody to parvovirus B19 in hemophiliacs and in the general population. *Zentralbl Bakteriol* **284:**232–240. PubMed
26. **Naides SJ.** 1998. Rheumatic manifestations of parvovirus B19 infection. *Rheum Dis Clin North Am* **24:**375–401. PubMed
27. **Naides SJ, Scharosch LL, Foto F, Howard EJ.** 1990. Rheumatologic manifestations of human parvovirus B19 infection in adults. Initial two-year clinical experience. *Arthritis Rheum* **33:**1297–1309. PubMed
28. **Naides SJ, Field EH.** 1988. Transient rheumatoid factor positivity in acute human parvovirus B19 infection. *Arch Intern Med* **148:**2587–2589. PubMed
29. **Meyer O.** 2003. Parvovirus B19 and autoimmune diseases. *Joint Bone Spine* **70:**6–11. PubMed
30. **Klouda PT, Corbin SA, Bradley BA, Cohen BJ, Woolf AD.** 1986. HLA and acute arthritis following human parvovirus infection. *Tissue Antigens* **28:**318–319. PubMed
31. **Woolf AD, Campion GV, Klouda PT, Chiswick A, Cohen BJ, Dieppe PA.** 1987. HLA and the manifestations of human parvovirus B19 infection. *Arth Rheum*. **30:**S52.
32. **Foto F, Saag KG, Scharosch LL, Howard EJ, Naides SJ.** 1993. Parvovirus B19-specific DNA in bone marrow from B19 arthropathy patients: evidence for B19 virus persistence. *J Infect Dis* **167:**744–748. PubMed

33. **Söderlund-Venermo M, Hokynar K, Nieminen J, Rautakorpi H, Hedman K.** 2002. Persistence of human parvovirus B19 in human tissues. *Pathol Biol* (Paris) **50:**307–316. PubMed
34. **Stahl HD, Seidl B, Hubner B, Altrichter S, Pfeiffer R, Pustowoit B, Liebert UG, Hofmann J, von Salis-Soglio G, Emmrich F.** 2000. High incidence of parvovirus B19 DNA in synovial tissue of patients with undifferentiated mono- and oligoarthritis. *Clin Rheumatol* **19:**281–286. PubMed
35. **Takahashi Y, Murai C, Shibata S, Munakata Y, Ishii T, Ishii K, Saitoh T, Sawai T, Sugamura K, Sasaki T.** 1998. Human parvovirus B19 as a causative agent for rheumatoid arthritis. *Proc Natl Acad Sci USA* **95:**8227–8232. PubMed
36. **Ray NB, Nieva DRC, Seftor EA, Khalkhali-Ellis Z, Naides SJ.** 2001. Human parvovirus B19 induces an invasive phenotype in normal human synovial fibroblasts. *Arth Rheum* **44:**1582–1586.
37. **Takasawa N, Munakata Y, Ishii KK, Takahashi Y, Takahashi M, Fu Y, Ishii T, Fujii H, Saito T, Takano H, Noda T, Suzuki M, Nose M, Zolla-Patzner S, Sasaki T.** 2004. Human parvovirus B19 transgenic mice become susceptible to polyarthritis. *J Immunol* **173:**4675–4683. PubMed
38. **Naides SJ, Weiner CP.** 1989. Antenatal diagnosis and palliative treatment of non-immune hydrops fetalis secondary to fetal parvovirus B19 infection. *Prenat Diagn* **9:**105–114. PubMed
39. **Chorba T, et al.** 1986. The role of parvovirus B19 in aplastic crisis and erythema infectiosum (fifth disease). *J Infect Dis* **154:**383–393. PubMed
40. **Kurtzman GJ, Cohen BJ, Field AM, Oseas R, Blaese RM, Young NS.** 1989. Immune response to B19 parvovirus and an antibody defect in persistent viral infection. *J Clin Invest* **84:**1114–1123. PubMed
41. **Frickhofen N, Abkowitz JL, Safford M, Berry JM, Antunez-de-Mayolo J, Astrow A, Cohen R, Halperin I, King L, Mintzer D, Cohen B, Young NS.** 1990. Persistent B19 parvovirus infection in patients infected with human immunodeficiency virus type 1 (HIV-1): a treatable cause of anemia in AIDS. *Ann Intern Med* **113:**926–933. PubMed
42. **Langnas AN, Markin RS, Cattral MS, Naides SJ.** 1995. Parvovirus B19 as a possible causative agent of fulminant liver failure and associated aplastic anemia. *Hepatology* **22:**1661–1665. PubMed
43. **Sokal EM, Melchior M, Cornu C, Vandenbroucke AT, Buts JP, Cohen BJ, Burtonboy G.** 1998. Acute parvovirus B19 infection associated with fulminant hepatitis of favourable prognosis in young children. *Lancet* **352:**1739–1741. PubMed
44. **Karetnyi YV, Beck PR, Markin RS, Langnas AN, Naides SJ.** 1999. Human parvovirus B19 infection in acute fulminant liver failure. *Arch Virol* **144:**1713–1724. PubMed
45. **Anonymous.** 1989. Leads from the MMWR. Risks associated with human parvovirus B19 infection. *JAMA* **261:**1406–1408. PubMed
46. **Bell LM, Naides SJ, Stoffman P, Hodinka RL, Plotkin SA.** 1989. Human parvovirus B19 infection among hospital staff members after contact with infected patients. *N Engl J Med* **321:**485–491. PubMed
47. **Wu CG, Mason B, Jong J, Erdman D, McKernan L, Oakley M, Soucie M, Evatt B, Yu MY.** 2005. Parvovirus B19 transmission by a high-purity factor VIII concentrate. *Transfusion* **45:**1003–1010. PubMed
48. **Cohen BJ, Mortimer PP, Pereira MS.** 1983. Diagnostic assays with monoclonal antibodies for the human serum parvovirus-like virus (SPLV). *J Hyg* (London) **91:**113–130. PubMed
49. **Anderson LJ, Tsou C, Parker RA, Chorba TL, Wulff H, Tattersall P, Mortimer PP.** 1986. Detection of antibodies and antigens of human parvovirus B19 by enzyme-linked immunosorbent assay. *J Clin Microbiol* **24:**522–526. PubMed
50. **Kajigaya S, Shimada T, Fujita S, Young NS.** 1989. A genetically engineered cell line that produces empty capsids of B19 (human) parvovirus. *Proc Natl Acad Sci USA* **86:**7601–7605. PubMed
51. **Patou G, Ayliffe U.** 1991. Evaluation of commercial enzyme linked immunosorbent assay for detection of B19 parvovirus IgM and IgG. *J Clin Pathol* **44:**831–834. PubMed
52. **Bruu A-L, Nordbø SA.** 1995. Evaluation of five commercial tests for detection of immunoglobulin M antibodies to human parvovirus B19. *J Clin Microbiol* **33:**1363–1365. PubMed
53. **Heegaard ED, Qvortrup K, Christensen J.** 2002. Baculovirus expression of erythrovirus V9 capsids and screening by ELISA: serologic cross-reactivity with erythrovirus B19. *J Med Virol* **66:**246–252. PubMed
54. **Pickering JW, Forghani B, Shell GR, Wu L.** 1998. Comparative evaluation of three recombinant antigen-based enzyme immunoassays for detection of IgM and IgG antibodies to human parvovirus B19. *Clin Diagn Virol* **9:**57–63. PubMed
55. **Naides SJ, Howard EJ, Swack NS, True CA, Stapleton JT.** 1993. Parvovirus B19 infection in human immunodeficiency virus type 1-infected persons failing or intolerant to zidovudine therapy. *J Infect Dis* **168:**101–105. PubMed
56. **Clewley JP, Cohen BJ.** 1995. Investigation of human parvovirus B19 infection using PCR, p 205–215. *In* Clewley JP (ed), *The polymerase chain reaction (PCR) for human viral diagnosis*. CRC Press, Inc, Boca Raton, Fla.
57. **Hicks KE, Beard S, Cohen BJ, Clewley JP.** 1995. A simple and sensitive DNA hybridization assay used for the routine diagnosis of human parvovirus B19 infection. *J Clin Microbiol* **33:**2473–2475. PubMed
58. **Bonvicini F, Manaresi E, Bua G, Venturoli S, Gallinella GJ.** 2013. Keeping pace with parvovirus B19 genetic variability: a multiplex genotype-specific quantitative PCR assay. *J Clin Microbiol* **51:**3753–3759.
59. **Bergallo M, Merlino C, Daniele R, Costa C, Ponzi AN, Cavallo R.** 2006. Quantitative competitive-PCR assay to measure human parvovirus B19-DNA load in serum samples. *Mol Biotechnol* **32:**23–29. PubMed
60. **McOmish F, Yap PL, Jordan A, Hart H, Cohen BJ, Simmonds P.** 1993. Detection of parvovirus B19 in donated blood: a model system for screening by polymerase chain reaction. *J Clin Microbiol* **31:**323–328. PubMed
61. **Enders M, Helbig S, Hunjet A, Pfister H, Reichhuber C, Motz M.** 2007. Comparative evaluation of two commercial enzyme immunoassays for serodiagnosis of human parvovirus B19 infection. *J Virol Methods* **146:**409–413. PubMed

Respiratory Viruses

DAVID J. SPEICHER, MOHSIN ALI, AND MAREK SMIEJA

63

Respiratory viruses are among the most common acute viral infections affecting humans and contribute appreciably to school and to work absenteeism. Globally, acute respiratory tract infections (ARTI) cause frequent morbidity and mortality among children under the age of 5 years, and are a major health care burden (1). Among the very young and the very old, as well as those with chronic medical conditions, respiratory viruses contribute substantially to medical visits, prescription of antibiotics and antivirals, hospitalizations, and deaths.

Most ARTI are caused by viruses, such as human metapneumovirus (hMPV), respiratory syncytial virus (RSV), influenza viruses (IFV), parainfluenza viruses (PIV), adenoviruses (AdV), human rhinoviruses (HRV), human bocavirus (HBoV) and human coronaviruses (HCoV), but bacteria also contribute to similar clinical syndromes. However, the etiology of up to 70% of ARTI remains unknown from a laboratory perspective (2). The diagnosis, prevention, and therapy of respiratory viruses, particularly influenza, has been a major imperative for virology laboratories, public health departments, and international public health authorities such as the World Health Organization. Therefore, this chapter discusses the common viruses manifesting as ARTI in humans, the clinical syndromes, and how these pathogens can be diagnosed. The explosion of knowledge regarding the etiologic agents involved has expanded faster than the methods to ascertain whether they are causal or colonizers and has far outstripped the ability to develop preventive or treatment methods. In coming years, the anticipated development of new vaccines and antiviral drugs for the more important respiratory viruses will increase the need for prompt diagnosis.

The recognition of new species of HRV (i.e., rhinovirus C, with ≥50 genotypes), HCoV (i.e., HCoV-NL63, HCoV-HKU1, and MERS-CoV), HBoV, and polyomaviruses (i.e., WUPyV, KIPyV, and BKPyV) suggests that our knowledge is accelerating. Nevertheless, the majority of adults with ARTI, and as many as half of the children, do not have an etiologic diagnosis. The large number of undiagnosed ARTI is due to inefficient application of suitable detection methods, inadequate sampling methods or delay in obtaining diagnostic specimens, and the limitations on viral testing in many laboratories. Most respiratory viruses cause similar clinical symptoms, from fever and myalgia to abdominal pain and respiratory symptoms (3). In mild to moderate disease there may be no perceived clinical need to make a specific etiologic diagnosis, thus hampering development and availability of appropriate diagnostics. Conversely, the recognition that these agents may play a more severe or more chronic role in the immunocompromised patient has necessitated the development of improved testing.

Diagnostic testing has improved markedly over the past 20 years. Previous detection methods included serology and isolation of viruses by cell culture, but neither is optimal for all respiratory viruses because they are cumbersome, require large turnaround times (up to 10 days to diagnose influenza), and are insensitive. As well, many viruses, such as HCoV, are fastidious (4). Immunochromatic methods for detecting virus-specific antigens are much faster than culture, providing results in minutes, and may provide acceptable diagnostic test accuracy, particularly in children and during known influenza or RSV circulation. Furthermore, newly developed molecular methods are faster than culture and more accurate than either culture or antigen detection, and thus are replacing traditional methods and have enhanced the laboratory diagnoses of respiratory viruses. These changes have enabled diagnosis of a broader group of viruses, with consequent challenges in interpretation of certain viruses and of multiple viral infections. Finally, the advances in viral diagnosis have not been accompanied by a parallel improvement in the diagnosis of bacterial respiratory infections. Since viral and bacterial infection may coexist, diagnosis of a viral infection does not necessarily rule out a clinically important and treatable bacterial coinfection. As a result, the role of viruses as the sole cause of many respiratory syndromes remains controversial, and unnecessary antibiotic prescriptions for viral syndromes remain common.

Clinicians will increasingly demand rapid, accurate, and broad-spectrum diagnostic testing for viruses, particularly for hospitalized patients. In choosing which diagnostic tests to offer, the laboratory director will need to balance clinical needs against the plethora of testing modalities, the different technical and capital costs required, and the changing clinical utility of these tests in driving antibiotic and antiviral use, patient isolation and other infection control treatments, and in forecasting prognosis. Ultimately, the cost-effectiveness of providing an accurate diagnosis in different clinical settings will affect the provision of appropriate services. These are likely to be a combination of point-of-care molecular tests or enhanced sensitivity

doi:10.1128/9781555818722.ch63

immunochromatographic assays to aid in making immediate decisions (such as hospital admission or use of influenza antiviral drugs), combined with high-throughput, batched multiplex syndromic panels (for making a definitive viral diagnosis for a broader number of viruses).

TAXONOMY AND DESCRIPTION OF AGENTS

The majority of respiratory viruses are RNA viruses: nonenveloped, positive-sense single-stranded RNA viruses (e.g., HRV); enveloped, negative-sense single-stranded RNA viruses (e.g., IFV and PIV); nonenveloped, negative-sense single-stranded RNA viruses (e.g., RSV and hMPV); or enveloped positive-sense RNA viruses (e.g., HCoV). The minority are DNA viruses, such as the nonenveloped double-stranded AdV, the nonenveloped single-stranded HBoV, or the enveloped human herpesviruses (HHVs).

Orthomyxoviruses: Influenza A, B, and C

Influenza viruses, belonging to the family *Orthomyxoviridae*, are the most clinically important respiratory viruses due to their role in severe lower respiratory tract infections (LRTI), explosive outbreaks and epidemics, and in occasional global pandemics. Influenza viruses are spherical or filamentous, enveloped, single-stranded RNA viruses containing seven or eight separate segments of RNA. These viruses attach to human respiratory epithelium via sialic acid residues, are internalized, and multiply in the cell nucleus. The hemagglutinin antigen (HA) is expressed on the viral envelope, interacts with cell surface receptors in attachment, and is a major target of the body's immune defenses. Vaccines against influenza A and B target the HA. The neuraminidase (NA) facilitates viral release from infected cells to enable subsequent new generations of infections and is inhibited by commonly used antiviral drugs such as oseltamivir and zanamivir. The M2 ion channel, which enables viral entry, is a target of the drugs amantadine and rimantadine and is found only in influenza A but not in influenza B (5). Only influenza A causes pandemics, usually due to a genetic reassortment of HA and NA subtypes to confer a novel virus for which humans have limited immunity. Both influenza A and B cause seasonal outbreaks, whereas influenza C causes milder disease that is rarely specifically diagnosed.

Paramyxoviruses: RSV, hMPV, and PIV-1 to -4

The family *Paramyxoviridae* is a large family of negative-sense, single-stranded RNA viruses that cause measles, mumps, and respiratory infections. The associated respiratory viruses include RSV (subfamily *Pneumovirinae*, genus *Pneumovirus*), hMPV (genus *Metapneumovirus*), and four PIV types (PIV-1 and PIV-3 belong to the genus *Respirovirus* while PIV-2 and PIV-4 belong to the genus *Rubulavirus*). This group of viruses is the most clinically important after influenza. RSV is named after its propensity to cause syncytia formation in cell culture and is a common cause of childhood infections and hospitalizations. hMPV was discovered in 2001 and has four subtypes with a different subtype predominating in each year (6). PIV types 1 to 4 cause similar respiratory diseases but are generally less severe than RSV.

Picornaviruses: HRV and EV

The small, nonenveloped, positive-sense, single-stranded RNA viruses in the order *Picornavirales*, family *Picornaviridae*, genus *Enterovirus*, include the respiratory pathogens HRV and enterovirus (EV). Some authors refer to human enteroviruses with the abbreviation HEV, which is also used for hepatitis E virus and, as such, is ambiguous. Further confusion arises from the reclassification of HRV into the genus *Enterovirus*, with recognition of three rhinovirus species (A, B, and C), and five enterovirus species (A to E). HRV causes outbreaks of upper respiratory tract infections (URTI), as rhinovirus A and B infect respiratory epithelial cells via the ICAM-1 or LDL-receptors. The receptor for rhinovirus C viruses is unknown. HRVs are acid labile and grow best at 33°C. The EVs cause gastrointestinal, respiratory, and systemic diseases. The EVs have a larger genome than HRV, use a wide variety of receptors for cell entry, and are acid stable.

Coronaviruses: HCoV

Members of the family *Coronaviridae*, genus *Coronavirus*, are large (120 to 160 nm), roughly spherical, enveloped viruses, which carry a positive-sense-strand RNA genome approximately 30 kb in length. The name "coronavirus" is derived from the crown-like appearance of these viruses when examined using electron microscopy. This appearance is due to an envelope studded with long, petal-shaped spikes of glycoprotein (7, 8). Four HCoVs are in circulation.

HCoV-OC43 and HCoV-229E were initially identified in the 1960s and are responsible for up to 30% of common cold symptoms but have received little attention as serious human pathogens (7, 9, 10). HCoVs were overlooked in diagnosis because they were thought to only cause outbreaks of URTI and are difficult to culture (11). This view was dramatically altered in November 2002 when the newly identified severe acute respiratory syndrome (SARS) CoV was associated with severe pneumonia in more than 8,000 people, contributing to over 800 deaths worldwide (12, 13). Since the outbreak of SARS-CoV, two novel HCoVs (HCoV-NL63 and HCoV-HKU1) have been discovered in association with LRTI. Research has also shown that HCoVs have a marked seasonal distribution (14, 15). HCoV-NL63 was first isolated from a 7-month-old child suffering from bronchiolitis, conjunctivitis, and fever in April 2004 in the Netherlands and was placed in group 1 based on genetic similarity to HCoV-229E (16). Since the discovery of HCoV-NL63, a seasonal distribution has been identified among HCoV-OC43 and HCoV-NL63 which peaks during late winter (15, 17, 18). HCoV-HKU1 was initially discovered as a codetection of severe LRTI in two patients in Hong Kong in January 2005 and has since been found to cause community-acquired pneumonia in winter and spring with a 2.4% incidence (19–21). HCoV-HKU1 has been classified as a group 2 HCoV based on genomic analyses (22). More recently, the Middle Eastern respiratory syndrome (MERS) CoV was identified in 2012 in the Netherlands from a Saudi Arabian patient who died with severe respiratory illness.

DNA Respiratory Viruses: AdV, HBoV, and Others

The nonenveloped AdV is a double-stranded DNA virus containing 51 serotypes. These are small viruses that multiply in the cell nucleus and invade respiratory epithelium and the gastrointestinal tract as well as the systemic circulation and heart.

HBoV is a single-stranded DNA virus which was the first member of the family *Parvoviridae*, genus *Bocaparvovirus*, to cause disease among humans and has been suggested to cause respiratory and gastrointestinal disease in children (23). There are four known serotypes. Infections often occur as dual infections together with another respiratory virus (21).

Newly described polyomaviruses (WUPyV, KIPyV, and BKPyV) have been associated with respiratory disease symptoms (24, 25). Their role remains undefined.

Other DNA viruses causing respiratory disease include the HHVs, particularly cytomegalovirus (CMV), but also varicella-zoster virus (VZV). CMV is more commonly recognized in the immunocompromised host. HHV-6 and HHV-8 have also been associated with respiratory symptoms.

Other Viruses and Bacteria

Other RNA viruses such as measles and mumps can cause respiratory symptoms. Bacteria such as *Chlamydophila* (formerly *Chlamydia*) *pneumoniae* and *Mycoplasma pneumoniae*, while not viruses, overlap clinical syndromes caused by viruses and may be diagnosed in virology and molecular laboratories. *C. pneumoniae* is an obligate intracellular bacterium infecting respiratory epithelial cells. *Mycoplasma* spp. are cell-wall-free bacteria infecting the upper and lower respiratory tract. Both are sensitive to antibiotics, and, as part of the differential of upper and lower respiratory tract infection, both are included in some viral multiplex panels for laboratory detection. Finally, *Bordetella pertussis*, the bacterium that causes whooping cough, presents initially as URTI ,with antibiotics being effective only if started during the "catarrhal" stage of illness. Some molecular respiratory panels include *B. pertussis* as a target.

EPIDEMIOLOGY, TRANSMISSION, AND PATHOGENESIS

Respiratory viruses cause acute, self-limited infections spread person to person via infected hands, infected objects in the environment (fomites), large droplets from sneezing or coughing, and potentially via small-particle aerosols. Incubation times vary from as little as 10 hours for HRV, to 1 to 4 days for influenza, and up to 14 days for AdV and HCoV.

The transmission of respiratory viruses is highly seasonal in temperate and subtropical climates but may be year-round in tropical climates. In temperate and subtropical climates, influenza, RSV and other paramyxoviruses, and HCoVs predominate in the winter and spring. In North America, influenza is most common between December and April, whereas HRV is present year-round but peaks in the spring and early fall, and EV is most common in the summer months. In Australia, the "cold and flu season" starts as the prevalence of influenza peaks from late June to early August (early to mid-winter in the Southern Hemisphere) and is followed with a peak in HCoV prevalence in August (late winter), when they can be detected in 22% of specimens tested (15). The epidemic peak of hMPV is from August (late winter) to November (late spring) with a change in predominant viral genotype seen in most years (26). Seasonality also differs by serotypes (e.g., PIV-1 versus PIV- 3), and there are both synergistic and potentially antagonistic relationships between viruses. Seasonality may reflect effects of temperature, humidity, and indoor exposure, as well as lower vitamin D levels in winter months. In North America, peaks of HRV in September have been associated with school return and spread among children.

Most respiratory viruses multiply initially in the upper respiratory tract, in respiratory epithelial cells in the nose, nasopharynx, oropharynx, tonsils, or trachea. HRV is characterized by infection of only small numbers of epithelial cells, and symptoms may result from inflammatory cytokines.

CLINICAL SIGNIFICANCE

Respiratory virus infections may be asymptomatic or symptomatic and may affect the upper respiratory tract and its related structures, the lower respiratory tract, the gastrointestinal tract, or occasionally other organs.

Asymptomatic or minimally symptomatic illness may occur with most respiratory viral infections and can be detected by asymptomatic seroconversion or as an incidental finding with testing of asymptomatic study subjects in epidemiologic studies or volunteer inoculation studies. Community cohort studies have demonstrated asymptomatic infection with influenza or HRV, with rates of asymptomatic infection estimated at 15 to 20% for influenza and up to 80% for HRV (27). Asymptomatic infection and/or prolonged carriage after initial infection likely occurs with most respiratory viruses, thus complicating the interpretation of causality when a virus is detected.

The most common symptomatic presentation of respiratory viruses is URTI, also known as the common cold. Nasal congestion, rhinorrhea, sneezing, coughing, and/or throat irritation occur for 1 to 9 days, with shedding of virus for 3 to 7 days and resolution of symptoms generally in about 10 days. Neutrophils are present in nasal secretions, along with mucous and water. While HRV is the most common cause of URTI, all respiratory viruses can cause URTI and may be clinically indistinguishable. AdV, influenza, or HCoV may be more commonly associated with fever in the context of URTI, but HRV and EV can also be associated with fever—particularly in young children.

Pharyngitis and tonsillitis may be viral (especially HRV, but also influenza, AdV, HCoV, and other respiratory viruses) or bacterial (especially *Streptococcus pyogenes*, also referred to as group A *Streptococcus*). Viral sore throat is more likely to be accompanied by nasal congestion and cough, whereas fevers and painful lymphadenopathy favor a bacterial etiology. Persisting symptoms may be a manifestation of primary Epstein-Barr virus infections (i.e., acute mononucleosis).

Otitis media, or infection of the middle ear, is more common in the setting of acute viral infection and may be due to the virus itself (as evidenced by isolation of virus from middle ear fluid), bacterial (as with *Streptococcus pneumoniae*), or a bacterial complication of an initial viral infection. AdV, which affects the tonsils and adenoids, may obstruct the Eustachian tubes that aerate the middle ear and may predispose the patient to a bacterial middle ear infection.

Sinusitis is common with concurrent URTI, and the infection may be referred to as "rhinosinusitis." The contiguous respiratory epithelium covers the nasal, pharyngeal, and sinus surfaces, and a large proportion of HRV and other viral URTI involve nasal and sinus cavities even in uncomplicated infections. Bacterial sinusitis may result later, often after 7 to 10 days, with exacerbation of fevers, sinus congestion, and nasal discharge.

Laryngitis, or inflammation of the larynx, may be viral, bacterial, or noninfectious. PIV, RSV, influenza, HRV, and AdV have all been associated with laryngitis, as have *Mycoplasma pneumoniae* and *Chlamydophila pneumoniae*. These are usually self-limited and accompanied by other signs of URTI or LRTI.

Influenza-like illness (ILI) is a syndrome characterized by upper and potentially lower respiratory tract symptoms. A combination of fever, abrupt onset of cough, and new-onset sore throat characterize ILI, which may also involve constitutional symptoms of muscle aches, tiredness, and loss of appetite. The diagnosis of ILI is not highly sensitive for influenza infections, which may present as URTI or pharyngitis

without fevers or as LRTI (see below) without fever, particularly in the elderly, nor is ILI specific for influenza, but it may be due to any respiratory virus including HRV. ILI remains a key tool for tracking potential influenza in the community, and, when influenza outbreaks occur, ILI incidence is a useful epidemiologic measure. From a health-care perspective, screening emergency departments and clinic patients for ILI enables timely testing and infection control in order to prevent infection of other patients and staff.

LRTI is a broad term for symptoms and clinical signs of infection below the level of the larynx. Infections of the trachea (tracheitis), bronchi (bronchitis), and smaller airways (bronchiolitis) are primarily due to viral infections, including influenza, PIV, RSV, hMPV, HCoV, and AdV. Infections of the lung parenchyma, or pneumonia, are often of bacterial origin, although pneumonia may be a mixed viral and bacterial infection or a sole viral infection. Increasingly, HRV is being recognized as a cause of lower respiratory tract infection, particularly in young children, the elderly, and those with immune deficiencies such as bone marrow or solid organ transplantation, chemotherapy, or advanced infection with the human immunodeficiency virus type 1 (HIV-1).

Bronchitis/tracheitis is common with influenza and other respiratory viruses and causes cough, pain on tracheal pressure, and exacerbation of preexisting chronic respiratory diseases such as asthma or chronic obstructive pulmonary disease (COPD). The presentation may be exacerbation of asthma or COPD. COPD exacerbations are often accompanied by increased sputum production suggestive of a bacterial infection, and physicians will often treat with antibiotics since tests do not clearly rule out bacterial infection.

Croup, or laryngotracheobronchitis, is a common ARTI caused by PIV and other respiratory viruses. It affects young children, who develop acute difficulty with breathing out and develop a characteristic "seal-like" barking cough. Children are often brought to an emergency department and may require observation, with treatments consisting of oxygen and antiinflammatory corticosteroids for moderate to severe disease. The disease is self-limited and mortality is rare.

Bronchiolitis is an acute and potentially life-threatening illness and can be particularly severe in young children and premature infants or in infants with heart or lung disease. Bronchiolitis is characterized by fever, rapid and labored breathing, difficulty with oxygen exchange (resulting in lower oxygen saturation), and wheezing. RSV is the most common cause, although hMPV, PIV, and HRV can also cause bronchiolitis. Virtually all children are infected with RSV by 2 years of age, as evidenced by seroprevalence studies, and younger children are more likely to develop severe disease. RSV causes bronchiolitis and may require hospitalization. Severe disease may lead to intensive care unit admissions with therapies that include intravenous hydration, bronchodilators, antibiotics, oxygen, and even intubation and mechanical ventilation. Intravenous or inhaled ribavirin may be used in severe disease, although its effectiveness remains controversial. No vaccine is available for prevention of RSV, but RSV immunoglobulin is used to prevent severe disease among infants under the age of 2 years who are at high risk of developing severe RSV bronchiolitis and pneumonia. Risk groups include premature infants and those with severe heart or lung disease. RSV immunoglobulin is given monthly throughout the RSV season in a given community. While effective for preventing disease, RSV immunoglobulin is not effective for treatment once symptoms are established. Development of effective antivirals is currently being researched and is a high priority for the medical community.

Episodes of wheezing with respiratory viral infections in young children may be labeled as reactive airway disease, as airways in the young child do not have sufficient smooth muscle to cause bronchospasm characteristic of asthma. However, children with severe RSV or HRV bronchiolitis/reactive airway disease are more likely to manifest with childhood asthma by 6 years of age, although the role of these viruses in causing—as opposed to unmasking—asthma remains unclear. In younger children, all respiratory viruses can cause asthma exacerbations, including live attenuated influenza vaccine (which is not recommended for children with moderate to severe asthma). In older children and in adults, both HRV and EV are common causes of asthma exacerbations. In the late summer and fall of 2014, a serotype of Enterovirus, EV-D68, was associated with an outbreak of asthma exacerbations in hospitalized children in Kentucky, Colorado, and Canada (28). EV-D68 had been previously associated with similar outbreaks in the Philippines and in the Netherlands. The virus was first identified in California in 1962, and the cause for its recent increased activity is unknown.

Pneumonia is an infection of the lung parenchyma, with fluid, pus, and often bacteria in the alveoli affecting oxygen exchange by the lungs. Patients may need oxygen, fluids, hospital admission, and occasionally mechanical ventilation. In industrialized countries, pneumonia is a rare cause of death in children but remains a common cause of death in the elderly and immunocompromised. Viral pneumonia occurs with influenza and with most respiratory viruses and may be severe and result in diffuse lung white-out and severe difficulty with oxygen transport. Viruses such as influenza also predispose to bacterial pneumonia, often *Streptococcus pneumoniae*, *Staphylococcus aureus*, or *Streptococcus pyogenes*. *Haemophilus influenzae*, first associated with pneumonia during the H1N1 influenza pandemic of 1918, is now a rare cause of pneumonia since the onset of childhood vaccination against *H. influenza* type B (29, 30).

In 2009, a novel reassortment of animal and human viruses resulted in the pandemic H1N1 virus that originated in Mexico. Within 3 months, the pH1N1 virus spread worldwide and rapidly infected populations including children and adults. While the elderly were relatively spared and overall hospitalizations and deaths were lower than in the H3N2 years, there was an excess of deaths in children and young adults. Overall, the combined category of influenza and pneumonia remains the eighth most common cause of adult death in the United States, and the prevention, diagnosis, and treatment of influenza remain key health priorities.

Prevention of influenza includes annual vaccination of at-risk groups, such as young children, the elderly, and those with heart, lung, or immune diseases. Health care workers are recommended for vaccination to prevent hospital-based outbreaks. Universal vaccination of all children over 6 months of age, and of all adults, has long been recommended in jurisdictions such as the Province of Ontario and has recently been recommended in the United States by the Centers for Disease Control and Prevention (31). Universal influenza vaccination has been associated with a reduction in hospitalizations and complications among the elderly. A vaccination strategy targeting children was shown to reduce infection in the elderly in Japan, and more recently in a cluster-randomized clinical trial in Canada (32), the key role of children in spreading influenza in the community was demonstrated. Antiviral prophylaxis and treatment of

influenza includes amantadine and rimantadine, which are rarely used today because of drug resistance, and the neuraminidase inhibitors oseltamivir, zanamivir, and peramivir. Used early, these drugs are highly effective for the prevention or treatment of influenza (33).

Other influenza strains also occasionally cause human disease. In 1998, a novel H5N1 avian influenza virus infected 18 people in Hong Kong and was controlled by the culling of millions of birds. Since 2003, H5N1 continues to circulate among birds, with sporadic zoonotic infections of humans from bird markets or from direct exposure to dead birds. Person-to-person spread has only rarely been documented, and a total of 844 cases and 449 (53%) deaths have been recorded as of July 2015 (34). The most affected countries have been Egypt, Indonesia, and Vietnam, each with over 100 human cases. Other novel influenza viruses have infected humans exposed to bird markets in China, such as H7N9 in 2013 to 2015. Both H5N1 and H7N9 human cases have occasionally been imported into North America.

In 2002/2003, a novel CoV in China caused SARS, which affected 8,800 people in 29 countries and resulted in over 800 deaths (12, 13). The lungs and gastrointestinal tract were heavily infected in those who died and underwent autopsy. Diagnosis was complicated by the nonspecific nature of the illness, the frequent absence of virus in upper respiratory tract samples, and the delay to seroconversion among infected patients. Serology or molecular testing of lower respiratory tract specimens was helpful in making the diagnosis. Treatment was supportive, and the pandemic was controlled with careful infection control and other public health measures.

In 2012, a novel CoV was associated with severe respiratory disease in Saudi Arabia. Since then, MERS-CoV has infected over 1,000 people in Saudi Arabia and the Middle East, with occasional importation and secondary spread in the United States, United Kingdom and elsewhere. Serologic studies in Saudi Arabia suggested that 0.15% of surveyed people had serologic exposure to disease, with higher rates among shepherds (35). In June 2015, an outbreak in South Korea affected 186 patients, with 36 deaths, with at least three generations of infections (36). As of July 2015, over 16,500 South Koreans were transiently in quarantine, with concern for the potential of a much broader MERS-CoV outbreak.

Respiratory viruses can also contribute to extrapulmonary disease. In young children, respiratory viruses can also cause nausea, vomiting, and diarrhea. Extrapulmonary disease is also common with EV and AdV, with occasional involvement of the central nervous system (enterovirus meningitis, encephalitis, and acute flaccid paralysis), heart (myocarditis), liver (hepatitis), or muscle (myositis). Influenza, particularly influenza B, has been associated with myositis.

The respiratory illness in 2014 due to EV-D68 was also associated with neurologic disease, including acute flaccid paralysis—mimicking poliomyelitis—during the same time period. Virus was demonstrated in respiratory secretions in half of the examined children but could not be detected either in cerebrospinal fluid or in stools (37).

COLLECTION, TRANSPORT, AND STORAGE

Whom To Test

When considering testing, the first consideration is the patient. A young child, an elderly patient, or an immunocompromised patient would be at high risk for respiratory virus infections including severe disease or chronic/complicated disease. If admitted to hospital, they would be a potential source of infection for staff, visitors, and other patients. Any individual who is part of an institutional outbreak should be tested to guide prevention and treatment strategies. Travelers may warrant testing for exotic causes of their illness but will benefit from standard testing as well. Knowledge of worldwide outbreaks such as MERS-CoV in Saudi Arabia and other Middle Eastern countries, or H7N9 influenza in China, may direct specific testing and will require higher biosafety levels for specimen collection, transport, and laboratory testing.

When To Test

The second issue becomes when to test, although timing is often dictated by the point of contact between the patient and the medical system. Generally, viruses are shed from the upper respiratory tract for 3 to 7 days with many respiratory viral infections, but may be shed longer with certain viruses or in certain hosts (the young, the elderly, and the immunocompromised). Certain specimen types (e.g., nasopharyngeal swab [NPS]) may be positive early in the disease but do not rule out LRTI later in the disease. Similarly, transient viremia has been noted with influenza and with other viral infections, but blood is not commonly used as a direct test for infections in general. Wherever possible, samples should be obtained early in the disease, and certainly within the first 3 to 5 days of symptom onset. Children and the immunocompromised may shed viruses for weeks and may be tested if clinically relevant to guide decisions regarding etiology, isolation, and treatment. Testing for unusual infections such as novel influenza hemagglutinin serotypes may include acute and convalescent sera, although such testing requires prolonged turnaround time and is rarely helpful in treatment and infection control decisions for the patient.

Choice of Specimen Type

The next issue is the specimen type. Most commonly used specimens include NPSs and nasopharyngeal aspirates (NPAs). Nasal/mid-turbinate swabs (38), nasal washes, throat swabs or washes, and lower respiratory tract samples (tracheal aspirates or bronchoalveolar lavage samples) may all be submitted for respiratory virus testing. Choice of specimen type will involve decisions regarding the patient population (children versus adults, outpatients versus inpatients), the skills of the collecting nurse or physician, or the preference for self-collection or parental-collection of samples. In general, nasopharyngeal swabs or aspirates are the specimens of choice for acute diagnosis, with the exception of intubated patients, in whom supplementation with a lower respiratory tract specimen (such as bronchoalveolar lavage) is recommended (39). However, a lower respiratory tract specimen should not substitute for an upper respiratory tract specimen, as the latter is generally more sensitive.

Choice of Swab Type

Flocked swabs may be preferred to conventional nylon swabs and have been shown to be superior in collecting more respiratory epithelial cells and more infected cells (40). Viral transport media enable preservation of virus for antigen testing, culture, or molecular detection, and certain commercial media have demonstrated stability at room temperature for up to 3 weeks (41). Unless the stability characteristics of the viral transport medium are known, however, refrigeration of the sample at 2 to 8°C and processing of the sample within 48 hours are recommended. Samples can be stored for a prolonged period at −70°C but may be less stable to storage at −20°C.

Test Ordering

Test orders for respiratory virus detection may be limited (e.g., influenza alone by rapid antigen detection), expanded (e.g., influenza, PIV, RSV, hMPV, and AdV by direct fluorescent antibody and rapid shell vial culture), or comprehensive (multiplex PCR for 12 to 22 viruses and bacteria). These may be offered by setting (more limited for outpatients, more comprehensive for inpatients), patient comorbidities (immunocompromised), travel history, or physician ordering preference. However, the complexity of the ordering algorithm may be confusing and delay appropriate diagnosis, whereas an unrestricted policy of ordering comprehensive multiplex panels is costly and may result in overdiagnosis of incidental viral shedding unrelated to the current illness.

Test Utility

A diagnostic test for respiratory viruses may decrease the number of ancillary tests performed, affect decisions to admit a patient to the hospital, alter the degree of respiratory isolation required, and influence the choice of antiviral and antibacterial treatments for an overall cost savings (42). However, as respiratory viruses and bacteria may coexist, the cost savings may be exaggerated, as most physicians will continue to prescribe antibiotics in the setting of proven respiratory viruses amongst patients admitted to the hospital. Thus, in a retrospective review, 90% of adult inpatients with laboratory-confirmed influenza received antibiotics in our hospital, whereas, disturbingly, only 30% received antivirals (43). During known influenza activity in the community, we advise starting all admitted or high-risk patients with influenza-like illness on appropriate antiviral drugs, and discontinuing antivirals if subsequent batched multiplex PCR (generally available within 6 to 12 hours) proves negative for influenza A or B. Antibiotics are used for clinical or radiographic suspicion of pneumonia or for suspected bacteremia/sepsis.

Preanalytic Quality Control

Minimization of the number and types of swabs and transport media distributed throughout a hospital system may enable better inventory and quality control. Viral transport media may require refrigeration or be stable at room temperature, and many have a pH-dependent indicator dye to identify acid and unusable media in addition to an expiry date. In the future, as molecular testing replaces antigen and culture testing, simpler transport media enabling optimized molecular testing may extend shelf life and facilitate inventory and quality control. However, methods such as culture will still be required on a proportion of patients to enable characterization of a random sampling of influenza isolates each year, for travelers or others potentially exposed to novel influenza strains, or for phenotypic antiviral testing. One option may be to use molecular specific transport media routinely and to take additional specimens for culture when epidemiologic risk factors dictate the need.

Biohazard

Sample collection may entail a biohazard to the medical personal collecting the specimen as well as to laboratory personnel processing the sample. Thus, NPS and NPA collection may cause sneezing or coughing, with potential droplet and even aerosol spread of the virus to mucous membranes including the conjunctiva. Appropriate droplet precautions, including a gown, surgical mask, and eye protection, should be worn by clinical personnel when taking a nasopharyngeal specimen. Where a biosafety level 3 or higher pathogen is suspected (e.g., MERS-CoV, H5 influenza), enhanced biosafety during collection and laboratory processing will be required. Respiratory virus collection should be avoided altogether among patients with a suspected biosafety level 4 pathogen such as Ebola virus.

DIRECT FLUORESCENT ANTIBODY TESTING AND RAPID SHELL VIAL CULTURE

Conventional tube culture was the mainstay of respiratory virus diagnostics for many years. Both primary and continuous cell lines were used, including green monkey and rhesus monkey kidney cells, MDCK cells, A535, mink lung cells, or embryonal lung cells. These cells required considerable expertise to maintain and interpret and were time consuming, requiring daily examination and maintenance and taking 5 to 10 or more days to grow and identify viruses. Cytopathic effect of the viruses on the cell line, hemagglutination, or monoclonal antibody staining was used to verify detection of a virus. Tube culture methods continue to be used by some reference laboratories to prepare control material and to grow viruses for antigen characterization. However, they are generally impractical for clinical laboratories requiring a diagnosis to aid individual patient treatment or infection control.

Many clinical laboratories replaced conventional tube culture with rapid shell vial culture, in which one or more cell lines are placed below a cover slip, with a centrifuged patient sample, and incubated for 24 to 48 hours. The sample is then stained with a monoclonal antibody conjugated to FITC, and typical intranuclear or intracytoplasmic apple-green fluorescence is identified under a UV microscope.

Antigen detection using pools or individual monoclonal antibodies is available for influenza A, B, PIV-1, -2 and -3, RSV, hMPV, AdV, and EV. Commercial mixes of two or more cells are available, such as R-Mix, R-Mix-Too, or E-Mix shell vials (Diagnostic Hybrids). Antigen can be detected in a primary sample prior to culture, known as direct fluorescent antibody (DFA), enabling rapid identification in 90 to 120 minutes. Negative specimens are then inoculated into shell vial culture, and staining is repeated after 24 and 48 hours of culture, as described above.

The sensitivity of DFA is ~75% compared with culture, with a lower yield if insufficient numbers of respiratory epithelial cells are visible on the slide. Insufficient quantity would be reported, with an indication on the report that a negative could be a false-negative due to poor specimen adequacy. True sensitivity of DFA/culture, compared with a molecular test reference standard, is approximately 10% lower. The specificity of DFA approaches 100% but requires specialized equipment and experienced laboratory technologists. The requirement for fluorescent microscopy limits the daily throughput, although a result can be available as soon as 90 minutes after the specimen arrives in the laboratory.

Today, some laboratories may continue providing DFA/shell vial culture for respiratory virus detection, particularly for patients who are less urgent or in whom influenza has been excluded by molecular tests (described in "Molecular Tests for Respiratory Viruses" below).

IMMUNOCHROMATOGRAPHIC ASSAYS FOR INFLUENZA

Rapid methods for the identification of influenza and RSV have involved the detection of antigen using specific monoclonal antibodies raised in animals. Detection from an NPS

with a rapid immunochromatographic assay can be done in as little as 10 minutes, potentially enabling rapid institution of antiviral therapy and infection control procedures. Furthermore, monitoring of respiratory specimens in aggregate can identify when influenza is highly active. These assays are considerably less expensive than current multiplex molecular panels.

A representative sampling of currently available antigen assays is summarized in Table 1. The sensitivity of these assays is highly variable (44). Sensitivity of 60 to 90% compared with conventional or shell vial culture has been documented but depends on the patient's age (child versus adult), specimen type (NPS or NPA versus nasal swabs), duration of illness, and sensitivity of the reference standard (culture versus molecular). Compared with molecular reference standards, which are more sensitive than culture, antigen detection is appreciably less sensitive analytically and clinically. During pH1N1, it was estimated that rapid antigen detection had a very poor sensitivity of 20 to 40% (45).

Specificity of rapid antigen testing, however, is quite high at >90%, and the positive predictive value is >90% during influenza season. Thus, during known circulation of influenza in a community, a positive rapid antigen test would confirm the presence of influenza. However, at times without circulating influenza, the positive predictive value (which is a function of prevalence) would be much lower, and a second method (such as culture or molecular testing) would be required to verify the presence of influenza.

Two new, higher-sensitivity influenza assays have been cleared by the U.S. Food and Drug Administration (FDA): the Sofia Influenza A+B fluorescent immunoassay (Quidel Corp) and the BD Veritor Systems Flu A+B (46–49). These use analyzers that improve reliability, use signal-amplification methods, and incorporate algorithms to improve the sensitivity of the immunochromatographic influenza assays. These take 10 to 15 minutes to give results and are low-complexity assays requiring minimal sample preparation. These offer 80 to 90% sensitivity and 90 to 95% specificity, with higher sensitivity for children versus adults and for influenza A versus influenza B. The BD Veritor is low complexity and Clinical Laboratory Improvement Amendments (CLIA)-waived for NPSs and nasal swabs. The Sofia Influenza A+B is CLIA-waived for NPSs or nasal swabs but is classified as moderate complexity for NPAs or washes. Quidel has also introduced a Sofia RSV assay.

In settings in which viral load is high, such as early disease in children, these assays are likely to perform adequately. They are rapid, simple, and appreciably cheaper than molecular assays. However, among adults, or with any genetic drift in the virus, these assays may perform suboptimally. In a point–counterpoint, Dunn and Ginocchio argue for and against the use of these rapid immunochromatographic assays (50).

Antigen assays may still have a role in the diagnosis of infected children (particularly if not requiring hospital admission), in outbreaks (in which a single positive would suggest that the entire outbreak is due to the same infection), and in remote communities (in which a single viral infection may predominate, and knowledge of the circulation of influenza or RSV would enable appropriate decision making and treatment in other community members). Thus, an "ecologic" or "cluster" diagnostic tool, with imperfect abilities to diagnose (especially to exclude illness) in an individual, may still be highly useful in these particular group settings.

If antigen-based tests are to be used for influenza diagnosis, the two newer, higher-sensitivity tests would be preferred. Testing children during known influenza activity, or multiple individuals involved in an outbreak, may be a cost-effective use for these assays. However, decisions on treatment and isolation for individual patients, particularly for adults with comorbidities and among inpatients, should ideally rely on the more sensitive molecular diagnostics, described below. The FDA has proposed annual retesting for influenza assays, and these assays should not be relied upon for novel influenza strains until adequate validation has been performed.

Rapid immunochromatographic assays, including the newer, higher-sensitivity Sofia assay from Quidel, are also available for RSV. As with influenza antigen detection assays, both low-complexity immunochromatographic assays, as well as more complex enzyme immunoassays that are more amenable to high-throughput batch processing, are

TABLE 1 Reported ranges of sensitivity and specificity of a representative selection of influenza rapid antigen detection kits[1]

Kit (manufacturer)	Targets		Sensitivity (%)	Specificity (%)
	Flu A	Flu B		
Actim Influenza A&B (Medix Biochemica)	X	X	65–77	99–100
BD Veritor System for Flu A+B (Becton-Dickinson)	X	X	70–94	99–100
BinaxNOW Flu A and Flu B (Alere)	X	X	44–65	92–100
BinaxNOW Influenza A&B (Alere)	X	X	4–82	92–100
Directigen Flu A (Becton-Dickinson)	X		61–100	85–100
Directigen Flu A+B (Becton-Dickinson)	X	X	22–80	92–100
ESPLINE Influenza A&B-N (Fujirebio)	X	X	23–91	72–100
FLU OIA (BioStar)	X	X	41–93	83–95
QuickVue Influenza Test (Quidel)	X	X	22–96	75–100
QuickVue Influenza A+B Test (Quidel)	X	X	4–75	84–100
SD Bioline Influenza (Standard Diagnostics)	X	X	45–70	98–100
Sofia Influenza A+B FIA[2] (Quidel)	X	X	62–98	96–100
ZstatFlu (ZymeTx)	X	X	37–96	77–97

[1]Adapted from references 44 and 50.
[2]FIA, fluorescent immunoassay.

available. Sensitivities are reported at 70 to 90%, although a study comparing a rapid assay with PCR found only 41% sensitivity (51).

MOLECULAR TESTS FOR RESPIRATORY VIRUSES

Molecular tests for respiratory viruses have been extensively developed since 2005. Uniplex or multiplex testing for influenza A alone, A and B, or for influenza and RSV, has been instituted by many clinical virology laboratories around the world, using laboratory-developed tests (LDTs), published primers from the Centers for Disease Control and Prevention, commercially available analyte-specific reagents (ASRs), or commercially available *in vitro* diagnostic kits for diagnosis of one or more respiratory viruses. Use of molecular diagnostics greatly accelerated after the pandemic H1N1 influenza of 2009, at which time nonmolecular methods were found to have poor sensitivity.

Most of these LDTs, ASRs, and multiplex kits require manual or automated nucleic acid extraction, followed by reverse transcription (RT), amplification (usually using PCR), and then detection of amplicon using gels, real-time instruments and SYBR Green intercalating dyes, or specific hydrolysis probes. These methods generally take 3 to 8 hours, are moderately or highly complex, and are most appropriate for a skilled molecular laboratory. Unidirectional, three-phase workflows with separate reagent preparation, amplification, and detection areas are essential to prevent false positives from specimen or amplicon contamination (52). Contamination has also been minimized by the use of closed tubes and uracil-*N*-glycosylase as well as proper training of laboratory staff.

There are a number of FDA-approved molecular assays for the diagnosis of influenza A and B (Table 2). Many of the approved assays can differentiate influenza A from B, and can also differentiate influenza A H1, H3, and pandemic H1 subtypes (53). Three of the listed assays detect both influenza and RSV, whereas four diagnostic kits (from three manufacturers) were multiplex panels for a larger number of viral targets.

Most assays are RT-PCR assays requiring initial nucleic acid extraction followed by amplification and detection. Most assays take 4 to 8 hours to results. Two exceptions are the Cepheid Xpert for influenza A and B, with or without RSV, and the Alere iNAT Flu A/B assay (54). The Cepheid assay is cartridge-based, with self-contained extraction and multiplex PCR on a dedicated, expandable instrument.

TABLE 2 Representative molecular assays for influenza cleared by the U.S. FDA[a]

Product (Manufacturer)	Targets			Specimens	Time	Complexity
	Flu A	Flu B	Other			
iNAT Flu A/B (Alere)	X	X		Nasal	0.25 h	Low[b]
CDC RT-PCR	X	X		NS, NPS, NA, BAL	4 h	High
Xpert Flu (Cepheid)	X	X		NPS, NA, NW	1 h	Moderate
Xpert Flu/RSV	X	X	RSV	NPS, NA, NW	1 h	Moderate
eSensor Respiratory Viral Panel (GenMark)	X	X	RSV, PIV, hMPV, AdV, RV	NPS	8 h	High
FilmArray Respiratory Panel (BioFire/ BioMérieux)	X	X	RSV, PIV, hMPV, HRV/ EV, AdV, HCoV	NPS	1 h	Moderate
IMDx Flu A/B (Abbott)	X	X		NPS	8 h	High
Prodesse ProFlu (Hologic)	X	X	RSV	NPS	4 h	High
Prodesse ProFAST	X	X		NPS	4 h	High
Influenza A+B (Quidel)	X	X		NPS, NS	4 h	High
Artus Influenza A/B (Qiagen)	X	X		NPS	4 h	High
Verigene Respiratory Virus (Nanosphere)	X	X	RSV	NPS	4 h	Moderate
xTAG Respiratory Viral Panel (Luminex)	X	X	RSV, PIV, MPV, RV, AdV	NPS	8 h	High
xTAG Respiratory Viral Panel FAST (Luminex)	X	X	RSV, MPV, RV, AdV	NPS	6 h	High

[a]Adapted from reference 53. BAL, bronchoalveolar lavage; NA, nasal aspirates; NPS, nasopharyngeal swabs; NW, nasal wash.
[b]CLIA-waived.

Amplicon is identified with real-time detection in about one hour, and the instrument can be expanded to take a small, medium, or large number of cartridges simultaneously. The Alere iNAT is even faster; using a rapid isothermal molecular amplification method, this CLIA-waived, low-complexity assay for Influenza A and B requires only 15 minutes to results. Sensitivity was similar to culture, although more extensive evaluation versus the "gold standard" RT-PCR methods is needed. Nevertheless, such "point-of-care" molecular assays appear attractive, particularly in settings where immunochromatographic assays are currently used, such as in physicians' offices or emergency departments. While most diagnostic tests are approved for various specimen types, the Alere is approved for nasal swabs, which may be the most practical and easily obtained specimen in the outpatient setting.

The development of multiplex commercial panels started with the introduction of the TM Bioscience (now Luminex) xTAG Respiratory Viral Panel (RVP), which detects influenza A (with subtyping of H1 and H3), influenza B, RSV (subtyping of A and B), hMPV, PIV 1 to 4, HRV/EV, AdV, and four HCoV (NL63, 229E, OC43, and HKU1) (55). As with many uniplex PCR assays, the xTAG RVP assay required initial extraction of sample (via the bioMérieux NucliSENS easyMag), followed by reverse transcription and multiplex PCR, and then followed by hybridization to tagged oligonucleotide beads. Detection used the Luminex-100 with dual lasers. The process was highly complex and required 8 hours to run. A newer version of the assay, RVP FAST, decreased run time to 6 hours.

The eSensor Respiratory Viral Panel from GenMark detects influenza A and B (with subtyping A into H1, H3, and pandemic H1); RSV (subtype A or B), PIV 1 to 3, hMPV, AdV, and HRV. The assay takes approximately 8 hours and is of high complexity.

The final FDA-cleared assay is considerably less complex and much faster. The FilmArray from BioFire (now part of bioMérieux) is a self-contained, nested RT-PCR assay for influenza A (H1, H3, pandemic H1), RSV, PIV 1 to 4, hMPV, HRV/EV, AdV, and HCoV (HKU1 and NL63). This is a moderate-complexity assay requiring 2 minutes to set up and 1 hour to results. Each instrument processes one sample at a time and is best suited for ongoing, small-volume testing near the point of care. With one-hour turnaround time, the results can be used to influence antiviral treatment, admission, and isolation decisions. However, a large number of instruments are needed to run multiple specimens, and the tests are more expensive than many other molecular platforms.

A comparison of Luminex RVP and RVP FAST, GenMark eSensor, and BioFire FilmArray found sensitivity of 84 to 98% and specificity of 99 to 100%. Adenovirus and influenza B were the most likely to be false negative (56).

Other multiplex PCR diagnostic kits have been developed by Seegene and Qiagen and have CE-mark approval for sale in the European Community.

PHENOTYPING, GENOTYPING, ANTIVIRAL SUSCEPTIBILITY

While culture is increasingly rare in the clinical virology laboratory, it will continue to be used in some academic research laboratories and in reference laboratories. Culture continues to be important for the characterization of influenza for vaccination preparation and for phenotypic characterization of antiviral sensitivity. Neutralization assays for serologic testing also require culture of the relevant virus. However, molecular methods for both virus characterization and drug susceptibility are increasingly performed with Sanger sequencing of partial and whole genomes.

Antiviral susceptibility testing remains important for monitoring influenza antivirals. Between 2007 and 2009, increasing resistance to oseltamivir in seasonal H1N1 viruses was found, as well as amantadine resistance of H3N2. Subtyping was essential in severely ill, hospitalized patients to guide therapy and prophylaxis. Since 2009, amantadine resistance of all influenza A (influenza B is naturally resistant), but only minimal resistance to oseltamivir or zanamivir, has been seen. Resistance may emerge during treatment of severe disease, particularly among the immunocompromised, and can be measured with phenotypic or genotypic testing. The signature mutation for H1N1 is H275Y, but other mutations could also contribute to antiviral resistance. Resistance testing is primarily performed at reference laboratories by sequencing of the neuraminidase gene (57).

EVALUATION, INTERPRETATION, AND REPORTING OF RESULTS

The result of a respiratory virus molecular or immunochromatographic test may indicate the presence of virus (nucleic acids or antigen). The detection of virus does not prove that the virus is the cause of the current respiratory symptoms, nor does it exclude the coinfection of multiple viruses or concurrent bacterial infections. Thus, results will need to be interpreted in the appropriate clinical context. Multiplex PCR has demonstrated frequent coinfection with multiple viruses, particularly in children. Detection of more than one virus has unknown clinical consequences but may be of value to prevent cohorting of children with multiple viruses.

While a positive result indicates the presence of virus, as long as all quality controls are adequate, a negative or nonreactive result does not entirely rule out the absence of a viral infection. This is true particularly for the antigen-based assays, which have lower analytical sensitivity compared with molecular assays, and particularly in adults or in patients several days after symptom onset. However, even in children, inadequate collection of specimen could lead to false negatives. Inadequate extraction or inhibition would also lead to false negatives. These are controlled with most molecular assays by the addition of exogenous nucleic acid, such as MS2 phage, to the sample prior to extraction. Detection of MS2 will then control for extraction, reverse transcription, as well as amplification.

With individual tests, each can be reported as positive, negative, or indeterminate. For indeterminate results, a protocol is required for resolving these, which may include repeat testing before the report is finalized, reflexing to supplementary tests, or requesting a repeat or alternative sample.

For assay panels with a long list of tested analytes, a potential issue is how to report all of the results. A report in which each analyte is listed, and a "positive" or "negative," would be the simplest solution. However, clinicians may object to a long list of results, and a positive result may not be quickly apparent from a cursory glance at the report. An alternative is to report as "positive" for the individual viruses detected, or "negative for all tested viruses," and to list all the viruses tested at the bottom of the report. The latter solution may be clearer for clinicians to interpret. Some infections, such as influenza, are reportable to public health authorities, and this should be documented on the report as well.

The assay used for testing should be reported, whether an LDT, ASR, or commercial IVD. The source of the material, and version of the test, should be specified. Laboratories should consider assigning version codes to protocols using LDTs and ASRs, and should include a comment regarding the target of the assay. Finally, comments are added such as "Positive for rhinovirus/enterovirus by PCR. This assay does not distinguish rhinovirus from enterovirus. Please request additional testing if clinically relevant." Additional testing is then offered if enterovirus typing is clinically relevant.

Antigen-based assays, culture, or qualitative molecular assays would be reported as positive/negative or as detected/not detected. However, many LDTs, ASRs, and commercial assays will give a continuous outcome measure such as a cycle threshold or viral load. In the absence of a clear clinically important interpretation, these should generally not be reported. However, we choose to report these verbally to the infectious-diseases consultant in settings of apparent serial testing and nonresponse, as a marker for potential antiviral resistance for infections such as influenza.

All molecular tests are run with internal controls such as MS2, which indicate extraction, reverse transcription, and amplification. The presence of target indicates generally adequate extraction, reverse transcription, and amplification, but cannot rule out target-specific or relative (incomplete) inhibition of the reaction. Most current methods do not include a method for ascertaining specimen adequacy, which was done by laboratories using DFA by noting whether adequate epithelial cells were seen. While molecular methods are more tolerant of poor sample collection, validated methods for ascertainment of sample adequacy, such as measurement of beta-actin or GAPDH DNA or RNase P, may help identify inadequate specimens, although thresholds for specimen adequacy have not been well established. Ideally, multiplex assays will include a specimen-adequacy marker, such that an inadequate concentration could be reported as "Inadequate specimen collected, which may result in false negative results. Please repeat if clinically necessary."

Laboratories conducting respiratory virus testing must be attuned to regional and global outbreaks with novel strains of virus and must be aware of whether their current tests are capable of detecting currently circulating strains. Assays prone to changing diagnostic accuracy may require annual recertification by the FDA in the future; such recertification may be less important for molecular diagnostics which are capable of detecting broad targets such as influenza A matrix gene.

THE FUTURE OF RESPIRATORY VIRUS TESTING

Laboratory-developed and commercial assays are utilizing extraction-free methods and exploring the potential of alternate enzymes and isothermal conditions, such as loop-mediated isothermal amplification or helicase-dependent amplification. These may be faster and cheaper than conventional and real-time PCR-based molecular tests, although they currently have severe limitations for multiplexing targets. There will likely be many new assays available using the "molecular point of care" model of near-patient rapid testing.

Further into the future, chips and microarrays will be increasingly used for broad testing of viruses, bacteria, fungi, and parasites. Nucleic acids are applied to microarrays, and the hybridized products are detected. The very broad range of detection is offset by the expense and limited analytical sensitivity of these systems, but improvements are likely in the next few years and these methods may eventually be feasible in the clinical virology laboratory.

Finally, viral metagenomics with "shotgun" sequencing of all nucleic acids in a given clinical sample may obviate the need for pathogen-specific diagnostic testing. Rather, extraction of a specimen followed by amplification and sequencing of all nucleic acid material, using next-generation sequencing instruments such as the Thermo Fisher Scientific Ion Torrent or Illumina HiSeq, will enable identification of all potential infections in a sample. Currently, these methods remain highly complex, requiring extensive preparation and postanalysis bioinformatics manipulation, and analytical sensitivity remains inferior to uniplex or multiplex PCR. However, these methods will continue to develop and will increasingly supplement detection in a multiplex test-negative sample, where clinically relevant.

The development of respiratory virus diagnostics in the past decade has been dramatic, and the pace of change is accelerating. The dominance of rapid antigen detection and rapid culture has largely been replaced by molecular testing for influenza alone or with multiplex panels for various respiratory viruses. Molecular testing has been demonstrated to be more sensitive than antigen detection or culture, compatible with high specimen throughput, and more adaptable to new viruses and to new variants of old viruses.

The coming years are likely to see further development of uniplex assays, limited panels, and large multiplex panels. One type of test will be a new point-of-care rapid molecular test, performed in the emergency department or in a core laboratory and available in time to influence treatment and hospitalization decisions. Conversely, there will continue to be a need for high-throughput, batched testing for large numbers of viruses. On a more limited basis, reference laboratories will continue to use viral culture or more complex molecular methods for characterization of novel viruses and viral strains and for elucidation of antigens for vaccination and mutations for drug resistance.

Most importantly, the improved detection of viruses will drive a greater demand for effective prevention and therapy, which in turn will mandate improved detection. Currently, effective prevention and treatment strategies exist only for influenza. Laboratory directors should pay attention to the development of vaccines or drugs for common infections such as RSV or HRV, both common causes of morbidity and occasional mortality in young children and in the elderly. The demand for rapid testing will further accelerate in the future when specific antivirals are available.

REFERENCES

1. **Fouchier RA, Hartwig NG, Bestebroer TM, Niemeyer B, de Jong JC, Simon JH, Osterhaus AD.** 2004. A previously undescribed coronavirus associated with respiratory disease in humans. *Proc Natl Acad Sci USA* **101:**6212–6216. PubMed
2. **Fine MJ, Stone RA, Singer DE, Coley CM, Marrie TJ, Lave JR, Hough LJ, Obrosky DS, Schulz R, Ricci EM, Rogers JC, Kapoor WN.** 1999. Processes and outcomes of care for patients with community-acquired pneumonia: results from the Pneumonia Patient Outcomes Research Team (PORT) cohort study. *Arch Intern Med* **159:**970–980. PubMed
3. **Arden KE, Nissen MD, Sloots TP, Mackay IM.** 2005. New human coronavirus, HCoV-NL63, associated with severe lower respiratory tract disease in Australia. *J Med Virol* **75:**455–462. PubMed

4. **Mahony JB, Petrich A, Smieja M.** 2011. Molecular diagnosis of respiratory virus infections. *Crit Rev Clin Lab Sci* **48:**217–249. PubMed
5. **Sugrue RJ, Hay AJ.** 1991. Structural characteristics of the M2 protein of influenza A viruses: evidence that it forms a tetrameric channel. *Virology* **180:**617–624. PubMed
6. **Mackay IM, Bialasiewicz S, Jacob KC, McQueen E, Arden KE, Nissen MD, Sloots TP.** 2006. Genetic diversity of human metapneumovirus over 4 consecutive years in Australia. *J Infect Dis* **193:**1630–1633. PubMed
7. **Hamre D, Kindig DA, Mann J.** 1967. Growth and intracellular development of a new respiratory virus. *J Virol* **1:**810–816. PubMed
8. **Maertzdorf J, Wang CK, Brown JB, Quinto JD, Chu M, de Graaf M, van den Hoogen BG, Spaete R, Osterhaus AD, Fouchier RA.** 2004. Real-time reverse transcriptase PCR assay for detection of human metapneumoviruses from all known genetic lineages. *J Clin Microbiol* **42:**981–986. PubMed
9. **Tyrrell DA, Bynoe ML.** 1965. Cultivation of a novel type of common-cold virus in organ cultures. *BMJ* **1:**1467–1470. PubMed
10. **Enserink M.** 2003. Infectious diseases. Calling all coronavirologists. *Science* **300:**413–414. PubMed
11. **Vabret A, Mourez T, Gouarin S, Petitjean J, Freymuth F.** 2003. An outbreak of coronavirus OC43 respiratory infection in Normandy, France. *Clin Infect Dis* **36:**985–989. PubMed
12. **Peiris JS, Chu CM, Cheng VC, Chan KS, Hung IF, Poon LL, Law KI, Tang BS, Hon TY, Chan CS, Chan KH, Ng JS, Zheng BJ, Ng WL, Lai RW, Guan Y, Yuen KY, HKU/UCH SARS Study Group.** 2003. Clinical progression and viral load in a community outbreak of coronavirus-associated SARS pneumonia: a prospective study. *Lancet* **361:**1767–1772. PubMed
13. **Peiris JS, Lai ST, Poon LL, Guan Y, Yam LY, Lim W, Nicholls J, Yee WK, Yan WW, Cheung MT, Cheng VC, Chan KH, Tsang DN, Yung RW, Ng TK, Yuen KY, SARS study group.** 2003. Coronavirus as a possible cause of severe acute respiratory syndrome. *Lancet* **361:**1319–1325. PubMed
14. **Garbino J, Gerbase MW, Wunderli W, Deffernez C, Thomas Y, Rochat T, Ninet B, Schrenzel J, Yerly S, Perrin L, Soccal PM, Nicod L, Kaiser L.** 2004. Lower respiratory viral illnesses: improved diagnosis by molecular methods and clinical impact. *Am J Respir Crit Care Med* **170:**1197–1203. PubMed
15. **Mackay IM, Arden KE, Speicher DJ, O'Neil NT, McErlean PK, Greer RM, Nissen MD, Sloots TP.** 2012. Co-circulation of four human coronaviruses (HCoVs) in Queensland children with acute respiratory tract illnesses in 2004. *Viruses* **4:**637–653. PubMed
16. **van der Hoek L, Pyrc K, Jebbink MF, Vermeulen-Oost W, Berkhout RJ, Wolthers KC, Wertheim-van Dillen PM, Kaandorp J, Spaargaren J, Berkhout B.** 2004. Identification of a new human coronavirus. *Nat Med* **10:**368–373. PubMed
17. **Bastien N, Robinson JL, Tse A, Lee BE, Hart L, Li Y.** 2005. Human coronavirus NL-63 infections in children: a 1-year study. *J Clin Microbiol* **43:**4567–4573. PubMed
18. **Chiu SS, Chan KH, Chu KW, Kwan SW, Guan Y, Poon LL, Peiris JS.** 2005. Human coronavirus NL63 infection and other coronavirus infections in children hospitalized with acute respiratory disease in Hong Kong, China. *Clin Infect Dis* **40:**1721–1729. PubMed
19. **Woo PC, Lau SK, Chu CM, Chan KH, Tsoi HW, Huang Y, Wong BH, Poon RW, Cai JJ, Luk WK, Poon LL, Wong SS, Guan Y, Peiris JS, Yuen KY.** 2005. Characterization and complete genome sequence of a novel coronavirus, coronavirus HKU1, from patients with pneumonia. *J Virol* **79:**884–895. PubMed
20. **Woo PC, Lau SK, Tsoi HW, Huang Y, Poon RW, Chu CM, Lee RA, Luk WK, Wong GK, Wong BH, Cheng VC, Tang BS, Wu AK, Yung RW, Chen H, Guan Y, Chan KH, Yuen KY.** 2005. Clinical and molecular epidemiological features of coronavirus HKU1-associated community-acquired pneumonia. *J Infect Dis* **192:**1898–1907. PubMed
21. **Sloots TP, McErlean P, Speicher DJ, Arden KE, Nissen MD, Mackay IM.** 2006. Evidence of human coronavirus HKU1 and human bocavirus in Australian children. *J Clin Virol* **35:**99–102. PubMed
22. **Woo PC, Lau SK, Huang Y, Tsoi HW, Chan KH, Yuen KY.** 2005. Phylogenetic and recombination analysis of coronavirus HKU1, a novel coronavirus from patients with pneumonia. *Arch Virol* **150:**2299–2311. PubMed
23. **Allander T, Tammi MT, Eriksson M, Bjerkner A, Tiveljung-Lindell A, Andersson B.** 2005. Cloning of a human parvovirus by molecular screening of respiratory tract samples. *Proc Natl Acad Sci USA* **102:**12891–12896. PubMed
24. **Bialasiewicz S, Whiley DM, Lambert SB, Jacob K, Bletchly C, Wang D, Nissen MD, Sloots TP.** 2008. Presence of the newly discovered human polyomaviruses KI and WU in Australian patients with acute respiratory tract infection. *J Clin Virol* **41:**63–68. PubMed
25. **Gaynor AM, Nissen MD, Whiley DM, Mackay IM, Lambert SB, Wu G, Brennan DC, Storch GA, Sloots TP, Wang D.** 2007. Identification of a novel polyomavirus from patients with acute respiratory tract infections. *PLoS Pathog* **3:**e64. PubMed
26. **Sloots TP, Mackay IM, Bialasiewicz S, Jacob KC, McQueen E, Harnett GB, Siebert DJ, Masters BI, Young PR, Nissen MD.** 2006. Human metapneumovirus, Australia, 2001–2004. *Emerg Infect Dis* **12:**1263–1266. PubMed
27. **Granados A, Goodall EC, Luinstra K, Smieja M, Mahony J.** 2015. Comparison of asymptomatic and symptomatic rhinovirus infections in university students: incidence, species diversity, and viral load. *Diagn Microbiol Infect Dis* **82:**292–296. PubMed
28. **Hatchette TF, Drews SJ, Grudeski E, Booth T, Martineau C, Dust K, Garceau R, Gubbay J, Karnauchow T, Krajden M, Levett PN, Mazzulli T, McDonald RR, McNabb A, Mubareka S, Needle R, Petrich A, Richardson S, Rutherford C, Smieja M, Tellier R, Tipples G, LeBlanc JJ.** 2015. Detection of enterovirus D68 in Canadian laboratories. *J Clin Microbiol* **53:**1748–1751. PubMed
29. **Jain S, Self WH, Wunderink RG, Fakhran S, Balk R, Bramley AM, Reed C, Grijalva CG, Anderson EJ, Courtney DM, Chappell JD, Qi C, Hart EM, Carroll F, Trabue C, Donnelly HK, Williams DJ, Zhu Y, Arnold SR, Ampofo K, Waterer GW, Levine M, Lindstrom S, Winchell JM, Katz JM, Erdman D, Schneider E, Hicks LA, McCullers JA, Pavia AT, Edwards KM, Finelli L, CDC EPIC Study Team.** 2015. Community-acquired pneumonia requiring hospitalization among U.S. adults. *N Engl J Med* **373:**415–427. PubMed
30. **Jain S, Williams DJ, Arnold SR, Ampofo K, Bramley AM, Reed C, Stockmann C, Anderson EJ, Grijalva CG, Self WH, Zhu Y, Patel A, Hymas W, Chappell JD, Kaufman RA, Kan JH, Dansie D, Lenny N, Hillyard DR, Haynes LM, Levine M, Lindstrom S, Winchell JM, Katz JM, Erdman D, Schneider E, Hicks LA, Wunderink RG, Edwards KM, Pavia AT, McCullers JA, Finelli L, CDC EPIC Study Team.** 2015. Community-acquired pneumonia requiring hospitalization among U.S. children. *N Engl J Med* **372:**835–845. PubMed
31. **Centers for Disease Control and Prevention (CDC).** 2011. Prevention and control of influenza with vaccines: recommendations of the Advisory Committee on Immunization Practices (ACIP), 2011. *MMWR Morb Mortal Wkly Rep* **60:**1128–1132. PubMed

32. **Loeb M, Russell ML, Moss L, Fonseca K, Fox J, Earn DJ, Aoki F, Horsman G, Van Caeseele P, Chokani K, Vooght M, Babiuk L, Webby R, Walter SD.** 2010. Effect of influenza vaccination of children on infection rates in Hutterite communities: a randomized trial. *JAMA* **303:**943–950. PubMed
33. **Dobson J, Whitley RJ, Pocock S, Monto AS.** 2015. Oseltamivir treatment for influenza in adults: a meta-analysis of randomised controlled trials. *Lancet* **385:**1729–1737. PubMed
34. **World Health Organization (WHO).** 2015. Cumulative number of confirmed human cases for avian influenza A(H5N1) reported to WHO, 2003–2015. http://www.who.int/influenza/human_animal_interface/EN_GIP_20150717cumulativeNumberH5N1cases.pdf?ua=1. Accessed 7 August 2015.
35. **Müller MA, Meyer B, Corman VM, Al-Masri M, Turkestani A, Ritz D, Sieberg A, Aldabbagh S, Bosch BJ, Lattwein E, Alhakeem RF, Assiri AM, Albarrak AM, Al-Shangiti AM, Al-Tawfiq JA, Wikramaratna P, Alrabeeah AA, Drosten C, Memish ZA.** 2015. Presence of Middle East respiratory syndrome coronavirus antibodies in Saudi Arabia: a nationwide, cross-sectional, serological study. *Lancet Infect Dis* **15:**559–564. PubMed
36. **World Health Organization.** 2015. Middle East respiratory syndrome coronavirus (MERS-CoV)–Republic of Korea. Disease outbreak news. WHO, Geneva, Switzerland. http://www.who.int/csr/don/03-july-2015-mers-korea/en/
37. **Khan F.** 2015. Enterovirus D68: acute respiratory illness and the 2014 outbreak. *Emerg Med Clin North Am* **33:**e19–e32. PubMed
38. **Smieja M, Castriciano S, Carruthers S, So G, Chong S, Luinstra K, Mahony JB, Petrich A, Chernesky M, Savarese M, Triva D.** 2010. Development and evaluation of a flocked nasal midturbinate swab for self-collection in respiratory virus infection diagnostic testing. *J Clin Microbiol* **48:**3340–3342. PubMed
39. **Wurzel DF, Marchant JM, Clark JE, Mackay IM, Wang CY, Sloots TP, Upham JW, Yerkovich ST, Masters IB, Baker PJ, Anderson-James S, Chang AB.** 2013. Respiratory virus detection in nasopharyngeal aspirate versus bronchoalveolar lavage is dependent on virus type in children with chronic respiratory symptoms. *J Clin Virol* **58:**683–688. PubMed
40. **Daley P, Castriciano S, Chernesky M, Smieja M.** 2006. Comparison of flocked and rayon swabs for collection of respiratory epithelial cells from uninfected volunteers and symptomatic patients. *J Clin Microbiol* **44:**2265–2267. PubMed
41. **Luinstra K, Petrich A, Castriciano S, Ackerman M, Chong S, Carruthers S, Ammons B, Mahony JB, Smieja M.** 2011. Evaluation and clinical validation of an alcohol-based transport medium for preservation and inactivation of respiratory viruses. *J Clin Microbiol* **49:**2138–2142. PubMed
42. **Mahony JB, Blackhouse G, Babwah J, Smieja M, Buracond S, Chong S, Ciccotelli W, O'Shea T, Alnakhli D, Griffiths-Turner M, Goeree R.** 2009. Cost analysis of multiplex PCR testing for diagnosing respiratory virus infections. *J Clin Microbiol* **47:**2812–2817. PubMed
43. **Herman M, Smieja M, Carruthers S, Loeb M.** 2014. Oseltamivir use amongst hospitalized patients infected with influenza. *Influenza Other Respi Viruses* **8:**547–548. PubMed
44. **Chartrand C, Leeflang MM, Minion J, Brewer T, Pai M.** 2012. Accuracy of rapid influenza diagnostic tests: a meta-analysis. *Ann Intern Med* **156:**500–511. PubMed
45. **Hatchette TF, Bastien N, Berry J, Booth TF, Chernesky M, Couillard M, Drews S, Ebsworth A, Fearon M, Fonseca K, Fox J, Gagnon JN, Guercio S, Horsman G, Jorowski C, Kuschak T, Li Y, Majury A, Petric M, Ratnam S, Smieja M, Van Caeseele P, Pandemic Influenza Laboratory Preparedness Network.** 2009. The limitations of point of care testing for pandemic influenza: what clinicians and public health professionals need to know. *Can J Public Health* **100:**204–207. PubMed
46. **Rath B, Tief F, Obermeier P, Tuerk E, Karsch K, Muehlhans S, Adamou E, Duwe S, Schweiger B.** 2012. Early detection of influenza A and B infection in infants and children using conventional and fluorescence-based rapid testing. *J Clin Virol* **55:**329–333. PubMed
47. **Leonardi GP, Wilson AM, Zuretti AR.** 2013. Comparison of conventional lateral-flow assays and a new fluorescent immunoassay to detect influenza viruses. *J Virol Methods* **189:**379–382. PubMed
48. **Hassan F, Nguyen A, Formanek A, Bell JJ, Selvarangan R.** 2014. Comparison of the BD Veritor system for Flu A+B with the Alere BinaxNOW influenza A&B card for detection of influenza A and B viruses in respiratory specimens from pediatric patients. *J Clin Microbiol* **52:**906–910. PubMed
49. **Nam MH, Jang JW, Lee JH, Cho CH, Lim CS, Kim WJ.** 2014. Clinical performance evaluation of the BD Veritor system Flu A+B assay. *J Virol Methods* **204:**86–90. PubMed
50. **Dunn JJ, Ginocchio CC.** 2015. Can newly developed, rapid immunochromatographic antigen detection tests be reliably used for the laboratory diagnosis of influenza virus infections? *J Clin Microbiol* **53:**1790–1796. PubMed
51. **Khanom AB, Velvin C, Hawrami K, Schutten M, Patel M, Holmes MV, Atkinson C, Breuer J, Fitzsimons J, Geretti AM.** 2011. Performance of a nurse-led paediatric point of care service for respiratory syncytial virus testing in secondary care. *J Infect* **62:**52–58. PubMed
52. **Ratcliff RM, Chang G, Kok T, Sloots TP.** 2007. Molecular diagnosis of medical viruses. *Curr Issues Mol Biol* **9:**87–102. PubMed
53. **Centers for Disease Control and Prevention.** *Table 1. FDA-cleared RT-PCR Assays and Other Molecular Assays for Influenza Viruses*. http://www.cdc.gov/flu/pdf/professionals/diagnosis/table1-molecular-assays.pdf. Accessed 7 August 2015.
54. **Hazelton B, Gray T, Ho J, Ratnamohan VM, Dwyer DE, Kok J.** 2015. Detection of influenza A and B with the Alere i Influenza A & B: a novel isothermal nucleic acid amplification assay. *Influenza Other Respi Viruses* **9:**151–154. PubMed
55. **Mahony J, Chong S, Merante F, Yaghoubian S, Sinha T, Lisle C, Janeczko R.** 2007. Development of a respiratory virus panel test for detection of twenty human respiratory viruses by use of multiplex PCR and a fluid microbead-based assay. *J Clin Microbiol* **45:**2965–2970. PubMed
56. **Popowitch EB, O'Neill SS, Miller MB.** 2013. Comparison of the Biofire FilmArray RP, Genmark eSensor RVP, Luminex xTAG RVPv1, and Luminex xTAG RVP fast multiplex assays for detection of respiratory viruses. *J Clin Microbiol* **51:**1528–1533. PubMed
57. **Hurt AC, Chotpitayasunondh T, Cox NJ, Daniels R, Fry AM, Gubareva LV, Hayden FG, Hui DS, Hungnes O, Lackenby A, Lim W, Meijer A, Penn C, Tashiro M, Uyeki TM, Zambon M, WHO Consultation on Pandemic Influenza A (H1N1) 2009 Virus Resistance to Antivirals.** 2012. Antiviral resistance during the 2009 influenza A H1N1 pandemic: public health, laboratory, and clinical perspectives. *Lancet Infect Dis* **12:**240–248. PubMed

Measles, Mumps, and Rubella Viruses

DIANE S. LELAND AND RYAN F. RELICH

64

Measles virus, also called rubeola, and mumps virus are both RNA viruses of the family *Paramyxoviridae*, subfamily *Paramyxovirinae*; measles is in the *Morbillivirus* genus, and mumps virus is in the *Rubulavirus* genus. Rubella virus is also an RNA virus but is a member of the *Togaviridae* family. These three viruses, despite differences in their families and genera, are often considered together because the epidemiology of the infections they produce in humans and the preventive measures used against them are similar for all three. Measles and rubella, both of which produce rash-associated illness, and mumps, which typically infects the parotid glands, were all included among the expected illnesses of childhood in the United States prior to the introduction of vaccination programs in the late 1960s. Measles epidemics involving 500,000 to 700,000 cases occurred every 2 years (1), approximately 180,000 cases of mumps were reported annually (2), and approximately 58,000 rubella cases that included 60 congenital rubella syndrome (CRS) cases (3) were seen annually.

Individual vaccines for mumps (Mumpsvax, licensed in 1967), measles (Attenuvax, licensed in 1967), and rubella (Meruvax, licensed in 1969), all from Merck and Company, Inc., started the downward trend in numbers of infections. With the licensing of the first measles/mumps/rubella (MMR) vaccine in 1971, the epidemiology of measles, mumps, and rubella virus changed dramatically, with the number of cases in the United States decreasing rapidly throughout the 1970s and 1980s. In 1986 and 1987 in the U.S., there was a brief resurgence of mumps cases that peaked at 8,000 to 12,000 cases. A similar resurgence in the number of measles cases occurred from 1989 to 1991, peaking at nearly 30,000 cases. Resurgences were attributed to susceptible populations of children under 5 years of age residing in urban settings and to an accumulation of underimmunized children born between 1967 and 1977 (1).

Following measles and mumps resurgences, a two-dose schedule was implemented for the MMR vaccine in the United States. The first dose is given between 12 and 15 months and the second between 4 and 6 years of age (4). Although measles was declared eliminated from the U.S. in 2000, sporadic outbreaks continue to occur due to importation of infection from areas of the world in which measles remains endemic (5). Sporadic outbreaks are also seen with mumps, with infections sometimes seen in fully vaccinated individuals, although there is no longer endemic transmission of measles, mumps, or rubella in the U.S.

With the decrease in incidence of measles, mumps, and rubella, the demand for diagnostic services has changed. Although previously diagnosed on clinical grounds alone, these infections are now so rare that they are not readily recognized by physicians. Likewise, they may occur in underimmunized individuals or in immunocompromised individuals, in whom typical clinical signs and symptoms are absent. Laboratory-based confirmation of infection is essential to ensure an accurate diagnosis (6), but most hospital diagnostic laboratories do not offer testing to confirm current infection, focusing instead on immune-status evaluations. Each of these viruses continues to present unique epidemiologic and diagnostic challenges, so measles, mumps, and rubella viruses are discussed separately in the pages that follow.

MEASLES

Measles is a leading cause of vaccine-preventable death among children around the world, having killed approximately 139,000 people in 2010, most younger than 5 years old (7). Although seldom fatal in developed countries, measles is especially deadly in resource-challenged countries where death rates may reach 10 to 30% among young children, most of whom have not received vaccine (7). In the U.S., measles cases decreased to an average of 63 cases per year between 2000 and 2007 but increased in 2008 to the highest level in more than a decade; half of the cases were in children whose parents had refused to have them vaccinated. During 2011, there were 222 measles cases in the U.S., 200 of which were associated with importations from other countries and occurred in unvaccinated individuals (8). In the first 3 months of 2013, England experienced 587 confirmed measles cases, which is twice the number in the same period the previous year. Experts describe these cases as "the 'legacy' of unvaccinated children in the 10 to 16 age bracket who missed out on vaccination in the late 1990s and early 2000s when there was widespread concern over the now discredited link between autism and the MMR vaccine" (9).

Measles virus causes classic 7-day measles. In measles infection, after 1 to 2 weeks of incubation, fever, rhinorrhea, cough, and conjunctivitis appear, followed by a maculopapular rash and Koplik spots (1- to 3-mm red spots with a bluish-white speck in the center located on the buccal mucosa—pathognomonic for measles). The rash usually lasts

doi:10.1128/9781555818722.ch64

7 days, and recovery is rapid and complete. The complications of measles may include otitis media, lower respiratory infections, confusion, and seizures. Subacute sclerosing panencephalitis (SSPE) is believed to be a persistent measles infection of the central nervous system. Onset is 4 to 7 years after the initial measles episode and is characterized by personality changes, mental deterioration, involuntary movements, and muscular rigidity, invariably ending in death (1). The incidence of SSPE has been estimated as 1 per 11,000 measles cases (10). However, SSPE has been largely eliminated in countries like the United States in which measles has been reduced to low levels for more than a decade.

Transplacental transfer of antibodies traditionally provided protection from measles for infants for 6 months or longer after birth. Currently, the level of transplacental antibody is lower at birth, and infants are more susceptible because mothers whose measles immunity is vaccine induced have lower levels of antibodies. By 6 months of age, only 18% of infants born to vaccinated mothers were shown to have protective levels of measles antibodies; this is in contrast to the 50% of infants born to naturally infected mothers (11). Premature infants (<32 weeks gestation and weighing less than 1,000 g) may demonstrate seronegativity of 45% for measles, with further deterioration of immunity over the next 3 months, resulting in seronegativity of 94% for measles (12).

Interestingly, despite the lower measles-specific antibody levels following vaccination compared to those after natural infection, antibody in vaccinated individuals has been shown to persist (13). Measles antibody has been detected in two-dose MMR recipients 26 to 33 years after vaccine administration, with 92% of these individuals showing antibody at protective levels. Measles occurs very rarely in vaccinated individuals.

DIAGNOSTIC STRATEGIES FOR MEASLES

For measles, both current infection and immune status may need to be determined. For confirmation of current infection, virus isolation in culture, detection of viral RNA by reverse transcriptase polymerase chain reaction (RT-PCR), or confirmation of measles-specific IgM is needed. Throat or nasopharyngeal swabs are usually the preferred sample for virus isolation and RT-PCR, although urine may also contain virus (14). Oral fluids, buccal swabs, and blood are sometimes used in testing. Measles virus can be isolated in Vero/hSLAM cells. These are Vero cells transfected with a plasmid encoding the gene for human signaling lymphocyte activation molecular (hSLAM) protein, which is a receptor for both wild-type and laboratory-adapted strains of measles. Measles virus produces the cytopathic effect of syncytium formation in these cells (15). These cells are available to World Health Organization (WHO) laboratories. Measles virus may also proliferate in B95a cells, another cell type not used routinely in most hospital laboratories. Virus isolation typically takes several days or weeks.

Efficient and timely molecular testing by real-time RT-PCR performed directly on the specimen is likely the most effective approach for detecting current infections. Several RT-PCR methods have been developed (16–19), including one that simultaneously detects measles and rubella RNA (20). Sensitivities and specificities vary among methods, with typical lower limits of detection estimated as 10 (18) to 20 (19) copies per reaction. Specificity has been confirmed by testing with samples positive for respiratory viruses (respiratory syncytial virus, influenza A and B, and human metapneumovirus) (18, 19), mumps (18, 19), and enteroviruses (19). Some RT-PCR methods also provide quantitation and genotyping information. In addition to the types of samples listed previously, lysates of measles-infected cells dried onto filter paper can be used for molecular testing (15).

Detection of measles-specific IgM in blood or oral fluid is another accepted method for laboratory confirmation of suspected cases. In natural measles infection (in an unimmunized host), IgM is detectable initially within 3 to 4 days of appearance of clinical symptoms and persists for 8 to 12 weeks. IgM is most effectively detected between day 4 and 28 after the onset of rash; in the first 72 hours after the appearance of the rash, up to 30% of tests for measles IgM may be falsely negative (14). Enzyme immunoassay (EIA) methods for measles IgM detection in serum have been estimated to have a false-positive rate of 4%, with false-positives occurring in patients with parvovirus B19 and rubella (21, 22).

A significant increase in IgG between two samples, one collected at or near the time of the rash and the second collected 2 weeks later, can be confirmation of current infection. IgG is detectable within 7 to 10 days of the onset of symptoms, is maintained at high levels for years, and remains detectable for life. Confirmation of current measles infection by IgG measurements is slow and may be complicated by obtaining samples at the appropriate intervals.

Measles infection in vaccinated individuals is rare but presents a diagnostic challenge. Clinical signs and symptoms may be different from those seen in unvaccinated individuals, and laboratory confirmation of infection is more complicated. IgM and the virus itself may be difficult to detect. IgG avidity determinations may be useful in these cases to differentiate measles IgG produced in the new infection from IgG related to previous immunization. Commercially available measles-specific IgG assays can be modified to determine IgG avidity and have shown 91.9% sensitivity and 98.4% specificity in differentiating low-avidity (new infection) IgG from high-avidity (previous immunization) IgG (23). Avidity determinations, in addition to measurement of measles-neutralizing antibody levels, may be needed to confirm infection in previously vaccinated individuals (21). Unfortunately, at this writing, measles avidity assays remain as research or investigational tools. Further standardization of control materials and implementation of guidelines for use are needed (25).

Testing for measles immune status, rather than for current infection, is the focus of most hospital laboratories. Although antibodies are produced against various measles proteins, protection is most closely correlated with antibodies to the measles virus hemagglutinin (H) protein. Most assays use whole virus or viral extract antigens that will detect antibodies of various specificities, but most detect antibodies against the measles H proteins effectively.

The most widely used methods in measles antibody detection are EIA, indirect immunofluorescence (IFA), and multiplex bead fluorescence immunoassays (FIA) that simultaneously detect IgG antibodies to measles, mumps, rubella, and varicella zoster viruses. EIAs, IFAs, and FIAs can be designed to detect either IgG or IgM. U.S. Food and Drug Administration (FDA)-cleared EIA, IFA, and FIA kits are readily available commercially, and testing is not difficult to perform. Most EIAs and FIAs are fully automated, so they are optimal for large-volume testing. The IFAs are performed manually and require expertise for microscopic evaluation and interpretation.

Complement fixation (CF), hemagglutination inhibition (HI), neutralization (NT), and plaque reduction neutralization (PRN) are seldom used in diagnostic laboratories

but may be available at reference or research facilities. PRN can be modified to allow a comparison of IgM and IgG levels, as well as to measure total (IgG + IgM) response. The other methods detect total response and do not distinguish between IgG and IgM. CF, HI, NT, and PRN assays are more complicated, requiring a variety of reagents and considerable expertise on the part of the technologist. These are used primarily for difficult cases that are not resolved with routine testing methods.

Comparisons of IgG or total antibody (IgM and IgG together) levels can be achieved with IgG-specific EIA, IFA, and FIA or by total antibody detection by CF, HI, NT, or PRN. With assays performed in serial 2-fold dilutions, a 4-fold increase in antibody level between acute- and convalescent-phase samples confirms infection. With methods such as EIA that are not performed in serial dilutions, the manufacturer must provide guidelines for defining significant differences in antibody level. No standardized interpretation is available for these assays. EIA results show very good correlation with HI and PRN in testing of paired serum samples to detect rises in IgG (14).

The laboratory confirmation of SSPE is less straightforward. Measles virus often cannot be isolated due to its defective nature, and antibodies are detectable but in abnormally high quantities. A comparison of antibody levels in serum and cerebrospinal fluid (CSF) shows greater elevations in the CSF than in the serum (26).

Most commercially available FDA-cleared EIAs, IFAs, and FIAs have shown acceptable sensitivity and specificity for immune status determinations. However, endpoints of these assays are usually set to maximize confidence in positive results, causing these methods to yield false-negative results in low-titered immunity (26). In situations where very low levels of antibody are suspected, testing for measles antibodies by the NT, HI, or PRN assays—performed at a reference or research laboratory—may be needed.

TECHNOLOGY FOR MEASLES TESTING

Molecular Methods

After the appearance of the measles rash, RT-PCR methods are often able to detect measles virus for 3 to 4 days beyond the time of successful virus isolation. Typical samples such as nasal pharyngeal swabs, oral fluids, and blood can be tested. Oral fluid sampling devices which include a preservative for stabilizing IgM should not be used for collection of RT-PCR samples (14). None of the measles RNA real-time RT-PCR assays are FDA-cleared for *in vitro* diagnostic testing, but several published methods have been shown to be effective. Most of these use TaqMan technology to detect measles RNA alone (16–19) or in combination with rubella RNA (20). The multiplex assay detects measles and rubella RNA in a single tube as effectively as individual RT-PCR for measles alone or rubella alone. Primers and probes for the multiplex assay are based on highly conserved regions of the complete measles nucleoprotein (N) gene sequences available in GenBank; the assay has a lower limit of detection of 100 copies per reaction. A multiplex RT-PCR has been developed that identifies the RNAs of measles virus, rubella virus, parvovirus B19, enterovirus, human herpes virus type 6 (HHV-6), and human herpes virus type 7 (HHV-7). Infections with each of these viruses can be accompanied by a "measles-like rash." In 26 patients clinically diagnosed with measles, measles virus was detected in only eight; parvovirus was detected in two, HHV-6 in three, and HHV-7 in one (27).

Serologic Methods

Sample requirements: The specimen collection guidelines are similar for most serologic assays: collect whole blood, separate serum, store the serum in the refrigerator (2 to 8°C) for up to 48 h, and freeze the serum (−20°C) if testing will be performed after 48 h. For most methods, heat inactivation of the serum (incubation at 56°C for 30 min) is not required. Some methods specify that heat-inactivated samples cannot be used. In general, contaminated, hemolyzed, lipemic, or icteric specimens should not be used.

An alternative to serum collected by venipuncture is whole blood obtained by finger stick or heel prick, spotted on Whatman filter paper, air dried, sealed in air-tight packets, and stored at 2 to 8°C. Venous blood collected by venipuncture may also be spotted on filter paper and stored. Following elution and dilution of the dried blood sample, commercial EIAs may be used to test the sample. Results of EIA testing for measles IgG and IgM from dried blood spots have shown excellent correlation with those of fresh serum or plasma testing (28–31). Storage of blood spots for up to 24 months without significant change in antibody testing results has been demonstrated, although storage for 6 months or less is recommended (32). Prior to testing, the dried blood is eluted from the filter paper using phosphate buffered saline (PBS) with Tween 20 at room temperature for 30 minutes. The eluted sample is then diluted in PBS containing 5% fat-free milk powder before testing by EIA (28).

EIA

Most diagnostic laboratories use FDA-cleared, commercially supplied measles antibody EIA testing systems and follow protocols provided and validated by the manufacturer. The typical configuration involves an antigen-coated solid phase (often microwells). The antigen may be an extract of cells infected with virus (often Edmonston strain for measles) or a recombinant protein. Testing is performed either manually or with an automated system. All controls are supplied by the manufacturer to ensure accuracy and reproducibility. Most EIAs detect only IgG, but IgM-specific EIAs are available. IgM-specific assays may include a serum pretreatment step to eliminate interference from virus-specific IgG and rheumatoid factor or an "IgM capture" step featuring microwells coated with antibodies against human IgM. In the first step of a capture assay, patient's serum is added to the antibody-coated microwell, and any IgM present in the sample is bound or captured. In subsequent steps, reagents are added to confirm that the captured IgM is, indeed, specific for the virus. Most large reference laboratories list measles-specific IgM testing in their menus.

IFA

IFA can be used for measles antibody detection. Written procedures, along with proper reagents and controls, are included with each FDA-cleared commercial product, and manufacturer's guidelines must be followed. Like the EIAs, most IFAs are designed to detect IgG antibodies but can be used for IgM detection. As described above for IgM-specific EIAs, IgM-specific IFA testing is preceded by a serum pretreatment step to aid in eliminating interference from IgG and rheumatoid factors.

FIA

Automated FIA technology is comparatively new to the diagnostic laboratory. Sets of tiny polystyrene beads are dyed various shades of color with fluorescent dyes, and each bead set is coated with a particular antigen. Beads from each set

are combined in a single reaction vessel to which the patient's serum is added. Following incubation and washing, a fluorescein-labeled antibody (either antihuman IgG or antihuman IgM) is added that binds to patient's IgG or IgM that bound to the antigen on the bead during the first incubation. After washing to remove unbound conjugate, beads are analyzed (up to 20,000 per second) by a dual-beam laser system. One laser identifies the bead set (by color of the bead), and the other laser measures bound conjugate to determine if the patient's antibody bound to the antigen on the bead surface. One multiplex bead FIA by BioRad Inc, the BioPlex 2200, features an FDA-cleared multiplex assay that simultaneously detects antibodies to measles, mumps, rubella, and varicella antibodies. The system is totally automated.

CF

CF depends on the binding of antibodies to the viral antigen to make antigen–antibody complexes that bind complement, thus making it unavailable for lysis of sensitized indicator red blood cells. CF is a lengthy and cumbersome method of antibody detection, requiring multiple reagents and an overnight incubation period (33–35). Few diagnostic laboratories currently use this method for measles antibody determinations because the EIAs, IFAs, and FIAs are more sensitive and so much easier to perform.

NT

Virus NT measures the capacity of serum antibody to neutralize live virus, thus preventing it from infecting susceptible cell cultures. NT testing requires laboratory facilities suitable for management of live, infectious viruses and cell cultures. The virus must be quantitated prior to the start of the assay, and cell cultures are observed to determine the result (36). This method is sometimes considered the reference method against which other assays should be compared because neutralizing antibodies, which are the type of antibody considered protective for infection, are measured.

HI

An overview of the HI test for measles (and mumps) antibodies is presented below. A detailed procedure was published previously (26, 37).

Antigens

Commercially purchased measles and mumps virus hemagglutinating antigens are used. Antigen suspensions must be treated to break up antigenic particles and titrated to determine a challenge dose of two 50% hemagglutinating units.

Erythrocytes

For measles antibody testing, African green, Patas, or rhesus monkey erythrocytes are used. For mumps antibody testing, chick, goose, or monkey cells are used.

Specimen Preparation

Serum, plasma, or CSF may be used. Nonspecific inhibitors of agglutination must be removed from serum or plasma by treatment with saturated ammonium sulfate, and nonspecific agglutinins must also be removed by mixing inhibitor-free sample with packed erythrocytes. CSF is usually free of nonspecific inhibitors and agglutinins.

Performance of the Test

A U-bottom microwell plate may be used to prepare serial 2-fold dilutions (from 1:2 to 1:2,048) of test serum. Add prepared, titrated hemagglutinating antigen to serum dilutions, incubate, and add a 0.5% erythrocyte suspension to all wells. Allow erythrocytes to settle. Read for hemagglutination.

IgG and IgM titers can be determined separately in a series of three titrations. The first is carried out as described above. The second titration uses serum that has been extracted with *Staphylococcus aureus* protein A, and the third titration is conducted on sera that have been further treated for 30 min with 0.2 volume of 1 M 2-mercaptoethanol. The IgG level is the difference between the arithmetic titers of the first two tests, and the IgM level is the difference between those of the second and third tests. IgG3 and IgA remain in the third test.

PRN

The PRN assay is used for detecting measles antibodies only. An overview of the PRN test is presented below. A detailed procedure was published previously (26, 37).

Challenge Virus

Use a low-pass measles virus (previously titrated).

Cell Cultures

Use Vero cells grown to confluence in 24-well (16-mm-diameter) plates.

Performance of the Test

Mix portions of serial dilutions of inactivated serum with an equal volume of virus containing 125 PFU. Incubate mixtures for 1 h at 37°C. Inoculate this mixture into cell cultures drained of their medium. Incubate cultures for 1 h at 37°C. Replace the inoculum with agarose overlay. Incubate for 4 to 7 days, with timing determined by plaque formation. Remove the overlay, stain the cells with neutral red diluted in cell culture medium, and count. A 50% reduction in plaque count, relative to controls, is considered the endpoint.

INTERPRETATION OF MEASLES TESTING

Isolation of measles virus in culture or the presence of measles RNA in clinical samples is the preferred approach for confirming current or very recent infection or vaccination. If the serologic approach is used for diagnosis of current or very recent infection, serum is tested for measles IgM. The presence of IgM indicates current or recent experience with the virus, either through infection or vaccination. Timing of collection of samples for IgM testing relative to onset of symptoms is important for accurate detection. Both false-positive and false-negative results are possible.

Interpreting a positive IgM result from a person with suspected measles can be difficult if the person has recently received measles vaccine. Because measles-specific IgM may appear as early as 8 days after vaccination and persists for at least 8 weeks after primary vaccination, IgM-positive results obtained during this time should not be assumed to confirm infection (38). IgM is not produced routinely upon revaccination of those previously immunized but may be detected following clinical measles in these individuals (1). An absence of IgM does not rule out measles infection. Samples collected within 72 h after onset of rash may not yet contain detectable IgM, and IgM may not be produced in infection of those previously immunized (1).

A significant increase in IgG level between acute- and convalescent-phase samples is also indicative of infection or vaccination but may be seen in those with a history of natural infection or vaccination when they are again exposed

to the virus. Failure to detect a significant increase between acute- and convalescent-phase samples in infection may occur if the samples are collected too long after the onset of symptoms. This approach is slower than the other approaches and is, thus, the least desirable.

The U.S. Centers for Disease Control and Prevention (CDC) currently recommends collection of respiratory specimens for culture or RNA testing and blood for serologic testing in suspected measles cases. Clinical and epidemiological information should also be considered in the final interpretation of test results (25).

Most measles serologic testing in U.S. laboratories is for determination of immune status. Testing of a single serum sample for measles IgG is sufficient for this purpose. A positive (antibody detected) result by any of the many U.S. FDA-cleared methods correlates with immunity.

MUMPS

Mumps virus causes the infection known simply as "mumps," which typically involves swollen parotid glands. This infection is clinically unapparent in 25 to 30% of cases, is typically mild, and is characterized by slightly elevated temperature and enlargement of one or both parotid glands. Complications of mumps include meningoencephalitis (up to 15% of cases) and, in postpubertal individuals, orchitis (20 to 30% of males) and oophoritis (7% of females) (39). Mumps remains common throughout much of the world.

Although numbers of mumps cases in the U.S. diminished rapidly with the success of the MMR vaccine, isolated outbreaks continue to occur. Only 231 mumps cases were reported in the United States in 2002 (40), but the largest U.S. outbreak in 2 decades occurred in the Midwestern states in 2006 (41). More than 6,500 cases were involved in this outbreak, and a high percentage of the cases had received two doses of mumps vaccine. Waning immunity and incomplete vaccine-induced immunity to circulating wild-type virus were suspected as causes (41). The overall estimate of mumps antibody seroprevalence in the U.S. in 1999 through 2004 was 90%, which is the lower end of the level of immunity (90 to 92%) needed to achieve herd immunity (42).

During 2009 and 2010, another mumps outbreak occurred in the U.S involving 3,502 cases of mumps (43). As with the 2006 outbreaks, a high percentage of infected individuals had received either one (14%) or two (76%) doses of the MMR vaccine, so waning of vaccine-induced protection against mumps was again suggested as a contributing factor. It was also concluded that the level of immunity required to protect against clinical mumps may depend on the size of the inoculum of virus involved in the exposure, indicating that a particular antibody titer versus protection from infection is not absolute (43). However, there is evidence that individuals with lower antibody titers are more likely to become infected (44).

At this writing, the incidence of mumps has returned to its pre-2006 outbreak levels, but it remains unclear whether a change in the vaccine itself or in vaccine administration schedules will be needed to prevent future outbreaks in the United States. Mumps remains common throughout much of the world, usually infecting 6- to 10-year-old children in the spring in unvaccinated populations.

Similar to measles antibodies, mumps antibodies transplacentally transferred from vaccinated mothers are at lower levels at birth, and infants are more susceptible to infection than in the prevaccine era when mothers experienced natural infection. Premature infants may demonstrate seronegativity of 55% for mumps, with further deterioration of immunity over the next 3 months, resulting in seronegativity of 100% for mumps (12).

DIAGNOSTIC STRATEGIES FOR MUMPS

Both current infection and immune status may need to be confirmed for mumps. Virus isolation, RNA detection, and detection of mumps-specific IgM are evidence of current infection. Saliva, blood, urine, and CSF are suitable specimens for virus isolation and RNA testing. Mumps virus proliferates in several cell lines routinely used in viral diagnostic laboratories, including primary monkey kidney, human neonatal kidney, HeLa, and Vero cells. Better proliferation may be obtained in B95a and Vero/hSLAM cells, but these lines are not available at most diagnostic laboratories. The process of virus isolation is slow, and reagents may not be available for confirmation at most laboratories.

Molecular techniques are the method of choice for confirmation of current infection. The assays are more sensitive than virus isolation in culture and can provide sequence information needed for genotyping. RT-PCR methods can detect mumps RNA in oral fluids, CSF (45, 46), saliva/throat, and urine specimens (45, 47). There are currently no FDA-cleared molecular assays for mumps detection.

Mumps IgM is detectable initially within 3 to 4 days of appearance of clinical symptoms and persists for 8 to 12 weeks. Detection of mumps-specific IgM is one of the ways to confirm current infection. However, there is cross-reactivity of mumps antibodies and antibodies against other related viruses (human parainfluenza viruses, types 1, 2, 3, and 4 and others), so falsely positive results may be encountered. Samples collected too soon after infection may be falsely negative in IgM testing.

Mumps IgG is detectable within 7 to 10 days of the onset of symptoms, is maintained at high levels for years, and remains detectable for life. Confirmation of a significant increase in antibody level between two samples collected 2 weeks apart supports current infection, but—as seen in mumps IgM assays—increases in IgG may be seen in patients infected with related viruses. In general, cross-reactivity with related viruses can be ruled out by testing for antibodies to the related viruses in parallel with mumps virus antibody testing. The greatest increase in antibody level should identify the true infection. Given the lack of serologic test specificity, virus isolation and RNA detection in clinical samples remain the most effective ways to confirm infection in unvaccinated individuals.

Confirmation of current mumps infection in previously infected or immunized individuals is very difficult. Virus isolation and RNA detection have been recommended for mumps diagnosis in these individuals. Buccal swabs should be procured early (within 3 days of parotitis onset), as the duration of viral replication is likely to be shorter in these hosts. Virus isolation in culture or RNA detection can be variable, presumably due to low viral loads. IgM is not consistently observed in this situation, so it is not a reliable indicator of recent infection. IgM may be produced weakly or not at all in a secondary immune response. In a recent outbreak, mumps virus IgM antibodies were detected in fewer than 15% of mumps virus-infected persons who were previously immunized, and 95% of these patients were positive for mumps virus IgG (48). The CDC provides guidance online for mumps testing in both previously vaccinated and unvaccinated individuals (http://www.cdc.gov/mumps/lab/qa-lab-test-infect.html).

Because standard diagnostic tests for mumps that detect virus or virus-specific antibody perform inconsistently for

individuals with prior immune exposure via either immunization or natural infection, an alternate approach has been developed. Detection of activated mumps-specific antibody-secreting memory B cells (ASCs/plasmablasts) by EIA has been shown to be a more reliable test (49). ASCs are detectable in circulation only following recent activation by antigen. In testing for ASCs, peripheral blood mononuclear cells are cultured in the presence of polyclonal mitogens, and the ASCs are detected by exposure to viral antigen. Trials with this method detected mumps ASCs in recently MMR-vaccinated individuals and in those with clinical mumps during a mumps outbreak. Detection of ASCs appears to be more sensitive for longer periods of time than RT-PCR or IgM EIA and may be useful for diagnosing mumps cases that cannot be confirmed with standard methods and for testing asymptomatic case contacts in an outbreak. Interestingly, mumps ASCs appear to be produced in lower numbers than measles or rubella ASCs, suggesting that mumps infection may not generate robust B-cell memory (49).

As with measles, most mumps antibody testing in the United States involves immune status determinations using FDA-cleared, commercially available EIA, IFA, and FIA test kits. Because these methods may yield falsely negative results in low-titered immunity, NT and HI assays for mumps antibodies may be needed but are available only at reference or specialty laboratories.

TECHNOLOGY FOR MUMPS TESTING

Molecular Methods

At present, there are no FDA-cleared methods for mumps RNA detection, but high-quality reagents are available. Two RT-PCR assays have been developed and standardized by the CDC, with information available online. Step-by-step procedures are provided and commercial sources of reagents are identified for one standard RT-PCR that detects the SH gene of mumps virus (http://www.cdc.gov/mumps/downloads/lab-rt-pcr.doc) and for one real-time RT-PCR assay (http://www.cdc.gov/mumps/downloads/lab-rt-pcr-assay-detect.doc). Molecular assays are more sensitive than virus isolation in culture and can provide sequence information for the coding region of the SH gene that is needed to determine the viral genotype. Laboratories with advanced molecular assay capabilities may be able to offer mumps detection by RT-PCR, but most routine virology laboratories rely on mumps virus isolation as the standard method for diagnosing mumps virus infection.

Serologic Methods

As presented above for measles serologic methods, serum sample collection, processing, and storage are similar for most serologic assays. Blood spotted onto Whatman filter paper can be eluted and tested for mumps antibodies. Results of EIA testing for mumps (28) IgG and IgM from dried blood spots have shown excellent correlation with those of fresh serum or plasma testing. Protection from infection is most closely correlated with antibodies to the mumps virus hemagglutinin/neuraminidase (HN) protein. Most assays use whole virus or viral extract antigens that will detect antibodies of various specificities, but most detect antibodies against the mumps HN proteins effectively.

EIA, IFA, and FIA

FDA-cleared, commercially available EIA, IFA, and FIA kits are used by most laboratories for mumps antibody testing (as described above for measles EIA). Most EIAs and FIAs use either an extract of cells infected with Enders strain of mumps virus or a recombinant protein as the antigen in the system. IFA methods use mumps-infected cells fixed on a microscope slide as the antigen. Various configurations are available and may test for IgM alone, IgG alone, or IgM and IgG together. An IgM-capture EIA was used recently for detection of mumps virus IgM (48).

CF, NT, and HI

CF, NT, and HI can be used to detect mumps antibodies. All are cumbersome technologies seldom used in routine laboratories. The CF technique can be used with two different mumps virus antigens, V and S. Antibodies against the S antigen appear earlier and rise quickly, in contrast to the antibodies to the V antigen, which appear later. The presence of both V and S antibodies is thought to signal a recent past infection, while V antibodies alone signal a long-past infection (50). A detailed procedure for mumps virus antibody HI testing was published previously (26, 37). The NT method was described above for measles antibody detection (36).

INTERPRETATION OF MUMPS TESTING

As with measles virus infection, isolation of mumps virus or the presence of mumps RNA in clinical samples is evidence for current or very recent infection or vaccination. However, the interpretation of mumps antibody testing results is less straightforward than that of measles. Mumps IgM maybe detected, along with significant increases in IgG, in patients infected with related viruses such as the paramyxoviruses. In general, cross reactivity with related viruses can be ruled out by testing for these antibodies in parallel with mumps antibody testing. The greatest increase in antibody level should identify the true infection. Virus isolation and RT-PCR are the most accurate methods for resolving this issue. Interpretation of mumps serology can be obscured in patients previously vaccinated. Various therapeutic treatment regimens such as chemotherapy may result in a decrease in seropositivity for measles and mumps. Additional precautions in interpretation of testing results in diseases of low prevalence such as mumps are presented at the end of this chapter.

Testing for mumps IgG by various U.S. FDA-cleared methods is used to determine mumps immune status. Detection of IgG in a single serum sample is indicative of immunity.

RUBELLA

Rubella virus is the cause of a contagious, acute infectious disease called rubella, which is often colloquially referred to as German measles and 3-day measles. The rubella virus is principally transmitted by contact with infectious respiratory secretions and through inhalation of droplet nuclei, but vertical transmission is also possible. In symptomatic postnatal infections, the disease is characterized by mild fever, lymphadenopathy of suboccipital, postauricular, and posterior cervical nodes, and a discrete maculopapular rash that follows an incubation period averaging 16 to 18 days (range 10 to 21 days). Some patients may also experience conjunctivitis, arthralgia or arthritis (51). The disease is most often self-limited and without postinfectious sequelae, but rare complications including encephalitis (52, 53), polyradiculoneuritis (53), and thrombocytopenia (54) have been reported. Infection of pregnant women with rubella virus can lead to potentially devastating

consequences for the fetus. Congenital rubella syndrome has been associated with miscarriages, stillbirths, and a host of birth defects that include developmental delays, cataracts, hearing impairment, and congenital heart disease, among others. The risk of CRS appears to be greatest if infection occurs during the first trimester of gestation, and the risk declines after 12 weeks gestational age, with rare defects presenting in fetuses at risk of infection equal to or older than 20 weeks gestation.

The implementation of stringent vaccination campaigns such as The Measles and Rubella Initiative (http://www.measlesrubellainitiative.org/), a multicollaborator global partnership geared toward the eradication of measles and rubella, has essentially eliminated the endemic spread of rubella virus in the Americas. However, cases are still reported in many regions of the Western Hemisphere as a result of importation of cases from areas of endemicity. In other parts of the world, the disease remains endemic and, in 2012 alone, approximately 94,000 cases were reported to the World Health Organization by reporting countries (55).

Strict infection control precautions are mandatory to avoid transmission of the highly infectious rubella virus. Studies have demonstrated the presence of rubella virus in nasopharyngeal secretions 1 week prior to and 2 weeks following rash onset in postnatal cases. Because infected infants can remain infectious for 1 year or longer, enrollment of these children in daycare should be avoided, and isolation precautions should be implemented when they present to healthcare institutions (47).

DIAGNOSTIC STRATEGIES FOR RUBELLA

For rubella, laboratory testing to confirm acute or recent rubella infection, CRS, and immune status is needed. Immune status testing is straightforward and widely available at most diagnostic laboratories. As described above for measles and mumps immune status determinations, a single serum sample collected at random and tested by a rubella IgG-specific method such as EIA or FIA is all that is needed.

For diagnosis of current postnatal infections, serologic testing for rubella virus-specific IgG and IgM is the usual approach, although virus isolation in culture and detection of rubella virus RNA are useful. For serologic testing, a serum sample should be collected as soon as possible (within 7 to 10 days) after onset of illness and another collected 2 to 3 weeks later. If IgM antibodies are detected in the first sample, a diagnosis of rubella infection is supported; however, persons infected with parvovirus, those demonstrating the heterophile antibodies of infectious mononucleosis, or those who test positive for rheumatoid factors may have false-positive results for rubella IgM. Follow-up testing for these other analytes should be done if a false-positive rubella IgM result is suspected (57). A negative rubella IgM test may be encountered if the sample is collected before day 5 after rash onset, and testing should be repeated on another sample collected later. A significant increase in IgG levels between the first and second sample supports current rubella infection. Assays for IgG avidity can aid in distinguishing between recent and past rubella infections, with low avidity associated with recent primary infection and high avidity associated with past infection. These assays are most often performed in reference laboratories.

For investigation of rubella infection in pregnant women, rapid and accurate diagnosis is imperative. For patients who develop clinical signs, serum should be collected immediately and tested for the presence of anti-rubella IgM by EIA (58, 59). If a rubella IgM test result is positive in a woman with no history of illness and low or no risk of exposure to rubella, additional laboratory evaluation should be completed (57).

In current postnatal infection the virus can be isolated in culture. Virus shedding is greatest up to day 4 after rash onset, but virus may be isolated 1 to 2 weeks after rash onset. Throat swabs are the specimen of choice for isolation, although virus can be isolated from nasal, urine, and cataract specimens (57). RT-PCR provides a result more quickly than viral culture. Detection of rubella RNA confirms current infection. RT-PCR can be performed on the same specimens used for virus isolation.

Isolation of rubella virus in culture is not routinely performed since most diagnostic laboratories lack both the expertise and the technical capacity for it. In addition, rubella virus culture is quite slow, so most laboratories have abandoned cultivation-based methods in favor of faster and less challenging approaches such as serologic and nucleic acid amplification assays. For culture, many cell lines are permissive for rubella virus infection and include African green monkey kidney (AGMK), BHK21, RK-13, and Vero (51, 60). Detection of rubella virus in infected cell cultures has historically proved difficult because of the lack of apparent cytopathology in first-passage wild-type virus cultures. Interestingly, assays exploiting the fact that the rubella virus infectious cycle interferes with the replication of cytopathogenic enteroviruses have been devised to improve rubella virus detection. However, these assays are beyond the technical capability of most clinical laboratories. The availability of high-quality reagents and easily reproducible assays, such as viral antigen-specific IFAs and PCR, has replaced these older methods for detecting rubella virus in cell cultures. Also, reverse transcription-loop-mediated isothermal amplification (RT-LAMP) has been used for the detection of rubella virus RNA in media from infected cell cultures (61). The CDC provides guidance online for culture-based detection of rubella virus using Vero cells (http://www.cdc.gov/rubella/lab/ifa_protocol.html).

Diagnostic tests used to confirm CRS include serologic assays, isolation of the virus, and detection of rubella virus by RT-PCR. A positive IgM result in the infant's cord blood or serum supports the diagnosis of CRS. In CRS, IgM antibody is expected to persist for 6 to 12 months but may not be detectable until at least 1 month of age. Infants with symptoms suspicious for CRS but testing negative for IgM shortly after birth should be retested at 1 month of age (57). Persistence of rubella IgG beyond 6 months of age also supports CRS. The virus may be isolated from the throat and urine of CRS infants, but chances for isolation are best in samples collected before 5 months of age (57). Molecular detection by RT-PCR and molecular typing are recommended because epidemiologic information is needed to track rubella in the U.S. By comparing virus sequences from new cases with sequences from other cases, the origin of particular virus types in this country can be tracked (56).

Historically, serologic diagnosis of postnatal rubella and CRS as well as demonstration of immunity to rubella has been performed by a number of methods, including EIA, FIA, IFA, CF, HI, passive hemagglutination (PHA), latex agglutination (LA), hemolysis in gel, radioimmunoassay, and a variety of IgM detection assays. However, FDA-cleared, commercially available EIAs for detection of IgG and IgM are used by most laboratories for rubella antibody testing.

TECHNOLOGY FOR RUBELLA TESTING

Molecular Methods

Currently, there are no FDA-cleared assays for the detection of rubella virus RNA in clinical specimens. However, numerous laboratory-developed assays have been extensively evaluated for detection of viral RNA from clinical samples, including conventional and real-time reverse transcription-PCR methods (57) that test for rubella virus alone or in multiplex with other analytes. Specimens from which rubella RNA can be detected include blood, CSF, nasal and throat swabs, and urine (57).

Serologic Methods

Sample requirements: As discussed above for serologic methods for measles and mumps, serum sample collection, processing, and storage are similar for most rubella serologic assays. In addition, detection of anti-rubella virus IgM and IgG has been successful using eluates from dried blood spots (29). In general, sera should be rejected if they are grossly lipemic, icteric, contaminated, or hemolyzed. For many EIAs, heat-inactivated specimens should also be rejected. Always follow assay manufacturer guidelines for the collection, processing, and storage of specimens for rubella serology.

EIA and FIA

As with measles and mumps serology, most diagnostic laboratories use FDA-cleared commercial EIA testing systems for the detection of antibodies produced against rubella virus. These assays are perhaps the most inexpensive, widely available, and most commonly used assays for detection of anti-rubella IgM and IgG. All commercial systems are solid-phase (often microwells, beads, microparticles, or filters) capture assays that detect antibodies to rubella virus capsid and/or envelope antigens in serum or other clinical specimens (e.g., oral fluid). Both manual and automated rubella EIA testing platforms are available, and many of the tests are either quantitative or semiquantitative and have built-in controls.

IFA

IFA assays can be used for detection of antibodies against rubella. Historically, chronically infected rhesus monkey kidney cells (LLC-MK2 cells) fixed to glass slides have served as the solid-phase antigen (62) to which aliquots of patient sera are added followed by fluorescein isothiocyanate-conjugated antihuman secondary antibodies. Other sources of rubella antigen, including purified viral proteins, have also been used for IFA assays. Because IFA assays are read visually using a fluorescence microscope, subjective interpretation of results is possible. As with any other diagnostic test, controls should always be run in parallel with patient specimens to ensure validity of results and to provide standards for comparison.

CF and HI

CF testing for rubella antibody detection is performed by a standard technique (33). An excellent overview of HI testing for rubella antibodies has been published previously (63).

PHA and LA

PHA and LA assays use either erythrocytes or latex particles as carriers for rubella virus antigens in the test system. Anti-rubella antibodies react with rubella antigen coated on the particle to cause agglutination. Antibodies produced against both structural and nonstructural viral proteins usually remain measurable for years following natural infection or immunization. PHA is performed in a V-shaped microwell plate, and hemagglutination appears as a dispersed settling of erythrocytes within a plate well. Formation of an erythrocyte button in the bottom of the microwell is interpreted as negative. LA methods, which are routinely performed on slides, are read macroscopically for clumping of coated latex particles by rubella antibodies. Both PHA and LA have largely been replaced by EIA for detection of rubella antibodies.

INTERPRETATION OF RUBELLA TESTING

The isolation of rubella virus or the presence of rubella virus RNA in clinical samples, including those from infants with suspected congenital rubella, indicates current or very recent infection. Demonstration of a 4-fold rise in anti-rubella antibody titers in paired sera also indicates current or recent infection with rubella virus.

Because the incidence of rubella virus infection in the Western Hemisphere is very low, the majority of positive rubella IgM tests most likely represent false-positive results that must be confirmed by additional methods (57). Infection with other viruses and the presence of cross-reacting IgM class antibodies and rheumatoid factors have been shown to produce biological false-positive results (64, 65). If there is a likelihood that these substances may be present, additional testing, such as antibody avidity testing, is needed to confirm rubella infection. Care should also be taken when interpreting rubella serology data from pregnant women exposed to rubella; the CDC has constructed an algorithm to facilitate the serologic evaluation of such patients (available at http://www.cdc.gov/vaccines/pubs/surv-manual/chpt14-rubella.html#f20).

Interpretation/Applications of Laboratory Results in Diseases of Low Prevalence

Even assays of high specificity will have a low positive predictive value in populations with low prevalence (less than 1%) of infection, making a high percentage of positive results "false-positives" (66). This precautionary note fits well with the current status of measles, mumps, and rubella infections in the United States, suggesting that a single positive laboratory value should be carefully scrutinized. Thorough clinical histories and confirmatory laboratory testing are warranted in order to differentiate true- from false-positive laboratory findings. For example, a single positive measles IgM result should be supported/confirmed with follow-up measles IgG testing to demonstrate seroconversion from negative to positive or a significant increase in IgG titer. Also, in such cases, detecting viral RNA in clinical samples would give the necessary confirmation and would do so more quickly than monitoring the IgG level.

REFERENCES

1. **Bellini WJ, Rota PA.** 1999. Measles (rubeola) virus, p 603–621. *In* Lennette EH, Smith TF (ed), *Laboratory Diagnosis of Viral Infections*, 3rd ed. Marcel Dekker, Inc, New York.
2. **Centers for Disease Control (CDC).** 1983. Mumps—United States, 1980–1983. *MMWR Morb Mortal Wkly Rep* **32:**545–547. PubMed
3. **Reef SE, Frey TK, Theall K, Abernathy E, Burnett CL, Icenogle J, McCauley MM, Wharton M.** 2002. The changing epidemiology of rubella in the 1990s: on the

verge of elimination and new challenges for control and prevention. *JAMA* **287:**464–472. PubMed
4. **Watson JC, Hadler SC, Dykewicz CA, Reef S, Phillips L, Centers for Disease Control and Prevention (CDC).** 1998. Measles, mumps, and rubella—vaccine use and strategies for elimination of measles, rubella, and congenital rubella syndrome and control of mumps: recommendations of the Advisory Committee on Immunization Practices (ACIP). *MMWR Recomm Rep* **47**(RR-8)**:**1–57. PubMed
5. **Orenstein WA, Papania MJ, Wharton ME.** 2004. Measles elimination in the United States. *J Infect Dis* **189**(Suppl 1)**:**S1–S3. PubMed
6. **Hutchins SS, Papania MJ, Amler R, Maes EF, Grabowsky M, Bromberg K, Glasglow V, Speed T, Bellini WJ, Orenstein WA.** 2004. Evaluation of the measles clinical case definition. *J Infect Dis* **189**(Suppl 1)**:**S153–S159. PubMed
7. **Centers for Disease Control and Prevention (CDC) Global Health.** Why reducing measles, rubella, and congenital rubella syndrome (CRS) worldwide is important. http://www.cdc.gov/globalhealth/measles/why/. Viewed 29 August 2013.
8. **Centers for Disease Control and Prevention (CDC).** 2012. Measles—United States, 2011. *MMWR Morb Mortal Wkly Rep* **61:**253–257. PubMed
9. **Public Health England.** Measles cases in England: January to March 2013. www.hpa.org.uk/webc/HPAwebFile/HPAweb_c/1317138802384 (select "View item you were looking for").
10. **Bellini WJ, Rota JS, Lowe LE, Katz RS, Dyken PR, Zaki SR, Shieh W-J, Rota PA.** 2005. Subacute sclerosing panencephalitis: more cases of this fatal disease are prevented by measles immunization than was previously recognized. *J Infect Dis* **192:**1686–1693. PubMed
11. **Szenborn L, Tischer A, Pejcz J, Rudkowski Z, Wójcik M.** 2003. Passive acquired immunity against measles in infants born to naturally infected and vaccinated mothers. *Med Sci Monit* **9:**CR541–CR546. PubMed
12. **Glick C, Feldman S, Norris MR, Butler J.** 1998. Measles, mumps, and rubella serology in premature infants weighing less than 1,000 grams. *South Med J* **91:**159–160. PubMed
13. **Dine MS, Hutchins SS, Thomas A, Williams I, Bellini WJ, Redd SC.** 2004. Persistence of vaccine-induced antibody to measles 26-33 years after vaccination. *J Infect Dis* **189**(Suppl 1)**:**S123–S130. PubMed
14. **Centers for Disease Control and Prevention.** 2007. *WHO Manual for the Laboratory Diagnosis of Measles and Rubella Virus Infection*, 2nd ed. World Health Organization, Geneva, Switzerland. http://apps.who.int/iris/handle/10665/70211. Accessed 30 August 2013.
15. **Rota PA, Brown KE, Hübschen JM, Muller CP, Icenogle J, Chen M-H, Bankamp B, Kessler JR, Brown DW, Bellini WJ, Featherstone D.** 2011. Improving global virologic surveillance for measles and rubella. *J Infect Dis* **204**(Suppl 1)**:**S506–S513. PubMed
16. **Ozoemena LC, Minor PD, Afzal MA.** 2004. Comparative evaluation of measles virus specific TaqMan PCR and conventional PCR using synthetic and natural RNA templates. *J Med Virol* **73:**79–84. PubMed
17. **El Mubarak HS, De Swart RL, Osterhaus AD, Schutten M.** 2005. Development of a semi-quantitative real-time RT-PCR for the detection of measles virus. *J Clin Virol* **32:**313–317. PubMed
18. **Hummel KB, Lowe L, Bellini WJ, Rota PA.** 2006. Development of quantitative gene-specific real-time RT-PCR assays for the detection of measles virus in clinical specimens. *J Virol Methods* **132:**166–173. PubMed
19. **Thomas B, Beard S, Jin L, Brown KE, Brown DW.** 2007. Development and evaluation of a real-time PCR assay for rapid identification and semi-quantitation of measles virus. *J Med Virol* **79:**1587–1592. PubMed
20. **Hübschen JM, Kremer JR, De Landtsheer S, Muller CP.** 2008. A multiplex TaqMan PCR assay for the detection of measles and rubella virus. *J Virol Methods* **149:**246–250. PubMed
21. **Jenkerson SA, Beller M, Middaugh JP, Erdman DD.** 1995. False positive rubeola IgM tests. *N Engl J Med* **332:**1103–1104. PubMed
22. **Thomas HI, Barrett E, Hesketh LM, Wynne A, Morgan-Capner P.** 1999. Simultaneous IgM reactivity by EIA against more than one virus in measles, parvovirus B19 and rubella infection. *J Clin Virol* **14:**107–118. PubMed
23. **Mercader S, Garcia P, Bellini WJ.** 2012. Measles virus IgG avidity assay for use in classification of measles vaccine failure in measles elimination settings. *Clin Vaccine Immunol* **19:**1810–1817. PubMed
24. **Hickman CJ, Hyde TB, Sowers SB, Mercader S, McGrew M, Williams NJ, Beeler JA, Audet S, Kiehl B, Nandy R, Tamin A, Bellini WJ.** 2011. Laboratory characterization of measles virus infection in previously vaccinated and unvaccinated individuals. *J Infect Dis* **204**(Suppl 1)**:**S549–S558. PubMed
25. **Bellini WJ, Icenogle JP.** 2015. Measles and rubella viruses, p 1519–1535. *In* Jorgensen JH, Pfaller MA, Carroll KC, Funke G, Landry ML, Richter SS, Warnock DW (ed), *Manual of Clinical Microbiology*, 11th ed. ASM Press, Washington, DC.
26. **Black FL.** 1997. Measles and mumps, p 688–692. *In* Rose NR, de Macario EC, Folds JD, Lane HC, Nakamura RM (ed), *Manual of Clinical Laboratory Immunology*, 5th ed. ASM Press, Washington, DC.
27. **Takao S, Shigemoto N, Shimazu Y, Tanizawa Y, Fukuda S, Matsuo T.** 2012. Detection of exanthematic viruses using a TaqMan real-time PCR assay panel in patients with clinically diagnosed or suspected measles. *Jpn J Infect Dis* **65:**444–448. PubMed
28. **Condorelli F, Scalia G, Stivala A, Gallo R, Marino A, Battaglini CM, Castro A.** 1994. Detection of immunoglobulin G to measles virus, rubella virus, and mumps virus in serum samples and in microquantities of whole blood dried on filter paper. *J Virol Methods* **49:**25–36. PubMed
29. **Helfand RF, Keyserling HL, Williams I, Murray A, Mei J, Moscatiello C, Icenogle J, Bellini WJ.** 2001. Comparative detection of measles and rubella IgM and IgG derived from filter paper blood and serum samples. *J Med Virol* **65:**751–757. PubMed
30. **Chakravarti A, Rawat D, Yadav S.** 2003. Whole blood samples as an alternative to serum for detection of immunity to measles virus by ELISA. *Diagn Microbiol Infect Dis* **47:**563–567. PubMed
31. **El Mubarak HS, Yüksel S, Mustafa OM, Ibrahim SA, Osterhaus AD, de Swart RL.** 2004. Surveillance of measles in the Sudan using filter paper blood samples. *J Med Virol* **73:**624–630. PubMed
32. **Riddell MA, Leydon JA, Catton MG, Kelly HA.** 2002. Detection of measles virus-specific immunoglobulin M in dried venous blood samples by using a commercial enzyme immunoassay. *J Clin Microbiol* **40:**5–9. PubMed
33. **Health, Education, and Welfare.** 1965. *Public Health Monograph No. 74—Standardized Diagnostic Complement Fixation Method and Adaptation to Micro Test*. Department of Health, Education, and Welfare, Public Health Service, Health Resources Administration, Hyattsville, MD.
34. **Hawkes RA.** 1979. General principles underlying laboratory diagnosis of viral infections, p 3–48. *In* Lennette EH, Schmidt NJ (ed), *Diagnostic Procedures for Viral, Rickettsial and Chlamydial Infections*, 5th ed. American Public Health Association, Washington, DC.
35. **Stark LM, Lewis AL.** 1992. Complement fixation test, p 203–228. *In* Specter S, Lancz G (ed), *Clinical Virology Manual*, 2nd ed. Elsevier, New York, NY.

36. **Ballew HC.** 1992. Neutralization, p 229–241. *In* Specter S, Lancz G (ed), *Clinical Virology Manual*, 2nd ed. Elsevier, New York, NY.
37. **Leland DS.** 2002. Measles and mumps, p 682–686. *In* Rose NR, Hamilton RG, Detrick B (ed), *Manual of Clinical Laboratory Immunology*, 6th ed. ASM Press, Washington, DC.
38. **Helfand RF, Kebede S, Gary HE, Beyene H, Bellini WJ.** 1999. Timing of development of measles-specific immunoglobulin M and G after primary measles vaccination. *Clin Diagn Lab Immunol* **6**: 178-180.30.
39. **Centers for Disease Control (CDC).** 1989. Mumps prevention. *MMWR Morb Mortal Wkly Rep* **38:**388–392, 397–400. PubMed
40. **Centers for Disease Control and Prevention.** 2004. Summary of notifiable diseases, US, 2002. [Online.] http://www.cdc.gov/mmwr/preview/mmwrhtml/mm5153a1.htm.
41. **Dayan GH, Quinlisk MP, Parker AA, Barskey AE, Harris ML, Schwartz JM, Hunt K, Finley CG, Leschinsky DP, O'Keefe AL, Clayton J, Kightlinger LK, Dietle EG, Berg J, Kenyon CL, Goldstein ST, Stokley SK, Redd SB, Rota PA, Rota J, Bi D, Roush SW, Bridges CB, Santibanez TA, Parashar U, Bellini WJ, Seward JF.** 2008. Recent resurgence of mumps in the United States. *N Engl J Med* **358:**1580–1589. PubMed
42. **Kutty PK, Kruszon-Moran DM, Dayan GH, Alexander JP, Williams NJ, Garcia PE, Hickman CJ, McQuillan GM, Bellini WJ.** 2010. Seroprevalence of antibody to mumps virus in the US population, 1999–2004. *J Infect Dis* **202:**667–674. PubMed
43. **Barskey AE, Schulte C, Rosen JB, Handschur EF, Rausch-Phung E, Doll MK, Cummings KP, Alleyne EO, High P, Lawler J, Apostolou A, Blog D, Zimmerman CM, Montana B, Harpaz R, Hickman CJ, Rota PA, Rota JS, Bellini WJ, Gallagher KM.** 2012. Mumps outbreak in Orthodox Jewish communities in the United States. *N Engl J Med* **367:**1704–1713. PubMed
44. **Cortese MM, Barskey AE, Tegtmeier GE, Zhang C, Ngo L, Kyaw MH, Baughman AL, Menitove JE, Hickman CJ, Bellini WJ, Dayan GH, Hansen GR, Rubin S.** 2011. Mumps antibody levels among students before a mumps outbreak: in search of a correlate of immunity. *J Infect Dis* **204:**1413–1422. PubMed
45. **Poggio GP, Rodriguez C, Cisterna D, Freire MC, Cello J.** 2000. Nested PCR for rapid detection of mumps virus in cerebrospinal fluid from patients with neurological diseases. *J Clin Microbiol* **38:**274–278. PubMed
46. **Pabbaraju K, Tokaryk KL, Wong S, Fox JD.** 2008. Comparison of the Luminex xTAG respiratory viral panel with in-house nucleic acid amplification tests for diagnosis of respiratory virus infections. *J Clin Microbiol* **46:**3056–3062. PubMed
47. **Afzal MA, Buchanan J, Dias JA, Cordeiro M, Bentley ML, Shorrock CA, Minor PD.** 1997. RT-PCR based diagnosis and molecular characterisation of mumps viruses derived from clinical specimens collected during the 1996 mumps outbreak in Portugal. *J Med Virol* **52:**349–353. PubMed
48. **Bitsko RH, Cortese MM, Dayan GH, Rota PA, Lowe L, Iversen SC, Bellini WJ.** 2008. Detection of RNA of mumps virus during an outbreak in a population with a high level of measles, mumps, and rubella vaccine coverage. *J Clin Microbiol* **46:**1101–1103. PubMed
49. **Latner DR, McGrew M, Williams N, Lowe L, Werman R, Warnock E, Gallagher K, Doyle P, Smole S, Lett S, Cocoros N, DeMaria A, Konomi R, Brown CJ, Rota PA, Bellini WJ, Hickman CJ.** 2011. Enzyme-linked immunospot assay detection of mumps-specific antibody-secreting B cells as an alternative method of laboratory diagnosis. *Clin Vaccine Immunol* **18:**35–42. PubMed
50. **Leland D.** 2011. Parainfluenza and mumps viruses, p 1347–1356. *In* Versalovic J, Carroll KC, Funke G, Jorgensen JH, Landry ML, Warnock DW (ed), *Manual of Clinical Microbiology*, 10th ed, vol 2. ASM Press, Washington, DC.
51. **Bellini WJ, Icenogle JP.** 2011. Measles and rubella viruses, p 1372–1387. *In* Versalovic J, Carroll KC, Funke G, Jorgensen JH, Landry ML, Warnock DW (ed), *Manual of Clinical Microbiology*, 10th ed, vol 2. ASM Press, Washington, DC.
52. **Lau KK, Lai ST, Lai JY, Yan WW, So TMK, Wong TY.** 1998. Acute encephalitis complicating rubella. *Hong Kong Med J* **4:**325–328. PubMed
53. **Chang DI, Park JH, Chung KC.** 1997. Encephalitis and polyradiculoneuritis following rubella virus infection—a case report. *J Korean Med Sci* **12:**168–170. PubMed
54. **Morse EE, Zinkham WH, Jackson DP.** 1966. Thrombocytopenic purpura following rubella infection in children and adults. *Arch Intern Med* **117:**573–579. PubMed
55. **World Health Organization.** 2013. Reported cases of selected vaccine preventable diseases (VPDs). http://apps.who.int/immunization_monitoring/globalsummary/timeseries/tsincidencerubella.html. Accessed 25 September 2013.
56. **McLean H, Redd S, Abernathy E, Icenogle J, Wallace G.** 2012. *Manual for the Surveillance of Vaccine-Preventable Diseases*, 5th ed. Chapter 15: Congenital rubella syndrome. http://www.cdc.gov/vaccines/pubs/surv-manual/chpt15-crs.html. Accessed 30 September 2013.
57. **McLean H, Redd S, Abernathy E, Icenogle J, Wallace G.** 2012. *Manual for the Surveillance of Vaccine-Preventable Diseases*, 5th ed. Chapter 14: Rubella. http://www.cdc.gov/vaccines/pubs/surv-manual/chpt14-rubella.html. Viewed 30 September 2013.
58. **Abbott GG, Safford JW, MacDonald RG, Craine MC, Applegren RR.** 1990. Development of automated immunoassays for immune status screening and serodiagnosis of rubella virus infection. *J Virol Methods* **27:**227–239. PubMed
59. **Best JM, Palmer SJ, Morgan-Capner P, Hodgson J.** 1984. A comparison of Rubazyme-M and MACRIA for the detection of rubella-specific IgM. *J Virol Methods* **8:**99–109. PubMed
60. **Stewart GL, Parkman PD, Hopps HE, Douglas RD, Hamilton JP, Meyer HM Jr.** 1967. Rubella-virus hemagglutination-inhibition test. *N Engl J Med* **276:**554–557. PubMed
61. **Mori N, Motegi Y, Shimamura Y, Ezaki T, Natsumeda T, Yonekawa T, Ota Y, Notomi T, Nakayama T.** 2006. Development of a new method for diagnosis of rubella virus infection by reverse transcription-loop-mediated isothermal amplification. *J Clin Microbiol* **44:**3268–3273. PubMed
62. **Brown GC, Maassab HF, Veronelli JA, Francis TJ Jr.** 1964. Rubella antibodies in human serum: detection by the indirect fluorescent-antibody technique. *Science* **145:**943–945. PubMed
63. **Mahony JR.** 2006. Rubella virus, p 712–718. *In* Detrick B, Hamilton RG, Folds JD (ed), *Manual of Molecular and Clinical Laboratory Immunology*, 7th ed. ASM Press, Washington, DC.
64. **Kurtz JB, Anderson MJ.** 1985. Cross-reactions in rubella and parvovirus specific IgM tests. *Lancet* **2:**1356. PubMed
65. **Morgan-Capner P.** 1991. False positive tests for rubella-specific IgM. *Pediatr Infect Dis J* **10:**415–416. PubMed
66. **Bellini WJ, Helfand RF.** 2003. The challenges and strategies for laboratory diagnosis of measles in an international setting. *J Infect Dis* **187**(Suppl 1)**:**S283–S290. PubMed

Viral Hepatitis

HUBERT G. M. NIESTERS, ANNELIES RIEZEBOS-BRILMAN,
AND CORETTA C. VAN LEER-BUTER

65

The term "hepatitis" refers to the inflammation of the liver, and in this chapter the five so-called major or primary viruses that cause this inflammation are described. These are the viruses hepatitis A virus (HAV), hepatitis B virus (HBV), hepatitis C virus (HCV), hepatitis delta virus (HDV), and hepatitis E virus (HEV). In Table 1, the characteristics of these hepatitis viruses are described. Although there are also secondary viruses that can infect the liver and cause hepatitis, such as cytomegalovirus, Epstein-Barr virus, herpes simplex virus 1, and enterovirus, the five primary viruses account for at least 95% of hepatitis virus infections. They primarily cause an infection of the liver and may infect other organs, while the secondary viruses infect the liver only during the course of a systemic infection.

The initial diagnosis of hepatitis is based on biochemical parameters that give information on the function and integrity of the liver. Alanine aminotransferase (ALT) and aspartate transaminase (AST) are the most important enzymes and are easy to measure in serum because their levels are indicators for hepatocellular damage and inflammation. But these biochemical parameters do not give any information about the presence of viruses involved, since damage to the liver may also be caused by other routes, like medication or autoimmune hepatitis.

Clinically, hepatitis can be divided into acute infection and persistent or chronic infection. The latter is defined as infection lasting >6 months as established by the presence of the surface antigen of HBV, known as HBsAg, or by the detection of viral RNA in the case of a chronic or persistent HCV infection. In some immunocompromised patients, HEV can also cause a chronic infection. Symptoms can also be variable, from mild, subclinical infection without jaundice to fulminant infection, as well as chronic hepatitis. Fulminant hepatitis is a rare form of acute hepatitis associated with liver failure and may lead to death of the patient or the need for liver transplantation. A summary of the different forms of viral hepatitis is given in Table 2. The immune system plays a very important role in the pathogenesis of these viruses, because the immune system attacks the infected hepatocytes, which express viral antigens. Therefore, in those individuals in whom the immune system is suppressed, the manifestation of the infection can be less severe and less obvious. Also, in an infection that occurs prenatally or perinatally, as in many cases of HBV, the immune system does not attack the infected hepatocytes and the infection is very likely to become chronic. The immune system is crucial for clearing the viral infection, and thus it is obvious that in patients who are immunosuppressed, whether by HIV infection or immunosuppressive treatment, it is more difficult to cure the infection.

Both HAV and HEV are transmitted mainly by the fecal-oral route, while HBV (potentially accompanied by HDV) and HCV are blood-borne viruses (see Table 1). This implies that these viruses can be transmitted through activities in which blood is exchanged (e.g., medical procedures, tattooing, sexual contact, bites, and exchange of infected needles). In particular, HBV can persist with a high viral load in chronically infected individuals.

In general, HBV and HCV are the only viruses that can become chronic, although in the immunocompromised host (e.g., an organ transplant patient), HEV also has the ability to result in a chronic infection.

The importance of the five major hepatitis viruses (HAV, HBV, HCV, HDV, and HEV) is high due to their impact on global health issues. Billions of people are or have been in contact with one of these five viruses, and hundreds of millions are chronically infected with HBV or HCV. For HEV, the World Health Organization (WHO) estimates that every year ~20 million people are infected, with 3 million symptomatic cases and 56,600 HEV-related deaths. The numbers for HBV are even higher, with 240 million people chronically infected and 780,000 persons dying every year from HBV-related disease. HDV is actually a companion virus of HBV in some areas of the world. For HCV, it is estimated by the WHO that 180 million people are chronically infected, with 500,000 HCV-related deaths annually. For HAV, these figures are not completely known, but in developing countries ~90% of children are infected at a young age due to poor sanitation and unclean and unsafe drinking water. Generally, HAV does not cause a chronic disease and fatal cases are rare.

Because globally so many people are at risk of contact with a hepatitis virus, it is logical that diagnostic laboratories are involved in the detection of these viruses. With the availability of vaccines for HAV, HBV, and soon HEV, as well as different antiviral strategies to combat viruses like HBV and HCV, diagnostic laboratories are involved in monitoring treatment options and in the quantitation of viral genomes during different intervention strategies using molecular diagnostic assays, real-time genome amplification and detection, and sequencing strategies to understand the epidemiology as

doi:10.1128/9781555818722.ch65

TABLE 1 Characteristics of the five primary hepatitis viruses

Virus	Nucleic acid	Type of infection	Route of transmission	Incubation period (days)	Antigens
HAV	RNA	Self-limiting	Fecal-oral	15–45	HAV antigen
HBV	DNA	Self-limiting or persistent	Parenteral, other	40–180	HBsAg, HBcAg, and HBeAg
HCV	RNA	Self-limiting or persistent	Parenteral, other	15–150	HCV antigen
HDV	RNA	Self-limiting or persistent	Parenteral, other	30–50	HDV antigen
HEV	RNA	Self-limiting	Fecal-oral	15–60	HEV antigen

well as resistance against antivirals. But it must also be noted that one of the difficulties with the primary hepatitis viruses is the inability to grow them in culture for diagnostic purposes, and therefore serology and molecular methods are the only diagnostic instruments that laboratories have. Although this was a drawback in the earlier days of diagnostics, these methods are now common in clinical virology.

GENERAL CHARACTERISTICS OF DIAGNOSTIC PROCEDURES

Diagnostic procedures can be handled using serology or molecular methods. During the last decade, molecular technologies have been implemented in laboratories worldwide, although there are different regulations in different countries and continents. Serological markers can be analyzed using automated systems, and for most targets, including HAV, HBV, and HCV, these systems are generally available. The assays must be Food and Drug Administration (FDA) cleared/approved in the United States and CE-IVD marked in Europe, using serum and plasma as the materials of choice. Serum and plasma are readily available. There is a marked difference between CE-IVD-marked and CE-marked assays; in the latter case more attention is given to the manufacturing of the assays, while in CE-IVD as well as in FDA-cleared/approved assays, more information should be provided on the analytical and clinical performance and utility of the assays.

In the case of HEV serology, a number of serum- and plasma-based assays are available, used mostly in Europe and Asia; in Europe these serological assays are CE marked. Performance of the different assays varies, resulting in different epidemiological outcomes as well as differences in diagnostic decisions. They need to be used in laboratories with special interest and expertise in hepatitis. A similar situation exists with serological assays for HDV; they are of greater interest in specific cases or regions where HDV is more prevalent and less available in routine diagnostic laboratories.

TABLE 2 Clinical forms of hepatitis

Name	Clinical signs
Acute hepatitis	Typically associated with jaundice (icteric phase) and seroconvalescence. Infection will resolve.
Fulminant hepatitis	Severe infection with hepatic failure. High mortality.
Subclinical hepatitis	No jaundice, no clinical signs. Antibodies demonstrable in serum. Will resolve. Example: HEV.
Chronic hepatitis	Infection of the liver for a period of >6 months (rule of thumb). Caused by HBV (age dependent) and HCV. Chronic inflammation of the liver and higher risk for necrosis, fibrosis, and HCC. Chronic infections of HEV are described in specific patient groups.

Molecular methods have changed tremendously in recent decades. With the development of real-time detection systems for HBV and HCV, more information has become available for understanding the pathogenesis of these viruses. At the same time, diagnostic tools to monitor the effect of treatment using antiviral agents have become accessible to monitor the development of antiviral resistance, to characterize the genotype of the virus for epidemiological reasons, and to acquire insight into the route of transmission. Initially, these assays were used by laboratories with interest in hepatitis, but now they are more common in more and more laboratories worldwide. With the availability of WHO international standards for these viruses, the standardization of these molecular—mostly real-time-based—assays has made huge progress, although differences in genotype detection can sometimes still be a challenge. All of these assays can be used with serum or plasma, but it is of importance that the blood taken is handled quickly for transport to the laboratory and stored at low temperatures. These assays are also FDA cleared/approved and CE-IVD marked, and some of them can be used for the detection of these viruses in blood donations.

The use of molecular methods for detection of the other hepatitis viruses, meaning HAV, HDV, and HEV, is less common, and these assays are performed mainly in specialized reference laboratories or centers specializing in the treatment of hepatitis-infected patients. These viruses can be detected in both serum and plasma; however, HAV and HEV are also detectable in fecal samples. This can be used to understand how long treatment in the case of HEV infection should be continued; however, no clear guidelines are currently available.

Aside from detection, further characterization of these viruses is performed mostly in specialized laboratories, like the determination of the genotype and subtype, relevant for assessing treatment options for HBV and HCV. Now that sequencing technologies, including next-generation sequencing, are becoming more readily available, it is expected that this genetic characterization will be performed in more laboratories in the near future.

Diagnostics and Quality Control

Whether an assay is FDA cleared/approved, CE-IVD marked, or CE marked, the laboratory has to validate or verify the performance of the assay itself, and there might be special requirements in different countries or U.S. states. Laboratories have to be accredited or certified, and these regulations by official agencies will become more stringent in the years to come. Important parts of these regulations include quality assurance of the diagnostic performance in laboratories,

participation in proficiency programs, risk analyses, and dedicated responsibilities for the people involved in the complete workflow. Taking regional differences into account, different guidelines are available and continuously updated. Laboratories therefore will have to select the suitable guideline and make quality control and accreditation efforts accordingly. The ISO 15189:2012 guideline for medical laboratories is available in a number of countries.

HEPATITIS A VIRUS

HAV is a very small, nonenveloped, icosahedral RNA virus (size, ~27 to 32 nm) with a single-stranded and linear, positive-sense RNA genome. This RNA genome is ~7,500 bases in length and has only one open reading frame (ORF), two untranslated regions (UTRs) at the 5′ and 3′ ends, and a poly(A) tail. It is the prototype virus of the *Hepatovirus* genus within the *Picornaviridae* family. The virus is present worldwide and is more common in developing countries, where ~90% of the population may have been exposed to it. It has a tropism for the liver and is thermally very stable.

All human HAV strains belong to only one serological group; however, genetic analysis has shown that there are as many as six distinct genotypes, which correlate with geographic origin. Genotype I is the most common type worldwide, and in particular genotype IA.

Pathogenesis

The virus has an average incubation time of 30 days, with a range between 15 and 45 days. The prodromal period is normally 4 to 6 days and is characterized by nonspecific symptoms, like general malaise, vomiting, abdominal pain, loss of appetite, and headache. Transmission is via the fecal-oral route, and therefore poor hand hygiene and bad sanitation are strong contributing factors for exposure. It is estimated that ~1.5 million cases are reported annually worldwide. Transmission through water, food, and food additives is well known. Food may not only become contaminated during preparation, but contamination may also occur via HAV-contaminated water or ice. Alternatively, shellfish caught in HAV-contaminated water is a source of infection, particularly if contaminated sewage is dumped into the water. Person-to-person transmission is rare but may occur under poor hygienic circumstances.

Most infections are self-limiting, with no long-term sequelae or chronicity of the infection. An HAV infection may be more symptomatic in older patients due the maturity of the immune system, and fulminant hepatitis due to an acute HAV infection may occur, often accompanied with fever over 40°C, possibly resulting in liver transplantation or death (1). HAV infections occur outside the developing world in outbreaks surrounding a common source, or sporadically when visitors acquire the infection in countries where the virus is more prevalent. The virus can also be transmitted sexually, and epidemiological data have identified particular risk groups in which the virus can be easily transmitted (2, 3).

The virus invades the liver and subsequently replicates extensively in hepatocytes. As a result of this replication, huge amounts of virus are produced and the hepatocytes are damaged, resulting in the release of several biochemical markers in serum like ALT and to a lesser degree AST, which roughly correlates with the severity of the disease. No extrahepatic replication sites for HAV are clearly identified. Virus is already shed into the gastrointestinal tract towards the end of the incubation period, before clinical symptoms are observed; fecal shedding is at its highest just before the onset of clinical symptoms, and HAV RNA may be detected in feces for up to several months (4). During the prodromal phase, nonspecific symptoms may occur, like vomiting, abdominal pain, malaise, loss of appetite, headache, and fever, as well as some constipation and diarrhea. These symptoms disappear with the onset of jaundice; however, in 15% of cases, no prodromal symptoms are observed. The icteric phase that follows is marked by symptoms accompanying jaundice, such as scleral icterus, dark brown urine, clay-colored stool, and interestingly, a clearly decelerated heart rate. The icteric phase typically lasts for up to 3 weeks.

Viremia is present from a few days before and during the early acute phase of the infection when ALT and AST are high. The level of viremia is estimated to parallel the shedding of the virus in stool, albeit at a lower magnitude. But blood, serum, or plasma may be used to detect the viral RNA during the onset of disease using molecular amplification methods. The viral RNA can also be detected in stool samples. The typical course of the immunological events in symptomatic patients is described in Fig. 1, in which the similarity between HAV and HEV infections is depicted.

Diagnostics for HAV: Serology

Serological testing is necessary to distinguish an HAV infection from other viral infections and noninfectious causes

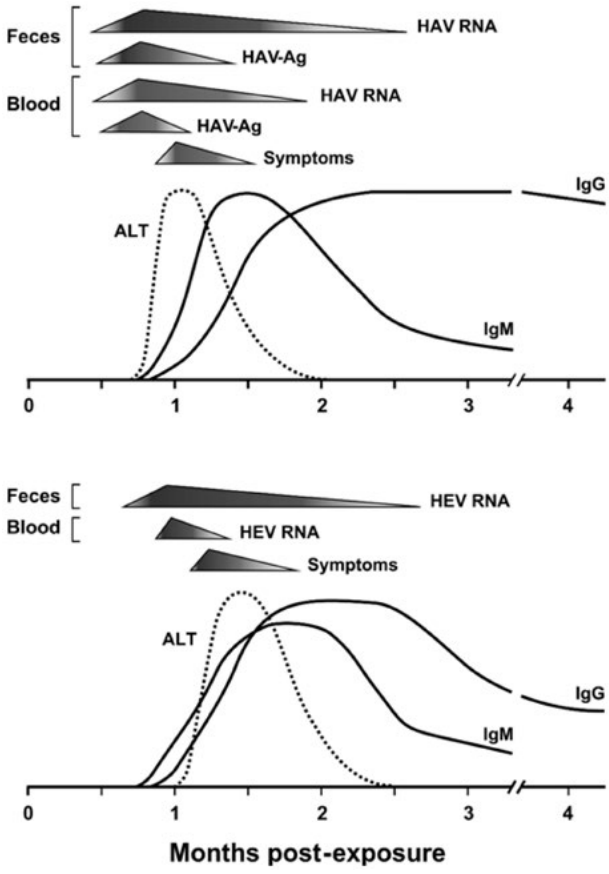

FIGURE 1 Typical course of the virological and immunological manifestations of HAV (top) and HEV (bottom). Neither of these viruses results in a chronic infection in the immunocompetent host. Infections with both viruses are in most cases asymptomatic. The virological parameters for both viruses are very similar. Both viruses are transmitted through the fecal-oral route.

of hepatitis, like autoimmune diseases or toxicity caused by medication or drugs. At the onset of symptoms, anti-HAV IgM antibodies are present in almost all patients, as well as viral RNA which can be detected in stool and in blood (serum or plasma) samples. The IgM antibodies disappear in about 3 to 6 months, but in some cases of relapsing hepatitis A, these IgM antibodies can be detected for a period of up to 1 year. One should keep in mind that IgM antibodies might not be caused by an acute HAV infection, although commercial assays to detect anti-HAV IgM antibodies are very sensitive and specific, nearly 100%. The detection of anti-HAV IgG antibodies coincides in most cases with the appearance of anti-HAV IgM antibodies, but the comparison of these two classes of antibodies has no added diagnostic value. If the anti-HAV IgM antibody titer is very low in a patient with a fulminant liver failure, one needs to confirm that the infection is truly caused by HAV. This could warrant an amplification-based RNA detection assay on stool or serum or plasma. Serum is usually available and so might be the first choice for additional diagnostics. In general, one must remember that the diagnostics for acute HAV infection must be carefully considered based on a single serological assay, but should always be viewed in correlation with the clinical data, like the onset of symptoms like jaundice, as well as the elevated biochemical parameters (ALT and AST). Furthermore, it is also important to determine whether there is a risk factor for this infection, e.g., shellfish consumption, travel to developing countries, or homosexual contact. For an algorithm of laboratory tests for HAV infection, see Table 3.

Diagnostics for HAV: Molecular Detection

Molecular detection methods are based on real-time amplification of viral RNA by PCR, enabling the detection of a few copies per reaction. Molecular detection is useful for epidemiological purposes and to supplement the diagnosis of an HAV infection when, for instance, the IgM ratio is low and one cannot be sure this is really a specific signal, as well as for blood safety. Detection methods based on amplification are being implemented more and more frequently in diagnostic laboratories, and currently there is a WHO international standard available for the detection of HAV RNA; this standard contains genotype IA (2nd WHO International Standard for Hepatitis A Virus for Nucleic Acid Amplification Techniques, NIBSC code 00/562) (5). This should be very helpful for standardizing real-time assays for the detection in blood or blood products, food samples, as well as environmental samples. The best region for diagnostic testing is the 5′ UTR of the virus, as it is for other *Picornaviridae*.

The transmission of HAV by blood or blood products is rare but has been described, despite the fact that currently one can implement enough inactivation and filtration steps to eliminate this virus from blood products. Some European countries and the United States have started to test pooled plasma samples from blood donors, as has been done already for other blood-borne viruses. The currently available commercial molecular detection assays are not registered for blood screening purposes and have some limitations in the detection of the most common genotypes. The LightCycler HAV quantitation assay (Roche Diagnostics, Indianapolis, IN) is not registered for diagnostics, while the RealArt HAV assay (QIAGEN Diagnostics, Valencia, CA) seems to be less sensitive for the detection of genotype I. Adaptations to these commercial assays have been made to overcome sensitivity issues in detecting the different genotypes of HAV. It is expected that more commercial assays will become available in the near future (6–8). Also, an External Quality Assessment program has been set up by Quality Control for Molecular Diagnostics (QCMD) (Glasgow, United Kingdom) to assess the performance of laboratories (9). Currently, no FDA-approved molecular assays exist.

Epidemiology

While the detection of HAV is based on the 5′ UTR, typing of *Picornaviridae* is based on the sequencing of the VP1/2A junction. Sequence analysis is the method of choice and is getting easier every year. Currently six genotypes are described based on sequence homology in the complete VP1 protein gene. Genotypes I, II, and III can each be divided into subtypes A and B. They all can infect humans and correlate with geographic regions. The most prevalent genotype, IA, is present in North, Central, and South America, China, Japan, Thailand, and Europe, while genotype IB is found in the Mediterranean, South Africa, and Turkey. Genotype IIIA is prevalent in India, Nepal, and South Korea. Genotypes IIA, IIB, and IIIB are rarely found.

Molecular epidemiological investigation, including phylogenetic analysis, allows the linkage of HAV cases to one another as well as back to a common source in outbreaks. With the globalization of food and food components, it has been shown to be a useful means to identify infectious products, as has been illustrated by a case of acute liver failure and liver transplantation after the consumption of

TABLE 3 Algorithm and interpretation of serological and molecular tests for the detection of HAV

Sample type	Test and result	Interpretation
Serum/plasma	IgM anti-HAV negative; IgG anti-HAV negative	No indication for HAV infection. No protection against HAV.
Serum/plasma	IgM anti-HAV negative; **IgG anti-HAV positive**	Past HAV infection or vaccinated against HAV. Protected.
Serum/plasma	**IgM anti-HAV positive; IgG anti-HAV positive**	Indications for a recent or acute infection with HAV. Check with clinical parameters and epidemiological factors. If ratio of IgM is low, measurement of RNA in serum/plasma or stool supportive for diagnostics to determine whether there is an acute infection.
Plasma/stool	**HAV RNA positive**	Indication for an acute infection with HAV.

contaminated food (1). Furthermore, these epidemiological investigations are helpful to understand local epidemics that may occur when there is an introduction of a strain, e.g., by travelers, as well as for investigating the distribution of strains among specific susceptible populations, like men who have sex with men (2). Indeed, it has been shown that HAV strains can be transmitted within networks of people who have the same risk factor.

The continuous surveillance of HAV strains among the populations in different countries enables better anticipation of public health questions that may arise. Subsequently, intervention strategies, like vaccination of at-risk groups, can be implemented if these risk groups are not already part of other vaccination programs. Despite the fact that HAV infections can be prevented by vaccination, there is still a public health concern among some populations who have more recently been identified as being at risk (10).

HEPATITIS B VIRUS

Introduction

HBV is the major virus causing hepatitis worldwide. It is estimated that ~2 billion people have been in contact with the virus, as demonstrated by the detection of antibodies (anti-HBc) against the virus. The WHO estimates that ~240 million people are chronically infected, defined as having detectable HBsAg for a period of >6 months. Other findings suggest that the number must be higher and that >350 million persons are chronically infected. It is estimated that >780,000 persons die every year from complications of HBV infection. The virus is transmitted through contact with blood or other body fluids, for instance, during sexual activity, and is an important occupational risk factor for health care workers. However, a very good and safe vaccine has been available since the early 1980s.

The virus was discovered in the 1960s and 1970s when it was recognized that a virus must have been the cause of hepatitis in indigenous Australians. Once the connection with the so-called Australia antigen (discovered in 1966), now known as HBsAg, was established, studies using electron microscopy by Dane et al. (11) and Almeida and Waterson (12) in 1970 led to the visualization of the infectious virus (known as Dane particle) and the nucleocapsid. Later, the virus was better studied, the genome was analyzed, and the serological profiles were described in more detail in both acutely as well as chronically infected individuals. The connection between HBV and the development of hepatocellular carcinoma (HCC) followed soon thereafter (13).

HBV is the prototype human virus of the family *Hepadnaviridae* and belongs to the genus *Hepadnavirus*, which also contains the woodchuck hepatitis virus and the duck hepatitis virus. Primates can also be infected with HBV-like strains.

HBV has interesting biological characteristics. It has a partially double-stranded circular DNA genome ~3,200 bp in length. The virion particle contains a membrane. Replication occurs mostly within the hepatocytes, although extrahepatic sites are also known. After the virus enters the cell, a double-stranded covalently closed circular DNA is generated (called cccDNA). This cccDNA is the template for the host RNA polymerase II, and it generates an RNA molecule longer than the genome, known as pgRNA. Interestingly, the large HBV polymerase which is generated has essentially three functional domains: a terminal protein involved in priming; a reverse transcriptase (unique for hepadnaviruses since they are essentially DNA viruses); and an RNAse H domain, which degrades the pgRNA while the new partially double-stranded HBV DNA is formed. The reverse transcriptase activity of HBV polymerase is remarkable because it has been shown that some nucleotide inhibitors against the reverse transcriptase of HIV-1 could also inhibit the replication of HBV. Another remarkable feature of the HBV genome is its compact size, resulting in the fact that most of the nucleotides encode two proteins and thus the genes of HBV have overlapping coding sequences. The reverse transcriptase of HBV takes up ~75% of the genome and overlaps sequences for the surface protein HBsAg and the core protein known as HBcAg.

During viral replication, the surface glycoprotein HBsAg is produced in three forms, i.e., as preS1-HBsAg, preS2-HBsAg, and an excessive amount of HBsAg. This overproduction of HBsAg results in free protein in the bloodstream, and the HBsAg is present as large tubular as well as spherical aggregates without the presence of infectious DNA. Furthermore, HBeAg is produced and part of it is cleaved off to produce the core protein used within the virion. The HBeAg protein is released from infected hepatocytes and circulates freely in the bloodstream. This protein can be used as a marker of infectivity or replication of HBV, since its presence is accompanied by a high viral load. However, mutants are present in certain genotypes and populations that result in no production of HBeAg. In that case, HBV DNA viral load is high in the absence of HBeAg or anti-HBeAg. Aside from replication of HBV, the virus can also integrate into the host DNA as a nonreplicating particle (14, 15).

Clinical Parameters

Most primary infections with HBV do not result in detectable disease; this results in an asymptomatic seroconversion and is known as subclinical hepatitis.

In the case that there is damage to the liver, the patient initially presents clinically with acute hepatitis; this is observed in ~5% of perinatal infections and up to 30% of adult infections. These acute infections often have a preicteric phase during which the patient may have specific complaints such as loss of appetite, nausea, fever, and loss of tolerance to alcohol. After this, the liver damage is more severe and functions fail, such as the processing of pigments derived from hemoglobin in the blood and subsequent extraction of the products into the bile and feces. This results in clinical signs of jaundice caused by the excess of bile in circulation. These pigments are now filtered by the kidney, and the urine becomes darker. These acute infections often resolve within a few months (it can take up to 6 months).

During acute infections, HBsAg can be readily detected from about 4 weeks after the initial infection (Fig. 2A). HBV DNA can also be detected after 4 weeks using molecular techniques, and viral load can rise up to 1 billion to 5 billion IU per ml of serum or plasma. HBeAg, which is only produced during active replication of HBV, can be detected easily using immunological methods. As long as HBsAg is detectable, the patient is infectious. Resolution of the infection is accompanied by the appearance of antibodies against HBsAg or anti-HBsAg, the appearance of anti-HBeAg antibodies, and the decrease to low and subsequently undetectable levels of HBV DNA. During the course of an HBV infection, the first antibodies directed against HBV are antibodies against HBcAg. These antibodies appear within a few weeks after the appearance of HBsAg and they remain detectable a very long period and even lifelong. The appearance of IgM anti-HBcAg is detected at a very early stage of infection and may give information about whether the infection occurred recently. IgM anti-HBcAg titers rise

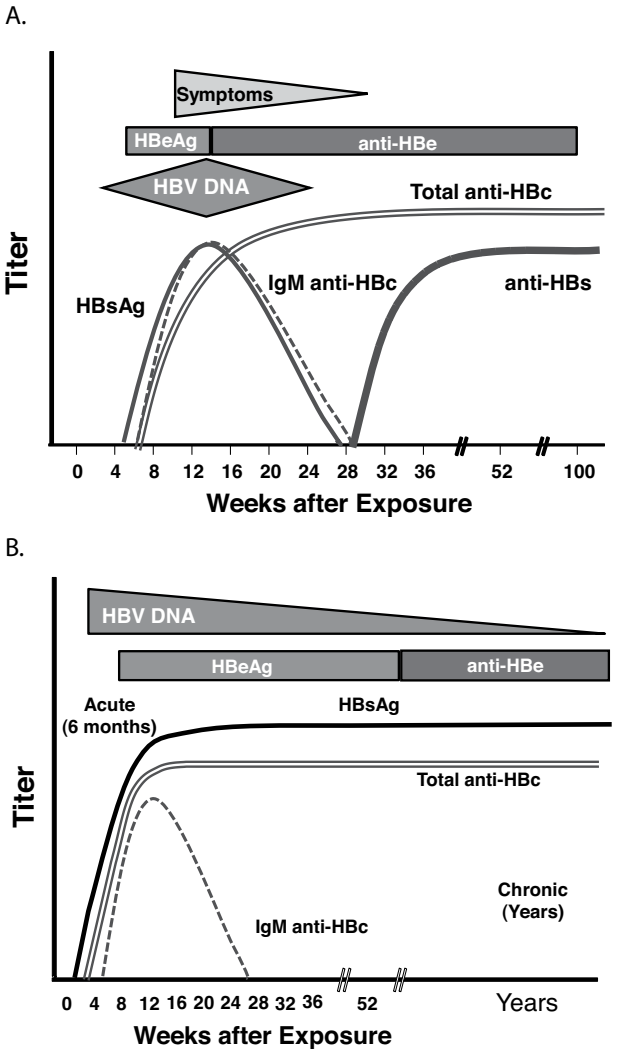

FIGURE 2 Virological profiles observed in patients infected with HBV. (A) Typical profiles in individuals with an acute HBV infection and subsequent resolution of the infection. HBV DNA is detected during a limited period of time and is ultimately undetectable using molecular techniques. Similarly, HBsAg is not detected anymore. The resolution of the infection and symptoms results in the presence anti-HBsAg antibodies, which is a marker for protection. (B) Profiles observed in individuals with a chronic HBV infection. In these cases, HBsAg and anti-HBc remain positive, while the patterns of HBeAg and anti-HBeAg may vary in time. The latter might be absent in the case of a precore mutation. HBV DNA is detectable at high levels during the whole period of the chronic infection.

rapidly in the acute phase of the infection but disappear in most patients after 3 to 6 months, although they may persist longer in some patients.

Since an excess of HBsAg is produced and also shed as noninfectious particles into the blood, the initial anti-HBsAg will form complexes and might give a negative value in the early stage of seroconversion. This anti-HBsAg has neutralizing activity against the virus and its levels rise when the infection is controlled by the immune system. Often, protective values of >1,000 IU/ml are reached.

A number of patients, especially those who acquired the infection at an early age, are not able to suppress the virus, which is recognizable by the continued production of HBsAg and no detectable anti-HBeAg antibodies. These patients continue to have replication of HBV in the liver and HBV DNA blood levels remain high. Chronicity of HBV infection is defined as having HBsAg present for a period of >6 months. Chronic infections also include partly suppressed infections, which can be distinguished by the presence of anti-HBe antibodies and usually low HBV DNA levels. During chronic infections there will be fluctuations of HBV DNA levels, notably when ALT levels are changing during so-called flares, while also IgM anti-HBc antibody can reoccur and fluctuate. These high levels of HBV replication result in a continuous infection of hepatocytes and ultimately may result in fibrosis and cirrhosis of the liver and in HCC. For a serological profile of a chronic HBV infection, see Fig. 2B. Persistent and chronic HBV infections may resolve spontaneously, but this is rare, occurring at a rate of ~1% per year.

The different HBV profiles are summarized in Table 4. Serology is the keystone in diagnostics, since it gives information on the presence or absence of the virus. Information on protection can be obtained by measuring anti-HBsAg levels. Anti-HBsAg is obtained after vaccination or after resolving a mostly acute HBV infection. In the latter case, anti-HBcAg is also detected. Anti-HBs levels of >10 IU/ml are considered protective. Following vaccination, levels of >1,000 IU/ml are not unusual. Serology is a relatively inexpensive diagnostic method, and serum or plasma is readily available. However, there may be more-complicated serological profiles in which the measurement of HBV DNA levels can be of assistance.

In the rare cases that only HBV DNA is measured and no other serological parameters are present, we describe this as an occult infection. The diagnosis of these infections remains a challenge, but they have been described in the absence of measurable HBsAg and/or anti-HBc (16–18). The measurement of HBsAg in the presence of naturally occurring mutants was shown in previous years to be a problem, but with the current commercial assays this has been resolved.

Cases in which only anti-HBc is detected need additional testing using sensitive molecular techniques, as these could be the result of low and undetectable levels of HBsAg or undetectable levels of anti-HBs, but also false-positive tests.

The loss of HBeAg followed by the appearance of anti-HBeAg signals seroconversion and suppression of the infection. HBV DNA levels decrease during HBeAg seroconversion, and levels of <20,000 IU/ml are indicative of this seroconversion. However, there are also known mutations in the HBV DNA, and particularly in the so-called precore protein, like the G1896A guanine-to-adenine substitution, which will result in the TAG stop codon and prevention of the production of HBeAg. The second known and prevalent dual mutation involves two substitutions at positions A1762T and G1674A. Both mutations result in high HBV DNA levels and no detection of HBeAg and anti-HBeAg in chronic HBV infections. They are more prevalent in HBV genotypes B, C, and D and less in HBV genotype A. There are data indicating that these mutations coexist together with the wild-type virus. With this profile it must be considered to include the measurement of HBV DNA, since many chronically infected patients do not have elevated ALT levels (13, 19, 20).

Molecular Methods: Measurement of HBV DNA

The measurement of HBV DNA is useful in cases in which patients are treated with antiviral therapy, and the viral load is indicative of the success as well as failure of

TABLE 4 Algorithm and interpretation of serological and molecular tests for the detection of HBV

Status, matrix is serum (usual)/plasma	HBsAg	Anti-HBsAg	IgM anti-HBc	Anti-HBc	HBeAg	Anti-HBeAg	HBV DNA
Susceptible to HBV	Negative	Negative	Negative	Negative	Negative	Negative	Negative
Immune after natural HBV infection	Negative	**Positive**		**Positive**			Negative
Immune after HBV vaccination	Negative	**Positive**					Negative
Acute HBV infection	**Positive**	Negative	**Positive**	**Positive**	**Positive**	Negative	**Positive**
Chronic HBV infection, high viral load	**Positive**	Negative	Negative	**Positive**	**Positive**	Negative	**Positive**
Chronic HBV infection, low viral load	**Positive**	Negative	Negative	**Positive**	Negative	**Positive**	**Positive**
Chronic HBV infection, look for HBeAg variant	**Positive**	Negative	Negative	**Positive**	Negative	Negative	**Positive**
Anti-HBc only	Negative	Negative		**Positive**			
Occult HBV infection	Negative						**Positive**

treatment. The latter can be the case in those instances in which, for instance, resistance to antiviral drugs is observed with an increase in viral HBV DNA levels. Also, when no HBeAg as well as no anti-HBeAg is observed, the measurement of HBV DNA is useful to identify those cases in which precore mutations are present, resulting in no production of HBeAg.

During the past decade, several commercial assays for the quantitation of HBV DNA have been introduced, in most cases based on real-time amplification assays with a decreasing limit of detection with every new test and a large linear range, currently up to 100 million IU/ml and down to <10 IU/ml. To improve consistency of measurement between laboratories, the WHO established a standard preparation from a high-titer HBV DNA genotype A (code 97/746) sample with an assigned potency of 1 million IU/ml (1 IU/ml equals in this case ~5.4 genome equivalents). The proposal is that all results should be reported in IU per milliliter (20–23). These levels of replication described in IU per milliliter are important parameters to define and select patients who need treatment, also taking into account ALT levels, liver histology, and age. In the United States, the updated HBV algorithm for the management of chronic HBV infection even mentions specifically which assays need to be used routinely, both of which are real-time amplification assays (13). Important threshold levels are 2,000 and 20,000 IU/ml, which need to be identified accurately, since these levels are pivotal in identifying patients who require treatment and patients who could achieve HBeAg seroconversion.

Since measurement of HBV DNA is important in treatment strategies, it is also important in follow-up of patients who are receiving treatment with antivirals, whether it is to identify resistance variants, viral breakthrough, or success of treatment by looking at kinetic patterns (24–28). When treatment is started, serum HBV DNA levels should be monitored at week 12 to identify primary treatment failure, which is defined as a reduction of <1 log. Continued follow-up at week 24 is recommended to ensure virological suppression. Continued monitoring every 3 to 6 months is recommended to prove viral suppression or to identify viral breakthrough. Viral breakthrough is defined as an increase of HBV DNA levels by >1 log above nadir after achieving a virological response during treatment. A real viral rebound is defined as HBV DNA levels of >20,000 IU/ml or above the pretreatment level. Since HBV DNA levels are often measured in reference laboratories, strategies in which HBsAg is measured quantitatively can also be used as a rapid and cheaper way to predict HBeAg seroconversion or to measure the effect of antiviral treatment (29, 30).

HBV Sequencing: Epidemiology, Typing, and Mutation Detection

HBV was initially classified into several immunological serotypes, based on determinants in the so-called antigenic determinant (designated *a*), present in all serotypes, in combination with a second determinant that is present in two forms, i.e., *d-y* or *w-r*. This resulted in the serotypes *adw*, *adr*, *ayw*, and *ayr*. However, since there is only one serotype of HBV, this was initially used for epidemiological purposes. With the availability of sequencing technologies, HBV can now be analyzed according to sequence homology. There are currently eight genotypes described. Genotype A is present globally, while genotypes B and C are more prevalent in Asia, and genotype D more prevalent in southern Europe and Turkey; genotype E is present in Africa, genotype F in the Americas, genotype G in the United States and France, and genotype H in Central America. Moreover, several subgenotypes have been described. The relation between genotype and response to therapy is of greatest importance, but genotyping may also predict the occurrence of HBeAg mutations, resistance to antiviral drugs, the likelihood of achieving resolution of an infection, and the development of HCC. There are different potential responses to antiviral treatment among the HBV genotypes, and this is used for selecting the optimal strategy. Patients with genotype A, for instance, are better responders to pegylated interferon α-2b compared to genotypes B, C, and D (31). There are several options to determine the genotype, whether by Sanger sequencing of part of the genome or by performing a line probe assay (32, 33).

Currently, sequencing technologies are developing very quickly and becoming more easily accessible. Minor variants can be detected by using ultradeep pyrosequencing or next-generation deep-sequencing technologies. But they all have to be used as fit-for-purpose, and most of them are still for research use only. At this time, standard population sequencing techniques can be used to identify variants (if present above 20 to 25%), precore mutations, or HBV genotypes (13, 34, 35).

HEPATITIS C VIRUS

In the late 1970s, blood and blood products could be screened relatively easily for HAV and HBV, but a number of cases of blood transfusion-related hepatitis were still observed that tested negative for the two above-mentioned viruses. This infection was classified as non-A, non-B hepatitis until 1989, when the virus was discovered by Kuo and coworkers as the causative agent of this parenterally transmitted hepatitis (36). The positive-stranded RNA virus was

named hepatitis C virus. HCV is an important cause of liver disease, cirrhosis, and HCC worldwide. Humans are known to be the only natural reservoir of the virus.

HCV belongs to the genus *Hepacivirus* and is the only member of this group, within the family *Flaviviridae*. Other genera within the *Flaviviridae* are *Pestivirus* and *Flavivirus*. It is an enveloped, positive-sense RNA virus with a genome of 9.6 kb in length that encodes a single long ORF of ~3,000 amino acids, flanked by short UTRs at the 5′ and 3′ ends. The viral genome is translated directly into a polyprotein that is cleaved both post- and cotranslationally by viral and cellular proteases to generate 10 gene products. HCV particles are 40 to 80 nm in diameter and are pleomorphic, without apparent symmetry.

The amino-terminal part of the polyprotein encodes the structural proteins, i.e., the capsid-forming "core" protein and the envelope glycoproteins E1 and E2. The carboxy-terminal two-thirds of the polyprotein encodes the nonstructural proteins, i.e., p7 (an ion channel), NS2 (a transmembrane protein), NS3 (the protease and RNA helicase), NS4A and NS4B (cofactors), NS5A (a phosphoprotein), and NS5B (the viral RNA-dependent RNA polymerase).

The lack of suitable culture systems has hampered research into the interactions between host and virus. Therefore, essential details required for more advanced understanding of virus entry, replication, interaction with the immune system, and virus assembly are still unknown. A striking feature of infectious HCV particles is their association with lipoproteins. These are particles, produced in the liver, that serve to transport lipids between liver and tissues. The apolipoproteins are a group of molecules, present on the surface of lipoproteins, that act as chaperones directing the trafficking of lipids throughout the body. Serum-derived HCV particles have been found to associate with apolipoproteins A1 (apoA1), apoB-4B, apoB100, apoC-1, and apoE. This interaction suggests that HCV forms hybrid lipoviral particles, which facilitate virus entry into hepatocytes and possibly protect the virus from antibody neutralization (37). Moreover, the apoproteins may have a role in virus entry into the host cell. HCV has been shown to use the low-density lipoprotein receptor for attachment, and this receptor also interacts with apoE. However, other cell surface molecules are needed in the entry process, of which the precise mechanisms are still under debate. HCV shows distinct tropism for hepatocytes but also replicates in lymphoid cells, circulating plasmacytoid dendritic cells, and other cell types.

Pathogenesis

In primary infections, the virus usually becomes detectable in blood within 1 to 3 weeks and peaks a few weeks later; then the viral load in plasma gradually declines over the following months. Just before and shortly after seroconversion, the load of HCV in plasma can fluctuate extensively and drops to very low levels. In this phase, spontaneous clearance of primary infections has been observed and the infection becomes self-limiting. However, in the majority of patients, up to 85%, the infection becomes persistent. Modulations in HCV load and clearance of the virus (when it occurs) are believed to result from the host's immune response, which is slower than in most other systemic viral

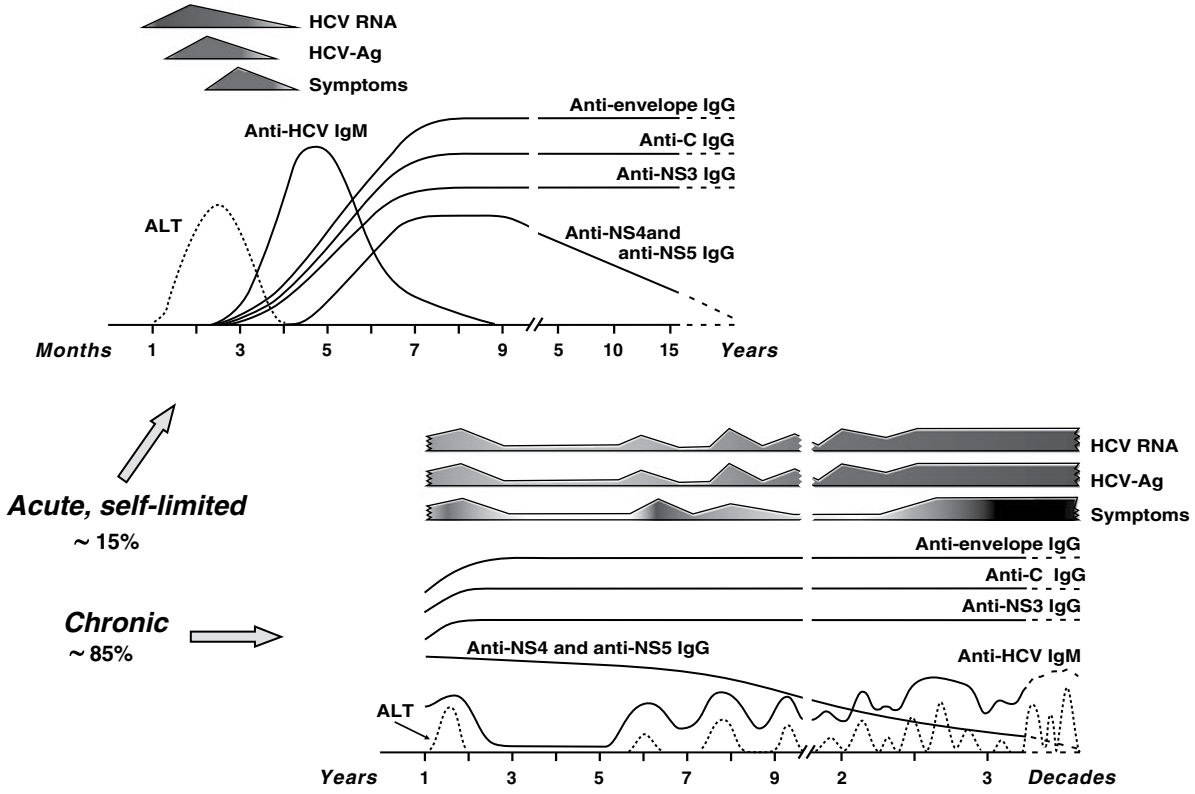

FIGURE 3 Virological profiles observed in patients infected with HCV: the course of an HCV infection and the immunological events that follow. Most patients become chronically infected, while a limited number are able to resolve the infection spontaneously. Many patients, whether acutely or chronically infected, do not know that they are infected or are having overt signals of the disease. They do, however, follow these patterns and those who are chronically infected will have clinical symptoms later in life.

infections. As a result, seroconversion may take as long as 9 months to a year. In most individuals, antibodies are nevertheless detectable within 2 months following infection. In Fig. 3, the typical immunological and virological profiles are presented both for the acute and self-limiting as well as for the chronically infected patient. Recently some host factors have been described that are associated with spontaneous clearance of acute infections. Individuals carrying a single nucleotide polymorphism of the interleukin-28B gene are more likely to clear the infection with and without treatment, and they are less likely to develop complications of chronic HCV infections (38). The C/C genotype, which is associated with a more favorable outcome, occurs to different degrees in different populations in the world. The C allele is the most prevalent in Asia, whereas in Africa the T allele is more prevalent. In Western Europe and North America, the C allele has an intermediate frequency. In addition to this polymorphism, a number of markers such as levels of particular cytokines and apolipoproteins have now been identified to be associated with spontaneous clearance of the infection (39, 40). Spontaneous clearance of HCV is rare in HIV-positive individuals, of whom it is estimated that 25% worldwide are coinfected with HCV.

In chronically infected individuals, up to 10^{10} to 10^{12} viral particles per day are produced and cleared. Levels of circulating HCV usually remain fairly constant over time, although they may fluctuate. HCV levels hardly ever fall below the detection levels of molecular assays. Spontaneous clearance of chronically established HCV infections has rarely been reported.

Acute infections are often mild or without clear symptoms, with ALT levels typically <1,000 IU/liter. Fulminant liver failure is seldom reported. Acute infections develop following an incubation period of 4 to 20 weeks and are frequently unnoticed. It is generally accepted that signs and symptoms of acute HCV infections are caused by the immune system, and the finding that symptomatic infections are more frequently associated with spontaneous clearance is in accordance with this.

Most individuals who have acquired the infection are not diagnosed due to the lack of symptoms, and may not become aware of the infection unless they are tested for other reasons. The long-term persistence of the virus nevertheless leads to damage to the liver, which progresses even without symptoms. In about a third of chronic infections, ALT levels remain normal for prolonged periods. Most patients start to show intermittently or persistently elevated levels of ALT and progressively deteriorated liver functions after 2 or 3 decades of infection, and up to 20% go on to develop cirrhosis. HCC can develop in 10% of cirrhotic livers. Male gender, old age at the time of infection, alcohol intake, elevated ALT levels, and coinfection with HBV and/or HIV-1 are all factors that negatively affect prognosis.

A significant proportion of patients acquire HCV in the absence of risk factors. Case control studies show that these cases, which are designated community acquired or sporadic, are associated with hospitalization, invasive medical procedures such as endoscopy, receiving injections in an outpatient setting, participating in contact sports, and beauty treatments (41, 42).

With no existing HCV vaccine and no demonstrated activity of postexposure prophylaxis in the form of immunoglobulins or drugs, the key to prevention of HCV lies in prevention of transmission. Needle-exchange programs for intravenous drug users have had mixed results, with some countries reporting a significant decrease in transmission and others no effect (43, 44). With a majority of HCV carriers being unaware of their HCV status, screening may well represent the way forward (45). Treatment options for chronic HCV infections have improved enormously in recent years and will continue to do so in the next few years, as new drugs become available in more countries. Treatment as prevention is already being considered in some settings (46). For now, unfortunately, the expense of the newly available regimens limits these prospects to high-income countries.

Diagnostics for HCV: Serology Combined with Molecular Testing

Anti-HCV screening is the first step in the diagnostic algorithm for HCV infection. Improvements in assay performance have been achieved in the past 2 decades, resulting in higher sensitivity and specificity of the tests currently in use. Due to delayed antibody formation in hepatitis C infection compared to other viral infections, the serological window period still is 4 to 6 weeks with the third-generation tests that are widely used. These third-generation assays can detect antibodies directed against the core gene as well against the nonstructural proteins NS3, NS4A, and NS5B. They are all enzyme immunoassays (EIAs) or chemiluminescence assays and have a sensitivity as well as specificity close to 100%. A negative screening test, however, does not exclude an acute hepatitis C infection, and testing blood for the presence of virus either by nucleic acid amplification techniques or by antigen testing is necessary for cases of suspected acute hepatitis C infection within the last 6 months. Also, for patients who are immunosuppressed, HCV RNA testing might be considered. However, under normal circumstances and without any risk factors, a negative result using HCV antibody testing with the third generation of serology testing implies no further investigation (47).

For patients at high risk of infection, who present with elevated ALT levels and high anti-HCV reactivity, supplemental anti-HCV testing can be skipped, since the correlation between a positive screening test and infection is nearly 100%. In all other cases a confirmatory test is essential. While some laboratories rely on a second immunological assay in these cases, other laboratories proceed to viremia testing, as recommended by the updated Centers for Disease Control and Prevention guidelines (48). For an algorithm for HCV detection, see Table 5.

If laboratories want to perform a serological confirmation, this usually involves immunoblotting, which allows dissection of antibodies directed to different viral determinants. Sera that react with products derived from at least two viral genes are considered positive, and those that are reactive with a single protein are indeterminate; reactivity to the carrier polypeptide fused to recombinant antigens shows that the positivity might be nonspecific. Indeterminate immunoblots may be indicative of false positivity, especially in low-risk individuals. Immunocompromised individuals with HCV infection nevertheless often show reactivity only to C and NS3 antigens, which may yield indeterminate results. Antibodies in response to NS4 and NS5 tend to be produced later during the infection, and these antibodies also wane earlier following spontaneous or posttreatment resolution of infection.

Testing for Viral Antigen

Immunoassays for HCV antigen detection and quantification have become available as an alternative to nucleic acid testing. Classical EIAs target the core antigen of HCV. The tests are highly specific and have a lower detection limit of 1,000 IU of HCV RNA per ml. They can be carried out in

TABLE 5 Algorithm and interpretation of serological and molecular tests for the detection of HCV

Sample type	Test and result	Interpretation
Serum/plasma	Total anti-HCV negative/ nonreactive	No HCV antibody detected. No indication for an HCV infection. If patient is immunosuppressed, HCV RNA testing can be considered. If exposed to possible HCV infection during the past 6 months, follow-up antibody testing or HCV RNA is recommended.
Serum/plasma	**Total anti-HCV positive;** HCV RNA negative	No indication for a current HCV infection. Repeat HCV RNA testing might be considered if exposure to HCV suspected within the past 6 months or clinical evidence of HCV disease, or if there are concerns with storage and handling of test specimen.
Serum/plasma	**Total anti-HCV positive; HCV RNA positive**	This is a current HCV infection and should be linked to care of the patient.

automated systems that give a result in 60 min. Therefore, they are faster but also less expensive than PCR assays. The assays have a role in the diagnosis of hepatitis C infection after anti-HCV antibodies have been detected. HCV core antigen tests nevertheless become positive a few days after the appearance of HCV RNA. These tests, which are available for testing on blood or saliva, have been evaluated for screening of high-risk individuals. In these settings, these rapid tests provide sensitivity and specificity comparable to that of the HCV EIAs, and provide a low-cost, easy-to-use assay alternative that can be used outside traditional laboratories (49).

Testing for Viral RNA

Methods of accurate quantification of HCV RNA levels are essential for the clinical management of patients with hepatitis C infection. Serum and plasma are routinely used, but recent research has shown good results using dried blood spots, which are easily transportable. Several automated, closed devices are available for nucleic acid extraction, detection, and quantitation while maintaining high sensitivity and specificity of tests. The benefits of these automated systems include minimal hands-on time and minimal potential for contamination of samples. The detection limits are as low as 12 to 50 IU/ml, and intra- and interassay variabilities are small. The available automated platforms have minor differences in detection of HCV RNA levels of different HCV genotypes. Underestimation of HCV RNA levels is most likely due to sequence polymorphisms in one of the primer or probe target regions. Quantification of HCV RNA is essential not only for making a decision to treat a patient but especially for monitoring the response to therapy.

In contrast with the relatively long serological window following infection, HCV RNA is usually detectable within just 1 week after infection. Viral RNA levels may reach 10^7 IU/ml, but commonly levels of 10^5 to 10^6 IU/ml are measured. Although there is some evidence that links plasma RNA levels to viral replication in the liver, the determination of HCV RNA is most relevant in response-guided treatment, where it is currently the standard procedure for measuring response to HCV treament. Quantitative HCV viral load testing is recommended at week 4 after the start of treatment and at 12 weeks after the therapy is completed. Antiviral therapy should not be interrupted or stopped if HCV RNA measurement has not yet been performed. If viral load has not been successfully reduced at week 4, the testing can be repeated at week 6 or week 8. Any increase in viral load is indicative of failure of treatment. Expressing the viral loads in IU has allowed comparison of results obtained by different methods, but quantitative differences between the different assay systems are such that in follow-up of patients the same method should be used throughout. Currently, levels of 12 IU/ml can be measured with high accuracy.

In a prospective study that followed a cohort of high-risk individuals for acute hepatitis C infections, it was shown that 28% had very low to undetectable HCV RNA levels at the time of the first serologically positive blood sample.

Detection of HCV: Epidemiology and Viral Genotype

Diversity among HCV isolates is minimal in the 5′ UTR and maximal in the E2 glycoprotein, where a stretch of 31 amino acids, the hypervariable region, has been proposed as a decoy for the immune system. Six major genotypes can be distinguished, designated 1 through 6. A genotype 7 has also been described (50). Each genotype can be divided into subtypes designated by lowercase letters. Intergenotype recombinants and more recently intragenotype recombinants have been reported (51, 52), of which so far only one, i.e., the 2k/1b intergenotype recombinant, has been transmitted (53). In addition to their epidemiological purposes, the subtypes have been shown to influence the response to certain therapeutic regimens.

About 3% of the world population is estimated to be infected, with prevalence rates ranging from <1% in some Western European countries to >10% in some African countries. The highest prevalence is found in Egypt, where 14.7% of the population is infected. Because the infection is asymptomatic in many individuals, the virus may continue to spread. The risk of transmission of HCV through blood transfusion is currently extremely low due to the use of molecular detection of HCV RNA in pooled blood donations. Intravenous drug use, tattooing, acupuncture, body piercing, and any other practice that involves contact with contaminated blood account for most of the new infections. Mother-to-child transmission, which is generally believed to be inefficient, still leads to infection of 1 in 20 children born from HCV-positive mothers, concurrent HIV infection being the most important predictor of HCV transmission in this group. Transmission to household contacts is rare, and there is no evidence for transmission through insect bites. Humans are the only known reservoir of HCV.

The prevalence of the genotypes depends largely on the population in which the screening was performed. Genotype 1 is most prevalent in Western Europe, North America, Central and South America, Australia, Indonesia, and Japan. Genotype 2 does not form the most prevalent genotype anywhere in the world, while genotype 3 infections are highly prevalent in the United Kingdom, Russia, India, and Brazil. Genotype 4 is prevalent almost exclusively in Egypt and surrounding countries; genotype 5 is found mostly in South Africa; and genotype 6 is so far found only in Southeast Asia, where this genotype is highly prevalent, and in Southeast Asian populations elsewhere in the world. The newly described genotype 7 was isolated from an individual from the Congo (50). Determining the viral genotype and subtype is essential for optimizing both treatment regimen and duration of treatment with current treatment protocols.

Until very recently the combination of ribavirin and pegylated alpha interferon formed the mainstay of treatment, with differences in dosing and duration depending on the genotype. Recently, new direct-acting antivirals have become available, which as a whole have improved the prospects of cure for all genotypes, but differences in response to different agents exist depending on the genotype. The new direct-acting antivirals are not universally available yet, because treatment of HCV infections with these agents is considered too expensive, even for many high-income countries. It is expected that direct-acting antivirals will continue to be introduced in Western countries but that their use will be restricted to some patient categories. Predicting the a priori chance that a patient will respond, and the subsequent adaptation of treatment and regimen to optimize treatment success, is expected to become the mainstay of HCV treatment. The need for reliable genotyping is therefore only becoming more obvious. Sequence analysis of the viral genome is the gold standard for any genotype determination, and in the case of HCV sequencing, the 5′-UTR region was historically chosen as the main target. Studies have shown more recently that analysis of the 5′ UTR unfortunately has its limitations for subtyping due to its high genetic conservation. Moreover, some genotype 1b subtypes and several genotype 6 subtypes have identical 5′-UTR sequences and are therefore indistinguishable by 5′-UTR analysis. For genotype and subtype sequencing, the core and NS5B regions are better targets, providing optimal genotype and subtype resolution. Methods such as reverse transcriptase PCR assays that amplify and detect portions of both 5′-UTR and NS5B regions have much better performance than methods that rely on amplification of 5′ UTR only. A frequently used commercial test exploits the ability of 5′-UTR amplicons to hybridize to type-specific probes immobilized on nitrocellulose strips (line probe assay). The line probe assay has a reasonable concordance with genotypes that have been identified by nucleotide sequencing; it misclassifies the subtypes of 10 to 40% of isolates, depending on genotype (54–56). At this time, all commercially available assays that aim to reduce hands-on time and are suitable for routine laboratories have significant shortcomings in accuracy (57).

Testing for Antiviral Resistance

Even before the introduction of the first direct-acting antiviral agents, reports showed the appearance of drug resistance mutations in regions targeted by antiviral agents. It has become clear that preexisting mutations are prevalent in treatment-naive patients and that this affects success rates of particular antiviral regimens (58). Early studies with the first protease inhibitors showed that the preexisting mutations were more common in treatment-naive patients with genotype 1a than with 1b (59). The major resistance mutation R155K, which is associated with treatment failure, required two nucleotide changes in subtype 1b strains and only one nucleotide change in subtype 1a strains (60). This resistance mutation confers resistance to all protease inhibitors currently on the market.

Following the introduction of protease inhibitors as the first direct-acting antiviral agents, the second class to become available were the polymerase inhibitors, of which sofosbuvir was the first available drug. This agent appears to possess a very high genetic barrier. The S282T mutation is most frequently seen, but it occurs in few patients with early relapses (61, 62).

The third class is the NS5A inhibitors, with daclatasvir and ledipasvir as the first representatives. Similarly to what was seen for protease inhibitors, resistance mutations are frequently seen in patients who have failed treatment, and preexisting drug resistance mutations are found in small percentages of treatment-naive patients.

The existence of preexisting mutations to certain direct-acting antiviral agents, together with the high prevalence of mutations in pretreated individuals and the high cost of modern hepatitis treatment options, is likely going to increase the demand for resistance testing. Some methods for targeted genotyping are now being explored, which could facilitate detection of resistance mutations more efficiently. Sequencing, however, remains the most commonly used method (63–65).

HEPATITIS DELTA VIRUS

HDV, initially called the delta agent, was described for the first time in 1977 in patients in Italy with a more severe form of HBV infection (66). It was found to resemble certain subviral agents of plants. Strictly it is not a virus since it requires the HBV surface protein HBsAg as its outer envelope protein, and is therefore called a subviral or satellite virus. There is no nucleotide homology between HBV and HDV. HDV has a single-stranded RNA genome structure of ~1,700 nucleotides and its infectious particles contain a ribonucleoprotein in a complex with ~70 copies of the delta antigen (HDV-Ag), which is the only protein encoded by its genome. This is the smallest circular RNA viral genome known in humans, and it forms an imperfect duplex by roughly 75% pairing of its nucleotides. Because of its small size, it is interesting to note that the replication of this genome is done by the host's RNA polymerase II and takes place in the nucleus of the cell. HDV replicates only in the liver, and no extrahepatic sites are known.

Pathogenesis

HDV infections can be more severe and may result in a more progressive liver disease, resulting in cirrhosis and liver failure, compared to HBV infections alone. An infection with HDV may be acquired at the same time as the HBV infection (coinfection) or may be acquired as a superinfection in a person already infected with HBV. The course of the infection is different in the two cases. With a coinfection, the number of HBsAg particles is low in the beginning, having an impact on the replication of HDV. This HDV infection therefore peaks at lower levels and has no influence on the replication of HBV itself. In superinfection, HBsAg is already abundantly present in the blood, and the replication of HDV is at full speed to begin with, in contrast with the

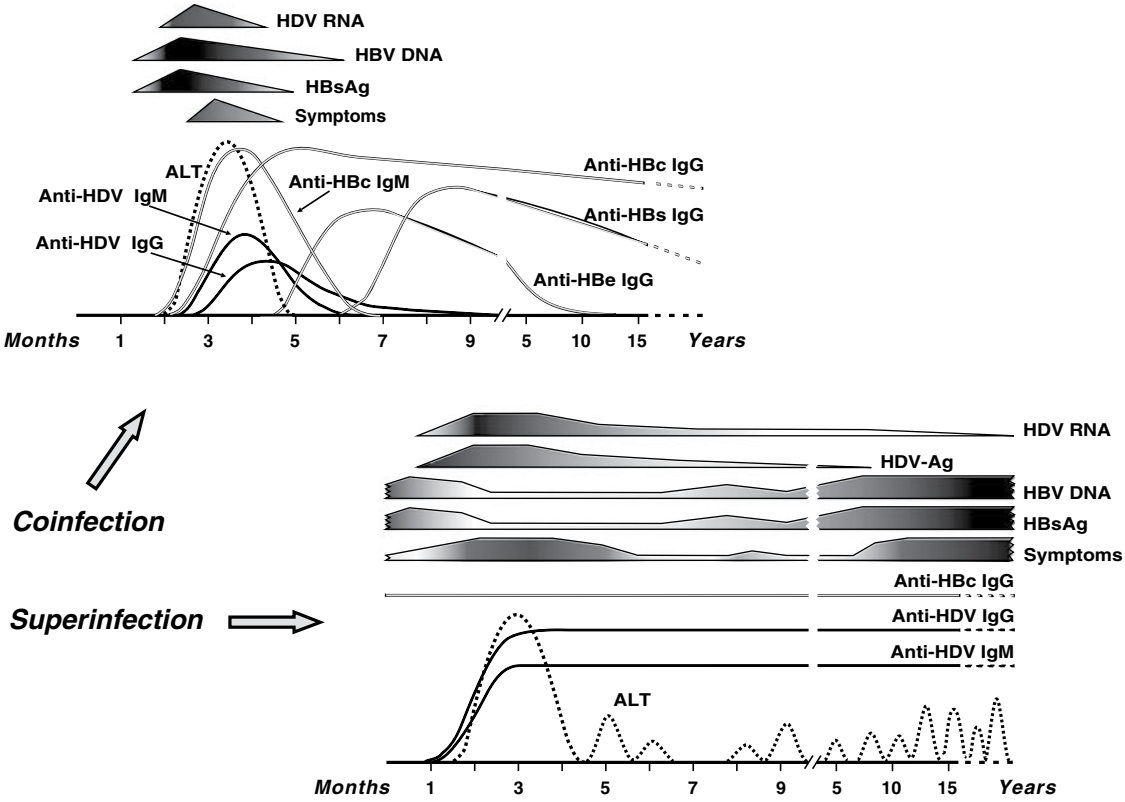

FIGURE 4 Virological profiles observed in patients infected with HDV. There are two routes of HDV infections. (Top) In the first one, HBV and HDV coinfect the same individual at the same time. Since the individual has not been infected previously with HBV, the replication of HBV and the production of HBsAg control the replication of HDV. As soon as the level of HBsAg is reduced due to the presence of anti-HBsAg, the replication of both HBV and HDV is dramatically reduced, and eventually both HBV DNA and HDV RNA are no longer detected in serum or plasma. Anti-HDV antibodies are present. (Bottom) In the case of a superinfection, HDV replication is enhanced from the beginning since an abundant amount of HBsAg is present in the liver. HDV RNA is detected by real-time amplification technologies as long as HBV replication and thus the production of HBsAg continue. In the case of this chronic infection with HDV, anti-HDV is also detected.

coinfection. It briefly causes a suppression of the replication of HBV. In the case of a superinfection with HDV, it may even worsen the HBV infection itself. For a typical course of these infections, see Fig. 4, in which the differences in profiles of coinfection and superinfection are described.

Diagnostics for HDV

Serology

Serological markers for the diagnosis of HDV are HDV-Ag and the anti-HDV antibody. Although IgM antibodies are detectable during the window phase of the infection, most diagnostics are based on the detection of total anti-HDV antibodies. The detection of IgM antibodies against HDV is only available in a limited number of reference laboratories. Total anti-HDV is indicative of an infection and may persist for several years even after the clearance of the infection. Patients with HBsAg-positive results from regions where HDV is endemic should be tested. HBV serological markers and HBV DNA levels can be of assistance in deciding whether treatment of the HBV infection is required. During an acute infection with HDV, HDV-Ag is detected in the early phase in serum or plasma but also disappears relatively quickly, making IgG anti-HDV in combination with HDV RNA the method of choice to establish the proper diagnosis. HDV-Ag can be detected in liver biopsy specimens using standard technologies (staining with anti-HDV-Ag peroxidase). The use of IgM antibodies as well as HDV-Ag is limited since its value can only be shown in the early phase of the acute super- or coinfection of HDV with HBV. During an acute coinfection with HBV, the IgM anti-HBcAg marker can be used. In conclusion, the detection of IgG anti-HDV is the most suitable test and can be viewed as a marker of exposure to the delta particle. For an algorithm of laboratory tests for HDV infection, see Table 6. The virological profiles are also summarized in Fig. 4. The first test to be performed has to show that indeed an HBV infection is also present by detecting HBsAg and anti-HBcAg, since HBsAg is needed for HDV replication.

Molecular Methods

The most efficient diagnostic parameter is the detection of HDV RNA as a result of viral replication. In the case of a coinfection of HDV with HBV, the resolution of HBV as determined by the presence of anti-HBsAg will also result in the resolution of HDV RNA. In the case of a superinfection with HDV when an HBV infection is already present chronically, HDV RNA is detected in most patients, if not

TABLE 6 Algorithm and interpretation of serological and molecular tests for the detection of HDV

Sample type	Test and result	Interpretation
Serum/plasma	IgM anti-HDV negative; total anti-HDV negative	No indication for an HDV infection. Determine HBV serological markers.
Serum/plasma	IgM anti-HDV negative; **total anti-HDV positive**	If HBsAg is negative and anti-HBsAg is positive, this is a past infection. HDV RNA will be negative. If HBsAg is positive and anti-HBsAg is negative, this is an acute HBV/HDV coinfection (early phase) or a chronic infection. Determine presence of IgM anti-HBc and HDV RNA.
Serum/plasma	**IgM anti-HDV positive; total anti-HDV positive**	Based on IgM anti-HDV positivity, this is most likely an acute HDV infection. Determine HDV RNA and HBV parameters (HBsAg, IgM anti-HBc). Total anti-HDV may be present for a long period of time and without clearance of HBV parameters.
Serum/plasma	**HDV RNA positive**	Indication for an active infection with HDV. Might be acute in early phase if IgM anti-HBcAg is positive.

all, continuously. The replication of HDV can be monitored by the detection of HDV RNA in serum or plasma, and with the availability of a WHO international standard, quantitative assays can be made more reliable, although no commercial assay is available at this moment. Currently, laboratory-developed tests based on real-time detection are available in laboratories with a special interest in diagnostics for hepatitis viruses. There are limited commercial assays available for the detection of HDV, but their performance and detection of the different HDV genotypes are not yet completely established (67–69).

Detection of HDV: Epidemiology

HDV was initially discovered in Italy and is more common in southern European countries (70). The particle has also been shown to be more endemic in certain parts of South America, in indigenous tribes living in the Amazon, and some parts of Asia. In North America and Western Europe, most of the infections are in intravenous drug users and their partners, and it coincides with the prevalence of HBV infections. It is estimated that in the United States, ~70,000 individuals are infected with HDV. These infections are all chronic. However, with increased vaccination against HBV in at-risk populations, the incidence of HDV infections is also decreasing in those countries. One has to be aware, however, that through migration of individuals from areas where HDV is endemic, the infection can still spread relatively easily and be maintained in specific populations like intravenous drug users, homosexuals, and practitioners of high-risk practices like tattooing or piercing, which are not often checked for their HBV vaccination status.

In the Asian-Pacific region, there is concern over an increase of HDV infections in Pakistan, Iran, and countries of Southeast Asia, where there is a higher prevalence of HBV and registration of HBV and HDV is absent. In Africa, too, the prevalence of HBV is high, and HDV is endemic in a number of countries, although this may not give a complete picture. HDV is known to be present in the Congo, Equatorial Guinea, Nigeria, and Cameroon. Phylogenetic data from Cameroon show that there are four different genotypes of HDV present, of which genotype 1 is the most prevalent (71–75).

HEPATITIS E VIRUS

HEV is an enterically transmitted hepatitis virus, similar to hepatitis A virus. It is a small (32 to 34 nm in diameter), nonenveloped, single-stranded, positive-sense RNA virus of ~7,200 bases that is capped and polyadenylated at the 5′ and 3′ termini and is organized in three ORFs. The first ORF codes for the nonstructural proteins and contains methyltransferase-, cysteine protease-, macrodomain-, RNA helicase-, and RNA-dependent RNA polymerase-encoding sequences. The second and third ORFs overlap and encode the structural proteins of the virus. ORF2 codes for the viral capsid protein and consists of three linear domains: the shell domain (S), a middle domain (M, also called P1), and a protruding domain (P, also called P2). The protein translated from ORF3 is a small phosphoprotein involved in virion morphogenesis and release.

The virus was discovered in the 1980s during a military campaign in Afghanistan among Soviet soldiers who had an unexplained hepatitis not caused by HAV. Its transmission route was discovered by a successful transmission to a human volunteer via the fecal-oral route with a stool sample from a non-A, non-B hepatitis patient. The logical next letter was E. Viral-like particles were seen by electron microscopy. HEV was already known to cause waterborne epidemics in developing countries, and it was also known that it coincided with a high fatality rate among pregnant women. There were also reports of outbreaks of jaundice caused by HEV in Europe with coincident fatalities among pregnant women, which is typically related to HEV genotype 1 (76).

HEV was initially classified in the family *Caliciviridae*, genus *Calicivirus*, based on the clinical symptoms and structural features. However, after subsequent studies, the virus is now a member of the family *Hepeviridae* and the genus *Orthohepevirus A* (formerly *Hepevirus*). Within this group of

Orthohepevirus A, there are four genotypes known (named 1 to 4) that can infect humans.

HEV genotypes 1 and 2 are strictly human viruses and mostly prevalent in areas of poor sanitation, causing endemic acute hepatitis in developing countries and resource-limited countries, resulting in occasional large waterborne outbreaks, and travel-related cases in developed countries. HEV genotype 1 is mainly present in Asia and Africa and genotype 2 in Mexico. Genotypes 3 and 4 have a zoonotic origin with a main reservoir in domestic pigs. Genotype 3 has a worldwide distribution, while genotype 4 is mostly found in Asia. These latter two genotypes, and in particular genotype 3, are drawing more and more interest as there is growing evidence of their zoonotic potential. Epidemics caused by genotypes 3 and 4 are rare. All four HEV genotypes belong to one serotype.

Pathogenesis

The clinical features of HEV infections range from asymptomatic infection to mild hepatitis to subacute liver failure. Following an incubation period of 15 to 60 (average, 40) days, patients may present with fever, nausea, jaundice, abdominal pain, vomiting, anorexia, malaise, and hepatomegaly. There are some differences in the clinical course between the developing and developed countries due to the different genotypes. In developing countries, hence mainly genotype 1 and 2 infections, most infected individuals present in their young adulthood with a mild self-limiting hepatitis. The fatality rate is low, but may still be up to 2% due to fulminant hepatitis. Exceptions are patients with underlying chronic liver disease. A unique feature of HEV infection is the high mortality rate, up to 25%, exclusively found among pregnant women in their third trimester and/or their unborn babies. The mechanisms of this fulminant hepatitis are still unknown. There have been no reports of such high mortality among pregnant women with infections of HEV genotype 3 or 4.

In developed countries, genotypes 3 and 4 are more prevalent. Symptomatically infected individuals are usually middle-aged and elderly males. Besides small clusters of cases due to a single food-related source, large outbreaks have not been documented. Most patients present, however, with a self-limiting hepatitis with elevated ALT levels up to 3,000 IU/liter. In contrast, HEV genotype 3 may cause a chronic infection that may lead to rapidly progressive cirrhosis in immunocompromised patients such as solid organ transplant recipients, individuals with HIV infection, or patients with a hematologic malignancy. This chronic infection, due to its often asymptomatic course, may be mistaken for drug-induced liver injury. Also, extrahepatic manifestations have been documented, including neurological syndromes, renal manifestations, pancreatitis, and hematologic disorders.

Transmission of HEV

HEV genotypes 1 and 2 are transmitted via contaminated water due to fecal shedding of HEV-infected individuals; transmission occurs from human to human through an environmental reservoir. In contrast, transmission of HEV genotypes 3 and 4 occurs mainly via an animal reservoir. HEV strains from domestic pigs, wild boar, deer, and rabbits have been identified as zoonotic causative agents for human infections. This is supported by phylogenetic studies showing that HEV strains circulating in pigs and humans are very closely related (77, 78). The main zoonotic transmission route is via consumption of undercooked meat of infected animals, yet persons with direct contact with infected animals are also at risk (79). Besides zoonotic transmission, waterborne infection and transfusion-transmitted HEV infection have been documented. Overall, clinicians should be aware of the fact that HEV diagnostics should be considered if elevated liver enzymes are detected, and that this should not be always travel related (80).

HEV RNA-positive blood products have been described repeatedly, and in almost all cases, HEV genotype 3 is involved, and to a much lesser extent genotype 4 (81–84). Only a limited number of transfusion-related transmissions have been reported, but there are more data suggesting that such transmissions may happen frequently. The incidence of HEV RNA-positive blood varies among countries, and rates of 1 in 1,000 blood donations have been reported (84). One should keep in mind that in most cases, blood and blood products are given to patients who already have an underlying condition that may cause immunodeficiency, such as hematological disease or transplantation. This may be one explanation why chronic HEV infections, which by definition are infections of >6 months, have been described in those immune-suppressed patients. The scale of the problem is still not known. A growing number of blood banks have begun to screen for HEV RNA by PCR to provide an indication of the problem of whether and how often viremic HEV-positive blood is drawn from a donor. There is growing evidence that HEV infections might be transmitted through blood transfusion, because HEV RNA can be detected in plasma pool samples (85, 86).

Diagnostics for HEV

Serology

As with other forms of hepatitis, HEV infection can be diagnosed either indirectly by using serology to detect anti-HEV antibodies in serum or directly by detecting the HEV genome in blood or stool. The serological profile is similar to that for infection with HAV, depicted in Fig. 1. After an incubation period of 2 to 6 weeks, antibodies can be detected. First, IgM antibodies appear as a marker of a recent infection; their levels may remain high for up to 8 weeks after an acute infection. IgG antibodies peak around week 4 and can remain high for >1 year (87). In immunocompetent individuals, these antibodies appear at the time of clinical onset of disease. There are several commercial EIAs based on ORF2/ORF3 peptides or recombinant antigens mainly from HEV genotypes 1 and 2, varying widely in sensitivity and specificity. Only one assay uses the combination of HEV genotype 1 and 3 antigens (88, 89). A WHO reference reagent for hepatitis E serum IgG (NIBSC code 95/584) can be used for evaluating the analytical sensitivity of anti-HEV IgG assays (90). Since many infections with HEV have occurred years before a serological assay is performed, one has to consider that the detection of antibodies may represent past infections. Moreover, some assays appear to have sensitivity problems for some genotypes, which may result in an underestimation of the seroprevalence in certain populations. Western blotting is still used in small-scale studies. There are assays available that use a specific pE2 peptide (amino acid residues 394 to 606), which is superior to alternative assays using shorter E2 peptides because of the stabilizing effect a 60-amino-acid extension has on the dimer formation of this antigen. This assay also uses a μ-chain capture strategy, which is known to improve both sensitivity as well as specificity of assays by combining the results of IgM and IgG assays (91). However, one has to keep in mind that not all IgM positive samples are also viremic for HEV. In those cases, HEV RNA has to be detected. For an algorithm of laboratory tests for HEV infection, see Table 7.

TABLE 7 Algorithm and interpretation of serological and molecular tests for the detection of HEV

Sample type	Test and result	Interpretation
Serum/plasma	IgM anti-HEV negative; IgG anti-HEV negative	No indication for an HEV infection.
Serum/plasma	IgM anti-HEV negative; **IgG anti-HEV positive**	Past HEV infection. If immunosuppressed, HEV RNA should be determined (like in transplant patients).
Serum/plasma	**IgM anti-HEV positive; IgG anti-HEV positive**	Indications for a recent or acute HEV infection. Check with clinical parameters and epidemiological factors. Measurement of RNA in serum/plasma or stool supportive for diagnostics to determine whether there is an acute infection.
Plasma/stool	**HEV RNA positive**	Indication for an acute infection with HEV. May be chronic in specific patient populations, like immunosuppressed patients (transplant).

Molecular Methods

In immunocompromised individuals, antibody production may be delayed or even absent, making detection of the HEV genome essential for diagnosing HEV infection. Most detection assays that are currently used are laboratory-developed tests, a phenomenon that is seen globally as the development of commercial assays is always behind the development needed in clinical practice. It has been shown that standardization is needed to enable a better comparison as well as to monitor the effect of antiviral treatment. A WHO international standard for nucleic acid testing of HEV genotype 3 is available (92), and a WHO genotype-specific reference panel will be made available in 2016. Also, an External Quality Assessment program is organized through the QCMD (9). However, one has to realize that laboratory-developed assays are currently used to screen blood and blood products, as no commercial assay is approved for screening these products for HEV RNA.

The existing commercial HEV viral load assays appear to have good sensitivity and specificity (93, 94). In immunocompetent patients, viremia peaks during the incubation period and during the first phase of disease. The window of HEV RNA detection may be rather short (3 to 6 weeks) in these patients; therefore, a negative HEV RNA result does not exclude a recent infection. On the other hand, in immunocompromised patients, HEV RNA testing is necessary to monitor for a chronic infection and to further characterize, using sequence analysis, the virus. If the HEV RNA remains detectable for 3 months, it is unlikely that the patient will spontaneously clear the infection without therapeutic intervention (95, 96). HEV RNA is less stable compared to HAV RNA, and therefore precautions have to be taken to ensure the integrity of the material, like storage at –80°C and rapid transportation of clinical materials to the diagnostic laboratory.

Treatment Options for HEV

HEV infections in developing countries can be prevented by good sanitary infrastructure and clean drinking water. As mentioned previously, most of these outbreaks of HEV are caused by genotype 1 or 2. Despite the clinical and epidemiological differences among the four different genotypes, cross-neutralization occurs, indicating that they belong to a single serotype (97). HEV infection is preventable by vaccination. Two recombinant genotype 1 HEV vaccines have been developed and have been shown to be safe and immunogenic in clinical trials. Immunizations resulted in cross-protection against different HEV genotypes (98, 99). All the trials were carried out in China and showed that the vaccines are well tolerated. These vaccines are very promising, although there are no data yet on their efficacy against emerging strains of HEV—including the animal strains with zoonotic potential—or in prevention of the infections seen in high-risk groups, specifically those caused by genotype 3.

For HEV infections in developed countries, a better understanding of the route of transmission and the relation to the zoonotic origin is needed to effectively prevent transmission. Discussion is ongoing on the exact routes of transmission, although eating of uncooked meat is certainly one such route, and contaminated water has also been seen as a source. The use of blood or blood products has been implicated for people in high-risk groups, although the virus might be inactivated during preparation of blood products as it is less stable than, for instance, HAV.

The first step in the treatment of chronic HEV infection in solid organ transplant recipients is to reduce the dose of immunosuppressive medications. This may result in viral clearance in nearly one-third of patients (100). For antiviral treatment of HIV-infected patients, patients with hematologic conditions, solid organ transplant recipients, or patients with severe acute infection, the first line of treatment is oral ribavirin. In addition, pegylated interferon α-2b has also been described as a potentially effective treatment of HEV infection (101). Recently several cell culture systems have been developed for HEV genotypes 3 and 4, making it possible to further analyze the basic biology of HEV (102, 103).

FINAL CONCEPT: THE DIAGNOSTICS OF HEPATITIS CAUSED BY THE PRIMARY FIVE HEPATITIS VIRUSES

In normal circumstances, the determination of the cause of viral hepatitis of unknown origin is not focused on a single determinant, but a combined testing scheme is used. For this purpose, low-cost serological screening methods could be used. Follow-up of viral infections after diagnosis is rather specific for each pathogen. When liver function tests are severely abnormal, or when specific risk factors in a patient

are identified such as travel history, vaccination status, and alcohol and drug use, more specific tests are appropriate.

In the case of fulminant hepatitis, serology for HAV and HBV is recommended, as IgM directed against HAV is generally present in the acute phase, and in the case of acute HBV infection, HBsAg is detectable. Serology for HCV usually does not contribute in this context, as HCV is an extremely rare cause of fulminant hepatitis and acute infections are not diagnosed by serological testing. HCV RNA testing could be considered when other infections have been excluded. In some countries, HEV serology is appropriate in patients presenting with fulminant hepatitis, depending on local epidemiology of the circulating genotypes. If needed, PCR against HAV and HEV can be carried out in those cases where it is not clear.

In cases where chronic hepatitis is suspected, it is obvious to start with detection of IgG antibodies against anti-HBc, anti-HCV, anti-HAV, anti-HEV, and HBsAg. If HBsAg is positive, reflex testing should be performed to determine HBeAg and anti-HBe. In cases where antibodies are positive against HBV and HCV, viral load is needed to determine the need for treatment. IgG anti-HEV in the immunocompromised is frequently absent even in chronic infections. The detection of IgM has to be complemented by an HEV PCR in these patients, and HEV PCR may even have to be considered without any serological markers compatible with HEV infection.

An important point is that new and acute infections of HAV, HBV, HCV, and in some countries even HEV must be reported to public health authorities. This should be done in countries where the prevalence of these viruses is low as well as in high-prevalence areas. Due to the high infectivity of primary hepatitis viruses, reporting is a first step in controlling continuous transmission.

REFERENCES

1. **Chi H, Haagsma EB, Riezebos-Brilman A, van den Berg AP, Metselaar HJ, de Knegt RJ.** 2014. Hepatitis A related acute liver failure by consumption of contaminated food. *J Clin Virol* **61:**456–458. PubMed
2. **Stene-Johansen K, Tjon G, Schreier E, Bremer V, Bruisten S, Ngui SL, King M, Pinto RM, Aragonès L, Mazick A, Corbet S, Sundqvist L, Blystad H, Norder H, Skaug K.** 2007. Molecular epidemiological studies show that hepatitis A virus is endemic among active homosexual men in Europe. *J Med Virol* **79:**356–365. PubMed
3. **Tjon GM, Götz H, Koek AG, de Zwart O, Mertens PL, Coutinho RA, Bruisten SM.** 2005. An outbreak of hepatitis A among homeless drug users in Rotterdam, The Netherlands. *J Med Virol* **77:**360–366. PubMed
4. **Bower WA, Nainan OV, Han X, Margolis HS.** 2000. Duration of viremia in hepatitis A virus infection. *J Infect Dis* **182:**12–17. PubMed
5. **Fryer JF, Heath AB, Morris CL, Collaborative Study Group.** 2013. *Collaborative Study to Evaluate the Proposed 2nd WHO International Standard for Hepatitis A Virus (HAV) for Nucleic Acid Amplification Technology (NAT)-Based Assays*. WHO ECBS report WHO/BS/2013.2225. World Health Organization, Geneva, Switzerland. http://www.who.int/biologicals/expert_committee/BS_2225_2nd_HAV_IS.pdf.
6. **Henriques I, Monteiro F, Meireles E, Cruz A, Tavares G, Ferreira M, Araújo F.** 2005. Prevalence of Parvovirus B19 and Hepatitis A virus in Portuguese blood donors. *Transfus Apher Sci* **33:**305–309. PubMed
7. **Müller MM, Fraile MI, Hourfar MK, Peris LB, Sireis W, Rubin MG, López EM, Rodriguez GT, Seifried E, Saldanha J, Schmidt M.** 2013. Evaluation of two, commercial, multi-dye, nucleic acid amplification technology tests, for HBV/HCV/HIV-1/HIV-2 and B19V/HAV, for screening blood and plasma for further manufacture. *Vox Sang* **104:**19–29. PubMed
8. **Heitmann A, Laue T, Schottstedt V, Dotzauer A, Pichl L.** 2005. Occurrence of hepatitis A virus genotype III in Germany requires the adaptation of commercially available diagnostic test systems. *Transfusion* **45:**1097–1105. PubMed
9. **Quality Control for Molecular Diagnostics.** EQA programmes. Quality Control for Molecular Diagnostics, Glasgow, United Kingdom. http://www.qcmd.org/index.php?pageId=3&pageVersion=EN.
10. **Ly KN, Klevens RM.** 2015. Trends in disease and complications of hepatitis A virus infection in the United States, 1999-2011: a new concern for adults. *J Infect Dis* **212:**176–182. PubMed
11. **Dane DS, Cameron CH, Briggs M.** 1970. Virus-like particles in serum of patients with Australia-antigen-associated hepatitis. *Lancet* **1:**695–698. PubMed
12. **Almeida JD, Waterson AP.** 1970. [The Australia antigen and its relation to hepatitis]. *Internist (Berl)* **11:**73–77. (In German.) PubMed
13. **Martin P, Lau DT, Nguyen MH, Janssen HL, Dieterich DT, Peters MG, Jacobson IM.** 2015. A treatment algorithm for the management of chronic hepatitis B virus infection in the United States: 2015 update. *Clin Gastroenterol Hepatol* **13:**2071–2087.e16. doi:10.1016/j.cgh.2015.07.007. PubMed
14. **Yan H, Yang Y, Zhang L, Tang G, Wang Y, Xue G, Zhou W, Sun S.** 2015. Characterization of the genotype and integration patterns of hepatitis B virus in early- and late-onset hepatocellular carcinoma. *Hepatology* **61:**1821–1831. PubMed
15. **Amaddeo G, Cao Q, Ladeiro Y, Imbeaud S, Nault JC, Jaoui D, Gaston Mathe Y, Laurent C, Laurent A, Bioulac-Sage P, Calderaro J, Zucman-Rossi J.** 2015. Integration of tumour and viral genomic characterizations in HBV-related hepatocellular carcinomas. *Gut* **64:**820–829. PubMed
16. **Lieshout-Krikke RW, van Kraaij MG, Danovic F, Zaaijer HL.** 2015 Nov 11. Rare transmission of hepatitis B virus by Dutch donors with occult infection. *Transfusion* doi:10.1111/trf.13401. PubMed
17. **Kim H, Gong JR, Lee SA, Kim BJ.** 2015. Discovery of a novel mutation (X8Del) resulting in an 8-bp deletion in the hepatitis B virus X gene associated with occult infection in Korean vaccinated individuals. *PLoS One* **10:**e0139551. doi:10.1371/journal.pone.0139551. PubMed
18. **Vargas JI, Jensen D, Sarmiento V, Peirano F, Acuña P, Fuster F, Soto S, Ahumada R, Huilcaman M, Bruna M, Jensen W, Fuster F.** 2015 Sep 18. Presence of anti-HBc is associated to high rates of HBV resolved infection and low threshold for occult HBV infection in HIV patients with negative HBsAg in Chile. *J Med Virol* doi:10.1002/jmv.24384.
19. **Ghosh M, Nandi S, Dutta S, Saha MK.** 2015. Detection of hepatitis B virus infection: a systematic review. *World J Hepatol* **7:**2482–2491. PubMed
20. **Vivekanandan P, Singh OV.** 2010. Molecular methods in the diagnosis and management of chronic hepatitis B. *Expert Rev Mol Diagn* **10:**921–935. PubMed
21. **Yeh ML, Huang CF, Hsieh MY, Huang JF, Dai CY, Yu ML, Chuang WL.** 2014. Comparison of the Abbott RealTime HBV assay with the Roche Cobas AmpliPrep/Cobas TaqMan HBV assay for HBV DNA detection and quantification. *J Clin Virol* **60:**206–214. PubMed
22. **Pol J, Le Pendeven C, Beby-Defaux A, Rabut E, Jais JP, Pilloux M, Osada C, Zatla F, Assami H, Grange JD, Kremsdorf D, Nicolas JC, Soussan P.** 2008. Prospective

comparison of Abbott RealTime HBV DNA and Versant HBV DNA 3.0 assays for hepatitis B DNA quantitation: impact on HBV genotype monitoring. *J Virol Methods* **154:**1–6. PubMed

23. **Allice T, Cerutti F, Pittaluga F, Varetto S, Gabella S, Marzano A, Franchello A, Ghisetti V.** 2008. Comparison of the Cobas Ampliprep/Cobas TaqMan HBV Test versus the Cobas Amplicor HBV monitor for HBV-DNA detection and quantification during antiviral therapy. *New Microbiol* **31:**27–35. PubMed
24. **Caviglia GP, Abate ML, Pellicano R, Smedile A.** 2015. Chronic hepatitis B therapy: available drugs and treatment guidelines. *Minerva Gastroenterol Dietol* **61:**61–70. PubMed
25. **Zeng T, Xu H, Liu JY, Lei Y, Zhong S, Zhou Z.** 2014. Entecavir plus adefovir combination therapy versus lamivudine add-on adefovir for lamivudine-resistant chronic hepatitis B: a meta-analysis. *J Clin Pharmacol* **54:**959–967. PubMed
26. **Corsa AC, Liu Y, Flaherty JF, Mitchell B, Fung SK, Gane E, Miller MD, Kitrinos KM.** 2014. No resistance to tenofovir disoproxil fumarate through 96 weeks of treatment in patients with lamivudine-resistant chronic hepatitis B. *Clin Gastroenterol Hepatol* **12:**2106–2112.e1. doi:10.1016/j.cgh.2014.05.024. PubMed
27. **Reijnders JG, Deterding K, Petersen J, Zoulim F, Santantonio T, Buti M, van Bömmel F, Hansen BE, Wedemeyer H, Janssen HL, VIRGIL Surveillance Study Group.** 2010. Antiviral effect of entecavir in chronic hepatitis B: influence of prior exposure to nucleos(t)ide analogues. *J Hepatol* **52:**493–500. PubMed
28. **Kim HS, Yim HJ, Jang MK, Park JW, Suh SJ, Seo YS, Kim JH, Kim BH, Park SJ, Lee SH, Kim SG, Kim YS, Lee JI, Lee JW, Kim IH, Kim TY, Kim JW, Jeong SH, Jung YK, Park H, Hwang SG, Antiviral Resistance Study Group.** 2015. Management of entecavir-resistant chronic hepatitis B with adefovir-based combination therapies. *World J Gastroenterol* **21:**10874–10882. PubMed
29. **Yang J, Chen J, Ye P, Jin L, Wu W, Sheng G, Li LJ.** 2014. HBsAg as an important predictor of HBeAg seroconversion following antiviral treatment for HBeAg-positive chronic hepatitis B patients. *J Transl Med* **12:**183. doi:10.1186/1479-5876-12-183. PubMed
30. **Kim JH, Moon HW, Ko SY, Choe WH, Kwon SY.** 2014. Hepatitis B surface antigen levels at 6 months after treatment can predict the efficacy of lamivudine-adefovir combination therapy in patients with lamivudine-resistant chronic hepatitis B. *Clin Mol Hepatol* **20:**274–282. PubMed
31. **Janssen HL, van Zonneveld M, Senturk H, Zeuzem S, Akarca US, Cakaloglu Y, Simon C, So TM, Gerken G, de Man RA, Niesters HG, Zondervan P, Hansen B, Schalm SW, HBV 99-01 Study Group, Rotterdam Foundation for Liver Research.** 2005. Pegylated interferon alfa-2b alone or in combination with lamivudine for HBeAg-positive chronic hepatitis B: a randomised trial. *Lancet* **365:**123–129. PubMed
32. **Pas SD, Tran N, de Man RA, Burghoorn-Maas C, Vernet G, Niesters HG.** 2008. Comparison of reverse hybridization, microarray, and sequence analysis for genotyping hepatitis B virus. *J Clin Microbiol* **46:**1268–1273. PubMed
33. **Niesters HG, Pas S, de Man RA.** 2005. Detection of hepatitis B virus genotypes and mutants: current status. *J Clin Virol* **34**(Suppl 1)**:**S4–S8. PubMed
34. **Lupo J, Larrat S, Hilleret MN, Germi R, Boyer V, Nicod S, Barguès G, Leroy V, Seigneurin JM, Zarski JP, Morand P.** 2009. Assessment of selective real-time PCR for quantitation of lamivudine and adefovir hepatitis B virus-resistant strains and comparison with direct sequencing and line probe assays. *J Virol Methods* **156:**52–58. PubMed
35. **Lee JH, Hong SP, Jang ES, Park SJ, Hwang SG, Kang SK, Jeong SH.** 2015. Analysis of HBV genotype, drug resistant mutations, and pre-core/basal core promoter mutations in Korean patients with acute hepatitis B. *J Med Virol* **87:**993–998. PubMed
36. **Miyamura T, Saito I, Katayama T, Kikuchi S, Tateda A, Houghton M, Choo QL, Kuo G.** 1990. Detection of antibody against antigen expressed by molecularly cloned hepatitis C virus cDNA: application to diagnosis and blood screening for posttransfusion hepatitis. *Proc Natl Acad Sci USA* **87:**983–987. PubMed
37. **Lindenbach BD, Rice CM.** 2013. The ins and outs of hepatitis C virus entry and assembly. *Nat Rev Microbiol* **11:**688–700. PubMed
38. **De Re V, Gragnani L, Fognani E, Piluso A, Izzo F, Mangia A, Crovatto M, Gava G, Casarin P, Sansonno D, Racanelli V, De Vita S, Pioltelli P, Caggiari L, De Zorzi M, Berretta M, Gini A, Zucchetto A, Buonaguro FM, De Paoli P, Zignego AL.** 2014. Impact of immunogenetic IL28B polymorphism on natural outcome of HCV infection. *BioMed Res Int* **2014:**710642. doi:10.1155/2014/710642. PubMed
39. **Riva A, Laird M, Casrouge A, Ambrozaitis A, Williams R, Naoumov NV, Albert ML, Chokshi S.** 2014. Truncated CXCL10 is associated with failure to achieve spontaneous clearance of acute hepatitis C infection. *Hepatology* **60:**487–496. PubMed
40. **Laird ME, Mohsen A, Duffy D, Mamdouh R, LeFouler L, Casrouge A, El-Daly M, Rafik M, Abdel-Hamid M, Soulier A, Pawlotsky JM, Hézode C, Rosa I, Renard P, Mohamed MK, Bonnard P, Izopet J, Mallet V, Pol S, Albert ML, Fontanet A.** 2014. Apolipoprotein H expression is associated with *IL28B* genotype and viral clearance in hepatitis C virus infection. *J Hepatol* **61:**770–776. PubMed
41. **Karmochkine M, Carrat F, Dos Santos O, Cacoub P, Raguin G.** 2006. A case-control study of risk factors for hepatitis C infection in patients with unexplained routes of infection. *J Viral Hepat* **13:**775–782. PubMed
42. **Saleh DA, Shebl FM, El-Kamary SS, Magder LS, Allam A, Abdel-Hamid M, Mikhail N, Hashem M, Sharaf S, Stoszek SK, Strickland GT.** 2010. Incidence and risk factors for community-acquired hepatitis C infection from birth to 5 years of age in rural Egyptian children. *Trans R Soc Trop Med Hyg* **104:**357–363. PubMed
43. **Martin NK, Hickman M, Hutchinson SJ, Goldberg DJ, Vickerman P.** 2013. Combination interventions to prevent HCV transmission among people who inject drugs: modeling the impact of antiviral treatment, needle and syringe programs, and opiate substitution therapy. *Clin Infect Dis* **57**(Suppl 2)**:**S39–S45. PubMed
44. **Iversen J, Wand H, Topp L, Kaldor J, Maher L.** 2013. Reduction in HCV incidence among injection drug users attending needle and syringe programs in Australia: a linkage study. *Am J Public Health* **103:**1436–1444. PubMed
45. **Panneer N, Lontok E, Branson BM, Teo CG, Dan C, Parker M, Stekler JD, DeMaria A Jr, Miller V.** 2014. HIV and hepatitis C virus infection in the United States: whom and how to test. *Clin Infect Dis* **59:**875–882. PubMed
46. **Martin NK, Vickerman P, Goldberg D, Hickman M.** 2015. HCV treatment as prevention in prison: key issues. *Hepatology* **61:**402–403. PubMed
47. **Kamili S, Drobeniuc J, Araujo AC, Hayden TM.** 2012. Laboratory diagnostics for hepatitis C virus infection. *Clin Infect Dis* **55**(Suppl 1)**:**S43–S48. PubMed
48. **Centers for Disease Control and Prevention (CDC).** 2013. Testing for HCV infection: an update of guidance for clinicians and laboratorians. *MMWR Morb Mortal Wkly Rep* **62:**362–365. PubMed
49. **Scalioni LP, Cruz HM, de Paula VS, Miguel JC, Marques VA, Villela-Nogueira CA, Milagres FA, Cruz MS, Bastos FI, Andrade TM, Motta-Castro AR, Lewis-Ximenez LL, Lampe E, Villar LM.** 2014. Performance of rapid hepatitis C virus antibody assays among high- and low-risk populations. *J Clin Virol* **60:**200–205. PubMed

50. **Smith DB, Bukh J, Kuiken C, Muerhoff AS, Rice CM, Stapleton JT, Simmonds P.** 2014. Expanded classification of hepatitis C virus into 7 genotypes and 67 subtypes: updated criteria and genotype assignment web resource. *Hepatology* **59:**318–327. PubMed
51. **Du H, Qi Y, Hao F, Huang Y, Mao L, Ji S, Huang M, Qin C, Yan R, Zhu X, Zhang C.** 2012. Complex patterns of HCV epidemic in Suzhou: evidence for dual infection and HCV recombination in East China. *J Clin Virol* **54:**207–212. PubMed
52. **Gededzha MP, Selabe SG, Kyaw T, Rakgole JN, Blackard JT, Mphahlele MJ.** 2012. Introduction of new subtypes and variants of hepatitis C virus genotype 4 in South Africa. *J Med Virol* **84:**601–607. PubMed
53. **Raghwani J, Thomas XV, Koekkoek SM, Schinkel J, Molenkamp R, van de Laar TJ, Takebe Y, Tanaka Y, Mizokami M, Rambaut A, Pybus OG.** 2012. Origin and evolution of the unique hepatitis C virus circulating recombinant form 2k/1b. *J Virol* **86:**2212–2220. PubMed
54. **Verbeeck J, Stanley MJ, Shieh J, Celis L, Huyck E, Wollants E, Morimoto J, Farrior A, Sablon E, Jankowski-Hennig M, Schaper C, Johnson P, Van Ranst M, Van Brussel M.** 2008. Evaluation of Versant hepatitis C virus genotype assay (LiPA) 2.0. *J Clin Microbiol* **46:**1901–1906. PubMed
55. **Nakatani SM, Santos CA, Riediger IN, Krieger MA, Duarte CA, do Carmo Debur M, Carrilho FJ, Ono SK.** 2011. Comparative performance evaluation of hepatitis C virus genotyping based on the 5′ untranslated region versus partial sequencing of the NS5B region of Brazilian patients with chronic hepatitis C. *Virol J* **8:**459. doi:10.1186/1743-422X-8-459. PubMed
56. **Yang R, Cong X, Du S, Fei R, Rao H, Wei L.** 2014. Performance comparison of the Versant HCV genotype 2.0 assay (LiPA) and the Abbott Realtime HCV genotype II assay for detecting hepatitis C virus genotype 6. *J Clin Microbiol* **52:**3685–3692. PubMed
57. **Mallory MA, Lucic DX, Sears MT, Cloherty GA, Hillyard DR.** 2014. Evaluation of the Abbott Realtime HCV genotype II RUO (GT II) assay with reference to 5′UTR, core and NS5B sequencing. *J Clin Virol* **60:**22–26. PubMed
58. **Wu S, Kanda T, Nakamoto S, Imazeki F, Yokosuka O.** 2013. Hepatitis C virus protease inhibitor-resistance mutations: our experience and review. *World J Gastroenterol* **19:**8940–8948. PubMed
59. **Kuntzen T, Timm J, Berical A, Lennon N, Berlin AM, Young SK, Lee B, Heckerman D, Carlson J, Reyor LL, Kleyman M, McMahon CM, Birch C, Schulze Zur Wiesch J, Ledlie T, Koehrsen M, Kodira C, Roberts AD, Lauer GM, Rosen HR, Bihl F, Cerny A, Spengler U, Liu Z, Kim AY, Xing Y, Schneidewind A, Madey MA, Fleckenstein JF, Park VM, Galagan JE, Nusbaum C, Walker BD, Lake-Bakaar GV, Daar ES, Jacobson IM, Gomperts ED, Edlin BR, Donfield SM, Chung RT, Talal AH, Marion T, Birren BW, Henn MR, Allen TM.** 2008. Naturally occurring dominant resistance mutations to hepatitis C virus protease and polymerase inhibitors in treatment-naïve patients. *Hepatology* **48:**1769–1778. PubMed
60. **McCown MF, Rajyaguru S, Kular S, Cammack N, Nájera I.** 2009. GT-1a or GT-1b subtype-specific resistance profiles for hepatitis C virus inhibitors telaprevir and HCV-796. *Antimicrob Agents Chemother* **53:**2129–2132. PubMed
61. **Lawitz E, Mangia A, Wyles D, Rodriguez-Torres M, Hassanein T, Gordon SC, Schultz M, Davis MN, Kayali Z, Reddy KR, Jacobson IM, Kowdley KV, Nyberg L, Subramanian GM, Hyland RH, Arterburn S, Jiang D, McNally J, Brainard D, Symonds WT, McHutchison JG, Sheikh AM, Younossi Z, Gane EJ.** 2013. Sofosbuvir for previously untreated chronic hepatitis C infection. *N Engl J Med* **368:**1878–1887. PubMed
62. **Vermehren J, Susser S, Lange CM, Forestier N, Karey U, Hughes E, Ralston R, Tong X, Zeuzem S, Sarrazin C.** 2012. Mutations selected in the hepatitis C virus NS3 protease domain during sequential treatment with boceprevir with and without pegylated interferon alfa-2b. *J Viral Hepat* **19:**120–127. PubMed
63. **de Carvalho IM, Alves R, de Souza PA, da Silva EF, Mazo D, Carrilho FJ, Queiroz AT, Pessoa MG.** 2014. Protease inhibitor resistance mutations in untreated Brazilian patients infected with HCV: novel insights about targeted genotyping approaches. *J Med Virol* **86:**1714–1721. PubMed
64. **Nishiya AS, de Almeida-Neto C, Ferreira SC, Alencar CS, Di-Lorenzo-Oliveira C, Levi JE, Salles NA, Mendrone A Jr, Sabino EC.** 2014. HCV genotypes, characterization of mutations conferring drug resistance to protease inhibitors, and risk factors among blood donors in São Paulo, Brazil. *PLoS One* **9:**e86413. doi:10.1371/journal.pone.0086413. PubMed
65. **Paolucci S, Fiorina L, Mariani B, Gulminetti R, Novati S, Barbarini G, Bruno R, Baldanti F.** 2013. Naturally occurring resistance mutations to inhibitors of HCV NS5A region and NS5B polymerase in DAA treatment-naïve patients. *Virol J* **10:**355. doi:10.1186/1743-422X-10-355. PubMed
66. **Sagnelli E, Sagnelli C, Pisaturo M, Macera M, Coppola N.** 2014. Epidemiology of acute and chronic hepatitis B and delta over the last 5 decades in Italy. *World J Gastroenterol* **20:**7635–7643. PubMed
67. **Karataylı E, Altunoğlu YÇ, Karataylı SC, Alagöz SG, Cınar K, Yalçın K, Idilman R, Yurdaydın C, Bozdayı AM.** 2014. A one step real time PCR method for the quantification of hepatitis delta virus RNA using an external armored RNA standard and intrinsic internal control. *J Clin Virol* **60:**11–15. PubMed
68. **Kodani M, Martin A, Mixson-Hayden T, Drobeniuc J, Gish RR, Kamili S.** 2013. One-step real-time PCR assay for detection and quantitation of hepatitis D virus RNA. *J Virol Methods* **193:**531–535. PubMed
69. **Brichler S, Le Gal F, Butt A, Chevret S, Gordien E.** 2013. Commercial real-time reverse transcriptase PCR assays can underestimate or fail to quantify hepatitis delta virus viremia. *Clin Gastroenterol Hepatol* **11:**734–740. PubMed
70. **Romeo R, Perbellini R.** 2015. Hepatitis delta virus: making the point from virus isolation up to 2014. *World J Hepatol* **7:**2389–2395. PubMed
71. **Makuwa M, Caron M, Souquière S, Malonga-Mouelet G, Mahé A, Kazanji M.** 2008. Prevalence and genetic diversity of hepatitis B and delta viruses in pregnant women in Gabon: molecular evidence that hepatitis delta virus clade 8 originates from and is endemic in central Africa. *J Clin Microbiol* **46:**754–756. PubMed
72. **Makuwa M, Mintsa-Ndong A, Souquière S, Nkoghé D, Leroy EM, Kazanji M.** 2009. Prevalence and molecular diversity of hepatitis B virus and hepatitis delta virus in urban and rural populations in northern Gabon in central Africa. *J Clin Microbiol* **47:**2265–2268. PubMed
73. **Foupouapouognigni Y, Noah DN, Sartre MT, Njouom R.** 2011. High prevalence and predominance of hepatitis delta virus genotype 1 infection in Cameroon. *J Clin Microbiol* **49:**1162–1164. PubMed
74. **Casey JL, Niro GA, Engle RE, Vega A, Gomez H, McCarthy M, Watts DM, Hyams KC, Gerin JL.** 1996. Hepatitis B virus (HBV)/hepatitis D virus (HDV) coinfection in outbreaks of acute hepatitis in the Peruvian Amazon basin: the roles of HDV genotype III and HBV genotype F. *J Infect Dis* **174:**920–926. PubMed
75. **Arakawa Y, Moriyama M, Taira M, Hayashi N, Tanaka N, Okubo H, Sugitani M.** 2000. Molecular analysis of hepatitis D virus infection in Miyako Island, a small Japanese island. *J Viral Hepat* **7:**375–381. PubMed

76. **Ijaz S, Arnold E, Banks M, Bendall RP, Cramp ME, Cunningham R, Dalton HR, Harrison TJ, Hill SF, Macfarlane L, Meigh RE, Shafi S, Sheppard MJ, Smithson J, Wilson MP, Teo CG.** 2005. Non-travel-associated hepatitis E in England and Wales: demographic, clinical, and molecular epidemiological characteristics. *J Infect Dis* **192:**1166–1172.
77. **Fu H, Li L, Zhu Y, Wang L, Geng J, Chang Y, Xue C, Du G, Li Y, Zhuang H.** 2010. Hepatitis E virus infection among animals and humans in Xinjiang, China: possibility of swine to human transmission of sporadic hepatitis E in an endemic area. *Am J Trop Med Hyg* **82:**961–966. PubMed
78. **Norder H, Sundqvist L, Magnusson L, Østergaard Breum S, Löfdahl M, Larsen LE, Hjulsager CK, Magnius L, Böttiger BE, Widén F.** 2009. Endemic hepatitis E in two Nordic countries. *Euro Surveill* **14:**pii=19211. http://www.eurosurveillance.org/ViewArticle.aspx?ArticleId=19211.
79. **Meng XJ.** 2011. From barnyard to food table: the omnipresence of hepatitis E virus and risk for zoonotic infection and food safety. *Virus Res* **161:**23–30. PubMed
80. **Drobeniuc J, Greene-Montfort T, Le NT, Mixson-Hayden TR, Ganova-Raeva L, Dong C, Novak RT, Sharapov UM, Tohme RA, Teshale E, Kamili S, Teo CG.** 2013. Laboratory-based surveillance for hepatitis E virus infection, United States, 2005-2012. *Emerg Infect Dis* **19:**218–222, quiz 353. PubMed
81. **Matsubayashi K, Kang JH, Sakata H, Takahashi K, Shindo M, Kato M, Sato S, Kato T, Nishimori H, Tsuji K, Maguchi H, Yoshida J, Maekubo H, Mishiro S, Ikeda H.** 2008. A case of transfusion-transmitted hepatitis E caused by blood from a donor infected with hepatitis E virus via zoonotic food-borne route. *Transfusion* **48:**1368–1375. PubMed
82. **Adlhoch C, Kaiser M, Pauli G, Koch J, Meisel H.** 2009. Indigenous hepatitis E virus infection of a plasma donor in Germany. *Vox Sang* **97:**303–308. PubMed
83. **Colson P, Coze C, Gallian P, Henry M, De Micco P, Tamalet C.** 2007. Transfusion-associated hepatitis E, France. *Emerg Infect Dis* **13:**648–649. PubMed
84. **Slot E, Hogema BM, Riezebos-Brilman A, Kok TM, Molier M, Zaaijer HL.** 2013. Silent hepatitis E virus infection in Dutch blood donors, 2011 to 2012. *Euro Surveill* **18:**20550. http://dx.doi.org/10.2807/1560-7917.ES2013.18.31.20550. PubMed
85. **Hewitt PE, Ijaz S, Brailsford SR, Brett R, Dicks S, Haywood B, Kennedy IT, Kitchen A, Patel P, Poh J, Russell K, Tettmar KI, Tossell J, Ushiro-Lumb I, Tedder RS.** 2014. Hepatitis E virus in blood components: a prevalence and transmission study in southeast England. *Lancet* **384:**1766–1773. PubMed
86. **Cleland A, Smith L, Crossan C, Blatchford O, Dalton HR, Scobie L, Petrik J.** 2013. Hepatitis E virus in Scottish blood donors. *Vox Sang* **105:**283–289. PubMed
87. **Huang S, Zhang X, Jiang H, Yan Q, Ai X, Wang Y, Cai J, Jiang L, Wu T, Wang Z, Guan L, Shih JW, Ng MH, Zhu F, Zhang J, Xia N.** 2010. Profile of acute infectious markers in sporadic hepatitis E. *PLoS One* **5:**e13560. doi:10.1371/journal.pone.0013560. PubMed
88. **Bendall R, Ellis V, Ijaz S, Ali R, Dalton H.** 2010. A comparison of two commercially available anti-HEV IgG kits and a re-evaluation of anti-HEV IgG seroprevalence data in developed countries. *J Med Virol* **82:**799–805. PubMed
89. **Pas SD, Streefkerk RH, Pronk M, de Man RA, Beersma MF, Osterhaus AD, van der Eijk AA.** 2013. Diagnostic performance of selected commercial HEV IgM and IgG ELISAs for immunocompromised and immunocompetent patients. *J Clin Virol* **58:**629–634. PubMed
90. **Ferguson M, Walker D, Mast E, Fields H.** 2002. Report of a collaborative study to assess the suitability of a reference reagent for antibodies to hepatitis E virus. *Biologicals* **30:**43–48. PubMed
91. **Pas SD, Streefkerk RH, Pronk M, de Man RA, Beersma MF, Osterhaus AD, van der Eijk AA.** 2013. Diagnostic performance of selected commercial HEV IgM and IgG ELISAs for immunocompromised and immunocompetent patients. *J Clin Virol* **58:**629–634. PubMed
92. **Baylis SA, Blümel J, Mizusawa S, Matsubayashi K, Sakata H, Okada Y, Nübling CM, Hanschmann KM, HEV Collaborative Study Group.** 2013. World Health Organization International Standard to harmonize assays for detection of hepatitis E virus RNA. *Emerg Infect Dis* **19:**729–735. PubMed
93. **Abravanel F, Chapuy-Regaud S, Lhomme S, Dubois M, Peron JM, Alric L, Rostaing L, Kamar N, Izopet J.** 2013. Performance of two commercial assays for detecting hepatitis E virus RNA in acute or chronic infections. *J Clin Microbiol* **51:**1913–1916. PubMed
94. **Mokhtari C, Marchadier E, Haïm-Boukobza S, Jeblaoui A, Tessé S, Savary J, Roque-Afonso AM.** 2013. Comparison of real-time RT-PCR assays for hepatitis E virus RNA detection. *J Clin Virol* **58:**36–40. PubMed
95. **Kamar N, Rostaing L, Legrand-Abravanel F, Izopet J.** 2013. How should hepatitis E virus infection be defined in organ-transplant recipients? *Am J Transplant* **13:**1935–1936. PubMed
96. **Kamar N, Izopet J, Dalton HR.** 2013. Chronic hepatitis E virus infection and treatment. *J Clin Exp Hepatol* **3:**134–140. PubMed
97. **Tang X, Yang C, Gu Y, Song C, Zhang X, Wang Y, Zhang J, Hew CL, Li S, Xia N, Sivaraman J.** 2011. Structural basis for the neutralization and genotype specificity of hepatitis E virus. *Proc Natl Acad Sci USA* **108:**10266–10271.
98. **Zhang J, Liu CB, Li RC, Li YM, Zheng YJ, Li YP, Luo D, Pan BB, Nong Y, Ge SX, Xiong JH, Shih JW, Ng MH, Xia NS.** 2009. Randomized-controlled phase II clinical trial of a bacterially expressed recombinant hepatitis E vaccine. *Vaccine* **27:**1869–1874. PubMed
99. **Zhu FC, Zhang J, Zhang XF, Zhou C, Wang ZZ, Huang SJ, Wang H, Yang CL, Jiang HM, Cai JP, Wang YJ, Ai X, Hu YM, Tang Q, Yao X, Yan Q, Xian YL, Wu T, Li YM, Miao J, Ng MH, Shih JW, Xia NS.** 2010. Efficacy and safety of a recombinant hepatitis E vaccine in healthy adults: a large-scale, randomised, double-blind placebo-controlled, 3 trial. *Lancet* **376:**895–902. PubMed
100. **Kamar N, Garrouste C, Haagsma EB, Garrigue V, Pischke S, Chauvet C, Dumortier J, Cannesson A, Cassuto-Viguier E, Thervet E, Conti F, Lebray P, Dalton HR, Santella R, Kanaan N, Essig M, Mousson C, Radenne S, Roque-Afonso AM, Izopet J, Rostaing L.** 2011. Factors associated with chronic hepatitis in patients with hepatitis E virus infection who have received solid organ transplants. *Gastroenterology* **140:**1481–1489. PubMed
101. **Kamar N, Dalton HR, Abravanel F, Izopet J.** 2014. Hepatitis E virus infection. *Clin Microbiol Rev* **27:**116–138. PubMed
102. **Takahashi M, Tanaka T, Takahashi H, Hoshino Y, Nagashima S, Jirintai, Mizuo H, Yazaki Y, Takagi T, Azuma M, Kusano E, Isoda N, Sugano K, Okamoto H.** 2010. Hepatitis E virus (HEV) strains in serum samples can replicate efficiently in cultured cells despite the coexistence of HEV antibodies: characterization of HEV virions in blood circulation. *J Clin Microbiol* **48:**1112–1125. PubMed
103. **Shukla P, Nguyen HT, Faulk K, Mather K, Torian U, Engle RE, Emerson SU.** 2012. Adaptation of a genotype 3 hepatitis E virus to efficient growth in cell culture depends on an inserted human gene segment acquired by recombination. *J Virol* **86:**5697–5707. PubMed

Viral Agents of Gastroenteritis

GABRIEL I. PARRA AND KIM Y. GREEN

66

The healthy human enteric tract is populated by a complex community of microbiota in synergistic balance with its host. Infection with a pathogenic virus can cause intestinal damage, inflammation, and diarrhea that alter the gut environment. The ability to diagnose pathogenic viruses rapidly and accurately is important in providing appropriate patient care and in controlling virus spread.

Diagnostic virology is riding the wave of a technologic revolution. The increasing ability to assay small amounts of nucleic acid and protein in a clinical sample offers tremendous opportunity to identify viruses that were previously below the threshold of detection. However, this technology also presents new challenges in sorting through massive data sets and establishing etiologic significance. Multipathogen detection panels for gastrointestinal viruses will cast a wider net that will help establish the true incidence of viruses that have never been fully surveyed. However, they may also increase the number of diagnosed mixed infections, again demanding the ability to distinguish between symptomatic and asymptomatic infection and establishing the true etiologic agent of a diarrheal illness.

The purpose of this chapter is to review current techniques that are available for the specific detection and genotyping of major viral enteric pathogens associated with gastroenteritis, focusing on the rotaviruses, noroviruses, sapoviruses, astroviruses, and adenoviruses. Key features of these viruses and other enteric viral pathogens detected in stool are summarized in Table 1. Although the field of diagnostic virology is advancing rapidly, with multipathogen formats gaining widespread use, the techniques described here for individual viral pathogens will continue to provide important information on the epidemiology, natural history, and evolution of these viruses.

ROTAVIRUSES

Overview

Rotaviruses are a major cause of acute gastroenteritis in humans and animals. They have a double-stranded RNA genome divided into 11 segments that encode the viral proteins: 6 structural proteins (VP1 to VP4, VP6, and VP7) and at least 5 nonstructural proteins (NSP1 to NSP5) (Fig. 1A) (1). The rotavirus segmented genome is enclosed within a triple-layered protein icosahedral capsid, in which the inner capsid is formed by the VP2, the intermediate capsid by the VP6, and the outer capsid by the VP7 and VP4 (Fig. 1A). Based on differences within the VP6 protein, rotaviruses can be divided into nine groups (A to I) (2), with group A rotavirus (RVA) the most prevalent (>99% of the isolates) in humans (1).

Antigenic and genetic differences within the two outermost proteins, VP4 and VP7, have been used to classify RVA by a dual nomenclature system into P and G types, respectively. Currently, 37 P types and 27 G types have been described in different animal species (3, 4). Surveillance of RVA in humans has shown that five strains (G1P[8], G2P[4], G3P[8], G4P[8], and G9P[8]) are the most common (Fig. 1B), but temporal and geographic changes in strain prevalence as well as the emergence of strains bearing unusual G types (e.g., G8, G10, or G12) have been observed (1, 5). Based on full-genome sequencing and differences within each of the 11 segments, a comprehensive classification system has been established for RVA. This system recognizes the genomic characteristics of RVA from different species and defines the presence of three major genomic constellations, with two prevalent in humans (WA-like and DS1-like) and one in animals (AU1-like) (6).

Two RVA vaccines, Rotarix (monovalent G1P[8]) and Rotateq (pentavalent G1 to G4 and P[8]), are currently licensed for use in children. Both vaccines are highly effective against severe rotavirus gastroenteritis in high- and middle-income countries, which has reduced the public health burden of RVA (7). Interestingly, vaccination of children has been associated with a reduction in disease prevalence in older children and adults (8). Vaccination in low-income countries has been less effective (reviewed in reference 9).

Detection and Characterization

Nucleic Acid-Based

Early detection methods relied on direct visualization of RVA virions in stool by electron microscopy, as the virus (70 nm in diameter) is often abundant and exhibits a distinct morphology. The migration of rotavirus double-stranded RNA genome segments by PAGE (known as electropherotyping) became a popular technique during the 1980s and early 1990s. Depending on the mobility of segment 11, two electropherotypes have been described for RVA (i.e., long or short). In humans, strains with "short" electropherotypes

doi:10.1128/9781555818722.ch66

TABLE 1 Common viral agents of gastroenteritis identified in stool[a]

Virus	Classification	Nucleic acid	Characteristic epidemiologic features
Rotavirus	*Reoviridae*	Segmented, double-stranded RNA	Pediatric diarrhea
Norovirus	*Caliciviridae*	Nonsegmented, single-stranded RNA	Sporadic diarrhea and outbreaks in all age groups
Sapovirus	*Caliciviridae*	Nonsegmented, single-stranded RNA	Pediatric diarrhea
Astrovirus	*Astroviridae*	Nonsegmented, single-stranded RNA	Pediatric diarrhea
Adenovirus	*Adenoviridae*	Nonsegmented, double-stranded DNA	Pediatric diarrhea
Bocavirus	*Parvoviridae*	Nonsegmented, single-stranded DNA	Pediatric diarrhea (human bocavirus-2, -3, and -4)
Aichivirus A	*Picornaviridae*	Nonsegmented, single-stranded RNA	Sporadic diarrhea in all age groups

[a]Common features of these viruses are as follows. (i) They are nonenveloped, icosahedral particles; (ii) infectious virions are shed in stool; (iii) viruses have a global distribution with multiple genotypes or serotypes; and (iv) severe cases occur most often in young individuals and immunocompromised patients. Currently, vaccines are available only for the rotaviruses.

usually correspond to G2P[4] or G9P[6] strains, and those with "long" electropherotypes to G1P[8], G3P[8], G4P[8], or G9P[8] strains (1, 5).

The most widely used current technique for the detection and characterization of RVA double-stranded RNA is a multiplex reverse transcription-PCR (RT-PCR) that targets either the VP4 or the VP7 gene. Briefly, the strategy utilizes an anchoring cross-reactive primer and a pool of genotype-specific primers in the PCR reaction. Each genotype-specific primer yields an amplicon of defined length, so that the genotype can be assigned following sizing of the products by electrophoresis (Fig. 2). Two RT-PCR strategies have been reported for identification of the most common G types in humans (10, 11) and one for the most common P types (12). RT-PCR methods for detection of G and P types characteristically found in RVA strains infecting animals are also available (13) and have the potential to be multiplexed with human RVA typing assays. A modified scheme developed by Das et al. (11) for G typing is illustrated in Fig. 2. Although these multiplex RT-PCR assays are widely used, it is recommended that the results be validated by sequencing or an alternative strategy such as hybridization. Intragenotypic diversification could lead to mutations in the primer-binding sites, which might result in negative results or the misidentification of the genotype (14, 15). The state-of-the-art method for the complete genetic characterization of RVA strains is full-genome (or nearly full) sequencing analysis (6, 16).

Quantitative real-time RT-PCR (RT-qPCR) assays have been developed for rotaviruses that enhance the sensitivity of detection and that also allow the quantification of virus genome (17, 18). The use of RT-qPCR is advantageous in the analysis of environmental or food samples containing small amounts of virus. However, its higher cost often limits its general use because cheaper assays (antigen-based or multiplex RT-PCR) work well to detect the high levels of rotaviruses often present in patient stool. Recently, Bennett et al. have reported a correlation between low threshold cycle values and more severe infections when testing for the presence of rotavirus RNA in stool samples (17). This type of test could prove useful as a quantitative readout in vaccine efficacy studies that score disease severity.

Antigen-Based

Multiple tests are commercially available for the detection of rotavirus antigen in stool samples. Most are based on the use of antibodies directed to the VP6 (inner capsid protein), which is highly conserved among rotavirus strains from the same group (19). Most kits provide results within 2 h, and some strip-based kits provide detection of rotaviruses within the first 10 min. The method used for the interpretation of results can vary from visual inspection to spectrophotometric reading of the wells. The antigen-based methods present higher sensitivity than the molecular methods (like RT-PCR or PAGE); however, they are limited by the specificity of the antibodies, which in some cases may fail to detect certain strains.

NOROVIRUSES

Overview

Noroviruses are a major cause of acute gastroenteritis in humans and have gained increasing importance after the successful introduction of rotavirus vaccines in different countries worldwide (20, 21). Currently, noroviruses are the major cause of hospitalizations and emergency visits due to acute gastroenteritis in the United States (20), and it is estimated that they are responsible for up to 200,000 deaths per year, predominantly in children <5 years of age in developing countries (22). These viruses are known to cause outbreaks in semi-enclosed settings such as child care facilities, schools, universities, nursing homes, family events, and cruise ships. Norovirus outbreaks often occur during the coolest months of the year, and the illness has been called "stomach flu" and "winter vomiting disease" (23).

Noroviruses possess a single-stranded, positive-sense RNA genome organized into three open reading frames (ORFs) that are flanked by 5′- and 3′-end nontranslated regions (NTRs). ORF1 encodes the nonstructural proteins required for replication, including the RNA-dependent RNA polymerase (RdRp); ORF2 encodes the major capsid protein (VP1); and ORF3 encodes a minor capsid protein (VP2) (Fig. 3A) (23). The current norovirus classification scheme is based on differences in the genes encoding RdRp (polymerase or P genotype) and the VP1 (capsid or C genotype). Currently, at least 7 genogroups (GI to GVII) and >30 genotypes have been defined (24). Noroviruses in GI, GII, and GIV infect humans, and GII.4 strains are the most prevalent worldwide (Fig. 3B) (25). Because noroviruses can undergo recombination near the ORF1/ORF2 junction during coinfection, recombinant strains with different P and C genotypes are not unusual (26). The interchange of P and C genotypes occurs almost

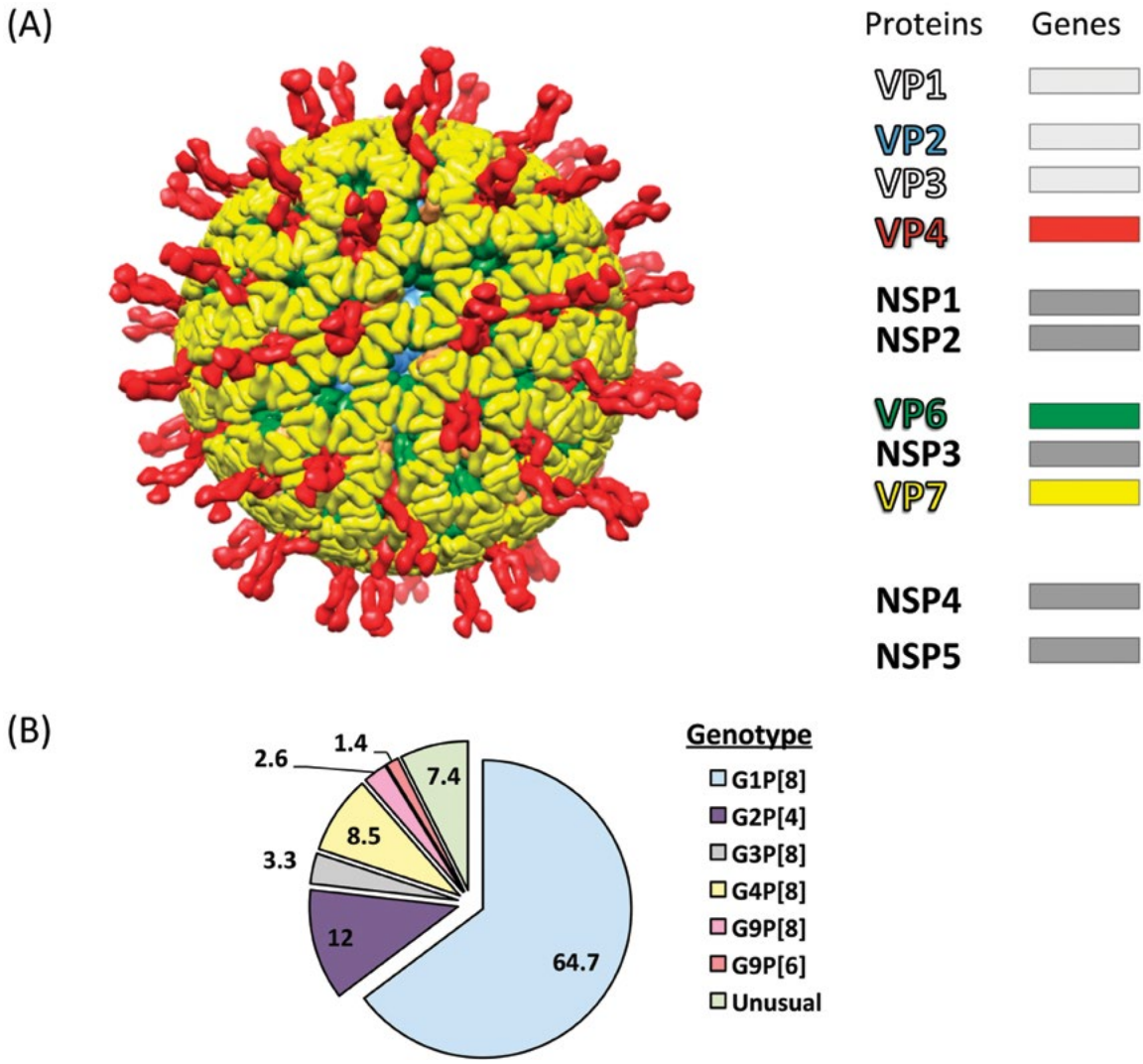

FIGURE 1 Rotavirus genome and genotype distribution. (A) Representation of rotavirus virion, proteins, and double-stranded RNA gene segments. Proteins are color coded, and genes used for typing are highlighted with corresponding colors. The rotavirus virion was modeled using crystal coordinates from VP2, VP6, VP7, and VP4 proteins (PDBs: 3IYU and 3N09) and visualized in Chimera. (B) Global incidence of the most predominant rotavirus strains in humans according to genotype. Numbers represent the percentage of total strains included (n = 16,474). (Adapted from reference 5.)

exclusively between strains within the same genogroup (i.e., intragenogroup recombinants).

The absence of a robust *in vitro* cell culture system or small animal disease model to study human noroviruses has been a roadblock in the field. The major capsid protein VP1 self-assembles into virus-like particles (VLPs) in several *in vitro* expression systems, and VLPs have been employed in the study of virus structure, antigenic diversity, diagnostics development, and virus-cell interactions. Furthermore, VLPs are currently under investigation as a promising vaccine candidate (27, 28).

Detection and Characterization

Nucleic Acid-Based

The detection of viral RNA in stool is currently the most widely used diagnostic method for the noroviruses (reviewed in reference 29), and commercial kits for RT-PCR are available. The two most common RT-PCR-based techniques require the initial isolation of highly purified viral RNA from stool specimens that is free of PCR inhibitors. In the first technique, RNA is subjected to RT-PCR with primers targeted to conserved regions of the genome (Fig. 3A) and the amplicon is directly sequenced (30–32). Sequences can be interrogated against an extensive norovirus database with the Norovirus Genotyping Tool (http://www.rivm.nl/mpf/norovirus/typingtool), and the P and/or C genotype assigned. Furthermore, sequence analysis provides the ability to track the emergence of new norovirus variants and recombinants. In the second technique, viral RNA is analyzed by RT-qPCR for virus detection and, if desired, quantification of genome copies. This method is sensitive and fast and provides the identity of genogroup (but not genotype, which requires sequence analysis of genomic RNA).

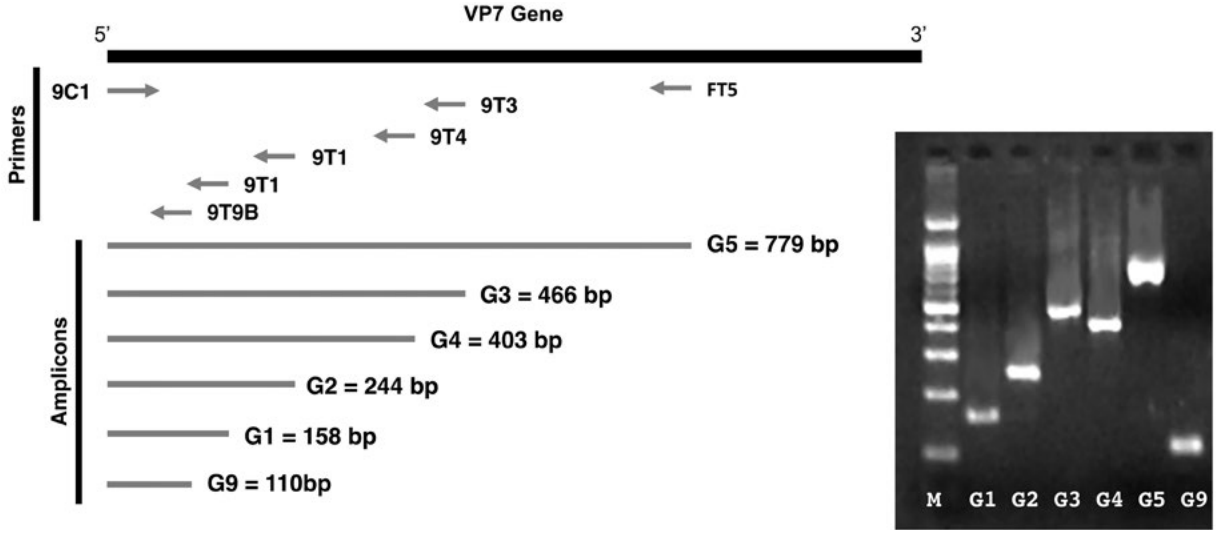

FIGURE 2 Representation of the RT-PCR genotyping strategy for human rotaviruses based on amplicon sizing. Genotype-specific primers annealing at different regions of the VP7 gene produce different-sized amplicons, which allows the genotype identification after electrophoresis of the PCR products. The molecular size marker (100-bp ladder) is shown in the first lane. (Primers were designed using reference strains and adapted from references 11 and 13.)

Antigen-Based

Although noroviruses are antigenically diverse, many strains within GI or GII share cross-reactive epitopes that have proven useful in the development of antigen-based diagnostic assays (33). Over the last decade, a number of commercial diagnostic immunoassays have become available that are generally based on an antigen capture step with cross-reactive antibodies (29). These assays can prove useful when rapid diagnosis is especially beneficial, such as during an outbreak investigation when the implementation of infection control measures is needed to limit virus spread.

SAPOVIRUSES

Overview

The association of sapoviruses with pediatric diarrhea was recognized long before their better-known calicivirus relatives the noroviruses. The sapoviruses (30 to 38 nm in diameter) were described initially as "classical caliciviruses" because of their distinct virion morphology that was similar to that of prototype animal caliciviruses such as feline calicivirus. The molecular characterization of the sapovirus viral genome showed that it was phylogenetically distinct from that of norovirus. Furthermore, the first ORF of sapovirus encodes a long, nonstructural, polyprotein-capsid protein fusion that is proteolytically processed to release the individual proteins, including the major capsid protein VP1. The second ORF encodes the putative minor capsid protein VP2 (34). Like noroviruses, the classification of sapoviruses is based on genetic differences within the RdRp and the major capsid protein VP1 genes (reviewed in reference 34). There are presently five major capsid-based genogroups (GI to GV), with human sapoviruses belonging to GI, GII, GIV, and GV. The GI and GII groups are further divided into genotypes, with GI.2 reported as predominant for a number of years (35). The dominance of a particular sapovirus genogroup varies according to region and year, and increased global tracking will be needed to fully establish the molecular epidemiology. Both intergenogroup and intragenogroup recombinant sapovirus strains have been described (36, 37), with the junction between the RdRp and VP1 genes as a major breakpoint for recombination.

Detection and Characterization

Nucleic Acid-Based

The detection of viral RNA in stool is the most widely used diagnostic method for sapoviruses. A number of primer pairs have been described for sapovirus RT-PCR assays that recognize the RdRp, the capsid, or the overlapping genomic region between the two genes, and these are reviewed by Oka et al. (34). Genotype identification requires sequence analysis of the full-length VP1 gene and comparison with sapovirus reference strains (34). A number of RT-qPCR assays have been developed to detect sapovirus RNA in stool, with some of these offered by commercial companies as part of a multipathogen array (38, 39).

Antigen-Based

Immunoassays have been developed for the detection of human sapoviruses in stool samples based on antibodies raised against VLPs (40, 41), but these are not yet commercially available.

ASTROVIRUSES

Overview

Soon after the discovery of rotaviruses and noroviruses, two groups independently reported the presence of small viruses (~28 nm in diameter) in fecal samples from children with acute gastroenteritis (42, 43). These viruses received the name "astrovirus" for their star-like (*astron* = "star" in Greek) appearance under the electron microscope, and early detection methods relied on this unique morphology for detection. Although initially described in humans, a

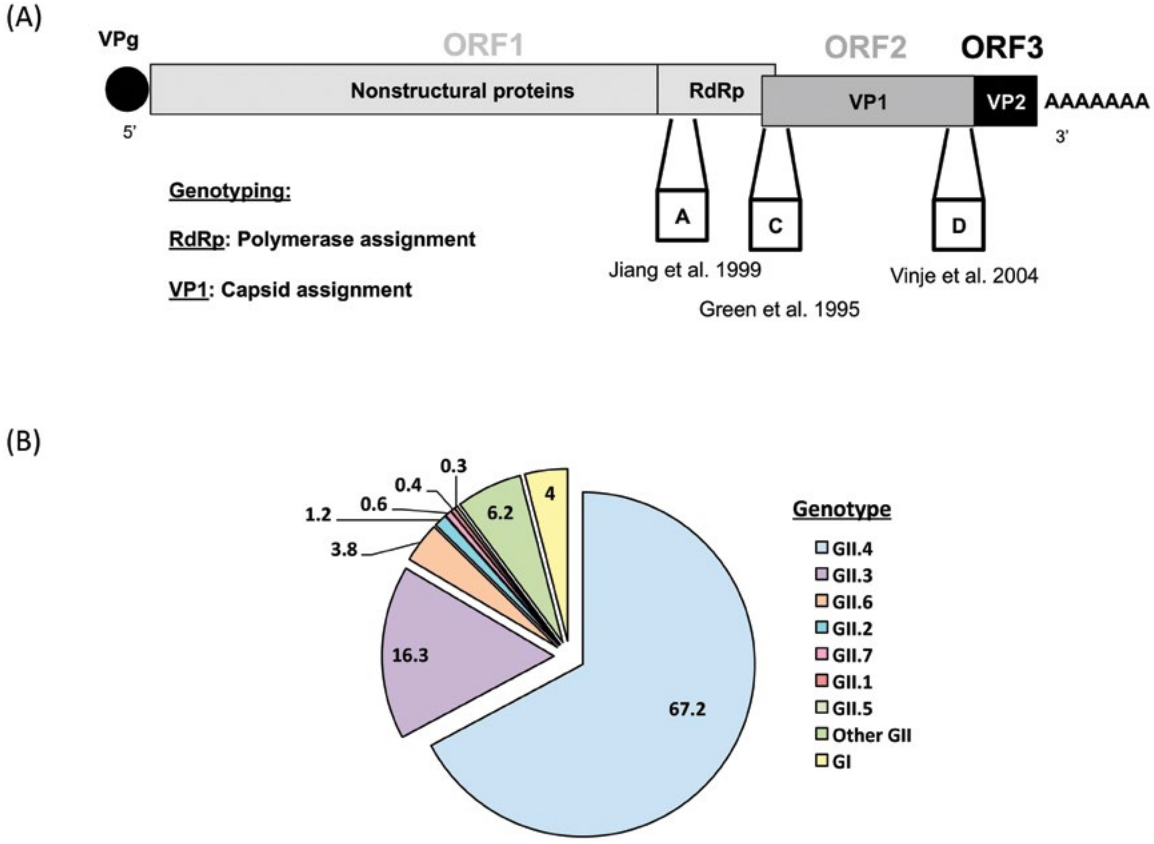

FIGURE 3 Norovirus genome and capsid genotype distribution. (A) Schematic representation of the norovirus positive-sense, single-stranded RNA genome (~7.5 to 7.6 kb) showing three of the major target regions for norovirus identification and characterization (regions A, C, and D) (30–32). The ORFs; the virus protein, genome-linked (VPg); and the poly(A) tail are indicated. (B) Prevalence of norovirus capsid genotypes in humans. Numbers represent the percentage of total number of strains tested (n = 2,968). (Adapted from reference 25.)

wide variety of astroviruses have been reported in different mammals (including pigs, cattle, sheep, minks, dogs, cats, bats, mice, and sea mammals) and birds (including chickens, ducks, pigeons, and turkeys) (44, 45). Astroviruses are an important cause of gastroenteritis in children and animals, but they have been also associated with neurological disease in immunocompromised patients or mammals, and fatal hepatitis in ducklings (44, 46–50).

Astroviruses are nonenveloped viruses with a single-stranded, positive-sense RNA genome that varies in length from 6.2 to 7.8 kb. The genome contains three overlapping ORFs and a 5′- and 3′-end NTR. ORF1a encodes multiple proteins required for replication, including a helicase, protease, and genome-linked viral protein (VPg). ORF1b encodes the RdRp, and ORF2 the proteins that form the viral capsid (44, 45). The proteolytic cleavage of the primary translation product (VP90) is required for maturation of the virion, which comprises VP34 (the highly conserved N-terminal region of ORF2) and VP27/29 and VP25/26 (both the variable C-terminal region of ORF2) (45).

Astroviruses can be cultured in LLC-MK2 (monkey kidney) cells and Caco-2 (human colorectal adenocarcinoma) cells (45). Based on their reactivity with type-specific rabbit antisera and neutralization assays, human astroviruses (HAstVs) have been classified into eight serotypes (HAstV-1 through HAstV-8) (45). The genetic characterization of the capsid gene (ORF2) of these viruses confirmed the presence of eight genotypes that correlated with the serotype designation (45). Epidemiological studies have shown that HAstV-1 is the most prevalent type in children with diarrhea, but outbreaks with different genotypes have been reported in various settings (45). Recently, two HAstV strains that were phylogenetically distinct from all other genotypes were detected by next-generation sequencing methods in stools from children with diarrhea in Australia (HAstV-MLB) and Virginia (HAstV-VA) (51, 52).

Detection and Characterization

Nucleic Acid-Based

Conventional RT-PCR is the method chosen by most research groups for screening and characterization of astroviruses. There are multiple primer pairs designed to detect HAstVs in stool samples (reviewed in reference 53). Most diagnostic primers target the conserved genomic regions encoding nonstructural proteins (ORF1a or ORF1b), while genotyping primers target the ORF2 region. The capsid genotyping primers flank a region of genomic variability near the 3′ end of ORF2 that is most commonly analyzed for typing (45, 53–55). Matsui et al. (55) developed a hemi-nested RT-PCR that in a first step amplifies the entire ORF2 with primers that anneal to the conserved 5′ and 3′ ends.

The resulting amplicon is then used as a template in a second PCR step with eight genotype-specific primers that allow typing based on size of the amplicon (a strategy similar to the one developed for rotavirus genotyping). This PCR strategy has been shown to be orders of magnitude ($\geq 10^5$) more sensitive than enzyme immunoassay (54). Sequence analysis of ORF2 amplicons provides definitive identification and can be used to monitor viral evolution.

There are several different RT-qPCR assays developed for astroviruses, with many of them part of multipathogen screening systems. The advantage of the RT-qPCR is that in some cases results can be obtained in <2 h. Several companies offer standardized RT-qPCR assays for astrovirus or multivirus screening in stool samples (38, 39).

Antigen-Based

Antigen-based detection kits for astroviruses offer the advantage of providing results within 1 or 2 h. Most of the tests use a combination of hyperimmune antisera as capture antibody and a panel of monoclonal antibodies that specifically detect the capsid protein of each of eight HAstV serotypes. The enzyme immunoassay tests for astroviruses have demonstrated high sensitivity and specificity (>90%) for the most common astroviruses circulating in humans (56, 57), although they do not detect the newly discovered HAstV-MLB and HAstV-VA viruses.

ADENOVIRUSES

Overview

Adenoviruses were first detected in individuals with respiratory disease, and their name derives from their initial isolation from human adenoids (nasopharyngeal tonsil) (58, 59). Adenoviruses can cause a variety of symptoms including respiratory distress, conjunctivitis, gastroenteritis, renal failure, and, to a lesser extent, neurological diseases.

Adenoviruses are medium-sized (90 to 100 nm in diameter), nonenveloped viruses with an icosahedral capsid that contains a long (34- to >37-kbp), double-stranded DNA genome. The genome is covalently linked at both ends to a 55-kDa protein that is required for the initiation of viral replication. Upon interaction with the cellular receptor, human adenovirus enters the cell by endocytosis and the genome is translocated to the nucleus to start replication. The "early" genes are mostly involved in viral DNA replication, while the "late" genes mediate viral assembly (59, 60).

Adenoviruses possess a complex capsid that is composed of multiple proteins, with three of them (hexon, penton, and fiber) containing the major antigen determinants (Fig. 4A). The most abundant protein in the virion is the hexon (240 trimers), and therefore most of the neutralizing antibodies are directed against the loops (outermost region) of this protein (Fig. 4A). Neutralizing epitopes are also present

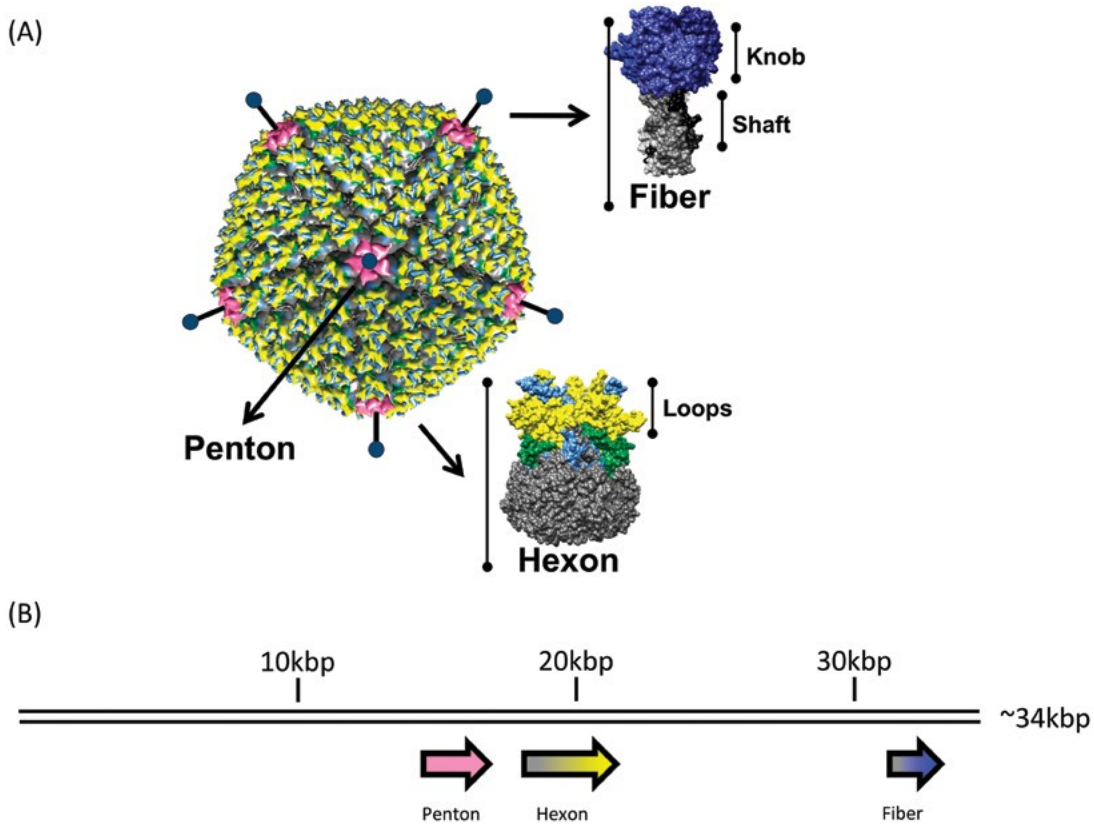

FIGURE 4 Adenovirus proteins and genome. (A) Capsid of adenovirus showing the three major external proteins: penton (pink), hexon (light gray), and fiber (shaft domain: gray; knob domain: navy blue). The three external loops of the hexon are indicated by yellow, green, and light blue. The model was visualized using Chimera and the structural coordinates from adenovirus type 5 (PDB: 3IYN) and adenovirus type 2 (PDB: 1QIU). (B) Schematic representation of the adenovirus double-stranded DNA genome (34 to 37 kbp) showing the position of the penton, hexon, and fiber genes used for molecular characterization.

in the penton and fiber proteins (61). The fiber protein is divided into two structural domains, the shaft and the knob, with the latter involved in interactions with the cellular receptor. The classification of adenoviruses is based on the biological and antigenic characteristics of these three proteins (59).

Based on genomic analyses, serological differences, and pathology, human adenoviruses can be divided into seven species (A to G) and >50 serotypes/genotypes (59, 60). Although different species of adenoviruses can be found in stool samples, species F (types 40 and 41) and G (type 52) have been directly associated with gastroenteritis in humans (59). In general, the incidence of enteric adenovirus in sporadic cases of diarrhea in children and adults is low (~5%), but adenovirus requires special attention in immunocompromised individuals, who can develop severe complications during infection (60).

Detection and Characterization

Nucleic Acid-Based

Because serotyping was expensive and time-consuming and required type-specific sera, the analyses of the DNA fragment patterns obtained by restriction enzymatic fragmentation of the whole genome became widely used in the 1990s. This technique was replaced by the amplification and sequencing of the genes encoding the hexon, penton, or fiber (Fig. 4B), which allowed the faster detection and characterization of clinical isolates (60). A qPCR that uses primers that anneal in a conserved region of the hexon gene proved to detect >50 different adenovirus prototype strains in different samples (62). Detection of adenovirus is also included in multiplex assays for screening stool samples (38, 39).

Cell Culture- and Antigen-Based

Isolation and propagation of clinical adenoviruses can be achieved in different continuous cell lines, including but not limited to HEp-2, HeLa, KB, and HEK 293. Upon infection, cells round, swell, and form grape-like clusters, which is the characteristic cytopathic effect. Adenoviruses were initially characterized and classified into serotypes by cross-neutralization or hemagglutination inhibition assays. Serum neutralization and hemagglutination inhibition serotyping assays correlate well for adenovirus strains that share hexon, penton, and fiber specificity. However, because hemagglutination specificity is conferred by the fiber protein, such correlation may not be seen in recombinant strains that bear a unique fiber protein (59, 60).

The hexon protein is the most abundant in the virion and is the major target for immunoassays developed to detect adenoviruses in stool. Although the tests are faster and require less equipment and training, they present lower sensitivity as compared to the nucleic acid-based tests (57).

SUMMARY

Multiplex nucleic acid-based tests are rapidly gaining widespread use in diagnostic laboratories. These multipathogen formats provide positive identification of the pathogen and may eventually provide in-depth information on the identity of the virus genotype. Next-generation sequencing and genome assembly is another emerging technology that is becoming more cost-effective and that will allow the ability to track viral evolution at the nucleotide level. Point-of-care diagnostics that are rapid and inexpensive and based on the detection of viral antigens in stool will undoubtedly continue as a popular and practical choice as these assays improve in specificity and sensitivity. The comparison of acute (or preinfection) and convalescent immune responses following infection will remain instructive in establishing the etiology of viral gastroenteritis when paired samples are available. This chapter reviewed key aspects of several viral diarrheal pathogens that are important in the development of diagnostic assays and in virus characterization. Basic information on virus structure and diversity, coupled with the clinical features and epidemiology of a pathogen, will also continue to be important parameters in the establishment of the etiology of viral gastroenteritis.

This writing of this review was funded by the Division of Intramural Research, National Institute of Allergy and Infectious Diseases, National Institutes of Health, Department of Health and Human Services.

REFERENCES

1. **Estes M, Greenberg HB.** 2013. Rotaviruses, p 1347–1401. *In* Knipe DM, Howley PM, Cohen JI, Griffin DE, Lamb RA, Martin MA, Racaniello VR, Roizman B (ed), *Fields Virology*, 6th ed, vol 2. Lippincott Williams & Wilkins, Philadelphia, PA.
2. **Mihalov-Kovács E, Gellért Á, Marton S, Farkas SL, Fehér E, Oldal M, Jakab F, Martella V, Bányai K.** 2015. Candidate new rotavirus species in sheltered dogs, Hungary. *Emerg Infect Dis* **21:**660–663. PubMed
3. **Matthijnssens J, Ciarlet M, McDonald SM, Attoui H, Bányai K, Brister JR, Buesa J, Esona MD, Estes MK, Gentsch JR, Iturriza-Gómara M, Johne R, Kirkwood CD, Martella V, Mertens PP, Nakagomi O, Parreño V, Rahman M, Ruggeri FM, Saif LJ, Santos N, Steyer A, Taniguchi K, Patton JT, Desselberger U, Van Ranst M.** 2011. Uniformity of rotavirus strain nomenclature proposed by the Rotavirus Classification Working Group (RCWG). *Arch Virol* **156:**1397–1413. PubMed
4. **Trojnar E, Sachsenröder J, Twardziok S, Reetz J, Otto PH, Johne R.** 2013. Identification of an avian group A rotavirus containing a novel VP4 gene with a close relationship to those of mammalian rotaviruses. *J Gen Virol* **94:**136–142. PubMed
5. **Santos N, Hoshino Y.** 2005. Global distribution of rotavirus serotypes/genotypes and its implication for the development and implementation of an effective rotavirus vaccine. *Rev Med Virol* **15:**29–56. PubMed
6. **Matthijnssens J, Ciarlet M, Heiman E, Arijs I, Delbeke T, McDonald SM, Palombo EA, Iturriza-Gómara M, Maes P, Patton JT, Rahman M, Van Ranst M.** 2008. Full genome-based classification of rotaviruses reveals a common origin between human Wa-like and porcine rotavirus strains and human DS-1-like and bovine rotavirus strains. *J Virol* **82:**3204–3219. PubMed
7. **Lopman BA, Payne DC, Tate JE, Patel MM, Cortese MM, Parashar UD.** 2012. Post-licensure experience with rotavirus vaccination in high and middle income countries; 2006 to 2011. *Curr Opin Virol* **2:**434–442. PubMed
8. **Lopman BA, Curns AT, Yen C, Parashar UD.** 2011. Infant rotavirus vaccination may provide indirect protection to older children and adults in the United States. *J Infect Dis* **204:**980–986. PubMed
9. **Glass RI, Parashar U, Patel M, Gentsch J, Jiang B.** 2014. Rotavirus vaccines: successes and challenges. *J Infect* **68**(Suppl 1)**:**S9–S18. PubMed
10. **Gouvea V, Glass RI, Woods P, Taniguchi K, Clark HF, Forrester B, Fang ZY.** 1990. Polymerase chain reaction amplification and typing of rotavirus nucleic acid from stool specimens. *J Clin Microbiol* **28:**276–282. PubMed
11. **Das BK, Gentsch JR, Cicirello HG, Woods PA, Gupta A, Ramachandran M, Kumar R, Bhan MK, Glass RI.** 1994.

Characterization of rotavirus strains from newborns in New Delhi, India. *J Clin Microbiol* **32:**1820–1822. PubMed
12. **Gentsch JR, Glass RI, Woods P, Gouvea V, Gorziglia M, Flores J, Das BK, Bhan MK.** 1992. Identification of group A rotavirus gene 4 types by polymerase chain reaction. *J Clin Microbiol* **30:**1365–1373. PubMed
13. **Gouvea V, Santos N, Timenetsky MC.** 1994. Identification of bovine and porcine rotavirus G types by PCR. *J Clin Microbiol* **32:**1338–1340. PubMed
14. **Iturriza-Gómara M, Kang G, Gray J.** 2004. Rotavirus genotyping: keeping up with an evolving population of human rotaviruses. *J Clin Virol* **31:**259–265. PubMed
15. **Parra GI, Espinola EE.** 2006. Nucleotide mismatches between the *VP7* gene and the primer are associated with genotyping failure of a specific lineage from G1 rotavirus strains. *Virol J* **3:**35. PubMed
16. **Fujii Y, Shimoike T, Takagi H, Murakami K, Todaka-Takai R, Park Y, Katayama K.** 2012. Amplification of all 11 RNA segments of group A rotaviruses based on reverse transcription polymerase chain reaction. *Microbiol Immunol* **56:**630–638. PubMed
17. **Bennett A, Bar-Zeev N, Jere KC, Tate JE, Parashar UD, Nakagomi O, Heyderman RS, French N, Iturriza-Gomara M, Cunliffe NA.** 2015. Determination of a viral load threshold to distinguish symptomatic versus asymptomatic rotavirus infection in a high-disease-burden African population. *J Clin Microbiol* **53:**1951–1954. PubMed
18. **Freeman MM, Kerin T, Hull J, McCaustland K, Gentsch J.** 2008. Enhancement of detection and quantification of rotavirus in stool using a modified real-time RT-PCR assay. *J Med Virol* **80:**1489–1496. PubMed
19. **Eing BR, May G, Baumeister HG, Kühn JE.** 2001. Evaluation of two enzyme immunoassays for detection of human rotaviruses in fecal specimens. *J Clin Microbiol* **39:**4532–4534. PubMed
20. **Payne DC, Vinjé J, Szilagyi PG, Edwards KM, Staat MA, Weinberg GA, Hall CB, Chappell J, Bernstein DI, Curns AT, Wikswo M, Shirley SH, Hall AJ, Lopman B, Parashar UD.** 2013. Norovirus and medically attended gastroenteritis in U.S. children. *N Engl J Med* **368:**1121–1130. PubMed
21. **Becker-Dreps S, Bucardo F, Vilchez S, Zambrana LE, Liu L, Weber DJ, Peña R, Barclay L, Vinjé J, Hudgens MG, Nordgren J, Svensson L, Morgan DR, Espinoza F, Paniagua M.** 2014. Etiology of childhood diarrhea after rotavirus vaccine introduction: a prospective, population-based study in Nicaragua. *Pediatr Infect Dis J* **33:**1156–1163. PubMed
22. **Patel MM, Widdowson MA, Glass RI, Akazawa K, Vinjé J, Parashar UD.** 2008. Systematic literature review of role of noroviruses in sporadic gastroenteritis. *Emerg Infect Dis* **14:**1224–1231. PubMed
23. **Green KY.** 2013. *Caliciviridae*: the noroviruses, p 582–608. *In* Knipe HP, Howley PM, Cohen JI, Griffin DE, Lamb RA, Martin MA, Racaniello VR, Roizman B (ed), *Fields Virology*, 6th ed. Lippincott Williams & Wilkins, Philadelphia, PA.
24. **Kroneman A, Vega E, Vennema H, Vinjé J, White PA, Hansman G, Green K, Martella V, Katayama K, Koopmans M.** 2013. Proposal for a unified norovirus nomenclature and genotyping. *Arch Virol* **158:**2059–2068. PubMed
25. **Hoa Tran TN, Trainor E, Nakagomi T, Cunliffe NA, Nakagomi O.** 2013. Molecular epidemiology of noroviruses associated with acute sporadic gastroenteritis in children: global distribution of genogroups, genotypes and GII.4 variants. *J Clin Virol* **56:**185–193. PubMed
26. **Bull RA, Tanaka MM, White PA.** 2007. Norovirus recombination. *J Gen Virol* **88:**3347–3359. PubMed
27. **Atmar RL, Bernstein DI, Harro CD, Al-Ibrahim MS, Chen WH, Ferreira J, Estes MK, Graham DY, Opekun AR, Richardson C, Mendelman PM.** 2011. Norovirus vaccine against experimental human Norwalk virus illness. *N Engl J Med* **365:**2178–2187. PubMed
28. **Richardson C, Bargatze RF, Goodwin R, Mendelman PM.** 2013. Norovirus virus-like particle vaccines for the prevention of acute gastroenteritis. *Expert Rev Vaccines* **12:**155–167. PubMed
29. **Vinjé J.** 2015. Advances in laboratory methods for detection and typing of norovirus. *J Clin Microbiol* **53:**373–381. PubMed
30. **Green SM, Lambden PR, Deng Y, Lowes JA, Lineham S, Bushell J, Rogers J, Caul EO, Ashley CR, Clarke IN.** 1995. Polymerase chain reaction detection of small round-structured viruses from two related hospital outbreaks of gastroenteritis using inosine-containing primers. *J Med Virol* **45:**197–202. PubMed
31. **Jiang X, Huang PW, Zhong WM, Farkas T, Cubitt DW, Matson DO.** 1999. Design and evaluation of a primer pair that detects both Norwalk- and Sapporo-like caliciviruses by RT-PCR. *J Virol Methods* **83:**145–154. PubMed
32. **Vinjé J, Hamidjaja RA, Sobsey MD.** 2004. Development and application of a capsid VP1 (region D) based reverse transcription PCR assay for genotyping of genogroup I and II noroviruses. *J Virol Methods* **116:**109–117. PubMed
33. **Parra GI, Azure J, Fischer R, Bok K, Sandoval-Jaime C, Sosnovtsev SV, Sander P, Green KY.** 2013. Identification of a broadly cross-reactive epitope in the inner shell of the norovirus capsid. *PLoS One* **8:**e67592. doi:10.1371/journal.pone.0067592. PubMed
34. **Oka T, Wang Q, Katayama K, Saif LJ.** 2015. Comprehensive review of human sapoviruses. *Clin Microbiol Rev* **28:**32–53. PubMed
35. **Svraka S, Vennema H, van der Veer B, Hedlund KO, Thorhagen M, Siebenga J, Duizer E, Koopmans M.** 2010. Epidemiology and genotype analysis of emerging sapovirus-associated infections across Europe. *J Clin Microbiol* **48:**2191–2198. PubMed
36. **Hansman GS, Ishida S, Yoshizumi S, Miyoshi M, Ikeda T, Oka T, Takeda N.** 2007. Recombinant sapovirus gastroenteritis, Japan. *Emerg Infect Dis* **13:**786–788. PubMed
37. **Mikula C, Springer B, Reichart S, Bierbacher K, Lichtenschopf A, Hoehne M.** 2010. Sapovirus in adults in rehabilitation center, upper Austria. *Emerg Infect Dis* **16:**1186–1187. PubMed
38. **Khare R, Espy MJ, Cebelinski E, Boxrud D, Sloan LM, Cunningham SA, Pritt BS, Patel R, Binnicker MJ.** 2014. Comparative evaluation of two commercial multiplex panels for detection of gastrointestinal pathogens by use of clinical stool specimens. *J Clin Microbiol* **52:**3667–3673. PubMed
39. **van Maarseveen NM, Wessels E, de Brouwer CS, Vossen AC, Claas EC.** 2010. Diagnosis of viral gastroenteritis by simultaneous detection of Adenovirus group F, Astrovirus, Rotavirus group A, Norovirus genogroups I and II, and Sapovirus in two internally controlled multiplex real-time PCR assays. *J Clin Virol* **49:**205–210. PubMed
40. **Nakata S, Honma S, Numata K, Kogawa K, Ukae S, Adachi N, Jiang X, Estes MK, Gatheru Z, Tukei PM, Chiba S.** 1998. Prevalence of human calicivirus infections in Kenya as determined by enzyme immunoassays for three genogroups of the virus. *J Clin Microbiol* **36:**3160–3163. PubMed
41. **Hansman GS, Guntapong R, Pongsuwanna Y, Natori K, Katayama K, Takeda N.** 2006. Development of an antigen ELISA to detect sapovirus in clinical stool specimens. *Arch Virol* **151:**551–561. PubMed
42. **Appleton H, Higgins PG.** 1975. Letter: viruses and gastroenteritis in infants. *Lancet* **1:**1297. PubMed
43. **Madeley CR, Cosgrove BP.** 1975. Letter: 28 nm particles in faeces in infantile gastroenteritis. *Lancet* **2:**451–452. PubMed

44. **De Benedictis P, Schultz-Cherry S, Burnham A, Cattoli G.** 2011. Astrovirus infections in humans and animals—molecular biology, genetic diversity, and interspecies transmissions. *Infect Genet Evol* **11:**1529–1544. PubMed
45. **Bosch A, Pintó RM, Guix S.** 2014. Human astroviruses. *Clin Microbiol Rev* **27:**1048–1074. PubMed
46. **Gough RE, Collins MS, Borland E, Keymer LF.** 1984. Astrovirus-like particles associated with hepatitis in ducklings. *Vet Rec* **114:**279. PubMed
47. **Li L, Diab S, McGraw S, Barr B, Traslavina R, Higgins R, Talbot T, Blanchard P, Rimoldi G, Fahsbender E, Page B, Phan TG, Wang C, Deng X, Pesavento P, Delwart E.** 2013. Divergent astrovirus associated with neurologic disease in cattle. *Emerg Infect Dis* **19:**1385–1392. PubMed
48. **Herrmann JE, Taylor DN, Echeverria P, Blacklow NR.** 1991. Astroviruses as a cause of gastroenteritis in children. *N Engl J Med* **324:**1757–1760. PubMed
49. **Quan PL, Wagner TA, Briese T, Torgerson TR, Hornig M, Tashmukhamedova A, Firth C, Palacios G, Baisre-De-Leon A, Paddock CD, Hutchison SK, Egholm M, Zaki SR, Goldman JE, Ochs HD, Lipkin WI.** 2010. Astrovirus encephalitis in boy with X-linked agammaglobulinemia. *Emerg Infect Dis* **16:**918–925. PubMed
50. **Naccache SN, Peggs KS, Mattes FM, Phadke R, Garson JA, Grant P, Samayoa E, Federman S, Miller S, Lunn MP, Gant V, Chiu CY.** 2015. Diagnosis of neuroinvasive astrovirus infection in an immunocompromised adult with encephalitis by unbiased next-generation sequencing. *Clin Infect Dis* **60:**919–923. PubMed
51. **Finkbeiner SR, Li Y, Ruone S, Conrardy C, Gregoricus N, Toney D, Virgin HW, Anderson LJ, Vinjé J, Wang D, Tong S.** 2009. Identification of a novel astrovirus (astrovirus VA1) associated with an outbreak of acute gastroenteritis. *J Virol* **83:**10836–10839. PubMed
52. **Finkbeiner SR, Allred AF, Tarr PI, Klein EJ, Kirkwood CD, Wang D.** 2008. Metagenomic analysis of human diarrhea: viral detection and discovery. *PLoS Pathog* **4:**e1000011. doi:10.1371/journal.ppat.1000011. PubMed
53. **Guix S, Bosch A, Pintó RM.** 2005. Human astrovirus diagnosis and typing: current and future prospects. *Lett Appl Microbiol* **41:**103–105. PubMed
54. **Saito K, Ushijima H, Nishio O, Oseto M, Motohiro H, Ueda Y, Takagi M, Nakaya S, Ando T, Glass R, et al.** 1995. Detection of astroviruses from stool samples in Japan using reverse transcription and polymerase chain reaction amplification. *Microbiol Immunol* **39:**825–828. PubMed
55. **Matsui M, Ushijima H, Hachiya M, Kakizawa J, Wen L, Oseto M, Morooka K, Kurtz JB.** 1998. Determination of serotypes of astroviruses by reverse transcription-polymerase chain reaction and homologies of the types by the sequencing of Japanese isolates. *Microbiol Immunol* **42:**539–547. PubMed
56. **Noel JS, Lee TW, Kurtz JB, Glass RI, Monroe SS.** 1995. Typing of human astroviruses from clinical isolates by enzyme immunoassay and nucleotide sequencing. *J Clin Microbiol* **33:**797–801. PubMed
57. **Rovida F, Campanini G, Sarasini A, Adzasehoun KM, Piralla A, Baldanti F.** 2013. Comparison of immunologic and molecular assays for the diagnosis of gastrointestinal viral infections. *Diagn Microbiol Infect Dis* **75:**110–111. PubMed
58. **Rowe WP, Huebner RJ, Gilmore LK, Parrott RH, Ward TG.** 1953. Isolation of a cytopathogenic agent from human adenoids undergoing spontaneous degeneration in tissue culture. *Proc Soc Exp Biol Med* **84:**570–573. PubMed
59. **Wold WS, Ison MG.** 2013. Adenoviruses, p 1733–1767. *In* Knipe DM, Howley PM, Cohen JI, Griffin DE, Lamb RA, Martin MA, VR, Roizman B (ed), *Fields Virology*, 6th ed, vol 2. Lippincott Williams & Wilkins, Philadelphia, PA.
60. **Lion T.** 2014. Adenovirus infections in immunocompetent and immunocompromised patients. *Clin Microbiol Rev* **27:**441–462. PubMed
61. **Sumida SM, Truitt DM, Lemckert AA, Vogels R, Custers JH, Addo MM, Lockman S, Peter T, Peyerl FW, Kishko MG, Jackson SS, Gorgone DA, Lifton MA, Essex M, Walker BD, Goudsmit J, Havenga MJ, Barouch DH.** 2005. Neutralizing antibodies to adenovirus serotype 5 vaccine vectors are directed primarily against the adenovirus hexon protein. *J Immunol* **174:**7179–7185. PubMed
62. **Heim A, Ebnet C, Harste G, Pring-Akerblom P.** 2003. Rapid and quantitative detection of human adenovirus DNA by real-time PCR. *J Med Virol* **70:**228–239. PubMed

Arboviruses

ROBERT S. LANCIOTTI AND JOHN T. ROEHRIG

67

The arthropod-borne viruses (arboviruses) represent a diverse amalgam of more than 500 animal viruses that are grouped together because of their ability to replicate in both vertebrates and arthropods. While more than 150 arboviruses are known to cause human illness or infection, the list of the most medically important viruses is considerably shorter (Table 1) (1–3). Because of the vast number of agents that potentially should be considered in a differential diagnosis, the use of epidemiologic, ecologic, and clinical data to guide the choice and interpretation of clinical laboratory diagnostic tests is essential. Most arboviruses are transmitted seasonally in specific geographic locations or ecological habitats. The patient's history of travel, activities, and potential exposures to arthropods or habitats associated with arbovirus transmission provides vital data for selection of appropriate antigens and relevant diagnostic approaches. Knowledge of the patient's immunizations against yellow fever (YF), Japanese encephalitis (JE), or tick-borne encephalitis (TBE) viruses is also important for the proper interpretation of serological results. Although the laboratory diagnosis of arboviral infections still relies chiefly on serology, other approaches that directly detect viral antigen or genomic material and not antibodies are now routine.

METHODS

Antibody Detection

IgM ELISA

Assays that detect virus-elicited immunoglobulin M (IgM) are useful because they detect antibodies produced within days of a primary viral infection. IgM antibody capture enzyme-linked immunosorbent assay (MAC-ELISA) is the preferred approach to IgM detection because it is simple, sensitive, and applicable to serum and cerebrospinal fluid (CSF) samples. False-positive reactions due to rheumatoid factor also are minimized (4, 5). While most ELISAs are based on a 96-well microplate format, assays have been developed and adapted to microsphere-based systems (6, 7). These new systems require very small volumes of test specimens and permit antigen multiplexing, resulting in a considerable savings of time and money (8, 9).

IgM from serum or CSF is first captured onto the solid phase with μ-chain-specific antispecies antibody. IgM antibodies of all reactivities are thus concentrated, but during an acute infection, IgM antibodies directed at the etiologic agent are the principal circulating species. Virus antigen is next added, and if virus-specific IgM is present, viral antigen is bound to the plate. A variety of antigen sources such as virus-infected mouse brain, lysed cells, cell culture supernatant, or recombinant antigen can be employed. The bound antigen can be detected by a variety of means; however, the most practical approach is to use an enzyme-labeled antiviral monoclonal antibody (MAb). Since the reactivity of the patient's IgM with the test antigen in part defines the specificity of the assay, broadly reactive labeled antibodies can be used as detectors for most of the medically important arboviruses, e.g., monoclonal antibodies reactive against flavivirus group (6B6C-1), alphavirus group (2A2C-3), and California serogroup (10G5.4) (Table 2) (10).

Approximately 75% of patients with flavivirus encephalitis (e.g., JE or St. Louis encephalitis [SLE]) have detectable IgM in serum or CSF in the first 4 days of illness, and nearly 100% of samples are reactive by 7 days. Similar levels of sensitivity have been reported for patients with LaCrosse (LAC) encephalitis or alphavirus encephalitis and in patients with dengue (DEN) or YF. For patients with central nervous system (CNS) infections, greater sensitivity and specificity are obtained by also testing CSF.

The specificity of the MAC-ELISA is similar to that of the complement fixation (CF) test, and heterologous antibodies to related viruses may interfere with interpretation, particularly in patients with previous related infections. To improve diagnostic specificity, ratios of absorbances to related viruses can be calculated, yielding indices that are better discriminators than the individual absorbances alone. For example, antibodies to DEN and JE viruses cross-react in hemagglutination inhibition (HI) tests and ELISAs, but patients with the respective infections can be identified by calculating ratios of ELISA absorbances to the two viruses. Similarly, ratios of absorbances in IgM and IgG capture tests have a high predictive value in discriminating recent from previous infections with these viruses (11).

Although levels of IgM antibodies generally decline after 2 to 4 weeks and are absent after 90 to 120 days, IgM persists for a year or more after infection in some patients. This phenomenon has been reported for patients with JE, SLE, West Nile (WN) encephalitis, Murray Valley encephalitis (MVE), LAC encephalitis, and Sindbis and Ross River (RR) virus polyarthropathy, and it is common in patients

doi:10.1128/9781555818722.ch67

TABLE 1 Characteristics of selected medically important arbovirus disease

Disease	Viral agent	Arthropod vector or source	Clinical syndrome(s)	Geographic distribution	Risk factor(s)	Case-fatality ratio (%)
EEE	Alphavirus	Mosquito	CNS infection	Eastern United States, Central and South America	Advanced age	30
JE	Flavivirus	Mosquito	CNS infection	Asian rice-growing areas	Exposure to rural areas	15–30
LAC encephalitis	Bunyavirus	Mosquito	CNS infection	East-central United States (children)	Males > females; agricultural occupations	<1
Rocio encephalitis	Flavivirus	Mosquito	CNS infection	Sao Paulo state, Brazil	Males > females; agricultural occupations	5
SLE	Flavivirus	Mosquito	CNS infection	North, Central, and South America	Advanced age	7
TBE	Flavivirus	Tick	CNS infection	Europe, Asia	Forest exposure	1–10
Powassan encephalitis	Flavivirus	Tick, mosquito	CNS infection	Canada, United States, Russia, China	Forest exposure	10
WEE	Alphavirus	Mosquito	CNS infection	Western United States, South America, Canada, Mexico	Males > females; extremes of age	5
CTF	Coltivirus	Tick	Febrile grippe	Rocky Mountain states, South Dakota, California, western Canada	Exposure to areas >5,000 ft (ca. 1,500 m) in elevation	<1
DEN	Flavivirus	Mosquito	Febrile grippe and rash; hemorrhagic fever	Tropical locations worldwide	Urban, peridomestic exposure	5
WN fever	Flavivirus	Mosquito	Febrile grippe and rash; encephalitis	United States, Africa, Europe, Asia	Advanced age	<1
Oropouche fever	Bunyavirus	Midge	Febrile grippe	Central and South America	Agricultural occupation	<1
Phlebotomus fever	Phlebovirus	Phlebotomine fly	Febrile grippe	Europe, Africa, Asia	Peridomestic exposure	<1
Chikungunya	Alphavirus	Mosquito	Febrile polyarthropathy and rash; rarely hemorrhagic fever	Africa, Asia	Urban, peridomestic exposure	<1
Mayaro fever	Alphavirus	Mosquito	Febrile polyarthropathy and rash	Central, South America	Males > females; forest exposure	<1
RR arthropathy	Alphavirus	Mosquito	Febrile polyarthropathy and rash	Australia, Pacific	Females > males	<1
Sindbis virus fever	Alphavirus	Mosquito	Febrile polyarthropathy and rash	Africa, Europe, Asia	Woodland exposure	<1
Crimean-Congo hemorrhagic fever	Nairovirus	Tick, infected blood	Hemorrhagic fever	Africa, Europe, Asia	Animal husbandry; agricultural and medical occupations	10–50
Rift Valley fever	Phlebovirus	Mosquito, infected blood	Febrile grippe; hemorrhagic fever	Africa, Middle East	Animal husbandry; butchering	<1
YF	Flavivirus	Mosquito	Febrile grippe; hemorrhagic fever	South America, West and Central Africa	Forest or rural exposure	15

TABLE 2 Selected arbovirus monoclonal antibodies for serologic and antigen detection assays[a]

Antibody[b]	Prepared against:	Reactivity	Use
6B6C-1	SLE virus (MSI-7)	Flavivirus group	As HRP[c] conjugate in antigen capture and IgM capture ELISAs
4G2	DEN virus 2 (New Guinea C)	Flavivirus group	Viral identification by IF or ELISA; ELISA capture antibody
6B4A-10	JE virus (Nakayama)	JE-SLE-WN-MVE complex	Capture antibody in antigen capture ELISA
JE314H52	JE virus (Nakayama)	JE virus specific	Viral identification by IF or ELISA
6B5A-2	SLE virus (MSI-7)	SLE virus specific	Viral identification by IF and neutralization
4A4C-4	SLE virus (MSI-7)	SLE virus specific	Capture antibody in antigen capture ELISA
4B6C-2	MVE virus (original)	MVE virus specific	Viral identification by IF or ELISA
D2-1F-3	DEN virus 1 (Hawaii)	DEN virus 1 specific	Viral identification by IF or ELISA
3H5-1-21	DEN virus 2 (New Guinea C)	DEN virus 2 specific	Viral identification by IF or ELISA
D6-8A1-12	DEN virus 3 (H87)	DEN virus 3 specific	Viral identification by IF or ELISA
1H10-6-7	DEN virus 4 (H-241)	DEN virus 4 specific	Viral identification by IF or ELISA
5E-3	YF virus (17D)	YF virus specific	Capture antibody in antigen capture ELISA
117	YF virus (Asibi)	YF wild-type virus specific	Viral identification by IF
864	YF virus (17D)	YF vaccine virus specific	Identification of vaccine strains by IF
4D9	TBE virus	Tick-borne flavivirus complex	Viral identification by IF or ELISA
H5.46	WN virus	WN virus specific	Viral identification by IF or ELISA
2A2C-3	WEE virus (McMillan)	Alphavirus group	As HRP conjugate in antigen and IgM capture ELISAs
2A3D-5	WEE virus (McMillan)	WEE complex	Capture antibody for WEE and HJ antigen capture ELISA
2B1C-6	WEE virus (McMillan)	WEE virus specific	Viral identification by IF or ELISA; as HRP conjugate in antigen capture ELISA
1B5C-3	EEE virus (NJ 60)	EEE North American virus specific	Viral identification by IF or ELISA; as HRP conjugate in antigen capture ELISA
1C1J-4	EEE virus (BeAn 5122)	EEE South American virus specific	Viral identification by IF or ELISA
1B1C-4	EEE virus (BeAn 5122)	EEE complex specific	Viral identification by IF or ELISA
2D4-1	Highlands J virus (B230)	Highlands J virus specific	Viral identification by IF or ELISA; as HRP conjugate in antigen capture ELISA
1A2B-10	VEE virus (E2 peptide)	VEE complex	Viral identification by IF or ELISA
5B4D-6	VEE virus (TC-83)	TC-83 (vaccine) specific	Viral identification by IF or ELISA
1A3A-5	VEE virus (IC)	Epizootic VEE virus	Viral identification by IF or ELISA
1A1B-9	VEE virus (IE)	Enzootic VEE virus	Viral identification by IF or ELISA
807-18	LAC virus (original)	LAC virus specific	Viral identification by HI, neutralization, or ELISA
10G5.4	LAC virus (original)	California serogroup reactive	Viral identification by ELISA

[a]Adapted from reference 35.
[b]Antibodies and/or conjugates are available from the Centers for Disease Control and Prevention.
[c]HRP, horseradish peroxidase.

with YF or after YF vaccination. This observation is of diagnostic importance, because in areas where the diseases are endemic, IgM from infection during a previous transmission season could be mistaken as evidence of recent infection. For this reason, demonstration of IgM in a single serum sample alone does not necessarily indicate a recent infection. Virus-specific IgM in CSF has been detected 50 to 180 days after onset of acute JE, indicating continuing intrathecal production of antibody and the possibility of persistent CNS infection. However, these appear to be unusual cases, and in most circumstances, detection of arbovirus-specific IgM in CSF is a reliable indication of recent infection.

A practical problem in implementing the MAC-ELISA is the unavailability of human positive-control sera containing IgM for all the antigens of interest. Although reactive human sera for many of the common arbovirus infections are available from the Centers for Disease Control and Prevention and other laboratories, human positive-control sera for less prevalent infections are unavailable. To solve this problem, chimeric murine/human IgM and IgG MAbs (cMAbs) have been developed for both alphaviruses and flaviviruses (12–14). These cMAbs are based on the broad flavivirus- and alphavirus-reactive MAbs, 6B6C-1 and 1A4B-6, respectively, Due to the presence of a human Fc region in these cMAbs, they react like human antibodies in ELISA and other binding assays, e.g., indirect immunofluorescence assay.

Reference laboratories can also provide testing panels of serum for quality control of test performance. Unlike the

HI, CF, and neutralization tests described below, in which mouse immune fluids can be used as controls, the MAC-ELISA incorporates a species-specific capture antibody and requires reactive human samples. MAC-ELISAs for agents of arbovirus encephalitis are offered by commercial reference laboratories, and a kit for TBE diagnosis is available in Europe. Commercial MAC-ELISAs for human WN and dengue infections that have U.S. Food and Drug Administration (FDA) approval are also available. Commercial dot blot kits for DEN and JE are available in Asia, but their sensitivity and specificity require further characterization.

The original source of flaviviral antigen (virus-infected mouse brain) used in ELISA protocols has been replaced for some flaviviruses with virus-like particles (VLPs) also known as recombinant soluble particles (15). These antigens are either transiently or stably secreted from animal cells (e.g., primate COS-1 cells) that have been transformed with a plasmid containing the flaviviral prM and envelope (E) glycoproteins. The prM and E proteins self-assemble into particles with a structure similar, but not identical, to virus without the nucleocapsid. The viral antigenic properties are retained in the VLP, so they are satisfactory substitutes for virus in binding assays, since the major antibody responses are against these viral surface proteins. Some VLPs have been modified to remove major flavivirus cross-reactive E protein epitopes, thus improving virus specificity (16).

IgG ELISA

IgG ELISA has replaced the HI test for the diagnosis of most infections because the procedure is less cumbersome and titration curves for the two procedures are similar. Various indirect procedures to measure the levels of IgG antibodies to arboviruses differ chiefly in the procedures for antigen preparation and methods for their attachment to the solid phase. Conventional mouse brain antigens extracted with sucrose and acetone generally do not have adequate potency as antigens unless they are first captured and concentrated onto the solid phase with antibody (mouse monoclonal or polyclonal ascitic fluid) (10). Dot ELISAs, in which antigens are adsorbed to nitrocellulose or other membranes, also have been used successfully. The sensitivities of IgG ELISAs generally are similar to or greater than those of HI tests, and their specificities correspondingly are equal or lower.

IF Test

The procedures for arbovirus diagnosis generally use virus-infected Vero or other cells fixed onto slides in monovalent or polyvalent preparations. Commercially available spot slides with SLE, western equine encephalitis (WEE), eastern equine encephalitis (EEE), and LAC virus-infected cells make it possible to screen a serum sample simultaneously against several arbovirus agents of encephalitis in the United States. A similar polyvalent slide is available to screen patients with suspected viral hemorrhagic fever for antibodies against Crimean-Congo and Rift Valley fever (RVF) viruses, two strains of Ebola virus, and Lassa and Marburg viruses in a single CRE_2LM (derived from the names of the viruses) slide. Virus-specific IgM and IgG antibodies in CSF also can be measured by immunofluorescence (IF), although the titers generally are lower than in serum. With all indirect tests for IgM, the confounding effects of IgM rheumatoid factors should be controlled.

Indirect IF, HI, and neutralization tests have similar sensitivities, but IF is less sensitive than ELISA. The indirect IF test for antibodies to most arboviruses is as specific as or less specific than the HI test. Indirect IF cannot be relied upon to distinguish infections among the flaviviruses, among the alphaviruses, or among viruses in bunyavirus serogroups. However, the broad reactivity of IF can be exploited in screening tests and in epidemiologic studies.

HI and CF Tests

Classical serodiagnosis of arbovirus infections relied on the HI and CF tests. These technically demanding assays rely on the availability of goose or other erythrocytes and have largely been abandoned in favor of the more readily standardizable IgM and IgG ELISAs except in the largest diagnostic reference laboratories (17). The major advantage of both the HI and the CF test is that species-specific positive-control reagents are not necessary. Consequently, more readily available, experimentally derived antiviral antibodies from mice, rabbits, or goats can be used in these tests.

HI antibodies are long-lived, and for this reason HI has often been used as a screening test, especially in serosurveys. After infection, HI antibodies rise within the first week, peak by the third week, and decline to low levels that may persist for years or decades. HI antibodies arising from a primary infection are relatively specific; however, with second and repeated flavivirus infections (superinfection), such as with DEN, YF, or JE virus, the antibody response broadens and heterologous reactions preclude differentiation of the most recent infection from previous infections. Patients with repeated exposures to flaviviruses routinely develop heterologous antibodies to agents to which they have never been exposed. Often, these heterologous reactions have titers that are equal to or higher than those of the presumed homologous reaction. More specific assays, described below, are required to differentiate these cross-reactions.

The CF test provides a level of specificity intermediate between those of HI and neutralization tests (17). CF antibody levels usually are late to rise, and in some patients they are not detectable until 6 weeks after infection. In up to one-third of proven SLE patients, no CF antibodies can be detected. Because of its insensitivity, the CF test should not be used alone as a diagnostic procedure. The test remains useful for viruses that do not hemagglutinate, such as Colorado tick fever (CTF) virus. The kinetics of the rise and fall (half-life of 2 years) of CF antibody levels can be exploited to identify infections that have occurred relatively recently, in the period after which IgM antibodies have disappeared. The test also is relatively specific in differentiating natural from vaccine-induced immunity to YF virus. Immunized patients generally do not produce detectable CF antibodies to YF virus unless they have had previous flavivirus infections.

Neutralization Test

The serum neutralization test is the most virus-specific test for serologic diagnosis and is used to confirm other serologic testing results (17). The serum dilution-plaque reduction neutralization test performed in cell culture is the standard method; however, animal, especially mouse, protection tests follow the same principle. A detailed description of the plaque-reduction neutralization test for DEN viruses has been published (18). Dilutions of heat-inactivated serum are added to equal volumes of a viral preparation known to contain a predetermined viral input dose from previous infectivity titrations. The resulting mixtures of serum, beginning at a 1:10 final dilution, and virus (100 plaques for 35-mm-diameter wells and 25 plaques for 16-mm-diameter wells) are incubated either overnight at 4°C or for 1 h at 37°C for viral neutralization to proceed. The resulting mixtures are used to inoculate confluent cell monolayers and are overlaid with a nutrient semisolid or solid medium (methylcellulose, agarose, gum

tragacanth, or agar can be used); after a suitable interval (e.g., 2 to 7 days, depending on the virus), when plaques have formed, a vital stain is added to differentiate infected nonviable cells, which appear as unstained plaques, from the uninfected stained monolayer. Neutral red in agar or as a liquid solution is conventionally used, but when removable semisolid overlays are used, a permanent record of the test can be made by fixing the monolayer and staining it with amido black or crystal violet.

Numerous variations of the procedure have been described, including (i) the use of DEAE-dextran or other cationic polymers to reduce electrostatic charges on agar that interfere with virus–cell interactions, and (ii) the addition of complement or normal human or animal serum to serum–virus mixtures to increase the sensitivity of neutralization.

The last serum dilution that significantly reduces the input dose of virus is the end point (80 to 90% reduction of the plaque count in the virus control). End points in animal protection assays are calculated by the Reed-Muench or Karber method, and six animals per serum dilution should be the minimum number used.

Neutralizing-antibody levels generally rise within days of the onset of illness, peak in the second week, and decline slowly to moderate or low levels, where they persist for years and often a lifetime. The sensitivity of the test is high, usually equal to that of HI or IF tests, but, most importantly, no other approach is as virus specific.

An alternative approach to measuring the neutralizing power of a serum is the constant serum-varying virus dilution test, resulting in a log neutralization index. This procedure has fallen into disuse because it is somewhat less specific than the serum dilution method and large quantities of serum are needed.

One of the most significant improvements in the plaque reduction neutralization test for pathogenic or poorly growing viruses has been the creation of chimeric viruses using recombinant DNA technology and full-length infectious cDNA clones of viruses (19). This technique has been applied most to flaviviruses. Chimeric flaviviruses that encode the nucleocapsid and nonstructural proteins of one virus (e.g., YF virus) and the prM E protein of a second flavivirus (e.g., WN virus) yield a chimeric, usually attenuated virus that maintains the growth parameters of YF virus and the serological reactivity of WN virus. This approach permits construction of chimeric viruses that have similar growth characteristics, but with differing serological attributes. By preparing chimeric viruses for all four DEN virus serotypes, the improved chimeric virus growth characteristics have resulted in a more robust and reproducible DEN virus plaque reduction neutralization test.

Antigen Detection

Certain arboviruses produce a viremia of sufficient magnitude and duration that the viruses can be isolated from blood during the acute phase of illness, e.g., 0 to 5 days after onset. Epidemiologically, this is significant because during the period of viremia, the viruses may be transmitted from person to person by biting vectors. Examples of these viruses include the agents of YF, DEN, chikungunya, sandfly, RR, and Oropouche fevers. The viremia in CTF is unique because it can extend for weeks or months and infection has been transmitted by transfusion. Recently, several commercial assays have been developed for the detection of soluble NS1 DEN antigen (20).

While Venezuelan equine encephalitis (VEE) virus can be recovered from the throat of one-fourth of patients, person-to-person spread has not been conclusively proven. SLE virus and certain hantaviruses can be detected in urine (see below). Many encephalitogenic arboviruses can be recovered from CSF obtained during the acute phase of illness, and, rarely, SLE, JE, WEE, and EEE viruses have been recovered from blood. The virus of TBE commonly contaminates milk of infected sheep, cows, and goats, but its occurrence in human milk has not been reported.

Antigen Capture ELISA

Antigen capture ELISA has been used to directly detect antigens of YF, DEN, sandfly fever, Rift Valley fever, Sindbis, and chikungunya viruses directly in blood. In some cases, viral antigens complexed with antibody must first be dissociated by use of a reducing agent, e.g., dithiothreitol. Generally, an overnight incubation of antigen maximizes sensitivity, which approaches 10^3 PFU/0.1 ml. The sensitivity of antigen capture ELISA for YF virus is similar to that of viral isolation from cell cultures, mosquitoes, or mice and is accomplished 3 to 7 days more quickly.

Antigen capture ELISA also has proved useful in epidemiologic surveillance of arbovirus infection rates in vector mosquitoes. A single infected mosquito in a pool can be detected rapidly and cheaply by the direct detection of antigen, allowing greater flexibility and time to implement emergency vector-control measures. This approach has been applied to SLE, WN, EEE, and LAC viruses (21). The SLE and EEE virus tests have been converted to a commercial dipstick format. Other arbovirus antigens have been detected directly in sandflies and ticks.

Immunohistochemical Staining

Certain arbovirus infections can be rapidly diagnosed by direct detection of virus-infected cells by IF or other histochemical techniques. The various causes of potentially fatal viral hemorrhagic fever, including DEN virus, cannot be reliably differentiated on a clinical basis, and immunohistochemical examination of liver tissues is a means by which a specific diagnosis can be reached. When liver biopsy specimens from patients with suspected YF are available, ordinary histopathological examination should be supplemented with more specific immunohistochemical techniques such as indirect IF. Similarly, IF and immunoperoxidase staining of brain biopsy or autopsy specimens have been helpful in differentiating arbovirus infections such as WEE, EEE, and LAC virus infections from other causes of encephalitis.

In disseminated infections such as YF and DEN, viral antigen has been demonstrated in various sites, including myocardium and kidney (YF) and bone marrow, spleen, lymph nodes, and dermal mononuclear cells (DEN) (22).

The CTF virus is unusual because it infects erythrocyte precursors, and infected erythrocytes can be detected in peripheral blood for the life of the infected cells. Examination of peripheral blood smears by IF is the most rapid approach to diagnosis and is more sensitive than serology. For patients with RR virus polyarthropathy, IF viral antigen has been found in monocytes and macrophages of synovial exudates, and it has been possible to rapidly identify infected patients by examining fluid from inflamed joints. Peripheral blood mononuclear cells are a principal replicative site for DEN virus and other flaviviruses. DEN and JE virus-infected mononuclear cells have been detected in peripheral blood by IF, and JE virus-infected cells have been found in CSF, making a specific diagnosis possible within hours of a diagnostic lumbar puncture. SLE virus-infected cells have been detected by IF in urinary sediment of some patients, and free viral particles were visualized by electron microscopy; however, virus was not recovered from urine. Patients with

suspected viruria had urinary incontinence and other symptoms possibly associated with myelitis.

IF is the simplest approach to identifying viral isolates recovered from clinical samples. The source of the isolate, the rapidity and characteristics of viral growth in cell culture, and mortality patterns and average survival time in mice may provide clues to its identity; e.g., alphaviruses kill suckling mice and produce plaques in cell culture within 1 to 5 days. The basic approach to viral identification is to prepare spot slides with an infected cell culture suspension. After being dried, the slides are fixed in acetone and stained by the indirect method with a series of mouse ascitic grouping fluids containing antibodies to various groups of arboviruses (National Institutes of Health grouping fluids) or broadly cross-reactive monoclonal antibodies (Table 2). A positive reaction to a single grouping fluid is followed by further IF and neutralization tests with monospecific ascitic fluids or monoclonal antibodies until the virus is identified (23–27). Inoculated cell cultures that do not show cytopathic effects still should be tested by the aforementioned method because arboviruses may not be lytic in every cell line. Alternatively, frozen brain sections of intracerebrally inoculated suckling mice or squashes of intrathoracically inoculated mosquitoes can be stained by the same procedure. Morphologic characteristics of the isolate should be confirmed by electron microscopy, but definitive antigenic classification requires the production of a homologous antibody (immune mouse ascitic fluid) and cross-serologic tests, especially cross-neutralization tests, with antigenically related agents.

In situ ELISA combines the sensitivity of cell culture systems for viral isolation with the rapidity of ELISA to identify the amplified isolates. Virus in clinical specimens is amplified briefly by growth in cell culture in 96-well panels; after fixation, the resulting amplified cell-associated antigens are detected directly by ELISA in the same vessel. Infected cell cultures can be identified within 24 to 72 h after inoculation, depending on the titer of the inoculum and viral growth characteristics. The approach is especially useful for mass screening, such as for inhibitory effects of candidate antiviral drugs and for viruses that do not produce cytopathic effects. If a long-working-distance objective is available, the monolayer also can be examined microscopically for infected foci.

Detection of Viral Genomic Sequences

In Situ Hybridization

In situ hybridization has been used to identify genomic sequences of LAC virus and other bunyaviruses, SIN virus, and DEN virus in mosquitoes; bluetongue virus in sandflies; and DEN and YF virus genomic sequences in formalin-fixed, paraffin-embedded liver tissue (28).

The principal advantage of *in situ* hybridization over immunohistochemical detection of viral proteins is the greater stability of viral RNA than of viral protein antigens in fixed, embedded specimens. Paraffin-embedded liver samples that had been stored at ambient temperatures for 23 years still had detectable viral RNA when viral antigens were undetectable by immunohistochemical stains. Non-isotopelabeled probes, such as biotin, have been used for the detection of DEN virus in human tissues.

Nucleic Acid Amplification Tests (NAAT) for the Detection of Arboviruses

A variety of nucleic acid amplification platforms have been successfully utilized for the detection of arboviruses, including standard reverse transcriptase PCR (RT-PCR) (with agarose gel analysis), real-time RT-PCR using fluorescent probes, nucleic acid sequence-based amplification (NASBA), and reverse transcription loop-mediated isothermal amplification (RT-LAMP). More recently, next-generation sequencing technologies have been described for the sequence-based identification of arboviruses (29). Because no prior sequence information is needed to employ this approach, it is anticipated that next-generation sequencing will be used more in the future both for virus identification as well as virus discovery. Several of these technologies will be described below; however, important issues common to each approach will be presented first. In general, the sensitivity of any of the NAATs in identifying arboviruses has been shown to be equal to or greater than that of the most sensitive viral isolation procedures (either in cultured cells or in neonatal mice) while providing equal specificity in identifying specific viruses. The dynamics of *in vivo* viral replication and tissue tropisms must be carefully considered so that the utility of a NAAT to a particular arbovirus can be properly applied and interpreted. For example, the encephalitic flaviviruses (i.e., WN, SLE, and JE viruses) demonstrate a short viremia which is often low or absent at the time of clinical presentation of CNS symptoms. With these viruses, the detection of virus in serum by NAAT (or any method) is typically unproductive and a negative result is not informative. Detection of virus in CSF obtained from meningitis or encephalitis patients is often better. In one study of WN encephalitis patients, virus was detected by a real-time RT-PCR in 14% of acute-phase serum specimens and 57% of CSF specimens (30). In contrast, the DEN viruses often achieve a much higher viremia of longer duration which can be detected by virus isolation or NAAT methods; as a result, NAATs are a good choice for detecting and serotyping the DEN viruses. In general, the alphaviruses demonstrate replication kinetics similar to those of the flaviviruses and are not commonly detected in acute-phase serum and/or CSF specimens, although detection is generally greater than with the flaviviruses. In contrast, NAATs have been highly successful in detecting arboviruses from tissues obtained from fatal human cases when the appropriate tissue target is known and assayed (i.e., brain tissue for WN virus, LAC or EEE virus cases, liver tissue from YF cases, etc.).

The use of NAATs for the detection of arboviruses in surveillance protocols is highly successful, in particular the testing of field-collected mosquitoes. In this application, NAATs have often demonstrated superior sensitivity compared to virus isolation or antigen detection assays. With the addition of automation, these NAAT approaches have been used to test hundreds of mosquito specimens in a single day (31). NAATs have also been successfully utilized in environmental surveillance by detecting arboviruses from tissues obtained from field-collected vertebrate hosts. Detection of WN virus in field-collected dead birds and detection of EEE virus from fatal equine cases are typical applications of this technology.

RNA Extraction and Purification

Most arboviruses have a single-stranded RNA genome, and as a result the sensitivity and specificity of all amplification strategies depend upon the efficient extraction and purification of the target RNA template. In the past, RNA extraction protocols were developed primarily in-house and suffered from inconsistency due to RNA degradation during purification; however, a variety of highly efficient RNA extraction and purification protocols which allow for more rapid, consistent, and high-volume sample processing are

now commercially available. Most of these utilize a chaotropic lysis buffer for efficient solubilization and stabilization of RNA from a variety of sources, followed by binding to silica, subsequent washing, and then elution in a low-salt solution. This approach also has been automated, and hundreds of samples can be processed within a single day (31). The use of a chaotropic lysis buffer has also enabled the efficient extraction of intact RNA from a variety of sources, including serum or plasma, whole blood, CSF, tissues, and homogenized ticks or mosquitoes. The last are particularly useful for environmental surveillance of arboviruses.

Testing Algorithms and Interpretation

Sound testing algorithms for NAATs are necessary to ensure that results have a high degree of confidence. The most desirable testing algorithm is one in which the amplification assays are complemented by another virus detection assay, such as an alternate NAAT, virus isolation, antigen capture ELISA, or direct IF assay. At a minimum, NAAT-positive results should be confirmed by retesting using the same technology with an additional primer set. NAAT assays must also incorporate the appropriate controls to ensure against false-positive or false-negative results. At a minimum, clinical samples should be tested in duplicate. Positive controls included in each assay should contain various levels of target RNA (high, medium, low, etc.) to evaluate the sensitivity of each test in comparison with previous tests. An internal positive control also can be very useful when specimens that may contain inhibitors of RT-PCR (i.e., blood, mosquito lysates, etc.) are tested. In all amplification-based technologies, it is essential that proper laboratory procedures be followed that prevent cross-contamination of nascent samples with amplified DNA (amplicon) from previous tests, resulting in the generation of false-positive results. In general, there should be complete physical separation of pre- and post-amplification laboratory space and equipment. Of particular importance is the use of several no-template (negative) controls spaced randomly throughout the assay to monitor for amplicon contamination.

RT-PCR

Standard RT-PCR-based assays (compared to the real-time assays described below) to detect arbovirus genomic sequences have been developed for a number of agents (32). These assays use either virus-specific primers or consensus primers that are designed to amplify genetically related viruses. These "first-generation" assays typically involve RT-PCR amplification followed by agarose gel electrophoresis with DNA visualization by staining with ethidium bromide to characterize the amplified DNA by molecular weight. Obtaining a DNA fragment of the predicted size is considered by some to be diagnostic. However, note that in some instances nonspecific amplification can generate DNA products with mobility on agarose gels similar or identical to that of the predicted fragment, which would lead to a false-positive interpretation of results. Greater specificity can be achieved by using sequence-specific approaches for detecting and confirming the identity of the amplified DNA, including hybridization with virus-specific probes (e.g., Southern blot, dot blot, or microtiter plate hybridization), PCR amplification with additional primers internal to the original primers (nested or seminested PCR), restriction endonuclease digestion of the DNA product, or nucleic acid sequence analysis. When consensus primers are utilized, a sequence-specific detection method such as one of those described above must be employed to specifically identify the resulting DNA, since by the design of the assay all related viruses would all be amplified. Consensus RT-PCR assays have been described for alphaviruses, flaviviruses, and the California and Bunyamwera serogroup bunyaviruses (33–36). Virus-specific assays include assays for the DEN viruses; the YF, JE, WEE, EEE, SLE, MVE, Powassan, TBE, and WN viruses; the California serogroup viruses; and the RR and Ockelbo and CTF viruses.

Real-Time 5′-Exonuclease Fluorogenic Assays

Real time RT-PCR assays combine RT-PCR amplification with fluorescently labeled virus-specific probes able to detect amplified DNA during the amplification reaction. These assays offer numerous advantages over standard RT-PCR, namely, increased sensitivity and specificity, quantitation of initial target RNA, high throughput, and rapid turnaround of results. The increased specificity of the TaqMan assay compared to that of standard RT-PCR is due to the use of the virus-specific internal probe during the amplification. The hybridization of this probe to the target sequence is detectable by the increase in fluorescence in real time. This sequence-specific detection obviates the need for any post-amplification characterization of the amplified DNA. As a result, amplified DNA is not manipulated in the laboratory as occurs with standard RT-PCR, thus greatly reducing the likelihood of amplicon contamination. Real-time fluorogenic assays also offer the advantage of the ability to detect multiple targets at the same time in the same amplification reaction (multiplexing). This can be accomplished by using multiple oligonucleotide probes (up to four in some instruments), each labeled with fluorescent reporter dyes with discrete emission spectra. Several TaqMan assays for the detection of arboviruses have been described, including assays for WN, SLE, CHIK, TBE, DEN, EEE, WEE, and LAC viruses (37–40).

NASBA

Another amplification technology which has successfully been used for the detection and identification of arboviruses is NASBA. This approach shows some similarities to RT-PCR at the initial stages. However, there are several significant differences; namely, the reaction is isothermic (41°C); the enzymes utilized are RT, RNase H, and T7 RNA polymerase; and the final amplification product is single-stranded RNA. Amplified RNA can be detected in a sequence-specific manner either by utilizing an electrochemiluminescence probe detection format or by using a fluorescently labeled molecular beacon probe in real time. These approaches have been successfully employed for the detection of a number of arboviruses, including WN, SLE, EEE, WEE, LAC, and DEN viruses (37, 41, 42).

RT-LAMP

A number of reports describing the detection of arboviruses by reverse-transcriptase loop mediated amplification have recently been described in the literature (43). The amplification is based upon strand-displacement DNA polymerization utilizing six target-specific oligonucleotide primers. After reverse transcription, isothermal DNA amplification proceeds using a DNA polymerase with high displacement activity (Bst DNA polymerase). The LAMP strategy generates double-stranded DNA stem-loop molecules of varying stem lengths based upon primer design, specifically the incorporation of complimentary target sequences into the 5′ region of some of the primers. The final DNA products can

be visualized as a DNA "ladder" on an agarose gel. Alternatively, amplification can be detected in real time by measuring the turbidity (using a photometer/turbidimeter) of the reaction mixture, which increases with the amount of DNA synthesized due to the accumulation of magnesium pyrophosphate. The specificity in LAMP is due to the binding of the six oligonucleotide primers; therefore, specific identification of the amplified DNA is not considered necessary, and the final detection can be accomplished by turbidity. LAMP reagent kits and detection equipment are available commercially, and the overall reaction costs are similar to those for real-time PCR reactions. LAMP assays have been described for the detection of WNV, RVFV, CHIK, JE, YF, CCHF, TBE, and DEN (44–50).

SELECTION AND SEQUENCE OF TESTS

The laboratory diagnosis of an arbovirus infection presents a unique set of problems because of the large number of arbovirus agents that must be considered in a differential diagnosis. The approach is simplified by first considering the viruses according to the clinical illness they produce, e.g., viruses that produce principally CNS infection, hemorrhagic fever, polyarthritis, or nonspecific febrile illnesses with or without a rash (Table 1). The geographic distribution of certain arboviruses may be restricted to certain countries or regions, and the choice of antigens to be included in a diagnostic battery can be reduced further by including only those that are relevant to the patient's history of travel and exposure. If the patient gives a history of exposure to a specific vector, the choice of antigens can be narrowed further; e.g., if the patient reports an attached tick or tick exposure, antigens of tick-borne viruses should be emphasized.

When brain or liver specimens are available from patients with encephalitis or hemorrhagic fever, respectively, the tissues should be submitted for viral isolation and detection of viral genome or antigens. The tissue should be divided, and portions should be fixed in buffered formalin for histochemical staining and frozen in liquid N_2 on dry ice or in a mechanical freezer at −70°C for viral isolation or molecular detection. If sufficient quantities are available, tissues in 10% (wt/vol) suspensions should be used to inoculate cell cultures and to intracerebrally inoculate suckling mice for viral isolation. While areas of the cerebral cortex have served as good sources of virus and antigen for many arboviruses, recent experience with WN virus suggested that more virus and antigen can be obtained from the brain stem and spinal cord. This observation is supported by the flaccid paralysis demonstrated by WN virus-infected patients.

Although a probable diagnosis sometimes can be made serologically from a single serum specimen, paired sera should always be used when possible. In patients with a CNS infection, an accompanying CSF sample should be requested routinely. The MAC-ELISA is more sensitive when CSF samples are tested, and IgM can often be demonstrated in CSF slightly earlier than in acute-phase serum. MAC-ELISA is now the serologic test of first choice in the laboratory diagnosis of arbovirus infections because of its sensitivity and the possibility that a presumptive diagnosis can be made in an early stage of infection.

The conventional sequence of serologic testing, which is still a valid and sensitive approach, is to test paired sera to quantify a change in antibody titer. Often, an elevated titer in an acute-phase serum sample is sufficient information upon which to make a presumptive diagnosis. If heterologous reactions are present, the sera are tested subsequently by neutralization to better elucidate the cause of infection.

INTERPRETATION OF RESULTS

Serologic test results should be interpreted in the context of the clinical and epidemiologic features of the case. Heterologous antibodies from previous infections or from immunizations (namely, to YF) may interfere with the correct interpretation of a result, especially if serum specimens are tested by a single screening assay. For example, anti-SLE virus antibody may be present in people who previously were infected with DEN virus during travel or residence in tropical countries of South or Central America or Asia. Unless changes in antibody titer or specific IgM antibody levels are demonstrable or more specific tests are done, it may be difficult to differentiate these reactions. Epidemiologically and clinically, 4-fold changes in serum antibody titer or the presence of virus-specific IgM in CSF confirms a recent infection.

Until the introduction of WN virus into the United States, the incidence of arbovirus infections had been low and the diseases occurred in certain geographic locations or episodically. Seroprevalence remains low, except in areas where WN virus outbreaks have been documented or where LAC virus is transmitted in an endemic pattern. Therefore, the discovery of specific arbovirus antibodies in a single serum specimen of an ill patient is likely to be associated with a recent infection. The recent introduction of WN virus into the United States has also complicated the serodiagnosis of SLE virus infections in regions where these viruses may cocirculate. Seroprevalence to EEE virus is the lowest among all the domestic arboviruses, and the positive predictive value of a single seroreactive serum sample for other arboviruses depends on the clinical and epidemiological circumstances of the case. For example, the majority of SLE virus infections are asymptomatic or result in mild symptoms of headache and fever. The probability of SLE in seroreactive patients without frank signs of CNS infection normally is low, but in an epidemic, seroreactions in patients with less distinctive symptoms, such as acute fever and headache, may have a high predictive value.

The interpretation of ELISA results is not standardized, and the significance of raw absorbance values has been determined by methods established in individual laboratories. Thorough evaluations of the operating characteristics of arbovirus ELISAs have been hampered by the large number of agents for which assays must be established and the scarcity of positive human specimens for rare infections. A frequently used standard for a positive absorbance value is 3 standard errors above the mean absorbance of a sample of known negative sera. An alternative approach is to calculate the ratio of the sample absorbances with test (positive) and control (negative) antibodies (positive-to-negative ratio). With the diagnosis of RR and JE virus infections, a binding index, in which the sample absorbance is expressed in units in relation to the absorbance of a known positive sample, has also been used.

The isolation and identification of an arbovirus or its antigen or viral genomic sequences in a clinical sample generally are specific evidence of a recent infection. With few exceptions, arboviruses cause acute self-limited infections without persistence or latency. Certain flavivirus infections, however, cause subacute or persistent CNS infection. A progressive degenerative infection of the brain stem and cervical spinal cord leading to paralysis and atrophy of the shoulder girdle and upper arm after infection with viruses of the tick-borne flavivirus complex has been described, and in a small proportion of patients with JE, clearance from the CNS is delayed for several months after the onset of acute illness. Experimental infection of monkeys with WN virus, another flavivirus, also results in persistent CNS infection.

IgM antibodies to YF virus remain detectable in a large proportion of patients for years or decades following infection or immunization, leading to the suspicion that this flavivirus persists in some individuals. Infections with certain viruses of the *Bunyaviridae* family also are followed by persistent silent infections in animals, of which the clearest examples are the lifelong infections of rodents with Hantaan, Seoul, and Prospect Hill viruses and other hantaviruses. There is no evidence, however, of persistent bunyavirus infections in humans.

CONCLUSIONS

Arbovirus infections in the wealthy countries of the world are usually rare events. As a result, funding for research on arboviruses had fallen dramatically, resulting in only small advances and improvements in the diagnosis of arboviral infections. Two events which have shifted these priorities have occurred in recent years. One is the renewed emphasis on preparedness for bioterrorist events. Three of these arboviruses (VEE, EEE, and WEE viruses) have been classified as possible biological threats. This designation has renewed interest in rapid and sensitive diagnosis of alphaviruses. The second event was the introduction of WN virus into the Western Hemisphere for the first time, reminding us of the ease with which new and emerging infections can travel great distances. As mentioned above, the introduction of a second mosquito-borne flaviviral encephalitis virus into the United States resets the diagnostic algorithms. It will be imperative for the diagnostic virologist to keep close watch for new, faster, and more sensitive diagnostic methods, which will undoubtedly result from this new level of recognition of this group of viral pathogens.

REFERENCES

1. **Karabatsos N.** 1985. *International Catalogue of Arboviruses*. American Society for Tropical Medicine and Hygiene, San Antonio, TX.
2. **Monath TP.** 1988. *Arboviruses: Epidemiology and Ecology*, vol 1. CRC Press, Boca Raton, FL.
3. **Tsai TF.** 1995. Arboviruses, p 980–996. *In* Murray PR, Baron EJ, Pfaller MA, Tenover FC, Yolken RH (ed), *Manual of Clinical Microbiology*, 6th ed. American Society for Microbiology, Washington, DC.
4. **Burke DS, Nisalak A, Ussery MA, Laorakpongse T, Chantavibul S.** 1985. Kinetics of IgM and IgG responses to Japanese encephalitis virus in human serum and cerebrospinal fluid. *J Infect Dis* **151:**1093–1099. PubMed
5. **Roehrig JT, Brown TM, Johnson AJ, Karabatsos N, Martin DM, Mitchell CJ, Nasci R.** 1998. Alphaviruses, p 7–18. *In* Stephenson JR, Warnes A (ed), *Methods in Molecular Biology: Diagnostic Virology Protocols*. Humana Press, Totowa, NJ.
6. **Wong SJ, Boyle RH, Demarest VL, Woodmansee AN, Kramer LD, Li H, Drebot M, Koski RA, Fikrig E, Martin DA, Shi PY.** 2003. Immunoassay targeting nonstructural protein 5 to differentiate West Nile virus infection from dengue and St. Louis encephalitis virus infections and from flavivirus vaccination. *J Clin Microbiol* **41:**4217–4223. PubMed
7. **Wong SJ, Demarest VL, Boyle RH, Wang T, Ledizet M, Kar K, Kramer LD, Fikrig E, Koski RA.** 2004. Detection of human anti-flavivirus antibodies with a west nile virus recombinant antigen microsphere immunoassay. *J Clin Microbiol* **42:**65–72. PubMed
8. **Basile AJ, Horiuchi K, Panella AJ, Laven J, Kosoy O, Lanciotti RS, Venkateswaran N, Biggerstaff BJ.** 2013. Multiplex microsphere immunoassays for the detection of IgM and IgG to arboviral diseases. *PLoS One* **8(9):**e75670. doi:10.1371/journal.pone.0075670
9. **Johnson AJ, Noga AJ, Kosoy O, Lanciotti RS, Johnson AA, Biggerstaff BJ.** 2005. Duplex microsphere-based immunoassay for detection of anti-West Nile virus and anti-St. Louis encephalitis virus immunoglobulin m antibodies. *Clin Diagn Lab Immunol* **12:**566–574.
10. **Johnson AJ, Martin DA, Karabatsos N, Roehrig JT.** 2000. Detection of anti-arboviral immunoglobulin G by using a monoclonal antibody-based capture enzyme-linked immunosorbent assay. *J Clin Microbiol* **38:**1827–1831. PubMed
11. **Innis BL, Nisalak A, Nimmannitya S, Kusalerdchariya S, Chongswasdi V, Suntayakorn S, Puttisri P, Hoke CH.** 1989. An enzyme-linked immunosorbent assay to characterize dengue infections where dengue and Japanese encephalitis co-circulate. *Am J Trop Med Hyg* **40:**418–427. PubMed
12. **Thibodeaux BA, Liss NM, Panella AN, Roehrig JT.** 2011. Development of a human-murine chimeric immunoglobulin M for use in the serological detection of human alphavirus antibodies. *Clin Vaccine Immunol* **18:**2181–2182.
13. **Thibodeaux BA, Panella AN, Roehrig JT.** 2010. Development of human-murine chimeric immunoglobulin G for use in the serological detection of human flavivirus and alphavirus antibodies. *Clin Vaccine Immunol* **17:**1617–1623.
14. **Thibodeaux BA, Roehrig JT.** 2009. Development of a human-murine chimeric immunoglobulin M antibody for use in the serological detection of human flavivirus antibodies. *Clin Vaccine Immunol* **16:**679–685.
15. **Davis BS, Chang GJ, Cropp B, Roehrig JT, Martin DA, Mitchell CJ, Bowen R, Bunning ML.** 2001. West Nile virus recombinant DNA vaccine protects mouse and horse from virus challenge and expresses in vitro a noninfectious recombinant antigen that can be used in enzyme-linked immunosorbent assays. *J Virol* **75:**4040–4047. PubMed
16. **Chiou SS, Fan YC, Crill WD, Chang RY, Chang GJ.** 2012. Mutation analysis of the cross-reactive epitopes of Japanese encephalitis virus envelope glycoprotein. *J Gen Virol* **93**(Pt 6)**:**1185–1192.
17. **Beaty BJ, Calisher CH, Shope RW.** 1989. Arboviruses, p 797–856. *In* Schmidt NJ, Emmons RW (ed), *Diagnostic Procedures for Viral, Rickettsial and Chlamydial Infections*, 6th ed. American Public Health Association, Washington, DC.
18. **Roehrig JT, Hombach J, Barrett AD.** 2008. Guidelines for plaque-reduction neutralization testing of human antibodies to dengue viruses. *Viral Immunol* **21:**123–132.
19. **Johnson BW, Kosoy O, Wang E, Delorey M, Russell B, Bowen RA, Weaver SC.** 2011. Use of sindbis/eastern equine encephalitis chimeric viruses in plaque reduction neutralization tests for arboviral disease diagnostics. *Clin Vaccine Immunol* **18:**1486–1491. PubMed
20. **Dussart P, Petit L, Labeau B, Bremand L, Leduc A, Moua D, Matheus S, Baril L.** 2008. Evaluation of two new commercial tests for the diagnosis of acute dengue virus infection using NS1 antigen detection in human serum. *PLoS Negl Trop Dis* **2(8):**e280. doi:10.1371/journal.pntd.0000280
21. **Tsai TF, Bolin RA, Montoya M, Bailey RE, Francy DB, Jozan M, Roehrig JT.** 1987. Detection of St. Louis encephalitis virus antigen in mosquitoes by capture enzyme immunoassay. *J Clin Microbiol* **25:**370–376. PubMed
22. **De Brito T, Siqueira SA, Santos RT, Nassar ES, Coimbra TL, Alves VA.** 1992. Human fatal yellow fever. Immunohistochemical detection of viral antigens in the liver, kidney and heart. *Pathol Res Pract* **188:**177–181. PubMed
23. **Hunt AR, Roehrig JT.** 1985. Biochemical and biological characteristics of epitopes on the E1 glycoprotein of western equine encephalitis virus. *Virology* **142:**334–346. PubMed

24. **Roehrig JT.** 1986. The use of monoclonal antibodies in studies of the structural proteins of alphaviruses and flaviviruses, p 251–278. *In* Schlesinger S, Schlesinger MJ (ed), *The Viruses: The Togaviridae and Flaviviridae*. Plenum Press, New York, NY.
25. **Roehrig JT, Bolin RA.** 1997. Monoclonal antibodies capable of distinguishing epizootic from enzootic varieties of subtype 1 Venezuelan equine encephalitis viruses in a rapid indirect immunofluorescence assay. *J Clin Microbiol* **35:**1887–1890. PubMed
26. **Roehrig JT, Hunt AR, Chang GJ, Sheik B, Bolin RA, Tsai TF, Trent DW.** 1990. Identification of monoclonal antibodies capable of differentiating antigenic varieties of eastern equine encephalitis viruses. *Am J Trop Med Hyg* **42:**394–398. PubMed
27. **Roehrig JT, Mathews JH, Trent DW.** 1983. Identification of epitopes on the E glycoprotein of Saint Louis encephalitis virus using monoclonal antibodies. *Virology* **128:**118–126. PubMed
28. **Monath TP, Ballinger ME, Miller BR, Salaun JJ.** 1989. Detection of yellow fever viral RNA by nucleic acid hybridization and viral antigen by immunocytochemistry in fixed human liver. *Am J Trop Med Hyg* **40:**663–668. PubMed
29. **Lanciotti RS, Kosoy OI, Bosco-Lauth AM, Pohl J, Stuchlik O, Reed M, Lambert AJ.** 2013. Isolation of a novel orthobunyavirus (Brazoran virus) with a 1.7 kb S segment that encodes a unique nucleocapsid protein possessing two putative functional domains. *Virology* **444:**55–63. PubMed
30. **Lanciotti RS, Kerst AJ, Nasci RS, Godsey MS, Mitchell CJ, Savage HM, Komar N, Panella NA, Allen BC, Volpe KE, Davis BS, Roehrig JT.** 2000. Rapid detection of west nile virus from human clinical specimens, field-collected mosquitoes, and avian samples by a TaqMan reverse transcriptase-PCR assay. *J Clin Microbiol* **38:**4066–4071. PubMed
31. **Shi PY, Kauffman EB, Ren P, Felton A, Tai JH, Dupuis AP II, Jones SA, Ngo KA, Nicholas DC, Maffei J, Ebel GD, Bernard KA, Kramer LD.** 2001. High-throughput detection of West Nile virus RNA. *J Clin Microbiol* **39:**1264–1271. PubMed
32. **Kuno G.** 1998. Universal diagnostic RT-PCR protocol for arboviruses. *J Virol Methods* **72:**27–41. PubMed
33. **Kuno G, Mitchell CJ, Chang GJ, Smith GC.** 1996. Detecting bunyaviruses of the Bunyamwera and California serogroups by a PCR technique. *J Clin Microbiol* **34:**1184–1188. PubMed
34. **Lanciotti RS, Calisher CH, Gubler DJ, Chang GJ, Vorndam AV.** 1992. Rapid detection and typing of dengue viruses from clinical samples by using reverse transcriptase-polymerase chain reaction. *J Clin Microbiol* **30:**545–551. PubMed
35. **Pfeffer M, Proebster B, Kinney RM, Kaaden OR.** 1997. Genus-specific detection of alphaviruses by a semi-nested reverse transcription-polymerase chain reaction. *Am J Trop Med Hyg* **57:**709–718. PubMed
36. **Scaramozzino N, Crance J-M, Jouan A, DeBriel DA, Stoll F, Garin D.** 2001. Comparison of *flavivirus* universal primer pairs and development of a rapid, highly sensitive heminested reverse transcription-PCR assay for detection of flaviviruses targeted to a conserved region of the NS5 gene sequences. *J Clin Microbiol* **39:**1922–1927. PubMed
37. **Lambert AJ, Martin DA, Lanciotti RS.** 2003. Detection of North American eastern and western equine encephalitis viruses by nucleic acid amplification assays. *J Clin Microbiol* **41:**379–385. PubMed
38. **Lanciotti RS, Kosoy OL, Laven JJ, Panella AJ, Velez JO, Lambert AJ, Campbell GL.** 2007. Chikungunya virus in US travelers returning from India, 2006. *Emerg Infect Dis* **13:**764–767. PubMed
39. **Laue T, Emmerich P, Schmitz H.** 1999. Detection of dengue virus RNA in patients after primary or secondary dengue infection by using the TaqMan automated amplification system. *J Clin Microbiol* **37:**2543–2547. PubMed
40. **Wicki R, Sauter P, Mettler C, Natsch A, Enzler T, Pusterla N, Kuhnert P, Egli G, Bernasconi M, Lienhard R, Lutz H, Leutenegger CM.** 2000. Swiss Army Survey in Switzerland to determine the prevalence of *Francisella tularensis*, members of the *Ehrlichia phagocytophila* genogroup, *Borrelia burgdorferi* sensu lato, and tick-borne encephalitis virus in ticks. *Eur J Clin Microbiol Infect Dis* **19:**427–432. PubMed
41. **Wu SJ, Lee EM, Putvatana R, Shurtliff RN, Porter KR, Suharyono W, Watts DM, King CC, Murphy GS, Hayes CG, Romano JW.** 2001. Detection of dengue viral RNA using a nucleic acid sequence-based amplification assay. *J Clin Microbiol* **39:**2794–2798. PubMed
42. **Lanciotti RS, Kerst AJ.** 2001. Nucleic acid sequence-based amplification assays for rapid detection of West Nile and St. Louis encephalitis viruses. *J Clin Microbiol* **39:**4506–4513. PubMed
43. **Mori Y, Kanda H, Notomi T.** 2013. Loop-mediated isothermal amplification (LAMP): recent progress in research and development. *J Infect Chemother* **19:**404–411.
44. **Hayasaka D, Aoki K, Morita K.** 2013. Development of simple and rapid assay to detect viral RNA of tick-borne encephalitis virus by reverse transcription-loop-mediated isothermal amplification. *Virol J* **10:**68.
45. **Kwallah AO, Inoue S, Muigai AW, Kubo T, Sang R, Morita K, Mwau M.** 2013. A real-time reverse transcription loop-mediated isothermal amplification assay for the rapid detection of yellow fever virus. *J Virol Methods* **193:**23–27.
46. **Le Roux CA, Kubo T, Grobbelaar AA, van Vuren PJ, Weyer J, Nel LH, Swanepoel R, Morita K, Paweska JT.** 2009. Development and evaluation of a real-time reverse transcription-loop-mediated isothermal amplification assay for rapid detection of Rift Valley fever virus in clinical specimens. *J Clin Microbiol* **47:**645–651.
47. **Li S, Fang M, Zhou B, Ni H, Shen Q, Zhang H, Han Y, Yin J, Chang W, Xu G, Cao G.** 2011. Simultaneous detection and differentiation of dengue virus serotypes 1-4, Japanese encephalitis virus, and West Nile virus by a combined reverse-transcription loop-mediated isothermal amplification assay. *Virol J* **8:**360.
48. **Osman HA, Eltom KH, Musa NO, Bilal NM, Elbashir MI, Aradaib IE.** 2013. Development and evaluation of loop-mediated isothermal amplification assay for detection of Crimean Congo hemorrhagic fever virus in Sudan. *J Virol Methods* **190:**4–10.
49. **Parida MM, Santhosh SR, Dash PK, Tripathi NK, Lakshmi V, Mamidi N, Shrivastva A, Gupta N, Saxena P, Babu JP, Rao PV, Morita K.** 2007. Rapid and real-time detection of Chikungunya virus by reverse transcription loop-mediated isothermal amplification assay. *J Clin Microbiol* **45:**351–357.
50. **Teoh BT, Sam SS, Tan KK, Johari J, Danlami MB, Hooi PS, Md-Esa R, AbuBakar S.** 2013. Detection of dengue viruses using reverse transcription-loop-mediated isothermal amplification. *BMC Infect Dis* **13:**387. PubMed

Diagnosis of Hantavirus Infections

WILLIAM MARCIEL DE SOUZA AND LUIZ TADEU MORAES FIGUEIREDO

68

Hantavirus is a genus in the family *Bunyaviridae* that includes small mammal-borne viruses. These viruses are causative of severe human diseases such as hemorrhagic fever with renal syndrome (HFRS) in Asia and Europe and cardiopulmonary syndrome (HCPS) in the Americas. Hantaviruses are 80- to 120-nm enveloped RNA viruses. Their negative-sense single-stranded genome has approximately 12,000 nucleotides and is divided into three fragments named S (small), M (medium), and L (large) (1). The S fragment encodes the nucleoprotein (N), the M segment encodes the envelope glycoproteins (Gn and Gc), and the viral RNA (vRNA)-dependent RNA polymerase (RdRp), the largest viral protein (250 to 280 kDa), is codified by the L segment. The viral RNA segments are circular, include base-paired inverted complementary sequences at the 3′ and 5′ ends, and wrap up by the N protein (1). An open reading frame encoding NSs can be found in American hantavirus and in the vole-borne Puumala and Tula viruses, all evolutionarily related (2, 3).

Hantaviruses are emergent zoonotic pathogens harbored by rodents and other small mammals (shrews, moles, and bats). Small mammals infected by hantavirus can be observed in the subtropics and tropics worldwide and transmit these pathogens to humans by inhalation of aerosols containing particles of their feces, urine, or other excreta (4, 5). The virus remains infectious in the environment for several weeks depending on humidity, temperature, and association with protective proteins (6). Risk factors for hantavirus infection include involvement in rural and forest-related activities, cohabitation with domestic and peridomestic rodents, exposure to potentially infected dust, and field military training (4). Additionally, in Argentina and Chile, human-to-human transmission of Andes hantavirus was reported (7–9). Different trends of hantavirus case numbers have been observed; whereas in China about 10,000 HFRS cases occur every year, even after implementation of a vaccination program, the number of cases in the Americas is much lower, about 500 HCPS cases per year (1, 10).

Hantaviruses produce acute febrile diseases, HFRS and HCPS. More severe than HFRS, HCPS produces 35 to 50% case fatalities. The pathogenesis of these hantavirus diseases includes capillary leakage of intravascular fluid into interstitium tissues that leads to respiratory and renal failure and shock (1). In fact, a comparative analysis of hantavirus diseases has revealed that HFRS and HCPS are mostly didactic names. Considering that most American HCPS patients also have renal failure and many HFRS European or Asiatic patients also have respiratory failure, it has been recently proposed to use the term hantavirus fever worldwide (11).

We present here laboratory diagnostic techniques used for diagnosis of hantavirus infections (summarized in Table 1).

LABORATORY DIAGNOSIS

Most hantavirus diseases (HCPS and HFRS) are rapidly progressive and often confused with other severe diseases, such as bacterial sepsis with respiratory failure, pneumocystosis, and leptospirosis. Blood biochemistry findings that may be helpful for clinical diagnosis of HCPS are low albumin levels in serum (<3.5 g/dl), thrombocytopenia (<130,000 platelets/μl), leukocytosis, and increased creatinine levels in serum (12, 13). However, specific and rapid laboratory assays should be used to confirm the clinical suspicion of a hantavirus disease. Laboratorial techniques confirm hantavirus infection based on (i) the presence of hantavirus-specific IgM or more than 2-fold rising titers of IgG in paired sera, (ii) the detection of hantavirus RNA by RT-PCR, and (iii) the detection of hantavirus antigens in tissues by immunohistochemistry. Other classical techniques such as hantavirus isolation in cell culture and neutralization assay are not routine procedures in laboratory diagnosis because they are laborious and time-consuming and can be performed only in laboratories of biosafety level 3 (BSL-3) by trained personnel (1). To develop fast, easy, reliable, and specific assays for diagnoses of hantavirus that infect humans and could be used in the laboratory routine is a major task for the next decade. We show below procedures used in each hantavirus diagnostic method.

SPECIMENS FOR DIAGNOSIS

Clinical specimens required for serological testing should be blood drawn into a silicone-coated tube containing no additive. For ideal diagnostic purposes, the sample should be collected at or immediately after hospital admission. A second specimen should be collected 2 or 3 weeks later, in the convalescent phase of the disease. Blood collected from the heart in autopsy should also be collected in tubes as mentioned above. Blood samples should be centrifuged, and the serum should be aliquoted and stored at 4°C when it is

doi:10.1128/9781555818722.ch68

TABLE 1 Laboratory methods used for hantavirus diagnosis[a]

Methods	Advantages	Disadvantages	Future perspectives
Virological			
Hantavirus isolation in cell culture	Allows studies on viral ultrastructure, replication, and genomics and infection of experimental models	Laborious and time-consuming Can only be performed by trained personnel in BSL-3 laboratories Far from being always successful	New cell cultures and techniques to enhance hantavirus isolation
Detection of hantavirus antigens (immunohistochemistry) by immunofluorescent test and enzyme immunoassay	Allows diagnosis on infected tissues of organs (lungs, heart, salivary glands, etc.)	Allows mostly diagnosis postmortem Requires laborious preparations	Improve the technique to process *in vivo* blood or organ tissues
Molecular			
Conventional RT-PCR	Fast, sensitive, and specific technique using primers selected for matching high-homology regions of the genome Allows diagnosis of hantavirus infection in the viremic phase Allows sequencing of amplicon nucleotides of the viral genome	Does not allow diagnosis of hantavirus infection after the viremic phase More expensive than serologic methods	Future improvements are likely
Real-time RT-PCR	Allows faster results than those from conventional RT-PCR Higher levels of sensitivity and specificity than conventional RT-PCR Lower risk of contamination than conventional RT-PCR Informs on the specific virus causing the infection and the viral load	More expensive than conventional RT-PCR Requires further procedure to obtain amplicon for nucleotide sequencing	Increase the specificity of the test using multiple targets
Hantavirus detection DNA microarray	Fast, sensitive, and specific Allows simultaneous detection of tens to thousands of virus genes	Still too expensive and complex for routine use	Increase in targets Reduction of costs Simplification of data analysis
Serological			
Indirect immunofluorescence assay	Allows detection of IgG and IgM antibodies to hantavirus	Low sensitivity Result of the test depends on a subjective analysis of microscopy	Increase the use of this technique with distinct and simultaneous fluorescent targets for research on viral replication and pathogenesis of hantavirus infections
Indirect IgG and IgM ELISAs and IgM capture ELISAs	Can be used in the acute viremic phase of the disease Sensitive Low cost and easy to perform Provides cross-reacting results among hantaviruses	Cross-reacting results among hantaviruses create difficulties in identifying the hantavirus species	Improvement of antigens that allow hantavirus-specific antibody detection
Neutralization test	The most specific of serological tests	Laborious, time-consuming, and expensive	New approaches to facilitate reading of results of the test
Immunoblotting	More sensitive and specific than ELISA Allows detection of antibody response to distinct viral antigens	Expensive and time-consuming	Improvement of the technique for hantavirus-specific antibody detection
Immunochromatographic test for diagnosis of hantavirus disease	Rapid test (15–30 min) detects IgM and IgG antibodies in patient sera Easy to perform Low cost	Cross-reacting results among hantaviruses create difficulties in identifying the hantavirus species	Improvement of antigens allowing increase in sensitivity and hantavirus-specific antibody detection

[a]Table adapted from Kruger et al., 2014 (5).

to be processed within 24 h or frozen at −70°C for later use. Shipped samples should be either frozen or stored with an ice pack. These samples are not considered as having "etiologic agents" for purposes of shipment even if a hantavirus has been previously diagnosed in the donor patient.

SEROLOGICAL TESTS

Immunofluorescence Assays

Immunofluorescence assays (IFA) have been widely used for hantavirus diagnosis. Advantages of IFA include low cost, simplicity, and a possibility of quantitative detection of either IgM or IgG. After the discovery of Hantaan virus, IFA was the first method used for diagnosis of HFRS in Europe and Asia (outbreaks in China or Korea) (1, 14).

The indirect type of IFA has been used to detect antibodies to hantavirus. For the assay, Vero-E6 cells in culture, which are normally susceptible to the hantavirus, are infected, collected, and fixed on glass microscope slides. Dilutions of the test serum are added to the slide, which is incubated and washed to remove the excess. In sequence, specific antibody-antigen complexes are detected by adding an anti-human IgG or IgM antibody conjugated to fluorescein isothiocyanate. This fluorescent dye is used because the human eye is more sensitive to the green portion of the spectrum; the background autofluorescence of clinical specimens is commonly red, highlighting the green fluorescence. The nonspecific background caused by the fluorescent dye can be blocked by Evans blue or dark stain. Finally, the slides are washed, dried, and examined under UV light in a fluorescence microscope. The results of immunofluorescence assays are subjective and usually require evaluation by an experienced technician. This is because the number of positive-fluorescing cells and the quality and intensity of the fluorescence must be carefully compared with those of uninfected cells. The direct-type IFA using positive sera has been used to detect infected cells and thus confirm the isolation of hantavirus or to look for the virus in human and animal tissues.

Major disadvantages of immunofluorescent assays for diagnosis of hantavirus are that (i) the preparation of hantavirus antigens for serologic testing is usually difficult because cell culture infections result in low virus yield, (ii) handling of hantavirus for concentration and purification procedures can be performed only in BSL-3 facilities, (iii) nonspecific binding of antibodies occurs, (iv) the procedure requires a darkroom and a fluorescence microscope, and (v) it may be difficult to read and interpret the test results. Currently, an approach used for IFA is a multiparametric IFA-based detection of hantavirus IgG and IgM available commercially by Euroimmun (Luebeck, Germany). This assay is performed with serum samples diluted 1:100 added into biochips containing either cells infected with Puumala virus (PUUV), Saaremaa virus (SAAV), Dobrava-Belgrade virus (DOBV), Hantaan virus (HTNV), or Seoul virus (SEOV) or uninfected cells. The cells are fixed by acetone and sterilized by gamma irradiation. These commercial assays do not depend on propagation of hantavirus in cell culture and can be used in any laboratory able to perform IFA-based diagnostics (15). Another test commercially available is a PUUV-IFA (Progen, Heidelberg, Germany), which requires only a positive reaction in sera diluted 1:32.

Neutralization Assays

Neutralization assays (NTs) are the most specific among all serologic tests, and that is why these assays are included in the four criteria of the International Committee on Taxonomy of Viruses (ICTV) to delineate new species of hantavirus. NTs can detect the ability of a serum to neutralize the infectivity and replication of the virus in cell culture. Also, NT is important to differentiate species of hantavirus in serological tests. This is necessary because in serological assays for hantavirus, cross-reaction between species is common. However, usually, high titers of neutralizing antibodies are found only against the hantavirus that is infecting the patient (16).

In the NT node focus reduction neutralization test (FRNT), a defined quantity of viable virus is mixed to test serum. Thus, heat-inactivated serum specimens (56°C for 30 minutes) are diluted 2-fold (1:10 to 1:160) in minimum essential medium (MEM), and 250 μl of each serum dilution is added to a mixture of the same volume containing a constant amount of virus (e.g., 100 PFU). Also, it is important to test negative sera as controls of the assay. Following the incubation to allow neutralizing antibodies to bind with the virus, the mixture is inoculated into Vero E6 cultured cells that are further incubated for 6 to 14 days, in order to present a visible focus of virus-induced cell death. At this moment, the cell monolayer is stained with naphthalene black, and the focus of dead cells is visualized and counted under microscope. The neutralizing antibody titer is defined as the reciprocal dilution of the serum able to reduce more than 5-fold the number of foci (microplaques) in comparison with the virus titer without serum (17, 18). Another NT is based on the cytopathic effect (CPE) produced by the hantavirus infecting Vero E6 cells. The test is performed as described above and after incubation, in order for the infected cells to present CPE (18).

The major disadvantages of NTs for routine diagnosis of hantavirus are that these in-house tests (i) are cumbersome, (ii) are expensive, (iii) are time-consuming, (iv) and require BSL-3 facilities for handling hantavirus and that (v) hantavirus infection in cell culture usually produces little or minimal CPE and development of plaques in the monolayer.

Alternatively, the FRNT for hantaviruses can be read using a chemiluminescent substrate. This assay is based on the conversion of a substrate into a luminescent product by peroxidase-antibody conjugates; the emitted light of infected cell foci can easily be recorded by autoradiography or video imaging, providing a hard copy for documentation. The main advantage of this method compared to conventional immunochemical staining is higher detection sensitivity due to the magnification effect of luminescence, which produces a boost in focal image and intensity. This technique enables reduction of the incubation period for the virus-infected cells and also reduces the amount of antibody necessary for antigen detection in foci (19). Another alternative method for NT of hantavirus is the replication reduction neutralization test (RRNT), which uses a quantitative reverse transcriptase (qRT)-PCR-based system. This assay is performed as previously described, but after an incubation of 2 weeks, virus titers are determined by qRT-PCR (20). Last, there is a recently published NT using recombinant pseudotyped lentivirus bearing the envelope glycoproteins of hantavirus (21).

Immunoblotting

Immunoblotting is basically used to detect antibodies to specific hantavirus proteins previously separated and immobilized after electrophoresis. In Western blotting, whole-virus lysates containing inactivated and disrupted viral proteins are separated by electrophoresis according to their molecular weight or relative mobility as they migrate

through a polyacrylamide gel in the presence of sodium dodecyl sulfate. The resolved protein bands are transferred to a nitrocellulose membrane that is cut into strips that are used in reaction with serum specimens. Hantavirus-specific antibodies bind to the viral proteins separated, and this produces bands in the nitrocellulose paper. The bands are directly visualized by using an enzyme-labeled anti-human antibody followed by a chromogenic substrate. The test results are determined by comparison of the nitrocellulose strip with those containing positive and negative controls (22). Western blotting produces a lower background and has a higher specificity than does IFA.

To minimize the use of infected cell culture in Western blotting, recombinant proteins of hantavirus have been used as antigens to detect IgM and IgG specific antibodies in human and small mammal sera. The sera of infected patients or animals commonly show antibodies to recombinant nucleocapsid protein of hantavirus, and that is why it is commonly used in diagnosis by Western blotting. The major disadvantages of this technique for routine diagnosis of hantavirus are that it (i) is labor-intensive, (ii) is expensive, (iii) is time-consuming, and (iv) requires BSL-3 facilities for handling of hantavirus.

Enzyme-Linked Immunosorbent Assays

Indirect enzyme-linked immunosorbent assays (ELISAs) IgM-ELISA, IgG-ELISA, and IgM capture ELISA are the most frequently used serological tests for diagnosis of hantavirus infections. ELISAs are capable of detecting hantavirus-specific IgM antibodies in human acute infections (HCPS and HFRS), since these antibodies are detectable starting on the first days of disease. The detection of IgG by ELISA is used in epidemiological surveys worldwide. ELISAs can use, as hantavirus antigens, infected cell lysates or viral proteins purified or produced by recombinant molecular techniques. The Nucleocapsid protein (N), which is the most immunogenic viral protein, is commonly used as the antigen in these tests. Recombinant N proteins have been produced in *Escherichia coli* or baculovirus (23, 24).

For the indirect ELISA, 96-well polystyrene plates are coated with hantavirus antigens and incubated at 4°C for 16 hours. These plates can be held for up to 7 days. The plate wells are washed with phosphate-buffered saline (PBS), blocked with milk or gelatin, and incubated at room temperature. The wells are washed with pure PBS or with PBS containing Tween-20. Following this, PBS-diluted serum samples to be tested are added to the wells. After another incubation, an anti-IgM or anti-IgG antibody conjugated with an enzyme, such as peroxidase, is added. The plates are incubated, the wells are washed with PBS, and a substrate, either 3,3′,5,5′-tetramethylbenzidine (TMB) or 2,2′-azinobis(3-ethylbenzthiazolinesulfonic acid) (ABTS) peroxide, is added to the wells. The optical density (OD) of the color generated in the reaction can be read visually or in the spectrophotometer. The capture-IgM ELISA is similar to the indirect IgM-ELISA, except that the wells of the plate are first coated with an anti-human IgM mu chain antibody and the plates are incubated overnight. At this point, plates may be prepared weekly and stored. The proper assay begins by adding the hantavirus antigen into the rows of wells A through D. A negative cell extract is added to rows E through H. Following this, the serum for test diluted is added. After incubation and washing, an enzyme (such as horseradish peroxidase) conjugated to an anti-human IgM is added to the wells. Finally, after incubation and washing, a substrate (ABTS) is added and the color reaction is read visually and/or spectrophotometrically. The washing steps of the plate wells are used to remove unspecific IgG and unwanted immune complexes, thus reducing background and improving the accuracy of the test. IgM capture assays are considered more sensitive and specific than those of indirect IgM-ELISA formats.

ELISAs are fast (4 to 6 hours) and sensitive, are simple to perform, allow titration of IgM or IgG, and do not require a BSL-3 laboratory, viral isolation in culture cells, or use of a darkroom or fluorescence microscope. The specificity of the assay depends on the virus antigen used. The rapid capture IgM-ELISA developed by the U.S. Army Medical Research Institute of Infectious Diseases and the Centers for Disease Control and Prevention is effective for diagnosis of HFRS and HCPS (1). In addition, other ELISAs have been developed for many species of hantavirus worldwide.

Other enzyme immunoassays (EIA) for detection of IgM or IgG to hantavirus are available commercially. The Reagena EIA (Finland) is able to detect IgM and IgG antibodies to PUUV, DOBV, and HTNV in human serum. The IgM antibodies for PUUV are captured in the microtiter plate and are detected by a horseradish peroxidase coupled to recombinant PUUV N protein. Finally, the color is developed by TMB substrate. The test requires 2.5 hours. The Hantavirus IgG Dx Select ELISA (Focus Diagnostics, Cypress, CA, USA) is supposed to detect all known European hantaviruses and is used for initial screening of sera. This assay has high specificity and sensitivity and is a suitable solution for routine testing in a reference laboratory.

Immunochromatographic Test

Highly sensitive and fast serodiagnostic tests for hantavirus include those using immunochromatography and stain revelation with protein A-labeled colloidal gold. This technique using representative antigens of different hantaviruses is an effective tool for screening the infection in humans (25).

Currently, three commercial immunochromatographic assays are used for hantavirus diagnosis. The recomLine Bunyavirus IgG/IgM test kit (Mikrogen, Neuried, Germany) evaluates serum samples diluted 1:100, incubated on test strips with six lines containing nucleocapsid proteins from HTNV and PUUV or a recombinant N terminus of the nucleocapsid antigen of PUUV, HTNV, DOBV, and SEOV and a control band for IgG or IgM. The rapid immunoblot strip assay (RIBA) (Novartis Vaccines and Diagnostics, Cambridge, MA, USA) employs combinations of recombinant N and/or G1 antigens from at least six different hantavirus serotypes, including HTNV, PUUV, SEOV, DOBV, Sin Nombre virus, and Andes virus. In Europe, there is also the POC PUUMALA test (Reagena Ltda, Finland), which uses a lateral-flow membrane-based assay technology, in which baculovirus-expressed highly purified PUUV N antigen is immobilized in a nitrocellulose membrane (23). The test result is visualized by using gold-conjugated rabbit anti-human IgM antibodies. These methods provide highly accurate results and allow the detection of infection so that treatment can be administered and death avoided. However, Western blot assays commonly have a limited use as a supplemental assay to confirm results obtained by other serologic tests.

Interpretation of Results of Serologic Tests

In patients having hantavirus fever, the appearance of IgM antibodies is detected until 3 days after the onset of symptoms. IgG antibodies to hantavirus are usually detected later than IgM. Therefore, specific IgM antibodies are used to diagnose hantavirus fever.

In order to improve control measures in serologic assays detecting IgM to hantavirus, tests of positive samples, besides the test with negative antigen control, should be performed

in duplicate, and their results should also be compared to the results observed with positive and negative controls. Positive results should be determined by subtracting of the OD value of a serum diluted 1:100 or more in the well containing the hantavirus antigen from the OD of the same serum under the same conditions, tested to the negative antigen. The result of this difference must be greater than 0.1. A good-quality test should have low fluctuation of OD values among replicates of positive and negative controls.

Besides the detection of specific IgM antibodies in serum, the conversion of IgG-negative serum obtained in the acute phase of disease into IgG-positive in serum obtained at the convalescent phase can be diagnostic of recent infection by hantavirus. Likewise, 4-fold or greater rises in IgG antibody titers in the serum obtained at the convalescent phase may support the diagnosis of recent infection. Unchanged titers of specific antibodies in paired sera indicate an old hantavirus infection or a vaccine. Negative tests in paired sera may exclude infection by hantavirus. However, the results of serologic tests for detection of hantavirus-specific antibodies must be interpreted with caution. A lack or delay in production of IgM or IgG antibodies in the serum may occur, giving false-negative results in the acute phase of hantavirus disease. IgM antibodies also may persist for extended periods after primary infection, giving false-positive results in infections by other pathogens. Significant rises in IgG antibodies do not always occur as a result of recurrent infections or exogenous reinfection. There is no "gold standard" to which any serological assay can be compared. Therefore, many caveats related to the serologic diagnosis of hantavirus infections indicate that the direct methods of detecting viral antigens or nucleic acids are more reliable.

MOLECULAR METHODS

Rapid diagnosis is essential for management of patients with severe diseases caused by hantavirus, such as HCPS, which produce respiratory failure, shock, and high case fatality rates. Thus, fast and highly sensitive diagnostic tests have been developed based on detection of the virus genome. This genome can be rapidly detected in clinical samples, such as blood, serum, or organ fragments, by reverse transcription (RT)-PCR. Hantavirus genome detection can be allowed starting on the first day of onset of symptoms. Detection of the hantavirus genome has been reported in patients before the first day of symptoms. However, the low levels of viral RNA present in human and rodent tissue samples can sometimes require the nested-RT-PCR or, alternatively, the real-time RT-PCR amplifying regions of high homology in the hantavirus genome. A large number of potential variants of RT-PCRs are available, including those involving different primer combinations. A representative procedure for these methods is described below.

Reverse Transcription-PCR

RT-PCR is a molecular method commonly used worldwide for diagnosis of hantavirus infections. This technique allows detection of the virus RNA in serum, in blood clots, in nucleated blood cells, and in lung tissues. However, RT-PCR is very prone to cross-contamination and meticulous care must be taken to avoid this contamination. For RT-PCR, it is essential to use specific primer sets for hantavirus. The small (S) genomic segment is a common place for selection of suitable primers for routine diagnostic work. However, for increasing the specificity and the sensitivity of the RT-PCR, it is recommended to perform an additional assay using primers for the M segment of the hantavirus genome (1, 26).

For the extraction of RNA from serum or plasma, there are commonly used commercial kits or TRIzol. A positive-control RNA, a negative-control RNA, and negative-control water are required for the interpretation of RT-PCR results. Hantaviruses are RNA viruses; they require a previous reaction of reverse transcription to make the cDNA, which in sequence is added into a mixture for PCR containing a heat-stable Taq-DNA polymerase, an excess of deoxynucleoside triphosphates, and forward and reverse oligonucleotide primers that flank the DNA sequence of interest. The PCR process is then performed during repeated cycles of heating and cooling of the reaction mixture, when the double-stranded target DNA (dsDNA) is heat denatured and cooled, enabling forward and reverse primers to anneal to complementary sequences on each target in the DNA strand. The primers are extended by the DNA polymerase and create double-stranded copies of the target DNA, which can act as templates for new DNA amplifications. In some cases, when the concentration of RNA of hantavirus is low or when a virus-specific detection is required, a second-turn PCR using internal primers to those of the first round (nested PCR) enables a more sensitive new amplification that could also be more specific, depending on the primers. The PCR products amplified from the hantavirus genome are visualized under UV light, in an agarose gel previously subjected to electrophoresis (26–28).

Currently, the number of commercial assays for hantavirus diagnosis is limited, and this leads to an extensive use of "in-house" protocols of RT-PCR. Subjective result interpretation, high cost, and laborious performance are limitations of the PCR technique. Additionally, in the nested PCR, manipulations of all reagents should be carried out exclusively with plugged pipette tips. Great caution must be taken to separate pre-PCR from post-PCR steps, including the use of separate pipettes and pipette tips and different bench or hood spaces.

Real-Time RT-PCR

The advent of real-time PCR represents a remarkable leap in DNA amplification technology. Therefore, numerous real-time PCR protocols have been described worldwide (29–33). Briefly, real-time PCR is achieved through the use of fluorescent detection technology. Fluorescent molecules are added to the reaction mixture and interact with the PCR product to produce an increase in fluorescent signal while DNA amplification occurs. This fluorescent signal is measured during each thermal cycle and monitored in real time.

There are two main types of fluorescent technologies used in real-time PCR. One uses DNA intercalating dyes, such as SYBR green, which bind nonspecifically into dsDNA; upon intercalation into dsDNA, SYBR green emits a fluorescent signal, which can be observed by a fluorescent reader. Thus, the SYBR green technology is a very simple and quick method for real-time monitoring of the cDNA amplification of hantavirus by PCR. The main disadvantage of SYBR green is its binding into any dsDNA, including nonspecific PCR products, such as primer dimer, and it requires an additional analysis of the melting curve for assay specificity (32–34). The other real-time PCR fluorescent technology is the TaqMan system that uses reporter fluorescent dye covalently coupled specifically into probes. The probe is degraded when it is found by Taq polymerase, and it hybridizes into a strand of the amplimer. In sequence, an endonuclease breaks the probe into shorter fragments, thus liberating the reporter fluor. The sequence detection system continuously interrogates each tube by using light

and simultaneously monitors the intensity of light in the wavelength emitted as fluor response (29–31).

Thus, real time RT-PCR provides numerous advantages over conventional RT-PCR. From a practical perspective, real-time PCR removes the need for a separate detection step, which significantly reduces test time. Also, the system is closed, reducing the potential for carryover contamination. Additionally, this technology allows the establishment of a parallel standard curve using a template molecule of known concentration and thus the determination of the quantity of the viral RNA in a sample (qRT-PCR). However, the equipment for the test is still expensive, and the real-time RT-PCR method for diagnosis of hantavirus has not been widely used in diagnostic laboratories.

Interpretation of RT-PCR Results

The RNA of hantavirus is present in samples from viremic symptomatic patients at the acute phase of infection. However, in later phases of illness, viral RNA becomes increasingly less abundant until it is undetectable, usually within 7 to 12 days after hospitalization. Using serum samples as the RNA source, nested PCR can detect viral genetic material in about 70% of acute-phase samples. Because RT-PCR assays are positive only in the acute phase of hantavirus infection, RT-PCR and qRT-PCR should be performed together with other diagnostic tests, such as IgM-ELISA. RT-PCR assays are fundamental for molecular epidemiology, including identification of emergent hantavirus genotypes in a region, and also for studies of pathogenesis.

NEW PLATFORMS FOR DIAGNOSIS

Microarray

A hantavirus-specific microarray was developed to detect amplicons from independent-sequence PCR amplifications. Nordström et al. developed a diagnostic DNA microarray specific for detection of PUUV, Prospect Hill virus, SNV, DOBV, SEOV, and HTNV. The array contains RNA fragments of S and M segments of 12 hantaviruses. The assay is performed with purified PCR products, and the amplicons from viral sequences contain nucleotides Cy3-dCTP or Cy5-dCTP (Amersham Biosciences). These amplicons are then annealed to a microarray chip, which is read by the GSI Lumonics Scanarray 4000 confocal laser scanner (GSI Lumonics, Billerica, MA). The slide produces TIFF images, which are quantified using ImaGene 4.0 (Biodiscovery, Inc., Marina del Rey, CA), identified (CloneTracker 1.3; Biodiscovery, Inc.), and analyzed (Microsoft Excel 2000; Microsoft Corp.) (35). The microarray possesses a large number of specific primers that can be used for detection of a panel of hantaviruses based on their diversity. However, this assay (i) is cumbersome, (ii) is highly expensive, (iii) requires laborious analysis, and (iv) has a high risk of contamination. Thus, the microarray is still an experimental method, which currently is not attractive and competitive for the clinical routine laboratory.

Flow Cytometry

Flow cytometry can be used for detection and titration of hantavirus. This technique was developed using an anti-N monoclonal antibody for detection of viral nucleocapsid protein (N). The flow cytometry method was used in cells infected with Andes virus. The viral titer was calculated based on the percentage of cells tagged for the nucleocapsid protein of hantavirus, and the results of flow cytometry were corroborated by viral titers obtained in the focus assay. This new assay for hantavirus is highly sensitive and a suitable tool to detect and quantify the virus in human samples. It also can be a fast quantitative method, applicable to studies on antiviral drugs (36). Although providing the advantage of circumventing the use of BSL-3 laboratories, flow cytometry requires expensive cytometers and labeled monoclonal antibodies.

Luminex

The Luminex system can be utilized for detection of many pathogens. When used for diagnosis, nucleic acid or protein probes of the pathogen are usually conjugated to distinct bead types and a mixture of these beads is used in an array for detection and differentiation, based on the products that are bead linked. Recently, it was established that a multiplexed Luminex-based immunoassay simultaneously detected the IgG antibodies produced in hemorrhagic fever, including those produced by Hantaan virus, Seoul virus, Puumala virus, Andes virus, Sin Nombre virus, Crimean-Congo hemorrhagic fever virus, Rift Valley fever virus, Severe fever with thrombocytopenia syndrome virus, bunyavirus, and dengue virus. This assay uses recombinant N proteins of each hantavirus linked into microspheres that are analyzed by lasers in the Luminex, allowing identification of the specific bead and also any IgG binding into the bead. The evaluation of this new method with clinical serum samples showed 98.04% diagnostic sensitivity for HFRS and a specificity ranging from 66.67 to 100% (37). The Luminex x MAP technology is rapid and sensitive and detects multiple pathogens. It is a high-throughput method but is still too expensive for use in clinical routine laboratories.

REFERENCES

1. **Jonsson CB, Figueiredo LT, Vapalahti O.** 2010. A global perspective on hantavirus ecology, epidemiology, and disease. *Clin Microbiol Rev* **23:**412–441. PubMed
2. **Jääskeläinen KM, Kaukinen P, Minskaya ES, Plyusnina A, Vapalahti O, Elliott RM, Weber F, Vaheri A, Plyusnin A.** 2007. Tula and Puumala hantavirus NSs ORFs are functional and the products inhibit activation of the interferon-beta promoter. *J Med Virol* **79:**1527–1536. PubMed
3. **Vera-Otarola J, Solis L, Soto-Rifo R, Ricci EP, Pino K, Tischler ND, Ohlmann T, Darlix JL, López-Lastra M.** 2012. The Andes hantavirus NSs protein is expressed from the viral small mRNA by a leaky scanning mechanism. *J Virol* **86:**2176–2187. PubMed
4. **Watson DC, Sargianou M, Papa A, Chra P, Starakis I, Panos G.** 2014. Epidemiology of Hantavirus infections in humans: a comprehensive, global overview. *Crit Rev Microbiol* **40:**261–272. PubMed
5. **Kruger DH, Figueiredo LT, Song JW, Klempa B.** 2015. Hantaviruses—globally emerging pathogens. *J Clin Virol* **64:**128–136. PubMed
6. **Kallio ER, Klingström J, Gustafsson E, Manni T, Vaheri A, Henttonen H, Vapalahti O, Lundkvist A.** 2006. Prolonged survival of Puumala hantavirus outside the host: evidence for indirect transmission via the environment. *J Gen Virol* **87:**2127–2134. PubMed
7. **Padula PJ, Edelstein A, Miguel SD, López NM, Rossi CM, Rabinovich RD.** 1998. Hantavirus pulmonary syndrome outbreak in Argentina: molecular evidence for person-to-person transmission of Andes virus. *Virology* **241:**323–330. PubMed
8. **Martinez VP, Bellomo C, San Juan J, Pinna D, Forlenza R, Elder M, Padula PJ.** 2005. Person-to-person transmission of Andes virus. *Emerg Infect Dis* **11:**1848–1853. PubMed
9. **Martinez-Valdebenito C, Calvo M, Vial C, Mansilla R, Marco C, Palma RE, Vial PA, Valdivieso F, Mertz G,**

Ferrés M. 2014. Person-to-person household and nosocomial transmission of Andes hantavirus, Southern Chile, 2011. *Emerg Infect Dis* **20:**1629–1636. PubMed
10. **Figueiredo LT, Souza WM, Ferrés M, Enria DA.** 2014. Hantaviruses and cardiopulmonary syndrome in South America. *Virus Res* **187:**43–54. PubMed
11. **Clement J, Maes P, Van Ranst M.** 2014. Hemorrhagic fever with renal syndrome in the New, and hantavirus pulmonary syndrome in the Old World: paradi(se)gm lost or regained? *Virus Res* **187:**55–58. PubMed
12. **Sargianou M, Watson DC, Chra P, Papa A, Starakis I, Gogos C, Panos G.** 2012. Hantavirus infections for the clinician: from case presentation to diagnosis and treatment. *Crit Rev Microbiol* **38:**317–329. PubMed
13. **Knust B, Macneil A, Rollin PE.** 2012. Hantavirus pulmonary syndrome clinical findings: evaluating a surveillance case definition. *Vector Borne Zoonotic Dis* **12:**393–399. PubMed
14. **Lee HW, Lee PW, Johnson KM.** 1978. Isolation of the etiologic agent of Korean hemorrhagic fever. *J Infect Dis* **137:**298–308. PubMed
15. **Lederer S, Lattwein E, Hanke M, Sonnenberg K, Stoecker W, Lundkvist Å, Vaheri A, Vapalahti O, Chan PK, Feldmann H, Dick D, Schmidt-Chanasit J, Padula P, Vial PA, Panculescu-Gatej R, Ceianu C, Heyman P, Avšič-Županc T, Niedrig M.** 2013. Indirect immunofluorescence assay for the simultaneous detection of antibodies against clinically important old and new world hantaviruses. *PLoS Negl Trop Dis* **7:**e2157. PubMed
16. **Valdivieso F, Vial P, Ferres M, Ye C, Goade D, Cuiza A, Hjelle B.** 2006. Neutralizing antibodies in survivors of Sin Nombre and Andes hantavirus infection. *Emerg Infect Dis* **12:**166–168. PubMed
17. **Niklasson B, Jonsson M, Lundkvist A, Horling J, Tkachenko E.** 1991. Comparison of European isolates of viruses causing hemorrhagic fever with renal syndrome by a neutralization test. *Am J Trop Med Hyg* **45:**660–665. PubMed
18. **Tanishita O, Takahashi Y, Okuno Y, Yamanishi K, Takahashi M.** 1984. Evaluation of focus reduction neutralization test with peroxidase-antiperoxidase staining technique for hemorrhagic fever with renal syndrome virus. *J Clin Microbiol* **20:**1213–1215. PubMed
19. **Heider H, Ziaja B, Priemer C, Lundkvist A, Neyts J, Krüger DH, Ulrich R.** 2001. A chemiluminescence detection method of hantaviral antigens in neutralisation assays and inhibitor studies. *J Virol Methods* **96:**17–23. PubMed
20. **Maes P, Keyaerts E, Li S, Nlandu-Masunda V, Clement J, Van Ranst M.** 2009. Replication reduction neutralization test, quantitative RT-PCR-based technique for the detection of neutralizing hantavirus antibodies. *J Virol Methods* **159:**295–299. PubMed
21. **Yu L, Bai W, Wu X, Zhang L, Zhang L, Li P, Wang F, Liu Z, Zhang F, Xu Z.** 2013. A recombinant pseudotyped lentivirus expressing the envelope glycoprotein of Hantaan virus induced protective immunity in mice. *Virol J* **10:**301. PubMed
22. **Yoshimatsu K, Arikawa J, Li H, Kariwa H, Hashimoto N, Suzuki N.** 1996. Western blotting using recombinant Hantaan virus nucleocapsid protein expressed in silkworm as a serological confirmation of hantavirus infection in human sera. *J Vet Med Sci* **58:**71–74. PubMed
23. **Vapalahti O, Lundkvist A, Kallio-Kokko H, Paukku K, Julkunen I, Lankinen H, Vaheri A.** 1996. Antigenic properties and diagnostic potential of Puumala virus nucleocapsid protein expressed in insect cells. *J Clin Microbiol* **34:**119–125. PubMed
24. **Figueiredo LT, Moreli ML, Borges AA, Figueiredo GG, Souza RL, Aquino VH.** 2008. Expression of a hantavirus N protein and its efficacy as antigen in immune assays. *Braz J Med Biol Res* **41:**596–599. PubMed
25. **Amada T, Yoshimatsu K, Koma T, Shimizu K, Gamage CD, Shiokawa K, Nishio S, Ahlm C, Arikawa J.** 2014. Development of an immunochromatography strip test based on truncated nucleocapsid antigens of three representative hantaviruses. *Virol J* **11:**87. PubMed
26. **Moreli ML, Sousa RL, Figueiredo LT.** 2004. Detection of Brazilian hantavirus by reverse transcription polymerase chain reaction amplification of N gene in patients with hantavirus cardiopulmonary syndrome. *Mem Inst Oswaldo Cruz* **99:**633–638. PubMed
27. **Ahn C, Cho JT, Lee JG, Lim CS, Kim YY, Han JS, Kim S, Lee JS.** 2000. Detection of Hantaan and Seoul viruses by reverse transcriptase-polymerase chain reaction (RT-PCR) and restriction fragment length polymorphism (RFLP) in renal syndrome patients with hemorrhagic fever. *Clin Nephrol* **53:**79–89. PubMed
28. **Kim EC, Kim IS, Choi Y, Kim SG, Lee JS.** 1994. Rapid differentiation between Hantaan and Seoul viruses by polymerase chain reaction and restriction enzyme analysis. *J Med Virol* **43:**245–248. PubMed
29. **Aitichou M, Saleh SS, McElroy AK, Schmaljohn C, Ibrahim MS.** 2005. Identification of Dobrava, Hantaan, Seoul, and Puumala viruses by one-step real-time RT-PCR. *J Virol Methods* **124:**21–26. PubMed
30. **Maes P, Li S, Verbeeck J, Keyaerts E, Clement J, Van Ranst M.** 2007. Evaluation of the efficacy of disinfectants against Puumala hantavirus by real-time RT-PCR. *J Virol Methods* **141:**111–115. PubMed
31. **Evander M, Eriksson I, Pettersson L, Juto P, Ahlm C, Olsson GE, Bucht G, Allard A.** 2007. Puumala hantavirus viremia diagnosed by real-time reverse transcriptase PCR using samples from patients with hemorrhagic fever and renal syndrome. *J Clin Microbiol* **45:**2491–2497. PubMed
32. **Jakab F, Sebok J, Ferenczi E, Horváth G, Szucs G.** 2007. First detection of Dobrava hantavirus from a patient with severe haemorrhagic fever with renal syndrome by SYBR Green-based real time RT-PCR. *Scand J Infect Dis* **39:**902–906. PubMed
33. **Machado AM, de Souza WM, de Pádua M, da Silva Rodrigues Machado AR, Figueiredo LT.** 2013. Development of a one-step SYBR Green I real-time RT-PCR assay for the detection and quantitation of Araraquara and Rio Mamore hantavirus. *Viruses* **5:**2272–2281. PubMed
34. **Mossbrugger I, Felder E, Gramsamer B, Wölfel R.** 2013. EvaGreen based real-time RT-PCR assay for broad-range detection of hantaviruses in the field. *J Clin Virol* **58:**334–335. PubMed
35. **Nordström H, Johansson P, Li QG, Lundkvist A, Nilsson P, Elgh F.** 2004. Microarray technology for identification and distinction of hantaviruses. *J Med Virol* **72:**646–655. PubMed
36. **Barriga GP, Martínez-Valdebenito C, Galeno H, Ferrés M, Lozach PY, Tischler ND.** 2013. A rapid method for infectivity titration of Andes hantavirus using flow cytometry. *J Virol Methods* **193:**291–294. PubMed
37. **Wu W, Zhang S, Qu J, Zhang Q, Li C, Li J, Jin C, Liang M, Li D.** 2014. Simultaneous detection of IgG antibodies associated with viral hemorrhagic fever by a multiplexed Luminex-based immunoassay. *Virus Res* **187:**84–90. PubMed

Rabies Virus

D. CRAIG HOOPER

69

Rabies virus (RABV) and RABV-related lyssaviruses are the causative agents of zoonotic viral encephalitis, with a case/fatality ratio approaching 1:1. These viruses are endemic in a number of terrestrial mammals and bat species throughout much of the world. Lyssaviruses (family *Rhabdovirus*, order *Mononegavirales*, of which RABV is the type species) are characteristically bullet-shaped particles averaging 75 by 180 nm with a single-stranded, negative-sense RNA genome encoding five proteins. In genome order, these proteins are nucleoprotein (N), which tightly encapsulates the genome; phosphoprotein (P), which was formerly referred to as the nonstructural (NS) protein; matrix (M) protein; glycoprotein (G), the primary target of neutralizing antibodies, which is found spread over the surface of the virus; and polymerase (L), the RNA-dependent RNA polymerase. Genetically and antigenically more diverse in glycoprotein than in nucleoprotein, the different lyssavirus variants are each associated with a particular host species. The major reservoir of RABV in Asia is the dog, historically and currently the cause of most human rabies cases; wildlife, including foxes, coyotes, skunks, raccoons, and bats, carry RABV or RABV-related viruses in diverse geographic regions. Effective vaccines and postexposure prophylaxis (PEP) regimens consisting of active and passive vaccination have been available for some time, and where animal reservoirs of the virus have been controlled by vaccination and PEP is readily available, human rabies is no longer the well-known disease of antiquity. However, in Asia, where dog rabies persists, human rabies is not uncommon, with cases estimated to occur at a rate of over 50,000 a year. Elsewhere, human rabies is sporadic, generally resulting from the bite of an infected dog while a traveler is in a region where rabies is endemic or from an interaction with an infected animal when the possibility of virus transmission is not recognized. As RABV can infect all mammals, the virus may be transmitted between a reservoir species and humans by intermediate species that are not normally associated with rabies, such as cats. However, the more common cause of unrecognized infection is through contact with an infected bat. In such cases, the bite or scratch responsible for the infection may be so minor as to go unnoticed.

HUMAN RABIES AND ITS PREVENTION

Historical evidence that the highest rabies mortality results from the bite of an infected animal on the head and face (1, 2) suggests that the lethality of RABV infection is related to the distance between the inoculation site and central nervous system (CNS). Generally, the initial signs of disease appear 2 to 6 weeks after exposure, but there have been occasional cases that developed a number of years after exposure (3, 4). Clinical rabies becomes apparent initially in nonspecific symptoms, which may include general malaise, chills, fever, headache, photophobia, anorexia, sore throat, cough, and musculoskeletal pain. In the case of a bite, there is often a prodromal period generally lasting from 2 to 10 days, with itching, burning, numbness, or paresthesia around the site. An acute neurologic phase in which patients manifest signs of neurological dysfunction, such as anxiety, agitation, paralysis, or episodes of delirium, follows. Various proportions of patients exhibit the classical pathognomonic sign of rabies, hydrophobia. Disease progression is variable but usually proceeds through coma to death from respiratory arrest by approximately 30 to 60 days after infection. The prolonged incubation period between infection and the development of the first clinical signs of rabies in humans led Louis Pasteur to speculate that the virus required time to spread from the inoculation site to the brain and that vaccination during this period might be protective (5). His proof of this principle is the foundation for PEP, which continues to be widely used where RABV exposure is suspected (6). Rabies PEP is highly effective in preventing the development of clinical rabies if administered in the first days after exposure but is ineffective once clinical signs of rabies appear, and the infection most often has a lethal outcome (7, 8). However, a number of individuals treated by the Milwaukee protocol, an experimental intervention that includes supportive care along with administration of neuroprotective and antiviral agents, have survived confirmed rabies (9, 10). Moreover, immune mechanisms capable of clearing RABV from CNS tissues have been described in animal models (11–14).

Human rabies is minimized by control of reservoirs of the virus, for example by vaccinating dogs, and by promptly providing PEP to individuals who may have been exposed. Recognition of potential exposure is the most important criterion for successful PEP, which entails the passive administration of RABV-neutralizing antibodies (VNA) and immunization with a potent vaccine. In the case of contact through broken skin or mucosal surfaces with the saliva of a suspect animal, as would occur with a bite, the decision to

doi:10.1128/9781555818722.ch69

administer PEP can be based on testing of the animal, if it is available. For a domestic animal that should have been vaccinated against rabies, confirmation of adequate VNA titers by serology is warranted. For wildlife, if the animal can be caught, the general approach is to have its neural tissues tested for RABV by immunohistochemistry or molecular techniques. Delaying the administration of PEP while tests are being conducted or the animal is observed for the development of clinical rabies is not advised. If the animal cannot be captured and the species is known to carry rabies in the area, PEP is recommended. Modern PEP is safe and effective, generally with minimal side effects, and should be commenced within the first several days of a possible exposure.

Bats present a unique problem with respect to human rabies, as the RABV and RABV-related lyssavirus reservoirs in these animals are difficult to eliminate through vaccination and the event transferring the virus between bat and human is often not recognized as the potential cause of an infection. Human deaths from bat RABV variants have been reported in North America and Europe and from the RABV-related Australian bat lyssavirus in Australia. In some cases where there was no history of possible exposure, "cryptic" rabies cases were initially classified as encephalitis of unknown origin and correctly identified as rabies only in the terminal stages of the disease or postmortem. As an infected individual presents a risk of infection to others, this can greatly expand the numbers of people who might be exposed to the virus and must receive PEP.

Because of the lack of specificity of the clinical signs of rabies, diagnosis of the disease requires immunohistochemical or molecular analysis of infected tissues. The failure to test for rabies when tissues from subjects who die of unexplained encephalitis are used for transplantation can have lethal consequences for recipients. Cornea, kidney, kidney/pancreas, liver, lung, and a segment of iliac artery are among the tissues known to have transmitted RABV to recipients (15–18). In one case, rabies was not suspected in the donor until the disease manifested in a recipient over a year later (18). RABVs originating in dogs, bats, and raccoons have all been implicated in the transmission of rabies by transplantation (15–18). Analysis of the donors' brain tissues for RABV by immunohistochemistry or molecular approaches would likely have prevented these deaths.

Due to the importance of rabies surveillance, a number of national and international agencies maintain recommendations for assessing RABV infection and immunity as well as guidelines for what to do in the case of a possible exposure. These are available on the Internet from the World Health Organization (WHO) at http://www.who.int/rabies/ and the United States Centers for Disease Control and Prevention (CDC) at http://www.cdc.gov/rabies/.

LABORATORY DIAGNOSIS

Immunohistochemistry and Immunofluorescence

Historically, the diagnosis of rabies was most often validated postmortem by histological examination of brain tissue for the intraneuronal cytoplasmic inclusions of RABV nucleocapsid particles (RNP) called Negri bodies. The presence of infectious virions may be confirmed by injecting suspect material into suckling mouse brain and looking for Negri bodies when the animal succumbs several days later. However, Negri bodies are not always present in RABV-infected brain tissue or may be confused with other viral inclusion bodies. Thus, more-specific immunohistochemical and immunofluorescence techniques have supplanted simple histology in testing of tissue specimens for evidence of RABV. The greater sensitivity of these approaches also allows RABV antigens to be detected in antemortem samples, including neural tissue biopsy specimens, skin biopsy specimens, saliva, and corneal impressions from individuals with rabies.

Since nucleoprotein antigens are more conserved among different RABV isolates than glycoprotein antigens, nucleoprotein-specific antibodies are normally used to detect RABV in histological specimens. The most widely employed methods for the general diagnosis of RABV infection utilize monoclonal anti-nucleoprotein-specific antibodies. A variety of different antibody-based tests have been developed to provide specificity and improve the sensitivity of RABV antigen detection in specimens. The method of choice for the detection of RABV infection in postmortem samples from either animals or humans is the direct fluorescent-antibody (dFA) test, which utilizes fluorescein isothiocyanate-conjugated RABV nucleoprotein-specific antibodies to detect viral antigen. The dFA test is more sensitive and specific than histochemical visualization of Negri bodies in CNS tissues, allowing a specific diagnosis to be made earlier in the infection, provided that appropriate samples are available. This methodology can detect RABV antigen in a variety of samples, including fixed and frozen material of varied quality. A positive dFA test on brain tissue sections, impressions, or smears (brain stem and cerebellum are preferred) is the minimum standard for the diagnosis of RABV infection in the United States (19, 20).

The fluorescein-conjugated N-specific monoclonal antibodies capable of detecting all known RABV variants that are used for dFA tests are commercially available. Such antibodies can also detect Australian bat lyssavirus as well (21). Preparation of samples from field specimens and clinical isolates for dFA analysis has been extensively detailed elsewhere (22), and a detailed protocol for the postmortem diagnosis of rabies in animals by the dFA test that includes sample preparation and the test procedure as well as a list of reagent suppliers can be found on the CDC website http://www.cdc.gov/rabies/.

The requirement for a fluorescence microscope for the dFA test and related technologies can be problematic in certain regions and in the field. Consequently, immunohistochemistry (IHC) techniques that can be performed with a light microscope have been developed (23). Through the use of enzyme-labeled, RABV-specific antibodies and substrate, IHC is as specific as the dFA test and may be preferable for fixed tissue specimens.

ELISA-Based Tests for Detection of RABV Antigen

The need to test tissue samples for RABV infection in the field where sophisticated technology is unavailable has led to the development of several enzyme-linked immunosorbent assay (ELISA)-based methods that enable the detection of RABV antigens by direct visual examination. The rapid rabies enzyme immunodiagnosis (RREID) assay and its many variants are essentially ELISAs in which RABV antigens are detected by a substrate reaction, the product of which, under optimal conditions, is readily visible. In RREID, plates coated with anti-N antibodies are used to trap RNP from specimen preparations, which is then detected using additional enzyme-conjugated anti-N antibodies and conventional ELISA. The sensitivity of the technique can be improved by the use of biotinylated N-specific antibodies for detection and peroxidase-streptavidin (24). Both the sensitivity and the specificity of these approaches are generally considered to be somewhat lower than those of

the dFA test with appropriately prepared samples. However, sample quality may be less critical than for the dFA test and the assay may be structured such that positive results can be visualized without microscopy (24, 25). Moreover, ELISA-based assays are more readily amenable to the quantitation of antigen content than is dFA analysis (26).

Detection of Rabies Viral RNA by RT-PCR

While dFA is the current standard for the analysis of both post- and antemortem samples from animals and humans suspected of having rabies, molecular technologies are increasingly used to confirm and assess RABV infection. Reverse transcription-PCR (RT-PCR) for RABV genomic RNA or mRNA can rapidly confirm a diagnosis from a relatively small amount of an infected sample, which has important implications for patient management, particularly with respect to transplantation and PEP of a patient's contacts. A number of different procedures for RT-PCR detection and characterization of RABV RNA using a variety of oligonucleotide primers and probes specific for conserved or strain-specific sequences have been developed (27–34). In addition, certain well-established RT-PCR-based technologies, such as real-time quantitative RT-PCR (QRT-PCR), are useful for the analysis of poor-quality specimens and archived material.

RT-PCR for RABV RNAs has been shown to sensitively detect evidence of infection in tissues from experimentally infected animals as well as in human autopsy material, including fresh, snap-frozen, formalin-fixed, and paraffin-embedded material (see, e.g., references 28, 29, 32, and 33). RNA purified from these specimens by conventional technology, or *in situ*, can be subjected to RT-PCR or nested RT-PCR if greater sensitivity and specificity is required. Through the use of the appropriate primer or primer/probe combinations, RT-PCR-based techniques can be used to screen for RABV infection as well as identify RABV strains associated with a particular reservoir species (see below). In addition, individual viral isolates can be identified by sequencing RT-PCR products (27).

For general screening for RABV infection, as is the case for antibody-based techniques, RT-PCR approaches commonly test samples for the presence of the more conserved nucleoprotein gene. For conventional RT-PCR, primers derived from the nucleoprotein gene sequence, such as a sense primer near the initial methionine codon of N and an antisense primer close to the initial methionine residue of the NS protein (Table 1), are appropriate for amplifying RABV RNA from a range of street virus isolates (22). This pair of primers will amplify a fragment of 1.4 kb. For increased sensitivity and specificity, nested PCR can be performed on this product (34). The lack of a product should not be considered confirmation that there is no infection. The quality of the RNA should be assessed by examining the expression of a cell housekeeping gene, such as those for β-actin, glyceraldehyde-3-phosphate dehydrogenase (GAPDH), and ribosomal L13a, etc., as RNA degradation is not uncommon, particularly in field specimens. In this case, an RT-PCR reaction targeting a smaller RNA fragment may have greater success. For example, primers RabNfor and RabNbatl.l (Table 1) amplify a fragment of about 200 nucleotides of RNA from a large variety of RABV strains, including a silver-haired bat RABV (35). PCR amplification of viral mRNA can also be performed but is usually limited to research specimens, as opposed to field specimens.

QRT-PCR is well suited for the analysis of samples for RABV genome RNA or mRNA. This technology is based upon the replication of only a relatively short stretch of RNA (120 to 150 nucleotides) and therefore has utility for a wide variety of samples of varying quality, including archived paraffin tissue sections. As is the case for other

TABLE 1 Primer and probe sets for PCR for rabies N protein mRNA[a]

Test and direction of primer (name)	Primer or probe sequence	Virus strain(s)
Conventional PCR		Multiple
Forward	5′-CTACAATGGATGCCCAC-3′	1.4-kb product
Reverse	5′-TTGACGAAGATCTTGCTCAT-3	
Forward (RabNfor)	5′-TTGT(AG)GA(TC)CAATATGAGTACAA-3′	~200-nt product
Reverse (RabNbatl.l)	5′-TTCCATAGCTGGTCCAGTCA-3′	
QRT-PCR		CVS/SHBRV
Forward	5′-CACTTCCGTTCACTAGGCTTGA-3′	
Reverse	5′-GACCCATGTAGCATCCAACAA-3′	
Probe	5′-FAM-TGAACACATGACCGACAGCATTCGA-BHQ-3′	+++/−
Forward	5′-TGTGCCCTAACTGGAGTACCA-3′	
Reverse	5′-GTGCCTACCCTAATTGCTGAA-3′	
NA (probe)	5′-FAM-CCGAACTTCAGATTCCTAGCTGGAACC-BHQ-3′	−/+++

[a]Primers and probes for QRT-PCR were designed from the N mRNA sequences of a CVS (NCBI accession no. AF406696) and SHBRV-18 (NCBI accession no. AY705373). FAM, carboxyfluorescein; BHQ, Black Hole Quencher; NA, not applicable; nt, nucleotides. +++ indicates a strong reaction and – indicates none, such that +++/– means that CVS is detected but not SHBRV and –/+++ means that CVS is not detected but SHBRV is. QRT-PCR was performed with a Bio-Rad iCycler on samples of mouse brain infected with CVS-24, CVS-N2C, CVS-F3, and a silver-haired bat rabies virus (SHBRV) isolate obtained from a human rabies case.

technologies, the choice of primers and probes for QRT-PCR (Table 2) is of paramount importance because of the extensive variability between RABV strains. The product may be detected nonspecifically using SYBR Green or with a sequence-specific probe, with the latter offering greater specificity and sensitivity. As is the case for conventional RT-PCR, the quality of the sample and the success of RNA extraction are assessed by examining the levels of expression of a housekeeping gene. Using the level of expression of a housekeeping gene as a measure of the quantity of the sample, QRT-PCR readily provides information about the extent of infection. To accurately assess the amount of RABV in a sample (genomic RNA) or extent of replication (mRNA) and provide a positive control for the reaction, synthetic DNA templates are advantageous. Using these, the absolute number of copies of RABV genomic RNA or mRNA in a sample can be determined and normalized to the quality of tissue studied.

RABV Characterization with Monoclonal Antibodies

A wide variety of monoclonal antibodies that can be used to antigenically phenotype different RABV isolates have been produced by a wide variety of laboratories (42–47). Since RABV glycoprotein has greater antigenic variability than nucleoprotein, glycoprotein-specific monoclonal antibodies have greater utility for the identification of diverse RABV and RABV-related lyssaviruses (48). While the dFA test, IHC, and other antibody-based technologies can be used to phenotype RABV, panels of antibodies for this purpose are not readily available, and more detailed characterization of isolates is generally performed using molecular approaches.

Molecular Characterization of RABV

Since each animal and bat species carries unique RABV strains, molecular analysis can determine the origin of an infecting virus, which is important in understanding the etiology of a human infection such that appropriate risk management strategies can be implemented. Conventional and real-time quantitative RT-PCR analyses using strain-specific primers or primer/probe combinations are now extensively used for this purpose. A number of these and their specificities have been reviewed elsewhere (34). Through analysis of areas of the genome that are highly variable, such as the pseudogene found between the G and L cistrons (32), individual RABV isolates may be identified. Sequencing the RT-PCR product of primers surrounding a region of interest is useful for this purpose.

PREPARATION OF RABV

Isolation

Wild-type (street) RABVs are highly neuronotropic and have limited potential to replicate in most common cell lines. Consequently, isolates of wild-type RABVs have historically been prepared by injecting the homogenate of an infected tissue sample or infected saliva into the brains of 1- to 3-day-old suckling mice, waiting over the next few days for neurological signs to manifest, and testing the tissues for the presence of virus by the dFA test or by titration as described below. However, many RABV variants, including all wild-type virus isolates tested so far, also replicate in cultures of neuroblastoma cells, such as mouse NA Cl300 cells (NB41A3, ATCC CCL-147). The dFA test is also the

TABLE 2 Primer and probe sets for QRT-PCR for RABV strains

Virus strain(s) and protein	Primer and probe set[a]	Apparatus (manufacturer)	Reference
SHBRV N protein	5′-TGTGCGCTAACTGGAGTACCA-3′ (forward) 5′-GTGCCTACCCTAAATTGCTGAA-3′ (reverse) 5′-FAM-CCGAACTTCAGATTCCTAGCTGGAACC-BHQ-3′ (probe)	iCycler (Bio-Rad)	36
CVS-F3 N protein	5-'CACTTCCGTTCACTAGGCTTGA-3′ (forward) 5′-GACCCATGTAGCATCCAA-3′ (reverse) 5′-HEX/FAM-TGAACACATGACCGACAGCATTCGA-BHQ-3′ (probe)	iCycler	12
Dog isolates	5′-CTGGCAGACGACGGAACC-3′ (forward) 5′-CATGATTCGAGTATAGACAGCC-3′ (reverse) 5′-FAM-TCAATTCTGATGACGAGGATTACTTCTCCGG-TAMRA-3′ (probe)	LightCycler 2.0 (Roche)	37
Dog rabies virus from Mexico	5′-GGAAAAGGGACATTTGAAAGAA-3′ (forward) 5′-AGTCCTCGTCATCAGAGTTGAC-3′ (reverse)	Mx3000P (Stratagene)	38
Fujian strain N protein	5′-GTGGGTACTGTTGTCACTGCTTA-3′ (forward) 5′-GTGAGATTTATCTGCTTTATGAACCCTGTA-3′ (reverse) FAM-TCCTGAGCAATCTTC-NFQ (probe)	Mx3005P	39
DRV-4 N protein	5′-CAGGCATGAACGCTTCCAAA-3′ (forward) 5′-CGTCAGTGCGCTTTATCTCCAA-3′ (reverse) FAM-5′-GATCCCGATGATGTATGCTCCTACTTGGC-3′-TAMRA (probe)	iCycler	40
Silver-haired-bat-associated RABV strain SHBRV-18	5′-AGGAAAAGCCCCTGACTTG-3′ (forward) 5′-TGCTCCCTCAAAGAACTGC-3′ (reverse) FAM-5′-GCTCGACCCTGATGATGTATGCTCTTATCT-3′-6-TAMRA (probe)	LightCycler 1.5	41

[a]HEX, hexachlorofluorescein; TAMRA, 6-carboxytetramethylrhodamine.

method of choice to confirm that cultured cells are infected. General methodologies for the isolation of RABV by mouse inoculation and in cell culture can be found elsewhere (22).

Production

For preparation of virus for VNA assays or of antigen for serology or more-detailed analysis, RABV may be produced *in vitro*. Wild-type and certain animal-passaged RABVs generally exist as quasispecies, and their culture in different cell types can cause the ratios of the different RABV variants to vary widely (49). Consequently, when stocks of wild-type RABVs must be expanded with minimal selection pressure, the method of choice is to infect suckling mice intracranially and to prepare virus from these tissues several days later.

Due to their antigenic cross-reactivity with most RABVs and related viruses and their capacity to infect and replicate in cell lines, fixed laboratory strains of RABV, such as challenge virus standard (CVS) strain 11 (CVS-11) and Evelyn-Rokitnicki-Abelseth, are normally used for these purposes. Unlike wild-type RABVs, these laboratory strains readily infect and can replicate to high titer in BHK cells (BHK-21[C-13]; ATCC CCL-10) and BSR cells, an interferon-incompetent clone of BHK cells which are widely used for virus production in laboratories. The WI-38 human diploid lung fibroblast cell line or Vero cells, an African green monkey kidney epithelial cell line, are generally used to produce virus for human vaccines using the Pitman-Moore or Pasteur RABV strains. Other cell lines, such as mouse NA cells, are more permissive for the growth of diverse RABV isolates but more fastidious and do not readily support high-titer virus production.

For small-batch production of RABVs, confluent cultures of BHK or BSR cells are infected with seed RABVs at 37°C in Dulbecco's modified Eagle's medium-bovine serum albumin and then cultured at 34°C. Since many of these viruses have limited pathogenicity for the cells, virus-containing supernatants can often be collected twice at 3- to 4-day intervals. The supernatant is concentrated, for example by tangential-flow filtration, and the virus purified by centrifugation in a sucrose gradient, followed by centrifugation at 24,000 rpm for 1 h at 5°C. The virus is then resuspended in Tris-saline buffer and stored at −80°C. Virus stability can be greatly enhanced by including low concentrations of bovine serum albumin in the buffer.

Titration of RABV: The Fluorescent-Focus Assay

RABVs in general and wild-type RABVs in particular have limited cytotoxicity *in vivo* and *in vitro* (50, 51). Due to the nonlytic nature of the virus, conventional plaque assays are not possible and titration of the virus in cell culture is routinely performed by visualizing foci of infected cells with fluorescein-conjugated rabies antigen-specific antibodies. For example, in brief, 10-fold dilutions of sample containing virus are made in medium (e.g., 10 μl to 90 μl), and 90 μl is added to 30 μl of BHK or NA cells in suspension (approximately 2.5×10^6 cells per ml). The mixtures are transferred to the wells of flat-bottom 96-well microtiter plates and incubated for 24 to 48 h at 34°C, washed once with phosphate-buffered saline, and fixed with ice-cold 80% acetone for 20 to 30 min. The acetone is then removed, the plates are dried, and the cell monolayers are stained with fluorescein-labeled anti-RABV antibodies. Nucleoprotein-specific antibodies are preferred for virus detection because wild-type RABV strains tend to express relatively low levels of glycoprotein (52), and as noted above, the antigenic structure of nucleoprotein is more conserved than that of glycoprotein. The results of the assay, with each initially infecting virion being represented by a fluorescent focus of cells into which the virus has spread, are read with a fluorescence microscope. The RABV titer is then reported in focus-forming units (FFU).

SEROLOGIC ASSESSMENT OF RABV IMMUNITY

Titration of Rabies VNA by Fluorescent-Focus Reduction Assays

RABV-neutralizing antibodies are the principal effectors of RABV immunity, and serum VNA levels are universally used to assess the level of protective immunity in individuals vaccinated either due to an occupational risk of exposure or due to contact with a suspect animal. Determination of a domestic animal's RABV immune status is also appropriate if it has been involved in an event consistent with exposure. RABVs do not lyse but bud from infected cells; therefore, a fluorescent-focus assay, measuring FFU, rather than a plaque assay, is used for quantifying virus levels and the reduction in FFU is generally used to titer serum levels of rabies VNA. While there are many variations and adaptations of this fluorescent-antibody virus neutralization (FAVN) technique in practice, the basic principle is the same. Generally, a known titer of fixed, tissue culture-adapted virus (Table 3) is incubated with dilutions of sera and then added to cultures of a susceptible cell line (e.g., BHK, BSR, or NA cells) prior to measurement of FFU, visualized using fluorescein-conjugated antibodies to RABVs and a fluorescence microscope (53). RABV N-specific antibodies are normally used due to the more highly conserved antigen structure of N. With these reagents, the capacity of sera to neutralize essentially any RABV strain can be assessed. A widely used RABV neutralization assay is the rapid fluorescent-focus inhibition test (RFFIT). A representative microculture RFFIT protocol is as follows. Test sera (inactivated at 56°C for 30 min) or antibody preparations are serially diluted (e.g., 3-fold, starting at a 1:5 dilution) in medium to give a final volume of 30 μl and added to an equal volume of RABV, prediluted to contain sufficient virus to infect 50 to 70% of 30 μl of a 2.5×10^6/ml suspension or a monolayer of BHK, BSR, or NA cells (e.g., 5 to 10 FFU per cell). Virus plus cells in media alone is used as an infection control, and reference sera are used to establish potency in international units (IU). The mixtures are incubated in the wells of a microtiter plate at 37°C for 60 min and then added to 30 μl of a 1×10^6 to 2×10^6 BHK, BSR, or NA cell suspension for overnight culture at 37°C in 96-well flat-bottom microtiter plates. Following incubation, the plates are washed once with phosphate-buffered saline and then fixed and stained as described for the fluorescent-focus assay described above. The numbers of infected cells are read using a fluorescence microscope. The virus-neutralizing antibody titer is defined as the highest antibody dilution causing a 50% reduction in infected cells. A standard antirabies serum (e.g., the WHO reference serum) with a virus-neutralizing titer of at least 2 IU per ml should be included in each test so that the assays can be standardized.

To take into account variables in the assay, such as the percent infection obtained in the control and the reference serum titer, the RFFIT results may be calculated as follows:

1. Determine the average percentage of infected cells in the control wells (C; virus plus cells without serum).
2. Determine the dilution of the reference serum that causes 50% of the number of control infected cells (C/2) in wells containing infected cells plus reference

TABLE 3 Selected laboratory (fixed) strains of rabies virus

Virus designation	Origin
CVS	Thought to be derived from the original Pasteur rabies virus isolate passaged in rabbit brain and then in mouse brain; several variants exist in different laboratories (e.g., CVS-11, passaged in cell culture, and CVS-24, passaged in mouse brain)
Evelyn-Rokitnicki-Abelseth	Derived from Street Alabama Dufferin by passage in mouse brain
Flury (low and high passage numbers in eggs)	Isolated from a human with rabies by mouse brain inoculation and then passaged in chick brain and a chicken embryo
Kelev	Isolated from a rabid dog by mouse brain inoculation and then passaged in a chicken embryo
Louis Pasteur	Isolated from a rabid cow infected by a dog bite; passaged in rabbit brain and then cultured in primary hamster kidney cells
Pitman-Moore	Thought to be derived from a rabbit brain-passaged isolate from the original Pasteur virus, adapted to cell culture
Street Alabama Dufferin	Isolated from a rabid dog by mouse brain inoculation and then passaged in a chicken embryo and cultured in cells

serum dilutions. Determine the percentage of infection in wells containing the next-higher dilution of serum (A) as well as the percentage of infection in wells containing the next-higher concentration of serum (B). The 50% dilution point of the reference serum is calculated as follows: the dilution of serum giving $A - \{[(C/2 - B)/(A - B)] \times$ (the dilution of serum giving B – the dilution of serum giving A)$\}$. This number represents the dilution of reference serum that contains 2 IU (S).

3. Calculate the 50% dilution point in the test serum using the same formula and substituting the test values of A and B and their respective dilutions (the result of this calculation is T).
4. The titer of the test serum can now be expressed in international units by the following relationship: the titer of test serum (IU) $= 2 \times S \times (1/T)$.

The FAVN test, based on the fluorescence principle used in the RFFIT but with an endpoint titer determined by the absence of fluorescence, has also been described (54). No significant differences in specificity or sensitivity between the RFFIT and FAVN test were detected in comprehensive comparisons (55, 56), and the assessment of fluorescence in both assays has been automated (55), which is highly advantageous in the screening of large numbers of serum samples.

For humans vaccinated against rabies, WHO guidelines recommend that effectiveness of immunization, as well as the persistence of immunity, be assessed by virus neutralization at 6-month intervals and that a booster vaccination be administered if the neutralizing titer drops below 0.5 IU/ml (20; (http://www.who.int/rabies/vaccines/other_rabies_biolog_product/en/).

Analysis of RABV-Specific Antibody by ELISA

ELISA can be used for the general assessment of RABV-specific antibody titers. While the majority of antibodies are generally specific for the virus glycoprotein, substantial amounts of antibodies to the nucleoprotein and other components may be present. The majority of antibodies specific for RABV nucleoprotein and other viral proteins fail to neutralize the virus yet are readily detectable by ELISA. Thus, ELISA with virus as the capture reagent should not be taken as a surrogate for neutralization assays. On the other hand, glycoprotein-specific antibody titers determined by ELISA with glycoprotein-coated plates generally parallel virus-neutralizing antibody titers. Since RABV nucleoprotein is highly antigenically conserved and a significant segment of the humoral response to RABV is directed against the nucleoprotein, detection of these antibodies by ELISA may have particular utility where the virus that elicited the antibody is unknown or antigenically distinct from those available in the laboratory. A situation in which ELISA for RABV-specific antibodies may also be more advantageous than a neutralization test is for the screening of serum and CSF from individuals with encephalitis of unknown origin. Late in the disease process, individuals infected with RABVs often produce some RABV-specific antibodies. ELISA can sensitively detect these antibodies regardless of whether they are neutralizing, with increasing titers of RABV-specific antibodies in consecutive serum samples or the appearance of such antibodies in CSF being indicative of an active infection. ELISA is more suited than neutralization tests for automated screening. Moreover, ELISA can be used to profile the RABV-specific antibody isotypes produced, which provides valuable insight into the nature of the immune response responsible for their generation. For example, conventional killed RABV vaccines predominantly elicit Th2 antibodies (IgG2 and IgG4 in humans, IgG1 in mice), while infection elicits Th1 antibodies (IgG1 and IgG3 in humans, IgG2a in mice).

ELISA for RABV-specific antibody is straightforward. ELISA plates can readily be coated with purified inactivated (β-propiolactone or UV) virus, isolated virus RNP (for nucleoprotein-specific antibodies), or isolated or recombinant-expressed glycoprotein and nucleoprotein. Plates can also be sensitized with rabies antigen-specific antibodies to trap antigens from crude preparations containing the virus (e.g., infected suckling mouse brain) as long as cross-reactivity between the different trapping, primary, and secondary antibodies is avoided. After incubation with serum, bound antibodies can be detected and their isotypes characterized by conventional methods using secondary peroxidase- or alkaline phosphatase-conjugated antibodies. Commercial ELISA kits for the detection of RABV-specific antibodies are available.

QUALITY CONTROL AND INTERPRETATION

Natural RABV infection can be difficult to diagnose, the gold standard being the immunofluorescent detection of viral nucleoprotein in patient samples, such as neural tissue biopsy specimens, skin biopsy specimens, saliva, and corneal impressions. Detection of viral mRNA in these specimens is also useful for diagnosis and can provide additional information about the origin of the virus strain. Infection with wild-type RABVs, which spread with minimal glycoprotein production, may progress through the nervous system without producing substantial immunostimulatory antigen, depending upon the initial site of virus entry and the amount of viral antigen present in the initial inoculum. Thus, serum antibodies, which begin to appear 6 to 8 days after optimal immunization and generally peak at about 3 to 4 weeks, may not be detected until near the end stage of rabies in humans if at all. Rabies serology is therefore more useful in confirming that immunization has been successful than in diagnosis. The assessment of RABV-specific neutralizing antibody titers by fluorescent-focus inhibition tests like the RFFIT requires technical expertise. With variability in the quality of the cell culture and the percentages of cells infected by the assay virus in the absence of antibody and with changes in the appearance of the fluorescent signal when different assay viruses are used, individual assays give results which can be difficult to interpret and must be equilibrated using antibody standards. Observation of the correct staining pattern is important for both the dFA test and RFFIT. As nucleoprotein-specific antibodies are generally used, the staining pattern should be punctate intracellular, reflecting the detection of the RNP aggregates of Negri bodies, as opposed to a surface stain. NA cells infected with CVS-11, the positive control in an RFFIT, are shown in Fig. 1. ELISA-based technologies are relatively straightforward technically but cannot discriminate between neutralizing and non-neutralizing antibodies. Thus, while it is generally accepted that the level of glycoprotein-specific antibodies parallels the neutralization capacity of sera, ELISA cannot directly be used to assess protective immunity. However, quantitation by ELISA of RABV N produced by cells cultured with RABV in the presence and absence of antiserum can be used to provide an estimate of antibody neutralizing activity. Nevertheless, these and similar assays in which virus replication is assessed by RT-PCR have not been generally accepted. For both antibody and molecular analysis of RABV infection and immunity, antigenic and sequence disparities between different RABVs must always be taken into account. False negatives can occur where the antigenic cross-reactivity or sequence homology between assays and field viruses differ substantially. The use of nucleoprotein-specific antibodies and targeting highly conserved sequences for molecular analysis should always be the starting points for dealing with an unknown infection. Should RABV be identified as a possibility, strategies and reagents to more completely characterize the origin of the virus are readily available.

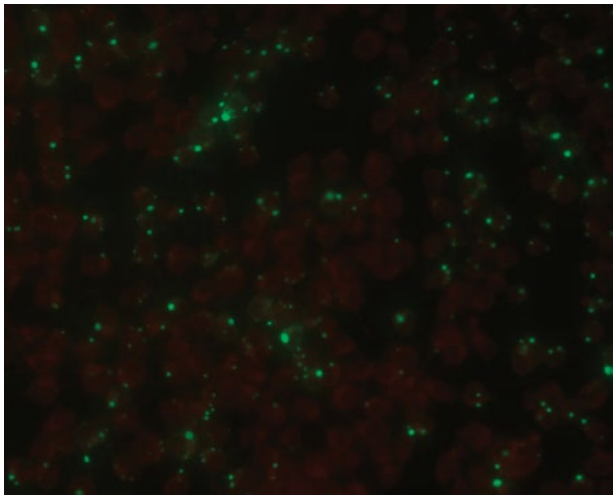

FIGURE 1 Mouse NA cells infected with CVS-11. Cells were infected and stained as described for an RFFIT in the text.

CONSIDERATIONS FOR WORKING WITH RABV

The U.S. Department of Health and Human Services, Public Health Service, CDC, and National Institutes of Health recommend biosafety level 2 practices and facilities for all activities with materials infected or potentially infected with RABV. Immunization is recommended for individuals whose occupations or other activities may predispose them to exposure to RABV. It is noteworthy in this regard that antigenic cross-reactivity between RABV G and human immunodeficiency virus type 1 (HIV-1) gp120 has been described, and sera from rabies-immune individuals have occasionally cross-reacted with HIV-1 gp120 in ELISAs (57).

REFERENCES

1. **Baltazard M, Ghodssi M.** 1954. Prevention of human rabies; treatment of persons bitten by rabid wolves in Iran. *Bull World Health Organ* **10:**797–803. PubMed
2. **Lakhanpal U, Sharma RC.** 1985. An epidemiological study of 177 cases of human rabies. *Int J Epidemiol* **14:**614–617.
3. **Smith JS, Fishbein DB, Rupprecht CE, Clark K.** 1991. Unexplained rabies in three immigrants in the United States. A virologic investigation. *N Engl J Med* **324:**205–211. PubMed
4. **Shankar SK, Mahadevan A, Sapico SD, Ghodkirekar MSG, Pinto RGW, Madhusudana SN.** 2012. Rabies viral encephalitis with probable 25 year incubation period! *Ann Indian Acad Neurol* **15:**221–223.
5. **Pasteur L.** 1885. Séance du 27 octobre 1885. Bull Acad Med, 2nd ser **XIV:**1431–1439.
6. **Manning SE, Rupprecht CE, Fishbein D, Hanlon CA, Lumlertdacha B, Guerra M, Meltzer MI, Dhankhar P, Vaidya SA, Jenkins SR, Sun B, Hull HF, Advisory Committee on Immunization Practices, Centers for Disease Control and Prevention (CDC).** 2008. Human rabies prevention—United States, 2008: recommendations of the Advisory Committee on Immunization Practices. *MMWR Recomm Rep* **57**(RR-3)**:**1–28. PubMed
7. **Krebs JW, Long-Marin SC, Childs JE.** 1998. Causes, costs, and estimates of rabies postexposure prophylaxis treatments in the United States. *J Public Health Manag Pract* **4:**56–62. PubMed
8. **Wilde H.** 2007. Failures of post-exposure rabies prophylaxis. *Vaccine* **25:**7605–7609. PubMed
9. **Willoughby RE Jr, Tieves KS, Hoffman GM, Ghanayem NS, Amlie-Lefond CM, Schwabe MJ, Chusid MJ, Rupprecht CE.** 2005. Survival after treatment of rabies with induction of coma. *N Engl J Med* **352:**2508–2514. PubMed
10. **Centers for Disease Control and Prevention.** 2011. Recovery of a patient from clinical rabies—California, 2011. *MMWR Morb Mortal Wkly Rep* **61:**61–65.
11. **Hooper DC, Morimoto K, Bette M, Weihe E, Koprowski H, Dietzschold B.** 1998. Collaboration of antibody and inflammation in clearance of rabies virus from the central nervous system. *J Virol* **72:**3711–3719. PubMed

12. **Phares TW, Kean RB, Mikheeva T, Hooper DC.** 2006. Regional differences in blood-brain barrier permeability changes and inflammation in the apathogenic clearance of virus from the central nervous system. *J Immunol* **176:**7666–7675. PubMed
13. **Roy A, Hooper DC.** 2007. Lethal silver-haired bat rabies virus infection can be prevented by opening the blood-brain barrier. *J Virol* **81:**7993–7998. PubMed
14. **Hooper DC, Phares TW, Fabis MJ, Roy A.** 2009. The production of antibody by invading B cells is required for the clearance of rabies virus from the central nervous system. *PLoS Negl Trop Dis* **3:**e535. PubMed
15. **Centers for Disease Control and Prevention (CDC).** 2004. Investigation of rabies infections in organ donor and transplant recipients—Alabama, Arkansas, Oklahoma, and Texas, 2004. *MMWR Morb Mortal Wkly Rep* **53:**586–589. PubMed
16. **Centers for Disease Control and Prevention.** 2004. Update: investigation of rabies infections in organ donor and transplant recipients—Alabama, Arkansas, Oklahoma, and Texas. *MMWR Morb Mortal Wkly Rep* **53:**615–616.
17. **Johnson N, Brookes SM, Fooks AR, Ross RS.** 2005. Review of human rabies cases in the UK and in Germany. *Vet Rec* **157:**715. PubMed
18. **Vora NM, Basavaraju SV, Feldman KA, Paddock CD, Orciari L, Gitterman S, Griese S, Wallace RM, Said M, Blau DM, Selvaggi G, Velasco-Villa A, Ritter J, Yager P, Kresch A, Niezgoda M, Blanton J, Stosor V, Falta EM, Lyon GM III, Zembower T, Kuzmina N, Rohatgi PK, Recuenco S, Zaki S, Damon I, Franka R, Kuehnert MJ, Transplant-Associated Rabies Virus Transmission Investigation Team.** 2013. Raccoon rabies virus variant transmission through solid organ transplantation. *JAMA* **310:**398–407.
19. **Dean DJ, Abelseth MK.** 1973. Laboratory techniques in rabies: the fluorescent antibody test. *Monogr Ser World Health Organ* **23:**73–84. PubMed
20. **WHO Expert Committee on Rabies.** 1992. WHO Expert Committee on Rabies, 8th report. WHO Technical Report Series no. 824. WHO, Geneva, Switzerland.
21. **Warrilow D, Harrower B, Smith IL, Field H, Taylor R, Walker C, Smith GA.** 2003. Public health surveillance for Australian bat lyssavirus in Queensland, Australia, 2000–2001. *Emerg Infect Dis* **9:**262–264. PubMed
22. **Smith J.** 1999. Rabies virus, p 1099–1106. *In* Murray PR, Baron EJ, Pfaller MA, Tenover FC, Yolken RH (ed), *Manual of Clinical Microbiology,* 7th ed. ASM Press, Washington, DC.
23. **Dyer JL, Niezgoda M, Orciari LA, Yager PA, Ellison JA, Rupprecht CE.** 2013. Evaluation of an indirect rapid immunohistochemistry test for the differentiation of rabies virus variants. *J Virol Methods* **190:**29–33. PubMed
24. **Perrin P, Gontier C, Lecocq E, Bourhy H.** 1992. A modified rapid enzyme immunoassay for the detection of rabies and rabies-related viruses: RREID-Lyssa. *Biologicals* **20:**51–58. PubMed
25. **Jayakumar R, Thirumurugan G, Nachimuthu K, Padmanaban VD.** 1996. Detection of rabies virus antigen in animals by avidin-biotin dot ELISA. *Zentralbl Bakteriol* **285:**82–85. PubMed
26. **Katayama S, Yamanaka M, Ota S, Shimizu Y.** 1999. A new quantitative method for rabies virus by detection of nucleoprotein in virion using ELISA. *J Vet Med Sci* **61:**411–416. PubMed
27. **Arai YT, Yamada K, Kameoka Y, Horimoto T, Yamamoto K, Yabe S, Nakayama M, Tashiro M.** 1997. Nucleoprotein gene analysis of fixed and street rabies virus variants using RT-PCR. *Arch Virol* **142:**1787–1796. PubMed
28. **Heaton PR, McElhinney LM, Lowings JP.** 1999. Detection and identification of rabies and rabies-related viruses using rapid-cycle PCR. *J Virol Methods* **81:**63–69. PubMed
29. **Kulonen K, Fekadu M, Whitfield S, Warner CK.** 1999. An evaluation of immunofluorescence and PCR methods for detection of rabies in archival Carnoy-fixed, paraffin-embedded brain tissue. *Zentralbl Veterinarmed B* **46:**151–155. PubMed
30. **Nadin-Davis SA, Huang W, Wandeler AI.** 1996. The design of strain-specific polymerase chain reactions for discrimination of the raccoon rabies virus strain from indigenous rabies viruses of Ontario. *J Virol Methods* **57:**1–14. PubMed
31. **Sabouraud A, Smith JS, Orciari LA, de Mattos C, de Mattos C, Rohde R.** 1999. Typing of rabies virus isolates by DNA enzyme immunoassay. *J Clin Virol* **12:**9–19. PubMed
32. **Sacramento D, Bourhy H, Tordo N.** 1991. PCR technique as an alternative method for diagnosis and molecular epidemiology of rabies virus. *Mol Cell Probes* **5:**229–240. PubMed
33. **Warner CK, Whitfield SG, Fekadu M, Ho H.** 1997. Procedures for reproducible detection of rabies virus antigen mRNA and genome in situ in formalin-fixed tissues. *J Virol Methods* **67:**5–12. PubMed
34. **Fischer M, Wernike K, Freuling CM, Müller T, Aylan O, Brochier B, Cliquet F, Vázquez-Morón S, Hostnik P, Huovilainen A, Isaksson M, Kooi EA, Mooney J, Turcitu M, Rasmussen TB, Revilla-Fernández S, Smreczak M, Fooks AR, Marston DA, Beer M, Hoffmann B.** 2013. A step forward in molecular diagnostics of lyssaviruses—results of a ring trial among European laboratories. *PLoS One* **8:**e58372. PubMed
35. **Nadin-Davis SA.** 1998. Polymerase chain reaction protocols for rabies virus discrimination. *J Virol Methods* **75:**1–8. PubMed
36. **Prosniak M, Zborek A, Scott GS, Roy A, Phares TW, Koprowski H, Hooper DC.** 2003. Differential expression of growth factors at the cellular level in virus-infected brain. *Proc Natl Acad Sci U S A* **100:**6765–6770. PubMed
37. **Wacharapluesadee S, Tepsumethanon V, Supavonwong P, Kaewpom T, Intarut N, Hemachudha T.** 2012. Detection of rabies viral RNA by TaqMan real-time RT-PCR using non-neural specimens from dogs infected with rabies virus. *J Virol Methods* **184:**109–112. PubMed
38. **Chai Q, He WQ, Zhou M, Lu H, Fu ZF.** 2014. Enhancement of blood-brain barrier permeability and reduction of tight junction protein expression are modulated by chemokines/cytokines induced by rabies virus infection. *J Virol* **88:**4698–4710. PubMed
39. **Zhao P, Zhao L, Zhang K, Feng H, Wang H, Wang T, Xu T, Feng N, Wang C, Gao Y, Huang G, Qin C, Yang S, Xia X.** 2012. Infection with street strain rabies virus induces modulation of the microRNA profile of the mouse brain. *Virol J* **9:**159. PubMed
40. **Li J, Ertel A, Portocarrero C, Barkhouse DA, Dietzschold B, Hooper DC, Faber M.** 2012. Postexposure treatment with the live-attenuated rabies virus (RV) vaccine TriGAS triggers the clearance of wild-type RV from the central nervous system (CNS) through the rapid induction of genes relevant to adaptive immunity in CNS tissues. *J Virol* **86:**3200–3210. PubMed
41. **Pulmanausahakul R, Li J, Schnell MJ, Dietzschold B.** 2008. The glycoprotein and the matrix protein of rabies virus affect pathogenicity by regulating viral replication and facilitating cell-to-cell spread. *J Virol* **82:**2330–2338. PubMed
42. **Dietzschold B, Gore M, Casali P, Ueki Y, Rupprecht CE, Notkins AL, Koprowski H.** 1990. Biological characterization of human monoclonal antibodies to rabies virus. *J Virol* **64:**3087–3090. PubMed
43. **Champion JM, Kean RB, Rupprecht CE, Notkins AL, Koprowski H, Dietzschold B, Hooper DC.** 2000. The development of monoclonal human rabies virus-neutralizing

antibodies as a substitute for pooled human immune globulin in the prophylactic treatment of rabies virus exposure. *J Immunol Methods* **235:**81–90. PubMed

44. **Hanlon CA, DeMattos CA, DeMattos CC, Niezgoda M, Hooper DC, Koprowski H, Notkins A, Rupprecht CE.** 2001. Experimental utility of rabies virus-neutralizing human monoclonal antibodies in post-exposure prophylaxis. *Vaccine* **19:**3834–3842. PubMed
45. **Prosniak M, Faber M, Hanlon CA, Rupprecht CE, Hooper DC, Dietzschold B.** 2003. Development of a cocktail of recombinant-expressed human rabies virus-neutralizing monoclonal antibodies for postexposure prophylaxis of rabies. *J Infect Dis* **188:**53–56. PubMed
46. **Sloan SE, Hanlon C, Weldon W, Niezgoda M, Blanton J, Self J, Rowley KJ, Mandell RB, Babcock GJ, Thomas WD Jr, Rupprecht CE, Ambrosino DM.** 2007. Identification and characterization of a human monoclonal antibody that potently neutralizes a broad panel of rabies virus isolates. *Vaccine* **25:**2800–2810. PubMed
47. **Müller T, Dietzschold B, Ertl H, Fooks AR, Freuling C, Fehlner-Gardiner C, Kliemt J, Meslin FX, Franka R, Rupprecht CE, Tordo N, Wanderler AI, Kieny MP.** 2009. Development of a mouse monoclonal antibody cocktail for post-exposure rabies prophylaxis in humans. *PLoS Negl Trop Dis* **3:**e542. PubMed
48. **Warner C, Fekadu M, Whitfield S, Shaddock J.** 1999. Use of anti-glycoprotein monoclonal antibodies to characterize rabies virus in formalin-fixed tissues. *J Virol Methods* **77:**69–74. PubMed
49. **Morimoto K, Hooper DC, Carbaugh H, Fu ZF, Koprowski H, Dietzschold B.** 1998. Rabies virus quasispecies: implications for pathogenesis. *Proc Natl Acad Sci U S A* **95:**3152–3156.
50. **Murphy FA.** 1977. Rabies pathogenesis. *Arch Virol* **54:**279–297. PubMed
51. **Dietzschold B, Li J, Faber M, Schnell M.** 2008. Concepts in the pathogenesis of rabies. *Future Virol* **3:**481–490. PubMed
52. **Morimoto K, Hooper DC, Spitsin S, Koprowski H, Dietzschold B.** 1999. Pathogenicity of different rabies virus variants inversely correlates with apoptosis and rabies virus glycoprotein expression in infected primary neuron cultures. *J Virol* **73:**510–518. PubMed
53. **Wiktor TJ, Macfarlan RI, Foggin CM, Koprowski H.** 1984. Antigenic analysis of rabies and Mokola virus from Zimbabwe using monoclonal antibodies. *Dev Biol Stand* **57:**199–211. PubMed
54. **Cliquet F, Aubert M, Sagné L.** 1998. Development of a fluorescent antibody virus neutralisation test (FAVN test) for the quantitation of rabies-neutralising antibody. *J Immunol Methods* **212:**79–87. PubMed
55. **Briggs DJ, Smith JS, Mueller FL, Schwenke J, Davis RD, Gordon CR, Schweitzer K, Orciari LA, Yager PA, Rupprecht CE.** 1998. A comparison of two serological methods for detecting the immune response after rabies vaccination in dogs and cats being exported to rabies-free areas. *Biologicals* **26:**347–355. PubMed
56. **Péharpré D, Cliquet F, Sagné E, Renders C, Costy F, Aubert M.** 1999. Comparison of visual microscopic and computer-automated fluorescence detection of rabies virus neutralizing antibodies. *J Vet Diagn Invest* **11:**330–333. PubMed
57. **Bracci L, Ballas SK, Spreafico A, Neri P.** 1997. Molecular mimicry between the rabies virus glycoprotein and human immunodeficiency virus-1 GP120: cross-reacting antibodies induced by rabies vaccination. *Blood* **90:**3623–3628. PubMed

Human T-Cell Lymphotropic Virus Types 1 and 2

BREANNA CARUSO, RAYA MASSOUD, AND STEVEN JACOBSON

70

INTRODUCTION

Discovery and General Characteristics

Human T-cell lymphotropic virus type 1 (HTLV-1) was the first pathogenic human retrovirus to be discovered. It was isolated in 1979 from the peripheral blood lymphocytes of a patient with adult T-cell leukemia/lymphoma (ATLL) (1). Following years of research to find a retroviral agent involved in ATLL, Yoshida and Yamamato isolated a retrovirus from an ATLL patient in 1986 that they named adult T-cell leukemia virus. Soon, the similarities between HTLV-1 and adult T-cell leukemia virus were confirmed, and the name HTLV-1 was chosen. Shortly thereafter, the closely related virus HTLV-2 was isolated from the splenic cells of an individual with hairy cell T-cell leukemia (2).

HTLV-1 and -2 belong to the *Deltaretrovirus* genus of the *Retroviridae* family and share approximately 70% nucleotide sequence homology. This genus also includes HTLV-3 and -4, simian T-cell lymphotropic virus types 1, 2, and 3, and bovine leukemia virus, all of which are characterized by an extra genomic region, pX, between the envelope gene (*env*) and the 3′ long terminal repeat (3′ LTR). pX encodes regulatory and accessory proteins that are implicated in pathogenesis. Both viruses also produce negative-strand transcripts: HBZ for HTLV-1 and APH-2 for HTLV-2.

Free virions of HTLV-1 and -2 are poorly infectious. Their transmission requires the transfer of live infected cells followed by the formation of specialized cell-to-cell contacts called virological synapses, which favor the infection of new cells (3). Despite a wide range of target cells *in vitro*, *in vivo* HTLV-1 primarily infects $CD4^+$ T cells, and HTLV-2 primarily infects $CD8^+$ T cells (4). Additionally, there is evidence that dendritic cells, B cells, and monocytes can be infected in individuals with HTLV-1 and -2 (5). HTLV-1 and -2 replicate mainly through clonal expansion of the infected cells; therefore, they both predominantly utilize the cellular DNA polymerase rather than the viral reverse transcriptase, which is less reliable, to duplicate their genomes. As a result, HTLV-1 and -2 are genetically stable, unlike other retroviruses.

Epidemiology and Geographic Distribution

It is estimated that 20 million people worldwide are infected with HTLV-1 (6). HTLV-1 is not ubiquitous but instead is found in clusters in areas where it is highly endemic, which include southwestern Japan (where the virus was first isolated from patients with ATLL), the Caribbean islands, equatorial Africa, and foci in South America (Colombia, French Guyana, and Brazil), the Middle East (the Mashad region in Iran), and Melanesia. In North America and Australia, the highest prevalence is among the indigenous populations. In Europe, the highest prevalence is in Romania.

Variations in the LTR region of HTLV-1 led to the discovery of four major subtypes of HTLV-1 (A, B, C, and D) based upon geographic origins. The cosmopolitan subtype A is the most widespread and is endemic in Japan, the Caribbean, Central and South America, North and West Africa, and parts of the Middle East. The other three subtypes are endemic to the areas specified by their names: Central African subtype B, Melanesian subtype C, and Central African/Pygmies subtype D. There have also been reports of other rare subtypes (E, F, and G) found only in Central Africa (7). Interestingly, these rare subtypes tend to cluster in areas where simian isolates have also been found, suggesting a possible simian-to-human transmission. Moreover, an African origin of HTLV-1 has been suggested, as Africa is the only continent where all the HTLV-1 subtypes and their simian counterparts have been found. Phylogenetic studies estimate that the virus originated in Africa about 27,000 years ago (8).

Currently, the prevalence of HTLV-2 infection remains unknown. HTLV-2 is endemic among Amerindian populations and intravenous drug users (IDUs) in the United States, Europe, South America, and Asia. There are four known subtypes of HTLV-2 (A, B, C, and D), with specific geographic distributions. Subtypes A and B are found throughout the Americas and in Europe. In the Americas, subtype A is found mostly in IDU populations, and subtype B is found predominantly in Amerindian populations. In Europe, subtype B is more common in IDUs in Italy and Spain, but subtype A is more common in IDUs in Ireland and Sweden. Subtype C is found exclusively in the indigenous populations of the Amazon region of Brazil, and subtype D is found in the indigenous populations of Central Africa. The discoveries of HTLV-2D and simian T-cell lymphotropic virus type 2 support an African origin for HTLV-2 as well (7).

Transmission

Transmission of HTLV-1 and -2 requires the transfer of live infected T cells via one of the following three routes:

doi:10.1128/9781555818722.ch70

mother to child, intravenous exposure to infected cells, and sexual contact.

For HTLV-1, mother-to-child transmission, mainly through breastfeeding, is the major mode of infection in areas of endemicity, with an infection rate as high as 35% when breastfeeding is prolonged beyond 6 months (9). Fewer than 5% of mother-to-child transmissions occur *in utero* or at birth (10). Intravenous exposure to infected cells also transmits HTLV-1 very efficiently, with reported seroconversion rates of 40 to 60% following transfusion of HTLV-1-contaminated blood products. Another currently more prevalent mode of parenteral transmission is through sharing of contaminated needles and syringes (11). Transmission through sexual contact appears to be more efficient from male to female because of infected T cells present in semen, though transmission in the reverse direction also occurs (12). HTLV-2 is transmitted similarly to HTLV-1, but much less is known about the specific modes and efficiency of transmission of this virus.

Pathogenesis

The majority of HTLV-1-infected subjects remain lifetime asymptomatic carriers of the virus; however, rarely, HTLV-1 can lead to serious neoplastic and inflammatory conditions. The outcome of the infection is influenced by several factors, including the route of transmission, genetic background, and age.

The two major HTLV-1-related conditions are ATLL and HTLV-1-associated myelopathy/tropical spastic paraparesis (HAM/TSP) (13). Other associations include uveitis, infective dermatitis, and polymyositis (13).

ATLL is a lymphoproliferative malignancy of T cells that was first described in Japan in 1977 (14). It occurs in up to 5% of HTLV-1-infected subjects, is more common in males, and typically occurs 20 to 30 years after infection, which explains the higher risk for subjects infected via vertical transmission (15). ATLL can be divided into four types: smoldering, chronic, lymphoma, and acute. Clinical characteristics and laboratory features include subacute or chronic leukemia with a rapidly progressive terminal course, frequent leukemic cells with indented lobulated nuclei, skin involvement, lymphadenopathy, hepatosplenomegaly, and a high frequency of hypercalcemia (16).

In 1985, Gessain and colleagues suggested an association between HTLV-1 seropositivity and a myelopathy endemic to the tropics known as tropical spastic paraparesis (TSP) (17). Independently, a group in Japan recognized HTLV-1 infection and its association with a similar disorder that they called HTLV-1-associated myelopathy (HAM) (18). An international consensus conference sponsored by the World Health Organization in 1988 determined that these two syndromes were the same. The combined name HAM/TSP was selected, and diagnostic criteria for the disease were established (19). HAM/TSP is a chronic and progressive myelopathy that primarily affects the spinal cord. Patients typically present with weakness of the lower extremities, back pain, bladder dysfunction, constipation, sexual dysfunction, and sensory disturbances, including paresthesias of the lower extremities. HAM/TSP occurs more frequently in females than in males and is associated with transmission from sexual intercourse or blood transfusion.

Unlike the case for HTLV-1, the role of HTLV-2 in disease remains poorly understood. Some studies have suggested that HTLV-2 can be associated with a disorder similar to HAM/TSP, and others have suggested a relationship with other neurological disorders (20–22). Establishing a clear association of HTLV-2 with disease has been difficult to assess because of confounding factors, such as intravenous drug use or concomitant HIV-1 infection. Therefore, the clinical significance of HTLV-2 infections is an area of ongoing study.

INDICATIONS FOR HTLV-1 AND -2 TESTING

Testing for HTLV-1 is indicated for patients with clinical conditions that can be related to HTLV-1, such as myelitis, uveitis, arthritis, or $CD4^+$ T-cell leukemia, and can inform prognostic and therapeutic choices. Testing is especially indicated for high-risk individuals, such as those from areas of endemicity or with possible exposure to HTLV-1 or -2. Importantly, HTLV-1/2 testing is offered to asymptomatic at-risk subjects, such as sexual partners of known infected people, to help formulate specific counseling advice.

In Japan, a country where HTLV-1 is endemic, there is a nationwide public health policy requiring the screening of all pregnant women during antenatal care. This is aimed at decreasing the risk of mother-to-child transmission and subsequent ATLL. Unfortunately, other areas of endemicity still lack such policies. Finally, given that HTLV-1 and -2 can be transmitted by blood transfusion and solid organ/tissue transplantation, testing for these agents has become routine in these settings.

Screening for HTLV is based on the detection of anti-HTLV antibodies, which develop 1 to 3 months after infection and persist for life. In a clinical setting, this is typically done by use of enzyme-linked immunosorbent assays (ELISAs), which are very sensitive but lack specificity for low-prevalence populations. Samples that are positive twice by ELISA are referred to as "repeat reactive." There is currently no FDA-licensed HTLV-confirmatory test, and confirmation is based on any of several available, more specific tests, including a second manufacturer's enzyme immunosorbent assay, Western blotting (WB), and a specific line immunoassay, which can differentiate between HTLV-1 and -2 by identifying specific viral proteins. PCR, a nucleic acid sequence-based amplification test, can also be used to diagnose the infection and quantify the proviral load (PVL).

LABORATORY ASSAYS FOR HTLV-1 AND -2 DETECTION

Particle Agglutination

Particle agglutination was the first commercially available assay for HTLV screening. This method traditionally tests for HTLV-1 infection, so it is most useful in areas where HTLV-2 is not endemic, such as Japan. The assay is based on the ability of antibodies to cross-link their target antigens. This cross-linking allows the formation of a lattice due to antibody interactions with multivalent antigens.

Particle agglutination utilizes a particulate form of the target antigen, such as whole bacterial cells, antigen-coated red blood cells, or an inert particle sensitized with the target antigen. The test for HTLV-1 uses gelatin particles sensitized with antigen for HTLV-1 purified from concentrated culture fluid of an HTLV-1-producing cell line. This strategy uses whole-virion antigens and enriched whole Env proteins, which yields a greater sensitivity to HTLV-1 infection (23). Sensitized gelatin particles are preferred over antigen-coated red blood cells because they do not show nonspecific agglutination (24). If the test is negative, the suspension will remain homogenous and opaque. If the test is positive, the suspension will become clear with visible aggregates. The test is graded based upon the pattern and size of agglutination, on a scale of 1+ to 4+. A score of 2+ or higher is considered positive for HTLV-1 antibody (25).

In order for visible clumping to occur, the proportion of antigen to antibody should allow sufficient lattice formation. In the case of excess antibody in the sample, cross-linking is not observed because each antigen molecule can bind to a single antibody, and thus no lattices are formed, yielding a false-negative result. On the other hand, if there is very little antibody, then there may be no visible agglutination because there are insufficient antibodies for cross-linking to occur. Therefore, it is advisable to run samples at multiple dilutions to avoid these concentration issues (25).

Enzyme-Linked Immunosorbent Assay

The first ELISA developed for the detection of HTLV-1 and -2 became available in the mid-1980s (26). ELISAs do not differentiate between HTLV-1 and -2 infections but are useful for initial screening because of their low cost and easy adaptation for large-scale use. The first assay used whole-virus lysates from HTLV-1-infected cells, relying upon cross-reactivity to detect HTLV-2 (26). As a result, there was a high rate of false-positive reactions and a poor sensitivity for detecting HTLV-2 infections (27). Second-generation ELISAs combined HTLV-1 lysates with synthetic HTLV-1 peptides and recombinant proteins. One of the biggest developments was the addition of a recombinant envelope protein, rgp21e, which increased the detection of HTLV-2 infections. Although these second-generation ELISAs performed better, they still required a confirmatory test to eliminate false-positive reactions (26, 28). The third generation of ELISAs that are now available make use of the "sandwich" format for the detection of antibody. There have been additional improvements in sensitivity and specificity through the use of both HTLV-1 and HTLV-2 lysates, artificial proteins, recombinant proteins, and synthetic peptides (27, 29, 30).

Microwells included in assay kits have been coated with HTLV antigens. The exact components differ by kit: some include purified viral lysates, recombinant proteins, and/or synthetic peptides. Each assay kit includes a second recombinant HTLV antigen that has been conjugated to horseradish peroxidase, the enzyme used as a color indicator for this assay. Samples that are negative for HTLV infection remain colorless, while positive samples contain a yellow product that is proportional to the amount of antibodies present in the specimen.

One difficulty with interpreting ELISA results has been determining the cutoff value for differentiating between negative and positive results. The third-generation ELISAs show much higher specificities than those of their predecessors, and the majority of HLTV-infected specimens show very strong signals, making these assays suitable for use for screening (27, 30). However, these assays still show some false-positive results (23). Some researchers believe that optimization of the cutoff value can eliminate many of the false-positive reactions that have been reported (23, 30). It is still necessary that repeat reactive samples be tested using a confirmatory assay to differentiate between HTLV-1 and -2 infections. More problematic than the false-positive results by ELISA are the false-negative results that have been reported. Studies have shown that anywhere from 1 to 7.5% of ELISA-negative samples are actually positive for HTLV-1 or -2 by PCR (26, 31). One possible explanation for these false-negative ELISA reactions is a mutation in the MTA1 envelope gene which causes a truncated protein that results in false-negative ELISA outcomes (32). This is a significant concern in areas where HTLV is endemic. The use of a dual-ELISA screening assay can help to eliminate false-positive results and catch false-negative ones, which is an appealing solution in areas where access to confirmatory assays is more difficult due to the higher costs associated with these tests (33, 34).

Western Blotting

In 1994 and 1995, a commercially available WB kit became available to confirm all ELISA-reactive HTLV samples (26). The current WB kit contains nitrocellulose strips that contain HTLV-1 and -2 proteins derived from native inactivated viral particles and genetically engineered proteins. The development of recombinant proteins has been important in clarifying the interpretation of WB patterns. The older WB kits contained a native form of gp46 which was not recognized by almost half of HTLV-1 infections and most HTLV-2 infections (30). In recent years, a new clone was developed that produces a more specific recombinant envelope protein, GD21 (rgp21), which permits the detection of antibodies to envelope proteins in all HTLV-1 and -2 infections. The addition of rgp46-I (MTA1), a unique recombinant HTLV-1 envelope protein, and rgp46-II (K55), a unique recombinant HTLV-2 envelope protein, has allowed for more accurate differentiation between HTLV-1 and -2 (30).

Samples are considered HTLV-1 positive when reactivity to two Env proteins (GD21 and MTA1) and two Gag proteins (p19 with or without p24) is present (Fig. 1). Samples are considered HTLV-2 positive when reactivity to two Env proteins (GD21 and K55) and two Gag proteins (p24 with or without p19) is present (Fig. 1) (26, 30). HTLV seropositivity can be confirmed if reactivity to GD21, p19, and p24 is present, but further investigation is needed to differentiate between HTLV-1 and -2 (30). All other banding patterns are indeterminate (some examples are shown in Fig. 1); however, follow-up is recommended if reactivity to GD21 is present, because this pattern may correspond to recent seroconversion (16, 35).

A major concern in interpreting WB results is the presence of indeterminate patterns. Studies have shown that a surprisingly large proportion of ELISA-positive sera display indeterminate WB profiles. This is especially true for sera from areas of endemicity in Melanesia (36), Africa (37, 38), Brazil (34), and tropical areas (39). Estimates for WB seroindeterminate status range from as high as 67% for patients from Zaire with neurologic disease (38) to 4.1% for HIV-positive patients from Brazil (40) and $<0.1\%$ for healthy blood donors from Argentina (41). However, the true incidence of indeterminate WB results may be higher than estimated, because ELISA-negative individuals could also have a seroindeterminate status (35, 38). The clinical significance of a seroindeterminate status is still unclear. Occasionally, HTLV-1 or -2 has been confirmed by PCR for those with a seroindeterminate status, indicating that at least some cases are due to early seroconversion or low antibody titers (16, 38, 42). Others have found an indeterminate status in those exposed to HTLV-infected blood products without seroconverting (35). Still others believe that it could be due to the presence of a viral variant, but studies using PCR have not supported this claim (43). This difficulty, combined with the high cost associated with running the assay, does not make WB a good first-line screening assay for large-scale use, especially in areas of endemicity; however, WB remains a useful secondary confirmation test (26, 44).

Line Immunoassay

Recently, a highly sensitive and specific line immunoassay was developed for the confirmation and differentiation of HTLV-1 and -2 infections. The assay uses a combination of recombinant antigens and synthetic peptides derived from

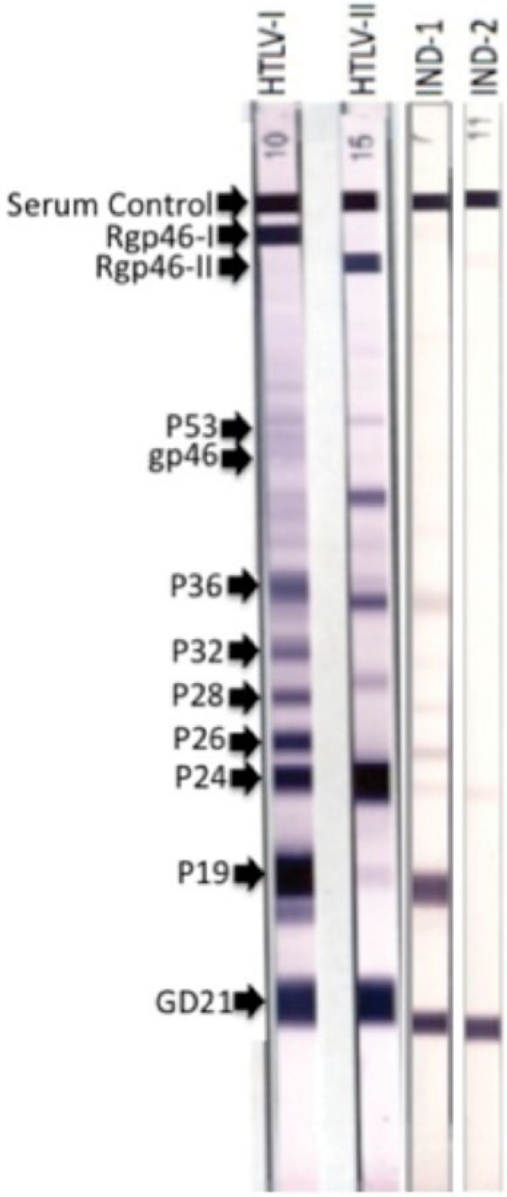

FIGURE 1 Representative examples of HTLV-1-positive and HTLV-2-positive WB patterns. WB patterns can also demonstrate indeterminate reactivity, and two examples of this are shown here (IND-1 and -2). This can complicate the interpretation of results.

HTLV-1 and -2 immunodominant protein sequences that are purified and fixed on a nylon membrane. It is designed to allow the detection of antibodies with a wide specificity to all known isolates of the HTLV strains, while also providing the ability to distinguish between HTLV-1 and -2. The manufacturers included antigens for Gag (p19 and p24) and Env (gp46 and gp21) that are common between HTLV-1 and -2, along with antigens that are type specific (Gag p19-1 and Env gp46-1 for HTLV-1 and Env gp46-2 for HTLV-2). The strips also contain four control lines: one negative-control line and three positive-control lines that include strong (3+), moderate (1+), and weak (cutoff) lines to allow for semiquantitative interpretation of results.

To evaluate the pattern on a strip, the color development of each line is compared to that on the control lines, and the intensity is scored. Results are considered positive if there is reactivity above the cutoff line with at least one envelope antigen (gp21 or gp46) and one Gag antigen (p19 or p24) or both envelope antigens. Positive results are classified as HTLV-1 if the sum of the gp46-1 and p19-1 band intensities is greater than the gp46-2 band intensity, HTLV-2 if the gp46-2 band intensity is greater than the gp46-1 band intensity or the sum of the gp46-1 and p19-1 band intensities, and nontypeable if the band intensities do not meet the criteria for HTLV-1 or -2. The results are considered indeterminate if gp21 is reactive or if any two bands are reactive without a detectable gp21 band.

Like WB, line immunoassays can have indeterminate results; however, research has suggested that line immunoassays produce a much smaller number of seroindeterminate results than the most current WB (45, 46). The line immunoassay is also more sensitive than WB for the verification of HTLV-2 infection (26). Because each strip contains three internal positive controls, comparing each band to the controls allows for more accurate differentiation between a band that is reactive and a band that is below the reactivity threshold. Researchers believe that this has helped to eliminate some false-positive and indeterminate results that are due to the subjectivity of scoring (45, 46). To help further reduce the subjectivity, companies have developed software that rates each band's intensity to create a report for each individual strip. The strips can be scanned and uploaded in batches for more efficient, high-throughput analyses. There are also options for automation available to facilitate large-scale use of this assay. Line immunoassays are cheaper than WB, making them a more economical option for use in screening donor populations. Several researchers have suggested making line immunoassays the standard confirmatory assay for HTLV-1 and -2, with WB becoming a secondary confirmation assay when needed (26, 45, 46).

Polymerase Chain Reaction

PCR is a DNA amplification technique that was developed in the 1980s for the detection and analysis of specific sequences of DNA (47). It has changed the field of viral diagnostics by allowing the sensitive detection and quantification of viral infections based on amplification of specific viral nucleic acid sequences. Several types of PCR are currently used for the detection of HTLV-1 or -2.

Nested PCR

Nested PCR increases the specificity of DNA amplification by reducing nonspecific amplification of DNA. In this technique, two sets of primers are used in two successive PCRs (48). In the first PCR, one set of primers is used to amplify the intended product but the reaction mixture may also contain nonspecific DNA products. Some of the product from the first PCR is added to a second PCR mixture that has a different set of PCR primers specific for the target sequence (49). The products are then analyzed on an agarose gel for the presence of a band at the predicted product size. Different PCR primers can be designed in order to differentiate between HTLV-1 and -2 infections (49).

Nested PCR is very sensitive because it utilizes two separate amplification reactions with two different primer sets. This makes it useful for situations where the HTLV status is in question, such as for samples that are seroindeterminate by WB. Faintly positive samples by WB are typically the most difficult to amplify by PCR because they generally have low antibody titers, which may be indicative of low viral loads. For this reason, several studies have suggested that

nested PCR be used for the analysis of seroindeterminate samples (30, 48, 49). On the downside, the sensitive nature of nested PCR makes it prone to contamination, which can complicate the interpretation of results.

Quantitative Real-Time PCR

Although several methods existed for detecting viruses, it was not until the advent of quantitative real-time PCR (qPCR) in the 1990s that scientists were able to quantify viral loads in HTLV-infected patients. Quantification of the HTLV-1 PVL has contributed to the understanding of HTLV-1 pathogenesis. In particular, it highlighted the association between an elevated PVL and the development of HTLV-1-related disease in infected subjects. Currently, a PVL of >1% is recognized as a risk factor for HAM/TSP and ATLL in infected subjects (50, 51). Additionally, the HTLV-1 PVL is an important biomarker in clinical trials for both HAM/TSP and ATLL (50, 52–54).

For qPCR, a single PCR mixture is prepared that contains primers complementary to a portion of the viral genome and a probe with a fluorescent reporter molecule attached. The most commonly examined genes for HTLV-1 detection are the *tax* and *pol* genes (Table 1). The most commonly examined genes for HTLV-2 detection are the *pol*, *tax*, and LTR genes (Table 1).

While the sample undergoes PCR, the qPCR instrument monitors and detects fluorescence to produce an amplification plot. All qPCR assays are characterized by the quantification cycle (C_q), which represents the number of cycles needed to reach a threshold fluorescence signal. To calculate the C_q, a threshold is set by a software-determined algorithm or manually by the user. However, the C_q can be affected by the efficiency of PCR amplification, the efficiency of hybridization of the fluorescent probe, and the sensitivity of detection. In order to determine the amplification efficiency, a standard curve is created by using HTLV-1- or -2-infected material. Different labs use different reference materials for their standard curves, including various infected cell lines or plasmids (Table 1) (54–56). Importantly, the use of a standard curve also allows for the quantification of HTLV-1 or -2. Typically, a lower C_q correlates with a larger amount of viral DNA and a higher C_q correlates with a smaller amount of viral DNA.

Due to the nature of detection, multiple target products can be analyzed in parallel by using different fluorophores. Therefore, it is common for a viral gene and a housekeeping gene to be examined for each sample. There are many different housekeeping genes that can be quantified, including albumin, β-actin, and β-globin. The housekeeping gene allows for normalization of the amount of virus detected in a sample to the amount of input DNA, which can then be translated into the PVL as a percentage of infected cells.

Like nested PCR, qPCR has been a useful tool for differentiating between HTLV-1 and -2 infections in seroindeterminate cases (29, 56–58). Moreover, qPCR has acceptable intra- and interassay reproducibility, making it a good method for quantifying PVL in patient samples (55, 56).

The major problem with qPCR, however, is the lack of standardization. Currently, different laboratories use different viral target genes and a variety of internal controls (Table 1). In addition, laboratories also use different reference materials for the creation of their standardized curves, which can affect the relative quantification of virus (Table 1). Taken together, these factors create known laboratory-to-laboratory variations in PVL quantification, limiting the relevance of this measure as a "gold standard" biomarker. In particular, this hinders the establishment of a threshold that differentiates asymptomatic carriers from those with disease, and it also complicates the use of PVL as a diagnostic criterion (46, 59, 60). In addition, the use of qPCR remains inconvenient for large-scale screening, impeding its implementation in blood banks as a confirmatory test (46).

TABLE 1 Viral target regions and reference materials for quantification of HTLV-1 and -2 by qPCR[a]

Virus	Target region	Viral reference material	Reference
HTLV-1	pX	MT2 cell line	51
	tax	Plasmid	63
	pol	Plasmid	54
	pX	TARL-2 cell line	64
	pol	MT2 cell line	29
	pX	TARL-2 cell line	56
	tax	MT2 cell line	55
HTLV-2	LTR	C3-44 cell line	65
	pol	Plasmid	29
	tax	Transfected cell line	66

[a]Several different viral target regions and viral reference materials are used for the quantification of HTLV-1 and -2 by qPCR. This lack of standardization makes comparison across laboratories challenging.

Droplet Digital PCR

Droplet digital PCR (ddPCR) was developed in 2011 and is considered the third generation of PCR, which allows for the direct absolute quantification of target genes. The reagents used in ddPCR are very similar to those used for qPCR; therefore, primer and probe sets specific for the detection of HTLV-1 or -2 can be designed to allow for differentiation of these viruses. Unlike qPCR, which amplifies mixtures in single wells in duplicate or triplicate, in ddPCR each PCR mixture is randomly partitioned into 20,000 nanoliter-sized droplets. PCR amplification of the template occurs in each droplet and is then analyzed for fluorescence in a flow cytometer, and the sample is designated either PCR positive or PCR negative based upon the level of fluorescence. As in qPCR, multiple genes can be analyzed simultaneously by using fluorophores that can be read on different channels of the flow cytometer. Because of the randomization of the sample partitioning and the large number of events queried, the data meet the criteria for analysis by Poisson statistics. The fraction of positive droplets is fitted to a Poisson distribution to directly determine the amount of template in the sample, most importantly without the need for a standard curve (61). The quantification of the HTLV-1 or -2 gene together with a housekeeping gene is sufficient to calculate the PVL.

Because of the statistical nature of the quantification, ddPCR has the ability to detect and quantify virus even in samples with very low viral copy numbers (61). Moreover, it is a highly precise and reproducible method of viral detection and quantification because it lacks the variability of relative quantification by qPCR (62). Because ddPCR is a novel technology, the ddPCR machinery is still expensive and the procedure is time-consuming, which limit the large-scale implementation and use of ddPCR as a confirmatory assay. However, it is a useful tool for monitoring patient PVL and for analyzing therapeutic interventions (62).

REFERENCES

1. **Poiesz BJ, Ruscetti FW, Gazdar AF, Bunn PA, Minna JD, Gallo RC.** 1980. Detection and isolation of type C retrovirus particles from fresh and cultured lymphocytes of

a patient with cutaneous T-cell lymphoma. *Proc Natl Acad Sci USA* **77:**7415–7419. PubMed
2. **Kalyanaraman VS, Sarngadharan MG, Robert-Guroff M, Miyoshi I, Golde D, Gallo RC.** 1982. A new subtype of human T-cell leukemia virus (HTLV-II) associated with a T-cell variant of hairy cell leukemia. *Science* **218:**571–573. PubMed
3. **Nejmeddine M, Negi VS, Mukherjee S, Tanaka Y, Orth K, Taylor GP, Bangham CR.** 2009. HTLV-1-Tax and ICAM-1 act on T-cell signal pathways to polarize the microtubule-organizing center at the virological synapse. *Blood* **114:**1016–1025. PubMed
4. **Nagai M, Brennan MB, Sakai JA, Mora CA, Jacobson S.** 2001. CD8(+) T cells are an in vivo reservoir for human T-cell lymphotropic virus type I. *Blood* **98:**1858–1861. PubMed
5. **Lal RB, Owen SM, Rudolph DL, Dawson C, Prince H.** 1995. In vivo cellular tropism of human T-lymphotropic virus type II is not restricted to CD8+ cells. *Virology* **210:**441–447. PubMed
6. **de Thé G, Kazanji M.** 1996. An HTLV-I/II vaccine: from animal models to clinical trials? *J Acquir Immune Defic Syndr Hum Retrovirol* **13**(Suppl 1)**:**S191–S198. PubMed
7. **Verdonck K, González E, Van Dooren S, Vandamme AM, Vanham G, Gotuzzo E.** 2007. Human T-lymphotropic virus 1: recent knowledge about an ancient infection. *Lancet Infect Dis* **7:**266–281. PubMed
8. **Cooper SA, van der Loeff MS, Taylor GP.** 2009. The neurology of HTLV-1 infection. *Pract Neurol* **9:**16–26. PubMed
9. **Ureta-Vidal A, Angelin-Duclos C, Tortevoye P, Murphy E, Lepère JF, Buigues RP, Jolly N, Joubert M, Carles G, Pouliquen JF, de Thé G, Moreau JP, Gessain A.** 1999. Mother-to-child transmission of human T-cell-leukemia/lymphoma virus type I: implication of high antiviral antibody titer and high proviral load in carrier mothers. *Int J Cancer* **82:**832–836. PubMed
10. **Fujino T, Nagata Y.** 2000. HTLV-I transmission from mother to child. *J Reprod Immunol* **47:**197–206. PubMed
11. **Manns A, Wilks RJ, Murphy EL, Haynes G, Figueroa JP, Barnett M, Hanchard B, Blattner WA.** 1992. A prospective study of transmission by transfusion of HTLV-I and risk factors associated with seroconversion. *Int J Cancer* **51:**886–891. PubMed
12. **Kajiyama W, Kashiwagi S, Ikematsu H, Hayashi J, Nomura H, Okochi K.** 1986. Intrafamilial transmission of adult T cell leukemia virus. *J Infect Dis* **154:**851–857. PubMed
13. **Proietti FA, Carneiro-Proietti AB, Catalan-Soares BC, Murphy EL.** 2005. Global epidemiology of HTLV-I infection and associated diseases. *Oncogene* **24:**6058–6068. PubMed
14. **Uchiyama T, Yodoi J, Sagawa K, Takatsuki K, Uchino H.** 1977. Adult T-cell leukemia: clinical and hematologic features of 16 cases. *Blood* **50:**481–492. PubMed
15. **Blattner WA, Nomura A, Clark JW, Ho GY, Nakao Y, Gallo R, Robert-Guroff M.** 1986. Modes of transmission and evidence for viral latency from studies of human T-cell lymphotrophic virus type I in Japanese migrant populations in Hawaii. *Proc Natl Acad Sci USA* **83:**4895–4898. PubMed
16. **Manns A, Blattner WA.** 1991. The epidemiology of the human T-cell lymphotrophic virus type I and type II: etiologic role in human disease. *Transfusion* **31:**67–75. PubMed
17. **Gessain A, Barin F, Vernant JC, Gout O, Maurs L, Calender A, de Thé G.** 1985. Antibodies to human T-lymphotropic virus type-I in patients with tropical spastic paraparesis. *Lancet* **ii:**407–410. PubMed
18. **Kitajima I, Osame M, Izumo S, Igata A.** 1988. Immunological studies of HTLV-I associated myelopathy. *Autoimmunity* **1:**125–131. PubMed
19. **World Health Organization Regional Office for the Western Pacific.** 1989. *Scientific Group on HTLV-I Infections and Associated Diseases: Report*. World Health Organization Regional Office for the Western Pacific, Manila Philippines.
20. **Araujo A, Hall WW.** 2004. Human T-lymphotropic virus type II and neurological disease. *Ann Neurol* **56:**10–19. PubMed
21. **Jacobson S, Lehky T, Nishimura M, Robinson S, McFarlin DE, Dhib-Jalbut S.** 1993. Isolation of HTLV-II from a patient with chronic, progressive neurological disease clinically indistinguishable from HTLV-I-associated myelopathy/tropical spastic paraparesis. *Ann Neurol* **33:**392–396. PubMed
22. **Lehky TJ, Flerlage N, Katz D, Houff S, Hall WH, Ishii K, Monken C, Dhib-Jalbut S, McFarland HF, Jacobson S.** 1996. Human T-cell lymphotropic virus type II-associated myelopathy: clinical and immunologic profiles. *Ann Neurol* **40:**714–723. PubMed
23. **Fujiyama C, Fujiyoshi T, Matsumoto D, Tamashiro H, Sonoda S.** 1995. Evaluation of commercial HTLV-1 test kits by a standard HTLV-1 serum panel. *Bull World Health Organ* **73:**515–521. PubMed
24. **Stanley J.** 2002. *Essentials of Immunology and Serology*. Delmar Thomson Learning, Clifton Park, NY.
25. **Anushka S, Balram P, Mathai J, Shanumugam J.** 2012. Serological evidence of HTLV-1 infection among voluntary blood donors and cancer patients from Kerala State. *J Int Med Sci Acad* **25:**85–86.
26. **Thorstensson R, Albert J, Andersson S.** 2002. Strategies for diagnosis of HTLV-I and -II. *Transfusion* **42:**780–791. PubMed
27. **Vrielink H, Reesink H, Habibuw M, Schuller M, van der Meer C, Lelie P.** 1999. Comparison of four HTLV-I and HTLV-I + II ELISAs. *Vox Sang* **76:**187–191. PubMed
28. **Vrielink H, Reesink HW.** 2004. HTLV-I/II prevalence in different geographic locations. *Transfus Med Rev* **18:**46–57. PubMed
29. **Andrade RG, Ribeiro MA, Namen-Lopes MS, Silva SM, Basques FV, Ribas JG, Carneiro-Proietti AB, Martins ML.** 2010. Evaluation of the use of real-time PCR for human T cell lymphotropic virus 1 and 2 as a confirmatory test in screening for blood donors. *Rev Soc Bras Med Trop* **43:**111–115. PubMed
30. **Couroucé AM, Pillonel J, Saura C.** 1999. Screening of blood donations for HTLV-I/II. *Transfus Med Rev* **13:**267–274. PubMed
31. **Verdonck K, González E, Maldonado F, Agapito D, Van Dooren S, Vandamme AM, Silva-Santisteban A, Vanham G, Clark D, Gotuzzo E.** 2009. Comparison of three ELISAs for the routine diagnosis of human T-lymphotropic virus infection in a high-prevalence setting in Peru. *Trans R Soc Trop Med Hyg* **103:**420–422. PubMed
32. **Abbaszadegan MR, Jafarzadeh N, Sankian M, Varasteh A, Mahmoudi M, Sadeghizadeh M, Khatami F, Mehramiz N.** 2008. Truncated MTA-1: a pitfall in ELISA-based immunoassay of HTLV-1 infection. *J Biomed Biotechnol* **2008:**846371. PubMed
33. **Berini CA, Susana Pascuccio M, Bautista CT, Gendler SA, Eirin ME, Rodriguez C, Pando MA, Biglione MM.** 2008. Comparison of four commercial screening assays for the diagnosis of human T-cell lymphotropic virus types 1 and 2. *J Virol Methods* **147:**322–327. PubMed
34. **Jacob F, Santos-Fortuna EL, Azevedo RS, Caterino-de-Araujo A.** 2007. Performances of HTLV serological tests in diagnosing HTLV infection in high-risk population of São Paulo, Brazil. *Rev Inst Med Trop Sao Paulo* **49:**361–364. PubMed
35. **Yao K, Hisada M, Maloney E, Yamano Y, Hanchard B, Wilks R, Rios M, Jacobson S.** 2006. Human T

lymphotropic virus types I and II Western blot seroindeterminate status and its association with exposure to prototype HTLV-I. *J Infect Dis* **193:**427–437. PubMed
36. **Yanagihara R, Garruto RM, Miller MA, Leon-Monzon M, Liberski PP, Gajdusek DC, Jenkins CL, Sanders RC, Alpers MP.** 1990. Isolation of HTLV-I from members of a remote tribe in New Guinea. *N Engl J Med* **323:**993–994. PubMed
37. **Delaporte E, Monplaisir N, Louwagie J, Peeters M, Martin-Prével Y, Louis JP, Trebucq A, Bedjabaga L, Ossari S, Honoré C.** 1991. Prevalence of HTLV-I and HTLV-II infection in Gabon, Africa: comparison of the serological and PCR results. *Int J Cancer* **49:**373–376. PubMed
38. **Garin B, Gosselin S, de Thé G, Gessain A.** 1994. HTLV-I/II infection in a high viral endemic area of Zaire, Central Africa: comparative evaluation of serology, PCR, and significance of indeterminate Western blot pattern. *J Med Virol* **44:**104–109. PubMed
39. **Gessain A, Mathieux R.** 1995. HTLV-I "indeterminate" Western blot patterns observed in sera from tropical regions: the situation revisited. *J Acquir Immune Defic Syndr Hum Retrovirol* **9:**316–319. PubMed
40. **Caterino-de-Araujo A, de los Santos-Fortuna E, Meleiro MC, Suleiman J, Calabrò ML, Favero A, De Rossi A, Chieco-Bianchi L.** 1998. Sensitivity of two enzyme-linked immunosorbent assay tests in relation to Western blot in detecting human T-cell lymphotropic virus types I and II infection among HIV-1 infected patients from São Paulo, Brazil. *Diagn Microbiol Infect Dis* **30:**173–182. PubMed
41. **Mangano AM, Remesar M, del Pozo A, Sen L.** 2004. Human T lymphotropic virus types I and II proviral sequences in Argentinian blood donors with indeterminate Western blot patterns. *J Med Virol* **74:**323–327. PubMed
42. **Medrano FJ, Soriano V, Calderón EJ, Rey C, Gutiérrez M, Bravo R, Leal M, González-Lahoz J, Lissen E.** 1997. Significance of indeterminate reactivity to human T-cell lymphotropic virus in Western blot analysis of individuals at risk. *Eur J Clin Microbiol Infect Dis* **16:**249–252. PubMed
43. **Busch MP, Switzer WM, Murphy EL, Thomson R, Heneine W.** 2000. Absence of evidence of infection with divergent primate T-lymphotropic viruses in United States blood donors who have seroindeterminate HTLV test results. *Transfusion* **40:**443–449. PubMed
44. **Roberts BD, Foung SK, Lipka JJ, Kaplan JE, Hadlock KG, Reyes GR, Chan L, Heneine W, Khabbaz RF.** 1993. Evaluation of an immunoblot assay for serological confirmation and differentiation of human T-cell lymphotropic virus types I and II. *J Clin Microbiol* **31:**260–264. PubMed
45. **Sabino EC, Zrein M, Taborda CP, Otani MM, Ribeiro-Dos-Santos G, Sáez-Alquézar A.** 1999. Evaluation of the INNO-LIA HTLV I/II assay for confirmation of human T-cell leukemia virus-reactive sera in blood bank donations. *J Clin Microbiol* **37:**1324–1328. PubMed
46. **Zrein M, Louwagie J, Boeykens H, Govers L, Hendrickx G, Bosman F, Sablon E, Demarquilly C, Boniface M, Saman E.** 1998. Assessment of a new immunoassay for serological confirmation and discrimination of human T-cell lymphotropic virus infections. *Clin Diagn Lab Immunol* **5:**45–49. PubMed
47. **Mullis KB, Faloona FA.** 1987. Specific synthesis of DNA in vitro via a polymerase-catalyzed chain reaction. *Methods Enzymol* **155:**335–350. PubMed
48. **Defer C, Coste J, Descamps F, Voisin S, Lemaire JM, Maniez M, Couroucé AM, Retrovirus Study Group of the French Society of Blood Transfusion.** 1995. Contribution of polymerase chain reaction and radioimmunoprecipitation assay in the confirmation of human T-lymphotropic virus infection in French blood donors. *Transfusion* **35:**596–600. PubMed
49. **Gallego S, Mangano A, Gastaldello R, Sen L, Medeot S.** 2004. Usefulness of a nested-polymerase chain reaction for molecular diagnosis of human T-cell lymphotropic virus type I/II. *Mem Inst Oswaldo Cruz* **99:**377–380. PubMed
50. **Kira J, Koyanagi Y, Yamada T, Itoyama Y, Goto I, Yamamoto N, Sasaki H, Sakaki Y.** 1991. Increased HTLV-I proviral DNA in HTLV-I-associated myelopathy: a quantitative polymerase chain reaction study. *Ann Neurol* **29:**194–201. PubMed
51. **Nagai M, Usuku K, Matsumoto W, Kodama D, Takenouchi N, Moritoyo T, Hashiguchi S, Ichinose M, Bangham CR, Izumo S, Osame M.** 1998. Analysis of HTLV-I proviral load in 202 HAM/TSP patients and 243 asymptomatic HTLV-I carriers: high proviral load strongly predisposes to HAM/TSP. *J Neurovirol* **4:**586–593. PubMed
52. **Demontis MA, Hilburn S, Taylor GP.** 2013. Human T cell lymphotropic virus type 1 viral load variability and long-term trends in asymptomatic carriers and in patients with human T cell lymphotropic virus type 1-related diseases. *AIDS Res Hum Retroviruses* **29:**359–364. PubMed
53. **Matsuzaki T, Nakagawa M, Nagai M, Usuku K, Higuchi I, Arimura K, Kubota H, Izumo S, Akiba S, Osame M.** 2001. HTLV-I proviral load correlates with progression of motor disability in HAM/TSP: analysis of 239 HAM/TSP patients including 64 patients followed up for 10 years. *J Neurovirol* **7:**228–234. PubMed
54. **Olindo S, Lézin A, Cabre P, Merle H, Saint-Vil M, Edimonana Kaptue M, Signate A, Césaire R, Smadja D.** 2005. HTLV-1 proviral load in peripheral blood mononuclear cells quantified in 100 HAM/TSP patients: a marker of disease progression. *J Neurol Sci* **237:**53–59. PubMed
55. **Castro GM, Balangero MC, Maturano E, Mangeaud A, Gallego SV.** 2013. Development and validation of a real-time PCR assay for a novel HTLV-1 tax sequence detection and proviral load quantitation. *J Virol Methods* **189:**383–387. PubMed
56. **Rosadas C, Cabral-Castro MJ, Vicente AC, Peralta JM, Puccioni-Sohler M.** 2013. Validation of a quantitative real-time PCR assay for HTLV-1 proviral load in peripheral blood mononuclear cells. *J Virol Methods* **193:**536–541. PubMed
57. **Rafatpanah H, Fathimoghadam F, Shahabi M, Eftekharzadeh I, Hedayati-Moghaddam M, Valizadeh N, Tadayon M, Shamsian SA, Bidkhori H, Miri R, Bazarbachi A.** 2013. No evidence of HTLV-II infection among immunoblot indeterminate samples using nested PCR in Mashhad, Northeast of Iran. *Iran J Basic Med Sci* **16:**229–234. PubMed
58. **Santos TJ, Costa CM, Goubau P, Vandamme AM, Desmyter J, Van Doren S, Mota RM, de Castro Costa FB, Oliveira AC, Barreto V, Gomes AF, Carneiro-Proietti AB, de Bruin VM, de Sousa FC, Oriá RB.** 2003. Western blot seroindeterminate individuals for human T-lymphotropic virus I/II (HTLV-I/II) in Fortaleza (Brazil): a serological and molecular diagnostic and epidemiological approach. *Braz J Infect Dis* **7:**202–209. PubMed
59. **Grassi MF, Olavarria VN, Kruschewsky RA, Yamano Y, Jacobson S, Taylor GP, Martin F, Galvão-Castro B.** 2013. Utility of HTLV proviral load quantification in diagnosis of HTLV-1-associated myelopathy requires international standardization. *J Clin Virol* **58:**584–586. PubMed
60. **Kamihira S, Yamano Y, Iwanaga M, Sasaki D, Satake M, Okayama A, Umeki K, Kubota R, Izumo S, Yamaguchi K, Watanabe T.** 2010. Intra- and inter-laboratory variability in human T-cell leukemia virus type-1 proviral load quantification using real-time polymerase chain reaction assays: a multi-center study. *Cancer Sci* **101:**2361–2367. PubMed
61. **Pinheiro LB, Coleman VA, Hindson CM, Herrmann J, Hindson BJ, Bhat S, Emslie KR.** 2012. Evaluation

of a droplet digital polymerase chain reaction format for DNA copy number quantification. *Anal Chem* **84:**1003–1011. PubMed

62. **Brunetto GS, Massoud R, Leibovitch EC, Caruso B, Johnson K, Ohayon J, Fenton K, Cortese I, Jacobson S.** 2014. Digital droplet PCR (ddPCR) for the precise quantification of human T-lymphotropic virus 1 proviral loads in peripheral blood and cerebrospinal fluid of HAM/TSP patients and identification of viral mutations. *J Neurovirol* **20:**341–351. PubMed
63. **Kamihira S, Dateki N, Sugahara K, Hayashi T, Harasawa H, Minami S, Hirakata Y, Yamada Y.** 2003. Significance of HTLV-1 proviral load quantification by real-time PCR as a surrogate marker for HTLV-1-infected cell count. *Clin Lab Haematol* **25:**111–117. PubMed
64. **Silva MT, Harab RC, Leite AC, Schor D, Araújo A, Andrada-Serpa MJ.** 2007. Human T lymphotropic virus type 1 (HTLV-1) proviral load in asymptomatic carriers, HTLV-1-associated myelopathy/tropical spastic paraparesis, and other neurological abnormalities associated with HTLV-1 infection. *Clin Infect Dis* **44:**689–692. PubMed
65. **Estes MC, Sevall JS.** 2003. Multiplex PCR using real time DNA amplification for the rapid detection and quantitation of HTLV I or II. *Mol Cell Probes* **17:**59–68. PubMed
66. **Waters A, Oliveira AL, Coughlan S, de Venecia C, Schor D, Leite AC, Araújo AQ, Hall WW.** 2011. Multiplex real-time PCR for the detection and quantitation of HTLV-1 and HTLV-2 proviral load: addressing the issue of indeterminate HTLV results. *J Clin Virol* **52:**38–44. PubMed

Diagnosis of Prion Diseases

RICHARD RUBENSTEIN, ROBERT B. PETERSEN,
AND THOMAS WISNIEWSKI

71

Prion diseases, or transmissible spongiform encephalopathies (TSEs), are a large group of transmissible, progressive, and invariably fatal neurodegenerative conditions that affect both animals and humans (1–5). Prion diseases are unique in that they can be inherited, occur sporadically, or can be acquired by infection (1, 3–5). As described below, the infectious agent in the prion disease is composed mainly or entirely of an abnormal conformation of a host-encoded glycoprotein called the cellular prion protein (PrP^{C}). The replication of prions involves the recruitment of the normally expressed prion protein (PrP^{C}) structure, which is largely alpha-helical, into a disease-specific conformation (PrP^{Sc}) that is rich in beta-sheets and that can adopt a fibrillar aggregated structure that is characteristic of many of the deposits found in the brains of TSE-affected species. In contrast to the protease-sensitive PrP^{C}, the beta-sheet conformation along with the aggregation properties of PrP^{Sc} makes this protein partially resistant to proteolytic digestion (6). Furthermore, this posttranslational modification of PrP^{C} into the abnormal, infection-associated isoform, PrP^{Sc}, is believed to be the principal molecular basis underlying prion diseases. Animal prion diseases include scrapie of sheep and goats, bovine spongiform encephalopathy (BSE) or mad cow disease, chronic wasting disease (CWD) of cervids (predominantly mule deer and elk), transmissible mink encephalopathy (TME), feline spongiform encephalopathy, exotic ungulate spongiform encephalopathy, and spongiform encephalopathy of nonhuman primates. Although some cases of sporadic atypical scrapie and BSE have also been reported, most animal prion diseases occur via the acquisition of infection from contaminated feed or via exposure to environmental contaminants. Scrapie and CWD are naturally sustaining epidemics. The human prion diseases can be sporadic, inherited, or acquired. Sporadic human prion diseases include Creutzfeldt-Jakob disease (sCJD), fatal insomnia, and variably protease-sensitive prionopathy (VPSPr) (3, 4). Genetic prion diseases are caused by inheritance of autosomal dominant mutations in the host *PRNP* gene, which encodes the normal cellular PrP^{C} and includes genetic CJD (gCJD), fatal familial insomnia (FFI), and Gerstmann-Sträussler-Scheinker syndrome (GSS) (3, 4). Acquired human prion diseases account for only 5% of cases of human prion disease. They include kuru, iatrogenic CJD (iCJD), and variant CJD (vCJD) (3, 4), which was transmitted to humans from affected cattle via meat consumption. The transmission of BSE to humans has resulted in more than 200 cases of vCJD and has raised serious public health concerns. All prion diseases have long incubation periods but are typically rapidly progressive once clinical symptoms begin. Currently, there are no effective treatments for prion diseases, although increased understanding of their pathogenesis has recently led to the promise of effective therapeutic interventions. Numerous therapeutic approaches are under development both for the prevention of prion disease prior to or shortly after exposure and for treatment of already symptomatic disease (2, 7–10).

ETIOLOGY OF PrP-RELATED DISEASES

Highly divergent hypotheses have been put forward regarding the makeup of the prions, including the existence of a nucleic acid-derived agent, the protein-only hypothesis, that they lack both proteins and nucleic acids, and that the prion is a polysaccharide. The most widely accepted hypothesis, first described by Griffith (11) and more explicitly detailed by Stanley Prusiner, is the protein-only hypothesis (1, 12). Prusiner introduced the term "prion" to indicate that scrapie is related to a proteinaceous infectious particle (i.e., PrP) (1, 13).

This prion hypothesis was initially greeted with great skepticism by the scientific community. Now it represents the current dogma, with Prusiner winning the 1997 Nobel Prize in Physiology and Medicine. This hypothesis suggests that prions contain no nucleic acid and are composed predominantly, if not entirely, of the conformationally modified prion protein PrP^{Sc}. PrP^{C} is found on the surface of many cells, in particular neurons. PrP^{Sc}, when introduced into normal healthy cells, causes the conversion of PrP^{C} into PrP^{Sc}, initiating a self-perpetuating vicious cycle (1, 12). PrP^{Sc} originates from an exogenous source in acquired prion diseases and, presumably, from a spontaneous somatic conformational change in sporadic disease. In recent years, it has become clear that the prion hypothesis is an epigenetic mechanism of transmitting information on protein conformation and can be applied to numerous other biological and pathological situations (14–19). If one defines a "prion" more broadly as a protein-based inheritance unit that confers a trait based on a posttranslational switch involving the acquisition of increased β-sheet structure, along with an increased propensity for aggregation, then a number

doi:10.1128/9781555818722.ch71

of yeast proteins can be viewed as prions, such as Ure2p, Sup35p, Rinq1p, and HETs (the respective prion forms are URE2, PSI+, PIN+, and Het-s) (16, 17). These yeast "prions" are not associated with disease but serve as an epigenetic mechanism for cellular responses to environmental stress (20, 21). It has also been demonstrated that long-term potentiation is regulated by a prion-like switch in *Aplysia*, involving the cytoplasmic polyadenylation element binding protein (CPEB) (18, 19). In addition, a "prion-like" spread of pathology has been invoked to explain the behavior of numerous proteins involved in a broad spectrum of neurodegenerative disorders, including amyloid β (Aβ), tau, TDP-43, FUS, α-synuclein, and huntingtin (which are associated with Alzheimer's disease [AD] [Aβ and tau] , frontotemporal dementia [tau, TDP-43, and FUS], Parkinson's disease [α-synuclein], and Huntington's disease) (12, 13). The specific targeting of the shared pathological prion-like conformation of these different neurodegenerative disease-associated proteins is currently being investigated as a novel therapeutic approach (22–25).

CELL BIOLOGY OF PRIONS

Function(s) of PrP^C

The human PrP gene (*PRNP*) is found on chromosome 20 and encodes a protein of 253 amino acids. PrP^C is a glycosylphosphatidylinositol-anchored cell surface glycoprotein with numerous suggested roles, although its exact cellular function(s) remains unknown. Expression of PrP^C is a prerequisite for prion replication and the development of pathology (26). The N-terminal region of PrP^C contains a segment of 5 repeats of an 8-amino-acid sequence (i.e., an octapeptide repeat region) that contains a high-affinity binding site for metal ions; hence, PrP^C may have a role in copper and manganese transport or metabolism (27). PrP^C has also been reported to facilitate uptake of zinc into neuronal cells at the synaptic cleft (28, 29). Metal imbalance has been reported as an early change during prion infections (30, 31). Chelation of both copper and manganese has been shown to prolong the incubation period of prion infection (32, 33). Immunological functions have also been suggested for PrP^C, such as involvement in T-cell development and macrophage phagocytosis (34). PrP^C and/or Shadoo (a PrP^C-like protein) have also been shown to be important for early mouse embryogenesis and trophoblastic development (35, 36). A surprising recently identified role for PrP^C is as a receptor for Aβ oligomers, in part mediating their toxicity (37–39). At least some of the function(s) of PrP^C is likely to be important because PrP^C is highly conserved among mammals and is found in all tetrapods and birds (5, 40, 41), although PrP^C knockout mice are viable (42).

PrP^C is found in most tissues of the body but is expressed at the highest levels in the central nervous system (CNS), especially in neurons. PrP^C is also expressed widely on cells of the immune system. PrP^C knockout mice, which were engineered to block expression of the PrP gene, show no obvious pathological phenotype (42). However, these mice have been shown to have abnormalities in synaptic physiology (43) and in circadian rhythms and sleep (44).

An amino acid polymorphism at codon 129 of *PRNP* is an important genetic risk modifier for human prion disease. Among Caucasian populations, about 51% of individuals are methionine-valine (MV) heterozygous, 38% are MM homozygous, and 11% are VV homozygous (45–47). MM homozygotes are significantly overrepresented among sCJD patients, as are, to a lesser extent, VV homozygotes. MV heterozygotes are relatively protected. For example, among 300 cases of reported sCJD cases from the United States and Europe, 71.6% were MM, 16.7% were VV, and only 11.7% were MV (46). Furthermore, all confirmed cases of vCJD have been MM homozygotes, with only one potential case of vCJD being an MV heterozygote (48).

The secondary structure of PrP^C was first elucidated by nuclear magnetic resonance (NMR) imaging using recombinant mouse PrP (49, 50). NMR was subsequently performed using recombinant hamster and human PrP as well (51–53). These studies showed that PrP^C is about 40% alpha-helix and about 3% beta-sheet. No high-resolution structural studies, such as NMR imaging, have been performed on PrP^{Sc} due to its insolubility and aggregation, which are properties that preclude the use of these techniques (54). However, less exact structural methods, such as circular dichroism and Fourier transform infrared spectroscopy, demonstrated that PrP^{Sc} contains about 45% beta-sheet and 30% alpha-helix (54–56). The high beta-sheet content correlates with PrP^{Sc} resistance to enzymatic digestion and infectivity.

Prion Strains and the Species Barrier

Many lines of evidence support the protein-only hypothesis of prion propagation. However, the protein-only hypothesis has had difficulty explaining the existence of several distinct isolates or strains of prions that can be stably passaged among inbred mice of the same genotype (1, 5, 57). The existence of strains suggests that PrP^{Sc} may adopt multiple distinct pathological conformations. Strains are defined by their incubation time, distribution of CNS involvement, and the pattern of proteolytic cleavage of PrP^{Sc} following proteinase K (PK) digestion (14, 58). For example, at least 14 significantly different scrapie strains have been isolated from natural sheep scrapie by passage into mice (57, 59). Each strain of prion has a characteristic range of infectivity. For example, strain 263K is pathogenic for hamsters but does not infect mice (60). This effect is called a species barrier and is related to PrP^{Sc} being an effective template for homologous PrP^C and a poor template for heterologous PrP^C; hence, mouse PrP^{Sc} can effectively convert mouse PrP^C but is a very poor template for human or hamster PrP^C. The species barrier is not absolute, as illustrated by the emergence of BSE.

Among the best-studied strain differences are the two strains of TME called hyper (HY) and drowsy (DY) (61, 62). The truncated DY PrP^{Sc} fragments (PrP27-30) migrate 1 to 2 kDa faster than similar preparations of HY because the sites of PK cleavage differ. The two strains also differ in the amount of beta-sheet content (61–64). Parchi et al. (47, 65, 66) defined two distinct types of sCJD based on the pattern of sodium dodecyl sulfate-polyacrylamide (SDS-PAGE) migration of the PrP27-30 fragment. Type 1 sCJD has a molecular mass of the deglycosylated PrP27-30 of about 21 kDa, while type 2 has a mobility of about 19 kDa. This allows the division of sCJD into six major phenotypic subtypes with distinctive clinicopathological features based on the genotype at the polymorphic codon 129 (M/M, M/V, or V/V genotype) in the prion protein gene, as well as the type 1 or 2 electrophoretic migration pattern. Collinge et al. (67, 68) reported two further types related to infectious CJD.

How Prion Agents Reach the CNS

Acquired prion diseases are naturally transmitted via peripheral routes, most commonly orally (69), but transcutaneous (70–73) or aerosol (74–77) transmission is also possible. Consequently, determining the route that prions employ to reach the CNS is an important issue. Aerosol transmission

has been identified to have a major role in CWD, which is the most infectious prionosis to date (74, 75, 77–79). Although the prion diseases are neurological conditions, critical events in their pathogenesis take place in restricted sites out of the nervous system, especially in peripheral lymphoid organs (80–83).

Lymphoid organs have long been known to be involved in the early stages of prion diseases (83–86). In particular, the spleen and lymph nodes were demonstrated to be the first sites of PrP^{Sc} replication after infection by peripheral routes, and they are also significantly involved following intracerebral challenge (87, 88). Their importance for neuroinvasion after peripheral inoculation was suggested by studies showing that splenectomy and other methods that reduce peripheral lymphoid structures delay clinical manifestations (85). Replication in the lymphoid organs is particularly important for specific prionoses, which are more "lymphotrophic"; these include scrapie, CWD, BSE, and vCJD (89–92). The lymphotrophic nature of vCJD allows the use of tonsil biopsy for its preclinical diagnosis and for analysis of appendices in nationwide prevalence screening studies (93–95). Following oral exposure, which is thought to be the most common route for acquired prionoses such as vCJD, BSE, and CWD, prions are able to resist exposure to digestive enzymes due to their protease resistance. Prions are able to cross the epithelial gut barrier and accumulate rapidly in Peyer's patches prior to colonization of the spleen (69). Susceptibility to prion infection following an oral challenge is correlated with the number of Peyer's patches present in the small intestine (96). At the epithelial level, three cell types can be involved in PrP^{Sc} entry in non-mutually exclusive pathways: enterocytes, dendritic cells (DCs), and microfold (M) cells (82, 83). Enterocytes express the 37-kDa/67-kDa laminin receptor (LRP/LR) on their apical brush border, which has been shown to bind PrP^{Sc} (96–98). It has also been shown that human enterocytes internalize BSE PrP^{Sc} via the LRP/LR receptor (99). M cells are unique epithelial cells that specialize in the transcytosis of particles. Coculture systems have been used to demonstrate that M cells are able to facilitate transcytosis of PrP^{Sc} (100) and that M cell depletion inhibits prion infection after oral challenge (101). DCs are known to patrol the gut-associated lymphoid tissue and are able to transcytose antigens for presentation to B and T cells. Depletion of $CD11c^+$ DCs was shown to inhibit PrP^{Sc} accumulation in the gut-associated lymphoid tissue and spleen, reducing susceptibility to prion infection after an oral challenge (102).

Once PrP^{Sc} gains entry and replicates in the secondary lymphoid organs, further spread to the CNS occurs via the autonomic nervous system (69, 103). Hence, following intraperitoneal or oral delivery of prions, onset of disease can be delayed by sympathectomy or can be accelerated by sympathetic hyperinnervation of lymphoreticular organs (104). Prions can also gain entry to the CNS via the circulation. The hematogenic spread of prions to the CNS is suggested by experiments that show BSE and CWD to be transmissible from sheep to sheep and deer to deer, respectively, by blood transfusion (105, 106). Three cases of vCJD infection associated with blood transfusion have also been identified (48). All received nonleucodepleted red blood cells and were homozygous for methionine at codon 129 of the *PRNP* gene, similar to all other vCJD cases (see discussion of vCJD below). The first patient developed vCJD in 2003, 6.5 years following transfusion from a donor who developed vCJD 3.5 years after donating blood. The second patient developed vCJD in 2006, 7.8 years after transfusion from a donor who was diagnosed with vCJD about 20 months after donation. One additional case received vCJD-contaminated red blood cells and died of causes unrelated to vCJD; however, at autopsy PrP^{Sc} was found in the spleen and cervical lymph nodes but not in the brain. Interestingly, this case was MV heterozygous at codon 129 (107). These cases raise the possibility of future human prion disease cases related to transmission through blood or blood products. Hematogenic neuroinvasion has been shown to be dependent on the presence of B lymphocytes (108). However, because expression of PrP^C by B cells is not required for neuroinvasion, some have suggested that their main function is to allow maintenance of follicular dendritic cells (109). A number of studies have implicated follicular dendritic cells as having a critical role in the replication of lymphotrophic strains of prions (85). Other studies have also implicated a distinct $CD11c^+$ dendritic cell population in prion neuroinvasion (110).

Establishing a better understanding of how PrP^{Sc} gains entry via the gut and ultimately into the CNS may lead to novel therapeutic approaches to prevent prion infection. A *Salmonella*-based vaccine applied orally to wild-type mice was observed to induce a specific anti-PrP mucosal immune response that can prevent prion infection after oral challenge in mice (111). More recently, a similar approach was shown to give partial protection to white-tailed deer immunized with a *Salmonella* vaccine strain expressing cervid PrP from oral challenge with CWD (112).

ANIMAL PRION DISEASES

The first of the animal diseases to be described was scrapie in the United Kingdom over 250 years ago (113). Referred to as scrapie based on the disheveled appearance of the affected sheep, at that time diagnosis relied solely on a physical description. Scrapie was subsequently found to affect goats as well. This illness, manifested by hyperexcitability, itching, and ataxia, leads to paralysis and death. It is called scrapie because of the tendency of affected animals to rub against the fences of their pens in order to stay upright, reflecting their cerebellar dysfunction. In the 1930s, scrapie was shown to be transmissible (114). The transmission of this disease was further demonstrated in 1943, when a population of Scottish sheep was accidentally inoculated against a common virus using a formalin extract of lymphoid tissue from an animal with scrapie. Accidental transmission of prions is a recurrent event in the history of these agents and is related to their unusual biophysical properties.

The observation that some strains of sheep were more susceptible to infection than others led to the hypothesis that scrapie may be inheritable as well (115). We now know that there are polymorphic sites in the protein underlying the disease, and genetic analysis of flocks is done to assess the risk of scrapie (http://www.aphis.usda.gov/animal_health/animal_diseases/scrapie/index2.shtml). At about the same time, TME, a disease in farmed mink, which presumably resulted from feeding scrapie-infected sheep to mink, arose (116), although recent speculation is that the source may actually have been an uncommon type of BSE (117).

The transmissible nature of the disease was used to create a bioassay in which brain homogenates from suspect animals were used to infect a test animal, of late typically transgenic mice (118). An important concept that arose from the transmission studies was, as mentioned above, that of the species barrier, i.e., the increased latency or inability to transmit disease between some species (119). One of the principal determinants of species barrier is the difference in the primary amino acid sequences of the PrP of the infected species and the PrP of the uninfected new host.

Of greater impact than any of the previously identified diseases was the identification of BSE as a prion disease (120). Primarily limited to the United Kingdom, a few cases traced to imported cattle from the United Kingdom were also identified in continental Europe. The suspected etiology was the ingestion of scrapie-contaminated feed, which may be linked to a change in rendering practices (121). Others have speculated that the origin of BSE may be linked to a mutation in an animal that initiated the epidemic. The origin of CWD in North America, while unknown, may also be linked to contaminated feed given to farmed deer and elk, which escaped to infect wild populations of cervids, although this is less certain (122). The spread of CWD throughout North America and to South Korea was facilitated by the transport of captive animals.

Unifying all of these diseases is its transmissibility, whether through vertical transmission from mother to offspring or by contaminants in the environment. Characterization of the pathogen indicated that it was resistant to those treatments that eliminate most infectious agents (UV inactivation, nucleases, heat, etc.) (123, 124), leading to the proposal that the prion agent may be composed solely of protein (13). Of note, while protease treatment reduced the titers of the agent, the partially protease-resistant PrP^{Sc} (also called PrP27-30 or PrP^{res}) could be detected in the CNS from infected animals (125) and has been subsequently used as a biomarker to identify infected animals (see below).

Diagnosis of Animal Prion Diseases

On the diagnostic front, the first neuropathological description of animal prion diseases characterized the vacuole-laden neurons found in scrapie-affected sheep (126). At that time, based on the transmissible nature of the diseases, they became known as TSEs. Another diagnostic feature was the presence of scrapie-associated fibrils (SAFs) in the detergent extract of brains from infected animals observed by negative-stain electron microscopy (127). However, it was the purification of the disease-linked PrP^{Sc} and the discovery that it was encoded by the PRNP gene that opened up a new age in prion disease diagnosis (125, 128, 129).

Purification of SAFs or PrP27-30, the PK-resistant core of the prion, permitted the development of PrP-specific antibodies (Abs) (130, 131). An early application to diagnosis that entailed performing PK treatment (a necessary step since PrP-specific Abs do not distinguish between PrP^{C} and PrP^{Sc}) prior to Western blotting was proposed (132). An alternative method using immunohistochemistry (IHC) was quickly adopted as the "gold standard" for diagnosis of TSEs (133) for its greater sensitivity. IHC staining used protease treatment or formic acid pretreatment of tissue to remove PrP^{C} before addition of Abs, while Western blotting required protease pretreatment. These tests were largely confined to academic laboratories and regulatory agencies monitoring scrapie. Table 1 lists the animal diseases and the clinical and pathological symptoms used to diagnose them as prion diseases. Final diagnosis depends on demonstrating PrP^{Sc} by Western blotting or IHC staining of fixed tissue.

The identification of vCJD in 1996 (134) and the link to BSE dramatically affected the demand for sensitive diagnostic tests for prion diseases to screen cattle. The diagnostic needs were 2-fold. First, there was a need for epidemiologic screening, and second, there was a need for a test to ensure food safety. While the nature of the infectious agent was still under debate, the utility of diagnosis based on the presence of PrP^{res} in brain was quickly accepted. Up to this point, animal bioassays using mice or hamsters were viewed as the definitive test. However, the long latency between intracerebral inoculation and infection, a minimum of 90 days in hamsters and >120 days in mice, and the cost of these studies made them impractical for screening samples from the abattoir. The

TABLE 1 Animal prion diseases

Species	Disease	Route	Clinical symptoms	Pathology	Genetics
Sheep, goats	Scrapie	Environmental contamination; vertical transmission	Ataxia, tremors, behavioral changes, pruritus	Spongiosis, astrogliosis, PrP^{Sc} deposition in CNS, tonsil, spleen, lymph nodes, nictating membrane (third eyelid), muscle, placenta, distal ileum, proximal colon	Polymorphisms at codons 136, 154, and 171 affecting susceptibility
Mink	Transmissible mink encephalopathy	Contaminated feed (MBM)[a]	Behavior, neglected grooming, ataxia, compulsive biting	Spongiosis in CNS as well as astrogliosis	
Cattle	Bovine spongiform encephalopathy	Contaminated feed (MBM)	Gait abnormalities, tremors, aggressiveness, hyperreactivity	Spongiosis, PrP^{Sc} deposition in CNS, spinal cord, retina, dorsal root and thoracic ganglia, and trigeminal ganglion	
Deer, elk, moose	Chronic wasting disease	Environmental contamination; contaminated feed (MBM)	Ataxia, tremor, teeth grinding, polyuria, polydipsia	Spongiosis in thalamus, hypothalamus, midbrain, pons, medulla oblongata, olfactory bulb, and cortex. PrP^{Sc} and infectivity found in virtually all tissues and fluids	Polymorphisms at codons 96, 132, and 225 affecting susceptibility
Domestic cats, large cats and exotic ungulates	Spongiform encephalopathy	Probably BSE-contaminated feed (MBM)	Behavioral changes, ataxia, loss of coordination, aggressiveness	Spongiosis in neuropil of brain and spinal cord. Plaques in CNS, PNS, retina, lymphoreticular system, kidney, and adrenal gland	

[a]MBM, meat and bone meal.

European Food Safety Agency (EFSA) approved 3 postmortem diagnostic screening tests for cattle from 1999 to 2001 (Table 2). These approved tests depended on the difference in protease sensitivity between PrP^{C} and PrP^{Sc} to remove the normal prion protein in the sample. Although there have been claims of PrP^{Sc}-specific monoclonal antibodies (MAbs), the difference in affinity was not sufficient for use in assays with samples that had not been treated with protease, given the great excess of PrP^{C} in the samples (135, 136).

The major time factor in testing was delivery of samples from the abattoir to the testing facility. Turnaround time was typically >24 hours and, depending on the site of the abattoir, could range to >3 days. While point-of-slaughter testing was never adopted, Prionics and Prion Developmental Laboratories developed capillary flow test devices that could have been used in that application (see below). For all of these tests, sample isolation and preparation were a significant issue. Unlike conventional infectious agents that are detected in body fluids, the highest titer, and hence greatest sensitivity, is obtained from solid CNS tissue. A key determinant of assay sensitivity in the postmortem tests was identification of the tissue region containing the highest amount of PrP^{Sc}. For BSE testing, a precisely defined section of the brain stem, the obex, was sampled, homogenized, treated with protease, and then analyzed (https://www.gov.uk/government/statistics/cattle-tse-surveillance-statistics). To facilitate higher throughput for sample processing, homogenization of tissue samples used devices such as the ribolyzer to produce homogenates from multiple samples simultaneously. The ribolyzer incorporates ceramic beads in a microcentrifuge tube and a modified centrifuge that shakes while it rotates to produce the homogenate. The Prionics Western blot used SDS gels to separate proteins before transfer to membrane for probing with MAb 6H4. One potential advantage of this system is the ability to create "glycoform" profiles; the PrP contains two nonobligatory N-linked glycosylation sites that potentially yield information about specific strains (137). Subsequently, the glycoform profile has also been used to distinguish natural scrapie from potentially BSE-infected ruminants (138). The two enzyme-linked immunosorbent assay (ELISA)-based tests prepared the sample in the same way as did Prionics except that they used a sandwich assay comprised of two Abs to detect the residual PrP^{Sc}. The Enfer test differed from the CEA/BioRad in that the second Ab used in the Enfer assay was fluorescently labeled.

In further rounds, the EFSA validated additional rapid postmortem BSE tests as well as rapid TSE tests for ovine and caprine animals (see the report entitled "Scientific Opinion on the Evaluation of new TSE rapid test submitted in the framework of the Commission Call for expression of interest 2007/S204-247339 2012" from the EFSA [http://www.efsa.europa.eu/en/efsajournal/pub/2660] and references therein). With the exception of the Prionics PrioStrip, the tests approved were largely variants on the ELISA platform. The PrioStrip is a chromatographic assay that employs a capture Ab in the well of a 96-well plate and a dipstick containing two immobilized Abs, one of which is PrP specific and the second an IgG control to demonstrate the integrity of the test strip. While not as sensitive as the ELISAs, the robust nature of this testing modality could have allowed on-site testing, although this was never done. As originally, all of these tests were dependent on protease treatment to remove the PrP^{C} from the sample.

TABLE 2 Postmortem diagnostic tests[a]

Company	Assay	Time (h)	Sensitivity (dilution)
Prionics	Western blot	6–7 (total)	~1:100
CEA/BioRad	ELISA	5	~1:1,000
Enfer	ELISA	3 (after sample preparation)	~1:100

[a]Data from http://eurlex.europa.eu/LexUriServ/LexUriServ.do?uri=OJ:L:2001:147:0001:0040:EN:PDF.

An alternative diagnostic modality is provided by the conformational difference between PrP^{C} and PrP^{Sc}. Caughey and colleagues demonstrated that PrP^{Sc} could serve as a seed for converting PrP^{C} to a protease-resistant form (139). The observation that PrP^{Sc} could seed conversion *in vitro* led to the development of the cyclic protein-refolding assays PMCA (protein misfolding cyclic amplification) and QuIC (quaking-induced conversion), which "amplify" the conformationally altered structure in a PrP^{C} substrate. In these assays, the test sample is added to PrP^{C}, generally bacterially produced recombinant protein, to determine whether there is a prion-associated seeding activity in the sample (140, 141). The major difference between the two techniques, and the variants thereof, is that PMCA uses Western blotting of amplified, protease-treated samples for detection and in its most recent iteration RT-QuIC is a real-time assay employing thioflavin T to assess the accumulation of amyloid in the sample (142). A further refinement to the RT-QuIC assay was an immunoprecipitation step to concentrate the seed before addition use (143). In addition to concentrating the seed, this step also removes inhibitory substances from the sample that prevents conversion, which has been a particular problem with blood samples. The sensitivity of PMCA has been enhanced by the adoption of a novel detection platform, surround optical fiber immunoassay (SOFIA), which has provided detection as low as 10 attograms (144). SOFIA is based on a sandwich ELISA and also uses Rhodamine Red-X coupled to streptavidin. Specially designed hardware that enables maximum light collection and very high sensitivity of the method at the same time makes SOFIA less accessible for widespread use. However, the significance of this is that improving sensitivity at the level of the detection equipment can reduce the number of cycles required for amplification, which in turn reduces the number of false positives. PMCA-SOFIA has been used to demonstrate prion-associated seeding activity in blood (145), urine (146), and semen (147). The major limitation of this assay is that the detection equipment is still in prototype form. For the first time, however, the conformation-based assays offer the possibility of antemortem testing for prion diseases (Table 3).

While they represent a significant improvement in sensitivity relative to Western blotting of samples or ELISAs, the conformation-based tests do have some limitations. First, test results take a minimum of 1 day and range up to as long as 16 days. Second, the tests have been difficult to reproduce when moved to new laboratories. In many cases, lab personnel needed to visit the lab of the assay developers to successfully achieve results similar to those published. One reason may be the importance of the PrP^{C} preparation (B. Caughey, personal communication). Another difficulty with these tests is, like PCR in the early stages of development, the generation of false positives due to the sensitivity of the tests and the tendency for PrP^{C} to spontaneously undergo conversion to an abnormal isoform *in vitro*. The difficulty in standardizing the sonication step in PMCA (148) and the inherent tendency of PrP^{C} to undergo spontaneous fibrillization in QuIC remain as outstanding problems.

Finally, another test based on conformation that depends on epitope masking in structural variants of a protein was

TABLE 3 Conformation based tests[a]

Test name	Time/sensitivity[b]	Samples	Detection method
Protein misfolding cyclic amplification (PMCA)	1–16 days/1 attogram	Brain, blood, CSF, urine, semen	Western blotting, SOFIA
Quaking-induced conversion (QuIC)	1–3 days/1 attogram	Brain, blood, CSF, nasal fluids	Western blotting, thioflavin T detection
Conformation-dependent immunoassay (CDI)	2.5–4 h/≤1 ng/ml	Brain, plasma	Fluorescence, europium-labeled Ab

[a]Data from references 267 and 271–287.
[b]Sensitivity depends on the strain/species tested.

developed by Safar and colleagues (149). In this assay, Abs are added to samples in a native state or following denaturation. An Ab that reacts with native PrP^{C} but not PrP^{Sc} would show different amounts of reaction with native or denatured samples. The difference in signal reflects the amount of PrP^{Sc} in the sample. Sensitivity can be enhanced by the selective precipitation of PrP^{Sc} using sodium phosphotungstate (150). In addition, recent studies have demonstrated that there are protease-sensitive forms of PrP^{Sc} that are associated with prion disease (151–153).

HUMAN PRION DISEASES

A unifying feature of all the human prionoses is their neuropathology. These illnesses tend to affect the gray matter of the CNS, producing neuronal loss, gliosis, and characteristic spongiform change (1, 3, 4). The latter is a vacuolation of the neuropil and, to a variable degree, of the neurons. In addition, plaques with the typical staining properties of amyloid (e.g., apple-green birefringence after Congo Red staining when viewed under polarized light) are observed in many of these conditions. In approximately 10% of patients with sCJD, amyloid is present in the cerebellum or in the cerebral hemispheres. All cases of GSS are associated with multicentric cerebellar plaques. These amyloid plaques are immunoreactive with Abs to PrP and are not immunoreactive with Abs to other amyloidogenic proteins, such as Aβ (which is deposited in AD).

Several different forms of human prion disease exist (Table 4). As described above, human prion diseases are classified into three groups: sporadic (~85 to 90%), genetic (~10 to 15%), and acquired (~1 to 3%) (3, 4).

Kuru

The first human prionosis to be described is called kuru (154, 155). This is an illness of the Fore people living in the highlands of New Guinea that is thought to be linked to ritualistic cannibalism. Presumably, this illness originated with the consumption of an initial tribe member that died of sCJD. Kuru was once a major cause of death among Fore people; however, the disease has virtually disappeared with the end of cannibalistic rituals in the 1950s. A peak annual mortality of more than 2% was recorded in some Fore villages (155, 156). Human prion diseases have no gender preponderance, with kuru being the exception. Women had a greater tendency than men to develop kuru because it was part of the ritual cannibalism for women to prepare and eat the brains (neural tissue has the highest titer of PrP^{res}); some Fore villages became largely devoid of young women at the peak of the epidemic. Exhibiting symptoms similar to those of scrapie, patients present clinically with difficulty walking, and they develop progressive signs of cerebellar dysfunction ("kuru" means shivering in the Fore language). Death occurs approximately 1 year following the onset of symptoms. Between July 1996 and June 2004, 11 new cases of kuru were documented, suggesting that the incubation period of human prion disease can last as long as 56 years (that being the length of time following the last known cannibalism-related exposure and the onset of clinically symptomatic kuru) (157). This is an important fact to consider when evaluating the potential risks to humans for new animal prion diseases such as CWD, which have an unclear zoonotic potential (2, 78, 112).

The neuropathology of kuru, in common with all prionoses to a variable extent, includes widespread spongiform change and astrocytosis, as well as neuronal loss affecting the cerebral hemispheres and cerebellum. More intraneuronal vacuolation is observed in kuru than in sCJD (see below). In about 70% of cases, amyloid plaques are found, with amyloid deposition being a common, but not invariable, accompaniment of the prionoses. Carlton Gajdusek's detailed description of this illness led the scrapie scientist W. J. Hadlow to suggest that kuru might be the human homologue of scrapie (158). This in turn inspired Gajdusek and his team to test whether kuru was also transmissible. In 1965, they first showed that kuru was transmissible to chimpanzees, after a long incubation (159), and Gajdusek was awarded the Nobel Prize in 1976 for this work.

Similar to what is seen in sCJD, MM or VV homozygosity at codon 129 is overrepresented in kuru. Interestingly, among Fore women over 50 years of age who survived the kuru epidemics of the 1950s, there is a marked overrepresentation of the resistant MV genotype at codon 129 (160,

TABLE 4 Human prion diseases

Disease	Mechanism
Kuru	Cannibalism
sCJD	Spontaneous PrP^{C}-to-PrP^{Sc} conversion or somatic mutation
iCJD	Infection from prion-containing material (e.g., dura mater, cornea, electrode, hormones)
gCJD	Mutations in the PRNP gene
vCJD	Infection from consumption of BSE-infected meat
GSS	Mutations in the PRNP gene
FFI	D178N mutation in the PRNP gene with M129 polymorphism
Sporadic fatal insomnia (or sCJD MM2 thalamic type)	Spontaneous PrP^{C}-to-PrP^{Sc} conversion or somatic mutation
VPSPr	Spontaneous PrP^{C}-to-PrP^{Sc} conversion or somatic mutation

161). A novel *PRNP* variant, G127V, was found exclusively among people living in the region where kuru was prevalent and was present in ~50% of otherwise susceptible women from regions of highest exposure, who were homozygous for methionine at codon 129. This polymorphism was not found in patients with kuru or unexposed population groups worldwide (156). This is an example of recent human genotype evolution resulting from the selection pressures of an infectious human prion disease.

Sporadic Creutzfeldt-Jakob Disease

By far, the most common human prion disease is sCJD, accounting for about 85% of all human prion diseases. sCJD is found throughout the world, with an incidence of about 1 to 1.5 cases per million population per year (3). The peak age of onset of sCJD is ~68 years, with a wide range of 12 to 98 years (162, 163). However, sCJD patients that are <30 years old are rarely presented (164). The median duration of disease is from 4 to 6 months, with death occurring within 1 year in 90% of cases and another 5% dying in the second year of disease (165). Jakob initially described CJD in 1921 (166); ironically, the case reported by Creutzfeldt a year earlier is probably unrelated to the disease that carries his name.

An issue that has not been fully resolved is how sCJD arises. This has been suggested to be the result of either a random somatic mutation in the *PRNP* gene or more commonly a spontaneous conformational conversion of PrP^{C} to PrP^{Sc} (167, 168). Aging is recognized to contribute to protein quality control failure in the CNS, and this may be a factor in sCJD being an age-related disease. In fact, a recent therapeutic avenue for prion disease, which has shown some promise in mouse models, is ameliorating an aberrant unfolded protein response (169, 170). An argument in favor of the spontaneous-conversion hypothesis is the uniform worldwide occurrence of sCJD with no convincing geographic clustering, with the exception being areas with an increased incidence of genetic forms of CJD (i.e., gCJD). However, some case-control studies suggest that at least a portion of "sporadic" CJD can in fact be related to surgical procedures much earlier in life (hence in fact representing acquired CJD, i.e., iCJD). In a comparison of 241 patients with sCJD from the Australian CJD registry to 784 controls, there was an association with past surgical treatments that increased with the number to a maximum of three procedures producing an odds ratio of 2.13 (171). In another case-control study, using Danish and Swedish registries of 167 CJD patients compared to 3,059 controls, a similar association was found with past surgical procedures (172). The authors conclude, "We provide evidence to indicate that surgery, acting with long incubation periods, has constituted a risk factor for sCJD." A more recent risk-based classification of surgical interventions found that past procedures involving the retina and optic nerve as well as peripheral nerves were particularly associated with an increased risk of CJD (173). As mentioned above, PrP^{Sc} is known to be highly resistant to inactivation. Even ashing of the agent at 600°C does not result in complete inactivation (174). PrP^{Sc} is also known to bind to metals with a very high affinity (27, 175), hence perhaps allowing for the low-level contamination of some surgical instruments. This may be related to the reported association of "sporadic" CJD to prior surgical procedures, in particular, those related to the nervous system, many years prior to clinical presentation, discussed above. This issue requires further investigation.

Clinically, sCJD is classically characterized by a rapidly progressive dementia associated with myoclonic jerks, as well as a variable constellation of pyramidal, extrapyramidal, and cerebellar signs. However, the clinical presentation can be quite variable and is in part a feature of the six molecular subtypes that are based on the *PRNP* codon 129 polymorphism (MM, MV, or VV) and the type 1 or type 2 banding pattern of PrP^{res} on SDS-PAGE (as introduced above) (49, 68, 176–178). The most common phenotypes are the MM1 and MV1 variants, which are combined because they are very similar clinically. Together they account for ~50% of all sCJD cases (47, 176–178). The onset of symptoms is at a mean age of 65 years, and the average clinical duration is 4 months. Clinical signs typically include rapid cognitive decline at onset in almost all cases, with ataxia in about 50% of cases, as well as myoclonus and visual abnormalities. Periodic sharp wave complexes (PSWCs) are seen on electroencephalograms (EEG) in >80% of cases, usually in the first 3 months of onset of symptoms (179). Diffusion-weighted (DW) magnetic resonance imaging (MRI) shows increased signal in the basal ganglia in ~70% of cases and involvement of ≥3 cerebral cortical areas in ~50% of cases (180). The neuropathology displays the classical features of spongiform change, consisting of small vacuoles (2 to 10 μm) throughout the cortical neutrophil, with the basal ganglia and thalamus also affected. Often, the hippocampus and the brainstem are spared. The cerebellum typically shows focal spongiform change in the molecular layer. IHC with anti-PrP Ab shows a pattern of synaptic type (178). The next most frequent type is VV2, also called the ataxic variant, consisting of ~15% of cases (47, 176–178). The mean age at onset is 60 years, and the mean duration is 6.5 months. Typically, patients exhibit ataxia with dementia quickly developing in the course of the disease. Prominent myoclonus is a feature in one-third of the patients. Most patients lack the PSWC on EEG. DW MRI sequences commonly show increased signal in the basal ganglia and thalamus, while cortical signal changes are typically limited to the limbic cortex. The spongiform change is of similar fine vacuoles as in the MM1/MV1 type, but in the cortex it is often laminar and involves mainly the deeper layers. Immunostaining with anti-PrP antibodies shows plaque-like reactive deposits; however, these are Congo red and thioflavin S negative (and therefore not amyloid). The third most common type is MV, type 2, comprising ~8% of cases. This type is also called the kuru plaque variant. The mean age and clinical course are 59 years and 18 months, respectively. Clinically, both ataxia and dementia are prominent at disease onset. The longer duration of disease can cause diagnostic confusion. It is not usual for these patients to survive >2 years. Typically, there are no PSWCs on EEG. The DW MRI sequences, like the VV2 type, show abnormal signal in the basal ganglia and thalamus. Specifically, the thalamic signal hyperintensity is most commonly seen in the pulvinar, sometimes displaying the "pulvinar sign" (181). Neuropathologically, a distinctive feature is kuru-like plaques in the cerebellum, which are round, dense PrP^{Sc} immunoreactive deposits that are Congo red positive and are also easily seen on hematoxylin and eosin stains. These are abundant in the molecular and granular layers of the cerebellum but are rare in other cerebral locations. Two distinct clinical phenotypes can occur among individuals who are MM type 2. The first phenotype, MM2-cortical or MM2C, affects ~1% of patients. The mean age at onset is 65 years, with an average duration of ~17 months. These patients present with cognitive deficits and myoclonus, but typical EEG findings and visual symptoms are typically absent. Ataxia is mild or absent, even late in the clinical course. DW MRI hyperintensity is typically seen involving the temporal lobes, while basal ganglia involvement is

absent or limited. Thalamic hyperintensity may be present. The neuropathological changes are distinct by the lack of cerebellar involvement and by the spongiform change typically consisting of larger and coarser vacuoles. PrP^{Sc} immunoreactivity is often found at the rim of these coarse vacuoles. The second clinical phenotype associated with the MM2 type is also referred to as the sporadic form of fatal insomnia or MM2 thalamic type. This variant affects <1% of sCJD patients and is clinically characterized by insomnia and psychomotor hyperactivity. Motor signs may include diplopia, dysarthria, dysphagia, pyramidal tract signs, and gait abnormalities. Myoclonus is a typical finding. Typically, there are no PSWCs on EEG and there are no signal abnormalities on DW MRI. However, evidence of hypometabolism and/or gliosis may be found by fluorodeoxyglucose positron emission tomography (FDG-PET) and MR spectroscopy, respectively. The neuropathological changes principally affect the thalamus and inferior olive, consisting of atrophy of these structures, neuronal loss, and gliosis. Spongiform change can be absent or limited to focal areas of the cerebral cortex. PrP^{Sc} immunoreactivity may be limited to the entorhinal cortex. The least common molecular phenotype of sCJD is VV1, type 1, also called "early onset sCJD," since the average age at onset is ~39 years, with a disease duration of ~15 months (47, 176). Clinically, there is a progressive dementia at onset, often with features of a frontotemporal dementia. PSWCs are typical absent on EEG. Neuropathologically, there is severe fine spongiform change affecting the cortex and striatum with relative sparing of the cerebellum. PrP immunostaining shows a fine punctuate pattern in the cerebral cortex.

Other classical sCJD clinical phenotypes have been recognized. The Heidenhain variant, seen in ~10% of sCJD patients, mostly with the MM1 molecular subtype, is characterized by visual symptoms at presentation, typically visual hallucinations, cortical visual deficits, and/or oculomotor apraxias (182, 183). The Brownell-Oppenheimer variant has ataxia as its major feature, with a typical lack of PSWCs on EEG and with striatal DW MRI hyperintensities (182, 184). This variant is associated mostly with the MV2 molecular subtype. In addition, there is a panencephalopathic form, which has significant involvement of the white matter, along with severe global atrophy and status spongiosus (185–187). This form has been reported primarily in Japan, and some have suggested that this type of sCJD is related to Wallerian degeneration in the white matter, which may occur in patients with a prolonged survival, found among cultures in which more extraordinary life extending measures are taken (3).

In 2008, a new type of sCJD was described, termed variable proteinase-sensitive proteinopathy (VPSPr) (151, 188). The defining feature of VPSPr is the Western blot profile of PrP^{Sc} after PK digestion containing a ladder-like banding pattern including at least 4 bands. Relatively few cases have been described in the literature so far (151, 188–193). Diagnostic criteria for VPSPr remain to be determined, and most cases are diagnosed postmortem. The disease affects all three codon 129 genotypes, with slightly increased susceptibility with expression of valine. Symptoms include aphasia, parkinsonism, cognitive dysfunction, and ataxia. The 14-3-3 protein in the cerebrospinal fluid (CSF) is typically negative, and most cases do not have cerebral DW MRI hyperintensities. Neuropathologically, there is widespread spongiform change consisting of relatively large vacuoles. Small amyloid plaques containing PrP^{Sc} are often present in the cerebellar molecular layer among the MM and MV subjects. In these subjects, the PrP^{Sc} immunoreactivity is of target-like rounded clusters of granules, while in MM subjects a more plaque-like pattern like the one seen in VV2 sCJD is found (178).

Diagnosis of sCJD

Neuroimaging

Currently, the single most accurate method for the diagnosis of sCJD is by MRI using DWI (diffusion-weighted imaging) and apparent diffusion coefficient sequences, with a reported sensitivity of 91 to 96% and a specificity of 92 to 94% (3, 177, 194, 195). The major patterns of DWI MRI hyperintensities are cortical and subcortical (68% of cases), mainly cortical (24%), and predominantly striatal, with or without thalamic involvement (5%) (196). MRI abnormalities are often seen very early in the disease course, but in some cases these will appear only after repeated studies (197). MRI criteria for the diagnosis of sCJD have been published (194).

EEG

The classical EEG pattern in sCJD is PSWCs consisting of sharp or triphasic waves that occur about once per second. This pattern occurs in about two-thirds of sCJD patients, usually after serial EEGs are performed (197). PSWCs, although helpful in making an sCJD diagnosis, can also be seen in other conditions, such as Lewy body dementia, toxic-metabolic states, anoxic encephalopathy, progressive multifocal leukoencephalopathy, AD, and autoimmune encephalitis (197, 198).

Surrogate Biomarkers

The ultimate goal of TSE diagnosis is an antemortem test that would be sensitive enough to detect prions in body fluids such as blood, CSF, or urine. The standard CSF analysis of cell count, protein, and glucose is typically normal in sCJD. For antemortem diagnosis of sCJD, different proteins have been employed in tests that reach high sensitivity and are often used to complement clinical neurological assessment. However, none of these tests is 100% specific for prion diseases, and so far their use in diagnostics has been limited to the advanced stages of disease. In current clinical practice, the two widely used markers are CSF 14-3-3 protein and total tau. The American Academy of Neurology recommends ordering a CSF 14-3-3 protein when CJD is suspected (199). The 14-3-3 proteins are a group of cytosolic proteins that are released into the CSF as a result of neuronal damage; hence, all conditions with acute neuronal damage exhibit elevated CSF 14-3-3, including autoimmune, viral, paraneoplastic, or Hashimoto's encephalitis or a recent stroke (178). Rapidly progressive AD or Lewy body dementia may also elevate 14-3-3 (200, 201). A systematic review indicated that the sensitivity of 14-3-3 was 92% and the specificity was 80%. Total tau is also used as a marker of neuronal damage. Using a cutoff of >1,150 pg/ml of total tau in CSF, the reported sensitivity and specificity are >90% (202, 203). Other markers for neuronal damage have also been explored, such as neuronal specific enolase (a glycolytic enzyme) and S-100β protein (a glial protein), but they do not offer any advantage over 14-3-3 or total tau (201). The use of existing biomarkers, such as PrP^{Sc}, and the development of new biomarkers and/or methods that would enable their detection during preclinical stages will be important in the future for antemortem diagnosis of prion diseases. PMCA has been reported to be an efficient method for the amplification of PrP^{Sc} in human tissues and body fluids and thus can increase the sensitivity of disease diagnosis (204, 205). To lower the detection limit even further,

SOFIA was used in conjunction with PMCA for detection of PrP^{Sc} in human CSF from CJD (206).

As described above for animal prion diseases, the human prion diseases can also be diagnosed using immunochemical assays (IHC, Western blotting). Because of the abundance of PrP^{Sc}, CNS tissue is the most common and reliable diagnostic material. These methods exploit the physicochemical differences between PrP^{C} and PrP^{Sc}, namely, the resistance of PrP^{Sc} to denaturation and proteolytic degradation. However, PK digestion has in recent years become somewhat controversial since studies have identified PK-sensitive PrP^{Sc} that may comprise as much as 80% of the PrP^{Sc} population (151). Further, it is still debated whether PrP^{TSE} is unequivocally associated with prion infectivity, as there are occasions in which PrP^{Sc} is either not associated with infectivity (207) or absent in infected hosts (208). Despite these limits, PrP^{Sc} remains the best available choice for confirming the diagnosis of prion diseases and for the identification of prion-associated infectivity in tissues and body fluids. Moreover, the profile that PrP^{Sc} generates in Western blotting, reflecting different pathological conformations, is of great help in making a correct molecular diagnosis of sCJD and for differentiating sporadic from variant CJD (209).

In addition to PMCA, QuIC (210) and then real-time QuIC (RT-QuIC) have been used for amplification of human PrP^{Sc} (142, 210, 211). The two disadvantages of RT-QuIC are the relatively poor performance in amplifying PrP^{Sc} from vCJD tissues (211) and the failure to reproduce the original PrP^{Sc} signature, thus impeding the molecular diagnosis of sCJD and the distinction between sCJD and vCJD.

Safar and colleagues (150) developed an ELISA-formatted, dissociation-enhanced time-resolved fluorescence detection system, known as the conformation-dependent immunoassay, based on specific antibody binding to epitopes that are accessible in PrP^{C} but that are unmasked only after denaturation of PrP^{Sc}. This method does not require PK treatment and is able to recognize different PrP^{Sc} conformations. The assay was able to discriminate PrP^{Sc} signatures in different molecular forms of sCJDs, iCJDs, and genetic TSEs (212) with a detection limit at a 10^{-5} dilution of PrP^{Sc} from vCJD brain used for spiking human normal plasma (213, 214).

Brain Biopsy

The only definitive diagnosis of sCJD is by brain biopsy. However, this procedure is currently done less often, given the availability of the diagnostic methods discussed above. Current neuropathological diagnostic criteria require positive PrP^{Sc} immunoreactivity and the presence of spongiform change (215).

Genetic Prion Diseases

The genetics, clinical presentation, and pathological features of genetic prion diseases divide them into four types: genetic CJD (gCJD), GSS, FFI, and the newly described prion disease associated with diarrhea and autonomic neuropathy (3, 12, 216–218). Genetic prion diseases are sometimes referred to as familial; however, this often is not accurate, as studies have shown that up to 60% of genetic prion disease cases have no positive family history (219). In these cases, previous generations' family members may have been misdiagnosed with other neurodegenerative diseases such as AD. Alternatively, there can be an age-dependent penetrance or there may be incomplete information on the family history.

More than 20 CJD-associated point and octapeptide repeat mutations of PRNP are known. gCJD has been linked to point mutations leading to amino acid substitutions or deletion/insertions in the number of octapeptide repeats (3, 220). The clinical features of gCJD are extremely variable, with inter- and intrafamily differences reported (234, 235). A number of gCJD-associated point mutations have been reported, including G131V, D178N (with V129), V180I, T183A, H187R, T188K, E196K, E200K, D202N, V203I, R208H, V210I, E211Q, Q212P, and M232R (216, 217). On average, gCJD is associated with an earlier age at onset (<55 years) and a much longer clinical course. However, onset may be as late as the 9th decade of life. The codon E200K mutation (which is the most common *PRNP* mutation worldwide) is unusual in that it has been described in several unaffected elderly individuals, suggesting that the penetrance of this mutation is incomplete (3, 221). The penetrance has been calculated to be ~1% at age 40 but is closer to 100% after the 9th decade of life (222, 223). CSF, EEG, and brain MRI markers are not as sensitive in gCJD as in sCJD (3, 217, 220).

GSS was initially described in a large kindred in 1936 and is a slowly progressive autosomal dominant disease (224). It was the first human prion disease in which a mutation in the PRNP gene was discovered (225). The disease is rare, with a prevalence in the range of 1 and 10 per 100 million (12). GSS is most often caused by the P102L mutation in the *PRNP* gene, but additional mutations at codons 105, 117, 131, 198, 202, 212, 217, and 218 and insert mutations can also cause the syndrome. Patients with this illness present with a slowly progressive limb and truncal ataxia, as well as dementia. Death occurs 2 to 12 years following presentation. The prominent involvement of the brainstem often leads to symptoms suggestive of olivopontocerebellar degeneration. The neuropathology of GSS is remarkable in that extensive and invariable amyloid deposition occurs, in addition to the typical spongiform change, gliosis, and neuronal loss. The amyloid deposits are large and often multicentric. On Western blots, the PrP^{Sc} of GSS typically shows a 7- to 8-kDa or an 11-kDa band, distinct from the type 1 or 2 banding patterns seen in sCJD (226, 227). These lower-molecular-mass bands are most prominent in areas of the brain with the most abundant amyloid deposits. Interestingly, in several kindreds of GSS, extensive neurofibrillary tangle (NFT) formation is found (in association with mutations Y145X, F198S, Q217R, and Y218N) (228–230). NFTs are an essential feature of AD but are also observed in other neurodegenerative conditions.

FFI is only associated with the D178N mutation with a methionine at codon 129 (231). Patients with FFI present with intractable insomnia, dysautonomia (i.e., hyperthermia, hypertension, tachycardia, tachypnea, hyperhydrosis), dementia, and motor paralysis. However, the phenotypic expression is quite variable even within the same family (217, 221, 222, 232). The age of onset is also variable, ranging from 18 to 60 years, but occurs most commonly between 40 and 50 years of age. Once symptoms begin, the disease course ranges from 6 months to 3 years. Because of the diversity of clinical presentations of this disorder, genotyping is very important for definitive diagnosis. FDG-PET can also be helpful in the diagnosis, as a selective hypometabolism can typically be seen within the thalamus (221, 222). Neuropathologically, marked atrophy of the anterior ventral and mediodorsal thalamic nuclei occurs because of neuronal loss and gliosis. Unlike other prionoses, spongiform change can be a minor feature or can be absent altogether.

Recently, a novel human prion disease associated with diarrhea and autonomic neuropathy has been described (218). This condition is linked to a Y163X truncation mutation in the PRNP gene. The syndrome begins clinically with a chronic diarrhea in the patient's 30s. Next, symptoms of a length-dependent axonal and mainly sensory peripheral neuropathy begin. Cognitive decline and seizures occur in patients in their 40s and 50s. There is systemic deposition of PrP amyloid systemically including peripheral nerves and the gut, corresponding to the clinical symptoms. Neuropathologically, there are extensive cortical PrP amyloid plaques, PrP-related cerebral amyloid angiopathy, and a tauopathy. Spongiform change appears to be more limited, mainly to superficial cortical areas. The PrP banding pattern after PK digestion is distinct, with a ladder of protease-resistant fragments ranging in masses from 10 kDa to >100 kDa (218). Typical MRI findings are not present in these patients. Elevated total tau and 14-3-3 levels were found in one patient with advanced disease (218).

Iatrogenic Creutzfeldt-Jakob Disease

iCJD was first described in 1974 in a patient who received a cadaveric corneal transplant from a patient who was subsequently diagnosed with CJD (233). More than 400 cases of iCJD have been reported worldwide related to use of cadaver-derived human pituitary hormones (growth hormones [hGH] and gonadotrophic hormones [hPGJ), dura mater grafts, corneal transplants, EEG electrodes, or neurosurgical instruments (234, 235). The greatest number of cases of iCJD are related to either hGH (226 cases, mainly in France) or dural grafts (228 cases, mainly in Japan) (234, 235). As noted with sCJD, susceptibility to infection is linked to the codon 129 polymorphism, with the majority of iCJD cases being MM homozygous (12, 184). Between the late 1950s and 1985, about 30,000 children were treated with hGH; it is estimated that about 1/100 may have developed iCJD. Presumably, this was due to contamination by a cadaveric pituitary infected with sCJD during the batch processing (which included 5,000 to 20,000 cadaveric pituitaries in a single batch). With the availability of recombinant hormones, this source of iCJD is no longer an issue. The initiation of separate processing of individual dura mater grafts since 1987 has also eliminated this source of iCJD. The clinical and pathological features of iCJD linked to hGH were more similar to those of kuru, with prominent cerebellar signs at the onset, with dementia only late in the course of disease (184, 236). The incubation period range was from 4.5 to over 25 years, with a mean of 12 years. The features of iCJD linked to dural grafts were more similar to those of sCJD, with the incubation period being 1.5 to 18 years with a mean of ~6 years (234, 235). iCJD cases have been greatly reduced in number by increased surveillance in recent years (235). However, one caveat noted in the discussion above ("Diagnosis of sCJD") is that some epidemiological evidence suggests that a portion of apparently sporadic CJD cases may be acquired, related to surgeries much earlier in life (171–173).

Variant Creutzfeldt-Jakob Disease

vCJD is a novel human prionosis linked to BSE or "mad cow disease" (48). BSE caused more than 180,000 cattle deaths, mainly in the United Kingdom (3, 48, 237). This disease is thought to be caused by meat and bone meal dietary supplements to cattle that were contaminated with scrapie-infected sheep or to cattle with BSE. Extensive evidence suggests that BSE caused a new type of CJD called vCJD (48, 238). The first cases of vCJD were reported in 1995, when CJD was found in 2 British teenagers (48, 239, 240). The incidence of BSE has greatly declined since 1992 (48). Up to November 2013, 225 cases (http://www.cjd.ed.ac.uk) were reported worldwide, with no new cases in the United Kingdom in 2012 or 2013. All cases of vCJD have been methionine homozygous at codon 129, with the possible exception of one vCJD case (48, 241). vCJD patients differ from sCJD patients in that they are typically younger, with a median age of ~27 years (range, 12 to 74 years) (48). The disease duration is longer, ~14.5 months, and prominent psychiatric symptoms are often the presenting feature of vCJD, often for >6 months before clear neurological symptoms develop. An EEG rarely shows classic PSWCs. The brain MRI typically shows the "pulvinar sign," whereby the pulvinar nucleus of the thalamus has hyperintense signal on DWI MRI. This MRI finding is present in >85% of vCJD cases on the first examination (242). The definitive diagnosis of vCJD is dependent on PrP^{Sc} identification on brain biopsy or autopsy. PrP^{Sc} can also be identified in the lymphorecticular system, such as the tonsil (48). Neuropathologically, vCJD shows abundant PrP^{Sc} deposition in multiple fibrillary plaques surround by a halo of spongiform vacuoles, called "florid plaques" (48). Although the number of vCJD patients is declining, as discussed above, three cases of vCJD infection associated with blood transfusion have also been reported (48). Furthermore, a recent survey of 32,441 appendix samples in the United Kingdom has indicated a vCJD subclinical infection rate of ~1:2,000 (95), largely consistent with four prior prevalence surveys (94, 243–245). This suggests that a substantial number of United Kingdom individuals might be carriers of vCJD. It is unclear if any of these subclinically infected individuals will ever develop clinical vCJD. However, this represents a substantial pool of patients for a possible secondary spread of prion infection. At present, no effective method for screening blood for vCJD contamination exists (246, 247), although such assays are under development (248, 249). Therefore, the risk of further cases of vCJD occurring due to blood transfusion remains a distinct possibility. This highlights the need to develop better diagnostic means for the specific identification of PrP^{Sc} or prion-associated seeding activity in biological fluids.

EMERGING RISKS OF FUTURE NOVEL PRION DISEASES

The divergent clinical and neuropathological features of the more recent additions to the list of human prion diseases, such as FFI, VPSPr, and the recently described prion disease associated with diarrhea and autonomic neuropathy, highlight the wide spectrum of diseases associated with PrP^{Sc} accumulation and suggest that there may be other human illnesses that have yet to be recognized as a prionosis. Furthermore, a significant area of concern for a further outbreak of human prion disease relates to CWD in North America. CWD appears to be the most infectious prionosis to date, affecting free-ranging and farmed ungulates (white-tailed deer, mule deer, elk, and moose) (78, 250–252). CWD was first described in 1967 and was recognized to be a prion disease in 1978 on the basis of brain histopathology (78, 250, 252–254). CWD has been detected in 19 states in the United States, two Canadian provinces, and South Korea (78, 252, 255). Up to 90% of captive cervids have been reported to be prion positive, while in the wild the prion infection prevalence has been reported to be as high as 50%. The cervid population in the United States is estimated to be ~33 million, a large at-risk population. Transmission of CWD is mainly horizontal via a mucosal/oral route (252, 256, 257). CWD has been shown to be transmissible to

nonhuman primates (squirrel monkeys) by two groups using intracerebral inoculation (258, 259). Significantly, a recent study also showed CWD to be orally transmissible to squirrel monkeys (259). Interestingly, the clinical symptoms of CWD infection in the CWD-infected monkeys resembled a wasting syndrome rather than more typical symptoms such as ataxia, leading to the speculation that if CWD was transmitted to humans and presented in a similar manner, the disease would not be identified as a prion disease without neuropathological evaluation (something that is done on a very small proportion of patient deaths) (259). CWD has also been shown to be transmissible to sheep, cattle, fallow deer, reindeer, and several North American rodents (prairie voles, mice, and ferrets), which can scavenge on CWD carcasses (260–265). These animals can enter the human food chain directly or indirectly by accidental inclusion in grain and forage. Large predators of cervids in the wild are, not surprisingly, preferentially killing incapacitated CWD-infected animals, raising the possibility of further cross-species spread (266). Thus far, studies using transgenic mice expressing human PrP^{C} have failed to show transmission of CWD, indicating that this presents a more significant species barrier than BSE to human transmission (267–269). On the other hand, two different strains of CWD have been identified to date, with the likelihood that there may be more (79, 270). The possibility that these other, future strains of CWD will have greater potential for human spread remains to be explored. Recent studies have also shown evidence for strain-dependent, peripheral infection in humanized transgenic mice challenged by cervid prions (Q. Kong, unpublished results). Hence, CWD presents a significant threat to human populations, again highlighting the need to develop assays that can specifically detect PrP^{Sc} infection in biological fluids. Recent technologies that include PMCA-SOFIA and RT-QuIC are showing great promise at fulfilling this critical need.

CONCLUSION

Prion diseases continue to present a diagnostic and therapeutic challenge to clinicians and researchers worldwide. There are many aspects of prion biology that remain unclear; we still do not know the precise physical nature of the infectious agent, the molecular and biochemical mechanisms underlying associated neurodegeneration, or the physiological function of PrP^{C}. Current diagnostic methods are based mainly on the physicochemical differences between PrP^{C} and PrP^{Sc}, which, to date, are the only reliable markers for TSEs. The tests differ mainly at the level of the detection methods. Although the diagnostic tools currently available for prion diseases are less sensitive than those available for other infectious diseases, continued technological advances are being made. In addition, the search for additional markers for the detection of TSEs is of utmost importance. Several approaches to detect additional surrogate markers have already been undertaken. Furthermore, assessment of therapeutic advances are dependent on disease diagnosis and biomarker monitoring. Interestingly, with increasing understanding of neurodegenerative processes, it appears that protein misfolding and subsequent propagation of rogue proteins are a generic phenomenon shared with diseases caused by tau, α-synucleins, and β-amyloid proteins. Consequently, effective antiprion agents may have wider implications. In the past decade, research on prion diseases has advanced our knowledge and understanding of basic prion biology, and this trend will trigger further advances in disease diagnosis and therapeutics.

This work was supported in part by the SUNY Downstate Medical Center, DoD grant DM102153, and NIH grants NS47433 and NS73502.

Publisher's Note: References 101–287 are available as supplemental material at http://www.asmscience.org/files/MMCLI8.ch71.Rubenstein.pdf.

REFERENCES

1. **Colby DW, Prusiner SB.** 2011. Prions. *Cold Spring Harb Perspect Biol* **3:**a006833. PubMed
2. **Wisniewski T, Goñi F.** 2012. Could immunomodulation be used to prevent prion diseases? *Expert Rev Anti Infect Ther* **10:**307–317. PubMed
3. **Takada LT, Geschwind MD.** 2013. Prion diseases. *Semin Neurol* **33:**348–356. PubMed
4. **Head MW.** 2013. Human prion diseases: molecular, cellular and population biology. *Neuropathology* **33:**221–236. PubMed
5. **Kretzschmar H, Tatzelt J.** 2013. Prion disease: a tale of folds and strains. *Brain Pathol* **23:**321–332. PubMed
6. **DeArmond SJ, Bouzamondo E.** 2002. Fundamentals of prion biology and diseases. *Toxicology* **181-182:**9–16. PubMed
7. **Forloni G, Artuso V, Roiter I, Morbin M, Tagliavini F.** 2013. Therapy in prion diseases. *Curr Top Med Chem* **13:**2465–2476. PubMed
8. **Roettger Y, Du Y, Bacher M, Zerr I, Dodel R, Bach J-P.** 2013. Immunotherapy in prion disease. *Nat Rev Neurol* **9:**98–105. PubMed
9. **Sim VL.** 2012. Prion disease: chemotherapeutic strategies. *Infect Disord Drug Targets* **12:**144–160. PubMed
10. **Trevitt CR, Collinge J.** 2006. A systematic review of prion therapeutics in experimental models. *Brain* **129:**2241–2265. PubMed
11. **Griffith JS.** 1967. Self-replication and scrapie. *Nature* **215:**1043–1044. PubMed
12. **Prusiner SB, Scott MR, DeArmond SJ, Cohen FE.** 1998. Prion protein biology. *Cell* **93:**337–348. PubMed
13. **Prusiner SB.** 1982. Novel proteinaceous infectious particles cause scrapie. *Science* **216:**136–144. PubMed
14. **Prusiner SB.** 2012. Cell biology. A unifying role for prions in neurodegenerative diseases. *Science* **336:**1511–1513. PubMed
15. **Prusiner SB.** 2013. Biology and genetics of prions causing neurodegeneration. *Annu Rev Genet* **47:**601–623. PubMed
16. **Wickner RB, Edskes HK, Kryndushkin D, McGlinchey R, Bateman D, Kelly A.** 2011. Prion diseases of yeast: amyloid structure and biology. *Semin Cell Dev Biol* **22:**469–475. PubMed
17. **Wickner RB, Edskes HK, Bateman DA, Kelly AC, Gorkovskiy A, Dayani Y, Zhou A.** 2013. Amyloids and yeast prion biology. *Biochemistry* **52:**1514–1527. PubMed
18. **Si K, Choi YB, White-Grindley E, Majumdar A, Kandel ER.** 2010. Aplysia CPEB can form prion-like multimers in sensory neurons that contribute to long-term facilitation. *Cell* **140:**421–435. PubMed
19. **Raveendra BL, Siemer AB, Puthanveettil SV, Hendrickson WA, Kandel ER, McDermott AE.** 2013. Characterization of prion-like conformational changes of the neuronal isoform of Aplysia CPEB. *Nat Struct Mol Biol* **20:**495–501. PubMed
20. **Halfmann R, Jarosz DF, Jones SK, Chang A, Lancaster AK, Lindquist S.** 2012. Prions are a common mechanism for phenotypic inheritance in wild yeasts. *Nature* **482:**363–368. PubMed
21. **Newby GA, Lindquist S.** 2013. Blessings in disguise: biological benefits of prion-like mechanisms. *Trends Cell Biol* **23:**251–259. PubMed
22. **Goñi F, Herline K, Peyser D, Wong K, Ji Y, Sun Y, Mehta P, Wisniewski T.** 2013. Immunomodulation targeting of

both Aβ and tau pathological conformers ameliorates Alzheimer's disease pathology in TgSwDI and 3xTg mouse models. *J Neuroinflammation* **10:**150. PubMed
23. **Wisniewski T, Goñi F.** 2014. Immunotherapy for Alzheimer's disease. *Biochem Pharmacol* **88:**499–507. PubMed
24. **Goñi F, Prelli F, Ji Y, Scholtzova H, Yang J, Sun Y, Liang F-X, Kascsak R, Kascsak R, Mehta P, Wisniewski T.** 2010. Immunomodulation targeting abnormal protein conformation reduces pathology in a mouse model of Alzheimer's disease. *PLoS One* **5:**e13391. PubMed
25. **Rasool S, Martinez-Coria H, Milton S, Glabe CG.** 2013. Nonhuman amyloid oligomer epitope reduces Alzheimer's-like neuropathology in 3xTg-AD transgenic mice. *Mol Neurobiol* **48:**931–940. PubMed
26. **Brandner S, Raeber A, Sailer A, Blättler T, Fischer M, Weissmann C, Aguzzi A.** 1996. Normal host prion protein (PrP^C) is required for scrapie spread within the central nervous system. *Proc Natl Acad Sci USA* **93:**13148–13151. PubMed
27. **Brown DR.** 2011. Prions and manganese: A maddening beast. *Metallomics* **3:**229–238. PubMed
28. **Watt NT, Taylor DR, Kerrigan TL, Griffiths HH, Rushworth JV, Whitehouse IJ, Hooper NM.** 2012. Prion protein facilitates uptake of zinc into neuronal cells. *Nat Commun* **3:**1134. PubMed
29. **Watt NT, Griffiths HH, Hooper NM.** 2013. Neuronal zinc regulation and the prion protein. *Prion* **7:**203–208. PubMed
30. **Thackray AM, Knight R, Haswell SJ, Bujdoso R, Brown DR.** 2002. Metal imbalance and compromised antioxidant function are early changes in prion disease. *Biochem J* **362:**253–258. PubMed
31. **Singh A, Haldar S, Horback K, Tom C, Zhou L, Meyerson H, Singh N.** 2013. Prion protein regulates iron transport by functioning as a ferrireductase. *J Alzheimers Dis* **35:**541–552. PubMed
32. **Sigurdsson EM, Brown DR, Alim MA, Scholtzova H, Carp R, Meeker HC, Prelli F, Frangione B, Wisniewski T.** 2003. Copper chelation delays the onset of prion disease. *J Biol Chem* **278:**46199–46202. PubMed
33. **Brazier MW, Volitakis I, Kvasnicka M, White AR, Underwood JR, Green JE, Han S, Hill AF, Masters CL, Collins SJ.** 2010. Manganese chelation therapy extends survival in a mouse model of M1000 prion disease. *J Neurochem* **114:**440–451. PubMed
34. **Linden R, Martins VR, Prado MA, Cammarota M, Izquierdo I, Brentani RR.** 2008. Physiology of the prion protein. *Physiol Rev* **88:**673–728. PubMed
35. **Young R, Passet B, Vilotte M, Cribiu EP, Béringue V, Le Provost F, Laude H, Vilotte J-L.** 2009. The prion or the related Shadoo protein is required for early mouse embryogenesis. *FEBS Lett* **583:**3296–3300. PubMed
36. **Passet B, Young R, Makhzami S, Vilotte M, Jaffrezic F, Halliez S, Bouet S, Marthey S, Khalifé M, Kanellopoulos-Langevin C, Béringue V, Le Provost F, Laude H, Vilotte JL.** 2012. Prion protein and Shadoo are involved in overlapping embryonic pathways and trophoblastic development. *PLoS One* **7:**e41959. PubMed
37. **Um JW, Nygaard HB, Heiss JK, Kostylev MA, Stagi M, Vortmeyer A, Wisniewski T, Gunther EC, Strittmatter SM.** 2012. Alzheimer amyloid-β oligomer bound to postsynaptic prion protein activates Fyn to impair neurons. *Nat Neurosci* **15:**1227–1235. PubMed
38. **Chung E, Ji Y, Sun Y, Kascsak R, Kascsak RB, Mehta PD, Strittmatter SM, Wisniewski T.** 2010. Anti-PrP^C monoclonal antibody infusion as a novel treatment for Aβ oligomer cognitive deficits. *BMC Neurosci* **11:**130. PubMed
39. **Um JW, Kaufman AC, Kostylev MA, Heiss JK, Stagi M, Takahashi H, Kerrisk ME, Vortmeyer A, Wisniewski T, Koleske AJ, Gunther EC, Nygaard HB, Strittmatter SM.** 2013. Metabotropic glutamate receptor 5 mediates signaling from Alzheimer Aβ oligomer bound to prion protein. *Neuron* **79:**887–902. PubMed
40. **Harris DA, Huber MT, van Dijken P, Shyng SL, Chait BT, Wang R.** 1993. Processing of a cellular prion protein: identification of N- and C-terminal cleavage sites. *Biochemistry* **32:**1009–1016. PubMed
41. **Windl O, Dempster M, Estibeiro P, Lathe R.** 1995. A candidate marsupial PrP gene reveals two domains conserved in mammalian PrP proteins. *Gene* **159:**181–186. PubMed
42. **Büeler H, Aguzzi A, Sailer A, Greiner RA, Autenried P, Aguet M, Weissmann C.** 1993. Mice devoid of PrP are resistant to scrapie. *Cell* **73:**1339–1347. PubMed
43. **Collinge J, Whittington MA, Sidle KC, Smith CJ, Palmer MS, Clarke AR, Jefferys JGR.** 1994. Prion protein is necessary for normal synaptic function. *Nature* **370:**295–297. PubMed
44. **Tobler I, Gaus SE, Deboer T, Achermann P, Fischer M, Rülicke T, Moser M, Oesch B, McBride PA, Manson JC.** 1996. Altered circadian activity rhythms and sleep in mice devoid of prion protein. *Nature* **380:**639–642. PubMed
45. **Windl O, Dempster M, Estibeiro JP, Lathe R, de Silva R, Esmonde T, Will R, Springbett A, Campbell TA, Sidle KC, Palmer MS, Collinge J.** 1996. Genetic basis of Creutzfeldt-Jakob disease in the United Kingdom: a systematic analysis of predisposing mutations and allelic variation in the PRNP gene. *Hum Genet* **98:**259–264. PubMed
46. **Windl O, Giese A, Schulz-Schaeffer W, Zerr I, Skworc K, Arendt S, Oberdieck C, Bodemer M, Poser S, Kretzschmar HA.** 1999. Molecular genetics of human prion diseases in Germany. *Hum Genet* **105:**244–252. PubMed
47. **Parchi P, Giese A, Capellari S, Brown P, Schulz-Schaeffer W, Windl O, Zerr I, Budka H, Kopp N, Piccardo P, Poser S, Rojiani A, Streichemberger N, Julien J, Vital C, Ghetti B, Gambetti P, Kretzschmar H.** 1999. Classification of sporadic Creutzfeldt-Jakob disease based on molecular and phenotypic analysis of 300 subjects. *Ann Neurol* **46:**224–233. PubMed
48. **Ironside JW.** 2012. Variant Creutzfeldt-Jakob disease: an update. *Folia Neuropathol* **50:**50–56. PubMed
49. **Riek R, Hornemann S, Wider G, Billeter M, Glockshuber R, Wüthrich K.** 1996. NMR structure of the mouse prion protein domain PrP(121-231). *Nature* **382:**180–182. PubMed
50. **Riek R, Hornemann S, Wider G, Glockshuber R, Wüthrich K.** 1997. NMR characterization of the full-length recombinant murine prion protein, *m*PrP(23-231). *FEBS Lett* **413:**282–288. PubMed
51. **Hosszu LLP, Baxter NJ, Jackson GS, Power A, Clarke AR, Waltho JP, Craven CJ, Collinge J.** 1999. Structural mobility of the human prion protein probed by backbone hydrogen exchange. *Nat Struct Biol* **6:**740–743. PubMed
52. **James TL, Liu H, Ulyanov NB, Farr-Jones S, Zhang H, Donne DG, Kaneko K, Groth D, Mehlhorn I, Prusiner SB, Cohen FE.** 1997. Solution structure of a 142-residue recombinant prion protein corresponding to the infectious fragment of the scrapie isoform. *Proc Natl Acad Sci USA* **94:**10086–10091. PubMed
53. **Knaus KJ, Morillas M, Swietnicki W, Malone M, Surewicz WK, Yee VC.** 2001. Crystal structure of the human prion protein reveals a mechanism for oligomerization. *Nat Struct Biol* **8:**770–774. PubMed
54. **Diaz-Espinoza R, Soto C.** 2012. High-resolution structure of infectious prion protein: the final frontier. *Nat Struct Mol Biol* **19:**370–377. PubMed
55. **Pan KM, et al.** 1993. Conversion of alpha-helices into β-sheets features in the formation of the scrapie prion proteins. *Proc Natl Acad Sci USA* **90:**10962–10966. PubMed
56. **Aucouturier P, Kascsak RJ, Frangione B, Wisniewski T.** 1999. Biochemical and conformational variability of

human prion strains in sporadic Creutzfeldt-Jakob disease. *Neurosci Lett* **274:**33–36. PubMed
57. **Baron T.** 2002. Identification of inter-species transmission of prion strains. *J Neuropathol Exp Neurol* **61:**377–383. PubMed
58. **Kascsak RJ, Rubenstein R, Merz PA, Carp RI, Robakis NK, Wisniewski HM, Diringer H.** 1986. Immunological comparison of scrapie-associated fibrils isolated from animals infected with four different scrapie strains. *J Virol* **59:**676–683. PubMed
59. **Carp RI, Rubenstein R.** 1991. Diversity and significance of scrapie strains. *Semin Virol* **2:**203–213.
60. **Kimberlin RH, Walker CA.** 1978. Evidence that the transmission of one source of scrapie agent to hamsters involves separation of agent strains from a mixture. *J Gen Virol* **39:**487–496. PubMed
61. **Bessen RA, Marsh RF.** 1994. Distinct PrP properties suggest the molecular basis of strain variation in transmissible mink encephalopathy. *J Virol* **68:**7859–7868. PubMed
62. **Caughey B, Raymond GJ, Bessen RA.** 1998. Strain-dependent differences in β-sheet conformations of abnormal prion protein. *J Biol Chem* **273:**32230–32235. PubMed
63. **Schutt CR, Bartz JC.** 2008. Prion interference with multiple prion isolates. *Prion* **2:**61–63. PubMed
64. **Shikiya RA, Ayers JI, Schutt CR, Kincaid AE, Bartz JC.** 2010. Coinfecting prion strains compete for a limiting cellular resource. *J Virol* **84:**5706–5714. PubMed
65. **Parchi P, Castellani R, Capellari S, Ghetti B, Young K, Chen SG, Farlow M, Dickson DW, Sima AAF, Trojanowski JQ, Petersen RB, Gambetti P.** 1996. Molecular basis of phenotypic variability in sporadic Creutzfeldt-Jakob disease. *Ann Neurol* **39:**767–778. PubMed
66. **Parchi P, de Boni L, Saverioni D, Cohen ML, Ferrer I, Gambetti P, Gelpi E, Giaccone G, Hauw JJ, Höftberger R, Ironside JW, Jansen C, Kovacs GG, Rozemuller A, Seilhean D, Tagliavini F, Giese A, Kretzschmar HA.** 2012. Consensus classification of human prion disease histotypes allows reliable identification of molecular subtypes: an inter-rater study among surveillance centres in Europe and USA. *Acta Neuropathol* **124:**517–529. PubMed
67. **Collinge J, Sidle KCL, Meads J, Ironside J, Hill AF.** 1996. Molecular analysis of prion strain variation and the aetiology of 'new variant' CJD. *Nature* **383:**685–690. PubMed
68. **Wadsworth JD, Powell C, Beck JA, Joiner S, Linehan JM, Brandner S, Mead S, Collinge J.** 2008. Molecular diagnosis of human prion disease. *Methods Mol Biol* **459:**197–227. PubMed
69. **Kimberlin RH, Walker CA.** 1989. Pathogenesis of scrapie in mice after intragastric infection. *Virus Res* **12:**213–220. PubMed
70. **Carp RI.** 1982. Transmission of scrapie by oral route: effect of gingival scarification. *Lancet* **1:**170–171. PubMed
71. **Mohan J, Brown KL, Farquhar CF, Bruce ME, Mabbott NA.** 2004. Scrapie transmission following exposure through the skin is dependent on follicular dendritic cells in lymphoid tissues. *J Dermatol Sci* **35:**101–111. PubMed
72. **Glaysher BR, Mabbott NA.** 2007. Role of the draining lymph node in scrapie agent transmission from the skin. *Immunol Lett* **109:**64–71. PubMed
73. **Denkers ND, Telling GC, Hoover EA.** 2011. Minor oral lesions facilitate transmission of chronic wasting disease. *J Virol* **85:**1396–1399. PubMed
74. **Denkers ND, Seelig DM, Telling GC, Hoover EA.** 2010. Aerosol and nasal transmission of chronic wasting disease in cervidized mice. *J Gen Virol* **91:**1651–1658. PubMed
75. **Denkers ND, Hayes-Klug J, Anderson KR, Seelig DM, Haley NJ, Dahmes SJ, Osborn DA, Miller KV, Warren RJ, Mathiason CK, Hoover EA.** 2013. Aerosol transmission of chronic wasting disease in white-tailed deer. *J Virol* **87:**1890–1892. PubMed
76. **Haybaeck J, Heikenwalder M, Klevenz B, Schwarz P, Margalith I, Bridel C, Mertz K, Zirdum E, Petsch B, Fuchs TJ, Stitz L, Aguzzi A.** 2011. Aerosols transmit prions to immunocompetent and immunodeficient mice. *PLoS Pathog* **7:**e1001257. PubMed
77. **Nichols TA, Spraker TR, Rigg TD, Meyerett-Reid C, Hoover C, Michel B, Bian J, Hoover E, Gidlewski T, Balachandran A, O'Rourke K, Telling GC, Bowen R, Zabel MD, VerCauteren KC.** 2013. Intranasal inoculation of white-tailed deer (Odocoileus virginianus) with lyophilized chronic wasting disease prion particulate complexed to montmorillonite clay. *PLoS One* **8:**e62455. PubMed
78. **Saunders SE, Bartelt-Hunt SL, Bartz JC.** 2012. Occurrence, transmission, and zoonotic potential of chronic wasting disease. *Emerg Infect Dis* **18:**369–376. PubMed
79. **Daus ML, Beekes M.** 2012. Chronic wasting disease: fingerprinting the culprit in risk assessments. *Prion* **6:**17–22. PubMed
80. **Aucouturier P, Carp RI, Carnaud C, Wisniewski T.** 2000. Prion diseases and the immune system. *Clin Immunol* **96:**79–85. PubMed
81. **Mabbott NA, MacPherson GG.** 2006. Prions and their lethal journey to the brain. *Nat Rev Microbiol* **4:**201–211. PubMed
82. **Natale G, Ferrucci M, Lazzeri G, Paparelli A, Fornai F.** 2011. Transmission of prions within the gut and towards the central nervous system. *Prion* **5:**142–149. PubMed
83. **Aguzzi A, Nuvolone M, Zhu C.** 2013. The immunobiology of prion diseases. *Nat Rev Immunol* **13:**888–902. PubMed
84. **Eklund CM, Kennedy RC, Hadlow WJ.** 1967. Pathogenesis of scrapie virus infection in the mouse. *J Infect Dis* **117:**15–22. PubMed
85. **Fraser H, Dickinson AG.** 1978. Studies of the lymphoreticular system in the pathogenesis of scrapie: the role of spleen and thymus. *J Comp Pathol* **88:**563–573. PubMed
86. **Kimberlin RH, Walker CA.** 1979. Pathogenesis of mouse scrapie: dynamics of agent replication in spleen, spinal cord and brain after infection by different routes. *J Comp Pathol* **89:**551–562. PubMed
87. **Fraser H, Dickinson AG.** 1970. Pathogenesis of scrapie in the mouse: the role of the spleen. *Nature* **226:**462–463. PubMed
88. **Kimberlin RH, Walker CA.** 1989. The role of the spleen in the neuroinvasion of scrapie in mice. *Virus Res* **12:**201–211. PubMed
89. **Pattison IH, Millson GC.** 1960. Further observations on the experimental production of scrapie in goats and sheep. *J Comp Pathol* **70:**182–193. PubMed
90. **Sigurdson CJ, Williams ES, Miller MW, Spraker TR, O'Rourke KI, Hoover EA.** 1999. Oral transmission and early lymphoid tropism of chronic wasting disease PrPres in mule deer fawns (Odocoileus hemionus). *J Gen Virol* **80:**2757–2764. PubMed
91. **Espinosa JC, Morales M, Castilla J, Rogers M, Torres JM.** 2007. Progression of prion infectivity in asymptomatic cattle after oral bovine spongiform encephalopathy challenge. *J Gen Virol* **88:**1379–1383. PubMed
92. **Hilton DA, Sutak J, Smith ME, Penney M, Conyers L, Edwards P, McCardle L, Ritchie D, Head MW, Wiley CA, Ironside JW.** 2004. Specificity of lymphoreticular accumulation of prion protein for variant Creutzfeldt-Jakob disease. *J Clin Pathol* **57:**300–302. PubMed
93. **Hill AF, Zeidler M, Ironside J, Collinge J.** 1997. Diagnosis of new variant Creutzfeldt-Jakob disease by tonsil biopsy. *Lancet* **349:**99–100. PubMed
94. **Hilton DA, Ghani AC, Conyers L, Edwards P, McCardle L, Ritchie D, Penney M, Hegazy D, Ironside JW.** 2004. Prevalence of lymphoreticular prion protein accumulation in UK tissue samples. *J Pathol* **203:**733–739. PubMed

95. **Gill ON, Spencer Y, Richard-Loendt A, Kelly C, Dabaghian R, Boyes L, Linehan J, Simmons M, Webb P, Bellerby P, Andrews N, Hilton DA, Ironside JW, Beck J, Poulter M, Mead S, Brandner S.** 2013. Prevalent abnormal prion protein in human appendixes after bovine spongiform encephalopathy epizootic: large scale survey. *BMJ* **347:**f5675. PubMed
96. **Prinz M, Huber G, Macpherson AJ, Heppner FL, Glatzel M, Eugster HP, Wagner N, Aguzzi A.** 2003. Oral prion infection requires normal numbers of Peyer's patches but not of enteric lymphocytes. *Am J Pathol* **162:**1103–1111. PubMed
97. **Rieger R, Edenhofer F, Lasmézas CI, Weiss S.** 1997. The human 37-kDa laminin receptor precursor interacts with the prion protein in eukaryotic cells. *Nat Med* **3:**1383–1388. PubMed
98. **Shmakov AN, Ghosh S.** 2001. Prion proteins and the gut: une liaison dangereuse? *Gut* **48:**443–447. PubMed
99. **Morel E, Andrieu T, Casagrande F, Gauczynski S, Weiss S, Grassi J, Rousset M, Dormont D, Chambaz J.** 2005. Bovine prion is endocytosed by human enterocytes via the 37 kDa/67 kDa laminin receptor. *Am J Pathol* **167:**1033–1042. PubMed
100. **Heppner FL, Christ AD, Klein MA, Prinz M, Fried M, Kraehenbuhl JP, Aguzzi A.** 2001. Transepithelial prion transport by M cells. *Nat Med* **7:**976–977. PubMed

Principles and Procedures of Human Immunodeficiency Virus Diagnosis

KELLY A. CURTIS, JEFFREY A. JOHNSON, AND S. MICHELE OWEN

72

HISTORICAL PERSPECTIVE

The human immunodeficiency virus (HIV) is the etiologic agent of AIDS. The clinical manifestations of AIDS were first recognized in 1981 (1). Search for the cause of this severe cellular immune dysfunction led to isolation of lymphadenopathy-associated virus in 1983 (2). The following year, additional researchers isolated cytopathic retroviruses from persons with AIDS, which they termed human T-lymphotrophic virus type III (3, 4). These viruses were soon confirmed to be identical, and in 1986 the International Committee on Taxonomy of Viruses named the virus causative of AIDS HIV (5). Genetic sequences of HIV have been identified retrospectively in human plasma specimens from as early as 1959 (6). It is estimated that approximately 75 million people worldwide have become infected with HIV. In the United States, the Centers for Disease Control and Prevention (CDC) estimates that 1.1 million persons are living with HIV.

HIV exists as two major viral species. Both are members of the genus *Lentivirus* within the family *Retroviridae*. HIV type 1 (HIV-1), identified first, is the more virulent of the two and responsible for the majority of AIDS cases worldwide. HIV-2, first isolated in 1986, has biological and morphologic properties similar to those of HIV-1 but differs from HIV-1 in some of its antigenic components (7). HIV-2 is less pathogenic and has a more limited geographic distribution than HIV-1. Both HIV-1 and HIV-2 are related to simian immunodeficiency viruses, which are found in 26 different species of African primates but do not cause disease in their native hosts (8). A schematic of virus structure is shown in Fig. 1. HIV-2 has a comparable structure, and the major proteins of diagnostic significance for each virus type are shown in Table 1.

Laboratory Markers of HIV Infection

Analyses of specimens from seroconversion panels have established the dynamics of HIV-1 viremia after infection and the sequential appearance of different laboratory markers. The approximate times at which different markers appear have been estimated from multiple sources and are outlined schematically in Fig. 2 (9–12).

Immediately after HIV infection, low levels of HIV-1 RNA might be present intermittently, but no viral markers are consistently detectable in plasma (13). Within approximately 5 to 28 days after infection (median, ~10 days), HIV-1 RNA becomes detectable by nucleic acid testing (NAT) in plasma, and quantities increase to very high levels (9, 10). Next, HIV-1 p24 antigen is expressed, and quantities rise to levels that can be detected by antigen/antibody combo immunoassays within 4 to 10 days after the initial detection of HIV-1 RNA (11, 12). However, p24 antigen detection is transient because, as antibodies begin to develop, they bind to the p24 antigen and form immune complexes that interfere with p24 assay detection unless the assay includes steps to disrupt the antigen-antibody complexes (14, 15). Next, immunoglobulin M (IgM)-class antibodies, which can be detected by antigen/antibody combo, and antibody immunoassays, which detect IgM, are expressed 3 to 5 days after p24 antigen is first detectable, 10 to 13 days after the appearance of viral RNA (10–12, 16). Finally, IgG-class antibodies emerge and persist throughout the course of HIV infection. Immunoassays designed to detect only IgG exhibit considerable variability in their sensitivities during early infection, becoming reactive 18 to 38 days or more after the initial detection of viral RNA (10, 12). The antigenic targets for the majority of the circulating antibodies directed against the virus are shown in Table 1.

The pattern of emergence of laboratory markers is highly consistent and allows classification of HIV infection into distinct laboratory stages. The phases are as follows. (i) The eclipse period is the interval after infection with HIV when no laboratory markers are consistently detectable. (ii) Acute HIV infection is the interval between the appearance of detectable HIV RNA and the first detection of antibodies. Its duration depends on the design of the antibody immunoassay used and the sensitivity of the immunoassay during seroconversion. (iii) The seroconversion window period is the interval between infection with HIV and the first detection of antibodies. Its duration depends on the design of the antibody immunoassay and the sensitivity of the immunoassay during seroconversion. (iv) Established HIV infection is the stage characterized by a fully developed IgG antibody response sufficient to meet the interpretive criteria for a positive Western blot or immunofluorescence assay (IFA) (17).

HIV Testing Algorithms

Accurate laboratory diagnosis of HIV infection relies on testing algorithms that maximize overall sensitivity and specificity by employing a sequence of tests in combination and applying decision rules for resolving discordant test results. Beginning in 1989, the diagnostic algorithm

doi:10.1128/9781555818722.ch72

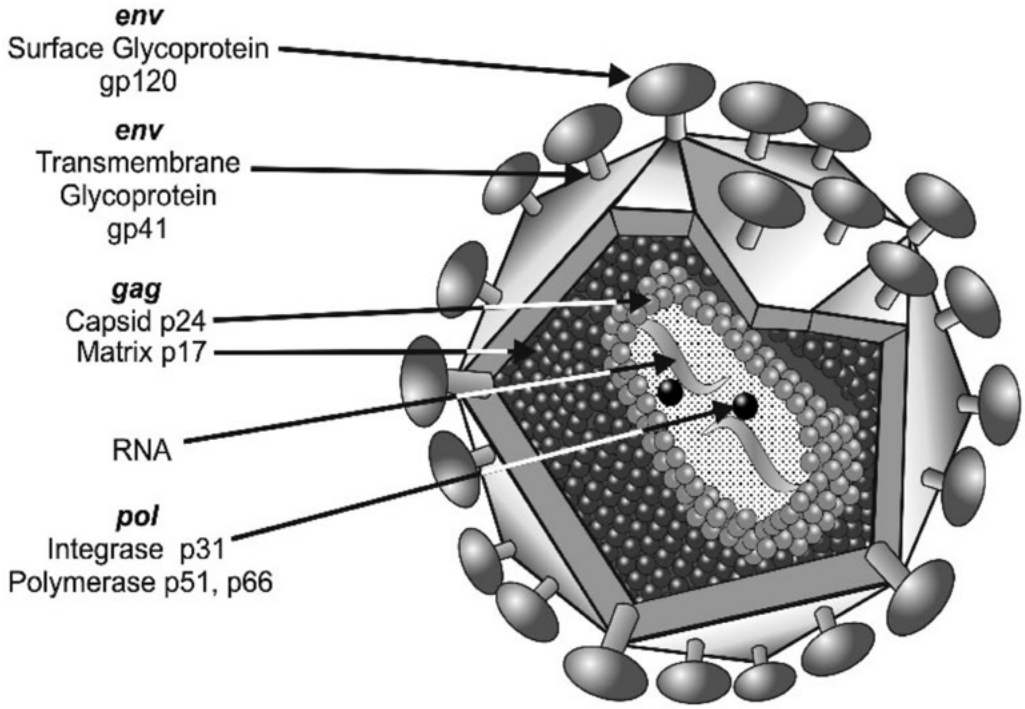

FIGURE 1 Structure of the HIV virion. The HIV genome consists of three major genes that encode the viral enzymatic and structural proteins: group-specific antigens or capsid proteins (Gag), polymerase, protease, and integrase enzymes (Pol), and envelope glycoproteins (Env). The nomenclature of viral proteins indicates either "gp" for glycoprotein or "p" for protein, followed by a number indicating its molecular weight in thousands. The major components of diagnostic utility for HIV-1 include envelope proteins (gp160, gp120, gp41), the *gag* core gene proteins (p55, p24, p17), and polymerase gene proteins (p66, p51, p31). HIV-2 proteins are similar but differ somewhat in the molecular weights of the three gene products (refer to Table 1).

for HIV testing in the United States, recommended by the CDC and the Association of Public Health Laboratories (APHL), began with screening using a sensitive HIV-1 antibody immunoassay. Specimens with repeatedly reactive initial immunoassays were then tested with a more specific HIV-1 antibody test, either the HIV-1 Western blot or the HIV-1 indirect IFA, to validate those results (18). In 1992, the CDC recommended specific testing for both HIV-1 and HIV-2 antibodies if demographic or behavioral information suggested that HIV-2 infection might be present, if there was clinical evidence or suspicion of HIV disease in the absence of a positive test for antibodies to HIV-1, and in cases in which the HIV-1 Western blot exhibited an unusual indeterminate pattern. At that time, the CDC also recommended that laboratories initiating testing with an HIV-1/HIV-2 antibody immunoassay conduct additional, more-specific tests to detect the presence of antibodies against HIV-2 if the HIV-1 Western blot was negative or indeterminate (19). In 2004, the CDC recommended confirmation of all reactive rapid HIV test results by either HIV-1 Western blotting or the HIV-1 IFA, irrespective of results of intermediate immunoassays that may have been conducted (20).

TABLE 1 Major HIV proteins of diagnostic significance

HIV gene and products	Viral protein in:	
	HIV-1	HIV-2
env		
Precursor	gp160	gp125
External glycoprotein	gp120	gp105
Transmembrane glycoprotein	gp41	gp36
pol		
Reverse transcriptase	p66	p68
Reverse transcriptase	p51	p53
Endonuclease	p31	p31[a]
gag		
Precursor	p55	p56
Core	p24	p27
Matrix	p17	p16

[a]The molecular weight of p31 is 34,000.

Since those recommendations were issued, improved immunoassays, an HIV-1 NAT and differentiation immunoassays that distinguish HIV-1 from HIV-2 antibodies, received FDA approval for use in the diagnosis of HIV infections (43, 44). These developments resulted in the CDC and APHL issuing updated recommendations for laboratory HIV diagnostic testing in 2014. The updated algorithm employs an initial HIV-1/2 antibody/p24 antigen combination immunoassay followed by an antibody assay that differentiates HIV-1 from HIV-2 and, if necessary, a NAT to identify HIV RNA before antibodies develop. The currently recommended laboratory algorithm was designed to improve detection of acute/early HIV infection, improve diagnosis of HIV-2 (important for appropriate clinical management),

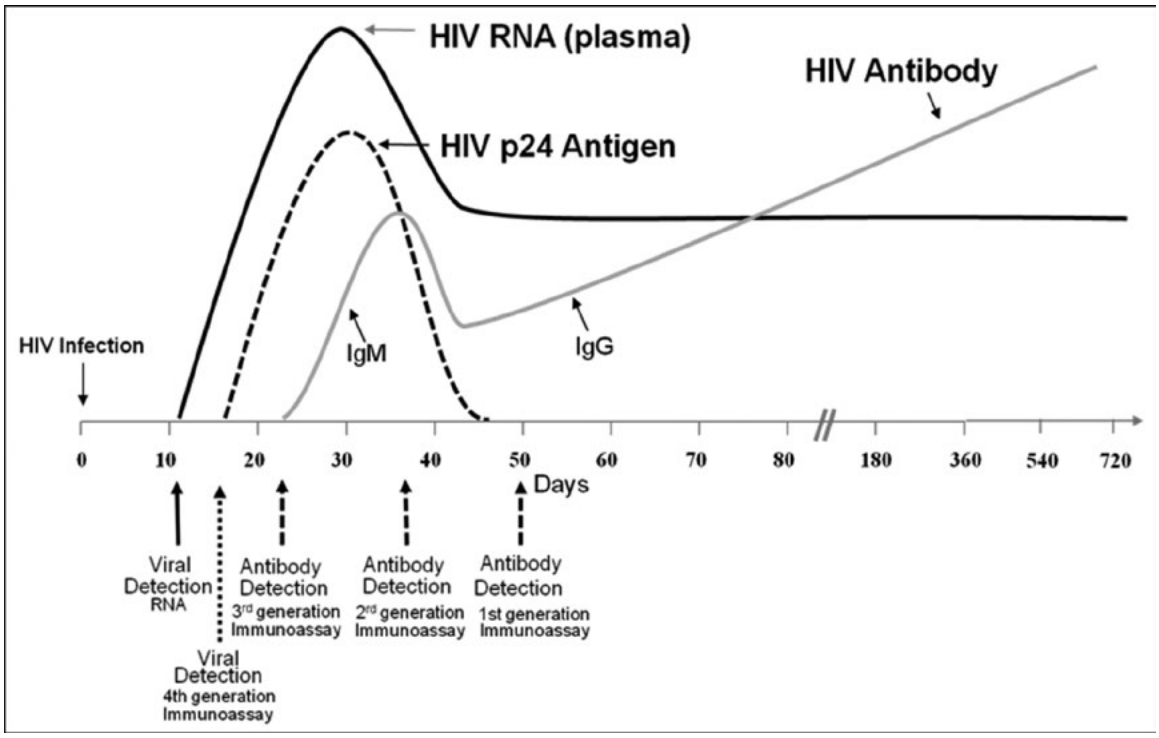

FIGURE 2 Time course of appearance of laboratory markers for HIV-1 infection. Units for vertical axis not given because the magnitude differs for RNA, p24 antigen, and antibody. Adapted data from reference 9 and updated with data from references 10–12.

decrease result turnaround time, allow more locations to conduct the first supplemental test, and not significantly increase the cost of HIV testing. A schematic diagram of the current laboratory algorithm recommended by the CDC and APHL is shown in Fig. 3, and the full set of guidelines (82) can be found at the following link: http://www.cdc.gov/hiv/pdf/hivtestingalgorithmrecommendation-final.pdf.

In addition to diagnostic assays, genotypic and phenotypic resistance assays guide the selection of antiretroviral regimens, and quantitative viral load assays that can detect fewer than 50 viral copies per ml are useful for prognosis and to monitor the response to therapy. These tests, while not strict diagnostic assays, are very important prognostic testing tools for monitoring and guiding the health care of HIV-infected individuals.

SEROLOGIC TESTS

As mentioned above, diagnosis of HIV infection has typically been accomplished via detection of HIV antibody using a sensitive initial immunoassay validated by a subsequent supplemental test. Because HIV infection typically persists for the lifetime of the individual and the initial infection may be minimally symptomatic, most patients who are identified by antibody detection are in the clinically latent or later phases of the illness. Immunoassays for HIV antibody are rapid and economical, but they suffer an important limitation because of the window period, i.e., the time between initial infection and the expression of detectable antibody. During the eclipse and window period, active viral replication and high levels of viremia occur. Different types of antibody immunoassays have different window periods, as indicated in Fig. 2, but all tests based on detection of antibody miss patients during early infection. Recognition that the risk of transmission from persons with acute infection is much higher than that from persons with established infection and indications of the clinical benefits from antiretroviral treatment during acute HIV infection have served as the impetus to adopt techniques that detect HIV earlier after initial infection (21–26). Antigen/antibody combination immunoassays and an HIV-1 NAT that allow earlier detection of HIV have received FDA approval and are now considered essential components in HIV diagnosis.

Laboratory Assays

HIV immunoassays based on different design principles are generally grouped into generations. Immunoassays for laboratory use consist of enzyme immunoassay (EIA) and chemiluminescence immunoassay (CIA) methods. Most of the commonly used assays incorporate specific antigens for the detection of HIV-1 group M and O and HIV-2. HIV antigens (and, in fourth-generation assays, anti-p24 antibodies) are adsorbed to a solid phase, usually plates, beads, or tubes, which bind HIV antibodies (or p24 antigen) in the specimens. Antibodies (and, with fourth-generation assays, p24 antigen) are conjugated to enzymes (alkaline phosphatase or horseradish peroxidase) or to acridinium esters. The indirect EIA format uses an enzyme-labeled antiglobulin conjugate (first- and second-generation assays); the antigen sandwich EIA and CIA formats used in third- and fourth-generation assays use a conjugate with enzyme-labeled HIV antigens (or anti-p24 monoclonal antibodies). With an EIA, the result is a color change, measured as optical density by a spectrophotometer, proportional to the amount of antibody (or antigen) in the specimen. CIA results are expressed in relative light units, also proportional to the amount of antibody (or antigen) in the specimen. Results are compared to internal control values; a result with a signal-to-cutoff ratio of >1.0

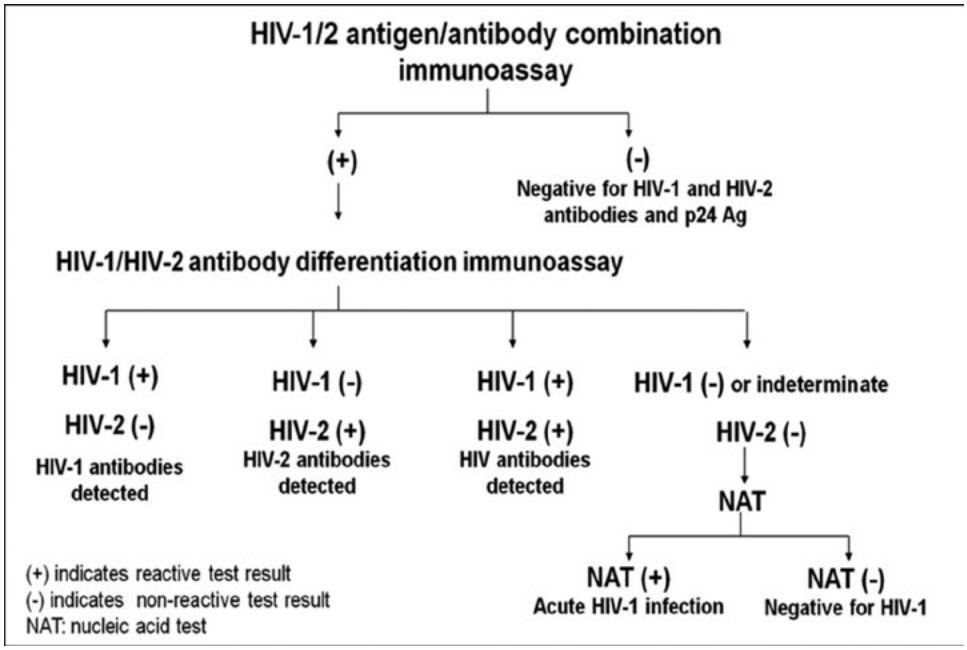

FIGURE 3 CDC and APHL recommended laboratory diagnostic HIV testing algorithm showing sequence of follow-up testing. Ag, antigen.

is considered to be reactive. Both EIAs and CIAs are suitable for automation. CIAs generally have a shorter processing time and wider dynamic range than EIAs. They have also been developed for random-access immunochemistry platforms with the potential to make laboratory-based HIV testing simpler and faster. In fact, some CIAs can produce results in a time frame similar to those of non-laboratory rapid tests and are a good alternative to rapid tests in situations where blood can be drawn and processed.

All third-generation antibody assays and the fourth-generation antigen/antibody assays report 100% sensitivity in their package inserts for specimens known to have HIV antibodies. For the fourth-generation antigen/antibody assays, the analytical sensitivity for p24 is reported to be between 5.2 and 18.39 pg/ml of p24. The specificity range reported for the third-generation assays is 99.58 to 99.92%. The specificities reported by the manufacturers for the antigen/antibody combo assays range from 99.72 to 99.87%. Analyses of specimens from seroconversion panels have established the approximate time of detection by the different generations of immunoassays. Estimates derived from several data sources are outlined schematically in Fig. 2 (9–12). Commercial assays currently available in the United States are summarized in Table 2.

Cautionary Remarks

The prevalences of HIV-1 group M subtypes and circulating recombinant forms (CRFs) vary geographically. All subtypes and most CRFs are found in sub-Saharan Africa. Subtype B is the predominant strain in the United States, Europe, Canada, and Australia. However, the prevalence of non-B subtypes in these countries is increasing. The most recent estimates for the United States indicate that non-B infections account for approximately 3 to 5% of HIV infections (27, 28). Current HIV immunoassays reliably detect the overwhelming majority of HIV-1 group M, B, and non-B subtype infections (11, 12). Group O infections remain rare in the United States. While HIV-1 group O infections can be missed by immunoassays that do not contain specific reagents for the detection of antibody to group O, most currently available assays now incorporate group O peptides (Table 2).

Immunoassays specific for the detection of HIV-1 antibodies can detect HIV-2 infections due to cross-reactivity to HIV-1 antigen present in the assay. However, levels of detection of HIV-2 infection by HIV-1-only immunoassays are highly varied: different assays detect 51 to 100% of HIV-2 infections (11). The ability of HIV-1/2 and HIV-2 assays to detect HIV-2 infections must be demonstrated for the assays to obtain approval by regulatory agencies, and most currently available FDA-approved HIV-1/2 assays incorporate gp36 antigen for reliable detection of HIV-2 (Table 2).

As with any assay capable of processing large numbers of test specimens at any one time, immunoassay methodology is subject to a number of technical drawbacks that should be considered. These range from procedural errors in the handling of samples, such as mislabeling of specimens, to deficiencies in the manual or automated performance of sample processing, such as well-to-well carryover during pipetting and the resultant contamination of neighboring wells. A false-positive result can also be caused by inadequate washing of the specimen or incorrect dilution of the sample or of any one of the assay reagents. Usually such false-positive reactions are corrected either by repeating the assay or by testing with another manufacturer's enzyme-linked immunosorbent assay kit. Apart from these purely technical considerations, the causes of false-positive immunoassay results may be both varied and obscure.

Rapid Immunoassays

The logistics of conventional laboratory HIV immunoassays require phlebotomy and, typically, a follow-up visit for test results after the specimen has been processed. This complicates HIV testing for many hard-to-reach populations for which phlebotomy is impractical; many persons may also fail to return for their test results. In addition, an immediate

TABLE 2 FDA-approved conventional laboratory HIV immunoassays

Test	Markers used for detection	Analyte(s) detected	Generation
Conventional EIAs			
Avioq HIV-1 Microelisa system	Viral lysate, native gp160	IgG antibodies	2nd
Bio-Rad GS HIV-1/2 *PLUS* O	Recombinant p24, gp160, HIV-2 gp36, synthetic group O peptide	IgG and IgM antibodies	3rd
Bio-Rad GS HIV Combo Ag/Ab EIA	Synthetic gp41, recombinant gp160, HIV-2 gp36, synthetic group O peptide, p24 monoclonal antibodies	IgG and IgM antibodies, p24 antigen	4th
Chemiluminescence assays			
Abbott Architect HIV Ag/Ab Combo	Synthetic and recombinant gp41 and HIV-2 gp36, group O peptide, p24 monoclonal antibodies	IgG and IgM antibodies, p24 antigen	4th
Ortho Vitros Anti-HIV 1+2	Recombinant p24, gp41, gp41/120, HIV-2 gp36	IgG and IgM antibodies	3rd
Bio-Rad BioPlex 2200 HIV Ag-Ab[a]	Recombinant gp160, synthetic HIV-1 group O peptide, HIV-2 gp36 peptide, p24 monoclonal antibodies	IgG and IgM antibodies, p24 antigen	4th
Siemens Advia Centaur HIV 1/O/2	Recombinant gp41/120, p24, HIV-2 gp36, synthetic group O peptide	IgG and IgM antibodies	3rd
Siemens Advia Centaur HIV Ag/Ab Combo	Recombinant HIV-1 and HIV-2 antigens, HIV-1 group O peptide antigen, anti-p24 antibodies	IgG and IgM antibodies, p24 antigen	4th

[a]This assay has the ability to differentiate between analyte reactivities.

HIV test result is medically desirable under certain circumstances when antiretroviral prophylaxis should be initiated promptly, for example, in assessment of the source patient after an occupational blood or body fluid exposure and for pregnant women in labor whose HIV status is unknown. To meet these needs, rapid HIV tests that are suitable for use at the point of care (POC) as well as in clinical laboratories have been developed.

Rapid HIV immunoassays are single-use devices that use either immunoconcentration (flowthrough) or immunochromatographic (lateral-flow) principles (29). Flowthrough assays require the sequential addition of specimen, conjugate reagent, and a clarifying buffer through a membrane. Lateral-flow assays contain all necessary reagents and are extremely simple to perform because they require the addition of only specimen or specimen and buffer. Rapid tests differ in their required specimen volumes (range, 3 μl to 50 μl for whole blood, serum, or plasma) and processing times (range, 1 to 20 min). Rapid tests that can use direct, unprocessed specimens (whole blood or oral fluid) have been classified as CLIA waived by FDA and are regulated differently under the Clinical Laboratory Improvement Amendments (CLIA) (83); they are especially well suited for testing outside traditional laboratory settings. There are currently nine rapid HIV antibody tests that are FDA approved in the United States and a multitude of other assays that are available outside the United States. Descriptions of the currently FDA-approved tests are shown in Table 3. Furthermore, one of these tests, OraQuick by OraSure Technologies, has been FDA approved for over-the-counter purchase and home use with oral fluid specimens (30, 31).

Cautionary Remarks

Disadvantages of rapid assays include their subjective interpretation, possible errors if the reader has vision problems, such as color blindness, and the potential for procedural errors when performed by less-skilled personnel (32, 33). Accurate specimen volumes must be dispensed and tests read within specified time limits, control lines must be observed, and instructions must be followed carefully. Rapid tests are useful primarily for small-volume testing. Accurate timing of steps can be adversely affected when multiple specimens are tested simultaneously. Nevertheless, rapid HIV tests have become valuable tools for clinical situations in which rapid results are essential and for outreach settings (34).

Published studies suggest that rapid HIV antibody immunoassays perform similarly to laboratory-based conventional immunoassays in identifying established HIV infection (35). For example, package inserts state that sensitivities range from 99.6 to 100% for all of the available rapid tests when used with blood specimens known to contain HIV antibodies. Specificities for antibody-only rapid tests range from 99.7 to 100% according to package inserts. However, most use colloidal gold bound to protein A for detection of IgG antibodies; the sensitivity of plasma seroconversion panels is similar to those of second-generation conventional immunoassays. Comparative studies of rapid tests performed on oral fluid, whole blood, and serum demonstrate that rapid tests identify fewer HIV infections than conventional laboratory immunoassays, and sensitivity with oral fluid specimens is lower than that with whole blood or serum in persons from populations with increased prevalences of early HIV infection (36, 37). One rapid HIV test that detects and distinguishes HIV antibodies and p24 antigen, the Alere Determine HIV Combo, has received FDA approval (Table 3). Its overall sensitivity is similar to those of third-generation assays; the sensitivity of the antigen component is lower than those of laboratory-based fourth-generation assays (37–39).

Alternative Specimens for Antibody Testing

Alternative specimens to blood, serum, or plasma for HIV antibody testing include oral fluid, urine, and dried blood spots (DBS). These may be useful in testing patients who are reluctant to undergo phlebotomy or who have poor vascular access, in mass-screening settings, in locations in

TABLE 3 FDA-approved rapid and POC HIV tests

Test	Manufacturer	Specimen types	CLIA category	Antigen(s) represented	Yr of FDA approval
OraQuick Advance rapid HIV-1/2 antibody test	OraSure Technologies, Inc.	Oral fluid, whole blood, plasma	Waived; moderate complexity	gp41, gp36	2002
Reveal G3 Rapid HIV-1 antibody test	MedMira, Inc.	Serum, plasma	Moderate complexity	gp41, gp120	2003
Uni-Gold Recombigen HIV-1/2	Trinity Biotech	Whole blood, serum, plasma	Waived; moderate complexity	gp41, gp120, gp36	2003
Multispot HIV-1/HIV-2 rapid test[a]	Bio-Rad Laboratories	Serum, plasma	Moderate complexity	gp41, gp36	2004
Alere Clearview HIV 1/2 Stat Pak	Alere	Whole blood, serum, plasma	Waived; moderate complexity	gp41, gp120, gp36	2006
Alere Clearview Complete HIV 1/2	Alere	Whole blood, serum, plasma	Waived; moderate complexity	gp41, gp120, gp36	2006
INSTI HIV-1 antibody test kit	bioLytical Laboratories	Whole blood, serum, plasma	Waived; moderate complexity	gp41, gp36	2010
Chembio DPP HIV 1/2 assay	Chembio Diagnostics	Oral fluid, whole blood, serum, plasma	Moderate complexity	gp 41, gp120, gp36	2012
Alere Determine HIV 1/2 Ag/Ab combo	Alere Scarborough	Whole blood, serum, plasma	Moderate complexity	gp41, gp120, gp36; p24 antibodies	2013
Bio-Rad Geenius[b]	Bio-Rad Laboratories	Whole blood, serum, plasma	Moderate complexity	gp41	2014

[a]This assay was FDA approved for screening or as a supplemental assay. The interpretive criteria used differ depending on the application.
[b]This assay was FDA approved for supplemental testing only.

which phlebotomy is impossible, in infants, and for seroprevalence studies. It is essential to employ only specimen collection systems and testing methods designed and validated for the specific specimen type. Oral fluid is a complex mixture of secretions from several different sets of glands, as well as transudated plasma from the capillaries of the gum and mucosa. Glandular secretions of saliva contain primarily secretory IgA, which is not a reliable target for diagnostic testing. Most IgG in the oral cavity derives from the crevicular space between the gums and the teeth and not from salivary glands, or can be obtained by inducing an oral mucosal transudate. The OraSure specimen collection device is designed to collect oral mucosal transudate for conventional testing with an FDA-approved oral-fluid-based HIV-1 EIA and Western blot. Two rapid tests are FDA approved for use with oral fluid as well as whole blood and plasma specimens (Table 3). DBS, after appropriate elution, can be tested for HIV antibody, p24 antigen, and HIV RNA and produce results comparable to those from matched serum or plasma specimens when the reduced sample volumes contained in DBS are taken into consideration.

Cautionary Remarks

None of the newer immunoassays that allow detection of IgM antibodies and p24 are approved for use with DBS (Table 2). Data indicate that infection is detected later when oral fluid specimens are used than when blood specimens are used (36, 40).

DIRECT DETECTION

p24 Antigen Assays

In the early days of the AIDS epidemic, p24 antigen testing played an important role as a tool for the diagnosis, prognosis, and evaluation of antiretroviral activity and for monitoring of HIV-1-infected cultures. In 1996, the FDA approved the Coulter HIV-1 p24 antigen assay (Coulter Co., Miami, FL) for screening blood products. This test was used for screening blood and plasma donors in the United States for a few years until it was replaced with more-sensitive nucleic acid tests in 1999 (55). Currently, there are no FDA-approved, stand-alone p24 antigen tests, and the use of individual p24 antigen assays is very limited in the United States. However, standalone p24 assays are still utilized by laboratories in various other countries as part of their HIV testing algorithm.

NUCLEIC ACID TESTING

HIV RNA Qualitative Assays

Aptima HIV-1 RNA Qualitative Assay

Presently, the Aptima HIV-1 RNA qualitative assay is the only nucleic acid test (NAT) that is FDA approved for diagnosis of HIV-1. The assay is intended for detection of HIV-1 in serum and plasma, which has utility for the identification of acute and neonatal HIV-1 infection. The sample preparation, amplification, and amplicon detection steps occur in a single tube. During the sample preparation step, HIV-1 RNA is isolated from clinical specimens by hybridization to target-specific, oligonucleotide-bound magnetic microparticles. The target RNA is amplified via transcription-mediated amplification, followed by detection of the amplified material by a hybridization protection assay (HPA), which involves capture via a chemiluminescent labeled oligonucleotide complementary to the amplicon sequence. The assay is capable of detecting virus sequences within HIV-1 groups M, N, and O, with a limit of detection of 30 RNA copies/ml. The Aptima assay does not detect HIV-2.

NAT Platforms on the Horizon for HIV Testing

Point-of Care NATs

NAT is restricted primarily to centralized laboratories, since the platform characteristics preclude testing in developing countries or other resource-limited settings. Viral load platforms are costly and require extensive training and laboratory resources, including space for the dedicated equipment. Although the platforms are typically high-throughput platforms, the turnaround time is relatively high and test results cannot be provided during the same office visit. Sample collection, storage, and shipment present a challenge for most POC settings, especially since care must be taken in order to preserve the integrity of the RNA for viral load testing. Dried blood spots have improved sample collection in resource-limited settings, as they are easier to transport and are stable at room temperature; however, they still must be shipped to a centralized laboratory for testing. Implementation of viral load testing at the POC is critical in order to avoid loss to follow-up and clinical progression. Thus far, NAT at the POC is not feasible, though several rapid NAT technologies are in development or in the early stages of commercialization. To highlight a few promising technologies, the following rapid NAT platforms are available commercially for other pathogens and are currently in development or in early-phase distribution for HIV: Alere q HIV-1/2 Detect (Alere Technologies, Jena, Germany), Liat HIV (Roche Molecular Branchburg, NJ), GeneXpert (Cepheid, Sunnyvale, CA), and a simple amplification-based assay (SAMBA) (Cambridge, United Kingdom). Currently, none of the HIV tests are FDA approved or available for purchase in the United States, but several have received CE marks (Alere, Cepheid, and SAMBA).

Alere q HIV-1/2 Detect

The Alere q HIV-1/2 Detect is a fully automated, portable real-time PCR platform for quantitative detection of HIV-1 and HIV-2 in whole blood or plasma. The assay is intended for detection of early infant diagnosis and acute/early infection at the POC or in resource-limited settings (41). A total of 25 μl of blood from a finger stick, venous blood, or plasma is added directly to the preloaded test cartridge, and the cartridge is immediately placed in the analyzer. The analyzer has a touchscreen interface and integrated battery for use if electricity is not available. The total run time for detection of HIV-1 and HIV-2 results is approximately 1 h. Internal controls are incorporated into each test cartridge. The Alere q is optimized to detect group M (A to H), group N, group O, CRFs, and HIV-2 groups A and B.

Liat

Like the Alere q HIV-1/2 Detect, the Liat (lab-in-a-tube) HIV Quant VL assay is a fully automated platform that can be used with either whole blood or plasma (42, 43). The sample preparation, target amplification, and amplicon detection occur in a single disposable tube, which is encoded with a barcode. All of the assay reagents, along with an internal RNA control, are prepackaged in segments of the Liat tube, which are separated by peelable seals. The clinical sample is added directly to the Liat tube with a disposable pipette, the barcode on the tube is scanned by the Liat analyzer, and the tube is placed in the analyzer. The tube compartments are compressed by an actuator in the analyzer to expose the reagents needed for the next step in the process. Sample processing involves silica magnetic bead extraction, followed by multiplexed real-time reverse transcription-PCR (RT-PCR) amplification. The Liat analyzer has a display screen with a keypad that indicates test time remaining and final test result, which is achieved within 30 to 35 min. One of the drawbacks of the current Liat platform for POC use is that the testing cartridges require cold storage at 4°C. Both qualitative and quantitative assays are being finalized.

GeneXpert

The GeneXpert is a fully automated rapid real-time PCR platform. The sample processing, amplification, and fluorescence-based detection are all performed in a single-use, microfluidic cartridge, which is preloaded with all of the test reagents. The GeneXpert platform is currently available in 1-, 2-, 4-, 16-, 48-, or 80-module configurations to customize throughput. The modules are stackable to reduce space requirements. For HIV-1 detection, the GeneXpert platform supports a qualitative and quantitative version of the assay, the Xpert HIV-1 Qual and Xpert HIV-1 viral load assays, respectively. For the HIV-1 Qual assay, 100 μl of blood and 750 μl of sample reagent are added to the test cartridge, while the HIV-1 viral load assay requires 1 ml of plasma. After transfer of the clinical specimen to the cartridge, the cartridge is scanned and placed in the module to begin the run. The GeneXpert platform can also be used with dried blood spots. Unlike the Alere q and Liat analyzers, the GeneXpert modules do not contain a display screen but communicate with an external computer. The total test time is approximately 90 min for both the Xpert HIV-1 Qual and Xpert HIV-1 viral load assay. A new, even-more-simplified instrument for running Cepheid GeneXpert assays (Omni) is projected to be available in 2016 and will be capable of easy transport and battery-powered operation.

Simple Amplification-Based Assay

The SAMBA is available in two different formats: SAMBA I and II. SAMBA I is intended for semiautomated batch testing and can run four samples at a time or 24 to 48 samples a day (44, 45). SAMBA II is fully automated, and individual assay modules can be added to the system to customize throughput. The assay modules are controlled by a display module, which is linked via Bluetooth. Each display module can support up to 16 assay modules. The SAMBA platform supports the following tests: whole-blood qualitative, plasma semiquantitative, and whole-blood semiquantitative. The intended use for the whole-blood qualitative test is early infant and acute-infection diagnosis, while the plasma semiquantitative and whole-blood semiquantitative assays are for therapy monitoring. The display module contains an integrated barcode scanner, which is used to scan the barcode on the cartridge box to identify the specific test and to scan the sample identifier. Unlike with most other rapid NAT platforms, the SAMBA involves isothermal amplification of target sequences. Test results are obtained within 90 min by a lateral-flow-based visual readout. The disposable, preloaded cartridges are stable at room temperature and have been shown to maintain stability at room temperature or at 37°C for up to a year.

Cautionary Remarks

HIV NAT testing has utility in screening high-risk individuals suspected of having had recent exposures, since RNA is the first marker of infection that can be detected in plasma (9). However, it is known that RNA detection is not always reliable in persons with established infections. It has been shown that approximately 2 to 4% (46) of specimens from

patients with established HIV infections are not reactive/positive for HIV RNA (11, 47).

Supplemental Assays for HIV

Initial screening immunoassays for HIV are optimized to provide very high sensitivity, often at the expense of specificity. HIV diagnostic testing therefore relies on a sequence of tests used in combination to improve the accuracy of HIV laboratory diagnosis. Specimens that are nonreactive in the initial immunoassay are generally considered HIV negative. If the initial immunoassay result is reactive, it must be followed by one or more supplemental tests. Four assay methods are FDA approved as supplemental tests: HIV-1 Western blotting, indirect IFA, HIV-1/HIV-2 antibody differentiation assay, and qualitative HIV-1 RNA assay. The following Web link lists licensed and approved tests: http://www.fda.gov/BiologicsBloodVaccines/BloodBloodProducts/ApprovedProducts/LicensedProductsBLAs/BloodDonorScreening/InfectiousDisease/UCM080466. Both the Western blot and the IFA are highly specific, but because they rely on viral lysate antigens and anti-human IgG conjugates, they detect HIV-1 later during seroconversion than most currently available conventional initial immunoassays and thus may produce false-negative or indeterminate results (9, 10). In addition, because of cross-reactivity, the HIV-1 Western blot has been interpreted as positive for HIV-1 in 46 to 85% of specimens from persons infected with HIV-2 (48–50). An HIV-1/HIV-2 antibody differentiation assay was approved by the FDA in 2013 for use as a supplemental test and for differentiation of HIV-1 and HIV-2 antibodies. Because the differentiation assay uses an indirect EIA format with an anti-human IgG conjugate, it also detects HIV antibodies later during seroconversion than most currently available conventional initial immunoassays (51, 52).

Historically, the HIV-1 Western blot has been the gold standard for HIV diagnosis (18). The Western blot owes its specificity to separation and concentration of viral components. A viral lysate of HIV is applied in a gel under an electric field; the mixture of viral components is separated by their molecular weights into specific "bands." Each viral component becomes relatively pure as it is separated. Components are blotted separately onto a membrane which is cut into strips. The testing laboratory incubates the strips with patient serum, plasma, or dried blood spot eluates and then develops the reaction with an enzyme-labeled anti-human antibody. Antibodies to the following HIV-1-associated antigens can be detected: gp160, gp120, p66, p55, p51, gp41, p31, p24, p17, and p15. Additional viral bands may be described by some manufacturers, and the molecular weights of some antigens might vary slightly between assays produced by different manufacturers. Because Western blot antigens are prepared from HIV grown in cell culture, non-viral cellular proteins may be present on the nitrocellulose strip and lead to nonspecific reactions. The interpretation of HIV-1 Western blots predominantly follow CDC guidelines. A positive result requires detection of at least two of three antigens: p24, gp41, and gp120/gp160 (18). The absence of all bands is a negative result. The presence of HIV-associated bands not meeting the criteria for positivity or the presence of nonviral bands is interpreted as an indeterminate result. After a reactive initial HIV-1/HIV-2 immunoassay, additional negative or indeterminate HIV-1 Western blot testing specific for HIV-2 antibodies was recommended (19). Western blots that include HIV-2 antigens (e.g., gp36 or gp105) are available outside the United States, but none are FDA approved. Line immunoassays employ a principle similar to that of the Western blot, but recombinant or synthetic antigens are placed on the strip instead of viral lysate antigens from an electrophoretic gel. This approach has the advantage of using only viral antigens in the reaction mixture, eliminating the background from cross-reactivity with nonspecific cellular proteins. The manufacturer also has control over the quantity and type of antigens represented and can include HIV-2 and group O antigens to confirm these infections with a single assay (53). The INNO-LIA HIV I/II Score test (Innogenetics, Ghent, Belgium) is a line immunoassay widely available outside the United States.

The Fluorognost HIV-1 IFA (Sanochemia) has been used as both an initial screening test and a supplemental test for HIV-1 infection with serum, plasma, and dried blood spot eluates. HIV-infected and uninfected lymphocytes are fixed on a slide. The slide is incubated first with patient serum and then with a fluorescently labeled anti-human antibody (54). For interpretation, patterns of fluorescence in infected and uninfected cells are compared for each patient specimen; fluorescence on the infected lymphocytes that exceeds that from nonspecific antibody binding on the uninfected lymphocytes is interpreted as a positive result. Considerable skill is required, and indeterminate results can be produced for patients with autoantibodies and other conditions. In addition to being used as an independent supplemental test, IFA can be used to resolve indeterminate HIV-1 Western blots. An HIV-2-specific IFA has been described, but it is not FDA approved.

The Multispot HIV-1/HIV-2 rapid test (Bio-Rad Laboratories, Redmond, WA) is a flowthrough rapid EIA that differentiates HIV-1 and HIV-2 antibodies in a single-use cartridge. Microscopic particles are coated separately with a synthetic gp41 peptide and recombinant gp41 antigen for HIV-1 and a synthetic gp36 peptide for HIV-2. The microparticles are immobilized separately on the reaction membrane in three separate test spots. Antibodies against HIV-1 or HIV-2 in the test specimen bind to the antigens in the spots on the membrane. Alkaline phosphatase-labeled goat anti-human IgG is added to the cartridge and binds to the antibody/antigen complexes immobilized in the spots. When development reagent is added to the cartridge, a purple color develops at the spots in proportion to the amount of antibodies present. The membrane is examined visually for the presence of purple color on the test spots. Reactivity at both gp41 spots is required to define a positive supplemental HIV-1 test result; reactivity at only one HIV-1 spot is interpreted as indeterminate. The sensitivity of the Multispot antibody differentiation assay for established HIV infection is comparable to that of the HIV-1 Western blot, but it produces fewer indeterminate results and accurately identifies HIV-2 antibodies, including those in specimens misclassified as HIV-1 by the HIV-1 Western blot (51, 52, 55, 56). Because of cross-reactivity, approximately 0.4% of reactive specimens remain dually reactive at the HIV-1 and HIV-2 spots after recommended dilution procedures (52). Although most dually reactive specimens represent HIV-1 infections with cross-reactivity to HIV-2 (57), one U.S. study of five dually reactive specimens found detectable HIV-2 RNA in the one specimen with strong HIV-2 reactivity, suggesting that strong reactivity at the HIV-2 spot indicated the need for further investigation with HIV-2 NAT (56).

Recently, another rapid assay designed for differentiation of HIV-1 and HIV-2 antibodies has been FDA approved as a supplemental test. This test, the Geenius HIV 1/2 supplemental assay (Bio-Rad Laboratories, Redmond, WA) is an

immunochromatographic test. The Geenius HIV 1/2 supplemental assay cassette contains antibody-binding protein A, which is conjugated to colloidal gold dye particles, and HIV-1 and HIV-2 antigens (gp36 HIV-2 envelope peptide, gp140 HIV-2 envelope peptides, p31 HIV-1 polymerase peptide, gp160 HIV-1 envelope recombinant protein, gp41 group M and O HIV-1 envelope peptides, and p24 HIV-1 core recombinant protein), which are bound to the membrane's solid phase. The sample is applied to the sample-plus-buffer well. After the sample and buffer have migrated onto the test strip, additional buffer is added to the buffer well. The buffer causes the specimens and reagents to flow laterally and facilitates the binding of antibodies to the antigens. In a reactive sample, the antibodies are captured by the antigens immobilized in the test area. The protein A-colloidal gold binds to the captured antibodies, causing development of pink/purple lines. When there are no HIV antibodies, there are no pink/purple lines in the test area. The sample continues to migrate through the membrane, and a pink/purple line develops in the control (C) area, which contains protein A. In the FDA-approved version, the results are read with a reader that incorporates a standardized algorithm to make a final determination of HIV-1 or HIV-2 reactivity (58, 59).

The Aptima HIV-1 qualitative assay is FDA approved for detection of HIV-1. HIV-1 RNA in the test specimen is hybridized to capture nucleotides homologous to highly conserved regions of HIV-1. The hybridized target is then captured onto magnetic microparticles and separated from plasma in a magnetic field. Target amplification occurs via a transcription-based nucleic acid amplification. Detection is achieved by chemiluminescence-labeled nucleic acid probes that hybridize specifically to the amplicon. The chemiluminescent signal, measured in a luminometer, is reported as relative light units. Analytical sensitivity is 30 copies/ml of HIV-1 RNA. The HIV-1 qualitative RNA assay can be used for the diagnosis of acute HIV-1 infection in serum or plasma from patients without antibodies to HIV-1 and as a supplemental test, with specimens repeatedly reactive for HIV antibodies.

Cautionary Notes

Some tests, such as Western blotting and the Geenius assay, are designed to be used only as supplemental assays. Use of either of these tests as screening assays may result in false-positive or false-negative results.

While HIV-1 RNA levels are generally very high in recently infected individuals, HIV-1 is undetectable in 2 to 4% of HIV-1 Western blot-positive specimens from infected persons (11, 46, 47, 59) and thus one of the reasons why NAT is currently not the second step in the lab diagnostic algorithm recommended for use in the United States. Quantitative HIV-1 and HIV-2 RNA and DNA NAT are also available but are not FDA approved for HIV diagnosis http://www.fda.gov/BiologicsBloodVaccines/BloodBloodProducts/ApprovedProducts/LicensedProductsBLAs/BloodDonorScreening/InfectiousDisease/UCM080.

Nucleic acid testing technology is subject to contamination due to the highly sensitive nature of the technique. Extreme care should be taken to separate pre- and postamplification specimens and reagents.

PROGNOSTIC HIV TESTING

Following HIV-1 diagnosis or presentation of clinical symptoms associated with infection, HIV RNA viral load assays are used as a clinical tool to monitor disease prognosis. Viral load assays measure HIV-1 RNA in plasma as a means of monitoring the response to antiretroviral therapy, adherence to treatment, or virological failure, which, in turn, aids clinicians in making decisions about treatment changes. Studies strongly indicate that HIV-1 RNA levels are predictive of transmission risk; therefore, viral load assays may be used to guide treatment-for-prevention interventions (60). In the United States, viral load testing is the standard for assessing care in patients (61, 62), and five commercial assays are FDA approved for the quantification of HIV-1 RNA in plasma; however, only three of these assays can still be obtained in the United States from the manufacturer: Abbott RealTime HIV-1, Roche COBAS AmpliPrep/COBAS TaqMan HIV-1 v2.0, and Roche Amplicor HIV-1 Monitor v1.5. None of the viral load platforms are intended for diagnosis, donor screening, or detection of HIV-2 (Table 4).

RealTime HIV-1

The RealTime HIV-1 assay is an RT-PCR-based, automated platform that quantitates HIV-1 RNA in human plasma. The automated m2000 system includes two components: the m2000sp for sample preparation and the m2000rt for real-time amplification and detection. Prior to sample processing, an internal control RNA sequence is added to the clinical specimen to ensure quality control of sample processing and amplification steps. Magnetic particles capture RNA in the sample, and bound nucleic acids are washed, eluted, and transferred to a 96-well plate. At this point, the assay plate is transferred to the m2000rt component for amplification of the target by real-time RT-PCR. Detection of the amplicon is mediated by a 5′ fluorochrome-labeled oligonucleotide probe that is complementary to the target sequence. In the absence of the target amplicon, the probe is bound to a shorter complementary sequence that contains a quencher molecule at the 3′ end. In the presence of target amplicon, the probe will preferentially bind the amplicon and dissociate from the quencher sequence, allowing fluorescence emission. Quantitation is based on a standard curve generated from two controls included in the assay kit.

There are several advantages to the RealTime HIV-1 assay. The test is designed to quantify all group M, N, and O viruses and CRFs, with a broad linear range of 40 to 10,000,000 RNA copies/ml. There is also a reduced risk for carryover amplicon contamination since the amplification and detection steps are carried out in a sealed 96-well optical plate.

COBAS AmpliPrep/COBAS TaqMan HIV-1

The COBAS AmpliPrep/COBAS TaqMan HIV-1 test version 2.0 is an automated platform based on real-time TaqMan technology for detection of HIV-1 in plasma. Automated sample processing is performed by the COBAS AmpliPrep instrument, and automated amplification/detection is carried out on the COBAS TaqMan analyzer or COBAS TaqMan 48 analyzer. Docking the COBAS TaqMan analyzer to the AmpliPrep instrument creates a fully automated system. Alternatively, the amplification tubes can be manually loaded into the COBAS TaqMan 48 analyzer. Sample processing involves a silica-based extraction method. The target RNA binds to silica-coated magnetic glass particles. An internal-control quantitation standard is added to the clinical sample along with the lysis buffer. After sample processing, the target RNA is added to the amplification mixture and transferred to the COBAS TaqMan analyzer or COBAS TaqMan 48 analyzer for amplification and detection, involving a fluorochrome-labeled oligonucleotide probe/quencher pair. Viral load is quantitated based on the threshold cycle of the QS standard, which is added at a

TABLE 4 Nucleic acid tests

Type of test	Test(s)	Manufacturer	Intended use	Amplification method	Detection range (no. of RNA copies/ml)[d]	Specificities
Qualitative RNA	Aptima HIV-1 RNA qualitative assay[a]	Gen-Probe, Inc., San Diego, CA	Diagnostic	Transcription-mediated amplification	30–ND	HIV-1 groups M, N, and O
Viral load	RealTime HIV-1[b]	Abbott Molecular, Des Plaines, IL	Patient monitoring, quantification	Real-time RT-PCR	40–10,000,000	HIV-1 groups M and O, CRFs
	COBAS AmpliPrep/ COBAS TaqMan HIV-1 version 2.0[b]	Roche Diagnostics, Indianapolis, IN	Patient monitoring, quantification	Real-time RT-PCR	20–10,000,000	HIV-1 groups M and O, CRFs
	Amplicor HIV-1 Monitor version 1.5	Roche Diagnostics, Indianapolis, IN	Diagnosis of HIV, qualitative	RT-PCR	400–750,000 (standard), 50–100,000 (ultrasensitive)	HIV-1 group M
Point of care	Alere q HIV-1/2 Detect[c]	Alere, Technologies, Jena, Germany	Proposed diagnostic use and patient monitoring	Real-time RT-PCR	ND	HIV-1 groups M, N, and O, CRFs, HIV-2 groups A and B
	Liat system[c]	Roche Molecular Diagnostics, Branchburg, NJ	Proposed diagnostic use and patient monitoring	Real-time RT-PCR	100–1,500,000	HIV-1 groups M and O, HIV-2
	GeneXpert (Xpert HIV-1 viral load and Xpert HIV-1 Qual)[c]	Cepheid, Sunnyvale, CA	Proposed diagnostic use and patient monitoring	Real-time RT-PCR	40–10,000,000 (Xpert HVI-1 viral load)	HIV-1 groups M, N, and O
	SAMBA (SAMBA I and SAMBA II)[c]	Diagnostics for the Real World, Ltd., Cambridge, United Kingdom	Proposed diagnostic use and patient monitoring	Isothermal amplification	ND	HIV-1 groups M and O

[a]Currently FDA approved for diagnostic use.
[b]Currently FDA approved for patient monitoring (viral load).
[c]Not currently FDA approved.
[d]ND, not determined.

constant concentration to each sample. Like the RealTime HIV-1 assay, the COBAS AmpliPrep/COBAS TaqMan HIV-1 assay has the ability to quantify all group M, N, and O viruses, including CRFs4, with a broad detection range of 48 to 10,000,000 copies/ml.

Amplicor HIV-1 Monitor

The Amplicor HIV-1 Monitor can be performed with the standard or UltraSensitive specimen processing procedure, which quantitates HIV-1 RNA in plasma over a range of 400 to 750,000 copies/ml or 50 to 75,000 copies/ml, respectively. The standard procedure includes a sample lysis step, followed by RNA precipitation with alcohol, while the ultrasensitive procedure involves ultracentrifugation of the virus particles in the sample prior to lysis and precipitation of the nucleic acid. A known concentration of QS RNA is added to each specimen along with the lysis reagent for quality control. Amplification of HIV-1 RNA in the plasma is mediated by RT-PCR, followed by PCR of the cDNA. One of the advantages of the Amplicor assay is the use of dUTP in the deoxynucleoside triphosphate mix. The enzyme uracil-*N*-glycosylase is added in the master mix reagent, which catalyzes the cleavage of DNA containing dUTP. Any contaminating amplicon from prior amplification reactions is destroyed at the start of the reaction, but the target amplicon is not affected. Colorimetric detection of the target amplicon is mediated by a probe-bound microplate containing sequences complementary to the target and QS. RNA is quantitated relative to the QS, which is a noninfectious RNA molecule with the same sequence as the target. The probe-binding sequence on the microplate distinguishes the QS amplicon from the target amplicon. A disadvantage of the Amplicor HIV-1 Monitor is that the assay has a smaller dynamic range than the RealTime HIV-1 and COBAS AmpliPrep/COBAS TaqMan HIV-1 assays. The Amplicor assay is also optimized for the detection of group M subtypes only.

Cautionary Remarks

Biological variation of HIV-1 RNA levels among clinically stable patients has been estimated to be approximately 0.3

$\log_{10}$. The abilities of commercial assays to be reproduced range from 0.1 to 0.3 $\log_{10}$ depending on the region of the assay's dynamic range. Numerous studies comparing the performances of the conventional FDA-approved viral load assays show high correlations between assays in terms of net changes in plasma RNA levels after antiretroviral therapy (63–65). Early assays showed larger variations in absolute values between assays with the same sample, but current-generation assays have been standardized so that the differences in values between assays are narrowing. The two real-time RT-PCR assays show improved correlation and agreement between viral load values (66). Although there is improved overall agreement between the different viral load assays, it is still considered optimal for patient care to monitor viral load values over time with the same assay.

HIV-1 RNA load testing is sometimes requested to resolve equivocal serologic findings, to facilitate the diagnosis of HIV-1 infection during the acute phase of infection, or to diagnose disease in children. Viral load tests can be performed for these purposes with a physician's order, but they are not approved by the FDA for the diagnosis of HIV-1 infection and they should be validated within a laboratory prior to routine use for these purposes. False-positive results can be obtained because of contamination during specimen processing, carryover of amplified products, or selection of incorrect thresholds for defining positivity.

ANTIVIRAL SUSCEPTIBILIES

Drug Resistance Testing

Antiviral drug resistance testing is an essential element in the management of antiretroviral therapy. Testing is important for the selection of initial regimens because of the prevalence of transmitted drug resistance in therapy-naive patients and is a recommendation of the Department of Health and Human Services (HHS). The HHS recommendations are updated periodically and can be found in reference 62. Drug resistance testing is also important for the selection of alternative antiretroviral treatment for patients who are failing their current regimen due to the development of antiviral resistance.

The clinical utility of HIV resistance testing has been evaluated in a number of prospective randomized clinical trials (67–69). Patients whose antiretroviral treatment was based on the results of resistance testing had greater decreases in viral load than patients in whom the antiretroviral regimen was based on prior antiretroviral usage, and the use of resistance testing to guide treatment is cost-effective (70, 71). Two types of methods are available to assay for HIV resistance. Genotyping tests examine the population of viral genomes in the patient sample for the presence of mutations known to confer decreased susceptibility to antiretroviral drugs. Phenotypic assays measure viral replication of the patient's virus in the presence of antiretroviral drugs. In addition, HIV tropism assays have become important to evaluate susceptibility to HIV entry inhibitors that inhibit viruses using the CCR5 coreceptor for cell entry. Table 5 provides a list of the currently available commercial HIV-1 resistance and tropism assays.

Genotyping Assays

The initial steps of genotypic assays for antiviral drug resistance include extraction of viral RNA from plasma and RT-PCR to amplify viral RNA sequences which code for portions of the viral genome that are targeted by antiretroviral drugs. These sequences include genes in the *pol* region of the virus for reverse transcriptase, protease, and integrase, as well as envelope regions related to the entry inhibitors. The nucleotide sequence is determined and examined for the presence of known resistance mutations. This can be accomplished most commonly using automated sequencing technology. The nucleotide sequence of the gene(s) of interest is obtained and compared to the sequence of wild-type virus to identify resistance mutations. The process requires alignment and editing of the sequence, comparison to the wild-type sequence, and final interpretation to identify mutations associated with resistance to specific antiretroviral drugs. FDA-approved kits containing sequencing reagents and the software programs required for sequence alignment and interpretation are commercially available. The Trugene HIV-1 genotyping kit, the OpenGene DNA sequencing system (Siemens Healthcare Diagnostics), and the ViroSeq HIV-1 Genotyping System (Abbott Molecular) have been found to perform in equivalent manners (72), although the Trugene kit may be coming off the market. These tests detect mutations in the reverse transcriptase and protease genes but do not detect mutations associated with resistance to the integrase or CCR5 inhibitors. The databases used for interpretation of resistance mutations require regular updating, as the number of new antiretroviral drugs continues to expand (http://hivdb.stanford.edu/).

One limitation of genotypic assays is that they are able to detect only mutants comprising major fractions of the patient's virus; resistant variants must constitute at least 25 to 30% of the virus population (73). Although the clinical significance of resistance mutations present at low levels remains to be fully elucidated, there is evidence that minor mutations which are missed by standard genotyping assays can lead to failure of subsequent treatments (74). Because standard genotyping assays lack sensitivity for low-frequency drug resistance mutations, efforts are under way to increase sensitivity by various methods, including PCR-based assays (75) and single-genome analysis (76). These techniques are not FDA approved, and the single-genome sequencing approach is not yet a practical clinical tool because the process is expensive and labor-intensive. However, next-generation sequencing technologies offer the promise of decreasing the cost of sequencing, and evaluations of this approach for clinical laboratories are under way (77).

Phenotyping Assays

Phenotyping assays measure the ability of HIV-1 to grow in the presence of various concentrations of an antiretroviral agent. The amount of drug required to inhibit virus replication by 50% or by 90% is determined and given as a 50% or 90% inhibitory concentration (IC_{50} or IC_{90}). The IC_{50} or IC_{90} obtained with the patient sample is compared to that of a control wild-type virus, and the result is reported as a relative difference. Early phenotypic resistance assays were labor-intensive because they necessitated the isolation and culture of HIV from the patient's specimen. Currently, commercially available methods use HIV-1 RNA amplified from plasma and are based on recombinant DNA technology. These phenotypic assays are automated but remain labor-intensive and technically complex. One such commercial assay is available from Monogram Biosciences (South San Francisco, CA). The first step involves extraction of HIV-1 RNA from plasma. Reverse transcription and PCR amplification of the protease and reverse transcriptase genes follow. The amplified genes from the patient's specimen are then inserted into vectors, and recombinants are used in culture to examine resistance against a drug concentration gradient. The PhenoSense assay (Monogram Biosciences) uses an HIV-1 vector

TABLE 5 Assays for drug resistance and cell tropism determination

Test(s) (manufacturer)	Format	Description
Trugene HIV-1 genotyping kit and OpenGene DNA sequencing system (Siemens Healthcare Diagnostics, Tarrytown, NY)	Genotypic resistance	Detects mutations known to be associated with protease and reverse transcriptase drug resistance
ViroSeq HIV-1 Genotyping System (Abbott Molecular, Des Plaines, IL)	Genotypic resistance	Detects mutations known to be associated with protease and reverse transcriptase drug resistance
Integrase and envelope genotypes (various commercial labs)	Genotypic resistance	Sequence analysis of integrase or envelope genes to identify mutations associated with resistance to integrase inhibitors or the fusion in inhibitor enfuvirtide (Fuzeon)
PhenoSense HIV (reverse transcriptase and protease inhibitors) (Monogram Biosciences, South San Francisco, CA)	Phenotypic resistance	Measures decrease in virus replication in the presence of reverse transcriptase and protease inhibitors
PhenoSense for entry inhibitor susceptibility (Monogram Biosciences, South San Francisco, CA)	Phenotypic resistance	Measures decrease in virus replication in the presence of entry inhibitors
PhenoSense integrase (Monogram Biosciences, South San Francisco, CA)	Phenotypic resistance	Measures decrease in virus replication in the presence of integrase inhibitors
SensiTrop II HIV coreceptor tropism (Pathway Diagnostics, Malibu, CA)	Genotypic cell tropism	Virus gene sequences used to predict CCR5 cell tropism
Trofile coreceptor tropism (Monogram Biosciences, Inc., South San Francisco, CA)	Phenotypic cell tropism	Single-round virus replication assay which uses envelop sequences from patient viruses to determine the ability to replicate in cells with CCR5, CXCR4, or both coreceptors

with a luciferase reporter gene that replaces the viral envelope gene, allowing viral replication to be quantified by measuring luciferase activity. PhenoSense tests are also available to measure resistance to the entry inhibitor and integrase inhibitors. As with genotypic testing, the phenotypic assays can detect only mutant variants that comprise at least 25% of the viral population. The combination of genotyping and phenotyping tests may offer a benefit to patients by better resolving potentially conflicting test results.

Tropism Assays

A new CCR5 inhibitor, maraviroc, has brought about a need for a tropism assay, because the drug is effective only against virus that uses CCR5 as a coreceptor for entry. The drug is not active against CXCR4-tropic virus or dual-tropism or mixed-tropism virus. The tropism assay must be performed prior to initiating maraviroc or any other CCR5 inhibitor to determine whether the virus is CCR5 tropic. As with drug resistance assays, there are two general approaches in use, and two tropism assays are commercially available. The Trofile (Monogram Biosciences) uses the phenotypic approach, and the SensiTrop II HIV coreceptor tropism assay (Pathway Diagnostics, Malibu, CA) uses the genotypic approach. For the Trofile assay, the *env* gene from the patient is amplified and used to construct pseudoviruses. Coreceptor tropism is then determined by measuring the ability of the pseudoviral population to infect CD41/U87 cells that express either CXCR4 or CCR5. Depending on which cells they infect, the viruses are then designated CXCR4 tropic, CCR5 tropic, or tropic to both. The SensiTrop assay uses a heteroduplex tracking assay combined with sequence analysis to identify minor viral populations that may be CXCR4 tropic. Only patients that are solely CCR5 tropic are candidates for a CCR5 inhibitor. Resistance to maraviroc has been reported and results from the development of mutations that allow the virus to use CXCR4 coreceptors or mutations that lead to structural changes in the envelope that prevent the drug from being effective (78, 79). In addition to the commercially available tropism assays, research tools are being developed for the prediction of virus tropism, including prediction of affinity for CCR5 binding (80) and next-generation sequencing to predict viral quasi-species binding to CXCR4 (81).

QUALITY ASSURANCE PROGRAM

All laboratories that report results for clinical care must have a quality assurance program in place. This includes quality control and proficiency testing to ensure the accuracy of laboratory results. Such a program consists of written policies and procedures that the laboratory has implemented to ensure that its performance is acceptable to its clients and regulatory agencies. Information related to the Clinical Laboratory Improvement Act can be found at the Web link https://www.cms.gov/Regulations-and-Guidance/Legislation/CLIA/index.html?redirect=/clia/.

CONCLUSIONS

HIV diagnostic and prognostic assays have continued to evolve as information has been gained about virus replication, therapy, and the importance of timely diagnosis and monitoring. As a result of this evolution, new tests and algorithms that allow for earlier diagnosis of infection and improved patient monitoring are available.

REFERENCES

1. **Masur H, Michelis MA, Greene JB, Onorato I, Stouwe RA, Holzman RS, Wormser G, Brettman L, Lange M, Murray HW, Cunningham-Rundles S.** 1981. An outbreak of community-acquired *Pneumocystis carinii* pneumonia:

initial manifestation of cellular immune dysfunction. *N Engl J Med* **305:**1431–1438. PubMed
2. **Barré-Sinoussi F, Chermann JC, Rey F, Nugeyre MT, Chamaret S, Gruest J, Dauguet C, Axler-Blin C, Vézinet-Brun F, Rouzioux C, Rozenbaum W, Montagnier L.** 1983. Isolation of a T-lymphotropic retrovirus from a patient at risk for acquired immune deficiency syndrome (AIDS). *Science* **220:**868–871. PubMed
3. **Gallo RC, Salahuddin SZ, Popovic M, Shearer GM, Kaplan M, Haynes BF, Palker TJ, Redfield R, Oleske J, Safai B, White G, Foster P, Markham PD.** 1984. Frequent detection and isolation of cytopathic retroviruses (HTLV-III) from patients with AIDS and at risk for AIDS. *Science* **224:**500–503. PubMed
4. **Levy JA, Hoffman AD, Kramer SM, Landis JA, Shimabukuro JM, Oshiro LS.** 1984. Isolation of lymphocytopathic retroviruses from San Francisco patients with AIDS. *Science* **225:**840–842. PubMed
5. **Coffin J, Haase A, Levy JA, Montagnier L, Oroszlan S, Teich N, Temin H, Toyoshima K, Varmus H, Vogt P, Weiss R.** 1986. What to call the AIDS virus? *Nature* **321:**10. PubMed
6. **Zhu T, Korber BT, Nahmias AJ, Hooper E, Sharp PM, Ho DD.** 1998. An African HIV-1 sequence from 1959 and implications for the origin of the epidemic. *Nature* **391:**594–597. PubMed
7. **Clavel F, Guétard D, Brun-Vézinet F, Chamaret S, Rey MA, Santos-Ferreira MO, Laurent AG, Dauguet C, Katlama C, Rouzioux C, Klatzmann D, Champalimaud JL, Montagnier L.** 1986. Isolation of a new human retrovirus from West African patients with AIDS. *Science* **233:**343–346. PubMed
8. **Hahn BH, Shaw GM, De Cock KM, Sharp PM.** 2000. AIDS as a zoonosis: scientific and public health implications. *Science* **287:**607–614. PubMed
9. **Busch MP, Satten GA.** 1997. Time course of viremia and antibody seroconversion following human immunodeficiency virus exposure. *Am J Med* **102**(5B)**:**117–126. PubMed
10. **Fiebig EW, Wright DJ, Rawal BD, Garrett PE, Schumacher RT, Peddada L, Heldebrant C, Smith R, Conrad A, Kleinman SH, Busch MP.** 2003. Dynamics of HIV viremia and antibody seroconversion in plasma donors: implications for diagnosis and staging of primary HIV infection. *AIDS* **17:**1871–1879. PubMed
11. **Owen SM, Yang C, Spira T, Ou CY, Pau CP, Parekh BS, Candal D, Kuehl D, Kennedy MS, Rudolph D, Luo W, Delatorre N, Masciotra S, Kalish ML, Cowart F, Barnett T, Lal R, McDougal JS.** 2008. Alternative algorithms for human immunodeficiency virus infection diagnosis using tests that are licensed in the United States. *J Clin Microbiol* **46:**1588–1595. PubMed
12. **Masciotra S, McDougal JS, Feldman J, Sprinkle P, Wesolowski L, Owen SM.** 2011. Evaluation of an alternative HIV diagnostic algorithm using specimens from seroconversion panels and persons with established HIV infections. *J Clin Virol* **52**(Suppl 1)**:**S17–S22. PubMed
13. **Fiebig EW, Heldebrant CM, Smith RI, Conrad AJ, Delwart EL, Busch MP.** 2005. Intermittent low-level viremia in very early primary HIV-1 infection. *J Acquir Immune Defic Syndr* **39:**133–137. PubMed
14. **Bollinger RC Jr, Kline RL, Francis HL, Moss MW, Bartlett JG, Quinn TC.** 1992. Acid dissociation increases the sensitivity of p24 antigen detection for the evaluation of antiviral therapy and disease progression in asymptomatic human immunodeficiency virus-infected persons. *J Infect Dis* **165:**913–916. PubMed
15. **Schüpbach J, Tomasik Z, Knuchel M, Opravil M, Günthard HF, Nadal D, Böni J, Swiss HIV Cohort Study, Swiss HIV Mother and Child Cohort Study.** 2006. Optimized virus disruption improves detection of HIV-1 p24 in particles and uncovers a p24 reactivity in patients with undetectable HIV-1 RNA under long-term HAART. *J Med Virol* **78:**1003–1010. PubMed
16. **Cooper DA, Imrie AA, Penny R.** 1987. Antibody response to human immunodeficiency virus after primary infection. *J Infect Dis* **155:**1113–1118. PubMed
17. **CLSI.** 2011. *Criteria for Laboratory Testing and Diagnosis of Human Immunodeficiency Virus Infection. Approved Guideline.* Clinical and Laboratory Standards Institute, Wayne, PA.
18. **Centers for Disease Control (CDC).** 1989. Interpretation and use of the western blot assay for serodiagnosis of human immunodeficiency virus type 1 infections. *MMWR Morb Mortal Wkly Rep* **38**(Suppl 7)**:**1–7. PubMed
19. **O'Brien TR, George JR, Epstein JS, Holmberg SD, Schochetman G.** 1992. Testing for antibodies to human immunodeficiency virus type 2 in the United States. *MMWR Recomm Rep* **41**(RR-12)**:**1–9. PubMed
20. **Centers for Disease Control and Prevention.** 2004. Protocol for confirmation of rapid HIV tests. *MMWR Morb Mortal Wkly Rep* **53:**221–222. PubMed
21. **Koopman JS, Jacquez JA, Welch GW, Simon CP, Foxman B, Pollock SM, Barth-Jones D, Adams AL, Lange K.** 1997. The role of early HIV infection in the spread of HIV through populations. *J Acquir Immune Defic Syndr* **14:**249–258.
22. **Hollingsworth TD, Anderson RM, Fraser C.** 2008. HIV-1 transmission, by stage of infection. *J Infect Dis* **198:**687–693. PubMed
23. **Brenner BG, Roger M, Routy JP, Moisi D, Ntemgwa M, Matte C, Baril JG, Thomas R, Rouleau D, Bruneau J, Leblanc R, Legault M, Tremblay C, Charest H, Wainberg MA, Quebec Primary HIV Infection Study Group.** 2007. High rates of forward transmission events after acute/early HIV-1 infection. *J Infect Dis* **195:**951–959. PubMed
24. **Prabhu VS, Hutchinson AB, Farnham PG, Sansom SL.** 2009. Sexually acquired HIV infections in the United States due to acute-phase HIV transmission: an update. *AIDS* **23:**1792–1794. PubMed
25. **Hecht FM, Wang L, Collier A, Little S, Markowitz M, Margolick J, Kilby JM, Daar E, Conway B, Holte S, Network A, AIEDRP Network.** 2006. A multicenter observational study of the potential benefits of initiating combination antiretroviral therapy during acute HIV infection. *J Infect Dis* **194:**725–733. PubMed
26. **Smith MK, Rutstein SE, Powers KA, Fidler S, Miller WC, Eron JJ Jr, Cohen MS.** 2013. The detection and management of early HIV infection: a clinical and public health emergency. *J Acquir Immune Defic Syndr* **63**(Suppl 2)**:**S187–S199. PubMed
27. **Bennett D.** 2005. HIV [corrected] genetic diversity surveillance in the United States. *J Infect Dis* **192:**4–9. PubMed
28. **Brennan CA, Yamaguchi J, Devare SG, Foster GA, Stramer SL.** 2010. Expanded evaluation of blood donors in the United States for human immunodeficiency virus type 1 non-B subtypes and antiretroviral drug-resistant strains: 2005 through 2007. *Transfusion* **50:**2707–2712. PubMed
29. **Branson BM.** 2003. Point-of-care rapid tests for HIV antibodies. *J Lab Med* **27:**288–295.
30. **Paltiel AD, Walensky RP.** 2012. Home HIV testing: good news but not a game changer. *Ann Intern Med* **157:**744–746. PubMed
31. **Koval CE.** 2012. Home testing for HIV: hopefully, a step forward. *Cleve Clin J Med* **79:**713–716. PubMed
32. **Granade TC, Parekh BS, Phillips SK, McDougal JS.** 2004. Performance of the OraQuick and Hema-Strip rapid HIV antibody detection assays by non-laboratorians. *J Clin Virol* **30:**229–232. PubMed
33. **Gray RH, Makumbi F, Serwadda D, Lutalo T, Nalugoda F, Opendi P, Kigozi G, Reynolds SJ, Sewankambo NK,**

Wawer MJ. 2007. Limitations of rapid HIV-1 tests during screening for trials in Uganda: diagnostic test accuracy study. *BMJ* **335:**188. PubMed
34. **Campbell S, Fedoriw Y.** 2009. HIV testing near the patient: changing the face of HIV testing. *Clin Lab Med* **29:**491–501. PubMed
35. **Delaney KP, Branson BM, Uniyal A, Phillips S, Candal D, Owen SM, Kerndt PR.** 2011. Evaluation of the performance characteristics of 6 rapid HIV antibody tests. *Clin Infect Dis* **52:**257–263. PubMed
36. **Stekler JD, O'Neal JD, Lane A, Swanson F, Maenza J, Stevens C, Coombs RW, Dragavon J, Swenson PD, Golden M, Branson BM.** 2013. Relative accuracy of serum, whole blood, and oral fluid HIV tests among Seattle men who have sex with men. *J Clin Virol* **58**(Suppl 1)**:**e119–e122.
37. **Pilcher CD, Louie B, Facente S, Keating S, Hackett J Jr, Vallari A, Hall C, Dowling T, Busch MP, Klausner JD, Hecht FM, Liska S, Pandori MW.** 2013. Performance of rapid point-of-care and laboratory tests for acute and established HIV infection in San Francisco. *PLoS One* **8:**e80629. PubMed
38. **Masciotra S, Luo W, Youngpairoj AS, Kennedy MS, Wells S, Ambrose K, Sprinkle P, Owen SM.** 2013. Performance of the Alere Determine™ HIV-1/2 Ag/Ab Combo Rapid Test with specimens from HIV-1 seroconverters from the US and HIV-2 infected individuals from Ivory Coast. *J Clin Virol* **58**(Suppl 1)**:**e54–e58. PubMed
39. **Laperche S, Leballais L, Ly TD, Plantier JC.** 2012. Failures in the detection of HIV p24 antigen with the Determine HIV-1/2 Ag/Ab Combo rapid test. *J Infect Dis* **206:**1946–1947. (Author Reply, **206:**1949–1950.)
40. **Luo W, Masciotra S, Delaney KP, Charurat M, Croxton T, Constantine N, Blattner W, Wesolowski L, Owen SM.** 2013. Comparison of HIV oral fluid and plasma antibody results during early infection in a longitudinal Nigerian cohort. *J Clin Virol* **58**(Suppl 1)**:**e113–e118. PubMed
41. **Jani IV, Meggi B, Mabunda N, Vubil A, Sitoe NE, Tobaiwa O, Quevedo JI, Lehe JD, Loquiha O, Vojnov L, Peter TF.** 2014. Accurate early infant HIV diagnosis in primary health clinics using a point-of-care nucleic acid test. *J Acquir Immune Defic Syndr* **67:**e1–e4. PubMed
42. **Scott L, Gous N, Carmona S, Stevens W.** 2015. Laboratory evaluation of the Liat HIV Quant (IQuum) whole-blood and plasma HIV-1 viral load assays for point-of-care testing in South Africa. *J Clin Microbiol* **53:**1616–1621. PubMed
43. **Tanriverdi S, Chen L, Chen S.** 2010. A rapid and automated sample-to-result HIV load test for near-patient application. *J Infect Dis* **201**(Suppl 1)**:**S52–S58. PubMed
44. **Lee HH, Dineva MA, Chua YL, Ritchie AV, Ushiro-Lumb I, Wisniewski CA.** 2010. Simple amplification-based assay: a nucleic acid-based point-of-care platform for HIV-1 testing. *J Infect Dis* **201**(Suppl 1)**:**S65–S72. PubMed
45. **Ritchie AV, Ushiro-Lumb I, Edemaga D, Joshi HA, De Ruiter A, Szumilin E, Jendrulek I, McGuire M, Goel N, Sharma PI, Allain JP, Lee HH.** 2014. SAMBA HIV semiquantitative test, a new point-of-care viral-load-monitoring assay for resource-limited settings. *J Clin Microbiol* **52:**3377–3383. PubMed
46. **Ren A, Louie B, Rauch L, Castro L, Liska S, Klausner JD, Pandori MW.** 2008. Screening and confirmation of human immunodeficiency virus type 1 infection solely by detection of RNA. *J Med Microbiol* **57:**1228–1233. PubMed
47. **Patel P, Mackellar D, Simmons P, Uniyal A, Gallagher K, Bennett B, Sullivan TJ, Kowalski A, Parker MM, LaLota M, Kerndt P, Sullivan PS, Centers for Disease Control and Prevention Acute HIV Infection Study Group.** 2010. Detecting acute human immunodeficiency virus infection using 3 different screening immunoassays and nucleic acid amplification testing for human immunodeficiency virus RNA, 2006–2008. *Arch Intern Med* **170:**66–74. PubMed
48. **Torian LV, Eavey JJ, Punsalang AP, Pirillo RE, Forgione LA, Kent SA, Oleszko WR.** 2010. HIV type 2 in New York City, 2000–2008. *Clin Infect Dis* **51:**1334–1342. PubMed
49. **Nasrullah M, Ethridge SF, Delaney KP, Wesolowski LG, Granade TC, Schwendemann J, Boromisa RD, Heffelfinger JD, Owen SM, Branson BM.** 2011. Comparison of alternative interpretive criteria for the HIV-1 Western blot and results of the Multispot HIV-1/HIV-2 Rapid Test for classifying HIV-1 and HIV-2 infections. *J Clin Virol* **52**(Suppl 1)**:**S23–S27. PubMed
50. **Centers for Disease Control and Prevention (CDC).** 2011. HIV-2 infection surveillance—United States, 1987–2009. *MMWR Morb Mortal Wkly Rep* **60:**985–988. PubMed
51. **Styer LM, Sullivan TJ, Parker MM.** 2011. Evaluation of an alternative supplemental testing strategy for HIV diagnosis by retrospective analysis of clinical HIV testing data. *J Clin Virol* **52**(Suppl 1)**:**S35–S40. PubMed
52. **Pandori MW, Westheimer E, Gay C, Moss N, Fu J, Hightow-Weidman LB, Craw J, Hall L, Giancotti FR, Mak ML, Madayag C, Tsoi B, Louie B, Patel P, Owen SM, Peters PJ.** 2013. The Multispot rapid HIV-1/HIV-2 differentiation assay is comparable with the Western blot and an immunofluorescence assay at confirming HIV infection in a prospective study in three regions of the United States. *J Clin Virol* **58**(Suppl 1)**:**e92–e96. PubMed
53. **Mingle JA.** 1997. Differentiation of dual seropositivity to HIV 1 and HIV 2 in Ghanaian sera using line immunoassay (INNOLIA). *West Afr J Med* **16:**71–74. PubMed
54. **Blumberg RS, Sandstrom EG, Paradis TJ, Neumeyer DN, Sarngadharan MG, Hartshorn KL, Byington RE, Hirsch MS, Schooley RT.** 1986. Detection of human T-cell lymphotropic virus type III-related antigens and anti-human T-cell lymphotropic virus type III antibodies by anticomplementary immunofluorescence. *J Clin Microbiol* **23:**1072–1077. PubMed
55. **Torian LV, Forgione LA, Punsalang AE, Pirillo RE, Oleszko WR.** 2011. Comparison of Multispot EIA with Western blot for confirmatory serodiagnosis of HIV. *J Clin Virol* **52**(Suppl 1)**:**S41–S44. PubMed
56. **Ramos EM, Harb S, Dragavon J, Coombs RW.** 2013. Clinical performance of the Multispot HIV-1/HIV-2 Rapid Test to correctly differentiate HIV-2 from HIV-1 infection in screening algorithms using third and fourth generation assays and to identify cross reactivity with the HIV-1 Western blot. *J Clin Virol* **58**(Suppl 1)**:**e104–e107.
57. **Gottlieb GS, Sow PS, Hawes SE, Ndoye I, Coll-Seck AM, Curlin ME, Critchlow CW, Kiviat NB, Mullins JI.** 2003. Molecular epidemiology of dual HIV-1/HIV-2 seropositive adults from Senegal, West Africa. *AIDS Res Hum Retroviruses* **19:**575–584. PubMed
58. **Mor O, Mileguir F, Michaeli M, Levy I, Mendelson E.** 2014. Evaluation of the Bio-Rad Geenius HIV 1/2 assay as an alternative to the INNO-LIA HIV 1/2 assay for confirmation of HIV infection. *J Clin Microbiol* **52:**2677–2679. PubMed
59. **Malloch L, Kadivar K, Putz J, Levett PN, Tang J, Hatchette TF, Kadkhoda K, Ng D, Ho J, Kim J.** 2013. Comparative evaluation of the Bio-Rad Geenius HIV-1/2 Confirmatory Assay and the Bio-Rad Multispot HIV-1/2 Rapid Test as an alternative differentiation assay for CLSI M53 algorithm-I. *J Clin Virol* **58**(Suppl 1)**:**e85–e91. PubMed
60. **Novitsky V, Essex M.** 2012. Using HIV viral load to guide treatment-for-prevention interventions. *Curr Opin HIV AIDS* **7:**117–124. PubMed
61. **Aberg JA, Gallant JE, Ghanem KG, Emmanuel P, Zingman BS, Horberg MA, Infectious Diseases Society of**

America. 2014. Primary care guidelines for the management of persons infected with HIV: 2013 update by the HIV medicine association of the Infectious Diseases Society of America. *Clin Infect Dis* **58:**e1–e34. PubMed

62. **Panel on Antiretroviral Guidelines for Adults and Adolescents.** 28 January 2016. *Guidelines for the Use of Antiretroviral Agents in HIV-1-Infected Adults and Adolescents*. AIDSinfo, Department of Health and Human Services, Washington, DC. http://www.aidsinfo.nih.gov/ContentFiles/AdultandAdolescentGL.pdf.
63. **Hecht FM, Busch MP, Rawal B, Webb M, Rosenberg E, Swanson M, Chesney M, Anderson J, Levy J, Kahn JO.** 2002. Use of laboratory tests and clinical symptoms for identification of primary HIV infection. *AIDS* **16:**1119–1129. PubMed
64. **Gueudin M, Plantier JC, Lemée V, Schmitt MP, Chartier L, Bourlet T, Ruffault A, Damond F, Vray M, Simon F.** 2007. Evaluation of the Roche Cobas TaqMan and Abbott RealTime extraction-quantification systems for HIV-1 subtypes. *J Acquir Immune Defic Syndr* **44:**500–505. PubMed
65. **Lin HJ, Pedneault L, Hollinger FB.** 1998. Intra-assay performance characteristics of five assays for quantification of human immunodeficiency virus type 1 RNA in plasma. *J Clin Microbiol* **36:**835–839. PubMed
66. **Karasi JC, Dziezuk F, Quennery L, Förster S, Reischl U, Colucci G, Schoener D, Seguin-Devaux C, Schmit JC.** 2011. High correlation between the Roche COBAS® AmpliPrep/COBAS® TaqMan® HIV-1, v2.0 and the Abbott m2000 RealTime HIV-1 assays for quantification of viral load in HIV-1 B and non-B subtypes. *J Clin Virol* **52:**181–186. PubMed
67. **Dykes C, Demeter LM.** 2007. Clinical significance of human immunodeficiency virus type 1 replication fitness. *Clin Microbiol Rev* **20:**550–578. PubMed
68. **Cohen CJ, Hunt S, Sension M, Farthing C, Conant M, Jacobson S, Nadler J, Verbiest W, Hertogs K, Ames M, Rinehart AR, Graham NM, Team VS, VIRA3001 Study Team.** 2002. A randomized trial assessing the impact of phenotypic resistance testing on antiretroviral therapy. *AIDS* **16:**579–588. PubMed
69. **Meynard JL, Vray M, Morand-Joubert L, Race E, Descamps D, Peytavin G, Matheron S, Lamotte C, Guiramand S, Costagliola D, Brun-Vézinet F, Clavel F, Girard PM, Narval Trial Group.** 2002. Phenotypic or genotypic resistance testing for choosing antiretroviral therapy after treatment failure: a randomized trial. *AIDS* **16:**727–736. PubMed
70. **Weinstein MC, Goldie SJ, Losina E, Cohen CJ, Baxter JD, Zhang H, Kimmel AD, Freedberg KA.** 2001. Use of genotypic resistance testing to guide HIV therapy: clinical impact and cost-effectiveness. *Ann Intern Med* **134:**440–450. PubMed
71. **Snedecor SJ, Khachatryan A, Nedrow K, Chambers R, Li C, Haider S, Stephens J.** 2013. The prevalence of transmitted resistance to first-generation non-nucleoside reverse transcriptase inhibitors and its potential economic impact in HIV-infected patients. *PLoS One* **8:**e72784. PubMed
72. **Erali M, Page S, Reimer LG, Hillyard DR.** 2001. Human immunodeficiency virus type 1 drug resistance testing: a comparison of three sequence-based methods. *J Clin Microbiol* **39:**2157–2165. PubMed
73. **Günthard HF, Wong JK, Ignacio CC, Havlir DV, Richman DD.** 1998. Comparative performance of high-density oligonucleotide sequencing and dideoxynucleotide sequencing of HIV type 1 pol from clinical samples. *AIDS Res Hum Retroviruses* **14:**869–876. PubMed
74. **Johnson JA, Li JF, Wei X, Lipscomb J, Irlbeck D, Craig C, Smith A, Bennett DE, Monsour M, Sandstrom P, Lanier ER, Heneine W.** 2008. Minority HIV-1 drug resistance mutations are present in antiretroviral treatment-naïve populations and associate with reduced treatment efficacy. *PLoS Med* **5:**e158. PubMed
75. **Johnson JA, Li JF, Wei X, Lipscomb J, Bennett D, Brant A, Cong ME, Spira T, Shafer RW, Heneine W.** 2007. Simple PCR assays improve the sensitivity of HIV-1 subtype B drug resistance testing and allow linking of resistance mutations. *PLoS One* **2:**e638. PubMed
76. **Palmer S, Kearney M, Maldarelli F, Halvas EK, Bixby CJ, Bazmi H, Rock D, Falloon J, Davey RT Jr, Dewar RL, Metcalf JA, Hammer S, Mellors JW, Coffin JM.** 2005. Multiple, linked human immunodeficiency virus type 1 drug resistance mutations in treatment-experienced patients are missed by standard genotype analysis. *J Clin Microbiol* **43:**406–413. PubMed
77. **Avidor B, Girshengorn S, Matus N, Talio H, Achsanov S, Zeldis I, Fratty IS, Katchman E, Brosh-Nissimov T, Hassin D, Alon D, Bentwich Z, Yust I, Amit S, Forer R, Vulih Shultsman I, Turner D.** 2013. Evaluation of a benchtop HIV ultradeep pyrosequencing drug resistance assay in the clinical laboratory. *J Clin Microbiol* **51:**880–886. PubMed
78. **MacArthur RD, Novak RM.** 2008. Reviews of anti-infective agents: maraviroc: the first of a new class of antiretroviral agents. *Clin Infect Dis* **47:**236–241. PubMed
79. **Tsibris AM, Sagar M, Gulick RM, Su Z, Hughes M, Greaves W, Subramanian M, Flexner C, Giguel F, Leopold KE, Coakley E, Kuritzkes DR.** 2008. In vivo emergence of vicriviroc resistance in a human immunodeficiency virus type 1 subtype C-infected subject. *J Virol* **82:**8210–8214. PubMed
80. **Chikere K, Chou T, Gorry PR, Lee B.** 2013. Affinofile profiling: how efficiency of CD4/CCR5 usage impacts the biological and pathogenic phenotype of HIV. *Virology* **435:**81–91. PubMed
81. **Raymond S, Saliou A, Nicot F, Delobel P, Dubois M, Carcenac R, Sauné K, Marchou B, Massip P, Izopet J.** 2013. Characterization of CXCR4-using HIV-1 during primary infection by ultra-deep pyrosequencing. *J Antimicrob Chemother* **68:**2875–2881. PubMed
82. **Centers for Disease Control and Prevention and Association of Public Health Laboratories.** 2014. *Laboratory Testing for the Diagnosis of HIV Infection: Updated Recommendations*. Centers for Disease Control and Prevention, Atlanta, GA. http://stacks.cdc.gov/view/cdc/23447.
83. **Centers for Medicare and Medicaid Services.** 2 February 2016. *Clinical Laboratory Improvement Amendments (CLIA)*. Centers for Medicare and Medicaid Services, Baltimore, MD. https://www.cms.gov/Regulations-and-Guidance/Legislation/CLIA/index.html?redirect=/clia/.

Immunodeficiency Diseases

section K

VOLUME EDITOR: BARBARA DETRICK

SECTION EDITORS: KATHLEEN E. SULLIVAN AND HOWARD M. LEDERMAN

The Primary Immunodeficiency Diseases

HOWARD M. LEDERMAN

73

Patients with primary immunodeficiency diseases most often are recognized because of their increased susceptibility to infection (chronic or recurrent infections without other explanation, infection with an organism of low virulence, or infection of unusual severity). However, these patients may also present with autoimmune or inflammatory disorders (e.g., hemolytic anemia, inflammatory bowel disease, vasculitis, or systemic lupus erythematosus) or as part of a syndrome complex (Table 1). Finally, in the future we will see an increasing number of people who are identified as having an immunodeficiency because of an abnormal newborn-screening test for T-cell receptor-excision circles (TRECs) or a mutation identified by genome sequencing.

SYMPTOMS OFTEN CAN GUIDE THE LABORATORY EVALUATION

The type of pathogen and the location of the infection may give valuable insight into the nature of the immunologic defect. For example, individuals with antibody deficiencies are unusually susceptible to encapsulated bacteria and enteroviruses, which cause infections along mucosal surfaces. Individuals with defects in cell-mediated immunity can have problems with almost any microorganism, including opportunistic pathogens. Individuals with complement deficiencies most often present with bacteremia, septic arthritis, and meningitis, caused by encapsulated bacteria. Phagocytic disorders are characterized by bacterial and fungal infections of the skin and abscesses in the reticuloendothelial system (lymph nodes, spleen, and liver). Defects in natural killer cell function cause life-threatening viral infections and hemophagocytic lymphohistiocytosis (HLH).

Autoimmune and inflammatory diseases are more commonly seen in particular primary immunodeficiency diseases, most notably common variable immunodeficiency, selective immunoglobulin A (IgA) deficiency, chronic mucocutaneous candidiasis, and deficiencies of early components of the classical complement pathway (C1 to C4).

When immunodeficiency is part of a constellation of signs and symptoms in a syndrome complex, the diagnosis of immunodeficiency may be made before there are any clinical manifestations of that deficiency. For instance, children with DiGeorge syndrome are most often first identified because of the neonatal presentation of congenital heart disease and/or hypocalcemic tetany. This should lead to T-lymphocyte evaluation prior to the onset of opportunistic infections. Similarly, a diagnosis of Wiskott-Aldrich syndrome can often be made in young boys with eczema and thrombocytopenia even prior to the onset of infections.

LABORATORY EVALUATION

Although immune system dysfunction can be suspected by the clinician after careful review of the history and physical exam, specific diagnoses are rarely evident without the use of the laboratory. However, the types of infections and other symptoms should help to focus the laboratory workup on specific compartments of the immune system (Table 2).

TABLE 1 Examples of immunodeficiency syndromes

Syndrome	Usual clinical presentation(s)	Immunologic abnormality
DiGeorge syndrome	Congenital heart disease, hypoparathyroidism, abnormal facies	Thymic hypoplasia
Wiskott-Aldrich syndrome	Thrombocytopenia, eczema	Variable B- and T-lymphocyte dysfunction
Ataxia-telangiectasia	Ataxia, telangiectasia	Variable B- and T-lymphocyte dysfunction
Ivemark syndrome	Congenital heart disease, bilateral three-lobed lungs	Asplenia
Polyendocrinopathy syndrome	Endocrine organ dysfunction	Chronic mucocutaneous candidiasis

doi:10.1128/9781555818722.ch73

TABLE 2 Patterns of illness associated with primary immunodeficiency

Disorder	Illnesses	
	Infection	Other
Antibody	Sinopulmonary (pyogenic bacteria) Gastrointestinal (enterovirus, giardiasis)	Autoimmune disease (autoantibodies, inflammatory bowel disease)
Cell-mediated immunity	Pneumonia (pyogenic bacteria, *Pneumocystis jiroveci*, and viruses) Gastrointestinal (viruses) Skin, mucous membranes (fungi)	
Complement	Sepsis and other blood-borne infections (streptococci, pneumococci, and neisseriae)	Autoimmune disease (systemic lupus erythematosus, glomerulonephritis)
Phagocytosis	Skin, reticuloendothelial system, abscesses (*Staphylococcus*, enteric bacteria, fungi, and mycobacteria)	
Natural killer cells	Herpes family and papilloma viruses	Hemophagocytic lymphohistiocytosis

Screening tests that should be performed for almost all patients include a complete blood count with differential, and quantitative measurement of serum immunoglobulins. Other tests should be guided by the clinical features of the patient (Table 3). Finally, whenever primary immunodeficiency is suspected, consideration must also be given to secondary causes of immunodeficiency, including infections (e.g., HIV and Epstein-Barr virus), therapy with anti-inflammatory or immunosuppressive medications (e.g., corticosteroids, rituximab), and other underlying illnesses (e.g., lymphoreticular neoplasms and protein-losing enteropathy). Details about the selection and performance of specific laboratory tests are discussed in the following chapters, organized by immunologic compartment: antibody, cell-mediated immunity (severe combined immunodeficiency), complement, phagocytes, and natural killer cells.

TABLE 3 Screening tests for primary immunodeficiency

Suspected abnormality	Diagnostic test(s)
Antibody	Quantitative immunoglobulins (IgG, IgA, and IgM) Antibody response to immunization
Cell-mediated immunity	Lymphocyte count T-lymphocyte enumeration (CD4 and CD8) HIV serology Delayed-type hypersensitivity tests
Complement	Total hemolytic complement
Phagocytosis	Neutrophil count Nitroblue tetrazolium dye test or equivalent
Natural killer (NK) cells	NK cell enumeration NK function, measurement of intracellular perforin

SUGGESTED READING

1. **Al-Herz W, Bousfiha A, Casanova JL, Chatila T, Conley ME, Cunningham-Rundles C, Etzioni A, Franco JL, Gaspar HB, Holland SM, Klein C, Nonoyama S, Ochs HD, Oksenhendler E, Picard C, Puck JM, Sullivan K, Tang ML.** 2014. Primary immunodeficiency diseases: an update on the classification from the international union of immunological societies expert committee for primary immunodeficiency. *Front Immunol* **5:**162.
2. **Chou J, Ohsumi TK, Geha RS.** 2012. Use of whole exome and genome sequencing in the identification of genetic causes of primary immunodeficiencies. *Curr Opin Allergy Clin Immunol* **2:**623–628.
3. **Ochs HD, Hagin D.** 2014. Primary immunodeficiency disorders: general classification, new molecular insights, and practical approach to diagnosis and treatment. *Ann Allergy Asthma Immunol* **112:**489–495.
4. **Oliveira JB, Fleisher TA.** 2010. Laboratory evaluation of primary immunodeficiencies. *J Allergy Clin Immunol* **125:**S297–S305.
5. **Rozenzweig SD, Fleisher TA.** 2014. Overview of laboratory studies for evaluating primary immune deficiency disorders, p 61–72. *In* Sullivan KE, Stiehm ER (ed), *Stiehm's Immune Deficiencies*. Elsevier Academic Press, Amsterdam, The Netherlands.

Severe Combined Immune Deficiency: Newborn Screening

JAMES W. VERBSKY AND JOHN M. ROUTES

74

PURPOSE AND BENEFIT OF NEWBORN SCREENING

The history of newborn screening (NBS) in the United States began in 1963, when Guthrie demonstrated that phenylketonuria (PKU) can be detected using dried blood spots (DBSs) on filter paper from newborns (1). Neonatal testing for PKU proved to be inexpensive, sensitive, specific, and amenable to high-throughput screening. The ability to screen neonates for other serious diseases increased dramatically, and in 1968, Wilson and Jungner published a landmark report that included guidelines for population-based health screening (Table 1) (2). This report tried to balance the desire for early detection and treatment of disease with the potential harms to patients, family, and society. The report defined principles for NBS programs and has undergone revisions to address concerns for both newborn screening and population-based screening programs in general (Table 1) (3–5).

SCID as a Model Disorder for NBS

Severe combined immunodeficiency (SCID) is a genetically heterogeneous group of disorders with a common phenotype characterized by profound deficiencies in cellular and humoral immunity (6–9). The vast majority of infants with SCID lack lymphoid tissue. However, this finding is frequently missed on routine physical examination, and most infants otherwise appear physically normal at birth. Subsequently, these infants develop failure to thrive, severe infections, and ultimately death, without intervention. Absent NBS, the median age of diagnosis of SCID is 6.6 months, with an average delay of 2 months from the onset of symptoms to diagnosis (10, 11). Viral and opportunistic infections acquired in the first few months of life can be persistent and fatal, even with aggressive treatment (9, 11, 12). Importantly, the current Centers for Disease Control and Prevention recommendation for vaccinations includes the live attenuated rotavirus vaccine at 2 months, which causes life-threatening rotavirus infection in children with undiagnosed SCID (13–16).

SCID is estimated to occur in 1 in 50,000 to 100,000 live births (17). More recent estimates based on preliminary data by NBS screening programs in the United States put the incidence closer to 1:40,000 to 1:60,000 (18–20). SCID is treated through immunologic reconstitution by hematopoietic stem cell transplantation (HSCT) (6) or, in certain cases, gene therapy (e.g., X-linked SCID, adenosine-deaminase [ADA] deficiency) (21, 22). ADA deficiency can also be treated with enzyme replacement (23). Children who receive HSCT early in life, before the development of severe infections, have improved survival and immune reconstitution (6, 10, 24). For example, at one center, infants who received HSCT before 3.5 months had a 95% survival rate, compared with a 76% survival rate for those who received HSCT later (6).

There are several characteristics that fulfill the criteria proposed by Wilson and Jungner and that make SCID an ideal disease for NBS (2). The incidence of the disease is high enough to warrant screening, there is a test amenable to population-based screening that detects SCID (i.e., the T-cell receptor excision circle [TREC] assay), and there is a definitive and potentially curative treatment for the disease. Finally, the cost associated with screening all infants and the treatment of the infants found to have SCID needs to be considered. This is a complex question and can be definitively answered only when NBS screening for SCID is widely used. However, there are studies that have modeled NBS for SCID, taking into account numerous factors, and indicate that it is cost effective if the screening test is sufficiently robust and relatively inexpensive (25).

BRIEF OVERVIEW OF TYPES OF SCREENING AND METHODOLOGY

Newborn screening refers to any testing done on all infants during the newborn period and includes both blood-based and other modalities. For example, NBS for hearing defects is performed in a number of states. Blood-based screening tests include sickle cell anemia, hypothyroidism, and cystic fibrosis. With the advent of tandem mass spectroscopy, the number of metabolic disorders screened at birth increased greatly. SCID is the first disease in which the NBS assay uses DNA-based technology.

Current NBS programs in the United States and elsewhere (Brazil, Canada) use the TREC assay to screen neonates for SCID. However, other methods of screening for SCID have been proposed, such as determining the absolute lymphocyte count from a complete blood count (CBC) or by flow cytometry (9, 26). These screening modalities have significant shortcomings, including the cost of a CBC and the need to obtain, transport, and analyze an additional blood sample. A normal absolute lymphocyte count will

doi:10.1128/9781555818722.ch74

TABLE 1 Criteria for newborn screening[a]

The incidence of the disease should be sufficiently high to warrant screening.
The disorder should not be readily identifiable by physical examination.
The disorder should cause serious medical complications.
There should be an accepted treatment for patients with recognized disease.
There must be a sensitive and specific screening test.
The screening test should be economically viable.
There should be a definitive confirmatory test.

[a]Adapted from reference 55.

result in a small but significant rate of false negatives in infants with SCID due to maternal engraftment of T cells, certain subtypes of SCID that have normal numbers of B and NK cells, or SCID due to hypomorphic mutations that result in expansion of a few clones of T cells (9, 27, 28).

Other modalities to detect SCID have been proposed, including assays to detect interleukin-7 (IL-7) or T cell-specific proteins in the peripheral blood. High IL-7 levels are associated with T-lymphopenic states, and one study demonstrated that 11 of 13 infants with SCID had high levels of IL-7 in the serum or extracts from DBSs (29). The use of the IL-7 assay to detect SCID has not been replicated to date. Other studies have evaluated serum levels of T cell-specific proteins, including CD3 or CD45 (30). These modalities have not been implemented as population-based screening tests, but have been proposed as ancillary or follow-up testing.

The TREC Assay

The TREC assay is currently the test used for neonatal screening for SCID and relies on the fact that all forms of SCID lead to a reduction in the number of naive T cells in the affected infant. The theoretical basis of the TREC assay is as follows. In order to exit the thymus, all T cells must express a functional T cell receptor (TCR). In the normal development of T cells, the variable (V), diverse (D), and joining (J) segments of the TCR genes undergo a process of DNA rearrangement that involves DNA breakage and repair. This rearrangement process brings distant segments of the TCR genes together (VDJ rearrangement). The by-products of this process are small, circular, nonreplicating pieces of DNA known as TRECs. The δRec-ψJα TREC is produced by approximately 70% of all T cells that express the α/β T cell receptor, which is the most common type of TCR produced by the thymus (31). By performing RT-qPCR using DNA extracted from the DBS, the TREC assay enumerates the copy number of the δRec-ψJα TREC (32). Since TRECs do not replicate, the number of TRECs per cell is diluted as T cells divide into memory T cells. Consequently, TRECs serve as a biomarker of naive T cells (33).

The ability of the TREC assay to serve as a biomarker for naive T cells is extremely important. In some cases of SCID or so-called "leaky" SCID, the specific mutation may result in a gene that encodes for a protein that has partial activity. Consequently, a small number of T cells may be generated in the thymus and then expand in the periphery of the affected infant and cause disease (e.g., Omenn's syndrome). In other cases, T cells from the mother may engraft in the infant. Infants with hypomorphic mutations in genes that cause SCID or Omenn's syndrome, or infants with maternally engrafted T cells, may not have profound T cell lymphopenia. However, the majority of T cells in these infants will have expanded by cellular division and are memory T cells (CD45RO+). TRECs do not replicate, and therefore the number of TRECs enumerated by the TREC assay will be abnormally low. Thus, regardless of the molecular cause, in all forms of SCID there is a profound reduction of naive T cells that will be detected by the TREC assay (28, 31, 34). It is important to acknowledge that the TREC assay will detect SCID as well as known and unknown causes of T cell lymphopenia (TCL).

NBS cards are sent to central labs in extremely variable environmental conditions, which may result in poor DNA template integrity. In addition, the DBS may contain substances that inhibit the PCR component of the TREC assay. For example, there are times when the blood is obtained through an intravenous line rather than the conventional heel stick (35). In either of these cases, the resulting TREC number may be falsely low. This important issue is addressed by performing RT-qPCR using the same DNA as the TREC assay on a housekeeping gene such as β-actin.

Optimization and Validation of the RT/PCR Reaction for TRECs

Successful implementation of NBS for SCID using the TREC assay requires careful optimization of the assay to ensure sensitivity and reproducibility. Optimizing the yield of DNA extracted from DBSs, as well as amplification efficiency of the RT-qPCR reaction, is essential. Once optimized, reproducibility of the assay should be determined on DNA isolated from DBSs. Finally, the sensitivity of the assay should be determined. This is ideally determined with blood spots with specific amounts of TRECs added, which can be accomplished with leukocyte-poor blood or blood from a known SCID patient. Attempts have been made to standardize the TREC assay with cell lines that express a single TREC per cell (36). Finally, a pilot study using large numbers of anonymized NBS cards should be performed to determine the range and variability of the assay (34).

Determination of TREC Cutoff Value and Sensitivity

As NBS for SCID moves forward in other states and countries, the number of TRECs considered abnormally low as determined by the TREC assay must be determined empirically. The different laboratories performing the TREC assay use different methodologies of DNA extraction and RT-qPCR. Even laboratories utilizing the very similar methodologies have reported different sensitivities in the TREC assay. Thus, before implementation for NBS, it is important that each laboratory establish its unique TREC cutoff values. In Wisconsin, the number of TRECs considered abnormally low was empirically determined based on a pilot study of 10,000 anonymized blood spots (34). In addition, the cutoff value for the TREC assay needs to be adjusted longitudinally, as small changes in any component of the assay may result in slightly enhanced or reduced assay efficiency.

During the first 5 years of screening for SCID in Wisconsin, 340,037 infants were screened; 0.03% of term births and 0.48% of preterm births (<37 weeks adjusted gestational age [AGA]) were abnormal on initial testing (Table 1) (20). The rate of inconclusive results due to a low β-actin level was 0.03% in term infants and 1.25% in preterm infants. Thus, the repeat testing rate of preterm infants (inconclusive and abnormal results) and full-term infants (inconclusive results) was 0.18%. In total, 110 infants were ultimately classified as abnormal after repeat screening of inconclusive results (20).

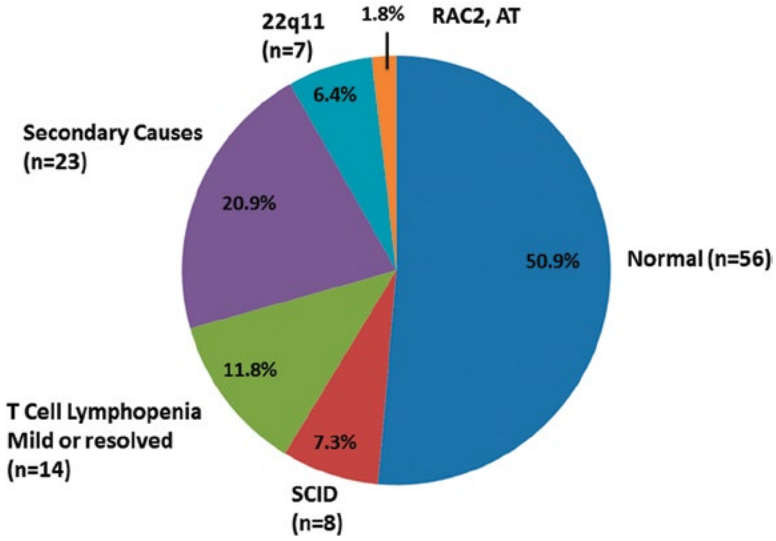

FIGURE 1 Final diagnoses of 110 infants with abnormal TREC screen for SCID. Secondary causes include metabolic disorders, chromosomal abnormalities, infections (e.g., necrotizing enterocolitis, sepsis). 22q11, 22q11 deletion syndrome; AT, ataxia telangiectasia.

Of these, 56 infants were ultimately found to be normal, resulting in a false-positive rate of 0.016% and a specificity of 99.98% (Fig. 1). Fifty-four infants were found to have TCL of varying degrees, giving a positive predictive value of the TREC assay predicting TCL of 49%.

FOLLOW-UP ALGORITHM AND RESULTS OF NBS FOR SCID

In Wisconsin, an algorithm was developed that established a standard operating protocol for the TREC assay, and this was in part based on the high false-positive rate of preterm infants (35). Briefly, full-term infants with a TREC level below the cutoff were first tested for DNA integrity by analyzing β-actin by RT-qPCR. If the β-actin level was normal with abnormally low TRECs, an abnormal report was issued, and the primary care provider was contacted for confirmatory testing by flow cytometry. If the β-actin result was low, an inconclusive report was issued, and the screening test was repeated with a new newborn screening card. For preterm infants with an abnormal or inconclusive TREC assay, the screening test was repeated either until it was normal or until the infant reached 37 weeks AGA, at which time the infant's results were reclassified as an abnormal. Lymphocyte subset analysis by flow cytometry was recommended on all full-term infants and all preterm infants with an AGA of 37 weeks with an abnormal TREC assay. Infants with an abnormal flow cytometry were then referred for evaluation by a clinical immunologist.

Each state that has implemented NBS for SCID has generated an algorithm for follow up of positive NBS results. In some states, DNA integrity is determined using a control gene (β-actin or RNase P) at the time of the initial TREC analysis using multiplex assays (37). In contrast, other states such as Wisconsin check DNA integrity only if the TREC assay is abnormal (19, 35). Determining DNA integrity at the time of TREC analysis is convenient, but it may increase the cost of the assay due to the need for extra primers and fluorescent probes. In Wisconsin, a repeat TREC assay is performed using DNA obtained from a different part of the DBS on all abnormal TREC assays. By repeating abnormal TREC assays and retesting infants until they reach an AGA of 37 weeks, the number of infants who have needed the much more costly lymphocyte subset analysis performed by flow cytometry has been reduced.

Findings in 5 Years of NBS in Wisconsin

Of infants with an abnormal TREC assay who were found to have TCL, 43% ($n = 23$) had secondary causes for their TCL such as anatomic abnormalities of the lymphatics, chromosomal abnormalities, multiple congenital anomalies, infections (necrotizing enterocolitis or sepsis), or a presumed metabolic disorder (Table 2). The remaining 30 infants had primary TCL, including 7 infants with 22q11.2 deletion syndrome, 14 infants with idiopathic mild TCL, 8 infants with SCID/severe TCL, 1 infant with ataxia telangiectasia, and 1 infant with a *RAC2* mutation. Of note, no known cases of SCID have been identified in infants screened in Wisconsin since the implementation of neonatal screening in 2008. For comparison, we show the results of 2 years of NBS for SCID of 993,724 infants in California (Table 3).

TABLE 2 Initial screening results and results of confirmatory flow cytometry[a]

Testing	Abnormal	Inconclusive
Initial testing (340,037 births)		
Preterm (30,664; 9%)	147 (0.48%)	382 (1.25%)
Term (309,373; 91%)	99 (0.03%)	90 (0.03%)
Second testing (110 abnormal)	54 (49%) (lymphopenic)	56

[a]Adapted from reference 55.

TABLE 3 Final diagnoses of patients with SCID or severe TCL from Wisconsin and California[a]

Wisconsin
4 T–B+NK+
3 Diagnosis unknown
1 Complete DiGeorge
4 T–B–NK+
1 RAG1−/−
2 Likely RAG1−/−
1 unknown
1 ADA
1 Ataxia telangiectasia
1 RAC2
California
5 T–B+NK–
4 IL2TG
1 Jak3
3 T–B–NK+
3 RAG1−/−
6 T–B+NK+
3 IL7R
1 Complete Digeorge
1 RMRP
1 Unknown

[a]Adapted from references 20 and 56.

LIMITATIONS WITH SCID AND NON-SCID IDENTIFICATION THROUGH NBS PROGRAMS

Vunerable Populations (Amish, Athabascans, etc.)

It is clear that the TREC assay is effective at identifying SCID. However, all mass screening programs require screening of all infants to ensure that these rare patients are not missed. This becomes problematic with certain populations that may be unwilling to undergo NBS, such as the Amish, Mennonite, or Navajo Indian populations. Due to consanguinity, these populations exhibit much higher rates of SCID than the general population (38). In these situations, babies with SCID may be missed until they have SCID-defining illnesses. It is essential that outreach programs approach these communities to inform them of the NBS assays, what they detect, and how these disorders are treated, in hopes of alleviating any fears regarding the screening program.

Immune Deficiencies Not Detected

Although the TREC assay detects a variety of causes of SCID and TCL, several serious immune defects could be missed by the TREC assay. In bare lymphocyte syndrome, there is a defect in HLA class II expression resulting in loss of development of CD4 T cells. Since CD8 cells are still present, these patients likely will express approximately one-third the level of TRECs present in a normal infant, which could be above the cutoff value. In this regard, an infant screened for SCID who had bare lymphocyte syndrome was not detected (39, 40). In delayed ADA deficiency, the initial TREC value at birth can be normal but become negative later in life (41). In addition, there are serious SCID-like illnesses that do not result in a lack of T cells. Defects in ORA1, STIM1, or CD25 result in illness with a severe propensity to opportunistic and other infections, but these disorders can have relatively normal T cell counts (42–45). Thus, primary immunodeficiencies should still be considered in children presenting with SCID-defining disorders (e.g., failure to thrive, opportunistic or severe infections), even if NBS for SCID was normal.

Since the TREC assay detects any form of TCL, it is not uncommon to detect an infant with a T cell level that is low but not at levels typically seen in SCID (<200 T cells/mm^3); these disorders can be considered combined immunodeficiencies (CID). The decision of whether to perform HSCT on infants with CID can be difficult, particularly if a specific genetic mutation known to cause CID is not identified. This illustrates why it is of the utmost importance that infants with SCID or CID identified by the TREC assay should be referred to centers of excellence in the diagnosis and treatment of primary immunodeficiencies.

The more widespread implementation of the NBS using the TREC assay has resulted in some unexpected findings. One infant was identified with immunodeficiency due to a *de novo* mutation in the *RAC2* gene, the second reported case of this primary immunodeficiency (46). The previously described case of a *RAC2* mutation resulted in immunodeficiency secondary to dysfunction of neutrophils (47). However, immunological assessment of the infant identified by neonatal screening for TCL demonstrated both neutrophil and T cell abnormalities. In addition, two cases of Jacobsen syndrome have been detected, and reports have linked this chromosomal abnormality with the development of common variable immunodeficiency (20, 48–50). Finally, a case of DOCK8 deficiency has been detected by the TREC assay (51). These cases illustrate that the NBS using the TREC assay will identify infants with known and unknown cellular immunodeficiencies.

Finally, the TREC assay will not detect defects in B cell development, such as x-linked agammaglobulinemia. A RT-qPCR-based assay has been developed that detects excision circles that are generated during B cell receptor formation. Similar to T cell receptor development, B cell receptors are generated by the rearrangement of the light chains of the B cell receptor (i.e., kappa and lambda chains) and the heavy chain of the B cell receptor, resulting in the production of circular episomal pieces of DNA known as kappa receptor excision circles (KRECs). The KREC assay is able to detect all forms of inherited agammaglobulinemia characterized by an absence or near absence of naive B cells (52, 53). Since the KREC assay is performed in a similar manner to the TREC assay, a TREC/KREC multiplexed assay could be used to screen for defects in both T and B cell development. This multiplexed assay could be performed with a minimal increase in cost, as only an extra primer pair and probe need to be added to the RT-qPCR assay. Although congenital agammaglobulinemias do not inevitably result in death, when they are undiagnosed they are associated with significant morbidity and mortality (54). As definitive therapy that may lead to a normal or near-normal life expectancy exists for congenital agammaglobulinemias (i.e., intravenous or subcutaneous immunoglobulin replacement), it appears that these disorders may fulfill the abridged criteria for NBS proposed by Wilson and Jungner. However, the KREC assay has yet to be implemented on a statewide basis, and the issue of fulfilling the NBS criteria is still a matter of debate.

SUMMARY

The establishment and implementation of the TREC assay for SCID has proven highly effective in the detection of SCID as well as other primary immune deficiencies. Successful implementation of this program requires a validated,

sensitive assay and appropriate algorithms for follow up of abnormal results. Since this assay detects a variety of defects other than SCID, and evaluating these infants can be difficult, referral to a clinical immunologist with expertise in the evaluation and treatment of SCID and other primary immune deficiencies is recommended. The DNA-based TREC assay is amenable to multiplex analysis, which allows the addition of other tests such as the KREC assay for B cell defects with incremental increases in cost.

REFERENCES

1. **Guthrie R, Susi A.** 1963. A simple phenylalanine method for detecting phenylketonuria in large populations of newborn infants. *Pediatrics*. **32:**338–343.
2. **Wilson JM, Jungner G.** 1968. *Principles and Practice of Screening for Disease*. World Health Organization, Geneva, Switzerland. http://www.who.int/bulletin/volumes/86/4/07-050112BP.pdf
3. **Andermann A, Blancquaert I, Beauchamp S, Déry V.** 2008. Revisiting Wilson and Jungner in the genomic age: a review of screening criteria over the past 40 years. *Bull World Health Organ* **86:**317–319. PubMed
4. **Andermann A, Blancquaert I, Beauchamp S, Costea I.** 2011. Guiding policy decisions for genetic screening: developing a systematic and transparent approach. *Public Health Genomics* **14:**9–16. PubMed
5. **Anonymous.** 2006. Newborn screening: toward a uniform screening panel and system. *Genet Med* **8**(Suppl 1)**:**1S–252S.
6. **Buckley RH, Schiff SE, Schiff RI, Markert L, Williams LW, Roberts JL, Myers LA, Ward FE.** 1999. Hematopoietic stem-cell transplantation for the treatment of severe combined immunodeficiency. *N Engl J Med* **340:**508–516. PubMed
7. **Buckley RH.** 2002. Primary cellular immunodeficiencies. *J Allergy Clin Immunol* **109:**747–757. PubMed
8. **Notarangelo LD.** 2010. Primary immunodeficiencies. *J Allergy Clin Immunol* **125**(Suppl 2)**:**S182–S194. PubMed
9. **Buckley RH.** 2004. Molecular defects in human severe combined immunodeficiency and approaches to immune reconstitution. *Annu Rev Immunol* **22:**625–655.
10. **Myers LA, Patel DD, Puck JM, Buckley RH.** 2002. Hematopoietic stem cell transplantation for severe combined immunodeficiency in the neonatal period leads to superior thymic output and improved survival. *Blood* **99:**872–878. PubMed
11. **Stephan JL, Vlekova V, Le Deist F, Blanche S, Donadieu J, De Saint-Basile G, Durandy A, Griscelli C, Fischer A.** 1993. Severe combined immunodeficiency: a retrospective single-center study of clinical presentation and outcome in 117 patients. *J Pediatr* **123:**564–572. PubMed
12. **Adeli MM, Buckley RH.** 2010. Why newborn screening for severe combined immunodeficiency is essential: a case report. *Pediatrics* **126:**e465–e469. PubMed
13. **Cortese MM, Parashar UD, Centers for Disease Control and Prevention.** 2009. Prevention of rotavirus gastroenteritis among infants and children: recommendations of the Advisory Committee on Immunization Practices (ACIP). *MMWR Recomm Rep* **58** (RR-2)**:**1–25. PubMed
14. **Patel NC, Hertel PM, Estes MK, de la Morena M, Petru AM, Noroski LM, Revell PA, Hanson IC, Paul ME, Rosenblatt HM, Abramson SL.** 2010. Vaccine-acquired rotavirus in infants with severe combined immunodeficiency. *N Engl J Med* **362:**314–319. PubMed
15. **Werther RL, Crawford NW, Boniface K, Kirkwood CD, Smart JM.** 2009. Rotavirus vaccine induced diarrhea in a child with severe combined immune deficiency. *J Allergy Clin Immunol* **124:**600. doi:10.1016/j.jaci.2009.07.005. PubMed
16. **Uygungil B, Bleesing JJ, Risma KA, McNeal MM, Rothenberg ME.** 2010. Persistent rotavirus vaccine shedding in a new case of severe combined immunodeficiency: A reason to screen. *J Allergy Clin Immunol* **125:**270–271. PubMed
17. **Villa A, Moshous D, deVillartay J-P, Notarangelo L, Candotti F.** 2014. Severe combined immunodeficiencies, p 88–143. *In* Sullivan KE, Stiehm ER (ed), *Stiehm's Immune Deficiencies*. Elsevier Academic Press, Amsterdam, The Netherlands.
18. **Kalman L, Lindegren ML, Kobrynski L, Vogt R, Hannon H, Howard JT, Buckley R.** 2004. Mutations in genes required for T-cell development: IL7R, CD45, IL2RG, JAK3, RAG1, RAG2, ARTEMIS, and ADA and severe combined immunodeficiency: HuGE review. *Genet Med* **6:**16–26. PubMed
19. **Kwan A, Church JA, Cowan MJ, Agarwal R, Kapoor N, Kohn DB, Lewis DB, McGhee SA, Moore TB, Stiehm ER, Porteus M, Aznar CP, Currier R, Lorey F, Puck JM.** 2013. Newborn screening for severe combined immunodeficiency and T-cell lymphopenia in California: results of the first 2 years. *J Allergy Clin Immunol* **132:**140–150. PubMed
20. **Verbsky JW, Baker MW, Grossman WJ, Hintermeyer M, Dasu T, Bonacci B, Reddy S, Margolis D, Casper J, Gries M, Desantes K, Hoffman GL, Brokopp CD, Seroogy CM, Routes JM.** 2012. Newborn screening for severe combined immunodeficiency; the Wisconsin experience (2008-2011). *J Clin Immunol* **32:**82–88. PubMed
21. **Hacein-Bey-Abina S, Hauer J, Lim A, Picard C, Wang GP, Berry CC, Martinache C, Rieux-Laucat F, Latour S, Belohradsky BH, Leiva L, Sorensen R, Debré M, Casanova JL, Blanche S, Durandy A, Bushman FD, Fischer A, Cavazzana-Calvo M.** 2010. Efficacy of gene therapy for X-linked severe combined immunodeficiency. *N Engl J Med* **363:**355–364. PubMed
22. **Aiuti A, Cattaneo F, Galimberti S, Benninghoff U, Cassani B, Callegaro L, Scaramuzza S, Andolfi G, Mirolo M, Brigida I, Tabucchi A, Carlucci F, Eibl M, Aker M, Slavin S, Al-Mousa H, Al Ghonaium A, Ferster A, Duppenthaler A, Notarangelo L, Wintergerst U, Buckley RH, Bregni M, Marktel S, Valsecchi MG, Rossi P, Ciceri F, Miniero R, Bordignon C, Roncarolo MG.** 2009. Gene therapy for immunodeficiency due to adenosine deaminase deficiency. *N Engl J Med* **360:**447–458. PubMed
23. **Chan B, Wara D, Bastian J, Hershfield MS, Bohnsack J, Azen CG, Parkman R, Weinberg K, Kohn DB.** 2005. Long-term efficacy of enzyme replacement therapy for adenosine deaminase (ADA)-deficient severe combined immunodeficiency (SCID). *Clin Immunol* **117:**133–143. PubMed
24. **Lipstein EA, Vorono S, Browning MF, Green NS, Kemper AR, Knapp AA, Prosser LA, Perrin JM.** 2010. Systematic evidence review of newborn screening and treatment of severe combined immunodeficiency. *Pediatrics* **125:**e1226–e1235. PubMed
25. **McGhee SA, Stiehm ER, McCabe ER.** 2005. Potential costs and benefits of newborn screening for severe combined immunodeficiency. *J Pediatr* **147:**603–608.
26. **Collier F, Tang M, Ponsonby AL, Vuillermin P.** 2013. Flow cytometric assessment of cord blood as an alternative strategy for population-based screening of severe combined immunodeficiency. *J Allergy Clin Immunol* **131:**1251–1252. PubMed
27. **Puck JM, SCID Newborn Screening Working Group.** 2007. Population-based newborn screening for severe combined immunodeficiency: steps toward implementation. *J Allergy Clin Immunol* **120:**760–768. PubMed
28. **Chan K, Puck JM.** 2005. Development of population-based newborn screening for severe combined immunodeficiency. *J Allergy Clin Immunol* **115:**391–398.
29. **McGhee SA, Stiehm ER, Cowan M, Krogstad P, McCabe ER.** 2005. Two-tiered universal newborn screening strategy for severe combined immunodeficiency. *Mol Genet Metab* **86:**427–430. PubMed

30. **Janik DK, Lindau-Shepard B, Comeau AM, Pass KA.** 2010. A multiplex immunoassay using the Guthrie specimen to detect T-cell deficiencies including severe combined immunodeficiency disease. *Clin Chem* **56:**1460–1465. PubMed
31. **Verschuren MC., Wolvers-Tettero IL, Breit TM, Noordzij J, van Wering ER, van Dongen JJ.** 1997. Preferential rearrangements of the T cell receptor-delta-deleting elements in human T cells. *J Immunol* **158:**1208–1216.
32. **McFarland RD, Douek DC, Koup RA, Picker LJ.** 2000. Identification of a human recent thymic emigrant phenotype. *Proc Natl Acad Sci USA* **97:**4215–4220. PubMed
33. **Douek DC, Vescio RA, Betts MR, Brenchley JM, Hill BJ, Zhang L, Berenson JR, Collins RH, Koup RA.** 2000. Assessment of thymic output in adults after haematopoietic stem-cell transplantation and prediction of T-cell reconstitution. *Lancet* **355:**1875–1881.
34. **Baker MW, Grossman WJ, Laessig RH, Hoffman GL, Brokopp CD, Kurtycz DF, Cogley MF, Litsheim TJ, Katcher ML, Routes JM.** 2009. Development of a routine newborn screening protocol for severe combined immunodeficiency. *J Allergy Clin Immunol* **124:**8272–8279.
35. **Routes JM, Grossman WJ, Verbsky J, Laessig RH, Hoffman GL, Brokopp CD, Baker MW.** 2009. Statewide newborn screening for severe T-cell lymphopenia. *JAMA* **302:**2465–2470.
36. **Punwani D, Gonzalez-Espinosa D, Comeau AM, Dutra A, Pak E, Puck J.** 2012. Cellular calibrators to quantitate T-cell receptor excision circles (TRECs) in clinical samples. *Mol Genet Metab* **107:**586–591. PubMed
37. **Comeau AM, Hale JE, Pai SY, Bonilla FA, Notarangelo LD, Pasternack MS, Meissner HC, Cooper ER, DeMaria A, Sahai I, Eaton RB.** 2010. Guidelines for implementation of population-based newborn screening for severe combined immunodeficiency. *J Inherit Metab Dis* **33**(Suppl 2)**:**S273–S281. PubMed
38. **Jones JF, Ritenbaugh CK, Spence MA, Hayward A.** 1991. Severe combined immunodeficiency among the Navajo. I. Characterization of phenotypes, epidemiology, and population genetics. *Hum Biol* **63:**669–682. PubMed
39. **Kuo CY, Chase J, Garcia Lloret M, Stiehm ER, Moore T, Aguilera MJ, Lopez Siles J, Church JA.** 2013. Newborn screening for severe combined immunodeficiency does not identify bare lymphocyte syndrome. *J Allergy Clin Immunol* **131:**1693–1695. PubMed
40. **Lev A, Simon AJ, Broides A, Levi J, Garty BZ, Rosenthal E, Amariglio N, Rechavi G, Somech R.** 2013. Thymic function in MHC class II-deficient patients. *J Allergy Clin Immunol* **131:**831–839. PubMed
41. **La Marca G, Canessa C, Giocaliere E, Romano F, Duse M, Malvagia S, Lippi F, Funghini S, Bianchi L, Della Bona ML, Valleriani C, Ombrone D, Moriondo M, Villanelli F, Speckmann C, Adams S, Gaspar BH, Hershfield M, Santisteban I, Fairbanks L, Ragusa G, Resti M, de Martino M, Guerrini R, Azzari C.** 2013. Tandem mass spectrometry, but not T-cell receptor excision circle analysis, identifies newborns with late-onset adenosine deaminase deficiency. *J Allergy Clin Immunol* **131:**1604–1610. PubMed
42. **Caudy AA, Reddy ST, Chatila T, Atkinson JP, Verbsky JW.** 2007. CD25 deficiency causes an immune dysregulation, polyendocrinopathy, enteropathy, X-linked-like syndrome, and defective IL-10 expression from CD4 lymphocytes. *J Allergy Clin Immunol* **119:**482–487. PubMed
43. **Sharfe N, Dadi HK, Shahar M, Roifman CM.** 1997. Human immune disorder arising from mutation of the alpha chain of the interleukin-2 receptor. *Proc Natl Acad Sci USA* **94:**3168–3171. PubMed
44. **Feske S, Prakriya M, Rao A, Lewis RS.** 2005. A severe defect in CRAC Ca2+ channel activation and altered K+ channel gating in T cells from immunodeficient patients. *J Exp Med* **202:**651–662. PubMed
45. **Picard C, McCarl CA, Papolos A, Khalil S, Lüthy K, Hivroz C, LeDeist F, Rieux-Laucat F, Rechavi G, Rao A, Fischer A, Feske S.** 2009. STIM1 mutation associated with a syndrome of immunodeficiency and autoimmunity. *N Engl J Med* **360:**1971–1980. PubMed
46. **Accetta D, Syverson G, Bonacci B, Reddy S, Bengtson C, Surfus J, Harbeck R, Huttenlocher A, Grossman W, Routes J, Verbsky J.** 2011. Human phagocyte defect caused by a Rac2 mutation detected by means of neonatal screening for T-cell lymphopenia. *J Allergy Clin Immunol* **127:**535–538.e1, 2. PubMed
47. **Ambruso DR, Knall C, Abell AN, Panepinto J, Kurkchubasche A, Thurman G, Gonzalez-Aller C, Hiester A, deBoer M, Harbeck RJ, Oyer R, Johnson GL, Roos D.** 2000. Human neutrophil immunodeficiency syndrome is associated with an inhibitory Rac2 mutation. *Proc Natl Acad Sci USA* **97:**4654–4659.
48. **Fernández-San José C, Martín-Nalda A, Vendrell Bayona T, Soler-Palacín P.** 2011. Hypogammaglobulinemia in a 12-year-old patient with Jacobsen syndrome. *J Paediatr Child Health* **47:**485–486. PubMed
49. **Puglisi G, Netravali MA, MacGinnitie AJ, Bonagura VR.** 2009. 11q terminal deletion disorder and common variable immunodeficiency. *Ann Allergy Asthma Immunol* **103:**267–268. PubMed
50. **von Bubnoff D, Kreiss-Nachtsheim M, Novak N, Engels E, Engels H, Behrend C, Propping P, de la Salle H, Bieber T.** 2004. Primary immunodeficiency in combination with transverse upper limb defect and anal atresia in a 34-year-old patient with Jacobsen syndrome. *Am J Med Genet A* **126A:**293–298. PubMed
51. **Dasouki M, Okonkwo KC, Ray A, Folmsbeel CK, Gozales D, Keles S, Puck JM, Chatila T.** 2011. Deficient T Cell Receptor Excision Circles (TRECs) in autosomal recessive hyper IgE syndrome caused by DOCK8 mutation: implications for pathogenesis and potential detection by newborn screening. *Clin Immunol* **141:**128–132. PubMed
52. **Borte S, von Döbeln U, Fasth A, Wang N, Janzi M, Winiarski J, Sack U, Pan-Hammarström Q, Borte M, Hammarström L.** 2012. Neonatal screening for severe primary immunodeficiency diseases using high-throughput triplex real-time PCR. *Blood* **119:**2552–2555. PubMed
53. **Nakagawa N, Imai K, Kanegane H, Sato H, Yamada M, Kondoh K, Okada S, Kobayashi M, Agematsu K, Takada H, Mitsuiki N, Oshima K, Ohara O, Suri D, Rawat A, Singh S, Pan-Hammarström Q, Hammarström L, Reichenbach J, Seger R, Ariga T, Hara T, Miyawaki T, Nonoyama S.** 2011. Quantification of κ-deleting recombination excision circles in Guthrie cards for the identification of early B-cell maturation defects. *J Allergy Clin Immunol* **128:**223–225.e2. PubMed
54. **Winkelstein JA, Marino MC, Lederman HM, Jones SM, Sullivan K, Burks AW, Conley ME, Cunningham-Rundles C, Ochs HD.** 2006. X-linked agammaglobulinemia: report on a United States registry of 201 patients. *Medicine (Baltimore)* **85:**193–202.
55. **Verbsky J, Thakar M, Routes J.** 2012. The Wisconsin approach to newborn screening for severe combined immunodeficiency. *J Allergy Clin Immunol* **129:**622–627. PubMed
56. **Kwan A, Church JA, Cowan MJ, Agarwal R, Kapoor N, Kohn DB, Lewis DB, McGhee SA, Moore TB, Stiehm ER, Porteus M, Aznar CP, Currier R, Lorey F, Puck JM.** 2013. Newborn screening for severe combined immunodeficiency and T-cell lymphopenia in California: results of the first 2 years. *J Allergy Clin Immunol* **132:**140–150. PubMed

Combined Immunodeficiencies

CHRISTINE SEROOGY AND MELISSA ELDER

75

This chapter is dedicated to describing combined immunodeficiencies (CIDs) and useful diagnostic assays. Here, a CID is defined as a defect that affects the two most prominent arms of the adaptive immune system: T cells and B cells. The molecular defect may directly affect both cell types or just one cell type, specifically T lymphocytes, with indirect effects on B-cell function. CIDs are distinguished from severe combined immunodeficiencies (SCIDs) because T-cell numbers and function are higher than per established criteria for SCID and thus may not be detected on SCID newborn screening (NBS). Several CIDs are attributed to distinct genetic mutations in SCID-associated genes. In recent years, the field of immunology has witnessed increased reporting of unique CIDs affecting isolated families or small numbers of individuals. This increase is attributable to the advent of improved genetic testing, such as whole-exome sequencing. In Table 1, we provide a comprehensive list of CIDs, their immunophenotypes, and useful diagnostic tests. Common themes for CIDs include aberrant T-cell development, function, cytoskeletal regulation, and survival. These defects translate to clinical problems secondary to immune deficiency and, in many instances, immune dysregulation. This chapter does not include in-depth description of all CIDs but rather focuses on categorical descriptions and highlights more prevalent genetic abnormalities along with overviews of diagnostic assays for CID confirmation.

ABNORMALITIES OF THYMOPOIESIS

Defects in T-Cell Development

T-cell development occurs in the thymus over a period of 2 weeks in humans and via a complex series of gene rearrangements and productive T-cell signals mediated by interactions between thymic stromal cells, bone marrow-derived antigen-presenting cells, and developing thymocytes. These interactions provide signals to developing thymocytes to survive, proliferate, and egress from the thymus to the periphery. Profound defects in any of these pathways result in severely diminished T-cell development and a SCID immunophenotype. Defects that partially affect T-cell development result in CID.

MHC Class I and II Deficiencies

A number of genetic defects have been described for both major histocompatibility complex (MHC) class I and II deficiencies with an associated broad spectrum of clinical phenotypes, ranging from mild defects to severe and life-threatening (Table 1). Defects in MHC-I affect $CD8^+$ T-cell development without impairing $CD4^+$ T cells (1), while defects in MHC-II affect $CD4^+$ T-cell development and spare $CD8^+$ T cells (2). The most common cause of MHC-I deficiency is a homozygous inactivating mutation in one of the two subunits of the protein transporter associated with MHC-I endoplasmic reticulum processing (*TAP1* and *TAP2*). Severe clinical phenotypes of MHC-II deficiency or "bare lymphocyte syndrome" that would be classified as SCID are most often due to homozygous mutations in essential transcription factor genes, such as *CIITA*, required for MHC-II gene transcription. Interestingly, MHC-II deficiency is not detected on SCID NBS (3). Genetic mutations in *CD8A*, encoding the CD8α chain, have been described in one family and represent another example of a critical interaction between T-cell surface receptors and MHC molecules on thymic stromal cells during T-cell development (4).

Diagnostic Evaluation

MHC-I deficiency. Flow cytometry for lymphocyte subset enumeration demonstrates decreased peripheral blood $CD8^+$ T cells, and diagnosis is supported by unsuccessful serological HLA class I typing but normal molecular typing or observation of significantly diminished cell surface expression of MHC-I antigens by flow cytometry using a pan-anti-HLA class I antibody (such as clone W6/32). These patients are often from consanguineous families and have homozygous HLA genotyping. Rare causes of MHC-I deficiency, including transcription defects, may be characterized using Epstein-Barr virus (EBV)-transformed B-cell lines before and after incubation with proinflammatory cytokines.

MHC-II deficiency. Decreased $CD4^+$ T cells by flow cytometry and diminished *in vitro* T-cell responses to foreign antigens in proliferative assays or in mixed lymphocyte culture are seen. Hypogammaglobulinemia with inability to make specific antibody is typical despite normal B-cell numbers. Diagnosis is confirmed by absence of cell surface expression of MHC-II antigens on peripheral blood mononuclear cells (PBMCs) and EBV-transformed B-cell lines by flow cytometry or by serological HLA class II typing.

doi:10.1128/9781555818722.ch75

TABLE 1 CIDs, their immunophenotypes, and useful diagnostic tests

Combined immunodeficiency disease	Gene mutation(s)	Immunophenotype	Useful diagnostic tests	Reference(s)
Defects in T-cell development				
MHC-II deficiency	*CIITA* (*MHC2TA*), *RFX5*, *RFXAP*, *RFXANK*	Absent MHC-II expression, low $CD4^+$ T cells, diminished T-cell-antigen-specific function	Flow cytometry, T-cell function	2, 43
MHC-I deficiency	*TAP1*, *TAP2*, *TAPBP*	Diminished $CD8^+$ T cells	Flow cytometry	1
CD8α deficiency	*CD8A*	Absent CD8 T cells, increased $CD3^+CD4^-CD8^-$ $TCR\alpha\beta^+$ T cells	Flow cytometry	4
Cartilage hair hypoplasia	*RMRP*	T-cell lymphopenia	T-cell function, flow cytometry, TREC	5
Defects in DNA repair and recombination				
Rag1/2 hypomorphic mutations	*RAG1*, *RAG2*	$CD4^+$ T-cell lymphopenia, normal Vβ gene usage	Flow cytometry	8, 44–46, 72
Ataxia telangiectasia	*ATM*	T-cell lymphopenia, variable T- and B-cell dysfunction	Flow cytometry, T-cell function	12, 47
Omenn syndrome	*RAG1*, *RAG2*, *IL7RA*, *DCLRE1C*, *AK2*	Oligoclonal and activated T cells, poor T-cell function, hyper-IgE, hypereosinophilia	T-cell proliferation, spectratyping, TREC, flow cytometry	8–11, 21, 48
Defects in proximal T-cell activation				
ORAI-1 deficiency (CRAC channel defect)	*ORAI1*	Normal lymphocyte numbers, diminished T-cell function	T-cell calcium flux	49, 50
Stromal interaction molecule (STIM-1) deficiency	*STIM1*	Normal lymphocyte numbers, diminished T-cell function	T-cell calcium flux	50
CD3γ deficiency	*CD3G*	Mild T-cell lymphopenia, diminished T-cell function, diminished naive T cells	Flow cytometry, TREC, T-cell function	13, 51
TCRα deficiency	*TRAC*	Defective surface expression of TCRαβ, diminished T-cell function, intact humoral function	Flow cytometry, T-cell function	52
Hyper-IgM (CD40 ligand deficiency)	*CD40LG*	Hyper-IgM, hypogammaglobulinemia	Flow cytometry	16, 53
Defects in T-cell signal transduction pathways				
Lymphocyte-specific protein kinase (Lck) deficiency	*LCK*	$CD4^+$ T-cell lymphopenia, defective T-cell activation, low-level CD4 and CD8 surface expression	Flow cytometry, T-cell function, spectratyping	18, 54
ζ chain-associated protein of 70 kDa (ZAP-70) deficiency	*ZAP-70*	Absent CD8 T cells, defective TCR signaling, defective specific humoral antibody response	Flow cytometry, T-cell function	19
Uncoordinated 119 (Unc119) deficiency	*UNC119*	$CD4^+$ T-cell lymphopenia, defective T-cell activation, intact humoral function	Flow cytometry, T-cell function	17, 20

Defects in cytokine signaling pathways				
IL-21R deficiency	*IL21R*	Poor B-cell differentiation, diminished T-cell cytokine production, defective NK-cell function	Flow cytometry	55
Autosomal dominant hyper-IgE syndrome	*STAT3*	Impaired T-cell memory, impaired Th17 differentiation, impaired T-cell function	Memory-T-cell enumeration, Th17 differentiation, T-cell function	27, 28, 56, 57
JAK3 G2775(+3)C	*JAK3*	Lymphoproliferation, skewed TCR repertoire	Flow cytometry, Vβ gene usage	23
STAT5b deficiency	*STAT5B*	T-cell lymphopenia, diminished lymphocyte proliferation, decreased Treg-cell number	Treg-cell function and enumeration, T-cell function	26, 58
CD25 deficiency	*IL2RA*	Lymphoproliferation, increased T-cell activation markers, diminished antigen-specific T-cell responses	Flow cytometry, Treg-cell function and enumeration	24, 59, 60
Common γ chain, p.R222C	*IL2RG*	Normal T-, B-, and NK-cell numbers, normal T-cell function, normal immunoglobulins with diminished vaccine response	IL-2 response, vaccine antibody response	22, 61
Defects in T-cell survival				
Mammalian sterile 20-like protein (MST1) deficiency	*STK4*	Defective naive-T-cell survival, possible impaired thymic egress	Flow cytometry, TREC, T-cell function, apoptosis assay	6, 62, 63
Coronin-1A deficiency	*CORO1A*	Naive CD4 T-cell lymphopenia, EBV lymphoproliferation	Flow cytometry	7, 64
Purine nucleoside phosphorylase deficiency	*PNP*	T-cell lymphopenia	T-cell function, serum uric acid, flow cytometry	29
Defects in NF-κB activation				
Caspase recruitment domain family member 11 (CARD11) deficiency	*CARD11*	Mild lymphopenia (T and NK), blocked B-cell differentiation, defective T-cell activation	Flow cytometry, T-cell function	66, 67
Caspase-8 deficiency state (CEDS)	*CASP8*	Diminished $CD4^+$ T-cell numbers, diminished T- and NK-cell function	Flow cytometry, T-cell function, apoptosis assay	68, 69
X-linked anhidrotic ectodermal dysplasia with immunodeficiency (X-ED-ID)	*NEMO*	Hyper-IgA/IgM, normal T- and B-cell numbers, variable T-cell function, hypogammaglobulinemia with poor polysaccharide antibody responses, impaired production of cytokines	T-cell function, flow cytometry, immunoglobulins	30–32, 70, 71
Defects in cytoskeletal and migration pathways				
Wiskott-Aldrich syndrome	*WASP*	T-cell lymphopenia, defective TCR signaling, impaired immune synapse, impaired NK-cell function	Flow cytometry, T-cell functional studies	33, 73
WASp-interacting protein deficiency	*WIP*	Defective TCR signaling, impaired immune synapse, impaired NK-cell function	Flow cytometry, T-cell functional studies	74

(Continued on next page)

TABLE 1 CIDs, their immunophenotypes, and useful diagnostic tests *(Continued)*

Combined immunodeficiency disease	Gene mutation(s)	Immunophenotype	Useful diagnostic tests	Reference(s)
Warts, hypogammaglobulinemia, infections, myelokathexis syndrome (WHIM)	*CXCR4*	Lymphopenia, decreased naive T cells and memory B cells, hypogammaglobulinemia, impaired chemotaxis, impaired thymic output	Flow cytometry, TREC, immunoglobulins	75
Ras homology family member H (RHOH) deficiency	*RHOH*	Skewing toward effector memory T cells, impaired TCR signaling, diminished β7 integrin expression on circulating T cells	T-cell function, flow cytometry	76
Dedicator of cytokinesis 8 (DOCK8) deficiency	*DOCK8*	Hyper-IgE, T-cell lymphopenia, eosinophilia, impaired T-cell survival, impaired immune synapse, impaired NKT-cell survival	TREC, T-cell function, flow cytometry	34, 35, 65
Combined immunodeficiencies with narrow clinical phenotypes				
X-linked with magnesium defect Epstein-Barr virus infection and neoplasia (XMEN)	*MAGT1*	$CD4^+$ T-cell lymphopenia, defective T-cell activation	Flow cytometry, T-cell Mg^{2+} and Ca^{2+} flux	77, 78
CD27 deficiency	*CD27*	Absent memory B cells, hypogammaglobulinemia	Flow cytometry	79, 80
X-linked lymphoproliferative (XLP) disease	*SH2D1A*	Low numbers of NKT cells, hypogammaglobulinemia, impaired T-cell apoptosis	Apoptosis assay	36, 37, 41
X-linked inhibitor of apoptosis (XIAP) deficiency	*BIRC4*	Enhanced lymphocyte apoptosis, low numbers of invariant NKT cells, hypogammaglobulinemia	Flow cytometry, apoptosis assay	38–41

Cartilage Hair Hypoplasia

During thymopoiesis, in addition to critical interactions between MHC molecules and T-cell receptors (TCRs), T-cell proliferation is essential for T-cell development. Defects in cell activation or cell cycle progression can dramatically affect T-cell development. One T-cell proliferation defect shown to directly impact thymopoiesis results from mutations in the gene encoding the RNA component of the mitochondrial RNA-processing endoribonuclease (*RMRP*), which is the genetic basis of cartilage hair hypoplasia (5). RMRP is important for ribosomal assembling, telomere stability, and cell cycle control.

Diagnostic Evaluation

Although the immunologic and clinical phenotype of cartilage hair hypoplasia is broad, decreased T-cell numbers by flow cytometry, diminished thymic function by TCR excision circles (TREC) analysis, and reduced *in vitro* T-cell function are usually seen. Unlike MHC-I and MHC-II deficiencies, discussed above, severe *RMRP* mutations are detected by SCID NBS.

MST1 and *CORO1A* Mutations

Another mechanism that may affect T-cell development is impaired thymic egress of single-positive T cells. This abnormality has been described in several distinct CIDs, including hypomorphic mammalian sterile 20-like protein (*MST1*) mutations (6) and *CORO1A* mutations, encoding coronin-1A (7). Coronin-1A regulates actin cytoskeletal rearrangement and may be the mechanism for impaired egress of T cells from the thymus. MST1 is a kinase important for activating Rho family GTPases and as such impacts actin cytoskeleton. However, the underlying mechanisms for impaired thymic egress have not been fully delineated, and other functional defects have been described with these genetic mutations, such as decreased survival of naive T cells in apoptosis assays (6, 7). Homozygous *MST1* mutations are characterized by progressive $CD4^+$ T lymphopenia with few naive T cells in the peripheral blood. Patients with *CORO1A* mutations exhibit decreased T-cell but not B-cell or NK-cell numbers as well as poor T- and B-cell function.

Diagnostic Evaluation

TREC analysis as a measurement of thymic output, characterization of T-cell surface antigens by flow cytometry that differentiate naive ($CD45RA^+CCR7^+$) from memory ($CD45RO^+$) T cells produced in the periphery, and determination of TCRαβ and TCRγδ expression as well as TCR Vβ repertoire by TCR Vβ spectratyping provide information about thymic function. Expected abnormalities of thymic function and egress include T-cell lymphopenia, diminished frequency of naive T cells, increased memory and activated T cells, and possibly a restricted or skewed TCR Vβ repertoire. *In vitro* proliferative responses to TCR stimulation using anti-CD3 or phytohemagglutinin (PHA) are diminished. Apoptosis of MST1-deficient T cells is increased and survival decreased by annexin flow cytometry-based assays (6).

Defects in DNA Repair and Recombination

Omenn Syndrome

In addition to adequate cell activation and migration, T-cell development requires tightly regulated DNA cleavage and repair during thymopoiesis. Complete abrogation of nonredundant DNA repair gene activity results in SCID, while hypomorphic mutations in SCID-associated genes involved in these pathways are associated with CIDs. The best examples are hypomorphic mutations in the *RAG1* and *RAG2* genes. The classical presentation of hypomorphic *RAG1/2* mutations results in the CID termed Omenn syndrome (8). This is often described as a "leaky" SCID and is a disease that is universally fatal in the first 2 years of life without hematopoietic stem cell replacement. The classic features of Omenn syndrome include dermatitis, hepatomegaly, eosinophilia, elevated IgE, and expansion of oligoclonal T cells. Hypomorphic mutations in other SCID-associated genes have also been described in Omenn syndrome patients (*IL7RA* [9], *DCLRE1C* [10], and *AK2* [11]). The overarching paradigm in Omenn syndrome is a profound immune deficiency with immune dysregulation. More recently, hypomorphic *RAG1* and *RAG2* mutations have also been identified in older patients with CID and have been associated with a spectrum of clinical phenotypes distinct from Omenn syndrome (81).

Diagnostic Evaluation

Initial immunologic testing for DNA repair and recombination defects includes flow cytometry, TCR Vβ spectratyping, TREC analysis, and T-cell functional studies. Expected abnormalities include diminished T-cell numbers, restricted T-cell repertoire by TCR Vβ spectratyping, reduced thymopoiesis by TREC analysis, and diminished T-cell functionality (determined by *in vitro* mitogen responses and expression of lymphocyte activation markers by flow cytometry). Sequencing of known SCID genes would be required to confirm the underlying mutation(s).

Ataxia Telangiectasia

Ataxia telangiectasia (AT) is characterized by cerebellar ataxia, oculocutaneous telangiectasia, cellular radiosensitivity, and predisposition to malignancy and CID and is due to mutations in ataxia telangiectasia mutated (*ATM*), a phosphatidylinositol 3-like protein kinase critical for activation of the complex cellular response to double-strand DNA breaks and for cellular homeostasis. AT is characterized by progressive cerebellar degeneration in association with variable and progressive cellular and humoral immune dysfunction and predisposition to T- and B-cell malignancies. Most symptoms are the result of defective cellular responses to physiological and induced double-strand DNA breaks. AT patients are lymphopenic, with selective loss of $CD4^+$ T cells, T-cell dysfunction, and progressive hypogammaglobulinemia due to defects in the DNA damage and repair responses including phosphorylation of NF-κB essential modulator (NEMO) during NF-κB activation and multiple other signaling events involved in cell survival and cell death (12). The neurologic symptoms are the typical presenting symptom leading to a diagnosis of AT.

Diagnostic Evaluation

Initial immunologic screening includes lymphocyte subsets by flow cytometry, *in vitro* mitogen and antigen proliferative responses, immunoglobulin levels, and specific antibody production. As mentioned, the spectrum of immune defects and function is broad. In general, AT patients are expected to have decreased T-cell numbers, diminished B-cell function (in particular, polysaccharide antibody responses), and relatively intact T-cell function. SCID NBS has picked up infants with AT (82).

T-CELL ACTIVATION, SIGNAL TRANSDUCTION, AND SURVIVAL

Defects in Proximal T-Cell Activation

The TCR is a multisubunit complex consisting of a disulfide-linked αβ heterodimer noncovalently associated with the CD3 γ, δ, and ε chains and a ζζ homodimer (CD247). Defects in proximal T-cell activation include abnormal cell surface expression of TCR and CD3 subunits ε, γ, or δ (5, 13–15). Defective CD3 expression may present as SCID or CID depending on the affected subunit and mutation severity.

Patients with typical (complete) CD3δ deficiency have virtually no αβ or γδ T cells and present as SCID with absent T-cell function. The phenotype of CD3ε deficiency is dependent on the level of residual CD3ε expression. Absence of CD3ε causes $T^-B^+NK^+$ SCID, while partial CD3ε expression results in CID with decreased T-cell numbers and variably reduced mitogen responses *in vitro*. Mutations in CD3γ and ζζ usually result in defective, but not absent, T-cell numbers and function, although SCID has been reported.

Diagnostic Evaluation

A diagnosis of defective CD3 expression is usually suggested by moderately to severely decreased numbers of peripheral T cells that weakly express TCRαβ and CD3 by flow cytometry using a range of monoclonal antibodies (MAbs) to all subunits. Measurement of the mean fluorescence intensity of the TCR complex on the T-cell surface is critical to determining which subunit is affected. TCR Vβ usage is often restricted, with some skewing of percentages of TCRαβ versus TCRγδ cells. Most peripheral T cells are not recent thymic emigrants by TREC analysis or naive by flow cytometry. It is unknown if CD3γ or partial CD3ε mutations would be detected in SCID NBS. As with other forms of CID and SCID, gene sequencing is required to confirm mutations in a CD3 subunit.

Hyper-IgM Syndromes

Hyper-IgM (HIGM) syndromes are characterized by low serum IgG, IgA, and IgE with normal or elevated IgM as a result of failure to complete immunoglobulin class switch recombination due to defects in the CD40 ligand/CD40 signaling pathway. X-linked HIGM (X-HIGM) is due to CD40 ligand (CD154) deficiency, often with absent expression of CD40 ligand on $CD4^+$ T cells or failure of mutant CD40 ligand to bind CD40 on B cells and antigen-presenting cells (16). The inability to signal via CD40 interrupts activation of NEMO (nuclear factor κB essential modulator) and thus NF-κB, preventing immunoglobulin class switching, somatic hypermutation, and development of memory B cells. In addition, the interaction of CD40 ligand with CD40 is important for T-cell costimulation and cytokine responses involving gamma interferon (IFN-γ) and interleukin-12 (IL-12). Abnormal CD40 ligand signaling leads to impaired T-cell function with defects in T-cell priming and differentiation and increased susceptibility to opportunistic infections, particularly *Pneumocystis jirovecii* and *Cryptosporidium parvum*. As a result of chronic cryptosporidial infection of the biliary tract, boys with X-HIGM develop sclerosing cholangitis and tumors of the biliary tract, and liver autoimmunity and neutropenia are common.

The autosomal recessive (AR) forms (AR-HIGM) are caused by defects in CD40 or in downstream signaling molecules and are most often due to mutations in the *AICDA* gene, encoding activation-induced cytidine deaminase, but also may be due to mutations in *CD40*, *PMS2* (postmeiotic segregation increased 2), or *UNG* (uracil-*N*-glycosylase) (16). As expected, HIGM is also a frequent consequence of AT, NEMO deficiency, gain-of-function mutations in the IkBα subunit of the IκB kinase (IKK) complex, and Nijmegen breakage syndrome.

Diagnostic Evaluation

Initial screening includes lymphocyte subset enumeration for presence of B cells, measurement of serum immunoglobulins, and specific antibody titers. A rapid screening test for X-HIGM uses the knowledge that CD40 ligand is a T-cell activation surface marker easily detected by flow cytometry on PHA- or phorbol myristic acetate (PMA)-stimulated PBMCs using CD25 and CD69 expression to document T-cell activation (see below for more detailed protocol). Although deficient expression of CD40 ligand on activated $CD4^+$ T cells by flow cytometry is often seen in X-HIGM, genotyping may be required to confirm a *CD40L* mutation, especially in non-informative families. CD40 expression on PBMCs can also be determined by flow cytometry. In contrast to X-HIGM, AR-HIGM due to CD40 deficiency is characterized by absent CD40 expression on B cells and monocytes but normal expression of CD40 ligand on activated T cells. Genotyping is usually required to confirm diagnosis of AR-HIGM, particularly when CD40 expression is normal on B cells.

Defects in T-Cell Signal Transduction Pathways

The polymorphic TCRαβ chains are responsible for recognition of peptide bound to self-MHC molecule; these chains lack signaling capability. In contrast, the ζ and CD3 proteins are able to transduce extracellular antigen-binding events to intracellular signaling pathways through associations with cytoplasmic protein tyrosine kinases via conserved immunoreceptor tyrosine-based activation motifs (ITAMs) within their extensive cytoplasmic domains. Propagation of antigen-binding signals from the TCR to the nucleus is dependent on the recruitment and activation of two protein tyrosine kinases, lymphocyte-specific protein kinase (Lck) and ζ chain-associated protein of 70 kDa (ZAP-70), whose functions are critical for lymphocyte responses to antigens. Lck and ZAP-70 are also required for normal TCR signaling, CD4 versus CD8 selection in the thymus, and lymphocyte proliferation in the periphery.

Recruitment of Lck to the plasma membrane and its subsequent activation is dependent on activity of the signaling adapter protein Uncoordinated 119 (Unc119) (17). Roles of Unc119 include activation of the GTPase Rab11 to facilitate transport of Lck from perinuclear endosomes to the plasma membrane in resting T cells, and also as an SH3 ligand for Lck activation during early TCR signaling. Once activated, Lck mediates ITAM phosphorylation and recruitment of ZAP-70 to the TCR. Activation of first Lck and then ZAP-70 triggers phosphorylation of phospholipase Cγ1 via recruitment of numerous proteins to the signaling complex, referred to as the signalosome. The recruited downstream proteins include linker for activation of T cells (LAT) and SH2 domain-containing leukocyte protein of 76 kDa (SLP-76). Formation of these protein complexes at the plasma membrane is dependent on Unc119 function (17), and the resulting TCR-mediated signal amplification culminates in transcription of genes essential for T-cell activation and initiation of T-cell-specific responses.

Lck Deficiency

Lck is expressed at high levels in peripheral T cells and in thymocytes at all stages of maturation. Disruption of Lck in

humans usually presents with a selective CD4 lymphopenia and normal numbers of $CD3^+$ and $CD8^+$ T cells (18) and may be missed by SCID NBS. B-cell and NK-cell numbers are normal, but hypogammaglobulinemia and defective functional antibody responses are typical. The clinical presentation of selective CD4 lymphopenia due to Lck deficiency is variable and typical of CID, although SCID has been seen.

Diagnostic Evaluation

Despite CD4 lymphopenia, Lck-deficient T cells do proliferate, although not fully, to mitogens (phytohemagglutinin [PHA], concanavalin A [ConA], pokeweed mitogen [PWM]), anti-CD3, and IL-2 *in vitro*, and demonstrate normal alloantigen responses. Genotyping is required for diagnosis in most patients, but the underlying genetic defects resulting in decreased Lck function in a few sporadic cases of CD4 lymphopenia are unknown but may include patients with mutations in *UNC119* (uncoordinated 119 protein) or *MAGT1* (magnesium transporter 1) genes (see below and Table 1).

ZAP-70 Deficiency

ZAP-70 is expressed in all thymocyte subpopulations, peripheral T cells, NK cells, and also aberrantly in a subpopulation of human B-cell chronic lymphocytic leukemia. In contrast to ZAP-70-deficient mice, human ZAP-70 deficiency is characterized by the selective absence of $CD8^+$ T cells but with abundant nonfunctional $CD4^+$ T cells in the peripheral blood (19). B-cell numbers are normal, but serum immunoglobulins and specific antibody responses are defective due to lack of T-cell function in the majority of patients. The diagnosis of ZAP-70 deficiency is suggested by a clinical phenotype of SCID requiring hematopoietic stem cell transplantation but with normal numbers of $CD3^+$ and $CD4^+$ T cells and absent $CD8^+$ T cells in the peripheral blood. Therefore, ZAP-70 deficiency is missed by SCID NBS.

Diagnostic Evaluation

Diagnosis of ZAP-70 deficiency is suggested by lack of T-cell proliferation *in vitro* to mitogens and TCR stimuli (PHA, ConA, PWM, or anti-CD3) but normal proliferative responses to PMA plus ionomycin, agents that bypass proximal TCR signaling events by mimicking actions of the second messengers Ras, in the case of PMA, and $[Ca^{2+}]_i$ for ionomycin. Further studies to confirm a proximal TCR signaling defect include defective $[Ca^{2+}]_i$ mobilization by fluorimetry or flow cytometry and abnormal tyrosine phosphoprotein induction after anti-CD3 stimulation on immunoblots or by flow-based methods using phospho-site-specific antibodies (phosphoepitope flow cytometry; see below). IL-2 production is also absent in anti-CD3- or PHA-simulated, ZAP-70-deficient T cells but normal using PMA plus ionomycin. In most cases, Western blotting or intracellular flow cytometry using permeabilized PBMCs demonstrates lack of ZAP-70 protein. DNA sequencing is required to confirm two mutant *ZAP-70* alleles in patients with SCID characterized by a paucity of circulating $CD8^+$ T cells.

Unc119 Deficiency

Unc119 is essential for Lck activity, and its deficiency results in a rare form of idiopathic CD4 lymphopenia. The dominant-negative Unc119 mutation (G22V) interferes with both Lck recruitment to the plasma membrane and its activation, resulting in impaired immunologic synapse formation, defective T-cell activation and proliferation, and a CID phenotype on diagnostic testing (20). SCID is not seen, possibly due to a less critical role for Unc119 in Lck activation during thymocyte development.

Diagnostic Evaluation

Genotyping of the *UNC119* gene is reserved for the rare patients with reproducible CD4 lymphopenia, reduced T-cell proliferation to mitogens and antigens *in vitro*, and defective Lck activity but normal Lck gene sequencing.

Defects in Cytokine Signaling Pathways

Partial Common γ-Chain Defects

Mutations in the γ chain (γc) common to the receptors for IL-2, IL-4, IL-7, IL-9, and IL-15 are found in boys with X-linked recessive SCID (SCID-X1). The γc molecule is essential for the intracellular transmission of cytokine signals and is required for T-cell development. Absence of γc-containing cytokine receptor complexes usually results in SCID with early arrest of T- and NK-cell development and normal numbers of immature B cells exhibiting defective isotype switching. However, at least one hypomorphic γc mutation, R222C, only partially blocks T-cell development, resulting in a variant form of Omenn syndrome (21). In such patients, normal numbers and subset distribution of T, B, and NK cells as well as levels of serum immunoglobulins are observed, but specific antibody production is absent.

Diagnostic Evaluation

Unlike in SCID-X1 patients, normal expression of the γc chain of the IL-2 receptor (IL-2RG; CD132) by flow cytometry is seen and T-cell proliferation to PHA and anti-CD3 *in vitro* is normal. However, addition of exogenous IL-2 to mitogen-stimulated T cells *in vitro* does not increase proliferation further, as would be expected (22). Genotyping is required to confirm two hypomorphic R222C mutations.

Partial JAK3 Deficiency

Females, as well as some males with the typical SCID-X1 phenotype, do not have mutations in γc. Instead, these patients have autosomal recessive SCID due to mutations in the downstream cytoplasmic tyrosine kinase Janus kinase 3 (JAK3), whose activation is required for transduction of ligand-binding signals from γc-containing cytokine receptors. Like CID due to the R222C mutation in γc, the clinical spectrum of JAK3 deficiency may include CID rather than SCID if due to hypomorphic mutations, such as A96G or G2775(+3)C (23).

Diagnostic Evaluation

Affected patients exhibit CD4 T-cell lymphopenia and reduced mitogen proliferative responses *in vitro* that are variably increased with addition of exogenous IL-2 despite poor IL-2-dependent signal transducer and activator of transcription (STAT) 5 phosphorylation on immunoblots or by phosphoepitope flow cytometry (23). However, affected T cells do not upregulate Fas ligand in response to IL-2 by flow cytometry. Genotyping is needed to confirm a hypomorphic *JAK3* mutation.

CD25 Deficiency

The IL-2R is composed of three chains: α (IL-2Rα, CD25), β (IL-2Rβ, CD122), and γc (IL-2Rγ, CD132) (3), and only CD25 binds IL-2 exclusively. Due to its roles in IL-2-mediated effector-T-cell responses and regulation of $CD4^+CD25^+Foxp3^+$ T regulatory cell (Treg) responses in homeostasis, CD25 deficiency results in both chronic viral infections and severe autoimmunity (24), somewhat resembling the immune dysregulation, polyendocrinopathy, enteropathy, X-linked (IPEX) syndrome, caused by mutations in the *FOXP3* gene (25). Patients with CD25 deficiency

tend to have normal numbers of $CD4^+$ T cells, unlike in IPEX, but elevated $CD8^+$ T cells, possibly from chronic viral infections, inverting their CD4/CD8 ratio.

Diagnostic Evaluation

Absence of CD25 expression on T-cell subpopulations and impaired IL-2 production can be demonstrated by cell surface and intracellular flow cytometry. *In vitro* proliferative responses to TCR stimuli are poor but can be partially rescued by exogenous IL-2, unlike specific viral and antigen responses, which are consistently absent. As expected, phosphorylation and activation of the transcription factor STAT5b is markedly reduced in the presence of IL-2 but is normal with other cytokines. Diagnostic tests to document CD25 deficiency include flow cytometry, phosphoepitope flow cytometry, soluble CD25 and cytokine production, and T-cell function including cytotoxicity and proliferation to mitogens and specific antigens *in vitro*.

STAT5b Deficiency

STAT5b is a critical downstream effector of JAK-mediated signal transduction, including for γc-containing cytokines, growth hormone, and erythropoietin, and is involved in the pathogenesis of a variety of human diseases. The phosphorylation of JAK3 and STAT5b is required for normal IL-2 signaling, and disruption of these events results in impaired development, immune homeostasis, and proliferation of most lymphocyte populations. Engagement of the high-affinity IL-2R on T cells results in activation of JAK3 with subsequent phosphorylation and activation of STAT5b. In the nucleus, phosphorylated STAT5b initiates transcription of multiple genes, including *FOXP3* and *CD25*, required for Treg development. As a result, the rare patients with STAT5b deficiency have chronic diarrhea, atopic dermatitis, recurrent herpesvirus infections, and autoimmunity and are very short due to growth hormone insensitivity (26). All patients have been from consanguineous families.

Diagnostic Evaluation

The immunophenotype may include SCID or CID with pan-lymphopenia, significantly decreased numbers of Treg cells by flow cytometry, and diminished Treg-cell suppressor function *in vitro*. Gene sequencing is required to confirm the diagnosis.

STAT3 Deficiency (Autosomal Dominant Hyper-IgE Syndrome)

In contrast to STAT5b, heterozygous mutations in *STAT3* cause the autosomal dominant form of hyper-IgE syndrome (AD-HIES), which is characterized by recurrent severe lung and skin infections with pneumatocele formation; staphylococcal abscesses; generalized eczema; mucocutaneous candidiasis; and abnormalities of bone, teeth, and connective tissue in association with markedly elevated serum IgE (27).

Diagnostic Evaluation

In addition to measurement of serum IgE, quantification of IL-17-producing $CD4^+$ T cells (Th17) by intracellular flow cytometry after mitogen stimulation has proven to be a useful diagnostic test for HIES (28, and see below). A severe reduction or absence of Th17 cells is characteristic of AD-HIES.

Defects in T-Cell Survival

PNP Deficiency

Purine nucleoside phosphorylase (PNP) deficiency is associated with both immune defects and neurological symptoms, including developmental delay and behavioral and motor problems (29). Immunologic features of PNP deficiency include lymphopenia, severely decreased T-cell numbers, poor *in vitro* T-cell function, and attrition of B cells over time. Despite significant decline in B-cell function, many patients develop autoimmune disease and are at increased risk for lymphoma or other malignancies.

Diagnostic Evaluation

Initial immunologic tests include flow cytometry for T- and B-cell enumeration and T-cell functional studies (e.g., *in vitro* mitogen proliferation). Absent PNP function results in an undetectable serum uric acid level, which can be used to screen for the disorder with measurement of erythrocyte or lymphocyte PNP activity for confirmation of the diagnosis.

Defects in NF-κB Activation

NEMO Deficiency (X-linked Anhidrotic Ectodermal Dysplasia with Immunodeficiency)

Anhidrotic ectodermal dysplasia with immunodeficiency (HED-ID or X-ED-ID) is caused by hypomorphic mutations in NEMO (IκKγ). NEMO functions as a regulatory subunit of the IκB kinase complex, which tightly controls activation of the NF-κB/Rel transcription factor pathways by promoting phosphorylation and degradation of cytosolic IκB. Null mutations in the NEMO gene *IKBG* cause incontinentia pigmenti in females and are lethal in males *in utero*. In contrast, hypomorphic mutations are associated with broad phenotypic variability, depending on the localization of the mutation and effect on NEMO function (30, 31). Affected males usually have ectodermal dysplasia and tooth abnormalities and may present with life-threatening pyogenic and mycobacterial infections and autoimmune disease, especially inflammatory colitis (30, 31).

Diagnostic Evaluation

Defective NF-κB/Rel activation in NEMO patients leads to a wide range of immune defects, including hypogammaglobulinemia with hyper-IgM due to failure to undergo CD40-mediated class switch recombination, defective CD40 ligand-mediated IL-12 and tumor necrosis factor alpha production, deficient NK cytotoxicity, and impaired polysaccharide antibody responses, particularly to *Pneumococcus*. Sequencing of the *IKBG* gene is required for diagnosis, particularly since phenotype of NEMO deficiency is dependent on location and severity of the underlying mutation. A similar phenotype can be seen with a hypermorphic (gain-of-function) mutation in the gene encoding the IkBα subunit of the IKK complex (32).

DEFECTS IN CYTOSKELETAL AND MIGRATION PATHWAYS

Optimal activation of immune cells requires a dynamic and intimate interaction between immune cells. This is best exemplified by the immunologic synapse. The immunologic synapse is a physical and dynamic engagement of immune cells typically with other immune cells brought together by receptor-ligand recognition, resulting in numerous outcomes, such as T-cell activation, differentiation, or death. A basic fundamental process underlying this critical engagement is proper actin cytoskeletal rearrangement. Defects in the actin cytoskeleton can have profound effects on immune function, including aberrant immunologic synapse formation, as well as diminished effector function. The characterization of immunologic synapse formation, chemotaxis, adhesion, and

cell migration remains research-use-only applications that have greatly enhanced the biologic knowledge of the role of the actin cytoskeleton in immune function and the essential proteins for key functions. Readily available functional immunologic testing for the CIDs with actin cytoskeletal defects includes functional tests of B and T cells, including proliferation assays and flow cytometric analysis for protein expression and immune phenotype.

Wiskott-Aldrich Syndrome

The most prevalent example of an actin cytoskeletal defect resulting in CID is Wiskott-Aldrich syndrome (WAS), caused by mutations in the gene encoding the Wiskott-Aldrich syndrome protein (*WASP*). WASp is an important regulator of the actin cytoskeleton, and loss of WASp activity results in impaired hematopoietic cell migration, impaired phagocytosis, and impaired immune cell synapse formation. The immunologic defects and clinical findings in WAS are broad, and *WASP* mutations causing the full spectrum of WAS simultaneously result in immune deficiency and autoimmunity.

Diagnostic Evaluation

Initial immunologic assays for immune defects that affect cytoskeletal and migration pathways include flow cytometry, T-cell function, immunoglobulin levels, specific antibody production, and TREC analysis. Platelet volume can be used to screen for WAS; unlike immune thrombocytopenia, in which platelet size is large, platelet volume is small in WAS. Genetic sequencing is done if rapid screening for detection of WASp in PBMCs by intracellular flow cytometry is abnormal (33).

DOCK8 Deficiency

Dedicator of cytokinesis 8 (DOCK8) loss-of-function mutations are a recently described CID that is often categorized as an autosomal recessive form of hyper-IgE syndrome (34). DOCK8 is a member of the DOCK180 family of guanine exchange factors important for activating Rho family GTPases. DOCK8 is important for actin cytoskeletal regulation and has been shown to interact with WASp. Similar to *WASP* mutations, *DOCK8* mutations impact immune function broadly. A full mechanistic understanding of the role of DOCK8 in immune function is still an area of active investigation. Other rarer mutations have been described that affect cytoskeletal and migration pathways (*RHOH*, *WIP*, *WHIM*, and *CORO1A*; see Table 1).

Diagnostic Evaluation

In addition to the initial immunologic screening tests listed above for WAS, serum IgE level is increased in DOCK8 deficiency, unlike in WAS. Interestingly, DOCK8-deficient patients have been detected by SCID NBS (35). This supports a nonredundant role for DOCK8 in naive-T-cell survival and T-cell egress from the thymus. Whereas WAS is generally not picked up by SCID NBS, retrospective TREC analysis revealed diminished values in a subset of WAS patients (83).

COMBINED IMMUNODEFICIENCIES WITH NARROW CLINICAL PHENOTYPES

X-Linked Lymphoproliferative Syndromes

X-linked lymphoproliferative syndrome (XLP) is characterized by overwhelming susceptibility to EBV infection, leading to life-threatening complications such as hemophagocytic lymphohistiocytosis (HLH), fulminant infectious mononucleosis, and B-cell lymphoma. Two different genetic defects cause XLP. Most cases of XLP (XLP type 1) are due to mutations in *SH2D1A*, the gene encoding the signaling lymphocyte activation molecule (SLAM)-associated protein (SAP) (36, 37). SAP is a cytoplasmic adapter protein critical to normal lymphocyte signal transduction, and its deficiency affects the development and effector functions of T-, NK-, and NKT-lymphocyte populations. Observed defects in humoral immunity, including dysgammaglobulinemia, are due in large part to lack of T-cell help, particularly failure of $CD4^+$ T cells to produce IL-10 required for generation of memory B cells and isotype class switching.

X-linked inhibitor of apoptosis (XIAP) is a member of the inhibitor of apoptosis family of proteins and is encoded by *XIAP/BIRC4*, which is mutated in XLP type 2 and the cause of X-linked familial HLH (38, 39). In XIAP deficiency, EBV-associated HLH is the most common presentation and dysgammaglobulinemia is seen less often (40). The development of HLH is related to overproduction of IL-18 and other proinflammatory cytokines by activated T cells and monocytes.

Diagnostic Evaluation

Initial immunologic testing includes enumeration of immune cell numbers and ascertainment of EBV levels and antibody response, as well as apoptosis assays. Flow cytometry and immunoblotting can be used to analyze intracellular expression of SAP and XIAP and support a diagnosis of XLP (40). However, genotyping is required to confirm mutations in either *SH2D1A* or *XIAP/BIRC4*, and clinically it is important to make this distinction since XLP type 1 is associated with malignancy and the clinical features are not overlapping.

DIAGNOSTIC ASSAYS

Flow Cytometry

The invention of flow cytometry and its entry into the clinical laboratory has revolutionized the field of immunology. The past 30-plus years in which flow cytometry has been available as a clinical laboratory tool have been witness to a growing list of quantitative and qualitative assays. With ongoing development of novel suitable antibodies, discovery of new immunologic disorders, and development of new platforms for cytometry such as mass cytometry, or CyTOF, the clinical diagnostic utility of flow cytometry will undoubtedly continue to expand.

Enumeration of Lymphocyte Cell Populations

Flow cytometry for immune cell quantification is a widely used and easily standardized diagnostic test for initial CID evaluation. Clinically useful cell surface and intracellular expression determination of various proteins can be achieved with appropriate controls and proper maintenance of a four-color flow cytometer. Essentially every initial diagnostic screen for CID includes quantification of T cells, B cells, and NK cells using various antibodies that recognize surface antigens.

1. Peripheral blood should be collected in sterile Vacutainer tube or syringe containing anticoagulant. Samples should be kept at ambient temperature without agitation until processing. Samples should be processed within 24 h of collection. In the clinical setting, fresh samples are typically used. If a sample is being shipped for flow cytometry analysis at another site, it is important for the submitting institution

to obtain a complete blood count prior to shipment. The flow cytometry analysis determines the frequency of the stained population. If the sample cannot be processed within 24 h of collection, many adaptive immune cells are amenable to flow cytometry analysis after recovery from viably frozen samples.

2. For convenience, whole blood with anticoagulant is stained and red blood cells are removed by osmotic lysis prior to sample acquisition on the flow cytometer when surface staining is performed in unmanipulated samples. Determine the number of staining conditions needed; wash 0.5 ml of blood per FACS staining tube needed with 5 ml of phosphate-buffered saline (PBS) containing heparin. Centrifuge at 400 × *g* for 10 min and aspirate carefully. Mix cell suspension well by flicking the tube and repeat the wash. Resuspend cells in 50 μl of fluorescence-activated cell sorter (FACS) staining buffer (e.g., PBS with bovine calf serum and azide)/staining tube. Add 10 μl of human IgG (12 mg/ml) to block nonspecific staining and incubate for 15 min at 4°C.

3. Add desired antibody cocktail. Manufacturers provide recommendations on the amount of antibody used to stain a sample, but it is critical that the operator determine the optimal antibody concentration in their laboratory since results can vary. This can be achieved by using a fixed number of cells and incubating with a range of concentrations that are above and below the manufacturer's recommended amount. This becomes particularly important for intracellular staining (see below). Mix tube by flicking and incubate at 4°C for 30 min in the dark.

4. Add 3.5 ml of FACS buffer and centrifuge.

5. Discard supernatant and resuspend in fixation/red blood cell lysis buffer (for example, 1× FACSLyse; BD Biosciences, San Jose, CA). Invert all tubes and centrifuge at 1,300 rpm for 10 min. Keep samples cold and protected from light. The samples can be run on flow cytometer between 30 min after fix to after an overnight incubation.

6. Run on flow cytometer with appropriate compensation tubes.

Interpretation

The frequency of the targeted populations can be determined using compatible software for analysis of acquired data. The absolute lymphocyte count from the submitting institution is used to determine the absolute values of the various lymphocytic cell subsets determined by the flow analysis. Age-adjusted normal ranges are available from the published literature (84). Determination of T-, B-, and NK-cell subsets is by a standard flow cytometry panel used to screen for CIDs. Inclusion of additional antibodies against various surface molecules can broaden the utility of flow cytometry surface staining. Depending on the staining panel used and commercially available antibody conjugates, acquisition beyond four-color flow cytometry may be necessary.

Thymic function and egress can be determined indirectly by quantification of CD45RA and CD45RO isoform distribution on peripheral blood lymphocytes with interpretation of the frequencies using age-related controls. This is commonly added to screening panels for CIDs and does not require flow cytometer upgrade. Determination of TCRαβ and -γδ expression and distribution can provide additional information on thymic function and is feasible with the flow cytometer platform. Additionally, interrogation of the T-cell memory compartment can be done by flow cytometry using a combination of antibodies for T-cell resting and activated surface receptors. Naive T cells are defined as $CD45RA^{+}CCR7^{+}$, central memory ($CD45RA^{-}CCR7^{+}$), effector memory ($CD45RA^{-}CCR7^{-}$), or effector memory RA (TEMRA; $CD45RA^{+}CCR7^{-}$) cells.

Intracellular Protein Expression and T-Cell Differentiation

Flow cytometry has been essential for expanding diagnostic testing aimed at determining T-cell differentiation and quantification of critical intracellular proteins (e.g., transcription factor Foxp3 or cytosolic WASp) and has proven to be a useful diagnostic tool. These more in-depth flow cytometry analyses require cellular manipulation and increased flow cytometer capability. Example protocols, outlined below, include intracellular staining for Th17 cells, which is a useful screening test for AD STAT3 HIES. Intracellular and extracellular staining for Treg quantification is discussed and serves as a useful screening test for IPEX and STAT5 or CD25 deficiency. Intracellular staining for WASp, SAP, or XIAP is used to screen for affected males with WAS or XLP and also to screen for carrier females.

Intracellular Cytokine Staining (IL-17)

1. Peripheral blood should be collected, stored, and processed as described above. One exception is that the anticoagulant used should be sodium heparin since EDTA can interfere with the activity of the stimulant. Whole blood with anticoagulant can be used for intracellular staining of unmanipulated cells or stimulated cells. However, PBMCs are used more routinely to decrease the volume of the sample to allow for more accuracy in cell numbers. PBMCs are isolated using a density gradient as described elsewhere. If the sample cannot be processed within 24 h of collection, many adaptive immune cells are amenable to flow cytometry analysis after recovery from viably frozen samples.

2. Plate 2×10^6 cells/well in appropriate culture media (e.g., RPMI-1640 plus 10% fetal calf serum, 100 μg/ml penicillin, 100 U/ml streptomycin, and 2 mM L-glutamine) with stimulant; options include 1 μg/ml *Staphylococcus* enterotoxin B or PMA (100 ng/ml) + ionomycin (1 μg/ml) and 2.5 μg/ml brefeldin A at 37°C for 5 h. Unstimulated wells should be included as an appropriate control.

3. Wash cells with FACS buffer. Add predetermined concentration of antibody cocktail for surface proteins (e.g., CD3, CD4, and CD45RO) and incubate for 30 min at 4°C.

4. Wash the cells once with 2 volumes of FACS buffer, followed by resuspension in 2% paraformaldehyde, and incubate for 20 min at room temperature.

5. Wash cells in 1× permeabilization (Perm) buffer (commercially available products for intracellular cytokine staining work consistently, such as from eBioscience, San Diego, CA), then resuspend in 100 μl of 1× Perm buffer containing blocking antibody (e.g. human IgG) and incubate at room temperature for 10 min.

6. Add predetermined amount of anti-IL-17A (e.g., clone N49-653) and anti-IFN-γ (e.g., clone B27) and incubate for 60 min at room temperature. Appropriate control tubes should include fluorescence minus one (FMO) and/or isotype controls for the intracellular protein. An FMO is a staining tube that contains all fluorescent antibodies in a panel except for one and controls for spread of fluorochromes into the channel of interest. These controls assist with gate setting in data analysis.

7. Wash twice with 1× Perm buffer, resuspend in FACS buffer, and proceed to flow cytometer.

Interpretation

In this assay, IL-17A cytokine production by memory Th17 cells is triggered in polyclonally activated PBMCs in the presence of brefeldin A to block endoplasmic reticulum release of secretory proteins, thus trapping cytokines

produced during activation inside the cells. Determination of the frequency of Th17 cells is used as a screening test in HIES. Th1 cells (IFN-γ) should not be affected in HIES patients.

Foxp3 Analysis

Whole blood or isolated PBMCs can be used. A PBMC protocol is presented below.

1. Peripheral blood should be collected, stored, and processed as described above for IL-17 staining. PBMCs should be resuspended in FACS buffer at a concentration of 1×10^7 cells/ml.
2. Place 1×10^6 cells/FACS staining tube and incubate for 15 min at 4°C. Appropriate control tubes must be included to account for background staining and assist with setting gates in data analysis, for example, isotype control for Foxp3 antibody.
3. Add surface staining antibody cocktail containing predetermined concentrations. A standard cocktail for Treg surface staining includes CD3, CD4, CD127, and CD25 antibodies. Incubate for 60 min at 4°C in the dark.
4. Add 2 ml of FACS buffer/tube. Spin at 1,300 rpm for 10 min at 4°C. Remove supernatant.
5. Add 1 ml of 1× fix/perm buffer to each tube (commercially available from BioLegend or eBioscience and should be compared by the investigator). Incubate for 30 min at room temperature in the dark.
6. Spin at 1,300 rpm for 10 min at 4°C and resuspend in 1 ml of 1× Perm buffer/tube. Repeat. Remove supernatant, leaving residual 50-100 μl/tube. Add 10 μl human IgG (12 mg/ml) to block, and incubate 10 min at 4°C in the dark.
7. Add predetermined anti-FoxP3 (e.g., clone 206D) or isotype control (e.g., clone MOPC21) to appropriate tube. Incubate for 60 min at room temperature in the dark.
8. Add 1 ml of 1× Perm buffer/tube. Spin at 1,300 rpm for 10 min at 4°C. Remove supernatant and repeat with FACS buffer.
9. Resuspend in 1% paraformaldehyde and store at 4°C in the dark until acquired on flow cytometer.

Interpretation

Tregs are defined as $CD4^+CD25^+CD127^{lo/-}Foxp3^+$. Both CD25 and Foxp3 can be upregulated on activated conventional T cells (CD25 routinely and Foxp3 transiently and at lower levels than bona fide Treg cells). This assay is a helpful screening test in inherited immunodeficiency/immune dysregulation states that are secondary to Treg abnormalities, such as STAT5b deficiency or CD25 deficiency. This approach determines Treg cell numbers but does not address functionality.

WASp, SAP, or XIAP Expression

Whole blood or PBMCs can be used. Below is an example protocol for PBMCs. This assay protocol follows the same principles as Foxp3 staining for Treg analysis.

1. Stain 1×10^6 cells/tube for surface markers with predetermined concentration of antibodies in FACS buffer for 30 min at 4°C in the dark.
2. Fix cells with 2% paraformaldehyde.
3. Resuspend cells in 1× Perm buffer; incubate for 15 min at 4°C in the dark. Wash once and resuspend in 1× Perm buffer.
4. Incubate with predetermined amount of antibody for protein of interest and include tubes for appropriate controls (isotype controls).
   a. Mouse anti-WASp MAb (e.g., clone 5A5)
   b. Monoclonal anti-SAP (e.g., clone EPR3168)
   c. Anti-XIAP (e.g., clone 48)

   Incubate 60 min at 4°C in the dark.
5. Wash with 1× Perm buffer. These antibodies are not available with directly conjugated fluorophore and thus require stain with appropriate fluorophore-conjugated secondary antibody for 30 min at 4°C in the dark.
6. Wash once with 1× Perm buffer, followed by FACS buffer, then resuspend in 1% paraformaldehyde and store at 4°C in the dark until acquired on flow cytometer.

Interpretation

WASp is expressed in many hematopoietic cells including platelets, neutrophils, monocytes, and lymphocytes. WASp protein expression in lymphocytes and monocytes can be determined after gating by a distribution pattern in the forward and side scatter. Protein positivity is compared to isotype control and with the results of a healthy control. If the sample was shipped, it is critical that a healthy shipping control be included with the test sample.

SAP can be detected in T and NK cells. Patients with SAP deficiency typically have severely diminished SAP expression detected by flow cytometry. XIAP is detectable in neutrophils, monocytes, and all lymphocyte subsets. Reported patients with XIAP mutations can have absent or decreased protein expression depending on the mutation. Female carriers display bimodal distribution of SAP and XIAP expression. Skewing toward XIAP-positive cells has been observed and suggests a selective survival advantage in XIAP-expressing cells and can complicate carrier testing by this methodology (41).

T-Cell Activation

1. Whole blood or PBMCs have been successfully used for this assay. Ideally, the anticoagulant should be sodium heparin.
2. Stimulate the cells with PMA 15 ng/ml + ionomycin 300 ng/ml (should determine optimal dose in your facility with dose-response curve) for 4 h in appropriate culture media at 37°C.
3. Wash in FACS staining buffer.
4. Stain with anti-CD3, anti-CD8, anti-CD154, and anti-CD69 antibodies and appropriate controls. Here is an example template.
   a. Tube 1: anti-CD3, anti-CD8, and isotype control (for anti-CD154)
   b. Tube 2: anti-CD3, anti-CD8, and anti-CD154 (e.g., clone TRAP-1)
   c. Tube 3: anti-CD3, anti-CD8, and anti-CD69

   Incubate for 20 min at room temperature in the dark.
5. Wash cells with FACS staining buffer.
6. Resuspend in 1% paraformaldehyde and store at 4°C in the dark until acquired on flow cytometer.

Interpretation

For screening of X-HIGM, peripheral blood T cells stimulated first with PMA and ionomycin are stained for T-cell surface markers such as CD69 and CD40 ligand (CD154). Cell surface markers of T-cell activation may be analyzed by flow cytometry to investigate adequate T-cell activation and the ability of T cells to upregulate critical costimulatory molecules. CD69, a member of the C-type lectin domain family, is a surface receptor upregulated within hours of T-cell

activation and can serve as a positive control or marker for adequate T-cell activation and is routinely used in screening for CIDs such as X-HIGM. Since CD69 and CD154 are not present on resting T cells and are activation markers with similar kinetics of expression, CD69 staining serves as a suitable positive control for adequate culture stimulation conditions. Additionally, since CD69 expression is dependent on activation of the Ras/mitogen-activated protein kinase pathway, absence of CD69 expression on activated T cells may suggest a proximal signal transduction defect. If CD154 is detected but the clinical suspicion is still high for HIGM, use of soluble biotinylated CD40:Fc can determine the functionality of the expressed protein; however, this reagent is more difficult to acquire.

Tyrosine Phosphorylation by Flow Cytometry (Phosphoepitope Analysis)

A number of suitable reagents are now available to stain for phosphorylation of essential signaling molecules by flow cytometry rather than more labor-intensive immunoblotting methods and can offer more information since single cells can be analyzed for multiple parameters (42).

1. PBMCs should be isolated as detailed elsewhere.
2. Stimulate PBMCs to induce the desired phosphorylation step. For example, to screen for signaling defects in the IL-2–IL-2R axis, PBMCs are incubated with 1,000 U of recombinant IL-2 and then stained intracellularly with a fluorophore-conjugated anti-phospho-STAT5 antibody (26). A proper control includes unstimulated cells.
3. Wash cells and stain with predetermined concentration of desired antibodies against surface receptors. Incubate for 30 min at 4°C in the dark. Wash with FACS buffer.
4. Fix cells with 2% paraformaldehyde for 30 min at room temperature in the dark. Wash cells with FACS buffer.
5. Permeabilize cells with ice-cold methanol and incubate at 4°C in the dark for 15 min. Wash with FACS buffer × 2.
6. Stain cells with predetermined concentration of antibodies that recognize intracellular protein of interest as well as antibodies specific for the phosphorylated form of the protein of interest in FACS buffer for 30 min at room temperature in the dark. Proper controls include an isotype control.
7. Acquire data on flow cytometer.

Interpretation

Analysis of tyrosine phosphoproteins is indicated if a defect in proximal antigen receptor signaling is suggested by defective lymphocyte proliferation or $[Ca^{2+}]_i$ mobilization with CD3 cross-linking. The development of these tools has resulted in more-rapid screening techniques for CIDs, decreased sample volume requirements, and increased sensitivity compared with immunoblot assays. STAT5b deficiency provides an excellent example for the use of phosphoepitope flow cytometry. In this CID, stimulation with IL-2 demonstrates diminished phospho-STAT5 based on frequency of positive cells determined with isotype control and compared to control cells. With flow cytometry the amount of protein per cell can be determined with various software analysis programs and is expressed at median fluorescence intensity. Ratios between phosphorylated and nonphosphorylated protein can be determined with the experimental approach. This is a rapid screening test, and positive results should be confirmed at the genetic level.

T-Cell Proliferation Assays

Lymphocyte proliferation response *in vitro* can be assessed by [^{3}H]thymidine incorporation and liquid scintillation or by flow cytometry using 5-ethynyl-2′-deoxyuridine. Alternatively, carboxyfluorescein succimidyl ester dilution can simultaneously determine cell proliferation and cell division number by flow cytometry (43). Typical T-cell stimulants include mitogens such as PHA, vaccine antigens (e.g., tetanus toxoid), PMA plus ionomycin, or antibodies that cross-link the TCR complex (i.e., anti-CD3 clone OKT3). The response to the stimulant can provide useful information on the extent of the T-cell dysfunction and provide guidance for additional studies. For example, T-cell proliferation to PMA plus ionomycin may be used to screen for proximal TCR signaling defects. Since PMA plus ionomycin bypasses the need for TCR expression or function, a significantly diminished response to PHA or CD3 cross-linking but normal PMA plus ionomycin response is suggestive of abnormalities in the TCR complex or in very early TCR signaling events.

Lymphocyte Proliferation

1. Suspend PBMCs in appropriate culture media (e.g., RPMI-1640 plus 10% fetal calf serum, 100 μg/ml penicillin, 100 U/ml streptomycin, and 2 mM L-glutamine) at a concentration of 1×10^6 cells/ml.
2. Incubate 1×10^4 cells in 200 μl at 37°C in flat-bottomed 96-well plates with 50 ng/ml anti-CD3 antibody (agonistic clone, e.g., UCHT1), 5 μg/ml PHA (Burroughs Wellcome, Research Triangle Park, NC), or 0.5 ng/ml PMA plus 1 μM ionomycin for 72 h.
3. Pulse wells with 0.96 μCi/well of [^{3}H]thymidine for 6 h, harvest, and count in a scintillation counter.

More-nuanced T-cell proliferation studies can be performed by adding cytokines to the culture alongside CD3 cross-linking. For example, the addition of IL-2 increases the proliferative response above CD3 stimulation alone. The absence of an increased proliferative response would be suggestive of a defect in the IL-2–IL-2R axis, such as STAT5b deficiency, CD25 deficiency, or JAK3/common γ-chain hypomorphic mutations. Another example is the addition of IL-7 or IL-15 to the culture media alongside CD3 cross-linking. The absence of additional proliferation with IL-7 suggests a defect in the IL-7–IL-7R axis or impaired differentiation or maintenance of T-cell memory, as seen in STAT3 deficiency.

Recall response to vaccine antigens can be determined by all of the methodologies listed above. The responding T-cell frequency is diminished and will require longer incubation times and ideally acquisition of high event counts for flow cytometry-based methods. Diminished recall response is seen in CIDs with global T-cell functional defects, as well as in CIDs with intact T-cell function with global stimulants, e.g., PHA, but impaired T-cell memory differentiation or maintenance.

Ca^{2+} Flux Assays

If T-cell proliferation is diminished with CD3 cross-linking, measurements of $[Ca^{2+}]_i$ mobilization may be indicated in order to localize a putative signaling defect, calcium channel dysfunction, or store-operated Ca^{2+} entry defect. $[Ca^{2+}]_i$ flux assays may be done either by fluorimetry or by flow cytometry. Fluorimetric methods require more cells but do not require concomitant cell staining with potentially stimulatory antibodies. The advantages of flow cytometry $[Ca^{2+}]_i$ flux assays include smaller cell number requirement, and they more easily allow for continuous monitoring of $[Ca^{2+}]_i$ flux alongside other immune markers. To test for proximal signaling defects, depletion of intracellular Ca^{2+} stores is monitored after cross-linking of surface TCR (with agonistic antibody such

as clone UCHT1) in cells loaded with a ratiometric Ca^{2+} indicator dye (e.g., Indo-1). In patients with defects in calcium channels or store-operated Ca^{2+} entry defects, after depletion of intracellular Ca^{2+} stores with activation, Ca^{2+} is added to the analysis tube and reentry is monitored (42).

Fluorimetric Assay

1. Suspend PBMCs at 2×10^7 cells/ml in complete RPMI and load with 3 μM Indo-1 acetomethoxy (AM) for 30 min at 37°C.

2. Wash cells in calcium-containing buffer (e.g., Hanks balanced salt solution plus 1% bovine serum albumin, 1 mM $CaCl_2$, and 0.5 mM $MgCl_2$), resuspend at 5×10^6 cells/ml in calcium-containing buffer, and keep on ice until use.

3. Warm 400 μl of cell suspension at 37°C for 2 min before analysis. Measure absorbance at an excitation wavelength of 355 nm and emission wavelengths of 400 nm and 500 nm using a fluorescence spectrophotometer. Maximal fluorescence is determined after cell lysis with 5 μl of 10% Triton X-100 detergent; minimal fluorescence is determined after addition of 50 μl of 1 M Tris base and 15 μl of 0.4 M EGTA.

4. Recordings are made before and after cells are stimulated by TCR cross-linking. For T-cell analysis, add 2 μl of biotinylated anti-CD3 antibody (agonistic antibody such as clone UCHT1) plus 5 μg/ml streptavidin, or a purified anti-CD3 antibody followed by IgM MAb to TCR to cross-link surface may be used instead. To ensure proper loading of Indo-1, add 1 μl of 1 mM ionomycin to nonresponding cell suspensions after 5 min.

Flow Cytometric Assay

1. Stain 2×10^7 PBMCs with a purified, azide-free anti-CD3 antibody for 30 min in the dark at room temperature, wash, and resuspend 2×10^6 cells in 1 ml calcium/magnesium-free RPMI or Hanks balanced salt solution.

2. Incubate PBMCs for 30 min at 37°C in 3 μM Indo-1 AM, wash, and resuspend in 1 ml calcium/magnesium-free RPMI.

3. Measure baseline fluorescence of gated $CD3^+$ for 1 to 2 min, followed by recordings for 10 min of fluorescence after addition of an anti-CD3 cross-linking antibody.

4. Change in calcium flux after stimulation is calculated as fluorescence intensity peak increase by subtracting fluorescence intensity value before stimulation from the value after stimulation.

Protein Tyrosine Phosphorylation by Immunoblotting

Analysis of tyrosine phosphoproteins is indicated if a defect in proximal antigen receptor signaling is suggested by defective lymphocyte proliferation or $[Ca^{2+}]_i$ mobilization to TCR stimulation.

1. Incubate 100 μl of 2×10^6 PBMCs or enriched for CD2 using magnetic bead selection (Dynal, Life Technologies) for 20 min on ice with 2 μl each of biotinylated anti-CD3 MAb plus biotinylated anti-CD4 MAb or PBS alone. Wash cells, resuspend in 100 μl PBS, and cross-link with 5 μg/ml avidin for 4 min at 37°C.

2. Lyse cells in 45 μl of NP-40 buffer (1% NP-40 plus 10 mM Tris [pH 7.6], 150 mM NaCl, 0.5 mM EDTA, 10 mM NaF, 1 mM phenylmethylsulfonyl fluoride, 1 μg/ml pepstatin A, 10 μg/ml leupeptin, 1 μg/ml aprotonin, and 1 mM Na_3VO_4) for 30 min at 4°C. Centrifuge cells at $12{,}000 \times g$ at 4°C for 10 min, collect supernatants, and mix with 15 μl of 4× sample buffer dye (2% SDS, 5% 2-mercaptoethanol, 250 mM Tris, 10% glycerol, and 1 mg/ml bromophenol blue [pH 6.8]). Boil at 90°C for 5 min prior to separation by SDS–12% PAGE under reducing conditions.

3. Electrophoretically transfer separated protein bands to Immobilon-P membranes (Millipore), block in blotting buffer (Tris-buffered saline plus 0.1% Tween) plus 3% bovine serum albumin, and incubate at room temperature for 1 h in blotting buffer with 4G10 (anti-phosphotyrosine MAb; Upstate Biotechnology, Millipore).

4. Wash filters three times in blotting buffer, and incubate with horseradish peroxidase-conjugated goat anti-mouse MAb (Southern Biotechnology Associates, Birmingham, AL) for 1 h at room temperature. Phosphoproteins are assayed using an enhanced chemiluminescence detection system (e.g., ECL; GE Healthcare, Piscataway, NJ).

Apoptosis

Apoptosis, or activation-induced cell death, is a normal consequence of T-cell activation and serves to maintain T-cell homeostasis. Defects in apoptosis are observed in several CIDs. The clinical consequences of impaired apoptosis include lymphoproliferation (e.g., SAP deficiency), impaired T-cell survival (e.g., MST1 deficiency), and possibly impaired $CD8^+$ T-cell effector responses (e.g., XIAP deficiency).

In vitro induction of apoptosis is routinely performed using T-cell restimulation. PHA T-cell blasts are first generated *in vitro*, followed by CD3 cross-linking that typically would induce apoptosis in a proportion of the blasting T cells. T cells are subsequently stained for annexin V (AV; surface phosphatidylserine is an early marker of apoptosis) and a marker for necrosis (typically propidium iodide [PI]). Survival is determined as the percentage of AV-PI-negative cells. It is essential to run healthy controls alongside the subject's cells. T-cell survival above or below healthy control is suggestive of an apoptosis defect. This activation-induced cell death is Fas (CD95) dependent, and CD95 cross-linking can be a suitable alternative to CD3.

Apoptosis assays are a useful screening tool for some CIDs, but correlation with clinical disease is not always apparent. Therefore, normal apoptosis results should not strongly influence decision making for confirmatory genetic testing or additional immunologic studies in cases with abnormal immunophenotyping and suggestive CID-associated clinical disease (40).

REFERENCES

1. **Zimmer J, Andrès E, Donato L, Hanau D, Hentges F, de la Salle H.** 2005. Clinical and immunological aspects of HLA class I deficiency. *QJM* **98:**719–727. PubMed
2. **Griscelli C.** 1991. Combined immunodeficiency with defective expression in major histocompatibility complex class II genes. *Clin Immunol Immunopathol* **61:**S106–S110. PubMed
3. **Lev A, Simon AJ, Broides A, Levi J, Garty BZ, Rosenthal E, Amariglio N, Rechavi G, Somech R.** 2013. Thymic function in MHC class II-deficient patients. *J Allergy Clin Immunol* **131:**831–839. PubMed
4. **de la Calle-Martin O, Hernandez M, Ordi J, Casamitjana N, Arostegui JI, Caragol I, Ferrando M, Labrador M, Rodriguez-Sanchez JL, Espanol T.** 2001. Familial CD8 deficiency due to a mutation in the *CD8α* gene. *J Clin Invest* **108:**117–123. PubMed
5. **de la Fuente MA, Recher M, Rider NL, Strauss KA, Morton DH, Adair M, Bonilla FA, Ochs HD, Gelfand EW, Pessach IM, Walter JE, King A, Giliani S, Pai SY, Notarangelo LD.** 2011. Reduced thymic output, cell cycle abnormalities, and increased apoptosis of T lymphocytes in patients with cartilage-hair hypoplasia. *J Allergy Clin Immunol* **128:**139–146. PubMed
6. **Nehme NT, Pachlopnik Schmid J, Debeurme F, André-Schmutz I, Lim A, Nitschke P, Rieux-Laucat F, Lutz P,**

Picard C, Mahlaoui N, Fischer A, de Saint Basile G. 2012. MST1 mutations in autosomal recessive primary immunodeficiency characterized by defective naive T-cell survival. *Blood* **119:**3458–3468. PubMed

7. **Shiow LR, Paris K, Akana MC, Cyster JG, Sorensen RU, Puck JM.** 2009. Severe combined immunodeficiency (SCID) and attention deficit hyperactivity disorder (ADHD) associated with a Coronin-1A mutation and a chromosome 16p11.2 deletion. *Clin Immunol* **131:**24–30. PubMed
8. **Villa A, Santagata S, Bozzi F, Giliani S, Frattini A, Imberti L, Gatta LB, Ochs HD, Schwarz K, Notarangelo LD, Vezzoni P, Spanopoulou E.** 1998. Partial V(D)J recombination activity leads to Omenn syndrome. *Cell* **93:**885–896. PubMed
9. **Giliani S, Bonfim C, de Saint Basile G, Lanzi G, Brousse N, Koliski A, Malvezzi M, Fischer A, Notarangelo LD, Le Deist F.** 2006. Omenn syndrome in an infant with *IL7RA* gene mutation. *J Pediatr* **148:**272–274. PubMed
10. **Mancebo E, Recio MJ, Martínez-Busto E, González-Granado LI, Rojo P, Fernández-Díaz E, Ruiz-Contreras J, Paz-Artal E, Allende LM.** 2011. Possible role of Artemis c.512C>G polymorphic variant in Omenn syndrome. *DNA Repair (Amst)* **10:**3–4. PubMed
11. **Henderson LA, Frugoni F, Hopkins G, Al-Herz W, Weinacht K, Comeau AM, Bonilla FA, Notarangelo LD, Pai SY.** 2013. First reported case of Omenn syndrome in a patient with reticular dysgenesis. *J Allergy Clin Immunol* **131:**1227–1230.
12. **Shiloh Y, Ziv Y.** 2013. The ATM protein kinase: regulating the cellular response to genotoxic stress, and more. *Nat Rev Mol Cell Biol* **14:**197–210.
13. **Arnaiz-Villena A, Timon M, Corell A, Perez-Aciego P, Martin-Villa JM, Regueiro JR.** 1992. Brief report: primary immunodeficiency caused by mutations in the gene encoding the CD3-γ subunit of the T-lymphocyte receptor. *N Engl J Med* **327:**529–533. PubMed
14. **Dadi HK, Simon AJ, Roifman CM.** 2003. Effect of CD3δ deficiency on maturation of α/β and γ/δ T-cell lineages in severe combined immunodeficiency. *N Engl J Med* **349:**1821–1828. PubMed
15. **Soudais C, de Villartay JP, Le Deist F, Fischer A, Lisowska-Grospierre B.** 1993. Independent mutations of the human CD3-ε gene resulting in a T cell receptor/CD3 complex immunodeficiency. *Nat Genet* **3:**77–81. PubMed
16. **Qamar N, Fuleihan RL.** 2014. The hyper IgM syndromes. *Clin Rev Allergy Immunol* **46:**120–130. PubMed
17. **Gorska MM, Liang Q, Karim Z, Alam R.** 2009. Uncoordinated 119 protein controls trafficking of Lck via the Rab11 endosome and is critical for immunological synapse formation. *J Immunol* **183:**1675–1684. PubMed
18. **Goldman FD, Ballas ZK, Schutte BC, Kemp J, Hollenback C, Noraz N, Taylor N.** 1998. Defective expression of p56lck in an infant with severe combined immunodeficiency. *J Clin Invest* **102:**421–429. PubMed
19. **Elder ME, Lin D, Clever J, Chan AC, Hope TJ, Weiss A, Parslow TG.** 1994. Human severe combined immunodeficiency due to a defect in ZAP-70, a T cell tyrosine kinase. *Science* **264:**1596–1599. PubMed
20. **Gorska MM, Alam R.** 2012. A mutation in the human Uncoordinated 119 gene impairs TCR signaling and is associated with CD4 lymphopenia. *Blood* **119:**1399–1406. PubMed
21. **Poliani PL, Facchetti F, Ravanini M, Gennery AR, Villa A, Roifman CM, Notarangelo LD.** 2009. Early defects in human T-cell development severely affect distribution and maturation of thymic stromal cells: possible implications for the pathophysiology of Omenn syndrome. *Blood* **114:**105–108. PubMed
22. **Sharfe N, Shahar M, Roifman CM.** 1997. An interleukin-2 receptor γ chain mutation with normal thymus morphology. *J Clin Invest* **100:**3036–3043. PubMed
23. **Frucht DM, Gadina M, Jagadeesh GJ, Aksentijevich I, Takada K, Bleesing JJ, Nelson J, Muul LM, Perham G, Morgan G, Gerritsen EJ, Schumacher RF, Mella P, Veys PA, Fleisher TA, Kaminski ER, Notarangelo LD, O'Shea JJ, Candotti F.** 2001. Unexpected and variable phenotypes in a family with JAK3 deficiency. *Genes Immun* **2:**422–432. PubMed
24. **Sharfe N, Dadi HK, Shahar M, Roifman CM.** 1997. Human immune disorder arising from mutation of the α chain of the interleukin-2 receptor. *Proc Natl Acad Sci USA* **94:**3168–3171. PubMed
25. **Bennett CL, Christie J, Ramsdell F, Brunkow ME, Ferguson PJ, Whitesell L, Kelly TE, Saulsbury FT, Chance PF, Ochs HD.** 2001. The immune dysregulation, polyendocrinopathy, enteropathy, X-linked syndrome (IPEX) is caused by mutations of *FOXP3*. *Nat Genet* **27:**20–21. PubMed
26. **Bernasconi A, Marino R, Ribas A, Rossi J, Ciaccio M, Oleastro M, Ornani A, Paz R, Rivarola MA, Zelazko M, Belgorosky A.** 2006. Characterization of immunodeficiency in a patient with growth hormone insensitivity secondary to a novel *STAT5b* gene mutation. *Pediatrics* **118:**e1584–e1592.
27. **Holland SM, DeLeo FR, Elloumi HZ, Hsu AP, Uzel G, Brodsky N, Freeman AF, Demidowich A, Davis J, Turner ML, Anderson VL, Darnell DN, Welch PA, Kuhns DB, Frucht DM, Malech HL, Gallin JI, Kobayashi SD, Whitney AR, Voyich JM, Musser JM, Woellner C, Schäffer AA, Puck JM, Grimbacher B.** 2007. *STAT3* mutations in the hyper-IgE syndrome. *N Engl J Med* **357:**1608–1619. PubMed
28. **Woellner C, Gertz EM, Schäffer AA, Lagos M, Perro M, Glocker EO, Pietrogrande MC, Cossu F, Franco JL, Matamoros N, Pietrucha B, Heropolitańska-Pliszka E, Yeganeh M, Moin M, Español T, Ehl S, Gennery AR, Abinun M, Breborowicz A, Niehues T, Kilic SS, Junker A, Turvey SE, Plebani A, Sánchez B, Garty BZ, Pignata C, Cancrini C, Litzman J, Sanal O, Baumann U, Bacchetta R, Hsu AP, Davis JN, Hammarström L, Davies EG, Eren E, Arkwright PD, Moilanen JS, Viemann D, Khan S, Maródi L, Cant AJ, Freeman AF, Puck JM, Holland SM, Grimbacher B.** 2010. Mutations in *STAT3* and diagnostic guidelines for hyper-IgE syndrome. *J Allergy Clin Immunol* **125:**424–432.e8. doi:10.1016/j.jaci.2009.10.059.
29. **Grunebaum E, Cohen A, Roifman CM.** 2013. Recent advances in understanding and managing adenosine deaminase and purine nucleoside phosphorylase deficiencies. *Curr Opin Allergy Clin Immunol* **13:**630–638. PubMed
30. **Jain A, Ma CA, Liu S, Brown M, Cohen J, Strober W.** 2001. Specific missense mutations in NEMO result in hyper-IgM syndrome with hypohydrotic ectodermal dysplasia. *Nat Immunol* **2:**223–228. PubMed
31. **Zonana J, Elder ME, Schneider LC, Orlow SJ, Moss C, Golabi M, Shapira SK, Farndon PA, Wara DW, Emmal SA, Ferguson BM.** 2000. A novel X-linked disorder of immune deficiency and hypohidrotic ectodermal dysplasia is allelic to incontinentia pigmenti and due to mutations in *IKK-gamma* (*NEMO*). *Am J Hum Genet* **67:**1555–1562. PubMed
32. **Courtois G, Smahi A, Reichenbach J, Döffinger R, Cancrini C, Bonnet M, Puel A, Chable-Bessia C, Yamaoka S, Feinberg J, Dupuis-Girod S, Bodemer C, Livadiotti S, Novelli F, Rossi P, Fischer A, Israël A, Munnich A, Le Deist F, Casanova JL.** 2003. A hypermorphic IκBα mutation is associated with autosomal dominant anhidrotic ectodermal dysplasia and T cell immunodeficiency. *J Clin Invest* **112:**1108–1115. PubMed
33. **Ariga T, Nakajima M, Yoshida J, Yamato K, Nagatoshi Y, Yanai F, Caviles AP, Nelson DL, Sakiyama Y.** 2004. Confirming or excluding the diagnosis of Wiskott-Aldrich syndrome in children with thrombocytopenia of an unknown etiology. *J Pediatr Hematol Oncol* **26:**435–440. PubMed

34. **Su HC.** 2010. Dedicator of cytokinesis 8 (DOCK8) deficiency. *Curr Opin Allergy Clin Immunol* **10:**515–520. PubMed
35. **Dasouki M, Okonkwo KC, Ray A, Folmsbeel CK, Gozales D, Keles S, Puck JM, Chatila T.** 2011. Deficient T Cell Receptor Excision Circles (TRECs) in autosomal recessive hyper IgE syndrome caused by DOCK8 mutation: implications for pathogenesis and potential detection by newborn screening. *Clin Immunol* **141:**128–132. PubMed
36. **Coffey AJ, Brooksbank RA, Brandau O, Oohashi T, Howell GR, Bye JM, Cahn AP, Durham J, Heath P, Wray P, Pavitt R, Wilkinson J, Leversha M, Huckle E, Shaw-Smith CJ, Dunham A, Rhodes S, Schuster V, Porta G, Yin L, Serafini P, Sylla B, Zollo M, Franco B, Bolino A, Seri M, Lanyi A, Davis JR, Webster D, Harris A, Lenoir G, de St Basile G, Jones A, Behloradsky BH, Achatz H, Murken J, Fassler R, Sumegi J, Romeo G, Vaudin M, Ross MT, Meindl A, Bentley DR.** 1998. Host response to EBV infection in X-linked lymphoproliferative disease results from mutations in an SH2-domain encoding gene. *Nat Genet* **20:**129–135. PubMed
37. **Sayos J, Wu C, Morra M, Wang N, Zhang X, Allen D, van Schaik S, Notarangelo L, Geha R, Roncarolo MG, Oettgen H, De Vries JE, Aversa G, Terhorst C.** 1998. The X-linked lymphoproliferative-disease gene product SAP regulates signals induced through the co-receptor SLAM. *Nature* **395:**462–469. PubMed
38. **Marsh RA, Madden L, Kitchen BJ, Mody R, McClimon B, Jordan MB, Bleesing JJ, Zhang K, Filipovich AH.** 2010. XIAP deficiency: a unique primary immunodeficiency best classified as X-linked familial hemophagocytic lymphohistiocytosis and not as X-linked lymphoproliferative disease. *Blood* **116:**1079–1082. PubMed
39. **Rigaud S, Fondanèche MC, Lambert N, Pasquier B, Mateo V, Soulas P, Galicier L, Le Deist F, Rieux-Laucat F, Revy P, Fischer A, de Saint Basile G, Latour S.** 2006. XIAP deficiency in humans causes an X-linked lymphoproliferative syndrome. *Nature* **444:**110–114. PubMed
40. **Speckmann C, Lehmberg K, Albert MH, Damgaard RB, Fritsch M, Gyrd-Hansen M, Rensing-Ehl A, Vraetz T, Grimbacher B, Salzer U, Fuchs I, Ufheil H, Belohradsky BH, Hassan A, Cale CM, Elawad M, Strahm B, Schibli S, Lauten M, Kohl M, Meerpohl JJ, Rodeck B, Kolb R, Eberl W, Soerensen J, von Bernuth H, Lorenz M, Schwarz K, Zur Stadt U, Ehl S.** 2013. X-linked inhibitor of apoptosis (XIAP) deficiency: the spectrum of presenting manifestations beyond hemophagocytic lymphohistiocytosis. *Clin Immunol* **149:**133–141. PubMed
41. **Marsh RA, Bleesing JJ, Filipovich AH.** 2010. Using flow cytometry to screen patients for X-linked lymphoproliferative disease due to SAP deficiency and XIAP deficiency. *J Immunol Methods* **362:**1–9. PubMed
42. **Krutzik PO, Irish JM, Nolan GP, Perez OD.** 2004. Analysis of protein phosphorylation and cellular signaling events by flow cytometry: techniques and clinical applications. *Clin Immunol* **110:**206–221. PubMed
43. **Wiszniewski W, Fondaneche MC, Le Deist F, Kanariou M, Selz F, Brousse N, Steimle V, Barbieri G, Alcaide-Loridan C, Charron D, Fischer A, Lisowska-Grospierre B.** 2001. Mutation in the class II *trans*-activator leading to a mild immunodeficiency. *J Immunol* **167:**1787–1794. (Erratum, **169:**607, 2002.) PubMed
44. **Schuetz C, Huck K, Gudowius S, Megahed M, Feyen O, Hubner B, Schneider DT, Manfras B, Pannicke U, Willemze R, Knüchel R, Göbel U, Schulz A, Borkhardt A, Friedrich W, Schwarz K, Niehues T.** 2008. An immunodeficiency disease with *RAG* mutations and granulomas. *N Engl J Med* **358:**2030–2038. PubMed
45. **Avila EM, Uzel G, Hsu A, Milner JD, Turner ML, Pittaluga S, Freeman AF, Holland SM.** 2010. Highly variable clinical phenotypes of hypomorphic *RAG1* mutations. *Pediatrics* **126:**e1248–e1252. doi:10.1542/peds.2009-3171. PubMed
46. **Kuijpers TW, Ijspeert H, van Leeuwen EM, Jansen MH, Hazenberg MD, Weijer KC, van Lier RA, van der Burg M.** 2011. Idiopathic $CD4^+$ T lymphopenia without autoimmunity or granulomatous disease in the slipstream of *RAG* mutations. *Blood* **117:**5892–5896. PubMed
47. **Ambrose M, Gatti RA.** 2013. Pathogenesis of ataxia-telangiectasia: the next generation of ATM functions. *Blood* **121:**4036–4045. PubMed
48. **Felgentreff K, Perez-Becker R, Speckmann C, Schwarz K, Kalwak K, Markelj G, Avcin T, Qasim W, Davies EG, Niehues T, Ehl S.** 2011. Clinical and immunological manifestations of patients with atypical severe combined immunodeficiency. *Clin Immunol* **141:**73–82. PubMed
49. **Feske S, Gwack Y, Prakriya M, Srikanth S, Puppel SH, Tanasa B, Hogan PG, Lewis RS, Daly M, Rao A.** 2006. A mutation in Orai1 causes immune deficiency by abrogating CRAC channel function. *Nature* **441:**179–185. PubMed
50. **Feske S, Picard C, Fischer A.** 2010. Immunodeficiency due to mutations in *ORAI1* and *STIM1*. *Clin Immunol* **135:**169–182. PubMed
51. **Tokgoz H, Caliskan U, Keles S, Reisli I, Guiu IS, Morgan NV.** 2013. Variable presentation of primary immune deficiency: two cases with CD3 gamma deficiency presenting with only autoimmunity. *Pediatr Allergy Immunol* **24:**257–262. PubMed
52. **Morgan NV, Goddard S, Cardno TS, McDonald D, Rahman F, Barge D, Ciupek A, Straatman-Iwanowska A, Pasha S, Guckian M, Anderson G, Huissoon A, Cant A, Tate WP, Hambleton S, Maher ER.** 2011. Mutation in the TCRα subunit constant gene (*TRAC*) leads to a human immunodeficiency disorder characterized by a lack of $TCR\alpha\beta^+$ T cells. *J Clin Invest* **121:**695–702. PubMed
53. **Korthäuer U, Graf D, Mages HW, Brière F, Padayachee M, Malcolm S, Ugazio AG, Notarangelo LD, Levinsky RJ, Kroczek RA.** 1993. Defective expression of T-cell CD40 ligand causes X-linked immunodeficiency with hyper-IgM. *Nature* **361:**539–541. PubMed
54. **Hauck F, Randriamampita C, Martin E, Gerart S, Lambert N, Lim A, Soulier J, Maciorowski Z, Touzot F, Moshous D, Quartier P, Heritier S, Blanche S, Rieux-Laucat F, Brousse N, Callebaut I, Veillette A, Hivroz C, Fischer A, Latour S, Picard C.** 2012. Primary T-cell immunodeficiency with immunodysregulation caused by autosomal recessive LCK deficiency. *J Allergy Clin Immunol* **130:**1144–1152.e11. doi:10.1016/j.jaci.2012.07.029. PubMed
55. **Kotlarz D, Ziętara N, Uzel G, Weidemann T, Braun CJ, Diestelhorst J, Krawitz PM, Robinson PN, Hecht J, Puchałka J, Gertz EM, Schäffer AA, Lawrence MG, Kardava L, Pfeifer D, Baumann U, Pfister ED, Hanson EP, Schambach A, Jacobs R, Kreipe H, Moir S, Milner JD, Schwille P, Mundlos S, Klein C.** 2013. Loss-of-function mutations in the IL-21 receptor gene cause a primary immunodeficiency syndrome. *J Exp Med* **210:**433–443. PubMed
56. **Siegel AM, Heimall J, Freeman AF, Hsu AP, Brittain E, Brenchley JM, Douek DC, Fahle GH, Cohen JI, Holland SM, Milner JD.** 2011. A critical role for STAT3 transcription factor signaling in the development and maintenance of human T cell memory. *Immunity* **35:**806–818. PubMed
57. **Milner JD, Brenchley JM, Laurence A, Freeman AF, Hill BJ, Elias KM, Kanno Y, Spalding C, Elloumi HZ, Paulson ML, Davis J, Hsu A, Asher AI, O'Shea J, Holland SM, Paul WE, Douek DC.** 2008. Impaired T_H17 cell differentiation in subjects with autosomal dominant hyper-IgE syndrome. *Nature* **452:**773–776. PubMed
58. **Nadeau K, Hwa V, Rosenfeld RG.** 2011. STAT5b deficiency: an unsuspected cause of growth failure, immunodeficiency, and severe pulmonary disease. *J Pediatr* **158:**701–708. (Erratum, **159:**356, 2011.) PubMed

59. **Goudy K, Aydin D, Barzaghi F, Gambineri E, Vignoli M, Ciullini Mannurita S, Doglioni C, Ponzoni M, Cicalese MP, Assanelli A, Tommasini A, Brigida I, Dellepiane RM, Martino S, Olek S, Aiuti A, Ciceri F, Roncarolo MG, Bacchetta R.** 2013. Human *IL2RA* null mutation mediates immunodeficiency with lymphoproliferation and autoimmunity. *Clin Immunol* **146:**248–261. PubMed
60. **Caudy AA, Reddy ST, Chatila T, Atkinson JP, Verbsky JW.** 2007. CD25 deficiency causes an immune dysregulation, polyendocrinopathy, enteropathy, X-linked-like syndrome, and defective IL-10 expression from CD4 lymphocytes. *J Allergy Clin Immunol* **119:**482–487. PubMed
61. **Schmalstieg FC, Leonard WJ, Noguchi M, Berg M, Rudloff HE, Denney RM, Dave SK, Brooks EG, Goldman AS.** 1995. Missense mutation in exon 7 of the common γ chain gene causes a moderate form of X-linked combined immunodeficiency. *J Clin Invest* **95:**1169–1173. PubMed
62. **Abdollahpour H, Appaswamy G, Kotlarz D, Diestelhorst J, Beier R, Schäffer AA, Gertz EM, Schambach A, Kreipe HH, Pfeifer D, Engelhardt KR, Rezaei N, Grimbacher B, Lohrmann S, Sherkat R, Klein C.** 2012. The phenotype of human STK4 deficiency. *Blood* **119:**3450–3457. PubMed
63. **Mou F, Praskova M, Xia F, Van Buren D, Hock H, Avruch J, Zhou D.** 2012. The Mst1 and Mst2 kinases control activation of rho family GTPases and thymic egress of mature thymocytes. *J Exp Med* **209:**741–759. PubMed
64. **Moshous D, Martin E, Carpentier W, Lim A, Callebaut I, Canioni D, Hauck F, Majewski J, Schwartzentruber J, Nitschke P, Sirvent N, Frange P, Picard C, Blanche S, Revy P, Fischer A, Latour S, Jabado N, de Villartay JP.** 2013. Whole-exome sequencing identifies Coronin-1A deficiency in 3 siblings with immunodeficiency and EBV-associated B-cell lymphoproliferation. *J Allergy Clin Immunol* **131:**1594–1603. PubMed
65. **Crawford G, Enders A, Gileadi U, Stankovic S, Zhang Q, Lambe T, Crockford TL, Lockstone HE, Freeman A, Arkwright PD, Smart JM, Ma CS, Tangye SG, Goodnow CC, Cerundolo V, Godfrey DI, Su HC, Randall KL, Cornall RJ.** 2013. DOCK8 is critical for the survival and function of NKT cells. *Blood* **122:**2052–2061. PubMed
66. **Stepensky P, Keller B, Buchta M, Kienzler AK, Elpeleg O, Somech R, Cohen S, Shachar I, Miosge LA, Schlesier M, Fuchs I, Enders A, Eibel H, Grimbacher B, Warnatz K.** 2013. Deficiency of caspase recruitment domain family, member 11 (CARD11), causes profound combined immunodeficiency in human subjects. *J Allergy Clin Immunol* **131:**477–485.e1. doi:10.1016/j.jaci.2012.11.050. PubMed
67. **Greil J, Rausch T, Giese T, Bandapalli OR, Daniel V, Bekeredjian-Ding I, Stütz AM, Drees C, Roth S, Ruland J, Korbel JO, Kulozik AE.** 2013. Whole-exome sequencing links caspase recruitment domain 11 (CARD11) inactivation to severe combined immunodeficiency. *J Allergy Clin Immunol* **131:**1376–1383.e3. doi:10.1016/j.jaci.2013.02.012. PubMed
68. **Chun HJ, Zheng L, Ahmad M, Wang J, Speirs CK, Siegel RM, Dale JK, Puck J, Davis J, Hall CG, Skoda-Smith S, Atkinson TP, Straus SE, Lenardo MJ.** 2002. Pleiotropic defects in lymphocyte activation caused by caspase-8 mutations lead to human immunodeficiency. *Nature* **419:**395–399. PubMed
69. **Lenardo MJ, Oliveira JB, Zheng L, Rao VK.** 2010. ALPS—ten lessons from an international workshop on a genetic disease of apoptosis. *Immunity* **32:**291–295. PubMed
70. **Puel A, Picard C, Ku CL, Smahi A, Casanova JL.** 2004. Inherited disorders of NF-κB-mediated immunity in man. *Curr Opin Immunol* **16:**34–41. PubMed
71. **Uzel G.** 2005. The range of defects associated with nuclear factor κB essential modulator. *Curr Opin Allergy Clin Immunol* **5:**513–518. PubMed
72. **Lee YN, Frugoni F, Dobbs K, Walter JE, Giliani S, Gennery AR, Al-Herz W, Haddad E, LeDeist F, Bleesing JH, Henderson LA, Pai SY, Nelson RP, El-Ghoneimy DH, El-Feky RA, Reda SM, Hossny E, Soler-Palacin P, Fuleihan RL, Patel NC, Massaad MJ, Geha RS, Puck JM, Palma P, Cancrini C, Chen K, Vihinen M, Alt FW, Notarangelo LD.** 2014. A systematic analysis of recombination activity and genotype-phenotype correlation in human recombination-activating gene 1 deficiency. *J Allergy Clin Immunol* **133:**1099–1108. PubMed
73. **Massaad MJ, Ramesh N, Geha RS.** 2013. Wiskott-Aldrich syndrome: a comprehensive review. *Ann N Y Acad Sci* **1285:**26–43. PubMed
74. **Lanzi G, Moratto D, Vairo D, Masneri S, Delmonte O, Paganini T, Parolini S, Tabellini G, Mazza C, Savoldi G, Montin D, Martino S, Tovo P, Pessach IM, Massaad MJ, Ramesh N, Porta F, Plebani A, Notarangelo LD, Geha RS, Giliani S.** 2012. A novel primary human immunodeficiency due to deficiency in the WASP-interacting protein WIP. *J Exp Med* **209:**29–34. PubMed
75. **Gulino AV, Moratto D, Sozzani S, Cavadini P, Otero K, Tassone L, Imberti L, Pirovano S, Notarangelo LD, Soresina R, Mazzolari E, Nelson DL, Notarangelo LD, Badolato R.** 2004. Altered leukocyte response to CXCL12 in patients with warts hypogammaglobulinemia, infections, myelokathexis (WHIM) syndrome. *Blood* **104:**444–452. PubMed
76. **Crequer A, Troeger A, Patin E, Ma CS, Picard C, Pedergnana V, Fieschi C, Lim A, Abhyankar A, Gineau L, Mueller-Fleckenstein I, Schmidt M, Taieb A, Krueger J, Abel L, Tangye SG, Orth G, Williams DA, Casanova JL, Jouanguy E.** 2012. Human RHOH deficiency causes T cell defects and susceptibility to EV-HPV infections. *J Clin Invest* **122:**3239–3247. PubMed
77. **Li FY, Chaigne-Delalande B, Kanellopoulou C, Davis JC, Matthews HF, Douek DC, Cohen JI, Uzel G, Su HC, Lenardo MJ.** 2011. Second messenger role for Mg^{2+} revealed by human T-cell immunodeficiency. *Nature* **475:**471–476. PubMed
78. **Li FY, Chaigne-Delalande B, Su H, Uzel G, Matthews H, Lenardo MJ.** 2014. XMEN disease: a new primary immunodeficiency affecting Mg^{2+} regulation of immunity against Epstein-Barr virus. *Blood* **123:**2148–2152. PubMed
79. **van Montfrans JM, Hoepelman AI, Otto S, van Gijn M, van de Corput L, de Weger RA, Monaco-Shawver L, Banerjee PP, Sanders EA, Jol-van der Zijde CM, Betts MR, Orange JS, Bloem AC, Tesselaar K.** 2012. CD27 deficiency is associated with combined immunodeficiency and persistent symptomatic EBV viremia. *J Allergy Clin Immunol* **129:**787–793.e6. doi:10.1016/j.jaci.2011.11.013. PubMed
80. **Salzer E, Daschkey S, Choo S, Gombert M, Santos-Valente E, Ginzel S, Schwendinger M, Haas OA, Fritsch G, Pickl WF, Förster-Waldl E, Borkhardt A, Boztug K, Bienemann K, Seidel MG.** 2013. Combined immunodeficiency with life-threatening EBV-associated lymphoproliferative disorder in patients lacking functional CD27. *Haematologica* **98:**473–478. PubMed
81. **Geier CB, Piller A, Linder A, Sauerwein KM, Eibl MM, Wolf HM.** 2015. Leaky RAG deficiency in adult patients with impaired antibody production against bacterial polysaccharide antigens. *PLoS One* **10:**e0133220. doi:10.1371/journal.pone.0133220.
82. **Mallott J, Kwan A, Church J, Gonzalez-Espinosa D, Lorey F, Tang LF, Sunderam U, Rana S, Srinivasan R, Brenner SE, Puck J.** 2013. Newborn screening for SCID identifies patients with ataxia telangiectasia. *J Clin Immunol* **33:**540–549.
83. **Borte S, Fasth A, von Döbeln U, Winiarski J, Hammarström L.** 2014. Newborn screening for severe T and B cell lymphopenia identifies a fraction of patients with Wiskott-Aldrich syndrome. *Clin Immunol* **155:**74–78.
84. **Shearer WT, Rosenblatt HM, Gelman RS, Oyomopito R, Plaeger S, Stiehm ER, Wara DW, Douglas SD, Luzuriaga K, McFarland EJ, Yogev R, Rathore MH, Levy W, Graham BL, Spector SA; Pediatric AIDS Clinical Trials Group.** 2003. Lymphocyte subsets in healthy children from birth through 18 years of age: the Pediatric AIDS Clinical Trials Group P1009 study. *J Allergy Clin Immunol* **112:**973–980.

Antibody Deficiencies

KIMBERLY C. GILMOUR, ANITA CHANDRA, AND D.S. KUMARARATNE

76

DISORDERS CHARACTERIZED BY ANTIBODY DEFICIENCY

Antibody deficiency can be defined as a condition characterized by a reduction in serum immunoglobulin concentrations below the fifth centile for age. Antibody deficiency may affect all classes of immunoglobulins or may be confined to a single isotype.

WHO SHOULD BE INVESTIGATED FOR ANTIBODY DEFICIENCY: CLINICAL MANIFESTATIONS OF ANTIBODY DEFICIENCY

Key Concepts

1. Patients with antibody deficiency typically develop recurrent infection with encapsulated bacteria such as *Streptococcus pneumoniae* and *Haemophilus influenzae* type B. The common sites affected are the upper and lower respiratory tracts and the middle ear. From these sites, infection can spread via the bloodstream to produce metastatic infections, for example meningitis or bone and joint infection.

2. Structural lung damage (bronchiectasis, pulmonary fibrosis) can be a consequence of recurrent respiratory tract infections in untreated or inadequately treated, antibody-deficient patients, and contributes to morbidity and mortality. Once respiratory tract damage is established, patients are prone to sinopulmonary sepsis caused by nontypeable *Haemophilus influenzae* strains and with other bacterial species like *Pseudomonas*. Granulomatous lesions may affect the lungs, giving rise to a sarcoid-like state with impaired gas transfer and secondary fibrosis, or they may affect other organs like the liver, spleen, kidneys, or lymph nodes.

3. Diarrhea and malabsorption may occur due to chronic infection with intestinal pathogens including *Giardia*, *Campylobacter*, *Salmonella*, or Norovirus, or as a consequence of bacterial overgrowth in the small intestine.

4. In general, the course of uncomplicated viral infection (chicken pox, measles, etc.) is not significantly different from that in normal individuals, except for the rare occurrence of enteroviral infections; ECHO viruses or Coxsakie viruses can cause meningoencephalitis or dermatomyositis-like conditions. Oral polio vaccine-associated poliomyelitis has also been rarely reported in patients with antibody deficiency.

5. Arthritis has been reported in about 20% of patients and may be septic, caused by *Haemophilus influenzae* type b, *S. pneumoniae*, or *Mycoplasma/ureoplasma*, or aseptic, resembling seronegative rheumatoid arthritis.

6. Fungal and intracellular bacterial infections are not a feature of antibody deficiency.

7. About one-fifth of patients with antibody deficiency due to common variable immunodeficiency (CVID) develop autoimmune disorders. These include autoimmune hematological disorders (hemolytic anemia, autoimmune thrombocytopenia, pernicious anemia), autoimmune endocrinopathies (e.g., thyroid disease) or neurological diseases such as Guillain Barre Syndrome, and, rarely, a lupus-like syndrome.

8. Infants with antibody deficiency may present with failure to thrive.

MAJOR CATEGORIES OF PRIMARY ANTIBODY DEFICIENCY

Antibody deficiency may occur on its own or as part of a syndrome of severe combined immunodeficiency or combined B- and T-cell immunodeficiency. The latter two conditions are outside the scope of this chapter. The main features of primary antibody deficiencies are summarized in Tables 1 and 2.

APPROACH TO EVALUATION OF PATIENTS WITH SUSPECTED ANTIBODY DEFICIENCY

Antibody deficiency should be considered in patients with the following problems:

1. Recurrent, severe, or persistent sinopulmonary infections
2. Invasive encapsulated bacterial infections
3. Chronic diarrhea, malabsorption, or occasionally inflammatory bowel disease
4. Infants with failure to thrive

Suspected antibody deficiency should be confirmed with:

1. Measurement of serum IgG, IgA and IgM (IgG subclasses), and comparison with age-specific normal ranges to determine if these levels are below the 5th centile.

doi:10.1128/9781555818722.ch76

TABLE 1 The main phenotypes of primary antibody deficiencies[a]

Phenotype	Main clinical features	Main B-cell biological features	Known affected proteins
Pan-agammaglobulinemia (absence of IgM, IgG, and IgA)	Bacterial infections with encapsulated organisms (mainly respiratory tract) and enteroviral infections	Absence of $CD19^+$ B cells	λ5, BLNK, BTK, Cμ, Igα, Igβ, and PI3Kα May have trisomy 7 or 8 or dyskeratosis congenita
Pan-agammaglobulinemia in association with thymoma	Bacterial and opportunistic infections; autoimmunity	Decreased number of pro-B cells	Unknown
Variable pan-hypogammaglobulinemia (CVID)	Bacterial infections (affecting respiratory tract and GI system), autoimmunity, lymphoproliferation, and systemic granulomata	Decreased frequency of $CD27^+$ memory B cells; defective plasma cells in tissues	CD19, CD20, CD21, CD27, CD81, DNMT3B, ZBTB24, ICOS, SAP, XIAP, TACI, BAFFR
CSR deficiencies: reduced or absent IgG and IgA with normal or low IgM	Bacterial and opportunistic infections	Decreased frequency of $CD27^+$ memory B cells	CD40 and CD40L
	Bacterial infections, autoimmunity and lymphadenopathies	Normal frequency of $CD27^+$ B cells	AID and UNG, PMS2, PI3Kδ, NEMO
Isotype or light chain deficiencies:			
Variable low Igs	May be asymptomatic		Mutation or chromosomal deletion at 14q32
All Igs have lambda light chain	Asymptomatic		Mutations in κ constant gene
Isolated IgG subclass deficiency	Usually asymptomatic; minority poor Ab response to specific antigen and recurrent viral/bacterial infections	Normal B-cell numbers	Unknown
IgA with IgG subclass deficiency	Recurrent bacterial infections		Unknown
Selective IgA deficiency	Majority asymptomatic; some have recurrent bacterial infections with poor Ab responses; may have allergies or autoimmune disease		Unknown
Specific antibody deficiency (normal Ig concentrations)	Bacterial infections after 2 years of age associated with defective polysaccharide-specific Ab production	Normal B-cell numbers	NF-κB pathway proteins (CARD11, HOIL1, IκBα, and NEMO), BTK, LRBA, and CD20

[a]Abbreviations: AID, activation-induced cytidine deaminase; BAFFR, BAFF receptor; BTK, Bruton's tyrosine kinase; BLNK, B-cell linker; Cμ, constant region μ; CD40L, CD40 ligand; CSR, class switch recombination; CVID, common variable immunodeficiency; ICOS, inducible T-cell c-stimulator; NF-κB, nuclear factor κB; PI3K, phosphoinositide 3-kinase; SAP, SLAM-associated protein; TACI, transmembrane activator and CAML interactor; UNG, uracil *N*-glycosylase; PMS2, postmeiotic segregation 2; LRBA, lipopolysaccharide beige-like anchor protein; Ab, antibody.

2. In those above 20 years of age, serum protein electrophoresis, and if required, immunofixation should be carried out for the exclusion of paraproteinemia.
3. Assess response to immunization with T-cell-dependent (tetanus toxoid, haemophilus B conjugate), and T-cell-independent (polyvalent pneumococcal polysaccharide) (if >2 years of age) vaccines. The use and interpretation of these vaccine responses or the diagnosis of antibody deficiency is described in Orange et al., 2012 (1).

Antibody Deficiency Associated with Absent B Cells

B-cell maturation beyond the pre-B-cell stage found in the bone marrow requires signals received through the pre-B-cell receptor complex. The pre-B-cell receptor is composed of the μ chains, surrogate light chains (heterodimers of λ constant region with V pre-β), and the signal-transducing components Igα and Igβ. The activities of the protein Bruton's tyrosine kinase (BTK) and B-cell linker protein (BLNK) are also essential for the transduction of signals received via the B-cell (and pre-B-cell) receptors. Therefore, it is not surprising that mutations in each of these elements cause early onset antibody deficiency associated with lack of circulating B cells.

Ninety percent of all such cases occur in boys due to mutation of the *BTK* gene (2), which maps to the X chromosome (Xp22). This condition is called X-linked agammaglobulinemia, which was the first immunodeficiency to be described in 1952 by Colonel Ogden Bruton. Mutations in the genes, including μ (3), λ5 (4), Igα (5), Igβ (6), and BLNK (7) cause rare autosomal recessive forms of early onset antibody deficiency with severe B lymphopenia.

TABLE 2 Inheritance of antibody deficiencies

Disease	Gene affected	Inheritance	Online Mendelian Inheritance in Man (OMIM) number	Reference
BTK deficiency	*BTK*	X linked	300300	Vetrie et al., 1993 (2)
μ heavy chain deficiency	μ heavy chain	AR	147020	Yel et al., 1996 (3)
λ5 deficiency	λ5 part of surrogate light chain	AR	146770	Minegishi et al., 1998 (4)
Igα deficiency	*CD79a*	AR	112205	Minegishi et al., 1999 (18)
Igβ deficiency	*CD79b*	AR	147245	Ferrari et al., 2007 (9)
BLNK deficiency	*BLNK*	AR	604615	Minegishi et al., 1999 (7)
PI3k p85 alpha deficiency	*PI3KR1*	AR	171833	Conley et al., 2012 (19)
CD19 deficiency	*CD19*	AR	107265	van Zelm et al., 2006 (20)
CD20 deficiency	*CD20*	AR	112210	Kuijpers et al., 2010 (21)
CD21 deficiency	*CD21*	AR	120650	Thiel et al., 2012 (22)
CD81 deficiency	*CD81*		186845	van Zelm et al., 2010 (23)
DNMT3B deficiency (ICF1)	*DNMT3B*	AR	242860	Xu et al., 1999 (24)
ZBTB24 (ICF2)	*ZBTB24*	AR	242860	de Greef et al., 2011 (25)
ICOS deficiency	*ICOS*	AR	604558	Grimbacher et al., 2003 (26)
SAP deficiency	*SH2D1A*	XL	308240	Sayos et al., 1998 (27)
XIAP deficiency	*XIAP*	XL	300635	Rigaud et al., 2006 (28)
TACI deficiency	*TNFRSF13B*	AR, AD, or complex	604907	Castigli et al., 2005 (29)
BAFFR deficiency	*TNFRSF13C*	AR	606269	Warnatz et al., 2009 (30)
CD40 deficiency (HIGM3)	CD40	AR	109535	Ferrari et al., 2001 (9)
CD40L deficiency (HIGM1)	CD40L	XL	300386	Korthäuer et al., 1993 (8)
AID deficiency (HIGM2)	*AICDA*	AR	605257	Revy et al., 2000 (31)
UNG (HIGM5) deficiency	*UNG*	AR	191525	Imai et al., 2003 (32)
PMS2 deficiency	*PMS2*	AR	600259	Péron et al., 2008 (33)
Activated PI3kinase-delta syndrome (APDS)	*PI3KCD*	AD	602839	Angulo et al., 2013 (10)
CARD11 deficiency	*CARD11*	AD and AR	607210	Stepensky et al., 2013 (34)
HOIL1 deficiency	*RBCK1*	AR	610924	Boisson et al., 2012 (35)
NEMO deficiency	*IKBKG*	XL	300291, 300584, 300301	Döffinger et al., 2001 (36)
IκBα deficiency	*IKBA*	AD	612132	Courtois et al., 2003 (37)

Antibody Deficiency Due to Defect in Immunoglobulin Isotope Switching

During primary antibody responses, B cells initially produce IgM and later on in the response switch to the production of IgG, IgA, and IgE.

During the so-called immunoglobulin class-switching process, the heavy-chain constant region changes while antigen specificity is maintained. Immunoglobulin class switch takes place within germinal centers contained within B-cell follicles of the secondary lymphoid organs. Another process that occurs within germinal centers is somatic hypermutation, which results in the sequential accumulation of point mutations in the Ig variable-region gene. If the point mutation(s) result in increased binding affinity to the inducing antigen, the B-cell blasts (centrocytes) survive, proliferate, and eventually give rise to memory B cells and plasma cells that secrete high-affinity antibody (this process is called affinity maturation). Through these processes, memory B cells are generated within germinal centers.

Defects in genes encoding molecules required for the above processes, which operate within germinal centers, result in a form of antibody deficiency with elevated (or normal) IgM levels but lacking IgG, IgA, and IgE. These conditions are called hyper-IgM syndromes (HIGM). A key requirement for germinal center formation and function is the interaction of CD40 (belonging to the TNF-receptor superfamily) found on the surface of B cells with an "activation induced" CD40-ligand (CD40L) protein expressed on the surface of CD4 lymphocytes. Mutations in the *CD40L* (8) gene or the *CD40* (9) gene result in X-linked (relatively

common) and autosomal recessive (rare) HIGM, respectively. Patients with the CD40L deficiency suffer from recurrent bacterial infections typical of antibody deficiency. However, because CD40L function is required for optimal T-cell immunity, they also suffer from opportunistic infections characteristic of T-cell deficiency. About one-third of patients with CD40L deficiency develop *Pneumocystis pneumonia*. Infections with cryptosporidiosis, toxoplasmosis, and nontuberculous mycobacteria also occur in this condition. These opportunistic infections can be explained on the basis that the interaction of CD40L on activated T cells with CD40 expressed on the surface of macrophages and dendritic cells, which in turn undergo maturation and activation, is required for the optimum expression of antimicrobial immunity.

A high proportion of CD40L-deficient patients develop progressive liver damage (sclerosing cholangitis), probably the result of cryptosporidial infection of the bile ducts.

Defects in the RNA-editing enzymes, activation-induced cytidine deaminase (AID), and uracil-DNA glycosylase (UNG) result in two further types of hyper-IgM syndromes: defective class switching and affinity maturation. Mutations in the gene encoding the PMS2 component of the mismatch repair machinery cause a variable but significant defect in class-switch recombination.

Signaling through CD40, which belongs to the TNF-receptor superfamily, depends on the activation of the inhibitor of κ kinase complex, resulting in the induction of NF-κB. Hypomorphic mutations of the gamma subunit of the inhibitor of κ kinase complex, which is called NEMO (NF-κB essential modulator), impair NF-κB activation. Patients with mutations in NEMO develop a complex immunodeficiency, which includes features of the hyper-IgM syndrome.

An activating heterozygous mutation in PI3 kinase δ is responsible for about 10% of cases of hyper-IgM syndrome without one of the genetic defects described above, and is characterized by IgG2 subclass deficiency, normal or modestly elevated serum IgM levels, impaired specific antibody responses to bacterial capsular polysaccharides, and recurrent respiratory infection with progressive lung damage (10).

Common Variable Immune Deficiency

Most patients with primary antibody deficiency are collected under the heading "common variable immune deficiency," which is a condition characterized by low serum IgG and IgA and a variable decrease in IgM and the impaired production of specific antibodies following natural microbial exposure or immunization. The estimated prevalence of CVID is between 1 in 10,000 and 1 in 50,000. Clinically, CVID is dominated by the effects of antibody deficiency. About 20% of patients with CVID develop autoimmune disorders (arthritis, cytopenias, endocrinopathies). Some patients with CVID develop noncaseating sarcoidlike granulomata infiltrating various organs (lungs, liver, spleen, skin). The mechanisms underlying autoimmunity and granulomatous disease in CVID are unknown.

The immunological phenotype of CVID is heterogeneous with documented defects in B-cell survival, generation of B memory cells, and *in vitro* B- and T-cell activation. About 10% of cases of CVID are familial, with a predominance of autosomal dominant or autosomal recessive inheritance. CVID or selective IgA deficiency can affect different members of the same kindred. Recently, a number of gene defects have been identified in CVID patients, accounting for about 10 to 15% of the total patient pool.

The most common defect (in approximately 10% of CVID patients) is a mutation of the gene TACI (transmembrane activator and calcium modulator and cyclophilin ligand interacter). TACI, which belongs to the TNF-receptor superfamily, is a ligand for the cytokines BAFF (B-cell-activating factor of the TNF family) and APRIL (a proliferation-induced ligand), which induce immunoglobulin class-switch recombination.

Mice deficient in BAFF or its receptor have impaired B-cell development and antibody deficiency. TACI$^{-/-}$ mice have reduced serum IgA and IgM levels, reduced antibody responses to T-cell-independent antigens, and tend to develop autoimmunity and B lymphoproliferation. Mutations in TACI have been found in CVID patients and their relatives, with selective IgA deficiency, indicating variable penetrance of this gene defect. In the majority of currently documented patients, TACI mutations affect only one allele, indicating a dominant negative effect of the mutated gene. A possible explanation is that TACI, like other members of the TNF-receptor family, undergo ligand-independent preassociation and function as multimeric units. Thus, incorporation of a mutated TACI chain in this multimeric complex may disrupt ligand binding or signal-transducing capacity. Recent studies have found that family members of CVID patients possessing heterozygous TACI mutations may have completely normal serum immunoglobulin levels and "*in vitro*" B-cell function. This leads to the conclusion that the development of antibody deficiency in those carrying heterozygous TACI mutations may depend on modifier genes or environmental factors.

Inducible costimulating receptor (ICOS) is a costimulatory T-cell molecule that induces cytokines required for supporting class-switch recombination, Ig production, and terminal B-cell differentiation. ICOS$^{-/-}$ and ICOS ligand$^{-/-}$ mice exhibit defective germinal center formation and antibody production. Mutations in the ICOS gene account for about 1% of CVID patients.

A single CVID patient was identified as having a mutation on the gene encoding the BAFF receptor, a finding that could be predicted from observations in BAFF$^{-/-}$ mice.

CD19 deficiency has been described in two families with CVID. CD19 is a B-cell accessory molecule that is required for B-cell activation, proliferation, and hence B-cell development. CD19$^{-/-}$ mice exhibit hypogammaglobulinemia and poor antibody responses to protein antigens. Deficiency of CD20, CD21, CD27, CD81, DNMT3B, and ZBTB24 have also been reported in rare patients with antibody deficiency.

In the case of the large majority of patients with CVID, the underlying molecular defect is unknown.

IgA Deficiency

IgA deficiency is characterized by reduced (<0.07 g/liter) or absent serum IgA levels. IgA deficiency is the most common form of primary antibody deficiency and affects about 1 in 700 Caucasians. IgA deficiency is rare in some racial groups (Japanese, Africans). The majority of IgA-deficient individuals remain free of infection due to the ability of IgG and IgM to compensate for the lack of IgA. Long-term studies have shown that a small proportion of IgA-deficient patients develop recurrent sinopulmonary or gastrointestinal infections. Most infection-prone IgA-deficient patients have concomitant IgG2 subclass deficiency and a selective inability to produce antibodies against bacterial capsular polysaccharides. IgA deficiency is associated with an increased incidence of atopy, celiac disease, and a range of autoimmune diseases, including arthritis, "lupus-like" syndrome, autoimmune endocrinopathies, and autoimmune cytopenias.

IgA-deficient patients with serum levels below 0.07 g/liter are at the risk of developing anti-IgA antibodies after receiving blood products. Such individuals are at risk of developing anaphylaxis on receiving blood products.

IgA deficiency and CVID can affect different members of the same kindred. Rarely, IgA deficiency can precede the development of CVID. Therefore, in some instances, the molecular mechanisms underlying CVID and IgA deficiency may be identical. TACI deficiency can cause IgA deficiency in some family members while others develop CVID. However, the molecular basis of IgA deficiency in most cases is largely unknown.

Genetic analyses of kindred with CVID and IgA deficiency have highlighted the existence of susceptibility loci within the MHC region of chromosome 6. The strongest linkage lies within the DR/DQ within the MHC class II region.

IgG Subclass Deficiency

Serum IgG comprises four subclasses, called IgG1, IgG2, IgG3, and IgG4, reflecting the relative abundance of these isotypes in the serum. IgG subclass deficiency is diagnosed on finding a reduction in the serum concentration of IgG subclasses, of more than two standard deviations below the mean value for age, despite the total IgG level being normal. In practice, IgG subclass assays are difficult to standardize due to the lack of an internationally accepted reference preparation. Furthermore, genetic variations that influence serum IgG subclass levels exist among different ethnic groups. Hence, age- and population-related normal ranges are not always available.

Some individuals with IgG subclass deficiencies are asymptomatic. Others with IgG subclass deficiencies are prone to recurrent sinopulmonary infections. Such infection-prone patients exhibit reduced antibody responses to bacterial capsular polysaccharides. Defective antipolysaccharide antibody responses are most often seen in individuals with IgG2 subclass deficiency with or without concomitant IgA deficiency. The molecular mechanisms underlying IgG subclass deficiencies are unknown.

THE LABORATORY INVESTIGATION OF PRIMARY ANTIBODY DEFICIENCY

Figure 1 shows an algorithm for suggested laboratory investigations.

Methods

Flow Cytometry

Flow cytometry is a widely available technology that can be used to examine surface markers (extracellular staining) and intracellular proteins (intracellular staining). Extracellular fluorescent staining for lymphocyte markers (CD3, CD19, $CD56^{+}16$, CD4, CD8) is readily available.

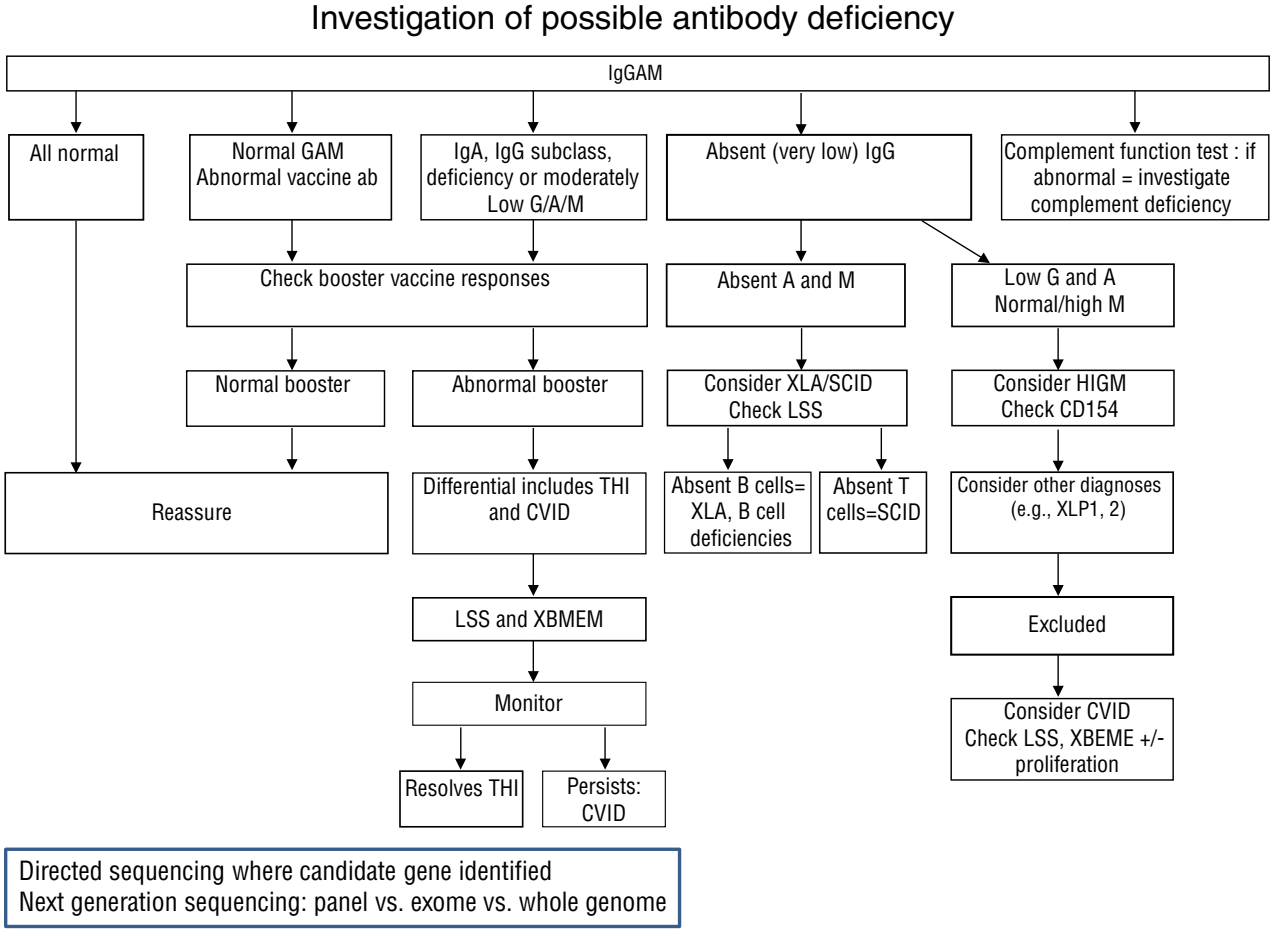

FIGURE 1 Investigation of possible antibody deficiency. This picture shows laboratory investigations in patients suspected of antibody deficiency.

Extended B-Cell Immunophenotyping

Extended B-cell immunophenotyping enables the measurement of different subtypes of B cells, which aids in the classification of CVID as patients with few switched memory B cells may have defects in genes such as ICOS and CD40L, those with increased transitional B cells tend to have lymphadenopathy, and the presence of elevated CD21low B cells correlates with splenomegaly (11).

Materials and Reagents

5-ml FACS tubes (VWR, catalog no. 734-0442)
CD27 (V500) (Becton Dickinson, catalog no. 561222)
CD38 (PerCp Cy5.5) (Becton Dickinson, catalog no. 551400)
IgM (Alexa 647) (Stratech Scientific, catalog no. 309-605-095)
CD19 (Pe-Cy7) (Becton Dickinson, catalog no. 341113)
IgD (FITC) (Life Technologies, catalog no. H15501)
CD21 (PE) (Becton Dickinson, catalog no. 555422)
FACS Lyse (Becton Dickinson, catalog no. 349202)
Cell Wash (Becton Dickinson, catalog no. 349524)
Cell Fix (Becton Dickinson, catalog no. 340181)
300 μl of EDTA blood from the patient – should be stained within 72 hours of collection

Procedure

1. Label tube with patient identifiers.
2. Add 300 μl of whole blood to a FACS tube. Mark the volume on the side of the tube.
3. Add 3 ml of Cell Wash and mix.
4. Spin for 45 seconds in the bench-top centrifuge at 1,000 rpm (relative centrifugal force of 800).
5. Using a Pasteur pipette, remove the supernatant, leaving the packed cells.
6. Add 3 ml of Cell Wash and resuspend the cell pellet.
7. Spin for 45 seconds in the centrifuge.
8. Using a Pasteur pipette, remove the supernatant, leaving the packed cells.
9. Add 3 ml of Cell Wash and resuspend the cell pellet.
10. Spin for 45 seconds in the centrifuge.
11. Using a Pasteur pipette, remove the supernatant, leaving the packed cells.
12. Resuspend using cell wash to the marked line on the tube.
13. Add 2 μl of antibodies (predilute IgM 1/100) to the bottom of a new tube.
14. Add 100 μl of washed blood to the bottom of the tube.
15. Mix all of the tubes well and incubate at room temperature in the dark for 10 minutes.
16. Add 1 ml of FACS Lyse to all of the tubes, mix well, and incubate at room temperature in the dark for 10 minutes.
17. At the end of the incubation, wash with the centrifuge: centrifuge on high for 45 s, and tip the supernatant off and blot the tubes on tissue. Mix all of the tubes to resuspend, and add 1 ml of Cell Wash. Centrifuge on high for 45 s, tip the supernatant off, and blot the tubes on tissue.
18. Resuspend in 500 μl Cell Wash or 500 μl Cell Fix.
19. Acquire on the day of staining using a flow cytometer that can detect 8 or more colors.
20. Analyze by gating on lymphocytes and then $CD19^+$ cells and then the different B-cell populations (see Fig. 2).

Adult normal ranges are the following: naive B cells, 43 to 82%; non-switched memory B cells, 7 to 32%; class switched memory B cells, 6.5 to 29%; $CD21^{Low}$ $CD38^{Low}$ B cells, 09 to 7.6%; transitional B cells, 0.6 to 3.5%; and plasmablasts, 0.4 to 3.6% (11). It is important to remember that memory B cells increase with age in children, and the younger the child, the more naive B cells he or she will have (12).

CD40L (CD154) Expression for Diagnosis of X-linked Hyper IgM Syndrome (HIGM)

Absence of CD154 expression is indicative of X-linked hyper-IgM syndrome (13). Whole blood is incubated with phorbol myristate acetate (PMA) and phytohemagglutinin (PHA) to stimulate the lymphocytes. Monoclonal antibodies conjugated with fluorochromes are then added, the red blood cells are lysed, and the results are acquired and analyzed by flow cytometry.

Materials and Reagents

FACS capped Tubes (VWR, catalog no. 734-0443)
5-ml FACS tubes (VWR, catalog no. 734-0442)
CD25 PE (Becton Dickinson, catalog no. 36793)
CD154 FITC (Ancell, catalog no. 353040)
CD45 PerCP (Becton Dickinson, catalog no. 347464)
CD4 APC (Becton Dickinson, catalog no. 58505)
FACS Lyse (Becton Dickinson, catalog no. 349202)
Cell Wash (Becton Dickinson, catalog no. 349524)
Cell Fix (Becton Dickinson, catalog no. 340181)
Culture media (RPMI + 10% FCS)
PHA (working solution, 320 μg/ml) (Bio-Stat Diagnostics, catalog no. HA17)
PMA (working solution, 5 μg/ml) (Sigma, catalog no. P8139)
1 ml lithium heparinized patient blood
1 ml lithium heparinized control blood (blood from any healthy adult)

Samples should be stimulated on the day the blood is taken and must be stained the day after stimulation, but the whole blood may be left at room temperature and set up to two days later as long as it has been diluted 50:50 in culture medium and kept at room temperature. These results are not as clear as samples set up on the day of receipt, and so this should be avoided if possible.

Procedure

1. Two FACS capped tubes per sample are required. In a tissue culture cabinet while following aseptic techniques, label tube one "Unstim" plus patient or control details. Label tube two "Stim" plus patient or control details.
2. Add 0.5 ml of culture medium and 0.5 ml of patient or control whole blood to each tube.
3. Add 18.5 μl of PHA working solution (final 6 μg/ml) and 4 μl of PMA working solution (final 20 ng/ml) to the "Stim" tubes. Mix gently.
4. Secure the caps loosely and incubate overnight at 37°C in CO_2.
5. Label two FACS tubes with the patient's initials and antibody combination plus 'S' for stimulated or 'U' for unstimulated. Do the same for the control. Stain both 'Stim' and 'Unstim' tubes, using CD154-FITC, CD25-PE, CD4-APC, and CD45-Percp.
6. Add 5 μl of antibody to the bottom of each tube, except for CD154.

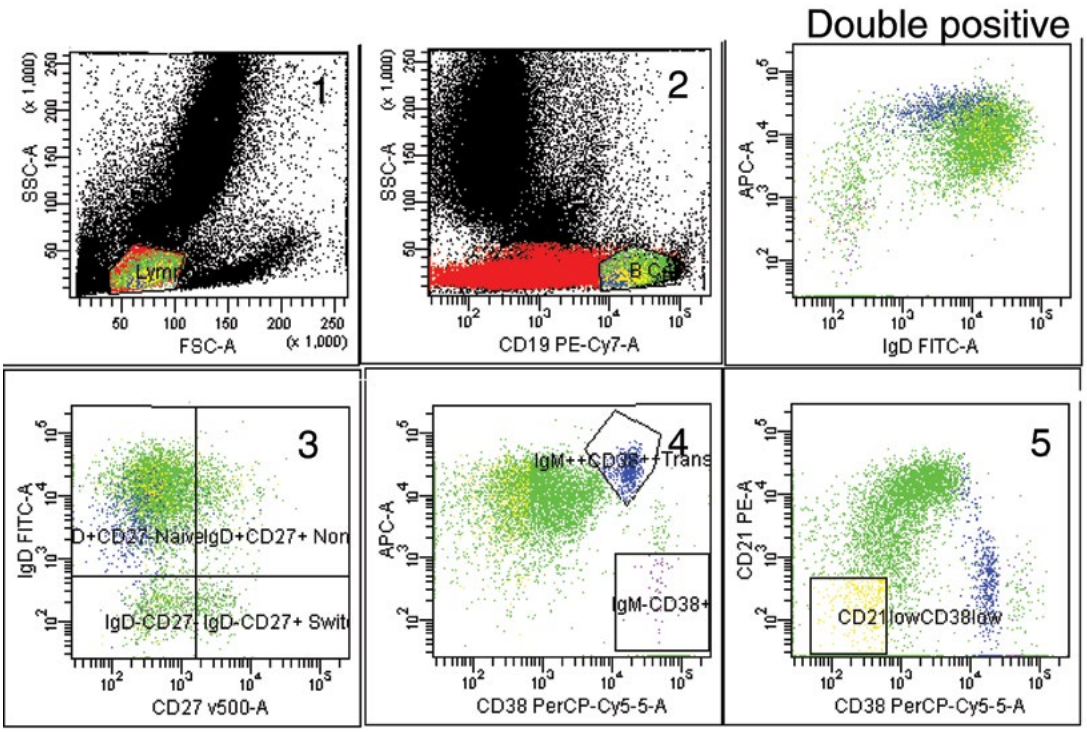

FIGURE 2 Extended B-cell immunophenotyping. The FACS plots demonstrate the gating strategy for B-cell immunophenotyping. Lymphocytes are gated based on forward (FSC) versus side scatter (SSC) (panel 1). The lymphocyte population is then used to gate B cells (CD19 versus side scatter) (panel 2). Using quadrants, naive B cells are defined as $IgD^+/CD27^-$, $IgD^+/CD27^+$ are non-switched memory B cells, and $IgD^-/CD27^+$ are switched memory B cells (panel 3). Transitional B cells are defined as $IgM^{++}CD38^+$ and IgM-$CD38^+$ B cells and plasmablasts as IgM-$CD38^+$ (panel 4). CD21low/CD38low B cells are indicated in panel 5. The presence of double-positive B cells greatly decreases the possibility of mutations in the AID gene, and they are used for back gating to confirm the IgM status of naive, switched, and non-switched memory B cells.

7. Dilute the CD154 with Cell Wash according to the manufacturer's instructions, usually 1:50. Add 80 μl of this dilution to the appropriate tubes.
8. Add 200 μl of blood/culture media to the bottom of each FACS tube. Mix thoroughly and leave to incubate at room temperature for 10 minutes.
9. Add 1 ml of 1× FACS lysing solution. Mix thoroughly (important) and leave to incubate at room temperature for 10 minutes.
10. Centrifuge on high for 45 s (1,000 rpm), tip the supernatant off, and blot the tubes on tissue.
11. Mix to resuspend. Add 1 ml of Cell Wash.
12. Centrifuge on high for 45 s, tip the supernatant off, and blot the tubes on tissue.
13. Resuspend in 500 μl of Cell Fix.
14. Acquire using a FACS that can detect four or more colors.

To analyze, compare unstimulated with stimulated scattergrams and set the quads using the unstimulated tubes. Check that cells have activated using CD25 and CD4 expression as a guide. A good stimulation should produce over 70% CD25-positive cells. Weak and absent expression with less than 70% activation should be interpreted with caution. (See Fig. 3 for examples of normal and absent CD154 expression.)

Diagnosis of X-Linked Lymphoproliferative Syndrome 1 (XLP1), X-Linked Lymphoproliferative Syndrome 2 (XLP2), and X-Linked Antibody Deficiency (XLA)

Intracellular FACS is a rapid and reliable technique for screening patients suspected of having XLP1, XLP2, or XLA. If the protein is absent or abnormal, then genetic analysis can focus on analyzing that single gene. In addition, many carriers of these X-linked conditions may be detected using this technique.

Materials

FACS capped Tubes (VWR, catalog no. 734-0443)
Anti-SLAM-associated protein (Anti-SAP) (Stratech Scientific, catalog no. H00004068-MO1)
Anti-mouse IgG1 FITC (Dako, catalog no. F0479)
Anti-BTK (gift of Toshio Miyakawi, clone 48-2H)
Anti-CD14 PE (Becton Dickinson, catalog no. 345785)
Anti-XIAP (Becton Dickinson, catalog no. 610763)
IgG1 isotype control (Becton Dickinson, catalog no. 349040)
Anti-CD56 PE (Becton Dickinson, catalog no. 345810)
Anti-CD8 PerCP (Becton Dickinson, catalog no. 345774)

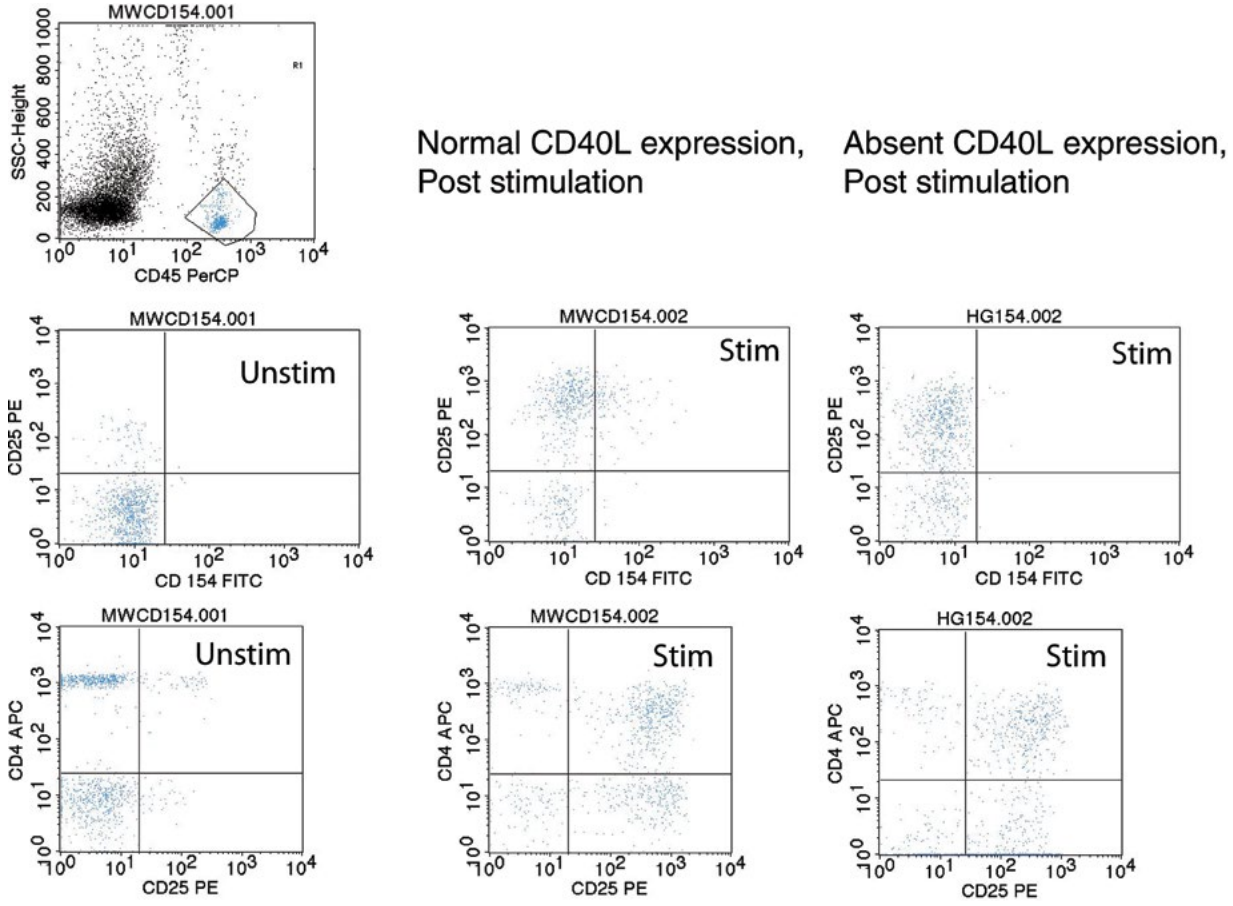

FIGURE 3 CD40L expression. Lymphocytes are defined by CD45 versus SSC. Prior to stimulation, there is limited CD25 and CD40L (CD154) expression ("Unstim" panels). Post stimulation in healthy individuals, there is an increase in both CD40L and CD25 expression (middle "Stim" panels). In patients with XHIM, although there is significant upregulation of CD25 (bottom right "Stim" panel), there is no increase in CD40L expression (top right "Stim" panel).

Anti-CD3 APC (Becton Dickinson, catalog no. 345767)
Intraprep Perm/Fix (Beckman Coulter, catalog no. A07802)
PBS/0.5% BSA/0.1 μM EDTA (SAP wash)
Cell Fix (Becton Dickinson, catalog no.340181)
DMEM/10% FCS (block)
SAP wash: phosphate-buffered saline plus 0.2 mM EDTA plus 1.0% bovine serum albumin
0.6 ml EDTA patient blood
0.6 ml EDTA control blood

Procedure

1. Label each tube with control (C) or the patient's initials and isotype (I), BTK (B), SAP (S), or XIAP (X). Add 50 μl of blood to the bottom of each tube. If BTK and SAP/XIAP expression are analyzed for the same patient, set up two isotype tubes labeled I-S/X and I-B.
2. Add 100 μl of Intraprep solution 1 to each tube and mix immediately upon addition. Incubate at room temperature for 15 minutes.
3. Add 1 ml of SAP wash, mix, add a further 2 ml of SAP wash, spin for 45 seconds in the bench top centrifuge (1,000 rpm), decant, and drain well.
4. Add 100 μl of Intraprep solution 2. Do NOT mix, but let diffuse naturally into cell pellet. Incubate at room temperature for 5 minutes.
5. Disperse the cell pellet and add 1 μl of BTK antibody, 0.5 μl of SAP antibody, 1 μL of XIAP antibody or 6 μl mouse isotype control antibody to the bottom of appropriate tubes. Incubate at room temperature for 15 minutes. Make up secondary solution during this incubation.
6. Wash two times with 2 ml of SAP wash per wash.
7. Add 100 μl of secondary solution (anti-mouse IgG FITC/SAP block/SAP wash [1 μl/10 μl/90 μl]) and incubate for 15 minutes.
8. Wash two times with 2 ml of SAP wash.
9. Add 5 μl of CD56-PE, CD8-PerCP, and CD3-APC to each tube except for the BTK and isotype tube I-B, into which 5 μl CD14 should be added instead.
10. Incubate at room temperature for 10 minutes.
11. Wash two times with 1 ml of SAP wash per wash.
12. Add 250 μl Cell Fix.
13. On a four-color FACS, acquire 20,000 $CD3^+$ events for the SAP/XIAP/isotype tubes or 20,000 $CD14^+$ events for the BTK/isotype tubes. Once fixed, samples are stable for 72 hours.

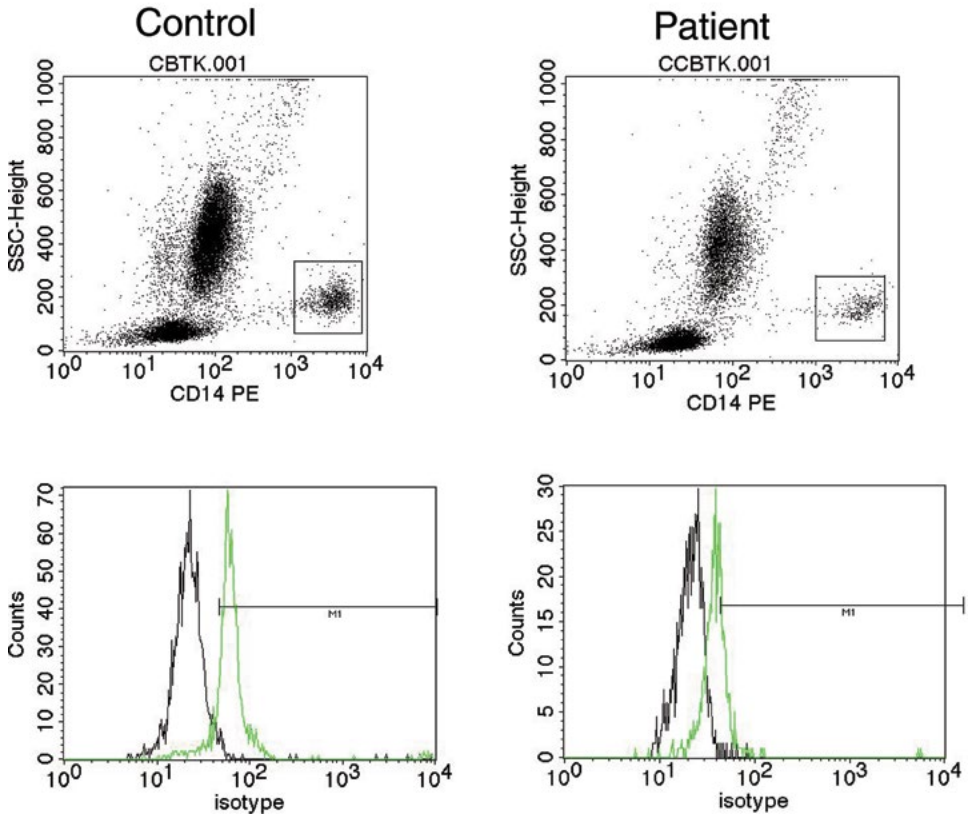

FIGURE 4 BTK analysis by FACs. Monocytes are gated by $CD14^+$ versus SSC. Histograms showing isotype staining and BTK staining are then overlaid. Many hypomorphic mutations in BTK show a partial overlay as shown in the patient sample.

14. For BTK, gate on monocytes as defined by CD14 versus SSC and then compare isotype against BTK by overlaid histograms (see Fig. 4). For the SAP/XIAP, gate on lymphocyte followed by CD8 T cells and then analyze using overlaid histogram (see Fig. 5).

GENETIC ANALYSIS

For many PIDs, a genetic diagnosis enables optimal management of the condition as well as offering carrier testing and prenatal screening. Until recently, direct sequencing (also known as Sanger sequencing) of exons and exon/intron boundaries was the method of choice.

Direct Sequencing

In direct sequencing, the exons or other regions of interest are amplified by PCR using fluorescently labeled oligonucleotides as primers. The primers bind to specific regions of DNA and enable those regions to be amplified many times. The amplified product is then separated by size and an automated reader identifies each nucleotide, resulting in a trace that shows each nucleotide in sequence order. Direct sequencing is rapid for smaller genes and detects not only nucleotide changes but also small deletions. It is a recommended method of genetic analysis for single genes (14). However, if multiple genes need to be sequenced, direct sequencing can be costly and time consuming. Direct sequencing cannot detect single chromosomal deletions, duplications, or inversions.

MPLA and aCGH

Multiplex ligation-dependent probe amplification (MLPA) is a new technique used to detect copy number variation (deletions or extra copies of a gene) (15). It is ideal for examining gene deletions in targeted genes. Like direct sequencing, the gene to be analyzed must be known. MPLA is based on denaturing the DNA and oligonucleotides, letting the oligonucleotides bind the DNA, ligating (joining) the oligonucleotides together, amplifying the product by PCR, and running and analyzing the products on a gel. MPLA can also be used to detect point mutations (single nucleotide changes), by designing the probe so that it will only bind with a normal sequence. This is useful for detecting common point mutations. MPLA is routinely used to detect deletions in the SH2DAI (XLP1) gene where exon 2 and other deletions are common.

Although relatively few antibody deficiencies are due to large deletions and duplications, array comparative genomic hybridization (aCGH) is a useful screening tool to detect copy number variation in the entire genome. Patients with chromosomal abnormalities including Down syndrome may have abnormal B cells and/or impaired antibody production (16). aCGH can detect changes in copy number where the deletion or additional copy is 100 kilobases or greater and is unbalanced. It is particularly useful for detecting deletions and duplications. There is a consensus group (the International Standards for Cytogenomic Arrays Consortium) that provides guidance as to best practice for running and interpreting this technique (www.iscaconsortium.org). The

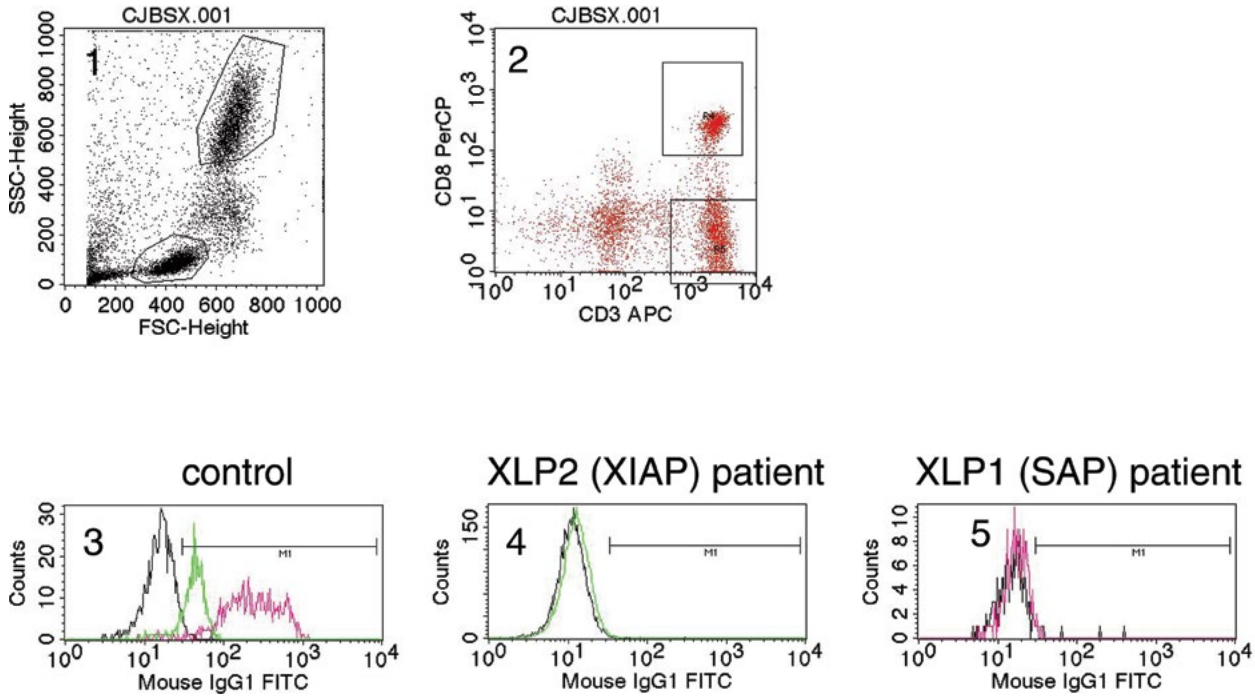

FIGURE 5 XIAP and SAP by FACs. Lymphocytes are defined based on FSC vs. SSC (panel 1). $CD8^+$ T cells are then gated based on $CD3^+/CD8^+$ (panel 2). Isotype, XIAP (green), and SAP (pink) are analyzed as overlaid histograms (panel 3), where the XIAP shift about 1 log and the SAP about 2 logs. An XLP2 patient lacks XIAP (panel 4). An XLP1 patient lacks SAP (panel 5).

basis of aCGH is that it compares the patient's genome to a reference genome and any differences are identified. Both genomes are labeled with different fluorescent probes, hybridized to normal sequence probes spanning the genome, and then measured. If the patient's sample shows decreased fluorescence in a particular area, it indicates a deletion; if the patient's sample shows an increased signal, then a duplication is identified.

NEXT-GENERATION SEQUENCING

(See reference 17 for a fuller discussion of this topic.)

Next-generation sequencing (NGS), also known as high-throughput sequencing, is a method for rapidly sequencing a large number of genes from a number of patients. The advantage of NGS is the amount of data that are rapidly generated. The entire human genome can be sequenced in less than three weeks. The main disadvantages are the analysis and storage of the data as well as the ethical considerations regarding incidental findings (also known as unsolicited information). These are the discovery of a mutation in a gene that the clinician was not expecting (e.g., finding a breast cancer mutation in a PID patient). For NGS, DNA is isolated, fragmented, and then hybridized to a library of interest. This library contains fragments of a defined list of genes or might represent the entire human exome. The hybridized fragments are then selected, and nonselected DNA is washed away. The selected DNA is then sequenced, the data generated are checked for quality and aligned to a defined human genome, and then sequence variants can be identified. Once these variants are identified, they can be compared to known databases to eliminate known variants; unknown variants can then be assessed for likely pathogenicity *in silico* and based on known gene function. The variants are then confirmed by direct sequencing, and functional assays can be performed to demonstrate that a variant is the likely cause of the disease of interest. To speed up analysis, provide better coverage, and avoid the possibility of incidental findings, a number of groups are using targeted NGS where only a subset of genes is analyzed. This is less expensive than exome sequencing, the analysis time is much more rapid, and it meets the guidelines of the European Society of Human Genetics (14). For PIDs, several groups are using the targeted approach and have identified a number of patients with mutations in rare PID genes (Dury et al., manuscript in preparation). The current approach is to use targeted NGS to rapidly screen known PID genes, and where no mutation is identified, to then undertake whole-exome sequencing.

REFERENCES

1. **Orange JS, Ballow M, Stiehm ER, Ballas ZK, Chinen J, De La Morena M, Kumararatne D, Harville TO, Hesterberg P, Koleilat M, McGhee S, Perez EE, Raasch J, Scherzer R, Schroeder H, Seroogy C, Huissoon A, Sorensen RU, Katial R.** 2012. Use and interpretation of diagnostic vaccination in primary immunodeficiency: a working group report of the Basic and Clinical Immunology Interest Section of the American Academy of Allergy, Asthma & Immunology. *J Allergy Clin Immunol* **130**(Suppl)**:**S1–S24. PubMed
2. **Vetrie D, Vorechovský I, Sideras P, Holland J, Davies A, Flinter F, Hammarström L, Kinnon C, Levinsky R, Bobrow M, et al.** 1993. The gene involved in X-linked agammaglobulinaemia is a member of the src family of protein-tyrosine kinases. *Nature* **361:**226–233. PubMed
3. **Yel L, Minegishi Y, Coustan-Smith E, Buckley RH, Trübel H, Pachman LM, Kitchingman GR, Campana D, Rohrer J, Conley ME.** 1996. Mutations in the mu

heavy-chain gene in patients with agammaglobulinemia. *N Engl J Med* **335:**1486–1493. PubMed

4. **Minegishi Y, Coustan-Smith E, Wang YH, Cooper MD, Campana D, Conley ME.** 1998. Mutations in the human lambda5/14.1 gene result in B cell deficiency and agammaglobulinemia. *J Exp Med* **187:**71–77. PubMed
5. **Minegishi Y, Hendershot LM, Conley ME.** 1999. Novel mechanisms control the folding and assembly of lambda5/14.1 and VpreB to produce an intact surrogate light chain. *Proc Natl Acad Sci USA* **96:**3041–3046. PubMed
6. **Ferrari S, Lougaris V, Caraffi S, Zuntini R, Yang J, Soresina A, Meini A, Cazzola G, Rossi C, Reth M, Plebani A.** 2007. Mutations of the Igbeta gene cause agammaglobulinemia in man. *J Exp Med* **204:**2047–2051. PubMed
7. **Minegishi Y, Rohrer J, Coustan-Smith E, Lederman HM, Pappu R, Campana D, Chan AC, Conley ME.** 1999. An essential role for BLNK in human B cell development. *Science* **286:**1954–1957. PubMed
8. **Korthäuer U, Graf D, Mages HW, Brière F, Padayachee M, Malcolm S, Ugazio AG, Notarangelo LD, Levinsky RJ, Kroczek RA.** 1993. Defective expression of T-cell CD40 ligand causes X-linked immunodeficiency with hyper-IgM. *Nature* **361:**539–541. PubMed
9. **Ferrari S, Giliani S, Insalaco A, Al-Ghonaium A, Soresina AR, Loubser M, Avanzini MA, Marconi M, Badolato R, Ugazio AG, Levy Y, Catalan N, Durandy A, Tbakhi A, Notarangelo LD, Plebani A.** 2001. Mutations of CD40 gene cause an autosomal recessive form of immunodeficiency with hyper IgM. *Proc Natl Acad Sci USA* **98:**12614–12619. PubMed
10. **Angulo I, Vadas O, Garçon F, Banham-Hall E, Plagnol V, Leahy TR, Baxendale H, Coulter T, Curtis J, Wu C, Blake-Palmer K, Perisic O, Smyth D, Maes M, Fiddler C, Juss J, Cilliers D, Markelj G, Chandra A, Farmer G, Kielkowska A, Clark J, Kracker S, Debré M, Picard C, Pellier I, Jabado N, Morris JA, Barcenas-Morales G, Fischer A, Stephens L, Hawkins P, Barrett JC, Abinun M, Clatworthy M, Durandy A, Doffinger R, Chilvers ER, Cant AJ, Kumararatne D, Okkenhaug K, Williams RL, Condliffe A, Nejentsev S.** 2013. Phosphoinositide 3-kinase δ gene mutation predisposes to respiratory infection and airway damage. *Science* **342:**866–871. PubMed
11. **Wehr C, Kivioja T, Schmitt C, Ferry B, Witte T, Eren E, Vlkova M, Hernandez M, Detkova D, Bos PR, Poerksen G, von Bernuth H, Baumann U, Goldacker S, Gutenberger S, Schlesier M, Bergeron-van der Cruyssen F, Le Garff M, Debré P, Jacobs R, Jones J, Bateman E, Litzman J, van Hagen PM, Plebani A, Schmidt RE, Thon V, Quinti I, Espanol T, Webster AD, Chapel H, Vihinen M, Oksenhendler E, Peter HH, Warnatz K.** 2008. The EUROclass trial: defining subgroups in common variable immunodeficiency. *Blood* **111:**77–85. PubMed
12. **Morbach H, Eichhorn EM, Liese JG, Girschick HJ.** 2010. Reference values for B cell subpopulations from infancy to adulthood. *Clin Exp Immunol* **162:**271–279. PubMed
13. **Gilmour KC, Walshe D, Heath S, Monaghan G, Loughlin S, Lester T, Norbury G, Cale CM.** 2003. Immunological and genetic analysis of 65 patients with a clinical suspicion of X-linked hyper-IgM. *Mol Pathol* **56:**256–262.
14. **van El CG, Cornel MC, Borry P, Hastings RJ, Fellmann F, Hodgson SV, Howard HC, Cambon-Thomsen A, Knoppers BM, Meijers-Heijboer H, Scheffer H, Tranebjaerg L, Dondorp W, de Wert GM, ESHG Public and Professional Policy Committee.** 2013. Whole-genome sequencing in health care. Recommendations of the European Society of Human Genetics. *Eur J Hum Genet* **21**(Suppl 1)**:**S1–S5. PubMed
15. **Schouten JP, McElgunn CJ, Waaijer R, Zwijnenburg D, Diepvens F, Pals G.** 2002. Relative quantification of 40 nucleic acid sequences by multiplex ligation-dependent probe amplification. *Nucleic Acids Res* **30:**e57. PubMed
16. **Ram G, Chinen J.** 2011. Infections and immunodeficiency in Down syndrome. *Clin Exp Immunol* **164:**9–16. PubMed
17. **Yang Y, Muzny DM, Reid JG, Bainbridge MN, Willis A, Ward PA, Braxton A, Beuten J, Xia F, Niu Z, Hardison M, Person R, Bekheirnia MR, Leduc MS, Kirby A, Pham P, Scull J, Wang M, Ding Y, Plon SE, Lupski JR, Beaudet AL, Gibbs RA, Eng CM.** 2013. Clinical whole-exome sequencing for the diagnosis of mendelian disorders. *N Engl J Med* **369:**1502–1511. PubMed
18. **Minegishi Y, Coustan-Smith E, Rapalus L, Ersoy F, Campana D, Conley ME.** 1999. Mutations in Igalpha (CD79a) result in a complete block in B-cell development. *J Clin Invest* **104:**1115–1121. PubMed
19. **Conley ME, Dobbs AK, Quintana AM, Bosompem A, Wang Y-D, Coustan-Smith E, Smith AM, Perez EE, Murray PJ.** 2012. Agammaglobulinemia and absent B lineage cells in a patient lacking the p85α subunit of PI3K. *J Exp Med* **209:**463–470. PubMed
20. **van Zelm MC, Reisli I, van der Burg M, Castaño D, van Noesel CJ, van Tol MJ, Woellner C, Grimbacher B, Patiño PJ, van Dongen JJ, Franco JL.** 2006. An antibody-deficiency syndrome due to mutations in the CD19 gene. *N Engl J Med* **354:**1901–1912. PubMed
21. **Kuijpers TW, Bende RJ, Baars PA, Grummels A, Derks IAM, Dolman KM, Beaumont T, Tedder TF, van Noesel CJM, Eldering E, van Lier RAW.** 2010. CD20 deficiency in humans results in impaired T cell-independent antibody responses. *J Clin Invest* **120:**214–222. PubMed
22. **Thiel J, Kimmig L, Salzer U, Grudzien M, Lebrecht D, Hagena T, Draeger R, Voelxen N, Bergbreiter A, Jennings S, Gutenberger S, Aichem A, Illges H, Hannan JP, Kienzler A-K, Rizzi M, Eibel H, Peter H-H, Warnatz K, Grimbacher B, Rump J-A, Schlesier M.** 2012. Genetic CD21 deficiency is associated with hypogammaglobulinemia. *J Allergy Clin Immunol* **129:**801–810.e6. PubMed
23. **van Zelm MC, Smet J, Adams B, Mascart F, Schandené L, Janssen F, Ferster A, Kuo C-C, Levy S, van Dongen JJM, van der Burg M.** 2010. CD81 gene defect in humans disrupts CD19 complex formation and leads to antibody deficiency. *J Clin Invest* **120:**1265–1274. PubMed
24. **Xu GL, Bestor TH, Bourc'his D, Hsieh CL, Tommerup N, Bugge M, Hulten M, Qu X, Russo JJ, Viegas-Péquignot E.** 1999. Chromosome instability and immunodeficiency syndrome caused by mutations in a DNA methyltransferase gene. *Nature* **402:**187–191. PubMed
25. **de Greef JC, Wang J, Balog J, den Dunnen JT, Frants RR, Straasheijm KR, Aytekin C, van der Burg M, Duprez L, Ferster A, Gennery AR, Gimelli G, Reisli I, Schuetz C, Schulz A, Smeets DF, Sznajer Y, Wijmenga C, van Eggermond MC, van Ostaijen-Ten Dam MM, Lankester AC, van Tol MJ, van den Elsen PJ, Weemaes CM, van der Maarel SM.** 2011. Mutations in ZBTB24 are associated with immunodeficiency, centromeric instability, and facial anomalies syndrome type 2. *Am J Hum Genet* **88:**796–804. PubMed
26. **Grimbacher B, Hutloff A, Schlesier M, Glocker E, Warnatz K, Dräger R, Eibel H, Fischer B, Schäffer AA, Mages HW, Kroczek RA, Peter HH.** 2003. Homozygous loss of ICOS is associated with adult-onset common variable immunodeficiency. *Nat Immunol* **4:**261–268. PubMed
27. **Sayos J, Wu C, Morra M, Wang N, Zhang X, Allen D, van Schaik S, Notarangelo L, Geha R, Roncarolo MG, Oettgen H, De Vries JE, Aversa G, Terhorst C.** 1998. The X-linked lymphoproliferative-disease gene product SAP regulates signals induced through the co-receptor SLAM. *Nature* **395:**462–469. PubMed
28. **Rigaud S, Fondanèche M-C, Lambert N, Pasquier B, Mateo V, Soulas P, Galicier L, Le Deist F, Rieux-Laucat F, Revy P, Fischer A, de Saint Basile G, Latour S.** 2006.

XIAP deficiency in humans causes an X-linked lymphoproliferative syndrome. *Nature* **444:**110–114. PubMed

29. **Castigli E, Wilson SA, Garibyan L, Rachid R, Bonilla F, Schneider L, Geha RS.** 2005. TACI is mutant in common variable immunodeficiency and IgA deficiency. *Nat Genet* **37:**829–834. PubMed
30. **Warnatz K, Salzer U, Rizzi M, Fischer B, Gutenberger S, Böhm J, Kienzler A-K, Pan-Hammarström Q, Hammarström L, Rakhmanov M, Schlesier M, Grimbacher B, Peter H-H, Eibel H.** 2009. B-cell activating factor receptor deficiency is associated with an adult-onset antibody deficiency syndrome in humans. *Proc Natl Acad Sci USA* **106:**13945–13950. PubMed
31. **Revy P, Muto T, Levy Y, Geissmann F, Plebani A, Sanal O, Catalan N, Forveille M, Dufourcq-Labelouse R, Gennery A, Tezcan I, Ersoy F, Kayserili H, Ugazio AG, Brousse N, Muramatsu M, Notarangelo LD, Kinoshita K, Honjo T, Fischer A, Durandy A.** 2000. Activation-induced cytidine deaminase (AID) deficiency causes the autosomal recessive form of the Hyper-IgM syndrome (HIGM2). *Cell* **102:**565–575. PubMed
32. **Imai K, Slupphaug G, Lee W-I, Revy P, Nonoyama S, Catalan N, Yel L, Forveille M, Kavli B, Krokan HE, Ochs HD, Fischer A, Durandy A.** 2003. Human uracil-DNA glycosylase deficiency associated with profoundly impaired immunoglobulin class-switch recombination. *Nat Immunol* **4:**1023–1028. PubMed
33. **Péron S, Metin A, Gardès P, Alyanakian MA, Sheridan E, Kratz CP, Fischer A, Durandy A.** 2008. Human PMS2 deficiency is associated with impaired immunoglobulin class switch recombination. *J Exp Med* **205:**2465–2472. PubMed
34. **Stepensky P, Keller B, Buchta M, Kienzler A-K, Elpeleg O, Somech R, Cohen S, Shachar I, Miosge LA, Schlesier M, Fuchs I, Enders A, Eibel H, Grimbacher B, Warnatz K.** 2013. Deficiency of caspase recruitment domain family, member 11 (CARD11), causes profound combined immunodeficiency in human subjects. *J Allergy Clin Immunol* **131:**477–485.e1. PubMed
35. **Boisson B, Laplantine E, Prando C, Giliani S, Israelsson E, Xu Z, Abhyankar A, Israël L, Trevejo-Nunez G, Bogunovic D, Cepika A-M, MacDuff D, Chrabieh M, Hubeau M, Bajolle F, Debré M, Mazzolari E, Vairo D, Agou F, Virgin HW, Bossuyt X, Rambaud C, Facchetti F, Bonnet D, Quartier P, Fournet J-C, Pascual V, Chaussabel D, Notarangelo LD, Puel A, Israël A, Casanova J-L, Picard C.** 2012. Immunodeficiency, autoinflammation and amylopectinosis in humans with inherited HOIL-1 and LUBAC deficiency. *Nat Immunol* **13:**1178–1186. PubMed
36. **Döffinger R, Smahi A, Bessia C, Geissmann F, Feinberg J, Durandy A, Bodemer C, Kenwrick S, Dupuis-Girod S, Blanche S, Wood P, Rabia SH, Headon DJ, Overbeek PA, Le Deist F, Holland SM, Belani K, Kumararatne DS, Fischer A, Shapiro R, Conley ME, Reimund E, Kalhoff H, Abinun M, Munnich A, Israël A, Courtois G, Casanova JL.** 2001. X-linked anhidrotic ectodermal dysplasia with immunodeficiency is caused by impaired NF-kappaB signaling. *Nat Genet* **27:**277–285. PubMed
37. **Courtois G, Smahi A, Reichenbach J, Döffinger R, Cancrini C, Bonnet M, Puel A, Chable-Bessia C, Yamaoka S, Feinberg J, Dupuis-Girod S, Bodemer C, Livadiotti S, Novelli F, Rossi P, Fischer A, Israël A, Munnich A, Le Deist F, Casanova J-L.** 2003. A hypermorphic IkappaBalpha mutation is associated with autosomal dominant anhidrotic ectodermal dysplasia and T cell immunodeficiency. *J Clin Invest* **112:**1108–1115. PubMed

Hereditary and Acquired Complement Deficiencies

PATRICIA C. GICLAS

77

Complement deficiencies comprise a small but important category of primary immune deficiency diseases. Complement deficiency states can also be acquired from *in vivo* activation or inhibition of the complement system, temporarily depleting components faster than they can be replaced or causing changes in control of the system. Complement plays an important role in the host's response to infection by directly killing bacteria, neutralizing viruses, or coating microbial surfaces with complement fragments that enhance uptake and killing by phagocytes, a process called opsonization that ensures that objects identified as foreign by complement are dealt with quickly and efficiently. Complement serves as a link between many of the activities of acquired immunity, with ties to diverse cell signal responses and other defense mechanisms, as an ever-increasing number of related conditions are identified (1).

Activation of the complement enzyme cascade produces fragments that exhibit proinflammatory properties, including chemotactic activity and the ability to regulate local blood flow and vascular permeability and cause smooth muscle contraction or relaxation. These properties are species and tissue dependent. Complement also has "housekeeping" activities, such as clearance of immune complexes, effete and apoptotic cells, and cellular debris. Deficiencies or mutations of complement components, whether inherited or acquired, create a predisposition to infections, autoimmune diseases, impaired immune responses, and diverse conditions such as acute and chronic renal disease, vasculitis, allergic reactions, hereditary angioedema (HAE), and age-related macular degeneration (AMD). The discussion that follows touches on examples of these and other complement-related functions that go awry when one or more of the proteins in a pathway is missing or functions abnormally. Figure 1 depicts the complement pathways for review of the steps and proteins involved.

Measurement of most of the complement components in the circulation can be done by standard immunochemical techniques. If the protein concentration is relatively high (milligrams per milliliter), then nephelometry or turbidimetry can be used, but when the concentrations are lower (micrograms per milliliter down to nanograms or picograms per milliliter), radial immunodiffusion, radioimmunoassay, and enzyme-linked immunosorbent assay are the methods of choice. Newer variations on the latter include bead-based multiplex tests that allow the measurement of several different proteins at a time. Flow cytometry is used to evaluate the cell-bound complement control proteins such as membrane cofactor protein (MCP; CD46) and decay accelerating factor (CD55), as well as receptors for C3 and C4 fragments such as CR1 (CD35) and CR3 (CD11b/CD18).

Measuring the functions of the complement pathways and their individual components presents challenges for the clinical laboratory. Except for a few tests, the methods and reagents used are, for the most part, not sold commercially, and the procedures are done manually. The temperature sensitivity of the proteins makes it difficult to maintain the serum samples at 0°C during the time required for the test setup.

The first functional assay for complement was done by bactericidal measurements, either *in vivo* in guinea pigs or *in vitro* using serum from guinea pigs, humans, or other species. The CH50 was developed around 1900 as an easy method using available supplies (2–5). The AH50 was built on the model of the CH50 except that it required a different target cell. For human serum, either guinea pig or rabbit red blood cells have been used for the AH50. The two tests, described below, cover the function of complement except for the lectin pathways (LPs), which are described in chapter 14.

HEMOLYTIC ASSAYS FOR COMPLEMENT FUNCTION

The CH50 assay (name derived from "CP hemolytic 50%") depends on the sequential activation of each of the 11 classical pathway (CP) components: C1q, C1r, C1s, C4, C2, C3, C5, C6, C7, C8, and C9, in that order, ending in lysis of sensitized sheep erythrocytes (E) that have been coated with polyclonal rabbit IgM or IgG anti-sheep E antibodies (A). The antibody-treated cells are referred to as "sensitized," and the abbreviation EA is used in the following description of the assay.

The AH50 assay (name derived from "AP hemolytic 50%") relies on lysis of rabbit red blood cells (E_{rab}) that have a natural charge on their surface that promotes antibody-independent activation of the human alternative pathway (AP). The AH50 relies on the same terminal pathway components (C3, and C5 through C9) as those of the CP, but there are unique components in the initiation phase: preformed C3b, factor D (FD), and factor B (FB) are necessary to generate the C3bBb enzyme complex that cleaves C3, and properdin (P) has a unique role in stabilizing the C3bBb

doi:10.1128/9781555818722.ch77

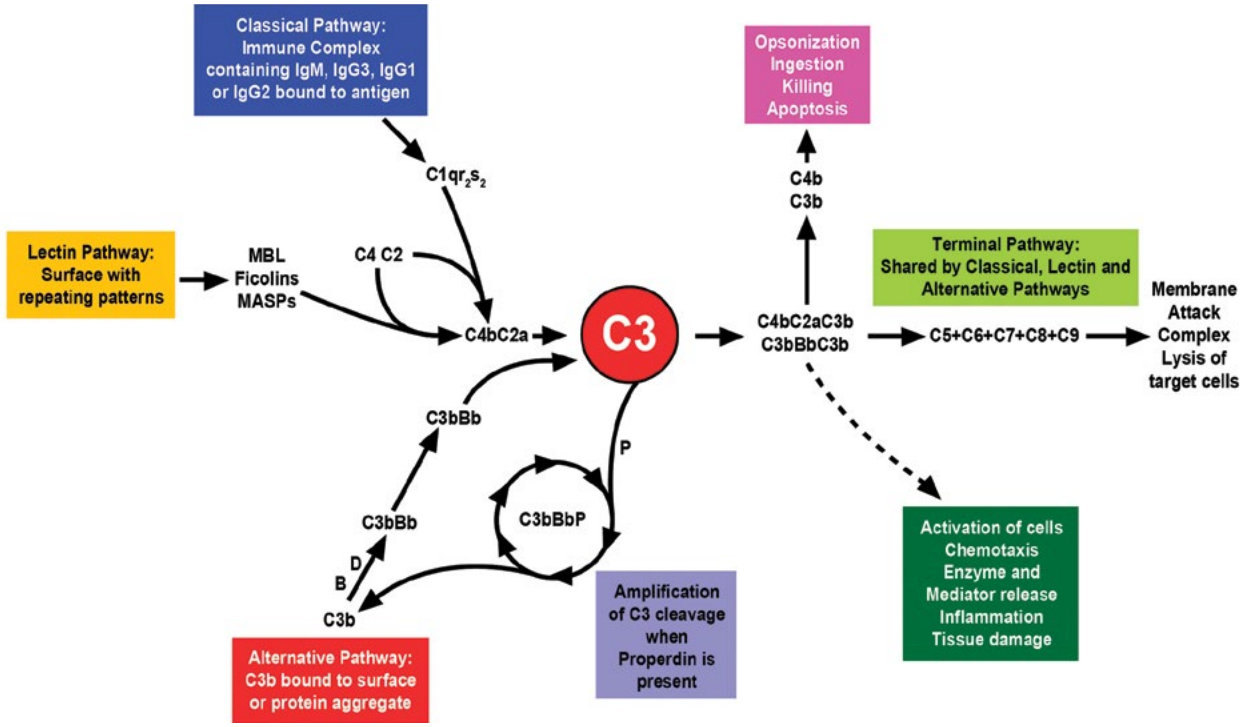

FIGURE 1 Complement was one of the earliest members of the innate immune system to evolve, and, as such, different forms of pattern recognition allowed it to become active against a variety of organisms and substances without the need for prior exposure. The three boxes to the left (classical pathway [CP], blue; lectin pathway [LP], orange; alternative pathway [AP], red) indicate examples of one of the triggers for activation of each pathway. As drawn, the C3 molecule is the central target for all three pathways. Activation of the CP by immune complexes, or the LP by a recognized target pattern, results in cleavage of C3, C4, and C2. Clearance of the complex or LP target from the circulation occurs through interaction of the phagocytes in the liver and spleen with the C4b and C3b bound to the complex. The alternative pathway is different. In the AP, the unique protein properdin allows the formation of an amplification process (shown as circle of arrows) in which a very large amount of C3 but not C4 becomes rapidly cleaved. The resulting C3b from this process becomes covalently bound to the surface of nearby proteins, microbes, and cells and flags them as targets for destruction by the immune system. The fragments of C3 and C4 form the major opsonins that are used by cells such as phagocytes and lymphocytes to clear the C3 and C4 fragments. Note that complement fragments can be useful in the laboratory to identify the pathway involved in a reaction. Note also that a large decrease in serum C3 but not C4 is indicative of AP activation. The majority of the physiological effects of complement activation are due to the inflammatory properties of the fragments. These include opsonization, chemotaxis, mediator release, priming of phagocytes and lymphocytes, apoptosis, and direct killing of microbes by lysis.

to prolong its half-life and promote the amplification of the C3 cleavage process.

The AH50 assay described below depends on AP-dependent lysis of unsensitized (i.e., no antibody) E_{rab} by human serum complement. Activation of the calcium-dependent CP or LP is prevented by adding a calcium chelator, EGTA, to the AH50 buffer along with magnesium, necessary for the AP activity. In an endpoint titration of the patient's serum using serial dilutions, complement activity is quantitated by determining the dilution of serum it takes to lyse 50% of the EA in the assay mixture, and the results are expressed as the reciprocal of this dilution, in CH50 units (U) per milliliter. Thus, if a dilution of 1/20 lyses half the cells, the CH50 reported would be 20 units. There are some commercially available reagents such as buffers for performing the CH50 assay, or you can prepare your own.

The CH50 and AH50 are dose-response methods. The test article (serum) is tested at different concentrations until the amount that gives a 50% effect is found.

CH50 Assay

Sample Requirements

The CH50 assay requires 0.5 ml of serum from blood collected in a red-top Vacutainer tube or serum separator tube, allowed to clot for 30 to 60 min at 37°C or room temperature, and centrifuged to separate the serum from the clot. The minimum serum requirement from an infant or to allow for repeat of the assay is 50 μl. The serum should be transferred without cellular contamination to a clean plastic tube, capped tightly, and frozen at −70°C until the assay is performed. Transportation of the serum to another location for CH50 or AH50 analysis should use a box containing enough dry ice to keep it frozen until it reaches its destination.

Both the CP and AP contain factors that are heat labile, so care must be taken that the specimen to be tested has been collected and stored properly. Repeated freeze-thaw cycles or allowing specimens to stand at room temperature

for long periods of time (>30 min) can cause erroneously low results. Patients with low CH50 may have immune complexes, cryoglobulins, bacteria, or other complement activators in their serum that continue to activate the complement after the blood is drawn, so in the case of a low CH50, the assay should be repeated with a fresh specimen from the patient for confirmation at a later date.

Materials

Chipped or crushed ice: essential for keeping buffers, dilution tubes, and sera cold while the assay is being set up. A tube will stay upright if pushed down in chipped ice, but not if ice cubes are used. A mixture of ice and water will stay at 0°C as long as there is still ice present.

Container for ice such as ice bucket, Styrofoam box, or other insulated container

Plastic dishpans about 10 by 14 in. and at least 4 in. deep, or other similar-sized trays to hold racks for dilution tubes

Disposable borosilicate glass or clear plastic culture tubes (12 by 75 mm) for preparing the dilutions of serum: 10 tubes to run each specimen in duplicate, including standard and controls

Racks to hold tubes (12 by 75 mm): separate racks for making dilutions and for incubating serum dilutions with EA

2 conical-bottom 50-ml plastic tubes with screw caps

Equipment and Instruments

Pipettors with volume ranges covering 10 μl to 1 ml

37°C water bath

Centrifuge

Spectrophotometer capable of reading visible light

Buffers, Sera, and Other Reagents

Human serum complement standard (available at Quidel Corp., San Diego, CA). Normal human serum, pooled and standardized for hemolytic assays: need 50 μl per test run. Store in 60-μl aliquots so you can recover 50 μl and discard the rest. Do not refreeze after thawing.

Normal human serum controls: 50 μl of high, medium, and low controls. Prepare these sera from individual or pool of donors, making enough individual aliquots as above to last for a few months at −70°C. Aliquots of serum at 60 μl each can be prepared and stored safely in small Eppendorf tubes at −70°C for up to 1 year. The same sera should be used each time the assay is run for control of interassay variability. The run-to-run coefficient of variation should be 10% or less.

Test sera: 50 μl each; sera from patients to be tested should be run in duplicate

Ice-cold saline: 0.15 M NaCl, 12 ml per sample

Sheep's whole blood in Alsever's solution (Colorado Serum Co., Denver, CO)

Buffer (gelatin-Veronal buffer with metal ions; GVB^{2+}): 200 ml of ice-cold Veronal-buffered saline with gelatin, calcium, and magnesium (Veronal is another name for barbital)

Hemolysin: rabbit anti-sheep E antiserum (Colorado Serum Co.). This is usually whole rabbit serum, so it must be heat-inactivated before being used: incubate it at 56°C for 30 min to inactivate the rabbit complement. The heat-treated hemolysin can be stored for months at −20°C.

Buffer Preparation

1. For 2 liters of 5× stock GVB^{2+}, dissolve 83.0 g of NaCl and 10.19 g of Na-5,5′-diethyl barbiturate in about 1.5 liters of warm (75 to 85°C) distilled water, add 10 g of gelatin, and continue to stir until it is dissolved. Add 2 ml of calcium chloride (0.3 M) and 2 ml of magnesium chloride (2.0 M), followed by 4 ml of 10% (wt/vol) sodium azide.

2. Mix well, and bring the pH to 7.35 ± 0.05 with a small amount of 1 N HCl or NaOH, as needed. Bring the volume to 2.0 liters with distilled water. Store at room temperature for up to 1 month. Discard buffer stock if it becomes cloudy or develops a strong odor. Aliquots of 40 ml can be frozen at −20°C in 50-ml conical-bottom centrifuge tubes if the assay is not done frequently.

3. For 1× working buffer, mix 1 part stock with 4 parts distilled water.

Sensitized Sheep Cells (EA)

1. Wash the cells. To obtain about 20 ml of EA at 2×10^8 cells per ml, gently mix the bottle of sheep's blood (Colorado Serum Co.) and take out 4 ml with a syringe. Put it into a 50-ml conical-bottom plastic centrifuge tube and add enough GVB^{2+} to bring the volume to 40 ml. Invert the tube a few times to mix, and then centrifuge the cells for 5 to 10 min at 1,250 × *g*. Remove the supernatant and buffy coat cells. Add more GVB^{2+} to bring the volume to 40 ml and centrifuge again. Repeat wash three or four times until the supernatant is clear.

2. Make 5% suspension. Measure the volume of packed E after the last centrifugation, and add enough GVB^{2+} to give a 5% cell suspension, by volume. To determine the actual concentration of cells, remove 100 μl of the 5% cell suspension and add it to 1.4 ml of distilled water and mix to lyse the cells. Read the optical density (OD) of the lysate at 541 nm (OD_{541}). If the cells are at 1×10^9 per ml, the OD_{541} should be 0.700. Adjust the cell suspension by adding more buffer if the OD_{541} is >0.700, or spin the E down and resuspend them in less buffer if the OD_{541} is <0.700.

3. Once the cells are at 1×10^9 cells per ml, put 4 ml of the E into a conical-bottom plastic tube. In another tube, put 4 ml of GVB^{2+} and add enough hemolysin to obtain the optimum dilution for sensitizing the E (1). Prewarm the E and the diluted hemolysin to 37°C; then add the hemolysin all at once to the E and quickly mix thoroughly. Incubate at 37°C for 20 min. Centrifuge as described above, decant the supernatant, and resuspend the E to 20 ml with ice-cold GVB^{2+}. At this point, the E should be at 2×10^8 per ml and ready to use for the CH50. Keep cells on ice or in refrigerator or cold room (temperature maintained at 2 to 8°C until needed for assay). If kept cold, the E should be stable for 1 to 2 weeks. Discard if the background lysis exceeds 10% of the total lysis.

Procedure for CH50 Assay

Once starting the assay, proceed quickly. Thaw serum tubes rapidly at 37°C; then put them on ice once they are thawed. Keep the cells and buffer on ice.

1. Prepare two test tube racks, one for making the serum dilutions and one for the assay tubes. For each sample you will need five tubes in the dilution rack and duplicate rows of five tubes in the assay rack. Label each tube with its dilution and a code for the sample to be tested. Add four additional control tubes to the assay rack: two for 0% (background lysis) and two for 100% (total lysis) controls. Place both racks into a slushy ice bath so that the bottom inch or so of each tube is below the ice-water level.

2. Put 150 μl of GVB^{2+} into each of the tubes in the dilution rack and add an extra 135 μl to the first tube in each series. Add 15 μl of the appropriate undiluted test, control, or standard serum to the first tube of its series and vortex to mix well. To make doubling dilutions, transfer 150 μl from the first tube to the second, vortex to mix well, transfer 150 μl from the second tube to the third, etc. The final dilutions will be 1/20, 1/40, 1/80, 1/160, and 1/320.

3. When all the serum samples have been diluted, quickly transfer 50 μl of each dilution into the duplicate tubes in the assay rack, starting from the most dilute and ending with the least dilute. Put 50 μl of GVB^{2+} into the 0% tubes and 50 μl of distilled water into the 100% tubes. Once all the samples have been transferred, add 50 μl of EA at 2×10^8 cells per ml to each tube. A repeating pipettor works well for this purpose. Remove the rack from the ice bath, cover with Parafilm, and shake it vigorously to mix the cells with the serum dilutions.

4. Place the rack in the 37°C water bath and incubate for 30 min at 37°C, with shaking two or three times during that time to keep the EA suspended (a shaking water bath can be used). Add 1.2 ml of ice-cold saline to each of the tubes except the 100% lysis controls, to which 1.2 ml of distilled water should be added. Centrifuge all tubes at $1{,}250 \times g$ for 5 min to pellet the unlysed EA and read the OD_{412} of the supernatants. Use distilled water or GVB^{2+} as the blank to zero the spectrophotometer. Calculate the percent lysis for each tube (divide its OD_{412} by the OD_{412} of the 100% lysis control tube and multiply by 100). *Note: lysis of the background (0%) tube should be <10% of total lysis*. Average the results of the duplicate tubes for calculations. Some spectrophotometers can be programmed to do this step.

5. Data calculations: Manual method: Plot the data on 3 log-cycle probability paper (Keuffel & Esser, Morristown, NJ). Plot the reciprocal serum dilutions on the logarithmic *y* axis, using the percentage scale at the top of the page. Draw the best-fit line through the points and locate the corresponding *y* value where it crosses the line at 50% lysis. The reciprocal of the dilution at this point is the CH50 value (5). Note that lysis of >85% or <15% of the cells tends to fall off the straight line formed by the points between these values, so use only the points that fall within this linear range for calculations. If a computer or calculator with linear regression capability is available, the data can be calculated using the natural logarithm of the reciprocal dilution as the independent variable (x) and the percent lysis as the dependent variable (y). Once the best-fit line [$y = m * \ln(x) + b$] is determined, the 50% lysis point can be calculated from its slope (m) and intercept (b). For the CH50, the value of $y = 50\%$, so $x =$ the anti-ln of $[(50 - b)/m]$. The correlation coefficient, R^2, for the line should be >0.95.

6. The results are reported as the number of CH50 units per milliliter, where the CH50 unit (U) is defined as the reciprocal of the dilution of serum. Thus, a sample that lyses 50% of the EA at a dilution of 1:150 will be reported as 150 CH50 U/ml. Because different laboratories do CH50 assays using different cell concentrations and conditions, the ranges for normal sera vary from one laboratory to the next, and when you are setting the test up, you must establish your own normal range. Interassay variability can be controlled by using a calibrated serum standard each time you do the test. The experimental CH50 value obtained for the standard in the current run is divided by its established value, and the resulting factor is used to correct the CH50 values of the other samples in the run. This allows comparisons to be made between tests run over a long period of time. The corrected values for the controls should not vary by more than ±10% from run to run for the data to be acceptable.

AH50 Assay

Materials and Reagents (Sources)

Materials and reagents are the same as for the CH50 procedures except as follows.

Buffer ($GVB\text{-}Mg^{2+}$–EGTA): prepare stock GVB as described above for the CH50 procedure, except leave out the calcium and add 160 ml of 0.1 M EGTA solution and 10 ml of 2.0 M $MgCl_2$ before bringing to 2 liters with distilled water

Calibrated standard serum: same as for CH50 except use the AH50 value assigned to it

Control sera: normal serum pool or sera from individual donors with normal AH50 values. As above, high, middle, and low controls should be collected and aliquoted for one-time use.

Starting with rabbit whole blood in Alsever's solution (Colorado Serum Co.), prepare E_{rab} at 2×10^8/ml as for the CH50 procedure preparation of sheep E. Use the $GVB\text{-}Mg^{2+}$–EGTA buffer for washing the cells.

Equipment and Instruments

Equipment and instruments are the same as for the CH50 procedure.

Procedure for AH50 Assay

Apart from the difference in the target cells and the buffer, the main difference between the CH50 and the AH50 is that the latter is more sensitive to dilution. For this reason, the volumes and dilutions are different for the AH50. Activity is lost at higher dilutions than those given.

1. Use disposable glass tubes (12 by 75 mm) for the test and dilutions. Set up two racks of tubes, one for making the dilutions and one for the assay itself. In the dilution rack, put five tubes for each serum sample you want to test (plus serum pool or other controls). In the assay rack, put duplicate rows of the five tubes each for the sera. Label each row with the name of its sample and dilution. Place the rack of dilution tubes into a slushy ice bath. Put 600 μl of $GVB\text{-}Mg^{2+}$–EGTA in the first tube of each series and 200 μl into each of the remaining four tubes. Make 1.5-fold dilutions in each row beginning with 1/4 dilution: add 200 μl of serum to the first tube, and transfer 400 μl from tube 1 to tube 2, etc., for the serial dilutions. Transfer 50 μl of each dilution into the duplicate tubes for the appropriate sample in the assay rack. Also include the following controls for each assay: two tubes for 100% cell lysis (substitute 100 μl of distilled H_2O for buffer and serum) and two tubes for background lysis (100 μl of buffer only but no serum). Background should not exceed 10% of the total lysis.

2. Add 50 μl of the E_{rab} suspension to each of the serum dilution tubes and transfer the rack to a water bath at 37°C.

3. Incubate for 60 min, with occasional shaking to keep the cells in suspension.

4. Add 1.2 ml of ice-cold saline to each tube to stop the reaction and spin the cells down ($1{,}000 \times g$ for 5 to 10 min). Read the OD_{412} of each supernatant. If the spectrophotometer you are using has the ability to calculate concentration of samples versus a standard, enter 100 as the value of the standard and read the OD of the 100% lysis tubes. Next, read the OD of the background tubes and rezero the machine so

that this background will be subtracted from each of the test samples to follow.

Calculate Results

1. Using probability paper, plot the percent lysis on the *x* axis (use the percentage scale at the top of the page) versus the log of the dilution on the *y* axis. Draw the best-fit straight line between the points, excluding those for percent lysis >85% or <15%, since the curve is nonlinear at the ends. The AH50 is the corresponding point on the *y* axis where the line crosses 50% and is the reciprocal of the dilution that caused 50% lysis in the test. Since the volumes used were 50 μl, the result can be converted to units per milliliter by multiplying the answer by 20.

2. An alternative method for calculating results is as follows. Calculate $y/(1-y)$ and graph the results on log paper, using the reciprocal of the serum dilution on the *y* axis and the value of $y/(1-y)$ on the *x* axis, where *y* is the fraction of cells lysed (3). The AH50 value is then read off the graph as the reciprocal of the dilution where $y/(1-y) = 1$ (50% of the cells lysed). Use a linear regression program to determine the best-fit line for the data [*x* = percent lysis and *y* = ln(dilution)] as described for the CH50 method.

Standardizing the Results

To minimize the variability of the test from one batch of cells and reagents to the next, use a correction factor based on your calibrator serum or serum pool so that interassay comparisons can be made. Determine the average value for your serum pool (from 10 or more assays) or use the given value for the calibrated standard or other serum with known AH50 titer. Divide the answer obtained in your assay for the standard by the value of the standard obtained as described above, and use the resulting factor to multiply all other results in that run. This will bring the amount of interassay variability to within the desired limits of ±10%.

Controls

A control serum with predetermined (from 10 to 20 tests) CH50 or AH50 units per milliliter should be included with each batch of test sera. Ideally, sera with high and low activities should be used to control for variability at each end of the CH50 or AH50 range. The background lysis (0%) and total lysis (100%) controls define the OD range that is acceptable for the assay. The 0% control should be <10% of the total lysis.

Standardization, Quality Control, and Quality Assurance

A calibrated standard serum must be included with each run. This can be a serum that is obtained from another laboratory that is using a similar method or prepared in-house. To obtain enough to last for a reasonable length of time, prepare a pool of sera from 10 or more donors and store it in aliquots of 50 to 100 μl each at −70°C. Perform the CH50 or AH50 assay on this standard pool of serum at least 10 times and calculate the average CH50 or AH50 value. The coefficient of variation should be within 10% for these values if the assay is working well. The average is then defined as the CH50 or AH50 value for the serum pool. Quality control should include Levy-Jennings plots of the control sera for each assay run, and Westgard rules should be followed. A normal range should be established from 50 to 120 serum samples obtained from healthy individuals. The range to be used for the assay is the mean ± 2 standard deviations, and any abnormal test results that are >3 standard deviations from the mean should be verified by repeat assay.

Preanalytical Concerns

Proper collection of samples is critical for the CH50 and AH50 assays. Serum should be collected and frozen at −70°C or placed on dry ice within 1 to 2 h from the time the blood is drawn. If the assay is to be done in-house on the same day, the serum can be kept on wet ice until the assay, or it may be frozen overnight at −20°C in a non-frost-free freezer. Prolonged storage at temperatures above −70°C will result in loss of complement activity, whereas sera stored at −70°C or below are stable for years. Ship specimens for CH50 and AH50 assay by overnight mail in a well-insulated package with enough dry ice to last 48 h. *Note: if the patient has cryoglobulinemia, the serum must be kept at 37°C and the testing must be done with cells and buffers at that temperature within a few hours.*

Analytical Concerns

These assays work best when all reagents and serum dilutions are kept on ice. The control sera and the standard serum must be stored at −70°C in small aliquots that can be thawed once for the assay and discarded afterward. *Do not refreeze and reuse the sera more than one time.* Patients' sera to be tested should be stored at −70°C and thawed just before the test is to be performed. If the test needs to be repeated, make a few small aliquots of the patient's serum, so that the main tube does not undergo repeated freeze-thaw cycles. Do not reuse diluted sera, but prepare new dilutions for repeat assays.

The sheep blood and rabbit blood in Alsever's solution are stable for 4 to 6 weeks in the cold (2 to 8°C). If the cells continue to lyse during the washing process, discard them and obtain a fresh supply. Hemolysin can be stored at −20°C for several years in a non-frost-free freezer.

Postanalytical Concerns

Test results should be analyzed as described earlier. If only a few specimens are to be tested, the probability paper plotting method is the simplest way to obtain the results. For larger runs, use the linear regression program on a personal computer.

Normal ranges can be established from 30 to 50 serum samples obtained from healthy individuals. The distribution should be normal for this population.

Quality control for these assays includes the high (top 10% of reference range) and low (lowest 20% of reference range) serum controls and the background lysis (0%). The total lysis (100%) should be within the interassay variability range as well. Because there is no established proficiency testing available from the College of American Pathologists or other organizations, in-house proficiency testing should be performed on a regular basis. Specimens for this could include repeated testing of a patient's sample, especially if abnormal, or varied proficiency test samples prepared in-house. For example, serum from a healthy individual, treated by dilution (1/2 or 1/5), by heat inactivation (56°C, 30 min), or by activation with a known complement activator such as zymosan (1 to 10 mg/ml, 20 min, 37°C), will have low or completely blocked CH50 or AH50 values. Specimens with elevated CH50 or AH50 results can be obtained by testing acute-phase sera or by gently concentrating normal sera.

Pitfalls and Troubleshooting

The most common problem encountered with functional complement tests is improper sample collection and handling. This occurs often when the blood is collected off-site and is allowed to stand for hours with the cells and clot present or when the serum is collected and then put into a

TABLE 1 Testing for complement deficiency or dysfunction[a]

First order of testing	CH50 and AH50			MBL
Results	CH50 low or absent; AH50 normal	AH50 low or absent; CH50 normal	Both CH50 and AH50 low or absent	MBL low or absent; CH50 normal; AH50 normal
	▼	▼	▼	▼
Interpretation	Likely classical component deficiency	Likely alternative component deficiency	Likely terminal component deficiency	Likely lectin component deficiency
	▼	▼	▼	
Next steps	C1, C2, and C4 function and level	Factor B and factor D level or function	C3, C5, C6, C7, C8, C9 levels or functions	
	C1-INH level or function	Properdin level or function	Factor H, factor I levels and H function	
Final step	Genetic analysis of complement components in pathway identified			

[a]Because genetic mutations alter the function but not the level of the protein, testing for both the level and the function can reveal a defect that the level alone does not pick up. If these tests are inconclusive, consider testing for complement autoantibodies against C1q, C1-INH, Factor H, FB, C3NeF, FI, and others.

refrigerator where it may be kept for days before it reaches the laboratory. The major problem with running the CH50 assay is failure to sensitize the E correctly. The hemolysin should be titrated before it is used, but once the titer of a given hemolysin is known, the titration does not need to be repeated for each test (5). Buffers should be made up fresh for each assay and discarded after 24 h.

Interpretation

The CH50 and AH50 assays reflect the sequential interaction of all of the components of the CP and AP, respectively. If any single component is missing, the resulting CH50 or AH50 value will be 0 U/ml. Because the pathways share the same terminal components (C3, C5, C6, C7, C8, and C9), a deficiency of one of these will lead to the loss of both CH50 and AH50 activity. Using the algorithm in Table 1, the physician can decide on the best set of assays to use for a patient with a suspected complement deficiency. Thus, if only the CP is 0, there is no need to look at late components or AP components. If both pathways are blocked, then one of the late components is likely to be missing. When the CH50 and/or AH50 value is between 0 and the low end of the normal range, the most likely cause is *in vivo* activation. This can be verified in two ways: (i) assays of individual components will show that more than one is decreased, or (ii) results obtained with assays of complement split products will be elevated (see chapter 15). The primary pathway that has been activated can be determined by which component levels are decreased or which split product levels are elevated.

The CH50 and AH50 assays are excellent screens for total complement activity but are relatively insensitive to small changes that may occur because of complement activation. Much more sensitive assays exist to look at ongoing inflammatory processes or involvement of complement in disease states, as described in chapter 15 of this volume.

The basic screening tests should include hemolytic CH50 and AH50 tests that measure total CP and AP activity, respectively, or their equivalents that have been developed for CP and AP function by enzyme-linked immunosorbent assay, liposome lysis, or other methods. Additional tests for LP function are available for mannose-binding lectin (MBL) (chapter 14), and tests for other LP proteins are in development that will further narrow the search for abnormal proteins in this important system (6). Since all three initiating pathways, CP, AP, and LP, feed into the same terminal pathway, a missing component unique to any one of the pathways blocks progression of the reaction of the affected pathway and thus no lysis occurs when that pathway is activated. The other pathways are unaffected. A block in the late components that make up the terminal pathway affects all of the others.

An algorithm depicting a useful sequence for testing is given in Table 1. Exceptions to this might be for a patient with HAE due to C1-INH deficiency, for whom the testing should include C4 level and C1-INH level and function, or a patient with one of the C3 glomerulopathies due to AP dysregulation, for whom testing might also include C3, factor H (FH), factor I (FI), CD46, C3 nephritic factor, or antibodies to FH.

As with other laboratory tests, care must be taken with specimen collection, handling, and shipping. The best policy to follow is to minimize the amount of time that a given specimen spends at room temperature, from the time it is collected from the patient to the time it is processed and safely stored (e.g., frozen at −70°C). Because specimens from patients may contain bacteria, immune complexes, cryoglobulins, drugs, and other potential activators of complement, the reaction can continue long after the blood has been drawn and result in misleading results when tested in the laboratory. It is strongly advised to contact the

laboratory to which the specimen will be sent for instructions for specific assays.

DEFICIENCIES OF CP PROTEINS: C1q, C1r, C1s, C2, AND C4

The CP is critical for the clearance of immune complexes, the removal of apoptotic cells, and the defense against certain bacterial and viral infections. The phenotype of CP component deficiencies is closely linked to diseases in which these processes are impaired, such as systemic lupus erythematosus (SLE), rheumatoid arthritis, anaphylactoid purpura, vasculitis, and infections with encapsulated bacteria (7). SLE patients with C1q or C4 deficiencies have characteristic features such as earlier age of onset, prominent photosensitivity, lower frequency of renal disease, variable antinuclear antibody titers, and a nearly equal male-to-female ratio. In addition to SLE and other immune complex diseases, CP deficiencies also lead to recurrent infections with streptococcal, staphylococcal, and other common encapsulated bacteria and should not be overlooked in the workup for immune dysfunction. Infections with Gram-negative organisms, especially *Neisseria*, are associated with the terminal pathway, and the CH50 or equivalent assays are the best initial screens for these deficiencies, followed by tests for individual components, since the absence of any one of the CP proteins prevents lysis by CP activity (8).

The gene for human C1q is located on chromosome 1, at 1p34-1p36.3 (9). The protein is related to the collectin family, possessing both collagen-like and globular pattern recognition structures. There are six each of three different polypeptide chains, A, B, and C, in the intact 460-kDa molecule. These chains are combined to form six triple-chain helices that make up the collagen-like "stalk" of the molecule. The stalks branch at flexible hinge regions midway along their length, and their ends are capped with globular protein head regions. The molecule has been described as a bunch of six tulips, based on electron micrographs. This complex structure is highly labile and becomes denatured if subjected to temperatures above 56°C or to repeated freeze-thaw cycles.

Cells of monocyte/macrophage lineage are responsible for most of the circulating C1q that is produced, while follicular dendritic cells provide a secondary site of synthesis. C1q deficiency is an autosomal recessive condition, with deficient patients having little or no detectable protein or C1q function in the circulation. Mutations have been identified in the genes for each of the three chains. Almost all patients with documented C1q deficiency have developed SLE-like disease, and linkage studies demonstrate that the C1q gene is close to that for other proposed SLE susceptibility genes on chromosome 1 in humans (10, 11). Acquired C1q deficiency occurs when autoantibodies are produced against the collagen-like region of the C1q molecule. These anti-C1q antibodies are associated with SLE and also with hypocomplementemic urticarial vasculitis syndrome (12). C1q can also be temporarily reduced in the circulation by ongoing CP activation *in vivo*, as well as activation in the specimen after blood is drawn if the patient has an immune complex burden, cryoglobulinemia, bacteremia, or other condition likely to activate complement.

The genes for C1r and C1s are located on chromosome 12, at 12p13, where the two genes lie in tandem (13). C1r and C1s are synthesized as single-chain proenzyme molecules that, with C1q, form a calcium-dependent complex: $C1q_1C1r_2C1s_2$. During activation of the CP, each proenzyme is activated by cleavage of a single bond that produces two disulfide-linked peptides, the smaller of which has esterase activity. C1r has very limited trypsin-like activity and undergoes autoactivation followed by cleavage of C1s. C1s has trypsin-like activity against C4 and C2, each of which it cleaves into two fragments: C4a and C4b, and C2a and C2b.

C1r and C1s are synthesized primarily by hepatocytes, but monocytes, macrophages, epithelial and endothelial cells, and some cells of the central nervous system provide secondary synthesis sites. Deficiencies of C1r and C1s are very rare and may be partial or combined. They predispose the patient to recurrent pyogenic infections as well as immune complex disease and are associated with SLE and other autoimmune disorders (14). Without C1r and C1s, the CP cannot be activated.

The proteins C4 and C2 are required for formation of the C3 convertase of the CP (C4bC2a). C4b has cofactor activity required for the enzyme function of C2a. The absence of either protein leads to a complete block of CP activity and is associated with recurrent infections and immune complex disease as described above. In spite of this, many patients with C2 deficiency remain asymptomatic for long periods, if not for life. A bypass mechanism is provided by the LP that allows direct C3 cleavage by the MBL-associated serine proteases (MASPs), generating C3b for AP activation without the need for C2 or C4, and explaining why some patients have milder disease. Those who do have recurrent severe infections may have undetected LP or other defects as well. The wider availability of functional assays for the lectins and their enzymes will help to answer this question (15, 16).

The genes for C4 and C2, along with those for FB, are found in the major histocompatibility complex (MHC) on chromosome 6, in the class III MHC genes. The null allele for C2 deficiency is linked to HLA-A25, B18 haplotype (17, 18).

C4 is produced primarily by hepatocytes but can also be made by other cells. It is synthesized as a single chain that undergoes posttranslational modification to three chains, α, β, and γ, that are disulfide linked. The α chain contains an internal thioester linkage that is transiently exposed and forms a covalent bond with nearby substances when C4a is clipped off the N-terminal end during activation. This bond provides a means for attachment of C4b to the nearest protein or carbohydrate group when activation occurs, and results in long-lasting deposition of C4b and its breakdown fragment, C4d, on the activator or nearby cells.

Human C4 exists in two forms called C4A and C4B, coded for by different genes. Approximately 75% of the Caucasian population has two alleles for each C4 haplotype (19). The differences between the two forms of C4 are in a few amino acids near the thioester group, and they alter the ability of the C4b fragment to bind covalently to nearby surfaces when C4 is cleaved during activation. C4A binds best to amino groups on proteins such as antibodies, and C4B binds to carbohydrate on cell surfaces. The naming of these haplotypes is unfortunate, since the uppercase A and B are confused with the lowercase in C4a and C4b. Standard assays for C4 do not distinguish between these forms. Variation in C4 gene copy number is not uncommon, and the number can range from none to eight or more copies, giving this protein a wide range of concentrations in the general population (19, 20). More than 100 different polymorphisms in the C4 protein make it one of the most variable proteins in the circulation.

Most of the partial C4 deficiencies are without consequence, but some individuals have a total deficiency of one haplotype and not the other. C4A deficiency is increased (8 to 12%) in Caucasian lupus patients compared to control individuals (1 to 3%), resulting in decreased binding of C4b to protein antigens and antibodies and consequently

difficulty with immune complex clearance. An increased incidence of C4B null alleles was recently reported for patients with Henoch-Schönlein purpura (21). A report in 2010 described two siblings who developed membranoproliferative glomerulonephritis type III. The brother was diagnosed with Henoch-Schönlein purpura with proliferative glomerulonephritis at age 14 and died on dialysis at age 28. The lab results and biopsy were not available. The sister, age 28, presented with proliferative glomerulitis with confirmed C4B deficiency. The biopsy showed 3+ staining for C4 and IgG, 2+ for C1 and IgM, and weak IgA and C3 (22). This case illustrates the need for both protein and genetic analysis to arrive at the diagnosis.

Many cell types produce C2, including hepatocytes, monocytes, macrophages, fibroblasts, astroglioma cells, and alveolar type II cells. It is synthesized as a single-chain proenzyme that expresses its esterase activity only after it has been cleaved. This activity is very weak in the fluid phase but becomes efficient when, in the presence of magnesium, the C2a fragment binds to C4b that is fixed on a surface. C2a that has been dissociated from C4b is rapidly inactivated in the fluid phase, and native C2 protein, like C1q, is rapidly degraded at temperatures near or above 50°C.

Children and infants with C2 deficiency have increased susceptibility to infections such as streptococcal pneumonia and other encapsulated bacteria, as well as the previously mentioned association with immune complex diseases. In Caucasian patients with rheumatologic disorders such as SLE, the incidence of C2 deficiency approaches 1/100, as opposed to the general population, where the incidence is estimated to be 1/10,000 (23, 24). There are two forms of C2 deficiency. Type I C2 deficiency, which affects >90% of patients, results from a complete lack of protein in the circulation, while type II C2 deficiency comes from the production of protein that is incapable of normal function but that can be detected in the circulation by immunochemical assays. The former deficiency is caused by a 28-base-pair deletion that stops production of the protein, while the latter occurs from single nucleotide polymorphisms or point mutations identified by sequencing. Because some of the latter mutations result in production of normal levels of dysfunctional protein that reacts with the antibodies used in C2 analysis, similar to the situation in type II C1-INH deficiency, C2 should also be tested by a functional assay. With the increased availability of genetic tests, it is likely that the percentage of cases identified as type II C2 deficiency will increase in the next few years.

DEFICIENCIES OF THE LP: MBL, FICOLINS, AND MASPs

The family of proteins that make up the LP are ancient conserved pattern recognition molecules that recognize danger signals such as microbes as well as altered self surfaces. They are involved in clearance of infectious organisms, damaged tissues, and inflammatory responses. MBL was the first characterized, and the pathway was initially called the MBL pathway. Similar in structure to C1q, it is made up of trimers of single polypeptide subunits, two to six of which combine to form oligomers. The head group of each trimer has specificity for sugars and binds with high affinity to mannose, peptidoglycan, and *N*-acetylglucosamine residues that are found on the surfaces of bacteria, yeasts, and fungi (25). Like C1q, it is associated with serine proteases called MASPs that become active when MBL is bound to a surface (26). In addition to activating complement, MBL may be able to act as an opsonin by interacting directly with cell surface receptors.

The gene for MBL is found on chromosome 10, at 10q11.2-q21, with another gene that encodes a truncated protein at 10q22.2-22.3. There is a wide range of serum concentrations of MBL, due in part to the presence of gene variants that produce different amounts of the protein. Approximately 5 to 10% of individuals studied to date are MBL deficient (27). Because complement activation by the LP is antibody and C1 independent, it is thought to play an important role in innate immunity during infancy at the time when maternal antibodies are disappearing and before the infant's own adaptive immune responses are mature (28, 29). Deficiency of MBL has been linked to an increased frequency of pyogenic infections and sepsis, particularly in neonates and young children. It has been implicated as a risk factor in ischemia-reperfusion injury, Behçet's disease, cystic fibrosis, severe acute respiratory syndrome, and other respiratory infections (30–34). There is a 2- to 3-fold increase in MBL deficiency in those lupus patients who tend to have more frequent and severe infections. Worse outcomes are also observed in rheumatoid arthritis patients with MBL deficiency. Autoantibodies that reacted with MBL were found in a Japanese study of patients with SLE, but the significance of the antibodies was not evident from the disease characteristics of the patients (35). A recent report from Denmark linked deficiency of MBL (<100 ng/ml) and low levels of MASP-2 along with the *MBL2* YA two-marker haplotype in a group of patients with panic disorder, and the *MBL2* LXPA haplotype and low MASP-2 levels in patients with bipolar disorder. Both disorders are associated with infections and inflammation (36).

The ficolins are also similar to C1q and MBL, with four or more trimers bound together in a collagen-like tail region and a C-terminal fibrinogen domain that is thought to be the ligand-binding site for *N*-acetylglucosamine (37). Three ficolins have been described: ficolin-1 (previously M-ficolin), ficolin-2 (previously L-ficolin), and ficolin 3 (previously H-ficolin, also known as Hakata antigen). The genes for ficolin-1 and ficolin-2 are at chromosome 9q34 and are similar, suggesting gene duplication in their past. The gene for ficolin-3 is found at 1p36.11. The ficolin-1 and ficolin-2 proteins are 80% homologous with each other, while the ficolin-3 protein is only 48% homologous with ficolin-1 and ficolin-2. The carbohydrate binding sites differ in that ficolin-1 and ficolin-3 have a single domain but ficolin-2 has four distinct binding sites. Ficolin-1 is expressed in monocytes and is present in the spleen and type II alveolar cells. Ficolin-2 is expressed primarily in the liver, but low levels of mRNA can be found in the bone marrow, tonsils, intestine, and the fetal lung. It is not known if these represent synthesis sites. Ficolin-3 is produced in the liver and the lung, with low levels found also in the heart, kidney, spleen, pancreas, and placenta. Low levels of mRNA have been seen in the brain and in a human glioma cell line. The levels in the lung exceed those in the liver, suggesting a role for ficolin-3 in lung defense. Hereditary deficiencies of the ficolins are extremely rare, but polymorphisms that affect the level and concentration of ficolin-2 are relatively common. A frameshift mutation was found in ficolin-3, resulting in a truncated protein. The patient had recurrent lower respiratory infections since childhood. He later developed cerebral abscesses (38).

The MASP enzymes also associate with the ficolins, with MASP-2 being the primary initiator for activation. MASP-1 and MASP-2 are also capable of cleaving prothrombin and fibrinogen and generating a fibrin clot (39, 40).

All forms have similar opsonizing capacities for pathogens and are associated with the MASP enzymes found with MBL. Although the ficolins were first described as opsonins

in 1996, little is known of the prevalence or phenotype of ficolin deficiencies.

The four MASP proteins, MASP-1, MASP-2, MASP-3, and Map19, are encoded by two genes. Structurally they are similar to C1r and C1s, with a serine protease domain in the B chain. MASP-1 and MASP-3 are alternative splice products of one gene (*MASP-1/3*) that have the same A chain but different B chains. A different gene encodes MASP-2 and Map19, the latter of which has only the first two domains of MASP-2 plus an additional four amino acids. MASP-2 is responsible for the cleavage of C4 and C2, making it analogous to C1s in function. Although there have been mutations found in the genes for the MASP proteins, the mutations in MBL that prevent the assembly of the complete complex are the major known cause of functional deficiency of these proteins (29, 41).

DEFICIENCIES OF THE CP AND LP CONTROL PROTEINS: C1-INH AND C4BP

The active enzyme forms of C1r and C1s are regulated solely by C1-INH, a member of the SERPIN family of serine protease inhibitors. C1-INH also contributes to the control of other enzymes, including coagulation factors XIa, XIIa, plasmin, and plasma kallikrein. When the enzyme and inhibitor interact, the enzyme binds to and cleaves a "bait-sequence" on the inhibitor and the resulting change in conformation forms a tight complex, rendering the enzyme inactive. The enzyme-inhibitor complexes formed in these reactions are cleared from the circulation by cells of the reticuloendothelial system. If the inhibitor is present in low levels, if it has a defect that makes it nonfunctional, or if there is an autoantibody that binds to and inactivates the C1-INH, then symptoms of angioedema are likely to occur.

C1-INH deficiency can be of hereditary origin (HAE) or acquired (AAE). Clearance of inhibitor-enzyme complexes that result from complement activation or action of autoantibodies that react with the inhibitor and result in its inappropriate cleavage can decrease the available amount of C1-INH present at a given time. Symptoms are similar regardless of the cause of the deficiency, so careful evaluation is required to distinguish between HAE and AAE. In the past few years, other forms of HAE have been recognized that are not associated with C1-INH deficiency. Konrad Bork, working in Germany, found numerous patients, most of whom were women, with HAE but normal levels and function of C1-INH. A subgroup of these patients was shown to have a mutation in factor XII of the contact coagulation pathway. Since his publication, other families with the same mutation have been identified (42, 43). The biochemical mediator of C1-INH deficiency-related HAE, as well as the factor XII-related form, has been identified as bradykinin. C1-INH is also involved in the coagulation pathway as an inhibitor of factor XIIa, kallikrein, plasmin, and other enzymes, so decreased amounts of the C-INH would allow increased production of bradykinin. The mutation in factor XII makes it less susceptible to control by C1-INH, which can also lead to more bradykinin. The fact that both kinds of patients respond to inhibition of bradykinin or its receptor supports this assumption.

C1-INH is inherited in an autosomal codominant pattern in which each allele produces approximately half of the protein in the circulation, although increased catabolism often causes decreases of the normal gene product to below the predicted 50% level. To date, very few patients with homozygous deficiency of C1-INH (both alleles defective) have been reported, and the heterozygous state determines the dominant phenotype (44). Patients with C1-INH deficiency suffer various degrees of intermittent angioedema characterized by nonpainful, nonpruritic, and nonerythematous subcutaneous and submucosal swelling that spontaneously subsides within 72 h (45, 46). Swelling may arise sporadically and spontaneously, or it may be triggered by mild trauma or psychological stress. It is not accompanied by urticaria and is not responsive to antihistamines, steroids, or β agonists. Symptoms usually begin in adolescence and range in severity from mild edema of the extremities to life-threatening laryngeal edema. Edema of the bowel wall results in severe colicky abdominal pain, nausea, and vomiting that can be distinguished from acute abdominal syndromes by the absence of fever, peritoneal signs, and elevated white blood cell count. Angiotensin inhibitors may increase attack frequency and severity. In one case report, an underlying autoantibody to the C1-INH was "unmasked" by an angiotensin-converting enzyme inhibitor, greatly enhancing the patient's symptoms.

Genetic defects in C1-INH range from single nucleotide polymorphisms that may alter the function of the protein produced to inappropriate stop codons resulting in large deletions and no protein production. Since most patients are heterozygous for the deficiency, each patient has one normal allele and one abnormal allele, and he or she will have variable amounts of C1-INH protein in the circulation, from very low to elevated, depending on the particular mutation in the affected gene. In the majority of patients, low levels of C1-INH are indicative of the defect, but final diagnosis of HAE should be based on the functional activity of C1-INH protein in conjunction with decreased levels of C4, the clinical presentation, and family history. Spontaneous mutations in C1-INH genes have been documented in about 20% of cases, so the lack of family history does not rule out the defect (47, 48). The prevalence of C1-INH deficiency is 1/10,000 in Caucasian populations. MASP-1 and MASP-2 are controlled in a 1:1 manner by C1-INH, in the same way that C1r and C1s are controlled. The control of MASP-3 is not known at this time.

The classification of HAE is undergoing scrutiny by several consensus groups that are trying to define the disease based on its genetics, symptoms, and response to treatment. The two "classical" forms of HAE appear the same clinically. Type I HAE (80% of patients) is defined by a reduction of C1-INH to less than half of normal antigenic and functional levels. Type II patients have normal or elevated C1-INH antigenic levels but synthesize a dysfunctional protein that results in reduced C1-INH function. Recent studies have identified other forms in which the patients, all women, have clinical findings consistent with HAE but normal C1-INH level and function (49, 50). The underlying estrogen-dependent defect has not been identified. In some families, a gain-of-function mutation in coagulation factor XII has been associated with the HAE (28).

Several forms of AAE have been described, depending on the underlying cause. Patients with B-cell lymphoproliferative diseases that produce circulating anti-idiotype antibodies generate immune complexes that cause a persistent activation of complement and result in profound C1-INH depletion as the enzyme-inhibitor complexes are cleared (51, 52). In this form of AAE, the C1q level is decreased due to the activation, whereas in the hereditary forms it is not, making the measurement of the C1q protein a method for identifying these patients. Another form of AAE results from inactivation of C1-INH caused by autoantibodies to the C1-INH protein (53). In these patients, the C1-INH level can be normal by immunoassay but the protein's function is blocked, similar to type II HAE. The autoantibody can be detected by enzyme-linked immunosorbent assay,

and a cleaved form of the C1-INH molecule can be detected by Western blotting.

The good news about HAE is the availability of new treatments for patients, and more rapid diagnosis so that they can get help sooner. Human plasma-derived purified C1-INH and recombinant human C1-INH protein preparations are now available for infusion or subcutaneous administration. There is also a drug that blocks the receptor for bradykinin and another that acts on the bradykinin itself. The interest that the pharmaceutical industry has shown in orphan diseases has increased greatly in the past 10 years and resulted in benefits for other complement-related diseases as well.

The fluid-phase control of C4aC2b, the C3 convertase of the CP and LP, is accomplished through the combined effects of C4b-binding protein (C4BP) and FI. Also known as proline-rich protein, human C4BP is a member of the gene family called regulators of complement activation (RCA). Characterized by multiple short consensus repeat motifs, also referred to as complement control protein (CCP) units, the RCA proteins bind C3b and C4b fragments and possess various control properties that are critical for regulation of complement activity. These small globular CCP units are typically connected in linear fashion like beads on a string. They occur in all of the RCA and many other complement proteins in various numbers.

C4BP has several isomers made up of two types of subunits: six or seven α chains and zero or one β chain. These are connected at a central joining region and radiate outward, giving the molecule a spider-like appearance in electron micrographs. The α chains bind to C4b and accelerate the dissociation of C4bC2a to form free C2a and C4b-C4BP. C2a is unable to bind to newly formed C4b and becomes inactivated, while C4b undergoes degradation by FI (with C4BP as a cofactor) to form C4c and C4d (54). C3 convertase activity by the CP enzyme is short-lived due in part to the efficiency of C4BP. For this reason, activation of the CP does not produce a large amount of C3 fragments and activation often stops at this point in the cascade unless enough C3b is generated to allow the AP to be activated. In autoimmune diseases such as SLE and rheumatoid arthritis, the ratio of C4 to C3 is used to determine the state of complement activation in the patient: low C4 but normal C3 implies low-level CP activity. Another method of looking at the amount of activation is to measure the amounts of C4d and C3d that are deposited on platelets, erythrocytes, and other cells that are in the vicinity of complement activation. Flow cytometry is used for evaluation of these markers for complement activation (55, 56).

In the absence of C1-INH, it is the control of C4bC2a activity by C4BP and FI that accounts for the stability of C3 in HAE patients in spite of decreased C4 and C2 (57). The β chain has a binding site for the anticoagulant protein S and plays a role in control of coagulation (58).

C4BP is synthesized by hepatocytes. The genes for the C4BP α and β chains are located in the RCA gene cluster on chromosome 1, at 1q32. Circulating concentrations of C4BP vary according to genetic determinants as well as fluctuations due to consumption during disease states. Deficiencies of C4BP are very rare and would logically be associated with uncontrolled activation of C3 through the CP. The only documented case was a patient with an atypical form of Behçet's disease and angioedema (59).

DEFICIENCIES OF THE AP: FD, FB, AND P

FD is the smallest of the complement proteins and is the only serine protease of the system that does not require enzymatic cleavage in order to become active. Instead, its enzyme activity is a function of its conformational state, and it can flip between the active and inactive forms depending on its proximity to its substrate: C3b-bound FB (60). Monocytes and their lineage synthesize some of the FD found in the circulation, but the major source is in adipose tissue. FD has another role apart from its complement duties, in that it is known as adipsin and acts as a regulator of fat metabolism. Likewise, C3a is known as acylation-stimulating protein, or ACP (61). FD is the only initiating enzyme for the AP. It binds to and cleaves FB only when the FB is bound to C3b. The resulting complex, C3bBb, is the AP C3 convertase.

The gene for FD is located on chromosome 19. FD deficiency is extremely rare. One family with FD deficiency has been described to date. In five generations of family members, the propositus was a 23-year-old woman who presented with meningococcemia from *Neisseria meningitidis*. Three relatives had FD deficiency with no health problems, and a deceased family member had a history of meningitis in his twenties and died from pneumonia and meningitis caused by *Streptococcus pneumoniae* at age 81 (62). Complement studies for the patient and family members included C3 and C4 levels and CH50 (normal in all). The AH50 was <10% of normal in homozygous deficient individuals but was normal in all others, including those heterozygous for the deficiency. When FD was analyzed, it was found to be slightly elevated in those members who were homozygous for the wild-type FD gene, about half the normal level in those heterozygous for the mutation, and undetectable in the four patients homozygous for the mutation.

In addition to its participation in the AP of complement, FD plays a role in fatty acid metabolism, and the $C3a_{desArg}$ fragment produced by FD-mediated cleavage of C3 has been identified as the autocrine mediator of hyperapobetalipoproteinemia (61, 63). It is tempting to speculate that this involvement with lipid metabolism may be impaired or dysregulated somehow in those rare patients with partial lipodystrophy who have increased cleavage of C3 due to the presence of autoantibodies to the C3bBb complex (C3 nephritic factors) (64). Another question that is receiving attention in this regard is the role of complement in cardiometabolic disease or type 2 diabetes (121).

FB has been known variably as glycine-rich β-glycoprotein, properdin factor B, and C3 proactivator. The gene for FB is in the MHC complex on chromosome 6, at 6p21.1-6p21.3, 3′ to the C2 gene (65). It is synthesized primarily in the liver, with additional protein produced by cells of monocyte/macrophage lineage, fibroblasts, endothelial cells, and alveolar type II epithelial cells. Secreted as a single polypeptide chain proenzyme, FB is activated only when it is bound to C3b and cleaved by FD. Its activity is specific for C3 and C5, but it requires C3b as a cofactor to cleave the former and an additional C3b to cleave the latter. The hydrolyzed form of C3 known as $C3(H_2O)$ can also serve as the first ligand for FB binding.

FB is an acute-phase protein and increases during inflammation. There are two polymorphic forms of FB, FB*F and FB*S, based on their electrophoretic mobilities on immunoelectrophoresis. The amount of FB in the circulation is higher in individuals homozygous for the former and lower in individuals homozygous for the latter, with heterozygous individuals intermediate (66). A recent letter to the *New England Journal of Medicine* described an FB deficiency due to a nonsense mutation inherited from the patient's father and a frameshift mutation from the mother. The patient had normal CH50 and no AH50 activity, while the parents both

had normal activity for both assays. The patient had recurrent pneumococcal and meningococcal infections, starting at age 2 years (67).

P is a unique protein that acts as a stabilizer for the AP C3 convertase and makes possible the amplification loop that very efficiently cleaves C3 when the AP is activated. This unique property makes it the only positive regulator in the complement system. P is a single-chain linear molecule with no enzyme activity, but it forms head-to-tail polymers, about half of which are trimers, with dimers and tetramers making up the remainder. P binds to C3b with increasing avidity depending on the number of C3b molecules in a cluster, and its affinity increases when Bb is present (68, 69). In some cases, P binds to the activator surface before any other complement proteins, providing a nucleus on which the C3bBbP complex can form and start the amplification loop for deposition of C3b (70, 71).

P is the only complement protein that is X-linked, with its gene at Xp11.3-Xp11.23 (72, 73). The protein is synthesized by monocytes, granulocytic cells, and T cells. Three types of P deficiency have been described. Type I deficiency is associated with fulminant meningococcal infections, with little or no P detectable in the circulation. Partial P deficiency found in another family with neisserial septicemia was characterized by about 10% of normal levels of P in the serum (74). Several dysfunctional mutant forms of the protein have been identified that result in decreased AP function, making this type III deficiency (75). P deficiency increases the susceptibility to bacterial infections, including *Neisseria* infections. Carriers of a defective or absent P gene cannot be reliably identified from the protein's level in the circulation or by other lab tests, and genetic typing is necessary to provide evidence of the carrier state (76).

CONTROL PROTEINS OF THE AP: FH, FI, MCP (CD46), AND CR1 (CD35)

The amplification, or feedback, loop of the AP makes it one of the most efficient enzyme systems in the circulation (77). As long as P can continue to stabilize the C3 convertase (C3bBbP), C3 cleavage continues unchecked. This leads to deposits of C3 clusters on the surface of nearby cells, close to where the C3bBb is bound, and greatly enhances opsonization and other inflammatory cell interactions with the C3-coated particles due to the increased avidity provided by multiple closely spaced C3 fragments for C3 receptor interaction. The two major controls of the fluid-phase activation of the AP are FH and FI. The former is a member of the RCA family with the ability to bind C3b, and the latter is a serine protease with specificity for cleaving C3b. When C3bBb is formed, FH can bind to the C3b, displacing the Bb. FI can then cleave the C3b in two places on the α chain to create the fragments: iC3b and C3f (78). FI can then further degrade the fragments to C3c, C3dg, and C3d. C3 degradation prevents the reuse of the C3b in forming another C3bBb enzyme. On cell surfaces, two membrane proteins act in a manner similar to FH. CR1 (CD36) and MCP (CD46) are found on the surface of most cells in the body and possess cofactor activity for FI in degradation of C3b and C4b. While decay accelerating factor (CD55) can dissociate the C3 convertases of the CP and AP, it does not provide cofactor function for FI, so the dissociated C4b and C3b can reenter the activation process with a new partner (79).

FH binds to many anions including those on endothelial and other cell surfaces. Thus it can provide local backup control on a surface where complement activation is causing tissue damage, such as in the kidney or the eye. When the FH is compromised by a genetic defect that prevents it from binding to the surface, there is less help provided and the damage proceeds unchecked. The same result is seen when one of the other proteins in the pathway is not fully functional or has a gain-of-function defect that allows it to evade control. This has been shown to be true for mutations in FB and C3, and the resulting loss of regulation of the AP is seen in the development of uncontrolled deposition of C3b in sites such as the macula of the eye, contributing to AMD, or in the kidney, generating damage that impairs kidney function. The list of complement-related risk factors for developing these diseases includes mutations in factors H, I, B, C3, and thrombomodulin.

The important complement control protein FH is synthesized as a single chain comprising 20 CCP modules. The gene for FH is located in the RCA cluster of genes on chromosome 1, at 1q32 (80). FH is produced primarily in the liver, but monocytes, macrophages, fibroblasts, endothelial cells, and myoblasts can also produce it. There are several variant forms of FH, referred to as FH-like (FHL1) or FH-related (FHR1 to -5) proteins, that differ in size and function from FH. In humans, these different forms of FH appear to represent products of alternative splicing of the FH gene rather than separate genes (81).

FH has multiple binding sites that interact with C3b, heparin, chondroitin sulfate and other polyanions, bacterial surface components, DNA and other nucleotides, and endothelial cells. Its mode of action as a control protein is to bind to C3b and displace the Bb enzyme component of the AP C3 convertase. If additional C3b fragments are bound to or near the convertase, the avidity of this binding is increased. Once Bb has been removed, FI can use FH as a cofactor in cleaving C3b to form iC3b, C3dg, and C3c, thus preventing the C3b from interacting with B to form a new convertase. The fragments iC3b and C3dg can interact with CR3 receptors on phagocytic cells and with CR2 receptors on B cells and dendritic cells, respectively. In addition to its function as a fluid-phase control protein, FH has been reported to have chemotactic activity for monocytes (82, 83). It also functions as an adhesion protein for neutrophils, possibly through the RGD sequence in the fourth CCP module. FH binds to many cell types, including endothelial cells, through its polyanion binding regions and can serve as a cell surface control protein in this capacity.

FH deficiency involves compromise of the complement regulatory action, which can be severe in patients who lack FH protein completely. These patients have varied presentations, including recurrent infections, membranoproliferative glomerulonephritis, SLE, and atypical hemolytic-uremic syndrome (aHUS) (84–86). Initial lab results may identify them as C3 deficient, since without functional FH, the C3 in their circulation is diminished or absent. More-subtle deficiencies stem from point mutations in the *CFH* gene and result in decreased ability of the FH to control complement on cell surfaces, particularly in the kidney (aHUS) and in the eye (AMD) (87–92). In the latter case, the Y402H mutation is strongly associated with the susceptibility to AMD. In a recent study by Hageman and colleagues (88), the result of combining the genetic information with the fundus phenotype, age, and smoking history provided better ability to predict geographic atrophy or choroidal neovascularization as the endpoint. The genes analyzed included *ARMS2*, *CFH*, *C3*, *C2*, *FB*, *CFHR4*, *CFHR5*, and *F13B*.

An acquired form of aHUS is associated with anti-FH autoantibodies (93, 94). The list of complement gene mutations that are risk factors for AMD and renal disease includes *FI*, *MCP* (*CD46*), as well as missense mutations in

C3 and *FB* that make them unable to allow FH binding and thus evade control (95).

Another disease-related property of FH is the prevalence of bacterial or viral binding surface proteins that have evolved to bind it and thus wrap the microbe in a protective coating that prevents complement activation on their surfaces. Among the microbes that use this scheme to escape complement attack are strains of *Borrelia*, *Streptococcus*, *Yersinia*, and *Neisseria* (96–98). This method of acquiring serum resistance also includes binding of other regulatory proteins (C4BP and MCP) as well as RCA-like proteins encoded by the microbial DNA and expressed on the surface.

FI, also known in the older literature as C3b-inactivator and KAF (conglutinogen-activating factor), is a single-chain serine protease that cleaves two sites on the α chains of both C4b and C3b: one on either side of the thioester bond region. This stops further participation of these molecules in complement activation and creates first iC4b or iC3b, followed by the final breakdown fragments C4c and C4d, and C3c and C3dg. FI requires C4BP (for C4b cleavage) or FH (for C3b cleavage) for cofactor activity in the fluid phase. On cell surfaces, the complement receptors CR1 and CR3 and MCP can fill this role as cofactors (99). FI production occurs in many different cell types: hepatocytes, monocytes, fibroblasts, endothelial cells, myoblasts, glial cells, and Raji cells. The gene for FI is on chromosome 4, at 4q25. FI deficiency was first identified in a patient with little or no C3 in the circulation (100, 101). FI deficiencies, like those of FH, are characterized by low or absent C3 in the circulation. FI deficiency is associated with recurrent severe pyogenic infections, vasculitis, glomerulonephritis, and aHUS (54, 102, 103).

DEFICIENCIES OF THE TERMINAL PATHWAY COMPONENTS: C3, C5, C6, C7, C8, AND C9

Because C3 occupies the central position where the three initiating pathways merge with the terminal pathway, it is critical in the functioning of the system as a whole. C3 is an acute-phase reactant, increasing as much as 2-fold during inflammation. This increase may mask decreases due to activation, making it difficult to determine what is actually happening *in vivo*. Cleavage of C3 during complement activation produces a sequence of fragments, most of which have biological activities associated with opsonization, phagocytosis, immune adherence, effects on local vasodilation, smooth muscle contraction, and induction of mediator release, including histamine from inflammatory cells. The absence of C3, due to either an inherited defect or an acquired condition, renders the individual highly susceptible to bacterial infections, membranoproliferative glomerulonephritis, and immune complex-mediated diseases such as lupus. The internal thioester bond in C3 is like that described earlier for C4 and leads to permanent attachment of the C3b and C3d fragments to the surface of the activating particle or molecule.

Most of the C3 in the circulation comes from hepatocytes, but many other cells can produce C3 and contribute to the local supply. The gene for human C3 is located on chromosome 19, at 19p13.3-p13.2 (104). Inheritance follows an autosomal recessive pattern in which the C3 protein is undetectable in the homozygous state and is approximately half the normal level in heterozygous individuals. The acquired forms of C3 deficiency can be profound and have been mistaken for genetic C3 deficiency on occasion. The usual causes of acquired C3 deficiency are secondary to deficiencies of FI or FH, or the presence of autoantibodies to either of the C3 convertases, C3 or C4 nephritic factors, resulting in uncontrolled C3 cleavage in the circulation. In these cases, C3 fragments (iC3b, C3c, or C3a) can usually be detected in the circulation, and incubation of the patient's serum with normal serum or with purified C3 leads to C3 cleavage in the normal serum.

C5 is structurally similar to C3 but lacks the internal thioester bond that characterizes C3 and C4. When cleaved during activation, C5 also gives rise to similar fragments, but their activities are different from those for C3 and C4: C5b participates in the initiation and formation of the lytic complex (C5b-9) that inserts into the membrane of the target cells, and C5a is one of the most potent chemoattractants for neutrophils and other inflammatory cells. As anaphylatoxins, C5a and C3a induce changes in vascular permeability; smooth muscle contraction; cell activation; upregulation of adherence molecules; and release of enzymes, mediators such as histamine, and cytokines.

Like C3, C5 is produced mainly in the liver but can also be synthesized by cells in the lung, spleen, and intestine, as well as by monocytes, macrophages, and alveolar type II cells. The gene for C5 is located on the ninth chromosome, at 9q33. Several strains of mice have spontaneously occurring C5 deficiency. Homozygous deficiency of C5 is associated with severe infections, often from *N. meningitidis* or *Neisseria gonorrhoeae*. C5-deficient individuals lack bactericidal activity and are unable to mobilize their neutrophils and other inflammatory cells to respond to bacterial infections. Other presentations have included discoid lupus and Sjögren's syndrome (105–107).

An interesting phenomenon is occurring in laboratories measuring C5 levels and function. The number of patients with little or no C5 function is increasing due to the increased use of the humanized anti-C5 antibody eculizumab for treatment of paroxysmal nocturnal hemoglobinuria and aHUS. Other conditions that are being considered for eculizumab treatment include phospholipid antibody syndrome, lupus nephritis, and kidney transplantation, so the frequency of low C5 results will probably continue to increase (108).

C6 and C7 are similar proteins that are encoded by genes on the fifth chromosome, at 5p12-14. Another complement gene, C9, is close to this locus as well. Unlike the previously discussed complement proteins up through C5 in the activation pathways, none of the late components (C6, C7, C8, and C9) is cleaved during activation, but all are critical for the formation of C5b-9, the membrane attack complex (MAC), also called the terminal complement complex. When C5 is cleaved by the C5 convertase (C4bC2aC3b), a neoepitope is exposed on C5b, allowing C6 to bind to it and form a C5b6 complex that is rapidly expanded to C5b-7 by the addition of C7. The final complex formation occurs on a membrane surface when C8 binds and multiple C9 molecules polymerize to form the membranolytic complement lesion, C5b-9, on the cell surface, leading to osmotic lysis of the cell.

Deficiencies of C6 and C7 are associated with recurrent severe neisserial infections as well as infections caused by other pyogenic bacteria, although there have been reports of lupus in individuals with these deficiencies as well. A number of cases of combined deficiency of C6 and C7 have been reported, as well as the influence of one gene upon the synthesis rate of the other, leading to decreased production of one of the proteins from an otherwise normal gene. Subtotal deficiencies of both proteins were accompanied in one patient by a lower-molecular-weight form of C6 that was associated with a defect in the 5′ splice donor site of intron 15 of the C6 gene. The same patient had low C7 as well, with the C7 protein containing an Arg→Ser substitution that altered the protein's isoelectric point. Patients with complete

deficiency of C6 or C7 lack measurable protein and have little or no hemolytic activity in the CH50 or AH50 assays. Subtotal deficiencies of C6 or C7 are similar, although loss of hemolytic function is not complete (109).

C8 is a complex protein made up of three nonidentical polypeptide chains: a disulfide-linked α-γ pair and a non-covalently linked β chain. Each one of the chains is coded for by a separate gene and the protein is assembled intracellularly, although there is evidence from deficiencies that C8α-γ and C8β may be produced and secreted independently. The intact molecule is required for function in the lysis of the target cell (110).

The genes for the C8 subunits are located on the first (C8α and C8β at 1p32) and ninth (C8γ at 9q34.4) chromosomes. The three chains of C8 are interesting in that C8α and C8β are similar to C6, C7, and C9 in their structure, while C8γ is more closely related to the lipocalin family of proteins that bind and transport small hydrophobic ligands (111). Because C8 deficiency is due to decreased or no synthesis of only part of the complex molecule (C8α chain or C8β chain), the part of the molecule that is produced is still recognized by the antisera used for measuring C8 levels in serum, giving, in effect, a false-positive result. This makes it necessary to use caution in diagnosing C8 deficiency from protein levels alone, and a functional test should be done as well. C8 deficiency, like that of other MAC proteins, is characterized by recurrent infections, most often caused by neisserial species. C8 is synthesized primarily by hepatocytes, although it can also be produced by cells of monocyte/macrophage lineage, astrocytes, oligodendrocytes, fibroblasts, and endothelial cells.

As the MAC is assembled on the cell surface, the C5 to C8 proteins are joined by C9, the final protein in the terminal complement pathway. The C9 protein unfolds to form polymers that penetrate the membrane and create perturbations that lead to osmotic lysis of the target cells. Estimates of the number of C9 molecules required to form a lytic pore range from 6 to 18 (112). C9 is produced primarily by hepatocytes and secondarily by monocytes, glial cells, fibroblasts, and other local cells at sites of inflammation. It is an acute-phase protein and is coded for by a gene at 5p13, close to the genes for C5 and C6.

Many cases of C9 deficiency have been reported, and the remarkable thing is the lack of strong association of disease phenotypes with this complement deficiency. Although there have been scattered reports of neisserial infections, most C9-deficient patients appear to be healthy. This is most likely because C9 is not absolutely required for lysis of the target cell. C9 is the most common complement component deficiency in Japan and other Asian populations as well (113, 114).

CONTROL PROTEINS OF THE TERMINAL PATHWAY: VN, CN, AND CD59

Protection of host cells from "bystander lysis" caused by insertion of fluid-phase C5b-9 (MAC) complexes is accomplished by several mechanisms. Two proteins, Vn (vitronectin; formerly S-protein) and Cn (formerly clusterin, SP 40,40, or apolipoprotein J), act as solubilizing factors to bind the MAC and block its hydrophobic insertion into the membranes of nearby cells. These proteins can bind to C5b-7 and C5b-8 in the fluid phase, preventing membrane interaction and C9 polymerization, although at least one C9 molecule is associated with the final sC5b-9 complexes detected in the circulation. This complex is relatively long-lived and serves as a marker for complement activation when most other complement fragments (C3a, C5a, etc.) have been cleared from the circulation. No deficiency of either of these proteins has been identified to date.

CD59 is a membrane-bound glycoprotein that inhibits the polymerization of C9 and the lytic activity of the MAC. It is expressed on a wide variety of cell types, including erythrocytes. Because it is species specific, it is the primary cell surface protector against lysis mediated by homologous complement. CD59 is linked to the cell membrane by a glycophosphatidylinositol anchor that is variably lost from cells in patients with paroxysmal nocturnal hemoglobinuria; loss of CD59 provides one of the mechanisms for hemolysis in these patients. Inherited CD59 deficiency is rare and is associated with chronic hemolysis and infections (115).

THERAPY FOR COMPLEMENT DEFICIENCIES

Treatment of patients with complement deficiencies has been limited to prophylactic antibiotics, vaccination for relevant organisms, and treatment of infection and autoimmunity. Replacement of the missing component with fresh frozen plasma at this point in time, or the use of recombinant components for a completely deficient patient, is possible, but the hurdles of economics and potential for immune responses to the recombinant proteins make this tactic unlikely to succeed. Blood transfusion to replace C2 has been used with some success in two SLE patients and early in aHUS patients with FH deficiency (84, 116). Purified plasma C1-INH has been successful at the time of attacks, but other possible drugs are currently available or in the pipeline, including recombinant C1-INH and a specific inhibitor of the bradykinin receptor BK2.

Recombinant or monoclonal antibody complement inhibitors have been used in ischemia-reperfusion injury, cardiopulmonary bypass surgery, and autoimmune disorders. Soluble CR1 acts against the C3 and C5 convertases of both the AP and CP (117, 118). The humanized anti-C5 monoclonal antibody eculizumab prevents cleavage of C5 to C5a and C5b and has been effective in treatment of paroxysmal nocturnal hemoglobinuria and aHUS as well as other complement-mediated kidney disease. As seen with the expanding uses of eculizumab and C1-INH drugs in patients with diverse conditions, there will be continued production and modification of the current inhibitors as well as development of novel solutions for treating patients with deficiencies as well as dysfunctional complement pathways (119, 120). Given this beginning, it seems only a matter of time until most patients with complement deficiencies can be helped by compounds that will reverse the acute symptoms as well as provide long-term prevention of the often devastating diseases associated with malfunction of this important immune pathway.

REFERENCES

1. **Ricklin D, Lambris JD.** 2013. Complement in immune and inflammatory disorders: pathophysiological mechanisms. *J Immunol* **190:**3831–3838. PubMed
2. **Giclas PC.** 1997. Complement tests, p 181–186. *In* Rose NR, Conway de Macario E, Folds JD, Lane HC, Nakamura RM (ed), *Manual of Clinical Laboratory Immunology*, 5th ed. ASM Press, Washington, DC.
3. **Giclas PC.** 2001. Classical pathway evaluation. *Curr Protoc Immunol* **Chapter 13:**Unit 13.1. doi:10.1002/0471142735.im1301s09.
4. **Giclas PC.** 2001. Alternative pathway evaluation. *Curr Protoc Immunol* **Chapter 13:**Unit 13.2. doi:10.1002/0471142735.im1302s09.
5. **Giclas PC.** 2002. Choosing complement tests: differentiating between hereditary and acquired deficiency, p

111–116. *In* Rose NR, Hamilton RG, Detrick B (ed) *Manual of Clinical Laboratory Immunology*, 6th ed. ASM Press, Washington, DC.
6. **Varga L, Széplaki G, Laki J, Kocsis A, Kristóf K, Gál P, Bajtay Z, Wieslander J, Daha MR, Garred P, Madsen HO, Füst G, Farkas H.** 2008. Depressed activation of the lectin pathway of complement in hereditary angioedema. *Clin Exp Immunol* **153:**68–74. PubMed
7. **Figueroa JE, Densen P.** 1991. Infectious diseases associated with complement deficiencies. *Clin Microbiol Rev* **4:**359–395. PubMed
8. **Giclas PC.** 2002. Choosing complement tests: differentiating between hereditary and acquired deficiency, p 111–116. *In* Rose NR, Hamilton RG, Detrick B (ed), *Manual of Clinical Laboratory Immunology*, 6th ed. ASM Press, Washington, DC.
9. **Sellar GC, Cockburn D, Reid KB.** 1992. Localization of the gene cluster encoding the A, B, and C chains of human C1q to 1p34.1-1p36.3. *Immunogenetics* **35:**214–216. PubMed
10. **Shen N, Tsao BP.** 2004. Current advances in the human lupus genetics. *Curr Rheumatol Rep* **6:**391–398. PubMed
11. **Tsao BP.** 2000. Lupus susceptibility genes on human chromosome 1. *Int Rev Immunol* **19:**319–334. PubMed
12. **Wisnieski JJ, Jones SM.** 1992. Comparison of autoantibodies to the collagen-like region of C1q in hypocomplementemic urticarial vasculitis syndrome and systemic lupus erythematosus. *J Immunol* **148:**1396–1403. PubMed
13. **Kusumoto H, Hirosawa S, Salier JP, Hagen FS, Kurachi K.** 1988. Human genes for complement components C1r and C1s in a close tail-to-tail arrangement. *Proc Natl Acad Sci USA* **85:**7307–7311. PubMed
14. **Morgan BP, Walport MJ.** 1991. Complement deficiency and disease. *Immunol Today* **12:**301–306. PubMed
15. **Selander B, Mårtensson U, Weintraub A, Holmström E, Matsushita M, Thiel S, Jensenius JC, Truedsson L, Sjöholm AG.** 2006. Mannan-binding lectin activates C3 and the alternative complement pathway without involvement of C2. *J Clin Invest* **116:**1425–1434. PubMed
16. **Atkinson JP, Frank MM.** 2006. Bypassing complement: evolutionary lessons and future implications. *J Clin Invest* **116:**1215–1218. PubMed
17. **Mortensen JP, Buskjaer L, Lamm LU.** 1980. Studies on the C2-deficiency gene in man. *Immunology* **39:**541–549. PubMed
18. **Atkinson JP.** 1999. Genetic susceptibility and class III complement genes, p 91–104. *In* Lahita RG (ed), *Systemic Lupus Erythematosus*. Academic Press, San Diego, CA.
19. **Yu CY, Blanchong CA, Chung EK, Rupert KL, Yang Y, Yang Z, Zhou B, Moulds JM.** 2002. Molecular genetic analysis of human complement components C4A and C4B, p 117–131. *In* Rose NR, Hamilton RG, Detrick B (ed), *Manual of Clinical Laboratory Immunology*, 6th ed. ASM Press, Washington, DC.
20. **Yang Y, Chung EK, Zhou B, Blanchong CA, Yu CY, Füst G, Kovács M, Vatay A, Szalai C, Karádi I, Varga L.** 2003. Diversity in intrinsic strengths of the human complement system: serum C4 protein concentrations correlate with C4 gene size and polygenic variations, hemolytic activities, and body mass index. *J Immunol* **171:**2734–2745. PubMed
21. **Stefansson Thors V, Kolka R, Sigurdardottir SL, Edvardsson VO, Arason G, Haraldsson A.** 2005. Increased frequency of C4B*Q0 alleles in patients with Henoch-Schönlein purpura. *Scand J Immunol* **61:**274–278. PubMed
22. **Soto K, Wu YL, Ortiz A, Aparício SR, Yu CY.** 2010. Familial C4B deficiency and immune complex glomerulonephritis. *Clin Immunol* **137:**166–175. PubMed
23. **Atkinson JP.** 1989. Complement deficiency: predisposing factor to autoimmune syndromes. *Clin Exp Rheumatol* **7**(Suppl 3)**:**S95–S101. PubMed
24. **Johnson CA, Densen P, Wetsel RA, Cole FS, Goeken NE, Colten HR.** 1992. Molecular heterogeneity of C2 deficiency. *N Engl J Med* **326:**871–874. PubMed
25. **Turner MW.** 2003. The role of mannose-binding lectin in health and disease. *Mol Immunol* **40:**423–429. PubMed
26. **Matsushita M, Endo Y, Fujita T.** 2000. Cutting edge: complement-activating complex of ficolin and mannose-binding lectin-associated serine protease. *J Immunol* **164:**2281–2284. PubMed
27. **Casanova JL, Abel L.** 2004. Human mannose-binding lectin in immunity: friend, foe, or both? *J Exp Med* **199:**1295–1299. PubMed
28. **Bork K, Wulff K, Witske G, Staubach P.** 2009. Hereditary angioedema caused by missense mutations in the factor XII gene: clinical features, trigger factors, and therapy. *J Allergy Clin Immunol* **124:**129–134. PubMed
29. **Turner MW.** 2003. The role of mannose-binding lectin in health and disease. *Mol Immunol* **40:**423–429. PubMed
30. **Carlsson M, Sjöholm AG, Eriksson L, Thiel S, Jensenius JC, Segelmark M, Truedsson L.** 2005. Deficiency of the mannan-binding lectin pathway of complement and poor outcome in cystic fibrosis: bacterial colonization may be decisive for a relationship. *Clin Exp Immunol* **139:**306–313. PubMed
31. **Gadjeva M, Paludan SR, Thiel S, Slavov V, Ruseva M, Eriksson K, Löwhagen GB, Shi L, Takahashi K, Ezekowitz A, Jensenius JC.** 2004. Mannan-binding lectin modulates the response to HSV-2 infection. *Clin Exp Immunol* **138:**304–311. PubMed
32. **Hart ML, Ceonzo KA, Shaffer LA, Takahashi K, Rother RP, Reenstra WR, Buras JA, Stahl GL.** 2005. Gastrointestinal ischemia-reperfusion injury is lectin complement pathway dependent without involving C1q. *J Immunol* **174:**6373–6380. PubMed
33. **Inanc N, Mumcu G, Birtas E, Elbir Y, Yavuz S, Ergun T, Fresko I, Direskeneli H.** 2005. Serum mannose-binding lectin levels are decreased in behcet's disease and associated with disease severity. *J Rheumatol* **32:**287–291. PubMed
34. **Ip WK, Chan KH, Law HK, Tso GH, Kong EK, Wong WH, To YF, Yung RW, Chow EY, Au KL, Chan EY, Lim W, Jensenius JC, Turner MW, Peiris JS, Lau YL.** 2005. Mannose-binding lectin in severe acute respiratory syndrome coronavirus infection. *J Infect Dis* **191:**1697–1704.
35. **Takahashi R, Tsutsumi A, Ohtani K, Goto D, Matsumoto I, Ito S, Wakamiya N, Sumida T.** 2004. Anti-mannose binding lectin antibodies in sera of Japanese patients with systemic lupus erythematosus. *Clin Exp Immunol* **136:**585–590. PubMed
36. **Foldager L, Köhler O, Steffensen R, Thiel S, Kristensen AS, Jensenius JC, Mors O.** 2014. Bipolar and panic disorders may be associated with hereditary defects in the innate immune system. *J Affect Disord* **164:**148–154. PubMed
37. **Lu J.** 1997. Collectins: collectors of microorganisms for the innate immune system. *BioEssays* **19:**509–518. PubMed
38. **Munthe-Fog L, Hummelshøj T, Honoré C, Madsen HO, Permin H, Garred P.** 2009. Immunodeficiency associated with *FCN3* mutation and ficolin-3 deficiency. *N Engl J Med* **360:**2637–2644. PubMed
39. **Krarup A, Wallis R, Presanis JS, Gál P, Sim RB.** 2007. Simultaneous activation of complement and coagulation by MBL-associated serine protease 2. *PLoS One* **2:**e623 10.1371/journal.pone.0000623. PubMed
40. **Gulla KC, Gupta K, Krarup A, Gal P, Schwaeble WJ, Sim RB, O'Connor CD, Hajela K.** 2010. Activation of mannan-binding lectin-associated serine proteases leads to generation of a fibrin clot. *Immunology* **129:**482–495. PubMed
41. **Schwaeble W, Dahl MR, Thiel S, Stover C, Jensenius JC.** 2002. The mannan-binding lectin-associated serine

proteases (MASPs) and MAp19: four components of the lectin pathway activation complex encoded by two genes. *Immunobiology* **205:**455–466. PubMed
42. **Bork K.** 2013. Hereditary angioedema with normal C1 inhibitor. *Immunol Allergy Clin North Am* **33:**457–470. PubMed
43. **Cicardi M, Aberer W, Banerji A, Bas M, Bernstein JA, Bork K, Caballero T, Farkas H, Grumach A, Kaplan AP, Riedl MA, Triggiani M, Zanichelli A, Zuraw B, HAWK under the patronage of EAACI (European Academy of Allergy and Clinical Immunology).** 2014. Classification, diagnosis, and approach to treatment for angioedema: consensus report from the Hereditary Angioedema International Working Group. *Allergy* **69:**602–616. PubMed
44. **Frank MM.** 2006. Hereditary angioedema: the clinical syndrome and its management in the United States. *Immunol Allergy Clin North Am* **26:**653–668.
45. **Davis A.** 1998. C1 inhibitor gene and hereditary angioedema, p 229–283. *In* Volanakis JE, Frank MM (ed), *The Human Complement System in Health and Disease*. Marcel Dekker, New York, NY.
46. **Frank MM, Gelfand JA, Atkinson JP.** 1976. Hereditary angioedema: the clinical syndrome and its management. *Ann Intern Med* **84:**580–593. PubMed
47. **Cicardi M, Agostoni A.** 1996. Hereditary angioedema. *N Engl J Med* **334:**1666–1667. PubMed
48. **Bowen B, Hawk JJ, Sibunka S, Hovick S, Weiler JM.** 2001. A review of the reported defects in the human C1 esterase inhibitor gene producing hereditary angioedema including four new mutations. *Clin Immunol* **98:**157–163. PubMed
49. **Binkley KE, Davis AE III.** 2003. Estrogen-dependent inherited angioedema. *Transfus Apheresis Sci* **29:**215–219. PubMed
50. **Kränke B, Salmhofer W, Aberer W.** 2000. Hereditary angioedema and normal C1-inhibitor activity in women. *Lancet* **356:**1440–1441. PubMed
51. **Melamed J, Alper CA, Cicardi M, Rosen FS.** 1986. The metabolism of C1 inhibitor and C1q in patients with acquired C1-inhibitor deficiency. *J Allergy Clin Immunol* **77:**322–326. PubMed
52. **Castelli R, Deliliers DL, Zingale LC, Pogliani EM, Cicardi M.** 2007. Lymphoproliferative disease and acquired C1 inhibitor deficiency. *Haematologica* **92:**716–718. PubMed
53. **Jackson J, Sim RB, Whaley K, Feighery C.** 1989. Autoantibody facilitated cleavage of C1-inhibitor in autoimmune angioedema. *J Clin Invest* **83:**698–707. PubMed
54. **Fujita T, Gigli I, Nussenzweig V.** 1978. Human C4-binding protein. II. Role in proteolysis of C4b by C3b-inactivator. *J Exp Med* **148:**1044–1051. PubMed
55. **Liu CC, Manzi S, Kao AH, Navratil JS, Ruffing MJ, Ahearn JM.** 2005. Reticulocytes bearing C4d as biomarkers of disease activity for systemic lupus erythematosus. *Arthritis Rheum* **52:**3087–3099. PubMed
56. **Kao AH, Navratil JS, Ruffing MJ, Liu CC, Hawkins D, McKinnon KM, Danchenko N, Ahearn JM, Manzi S.** 2010. Erythrocyte C3d and C4d for monitoring disease activity in systemic lupus erythematosus. *Arthritis Rheum* **62:**837–844. PubMed
57. **Gronski P, Bodenbender L, Kanzy EJ, Seiler FR.** 1988. C4-binding protein prevents spontaneous cleavage of C3 in sera of patients with hereditary angioedema. *Complement* **5:**1–12. PubMed
58. **Blom AM, Villoutreix BO, Dahlbäck B.** 2004. Functions of human complement inhibitor C4b-binding protein in relation to its structure. *Arch Immunol Ther Exp (Warsz)* **52:**83–95. PubMed
59. **Trapp RG, Fletcher M, Forristal J, West CD.** 1987. C4 binding protein deficiency in a patient with atypical Behçet's disease. *J Rheumatol* **14:**135–138. PubMed
60. **Volanakis JE, Narayana SV.** 1996. Complement factor D, a novel serine protease. *Protein Sci* **5:**553–564. PubMed
61. **White RT, Damm D, Hancock N, Rosen BS, Lowell BB, Usher P, Flier JS, Spiegelman BM.** 1992. Human adipsin is identical to complement factor D and is expressed at high levels in adipose tissue. *J Biol Chem* **267:**9210–9213. PubMed
62. **Biesma DH, Hannema AJ, van Velzen-Blad H, Mulder L, van Zwieten R, Kluijt I, Roos D.** 2001. A family with complement factor D deficiency. *J Clin Invest* **108:**233–240. PubMed
63. **Kildsgaard J, Zsigmond E, Chan L, Wetsel RA.** 1999. A critical evaluation of the putative role of C3adesArg (ASP) in lipid metabolism and hyperapobetalipoproteinemia. *Mol Immunol* **36:**869–876. PubMed
64. **Cianflone K, Xia Z, Chen LY.** 2003. Critical review of acylation-stimulating protein physiology in humans and rodents. *Biochim Biophys Acta* **1609:**127–143. PubMed
65. **Carroll MC, Campbell RD, Bentley DR, Porter RR.** 1984. A molecular map of the human major histocompatibility complex class III region linking complement genes C4, C2 and factor B. *Nature* **307:**237–241. PubMed
66. **Mortensen JP, Lamm LU.** 1981. Quantitative differences between complement factor-B phenotypes. *Immunology* **42:**505–511. PubMed
67. **Slade C, Bosco J, Unglik G, Bleasel K, Nagel M, Winship I.** 2013. Deficiency in complement factor B. *N Engl J Med* **369:**1667–1669. PubMed
68. **Farries TC, Lachmann PJ, Harrison RA.** 1988. Analysis of the interaction between properdin and factor B, components of the alternative-pathway C3 convertase of complement. *Biochem J* **253:**667–675. PubMed
69. **Farries TC, Lachmann PJ, Harrison RA.** 1988. Analysis of the interactions between properdin, the third component of complement (C3), and its physiological activation products. *Biochem J* **252:**47–54. PubMed
70. **Cortes C, Ohtola JA, Saggu G, Ferreira VP.** 2012. Local release of properdin in the cellular microenvironment: role in pattern recognition and amplification of the alternative pathway of complement. *Front Immunol* **3:**412. doi:10.3389/fimmu.2012.00412. PubMed
71. **Hourcade DE.** 2006. The role of properdin in the assembly of the alternative pathway C3 convertases of complement. *J Biol Chem* **281:**2128–2132. PubMed
72. **Sjöholm AG, Braconier JH, Söderström C.** 1982. Properdin deficiency in a family with fulminant meningococcal infections. *Clin Exp Immunol* **50:**291–297. PubMed
73. **Goundis D, Holt SM, Boyd Y, Reid KB.** 1989. Localization of the properdin structural locus to Xp11.23-Xp21.1. *Genomics* **5:**56–60. PubMed
74. **Frémeaux-Bacchi V, Le Coustumier A, Blouin J, Kazatchkine MD, Weiss L.** 1995. [Partial properdin deficiency revealed by a septicemia caused by *Neisseria meningitidis*.]. *Presse Med* **24:**1305–1307. (In French.) PubMed
75. **Westberg J, Fredrikson GN, Truedsson L, Sjöholm AG, Uhlén M.** 1995. Sequence-based analysis of properdin deficiency: identification of point mutations in two phenotypic forms of an X-linked immunodeficiency. *Genomics* **29:**1–8. PubMed
76. **Kölble K, Cant AJ, Fay AC, Whaley K, Schlesinger M, Reid KB.** 1993. Carrier detection in families with properdin deficiency by microsatellite haplotyping. *J Clin Invest* **91:**99–102. PubMed
77. **Fearon DT.** 1979. Activation of the alternative complement pathway. *CRC Crit Rev Immunol* **1:**1–32. PubMed
78. **Harrison RA, Farries TC, Northrop FD, Lachmann PJ, Davis AE.** 1988. Structure of C3f, a small peptide specifically released during inactivation of the third component of complement. *Complement* **5:**27–32. PubMed
79. **Liszewski MK, Post TW, Atkinson JP.** 1991. Membrane cofactor protein (MCP or CD46): newest member of the

regulators of complement activation gene cluster. *Annu Rev Immunol* **9:**431–455. PubMed
80. **Hing S, Day AJ, Linton SJ, Ripoche J, Sim RB, Reid KB, Solomon E.** 1988. Assignment of complement components C4 binding protein (C4BP) and factor H (FH) to human chromosome 1q, using cDNA probes. *Ann Hum Genet* **52:**117–122. PubMed
81. **Estaller C, Schwaeble W, Dierich M, Weiss EH.** 1991. Human complement factor H: two factor H proteins are derived from alternatively spliced transcripts. *Eur J Immunol* **21:**799–802. PubMed
82. **Nabil K, Rihn B, Jaurand MC, Vignaud JM, Ripoche J, Martinet Y, Martinet N.** 1997. Identification of human complement factor H as a chemotactic protein for monocytes. *Biochem J* **326:**377–383. PubMed
83. **Ohtsuka H, Imamura T, Matsushita M, Tanase S, Okada H, Ogawa M, Kambara T.** 1993. Thrombin generates monocyte chemotactic activity from complement factor H. *Immunology* **80:**140–145. PubMed
84. **Ault BH.** 2000. Factor H and the pathogenesis of renal diseases. *Pediatr Nephrol* **14:**1045–1053. PubMed
85. **Moseley HL, Whaley K.** 1980. Control of complement activation in membranous and membranoproliferative glomerulonephritis. *Kidney Int* **17:**535–544. PubMed
86. **Nielsen HE, Christensen KC, Koch C, Thomsen BS, Heegaard NH, Tranum-Jensen J.** 1989. Hereditary, complete deficiency of complement factor H associated with recurrent meningococcal disease. *Scand J Immunol* **30:**711–718. PubMed
87. **Edwards AO, Ritter R III, Abel KJ, Manning A, Panhuysen C, Farrer LA.** 2005. Complement factor H polymorphism and age-related macular degeneration. *Science* **308:**421–424. PubMed
88. **Hageman GS, Anderson DH, Johnson LV, Hancox LS, Taiber AJ, Hardisty LI, Hageman JL, Stockman HA, Borchardt JD, Gehrs KM, Smith RJ, Silvestri G, Russell SR, Klaver CC, Barbazetto I, Chang S, Yannuzzi LA, Barile GR, Merriam JC, Smith RT, Olsh AK, Bergeron J, Zernant J, Merriam JE, Gold B, Dean M, Allikmets R.** 2005. A common haplotype in the complement regulatory gene factor H (HF1/CFH) predisposes individuals to age-related macular degeneration. *Proc Natl Acad Sci USA* **102:**7227–7232. PubMed
89. **Haines JL, Hauser MA, Schmidt S, Scott WK, Olson LM, Gallins P, Spencer KL, Kwan SY, Noureddine M, Gilbert JR, Schnetz-Boutaud N, Agarwal A, Postel EA, Pericak-Vance MA.** 2005. Complement factor H variant increases the risk of age-related macular degeneration. *Science* **308:**419–421. PubMed
90. **Klein RJ, Zeiss C, Chew EY, Tsai JY, Sackler RS, Haynes C, Henning AK, SanGiovanni JP, Mane SM, Mayne ST, Bracken MB, Ferris FL, Ott J, Barnstable C, Hoh J.** 2005. Complement factor H polymorphism in age-related macular degeneration. *Science* **308:**385–389. PubMed
91. **Richards A, Goodship JA, Goodship TH.** 2002. The genetics and pathogenesis of haemolytic uraemic syndrome and thrombotic thrombocytopenic purpura. *Curr Opin Nephrol Hypertens* **11:**431–435. PubMed
92. **Richards A, Kemp EJ, Liszewski MK, Goodship JA, Lampe AK, Decorte R, Müslümanoğlu MH, Kavukcu S, Filler G, Pirson Y, Wen LS, Atkinson JP, Goodship TH.** 2003. Mutations in human complement regulator, membrane cofactor protein (CD46), predispose to development of familial hemolytic uremic syndrome. *Proc Natl Acad Sci USA* **100:**12966–12971. PubMed
93. **Dragon-Durey MA, Blanc C, Garnier A, Hofer J, Sethi SK, Zimmerhackl LB.** 2010. Anti-factor H autoantibody-associated hemolytic uremic syndrome: review of literature of the autoimmune form of HUS. *Semin Thromb Hemost* **36:**633–640. PubMed
94. **Skerka C, Józsi M, Zipfel PF, Dragon-Durey MA, Fremeaux-Bacchi V.** 2009. Autoantibodies in haemolytic uraemic syndrome (HUS). *Thromb Haemost* **101:**227–232. PubMed
95. **Roumenina LT, Roquigny R, Blanc C, Poulain N, Ngo S, Dragon-Durey MA, Frémeaux-Bacchi V.** 2014. Functional evaluation of factor H genetic and acquired abnormalities: application for atypical hemolytic uremic syndrome (aHUS). *Methods Mol Biol* **1100:**237–247. PubMed
96. **China B, Sory MP, N'Guyen BT, De Bruyere M, Cornelis GR.** 1993. Role of the YadA protein in prevention of opsonization of *Yersinia enterocolitica* by C3b molecules. *Infect Immun* **61:**3129–3136. PubMed
97. **Horstmann RD, Sievertsen HJ, Knobloch J, Fischetti VA.** 1988. Antiphagocytic activity of streptococcal M protein: selective binding of complement control protein factor H. *Proc Natl Acad Sci USA* **85:**1657–1661. PubMed
98. **McDowell JV, Wolfgang J, Tran E, Metts MS, Hamilton D, Marconi RT.** 2003. Comprehensive analysis of the factor h binding capabilities of *borrelia* species associated with lyme disease: delineation of two distinct classes of factor h binding proteins. *Infect Immun* **71:**3597–3602. PubMed
99. **Roversi P, Johnson S, Caesar JJ, McLean F, Leath KJ, Tsiftsoglou SA, Morgan BP, Harris CL, Sim RB, Lea SM.** 2011. Structural basis for complement factor I control and its disease-associated sequence polymorphisms. *Proc Natl Acad Sci USA* **108:**12839–12844. PubMed
100. **Abramson N, Alper CA, Lachmann PJ, Rosen FS, Jandl JH.** 1971. Deficiency of C3 inactivator in man. *J Immunol* **107:**19–27. PubMed
101. **Alper CA, Abramson N, Johnston RB Jr, Jandl JH, Rosen FS.** 1970. Studies in vivo and in vitro on an abnormality in the metabolism of C3 in a patient with increased susceptibility to infection. *J Clin Invest* **49:**1975–1985. PubMed
102. **Genel F, Sjöholm AG, Skattum L, Truedsson L.** 2005. Complement factor I deficiency associated with recurrent infections, vasculitis and immune complex glomerulonephritis. *Scand J Infect Dis* **37:**615–618. PubMed
103. **Vyse TJ, Morley BJ, Bartok I, Theodoridis EL, Davies KA, Webster AD, Walport MJ.** 1996. The molecular basis of hereditary complement factor I deficiency. *J Clin Invest* **97:**925–933. PubMed
104. **Whitehead AS, Solomon E, Chambers S, Bodmer WF, Povey S, Fey G.** 1982. Assignment of the structural gene for the third component of human complement to chromosome 19. *Proc Natl Acad Sci USA* **79:**5021–5025. PubMed
105. **Schoonbrood TH, Hannema A, Fijen CA, Markusse HM, Swaak AJ.** 1995. C5 deficiency in a patient with primary Sjögren's syndrome. *J Rheumatol* **22:**1389–1390. PubMed
106. **Ramos-Casals M, Brito-Zerón P, Yagüe J, Akasbi M, Bautista R, Ruano M, Claver G, Gil V, Font J.** 2005. Hypocomplementaemia as an immunological marker of morbidity and mortality in patients with primary Sjogren's syndrome. *Rheumatology (Oxford)* **44:**89–94. PubMed
107. **Asghar SS, Venneker GT, van Meegen M, Meinardi MM, Hulsmans RF, de Waal LP.** 1991. Hereditary deficiency of C5 in association with discoid lupus erythematosus. *J Am Acad Dermatol* **24:**376–378. PubMed
108. **Salvadori M, Bertoni E.** 2013. Update on hemolytic uremic syndrome: diagnostic and therapeutic recommendations. *World J Nephrol* **2:**56–76. PubMed
109. **Fernie BA, Würzner R, Orren A, Morgan BP, Potter PC, Platonov AE, Vershinina IV, Shipulin GA, Lachmann PJ, Hobart MJ.** 1996. Molecular bases of combined subtotal deficiencies of C6 and C7: their effects in

combination with other C6 and C7 deficiencies. *J Immunol* **157:**3648–3657. PubMed

110. **Tedesco F, Densen P, Villa MA, Petersen BH, Sirchia G.** 1983. Two types of dysfunctional eighth component of complement (C8) molecules in C8 deficiency in man. Reconstitution of normal C8 from the mixture of two abnormal C8 molecules. *J Clin Invest* **71:**183–191. PubMed
111. **Kaufman KM, Sodetz JM.** 1994. Genomic structure of the human complement protein C8 gamma: homology to the lipocalin gene family. *Biochemistry* **33:**5162–5166. PubMed
112. **Müller-Eberhard HJ.** 1985. The killer molecule of complement. *J Invest Dermatol* **85**(Suppl)**:**47s–52s. PubMed
113. **Fukumori Y, Yoshimura K, Ohnoki S, Yamaguchi H, Akagaki Y, Inai S.** 1989. A high incidence of C9 deficiency among healthy blood donors in Osaka, Japan. *Int Immunol* **1:**85–89. PubMed
114. **Kang HJ, Kim HS, Lee YK, Cho HC.** 2005. High incidence of complement C9 deficiency in Koreans. *Ann Clin Lab Sci* **35:**144–148. PubMed
115. **Hobart MJ, Fernie BA, Würzner R, Oldroyd RG, Harrison RA, Joysey V, Lachmann PJ.** 1997. Difficulties in the ascertainment of C9 deficiency: lessons to be drawn from a compound heterozygote C9-deficient subject. *Clin Exp Immunol* **108:**500–506. PubMed
116. **Barrett DJ, Boyle MD.** 1984. Restoration of complement function in vivo by plasma infusion in factor I (C3b inactivator) deficiency. *J Pediatr* **104:**76–81.
117. **Perry G, Eisenberg PR, Zimmerman JL, Levin J.** 1998. Phase I safety trial of soluble complement receptor type (TP 10) on acute myocardial infarction. *J Am Coll Cardiol* **31**(2s2)**:**411A.
118. **Quigg RJ, Kozono Y, Berthiaume D, Lim A, Salant DJ, Weinfeld A, Griffin P, Kremmer E, Holers VM.** 1998. Blockade of antibody-induced glomerulonephritis with Crry-Ig, a soluble murine complement inhibitor. *J Immunol* **160:**4553–4560. PubMed
119. **Ricklin D, Lambris JD.** 2013. Complement in immune and inflammatory disorders: therapeutic interventions. *J Immunol* **190:**3839–3847. PubMed
120. **Lachmann PJ, Smith RA.** 2009. Taking complement to the clinic—has the time finally come? *Scand J Immunol* **69:**471–478. PubMed
121. **Hertle E, Stehouer CDA, van Greevenbroek MMJ.** 2014. The complement system in human cardiometabolic disease. *Mol Immunol* **61:**135–148.

Neutropenia and Neutrophil Defects

STEVEN M. HOLLAND

78

Concern about the neutrophil status of a patient is usually raised on the basis of the frequency, severity, and distribution of a specific infectious agent(s) involved in one or more episodes that are, or are thought to be, infectious. The clinical presentations of patients with neutrophil disorders usually share a few common features: gingivitis, periodontal disease, and oral ulceration. Cutaneous infections with *Staphylococcus aureus* are often recurrent and can be severe. In neutrophil disorders characterized by inadequate inflammation (neutropenia, leukocyte adhesion deficiency [LAD], Chédiak-Higashi syndrome, and specific granule deficiency), infections can extend locally and subcutaneously with little reaction until marked destruction has taken place. Clinically relevant neutrophil abnormalities fall into several broad categories: neutropenia, abnormalities of neutrophil adherence and locomotion, abnormalities of neutrophil granule formation or content, and abnormalities of killing. With the widespread use of therapies which modulate the immune system either by design (e.g., steroids and monoclonal antibodies) or incidentally (e.g., cytotoxic chemotherapy), the most common causes of immunodeficiency are iatrogenic. The recognition, characterization, identification, and cloning of disease-related genes and, in some cases, genetic correction of immune defects are progressing rapidly. As specific and genetic treatments become available, making the correct diagnosis early takes on greater therapeutic importance (1).

The clinical history should include type, location, microbiology, severity, and frequency of infections; family history with specific questioning as to consanguinity; and physical examination of the oral mucosa and any lesions or scars. A complete peripheral blood count with differential and examination of the peripheral smear are necessary initial studies to determine whether the patient has a quantitative, qualitative, or combined abnormality of neutrophils.

NEUTROPENIA

The normal neutrophil count in peripheral blood is about 4,000/mm^3, with a large variation among racial and ethnic groups, especially certain West Indian and African blacks and Yemeni Jews, who may have much lower neutrophil counts. Neutropenia is determined by the presence of fewer than 1,500 neutrophils/mm^3. Increased risk of infections does not occur until the absolute neutrophil count (the sum of mature and band-form neutrophils) falls below 1,000/mm^3; risk of serious infections occurs below 500 neutrophils/mm^3. Since about 90% of the body's neutrophils are kept in reserve in the bone marrow, neutropenias with impaired marrow stores are associated with greater infection risk than neutropenias with normal marrow stores. Thus, acute neutropenias associated with a lack of marrow reserves, such as those induced by cancer chemotherapy, are usually associated with greater infectious complications than chronic neutropenias (2).

There are three basic mechanisms by which neutropenia can occur: decreased neutrophil production, increased neutrophil destruction, or abnormal neutrophil trafficking (either defective release of neutrophils from the bone marrow or an abnormal increase in the marginated or tissue pools). Recently, an autosomal dominant disorder with mild neutropenia due to neutrophil retention in the bone marrow (myelokathexis) has been molecularly characterized. The syndrome of warts, hypogammaglobulinemia, infections, and myelokathexis (WHIM) is due to mutations in the chemokine receptor CXCR4 which lead to retention of mature neutrophils on their marrow-expressed ligand stromal cell-derived factor 1 (SDF1; CXCL12). Major causes of intrinsic, acquired, and apparent neutropenia are listed in Table 1. An acquired cause of neutrophil destruction is antineutrophil antibodies. These antibodies can be detected in the clinical laboratory by either immunofluorescence or agglutination, procedures which are readily available in most laboratories (2).

Methods of neutrophil preparation and isolation are reviewed in chapter 33 of this volume.

Antineutrophil Antibodies

Principle

Antineutrophil antibodies may cause neutrophils to be more susceptible to complement-mediated lysis, enhance neutrophil sequestration via Fc receptors on tissue macrophages, or affect the maturation and development of myeloid precursors. Detection of these antibodies in a flow cytometer relies upon demonstration of specific binding of patient immunoglobulin G (IgG) and IgM to neutrophils (3). Many of these antibodies are directed against Fcγ RIII (CD16). Techniques which are not dependent on flow cytometry are more difficult to interpret.

doi:10.1128/9781555818722.ch78

Specimen Collection

Patient serum, stored at −70°C, 1 ml

Pooled normal sera from several donors, stored at −70°C, 200-μl aliquots

Neutrophils isolated from three healthy donors, prepared as described above (≥10^7 neutrophils per serum sample to be assayed)

Reagents and Equipment

Phosphate-buffered saline, pH 7.2 (PBS), 1×

Bovine serum albumin (BSA), 0.22% (1 ml of 22% BSA plus 99 ml of PBS; make it fresh and keep it stable for 1 week at 4°C)

Paraformaldehyde, 4% stock solution (2 g of paraformaldehyde in 45 ml of 0.85% normal saline; warm to 70°C with dropwise addition of 1 N NaOH solution, adjust final pH to 7.2 with dropwise addition of 1 N HCl, bring volume to 50 ml, and store in the dark at 4°C) and 1% working solution (1 volume of 4% stock solution in 3 volumes of PBS; can be stored for 1 week at 4°C)

Fluorescein isothiocyanate-conjugated goat anti-human IgG and IgM, diluted 1:10 with PBS

Microcentrifuge

Flow cytometer

Procedure

1. Label triplicate pairs of microcentrifuge tubes for each serum sample to be assayed (i.e., assays for antineutrophil IgG and IgM with each of three normal donor neutrophil preparations).
2. Dilute the patient and control sera 1:1 with PBS.
3. Resuspend the healthy-donor neutrophils in PBS and sediment them at 300 × *g* for 7 min.
4. Remove and discard the supernatants and resuspend the neutrophils in 2 ml of 1% paraformaldehyde; allow this to stand for 5 min at room temperature.
5. Resuspend the neutrophils in 20 ml of PBS and sediment them at 300 × *g* for 7 min.
6. Resuspend treated cells in PBS to 3 × 10^7 neutrophils/ml.
7. Transfer 50 μl of each diluted serum sample to the appropriate microcentrifuge tube.
8. Add 50 μl of the neutrophil suspension to the appropriate microcentrifuge tube and incubate it at 4°C for 30 min.
9. Wash the suspension twice with ice-cold 0.22% BSA, sedimenting the cells for 10 s in a microcentrifuge.
10. Remove and discard the supernatants, add 50 μl of the diluted conjugated anti-human IgG or IgM to the appropriate tube, and incubate the tube at 4°C for 30 min.
11. Wash the cells once with ice-cold 0.22% BSA, sedimenting them for 10 s in a microcentrifuge.
12. Remove and discard the supernatants, resuspend the pellets in 1 ml of PBS, and transfer the suspension to tubes appropriate for analysis in the flow cytometer (usually 12 by 75 mm).

Interpretation

Patient sera are examined for a distinct shift in the peak fluorescence relative to that of the control samples run the same day. Modest and great shifts of fluorescence should be noted through both the histograms and the determinations of channel fluorescence. Increased binding of IgG or IgM over that in the normal control sera is considered abnormal and is reported. The report should be descriptive, including the antibody subclass implicated and the number of normal donors (out of the day's controls) to which it bound.

NEUTROPHIL DYSFUNCTION

The determination of a qualitative defect of neutrophil function is more complex than the simple determination of neutropenia, since it requires the demonstration of a dysfunctional phenotype. Methods for diagnosis of these abnormalities range from inspection of the peripheral blood smear to fluorescence-activated cell sorting (FACS). Some of these diseases simultaneously affect several limbs of neutrophil function, making prior determination of the single-best diagnostic test in a given case important. The clinical history, peripheral blood neutrophil count, and inspection of the peripheral smear readily indicate the direction of further evaluation of a possible neutrophil functional abnormality.

The major classes of neutrophil defects highlight the major neutrophil functions: adhesion, chemotaxis, phagocytosis, degranulation, and killing (Table 2). General features which suggest clinically relevant neutrophil disorders include recurrent, severe infections often requiring intravenous antibiotics, hospitalization, or surgery. Cutaneous and oral infections are common. The microbiology of specific infectious episodes may be quite informative: infections with *Burkholderia* (*Pseudomonas*) *cepacia*, *Serratia marcescens*, *Chromobacterium violaceum*, *Nocardia* species, *Aspergillus* species, or *Paecilomyces* species, or hepatic abscesses with *S. aureus*, suggest the diagnosis of chronic granulomatous disease (CGD) (4).

Adhesion Disorders

A normal neutrophil exits the bone marrow and remains in the circulation for about 7 h before entering the tissue, the intestinal lumen, or the oral cavity. During its time in the peripheral circulation, it is frequently "rolling" along and sampling the endothelium for evidence of infection or tissue damage. The low-affinity rolling of the neutrophil along the postcapillary endothelium is mediated by interacting glycoproteins on the endothelial surface (endothelial selectin [E-selectin] and platelet selectin [P-selectin]) and the neutrophil surface (sialyl-Lewis^x, CD15s). When the neutrophil encounters endothelium activated by chemokines or other stimuli, it adheres to specific molecules (intercellular adhesion molecules 1 and 2 [ICAM 1 and 2]) by way of the heterodimeric leukocyte integrins (leukocyte functional antigen 1 [LFA-1] and Mac-1 or complement receptor 3 [CR3]), which contain CD18 as their common β chain. Disorders in both of these critical pathways have been described as LADs. LAD type 1 (LAD1) is due to loss of leukocyte integrin function secondary to CD18 deficiency (5); LAD2 is due to loss of neutrophil selectin binding due to loss of CD15s. LAD3 is quite rare and due to mutations in *FERMT3*, which encodes the protein KINDLIN-3 (6). These diseases lead to profound impairment of the ability of neutrophils to exit the circulation to sites of infection. One of the CD18-containing molecules (CD18/CD11b, Mac-1, or CR3) also serves as the receptor for the cleaved, inactivated third component of complement (C3bi). Therefore, the absence of CD18-containing leukocyte integrins leads to the inability of neutrophils to perform complement-mediated phagocytosis as well. The cellular signal from CD18 ligation leads to adherence and movement toward the ligand. Rac2 is the G protein that tethers CD18 to cytoskeletal actin. In Rac2 deficiency, CD18 expression is

TABLE 1 Causes of neutropenia[a]

Disease	Clinical features	Mechanism(s)	Diagnosis	Treatment
Intrinsic				
Severe chronic neutropenia (Kostmann syndrome)	Neutropenia (<200 PMN/mm^3) at birth; recurrent, severe infections, autosomal dominant and recessive	Mutations in neutrophil elastase gene (*ELANE*), *HAX-1*, and GFI1	Bone marrow aspiration shows maturation defect at promyelocyte/myelocyte stage	G-CSF
Cyclic neutropenia (cyclic hematopoiesis)	Severe neutropenia ca. every 21 days for about 4–5 days; fever, cutaneous oral infections; autosomal dominant, spontaneous, and acquired forms	Mutations in neutrophil elastase gene (*ELANE*)	Serial blood counts (6 wk) at least every 3 days; mutation detection	G-CSF
Warts, hypogammaglobulinemia, infections, myelokathexis (WHIM)	Neutropenia; hypogammaglobulinemia, warts; familial cases reported	Mutations in *CXCR4*	Bone marrow aspiration, no evidence of peripheral destruction, abnormal marrow release on steroid challenge	G-CSF
Shwachman-Diamond syndrome	Moderate to severe neutropenia, anemia, growth retardation, exocrine pancreatic insufficiency, bone abnormalities; some patients may develop aplastic anemia or malignancy	Mutations in *SDBS*	Demonstration of fatty infiltration of the pancreas	G-CSF
Benign chronic neutropenia	Infantile severe neutropenia (<200 PMN/mm^3) without serious infections; can last for years	Unknown	Bone marrow aspiration shows normal morphology and development of myeloid series	None
Chédiak-Higashi syndrome	Mild to moderate neutropenia, partial oculocutaneous albinism, recurrent cutaneous, pulmonary infections; fatal lymphoproliferative syndrome in some cases; autosomal recessive	Mutations in *CHS1*	Demonstration of giant primary granules in peripheral blood neutrophils and in other lysosome-containing cells	Supportive; bone marrow transplantation
Reticular dysgenesis	Neonatal neutropenia, hypogammaglobulinemia, thymic abnormalities, lymphopenia, deafness; fatal without bone marrow transplantation	Mutations in *AK2*	Absent myeloid development in bone marrow; other lines may be normal	Supportive; bone marrow transplantation
GATA2 deficiency	Neutropenia, warts, lymphedema, mycobacterial diseases	Mutations in *GATA2*	Hypoplastic marrow, dysplastic megakaryocytes	Supportive; bone marrow transplantation
Acquired				
Cytotoxic chemotherapy	Severity of neutropenia depends on dose and specific agent, commonly profound; neutropenia onset variable after treatment; fevers, oral ulcers, bacteremia (e.g., cyclophosphamide)	Reduction of dividing cells	Clinical history	Supportive; G- or GM-CSF in some cases

Drug induced				
Immune	Requires sensitization of neutrophils to antibody (e.g., β-lactams); antibodies may cross placenta	Peripheral destruction of neutrophils	Demonstration of antineutrophil antibodies	Discontinuation of drug, supportive, G-CSF in some cases
Nonimmune	Dose-related or idiopathic reaction to drug, may cause profound neutropenia (e.g., chloramphenicol or clozapine)	Suppression of bone marrow precursors	Clinical history	Supportive; G-CSF in some cases
Isoimmune	Neonatal neutropenia due to maternal alloimmunization; lasts for several weeks; may be moderate to severe; predominantly cutaneous infections	Antibody-mediated peripheral destruction of neutrophils; against FcγRIII (CD16)	Clinical history, demonstration of antineutrophil antibodies epitopes	Supportive; G-CSF in some cases
Autoimmune	Antibody-mediated neutropenia during collagen vascular diseases (e.g., rheumatoid arthritis with splenomegaly, Felty syndrome; systemic lupus erythematosus)	Sequestration, peripheral destruction of neutrophils	Clinical history, demonstration of antineutrophil antibodies	Treatment of underlying disease; splenectomy in Felty syndrome; steroids in some cases; G-CSF in some cases
Splenomegaly	Mild to moderate neutropenia with moderate to massive splenomegaly due to mechanical (e.g., portal hypertension), infectious (e.g., chronic malaria), or neoplastic causes; often accompanied by anemia and thrombocytopenia	Sequestration with or without destruction of neutrophils	Clinical history and exam, normal bone marrow examination	Treatment of underlying disease; no specific therapy usually required
LGL induced	Moderate to severe acquired cyclic neutropenia; onset usually in adulthood	Clonal proliferation of T cells; probably acts on stem cells	LGL, serial blood sampling, demonstration of LGL proliferation	Treatment of underlying disease; supportive; G-CSF, steroids, or immunosuppression in some cases
Nutritional deficiency	Mild to severe neutropenia associated with vitamin B_{12}, folate, or copper deficiency; protein energy malnutrition (marasmus)	Ineffective myelopoiesis	Clinical history, determination of specific nutrient levels	Treatment of underlying disease; supportive
AIDS	Moderate to severe neutropenia in AIDS; pyomyositis and aspergillosis seen	HIV related; treatment related (e.g., zidovudine and ganciclovir)	Demonstration of HIV infection; drug history	Discontinuation of drug if possible; G-CSF
Apparent				
Severe infections	Mild neutropenia seen early in severe infections; resolves relatively rapidly	Increase in marginated tissue neutrophil pools	Demonstration of acute infection (e.g., Gram-negative sepsis)	Treatment of underlying infection
Hemodialysis	Mild to moderate neutropenia seen during hemodialysis; resolves off dialyzer	C5a-induced stiffening of neutrophils leads to transient trapping in lung	Clinical history, no evidence of acute infection	None

[a]G-CSF, granulocyte colony-stimulating factor; GM-CSF, granulocyte-macrophage colony-stimulating factor; HIV, human immunodeficiency virus; LGL, large granular lymphocyte; PMN, polymorphonuclear leukocytes.

TABLE 2 Neutrophil defects[a]

Disease	Clinical features	Mechanism(s)	Diagnosis	Treatment
Adhesion disorders				
LAD1	Neutrophilia (>15,000 PMN/mm^3), delayed umbilical stump separation; recurrent, severe infections; autosomal recessive	Defective leukocyte integrin expression; neutrophils unable to exit circulation to sites of infection	FACS analysis for CD18 and the integrins it constitutes: LFA-1 (CD18/CD11a), Mac-1/CR3 (CD18/CD11b), and p150,95 (CD18/CD11c); abnormal complement-mediated phagocytosis; impaired chemotaxis	Supportive; bone marrow transplantation
LAD2	Neutrophilia, short stature, abnormal facies, mental retardation, recurrent infections; autosomal recessive	Defective neutrophil selectin ligand (CD15s)	FACS analysis for sialyl-Lewis^x (CD15s) on neutrophils	Supportive
LAD3	Neutrophilia, recurrent infections, recurrent bleeding	Defective KINDLIN-3 due to mutations in *FERMT3*	Demonstration of absent KINDLIN-3 or mutation in *FERMT3*	Supportive; bone marrow transplantation
Rac2 deficiency	Neutrophilia, recurrent infections	*RAC2* defect	Defective adhesion; defective chemotaxis; absence of Rac2 on immunoblot	Supportive; bone marrow transplantation
Granule disorders				
Chédiak-Higashi syndrome	Mild to moderate neutropenia, partial oculocutaneous albinism, recurrent cutaneous or pulmonary infections, fatal lymphoproliferative syndrome in some cases; autosomal recessive	LYST defect due to mutations in *CHS1*	Demonstration of giant primary granules in peripheral blood neutrophils and in other lysosome-containing cells; delayed staphylococcal killing	Supportive; bone marrow transplantation
Specific granule deficiency	Recurrent infections, poor inflammatory response; rare; autosomal recessive	C/EBPε mutation; absence of neutrophil secondary granules and defensins	Absent secondary granules; bi- and trilobed neutrophil nuclei; absence of neutrophil lactoferrin defensins; impaired chemotaxis	Supportive; bone marrow transplantation
Chemotactic disorder				
Actin dysfunction	Recurrent infections, poor inflammatory response; rare; autosomal recessive	Defective actin polymerization	Impaired chemotaxis and staphylococcal killing; absence of 47-kDa protein	Supportive; bone marrow transplantation
Oxidative metabolism disorders				
MPO deficiency	No clinical phenotype except in diabetics, in whom severe *Candida* infections occur; most common neutrophil abnormality; autosomal recessive	Abnormalities in MPO gene	Absence of peroxidase staining of peripheral blood neutrophils; impaired candidacidal activity	No treatment needed in most cases
CGD	Recurrent life-threatening infections with catalase-positive organisms; tissue granuloma formation; X-linked and autosomal recessive forms	Defective superoxide formation	Impaired superoxide production: abnormal NBT test, chemiluminescence, DHR oxidation, or cytochrome *c* reduction; impaired staphylococcal killing	Supportive; antibiotic, antifungal and interferon gamma prophylaxis; bone marrow transplantation

[a]PMN, polymorphonuclear leukocytes; LYST, lysosomal transporter.

intact, but adherence is reduced and the clinical presentation is like that of LAD1.

Diagnosis of LAD1 should be made by FACS staining for CD18 and its associated alpha chains, CD11a, CD11b, and CD11c. The functional assays below can help to suggest the diagnosis. LAD2 is rarer and clinically distinct; it can be definitively diagnosed by FACS staining for sialyl-Lewis^x (CD15s). The diagnosis of Rac2 deficiency requires specialized research laboratory resources (6).

Neutrophil Adherence to Nylon Wool

Principle

Normal neutrophils adhere to several synthetic surfaces, including glass, plastic, and nylon wool, in addition to the endothelium. This adherence is impaired in LAD1 and by aspirin, ethanol, and prednisone.

Specimen Collection

Heparinized blood, 5 ml each from the patient and three healthy subjects, is used.

Reagents and equipment

Analytical balance

Apparatus for counting leukocytes and performing differential counts

Scrubbed nylon fiber (3 denier, 4 cm, type 200; Fenwal Laboratories, Morton Grove, IL)

Tuberculin syringes, 1 ml, without needle (three per sample)

Small collecting tubes (polypropylene is preferred)

Procedure

1. Weigh out 40 mg of nylon wool/column to be used.
2. Using a plunger, pack each column with the 40 mg of nylon wool to the 0.4-ml mark on the syringe.
3. Aliquot and reserve 1 ml of blood from each sample for total leukocyte and differential counts ("precolumn" sample).
4. Place the packed syringes in a rack with their tips inside but not touching the sides or bottom of the small tubes.
5. Add 1.0 ml of heparinized blood to the column and allow it to filter by gravity for 10 min at room temperature.
6. Discard the columns.
7. Determine complete and differential leukocyte counts of the pre- and postcolumn samples.

Interpretation

The percent neutrophils adherent to the nylon wool is calculated as follows: 100% – ([cells per milliliter postcolumn/cells per milliliter precolumn] × 100) = percent cells adherent. Normally, 68% ± 7% neutrophils adhere in this assay. Adherence of a significantly lower percentage of neutrophils is suggestive of an adherence defect. Neutrophil adherence to plastic or glass requires more-specialized techniques and is described elsewhere (5).

Flow Cytometric Determination of LAD

FACS analysis (chapter 33) of peripheral blood or isolated neutrophils is required for definitive diagnosis of LAD1 or LAD2. In LAD1, levels of CD18 are profoundly reduced on neutrophils and monocytes, leading to low levels of the associated molecules CD11a, CD11b, and CD11c (the method is given in chapter 33). Levels of CD18 expression below 0.5% of normal are seen in the "severe" phenotype and are associated with more devastating disease and earlier mortality in the absence of bone marrow transplantation than with other phenotypes. Levels of CD18 expression between 0.5 and 10% of normal are associated with the "moderate" phenotype of LAD1 and are associated with a better rate of survival. The display of CD18/CD11 complexes, which are stored in secondary granules, is upregulated by neutrophil activation.

Demonstration of sialyl-Lewis^x (CD15s) deficiency on neutrophils confirms the diagnosis of LAD2. These patients also have the relatively rare Bombay (Hh) blood type, another manifestation of the underlying genetic defect in fucosylation caused by mutations in the GDP-fucosyl transferase. This disease is also now named congenital disorder of glycosylation IIc. LAD3 is confirmed by reduced levels of KINDLIN-3 when blotted or by mutations in *FERMT3*. Rac2 deficiency should be suspected in cases in which the surface display of CD18 and CD15s is normal but adherence is impaired, as is superoxide production (6).

Granule Disorders

In the normal course of neutrophil ontogeny, the large (about 0.8 μm in diameter) azurophilic or primary granules, containing myeloperoxidase (MPO), lysozyme, β-glucuronidase, and defensins, among others, appear at the promyelocyte stage; the smaller (about 0.5 μm in diameter) specific or secondary granules, containing lactoferrin, vitamin B_{12}-binding protein, cytochrome b_{558}, and CR3, among others, appear during the myelocyte stage.

In Chédiak-Higashi syndrome, neutrophil primary granulogenesis is initially normal, but the primary granules readily fuse to each other and subsequently to some secondary granules as well, resulting in giant primary granules that are easily appreciated under a light microscope. Chédiak-Higashi syndrome is due to autosomal recessive mutations in the gene lysosomal transporter (*LYST* or *CHS1*). Neutrophils from Chédiak-Higashi syndrome patients show delayed bactericidal activity against *S. aureus*. Other clinical features include partial oculocutaneous albinism, irregular melanization of hair, peripheral neuropathy later in life, and an eventual lymphoma-like "accelerated phase" in most patients.

In specific granule deficiency, the secondary granules are rare or absent, as are secondary granule proteins, such as lactoferrin. One form of secondary (specific) granule deficiency is due to an autosomal recessive mutation in the CCAAT/enhancer binding protein C/EBPε. Since lactoferrin is present in other secretions, it appears to be a tissue-specific phenomenon. Levels of defensins, a primary granule product, are also low to absent, because the defect is in a transcription factor important in neutrophil ontogeny and granule protein expression. Careful inspection of the peripheral smear suggests the diagnosis, as these neutrophils are larger and paler than normal. The diagnosis is confirmed by electron microscopy, showing an absence of secondary granules, or demonstration of the absence of lactoferrin in patient neutrophils by direct immunofluorescence or enzyme-linked immunosorbent assay. Methods for the detection of lactoferrin and other secondary and primary granule proteins are detailed elsewhere (5).

Chemotaxis

The neutrophil's ability to locomote up a chemoattractant gradient is chemotaxis, whereas the stimulation of shape change and random locomotion induced by a uniform concentration of a chemoattractant is chemokinesis. These properties are critical for the neutrophil response to

infection. Disorders involving chemotaxis are found in only a few diseases; secondary causes of depressed chemotaxis are more common (e.g., aspirin, prednisone, and ethanol). Actin dysfunction, Chédiak-Higashi syndrome, LAD1, Rac2 deficiency, secondary granule deficiency, and Job's syndrome (intermittently) all show decreased chemotaxis, although the mechanisms are quite disparate. In none of these disorders is the demonstration of a chemotactic defect diagnostic. The several assays of chemotaxis all require fresh neutrophils and an experienced laboratory technician. The sensitive techniques (Boyden chamber migration or the multiwell chamber) require highly specialized equipment, radioactivity, or both (5). In view of the complexity of the current chemotactic assays and their extremely limited diagnostic value, I recommend that for cases in which chemotactic determination appears to be appropriate, specialty reference or research laboratories be contacted. Chemotaxis assays are discussed in reference 6.

Oxidative Metabolism Disorders

Neutrophils, eosinophils, and macrophages use the NADPH oxidase enzyme complex to augment molecular oxygen by one electron, yielding superoxide (O_2^-). This in turn is converted to hydrogen peroxide (H_2O_2) by superoxide dismutase. H_2O_2 is combined with halide (X^-) by MPO to produce hypohalous acid (HOX); in the neutrophil, which uses chloride for its halide, this is bleach (HOCl). Defects in the proximal portion of this pathway, at the level of the NADPH oxidase, lead to life-threatening infections in CGD; defects in the latter portion of the pathway caused by MPO deficiency are clinically quite inapparent and lead to infectious problems only when coupled to other diseases, such as diabetes mellitus.

CGD is a genetic disorder estimated to occur in about 1/250,000 persons and is characterized by severe, recurrent life-threatening infections with catalase-producing bacteria and fungi and tissue granuloma formation (7). Five separate genotypes (one X chromosome linked, gp91^{phox}; four autosomal recessive, p22^{phox}, p47^{phox}, p67^{phox}, and p40^{phox}) can give rise to the phenotype of CGD, but there are slight differences in clinical phenotype and obvious differences in genetic transmission and associated counseling. Since all of the relevant genes have been cloned and characterized, a definitive molecular diagnosis can be made. Molecular diagnoses can be performed by reference and commercial laboratories. All patients with CGD should be referred for definitive molecular characterization of their CGD to help with genetic counseling and prognosis (8).

Several methods are available for diagnosis of CGD. Nitroblue tetrazolium (NBT) reduction and dihydrorhodamine (DHR) oxidation are the simplest tests available and are discussed here. Chemiluminescence and staphylococcal killing are also discussed since they not only are used in the demonstration of CGD functional defects but also occasionally may help in diagnosis (4). Superoxide production, hydrogen peroxide production, and cytochrome *c* reduction are other techniques which bear on the integrity of oxidative metabolism covered elsewhere in this text (chapter 33).

NBT Test

Principle

Superoxide produced by neutrophils reduces NBT from a soluble yellow dye to blue-black formazan, which is readily apparent as a cytoplasmic precipitate. Neutrophils unable to produce superoxide fail to reduce NBT and are therefore free of precipitate. Because this assay is read by light microscopy, individual cells reducing or not reducing NBT can be recognized. Mothers of patients with X chromosome-linked CGD show mosaicism of peripheral blood neutrophil NBT reduction, since X chromosome inactivation (lyonization) occurs randomly in hematopoietic precursors.

Interpretation

More than 95% of normal neutrophils will reduce NBT, showing orange nuclei with clumps of blue-black precipitate in the cytoplasm. In a patient with CGD, there is usually no NBT reduction. Since X chromosome inactivation is thought to be random in females, there should be two populations of neutrophils in the peripheral blood of X-linked carriers, NBT reducing (normal) and non-NBT reducing (CGD). This mosaic pattern can range anywhere from 0.001 to 97% of neutrophils, although most carriers will fall within a range of about 20 to 80% NBT-reducing neutrophils. At the extremes of lyonization, these X-linked carriers are indistinguishable from CGD patients or healthy subjects, respectively. It is best to report the results as percent NBT-reducing neutrophils to avoid the confusion surrounding the terms positive and negative in this setting. The drug D-penicillamine can act as a superoxide-generating source when oxidized and therefore can cause unreliable NBT results.

The X-linked form of CGD is the most common (about 65% of cases in outbred populations). One can often rapidly determine whether a male patient is X linked or autosomal recessive by analysis of the mother's blood at the time of the initial NBT test. In this way, the genotype can be approximated at the same time as the phenotype in most cases.

There are several reports of patients with variant forms of X-linked CGD in whom a dysfunctional gp91^{phox} protein is normally expressed. These patients may have apparently normal NBT reduction. In cases in which the clinical suspicion is high, testing by DHR oxidation, quantitative superoxide generation, or bactericidal activity should be pursued.

DHR Oxidation

Principle

DHR 123 is oxidized to rhodamine 123 by H_2O_2 and O_2^-, with the emission of bright fluorescence upon stimulation by blue light (488 nm). This dye is freely able to permeate cells and can be used in whole blood to determine whether granulocytes produce H_2O_2 and O_2^-, upon stimulation with phorbol myristate acetate (PMA), a potent stimulus of NADPH oxidase activity.

This technique is simple, sensitive, and quantitative and can be performed on whole blood shipped overnight. PMA-stimulated and unstimulated samples are run simultaneously.

Specimen Collection

Collect 1 ml of heparin-anticoagulated peripheral blood in plastic, endotoxin-free tubes.

Reagents

Lysis buffer (store at room temperature)

Ammonium chloride	4.15	g
Sodium bicarbonate	0.84	g
0.5 M EDTA (pH 8.0)	1	ml
Distilled water	500	ml

Suspension buffer (store at room temperature)

Hanks' balanced salt solution (HBSS) (without Ca^{2+}, Mg^{2+}, or phenol red)	500	ml

Albumin (human fraction V)	0.5	g
0.5 M EDTA, pH 8.0	1	ml

Catalase stock solution (1,400 U/μl)

Catalase (C40; Sigma)	28	mg
Suspension buffer	400	μl

Store 10-μl aliquots at −70°C. For catalase working solution, dilute 10 μl of stock with 130 μl of suspension buffer immediately before use. Use 5 liters for each 500-μl tube (final concentration, 1,000 U/ml).

PMA stock (2 μg/μl)

PMA (P8139; Sigma)	1	mg
Dimethyl sulfoxide (DMSO) (D2650; Sigma)	500	μl

Store 10-μl aliquots at −70°C. PMA working solution (1:1,000 dilution) consists of 2 μl of PMA stock solution combined with 1,998 μl of suspension buffer immediately before use. Add 100 μl to tubes for a final concentration of 400 ng/ml.

DHR stock (29 mM)

DHR 123 (catalog no. D-632; Molecular Probes, Eugene, OR)	10	mg
DMSO	1	ml

Store 25-μl aliquots at −70°C. Add 1.8 μl of stock to each reaction tube.

Procedure

The procedure for DHR oxidation is as follows.

1. Add 4 ml of prewarmed, 37°C lysis buffer to polypropylene tubes.
2. Add 100 to 300 μl of whole blood to each of two tubes for each sample to be assayed, mix by inversion, and let stand for 5 min at room temperature.
3. Centrifuge at 800 × *g* at room temperature for 5 min to pellet leukocytes.
4. Discard the supernatant and blot the tubes.
5. Resuspend the leukocyte pellet in 4 ml of suspension buffer and centrifuge as described above.
6. Discard the supernatant, blot the tubes, and resuspend the pellet in 400 μl of suspension buffer.
7. Add 5 μl of the catalase working solution.
8. Add 1.8 μl of DHR 123 stock solution and incubate the tubes for 5 min in a 37°C shaking water bath.
9. Add 100 μl of PMA working solution to one tube and 100 μl of suspension buffer to the other (unstimulated) tube.
10. Incubate for 15 min in a 37°C shaking water bath.
11. Analyze by flow cytometry, collecting forward and side scatter.

Interpretation

Histograms are compared for unstimulated and PMA-stimulated tubes. In normal neutrophils, PMA-stimulated DHR oxidation yields between 50- and 200-fold more mean channel fluorescence than unstimulated DHR oxidation. CGD neutrophils usually show less than 10-fold augmentation of DHR oxidation by PMA. X-linked carriers show two distinct populations of neutrophils, those which oxidize normally in the presence of PMA and those which do not. This technique is sensitive to at least 0.01% normal cells among 99.99% CGD cells and is therefore able to identify highly lyonized carriers (4). Given the general availability of FACS machines and the ease, sensitivity, and reproducibility of this assay, this test should be widely applied for the diagnosis of CGD. It is important to recognize some diagnostic overlap in the DHR assay with myeloperoxidase deficiency (7).

Chemiluminescence

Principle

In the normal neutrophil, stimulation of the NADPH oxidase leads to the generation of H_2O_2, which couples with hypochlorite (OCL^-) to produce singlet oxygen ($^1O_2$), water, and chloride (Cl^-). Singlet oxygen is molecular oxygen with an electron lifted to a higher orbit with inversion of spin. The return of this electron to its ground state is associated with light emission, which can be measured as chemiluminescence with several different reagents (9).

Specimen Collection

Isolated neutrophils, 2×10^4/ml, are used.

Reagents and Equipment

Chemiluminometer or fluorometer with only one photomultiplier tube or a beta counter that can be shifted to only one photomultiplier tube, since the coincidence sum cannot be used. Use the ^3H channel; background is usually 25,000 to 50,000 cpm.

Twenty-milliliter glass scintillation vials (keep in the dark) or microtiter plates

37°C incubator with rotator

Luminol stock solution (A8511; Sigma) (275 μM in DMSO stored at room temperature in the dark; the final concentration for the assay is 1 μM) or lucigenin stock solution (M8010; Sigma) (6.88 μM in distilled water stored at room temperature in the dark; the final concentration for the assay is 25 μM)

PMA stock solution (P8139; Sigma) (200 μg/ml in DMSO, aliquot and store at −70°C)

Zymosan stock solution (Z4250)

Zymosan	500	mg
PBS	50	ml

Boil for 1 h and then cool. Centrifuge at 500 × *g* for 10 min and discard the supernatant. Resuspend the pellet in 10 ml of PBS and keep at 4°C in the dark.

Opsonized zymosan: on the day of use, suspend 1 part zymosan stock in 9 parts pooled human serum. Rotate for 15 min at 37°C. Centrifuge at 500 × *g* for 10 min and discard the supernatant. Resuspend to 1.25 mg/ml in $HBSS^+$ HBSS (with $Ca^{2+}$and Mg^{2+}).

Procedure

1. To each vial add 400 μl of opsonized zymosan or 55 μl of PMA, 20 μl of luminol solution, and $HBSS^+$ to 4.5 ml.
2. Place scintillation vials in a counter in the dark for at least 20 min before adding the cells.
3. Arrange control vials as follows:
   HBSS plus luminol
   HBSS plus luminol plus zymosan or PMA
   HBSS plus luminol plus cells
4. Record the background chemiluminescence of the vials.

5. At 1-min intervals, add 1 ml of cells to each vial sequentially, swirling each vial for 30 s before replacing the vial in the counter.
6. Count vials sequentially for 1-min periods continuously for 1 h.
7. Plot the counts per minute versus time.

Interpretation

The normal range of chemiluminescence values is 300,000 to 600,000 cpm, with peak values obtained between 8 and 12 min. Chemiluminescence is not entirely specific for singlet oxygen, but it is a sensitive technique for detecting abnormalities in oxidative metabolism. Very low chemiluminescence is consistent with CGD. Heterozygotes can be detected as intermediate between those of normal subjects and CGD patients. If performed with opsonized zymosan instead of PMA, this assay can detect abnormalities of phagocytosis, such as in LAD1, in which the receptor for C3bi (CR3 or CD18/CD11b) is deficient (5).

The assay given here is adaptable to laboratories without highly specialized equipment. These procedures are now routinely performed in many laboratories with microtiter plates on specialized chemiluminometers. Recently, an enhancer of chemiluminescence has been marketed (Diogenes, order no. CL-202; National Diagnostics, Atlanta, GA), which allows ≥100-fold amplification of the chemiluminescent signal using essentially the same protocol. For experiments using B cells or cell lines which produce small amounts of superoxide or very low numbers of neutrophils, the Diogenes system should be considered.

Myeloperoxidase

MPO is the enzyme that makes pus green and catalyzes the conversion of hydrogen peroxide to bleach in the neutrophil. Deficiency of MPO is the most common neutrophil disorder, occurring in about 1/2,000 persons. Despite the important role of MPO in neutrophils, clinical disease from MPO deficiency is quite rare and has been reported mostly for diabetics with disseminated *Candida* infections. MPO is an important marker of myeloid maturation, appearing at the promyelocyte stage of development. This procedure will stain peroxidase-containing granules in neutrophils, eosinophils, and monocytes.

Specimen Collection

Cytocentrifuged neutrophils on glass slides are preferred, but peripheral blood can be used.

Reagents and Equipment

Fixative, 10% formyl ethanol

Ethanol (absolute)	90	ml
Formaldehyde (37%)	10	ml

Stain, pH 5.8 to 6.5

Ethanol (30%)	100	ml
Benzidine hydrochloride (carcinogen)	0.3	g
Zinc sulfate · $7H_2O$ (3.6%)	1.0	ml
Sodium acetate	1.0	g
Hydrogen peroxide (30%)	70	μl
Safranin O	0.2	g

Mix reagents well in the order listed. The benzidine hydrochloride may leave a slight residue, which will not dissolve. A precipitate forms upon the addition of the zinc sulfate, which will dissolve with addition of the remaining reagents. Filter and store the solution capped at room temperature. This solution is good for 6 months.

Procedure

1. Fix the slide in formyl ethanol for 60 s.
2. Rinse the slide thoroughly to remove residual formyl ethanol, since this can inactivate the benzidine hydrochloride stain.
3. Place the slide in the stain for 45 s.
4. Rinse the slide thoroughly, and allow it to air dry.

Interpretation

Neutrophils show a blue cytoplasm with discrete blue granules, monocytes stain more weakly but still display discrete granules, and eosinophils stain most intensely, often tinged brown-black or green-black. Lymphocytes, basophils, and platelets do not stain. Cells from patients with MPO deficiency do not stain (7).

Other techniques related to neutrophil function and measurement are reviewed by Metcalf et al. (10).

This research was supported by the Intramural Research Program of the National Institute of Allergy and Infectious Diseases, National Institutes of Health.

REFERENCES

1. **Rosenzweig SD, Holland SM.** 2011. Recent insights into the pathobiology of innate immune deficiencies. *Curr Allergy Asthma Rep* **11:**369–377. PubMed
2. **Newburger PE, Dale DC.** 2013. Evaluation and management of patients with isolated neutropenia. *Semin Hematol* **50:**198–206. PubMed
3. **Akhtari M, Curtis B, Waller EK.** 2009. Autoimmune neutropenia in adults. *Autoimmun Rev* **9:**62–66. PubMed
4. **Leiding JW, Holland SM.** 2013. Chronic granulomatous disease, p 1993–2013. *In* Pagon RA, Adam MP, Bird TD, Dolan CR, Fong CT, Stephens K (ed), *GeneReviews*. University of Washington, Seattle, Seattle, WA.
5. **Elloumi HZ, Holland SM.** 2007. Diagnostic assays for chronic granulomatous disease and other neutrophil disorders. *Methods Mol Biol* **412:**505–523. PubMed
6. **van de Vijver E, van den Berg TK, Kuijpers TW.** 2013. Leukocyte adhesion deficiencies. *Hematol Oncol Clin North Am* **27:**101–116, viii. PubMed
7. **Mauch L, Lun A, O'Gorman MR, Harris JS, Schulze I, Zychlinsky A, Fuchs T, Oelschlägel U, Brenner S, Kutter D, Rösen-Wolff A, Roesler J.** 2007. Chronic granulomatous disease (CGD) and complete myeloperoxidase deficiency both yield strongly reduced dihydrorhodamine 123 test signals but can be easily discerned in routine testing for CGD. *Clin Chem* **53:**890–896. PubMed
8. **Kuhns DB, Alvord WG, Heller T, Feld JJ, Pike KM, Marciano BE, Uzel G, DeRavin SS, Priel DA, Soule BP, Zarember KA, Malech HL, Holland SM, Gallin JI.** 2010. Residual NADPH oxidase and survival in chronic granulomatous disease. *N Engl J Med* **363:**2600–2610. PubMed
9. **Segal BH, Leto TL, Gallin JI, Malech HL, Holland SM.** 2000. Genetic, biochemical, and clinical features of chronic granulomatous disease. *Medicine (Baltimore)* **79:**170–200. PubMed
10. **Metcalf JA, Gallin JI, Nauseef WM, Root RK.** 1986. *Laboratory Manual of Neutrophil Function*. Raven Press, New York, NY.

Evaluation of Natural Killer (NK) Cell Defects

KIMBERLY RISMA AND REBECCA MARSH

79

CLINICAL INDICATIONS FOR EVALUATION OF NK CELL FUNCTION

Genetic defects in natural killer (NK) cell and cytotoxic T lymphocyte (CTL) function generally lead to one of two outcomes: (i) life-threatening and/or severe chronic infections with viruses, particularly from the *Herpesviridae* family member viruses Epstein-Barr virus, cytomegalovirus, herpes simplex viruses, and varicella-zoster virus but also other viruses such as human papillomaviruses; or (ii) a life-threatening hyperinflammatory disorder called hemophagocytic lymphohistiocytosis (HLH).

The first clinical indication to measure cytotoxic function is in the patient presenting with severe herpesviral infections. Such infections are noted in many primary immunodeficiencies in which the gene defect disrupts both NK and CTL interaction with target cells. An extensive list of gene defects associated with abnormal cytotoxic function in NK and CTL has recently been compiled (1). Recently, NK-specific disorders have been described (Table 1). The typical starting point for evaluation of NK cell function in children or adults with severe or persistent herpesviral infections includes NK cell enumeration and an NK cell functional assay. Conditions associated with a specific deficiency of NK cell numbers are sometimes referred to as "classical NK cell deficiency," whereas "functional NK cell deficiency" implies the presence of NK cells but abnormal function.

The second clinical indication for evaluation of NK cell function is the development of HLH. HLH is a systemic hyperinflammatory disorder that arises when CTL and NK function is severely impaired and/or absent due to genetic defects in the perforin-mediated cytotoxic pathway (Table 2) (2). HLH may be triggered by viral infections, especially herpes virus family members; however, the pathophysiology of the disease is distinct. Patients have uncontrolled T cell and macrophage activation due to a failure of elimination of antigen-presenting cells. Patients presenting with symptoms of HLH (fever, rash, pancytopenia, lymphoproliferation [lymphadenopathy and splenomegaly], and multisystem organ failure) require prompt diagnosis and recognition, as the disease is fatal if immunosuppressive therapy is not urgently initiated (3).

The first tests performed for the rapid evaluation of patients with HLH also include enumeration of NK cells and one or more NK cell functional assays but, uniquely, should also include measurement of intracellular perforin. These tests can be performed on even limited blood samples from patients with suspected disease. Additional testing (generally from a second blood draw due to limitations of volume in young children) should include genetic testing which can be guided by the initial immune findings. Of note, males with X-linked lymphoproliferative disease (XLP) may present with HLH despite normal NK numbers and preserved NK function (against K562 cells) due to X-linked inheritance of gene mutations in *SH2D1A* (XLP type 1) or *XIAP/BIRC4* (XLP type 2). Therefore, flow cytometric evaluation of signaling lymphocyte activation molecule-associated protein (SAP) and XIAP protein is recommended for boys to rule out either form of XLP as a cause of HLH (4, 5). The cytotoxic defect associated with SAP deficiency appears to be restricted to Epstein-Barr virus-infected B cells (6), whereas no cytotoxic defect has been described in boys with XIAP deficiency (7–9).

DEFECTS IN NK CELLS ASSESSED BY ENUMERATION

Patients may be noted to have quantitative defects in NK cell number (if the NK number is <1% of all lymphocytes) due to a primary disorder in NK generation or from secondary etiologies. Primary defects in the number of NK cells are rare and have been described thus far only in relationship to two genes, *GATA2* and *MCM4*, as recently reviewed (1). NK cell lymphopenia is also described in numerous other primary immune deficiencies, including severe combined immunodeficiency due to a failure in interleukin-15 signaling (common gamma chain or JAK3 deficiency) or adenosine deaminase deficiency, and for unknown reasons in common variable immunodeficiency (10, 11). Patients with primary quantitative disorders present largely with recurrent and/or severe viral infections rather than HLH. Quantitative defects in NK cells (generally transient) can also be observed at the time of presentation with HLH (12), unfortunately delaying diagnosis due to the inadequacy of NK function and protein expression testing when numbers are limited.

Secondary defects in NK cell number may also be noted incidentally upon evaluation of lymphocyte subpopulations in children with lymphopenia unrelated to NK functional defects. For example, reduced or absent peripheral and lung NK cells may be a transient phenomenon during viral infections, as described in infants with life-threatening varicella-zoster virus (13) and respiratory viral infections, including respiratory syncytial virus (RSV) (14, 15). The mechanism for

doi:10.1128/9781555818722.ch79

TABLE 1 Primary immunodeficiencies presenting with severe herpesvirus and/or human papillomavirus infections due to exclusive NK defects

Gene	Clinical disorder	Abnormal immunologic assays
GATA2	Classical NK defect type 1	Enumeration and phenotype (reduced CD56dim and CD56bright) Cr^{51} release (K562)
MCM4	Classical NK defect type 2	Enumeration and phenotype (reduced CD56dim) Cr^{51} release (K562)
CD16	Functional NK defect type 1	CD16 flow cytometry (with antibody clone B73.1) Cr^{51} release (K562)

quantitative deficiency may be related to abnormal trafficking to inflamed organs or apoptosis, as theorized to occur upon influenza virus infection of human NK cells (described *in vitro* only in human cells) (16). Shown in Fig. 1 is a 2.5-year-old child with life-threatening RSV who was initially noted to be mildly lymphopenic. Lymphocyte subpopulation analysis revealed absent NK cells and normal T cells. Repeat testing revealed that this was a transient phenomenon, with reappearance of NK in the blood (at reduced numbers) at 2 days, coincident with improvement in clinical symptoms. It is unknown whether the low NK cells played any role in his primary disease; however, it illuminates the need for serial testing when abnormal NK cell quantification is noted.

DEFECTS IN NK CELL FUNCTION ASSESSED BY PERFORIN STAINING

When patients present with HLH, an immediate diagnosis of perforin deficiency may be made by flow cytometric evaluation of intracellular perforin in NK and CTL. Perforin is required for cytotoxic granule contents from NK cells and CTL to penetrate the outer cell membrane of target cells (17). Blood samples are stained to identify CTL (CD3 and CD8 positive) and NK cells (CD3 negative and CD56 and/or CD16 positive), and perforin is assessed on both populations. $CD8^+$ T cells express perforin and granzymes only after they have differentiated into CTL effectors and/or memory cells (18, 19). This is an age-dependent phenomenon due to exposure to antigen followed by acquisition of secretory granules that store perforin and granzymes. Therefore, in young babies, the amount of perforin in $CD8^+$ cells may be nearly zero physiologically. In contrast, at birth, essentially all NK cells are perforin positive in healthy individuals. Therefore, this population is the easiest in which to diagnose perforin deficiency (biallelic mutations) as well as detect heterozygous carriers of *PRF1* defects. As shown in Fig. 2A, when biallelic *PRF1* mutations are present, perforin staining is absent. Heterozygous carriers of defective alleles often have one-half of the normal or reduced expression. For a detailed description of lytic granule content procedure, refer to chapter 32 of this volume.

As intracellular perforin staining is dependent upon the presence of secretory granules, an internal control protein such as granzyme B is also typically stained when assessing patients for perforin expression. Interestingly, in patients with active HLH, this protein is markedly upregulated in both CTL and NK cells (19), suggesting that the cytotoxic lymphocytes are chronically activated by the presence of ongoing antigenic stimulation. In fact, in patients with HLH related to inherited defects in degranulation (*UNC13D* and *STXBP2*), both granzyme B and perforin are detected at higher levels in NK and CTL during active disease. These levels normalize with immunosuppressive therapy.

DEFECTS IN NK CELL FUNCTION ASSESSED BY Cr^{51} RELEASE ASSAY

Historically, the first-line test for assessing NK cell cytotoxic function in patients with suspected immunodeficiency has been the Cr^{51} release assay. Briefly, peripheral blood mononuclear cells (PBMC) are prepared from a blood sample and coincubated at various ratios with tumor cell line target cells preincubated with Cr^{51}. After 4 hours, the supernatant is assayed for the amount of Cr^{51} released due to cell death. The result is reported as a percentage

TABLE 2 Primary immunodeficiency presenting with development of HLH

Gene	Clinical disorder	Abnormal immunologic assays
PRF1	Familial HLH type 2	Perforin protein (flow cytometry) Cr^{51} release (K562)
UNC13D	Familial HLH type 3	Cr^{51} release (K562) CD107 degranulation assay (K562)
STX11	Familial HLH type 4	Cr^{51} release (K562) CD107 degranulation assay (K562)
STXBP2	Familial HLH type 5	Cr^{51} release (K562) CD107 degranulation assay (K562)
RAB27A	Griscelli syndrome type 2	Cr^{51} release (K562) CD107 degranulation assay (K562)
LYST	Chédiak-Higashi syndrome	Cr^{51} release (K562) CD107 degranulation assay (K562)
SH2D1A[a]	X-linked lymphoproliferative syndrome type 1	SAP protein (flow cytometry)
XIAP/BIRC4[a]	X-linked lymphoproliferative syndrome type 2	XIAP protein (flow cytometry)

[a]Cytotoxic function against K562 target cells is preserved.

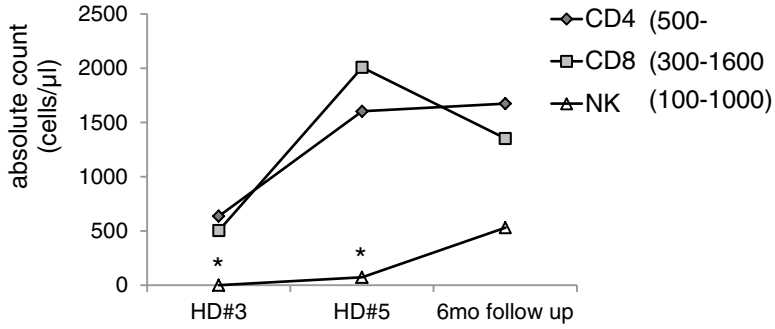

FIGURE 1 Transient NK lymphopenia. A two-and-a-half-year-old child with life-threatening RSV infection was evaluated for low lymphocyte counts on hospital days (HD) 3 and 5. No detectable NK cells in the peripheral blood were seen in the first sample, and a reduced number was noted (<1%) 2 days later. In contrast, CD8 and CD4 T cells were in the normal range. NK cell numbers were normal at follow-up (age-appropriate normal ranges are shown in parentheses).

of maximum release from a detergent-treated, target cell, typically K562 cells.

As shown in Fig. 2B, when patients have biallelic *PRF1* mutations, cytotoxic function is absent. Carriers of a single *PRF1* mutation have one-half of the normal function but do not develop HLH and are not known to be at any increased risk of cancer, autoimmunity, or viral disease. Absent cytotoxicity is also observed in patients with profound defects in NK degranulation (Table 2) leading to HLH. The development of HLH is dependent upon a fundamental defect

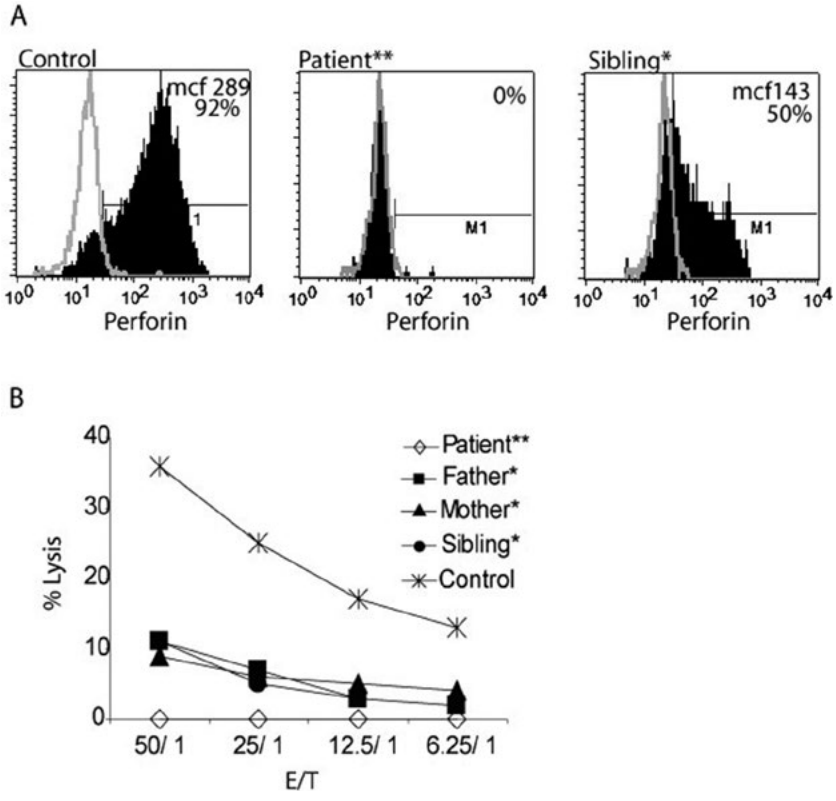

FIGURE 2 Example of assessment of perforin staining and NK cell functional testing by Cr^{51} release assay. (A) Intracellular perforin staining on NK cells is performed by flow cytometry using whole-blood samples. Gating on $CD56^+$ lymphocytes, histograms from a healthy control, a patient with biallelic *PRF1* mutations, and a representative, heterozygous carrier (family member) of *PRF1* mutations are shown. The patient's perforin is not detectable, whereas the sibling has one-half the normal perforin detection. (B) NK function against K562 target cells as measured by Cr^{51} release is measured by preparing peripheral blood mononuclear cells (PBMC) from the patient and family members as described for panel A. PBMC were diluted at ratios of 50:1 down to 6.25:1 target cells. K562 target cells release Cr^{51} to the supernatant upon death in a 4-h assay. Family members with one-half the normal perforin protein have reduced function compared to healthy controls but are not at risk for developing HLH. E/T, effector/target cell ratio.

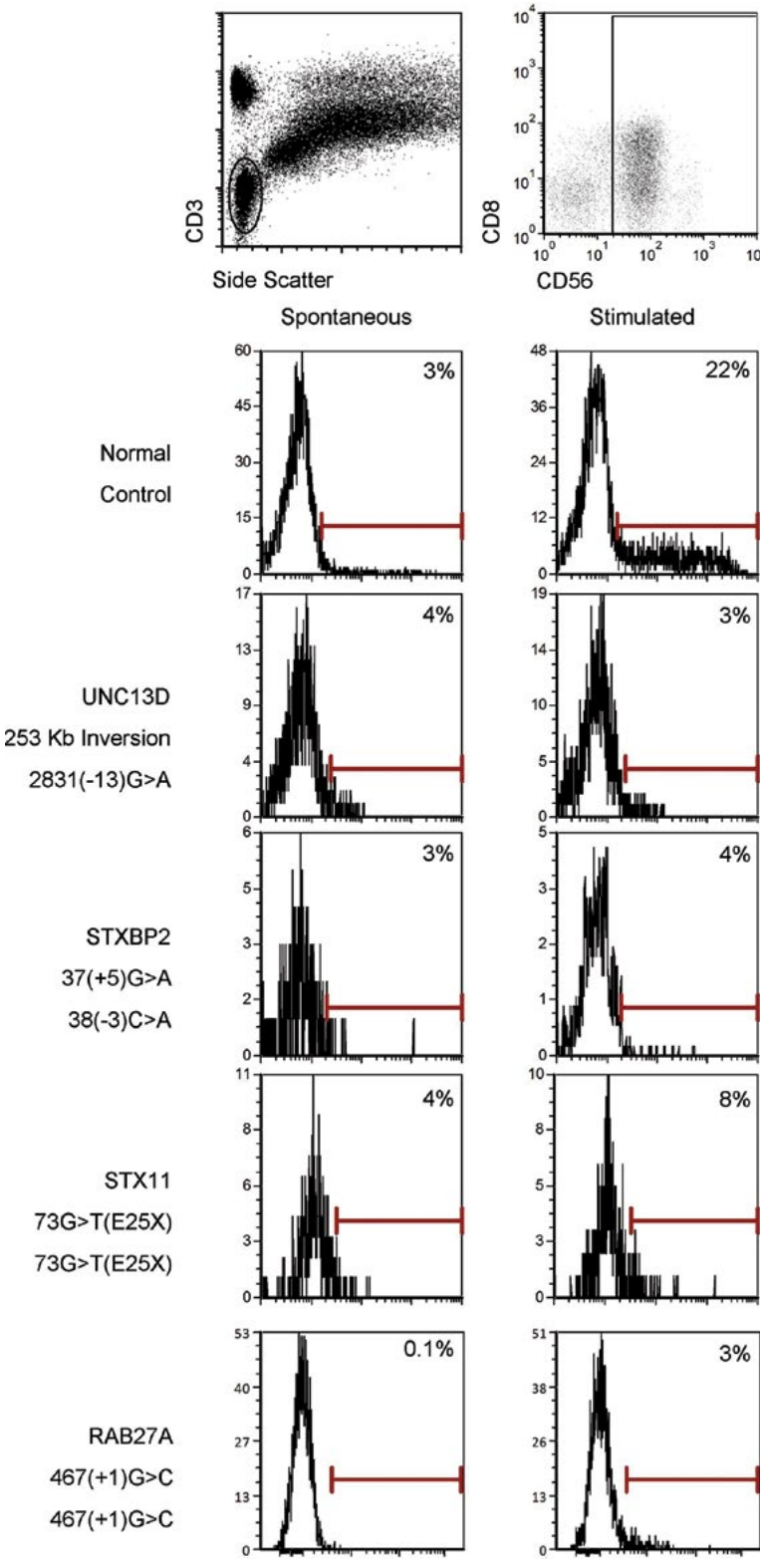

FIGURE 3 Examples of assessment of NK cell degranulation in a representative control and in patients with genetic forms of HLH. Peripheral blood mononuclear cells from a representative control and patients with UNC13D, STXBP2, STX11, and RAB27A mutations were incubated with target cells in medium containing a fluorochrome-labeled antibody directed against CD107a in the presence of monensin. Following that, cells were surface stained for CD3 and CD56. NK cells were identified as CD3-negative, CD56-positive lymphocytes. CD107a detection following incubation (Stimulated) was quantified in the NK cells by flow cytometric analysis in comparison to baseline CD107a expression (Spontaneous) and isotype control staining (not shown). Examples courtesy of the Diagnostic Immunology Laboratory, Cincinnati Children's Hospital.

in CTL and NK function. Therefore, reduced NK function as an isolated finding does not lead to HLH. A mutation in CD16 that impairs costimulation through CD2 has been described as an exclusive NK defect (20). The phenotype is not associated with HLH, as CTL do not express CD16.

The Cr^{51} assay is also impacted by cell number and the type of NK cells circulating in the peripheral blood, as the sample typically measures lysis from a total PBMC sample, not isolated NK cells. Human circulating NK cells are distinguished by cell surface markers CD56 and CD16. There are two subtypes, CD56dim and CD56bright. The former population is thought to possess the cytotoxic function required for removal of tumor or virally infected cells. A pitfall in assessing function may occur if the total number of NK cells (bright and dim) is not determined at the same time as testing for cytotoxic function by Cr^{51} release assay. NK function may be low or absent if CD56dim cells are low in the patient sample at the time of testing, as seen in patients with functional defects in NK development (Table 1) (1).

A major obstacle to assessing NK function for most clinical labs is the use of radioactivity. Therefore, the development of flow-based assays represents an alternative method for testing. For a detailed description of NK cell procedure, refer to chapter 32.

In research labs, a variety of methods are available to assess markers of apoptosis and death (annexin staining, propidium iodide, or 7-aminoactinomycin D uptake); however, these approaches have not been readily adapted to the clinical lab. One of the major difficulties is in timing: measurements at early time periods (15 to 45 minutes after coincubation) capture apoptotic events but are not sensitive enough for quantification. Late measurements (90 to 240 minutes) are problematic, as cells are routinely "lost" upon death. Commercially available reagents can assess granzyme B delivery to the target cells using a fluorescent probe that is cleaved by granzyme B. This method is effective to detect NK function defects (data not shown); however, the number of samples required for replicate testing at multiple effector/target ratios has prevented routine use in the clinical lab, where the 96-well Cr^{51} assay is straightforward. A nonradioactive 96-well microplate assay would be desirable but has not yet been described. Additionally, patients may have cytotoxic defects that are not detected against the tumor target cell in routine usage in the diagnostic immunology lab (K562), such as those observed in boys with SAP deficiency.

DEFECTS IN NK CELL FUNCTION ASSESSED BY DEGRANULATION ASSAY

The measurement of degranulation of NK cells is an attractive method to evaluate NK function when perforin detection is normal and Cr^{51} release is abnormal, or in addition to or in place of traditional Cr^{51} release studies. According to this method, patient PBMC are coincubated with tumor target cells and CD107a is detected by flow cytometry on the cell surface. CD107a is normally detected on the inner aspect of the cytotoxic granule and therefore detected on the cell surface only when NK have recognized a target cell and degranulated in response to immune synapse formation. This method is sensitive to detect defects in the machinery required for NK degranulation, such as MUNC 13-4 (21), STXBP2 (22), STX11 (23), or RAB27A (24), and offers greater than 85% sensitivity for identifying patients with the various genetic causes of HLH due to degranulation defects (25). Shown in Fig. 3 are examples of patients with genetic forms of HLH.

CONCLUSION

Assessment of NK phenotype and function in humans relies on flow cytometry and radioactive assays in the diagnostic immunology lab. In the setting of recurrent or severe viral infections, these assays may be repeated to ensure that the findings are not transient. In the clinical setting of HLH, these assays may be reported within 24 hours, facilitating rapid diagnosis and treatment. It is often difficult to assess the results of functional assays if enumeration and phenotyping of NK cells are not performed at the same time. The development of nonradioactive, microplate assays is desirable to evaluate NK function, and additional information may be obtained if future clinical assays were to include more than one type of target cell for testing function.

REFERENCES

1. **Orange JS.** 2013. Natural killer cell deficiency. *J Allergy Clin Immunol* **132:**515–525, quiz 526. PubMed
2. **de Saint Basile G, Ménasché G, Latour S.** 2011. Inherited defects causing hemophagocytic lymphohistiocytic syndrome. *Ann N Y Acad Sci* **1246:**64–76. PubMed
3. **Jordan MB, Allen CE, Weitzman S, Filipovich AH, McClain KL.** 2011. How I treat hemophagocytic lymphohistiocytosis. *Blood* **118:**4041–4052. PubMed
4. **Tabata Y, Villanueva J, Lee SM, Zhang K, Kanegane H, Miyawaki T, Sumegi J, Filipovich AH.** 2005. Rapid detection of intracellular SH2D1A protein in cytotoxic lymphocytes from patients with X-linked lymphoproliferative disease and their family members. *Blood* **105:**3066–3071. PubMed
5. **Marsh RA, Villanueva J, Zhang K, Snow AL, Su HC, Madden L, Mody R, Kitchen B, Marmer D, Jordan MB, Risma KA, Filipovich AH, Bleesing JJ.** 2009. A rapid flow cytometric screening test for X-linked lymphoproliferative disease due to XIAP deficiency. *Cytometry B Clin Cytom* **76:**334–344. PubMed
6. **Cannons JL, Tangye SG, Schwartzberg PL.** 2011. SLAM family receptors and SAP adaptors in immunity. *Annu Rev Immunol* **29:**665–705. PubMed
7. **Marsh RA, Villanueva J, Kim MO, Zhang K, Marmer D, Risma KA, Jordan MB, Bleesing JJ, Filipovich AH.** 2009. Patients with X-linked lymphoproliferative disease due to BIRC4 mutation have normal invariant natural killer T-cell populations. *Clin Immunol* **132:**116–123. PubMed
8. **Rigaud S, Fondanèche MC, Lambert N, Pasquier B, Mateo V, Soulas P, Galicier L, Le Deist F, Rieux-Laucat F, Revy P, Fischer A, de Saint Basile G, Latour S.** 2006. XIAP deficiency in humans causes an X-linked lymphoproliferative syndrome. *Nature* **444:**110–114. PubMed
9. **Yang X, Kanegane H, Nishida N, Imamura T, Hamamoto K, Miyashita R, Imai K, Nonoyama S, Sanayama K, Yamaide A, Kato F, Nagai K, Ishii E, van Zelm MC, Latour S, Zhao XD, Miyawaki T.** 2012. Clinical and genetic characteristics of XIAP deficiency in Japan. *J Clin Immunol* **32:**411–420. PubMed
10. **Aspalter RM, Sewell WA, Dolman K, Farrant J, Webster AD.** 2000. Deficiency in circulating natural killer (NK) cell subsets in common variable immunodeficiency and X-linked agammaglobulinaemia. *Clin Exp Immunol* **121:**506–514. PubMed
11. **Trujillo CM, Muskus C, Arango J, Patiño PJ, Montoya CJ.** 2011. Quantitative and functional evaluation of innate immune responses in patients with common variable immunodeficiency. *J Investig Allergol Clin Immunol* **21:**207–215. PubMed
12. **Mazodier K, Marin V, Novick D, Farnarier C, Robitail S, Schleinitz N, Veit V, Paul P, Rubinstein M, Dinarello CA, Harlé JR, Kaplanski G.** 2005. Severe imbalance of

IL-18/IL-18BP in patients with secondary hemophagocytic syndrome. *Blood* **106:**3483–3489. PubMed

13. **Vossen MT, Biezeveld MH, de Jong MD, Gent MR, Baars PA, von Rosenstiel IA, van Lier RA, Kuijpers TW.** 2005. Absence of circulating natural killer and primed CD8+ cells in life-threatening varicella. *J Infect Dis* **191:**198–206. PubMed
14. **De Weerd W, Twilhaar WN, Kimpen JL.** 1998. T cell subset analysis in peripheral blood of children with RSV bronchiolitis. *Scand J Infect Dis* **30:**77–80. PubMed
15. **Welliver TP, Reed JL, Welliver RC Sr.** 2008. Respiratory syncytial virus and influenza virus infections: observations from tissues of fatal infant cases. *Pediatr Infect Dis J* **27**(Suppl)**:**S92–S96. PubMed
16. **Mao H, Tu W, Qin G, Law HK, Sia SF, Chan PL, Liu Y, Lam KT, Zheng J, Peiris M, Lau YL.** 2009. Influenza virus directly infects human natural killer cells and induces cell apoptosis. *J Virol* **83:**9215–9222. PubMed
17. **Lieberman J.** 2010. Anatomy of a murder: how cytotoxic T cells and NK cells are activated, develop, and eliminate their targets. *Immunol Rev* **235:**5–9. PubMed
18. **Kogawa K, Lee SM, Villanueva J, Marmer D, Sumegi J, Filipovich AH.** 2002. Perforin expression in cytotoxic lymphocytes from patients with hemophagocytic lymphohistiocytosis and their family members. *Blood* **99:**61–66. PubMed
19. **Mellor-Heineke S, Villanueva J, Jordan MB, Marsh R, Zhang K, Bleesing JJ, Filipovich AH, Risma KA.** 2013. Elevated granzyme B in cytotoxic lymphocytes is a signature of immune activation in hemophagocytic lymphohistiocytosis. *Front Immunol* **4:**72. PubMed
20. **Grier JT, Forbes LR, Monaco-Shawver L, Oshinsky J, Atkinson TP, Moody C, Pandey R, Campbell KS, Orange JS.** 2012. Human immunodeficiency-causing mutation defines CD16 in spontaneous NK cell cytotoxicity. *J Clin Invest* **122:**3769–3780. PubMed
21. **Marcenaro S, Gallo F, Martini S, Santoro A, Griffiths GM, Aricó M, Moretta L, Pende D.** 2006. Analysis of natural killer-cell function in familial hemophagocytic lymphohistiocytosis (FHL): defective CD107a surface expression heralds Munc13-4 defect and discriminates between genetic subtypes of the disease. *Blood* **108:**2316–2323. PubMed
22. **zur Stadt U, Rohr J, Seifert W, Koch F, Grieve S, Pagel J, Strauss J, Kasper B, Nürnberg G, Becker C, Maul-Pavicic A, Beutel K, Janka G, Griffiths G, Ehl S, Hennies HC.** 2009. Familial hemophagocytic lymphohistiocytosis type 5 (FHL-5) is caused by mutations in Munc18-2 and impaired binding to syntaxin 11. *Am J Hum Genet* **85:**482–492. PubMed
23. **Marsh RA, Satake N, Biroschak J, Jacobs T, Johnson J, Jordan MB, Bleesing JJ, Filipovich AH, Zhang K.** 2010. STX11 mutations and clinical phenotypes of familial hemophagocytic lymphohistiocytosis in North America. *Pediatr Blood Cancer* **55:**134–140. PubMed
24. **Wood SM, Meeths M, Chiang SC, Bechensteen AG, Boelens JJ, Heilmann C, Horiuchi H, Rosthøj S, Rutynowska O, Winiarski J, Stow JL, Nordenskjöld M, Henter JI, Ljunggren HG, Bryceson YT.** 2009. Different NK cell-activating receptors preferentially recruit Rab27a or Munc13-4 to perforin-containing granules for cytotoxicity. *Blood* **114:**4117–4127. PubMed
25. **Bryceson YT, Pende D, Maul-Pavicic A, Gilmour KC, Ufheil H, Vraetz T, Chiang SC, Marcenaro S, Meazza R, Bondzio I, Walshe D, Janka G, Lehmberg K, Beutel K, zur Stadt U, Binder N, Arico M, Moretta L, Henter JI, Ehl S.** 2012. A prospective evaluation of degranulation assays in the rapid diagnosis of familial hemophagocytic syndromes. *Blood* **119:**2754–2763. PubMed

Allergic Diseases *section L*

VOLUME EDITOR: ROBERT G. HAMILTON
SECTION EDITOR: PAMELA A. GUERRERIO

Introduction

PAMELA GUERRERIO

80

The prevalence of allergic diseases has risen dramatically throughout the world in recent years, creating a major health care burden. While immunoglobulin E (IgE) has been recognized to play a central role in the pathogenesis of human allergic conditions since 1967, a multitude of inflammatory mediators and cells are now known to contribute to these common phenotypes. Section L covers laboratory investigations useful in the diagnosis and management of allergic disorders. Important topics covered include the allergen, *in vivo* and *in vitro* assays to screen for the presence of allergen-specific IgE and other mediators of allergic inflammation, and analytic approaches to diagnosing food allergy, hypereosinophilic syndromes, and mast cell disorders.

Chapter 81, by Rabin et al., examines the quantification and standardization of allergens. Although hundreds of allergen extracts are commonly used clinically for both diagnosis and treatment (immunotherapy) of allergic diseases, only 19 allergen extracts are currently standardized for allergen potency in the United States. This chapter describes the major *in vivo* and *in vitro* assays used to assess the potency of manufactured allergen products. These include quantitation of erythema size following serial intradermal skin testing of highly allergic individuals, quantitation of total protein content or specific major allergens within the extract, and inhibition of IgE binding from pooled allergic sera to a reference allergen extract. The potential utility of research-based assays, including basophil histamine release and expression of basophil activation markers by flow cytometry, for characterizing allergen extracts is also discussed.

Chapter 82, by Hamilton, describes the immunoassays performed by clinical immunology laboratories that can aid in the diagnosis, management, and research of allergic conditions. This chapter details the methods used to quantify serum levels of total IgE and allergen-specific IgE, including the use of allergenic components that can be used to identify cross-reactivity among different allergens. Methods to quantify the levels of antigen-specific IgG and IgG4, which may have utility as a biomarker for successful immunotherapy, are also discussed.

Chapter 83, by Schroeder et al., examines the major cells and mediators of allergic inflammation. The most recent approaches for measuring histamine, leukotriene C4, prostaglandin D2, tryptase, and Th2 cytokines (interleukins 4 and 13) are covered, as well as flow-based assays used to monitor basophil activation. Cellular assays utilized to study the role of basophils and dendritic cells in allergic responses are described. This chapter also includes a detailed discussion of the procedures and allergen reagents needed for prick/puncture and intradermal skin testing, both of which are commonly used by clinicians to identify allergens to which a patient is sensitized. However, the diagnosis of an allergic disorder additionally requires a clinical history that supports a causal relationship between exposure to the allergen and the development of allergic symptoms. Chapter 83 concludes with a discussion of *in vivo* provocation tests, focusing primarily on airway challenges, which can be used to further define the relationship between a patient's allergen sensitivities and their development of clinical respiratory symptoms.

Chapter 84, by Santos et al., examines the diagnostic tools used in the evaluation of patients with food allergy. Topics that are examined include prick/puncture and intradermal skin testing, fresh-food skin prick testing, atopy patch testing, food-specific IgE serology testing, elimination diets, and the double-blind placebo-controlled food challenge, which remains the gold standard for diagnosing food allergy. The performance, interpretation, advantages, and limitations of each approach are discussed. The authors discuss component-resolved diagnostic testing that may improve the accuracy of food allergy testing, as well as highlighting the lack of utility of total IgE and food-specific IgG testing in food allergy diagnosis. Chapter 84 concludes with a discussion of research-based assays and their potential role in the diagnosis and management of food allergy, including specific epitope analysis, serum tryptase, and basophil histamine release assays.

Chapter 85, by Akin et al., overviews the laboratory analyses used in the evaluation of patients with suspected hypereosinophilic syndromes (HES). The authors present the clinical features and diagnostic criteria for the HES variants, as well as the controversies surrounding the diagnosis of HES and its classification into subtypes. Eosinophilic gastrointestinal diseases (EGID) are a family of disorders characterized by excessive eosinophilic inflammation in the gastrointestinal tract. The prevalence of EGID appears to be increasing in recent years in both children and adults. The authors detail the major clinical and pathologic features of EGID and current treatment approaches. Chapter 85 concludes with a discussion of the clinical presentation, classification, diagnostic approach, and treatment of mast cell disorders.

doi:10.1128/9781555818722.ch80

Quantitation and Standardization of Allergens

RONALD L. RABIN, LYNNSEY RENN, AND JAY E. SLATER

81

Allergic reactions and allergic diseases are the most common human disorders of immune regulation. Diseases may include localized responses in the skin and various portions of the airway, or systemic responses characterized by extensive skin involvement, severe airway compromise, or cardiovascular collapse. Mechanisms include mast cell or basophil activation by the cross-linking of allergen-specific homocytotropic IgE, cellular infiltration following mast cell or basophil mediator release, complement activation, the deposition of immune complexes in susceptible tissues, or the infiltration of activated T-lymphocytes. The degree of impairment from allergic disease varies widely, with most reactions posing minor inconvenience, but with rare episodes requiring intensive—and sometimes unsuccessful—interventions to prevent death.

While the treatment of allergic diseases often includes highly effective and specific pharmacotherapy, for many allergic disorders allergen avoidance and allergen immunotherapy remain the best and safest options. Specific *allergen diagnosis*, which is a prerequisite for effective avoidance or immunotherapy, may be achieved by confirmation of a suggestive clinical history using a controlled *in vivo* allergen challenge (skin testing or, less often, ocular or respiratory challenge) or using *in vitro* methods such as serological assays for IgE antibody, basophil histamine release assays, or lymphocyte stimulation analysis. Specific *allergen immunotherapy* involves a graded administration of the identified allergen specificities to which the individual is sensitized. The goal of immunotherapy is to achieve a temporary reduction in the individual's allergic response, either through receptor saturation, antibody depletion, the formation of blocking antibodies, or T-cell tolerance. Remarkably, the purity of the allergen being tested is not essential for diagnostic or therapeutic efficacy. In fact, purity has not been achieved for any commercially available allergen preparations. However, for each of these evaluations or treatments, it is critical that the allergen used be correctly identified and that it is present in a sufficient bioactive form to achieve the expected diagnostic or therapeutic performance. Thus, for the successful use of allergens in allergy diagnosis or immunotherapy, it is important that we are able to *identify* and *measure* the allergen being used.

Allergens are molecules that elicit allergic reactions in susceptible individuals. Typically, allergens are naturally occurring proteins or glycoproteins derived from plants or animals, but biomolecules derived from single-cell organisms, synthetic compounds, metals, and small molecules may elicit significant allergic reactions as well. In this chapter, we limit our discussion to *natural or recombinant proteins or glycoproteins used in the diagnosis and/or treatment of IgE-mediated allergic disease*.

Allergen extracts are manufactured and sold worldwide for the diagnosis and treatment of IgE-mediated allergic disease. Crude extracts are composed of natural animal or plant source materials, and they are complex mixtures of natural biomaterials. Each extract contains proteins, carbohydrates, enzymes, and pigments of which the allergens—presumably the active ingredients—may constitute only a small proportion (1).

All current U.S. allergenic products were licensed prior to the efficacy requirements that were established for biologics in 1972. The safety, efficacy, and labeling of these products were evaluated by a Review Panel in the 1970s, which considered all of the products available at that time and made separate recommendations for the diagnosis and therapy indications of these products (2). Although some allergenic products have been removed from the market following the Panel's deliberations, most have been deemed presumptively safe and effective for therapy and/or diagnosis (3).

Traditionally, allergen extracts have been labeled either with a designation of extraction ratio (wt/vol) or with a protein unit designation (protein nitrogen units/milliliter) that is determined using the Kjeldahl method. However, little correlation has been detected between these two designations and biological measures of allergen potency (4, 5). In the absence of a concerted effort to maintain product consistency, lot-to-lot variations in allergen content may be considerable. Product consistency may be enhanced by the inherent nature of the raw materials. For example, pollen and pure mite extracts (6) generally have greater lot-to-lot consistency than mold, house dust, and insect extracts (7). In addition, manufacturers can increase the consistency of their products by controlled collection, storage, and processing of the raw materials; by reproducible and optimized extraction and manufacturing techniques; and by setting expiration dates based on real-time stability data. However, consistency can only be assured by measuring the potency of each lot of extract, and by marketing only those lots whose potency falls within a pre-defined acceptable range. When such additional tests and specifications are applied to similar products from more than one manufacturer, those products are said to be *standardized*.

doi:10.1128/9781555818722.ch81

FDA's allergen standardization regulation (21 CFR 680.3(e)) mandates that when an appropriate potency test exists, manufacturers must test each lot of an allergen extract for potency prior to distribution. In practice, the FDA has provided manufacturers with a U.S. reference standard for 19 products to which each new lot of allergen extract may be compared. The purpose of allergen standardization is to ensure that the allergen extracts are consistent in terms of allergen content and that variation between lots is minimized, even among different manufacturers (8). Since standardized allergenic extracts are compared to a single, national potency standard, patients and their physicians can switch from one manufacturer's product to another with minimized risk of adverse reaction.

The 19 standardized allergen extracts currently available in the U.S. are presented in Table 1. For each of these products, there is a U.S. standard of potency to which each lot is compared prior to release for sale to the public. The potency measures, and the assays used to determine these measures, are specified in the approved product-license applications submitted by each manufacturer for each product.

Overview of *In Vivo* Assessments of Allergen Potency

Allergen standardization in the U.S. comprises two important components: the selection of a reference allergenic extract and the selection of the procedures to compare manufactured products to the reference extract (9–11). In the U.S., the use of a biological model of allergen standardization has permitted the assignment of "bioequivalent allergen units" or BAUs for most standardized allergens (10). Once a specific unitage is assigned to a reference, then all allergenic extracts from the same allergenic source can be assigned units based on the relative potency (RP) with respect to the reference, using an established quantitative *in vitro* potency method (12).

In theory, standardizing an allergenic extract might involve purifying each allergenic component in the extract and establishing with precision the importance of these allergens. However, most allergenic extracts are complex mixtures of several relevant allergens of as yet uncertain immunodominance. In addition, an individual allergen in a particular lot may be less likely to elicit an allergic or immunotherapeutic response due to instability or denaturation.

The choice of the best potency test depends on the extract that is being standardized. In the absence of data supporting the safety of potency designations based on single allergen content, a measure of overall allergenicity may be a better predictor of safe dosing. For two allergenic extracts (short ragweed and cat hair), data have supported the use of single allergen determinations (Amb a 1 and Fel d 1, respectively). For extracts of cat pelt and hymenoptera venoms, the presence of two allergens (Fel d 1 and albumin for cat pelt; hyaluronidase and phospholipase A2 for hymenoptera venoms) is verified for each lot. For extracts of dust mites and grass pollens, overall allergenicity is determined.

For initial overall allergenicity assessment, the Center for Biologics Evaluation and Research (CBER) developed a method using erythema size following serial intradermal testing of highly allergic individuals. Intradermal testing was chosen over prick/puncture testing to achieve greater dosing accuracy. The erythema size was chosen over wheal size to achieve greater accuracy in reaction measurements (12). This method is called IntraDermal dilution for 50 mm sum of Erythema determines the bioequivalent ALlergy units ($ID_{50}EAL$), and it can be used to compare the allergenicity of extracts regardless of their source. Subsequent comparisons of extracts from the same source material are made by a variant analysis called the parallel line bioassay. Both of these methods are described in CBER's Methods of the Allergenic Products Testing Laboratory (13).

In the $ID_{50}EAL$ method, allergenic extracts are evaluated in subjects maximally reactive to the respective reference concentrates. Each subject is tested with serial 3-fold dilutions of the reference extract. After 15 minutes, the sum of the longest and midpoint orthogonal diameters of erythema (ΣE) is determined at each dilution, and the log dose producing a 50-mm ΣE response (D_{50}) is calculated (12) (Fig. 1).

Extracts that produce similar D_{50} responses can be considered bioequivalent and are assigned similar units, the bioequivalent-allergy unit (BAU). Because the modal D_{50} of a series of allergen extracts was 14 (a 3^{-14} or 1:4.8 million dilution), extracts with a mean D_{50} of 14 were arbitrarily assigned the value of 100,000 BAU/ml (10). Thus, the formula for the determination of potency from the D_{50} is:

$$\text{Potency} = 3^{-(14-\text{ mean D50})} * 100{,}000 \text{ BAU/ml.}$$

By a similar technique and analysis, bioequivalent doses of test extracts from the same source as the reference extract can be determined by the parallel-line bioassay (14). The inverse ratio of the doses of test extract required to produce identical D_{50} responses to a reference extract is the RP of that extract. This analysis requires that the log dose-response curves of the test extract and the reference extract be parallel. If the two dose-response lines are not parallel, then the ratio of skin test doses for identical responses and the reference preparation will vary with the dose. In this situation, which strongly suggests compositional differences between the two extracts, the distance between the two lines is different at each dose and a meaningful RP cannot be determined (9, 15) (Fig. 2).

In the original 1994 protocol, the mean D_{50} for 15 highly allergic individuals was used to determine the D_{50} for the extract. In a later re-analysis of the statistical considerations underlying such potency studies, Rabin et al. (16) applied the following formula for the number of study subjects, n, that would be required:

$$n = 2\left(\frac{\sigma}{\delta}\right)^2 (z_{1-\alpha} + z_{1-\beta/2})^2$$

where σ is the standard deviation of the measurement, δ is the acceptable difference in D_{50}s of two equivalent products, and the z values are the critical values from the cumulative normal distribution table for a significance level α and a power of $1 - \beta$ (17). From this formula, n is a function of the *squares* of σ and δ. The value of n will depend on the particular allergen to be tested, but, for typical values of σ and δ, n will usually be larger than 15.

In Europe, the Committee for Proprietary Medicinal Products issued a Guideline on Allergen Products: Production and Quality Issues that was revised in 2009 (18). The European system for standardizing allergens and determining allergenic extract potency is different from the system used in the U.S. The differences are as follows:

1. Manufacturers ensure batch-to-batch consistency using an in-house standard. The in-house standard may be characterized by a number of physico-chemical and immunologic assays, with demonstration of the presence of individual allergens preferred.

2. There are no external reference standards to ensure consistency among manufacturers.

TABLE 1 Allergenic extracts currently standardized in the U.S.

Allergen extract	Current lot-release tests	Labeled unitage	Current standard (date placed in service)	Method to establish equivalence to previous standard
Dust mite (*Dermatophagoides farinae*)	Competition ELISA Protein	AU/ml (equivalent to BAU/ml)	E11-Df (2012)	Competition ELISA
Dust mite (*Dermatophagoides pteronyssinus*)			E11-Dp (2011)	Competition ELISA
Cat pelt (*Felis domesticus*)	Fel d 1 (RID)	BAU/ml	E6-cat pelt (2012)	RID, IEF
Cat hair (*Felis domesticus*)	IEF Protein	5-9.9 Fel d I U/ml = 5,000 BAU/ml 10-19.9 Fel d I U/ml = 10,000 BAU/ml	E8-cat hair (2015) C13-cat (calibration set, 2012)	RID, IEF
Bermuda grass (*Cynodon dactylon*)	Competition ELISA	BAU/ml	E12-Ber (2016)	Competition ELISA
Red-top grass (*Agrostis alba*)	IEF Protein		E7-Rt (2016)	
June (Kentucky blue) grass (*Poa pratensis*)			E8-Jkb (2016)	
Perennial ryegrass (*Lolium perenne*)			E15-Rye (2015)	
Orchard grass (*Dactylis glomerata*)			E6-Or (2013)	
Timothy grass (*Phleum pretense*)			E10-Ti (2014)	
Meadow-fescue grass (*Festuca elatior*)			E6-Mf (2014)	
Sweet vernal grass (*Anthoxanthum odoratum*)			E7-Sv (2015)	
Short ragweed (*Ambrosia artemisiifolia*)	Amb a 1 (RID)	Amb a 1 units	E15-Ras C14-Ras (calibration set, 2011)	RID
Yellow hornet (*Vespa* spp.)	Hyaluronidase and phospholipase activity	μg protein	V4-HB (2015)	
Wasp (*Polistes* spp.)				
Honey bee (*Apis mellifera*)				
White-faced hornet (*Vespa* spp.)				
Yellow jacket (*Vespula* spp.)				
Mixed vespid (*Vespa* + *Vespula* spp.)				

ELISA, enzyme-linked immunosorbent assay; AU/ml, absorbance units/milliliter; BAU/ml, Bioequivalency Allergy Units/milliliter; RID, radial immunodiffusion assay; IEF, isoelectric focusing

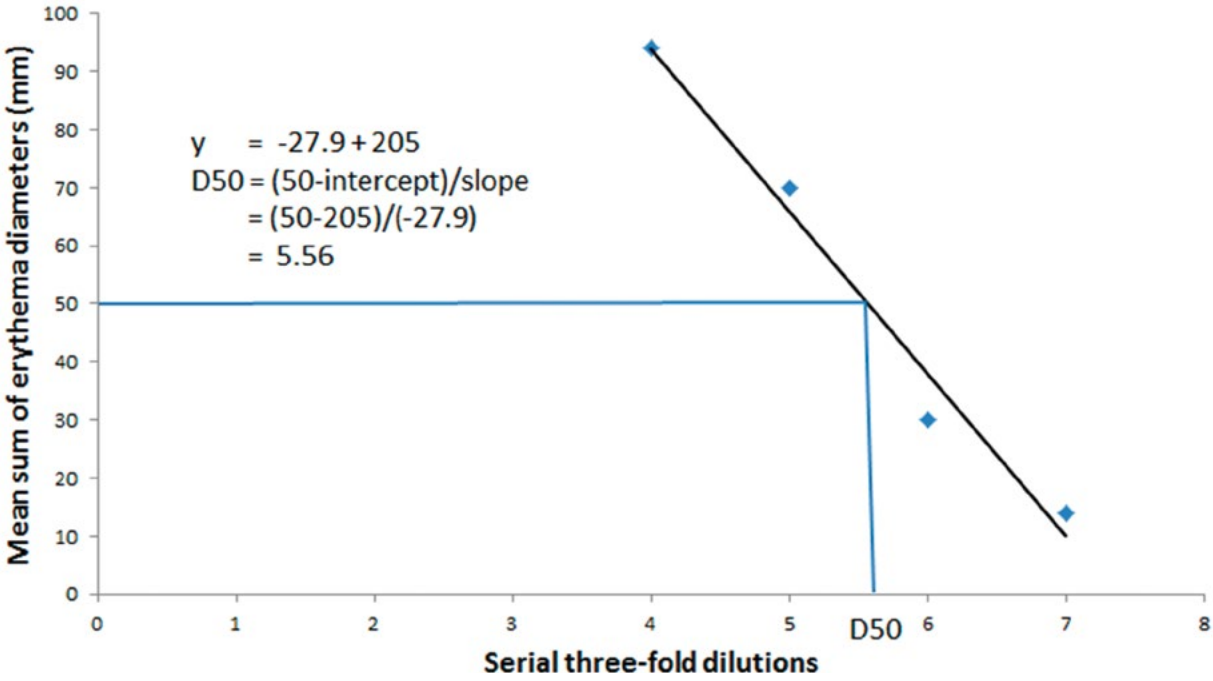

FIGURE 1 Sample calculation of D_{50}. Serial 3-fold dilutions of test material—in this example, histamine base—were injected and the ΣE responses were plotted against the negative log dilutions. The D_{50} is determined from the best-fit line using the formula: D_{50} = (50 - Intercept)/slope. The calculated D_{50} of 5.56 corresponds to a value of $-3^{-(14-5.56)}$ * 100,000 BAU/ml = 9.4 BAU/ml.

3. Potency may be determined by any validated measure of *in vitro* IgE binding or other immunoassay. The potency of the in-house standard may also be tested by a skin test technique.

4. An *in vivo* method by which European products may be tested is called the Nordic technique (19). This skin test method differs from the U.S. FDA CBER $IDE_{50}AL$ method in its use of prick skin tests rather than intradermal tests; its focus on wheal size rather than erythema; its choice of study subjects; and its use of a histamine dose-response curve to determine unitage. The method likely provides a reasonable estimate of extract potency. In theory, the comparison of the skin test reactivity of all allergens to a single standard (histamine dihydrochloride 10 mg/ml) allows the assignment of universal unitage without the development or maintenance of specific allergen reference standards. However, the European guideline does not prescribe the skin test technique to be used, and manufacturers are free to modify it as needed as long as the test is validated. Thus, as applied in Europe, this method cannot provide a level of standardization among the different manufacturers that market products in the European Union.

$ID_{50}EAL$ Test (12, 20)

Study Sequence

1. Identify three to four testing sites to achieve geographic and ethnic diversity of study populations.
2. Recruit 6 to 10 subjects per tester for proficiency testing (subjects need not be atopic). In order to generate useful data, the $ID_{50}EAL$ and parallel line bioassay methods must be performed by individuals proficient in the accurate and reproducible delivery of intradermal skin test doses, and the precise measurement of the skin test responses. Hence, a proficiency program has been developed to qualify personnel. This program, which is not described in detail here, involves puncture skin testing with histamine at 0.1 mg/ml and intradermal testing with eight serial 3-fold dilutions of histamine. The tester then analyzes the data and compares the results with normative data. Thus, the proficiency program examines the tester's ability to prepare accurate dilutions, administer the skin tests with precision, and record and analyze the data properly.
3. Recruit 10 to 20 study subjects for initial allergen skin testing.
4. Skin-test subjects and analyze the intradermal skin test data. Analysis will include determination of σ for intradermal testing.
5. Based upon initial data, determine the final study size.
6. Recruit study subjects, skin-test subjects, and analyze skin test data.
7. Prepare final study report.

Selection of subjects. Select individuals within the target-age range with a history of allergic disease relevant to the allergen being tested. Subjects must have a puncture sum of erythema diameter responses (ΣE) to the allergen concentrate of at least 30 mm. Exclude individuals with asthma whose peak flow is less than 75% of predicted at the time of testing; whose skin coloring or skin condition would preclude the measurement of erythema responses; who are dermographic; or who are currently using antihistamines, tricyclic antidepressants, monoamine oxidase (MAO) inhibitors, and beta-blockers.

Dilution of allergens for skin testing. Starting with the undiluted or reconstituted lyophilized extract, prepare serial 3-fold dilutions using sterile technique, down to a dilution

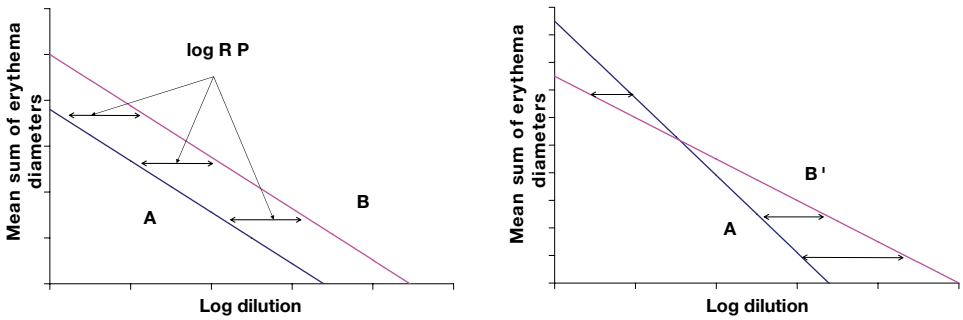

FIGURE 2 Hypothetical parallel line bioassay curves. In panel A, the bioassay curves are parallel, and the difference of log dilutions resulting in the same diameters is constant at all diameters. The log relative potency (log RP) of test sample B compared to reference A is represented by the difference. In panel B, the curves are not parallel, and the differences vary with the strength of the reaction. Thus, the log RP of B′ compared to A cannot be calculated.

of 3^{-17}. For convenience, label the dilution by the $\log_3$ doses: undiluted extract is labeled "0" and the 3^{-17} dose is labeled "17".

Preparation of subject. Skin tests may be placed on the back or the glabrous skin of the volar surface of the arms, avoiding a 1-inch area above and below the antecubital fossa and a 1-inch area above the wrist. For consistency, the back should be used for final titrations.

Injection technique. The volume of solution to be injected is 0.05 ml. Insert the needle of a 27-gauge 0.5 ml syringe at a 30° angle, bevel down. A distinct injection bleb should be observed. Injections in which gross leakage of extract around the needle, an indistinct bleb, or a subcutaneous injection occur should be repeated at a different site.

Measurement of skin tests. THIS IS A TIME-DEPENDENT ASSAY. Exactly 15 minutes following injection, the wheal and erythema margins are outlined using a fine, roller-tip pen with washable ink. In order to make a permanent record of the skin test reaction, transparent surgical tape is placed on the skin over the skin test outline. Lifting of the tape from the skin results in transfer of the outline to the tape. The tape is then placed in a notebook for future reference.

The size of the skin response is obtained by measuring and recording the longest diameter of erythema and the orthogonal erythema diameter measured at one-half the longest erythema diameter (Fig. 3). The sum of the longest and orthogonal erythema diameters (ΣE) (or wheal [ΣW]) constitutes the skin response at that site. Measurements are made from the inner edge of the skin test outlines.

Skin test procedure. The dose-response line for each product is generated using four serial 3-fold dilutions with graded erythema responses that bracket ΣE = 50 mm and includes the endpoint where ΣE = 0 or ΣE ~ ΣW. The skin response (ΣE) should fall within the limits of ≤0 to <125 mm. Each more concentrated dilution should produce a graded erythema response. The four dilutions selected should span a wide range of ΣE (for example from 0–20 mm to 80–125 mm) and bracket ΣE of 50 mm.

Inject the test and reference extracts beginning with dilution #15. The expected change in ΣE going from one dilution to the next dilution is about 20 mm. Therefore, if dilution #15 is negative, proceeding to dilution #12 would not be expected to exceed a ΣE response of 60 mm. Similarly, if dilution #12 is negative, proceed to dilution #9. Do not inject reference extract dilutions more concentrated than #5 unless the extract is known to be of low potency. Apply each dilution in singlicate for each product and reference. Always include an intradermal diluent control test.

Overview of *In Vitro* Assays of Allergen Potency

Although skin testing is an essential component of the allergen standardization program, it is not intended for routine use in the testing of manufactured lots of extracts prior to release. *In vitro* potency assays that accurately predict the *in vivo* activity of extracts have been developed (15). Once an *in vivo* assay has been utilized to assign unitage to a reference extract, then an appropriate surrogate *in vitro* assay can be used to assign units to test extracts from the same sources. These methods can be based on quantitation of the *total protein* content (Hymenoptera venoms), the *specific allergen* content within the allergenic extract (short ragweed and cat), or the *inhibition of the binding of IgE* from pooled allergic sera to reference allergen (grasses, mites) (17). For the Hymenoptera venom allergens, the potency determination is also based on the content of the known principal allergens within the extract, hyaluronidase and phospholipase, which is determined by enzyme activity (see Table 1).

The potency units for short ragweed extracts were originally assigned based on their Amb a 1 content. Subsequent data suggested that 1 unit of Amb a 1 is equivalent to 1 μg of Amb a 1, and 350 Amb a 1 units/ml is equivalent to 100,000 BAU/ml. However, the original unitage has been retained.

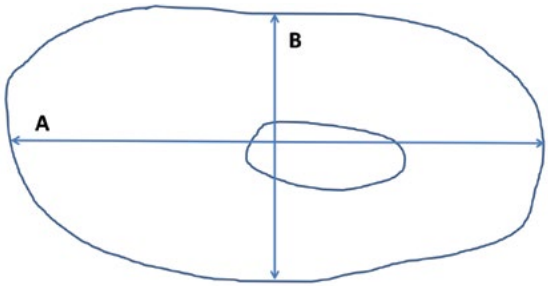

FIGURE 3 Diameters are measured from the inner margins of the penned outline. Longest (A) plus midpoint orthogonal diameters (B) and summed (A + B).

Grass pollen extracts are labeled in BAU/ml, based on ID_{50}EAL testing. In some cases, the assignment of potency units to standardized allergenic extracts in the U.S. has changed as better bioequivalence data have become available (12). Cat extracts were originally standardized based on their Fel d 1 content, with arbitrary unitage (AU/ml) tied to the Fel d 1 determinations. Subsequent ID_{50}EAL testing suggested that the 100,000 AU/ml cat extracts, which contained 10–19.9 Fel d 1 U/ml, should be relabeled as 10,000 BAU/ml (21). In addition, 20% of individuals allergic to cat were found to have antibody to non-Fel d 1 proteins (22), and the identification of a cat albumin band on isoelectric focusing (IEF) gel was added as a requirement for cat pelt extracts. Dust mite extracts were originally standardized (in AU/ml) based on IgE antibody-based inhibition assays. Subsequent ID_{50}EAL testing has indicated that the arbitrary unitage is statistically bioequivalent to BAU/ml (21, 23). Thus, in this case, the original unitage was retained (24).

Tests for Individual Allergens

Individual allergens may be measured and detected by various approaches using monospecific antisera or antibodies. Assay designs using these antisera include the radial immunodiffusion assay (RID), crossed immunoelectrophoresis/crossed radioimmunoelectrophoresis (CIE/CRIE), and enzyme-linked immunosorbent assay (ELISA) variants (direct, two-site, competition). Each of the assays utilizes monospecific antisera or antibodies to detect and quantify the specified allergen. The RID assay is currently applied to two standardized allergenic extracts, short ragweed and cat, in which the immunodominant allergens (Amb a 1 and Fel d 1, respectively) have been identified and defined. Sheep antisera are used for the RID performed at CBER/FDA, but polyclonal and monoclonal antibodies from several species have been used with success for many of these assays. Specifications for the antibodies vary with the assay system. For example, antibodies for the RID must form a discrete precipitin ring; the two antibodies for the two-site ELISA must recognize different epitopes on the allergen molecule; and, in all cases, the epitope(s) recognized must be present on the allergen and reflective of its bioactivity.

Antibodies

Monospecific antisera that recognize the allergen of interest may be purchased or, alternatively, obtained by inoculating an animal with the appropriate amounts of recombinant or purified allergen. Monoclonal antibodies or recombinant antibodies (such as scFv or Fabs) can also be generated for these assays.

RID

This assay is currently used by CBER and most U.S. allergen manufacturers to measure the allergen content of short ragweed and cat allergen extracts. Monospecific antiserum is added to an agar solution which is allowed to solidify. Wells are then cut into the agar and test allergen is placed in the wells. As the specific allergen diffuses out into the agar a precipitin ring forms. The precipitin area delineates the equivalence zone for antigen-antibody binding. The radius of the precipitin ring can then be measured. Since the antibody concentration in the agar is constant, the antigen concentration decreases with increasing distance from the well and is proportional to the log of the concentration of the applied test allergen in comparison to the reference extract (25).

1. Prepare a solution consisting of 1% Noble agar (Difco, Becton, Dickinson and Company, Franklin Lakes, NJ) and 1% sodium azide in water. Heat in a boiling water bath until the solution is clear. Allow the temperature to equilibrate in a 55°C water bath.

2. Once the solution has cooled to 55°C, add 0.2 ml monospecific antiserum to 2 ml of agar solution. Mix thoroughly but gently and pour onto a microscope slide that has been pre-coated with 0.01% Noble agar. Allow agar to solidify at room temperature (RT).

3. After the agar has hardened, place the slide on a sheet of graph paper that contains a template with five evenly spaced dots, approximately 1.5 mm apart. Cut wells into the agar over each dot with a gel cutter; and carefully pipette 8 μl of allergen test solutions into each well. Incubate the slides in a sealed humidified chamber at RT for 72 hours.

4. Fix the slides by soaking them in 10% acetic acid for 2 minutes, followed by a brief rinse in deionized water. The diameters of the precipitin rings can be measured to the nearest 0.1 mm using a calibrating viewer (Transidyne General Corporation, Ann Arbor, MI).

5. After measuring the diameter of the precipitin rings, the reference standard data are graphed on a semilog scale. The average ring size of the unknown can then be used to determine the amount of allergen by interpolation.

Troubleshooting the RID. Prior to performing this assay on an unknown, a dose-response curve should be performed to determine the antiserum concentration at which the ring diameter plateaus. If multiple RID assays are going to be compared, person-to-person variability should be established by direct comparison of an identical test profile. Likely sources of person-to-person variability may include 1) pipetting errors leading to spillover of samples applied to the wells, and 2) measurement errors using the calibrating viewer.

Sandwich ELISA

While CBER has been using the RID assay for over 20 years, individual variability, technical challenges, reagent consumption, and the difficulty in obtaining replacement calibrating viewers have led to recent efforts by CBER (26) to replace the RID with ELISA-based methods of specific-allergen measurement.

Antibody-sandwich ELISAs (sELISAs) are 2- to 5-fold more sensitive than ELISAs in which the antigen is bound directly to the plate. sELISAs use capture antibodies, such as recombinant single-chain variable fragments (scFvs), attached to a plate surface to detect sample antigens. sELISAs can be developed to quantify major allergens in test samples using allergen-specific antibodies.

sELISA Procedure

1. Avian scFv antibodies against Fel d 1 and Amb a 1 were generated and purified as described previously (27). scFv antibodies are stored at −20°C.

2. Prepare a coating solution consisting of 10 μg/ml purified monospecific scFv antibody diluted in 1X phosphate-buffered saline (PBS). Add 50 μl of the diluted coating solution to each well of a 96-well polystyrene plate and incubate overnight at 4°C.

3. Wash the plate with 1X PBS with 0.05% Tween (PBS-T) buffer using a Dynex Ultra Wash Plus (Dynex Technologies, Chantilly, VA) plate washer. Block the plate with 200 μl Pierce StartingBlock blocking buffer (Thermo Scientific, Middletown, VA) per well for 1–2 hours at RT.

4. Prepare a standard antigen dilution series in duplicate with an initial 1:3 dilution followed by serial 1:3 dilutions of

the antigen in PBS-T buffer. Positive displacement pipettes are used for diluting glycerinated allergenic extracts. Wash the plate with PBS-T, add 50 μl of the dilution series and incubate the plates for 1 hour at RT.

5. Prepare a 1:1,000 dilution of the sheep antiserum (containing the antigen-specific antibody) in StartingBlock. Wash the plate with PBS-T, add 50 μl diluted antiserum to each well and incubate for 1 hour at RT.

6. Prepare a 1:1,000 dilution of the rabbit anti-sheep horseradish peroxidase (HRP)-labeled antibody-enzyme conjugate (KPL; SeraCare Life Sciences, Gaithersburg, MD) in StartingBlock. Wash the plate with PBS-T, add 50 μl conjugate to each well, and incubate for 45 minutes at RT.

7. To develop the reaction, prepare a mix (1:1) of the peroxidase solution B and 3,3′,5,5′-tetramethylbenzidine (TMB)-peroxidase substrate from the microwell TMB Substrate System (KPL) and incubate the working substrate solution for 5 minutes at RT. Wash the plate with PBS-T, add 100 μl of substrate to each well and incubate for 5 minutes. Add 100 μl of 1 M phosphoric acid (H_3PO_4) stop solution to each well and measure the absorbance values (Abs_{450}) within 30 minutes using a Dynex MR 5000 plate reader or other microplate reader capable of measuring absorbance at 450 nm.

To analyze the data, the values obtained from the test samples are compared to the standard antigen dilution. Statistical tests, such as the Grubb's test, are used to mathematically remove outlier points from data sets prior to analysis. The four-parameter logistic regression (4PL) and associated statistical analysis is a commonly used analysis method for immunoassays. It provides an unbiased modeling method to determine testing parameters. The four parameters assessed in the analysis are the upper and lower asymptotes, hillslope, and inflection point.

ELISA results rely on the interpolation of data based on a standard curve. Methods for purification of natural allergens have made it possible to develop assays to quantify antigens using major allergens as reference standards. Therefore, natural allergens are useful as a reference reagent of known starting concentration to use to determine the concentration of a particular antigen in test extracts.

CIE/CRIE

In CIE, allergen extract is typically separated by electrophoresis on a 1% agarose gel, and a narrow strip of gel containing the separated antigen is then transferred to a clean glass plate. The remaining area of the plate is then filled with agarose containing poly-specific antisera against the antigen. A second electrophoresis is performed at right angles to the first one (hence "crossed" electrophoresis). Immune complexes form precipitin arcs that can be visualized by Coomassie blue staining (28, 29).

In CRIE, the unstained CIE preparation is incubated in the presence of appropriately diluted patient sera containing specific IgE, which is detected by overnight incubation in ^{125}I-labeled anti-IgE (30).

Enzyme Activity Assays

Hymenoptera venoms contain multiple glycoprotein enzymes, the most important of which are hyaluronidase and phospholipases A1 and A2. Venom allergenic extracts are standardized using enzymatic assays, which estimate hyaluronidase and phospholipase content based on their enzymatic activity. In these assays, an agar solution is prepared with the appropriate enzymatic substrate and test samples are then added to cut wells. As the enzyme present in the sample diffuses into the agar, it digests the substrate, forming clearing zones around the wells. The radius of the clear zones is then measured and calculated as the log of the concentration of the enzyme present in the sample (31).

Tests of Overall Potency

The potency of those standardized allergen extracts for which the immunodominant components have not been identified with certainty may be estimated using assays for IgE-antigen binding. These assays compare the overall IgE-binding properties of test and reference extracts, using pooled allergic sera. Initially, a radioallergosorbent test (RAST) inhibition assay was used for this purpose; CBER adopted the competition ELISA as its alternative standard assay because of its greater precision and convenience. After coating the wells of the polystyrene microtiter plate with the reference allergen and blocking the wells with bovine albumin, a mixture of the extract to be tested and a reference serum pool is added to the wells. The greater the amount of immunoreactive allergen in the mix, the less free IgE antibody will be available from the serum pool to bind to the immobilized allergen on the plate. The concentration of the allergens in the extract is determined by comparison to the reference allergen extract. However, since this assay does not explicitly measure a specific allergen, the allergen concentration is expressed as relative potency (RP), with the reference extract assigned an arbitrary RP of 1.0. Early studies showed an excellent correlation between RP assigned by titration skin testing and RP determined by RAST inhibition (10); subsequent studies showed the competition ELISA to be equivalent as well (32).

Method Summary: Inhibition Immunoassays

The inhibition immunoassays for the determination of overall allergen potency share basic design features:

1. Known allergens are bound to a solid-phase support.
2. The solid support is then exposed to serum containing IgE antibodies from an allergic individual, mixed with dilutions of unknown competing allergen.
3. IgE binds to the allergens on the solid phase forming antigen-allergen complexes. The competing (soluble) unknown allergen reduces the binding of specific IgE to the solid-phase allergen.
4. The unbound IgE is washed away. Labeled anti-IgE is allowed to bind to the antigen-IgE complexes. After a final wash, the label remaining bound to the antigen-allergen complex is related to the quantity of the IgE antibody present in the serum of the patient.
5. The results are then plotted and the 50% binding value determined is proportional to the potency of the extract. In addition to finding the 50% binding value, the slopes of different extracts can be compared; those extracts with similar slopes have similar antigen composition. The relative potency may then be determined as illustrated in Fig. 2, above.

RAST was first described in 1967 (33). In this assay, which is intended to determine the presence of specific IgE in a serum sample, allergen is bound to cyanogen bromide-activated paper disks, followed by incubation with patient serum. After unbound antibody is washed away, ^{125}I-radiolabeled anti-IgE is used to detect the bound IgE. Following the approach outlined above, RAST inhibition is used to establish the overall allergen content of an unknown extract.

Several IgE-antibody autoanalyzers have replaced the original paper disk-based RAST assay. These are the

ImmunoCAP (Thermofisher Scientific/Phadia division), and the Immulite (Siemens Healthcare). The ImmunoCAP system, which was introduced in 1990, has been used by CBER for allergen extract qualification. In place of the paper disk, it employs a sponge cellulose material to which allergen is covalently bound. The secondary antibody is an anti-human IgE-β-galactosidase conjugate. Substrate 4-methylumbelliferyl-β-D-galactoside is cleaved by the β-galactosidase, which generates a detectable fluorogen. The ImmunoCAP system has reported increased analytical sensitivity for some allergen specificities such as the Hymenoptera venoms (34, 35), cat (35–37), *Dermatophagoides pteronyssinus* (35–37), and *Alternaria alternata* (36, 37). Other studies failed to show a significant improvement in analytical sensitivity (38, 39). This assay can be used to measure overall allergen content in a manner similar to the past RAST assay.

Overview of ELISA Inhibition, or Competition ELISA

The competition ELISA is the one assay used by CBER and most U.S. allergen manufacturers to determine the relative potency of standardized grass pollen and dust mite allergenic extracts. In this assay, serial dilutions of an extract to be tested are placed in their respective wells that have been precoated with a known amount of reference extract. Optimal concentrations of the reference extract and the detecting antibody conjugate must be determined by checkerboard titration for each new set of reagents.

The detection antibody is a critical component of the assay. It is essential that the antibodies used reflect the broadest range of allergens considered relevant to the overall allergenicity of the allergenic extract being tested and should be evaluated by Western blot or a comparable technique. IgE is biologically relevant for allergic disease, but each batch of IgE-containing sera is likely to vary in the specificity profile of the IgE. Since most atopic donors will be multi-allergic, their sera may contain IgE molecules that recognize irrelevant allergens as well. Such extraneous IgE will only interfere in the assay to the degree that the coating allergen contains cognate irrelevant allergens. Human sera containing IgE antibodies should be collected from as many allergic individuals as possible, with a minimum of six, but preferably 10 to 20 (40). Other polyspecific antisera can also be utilized for these assays and are discussed above.

ELISA inhibition procedure (41, 42).

1. Coat the microplate wells with 100 μl/well of the reference extract and allow to bind at 4°C overnight. Wash the plates in 0.05% Tween in PBS (PBS-T).
2. Block at RT for 1 hour 30 minutes in blocking buffer (1% BSA in PBS-T), and wash in PBS-T.
3. Into duplicate wells, pipette 1:3 serial dilutions of the reference extract. Into the remaining wells, pipette 1:3 serial dilutions of the test extracts in duplicate.
4. Immediately add 50 μl of the detecting antibody at the appropriate concentration.
5. Incubate overnight at 4°C.
6. Wash the plate with PBS-T, develop, and read as appropriate.
7. The results are plotted with the values of the optical density along the *y*-axis and the log of the dilution factor along the *x*-axis. The 50%-binding value that is determined is proportional to the potency of the extract; the RP is estimated by comparing the *x*-intercepts of the test and reference extracts. The slopes of the different extracts can also be compared; those extracts with identical slopes as determined by the *t*-test are presumed to have similar antigen composition.

Basophil Activation

Basophil histamine release is an *in vitro* surrogate for skin testing. As with other assays based upon interactions between allergen and specific IgE, the release of histamine from sensitized human basophils may be used to measure the allergen content of an unknown solution. Histamine release assays have been performed on heparinized whole blood (43, 44), crude leukocyte preparations (45), purified basophils (46–48), cell lines (49, 50), and using RBL SX-38, a rat basophil cell line that expresses human FcεR1 (51). The drawbacks of this assay are that histamine release assays from whole or fractionated blood require large amounts of recently drawn blood, and specialized cell lines are not readily available. In addition, basophils from 20% or more of skin test-positive patients do not release histamine *in vitro* (52), even in the presence of cross-linking anti-IgE. However, these same individuals' serum IgE may still be used in histamine release experiments by passively sensitizing basophils from other donors with the heterologous IgE (53). In all variants of this assay, released histamine may be quantified by radioimmunoassay, fluorimetry (54), or measurement of radioactivity after pretreatment with tritiated 5-hydroxytryptamine. Although this technique and its variants have been used to assess allergen potency (55–57), it does not appear to have any advantage over other assays that depend upon specific allergen-antibody interactions (58). Basophil histamine release assays are discussed further in chapter 83 of this volume (Schroeder et al.).

Flow Cytometry

In the past 20 years, the discovery of basophil activation markers CD63, CD45, CD69, and CD203c have led to a flow cytometric approach that assesses the *in vitro* activation of basophils (59). Most commonly, CD63 and CD203c are used (60). CD63 is located on the membrane of intracellular secretory granules that fuse with the plasma membrane upon stimulation through high-affinity IgE receptor FcεRI. CD203c is weakly expressed on the plasma membrane of resting basophils, and is rapidly increased upon stimulation through FcεRI. While both of these surface antigens measure basophil activation, they may represent the end point of different molecular pathways, and the best choice appears to be dependent on the context of activation (59).

Identity Testing

The identity of an allergen extract may be verified by visualizing the separated allergen proteins based on their size and isoelectric points (1). The IEF assay is an important safety test in the lot release of grass pollen and cat extracts. The patterns produced by the crude allergen mixtures are reproducible enough to consistently indicate the presence of known allergens, to identify possible contaminants present in the extracts, and to check lot-to-lot variation (61). In addition, IEF is used to verify the presence of cat albumin in cat pelt extracts.

Method Summary: Identity Testing

IEF

Polyacrylamide gels IEF pH 3-10, Anode (Upper) and Cathode (Lower) Buffers, IEF pH 3-10 Sample Buffer,

cellophane-preserving sheets, and the electrophoresis unit are available from Invitrogen by ThermoFisher (Life Technologies Corporation, Carlsbad, CA).

1. Prepare Anode and Cathode buffers. Refrigerate for at least 6 hours.
2. Remove IEF pH 3-10 polyacrylamide gel from pouch and rinse with deionized water. Rinse the electrophoresis unit with deionized water and assemble the apparatus.
3. Mix equal volumes of extract and Sample Buffer and load into the appropriate wells on the gel. (Note that for cat pelt 0.6–0.8 Fel d 1 units must be used, and more may be needed for cat hair extracts.)
4. For each sample, a reference extract and an IEF pH 3-10 marker (Serva Electrophoresis GmbH) should also be run on the gel. For best results, the gel should be run initially for 60 minutes at 100 volts constant, then 60 minutes at 200 volts constant, and finally at 500 volts constant for 30 minutes. The expected current is 5 mA (start) and 6 mA (end). IEF is typically performed by increasing the voltage gradually and maintaining the final focusing voltage for 30 minutes. During IEF, proteins migrate in an electric field until a stable pH gradient is formed and proteins reach their isoelectric point (pI). At that point, a high finishing voltage is applied to focus the proteins into narrow zones. High voltage cannot be applied during the initial stages of IEF due to excessive heat generated by the movement of carrier ampholytes.
5. After the gel has been run, the gel is immediately fixed for 30 minutes in 12% trichloroacetic acid, washed with deionized water, and stained for 1 to 3 hours in SimplyBlue SafeStain (Invitrogen, Carlsbad, CA). Destain over a period of 16 to 24 hours with several exchanges of deionized water until the background is clear.
6. An image of the gel may be captured using a G-Box Gel Imaging and Analysis System (Syngene, Frederick, MD) and exported as a joint photographic experts group (JPEG) file or a tagged-image file (TIF). Alternatively, the gel may be photographed with high-contrast film and a yellow filter. To preserve the gel, incubate it in Gel-Dry gel drying solution (Novex ThermoFisher Scientific, Carlsbad, CA) for 10 to 20 minutes at room temperature. Place the gel on a gel drying frame (Novex ThermoFisher Scientific) between cellophane preserving sheets previously soaked in the Gel-Dry drying solution for 10 to 20 seconds. Allow the gel and cellophane to dry for 24 to 48 hours and store away from bright light.
7. The pI of the sample proteins can be determined by interpolation on a calibration curve utilizing the IEF marker that was resolved along with the sample.

This article is an informal communication and represents the best judgment of the authors. These comments do not bind or obligate the FDA.

The authors acknowledge the assistance of Cherry Geronimo, Sandra Menzies, and Susan Huynh in the development and improvement of the current generation of LIB potency and identity assays.

REFERENCES

1. **Yunginger JW.** 1983. Allergenic extracts: characterization, standardization, and prospects for the future. *Pediatr Clin North Am* **30:**795–805. PubMed
2. **Food and Drug Administration.** 1985. Biological Products; Allergenic Extracts; Implementation of Efficacy Review. *Fed Regist* **50:**3082.
3. **Slater JE, Menzies SL, Bridgewater J, Mosquera A, Zinderman CE, Ou AC, Maloney D, Cook CM, Rabin RL.** 2012. The US Food and Drug Administration review of the safety and effectiveness of nonstandardized allergen extracts. *J Allergy Clin Immunol* **129:**1014–1019. PubMed
4. **Baer H, Godfrey H, Maloney CJ, Norman PS, Lichtenstein LM.** 1970. The potency and antigen E content of commercially prepared ragweed extracts. *J Allergy* **45:**347–354. PubMed
5. **Baer H, Maloney CJ, Norman PS, Marsh DG.** 1974. The potency and Group I antigen content of six commercially prepared grass pollen extracts. *J Allergy Clin Immunol* **54:**157–164. PubMed
6. **Slater JE, Gam AA, Solanki MD, Burk SH, May FM, Pastor RW.** 1999. Statistical considerations in the establishment of release criteria for allergen vaccines in the USA. *Arb Paul Ehrlich Inst Bundesamt Sera Impfstoffe Frankf A M* **93:**47–55, discussion 56. PubMed
7. **Patterson ML, Slater JE.** 2002. Characterization and comparison of commercially available German and American cockroach allergen extracts. *Clin Exp Allergy* **32:**721–727. PubMed
8. **Yunginger JW.** 1988. Allergens: recent advances. *Pediatr Clin North Am* **35:**981–993. PubMed
9. **Turkeltaub PC.** 1988. *In-vivo* standardization, p 388–401. *In* Middleton EJ, Reed CE, Ellis EF (ed), *Allergy, Principles and Practice*, 3rd ed. CV Mosby Co, St. Louis, MO.
10. **Turkeltaub PC.** 1989. Biological standardization of allergenic extracts. *Allergol Immunopathol (Madr)* **17:**53–65. PubMed
11. **Turkeltaub PC.** 1997. Biological standardization. *Arb Paul Ehrlich Inst Bundesamt Sera Impfstoffe Frankf A M* **91:**145–156. PubMed
12. **Turkeltaub PC.** 1999. Allergen vaccine unitage based on biological standardization: clinical significance p 321–340. *In* Lockey R, Bukantz SC (ed), *Allergens and Allergen Immunotherapy*, 2nd ed. Marcel Dekker, Inc, New York, NY.
13. **Food and Drug Administration.** 1994. Methods of the allergenic products testing laboratory (Docket 94N-0012). *Fed Regist* **59:**60362–60363.
14. **Turkeltaub PC, Rastogi SC, Baer H, Anderson MC, Norman PS.** 1982. A standardized quantitative skin-test assay of allergen potency and stability: studies on the allergen dose-response curve and effect of wheal, erythema, and patient selection on assay results. *J Allergy Clin Immunol* **70:**343–352. PubMed
15. **Turkeltaub PC.** 1986. *In vivo* methods of standardization. *Clin Rev Allergy* **4:**371–387. PubMed
16. **Rabin RL, Slater JE, Lachenbruch P, Pastor RW.** 2003. Sample size considerations for establishing clinical bioequivalence of allergen formulations. *Arb Paul Ehrlich Inst Bundesamt Sera Impfstoffe Frankf A M* **94:**24–33. PubMed
17. **Schuirmann DJ.** 1987. A comparison of the two one-sided tests procedure and the power approach for assessing the equivalence of average bioavailability. *J Pharmacokinet Biopharm* **15:**657–680. PubMed
18. **Committee for Medicinal Products for Human Use.** 2008. Guideline on allergen products: production and quality issues, November 2008. European Medicines Agency. http://www.ema.europa.eu/docs/en_GB/document_library/Scientific_guideline/2009/09/WC500003333.pdf
19. **Malling HJ.** 1997. Skin prick testing in biological standardization of allergenic products. *Arb Paul Ehrlich Inst Bundesamt Sera Impfstoffe Frankf A M* **91:**157–163. PubMed
20. **Slater JE, James R, Pongracic JA, Liu AH, Sarpong S, Sampson HA, Satinover SM, Woodfolk JA, Mitchell HE, Gergen PJ, Eggleston PA.** 2007. Biological potency of

German cockroach allergen extracts determined in an inner city population. *Clin Exp Allergy* **37:**1033–1039. PubMed
21. **Matthews J, Turkeltaub PC.** 1992. The assignment of biological allergy units (AU) to standardized cat extracts. *J Allergy Clin Immunol* **89:**151.
22. **Turkeltaub PC, Matthews J.** 1992. Determination of compositional differences (CD) among standardized cat extracts by in vivo methods. *J Allergy Clin Immunol* **89:**151.
23. **Turkeltaub PC, Anderson MC, Baer H.** 1987. Relative Potency (RP), compositional differences (CD), and assignment of allergy units (AU) to mite extracts (Dp and Df) assayed by parallel line skin test (PLST). *J Allergy Clin Immunol* **79:**235.
24. **Turkeltaub PC.** 1994. Use of skin testing for evaluation of potency, composition, and stability of allergenic products. *Arb Paul Ehrlich Inst Bundesamt Sera Impfstoffe Frankf A M* **87:**79–87, 114–117. PubMed
25. Laboratory of Immunobiochemistry CBER FDA. Standard Operating Procedures - 5 and 6. 1993 Nov.
26. **Rabin RL, Allergenic Products Advisory Committee.** 2011. Meeting Materials, Allergenic Products Advisory Committee. http://www.fda.gov/AdvisoryCommittees/CommitteesMeetingMaterials/BloodVaccinesandOtherBiologics/AllergenicProductsAdvisoryCommittee/ucm247212.htm.
27. **deVore NC, Huynh S, Dobrovolskaia EN, Slater JE.** 2010. Multiplex microbead measurements for the characterization of cat and ragweed allergen extracts. *Ann Allergy Asthma Immunol* **105:**351–358. PubMed
28. **Weeke B.** 1973. Crossed immunoelectrophoresis. *Scand J Immunol Suppl* **1:**47–56. PubMed
29. **Weeke B.** 1973. A manual of quantitative immunoelectrophoresis. Methods and applications. 1. General remarks on principles, equipment, reagents and procedures. *Scand J Immunol Suppl* **1:**15–35. PubMed
30. **Løwenstein H.** 1978. Quantitative immunoelectrophoretic methods as a tool for the analysis and isolation of allergens. *Prog Allergy* **25:**1–62. PubMed
31. Laboratory of Immunobiochemistry CBER FDA. Standard Operating Procedures - 1 and 2. 1995 Jan.
32. **Lin Y, Miller CA.** 1997. Standardization of allergenic extracts: An update on CBER's standardization program. *Arb Paul Ehrlich Inst Bundesamt Sera Impfstoffe Frankf A M* **91:**127–130. PubMed
33. **Wide L, Bennich H, Johansson SG.** 1967. Diagnosis of allergy by an *in-vitro* test for allergen antibodies. *Lancet* **2:**1105–1107. PubMed
34. **Jeep S, Kirchhof E, O'Connor A, Kunkel G.** 1992. Comparison of the Phadebas RAST with the Pharmacia CAP system for insect venom. *Allergy* **47:**212–217. PubMed
35. **Leimgruber A, Lantin JP, Frei PC.** 1993. Comparison of two *in vitro* assays, RAST and CAP, when applied to the diagnosis of anaphylactic reactions to honeybee or yellow jacket venoms. Correlation with history and skin tests. *Allergy* **48:**415–420. PubMed
36. **Bousquet J, Chanez P, Chanal I, Michel FB.** 1990. Comparison between RAST and Pharmacia CAP system: A new automated specific IgE assay. *J Allergy Clin Immunol* **85:**1039–1043. PubMed
37. **Ewan PW, Coote D.** 1990. Evaluation of a capsulated hydrophilic carrier polymer (the ImmunoCAP) for measurement of specific IgE antibodies. *Allergy* **45:**22–29. PubMed
38. **Nalebuff DJ, Fadal RG, May BC.** 1993. A comparative study of the diagnostic characteristics of the modified RAST and Pharmacia CAP System. *Otolaryngol Head Neck Surg* **109:**601–605. PubMed
39. **Pastorello EA, Incorvaia C, Pravettoni V, Marelli A, Farioli L, Ghezzi M.** 1992. Clinical evaluation of CAP System and RAST in the measurement of specific IgE. *Allergy* **47:**463–466. PubMed
40. Laboratory of Immunobiochemistry CBER FDA. Standard Operating Procedures - 13. 1998 Oct.
41. Laboratory of Immunobiochemistry CBER FDA. Standard Operating Procedures - 7. 1998 Nov.
42. **Slater JE, Gam AA, Solanki MD, Burk SH, May FM, Pastor RW.** 1999. Statistical considerations in the establishment of release criteria for allergen vaccines in the USA. *Arb Paul Ehrlich Inst Bundesamt Sera Impfstoffe Frankf A M* **93:**47–55, discussion 56. PubMed
43. **Katz G, Cohen S.** 1941. Experimental evidence for histamine release in allergy. *JAMA* **117:**1782–1783.
44. **Noah JW, Brand A.** 1954. Release of histamine in the blood of ragweed-sensitive individuals. *J Allergy* **25:**210–214. PubMed
45. **Lichtenstein LM, Osler AG.** 1964. Studies on the mechanisms of hypersensitivity phenomena. IX. Histamine release from human leukocytes by ragweed pollen antigen. *J Exp Med* **120:**507–530. PubMed
46. **Gibbs BF, Noll T, Falcone FH, Haas H, Vollmer E, Vollrath I, Wolff HH, Amon U.** 1997. A three-step procedure for the purification of human basophils from buffy coat blood. *Inflamm Res* **46:**137–142. PubMed
47. **Kepley C, Craig S, Schwartz L.** 1994. Purification of human basophils by density and size alone. *J Immunol Methods* **175:**1–9. PubMed
48. **Tanimoto Y, Takahashi K, Takata M, Kawata N, Kimura I.** 1992. Purification of human blood basophils using negative selection by flow cytometry. *Clin Exp Allergy* **22:**1015–1019. PubMed
49. **Barsumian EL, Isersky C, Petrino MG, Siraganian RP.** 1981. IgE-induced histamine release from rat basophilic leukemia cell lines: isolation of releasing and nonreleasing clones. *Eur J Immunol* **11:**317–323. PubMed
50. **Lowe J, Jardieu P, VanGorp K, Fei DT.** 1995. Allergen-induced histamine release in rat mast cells transfected with the alpha subunits of Fc epsilon RI. *J Immunol Methods* **184:**113–122. PubMed
51. **Dibbern DA Jr, Palmer GW, Williams PB, Bock SA, Dreskin SC.** 2003. RBL cells expressing human Fc epsilon RI are a sensitive tool for exploring functional IgE-allergen interactions: studies with sera from peanut-sensitive patients. *J Immunol Methods* **274:**37–45. PubMed
52. **Asero R, Lorini M, Chong SU, Zuberbier T, Tedeschi A.** 2004. Assessment of histamine-releasing activity of sera from patients with chronic urticaria showing positive autologous skin test on human basophils and mast cells. *Clin Exp Allergy* **34:**1111–1114. PubMed
53. **Levy DA, Osler AG.** 1966. Studies on the mechanisms of hypersensitivity phenomena. XIV. Passive sensitization *in vitro* of human leukocytes to ragweed pollen antigen. *J Immunol* **97:**203–212. PubMed
54. **Siraganian RP, Brodsky MJ.** 1976. Automated histamine analysis for *in vitro* allergy testing. I. A method utilizing allergen-induced histamine release from whole blood. *J Allergy Clin Immunol* **57:**525–540. PubMed
55. **Hoffmann A, Vogel L, Scheurer S, Vieths S, Haustein D.** 1997. Potency determination of allergenic extracts using mediator release of rat basophil leukemia cells. *Arb Paul Ehrlich Inst Bundesamt Sera Impfstoffe Frankf A M* **91:**203–208. PubMed
56. **Kordash TR, Freshwater LL, Amend MJ.** 1995. Standardization of allergenic extracts by basophil histamine release. *Ann Allergy Asthma Immunol* **75:**101–106. PubMed
57. **Poulsen LK, Pedersen MH, Platzer M, Madsen N, Sten E, Bindslev-Jensen C, Dircks CG, Skov PS.** 2003. Immunochemical and biological quantification of peanut extract. *Arb Paul Ehrlich Inst Bundesamt Sera Impfstoffe Frankf A M* **94:**97–105, discussion 106. PubMed
58. **Chen X, Wang Q, El-Mezayen R, Zhuang Y, Dreskin SC.** 2013. Ara h 2 and Ara h 6 have similar allergenic activity

and are substantially redundant. *Int Arch Allergy Immunol* **160:**251–258. PubMed

59. **McGowan EC, Saini S.** 2013. Update on the performance and application of basophil activation tests. *Curr Allergy Asthma Rep* **13:**101–109. PubMed
60. **Ebo DG, Hagendorens MM, Bridts CH, Schuerwegh AJ, De Clerck LS, Stevens WJ.** 2004. *In vitro* allergy diagnosis: should we follow the flow? *Clin Exp Allergy* **34:**332–339. PubMed
61. **Yunginger JW, Adolphson CR.** 1992. Standardization of allergens, p 678–684. *In* Rose NR, de Macario EC, Fahey JL, Friedman H, Penn GM (ed), *Manual of Clinical Laboratory Immunology,* 4th ed. American Society for Microbiology, Washington, DC.

Immunological Methods in the Diagnostic Allergy Clinical and Research Laboratory

ROBERT G. HAMILTON

82

Nearly 50 years have passed since IgE was identified as the reagin or serum antibody that sensitizes skin mast cells and circulating basophils and mediates immediate-type hypersensitivity reactions in humans (1, 2). Since IgE's identification, the clinical immunology laboratory has provided the clinician with analytical measurements that aid in the diagnosis, management, and research of the natural history and epidemiology of IgE-mediated diseases. Total and allergen-specific IgE antibody are the primary analytes measured clinically to support the diagnosis of human allergic disease. Antigen-specific IgG antibodies are measured as a research analyte to identify chronic allergen exposure and to monitor potential blocking antibody activity following immunotherapy.

The goal of this chapter is to overview the status of immunological methods that are used in the quantification of total and allergen-specific IgE and research investigation of IgG antibodies. Other analytes that will not be discussed but that are occasionally measured in allergy and asthma patients include mast cell tryptase (see chapter 85 of this volume), cotenine (a metabolite of nicotine and indicator of passive smoke exposure), and the levels of indoor indicator aeroallergens from dust mites, house pets (cats and dogs), rodents (mice and rats), insects (cockroaches), and molds in surface dust, which help target avoidance therapy.

ANALYTES RELEVANT TO THE EVALUATION OF PATIENTS FOR ALLERGIC DISEASE

As discussed in chapters 83 and 84, immediate-type hypersensitivity manifests as a spectrum of symptoms that involve respiratory responses (asthma or rhinitis), ocular symptoms (conjunctivitis), skin reactions (urticaria, dermatitis), gastrointestinal symptoms, and/or life-threatening anaphylactic shock. These symptoms are produced as a result of the re-exposure of a previously sensitized (IgE antibody positive) individual to one or more sensitizing allergen(s). These allergens are ubiquitous proteins that are abundant in nature. They are released from pollens of grasses, weeds and trees, or antigenic proteins released from mites, rodents, domestic animals, insects, and mold spores and present in some drugs and generally well-tolerated foods. Allergenic proteins tend to form aggregates and vary in the symptoms that they induce based on their degree of stability to processing (heat) and enzymatic digestion. The more stable the allergenic molecule, the more likely it is able to evade destruction by the body's defenses (mucosal enzymatic digestion, gastrointestional pH denaturation) and induce serious allergic reactions.

IgE mediates allergic reactions by binding onto high-affinity epsilon Fc receptors on mast cells and basophils and initiating the release of vasoactive mediators following allergen binding and cell surface IgE antibody cross-linking (see chapter 83 of this volume) (2). Total serum IgE levels are used clinically by some immunologists as a diagnostic analyte because a moderately elevated total serum IgE reinforces the clinical diagnosis of atopic disorders, including allergic rhinitis, allergic asthma, and atopic dermatitis (3, 4). Moreover, high IgE levels are commonly observed in parasite infections (see chapter 54 of this volume) and are necessary in the definitive diagnosis of bronchopulmonary aspergillosis, Wiskott-Aldrich syndrome, and hyper-gammaglobulinemia E syndrome (Table 1). Serial total serum IgE levels can confirm an expected seasonal boost in serum IgE antibodies that is commonly seen after environmental exposure to the allergen to which the patient has become sensitized. However, the wide overlap in total serum IgE levels among atopic and non-atopic individuals and the age dependency diminishes its general diagnostic utility (3, 4). Thus, the clinician must refrain from discounting allergy when total IgE levels are low or from automatically inferring an allergic etiology when the total serum IgE level is high. Since the therapeutic Omalizumab (anti-IgE) was licensed in 2003 for the treatment of allergic asthma and, most recently, for idiopathic urticaria, total serum IgE measurements are needed to ensure that the patient is a candidate for anti-IgE therapy and to select the proper anti-IgE dose, which is based on the pre-treatment total serum IgE level (5). The required total serum IgE range for Omalizumab treatment is 30 and 700 kIU/liter (where 1 IU = 2.4 ng of IgE).

Allergen-specific IgE antibody has remained the primary analyte that is used to support the clinical history based diagnosis of IgE-mediated allergic disease (Table 1). IgE antibody can be detected *in vivo* using a puncture or an intradermal skin test that provokes IgE-mediated skin mast cell release and elicits a visible wheal and erythema, if positive, larger than the skin reaction produced by a saline control. Because skin testing is extensively discussed in chapter 81 in this volume, it will not be discussed further here. While skin testing is a biologically relevant response

doi:10.1128/9781555818722.ch82

TABLE 1 Clinical conditions in which serological determination of IgE and IgG antibodies may be useful in the differential diagnosis

Clinical condition	Total serum IgE	Allergen-specific IgE	Allergen-specific IgG
Atopic disorders: allergic rhinitis, allergic asthma, atopic dermatitis	Moderately elevated levels positively reinforce clinical diagnosis; however, low or normal IgE level is not incompatible with diagnosis	Positive allergen-specific IgE antibody level supports the diagnosis of IgE-mediated atopic disorders	In the absence of allergen immunotherapy, the allergen-specific IgG antibody can be low or undetectable
Intrinsic (non-allergic) asthma	Normal or low levels suggest that IgE mechanisms play only a minor role in the pathogenesis of asthma	Negative IgE antibody levels support the diagnosis of intrinsic asthma	Not useful in the definitive diagnosis of intrinsic asthma
Allergic bronchopulmonary Aspergillosis (ABPA)	Normal serum IgE levels virtually exclude diagnosis	Positive *Aspergillus*-specific IgE antibody is required for the definitive diagnosis of ABPA	Precipitating IgG antibodies are required for the definitive diagnosis of ABPA
Wiskott-Aldrich syndrome	Elevated levels are commonly found in patients who exhibit eczema		
Hypergammaglobulinemia E syndrome (elevated IgE, increased susceptibility to infection and dermatitis)	Very high serum IgE levels are necessary for the definitive diagnosis of hyper-IgE syndrome		
Parasitism	Many parasitic infections produce extreme elevations in serum IgE; a very high IgE in the absence of other explanations strongly suggests the possibility of parasitism	The presence of parasite-specific IgE antibodies confirms the diagnosis of parasitism	Parasite-specific IgG antibodies confirm a present or recent parasite infection
Eosinophilia	A normal IgE level makes the diagnosis of parasitism less likely as a cause of eosinophilia; eosinophilia with normal serum IgE is a common feature of non-allergic asthma		
Allergen immunotherapy	Same as atopic disorders (above)	Specific IgE antibodies are not helpful in monitoring patients on immunotherapy and assessing its clinical efficacy	Used in *Hymenoptera* venom immunotherapy to confirm adequate immunotherapy dosages and assess relative risk for reactions on resting

in the patient's skin, some generalized skin conditions such as eczema, dermagraphism, psoriasis, and urticaria make skin testing problematic. Moreover, skin testing of children younger than 10 can be difficult. There are also occasions when skin reactivity has been suppressed by prolonged use of antihistamines and other medications that cannot be stopped prior to skin testing. In all these cases or when a characterized allergen extract is not available for *in vivo* use, *in vitro* analysis of a serum specimen for allergen-specific IgE antibody may be preferred over skin testing in the diagnostic work-up of a suspected allergic patient (6).

The immunological methods used to quantify IgE antibody levels in serum have reached an elevated state in which highly quality-controlled reagents and computer-driven autoanalyzers are widely employed for clinical testing (7). There are, however, several recent trends in IgE antibody serology analyses. First, there is an increasing use of allergenic components to detect IgE antibodies that allow identification of cross-reactivity, especially among pollen and food allergens (8). This has had a particular impact on the evaluation of patients with suspected food allergies (see chapter 84). Microarrays have been introduced into the research laboratory that semi-quantitatively detect IgE antibody in more than 100 individual allergenic components from more than 70 allergen specificities. For select food allergen specificities such as peanut, the presence and level of IgE antibody specific for signature allergic components may aid in defining the relative risk of a patient experiencing a

mild versus severe systemic reaction. As discussed earlier, the presence of IgE antibody in serum is known to be a "risk factor" for, but not a guarantee of, allergic disease manifestation (9). The use of quantitative IgE antibody measurements has expanded the use of select food-specific IgE antibody levels in making predictions about the need for a food challenge to verify an allergic versus tolerant state (10).

One area in which the laboratory has limited useful analytes involves biomarkers for identifying successful immunotherapy treatment of allergic patients that leads to tolerance. Antigen-specific IgG and IgG4 antibody levels in serum have been historically considered markers of intentional or inadvertent chronic exposure in an individual exposed to potent antigens (11). They increase following repetitive antigenic exposure in parallel with a concomitant decrease in allergen-specific IgE antibody-facilitated binding to B cells (12, 13). IgG antibodies are known to bind circulating antigen and thus block allergen from binding cell-bound IgE antibody. Unfortunately, changing levels of allergen-specific IgG and IgG4 antibodies as well as the degree of inhibition of CD23-dependent facilitated IgE antibody binding to B-cells have each failed to correlate with improved clinical symptoms following immunotherapy (14). Thus, allergen-specific-IgG and IgG4 antibody and the degree of inhibition of facilitated IgE antibody binding to B cells are not routinely assayed clinically because of the lack of a clinical indication for these measurements (Table 1).

TOTAL SERUM IgE

Of the assays historically used to measure the total level of IgE in human serum, the two-site (sandwich) immunometric (labeled antibody) assays and nephelometric assays have emerged as the principal methods of choice for clinical immunology laboratories. Of these assays, the two-site immunometric assay has become the most widely used clinical and research assay for the quantification of total serum IgE (6). The first reported noncompetitive solid-phase two-site immunometric assay used polyclonal anti-human IgE covalently bound to a solid phase (paper disks) to bind IgE from unknown and calibrated reference and control sera (15). Following a buffer wash, radioiodinated anti-IgE detected bound IgE. The amount of radiolabeled anti-IgE bound was directly related to the IgE content in the original serum. The assay displayed excellent sensitivity (as low as 0.2 ng of IgE per ml) and precision (coefficients of variation [CV] $\leq$5%), and it was minimally affected by nonspecific serum factors. Clinical laboratories currently perform one of several U.S. FDA-cleared assays for measuring total serum IgE, and all display exceptional analytical sensitivity and reproducibility, as discussed elsewhere (6, 16).

Occasionally, researchers need to measure total serum IgE using a less expensive and more flexible assay design that can accommodate unusual specimens and varying dilutions. A research monoclonal antibody-based noncompetitive solid-phase two-site immunoenzymetric assay (IEMA) is one option for investigation of total IgE levels in serum. In this assay, monoclonal anti-human IgE that has been adsorbed onto plastic wells of a microtiter plate binds IgE from the specimen, and a second monoclonal anti-human IgE clone that is labeled detects bound IgE (6). More specifically, use of murine IgM monoclonal anti-human IgE Fc capture antibody (clone HP6061) and biotinylated murine IgG monoclonal anti-human IgE Fc detection antibody (clone HP6029; EMD-Millipore, La Jolla, CA) optimizes both assay sensitivity and specificity. The assay performs best with serum, but IgE levels can also be measured in plasma, tear fluid, bronchial alveolar lavage fluid, saliva, nasal washings, and peripheral blood cell culture supernatants. Appendix A describes the generic microtiter plate-based IEMA protocol in more detail.

The World Health Organization international reference preparation for human IgE 75/502 is nearly depleted, and its replacement 11/234 is currently being validated (17). Secondary total IgE standards can be cross-calibrated against these primary standards and used in routine clinical assays. The assay regularly achieves a working range from 1 to 200 IU/ml. The analytical sensitivity of 0.5 IU/ml (1.2 μg/liter) can be achieved, and agreement among replicates and between assays is usually excellent (CV $<$ 5% and CV $<$ 15%, respectively). Parallelism is also maintained with interdilutional CVs of $<$15%. The total serum IgE IEMA can be quality controlled by inclusion of two or three well-studied sera within each assay. The quality control sera should, minimally, have a low ($<$10 IU/ml), moderate (100 to 250 IU/ml), and high level of IgE ($>$1,000 IU/ml).

When interpreting the total serum IgE levels, non-atopic percentiles are known to be age-dependent. The level of IgE in cord serum is usually less than 2 IU/ml, since IgE does not cross the placental barrier in significant amounts. Mean serum IgE levels progressively increase in healthy children until 10 to 15 years of age (3, 4). Atopic infants have an earlier and steeper rise in serum IgE levels during the early years of life compared with non-atopic controls. An age-dependent decline in total serum IgE typically occurs from the second to eighth decade of life. Individuals with total serum IgE levels above the upper 95% confidence limit often have atopic disorders such as allergic rhinitis, extrinsic or allergic asthma, and atopic dermatitis (Table 1).

ALLERGEN-SPECIFIC IgE ANTIBODY

Historically, the first-generation assay for allergen-specific IgE antibody in human serum was the radioallergosorbent test (RAST) (15). This assay employed allergen extracts immobilized on paper disks to bind specific antibody of any immunoglobulin class from serum. The solid phase was then washed with buffer and radiolabeled anti-human IgE antibody detected bound IgE. The quantity of bound radioactivity directly correlated with the quantity of specific IgE antibody in the original serum. IgE antibody results were compared with a calibrated standard reference serum, and insolubilized allergen and radiolabeled anti-IgE antibody were used in molar excess.

Over the past 50 years or so, there have been major improvements in the design and performance of allergen-specific IgE assays. Commercially available allergen-specific IgE antibody autoanalyzers are now widely used in hospital and private clinical immunology laboratories. An overview of these commercial IgE antibody assays is presented elsewhere (6, 16). These assays have in common an allergen-containing reagent (typically a solid-phase allergosorbent); a panel of reference, control, and test human sera; and a labeled anti-human IgE reagent. As of this writing, the Thermofisher Scientific/Phadia ImmunoCAP system and the Siemens Healthcare Corporation Immulite 2000 have achieved the widest use throughout the world. Tight precision around the positive/negative threshold and a more rapid, robust chemistry have been achieved with computer-controlled automation. A third assay system called HyTech-288 by Hycor Biomedical is being replaced by a new instrument that is currently in development. With clinical use comes the need to analyze quality-control sera with IgE antibody levels across the measured dose-response curve range, from 1 to 100 kUa/

liter. As many as 15 quality-control sera containing different specificities and levels of IgE antibody are randomly sprinkled throughout the assay run to investigate quality. Daily monitoring of results from these positive control sera in the form of Levey-Jennings plots verifies that the instrument is performing accurately (16).

In the United States, the FDA regulates the sale of clinically used *in vitro* diagnostic products under regulation 21 CFR 809. This includes allergen-specific IgE antibody assay reagents that are intended for human use. Some allergen extracts that have been insolubilized on allergosorbents for use in allergen-specific IgE assays have not yet been cleared by the FDA. These are currently analyzed by clinical laboratories as research reagents under an "analyte-specific reagent" classification. These allergosorbents can be used by laboratories that are qualified to perform high-complexity testing; however, a disclaimer must be stated on the report indicating that a measurement was performed with an "analyte-specific reagent." The FDA now requires that manufacturers phase out ASRs from their reagent inventory, so all allergosorbents used in the future will be FDA-cleared.

Among the newest of the IgE antibody commercial assays is the ImmunoSorbent Allergen Chip or ISAC from Thermofisher Scientific/Phadia that uses a glass slide on which more than 100 purified allergenic components from more than 70 allergen specificities are spotted in triplicate in four separate matrices (18). Serum (35 μl) is incubated on the chip for 2 hours. Following a buffer wash, IgE (IgG or IgG4) antibodies are detected using a fluorescent-labeled anti-human IgE (IgG or IgG4) reagent. This is a remarkably sophisticated technology that involves inserting the completed chip into a fluoresecent scanner and obtaining antibody results within minutes that have been interpolated from an antibody reference curve. Depending on the allergen specificity, this multiplex chip has a more limited analytical sensitivity for IgE antibody than the singleplex autoanalyzers. It also reports in semiquantitative ISU units and has the disadvantage of not containing all the relevant allergen specificities for any given allergen source material.

Researchers sometimes have need of a more versatile immunoassay to measure allergen-specific IgE antibody than is available with the principal commercial autoanalyzers. A number of polymers have been used for allergen insolubilization, including carbohydrate matrices (Sephadex, agarose, and cellulose) and polystyrene test tubes and microtiter plates. Each of these polymers differs with respect to its allergen-binding capacity, nonspecific binding properties, stability, and ease of washing. The use of a solid phase with the highest allergen-binding capacity is often needed when maximum sensitivity is required or when sera from hyperimmunized patients with high levels of allergen-specific IgG blocking antibodies are being analyzed. For suitably equipped clinical laboratories with adequate facilities for centrifugation, aspiration, and pipetting, a carbohydrate particle matrix is preferred because of its high antigen-binding capacity. Alternatively, polystyrene microtiter plates can be satisfactory with allergens that are purified proteins. Plastic solid phases, however, display selectivity and variability with limited binding capacity, which make them less than ideal for use in IgE antibody immunoassays that involve crude allergen extracts with multiple protein antigens.

One versatile research assay has been effectively used for the measurement of both IgE and IgG antibodies that are specific for crude allergen mixtures. It is a noncompetitive radioallergosorbent test that uses an agarose carbohydrate solid phase (16, 19). In this assay, protein that is present in allergenic extracts is covalently coupled to agarose using CNBr chemistry. The immobilized allergen then binds specific antibody from the human specimen. Radiolabeled anti-human IgE is then used to detect bound IgE. An alternative assay uses a microtiter plate-based enzyme immunoassay to measure IgE antibodies that are specific for purified allergenic components. IgE antibodies can be detected using the assay format in Appendix A by replacing the immobilized anti-IgE with purified allergen that has been adsorbed onto the plate. This microtiter plate-based assay is not useful for detecting antibodies to complex allergen extracts that contain multiple proteins with different pIs and molecular weights. In this enzyme immunoassay, serum (neat to 1:5) is added to allergen-coated plates, and biotin-conjugated murine anti-human IgE detection antibody is used to detect bound allergen-specific IgE antibody. As in the total IgE assay, serum is the optimal specimen. IgE anti-allergen assay responses are interpolated from a total IgE reference curve by "heterologous interpolation" (20).

In terms of quality control, the most important region of the IgE antibody assay dose-response curve, from a clinical point of view, is its minimal detectable dose. Positive thresholds can differ according to the blank subtraction and reporting methods used. Therefore, each allergen-specific IgE antibody assay should contain one or more positive and negative serum controls that span the entire working range of the reference curve. All samples should be analyzed in duplicate to document reproducibility and minimize random errors. Since the quality of each antibody measurement depends on parallelism between the dilution curves of the reference serum and test sera under study, 2 or 3 dilutions of IgE antibody-positive test serum should be periodically analyzed to confirm assay parallelism.

Federally licensed clinical laboratories that perform allergen-specific IgE antibody assays are required to participate in an external proficiency testing program. The College of American Pathologists conducts the Diagnostic Allergy "SE" Survey, which submits five sera in each of three cycles per year to participating laboratories (7). The laboratory is required to analyze each serum, for a total serum IgE and IgE antibody to five allergen specificities that cycle among the weed, grass, and tree pollens; pet epidermals; molds; occupational allergens; and food allergens. Results are submitted to the survey's coordinating center, and performance of a participating laboratory is judged in relation to its peers that use the same assay.

The presence of allergen-specific IgE antibody in serum does not directly indicate allergic disease without a positive history (9). A positive IgE antibody result does indicate that the individual is sensitized to that allergen specificity and has an increased probability (or risk) of experiencing allergic symptoms if exposed to that allergen. The relative quantity of IgE antibody in serum may, but does not always, correlate with the relative risk of severe symptoms. The association between antibody quantity and allergic symptoms can be confounded by many variables, including the IgE antibody's affinity, the presence of IgG-blocking antibodies, and most important, the relative biochemical sensitivity, or "releasibility," of the subject's IgE-laden effector cells. Thus, IgE antibody is necessary but not sufficient for expression of allergic disease symptoms. For many food-, drug-, and insect venom-related allergies, only about half of individuals with IgE antibody react clinically when challenged. IgE results must therefore be carefully integrated with clinical history-based information for proper diagnostic interpretation.

ALLERGEN-SPECIFIC SERUM IgG AND IgG4 ANTIBODIES

Allergen-specific IgG and IgG4 antibodies are measured as research analytes to assess the status of the individual's humoral immune response to systematic exposure through immunotherapy or inadvertent accidental natural exposure. The levels of specific IgG antibodies are generally low (e.g., <1 ng/ml) or non-detectable in an unimmunized individual who has been naturally exposed to clinically important antigens (e.g., aeroallergens from weeds, grass, and tree pollens; dust mite, mold; and animal epidermal antigens). The analytical sensitivity and specificity of an IgG antibody assay that is used to assess these sera therefore becomes important because nanogram-per-milliliter levels of specific IgG must be measured in the presence of mg/ml levels of nonspecific IgG. In contrast, individuals who have received injections of an antigen, either by accidental exposure (e.g., bee sting, drug injection) or by active allergen immunotherapy, can produce high microgram-per-milliliter levels of specific IgG. At these levels, nonspecific binding and assay sensitivity become less critical, and assay parallelism, precision, and accuracy and human antibody standards become the focus of assay design.

The non-isotopic microtiter plate and monoclonal antibody-based enzyme immunoassay that has been described in Appendix A for total and allergen-specific IgE can be used to detect IgG antibodies specific for purified allergens. Although a crude aqueous extract can also be used as an antigen source, it contains many irrelevant proteins that readily adsorb onto plastic surfaces. In doing so, these occupy limited sites on the plastic surface that can be used to bind more relevant protein antigens. While serum is the specimen of choice for this assay, plasma and other body fluids (e.g., bronchial alveolar lavage, tears, nasal secretions) can be tested if the appropriate negative controls are analyzed in the same assay to identify the level of nonspecific binding.

The IgE ELISA procedure in Appendix A must be modified to allow the detection of IgG antibodies. This is accomplished by adsorbing purified antigen at 10 ug/ml in phosphate-buffered saline (PBS) (10 μg/ml, 0.1 ml/well) on the plate instead of anti-human IgE. After the buffer wash and blocking, 0.1 ml of antigen-specific IgG-containing reference, control, and test sera (diluted at least 1:50 in PBS-1% bovine serum albumin [BSA]) is added to their respective wells. Following a PBS-Tween buffer wash, horseradish peroxidase-conjugated/conjugated mouse anti-human IgG Fc (HP6043-HRP; EMD Millipore Corp., La Jolla, CA) is added (0.1 ml per well, 1 μg/ml in PBS-1% BSA). The plates are then processed in a similar manner, and response data is interpolated from the IgG anti-antigen reference curve.

The typical working range of the IgG antibody assays is 10 to 2,000 ng of specific IgG per ml. Both the sensitivity and working range of these assays are dependent on the density of the antigen on the solid phase, the dilution and affinity of the detection antibody, duration of the serum, conjugate and substrate incubations, and the relative amount of specific antibody of other isotypes (e.g., IgE, IgA, IgM) that compete for available solid-phase antigen epitopes. Parallelism between the reference and test serum dilution curves remains good over the working range of both assays, with interdilutional CVs typically <20%. The CV for within-experiment replicates typically averages 5%, and the CV for results between assays when all reagents remain constant should be 10% to 15%.

In terms of quality control, the minimum detectable concentration of the assay varies as a function of the negative serum subtraction and reporting methods used. Therefore, each assay should contain one or more positive and negative serum controls in addition to the reference serum dilution curve. All samples should be analyzed in duplicate to minimize systematic (procedural) and random errors. At present, there are no external proficiency surveys for assays that monitor allergen-specific human IgG antibody assays.

An IgG antibody measurement is commonly performed to document an exposure of an individual to an immunizing dose of antigen and to follow changes in antibody levels with long-term exposure. In select cases, it can serve as an indicator of the effectiveness of various antigen doses that are used to induce a specific IgG antibody response during immunotherapy. In research applications, specific IgG antibody levels are used to quantitatively monitor humoral immune response to an antigen to which a patient has been accidentally or intentionally exposed.

In the 1930s, allergen-specific IgG antibodies were identified as "blocking antibodies" that could block transfer of reaginic activity in the Prausnitz-Kustner reaction and basophil leukocyte histamine release assays. Presently, the only cited clinical application for IgG antibody measurements in the field of allergy is their use in the evaluation of Hymenoptera venom-allergic patients who are initiating venom immunotherapy or who have been receiving maintenance injections for a number of years. In a 1992 study (11), 211 insect sting challenges were performed in 109 patients over a 4-year period to investigate the clinical significance of venom-specific IgG levels. In individuals on immunotherapy for fewer than 4 years, systemic symptoms occurred in only 1.6% of individuals with venom-specific IgG levels greater than 3.5 μg/ml but 16% of individuals with levels lower than 3.5 μg/ml. The venom-specific IgG level had no predictive value for risk in patients who received therapy for more than 4 years. This study concluded that venom-specific IgG levels of <3.5 μg/ml were associated with an increased risk of allergic reactions upon resting during the first 4 years of immunotherapy with yellow jacket or mixed-vespid venoms. Other published studies of IgG antibody levels in patients receiving ragweed, grass, and dust mite immunotherapy have remained research observations that relate the antigen exposure to IgG (humoral) immune responses.

CONCLUDING THOUGHTS

In summary, the diagnostic allergy laboratory employs a number of immunoassay methods to quantify the levels of IgE and IgG antibodies in serum that can aid the clinician in the diagnosis and management of individuals with allergic disease. At present, there are no molecular biology techniques explicitly used by allergy laboratories to facilitate the diagnosis of allergic disease. Recombinant DNA technology to date has only been used in the generation of recombinant allergenic proteins that have become incorporated as component reagents in both the singleplex assays and multiplex microarray ISAC assay for IgE and IgG antibody. The laboratory analyses of allergen-specific IgE antibodies in serum identify a state of sensitization in support of a clinical history-based diagnosis of allergic disease, while allergen-specific IgG antibodies indicate antigenic exposure.

APPENDIX A

Total serum IgE IEMA procedure

The IEMA has been designed to balance good performance with a reasonable turnaround time.

1. Plastic 96-well microtiter plates are coated for 1 hour at room temperature (RT; ~23°C) and then overnight at 4°C with mouse

IgM monoclonal anti-human IgE Fc (clone HP6061, 100 μl/well) that has been diluted in PBS to 10 μg/ml just prior to use.

2. Each plate is washed once with PBS-Tween, and 0.3 ml of PBS-1% BSA is added to each well to block unreacted sites.

3. After a second wash (4x) with PBS-Tween 20, 0.1 ml of reference, control, or test serum is added to their respective wells. The standard curve is composed of 8 to 10 two-fold dilutions in duplicate of a reference serum, beginning with a concentration of 100 kIU/liter (1 IU of IgE = 2.4 ng). The plates are then incubated for 2 hours at 23°C. Two or three dilutions of high, medium, and low serum controls are analyzed in different regions of the plate to demonstrate that the assay is in control. The total IgE levels in the reference serum should be calibrated against the second WHO human IgE international reference preparation (IRP) 75/502 or the new third IgE IRP 11/234, which is currently being validated.

4. Following a PBS-Tween buffer wash (4x), biotin-conjugated mouse IgG anti-human IgE Fc (clone HP6029) is added (0.1 ml per well, 1 μg/ml in PBS-1% BSA), and the plates are incubated for 1 hour at 23°C.

5. The plates are washed with PBS-T buffer, strepavidin-horseradish peroxidase (avidin HRP) is added (0.1 ml per well, 1 μg/ml in PBS-1% BSA), and the plates are incubated for 1 hour at 23°C.

6. Plates are washed, and 0.1 ml of substrate is added. For routine analysis of human sera, 1 mM ABTS is prepared in 70 mM citrate-phosphate buffer. Immediately prior to use, 1 μl of 30% hydrogen peroxide is added per ml of ABTS required. The substrate is immediately pipetted into the plate (0.1 ml/well).

7. The peroxidase enzymatic reaction is stopped by adding 0.1 ml/well of 2 mM sodium azide when the top point on the standard curve reaches 1.5 to 2.0 OD. The plate is read on a microtiter plate reader at 410 nm, and optical densities of the unknown sera are interpolated from the standard curve in kIU/liter.

Note: This assay can be converted into an allergen-specific IgE, IgG, or IgG4 antibody assay by replacing the capture anti-human IgE reagent adsorbed to the microtiter plate with allergenic protein. Second, a monoclonal detection antibody with specificity for human IgE (HP6029-biotin), human IgG (HP6043-biotin), or human IgG4 (clone HP6023-biotin) needs to be used to detect IgE, IgG, or IgG4 antibodies, respectively. These monoclonal antibody reagents are available from EMD-Millipore, La Jolla, CA.

REFERENCES

1. **Bennich HH, Ishizaka K, Johansson SGO, Rowe DS, Stanworth DR, Terry WD.** 1968. Immunoglobulin E: a new class of human immunoglobulin. *Immunology* **15:**323–324. PubMed
2. **Saini SS, MacGlashan DW Jr, Sterbinsky SA, Togias A, Adelman DC, Lichtenstein LM, Bochner BS.** 1999. Down-regulation of human basophil IgE and FC epsilon RI alpha surface densities and mediator release by anti-IgE-infusions is reversible *in vitro* and *in vivo*. *J Immunol* **162:**5624–5630. PubMed
3. **Barbee RA, Halonen M, Lebowitz M, Burrows B.** 1981. Distribution of IgE in a community population sample: correlations with age, sex, and allergen skin test reactivity. *J Allergy Clin Immunol* **68:**106–111. PubMed
4. **Martins TB, Bandhauer ME, Bunker AM, Roberts WL, Hill HR.** 2014. New childhood and adult reference intervals for total IgE. *J Allergy Clin Immunol* **133:**589–591. PubMed
5. **Paterniti MO, Breslin LM, Courneya JP, Sterba PM, Hamilton RG, Macglashan DW Jr, Saini SS.** 2013. Differences in effects of Omalizumab on late-phase responses to allergen challenge in the skin and nose at the time of basophil hyporesponsiveness. *J Invest Dermatol* **134:**1743–1744. PubMed
6. **Hamilton RG.** 2006. Immunological methods in the diagnostic allergy clinical and research laboratory, p 955–963. *In* Detrick B, Hamilton RG, Folds JD (ed), *Manual of Molecular and Clinical Laboratory Immunology,* 7th ed. ASM Press, Washington, D.C.
7. **Hamilton RG.** 2010. Proficiency survey-based evaluation of clinical total and allergen-specific IgE assay performance. *Arch Pathol Lab Med* **134:**975–982. PubMed
8. **Valenta R, Lidholm J, Niederberger V, Hayek B, Kraft D, Grönlund H.** 1999. The recombinant allergen-based concept of component-resolved diagnostics and immunotherapy (CRD and CRIT). *Clin Exp Allergy* **29:**896–904. PubMed
9. **Hamilton RG.** 2014. Allergic sensitization is a key risk factor for but not synonymous with allergic disease. *J Allergy Clin Immunol* **134:**360–361. PubMed
10. **Sampson HA.** 2001. Utility of food-specific IgE concentrations in predicting symptomatic food allergy. *J Allergy Clin Immunol* **107:**891–896. PubMed
11. **Golden DBK, Lawrence ID, Hamilton RH, Kagey-Sobotka A, Valentine MD, Lichtenstein LM.** 1992. Clinical correlation of the venom-specific IgG antibody level during maintenance venom immunotherapy. *J Allergy Clin Immunol* **90:**386–393. PubMed
12. **Shamji MH, Ljørring C, Francis JN, Calderon MA, Larché M, Kimber I, Frew AJ, Ipsen H, Lund K, Würtzen PA, Durham SR.** 2012. Functional rather than immunoreactive levels of IgG4 correlate closely with clinical response to grass pollen immunotherapy. *Allergy* **67:**217–226. PubMed
13. **Varga EM, Francis JN, Zach MS, Klunker S, Aberer W, Durham SR.** 2009. Time course of serum inhibitory activity for facilitated allergen-IgE binding during bee venom immunotherapy in children. *Clin Exp Allergy* **39:**1353–1357. PubMed
14. **Shamji MH, Ljørring C, Würtzen PA.** 2013. Predictive biomarkers of clinical efficacy of allergen-specific immunotherapy: how to proceed. *Immunotherapy* **5:**203–206. PubMed
15. **Wide L, Bennich H, Johansson SG.** 1967. Diagnosis of allergy by an *in-vitro* test for allergen antibodies. *Lancet* **2:**1105–1107. PubMed
16. **Matsson P, Hamilton RG.** 2009. Evaluation methods and analytical performance characteristics of immunological assays for human IgE antibody of defined allergen specificities: Guideline, National Committee on Clinical Laboratory Standards 1/LA20-A.
17. **Thorpe SJ, Heath A, Fox B, Patel D, Egner W.** 2014. The 3rd International Standard for serum IgE: international collaborative study to evaluate a candidate preparation. *Clin Chem Lab Med* **52:**1283–1289. PubMed
18. **Hiller R, Laffer S, Harwanegg C, Huber M, Schmidt WM, Twardosz A, Barletta B, Becker WM, Blaser K, Breiteneder H, Chapman M, Crameri R, Duchêne M, Ferreira F, Fiebig H, Hoffmann-Sommergruber K, King TP, Kleber-Janke T, Kurup VP, Lehrer SB, Lidholm J, Müller U, Pini C, Reese G, Scheiner O, Scheynius A, Shen HD, Spitzauer S, Suck R, Swoboda I, Thomas W, Tinghino R, Van Hage-Hamsten M, Virtanen T, Kraft D, Müller MW, Valenta R.** 2002. Microarrayed allergen molecules: diagnostic gatekeepers for allergy treatment. *FASEB J* **16:**414–416. PubMed
19. **Hamilton RG, Sobotka AK, Adkinson NF Jr.** 1979. Solid phase radioimmunoassay for quantitation of antigen-specific IgG in human sera with 125I-protein A from *Staphylococcus aureus*. *J Immunol* **122:**1073–1079. PubMed
20. **Butler JE, Hamilton RG.** 1981. Quantitation of specific antibodies: methods of expression, standards, solid phase considerations and specific applications, chapter 9. *In* Butler JE (ed), *Immunochemistry of Solid Phase Immunoassays*. CRC Press, Boca Raton, FL.

Assay Methods for Measurement of Mediators and Markers of Allergic Inflammation

JOHN T. SCHROEDER, R. STOKES PEEBLES, JR., AND PAMELA A. GUERRERIO

83

Assays facilitating the measurement of mediators and markers of allergic inflammation have evolved during the past 40 years, arising from two primary discoveries: first, that immunoglobulin E (IgE) is the source of reaginic activity in serum, and second, that tissue mast cells and blood basophils—cells expressing the high-affinity receptor for IgE (FcεR1)—respond to allergen by releasing the most relevant mediators underlying immediate hypersensitivity reactions. Naturally, skin testing has long been used to assess the *in vivo* mast cell response to allergen. Basophils, however, by virtue of their accessibility and the fact that they are the sole source of many of these mediators among blood leukocytes, continue to dominate the performance of *in vitro* assays assessing IgE-mediated responses.

Histamine and leukotriene C_4 (LTC4) have potent vaso- and bronchoconstrictive properties and represent two classes of mediators released by mast cells and basophils that have long been at the core of assays used to assess allergic inflammation. Cytokines represent a third class of mediator released from cells expressing FcεR1, but unlike histamine and LTC4, they are generated *de novo* (1). In particular, human basophils secrete copious amounts of interleukin-4 (IL-4) and IL-13—arguably the two most important cytokines in allergic disease, given the primary role of these cytokines in regulating IgE synthesis from B cells. The importance of this has only recently been appreciated, with evidence that basophils *in vivo* are, indeed, a major source of this cytokine (2). Also, the activation-linked markers CD63 and CD203c continue to be popular as flow cytometry-based assays used as surrogate indicators of basophil degranulation and mediator release. Therefore, it has been the objective of this chapter during the last three editions of this manual to focus on the laboratory procedures commonly performed for measuring the release of these inflammatory mediators, both *in vitro* and in biological fluids. Rather than concentrating in detail on procedures that have changed little during the course of three decades, this chapter instead focuses more on recent approaches for measuring, for example, histamine, LTC4, cytokines, and markers but refers to previous editions when specific details are deemed necessary. Likewise, the assays used for the detection of tryptase (a mast cell product) and major basic protein (MBP, a product of eosinophils) have also changed little during the past 15 years or so and therefore are mentioned only briefly. Instead, some discussion of more novel cellular assays utilizing dendritic cells (DC) to assess the allergic condition is included. Of note, while several technical advances have made these *in vitro* detection assays more applicable for clinical use, some of these methods remain time-consuming and are presently useful only in specialized clinical situations or for research purposes.

While these types of *in vitro* assays provide an important means to evaluate the mechanisms and pathways that regulate allergic inflammation, a number of complementary *in vivo* assays are routinely used to facilitate the diagnosis and management of patients with allergic disease. Most of these assays are based on the simple idea of challenging subjects with antigenic material to reproduce a biological response. Prick-puncture and intradermal skin testing represent the most common methods for diagnosing immediate hypersensitivity to aeroallergens, food, venom, and medications in the clinic, while intranasal and whole-lung challenges are often used in the research setting to evaluate end-organ allergen sensitivity as it relates to clinical symptoms.

HISTAMINE

Commercial and Laboratory Assays

Commercial assays for measuring histamine have become mainstream compared with other approaches, such as the automated fluorometric technique. However, this shift has been driven by availability rather than dependability and ease in performance. For instance, an enzyme immunoassay (EIA) and an enzyme-linked immunosorbent assay (ELISA) are offered by Cayman Chemicals and Immuno-Biological Laboratories, respectively, for the detection of histamine in a variety of biological specimens, including culture supernatant, urine, and plasma. These assays are sensitive, do not require specialized equipment, require small sample volumes (e.g., 0.050 to 0.100 ml), are less affected by high-protein contamination than automated fluorometry (see below), and are cost-effective for low-throughput needs. On the other hand, their dynamic range (~20–1.000 pg/ml) remains quite limited compared with the flurometric approach (~0.5–100 ng/ml), which is less appealing when measuring histamine released from leukocyte/basophil suspensions.

The fluorometric approach was first automated in the mid-1970s, making it possible to analyze 45 to 60 samples per hour with today's machines. The chemistry behind the assay is described elsewhere (3). Briefly, histamine is first

doi:10.1128/9781555818722.ch83

extracted from the specimen and is coupled with ophthalaldehyde (OPT) using *n*-butanol from a salt-saturated, alkalinized solution to form a fluorescent product. Samples tested must be relatively free of protein and other interfering compounds such as histidine. Before the condensation step with OPT, histamine is back extracted into an aqueous solution of diluted HCl by adding heptane. The histamine-OPT complex is stable at an acid pH, which increases the fluorescence intensity of the compound. The chemicals utilized require that proper ventilation be used to house the machine. Relatively larger sample volumes (0.6 to 1.0 ml) are also required. The major advantage of automated fluorometry over other systems is its ability to rapidly process, with reproducibility and ease, a large quantity of samples, making it the method of choice when assaying histamine released from basophil or mast cell suspensions. It has also been useful for determining levels of histamine released at sites of experimental allergen challenge in the nose, lung, and skin by assaying fluids from lavages performed with normal saline. Fluorometric measurement of histamine in whole blood and in serum at concentrations greater than 10% requires extensive acid precipitation and/or dialysis to remove protein, cumbersome manipulations that lead to a loss of assay sensitivity.

The radioenzymatic assay (REA), which involves the transfer of ^{3}H- or ^{14}C-labeled methyl groups from *S*-adenosylmethionine to histamine by using the enzyme histamine *N*-methyltransferase, is essentially no longer used in measuring histamine. While highly sensitive in detecting histamine (10 pg/ml) and not interfered by high protein, the assay is rather cumbersome, requiring a series of extractions and back extractions that are not automated as in the fluorometric approach. The assay also requires a source of histamine *N*-methyltransferase, which is typically derived from crude extracts of rat kidney (Pel-Freez, Rogers, AR). The assay is relatively time-consuming and lacks the reproducibility achieved with the automated fluorometric system. Presently, one must also establish this assay in-house, since greater appeal of the ELISA and EIA have diminished the commercial availability of the REA.

The standards used in the fluorometric assay are made from stock solutions prepared by accurately weighing an appropriate amount of histamine dihydrochloride (see Appendix). Standard solutions are stable at 4°C when diluted in water containing 2% $HClO_4$. Commercial EIA and ELISA kits come with standards and should use diluent best representing the samples to be tested but in the absence of $HClO_4$, which interferes with the assay.

Clinical Indications for Measuring *In Vitro* BHR

Measurement of *in vitro* basophil histamine release (BHR) continues to serve as a valuable test for evaluating IgE-mediated reactions. In fact, the indications for the use of this method remain more extensive than those for any other *in vitro* test described in this chapter. Yet, because the parameters involved in the histamine release assay are extensively described in previous editions of this book, they will be mentioned only briefly here.

Evaluation of Allergic Status

In vitro BHR can serve as a dependable and precise indicator of the allergic status of an individual, with few false positives compared with skin-testing techniques. Nonetheless, the presence of allergen-specific IgE is not sufficient and must be combined with the clinical history to indicate the presence of disease, given the widespread prevalence of IgE specific to insect venoms, latex, and food allergens. Since many dilutions of an antigen can be tested for reactivity, the BHR assay can also be more quantitative than skin testing, which often relies on a somewhat less precise endpoint. Basophil analyses can be performed safely using "crude" allergens and products not yet approved for *in vivo* use. However, any clinical applicability is limited to a positive assay result, since *in vitro* BHR does not necessarily predict a negative skin test reaction. Due to the complexities of the assay, direct measures of specific IgE rather than histamine release are more commonly used in clinical practice (see chapter 82, this volume).

Demonstration of IgE Antibody Activity

Measuring BHR from normal donor leukocyte suspensions passively sensitized with IgE is a useful technique for detecting allergen-specific antibody in the sera (or plasma) of patients presenting with clinical symptoms (6). In fact, BHR has some advantages over the more commonly used serological assays used in the detection of allergen-specific IgE. First, it gives a quick and precise assessment of whether serum contains biologically active IgE. The serological assays for IgE antibody, although more easily standardized, simply quantify the amount of IgE antibody in serum. Second, very little antigen is often required to induce BHR. In contrast, the serological assay reagents require relatively larger quantities of allergen in order to be successfully bound to an insoluble matrix for subsequent binding of allergen-specific IgE from serum. Third, the BHR assay is excellent for studies investigating, by direct analysis and after passive sensitization, whether a patient has become sensitized to an uncommon allergen for which serological assay methods are not available. A disadvantage of these assays is their requirement for fresh leukocytes from a nonallergic subject whose cells can withstand the rigors of passive sensitization (see below) and retain responsiveness.

Quality Control of Prepared Allergens

It is often desirable to check the quality of allergens, whether commercially prepared or made in-house, by testing their ability to induce histamine release from leukocytes obtained from allergic donors. This is becoming particularly useful for immunotherapy studies for which modified allergens can be evaluated for biological activity or cross-reactivity prior to being used *in vivo*.

Alternative for Skin Testing

In some instances, it is desirable to avoid skin testing and to use the *in vitro* BHR assay as an alternative approach for evaluating allergic status. However, given the wide use of serological methods for detecting allergen-specific IgE, this particular indication is rarely practiced.

Test Procedures

Induction of Histamine Release from Washed Human Leukocytes: General Method

While there are presently many variations of the protocol originally described for inducing histamine release from basophils *in vitro*, these relate primarily to the method used for histamine analysis. Otherwise, little has changed in the 40 years since its first description (4). The reader is therefore directed to previous editions of this book for specific details, as this section emphasizes only certain aspects of the assay. Also, the techniques described herein are, for the most part, used when histamine is analyzed by automated fluorometry.

Blood is drawn into a plastic syringe, preferably by using a butterfly infusion set with the needle size reflecting the

desired volume required for the assay. Usually, 1 ml of blood per reaction tube provides total histamine levels of approximately 20 ng, with some variation occurring among donors. Dextran sedimentation remains the method of choice for preparing washed leukocytes for histamine release, as it requires little technical expertise and is the least manipulative of the cells. These issues are necessary to consider when both preparation time and retention of cell function are of greatest importance. In this instance, whole blood is immediately transferred into disposable 50-ml polypropylene centrifuge tubes (catalog no. 25330; Corning Incorporated, Corning, NY), each containing 12.5 ml of dextran, 5.0 ml of 0.1 M EDTA, and 375 mg of dextrose, which allows proper mixing for up to 20 ml of blood. After sitting for 60 to 90 min at room temperature (23 to 25°C), the leukocyte-rich plasma layer is carefully removed and centrifuged and the cell pellet is washed two or three times in PIPES [piperazine-*N*,*N*′-bis(2-ethanesulfonic acid)]-albuminglucose (PAG) buffer (see Appendix) to remove platelets. It is sometimes useful to do one or more washes in PAG containing EDTA (~4 mM), since this reagent chelates calcium and prevents platelet clumping. However, it is important that the final wash be done in the absence of EDTA, since histamine release requires calcium, and residual EDTA may prevent the reaction cascade. After the final wash, the cell pellet is resuspended in PAG buffer containing 1 mM $CaCl_2$ and 1 mM $MgCl_2$ (PAGCM) to a volume sufficient to allow the addition of the required amount of cells to each reaction tube, as per the protocol. Histamine release can be induced in almost any variety of test tube, but total reaction volumes usually range from 0.1 to 1.0 ml. The washed leukocytes in PAGCM and the reaction tubes are then warmed separately in a 37°C water bath before mixing with one another. The total histamine content (called "completes") is obtained by the lysis of cells in a duplicate set of reaction tubes using perchloric acid at a final concentration of 1.6%. The amount of histamine released spontaneously (usually less than 5% of the total) is determined by incubating cells in buffer alone. Reactions are allowed to proceed at 37°C for 30 to 45 min, at which time buffer is added to a 1-ml total volume, the cells are centrifuged, and the cell-free supernatants are decanted into 2-ml autoanalyzer cups (catalog no. 73.641; Sarstedt, Inc., Princeton, NJ) and stored at 4°C in plastic racks (Elkay Products Inc., Shrewsbury, MA). To prevent evaporation, samples should be frozen at −20°C if histamine cannot be analyzed within 2 weeks. Any samples requiring added protein during the reaction may require acid precipitation in order to prevent interference with histamine measurements using the automated fluorometric technique. In such instances, much of the protein can be precipitated prior to analysis by adding perchloric acid to the cell-free supernatant at a final concentration of 1.6%, incubating overnight at 4°C, and recentrifuging prior to analysis. Alternatively, histamine can be measured using either the REA or ELISA.

Inhibition of Histamine Release from Basophils

Inhibition of the standard BHR assay can be useful in monitoring whether a patient's serum contains an allergen-neutralizing blocking antibody (e.g., IgG antibody), as often happens during the course of immunotherapy (6). However, the assay has largely been replaced by immunoassays that directly measure specific IgG antibody. The reader is therefore directed to previous editions of this book for specific details of this assay. Although its clinical utility is somewhat limited, the inhibition of *in vitro* BHR is often used to determine the effectiveness of pharmacologic agents. This test also involves a modification of the standard release assay but differs slightly from that used in measuring IgG antibodies. In brief, washed leukocytes are mixed with PAGCM alone or with several concentrations of the drug diluted in buffer. Final drug concentrations of 10^{-4} M to 10^{-6} M are useful for initial screening. After preincubation (usually for 10 to 15 min) at 37°C, several concentrations of an allergen (or anti-IgE antibody) are added for an additional 45 min to induce BHR. Once again, it is best to use stimulus concentrations that cause roughly half of the maximal histamine release. In addition to the usual controls (completes and blanks), it is important to include cells incubated with drug alone to assess any lytic effects, as well as drugs diluted in buffer (no cells) to control for fluorescent compounds if the OPT-based assay is used.

Passive Sensitization of Basophils

The basophils isolated from some donors express sufficient numbers of unoccupied FcεR1 sites to enable these cells to be passively sensitized with IgE antibody from an unrelated source. Thus, the serum or plasma of an allergic individual can be tested for antigen-reactive IgE antibodies by sensitizing the basophils of a nonallergic donor and inducing BHR from these cells by using the antigen in question. The success of studies using this technique requires the use of nonallergic donors whose basophils normally release well in response to IgE-dependent stimulation and whose cells have naturally unoccupied FcεR1 sites that can be passively sensitized with IgE antibody. Since only an estimated 1 out of 20 nonallergic individuals has basophils that meet these criteria, lactic acid is often used to remove endogenous basophil-bound IgE, thereby increasing one's ability to passively sensitize cells. In fact, the details of performing this procedure are outlined elsewhere (6) and are also described in previous editions of this chapter. As a result, it seems appropriate to note here only a few considerations, since the reader can refer to the above-mentioned references for specific information. First, these assays are best done using mixed leukocytes containing basophils. The lactic acid solution (pH 3.9) can be used effectively at room temperature (25°C) or on ice (4°C) for as long as 5 min. However, only partial removal of IgE is expected when performed on ice and with shorter treatment times. Treated cells are immediately washed to remove unbound IgE before passive sensitization (30 min at 37°C) with an appropriate dilution of patient serum in PAG containing 10 U of heparin/ml and 4 mM EDTA. An important negative control includes acid-treated cells sensitized with an equal amount of irrelevant IgE in control serum. It is also important to leave a portion of cells untreated with acid solution in order to control for any effect this treatment may have on basophil responsiveness. After washing twice in PAG buffer, the leukocytes are tested for histamine release by using identical test conditions. The antigen-induced release of histamine by leukocytes passively sensitized with the patient's serum, but not with control serum, indicates positivity. Of course, non-passively sensitized cells should not react with the antigen, while cells subjected to all conditions of passive sensitization should still respond to anti-IgE used as a positive control.

LIPID MEDIATORS

Leukotriene C4

The secretion of LTC4 by basophils and mast cells is also rapid, nearly paralleling the release of histamine, and is essentially complete by 30 min after activation. IL-3 enhances LTC4 levels generated by basophils in response to

IgE-dependent activation by nearly 100-fold, and following IL-3 priming, release of LTC4 occurs with stimulation by C5a, a secretagogue that alone does not normally cause the release of this mediator. Essentially no release of prostaglandins from basophils occurs in response to activation, indicating that cyclooxygenase enzyme activity is not prominent in these cells. However, all human mast cells studied to date do produce prostaglandin D_2 (PGD2), and lung and mucosal cells secrete levels of LTC4 nearly identical to those secreted by basophils but usually only in response to IgE-dependent stimuli.

While competitive RIAs have long been used in detecting LTC4 (and PGD2), their requirement for radioactive isotopes and cumbersome protocols have given way to commercial ELISA kits (Assay Designs and Cayman Chemicals). These assays are also generally quite sensitive (~50 pg/ml) and exhibit only slight cross-reactivity with LTD4 and LTE4.

Clinical Indications

Evaluation of Allergic Status

LTC4 is generated from several cell types, including monocytes and eosinophils. However, the formation and secretion of this mediator from washed leukocytes can serve as an *in vitro* test of allergic status, since the basophil is the only cell in these preparations that responds to IgE-mediated stimulation. In practice, however, since histamine is released in parallel with LTC4 and the assays for measuring it are less cumbersome and more reliable, histamine is more often used as an index of allergen sensitivity. Nonetheless, measurements of LTC4 in biological specimens may be useful in assessing the inhibitory actions of the 5-lipoxygenase inhibitors, which do not affect histamine release.

Test Procedures

Washed leukocytes are prepared from peripheral blood using dextran sedimentation, as described above for BHR; LTC4 and histamine release are assessed simultaneously. However, the reactions are done in a total volume of 0.1 ml in PAGCM buffer. PAG buffer (0.2 ml) is added to all tubes at the end of the reaction, and after centrifugation, a portion of the supernatant (0.1 ml) is carefully removed for LTC4 analysis. An additional 0.5 to 0.8 ml of PAG buffer is then added to the reaction tubes, and following recentrifugation, the supernatant is obtained for histamine analysis by automated fluorometry, as described above. By measuring the release of these two mediators from the same aliquot of cells, the LTC4 levels can be normalized to the amount of histamine released (i.e., picograms of LTC4 per nanograms of histamine).

CYTOKINE GENERATION BY BASOPHILS

Evidence has emerged during the past 20 years showing basophils to be an important source of cytokines that are essential for allergic inflammation (1). In particular, basophils secrete IL-4 and IL-13—two cytokines critical in promoting IgE production from B-lymphocytes, activating endothelium for the selective adherence and transendothelial migration of eosinophils, and promoting development of the Th2 phenotype. The parameters important for the generation of these cytokines in basophils indicate that both proteins, much like histamine, are important correlates of immediate hypersensitivity. Both IL-4 and IL-13 are secreted following IgE cross-linking, and the concentration of a stimulus required for optimal release is nearly 10-fold less than that necessary for histamine release. IL-4 protein levels peak after 4 to 6 hours of activation, with IL-13 secretion being somewhat slower, beginning at about 4 hours and peaking after some 20 hours of incubation. The generation of both cytokines is inhibited by the addition of cycloheximide, suggesting that their production occurs *de novo* and that neither is stored and released during degranulation or produced minutes following stimulation, as is true for histamine and LTC4.

Clinical Indications for Measuring *In Vitro* Basophil IL-4 and IL-13 Secretion

The clinical indications for measuring IL-4 and IL-13 are much the same as those described for measuring BHR. Indeed, basophil cytokine production shows increased sensitivity to IgE-mediated stimulation and is somewhat specific for this type of activation: C5a and *N*-formyl-methionyl-leucyl phenylalanine (FMLP), which are potent stimuli for histamine release, do not normally induce IL-4 and IL-13. Basophils from allergic subjects have been shown to secrete greater levels of IL-13 in response to IL-3 compared with those from non-allergic individuals (7). This response is particularly evident following allergen exposure (8, 9). Overall, these findings suggest a novel indication for measuring basophil secretion of cytokines (particularly IL-13), since these cytokines are observed in the absence of BHR and may also be indicative of underlying systemic Th2-like responses occurring as a result of allergen exposure. Nonetheless, the clinical applicability of measuring IL-4 and IL-13 remains less than that of measuring BHR, since measuring these cytokines is time-consuming and requires multiple assay systems.

IL-4 and IL-13 Protein: Methods of Cytokine Detection

Measurements of IL-4 and IL-13 protein are most often done by ELISA, and many sources of commercial kits (or matched antibodies to make in-house plates) now exist with assay ranges of 1 pg/ml to 1 ng/ml. Since protocols described elsewhere in this manual are devoted to ELISA design, specific details will not be belabored here other than to make some general comments. First, when quantifying IL-4 and IL-13 protein by ELISA (as with any protein ELISA), problems may arise with inter-assay variation. This is particularly true since many assays, including commercially available kits, are supplied with standards that typically give different results among assays. It is important, therefore, to calibrate in-house standards against a variety of other available standards, ideally those set by World Health Organization specifications.

It has become increasingly popular to monitor cytokine generation at the single-cell level by using multicolor flow cytometry. The technique requires the inclusion of a protein transport inhibitor, such as brefeldin A (1–10 μg/ml), which is added to cell cultures during stimulation to prevent the secretion of cytokines from activated cells. Intracellular cytokines are subsequently detected in paraformaldehyde (4%)-fixed, detergent (e.g., saponin, 0.1%)-permeabilized cells using fluorescence-conjugated antibodies. With the use of a two-color staining protocol, basophils account for most of the IL-4 and IL-13 produced in peripheral blood mononuclear cell suspensions following *in vitro* stimulation with an allergen (10). While multicolor flow cytometry has significant potential as an analytical technique for monitoring cytokine generation in specific cell types, particularly those found in low frequencies, its success depends on antibodies

that are compatible with fixation and permeabilization. These steps are necessary in allowing intracellular access by fluorescence-conjugated antibodies. These procedures, however, can often affect antigenic binding sites, making cytokines unrecognizable by antibodies (particularly those monoclonal in nature) that would ordinarily detect native protein. When antibodies do stain, it is important to establish specificity by performing neutralization experiments with unlabeled antibody.

Preparation of Basophil Suspensions for Cytokine and/or Mediator Release

Enriched Suspensions

Basophil-enriched suspensions are prepared by density centrifugation on isotonic Percoll gradients to allow simultaneous assessment of cytokine secretion and histamine release. For IL-4 and IL-13 production, 5 ml of blood per reaction tube, approximately five times the amount required for histamine release, is anticoagulated with 10 mM EDTA. The plasma layer, obtained following centrifugation (300 × *g*; 15 min; 24°C), is aspirated without disturbing the leukocyte interface (buffy coat). The buffy coat interface is then removed and transferred into a tube containing an equal volume of PAG-EDTA buffer (approximately 20 ml of buffy coat per 50 ml of whole blood). Diluted buffy coat (20 ml) is then layered onto gradients consisting of 12.5 ml of 55% isotonic Percoll (approximate density, 1.072 g/ml) underlaid with 12.5 ml of 61% isotonic Percoll (d ≈ 1.082 g/ml), as illustrated in Fig. 1. Note that an alternative to performing this "double Percoll" approach is the simple use of the 61% Percoll solution for a "single Percoll" protocol. While this typically results in a basophil purity of less than 3%, it adequately removes excessive red cells, producing a leukocyte suspension suitable for investigating cytokine expression by flow cytometry. In any case, the gradients are centrifuged (700 × *g*; 20 min; 24°C). The cells banding at the 55% Percoll interface and penetrating the top half of this layer are removed and discarded. Basophils are present in the fraction consisting of the lower half of the 55% Percoll layer, the 61% interface, and the upper half of this layer. These leukocytes are immediately transferred into clean tubes containing 35 ml of PAG-EDTA buffer and centrifuged (150 × *g*; 10 min; 24°C). After combining and transferring the cells into 15-ml polypropylene tubes, the cells are washed twice in cold PAG (6 to 10 ml per wash). The mean percentage of basophils found in these fractions ranges from 5% to 50% (using the double Percoll approach), as determined by cell counts in Spiers-Levy chambers using alcian blue (11). Of note, these enriched suspensions allow concurrent analysis of multiple mediators within the same culture/tube simply because more total cells can be added without overcrowding, which is harder to do the more impure the suspension. When warranted, enriched suspensions also facilitate basophil purification by negative selection using commercial kits (e.g., Miltenyi Biotec, StemCell Technologies). And, while the need for pure basophil suspensions is often not necessary in assessing mediator release and cytokine secretion, having this technology enables testing of substances that potentially have a direct effect of function.

Culture Procedure

For cytokine protein secretion from basophils, leukocytes obtained directly or from Percoll gradients are resuspended in a culture medium such as Iscove's modified Dulbecco's medium, pH 7.4, supplemented with 5% heat-inactivated (56°C for 30 min) fetal bovine serum, nonessential amino acids, and 5 μg of gentamicin per ml (C-IMDM). For simultaneous analysis of histamine release and IL-4 protein secretion, basophil-enriched suspensions are prepared on Percoll gradients, and 100,000 to 200,000 basophils, accurately enumerated by counting of alcian blue-stained cells, are added per well in a 96-well microtiter plate. The cells are added in 125 μl of C-IMDM and are brought to 37°C in a CO_2 incubator (5% CO_2), after which 125 μl of C-IMDM with or without a stimulus (e.g., a specific antigen) at 37°C is added for a 4-hour incubation. The cultures are then centrifuged, and the cell-free supernatants are collected for analysis. A portion of the supernatant is obtained for histamine measurement by carefully removing the upper 25 to 50 μl of supernatant and adding this to 1 ml of PAG buffer containing 1.6% $HClO_4$. After precipitation of protein overnight at 4°C, the histamine in the samples is measured by automated fluorometry (note: histamine measurements

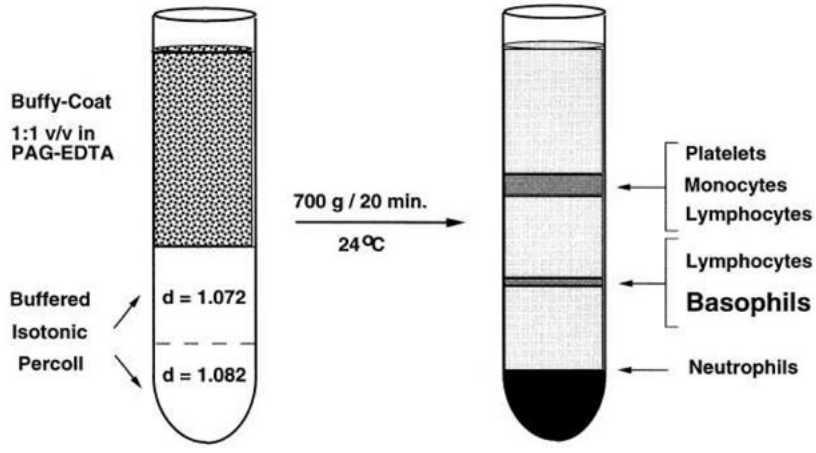

FIGURE 1 Diagrammatic representation of preparation of peripheral blood basophils by discontinuous Percoll density centrifugation. Leukocyte interface cells (buffy coat) are prepared from whole blood by centrifugation. Diluted buffy-coat cell suspensions are layered onto buffered isotonic gradients consisting of two Percoll densities (d) of 1.072 and 1.082 g/ml. Following centrifugation (700 × *g*, 20 min, at 24°C), basophils band on the 1.082-g/ml Percoll interface and range from 5 to 50% purity. v/v, vol/vol.

using ELISA must be free of $HClO_4$). Histamine release is reported as a percentage of the total histamine, which is measured by taking a portion of the starting leukocyte suspension, containing a number of basophils proportional to the amount of supernatant used for analysis, for direct lysis in 1 ml of acid solution. The supernatant remaining is then collected for IL-4 protein analysis by ELISA.

The conditions necessary for IgE-dependent secretion of IL-13 are essentially the same as those important for IL-4 secretion, with the only difference being that detection of the former cytokine requires an 8- to 20-hour incubation. Thus, the protocol described above for IL-4 also applies to IL-13 secretion, with the exception that longer incubation times are required.

BASOPHIL SURFACE ACTIVATION MARKERS: CLINICAL INDICATIONS

The so-called basophil activation markers (BAM), CD63, CD69, and CD203c have been put forward as surface markers that are sensitive to basophil activation after exposure to an allergen (CD63 and CD203c), exposure to IL-3 (CD69), or exposure to other degranulation stimuli such as FMLP and ionophores. In particular, the commercially available basophil activation test (BAT) reportedly assesses IgE-dependent activation of basophils *in vitro* by monitoring for the increased expression of CD63—a surrogate marker for BHR. This flow-based assay has become widely used, particularly in evaluating drug, food, and venom hypersensitivities. Likewise, CD203c (ectonucleotide pyrophosphatase/phosphodiesterase family member 3) is a marker of blood basophils in which increased expression was recently shown to associate both in food allergy and asthma (12, 13). The use of these activation markers as part of diagnostic evaluation of the presence of allergic reaction-specific IgE has been reported. However, several questions remain as to the specificity of these markers for diagnostic testing with specific allergens (14). As apparent from BHR assays, a broad range of allergen doses must be utilized to allow the use of these tests across a given population. Access to blood basophils for each individual allergen to be tested must be considered, as well as the potential that nearly 1 in 20 subjects may have non-responding basophils, which may hamper the ability to interpret the results. In addition, IL-3 is often added as an amplifier of IgE-dependent responses, yet this cytokine can often directly induce basophil responses, thus interfering with interpretations. The use of whole blood for assay of these surface markers is quite popular; however, the conditions used for the lysis of contaminating red cells (see below) may also deliver an activation stimulus to the basophils. Other isolation strategies such as Percoll isolation may be desirable, but negative selection procedures for highly purified basophil preparation may evoke nonspecific basophil activation due to prolonged handling of basophils. In addition, controls to monitor for false signals from other cell types that bear CD69 and CD63, such as adherent platelets, must be considered in these assays. Although some studies have shown expression of activation markers in parallel with histamine release from basophils, a very early study showed discordance between the elevation of activation marker expression and basophil histamine release in response to a polyclonal anti-IgE stimulus (15). Thus, concerns remain regarding the use of these surface markers as diagnostic tests in assessing allergic status.

Standard Assay Approach

BAM assays are often conducted using heparinized whole blood (0.1 ml/assay tube), which is added to reaction tubes (e.g., flow cytometry test tubes) containing negative controls (buffer alone), positive controls (e.g., anti-IgE, anti-FcεRI antibody), and several concentrations of the test antigen. Fluorescently labeled antibodies are then added for the detection of basophils and the BAM of interest. For example, phycoerythrin (PE)-labeled anti-CD123 (anti-CD123/PE) and fluorescein isothiocyanate (FITC)-labeled anti-CD303 (anti-CD303/FITC) readily identified basophils from other leukocytes (16). BAM are then detected using allophycocyanin (APC)-labeled antibodies (e.g., anti-CD63/APC). The presence or absence of other markers have also been useful in identifying basophils (e.g., $CCR3^+$, $CD203c^+$, MHC II^-), and may function equally as well depending on the application. Once labeling for the markers of choice is complete, red blood cells are lysed using commercially available reagents (e.g., PhosFlow, BD Biosciences), thus facilitating subsequent analysis by flow cytometry. BAM values are generally reported as the percent positive basophils above the negative control. Net mean fluorescence intensity (nMFI) is also often reported.

MAST CELL SPECIFIC MEDIATORS AND MARKERS

Tryptase

Tryptase is a neutral protease stored in large quantities in mast cells (roughly 10 pg per lung mast cell and up to 135 pg per skin mast cell). Several forms have been described (I, βII, III, α, and transmembrane tryptase), and all are found in mast cells. Only the mature form of tryptase, previously referred to as β-tryptase, and immature or protryptase, previously referred to as α-tryptase, are clinically relevant. Although tryptase is generally accepted as a mediator of immediate hypersensitivity, its biological role is not known. However, several *in vitro* activities of tryptase, such as its ability to sensitize smooth muscle to histamine and to stimulate fibroblast proliferation, have suggested a direct role for this enzyme in conditions ranging from asthma to wound healing.

Assessment of *In Vivo* Mast Cell Activation: Clinical Indications

The ability to detect tryptase in many types of biological specimens, such as serum, bronchial lavage fluid, nasal lavage fluid, skin blister fluid, and tears, has made this enzyme a valuable marker of *in vivo* mast cell activation. In conjunction with histamine measurements, the detection of tryptase is useful in determining the involvement of mast cells in immediate allergic responses occurring in many different reaction sites. Mature β-tryptase is released from mast cells within 15 min following *in vitro* degranulation and is the predominant form detected in the serum 1 to 2 hours following anaphylaxis (>1 μg/liter). However, immature α-protryptase is spontaneously secreted from mast cells and often elevated (>20 μg/liter) in mastocytosis patients, which reflects an increased mast cell burden. Quantifying ratios of the immature and mature forms of tryptase in serum provides the best indication of mast cell activation (16). Additional details regarding tryptase detection are found in chapter 85.

Test Procedures for Detection of Tryptase

Tryptase is often measured using ELISA, with anti-lung tryptase primary and biotinylated secondary antibodies in a two-site immunoenzymatic assay. Polyclonal antibodies are also useful for detecting tryptase by RIA, although nonspecific binding and protein interference are often problematic. Human lung mast cell tryptase is often used

as a standard in both the ELISA and RIA techniques and requires extensive purification protocols. Recombinant tryptase is available, but its usefulness as a standard has not been fully determined. It is also now possible to measure immature pro-tryptase using the commercially available ImmunoCAP assay (Thermofisher Scientific/Phadia, Uppsala, Sweden), which is designed as a sandwich immunoassay involving a cellulose-derivative solid-phase component. The assay is reported to be suitable for serum or nasal lavage specimens collected 15 min to 3 hours after mast cell activation.

Prostaglandin D2

PGD2 is a pro-inflammatory mediator released from mast cells (roughly 60 ng/10^6 cells) upon IgE-dependent activation and is capable of causing bronchoconstriction, dilation, and increased permeability of the microvasculature via binding to the DP1 receptor. Also, PGD2 is an important chemoattractant, selectively recruiting cells (e.g., eosinophils, basophils, Th2) expressing a second receptor, DP2, (also known as CRTH2). PGD2 assays should be performed as quickly as possible, especially when skin mast cells are involved, since this mediator is susceptible to degradation even when stored at –20°C. PGD2 is most often measured using a competitive RIA, either a commercially available or an in-house assay. Because of the technical problems observed, especially with high-protein-concentration fluids, some laboratories have developed gas chromatographic technology, which is considered the method of choice for detection of prostanoids in biologic fluids. Adding tetradeuterated standards overcomes problems of differential degradation, and chromatography of samples using Sep-Pak columns removes interfering proteins and other substances in biologic matrices. PGD2 is not regularly analyzed as a mediator of allergic inflammation, since tryptase is more readily detected in the same biological specimens and is generally accepted as a more specific marker of mast cell activation.

DENDRITIC CELLS: INNATE IMMUNE RESPONSES

Blood dendritic cell (DC) subtypes are gaining distinction in allergic disease for possessing impaired innate immune responses but also the capacity to induce Th2 responses. As a result, they are being increasingly used in cellular assays indicative of the allergic status (16). While the clinical applicability of these assays remains limited at this time, we discuss a few selected assays here because they are predicted to gain greater validation in the future.

IFN-α: Clinical Indication and Assay

Although plasmacytoid DCs (pDCs) constitute <0.5% of the PBMC isolated from blood, they are the predominant (if not sole) source of IFN-α and other type I IFNs upon stimulation with TLR7/9 agonists (18). Yet, there are now several reports indicating that this response is impaired among subjects suffering from allergic disease and that events occurring from the cross-linking of the IgE receptors expressed by these cells may account for this deficiency (19–22). Moreover, there is evidence suggesting that these responses improve in subjects undergoing allergen immunotherapy (IT) and therefore may become useful in monitoring one's course during this treatment (23). A straightforward assay to assess IFN-α production involves stimulating PBMCs (or the basophil-depleted cells on the 1.075-g/ml Percoll interface shown in Fig. 1) with DNA oligodeoxynucleotides (ODN) containing unmethylated CpG motifs, which activate pDC within the suspension via TLR9. In particular, ODN-2216 is a well-known type A ODN that induces potent IFN-α responses, especially when synthesized with a phosphothioated backbone to preserve its stability in culture. Its nucleotide sequence consists of two CpG motifs, and there are now several companies (e.g., TriLink Biotechnologies, San Diego, CA; IBA Inc., Göttingen, Germany; Coley Pharmaceutical-Pfizer, Wellesley, MA) that will synthesize various ODNs as stimuli of IFN-α production by pDC. We typically use ODN-2216 at 100 nM to activate PBMC (1.25 $\times$ 10^6 per 0.250 ml C-IMDM). After incubating cultures for 18 to 20 hours at 37°C, 5% CO_2, cell-free supernatants are harvested and assayed for IFN-α using commercial ELISAs. These IFN-α values are then normalized to picograms/10^6 pDCs by determining the frequency of $CD123^+BDCA2^+$ pDCs within an aliquot of the PBMC suspension using flow cytometry. TLR7-specific stimuli, including single-stranded RNA viruses (e.g., influenza A, rhinovirus) and synthetic compounds (e.g., R848), also induce potent IFN-α responses and have been used in assessing pDC responses. It is important to emphasize that there are now many (~20) different species of IFN-α. And while these potentially cross-react with detection antibodies, most ELISAs to date report specificity for IFNα2. Finally, both pDCs and myeloid DCs (mDCs) have been shown to support T-cell responses to allergen, suggesting that these adaptive immune responses may also function as assays to monitor allergic inflammation. Naturally, the requirement to purify these rare DC subtypes makes these assays technically challenging, thus lessening their clinical relevance at this time. As a result, the reader is referred elsewhere for an in-depth description of how these assays are performed (16), since they are beyond the scope of this chapter.

QUALITY ASSURANCE OF *IN VITRO* ASSAYS

The above assays are not regulated by the Clinical Laboratory Improvement Act of 1988. Therefore, inter-laboratory proficiency surveys are not available. However, there are critical steps that can be taken to ensure the validity of the analytical measurements. First, when the allergic status of an individual is evaluated, it is important to include controls to ensure basophil reactivity, especially when the challenging allergen does not induce the release of the mediator in question. For histamine and LTC4 release, but also BAM expression, this inclusion is most commonly achieved by stimulating basophils with anti-IgE antibody and/or with FMLP, which are both quite effective in inducing the release of these mediators from basophils obtained from most donors. For IL-4 and IL-13 protein, anti-IgE antibody alone is usually sufficient to induce the secretion of these cytokines from most donors' basophils. However, as noted above, a calcium ionophore (ionomycin or A23187) has been shown to be a potent and relatively specific stimulus for the secretion of both cytokines by basophils. The lack of reactivity with these stimuli could indicate that calcium is missing from the reaction buffer or that the temperature is not 37°C, but at ≥40°C. It is also important that IL-3 will often enhance the IgE-mediated release of all of the above-listed mediators and BAM and may be employed when basophils show marginal release in response to an antigen alone. In contrast, false-positive histamine release may occur as a result of cell lysis due to solvents found in allergen preparations. In this instance, it is important to include controls showing that, in the absence of allergen, the solvents cause no additional release above the spontaneous release (blanks). Similarly, in studies investigating substances that inhibit mediator release,

it is important to show that final concentrations of the solvent (e.g., dimethyl sulfoxide) have no effect on secretion.

There are several other factors to consider when performing the assays that directly measure mediators and markers of allergic inflammation. The first deals with the general use of standards for these assays. Stock solutions should always be prepared using established methodology to prevent inter-assay variability. Storing these in small aliquots avoids repeated freeze/thaw conditions that may result in loss of activity. It is also extremely important that the standards be prepared in diluent identical to or closely resembling that found in the test samples. For example, when culture supernatants are tested for IL-4 or IL-13 protein, it is important that the standards be diluted in medium identical to that used in the cultures, since medium-containing serum may produce different background levels compared with buffer containing little to no protein. Finally, data analysis for these assays is greatly facilitated by the use of computer application programs, which are often commercially available from equipment manufacturers. They are especially helpful for histamine measurements determined by automated fluorometry, in which many samples can be assayed at a given time and the data can be saved and stored for later access and rapid analysis.

IN VIVO DIAGNOSTIC ALLERGY TESTING: SKIN TESTING

Allergen skin testing is a convenient, rapid, and cost-effective screening modality for the detection of IgE-mediated conditions. A positive skin test indicates the presence of allergen-specific IgE bound to FcεRI on the surface of mast cells. Introduction of allergen into the skin either by prick-puncture or by needle injection crosslinks the allergen-specific IgE on the surface of local mast cells, leading to degranulation and mediator release, as described above, that produces a sharply demarcated area of edema (wheal) and an even larger area of erythema (flare). Some individuals also develop a late-phase reaction (LPR) at skin test sites, characterized by warmth, deep tissue edema, erythema, and pruritus that typically resolves over 24 to 48 hours. LPRs are instigated by mast cell-derived mediators but do not predict clinical symptoms and are therefore not useful in the diagnosis of allergic disease (24). Subjects harboring IgE specific to an allergen are said to be "sensitized" to that allergen. However, the diagnosis of an allergic disorder also requires a clinical history and/or allergen challenge that supports a causal relationship between exposure to the allergen and the development of allergic symptoms.

As noted above, alternatives to allergen skin testing are available, including serum assays that allow direct measurement of allergen-specific IgE antibodies (see chapter 82). Naturally, some situations mandate the use of in these *in vitro* assays over the use of skin testing, especially in individuals deemed to be at high risk for an anaphylactic reaction to testing, those with severe poorly controlled asthma, or patients who have experienced severe reactions following exposure to minute amounts of allergen. However, systemic reactions following prick-puncture testing are exceedingly rare (<0.001%), with only one case of fatal anaphylaxis ever reported (25, 26). Patients with extensive dermatitis or dermatographism as well as those who cannot withhold interfering medications (either those that interfere with interpretation of skin test results or those that inhibit treatment of anaphylaxis) may also not be candidates for skin testing. A recent episode of anaphylaxis can lead to false-negative results since skin mast cells can persist in a hypoactive state for at least 4 weeks following a severe allergic reaction. Assessment of basophil mediator release and expression of activation markers as described above is another strategy to investigate the role of IgE in clinical symptoms. The relative sensitivity of *in vivo* and *in vitro* testing varies, depending on the particular antigen being tested. Many early comparative studies suggested that skin testing is more sensitive than *in vitro* tests; however, most of these studies were performed with earlier generations of *in vitro* tests, and newer versions appear to give comparable diagnostic sensitivity and specificity (27).

Clinical Indications

Aeroallergen Assessment

Skin testing with a panel of aeroallergen extracts of clinical relevance to the geographical area where testing is performed or symptoms are experienced is a primary means of diagnosing allergic rhinitis, asthma, and conjunctivitis. Assessment using the prick-puncture method has excellent positive predictive value. A positive intradermal test for an aeroallergen in the setting of a negative prick-puncture test has low positive predictive value for predicting symptoms following allergen exposure (28).

Food Allergy Assessment

The use of *in vivo* tests for the diagnosis of food allergy are discussed in detail in chapter 84.

Stinging-Insect Assessment

The diagnosis of Hymenoptera venom allergy requires a clinical history of a sting that elicited a systemic allergic reaction, as well as evidence of venom-specific IgE. For *in vivo* testing, intradermal injection is required for definitive diagnosis when prick-puncture testing is negative. Initially, prick-puncture testing is started at 100 μg/ml. If negative, the protocol proceeds with intradermal testing with venom concentrations between 0.001–0.01 μg/ml, and injections are advanced in logarithmic increases to 1.0 μg/ml. Concentrations higher than 1.0 μg/ml may result in irritant reactions (29). If skin testing is negative in patients with a convincing history, *in vitro* testing should be performed and skin testing should be repeated in 6 to 12 weeks. These two methods of testing can provide complementary information, as up to 20% of skin test-positive patients have undetectable venom-specific IgE, and 10 to 20% of patients with negative skin tests have positive *in vitro* studies (30, 31). Together, skin testing and *in vitro* studies identify approximately 98% of patients who will develop a systemic allergic reaction to a subsequent sting.

Medications Adverse Reaction Assessment

Skin testing can be a helpful diagnostic tool when the adverse reaction to a medication is suspicious for an IgE-mediated mechanism. However, in many instances, the relevant antigen is not the parent compound and therefore is not commercially available for testing. Interpreters must keep in mind that the antigenic epitope responsible for the reaction may be a metabolized product of the parent compound. Currently, the only group of medications for which skin testing has been validated and standardized is beta-lactam antibiotics. Skin testing is the preferred method for identifying patients at risk for penicillin-induced anaphylactic reactions, because this method is more sensitive than *in vitro* assays for penicillin-specific IgE. The minimal reagents required for penicillin skin testing include the major determinant, penicilloyl-polylysine (Pre-Pen), and the minor determinant, penicillin G, although a minor determinant mixture that also includes

penicilloate and penilloate can be used if available. However, most studies have suggested that the negative predictive value of skin testing with Pre-Pen plus the minor determinant mixture was similar to Pre-Pen plus penicillin G alone (32, 33). Prick-puncture testing is usually performed first, followed by intradermal testing if the prick-puncture tests are negative. Approximately 50% of patients who have a positive skin test for penicillin develop an immediate-type allergic reaction following exposure to penicillin (33, 34–37). However, a negative test confers a 97 to 99% negative predictive value (32, 35, 37–39). While the availability of Pre-Pen had been plagued with manufacturing issues, this product became commercially available again in the United States in 2009.

Procedures

Several preparatory measures are required for successful testing outcomes. All interfering medications must be discontinued in order to achieve interpretable results. Second-generation H1 antihistamines (cetirizine, loratadine) should be discontinued for 7 days prior to testing, while 1 to 3 days is typically sufficient for first-generation nonselective antihistamines (diphenhydramine) (40). Hydroxyzine should be discontinued at least 96 hours prior to testing, H2 receptor antagonists (ranitidine, cimetidine) for 48 hours, and tricyclic antidepressants for 7 to 14 days (41). In general, systemic glucocorticoids, inhaled or intranasal glucocorticoids, decongestants, inhaled beta agonists, cromolyn, and leukotriene receptor antagonists do not affect skin test responses (42, 43). Topical steroids can transiently reduce the frequency of skin mast cells, and therefore, skin testing should be performed on non-treated areas of skin (44, 45). Finally, patients who received omalizumab, a humanized anti-IgE monoclonal antibody, may exhibit reduced skin test responses for as long as 6 months following discontinuation of the drug. *In vitro* assays should be considered an alternative in patients with dermatographism or active dermatitis, given the increased risk of obtaining false-positive results. Testing can be performed on pregnant patients but is not advisable unless the information gained from testing is deemed to outweigh the risk of adverse effects on the fetus if a systemic reaction occurs. Although systemic reactions are rare, a supervising physician and resuscitation materials should always be on hand. First-line treatment for a systemic reaction is 0.3 ml of 1:1000 aqueous epinephrine for adults and 0.01 ml/kg of body weight (up to 0.3 ml) for children, administered intramuscularly (46). Other resuscitative materials should include antihistamines, corticosteroids, oxygen, and normal saline for volume replacement. Patients with life-threatening reactions should be transported to the nearest emergency department. The risk of systemic reaction is higher with intradermal testing; therefore, a practical approach is to use prick-puncture testing for screening and intradermal testing for confirming equivocal or negative percutaneous tests (47). While intradermal testing does have much greater sensitivity, it also produces more false-positive results. Intradermal testing is primarily used in the diagnosis of venom allergy and is not recommended for diagnosing food or latex allergy due to an unacceptably high rate of systemic reactions to testing. The number of individual extracts tested is dependent on many variables, including the patient's clinical history, geographical area, age, and knowledge of antigen cross-reactivity. Skin testing can be performed at any age. Skin reactivity generally increases throughout childhood and then plateaus in the teenage years. Although both infants and older adults may exhibit smaller positive results, skin testing can still be clinically useful in these age groups (48, 49).

Testing sites are cleansed with 70% isopropyl alcohol and marked for identification. Using barrier precautions, allergen extracts of known composition are introduced into the skin, usually on the volar surface of the arm or the upper back. While the forearm may produce smaller wheals than the skin on the back, the difference is not thought to be clinically relevant (50). Individual tests should have sufficient spacing, usually 2.5 cm, and should not be placed within 5 cm of the wrist or 3 cm of the antecubital fossa. False-positive results from adjacent reactions are unlikely if there are at least 2 cm between individual test sites (50).

Controls

Positive and negative controls must be applied in the absence of interfering medications. Histamine as a positive control must be read at 10 to 15 min to achieve peak reactivity. Histamine dichloride (10 mg/ml for epicutaneous use and 0.001 mg/ml for intradermal use) is typically used as the positive control and the same diluent used for the allergen extracts (usually glycerinated saline) as the negative control.

Prick-Puncture Tests

Several devices and techniques can be used to perform the prick-puncture test. The purpose is to introduce a small quantity of allergen into the skin after interruption of the epidermal barrier. Disposable lancets on single or multi-tipped devices (which allow application of multiple allergens simultaneously) as well as various needles can be used for the prick-puncture technique. The type of testing device used can influence the results (51, 52). For example, multi-tipped devices generally produce more false-negative results than single-tipped devices, but can be useful for rapid testing of multiple allergens (51, 53, 54). Additional variables involved in testing include the angle and depth of penetration and the force applied by the applicator. Proper application should not cause excessive trauma or bleeding at the site. Single- and multi-tipped devices often simultaneously place a drop of allergen extract while puncturing the skin. If such devices are not used, a drop of extract is placed on the skin, and the needle or lancet is used to prick through the extract.

Intradermal Tests

Intradermal testing is usually performed on the volar aspect of the arm to allow application of a tourniquet in the event of a systemic reaction. The concentration used is usually 100- to 1,000-fold more dilute than the concentration used in the prick-puncture method. The skin test site is first cleansed and marked for allergen identification. Using a 26- or 27-gauge tuberculin needle, 0.01–0.05 ml of diluted extract is introduced into the skin. With the skin held taut, the needle is inserted bevel down at a 45-degree angle to the skin. After initial insertion, the syringe is lowered parallel to the skin and advanced only sufficiently to provide an intradermal injection. A small wheal about 3 mm in diameter is usually formed. A new needle is used for each injection.

Interpretation

Quality interpretation can depend on many variables, including skin color, testing site, skin reactivity, and reader skill. Histamine-positive controls are ideally read 10 min after application and allergen extracts after 15 to 20 min. Reporting in a standardized manner as recommended by the American College of Allergy, Asthma, and Immunology and the American Academy of Allergy, Asthma, and Immunology should include subject name and date of birth, longest diameter of wheal and flare in millimeters,

device used, time, date, reader, and extracts tested. A semi-quantitative manner of reporting using, for example, 1+, 2+, is not advised due to marked inter-physician variability in reporting results this way, other than for extreme positive results (55). A positive prick puncture test is defined as either a wheal equal to or larger in size than that elicited by the histamine control (which usually produces a wheal of at least 3 mm) or a wheal diameter of 3 mm or greater compared with the diluent control. For intradermal testing, a wheal of 5 mm or larger is considered positive; the clinical significance of smaller positive reactions has been debated (56). In general, prick-puncture testing is considered more specific but less sensitive than intradermal testing. False-positives with intradermal testing may be due to the presence of naturally occurring histamine or other vasoactive amines, endotoxin, or other skin irritants in the extracts, especially those for venom, molds, and food. Interpretation of all skin tests is dependent on clinical correlation and an understanding of testing limitations, since the presence of IgE antibodies does not always imply symptom culpability.

Reagents

Reconstitution, Stability, and Storage

The potency and quality of the allergen extracts used for testing can drastically alter the results. Currently, 19 allergens, including grass pollens, cat hair, dust mite, ragweed, and Hymenoptera venoms are standardized in potency units. However, the other extracts, including all commercially available food extracts, are not. Non-standardized extracts are supplied in weight per volume and, therefore, may have significant variation in lot-to-lot concentration (57). The thermal stability, compatibility, and cross-reactivity of allergen extracts are critical to consider when storing and mixing different reagents for testing and/or allergen immunotherapy. Allergen extract potency deteriorates with time, dilution, and increased temperature. Several studies have demonstrated extract degradation with higher temperatures, fungal and insect protease activity, and percent glycerin of diluent (58, 59). Glycerinated extracts protect unstable allergens from denaturation, inhibit protease degradation, and increase thermal stability. Diluted extracts need to be remixed every 2 to 3 months in buffered saline or normal saline diluent and every 6 months in 10% glycerin or human serum albumin diluent. Allergen extracts should be stored at 4°C.

A number of recombinant allergens are undergoing preclinical and clinical studies but are not yet licensed for use in skin testing or immunotherapy. Recombinant allergens may be advantageous since they can be produced with greater purity and stability, although critical antigen epitopes may be excluded when single recombinant allergens, versus their natural counterparts, are used. The diagnostic and therapeutic uses of recombinant allergens await further study (60, 61).

AIRWAY CHALLENGES

While both skin and serologic testing can provide insight into the antigens that elicit IgE-mediated reactions, these tests do not predict the nature or intensity of clinical symptoms in a given individual when exposed to those allergens. For this reason, allergen challenges of either the upper (intranasal) or lower (bronchial) airway can be done to further assess the relationship between a patient's allergen sensitivities and their development of rhinitis and/or asthma symptoms following allergen exposure.

Clinical Indications

Airway challenges, either intranasal or bronchial, can be used to determine whether a single allergen may be responsible for symptoms of either rhinitis or asthma or both conditions. In general, most allergists use a combination of patient-reported rhinitis symptoms and positive skin tests to identify the most likely culprit of allergic nasal symptoms. Intranasal challenges are more often used to determine the effect of anti-allergic drugs in an experimental setting. Bronchial challenge can be done to assess airway reactivity in the diagnosis of asthma but has also been utilized to determine the effectiveness of pharmacologic agents. Two bronchial challenge models that have been developed to mimic allergic asthma are the whole-lung and segmental antigen challenges. Segmental challenge involves installation of antigen solution through a bronchoscope into a sub-segment of the lung. Since it may be performed only by those trained in bronchoscopy and is used almost exclusively for research investigation, it will not be discussed further in this chapter. Whole-lung antigen challenge can be used both as a diagnostic and as a research tool and is useful in determining relevant environmental stimuli, including occupational exposures that may be provoking asthma symptoms in a patient who cannot define exacerbating factors. In addition to its diagnostic application, whole-lung antigen challenge is also used to determine the effects of treatment methods to block allergic physiologic changes and asthmatic symptoms. Bronchial challenge with nonspecific agents (e.g., methacholine, histamine) can also be used to assess bronchial reactivity and are discussed further in prior editions of this manual.

Both intranasal and whole-lung antigen challenges initiate allergic reactions and may precipitate bronchoconstriction. Therefore, these procedures should be performed only by trained personnel equipped to treat such emergencies. Neither intranasal nor whole-lung antigen challenges should be performed during asthma exacerbations, because doing so may make the flare worsen and may also lead to aberrant results due to the increase in nonspecific bronchial reactivity that can occur during asthma flares. In general, it is not recommended that whole-lung antigen challenge be performed if the forced expiratory volume in 1 s (FEV1) is <60% of predicted values (62). Other health problems such as underlying heart disease must also be considered, since whole-lung antigen challenge may result in prolonged bronchoconstriction and, potentially, hypoxia.

Test Procedures

Intranasal Challenge

Several methods have been developed to test the effect of antigen exposure on the nasal mucosal surface in allergic reactions. The decision of which allergens to test usually depends on the patient's clinical history and sensitivities as determined by skin testing and/or serologic testing. Nasal provocation tests using standardized allergens are usually started at an initial concentration of 1:1,000 and then increased at log or half-log intervals. For other allergens, 1/1,000 of the concentration that elicits a positive prick-puncture test can be used as the starting dose (63). Sequential dose increments are usually given in 10- to 15-min intervals, but this varies depending on the allergen and the patient's sensitivity. A diluent solution (in which the allergen is dissolved) is first applied to detect nonspecific responses, followed by application of the allergen. The allergen can be applied using several methods, but the most commonly used methods include a spray pump or nebulizer that instills allergen into the nares or a micropipette that

deposits the allergen solution directly on the inferior turbinate. The patient should be seated and hold his/her breath during application to prevent allergen from entering the lower respiratory tract. Several outcomes can be followed, including symptom scores (e.g., sneezes, itchiness, rhinorrhea, nasal obstruction, ocular symptoms), measurements of nasal patency by rhinometry, and inflammatory responses (e.g., cell differentials and inflammatory mediator concentrations in nasal lavage fluid, nasal brushings, or nasal biopsies) (64). The quantity and weight of nasal secretions can also be measured from paper disks placed on the nasal mucosa for a defined period of time. Alternatively, the weight and/or number of paper tissues into which a subject has blown his or her nose is determined (65). Generally, both a symptom score and an objective measure of nasal obstruction are recommended. Outcomes are typically assessed at baseline, following application of the inert diluent, and after each dose of allergen. Completion of the challenge protocol may be determined by a preordained level of symptoms or physiologic changes or by administration of a defined number of individual allergen concentrations.

Since there is no standardized protocol for intranasal challenge, and different investigators have used a wide variety of methods and doses of antigen instillation, the reproducibility of intranasal challenges is not well-established. To improve the reliability of results, the patient should be asymptomatic at the time of the challenge, the procedure should not be performed during the peak pollen season, and at least 1 week should be left between tests in order to reduce the "priming" effect, in which an exposure to an allergen augments the response to subsequent exposure to the same allergen.

Whole-Lung Antigen Challenge

Allergen inhalation challenges are invaluable to study the mechanisms of asthma and the potential of new asthma therapeutics but can induce severe bronchoconstriction. Therefore, the dose of allergen used must be chosen carefully so that it will induce a sufficient airway response but still be safe for the patient. The starting dose of allergen used is typically determined using end point dilution intradermal skin testing, in which 10-fold allergen dilutions are injected into a patient's skin, and the wheal measured 15 min later (66). The concentration given intradermally is then increased at 15-min intervals until a wheal response of 10 mm is obtained. One log higher than this concentration is used to initiate the inhaled challenge.

The choice of an apparatus to deliver aerosolized solutions is important for delivering test doses reliably. The Wright and DeVilbiss nebulizers are commonly used. The Wright nebulizer generates an aerosol that is inhaled by tidal breathing for 2 min for each dose. The flow rate on the nebulizer is adjusted to achieve an output of 0.13 ml/min. Optimal particle size from the nebulizer is 0.5 to 2 μm, which is ideal for allergen delivery to the small airways; larger particles are deposited in the mouthpiece and upper airway, and smaller particles are lost through exhalation (67). At the start of the procedure, baseline pulmonary function testing is performed, and the FEV1 is recorded. Next, the subject takes five breaths of sterile 10% phosphate-buffered saline solution used as a diluent via the nebulizer. Spirometry is performed 3 min later. If the FEV1 decreases by more than 10%, the study should be terminated since the specificity of the antigen challenge cannot be evaluated. Five breaths of the initial antigen concentration are then inhaled, and the FEV1 is measured 10 min later. Five breaths of half-log-increasing concentrations of antigen are inhaled at 10-min intervals until either a >20% decrease in FEV1 or the maximum dose is achieved. At this point, bronchodilators can be administered to immediately relieve the bronchoconstriction, or hourly pulmonary function measurements can be made to determine whether the subject experiences an asthmatic late-phase reaction. The presence of a late-phase reaction is defined as an FEV1 measurement 4 to 8 hours after the whole-lung antigen challenge that is <15% of the saline control FEV1 measurement. The physiologic mechanisms behind late-phase reactions are unclear but may involve smooth muscle constriction, airway edema, and mucus hyperproduction that causes airflow obstruction. Approximately 30% to 40% of subjects who have at least a 20% immediate decrease in FEV1 with whole-lung antigen challenge experience a late-phase reaction.

Whole-lung allergen challenges are considered to be the most definitive method to test the specificity of a particular antigen to cause bronchial reactions. False-positive reactions can occur when the antigen is given in high enough concentrations to cause asthma symptoms in allergic rhinitis patients or normal subjects who previously had never experienced asthma. The reproducibility of whole-lung allergen challenge from day to day is less than 2-fold in concentration and is improved if the prechallenge FEV1 is within 10% on the two challenges.

SUMMARY

It is now possible to measure a number of inflammatory mediators released from cells participating in allergic disease. Measurement of the release of preformed histamine from peripheral blood basophils challenged with a specific antigen is among several tests available, and histamine release remains a valuable *in vitro* correlate of immediate hypersensitivity reactions. However, other mediators that have a role in allergic inflammation, such as LTC4 and IL-4, are also generated by basophils upon IgE-dependent activation, and *in vitro* assays have recently been developed to measure these products. These assays, combined with those long used for *in vivo* assessment of immediate hypersensitivity reactions, have significantly added to our understanding of the parameters, mechanisms, and pharmacologic control of allergic inflammation.

APPENDIX

Special Reagents and Equipment

RFA 300 rapid flow analyzer for histamine measurement by fluorometry (Astoria-Pacific International, Clackamas, OR)

Filtered Reagents for Fluorometry

Phosphoric acid (0.73 M)

30% NaCl

5 N NaOH

1 N NaOH containing 1 mM EDTA

0.1 NHCl

Brij-saline-EDTA: 0.17 M NaCl, 1.5 mM EDTA, 0.015% Brij 35 (Perstorp Analytical, Silver Spring, MD)

Heptane

Butanol

OPT solution: 50 mg of OPT (Sigma, St. Louis, MO) recrystallized in ligroine solvent (Eastman Kodak Co., Rochester, NY), 1 ml of spectranalyzed methanol (Fisher Scientific, Pittsburgh, PA), and 99 ml of borate buffer (0.5 M)

Histamine Standards (for Fluorometry)

Histamine dihydrochloride (molecular weight, 184.1)

Histamine (molecular weight, 111.0)

Make a 1-mg/ml solution of histamine.

Note that 1 mg of histamine equals 1.66 mg of histamine dihydrochloride.

Dilute the 1-mg/ml solution 1/1,000 in 2% $HClO_4$ to give a 1-μg/ml stock and store at –20°C in 6-ml aliquots. Six milliliters of 1-μg/ml histamine added to 294 ml of 2% $HClO_4$ yields 20 ng/ml; 50 ml of 20-ng/ml standard added to 50 ml of 2% $HClO_4$ yields 10 ng/ml.

10× PIPES buffer, pH 7.4: 250 mM PIPES (Sigma Chemical Co.), 1.10 M NaCl, 50 mM KCl

PAG buffer: 10% 10× PIPES, 0.003% human serum albumin (Calbiochem-Behring Corp., La Jolla, CA), 0.1% D-glucose

PAG-EDTA buffer: PAG containing 4 mM EDTA

PAGCM buffer: PAG containing 1 mM $CaCl_2$ and 1 mM $MgCl_2$

Isotonic Percoll: 9 parts Percoll (Pharmacia, Piscataway, NJ) plus 1 part 10× PIPES

Lactic acid buffer (pH 3.9): 90.1 mg of lactic acid (Calbiochem-Behring Corp.), 817.6 mg of NaCl, 37.28 mg of KCl, 100 ml of distilled water

REFERENCES

1. **Schroeder JT.** 2011. Basophils: emerging roles in the pathogenesis of allergic disease. *Immunol Rev* **242:**144–160. PubMed
2. **Pulendran B, Artis D.** 2012. New paradigms in type 2 immunity. *Science* **337:**431–435. PubMed
3. **Siraganian RP.** 1974. An automated continuous-flow system for the extraction and fluorometric analysis of histamine. *Anal Biochem* **57:**383–394. PubMed
4. **Ishizaka T, De Bernardo R, Tomioka H, Lichtenstein LM, Ishizaka K.** 1972. Identification of basophil granulocytes as a site of allergic histamine release. *J Immunol* **108:**1000–1008. PubMed
5. **Aalberse RC, van der Gaag R, van Leeuwen J.** 1983. Serologic aspects of IgG4 antibodies. I. Prolonged immunization results in an IgG4-restricted response. *J Immunol* **130:**722–726. PubMed
6. **Pruzansky JJ, Grammer LC, Patterson R, Roberts M.** 1983. Dissociation of IgE from receptors on human basophils. I. Enhanced passive sensitization for histamine release. *J Immunol* **131:**1949–1953. PubMed
7. **Sin AZ, Roche EM, Togias A, Lichtenstein LM, Schroeder JT.** 2001. Nerve growth factor or IL-3 induces more IL-13 production from basophils of allergic subjects than from basophils of nonallergic subjects. *J Allergy Clin Immunol* **108:**387–393. PubMed
8. **Saini S, Bloom DC, Bieneman A, Vasagar K, Togias A, Schroeder J.** 2004. Systemic effects of allergen exposure on blood basophil IL-13 secretion and FcepsilonRIbeta. *J Allergy Clin Immunol* **114:**768–774. PubMed
9. **Schroeder JT, Beineman AP, Chichester KL, Bresline L, Xiao H-Q, Liu MC.** 2010. Pulmonary allergic responses augment IL-13 secretion by circulating basophils yet suppress IFN-alpha from plasmacytoid dendritic cells. *Clin Exp Allergy* **40:**745–754. PubMed
10. **Devouassoux G, Foster B, Scott LM, Metcalfe DD, Prussin C.** 1999. Frequency and characterization of antigen-specific IL-4- and IL-13- producing basophils and T cells in peripheral blood of healthy and asthmatic subjects. *J Allergy Clin Immunol* **104:**811–819. PubMed
11. **Gilbert HS, Ornstein L.** 1975. Basophil counting with a new staining method using alcian blue. *Blood* **46:**279–286. PubMed
12. **Ono E, Taniguchi M, Higashi N, Mita H, Kajiwara K, Yamaguchi H, Tatsuno S, Fukutomi Y, Tanimoto H, Sekiya K, Oshikata C, Tsuburai T, Tsurikisawa N, Otomo M, Maeda Y, Hasegawa M, Miyazaki E, Kumamoto T, Akiyama K.** 2010. CD203c expression on human basophils is associated with asthma exacerbation. *J Allergy Clin Immunol* **125:**483–489.e3. PubMed
13. **Ford LS, Bloom KA, Nowak-Węgrzyn AH, Shreffler WG, Masilamani M, Sampson HA.** 2013. Basophil reactivity, wheal size, and immunoglobulin levels distinguish degrees of cow's milk tolerance. *J Allergy Clin Immunol* **131:**180–6.e1, 3. PubMed
14. **Kleine-Tebbe J, Erdmann S, Knol EF, MacGlashan DW Jr, Poulsen LK, Gibbs BF.** 2006. Diagnostic tests based on human basophils: potentials, pitfalls and perspectives. *Int Arch Allergy Immunol* **141:**79–90. PubMed
15. **MacGlashan DW Jr.** 1995. Graded changes in the response of individual human basophils to stimulation: distributional behavior of events temporally coincident with degranulation. *J Leukoc Biol* **58:**177–188. PubMed
16. **Frischmeyer-Guerrerio PA, Schroeder JT.** 2012. Cellular immune response parameters that influence IgE sensitization. *J Immunol Methods* **383:**21–29. PubMed
17. **Schwartz LB, Metcalfe DD, Miller JS, Earl H, Sullivan T.** 1987. Tryptase levels as an indicator of mast-cell activation in systemic anaphylaxis and mastocytosis. *N Engl J Med* **316:**1622–1626. PubMed
18. **Siegal FP, Kadowaki N, Shodell M, Fitzgerald-Bocarsly PA, Shah K, Ho S, Antonenko S, Liu Y-J.** 1999. The nature of the principal type 1 interferon-producing cells in human blood. *Science* **284:**1835–1837. PubMed
19. **Tversky JR, Le TV, Bieneman AP, Chichester KL, Hamilton RG, Schroeder JT.** 2008. Human blood dendritic cells from allergic subjects have impaired capacity to produce interferon-alpha via Toll-like receptor 9. *Clin Exp Allergy* **38:**781–788. PubMed
20. **Gill MA, Bajwa G, George TA, Dong CC, Dougherty II, Jiang N, Gan VN, Gruchalla RS.** 2010. Counterregulation between the FcepsilonRI pathway and antiviral responses in human plasmacytoid dendritic cells. *J Immunol* **184:**5999–6006. PubMed
21. **Futata E, Azor M, Dos Santos J, Maruta C, Sotto M, Guedes F, Rivitti E, Duarte A, Sato M.** 2011. Impaired IFN-α secretion by plasmacytoid dendritic cells induced by TLR9 activation in chronic idiopathic urticaria. *Br J Dermatol* **164:**1271–1279. PubMed
22. **Schroeder JT, Bieneman AP, Xiao H, Chichester KL, Vasagar K, Saini S, Liu MC.** 2005. TLR9- and FcepsilonRI-mediated responses oppose one another in plasmacytoid dendritic cells by down-regulating receptor expression. *J Immunol* **175:**5724–5731. PubMed
23. **Tversky JR, Bieneman AP, Chichester KL, Hamilton RG, Schroeder JT.** 2010. Subcutaneous allergen immunotherapy restores human dendritic cell innate immune function. *Clin Exp Allergy* **40:**94–102. PubMed
24. **Bernstein IL, Storms WW.** 1995. Practice parameters for allergy diagnostic testing. Joint Task Force on Practice Parameters for the Diagnosis and Treatment of Asthma. The American Academy of Allergy, Asthma and Immunology and the American College of Allergy, Asthma and Immunology. *Ann Allergy Asthma Immunol* **75:**543–625. PubMed
25. **Bernstein DI, Wanner M, Borish L, Liss GM, Immunotherapy Committee, American Academy of Allergy, Asthma, and Immunology.** 2004. Twelve-year survey of fatal reactions to allergen injections and skin testing: 1990–2001. *J Allergy Clin Immunol* **113:**1129–1136. PubMed
26. **Norrman G, Fälth-Magnusson K.** 2009. Adverse reactions to skin prick testing in children - prevalence and possible risk factors. *Pediatr Allergy Immunol* **20:**273–278. PubMed

27. **Oppenheimer J, Nelson HS.** 2006. Skin testing. *Ann Allergy Asthma Immunol* **96**(Suppl 1)**:**S6–S12. PubMed
28. **Wood RA, Phipatanakul W, Hamilton RG, Eggleston PA.** 1999. A comparison of skin prick tests, intradermal skin tests, and RASTs in the diagnosis of cat allergy. *J Allergy Clin Immunol* **103:**773–779. PubMed
29. **Georgitis JW, Reisman RE.** 1985. Venom skin tests in insect-allergic and insect-nonallergic populations. *J Allergy Clin Immunol* **76:**803–807. PubMed
30. **Hamilton RG.** 2001. Responsibility for quality IgE antibody results rests ultimately with the referring physician. *Ann Allergy Asthma Immunol* **86:**353–354. PubMed
31. **Hamilton RG.** 2004. Diagnostic methods for insect sting allergy. *Curr Opin Allergy Clin Immunol* **4:**297–306. PubMed
32. **del Real GA, Rose ME, Ramirez-Atamoros MT, Hammel J, Gordon SM, Arroliga AC, Arroliga ME.** 2007. Penicillin skin testing in patients with a history of beta-lactam allergy. *Ann Allergy Asthma Immunol* **98:**355–359. PubMed
33. **Green GR, Rosenblum AH, Sweet LC.** 1977. Evaluation of penicillin hypersensitivity: value of clinical history and skin testing with penicilloyl-polylysine and penicillin G. A cooperative prospective study of the penicillin study group of the American Academy of Allergy. *J Allergy Clin Immunol* **60:**339–345. PubMed
34. **Adkinson NF Jr, Thompson WL, Maddrey WC, Lichtenstein LM.** 1971. Routine use of penicillin skin testing on an inpatient service. *N Engl J Med.* **285:**22–24.
35. **Caubet JC, Kaiser L, Lemaitre B, Fellay B, Gervaix A, Eigenmann PA.** 2011. The role of penicillin in benign skin rashes in childhood: a prospective study based on drug rechallenge. *J Allergy Clin Immunol* **127:**218–222.
36. **Macy E, Burchette RJ.** 2002. Oral antibiotic adverse reactions after penicillin skin testing: multi-year follow-up. *Allergy* **57:**1151–1158.
37. **Sogn DD, Evans R 3rd, Shepherd GM, Casale TB, Condemi J, Greenberger PA, Kohler PF, Saxon A, Summers RJ, Van Arsdel PP Jr, et al.** 1992. Results of the National Institute of Allergy and Infectious Diseases Collaborative Clinical Trial to test the predictive value of skin testing with major and minor penicillin derivatives in hospitalized adults. *Arch Intern Med.* **152:**1025–1032.
38. **Kamboj S, Yousef E, McGeady S, Hossain J.** 2011. The prevalence of antibiotic skin test reactivity in a pediatric population. *Allergy Asthma Proc.* **32:**99–105.
39. **Macy E, Mangat R, Burchette RJ.** 2003. Penicillin skin testing in advance of need: multiyear follow-up in 568 test result-negative subjects exposed to oral penicillins. *J. Allergy Clin. Immunol.* **111:**1111–1115.
40. **dos Santos RV, Magerl M, Mlynek A, Lima HC.** 2009. Suppression of histamine- and allergen-induced skin reactions: comparison of first- and second-generation antihistamines. *Ann Allergy Asthma Immunol.* **102:**495–499.
41. **Kupczyk M, Kuprys I, Bochenska-Marciniak M, Gorski P, Kuna P.** 2007. Ranitidine (150 mg daily) inhibits wheal, flare, and itching reactions in skin-prick tests. *Allergy Asthma Proc.* **28:**711–715.
42. **Des Roches A, Paradis L, Bougeard YH, Godard P, Bousquet J, Chanez P.** 1996. Long-term oral corticosteroid therapy does not alter the results of immediate-type allergy skin prick tests. *J Allergy Clin Immunol.* **98:**522–527.
43. **Hill SL 3rd, Krouse JH** (2003). The effects of montelukast on intradermal wheal and flare. *Otolaryngol Head Neck Surg.* **129:**199–203.
44. **Gradman J, Wolthers OD.** 2008. Suppressive effects of topical mometasone furoate and tacrolimus on skin prick testing in children. *Pediatr Dermatol.* **25:**269–270.
45. **Pipkorn U, Hammarlund A, Enerback L.** 1989. Prolonged treatment with topical glucocorticoids results in an inhibition of the allergen-induced weal-and-flare response and a reduction in skin mast cell numbers and histamine content. *Clin Exp Allergy* **19:**19–25.
46. **Simons FE, Gu X, Simons KJ.** 2001. Epinephrine absorption in adults: intramuscular versus subcutaneous injection. *J Allergy Clin Immunol.* **108:**871–873.
47. **Turkeltaub PC.** 2000. Percutaneous and intracutaneous diagnostic tests of IgE-mediated diseases (immediate hypersensitivity). *Clin Allergy Immunol.* **15:**53–87.
48. **Menardo JL, Bousquet J, Rodiere M, Astruc J, Michel FB.** 1985. Skin test reactivity in infancy. *J Allergy Clin Immunol.* **75:**646–651.
49. **Song WJ, Lee SM, Kim MH, Kim SH, Kim KW, Cho SH, Min KU, Chang YS.** 2011. Histamine and allergen skin reactivity in the elderly population: results from the Korean Longitudinal Study on Health and Aging. *Ann Allergy Asthma Immunol.* **107:**344–352.
50. **Nelson HS, Knoetzer J, Bucher B.** 1996. Effect of distance between sites and region of the body on results of skin prick tests. *J Allergy Clin Immunol.* **97:**596–601.
51. **Carr WW, Martin B, Howard RS, Cox L, Borish L, Immunotherapy Committee of the American Academy of Allergy, Asthma, and Immunology.** 2005. Comparison of test devices for skin prick testing. *J Allergy Clin Immunol.* **116:**341–346.
52. **Masse MS, Granger Vallee A, Chiriac A, Dhivert-Donnadieu H, Bousquet-Rouanet L, Bousquet PJ, Demoly P.** 2011. Comparison of five techniques of skin prick tests used routinely in Europe. *Allergy* **66:**1415–1419.
53. **Nelson HS, Kolehmainen C, Lahr J, Murphy J, Buchmeier A.** 2004. A comparison of multiheaded devices for allergy skin testing. *J Allergy Clin Immunol.* **113:**1218–1219.
54. **Nelson HS, Lahr J, Buchmeier A, McCormick D.** 1998. Evaluation of devices for skin prick testing. *J Allergy Clin Immunol.* **101:**153–156.
55. **McCann WA, Ownby DR.** 2002. The reproducibility of the allergy skin test scoring and interpretation by board-certified/board-eligible allergists. *Ann Allergy Asthma Immunol.* **89:**368–371.
56. **Bernstein IL, Li JT, Bernstein DI, Hamilton R, Spector SL, Tan R, Sicherer S, Golden DB, Khan DA, Nicklas RA, Portnoy JM, Blessing-Moore J, Cox L, Lang DM, Oppenheimer J, Randolph CC, Schuller DE, Tiles SA, Wallace DV, Levetin E, Weber R; American Academy of Allergy, Asthma and Immunology; American College of Allergy, Asthma and Immunology.** 2008. Allergy diagnostic testing: an updated practice parameter. *Ann Allergy Asthma Immunol.* **100:**S1–148.
57. **Nelson HS.** 2004. Preparing and mixing allergen vaccines. *Clin Allergy Immunol.* **18:**457–479.
58. **Esch RE, Grier TJ.** 2011. Allergen compatibilities in extract mixtures. *Immunol Allergy Clin North Am.* **31:**227–239, viii.
59. **Grier TJ, LeFevre DM, Duncan EA, Esch RE, Coyne TC.** 2012. Allergen stabilities and compatibilities in mixtures of high-protease fungal and insect extracts. *Ann Allergy Asthma Immunol.* **108:**439–447.
60. **Chapman MD, Briza P.** 2012. Molecular approaches to allergen standardization. *Curr Allergy Asthma Rep.* **12:**478–484.
61. **Valenta R, Niespodziana K, Focke-Tejkl M, Marth K, Huber H, Neubauer A, Niederberger V.** 2011. Recombinant allergens: what does the future hold? *J Allergy Clin Immunol.* **127:**860–864.
62. **Crapo RO, Casaburi R, Coates AL, Enright PL, Hankinson JJ, Irvin CG, MacIntyre NR, McKay RT, Wanger JS, Anderson SD, Cockcroft DW, Fish JE, Sterk PJ.** 2000. Guidelines for methacholine and exercise challenge testing-1999. This official statement of the American Thoracic Society was adopted by the ATS Board of Directors, July 1999. *Am J Respir Crit Care Med.* **161:**309–329.

63. **Melillo G, Bonini S, Cocco G, Davies RJ, de Monchy JG, Frolund L, Pelikan Z.** 1997. EAACI provocation tests with allergens. Report prepared by the European Academy of Allergology and Clinical Immunology Subcommittee on provocation tests with allergens. *Allergy* **52:**1–35.
64. **Dordal MT, Lluch-Bernal M, Sánchez MC, Rondón C, Navarro A, Montoro J, Matheu V, Ibáñez MD, Fernández-Parra B, Dávila I, Conde J, Antón E, Colás C, Valero A; SEAIC Rhinoconjunctivitis Committee.** 2011. Allergen-specific nasal provocation testing: review by the rhinoconjunctivitis committee of the Spanish Society of Allergy and Clinical Immunology. *J Investig Allergol Clin Immunol.* **21:**1–12; quiz follow 12.
65. **Doyle WJ, Skoner DP, Seroky JT, Fireman P.** 1995. Reproducibility of the effects of intranasal ragweed challenges in allergic subjects. *Ann Allergy Asthma Immunol.* **74:**171–176.
66. **Cockcroft DW, Murdock KY, Kirby J, Hargreave F.** 1987. Prediction of airway responsiveness to allergen from skin sensitivity to allergen and airway responsiveness to histamine. *Am Rev Respir Dis.* **135:**264–267.
67. **Boulet LP, Gauvreau G, Boulay ME, O'Byrne P, Cockcroft DW; Clinical Investigative Collaboration, Canadian Network of Centers of Excellence AllerGen.** 2007. The allergen bronchoprovocation model: an important tool for the investigation of new asthma anti-inflammatory therapies. *Allergy* **62:**1101–1110.

Tests for Immunological Reactions to Foods

CARAH B. SANTOS, DAVID M. FLEISCHER, AND ROBERT A. WOOD

84

Food allergy is defined as an adverse health effect arising from a specific immune response that occurs reproducibly on exposure to a given food protein, and is distinguished from food intolerance (e.g. lactose intolerance), which is typically non-immunologic in origin (1). Food allergic disorders can be divided into those that are immunoglobulin E (IgE)-mediated and those that are non-IgE mediated. Disorders with acute onset of symptoms, defined typically as occurring within 2 hours after ingestion, are usually mediated by IgE antibodies, while subacute and chronic food allergic disorders may be cell mediated (primarily T cell) or of mixed origin with both cell-mediated and IgE-associated mechanisms. The subacute and chronic food allergic disorders primarily affect the gastrointestinal tract. Table 1 lists examples of IgE-, cell-, and mixed IgE- and cell-mediated disorders.

The diagnosis of food allergy must first begin with a detailed medical and reaction history. The information gathered should guide the best mode of diagnosis, or the history alone may rule out a diagnosis of food allergy. In some studies, only about 40% of suspected food-induced allergic reactions could be verified by double-blind, placebo-controlled food challenges (DBPCFCs) (2). In cases of acute reactions, such as anaphylaxis and urticaria following the ingestion of an isolated food, the medical history has a much higher predictive value than in reactions secondary to chronic disorders, such as atopic dermatitis and eosinophilic gastrointestinal disease. The history should focus on the type and quantity of food(s) suspected of provoking the reaction, the nature of the symptoms attributed to food ingestion (acute versus chronic), the timing between ingestion and onset of symptoms, the patterns of reactivity, the most recent reaction, and whether associated activities (e.g., exercise or alcohol ingestion) play a role in inducing symptoms. Once a reaction history is established (see Table 2 for a list of signs and symptoms of food-induced allergic reactions), the likelihood that a food is causative must be considered. For example, food-allergic reactions account for about 20% of acute urticaria, 2% of chronic urticaria, and approximately 35% of moderate to severe atopic dermatitis in children, while food allergy is not a common cause of atopic dermatitis in adults (3, 4). Also, the prevalence of food allergy is greatest in the first few years of life, affecting about 3 to 8% of children and then decreasing to a prevalence of 1 to 3% in adults (5).

Furthermore, although any food may theoretically cause an allergic reaction, only a small number of foods account for approximately 90% of verified food reactions. These foods include milk, egg, soy, wheat, peanut, tree nuts, and fish in children, and peanuts, tree nuts, fish, and shellfish in adults. Finally, the majority of patients outgrow their food allergy, usually in childhood. While the natural history of food allergy varies by food, approximately 50 to 80% of patients with milk, egg, soy, or wheat allergy acquire tolerance to these foods by their teenage years (5). However, sensitivity to peanut, tree nuts, fish, and shellfish usually persist into adulthood. Some of the tests that will be discussed in this chapter not only aid in the diagnosis of food allergies but also are useful in monitoring the natural history of patients' food allergies over time, from diagnosis to oral tolerance.

The physical examination should focus on detecting other atopic features, such as atopic dermatitis, which are more common in patients with IgE-mediated food allergy. Information gathered during the history and physical exam can indicate the likelihood that the patient has true food allergy and whether an IgE-mediated or non-IgE-mediated mechanism is most likely responsible. IgE-mediated reactions, such as urticaria, angioedema, and wheezing, typically have a rapid onset, often immediately but usually within two hours after ingestion, whereas other presentations, such as vomiting, diarrhea, and bloody stools, may not develop for hours to days after ingestion of the allergen in non-IgE-mediated disorders. Once food allergy has been identified as the likely cause of a patient's symptoms, confirmation of the diagnosis and identification of the implicated food(s) can begin. There are a number of tools that aid in the diagnosis of food allergy, some of which are more commonly used than others, and they vary in their ability to provide an accurate diagnosis. In general, laboratory tests are more useful in determining the specific foods responsible for IgE-mediated reactions, whereas they are of limited value in non-IgE-mediated disorders. Available studies include *in vivo* tests, such as skin prick tests (SPTs), oral food challenges (OFCs), elimination diets, and patch testing, and *in vitro* tests, such as quantification of food-specific IgE antibodies in serum and basophil histamine release (BHR). The utility of these and other test modalities will be discussed in detail.

doi:10.1128/9781555818722.ch84

TABLE 1 Food allergy disorders

IgE-mediated
Gastrointestinal: pollen-food allergy syndrome, gastrointestinal anaphylaxis
Cutaneous: urticaria, angioedema, morbilloform rashes and flushing
Respiratory: acute rhinoconjunctivitis, wheezing
Generalized: anaphylactic shock
Mixed IgE- and cell-mediated
Gastrointestinal: eosinophilic esophagitis/gastroenteritis/colitis
Cutaneous: atopic dermatitis
Respiratory: asthma
Cell-mediated
Gastrointestinal: food protein-induced enterocolitis, proctocolitis, and enteropathy syndromes; celiac disease
Cutaneous: contact dermatitis, dermatitis herpetiformis
Respiratory: food-induced pulmonary hemosiderosis (Heiner syndrome)

IN VIVO TESTS

Skin Prick Tests

Skin prick tests are commonly used to screen patients with suspected IgE-mediated food reactions. While the patient is off antihistamines for an appropriate amount of time (short acting, 72 h; long acting, 5 to 7 days), a device, such as a bifurcated needle, lancet, plastic probe, or the tip of a small-gauge needle, is used to puncture the skin through a glycerinated food extract (1:10 or 1:20, wt/vol) into the epidermis. Positive (histamine) controls are used to show that the skin response is not blocked, and negative (saline-glycerin) controls are used to rule out false-positive results, such as those due to dermatographism, irritant and contact reactions from the diluent used to preserve allergen extracts, or poor technique of the tester. Testing should be limited to the most common foods that are suspected of provoking symptoms gathered on history since false-positive results are common (6). If food-specific antibody is present, mast cells with food-specific IgE bound to their surface degranulate and release mediators, such as histamine, that result in a local wheal-and-flare reaction within 15 to 20 min.

SPTs are generally considered positive if the mean wheal diameter is ≥3 mm after subtraction of the negative-control wheal. The mean diameter of the wheal is calculated by measuring the greatest diameter of the wheal and the largest diameter perpendicular to it, then averaging the sum of these diameters. The positive predictive accuracies of SPTs are <50% compared to those of DBPCFCs. Thus, when an SPT is positive, it indicates only a possible association between the food tested and the patient's reactivity to that food, rather than confirmation of a clinically relevant food allergy (7). On the other hand, negative responses virtually exclude the possibility of an IgE-mediated reaction, as the negative predictive value of SPTs exceeds 90% (3). Therefore, negative SPTs are an excellent means of excluding IgE-mediated food allergies, although they are not perfect, and positive SPTs are only suggestive of the presence of symptomatic allergy. However, a positive SPT is virtually diagnostic in patients who have experienced a systemic reaction to an isolated food (3).

Several key studies have looked at the performance characteristics of SPTs in predicting true food allergy at different wheal cutoffs compared to the outcome of DBPCFCs. Sampson (8), in a study of 87 patients (median age, 7.9 years) who all had atopic dermatitis and underwent DBPCFCs to rule out food hypersensitivities after SPTs, reported that a 3-mm wheal had a 96% diagnostic sensitivity in identifying children with cow's milk allergy, 98% with egg allergy, and 90% with peanut allergy, with corresponding diagnostic specificities of 51, 53, and 29%, respectively. Sporik et al. (9) showed corresponding diagnostic sensitivities for a 3-mm wheal of 74% for cow's milk, 84% for egg, and 96% for peanut, with respective diagnostic specificities of 79, 70, and 71% from 535 challenges in 467 children (median age, 3 years). For each food, the authors were also able to identify an SPT wheal diameter at and above which negative food challenges did not occur, thus in theory reducing the need for formal food challenges if the wheal size equaled or exceeded these values: 8 mm for cow's milk, 7 mm for egg, and 8 mm for peanut in a group of children with a median age of 3 years. For children 2 years of age or younger, the SPT wheal diameter cutoffs were lower: 6 mm for cow's milk, 5 mm for egg, and 4 mm for peanut. Finally, Eigenmann and Sampson (10) reevaluated SPTs in the diagnosis of food allergy in a group of children (median age, 4.6 years) with a history of atopic dermatitis. They used wheal sizes at the upper 95% confidence interval for food-tolerant patients as cutoffs; these were 5 mm for cow's milk, 4 mm for egg, and 6 mm for peanut. The corresponding diagnostic sensitivities were 89% for cow's milk, 98% for egg, and 63% for peanut, and the diagnostic specificities were 68, 61, and 71%, respectively.

When the test is appropriately performed, SPT results have been shown to be highly reproducible (8). The accuracy of SPTs does vary, however, depending on which food antigen is being studied, the quality of the food extract, and the technical skills of the tester. In addition, children <1 year old may have negative SPT responses but still have IgE-mediated disease, and infants <2 years old may have smaller wheals, which is presumably due to lower levels of food-specific IgE and skin reactivity.

SPTs have several advantages: they are quick, patients can see the reaction of a positive test result on the skin,

TABLE 2 Signs and symptoms of food-induced allergic reactions

Skin
Urticaria/angioedema
Flushing
Erythematous, pruritic rash
Atopic dermatitis
Gastrointestinal
Pruritus and/or swelling of the lips, tongue, or oral mucosa
Nausea
Abdominal pain or colic
Vomiting or reflux
Diarrhea
Respiratory
Nasal congestion
Rhinorrhea
Pruritus/sneezing
Laryngeal edema, staccato cough, and/or dysphonia
Wheezing/repetitive cough
Cardiovascular
Hypotension/shock
Dizziness
Other
Feeling of "impending doom"

and they are relatively inexpensive compared with serologic methods for allergy investigation. They are also safe. No lethal reactions have been reported after SPTs. However, SPTs are often not helpful in determining if a patient who was allergic to a particular food has achieved tolerance to that food, as skin tests often remain positive for years following attainment of clinical tolerance (7).

Intradermal Skin Tests

In 1978, Bock et al. (11) performed DBPCFCs on 76 children aged 5 months to 15 years who exhibited a wheal of 3.0 mm or greater in response to an SPT with one or more of 14 foods, regardless of whether or not they reported a history of an adverse reaction to that food. Positive SPTs with 1:20 (wt/vol) food extracts identified all subjects who exhibited adverse reactions during their challenges. In addition, intradermal skin tests (IDSTs) were performed with 1:1,000 (wt/vol) extracts. For each of the 14 foods, between 19 and 39 additional patients (mean, 26) who were negative by SPT had a 3.0 mm or greater wheal in response to intradermal testing. Using peanut as an example, 26 patients were identified by SPT, 12 of whom failed DBPCFCs. An additional 28 patients, all of whom had negative DBPCFCs, had positive intradermal tests. Based on this study, IDSTs with food extracts have no advantage over SPTs and appear to produce more false-positive tests than seen with the prick technique.

Fresh Food Skin Prick Tests

Fresh food skin prick tests (FFSPTs) are not commonly performed since the indications for doing so are limited. Some commercially prepared extracts frequently lack the labile proteins that are responsible for IgE-mediated sensitivity to many fruits and vegetables (e.g., apples, oranges, bananas, pears, melons, potato, carrots, and celery), as is seen in patients with pollen-food allergy syndrome, because the proteins are degraded or lose allergenicity during extract preparation (12). Negative SPTs with commercially available extracts that contradict a convincing history of a food-induced allergic reaction should be repeated with the fresh food before concluding that food-specific IgE is absent. Rosen et al. (13) also suggested that patients should be tested with the food in the form that caused the reaction (e.g., raw or cooked). FFSPTs are usually done in one of two manners, depending on the type of food. In the prick-to-prick technique, the needle or lancet device is first embedded in the fresh food and is then immediately used to prick the patient's skin. In the second technique, foods with a harder consistency, such as peanut, are often ground first and diluted in buffered saline.

Several studies have compared FFSPTs, SPTs with commercial extracts, food-specific IgE levels, and/or food challenges. In a study by Ortolani et al. (12), 100 patients with pollen-food allergy syndrome (previously termed oral allergy syndrome) and 32 nonallergic control subjects were enrolled. Patients had FFSPTs, commercial extract SPTs, and specific IgE testing using the Phadebas radioallergosorbent test (RAST). The results showed that FFSPTs provided better diagnostic sensitivity to many foods, including carrot, celery, cherry, apple, and potato, but commercial extract SPTs provided greater diagnostic sensitivity for peanut, almond, banana, and pea. Rosen et al. (13) confirmed the superiority of fresh food extracts in a study of 22 patients, including 9 children. Fourteen of the 22 patients presented with a history of anaphylactic reactions, and the remaining 8 presented with a history of pollen-food allergy syndrome. For 18 of the 22 patients, the foods presumed to be the offending allergens were not limited solely to fruits or vegetables, but included fish, crustaceans, mollusks, milk, egg, peanut, and tree nuts. All of the patients demonstrated a negative response to SPTs with commercial extracts to suspected foods but positive responses to SPTs with fresh food extracts. In this study, however, no food challenges were performed to confirm that these foods were the ones that caused the previous symptoms. Rance et al. (14), using commercial extracts and fresh foods, compared SPT results for milk, egg, and peanut to the results obtained with labial and/or oral challenge. They found that the overall correlation between positive SPT ($\geq$3 mm) and positive challenges was 58.8% using commercial extracts and 91.7% using fresh foods. They also observed that challenges were positive for 40.5% of subjects with negative commercial SPTs, while only 7.4% of challenges were positive for subjects with negative FFSPTs.

Atopy Patch Tests

Atopy patch tests (APTs) have been proposed as a mode of diagnosis of non-IgE-mediated food allergy and for identification of allergens in delayed-onset clinical reactions. APTs are performed epicutaneously, usually on a patient's back. A small amount of a food is placed on filter paper, which is then applied to uninvolved skin and covered by an aluminum cup. The application sites are checked after 15 to 20 min for immediate reactions and then are usually kept occluded for 48 h. Results are usually read 20 min after removal of the cups and again 24 h later for the final evaluation. Final reactions are then scored; a typical scoring system used is 1+ for erythema and slight infiltration, 2+ for erythema and papules, and 3+ for erythema and vesicles. Irritant reactions, which have been described as sharply defined, brownish erythema, blistering, and a lack of clear infiltration, are not regarded as positive reactions (15).

Although the exact pathomechanism of the APT is not known, APT reactions are thought to represent T-cell-mediated allergen-specific immune responses (16). The patch test reaction to aeroallergens seems to be specific for sensitized patients with atopic dermatitis, as it does not occur in healthy volunteers or in patients suffering from asthma or rhinitis (17).

The outcomes of APTs in different studies are often incongruent due to differences in patient selection and, more importantly, differences in method. At this time, there are large disparities in the type and concentration of allergens used and in the duration of application and reading time (17). Nonspecific irritation is a common finding in standard patch testing and therefore requires considerable skill in differentiating it from a positive reaction. These facts make interpretation of studies somewhat difficult due to reliability issues, but a number of investigators have examined the use of APTs in addition to SPTs for the diagnosis of mixed or non-IgE-mediated food allergy, primarily in atopic dermatitis and eosinophilic esophagitis (18).

Roehr et al. (15) studied 173 challenges in 98 patients with atopic dermatitis and used APTs, SPTs, and food-specific IgE levels with cow's milk, egg, soy, and wheat to see if the combination of a positive APT result plus a positive food-specific-IgE level, a positive SPT, or both would make DBPCFCs unnecessary. Patients were observed for 48 h on an inpatient basis after challenges to document late-phase reactions (>2 h post challenge). Observed reactions included eczema exacerbations, which were counted as positive challenges if they occurred either alone or in combination with early reactions. Positive APT results alone correlated with high positive predictive values (PPVs) for cow's milk (95%), hen's egg (94%), and wheat (94%) compared to positive DBPCFCs, but with

only a 50% PPV for soy (only 4 children reacted to soy). The combination of a positive APT with positive specific IgE for cow's milk (≥0.35 kilounits [kU_A] of antibody per liter) and for egg (≥17.5 kU_A/liter) increased the PPVs to 100%, thus making DBPCFCs superfluous. The addition of SPTs to the other two tests did not further improve results. A study by Mehl et al. (19) utilized similar methods in evaluating 437 children, 90% with atopic dermatitis, who underwent 873 OFCs to milk, egg, soy, and wheat. Using results from APTs in combination with SPTs and food-specific IgE levels led to improved diagnostic sensitivity and specificity compared to the individual tests, but the addition of APT made OFCs unnecessary in 0.5 to 14% of patients, thus only adding minimal predictive value to SPT and food-specific IgE measurements. Spergel et al. (20) studied 941 patients with biopsy-proven eosinophilic esophagitis and performed SPTs, followed by APTs if the SPT to a particular food was negative. Causative foods were identified in 319 patients. A comparison of a diet eliminating foods positive on SPT or APT to an empirically determined six-food elimination diet showed equal success rates based on posttreatment biopsies showing resolution of esophageal eosinophilia. However, fewer foods were removed based on the SPT/APT-directed elimination diet.

Elimination Diets

The purpose of an elimination diet is to determine whether a patient's symptoms will resolve when foods are restricted from the diet. Once certain foods are suspected of being responsible for a food-induced allergic disorder, an elimination diet is started as an attempt to support the diagnosis. If a patient's symptoms persist despite a very strict avoidance diet, it is unlikely that the food accounts for the patient's complaints. There are three types of elimination diets: elimination of one or more suspect foods, elimination of all but a defined group of allowed foods that are rarely antigenic (oligo-antigenic diet), and an elemental diet consisting of a hydrolyzed or amino acid-based formula. The type of diet chosen depends on the age of the patient, the clinical presentation being evaluated, and sometimes the results of food-specific skin or serological IgE antibody tests.

Elimination of one or more foods may be diagnostic and therapeutic in patients who experience an acute reaction to a food and have a positive test for IgE antibody to that food. It may also be especially helpful in evaluating infants who are on a very limited diet. In the oligo-antigenic diet, a large number of foods suspected to cause a chronic problem are removed, and the patient is given a list of allowed foods. This type of diet can be useful for evaluation of chronic disorders, such as atopic dermatitis or chronic urticaria. In the most extreme diet, the elemental diet, an amino acid-based formula (Neocate, EleCare, PurAmino) provides the entirety of a patient's nutrition. The elemental diet provides the most definitive trial, but it can be difficult to undertake and maintain, especially in patients beyond infancy, where tube feeding may be required. This diet may be necessary when less restrictive diets have failed but the suspicion for food-related illness remains high, especially in disorders such as eosinophilic gastrointestinal disease, which is often associated with multiple food allergies. If a patient's symptoms do not improve on an elemental diet, then it is very unlikely that ingested substances are the problem. The length of trial is dependent on the type of symptoms, but 6 weeks is usually sufficient to see clinical improvement (4).

If symptoms resolve on an elimination diet, some form of food challenge is generally warranted, especially in chronic disorders such as atopic dermatitis. One must be careful when a food to which the patient is sensitized is removed from the diet for a prolonged period, as reintroduction may induce severe reactions (3, 4). With gastrointestinal allergies such as eosinophilic gastrointestinal disease, endoscopy and biopsies performed after 6 to 8 weeks on an elimination diet that show resolution of pathology confirms that the implicated food(s) were likely responsible for the disorder.

Oral Food Challenges

OFCs are performed by feeding suspected foods in gradually increasing amounts over hours or days under the supervision of a physician. OFCs can be done openly, where both the physician and the patient are aware of the food being challenged, single-blind, where only the physician is aware, or double-blind, placebo-controlled, where neither patient nor physician knows the content being challenged. Open food challenges are best performed when there is not a high likelihood that symptoms will develop and when there are few to no psychological factors that may bias results. The DBPCFC is considered the "gold standard" for the diagnosis of food allergy, and it is the least prone to bias and confounding factors (21, 22). OFCs can be used to assess any kind of adverse response to foods. When several foods are under consideration, tests for food-specific IgE are positive, and an elimination diet results in resolution of symptoms, an OFC for each food may allow expansion of the diet. For acute anaphylactic reactions in which no specific IgE for the suspected food is found, an OFC would be indicated to confirm the diagnosis or to safely reintroduce the food in the case of a false-negative skin test or food-specific IgE. If an elimination diet does not alleviate symptoms and suspicion is still high for a food-related cause, then the OFC may be needed to resolve the issue. For those who have been previously diagnosed with an IgE-mediated food allergy, the OFC can also be used to determine whether the patients have outgrown their clinical reactivity. Finally, for non-IgE-mediated reactions, OFCs are often the only means of diagnosis due to the lack of reliable testing for these types of reactions.

To optimize challenge conditions, the suspected food should be eliminated from the diet for 1 to 2 weeks (and up to 8 to 12 weeks in some gastrointestinal disorders); potentially interfering medications, including antihistamines and β-agonists, should be withdrawn; and chronic diseases, such as asthma and atopic dermatitis, should be adequately controlled. Fresh or dehydrated foods can be used, and challenge vehicles should not contain fat, which can interfere with protein absorption. The OFC should be administered in the fasting state and proceed in a graded fashion, starting with a dose that is less than the expected threshold dose, such as the approximate dose the patient reacted to previously. In suspected IgE-mediated reactions, if there is no reaction with the starting dose, then increasing doses are given every 15 to 60 min (the interval time may need to be increased for more delayed reactions). The total cumulative dose given in the OFC should be equivalent to a regular, age-appropriate serving size of the food. Some suggestions include a total of 8 to 10 g of dry food, 16 to 20 g of meat or fish, or 100 ml of wet food (22). Another suggested graded dosing schedule, using weight of food protein, consists of 3-mg, 10-mg, 30-mg, 100-mg, 300-mg, 1,000-mg, and 3,000-mg food protein doses (21). Once the challenge is completed, patients should generally be observed for up to 2 h. Once the patient has tolerated one of the above amounts in the challenge, then clinical reactivity has generally been ruled out, since a negative challenge has a high negative predictive value. However, for blinded challenges, negative challenges should be confirmed by an open feeding

of the suspected food to eliminate the rare possibility of a false-negative challenge.

Although any constellation of symptoms may occur during a positive food challenge, Ahrens et al. (23) analyzed the outcomes of 1,843 OFCs performed in children and found that certain foods were more likely to cause organ-specific symptoms than others during OFCs. Namely, gastrointestinal symptoms were more likely to occur during OFCs to egg and peanut compared to milk, soy, or wheat. Additionally, respiratory symptoms were more likely to occur with peanut compared to milk, egg, soy, or wheat OFCs.

In suspected non-IgE-mediated food allergies, such as food protein-induced enterocolitis syndrome, there are no specific laboratory tests, and the OFC may be the only way to identify causative foods. In OFCs for food protein-induced enterocolitis syndrome, patients need to be observed for at least 4 h postchallenge since reactions can occur up to 2 h postingestion, and intravenous access should be established prior to challenge since severe vomiting, diarrhea, and hypotension are common responses in failed challenges (22). For other, less acute non-IgE mediated gastrointestinal food allergies, patients may require several feedings over a 1- to 3-day period and these food introductions can usually be done in the home setting.

The decision to perform OFCs should not be taken lightly, as severe anaphylactic reactions can occur, and the challenges are time-consuming, cost-intensive, and may be stressful to the patients and their families. To aid in making the decision of when to challenge, the SPT wheal-size cutoffs described above that indicate the likelihood of true allergy based upon DBPCFCs should be considered. Other tools that can help guide whether to challenge a patient will be mentioned later in this chapter when food-specific IgE levels are discussed. Recent and severe anaphylaxis after an isolated ingestion of a food to which the patient is sensitized is a relative contraindication to performing a challenge, as the history is so convincing for a true food allergy that further investigation is not warranted. Because of the risk of anaphylaxis, the physician must be prepared to treat a severe reaction with emergency medications and equipment. Patients must be examined before the challenge begins as well as frequently during the OFC for objective signs of a reaction, and challenges need to be terminated promptly when a reaction becomes apparent.

As with any diagnostic test, false-positive and false-negative results may occur in OFCs. In the United States, the average false-negative rate for the DBPCFC was approximated at 1 to 3% (3). Caffarelli and Petroccione (24) reported that 5 of 193 patients (3%) challenged by DBPCFCs had passed a DBPCFC and then reacted the next day to an open feeding of the same food at home. Occasionally, an open challenge is positive in the face of a negative blinded challenge. Several possibilities explain this phenomenon. First, patients' threshold responses may vary even from day to day, or the open challenge could have contained more allergen than the blinded challenge. Second, the allergenicity of the food may have been different because of the way it was prepared. Third, the graded challenge may have actually induced a degree of desensitization that was not present when the full serving of the food was eaten (21).

IN VITRO TESTS

Quantification of Food-Specific IgE Antibodies

Another way to identify food-specific IgE that is more widely available to the general practitioner is the measurement of food-specific IgE in the serum. Various immunometric assays to measure results have evolved over time. The first widely used assay, initially described in 1967, was the RAST. In this type of test, the allergen in question is bound to a solid matrix and exposed to the patient's serum. If there is specific IgE for that allergen in the patient's serum, it binds to the protein matrix. After a buffer wash to remove unbound serum proteins, bound human IgE antibodies are detected with a radiolabeled anti-human IgE Fc. The RAST has since been replaced by fluorescence enzyme-labeled assays with improved analytical sensitivity and overall improved assay performance. The term "RAST," therefore, should no longer be used to refer to specific IgE assays. The most commonly used assay is currently the ImmunoCAP system (Thermo Fisher Scientific, Waltham, MA), which uses standardized allergens and is calibrated against the World Health Organization IgE standard. In this assay, results are reported on a scale from <0.35 or <0.1 kU_A/liter (undetectable) to the upper limit of >100 kU_A/liter. Results using ImmunoCAP have been shown in key studies to be predictive of symptomatic IgE-mediated food hypersensitivity. These studies provided support that certain concentrations of food-specific IgE were associated with a high likelihood of reactions, or true allergy. The 90 or 95% predictive values have been used to establish diagnostic decision points (25).

In a retrospective study of 196 children and adolescents (mean age, 5.2 years) with atopic dermatitis, Sampson and Ho (26) compared the levels of food-specific IgE with the results of DBPCFCs and found that concentrations of ≥ 6 kU_A/liter for egg, ≥ 32 kU_A/liter for cow's milk, ≥ 15 kU_A/liter for peanut, and ≥ 20 kU_A/liter for codfish were 95% predictive of an allergic reaction, thereby providing the 95% PPV. Therefore, a patient with a food-specific-IgE level greater than the 95% PPV could be considered reactive and an OFC would not be warranted. If, however, the level of food-specific IgE was less than the 95% PPV, a patient may be reactive but would need an OFC to confirm the diagnosis. There are caveats with this study that affect its use in the general population. First, all patients had atopic dermatitis, and these patients tend to have higher IgE levels. Second, this group of patients had a much higher prevalence of food allergy than is seen in most populations. Because of these factors, Sampson (25) performed a prospective study of 100 children (median age, 3.8 years) not selected for atopic dermatitis (only 61% had this disorder), with similar results, except the 95% PPV cutoff was lower for milk at 15 kU_A/liter.

Different results were obtained in studies of younger infants and children with different clinical histories. Garcia-Ara et al. (27) showed that an even lower concentration of food-specific IgE to milk had a high predictive capability, although their study included a much younger patient population of 170 infants (mean age, 4.8 months) without atopic dermatitis or gastrointestinal allergy. They determined the 95% PPV cutoff to be >5 kU_A/liter but recommended ≥ 2.5 kU_A/liter as the cutoff to not challenge because it still had a high probability of a positive challenge (90%) without a significant reduction in sensitivity. Osterballe and Bindslev-Jensen (28) determined the 95% PPV for egg to be 1.5 kU_A/liter in a population of 56 children with atopic dermatitis and a median age of 2.2 years. Boyano et al. (29), in a population of 81 children under 2 years of age (43% with atopic dermatitis), determined that an OFC was unnecessary to establish the diagnosis of egg allergy if the egg-white-specific IgE was ≥ 0.35 kU_A/liter and the patient had a history of immediate hypersensitivity to egg. Finally, Peters et al. (30) evaluated 5,276 infants 11 to 15 months of age from a population-based, longitudinal food allergy

study in Australia in order to determine SPT and specific IgE thresholds with 95% PPVs for challenge-proven allergy to egg, peanut, sesame, cow's milk, and shrimp in this age group. Eighty-three percent of infants with detectable SPTs underwent OFC. For SPTs, 95% PPVs were ≥8 mm for peanut, ≥4 mm for egg, and ≥8 mm for sesame. For specific IgE, 95% PPVs were ≥34 kU_A/liter for peanut and ≥1.7 kU_A/liter for egg.

Food-specific-IgE concentrations can also be helpful in monitoring a patient's ongoing sensitivity on an annual basis because they provide numerical values that can be monitored from an initial reference point. Moreover, food-specific-IgE cutoff values have been defined that can guide when patients should undergo OFCs to determine if they have outgrown their allergy. Perry et al. (31) retrospectively reviewed the levels of specific IgE for five major foods at the time of 604 open OFCs carried out in 391 patients. Challenges were performed when oral tolerance was suspected due to the lack of any reaction to the suspect food within the previous year and, for most patients, when the food-specific-IgE level was <0.35 kU_A/liter or approached one-fourth of the previously established 95% PPVs for milk, egg, and peanut or one-fourth of the 50 and 75% PPVs for soy and wheat, respectively. For analysis, patients were divided into two groups as follows, based on their reaction history: group 1, patients who clearly had a history of an allergic reaction or had previously failed a challenge to that food; and group 2, patients who were avoiding the suspect food solely on the basis of a positive test for food-specific IgE or who had an unclear history of reaction, such as worsening atopic dermatitis. The study identified food-specific IgE levels at which 50% of patients would pass an OFC to milk, egg, and peanut, a pass rate acceptable to both physicians and parents given the risk, expense, and time that each challenge entails. The proposed cutoff level for milk-specific IgE was 2 kU_A/liter, below which 53% of patients passed their challenge. For egg-specific IgE, the 50% cutoff was also 2 kU_A/liter, below which 60% of patients passed their challenge both with and without a clear history of reaction. For peanut, they recommended that patients with a clear history of reaction be challenged when the peanut-specific IgE level is <2 kU_A/liter, whereas a cutoff level of 5 kU_A/liter should be used for those patients with no clear history of ingestion. Firm recommendations could not be provided for soy and wheat, a problem seen with other studies as well (25, 26). However, in general, challenges should be considered for patients with a wheat-specific IgE <10 kU_A/liter or a soy-specific IgE <5 kU_A/liter, although higher levels may be appropriate for some patients, depending on their clinical history.

There are several important points regarding food-specific-IgE levels that need to be mentioned. The level of food-specific IgE, like the size of the SPT, does not correlate with the severity or type of reaction a patient will have, but especially high concentrations are associated with a very high likelihood of reaction (25). Also, food-specific IgE serological testing is preferable to SPTs in patients with significant dermatographism or severe skin disease and patients who cannot discontinue antihistamines, which can all lead to false-positive tests. Finally, SPTs may be dangerous in patients with intense sensitivity to certain foods (26).

Component Resolved Diagnostics

Component resolved diagnostics (CRD) has recently emerged as a tool that may provide improved accuracy in food allergy testing. CRD uses individual, purified allergenic proteins, rather than crude, whole allergen extracts, in assaying for IgE antibody-dependent sensitivity. This may, therefore, reduce false-positive tests that result from pollen cross-reactivity and may identify sensitivity to proteins that are more allergenic than others. Any diagnostic test with improved accuracy may prevent the need for unnecessary OFCs.

Several studies have suggested CRD may improve the specificity of food allergy diagnosis and allow for the differentiation between allergy and tolerance. Data are most convincing for peanut allergy, where sensitization to different peanut components best predicts the likelihood of true peanut allergy in sensitized patients. Nicolaou et al. (32) evaluated 933 children at age 8 years from a population-based birth cohort. They found that 110 (11.8%) children were sensitized to peanut, based on SPT and/or specific IgE measurement. Only 22.4% of peanut-sensitized patients were clinically allergic to peanut based on DBPCFC. CRD detected significant differences in component recognition between children with peanut allergy and those who were able to tolerate peanut. Allergic children had higher Ara h 1 to 3 values compared to peanut-tolerant children, and the storage protein Ara h 2 was identified as the most important predictor of peanut allergy. Conversely, the peanut component Ara 8, which is homologous with Bet v 1 in birch pollen, has been associated with peanut tolerance or mild oral allergy symptoms in peanut allergy. Asarnoj et al. (33) evaluated 144 children sensitized only to Ara h 8 and none of the major peanut components (Ara h 1 to 3). All but one child demonstrated tolerance to peanut, and the subject who reacted on DBPCFC was reevaluated and was found to have a rising peanut IgE level as well as sensitivity to Ara h 6, a stable peanut allergen.

A study by D'Urbano et al. (34) utilized CRD to predict food-challenge outcomes in 58 children with suspected cow's milk allergy and 46 with suspected egg allergy. The authors found that the cow's milk allergen casein (Bos d 8) and the egg allergen ovomucoid (Gal d 1) were the most predictive of true food allergy to milk and egg, respectively. Their 95% clinical decision points, or the food-specific IgE level above which 95% of patients would react, provided improved accuracy compared to specific IgE to the whole extracts of these foods. With respect to soy allergy, Holzhauser et al. (35) performed DBPCFCs in subjects with suspected soy allergy and concluded that sensitization to the soy storage proteins β-conglycinin (Gly m 5) and glycinin (Gly m 6) are associated with severe reactions to soy. The additional analysis of IgE to Gly m 2S albumin in one Japanese pediatric cohort aided in the diagnosis of soybean allergy (36).

Ando et al. (37) have suggested that the measurement of specific IgE antibodies to ovomucoid is useful in differentiating between children who react to heated egg white and those who are able to tolerate heated egg. This study evaluated 108 children with suspected egg allergy; all subjects underwent ImmunoCAP testing to egg white and ovalbumin and underwent DBPCFC to both regular and baked egg. They concluded that while egg-white IgE is most useful in diagnosing allergy to unbaked egg, ovomucoid is superior in diagnosing baked egg allergy, with an ovomucoid IgE of 10.8 kU_A/liter having 96% specificity in predicting clinical reactivity. Similarly, for milk allergy, Caubet et al. (38) evaluated 225 children with suspected milk allergy. They assessed IgE levels to cow's milk, casein, and β-lactoglobulin and performed OFCs to baked and regular milk. The study found that casein-specific IgE had the best accuracy in predicting baked milk reactivity, with a casein IgE of 20.2 kU_A/liter having 95% specificity in predicting a clinical reaction to baked milk.

While CRD represents an exciting advance that is likely to improve the diagnosis of food allergy over time, further

study is still needed to define its role in clinical practice. Like previous studies mentioned above using standard ImmunoCAP assays, several of the studies using CRD did not employ OFCs but based the diagnosis on clinical history and serology, which likely led to false-positive diagnoses (32, 35). Additionally, the number of studies evaluating the clinical utility of CRD in predicting food challenge outcomes in allergic subjects, while informative, has been sparse.

Quantification of Food-Specific IgG

Overall, levels of food-specific IgG, including IgG_4 antibodies, rise in response to long-term exposure in both symptomatic and asymptomatic patients and may comprise a normal, physiologic response to repeated food exposure. There has been no strong evidence to link the presence of IgG_4 antibodies to the mechanism of histamine release from basophils *in vivo*. IgG_4 levels are generally elevated in patients with food allergy affecting the gastrointestinal tract, but their specificities typically reflect the type of foods ingested and are not indicative of food-related pathogenesis (39).

IgG_4 antibodies may also reflect the induction of immunologic tolerance to specific antigens, such as food. Savilahti et al. (40) compared serial serum samples from 11 children with persistent IgE-mediated cow's milk allergy to 12 children with a history of cow's milk allergy who attained tolerance by age 3 years. They found that tolerance to cow's milk protein was associated with increasing IgG_4 binding to milk protein epitopes. It has also been shown that IgG_4 food-specific antibodies increase in patients who have successfully completed oral immunotherapy for milk and peanut allergy (41, 42). In summary, food-specific IgG antibodies play no role in the diagnosis of food hypersensitivity reactions.

Total IgE

IgE concentrations in serum are highly age dependent, rising gradually through childhood until they peak between ages 10 and 15 and then steadily decline throughout adulthood. Klink et al. (43) analyzed serum IgE levels in 2,657 subjects grouped into skin test-positive or skin test-negative rhinitic, asthmatic, or asymptomatic individuals. They found that although serum IgE concentrations tended to be higher in allergic children and adults than in nonallergic individuals, the range of IgE in all groups was extremely wide. There is usually a large overlap in the ranges of IgE between atopic and nonatopic populations, resulting in no single level of IgE that clearly distinguishes the different groups at a level of precision that is clinically meaningful. This large overlap greatly limits the diagnostic sensitivity of total serum IgE as a diagnostic screening test for allergy.

There are many atopic conditions that may be associated with elevated total IgE levels. In the realm of food allergy, the most common is atopic dermatitis (44). Elevated total serum IgE levels can lead to additional confusion in the diagnosis of food allergy as they further increase the probability of detecting falsely positive food IgE tests.

Another question has been whether the ratio of specific to total IgE may enhance the accuracy of food allergy diagnosis. Mehl et al. (45) compared the ratio of food-specific to total IgE to food-specific IgE alone in 501 children (median age, 13 months) undergoing 992 OFCs. The sensitivity and specificity of the clinical decision points of the ratio were similar to those of IgE levels to milk, egg, and wheat. Therefore, the predictive value of the ratio for these foods did not offer any additional advantage over the measurement of food-specific IgE alone in diagnosing food allergy.

Basophil Responses

Various laboratory tests have been developed to examine basophil responses to allergens, including foods. Basophil activation testing (BAT) measures the level of activation after incubation with allergen by evaluating the expression of cell surface proteins, such as CD63 or CD203c, via flow cytometry (46). BAT was shown to be useful in predicting outcomes of oral food challenges in patients with cow's milk allergy, with superior predictive values compared to SPT and food-specific IgE testing (47). Another study found that the use of BAT in children with peanut or egg allergy may help distinguish between patients who are simply sensitized to these specific foods and those with true clinical reactivity (48).

Basophil histamine release (BHR) after stimulation by antigen has been proposed as another *in vitro* correlate to *in vivo* allergic responses. BHR as a method of diagnosing food allergy was reported by Sato et al. (49), who determined that the threshold of histamine release, defined as the minimum concentration of egg white, cow's milk, or wheat antigen necessary to induce a 10% net histamine release, was useful in diagnosing food allergy to these respective foods, based on OFC outcomes or recent convincing history of reaction. Wanich et al. (50) studied both milk-allergic and milk-tolerant subjects and found that the basophils of those tolerant to milk were significantly less responsive to milk allergen stimulation compared to the basophils of milk-allergic subjects, suggesting extrinsic suppression of milk-specific basophil reactivity in those with tolerance. However, another study by Sampson et al. (51) that compared BHR, SPTs, and DBPCFCs found that the BHR assay was no more effective in predicting clinical sensitivity than SPTs.

The clinical use of BHR and BAT is complicated by several factors: (i) neither test is widely available; (ii) the blood needs to be processed within a relatively short period of time to ensure cellular viability; (iii) there are no standardized methods for performing these tests; and (iv) basophils from up to 80% of children with atopic dermatitis and food allergy documented by DBPCFC (51) can spontaneously release histamine, although the use of whole blood in these flow assays may overcome this issue. At present, basophil response assays remain primarily research tools.

Serum Tryptase

An increased level of serum tryptase, a neutral protease found almost exclusively in mast cells, has been found to be an excellent marker of mast cell activation in anaphylactic reactions. Basophils, the only other cell type in which tryptase has been found, contain 100 to 1,000 times less tryptase than mast cells (52). Tryptase level elevations are believed to begin at 1 h after mast cell stimulation (53), and the half-life of tryptase in the circulation is approximately 2 h (52).

An increase in serum tryptase in food-induced anaphylaxis, however, is rarely seen and therefore is not a reliable marker of food-related allergic reactions. The absence of a substantial increase in mast cell tryptase in food-induced reactions suggests that other mediators from mast cells may play a more central role, or that basophils, which contain significantly less tryptase, are the critical players in these reactions. Other cell types, including macrophages, monocytes, and endothelial cells that express FcεRI, the high affinity receptor for IgE, may also play a role in the allergic reaction to foods (54).

Specific Epitope Analysis

Recent technological advances have enabled investigators to map allergenic epitopes of many major food allergens, including milk, egg, and peanut, and determine specifically

where a patient's IgE antibodies bind to those proteins. As a result, it was discovered that conformational and sequential (or linear) epitopes can both be responsible for allergic reactions. Furthermore, individuals who possess IgE antibodies to sequential epitopes react to the allergenic food in any form, whether extensively cooked or partially hydrolyzed, while patients with IgE antibodies to conformational epitopes appear to tolerate small amounts of the food after extensive cooking or partial hydrolysis because the tertiary structure of the allergenic protein is altered and the conformational epitopes are destroyed (3).

Additionally, in several studies of egg- and milk-allergic patients (55, 56), it was shown that certain patients with IgE antibodies to sequential epitopes have a propensity to have persistent allergy, while patients with IgE antibodies primarily to conformational epitopes tend to more rapidly develop clinical tolerance. Therefore, screening for antibodies to specific epitopes may prove useful in identifying children who will not outgrow their allergy and thus may be candidates for immunotherapy when it becomes available. Further analysis of epitope binding in peanut-allergic patients demonstrated that there are differences in peanut-allergenic epitope-recognition patterns between patients with symptomatic peanut allergy and those who are sensitized but clinically tolerant (57, 58). Therefore, the addition of epitope-specific IgE determinations might prove to be a more valuable tool for diagnosing symptomatic peanut allergy than even CRD if this can be developed for clinical use. It has also been demonstrated that patients with peanut allergy with IgE antibodies to many epitopes, called broad epitope diversity, tend to have more severe allergic reactions than those who have IgE binding to relatively few epitopes (58).

CONCLUSIONS

The diagnosis of immunological reactions to foods must begin with a thorough history and physical exam, as this provides the basis for making decisions of what testing, if any, should be done to confirm the history. A number of valid diagnostic tools exist for diagnosing IgE-mediated food reactions, both *in vivo* methods, such as skin testing and food challenges, and *in vitro* methods, including measurement of serum food-specific IgE concentrations. Both methods of testing have their advantages and limitations, depending on the clinical situation, but for non-IgE-mediated food reactions, elimination diets and OFCs may be the only means of diagnosis. Tests that have not proven helpful in food allergy diagnosis include quantification of food-specific IgG and IgG_4, total serum IgE levels, and serum tryptase concentrations. Tests that warrant further study but show promise include allergenic component-based CRD and epitope-specific IgE measurements, both of which may provide improved diagnostic specificity. The APT may aid in the diagnosis of non-IgE-mediated disorders and delayed reactions to foods, but further research and standardization is required. Regardless of the test chosen, the DBPCFC still remains the gold standard for diagnosing food allergy. Finally, important features of the studies mentioned in this chapter for the described tests that should be appreciated by clinicians are (i) that the data generated may be particular to the study population and test material, and (ii) that the age and clinical disease of the patients are important variables. Clinicians must therefore be careful in applying the results in these published studies to their own individual clinical situations.

REFERENCES

1. **Boyce JA, Assa'ad A, Burks AW, Jones SM, Sampson HA, Wood RA, Plaut M, Cooper SF, Fenton MJ, Arshad SH, Bahna SL, Beck LA, Byrd-Bredbenner C, Camargo CA Jr, Eichenfield L, Furuta GT, Hanifin JM, Jones C, Kraft M, Levy BD, Lieberman P, Luccioli S, McCall KM, Schneider LC, Simon RA, Simons FE, Teach SJ, Yawn BP, Schwaninger JM, NIAID-Sponsored Expert Panel.** 2010. Guidelines for the diagnosis and management of food allergy in the United States: report of the NIAID-sponsored expert panel. *J Allergy Clin Immunol* **126**(Suppl)**:**S1–S58. PubMed
2. **Bock SA, Atkins FM.** 1990. Patterns of food hypersensitivity during sixteen years of double-blind, placebo-controlled food challenges. *J Pediatr* **117:**561–567. PubMed
3. **Sicherer SH, Sampson HA.** 2010. Food allergy. *J Allergy Clin Immunol* **125**(Suppl 2)**:**S116–S125. PubMed
4. **Burks AW, Tang M, Sicherer S, Muraro A, Eigenmann PA, Ebisawa M, Fiocchi A, Chiang W, Beyer K, Wood R, Hourihane J, Jones SM, Lack G, Sampson HA.** 2012. ICON: food allergy. *J Allergy Clin Immunol* **129:**906–920.
5. **Longo G, Berti I, Burks AW, Krauss B, Barbi E.** 2013. IgE-mediated food allergy in children. *Lancet* **382:**1656–1664.
6. **Sicherer SH, Wood RA, American Academy of Pediatrics Section On Allergy And Immunology.** 2012. Allergy testing in childhood: using allergen-specific IgE tests. *Pediatrics* **129:**193–197. PubMed
7. **Burks AW, Jones SM, Boyce JA, Sicherer SH, Wood RA, Assa'ad A, Sampson HA.** 2011. NIAID-sponsored 2010 guidelines for managing food allergy: applications in the pediatric population. *Pediatrics* **128:**955–965. PubMed
8. **Sampson HA.** 1988. Comparative study of commercial food antigen extracts for the diagnosis of food hypersensitivity. *J Allergy Clin Immunol* **82:**718–726. PubMed
9. **Sporik R, Hill DJ, Hosking CS.** 2000. Specificity of allergen skin testing in predicting positive open food challenges to milk, egg and peanut in children. *Clin Exp Allergy* **30:**1540–1546. PubMed
10. **Eigenmann PA, Sampson HA.** 1998. Interpreting skin prick tests in the evaluation of food allergy in children. *Pediatr Allergy Immunol* **9:**186–191. PubMed
11. **Bock SA, Lee WY, Remigio L, Holst A, May CD.** 1978. Appraisal of skin tests with food extracts for diagnosis of food hypersensitivity. *Clin Allergy* **8:**559–564. PubMed
12. **Ortolani C, Ispano M, Pastorello EA, Ansaloni R, Magri GC.** 1989. Comparison of results of skin prick tests (with fresh foods and commercial food extracts) and RAST in 100 patients with oral allergy syndrome. *J Allergy Clin Immunol* **83:**683–690. PubMed
13. **Rosen JP, Selcow JE, Mendelson LM, Grodofsky MP, Factor JM, Sampson HA.** 1994. Skin testing with natural foods in patients suspected of having food allergies: is it a necessity? *J Allergy Clin Immunol* **93:**1068–1070. PubMed
14. **Rancé F, Juchet A, Brémont F, Dutau G.** 1997. Correlations between skin prick tests using commercial extracts and fresh foods, specific IgE, and food challenges. *Allergy* **52:**1031–1035. PubMed
15. **Roehr CC, Reibel S, Ziegert M, Sommerfeld C, Wahn U, Niggemann B.** 2001. Atopy patch tests, together with determination of specific IgE levels, reduce the need for oral food challenges in children with atopic dermatitis. *J Allergy Clin Immunol* **107:**548–553. PubMed
16. **Strömberg L.** 2002. Diagnostic accuracy of the atopy patch test and the skin-prick test for the diagnosis of food allergy in young children with atopic eczema/dermatitis syndrome. *Acta Paediatr* **91:**1044–1049. PubMed
17. **de Bruin-Weller MS, Knol EF, Bruijnzeel-Koomen CA.** 1999. Atopy patch testing—a diagnostic tool? *Allergy* **54:**784–791. PubMed

18. **Niggemann B, Reibel S, Wahn U.** 2000. The atopy patch test (APT)—a useful tool for the diagnosis of food allergy in children with atopic dermatitis. *Allergy* **55:**281–285. PubMed
19. **Mehl A, Rolinck-Werninghaus C, Staden U, Verstege A, Wahn U, Beyer K, Niggemann B.** 2006. The atopy patch test in the diagnostic workup of suspected food-related symptoms in children. *J Allergy Clin Immunol* **118:**923–929. PubMed
20. **Spergel JM, Brown-Whitehorn TF, Cianferoni A, Shuker M, Wang ML, Verma R, Liacouras CA.** 2012. Identification of causative foods in children with eosinophilic esophagitis treated with an elimination diet. *J Allergy Clin Immunol* **130:**461–467. PubMed
21. **Sampson HA, Gerth van Wijk R, Bindslev-Jensen C, Sicherer S, Teuber SS, Burks AW, Dubois AE, Beyer K, Eigenmann PA, Spergel JM, Werfel T, Chinchilli VM.** 2012. Standardizing double-blind, placebo-controlled oral food challenges: American Academy of Allergy, Asthma & Immunology-European Academy of Allergy and Clinical Immunology PRACTALL consensus report. *J Allergy Clin Immunol* **130:**1260–1274. PubMed
22. **Nowak-Wegrzyn A, Assa'ad AH, Bahna SL, Bock SA, Sicherer SH, Teuber SS, Adverse Reactions to Food Committee of American Academy of Allergy, Asthma & Immunology.** 2009. Work Group report: oral food challenge testing. *J Allergy Clin Immunol* **123**(Suppl)**:**S365–S383. PubMed
23. **Ahrens B, Niggemann B, Wahn U, Beyer K.** 2012. Organ-specific symptoms during oral food challenge in children with food allergy. *J Allergy Clin Immunol* **130:**549–551. PubMed
24. **Caffarelli C, Petroccione T.** 2001. False-negative food challenges in children with suspected food allergy. *Lancet* **358:**1871–1872. PubMed
25. **Sampson HA.** 2001. Utility of food-specific IgE concentrations in predicting symptomatic food allergy. *J Allergy Clin Immunol* **107:**891–896. PubMed
26. **Sampson HA, Ho DG.** 1997. Relationship between food-specific IgE concentrations and the risk of positive food challenges in children and adolescents. *J Allergy Clin Immunol* **100:**444–451. PubMed
27. **García-Ara C, Boyano-Martínez T, Díaz-Pena JM, Martín-Muñoz F, Reche-Frutos M, Martín-Esteban M.** 2001. Specific IgE levels in the diagnosis of immediate hypersensitivity to cows' milk protein in the infant. *J Allergy Clin Immunol* **107:**185–190. PubMed
28. **Osterballe M, Bindslev-Jensen C.** 2003. Threshold levels in food challenge and specific IgE in patients with egg allergy: is there a relationship? *J Allergy Clin Immunol* **112:**196–201. PubMed
29. **Boyano Martínez T, García-Ara C, Díaz-Pena JM, Muñoz FM, García Sánchez G, Esteban MM.** 2001. Validity of specific IgE antibodies in children with egg allergy. *Clin Exp Allergy* **31:**1464–1469. PubMed
30. **Peters RL, Allen KJ, Dharmage SC, Tang ML, Koplin JJ, Ponsonby AL, Lowe AJ, Hill D, Gurrin LC; for the HealthNuts study.** 2013. Skin prick test responses and allergen-specific IgE levels as predictors of peanut, egg, and sesame allergy in infants. *J Allergy Clin Immunol* **132:**874–880. PubMed
31. **Perry TT, Matsui EC, Kay Conover-Walker M, Wood RA.** 2004. The relationship of allergen-specific IgE levels and oral food challenge outcome. *J Allergy Clin Immunol* **114:**144–149. PubMed
32. **Nicolaou N, Poorafshar M, Murray C, Simpson A, Winell H, Kerry G, Härlin A, Woodcock A, Ahlstedt S, Custovic A.** 2010. Allergy or tolerance in children sensitized to peanut: prevalence and differentiation using component-resolved diagnostics. *J Allergy Clin Immunol* **125:**191–197. PubMed
33. **Asarnoj A, Nilsson C, Lidholm J, Glaumann S, Östblom E, Hedlin G, van Hage M, Lilja G, Wickman M.** 2012. Peanut component Ara h 8 sensitization and tolerance to peanut. *J Allergy Clin Immunol* **130:**468–472. PubMed
34. **D'Urbano LE, Pellegrino K, Artesani MC, Donnanno S, Luciano R, Riccardi C, Tozzi AE, Ravà L, De Benedetti F, Cavagni G.** 2010. Performance of a component-based allergen-microarray in the diagnosis of cow's milk and hen's egg allergy. *Clin Exp Allergy* **40:**1561–1570. PubMed
35. **Holzhauser T, Wackermann O, Ballmer-Weber BK, Bindslev-Jensen C, Scibilia J, Perono-Garoffo L, Utsumi S, Poulsen LK, Vieths S.** 2009. Soybean (*Glycine max*) allergy in Europe: gly m 5 (beta-conglycinin) and Gly m 6 (glycinin) are potential diagnostic markers for severe allergic reactions to soy. *J Allergy Clin Immunol* **123:**452–458. PubMed
36. **Ebisawa M, Brostedt P, Sjölander S, Sato S, Borres MP, Ito K.** 2013. Gly m 2S albumin is a major allergen with a high diagnostic value in soybean-allergic children. *J Allergy Clin Immunol* **132:**976–978. PubMed
37. **Ando H, Movérare R, Kondo Y, Tsuge I, Tanaka A, Borres MP, Urisu A.** 2008. Utility of ovomucoid-specific IgE concentrations in predicting symptomatic egg allergy. *J Allergy Clin Immunol* **122:**583–588. PubMed
38. **Caubet JC, Nowak-Węgrzyn A, Moshier E, Godbold J, Wang J, Sampson HA.** 2013. Utility of casein-specific IgE levels in predicting reactivity to baked milk. *J Allergy Clin Immunol* **131:**222–224. PubMed
39. **Stapel SO, Asero R, Ballmer-Weber BK, Knol EF, Strobel S, Vieths S, Kleine-Tebbe J, EAACI Task Force.** 2008. Testing for IgG4 against foods is not recommended as a diagnostic tool: EAACI Task Force Report. *Allergy* **63:**793–796. PubMed
40. **Savilahti EM, Rantanen V, Lin JS, Karinen S, Saarinen KM, Goldis M, Mäkelä MJ, Hautaniemi S, Savilahti E, Sampson HA.** 2010. Early recovery from cow's milk allergy is associated with decreasing IgE and increasing IgG4 binding to cow's milk epitopes. *J Allergy Clin Immunol* **125:**1315–1321. PubMed
41. **Skripak JM, Nash SD, Rowley H, Brereton NH, Oh S, Hamilton RG, Matsui EC, Burks AW, Wood RA.** 2008. A randomized, double-blind, placebo-controlled study of milk oral immunotherapy for cow's milk allergy. *J Allergy Clin Immunol* **122:**1154–1160. PubMed
42. **Jones SM, Pons L, Roberts JL, Scurlock AM, Perry TT, Kulis M, Shreffler WG, Steele P, Henry KA, Adair M, Francis JM, Durham S, Vickery BP, Zhong X, Burks AW.** 2009. Clinical efficacy and immune regulation with peanut oral immunotherapy. *J Allergy Clin Immunol* **124:**292–300, 300. PubMed
43. **Klink M, Cline MG, Halonen M, Burrows B.** 1990. Problems in defining normal limits for serum IgE. *J Allergy Clin Immunol* **85:**440–444. PubMed
44. **Stone KD, Prussin C, Metcalfe DD.** 2010. IgE, mast cells, basophils, and eosinophils. *J Allergy Clin Immunol* **125**(Suppl 2)**:**S73–S80. PubMed
45. **Mehl A, Verstege A, Staden U, Kulig M, Nocon M, Beyer K, Niggemann B.** 2005. Utility of the ratio of food-specific IgE/total IgE in predicting symptomatic food allergy in children. *Allergy* **60:**1034–1039. PubMed
46. **McGowan EC, Saini S.** 2013. Update on the performance and application of basophil activation tests. *Curr Allergy Asthma Rep* **13:**101–109. PubMed
47. **Rubio A, Vivinus-Nébot M, Bourrier T, Saggio B, Albertini M, Bernard A.** 2011. Benefit of the basophil activation test in deciding when to reintroduce cow's milk in allergic children. *Allergy* **66:**92–100. PubMed
48. **Ocmant A, Mulier S, Hanssens L, Goldman M, Casimir G, Mascart F, Schandené L.** 2009. Basophil activation tests for the diagnosis of food allergy in children. *Clin Exp Allergy* **39:**1234–1245. PubMed
49. **Sato S, Tachimoto H, Shukuya A, Ogata M, Komata T, Imai T, Tomikawa M, Ebisawa M.** 2011. Utility of the

peripheral blood basophil histamine release test in the diagnosis of hen's egg, cow's milk, and wheat allergy in children. *Int Arch Allergy Immunol* **155**(Suppl 1)**:**96–103. PubMed

50. **Wanich N, Nowak-Wegrzyn A, Sampson HA, Shreffler WG.** 2009. Allergen-specific basophil suppression associated with clinical tolerance in patients with milk allergy. *J Allergy Clin Immunol* **123:**789–94. PubMed
51. **Sampson HA, Broadbent KR, Bernhisel-Broadbent J.** 1989. Spontaneous release of histamine from basophils and histamine-releasing factor in patients with atopic dermatitis and food hypersensitivity. *N Engl J Med* **321:**228–232. PubMed
52. **Ohtsuka T, Matsumaru S, Uchida K, Onobori M, Matsumoto T, Kuwahata K, Arita M.** 1993. Time course of plasma histamine and tryptase following food challenges in children with suspected food allergy. *Ann Allergy* **71:**139–146. PubMed
53. **Lin RY, Schwartz LB, Curry A, Pesola GR, Knight RJ, Lee HS, Bakalchuk L, Tenenbaum C, Westfal RE.** 2000. Histamine and tryptase levels in patients with acute allergic reactions: an emergency department-based study. *J Allergy Clin Immunol* **106:**65–71. PubMed
54. **Sampson HA, Mendelson L, Rosen JP.** 1992. Fatal and near-fatal anaphylactic reactions to food in children and adolescents. *N Engl J Med* **327:**380–384. PubMed
55. **Chatchatee P, Järvinen KM, Bardina L, Beyer K, Sampson HA.** 2001. Identification of IgE- and IgG-binding epitopes on α(s1)-casein: differences in patients with persistent and transient cow's milk allergy. *J Allergy Clin Immunol* **107:**379–383. PubMed
56. **Järvinen KM, Beyer K, Vila L, Chatchatee P, Busse PJ, Sampson HA.** 2002. B-cell epitopes as a screening instrument for persistent cow's milk allergy. *J Allergy Clin Immunol* **110:**293–297. PubMed
57. **Beyer K, Ellman-Grunther L, Järvinen KM, Wood RA, Hourihane J, Sampson HA.** 2003. Measurement of peptide-specific IgE as an additional tool in identifying patients with clinical reactivity to peanuts. *J Allergy Clin Immunol* **112:**202–207. PubMed
58. **Lin J, Bruni FM, Fu Z, Maloney J, Bardina L, Boner AL, Gimenez G, Sampson HA.** 2012. A bioinformatics approach to identify patients with symptomatic peanut allergy using peptide microarray immunoassay. *J Allergy Clin Immunol* **129:**1321–1328. PubMed

Diagnosis of Rare Eosinophilic and Mast Cell Disorders

CEM AKIN, CALMAN PRUSSIN, AND AMY D. KLION

85

HYPEREOSINOPHILIC SYNDROMES (HES)

Whereas mild to moderate eosinophilia has been reported in as many as 0.1% of North American outpatients (1) and may be due to seasonal allergies, asthma, or other common conditions, marked eosinophilia (>1,500/mm^3) is relatively infrequent and should always prompt a diagnostic evaluation. The differential diagnosis of marked eosinophilia is broad and includes secondary causes of eosinophilia (Table 1), such as hypersensitivity reactions, helminth infection, and neoplastic and inflammatory disorders, as well as several disorders for which eosinophilia is thought to be the primary etiology. In many cases, a thorough diagnostic evaluation will reveal a secondary cause of the eosinophilia, and appropriate treatment can be instituted. In other instances, a well-defined, single-organ-restricted, primary eosinophil disorder, such as eosinophilic esophagitis, eosinophilic fasciitis, or eosinophilia cystitis, is identified. Once secondary causes and alternative diagnoses have been excluded, however, a systemic primary eosinophil disorder should be considered.

Definition of HES

The term hypereosinophilic syndromes (HES) was first used in 1968 by Hardy and Anderson to describe three patients with marked peripheral eosinophilia, hepatosplenomegaly, and cardiac and/or pulmonary symptoms (2). Diagnostic criteria for HES were first proposed in 1975 by Chusid et al. (3), and they included idiopathic hypereosinophilia (>1,500 eosinophils/mm^3) of >6 months' duration, with signs and symptoms of eosinophil-mediated or unexplained end organ damage. However, as more-sophisticated diagnostic testing has become available and subgroups of patients with HES of known causes have been described, the "idiopathic" nature of HES has been called into question. Furthermore, the availability of effective treatment for HES often leads to the resolution of eosinophilia before the requisite 6 months has elapsed. Finally, the classification of eosinophilic syndromes of unknown cause with distinctive clinical patterns, such as episodic angioedema and eosinophilia (4), which are not excluded by this definition, and marked eosinophilia without current evidence of end organ manifestations (hypereosinophilia of unknown significance [5]), which is excluded by this definition, remains unresolved (see below).

In view of the above-described issues, a number of newer definitions and classification systems have been proposed (6–8). For the purposes of this review, HES will be defined as (i) eosinophilia (>1,500 eosinophils/mm^3 on at least two occasions), (ii) the absence of a secondary cause of eosinophilia other than the primary hematologic abnormalities described below, and (iii) end organ manifestations attributable to eosinophilia. Using this definition, HES is a group of heterogeneous disorders that typically occur between the ages of 20 and 50 years but may present in childhood or advanced age. The overall prevalences appear to be equal in men and women. The previously described male predominance (9:1) was likely due to an overrepresentation of platelet-derived growth factor receptor alpha (*PDGFRA*)-positive disease in early series. The clinical manifestations of HES are extremely varied, ranging from nonspecific complaints, such as fatigue, myalgias, and rhinitis, to severe end organ damage, including endomyocardial fibrosis, restrictive pulmonary disease, and neuropathy (9, 10). Furthermore, some patients may remain asymptomatic for decades despite markedly elevated eosinophil counts (5, 11). Although data from a number of published case series suggest that cardiac, neurologic, and dermatologic manifestations are most common (9, 10), any organ can be affected. Notably, increased susceptibility to infection is not a feature of HES. Thus, a history of recurrent infection should prompt an investigation for secondary causes of eosinophilia, including malignancy and immunodeficiency.

Diagnosis of HES

The first step in the diagnosis of HES is to exclude other disorders associated with marked peripheral eosinophilia. These include parasitic infections, drug hypersensitivity reactions, neoplasms, and immunodysregulatory disorders associated with secondary eosinophilia (Table 1). Once it is established that the patient has eosinophilia of >1,500/mm^3 of unknown cause, it is important to determine if the patient has one of the identifiable subtypes of HES, as this determination has prognostic and therapeutic implications (Table 2).

It is beyond the scope of this chapter to provide a comprehensive diagnostic approach to eosinophil-associated disorders. Nevertheless, several general principles apply. First, a thorough clinical history and physical examination are essential and should include a detailed travel history, medication and dietary history (including the use of dietary and herbal supplements), past medical history (including

doi:10.1128/9781555818722.ch85

TABLE 1 Secondary causes of marked eosinophilia[a]

Category and disease(s)
Allergic disorders
Asthma and/or atopic disease (rare)
Allergic bronchopulmonary aspergillosis
Drug hypersensitivity reactions
Infectious diseases
Helminth infection
Ectoparasite infestations (scabies and myiasis)
Protozoal infection (rarely in isosporiasis and sarcocystis)
Fungal infection (especially coccidiomycosis)
HIV infection
Neoplasms
Leukemia, lymphoma, or adenocarcinoma
Hypoadrenalism
Diseases associated with immunodysregulation
Sarcoidosis, inflammatory bowel disease, or connective tissue disorders
Other
Cholesterol embolization, radiation exposure

[a]This list is not exhaustive.

risk factors for human immunodeficiency virus [HIV] infections), and family history. It should be noted that HES occurs in countries where helminth infections are common, and some helminth infections associated with marked eosinophilia, including strongyloidiasis, occur worldwide. Second, whenever possible, all medications and supplements should be discontinued for a minimum of 1 month (or longer, depending on the half-life of the particular agent). Finally, if routine laboratory results (including HIV testing) and diagnostic testing do not lead to an alternative diagnosis, computed tomography of the chest, abdomen, and pelvis, as well as a bone marrow examination, should be performed in all patients to exclude occult malignancy before a diagnosis of HES is confirmed.

Primary eosinophilic disorders affecting a single organ, such as eosinophilic gastrointestinal disorders (EGIDs), eosinophilic fasciitis, and chronic eosinophilic pneumonia, may be associated with peripheral eosinophilia of >1,500/mm^3. When this occurs, it can be difficult to determine whether the patient has HES with single-organ involvement or a distinct primary eosinophilic disorder. For the purposes of this review, EGIDs, irrespective of the peripheral eosinophil count, will be discussed in a separate section. It should be noted, however, that the initial evaluation of patients with a presumed single-organ eosinophilic disorder and peripheral eosinophilia of >1,500/mm^3 should include assessment for possible HES.

Classification of HES Subtypes

Although it has long been appreciated that HES are a heterogeneous group of disorders (3, 9, 10), it is only recently that advances in molecular and immunologic techniques have begun to delineate the precise pathogenesis of HES in some groups of patients. Of these defined groups, the most common appear to be a clonal myeloproliferative disorder associated with the constitutive activation of platelet-derived growth factor receptor alpha (PDGFRA) (12, 13) and a lymphocytic variant characterized by the presence of a clonal and/or aberrant population of lymphocytes (14, 15). An autosomal dominant familial form of HES that mapped to chromosome 5q31-33 has also been described, although the exact nature of the molecular abnormality remains to be elucidated (16, 17). Subtype identification is important since it has profound implications for the patient with respect to anticipated clinical manifestations, prognosis, and treatment.

Myeloproliferative HES

Epidemiology and Clinical Features

Approximately 30% of patients presenting with a clinical diagnosis of HES have features suggestive of myeloproliferative HES (MHES), including dysplastic eosinophils, elevated serum B_{12} levels, splenomegaly, anemia, thrombocytopenia, and bone marrow hypercellularity with reticulin fibrosis (18). The vast majority of these patients have a myeloproliferative neoplasm (MPN) associated with an interstitial deletion in chromosome 4, del(4)(q12q12), that results in the formation of a fusion tyrosine kinase, FIP1-like-1/platelet-derived growth receptor α (FIP1L1-PDGFRA) that is exquisitely sensitive to the tyrosine kinase inhibitor imatinib (12, 13, 18). Additional features of *PDGFRA*-associated MPN include a striking male predominance and almost universal involvement of the mast cell lineage, with elevated serum tryptase levels and increased numbers of spindle-shaped CD25-positive mast cells in the bone marrow (17). Although alternate fusion partners (19) and point mutations (20) in *PDGFRA* have been described for patients presenting with MHES, these abnormalities appear to be relatively infrequent, although this may be due in part to the fact that routine testing is not currently available. Other myeloproliferative disorders that

TABLE 2 Evaluation of patients presumed to have HES

Test(s) or measurement
Complete blood count with differential[a]
Bone marrow aspirate and biopsy (with staining for reticulin and tryptase)
Conventional cytogenetics
Assessment of end organ pathology
Echocardiogram
Pulmonary function tests
Skin or gastrointestinal biopsies, if indicated
Chest and abdomen computed tomography scan
Subtype differentiation for myeloproliferative disease
Examination of peripheral smear for myeloid precursors or dysplasia
Tryptase level in serum
Vitamin B_{12} level in serum
Testing for *FIP1L1-PDGFRA* fusion (by RT-PCR or FISH)
Testing for additional potential abnormalities (i.e., *PDGFRB*, *FGFR1*, *JAK2*)
Subtype differentiation for lymphoproliferative disease
Serum immunoglobulins, including IgE
Lymphocyte phenotyping[b]
TCR and B-cell receptor gene rearrangement analysis
TARC level in serum
Assessment of T-cell cytokine profile, if reliable assays are available

[a]A CBC with differential should be performed every 3 days for 1 month in the absence of steroid treatment (if possible) for patients presenting with angioedema to exclude episodic angioedema and eosinophilia.

[b]Antibodies specific for the following additional markers should be included if routine phenotyping is normal and the lymphocytic variant is suspected: CD2, CD5, CD6, CD7, CD8, CD25, CD27, CD45RO, TCR-α/β, TCR-γ/δ, HLA-DR, and CD95.

can present as MHES include chronic eosinophilic leukemia that is not otherwise specified and MPN associated with rearrangements or mutations involving other tyrosine kinases, the most common of which are *PDGFRB, JAK2* and *FGFR1*, and D816V *KIT*-associated systemic mastocytosis (19, 21). In rare cases, patients with lymphocytic leukemia can present with clinical and bone marrow features that are indistinguishable from MHES (22). Finally, it is important to recognize that, even in a research setting, causative abnormalities cannot be identified in all patients who present with a clinical picture consistent with MHES.

Diagnosis

A bone marrow examination is a crucial component of the diagnostic evaluation of presumed MHES and should include studies to exclude chronic eosinophilic leukemia not otherwise specified (see World Health Organization [WHO] diagnostic guidelines [7]) and D816V *KIT*-associated systemic mastocytosis (see the section on mastocytosis below). Routine cytogenetic analysis, fluorescent *in situ* hybridization (FISH) to look for rearrangements in *PDGFRB* and *FGFR1*, and V617F *JAK2* mutation testing are commercially available and should also be performed.

The *FIP1L1-PDGFRA* fusion gene can be detected in peripheral blood or bone marrow mononuclear cells by nested reverse transcription-PCR (RT-PCR) or FISH. The breakpoints in *FIP1L1* are varied but are typically located in a 40-kb region spanning introns 7 to 10 of *FIP1L1*. In contrast, the breakpoints in *PDGFRA* appear to be restricted to a region of exon 12 that contains the WW-like region of the juxtamembrane domain (23). Disruption of this WW-like domain has been shown to cause constitutive kinase activation in members of the PDGFR family of tyrosine kinases, including *PDGFRA* (23). This mutation is undetectable by standard cytogenetic analysis (12, 13). Although published data to date suggest that these methods have comparable sensitivities for the detection of the *FIP1L1-PDGFRA* fusion gene (24), FISH has the theoretical advantage of being able to detect cases with variant *FIP1L1* breakpoints, translocations, or alternative *PDGFRA* fusion partners that appear negative by nested RT-PCR. On the other hand, FISH is more technically challenging, and the high autofluorescence of eosinophil granules makes an exact quantification of the number of positive cells difficult. If neither of these tests is available, surrogate markers for *PDGFRA*-associated MPN can be used, as described below.

Nested RT-PCR for *FIP1L1-PDGFRA*

Following total RNA isolation from peripheral blood mononuclear cells by standard methods, first-strand cDNA is synthesized from 2 μg of total RNA by the use of random-hexamer primers. The fusion of *FIP1L1* to *PDGFRA* is detected by nested PCR. The first PCR amplifies 2 μl of cDNA in a 50-μl reaction mix, using primers FIP1L1-F1 (5′-ACCTGGTGCTGATCTTTCTGAT) and PDGFRA-R1 (5′-TGAGAGCTTGTTTTTCACTGGA) and the following cycle conditions: 3 min at 95°C followed by 35 cycles of 95°C for 30 s, 58°C for 30 s, and 72°C for 1 min and a final extension at 72°C for 4 min. The product is then diluted 1/100, and 1 μl is used in a second PCR with primers FIP1L1-F2 (5′-AAAGAGGATACGAATGGGACTTG) and PDGFRA-R2 (5′-GGGACCGGCTTAATCCATAG) and the same cycle conditions. Multiple bands are often present upon gel electrophoresis and represent splice variants (12, 18). The EOL-1 cell line (ACC386; available from the Deutsche Sammlung von Mikroorganismen und Zellkulturen [http://www.dsmz.de]) has been shown to possess the *FIP1L1-PDGFRA* mutation (13) and is useful as a positive control. RT-PCR for a housekeeping gene, such as the glyceraldehyde-3-phosphate dehydrogenase (GAPDH) gene, should also be performed as a control for the amount and quality of the RNA template.

Fluorescent *In Situ* Hybridization

Slides for FISH are prepared by standard methods. BAC clones 120K16 (mapped centromeric of *FIP1L1*), 3H20 (mapped between *FIP1L1* and *PDGFRA*), and 24O10 (mapped telomeric of *PDGFRA*) can be obtained from the RPCI11 Roswell Park Cancer Institute library (http://bacpac.chori.org) for three-color labeling by nick translation. Following hybridization, interphase nuclei are examined for the presence or absence of the 3H20 signal, which is lost as a result of the interstitial deletion in cells with the *FIP1L1-PDGFRA* fusion gene (12).

One-color FISH with a probe for the cysteine-rich hydrophobic domain 2 (*CHIC2*) locus situated between *FIP1L1* and *PDGFRA* on chromosome 4q was initially described as a surrogate for detection of the fusion gene to identify patients with the *FIP1L1-PDGFRA* fusion gene (21). Although it is less cumbersome, this method is not useful for the detection of the *FIP1L1-PDGFRA* fusion genes, in which there is a translocation. A two-color modification of this approach was recently reported by the same authors (25) and appears to be comparable to the three-color strategy outlined above. FISH assays using the same strategy but different probes are commercially available.

Other (Bone Marrow Features and Level of Tryptase in Serum)

Clinical and laboratory features supportive of a diagnosis of *PDGFRA*-associated MPN (18) may serve as surrogates if formal testing for the mutation is not available. These include male gender, elevated tryptase levels in serum, splenomegaly, clinical evidence of fibrotic end organ involvement, bone marrow features of myeloproliferative disease (including hypercellularity and reticulin fibrosis), increased and spindle-shaped bone marrow mast cells, anemia, thrombocytopenia, and elevated vitamin B_{12} levels in serum. Although none of these features is by itself diagnostic of the *FIP1L1-PDGFRA* fusion gene, the presence of an elevated tryptase level in serum and four or more of the above-described clinical features has correlated with the presence of the fusion gene in all of the patients evaluated at our center to date and is predictive of a response to imatinib. It should be noted that rare patients with *FIP1L1-PDGFRA*-associated MPN have normal tryptase levels and no apparent involvement of the mast cell lineage. Several commercial laboratories measure serum tryptase levels. Enzyme-linked immunosorbent assay (ELISA) kits are also available from a number of sources.

Imatinib-responsive patients with HES in whom the *FIP1L1-PDGFRA* mutation cannot be demonstrated have been reported in several studies (10, 24). Clinical and hematologic responses in these patients are generally slower and require higher doses of imatinib than responses in patients with *PDGFRA*-associated MPN. A recent study suggests that the best predictor of imatinib response in these patients is the presence of four or more of the above-described myeloproliferative features (103).

Although the bone marrow features and elevated serum tryptase seen in *PDGFRA*-associated MPN sometimes fulfill the diagnostic criteria for systemic mastocytosis (see the Mastocytosis section below), it is extremely important to distinguish these patients from those with c-*kit*

mutation-driven disease, since D816V, the most common c-*kit* mutation associated with systemic mastocytosis, leads to resistance to imatinib (21). In this regard, clinical features, including the ratio of serum tryptase level to the eosinophil number, can be very useful (26).

Therapy

The dismal survival rates reported in the early HES literature (9, 27) likely reflect the high mortality from cardiac and neurologic complications in patients with *PDGFRA*-associated MPN prior to the availability of imatinib. Clinical, hematologic, and molecular responses are rapidly achieved with imatinib treatment in patients with *PDGFRA*-associated MPN and appear to be sustained (12, 28, 29). Consequently, whereas conventional first-line therapy for HES in most patients (including patients with MHES who are *PDGFRA* negative) should continue to be steroids, patients with *PDGFRA*-associated MPN are typically resistant to steroids and should receive targeted therapy with imatinib mesylate. It should be noted that imatinib therapy is not without risk, as life-threatening complications have occurred in patients with eosinophilic cardiac disease (22, 30). Troponin levels in serum have been proposed as a pretreatment marker for the development of this complication (30). Although uncommon in *PDGFRA*-positive MPN, primary and secondary resistance to imatinib has been reported (31, 32). Since the most common cause appears to be a mutation (T674I) that is homologous to the well-described T315I mutation in BCR-ABL, tyrosine kinase inhibitors that are active against this mutation should be used in a setting of imatinib resistance. Allogeneic bone marrow transplantation is a potentially curative alternative for patients with aggressive or treatment-refractory disease (33).

Lymphocytic Variant HES

Epidemiology and Clinical Features

Despite isolated reports of clonal populations of T cells in patients with HES as early as 1994 (14, 15), it was not until 1999 that a distinct subgroup of patients with lymphocyte-driven HES (LHES) was first described (34). Hypereosinophilia in these patients is believed to occur in response to the production of eosinophilopoietic cytokines, particularly interleukin 5 (IL-5), by clonal populations of activated phenotypically abnormal T lymphocytes. Although the levels of IL-5 in the serum are often normal, an increased production of IL-5 by stimulated peripheral blood mononuclear cells and/or phenotypically abnormal T-cell populations can be demonstrated in most patients with LHES, consistent with this hypothesis (34–36). Other evidence of Th2 activation in patients with this variant includes elevations of immunoglobulin E (IgE) and thymus- and activation-regulated chemokine (TARC) in serum (10, 37). Cytogenetic abnormalities are occasionally present in patients with the lymphocytic variant, although no consistent pattern has been delineated (36).

LHES appears to account for approximately 20% of HES cases, and LHES cases are equally distributed between men and women (10, 36). Although the clinical manifestations of this subgroup of patients can be extremely varied, tissue fibrosis, including endomyocardial fibrosis, is uncommon. In addition, patients with LHES share several clinical characteristics, the most striking of which is the predominance of dermatologic manifestations, including pruritus, urticaria, angioedema, and erythroderma (36). Gastrointestinal symptoms and obstructive pulmonary disease are also extremely common. Many patients have a history of atopic disease, and elevated IgE and IgG levels are common, but not restricted, to this subgroup of patients with HES.

Despite the relatively low mortality rate for this subgroup, the morbidity, due both to the underlying disease and to secondary effects of treatment, is significant. Furthermore, progression to T-cell lymphoma appears to be most common in this subgroup of patients and should be suspected in the setting of increasing numbers of aberrant T cells and/or the development of lymphadenopathy (35, 36). Two features that appear to be associated with an increased likelihood of progression to lymphoma are the $CD3^-$ $CD4^+$ surface phenotype and the presence of cytogenetic abnormalities.

Diagnosis

The diagnosis of LHES is based on the identification of a clonal population of phenotypically abnormal T cells in the peripheral blood by flow cytometry (see chapter 17 of this *Manual*). The sensitivity of this assay depends to a large degree on the number of antibodies used and the ability of the laboratory to detect subtle changes in the surface phenotype. Although T-cell clonality is not always present in cases with a demonstrable population of aberrant lymphocytes and is not essential for the diagnosis of the lymphocytic variant, identification of a clonal population of T cells by T-cell receptor (TCR) rearrangement analysis is strongly supportive of this diagnosis. Other diagnostic tests that may be helpful in establishing the diagnosis include the measurement of TARC levels in serum and the assessment of the lymphocyte production of eosinophilopoietic cytokines. Serum levels of IL-5 may be undetectable or elevated in patients with LHES and have no diagnostic or prognostic value.

Lymphocyte Phenotype

Although the most common aberrant phenotype of the lymphocytic variant of HES appears to be $CD3^-$ $CD4^+$, several other surface phenotypes have been described, including $CD3^+$ $CD4^-$ $CD8^-$ and $CD2^-$ $CD3^+$ (34). In many cases, the aberrant population may be identifiable only by markers that are not included in routine panels (such as CD5, CD6, CD7, CD27, and CD95) or by slight alterations in staining intensity. Therefore, if the lymphocytic variant is suspected and routine lymphocyte phenotyping is normal, surface staining for additional markers, including CD5, CD6, CD7, and CD27, should be considered. Activation markers, such as CD25 and HLA-DR, are commonly increased on the surfaces of aberrant T cells, providing additional markers.

Other (TCR Rearrangement Analysis, Measurement of TARC Levels, and Cytokine Assays)

T-cell clonality can be assessed in peripheral blood or bone marrow samples by PCR evaluation of TCR usage and has been reported to be present in approximately 75% of patients with the lymphocytic variant of HES, as defined by flow cytometry. When present, the demonstration of clonality may be helpful, although false-negative results may occur when the clonal population is very small or involves clonal deletion of TCR chain genes (35). In addition, restricted (or oligoclonal) patterns of TCR usage are common in all forms of HES, necessitating a very strict interpretation of banding results.

TARC is a CC chemokine thought to be involved in Th2-mediated immune responses. TARC levels in serum can be measured reliably by using several commercially available ELISA kits and are markedly elevated (>1,000 pg/ml) in patients with lymphocytic HES (10, 37). TARC levels in serum are also markedly elevated in patients with

cutaneous T-cell lymphoma (38) (a disorder that may overlap HES in clinical presentation) and rarely in patients with helminth infection (39) or atopic dermatitis (40). Thus, although TARC levels in serum may be a useful surrogate marker for T-cell clonality in HES, the presence of elevated levels should not replace a thorough diagnostic evaluation.

The ultimate proof of lymphocyte-driven HES is the documentation of an increased production of eosinophilopoietic cytokines by circulating lymphocytes. Enhanced levels of IL-3, IL-5, and/or granulocyte-macrophage colony-stimulating factor have been detected by ELISA in supernatants from *in vitro* cultures of peripheral blood mononuclear cells or purified T cells from patients with the lymphocytic variant of HES (34–36). Increased percentages of lymphocytes positive for eosinophilopoietic cytokines have also been demonstrated by intracellular flow cytometry in these patients. Although these assays are not routinely available in clinical laboratories at this time, they may be helpful, particularly in situations where an abnormal surface phenotype is not detected by more-standard methods.

Treatment

Imatinib does not appear to be useful for treating patients with LHES (41) and should not be used as first-line therapy for these patients. Historically, steroids have been used successfully in the majority of cases to control clinical symptoms, and significant decreases in clonal populations in response to steroid therapy have been described (10, 35). In patients with steroid-refractory disease or who are intolerant of the side effects of steroid treatment, a number of immunomodulatory agents with effects on Th2 cytokine production and T-cell proliferation, including alpha interferon, cyclosporine, and intravenous immunoglobulin, have been shown to have a therapeutic effect. Although stable responses have been achieved with relatively low doses of alpha interferon over prolonged periods of time, *in vitro* data demonstrating an inhibition of apoptosis of clonal $CD3^-$ $CD4^+$ T cells (42) suggest that interferon monotherapy should be avoided for this subgroup of patients. Newer agents, such as antibody to IL-5, that directly target eosinophilopoietic cytokines are currently in clinical trials and appear promising. In fact, subgroup analysis of a double-blind, placebo-controlled clinical trial revealed that mepolizumab, a humanized antibody to IL-5, was equally effective as a steroid-sparing agent in subjects with LHES and those with idiopathic HES (43).

Other

Several other HES of unknown etiology have distinctive clinical patterns that appear to set them apart. One of the most intriguing of these is episodic angioedema and eosinophilia (Gleich's syndrome) (44). Gleich's syndrome is characterized by episodic, but pronounced, eosinophilia and angioedema. In most cases, the episodes occur monthly and last for 7 to 11 days. Cyclical increases in eosinophilopoietic cytokines, most often IL-5, can be demonstrated preceding the rise in peripheral eosinophil counts. Although some patients with this syndrome ultimately progress to HES and/or develop clonal populations of lymphocytes (45), the unique clinical presentation is suggestive of a common and distinct etiology for this clinical subgroup of patients. The diagnosis should be suspected in patients whose primary complaint is swelling and/or weight gain and confirmed by the measurement of eosinophil counts every 3 days for several weeks off therapy. Often, the periodicity is missed because of intermittent steroid use and the measurement of eosinophil counts only when symptoms are present. Clonal $CD3^-$ $CD4^+$ T-cell populations have been described to occur in this subgroup of patients and should be assessed by flow cytometry and TCR rearrangement analysis.

The occurrence of marked eosinophilia in multiple members of the same family is rare, with only a few reports in the literature to date (46). Autosomal dominant transmission appears to be the most common form of transmission. In one such family, the gene responsible for the eosinophilia has been mapped to chromosome 5q31-33 (47). Despite marked eosinophilia (2,000 to 6,000/mm^3) from birth, a minority of family members with familial eosinophilia develop eosinophil-mediated end organ damage (48). This paucity of clinical manifestations is associated with a relative lack of eosinophil activation compared to that in patients with nonfamilial HES. Whether the sudden disease progression in a small number of these patients after a lifetime of asymptomatic eosinophilia represents a second mutation remains unknown at this time.

Another less well defined clinical subgroup of patients presents with marked eosinophilia and clinical features highly suggestive of eosinophilic granulomatosis with polyangiitis (EGPA, formerly Churg Strauss syndrome), including a long history of asthma, paranasal sinus abnormalities, and recurrent pulmonary infiltrates, without demonstrable vasculitis. Although some of these patients likely have occult EGPA, in some cases biopsies of affected tissues repeatedly fail to show evidence of vasculitis, and antineutrophil cytoplasmic antibodies are undetectable in serum. The pathologic basis of end organ damage in this subgroup of patients remains to be elucidated.

Controversies

A number of controversies remain surrounding the diagnosis of HES and its classification into subtypes. These include (i) the classification of patients with marked eosinophilia and no evidence of end organ damage, (ii) the distinction between HES and other organ-specific eosinophilic disorders of unknown etiology (e.g., eosinophilic gastroenteritis or chronic eosinophilic pneumonia) in patients with concomitant peripheral eosinophilia, and (iii) the diagnostic classification of patients with known etiologies, including *PDGFRA*-associated MPN and clonal lymphocytic disorders. As the number of chemotherapeutic agents with specific molecular and immunologic targets continues to grow, the resolution of these issues will become increasingly important for the appropriate management of patients presenting with a clinical syndrome consistent with HES.

EOSINOPHIL-ASSOCIATED GASTROINTESTINAL DISORDERS

Definition of EGIDs

Eosinophil-associated gastrointestinal disorders (EGIDs) are a family of related diseases characterized by eosinophilic inflammation of the gastrointestinal tract. The two major forms of EGID, eosinophilic esophagitis (EoE) and eosinophilic gastroenteritis (EGE), differ with regard to the site of inflammation (esophagus versus stomach/small bowel) (49, 50). EoE is the most common and best-characterized form of EGID. EoE was first described as a distinct clinical entity in the early 1990s (51) and in the past 15 years has emerged as an increasingly common clinical entity in both children and adults. Peripheral blood eosinophilia is a common feature of EGID, although it is rarely elevated above 1,500/mm^3. EGE, although less common than EoE, is more highly associated with peripheral eosinophilia and should be considered in

patients presenting with peripheral eosinophilia and GI symptoms.

One of the most notable features of EGID, particularly well established for EoE, is its responsiveness to highly restricted or amino acid-based elemental diets. Multiple clinical studies have demonstrated that >90% of patients with EoE have both clinical and histological remission after 1 month on an elemental diet (52). Case series suggest a similar dietary responsiveness in at least a subpopulation of patients with EGE (53). In sum, these findings strongly support the idea that EGID is a food allergen-driven eosinophilic inflammatory gut disease.

In EGID, food allergens directly activate antigen-specific Th2 cells and possibly mast cells or basophils, driving IL-5 and IL-13 expression. These two cytokines cause increased bone marrow eosinophil production and eosinophil tissue localization, respectively. The chronic eosinophilic inflammation in EoE ultimately results in tissue fibrosis. Although the exact mechanism of fibrosis is the subject of ongoing investigation, a number of profibrotic cytokines, such as IL-13 and transforming growth factor β, are expressed in active EGID sites of disease (54).

Although EoE was initially characterized in pediatric patients, the idea that it can occur at any age has been appreciated more recently. The clinical presentations of EoE vary with age; elementary school and younger patients often present with nonspecific symptoms, such as regurgitation, spitting up, and chest pain, whereas older patients present predominantly with dysphagia (55, 56). This difference is likely due to a greater duration of untreated disease in older patients, leading to remodeling, fibrosis, and stricture formation, which manifests as dysphagia. As in pediatric disease, adult EoE is highly responsive to diet therapy (52).

Diagnosis of EGID

EoE is the most common type of EGID and is the only form of EGID having consensus guidelines for diagnosis and management (57). The diagnosis of EoE requires both clinical and pathological findings. Clinically, the patient must have symptoms related to esophageal dysfunction, although in children these can be quite nonspecific. The pathological diagnosis requires ≥15 eosinophils per high-powered field (hpf) in the most affected biopsy area, commonly referred to as the "peak eosinophil count."

Gastroesophageal reflux can also cause esophageal eosinophilia; thus, to make the diagnosis of EoE, reflux must be ruled out. In practice, this is most commonly done by treatment with twice-daily proton pump inhibitors (PPIs) for 2 months prior to the esophageal biopsy procedure (57). Alternatively, the absence of gastroesophageal reflux can be confirmed by esophageal pH monitoring. Often, in cases where there is a low index of suspicion for EoE, biopsy specimens are obtained without proton pump inhibitor therapy. In these cases, the finding of >15 eosinophils/hpf is not diagnostic for EoE, as the majority of these patients have PPI-responsive esophageal eosinophilia due to gastroesophageal reflux and do not have EoE (58). In most cases, it is important to make a definitive diagnosis, and a second procedure must be undertaken to obtain biopsy specimens while the patient is on proton pump inhibitors. EoE is associated with many gross endoscopic features, such as esophageal rings, furrows, and strictures. However, multiple studies have shown that none of these are specific for the diagnosis of EoE (59). This further underscores the need for careful pathological diagnosis.

If it can be done safely, patients suspected of having EoE should be taken off diet or corticosteroid therapy for at least a month prior to the diagnostic esophagoduodenoscopy procedure. EoE is a patchy disease, and the affected tissue often looks normal; thus, multiple biopsy specimens are required to avoid a sampling error. To maximize the potential to make the diagnosis, a total of 6 biopsy specimens, including in both the distal and the midesophagus, are taken (57). Eosinophils are visualized using standard hematoxylin and eosin staining. Biopsy slides are then scanned to identify areas with the greatest number of eosinophils, and the numbers per hpf are counted.

Analysis of tissue eosinophils using immunohistochemistry for eosinophil granule proteins, such as eosinophil peroxidase or major basic protein, may provide additional information (60). However, at the present time, such analyses are limited to research applications and are not part of routine clinical care.

Unlike EoE, there are no consensus guidelines for the diagnosis of EGE. The diagnosis is based on typical symptoms coupled with increased gastric or intestinal eosinophils, in the absence of other potential causes of GI eosinophilia. There is no consensus on the requisite number of eosinophils needed for the diagnosis. Based on studies of healthy controls, peak eosinophil counts of 30 eosinophils/hpf in the stomach and 50 eosinophils/hpf in the duodenum have been proposed for the diagnosis of eosinophilic gastritis and duodenitis, respectively (61, 62). Additional features, such as epithelial eosinophils, intraglandular eosinophils, and eosinophils in the muscularis, also weight toward the diagnosis of EGE. Endoscopic biopsy specimens should be obtained from 5 to 6 sites per affected site, in a manner similar to those of the consensus procedures in cases of EoE. In EGE patients with peripheral eosinophilia, analysis of stool specimens for ova and parasites and serologic testing for *Toxocara* species (in children) and *Strongyloides* should be performed.

Treatment of EGID

There are no drugs currently approved for the treatment of EGID. As noted above, dietary therapy is highly effective in patients with EoE and in at least a subpopulation of patients with EGE. Systemic corticosteroids are highly effective in all forms of EGID, but their long-term use often results in side effects. Topical corticosteroids, such as fluticasone and budesonide, provide local anti-inflammatory activity with minimal systemic effects (63).

Use of Laboratory Tests in the Management of EGID

There are two major processes driving EoE symptoms. First, inflammation may directly cause symptoms, presumably by direct action on esophageal motility (64). Second, chronic eosinophilic inflammation drives esophageal fibrosis, ultimately resulting in rings, strictures, and remodeling (54). Although symptomatic improvement is an important treatment endpoint, the suppression of esophageal fibrosis is equally important. To that end, the management of EoE focuses on the treatment and monitoring of eosinophilic inflammation as a means to decrease esophageal fibrosis and dysfunction. Although there are no consensus targets, a posttreatment reduction to ≤6 eosinophils/hpf has been considered a successful response in clinical studies (65, 66).

EGID is highly associated with other allergic diseases, and IgE sensitization is associated with multiple food allergens. Some research groups have attempted to use food allergen-specific IgE tests to identify culprit foods driving EGID; however, others have not found such testing predictive (52). Given its uncertain value in managing EGID,

food allergen-specific IgE testing should not be used as a tool in the routine management of EGID dietary therapy.

MASTOCYTOSIS

Definition

Mastocytosis is a disorder characterized by the accumulation of aberrant mast cells in tissues, such as skin, bone marrow, gastrointestinal tract, liver, spleen, and lymph nodes (67). Most cases of mastocytosis are associated with gain-of-function mutations in c-*kit*, the receptor for the major mast cell growth factor, stem cell factor (68).

Classification and Diagnostic Criteria

The current WHO classification divides mastocytosis into seven categories (Table 3) (69, 70). The symptoms, prognosis, and treatment options vary according to the category of disease.

Cutaneous Mastocytosis

Cutaneous mastocytosis is the most common presentation in children (71). It is usually diagnosed within the first year of life. The most common skin lesion is urticaria pigmentosa (UP). The lesions are fixed (as opposed to a classic urticarial lesion, which is evanescent) and maculopapular and may be slightly raised and hyperpigmented. The diameters range from a few millimeters to a few centimeters. The lesions are generally nonpruritic at baseline but may be induced to urticate by stroking (Darier's sign), pressure, temperature changes, and exercise. Sterile blistering may be noted within the first 3 years of life. Less common forms of cutaneous mastocytosis include a mastocytoma(s) of the skin and diffuse cutaneous mastocytosis (72). The diagnosis of cutaneous mastocytosis is confirmed by a skin biopsy demonstrating increased numbers of mast cells in the upper dermis, usually around blood vessels.

Cutaneous mastocytosis has a good prognosis, with approximately 90% of patients experiencing resolution or improvement of disease by adolescence. By definition, cutaneous mastocytosis involves only the skin. It should not be confused with UP in adults, which is usually associated with systemic disease (bone marrow involvement). However, due to the low pretest probability, a bone marrow biopsy is generally not recommended for children who are diagnosed within the first 2 years of life and who do not have signs of hematologic involvement (unexplained abnormalities in a complete blood count with differential, hepatosplenomegaly, or lymphadenopathy) or a persistently elevated tryptase level greater than 20 ng/ml. In addition to having cutaneous symptoms, such as flushing and itching, patients with cutaneous mastocytosis may display gastrointestinal cramping, nausea, vomiting, and diarrhea. Anaphylactic episodes resulting in loss of consciousness may occur after hymenoptera stings or without provocation, but their prevalence is not as high as in the adult population (73). The incidence of IgE-mediated allergy is believed to be similar to that in the general population (74).

Systemic Mastocytosis

According to WHO criteria, systemic mastocytosis is diagnosed when pathologic mast cells are demonstrated in an extracutaneous tissue. The most common procedure for diagnosis is a bone marrow biopsy and aspiration. The disease is occasionally diagnosed in gastrointestinal biopsy specimens (75); however, we are not aware of a case of isolated GI disease without bone marrow involvement. In order to fulfill WHO criteria for systemic mastocytosis, the major criterion plus at least one minor criterion or three minor criteria must be fulfilled.

TABLE 3 Classification of mastocytosis from reference 69

Cutaneous mastocytosis
Indolent systemic mastocytosis
Systemic mastocytosis with an AHNMD
Aggressive systemic mastocytosis
Mast cell leukemia
Mast cell sarcoma
Extracutaneous mastocytomas
B findings
Infiltration by mast cells of >30% in a bone marrow biopsy specimen and 1 of the following:
Tryptase level of >200 ng/ml
Myelodysplastic or myeloproliferative changes in bone marrow without fully meeting the WHO criteria for MDS[a] or MPNs
Hepatomegaly or splenomegaly without end organ dysfunction
C findings
Cytopenias (neutropenia of <1,000/μl, hemoglobin of <10 g/dl, platelets of <100,000/μl) with extensive bone marrow mast cell infiltration or splenomegaly
Liver pathology indicating portal hypertension, ascites, elevated LFTs, hyperbilirubinemia
GI pathology indicating diarrhea with malabsorption, hypoalbuminemia, and weight loss
Bone pathology showing large osteolytes with pathologic fractures

[a]MDS, myelodysplastic syndromes.

Major Criterion

A major criterion is multifocal clusters of at least 15 mast cells per cluster. Mast cells in normal marrow or in reactive mast cell hyperplasia occur singly. Clustering of mast cells is a pathologic hallmark of systemic mastocytosis (76). Some patients with milder disease burden and relatively low serum tryptase levels may not display the major criterion. In those patients, there may be a smaller number of mast cells per cluster; however, close examination of an appropriately stained bone marrow biopsy specimen and aspirate may reveal evidence of mast cell pathology, such as spindle-shaped mast cells, CD25 expression, and perivascular or paratrabecular dominance of mast cells. The preferred stain to visualize mast cells is an immunohistochemical stain for tryptase. Mast cells are the only cells in bone marrow stainable for tryptase. Metachromatic stains are unreliable in bone marrow biopsy specimens and should not be relied upon for diagnosis.

Minor Criterion 1

Morphologic aberrancies in mast cells include spindle-shaped bi- or multilobed nuclei, cytoplasmic projections, and hypogranulation. A normal bone marrow mast cell should be round, with a single central nucleus and heavy granulation obscuring the nucleus. Detailed depictions of mast cell morphologic abnormalities are published and should be referred to by hematopathologists, since aberrant mast cells can sometimes be overlooked (77). Both aspirate

smears and a bone marrow biopsy specimen should be examined. In order to fulfill the criterion, at least 25% of the mast cells in the infiltrate should be abnormally shaped.

Minor Criterion 2

Minor criterion 2 is aberrant expression of CD25 and CD2. CD25 is not expressed by normal or hyperplastic mast cells. A mast cell expressing CD25 is highly specific and sensitive for the diagnosis of mastocytosis (78, 79). The only other disorder in which mast cells have been described to express CD25 is PDGFRA-associated myeloproliferative neoplasm (18). CD25 expression can be detected by flow cytometry or immunohistochemistry. Immunohistochemistry has the advantage that it can be performed on stored biopsy specimens. We currently recommend CD25 staining in all cases of suspected systemic mastocytosis, since patients with mild disease may not have a pathologically increased number or clustering of mast cells. Activated lymphocytes in the bone marrow can also express CD25, but the level of expression is much lower than on pathologic mast cells. Furthermore, mast cells can be recognized based on their distinct morphology. Flow cytometry of the bone marrow aspirate is also very helpful in demonstrating pathologic CD25 expression in freshly obtained bone marrow aspirate samples but is technically more challenging than immunohistochemistry, as it requires collection of at least 500,000 events (preferably more in cases suspected of having a low mast cell burden) and special gating to demonstrate the mast cell population. A detailed discussion of the recommended gating strategies and various pitfalls of this technique can be found in previous publications (80, 81). CD2 is a less sensitive marker and may be absent in advanced forms of mastocytosis, such as aggressive systemic mastocytosis or mast cell leukemia (82).

Minor Criterion 3

Minor criterion 3 is a codon 816 c-kit mutation in blood, bone marrow, or lesional tissue. c-kit is the transmembrane receptor for stem cell factor, the major growth and differentiation factor for mast cells (83). Its extracellular domain encodes five immunoglobulin-like domains that bind cell-bound or soluble stem cell factor (SCF) homodimers. Its intracellular domain has intrinsic tyrosine kinase activity. Under physiologic circumstances, dimerization of Kit triggers autophosphorylation of tyrosine residues, which can act as docking sites for downstream signal transduction and adapter proteins. More than 90% of patients with systemic mastocytosis (84) and approximately 40% of patients with cutaneous mastocytosis (85) carry a D816V activating point mutation affecting the tyrosine kinase domain of the receptor, resulting in ligand-independent autophosphorylation. D816V is a somatic mutation, and its detection is influenced by the degree of enrichment of mast cells in the sample, whether non-mast cell hematopoietic lineages are involved, and by the technique used to detect the mutation. For example, detection techniques based on sequence analysis of bulk tissue have low sensitivities (less than 20%) compared to those of PCR-based techniques using D816V mutation-specific primers but may be suitable for analysis of skin lesions, mastocytomas, or mast cell leukemias, where neoplastic mast cells are found enriched if the typical D816V mutation is absent. Enrichment of mast cells usually yields the best sensitivity, although this technique is available only on a research basis (68). Flow cytometric enrichment of mast cells from bone marrow tissue (based on high CD117 and high FceR1 and CD25 expression) or bulk sorting using magnetic beads or flow cytometry and anti-CD25 antibody followed by RT-PCR of c-kit mRNA yields the most-sensitive results. Recently, a more sensitive real-time quantitative PCR (qPCR)-based technique has been described. Sensitivity for the detection of the D816V mutation in peripheral blood is reported to approach 100% using this technique (86). Real-time qPCR was performed with a forward primer (5′-AGAGACTTGGCAGCCAGAAA-3′) and a reverse primer (5′-TTAACCACATAATTAGAATC ATTCTTGATCA-3′) with an intended mismatch to reduce cross-reaction with the wild-type c-kit allele. The fluorescent probe 5′-6-FAM-TCCTCCTTACTCATGGTCGGATCA CA-TAMRA-3′ (where FAM is 6-carboxyfluorescein and TAMRA is 6-carboxytetramethylrhodamine) was used for detection. Real-time qPCR was performed with 50 cycles of denaturation at 95°C for 15 s and annealing and elongation at 60°C for 1 min.

Mutations in c-kit residues other than D816V have been described but are less common. One study reported that approximately 40% of patients with cutaneous mastocytosis had an activating c-kit mutation outside codon 816 when lesional skin was analyzed (86). The prognostic significance of these mutations remains to be elucidated, however, since they can occur in both benign and aggressive forms of disease. In patients with advanced categories of disease, c-kit mutations can be present in other hematopoietic lineages in addition to mast cells (87). Patients with multilineage involvement have a poorer prognosis that those with limited mast cell involvement (87).

Minor Criterion 4

Minor criterion 4 is an elevated baseline serum tryptase level of >20 ng/ml. Tryptase is a protease that is abundantly produced and stored in mast cell granules. Mature tryptases (beta tryptase) are released from mast cell granules, and levels are generally elevated after mast cell activation episodes, such as anaphylaxis, if checked within 4 h of the event. Protryptases (alpha tryptase and pro-beta tryptase) do not possess enzymatic activity and are released constitutively from mast cells. Therefore, the level of serum tryptase at baseline (i.e., without an anaphylactic event) correlates with total body mast cell burden (88). Commercially available tryptase immunoassays measure total tryptase, which is a combination of both pro- and mature tryptases. A normal median serum tryptase level is approximately 5 ng/ml. Conditions other than mastocytosis that can be associated with elevated tryptase levels include chronic renal and liver disease, parasitic diseases, bone marrow suppression states, myeloproliferative and myelodysplastic disorders, mast cell activation syndromes, and idiopathic tryptase elevations. The serum tryptase levels in these disorders generally do not exceed 40 ng/ml. On the other hand, a normal tryptase level, while significantly decreasing the odds, does not completely exclude a diagnosis of systemic mastocytosis. Patients with normal or slightly elevated tryptase levels usually lack the major diagnostic criterion, and therefore it is important to look for minor criteria in these patients (89).

Well-differentiated systemic mastocytosis is a rare morphologic variant that is usually seen in patients with a history of pediatric onset UP that does not resolve spontaneously before they reach adulthood (90, 91). In this variant, the mast cells do not display major morphologic aberrancies, such as spindling, and lack surface CD25 expression and the c-kit D816V mutation. The major diagnostic criterion is present, and tryptase is usually elevated.

Monoclonal mast cell activation syndrome is a recently described diagnostic category. Patients present with recurrent mast cell activation symptoms but meet only 1 or 2

minor criteria of clonality (CD25 expression and/or c-kit D816V expression) (92).

Systemic mastocytosis is further subdivided into 4 categories based on clinical findings (69, 70).

Indolent Systemic Mastocytosis

This is the most common category in adults. Patients are usually diagnosed after their 2nd decade of life and have a life expectancy comparable to that of the general age-matched population. They are usually bothered by symptoms caused by mediator release from mast cells, variably resulting in flushing, itching, gastrointestinal cramping, nausea, vomiting, diarrhea, and/or presyncopal or syncopal episodes associated with hypotension and tachycardia. The episodes may last from a few minutes to a few hours and generally improve with antihistamine and epinephrine treatment. Some patients also experience bone and soft tissue pain similar to that from fibromyalgia, fatigue, memory and concentration problems, and osteoporosis. The pathologic basis of these symptoms is not well understood. The risk of progression of indolent systemic mastocytosis to a more advanced category is thought to be less than 5%; however, these patients should still be periodically monitored for disease progression by a complete blood count with differential and tryptase levels.

Systemic smoldering mastocytosis is a subgroup characterized by high tissue mast cell burden and high tryptase levels but no evidence of a separately identifiable hematologic disorder (B findings in Table 1). Whether these patients have a higher likelihood of progression remains to be determined.

Systemic Mastocytosis with an Associated Clonal Hematologic Non-Mast Cell Disease (SM-AHNMD)

Approximately 20% of patients with systemic mastocytosis have evidence of another associated hematologic disease at the time of diagnosis. These disorders are diagnosed upon examination of bone marrow, lymph nodes, or peripheral blood according to their respective WHO diagnostic criteria. Myeloid disorders, such as chronic myeloproliferative diseases and myelodysplastic syndromes, are most common. Concomitant detection of JAK2 V617F and D816V c-kit mutations has also been described (93). These disorders have an increased likelihood of progression to acute myeloid leukemia and therefore carry a poorer prognosis. Since tryptase can be produced in small quantities by myeloid blasts, serum tryptase levels cannot be used as a diagnostic criterion for patients in this category (94). Lymphoproliferative disorders, including non-Hodgkin lymphoma and myeloma, have also been reported in association with mastocytosis, albeit much less often than myeloid disorders.

Patients with PDGFRA-associated MPN often present with mildly elevated tryptase levels and increased numbers of spindle-shaped, CD25-positive mast cells in bone marrow biopsy specimens (18). Although this can present a diagnostic challenge in some cases, the mast cells are typically interstitially distributed in PDGFRA-associated MPN, do not form clusters, and do not display the D816V c-kit mutation. Clinical symptomatology and the tryptase/absolute eosinophil count ratio are also helpful in distinguishing patients with PDGFRA-associated MPN from those with mastocytosis.

Symptoms in patients with SM-AHNMD include a combination of mast cell mediator symptoms and the symptoms specific to the AHNMD, such as anemia, thrombocytopenia, and infections. Skin lesions of UP may be absent, and mastocytosis is usually diagnosed based on bone marrow findings during the workup of the associated hematologic disorder.

Aggressive Systemic Mastocytosis

Patients with aggressive systemic mastocytosis (ASM) display a high degree of mast cell burden, as evidenced by markedly elevated tryptase levels (generally greater than 100 ng/ml) and marked bone marrow infiltration (generally greater than 20%) associated with signs and symptoms of end organ dysfunction (C findings in Table 1). Organs involved include the hematopoietic system, liver, bones, and GI tract, with end organ dysfunction manifesting as cytopenias, portal hypertension/ascites, pathologic bone fractures, and malabsorption/weight loss, respectively.

Mast Cell Leukemia

Mast cell leukemia (MCL) is a rare diagnosis characterized by the presence of >10% mast cells in peripheral blood or >20% in aspirate smears in an aspicular area (95). Tryptase levels are significantly elevated (sometimes over 1,000 ng/ml), and the bone marrow is markedly hypercellular (often >90% cellularity, with the majority of the infiltrate consisting of pathologic mast cells). Mast cells display very immature morphology, including marked hypogranulation, bi-or multilobulated nuclei, and even mitotic figures. Aleukemic MCL is diagnosed when circulating mast cells are <10%. Mast cells may carry atypical codon 816 mutations, such as D816Y or D816H, which are not detected by D816V-specific PCR-based assays. Patients may present with signs of ASM along with coagulopathies and gastrointestinal bleeding. The prognosis of MCL is extremely poor due to the lack of an effective cytoreductive therapy.

Extracutaneous Mastocytoma and MCS

Extracutaneous mastocytoma and mast cell sarcomas (MCS) is an extremely rare diagnosis, which denotes benign and malignant mast cell tumors. Experience is limited to a few case reports. Mast cell sarcomas have been reported to develop in the setting of prior UP and MCL (102). MCS is characterized by its propensity to invade, which is not seen in benign mast cell tumors.

Pitfalls in Diagnosis

Both overdiagnosis and underdiagnosis of mastocytosis can be a problem in clinical practice. Overdiagnosis is usually encountered when WHO diagnostic criteria are not carefully documented for a patient with unexplained mast cell activation symptoms and a slightly elevated tryptase level. Some patients are diagnosed based on increased numbers of mast cells in non-bone marrow sites, such as the GI tract. Whereas some of these patients do have systemic mastocytosis, it should be emphasized that mast cell numbers vary widely in normal and pathologic GI tissue, and the WHO criteria, such as clustering and CD25 expression, should still be applied rather than depending on the absolute numbers of mast cells for diagnosis (75). Conversely, underdiagnosis is usually encountered in the setting of a low mast cell burden and lower tryptase levels, when appropriate histopathologic, immunohistochemical, and molecular diagnostic tests are not performed. Patients with recurrent episodes of hypotensive anaphylaxis and those with a history of systemic reactions to hymenoptera stings should be evaluated for mastocytosis. The incidence of mastocytosis in patients with idiopathic anaphylaxis may be as high as 30% (89), and as many as 10% of patients with systemic hymenoptera venom-induced reactions have elevated tryptase levels, most of whom have a clonal mast cell disease (96).

Interestingly, patients presenting with angioedema and urticaria as the main manifestations of anaphylaxis have a lower likelihood of mastocytosis than those with hypotensive events (97). Therefore, some authors advocate bone marrow examination in patients who present with hypotensive anaphylaxis without urticaria or angioedema, regardless of tryptase levels. It should be noted that patients presenting with recurrent mast cell activation symptoms and normal or slightly elevated tryptase levels will most likely lack the major criterion (multifocal clusters of mast cells), and therefore, special attention should be paid to appropriately investigate the minor criteria.

Therapy

Management of mastocytosis incorporates 3 major concepts: (i) avoidance of triggers of mast cell activation, (ii) symptomatic anti-mast cell mediator pharmacotherapy, and (iii) mast cell cytoreductive therapy in selected cases (98).

Mast cell activation can be triggered by various stimuli, including temperature changes; heat, cold, exercise, emotional, or physical stress; irritation or friction of the skin; fever; alcohol; spicy foods; *Hymenoptera* stings; and certain medications, such as opioids, analgesics, nonsteroidal anti-inflammatory drugs (NSAIDs), and perioperative medications, including muscle relaxants, general anesthetics, and antibiotics (70). The triggers differ in individual patients, and the individual patient history and known tolerances are helpful in guiding the patient to avoid these factors. For example, there would be no need to avoid NSAIDs in a patient who has been able to tolerate these medications without a problem. A detailed list of medications that can potentially cause or enhance mast cell activation can be found in the mastocytosis society patient support website www.tmsforacure.org.

Antimediator pharmacotherapy depends on the patient's symptoms. H1 and H2 antihistamines, leukotriene blockers, oral cromolyn sodium, and glucocorticoids are the most frequently used treatment options. Multiple doses of self-injectable epinephrine should be prescribed to patients to be used in case of an anaphylactic event.

Cytoreductive therapy is indicated only for patients with advanced disease categories, including ASM, SM-AHNMD, MCL, and MCS (99). Some authors suggest a trial of cytoreductive therapy in patients with indolent disease if the patient has a history of multiple anaphylactic episodes unresponsive to antimediator maintenance therapy. The most commonly used cytoreductive therapies are cladribine and alpha interferon, although neither is curative. Imatinib is a tyrosine kinase inhibitor with the capacity to inhibit wild-type Kit. Unfortunately, the most common mutation in systemic mastocytosis, D816V c-kit, confers resistance to imatinib. Consequently, most patients with mastocytosis are not candidates for imatinib (83). Bone marrow transplantation has been reported to yield mixed results in various case reports (100, 101).

REFERENCES

1. **Brigden M, Graydon C.** 1997. Eosinophilia detected by automated blood cell counting in ambulatory North American outpatients. Incidence and clinical significance. *Arch Pathol Lab Med* **121:**963–967. PubMed
2. **Hardy WR, Anderson RE.** 1968. The hypereosinophilic syndromes. *Ann Intern Med* **68:**1220–1229. PubMed
3. **Chusid MJ, Dale DC, West BC, Wolff SM.** 1975. The hypereosinophilic syndrome: analysis of fourteen cases with review of the literature. *Medicine (Baltimore)* **54:**1–27. PubMed
4. **Gleich GJ, Schroeter AL, Marcoux JP, Sachs MI, O'Connell EJ, Kohler PF.** 1984. Episodic angioedema associated with eosinophilia. *N Engl J Med* **310:**1621–1626. PubMed
5. **Chen YK, Khoury P, Ware JM, Holland-Thomas NC, Stoddard JL, Gurprasad S, Waldner AJ, Klion AD.** 26 August 2013. Marked and persistent eosinophilia in the absence of clinical manifestations. *J Allergy Clin Immunol* doi:10.1016/j.jaci.2013.06.037.
6. **Simon HU, Rothenberg ME, Bochner BS, Weller PF, Wardlaw AJ, Wechsler ME, Rosenwasser LJ, Roufosse F, Gleich GJ, Klion AD.** 2010. Refining the definition of hypereosinophilic syndrome. *J Allergy Clin Immunol* **126:**45–49. PubMed
7. **Vardiman JW, Thiele J, Arber DA, Brunning RD, Borowitz MJ, Porwit A, Harris NL, Le Beau MM, Hellström-Lindberg E, Tefferi A, Bloomfield CD.** 2009. The 2008 revision of the World Health Organization (WHO) classification of myeloid neoplasms and acute leukemia: rationale and important changes. *Blood* **114:**937–951. PubMed
8. **Valent P, Klion AD, Horny HP, Roufosse F, Gotlib J, Weller PF, Hellmann A, Metzgeroth G, Leiferman KM, Arock M, Butterfield JH, Sperr WR, Sotlar K, Vandenberghe P, Haferlach T, Simon HU, Reiter A, Gleich GJ.** 2012. Contemporary consensus proposal on criteria and classification of eosinophilic disorders and related syndromes. *J Allergy Clin Immunol* **130:**607–612.e9. PubMed
9. **Weller PF, Bubley GJ.** 1994. The idiopathic hypereosinophilic syndrome. *Blood* **83:**2759–2779. PubMed
10. **Ogbogu PU, Bochner BS, Butterfield JH, Gleich GJ, Huss-Marp J, Kahn JE, Leiferman KM, Nutman TB, Pfab F, Ring J, Rothenberg ME, Roufosse F, Sajous MH, Sheikh J, Simon D, Simon HU, Stein ML, Wardlaw A, Weller PF, Klion AD.** 2009. Hypereosinophilic syndrome: a multicenter, retrospective analysis of clinical characteristics and response to therapy. *J Allergy Clin Immunol* **124:**1319–1325.e3. PubMed
11. **Helbig G, Hus M, Francuz T, Dziaczkowska-Suszek J, Soja A, Kyrcz-Krzemień S.** 2014. Characteristics and clinical outcome of patients with hypereosinophilia of undetermined significance. *Med Oncol* **31:**815. PubMed
12. **Cools J, DeAngelo DJ, Gotlib J, Stover EH, Legare RD, Cortes J, Kutok J, Clark J, Galinsky I, Griffin JD, Cross NCP, Tefferi A, Malone J, Alam R, Schrier SL, Schmid J, Rose M, Vandenberghe P, Verhoef G, Boogaerts M, Wlodarska I, Kantarjian H, Marynen P, Coutre SE, Stone R, Gilliland DG.** 2003. A tyrosine kinase created by fusion of the PDGFRA and FIP1L1 genes as a therapeutic target of imatinib in idiopathic hypereosinophilic syndrome. *N Engl J Med* **348:**1201–1214. PubMed
13. **Griffin JH, Leung J, Bruner RJ, Caligiuri MA, Briesewitz R.** 2003. Discovery of a fusion kinase in EOL-1 cells and idiopathic hypereosinophilic syndrome. *Proc Natl Acad Sci U S A* **100:**7830–7835. PubMed
14. **Brugnoni D, Airó P, Rossi G, Bettinardi A, Simon HU, Garza L, Tosoni C, Cattaneo R, Blaser K, Tucci A.** 1996. A case of hypereosinophilic syndrome is associated with the expansion of a $CD3^{[minus]}$ $CD4^{+}$ T-cell population able to secrete large amounts of interleukin-5. *Blood* **87:**1416–1422. PubMed
15. **Cogan E, Schandené L, Crusiaux A, Cochaux P, Velu T, Goldman M.** 1994. Brief report: clonal proliferation of type 2 helper T cells in a man with the hypereosinophilic syndrome. *N Engl J Med* **330:**535–538. PubMed
16. **Klion AD, Law MA, Riemenschneider W, McMaster ML, Brown MR, Horne M, Karp B, Robinson M, Sachdev V, Tucker E, Turner M, Nutman TB.** 2004. Familial eosinophilia: a benign disorder? *Blood* **103:**4050–4055. PubMed
17. **Rioux JD, Stone VA, Daly MJ, Cargill M, Green T, Nguyen H, Nutman T, Zimmerman PA, Tucker MA, Hudson T, Goldstein AM, Lander E, Lin AY.** 1998.

Familial eosinophilia maps to the cytokine gene cluster on human chromosomal region 5q31-q33. *Am J Hum Genet* **63:**1086–1094. PubMed

18. **Klion AD, Noel P, Akin C, Law MA, Gilliland DG, Cools J, Metcalfe DD, Nutman TB.** 2003. Elevated serum tryptase levels identify a subset of patients with a myeloproliferative variant of idiopathic hypereosinophilic syndrome associated with tissue fibrosis, poor prognosis, and imatinib responsiveness. *Blood* **101:**4660–4666. PubMed
19. **Bain BJ.** 2010. Myeloid and lymphoid neoplasms with eosinophilia and abnormalities of PDGFRA, PDGFRB or FGFR1. *Haematologica* **95:**696–698. PubMed
20. **Elling C, Erben P, Walz C, Frickenhaus M, Schemionek M, Stehling M, Serve H, Cross NC, Hochhaus A, Hofmann WK, Berdel WE, Müller-Tidow C, Reiter A, Koschmieder S.** 2011. Novel imatinib-sensitive PDGFRA-activating point mutations in hypereosinophilic syndrome induce growth factor independence and leukemia-like disease. *Blood* **117:**2935–2943. PubMed
21. **Pardanani A, Ketterling RP, Brockman SR, Flynn HC, Paternoster SF, Shearer BM, Reeder TL, Li CY, Cross NC, Cools J, Gilliland DG, Dewald GW, Tefferi A.** 2003. CHIC2 deletion, a surrogate for FIP1L1-PDGFRA fusion, occurs in systemic mastocytosis associated with eosinophilia and predicts response to imatinib mesylate therapy. *Blood* **102:**3093–3096. PubMed
22. **Robyn J, Noel P, Wlodarska I, Choksi M, O'Neal P, Arthur D, Dunbar C, Nutman T, Klion A.** 2004. Imatinib-responsive hypereosinophilia in a patient with B cell ALL. *Leuk Lymphoma* **45:**2497–2501. PubMed
23. **Irusta PM, DiMaio D.** 1998. A single amino acid substitution in a WW-like domain of diverse members of the PDGF receptor subfamily of tyrosine kinases causes constitutive receptor activation. *EMBO J* **17:**6912–6923. PubMed
24. **Vandenberghe P, Wlodarska I, Michaux L, Zachée P, Boogaerts M, Vanstraelen D, Herregods MC, Van Hoof A, Selleslag D, Roufosse F, Maerevoet M, Verhoef G, Cools J, Gilliland DG, Hagemeijer A, Marynen P.** 2004. Clinical and molecular features of FIP1L1-PDFGRA (+) chronic eosinophilic leukemias. *Leukemia* **18:**734–742. PubMed
25. **Pardanani A, Brockman SR, Paternoster SF, Flynn HC, Ketterling RP, Lasho TL, Ho CL, Li CY, Dewald GW, Tefferi A.** 2004. FIP1L1-PDGFRA fusion: prevalence and clinicopathologic correlates in 89 consecutive patients with moderate to severe eosinophilia. *Blood* **104:**3038–3045. PubMed
26. **Maric I, Robyn J, Metcalfe DD, Fay MP, Carter M, Wilson T, Fu W, Stoddard J, Scott L, Hartsell M, Kirshenbaum A, Akin C, Nutman TB, Noel P, Klion AD.** 2007. *KIT* D816V-associated systemic mastocytosis with eosinophilia and *FIP1L1/PDGFRA*-associated chronic eosinophilic leukemia are distinct entities. *J Allergy Clin Immunol* **120:**680–687. PubMed
27. **Parrillo JE, Fauci AS, Wolff SM.** 1978. Therapy of the hypereosinophilic syndrome. *Ann Intern Med* **89:**167–172. PubMed
28. **Klion AD, Robyn J, Akin C, Noel P, Brown M, Law M, Metcalfe DD, Dunbar C, Nutman TB.** 2004. Molecular remission and reversal of myelofibrosis in response to imatinib mesylate treatment in patients with the myeloproliferative variant of hypereosinophilic syndrome. *Blood* **103:**473–478. PubMed
29. **Gleich GJ, Leiferman KM, Pardanani A, Tefferi A, Butterfield JH.** 2002. Treatment of hypereosinophilic syndrome with imatinib mesilate. *Lancet* **359:**1577–1578. PubMed
30. **Pitini V, Arrigo C, Azzarello D, La Gattuta G, Amata C, Righi M, Coglitore S.** 2003. Serum concentration of cardiac Troponin T in patients with hypereosinophilic syndrome treated with imatinib is predictive of adverse outcomes. *Blood* **102:**3456–3457. (Author Reply, **102:**3457.) PubMed
31. **Simon D, Salemi S, Yousefi S, Simon HU.** 2008. Primary resistance to imatinib in Fip1-like 1-platelet-derived growth factor receptor alpha-positive eosinophilic leukemia. *J Allergy Clin Immunol* **121:**1054–1056. PubMed
32. **Lierman E, Michaux L, Beullens E, Pierre P, Marynen P, Cools J, Vandenberghe P.** 2009. FIP1L1-PDGFRalpha D842V, a novel panresistant mutant, emerging after treatment of FIP1L1-PDGFRalpha T674I eosinophilic leukemia with single agent sorafenib. *Leukemia* **23:**845–851. PubMed
33. **Halaburda K, Prejzner W, Szatkowski D, Limon J, Hellmann A.** 2006. Allogeneic bone marrow transplantation for hypereosinophilic syndrome: long-term follow-up with eradication of *FIP1L1-PDGFRA* fusion transcript. *Bone Marrow Transplant* **38:**319–320. PubMed
34. **Simon HU, Plötz SG, Dummer R, Blaser K.** 1999. Abnormal clones of T cells producing interleukin-5 in idiopathic eosinophilia. *N Engl J Med* **341:**1112–1120. PubMed
35. **Roufosse F, Schandené L, Sibille C, Willard-Gallo K, Kennes B, Efira A, Goldman M, Cogan E.** 2000. Clonal Th2 lymphocytes in patients with the idiopathic hypereosinophilic syndrome. *Br J Haematol* **109:**540–548. PubMed
36. **Roufosse F, Cogan E, Goldman M.** 2007. Lymphocytic variant hypereosinophilic syndromes. *Immunol Allergy Clin North Am* **27:**389–413. PubMed
37. **de Lavareille A, Roufosse F, Schmid-Grendelmeier P, Roumier AS, Schandené L, Cogan E, Simon HU, Goldman M.** 2002. High serum thymus and activation-regulated chemokine levels in the lymphocytic variant of the hypereosinophilic syndrome. *J Allergy Clin Immunol* **110:**476–479. PubMed
38. **Kakinuma T, Sugaya M, Nakamura K, Kaneko F, Wakugawa M, Matsushima K, Tamaki K.** 2003. Thymus and activation-regulated chemokine (TARC/CCL17) in mycosis fungoides: serum TARC levels reflect the disease activity of mycosis fungoides. *J Am Acad Dermatol* **48:**23–30. PubMed
39. **Katoh S, Matsumoto N, Matsumoto K, Tokojima M, Ashitani J, Nakamura-Uchiyama F, Matsushima K, Matsukura S, Nawa Y.** 2004. A possible role of TARC in antigen-specific Th2-dominant responses in patients with *Paragonimiasis westermani*. *Int Arch Allergy Immunol* **134:**248–252. PubMed
40. **Shimada Y, Takehara K, Sato S.** 2004. Both Th2 and Th1 chemokines (TARC/CCL17, MDC/CCL22, and Mig/CXCL9) are elevated in sera from patients with atopic dermatitis. *J Dermatol Sci* **34:**201–208. PubMed
41. **Musto P, Perla G, Minervini MM, Carella AM, Coco FL, Catalano G.** 2004. Imatinib-mesylate for all patients with hypereosinophilic syndrome? *Leuk Res* **28:**773–774. PubMed
42. **Schandené L, Roufosse F, de Lavareille A, Stordeur P, Efira A, Kennès B, Cogan E, Goldman M.** 2000. Interferon alpha prevents spontaneous apoptosis of clonal Th2 cells associated with chronic hypereosinophilia. *Blood* **96:**4285–4292. PubMed
43. **Roufosse F, de Lavareille A, Schandené L, Cogan E, Georgelas A, Wagner L, Xi L, Raffeld M, Goldman M, Gleich GJ, Klion A.** 2010. Mepolizumab as a corticosteroid-sparing agent in lymphocytic variant hypereosinophilic syndrome. *J Allergy Clin Immunol* **126:**828–835.e3. PubMed
44. **Gleich GJ, Schroeter AL, Marcoux JP, Sachs MI, O'Connell EJ, Kohler PF.** 1984. Episodic angioedema associated with eosinophilia. *N Engl J Med* **310:**1621–1626. PubMed
45. **Morgan SJ, Prince HM, Westerman DA, McCormack C, Glaspole I.** 2003. Clonal T-helper lymphocytes and elevated IL-5 levels in episodic angioedema and eosinophilia (Gleich's syndrome). *Leuk Lymphoma* **44:**1623–1625. PubMed

46. **Lin AY, Nutman TB, Kaslow D, Mulvihill JJ, Fontaine L, White BJ, Knutsen T, Theil KS, Raghuprasad PK, Goldstein AM, Tucker MA.** 1998. Familial eosinophilia: clinical and laboratory results on a U.S. kindred. *Am J Med Genet* **76:**229–237. PubMed
47. **Rioux JD, Stone VA, Daly MJ, Cargill M, Green T, Nguyen H, Nutman T, Zimmerman PA, Tucker MA, Hudson T, Goldstein AM, Lander E, Lin AY.** 1998. Familial eosinophilia maps to the cytokine gene cluster on human chromosomal region 5q31-q33. *Am J Hum Genet* **63:**1086–1094. PubMed
48. **Klion AD, Law MA, Riemenschneider W, McMaster ML, Brown MR, Horne M, Karp B, Robinson M, Sachdev V, Tucker E, Turner M, Nutman TB.** 2004. Familial eosinophilia: a benign disorder? *Blood* **103:**4050–4055. PubMed
49. **Abonia JP, Rothenberg ME.** 2012. Eosinophilic esophagitis: rapidly advancing insights. *Annu Rev Med* **63:**421–434. PubMed
50. **Rothenberg ME.** 2004. Eosinophilic gastrointestinal disorders (EGID). *J Allergy Clin Immunol* **113:**11–29. PubMed
51. **Attwood SE, Smyrk TC, Demeester TR, Jones JB.** 1993. Esophageal eosinophilia with dysphagia. A distinct clinicopathologic syndrome. *Dig Dis Sci* **38:**109–116. PubMed
52. **Vashi R, Hirano I.** 2013. Diet therapy for eosinophilic esophagitis: when, why and how. *Curr Opin Gastroenterol* **29:**407–415. PubMed
53. **Gonsalves N, Doerfler B, Yang GY, Hirano I.** 2009. A prospective clinical trial of six food elimination diets or elemental diet in the treatment of adults with eosinophilic gastroenteritis. *Gastroenterology* **136:**A280.
54. **Cheng E, Souza RF, Spechler SJ.** 2012. Tissue remodeling in eosinophilic esophagitis. *Am J Physiol Gastrointest Liver Physiol* **303:**G1175–G1187. PubMed
55. **Lucendo AJ, Sánchez-Cazalilla M.** 2012. Adult versus pediatric eosinophilic esophagitis: important differences and similarities for the clinician to understand. *Expert Rev Clin Immunol* **8:**733–745. PubMed
56. **Straumann A, Schoepfer AM.** 2012. Therapeutic concepts in adult and paediatric eosinophilic oesophagitis. *Nat Rev Gastroenterol Hepatol* **9:**697–704. PubMed
57. **Liacouras CA, Furuta GT, Hirano I, Atkins D, Attwood SE, Bonis PA, Burks AW, Chehade M, Collins MH, Dellon ES, Dohil R, Falk GW, Gonsalves N, Gupta SK, Katzka DA, Lucendo AJ, Markowitz JE, Noel RJ, Odze RD, Putnam PE, Richter JE, Romero Y, Ruchelli E, Sampson HA, Schoepfer A, Shaheen NJ, Sicherer SH, Spechler S, Spergel JM, Straumann A, Wershil BK, Rothenberg ME, Aceves SS.** 2011. Eosinophilic esophagitis: updated consensus recommendations for children and adults. *J Allergy Clin Immunol* **128:**3–22. PubMed
58. **Molina-Infante J, Ferrando-Lamana L, Ripoll C, Hernandez-Alonso M, Mateos JM, Fernandez-Bermejo M, Dueñas C, Fernandez-Gonzalez N, Quintana EM, Gonzalez-Nuñez MA.** 2011. Esophageal eosinophilic infiltration responds to proton pump inhibition in most adults. *Clin Gastroenterol Hepatol* **9:**110–117. PubMed
59. **Dellon ES, Speck O, Woodward K, Gebhart JH, Madanick RD, Levinson S, Fritchie KJ, Woosley JT, Shaheen NJ.** 2013. Clinical and endoscopic characteristics do not reliably differentiate PPI-responsive esophageal eosinophilia and eosinophilic esophagitis in patients undergoing upper endoscopy: a prospective cohort study. *Am J Gastroenterol* **108:**1854–1860. PubMed
60. **Kephart GM, Alexander JA, Arora AS, Romero Y, Smyrk TC, Talley NJ, Kita H.** 2010. Marked deposition of eosinophil-derived neurotoxin in adult patients with eosinophilic esophagitis. *Am J Gastroenterol* **105:**298–307. PubMed
61. **DeBrosse CW, Case JW, Putnam PE, Collins MH, Rothenberg ME.** 2006. Quantity and distribution of eosinophils in the gastrointestinal tract of children. *Pediatr Dev Pathol* **9:**210–218. PubMed
62. **Lwin T, Melton SD, Genta RM.** 2011. Eosinophilic gastritis: histopathological characterization and quantification of the normal gastric eosinophil content. *Mod Pathol* **24:**556–563. PubMed
63. **Lucendo AJ, Molina-Infante J.** 2014. Emerging therapeutic strategies for eosinophilic esophagitis. *Curr Treat Options Gastroenterol* **12:**1–17. PubMed
64. **Rieder F, Nonevski I, Ma J, Ouyang Z, West G, Protheroe C, Depetris G, Schirbel A, Lapinski J, Goldblum J, Bonfield T, Lopez R, Harnett K, Lee J, Hirano I, Falk G, Biancani P, Fiocchi C.** 2014. T-helper 2 cytokines, transforming growth factor beta1, and eosinophil products induce fibrogenesis and alter muscle motility in patients with eosinophilic esophagitis. *Gastroenterology* **146:**1266–1277.e9.
65. **Dellon ES, Sheikh A, Speck O, Woodward K, Whitlow AB, Hores JM, Ivanovic M, Chau A, Woosley JT, Madanick RD, Orlando RC, Shaheen NJ.** 2012. Viscous topical is more effective than nebulized steroid therapy for patients with eosinophilic esophagitis. *Gastroenterology* **143:**321–324.e1. PubMed
66. **Dohil R, Newbury RO, Aceves S.** 2012. Transient PPI responsive esophageal eosinophilia may be a clinical subphenotype of pediatric eosinophilic esophagitis. *Dig Dis Sci* **57:**1413–1419. PubMed
67. **Metcalfe DD.** 2008. Mast cells and mastocytosis. *Blood* **112:**946–956. PubMed
68. **Akin C.** 2006. Molecular diagnosis of mast cell disorders: a paper from the 2005 William Beaumont Hospital Symposium on Molecular Pathology. *J Mol Diagn* **8:**412–419. PubMed
69. **Valent P, Horny HP, Escribano L, Longley BJ, Li CY, Schwartz LB, Marone G, Nuñez R, Akin C, Sotlar K, Sperr WR, Wolff K, Brunning RD, Parwaresch RM, Austen KF, Lennert K, Metcalfe DD, Vardiman JW, Bennett JM.** 2001. Diagnostic criteria and classification of mastocytosis: a consensus proposal. *Leuk Res* **25:**603–625. PubMed
70. **Valent P, Akin C, Escribano L, Födinger M, Hartmann K, Brockow K, Castells M, Sperr WR, Kluin-Nelemans HC, Hamdy NA, Lortholary O, Robyn J, van Doormaal J, Sotlar K, Hauswirth AW, Arock M, Hermine O, Hellmann A, Triggiani M, Niedoszytko M, Schwartz LB, Orfao A, Horny HP, Metcalfe DD.** 2007. Standards and standardization in mastocytosis: consensus statements on diagnostics, treatment recommendations and response criteria. *Eur J Clin Invest* **37:**435–453. PubMed
71. **Carter MC, Metcalfe DD.** 2002. Paediatric mastocytosis. *Arch Dis Child* **86:**315–319. PubMed
72. **Hartmann K, Henz BM.** 2002. Cutaneous mastocytosis—clinical heterogeneity. *Int Arch Allergy Immunol* **127:**143–146. PubMed
73. **Brockow K, Jofer C, Behrendt H, Ring J.** 2008. Anaphylaxis in patients with mastocytosis: a study on history, clinical features and risk factors in 120 patients. *Allergy* **63:**226–232. PubMed
74. **Greenhawt M, Akin C.** 2007. Mastocytosis and allergy. *Curr Opin Allergy Clin Immunol* **7:**387–392. PubMed
75. **Hahn HP, Hornick JL.** 2007. Immunoreactivity for CD25 in gastrointestinal mucosal mast cells is specific for systemic mastocytosis. *Am J Surg Pathol* **31:**1669–1676. PubMed
76. **Horny HP, Valent P.** 2001. Diagnosis of mastocytosis: general histopathological aspects, morphological criteria, and immunohistochemical findings. *Leuk Res* **25:**543–551. PubMed
77. **Sperr WR, Escribano L, Jordan JH, Schernthaner GH, Kundi M, Horny HP, Valent P.** 2001. Morphologic properties of neoplastic mast cells: delineation of stages of maturation and implication for cytological grading of mastocytosis. *Leuk Res* **25:**529–536. PubMed

78. **Escribano L, Orfao A, Díaz-Agustin B, Villarrubia J, Cerveró C, López A, Marcos MA, Bellas C, Fernández-Cañadas S, Cuevas M, Sánchez A, Velasco JL, Navarro JL, Miguel JF.** 1998. Indolent systemic mast cell disease in adults: immunophenotypic characterization of bone marrow mast cells and its diagnostic implications. *Blood* **91:**2731–2736. PubMed
79. **Sotlar K, Horny HP, Simonitsch I, Krokowski M, Aichberger KJ, Mayerhofer M, Printz D, Fritsch G, Valent P.** 2004. CD25 indicates the neoplastic phenotype of mast cells: a novel immunohistochemical marker for the diagnosis of systemic mastocytosis (SM) in routinely processed bone marrow biopsy specimens. *Am J Surg Pathol* **28:**1319–1325. PubMed
80. **Escribano L, Diaz-Agustin B, López A, Núñez López R, García-Montero A, Almeida J, Prados A, Angulo M, Herrero S, Orfao A, Spanish Network on Mastocytosis (REMA), Proposals of the Spanish Network on Mastocytosis (REMA).** 2004. Immunophenotypic analysis of mast cells in mastocytosis: when and how to do it. *Cytometry B Clin Cytom* **58:**1–8. PubMed
81. **Akin C, Valent P, Escribano L.** 2006. Urticaria pigmentosa and mastocytosis: the role of immunophenotyping in diagnosis and determining response to treatment. *Curr Allergy Asthma Rep* **6:**282–288. PubMed
82. **Pardanani A, Kimlinger TK, Reeder TL, Li CY, Tefferi A.** 2003. Differential expression of CD2 on neoplastic mast cells in patients with systemic mast cell disease with and without an associated clonal haematological disorder. *Br J Haematol* **120:**691–694. PubMed
83. **Akin C, Metcalfe DD.** 2004. The biology of Kit in disease and the application of pharmacogenetics. *J Allergy Clin Immunol* **114:**13–20. PubMed
84. **Garcia-Montero AC, Jara-Acevedo M, Teodosio C, Sanchez ML, Nunez R, Prados A, Aldanondo I, Sanchez L, Dominguez M, Botana LM, Sanchez-Jimenez F, Sotlar K, Almeida J, Escribano L, Orfao A.** 2006. KIT mutation in mast cells and other bone marrow hematopoietic cell lineages in systemic mast cell disorders: a prospective study of the Spanish Network on Mastocytosis (REMA) in a series of 113 patients. *Blood* **108:**2366–2372. PubMed
85. **Bodemer C, Hermine O, Palmérini F, Yang Y, Grandpeix-Guyodo C, Leventhal PS, Hadj-Rabia S, Nasca L, Georgin-Lavialle S, Cohen-Akenine A, Launay JM, Barete S, Feger F, Arock M, Catteau B, Sans B, Stalder JF, Skowron F, Thomas L, Lorette G, Plantin P, Bordigoni P, Lortholary O, de Prost Y, Moussy A, Sobol H, Dubreuil P.** 2010. Pediatric mastocytosis is a clonal disease associated with D816V and other activating c-KIT mutations. *J Invest Dermatol* **130:**804–815. PubMed
86. **Kristensen T, Vestergaard H, Møller MB.** 2011. Improved detection of the KIT D816V mutation in patients with systemic mastocytosis using a quantitative and highly sensitive real-time qPCR assay. *J Mol Diagn* **13:**180–188. PubMed
87. **Yavuz AS, Lipsky PE, Yavuz S, Metcalfe DD, Akin C.** 2002. Evidence for the involvement of a hematopoietic progenitor cell in systemic mastocytosis from single-cell analysis of mutations in the c-kit gene. *Blood* **100:**661–665. PubMed
88. **Schwartz LB.** 2006. Diagnostic value of tryptase in anaphylaxis and mastocytosis. *Immunol Allergy Clin North Am* **26:**451–463. PubMed
89. **Akin C, Scott LM, Kocabas CN, Kushnir-Sukhov N, Brittain E, Noel P, Metcalfe DD.** 2007. Demonstration of an aberrant mast-cell population with clonal markers in a subset of patients with "idiopathic" anaphylaxis. *Blood* **110:**2331–2333. PubMed
90. **Akin C, Fumo G, Yavuz AS, Lipsky PE, Neckers L, Metcalfe DD.** 2004. A novel form of mastocytosis associated with a transmembrane c-kit mutation and response to imatinib. *Blood* **103:**3222–3225. PubMed
91. **Teodosio C, García-Montero AC, Jara-Acevedo M, Sánchez-Muñoz L, Alvarez-Twose I, Núñez R, Schwartz LB, Walls AF, Escribano L, Orfao A.** 2010. Mast cells from different molecular and prognostic subtypes of systemic mastocytosis display distinct immunophenotypes. *J Allergy Clin Immunol* **125:**719–726.e4. PubMed
92. **Akin C, Valent P, Metcalfe DD.** 2010. Mast cell activation syndrome: proposed diagnostic criteria. *J Allergy Clin Immunol* **126:**1099–1104.e4. PubMed
93. **Schwaab J, Schnittger S, Sotlar K, Walz C, Fabarius A, Pfirrmann M, Kohlmann A, Grossmann V, Meggendorfer M, Horny HP, Valent P, Jawhar M, Teichmann M, Metzgeroth G, Erben P, Ernst T, Hochhaus A, Haferlach T, Hofmann WK, Cross NC, Reiter A.** 2013. Comprehensive mutational profiling in advanced systemic mastocytosis. *Blood* **122:**2460–2466. PubMed
94. **Sperr WR, Jordan JH, Baghestanian M, Kiener HP, Samorapoompichit P, Semper H, Hauswirth A, Schernthaner GH, Chott A, Natter S, Kraft D, Valenta R, Schwartz LB, Geissler K, Lechner K, Valent P.** 2001. Expression of mast cell tryptase by myeloblasts in a group of patients with acute myeloid leukemia. *Blood* **98:**2200–2209. PubMed
95. **Georgin-Lavialle S, Lhermitte L, Dubreuil P, Chandesris MO, Hermine O, Damaj G.** 2013. Mast cell leukemia. *Blood* **121:**1285–1295. PubMed
96. **Bonadonna P, Perbellini O, Passalacqua G, Caruso B, Colarossi S, Dal Fior D, Castellani L, Bonetto C, Frattini F, Dama A, Martinelli G, Chilosi M, Senna G, Pizzolo G, Zanotti R.** 2009. Clonal mast cell disorders in patients with systemic reactions to Hymenoptera stings and increased serum tryptase levels. *J Allergy Clin Immunol* **123:**680–686. PubMed
97. **Alvarez-Twose I, González de Olano D, Sánchez-Muñoz L, Matito A, Esteban-López MI, Vega A, Mateo MB, Alonso Díaz de Durana MD, de la Hoz B, Del Pozo Gil MD, Caballero T, Rosado A, Sánchez Matas I, Teodósio C, Jara-Acevedo M, Mollejo M, García-Montero A, Orfao A, Escribano L.** 2010. Clinical, biological, and molecular characteristics of clonal mast cell disorders presenting with systemic mast cell activation symptoms. *J Allergy Clin Immunol* **125:**1269–1278.e2. PubMed
98. **Cardet JC, Akin C, Lee MJ.** 2013. Mastocytosis: update on pharmacotherapy and future directions. *Expert Opin Pharmacother* **14:**2033–2045. PubMed
99. **Valent P, Sperr WR, Akin C.** 2010. How I treat patients with advanced systemic mastocytosis. *Blood* **116:**5812–5817. PubMed
100. **Gromke T, Elmaagacli AH, Ditschkowski M, Hegerfeldt Y, Koldehoff M, Hlinka M, Ottinger H, Trenschel R, Beelen DW.** 2013. Delayed graft-versus-mast-cell effect on systemic mastocytosis with associated clonal haematological non-mast cell lineage disease after allogeneic transplantation. *Bone Marrow Transplant* **48:**732–733. PubMed
101. **Nakamura R, Chakrabarti S, Akin C, Robyn J, Bahceci E, Greene A, Childs R, Dunbar CE, Metcalfe DD, Barrett AJ.** 2006. A pilot study of nonmyeloablative allogeneic hematopoietic stem cell transplant for advanced systemic mastocytosis. *Bone Marrow Transplant* **37:**353–358. PubMed
102. **Ryan RJ, Akin C, Castells M, Wills M, Selig MK, Nielsen GP, Ferry JA, Hornick JL.** 2013. Mast cell sarcoma: a rare and potentially under-recognized diagnostic entity with specific therapeutic implications. *Mod Pathol* **26:**533–543. PubMed
103. **Khoury P, Desmond R, Pabon A, Holland-Thomas N, Ware JM, Arthur DC, Kurlander R, Fay MP, Maric I, Klion AD.** 2016. Clinical features predict responsiveness to imatinib in platelet derived growth factor receptor alpha-negative hypereosinophilic syndrome. *Allergy* Jan 21. doi:10.1111/all.12843. [Epub ahead of print]

Systemic Autoimmune Diseases

section M

VOLUME EDITOR: BARBARA DETRICK
SECTION EDITOR: WESTLEY H. REEVES

Introduction

WESTLEY H. REEVES

86

Systemic autoimmune diseases are often associated with the production of autoantibodies that recognize a diverse array of cytoplasmic and nuclear antigens. These autoantibodies are used as adjuncts in the diagnosis of autoimmune disease, for monitoring disease activity and severity, and for predicting the outcome of autoimmune disease. As the diagnosis of systemic autoimmune disease is not always straightforward, autoantibody testing has the potential to improve our ability to diagnose complex autoimmune disorders. However, autoantibody test results, particularly those based on enzyme-linked immunosorbent assays (ELISAs) and other solid-phase assays, must be interpreted with caution due to their high sensitivity and the possibility of false-positive results. It is important to interpret the results of autoantibody tests in light of both the clinical context and the methodology employed. In some cases, confirmatory testing, analogous to the use of Western blotting to verify positive ELISA test results for HIV infection, is warranted.

Conversely, it is important to understand that positive autoantibody tests can be harbingers of autoimmune disease in otherwise healthy individuals, especially in the case of disease-specific autoantibodies, which may appear months, years, or even decades before the onset of clinical symptoms. The detection of disease-specific autoantibodies or other immunological markers in asymptomatic individuals may permit early diagnosis and preventative treatment. Good examples are antimitochondrial antibodies in primary biliary cirrhosis, anti-Sm, RNP, Ro (SSA), and double-stranded DNA autoantibodies in systemic lupus erythematosus, and specific autoantibodies associated with rheumatoid arthritis, polymyositis, and scleroderma, all of which may appear prior to the onset of clinical manifestations. Thus, in the case of an unexpectedly positive autoantibody test, it is important to consider two possibilities: (i) that the test result is a false positive, or (ii) that the autoantibody is present, perhaps as the initial manifestation of an autoimmune disorder.

Autoantibody and immune testing for autoimmune diseases is an evolving field. Older autoantibody tests, such as double immunodiffusion in gels and agglutination assays, are highly specific but less sensitive than the more recently developed ELISAs, addressable bead assays, and autoantigen microarrays. The older tests also are frequently less amenable to automation, which has led to their rapid abandonment in favor of other tests. The past 20 years has seen a rapid shift from double immunodiffusion and agglutination assays to the ELISA format. Newer technologies are on the horizon, including fluorescence-based assays employing addressable beads and antigen arrays, which permit screening for multiple specificities in a single assay. Recent interest in the autoimmune biomarkers has led to the identification of molecular assays (e.g., the interferon signature) that may ultimately be employed clinically to subset patients and/or to choose appropriate therapies and/or the response to therapy. Assays for other markers, such as complement proteins/fragments, which have been used clinically for many years, are being refined and may be useful for novel clinical applications.

The chapters in this section reflect both the evolving technology and the need for reliable confirmatory tests, which frequently are older or more labor-intensive. Andrade and colleagues review the roles of a classical screening test, the fluorescent antinuclear antibody assay, versus solid-phase assays for antinuclear antibody screening in the serodiagnosis of systemic autoimmune disease. Although automated (ELISA) testing is widely available, it has not yet replaced the more labor-intensive fluorescence-based assay and is unlikely to do so in the near future. In the following chapter, Chan et al. discuss solid-phase assays, focusing on the use of recombinant autoantigens and peptides in ELISA, molecular line probe (LINE) assays, multiplex bead assays, and chemiluminescence assays. Following these methodology-focused reviews are a series of chapters outlining the approach to immunodiagnosis of major autoimmune syndromes, including the immunological evaluation of systemic lupus erythematosus in the clinical and research laboratory (Reeves et al.); autoimmune myopathies including polymyositis and dermatomyositis (Satoh et al.); scleroderma and its variants (Kuwana); rheumatoid arthritis (Chauffe and Bubb); antiphospholipid autoantibody syndrome (Murphy and Harris); and antineutrophil cytoplasmic antibody-associated vasculitis syndromes such as granulomatosis with polyangiitis (Wegener's granulomatosis), microscopic polyangiitis, eosinophilic granulomatosis with polyangiitis (Churg-Strauss syndrome), and levamisole-induced vasculitis (Burlingame et al.). These chapters are followed by a discussion by Stone of the immunological assessment of IgG4-related syndrome, a recently described and frequently misdiagnosed inflammatory disorder involving plasma cells that secrete IgG4-class antibodies. At present, it is unclear whether this disorder is "autoimmune" or "inflammatory" in origin. The section

doi:10.1128/9781555818722.ch86

includes a discussion of where the field of immune testing and disease biomarkers for rheumatic disease is moving in the future (Sokolove).

The identification of disease-specific autoantibodies over the past 30 or more years and the increasing sophistication of autoantibody testing have greatly facilitated the diagnosis of systemic autoimmune disease. Automation of autoantibody testing is a more recent development, raising hope that in the future, screening for these biological markers may be useful not only for confirming a clinical diagnosis but also for defining risk and establishing a diagnosis during the preclinical phase of the illness, when it may be more amenable to therapy. Gene expression analysis (e.g., for gene expression "signatures") and assessment of genetic disease susceptibility loci represent future directions that are likely to move into the clinical arena within the next decade.

Antinuclear Antibody Tests

ALESSANDRA DELLAVANCE, WILSON DE MELO CRUVINEL, PAULO LUIZ CARVALHO FRANCESCANTONIO, AND LUIS EDUARDO COELHO ANDRADE

87

HISTORICAL BACKGROUND

Autoantibodies are historical hallmarks in the establishment of the concept of autoimmunity and in the definition of the clinical limits of several autoimmune diseases. On a day-to-day basis, autoantibodies are helpful elements not only in the diagnosis of autoimmune diseases, but also frequently in the establishment of prognosis and in the monitoring of disease activity.

The first assay that allowed the detection of an antinuclear antibody was the LE cell test, originally reported by Hargraves et al. in 1948 (1). This assay takes advantage of the opsonization property of antibodies and complement. By mixing crushed and intact peripheral blood cells with the serum sample to be tested, one allows IgG antibodies to deoxynucleoprotein (nucleosomes) present in the serum to bind the exposed chromatin from crushed cells and pave the way for phagocytosis of the opsonized nuclei by intact phagocytes. The detection of several phagocytes with the nucleus compressed to the periphery of the cell by a large amorphous mass represents a positive LE cell assay (Fig. 1). This assay was soon recognized to be very specific and relatively sensitive for the diagnosis of systemic lupus erythematosus (SLE), being incorporated in the first edition of the American College of Rheumatology criteria for classification of SLE (2). The LE cell test remained useful for several decades and was eventually replaced by more sensitive and straightforward assays.

One decade later, Holborow et al. and Friou et al. adapted the recently reported indirect immunofluorescence methodology to the detection of autoantibodies (3, 4). These investigators showed that serum from SLE patients frequently contained high levels of antibodies reacting with the nuclei of cells from a variety of substrates, including human leukocytes and rodent tissue. This assay, named the indirect immunofluorescence antinuclear antibody (IIF-ANA) test, became progressively popular and presented higher sensitivity than the LE test for the diagnosis of SLE. In addition, it was also positive in other systemic autoimmune diseases, including systemic sclerosis (SSc), mixed connective tissue disease, polymyositis, dermatomyositis, and Sjögren's syndrome. Finally, the IIF-ANA test had the additional advantage of allowing the recognition of a few distinct immunofluorescence nuclear patterns, namely homogeneous, speckled, and nucleolar. In the late 1970s and into the 1980s, monolayers of human tumor cell lines grown onto glass slides were tested as the substrate for the IIF-ANA test, and progressively the HEp-2 cell line became the universal substrate for the IIF-ANA assay (5). The HEp-2 cell line (CCL-23; American Type Culture Collection) was characterized originally as derived from larynx epidermal carcinoma; however, there is evidence of contamination with the HeLa cell line (6). Some of the advantages of this substrate for the IIF-ANA test are listed in Table 1. The higher sensitivity in relation to rodent tissue allows positive results in the majority of patients with nontreated active SLE and other systemic autoimmune diseases. The IIF-ANA assay on HEp-2 cells allows the detection of autoantibodies against antigens in cellular compartments other than the nucleus, such as the cytoplasm and the mitotic apparatus. Therefore, the name "antinuclear antibody" does not correspond to the comprehensiveness of the test, and some authors have proposed that it be renamed "anticellular antibody" test. Despite the appearance of alternative methods, the IIF-ANA assay on HEp-2 cells remains the gold standard for the screening of antinuclear or anticellular antibodies (7).

METHODOLOGICAL PLATFORMS

Indirect Immunofluorescence Assay on HEp-2 Cells

The IIF-ANA assay is considered the gold standard for screening for antinuclear or anticellular antibodies in systemic autoimmune diseases (7). This very sensitive test allows the detection of a large number of autoantibodies relevant to a variety of clinical conditions (8) (Table 2). It offers three important pieces of information: (i) the presence or absence of autoantibodies in the sample, (ii) the titer, and (iii) the immunofluorescence pattern. The titer represents a semiquantitative assessment of the autoantibody concentration in serum, which is clinically valuable information. Since autoantibodies occur in a certain fraction of the general population, it is relevant that most nonautoimmune individuals with a positive IIF-ANA test present low titers, while patients with systemic autoimmune diseases frequently present moderate-to-high IIF-ANA titers (9–12). The IIF-ANA pattern adds valuable information because it helps to discriminate positive tests in nonautoimmune individuals and in autoimmune patients (12). In addition, the IIF-ANA pattern often indicates the autoantibody specificities most likely to be present in a given sample, thus guiding

doi:10.1128/9781555818722.ch87

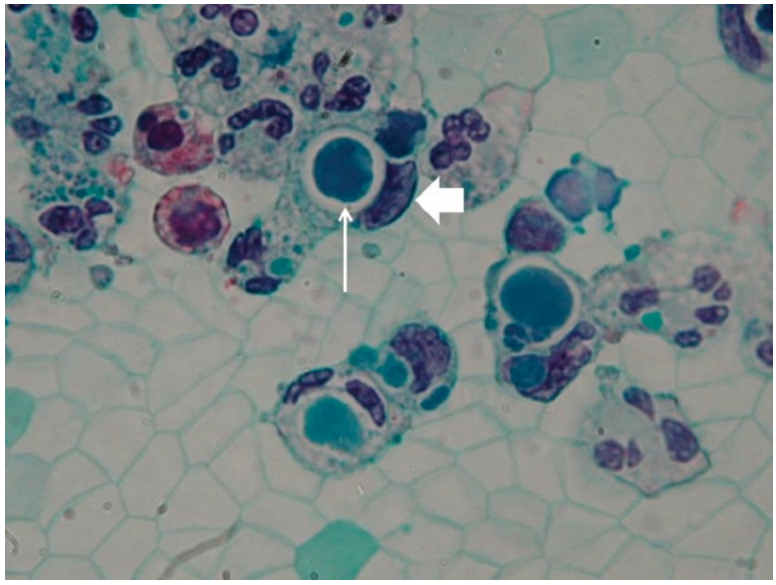

FIGURE 1 LE cell phenomenon. Viable neutrophils have their nucleus (thin arrow) displaced to the periphery of the cell due to the phagocytosis of a large piece of opsonized chromatin (wide arrow) from dead cells.

the next step in serologic analysis (8, 13–15). These aspects are discussed in "Interpretation of the IIF-ANA Test."

Automated Readers for the IIF-ANA Assay

The IIF-ANA assay is a labor-intensive, subjective, and reader-dependent procedure that requires highly skilled technicians. Several methodological factors affect intra- and interlaboratory result consistency of the IIF-ANA test. There is also considerable variability in the interpretation criteria of the several IIF-ANA patterns. In an attempt to overcome some of these limitations, efforts have been developed in applying digital technology to the acquisition and interpretation of IIF-ANA images. The automated ANA readers aim to minimize subjectivity and the requirement for expert microscopy analysts, as well as to assist on high-throughput operation. Conceptually, these devices can discriminate positive and negative reactivity, estimate the concentration of the autoantibodies (titer), and identify basic IIF-ANA patterns. The definition of the concentration of the autoantibodies is provided by the measurement of relative light units obtained with a given sample. Pattern recognition algorithms addressing basic IIF-ANA patterns are incorporated into the software for image analysis and help to determine the first-level approach in IIF-ANA pattern interpretation.

TABLE 1 Advantages of the ANA assay on HEp-2 cells

Monolayer arrangement of cells
Large nucleus, nucleoli, and cytoplasm
Possibility to appreciate fine details in the distribution of autoantigens
Figures at the various stages of the cell cycle
Absence of interstitial structures and extracellular matrix
Presentation of a vast array of autoantigens in optimal concentration
Easy handling and possibility of universal standardization of the substrate

Digitalized images are stored and available for analysis by the operator in order to supervise the preliminary classification provided by the automated device. Reliable positive/negative discrimination has been achieved with devices from different manufacturers, with an agreement rate in human reading of up to 96% (16–19). Several companies are involved in the development and upgrading of such systems, which represent a promising field, especially for high-throughput operation. However, it is controversial whether the available systems will be capable of determining all the subtle differences that exist in ANA patterns. At present, expert analyst supervision is required to a variable extent.

Enzyme-Based HEp-2 Cell ANA

An alternative method for the indirect immunofluorescence technique for ANA screening is the indirect enzyme-based HEp-2 cell ANA assay, in which the secondary antibody is conjugated to an enzyme instead of a fluorophore. Horseradish peroxidase and alkaline phosphatase are the main enzymes used in the available commercial kits. Reading requires a regular microscope with no need for a dark room. Slides can be kept as a permanent record since there is limited decay in comparison with the fluorescent dyes. The major limitations, however, are the low sensitivity and the low-resolution images compared to those obtained by the indirect immunofluorescence methodology. Therefore, the fine definition of IIF-ANA pattern nuances is not possible with the indirect enzyme-based ANA method.

Solid-Phase ANA

More recently, several companies have developed ingenious solid-phase assays intended for the screening of antinuclear or anticellular antibodies. The solid phase may be a standard polystyrene microtiter enzyme-linked immunosorbent assay plate, nitrocellulose strips, or beads made of a variety of materials. The autoantibody reactivity is usually detected by anti-human immunoglobulin antibodies conjugated to enzymes, fluorochromes, or chemiluminescent dyes. Regarding the antigenic substrate, these assays may be

TABLE 2 Ability of the ANA-HEp-2 test to detect clinically relevant autoantibodies[a]

Regularly detected	Sometimes not detected	Not detected
CENP-A, CENP-B , CENP-C, CENP-F	Actin	Acetylcholine receptor
p80-coilin and sp100/ PML	Aminoacyl-tRNA synthetase (Jo-1)	ANCA (MPO and PR3)
dsDNA	Centrosome/centriole	AQP-4
EEA-1 and GWB	Ku	ASCA
Fibrillarin and To/Th	La/SS-B	Cardiolipin
Golgi apparatus	Mi-2	Citrullinated peptides
Histones, nucleosome	PCNA	Desmoglein I and III
LEDGF/DFS 75	Ribosomal P proteins	Endomysial (IgG or IgA)
Mitochondria	Smooth muscle	LKM
Nuclear envelope (gp210, lamins, p63)	SS-A/Ro (Ro 60)	Lupus anticoagulant
NuMA	Tubulin	Rheumatoid factor
NOR-90 and PM/Scl	Vimentin SS-A/Ro(Ro-52)	Single-stranded DNA
RNA polymerase I, II, and III		SLA
Scl-70 (DNA topoisomerase 1)		
Sm and U1-RNP		Transglutaminase

[a]Abbreviations: EEA-1, early endosomal antigen 1; GWB, GW bodies; LEDGF, lens epithelium-derived growth factor; DFS, dense fine speckled pattern; NuMA, nuclear mitotic apparatus protein; ANCA, antineutrophil cytoplasm antibodies; AQP-4, aquaporin-4; MPO, myeloperoxidase; PR3, proteinase 3; ASCA, anti-*Saccharomyces cerevisiae* antibodies; LKM, liver kidney microsome; SLA, soluble liver antigen. Abbreviations not listed in this footnote are arbitrary designations.

divided into two general classes. One modality is based on cell extracts that may or may not be enriched with a particular set of autoantigens, therefore offering an unbiased and wide range of autoantigens. The other modality contains a predefined and limited array of recombinant or purified autoantigens for which the autoantibodies are clinically relevant. These arrays are usually built with the aim to address the screening for systemic autoimmune rheumatic diseases and usually include the following autoantigens: native DNA, Sm, U1-RNP, anti-Sjögren's syndrome antigen A (SS-A/Ro), SS-B/La, Jo-1, Scl-70, PM/Scl, Mi-2, CENP-B, and histones.

The antigen-unbiased method based on cell extracts has the advantage of allowing the recognition of a broad spectrum of autoantibodies, with the caveat of including some with uncertain clinical significance. In contrast, the methods based on arrays with a selected set of autoantigens tend to provide clinically specific results but may fail to recognize yet-undefined but clinically relevant autoantibodies. Usually, these assays attain lower sensitivity and higher specificity for the diagnosis of systemic autoimmune diseases than the ones based on whole-cell extract (7, 20, 21).

By proposing to replace the IIF-ANA test, the solid-phase ANA methods seek to provide the ability to detect most of the clinically relevant autoantigens present in the HEp-2 cell. These methods present some potential advantages, such as the lack of the subjectivity inherent to the microscopic analysis of IIF-ANA assay, the possibility of automation and high-throughput operation, and the possibility of quantitative analysis. In addition, these alternative methods do not require highly qualified personnel for the IIF-ANA slide interpretation. These features elicit great interest from industry and large laboratories. However, there are also important drawbacks inherent to this technology. The first one is that it is hard to reproduce the balanced dose of hundreds of autoantigens present in the HEp-2 cell. Also, detection of autoantibodies against poorly soluble autoantigens (e.g., lamins) is difficult in solid-phase assays. In addition, solid-phase immunoassays tend to detect low-avidity and low-concentration antibodies, causing considerable discrepancy with the IIF-ANA test, especially in the low-antibody-concentration range. Other elements that may affect the performance of solid-phase assays are the nature and purity of the antigenic substrate used to coat the solid phase, the binding capacity of the solid-phase scaffold, the nature of the blocking buffer, the stringency of the washing buffers, the quality of the conjugate, and the accuracy of the calibration curve. Not surprisingly, serious concerns have been raised about the appropriateness of this methodology at its present stage of development (22). Solid-phase-based assays may produce false-negative results, and this may be caused by the limited number of available autoantigens or by the absence of relevant autoepitopes in the available autoantigens. Several studies aiming to compare the diagnostic performances of the classical IIF-ANA and the solid phase-based methods were carried out. In general, it has been concluded that IIF-ANA has higher sensitivity and negative predictive value than the solid-phase-based tests (7, 21). A special task force designated by the American College of Rheumatology has produced a statement position document recommending that the IIF-ANA test should remain the gold standard for ANA testing and that the use of alternative methodology should be clearly stated in the laboratory report (7).

TECHNICAL RECOMMENDATIONS

There is a wide diversity of HEp-2 IIF-ANA commercial kits. Although the methodology sounds simple, careful slide processing is important to ensure reliable and consistent results, as small and important details can cause artifacts and misleading results. Here the procedure is detailed in successive steps with remarks for possible and common pitfalls.

Workspace

The procedure must be carried out in a temperature- and humidity-controlled, dust-free, and silent environment. The bench should be well illuminated, clean, and arranged with appropriate working equipment (pipettes, glassware, incubation tanks, reagents, etc.). The work maps with controlled identification of samples to be tested should be prepared in advance.

Standard Operating Procedure

It is recommended that each laboratory develop a standard operating procedure (SOP) document to be available at the bench with the detailed technical description of each step of the assay. This ensures that technicians follow the assay in a consistent fashion. The SOP document must be reviewed periodically by the technical supervisor or whenever there is any change in the technical procedure. This helps keep the SOP updated and consistent, avoiding potential deviations in the protocol.

Cell Substrate

Confluence of Cell Substrate

It is important that the distribution of cells be adequate for optimal visualization of all the cellular compartments, including the nucleus, nucleoli, cytoplasm, dividing cells, and mitotic apparatus. Cells should be neither overlapping nor scarce. In cases of excess of cells, appropriate visualization of cellular compartments is jeopardized. When the number of cells observed per field is low, the recognition of features that depend on specific stages of the cell cycle and mitotic figures may be affected. In addition, some features are best appreciated when there is some proximity among cells, such the characteristic "touch sign" observed in the nuclear envelope pattern.

Display of All Stages of the Cell Cycle

One of the advantages of using cell lines for the IIF-ANA test is the possibility of examining cells in all stages of the cell cycle, which allows the identification of cell cycle-related IIF-ANA patterns not seen in sections of animal tissue. The absence or paucity of cells undergoing division can hinder the proper interpretation of some IIF-ANA patterns, such as centromeric, nuclear dense fine speckled, and nuclear quasihomogeneous patterns and those associated with antibodies to Scl-70, fibrillarin, RNA polymerase I, NOR-90, NuMA, CENP-F, HsEg5, etc. To ensure that the substrate has an adequate number of dividing cells (3 to 5 mitotic figures per field at a magnification of ×200), each new batch of slides should be tested with appropriate control samples that highlight mitotic cells, such as those with antibodies to centromere, NuMA, or CENP-F.

Display of Relevant Autoantigens and IIF-ANA Patterns

Differences in the protocols used to grow, fix, and permeabilize cells can affect the availability of relevant epitopes and the natural location (vis-à-vis the IIF-ANA patterns) of some autoantigens (Fig. 2). Accordingly, several IIF-ANA patterns may show slight differences among different slide brands and even among different batches from the same supplier. For this reason, it is of paramount importance to use a panel of samples with known specificity to a variety of autoantigens in order to validate a new lot or a new slide brand. Adequate control samples can verify the availability of relevant epitopes in more fastidious autoantigens, such as SS-A/Ro, Jo-1, and P ribosomal proteins. In addition, a collection of known samples representing the several relevant IIF-ANA patterns helps to assess how these are represented in a new brand or batch of slides. Several reference serum samples systematized by the Autoantibody Standardization Committee affiliated to the International Union of Immunology Societies (IUIS) are distributed by the Centers for Disease Control and Prevention (CDC) (23). Such primary controls should be used to derive secondary controls that can then be used to assess each new slide batch from the same vendor or a new slide brand.

Assay Procedure

Controls

The use of control samples with known specificity and fluorescence intensity is essential in every run to ensure the quality of the reaction. The strong positive and negative controls usually provided in commercial kits may not be ideal because they characterize extremes that are not representative of most routine samples. It is recommended that a negative control and a low-intensity (1/80 to 1/160) positive control be assayed in each run. This will promote interassay consistency within the laboratory.

Samples

Blood samples should be collected in dry or separating gel-containing tubes. The serum may be stored under refrigeration (2°C to 8°C) for a maximum of 5 days. After this period, it is recommended that serum samples be kept at −20°C for some months or at −70°C for prolonged storage. Sodium azide (100 μg/ml) may be helpful in preventing bacterial and fungal contamination. Prolonged freezing may cause lyophilizing (resulting in titer increase) and successive freeze-thawing cycles may cause a decrease in antibody activity. It is important that the original serum tube and the working tubes be perfectly identified in order to preserve the traceability of samples. Samples showing fibrin clots and those with strong evidence of hemolysis or lipid content require caution because of possible interference with the reaction.

Sample Dilution

Most commercial kits provide salt sachet for reconstitution of phosphate-buffered saline (PBS) (0.15 M phosphate buffered saline, pH 7.2 to 7.4). It is highly recommended that the pH be checked after reconstitution and before each assay, because deviation from the pH 7.2 to 7.4 range can impair antibody reactivity drastically. Adding 0.5 mg/ml Tween 20 and 20 mg/ml bovine serum albumin to the dilution buffer may help with background reduction.

The recommended screening dilution is 1/80 to 1/160, and this range should account for variability in microscope and lighting conditions as well as peculiarities in IIF-ANA reactivity of normal individuals in different regions. Positive samples should be further tested using a geometric series of dilutions by the factor 2. Some authors recommend dilution up to the end titer, whereas others feel that there is no clinically significant gain in diluting samples above 1/1,280 (12, 14, 15).

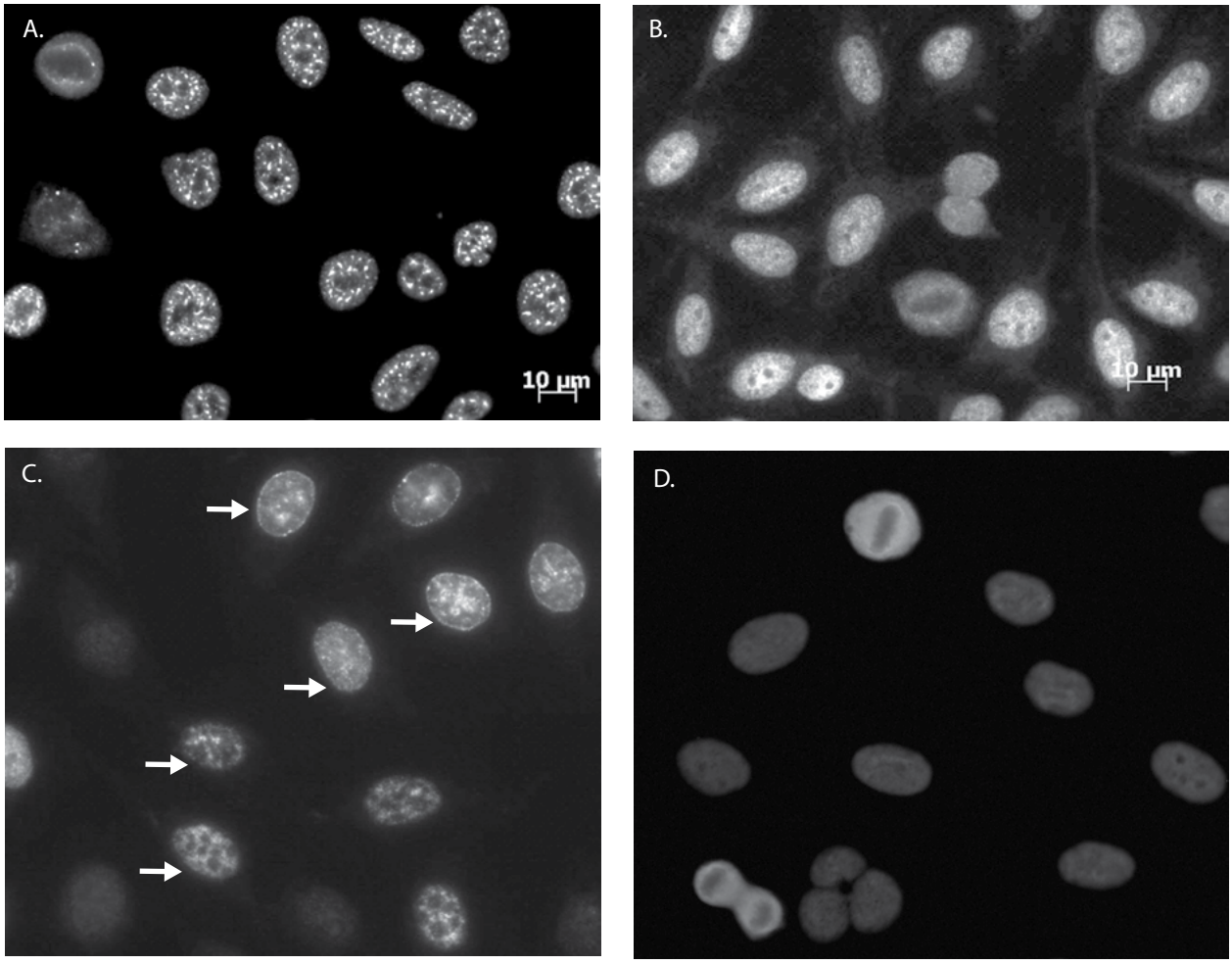

FIGURE 2 Influence of cell substrate on the ANA pattern. (A and B) Sample with anti-U1 RNP antibodies processed on slides from two different suppliers. The expected nuclear coarse speckled pattern is observed with the slide brand shown in panel A, whereas a nonspecific nuclear fine speckled pattern is observed the slide brand depicted in panel B. (C and D) Sample with anti-PCNA (proliferating cell nuclear antigen) antibody processed on slides from two different suppliers. The expected pleomorphic PCNA pattern is observed in the slide brand shown in panel C, whereas a nonspecific pattern is observed in the slide brand shown in panel D. Indirect immunofluorescence on HEp-2 cells; magnification, ×400.

Primary Antibody Incubation

Allow slides to reach room temperature over 30 min prior to opening their pouches and do not unpack them until immediately prior to pipetting the diluted samples. Slides must be kept in a humid chamber throughout the process since air drying may cause changes in the cell substrate and the appearance of spurious IIF-ANA patterns. Avoid touching the cell substrate with the pipette and ensure a perfect coverage of the cell carpet (usually, 30 µl is adequate). Be sure there is no overflow and contamination of neighboring wells. Incubation should proceed for 30 min in a humid chamber at room temperature or at 37°C, ensuring that no well dries out.

First Washing

With the slide at 45° to the table surface, a gentle stream of PBS is directed at the upper edge of the lower row of wells to remove the primary antibodies, avoiding contamination of neighboring wells. Rotate the slide and repeat the procedure for the other row of wells. Never aim the PBS stream directly on the cell carpet in order to prevent cell damage. Next, slides are immediately immersed in PBS for 5 to 10 minutes with shaking and one change of the PBS.

Incubation with Conjugate

Remove excess PBS from slides with a filter paper without touching the cell carpet, and immediately return the slides to the humid chamber. Never allow any well to dry out. If there are many slides being processed, it is recommended that a limited number at a time be transferred to the humid chamber and covered with conjugated secondary antibody. Conjugate incubation should occur for 30 min at room temperature in the dark, since light exposure promotes fluorochrome fading.

Affinity-purified anti-human γ heavy-chain plus κ and λ light-chain antibodies conjugated to fluorescein isothiocyanate are widely used. Kits usually provide ready-to-use conjugate. However, considering the wide variability in microscopes, lighting, and other operating conditions among laboratories, it is comprehensible that "one size may

not fit all." Therefore, it is recommended that the conjugate be titrated against preestablished laboratory controls prior to use for each new kit unit (Fig. 3).

Second Washing and Coverslip Mounting

Slides are briefly rinsed and washed in PBS for 10 min as before. If desired, adding 250 μg/ml Evans blue to the PBS will promote appropriate counterstaining. Remove PBS with filter paper without touching the cells, and pipette mounting medium onto each well, making sure that the cell carpet does not dry out. Kits provide mounting medium, which most often consists of alkaline-buffered glycerin. Specific antifading mounting medium is commercially available and may be useful when prolonged exposure is required. Gently position the coverslip onto the slide. Use clean high-quality glass coverslips. Avoid touching the surface of the coverslip to prevent fingerprints and fat deposition. It is important to inspect and remove air bubbles by placing a layer of filter paper over the assembled slide and gently "combing" the assembly by hand. Assembled slides should be read immediately at the microscope or may be kept at 2°C to 8°C in the dark for some days with little loss of fluorescence activity.

Semiautomated devices can assist on several of the above steps, saving on labor. These devices are particularly appropriate for laboratories with high-throughput operation. Some instruments can perform serum dilutions, and others can run the whole procedure up to the point of but not including the mounting of the coverslips. Naturally, the use of automated instruments is not a substitute for strict quality control procedures.

Microscope and Dark Room

Slides should be observed in an epifluorescence microscope equipped with filters appropriate for fluorescein detection. An objective with magnification of ×40 along with an eyepiece with magnification of ×10 (yielding a final magnification of ×400) allows optimal visualization of cell organelles and identification of most relevant IIF-ANA patterns. The microscope must be under routine preventive maintenance to ensure appropriate cleaning of filters, lenses, and eyepieces and monitoring of the lifetime of lamp bulbs. Lamps should be properly aligned to ensure perfect illumination of the entire microscopic field. A simple maneuver to assess lamp alignment is to place a piece of white paper on the stage with the lamp on and to look for the formation of a single well-defined circle. The formation of parallel or overlapping circles indicates the need to review the positioning of the lamp. The equipment must rest on a stable surface and should not be transported without proper monitoring to prevent misalignment of the optical system. Routine observation of the reactivity of control samples with known titer may help in detecting unexpected decay in the lamp

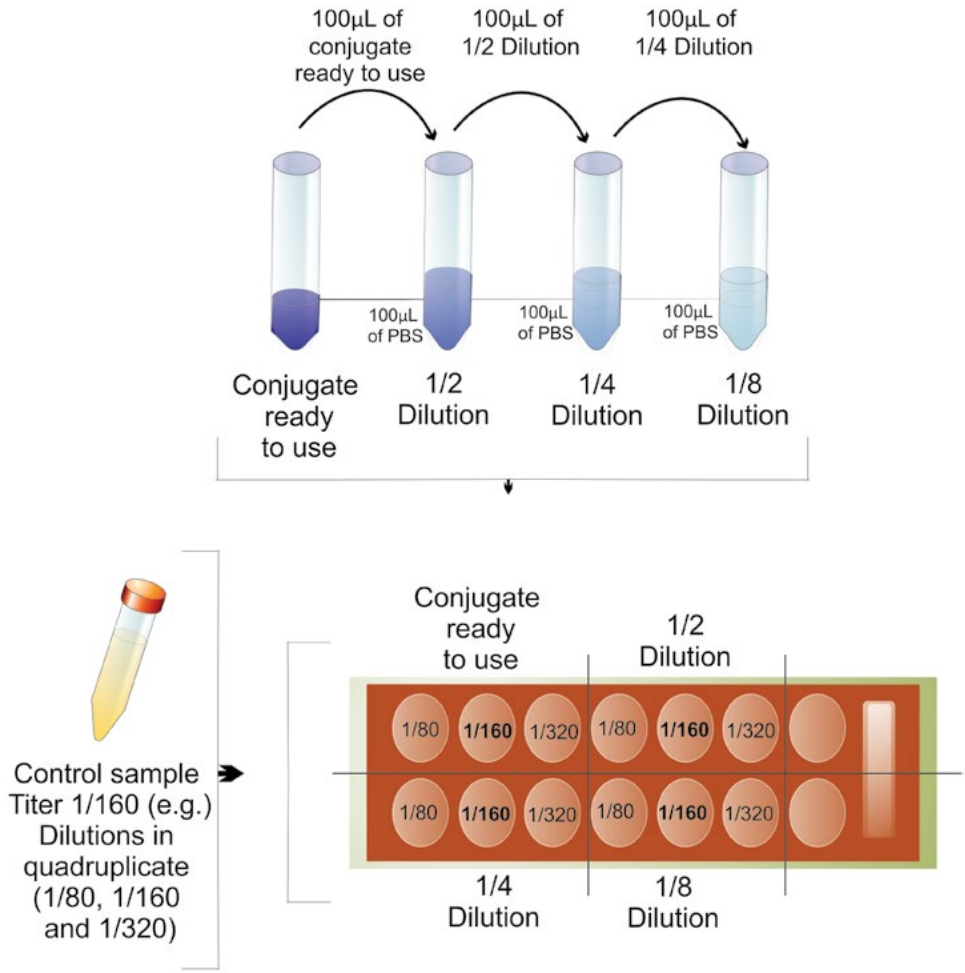

FIGURE 3 Checkerboard titration of the conjugate. A sample with known ANA titer is used to gauge the dilution of the conjugate that will reproduce the expected titer for that sample.

efficiency. The microscope should be in a dark room with a gentle spotlight at the bench to allow the analyst to make notes. Attachment of a digital camera allows recording images, and a network connection for laboratory computers simplifies working procedures.

READING THE IIF-ANA SLIDE

The IIF-ANA slide reading, especially the interpretation of morphological fluorescence patterns, is a highly complex activity that requires skilled analysts, the appropriate environment, and an organized strategy. The first step is the definition of what constitutes a positive reaction. Despite the inherent subjectivity, a common sense criterion is that a positive reaction should allow the determination of a well-defined IIF-ANA pattern. Low-intensity nonspecific staining usually does not allow a clear IIF-ANA pattern definition. Another helpful hint is that a positive reaction must appear as a minimally vivid green color, whereas low and nonspecific reactivity yields a dull greenish color. These criteria can also assist in determining the end titer for each sample.

It is important that each well be thoroughly examined. The periphery of the wells frequently stains stronger than central areas, and therefore, the definition of a positive reaction and end titer should not be estimated based on the peripheral areas. On the other hand, the examination of cells at the periphery of the well may be helpful in the definition of the IIF-ANA pattern in some cases. Focal areas of contamination with another sample, conjugate precipitation, drying of the well, and other unanticipated interferences may cause spurious staining in circumscribed areas of the well. This can be recognized by careful inspection of several areas of the well. It should be noted that some samples produce a diffuse low-intensity and poorly defined staining that cannot be defined as positive at the screening dilution but may become clearly positive at higher dilutions. If there is such a suspicion, the screening step should include two additional double dilutions.

A useful strategy for analyzing the IIF-ANA pattern is to follow a systematic sequence that includes the detailed inspection and registering of the staining of interphase and mitotic cells (Fig. 4). For interphase cells, specific attention must be paid to individual key cell elements: cytoplasm, nucleus, nuclear envelope, and nucleolus. The spatial distribution and the texture of the staining in each of these compartments must be carefully registered. For mitotic cells, one should focus on the metaphase and anaphase chromatin masses, the mitotic poles and centrosomes, mitotic spindles, intercellular bridge, and midbody.

The integrated analysis of the IIF-ANA pattern across the several cellular compartments along the sequential stages of the cell cycle increases the ability to identify the most probable autoantibodies in the sample. Several autoantigens occupy more than one cellular compartment and move across cellular compartments along the cell cycle. Such orchestrated and composite arrangements usually are not shared by many autoantigens and therefore narrow

Anti-Cellular Antibody Test (ANA)

Name: Gender: DOB:

Date:

Method: Indirect immunofluorescence on HEp-2 cells Biological specimen: serum

Reference range

Negative: no reactivity;

1/80: borderline;

1/160 – 1/320: weak reactivity;

1/640 – 1/1,280: moderate reactivity;

Above 1/1,280: strong reactivity;

Result

Nucleus: Fine speckled staining 1/320; Multiple discrete dots 1/2,560

Nucleolus: Not stained

Metaphase chromosome plate: Not stained

Mitotic apparatus: Not stained

Cytoplasm: reticular dotted mitochondria-like pattern 1/1,280

Interpretation

The sample contains multiple autoantibodies. Nuclear multiple discrete dots are suggestive of anti-sp100 antibodies. The cytoplasmic reticular dotted pattern is suggestive of anti-mitochondria antibodies. The nuclear fine speckled pattern has no specific association. Anti-sp100 and anti-mitochondria antibodies are strongly associated with primary biliary cholangitis.

FIGURE 4 Example of report of the IIF-ANA test.

TABLE 3 Specific composite IIF-ANA patterns

Composite IIF-ANA pattern	Features at interphase	Features at mitosis
Centromere	Discrete dots scattered in the nucleus	Discrete dots aligned at the chromatin mass
NuMA	Diffuse fine grainy staining of the nucleus	Sharp staining of the mitotic poles; delicate staining of the proximal parts of the mitotic spindles; nuclear staining in telophase cells; no staining of intercellular bridge and midbody
CENP-F	Variable-intensity fine speckled staining of the nucleus	Delicate centromere staining only in mitotic cells (prophase and metaphase); positive midbody staining
Scl-70	Nuclear diffuse fine grainy staining; nucleolar faint and inconsistent staining; cytoplasmic dot/ reticular network	The metaphase chromosome plate shows a diffuse fine grainy staining and a few (usually 1 to 5) bright discrete dots
RNA polymerase I and NOR-90	Nucleolar speckled staining	Few (usually 1 to 5) bright discrete dots

down the array of possible autoantibodies. In some cases, the composite IIF-ANA pattern is unique for one specific autoantigen. Examples of specific composite patterns are listed in Table 3.

In particular, the examination of the mitotic chromosome mass offers crucial clues for the nature of the autoantibodies in the sample because it is composed exclusively of chromatin and associated proteins. Therefore, a definite staining of the chromosome mass is compatible with autoantibodies to native DNA, nucleosomes (chromatin), histones, DNA topoisomerase I (Scl-70), LEDGF/p75, and other chromatin-associated autoantigens. The texture of the chromosome mass staining adds helpful information: a strong and hyaline staining of the chromosome mass is associated with antibodies to native DNA, nucleosomes, or histones (15); a fine grainy staining of the chromatin mass may be observed with antibodies to Scl-70 or nucleosomes (15, 24); a coarse speckled staining of the chromatin mass is most frequently due to anti-LEDGF/p75 antibodies (25). The observation of a few (usually 1 to 5) bright dots at the metaphase mass represents the staining of the nucleolar organizing regions (NOR) and indicates the possibility of antibodies to RNA polymerase I, DNA topoisomerase I (Scl-70), or NOR-90/human upstream binding factor (15).

The absence of staining of the mitotic chromosome mass, on the other hand, also provides valuable hints. For example, a nuclear speckled pattern with no staining of the metaphase mass argues against antibodies to chromatin-associated autoantigens and is frequently due to antibodies against RNA binding proteins, such as SS-A/Ro, SS-B/La, Sm, and U1-RNP. Additional information in such cases is obtained by observing the texture of the nuclear staining in interphase cells, since a coarse speckled pattern is usually associated with antibodies to Sm and U1-RNP, whereas a myriad discrete fine speckled pattern is most frequently caused by anti-SS-A/Ro 60-kDa autoantibodies (26). In contrast, a nonspecific fine speckled staining of the interphase nucleus with no staining of the metaphase plate may be due to several autoantibodies, including some of unknown specificity (Fig. 5).

It is important to bear in mind that one sample may contain more than one autoantibody specificity. In such cases, the resulting IIF-ANA pattern will be a mixture of the IIF-ANA patterns related to the individual autoantibodies in the sample. For example, the coexistence of antibodies to native DNA and U1-RNP renders a mix of the homogeneous and coarse speckled patterns in interphase nuclei and a homogeneous staining of the mitotic chromosome mass. The coexistence of more than one autoantibody specificity may preclude the definition of a standard IIF pattern. In such cases, it may be appropriate to define the IIF pattern as "mixed pattern" and indicate the possibility of more than one autoantibody specificity in the sample. However, if there is a difference in the concentration of the autoantibody specificities in the serum, it may be possible to identify individual IIF patterns along the several dilutions.

REPORT OF THE IIF-ANA TEST

The IIF-ANA test report should include information on the staining pattern and titer in each cell compartment, as follows: nucleus, nucleolus, metaphase plate, cytoplasm, and mitotic apparatus. More than one pattern may be reported

FIGURE 5 Panel of relevant IIF-ANA patterns. (A) Nuclear homogeneous pattern; (B) nuclear dense fine speckled pattern; (C) nuclear coarse speckled pattern; (D) nuclear SS-A/Ro pattern; (E) nuclear fine speckled pattern; (F) centromere pattern; (G) nuclear pleomorphic pattern; (H) ribosomal-P cytoplasmic pattern. Double arrows, cells in interphase; single arrow, cells in metaphase; arrowheads, cell nuclei with pleomorphic pattern and variable intensity. Indirect immunofluorescence using HEp-2 cells.

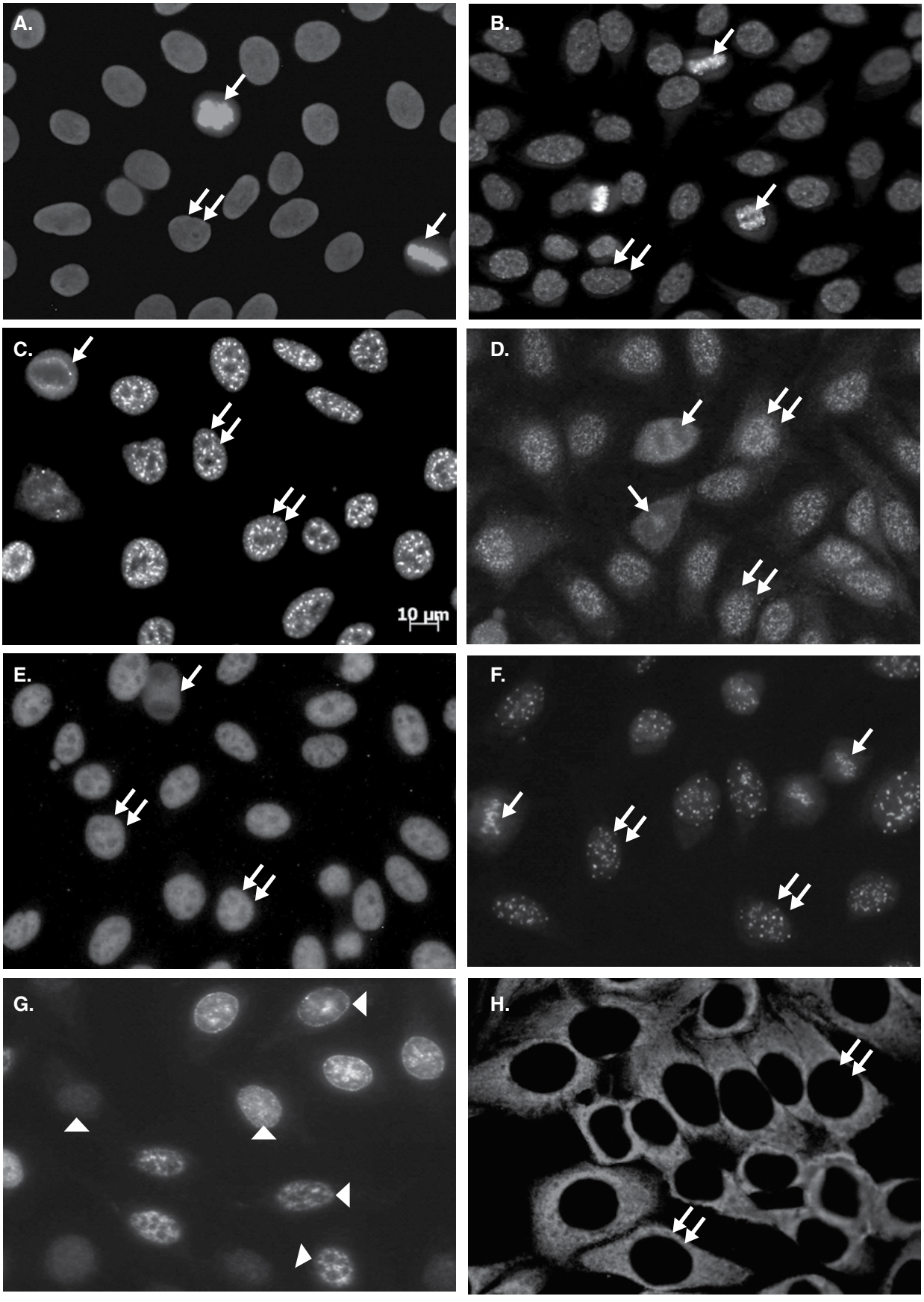
A.
B.
C.
10 µm
D.
E.
F.
G.
H.

in the same cell compartment (Fig. 4). Due to the great diversity of possible ANA patterns, it is recommended that the report contain an item dedicated to the interpretation of the findings. In this field of the report, the pathologist should comment on the possible autoantibody specificities associated with the reported ANA patterns and the possible clinical significance.

The method used in the test must be stated because there may be differences in results obtained by indirect immunofluorescence with HEp-2 cells, indirect enzyme with HEp-2 cells, and the various solid-phase-based assays. As for a reference range in the IIF-ANA test, it is generally agreed that 1/80 represents a borderline reactivity and 1/160 or higher represents a positive reaction. However, this needs to be established according to the peculiarities of each laboratory.

INTERPRETATION OF THE IIF-ANA TEST RESULT

The ANA test cannot be interpreted in a straightforward fashion as, for example, an HIV test can. A positive ANA test does not necessarily mean systemic autoimmune disease, and a negative ANA test does not exclude the possibility of a systemic autoimmune disease. The appropriate diagnostic decision must be based on the integration of the clinical context with nuances in the ANA pattern/titer and tests for disease marker autoantibodies.

When To Order an ANA Test

Ideally, an ANA test should be requested in individuals with clinical symptoms and signs consistent with a systemic autoimmune disease. In this context, a positive result may be interpreted as an additional element in the construction of the clinical diagnosis. However, at the early onset, systemic autoimmune diseases frequently present with nonspecific complaints and symptoms, and these patients are frequently first seen by a variety of medical specialists other than those mostly acquainted with systemic autoimmune diseases. Early diagnosis and treatment of systemic autoimmune diseases are relevant for higher remission rates, prognosis, and prevention of irreversible damage. A delay in diagnosis may have serious clinical consequences and represent an economic burden. A high degree of suspicion is necessary for early diagnosis of such cases, and a positive ANA result may represent a valuable hint to foster further investigation, especially when associated with a disease marker autoantibody. In this context, a study analyzing 10,550 consecutive patients sent to a university rheumatology laboratory by diverse medical specialists over a 3-year period showed that 21% of the ANA-positive samples had at least one disease marker autoantibody identified and 7.9% had multiple autoantibody specificities that contributed to the final diagnosis (27). However, a large proportion of ANA-positive samples were not associated with any disease marker autoantibodies. Therefore, judicious ordering and interpretation of the IIF-ANA test are of utmost importance.

On the other hand, the ANA test is not meant for general screening (check-up) in asymptomatic individuals. In addition, there is no formal evidence to support the use of the ANA test in monitoring treatment and disease activity of patients with an already established diagnosis. It is known that some autoantibodies do exhibit modulation in concentration in serum according to disease activity, including autoantibodies to native DNA, nucleosomes, ribosomal P protein, Jo-1, and Scl-70. In contrast, some autoantibodies have a rather stable concentration in serum irrespective of disease activity, including autoantibodies to SS-A/Ro, SS-B/La, Sm, and U1-RNP. Accordingly, ANA titer and pattern may change in some patients, but such a finding should be interpreted judiciously.

The Meaning of a Negative ANA Test

A negative IIF-ANA test is a strong (but not absolute) element against the diagnosis of systemic autoimmune diseases, such as drug-induced lupus, SLE, mixed connective tissue disease (MCTD), and SSc. On the other hand, the IIF-ANA test has a low negative predictive value for diseases such as systemic or local vasculitis, rheumatoid arthritis, Sjögren's syndrome, and polymyositis. It should be emphasized that a negative IIF-ANA test does not mean that the sample has no autoantibody. In fact, the ability of autoantigens to be recognized in the IIF-ANA assay on HEp-2 cells varies considerably (Table 2). Even for autoantigens regularly present in the HEp-2 cell, autoantibodies in some selected patients may recognize epitopes that are available in specific assays (e.g., double immunodiffusion or enzyme-linked immunosorbent assay) but may not be available in IIF-ANA on HEp-2 cells. Hoffman et al. analyzed 494 consecutive samples referred by rheumatologists and found that 4.1% of the IIF-ANA-negative samples had at least one disease marker autoantibody detected by other methods (28). Therefore, a negative IIF-ANA result in a patient with consistent suspicion of systemic autoimmune disease may require further testing for appropriate disease marker autoantibodies in specific assays.

The Meaning of a Positive ANA Test

Maybe due to historical reasons, there is a general misconception that a positive ANA test is strongly linked to the diagnosis of SLE. However, a positive IIF-ANA result simply means that there is a detectable concentration of autoantibodies in the sample. The clinical relevance of this finding depends on the clinical scenario, the specificity of the autoantibodies in the sample, and other laboratory findings. IIF-ANA is a very sensitive test capable of detecting low-concentration and low-avidity autoantibodies, some of which are not ordinarily associated with systemic autoimmunity. In other words, a positive ANA result per se is not enough for diagnosis or a final clinical decision.

One very important element for the interpretation of a positive IIF-ANA test is the pretest probability. This corresponds to the chance of a given disease to be present before the diagnostic test result is known. This concept is illustrated in Fig. 6, showing that a very sensitive test can yield a high or low positive predictive value depending on the pretest probability. Considering that a positive IIF-ANA occurs in roughly 13% of the general population, one can easily appreciate that indiscriminate ordering of the IIF-ANA test can yield positive results most probably not associated to systemic autoimmune disease, especially at low titer. These "false-positive results" may lead to undesirable consequences, including emotional distress, unnecessary and expensive laboratory investigation, and inappropriate treatment of the patient.

How To Deal with a Positive ANA Test without Clinical Evidence of Systemic Autoimmunity

The occurrence of a positive ANA test without clinical evidence of systemic autoimmunity has been designated the "idiopathic positive ANA syndrome." There are some

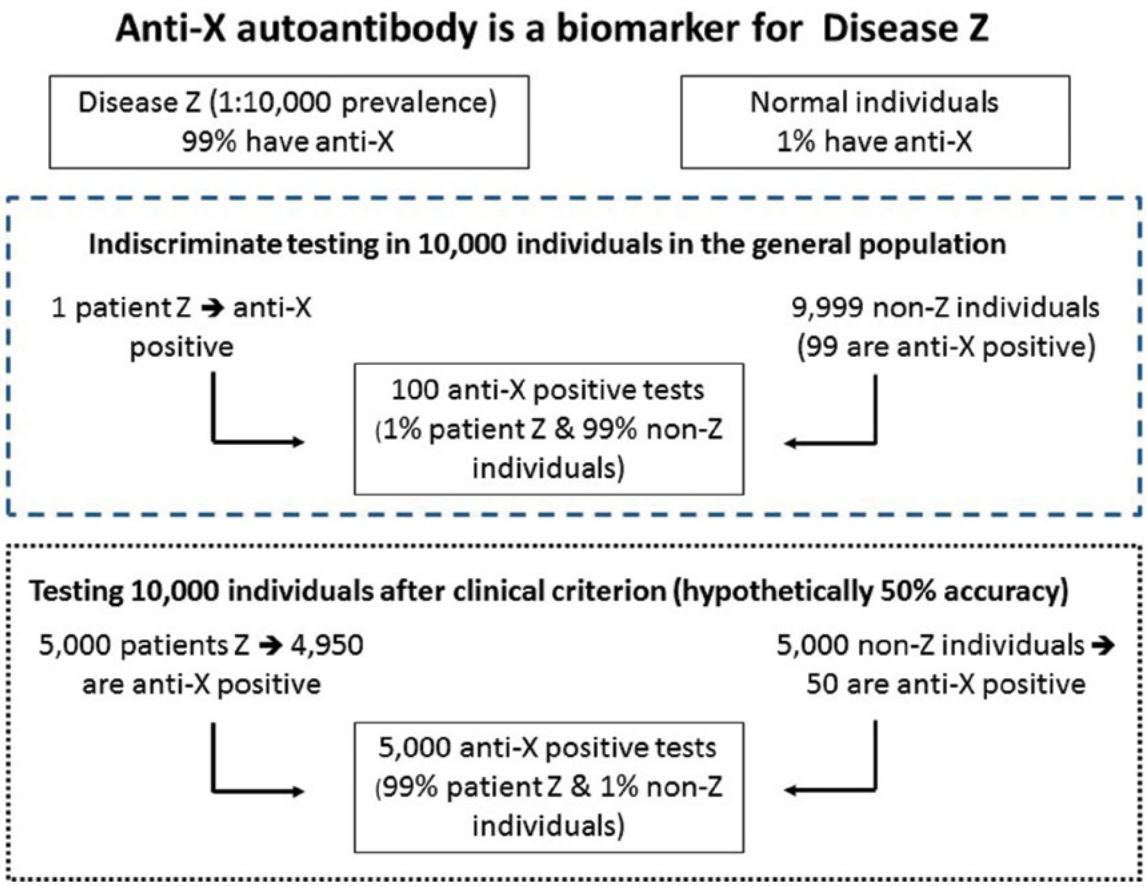

FIGURE 6 Pretest probability influences the diagnostic performance of tests. Anti-X antibody is a biomarker for the rare hypothetical disease Z and occurs in 1% of the general population. Indiscriminate testing for anti-X yields poor positive predictive value. Enrichment of the population sample to be tested according to clinical judgment restores the good performance of the anti-X antibody test.

possibilities to be considered for an individual with a positive ANA result and no apparent evidence of autoimmune disease:

- Impending autoimmune disease
- Nonautoimmune immunological derangement secondary to infection, cancer, or drug
- Minimal rank within the autoimmune disease spectrum or familial autoimmune trait
- Genuine "incidentaloma" (there is no immunological derangement at all)

In such scenarios, it may be helpful to analyze parameters that help to discriminate positive IIF-ANA results in patients with systemic autoimmune diseases and in nonautoimmune and healthy individuals. Two intrinsic dimensions of the IIF-ANA test are very useful in the interpretation of a positive result: the titer and the pattern. Although these correlations are not absolute, a high-titer IIF-ANA is more likely to be related to an underlying systemic autoimmune disease, and a low titer IIF-ANA is more likely to occur in nonspecific clinical scenarios. Exceptions do occur, as some autoimmune patients present low-titer ANA and some apparently healthy individuals present high-titer ANA. In this respect, it is important to bear in mind that some clinically relevant autoantibody specificities tend to yield high-titer ANA (e.g., anti-centromere, anti-U1-RNP) whereas some others may yield low- to medium-titer ANA (e.g., anti-native DNA) (29).

The second dimension of the IIF-ANA test, the IIF-ANA pattern, may be even more informative. The IIF-ANA pattern corresponds to the topographical distribution of the recognized autoantigens. This rationale may be used to distinguish autoantibodies to antigens belonging to the nucleus, nucleolus, and cytoplasm. A closer and more detailed observation allows the identification of several nuances in IIF-ANA patterns within each cellular compartment, and some of these subtle IIF-ANA patterns show strong association with a restricted set of autoantigens (Tables 3 and 4; Fig. 5). In fact, the topographical distribution of some autoantigens is peculiar enough to render the respective immunofluorescence pattern relatively specific for the autoantibodies reacting with that particular autoantigen (Table 4). The judicious interpretation of the IIF-ANA pattern may then direct further investigation of the appropriate autoantibody specificities, which will eventually help settle the diagnosis.

One particular IIF-ANA pattern, the nuclear dense fine speckled pattern (DFS), is of special importance because it is rather frequent, usually occurs at high titer, and is not associated with systemic autoimmune diseases. The DFS pattern (Fig. 5) is elicited by antibodies against the 75-kDa

TABLE 4 IIF-ANA patterns, targeted autoantigen, and disease associations[a]

ANA patterns	Autoantigen	Probable disease associations
Nuclear patterns		
Centromere	CENP-A/B/C	SSc (limited form), primary RP, PBC, SSj
Dense fine speckled	LEDGF	Usually denotes absence of systemic autoimmune disease. Interstitial cystitis, atopic dermatitis, asthma, prostate cancer.
Common fine speckled[b]	Unknown	Unknown clinical association
Type SS-A/Ro fine speckled	SS-A/Ro 60 kDa	Primary SSj, SLE, neonatal lupus, and subacute cutaneous lupus, SSc, polymyositis, PBC
Coarse speckled	Sm U1RNP	Anti-Sm: SLE Anti-U1 RNP: MCTD, SLE, SSc
Nuclear matrix-like[b]	hnRNP	Systemic autoimmune diseases and nonautoimmune diseases
Homogeneous	dsDNA, chromatin Histone	Anti-dsDNA and antinucleosome: SLE Antihistone: drug-induced LE, SLE, RA, oligoarticular JIA (especially with uveitis), Felty's syndrome, autoimmune hepatitis, PBC
Discrete nuclear dots[b]	p80 coilin sp100	Anti-p80 coilin: SSj, inflammatory conditions, HI Anti-sp100: PBC, autoimmune hepatitis
Nuclear envelope[b]	gp-210, p62 Lamin A/B/C, LBP	Anti-gp210 and anti-p62: PBC Nondefined autoantigens: PBC, autoimmune hepatitis, SLE, linear scleroderma, APS
Pleomorphic	PCNA	SLE
Nucleolar patterns		
Clumpy	Fibrillarin	SSc (diffuse and severe forms), hepatocellular carcinoma (rare)
Homogeneous	To/Th Nucleolin B23	Anti-To/Th: SSc (limited form with pulmonary hypertension) Antinucleolin: SLE, GVHD, hepatitis A, infectious mononucleosis Anti-B23 (nucleophosmin), SSc, APS, GVHD, cancer
Speckled	NOR-90; RNA pol I	SSc, cancer, SSj, RA, drug-induced LE, alcoholic liver disease SSc, rarely other systemic autoimmune diseases
Cytoplasmic patterns		
Fine speckled	tRNA synthetases	Jo-1 and other synthetases, specific for polymyositis, antisynthetase syndrome, rarely dermatomyositis
Dense fine speckled	PL7/PL12 Ribosomal P	Anti-PL7/PL12, polymyositis Anti-ribosomal P protein: SLE, type 1 autoimmune hepatitis
Golgi apparatus[b]	Golgin family	SLE, SSj, other systemic autoimmune diseases, idiopathic cerebellar ataxia, paraneoplastic cerebellar degeneration, viral infections.
Discrete dots[b]	EEA1 GWB	Anti-EEA1: subacute cutaneous LE, SLE, RA, primary RP Anti-GWB: SSj, motor/sensory neuropathy, ataxia, RA, PBC
Microfilaments[b]	Actin Myosin Keratin Vinculin Tropomyosin Vimentin	Antiactin: autoimmune hepatitis; cirrhosis Antimyosin: hepatitis C, hepatocellular cancer, MG, myocarditis Antikeratin: alcoholic hepatitis, inflammatory/infectious diseases Antivinculin: MG, Crohn's, ulcerative colitis Antitropomyosin: Crohn's disease, ulcerative colitis Antivimentin: nonspecific interstitial pneumonia.
Reticular/dots	Mitochondria	PBC; can be rarely found in isolated systemic sclerosis.
Mitotic apparatus patterns		
Centriole/centrosome[b]	Several	Several autoimmune and infectious diseases
Intercellular bridge[b]	Several	Various autoimmune conditions with low specificity
Mitotic spindles[b]	HsEg5 and others	Various autoimmune conditions with low specificity

[a]Abbreviations: SSc, systemic sclerosis; SLE, systemic lupus erythematosus; RP, Raynaud's phenomenon; PBC, primary biliary cholangitis; SSj, Sjögren's syndrome; MCTD, mixed connective tissue disease; RA, rheumatoid arthritis; HI, healthy individuals; APS, antiphospholipid syndrome; GVHD, graft-versus-host disease; MG, myasthenia gravis.

[b]When in low-to-moderate titer, may not have clinical relevance.

transcription coactivator LEDGF/p75 (30). Autoantibodies to LEDGF/p75 occur in 3 to 9% of the normal population (8, 30) and contribute to a sizable fraction of the cases of the idiopathic positive ANA syndrome, especially in those with high-titer ANA. Several studies have consistently shown that individuals with isolated anti-LEDGF/p75 antibodies do not present with systemic autoimmune diseases. In addition to apparently healthy individuals, the DFS pattern and anti-LEDGF/p75 antibodies have been reported in a variety of clinical scenarios, including interstitial cystitis, dermatitis atopica, asthma, and prostate cancer (30). Since the DFS pattern is clearly apparent only when anti-LEDGF/p75

antibodies are not overshadowed by the concomitant presence of significant levels of other autoantibodies, the identification of the DFS pattern has been considered an indication of absence of systemic autoimmune diseases (8, 25, 31).

In addition to the clinical context, the interpretation of the ANA result must take into account information from other tests, including the testing for autoantibody specificities associated with the particular IIF-ANA pattern observed. Useful tests include blood cell count, urinalysis, serum creatinine, liver function tests, acute-phase reactants, and the determination of the serum complement (CH50 and initial components of the classic pathway). The two following examples illustrate the integrated interpretation of information provided by the IIF-ANA test (titer and pattern), clinical context, and general laboratory tests. Patient A and patient B present with nonspecific musculoskeletal complaints and no other clinical finding. Patient A presents a 1:2,560 IIF-ANA with nuclear DFS pattern (with coarse staining of the metaphase plate). Patient B presents a 1:640 IIF-ANA test with a nuclear homogenous pattern (with strong hyaline staining of the metaphase plate). Patient A most probably presents no abnormality in blood cell count, urinalysis, acute-phase reactants, serum complement and creatinine, and liver tests and no reactivity in tests for disease marker autoantibodies, but it is highly probably that he/she presents positive reactivity to LEDGF/p75. For patient B, general laboratory exams may disclose unapparent abnormalities and specific tests for disease marker autoantibodies may reveal antibodies to native DNA, nucleosome, histone, Sm, or U1-RNP. Despite the higher-titer IIF-ANA, patient A most probably has no systemic autoimmune disease whereas patient B, despite moderate IIF-ANA titer, will probably develop evident SLE manifestations within the next few months or years. Patient A can be seen within 6 months for a "reassurance" visit and then discharged, but patient B must be closely followed with frequent laboratory investigation for impending SLE manifestations.

Limitations of the Test

Despite its recognized utility and its ranking as the gold standard for autoantibody screening, the IIF-ANA test presents some limitations and pitfalls. There is a high degree of inherent subjectivity in the definition of a positive test and in the interpretation of the ANA pattern. This can be minimized by delineating criteria for the establishment of a positive reaction and definition of each pattern. Continuous intra- and interlaboratory interaction among analysts is highly recommended. It is advisable that at least two analysts have the opportunity of examining each sample. The variability in the microscope and lighting conditions may contribute to nonreproducible results among laboratories. This can be partially overcome by the use of commercial precalibrated fluorescent beads. The heterogeneity in performance of the various slide brands may cause one sample to produce different results in different slides. This potential problem can be handled by validating each new slide lot or brand with an array of known samples representing diverse IIF-ANA patterns. In addition, some slide brands or some peculiar slide lots may yield spurious patterns not observed in other brands. This problem can be partially handled by retesting unusual patterns in more than one slide brand. Pattern recognition is a cognitive ability acquired by training and practice, which are obviously variable among analysts. This source of inconsistency must be overcome by continuous training and by exchanging experience within the group and with other groups.

Strategy for Ordering Autoantibody Tests in the Investigation of Autoimmune Diseases

The laboratory investigation strategy in autoimmune diseases varies according to the diagnostic hypotheses indicated by the clinical evaluation. There is a plethora of autoantibodies to be tested and an equally large array of methodological platforms, which may make the task difficult for those not familiar with the field. For systemic autoimmune diseases, the IIF-ANA test is useful as general screening for autoantibodies against antigens in several cellular compartments. Following the IIF-ANA test, additional tests are frequently necessary according to the clinical scenario and according to the IIF-ANA pattern. In case there is no firm evidence of a systemic autoimmune disease, a negative IIF-ANA test may be enough. In contrast, if there is compelling evidence of systemic autoimmunity, a negative IIF-ANA test must be complemented by the investigation of other autoantibodies. In fact, the ability of the IIF-ANA test in detecting the several autoantibodies varies substantially (Table 2). For example, it may be wise to test for anti-SS-A/Ro and anti-P ribosomal antibodies in patients with a suspicion of SLE and a negative IIF-ANA test. The same is true for anti-Jo-1 antibodies if the clinical scenario suggests polymyositis or antisynthetase syndrome. In addition, it is important to bear in mind that tissue-specific autoantigens are not available in HEp-2 cells. In such cases, specific tests for individual autoantibodies should be ordered. A corollary of that is that the ordering of autoantibody assays must obey a strategy dictated by the judicious analysis of the clinical scenario vis-à-vis the clinical associations of the several autoantibodies.

Quality Control

The careful execution of the standard operational protocol is of paramount importance, since it ensures appropriate elements for interpretation of the ANA reactivity and ANA patterns. In addition, a series of items are essential to ensure high-quality and consistent IIF-ANA results.

1. A set of controls should be used in each assay run, including (i) samples that clearly discriminate interphase and mitotic cells (e.g., centromeric, homogeneous, or dense fine speckled pattern) in dilution to present moderate fluorescence intensity, (ii) one sample with low fluorescence intensity (+/++++), and (iii) a negative sample. Samples with strong intensity of reaction yield beautiful images but do not add much information. The same set of controls should be used in each assay run in order to ensure day-to-day consistency.
2. A daily record should be registered with the results obtained with the set of controls used in each routine. Monitoring daily records of controls helps identify possible trends for deviation, allowing corrective actions to be implemented. These records should also register changes in PBS batch, lot of slides, and any unexpected event that may have occurred in the assay.
3. A panel of serum samples with reactivity to an array of autoantigens and representing several relevant ANA patterns should be used to validate any new lot or new brand of slides. Ideally, this validation panel should include samples reacting with SS-A/Ro, Jo-1, ribosomal P protein, LEDGF/p75 (DFS pattern), Scl-70, Sm/U1-RNP, mitochondria, sp-100, CENP-F, and PCNA. This panel can be constructed with secondary standards retrieved from the laboratory routine, exchange with expert laboratories, and samples obtained from the CDC.

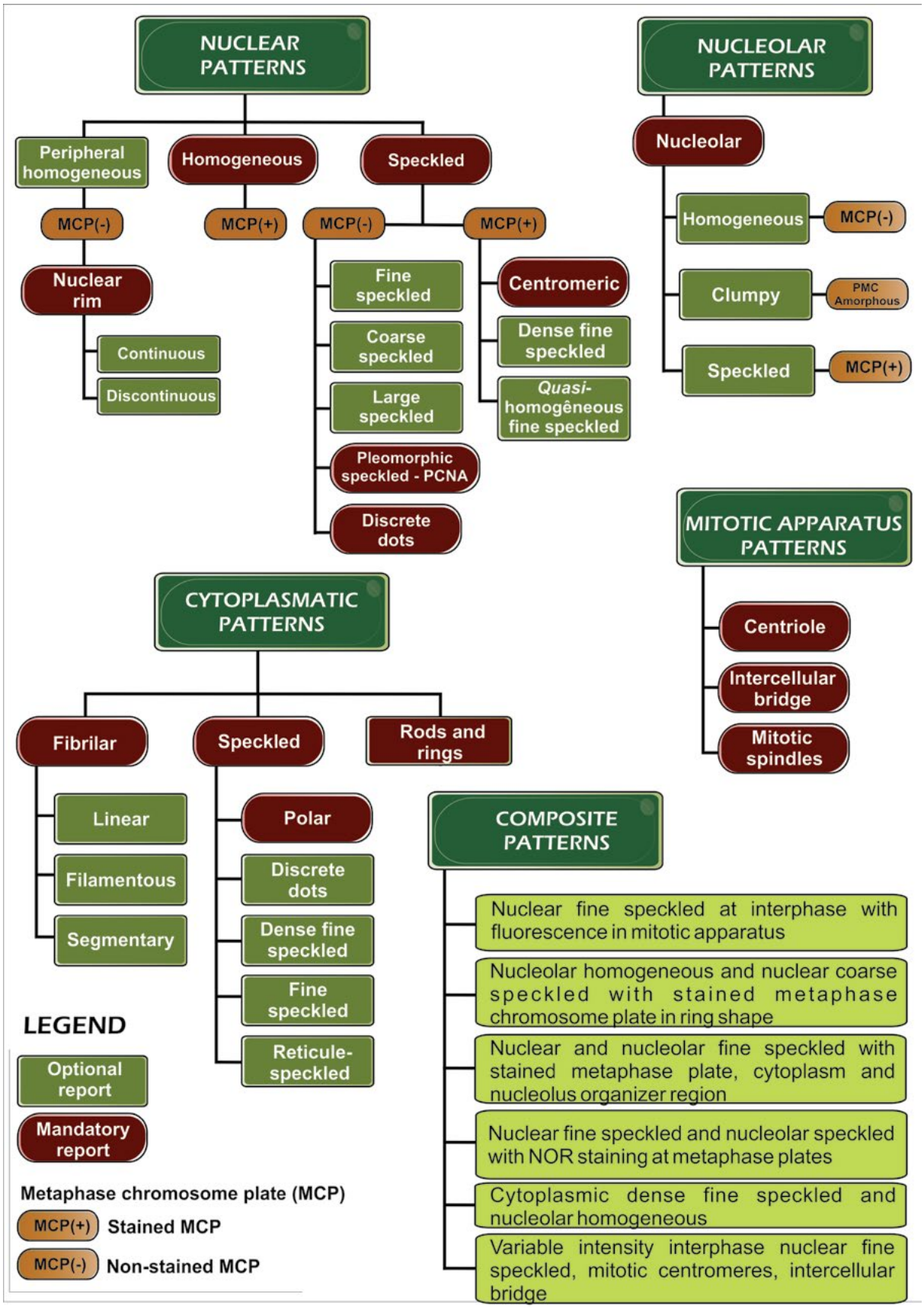

FIGURE 7 Decision-tree algorithm for classification of IIF-ANA patterns proposed by the IV Brazilian Consensus on ANA. MCP, metaphase chromatin plate.

4. Periodically, there should be checking of the PBS and mounting medium pH, microscope lamp lifetime, and the temperature of refrigerators used to store the kits and serum samples.
5. Regular preventive maintenance of microscopes to ensure the cleaning of filters, lenses, and eyepieces, centralization of lamps, and periodic calibration of automatic pipettes should be conducted.
6. Harmonization of the interpretation criteria among analysts. This can be achieved via a series of measures, including the following.
   a. Encouragement of discussion and sharing of routine IIF-ANA interpretation by analysts.
   b. The screening and titration steps should not be performed by the same analyst, ensuring that each positive ANA sample be seen by at least two analysts.
   c. Periodically, all analysts should blindly read and record a set of slides with various predefined patterns and titers; possible discrepancies may be identified and corrected.
   d. Continuous education and training of analysts.
7. Adherence to one of the available national and international external quality control programs is highly recommended. In addition, internal quality control can be implemented by assaying blinded samples with known reactivity.

There is a need to promote worldwide harmonization in the nomenclature of IIF-ANA patterns as well as in defining the characteristic features of each pattern, their immunologic associations, and their clinical relevance. A few consensus-building studies have been developed in different parts of the world (14, 15, 32) with the proposition of tree-decision algorithms for the classification of IIF-ANA patterns (Fig. 7). The International Consensus on ANA Patterns, recently launched during the 12th International Workshop on Autoantibodies and Autoimmunity held in Sao Paulo, Brazil, shall generate a continuous process of international harmonization and diffusing of useful information for those interested in performing and interpreting the IIF-ANA test (http://www.iwaa2014.org.br/home.html).

KEY MESSAGES

1. The designation "antinuclear antibody (ANA)" test should be updated to "anticellular antibody" test.
2. IIF-ANA on HEp-2 cells is the gold standard for autoantibody screening in systemic autoimmune diseases.
3. ANA testing in individuals with low pretest probability of systemic autoimmune disease often contributes to the idiopathic positive ANA syndrome. IIF-ANA is not recommended as general screening test (check-up).
4. A negative IIF-ANA speaks against, but does not formally exclude, the diagnosis of some systemic autoimmune diseases.
5. A positive ANA test by itself is not diagnostic of any autoimmune disease since patients with several other clinical conditions and even healthy people may present a positive ANA.
6. A high-titer ANA is most likely found in systemic autoimmune rheumatic diseases but may sometimes be found in apparently healthy individuals and in patients with nonautoimmune diseases.
7. Careful analysis of the IIF-ANA pattern provides valuable information regarding the possible autoantibody specificities in the sample.
8. The dense fine speckled (DFS) IIF-ANA pattern, even at high titer, is most likely found in healthy individuals and patients with nonautoimmune diseases.
9. The clinical significance of a positive IIF-ANA test must take into account the titer and pattern, the clinical scenario, and the results of other ancillary tests.

REFERENCES

1. **Hargraves M, Richmond H, Morton R.** 1948. Presentation of two bone marrow components; the tart cell and the L.E. cell. *Proc Staff Meet Mayo Clin* **27:**25–28.
2. **Tan EM, Cohen AS, Fries JF, Masi AT, McShane DJ, Rothfield NF, Schaller JG, Talal N, Winchester RJ.** 1982. The 1982 revised criteria for the classification of systemic lupus erythematosus. *Arthritis Rheum* **25:**1271–1277.
3. **Holborow EJ, Weir DM, Johnson GD.** 1957. A serum factor in lupus erythematosus with affinity for tissue nuclei. *BMJ* **2:**732–734. PubMed
4. **Friou GJ, Finch SC, Detre KD.** 1958. Interaction of nuclei and globulin from lupus erythematosis serum demonstrated with fluorescent antibody. *J Immunol* **80:**324–329. PubMed
5. **Fritzler MJ.** 1986. Autoantibody testing: procedures and significance in systemic rheumatic diseases. *Methods Achiev Exp Pathol* **12:**224–260. PubMed
6. **Nelson-Rees WA, Daniels DW, Flandermeyer RR.** 1981. Cross-contamination of cells in culture. *Science* **212:**446–452. PubMed
7. **Meroni PL, Schur PH.** 2010. ANA screening: an old test with new recommendations. *Ann Rheum Dis* **69:**1420–1422. PubMed
8. **Satoh M, Chan EK, Sobel ES, Kimpel DL, Yamasaki Y, Narain S, Mansoor R, Reeves WH.** 2007. Clinical implication of autoantibodies in patients with systemic rheumatic diseases. *Expert Rev Clin Immunol* **3:**721–738. PubMed
9. **Fritzler MJ, Pauls JD, Kinsella TD, Bowen TJ.** 1985. Antinuclear, anticytoplasmic, and anti-Sjogren's syndrome antigen A (SS-A/Ro) antibodies in female blood donors. *Clin Immunol Immunopathol* **36:**120–128. PubMed
10. **de Vlam K, De Keyser F, Verbruggen G, Vandenbossche M, Vanneuville B, D'Haese D, Veys EM.** 1993. Detection and identification of antinuclear autoantibodies in the serum of normal blood donors. *Clin Exp Rheumatol* **11:**393–397. PubMed
11. **Tan EM, Feltkamp TE, Smolen JS, Butcher B, Dawkins R, Fritzler MJ, Gordon T, Hardin JA, Kalden JR, Lahita RG, Maini RN, McDougal JS, Rothfield NF, Smeenk RJ, Takasaki Y, Wiik A, Wilson MR, Koziol JA.** 1997. Range of antinuclear antibodies in "healthy" individuals. *Arthritis Rheum* **40:**1601–1611. PubMed
12. **Mariz HA, Sato EI, Barbosa SH, Rodrigues SH, Dellavance A, Andrade LE.** 2011. Pattern on the antinuclear antibody-HEp-2 test is a critical parameter for discriminating antinuclear antibody-positive healthy individuals and patients with autoimmune rheumatic diseases. *Arthritis Rheum* **63:**191–200.
13. **Dellavance A, Gabriel A, Cintra AFU, Ximenes AC, Nuccitelli B, Taliberti BH, Moreira C, von Mühlen CA, Bichara CD, Santos CHR, Yano CM, Mangueira CLP, Carvalho DC, Bonfá ESDO, Doi EM, Guimarães FNC, Araújo FI, Mundim HM, Rego J, Vieira LEA, Poli L, Andrade LEC, Callado MR, Mesquita MM, Sugiyama M, Slhessarenko N, Silva NA, Carballo OG, Leser PG, Francescantonio PLC, Jarach R, Xavier RM, Levy RA, Neves SPF, Cruvinel WM, Santos WS.** 2003. II Brazilian consensus on antinuclear antibodies on HEp-2 cells. *Rev Bras Reumatol* **43:**129–140. (In Portuguese.)
14. **Sack U, Conrad K, Csernok E, Frank I, Hiepe F, Krieger T, Kromminga A, von Landenberg P, Messer G, Witte**

T, Mierau R, German EASI (European Autoimmunity Standardization Initiative). 2009. Autoantibody detection using indirect immunofluorescence on HEp-2 cells. *Ann N Y Acad Sci* **1173:**166–173. PubMed
15. **Wiik AS, Hoier-Madsen M, Forslid J, Charles P, Mayerowitsch.** 2010. Antinuclear antibodies: a contemporary nomenclature using HEp-2 cells. *J Autoimmun* **35:**276–290.
16. **Melegari A, Bonaguri C, Russo A, Luisita B, Trenti T, Lippi G.** 2012. A comparative study on the reliability of an automated system for the evaluation of cell-based indirect immunofluorescence. *Autoimmun Rev* **11:**713–716. PubMed
17. **Voigt J, Krause C, Rohwäder E, Saschenbrecker S, Hahn M, Danckwardt M, Feirer C, Ens K, Fechner K, Barth E, Martinetz T, Stöcker W.** 2012. Automated indirect immunofluorescence evaluation of antinuclear autoantibodies on HEp-2 cells. *Clin Dev Immunol* **2012:**651058. PubMed
18. **Copple SS, Jaskowski TD, Giles R, Hill HR.** 2014. Interpretation of ANA indirect immunofluorescence test outside the darkroom using NOVA view compared to manual microscopy. *J Immunol Res* **2014:**149316. PubMed
19. **Bizzaro N, Antico A, Platzgummer S, Tonutti E, Bassetti D, Pesente F, Tozzoli R, Tampoia M, Villalta D, Study Group on Autoimmune Diseases of the Italian Society of Laboratory Medicine, Italy.** 2014. Automated antinuclear immunofluorescence antibody screening: a comparative study of six computer-aided diagnostic systems. *Autoimmun Rev* **13:**292–298. PubMed
20. **Fenger M, Wiik A, Høier-Madsen M, Lykkegaard JJ, Rozenfeld T, Hansen MS, Samsoe BD, Jacobsen S.** 2004. Detection of antinuclear antibodies by solid-phase immunoassays and immunofluorescence analysis. *Clin Chem* **50:**2141–2147. PubMed
21. **Op De Beeck K, Vermeersch P, Verschueren P, Westhovens R, Mariën G, Blockmans D, Bossuyt X.** 2011. Detection of antinuclear antibodies by indirect immunofluorescence and by solid phase assay. *Autoimmun Rev* **10:**801–808. PubMed
22. **Bonilla E, Francis L, Allam F, Ogrinc M, Neupane H, Phillips PE, Perl A.** 2007. Immunofluorescence microscopy is superior to fluorescent beads for detection of antinuclear antibody reactivity in systemic lupus erythematosus patients. *Clin Immunol* **124:**18–21. PubMed
23. **Chan EKL, Fritzler MJ, Wiik A, Andrade LE, Reeves WH, Tincani A, Meroni PL, IUIS/WHO/AF/CDC Committee for the Standardization of Autoantibodies in Rheumatic and Related Diseases.** 2007. AutoAbSC .Org—Autoantibody Standardization Committee in 2006. *Autoimmun Rev* **6:**577–580. PubMed
24. **Dellavance A, Gallindo C, Soares MG, da Silva NP, Mortara RA, Andrade LEC.** 2009. Redefining the Scl-70 indirect immunofluorescence pattern: autoantibodies to DNA topoisomerase I yield a specific compound immunofluorescence pattern. *Rheumatology* (Oxford) **48:**632–637. PubMed
25. **Dellavance A, Viana VST, Leon EP, Bonfa ESDO, Andrade LEC, Leser PG.** 2005. The clinical spectrum of antinuclear antibodies associated with the nuclear dense fine speckled immunofluorescence pattern. *J Rheumatol* **32:**2144–2149. PubMed
26. **Dellavance A, Alvarenga RR, Rodrigues SH, Barbosa SH, Camilo AC, Shiguedomi HS, Rodrigues SS, Silva CG, Andrade LE.** 2013. Autoantibodies to 60kDa SS-A/Ro yield a specific nuclear myriad discrete fine speckled immunofluorescence pattern. *J Immunol Methods* **390:**35–40. PubMed
27. **Peene I, Meheus L, Veys EM, De Keyser F.** 2001. Detection and identification of antinuclear antibodies (ANA) in a large and consecutive cohort of serum samples referred for ANA testing. *Ann Rheum Dis* **60:**1131–1136. PubMed
28. **Hoffman IEA, Peene I, Veys EM, De Keyser F.** 2002. Detection of specific antinuclear reactivities in patients with negative anti-nuclear antibody immunofluorescence screening tests. *Clin Chem* **48:**2171–2176. PubMed
29. **Satoh M, Vázquez-Del Mercado M, Chan EK.** 2009. Clinical interpretation of antinuclear antibody tests in systemic rheumatic diseases. *Mod Rheumatol* **19:**219–228. PubMed
30. **Ochs RL, Muro Y, Si Y, Ge H, Chan EK, Tan EM.** 2000. Autoantibodies to DFS 70 kd/transcription coactivator p75 in atopic dermatitis and other conditions. *J Allergy Clin Immunol* **105:**1211–1220. PubMed
31. **Mahler M, Parker T, Peebles CL, Andrade LE, Swart A, Carbone Y, Ferguson DJ, Villalta D, Bizzaro N, Hanly JG, Fritzler MJ.** 2012. Anti-DFS70/LEDGF antibodies are more prevalent in healthy individuals compared to patients with systemic autoimmune rheumatic diseases. *J Rheumatol* **39:**2104–2110. PubMed
32. **Francescantonio PL, Cruvinel WM, Dellavance A, Andrade LE, Taliberti BH, von Mühlen CA, Bichara CD, Bueno C, Mangueira CL, Carvalho DG, Bonfá ES, Brito FA, Araújo FI, Rêgo J, Pereira KM, dos Anjos LM, Bissoli MF, Santiago MB, Maluf NZ, Alvarenga RR, Neves SP, Valim V, dos Santos WS.** 2014. IV Brazilian guidelines for autoantibodies on HEp-2 cells. *Rev Bras Reumatol* **54:**44–50. PubMed

Detection of Autoantibodies by Enzyme-Linked Immunosorbent Assay and Bead Assays

EDWARD K. L. CHAN, RUFUS W. BURLINGAME, AND MARVIN J. FRITZLER

88

Autoantibodies directed against intracellular antigens are characteristic features of a number of human autoimmune diseases and certain malignancies (1–3). Studies of systemic autoimmune rheumatic diseases have provided strong evidence that autoantibodies are maintained by antigen-driven responses (4, 5) and that autoantibodies can be reporters from the immune system, revealing the identities of antigens involved in disease pathogenesis. Historically, autoantibody detection and analysis have relied on a number of different technologies, such as hemagglutination and particle aggregation, immunodiffusion, indirect immunofluorescence (IIF), complement fixation, counterimmunoelectrophoresis (CIE), Western and dot blotting, immunoprecipitation (IP), and enzyme-linked immunosorbent assay (ELISA), and on functional assays that demonstrate inhibition of the catalytic or other functional activity of the antigen of interest. These technologies have limitations because they tend to be labor-intensive and time-consuming, are limited in throughput, are semiquantitative, and are not adaptable to leading-edge research. Immunodiffusion has been used for over 50 years, and it is still used in some clinical laboratories because it is inexpensive and has high specificity, but it lacks sensitivity and can take up to 48 h before precipitin lines are interpretable. Western blotting is more costly and time-consuming, and not all autoantibodies are detected by this technique. For example, in the SS-A/Ro system, it has been observed that IP techniques are required to identify some sera that contain antibodies reacting only with the "native" SS-A/Ro particle (6). IP protocols that use extracts from [^{35}S]methionine-labeled cells are not suitable for the detection of all autoantibodies, such as antibodies to Ro52/TRIM21 protein (7). ELISA techniques have rapidly advanced, but highly specific, sensitive, and reliable assays that use highly purified or recombinant proteins are limited by intermanufacturer and interlaboratory variation of results (8). Immunodiffusion and CIE generally favor high-titer sera and often cannot discriminate multiple autoantibody responses that are characteristic of systemic autoimmune rheumatic disease sera.

Despite the advantages of IP, CIE, and ELISA, IIF remains the least expensive and, perhaps, the screening assay of choice for many autoantibodies (9–11). HEp-2 cells are currently the most commonly used cell substrate in diagnostic autoantibody tests for systemic autoimmune rheumatic diseases. However, the use of IIF on HEp-2 cells to detect autoantibodies can be limited by a lack of specificity and sensitivity when the antigen in question is of low abundance or when epitopes are hidden or lost through cell fixation (12). These factors have resulted in variability in the clinical performance of commercial HEp-2 cell substrates (13). In addition to variation in kits produced by various manufacturers, significant lot-to-lot variation from single manufacturers has been noted, and variations in different batches from the same manufacturer have also been observed. Another limitation of current IIF substrates is that there is significant variation in the sensitivities of different commercially available substrates to detect different antibodies. This limitation can be compounded by sera that contain multiple autoantibodies, for which it is necessary to use other techniques to definitively identify as many autoantibodies as possible in a single serum.

Human sera contain autoantibodies that are notably heterogeneous with respect to antigen and epitope specificity and the polyclonality of the B cell response that leads to their formation. For example, it is common to find sera that show a complex pattern of IIF staining that might include reactivity with the nuclear envelope, mitochondria, and other intracellular structures and organelles. Further analysis of these sera with a variety of techniques confirms that there is reactivity with a variety of antigens that might include chromatin, Ro60, pyruvate dehydrogenase (pyruvate dehydrogenase complex or M2 antigen), nuclear pore complex antigens (14), and processing bodies (GW bodies) (15). Complex sera like those referenced here point to the need of multiplexed autoantigen arrays to provide an accurate picture of the autoantibody profile of any patient.

With the use of expression cloning and autoantibodies as probes to screen λ phage cDNA libraries, the identities of many autoantigens have been determined and validated. A logical strategy is to take advantage of the availability of recombinant autoantigens generated from the cDNA in *Escherichia coli* or other appropriate expression systems as the substrates for immunoassays such as ELISA and multiplex assays. More recently, protein and peptide microarrays and mass spectroscopy have been used to detect novel autoantibody reactivity (16). This chapter will focus on the purification of recombinant autoantigens used in the authors' laboratories and advances in multiplex immunoassays that are being used for autoantibody detection.

doi:10.1128/9781555818722.ch88

ANTIGEN TECHNOLOGY

A rapid expansion of new technologies developed by basic and applied immunology is making a significant impact on a broad spectrum of biomedical investigations (16, 17). The identification of biomarkers of disease onset, progression, and response to therapy is now made possible with the application of a variety of reagents in a number of novel platforms (18–21). Polyclonal, monoclonal, and single-component antibodies have become valuable tools in basic research and diagnostic technologies and have been used very successfully as therapeutics in patients with cancer, a broad spectrum of systemic rheumatic diseases, a variety of autoimmune conditions, and cell and organ transplantation. Accompanying these developments has been the appearance of a broad spectrum of DNA, RNA, and protein microarrays. Protein arrays in particular are gaining acceptance as an approach to multiplexed detection of autoantibodies in biological fluids and the detection of changes in cell physiology after various physiological triggers and therapeutic interventions (22). To capitalize on these advances, there has been a need for the parallel development of new technology platforms to produce and utilize the arrays in clinical settings. These have included novel adaptations of fluorescence-activated cell sorting, which is now a standard technique in most clinical immunology centers (23). Some of these emerging technologies include addressable laser beads, microfluidics and laboratory-on-a-chip platforms, chemiluminescence (17, 24), and nanotechnology (25–29). In addition, devices that produce protein arrays by spotting analytes of interest on solid-phase substrates have become a necessary technology of research-intensive institutions. The use of antigen arrays for the analyses of autoantibodies has been reported, but the technology remains mostly limited to research laboratory settings (30, 31).

Purification of Natural and Recombinant Autoantigens

One requirement in the development of a successful immunoassay for the detection of autoantibodies is that the antigen must be recognized efficiently. Many recombinant autoantigens generated in bacterial, viral, or eukaryotic expression systems can be used successfully for functional as well as immunological assays. In the analysis of systemic rheumatic diseases, recombinant human SS-B/La antigen is an excellent example, since most human anti-SS-B/La sera recognize multiple epitopes, most of which are readily expressed in recombinant forms. However, some recombinant autoantigens are found not suitable at all. For example, Sm D1 antigen generated in *E. coli* is not suitable for ELISA, while the same antigen expressed from a baculovirus system is suitable (32). Recombinant antigens derived from the bacterial expression system are often not suitable for the detection of autoantibodies because they may lack posttranslational modifications required directly or indirectly for the functionality of the epitope(s). Another example is the Ro60 antigen. Only a small fraction of anti-Ro60 sera are reactive to the recombinant protein generated from *E. coli*, unlike with the native-affinity-purified bovine Ro60 protein. It is not clear why the native preparation is more immunoreactive than the one derived from *E. coli*, but probable explanations are that the native antigen has a conformation, a posttranslational modification, or a cofactor that the recombinant protein made in *E. coli* lacks. It should be noted that recombinant Ro60 with apparently superior antigenicity is now available from a commercial source (33). Ribonucleoprotein (RNP) autoantibody targets are another instance where cloned antigens do not have as much reactivity as the native proteins. In this case, the increased reactivity with the native antigen is related to autoantibodies in patients with mixed connective tissue disease that react only with the quaternary structure found in the RNA-multiprotein complex and not in the individual components (34).

Use of Natural Autoantigens

There are a number of reasons that autoantigens purified from natural sources are preferred over recombinant proteins. Historical uses and costs are some of the issues that lead to the use of bovine chromatin preparations for the detection of antichromatin antibodies. Classical biochemical purification is still used for the purification of large quantities of different chromatin fractions as well as subunits that are useful for detecting a clinically relevant subset of antibodies (35). Additionally, it has been demonstrated that some diagnostically important autoantibodies react with epitopes present on the native histone-DNA complex found in chromatin. These epitopes are absent in DNA-free histones and histone-free DNA (36). The antigen tissue transglutaminase, recognized by people with celiac disease, is easily isolated by biochemical techniques from red blood cells. To obtain native autoantigens that are in relatively low abundance in animal tissue, affinity column purification using well-defined human autoantibodies coupled to solid-phase matrices is routinely used. Because it is possible to obtain the large quantities of tissue that are needed at a relatively low cost, bovine spleen and thymus are often the starting materials for native antigens. Examples in this category include extractable nuclear antigens, such as Sm, RNP, Ro60, SS-B/La, Scl-70, and Jo-1.

Use of Peptide Antigens

Patients with autoimmune diseases make a spectrum of autoantibodies to specific antigens, and some of these antibodies will react with small peptides derived or deduced from the target protein (37). Usually, these peptides are not as reactive as the whole protein in immunoassays and thus are not clinically useful. However, in a few instances, antibodies against peptides have been shown to be at least as clinically useful as antibodies against the corresponding native protein. In particular, the 23 C-terminal amino acids of ribosomal P proteins is the immunodominant peptide in certain patients with systemic lupus erythematosus (SLE) (38), as is a dimethylated peptide from SmD3 antigen (39, 40). Citrullinated peptides derived from filaggrin and other sources are highly reactive with sera from patients with rheumatoid arthritis (41).

Production of Recombinant Proteins

The strategy for the design of recombinant constructs is beyond the scope of this chapter; however, we will discuss briefly some key aspects related to the production of recombinant autoantigens. The production of recombinant proteins to be used in the detection of autoantibodies should take into consideration the suitability of the construct design and the ease of purification of resulting proteins. Earlier attempts in the production of recombinant proteins were faced with lengthy biochemical purification protocols to remove unwanted cellular proteins. More importantly, most of these protocols have to be specifically designed for each individual recombinant protein, and these invariably have distinctive biochemical characteristics. Currently, it is preferable to design recombinant proteins with an affinity tag that can be utilized for subsequent purification using a

one-step, solid-phase affinity chromatography protocol that can be utilized for most recombinant proteins largely independently of their biochemical properties. The preferred affinity tag should be short, such as the 6 histidine tag that can be attached to the N terminus or C terminus of the recombinant protein using vectors such as pET28 (Novagen/EMD Biosciences, Inc., San Diego, CA) or pDEST17 (Invitrogen, Carlsbad, CA). The glutathione *S*-transferase (GST) fusion proteins, although used by many investigators for the expression of autoantigens, may not be suitable for general use since anti-GST antibodies have been reported in some patients with autoimmune hepatitis (42). In contrast, human autoantibodies binding the histidine tag, a short peptide of 6 histidine residues, have not been reported to date.

In most designed recombinant autoantigens, full-length constructs are preferred so as to ensure that all the epitopes are well represented. In cases where the autoantigen is a large protein, such as the Golgi complex protein giantin, which has a molecular mass of ~350 kDa, it is technically difficult to produce the complete protein in *E. coli* or even in eukaryotic expression systems. Thus, overlapping fragments of giantin that can be used alone or as a mixture for the detection autoantibodies were produced (43).

Purification of Recombinant Proteins

It is beyond the scope of this chapter to discuss purification of different types of recombinant proteins, and thus, the following discussion represents two key modifications or improvements in overcoming problems encountered during the production of 6 histidine-tagged recombinant proteins for use in the detection of autoantibodies. The first concern is the purity of the preparation to ensure that there are no false-positive results caused by contamination from *E. coli* proteins. A modification of the established purification protocol for 6 histidine-tagged proteins has been used to achieve a higher degree of purity by repeating the affinity purification step (44). Preliminary studies showed that twice-purified recombinant proteins had lower background reactivity with normal human sera than once-purified preparations. This 2-fold affinity purification protocol has been used in several studies (43, 45). In brief, 6 histidine-tagged recombinant proteins are purified from *E. coli* lysates under denaturing conditions as described in the Qiagen manual *The QIAexpressionist* (44) and are eluted from a nickel affinity column using buffer E (8 M urea, 100 mM NaH_2PO_4, 10 mM Tris-HCl, pH 4.5). Fractions are pooled, the pH is adjusted to 8.0 with 1 M NaOH, and the nickel column is regenerated by washing it in 2 volumes of buffer A (6 M guanidine hydrochloride, 100 mM NaH_2PO_4, 10 mM Tris-HCl, pH 8.0). The second purification simply utilizes the pooled fraction and the regenerated affinity column identically to the first purification.

Use of Rosetta Bacteria for the Production of Large Recombinant Proteins

The second improvement addresses the low yield of recombinant protein in *E. coli*, especially when the recombinant protein to be produced has a high molecular mass. Most recombinant autoantigens up to ~70 kDa have been successfully produced in standard *E. coli* strain BL21(DE3) or JM109(DE3). Examples include SS-B/La, Ro60, and Ro52 proteins. Problems are often encountered when proteins of ~100 kDa or higher are generated in these *E. coli* strains. Figure 1 illustrates the problem encountered when the Golgi autoantigen p115 (115 kDa) was expressed in JM109(DE3) and the major products were only about 60 kDa. Similarly,

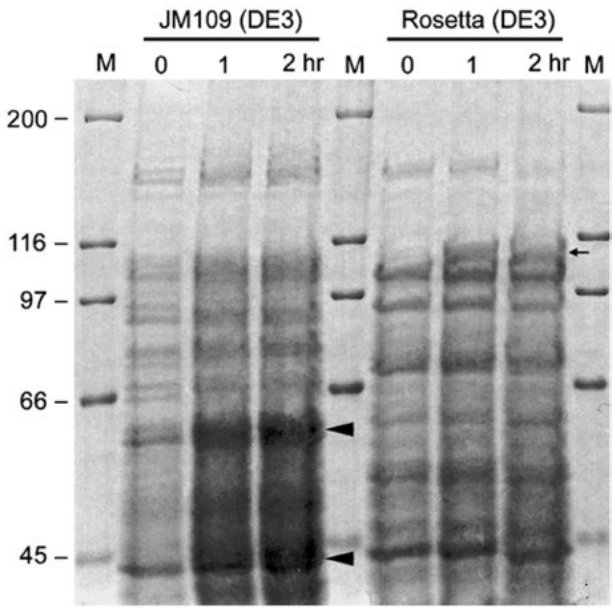

FIGURE 1 Enhanced expression of recombinant proteins is illustrated by the effect on the bacterial host. A construct, pET-p115, was transformed into either JM109(DE3) or Rosetta(DE3), and recombinant proteins were produced with the transformed bacteria using the same culture medium (2YT broth) and conditions. To the cultured bacteria was added 1 mM isopropyl-b-D-thiogalactopyranoside at time zero, and cells were harvested as pellets after 1 or 2 h, solubilized in gel sample buffer, and analyzed with SDS-PAGE using a 5% gel. Proteins were detected with Coomassie brilliant blue G-250 stain. Note that the recombinant JM109 culture generated major products of ~60 kDa (arrowhead) plus other lower-molecular-mass products, whereas the Rosetta culture yielded major products (arrow) corresponding to the native protein. Lane M, molecular mass markers (numbers at the left are masses in kilodaltons).

low-molecular-weight products were obtained with the BL21(DE3) bacteria. However, the expression was improved significantly using a new strain known as Rosetta(DE3), and a protein band corresponding to 115 kDa was generated (Fig. 1). Rosetta host strains from Novagen/EMD Biosciences, Inc. (La Jolla, CA), are BL21 *E. coli* derivatives engineered to increase the expression of eukaryotic proteins that contain codons rarely used in *E. coli*. These strains contain tRNA genes for AGG, AGA, AUA, CUA, CCC, and GGA on a chloramphenicol-resistant plasmid and thus provide for "universal" translation, which is otherwise limited by the codon usage of *E. coli*. Our experience is that the use of the Rosetta cells has made a significant positive impact on the production of recombinant human autoantigens in *E. coli*.

ADVANCES IN ASSAYS

Newer autoantibody assay systems include cell-based assays where selected tissue culture cells are transfected with the cDNAs of antigens of interest (46–48), "line" immunoassays (49, 50), solid-phase antigen arrays (51), addressable laser bead arrays, and paramagnetic bead arrays where relevant native or recombinant antigens are bound to a solid-phase matrix or to microbeads. The renewed interest in and use of cell-based immunoassays is due to the cellular overexpression of the autoantigen (i.e., particular cell surface or

transmembrane targets) in mammalian cells, where they are presented in a more native conformation (52). These advances are only the beginning of a rapid succession of newer technologies, such as microfluidics, lab-on-a-chip platforms, and nanotechnology (29). Comparison of the performance and costs of some of these technologies to those of conventional assays suggests that they are reliable, highly sensitive, and cost-effective. Clinical analyses suggest that gains in accuracy and repeatability obtained with these new technologies may be clouded by a need to reevaluate current paradigms of the diagnostic and prognostic specificities of autoantibodies (53). Each assay has limitations when determining the sensitivity, specificity and the positive predictive value for the detection of autoantibodies.

Bead-Based Immunoassays

Addressable Laser Beads

Addressable laser beads represent an application of array and flow technologies that has demonstrated flexibility in a variety of genomic, proteomic, ribonomic, and immunoassay applications (54). Although there are several applications of this technology, much experience has centered on the Luminex 100/200 platforms (Luminex Corp., Austin, TX), which incorporate laser-based flow technology that can analyze reactants in a microtiter plate format. A key component of this technology is the ability to differentiate more than 100 classes of microspheres based on various amounts of laser-reactive dyes embedded in each class, called 100 different colors for simplicity. This platform has been developed to measure antibodies in biological fluids (55, 56), screen supernatants for monoclonal antibodies of interest (57, 58), quantitate cytokines in cell extracts and biological fluids (59), detect bacterial pathogens, perform HLA typing, detect single nucleotide polymorphisms, track cell signaling responses, and monitor gene expression. The robust application of numerous technologies in this platform suggests that a future use may be to profile patients in a variety of diagnostic and therapeutic settings (54).

Addressable laser bead immunoassays (ALBIA) that utilize the Luminex LabMAP platform in research and clinical laboratory settings have been evaluated in a number of studies. In practice, an antigen of interest is chemically coupled to a specific colored microsphere. Other antigens are coupled to microspheres of different colors. After the coupling and stabilizing reactions, the antigen-coupled spheres are combined into a single microtiter well to provide a single assay that has the ability to detect multiple antibodies in a single specimen. The test samples (sera or other biological fluids) and a fluorochrome-coupled secondary antibody are added to the wells, and after an incubation time, they are analyzed. The principles of the assay are similar to those of flow cytometry, with one laser identifying the specific-antigen-coupled bead passing through the path and a second laser determining the presence and quantity of secondary antibody bound to the bead. The data are displayed in a number of formats but expressed as a quantitative analysis of multiple analytes and the relative amount of antibody bound to the antigen. We have found the development of our "in-house" assays to be easier, more efficient, and more economical than earlier technologies, such as Western blotting, IP, or ELISA. Research applications have included the development of assays to detect monoclonal antibodies and autoantibodies directed to a number of autoantigens, including early endosome antigen 1 (EEA1) (60, 61), GW182 (62, 63), the translocated promoter region (14), and valosin-containing protein (64).

In a clinical service laboratory setting, an autoantigen panel (Quanta Plex; INOVA Diagnostics, Inc.) based on that of ALBIA was evaluated and compared to the routine diagnostic protocol, which analyzed 870 sequential unselected sera received over a 6-month period (25). In this study, the sera were submitted primarily by clinicians who were considering a diagnosis of systemic rheumatic disease. The conventional serological algorithm used IIF on HEp-2 cell substrates (HEp-2000; Immuno Concepts, Inc.) to screen all sera. Antibodies to SS-A/Ro60 can be detected in this IIF assay because this substrate includes cells that are transfected with, and overexpress, the Ro60 autoantigen (47, 65). Sera that were found to be positive in this IIF assay were then evaluated by immunodiffusion for antibodies to Sm, U1-RNP, SS-A/Ro, SS-B/La, Scl-70 (topoisomerase I), and other saline-soluble autoantigens. Antibodies to double-stranded DNA (dsDNA) were detected by IIF on the *Crithidia luciliae* substrate (Immuno Concepts). This comparison showed that ALBIA results agreed with the conventional test result 92% of the time. An exception was a lack of high correlation of anti-dsDNA measured by the *Crithidia* assay and the ALBIA. Because of this, anti-dsDNA is no longer included in this profile. For some reason, the specificity of anti-dsDNA has been a problem with other ALBIA (i.e., TheraDiag FIDIS).

When the results of the ALBIA were compared to those of the conventional assay, it was noted that, on average, 25% of sera exhibited a positive result that was not detected by conventional autoantibody testing. The accuracy and validity of the ALBIA result might be confirmed by other techniques, such as IP and immunoblotting. This observed increase in the sensitivity of ALBIA was studied in various serological cohorts. The results of one such study are shown in Table 1; in that study were included 30 highly characterized sera that were previously shown to react with ribosomal P in at least one commercial ELISA (Euroimmun, MBL, Pharmacia Diagnostics) (66, 67). Comparison of the data show excellent agreement of ALBIA results with the ELISA results, including those that utilize the terminal C22 ribosomal P peptide (67).

Unselected sera from various disease cohorts were also studied to determine if the frequency of autoantibodies as detected by the ALBIA was consistent with the published frequency of autoantibodies (Table 2). This study showed that the frequencies of various autoantibodies in SLE, systemic sclerosis (SSc), Sjögren's syndrome (SjS), and rheumatoid arthritis were in keeping with those of published reports. Interesting exceptions included antibodies to Scl-70 (topoisomerase I), which were found in 8% of sera from SLE patients, and antibodies to Jo-1 (histidyl-tRNA synthetase), which were found in 15% of sera from SjS patients and 4% of sera from SSc patients. It was noted that the reactivity of sera from SLE patients with Scl-70 was in the borderline region of positivity. Similar observations were made with anti-Sm, which was found in 5% of sera from SSc patients, but all of these demonstrated a measurement of mean fluorescence units that was just above the cutoff. Follow-up testing of these sera found that none bound the SmD3 peptide, which is highly specific for SLE (39, 68). The observation that some sera from SLE patients bind Scl-70 is interesting in light of other reports that anti-Scl-70 antibodies were found in sera from SLE patients (69). Likewise, the finding of anti-Jo-1 antibodies in sera from SjS and SSc patients was surprising but may be related to more-recent observations that some sera with anti-Jo-1 antibodies contain antibodies to the Ro52/TRIM21 autoantigen (70). Early studies of ALBIA kits showed a high level (>90%) of agreement with antinuclear

TABLE 1 Comparison of results of ELISA and ALBIA detection of anti-ribosomal P autoantibodies in 30 sera[a]

Serum ID	ELISA result from indicated vendor (cutoff)			INOVA Quanta Plex ALBIA result (cutoff, ratio > 1)
	Euroimmun (ratio > 1)	MBL (11.6 U/ml)	INOVA (20 U)	
1	9.1	219	202	15
2	5.6	144	164	8
3	7.9	124	200	14
4	2.2	24	185	11
5	4.4	76	140	17
6	5.1	63	178	8
7	6.8	111	165	12
8	7.7	169	197	25
9	8.9	246	212	13
10	7.5	187	198	12
11	8.9	69	87	8
12	2.8	72	139	6
13	6.6	125	184	13
14	6.3	130	181	12
15	5.2	116	173	14
16	3.4	87	148	5
17	6.0	136	164	10
18	5.3	118	155	20
19	5.8	100	150	3
20	7.8	170	206	17
21	7.1	146	199	16
22	1.0[a]	11[a]	20	1.5
23	2.1	19	39	4
24	7.4	155	204	10
25	3.9	76	54	10
26	7.6	143	192	9
27	7.2	148	203	23
28	9.1	239	219	27
29	3.2	38	75	2
30	1.6	55	66	2

[a]ID, identifier. Data are extracted from reference 66 and rounded to the nearest whole number, except in the Euroimmun column. Units are defined as per the manufacturer's protocol.

antibody and conventional ELISA techniques. For example, in a study of 37 sera from SjS patients that compared a conventional ELISA to an ALBIA kit (Athena Multi-Lyte antinuclear antibody test system), a 99% concordance between the two assays was found (55).

Taken together, there are advantages and challenges that come with the adoption of the ALBIA platform to detect autoantibodies (Table 3). The capacity of one assay to analyze and detect a complex array of autoantibodies in a single small serum sample (>10 μl) with speed and precision is a significant advantage. There are now several ALBIA kits on the market that detect 10 or more autoantibodies relevant to systemic rheumatic diseases. In some kits, the secondary antibody is added with no subsequent washing of the bead required.

Chemiluminescence Immunoassay

Chemiluminescence immunoassay (CIA) is a relatively newly developed immunoassay platform that employs a fully automated chemiluminescent analyzer and a growing spectrum of autoantibody assays (QUANTA Flash; Inova Diagnostics Inc., San Diego, CA) designed for the Bio-Flash instrument (Biokit s.a., Barcelona, Spain). The principles of the Bio-Flash CIA have recently been described (71). CIAs are developed using native or recombinant antigens covalently coupled to paramagnetic beads. Prior to use, the lyophilized beads are suspended in a buffer. A patient serum sample is prediluted with a sample buffer in a small disposable plastic cuvette. Small amounts of the diluted patient serum, the beads, and the assay buffer are all combined into a second cuvette, mixed, and then incubated for 9.5 min at 37°C. The magnetized beads are sedimented using a strong magnet in the internal washing station and automatically washed several times; next, isoluminol-conjugated anti-human IgG is added, and then the mixture is incubated for 9.5 min at 37°C. The magnetized beads are sedimented and washed repeatedly. The isoluminol conjugate is oxidized when sodium hydroxide solution and peroxide solutions ("triggers") are added to the cuvette, and the flash of light produced from this reaction is measured as relative

TABLE 2 Frequency of autoantibodies detected by the INOVA Quanta Plex assay in cohorts of patients with systemic rheumatic diseases and multiple sclerosis and in controls[a]

Cohort antigen	Frequency (%) of autoantibodies detected in indicated patients						
	SLE (n = 200)	SSc (n = 100)	SjS (n = 100)	RA (n = 200)	IBD (n = 50)	MS (n = 100)	Normal (n = 50)
Chromatin	60	20	20	8	2	4	0
dsDNA[b]	48	0	0	2	0	0	0
U1 RNP	24	10	0	4	0	8	0
Sm	18	4*	0	0	0	1	0
Scl-70	6	24	0	0	0	4	0
SS-A/Ro60	34	24	35	0	0	5	0
SS-B/La	8	5	20	2	0	10	0
Jo-1	0	3	15	0	0	4	0
Rib-P	16	2	0	0.5	0	5	0

[a]Abbreviations: IBD, inflammatory bowel disease; MS, multiple sclerosis; RA, rheumatoid arthritis; RNP, ribonucleoprotein; SjS, primary Sjögren's syndrome; SLE, systemic lupus erythematosus; SSc, systemic sclerosis.
[b]Low positivity.

light units by the optical system. The relative light units are proportional to the amount of isoluminol conjugate that is bound to the human IgG, which is in turn proportional to the amount of autoantibodies bound to the antigen on the beads. The Bio-Flash CIA system also allows the user the option to reflex the individual assays of an autoantibody screening test, such as the QUANTA Flash using extractable nuclear antigen 7. In comparative studies with ELISA, the Bio-Flash CIA system performed very well (>93% agreement) (71, 72). Other advantages of the CIA system are the remarkable linearity of results throughout the dynamic range of the assay (72).

Advantages of Bead-Based Immunoassays

There are a number of advantages to bead-based immunoassays. First, test reports can be automatically generated through standard laboratory information systems and converted to standard encoded formats that can be directly uploaded into the patient's electronic medical record. Second, test results are generated very rapidly. In our laboratory, the turnaround time from receipt of the serum sample to generation of the laboratory report using the conventional technologies was 4 to 5 days. By comparison, the turnaround time using ALBIA and CIA is 1 to 2 days. This marked improvement is predicated on a laboratory algorithm that tests samples daily, as opposed to batch runs of ~90 sera. Last, although we have not performed detailed cost analyses, there is little additional cost because the sample throughput has been effectively doubled and this throughput was managed with the same staff complement as with the conventional protocols. In fact, the staff now has more time for quality assurance and research projects that were formerly delegated to other staff. The tradeoff for these apparent cost savings is more-expensive maintenance contracts, upgrades to software, and a budget allocation for replacement of lasers. However, it should be noted that one of us (M.J.F.) has been using Luminex technology for more than a decade, and laser replacement has not been required.

TABLE 3 Advantages, challenges, and opportunities relating to new array technologies

Advantage(s)[a]	Challenges and opportunities
Multiple autoantibodies are detected in a single assay	New clinical correlations and paradigms based on autoantibody and epitope profiling
Personnel costs	Costs of maintenance contracts and budgeting for laser replacement
Rapid test performance and automated test reporting	Medical centers not equipped or configured to accept digital reports can jeopardize rapid turnaround times
Small sample volumes	Adoption of new technologies that do not require conventional venipuncture
High correlation with other immunoassays, particularly ELISA	Low correlation with immunodiffusion
Ease of establishing new assays	Research and development required to provide broader spectrum of autoantigens (nucleolar, paraneoplastic, phospholipids)
Equipment and technology can be used for a variety of relevant assays: cytokine, SNP, HLA, gene activation, cell activation, drug discovery	Emergence of other microarray and nanotechnology platforms will complicate standardization

[a]SNP, single nucleotide polymorphism.

Challenges of Multiplexed Immunoassays

A major challenge and opportunity in the adoption of multiplexed autoantibody analyses is the breadth of autoantibody profiles provided in the laboratory reports (53). This increased amount of information presents a significant challenge to clinicians who are accustomed to dealing with one or two autoantibody results for any given patient. It is likely that with autoantibody profiling, a new wave of clinical studies and clinical correlations based on more-complete autoantibody profiles will emerge. The clinical picture may be enhanced by extending the breadth of this technology to epitope mapping and epitope spreading as an approach to monitoring disease progression or remission. Last, history has taught us that standardization of the new multiplexed platforms will be a significant challenge. The utilization of international reference sera for standardization of secondary antibodies to establish controls and cutoff values will be very important.

This work was supported in part by the Canadian Institutes for Health Research grant MOP-38034 and National Institutes of Health grants.

REFERENCES

1. **Chan EKL, Andrade LEC.** 1992. Antinuclear antibodies in Sjögren's syndrome. *Rheum Dis Clin North Am* **18:**551–570. PubMed
2. **Satoh M, Vázquez-Del Mercado M, Chan EKL.** 2009. Clinical interpretation of antinuclear antibody tests in systemic rheumatic diseases. *Mod Rheumatol* **19:**219–228. PubMed
3. **Mahler M, Pierangeli S, Meroni PL, Fritzler MJ.** 2014. Autoantibodies in systemic autoimmune disorders. *J Immunol Res* **2014:**263091. PubMed
4. **Tan EM, Chan EKL, Sullivan KF, Rubin RL.** 1988. Antinuclear antibodies (ANAs): diagnostically specific immune markers and clues toward the understanding of systemic autoimmunity. *Clin Immunol Immunopathol* **47:**121–141. PubMed
5. **Radic MZ, Weigert M.** 1994. Genetic and structural evidence for antigen selection of anti-DNA antibodies. *Annu Rev Immunol* **12:**487–520. PubMed
6. **Boire G, Lopez-Longo FJ, Lapointe S, Ménard HA.** 1991. Sera from patients with autoimmune disease recognize conformational determinants on the 60-kd Ro/SS-A protein. *Arthritis Rheum* **34:**722–730. PubMed
7. **Chan EKL, Buyon JP.** 1994. The SS-A/Ro antigen, p 1–18. *In* van Venrooij WJ, Maini RN (ed), *Manual of Biological Markers of Disease*. Kluwer Academic Publishers, Dordrecht, Netherlands.
8. **Tan EM, Smolen JS, McDougal JS, Fritzler MJ, Gordon T, Hardin JA, Kalden JR, Lahita RG, Maini RN, Reeves WH, Rothfield NF, Takasaki Y, Wiik A, Wilson M, Koziol JA.** 2002. A critical evaluation of enzyme immunoassay kits for detection of antinuclear autoantibodies of defined specificities. II. Potential for quantitation of antibody content. *J Rheumatol* **29:**68–74. PubMed
9. **Bizzaro N, Wiik A.** 2004. Appropriateness in anti-nuclear antibody testing: from clinical request to strategic laboratory practice. *Clin Exp Rheumatol* **22:**349–355. PubMed
10. **Wiik AS, Gordon TP, Kavanaugh AF, Lahita RG, Reeves W, van Venrooij WJ, Wilson MR, Fritzler M, IUIS/WHO/AF/CDC Committee for the Standardization of Autoantibodies in Rheumatic and Related Diseases.** 2004. Cutting edge diagnostics in rheumatology: the role of patients, clinicians, and laboratory scientists in optimizing the use of autoimmune serology. *Arthritis Rheum* **51:**291–298. PubMed
11. **Meroni PL, Schur PH.** 2010. ANA screening: an old test with new recommendations. *Ann Rheum Dis* **69:**1420–1422. PubMed
12. **Mahler M, Ngo JT, Schulte-Pelkum J, Luettich T, Fritzler MJ.** 2008. Limited reliability of the indirect immunofluorescence technique for the detection of anti-Rib-P antibodies. *Arthritis Res Ther* **10:**R131. PubMed
13. **Fritzler MJ, Wiik A, Fritzler ML, Barr SG.** 2003. The use and abuse of commercial kits used to detect autoantibodies. *Arthritis Res Ther* **5:**192–201. PubMed
14. **Ou Y, Enarson P, Rattner JB, Barr SG, Fritzler MJ.** 2004. The nuclear pore complex protein Tpr is a common autoantigen in sera that demonstrate nuclear envelope staining by indirect immunofluorescence. *Clin Exp Immunol* **136:**379–387. PubMed
15. **Chan EKL, Fritzler MJ (ed).** 2013. Ten years of progress in GW/P body research. Springer, New York, NY. PubMed
16. **Maecker HT, Lindstrom TM, Robinson WH, Utz PJ, Hale M, Boyd SD, Shen-Orr SS, Fathman CG.** 2012. New tools for classification and monitoring of autoimmune diseases. *Nat Rev Rheumatol* **8:**317–328. PubMed
17. **Mahler M, Meroni PL, Bossuyt X, Fritzler MJ.** 2014. Current concepts and future directions for the assessment of autoantibodies to cellular antigens referred to as anti-nuclear antibodies. *J Immunol Res* **2014:**315179. PubMed
18. **Chan-Hui PY, Stephens K, Warnock RA, Singh S.** 2004. Applications of eTag trade mark assay platform to systems biology approaches in molecular oncology and toxicology studies. *Clin Immunol* **111:**162–174. PubMed
19. **Illei GG, Tackey E, Lapteva L, Lipsky PE.** 2004. Biomarkers in systemic lupus erythematosus. I. General overview of biomarkers and their applicability. *Arthritis Rheum* **50:**1709–1720. PubMed
20. **Kantor AB, Wang W, Lin H, Govindarajan H, Anderle M, Perrone A, Becker C.** 2004. Biomarker discovery by comprehensive phenotyping for autoimmune diseases. *Clin Immunol* **111:**186–195. PubMed
21. **Sharp V, Utz PJ.** 2007. Technology insight: can autoantibody profiling improve clinical practice? *Nat Clin Pract Rheumatol* **3:**96–103. PubMed
22. **Robinson WH, DiGennaro C, Hueber W, Haab BB, Kamachi M, Dean EJ, Fournel S, Fong D, Genovese MC, de Vegvar HE, Skriner K, Hirschberg DL, Morris RI, Muller S, Pruijn GJ, van Venrooij WJ, Smolen JS, Brown PO, Steinman L, Utz PJ.** 2002. Autoantigen microarrays for multiplex characterization of autoantibody responses. *Nat Med* **8:**295–301. PubMed
23. **Thiel A, Scheffold A, Radbruch A.** 2004. Antigen-specific cytometry—new tools arrived! *Clin Immunol* **111:**155–161. PubMed
24. **Mahler M, Radice A, Yang W, Bentow C, Seaman A, Bianchi L, Sinico RA.** 2012. Development and performance evaluation of novel chemiluminescence assays for detection of anti-PR3 and anti-MPO antibodies. *Clin Chim Acta* **413:**719–726. PubMed
25. **Fritzler MJ, Conrad K, Meurer M, Sack U, Shoenfeld Y.** 2002. New technologies in the detection of autoantibodies, p 50–63. *In* Conrad K (ed), *Autoantigens, Autoantibodies, Autoimmunity*. Pabst Scientific Publishers, Lengerich, Germany.
26. **Joos TO, Stoll D, Templin MF.** 2002. Miniaturised multiplexed immunoassays. *Curr Opin Chem Biol* **6:**76–80. PubMed
27. **Xue Q, Wainright A, Gangakhedkar S, Gibbons I.** 2001. Multiplexed enzyme assays in capillary electrophoretic single-use microfluidic devices. *Electrophoresis* **22:**4000–4007. PubMed
28. **Templin MF, Stoll D, Bachmann J, Joos TO.** 2004. Protein microarrays and multiplexed sandwich immunoassays: what beats the beads? *Comb Chem High Throughput Screen* **7:**223–229. PubMed

29. **Utz PJ.** 2004. "Hot technologies" for clinical immunology research. *Clin Immunol* **111:**153–154. PubMed
30. **Olsen NJ, Li QZ, Quan J, Wang L, Mutwally A, Karp DR.** 2012. Autoantibody profiling to follow evolution of lupus syndromes. *Arthritis Res Ther* **14:**R174. PubMed
31. **Thibault DL, Chu AD, Graham KL, Balboni I, Lee LY, Kohlmoos C, Landrigan A, Higgins JP, Tibshirani R, Utz PJ.** 2008. IRF9 and STAT1 are required for IgG autoantibody production and B cell expression of TLR7 in mice. *J Clin Invest* **118:**1417–1426. PubMed
32. **Ou Y, Sun D, Sharp GC, Hoch SO.** 1997. Screening of SLE sera using purified recombinant Sm-D1 protein from a baculovirus expression system. *Clin Immunol Immunopathol* **83:**310–317. PubMed
33. **Schulte-Pelkum J, Fritzler M, Mahler M.** 2009. Latest update on the Ro/SS-A autoantibody system. *Autoimmun Rev* **8:**632–637. PubMed
34. **Satoh M, Richards HB, Hamilton KJ, Reeves WH.** 1997. Human anti-nuclear ribonucleoprotein antigen autoimmune sera contain a novel subset of autoantibodies that stabilizes the molecular interaction of U1RNP-C protein with the Sm core proteins. *J Immunol* **158:**5017–5025. PubMed
35. **Burlingame RW, Boey ML, Starkebaum G, Rubin RL.** 1994. The central role of chromatin in autoimmune responses to histones and DNA in systemic lupus erythematosus. *J Clin Invest* **94:**184–192. PubMed
36. **Burlingame RW, Rubin RL.** 1990. Subnucleosome structures as substrates in enzyme-linked immunosorbent assays. *J Immunol Methods* **134:**187–199. PubMed
37. **Kessenbrock K, Raijmakers R, Fritzler MJ, Mahler M.** 2007. Synthetic peptides: the future of patient management in systemic rheumatic diseases? *Curr Med Chem* **14:**2831–2838. PubMed
38. **Elkon K, Skelly S, Parnassa A, Moller W, Danho W, Weissbach H, Brot N.** 1986. Identification and chemical synthesis of a ribosomal protein antigenic determinant in systemic lupus erythematosus. *Proc Natl Acad Sci U S A* **83:**7419–7423. PubMed
39. **Mahler M, Stinton LM, Fritzler MJ.** 2005. Improved serological differentiation between systemic lupus erythematosus and mixed connective tissue disease by use of an SmD3 peptide-based immunoassay. *Clin Diagn Lab Immunol* **12:**107–113. PubMed
40. **Mahler M.** 2011. Sm peptides in differentiation of autoimmune diseases. *Adv Clin Chem* **54:**109–128. PubMed
41. **Schellekens GA, Visser H, de Jong BA, van den Hoogen FH, Hazes JM, Breedveld FC, van Venrooij WJ.** 2000. The diagnostic properties of rheumatoid arthritis antibodies recognizing a cyclic citrullinated peptide. *Arthritis Rheum* **43:**155–163. PubMed
42. **Kato T, Miyakawa H, Ishibashi M.** 2004. Frequency and significance of anti-glutathione S-transferase autoantibody (anti-GST A1-1) in autoimmune hepatitis. *J Autoimmun* **22:**211–216. PubMed
43. **Nozawa K, Fritzler MJ, von Mühlen CA, Chan EKL.** 2004. Giantin is the major Golgi autoantigen in human anti-Golgi complex sera. *Arthritis Res Ther* **6:**R95–R102. PubMed
44. **Qiagen.** 2003. *The QIAexpressionist. A Handbook for High-Level Expression and Purification of 6×His-Tagged Proteins*. Qiagen, Hilden, Germany.
45. **Zhang JY, Casiano CA, Peng XX, Koziol JA, Chan EKL, Tan EM.** 2003. Enhancement of antibody detection in cancer using panel of recombinant tumor-associated antigens. *Cancer Epidemiol Biomarkers Prev* **12:**136–143. PubMed
46. **Fritzler MJ, Miller BJ.** 1995. Detection of autoantibodies to SS-A/Ro by indirect immunofluorescence using a transfected and overexpressed human 60 kD Ro autoantigen in HEp-2 cells. *J Clin Lab Anal* **9:**218–224. PubMed
47. **Keech CL, McCluskey J, Gordon TP.** 1994. Transfection and overexpression of the human 60-kDa Ro/SS-A autoantigen in HEp-2 cells. *Clin Immunol Immunopathol* **73:**146–151. PubMed
48. **Melegari A, Bonaguri C, Russo A, Luisita B, Trenti T, Lippi G.** 2012. A comparative study on the reliability of an automated system for the evaluation of cell-based indirect immunofluorescence. *Autoimmun Rev* **11:**713–716. PubMed
49. **Meheus L, van Venrooij WJ, Wiik A, Charles PJ, Tzioufas AG, Meyer O, Steiner G, Gianola D, Bombardieri S, Union A, De Keyser S, Veys E, De Keyser F.** 1999. Multicenter validation of recombinant, natural and synthetic antigens used in a single multiparameter assay for the detection of specific anti-nuclear autoantibodies in connective tissue disorders. *Clin Exp Rheumatol* **17:**205–214. PubMed
50. **Yang JJ, Kim MH, Lee WI, Kang SY.** 2014. Relevance of indirect immunofluorescence patterns and autoantibodies identified via line immunoassay in patients with rheumatoid arthritis. *Lab Med* **45:**25–31. PubMed
51. **Scussel-Lonzetti L, Joyal F, Raynauld JP, Roussin A, Rich E, Goulet JR, Raymond Y, Senécal JL.** 2002. Predicting mortality in systemic sclerosis: analysis of a cohort of 309 French Canadian patients with emphasis on features at diagnosis as predictive factors for survival. *Medicine (Baltimore)* **81:**154–167. PubMed
52. **Radzimski C, Probst C, Teegen B, Rentzsch K, Blöcker IM, Dähnrich C, Schlumberger W, Stöcker W, Bogdanos DP, Komorowski L.** 2013. Development of a recombinant cell-based indirect immunofluorescence assay for the determination of autoantibodies against soluble liver antigen in autoimmune hepatitis. *Clin Dev Immunol* **2013:**572815. PubMed
53. **Fritzler MJ.** 2012. Toward a new autoantibody diagnostic orthodoxy: understanding the bad, good and indifferent. *Auto Immun Highlights* **3:**51–58. PubMed
54. **Earley MC, Vogt RF Jr, Shapiro HM, Mandy FF, Kellar KL, Bellisario R, Pass KA, Marti GE, Stewart CC, Hannon WH.** 2002. Report from a workshop on multianalyte microsphere assays. *Cytometry* **50:**239–242. PubMed
55. **Gilburd B, Abu-Shakra M, Shoenfeld Y, Giordano A, Bocci EB, delle Monache F, Gerli R.** 2004. Autoantibodies profile in the sera of patients with Sjogren's syndrome: the ANA evaluation—a homogeneous, multiplexed system. *Clin Dev Immunol* **11:**53–56. PubMed
56. **Rouquette AM, Desgruelles C, Laroche P.** 2003. Evaluation of the new multiplexed immunoassay, FIDIS, for simultaneous quantitative determination of antinuclear antibodies and comparison with conventional methods. *Am J Clin Pathol* **120:**676–681. PubMed
57. **Seideman J, Peritt D.** 2002. A novel monoclonal antibody screening method using the Luminex-100 microsphere system. *J Immunol Methods* **267:**165–171. PubMed
58. **Jia XC, Raya R, Zhang L, Foord O, Walker WL, Gallo ML, Haak-Frendscho M, Green LL, Davis CG.** 2004. A novel method of multiplexed competitive antibody binning for the characterization of monoclonal antibodies. *J Immunol Methods* **288:**91–98. PubMed
59. **Lynch HE, Sanchez AM, D'Souza MP, Rountree W, Denny TN, Kalos M, Sempowski GD.** 2014. Development and implementation of a proficiency testing program for Luminex bead-based cytokine assays. *J Immunol Methods* **409:**62–71. PubMed
60. **Selak S, Fritzler MJ.** 2004. Altered neurological function in mice immunized with early endosome antigen 1. *BMC Neurosci* **5:**2. PubMed

61. **Selak S, Mahler M, Miyachi K, Fritzler ML, Fritzler MJ.** 2003. Identification of the B-cell epitopes of the early endosome antigen 1 (EEA1). *Clin Immunol* **109:**154–164. PubMed
62. **Eystathioy T, Chan EKL, Mahler M, Luft LM, Fritzler ML, Fritzler MJ.** 2003. A panel of monoclonal antibodies to cytoplasmic GW bodies and the mRNA binding protein GW182. *Hybrid Hybridomics* **22:**79–86. PubMed
63. **Eystathioy T, Chan EK, Takeuchi K, Mahler M, Luft LM, Zochodne DW, Fritzler MJ.** 2003. Clinical and serological associations of autoantibodies to GW bodies and a novel cytoplasmic autoantigen GW182. *J Mol Med (Berl)* **81:**811–818. PubMed
64. **Miyachi K, Hirano Y, Horigome T, Mimori T, Miyakawa H, Onozuka Y, Shibata M, Hirakata M, Suwa A, Hosaka H, Matsushima S, Komatsu T, Matsushima H, Hankins RW, Fritzler MJ.** 2004. Autoantibodies from primary biliary cirrhosis patients with anti-p95c antibodies bind to recombinant p97/VCP and inhibit in vitro nuclear envelope assembly. *Clin Exp Immunol* **136:**568–573. PubMed
65. **Fritzler MJ, Hanson C, Miller J, Eystathioy T.** 2002. Specificity of autoantibodies to SS-A/Ro on a transfected and overexpressed human 60 kDa Ro autoantigen substrate. *J Clin Lab Anal* **16:**103–108. PubMed
66. **Mahler M, Kessenbrock K, Raats J, Fritzler MJ.** 2004. Technical and clinical evaluation of anti-ribosomal P protein immunoassays. *J Clin Lab Anal* **18:**215–223. PubMed
67. **Mahler M, Kessenbrock K, Raats J, Williams R, Fritzler MJ, Blüthner M.** 2003. Characterization of the human autoimmune response to the major C-terminal epitope of the ribosomal P proteins. *J Mol Med (Berl)* **81:**194–204. PubMed
68. **Mahler M, Fritzler MJ, Blüthner M.** 2005. Identification of a SmD3 epitope with a single symmetrical dimethylation of an arginine residue as a specific target of a subpopulation of anti-Sm antibodies. *Arthritis Res Ther* **7:**R19–R29. PubMed
69. **Gussin HA, Ignat GP, Varga J, Teodorescu M.** 2001. Anti-topoisomerase I (anti-Scl-70) antibodies in patients with systemic lupus erythematosus. *Arthritis Rheum* **44:**376–383. PubMed
70. **Venables PJ.** 1997. Antibodies to Jo-1 and Ro-52: why do they go together? *Clin Exp Immunol* **109:**403–405. PubMed
71. **Bentow C, Swart A, Wu J, Seaman A, Manfredi M, Infantino M, Benucci M, Lakos G, Mahler M.** 2013. Clinical performance evaluation of a novel rapid response chemiluminescent immunoassay for the detection of autoantibodies to extractable nuclear antigens. *Clin Chim Acta* **424:**141–147. PubMed
72. **Mahler M, Radice A, Sinico RA, Damoiseaux J, Seaman A, Buckmelter K, Vizjak A, Buchner C, Binder WL, Fritzler MJ, Cui Z.** 2012. Performance evaluation of a novel chemiluminescence assay for detection of anti-GBM antibodies: an international multicenter study. *Nephrol Dial Transplant* **27:**243–252. PubMed

Immunodiagnosis and Laboratory Assessment of Systemic Lupus Erythematosus

WESTLEY REEVES, SHUHONG HAN, JOHN MASSINI, AND YI LI

89

This chapter deals with immunological tests that are useful in the diagnosis and monitoring of systemic lupus erythematosus (SLE). We review the detection and quantification of antibodies against self-antigens (autoantibodies), measurement of complement levels, and the interferon gene expression signature.

SLE is a multisystem autoimmune disorder characterized by a combination of clinical and immunological features. It is the prototype of human immune complex disease, and the production of autoantibodies that form immune complexes with self-antigens leads to complement fixation and inflammation. Clinical manifestations include characteristic skin rashes, serositis (pleuritis, pericarditis), arthritis, central nervous system involvement, hematological abnormalities, and immune complex-mediated glomerulonephritis. Immunological features include the production of antinuclear or antiphospholipid antibodies, and low levels of certain complement proteins. The detection and clinical use of assays for antinuclear antibodies and antiphospholipid autoantibodies are reviewed elsewhere in this volume and will not be discussed further here. Likewise, general methodology ELISA, multiplex bead assays, and arrays for autoantibody detection are discussed elsewhere.

Antinuclear antibodies (ANA) are associated with systemic autoimmune disease, but also can be seen at low titers in healthy individuals (1). Thus, there has been considerable interest in identifying ANA subsets with higher diagnostic specificity for particular diseases. Autoantibodies specific for SLE, systemic sclerosis (SSc), polymyositis or dermatomyositis (PM/DM), and other systemic autoimmune disorders have been identified and are of considerable importance as diagnostic markers. Some of the more useful autoantibody markers for various diseases are summarized in Tables 1 and 2.

Several autoantibodies are produced uniquely in SLE. Anti-double-stranded DNA (dsDNA) antibodies are found in ~70% of SLE patients' sera at some point during their disease, and are 95% specific. Their levels may vary reciprocally with complement levels, serving as a marker of disease activity. Anti-Sm antibodies are produced by 7 to 25% of lupus patients depending on ethnic origin and, like anti-dsDNA, are virtually pathognomonic of SLE (1, 2). Unlike anti-DNA antibodies, levels of anti-Sm antibodies generally do not correlate with disease activity. Anti-nRNP antibodies, which recognize proteins associated with the Sm antigen, are associated with lupus and mixed connective tissue disease (MCTD) but are not disease specific (1). The frequency of anti-nRNP in SLE is 20 to 40%. All but a few sera containing anti-Sm also contain anti-nRNP autoantibodies. However, anti-nRNP antibodies frequently occur without anti-Sm.

Anti-ribosomal antibodies, which recognize the P0, P1, and P2 antigens are found in 5 to 15% of SLE patients and are associated with neuropsychiatric lupus (3). Anti-proliferating cell nuclear antigen (PCNA) (2 to 5% of patients) and anti-RNA helicase-A autoantibodies (5% of patients) are specific for SLE as well (4, 5). Other lupus-associated (but not disease-specific) autoantibodies include anti-Ro (SS-A) and La (SS-B) autoantibodies, which are associated with Sjogren's syndrome and other autoimmune diseases (SLE, rheumatoid arthritis [RA], PM/DM, and primary biliary cirrhosis), especially when they are accompanied by sicca symptoms. Anti-Ro (SS-A) antibodies are found in 10 to 50% of SLE and in 60 to 80% of primary Sjogren's syndrome sera (1, 6).

A nucleolar pattern on fluorescent antinuclear antibody testing is common in scleroderma (SSc). Nucleolar antigens recognized by SSc-specific autoantibodies include fibrillarin, the To/Th ribonucleoprotein, and RNA polymerases I and III (10 to 20% of patients, Tables 1 and 2) (7). The nucleoplasmic and nucleolar enzyme topoisomerase I (Scl-70) also is an important marker found in ~15% of patients. These autoantibodies are discussed elsewhere in this volume.

Autoantibodies to a set of cytoplasmic antigens, many of which are tRNA synthetases, are diagnostic markers for PM/DM (Tables 1 and 2). The detection and clinical significance of these autoantibodies, which are rare in the absence of myositis, are discussed elsewhere.

DETECTION AND QUANTIFICATION OF AUTOANTIBODIES

Anti-Sm and Anti-RNP Antibodies

In the clinic, anti-Sm and RNP autoantibodies are reliably detected by commercially available ELISA or multiplex bead assays (see chapter 88 of this volume). In a research setting, they can be detected by the radioimmunoprecipitation or luciferase immunoprecipitation methods. Anti-Sm and anti-nRNP antibodies recognize different subsets of the protein components of the U1 small nuclear ribonucleoprotein

doi:10.1128/9781555818722.ch89

TABLE 1 Some non-DNA/chromatin autoantibodies useful in the diagnosis of systemic autoimmune disease

Disease(s)	Autoantibody	Protein component(s)	RNA component(s)
SLE	Sm	B′/B (29/28 kDa), D1/2/3 (16 kDa), E/F/G (12, 11, 10 kDa)	U1, U2, U4–U6, U5
	Ribosomal P	P0, P1, P2 (38, 19, 17 kDa)	Ribosomal RNA
	PCNA	36 kDa	None
MCTD and others	RNP	70K (70 kDa), A (33 kDa), C (23 kDa)	U1
Sicca syndrome	Ro (SS-A)	Ro60 (60 kDa), Ro52 (52 kDa)	HY1, hY3, hY4, hY5
	La (SS-B)	48 kDa	8-2, 7-2, 7SL, 5S, hY1, hY3, hY4, hY5, tRNAs
SLE, MCTD, PM, SSC	Ku	Ku80 (80 kDa); Ku70 (70 kDa)	None
SLE, SSC	RNA pol II	240 (IIO), 220 (IIA), 140 (IIB) kDa	None
PM/DM	Various tRNA synthetases	His (50 kDa), Thr (80 kDa), Ala (110 kDa), Ile (150 kDa), Gly (75 kDa), Leu (130 kDa), Asp (65 kDa)	Corresponding tRNAs
	SRP	72, 68, 54, 19, 14, 9 kDa	7SL
SSc	Topo I	100 kDa	None
	Fibrillarin	34 kDa	U3
	RNA pol I/III	RNAP I: 190 (IA), 126 (IB) kDa; RNAP III: 155 (IIIA), 138 (IIIB) kDa	None
	To/Th	40 kDa (not readily visualized)	7-2, 8-2

(snRNP), an RNA-protein complex consisting of the proteins U1-70K (70 kDa), A (33 kDa), B′/B (29 and 28 kDa, respectively), C (23 kDa), D1/2/3 (16 kDa), E (12 kDa), F (11 kDa), and G (10 kDa). The proteins are associated with a single U1 small nuclear RNA molecule (1, 8). Proteins B′/B, D, E, F, and G assemble into a stable "Sm core particle" reactive with anti-Sm, but not anti-nRNP, antibodies. The Sm core particle is a component of additional snRNPs, each with a unique uridine-rich (U) RNA species as well as unique proteins. These include the U2, U4/U6, and U5 snRNPs, as well as other less abundant U snRNPs. Anti-Sm, but not anti-nRNP, antibodies immunoprecipitate unique 200 to 205 kDa proteins of the U5 snRNP, which are associated with the Sm core particle (Fig. 1).

Clinical Significance

Anti-Sm antibodies are highly specific for the diagnosis of SLE, and their production can predate the onset of clinical SLE (1, 9). They are one of the American College of Rheumatology criteria for the classification of SLE (10). In contrast, anti-nRNP antibodies are not disease-specific and are of limited utility in diagnosing SLE or predicting its course. However, anti-Sm as well as anti-RNP antibodies are strongly associated with the interferon signature (see below), suggesting that they may have a common pathogenesis.

Anti-Ro (SS-A) and Anti-La (SS-B) Antibodies

Sera containing anti-Ro (SS-A) autoantibodies may recognize two proteins: a 60-kDa protein (Ro60) that binds to the stem of four small RNAs designated hY1, hY3, hY4, and hY5 and a 52-kDa protein (Ro52) reactive with many, but not all, anti-Ro (SS-A) sera (1). It is controversial whether or not Ro52 interacts with Ro60 or the Y RNAs. Anti-Ro60 autoantibodies are readily detected by protein immunoprecipitation (Fig. 1). Anti-Ro52 autoantibodies are not efficiently immunoprecipitated and are most reliably detected by ELISA or other solid-phase assays. Commercial assays are widely available for anti-Ro60 and anti-La but are less readily available for anti-Ro52.

La (SS-B) antigen is a 47-kDa protein associated transiently with the precursors of several small RNAs synthesized by RNA polymerase III (1). It can be detected readily by protein immunoprecipitation (Fig. 1), but the band often is distorted because it migrates near the immunoglobulin heavy chain ("heavy chain artifact"). Anti-La (SS-B) autoantibodies are virtually always associated with anti-Ro (SS-A), whereas anti-Ro antibodies frequently are detected in the absence of anti-La (6).

Clinical Significance

Anti-Ro and anti-La antibodies are highly associated with sicca symptoms (xerostomia, keratoconjunctivitis sicca). Anti-La (SS-B) autoantibodies are produced by 10 to 20% of SLE patients, and at a somewhat higher frequency in Sjogren's syndrome. Additionally, anti-Ro/La antibodies are strongly associated with subacute cutaneous lupus.

In neonates, cardiac conduction abnormalities, including complete heart block, are caused by maternal antibody against the Ro (especially Ro52) and La antigens (11). Screening for these autoantibodies is important in pregnant women with systemic autoimmune disease. Since they may be present in asymptomatic individuals, screening also is carried out in mothers of children with congenital cardiac conduction abnormalities.

TABLE 2 Prevalence of some non-DNA/chromatin autoantibodies by disease

Autoantibody to:	Prevalence in disease subset (%)			
	SLE (n = 288)	Sjogren's (n = 50)	PM/DM (n = 30)	Scleroderma (n = 42)
Sm	10	0	0	0
RNP	39	6	0	12
Ribosomal P	2	0	0	0
PCNA	0.3	0	0	0
Ro60 (SS-A)	33	58	13	12
Ro52[a]	28	36	49	15
La (SS-B)	11	28	7	0
Jo-1[b]	1	ND[c]	22	0
Alanyl tRNA synthetase[b]	0	ND	6	ND
Ku	2	0	0	2
RNA polymerase I/III	0	0	0	21
RNA polymerase II	5	2	0	7
Scl-70 (Topo I)	0.3	0	0	7

[a]Recombinant antigen ELISA (SLE, n = 265; Sjogren's, n = 50; PM/DM, n = 35; scleroderma, n = 40).
[b]Recombinant antigen ELISA (SLE, n = 74; PM/DM, n = 51; scleroderma, n = 36).
[c]ND, not done.

Anti-Ribosomal P

Anti-ribosomal P antibodies recognize three proteins of ~38, 19, and 17 kDa (P0, P1, and P2) that are components of the large (60S) ribosomal subunit (Fig. 1). They recognize mainly a conserved epitope on the C-terminal 22 amino acids of P0, P1, and P2. Antibodies to the ribosomal P0, P1, and P2 antigens are highly specific for the diagnosis of SLE and have been linked with neuropsychiatric lupus, especially psychosis (3, 12). Immunoprecipitation is probably the gold standard test for this specificity, but commercial ELISA and immunoblotting assays also are reliable.

Anti-Proliferating Cell Nuclear Antigen (PCNA) and Anti-RNA Helicase A Autoantibodies

PCNA is a 36-kDa protein recognized by autoantibodies found in about 2 to 5% of SLE sera (4). Although unusual, these antibodies are quite specific for SLE. Immunoprecipitation is probably the most reliable way to detect them (Fig. 1). Autoantibodies to RNA helicase A are produced mainly by non-black SLE patients (3 to 7.5% of patients) (5). They are highly specific for SLE and are more common early in disease. The antigen is a 140-kDa member of the DExD/H box family that can be detected by immunoprecipitation (Fig. 1). Commercial assays are not widely available for either anti-PCNA or anti-RNA helicase A.

Method: Radioimmunoprecipitation

The protein and nucleic acid constituents of many lupus autoantigens were identified and characterized by radioimmunoprecipitation, and this technique remains useful for the analysis of autoantibodies in a research laboratory setting. Radiolabeled antigens are allowed to form immune complexes with autoantibodies and are purified onto protein A-Sepharose beads. After dissociating the immune complexes from the beads, the radiolabeled proteins are separated by sodium dodecyl sulfate (SDS)-polyacrylamide gel electrophoresis and detected by autoradiography (Fig. 1). A similar approach can be used to analyze the RNA components of small ribonucleoprotein particles (8). Required apparatus includes an electrophoresis power supply, vertical electrophoresis apparatus, tabletop centrifuge, CO_2 incubator, cell sonicator, and microcentrifuge.

Materials and Reagents

Phenylmethylsufonyl fluoride (PMSF, Sigma no. P7626), 50 mM in absolute ethanol stored at −20°C (= 100× stock)

Aprotinin (Sigma no. A6279), 24 TIU in H_2O (= 100× stock)

Protein A-Sepharose CL4B (PAS, Pharmacia no. 17-0780-01). Prepare the PAS as follows:

1. Add H_2O to 1.5 g of dry PAS in a 15-ml centrifuge tube and incubate with inversion for 20 to 30 min at room temperature to swell the beads.
2. Centrifuge for 1 min (1,500 rpm).
3. Wash three times with H_2O and centrifuge to pellet the beads.
4. To the packed beads, add an equal volume of H_2O. Add 2 M Tris-HCl (pH 8.0) to a final concentration of 20 mM (1:100). Add NaN_3 to a final concentration of 0.1%. The beads can be stored at 4°C in this buffer.

0.5 M NaCl NET/Nonidet P-40 (NP-40) buffer: 50 mM Tris-HCl (pH 7.5), 0.5 M NaCl, 2 mM EDTA, 0.3% NP-40

NET buffer: 50 mM Tris-HCl (pH 7.5), 0.15 M NaCl, 2 mM EDTA

3× sample buffer: mix 0.5 M Tris-HCl, pH 6.8 (6.0 ml), 1% bromophenol blue (0.6 ml), 2-mercaptoethanol (3.0 ml), 25% SDS (4.8 ml), glycerol (6.0 ml); store at −20°C until used.

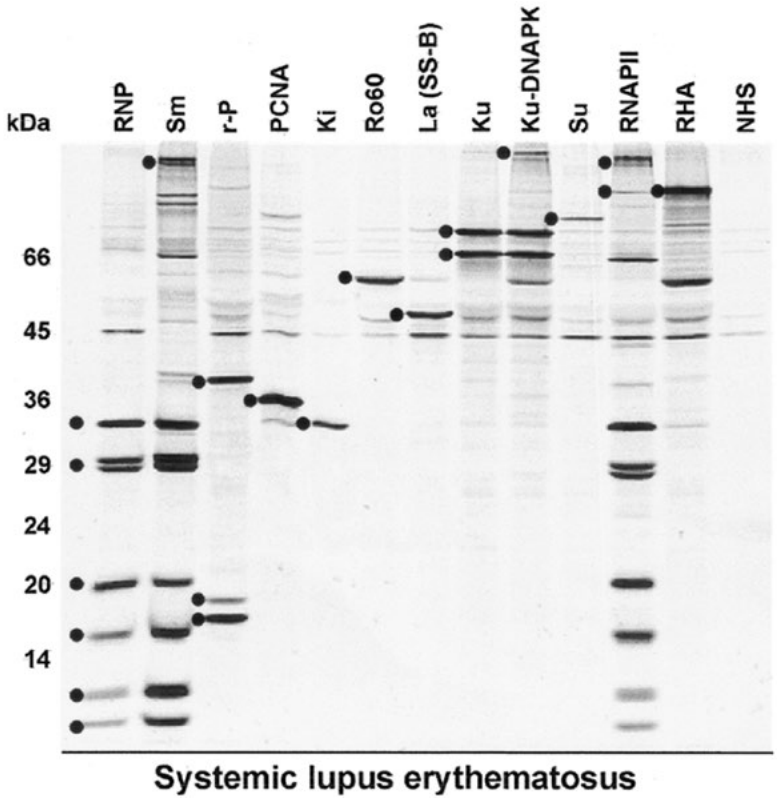

FIGURE 1 Protein immunoprecipitation for analyzing lupus autoantibodies. Sera were tested according to the protocol in the text, and immunoprecipitated proteins were resolved on a 12.5% gel. Sera containing the following autoantibodies were tested: anti-nRNP (RNP), anti-Sm, anti-ribosomal P (r-P), anti-proliferating cell nuclear antigen (PCNA), anti-Ki, anti-Ro60, anti-La (SS-B), anti-Ku, anti-Ku plus anti-DNA-PKcs, anti-Su, anti-RNA polymerase II (RNAPII), anti-RNA helicase A (RHA), and normal human serum (NHS). Positions of molecular weight standards are shown on the left (in kilodaltons). Protein components of the antigens are indicated (dots).

Sterile Dulbecco's phosphate-buffered saline (D-PBS)

D-PBS dialyzed fetal bovine serum: 50 ml fetal bovine serum is dialyzed for 3 days at 4°C against D-PBS (500 ml). Change the D-PBS twice daily.

[^{35}S]-Methionine/cysteine (DuPont/New England Nuclear NEG 072). Upon receipt, the isotope should be snap-frozen in small aliquots sufficient for one labeling reaction and stored at −80°C.

Methionine- and cysteine-free RPM1-1640 (Cellgro, Fisher no. 17-104-CI)

Penicillin (10,000 IU/ml)-streptomycin (10,000 μg/ml) (= 100× Pen-Strep, Gibco BRL no. 15140-031)

L-Glutamine, 200 mM (= 100×, Gibco BRL no. 25030-081)

[^{35}S]-Labeling medium is prepared as follows: 39 ml methionine- and cysteine-free medium, 4.5 ml D-PBS-dialyzed fetal bovine serum, 0.45 ml L-glutamine, 45 μl penicillin-streptomycin, 1.35 ml regular RPMI (for 10^8 cells).

Assay

Radiolabeled cell extract is prepared from log-phase K562 cells (ATCC no. CCL-243) grown at a density of 0.5 to 1.5 × 10^6/ml in RPMI 1640 plus L-glutamine (1:100), penicillin-streptomycin (1:100), and 10% fetal bovine serum in 750-ml tissue culture flasks at 37°C in a 5% CO_2 atmosphere. Rapidly growing cells are labeled more efficiently than slowly growing ones. *Note: K562 cells grow in small nonadherent or weakly adherent clusters when healthy.*

The night before use, collect the cells by centrifugation (1,000 rpm for 5 min), resuspend in 20 ml sterile D-PBS, and count. Cells should be adjusted to 10^8 cells per 45 ml of ^{35}S-labeling medium (recipe above) in a 250-ml flask. Add 2 mCi freshly thawed [^{35}S]methionine-cysteine and incubate the cells for 12 to 16 h at 37°C in a 5% CO_2 atmosphere. The following day, the cells are collected by centrifugation (1,000 rpm, 5 min). *Note: the level of RNA polymerase II antigen decreases after 16 h, so it is important not to label for too long.* After labeling, there should be ~1.8 × 10^8 cells. Collect by centrifugation. Make aliquots of 2 × 10^7 cells in 15-ml polypropylene centrifuge tubes. Centrifuge 5 min at 1,500 rpm and aspirate the supernatant. Freeze tubes with their cell pellets at −70°C. *Note: be sure to use polypropylene centrifuge tubes (e.g., Corning no. 430052) so they will not crack when frozen.*

Immunoprecipitation is carried out using serum that has been centrifuged (10,000 rpm for 5 min) to remove insoluble materials. Frozen serum samples (−20°C) should be recentrifuged before analysis. The procedure is as follows: in a 1.5-ml microfuge tube combine the following: 40 μl 50% PAS slurry in Tris-HCl (pH 8.0), 8 μl human serum, 500 μl 0.5 M NaCl NET/NP-40. The tube is rotated end-over-end at 4°C for 1 to 12 h or at room temperature for 1 to 3 h. *Avoid vortexing the beads at any stage of the procedure.* During incubation, prepare cell extract from radiolabeled K562 cells (see above, 2 × 10^6 radiolabeled cells per sample). Add 2 ml of 0.5 M NaCl NET/NP-40 + 1:100 (20 μl)

PMSF + 1:100 (20 μl) aprotinin to the pellet (final cell concentration, 10^7/ml). *Do not put PMSF directly on the cell pellet because the ethanol will denature the proteins.* Sonicate the cells for 1 min (duty cycle 30%, output 3). Place on ice for 1 min and then sonicate again for 1 min. *Avoid excessive heating of the cell suspension during sonication.* Transfer cell lysate to microfuge tubes and centrifuge at 10,000 rpm for 30 min. (4°C). Carefully collect the lysate and combine into one tube before dispensing. Extract from 2×10^7 cells is sufficient for 12 immunoprecipitations.

Pellet the serum-coated PAS beads by microfuging for 3 s. Aspirate the supernatant using a drawn-out Pasteur pipette attached to vacuum. Add 1 ml 0.5 M NaCl NET/NP-40 and microfuge for 3 s. Aspirate the supernatant. *Carefully remove any air bubbles on the surface of the samples first, since they may cause high background.* To each PAS pellet, add 150 to 160 μl of cell extract. Rotate end-over-end for 1 h at 4°C. Microfuge for 3 s and aspirate the supernatant. Wash beads three times with 1 ml 0.5 M NaCl NET/NP-40 and once more with NET. Carefully aspirate the supernatant. Add 50 μl 1× sample buffer to each pellet. Samples may be kept at −80°C for at least 1 month (half-life of ^{35}S is ~60 days). To analyze, boil the samples for 3 min, pellet the beads, and load 15 to 20 μl supernatant per lane of a 12.5% SDS-polyacrylamide gel. For large proteins (>100 kDa), resolution may be enhanced using a 10% or 8% gel. It usually takes 3 to 5 h for the tracking dye to reach the bottom of the gel at a constant voltage of 100 to 130 V. *Note: If performing immunoprecipitations with antibodies that do not bind protein A (e.g., human IgG3 or mouse IgG1), use protein G-Sepharose.*

Immunoprecipitated proteins are analyzed by SDS-polyacrylamide gel electrophoresis and fluorography. Reagents are as follows: 25% SDS (Fisher or BioRad) *[Note: filter this and all other stock solutions through a 0.45-μm bottle top filter]:*

Coomassie blue stain: Coomassie Brilliant Blue, R-250 (BioRad no. 161-0400) (5 g), methanol (1,200 ml), glacial acetic acid (400 ml); add distilled water to 4,000 ml

Destaining solution: 2 liters of glacial acetic acid, 7 liters of methanol, 11 liters of distilled water

2, 5 Diphenyloxazole (PPO) (Fisher no. D144-100), 20% (wt/vol) in dimethylsulfoxide (DMSO). *Note: PPO is carcinogenic.*

Glycerol

BioMax MR film (Eastman Kodak, catalog no. 870-1302)

5× Tris-glycine (for running buffer): 120 g Tris base plus 576 g glycine; add distilled water to 4 liters (no need to adjust pH, can be stored at room temperature).

Polyacrylamide minigels can be prepared "from scratch," or precast gels can be purchased from BioRad or other vendors. Run the gel as follows:

1. Make 1 liter of running buffer: 200 ml 5× Tris-glycine + distilled water to 1,000 ml; add 4 ml of 25% SDS and mix well.
2. Boil samples including molecular weight standards for 3 min in a water bath immediately before loading gel.
3. Carefully remove the comb and bottom spacer from the SDS-polyacrylamide gel.
4. Clamp gel to the gel apparatus and add running buffer to the top and bottom chambers to cover the top and bottom of the gel.
5. Remove air bubbles from the bottom of the gel using a syringe with a bent (90°) 18-gauge needle.
6. Gently wash out wells with running buffer using a Hamilton syringe.
7. Add 20 μl (or desired volume) of boiled sample per well.
8. Attach leads to the electrodes of the gel apparatus (proteins treated with SDS are negatively charged and will migrate toward the cathode).
9. Attach to power supply and run at 100 V until the blue tracking dye reaches the resolving gel. At this time, the voltage may be increased to 120 V.
10. Run the gel until the blue tracking dye reaches the bottom of the gel (do not run the dye off the gel).
11. Turn off the power, remove the electrodes, and unclamp the gel from the gel apparatus. Carefully pry the plates apart, leaving the gel adherent to one of the plates. Using a pizza cutter, cut off the stacking gel and diagonally cut off a small piece of the gel from the upper right hand corner to aid in orienting the gel.
12. Stain the gel for 20 min with Coomassie Blue solution. Destain and fix the gel with several changes of destaining solution.

After staining and fixation, the gel is fluorographed as follows:

1. Place the gel in a polyethylene or polypropylene (not polystyrene) container and remove as much of the destaining solution as possible. Immerse the gel in 100 to 200 ml of DMSO, cover the container, and rotate gently on a shaker for 30 min. Discard DMSO.
2. Transfer to 100 to 200 ml fresh DMSO, cover, and rotate for 30 min. After use, this DMSO solution is removed and can be saved for use as the first DMSO wash for another gel.
3. Add 100 to 200 ml of 20% PPO in DMSO (wt/vol), cover, and rotate gently for 60 min. Save the DMSO-PPO mixture. It can be reused for several gels, although the effectiveness gradually diminishes. *Note: PPO is a carcinogen and DMSO can penetrate standard laboratory gloves. Wear heavy rubber gloves (e.g., Playtex) and handle DMSO-PPO solution carefully.*
4. Wash the gel with several changes of water to rehydrate (at least 30 min). The PPO will precipitate in the gel. Add glycerol to the final wash to a concentration of ~3%. Remove the gel, which will have turned white and opaque, place on 3MM paper (Whatman), and dry using a vacuum gel dryer. Wash out the tray with ethanol to remove traces of PPO (which is insoluble in water). We use a BioRad gel dryer (model no. 583) at 60°C with the timer set to 3 h. After 1.5 h, the gel is removed. Vent the gel dryer and remove the gel and attached 3MM paper.
5. Tape dried gels to a used piece of X-ray film. If it is sticky, dust the gel lightly with talc to prevent sticking. Place this in a cassette and (in the darkroom) place in direct contact with BioMax MR film. *The film is coated on one side and the coated side must contact the gel.* Expose the gel to film for 3+ days at −70°C before developing.

QA/QC and Test Validation

Include a sample of normal human serum as a negative control and, if possible, a positive-control serum (reference serum). Expression of individual antigens may vary depending on the cell line used. Multiple weak bands using normal human serum may indicate problems with washing. Molecular weight standards (Sigma, catalog no. SDS-7 [low molecular

weight] or SDS-6H [high molecular weight]) also are run on the gel and stained with Coomassie blue. Migration of molecular weight standards and immunoglobulin heavy and light chains (~50 and 25 kDa, respectively) can be used to assess the quality of separation.

Radioimmunoprecipitation is a highly sensitive and specific technique for detecting a variety of autoantibodies. However, clinical application of this approach is limited because it is labor intensive, technically demanding, and requires the use of radioisotopes. Nevertheless, the immunoprecipitation technique is extremely useful for validating other assays, such as ELISAs.

Method: LIPS Assay for Anti-RNP

The luciferase immunoprecipitation system (LIPS) assay is a sensitive, nonradioactive variation on the immunoprecipitation method (13). A fusion protein comprised of a *Renilla* luciferase reporter and the test antigen is produced in mammalian cell culture, ensuring the addition of mammalian posttranslational modifications. Test serum is mixed with fusion protein and passed over immobilized protein A/G-agarose beads. After washing, the only luciferase-tagged antigens retained are those bound by specific antibodies, which can be quantified using chemiluminescence upon the introduction of coelenterazine. Due to the liquid-phase nature of the LIPS assay and the highly linear light output of the luciferase reporter, some antibodies can be detected over a dynamic range of 7 orders of magnitude. The protocol below for anti-U1A (RNP) autoantibodies can be adapted to detect other specificities.

Generation of *Renilla* Luciferase U1A (Ruc-U1A) Fusion Construct

A pET-28a(+) plasmid containing the human U1A cDNA sequence was ligated into *Bam*HI-Hind III-cut mammalian *Renilla* luciferase expression vector pREN2 and transformed into One Shot Top10 *E. Coli* (Invitrogen, catalog no. C4040-10). The pREN2-U1A plasmid was purified from bacterial lysates using a Qiagen Max kit and the integrity of the DNA construct was verified by sequencing.

Preparation of Antigen

Materials are as follows:

Buffer A: 20 mM Tris (pH 7.5), 150 mM NaCl, 5 mM $MgCl_2$, 1% Triton X-100

Sterile PBS

DMEM + 10% fetal bovine serum

Renilla luciferase assay system (Promega, catalog no. E2810)

96-well Multi Screen HTS filter plate (EMD Millipore, catalog no. MAFB N0B)

Protein A/G agarose beads (Santa Cruz Biotech, catalog no. SC-2003)

LUMIstar Omega plate reader (BMG Labtech)

Berthold Lumat LB9507

Lipofectamine 2000 (Invitrogen, catalog no. 11668)

Multi Screen HTS vacuum manifold (EMD Millipore).

Ruc-U1A fusion protein extracts are prepared as follows: one day before transfection, plate 2 to 6×10^6 293T cells in 15 ml of DMEM/10% FBS without antibiotics in a 100 mm dish. Allow the cells to become 90 to 95% confluent before transfecting.

Prepare Ruc-U1A plasmid DNA and Lipofectamine 2000 complex as follows: dilute 24 μg of DNA in 1.5 ml of serum-free DMEM. Mix Lipofectamine gently and dilute 60 μl into 1.5 ml of serum-free DMEM. Incubate for 5 min at room temperature and combine with the diluted DNA. Mix gently and incubate for 20 min at room temperature. Complexes are stable for 6 h. Add the complex drop by drop to the cells and gently rock the dish back and forth. Incubate cells at 37°C in a CO_2 incubator for 48 h. Remove the supernatant, add 1 ml of 1× *Renilla* luciferase assay lysis buffer, and incubate for 15 min on a rotary shaker at room temperature. Collect cell lysate into a 15 ml tube and sonicate for 15 s three times. Transfer the cell lysate into a 1.5-ml microfuge tube and centrifuge at maximum speed for 15 min at 4°C. Collect the cleared cell lysate and measure *Renilla* Luminometer Units (RUC) with a Berthold Lumat LB9507: 0.1 μl cell lysate should give ~5×10^7 RUC. Aliquot the Ruc-U1A extract and store at −80°C.

Determine the Appropriate Amount of Extract for Assay

Select a reference serum with high-titer anti-U1A antibodies and a normal control serum. In each well of a 96-well microtiter plate, add 50 μl of diluted Ruc-U1A fusion extract (0.1 μl Ruc-U1A fusion extract + 49.9 μl PBS) and 50 μl of serially diluted serum (2-fold dilutions from 1:500 to 1:64,000 in PBS/0.5% bovine serum albumin [BSA]). Incubate duplicate samples at 4°C overnight on a rotary shaker. Prepare a 96-well filter plate and add 10 μl of protein A/G beads (50% vol/vol in PBS). Transfer extract-serum mixture to the filter plate. Incubate for 2 h at 4°C on a rotary shaker, then attach filter plate to the MultiScreen HTS vacuum manifold. Protein A/G beads are washed under suction eight times with buffer A. Dry bottom of the plate and add 20 μl PBS. *Renilla* luciferase substrate is added and luciferase activity is measured in the LUMIstar Omega plate reader. The amount of cell extract can be varied to optimize signal-to-noise ratio at low serum concentrations. Once the assay is optimized, unknowns, reference sera, and normal control sera can be tested as above.

Anti-DNA Antibodies

Genomic DNA is packaged in histone and non-histone chromatin proteins. The histones form nucleosomes, consisting of two molecules each of H2A/H2B, H3, and H4, around which the DNA is coiled (145 base pairs per nucleosome). Between the nucleosomes is "linker" DNA, which is packaged in histone H1. Many lupus patients produce autoantibodies against nucleosomes, which recognize DNA-histones, H2A-H2B dimer, individual histones, single-stranded (ss) DNA, and double-stranded (ds) DNA. Anti-dsDNA antibodies are highly specific for the diagnosis of SLE (1, 14), whereas anti-ssDNA and anti-chromatin autoantibodies are not. The latter may be seen in drug-induced lupus and other systemic autoimmune diseases in addition to SLE. Anti-dsDNA antibodies have been implicated in the pathogenesis of lupus nephritis, and in some patients, their levels correlate with disease activity. Thus, assays for anti-dsDNA antibodies are more important clinically than anti-ssDNA assays. Anti-dsDNA antibodies are not reliably detected by immunoprecipitation. The most commonly used anti-dsDNA assays are ELISA, *Crithidia luciliae* kinetoplast staining assay, and radioimmunoassay (Farr assay). In anti-dsDNA antibody ELISAs and the Farr assay, it is important to treat the DNA with S1 nuclease to ensure the removal of contaminating ssDNA. This is unnecessary in the *Crithidia* assay, since the dsDNA substrate (the kinetoplast) is a closed circular DNA molecule packaged in histones. *Crithidia luciliae* organisms are fixed onto

microscope slides and incubated sequentially with serially diluted (1:10 to 1:160) patient serum followed by fluorescein isothiocyanate-conjugated goat anti-human immunoglobulin antibodies. A titer is determined as is done for the fluorescent ANA assay.

About 70% of SLE patients develop anti-dsDNA antibodies at some time in their disease. Although the clinical utility is somewhat controversial, anti-dsDNA antibody levels and complement component C3 and C4 levels vary reciprocally in some patients, with high anti-dsDNA and low C3 and C4 during flare-ups of disease activity (15). The affinity of anti-dsDNA antibodies may be important, and it has been suggested that the Farr assay (which measures only high-affinity antibodies) may be the assay most predictive of disease activity (15). Anti-dsDNA antibody levels may increase 10 or more weeks before a flare, and some would institute corticosteroid therapy at that time, although this remains controversial (16). The ELISA detects low-, intermediate-, and high-affinity anti-dsDNA antibodies, whereas the *Crithidia* assay detects moderate- and high-affinity anti-DNA antibodies. The Farr and *Crithidia* assays are relatively labor intensive and the Farr assay uses a radioisotope (^3H) to label the target DNA, although kits are available commercially. Most commercial laboratories employ either the ELISA or the *Crithidia* assay. We have developed an ELISA suitable for use in a research setting that correlates well with the *Crithidia* assay.

Method: Anti-dsDNA ELISA

The presence of anti-dsDNA antibodies using the following ELISA protocol generally correlates well with positivity by the *Crithidia* assay. We use this assay in a research setting. The following materials and reagents are used:

Reacti-Bind DNA coating solution (Pierce, catalog no. 17250)

S1 nuclease 100 U/μl (Promega, store at −20°C)

Calf thymus DNA (Sigma-Aldrich, catalog no. D-4522)

Alkaline phosphatase-conjugated goat anti-human IgG (Southern Biotechnology, catalog no. 2040-04)

TBS/Tween-20: 150 mM NaCl, 20 mM Tris (pH 7.5), 0.1% Tween-20 NET- NP-40: 150 mM NaCl, 2 mM EDTA, 50 mM Tris-HCl (pH 7.5), 0.3% Nonidet P-40

Diethanolamine buffer, pH 9.6: dissolve 97 ml diethanolamine, 0.1 g $MgCl_2 \cdot 6H_20$, and 0.2 g NaN_3 into ~900 ml dH_2O, and adjust pH to 9.6 with HCl. Adjust volume to 1 liter and filter. For ELISA substrate, dissolve one 5-mg phosphatase substrate (Sigma-Aldrich, catalog no. S-0942) in 5 ml diethanolamine buffer

96-Well flat-bottom Reacti-Bind plates (Pierce) or NUNC Immobilizer amino F96 plates.

Preparation of dsDNA

Carefully dissolve the DNA in sterile PBS. Mix by gentle pipetting (final concentration 0.5 mg/mL). Dialyze against 0.03 M sodium acetate, 0.1 M NaCl, 1 mM ZnCl, pH 4.4 at 4°C. Change buffer twice daily for 3 days then transfer the DNA into a 50-ml conical tube. Centrifuge at 3,000 rpm for 10 min to remove aggregates. Transfer supernatant into a clean tube and measure the optical density (A_{260}) of a small aliquot (1:200 in water). Add S1 nuclease to a final concentration of 0.1 U/μg of DNA and incubate for 3 h at 37°C in a water bath. After digestion, dialyze the DNA solution against PBS (3 days, change buffer twice daily). Centrifuge as before and determine A_{260} for calculating the final DNA concentration.

Assay

1. Coating of plates: adjust DNA to 6 μg/ml in distilled water, then dilute 1:2 with Reacti-Bind DNA coating solution in a glass tube (DNA/Reacti-Bind will stick to anything plastic). Final DNA concentration is 3 μg/ml. Mix gently on a shaker for 10 min. Dispense 100 μl/well of a 96-well microtiter plate. Incubate overnight at 4°C in the dark.
2. Wash the wells three times with TBS-Tween-20 and block for 3 h (150 μl/well NET/ NP-40, 0.5% BSA, 0.05% NaN_3).
3. Add diluted serum (100 μl/well, 2 h at room temperature protected from light). We use 1:500 patient serum in blocking buffer. To generate a standard curve, use high-titer anti-dsDNA serum at serial 5-fold dilutions (1:100 to 1:1,562,500 in blocking buffer). Wash three times with TBS-Tween-20.
4. Add second antibody (alkaline phosphatase-conjugated goat anti-human IgG, 1:1,000 in blocking buffer, 100 μl/well, 1 h at room temperature). Wash as before.
5. Add alkaline phosphatase substrate (100 μl/well) and measure OD_{405} nm 30 to 60 min afterward using an automated ELISA reader (e.g., VERSAmax, Molecular Devices). A standard curve is generated using serially diluted anti-dsDNA reference serum, and anti-DNA antibody levels (units) are calculated using a four-parameter logistic equation as part of the Softmax Pro 3.0 ELISA plate reader software. We use a group of 10 normal control serum samples to determine the cutoff for positive (mean + 2 SD).

EVALUATION OF COMPLEMENT IN SLE

The complement system links innate immunity to adaptive immunity. Complement can lyse cells via the pore-forming membrane attack complex (MAC), enhance phagocytosis through opsonization, and facilitate clearance of immune complexes and apoptotic cells by complement receptors on red blood cells and in the spleen (17, 18). Certain complement split products, such as C3a and C5a, act as chemoattractants for neutrophils and other phagocytes. There are three main pathways of complement activation: the classical, alternative, and lectin pathways. Most relevant to SLE is the classical pathway, in which C1q binds the Fc portion of membrane-bound IgM or IgG, leading to binding of C1r and C1s. Activated C1 cleaves C4 into C4a and C4b and cleaves C2 into C2a and C2b, forming C4b2a, the C3 convertase of the classical pathway. Cleavage of C5 initiates formation of the MAC (C5b-C9) and promotes inflammation (C5a). The role of late complement components and the MAC to lupus pathogenesis is unclear.

Importance of the Early Classical Complement Pathway in SLE

The early classical complement pathway plays a key role in immune complex clearance, and hereditary defects in C1, C2, C3, and C4 are associated with a substantially increased risk of SLE (18). Patients with homozygous C1q deficiency have approximately a 90% likelihood of developing lupus; those with C1r, C1s, or C4 deficiency have a ~75% risk; and those with homozygous C2 deficiency have a 10 to 30% risk. Interestingly, the female predominance in SLE is not seen in lupus-like disease associated with complement deficiency (18). Hereditary complement deficiencies are complex and have been reviewed recently (19). C4 deficiency is the most common hereditary complement deficiency in SLE. C4 is

encoded by two different but highly homologous genes: C4A and C4B, each of which exhibits copy number variation. Their products are indistinguishable using standard C4 assays. Complete C4A deficiency requires the absence of all copies of C4A/B and is very rare. Partial C4 deficiency (most commonly, C4A) is seen in ~10% of white SLE patients versus ~2% of controls (18).

Elevated levels of immune complexes in SLE also result in consumption of the early classical complement components with deposition of C4b and C3b in tissues, release of C3a/C5a, and MAC formation (18). Measurement of the early classical complement components can provide a measure of immune complex generation and disease activity. The total hemolytic complement (CH_{50}), a functional measure of the entire classical pathway, should be determined at least once in most SLE patients, as a defect in any of the individual components will be reflected in a low CH_{50}.

Assays of Complement Function

(More detailed descriptions of the complement assays [CH50 and assays for individual complement components] can be found in chapter 13 of this volume). The CH_{50} is used to assess integrity of the classical complement cascade (C1 to C9). Sheep erythrocytes are coated with rabbit anti-sheep erythrocyte antibodies (EA). Patient serum is added, leading to binding and activation of the C1 complex. This activates C3, leading ultimately to assembly of the membrane attack complex and erythrocyte lysis. The reciprocal of the serum dilution necessary to lyse 50% of the EA in the assay is defined as the CH_{50} (expressed as CH_{50} U per ml of serum). Reagents for performing this test are available commercially. The classical and lectin pathways are calcium ion dependent, whereas the alternative pathway is not. If the lysis of unsensitized rabbit erythrocytes is measured in the presence of ethylene glycol tetraacetic acid (EGTA) to chelate the calcium (with addition of Mg^{2+}), activation of the alternative and lectin pathways can be measured (AH_{50}). The CH_{50} and AH_{50} can be used to screen for hereditary complement deficiency (19). An absent or very low CH_{50} with a normal AH_{50} implies deficiency of C1q, C1r, C1s, C2, or C4. Subsequent testing should include assays for individual complement components.

Levels of Individual Complement Components

If a single component remains persistently low, a hereditary complement deficiency is likely (the exception being deficiency of a regulatory protein, such as C1-Inh). Immunoassays for measuring serum levels of complement components C1 to C9 are available. They measure component levels, but not function. Nephelometry, radial immunodiffusion, radioimmunoassay, and ELISA are the most common methodologies. Nephelometry is most commonly used to measure C3 and C4 levels, as these components are present in high concentrations in serum. Radial immunodiffusion and ELISA are used for components that are present at lower concentrations. Specificity of the antibodies used to measure complement components is critical for obtaining reliable results. Since certain complement components are acute-phase reactants produced in response to inflammation, it can be useful to measure complement split products as a measure of complement activation.

Testing for Activation Products

Complement deficiencies can be recognized by the presence of depressed individual component levels without increased complement breakdown/activation products. C3a, C3d, C4a, and C5a are measured using enzyme immunoassays or nephelometry. The main drawback is the short half-lives of most activation products. These assays are best performed on EDTA-anticoagulated plasma, which avoids generation of complement activation products *in vitro*. C3a has a half-life of 30 min, which limits its usefulness in clinical settings. C3dg has a half-life of 4 h but the assay is not widely available. C3dg is generated constitutively at a low level, so comparison with C3 (C3dg/C3) makes the measurement more informative. Complement activation products are present in low concentrations, making ELISA the most practical method for detecting them.

Lab Collection Techniques

Complement components are labile and spontaneously degrade, an important consideration when obtaining functional assays, such as the CH_{50}. The sample must be placed immediately on ice and brought to the lab immediately. Samples must be centrifuged within 30 min and frozen within 1 h. Sample collection is less critical in the case of immunoassays, which detect the protein (e.g., C3, C4) but are independent of function.

Monitoring Complement Activation in SLE

Although the CH_{50} is probably the best clinical test for monitoring complement activation in SLE, immunoassays for C3 and C4 are more practical in view of the difficulty of assuring proper handling of CH_{50} samples. There is not a consensus on the utility of monitoring complement levels in SLE, and hypocomplementemia is not one of the classification criteria for SLE. Nevertheless, many feel that low CH_{50}, C3, and/or C4 levels are a worthwhile measure of complement activation that may correlate with or precede increased activity of lupus nephritis or other manifestations. Active SLE also may be associated with high levels of the breakdown products C3d and C3dg.

Acquired Complement Component Deficiency in SLE

Acquired complement deficiency in SLE may be due to autoantibody production. Hypocomplementemic urticarial vasculitis (HUVS), a disorder caused by autoantibodies against C1q, is the best example (20). Autoantibodies against collagen-like region of C1q may be seen in up to 30% of SLE patients, though most patients do not develop HUVS. Clinically, HUVS is characterized by a leukocytoclastic cutaneous vasculitis (chronic urticaria lasting >24 h that resolves leaving hyperpigmented plaques) and activation of the classical complement pathway. Additional manifestations include glomerulonephritis, arthralgias, uveitis, and a severe form of chronic obstructive lung disease. HUVS can be suspected on clinical grounds, and diagnosis is based on skin biopsy and depressed C1q, C3, and C4 levels and CH_{50} with elevated activation products such as C3d. The detection of serum anti-C1q autoantibodies confirms the diagnosis.

MEASURING THE TYPE I INTERFERON GENE EXPRESSION SIGNATURE IN SLE

Type I interferons (IFN-I) include IFNα and IFNβ, which are produced by leukocytes, fibroblasts, and plasmacytoid dendritic cells. Their binding to the Type I interferon receptor leads to increased expression of 100 or so interferon-stimulated genes (ISGs). About 20 of these are involved in antiviral responses, and increased expression of these genes

in peripheral blood mononuclear cells is seen in SLE patients (21, 22). This "interferon signature," present in about two-thirds of adults and nearly all children with SLE, is associated with renal involvement and anti-dsDNA, Sm/nRNP, SSA/Ro, and SSB/La autoantibodies. There is considerable interest in using the interferon signature to monitor disease and/or disease susceptibility, although the clinical utility of doing so remains to be validated. Several assays are used, including the calculation of an "interferon score" by quantitative PCR (qPCR) (23), a bioassay using the induction of ISG expression in a standard cell line by patient serum (24), and flow cytometry-based assays for the expression of the proteins encoded by ISGs in blood leukocytes (25).

Method: Interferon Score by qPCR

An "interferon score" can be determined by quantifying the expression of three ISGs in peripheral blood leukocytes by qPCR (23). A number of the ISGs have been used for this purpose, but we generally use myxoma-resistant gene-1 (Mx1), interferon-inducible protein 44 (IFI44), and Ly6E (26). Human blood is collected in PAXgene tubes and RNA is isolated using the PAXgene RNA kit (Qiagen). The RNA (1 to 2 μg/sample) is treated with DNase I to remove contaminating genomic DNA and is then reverse transcribed (Superscript II First Strand Synthesis System, Invitrogen). Gene expression is quantified by real-time PCR (SYBR Green Core Reagent Kit, Applied Biosystems) using published forward and reverse primer sequences (26), and the expression is normalized to that of a housekeeping gene (β-actin) using the $2^{-\Delta\Delta Ct}$ method. Amplification conditions are: 95°C × 10 min, followed by 45 cycles of denaturation (94°C × 15 s), annealing (60°C × 25 s), and elongation (72°C × 25 s). After a final extension (72°C × 10 min), a melting curve analysis is performed to verify specificity of the products. Interferon scores are calculated as the number of standard deviations above or below the mean expression in a group or 10 healthy controls. The ISG score is calculated as follows: (Mx1 + Ly6E + IFI44) ÷ 3.

Method: Assessment of the Interferon by Flow Cytometry

Human peripheral blood monocytes constitutively express FcγRI (CD64), but expression is induced by IFN-I (and not other cytokines) (25). The level of CD64 expression on circulating $CD14^+$ monocytes can be measured rapidly by flow cytometry as a measure of total IFN-I production. IFN-I levels obtained by this assay correlate well with levels determined by the labor-intensive qPCR assay.

Reagents and Assay

PerCP-conjugated anti-CD14 (clone Mϕ P9) and phycoerythrin (PE)-conjugated anti-CD64 (clone X54-5/7.1.1), both from BD Bioscience, are used. Heparinized whole blood (100 μl) is incubated with labeled anti-CD64 + anti-CD14 antibodies for 20 min in the dark. Erythrocytes are lysed and the cells are washed with PBS/1% BSA/0.01% NaN_3 and fixed in 2% paraformaldehyde in PBS. Cells are analyzed by flow cytometry; gating on monocytes is based on their forward/side scatter and CD14 expression. At least 10^5 events are analyzed. Surface expression of CD64 is expressed as geometrical mean fluorescence intensity on monocytes. A PE-labeled irrelevant isotype control should be used. Since human $CD14^+$ monocytes constitutively express CD64, staining of peripheral blood from healthy controls should be carried out in parallel to define a normal range for CD64 mean fluorescence intensity. We have found that the monocyte CD64 expression level in heparinized blood is stable for at least 24 h at room temperature after blood collection.

REFERENCES

1. **Reeves WH, Li Y, Zhuang H.** 2011. Autoantibodies in systemic lupus erythematosus, p 1279–1288. *In* Hochberg MC, Silman AJ, Smolen JS, Weinblatt ME, Weisman MH (ed), *Rheumatology,* 5th ed. Mosby Elsevier, Philadelphia, PA.
2. **Craft J.** 1992. Antibodies to snRNPs in systemic lupus erythematosus. *Rheum Dis Clin North Am* **18:**311–335. PubMed
3. **Elkon KB, Bonfa E, Brot N.** 1992. Antiribosomal antibodies in systemic lupus erythematosus. *Rheum Dis Clin North Am* **18:**377–390. PubMed
4. **Fritzler MJ, McCarty GA, Ryan JP, Kinsella TD.** 1983. Clinical features of patients with antibodies directed against proliferating cell nuclear antigen. *Arthritis Rheum* **26:**140–145. PubMed
5. **Yamasaki Y, Narain S, Yoshida H, Hernandez L, Barker T, Hahn PC, Sobel ES, Segal MS, Richards HB, Chan EK, Reeves WH, Satoh M.** 2007. Autoantibodies to RNA helicase A: a new serologic marker of early lupus. *Arthritis Rheum* **56:**596–604. PubMed
6. **Mattioli M, Reichlin M.** 1974. Heterogeneity of RNA protein antigens reactive with sera of patients with systemic lupus erythematosus. Description of a cytoplasmic nonribosomal antigen. *Arthritis Rheum* **17:**421–429. PubMed
7. **Ho KT, Reveille JD.** 2003. The clinical relevance of autoantibodies in scleroderma. *Arthritis Res Ther* **5:**80–93. PubMed
8. **Lerner MR, Steitz JA.** 1979. Antibodies to small nuclear RNAs complexed with proteins are produced by patients with systemic lupus erythematosus. *Proc Natl Acad Sci USA* **76:**5495–5499. PubMed
9. **Arbuckle MR, McClain MT, Rubertone MV, Scofield RH, Dennis GJ, James JA, Harley JB.** 2003. Development of autoantibodies before the clinical onset of systemic lupus erythematosus. *N Engl J Med* **349:**1526–1533. PubMed
10. **Tan EM, Cohen AS, Fries JF, Masi AT, McShane DJ, Rothfield NF, Schaller JG, Talal N, Winchester RJ.** 1982. The 1982 revised criteria for the classification of systemic lupus erythematosus. *Arthritis Rheum* **25:**1271–1277. PubMed
11. **Buyon JP, Clancy RM, Friedman DM.** 2009. Cardiac manifestations of neonatal lupus erythematosus: guidelines to management, integrating clues from the bench and bedside. *Nat Clin Pract Rheumatol* **5:**139–148. PubMed
12. **Hanly JG, Urowitz MB, Siannis F, Farewell V, Gordon C, Bae SC, Isenberg D, Dooley MA, Clarke A, Bernatsky S, Gladman D, Fortin PR, Manzi S, Steinsson K, Bruce IN, Ginzler E, Aranow C, Wallace DJ, Ramsey-Goldman R, van Vollenhoven R, Sturfelt G, Nived O, Sanchez-Guerrero J, Alarcón GS, Petri M, Khamashta M, Zoma A, Font J, Kalunian K, Douglas J, Qi Q, Thompson K, Merrill JT, Systemic Lupus International Collaborating Clinics.** 2008. Autoantibodies and neuropsychiatric events at the time of systemic lupus erythematosus diagnosis: results from an international inception cohort study. *Arthritis Rheum* **58:**843–853. PubMed
13. **Burbelo PD, Ching KH, Issa AT, Loftus CM, Li Y, Satoh M, Reeves WH, Iadarola MJ.** 2009. Rapid serological detection of autoantibodies associated with Sjögren's syndrome. *J Transl Med* **7:**83. PubMed
14. **Weinstein A, Bordwell B, Stone B, Tibbetts C, Rothfield NF.** 1983. Antibodies to native DNA and serum complement (C3) levels. Application to diagnosis and classification of systemic lupus erythematosus. *Am J Med* **74:**206–216. PubMed

15. **Ter Borg EJ, Horst G, Hummel EJ, Limburg PC, Kallenberg CGM.** 1990. Measurement of increases in anti-double-stranded DNA antibody levels as a predictor of disease exacerbation in systemic lupus erythematosus. A long-term, prospective study. *Arthritis Rheum* **33:**634–643. PubMed
16. **Bootsma H, Spronk P, Derksen R, de Boer G, Wolters-Dicke H, Hermans J, Limburg P, Gmelig-Meyling F, Kater L, Kallenberg C.** 1995. Prevention of relapses in systemic lupus erythematosus. *Lancet* **345:**1595–1599. PubMed
17. **Pickering MC, Botto M, Taylor PR, Lachmann PJ, Walport MJ.** 2000. Systemic lupus erythematosus, complement deficiency, and apoptosis. *Adv Immunol* **76:**227–324. PubMed
18. **Ornstein BW, Atkinson JP, Densen P.** 2012. The complement system in pediatric systemic lupus erythematosus, atypical hemolytic uremic syndrome, and complocentric membranoglomerulopathies. *Curr Opin Rheumatol* **24:**522–529. PubMed
19. **Wen L, Atkinson JP, Giclas PC.** 2004. Clinical and laboratory evaluation of complement deficiency. *J Allergy Clin Immunol* **113:**585–593. PubMed
20. **Grotz W, Baba HA, Becker JU, Baumgärtel MW.** 2009. Hypocomplementemic urticarial vasculitis syndrome: an interdisciplinary challenge. *Dtsch Arztebl Int* **106:**756–763. PubMed
21. **Baechler EC, Batliwalla FM, Karypis G, Gaffney PM, Ortmann WA, Espe KJ, Shark KB, Grande WJ, Hughes KM, Kapur V, Gregersen PK, Behrens TW.** 2003. Interferon-inducible gene expression signature in peripheral blood cells of patients with severe lupus. *Proc Natl Acad Sci USA* **100:**2610–2615. PubMed
22. **Bennett L, Palucka AK, Arce E, Cantrell V, Borvak J, Banchereau J, Pascual V.** 2003. Interferon and granulopoiesis signatures in systemic lupus erythematosus blood. *J Exp Med* **197:**711–723. PubMed
23. **Feng X, Wu H, Grossman JM, Hanvivadhanakul P, FitzGerald JD, Park GS, Dong X, Chen W, Kim MH, Weng HH, Furst DE, Gorn A, McMahon M, Taylor M, Brahn E, Hahn BH, Tsao BP.** 2006. Association of increased interferon-inducible gene expression with disease activity and lupus nephritis in patients with systemic lupus erythematosus. *Arthritis Rheum* **54:**2951–2962. PubMed
24. **Hua J, Kirou K, Lee C, Crow MK.** 2006. Functional assay of type I interferon in systemic lupus erythematosus plasma and association with anti-RNA binding protein autoantibodies. *Arthritis Rheum* **54:**1906–1916. PubMed
25. **Li Y, Lee PY, Kellner ES, Paulus M, Switanek J, Xu Y, Zhuang H, Sobel ES, Segal MS, Satoh M, Reeves WH.** 2010. Monocyte surface expression of Fcgamma receptor RI (CD64), a biomarker reflecting type-I interferon levels in systemic lupus erythematosus. *Arthritis Res Ther* **12:**R90. PubMed
26. **Kellner ES, Lee PY, Li Y, Switanek J, Zhuang H, Segal MS, Sobel ES, Satoh M, Reeves WH.** 2010. Endogenous type-I interferon activity is not associated with depression or fatigue in systemic lupus erythematosus. *J Neuroimmunol* **223:**13–19. PubMed

Immunodiagnosis of Autoimmune Myopathies

MINORU SATOH, ANGELA CERIBELLI, MICHITO HIRAKATA, AND EDWARD K. L. CHAN

90

Certain autoantibodies can be clinically useful biomarkers associated with a particular disease and/or clinical features. Some of them, called disease marker antibodies, are highly specific for a particular diagnosis and have predictive value for the development of the disease, and they are included in classification criteria for systemic autoimmune rheumatic diseases (1, 2). The majority of disease-associated autoantibodies in systemic lupus erythematosus and scleroderma (systemic sclerosis) have been known for decades. However, autoantibody research in polymyositis/dermatomyositis (PM/DM) has been highly active in recent years as several new, clinically important autoantibody specificities with strong clinical impact have been identified, such as antibodies to transcription intermediary factor 1γ/α (TIF1γ/α; p155/140), which are frequently found in cancer-associated DM (3–5); and to melanoma differentiation-associated gene 5 (MDA5), associated with clinically amyopathic DM (CADM) with rapidly progressive interstitial lung disease (ILD) (6–9). Autoantibodies that are found in PM/DM are often classified into myositis-specific autoantibodies (MSAs) and myositis-associated autoantibodies (10, 11). MSAs are found almost exclusively in PM/DM among systemic rheumatic diseases, although some are also found in patients classified into idiopathic ILD, such as anti-PL-12 and anti-KS antibodies (12, 13).

Autoantibodies in PM/DM have been tested by a combination of immunoprecipitation (IP) analysis of proteins and RNA components of the target antigens along with enzyme-linked immunosorbent assay (ELISA) using purified or recombinant antigens, Western blot, and IP-Western blot as necessary (1, 14). In this chapter, we focus on experimental procedures of IP and ELISA using recombinant proteins, revising the previously published chapter of this manual (15). This chapter does not discuss details of molecular targets or the clinical significance of each autoantibody specificity, as many recent review articles on MSAs are available (11, 16–18).

IP ANALYSIS OF PROTEIN COMPONENTS

Radioimmunoprecipitation analysis of protein components of autoantigens using [^{35}S]methionine-labeled cell extract is a very powerful technique that allows screening for almost all known PM/DM autoantibodies in a single assay. Many of them can be interpreted almost conclusively, while a few may require additional techniques for confirmation (1). Advantages of IP include (i) screening of almost all known MSAs by a single assay, (ii) antigens being closer to the native condition compared with those in other immunoassays such as Western blot or ELISA, (iii) detection of multiproteins or multiprotein-nucleic acid complexes, and (iv) confirmation of the specific reactivity to the target antigen of the corresponding molecular weight (versus optical density [OD] in ELISA, which may not reflect the reactivity with the actual target in some cases).

Technology and Instrumentation

Antibodies in sera are affinity-purified onto beads coated with protein A or protein G. Beads with purified antibodies are mixed with radiolabeled cell extract. Antigens recognized by autoantibodies are affinity-purified onto the beads. Radiolabeled proteins are separated by SDS-PAGE and detected by autoradiography. A similar approach can be used to analyze the nucleic acid components of RNA-protein complex autoantigens. Required apparatus includes an electrophoresis power supply, vertical electrophoresis apparatus, tabletop centrifuge, CO_2 incubator, cell sonicator (Branson, Thomas Scientific, Swedesboro, NJ), and microcentrifuge.

Materials and Reagents

The following materials and reagents are needed.

1.5 g protein A-Sepharose CL4B (PAS) (17-0780-01; GE Healthcare, Little Chalfont, United Kingdom)

Prepare PAS stock solution as follows.

1. Add deionized H_2O (dH_2O) to 1.5 g of dry PAS in the vial, transfer to 15-ml centrifuge tubes, and let it swell by leaving at room temperature for 20 to 30 min.
2. Centrifuge for 30 s in a tabletop centrifuge (300 × *g*).
3. Aspirate water, add water to the top of the tube, and mix by inverting tubes. Wash the beads three times by centrifuging and aspirating supernatant.
4. Based on the volume of the beads, add dH_2O to make 50% (vol/vol) solution. Usually 14 to 15 ml of 50% (vol/vol) solution can be made from 1.5 g of PAS.
5. Add 1/100 amount of 2 M Tris-HCl (pH 7.5) to a final concentration of 20 mM and 10% NaN_3 to a final concentration of 0.1%. The beads can be stored at 4°C in this buffer.

doi:10.1128/9781555818722.ch90

Protein A, protein G, and protein A/G-Sepharose or -agarose beads are sold by many companies with variable binding capacity and nonspecific background. Although we have been using PAS for almost all IP experiments (including mouse IgG1 monoclonal antibodies), some mouse IgG1 and human IgG3 may not bind PAS efficiently; thus protein G or A/G may be more suitable for these.

0.5 M NaCl NET/IGEPAL buffer: 50 mM Tris-HCl (pH 7.5), 0.5 M NaCl, 2 mM EDTA, and 0.3% IGEPAL CA-630 (Sigma I3021; Sigma-Aldrich, St. Louis, MO). Nonionic, nondenaturing detergent Nonidet P-40 was replaced by IGEPAL CA-630, which is chemically indistinguishable from Nonidet P-40.

NET/IGEPAL buffer: 50 mM Tris-HCl (pH 7.5), 0.15 M NaCl, 2 mM EDTA, and 0.3% IGEPAL CA-630

Phenylmethylsulfonyl fluoride (PMSF) (Sigma P7626): 50 mM in absolute ethanol stored at −80°C

Aprotinin (Sigma A6279): Aprotinin from bovine lung aseptically filled solution in 0.9% NaCl and 0.9% benzyl alcohol. Activity: 3 to 7 trypsin inhibitor units (TIU)/mg protein; 5 to 10 TIU/ml solution.

3× sample buffer: mix 0.5 M Tris-HCl (pH 6.8) (6.0 ml), 1% bromophenol blue (0.6 ml), 2-mercaptoethanol (3.0 ml), 25% SDS (4.8 ml), and glycerol (6.0 ml). When it is used for IP samples, make 1× by mixing 1 volume of 3× sample buffer with 2 volumes of dH_2O.

Sterile phosphate-buffered saline (PBS)

[^{35}S]Methionine EXPRESS Protein Labeling Mix, [35S]-, 14 mCi (518 MBq), 50 mM Tricine (pH 7.4), and 10 mM 2-mercaptoethanol (NEG-072; PerkinElmer, Waltham, MA). Available in 2-, 7-, or 14-mCi vial.

Methionine- and cysteine-free culture medium RPMI 1640 (17-104-CI; Cellgro, ThermoFisher, Waltham, MA)

Penicillin (10,000 IU/ml)-streptomycin (= 100× Pen-Strep; Gibco BRL, ThermoFisher)

L-Glutamine, 200 mM (= 100× Gibco BRL catalog no. 25030-081)

HEPES (100×)

PBS-dialyzed fetal bovine serum (FBS) (SH3007902; HyClone, ThermoFisher)

^{35}S-labeling culture medium: 39 ml methionine- and cysteine-free RPMI, 4.5 ml PBS-dialyzed FBS, 0.45 ml L-glutamine, 0.45 ml HEPES, and 45 μl Pen-Strep

Assays: Cell Culture

Radiolabeled cell extract is prepared using K562 cells (human erythroleukemia cell line; ATCC CCL-243). The cells are thawed for 2 to 3 days before use and grown in RPMI 1640 with 10% FBS, 1:100 L-glutamine, 1:100 Pen-Strep, and 1:100 HEPES in a 5% CO_2 atmosphere at 37°C. Cells should be visually inspected carefully using an inverted microscope at high magnification for viability and contamination before labeling.

Note: K562 cells grow in clusters that can sometimes be quite large (20 to 30 to hundreds of cells per cluster) when they are proliferating rapidly. When clusters are smaller or rarely seen, with most of the cells as a single cell, proliferation may be slow and not optimal for efficient radiolabeling. When K562 cells start adhering, which indicates differentiation, expression of topoisomerase I (Scl-70) is very weak to deficient. When Plasmocin is used as an antibiotic in culture, cells proliferate normally without making any clusters. No clear differences in expression of known autoantigens are noted when K562 cells cultured with Plasmocin are used for radiolabeling and IP.

Radiolabeling

Collect cells by centrifuge (300 × *g* for 5 min in a tabletop centrifuge). Typically, 10^8 cells are cultured in 45 ml of complete methionine- and cysteine-free ^{35}S-labeling culture medium in a 250-ml flask. Add 3 mCi of [^{35}S]methionine (4.2 mCi as total radioactivity) and incubate cells for 12 to 14 h at 37°C in a 5% CO_2 atmosphere. After 12 to 14 h radiolabeling, add clean PBS to the culture and divide into 10 15-ml tubes, centrifuge (300 × *g*, 5 min), aspirate supernatant, and freeze at −80°C. Polypropylene tubes should be used to avoid cracking. Aliquots contain ~2×10^7 cells and can be used immediately or frozen at −80°C until use. After radiolabeling, there should be ~1.8×10^8 cells and the medium turns yellow. It is normal not to observe big clusters, and some apoptotic cells are seen after radiolabeling. However, contamination of bacteria and fungi should be carefully monitored after radiolabeling using high magnification.

Note: Levels of RNA polymerase II phosphorylated form were low after labeling for >16 h. It is better not to label for >14 h, though this also may depend on the condition of cells.

Preparation of PAS Beads with Purified Antibodies

Serum or plasma stored frozen or at 4°C can be used. Usually sera stored at 4°C with NaN_3 maintain their autoantibody reactivity for 10 to 15 years, though reduction of autoantibody reactivity in some sera was noticed. When sera are frozen, avoid repeat freezing and thawing. Clearing of sera by centrifuge is unnecessary. A heat-inactivated serum sample cannot be used because it causes very high background that makes interpretation of IP results impossible. This problem was not solved by microcentrifuging or filtering of sera.

Prepare labeled 1.6-ml microcentrifuge tubes and add 25 μl of 50% (vol/vol) PAS, followed by adding 8 μl of serum (or plasma). When serum is added, place the pipette tip in the PAS and pipette several times, as this will allow most IgG to bind to PAS immediately. Then add 500 μl of 0.5 M NaCl NET/IGEPAL. Microcentrifuge tubes are placed on a rack, which is then wrapped using plastic film and rotated for 1 h at 4°C up to 24 h.

Avoid vortexing the PAS beads at any stage of the procedure.

Preparation of Radiolabeled Cell Extract

When the beads are ready for washing, cell extract is prepared. Beads are washed and buffer aspirated while centrifuging the cell extract. For a standard reaction, radiolabeled cell extract from ~2×10^6 cells/sample is used. Add 2 ml of 0.5 M NaCl NET/IGEPAL to the frozen cell pellet (~2×10^7 cells; final cell concentration, 10^7/ml), then add 1:100 (20 μl) PMSF and aprotinin and leave on ice. Do not try to thaw at 37°C, as once the cells are thawed, they are disrupted and protein degradation commences. Also, avoid excessive heating of the cell suspension during sonication. With the above standard condition, heating is not a concern, but when the condition is changed, it will need to be carefully monitored for possible overheating. Do not put PMSF directly onto the frozen cell pellet because the 100% ethanol will denature the proteins. Sonicate the cells for 45 s (Branson Sonifier, duty cycle 25%, output 2.5), then place the tube on ice for 1 min, then sonicate again for 45 s. Transfer the cell lysate to microcentrifuge tubes and centrifuge at 9,000 × *g* for 30 min at 4°C. Carefully collect the

supernatant; avoid disturbing the small pellet that is usually seen at the bottom toward the outside. Combine all of the lysate in a 50-ml tube on ice. Use a 50-ml tube to avoid contamination of a pipette, as it is virtually impossible not to touch the inside wall with the pipette if a 15-ml tube is used.

Incubation with Cell Extract

Pellet the antibody-coated PAS beads by microcentrifuging for 8 s; aspirate the supernatant using a Pasteur pipette attached to a vacuum. For each aspiration step, carefully remove the bubbles on the surface of the liquid first since they may cause high background. Add 1 ml of 0.5 M NaCl NET/IGEPAL and microcentrifuge for 8 s and aspirate the supernatant. To each tube with PAS beads, add 160 μl of cell extract per sample. It is unnecessary to mix tubes as the beads and cell extract will be mixed completely during incubation. Make sure that caps are closed completely and tightly to prevent leaking of radioactive sample during incubation. Put tubes on a plastic rack, wrap with a plastic film, and rotate end over end to incubate for 1 h at 4°C.

Washing Beads

Microcentrifuge for 8 s, aspirate supernatant, add 1 ml of 0.5 M NaCl NET/IGEPAL, wash the inside of the cap by inverting once, and microcentrifuge for 8 s. Repeat washing three times and then once with NET/IGEPAL buffer. At each step, aspirate as completely as possible to reduce the background. Tubes can be aspirated in a horizontal position (versus vertical) for more complete aspiration. In the presence of proteins or detergent, PAS beads stay together and will not be easily aspirated (versus buffer without proteins or detergent such as PBS).

Add 50 μl of 1× SDS-PAGE sample buffer and freeze at −80°C or −20°C until running gels or proceed to boiling. Boiling could be before freezing or just before running gels. Boil samples for 3 min and absorb water around the cap using a paper towel immediately after boiling as it could get into the tubes when the air inside cools down and the pressure inside becomes negative. Microcentrifuge for 8 s and load 20 to 25 μl in each lane.

SDS-PAGE Gels

Since the smallest proteins that can be fractionated on 8% gels are ~25 kDa, while proteins of >100 kDa are not separated well on 12.5% gels, both 8 and 12.5% gels are run in routine screening of sera with unknown specificities. When running medium-size gels, it takes 3 to 5 h at a constant voltage of 100 to 130 V for the tracking dye front to reach to the bottom of the gels. For 8% gels, it is fine to let the dye front run out of the gels. For 12.5% gels, the thick blue dye band moves slower than the front of the samples; thus they need to be stopped when the thick blue dye band is 3 to 4 mm from the bottom. When a very thin blue line or a clear line at the sample front is seen, stop gels when it reaches the bottom of the gels.

SDS-PAGE Fluorography Reagents

Proteins immunoprecipitated are analyzed by SDS-PAGE, fluorography, and autoradiography after IP. Reagents are as follows.

25% SDS (Fisher, Sigma, or Bio-Rad, Hercules, CA). Filter this solution and all other stock solutions through a 0.45-μm bottle-top filter.

Coomassie blue stain (4 liters): Coomassie brilliant blue R-250 (catalog no. 161-0400; Bio-Rad) (5 g), methanol (1,200 ml), glacial acetic acid (400 ml), and dH_2O (2,400 ml)

Destaining solution (20 liters): 2 liters of glacial acetic acid, 7 liters of methanol, and 11 liters of dH_2O

2,5-Diphenyloxazole (PPO) (catalog no D144-100; Fisher), 20% (wt/vol) in dimethyl sulfoxide (DMSO). *Note:* PPO is carcinogenic.

Glycerol

BioMax MR film (catalog no. 870-1302; Eastman Kodak, Rochester, NY)

30% acrylamide–0.8% bisacrylamide stock: 30% (wt/vol) acrylamide (catalog no. BP 170-500; Fisher) plus 0.8% bisacrylamide (catalog no. 160-0201; Fisher) (wt/vol) in water (ratio, 37.5:1). Filter through a 0.45-μm bottle-top filter. Protein migration and mobility are affected by the ratio of acrylamide/bisacrylamide used. For detection of Ro52 protein, it is necessary to use acrylamide/bis = 166:1. Protein mobility on 12.5% acrylamide/bis = 166:1 gel is similar to 8% acrylamide/bis = 37.5:1 gel. However, 52-kDa Ro can be distinguished only on the former gel.

5× Tris-glycine (SDS-PAGE running buffer): 120 g of Tris base plus 576 g of glycine; add dH_2O to 4 liters (do not adjust pH; store at room temperature)

The procedure for preparing gels is as follows. *Note:* Precast minigels may be substituted for homemade ones. They can be purchased from Bio-Rad and other vendors. Identifying autoantibody specificities characterized by multiprotein complexes such as small nuclear ribonucleoproteins should not be difficult; however, a single protein autoantigen of close molecular weight (such as the ones of ~140 kDa [MDA5 and MJ; Table 1]) (19) will be difficult to differentiate with minigels.

If casting your own gels, keep in mind that acrylamide is a neurotoxin and suspected carcinogen. Gel plates, spacers, and rubber gaskets are washed thoroughly with detergent (e.g., PCC-54; Pierce, Rockford, IL), rinsed carefully, and wiped dry with ethanol. Gel plates should be assembled and clamped together with clips carefully to avoid leaking.

Preparation of SDS-PAGE Gels

We run both 12.5 and 8% SDS-PAGE for routine screening. Mix everything except 10% ammonium persulfate and TEMED (*N*,*N*,*N*′,*N*′-tetramethylethylenediamine; Bio-Rad) in 50-ml plastic tubes. Stacking gels are common regardless of the percentage of acrylamide in resolving gels. Add ammonium persulfate and TEMED to resolving gel solutions only to start polymerization. Mix thoroughly, but avoid excess bubbles by inverting the tubes several times. Pour the gel solution between glass plates. Usually bubbles go up to the surface, but when they stick to the glass in the middle, they can be removed by gently tapping the side of the plates. This needs to be done prior to overlaying ethanol. After checking bubbles, gently overlay 70% ethanol on the gel solution. Add from one site and avoid disturbing the gel solution. A spreading of ethanol on the surface with a clear border should be seen. Adding a 3- to 5-mm layer of ethanol is enough. Make sure the plates stand vertically at an ~90° angle to the bench and leave them without disturbing until the gels polymerize. Speed of polymerization depends on temperature but usually takes 30 to 40 min. The line between the overlaid ethanol and gel solution becomes unclear, and when it appears clearly again, it is a sign of polymerization.

After polymerization of resolving gels, pour out ethanol and rinse with dH_2O ~10 times to wash out ethanol, then completely remove water using small pieces of Whatman

TABLE 1 Identification of myositis autoantibodies by IP analysis

Autoantibodies	Target molecule	Function	Protein	RNA
Aminoacyl-tRNA synthetase				
Jo-1	Histidyl-tRNA synthetase	Incorporate histidine into proteins	50 kDa	$tRNA^{His}$
PL-7	Threonyl-tRNA synthetase	Incorporate threonine into proteins	80 kDa	$tRNA^{Thr}$
PL-12	Alanyl-tRNA synthetase	Alanine and aspartate biosynthesis and alanine incorporation into proteins	110 kDa	$tRNA^{Ala}$
EJ	Glycyl-tRNA synthetase	Glycine, serine, and threonine metabolism and aminoacyl-tRNA biosynthesis	75 kDa	$tRNA^{Gly}$
OJ	Isoleucyl-tRNA synthetase	Incorporate isoleucine into proteins	150 kDa (multienzyme complex, 170, 130, and 75 kDa)	$tRNA^{Iso}$
KS	Asparaginyl-tRNA synthetase	Glutamate, alanine, and aspartate metabolism	65 kDa	$tRNA^{Asp}$
ZO	Phenylalanyl-tRNA synthetase	Incorporate phenylalanine into proteins	60/70 kDa	$tRNA^{Phe}$
YRS (HA)	Tyrosyl-tRNA synthetase	Incorporate tyrosine into proteins	59 kDa	$tRNA^{Tyr}$
Anti-SRP	Signal recognition particle	Protein maturation in the ribosome	72, 68, 54, 19, 14, and 9 kDa	7SL RNA
Anti-Mi-2	Helicase protein	Transcriptional regulation	240, 150, 72, 65, 63, 50, and 34 kDa	
Anti-MDA5/ CADM140	MDA5	RNA-specific helicase that mediates the antiviral response	140 kDa	
Anti-TIF1γ/α (p155/140)	TIF1γ/α	Transcription and RNA metabolism	155 and 140 kDa	
Anti-MJ	NXP-2 (MORC3)	Transcriptional regulation and activation of the tumor suppressor p53	140 kDa	
Anti-SAE	SAE	Posttranslational modifications	90 and 40 kDa	
Anti-PMS1	PMS1 (postmeiotic segregation increased 1)	DNA mismatch repair enzyme	120 kDa	

filter paper. In particular, water tends to stay at each corner; thus, it should be removed completely until the sharp 90° angle can be seen. When plates are ready for stacking gels, add ammonium persulfate and TEMED to the stacking gel solution. Mix gently by inverting the tubes and pour the solution between glass plates. Insert combs, avoiding bubbles under the comb. If bubbles are seen under the comb, remove it and insert again. Resolving gels can be polymerized in 30 min. We usually leave gels at 4°C overnight because we feel the protein bands are sharper in 8% gels by this step. The polymerization step should be at room temperature.

SDS-PAGE Procedure

The gels are run as follows.

1. Make 1 liter of running buffer: 1 liter is used for a pair of gels; 200 ml of 5× Tris-glycine plus distilled water to make 1,000 ml; add 4 ml of 25% SDS and mix well by inverting a measuring cylinder.

2. Boil samples, including molecular weight marker if necessary. Prestained molecular weight marker is relatively expensive but convenient, as the quality and progress of running gels can be monitored.

3. Carefully remove the combs and silicone rubber spacer from the gel, and then remove clips.

4. Clamp the gel to the gel apparatus and add running buffer to the top and bottom chambers of the apparatus.

5. Flush out bubbles from the bottom of the gel immersed in the bottom chamber, using a 5- to 10-ml syringe with a bent (90°) 18-gauge needle.

6. Gently flush out each well with running buffer using a Hamilton microsyringe. Pieces of gels in the wells should be carefully removed.

7. Load a 20- to 25-μl sample to each well, using either a Hamilton syringe or pipette.

8. Attach leads to the electrodes of the gel apparatus (proteins treated with SDS are negatively charged and will migrate toward the cathode).

9. Attach the power supply and run at 100 V until the blue tracking dye reaches the resolving gel; the voltage can later be increased to 120 to 130 V.

10. Run the gel until the blue tracking dye reaches the bottom of the gel or to the appropriate level as discussed earlier.

11. Turn off the power, remove the electrodes, and unclamp the gel from the gel apparatus. Carefully pry the plates apart, leaving the gel adherent to one of the plates. Using a pizza cutter, cut off the stacking gel (leave 1 to 2 mm of stacking gel) and avoid cutting resolving gel. Also, diagonally cut off a small piece of the gel from the upper right-hand corner to aid in orienting the gel.

12. Stain the gel for 30 to 60 min with Coomassie blue solution in a box, making sure gels are not stacked together and freely moving on a shaker. Use low-speed orbital shaking. Prolonged staining makes gels fragile and should be avoided.

13. Gels can be destained in the solution overnight. Proteins can still be transferred to other gels at this stage if they stick together. Separating each gel in a small plastic box is ideal.

Fluorography

After staining and destaining, the gels are fluorographed as follows.

1. Place the first DMSO (100 to 150 ml, enough to cover all gels and allow them to move freely) in a Tupperware or similar (polyethylene or polypropylene, but not polystyrene) box and add gels after removing as much excess destaining solution as possible. Incubate in the first DMSO for 30 min on an oribital shaker at low speed.

2. Discard/save the first DMSO (can be reused for up to ~8 gels; keep in a glass bottle with a tight cap) and add 100 to 150 ml of the second DMSO and shake for another 30 min.

3. Discard/save the second DMSO and add 100 to 150 ml of 20% (wt/vol) PPO in DMSO and shake for 1 h. The second DMSO can be reused for up to ~8 gels and then can be used as a first DMSO.

4. Save the PPO-DMSO in brown glass bottles for reuse. It can be used a few times, though the effectiveness gradually diminishes.

5. Wash the gels with many changes of water (tap water is fine) to remove DMSO and make PPO precipitate in the gels. Clear gels will turn white and opaque upon washing with water. Repeat, changing water and putting on a shaker. Minimum washing will be 30 min, but it is important to change water frequently rather than keeping on a shaker with the same water. Removing DMSO is critical to make thinner, nonsticky gels after drying.

6. Add glycerol to a concentration of ~3%. Insert a piece of filter paper under the gel in a box, pick up, and set on a gel dryer (Bio-Rad model 583) at 60°C with the timer set to 3 h. Gels can be dried completely after 2 to 2.5 h; however, minor air leaking in the system or other reasons could delay this process. Thus, check the appearance of the water droplets inside of the vacuum tubing (large water droplets indicate gels are still wet) carefully prior to stopping the vacuum of the gel dryer. *Note:* Higher temperature should be avoided because PPO can be destroyed at >60°C.

7. Remove gels from gel dryer. Tape filter paper with the dried gel on a solid flat support, such as a used piece of X-ray film; avoid taping over the dried gels. If it is sticky, dust the gel lightly with talc powder to prevent sticking. Place the gels in a film cassette and place in direct contact with BioMax MR film in the darkroom. The film is coated on one side, and the coated side must contact the gel directly. Expose films for 3 to 5 days at −70°C before developing. Exposure time can be adjusted based on the decay of ^{35}S (half-life, 89 days) and the signals of the molecules of interest for the experiment. Wash the box used for PPO using 100% ethanol (PPO is insoluble to water) a few times to remove PPO.

Interpretation

As a basic rule in interpretation of IP, observation of any protein bands that are present in a particular lane but not in other lanes means that they are specifically recognized by autoantibodies to these proteins. Interpretation of specificity of autoantibodies by IP is based primarily on the migration of immunoprecipitated proteins, ideally by comparing with the size and the pattern of proteins immunoprecipitated by reference sera. Representative IP analysis of autoantigenic proteins is shown in Fig. 1. Molecular weight and other characteristics of each MSA are summarized (Tables 1 and 2). Identifying a multiprotein or multiprotein-nucleic acid complex characterized by a set of proteins, such as anti-OJ, anti-SRP (signal recognition particle), anti-Mi-2, anti-TIF1γ/α (p155/140), and anti-SAE (small ubiquitin-like modifier-1 [SUMO-1] activating enzyme), is usually not so difficult. Nevertheless, occasionally patterns that look similar to OJ or TIF1γ/α are seen. For identification of SAE, there are many other proteins recognized by sera close to 90 kDa and 40 kDa where components of SAE migrate; thus, the mobility of the candidate proteins needs to be carefully assessed. Conclusively identifying SRP72/68 and SRP54 is not always easy, as there are many proteins that are recognized by patients' sera in this range of molecular weight. Detecting a set of the smaller subunits of 19, 14, and 9 kDa appears more unique, though a high-percentage (e.g., 12.5%) gel is necessary to separate these components. Jo-1 is seen as a thin band of ~50 kDa that is shifted due to interference of IgG heavy chain (not shown; this effect is unclear in Fig. 1 due to a small amount of anti-Jo-1 serum used). The presence of Jo-1 can be suspected in most cases based on IP; however, confirmation by other tests such as ELISA or Western blot is necessary for anti-Jo-1. IP of an ~50-kDa thin band and confirmation of tRNA (it cannot be confirmed specifically as $tRNA^{His}$) is practically considered anti-Jo-1. Although interpretation of a single protein autoantigen needs to be done carefully, strong anti-PL-7 or -EJ can be easily interpreted by IP in most cases, though weak bands need additional confirmation. PL-12 also shows a strong band; however, there are several autoantigenic ~120-kDa proteins that migrate close to PL-12. Mobility of TIF1β is identical to that of PL-12; however, a good-quality gel can show a characteristic appearance of the band: a sharp line in the middle and diffuse band around it. MJ/NXP-2 (nuclear matrix protein 2) is a sharp thin band, and interpretation needs to be done carefully as MDA5 migrates very close and there are many other proteins of ~140 kDa recognized by some sera. IP-Western blot or ELISA will be necessary to confirm (19). Identification of MDA5 in IP is not easy, as the expression of MDA5 in culture cells varies and there are MJ and other proteins of ~140 kDa to be differentiated (7).

Quality Assurance, Quality Control, and Test Validation

Having positive controls is ideal, but running all references each time is not practical. As far as the cells in good condition are radiolabeled, expression of all autoantibodies discussed in this chapter appears consistent except MDA5 (7, 19). As there are proteins that are nonspecifically immunoprecipitated by virtually all sera, including negative controls is necessary.

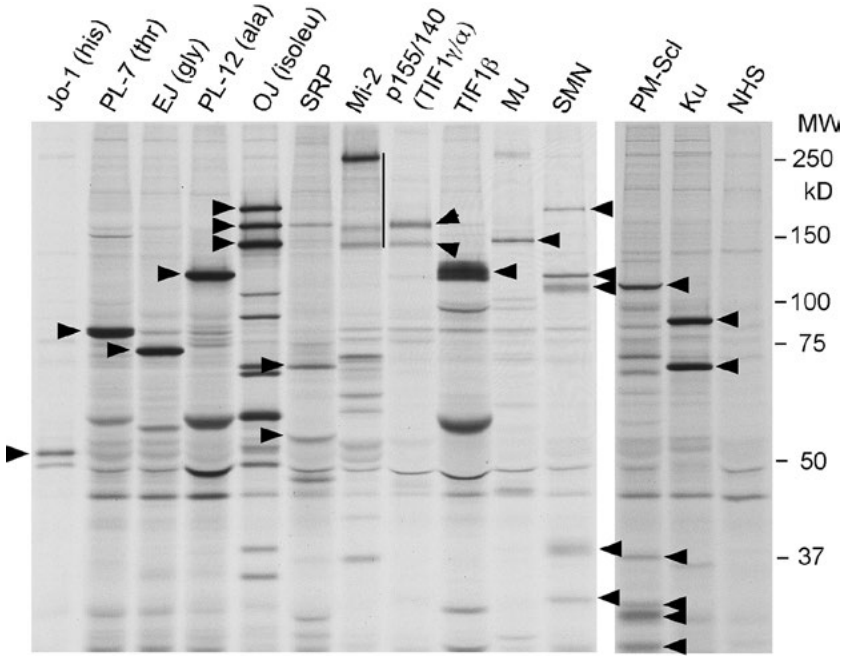

FIGURE 1 IP analysis of protein components of autoantigens recognized by autoantibodies in PM/DM. [^{35}S]Methionine-labeled K562 cell extract was immunoprecipitated by sera from patients with PM/DM. The main components of each autoantigen are indicated by arrowheads or a line drawn on the right (Mi-2). Jo-1, histidyl-tRNA synthetase; PL-7, threonyl-tRNA synthetase; EJ, glycyl-tRNA synthetase; PL-12, alanyl-tRNA synthetase; OJ, isoleucyl-tRNA synthetase multienzyme complex; SMN, survival of motor neuron; NHS, normal human serum; MW, molecular weight.

IP ANALYSIS OF SMALL RNAs

Small RNAs, components of autoantigens recognized by sera from patients, can be identified based on IP analysis of RNAs, similar to the IP procedure described above for proteins using radiolabeled K562 cells. The main differences are that (i) instead of [^{35}S]methionine-labeled cells, either unlabeled cells with silver staining of RNAs or [^{32}P]orthophosphate-labeled cells with autoradiography are used; and (ii) RNAs are extracted at the end of IP for analysis by urea-PAGE gels.

Due to concerns about strong β radiation produced by [^{32}P]orthophosphate-labeled cells, most laboratories working on autoantibody analysis switched from ^{32}P-radioimmunoprecipitation to silver staining analysis of RNAs. Thus, the method for the nonradioactive procedure is described in the following section.

In general, try to use autoclaved reagents and high-quality deionized water to avoid RNA degradation and reduce background in silver staining. Avoid any possible contamination of metal throughout the step because it will cause background in silver staining.

Steps for preparing PAS beads, stock, and incubation with sera are the same as the method for protein analysis by IP. Beads after incubation with sera can be refrigerated for several days in NET/IGEPAL buffer. Aspirate buffer before adding cell extract.

Cell Lysate

Unlabeled K562 cells (either frozen pellet or fresh cells; 5×10^6 cells/sample) are used. The number of cells necessary depends on specificities, but this number of cells is enough to detect RNA components for all MSAs that recognize RNA-protein complexes.

1. Add 2 ml of 0.5 M NaCl NET/IGEPAL plus PMSF (1:100) and aprotinin (1:100) to 50×10^6 cell pellets (20 μl each to 2 ml of the buffer). Final concentration: PMSF, 0.5 mM; aprotinin, 0.24 TIU/ml (Sigma). Do not put PMSF directly on cell pellets since ethanol will denature proteins. When frozen cell pellets are used, *do not* try to thaw cell pellets. Once the cells are thawed, cells will be disrupted and proteases and nucleases will be active. Also, it is unnecessary to mix and resuspend cells as they will be resuspended soon after sonication is started.

2. Sonicate cells for 45 s at duty cycle 25%, output control 2.5 (Branson Sonifier). Put on ice for 1 min. Sonicate again for 45 s. Keep samples on ice when it is possible. Transfer cell lysate to microfuge tubes. Microfuge for 30 min at 9,000 × *g* in a cold room (not at room temperature).

3. Wash PAS beads incubated with sera while clearing the cell lysate.

4. Carefully collect supernatant, avoiding the pellet. If there is more than one tube, pool all supernatant together in a tube before adding to samples. Add cell extract on beads (usually 200 μl/sample, but this can be adjusted depending on the experiment).

5. Put tubes on a plastic rack, wrap with a plastic film, and rotate at 4°C for 1 h.

Preparation of a Total RNA Sample as a Standard

1. Take 20 μl (extract from ~5×10^5 cells) and add 400 μl of NET/IGEPAL, 16 μl of 25% SDS, and 40 μl of 3 M Na acetate (pH 5.2). Add 400 μl of phenol/chloroform/isoamyl alcohol (25:24:1, pH 5.2) (Fisher). *Note:* Phenol/chloroform/isoamyl alcohol is available at pH 5.2 and pH 8.0. The pH 8.0 solution is supposed to allow extraction of both DNA and

TABLE 2 Prevalence and clinical association of myositis autoantibodies

Autoantibodies	Prevalence (%)	Clinical association/significance
Aminoacyl-tRNA		
Jo-1	15–30	Anti-synthetase syndrome (myositis, ILD, polyarthritis, Raynaud's phenomenon, mechanic's hands)
PL-7	<5	Myositis, ILD, DM-specific skin manifestations (heliotrope rash, Gottron's sign)
PL-12	<5	ILD, CADM, DM-specific skin manifestations (heliotrope rash, Gottron's sign)
EJ	<5	Myositis, ILD, DM-specific skin manifestations (heliotrope rash, Gottron's sign)
OJ	<5%	Anti-synthetase syndrome
KS	<5 (rare)	ILD
ZO	<1 (rare)	Myositis
YRS (HA)	<1 (rare)	Myositis
Anti-SRP	5	Myositis (necrotizing)
Anti-Mi-2	10	DM with typical skin lesions and mild myositis
Anti-MDA5/CADM140	15–20	CADM, rapidly progressive ILD, severe skin manifestations
Anti-TIFγ/α (p155/140)	10–15	Malignancy-associated DM
Anti-MJ/NXP-2	1–5	Adult and juvenile DM with severe skin disease
Anti-SAE	1	DM

RNA, whereas the pH 5.2 stock is designed mainly for RNA extraction.

2. Vortex vigorously for 1 min.

3. Spin for 1 min at room temperature at 9,000 × *g*.

4. Handle tubes very carefully and transfer supernatant to a clean new tube, avoiding the protein layer at the interphase between supernatant and phenol phase. Use a P200 pipette and harvest ~150 μl × 2 = ~300 μl.

5. Add 900 μl of 100% ethanol (200 proof) and *mix well by inverting tubes* (IMPORTANT).

6. Leave at −80°C overnight (>1 h is probably enough).

Washing Beads

1. After incubation of beads with cell extract, spin for 8 s and aspirate cell extract.

2. Add 1 ml of 0.5 M NaCl NET/IGEPAL. Wash the inside of the cap by inverting tubes.

3. Wash four times with 0.5 M NaCl NET/IGEPAL. Spin for 8 s.

4. Add 1 ml of NET/IGEPAL (50 mM Tris-HCl [pH 7.5], 150 mM NaCl, 2 mM EDTA, and 0.3% IGEPAL CA-630). Spin for 8 s and aspirate supernatant completely.

Extraction of RNAs

1. Mix 400 μl of NET/IGEPAL, 16 μl of 25% SDS, and 40 μl of 3M Na acetate (pH 5.2) and add 456 μl of the mixture to the beads.

2. Add 400 μl of phenol/chloroform/isoamyl alcohol (25:24:1). Vortex vigorously for 1 min.

3. Purify RNA as described above in "Preparation of a Total RNA Sample as a Standard."

Preparation of RNA Samples for Urea-PAGE

RNA samples in microcentrifuge tubes are spun at 9,000 × *g* for 15 min in a cold room. The supernatant can be discarded by gently pouring, and then carefully aspirate liquid using a thin Pasteur pipette (heat the thin part of the Pasteur pipette over a gas burner and pull to make a thin glass pipette).

The RNA pellet is usually not visible, but the RNA pellet will stay on the surface of the tubes if aspiration is along the opposite side of the tube, where the pellet is supposed to be. Leave tubes under a biological safety hood to dry.

Preparation of Urea-PAGE Gel

1. Wash a 100-ml glass beaker and stirrer using detergent and rinse very well with Milli-Q water.
2. Weigh 21 g of urea, add 20 ml of 30% acrylamide/bis and 5 ml of 10× Tris-borate-EDTA (TBE), and stir until urea is completely dissolved.
3. Wash a measuring cylinder, and rinse with Milli-Q water and transfer the above solution.
4. Adjust the volume to 50 ml using Milli-Q water. Make fresh 10% ammonium persulfate using Milli-Q water.

5. Add 300 μl of ammonium persulfate and 30 μl of TEMED and mix completely.
6. Pour between a pair of glass plates and a spacer, assembled using clips, and insert comb.

Urea-PAGE

1. Start running gel at a constant voltage of 480 to 500 V (current and watts at maximum position; adjust output by voltage). Check the temperature of the gel using a paper thermometer and try to keep the temperature between 55 and 60°C. This range of temperature can be reached with voltage between 480 and 500 V, but the necessary voltage could be different in different systems.
2. Add 50 μl of urea-PAGE sample buffer to each sample tube and vortex to dissolve RNA. Turn the power off. Load 20 μl of sample using thin plastic pipette tips with a P20 pipette, quickly before the gel cools down.
3. Before prerun and before loading samples, quickly flush each well using a Hamilton microsyringe. Urea emerges from the gel and may collect at the bottom of the wells, disturbing the sample.
4. Two dye bands are seen while running gels, a blue dye band of bromphenol blue and a purple dye band of xylene cyanol. Run until the xylene cyanol dye reaches the bottom of the gel (it may go out). It usually takes ~1.5 to 2 h to run with medium-size gels.

Silver Staining of Nucleic Acids (Silver Stain Plus; Bio-Rad)

Follow the manufacturer's instructions.

12% Urea-PAGE Gel for RNA Analysis

30% (acrylamide/bis = 37.5:1) acrylamide/bis	20 ml
10× TBE	5 ml
Urea	21 g

Bring the volume to 50 ml with Milli-Q water.

10% ammonium persulfate	300 μl
TEMED	30 μl

RNA Sample Buffer

10 M urea

0.025% bromophenol blue

0.025% xylene cyanol in 1× TBE

Make 1% dye solution and add 1/40 amount of bromophenol blue and xylene cyanol to 10 M urea to a final concentration of 0.025%.

10× TBE

900 mM Tris	108 g
900 mM boric acid	55 g
20 mM Na_2EDTA	40 ml of 0.5 M stock

Adjust final volume to 1 liter.

Interpretation

Detecting tRNAs in IP samples is not difficult; however, the only interpretable information is that the antibodies in the serum recognize autoantigen that has tRNA as a component; it is not possible to identify the specificity of tRNAs by IP. Nevertheless, it is reasonable and practical to conclude a specificity of anti-tRNA synthetase antibodies based on IP of protein of the right molecular weight corresponding to each tRNA synthetase combined with IP of the tRNA. Detection of 7SL RNA for anti-SRP is not difficult, though having a positive control is ideal. Detection of U small nuclear RNAs is easy with a positive control as well. Representative silver staining gel to analyze RNA components of autoantigens is shown in Fig. 2.

Quality Assurance, Quality Control, and Test Validation

Most small RNAs associated with MSA antigens can be detected easily with good-quality IP and staining. A positive control of anti-Jo-1 and negative controls are useful as a standard for quality control.

ELISA USING RECOMBINANT MYOSITIS AUTOANTIGENS

The following protocol is based on ELISA using recombinant Jo-1 antigen, but the same protocol can be used for any other myositis autoantibody ELISA using recombinant autoantigens.

When ELISA is performed for the detection of autoantibody, there will be differences in the reactivity between samples. However, it should be noted that it does not mean the observed OD reflects the actual recognition of the target autoantigen. Quality/purity of recombinant proteins and ELISA varies, and validation for each ELISA compared with results from a previously established standard method such as IP is necessary.

1. Coat a 96-well microtiter plate (Nunc Immobilizer Amino; Nunc/Thermo Fisher Scientific, Roskilde, Denmark) with purified recombinant Jo-1 antigen by adding 0.5 μg/ml in PBS, 50 μl/well, at room temperature for 2 h or at 4°C overnight. The concentration of antigens may need to be optimized by titration analysis and adjusted for each assay. Any other type of high-binding microtiter plate may be used. The Immobilizer Amino plate covalently cross-links proteins to the plastic surface at amino acid positions of lysine and cysteine. This cross-linking process will not work in the presence of amines such as Tris or glycine. Other types of plate may not be affected by amine.

2. Tap the side of the plate gently and make sure that the whole bottom area of the wells is covered with coating solution. With 50 μl/well it will not spread, but 100 μl/well or more will spread without tapping. Using 50 μl/well will save on the cost of reagent.

3. After the coating/cross-linking step, remove antigen solution completely by tapping on dry paper towels.

4. Block with 0.5% bovine serum albumin (BSA) NET/IGEPAL (150 mM NaCl, 2 mM EDTA, 50 mM Tris-HCl [pH 7.5], and 0.3% IGEPAL CA-630)–0.05% NaN_3, 150 μl/well, for 1 to 3 h at room temperature (or 4°C overnight).

5. Dump blocking buffer and tap on paper towels.

6. Add 100 μl/well of serum diluted in blocking buffer (0.5% BSA NET/IGEPAL–0.05% NaN_3, usually at 1:250 to 1:500, i.e., 2 μl of serum in 500 or 1,000 μl of blocking buffer). Incubate for 1 to 3 h at room temperature.

7. Wash plate three times with Tris-buffered saline (TBS)/Tween 20. There are many alternative types of washing buffer in common use.

8. Add 100 μl/well of alkaline phosphatase-conjugated goat F(ab)′2 anti-human IgG (γ-chain specific) second antibody at 1:1,000 in 0.5% BSA NET/IGEPAL–0.05% NaN_3. Incubate for 1 to 2 h at room temperature.

9. Wash three times with TBS/Tween 20.

10. Prepare the developing solution ~10 min before needed by adding 1 tablet (5 mg) of Sigma 104 substrate/5 ml

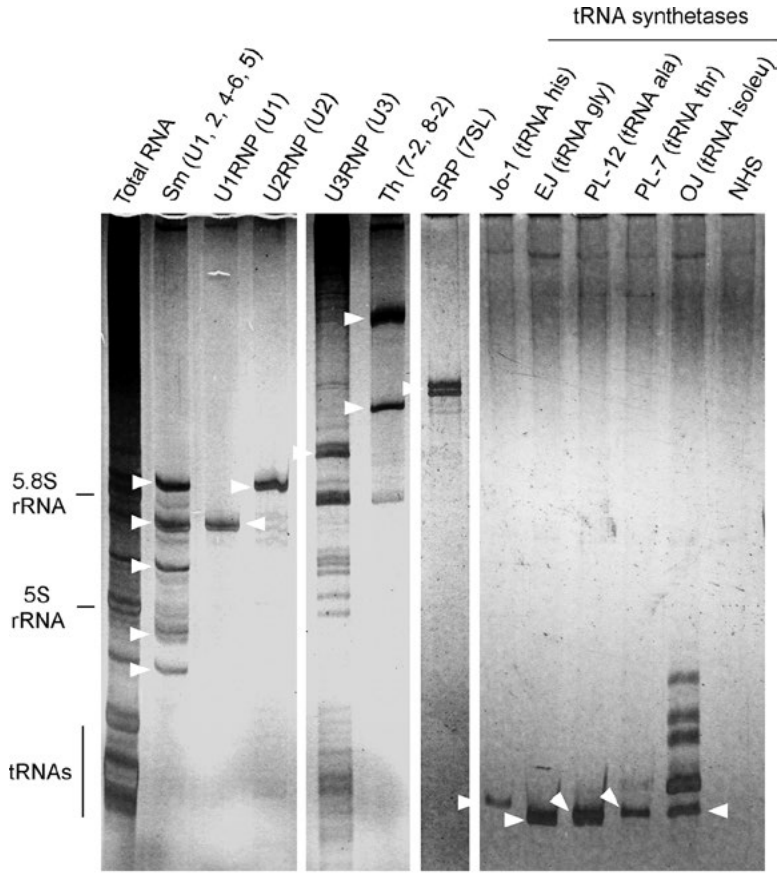

FIGURE 2 IP analysis of RNA components of autoantigens recognized by autoantibodies. K562 cell extract was immunoprecipitated by autoimmune sera. RNA components were extracted, fractionated on urea-PAGE, and silver stained. RNA components of autoantigen are indicated by arrowheads. Sm (U1, 2, 4-6, 5), U1, 2, 4-6, 5 small nuclear RNAs; U1RNP (U1), U1 small nuclear RNA; U2RNP (U2), U2 small nuclear RNA; U3RNP (U3), U3 small nucleolar RNA; Th (7-2, 8-2), 7-2 and 8-2 RNAs; SRP (7SL), 7SL RNAs; NHS, normal human serum. Y1-5 RNAs are also seen in the anti-OJ lane due to coexisting anti-Ro60 antibodies.

diethanolamine buffer. You need 10 ml/plate (100 μl/well × 96 wells = 9.6 ml). Put on rotator or shaker in a 50-ml tube to dissolve. Sigma 104 tablets are sensitive to temperature and humidity. Take the necessary amount quickly and do not leave the vial at room temperature for an extended period of time.

11. Develop plates by adding 100 μl/well of developing solution.

12. Read OD_{405} on a microtiter plate reader. Read OD more than once, including the one when the highest OD is ~1.5 to 2. If samples with low OD are important, overdevelop and read it again. Try to read at least twice for each plate.

VERY IMPORTANT: Do not push pipette all the way when developing solution is added because this will leave bubbles in the wells, which will directly and significantly affect the absorbance of wells. Depending on the operator's pipetting technique, there may still be bubbles. Check all wells for bubbles after pipetting and break them using a 25-gauge needle.

Blocking Buffer: NET/IGEPAL, 0.5% BSA, 0.05% NaN_3

0.15 M NaCl
2 mM EDTA
50 mM Tris-HCl (pH 7.5)
0.3% IGEPAL
0.5% BSA
0.05% NaN_3

Washing Buffer (TBS/Tween 20)

20 mM Tris-HCl (pH 7.5)
150 mM NaCl
0.1% Tween 20

Diethanolamine Buffer

Diethanolamine	97 ml
$MgCl_2 \cdot 6H_2O$	0.1 g
NaN_3	0.2 g
dH_2O	

Adjust pH to 9.6 with concentrated HCl, adjust volume to 1 liter with dH_2O, and filter using a 0.45-μm bottle-top filter.

Interpretation

It is ideal to set a cutoff in each laboratory based on a ROC (receiver operating characteristic) curve established by a large number of positive and negative controls.

Quality Assurance, Quality Control, and Test Validation

Quality and reliability of ELISA depend heavily on the quality of recombinant protein used. Positive controls selected based on conventional methods and negative controls are essential as standards for quality control. Weak but true positive versus false positive is often not easy to differentiate with ELISA.

FUTURE DIRECTIONS OF MSA TESTING

Currently anti-Jo-1 ELISA is the only widely available testing for most clinicians. Line immunoassay is available in certain countries but has not been used extensively. Although IP is a very powerful and reliable technique, it has been performed at only a limited number of laboratories and is not likely to become a routine assay in clinical practice. ELISAs and bead-based assays for several MSAs are currently under development and will become available in the future. Recently identified autoantibodies such as anti-TIF1 and anti-MDA5 have strong clinical significance, and development of commercial immunoassays is in progress. They will be widely available in the near future, and tests for these autoantibodies may become a part of standard tests in clinical practice for inflammatory myopathy.

REFERENCES

1. **Satoh M, Chan EK, Sobel ES, Kimpel DL, Yamasaki Y, Narain S, Mansoor R, Reeves WH.** 2007. Clinical implication of autoantibodies in patients with systemic rheumatic diseases. *Expert Rev Clin Immunol* **3:**721–738. PubMed
2. **Satoh M, Vázquez-Del Mercado M, Chan EK.** 2009. Clinical interpretation of antinuclear antibody tests in systemic rheumatic diseases. *Mod Rheumatol* **19:**219–228. PubMed
3. **Targoff IN, Mamyrova G, Trieu EP, Perurena O, Koneru B, O'Hanlon TP, Miller FW, Rider LG, Childhood Myositis Heterogeneity Study Group, International Myositis Collaborative Study Group.** 2006. A novel autoantibody to a 155-kd protein is associated with dermatomyositis. *Arthritis Rheum* **54:**3682–3689. PubMed
4. **Fujimoto M, Hamaguchi Y, Kaji K, Matsushita T, Ichimura Y, Kodera M, Ishiguro N, Ueda-Hayakawa I, Asano Y, Ogawa F, Fujikawa K, Miyagi T, Mabuchi E, Hirose K, Akimoto N, Hatta N, Tsutsui K, Higashi A, Igarashi A, Seishima M, Hasegawa M, Takehara K.** 2012. Myositis-specific anti-155/140 autoantibodies target transcription intermediary factor 1 family proteins. *Arthritis Rheum* **64:**513–522. PubMed
5. **Satoh M, Chan JY, Ross SJ, Li Y, Yamasaki Y, Yamada H, Vazquez-del Mercado M, Petri MH, Jara LJ, Saavedra MA, Cruz-Reyes C, Sobel ES, Reeves WH, Ceribelli A, Chan EK.** 2012. Autoantibodies to transcription intermediary factor TIF1β associated with dermatomyositis. *Arthritis Res Ther* **14:**R79. doi:10.1186/ar3802. PubMed
6. **Sato S, Hoshino K, Satoh T, Fujita T, Kawakami Y, Fujita T, Kuwana M.** 2009. RNA helicase encoded by melanoma differentiation-associated gene 5 is a major autoantigen in patients with clinically amyopathic dermatomyositis: association with rapidly progressive interstitial lung disease. *Arthritis Rheum* **60:**2193–2200. PubMed
7. **Sato S, Hirakata M, Kuwana M, Suwa A, Inada S, Mimori T, Nishikawa T, Oddis CV, Ikeda Y.** 2005. Autoantibodies to a 140-kd polypeptide, CADM-140, in Japanese patients with clinically amyopathic dermatomyositis. *Arthritis Rheum* **52:**1571–1576. PubMed
8. **Hoshino K, Muro Y, Sugiura K, Tomita Y, Nakashima R, Mimori T.** 2010. Anti-MDA5 and anti-TIF1-γ antibodies have clinical significance for patients with dermatomyositis. *Rheumatology (Oxford)* **49:**1726–1733. PubMed
9. **Nakashima R, Imura Y, Kobayashi S, Yukawa N, Yoshifuji H, Nojima T, Kawabata D, Ohmura K, Usui T, Fujii T, Okawa K, Mimori T.** 2010. The RIG-I-like receptor IFIH1/MDA5 is a dermatomyositis-specific autoantigen identified by the anti-CADM-140 antibody. *Rheumatology (Oxford)* **49:**433–440. PubMed
10. **Targoff IN.** 2000. Update on myositis-specific and myositis-associated autoantibodies. *Curr Opin Rheumatol* **12:**475–481. PubMed
11. **Nakashima R, Mimori T.** 2010. Clinical and pathophysiological significance of myositis-specific and myositis-associated autoantibodies. *Int J Clin Rheumatol* **5:**523–536.
12. **Targoff IN, Arnett FC.** 1990. Clinical manifestations in patients with antibody to PL-12 antigen (alanyl-tRNA synthetase). *Am J Med* **88:**241–251. PubMed
13. **Hirakata M, Suwa A, Nagai S, Kron MA, Trieu EP, Mimori T, Akizuki M, Targoff IN.** 1999. Anti-KS: identification of autoantibodies to asparaginyl-transfer RNA synthetase associated with interstitial lung disease. *J Immunol* **162:**2315–2320. PubMed
14. **Targoff IN.** 2002. Laboratory testing in the diagnosis and management of idiopathic inflammatory myopathies. *Rheum Dis Clin North Am* **28:**859–890, viii. PubMed
15. **Reeves WH, Satoh M, Lyons R, Nichols C, Narain S.** 2006. Detection of autoantibodies against proteins and ribonucleoproteins by double immunodiffusion and immunoprecipitation, p 1007–1018. *In* Rose NR, Hamilton RG, Detrick B, Reeves WH (ed), *Manual of Molecular and Clinical Laboratory Immunology*, 7th ed. ASM Press, Washington, DC.
16. **Betteridge ZE, Gunawardena H, McHugh NJ.** 2011. Novel autoantibodies and clinical phenotypes in adult and juvenile myositis. *Arthritis Res Ther* **13:**209. doi:10.1186/ar3275. PubMed
17. **Targoff IN.** 2008. Autoantibodies and their significance in myositis. *Curr Rheumatol Rep* **10:**333–340. PubMed
18. **Mammen AL.** 2011. Autoimmune myopathies: autoantibodies, phenotypes and pathogenesis. *Nat Rev Neurol* **7:**343–354. PubMed
19. **Ceribelli A, Fredi M, Taraborelli M, Cavazzana I, Franceschini F, Quinzanini M, Tincani A, Ross SJ, Chan JY, Pauley BA, Chan EK, Satoh M.** 2012. Anti-MJ/NXP-2 autoantibody specificity in a cohort of adult Italian patients with polymyositis/dermatomyositis. *Arthritis Res Ther* **14:**R97. doi:10.1186/ar3822. PubMed

Immunodiagnosis of Scleroderma

MASATAKA KUWANA

91

Systemic sclerosis (SSc) or scleroderma is a connective tissue disease characterized by excessive fibrosis, microangiopathy, and the presence of circulating autoantibodies to various cellular components (1). Clinical presentation is highly heterogeneous in patients with SSc: some have only Raynaud's phenomenon and sclerodactyly without any symptomatic organ involvement for >10 years, but others have progressive functional impairment in lungs, heart, kidneys, or gastrointestinal tract, leading to death. Distinct specificities of antinuclear antibodies (ANAs) are selectively detected in SSc patients and are associated with unique disease manifestations (2). The detection of individual SSc-related ANAs is useful in the diagnosis, disease subgrouping, and prediction of future organ involvement and prognosis. Therefore, SSc-related ANAs are important biomarkers in routine rheumatology practice.

A new group of autoantibodies reactive with cell-surface receptors or extracellular matrix proteins also have been identified in SSc patients. These include anti-platelet-derived growth-factor receptor, anti-angiotensin II type 1 receptor, anti-endothelin-1 type A receptor, and anti-fibrillin-1 antibodies, and appear to directly activate pathways that may contribute to tissue and vascular remodeling. However, reproducibility of the published reports is very poor, probably because of difficulty in reproducing antigenicity of the autoantigens with highly complicated conformation in the assays. This results in lack of reliable commercial assay kits for detection of these autoantibodies to functional molecules.

To date, at least 10 specificities were identified and characterized as ANAs specific to SSc. Two classic autoantibodies discovered in the late 1970's are anti-Scl-70 or anti-topoisomerase I (topo I) antibody, and anti-centromere antibody (ACA). Another group of antibodies, including anti-U1 ribonucleoprotein (RNP), anti-Ku, and anti-PM-Scl antibodies, were first identified using double immunodiffusion (DID). The remaining ANA specificities were discovered using immunoprecipitation (IP) assay. However, these conventional techniques are of limited use in routine clinical practice because they are labor-intensive and time-consuming, and are limited in throughput. DID, or the Ouchterlony, method has been used for more than 50 years and is still used in clinical laboratories because it is inexpensive and specific, but it lacks sensitivity and requires a large amount of reference serum and considerable experience in judging the assay results. The IP assay is a valuable detection method that is able to detect all SSc-related ANAs except ACA, but this assay requires complicated procedures using cellular extracts freshly prepared from radioisotope-labeled cultured human cells. Therefore, many efforts have been made to develop convenient and accurate assays for detection of individual SSc-related ANAs.

SSc-Related ANAs

ANAs are a hallmark of SSc, and are detected in >95% of the patients (2). The majority of autoantigens specifically recognized by SSc sera have been already identified. At this point, at least 10 ANA specificities associated with SSc have been reported and well characterized, and approximately 80% of SSc patients have one of those SSc-related ANAs in their circulation. These SSc-related ANAs target various nuclear components involved in essential cellular processes, such as cell division and transcription (Table 1). These autoantibodies are rarely seen in patients with other connective-tissue diseases without SSc features and thus are important diagnostic markers. In addition, detection of SSc-related ANAs is clinically useful in classifying SSc patients into subtypes that are almost exclusively associated with characteristic clinical phenotypes (Table 2). SSc-related ANAs are usually present at the onset of SSc symptoms and do not switch from one antibody to another during the course of the disease. These autoantibodies remain throughout the course of the disease regardless of whether patients receive treatment or not. Patients rarely have two or more SSc-related ANAs together, indicating mutual exclusiveness. Thus, SSc patients can be divided into a number of disease subsets stratified by SSc-related ANAs (Fig. 1).

Anticentromere Antibody (ACA)

The frequency of ACA in SSc patients has been reported to be 20% to 30% in many ethnic groups. ACA produces discrete speckled staining on indirect immunofluorescence (IIF). The recognition of kinetochore proteins located at the centromeric regions of individual metaphase chromosomes is highly specific to ACA. However, IIF using chromosomal spreads as the substrate is necessary to confirm the presence of ACA, especially when other high-titer ANA specificities coexist. ACA is sometimes detected in patients with primary Sjögren's syndrome or primary biliary cirrhosis as well as in individuals without an apparent connective

doi:10.1128/9781555818722.ch91

TABLE 1 Structure and function of molecules targeted by SSc-related ANAs

ANA specificity	Structure	Cellular localization	Main cellular function
Anticentromere	CENP-A, B, and C	Chromatin	Separation of chromosome
Anti-Scl-70	DNA topoisomerase I	Chromatin	Relaxation of supercoiled DNA
Anti-RNA polymerase III	Multi-subunit components of RNA polymerase III, including RPC155	Nucleoplasm	Transcription of small nuclear RNAs
Anti-U3 RNP/ fibrillarin	U3RNA and related components including fibrillarin	Nucleoli	Processing of pre-ribosomal RNAs
Anti-Th/To	RNase P/RNase MRP	Nucleoli	Processing of transfer RNAs and other small RNAs
Anti-U11/U12 RNP	U11/U12 RNA and related components	Nucleoplasm	Regulation of mRNA splicing
Anti-PM-Scl	Exosome complex containing PM-Scl-100 and PM-Scl-75	Nucleoli	Processing and degradation of RNAs
Anti-Ku	Ku80 and Ku70	Nucleoplasm	DNA repair
Anti-RuvBL1/2	Double hexamer consisting of RuvBL1 and RuvBL2	Nucleoplasm	DNA repair and chromatin remodeling
Anti-U1 RNP	U1RNA and related components including 70K, A, and C proteins	Nucleoplasm	mRNA splicing

tissue disease, who are almost always elderly. Non-SSc patients with ACA often lack Raynaud's phenomenon. The natural history of ACA-positive SSc patients includes long-standing Raynaud's phenomenon followed by appearance of puffy fingers. The presence of ACA in patients with Raynaud's phenomenon and/or nailfold capillary abnormalities is predictive of future development of SSc (3). Patients with ACA are often classified as having limited cutaneous SSc (lcSSc), in which skin sclerosis is restricted to distal to the elbows and knees in the presence or absence of facial skin sclerosis. Severe interstitial lung disease (ILD) or renal crisis almost never occurs in ACA-positive patients, but 10% to 20% of them develop pulmonary arterial hypertension (PAH) later in the course of the disease. Overall survival in SSc patients with ACA is better than those without, but PAH is the major cause of death in this subset.

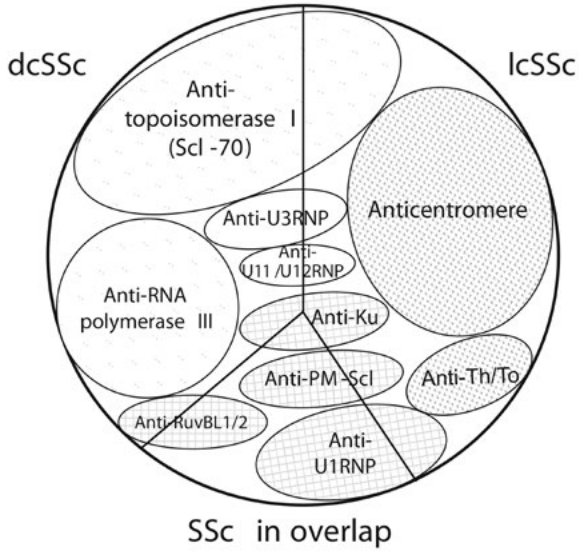

FIGURE 1 Diagram showing SSc subsets stratified by autoantibodies. Areas of individual circles represent approximate proportions in the entire SSc patients. dcSSc: diffuse cutaneous systemic sclerosis, lcSSc: limited cutaneous systemic sclerosis.

Anti-Topo I Antibody

Anti-topo I or anti-Scl-70 antibody is detected in 20 to 30% of SSc patients in many ethnic groups. The majority of anti-topo I-positive patients have diffuse cutaneous SSc (dcSSc), in which skin sclerosis extends to proximal to elbow or knee, but progression of skin thickening is slower than those with anti-RNA polymerase (RNAP) III antibody. Anti-topo I antibody is associated with a high risk for severe ILD and peripheral vascular complications, such as digital ulcers and gangrene, particularly early in the disease course. Anti-topo I antibody is considered to be a marker for poor prognosis, and patients typically die of ILD at an average of 10 years after onset of SSc.

Anti-RNAP III Antibody

Anti-RNAP III antibody often coexists with other classes of RNAP, such as RNAP I and II (4). Sera positive for anti-RNAP III antibody produce a speckled staining pattern with or without nucleolar staining on IIF. Frequency of anti-RNAP III antibody in SSc patients varies among ethnic groups: a higher frequency in North American Caucasian and British patients (20% to 25%) in comparison with French or Japanese patients (5%). Nearly all patients with this antibody have dcSSc with rapidly progressive skin thickening. Patients with anti-RNAP III antibody

TABLE 2 Methods for detection and clinical associations with SSc-related ANAs[a]

ANA specificity	Staining pattern on IF (ANA test)	Assay for detection	Disease subset	Clinical phenotype
Anticentromere (ACA)	Discrete speckled	IIF, IA	lcSSc	PAH Severe peripheral vascular disease
Anti-Scl-70	Speckled (with or without nucleolar staining)	IA, DID, IP	dcSSc	Severe ILD Severe peripheral vascular disease
Anti-RNA polymerase III	Speckled (with or without nucleolar staining)	IA, IP	dcSSc	Rapid progressive skin thickening Renal crisis
Anti-U3 RNP/ fibrillarin	Nucleolar	IP	dcSSc/lcSSc	ILD, PAH, renal crisis, small bowel disease
Anti-Th/To	Nucleolar	IP	lcSSc	ILD, PAH
Anti-U11/U12 RNP	Speckled	IP	dcSSc/lcSSc	Severe ILD
Anti-PM-Scl	Nucleolar	DID, IP	lcSSc (myositis overlap)	Mild myositis DM rash
Anti-Ku	Speckled	DID, IP	lcSSc (myositis overlap)	Mild myositis
Anti-RuvBL1/2	Speckled	IP	dcSSc (myositis overlap)	Mild myositis
Anti-U1 RNP	Speckled	IA, DID, IP	lcSSc ("MCTD")	Inflammatory arthritis, myositis, PAH

[a]DM, dermatomyositis; MCTD, mixed connective tissue disease.

have the highest risk for developing renal crisis, but they do not develop severe ILD. In many patients, skin thickening regresses over time even without treatment. Survival in patients with anti-RNAP III antibody is better than those with anti-topo I antibody since renal crisis is more easily treated with angiotensin-converting enzyme inhibitors than ILD. Several recent cohorts indicate that patients with anti-RNAP III antibody have better long-term survival rates compared with those with ACA or anti-Th/To antibody.

Anti-U3 RNP Antibody

Anti-U3 RNP antibody reacts with fibrillarin complexed with U3 RNA. This antibody produces bright nucleolar staining on IIF. Anti-U3 RNP antibody is found in 4% to 10% of patients with SSc, and is most frequent in African Americans (5). One third of the patients have lcSSc, but the remaining patients have typical features of dcSSc. Severe internal-organ involvement, including ILD, PAH, renal crisis, and small-bowel involvement with pseudo-obstruction and malabsorption is fairly common. Prognosis in this subset is comparable to that in patients with anti-topo I antibody. An unusual combination of PAH and renal crisis is occasionally found in patients with dcSSc and anti-U3 RNP antibody.

Anti-Th/To Antibody

Anti-Th/To antibody is one of SSc-related anti-nucleolar antibodies, and occurs in patients with lcSSc, although its frequency overall in SSc patients is only 2% to 5%. Like ACA-positive patients, anti-Th/To-positive patients are predominantly Caucasians, but tend to have a shorter duration of Raynaud's phenomenon before onset of other symptoms, such as puffy fingers. Digital ulcers and gangrene are infrequent, but patients with anti-Th/To antibody can have significant ILD or PAH, which occurs early in the disease course. This increased frequency and severity of pulmonary complications result in a decreased survival compared with lcSSc patients without this antibody (6).

Anti-U11/U12 RNP Antibody

Anti-U11/U12 RNP antibody is a rare antibody specificity found in 1% to 3% of patients with SSc (7). This antibody produces speckled nuclear staining on IIF, and sometimes is associated with low-titer anti-U1 RNP antibodies. Patients with this antibody are classified as having either dcSSc or lcSSc. A characteristic feature of patients with anti-U11/U12 RNP antibody is a high frequency of severe ILD, which is associated with a 2.25-fold greater risk of death

in comparison with anti-U11/U12 RNP-negative patients with ILD.

Anti-PM-Scl Antibody

Anti-PM-Scl antibody produces a homogenous nucleolar pattern, and is rarely found in non-Caucasian patients. The anti-PM-Scl-positive patients often present with the subacute onset of myositis, but also have typical Raynaud's phenomenon and scleroderma skin changes, usually lcSSc. A significant proportion of the patients have rashes consistent with dermatomyositis. This antibody is found in approximately 25% of SSc patients with myositis overlap, but in 2% of SSc patients overall. Serious internal-organ involvement is rare, leading to a favorable prognosis. Myositis is usually mild and shows a good response to moderate-dose corticosteroids.

Anti-Ku Antibody

Anti-Ku antibody is primarily detected in patients with SSc in overlap. The majority of patients have typical Raynaud's phenomenon and scleroderma skin changes, usually lcSSc. Concomitant myositis is common, but some have additional features of lupus. Anti-Ku antibody is rarely detected in patients with systemic lupus erythematosus without SSc features, but additional lupus-associated autoantibodies are always positive in such patients (8). Disease onset in these patients is usually younger than 50. Internal-organ involvement is infrequent and usually mild if present, but arthritis is common. Myositis is usually mild and shows a good response to moderate-dose corticosteroids, leading to favorable prognosis.

Anti-RuvBL1/2 Antibody

This newly identified antibody recognizes a double hexamer consisting of RuvBL1 and RuvBL2, which is located in nucleoplasm (9). Anti-RuvBL1/2 antibody is a rare antibody specificity detected in 1% to 2% of patients with SSc. This antibody produces speckled nuclear staining with a high antibody titer on IIF. Patients with this antibody have a unique combination of clinical features, including myositis overlap and diffuse cutaneous involvement. Internal-organ involvement is mild in general, but some patients develop severe myocardial dysfunction.

Anti-U1 RNP Antibody

Anti-U1 RNP antibody, which produces a pure speckled pattern with a high antibody titer, is primarily detected in patients with SSc in overlap. This antibody is preferentially detected in African Americans and Orientals. Anti-U1 RNP antibody was first described as a serologic marker for mixed connective-tissue disease. Disease onset in these patients is younger than others. The patients usually present with inflammatory symptoms, such as myositis and arthritis. Raynaud's phenomenon and puffy fingers occur early in the disease, but later these patients develop typical manifestations of SSc. Most of them have lcSSc, although approximately 20% develop dcSSc. Serious complications are relatively uncommon, but pulmonary complications, including PAH and ILD, are sometimes life-threatening. Prognosis is favorable, but PAH is the most common cause of death.

Screening of SSc-Related ANAs

A conventional method for ANA detection is IIF on cultured HEp-2 cell slides. This technique is recommended as the first ANA-screening test because it is highly sensitive and provides additional information on the antibody titer and staining pattern. Speckled staining is often detected in patients with dcSSc and suggests the presence of anti-topo I antibody in case of a high antibody titer ($\geq$1:320) or anti-RNAP III antibody in case of a low titer ($<$1:160). Anti-U1 RNP and anti-RuvBL1/2 antibodies, which are associated with SSc overlap, also produce the high-titer speckled pattern, while titers of anti-U11/U12 RNP antibody vary among the positive sera. A nucleolar pattern is fairly specific to SSc. The three major SSc-related anti-nucleolar antibodies are anti-U3 RNP, anti-Th/To, and anti-PM-Scl antibodies. Anti-RNAP III antibody also produces a nucleolar pattern when anti-RNAP I antibody coexists, but a concomitant speckled pattern is always present. A discrete speckled pattern is often detected in patients with lcSSc and suggests the presence of ACA, which recognizes a pair of dots located at the centromeric lesion of individual metaphase chromosomes. Serum dilution is an important issue for IIF used for the ANA screening. For immunofluorescence detection of ANAs on HEp-2 cells, a 1:10 or 1:20 dilution would produce a high false-positive rate from normal samples. Therefore, many clinical laboratories use a 1:40 dilution. Since the frequency of ANAs varies with age, it can be argued that a 1:160 dilution might be preferable for patients $>$65 years of age. However, this results in missing some clinically important low-titer ANAs, including anti-RNAP III antibody. It has been recommended that samples should be tested at both 1:40 and 1:160 dilutions (10).

Commercial solid-phase ANA assays have been available since the early 1990s, and might be viable alternatives to ANA detection on HEp-2 cells. This method has considerable potential, but it is of note that many SSc-related ANAs, including anti-RNAP III antibody and anti-nucleolar antibodies, are not identified with these assays, and thus are reported as "a negative ANA." This is because the sensitivity ultimately depends on the choice of autoantigens used. Therefore, it is currently recommended to use the conventional IIF for screening SSc-related ANAs.

Methods for Detection of Individual SSc-Related ANAs

Identification of individual SSc-related ANAs requires additional techniques, such as DID, IP assay, and specific immunoassays including enzyme immunoassay (EIA). The solid-phase immunoassays have several advantages over other traditional techniques in terms of simplicity, reproducibility, quickness, and ability to handle many samples at the same time. Typically, in immunoassays, the wells of plastic microwell strips are sensitized by passive absorption with the purified autoantigen. The test procedure involves three incubation steps with properly diluted test sera, enzyme-conjugated anti-human immunoglobulin antibodies, and an enzyme substrate. After the reaction is stopped, the color intensity of the solution is measured photometrically. The majority of commercially available immunoassays utilize recombinant autoantigens, which are expressed in the bacterial or eukaryotic system, while some assays still use native proteins purified from cellular extracts. However, solid-phase assay requires the availability of highly purified autoantigens that contain the major epitopes recognized by virtually all sera positive for given SSc-related ANAs. This is a critical limitation for developing immunoassays. For example, it is easy to prepare topo I as an antigenic source for immunoassays because the autoimmune target is a single molecule. However, the majority of autoantigens recognized by SSc-related ANAs are multiprotein complexes consisting of many constituents, and, in some cases, small RNAs. In this case, it is necessary to determine the antigenic subunit that is commonly recognized by autoantibodies. For example, RNAP III

exists as multiprotein complexes consisting of >12 subunits, requiring identification of the antigenic subunit recognized by all anti-RNAP III-positive sera. A series of experiments using individual subunits successfully identified the largest subunit RPC155 as the antigenic subunit, resulting in development of a sensitive immunoassay (11). Immunoassays for detection of ACA, anti-topo I, anti-RNAP III, and anti-U1 RNP antibodies are currently available in many countries (Table 3). Due to lack of comprehensive studies that compare sensitivity and specificity of individual commercial kits, it is not known which kit is the best.

EIA or enzyme-linked immunosorbent assay (ELISA), which uses enzyme-conjugated secondary anti-human immunoglobulin antibodies, has been the mainstream technique, but commercial kits utilizing chemiluminescent immunoassay (CIA) and fluorescence enzyme immunoassay (FEIA) have become available in recent years. CIA potentially shows a superior discrimination (signal-to-noise ratio) between the positive and negative samples (12). FEIA is a new assay system designed as a sandwich immunoassay. In this system, the enzyme conjugated to secondary antibodies transforms an added substrate into a fluorescent product.

TABLE 3 Commercially available kits for detection of anti-Scl-70, ACA, anti-RNAP III, and anti-U1RNP antibodies

SSc-related ANAs	Assay principle	Company	Brand name
Anti-Scl-70	EIA	INOVA Diagnostics	QUANTA Lite Scl-70 ELISA
		Diamedix Corporation	Is anti-Scl-70 Enzyme Immunoassay Test Kit
		DiaSorin	LIAISON ANA Screen LIAISON ENA Screen
		Immuno Concepts	RELISA ANA Screening System
		EUROIMMUN	Anti-Scl-70 ELISA
		MBL International	MESACUP-3 TEST Scl-70
	FEIA	Thermo Fisher Scientific	EliA Scl-70
	CIA	INOVA Diagnostics	QUANTA Flash SCL-70
	DID	INOVA Diagnostics	NOVA Gel Scl-70
	LIA	EUROIMMUN	EUROLine ANA Profile 3
	Multiplex bead assay	Bio-Rad Laboratories	BioPlex 2200 ANA Screen
		INOVA Diagnostics	Quanta Plex SLE Profile 8
		Zeus Scientific	AtheNA Multi-Lyte ANA III
ACA	EIA	Diamedix Corporation	Is ANA ELISA Screen
		DiaSorin	LIAISON ANA Screen LIAISON ENA Screen
		EUROIMMUN	Euroimmun Anti-centromere ELISA
		Trinity Biotech	Captia ANA Screen
		INOVA Diagnostics	QUANTA Lite Centromere (CENP-A & CENP-B)
		MBL International	MESACUP-2 TEST CENP-B
	FEIA	Thermo Fisher Scientific	EliA CENP
	CIA	INOVA Diagnostics	QUANTA Flash Centromere
	IIF	Immuno Concepts	Fluorescent Hep-2000
	LIA	EUROIMMUN	EUROLINE ANA Profile 3
	Multiplex bead assay	Bio-Rad Laboratories	BioPlex 2200 ANA Screen
		Zeus Scientific, Inc.	AtheNA Multi-Lyte ANA III
Anti-RNAP III	EIA	MBL International	Anti-RNA Polymerase III ELISA Kit
		INOVA Diagnostics	QUANTA Lite RNA Pol III ELISA
	LIA	EUROIMMUN	EUROLINE SSc Profile
Anti-U1RNP	EIA	INOVA Diagnostics	QUANTA Lite RNP ELISA
		Diamedix Corporation	Immunosimplicity anti-Sm/RNP Enzyme Immunoassay Test Kit
		Immuno Concepts	RELISA anti-Sm/RNP TEST SYSTEM
		MBL International	MESACUP-2 TEST RNP
	FEIA	Thermo Fisher Scientific	EliA U1RNP
	CIA	INOVA Diagnostics	QUANTA Flash RNP
	DID	INOVA Diagnostics	NOVA Gel Sm/RNP
	LIA	EUROIMMUN	EUROLINE SSc Profile
	Multiplex bead assay	Bio-Rad Laboratories	BioPlex 2200 ANA Screen
		Zeus Scientific	AtheNA Multi-Lyte ANA III

A recent study evaluating the sensitivity of a commercial autoantibody-screening method (EliA CTD screen, Thermo Fisher Scientific) revealed that the sensitivity is insufficient for the assay to be used as a screening test for anti-U3 RNP and anti-RNAP III antibodies, but appears to be satisfactory for ACA, anti-topo I, anti-PM-Scl, and anti-U1 RNP antibodies (13).

Assay Procedures of Immunoassays

Most commercial EIA kits contain the following components: antigen-sensitized microplates (usually 96-well plates), positive and negative control sera, serum calibrators, conjugated anti-human immunoglobulin antibodies, sample diluent, enzyme substrate, reaction-stop solution, and washing-buffer concentrate. Here is a general procedure, but instructions are somewhat different among kits. It is highly recommended to follow the instructions provided by the manufacturer.

1. Remove the individual components from storage and allow them to warm to room temperature (20–25°C).
2. It is better to use the entire kit all at once. When the number of samples is insufficient, some commercial kits allow use of a portion of the package. In this case, allow the required number of control/calibrator determinations, including blank, negative control, positive control, and calibrators. Return unused reagents to 4°C immediately after use.
3. Dilute serum samples as well as positive and negative control sera, and serum calibrators as indicated.
4. Incubate the plate at room temperature for the designated time period.
5. Wash the microwell strips either by manual or automated wash procedure. If necessary, the microwell plate may be inverted over a paper towel and tapped firmly to remove any residual wash solution from the microwells.
6. Add the conjugate solution to each well at the same rate and in the same order as the specimens were added.
7. Incubate the plate at room temperature for the designated time period.
8. Wash the microwells by following the procedure previously described in step 5.
9. Add substrate to each well, including reagent blank well, at the same rate and in the same order as the specimens were added.
10. Incubate the plate at room temperature for the designated time period.
11. Stop the reaction by adding stop solution to each well, including the reagent blank well, at the same rate and in the same order. Tap the plate several times to ensure that the samples are thoroughly mixed.
12. Set the microwell reader to read at the designated wavelength and measure the optical density of each well against the reagent blank. The plate should be read within 30 minutes after the addition of stop solution.
13. Calculate the autoantibody level as an index or unit according to the instruction. A cutoff value for positive samples is usually provided by the manufacturer.

Precautions

The human-serum controls are potentially hazardous materials despite the absence of known infectious agents such as HIV-1 and hepatitis B and C viruses. Adherence to the specified time and temperature of incubations is essential for accurate results. Ideally, serum samples that have been freshly collected should be used. Storage at 4°C is sufficient for samples analyzed up to a week after collection, while for longer periods storage at −20°C is preferable. Frequent thawing and freezing of the sample may lead to a decrease of the antibody activity. Addition of sodium azide (10 to 100 μg/ml) is recommended for storage for more than a month.

Quality Assurance, Quality Control, and Test Validation

It is best to assess the intra-assay and inter-assay variability of the test procedure. Specifically, a strong positive, a low positive, and a negative sample should be tested many times (usually at least 6) on each of three days. The coefficient of variance should be calculated for each sample, and it should be ≤10%. A positive and negative control, and reagent blank must also be included in each assay. At least one positive-control serum is included in the kit, but positive reference sera are also available from the Centers for Disease Control and Prevention (AF-CDC ANA Reference Lab, Immunology Branch, 17-3040, A25, Centers for Disease Control and Prevention, Atlanta, GA 30333) and commercially. It is convenient to develop a set of in-house positive and negative standards. Once appropriate sera are found, try to obtain a large amount (>10 ml) of each in order to maintain a stock that can be used over a period of several years. The antibody levels of each reference serum should be recorded to assess reproducibility. There are several national, international, and commercial quality-assurance schemes, including The College of American Pathologists (available at http://www.cap.org/) and The United Kingdom National External Quality Assessment Schemes for Autoimmune Serology (available at http://www.ukneqas.org.uk/). These schemes are widely used and cover the common autoantibodies. Samples are issued several times a year and a consensus report is produced so that individual laboratories can compare their performance with that of other participants.

Interpretation of Results

Results of immunoassays are not always reliable, although for the majority of commercial kits sensitivity and specificity are both >95%, in comparison with results measured by the gold-standard assay. One of the main reasons for false-negative results is insufficiency or lack of antigenicity of the antigens used for the assay. This is particularly the case in measurement of anti-topo I and anti-RNAP III antibodies. In some patients' sera, these antibodies recognize conformational epitopes present on native molecules alone. On the other hand, contaminants in the antigen preparation may cause the false-positive results. It has been previously reported that sera with anti-DNA antibodies occasionally provide a false-positive result on some anti-topo I antibody-assay kits because of contamination of native DNA in the purified topo I antigen preparation. This is not a problem anymore since nearly all commercially available immunoassays now utilize recombinant topo I as antigen. Specimens that give equivocal results should be repeated or evaluated using an alternate technique, such as DID and IP assay.

Multiplex Technologies for Detection of SSc-Related ANAs

During the last 20 years, several multiplex technologies have been developed and used in laboratory medicine (14). Line-blot immunoassay (LIA) is considered as the first-generation multianalyte immunoassay, and is commercially available for detection of a series of SSc-related ANAs

(EUROLINE, Euroimmune) (15). This system adopts the principle of immunoblots, in which membrane strips are coated with thin parallel lines of a panel of purified antigens. It can be performed manually, but automated systems have become available. LIA is principally a non-quantitative assay, but the intensity of the bands is shown to correlate with the antibody titer. The software has been developed to enable quantitative evaluation of test strips, to facilitate management of data, and to provide detailed documentation of results. One study reported that sensitivity and specificity of LIA were similar to those of immunoassays (EIA and FLIA) in terms of detection of ACA and anti-topo I antibody (16).

ANA-screening technology has become available as the next-generation multianalyte immunoassays based on multibead arrays, which can be measured by the newest flow cytometers, e.g., Luminex system (Luminex) and FACSarray (BD Biosciences) (17). Such systems allow for the screening of samples while at the same time providing semi-quantitative results on individual specificities for positive samples. However, the multiplex platforms are limited by their dependence on the autoantigens of choice. Currently, ACA and anti-topo I and anti-U1 RNP antibodies can be measured using commercially available platforms (18). Due to the infancy of multiplex systems, it is difficult to predict their impact on the preeminence of the conventional immunoassay.

Detection of Minor SSc-Related ANAs

At this moment, only a few research laboratories can identify a whole panel of SSc-related ANAs, because this can be done only by use of a cumbersome IP assay. Commercially available immunoassay kits are able to detect ACA, anti-topo I, anti-RNAP III, and anti-U1 RNP antibodies, but up to 20% of sera positive for known SSc-related ANAs will be missed. A recently developed LIA system is able to detect anti-U3 RNP, anti-Th/To, anti-PM-Scl, and anti-Ku antibodies (19), but side-by-side comparisons with the gold-standard IP assay have never been done. Our preliminary evaluations revealed that there may be some problems in sensitivity for detecting anti-U3 RNP and anti-Th/To, and in specificity for detecting anti-RNAP III, anti-PM-Scl, and anti-Ku antibodies. In this situation, old-fashioned DID is still useful for detection of anti-PM-Scl and anti-Ku antibodies. All SSc-related ANAs except ACA can be detectable by IP assays combined with electrophoretic detection of RNA and protein components, but availability of these techniques is restricted to special laboratories because of a complicated procedure involving a radioisotope. The RNA-IP assay was originally developed using ^{32}P-labeled cultures cells, but utilization of sensitive silver staining has enabled us to avoid use of radioisotope (20). This assay is capable of detecting anti-U3 RNP, anti-Th/To, and anti-U11/U12 RNP antibodies with high sensitivity and specificity, although identification of anti-RuvBL1/2 antibody still requires a protein-IP assay using ^{35}S methionine-labeled cultured cells. Recently, an immunoassay was developed to measure anti-Th/To antibody using Rpp25, one of the components of the Th/To complex, as an antigen (21). Anti-Th/To antibody detected by this immunoassay showed excellent agreement with anti-Th/To antibody detected by RNA-IP assay. An outline flowchart for identification of SSc-related ANAs including minor ones is shown in Fig. 2.

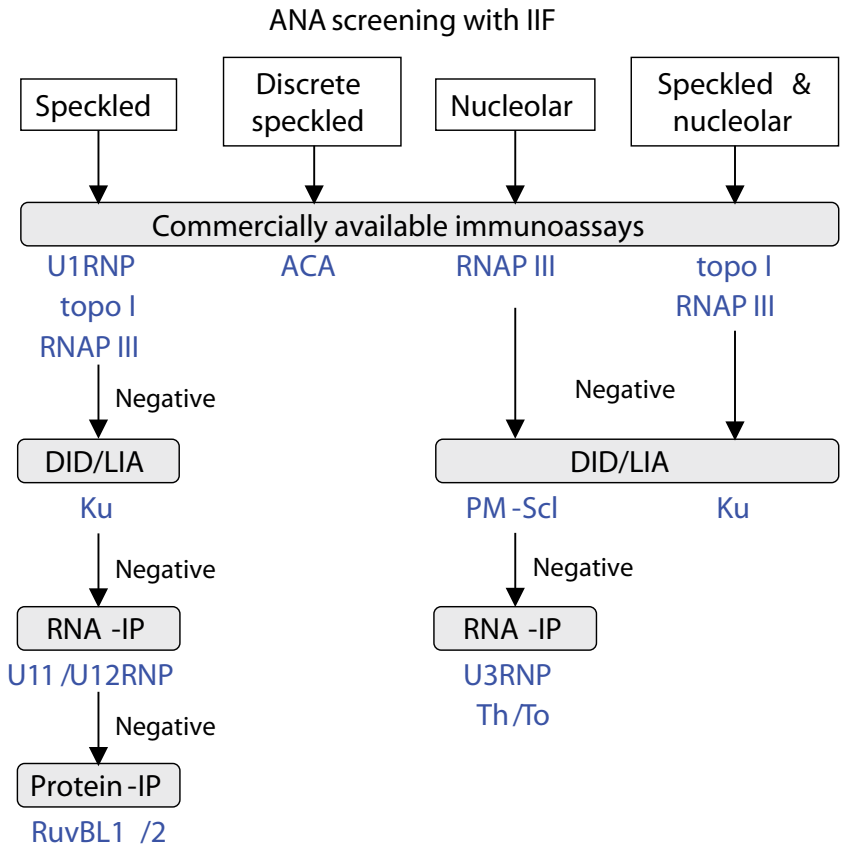

FIGURE 2 An outline flowchart for identification of SSc-related ANAs including minor ones.

TABLE 4 The American College of Rheumatology/European League Against Rheumatism criteria for the classification of SSc

Item	Sub-item(s)	Weight/ score
Skin thickening of the fingers of both hands extending proximal to the metacarpo-phalangeal joints	—	9
Skin thickening of the fingers (only count the higher score)	Puffy fingers Sclerodactyly of the fingers	2 4
Fingertip lesions (only count the higher score)	Digital tip ulcers Fingertip pitting scars	2 3
Telangiectasia	—	2
Abnormal nailfold capillaries	—	2
PAH and/or ILD (maximum score is 2)	PAH/ILD	2
Raynaud's phenomenon	—	3
SSc-related autoantibodies (maximum score is 3)	ACA Anti-topo I Anti-RNA polymerase III	3

[a]These criteria are applicable to any patient considered for inclusion in an SSc study. The criteria are not applicable to patients with skin thickening sparing the fingers or to patients who have a scleroderma-like disorder that better explains their manifestations. The total score is determined by adding the maximum weight (score) in each category. Patients with a total score of ≥9 are classified as having definite SSc.

CLINICAL SIGNIFICANCE OF MEASURING SSc-RELATED ANAs

Over the past decade, many studies have confirmed a strong association between ANA specificities and unique clinical phenotypes in SSc (1). However, it remains uncertain whether these autoantibodies play a direct pathogenic role or merely represent markers of particular disease manifestations. Measurement of SSc-related ANAs is essential in the clinical management of SSc patients. Because of the highly specific nature of SSc-related ANAs, their detection is useful in the diagnosis of SSc. In this regard, the presence of ACA, anti-topo I, or anti-RNAP III antibody is included in one of the criteria domains of a new classification system for SSc, which has been proposed by the American College of Rheumatology and the European League against Rheumatism (Table 4) (22). However, it is of note that a diagnosis should not be made solely on the basis of autoantibody-test results. Clinical features and prognosis in SSc patients are remarkably heterogeneous and grouping patients based on autoantibody profiles is a useful approach for clinicians. For example, the presence of anti-topo I antibody predicts future development of severe ILD; in contrast, patients with ACA should be monitored closely for development of PAH. It is generally believed that serial measurement of the antibody titers of SSc-related ANAs is not useful for assessment of disease severity and activity.

REFERENCES

1. **Steen VD.** 2008. The many faces of scleroderma. *Rheum Dis Clin North Am* **34:**1–15, v. PubMed
2. **Mehra S, Walker J, Patterson K, Fritzler MJ.** 2013. Autoantibodies in systemic sclerosis. *Autoimmun Rev* **12:**340–354. PubMed
3. **Koenig M, Dieudé M, Senécal JL.** 2008. Predictive value of antinuclear autoantibodies: the lessons of the systemic sclerosis autoantibodies. *Autoimmun Rev* **7:**588–593. PubMed
4. **Kuwana M, Kaburaki J, Mimori T, Tojo T, Homma M.** 1993. Autoantibody reactive with three classes of RNA polymerases in sera from patients with systemic sclerosis. *J Clin Invest* **91:**1399–1404. PubMed
5. **Aggarwal R, Lucas M, Fertig N, Oddis CV, Medsger TA Jr.** 2009. Anti-U3 RNP autoantibodies in systemic sclerosis. *Arthritis Rheum* **60:**1112–1118. PubMed
6. **Mitri GM, Lucas M, Fertig N, Steen VD, Medsger TA Jr.** 2003. A comparison between anti-Th/To- and anticentromere antibody-positive systemic sclerosis patients with limited cutaneous involvement. *Arthritis Rheum* **48:**203–209. PubMed
7. **Fertig N, Domsic RT, Rodriguez-Reyna T, Kuwana M, Lucas M, Medsger TA Jr, Feghali-Bostwick CA.** 2009. Anti-U11/U12 RNP antibodies in systemic sclerosis: a new serologic marker associated with pulmonary fibrosis. *Arthritis Rheum* **61:**958–965. PubMed
8. **Cavazzana I, Ceribelli A, Quinzanini M, Scarsi M, Airò P, Cattaneo R, Franceschini F.** 2008. Prevalence and clinical associations of anti-Ku antibodies in systemic autoimmune diseases. *Lupus* **17:**727–732. PubMed
9. **Kaji K, Fertig N, Medsger TA Jr, Satoh T, Hoshino K, Hamaguchi Y, Hasegawa M, Lucas M, Schnure A, Ogawa F, Sato S, Takehara K, Fujimoto M, Kuwana M.** 2014. Autoantibodies to RuvBL1 and RuvBL2: a novel systemic sclerosis-related antibody associated with diffuse cutaneous and skeletal muscle involvement. *Arthritis Care Res (Hoboken)* **66:**575–584. PubMed
10. **Tan EM, Feltkamp TE, Smolen JS, Butcher B, Dawkins R, Fritzler MJ, Gordon T, Hardin JA, Kalden JR, Lahita RG, Maini RN, McDougal JS, Rothfield NF, Smeenk RJ, Takasaki Y, Wiik A, Wilson MR, Koziol JA.** 1997. Range of antinuclear antibodies in "healthy" individuals. *Arthritis Rheum* **40:**1601–1611. PubMed
11. **Kuwana M, Kimura K, Kawakami Y.** 2002. Identification of an immunodominant epitope on RNA polymerase III recognized by systemic sclerosis sera: application to enzyme-linked immunosorbent assay. *Arthritis Rheum* **46:**2742–2747. PubMed
12. **Bentow C, Swart A, Wu J, Seaman A, Manfredi M, Infantino M, Benucci M, Lakos G, Mahler M.** 2013. Clinical performance evaluation of a novel rapid response chemiluminescent immunoassay for the detection of

autoantibodies to extractable nuclear antigens. *Clin Chim Acta* **424:**141–147. PubMed
13. **Parker JC, Bunn CC.** 2011. Sensitivity of the Phadia EliA connective tissue disease screen for less common disease-specific autoantibodies. *J Clin Pathol* **64:**631–633. PubMed
14. **Fritzler MJ, Fritzler ML.** 2006. The emergence of multiplexed technologies as diagnostic platforms in systemic autoimmune diseases. *Curr Med Chem* **13:**2503–2512. PubMed
15. **Damoiseaux J, Boesten K, Giesen J, Austen J, Tervaert JW.** 2005. Evaluation of a novel line-blot immunoassay for the detection of antibodies to extractable nuclear antigens. *Ann N Y Acad Sci* **1050:**340–347. PubMed
16. **Lee SA, Kahng J, Kim Y, Park YJ, Han K, Kwok SK, Park SH, Oh EJ.** 2012. Comparative study of immunofluorescent antinuclear antibody test and line immunoassay detecting 15 specific autoantibodies in patients with systemic rheumatic disease. *J Clin Lab Anal* **26:**307–314. PubMed
17. **Op De Beéck K, Vermeersch P, Verschueren P, Westhovens R, Mariën G, Blockmans D, Bossuyt X.** 2012. Antinuclear antibody detection by automated multiplex immunoassay in untreated patients at the time of diagnosis. *Autoimmun Rev* **12:**137–143. PubMed
18. **Copple SS, Martins TB, Masterson C, Joly E, Hill HR.** 2007. Comparison of three multiplex immunoassays for detection of antibodies to extractable nuclear antibodies using clinically defined sera. *Ann N Y Acad Sci* **1109:**464–472. PubMed
19. **Villalta D, Imbastaro T, Di Giovanni S, Lauriti C, Gabini M, Turi MC, Bizzaro N.** 2012. Diagnostic accuracy and predictive value of extended autoantibody profile in systemic sclerosis. *Autoimmun Rev* **12:**114–120. PubMed
20. **Forman MS, Nakamura M, Mimori T, Gelpi C, Hardin JA.** 1985. Detection of antibodies to small nuclear ribonucleoproteins and small cytoplasmic ribonucleoproteins using unlabeled cell extracts. *Arthritis Rheum* **28:**1356–1361. PubMed
21. **Mahler M, Gascon C, Patel S, Ceribelli A, Fritzler MJ, Swart A, Chan EK, Satoh M.** 2013. Rpp25 is a major target of autoantibodies to the Th/To complex as measured by a novel chemiluminescent assay. *Arthritis Res Ther* **15:**R50. PubMed
22. **van den Hoogen F, Khanna D, Fransen J, Johnson SR, Baron M, Tyndall A, Matucci-Cerinic M, Naden RP, Medsger TA Jr, Carreira PE, Riemekasten G, Clements PJ, Denton CP, Distler O, Allanore Y, Furst DE, Gabrielli A, Mayes MD, van Laar JM, Seibold JR, Czirjak L, Steen VD, Inanc M, Kowal-Bielecka O, Müller-Ladner U, Valentini G, Veale DJ, Vonk MC, Walker UA, Chung L, Collier DH, Csuka M, Fessler BJ, Guiducci S, Herrick A, Hsu VM, Jimenez S, Kahaleh B, Merkel PA, Sierakowski S, Silver RM, Simms RW, Varga J, Pope JE.** 2013. 2013 classification criteria for systemic sclerosis: an American College of Rheumatology/European League against Rheumatism collaborative initiative. *Arthritis Rheum* **65:**2737–2747. PubMed

Antibody and Biomarker Testing in Rheumatoid Arthritis

ANN DUSKIN CHAUFFE AND MICHAEL RAYMOND BUBB

92

Rheumatoid arthritis (RA) is a chronic systemic disease characterized by autoimmune-mediated joint destruction. RA affects 1% of the global population with a predilection for females. The pathogenesis of RA has not been fully elucidated; however, it is thought to be due to an environmental trigger stimulating an immune response in a genetically susceptible host. The resultant inflammatory cascade mediates synovial proliferation and ultimately joint destruction. Disease expression is not limited to the joints. Extra-articular manifestations occur in the lungs, eyes, skin, and the cardiovascular system culminating in significant morbidity and premature mortality (1). Moreover, numerous studies show substantial irreversible joint damage occurs within the first 2 years of disease onset. Thus, early diagnosis and aggressive treatment is paramount in preventing morbidity and mortality (2).

Risk factors associated with RA include female sex, Caucasian race, and tobacco use (3). Familial studies have also identified specific human leukocyte antigen (HLA) genotypes associated with disease development. HLA-DR4 has been recognized for more than 20 years as a risk factor. More recent data suggests a stronger association with particular DR4 alleles known as the "shared epitope," which confers the risk for more aggressive disease.

In 1958, the American Rheumatism Association developed a classification criterion for RA. This was revised by the American College of Rheumatism (ACR) in 1987. Importantly, the 1987 criterion was designed to identify a uniform population of patients with RA for research purposes. The criterion is effective at distinguishing between established RA and other arthritides, as most of the patients studied had long-standing disease. The utility of the diagnostic criterion was limited in clinical practice because it was not helpful in identifying early disease. Two of the seven criteria, nodules and radiographic changes, are infrequently evident early in the disease but rather accumulate with time. Additionally, the more recent discovery of an antibody that is highly associated with RA, anti-cyclic citrullinated peptide antibody (ACPA), was not part of the original criterion, as it had not been identified. In 2010 the ACR and the European League Against Rheumatism (EULAR) sought to rectify these issues and developed a new criterion with the express purpose of aiding in identifying early RA. The 2010 criteria includes a point system with the presence of synovitis in a pattern suggestive of RA, rheumatoid factor (RF) and ACPA serologic positivity, elevation of inflammatory markers (CRP and ESR), and duration of symptoms greater than 6 weeks. A score of at least 6 of 10 possible points from all four domains indicates RA (4). To date of this publication, studies have generally shown superiority of the 2010 criteria in identifying early RA while failing to identify the so-called "seronegative" patients, those lacking RF and ACPA. Thus, RF and ACPA seropositivity have been identified as independent predictors of disease development. Moreover, the presence of these antibodies also portends a more aggressive disease phenotype (5). A newer laboratory test, the multi-biomarker disease activity (MBDA) score, measures 12 proteins and has also been found to correlate with RA disease activity (6). The remainder of this chapter will further explore the array of diagnostic testing and serologic markers in RA.

RHEUMATOID FACTOR

Rheumatoid factor (RF) is an antibody that was first described by Waaler in 1939 when he noted that sera from RA patients caused agglutination of sheep erythrocytes coated with rabbit antibodies (7). RF was later found to be an antibody directed against the Fc portion of human IgG. RF-IgG immune complexes deposit in tissues and activate the classical complement pathway, perhaps contributing to the extra-articular manifestations of RA. Although RF may be IgG, IgM, IgA, or IgE, the IgM isotype is the most commonly measured in commercial assays. RF has a sensitivity of 68 to 81% and a specificity of 60 to 85% in RA (8). As previously mentioned, RF has prognostic value in RA. In general, RF-seropositive patients have a more aggressive joint disease course, as well as increased extra-articular manifestations, such as nodules and vasculitis (8). There are some reports that RF isotypes other than IgM are associated with particular disease manifestations, but these findings have not been widely applied in clinical testing. In the context of drug trials, a decrease in IgM-RF titers has been shown to correlate with clinical response, and serial measurements may be helpful in guiding response to treatment with disease-modifying anti-rheumatic drugs. Finally, loss of RF positivity confers improved prognosis (9).

However, RF has been identified in a host of other autoimmune conditions, such as Sjögren's syndrome, systemic lupus erythematosus (SLE), vasculitis, and idiopathic pulmonary

doi:10.1128/9781555818722.ch92

fibrosis. RF is also seen in 3 to 5% of young healthy individuals, as well as 10 to 30% of elders in good health (10). Tobacco smokers have also been found to have chronically elevated RF titers. Longitudinal data indicates that smoking a little as six to nine cigarettes per day for more than 20 years increases the risk of developing seropositive RA. In one study, female smokers had an odds ratio of 1.7 (95% confidence interval [CI], 1.2–2.3), while male smokers had an odds ratio of 1.9 (95% CI, 1.0–3.5). The risk of developing RA was proportionate to smoking intensity while the increased risk of RA was conserved for 10 to 19 years after cessation (11).

Clinical Interpretation of Rheumatoid Factor

Rheumatoid factor (RF) is a serological marker for RA. Although RF seropositivity is frequently misinterpreted as indicative of the diagnosis of RA, it is not, and the specificity of RF is limited to ~60%. The diagnosis of RA must include a consideration of clinical context that factors in pretest probability based on Bayes' theorem (12). Patients with other autoimmune diseases (Sjögren's, vasculitis) are often seropositive for RF. Interestingly, RF-positive Sjögren's patients have a worse prognosis, and significant changes in RF titer should alert the clinician to the development of lymphoma. It is important for the clinician to keep in mind that RF is often seen in other malignancies, such as Waldenström's macroglobulinemia, non-Hodgkin's lymphoma, other B-cell malignancies, and chronic lymphocytic leukemia, as the patients acquire monoclonal gammopathies with RF activity. RF seropositivity is also common in infections such as tuberculosis, leprosy, osteomyelitis, syphilis, bacterial endocarditis, infectious mononucleosis, and, most notably, hepatitis C virus (HCV) (13). The prevalence of RF in the HCV population is estimated to be 50%, but few patients have arthritis. RF is the major constituent of mixed cryoglobulins, which are often found in HCV patients. The cryoglobulins, or RF immunoglobulin-complement complexes, precipitate out of the serum in cool temperatures, leading to small vessel vasculitis. The typical manifestations include arthralgias, purpuric or ulcerative skin lesions, and membranoproliferative glomerulonephritis (14). Finally, RF frequently is positive in a substantial portion of the healthy population, particularly the elderly (10).

In RA, most patients are seropositive for RF within 6 months of onset of symptoms; however, studies have also identified seropositivity years prior to disease onset. RF functional avidity changes over time and persistently high levels of RF have been shown to be associated with more severe radiographic joint destruction. Although not often followed clinically, RF titers may correlate with RA disease activity. Changes in the RF concentration can reliably be measured by nephelometry and enzyme-linked immunosorbent assay (ELISA), but not agglutination (15).

ANTIBODIES AGAINST CITRULLINATED PROTEINS

Several apparently distinct autoantibodies have been described in RA over the last few decades. Gradually, several of these autoantibodies have been identified as recognizing related determinants containing peptides that have post-translational modification of the amino acid arginine to citrulline by enzymatic citrullination. These antibodies include anti-perinuclear factor (APF), anti-keratin antibody (AKA), anti-filaggrin (AFA), anti-Sa, and the synthetically produced anti-cyclic citrullinated peptide. Collectively, these antibodies are referred to as ACPAs, or anti-citrullinated protein antibodies (16).

Citrullination

Citrulline is produced when the enzyme peptidyl-arginine deiminase (PAD) modifies arginine with a corresponding change in charge from positive to neutral. There are four related isoforms of PAD in humans which can citrullinate arginine, and some proteins have a higher affinity for citrullination by the various isoforms of PAD. Moreover, the amino acids neighboring arginine residue influence its susceptibility to citrullination (17).

Citrullination is a normal physiological process that typically occurs in dying cells. The immune system does not typically encounter citrullinated proteins as these apoptic cells are quickly ingested by clearing cells such as macrophages. Several hypotheses are generally reported to explain the evolution of citrullinated antibodies in RA. In the first hypothesis, the immune trigger is due to inefficient or inadequate clearance of PAD enzymes and citrullinated proteins in highly inflammatory states. In support of this hypothesis, studies have identified citrullinated proteins at inflammatory sites (18).

An alternative hypothesis attributes citrullinated antibody production to aberrantly expressed PAD. The increased PAD generates additional citrullinated antigens in the synovium, thereby supplying the opportunity for immune recognition and stimulation. Studies have demonstrated genetic polymorphisms in one of the PAD genes (19). Moreover, this same PAD haplotype, PADI4, has been associated with RA susceptibility (17, 19).

A final theory suggests that citrullinated proteins are not pathologic. Rather, RA patients develop an abnormal humoral response to these proteins. Interestingly, citrullinated proteins have been identified in the synovium of RA patients, as well as in patients with osteoarthritis and reactive arthritis. There is strong evidence of a genetic predisposition to the development of citrullinated antibodies (20). This will be further discussed below in the Genetics section.

Specific Antibodies Against Citrullinated Proteins

APF was identified in 1964 when human buccal mucosal cells were evaluated under indirect immunofluorescence. In 1979, AKA was identified similarly as an IgG directed against rat esophageal epithelium. It was not until 1995 that APF and AKA were found to have a shared specificity for a cytokeratin-filament aggregating protein, filaggrin, and were designated AFA (21). Since then, the shared specificity was found to be more related to citrullination than the target protein. A diverse number of synthetic cyclical citrullinated peptides bind AFA, including 20 different epitopes on profilaggrin and the α- and β-chains of fibrin. AFA was found to be highly specific, 92 to 99%, for RA and present at disease onset. AFA testing has not been widely available as the original immunofluorescence assay was laborious and difficult to standardize. However, a more recently developed ELISA to the major epitopes of filaggrin has addressed this by providing automation and standardization (20).

In 1998, a synthetic antigen was developed for detection of citrullinated proteins known as ACPA. The synthetic antigen conformation was chosen to optimize antibody sensitivity and specificity and is not the natural antibody determinants. The cyclic conformation enables more efficient recognition of the citrullinated epitope by the antibody. The first-generation ELISA assay, anti-CCP1, used a filaggrin-derived cyclic peptide as the antigenic substrate. It had outstanding specificity for RA, 95%, but lacked in sensitivity, 53% (20). In 2002, a second-generation assay (anti-CCP2) was developed after screening 12 million peptides from dedicated synthetic peptide libraries against RA

sera. The best citrullinated peptides were incorporated into a new format and the assay captured the antigenic determinants for APF, AKA, AFA, and anti-CCP1. Anti-CCP2 has been found to have a greater sensitivity, 68%, than anti-CCP1 in diagnosis of RA. Moreover, there was no loss of specificity; 98% (20). A third-generation assay, anti-CCP3, was designed by combinatorial peptide engineering and contains multiple citrullinated epitopes displayed in a conformational structure to increase epitope exposure and thus immunoreactivity, particularly for early RA. The sensitivity of anti-CCP3 is slightly superior to anti-CCP2. Finally, another assay, anti-CCP3.1, has been developed to include the IgA isotype of anti-CCP to the standard IgG assay. The addition of IgA increased the sensitivity by 4.3% over anti-CCP2 (22).

Another autoantibody, anti-Sa, was named for the French-Canadian patient in which it was first identified. Anti-Sa was later found to react with citrullinated vimentin. Vimentin is a cytoskeletal protein widely expressed by macrophages and mesenchymal cells. It is modified in macrophages undergoing apoptosis and antibodies are thought to be generated when there is delayed clearance. Vimentin has been identified in the human placenta, spleen and, notably, in the pannus of rheumatoid patients (23). Likewise, anti-Sa is often found in patients with severe articular disease. In one study, anti-Sa was found to be three times more prevalent in patients with a highly destructive RA phenotype. Anti-Sa is least sensitive in early RA as titers increase as the disease progresses. Research has also demonstrated that the presence of anti-Sa predicts higher joint counts and requires more aggressive treatment (24).

As the technology for citrulline antibody testing evolves, new assays are being developed. One such test is the mutated (or modified) citrullinated vimentin, anti-MCV. An ELISA assay has been developed for anti-MCV but a systematic review found anti-MCV to have similar sensitivity to ACPA in the diagnosis of RA (25); however, anti-MCV has been identified in ACPA-seronegative RA patients. Thus, it may be useful in identifying RA in seronegative patients. Of particular interest in monitoring disease activity, one study found that anti-MCV titers decreased in conjunction with DAS-28 in patients receiving infliximab (26).

Fibrin binding globulin (FBG) is a glycoprotein found in blood plasma that is also a target of citrullination. During inflammation, the concentration of FBG increases from ~3 mg/ml to more than 7 mg/ml (27). It is hypothesized that the deimination of FBG that has been found in inflamed RA joints may be mediated by PAD (18, 19). Anti-FBG has not been widely studied outside of animal models, so its significance is not well characterized (27).

ACPA Clinical Significance

Testing for ACPA is now widely practiced, as about 35 to 40% of RF-negative RA patients are seropositive for ACPA (28). Likewise, there is a voluminous literature demonstrating the clinical significance of ACPA in RA (2, 28). Multiple studies have found ACPA to be more specific for RA than RF. Overall, the sensitivity and specificity of ACPA is ~60% and 95%, respectively. Moreover, ACPA seropositivity has been identified in healthy blood donors years before clinical disease activity was identified, demonstrating its positive predictive value in RA (29). Seropositivity for ACPA has also been associated with a heightened risk of destructive joint disease (28). The utility of ACPA for monitoring response to RA treatment is controversial. Levels for ACPA may decrease early in disease if prompt treatment is instituted. Although the literature is not completely clear, the preponderance of data suggests that patients with established RA do not experience sustained decreases in ACPA titers (26).

OTHER ANTIBODIES ASSOCIATED WITH RA

Anti-glucose-6-phosphate isomerase (anti-GPI) has been recognized in 64% of RA patients. Anti-GPI appears to be produced in the synovium, as titers have been found to be higher in the synovial fluid than the sera. Interestingly, anti-GPI has been identified in T-cell receptor-transgenic mice. Moreover, passive transfer of anti-GPI to healthy mice resulted in arthritis (30).

Anti-calpastatin antibodies have also been reported in RA. Calpains are ubiquitous calcium-dependent proteases. There are a diverse number of substrates for these enzymes, including cytoskeletal, nuclear, and extracellular proteins. Some researchers theorize that calpains play a role in cartilage destruction, as they have been identified in inflamed synovium (31). Calpastatin is the natural inhibitor of calpains. Thus, an antibody to calpastatin increases the protease. Immunoblot testing for anti-calpastatin has identified the antibody in 45% of RA patients, but also identified it in patients with SLE, myositis, and systemic sclerosis, as well as healthy controls (32).

Another antibody associated with RA is anti-RA33, an antibody to heterogeneous nuclear ribonucleoprotein A2. Anti-RA33 is found in approximately 35% of RA patients and is thus less specific than ACPA or RF in diagnosing RA. In one study it was also identified in 20% of SLE and 40% to 60% of mixed connective tissue disease patients. Interestingly, anti-RA33 has been identified in RF- and ACPA-seronegative RA patients. Moreover, anti-RA33 has been identified in early RA. Longitudinal studies have found patients with anti-RA33 to have a good prognosis, having less radiographic destruction than patients who are seropositive for ACPA or RF (33).

Binding immunoglobulin proteins (BiP) are molecular chaperones located in the lumen of the endoplasmic reticulum (ER), which play a critical role in maintaining cellular homeostasis. One such BiP is the 78-kDa glucose-regulated ER chaperone which has been identified as an autoantigen in RA (anti-BiP). This particular BiP is overexpressed in the synovium of rheumatoid joints, and anti-BiP has been identified in early and pre-disease sera. In addition, some have theorized that BiPs also have immunomodulatory properties and may represent a future therapeutic target (34).

ANTIBODIES LESS SPECIFIC FOR RA

A variety of other antibodies are seen in the sera of RA patients. However, these other antibodies are not very specific for RA. These include anti-collagen type II, antifibronectin, and anti-neutrophil cytoplasmic antibodies, which will be briefly discussed for the sake of completeness.

Antibodies against collagen type II (anti-CII) have been found in 30% of RA patients. Unfortunately, anti-CII has been found in nearly 50% of relapsing polychondritis, 20% of SLE, 15% of systemic sclerosis, and in 50% of those with leprosy. Thus, it is not specific for RA (35). Antifibronectin is a glycoprotein that interacts with collagens and adhesion molecules. Antifibronectin antibody has only been identified in 14% of RA patients, while being identified in 34% of SLE patients, thus it is not a good marker in RA (36). Anti-cytoplasmic antibodies are most notably associated with vasculitis. However, they were first identified in the sera of an RA patient and can be found in up to 30% of RA

TABLE 1 Summary of well-characterized autoantigens in rheumatoid arthritis

Class	Autoantigen
Citrullinated proteins	ACPA, Sa, vimentin, filaggrin, fibrin binding globulin
Articular cartilage	Collagen II
Serum protein	RF
Nuclear components	RA33
Enzymes	Calpastatin, glucose-6-phosphate isomerase
Stress protein	BiP
Glycoprotein	Fibronectin

patients, as well as in other autoimmune conditions and in a variety of infections (37). Table 1 summarizes the autoantigens associated with RA.

TESTING METHODS

There are several assays used to identify antibodies (Table 2). The original method of RF identification employed visible particle agglutination of human or rabbit IgG bound with a variety of substrates, including erythrocytes, latex, and charcoal. Another method, laser nephelometry, utilizes light scatter by latex particles coated with IgG. Finally, ELISA utilizes either the human or rabbit Fc region of IgG to bind the various RF subtypes (38). The latter two approaches are better suited for automation and consequently represent the bulk of commercially available testing. The antigen source for most RF assays is usually gamma globulin pools from humans, rabbits, or cattle. The various species' IgG fractions differ in RF binding capacity leading to result variability. The most commonly used IgG source is rabbit because it is more specific, although less sensitive, for RA when compared to other species (39).

Agglutination

The classical agglutination assay, the Waaler-Rose test, utilized sheep erythrocytes coated with rabbit IgG. If RF was present, the erythrocytes agglutinated (40). Testing was originally performed in test tubes with agglutination prompted by temperature-controlled incubation and centrifugation. A more rapid method involves quantification of agglutination on a glass slide, negating the need for incubation and centrifugation. IgM antibodies are more efficient in agglutination reactions, so it is most sensitive for the IgM RF isotype. The RF content is reported at the last doubling dilution at which agglutination can be visualized. The reciprocal of this dilution is known as the antibody titer. A major limitation of this method is the significant inconsistency in reported results due to condition variability and the subjective nature of determining when agglutination ceases (41).

Nephelometry

Laser nephelometry utilizes an antigen, heat-aggregated or chemically cross-linked IgG aggregates, which form antigen-antibody complexes. A beam of light is then passed through tubes containing fixed amounts of antibody and variable concentrations of antigen. The light scatter is a result of the formation of the concentration of immune complexes. Latex methods utilize IgG-coated latex particles, but again measure light scatter. Nephelometry is commonly used because it is automated and provides reliable results (15).

ELISA

ELISAs measure the amount of immunoglobulin that binds to target IgG absorbed to a solid phase, usually a polystyrene microtiter plate. Microwells are coated with the antigen, human IgG, and patient serum is added allowing the patient's RF to form antigen-antibody complexes. Unbound serum proteins are removed by washing the microwells. Enzyme-conjugated anti-human IgM (or IgG for IgG RF) is added to the wells. The enzyme conjugate binds to the antigen-antibody complex, and excess conjugate is washed away. Addition of a specific substrate begins a hydrolytic reaction with the bound enzyme conjugate, causing color

TABLE 2 Comparison of antibody assays

Assay	Equipment expense	Automation	Interlaboratory precision	Interferences	Sensitivity
Sheep cell agglutination	Low	No	Low	C1q, anti-rabbit IgG, anti-sheep erythrocytes	Low
Latex-fixation agglutination	Low	No	Low	C1q, fibrin	Medium
Nephelometry	High	Yes	High	Fibrin, cryoglobulins, other immune complexes if assay is polymer enhanced	High
ELISA	Moderate to high	Variable	Moderate	Nonspecific plastic binders heterophilic antibodies	High
Multiplex immunoassay	High	Yes	Moderate	RF, heterophilic antibodies	Medium

development. The intensity of the color change is proportional to the amount of IgM (or IgG) RF antibody. A spectrophotometer analyzes the result, which is expressed in international units per milliliter (IU/ml). There may be nonspecific binding of serum IgG to the plastic wells, a phenomenon known as "background binding." This is overcome by subtracting the optical density from wells that are blocked but not coated with antigen. In general, ELISA testing is considered reasonably precise (42).

Calibration

To promote consistency in IgM-RF identification, the World Health Organization (WHO) or the Centers for Disease Control and Prevention provide sera for nephelometer and ELISA calibration. The WHO standard does not contain IgG or IgA, so cannot be used for IgG or IgA RF. Each assay should be run with control sera; ideally, the control should detect one negative and two positive sera, one at a low positive cutoff and the other at a high positive cutoff (43). The WHO standard was developed in 1970 and its activity was projected to decrease by 50% over 8 years. However, it is not clear just how long the calibration sera is good for with ranges reported from 1 to 250 years (44).

Shortly after the first ELISA for ACPA was developed, multiple companies developed their own assays. Likewise, there is variance in the antigens utilized, making it difficult to compare the results. Euro-Diagnostica has proposed a freeze-dried standardized reference serum to the International Committee. The selected serum was tested in 12 commercially available ELISA-ACPA kits. Sera from 20 RA patients with variable antibody concentrations were analyzed, and the relative concentrations were calculated using both the kit's own curve and the six dilutions of the reference serum as a calibration curve. Additionally, sera from 50 healthy controls were used as cutoff values for the reference serum. Utilizing the reference serum led to significant reduction in variability of the results. The mean coefficient of variation (CV) was reduced from 76.4% to 27.9% ($P = 0.018$) and from 85.9% to 33.5% ($P = 0.028$) for the medium/high and negative samples, respectively. Low positive sera CV was also reduced, but to a smaller degree, from 82.5% to 55.5% ($P = 0.043$). Thus, this reference serum may be used in the future to establish a calibration curve and reduce the dispersion of antibody values, while allowing comparison of results from different manufacturer assays (45).

Multiplex Testing

Multiplex immunoassays test multiple antibodies simultaneously from the same specimen sample. Multiplex testing typically utilizes combinations of non-human-derived analyte-specific antibodies. Bead-based immunoassays can test up to 96 targets at once. A similar assay, cytometric bead assay (CBA), is based on membrane-based ELISA technology. Both of these techniques enable testing of multiple antibodies from one small-volume sample. Though these methods are efficient, there are technical concerns regarding the use of antibody-based technology in RF-positive RA. RF has specificity for antigenic epitopes on Fc portions of IgG. In states such as RA, where there are high titers of RF, there is the potential for RF interference. Excess RF can bind to the antibodies used to detect them, resulting in analyte-independent signaling. Heterophilic antibodies also have the potential to bind with analyte antibodies. Techniques to minimize the confounding effects of RF and heterophilic antibodies include blocking of IgG and IgG removal with PEG 6000 (Fluka). However, evaluation of bead-based multiplex assays with interference removing techniques has revealed high numbers of false positives. Not surprisingly, the low specificity was found to correlate with interfering antibody titers, with titers greater than 100 IU/ml escaping the interference removal mechanism. Surprisingly, the cytometric bead assay was not affected by the presence of RF, but the sensitivity of the assay was found to be quite low, missing true positives (46).

Multi-Biomarker Disease Activity Analyses

A multiplex assay has been developed to simultaneously measure multiple biomarkers of RA disease activity, with the result summarized in a single score from 1 to 100. This assay, known as Vectra DA (Crescendo Bioscience, California), measures 12 serum proteins to calculate an MBDA score. The 12 chosen biomarkers were screened from 396 candidate markers identified in 1900 RA sera samples. Biomarkers utilized were validated against disease activity scores (DAS28) (6). The selected biomarkers include: adhesion molecule, vascular cell adhesion molecule 1 (VCAM-1); growth factors, epidermal growth factor (EGF) and vascular endothelial growth factor A (VEGF-A); cytokine-related proteins, interleukin 6 (IL-6) and tumor necrosis factor receptor type I (TNF-RI); matrix metalloproteinases (MMP), MMP-1 and MMP-3; skeletal-related protein, human cartilage glycoprotein 39 (YKL-40); hormones, leptin and resistin; acute-phase proteins, serum amyloid A (SAA) and C-reactive protein (CRP). As would be expected from the additional information, the MBDA performs as well as or better than the CRP alone when assessing the level of RA activity over time and predicting radiographic progression (47). However, longitudinal follow-up is needed to assess the long-term effect of lowering MBDA scores on disease progression. Future studies are likely to prove that individual components of the MBDA (or assays not in the original MBDA) have utility in answering specific clinical questions regarding disease activity, prognosis, and response to individual therapy, raising the possibility that it is premature to focus on an aggregate compilation of these assay values at this time.

As previously discussed, multiplex assays are at risk for RF interference. The 12 biomarkers included in the Vectra DA have been evaluated for RF, human anti-mouse antibody, and antibody cross-reactivity interference. Analysis did not demonstrate significant interference in any of these domains. Additionally, testing was performed to assess for the possibility of pharmacologic interference. Testing did not identify any drug confounders in the MBDA score. Finally, freeze-thaw stability was evaluated. Assays chosen had less than 15% difference when compared to fresh samples (48).

FACTORS THAT INTERFERE WITH RF MEASUREMENTS

RF measurement can be obscured by several factors. In agglutination and nephelometric assays, high levels of C1q bind and cross-link with IgG, giving false-positive results. C1q is an acute-phase reactant and is often elevated in inflammatory disorders. Heating the serum to 56°C for 15 to 30 minutes circumvents this issue as C1q is heat labile. Complement inhibition can be avoided by adding polyvinyl sulfonate to the reaction mixture (49). Incompletely clotted serum, fibrin, and fibrinogen can interfere with or induce agglutination or aggregation in both nephelometric and agglutination assays, leading to false-positive or false-negative results. Nephelometric techniques that use polyethylene glycol or similar polymers to accelerate immune complex formation may give false-positive results from polymer-enhanced aggregation of fibrin, lipoproteins, cryoglobulins, or other immune complexes (50).

This can be avoided by subtracting background light scatter in specimens that are allowed to react in the absence of aggregated IgG target antigen or by simply avoiding the use of an accelerating polymer. Additionally, mixed cryoglobulins are composed mainly of RF, which can precipitate from the remainder of the serum at cool temperatures, resulting in a low titer or false negative (51). A plasma protein, histidine-rich glycoprotein, inhibits formation of RF complexes and enhances the solubility of RF-immune complexes, likely through competitive binding to IgG, leading to false negatives (52).

Heterophilic anti-immunoglobulin antibodies are naturally occurring polyreactive antibodies against poorly defined antigens. They generally demonstrate low affinity and weak binding. About 15% of the heterophilic antibodies recognize the Fc portion of IgG and are considered true positives. The remaining 85% recognize the Fab region of IgG and are not RF, rendering a false-positive result. Interference by heterophilic antibodies may be eliminated by using rabbit F(ab) or F(ab′)2 fragments, as there is little cross-reactivity (53).

GENETICS OF RA

Twin and family data suggest a heritability estimate of 60% for RA. Thus, more than genetic factors contribute to the variability in disease expression. The major histocompatibility complex (MHC) of chromosome 6 was explored as a potential candidate for RA because it was known to contribute to the strength and pattern of immune response (54). The genes for a particular human leukocyte antigen, HLA-DR, were first reported in 1976 by Stastny when he recognized an association with RA. Since then, a 5-amino-acid sequence motif in the allelic hypervariable region of the HLA-DR B chain has become known as the "shared epitope" (SE), as it is a major contributor to RA risk. The HLA-DRB1*0401 allele has been found to be the most strongly associated polymorphism in white patients with RA. Other alleles have seen been identified, including DRB1*1001, DQB1*0302, DQB1*0302, and DQB1*0501, which are associated with ACPA seropositivity. Likewise, these patients have more aggressive, erosive disease. Not surprisingly, studies combining RF and ACPA seropositivity and portions of the SE suggest that the presence of both is strongly predictive of the future development of RA (55). Interestingly, the contribution of HLA alleles to the genetic variance is 40% for ACPA-seropositive disease, but only 2% for ACPA-negative patients (56).

Genomic-wide association studies (GWAS) in RA have identified seven RA risk loci. These single nucleotide polymorphisms (SNPs) are in close proximity to genes associated with immune function (57). The susceptibility loci identified include: interlukin 2A and B (IL2RA and IL2RB, respectively); signal transducer activator of transcription 4 (STAT4); interferon-related factor 5 (IRF5); peptidylarginine-deiminase 4 (PADI4); protein tyrosine phosphatase, non-receptor type 22 (PTPN22); tumor necrosis factor receptor-associated factor 1(TRAF1); CD40; CC chemokine ligand 21 and CC chemokine receptor 6 (CCL21 and CCR6); CD2 and Fc gamma receptor (FCGR2A) (57).

ENVIRONMENTAL TRIGGERS

One feature of RA occurrence that seems to point to an environmental trigger is disease clustering. Population-based incidence studies have demonstrated trends in new cases. There have been a large number of infectious agents suspected to be linked to RA. Infection agents have included Epstein-Barr virus, parvovirus B-19, and mycoplasma. However, epidemiological studies have generally not found evidence to support this link. Additionally, seasonal variation has not been recognized (58).

Thus far, the only unequivocally identified risk factor for RA is a history of tobacco use (3). In particular, ACPA seropositivity has been linked with cigarette smoking. A major gene-environment interaction between smoking and the SE has been identified in ACPA-seropositive RA, but not for ACPA-negative RA. Moreover, the risk for RA increases 21-fold when patients have a history of smoking and double copies of the SE genes. As an interesting corollary, citrullinated antigens have been identified in the bronchoalveolar lavage of smokers (59).

COMBINED TESTING ACPA AND RF

The presence of certain autoantibodies, such as RF and ACPA, are distinguishing features in RA. They are incredibly valuable in making a prompt diagnosis of RA. The group of citrullinated antibodies, exemplified by ACPA, is highly specific for RA at 95%. Moreover, the sensitivity is 50% to 80%, similar to that of RF in RA (20). Although RF is less specific (75%), it is also very useful in making the diagnosis of RA. Both are particularly important in early synovitis, as RF and ACPA independently contribute to the diagnosis of RA. Thus, there is value in testing for both antibodies early in disease to maximize predictive value (38). The importance of early treatment has been well established, as delayed diagnosis often leads to delays in treatment. These antibodies are not only useful for diagnosis, but also in providing insight into prognosis. The use of these two antibodies together has an additive predictive value for the development of erosions (28). Likewise, patients who are seronegative for both RF and ACPA may have a different syndrome, as they typically have a milder disease course with less erosions and fewer extra-articular manifestations (60).

FINAL THOUGHTS

What laboratory tests should be performed in a patient presenting with synovitis? As outlined above, typically both RF and ACPA are evaluated. Inflammatory markers, such as CRP and ESR, and CBC, for evaluation of anemia that often is found in inflammatory states, are also useful to gauging the disease activity. A newer multi-biomarker disease activity (MBDA) test is also available as a tool to measure disease activity in RA, but its clinical role has yet to be established. Radiographs are often procured but typically are normal early in disease. Despite this, it is helpful to have a baseline study for future comparisons of disease activity. Although this chapter focused on serologic and laboratory evaluation of RA, the importance of history and physical cannot be overstated in making the correct diagnosis.

REFERENCES

1. **Turesson C, Jacobsson L, Bergström U, Truedsson L, Sturfelt G.** 2000. Predictors of extra-articular manifestations in rheumatoid arthritis. *Scand J Rheumatol* **29:**358–364. PubMed
2. **Hetland ML, Stengaard-Pedersen K, Junker P, Østergaard M, Ejbjerg BJ, Jacobsen S, Lottenburger T, Hansen I, Tarp U, Andersen LS, Svendsen A, Pedersen JK, Lauridsen UB, Ellingsen T, Lindegaard H, Pødenphant J, Vestergaard A, Jurik AG, Hørslev-Petersen K; CIMESTRA Study Group.** 2010. Radiographic progression and remission rates in early rheumatoid arthritis: MRI bone oedema

and anti-CCP predicted radiographic progression in the 5-year extension of the double-blind randomised CIMESTRA trial. *Ann Rheum Dis* **69:**1789–1795. PubMed

3. **Silman AJ, Newman J, MacGregor AJ.** 1996. Cigarette smoking increases the risk of rheumatoid arthritis. Results from a nationwide study of disease-discordant twins. *Arthritis Rheum* **39:**732–735. PubMed
4. **Aletaha D, Neogi T, Silman AJ, Funovits J, Felson DT, Bingham CO III, Birnbaum NS, Burmester GR, Bykerk VP, Cohen MD, Combe B, Costenbader KH, Dougados M, Emery P, Ferraccioli G, Hazes JM, Hobbs K, Huizinga TW, Kavanaugh A, Kay J, Kvien TK, Laing T, Mease P, Ménard HA, Moreland LW, Naden RL, Pincus T, Smolen JS, Stanislawska-Biernat E, Symmons D, Tak PP, Upchurch KS, Vencovský J, Wolfe F, Hawker G.** 2010. 2010 Rheumatoid arthritis classification criteria: An American College of Rheumatology/European League Against Rheumatism collaborative initiative. *Arthritis Rheum* **62:**2569–2581. PubMed
5. **Cornec D, Varache S, Morvan J, Devauchelle-Pensec V, Berthelot JM, Le Henaff-Bourhis C, Hoang S, Martin A, Chalè G, Jousse-Joulin S, Saraux A.** Comparison of ACR 1987 and ACR/EULAR 2010 criteria for predicting a 10-year diagnosis of rheumatoid arthritis. *Joint Bone Spine* **79:**581–585.
6. **Hirata S, Dirven L, Shen Y, Centola M, Cavet G, Lems WF, Tanaka Y, Huizinga TW, Allaart CF.** 2013. A multi-biomarker score measures rheumatoid arthritis disease activity in the BeSt study. *Rheumatology (Oxford)* **52:**1202–1207. PubMed
7. **Natvig JB, Tønder O.** 1998. The discovery of the rheumatoid factor. I. Erik Waaler. 1940. *Clin Exp Rheumatol* **16:**340–344. PubMed
8. **Bas S, Perneger TV, Seitz M, Tiercy JM, Roux-Lombard P, Guerne PA.** 2002. Diagnostic tests for rheumatoid arthritis: comparison of anti-cyclic citrullinated peptide antibodies, anti-keratin antibodies and IgM rheumatoid factors. *Rheumatology (Oxford)* **41:**809–814. PubMed
9. **Pope RM, Lessard J, Nunnery E.** 1986. Differential effects of therapeutic regimens on specific classes of rheumatoid factor. *Ann Rheum Dis* **45:**183–189. PubMed
10. **Shmerling RH, Delbanco TL.** 1991. The rheumatoid factor: An analysis of clinical utility. *Am J Med* **91:**528–534. PubMed
11. **Stolt P, Bengtsson C, Nordmark B, Lindblad S, Lundberg I, Klareskog L, Alfredsson L; EIRA Study Group.** 2003. Quantification of the influence of cigarette smoking on rheumatoid arthritis: results from a population based case-control study, using incident cases. *Ann Rheum Dis* **62:**835–841. PubMed
12. **Varache S, Cornec D, Morvan J, Devauchelle-Pensec V, Berthelot JM, Le Henaff-Bourhis C, Hoang S, Thorel JB, Martin A, Chalès G, Nowak E, Jousse-Joulin S, Youinou P, Saraux A.** 2011. Diagnostic accuracy of ACR/EULAR 2010 criteria for rheumatoid arthritis in a 2-year cohort. *J Rheumatol* **38:**1250–1257. PubMed
13. **Capra JD, Winchester RJ, Kunkel HG.** 1969. Cold-reactive rheumatoid factors in infectious mononucleosis and other diseases. *Arthritis Rheum* **12:**67–73. PubMed
14. **Ferri C, Giuggioli D, Cazzato M, Sebastiani M, Mascia MT, Zignego AL.** 2003. HCV-related cryoglobulinemic vasculitis: An update on its etiopathogenesis and therapeutic strategies. *Clin Exp Rheumatol* **21**(Suppl 32)**:**S78–S84. PubMed
15. **Roberts-Thomson PJ, McEvoy R, Langhans T, Bradley J.** 1985. Routine quantification of rheumatoid factor by rate nephelometry. *Ann Rheum Dis* **44:**379–383. PubMed
16. **Demoruelle MK, Deane K.** 2011. Antibodies to citrullinated protein antigens (ACPAs): clinical and pathophysiologic significance. *Curr Rheumatol Rep* **13:**421–430. PubMed
17. **Jones JE, Causey CP, Knuckley B, Slack-Noyes JL, Thompson PR.** 2009. Protein arginine deiminase 4 (PAD4): current understanding and future therapeutic potential. *Curr Opin Drug Discov Devel* **12:**616–627. PubMed
18. **Vossenaar ER, Zendman AJ, van Venrooij WJ, Pruijn GJ.** PAD, a growing family of citrullinating enzymes: genes, features and involvement in disease. *BioEssays* **25:**1106–1118.
19. **Suzuki A, Yamada R, Chang X, Tokuhiro S, Sawada T, Suzuki M, Nagasaki M, Nakayama-Hamada M, Kawaida R, Ono M, Ohtsuki M, Furukawa H, Yoshino S, Yukioka M, Tohma S, Matsubara T, Wakitani S, Teshima R, Nishioka Y, Sekine A, Iida A, Takahashi A, Tsunoda T, Nakamura Y, Yamamoto K.** 2003. Functional haplotypes of PADI4, encoding citrullinating enzyme peptidylarginine deiminase 4, are associated with rheumatoid arthritis. *Nat Genet* **34:**395–402. PubMed
20. **Avouac J, Gossec L, Dougados M.** 2006. Diagnostic and predictive value of anti-cyclic citrullinated protein antibodies in rheumatoid arthritis: A systematic literature review. *Ann Rheum Dis* **65:**845–851. PubMed
21. **Sebbag M, Simon M, Vincent C, Masson-Bessière C, Girbal E, Durieux JJ, Serre G.** 1995. The antiperinuclear factor and the so-called antikeratin antibodies are the same rheumatoid arthritis-specific autoantibodies. *J Clin Invest* **95:**2672–2679. PubMed
22. **dos Anjos LM, Pereira IA, d 'Orsi E, Seaman AP, Burlingame RW, Morato EF.** 2009. A comparative study of IgG second- and third-generation anti-cyclic citrullinated peptide (CCP) ELISAs and their combination with IgA third-generation CCP ELISA for the diagnosis of rheumatoid arthritis. *Clin Rheumatol* **28:**153–158. PubMed
23. **Després N, Boire G, Lopez-Longo FJ, Ménard HA.** 1994. The Sa system: A novel antigen-antibody system specific for rheumatoid arthritis. *J Rheumatol* **21:**1027–1033. PubMed
24. **Goldbach-Mansky R, Lee J, McCoy A, Hoxworth J, Yarboro C, Smolen JS, Steiner G, Rosen A, Zhang C, Ménard HA, Zhou ZJ, Palosuo T, Van Venrooij WJ, Wilder RL, Klippel JH, Schumacher HR Jr, El-Gabalawy HS.** Rheumatoid arthritis associated autoantibodies in patients with synovitis of recent onset. *Arthritis Res* **2:**236–243.
25. **Luime JJ, Colin EM, Hazes JM, Lubberts E.** 2010. Does anti-mutated citrullinated vimentin have additional value as a serological marker in the diagnostic and prognostic investigation of patients with rheumatoid arthritis? A systematic review. *Ann Rheum Dis* **69:**337–344. PubMed
26. **Bruns A, Nicaise-Roland P, Hayem G, Palazzo E, Dieudé P, Grootenboer-Mignot S, Chollet-Martin S, Meyer O.** Prospective cohort study of effects of infliximab on rheumatoid factor, anti-cyclic citrullinated peptide antibodies and antinuclear antibodies in patients with long-standing rheumatoid arthritis. *Joint Bone Spine* **76:**248–253.
27. **Rubin B, Sønderstrup G.** 2004. Citrullination of self-proteins and autoimmunity. *Scand J Immunol* **60:**112–120. PubMed
28. **Vallbracht I, Rieber J, Oppermann M, Förger F, Siebert U, Helmke K.** 2004. Diagnostic and clinical value of anti-cyclic citrullinated peptide antibodies compared with rheumatoid factor isotypes in rheumatoid arthritis. *Ann Rheum Dis* **63:**1079–1084. PubMed
29. **Nielen MM, van Schaardenburg D, Reesink HW, van de Stadt RJ, van der Horst-Bruinsma IE, de Koning MH, Habibuw MR, Vandenbroucke JP, Dijkmans BA.** 2004. Specific autoantibodies precede the symptoms of rheumatoid arthritis: A study of serial measurements in blood donors. *Arthritis Rheum* **50:**380–386. PubMed
30. **Schaller M, Burton DR, Ditzel HJ.** 2001. Autoantibodies to GPI in rheumatoid arthritis: linkage between an animal model and human disease. *Nat Immunol* **2:**746–753. PubMed
31. **Szomor Z, Shimizu K, Fujimori Y, Yamamoto S, Yamamuro T.** 1995. Appearance of calpain correlates with arthritis and

cartilage destruction in collagen induced arthritic knee joints of mice. *Ann Rheum Dis* **54:**477–483. PubMed
32. **Mimori T, Suganuma K, Tanami Y, Nojima T, Matsumura M, Fujii T, Yoshizawa T, Suzuki K, Akizuki M.** Autoantibodies to calpastatin (an endogenous inhibitor for calcium-dependent neutral protease, calpain) in systemic rheumatic diseases. *Proc Natl Acad Sci U S A* **92:**7267–7271.
33. **Nell VP, Machold KP, Stamm TA, Eberl G, Heinzl H, Uffmann M, Smolen JS, Steiner G.** 2005. Autoantibody profiling as early diagnostic and prognostic tool for rheumatoid arthritis. *Ann Rheum Dis* **64:**1731–1736. PubMed
34. **Corrigall VM, Bodman-Smith MD, Brunst M, Cornell H, Panayi GS.** 2004. Inhibition of antigen-presenting cell function and stimulation of human peripheral blood mononuclear cells to express an antiinflammatory cytokine profile by the stress protein BiP: relevance to the treatment of inflammatory arthritis. *Arthritis Rheum* **50:**1164–1171. PubMed
35. **Rönnelid J, Lysholm J, Engström-Laurent A, Klareskog L, Heyman B.** 1994. Local anti-type II collagen antibody production in rheumatoid arthritis synovial fluid. Evidence for an HLA-DR4-restricted IgG response. *Arthritis Rheum* **37:**1023–1029. PubMed
36. **Atta MS, Lim KL, Ala'deen DA, Powell RJ, Todd I.** 1995. Investigation of the prevalence and clinical associations of antibodies to human fibronectin in systemic lupus erythematosus. *Ann Rheum Dis* **54:**117–124. PubMed
37. **Mulder AH, Horst G, van Leeuwen MA, Limburg PC, Kallenberg CG.** 1993. Antineutrophil cytoplasmic antibodies in rheumatoid arthritis. Characterization and clinical correlations. *Arthritis Rheum* **36:**1054–1060. PubMed
38. **Lee AN, Beck CE, Hall M.** Rheumatoid factor and anti-CCP autoantibodies in rheumatoid arthritis: A review. *Clin Lab Sci* **21:**15–18.
39. **Houssien DA, Jónsson T, Davies E, Scott DL.** 1998. Rheumatoid factor isotypes, disease activity and the outcome of rheumatoid arthritis: comparative effects of different antigens. *Scand J Rheumatol* **27:**46–53. PubMed
40. **Waaler E.** On the occurrence of a factor in human serum activating the specific agglutination of sheep blood corpuscles. 1939. *APMIS* **115:**422–438; discussion 439.
41. **Butler VP Jr, Vaughan JH.** 1964. Hemagglutination by rheumatoid factor of cells coated with animal gamma globulins. *Proc Soc Exp Biol Med* **116:**585–593. PubMed
42. **Grunnet N, Espersen GT.** 1988. Comparative studies on RF-IgA and RF-IgM ELISA—human or rabbit IgG as antigen? *Scand J Rheumatol Suppl* **75:**36–39. PubMed
43. **Taylor RN, Fulford KM, Jones WL.** 1977. Reduction of variation in results of rheumatoid factor tests by use of a serum reference preparation. *J Clin Microbiol* **5:**42–45. PubMed
44. **Anderson SG, Bentzon MW, Houba V, Krag P.** 1970. International reference preparation of rheumatoid arthritis serum. *Bull World Health Organ* **42:**311–318. PubMed
45. **Bizzaro N, Pregnolato F, van Boekel MA, Villalta D, Tozzoli R, Tonutti E, Antico A, Borghi MO, Wiik A, Meroni PL.** 2012. Preliminary evaluation of the first international reference preparation for anticitrullinated peptide antibodies. *Ann Rheum Dis* **71:**1388–1392. PubMed
46. **Churchman SM, Geiler J, Parmar R, Horner EA, Church LD, Emery P, Buch MH, McDermott MF, Ponchel F.** 2012. Multiplexing immunoassays for cytokine detection in the serum of patients with rheumatoid arthritis: lack of sensitivity and interference by rheumatoid factor. *Clin Exp Rheumatol* **30:**534–542. PubMed
47. **Curtis JR, van der Helm-van Mil AH, Knevel R, Huizinga TW, Haney DJ, Shen Y, Ramanujan S, Cavet G, Centola M, Hesterberg LK, Chernoff D, Ford K, Shadick NA, Hamburger M, Fleischmann R, Keystone E, Weinblatt ME.** 2012. Validation of a novel multibiomarker test to assess rheumatoid arthritis disease activity. *Arthritis Care Res (Hoboken)* **64:**1794–1803. PubMed
48. **Zhao X, Qureshi F, Eastman PS, Manning WC, Alexander C, Robinson WH, Hesterberg LK.** 2012. Pre-analytical effects of blood sampling and handling in quantitative immunoassays for rheumatoid arthritis. *J Immunol Methods* **378:**72–80 10.1016/j.jim.2012.02.007. PubMed
49. **Borque L, Rus A, Ruiz R.** Automated turbidimetry of rheumatoid factor without heat inactivation of serum. *Eur J Clin Chem Clin Biochem* **29:**521–527.
50. **Virella G, Hipp WA, John JF Jr, Kahaleh B, Ford M, Fudenberg HH.** 1979. Nephelometric detection of soluble immune complexes: methodology and clinical applications. *Int Arch Allergy Appl Immunol* **58:**402–410. PubMed
51. **Sasso EH.** 2000. The rheumatoid factor response in the etiology of mixed cryoglobulins associated with hepatitis C virus infection. *Ann Med Interne (Paris)* **151:**30–40. PubMed
52. **Gorgani NN, Altin JG, Parish CR.** 1999. Histidine-rich glycoprotein prevents the formation of insoluble immune complexes by rheumatoid factor. *Immunology* **98:**456–463. PubMed
53. **Hennig C, Rink L, Fagin U, Jabs WJ, Kirchner H.** 2000. The influence of naturally occurring heterophilic anti-immunoglobulin antibodies on direct measurement of serum proteins using sandwich ELISAs. *J Immunol Methods* **235:**71–80. PubMed
54. **Benacerraf B.** 1981. Role of MHC gene products in immune regulation. *Science* **212:**1229–1238. PubMed
55. **Berglin E, Padyukov L, Sundin U, Hallmans G, Stenlund H, Van Venrooij WJ, Klareskog L, Dahlqvist SR.** 2004. A combination of autoantibodies to cyclic citrullinated peptide (CCP) and HLA-DRB1 locus antigens is strongly associated with future onset of rheumatoid arthritis. *Arthritis Res Ther* **6:**R303–R308. PubMed
56. **van der Woude D, Lie BA, Lundström E, Balsa A, Feitsma AL, Houwing-Duistermaat JJ, Verduijn W, Nordang GB, Alfredsson L, Klareskog L, Pascual-Salcedo D, Gonzalez-Gay MA, Lopez-Nevot MA, Valero F, Roep BO, Huizinga TW, Kvien TK, Martín J, Padyukov L, de Vries RR, Toes RE.** 2010. Protection against anti-citrullinated protein antibody-positive rheumatoid arthritis is predominantly associated with HLA-DRB1*1301: A meta-analysis of HLA-DRB1 associations with anti-citrullinated protein antibody-positive and anti-citrullinated protein antibody-negative rheumatoid arthritis in four European populations. *Arthritis Rheum* **62:**1236–1245. PubMed
57. **Stahl EA, Raychaudhuri S, Remmers EF, Xie G, Eyre S, Thomson BP, Li Y, Kurreeman FA, Zhernakova A, Hinks A, Guiducci C, Chen R, Alfredsson L, Amos CI, Ardlie KG; BIRAC Consortium, Barton A, Bowes J, Brouwer E, Burtt NP, Catanese JJ, Coblyn J, Coenen MJ, Costenbader KH, Criswell LA, Crusius JB, Cui J, de Bakker PI, De Jager PL, Ding B, Emery P, Flynn E, Harrison P, Hocking LJ, Huizinga TW, Kastner DL, Ke X, Lee AT, Liu X, Martin P, Morgan AW, Padyukov L, Posthumus MD, Radstake TR, Reid DM, Seielstad M, Seldin MF, Shadick NA, Steer S, Tak PP, Thomson W, van der Helm-van Mil AH, van der Horst-Bruinsma IE, van der Schoot CE, van Riel PL, Weinblatt ME, Wilson AG, Wolbink GJ, Wordsworth BP; YEAR Consortium, Wijmenga C, Karlson EW, Toes RE, de Vries N, Begovich AB, Worthington J, Siminovitch KA, Gregersen PK, Klareskog L, Plenge RM.** 2010. Genome-wide association study meta-analysis identifies seven new rheumatoid arthritis risk loci. *Nat Genet* **42:**508–514. PubMed
58. **Silman AJ.** 1997. Problems complicating the genetic epidemiology of rheumatoid arthritis. *J Rheumatol* **24:**194–196. PubMed
59. **Klareskog L, Stolt P, Lundberg K, Källberg H, Bengtsson C, Grunewald J, Rönnelid J, Harris HE, Ulfgren AK, Rantapää-Dahlqvist S, Eklund A, Padyukov L, Alfredsson L.** 2006. A new model for an etiology of rheumatoid arthritis: smoking may trigger HLA-DR (shared epitope)-restricted immune reactions to autoantigens modified by citrullination. *Arthritis Rheum* **54:**38–46. PubMed
60. **Sahatçiu-Meka V, Rexhepi S, Kukeli A, Manxhuka-Kërliu S, Pallaskas K, Murtezani A, Rexhepi M, Rexhepi B.** 2013. Course and prognosis in seropositive and seronegative rheumatoid arthritis. *Reumatizam* **60:**19–24. PubMed

Antiphospholipid Antibody Syndrome: Clinical Manifestations and Laboratory Diagnosis

MARTINA MURPHY AND NEIL HARRIS

93

BACKGROUND AND DIAGNOSTIC CRITERIA

Antiphospholipid antibody syndrome (APS) is an acquired thrombotic disorder caused by a heterogenous group of antibodies directed against plasma proteins that bind phospholipids. These are termed "antiphospholipid antibodies" (aPLs), and while they are required for the diagnosis for APS, they can also be detected in otherwise healthy individuals. The clinical manifestations of APS can be divided into thrombotic and obstetrical. Thrombotic complications include both venous and arterial thrombosis. Obstetrical complications include recurrent first trimester miscarriage and second trimester fetal demise, as well as other pregnancy complications like preeclampsia and placental insufficiency (1). APS is classified as "primary" when not associated with an underlying disease and accounts for over 50% of cases (2). Secondary APS is the distinction given to APS associated with an underlying autoimmune connective tissue disorder such as SLE.

The diagnosis of APS requires not only a clinical event but also the persistent presence of one or more of a unique set of antibodies that bind specific phospholipid binding proteins. Because aPLs can be detected in healthy individuals and in the setting of other disease states (e.g., infection, HIV, malignancy), it important that their persistence be documented in individuals suspected of having APS. While the presence of these antibodies is central to the diagnosis, the exact mechanisms by which they cause hypercoagulability are not well understood.

Most authorities diagnose APS based on the classification criteria (Sapporo criteria) as outlined in the International Symposium on Antiphospholipid Antibodies in 1998, which were subsequently updated in 2006 (3) (Table 1). The clinical criteria include objectively confirmed venous, arterial, or small vessel thrombosis or pregnancy complications that may be attributed to placental insufficiency, including pregnancy loss or premature birth. The laboratory criteria require that a moderate or strongly positive laboratory test for aPLs be found on 2 or more occasions at least 12 weeks apart. Low-level positivity for aPLs is thought to be nonspecific and nondiagnostic of the syndrome. The aPLs recognized in the international criteria include lupus anticoagulant (LA) detected according to guidelines published by the International Society on Thrombosis and Haemostasis, anticardiolipin (aCL) antibody (IgG or IgM) exceeding 40 IgG or IgM phospholipid units, or anti-β_2GPI antibody (IgG or IgM) at levels exceeding the 99th percentile. Patients who have aPLs not currently recognized in the diagnostic criteria (e.g., antiphosphotidylserine antibodies, antiprothrombin antibodies, IgA aCL, or anti-β_2GPI antibodies) or who have clinical manifestations other than thrombosis or pregnancy morbidity are not formally recognized as having APS at present, but diagnostic criteria continue to evolve. Testing for these alternative, noncriterial aPLs is not currently recommended in routine clinical practice.

The 2006 update included the advisement that patients be classified into those with positivity for only a single aPL and those that were positive for two or more laboratory criteria (present in any combination). The rationale for this change was the consensus that patients with single positivity carry a lower risk of thrombosis or pregnancy complications than those with multiple (especially triple) positivity (2).

CLINICAL MANIFESTATIONS

Virtually any organ system can be affected in APS, and recurrent thrombosis despite appropriate anticoagulation can be seen. The most common features seen in APS are venous thrombosis, thrombocytopenia, livedo reticularis, stroke, superficial thrombophlebitis, pulmonary embolism, fetal loss, transient ischemic attack, and hemolytic anemia (2, 4). In addition to the cerebrovascular system, the pulmonary, cardiovascular, renal, ocular, cutaneous, endocrine, gastrointestinal, and hematologic systems can be affected. APS in the background of SLE does not have a distinctly different array of clinical or laboratory manifestations. A small fraction of cases (<1%) may exhibit catastrophic APS (CAPS) resulting from widespread thrombosis in multiple organ systems, leading to organ failure and a mortality rate of nearly 50% (5). The distinction between APS and CAPS is important, as treatments are different and include consideration of immunosuppression as well as the addition of therapeutic plasmapheresis in patients with CAPS.

Fetal morbidity associated with APS typically occurs after 10 weeks of gestation (4, 6). Criteria for APS-associated fetal morbidity include three or more losses prior to the 10th week of gestation, one or more losses after the 10th week, or one or more premature deliveries at or before the 34th week because of preeclampsia, eclampsia, or placental insufficiency with the exclusion of other causes.

doi:10.1128/9781555818722.ch93

TABLE 1 Criteria for the diagnosis of antiphospholipid syndrome[a]

Clinical criteria
Vascular thrombosis (one or more episodes of arterial, venous, or small vessel thrombosis). For histopathologic diagnosis, there should be no evidence of inflammation in the vessel wall.
Pregnancy morbidities attributable to placental insufficiency, including (i) three or more otherwise unexplained recurrent spontaneous miscarriages, before 10 weeks of gestation, (ii) one or more fetal losses after the 10th week of gestation, (iii) stillbirth, and (iv) episode of preeclampsia, preterm labor, abruption placentae, intrauterine growth restriction, or oligohydramnios that is otherwise unexplained.
Laboratory criteria
Medium or high levels of anticardiolipin or anti-β2-glycoprotein I IgG and/or IgM antibodies present on two or more occasions at least 12 weeks apart as measured by standard ELISAs
Lupus anticoagulant in plasma on two or more occasions at least 12 weeks apart, detected according to the guidelines of the Subcommittee on Lupus Anticoagulant/Phospholipid-Dependent Antibodies of the Scientific and Standardization Committee of the International Society of Thrombosis and Haemostasis

[a]Definite antiphospholipid syndrome is considered to be present if at least one of the clinical criteria AND one of the laboratory criteria are met. Table modified from references 3 and 18.

LABORATORY ASPECTS OF TESTING FOR ANTIPHOSPHOLIPID SYNDROME

The laboratory definition of the antiphospholipid syndrome requires the presence of either a so-called "lupus anticoagulant" or a significant and persistent titer of antiphospholipid antibodies. A lupus anticoagulant is detected by an *in vitro* clot-based laboratory assay, while antiphospholipid antibodies are detected by immunoassay.

Lupus Anticoagulant Testing

A "lupus anticoagulant" is a laboratory-defined phenomenon by which *in vitro* clot-based assays (typically those dependent upon the intrinsic and common pathways) are prolonged by the presence of antiphospholipid antibodies. The LA phenomenon does not have an *in vivo* correlate. These antibodies are not "anticoagulants" *in vivo*; instead, they trigger inflammation and are capable of inducing a thrombophilic state. Lupus anticoagulant assays are performed on citrated platelet-poor plasma (7, 8). The assays are frequently formatted to have a screening step and a confirmatory step, and frequently there is an additional mixing study step (7–9). The classic lupus anticoagulant causes a prolongation of the activated partial thromboplastin time (APTT), which does not correct in a 1:1 mix with normal pooled plasma (NPP). In practice, APTT reagents vary in their sensitivity to LA; the more-sensitive assays are those that should be used for LA screening. Another commonly used assay is the dilute Russell Viper Venom time (dRVVT) assay, in which the common pathway is activated by a snake venom (from *Daboia russellii*) that converts Factor X to Xa (7, 8). The advantage of the dRVVT assay is that it is not affected by hemophilia, antibodies to factors VIII and IX, or an elevated FVIII. It is frequently recommended that both types of assays (APTT and dRVVT) be used in the diagnosis.

The dRVVT assay requires an initial baseline reaction (referred to as "screening") followed by a confirmatory step in which the reaction is supplemented by exogenous phospholipid (7, 8). A true LA shows shortening of the clotting time on phospholipid supplementation, while factor deficiencies are impervious to this step. Mixing studies with NPP are often incorporated into the reaction sequence. For example, a factor X or II deficiency may prolong the dRVVT screen; this prolongation does not respond to the addition of phospholipid in the confirmatory step, but the addition of NPP results in a significant shortening of the clotting time. As a cautionary note, weak lupus anticoagulants can show correction when normal plasma is added because the plasma dilutes the inhibitory antibody (9). For this reason, the mixing study should be used with caution and only if the confirmatory step shows no response to phospholipid. Because two reactions are carried out in the dRVVT assay, this type of approach is referred to as a "paired LA test."

Many dRVVT reagents contain a cationic heparin neutralizer that binds and inactivates unfractionated heparin in the therapeutic range. Polybrene (hexadimethrine bromide) is one of these. The aim is to prevent interference by heparin, which would otherwise prolong both the dRVVTs.

In order to assess if the clotting time of the confirmatory step is shortened relative to the screening step, it is common practice to establish a ratio of screening-to-confirm times (7–10). These ratios are typically accepted as positive for a lupus anticoagulant effect if they are greater than 1.2. The cutoff ratio may vary among different labs from 1.15 to 1.3. For example, a dRVVT screening time of 59 seconds and a confirm time of 45 seconds yield a ratio of 1.31, which would be deemed positive by most laboratories.

Recently, this approach has been modified by several national and international organizations such as the Clinical and Laboratory Standards Institute (CLSI) (7), the International Society on Haemostasis and Thrombosis, and the British Committee for Standards in Haematology. The important modification is that both the screening and confirm times themselves be converted to normalized ratios by dividing the clotting time of the patient specimen by the clotting time of normal plasma. The clotting time of the normal plasma can be determined by using either the NPP or the mean of the population reference interval (RI). The example below illustrates how this is performed for a dRVVT assay.

1. dRVVT patient screen time:	65 seconds
2. dRVVT (NPP or mean of RI) screen:	44 seconds
3. Normalized screen ratio:	1.48
4. dRVVT patient confirm time:	46 seconds
5. dRVVT (NPP or mean of RI) confirm:	41 seconds
6. Normalized confirm ratio:	1.12

Divide the value in no. 3 by the value in no. 6: 1.48/1.12
Final ratio = 1.32
This is greater than 1.2 and is therefore positive.

A third type of assay is available from a single vendor (STACLOT-LA Hexagonal Phospholipid Neutralization;

Diagnostica Stago) (7). This assay integrates the baseline and mixing assays. The reaction involves mixing the patient plasma specimen with NPP (to control for warfarin) as well as a heparin neutralizer (see above, to control for therapeutic heparin in the specimen). An APTT is initiated by recalcification and by a surface activator. A second independent reaction is performed as described above but with the addition of a specialized phospholipid preparation termed a "hexagonal (II) phase phospholipid." This is an alternative nonlamellar physical form of phospholipid. In this phase, the lipid (most commonly phosphatidylethanolamine) forms long tubes, with the polar head groups on the inside and the hydrophobic, hydrocarbon tails on the outside. Positivity is assessed by observing a significant difference between the two reactions (one with the hexagonal phase phospholipid and one without) of greater than 8 to 10 seconds.

ANTIPHOSPHOLIPID ANTIBODY TESTING

Antiphospholipid antibodies are those that interact with phospholipid-binding proteins. International guidelines recommend detection of either IgG or IgM antibodies to cardiolipin (aCL) or to beta2 glycoprotein I (aβ2GP1) (3). Antiphospholipid antibodies are identified by a solid-phase noncompetitive immunoassay that does not require activation of the coagulation pathway. These assays are commonly performed in enzyme-linked immunosorbent assay (ELISA) wells and are processed either manually or on a semiautomated platform. The wells are coated with the antigen. The specimen from the patient is added, and if the appropriate antibodies are present, they will bind to the target antigen. The remaining proteins are removed by a wash step, and the reaction is developed by adding labeled antibodies directed to human IgG or IgM.

In order to improve specificity of the assay, the guidelines focus on specificity, duration, and antibody level.

Specificity

The anticardiolipin assay should be β2GP1 dependent (11). This is achieved by supplementing the reaction with either human or bovine β2GP1, which acts a binding cofactor. The rationale behind this is that infections may induce transient aCL antibodies and these are typically not dependent on β2GP1.

Duration

The laboratory definition of antiphospholipid syndrome requires that a significant titer of aCL or aβ2GP1 persist for at least 12 weeks (3).

Antibody Level

International guidelines recommend that antibody levels should be at >99th percentile of the population reference range. One challenge is that levels are dependent upon the type of calibrator that is used. The original calibrators (Harris standards) utilized sera with defined concentrations of antibodies. One GPL unit and 1 MPL unit were defined as 1 μg/ml of affinity-purified IgG and 1 μg/ml of affinity-purified IgM, respectively. Use is now being made of the "Sapporo standards," which are monoclonal antibodies termed EY2C9 and HCAL for IgM and IgG, respectively. In the case of the latter, using the Inova QUANTA Lite anticardiolipin ELISA, 15 GPL would correspond to 0.0282 μg/ml of HCAL antibody, while 12.5 MPL would correspond to 0.0195 μg/ml of EY2C9 antibody. An important principle therefore is that anti-cardiolipin IgG values obtained with different manufacturers' assay methods may not be used interchangeably (12).

International standards are not available for aβ2GP1 testing, and these may be expressed as U/ml or SGU or SMU units.

Another challenge is that the guidelines set 2 different criteria for a significant level for anticardiolipin antibodies: (i) either >99th percentile or (ii) levels exceeding 40 units (3, 11). These may represent very different levels (13). In laboratory medicine, a population reference range either is the mean ± 1.96 standard deviations (if the distribution is Gaussian) or includes everything up to the 97.5% centile and down to the 2.5% centile (if the distribution of results is non-Gaussian). For example, in the case of one commonly used antiphospholipid antibody assay (Inova QUANTA Lite), 97.6% of "normals" are less than 15 GPL for aCL IgG. Only 1.4% of the normal population had aCL IgG levels above 20 GPL units, which would correspond to the 98.6th percentile. If one is therefore setting the cutoff at 40 GPL units, this is clearly a much higher level and more stringent criterion than the 99th percentile.

WHOM TO TEST

The diagnosis of APS should be considered in patients with venous/arterial thrombosis and/or a history of recurrent pregnancy loss in the absence of other clear risk factors. This is especially true in younger patients (<50 years of age), patients with thrombosis at unusual sites, patients with late pregnancy loss, and patients with autoimmune disorders experiencing thrombosis or pregnancy loss. Strong consideration should be given to testing in young patients with cerebral thrombosis including cerebrovascular accident without risk factors. The utility of testing is unclear in other neurologic symptoms such as chorea, migraines, etc.

CONSIDERATIONS WHEN TESTING

Accurate laboratory testing carries significant implications for patients who have suffered from one of the APS-defining clinical events. As such, it is important to take into consideration patient characteristics such as underlying medical comorbidities and medications when interpreting results of aPL studies. As previously discussed, aPLs are often identified in the elderly, patients with cirrhosis and other liver disease, patients with HIV, patients with autoimmune disease, and patients with cancer (14–17). In the absence of clinical sequelae of APS, the clinical significance of positive aPLs remains uncertain.

Several medications are associated with the development of aPLs, such as quinine, procainamide, phenothiazines, and anti-tumor necrosis factor drugs, but there has been no clear association with the use of these medications and the clinical syndrome of APS (18).

Importantly, it should be noted that several medications interfere with testing for aPLs, specifically testing for LA. Medications that prolong or have the potential to prolong the patient's baseline PTT may lead to false-positive aPL studies. This is particularly true of anticoagulant medications such as heparin, enoxaparin, or the targeted oral anticoagulants rivaroxaban, apixaban, dabigatran, and edoxaban.

REFERENCES

1. **Ortel TL.** 2012. Antiphospholipid syndrome: laboratory testing and diagnostic strategies. *Am J Hematol* **87**(Suppl 1)**:**S75–S81. PubMed

2. **Cervera R, Piette JC, Font J, Khamashta MA, Shoenfeld Y, Camps MT, Jacobsen S, Lakos G, Tincani A, Kontopoulou-Griva I, Galeazzi M, Meroni PL, Derksen RH, de Groot PG, Gromnica-Ihle E, Baleva M, Mosca M, Bombardieri S, Houssiau F, Gris JC, Quéré I, Hachulla E, Vasconcelos C, Roch B, Fernández-Nebro A, Boffa MC, Hughes GR, Ingelmo M, Euro-Phospholipid Project Group.** 2002. Antiphospholipid syndrome: clinical and immunologic manifestations and patterns of disease expression in a cohort of 1,000 patients. *Arthritis Rheum* **46:**1019–1027. PubMed
3. **Miyakis S, Lockshin MD, Atsumi T, Branch DW, Brey RL, Cervera R, Derksen RH, de Groot PG, Koike T, Meroni PL, Reber G, Shoenfeld Y, Tincani A, Vlachoyiannopoulos PG, Krilis SA.** 2006. International consensus statement on an update of the classification criteria for definite antiphospholipid syndrome (APS). *J Thromb Haemost* **4:**295–306.
4. **Levine JS, Branch DW, Rauch J.** 2002. The antiphospholipid syndrome. *N Engl J Med* **346:**752–763. PubMed
5. **Asherson RA, Cervera R, Piette JC, Font J, Lie JT, Burcoglu A, Lim K, Muñoz-Rodríguez FJ, Levy RA, Boué F, Rossert J, Ingelmo M.** 1998. Catastrophic antiphospholipid syndrome. Clinical and laboratory features of 50 patients. *Medicine* (Baltimore) **77:**195–207. PubMed
6. **Derksen RH, de Groot PG.** 2004. Clinical consequences of antiphospholipid antibodies. *Neth J Med* **62:**273–278. PubMed
7. **Clinical and Laboratory Standards Institute.** 2014. *H60—A Laboratory Testing for the Lupus Anticoagulant*. Approved Guideline. Clinical and Laboratory Standards Institute, Wayne, PA.
8. **Devreese K, Hoylaerts MF.** 2010. Challenges in the diagnosis of the antiphospholipid syndrome. *Clin Chem* **56:**930–940. PubMed
9. **Moore GW.** 2014. Commonalities and contrasts in recent guidelines for lupus anticoagulant detection. *Int J Lab Hematol* **36:**364–373. PubMed
10. **Moore GW, Brown KL, Bromidge ES, Drew AJ, Ledford-Kraemer MR.** 2013. Lupus anticoagulant detection: out of control? *Int J Lab Hematol* **35:**128–136. PubMed
11. **Devreese KMJ.** 2014. Antiphospholipid antibody testing and standardization. *Int J Lab Hematol* **36:**352–363. PubMed
12. **Forastiero R, Papalardo E, Watkins M, Nguyen H, Quirbach C, Jaskal K, Kast M, Teodorescu M, Lakos G, Binder W, Shums Z, Nelson V, Norman G, Puig J, Cox A, Vandam W, Hardy J, Pierangeli S.** 2014. Evaluation of different immunoassays for the detection of antiphospholipid antibodies: report of a wet workshop during the 13th International Congress on Antiphospholipid Antibodies. *Clin Chim Acta* **428:**99–105. PubMed
13. **Lakos G, Favaloro EJ, Harris EN, Meroni PL, Tincani A, Wong RC, Pierangeli SS.** 2012. International consensus guidelines on anticardiolipin and anti-β2-glycoprotein I testing: report from the 13th International Congress on Antiphospholipid Antibodies. *Arthritis Rheum* **64:**1–10.
14. **Cervera R, Asherson RA.** 2003. Clinical and epidemiological aspects in the antiphospholipid syndrome. *Immunobiology* **207:**5–11. PubMed
15. **Love PE, Santoro SA.** 1990. Antiphospholipid antibodies: anticardiolipin and the lupus anticoagulant in systemic lupus erythematosus (SLE) and in non-SLE disorders. Prevalence and clinical significance. *Ann Intern Med* **112:**682–698. PubMed
16. **Sebastiani GD, Galeazzi M, Tincani A, Piette JC, Font J, Allegri F, Mathieu A, Smolen J, de Ramon Garrido E, Fernandez-Nebro A, Jedryka-Goral A, Papasteriades C, Morozzi G, Bellisai F, De Pitá O, Marcolongo R.** 1999. Anticardiolipin and anti-beta2GPI antibodies in a large series of European patients with systemic lupus erythematosus. Prevalence and clinical associations. European Concerted Action on the Immunogenetics of SLE. *Scand J Rheumatol* **28:**344–351. PubMed
17. **Vila P, Hernández MC, López-Fernández MF, Batlle J.** 1994. Prevalence, follow-up and clinical significance of the anticardiolipin antibodies in normal subjects. *Thromb Haemost* **72:**209–213. PubMed
18. **Rand JH, Wolgast LR.** 2013. Antiphospholipid syndrome: pathogenesis, clinical presentation, diagnosis, and patient management, p 324–341. *In* Kitchens CS, Kessler CM, Konkle BA (ed), *Consultative Hemostasis and Thrombosis*, 3rd ed. Elsevier Saunders, Philadelphia, PA.

Antineutrophil Cytoplasmic Antibodies (ANCA) and Strategies for Diagnosing ANCA-Associated Vasculitides

R. W. BURLINGAME, C. E. BUCHNER, J. G. HANLY, AND N. M. WALSH

94

DISEASE DIAGNOSIS

Inflammation of and damage to blood vessel walls are the shared defining features of all vasculitides. The symptoms vary depending on the size of the vessels affected, the organs they serve, the underlying cause of the vasculitis, and the activity of the disease. The vasculitic diseases are rare. Since there are only 20 to 50 new cases of antineutrophil cytoplasmic antibodies (ANCA)-associated vasculitides per 1,000,000 people per year (1, 2), a systematic and thorough diagnostic algorithm is needed to correctly identify patients with the disease (3, 4). Missed or delayed diagnosis can result in permanent organ injury or even death (5, 6).

The most appropriate diagnostic criteria for the vasculitides are still the subject of debate (7). Classification criteria (8, 9, 10, 11, 12) are used in patients already diagnosed to ensure homogeneity of groups of patients with vasculitis enrolled in clinical studies. The new nomenclature for vasculitis (13) includes microscopic polyangiitis (MPA), which was not included in the earlier classifications by the American College of Rheumatology.

The patient's clinical history and physical examination are key factors in making a diagnosis of vasculitis since the symptoms are varied and the disease often takes a relapsing and remitting course. Exclusion of diseases other than vasculitis as the cause of the clinical presentation is necessary. Besides the normal careful patient workup, certain questions need to be answered by the patient if vasculitis is suspected. Has the patient traveled to any countries where they might have contracted an infectious disease associated with vasculitis? Is this patient taking any prescription drugs, such as propylthiouracil, or recreational drugs, such as cocaine, that sometimes cause vasculitis?

When feasible, a positive biopsy specimen provides the most robust evidence of vasculitis. The anatomical site of biopsy is guided by the presentation in a given patient. Common sites include skin, kidney, lung, nasal passage, temporal artery, and muscle. Biopsy of the kidney can be particularly important both for the initial diagnosis and to help direct treatment based on the histopathological evidence of disease activity, severity, and damage. For example, the histopathological diagnosis of crescentic necrotizing glomerulonephritis is a serious manifestation of several types of vasculitis and requires prompt treatment with corticosteroids and immunosuppressive therapy to avoid irreparable renal damage (5, 6).

The laboratory workup should be comprehensive in order to capture information about all potential organs involved and may have to be repeated if the disease is still in evolution and new manifestations of the illness appear (14). A complete blood count may indicate anemia, eosinophilia, or neutropenia. Urinalysis identifies proteinurea, hematuria, and red cell casts that are indicative of active renal disease as well as urinary tract infection. Laboratory markers of inflammation such as C-reactive protein and erythrocyte sedimentation rate are neither sensitive nor specific for vasculitis but if elevated may help monitor the activity of the disease. Both complement and cryoglobulins should be evaluated since low levels of complement proteins in the circulation correlate with active disease in immune complex mediated vasculitis such as cryoglobulinemia.

A workup for thrombophilia including measurement of anti-thrombin 3, protein C, and protein S, as well as evaluating autoantibodies to cardiolipin and beta-2 glycoprotein 1 and lupus anticoagulant, can help elucidate causes of thrombosis other than vasculitis. A careful search for infection, including hepatitis B and C as well as HIV infection, and underlying malignancy, including lymphoma, should be considered part of the differential diagnosis in all cases of systemic vasculitis.

TESTS FOR ANCA

A key diagnostic aid in certain types of vasculitis is the indirect immunofluorescent assay (IFA) to detect ANCA on ethanol-fixed neutrophils (15, 16, 17). Neutrophil-specific autoantibodies were first recognized by IFA in the mid-1960s, but their association with specific types of vasculitis and glomerulonephritis was not made until the mid-1980s (18). If the IFA on ethanol-fixed neutrophils is positive, follow-up testing with more-specific assays that detect autoantibodies against two proteins found in azurophilic granules, proteinase 3 (PR3) and myeloperoxidase (MPO), is necessary. These are the most diagnostically important ANCAs. Native PR3 antigen from human neutrophils appears to function better in solid-phase assays than recombinant PR3, possibly because the tertiary structure is preserved in the native antigen (3). The autoimmune diseases associated with them are discussed in detail later in this chapter. A previous edition of this *Manual* contained detailed instructions for making slides to test for ANCA by IFA (19) and

doi:10.1128/9781555818722.ch94

enzyme-linked immunosorbent assays (ELISAs) to detect specific autoantibodies (19, 20), so those procedures are not reproduced here. Slides with fixed neutrophils for ANCA testing are available from several commercial sources, as are specific solid-phase tests for detecting anti-PR3 and anti-MPO.

On ethanol-fixed neutrophils, antibodies to PR3 yield a characteristic granular cytoplasmic pattern (C-ANCA) with interlobular accentuation, consistent with its cellular location in azurophilic granules (Fig. 1A). Anti-MPO antibodies usually give a perinuclear pattern (P-ANCA) rather than a cytoplasmic pattern because MPO is cationic and migrates from cytoplasmic granules to the nucleus, where it binds anionic chromatin when the membranes around these organelles are dissolved during fixation (Fig. 2A). These and other antineutrophil nuclear autoantibodies (ANNA) are perhaps paradoxically still considered ANCA. The term ANNA, which is an alternative and more appropriate acronym for these antibodies, never became widely accepted. Autoantibodies to several other proteins from azurophilic granules also show P-ANCA by IFA because of the same phenomenon. Immunofluorescent patterns that are not C-ANCA or P-ANCA and are not directed to MPO or PR3 are considered atypical (A-ANCA). Some A-ANCA may be neutrophil-specific autoantibodies, and some react with the neutrophil nuclear membrane (21), while others may be caused by autoantibodies such as anti-DNA that are reactive to antigens found in many cell types. Patients without vasculitis may have autoantibodies that yield C-ANCA, P-ANCA, or A-ANCA patterns by IFA but are negative for anti-MPO and anti-PR3 by solid-phase assays, so it is absolutely necessary to perform follow-up testing for these specific autoantibodies (15, 16, 17, 21). Rarely, a PR3-ANCA yields a P-ANCA IFA pattern and an MPO-ANCA yields a C-ANCA pattern on ethanol-fixed neutrophils for unknown reasons.

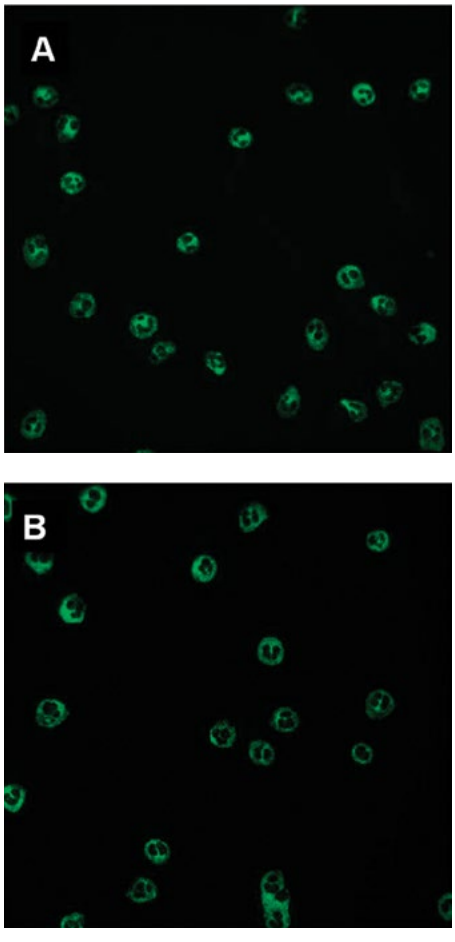

FIGURE 1 Indirect immunofluorescence of a PR3-ANCA-positive sample expressing cytoplasmic staining with interlobular accentuation on both ethanol-fixed (A) and formalin-fixed (B) neutrophils.

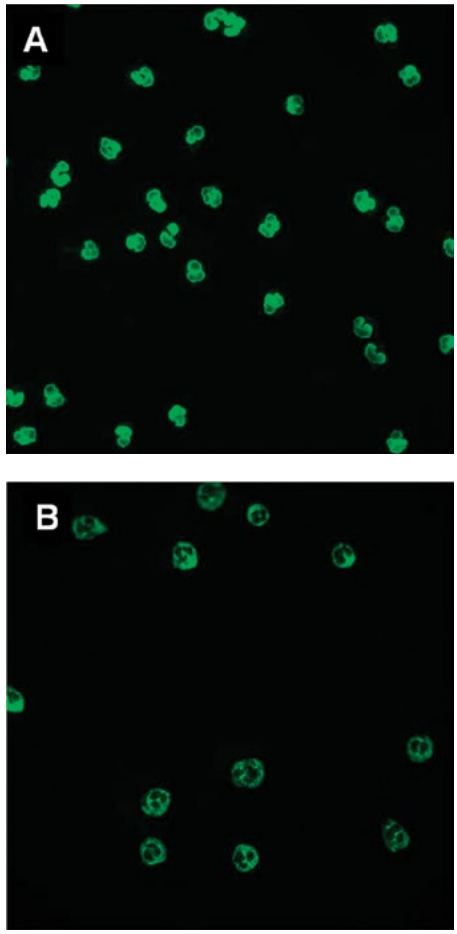

FIGURE 2 Indirect immunofluorescence of an MPO-ANCA-positive sample expressing perinuclear staining on ethanol-fixed neutrophils (A) and cytoplasmic staining with interlobular accentuation on formalin-fixed neutrophils (B).

It is useful to perform IFA on formalin-fixed neutrophils on samples that are positive on the initial IFA on ethanol-fixed neutrophils. PR3-ANCA remains positive with the C-ANCA pattern, while MPO-ANCA now shows a C-ANCA pattern since the antigens have been cross-linked in place by formalin fixation (Fig. 1B and 2B). The reactive epitopes of some A-ANCA antigens are destroyed by formalin fixation, so some of those samples become negative on formalin-fixed neutrophils.

If the ANCA IFA is positive but the specific anti-MPO and anti-PR3 follow-up tests are negative in patients in which vasculitis is suspected, it can be valuable to perform further tests to characterize the autoantibodies causing the positive ANCA IFA. A test for antinuclear antibodies, such as IFA on HEp-2 cells, can help differentiate neutrophil-specific antibodies from general ANA, with the caveat

that HEp-2 IFA is often performed at a 1:80 dilution while ANCA IFA is often performed at a 1:20 dilution, and thus the sensitivities of the two assays may be different. If the ANA assay is negative, which implies that the antibodies are neutrophil specific, follow-up testing for autoantibodies to other proteins found in azurophilic granules, such as elastase, lactoferrin, lysozyme, cathepsin G, and bacterial-permeability-increasing protein may be informative. Autoantibodies to these antigens have been found primarily in vasculitis induced by a wide class of therapeutic drugs (22, 23) or by levamisole-laced cocaine (24, 25) and in chronic liver disease (26) and other nonvasculitic diseases (27).

It is often necessary to test for a panel of other autoantibodies, since symptoms of vasculitis can be secondary to other autoimmune diseases such as systemic lupus erythematosus (SLE), rheumatoid arthritis (RA), and antiphospholipid syndrome. This panel should include tests for autoantibodies reactive with SS-A/Ro, SS-B/La, Sm, RNP, double-stranded DNA, chromatin, citrullinated proteins, rheumatoid factor, beta-2 glycoprotein 1, cardiolipin, and lupus anticoagulant.

In summary, the most accepted way to test for ANCA is to start with the IFA screen and to follow up positive results by specific ELISAs to MPO and PR3 autoantibodies. There are many commercially available kits to measure anti-MPO and anti-PR3 autoantibodies that have various sensitivities based on the cutoff chosen to differentiate positive and negative results rather than any inherent poor performance of the ELISA (28). However, different laboratories can get similar results if they standardize their testing with each other (15). One study suggests that a more cost-effective yet equally good strategy is to screen with the 2 ELISAs and follow up the positives with IFA on neutrophils (29). Native proteins are preferred over recombinant proteins (3) as the solid-phase antigens in ELISA. The capture PR3 ELISA has good performance (28), but it may not be better than the standard PR3 ELISA (29). Commercial kits to measure antibodies to the nonstandard proteins in the azurophilic granules mentioned above are available (Aesku Diagnostics, Wendelsheim, Germany). In-house ELISAs can be developed by following standard ELISA techniques (19, 20, 25, 27) with antigens from Athens Research and Technology, Athens, GA, USA, or other sources for individual antigens.

NOMENCLATURE OF VASCULITIS

The names of various forms of vasculitides have recently been revised to replace eponyms with key features of the disease (13). When a type of vasculitis is known to be caused by infectious agents, the name reflects that. Examples include rickettsial vasculitis, syphilitic aortitis, and aspergillus arteritis. Infectious organisms such as hepatitis C virus can induce cryoglobulinemia, which in turn indirectly causes vasculitis. The primary therapeutic strategy is with agents to remove infection and not with immunosuppressive agents. It is important that the diagnostic algorithm for vasculitis include tests to identify infections when the presentation suggests this as the most likely primary cause of the inflammation.

Large Vessel Vasculitis

Some types of vasculitis are not associated with ANCA. Large vessel vasculitis predominantly affects the aorta and large aortic root vessels. Smaller vessels within organs, particularly in the eyes, may also be affected. The etiologies of these diseases are not known. The two most common forms of large vessel vasculitis are Takayasu's arteritis and giant cell arteritis (GCA). It is not clear if these are separate diseases or represent a continuum of the same illness with different clinical phenotypes in different age groups. Takayasu's arteritis is found mainly in people younger than 50 (9), and GCA is seen in older individuals (10). A biopsy specimen of the temporal artery in patients with GCA is characterized histopathologically by a granulomatous inflammatory infiltrate of the inner muscular layer, where multinucleate giant cells are associated with fragmentation and destruction of the internal elastic lamina. Noninvasive tests such as magnetic resonance imaging, ultrasound, and positron emission tomography (30, 31) have been shown to be useful for diagnosing large vessel vasculitis.

Medium Vessel Vasculitis

Medium vessel vasculitis is found primarily in visceral arteries, though any size vessel may be affected. Histopathologically, there is acute inflammation and fibrinoid necrosis of vessel walls, which can culminate in aneurysm formation. Polyarteritis nodosa is the major medium vessel vasculitis. Symptoms include weight loss, fever, myalgia, rash, and neuropathy, and it is often associated with hepatitis B infection.

Kawasaki disease affects medium and small vessels but may also affect the coronary arteries. It is associated with the mucocutaneous lymph node syndrome and is predominantly found in children. Symptoms include fever, bilateral conjunctivitis, and erythema of the lips, palms of the hands, and soles of the feet. Mesenteric and renal angiograms and magnetic resonance imaging may be useful to detect gastrointestinal tract vasculitis and renal artery vasculitis (but not glomerulonephritis).

Small Vessel Vasculitis (SVV) and Non-ANCA SVV

As the name states, SVV primarily involves small vessels such as arterioles, capillaries, and venules. As all tissues contain small blood vessels, an appropriately directed biopsy based on clinical indication of affected sites is particularly useful to diagnose SVV. There are numerous types of non-ANCA-associated SVV that are described in detail in reference 13 and are briefly mentioned below. In one type of SVV, complement-fixing immune complexes are deposited within the vessel walls. These may be cryoglobulins induced by hepatitis C infection or immune complexes associated with systemic diseases like SLE or RA. Anti-glomerular basement membrane (GBM) disease, formerly Goodpasture's syndrome, is named after the specificity of the autoantibody typically found in patients with this disease. It must be diagnosed promptly and treated aggressively because of the severe pulmonary and renal symptoms that can progress rapidly. The autoantibodies in this disease bind to both GBM and pulmonary alveolar capillary basement membranes, linking the renal and pulmonary lesions to the specificity of the autoantibodies. Some patients with GBM disease are also ANCA positive. IgA vasculitis (IgAV), formerly Henoch-Schönlein purpura, is characterized by IgA immune complexes in the skin and gastrointestinal tract. Hypocomplementemic urticarial vasculitis is characterized by anti-C1q autoantibodies. Some non-ANCA SVVs are not systemic but are localized to a single organ such as the kidney or lung.

ANCA-ASSOCIATED VASCULITIS

ANCA-associated vasculitis (AAV) is characterized by ANCA that yield positive C-ANCA or P-ANCA patterns on IFA of ethanol-fixed neutrophils and react with MPO or PR3 antigens or, in the case of drug-induced vasculitis, with other proteins in the granules. The suggested nomenclature

includes the specific reactivity of the antibody: PR3-ANCA, MPO-ANCA, or ANCA negative. AAV is a necrotizing vasculitis of the small vessels with few or no immune deposits (Fig. 3). It typically affects the lungs and kidneys in addition to a skin rash, typically palpable or retiform purpura (Fig. 4). When AAV is suspected, it is strongly advised to perform IFA on ethanol-fixed neutrophils rather than just the specific solid-phase assays for anti-MPO and anti-PR3 because some patients with AAV are negative for MPO-ANCA and PR3-ANCA. This pattern of ANCA can be found in most patients with drug-induced vasculitis who have autoantibodies to other proteins in the azurophilic granule (22–25), in a minority of patients with granulomatosis with polyangiitis (GPA), formerly Wegener's granulomatosis, and in MPA patients (27). A positive ANCA IFA with negative results on the specific anti-PR3 and anti-MPO assays can also be found in nonvasculitic conditions such as inflammatory bowel disease (26, 27). In addition, some patients are ANCA negative but have all of the other features of AAV and follow the same disease course. These patients may have a seronegative vasculitic disease equivalent to seronegative SLE, RA, or antiphospholipid syndrome.

There is debate about the pathogenicity of MPO- and PR3-ANCA, in part because they may occur in the absence of vasculitis, implying that other factors besides the autoantibodies themselves are important. It is possible that the fine specificity of the autoantibodies may be different in ANCA-positive patients with and without AAV (3). Importantly, MPO and PR3 antigens are found on the surface of activated, but not resting, neutrophils, and MPO and PR3 autoantibodies can induce a reactive oxygen burst in these neutrophils. In a large cohort of 502 patients with vasculitis, it was found that three different classification systems, the Chapel Hill Consensus Nomenclature, the European Medicines Agency system, and MPO- or PR3-ANCA positivity, yielded different percentages of patients diagnosed with GPA and MPA (17). The best correlation with relapse was the presence of anti-PR3 autoantibodies, consistent with a pathogenic role for that autoantibody.

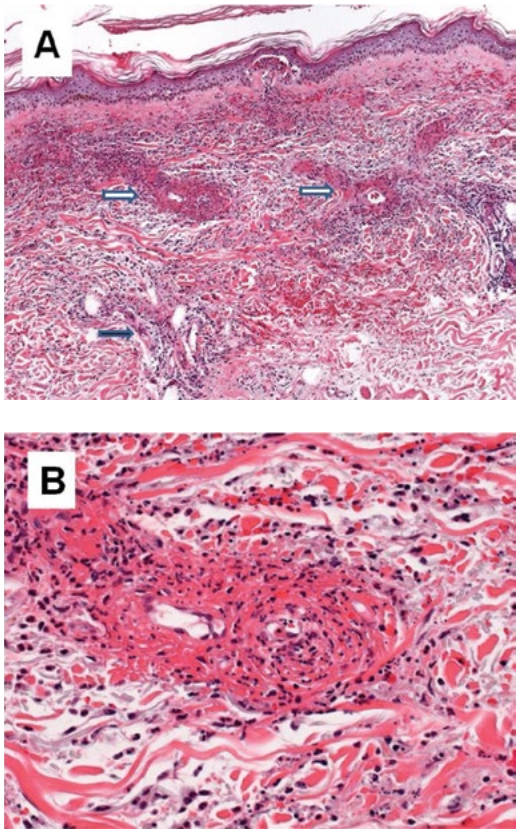

FIGURE 3 Photomicrograph of a skin biopsy displaying features of a leukocytoclastic vasculitis, such as that caused by ANCA. (A) At medium power, capillaries in the upper dermis, denoted by the white arrows, appear to have prominent thickened walls. These can be contrasted with normal dermal vessels denoted by the black arrow. Red blood cell extravasation is an additional feature. (B) At high power, the abnormal capillary wall displays fibrinoid change in association with a neutrophil-rich intramural inflammatory infiltrate.

FIGURE 4 Clinical photograph of a patient with palpable purpura on the legs. This is a cutaneous manifestation of a leukocytoclastic vasculitis, such as that caused by ANCA.

Granulomatosis with Polyangiitis

Patients with GPA have pauci-immune necrotizing granulomatous inflammation of the small to medium vessels, usually in the upper and lower respiratory tract (12, 13). Larger arteries are not frequently involved. Histopathology often shows extravascular inflammation with geographic zones of necrosis. Necrotizing crescentic glomerulonephritis without immune deposits is a serious manifestation. It should be noted that patients with GPA show the typical histopathology only 85% of the time (14), since not all specimens show granulomas and they are not present in all stages of the disease. So, patients with the correct clinical presentation and nonspecific inflammation on biopsy who are C-ANCA and PR3-ANCA positive are appropriately and frequently diagnosed with GPA (3, 12, 13). In some cases of GPA, the symptoms are very localized, such as in renal-limited necrotizing crescentic glomerulonephritis or pulmonary limited disease. These patients may still progress to systemic disease, so they must be closely monitored.

Similarly, with the correct clinical presentation and histopathologic features of vasculitis, albeit nongranulomatous, a patient can be diagnosed with GPA with negative ANCA since only approximately 85% of GPA patients are autoantibody positive (3, 13, 15, 17). In a GPA cohort derived from patients from 14 centers, 85% were ANCA positive by IFA. Approximately 65% were C-ANCA and/or PR3-ANCA positive, and 20% were P-ANCA and/or MPO-ANCA positive (15). Levels of ANCA fluctuate during the course of AAV,

so the ANCA-negative GPA patients may have been in a stage of decreased autoantibody production, or they may be true cases of seronegative GPA. There is evidence to support (32) and refute (33) the association between ANCA levels and clinical disease activity, but the majority of studies do not support the association. It was found that lung involvement and PR3-ANCA positivity were the best prognostic markers for the likelihood of disease flare in another GPA cohort (17).

Microscopic Polyangiitis

MPA is a pauci-immune necrotizing vasculitis that primarily affects small vessels, although medium vessels may also be involved. Necrotizing crescentic glomerulonephritis is a common feature and must be treated aggressively. One difference between GPA and MPA is that histopathology in MPA does not usually show granulomatous lesions or extravascular inflammation. In addition, the primary autoantibody in MPA is anti-MPO, which yields a P-ANCA pattern on IFA. P-ANCA and anti-MPO are found in nearly 60% of MPA patients, while C-ANCA and anti-PR3 are seen in about 25% (15).

EGPA, Formerly Churg-Strauss Syndrome

Eosinophilic granulomatosis with polyangiitis (EGPA) is a rare disease characterized by necrotizing vasculitis of the small and medium vessels of the respiratory tract. Eosinophilia in the blood, eosinophil-rich granulomatous inflammation on histopathology, and asthma are differentiating features (11). In some instances, EGPA is confined to the respiratory tract, while in other cases it may progress in 3 phases, with asthma followed by eosinophilic pneumonia or gastroenteritis and then necrotizing vasculitis. About 40% of EGPA patients show positive ANCA by IFA. Of these, about 70% are MPO-ANCA, 10% PR3-ANCA, and 20% atypical ANCA (34). A positive ANCA is strongly correlated with renal involvement.

Drug-Induced Vasculitis

Drug-induced vasculitis (DIV) presents with arthralgia, myalgia, skin rash, and autoantibodies to more than one protein found in azurophilic granules. These include human neutrophil elastase, cathepsin G, catalase K, bacterial-permeability-increasing protein, lactoferrin, and occasionally MPO (22–25). Usually, these are P-ANCA positive by IFA and negative for PR3-ANCA on follow-up specific-autoantibody testing. If the drug is continued for a substantial period after the onset of symptoms, severe manifestations that are the same as those seen in other AAV can occur.

Interestingly, many of the offending drugs can cause neutropenia. These include the thyroid drugs carbimazole, methimazole, and propylthiouracil, the antipsychotic clozapine, and the antihelminthic levamisole (22, 23). Several of these as well as other offending drugs have thiol groups. Propylthiouracil is the drug most frequently reported in the literature to be associated with DIV. Recently, levamisole-induced AAV has been reported in people using cocaine laced with levamisole (24, 25). When the patient stops taking the offending drug, the symptoms of drug-induced vasculitis usually resolve in a few weeks. If the disease is severe or the symptoms do not resolve, immunosuppressive therapy may be considered. However, treatment can be discontinued when the symptoms abate.

TREATMENT OF AAV

It is crucial to diagnose AAV as quickly as possible since many forms of the disease, including GBM, GPA, MPA, and EGPA, may rapidly progress to serious manifestations such as pulmonary hemorrhage or renal failure. Some DIV can quickly become life threatening (5, 35). Early and aggressive therapy with glucocorticoids and cyclophosphamide is necessary to bring acute manifestations under control (14, 17) with the goal of inducing remission as quickly as possible. This approach, which has been the standard therapy for over 40 years, has revolutionized the clinical outcome of AAV from a high probability of death to a low probability. Absolute and relative contraindications for aggressive treatment, such as concurrent infection, liver disease, pregnancy, or the desire to become pregnant, need to be addressed. After induction therapy, important clinical decisions are the types and dosages of drugs to maintain remission. In view of the significant comorbidity associated with the continued use of induction therapies over time, it is important to select treatment regimes with the least toxicity in striving to keep patients in remission.

A large, clinically well-characterized cohort of ANCA-positive vasculitis patients that were classified using the Chapel Hill system, using the European Medicines Agency system, or just on the basis of ANCA specificity were studied for prognostic markers of disease. The presence of PR3-ANCA was the best predictor of relapse regardless of the original diagnosis (17), with a nearly 2-fold increase in the likelihood of relapse. However, neither the presence of PR3-ANCA nor the level of autoantibody reliably predicts the time of onset of flare or relapse. Patients with GPA, MPA, or limited disease who were PR3-ANCA positive were more likely to have necrotizing granulomatous vasculitis, particularly in the lung, while those with MPO-ANCA were more likely to have limited disease, often confined to the kidney.

The Birmingham vasculitis activity score version 3 has been validated in a large cohort and can help define the current level of disease activity (6). It correlates well with the physician's global assessment of this parameter, but it does not predict relapse or remission.

Due to drug toxicity during long-term treatment with glucocorticoids and immunosuppressive drugs, there is a need to find alternative therapies. Biologic drugs have been explored with variable results (36). Tumor necrosis factor alpha inhibitors may be effective for the treatment of Takayasu's arteritis but not GCA, and their role in the treatment of other forms of vasculitis remains controversial. A large study showed that the addition of etanercept (Enbrel, another tumor necrosis factor alpha inhibitor) to standard treatment was not more effective than standard treatment alone in patients with GPA (37).

Early experience with rituximab (Rituxin), a drug that depletes circulating CD20-positive B cells, in the treatment of several forms of vasculitis has been quite promising, particularly in AAV. A single treatment of rituximab was as successful as continuous treatment with cyclophosphamide at inducing remission in patients with AAV (33). In addition, a single course of treatment with rituximab was statistically superior to cyclophosphamide at preventing relapse for 6 to 12 months, with comparable toxicity in the two groups (38). By 18 months, most patients had regained their circulating B cells, and while the rate of relapse in the rituximab group was still lower than in the cyclophosphamide-treated group, it did not reach statistical significance. An additional difference between these therapies was that rituximab was more effective in reducing the levels of PR3-ANCA. Fifty percent of patients became negative for PR3-ANCA following rituximab treatment, compared to 17% of patients treated with cyclophosphamide (33).

These new treatments are promising, but challenges remain. Individuals with the same disease may react differently to a particular drug, and a medication that is effective for one form of vasculitis may not be effective for another. Determining the right drug and correct dose for an individual with vasculitis is still a significant challenge.

NEUTROPHIL EXTRACELLULAR TRAPS

About 1 decade ago, a new antibacterial mechanism of neutrophils was discovered, neutrophil extracellular traps (NETs) (39). During a type of cell death termed NETosis, the neutrophil releases decondensed chromatin decorated with proteins from its azurophilic granules, effectively concentrating these proteins in the extracellular space. The NET can trap bacteria, stop them from spreading, and kill them with the associated proteins. Moreover, there are indications that in patients with AAV, this mechanism is involved in the autoantibody response and in thrombosis, as outlined below.

MPO, PR3, and other bactericidal proteins from azurophilic granules are found in NETs (40, 41, 42). The binding of these proteins to chromatin is a natural function of these proteins, required to concentrate these enzymes around the bacteria caught in the NETs. Thus, what was thought to be artifactual migration of MPO and other granule proteins to the nucleus during ethanol fixation of neutrophils, yielding the P-ANCA pattern on IFA, may actually be a normal expression of their chromatin binding capacity once the granule and nuclear membranes are destroyed by the fixation procedure.

When mice were injected with NETs, the NETs were taken up by dendritic cells and induced ANCA and vasculitis (40). Uptake by dendritic cells and autoimmunity were prevented when the NETs were first treated with DNase, suggesting that the structural integrity of the NETs was necessary for full expression of its antigenicity. The same study evaluated biopsies of skin lesions from MPO-ANCA-positive patients with MPA. The vascular inflammatory infiltrates were rich in neutrophils with MPO on their surface, and extracellular MPO was also detected, presumably attached to NETs. Myeloid dendritic cells were found in proximity to MPO-positive neutrophils, and some of the dendritic cells showed cytoplasmic MPO, consistent with uptake of NETs by these cells (40). Another group used immunofluorescence to study needle biopsy specimens of kidneys from 15 patients with SVV and acute renal failure (42). Extracellular chromatin decorated with MPO and PR3 was found in close proximity to neutrophil infiltrates in the glomeruli. These findings suggest a mechanism whereby MPO and PR3 could be presented to the immune system in a strongly antigenic form in a microenvironment with highly activated immune cells.

NETs can also induce thrombosis, which is likely a mechanism to encase bacteria trapped in NETs. An *in vitro* model system showed that platelets adhered to NETs and then became activated, and when blood flowed over this substrate, additional platelets adhered and aggregated in a self-perpetuating manner. Treatment with either DNase or heparin caused dismantling of NETs and prevented platelet aggregation (43). Tissue factor (TF), a critical component in the activation of the coagulation cascade, has recently been found in NETs from neutrophils isolated from patients with AAV (44). The neutrophils from patients with active disease based on the Birmingham vasculitis activity score (17 ± 7) before receiving immunosuppressive treatment spontaneously released NETs containing TF *in vitro*. After successful treatment, the release of NETs and the expression of TF decreased significantly to the levels of control subjects. TF and elastase that colocalized with extracellular DNA were found with specific staining of nasal biopsy specimens from the patients with active disease. The highest levels of TF colocalized with elastase and DNA, implying that TF was derived from neutrophils and trapped in NETs. In the same study of patients with active AAV, TF was identified in glomerular lesions from patients with kidney involvement (44). In a case report of a patient with MPA, histopathological evidence of NETs was found in glomerular crescents and thrombi. Extensive histone citrullination, which is a hallmark of histones in NETs, was found in the thrombus of this patient but not in control thrombi from patients without MPA (45).

Neutrophils are the main leukocytes found in histopathologic lesions in patients with AAV. Well-known properties of neutrophils such as the production of reactive oxygen species and recruitment of other mediators of the immune response can account for much of the inflammation observed in AAV. In addition, several aspects of AAV pathogenesis now can be linked to NETs, including the specificity of the autoantibodies, excess thrombosis, and possibly the initiation of the disease by bacterial infection. It has been proposed that MPO and PR3 autoantibodies are pathogenic because these antigens are on the surface of activated neutrophils, which can then become further activated by the autoantibodies. Adding the properties of NETs to this cycle of positive reinforcement of neutrophil activation by autoantibodies may explain more of the pathology found in these diseases.

REFERENCES

1. **Watts RA, Lane SE, Bentham G, Scott DG.** 2000. Epidemiology of systemic vasculitis: a ten-year study in the United Kingdom. *Arthritis Rheum* **43:**414–419.
2. **Mahr A, Guillevin L, Poissonnet M, Aymé S.** 2004. Prevalences of polyarteritis nodosa, microscopic polyangiitis, Wegener's granulomatosis, and Churg-Strauss syndrome in a French urban multiethnic population in 2000: a capture-recapture estimate. *Arthritis Rheum* **51:**92–99.
3. **Miller A, Chan M, Wiik A, Misbah SA, Luqmani RA.** 2010. An approach to the diagnosis and management of systemic vasculitis. *Clin Exp Immunol* **160:**143–160. PubMed
4. **Suresh E.** 2006. Diagnostic approach to patients with suspected vasculitis. *Postgrad Med J* **82:**483–488. PubMed
5. **Semple D, Keogh J, Forni L, Venn R.** 2005. Clinical review: vasculitis on the intensive care unit—part 1: diagnosis. *Crit Care* **9:**92–97. PubMed
6. **Suppiah R, Mukhtyar C, Flossmann O, Alberici F, Baslund B, Batra R, Brown D, Holle J, Hruskova Z, Jayne DR, Judge A, Little MA, Palmisano A, Stegeman C, Tesar V, Vaglio A, Westman K, Luqmani R.** 2011. A cross-sectional study of the Birmingham Vasculitis Activity Score version 3 in systemic vasculitis. *Rheumatology* (Oxford) **50:**899–905.
7. **Craven A, Robson J, Ponte C, Grayson PC, Suppiah R, Judge A, Watts R, Merkel PA, Luqmani RA.** 2013. ACR/EULAR-endorsed study to develop Diagnostic and Classification Criteria for Vasculitis (DCVAS). *Clin Exp Nephrol* **17:**619–621.
8. **Bloch DA, Michel BA, Hunder GG, McShane DJ, Arend WP, Calabrese LH, Edworthy SM, Fauci AS, Fries JF, Leavitt RY, Lie JT, Lightfoot RW, Masi AT, Mills JA, Stevens MB, Wallace SL, Zvaifler N.** The American College of Rheumatology 1990 criteria for the classification of vasculitis—patients and methods. *Arthritis Rheum* **33:**1068–1073.
9. **Arend WP, Michel BA, Bloch DA, Hunder GG, Calabrese LH, Edworthy SM, Fauci AS, Leavitt RY, Lie JT,**

Lightfoot RW Jr, Masi AT, McShane DJ, Mills JA, Stevens MB, Wallace SL, Zvaifler NJ. 1990. The American College of Rheumatology 1990 criteria for the classification of Takayasu arteritis. *Arthritis Rheum* **33:**1129–1134. PubMed

10. **Hunder GG, Bloch DA, Michel BA, Stevens MB, Arend WP, Calabrese LH, Edworthy SM, Fauci AS, Leavitt RY, Lie JT, Lightfoot RW, Masi AT, McShane DJ, Mills JA, Wallace SL, Zvzifler NJ.** 1990. The American College of Rheumatology 1990 criteria for the classification of giant cell arteritis. *Arthritis Rheum* **33:**1122–1128. PubMed
11. **Masi AT, Hunder GG, Lie JT, Michel BA, Bloch DA, Arend WP, Calabrese LH, Edworthy SM, Fauci AS, Leavitt RY, McShane DJ, Mills JA, Stevens MB, Wallace SL, Zvaifler NJ.** 1990. The American College of Rheumatology 1990 criteria for the classification of Churg-Strauss syndrome (allergic granulomatosis and angiitis). *Arthritis Rheum* **33:**1094–1100. PubMed
12. **Leavitt RY, Fauci AS, Bloch DA, Michel BA, Hunder GG, Arend P, Calabrese LH, Fries JF, Lie JT, Lightfoot RW Jr, Masi AT, McShane DJ, Mills JA, Stevens MB, Wallace SL, Zvaifler NJ.** 1990. The American College of Rheumatology 1990 criteria for the classification of Wegener's granulomatosis. *Arthritis Rheum* **33:**1101–1107.
13. **Jennette JC, Falk RJ, Bacon PA, Basu N, Cid MC, Ferrario F, Flores-Suarez LF, Gross WL, Guillevin L, Hagen EC, Hoffman GS, Jayne DR, Kallenberg CG, Lamprecht P, Langford CA, Luqmani RA, Mahr AD, Matteson EL, Merkel PA, Ozen S, Pusey CD, Rasmussen N, Rees AJ, Scott DG, Specks U, Stone JH, Takahashi K, Watts RA.** 2013. 2012 revised International Chapel Hill Consensus Conference Nomenclature of Vasculitides. *Arthritis Rheum* **65:**1–11. PubMed
14. **Mukhtyar C, Guillevin L, Cid MC, Dasgupta B, de Groot K, Gross W, Hauser T, Hellmich B, Jayne D, Kallenberg CGM, Merkel PA, Raspe H, Salvarani C, Scott DGI, Stegeman C, Watts R, Westman K, Witter J, Yazici H, Luqmani R, European Vasculitis Study Group.** 2009. EULAR recommendations for the management of primary small and medium vessel vasculitis. *Ann Rheum Dis* **68:**310–317. PubMed
15. **Hagen EC, Daha MR, Hermans J, Andrassy K, Csernok E, Gaskin G, Lesavre P, Lüdemann J, Rasmussen N, Sinico RA, Wiik A, van der Woude FJ.** 1998. Diagnostic value of standardized assays for anti-neutrophil cytoplasmic antibodies in idiopathic systemic vasculitis. EC/BCR Project for ANCA Assay Standardization. *Kidney Int* **53:**743–753.
16. **Stone JH, Talor M, Stebbing J, Uhlfelder ML, Rose NR, Carson KA, Hellmann DB, Burek CL.** 2000. Test characteristics of immunofluorescence and ELISA tests in 856 consecutive patients with possible ANCA-associated conditions. *Arthritis Care Res* **13:**424–434.
17. **Lionaki S, Blyth ER, Hogan SL, Hu Y, Senior BA, Jennette CE, Nachman PH, Jennette JC, Falk RJ.** 2012. Classification of antineutrophil cytoplasmic autoantibody vasculitides: the role of antineutrophil cytoplasmic autoantibody specificity for myeloperoxidase or proteinase 3 in disease recognition and prognosis. *Arthritis Rheum* **64:**3452–3462. PubMed
18. **van der Woude FJ, Rasmussen N, Lobatto S, Wiik A, Permin H, van Es LA, van der Giessen M, van der Hem GK, The TH.** 1985. Autoantibodies against neutrophils and monocytes: tool for diagnosis and marker of disease activity in Wegener's granulomatosis. *Lancet* **i:**425–429.
19. **Wiik A.** 2002. Antineutrophil cytoplasmic antibodies (ANCAs) and ANCA testing, p 981–986. *In* Rose NR, Hamilton RG, Detrick B (ed), *Manual of Clinical Laboratory Immunology*, 6th ed. ASM Press, Washington, DC.
20. **Burlingame RW, Rubin RL.** 2002. Enzyme-linked immunosorbent assays for diagnostically important antinuclear antibodies, p 951–960. *In* Rose NR, Hamilton RG, Detrick B (ed), *Manual of Clinical Laboratory Immunology*, 6th ed. ASM Press, Washington, DC.
21. **Wiik A.** 2003. Autoantibodies in vasculitis. *Arthritis Res Ther* **5:**147–152.
22. **Radić M, Martinović Kaliterna D, Radić J.** 2012. Drug-induced vasculitis: a clinical and pathological review. *Neth J Med* **70:**12–17. PubMed
23. **Bonaci-Nikolic B, Nikolic MM, Andrejevic S, Zoric S, Bukilica M.** 2005. Antineutrophil cytoplasmic antibody (ANCA)-associated autoimmune diseases induced by antithyroid drugs: comparison with idiopathic ANCA vasculitides. *Arthritis Res Ther* **7:**R1072–R1081.
24. **Wiesner O, Russell KA, Lee AS, Jenne DE, Trimarchi M, Gregorini G, Specks U.** 2004. Antineutrophil cytoplasmic antibodies reacting with human neutrophil elastase as a diagnostic marker for cocaine-induced midline destructive lesions but not autoimmune vasculitis. *Arthritis Rheum* **50:**2954–2965.
25. **Walsh NMG, Green PJ, Burlingame RW, Pasternak S, Hanly JG.** 2010. Cocaine-related retiform purpura: evidence to incriminate the adulterant, levamisole. *J Cutan Pathol* **37:**1212–1219. PubMed
26. **Lindgren S, Nilsson S, Nässberger L, Verbaan H, Wieslander J.** 2000. Anti-neutrophil cytoplasmic antibodies in patients with chronic liver diseases: prevalence, antigen specificity and predictive value for diagnosis of autoimmune liver disease. Swedish Internal Medicine Liver Club (SILK). *J Gastroenterol Hepatol* **15:**437–442.
27. **Talor MV, Stone JH, Stebbing J, Barin J, Rose NR, Burek CL.** 2007. Antibodies to selected minor target antigens in patients with anti-neutrophil cytoplasmic antibodies (ANCA). *Clin Exp Immunol* **150:**42–48.
28. **Holle JU, Hellmich B, Backes M, Csernok E.** 2005. Variations in performance characteristics of commercial enzyme immunoassay kits for detection of antineutrophil cytoplasmic antibodies: what is the optimal cutoff? *Ann Rheum Dis* **64:**1773–1779. PubMed
29. **Russell KA, Wiegert E, Schroeder DR, Homburger HA, Specks U.** 2002. Detection of anti-neutrophil cytoplasmic antibodies under actual clinical testing conditions. *Clin Immunol* **103:**196–203. PubMed
30. **Narváez J, Narváez JA, Nolla JM, Sirvent E, Reina D, Valverde J.** 2005. Giant cell arteritis and polymyalgia rheumatica: usefulness of vascular magnetic resonance imaging studies in the diagnosis of aortitis. *Rheumatology* (Oxford) **44:**479–483.
31. **Schmidt WA, Seifert A, Gromnica-Ihle E, Krause A, Natusch A.** 2008. Ultrasound of proximal upper extremity arteries to increase the diagnostic yield in large-vessel giant cell arteritis. *Rheumatology* (Oxford) **47:**96–101.
32. **Cartin-Ceba R, Golbin JM, Keogh KA, Peikert T, Sanchez-Menendez M, Ytterberg SR, Fervenza FC, Specks U.** 2012. Rituximab for remission induction and maintenance in refractory granulomatosis with polyangiitis (Wegener's): ten-year experience at a single center. *Arthritis Rheum* **64:**3770–3778. PubMed
33. **Stone JH, Merkel PA, Spiera R, Seo P, Langford CA, Hoffman GS, Kallenberg CG, St Clair EW, Turkiewicz A, Tchao NK, Webber L, Ding L, Sejismundo LP, Mieras K, Weitzenkamp D, Ikle D, Seyfert-Margolis V, Mueller M, Brunetta P, Allen NB, Fervenza FC, Geetha D, Keogh KA, Kissin EY, Monach PA, Peikert T, Stegeman C, Ytterberg SR, Specks U, RAVE-ITN Research Group.** 2010. Rituximab versus cyclophosphamide for ANCA-associated vasculitis. *N Engl J Med* **363:**221–232.
34. **Sinico RA, Di Toma L, Maggiore U, Bottero P, Radice A, Tosoni C, Grasselli C, Pavone L, Gregorini G, Monti S, Frassi M, Vecchio F, Corace C, Venegoni E, Buzio C.** 2005. Prevalence and clinical significance of antineutrophil

cytoplasmic antibodies in Churg-Strauss syndrome. *Arthritis Rheum* **52:**2926–2935.
35. **Papiris SA, Manali ED, Kalomenidis I, Kapotsis GE, Karakatsani A, Roussos C.** 2007. Bench-to-bedside review: pulmonary-renal syndromes—an update for the intensivist. *Crit Care* **11:**213–223.
36. **Chung SA, Seo P.** 2009. Advances in the use of biologic agents for the treatment of systemic vasculitis. *Curr Opin Rheumatol* **21:**3–9. PubMed
37. **Wegener's Granulomatosis Etanercept Trial (WGET) Research Group.** 2005. Etanercept plus standard therapy for Wegener's granulomatosis. *N Engl J Med* **352:**351–361. PubMed
38. **Specks U, Merkel PA, Seo P, Spiera R, Langford CA, Hoffman GS, Kallenberg CG, St Clair EW, Fessler BJ, Ding L, Viviano L, Tchao NK, Phippard DJ, Asare AL, Lim N, Ikle D, Jepson B, Brunetta P, Allen NB, Fervenza FC, Geetha D, Keogh K, Kissin EY, Monach PA, Peikert T, Stegeman C, Ytterberg SR, Mueller M, Sejismundo LP, Mieras K, Stone JH, RAVE-ITN Research Group.** 2013. Efficacy of remission-induction regimens for ANCA-associated vasculitis. *N Engl J Med* **369:**417–427.
39. **Brinkmann V, Reichard U, Goosmann C, Fauler B, Uhlemann Y, Weiss DS, Weinrauch Y, Zychlinsky A.** 2004. Neutrophil extracellular traps kill bacteria. *Science* **303:**1532–1535.
40. **Sangaletti S, Tripodo C, Chiodoni C, Guarnotta C, Cappetti B, Casalini P, Piconese S, Parenza M, Guiducci C, Vitali C, Colombo MP.** 2012. Neutrophil extracellular traps mediate transfer of cytoplasmic neutrophil antigens to myeloid dendritic cells toward ANCA induction and associated autoimmunity. *Blood* **120:**3007–3018. PubMed
41. **Knight JS, Carmona-Rivera C, Kaplan MJ.** 2012. Proteins derived from neutrophil extracellular traps may serve as self-antigens and mediate organ damage in autoimmune diseases. *Front Immunol* **3:**380. PubMed
42. **Kessenbrock K, Krumbholz M, Schönermarck U, Back W, Gross WL, Werb Z, Gröne HJ, Brinkmann V, Jenne DE.** 2009. Netting neutrophils in autoimmune small-vessel vasculitis. *Nat Med* **15:**623–625. PubMed
43. **Fuchs TA, Brill A, Duerschmied D, Schatzberg D, Monestier M, Myers DD Jr, Wrobleski SK, Wakefield TW, Hartwig JH, Wagner DD.** 2010. Extracellular DNA traps promote thrombosis. *Proc Natl Acad Sci USA* **107:**15880–15885.
44. **Kambas K, Chrysanthopoulou A, Vassilopoulos D, Apostolidou E, Skendros P, Girod A, Arelaki S, Froudarakis M, Nakopoulou L, Giatromanolaki A, Sidiropoulos P, Koffa M, Boumpas DT, Ritis K, Mitroulis I.** 2013. Tissue factor expression in neutrophil extracellular traps and neutrophil derived microparticles in antineutrophil cytoplasmic antibody associated vasculitis may promote thromboinflammation and the thrombophilic state associated with the disease. *Ann Rheum Dis* **73:**1854–1863.
45. **Nakazawa D, Tomaru U, Yamamoto C, Jodo S, Ishizu A.** 2012. Abundant neutrophil extracellular traps in thrombus of patient with microscopic polyangiitis. *Front Immunol* **3:**333. PubMed

IgG4-Related Disease: Diagnostic Testing by Serology, Flow Cytometry, and Immunohistopathology

JOHN H. STONE

95

IgG4-related disease (IgG4-RD) is a multiorgan immune-mediated condition that mimics many malignant, infectious, and inflammatory disorders (1–3). The diagnosis links numerous conditions once regarded as isolated, single-organ diseases that existed outside of any known underlying systemic condition (Table 1). The histopathological findings in IgG4-RD are consistent across the wide range of organ systems that can be involved. IgG4-RD is often confused with a malignancy upon presentation because it has a tendency to form mass lesions. In addition, IgG4-RD can mimic a host of immune-mediated conditions, e.g., primary sclerosing cholangitis, idiopathic interstitial lung disease, Sjögren's syndrome, granulomatosis with polyangiitis, and idiopathic membranous nephropathy.

CLINICAL FEATURES

IgG4-RD can affect essentially any organ in the body. The presentation of the disease is typically subacute, with symptoms and signs of organ dysfunction present months or even years before the diagnosis. Weight loss and fatigue are common but fevers and highly inflammatory presentations are not. Lymphadenopathy, when present, is seldom dramatic but can present in either a generalized form or as disease localized adjacent to an affected organ (4). The lymph nodes involved are generally 1 to 3 cm in diameter and non-tender.

The organ manifestations, organized according to anatomic location, are summarized briefly below:

Head and Neck

The brain parenchyma is seldom if ever involved, but IgG4-RD is among the most common causes of "idiopathic" hypertrophic pachymeningitis and can also cause hypophysitis. Dacryoadenitis leading to lacrimal gland enlargement is the most common feature of ophthalmic disease in IgG4-RD. Proptosis can result from combinations of orbital lesions, such as pseudotumors that do not affect the lacrimal gland and inflammation and thickening of the extraocular muscles. The triad of dacryoadenitis and enlargement of both the parotid and submandibular glands, once known as "Mikulicz's disease," is a classic presentation of IgG4-RD. Isolated submandibular gland enlargement is also a common finding in IgG4-RD.

The prevalence of atopy among IgG4-RD patients is similar to that of the general population, but a subset of nonatopic patients has peripheral blood eosinophilia and elevated IgE levels (5). Allergic rhinitis, nasal polyps, chronic sinusitis, nasal obstruction, and rhinorrhea are common in IgG4-RD. Mild to moderate peripheral eosinophilia and serum IgE concentration elevations that sometimes exceed ten times the upper limit of normal are common.

Mass lesions in the sinuses, destructive lesions in the middle ear and facial bones, midline destructive disease, and diffuse inflammation in the pharynx and hypopharynx, frequently associated with mass lesions, can all occur in IgG4-RD. Tracheal inflammation and vocal cord involvement have also been described. Riedel's thyroiditis is linked convincingly to IgG4-RD.

Chest

The lung is associated with a remarkable diversity of clinical and radiologic findings in IgG4-RD. IgG4-RD tends to track along bronchi and blood vessels, leading to thickening of the bronchovascular bundle on imaging studies. Pulmonary nodules, ground-glass opacities, pleural thickening, and interstitial lung disease can also occur. Fibrosing mediastinitis can lead to the compression of vital mediastinal structures from proliferation of invasive fibrous tissue.

IgG4-related aortitis is often diagnosed either on the basis of an incidental radiological finding or an unexpected finding at surgery. IgG4-related aortitis can lead to aneurysms or dissections in the thoracic aorta. Coronary artery lesions in IgG4-RD, sometimes associated with aneurysm formation, are observed in IgG4-RD.

Abdomen

The pancreas was the first organ recognized to be associated with elevated serum IgG4 concentrations (6, 7). AIP associated with IgG4-RD, sometimes termed type 1 (IgG4-related) AIP, demonstrates the classic histopathological findings of lymphoplasmacytic sclerosing pancreatitis. The most common clinical presentation of type 1 AIP is obstructive jaundice, induced by concomitant IgG4-related sclerosing cholangitis. IgG4-related sclerosing cholangitis must be differentiated from both primary sclerosing cholangitis and cholangiocarcinoma.

Retroperitoneum

Tubulointerstitial nephritis (TIN) is the most characteristic form of IgG4-related kidney disease (8). Computed tomographic scanning in IgG4-related TIN can reveal substantial

doi:10.1128/9781555818722.ch95

TABLE 1 Names of previously recognized conditions that comprise parts of the IgG4-related disease spectrum[a]

Mikulicz's disease (affecting the salivary and lacrimal glands)
Küttner's tumor (affecting the submandibular glands)
Riedel's thyroiditis
Eosinophilic angiocentric fibrosis (affecting the orbits and upper respiratory tract)
Lymphomatoid granulomatosis, grade 1 (commonly affecting the lungs)
Multifocal fibrosclerosis (commonly affecting the orbits, thyroid gland, retroperitoneum, mediastinum, and other tissues/organs)
Lymphoplasmacytic sclerosing pancreatitis/autoimmune pancreatitis
Inflammatory pseudotumor (orbits, lungs, kidneys, and other organs)
Mediastinal fibrosis
Retroperitoneal fibrosis
Sclerosing mesenteritis
Periaortitis/periarteritis
Inflammatory aortic aneurysm
Idiopathic hypocomplementemic tubulointerstitial nephritis with extensive tubulointerstitial deposits

[a]Modified with permission from the Massachusetts Medical Society (reference 29)

renal enlargement and hypodense lesions within the renal parenchyma. IgG4-related TIN is often distinguished from other organ manifestations of IgG4-RD by profound hypocomplementemia. The hypocomplementemia in IgG4-RD could result from the formation of immune complexes that contain IgG1 or IgG3, subclasses that bind complement more effectively and are often elevated to a lesser degree. Membranous glomerulonephropathy also occurs in IgG4-RD, but the pathophysiology of this entity appears to differ from that of IgG4-related TIN.

"Idiopathic" retroperitoneal fibrosis (RPF) is now considered to belong to a larger disease spectrum now known as chronic periaortitis. The three major components of chronic periaortitis are IgG4-related RPF, IgG4-related abdominal aortitis, and IgG4-related perianeurysmal fibrosis. IgG4-RD is responsible for most but not all (approximately two-thirds) of cases of "idiopathic" RPF. Sclerosing mesenteritis often appears to originate at the mesenteric root. The ensuing process often merges imperceptibly with RPF.

PATHOLOGY

IgG4-RD is characterized by the similarity of histologic appearance, regardless of the organ affected (9). The hallmark morphologic findings are a dense lymphoplasmacytic infiltrate rich in $IgG4^+$ plasma cells, an irregularly whorled fibrotic process referred to as "storiform" fibrosis, and obliterative phlebitis. A moderate tissue eosinophilia is also often observed. A disproportionate number of plasma cells within tissue lesions stain for IgG4.

PATHOPHYSIOLOGY

Many patients with IgG4-RD have striking elevations of serum IgG4 concentrations. In addition, except for advanced cases characterized primarily by fibrotic lesions, IgG4-positive plasma cells are nearly always present in abundance at sites of disease. Substantial elevations of plasmablasts have also been reported in IgG4-RD, and these cells appear to mirror disease activity (10, 11). Consequently, the IgG4 antibody and humoral immunity have been emphasized most prominently in discussions of pathophysiology thus far. However, the theory that IgG4 itself is a crucial player in disease etiology, which held sway for many years after the first recognition of the elevated serum IgG4 concentrations in "sclerosing pancreatitis," is now being revised.

The IgG4 Molecule

The IgG4 molecule has unique chemical properties that render it unlikely to play a central inflammatory role. The subclasses of IgG differ from each other in important ways, defined by the sequences of their heavy chain constant domains. IgG4 normally accounts for only about 4% of the total immunoglobulins among healthy individuals and is the least abundant of all of the IgG subclasses. IgG4 demonstrates weak binding to C1q and to Fc-gamma receptors because of a critical few amino acid differences in its CH2 domain (12, 13). Consequently, IgG4's ability to activate the classical complement pathway and participate in antibody-dependent cell-mediated cytotoxicity is attenuated substantially, compared, for example, to the capabilities of IgG1 (13).

IgG4 also has the unique ability to form "half-antibodies" through the process of Fab arm exchange. Amino acid variation at the hinge region of IgG4 permits the reduction of the disulfide bonds that join the two halves of an IgG4 molecule. Recombination of the dissociated arms leads to the random formation of "asymmetric antibodies" composed of half-antibody fragments directed against different antigens (12, 13). Fab-arm exchange results in the formation of IgG molecules with two different binding specificities (13). The consequence is a reduced ability to cross-link antigens and form immune complexes.

An alternative view of IgG4 is that its presence can be ascribed to a downregulatory role. The specific function of IgG4 in IgG4-RD may be to serve as a noninflammatory "antigen sink," "mopping up" antigen through its monovalent binding in a process that tends to dampen inflammation (2). Indeed, it has been demonstrated that the IgG4 response develops after chronic antigen exposure as a part of a tolerogenic response (12, 13).

The B-Cell Lineage

B cells and the cells of their lineage play important roles in IgG4-RD. Serum IgG4 concentrations decline swiftly following B-cell depletion, suggesting that the cells making most of the serum IgG4 are short-lived plasmablasts and plasma cells (14, 15). Plasmablasts are found in high concentrations in IgG4-RD, regardless of the serum IgG4 concentration (10, 11, 16). The roles of the B-cell lineage in IgG4-RD include not only infiltration into tissue sites of disease and the production of IgG4, but also antigen presentation to T cells. The circulating plasmablasts in IgG4-RD demonstrate intense somatic hypermutation, a hallmark of interaction with T cells within the germinal centers of lymph nodes (30). The fact that B-cell depletion does not lead to the complete normalization of serum IgG4 concentrations implies the presence of long-lived plasma cells that continue to make this immunoglobulin.

What Drives the Immunoglobulin Class Switch?

A T-follicular helper-cell response probably mediates the development of germinal centers within lymph nodes and other organs affected by IgG4-RD. T-follicular helper cells

may produce the cytokines (e.g., IL-4) that drive the IgG4 class-switch, culminating in the creation of IgG4-secreting plasmablasts and long-lived plasma cells.

T-Cell Pathways

T cells play a central role in IgG4-RD pathogenesis in a variety of ways, in addition to the class switch. $CD4^+$ T cells are typically dispersed throughout localized IgG4-RD lesions and are the most abundant cell found within affected tissues. Conflicting reports have implicated Th1 cells and Th2 cells in the pathophysiology of IgG4-RD (17, 18). Recent studies suggest that Th2 cells accumulate in the blood only in subjects with concomitant atopy (19).

A Novel "CD4 Killer" Cell

The recent identification of a clonally expanded population of $CD4^+$ cytotoxic T lymphocytes in both the peripheral blood and fibrotic lesions of IgG4-RD patients suggests that these cells are central to the disease. These cytotoxic T cells make products such as granzyme B and perforin that are associated more commonly with $CD8^+$ T cells. The T cells also elaborate interleukin-1, which may be an important mediator of the fibrosis.

TREATMENT

No randomized clinical trials evaluating the comparative effectiveness of different treatment regimens have been performed. Glucocorticoids are currently the first-line treatment for IgG4-RD. Most data on the use of glucocorticoids are derived from the treatment of IgG4-related pancreatitis (type 1 autoimmune pancreatitis) and have been extrapolated to the treatment of extrapancreatic IgG4-RD. Treatment of IgG4-related pancreatitis with glucocorticoids typically results in a symptomatic response within 2 weeks and remission within 2 to 3 months in most cases (20). However, the majority of patients relapse if the glucocorticoids are tapered or discontinued (20). Conventional immunosuppressive medications such as azathioprine and mycophenolate mofetil do not appear to have substantial efficacy in IgG4-RD in the absence of glucocorticoids (21). Treatment with rituximab to induce B-cell depletion has yielded promising results (14, 15, 22).

IMMUNODIAGNOSIS: TISSUE, SERUM, FLOW CYTOMETRY

Immunohistology of Tissue

"Positive" IgG4 immunostaining lends additional support to the diagnosis of IgG4-RD but is not diagnostic in and of itself. Neither the number of $IgG4^+$ plasma cells per high-power field (hpf) nor the $IgG4^+/IgG^+$ plasma cell ratio is specific for the diagnosis of IgG4-RD, and no number of $IgG4^+$ plasma cells within a biopsy sample is sufficient on its own to support the diagnosis of IgG4-RD. Rather, the finding of the characteristic histopathology in the right clinical context allows the pathologist and clinician to reach the diagnosis in collaboration.

The preponderance of plasma cells within tissue lesions stain for IgG4. An increase in the number of $IgG4^+$ plasma cells/hpf and an elevated $IgG4^+/IgG^+$ plasma cell ratio can therefore support the diagnosis of IgG4-RD, but careful clinicopathologic correlation and sound clinical judgment must be exercised in rendering the diagnosis of IgG4-RD. One may expect fewer $IgG4^+$ plasma cells in biopsies from patients with fibrotic lesions such as RPF because of the overwhelmingly fibrotic nature of the pathology at the time of biopsy in most patients. The $IgG4^+/IgG^+$ plasma cell ratio can also be a useful metric to aid in diagnosis. Most cases of documented IgG4-RD have an $IgG4^+/IgG^+$ plasma cell ratio >40% (9).

Performance and Evaluation of IgG4 Immunostaining of Tissue

Slides must be evaluated for immunohistochemistry for CD138 and IgG as well as for IgG4. IgG4 immunostaining is performed as follows: mouse monoclonal antihuman IgG4 antibody of IgG1/k isotype is diluted 1:200 for use in staining. Immunohistochemical studies are performed using appropriate controls to validate staining. Endogenous peroxidase activity is blocked by H_2O_2 before antibody incubation. Antigen retrieval is achieved by treating the tissue sections for 4 minutes with commercially available protease solutions prior to primary antibody incubations. The tissues sections are washed and incubated with the primary anti-IgG4 antibody for 24 minutes, followed by incubation with the antibody reagent. Three high-power fields with the most dense concentrations of IgG4-positive plasma cells are counted. One high-power field corresponds to a field area of 0.2375 mm^2 (10× eyepiece and 40× lens). Immunoreactive plasma cells are counted within the same three fields on the slide stained for IgG. The ratio of IgG4- to IgG-positive plasma cells is calculated.

SERUM IgG4 CONCENTRATIONS

A serum IgG4 level is often the first diagnostic test ordered when IgG4-RD is suspected. Although serum IgG4 measurements continue to play an important role in the diagnosis and management of IgG4-RD, several major considerations are important in interpreting serum IgG4 concentrations.

First, large elevations of serum IgG4 concentrations, e.g., measurements 6 to 8 times the upper limit of normal, strongly suggest the diagnosis. Serum IgG4 concentrations in patients with multiorgan disease sometimes have dramatic elevations, occasionally exceeding 4 mg/dl (16). The elevations of IgG4 are usually disproportionate to those of the other IgG subclasses, but the concentrations of IgG1, -2, and -3 are also increased in some patients (16).

Second, despite the frequently striking serum IgG4 concentrations observed in patients with this disease, elevated levels are far from universal among IgG4-RD patients. In fact, a large proportion of patients with biopsy-proven, clinically validated IgG4-RD have normal serum IgG4 concentrations, even before beginning treatment (16). Reliance upon serum IgG4 concentration elevations for diagnosis, therefore, can lead to a high rate of underdiagnosis.

Third, mild IgG4 elevations are common across a variety of conditions that can mimic IgG4-RD. Vasculitides such as granulomatosis with polyangiitis (formerly Wegener's) and eosinophilic granulomatosis with polyangiitis (formerly Churg-Strauss syndrome), bronchiectasis, biliary diseases such as primary sclerosing cholangitis, pancreatic cancer, and multiple others can have confoundingly high serum IgG4 concentrations, though they rarely if ever reach the highest values achieved by some patients with IgG4-RD (23).

Similar caveats apply to the use of serum IgG4 concentrations as a correlate of disease activity. Among patients with IgG4-RD whose serum IgG4 concentrations are elevated at the start of treatment, the serum IgG4 declines substantially in essentially all patients yet only normalizes entirely in about half. Declines in serum IgG4 concentration occur

quickly following the institution of treatment but continue for many weeks following clinical improvement.

In a large retrospective study of type 1 autoimmune pancreatitis from 17 centers in Japan (24), serum IgG4 levels declined in all patients following treatment with glucocorticoids but remained above the upper limit of normal in 63% of the patients despite good clinical responses. Thirty percent of the patients who relapsed had normal serum IgG4 levels at the time of relapse. Thus, serum IgG4 concentrations should not be relied upon exclusively as an indicator of disease activity.

Serum IgG4 Assays

Measurement of serum IgG4 has been performed using several different methodologies, including immunodiffusion and immunoelectrophoresis, immunonephelometry, enzyme-linked immunosorbent assay (ELISA) and liquid chromatography-tandem mass spectrometry (LC-MS/MS).

Early studies relied on the use of immunodiffusion and immunoelectrophoresis techniques. However, overall these methods lacked the necessary sensitivity and specificity required to detect IgG4 immunodeficiencies, had to be performed manually, and were time-consuming (25).

Most currently available serum IgG4 assays are nephelometry-based. As stated above, the original purpose for developing most IgG subclass assays was to detect immunodeficiencies. Thus, many of the original IgG4 assays were optimized for the detection of low serum IgG4 concentrations. The principles involved in nephelometry measure the amount of light scattered at a given wavelength by a particulate suspension. The amount of light scatter is dependent upon the size and amount of aggregates formed by the binding of antibodies present in the reagent to antigens (i.e., IgG4 in this case) present in the sample. However, this methodology is prone to antigen excess prozone effects in which the multi-fold elevations above the upper limit of normal that are frequently observed in IgG4-RD can result in falsely low values. The prozone effect can be circumvented by diluting the test sample to allow the antibody concentration to remain in excess of that of the antigen concentration. One study of serum IgG4 measurements in a patient population from one center found the prozone effect to be responsible for spurious IgG4 undermeasurement in 26% of samples. The same study also demonstrated that the use of nephelometric reagents from different vendors can lead to widely different results even when analyzed on the same instrument (26).

Commercially available 96-well ELISA formats are a suitable alternative to nephelometry and typically involve the binding of IgG4 in the patient sample to wells coated with antibody to IgG4 (27). The wells are washed, and the amount of bound IgG4 is detected by the formation of a colored product that is quantified versus a standard calibration curve of known concentrations of IgG4. Use of the ELISA format would address the issue of the prozone effect. In the case of high testing volumes, instrumentation allowing for automation of the assays could be added.

The newest methodology involves the use of LC-MS/MS as an alternative to the constraints of nephelometric analysis. The method involves the tryptic digestion of IgG subclass proteins followed by the analysis of subclass-specific peptides by LC-MS/MS. This assay is traceable to the results obtained by nephelometry and offers the simultaneous quantification of not only IgG4 but all of the subclasses and total IgG in a single analysis. Use of this method also overcomes interferences such as those due to the prozone effect as well as M-spikes from monoclonal gammopathies (28).

FLOW CYTOMETRY

Plasmablasts are found in high concentrations in IgG4-RD, regardless of the serum IgG4 concentration (10, 11, 16). Both total plasmablasts and IgG4+ plasmablasts are good biomarkers for disease activity in IgG4-RD, and their measurement might also be useful in diagnosis. Flow cytometry gating for these cells is not widely available at this time, even though transcriptional profiling of whole blood has proved useful in other disorders.

Flow Cytometry Assay for Plasmablasts

Fluorescence labeling for flow cytometry is performed by incubating cells in a staining buffer containing optimized concentrations of fluorochrome-conjugated antibodies. Monoclonal antibodies useful in flow cytometry for plasmablasts include those directed against CD19, CD27, CD38, CD24, and IgG4.

REFERENCES

1. **Kamisawa T, Zen Y, Pillai S, Stone JH.** 2015. IgG4-related disease. *Lancet* **385:**1460–1471. PubMed
2. **Mahajan VS, Mattoo H, Deshpande V, Pillai SS, Stone JH.** 2014. IgG4-related disease. *Annu Rev Pathol* **9:**315–347. PubMed
3. **Stone JH, Khosroshahi A, Deshpande V, Chan JK, Heathcote JG, Aalberse R, Azumi A, Bloch DB, Brugge WR, Carruthers MN, Cheuk W, Cornell L, Castillo CF, Ferry JA, Forcione D, Klöppel G, Hamilos DL, Kamisawa T, Kasashima S, Kawa S, Kawano M, Masaki Y, Notohara K, Okazaki K, Ryu JK, Saeki T, Sahani D, Sato Y, Smyrk T, Stone JR, Takahira M, Umehara H, Webster G, Yamamoto M, Yi E, Yoshino T, Zamboni G, Zen Y, Chari S.** 2012. Recommendations for the nomenclature of IgG4-related disease and its individual organ system manifestations. *Arthritis Rheum* **64:**3061–3067. PubMed
4. **Cheuk W, Chan JK.** 2012. Lymphadenopathy of IgG4-related disease: an underdiagnosed and overdiagnosed entity. *Semin Diagn Pathol* **29:**226–234. PubMed
5. **Della Torre E, Mattoo H, Mahajan VS, Carruthers M, Pillai S, Stone JH.** 2014. Prevalence of atopy, eosinophilia, and IgE elevation in IgG4-related disease. *Allergy* **69:**269–272. PubMed
6. **Kamisawa T, Egawa N, Nakajima H.** 2003. Autoimmune pancreatitis is a systemic autoimmune disease. *Am J Gastroenterol* **98:**2811–2812. PubMed
7. **Hamano H, Kawa S, Horiuchi A, Unno H, Furuya N, Akamatsu T, Fukushima M, Nikaido T, Nakayama K, Usuda N, Kiyosawa K.** 2001. High serum IgG4 concentrations in patients with sclerosing pancreatitis. *N Engl J Med* **344:**732–738. PubMed
8. **Cortazar F, Stone JH.** 2015. IgG4-related disease and the kidney. *Nat Rev Nephrology* **11:**599–609. PubMed
9. **Deshpande V, Zen Y, Chan JK, Yi EE, Sato Y, Yoshino T, Klöppel G, Heathcote JG, Khosroshahi A, Ferry JA, Aalberse RC, Bloch DB, Brugge WR, Bateman AC, Carruthers MN, Chari ST, Cheuk W, Cornell LD, Fernandez-Del Castillo C, Forcione DG, Hamilos DL, Kamisawa T, Kasashima S, Kawa S, Kawano M, Lauwers GY, Masaki Y, Nakanuma Y, Notohara K, Okazaki K, Ryu JK, Saeki T, Sahani DV, Smyrk TC, Stone JR, Takahira M, Webster GJ, Yamamoto M, Zamboni G, Umehara H, Stone JH.** 2012. Consensus statement on the pathology of IgG4-related disease. *Mod Pathol* **25:**1181–1192. PubMed
10. **Mattoo H, Mahajan VS, Della Torre E, Sekigami Y, Carruthers M, Wallace ZS, Deshpande V, Stone JH, Pillai S.** 2014 De novo oligoclonal expansions of circulating plasmablasts in active and relapsing IgG4-related disease. *J Allergy Clin Immunol* **134:**679–687.

11. **Wallace ZS, Mattoo H, Carruthers MN, Mahajan VS, Della Torre E, Lee H, Kulikova M, Deshpande V, Pillai S, Stone JH.** 2014. Plasmablasts as a biomarker for IgG4-related disease, independent of serum IgG4 concentrations. *Ann Rheum Dis* doi:10.1136/*annrheumdis*-2014-205233.rint.
12. **Nirula A, Glaser SM, Kalled SL, Taylor FR.** 2011. What is IgG4? A review of the biology of a unique immunoglobulin subtype. *Curr Opin Rheumatol* **23:**119–124. PubMed
13. **Aalberse RC, Stapel SO, Schuurman J, Rispens T.** 2009. Immunoglobulin G4: an odd antibody. *Clin Exp Allergy* **39:**469–477. PubMed
14. **Khosroshahi A, Carruthers MN, Deshpande V, Unizony S, Bloch DB, Stone JH.** 2012. Rituximab for the treatment of IgG4-related disease: lessons from 10 consecutive patients. *Medicine (Baltimore)* **91:**57–66. PubMed
15. **Carruthers MN, Topazian MD, Khosroshahi A, Witzig T, Wallace ZS, Hart P, Deshpande V, Smyrk T, Chari S, Stone JH.** 2015. RTX for IgG4-related disease: a prospective, open-label trial. *Nat Rev Nephrol* doi:10.1038/neneph. 2015.95.
16. **Wallace ZS, Deshpande V, Mattoo H, Mahajan V, Kulikova M, Pillai S, Stone JH.** 2015. IgG4-related disease: Baseline clinical and laboratory features in 125 patients with biopsy-proven disease. *Arthritis Rheumatol* **67:**2466–75.
17. **Zen Y, Fujii T, Harada K, Kawano M, Yamada K, Takahira M, Nakanuma Y.** 2007. Th2 and regulatory immune reactions are increased in immunoglobin G4-related sclerosing pancreatitis and cholangitis. *Hepatology* **45:**1538–1546. PubMed
18. **Okazaki K, Uchida K, Ohana M, Nakase H, Uose S, Inai M, Matsushima Y, Katamura K, Ohmori K, Chiba T.** 2000. Autoimmune-related pancreatitis is associated with autoantibodies and a Th1/Th2-type cellular immune response. *Gastroenterology* **118:**573–581. PubMed
19. **Mattoo H, Della-Torre E, Mahajan VS, Stone JH, Pillai S.** 2014. Circulating Th2 memory cells in IgG4-related disease are restricted to a defined subset of subjects with atopy. *Allergy* **69:**399–402. PubMed
20. **Masaki Y, Shimizu H, Sato Nakamura T, Nakamura T, Nakajima A, Iwao Kawanami H, Miki M, Sakai T, Kawanami T, Fujita Y, Tanaka M, Fukushima T.** 2014. IgG4-related disease: diagnostic methods and therapeutic strategies in Japan. *J Clin Exp Hematop* **54:**95–101. PubMed
21. **Hart PA, Kamisawa T, Brugge WR, Chung JB, Culver EL, Czakó L, Frulloni L, Go VL, Gress TM, Kim MH, Kawa S, Lee KT, Lerch MM, Liao WC, Löhr M, Okazaki K, Ryu JK, Schleinitz N, Shimizu K, Shimosegawa T, Soetikno R, Webster G, Yadav D, Zen Y, Chari ST.** 2013. Long-term outcomes of autoimmune pancreatitis: a multicentre, international analysis. *Gut* **62:**1771–1776. PubMed
22. **Khosroshahi A, Bloch DB, Deshpande V, Stone JH.** 2010. Rituximab therapy leads to swift decline of serum IgG4 levels and prompt clinical improvement in IgG4-related disease. *Arthritis Rheumatol* **62:**1755–1762.
23. **Ryu JH, Horie R, Sekiguchi H, Peikert T, Yi ES.** 2012. Spectrum of disorders associated with elevated serum IgG4 levels encountered in clinical practice. *Int J Rheumatol* **2012:**232960. PubMed
24. **Kamisawa T, Shimosegawa T, Okazaki K, Nishino T, Watanabe H, Kanno A, Okumura F, Nishikawa T, Kobayashi K, Ichiya T, Takatori H, Yamakita K, Kubota K, Hamano H, Okamura K, Hirano K, Ito T, Ko SB, Omata M.** 2014. Standard steroid treatment for autoimmune pancreatitis. 2009. *Gut* 58, 1504–1507.
25. **Hamilton RG.** 1987. Human IgG subclass measurements in the clinical laboratory. *Clin Chem* **33:**1707–1725. PubMed
26. **Khosroshahi A, Cheryk LA, Carruthers MN, Edwards JA, Bloch DB, Stone JH.** 2014. Brief Report: spuriously low serum IgG4 concentrations caused by the prozone phenomenon in patients with IgG4-related disease. *Arthritis Rheumatol* **66:**213–217. PubMed
27. **Nelson SL, Hynd BA.** 1993. ELISA kits measuring human IgG subclasses: cross-reactivity against IgG3 in an IgG1 ELISA. *Clin Chem* **39:**1919. PubMed
28. **Ladwig PM, Barnidge DR, Snyder MR, Katzmann JA, Murray DL.** 2014. Quantification of serum IgG subclasses by use of subclass-specific tryptic peptides and liquid chromatography–tandem mass spectrometry. *Clin Chem* **60:**1080–1088. PubMed
29. **Stone JH, Zen Y, Deshpande V.** 2012. IgG4-related disease. *N Engl J Med* **366:**539–551.
30. **Mattoo H, Mahajan VS, Della Torre E, Sekigami Y, Wallace ZS, Carruthers M, Della Torre E, Stone JH, Pillai S.** 2014. *De novo* oligoclonal expansions of circulating plasmablasts in active and relapsing IgG4-related disease. *J Allergy Clin Immunol* **134:**679–687.

Future Perspectives for Rheumatoid Arthritis and Other Autoimmune Diseases

JEREMY SOKOLOVE

96

Immunologic biomarkers are intrinsic to the field of rheumatology both for making a clinical diagnosis and in potentially detecting early signs of disease in at-risk individuals when symptoms are absent. In this brief chapter, we discuss developing and future directions in the use of biomarkers in rheumatology with an emphasis on rheumatoid arthritis. We discuss the role of the "mechanistic" biomarker, a subtype of the biomarker that measures a process directly linked to disease pathogenesis, thus increasing both diagnostic reliability and potentially identifying phenotype-targeted therapies. As such mechanistic biomarkers have begun a revolution in the approach to cancer, we attempt to provide parallels as to how such markers can be applied to diagnosis and targeted treatment in the rheumatic diseases.

DEFINITION OF A "BIOMARKER"

A biomarker is defined as a characteristic that can be objectively measured as an indicator of normal or pathologic biological processes or as an indicator of response to therapy (1). Although most commonly used to describe a biochemical variable, such as a circulating protein or other biomolecule, this definition can apply to many types of biological data. To this point, many biomarker studies focus on anatomical and structural variables visualized by conventional X-ray, ultrasound, computed tomography (CT) scanning (e.g., positron emission tomography), or magnetic resonance imaging (MRI), including functional MRI scans that can provide information about the biological activity in certain regions of the brain (2). Other variables that might be considered biomarkers include immune cells (number and/or type), genetic traits, and histolopathologic characteristics of diseased tissue, as well as proteins or RNA expressed at the tissue level. This review focuses primarily on the use of laboratory biomarkers, including autoantibodies, markers of inflammation, and genetic and cellular variables that might be of use for diagnosis and/or treatment of the rheumatic diseases.

MECHANISTIC BIOMARKERS

We would offer that the best biomarkers are those that are interlinked with the mechanism of a disease and refer to these as "mechanistic biomarkers." Notably, biomarkers need not be directly involved in disease pathogenesis to be useful. For example, erythrocyte sedimentation rate (ESR) and C-reactive protein (CRP) can be used as rough surrogates for the assessment of disease activity in rheumatoid arthritis (RA) and other inflammatory immune diseases. Nevertheless, such markers of inflammation are very nonspecific to any one inflammatory condition and can be seen in a variety of rheumatic as well as nonrheumatic inflammatory disorders, including infection and malignancy. Such markers often represent byproducts of disease pathophysiology rather than representing intrinsic players in disease pathogenesis. The usefulness of descriptive biomarkers is therefore limited, and alone they provide limited diagnostic and/or prognostic information (3). Furthermore, the utility of a mechanistic biomarker could be its ability to more specifically identify a disease process and, in addition, to differentiate otherwise subtle subtypes of the same disease and thus stratify them in terms of both expected outcome and optimal treatment. Such mechanistic biomarkers could serve as guideposts in the quest for more personalized treatment options as well as inform the development of future mechanism-based therapies.

Biomarkers linked to underlying disease pathophysiology have already proven invaluable in the treatment of multiple types of cancer with increasingly targeted therapies. Examples of such include the expected, but highly valuable observation that expression of the estrogen receptor indicates responsiveness to antiestrogen therapy in breast cancer (4, 5). Similarly, the presence of the pathogenic BCR-ABL translocation in chronic myelogenous leukemia was in part used to identify the therapeutic utility of tyrosine kinase inhibitors, including imatinib (6). Additional subphenotyping of cancers includes the observation that overexpression of the human epidermal growth factor receptor 2 (HER2) predicts responsiveness to specific anti-HER2 monoclonal antibodies (i.e., trastuzumab) and to specific tyrosine kinase inhibitors (i.e., lapatinib) in breast cancer (7). Other biomarkers that allow targeted therapy include several novel kinase mutations in patients with non-small-cell lung cancer. Mutations in kinases such as epidermal growth factor receptor (8) and anaplastic lymphoma kinase (9) have yielded targeted therapy effective for a small but clinically significant subpopulation of lung cancer patients.

Potential Mechanistic Biomarker in Rheumatology

Unlike the many cancers in which a specific mutation leads to a malignant clone (10) that can be identified, the

doi:10.1128/9781555818722.ch96

pathophysiology involved in both the generation of autoimmunity and the effector phase of disease such as RA and systemic lupus erythematosus (SLE) seems far more complex. Despite the lack of complete mechanistic understanding, many components of disease pathophysiology are being elucidated. For example, as discussed in the previous chapter, anti-citrullinated protein antibodies (ACPAs) have been utilized as both a specific diagnostic marker and a predictor in disease severity. They have similarly been suggested to differentiate a unique subphenotype of RA. In addition to clinical features typically characteristic of ACPA-associated RA, studies on RA suggest that ACPA could serve as a biomarker of responsiveness to methotrexate and to B-cell depletion therapy (11, 12).

If truly rooted in disease mechanism, these are biomarkers that can not only stratify disease but also provide a basis for selecting mechanism-based therapies. Allergy skin testing is perhaps the best current example in which mechanistic antibody biomarkers are utilized for antigen-specific therapy. For such testing, purified allergens are injected subcutaneously with the aim of identifying those antigens to which an individual is reactive, information that can guide the development of antigen-specific tolerizing immunotherapy. Though it would seem ideal to apply such an approach to autoimmune disease, efforts to this end have thus far been limited by the breadth and complexity of systemic autoimmunity. We attempt to evaluate the current status of mechanistic biomarkers in rheumatic disease, including their limitations and future potential.

Mechanistic Biomarkers in Rheumatic Diseases—Are We There Yet?

Studies of the pathogenesis of rheumatic diseases have just begun to identify potential mechanistic biomarkers. This is perhaps best exemplified by a group of rare and often genetically defined, autoinflammatory diseases including familial Mediterranean fever, Muckle Wells disease, the related cryopyrin-associated periodic fever syndrome, and systemic onset juvenile idiopathic arthritis, all of which have been tightly associated with activation of the inflammasome and production of interleukin-1 (IL-1) (13). As such, therapies targeting IL-1 have proven highly efficacious for each of these conditions. Unfortunately, neither levels of IL-1 in the blood nor levels of IL-1 derived from peripheral blood mononuclear cells have reliably predicted response to anti-IL-1 therapy (14), and thus biomarkers downstream of IL-1, such as IL-1-induced transcriptional profiles (15), are now being investigated.

Autoantibodies have long been a characteristic measurement in autoimmunity and especially the rheumatic diseases. Such autoantibodies are used both diagnostically and potentially for prediction of disease manifestation and/or severity. Recent evidence now links certain autoantibodies to underlying pathophysiology, suggesting that autoantibodies observed in diseases including RA and SLE could represent mechanistic biomarkers. For instance, in SLE, autoantibodies that target RNA-binding proteins (i.e., Ro, La, RNP) or DNA are associated with high interferon alpha (IFN-α) activity (16). By activating Toll-like receptor 9 (TLR9) (17, 18) and TLR7 (19, 20), respectively, immune complexes containing RNA or DNA can induce human plasmacytoid dendritic cells to produce type I IFN (21), a key player in SLE pathogenesis (22). Similarly, although measuring type I IFN directly is challenging because there are many different IFN isoforms, some groups are now measuring levels of transcripts induced by type I IFN as a surrogate of type I IFN burden. At the clinical level, increased levels of IFN-associated gene transcripts have been associated with SLE disease activity (23), and such transcriptional profiles have been proposed as surrogate measures of disease activity in early-phase clinical trials (24). Thus, levels of type I interferon or IFN-associated gene transcripts could prove to be mechanistic biomarkers for SLE and potentially identify subphenotypes of SLE patients most amenable to anti-IFN therapy.

In RA, anti-citrullinated protein autoantibodies can target a wide variety of citrullinated antigens, including citrullinated fibrinogen and citrullinated vimentin. Recent studies have suggested a potential mechanism by which these antibodies might mediate disease pathophysiology. For example, immune complexes comprising autoantibody-bound citrullinated fibrinogen can stimulate the production of tumor necrosis factor alpha by costimulating TLR4 and the Fc receptor (25), and anti-citrullinated vimentin antibodies have been associated with the development of erosive bone loss in RA (26). Thus, future studies will need to focus on mechanistic implications for these previously identified biomarkers.

Use of autoantibodies as predictive tools for the identification of disease before clinical onset has been limited in both rheumatic and nonrheumatic autoimmune diseases. However, early studies utilizing autoantibodies for prediction of disease onset are being conducted. Recent studies have suggested that the presence of ACPA identifies a population of early arthritis patients more likely to benefit from early initiation of methotrexate therapy (27), and RA prevention studies are ongoing and are for the most part being guided by currently available autoantibody biomarkers. Other studies have suggested that specific ACPA and cytokines present during the asymptomatic phase (28–30) may not only improve the identification of those at risk of developing clinical RA but also pinpoint the time closest to the onset of clinical RA—a time at which the disease may be most amenable to immunomodulatory intervention. In SLE, the core diagnostic autoantibodies, including ANA and anti-double-stranded DNA autoantibodies, have also been suggested to provide markers of responsiveness to belimumab, a monoclonal antibody that neutralizes the B-cell survival factor BLyS. Subgroup analysis of phase II trials showed that only those SLE subjects with an ANA titer of 80 or greater and/or a positive anti-double-stranded DNA test responded better to therapy than placebo (31). Though perhaps only serving to more clearly define those with active SLE, it provides a roadmap to the future use of immunologic correlates that might be most central to disease physiology.

THE FUTURE OF BIOMARKERS FOR RHEUMATIC DISEASES

As we develop a deeper understanding of rheumatic disease pathogenesis, we anticipate that we will uncover an increasing number of putative mechanistic biomarkers. It is anticipated that the use of immunologic biomarkers will both establish a primary diagnosis (RA, SLE, etc.) and potentially define a molecular taxonomy of disease guided by molecular subtypes, which cannot be ascertained by clinical phenotype alone. Given the heterogeneity in disease course, disease-related damage, and response to therapy, defining the molecular features of rheumatic diseases and identifying these subphenotypes could provide improved options for targeted therapeutic interventions.

Rheumatology has long been at the forefront of immunologic biomarker discovery; some of the currently known biomarkers may prove to be mechanistic (Table 1). But as our understanding of the molecular mechanisms underpinning

TABLE 1 Current and future biomarkers for rheumatoid arthritis: diagnosis and prediction[a]

Biomarker	Disease specificity	Mechanistic biomarker	Reference(s)
Current RA			
Rheumatoid factor	+++	++	5, 26, 32, 33
Anti-CCP			
ESR	++++	+++	
CRP	+	−	
	+	−	
Future RA			
ACPA subtypes	+++	+++	26, 30, 34–36
Novel autoantibodies	++	?	37–39
Multibiomarker disease activity test	++	++	40
Cytokines/chemokines	+	+++	28, 30, 41
MMPs	+	++	40
Genetic polymorphisms	+	+++	42–45
Functional cytometry	+	++	46

[a]CCP, cyclic citrullinated peptide; ESR, erythrocyte sedimentation rate; CRP, C-reactive protein; MMPs, matrix metalloproteinases.

the rheumatic diseases advances, so too will the identification of mechanistic biomarkers, some of which will have the capacity to guide more efficacious and targeted treatment of rheumatic disease.

REFERENCES

1. **Atkinson AJ, Biomarkers Definitions Working Group.** 2001. Biomarkers and surrogate endpoints: preferred definitions and conceptual framework. *Clin Pharmacol Ther* **69:**89–95. PubMed
2. **Logothetis NK.** 2008. What we can do and what we cannot do with fMRI. *Nature* **453:**869–878. PubMed
3. **van Leeuwen MA, van Rijswijk MH, van der Heijde DM, Te Meerman GJ, van Riel PL, Houtman PM, van De Putte LB, Limburg PC.** 1993. The acute-phase response in relation to radiographic progression in early rheumatoid arthritis: a prospective study during the first three years of the disease. *Br J Rheumatol* **32**(Suppl 3)**:**9–13. PubMed
4. **Higgins MJ, Baselga J.** 2011. Targeted therapies for breast cancer. *J Clin Invest* **121:**3797–3803. PubMed
5. **Vossenaar ER, van Venrooij WJ.** 2004. Citrullinated proteins: sparks that may ignite the fire in rheumatoid arthritis. *Arthritis Res Ther* **6:**107–111. PubMed
6. **Ernst T, La Rosée P, Müller MC, Hochhaus A.** 2011. BCR-ABL mutations in chronic myeloid leukemia. *Hematol Oncol Clin North Am* **25:**997–1008, v–vi. PubMed
7. **Sachdev JC, Jahanzeb M.** 2012. Blockade of the HER family of receptors in the treatment of HER2-positive metastatic breast cancer. *Clin Breast Cancer* **12:**19–29. PubMed
8. **Sequist LV, Martins RG, Spigel D, Grunberg SM, Spira A, Jänne PA, Joshi VA, McCollum D, Evans TL, Muzikansky A, Kuhlmann GL, Han M, Goldberg JS, Settleman J, Iafrate AJ, Engelman JA, Haber DA, Johnson BE, Lynch TJ.** 2008. First-line gefitinib in patients with advanced non-small-cell lung cancer harboring somatic EGFR mutations. *J Clin Oncol* **26:**2442–2449. PubMed
9. **Shaw AT, Engelman JA.** 2014. Ceritinib in ALK-rearranged non-small-cell lung cancer. *N Engl J Med* **370:**2537–2539. PubMed
10. **Gainor JF, Shaw AT.** 2013. Novel targets in non-small cell lung cancer: ROS1 and RET fusions. *Oncologist* **18:**865–875. PubMed
11. **Cohen SB, Emery P, Greenwald MW, Dougados M, Furie RA, Genovese MC, Keystone EC, Loveless JE, Burmester GR, Cravets MW, Hessey EW, Shaw T, Totoritis MC, REFLEX Trial Group.** 2006. Rituximab for rheumatoid arthritis refractory to anti-tumor necrosis factor therapy: results of a multicenter, randomized, double-blind, placebo-controlled, phase III trial evaluating primary efficacy and safety at twenty-four weeks. *Arthritis Rheum* **54:**2793–2806. PubMed
12. **Emery P, Fleischmann R, Filipowicz-Sosnowska A, Schechtman J, Szczepanski L, Kavanaugh A, Racewicz AJ, van Vollenhoven RF, Li NF, Agarwal S, Hessey EW, Shaw TM, DANCER Study Group.** 2006. The efficacy and safety of rituximab in patients with active rheumatoid arthritis despite methotrexate treatment: results of a phase IIB randomized, double-blind, placebo-controlled, dose-ranging trial. *Arthritis Rheum* **54:**1390–1400. PubMed
13. **Agostini L, Martinon F, Burns K, McDermott MF, Hawkins PN, Tschopp J.** 2004. NALP3 forms an IL-1beta-processing inflammasome with increased activity in Muckle-Wells autoinflammatory disorder. *Immunity* **20:**319–325. PubMed
14. **Gattorno M, Piccini A, Lasigliè D, Tassi S, Brisca G, Carta S, Delfino L, Ferlito F, Pelagatti MA, Caroli F, Buoncompagni A, Viola S, Loy A, Sironi M, Vecchi A, Ravelli A, Martini A, Rubartelli A.** 2008. The pattern of response to anti-interleukin-1 treatment distinguishes two subsets of patients with systemic-onset juvenile idiopathic arthritis. *Arthritis Rheum* **58:**1505–1515. PubMed
15. **Allantaz F, Chaussabel D, Stichweh D, Bennett L, Allman W, Mejias A, Ardura M, Chung W, Smith E, Wise C, Palucka K, Ramilo O, Punaro M, Banchereau J, Pascual V.** 2007. Blood leukocyte microarrays to diagnose systemic onset juvenile idiopathic arthritis and follow the response to IL-1 blockade. *J Exp Med* **204:**2131–2144. PubMed
16. **Niewold TB, Hua J, Lehman TJ, Harley JB, Crow MK.** 2007. High serum IFN-alpha activity is a heritable risk factor for systemic lupus erythematosus. *Genes Immun* **8:**492–502. PubMed
17. **Boulé MW, Broughton C, Mackay F, Akira S, Marshak-Rothstein A, Rifkin IR.** 2004. Toll-like receptor 9-dependent and -independent dendritic cell activation by chromatin-immunoglobulin G complexes. *J Exp Med* **199:**1631–1640. PubMed
18. **Means TK, Latz E, Hayashi F, Murali MR, Golenbock DT, Luster AD.** 2005. Human lupus autoantibody-DNA complexes activate DCs through cooperation of CD32 and TLR9. *J Clin Invest* **115:**407–417. PubMed

19. **Kelly KM, Zhuang H, Nacionales DC, Scumpia PO, Lyons R, Akaogi J, Lee P, Williams B, Yamamoto M, Akira S, Satoh M, Reeves WH.** 2006. "Endogenous adjuvant" activity of the RNA components of lupus autoantigens Sm/RNP and Ro 60. *Arthritis Rheum* **54:**1557–1567. PubMed
20. **Savarese E, Chae OW, Trowitzsch S, Weber G, Kastner B, Akira S, Wagner H, Schmid RM, Bauer S, Krug A.** 2006. U1 small nuclear ribonucleoprotein immune complexes induce type I interferon in plasmacytoid dendritic cells through TLR7. *Blood* **107:**3229–3234. PubMed
21. **Lövgren T, Eloranta ML, Kastner B, Wahren-Herlenius M, Alm GV, Rönnblom L.** 2006. Induction of interferon-alpha by immune complexes or liposomes containing systemic lupus erythematosus autoantigen- and Sjögren's syndrome autoantigen-associated RNA. *Arthritis Rheum* **54:**1917–1927. PubMed
22. **Niewold TB.** 2011. Interferon alpha as a primary pathogenic factor in human lupus. *J Interferon Cytokine Res* **31:**887–892. PubMed
23. **Hua J, Kirou K, Lee C, Crow MK.** 2006. Functional assay of type I interferon in systemic lupus erythematosus plasma and association with anti-RNA binding protein autoantibodies. *Arthritis Rheum* **54:**1906–1916. PubMed
24. **Yao Y, Richman L, Higgs BW, Morehouse CA, de los Reyes M, Brohawn P, Zhang J, White B, Coyle AJ, Kiener PA, Jallal B.** 2009. Neutralization of interferon-alpha/beta-inducible genes and downstream effect in a phase I trial of an anti-interferon-alpha monoclonal antibody in systemic lupus erythematosus. *Arthritis Rheum* **60:**1785–1796. PubMed
25. **Sokolove J, Zhao X, Chandra PE, Robinson WH.** 2011. Immune complexes containing citrullinated fibrinogen costimulate macrophages via Toll-like receptor 4 and Fcγ receptor. *Arthritis Rheum* **63:**53–62. PubMed
26. **Harre U, Georgess D, Bang H, Bozec A, Axmann R, Ossipova E, Jakobsson PJ, Baum W, Nimmerjahn F, Szarka E, Sarmay G, Krumbholz G, Neumann E, Toes R, Scherer HU, Catrina AI, Klareskog L, Jurdic P, Schett G.** 2012. Induction of osteoclastogenesis and bone loss by human autoantibodies against citrullinated vimentin. *J Clin Invest* **122:**1791–1802. PubMed
27. **van Dongen H, van Aken J, Lard LR, Visser K, Ronday HK, Hulsmans HM, Speyer I, Westedt ML, Peeters AJ, Allaart CF, Toes RE, Breedveld FC, Huizinga TW.** 2007. Efficacy of methotrexate treatment in patients with probable rheumatoid arthritis: a double-blind, randomized, placebo-controlled trial. *Arthritis Rheum* **56:**1424–1432. PubMed
28. **Deane KD, O'Donnell CI, Hueber W, Majka DS, Lazar AA, Derber LA, Gilliland WR, Edison JD, Norris JM, Robinson WH, Holers VM.** 2010. The number of elevated cytokines and chemokines in preclinical seropositive rheumatoid arthritis predicts time to diagnosis in an age-dependent manner. *Arthritis Rheum* **62:**3161–3172. PubMed
29. **Kokkonen H, Söderström I, Rocklöv J, Hallmans G, Lejon K, Rantapää Dahlqvist S.** 2010. Up-regulation of cytokines and chemokines predates the onset of rheumatoid arthritis. *Arthritis Rheum* **62:**383–391. PubMed
30. **Sokolove J, Bromberg R, Deane KD, Lahey LJ, Derber LA, Chandra PE, Edison JD, Gilliland WR, Tibshirani RJ, Norris JM, Holers VM, Robinson WH.** 2012. Autoantibody epitope spreading in the pre-clinical phase predicts progression to rheumatoid arthritis. *PLoS One* **7:**e35296. PubMed
31. **Stohl W, Hilbert DM.** 2012. The discovery and development of belimumab: the anti-BLyS-lupus connection. *Nat Biotechnol* **30:**69–77. PubMed
32. **Sokolove J, Johnson DS, Lahey LJ, Wagner CA, Cheng D, Thiele GM, Michaud K, Sayles H, Reimold AM, Caplan L, Cannon GW, Kerr G, Mikuls TR, Robinson WH.** 2014. Rheumatoid factor as a potentiator of anti-citrullinated protein antibody-mediated inflammation in rheumatoid arthritis. *Arthritis Rheumatol* **66:**813–821. PubMed
33. **Kay J, Morgacheva O, Messing SP, Kremer JM, Greenberg JD, Reed GW, Gravallese EM, Furst DE.** 2014. Clinical disease activity and acute phase reactant levels are discordant among patients with active rheumatoid arthritis: acute phase reactant levels contribute separately to predicting outcome at one year. *Arthritis Res Ther* **16:**R40. PubMed
34. **Sokolove J, Brennan MJ, Sharpe O, Lahey LJ, Kao AH, Krishnan E, Edmundowicz D, Lepus CM, Wasko MC, Robinson WH.** 2013. Brief report: citrullination within the atherosclerotic plaque: a potential target for the anti-citrullinated protein antibody response in rheumatoid arthritis. *Arthritis Rheum* **65:**1719–1724. PubMed
35. **El-Barbary AM, Kassem EM, El-Sergany MA, Essa SA, Eltomey MA.** 2011. Association of anti-modified citrullinated vimentin with subclinical atherosclerosis in early rheumatoid arthritis compared with anti-cyclic citrullinated peptide. *J Rheumatol* **38:**828–834. PubMed
36. **Syversen SW, Goll GL, van der Heijde D, Landewé R, Lie BA, Odegård S, Uhlig T, Gaarder PI, Kvien TK.** 2010. Prediction of radiographic progression in rheumatoid arthritis and the role of antibodies against mutated citrullinated vimentin: results from a 10-year prospective study. *Ann Rheum Dis* **69:**345–351. PubMed
37. **Thiele GM, Duryee MJ, Anderson DR, Klassen LW, Mohring SM, Young KA, Benissan-Messan D, Sayles H, Dusad A, Hunter CD, Sokolove J, Robinson WH, O'Dell JR, Nicholas AP, Tuma DJ, Mikuls TR.** 2015. Malondialdehyde-acetaldehyde adducts and anti-malondialdehyde-acetaldehyde antibodies in rheumatoid arthritis. *Arthritis Rheumatol* **67:**645–655. PubMed
38. **Charpin C, Martin M, Balandraud N, Roudier J, Auger I.** 2010. Autoantibodies to BRAF, a new family of autoantibodies associated with rheumatoid arthritis. *Arthritis Res Ther* **12:**R194. PubMed
39. **Shi J, Knevel R, Suwannalai P, van der Linden MP, Janssen GM, van Veelen PA, Levarht NE, van der Helm-van Mil AH, Cerami A, Huizinga TW, Toes RE, Trouw LA.** 2011. Autoantibodies recognizing carbamylated proteins are present in sera of patients with rheumatoid arthritis and predict joint damage. *Proc Natl Acad Sci USA* **108:**17372–17377. PubMed
40. **Curtis JR, van der Helm-van Mil AH, Knevel R, Huizinga TW, Haney DJ, Shen Y, Ramanujan S, Cavet G, Centola M, Hesterberg LK, Chernoff D, Ford K, Shadick NA, Hamburger M, Fleischmann R, Keystone E, Weinblatt ME.** 2012. Validation of a novel multibiomarker test to assess rheumatoid arthritis disease activity. *Arthritis Care Res* (Hoboken) **64:**1794–1803. PubMed
41. **Hughes-Austin JM, Deane KD, Derber LA, Kolfenbach JR, Zerbe GO, Sokolove J, Lahey LJ, Weisman MH, Buckner JH, Mikuls TR, O'Dell JR, Keating RM, Gregersen PK, Robinson WH, Holers VM, Norris JM.** 2013. Multiple cytokines and chemokines are associated with rheumatoid arthritis-related autoimmunity in first-degree relatives without rheumatoid arthritis: Studies of the Aetiology of Rheumatoid Arthritis (SERA). *Ann Rheum Dis* **72:**901–907. PubMed
42. **Plant D, Bowes J, Potter C, Hyrich KL, Morgan AW, Wilson AG, Isaacs JD, Barton A, Wellcome Trust Case Control Consortium, British Society for Rheumatology Biologics Register.** 2011. Genome-wide association study of genetic predictors of anti-tumor necrosis factor treatment efficacy in rheumatoid arthritis identifies associations with polymorphisms at seven loci. *Arthritis Rheum* **63:**645–653. PubMed
43. **Plant D, Thomson W, Lunt M, Flynn E, Martin P, Eyre S, Farragher T, Bunn D, Worthington J, Symmons D,**

Barton A. 2011. The role of rheumatoid arthritis genetic susceptibility markers in the prediction of erosive disease in patients with early inflammatory polyarthritis: results from the Norfolk Arthritis Register. *Rheumatology* (Oxford) **50:**78–84. PubMed

44. **Oliver J, Plant D, Webster AP, Barton A.** 2015. Genetic and genomic markers of anti-TNF treatment response in rheumatoid arthritis. *Biomarkers Med* **9:**499–512. PubMed
45. **Plant D, Wilson AG, Barton A.** 2014. Genetic and epigenetic predictors of responsiveness to treatment in RA. *Nat Rev Rheumatol* **10:**329–337. PubMed
46. **Galligan CL, Siebert JC, Siminovitch KA, Keystone EC, Bykerk V, Perez OD, Fish EN.** 2009. Multiparameter phospho-flow analysis of lymphocytes in early rheumatoid arthritis: implications for diagnosis and monitoring drug therapy. *PLoS One* **4:**e6703. PubMed

Organ-Localized Autoimmune Diseases *section N*

VOLUME EDITOR: JOHN L. SCHMITZ
SECTION EDITORS: C. LYNNE BUREK AND PATRIZIO CATUREGLI

Introduction

C. LYNNE BUREK

97

Autoimmunity is common, while autoimmune disease is not. It is not clear how or why a benign autoimmune response becomes "malignant," thereby leading to pathogenic changes of a target organ. Few autoimmune diseases fulfill the strict criteria by which the autoimmune response is directly related to pathogenesis. However, many findings, either cellular or humoral, can provide strong circumstantial evidence that autoimmunity is strongly associated with a particular disease. Often, the humoral responses detected in the laboratory are best considered to be markers rather than causes of disease. The autoantibodies are useful for diagnosis or prognosis, for excluding other conditions, for classifying disease, or for monitoring therapy. Whenever we test for autoimmune disease by evaluating autoantibodies, we must consider that individuals without evidence of disease may also exhibit these autoantibodies. Therefore, all results must be evaluated in context with the entire clinical picture; autoantibodies are rarely the sole criterion for disease. However, since autoantibodies are a significant marker of disease, often developing years before symptoms are present, the autoantibodies may indicate future disease.

Autoimmune diseases can be divided into two types. The first type, the systemic diseases, consists of conditions in which the whole body may be involved. They include such disorders as systemic lupus erythematosus and rheumatoid arthritis. The second category consists of the organ-specific autoimmunities. These conditions generally involve one particular organ of the body. In early editions of this *Manual*, the section covering organ-specific autoimmunity was small and was combined within the overall section on autoimmune diseases. In the 5th edition, organ-specific autoimmune diseases warranted their own section. In the 6th edition, the section was expanded approximately 25%. In the 7th edition, topics were expanded to include molecular methods of diagnosis. In this edition, many of the methodologies described use recombinant antigens in the assays. There are now many companies that offer FDA-approved test kits for the various autoantibody evaluations using these proprietary molecules. For other newly recognized autoimmune conditions, such as hypophysitis, laboratories still use the basic assay of indirect immunofluorescence since the antigen(s) has not been identified.

In certain chapters, such as the chapter on endocrinopathies, some things have changed only a little. As in the previous edition, the chapter on endocrinopathies contains collected descriptions of the various procedures currently used to detect circulating autoantibodies in patients with immune-mediated endocrine disease, e.g., thyroiditis, Graves' disease, insulin-dependent diabetes mellitus, Addison's disease, and pernicious anemia. Since the number of target-organ-specific diseases that display diagnostically important autoantibodies is ever expanding, we have included autoimmune hypophysitis. The test strategies change once individual antigens are identified. More and more of the assays are now based on enzyme-linked immunosorbent assay using purified antigens or recombinant antigens. However, there is still a role for the "older" assays, such as indirect immunofluorescence, that can be used for screening tests and for identification of antibodies for which the precise antigen is not yet known. Certain new assays use immunoblots of tissue extracts or digested purified antigens. These assays have promise for screening several antigens or epitopes simultaneously.

More and more commercial sources are producing reagents for assays in the form of FDA-approved kits for antigens that have been identified. However, manufacturers often use different processes to obtain components (e.g., native antigens versus recombinant peptides). There is no standardization among the assays. The result is that different antibody specificities may be recognized, which is one reason not all kits give identical results. Each commercial test kit used in the laboratory must be evaluated for quality assurance, including reproducibility, precision, and distinction of negative versus positive samples. The role of the clinical laboratory is changing from one in which new assays are developed to one of evaluating the new technologies. Yet, our goal of helping the patient remains the same.

doi:10.1128/9781555818722.ch97

Endocrinopathies: Chronic Thyroiditis, Addison Disease, Pernicious Anemia, Graves' Disease, Diabetes, and Hypophysitis

C. L. BUREK, N. R. ROSE, GIUSEPPE BARBESINO, JIAN WANG, ANDREA K. STECK, GEORGE S. EISENBARTH,† LIPING YU, LUDOVICA DE VINCENTIIS, ADRIANA RICCIUTI, ALESSANDRA DE REMIGIS, AND PATRIZIO CATUREGLI

98

AUTOANTIBODIES IN CHRONIC THYROIDITIS, ADDISON DISEASE, AND PERNICIOUS ANEMIA

(This section was written by C. L. Burek and N. R. Rose.)

Chronic lymphocytic thyroiditis (CLT), also known as Hashimoto thyroiditis, is an autoimmune disease characterized by lymphocytic infiltration of the thyroid gland, with the concomitant production of autoantibodies to thyroid antigens, primarily thyroglobulin and/or thyroperoxidase (TPO), formerly known as microsomal antigen (1). Although few epidemiological data are available, the prevalence of CLT is estimated to be 1 in 1,000 people, with an incidence of 0.2 to 2% and a female-to-male ratio of about 18:1 (1). Clinical signs and symptoms manifest slowly and may involve many systems of the body (1). Accumulations of hydrophilic mucoproteins with edema, a condition called myxedema, affects skin and connective tissue and can affect the appearance of the individual. Lethargy may ensue, with a loss of mental acuity. Systems commonly affected are the gastrointestinal tract, the hemopoietic system, the endocrine system, and the urogenital system (1). Enlargement of the thyroid gland due to lymphocyte invasion, called goiter, is a frequent manifestation, although there is an atrophic variation. Demonstration of autoantibodies to the thyroid antigens aids in the diagnosis of CLT, distinguishing it from other causes of hypothyroidism.

Antibodies to Thyroglobulin

Thyroglobulin is a 660-kDa homodimeric glycoprotein produced by the thyroid gland, which functions as a matrix for thyroid hormone synthesis and for storage of iodine (2).

Thyroglobulin antibodies have been demonstrated by several procedures, such as precipitation in agar, indirect immunofluorescence (IF), passive hemagglutination of cells coated with thyroglobulin, radioimmunoassay, and enzyme-linked immunosorbent assay (ELISA) (3). Precipitation in agar is simple to perform but of low sensitivity, detecting only antibodies present in relatively large amounts. Passive hemagglutination tests with the use of tanned erythrocytes (tanned-cell hemagglutination [TCH]) or chromic-chloride-treated erythrocytes (chromic-chloride hemagglutination [CCH]) are very sensitive and thus detect antibodies to thyroglobulin in patients with a variety of conditions other than thyroiditis, a possible disadvantage from the diagnostic point of view. ELISA procedures for thyroglobulin antibodies are also highly sensitive and demonstrate both agglutinating and nonagglutinating antibodies.

Recent evidence shows that the antigenic specificities of autoantibodies to thyroglobulin in patients with thyroiditis are different from those in people with antibody but no disease. The naturally occurring antibodies from healthy individuals are directed primarily to sites on the molecule that are shared among species (i.e., conserved sites), whereas those found primarily in patients are directed to human-specific regions (4). In the future, a test for thyroglobulin autoantibodies specific for those individuals with disease may be of more value in diagnosis.

Antibodies to TPO

The microsomal antigen of the thyroid epithelial cell has been identified as thyroid peroxidase (TPO) (5). TPO is a glycoprotein of 933 amino acids. It is an enzyme that catalyzes the oxidation of iodide and is essential for the incorporation of iodide onto tyrosine residues in thyroglobulin, a process known as organification, and for the coupling of iodotyrosyls to generate thyroid hormones (6). Formerly, the most commonly used tests for determining TPO antibodies were indirect IF and a commercially available tanned-cell hemagglutination assay or ELISA. Preparations of isolated thyroid microsomes are often contaminated with thyroglobulin. Therefore, the commercially prepared tanned-cell kit uses a special diluent containing thyroglobulin to block any antibody that may inadvertently react. Special attention must be paid to any serum that contains high titers of thyroglobulin autoantibodies. There may be insufficient thyroglobulin to remove all traces of the antithyroglobulin antibody, and the serum will give a false-positive result. Serum titers obtained by the indirect IF procedure may reach 1,200 or higher. Titers of TPO antibody obtained by TCH may reach well over 25,000 (7).

Newer technology for the detection of TPO antibodies uses recombinant TPO antigens in ELISAs, thereby removing the necessity of blocking any contaminating thyroglobulin. More details will be discussed below.

Newer Methodology for Thyroglobulin and TPO Autoantibodies

The earlier methods for detecting both thyroglobulin and TPO autoantibodies have virtually been superseded by

†Deceased.

doi:10.1128/9781555818722.ch98

commercially available FDA-approved test kits. Therefore, the detailed procedures for chromic-chloride hemagglutination, the ELISA for thyroglobulin autoantibodies, and the indirect immunofluorescence assay for TPO antibodies are not included in this edition of the *Manual*. Please refer to the seventh edition of the *Manual* for details of these procedures.

Several companies provide FDA-approved ELISA procedures for the semiquantitative detection of thyroid autoantibodies. Chemiluminescence-based tests are also available, allowing those laboratories with random-access instruments the benefit of automated testing platforms. The instructions provided by the vendor must be followed exactly.

There are many advantages in using these kits. The test procedures are identical for thyroglobulin and TPO autoantibodies, and the same serum sample can be used in both tests. Quality control reagents are provided. Interpretation guidelines are included. However, additional quality assurance procedures must be performed. For example, before the tests can be implemented in the laboratory, additional validation must be performed for precision and reproducibility. Additionally, 20 known-positive and 20 known-negative samples should be tested for determining performance parameters in a particular laboratory. Each laboratory should establish its own normal range according to established procedures. Furthermore, an additional external control should be included in every run to ensure that the kit is working properly. This control should be a known-positive serum that has been previously tested in the laboratory, aliquoted, and stored frozen at −20°C until used.

Interpretation

Interpretation of the results of the assays should follow the guidelines presented in the information provided by the individual vendors. Often, the results will be expressed in units. The units will generally be categorized in ranges for negative, weakly positive, moderately positive, and strongly positive reactions. The negative range suggests that only low levels or no antibodies to thyroid antigens are present. A positive result indicates that antibodies to thyroid antigens are present and suggests the possibility of CLT. The assays for thyroid autoantibodies are an aid in the diagnosis of CLT and are not diagnostic by themselves.

TPO antibodies are found in 90 to 95% of patients with CLT, while thyroglobulin antibodies are found in 60 to 80% (1).

In addition to being found in chronic-thyroiditis patients, these antibodies may be found in patients with other thyroid disorders, such as primary myxedema, hyperthyroidism, colloid goiter, nodular goiter, and thyroid tumors (3). Thyroid antibodies have also been observed in the sera of patients with pernicious anemia, adrenal insufficiency, type 1 diabetes mellitus, hypophysitis, and other autoimmune conditions. The presence of these antibodies is indicative of an ongoing pathology within the thyroid gland and subsequent end-stage CLT (1). Screening for thyroid autoantibodies in pregnant women represents an effective way to identify individuals who may develop postpartum thyroiditis (8). Approximately 7% of women develop postpartum thyroiditis within 6 months of delivery (1). This condition is detected by the presence of thyroid autoantibodies (1). The antibodies can be transient or a predictor of future hypothyroidism, so continuing to monitor for disease is indicated. Finally, antithyroid antibodies are seen in a certain proportion of healthy subjects (3). The prevalence of such antibodies in subjects without overt thyroid disease is higher in women than in men. The incidence also increases with age, so that 18% of women over 40 years old have antibodies to thyroglobulin. However, a word of caution: the continued presence of these antibodies does not necessarily mean that no disease activity is occurring within the thyroid. The autoantibodies may be a significant marker of later disease (9).

Antibodies to Adrenal Antigens

Primary Addison disease is a rare disorder, with prevalence estimates of 1 in 8,000 in Western countries (10). Autoimmunity accounts for 68 to 94% of the cases from the different studies, but the real prevalence is unknown (10). Clinical manifestations are often vague, so a diagnosis may take years. Typically, for chronic disease, signs and symptoms may include weakness, fatigue, weight loss, dizziness, and darkening of the skin (10). Acute disease may result in or manifest as nausea, vomiting, lethargy, coma, and shock (10).

Patients with idiopathic Addison disease have circulating antibodies to adrenal antigens. Such antibodies have been detected by a variety of procedures (3), but the method most commonly used is indirect IF. Antibodies detected by IF mark the cytoplasm of cells of the adrenal cortex and are directed to an antigen associated with the microsomes of these cells. The antibodies belong predominantly to the IgG class and, in general, have rather low titers (not higher than 100). Recent studies suggest that different steroidogenic enzymes of the cytochrome P-450 family may be the target antigens of autoimmune Addison disease. Sera from patients with autoimmune Addison disease contain autoantibodies to 21-hydroxylase (21-OH) or 17-c-hydroxylase (11–13). A sensitive radioimmunoassay using the 21-OH antigen has been developed, but its usage is limited (12). Patients with autoimmune polyendocrine syndrome type I (Addison disease plus hypoparathyroidism and chronic mucocutaneous candidiasis) have circulating autoantibodies to the P-450 cholesterol side chain cleavage enzyme. It is still uncertain whether these autoantigens are expressed on the surfaces of adrenal cells or are otherwise accessible to adrenal antibodies *in vivo*.

Indirect IF Test for Antibodies to Adrenal Antigens

Materials

1. Frozen sections (4-μm thick) of primate adrenal tissue (used as the substrate). These sections are available commercially from some venders that deal with autoimmune test kits. Positive- and negative-control sera can also be purchased commercially.
2. Phosphate-buffered saline (PBS), pH 7.2, and rabbit or goat antiserum to human immunoglobulins conjugated to fluorescein isothiocyanate (FITC conjugate). Most conjugates are commercial preparations, and information on the characteristics of a conjugate (i.e., an immunologic analysis of the conjugate to show its specificity, the antibody, protein, and fluorescein concentrations, and the fluorescein-to-protein ratio) are provided by the company. When a commercial conjugate is obtained, the lot number should be recorded, and the optimal dilution should be checked by testing several dilutions in a chessboard titration. One lot should then be used as long as possible.
3. Buffered glycerol. Mix 9 volumes of glycerol with 1 volume of phosphate buffer (pH 7.2).
4. Coverslips.

Procedure

1. Prepare 1:5 dilutions in PBS of all sera to be tested (unknown and positive and negative controls). Sera may be screened at 1:5 dilutions or titrated in serial 2-fold dilutions until the endpoint is reached.

2. Incubate diluted sera with cryostat-cut sections of tissue in a humid chamber at room temperature for 30 min.
3. Wash the slides in PBS for 30 min at room temperature. Effective washing can be performed by gently stirring the solution with a magnetic stirrer and changing the wash solution three times.
4. Incubate sections with the appropriate dilution of FITC conjugate in a humid chamber at room temperature for 30 min.
5. Wash the slides again for 30 min as described in step 3.
6. Mount the coverslip with buffered glycerol, and read the results with a microscope equipped for fluorescence microscopy.

Interpretation of Test Results

Antibodies to adrenocortical cells are detected in the sera of 38 to 60% of patients with idiopathic Addison disease (3, 12). The antibodies are present in 7 to 18% of patients with tuberculous Addison disease and in 1% of healthy subjects. The presence of antibodies to adrenocortical cells is an indication that the disease is idiopathic and not of tubercular or other nature. Different patterns of staining have been observed; most sera stain the whole cortex, with a brighter fluorescence in the glomerulosa zone (Fig. 1 and 2), but a few sera stain only the fasciculata and reticularis zones, not the glomerulosa zone. The latter pattern has been reported with sera that also stain the interstitial cells of the testis and the theca interna cells of the ovary.

Antibodies to Antigens of Ovary, Testis, and Placenta

Antibodies staining the cytoplasm of cells of the theca interna, interstitial, and corpus luteum cells of the ovary, interstitial cells of the testis, and trophoblast of the placenta have been detected in the sera of patients with Addison disease and of patients with premature ovarian failure (3, 12). The antigens involved have not been very well characterized, and the test itself is at present more of research than of diagnostic interest.

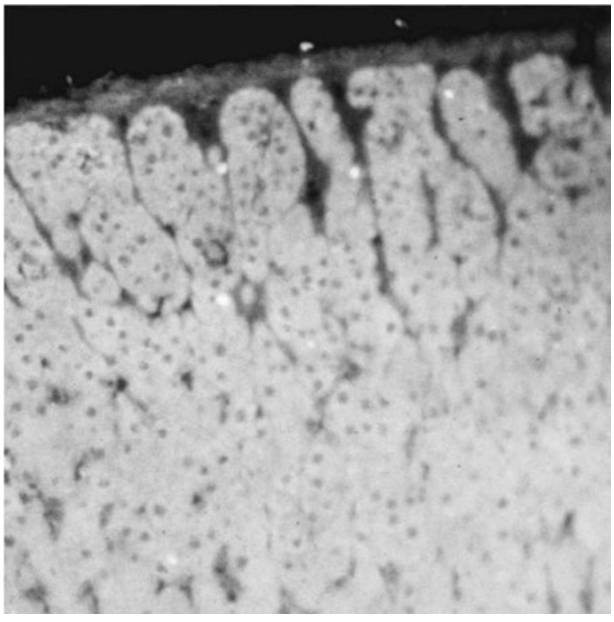

FIGURE 1 Indirect IF for antibodies to adrenal cortex using an unfixed, air-dried section of monkey adrenal cortex. All layers of the adrenal cortex are stained. Magnification, ×32.

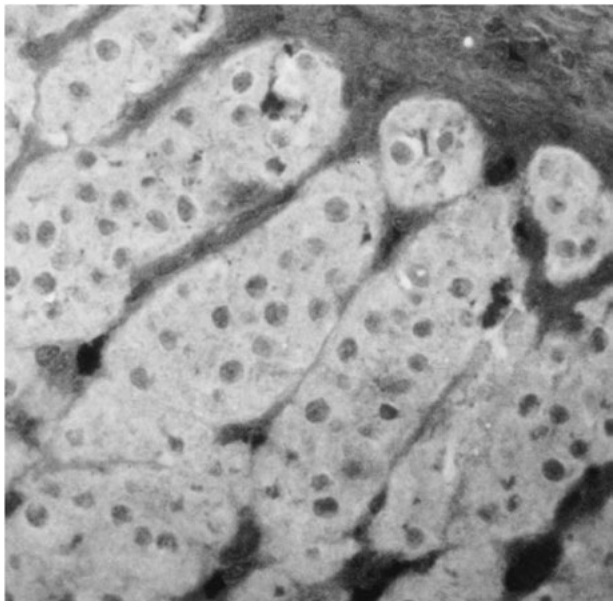

FIGURE 2 Same as Fig. 1 but at a higher magnification. Only the cytoplasm of the adrenal cells is attained. Magnification, ×80.

Antibodies to Gastric Parietal Cells

Autoimmune gastritis is a chronic condition that may be asymptomatic for many years before progression to end-stage disease resulting in depletion of vitamin B_{12} and the development of pernicious anemia. Pernicious anemia affects about 2% of the population over 60 years of age (14). Prevalence is estimated to be 151/100,000, with a 66% female preponderance (15). Clinical manifestations of end-stage disease result from complications of anemia, which include pallor and fatigue (14). However, the presence of parietal cell antibodies is indicative of an ongoing gastric pathology which may ultimately lead to end-stage disease (14).

Circulating autoantibodies to intracytoplasmic antigens of gastric parietal cells (parietal cell antibodies), to the B_{12} binding site of intrinsic factor, and to the intrinsic factor Blt complex occur with high frequency in patients with autoimmune gastritis leading to end-stage disease of pernicious anemia (16, 17). Antibodies to intrinsic factor may be detected by several radioassay procedures. However, these methods are not yet regularly performed in most hospitals. Parietal cell antibodies are detected primarily by indirect IF. Parietal cell antibodies, when detected by indirect IF, bind to the cytoplasm of parietal cells of the gastric fundal mucosae of humans and various animals, like monkeys, rats, and guinea pigs (Fig. 3). As noted above, the pattern of staining resembles that seen with mitochondrial antibodies; therefore, a control test on kidney should be performed. The autoantigens to which gastric parietal cell antibodies are directed have been identified as the alpha- and beta-subunits of the gastric H/K ATPase, the enzyme responsible for acid secretion in the stomach (17).

Indirect IF Test for Antibodies to Gastric Parietal Cells

Materials and Procedure

The materials used are the same as those described previously for IF tests to adrenal antibodies but starting at a 1:10 dilution of serum. Unfixed sections of rat stomach (gastric

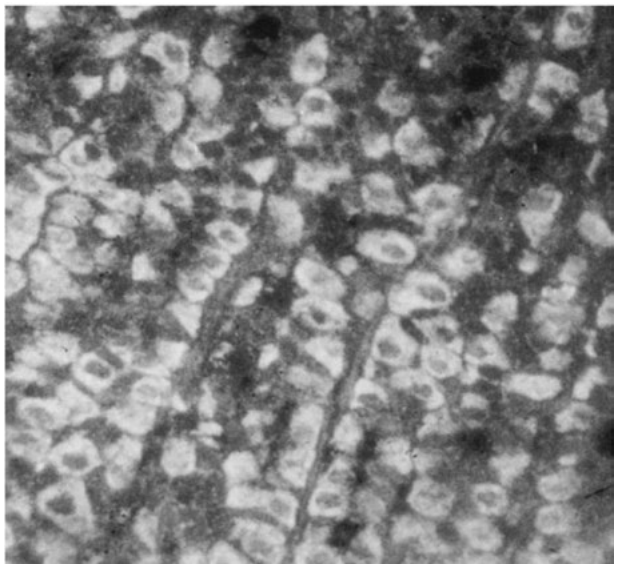

FIGURE 3 Indirect IF for antibodies to parietal cells using an unfixed, air-dried section of rodent stomach mucosa. The cytoplasm of only the parietal cells is stained. Magnification, ×100.

mucosa) are used as the substrate. Unfixed rat kidney sections are used as controls for staining because of mitochondrial antibodies.

Interpretation of Test Results

Parietal cell antibodies are found in about 90% of patients with pernicious anemia (16). These antibodies are also present in patients with a number of other conditions, such as chronic thyroiditis (33%), Sjogren's sicca syndrome (15%), atrophic gastritis (60%), and gastric ulcer (22%). Antibodies to parietal cells have been reported in about 20 to 30% of patients with *Helicobacter pylori*-associated gastritis, although the titers are usually lower than in patients with autoimmune gastritis (16). Whether *H. pylori* is an environmental agent triggering the autoimmune condition is still not known. Parietal cell antibodies are also found in the healthy population, with an incidence that varies according to age, i.e., from 2% in subjects younger than 20 years to 16% in subjects older than 60 years. They are more common in women than in men. It is also not known whether these antibodies are a biomarker of latent disease, as the interval between autoimmune gastritis with parietal cell antibodies and pernicious anemia may be as long as 20 to 30 years (16). As yet, no longitudinal studies have addressed this issue.

GRAVES' DISEASE, HYPERTHYROIDISM, AND ANTIBODIES TO THE THYROTROPIN RECEPTOR

(This section was written by Giuseppe Barbesino.)

Graves' disease (GD) is a relatively frequent and uniquely human autoimmune disease in which ongoing activation of the thyroid gland and hyperthyroidism is a consequence of circulating immunoglobulin capable of binding and activating the thyroid-stimulating hormone receptor (TSHR) on the surfaces of thyroid follicular cells. The TSHR is a cell-membrane receptor belonging to the superfamily of G protein-coupled receptors. The TSHR is closely related to the luteinizing and follicle-stimulating receptors in the same superfamily. The native TSHR is a 764-amino-acid protein. Posttranslational changes involve the cleavage of a 50-amino-acid peptide, yielding two subunits, termed A and B, linked by disulfide bonds and anchored to the thyroid cell membrane. The B subunit contains the seven membrane-spanning domains typical of all G protein-coupled receptors and a small intracellular domain. The A subunit is almost entirely extracellular (ectodomain) and contains nine leucine-rich repeats. Binding of TSH to this leucine-rich region results in structural changes along the whole receptor, ultimately resulting in the activation of the intracellular cyclic AMP (cAMP) cascade and initiation of the many TSH-dependent thyroid cell functions. The TSHR tightly controls all differentiated functions of the thyroid gland. These include transmembrane transport of iodine, the synthesis of thyroid hormone and its inclusion in the primary structure of thyroglobulin, and thyroid cell proliferation. The TSHR appears to have mild constitutive activity, in that some cAMP production occurs *in vitro* in the complete absence of the ligand.

The role of TSHR-blocking antibody (TRAb) in GD hyperthyroidism was first demonstrated with the discovery that hyperthyroidism could be caused in animals by the transfer of sera from GD patients (18). The serum factor, originally termed long-activating thyroid stimulator (LATS), was later identified as an immunoglobulin capable of stimulating the TSHR. It then became evident that while most patients with TRAb have hyperthyroidism, a subset of patients with TRAb but without TSHR-stimulating activity is capable of blocking the receptor and causing hypothyroidism (thyroid-blocking antibody [TBAb]) (19). Because of the heterogeneity of these antibodies and because of the different methods employed to determine them, the nomenclature has been the cause of some confusion. For the sake of simplicity, in this section I will abbreviate TSHR antibodies in general as TRAb, independently of their functional activity. Antibodies with TSHR-stimulating antibody will then be termed TSAb, while antibodies with blocking activity will be abbreviated TBAb, which partly follows recent recommendations (20).

In the decades since the discovery of LATS, both the TSHR and the TRAb have been studied extensively and have yielded a great deal of information on both molecules. Not only have these studies contributed tremendously to our understanding of thyroid dysfunction, but they have also resulted in the development of very sensitive and specific tests for the TRAb and expanded the clinical uses of such tests.

Nature and Properties of the TRAb

Human TRAbs are oligoclonal antibodies. Earlier studies suggested restriction to the IgG1 subclass (21), but it was subsequently suggested that TRAbs devoid of stimulating activity could also be found in the IgG2 and IgG3 subclasses (22). The ability of TSAbs to cause unremitting hyperthyroidism is due to their much longer half-life than that of TSH and to the absence of feedback regulation of thyroid hormone on plasma cells. Several monoclonal murine and human TRAbs are now available. These have been employed to gain understanding of the physiology of the TSHR and provided excellent tools in clinically useful assays for the detection of TRAbs, as described below. A large body of evidence suggests that TSAbs bind conformational epitopes on the A subunit of TSHR in a region also containing the TSH binding site (23). Early studies suggested that TSAb bound epitopes on the TSHR ectodomain but not necessarily epitopes coinciding with the TSH binding site (24).

Studies of the crystal structure of the complex TRAb-TSHR ectodomain later showed that TSH, TSAb, and TBAb bind the same region (23, 25). As a consequence, both TSAb and TBAb result in displacement of radiolabeled TSH from its receptor and are capable of competing with each other. It is interesting that the crystal structure of the bound TSHR ectodomain revealed no major conformational differences when either a TBAb or a TSAb was bound. However, the main orientations of bound Fab fragments were dramatically different when the two types of antibodies were examined (25). The mechanism for the difference in activity between TBAb and TSAb remains therefore somewhat obscure.

Assays for TRAb

Most autoantibodies in human autoimmune conditions really represent "markers" for the disease and therefore are associated with the disease with variable precision but are typically not necessary or sufficient for the clinical condition to be present. As a consequence, clinicians have to settle with limited diagnostic and predictive properties of such autoantibodies, even when excellent assays are available. Since TSAbs are the direct cause of true GD hyperthyroidism, they are expected to be present in all GD patients. On the basis of this rationale, great effort has been spent in designing and improving a TRAb assay for use in clinical practice. Indeed, over the past few decades, the performance of clinical assays for TRAb and TSAb has steadily improved, so that commercially available assays now provide outstanding tools in the management of GD. Based on the properties of TRAb, in general two types of assays are available: assays exploiting the completion of TRAb for the TSH receptor (binding assays) and assays exploiting the ability of TSAb to activate the TSH receptor (stimulating assays).

Binding Assays

Before the cloning of the human TSHR, binding assays relied on the use of human, porcine, or rodent thyroid membranes and analyzed the displacement of radiolabeled human or bovine TSH from the preparation (26, 27). These tests required fresh thyroid tissue from experimental animals or from cadaveric or surgical human thyroids and therefore were difficult to apply extensively in clinical practice. However, these studies provided fundamental information on the species specificities of TSAbs and on their binding properties. When binding data were compared with data from the bioassays available at the time, these early studies also provided evidence that the binding property of TRAb could in some cases be dissociated from the stimulating activity (26). With the cloning of the human TSHR, cell lines stably expressing the TSHR became available and provided a larger amount of the protein both for testing and for the immunization of animals (28). Monoclonal mouse TSHR antibodies thus obtained were then employed to immobilize the human or porcine TSHR to enzyme-linked immunosorbent assay plates or plastic tubes for use in solid-phase assays, with either radioactive, fluorescent, or chemiluminescent ligands, thus simplifying the assays, increasing the reproducibility of results, and making these assays available to a larger number of routine labs (29, 30). In the latest modification, TSH was replaced by a human biotinylated or enzyme-linked monoclonal TRAb (termed m22). m22 is a potent human TSAb demonstrated by crystallography to bind the TSH binding site on the TSHR (23, 31). Assays employing m22 as a ligand demonstrated greater analytical sensitivity in the low range (32) than assays employing biotinylated TSH. This translated to higher clinical sensitivity, approaching 100%, without loss in specificity (33).

TSAb Assays

The functional heterogeneity of TRAb has long been recognized. Hence, TRAb identified with binding assays may or may not also have TSAb properties. Historically, assays for TSAb were actually developed before TRAb assays. Soon after the discovery of LATS, McKenzie employed several variation bioassays in which the disappearance of radioiodine from mice's blood was measured after the infusion of GD sera (34), clearly a method not suitable for routine testing. Subsequently, *in vitro* systems employing primary thyroid cell monolayers, cryopreserved porcine thyroid cells, or a line of rat thyroid cancer cells, FRTL-5, were developed. The basic designs of these first-generation assays were similar: the patient's immunoglobulin fraction was obtained from the patient's serum and incubated with the cultured, thyroid-derived cells or tissues. The supernatant was then collected, and the cAMP production was measured by radioimmunoassay (35–38). The introduction of hypotonic medium allowed the use of serum directly, eliminating the fractionating step and allowing the use of smaller serum samples (39, 40). The cloning of the TSHR fostered the second generation of *in vitro* thyroid-stimulating immunoglobulin (TSI) assays. Chinese hamster ovary (CHO) cells were transfected with human recombinant TSHR. The transfected CHO cells were then used in the TSI tests in a manner very similar to that used for the assays described above (28, 41, 42). These assays certainly represented a major step forward but still required a laboratory to have nuclear medicine and cell culture capabilities. With the third-generation TSI assays, the need for measuring cAMP and therefore for a radioimmunoassay was eliminated. Cells were transfected with both the human TSHR and the luciferase gene, controlled by a cAMP response element. With this design, stimulation of the TSHR by the patients' sera results, as usual, in cAMP production and, in turn, transcription of the luciferase gene, which is then measured in a chemiluminescence assay (43). As an additional modification, a chimeric TSHR-luteinizing hormone receptor (LHR) has lately been introduced. In this chimeric receptor, the LHR binding site has been replaced with the homologous section of the TSHR. The rationale is that only TRAb with affinity to the TSHR binding domain will interact, while the remainder of the LHR guarantees posttranslational processing and a conformational structure similar to that of the native TSHR. This would eliminate interference from the patient's TRAb, which is devoid of stimulating activities but binds other regions of the TSHR and is capable of interfering with the detection of TSAb in the patient's oligoclonal mixture. While this assay displays excellent clinical performance in the published study (44), the theoretical basis for its advantage is not universally accepted (20).

TBAb Assays

Thyroid follicular cell destruction by the immune system is the cause of hypothyroidism in the vast majority of patients with hypothyroidism. However, in a minute fraction of patients, TBAb causes hypothyroidism. As mentioned before, TBAbs generally provide positive results and can be measured through a variation of the TSAb assay. Simply, the ability of TSH to stimulate the TSHR in any of the cellular systems used for TSAb is measured before and after the addition of the patient's serum (20). Although the assay is straightforward when the patient's serum contains only TBAb, there are analytical problems when the serum contains a mixture of TSAb and TBAb, a phenomenon that has been well documented in some cases (45). In such a situation, a mild TSAb level can act as a partial antagonist

and therefore yield positive inhibition results, even when its overall effect is as a stimulant (20).

Clinical Uses of TRAb

The major clinical use of a TRAb assay is in the differential diagnosis of hyperthyroidism. GD, the most common cause of hyperthyroidism in iodine-replete regions, can be clinically differentiated from other forms of hyperthyroidism by demonstrating a diffuse uptake of radioiodine. Indeed, in the presence of a suppressed TSH, such a finding unequivocally indicates the TSH-independent activation of all thyroid tissue by the same factor (hence the appellation toxic diffuse goiter). However, the thyroid uptake and scan test (radioactive iodine uptake) is expensive and time-consuming, unreliable when the patient has been exposed to large amounts of cold iodine, and contraindicated in pregnant patients. The recognition of TSAb as the causative factor has prompted extensive investigations into the clinical uses of TRAb assays as a diagnostic tool in the differential diagnosis of hyperthyroidism. First-generation assays, while contributing tremendous understanding of the pathophysiology and natural history of GD, were too insensitive, labor-intensive, and costly to warrant widespread clinical use: they were essentially clinical research tools. However, the last decade has brought tremendous technical advances with second- and third-generation assays, as detailed in the preceding sections. The clinical performance of these tests in accurately diagnosing GD in overtly hyperthyroid patients has now reached a sensitivity and specificity above 95% (46). The use of non-isotope-based methods has reduced costs significantly (47), while scanning for radioactive-iodine uptake remains an expensive test. As a consequence, it seems reasonable to adopt TRAb as the primary tool in the differential diagnosis of hyperthyroidism. This will allow us to accurately diagnose a large majority of patients with GD from the minority of patients with thyrotoxicosis from other causes. TRAb is particularly useful in differentiating GD from painless thyroiditis. In painless subacute thyroiditis, patients have hyperthyroidism and a diffuse nontender goiter, so the distinction from GD is difficult to make on clinical grounds alone (48). The distinction is also important, as patients with painless subacute thyroiditis will not benefit from radioiodine or antithyroid drugs (ATD), treatments used for GD. In the setting of hyperthyroidism, binding-based assays are equivalent to TSAb assays in terms of specificity and sensitivity. Patients with positive results will not need any additional tests, while a thyroid scan may still be useful in patients with negative TSAb (49). A few patients with painless thyroiditis also have a positive TSAb test. While it is important to be aware of potential false positives, this situation is quite rare. It should be noted that the clinical performance of TSAB has been studied only in patients with overt hyperthyroidism, so some caution should be exerted in extending these results to patients with subclinical hyperthyroidism.

TRAb tests can also be used in predicting which patients with GD have entered a remission and can therefore stop ATD. Patients with GD, as with many other autoimmune diseases, undergo remissions and flare-ups. Patients in remission do not need to continue ATD, while patients unable to achieve a remission while on these medications may prefer definitive treatment with surgery or radioactive iodine. Since ATD keep patients euthyroid independently of their GD activity, thyroid function tests are typically not helpful. TSAb can be employed in this situation, with some limitations. A negative test suggests that the patient is likely to remain euthyroid in the short term if ATD treatment is discontinued. However, such a result has limited efficiency in predicting which patient will remain euthyroid (i.e., free of relapses) in the long term. The cutoff for predicting remission was found to be somewhat higher than the cutoff used to diagnose Graves' disease (50, 51). This may indicate that the ongoing autoimmune process may reduce the thyroid capacity to respond to TSAb to some extent in some patients. It is also possible that during the natural history of the disease, some patients may develop a mixture of blocking and stimulating antibodies and would still test positive in a binding assay, but these circumstances may not be able to cause hyperthyroidism (52).

TRAb tests are also useful to screen GD women who are pregnant for the risk of fetal and neonatal hyperthyroidism. The mechanism for this condition is indeed the transplacental transfer of TSAb to the fetus. This event is clinically most relevant when the mother has undergone definitive treatment of her GD with radioactive iodine or surgery. In that situation, there is no maternal hyperthyroidism warning the clinician of the persistence of TSAb, and the absence of ATD treatment leaves the fetus unprotected. Several studies have shown that this dangerous syndrome occurs only in some mothers with high-titer TSAb (53). It is therefore recommended that mothers with a history of Graves' disease be screened by the TSAb assay at the 24th to 28th weeks of gestation (54) and that, in those with high titers (3 times the cutoff for a positive test), the fetus be monitored for fetal hyperthyroidism.

Conclusions

The past decades have greatly advanced our understanding of autoimmunity to the TSHR. These advancements have helped to unravel the molecular phenomena leading to the hyperthyroidism of GD but have also provided the basis for the development of reliable tests for diagnosing and monitoring GD. Both modern-day clinicians and clinical laboratorians should be familiar with these tests in order to exploit them to the full extent of their possibilities.

AUTOANTIBODIES IN DIABETES

(This section was written by Jian Wang, Andrea K. Steck, George S. Eisenbarth, and Liping Yu.)

Diabetes mellitus is made up of a heterogeneous group of metabolic disorders characterized by hyperglycemia. Approximately 10% of patients with diabetes mellitus have the immune-mediated form of the disease, now termed type 1A diabetes (American Diabetes Association [55]). Prior terms for this form of diabetes include juvenile-onset diabetes and insulin-dependent diabetes. Given that as many patients develop type 1A diabetes during their adult years as they do during childhood and that the disease results from a cellularly mediated autoimmune destruction of the β-cells of the pancreas, the term type 1A has been adopted to reflect disease etiology. A type 1B (idiopathic) form of diabetes represents severe loss of insulin secretion on a nonautoimmune basis, but at present, a clear example of this form of the disorder is lacking. Type 2 diabetes is characterized by insulin resistance and moderate loss of insulin secretory capacity, and the majority of patients with diabetes have this form of the disease. Finally, separate diabetes mellitus categories consist of gestational diabetes and "other specific types of diabetes," which include genetic defects, such as MODY (maturity onset of diabetes in the young) and diabetes due to an accompanying pathology (e.g., pancreatic abnormalities, endocrinopathies, drug-induced diabetes).

The great majority (>90%) of non-Hispanic Caucasian children and approximately 50% of Hispanic and African American children who develop diabetes have the type 1A form of the disease, while between 5 and 15% of adults presenting with diabetes (depending upon the population) have type 1A diabetes. Type 1A diabetes is highly associated with specific HLA class II (DR and DQ) alleles, with both high-risk and protective genotypes having been reported. In particular, DQ8 (DQA1*0301 DQB1*0302) and DQ2 (DQA1*0501 DQB1*0201) are present in 90% of Caucasian patients with the disease and 40% of the general population, and DQ6 (DQA1*0102 DQB1*0602) is present in 20% of the population and 1% of children with type 1A diabetes. The nomenclature and detailed associations of specific HLA alleles and additional genetic polymorphisms associated with type 1A diabetes can be found at www.barbaradaviscenter.org and in chapter 7 of *Type 1 Diabetes: Cellular, Molecular & Clinical Immunology* (56). There are no tests that can absolutely exclude a diagnosis of type 1A diabetes, and it is possible for individuals to have evidence of both type 1A diabetes (e.g., anti-islet autoantibodies) and type 2 diabetes (e.g., severe insulin resistance). In general, however, the presence of anti-islet autoantibodies measured with highly specific assays (≥99% specificity) in a patient with diabetes are pathognomonic of the disorder, and multiple autoantibodies are present in the majority of prediabetic individuals (57–59). The presence of anti-islet autoantibodies can be used to predict the disease, with varied positive predictive values depending on the number of autoantibodies expressed (Fig. 4) (60, 61). Though there is general agreement that T lymphocytes rather than autoantibodies are the primary pathogenic mechanism, at present there is a lack of assays for anti-islet T cells with sufficient specificity and sensitivity to contribute to laboratory diagnosis or disease prediction.

Autoantibodies

Anti-islet autoantibodies are usually present years before the clinical onset of type 1A diabetes. A decade ago, anti-islet autoantibody tests were limited to measuring cytoplasmic islet cell autoantibodies (ICA) and insulin autoantibodies (IAA). Currently, recombinant autoantibody assays with biochemically defined autoantigens, including insulin (62), glutamic acid decarboxylase (GAD) (63), insulinoma antigen-2 (IA-2 or ICA512) (64), a homologous antigen, I-A2β (phogrin), zinc transporter-8 (ZnT8) (65), and carboxypeptidase H, are available (Table 1).

Cytoplasmic ICA were first discovered in the early 1970s in patients with polyendocrine autoimmunity (66), and antibodies in the sera from these patients reacted with frozen sections of human pancreas. These polyendocrine patients with type 1A diabetes have ICA that frequently persist for decades, while in the majority of patients with type 1A diabetes, the ICA slowly disappear. The ICA were soon identified in patients with the more common form of type 1A diabetes and were found to be present long before the clinical onset of diabetes (67, 68). The Diabetes Prevention Trial—Type 1 (DPT-1) demonstrated that in relatives, all anti-islet autoantibodies tested for in the trial, including ICA, GAD autoantibodies (GAA), and IA-2 autoantibodies (IA-2A), were relatively stable, with 75 to 85% of all positivity (90 to 95% with high levels) confirmed during follow-up. ICA have been shown to be present in 70 to 80% of patients newly diagnosed with type 1A diabetes and are predictive for the development of diabetes in both relatives of patients with diabetes and the general population. ICA are a heterogeneous mixture of IgG isotype autoantibodies against a variety of islet cell molecules. To date, four autoantigens that contribute to ICA positivity, including GAD, IA-2/ICA512, ZnT8, and glycolipids, have been defined (63, 65, 69–72). However, there are likely other autoantibodies still to be identified (Fig. 5). Approximately 5% of ICA-positive individuals without biochemical autoantibodies in the DPT-1 trial progressed to diabetes, suggesting that there are other autoantigens playing roles in type 1A diabetes autoimmunity. We believe that the four current major autoantibody assays in general can replace the ICA test for initial screening even though there probably remains an additional unidentified ICA autoantigen(s) ("antigen X") (Fig. 5).

The first ICA antigen component to be determined was a 64-kDa protein that was later identified (62) as the enzyme GAD. GAD is present in all human islet cells (e.g., α, β, and δ) and other endocrinological organ tissues, like

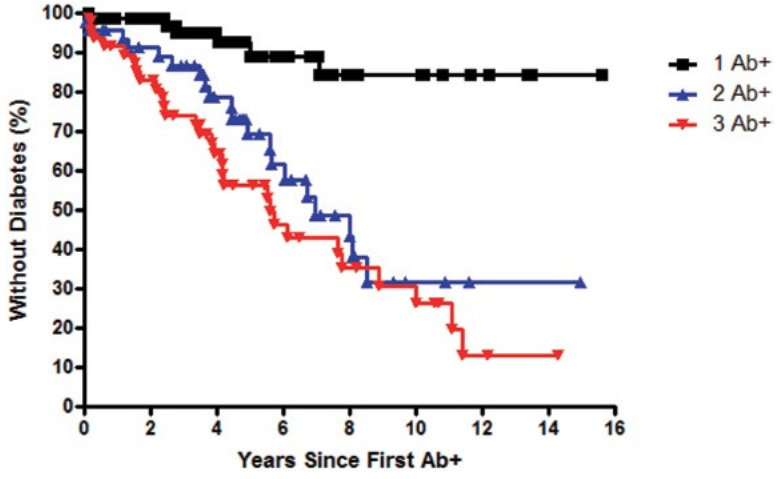

FIGURE 4 Progression to diabetes in children positive for anti-islet cell autoantibodies in DAISY (Diabetes Autoimmunity Study in the Young) relative to the number of anti-islet cell autoantibodies expressed (autoantibodies to GAD65 [glutamic acid decarboxylase], ICA512 [IA-2, insulinoma-associated antigen], and insulin). Adapted with permission from *Diabetes Care* (60).

TABLE 1 Biochemically characterized autoantigens

Autoantigen	% Sensitivity	Comment
Insulin	49–92	Higher levels in young children than in adults
GAD (glutamic acid decarboxylase)	84	High sensitivity for adult-onset type 1A
ICA512/IA-2	74	Tyrosine phosphatase-like molecule
ZnT8	70	Zinc transporter 8
IA-2β/phogrin	61	Tyrosine phosphatase-like molecule
Carboxypeptidase H	10	Infrequent
GLIMA38	14–38	Not yet sequenced
GM2-1	?	Ganglioside for chromatography assay
ICA69	?	Used in Western blot assay with poor specificity
ICA12	<20	Diabetes relatedness requires further study

testes, ovary, and neurons, though only pancreatic beta cells are destroyed in type 1A diabetes. The anti-GAA of patients with stiff-man syndrome (SMS) had been previously identified and are unusual in that they react with fixed sections of the brain and react with denatured GAD molecules on Western blots and with GAD protein fragments (73). In contrast, most diabetic sera target only GAD protein epitopes, depending on protein conformation, and do not bind GAD protein fragments or react with denatured GAD protein. There are two isomers of GAD, GAD65 and GAD67, which are 76% homologous in amino acid sequence. Autoantibodies to GAD65 are predominant over those to GAD67, and the autoantibodies binding to GAD67 in patients with diabetes seem to represent antibodies to epitopes shared with GAD65 (74).

The second-identified ICA antigen component was IA-2 (or ICA512), a protein tyrosine phosphatase (71, 72), and its homologous antigen IA-2β (phogrin). The two isomers are most homologous in their antigenic intracellular regions, to which essentially all of the autoantibodies are directed. Almost all autoantibodies to I-A2β also react with IA-2, while approximately 10% of patients with diabetes have autoantibodies reacting only with IA-2 and not with IA-2β. In addition, two differentially spliced ICA512 (IA-2) mRNAs are expressed in islets, with one form lacking exon 13, which includes the transmembrane region of the molecule (75). In our laboratory, an IA-2ic clone is used, but another clone (ICA512bdc) is still being used for some ongoing diabetes clinical trials. Approximately 10% of patients developing type 1 diabetes have autoantibodies reacting with only one of the two forms of alternatively spliced IA-2 molecules.

The most recently discovered ICA antigen component was ZnT8, a zinc transporter protein related to insulin secretion in humans coded by a gene, *SLC30A8* (65), and interestingly, certain alleles of this gene may increase the risk for developing type 2 diabetes (76). Most of the full-length molecule is hydrophobic, as it is within the membranes of secretory granules, and a highly specific and sensitive assay was achieved using the C terminus of the molecule (65). Of note, there are two major polymorphic variants of ZnT8, one with a tryptophan and the other with an arginine at position 325 of the molecule (77) (also, a glutamine variant is more common in African Americans). The majority of patients have autoantibodies recognizing both variants, but a subset have autoantibodies recognizing only one variant. Those recognizing the specific arginine variant are patients genetically homozygous for the arginine variant and vice versa for the tryptophan variant. This is a unique demonstration that islet autoimmunity in terms of epitopes recognized is truly autoimmune, with patients recognizing their own sequence.

To date, insulin is the only known beta-cell-specific autoantigen of humans (all other islet autoantigens are also produced by human non-beta islet cells). IAA were found by Palmer and coworkers (78) in patients with newly diagnosed type 1A diabetes and were soon demonstrated to be present for many years before the clinical onset of disease. IAA are so far the only autoantibodies dramatically age dependent in their prevalence and levels (79, 80). The levels of IAA inversely correlate with the age of disease onset (60, 80), and less than half of individuals developing type 1A diabetes after age 15 have detectable IAA levels. IAA is usually the first autoantibody to appear in young children developing type 1 diabetes (81, 82). For most patients, treatment with exogenous insulin also induces insulin antibodies (IA). The current IAA assay is not able to distinguish between natural insulin autoantibodies and induced insulin antibodies. In the rare insulin autoimmune syndrome (83), also termed Hirata syndrome, patients express high levels of IA, often with episodes of severe hypoglycemia.

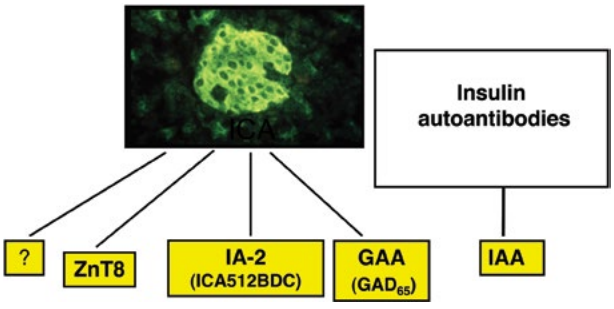

FIGURE 5 Current biochemical anti-islet autoantibody assays.

General Assay Methodology

The first useful islet autoantibody assay was the ICA test utilizing indirect immunofluorescence with frozen sections of human pancreas as the substrate. A standard for ICA utilizing a serial dilution of a calibrated serum with assigned Juvenile Diabetes Foundation (JDF) units was established. To date, the ICA test remains cumbersome, and Immunology of Diabetes Society (IDS) workshops demonstrated that there existed large variation between laboratories in terms of sera called ICA positive.

The current major format for determination of islet autoantibodies uses fluid-phase radioimmunobinding assays, applied to all four major islet autoantibody tests, including GAA, IA-2A, ZnT8A, and IAA. There is available a semi-automated format in which labeled antigen is incubated with patient sera, and then both are placed in 96-well filtration plates. The immune complex is precipitated with protein A- and/or protein G-coupled Sepharose, free radioactivity is separated by filtration washing, and then scintillation fluid is added directly to the 96-well filtration plates, and counting is performed on multichannel beta counters able to handle the plates (Fig. 6).

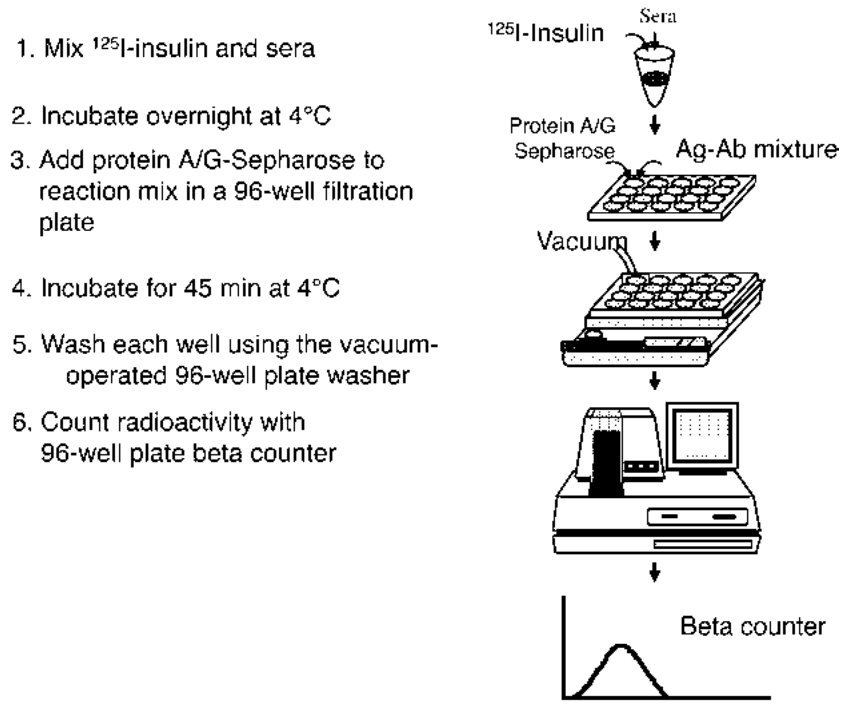

FIGURE 6 General outline of high-throughput fluid-phase 96-well plate assays for anti-insulin autoantibodies. In the illustrated example, ^{125}I-insulin is utilized, but the assay formats are identical for the GAD65, IA-2, and ZnT8 assays. Ag, antigen; Ab, antibody.

Given a lack of linear correlation between the laboratories, an islet autoantibody harmonization program (84) has been launched with the effort of an international collaborative group convened by the NIDDK. A standardized assay protocol and a set of common calibrator sera currently for GAA and IA-2A were developed to improve harmonization of measurement of these autoantibodies (84). The harmonization program eventually aims to have all islet autoantibody assays standardized, including those for IAA and ZnT8A. Utilization of the standard harmonized assays allows us to analyze and to compare the data between laboratories and between trials done by different laboratories, with expression of the assay results as NIDDK units.

ELISAs employing plate-bound antigen are the most common assay formats for basic immunologic research. In multiple diabetes autoantibody workshops, for either human or mouse models, standard ELISA formats lack both sensitivity and specificity compared to the fluid-phase radioassay formats, especially for the IAA assay. In the international workshop, a modified ELISA for GAA attained a level of specificity and sensitivity equivalent to that of the radioassays (85). In the 2012 Islet Autoantibody Standardization Program (IASP) workshop, a ZnT8A ELISA with an identical modified ELISA format was shown to have a level of sensitivity equivalent to that of the radioassay with less specificity.

It is recommended that all laboratories attempting to measure anti-islet autoantibodies take part in IASP workshops organized by the IDS and the NIDDK. As demonstrated with multiple workshops, although the majority of laboratories have excellent assays for GAA, IA-2A, and ZnT8, many laboratories have IAA assays with unacceptable sensitivities and specificities when evaluating in blind trials the IASP panel of 100 control sera and 50 sera from patients with type 1A diabetes of recent onset.

Determination of ICA by Indirect Immunofluorescence

Sample Requirements

Samples for indirect immunofluorescence were stored at −20°C or below until analyzed. Approximately 200 μl of serum per sample is needed for this assay. Hemolyzed or lipemic blood samples may have artificially low ICA titers and thus should not be used for analysis with this method. In order to obtain high-quality serum and prevent or decrease the possibility of hemolysis, the yellow-top gel serum separator tubes are recommended.

Materials, Reagents, and Equipment

- Cryostat
- Frozen 5-μm sections of human blood group O pancreas tissue
- Fluorescein-antibody conjugate [goat anti-human IgG $F(ab)_2$ fragment-FITC, rabbit fluorescein-conjugated antihuman IgG (Behringwerke AG, Marburg, Germany), or sheep anti-human IgG FITC conjugate (Sigma, St. Louis, MO, USA)]
- Fluorescence microscope with an epi-illumination 20× objective (Leica, Wetzlar, Germany)
- Reciprocal shaker

Principle

We highly recommend human pancreas with blood type O of cadaveric donors taken while the heart is still beating, because the pancreas is very prone to autolysis. Five-millimeter cubes of the pancreas are quickly frozen in isopentane at −70°C, sealed in a freezer container, and stored at −80°C. Five-micrometer-thick frozen sections are cut while the temperature of the cryostat is held between

−25 and −30°C, placed onto the glass microscope slides (usually four sections per slide), air-dried for 30 min with a fan, and then directly used or stored at −80°C. The freezer-stored slides must be brought up to room temperature with air-drying in front of a fan for 30 min before use. The slides to be used should be well labeled, and the sections on the same slide need to be isolated from each other with a hydrophobic marker. A serum sample is then applied to each section, and tissue-bound specific autoantibodies from the patient's serum will be revealed by an animal (goat, sheep, or rabbit) anti-human IgG-fluorescein conjugate under a fluorescence microscope with epi-illumination.

Procedure

1. In the initial experiment, 50 μl of undiluted serum is applied to each tissue section and incubated for 30 min at room temperature in a moisture chamber.
2. Each slide is rinsed gently with 0.5 M PBS (pH 7.4), with care taken not to damage or remove each tissue section.
3. The slides are completely submerged in 0.5 M PBS (pH 7.4) and gently washed on a reciprocal shaker for 5 min, and this wash step is repeated twice, each time in fresh PBS for 5 min.
4. Both sides of the slides are quickly dried with a low-lint Kim wipe, with care taken not to touch the tissue sections on each slide, and then placed back into the incubation chamber to prevent complete dehydration before the next step.
5. Each section is then covered with 50 μl of diluted (often a 1/20 dilution determined empirically) fluorescein-antibody conjugate in PBS (containing 1% bovine serum albumin [BSA]) and incubated for 30 min at room temperature in a moist chamber.
6. The slides are washed as in steps 2 and 3.
7. The slides are quickly dried as in step 4, and a slide cover is put on with a glycerol solution (90% glycerol-10% [wt/vol] PBS [the coverslip is applied and sealed with nail polish]).
8. Islet cell-specific fluorescence is observed under a fluorescence microscope fitted with 20× epi-illumination.
9. All samples with detectable ICA are titrated by retesting the serum in serial dilution. The endpoint titer is compared with the 80-JDF unit international standard used by the IDS workshops.

Standardization, Quality Control, and Quality Assurance

1. To determine the appropriate dilution of fluorescein-antibody conjugate, known-negative, weakly positive, and strongly positive sera need to be tested with various dilutions of conjugate, and the optimal dilution is the highest dilution that gives the strongest specific islet cell reaction with the least nonspecific staining.
2. A standardization procedure should be applied for each new lot of pancreas by serially diluting the 80-JDF unit standard in both negative sera and PBS. A five-point curve of standard diluted in negative serum versus standard diluted in PBS should be linear, and JDF units are calculated from this curve by interpolation of patient serum endpoint titers in PBS.
3. Strongly positive, weakly positive, and negative-control samples should be included in each assay. It is recommended that a known-positive serum sample be stored in aliquots and tested every 3 months to monitor assay drift. The ICA assay, including quality control samples, should be analyzed with the reader blind to the sample identity.

Biochemically Defined Autoantibody Radioassay

Sample Requirements

We recommend obtaining the serum from red-top or tiger-top (separator) blood-collecting tubes and ideally to be hemolysis and lipemia free. Only 5 μl of serum is required to measure GAA, IA-2A, or ZnT8A, and 12 μl of serum is required for micro-IAA (mIAA).

Materials, Reagents, and Equipment

- Human GAD65 cDNA clone
- Human IA-2 cDNA clone (the most utilized clone is IA-2ic [intracytoplasmic IA-2])
- TNT Sp6 coupled *in vitro* translation kit (Promega)
- RNasin RNase inhibitor (Promega)
- [^{35}S]methionine (PerkinElmer)
- ^{125}I-insulin (PerkinElmer)
- Protein A-Sepharose Fast Flow (GE Healthcare)
- Protein G-Sepharose Fast Flow (GE Healthcare)
- NAP-5 column (GE Healthcare)
- 96-Well PCR plate (Fisher)
- 96-Well filtration plates (Fisher)
- Bottle-Top 50-ml filter units (Fisher)
- TopSeal (PerkinElmer)
- Microscint-20 (PerkinElmer)
- TopCount β-counter (PerkinElmer)
- Plate autowasher (BioTek) or vacuum-operated 96-well plate washer (Millipore)
- 96-Well plate shaker (Wallac-Delfi)

GAA and IA-2A Assays

General Principle

The cDNA constructs used in the GAA and IA-2A assays are the full length of human GAD65 and an intracellular domain of IA-2 (IA2ic). The GADA and IA-2A assays are identical and use the NIDDK-harmonized standard protocol. Labeled GAD65 and IA-2 are produced by *in vitro* transcription/translation with [^{35}S]methionine. The patient serum is incubated with labeled antigen overnight, and antibody-bound labeled antigens are separated from unbound labeled antigens with protein-A Sepharose precipitation in a 96-well plate. Radioactivity is counted on a 96-well plate β-counter. Results are calculated with a standard curve from a set of NIDDK calibrator sera and expressed as standard NIDDK units. Many laboratories are currently still using their own index, which adjusts the counts per minute (cpm) of the test serum for the cpm of positive- and negative-control sera in each assay. A cutoff for positivity above the 99th percentile of normal controls is often utilized.

Procedure

Part I: *In Vitro* Transcription/Translation To Produce Labeled GAD65 and IA-2

Important notes. All reagents, tubes, and tips must be RNase free. All reagents should be kept on ice while on the bench. An incubation temperature of 30°C is critical for production efficiency. The reticulocyte lysate must be stored

at −80°C and thawed rapidly just before use. Each tube can be thawed only twice, after which there will be a significant decrease in its efficiency.

Procedure.

1. Follow the kit protocol for the one-step *in vitro* transcription/translation reaction. The total reaction volume can be adjusted, decreased, or increased, as needed.
2. Purify the labeled product with a NAP-5 column.
3. Analyze the activity of the labeled antigen by counting the activity in 5 μl of a 100-fold-diluted aliquot. The labeling efficiency significantly varies with different cDNAs and plasmids.

Part II: Radioassay (2 Days)

Day 1.

1. Prepare the buffers. The assay buffer consists of 20 mM Tris-HCl, 150 mM NaCl, and 0.15% Tween 20 (pH 7.4), and for the antigen buffer, add 0.1% BSA in assay buffer.
2. Prepare the antigen buffer solution. With the optimized conditions, 20,000 cpm in 50 μl of antigen buffer is usually applied per well. For a 96-well plate with 25% extra volume to ensure enough volume for aliquoting into each well, the total cpm is calculated as follows: $96 \times 20{,}000 \text{ cpm} \times 125\% = 2.4 \times 10^6$ cpm for either ^{35}S-GAD65 or ^{35}S-IA-2. The total volume is calculated as follows: $96 \times 50\ \mu l \times 125\% = 6$ ml.
3. Prepare the serial dilution of a calibrated standard serum with known NIDDK units. Calibrated standard sera with known NIDDK units in serial dilution are available from the NIDDK. We recommend a standard curve covering a wide range of antibody levels with a calibrated standard set of sera in each assay or every 4 plates if more than 4 plates are used in each assay.
4. In the incubation of serum with antigen buffer, duplicates are recommended for each sample. Add 2.5 μl of serum and 60 μl of antigen buffer solution containing either ^{35}S-GAD65 or ^{35}S-IA-2 into a 96-well PCR plate and incubate overnight at 4°C. The standard positive-control and negative-control serum samples for GAA or IA-2A must be included in each assay.
5. In preparing the 96-well filtration plates, coat the plate with BSA by adding 200 μl of antigen buffer to each well, put the plate on aluminum foil, and incubate it overnight at room temperature.
6. In preparing protein A-Sepharose, use only plastic tubes because protein A sticks to glass. Pull 20 ml of protein A-Sepharose into a 50-ml tube, spin the solution down at 1,000 × *g* for 3 min, remove the fluid phase, and resuspend it into assay buffer. Repeat this twice, and make a final 50% (vol/vol) solution of protein A-Sepharose/antigen buffer.

Day 2.

1. Remove the antigen buffer from the 96-well filtration plate and add 25 μl of well-mixed 50% protein A-Sepharose to each well.
2. Transfer 50 μl from each well of the overnight incubation to the 96-well filtration plate, and shake the plate on a plate shaker at low speed for 45 min at 4°C.
3. Place the plate on a plate washer, and wash the plate three times with 200 μl of assay buffer per well each time. Then remove the plate, add 100 μl of assay buffer per well, and shake the plate for at least 5 min at 4°C.
4. Wash the plate two more times with 200 μl of assay buffer per well each time, change the plate orientation, and wash the plate another two times.
5. Blot the plate with a paper towel, and place the plate under a lamp for about 15 min. After the plate is dry, add 25 μl of scintillation liquid (MicroScint-20) to each well, seal the plate with a piece of Top-Seal, and count the radioactivity of the plate on a TopCount β-counter.
6. Obtain the cpm for each well, and obtain mean cpm for each sample if duplicates are performed.
7. Calculate the index with the following formula: (cpm of the test serum – cpm of the negative serum)/(cpm of the positive serum – cpm of the negative serum).
8. Calculate NIDDK units. Using the cpm from the serial dilution (5 points) of a calibrated standard serum with known NIDDK units, plot a chart with log 2 NIDDK units versus cpm in an Excel sheet as in Fig. 7. With the curve formula, log 2 NIDDK units can be calculated for each test sample by replacing (*x*) in the formula with the cpm of the test sample and then converting log 2 units into NIDDK units by anti-log 2 (power of 2).

Standardization, Quality Control, and Quality Assurance

1. The laboratory should keep enough of the volume of the calibrated standard sera and the positive- and negative-control sera for long-term use. Each of these serum samples should be aliquoted and stored at −20°C.
2. All the assays are run in duplicate, with a standard curve for NIDDK unit calculation, and include high/low-positivity and negative-control samples for quality control purposes and for lab index calculation. In our assay, GAA positivity is any value greater than 20 NIDDK units and IA-2A positivity is greater than 5 NIDDK units.
3. The results of analysis of positive controls from each assay should be plotted in a preestablished Shewhart plot, with the mean ± 3 standard deviations (SD) to monitor the assay drift and evaluate assay performance. Our positive-control range for both GAA and IA-2A should be within 3 SD. The negative-control value must be less than the 99th-percentile value for

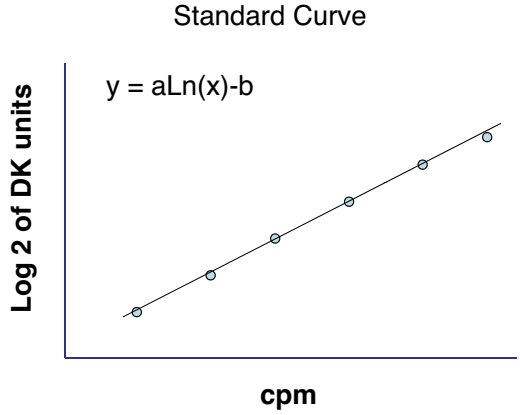

FIGURE 7 Standard curve for calculation of NIDDK units. The *x* axis is the number of cpm from the assay after removal of the background cpm, and the *y* axis is log 2 NIDDK units.

normal controls for the assay results to be valid (e.g., <20 [GAA] or <5 [IA-2A]).
4. Every positive sample in the first assay is confirmed by repeating that sample in a different assay. If the second confirmatory assay result is negative, a third run is performed. We utilize the results of two assays, which agree (−,− or +,+), for the determination of a positive or negative result.

mIAA Assay

General Principle

The mIAA assay is a competitive radioassay. The patient serum is incubated with ^{125}I-insulin with and without cold human insulin overnight, and antibody-bound labeled antigens are separated from unbound labeled antigens with protein A/G-Sepharose precipitation in a 96-well plate. Radioactivity is counted directly on a 96-well-plate β-counter for the βemission of ^{125}I. The levels are expressed as an index that adjusts the Δcpm of the test serum for the Δcpm of positive- and negative-control sera in a particular assay. An NIDDK unit is not available for IAA at present.

Procedure (2 Days)

Day 1.
1. Prepare the buffers. Assay buffer consists of 20 mM Tris-HCl, 150 mM NaCl, 0.15% Tween 20, 0.1% sodium azide, and 0.1% BSA (pH 7.4), and antigen buffer is the same as assay buffer except that it contains 1% BSA.
2. Prepare the ^{125}I-insulin-buffer solution with and without cold human insulin. Use 1 ml of 5% BSA in PBS to dissolve the powder of 10 μCi of ^{125}I-insulin as a stock solution. We utilize 20,000 cpm in 30 μl of antigen buffer per well. For a 96-well plate with 10% extra to ensure enough volume for aliquoting into each well, the total cpm equals 96 times 20,000 cpm times 110%, which equals 2.1 times 10^6 cpm or 160 μl of ^{125}I-insulin stock solution; the total volume is equal to 96 times 30 μl times 110% or 3.2 ml, which needs to be divided in half (half with and half without cold human insulin [100 U/ml]) as follows: 1,520 μl of buffer 1 plus 80 μl of ^{125}I-insulin (for a total of 1.6 ml) and 1,392 μl of buffer 1 plus 128 μl of cold insulin and 80 μl of ^{125}I-insulin (for a total of 1.6 ml).
3. Incubate the serum with antigen buffer. Four wells per serum sample will be used for both competition and noncompetition in duplicate. Add 6 μl of serum and 30 μl of antigen buffer into a 96-well PCR plate, mix well, leave the plate at room temperature for 2 h, and then incubate overnight at 4°C. The index positive control, low-positivity control, and negative-control serum samples must be included in each assay.
4. To prepare 96-well filtration plates, coat the plate with BSA by adding 200 μl of assay buffer to each well, put the plate on an aluminum foil sheet, and incubate it overnight at room temperature.
5. To prepare protein A/G-Sepharose, use only plastic tubes because protein A/G sticks to glass. Put 20 ml of protein A-Sepharose and 5 ml of protein G-Sepharose individually into two 50-ml tubes, spin the solution down at 1,000 × *g* for 3 min, remove the fluid phase, and resuspend it into assay buffer. Repeat this twice, and make a final 62.5% (vol/vol) solution for protein A-Sepharose with assay buffer and 40% (vol/vol) solution for protein G-Sepharose. Mix 4 parts of protein A-Sepharose solution with 1 part of protein G-Sepharose solution to form a final working solution with 50% (vol/vol) protein A-Sepharose and 8% protein G-Sepharose.

Day 2.
1. Remove the assay buffer from the 96-well filtration plate and add 50 μl of well-mixed protein A/G-Sepharose to each well.
2. Transfer 30 μl from each well of the overnight incubation to a corresponding well on the 96-well filtration plate, and shake the plate on a plate shaker at low speed for 45 min at 4°C.
3. Place the plate on a plate washer and wash the plate three times with 200 μl of assay buffer per well each time. Then remove the plate, add 100 μl of assay buffer per well, and shake the plate for at least 5 min at 4°C.
4. Wash the plate two more times with 200 μl of assay buffer per well each time, change the plate orientation, and wash the plate another two times.
5. Blot the plate on a paper towel and place the plate under a lamp for around 15 min. After it is dry, add 50 μl of scintillation liquid (MicroScint-20) to each well, seal the plate with a piece of TopSeal, and count the radioactivity of the plate on a TopCount β-counter.
6. Calculate the index with the following formula: (Δcpm of the test sample − Δcpm of the negative control)/(Δ cpm of the positive control − Δcpm of the negative control).

Standardization, Quality Control, and Quality Assurance

1. The laboratory should keep enough volume of the positive- and negative-control sera for long-term use. Each of these serum samples should be aliquoted and stored at −20°C.
2. All the assays are run in duplicate and must include positive/negative-control samples. An ultralow positive control just above the 99th percentile is highly recommended to be included in each mIAA assay, particularly to monitor the sensitivity of the assay. Our ultralow standard positive-control range is an index from 0.011 to 0.030. In our assay, a positive mIAA value is any value greater than the index value, 0.010, the 99th percentile of normal controls.
3. The results of the analysis of negative and positive controls from each assay should be plotted in a preestablished Shewhart plot with means ± 3 SD to monitor the assay drift and evaluate assay performance. Our positive-control range should be within 3 SD. The negative control must be <0.01 for results of the assay run to be utilized.
4. Every positive sample in the first run is confirmed to be positive by repeating that sample in a different assay. If the second confirmatory assay comes out negative, a third assay is necessary. The results of two assays that agree (e.g., +,+ or −,−) will be the final determination of a positive or negative result.

ZnT8A Assay

General Principle

The ZnT8A assay is similar to the GAA or IA-2A assay. The cDNA construct ZnT8RW is a dimmer of two identical intracellular domains of ZnT8, with one having arginine and the other tryptophan at amino acid position

325, representing two major polymorphisms in the white population that are important for antibody binding. Labeled ZnT8 protein is produced by *in vitro* transcription/translation with [^{35}S]methionine. The patient serum is incubated with labeled antigen overnight, and antibody-bound labeled antigens are separated from unbound labeled antigens with protein-A Sepharose precipitation in a 96-well plate. Radioactivity is counted on a 96-well plate β-counter. Results are calculated against our internal standard positive and negative controls and expressed as indexes. A cutoff for positivity above the 99th percentile of normal controls is often utilized.

Procedure

Part I: *In Vitro* Transcription/Translation To Produce Labeled ZnT8

Important notes. All reagents, tubes, and tips must be RNase free. All reagents should be kept on ice while on the bench. An incubation temperature of 30°C is critical for production efficiency. The reticulocyte lysate must be stored at −80°C and thawed rapidly just before use. Each tube can be thawed only twice, after which there will be a significant decrease in its efficiency.

Procedure.
1. Follow the kit protocol for the one-step *in vitro* transcription/translation reaction. The total reaction volume can be adjusted, decreased, or increased, as needed.
2. Purify the labeled product with a NAP-5 column.
3. Analyze the activity of the labeled antigen by counting the radioactivity in 5 μl of a 100-fold-diluted aliquot. The labeling efficiencies significantly vary with different cDNAs and plasmids.

Part II: Radioassay (2 Days)

Day 1.
1. Prepare the buffers. Assay buffer consists of 20 mM Tris-HCl, 150 mM NaCl, and 0.15% Tween 20 (pH 7.4). For antigen buffer, add 0.1% BSA to the assay buffer.
2. Prepare the antigen buffer solution. Under optimized conditions, 20,000 cpm in 50 μl of antigen buffer is usually applied per well. For a 96-well plate with 25% extra volume to ensure enough volume for aliquoting into each well, the total cpm is 96 times 20,000 cpm times 125%, which equals 2.4 times 10^6 cpm for [^{35}S]ZnT8; the total volume is 96 times 50 μl times 125%, or 6 ml.
3. Incubate the serum with antigen buffer. Duplicates are recommended for each sample. Add 2.5 μl of serum and 60 μl of antigen buffer solution containing ^{35}S-ZnT8 into a 96-well PCR plate and incubate it overnight at 4°C. The standard positive-control and negative-control serum samples for ZnT8A must be included in each assay.
4. Prepare 96-well filtration plates. Coat the plate with BSA by adding 200 μl of antigen buffer to each well, put the plate on aluminum foil, and incubate it overnight at room temperature.
5. Prepare the protein A-Sepharose. Use only plastic tubes because protein A sticks to glass. Pull 20 ml of protein A-Sepharose into a 50-ml tube, spin the solution down at 1,000 × *g* for 3 min, remove the fluid phase, and resuspend it into assay buffer. Repeat this twice, and make a final 50% (vol/vol) solution of protein A-Sepharose-antigen buffer.

Day 2.
1. Remove the antigen buffer from the 96-well filtration plate and add 25 μl of well-mixed 50% protein A-Sepharose to each well.
2. Transfer 50 μl from each well of the overnight incubation to the 96-well filtration plate, and shake the plate on a plate shaker at low speed for 45 min at 4°C.
3. Place the plate on a plate washer and wash the plate three times with 200 μl of assay buffer per well each time. Then remove the plate, add 100 μl of assay buffer per well, and shake the plate for at least 5 min at 4°C.
4. Wash the plate two more times with 200 μl of assay buffer per well each time, change the plate orientation, and wash the plate another two times.
5. Blot the plate on a paper towel and place the plate under a lamp for around 15 min. After the plate is dry, add 25 μl of scintillation liquid (MicroScint-20) to each well, seal the plate with a piece of TopSeal, and count the radioactivity on the plate on a TopCount β-counter.
6. Obtain the number of cpm for each well, and obtain mean numbers of cpm for each sample if duplicates are performed.
7. Calculate the index with the following formula: (cpm of the test serum − cpm of the negative serum)/(cpm of positive serum − cpm of the negative serum).

Standardization, Quality Control, and Quality Assurance

1. The laboratory should keep large enough volumes of the positive- and negative-control sera for long-term use. Each of these serum samples should be aliquoted and stored at −20°C.
2. All the assays are run in duplicate and must include positive- and negative-control samples for quality control purposes and for lab index calculation. In our assay, ZnT8A positivity is any value greater than an index of 0.020.
3. The results of analysis of negative and positive controls from each assay should be plotted in a preestablished Shewhart plot with means ± 3 SD to monitor the assay drift and evaluate the assay's performance. Our positive-control range should be within 3 SD. The negative control must be <0.020 for results of the assay run to be utilized.
4. The result for every positive sample in the first run is confirmed by repeating that sample in a different assay. If the second confirmatory assay comes out negative, a third assay is necessary. A result of two assays which agree (e.g., +,+ or −,−) will be the final determination of a positive or negative result.

New Technology

ECL Assay

We have recently developed a plate capture electrochemiluminescence (ECL) IAA assay and a GADA assay (86, 87), which are nonradioactive assays that may help to disseminate islet autoantibody testing possibly to the point of care. As shown in Fig. 8 for the ECL assay format, autoantibodies cross-link two antigen molecules,

one biotinylated and the other labeled with ruthenium, allowing plate capture with streptavidin. This assay detects high-affinity IAA and was more sensitive than the micro-IAA (mIAA) radioassays in the last (2013) Islet Autoantibody Standardization Program (IASP) workshop yet is equally specific, while the ECL GADA assay had sensitivity similar to that of the standard GADA radioassay. Interestingly, the ECL IAA assay antedated the detection of IAA in young DAISY (Diabetes Autoimmunity Study in the Young) children by a mean of 2.3 years (range, 0.3 to 7.2 years) in a comparison with the standard micro-IAA (mIAA) radioassay (88). Very remarkably, both the ECL IAA and ECL GADA assays were able to discriminate high-affinity, high-risk-diabetes-specific autoantibodies from those "low-risk" low-affinity signals; i.e., they are more disease specific since they are able to distinguish disease-associated antibodies from non- or less-disease-associated antibodies among single IAA- or GADA-positive subjects by radioassay (86, 87).

Materials, Reagents, and Equipment

- Human proinsulin
- Human GAD65
- Biotinylation kit (Thermo Scientific)
- Sulfo-Tag (Meso Scale Discovery [MSD])
- 96-well PCR plate (Fisher)
- Streptavidin-coated MSD plate (MSD)
- Zeba sizing spin column (ThermoScience)
- Blocker A buffer (MSD)
- Reader buffer (MSD)
- Chemicals: acetic acid, Tris base, HCl, 10× PBS buffer, BSA
- 96-Well plate shaker (Wallac-Delfi)
- Sector 2400 or Sector 6000 (MSD)
- Benchtop centrifuge with a bucket rotary (Beckman)

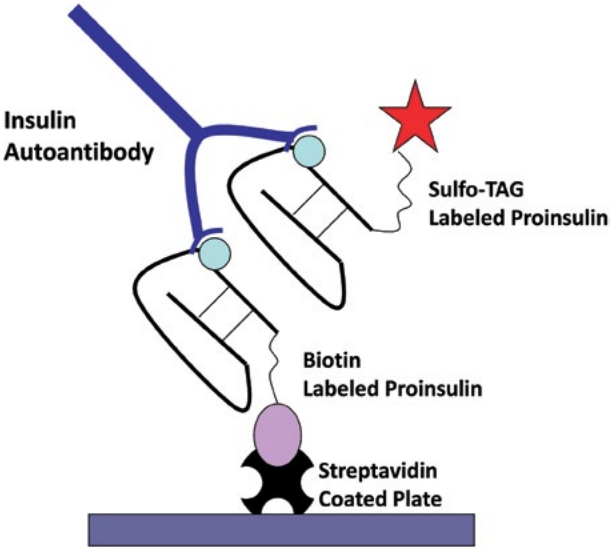

FIGURE 8 Format of the electrochemiluminescence (ECL) assay. In the illustrated example, biotin and Sulfo-Tag proinsulin were utilized, but the assay format is identical for GAD65. Adapted with permission from *Diabetes* (86).

ECL IAA Assay

General Principle

Given the need for improved IAA assays and the hypothesis that the binding of insulin to solid phases obscures a key determinant for recognition by human autoantibodies as seen also by Rojas et al. for specific murine monoclonals (89), we set out to immobilize "insulin" to a solid phase in a manner that preserved critical determinants recognized by human insulin autoantibodies. We had previously failed to develop a plate capture assay for human insulin autoantibodies, though we have developed such an assay (nonradioactive) for the insulin autoantibodies of the NOD mouse (90). The two fundamental components for our recent success were utilization of proinsulin rather than insulin and use of streptavidin rather than avidin for plate capture of biotinylated proinsulin (Fig. 8). The ruthenium assay system of MSD is a third important component. In our prior studies, all human insulin autoantibodies reacted with proinsulin in fluid-phase radioassays (91).

Procedure

Part I: Label Human Proinsulin with Biotin and Sulfo-Tags

Important notes. Biotin and Sulfo-Tag powder should be dissolved just before the labeling procedure every time. The proinsulin must be stored at −80°C and thawed on ice before use. The protein in either the Tris or glycine buffer system should be exchanged with 2-fold PBS buffer (pH 7.9) by sizing with a spin column.

Procedure.

1. Calculate the molar ratio of proinsulin with biotin or Sulfo-Tag. We recommend using a 1:5 molar ratio for proinsulin labeling.
2. Mix proinsulin with either biotin or Sulfo-Tag, cover the reaction tubes with aluminum foil to avoid light, and incubate them at room temperature for 1 h.
3. During the 1-h incubation, prepare a Zeba sizing spin column by washing the column three times with full-strength PBS buffer and centrifuging at 1,000 × *g* for 2 min each time in a centrifuge.
4. Stop the labeling reaction and purify labeled proinsulin by passing the reaction mixture through the prepared Zeba sizing spin columns at 1,000 × *g* for 2 min in a centrifuge.
5. Measure the protein concentration.
6. Aliquot the labeled proinsulin and store the samples in a −80°C freezer.

Part II: Plate Capture Assay (2 Days)

Day 1.

1. Prepare the buffers. The buffer is 0.5 M acetic acid with 1 M Tris-HCl (pH 9.0), and antigen buffer is full-strength PBS with 5% BSA. PBST is full-strength PBS with 0.05% Tween 20.
2. Treat the serum samples with acid. Mix 15 μl of serum with 18 μl of 0.5 M acetic acid and incubate it at room temperature for 45 min.
3. Prepare antigen buffer containing both biotin and Sulfo-Tag-labeled proinsulin with the same concentration of 100 ng/ml, and add to a new PCR plate 35 μl of solution per well.
4. Just before the completion of the 45-min incubation (step 2), add 8.3 μl of 1 M Tris (pH 9.0) buffer per well

into the antigen plate of step 3 (try to add it onto the side wall of each well; avoid complete mixing at this time); immediately afterwards, transfer 25 μl of the acid-treated serum of step 2 into the well, and then mix entirely. Cover the plate with sealing foil to avoid light.
5. Shake at room temperature on the low setting for 2 h.
6. Put in a 4°C refrigerator to incubate overnight (18 to 24 h).

Prepare the streptavidin plate.

1. Let MSD streptavidin plate(s) come to room temperature.
2. Add 150 μl of 3% blocker A (in PBS) per well.
3. Cover the plate with foil.
4. Incubate it in a 4°C refrigerator overnight.

Day 2.
1. Remove the streptavidin plate from the refrigerator. Dump out the buffer and bang the plate on a paper towel to dry it.
2. Wash it three times with 150 μl of PBST.
3. Transfer 30 μl of the serum-antigen mixture into the MSD streptavidin plate.
4. Cover it with foil to avoid light and shake it at room temperature for 1 h on the low speed setting.
5. Dump out the incubated contents and wash the plate three times with 150 μl of PBST.
6. Add 150 μl/well of 2-fold Read buffer (avoid any bubbles).
7. Count the reactivity on an MSD machine.

Standardization, Quality Control, and Quality Assurance

1. The mouse anti-human proinsulin monoclonal antibody is used as an internal-standard positive control. The monoclonal antibody should be diluted with normal human serum and treated identically as for human serum in the assay.
2. The laboratory should keep a high enough volume of the positive- and negative-control sera for long-term use. Each of these serum samples should be aliquoted and stored at −20°C.
3. All the assays are run in duplicate and must include positive- and negative-control samples for quality control purposes and for lab index calculation. In our assay, IAA positivity is any value greater than an index of 0.006.
4. The results of the analysis of negative and positive controls from each assay should be plotted in a preestablished Shewhart plot with means ± 3 SD to monitor the assay drift and evaluate assay performance. Our positive-control range should be within 3 SD. The negative control must be <0.006 for results of the assay run to be utilized,
5. The result for every positive sample in the first run is confirmed by repeating that sample in a different assay. If the second confirmatory assay comes out negative, a third assay is necessary. The results of two assays which agree (e.g., +,+ or −,−) will be the final determination of a positive or negative result.

ECL GADA Assay

General Principle

The format of the ECL GADA assay is adapted from the ECL IAA assay except for acid treatment of serum. In a way similar to that of the ECL IAA assay, the molecule of a full-length human GAD65 protein is set out to be immobilized to a solid phase in a manner that preserves all critical determinants recognized by human GAD65 autoantibodies.

Procedure

Part I: Label Human GAD65 with Biotin and Sulfo-Tag

Important notes. Biotin and Sulfo-Tag powder should be dissolved just before the labeling procedure every time. The GAD65 must be stored at −80°C and thawed on ice before use. The protein in either the Tris or glycine buffer system should be replaced with 2-fold PBS buffer with a pH of 7.9 with the sizing spin column.

Procedure.
1. Calculate the molar ratio of GAD65 with biotin or Sulfo-Tag. We recommend using a 1:20 molar ratio for GAD65 labeling.
2. Mix GAD65 with biotin or Sulfo-Tag, cover the reaction tubes with aluminum foil to avoid light, and incubate them at room temperature for 1 h.
3. During the 1-h incubation, prepare the Zeba sizing spin column by washing the column three times with full-strength PBS buffer and centrifuge at 1,000 × *g* for 2 min each time in a centrifuge.
4. Stop the labeling reaction and purify labeled GAD65 by passing the reaction mixture through the prepared Zeba sizing spin columns and centrifuging it at 1,000 × *g* for 2 min.
5. Measure the protein concentration.
6. Aliquot the labeled GAD65 and store the specimens in a −80°C freezer.

Part II: Plate Capture Assay (2 Days)

Day 1.
Prepare the serum samples.

1. Each serum is diluted five times with PBS.
2. Prepare antigen buffer containing both biotin and Sulfo-Tag-labeled GAD65 with a concentration of 125 ng/ml of Sulfo-Tag-labeled GAD65 and 500 ng/ml of biotin-labeled GAD65.
3. Mix 5 μl of diluted serum with 35 μl of labeled antigen solution per well in a PCR plate.
4. Cover the plate with sealing foil to avoid light.
5. Shake the plate at room temperature on the low setting for 1 to 2 h.
6. Put it in a 4°C refrigerator to incubate overnight (18 to 24 h).

Prepare the streptavidin plate.

1. Let an MSD streptavidin plate(s) come to room temperature.
2. Add 150 μl of 3% blocker A (in PBS) per well.
3. Cover the plate with foil.
4. Incubate it in a 4°C refrigerator overnight.

Day 2.
1. Remove the streptavidin plate from the refrigerator. Dump out the buffer and bang the plate on a paper towel to dry it.
2. Wash the plate three times with 150 μl of PBST.
3. Transfer 30 μl of the serum-antigen mixture into the MSD streptavidin plate.

4. Cover the plate with foil to avoid light and shake it at room temperature for 1 h on the low speed setting.
5. Dump out the incubates and wash the plate three times with 150 μl of PBST.
6. Add 150 μl/well of 2-fold Read buffer (avoid any bubbles).
7. Count the reactivity on an MSD machine.

Standardization, Quality Control, and Quality Assurance

1. The mouse anti-human GAD65 monoclonal antibody is used as an internal-standard positive control. The monoclonal antibody should be diluted with a normal human serum specimen and treated identically to human serum in the assay.
2. The laboratory should keep a large enough volume of the positive- and negative-control sera for long-term use. Each of these serum samples should be aliquoted and stored at −20°C.
3. All the assays are run in duplicate and must include positive- and negative-control samples for quality control purposes and for lab index calculation. In our assay, GAA positivity is any value greater than an index of 0.023.
4. The results of an analysis of negative and positive controls from each assay should be plotted in a preestablished Shewhart plot with means ± 3 SD to monitor the assay drift and evaluate the assay's performance. Our positive-control range should be within 3 SD. The negative control must be >0.023 for the results of the assay run to be utilized.
5. Every positive sample in the first run is confirmed by repeating that sample in a different assay. If the second confirmatory assay comes out negative, a third assay is necessary. The results of two assays which agree (e.g., +,+ or −,−) will be the final determination of a positive or negative result.

Other Technology

ELISA

For most autoimmune disorders and for basic immunologic research, ELISAs employing plate-bound antigen are popular. Many laboratories and biotech companies have adopted this method for anti-islet autoantibody assays, and different ELISA kits are available. Multiple workshops utilizing sera from patients with type 1 diabetes and multiple mouse strains have demonstrated that standard ELISA formats lack both sensitivity and specificity compared to fluid-phase radioassay formats (92). For insulin autoantibodies, the ELISA formats were able to detect high-capacity antibodies following insulin immunization (e.g., therapy with subcutaneous injections of human insulin) but not the insulin autoantibodies of prediabetic individuals. To date, in international workshops, a modified ELISA for GAA attained a level of specificity and sensitivity equivalent to those of the radioassays. This assay depends on using a free-antibody arm to capture biotinylated GAD (developed by Kronus and published in May of 2003 [85]). In brief, the ELISA plate was coated with GAD65 protein, and 25 μl of test sera was added to the plate before incubation with shaking for 1 h at room temperature. The wells were then washed three times with washing buffer, and 100 μl of biotinylated GAD65 was added. After another hour of incubation, the plate wells were washed three times and the plate was incubated for 20 min with 100 μl of streptavidin-peroxidase conjugate. A wash step was then followed by addition of 100 μl of tetramethylbenzidine and, after 20 min, 100 μl of 0.5-mol/liter H_2SO_4. Absorbance at 405 and 450 nm was then measured. This "ELISA" is actually a form of a fluid-phase reaction of labeled antigen with bound autoantibody, with specificity enhanced by the requirement for each arm of the immunoglobulin to react with antigen. Most recently, a ZnT8A ELISA kit by Kronus using a protocol format identical to that of the GAA ELISA kit has also achieved a sensitivity equivalent to that of the ZnT8A radioassay with less specificity than in the 2012 IASP international workshop.

Epitope Assays

Comparisons of the epitope repertoires of autoantibodies to insulin, GAD65, and IA-2 provide a tool to further analyze type 1 diabetes-related autoantibodies (75, 82, 93). Most type 1 diabetes sera target only GAD65 protein epitopes, dependent on protein conformation, and do not bind GAD65 protein fragments or react with denatured GAD65 protein with immunoblotting. In contrast, sera from patients with stiff-man syndrome (SMS) have antibodies that bind GAD65 protein fragments consisting of N-terminal, middle, and C-terminal regions (73). The majority of type 1 diabetes sera target more than two epitopes on IA-2 molecules, and epitope spreading may be an indicator of the risk of progression to type 1A diabetes (94). For the methodology of these epitope assays, laboratories usually use the same radioimmunoassay format as described above with cloned protein fragments containing the epitope to be utilized or with chimeric proteins (e.g., GAD65/GAD67), which contain epitopes of GAD65 and sequences of non-antibody-reactive GAD67 to retain protein conformation. For IAA epitope testing, proinsulin, insulin analogs, and insulin molecules from different species are used as competitive inhibitors in the regular IAA radioassay.

Autoantibody Subclass and Isotype Determination

Some reports have shown heterogeneity of immunoglobulin subclass antibodies to GAD65 in newly diagnosed type 1A diabetic patients and ICA-positive first-degree relatives who progressed or did not progress to diabetes (95). New-onset diabetic patients and progressors were found to have a predominance of IgG1, GAA, and ICA, while nonprogressors had predominantly IgG2 and/or IgG4 (94). A study on IAA also indicated that heterogeneity of IgG subclass is related to the risk of developing type 1A diabetes (96).

For the methodology of isotype analysis, a modified standard radioimmunoassay format is used. On day 1, reagent and serum mixtures are prepared for overnight incubation at 4°C in two separate tubes. In one tube, 2.5 μl of serum is incubated with 25 μl of radiolabeled antigen, and in the other tube, 5 μl of biotin-labeled anti-IgG subclass monoclonal antibody with 10 μl of streptavidin-Sepharose (per well) is added (BD Pharmingen), with shaking. On day 2, after the Sepharose incubation tube is washed three times, the contents of the two incubation tubes are mixed together in a 96-well filtration plate and incubated for 1 h at 4°C with shaking. The rest of the steps for washing and counting are the same as described above.

Interpretation

Analysis of Data

In general, it is important to utilize assays for anti-islet autoimmunity that have high specificity, usually defined as specificity of ≥99%. Even with specificities set at this level, if one measures three different anti-islet autoantibodies, 3% of the "normal" population will express one or more of the autoantibodies. Obviously, expression of multiple anti-islet

autoantibodies is a relatively rare event, though even for low-risk populations (for instance, 1/300 general-population children in the United States develop type 1 diabetes), there will be some individuals expressing anti-islet autoantibodies who may never progress to overt diabetes. As with all autoantibody tests, it is also important to recognize that a repeat assay of the same sample (particularly for levels just above the cutoff points of "positivity") may fail to confirm the presence of the autoantibody as often as one-third of the time (97). Repeat analysis of an independent sample is important to assess risk, as subjects with "transient" islet autoantibodies are at relatively low risk. After the onset of type 1A diabetes, a significant subset of patients lose (over decades) their GAD65, IA-2, and ZnT8 anti-islet autoantibodies.

A major caveat regarding insulin antibodies is that most individuals treated with subcutaneous insulin (even human insulin) will develop insulin antibodies. Thus, after approximately 10 days of insulin therapy, the presence of insulin antibodies (cannot be distinguished from autoantibodies with current assays) should not be used to diagnose type 1A diabetes.

Clinical Application

Anti-islet autoantibodies find their primary application in the differential diagnosis of the forms of diabetes and in predicting the risk of progression to overt diabetes.

It is clear that adults presenting with diabetes who express anti-islet autoantibodies (in particular, GAD65 autoantibodies) more rapidly progress to utilization of insulin than typical patients with type 2 diabetes (98). For many endocrinologists, having the diagnosis of autoimmune diabetes leads to the immediate initiation of insulin therapy rather than a trial of oral hypoglycemic agents. In children, anti-islet autoantibodies have become increasingly helpful in distinguishing the different forms of diabetes, as there have been increasing incidences of both type1A diabetes and type 2 diabetes (99) as well as an overall increase in obesity rates. Making the correct diagnosis is important not only for starting the correct treatment but also for monitoring of diabetes complications. A diagnosis of type 1A diabetes alerts one to the risk of accompanying autoimmune disorders (e.g., thyroid autoimmunity in 25% of patients, celiac disease in 5 to 10% of patients, and Addison's disease in approximately 1/200). Prediction of type 1A diabetes at present is based upon genetic, immunologic, and metabolic information. Though genetic markers can identify varying risk, it is only once autoimmunity has begun (marked by the presence of multiple autoantibodies to pancreatic beta-cell antigens, such as insulin, GAD65, IA-2, or ZnT8) that a high positive predictive value (>90%) can be achieved, and multiple autoantibodies are present in the great majority of prediabetics (57–59). Research studies such as DAISY have shown that children identified to be at risk for type 1A diabetes through islet autoantibody testing and educated about diabetes rarely present with ketoacidosis and have markedly lower glucose levels at diagnosis (100, 101).

HYPOPHYSITIS

(This section was written by Ludovica De Vincentiis, Adriana Ricciuti, Alessandra De Remigis, and Patrizio Caturegli.)

Detection of Pituitary Antibodies in Autoimmune Hypophysitis

The detection of serum antibodies recognizing the pituitary gland has been technically challenging, mainly because the targeted pituitary autoantigens still remain unknown (102) and because these antibodies seem to be present at titers that are low and decrease over time. After a brief review of autoimmune hypophysitis, the condition in which pituitary antibodies are predicted to be the highest, we will review the techniques used over the years to measure pituitary antibodies, focusing on indirect immunofluorescence (IF) because it remains the most widely used detection system.

Autoimmune Hypophysitis

The term pituitary autoimmunity comprises a spectrum of clinico-pathological conditions related to an autoimmune inflammation of the pituitary gland, ranging from biopsy-proven lymphocytic (autoimmune) hypophysitis to clinically suspected hypophysitis and to the sole finding of pituitary antibodies in patients with pituitary hormone deficiencies or other autoimmune diseases or even in healthy subjects. Autoimmune hypophysitis, first reported in 1962 by Goudie and Pinkerton (103), can affect either the anterior and/or posterior pituitary lobe, be present in isolation or in association with other autoimmune diseases (such as Hashimoto thyroiditis), and be primary, meaning without identifiable causes, or secondary to a traceable event, like the injection of a monoclonal antibody blocking cytotoxic T-lymphocyte antigen 4 (104). The disease is more common in women than in men; in women, it has a unique temporal association with pregnancy or the early postpartum condition (105), although some pathological variants, like the one related to IgG4-producing plasma cells, predominate in men (106). Autoimmune hypophysitis is rare but nevertheless clinically significant since it enters into the differential diagnosis of all the other non-hormone-secreting sellar masses, with which it shares similar clinical and radiological findings (107), especially the vastly more common condition of nonfunctioning pituitary adenoma. Currently, a diagnosis of certainty can be established only after pathological examination of a pituitary biopsy specimen, which is obtained through a relatively invasive procedure, such as transsphenoidal surgery. Theoretically, the demonstration of pituitary antibodies should be useful in distinguishing a mass that has an autoimmune pathogenesis from masses that arise through neoplastic, developmental, vascular, or infectious mechanisms. Practically, however, pituitary antibodies have not yet entered the clinical arena and are still detected predominantly in a research setting.

Techniques Used To Detect Pituitary Antibodies

Pituitary antibodies have been measured mainly by non-antigen-specific techniques, considering that the targeted pituitary autoantigens remain to be validated, but also by antigen-specific assays as novel candidate autoantigens are discovered. The first description in humans of antibodies recognizing pituitary antigens was made in 1965 using a complement consumption test based on protein homogenates prepared from human adenohypophysis (108). The authors tested 128 women with Sheehan syndrome before, at, and after delivery and reported that pituitary antibodies, absent at the end of pregnancy and delivery, developed in 23 (18%) puerperae between 5 and 7 months postpartum and later correlated with signs and symptoms of hypopituitarism. Following this initial report, which was not carried out further, the story of human pituitary antibodies really began in 1975, when they were measured by IF, and then unfolded to include newer techniques (Table 2). We will briefly review the less common techniques and then focus on IF, which remains the most widely published approach.

TABLE 2 Summary of techniques used to detect pituitary antibodies in human serum[a]

Technique	Initial paper		Total no. of papers
	Yr of publication	First author (reference)	
Non-antigen-specific techniques:			
Complement consumption	1965	Engelberth (108)	1
Indirect immunofluorescence	1975	Bottazzo (119)	118
Western blotting	1993	Crock (109)	20
ELISA	1998	Kobayashi (111)	6
Antigen-specific techniques:			
In vitro transcription/translation for:			
Growth hormone, PGSF1a, and PGSF2	2002	Tanaka (114)	1
Alpha-enolase	2003	Tatsumi (115)	1
Prohormone convertases 1, 2, and 7B2	2003	Tatsumi (115)	1
Tudor domain-containing protein 6	2007	Bensing (116)	1
Testis antigen 10	2011	Smith (117)	1
Corticotroph-specific transcription factor TPIT	2012	Smith (118)	1
Western blotting for:			
Corticotroph, thyrotroph, growth hormone	1993	Crock (109)	1
Growth hormone	2001	Takao (112)	1
Alpha-enolase	2002	O'Dwyer (113)	1
ELISA for:			
Growth hormone	1992	Wilkin (••)	1
Surface plasmon resonance for:			
Growth hormone	2013	German (••)	1

[a]The year and first author of the initial publication, as well as the overall number of publications, are indicated.

Western Blotting

In Western blotting, whole protein antigens are extracted from normal pituitary glands within a short period postmortem, size fractionated on a gel by electrophoresis, blotted onto a solid support, and then reacted with the patient's antibodies. Pituitary Western blotting was first reported in 1993 to study 19 children with idiopathic growth hormone deficiency, comparing their reactivities to those of 27 healthy controls (109). The authors found that 2 (10%) patients specifically recognized a 43- or 45-kDa pituitary membrane protein that was not recognized by healthy controls. Over the ensuing 2 decades, approximately 20 additional papers have studied pituitary antibodies by Western blotting. Results have been inconclusive, and it is overall safe to say that Western blotting, although useful in a discovery-driven mode, has not yet translated into clinically useful diagnostic tests for pituitary autoimmunity.

ELISA

In enzyme-linked immunosorbent assay (ELISA), wells of a microtiter plate are coated with proteins and incubated with the patient's antibodies. The binding is then detected by the addition of a commercial antibody that recognizes human immunoglobulins and that has been conjugated with a substance that allows color change detection. Whole pituitary protein extracts have been used to coat ELISA plates in an effort to express pituitary antibody results more quantitatively, rather than as binary values (present/absent) or titers. The first studies utilizing this approach were published in 1998 for patients with polyendocrine autoimmunity (110) or non-insulin-dependent diabetes mellitus (111). A few additional studies based on ELISA detection have been published since then. Overall, this ELISA has poor sensitivity and specificity, likely due to the use of crude pituitary protein extract as the antigen, and has no clinical value.

In Vitro Transcription/Translation Followed by Immunoprecipitation

In this assay, the cDNA encoding the protein of interest is incubated *in vitro* with the molecules necessary to synthesize mRNA and translate a protein in which the amino acid methionine is radiolabeled. The patient serum is then incubated with the radiolabeled protein, and the potential binding of antibodies to this protein is revealed by immunoprecipitation and counting of the radioactivity. It is a very useful approach to validate new candidate antigens as they are discovered through library screening or proteomics. It has been applied to numerous pituitary-gland-specific or -related targets: growth hormone (112), alpha-enolase (113), pituitary gland-specific factor 1a and 2 (114), prohormone convertases 1 and 2 and their regulatory protein 7B2 (115), tudor domain-containing protein 6 (116), testis antigen 10 (117), and the corticotroph transcription factor TPIT (118). As with Western blotting and ELISA, the *in vitro* transcription/translation technique, however, has not yet proven useful in the clinical arena since antibodies to the candidate antigens indicated above cannot reliably identify patients with autoimmune hypophysitis before surgery or distinguish them from patients with other, non-immune-related pituitary masses.

Indirect Immunofluorescence

The first successful detection of pituitary antibodies by IF was reported in 1975 by Bottazzo and colleagues in patients

with polyendocrine autoimmune diseases (119). Those authors found that 19 of 287 patients (7%) had serum antibodies recognizing cytosolic antigens in the human anterior pituitary gland. Using four of the strongest sera, they were then able to show that these antibodies recognized antigens contained in granules of prolactin-secreting cells but not prolactin itself (119). From 1975 to 2013, a total of 118 papers, 42 cohort studies, and 76 case reports have reported the measurement of pituitary antibodies by IF using the pituitary gland as the experimental substrate. These papers analyzed patients from a wide spectrum of conditions, ranging from biopsy-proven hypophysitis to cryptorchidism, often comparing results to a smaller group of healthy controls. Authors used different pituitary gland species (human, baboon, rat, *Macaca mulatta*, bovine, guinea pig, sheep, swine), different section fixatives, and different blocking solutions, in part explaining the large variability in the results. The IF protocol used in our laboratory (120) is presented below.

Pituitary Collection and Sectioning

Human pituitary glands are collected at autopsy within 24 h of death, embedded in optimal cutting temperature compound, and frozen on dry ice. Four- to 5-μm sections are then cut at the cryostat, attached to Superfrost Plus microscope slides, and allowed to air dry.

Fixation

Sections are fixed for 20 min at room temperature in alumina-filtered ice-cold acetone, with the goal of avoiding additional tissue breakdown during the staining procedure and thus maintaining a better tissue morphology. Fixation, instead, does not seem to negatively affect antigenicity (121).

Blocking of Unwanted Antibody Binding

The primary antibody (that is, the patient immunoglobulins) or the secondary fluorochrome-conjugated antibody can theoretically attach to tissue targets independently of their specific (Fab-mediated) binding sites. This "unwanted" attachment is thought to occur through two main mechanisms: the binding of the antibody tail (crystallizable fragment, Fc) to tissue Fc receptors (122) and the "adhesion" of the antibody to tissue macromolecules via ionic and hydrophobic interactions (123). Although the subject of blocking continues to remain the subject of considerable debate and some authors even question its utility (123), we block our sections for 1 h at room temperature in 0.25% casein.

Addition of Patient Serum

Sera are diluted 10 times in phosphate-buffered saline and then incubated for 1 h at room temperature on the sections.

Addition of the Fluorochrome-Conjugated Secondary Antibody

After three 2-min washes in phosphate-buffered saline supplemented with 0.2% Tween 20, sections are incubated for 1 h at room temperature in the dark with a fluorescein isothiocyanate (FITC)-conjugated $F(ab')_2$ anti-human IgG, diluted 1:400 in phosphate-buffered saline.

Nuclear Counterstaining and Quenching of Autofluorescence

Before the slide is coverslipped, sections are incubated for 10 min at room temperature in a solution of DAPI (4′,6-diamidino-2-phenylindole at 4 μl in 200 ml of phosphate-buffered saline), washed as described above, and then incubated under the same conditions in Sudan black B (0.3% in 70% ethanol), a dye known to quench autofluorescence (124).

Reporting of the Results

In addition to differing in substrate species, fixation, and blocking methods, publications have varied widely in the way IF results are reported. With IF being largely a subjective technique, it is important to develop an interpretation scheme that ensures consistency across samples and readers. After selecting intact and not peripherally located pituitary areas with a 10× objective, we scored sections for positivity using a 20× objective and considered positive those sections where stained cells were found in at least 2 of 10 fields. Positive sections were then classified according to area of involvement, cellular location, staining features, and staining intensity. The area of involvement can be classified as focal (Fig. 9A) or clustered (Fig. 9B) to indicate the staining of a few isolated cells within an acinus, or multiple aggregated cells. These two staining patterns have been identified since the very beginning of pituitary IF experiments and are called the type 1 (single-cell) or type 2 (multiple-cell) pattern by Pouplard and colleagues (125, 126). Cellular

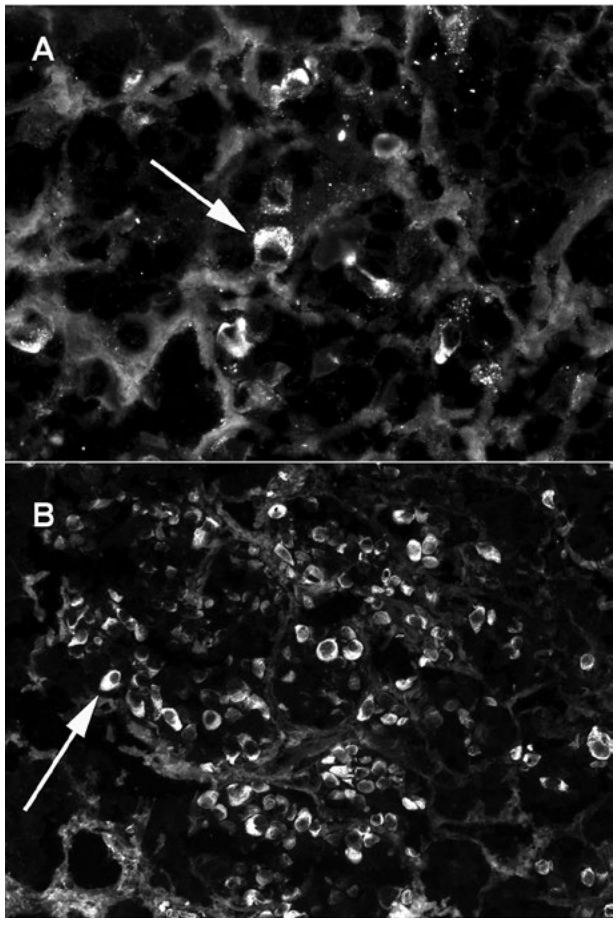

FIGURE 9 Detection of serum pituitary antibodies by indirect immunofluorescence using acetone-fixed cryostat sections cut from a human anterior pituitary gland. (A) A few isolated cells are recognized by the patient antibodies (type 1 pattern). The arrow shows the granularity, suggesting that antibodies recognize small vesicles scattered in the cytosol. (B) Multiple clustered cells are highlighted by the patient serum (type 2 pattern), which diffusely stains the entire cytosol (arrow).

location theoretically includes cytosolic, nuclear, plasma membrane, or nuclear membrane staining, although practically, pituitary antibodies stain predominantly the cytosol. The staining can be diffuse (homogeneous) when it involves uniformly the entire cytosol, granular when numerous small vesicles are seen in the cytosol, reticular when fine filaments are scattered throughout the cytosol, perinuclear when a ring of staining encircles the nucleus, and mixed for a combination of the above (Fig. 9). The staining intensity can be classified as weak (+), moderate (++), or strong (+++).

Double IF Staining

If needed, it is possible to identify the type of anterior pituitary cell recognized by the patient antibodies by adding a commercial antihormone antibody along with the patient serum during the primary incubation. This commercial antibody, directed, for instance, against growth hormone or prolactin, is raised in a nonhuman species, and its binding can be detected with a secondary antibody directed against the immunoglobulins of that species and conjugated with a fluorochrome that is different from the fluorochrome used on the anti-human antibody secondary reagent. Through these double-IF studies, investigators have shown that patient antibodies most often recognize antigens that are different from the hormone itself (119).

Clinical Significance and Utility of Pituitary Antibodies

During the past 5 decades, numerous studies have measured pituitary antibodies in a variety of diseases, with the goal of developing a biomarker that can aid in the diagnosis and prognosis of patients with pituitary autoimmunity. Results, thus far, have been somewhat disappointing. If we limit the analysis to IF, which remains the technique most commonly published (Table 2), and analyze the 42 papers that have used the pituitary gland as the experimental substrate, we note that pituitary antibodies are indeed more common in patients with biopsy-proven hypophysitis (57% prevalence) (Table 3) than in patients with other conditions. However, these antibodies are also found in patients with conditions not typically associated with pituitary autoimmunity, such as traumatic brain injury, as well as in patients with other autoimmune diseases. It thus seems that pituitary antibodies, although significantly more common in disease than in health, do not currently associate with a particular disease in a form strong enough to make it clinically useful. It is to be predicted that the diagnostic validity of pituitary antibody tests will improve once pathogenic pituitary autoantigens are discovered and confirmed in the clinical arena.

Additional information can be gathered by refining the interpretation of the pituitary antibody results, which are typically reported as present or absent without further specifications. It has been apparent since the early studies that patients produce antibodies recognizing different types of anterior pituitary endocrine cells (119), as well as different antigenic components within a given cell (127), so that type 1 (single-cell) and type 2 (multiple-cell) stainings have been described (125, 126). After almost 3 decades, these two staining patterns have been shown to possess clinical relevance. In fact, patients with type 1 antibodies go on to develop various degrees of hypopituitarism, whereas those with type 2 antibodies do not acquire pituitary function defects (128).

In summary, the field of pituitary antibodies remains a work in progress. Advances will be made in the near future when standardizations in IF techniques and result interpretation are integrated and in the more distant future when the pathogenic pituitary autoantigens are finally identified and related to the various clinical facets and stages of pituitary autoimmunity.

TABLE 3 Summary of 42 cohort studies using IF and pituitary gland substrate to detect the presence of serum pituitary antibodies

Diagnosis	No. of papers	No. of patients	No. of IF-positive patients	% IF-positive patients
None (healthy controls)	31	2,115	40	2
Other pituitary diseases	11	881	108	12
Miscellaneous diseases	18	911	116	13
Isolated pituitary hormone deficiencies	10	350	67	19
Other autoimmune diseases (nonpituitary)	20	2,737	541	20
Traumatic brain injury	3	115	39	34
Hypophysitis (clinically suspected)	3	66	25	38
Hypophysitis (biopsy proven)	1	14	8	57

REFERENCES

Autoantibodies in Chronic Thyroiditis, Addison Disease, and Pernicious Anemia

1. **Rocchi R, Rose NR, Caturegli P.** 2008. Hashimoto thyroiditis, p 217–220. *In* Shoenfeld Y, Cervera R, Gershwin ME (ed), *Diagnostic Criteria in Autoimmune Diseases*. Humana Press, Totowa, NJ.
2. **Targovnik HM.** 2013. Thyroglobulin structure, function, and biosynthesis, p 74–92. *In* Braverman LE, Cooper DS (ed), *Werner & Ingbar's The Thyroid*, 10th ed. Lippincott Williams & Wilkins, Philadelphia, PA.
3. **Bigazzi PE, Burek CL, Rose NR.** 1992. Antibodies to tissue-specific, endocrine, gastrointestinal, and surface-receptor antigens, p 765–774. *In* Rose NR, Conway de Macario E, Fahey JL, Friedman H, Penn GM (ed), *Manual of Clinical Laboratory Immunology*, 4th ed. American Society for Microbiology, Washington, DC.
4. **Bresler HS, Burek CL, Hoffman WH, Rose N.** 1990. Autoantigenic determinants on human thyroglobulin. II. Determinants recognized by autoantibodies from patients with chronic autoimmune thyroiditis compared to healthy subjects. *Clin Immunol Immunopathol* **54:**76–86.
5. **Czarnocka B, Ruf J, Ferrand M, Carayon P, Lissitzky S.** 1985. Purification of the human thyroid peroxidase and its identification as the microsomal antigen involved in autoimmune thyroid diseases. *FEBS Lett* **190:**147–152. PubMed
6. **Kopp P.** 2013. Thyroid hormone synthesis, p 48–74. *In* Braverman LE, Cooper DS (ed), *Werner & Ingbar's The Thyroid*, 10th ed. Lippincott Williams & Wilkins, Philadelphia, PA.
7. **Burek CL, Bigazzi PE, Rose NR.** 2006. Endocrinopathies, p 1062–1067. *In* Detrick B, Hamilton RG, Folds JD (ed), *Manual of Molecular and Clinical Laboratory Immunology*, 7th ed. ASM, Washington, DC.

8. **Lazarus JH.** 1998. Prediction of postpartum thyroiditis. *Eur J Endocrinol* **139:**12–13. PubMed
9. **Hutfless S, Matos P, Talor MV, Caturegli P, Rose NR.** 2011. Significance of prediagnostic thyroid antibodies in women with autoimmune thyroid disease. *J Clin Endocrinol Metab* **96:**E1466–E1471. PubMed
10. **De Carvalho JF, Brandao Neto RA.** 2008. Autoimmune Addison disease or autoimmune adrenalitis, p 251–254. *In* Shoenfeld Y, Cervera R, Gershwin ME (ed), *Diagnostic Criteria in Autoimmune Diseases*. Humana Press, Totowa, NJ.
11. **Betterle C, Zanchetta R.** 2014. Adrenalitis, p 587–604. *In* Rose NR, Mackay IR (ed), *The Autoimmune Diseases*, 5th ed. Elsevier, Oxford, United Kingdom.
12. **Betterle C, Coco G, Zanchetta R.** 2005. Adrenal cortex autoantibodies in subjects with normal adrenal function. *Best Pract Res Clin Endocrinol Metab* **19:**85–99. PubMed
13. **Weetman AP.** 1995. Autoimmunity to steroid-producing cells and familial polyendocrine autoimmunity. *Baillieres Clin Endocrinol Metab* **9:**157–174. PubMed
14. **Toh B, Whittingham S, Alderucci F.** 2008. Autoimmune gastritis, p 315–321. *In* Shoenfeld Y, Cervera R, Gershwin ME (ed), *Diagnostic Criteria in Autoimmune Diseases*. Humana Press, Totowa, NJ.
15. **Jacobson DL, Gange SJ, Rose NR, Graham NMH.** 1997. Epidemiology and estimated population burden of selected autoimmune diseases in the United States. *Clin Immunol Immunopathol* **84:**223–243. PubMed
16. **Toh BH, Alderuccio F.** 2004. Pernicious anaemia. *Autoimmunity* **37:**357–361. PubMed
17. **van Driel IR, Tu E, Gleeson PA.** 2014. Autoimmune gastritis and pernicious anemia, p 619–631. *In* Rose NR, Mackay IR (ed), *The Autoimmune Diseases*, 5th ed. Elsevier, Oxford, United Kingdom.

Graves' Disease, Hyperthyroidism, and Antibodies to the Thyrotropin Receptor

18. **Adams DD, Purves HD.** 1956. Abnormal responses in the assay of thyrotropin. *Proc Univ Otago Med Sch* **34:**11–15.
19. **Endo K, Kasagi K, Konishi J, Ikekubo K, Okuno T, Takeda Y, Mori T, Torizuka K.** 1978. Detection and properties of TSH-binding inhibitor immunoglobulins in patients with Graves' disease and Hashimoto's thyroiditis. *J Clin Endocrinol Metab* **46:**734–739. PubMed
20. **McLachlan SM, Rapoport B.** 2013. Thyrotropin blocking autoantibodies and thyroid stimulating autoantibodies: potential mechanisms involved in the pendulum swinging from hypothyroidism to hyperthyroidism or vice versa. *Thyroid* **23:**14–24.
21. **Weetman AP, Yateman ME, Ealey PA, Black CM, Reimer CB, Williams RC Jr, Shine B, Marshall NJ.** 1990. Thyroid-stimulating antibody activity between different immunoglobulin G subclasses. *J Clin Invest* **86:**723–727. PubMed
22. **Latrofa F, Chazenbalk GD, Pichurin P, Chen CR, McLachlan SM, Rapoport B.** 2004. Affinity-enrichment of thyrotropin receptor autoantibodies from Graves' patients and normal individuals provides insight into their properties and possible origin from natural antibodies. *J Clin Endocrinol Metab* **89:**4734–4745. PubMed
23. **Sanders J, Chirgadze DY, Sanders P, Baker S, Sullivan A, Bhardwaja A, Bolton J, Reeve M, Nakatake N, Evans M, Richards T, Powell M, Miguel RN, Blundell TL, Furmaniak J, Smith BR.** 2007. Crystal structure of the TSH receptor in complex with a thyroid-stimulating autoantibody. *Thyroid* **17:**395–410. PubMed
24. **Chazenbalk GD, Latrofa F, McLachlan SM, Rapoport B.** 2004. Thyroid stimulation does not require antibodies with identical epitopes but does involve recognition of a critical conformation at the N terminus of the thyrotropin receptor A-subunit. *J Clin Endocrinol Metab* **89:**1788–1793. PubMed
25. **Sanders P, Young S, Sanders J, Kabelis K, Baker S, Sullivan A, Evans M, Clark J, Wilmot J, Hu X, Roberts E, Powell M, Núñez Miguel R, Furmaniak J, Rees Smith B.** 2011. Crystal structure of the TSH receptor (TSHR) bound to a blocking-type TSHR autoantibody. *J Mol Endocrinol* **46:**81–99. PubMed
26. **Smith BR, Hall R.** 1974. Thyroid-stimulating immunoglobulins in Graves' disease. *Lancet* **ii:**427–431. PubMed
27. **Southgate K, Creagh F, Teece M, Kingswood C, Rees Smith B.** 1984. A receptor assay for the measurement of TSH receptor antibodies in unextracted serum. *Clin Endocrinol (Oxf)* **20:**539–548. PubMed
28. **Perret J, Ludgate M, Libert F, Gerard C, Dumont JE, Vassart G, Parmentier M.** 1990. Stable expression of the human TSH receptor in CHO cells and characterization of differentially expressing clones. *Biochem Biophys Res Commun* **171:**1044–1050. PubMed
29. **Bolton J, Sanders J, Oda Y, Chapman C, Konno R, Furmaniak J, Rees Smith B.** 1999. Measurement of thyroid-stimulating hormone receptor autoantibodies by ELISA. *Clin Chem* **45:**2285–2287. PubMed
30. **Costagliola S, Morgenthaler NG, Hoermann R, Badenhoop K, Struck J, Freitag D, Poertl S, Weglöhner W, Hollidt JM, Quadbeck B, Dumont JE, Schumm-Draeger PM, Bergmann A, Mann K, Vassart G, Usadel KH.** 1999. Second generation assay for thyrotropin receptor antibodies has superior diagnostic sensitivity for Graves' disease. *J Clin Endocrinol Metab* **84:**90–97. PubMed
31. **Sanders J, Jeffreys J, Depraetere H, Evans M, Richards T, Kiddie A, Brereton K, Premawardhana LD, Chirgadze DY, Núñez Miguel R, Blundell TL, Furmaniak J, Rees Smith B.** 2004. Characteristics of a human monoclonal autoantibody to the thyrotropin receptor: sequence structure and function. *Thyroid* **14:**560–570. PubMed
32. **Smith BR, Bolton J, Young S, Collyer A, Weeden A, Bradbury J, Weightman D, Perros P, Sanders J, Furmaniak J.** 2004. A new assay for thyrotropin receptor autoantibodies. *Thyroid* **14:**830–835. PubMed
33. **Kamijo K, Ishikawa K, Tanaka M.** 2005. Clinical evaluation of third generation assay for thyrotropin receptor antibodies: the M22-biotin-based ELISA initiated by Smith. *Endocr J* **52:**525–529. PubMed
34. **McKenzie JM.** 1958. The bioassay of thyrotropin in serum. *Endocrinology* **63:**372–382. PubMed
35. **Hinds WE, Takai N, Rapoport B, Filetti S, Clark OH.** 1981. Thyroid-stimulating immunoglobulin bioassay using cultured human thyroid cells. *J Clin Endocrinol Metab* **52:**1204–1210. PubMed
36. **Kasagi K, Konishi J, Arai K, Misaki T, Iida Y, Endo K, Torizuka K.** 1986. A sensitive and practical assay for thyroid-stimulating antibodies using crude immunoglobulin fractions precipitated with polyethylene glycol. *J Clin Endocrinol Metab* **62:**855–862. PubMed
37. **Kasagi K, Konishi J, Iida Y, Tokuda Y, Arai K, Endo K, Torizuka K.** 1987. A sensitive and practical assay for thyroid-stimulating antibodies using FRTL-5 thyroid cells. *Acta Endocrinol (Copenh)* **115:**30–36. PubMed
38. **Toccafondi RS, Aterini S, Medici MA, Rotella CM, Tanini A, Zonefrati R.** 1980. Thyroid-stimulating antibody (TSab) detected in sera of Graves' patients using human thyroid cell cultures. *Clin Exp Immunol* **40:**532–539. PubMed
39. **Vitti P, Chiovato L, Lopez G, Lombardi A, Santini F, Mammoli C, Bassi P, Gryczynska M, Schipani E, Tosti-Balducci M, Pinchera A.** 1988. Measurement of TSAb directly in serum using FRTL-5 cells. *J Endocrinol Invest* **11:**313–317. PubMed
40. **Kasagi K, Konishi J, Iida Y, Ikekubo K, Mori T, Kuma K, Torizuka K.** 1982. A new in vitro assay for human thyroid

stimulator using cultured thyroid cells: effect of sodium chloride on adenosine 3′,5′-monophosphate increase. *J Clin Endocrinol Metab* **54:**108–114. PubMed

41. **Morgenthaler NG, Pampel I, Aust G, Seissler J, Scherbaum WA.** 1998. Application of a bioassay with CHO cells for the routine detection of stimulating and blocking autoantibodies to the TSH-receptor. *Horm Metab Res* **30:**162–168. PubMed
42. **Vitti P, Elisei R, Tonacchera M, Chiovato L, Mancusi F, Rago T, Mammoli C, Ludgate M, Vassart G, Pinchera A.** 1993. Detection of thyroid-stimulating antibody using Chinese hamster ovary cells transfected with cloned human thyrotropin receptor. *J Clin Endocrinol Metab* **76:**499–503. PubMed
43. **Watson PF, Ajjan RA, Phipps J, Metcalfe R, Weetman AP.** 1998. A new chemiluminescent assay for the rapid detection of thyroid stimulating antibodies in Graves' disease. *Clin Endocrinol (Oxf)* **49:**577–581. PubMed
44. **Kamijo K, Murayama H, Uzu T, Togashi K, Olivo PD, Kahaly GJ.** 2011. Similar clinical performance of a novel chimeric thyroid-stimulating hormone receptor bioassay and an automated thyroid-stimulating hormone receptor binding assay in Graves' disease. *Thyroid* **21:**1295–1299. PubMed
45. **Evans M, Sanders J, Tagami T, Sanders P, Young S, Roberts E, Wilmot J, Hu X, Kabelis K, Clark J, Holl S, Richards T, Collyer A, Furmaniak J, Smith BR.** 2010. Monoclonal autoantibodies to the TSH receptor, one with stimulating activity and one with blocking activity, obtained from the same blood sample. *Clin Endocrinol (Oxf)* **73:**404–412. PubMed
46. **Tozzoli R, Bagnasco M, Giavarina D, Bizzaro N.** 2012. TSH receptor autoantibody immunoassay in patients with Graves' disease: improvement of diagnostic accuracy over different generations of methods. Systematic review and meta-analysis. *Autoimmun Rev* **12:**107–113. PubMed
47. **McKee A, Peyerl F.** 2012. TSI assay utilization: impact on costs of Graves' hyperthyroidism diagnosis. *Am J Manag Care* **18:**e1–e14. PubMed
48. **Yanagisawa T, Sato K, Kato Y, Shimizu S, Takano K.** 2005. Rapid differential diagnosis of Graves' disease and painless thyroiditis using total T3/T4 ratio, TSH, and total alkaline phosphatase activity. *Endocr J* **52:**29–36. PubMed
49. **Barbesino G, Tomer Y.** 2013. Clinical review: clinical utility of TSH receptor antibodies. *J Clin Endocrinol Metab* **98:**2247–2255. PubMed
50. **Carella C, Mazziotti G, Sorvillo F, Piscopo M, Cioffi M, Pilla P, Nersita R, Iorio S, Amato G, Braverman LE, Roti E.** 2006. Serum thyrotropin receptor antibodies concentrations in patients with Graves' disease before, at the end of methimazole treatment, and after drug withdrawal: evidence that the activity of thyrotropin receptor antibody and/or thyroid response modify during the observation period. *Thyroid* **16:**295–302. PubMed
51. **Massart C, Gibassier J, d'Herbomez M.** 2009. Clinical value of M22-based assays for TSH-receptor antibody (TRAb) in the follow-up of antithyroid drug treated Graves' disease: comparison with the second generation human TRAb assay. *Clin Chim Acta* **407:**62–66. PubMed
52. **Tamai H, Kasagi K, Takaichi Y, Takamatsu J, Komaki G, Matsubayashi S, Konishi J, Kuma K, Kumagai LF, Nagataki S.** 1989. Development of spontaneous hypothyroidism in patients with Graves' disease treated with antithyroidal drugs: clinical, immunological, and histological findings in 26 patients. *J Clin Endocrinol Metab* **69:**49–53. PubMed
53. **Kamijo K.** 2007. TSH-receptor antibodies determined by the first, second and third generation assays and thyroid-stimulating antibody in pregnant patients with Graves' disease. *Endocr J* **54:**619–624. PubMed
54. **Stagnaro-Green A, Abalovich M, Alexander E, Azizi F, Mestman J, Negro R, Nixon A, Pearce EN, Soldin OP, Sullivan S, Wiersinga W, American Thyroid Association Taskforce on Thyroid Disease During Pregnancy and Postpartum.** 2011. Guidelines of the American Thyroid Association for the diagnosis and management of thyroid disease during pregnancy and postpartum. *Thyroid* **21:**1081–1125. PubMed

Autoantibodies in Diabetes

55. **American Diabetes Association.** 2013. Diagnosis and classification of diabetes mellitus. *Diabetes Care* **36**(Suppl 1)**:**S67–S74. PubMed
56. **Steck AK, Pugliese A, Eisenbarth GS.** 2012. Chapter 7. Type 1 diabetes mellitus of man: genetic susceptibility and resistance. *In* Eisenbarth GS (ed), *Type 1 Diabetes: Cellular, Molecular & Clinical Immunology*. Barbara Davis Center for Childhood Diabetes, University of Colorado, Denver, CO. www.barbaradaviscenter.org.
57. **Bingley PJ, Gale EA, European Nicotinamide Diabetes Intervention Trial (ENDIT) Group.** 2006. Progression to type 1 diabetes in islet cell antibody-positive relatives in the European Nicotinamide Diabetes Intervention Trial: the role of additional immune, genetic and metabolic markers of risk. *Diabetologia* **49:**881–890. PubMed
58. **Orban T, Sosenko JM, Cuthbertson D, Krischer JP, Skyler JS, Jackson R, Yu L, Palmer JP, Schatz D, Eisenbarth G, Diabetes Prevention Trial-Type 1 Study Group.** 2009. Pancreatic islet autoantibodies as predictors of type 1 diabetes in the Diabetes Prevention Trial-Type 1. *Diabetes Care* **32:**2269–2274. PubMed
59. **Siljander HT, Simell S, Hekkala A, Lähde J, Simell T, Vähäsalo P, Veijola R, Ilonen J, Simell O, Knip M.** 2009. Predictive characteristics of diabetes-associated autoantibodies among children with HLA-conferred disease susceptibility in the general population. *Diabetes* **58:**2835–2842. PubMed
60. **Steck AK, Johnson K, Barriga KJ, Miao D, Yu L, Hutton JC, Eisenbarth GS, Rewers MJ.** 2011. Age of islet autoantibody appearance and mean levels of insulin, but not GAD or IA-2 autoantibodies, predict age of diagnosis of type 1 diabetes: diabetes autoimmunity study in the young. *Diabetes Care* **34:**1397–1399. PubMed
61. **Ziegler AG, Rewers M, Simell O, Simell T, Lempainen J, Steck A, Winkler C, Ilonen J, Veijola R, Knip M, Bonifacio E, Eisenbarth GS.** 2013. Seroconversion to multiple islet autoantibodies and risk of progression to diabetes in children. *JAMA* **309:**2473–2479. PubMed
62. **Williams AJK, Bingley PJ, Bonifacio E, Palmer JP, Gale EAM.** 1997. A novel micro-assay for insulin autoantibodies. *J Autoimmun* **10:**473–478. PubMed
63. **Baekkeskov S, Aanstoot HJ, Christgau S, Reetz A, Solimena M, Cascalho M, Folli F, Richter-Olesen H, De Camilli P.** 1990. Identification of the 64K autoantigen in insulin-dependent diabetes as the GABA-synthesizing enzyme glutamic acid decarboxylase. *Nature* **347:**151–156. PubMed
64. **Gianani R, Rabin DU, Verge CF, Yu L, Babu SR, Pietropaolo M, Eisenbarth GS.** 1995. ICA512 autoantibody radioassay. *Diabetes* **44:**1340–1344. PubMed
65. **Wenzlau JM, Juhl K, Yu L, Moua O, Sarkar SA, Gottlieb P, Rewers M, Eisenbarth GS, Jensen J, Davidson HW, Hutton JC.** 2007. The cation efflux transporter ZnT8 (Slc30A8) is a major autoantigen in human type 1 diabetes. *Proc Natl Acad Sci USA* **104:**17040–17045. PubMed
66. **Bottazzo GF, Florin-Christensen A, Doniach D.** 1974. Islet-cell antibodies in diabetes mellitus with autoimmune polyendocrine deficiencies. *Lancet* **ii:**1279–1283. PubMed
67. **Lendrum R, Walker G, Gamble DR.** 1975. Islet-cell antibodies in juvenile diabetes mellitus of recent onset. *Lancet* **i:**880–882. PubMed
68. **Maclaren NK, Huang SW, Fogh J.** 1975. Antibody to cultured human insulinoma cells in insulin-dependent diabetes. *Lancet* **i:**997–1000. PubMed

69. **Bleich D, Polak M, Chen S, Swiderek KM, Lévy-Marchal C.** 1999. Sera from children with type 1 diabetes mellitus react against a new group of antigens composed of lysophospholipids. *Horm Res* **52:**86–94. PubMed
70. **Colman PG, Nayak RC, Campbell IL, Eisenbarth GS.** 1988. Binding of cytoplasmic islet cell antibodies is blocked by human pancreatic glycolipid extracts. *Diabetes* **37:**645–652. PubMed
71. **Notkins AL, Lu J, Li Q, VanderVegt FP, Wasserfall C, Maclaren NK, Lan MS.** 1996. IA-2 and IA-2 beta are major autoantigens in IDDM and the precursors of the 40 kDa and 37 kDa tryptic fragments. *J Autoimmun* **9:**677–682. PubMed
72. **Rabin DU, Pleasic SM, Shapiro JA, Yoo-Warren H, Oles J, Hicks JM, Goldstein DE, Rae PMM.** 1994. Islet cell antigen 512 is a diabetes-specific islet autoantigen related to protein tyrosine phosphatases. *J Immunol* **152:**3183–3188. PubMed
73. **Daw K, Ujihara N, Atkinson M, Powers AC.** 1996. Glutamic acid decarboxylase autoantibodies in stiff-man syndrome and insulin-dependent diabetes mellitus exhibit similarities and differences in epitope recognition. *J Immunol* **156:**818–825. PubMed
74. **Hagopian WA, Michelsen B, Karlsen AE, Larsen F, Moody A, Grubin CE, Rowe R, Petersen J, McEvoy R, Lernmark A.** 1993. Autoantibodies in IDDM primarily recognize the 65,000-M(r) rather than the 67,000-M(r) isoform of glutamic acid decarboxylase. *Diabetes* **42:**631–636. PubMed
75. **Park YS, Kawasaki E, Kelemen K, Yu L, Schiller MR, Rewers M, Mizuta M, Eisenbarth GS, Hutton JC.** 2000. Humoral autoreactivity to an alternatively spliced variant of ICA512/IA-2 in type I diabetes. *Diabetologia* **43:**1293–1301. PubMed
76. **Sladek R, Rocheleau G, Rung J, Dina C, Shen L, Serre D, Boutin P, Vincent D, Belisle A, Hadjadj S, Balkau B, Heude B, Charpentier G, Hudson TJ, Montpetit A, Pshezhetsky AV, Prentki M, Posner BI, Balding DJ, Meyre D, Polychronakos C, Froguel P.** 2007. A genome-wide association study identifies novel risk loci for type 2 diabetes. *Nature* **445:**881–885. PubMed
77. **Wenzlau JM, Liu Y, Yu L, Moua O, Fowler KT, Rangasamy S, Walters J, Eisenbarth GS, Davidson HW, Hutton JC.** 2008. A common nonsynonymous single nucleotide polymorphism in the SLC30A8 gene determines ZnT8 autoantibody specificity in type 1 diabetes. *Diabetes* **57:**2693–2697. PubMed
78. **Palmer JP, Asplin CM, Clemons P, Lyen K, Tatpati O, Raghu PK, Paquette TL.** 1983. Insulin antibodies in insulin-dependent diabetics before insulin treatment. *Science* **222:**1337–1339. PubMed
79. **Eisenbarth GS, Gianani R, Yu L, Pietropaolo M, Verge CF, Chase HP, Redondo MJ, Colman P, Harrison L, Jackson R.** 1998. Dual-parameter model for prediction of type I diabetes mellitus. *Proc Assoc Am Physicians* **110:**126–135. PubMed
80. **Wang J, Miao D, Babu S, Yu J, Barker J, Klingensmith G, Rewers M, Eisenbarth GS, Yu L.** 2007. Prevalence of autoantibody-negative diabetes is not rare at all ages and increases with older age and obesity. *J Clin Endocrinol Metab* **92:**88–92. PubMed
81. **Yu L, Robles DT, Abiru N, Kaur P, Rewers M, Kelemen K, Eisenbarth GS.** 2000. Early expression of antiinsulin autoantibodies of humans and the NOD mouse: evidence for early determination of subsequent diabetes. *Proc Natl Acad Sci USA* **97:**1701–1706. PubMed
82. **Achenbach P, Koczwara K, Knopff A, Naserke H, Ziegler AG, Bonifacio E.** 2004. Mature high-affinity immune responses to (pro)insulin anticipate the autoimmune cascade that leads to type 1 diabetes. *J Clin Invest* **114:**589–597. PubMed
83. **Uchigata Y, Kuwata S, Tsushima T, Tokunaga K, Miyamoto M, Tsuchikawa K, Hirata Y, Juji T, Omori Y.** 1993. Patients with Graves' disease who developed insulin autoimmune syndrome (Hirata disease) possess HLA-Bw62/Cw4/DR4 carrying DRB1*0406. *J Clin Endocrinol Metab* **77:**249–254. PubMed
84. **Bonifacio E, Yu L, Williams AK, Eisenbarth GS, Bingley PJ, Marcovina SM, Adler K, Ziegler AG, Mueller PW, Schatz DA, Krischer JP, Steffes MW, Akolkar B.** 2010. Harmonization of glutamic acid decarboxylase and islet antigen-2 autoantibody assays for National Institute of Diabetes and Digestive and Kidney Diseases consortia. *J Clin Endocrinol Metab* **95:**3360–3367. PubMed
85. **Brooking H, Ananieva-Jordanova R, Arnold C, Amoroso M, Powell M, Betterle C, Zanchetta R, Furmaniak J, Smith BR.** 2003. A sensitive non-isotopic assay for GAD65 autoantibodies. *Clin Chim Acta* **331:**55–59. PubMed
86. **Yu L, Miao D, Scrimgeour L, Johnson K, Rewers M, Eisenbarth GS.** 2012. Distinguishing persistent insulin autoantibodies with differential risk: nonradioactive bivalent proinsulin/insulin autoantibody assay. *Diabetes* **61:**179–186. PubMed
87. **Miao D, Guyer KM, Dong F, Jiang L, Steck AK, Rewers M, Eisenbarth GS, Yu L.** 2013. GAD65 autoantibodies detected by electrochemiluminescence (ECL) assay identify high risk for type 1 diabetes. *Diabetes* **62:**4174–4178.
88. **Yu L, Dong F, Miao D, Fouts AR, Wenzlau JM, Steck AK.** 2013. Proinsulin/insulin autoantibodies measured with electrochemiluminescent assay are the earliest indicator of prediabetic islet autoimmunity. *Diabetes Care* **36:**2266–2270. PubMed
89. **Rojas M, Hulbert C, Thomas JW.** 2001. Anergy and not clonal ignorance determines the fate of B cells that recognize a physiological autoantigen. *J Immunol* **166:**3194–3200. PubMed
90. **Babaya N, Liu E, Miao D, Li M, Yu L, Eisenbarth GS.** 2009. Murine high specificity/sensitivity competitive europium insulin autoantibody assay. *Diabetes Technol Ther* **11:**227–233. PubMed
91. **Castaño L, Ziegler AG, Ziegler R, Shoelson S, Eisenbarth GS.** 1993. Characterization of insulin autoantibodies in relatives of patients with type I diabetes. *Diabetes* **42:**1202–1209. PubMed
92. **Liu E, Eisenbarth GS.** 2007. Accepting clocks that tell time poorly: fluid-phase versus standard ELISA autoantibody assays. *Clin Immunol* **125:**120–126. PubMed
93. **Ziegler AG, Hummel M, Schenker M, Bonifacio E.** 1999. Autoantibody appearance and risk for development of childhood diabetes in offspring of parents with type 1 diabetes: the 2-year analysis of the German BABYDIAB Study. *Diabetes* **48:**460–468. PubMed
94. **Bonifacio E, Scirpoli M, Kredel K, Füchtenbusch M, Ziegler AG.** 1999. Early autoantibody responses in prediabetes are IgG1 dominated and suggest antigen-specific regulation. *J Immunol* **163:**525–532. PubMed
95. **Couper JJ, Harrison LC, Aldis JJE, Colman PG, Honeyman MC, Ferrante A.** 1998. IgG subclass antibodies to glutamic acid decarboxylase and risk for progression to clinical insulin-dependent diabetes. *Hum Immunol* **59:**493–499. PubMed
96. **Achenbach P, Warncke K, Reiter J, Naserke HE, Williams AJ, Bingley PJ, Bonifacio E, Ziegler AG.** 2004. Stratification of type 1 diabetes risk on the basis of islet autoantibody characteristics. *Diabetes* **53:**384–392. PubMed
97. **Barker JM, Barriga KJ, Yu L, Miao D, Erlich HA, Norris JM, Eisenbarth GS, Rewers M, Diabetes Autoimmunity Study in the Young.** 2004. Prediction of autoantibody positivity and progression to type 1 diabetes: Diabetes Autoimmunity Study in the Young (DAISY). *J Clin Endocrinol Metab* **89:**3896–3902. PubMed

98. **Turner R, Stratton I, Horton V, Manley S, Zimmet P, Mackay IR, Shattock M, Bottazzo GF, Holman R, UK Prospective Diabetes Study Group.** 1997. UKPDS 25: autoantibodies to islet-cell cytoplasm and glutamic acid decarboxylase for prediction of insulin requirement in type 2 diabetes. *Lancet* **350:**1288–1293. PubMed
99. **Pinhas-Hamiel O, Zeitler P.** 1998. Type 2 diabetes in adolescents, no longer rare. *Pediatr Rev* **19:**434–435. PubMed
100. **Barker JM, Goehrig SH, Barriga K, Hoffman M, Slover R, Eisenbarth GS, Norris JM, Klingensmith GJ, Rewers M, DAISY Study.** 2004. Clinical characteristics of children diagnosed with type 1 diabetes through intensive screening and follow-up. *Diabetes Care* **27:**1399–1404. PubMed
101. **Triolo TM, Chase HP, Barker JM, DPT-1 Study Group.** 2009. Diabetic subjects diagnosed through the Diabetes Prevention Trial-Type 1 (DPT-1) are often asymptomatic with normal A1C at diabetes onset. *Diabetes Care* **32:**769–773. PubMed

Hypophysitis

102. **Caturegli P.** 2007. Autoimmune hypophysitis: an underestimated disease in search of its autoantigen(s). *J Clin Endocrinol Metab* **92:**2038–2040. PubMed
103. **Goudie RB, Pinkerton PH.** 1962. Anterior hypophysitis and Hashimoto's disease in a young woman. *J Pathol Bacteriol* **83:**584–585.
104. **Gutenberg A, Landek-Salgado MA, Tzou SC, Lupi I, Geis A, Kimura H, Caturegli P.** 2009. Autoimmune hypophysitis: expanding the differential diagnosis to CTLA-4 blockade. *Expert Rev Endocrinol Metab* **4:**681–698.
105. **Caturegli P, Newschaffer C, Olivi A, Pomper MG, Burger PC, Rose NR.** 2005. Autoimmune hypophysitis. *Endocr Rev* **26:**599–614. PubMed
106. **Caturegli P, Iwama S.** 2013. From Japan with love: another tessera in the hypophysitis mosaic. *J Clin Endocrinol Metab* **98:**1865–1868. PubMed
107. **Gutenberg A, Larsen J, Lupi I, Rohde V, Caturegli P.** 2009. A radiologic score to distinguish autoimmune hypophysitis from nonsecreting pituitary adenoma preoperatively. *AJNR Am J Neuroradiol* **30:**1766–1772. PubMed
108. **Engelberth O, Jezkova Z.** 1965. Autoantibodies in Sheehan's syndrome. *Lancet* **i:**1075. PubMed
109. **Crock P, Salvi M, Miller A, Wall J, Guyda H.** 1993. Detection of anti-pituitary autoantibodies by immunoblotting. *J Immunol Methods* **162:**31–40. PubMed
110. **Yabe S, Kanda T, Hirokawa M, Hasumi S, Osada M, Fukumura Y, Kobayashi I.** 1998. Determination of antipituitary antibody in patients with endocrine disorders by enzyme-linked immunosorbent assay and Western blot analysis. *J Lab Clin Med* **132:**25–31. PubMed
111. **Kobayashi T, Yabe S, Kanda T, Kobayashi I.** 1998. Studies on circulating anti-pituitary antibodies in NIDDM patients. *Endocr J* **45:**343–350. PubMed
112. **Takao T, Nanamiya W, Matsumoto R, Asaba K, Okabayashi T, Hashimoto K.** 2001. Antipituitary antibodies in patients with lymphocytic hypophysitis. *Horm Res* **55:**288–292. PubMed
113. **O'Dwyer DT, Smith AI, Matthew ML, Andronicos NM, Ranson M, Robinson PJ, Crock PA.** 2002. Identification of the 49-kDa autoantigen associated with lymphocytic hypophysitis as alpha-enolase. *J Clin Endocrinol Metab* **87:**752–757. PubMed
114. **Tanaka S, Tatsumi KI, Kimura M, Takano T, Murakami Y, Takao T, Hashimoto K, Kato Y, Amino N.** 2002. Detection of autoantibodies against the pituitary-specific proteins in patients with lymphocytic hypophysitis. *Eur J Endocrinol* **147:**767–775. PubMed
115. **Tatsumi KI, Tanaka S, Takano T, Tahara S, Murakami Y, Takao T, Hashimoto K, Kato Y, Teramoto A, Amino N.** 2003. Frequent appearance of autoantibodies against prohormone convertase 1/3 and neuroendocrine protein 7B2 in patients with nonfunctioning pituitary macroadenoma. *Endocrine* **22:**335–340. PubMed
116. **Bensing S, Fetissov SO, Mulder J, Perheentupa J, Gustafsson J, Husebye ES, Oscarson M, Ekwall O, Crock PA, Hökfelt T, Hulting AL, Kämpe O.** 2007. Pituitary autoantibodies in autoimmune polyendocrine syndrome type 1. *Proc Natl Acad Sci USA* **104:**949–954. PubMed
117. **Smith CJ, Oscarson M, Rönnblom L, Alimohammadi M, Perheentupa J, Husebye ES, Gustafsson J, Nordmark G, Meloni A, Crock PA, Kämpe O, Bensing S.** 2011. TSGA10—a target for autoantibodies in autoimmune polyendocrine syndrome type 1 and systemic lupus erythematosus. *Scand J Immunol* **73:**147–153. PubMed
118. **Smith CJ, Bensing S, Burns C, Robinson PJ, Kasperlik-Zaluska AA, Scott RJ, Kämpe O, Crock PA.** 2012. Identification of TPIT and other novel autoantigens in lymphocytic hypophysitis: immunoscreening of a pituitary cDNA library and development of immunoprecipitation assays. *Eur J Endocrinol* **166:**391–398. PubMed
119. **Bottazzo GF, Pouplard A, Florin-Christensen A, Doniach D.** 1975. Autoantibodies to prolactin-secreting cells of human pituitary. *Lancet* **ii:**97–101. PubMed
120. **Iwama S, Welt CK, Romero CJ, Radovick S, Caturegli P.** 2013. Isolated prolactin deficiency associated with serum autoantibodies against prolactin-secreting cells. *J Clin Endocrinol Metab* **98:**3920–3925. PubMed
121. **Stumpf WE, Roth LJ.** 1965. Thin sections cut at temperature of −70 degrees to −90 degree C. *Nature* **205:**712–713. PubMed
122. **Pouplard A, Bottazzo GF, Doniach D, Roitt IM.** 1976. Binding of human immunoglobulins to pituitary ACTH cells. *Nature* **261:**142–144. PubMed
123. **Buchwalow I, Samoilova V, Boecker W, Tiemann M.** 2011. Non-specific binding of antibodies in immunohistochemistry: fallacies and facts. *Sci Rep* **1:**28. PubMed
124. **Schnell SA, Staines WA, Wessendorf MW.** 1999. Reduction of lipofuscin-like autofluorescence in fluorescently labeled tissue. *J Histochem Cytochem* **47:**719–730.
125. **Pouplard A, Bigorgne JC, Chevalier JM, Rohmer V, Poron MF.** 1980. Pituitary insufficiency and auto-immunity. *Nouv Presse Med* **9:**1757–1760. (In French.) PubMed
126. **Pouplard-Barthelaix A, Lepinard V, Luxembourger L, Rohmer V, Berthelot J, Bigorgne JC.** 1984. Circulating pituitary autoantibodies against cells secreting luteinising and follicle stimulating hormones in children with cryptorchidism. *Lancet* **ii:**631–632. PubMed
127. **Yabe S, Murakami M, Maruyama K, Miwa H, Fukumura Y, Ishii S, Sugiura M, Kobayashi I.** 1995. Western blot analysis of rat pituitary antigens recognized by human antipituitary antibodies. *Endocr J* **42:**115–119. PubMed
128. **Bellastella G, Rotondi M, Pane E, Dello Iacovo A, Pirali B, Dalla Mora L, Falorni A, Sinisi AA, Bizzarro A, Colao A, Chiovato L, De Bellis A, Italian Autoimmune Hypophysitis Network Study.** 2010. Predictive role of the immunostaining pattern of immunofluorescence and the titers of antipituitary antibodies at presentation for the occurrence of autoimmune hypopituitarism in patients with autoimmune polyendocrine syndromes over a five-year follow-up. *J Clin Endocrinol Metab* **95:**3750–3757. PubMed

Myasthenia Gravis

ARNOLD I. LEVINSON AND ROBERT P. LISAK

99

Myasthenia gravis (MG) is a disease of striated muscles which clinically manifests as weakness. It is caused by impaired neuromuscular transmission due to a reduction in the number of receptors for the neurotransmitter acetylcholine (ACh) at the postsynaptic myoneural junction. This reduction is caused predominantly by the action of anti-acetylcholine receptor (anti-AChR) antibodies in most instances. The disease occurs with a reported prevalence of 0.5 to 5/100,000 and an incidence of 0.4/100,000/year. MG can occur at any age; however, it typically presents in the second and third decades of life, with a later peak occurring after age 50 (late-onset disease). A female preponderance (3:1 to 4:1) has been reported in the first 40 years of life; thereafter, the incidences are comparable between the sexes.

CLASSIFICATION

MG patients have typically been divided into those with generalized disease and those presenting with disease limited to the ocular muscles (1). Within these two groups, patients can be further subdivided on the basis of age of onset. Neonatal MG affects 10 to 20% of offspring born to myasthenic mothers. Disease manifestations are those of generalized MG (see below) but are transient, dissipating with the metabolism of maternal anti-AChR antibodies that had been transmitted across the placenta during the third trimester of pregnancy. Several congenital myasthenic syndromes have been described. In general, these manifest during the neonatal period, persist into adulthood, and do not have an autoimmune basis (2). Patients with juvenile MG present between 1 year of age and puberty. Apart from the age of onset, juvenile myasthenics, in general, behave like adult patients with MG.

Adults may present with ocular involvement or signs of more generalized disease. The ocular involvement is characterized by impaired ocular muscle motility and lid weakness, manifesting as diplopia and ptosis, respectively. Most MG patients experience ocular involvement, with roughly 50% of patients presenting with ocular signs at the time of diagnosis. If generalized disease does not develop in such patients by 2 years, the likelihood of its development is about 10 to 20%. If generalized disease does not develop by 5 years, the chances of developing generalized disease are probably no greater than 2 to 5% (3).

In the generalized-disease group, patients can be classified into those having mild, moderate, and severe disease on the basis of clinical activity. Any skeletal muscle group may be affected, but typically the palatal, pharyngeal, and upper esophageal muscles are involved. This results in dysarthria, dysphagia, and difficulty in handling secretions. Involvement of respiratory muscles, including intercostal muscles and the diaphragm, is seen in many individuals. Concomitant involvement of bulbar muscles may lead to "myasthenic crisis" requiring intubation. Involvement of muscles of the extremities and trunk occurs in 20 to 30% of patients at initial presentation and causes difficulties with activities of daily living. Sensory complaints accompanied by sensory findings are not a feature of MG. Autonomic nervous system-related complaints or problems with cognition or level of consciousness, in the absence of CO_2 narcosis or hypoxia, are also not part of the presentation of MG. While many patients report fatigue, fatigue in the absence of weakness is rarely, if ever, seen in MG and often reflects the confusion between fatigability of strength with sustained or repetitive effort (repetitive stimulation) and diffuse fatigue without any weakness, which more often represents systemic disease or depression. The hallmark of all muscle involvement in MG is its variability over time, with weakness usually exacerbated by repetitive use.

IMMUNOPATHOGENESIS OF AUTOIMMUNE MG

The Principal Autoantigen: Neuromuscular nAChR

The nicotinic AChR (nAChR) is a member of a larger family of ligand-gated ion channels. The muscle-type receptor, which is involved in myasthenia, can be subclassified further into mature junctional receptors and immature, extrajunctional or denervated receptors. The nAChR at a mature myoneural junction is composed of four subunits, labeled α, β, δ, and ε. In fetal muscle and adult denervated muscle or nonjunctional membrane, a γ subunit replaces the ε subunit found in mature innervated muscle endplates. This form of the receptor differs from the mature junctional form by its lower density (500 receptors/μm^2) and its distribution over most of the surface of the sarcolemma.

Two α subunits and one of each of the other subunits are assembled to form an asymmetric hourglass channel

doi:10.1128/9781555818722.ch99

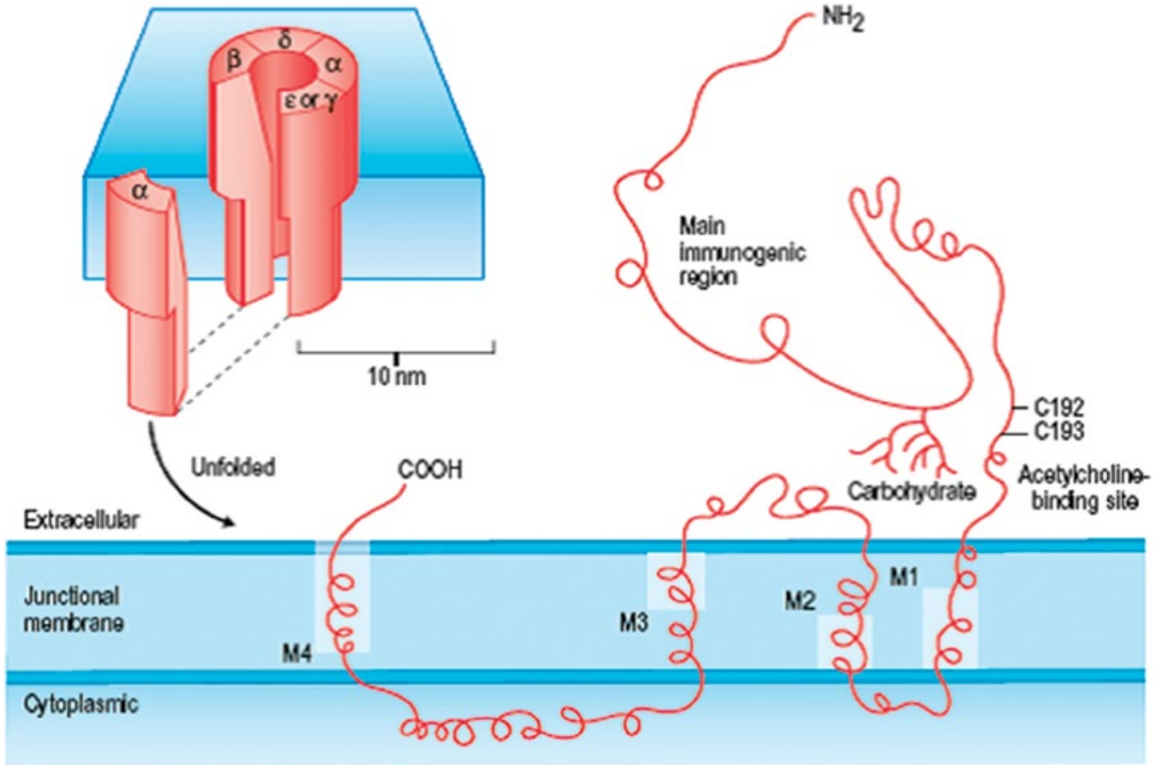

FIGURE 1 The AChR. The subunits of the AChR—α, β, δ, and γ or ε—are arranged like barrel staves around the central ion pore. Each subunit winds through the junctional membrane four times (sites M1, M2, M3, and M4). In the unfolded view of the α subunit, the amino-terminal end of the α subunit is extracellular, where it is accessible to ACh, which binds at the site shown (amino acids 192 and 193). In MG, autoantibodies may bind to various epitopes of all subunits, but a high proportion of antibodies bind to the main immunogenic region of the α subunit.

spanning the membrane (Fig. 1). Each subunit has a large amino terminus located extracellularly, four transmembrane regions, and a short cytoplasmic tail formed by a loop between the third and fourth transmembrane domains. The receptor appears as a dimer owing to disulfide bonding between the δ subunits of two receptors. The two α subunits are not contiguous in each receptor but are separated by another subunit. One ACh-binding site is found on each of the α subunits around the pair of cysteines at amino acids 192 and 193. The binding of ACh to the α subunits is believed to engender a conformational change, possibly resulting in rearrangement of charged groups. The binding of ACh to both α subunits increases the probability of transition of the channel to an open conformation. Binding of curare or α-bungarotoxin, a snake venom-derived neurotoxin, to the α subunits blocks this channel.

The receptors are concentrated at the top of the folds in the muscle endplate, adjacent to the nerve terminus, at a density of 10,000/μm^2 (Fig. 2) This localization reflects the action of agrin (4), an extracellular matrix protein secreted by neurons, which is critical in the development and maintenance of the neuromuscular junction. The AChRs are organized into clusters by rapsyn, a 43-kDa cytoplasmic protein (4). The clustered AChRs are linked to the cytoskeleton by connections between rapsyn and a dystrophin-glycoprotein complex.

PRINCIPAL EFFECTOR MOLECULES: ANTI-AChR ANTIBODIES

Properties of Anti-AChR Antibodies

Anti-AChR antibodies are detected in 80 to 90% of generalized MG patients and are responsible for the decreased number of nAChRs and impaired neuromuscular transmission (reviewed in reference 5). This statement is based on the following lines of evidence: (i) IgG, along with C3 and the terminal attack complex (C5-C9), is deposited at AChR-containing areas of the postsynaptic membrane; (ii) anti-AChR/AChR complexes can be extracted from the muscles of patients with MG; (iii) transfer of myasthenic serum from mother to fetus, or from human to mouse, results in symptoms or signs of myasthenia in the recipient; and (iv) plasmapharesis, which decreases anti-AChR antibody levels, is associated with clinical improvement.

Anti-AChR antibodies are predominantly IgG1 and IgG3, but IgG2 and IgG4 isotypes have also been found. IgA and IgM anti-AChR antibodies are present in some patients but never in the absence of IgG anti-AChR antibodies. The IgA and IgM anti-AChR antibodies tend to appear in patients whose disease is of longer duration and greater severity, and in association with high IgG titers. Pathogenic anti-AChR antibodies are considered to be directed at conformationally dependent structures.

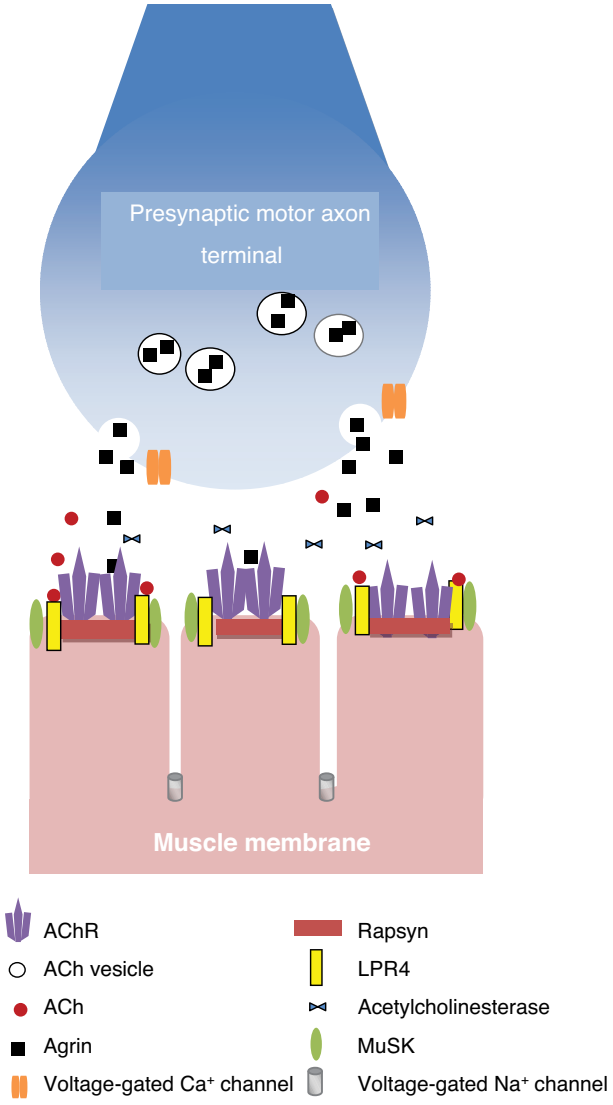

FIGURE 2 Schematic representation of the myoneural junction. Vesicles of ACh release their contents at active zones across from AChRs in response to impulses conducted down nerve axons. ACh diffuses across the synaptic cleft and binds to AChRs when not interdicted by AChE, with opening of the ion channel and the generation of endplate potentials. Action potential is propagated to muscle when sufficient amplitude of summated endplate potentials is attained. MuSK is a neuromuscular protein that anchors AChRs to the muscle membrane. LRP4 is a receptor for agrin, which activates clustering of MuSK and AChRs.

Approximately 60% of these antibodies are directed against the α subunit, particularly to a small region on the extracellular portion referred to as the main immunogenic region (6). Approximately 60% of the anti-AChR antibodies are directed against this region, which encompasses a set of overlapping epitopes clustered around amino acids 67 to 76 of the α subunit (7). However, not all disease-producing antibodies in humans or experimental rodents appear to be directed to this region. Many patients also have antibodies recognizing the γ-containing embryonic form of AChR. This observation has led to speculation about a nonmuscle source of sensitization.

Effector Mechanisms of Anti-AChR antibodies

Complement-Mediated Damage

As noted above, the critical problem in MG is the anti-AChR antibody-mediated reduction in the number of nAChRs at the myoneural junction. There are several possible mechanisms by which anti-AChR antibodies could lead to impaired neuromuscular transmission (8). Ultramicroscopy shows marked destructive changes in some endplates, particularly at the peaks of the postsynaptic folds, where AChR is usually present in greatest concentration. The architecture of the muscle endplate is simplified, with loss of junctional folds and widening of the synaptic cleft that contains membrane debris. C3, C9, and the membrane attack complex are deposited at the muscle endplate, suggesting a role for complement in membrane destruction (9). Indeed, the anti-AChR antibodies in many patients can fix complement *in vitro* when bound to skeletal muscle and can damage cultured rat myotubes, with a resultant decrease in AChR content. Although antibody-directed complement-mediated destruction is important in the pathophysiology of MG, it is not the entire story. The rapid clinical improvement in MG following certain therapeutic interventions and the lack of destructive changes in many neuromuscular junctions of symptomatic areas despite prominent immunoglobulin deposition suggest that a more readily reversible process is in play.

Acceleration of AChR Degradation

It is clear that anti-AChR antibodies can accelerate the rate of degradation of extrajunctional and junctional receptors (10). This reaction is complement independent and is due to the endocytosis of AChRs via shallow depressions, presumably clathrin-coated pits. The reaction can be mediated by $F(ab)_2$ fragments, but not Fab fragments, of anti-AChR antibodies. This indicates that cross-linking of adjacent AChRs is required.

Receptor Blockade

The inhibition of binding of α-bungarotoxin to AChRs by MG serum has been studied to detect so-called blocking anti-AChR antibodies. Such blocking antibodies are found in a variable number of MG sera. Blockade has been generally attributed to steric hindrance of the ligand-binding site, rather than direct binding to the ACh-binding site (11). The importance of these different antibodies in the pathophysiology of MG remains unclear. However, in one study, the functional ability of an individual serum to accelerate degradation and cause blockade of AChRs paralleled most closely the clinical status of the patient. The *in vivo* significance of such antibodies has also been demonstrated by passive transfer of certain rat monoclonal anti-AChR antibodies into chicks. Complete paralysis was observed within 1 h of the transfer, presumably before there was time for complement-mediated damage. It has been reasoned that in MG patients, such blocking antibodies could further diminish synaptic function already decreased owing to complement-mediated damage and/or accelerated receptor degradation. This could result in acute clinical deterioration or the rapid clinical improvement seen after plasmapharesis before the repair of damaged membrane and regeneration of new AChRs.

A number of other autoantibodies in the sera of MG patients have been described. Most of these autoantibodies are directed against other components of the neuromuscular junction. The mechanisms by which they may cause disease is still not completely understood. These autoantibodies as

well as some of the possible immunopathogenic mechanisms are discussed in the section below on diagnostic testing.

THE UNRESOLVED ROLE OF THE THYMUS

Interest in a primary role for the thymus in the pathogenesis of MG has been fueled by pathological, clinical, and immunological lines of evidence, although the nature of its involvement remains to be elucidated (reviewed in reference 12). The thymus is pathologically abnormal in 80 to 90% of MG patients. The majority of patients (65 to 75%) have thymic follicular hyperplasia with germinal center formation. The architecture of the hyperplastic thymi is generally preserved, with well-demarcated cortical and medullary regions. However, the medulla is crowded by numerous germinal centers that display the architectural features and cellular constituents of germinal centers in the secondary follicles of peripheral lymph nodes from normal individuals. Although these germinal centers in patients are generally thought to occupy an intraparenchymal position, some observers feel that they may actually lie extraparenchymally in the perivascular space.

Thymomas are seen in approximately 10% of MG patients who tend to be older than those with hyperplastic thymi (12). The thymomas are characterized by a loss of cortico-medullary demarcation and consist largely of neoplastic epithelial cells admixed with thymocytes. The affected epithelial cells belong to the cortical epithelial compartment, and the thymocytes have the immunophenotypic properties of normal immature cortical thymocytes.

Further evidence for a pathogenic role of the thymus comes from the results of empiric trials of thymectomy. Despite the absence of a controlled study, for years there has been general agreement that removal of the thymus, particularly in young patients with follicular hyperplasia, leads to clinical improvement. Very recently a controlled international multicenter study was completed which compared clinical outcome in MG patients treated with corticosteroid versus those treated with corticosteroid plus thymectomy. All patients were anti-AChR antibody positive and lacked thymoma. Those receiving thymectomy demonstrated a more favorable clinical outcome (personal communication). The underlying mechanism of the beneficial effect of thymectomy remains unknown.

INTRATHYMIC FACTORS POSSIBLY CONTRIBUTING TO LOCAL ANTI-ACHR ANTIBODY RESPONSE

The MG thymus, particularly hyperplastic thymus, is characterized by several unique features that strongly suggest that it plays a primary role in the immunopathogenesis of MG (reviewed in reference 12). It contains important constituents necessary for and indicative of an immune response directed against nAChRs. There is considerable evidence that resident cells in the thymus, including myoid cells and epithelial cells, express various subunits of AChR, including the α subunit. Additional factors found uniquely in hyperplastic MG thymus include increased expression of chemokines that attract immigrant $CD4^+$ T and B cells; the presence of nAChR-reactive B and $CD4^+$ T cells and anti-AChR antibody-secreting plasma cells; cytokines that can facilitate B cell activation, differentiation, and survival; and possibly decreased $CD4^+$ $CD25^+$ regulatory T cell function (12).

As yet it is not known whether or how such perturbations of the thymus lead to a breach in self-tolerance and the induction of anti-AChR antibodies. However, an understanding of this enduring mystery likely holds the key to unlocking the immunopathogenesis of this disease. The reader is referred elsewhere for a discussion of this topic (12).

DIAGNOSIS

In the appropriate clinical setting, the diagnosis of MG depends on combinations of clinical neurophysiological and/or pharmacological testing and immunological testing.

Clinical Neurophysiological Testing

The demonstration of a decrement in the amplitude of the muscle response to repetitive stimulation of a motor nerve at low rates of frequency (2 to 5 Hz) is highly diagnostic of MG. It is found in approximately 75% of patients with generalized MG and 50% of patients with purely ocular MG. Demonstration of a decline of 10% or more is highly diagnostic of a postsynaptic disorder, of which the most common is autoimmune MG. There are important technical considerations in performing this test, which are covered in basic clinical neurophysiology texts. Certainly, repetitive stimulation should be carried out for any patient who is seronegative and for some who are seropositive if the clinical picture is at all atypical. If serologic and classic repetitive nerve stimulation studies are negative, then single-fiber electromyography can prove useful. This technique, which requires considerable experience, allows measurement of neuromuscular transmission in individual muscle endplates (13).

Pharmacological Testing

The rationale behind the use of pharmacological agents as diagnostic probes in MG relates to our understanding of the physiology of neuromuscular transmission. Inhibition of acetylcholinesterase (AChE), the enzyme that is responsible for the breakdown of the transmitter ACh, results in increased amounts of ACh to bind to and activate AChR. In patients with MG, inhibition of AChE results in improvement in strength, which can then be demonstrated on the neurological examination or, if available, electrophysiological testing (reversal of decremental pattern following repetitive muscle stimulation). Edrophonium, an ultrashort-acting inhibitor of AChE, is given intravenously and improvement is sought in the clinical exam. However, this drug is currently very difficult to obtain for diagnostic testing. Pyridostimine or neostigmine, longer-acting AChE inhibitors used orally for treatment of MG, can also be used for diagnostic testing when given via the intramuscular route, along with atropine to reduce muscarinic side effects (13).

Immunological Testing

Anti-AChR Antibodies

As previously noted, 80 to 90% of patients with generalized MG have binding antibodies to nAChR, as do 50 to 70% of those with ocular MG. The presence or absence of AChR antibodies at onset does not predict the future clinical course. While some report that patients with ocular MG tend to have lower titers of AChR antibodies, there are enough exceptions to make the use of the binding antibody titer as a predictor of whether a patient will go on to have generalized MG not useful in individual patients. In addition, the titer or level of antibody does not correlate with severity of disease across patients. However, in an individual patient, an increase or decrease in anti-AChR antibody levels often accompanies deterioration or improvement, respectively, in clinical activity, particularly over the short-term response to plasmapheresis (reviewed in reference 14). Some laboratories also provide assays of the modulating antibodies and blocking

antibodies discussed previously, which may occasionally provide additional diagnostic information. Modulating and blocking antibodies are seen in 65 to 70% of patients with generalized MG. Only 0.4% of patients whose serum is negative for both binding and blocking anti-AChR antibodies have modulating antibodies. Testing for modulating antibodies, which some feel is important in prognosis (15, 16), involves incubating test serum with a human muscle sarcoma cell line, which serves as a target for anti-AChR antibodies. Radiolabeled bungarotoxin is then added to bind the remaining AChR. The bound fraction is separated from the free radiolabeled bungarotoxin and then quantified. The specificity of binding is assessed by preaddition of carbamylcholine agonist in parallel cultures. However, this test really measures both modulating and blocking antibodies. Measurement of only blocking antibodies, which is not widely employed, involves incubating test serum and calibrators with detergent-solubilized fetal and adult AChR along with ^{125}I-radiolabeled bungarotoxin. Blocking antibodies, if present, compete with the bungarotoxin for AChR. The AChR-blocking antibodies are precipitated. Radioactivity is inversely proportionate to the amount of blocking antibody. Commercial assays that detect complement-fixing AChR antibodies are not widely available for diagnostic testing. As noted previously, binding anti-AChR antibodies are predominately of the IgG1 and IgG3 isotypes.

The "gold standard" for detecting binding AChR antibodies is still the radioimmunoassay. The assay is widely available in the United States, Canada, Europe, the Middle East, Australia, New Zealand, and many parts of Asia. In this assay, serum is reacted with a nAChR preparation (generally human sourced) labeled with ^{125}I-α-bungarotoxin, a snake venom polypeptide that binds irreversibly to the receptor. Bound antibodies are immunoprecipitated by an anti-immunoglobulin reagent or staphylococcal protein A, and the quantity of antibodies detected is expressed in terms of the amount of α-bungarotoxin bound. Since sensitivity varies among laboratories, laboratories should provide the cutoff for normal, equivocal, and positive values. Many laboratories consider values of >0.5 nM/liter to indicate positivity, whereas some define positivity as >0.02 nM/liter. Specificity is also very high, although when a very sensitive assay for anti-AChR antibodies is used, it has been reported that as many as 11% of patients with neuromyelitis optica spectrum disorder have AChR antibodies, with 2% of these having concomitant MG (17). It has been recognized for more than 50 years that patients with MG have an increase in concomitant autoimmune diseases as well as other autoantibodies (18). Rarely, patients with Lambert-Eaton myasthenic syndrome (LEMS), an autoimmune disease of the neuromuscular junction caused by antibodies to the presynaptic P/Q voltage-gated calcium channel, have antibodies to AChR. Antibodies to AChR and/or cross-striational antibodies (antibodies that bind to molecules that are intracellular components of skeletal muscle) can be seen in up to 13% of patients with LEMS as well as in some other immune-mediated diseases (19, 20). It has been suggested that some patients have both MG and LEMS, but on the basis of clinical and clinical neurophysiological testing, there are no well-documented cases of patients with both clinical entities.

One laboratory has reported antibodies to AChR for some MG patients who do not have detectable AChR antibodies using the standard assays for detecting binding, blocking, and/or modulating antibodies. These presumably low-affinity antibodies can be detected by increasing the clustering of AChR on muscle cells in culture (21). This assay is not available on a commercial basis at this time.

Anti-MuSK Antibodies

Approximately 50% of patients with generalized MG and no detectable AChR antibodies have antibodies to muscle-specific kinase (MuSK) (22–24). MuSK is a neuromuscular junction protein that is important in anchoring AChR in the muscle membrane. Inhibition of MuSK negatively affects the availability of AChR. The currently available assay is a radioimmunoassay using recombinant human MuSK. The test is sometimes reported as negative (<1:10), borderline (1:10), or positive (≥1:20) without any further quantitation within the positive range. Other laboratories report the results as nanomolar concentration per liter, with values above 0.05 nM/liter being positive (25). In the appropriate clinical setting, a positive result confirms the diagnosis of MG. It is rare for a patient to have both anti-AChR and anti-MuSK antibodies. From the point of view of diagnosis, if a patient has anti-AChR antibodies, testing for anti-MuSK antibodies does not have diagnostic utility. Originally, anti-MuSK antibodies were described for patients with marked facial and bulbar weakness, including tongue weakness (24, 26), and respiratory involvement with relative sparing of upper- and lower-extremity muscles (24, 27). Ophthalmoparesis was also seen but was not a first symptom in at least one series of patients (28). Subsequently, it has become clear that patients with MuSK antibodies can also have a more traditional clinical phenotype similar to that seen with AChR patients. Most MuSK antibodies are of the non-complement-fixing IgG4 isotype. The pathogenic effects of MuSK antibodies are still not fully clear (23) but might result from inhibition of the effects of MuSK on normal AChR expression (29, 30).

Anti-LRP4 Antibodies

There are now three independent reports of serum from MG patients having antibodies binding to lipoprotein-related protein 4 (LRP4) (31–33). LRP4 is an important component of the neuromuscular junction, which serves as a receptor for agrin and which is required for agrin-induced activation of MuSK and AChR clustering. The prevalence of reactivity to LRP4 varied from 2 to 50% of patients who are negative for anti-AChR and MuSK antibodies (double seronegative), with the differences possibly being related to geography or ethnicity. Anti-LRP4 antibodies were found in the sera of 3% of patients with anti-MuSK antibodies in one study but otherwise were limited to double seronegative patients. Anti-LRP4 antibodies were not present in the sera of a large number of patients with other neurological diseases with the exception of neuromyelitis optica spectrum disorder, where 12.5% of patients had anti-LRP4 antibodies. If larger studies demonstrate that anti-LRP4 antibodies are found in MG patients without anti-AChR or MuSK antibodies and are rare in other neurological disorders, the test could become important in the diagnosis of MG. The antibodies are detected using enzyme-linked immunosorbent assay (ELISA) technique with recombinant human LRP4 by the three laboratories which have reported the findings (31–33). All three groups failed to find a positive test, as defined in their assays, for other diseases, but more experience is needed in order to be certain of the diagnostic utility of finding LRP4 antibodies in the serum. The assay is not commercially available at this time. LRP4 antibodies were able to inhibit LRP4-agrin interaction and/or alter AChR clustering in muscle cells *in vitro* (33).

Anti-Agrin Antibodies

Anti-agrin antibodies have recently been reported by two groups, often for MG patients with anti-AChR or anti-MuSK antibodies, but occasionally for MG patients who

are "triple seronegative" (AChR$^-$ MuSK$^-$ LRP4$^-$) (34, 35). These antibodies can be detected by cell-based assays (34) and by ELISA employing recombinant human agrin (35). In one study, no patients with other neurological disorders had agrin antibodies. Studies of larger numbers of patients and studies from other groups will be necessary to determine the prevalence of anti-agrin antibodies in triple seronegative MG patients as well as the degree of specificity for MG.

Other Autoantibodies

In addition to antibodies to neuromuscular junction molecules, MG patients may have antibodies to other autoantigens, some organ specific (thyroid, gastric parietal cells, red cells) as well as non-organ specific (antinuclear antibodies [ANA], double-stranded DNA, rheumatoid factor) even in the absence of evidence or presence of another autoimmune or immunologically mediated diseases (thyroiditis, pernicious anemia, hemolytic anemia, systemic lupus erythematosus, and rheumatoid arthritis). Some MG patients also have serum antibodies directed against one or more molecules that are specific for or relatively specific for skeletal muscle (36). In fact, antibodies that react with several intracellular muscle proteins were initially identified in patients with MG. Two of the many molecules that have been identified as antigens for these antibodies, titin and ryanodine receptors, may be important in indicating the presence of a thymoma (37) or as a factor in disease severity (38). Titin is a giant filamentous protein of striated muscle. Titin filaments are involved in muscle assembly and contribute to the muscle's ability to recoil following stimulation. Ryanodine receptors are Ca^{2+} release channels which are critically involved in muscle contraction. They are located in the sarcoplasmic reticulum of striated muscles. An antibody ELISA is commercially available for titin, and increased levels (>0.6), like that of anti-striational (skeletal muscle) antibodies (see below), are associated with thymoma or "elderly onset." Ryanodine receptors are not used for diagnosis and are rarely used for management of patients with MG, although an immunoblot test is available through a Swedish company. Striational-antibody (skeletal muscle antibody) assays are available from several commercial laboratories. Demonstration of increased titers of cross-striational (skeletal muscle) antibodies were first demonstrated using immunofluorescent techniques with frozen muscle and raises the likelihood that a patient with MG has a thymoma. Some laboratories continue to employ the indirect immunofluorescent assay using monkey skeletal muscle as the substrate. An ELISA employing proteins extracted from rat skeletal muscle is used, and the results are expressed as antibody titer in comparison to those of 4 normal sera run in each assay (20). Striational antibodies are also seen in MG patients with elderly onset (39, 40) and have also been reported for patients with thymoma who were said to not have MG as well as in other disorders (20, 41, 42).

REFERENCES

1. **Lisak RP, Barchi RL.** 1982. Myasthenia gravis, p 5–36. *In* Walton JN (ed), *Major Problems in Neurology,* vol 11. WB Saunders, Philadelphia, PA.
2. **Engel AG, Shen XM, Selcen D, Sine S.** 2012. New horizons for congenital myasthenic syndromes. *Ann N Y Acad Sci* **1275:**54–62. PubMed
3. **Watson D, Lisak R.** 1994. Myasthenia gravis: an overview, p 1–20. *In* Lisak R (ed), *Handbook of Myasthenia Gravis and Myasthenic Syndromes*. Marcel Dekker, New York, NY.
4. **Sanes JR, Apel ED, Gautam M, Glass D, Grady RM, Martin PT, Nichol MC, Yancopoulos GD.** 1998. Agrin receptors at the skeletal neuromuscular junction. *Ann N Y Acad Sci* **841:**1–13. PubMed
5. **Levinson AI, Zweiman B, Lisak RP.** 1987. Immunopathogenesis and treatment of myasthenia gravis. *J Clin Immunol* **7:**187–197. PubMed
6. **Tindall RS.** 1981. Humoral immunity in myasthenia gravis: biochemical characterization of acquired antireceptor antibodies and clinical correlations. *Ann Neurol* **10:**437–447. PubMed
7. **Papadouli I, Sakarellos C, Tzartos SJ.** 1993. High-resolution epitope mapping and fine antigenic characterization of the main immunogenic region of the acetylcholine receptor. Improving the binding activity of synthetic analogues of the region. *Eur J Biochem* **211:**227–234. PubMed
8. **Drachman DB, Adams RN, Josifek LF, Pestronk A, Stanley EF.** 1981. Antibody-mediated mechanisms of ACh receptor loss in myasthenia gravis: clinical relevance. *Ann N Y Acad Sci* **377:**175–188. PubMed
9. **Engel AG, Sahashi K, Fumagalli G.** 1981. The immunopathology of acquired myasthenia gravis. *Ann N Y Acad Sci* **377:**158–174. PubMed
10. **Drachman DB, Angus CW, Adams RN, Michelson JD, Hoffman GJ.** 1978. Myasthenic antibodies cross-link acetylcholine receptors to accelerate degradation. *N Engl J Med* **298:**1116–1122. PubMed
11. **Richman DP, Wollmann RL, Maselli RA, Gomez CM, Corey AL, Agius MA, Fairclough RH.** 1993. Effector mechanisms of myasthenic antibodies. *Ann N Y Acad Sci* **681:**264–273. PubMed
12. **Levinson AI.** 2013. Modeling the intrathymic pathogenesis of myasthenia gravis. *J Neurol Sci* **333:**60–67. PubMed
13. **Sanders DB.** 1994. Electrophysiological and pharmacological tests in neuromuscular junction disorders, p 103–148. *In* Lisak RP (ed), *Handbook of Myasthenia Gravis and Myasthenic Syndromes*. Marcel Dekker, New York, NY.
14. **Leite MI, Waters P, Vincent A.** 2010. Diagnostic use of autoantibodies in myasthenia gravis. *Autoimmunity* **43:**371–379. PubMed
15. **Drachman DB, Adams RN, Josifek LF, Self SG.** 1982. Functional activities of autoantibodies to acetylcholine receptors and the clinical severity of myasthenia gravis. *N Engl J Med* **307:**769–775. PubMed
16. **Howard FM Jr, Lennon VA, Finley J, Matsumoto J, Elveback LR.** 1987. Clinical correlations of antibodies that bind, block, or modulate human acetylcholine receptors in myasthenia gravis. *Ann N Y Acad Sci* **505:**526–538. PubMed
17. **McKeon A, Lennon VA, Jacob A, Matiello M, Lucchinetti CF, Kale N, Chan KH, Weinshenker BG, Apiwattinakul M, Wingerchuk DM, Pittock SJ.** 2009. Coexistence of myasthenia gravis and serological markers of neurological autoimmunity in neuromyelitis optica. *Muscle Nerve* **39:**87–90. PubMed
18. **Simpson JA.** 1966. Myasthenia gravis as an autoimmune disease: clinical aspects. *Ann N Y Acad Sci* **135:**506–516. PubMed
19. **Lennon VA, Lambert EH, Whittingham S, Fairbanks V.** 1982. Autoimmunity in the Lambert-Eaton myasthenic syndrome. *Muscle Nerve* **5**(9S)**:**S21–S25. PubMed
20. **Cikes N, Momoi MY, Williams CL, Howard FM Jr, Hoagland HC, Whittingham S, Lennon VA.** 1988. Striational autoantibodies: quantitative detection by enzyme immunoassay in myasthenia gravis, thymoma, and recipients of D-penicillamine or allogeneic bone marrow. *Mayo Clin Proc* **63:**474–481. PubMed
21. **Leite MI, Jacob S, Viegas S, Cossins J, Clover L, Morgan BP, Beeson D, Willcox N, Vincent A.** 2008. IgG1 antibodies to acetylcholine receptors in 'seronegative' myasthenia gravis. *Brain* **131:**1940–1952. PubMed
22. **Hoch W, McConville J, Helms S, Newsom-Davis J, Melms A, Vincent A.** 2001. Auto-antibodies to the

receptor tyrosine kinase MuSK in patients with myasthenia gravis without acetylcholine receptor antibodies. *Nat Med* **7:**365–368. PubMed

23. **McConville J, Farrugia ME, Beeson D, Kishore U, Metcalfe R, Newsom-Davis J, Vincent A.** 2004. Detection and characterization of MuSK antibodies in seronegative myasthenia gravis. *Ann Neurol* **55:**580–584. PubMed
24. **Zhou L, McConville J, Chaudhry V, Adams RN, Skolasky RL, Vincent A, Drachman DB.** 2004. Clinical comparison of muscle-specific tyrosine kinase (MuSK) antibody-positive and -negative myasthenic patients. *Muscle Nerve* **30:**55–60. PubMed
25. **Matthews I, Chen S, Hewer R, McGrath V, Furmaniak J, Rees Smith B.** 2004. Muscle-specific receptor tyrosine kinase autoantibodies—a new immunoprecipitation assay. *Clin Chim Acta* **348:**95–99. PubMed
26. **Farrugia ME, Robson MD, Clover L, Anslow P, Newsom-Davis J, Kennett R, Hilton-Jones D, Matthews PM, Vincent A.** 2006. MRI and clinical studies of facial and bulbar muscle involvement in MuSK antibody-associated myasthenia gravis. *Brain* **129:**1481–1492. PubMed
27. **Vincent A, Leite MI.** 2005. Neuromuscular junction autoimmune disease: muscle specific kinase antibodies and treatments for myasthenia gravis. *Curr Opin Neurol* **18:**519–525. PubMed
28. **Sanders DB, El-Salem K, Massey JM, McConville J, Vincent A.** 2003. Clinical aspects of MuSK antibody positive seronegative MG. *Neurology* **60:**1978–1980. PubMed
29. **Cole RN, Reddel SW, Gervásio OL, Phillips WD.** 2008. Anti-MuSK patient antibodies disrupt the mouse neuromuscular junction. *Ann Neurol* **63:**782–789. PubMed
30. **Morsch M, Reddel SW, Ghazanfari N, Toyka KV, Phillips WD.** 2012. Muscle specific kinase autoantibodies cause synaptic failure through progressive wastage of postsynaptic acetylcholine receptors. *Exp Neurol* **237:**286–295. PubMed
31. **Higuchi O, Hamuro J, Motomura M, Yamanashi Y.** 2011. Autoantibodies to low-density lipoprotein receptor-related protein 4 in myasthenia gravis. *Ann Neurol* **69:**418–422. PubMed
32. **Pevzner A, Schoser B, Peters K, Cosma NC, Karakatsani A, Schalke B, Melms A, Kröger S.** 2012. Anti-LRP4 autoantibodies in AChR- and MuSK-antibody-negative myasthenia gravis. *J Neurol* **259:**427–435. PubMed
33. **Zhang B, Tzartos JS, Belimezi M, Ragheb S, Bealmear B, Lewis RA, Xiong WC, Lisak RP, Tzartos SJ, Mei L.** 2012. Autoantibodies to lipoprotein-related protein 4 in patients with double-seronegative myasthenia gravis. *Arch Neurol* **69:**445–451. PubMed
34. **Cossins J, Belaya K, Zoltowska K, Koneczny I, Maxwell S, Jacobson L, Leite MI, Waters P, Vincent A, Beeson D.** 2012. The search for new antigenic targets in myasthenia gravis. *Ann N Y Acad Sci* **1275:**123–128. PubMed
35. **Zhang B, Shen C, Bealmear B, Ragheb S, Xiong W-C, Lewis RA, Lisak RP, Mei L.** 2014. Autoantibodies to agrin in myasthenia gravis patients. *PLoS One* **9:**e91816. PubMed
36. **McKeon A, Lennon VA, LaChance DH, Klein CJ, Pittock SJ.** 2013. Striational antibodies in a paraneoplastic context. *Muscle Nerve* **47:**585–587. PubMed
37. **Mygland A, Tysnes OB, Matre R, Volpe P, Aarli JA, Gilhus NE.** 1992. Ryanodine receptor autoantibodies in myasthenia gravis patients with a thymoma. *Ann Neurol* **32:**589–591. PubMed
38. **Romi F, Skeie GO, Aarli JA, Gilhus NE.** 2000. The severity of myasthenia gravis correlates with the serum concentration of titin and ryanodine receptor antibodies. *Arch Neurol* **57:**1596–1600.
39. **Skeie GO, Mygland A, Aarli JA, Gilhus NE.** 1995. Titin antibodies in patients with late onset myasthenia gravis: clinical correlations. *Autoimmunity* **20:**99–104. PubMed
40. **Aarli JA.** 2008. Myasthenia gravis in the elderly: is it different? *Ann N Y Acad Sci* **1132:**238–243. PubMed
41. **Strauss AJ.** 1968. Myasthenia gravis, autoimmunity and the thymus. *Adv Intern Med* **14:**241–280. PubMed
42. **Vernino S, Lennon VA.** 2004. Autoantibody profiles and neurological correlations of thymoma. *Clin Cancer Res* **10:**7270–7275. PubMed

Autoantibodies to Glycolipids in Peripheral Neuropathy

HUGH J. WILLISON

100

Peripheral neuropathies constitute a diverse group of diseases caused by a wide range of genetic, toxic, metabolic, and inflammatory insults to the peripheral nervous system. A considerable proportion of neuropathies are believed to have an autoimmune basis, either as a feature of systemic autoimmune diseases, vasculitides, or paraneoplastic or postinfectious syndromes, in association with lymphoproliferative diseases, or as isolated peripheral nerve syndromes. In clinical practice, the cause of sporadic neuropathies is often obscure, resulting in the frequent use of multiple screening tests to aid in diagnosis. Over the last 20 years, there has been a widespread increase in the use of antiganglioside antibody assays as diagnostic tools, based on the recognition from research studies that gangliosides are important autoantigens in many patients with autoimmune peripheral nerve disorders (1).

Early progress in this field stemmed from the discovery that IgM paraproteins with anti-myelin-associated glycoprotein (anti-MAG) activity present in patients with IgM paraproteinemic neuropathy also reacted with carbohydrate epitopes on a sulfated glucuronic acid-containing glycosphingolipid termed sulfated glucuronyl paragloboside (SGPG) (2). Further studies soon showed that cases of IgM paraproteinemic neuropathy that were anti-MAG/SGPG antibody negative often had antibodies reactive to various other glycolipid and ganglioside antigens.

Anti-GM1 ganglioside IgM antibodies were then found in a large proportion of patients with a syndrome termed multifocal motor neuropathy (MMN), thereby catalyzing a vast body of clinical research into the association between anti-GM1 antibodies and other motor nerve syndromes (3). At the same time, interest centered on identifying antiganglioside antibodies in Guillain-Barré syndrome (GBS) and its variant forms, including Miller Fisher syndrome (MFS) (4, 5), and these areas of research remain highly topical.

Both preceding and in parallel with this evolving field of neuropathy research and clinical practice, antiganglioside and antiglycolipid antibodies have also been reported for a vast range of other diseases and syndromes, including normal health (6, 7). Antiglycolipid antibodies are viewed as forming an important part of the natural autoantibody repertoire directed towards microbial carbohydrate structures, which has the potential to be expanded in both specific and nonspecific ways (8). This may explain their ubiquitous presence in both healthy and diseased patient populations and may account for some of the potentially misleading studies that have claimed disease-specific associations, which are further confounded by technical difficulties in antiganglioside antibody measurement. This chapter addresses only their relationship to autoimmune neuropathy, for which diagnostic testing is widespread.

Table 1 displays the main clinical syndromes for which a well-defined antiglycolipid antibody specificity has been identified. In patients with IgM paraproteinemic demyelinating neuropathy, paraproteins with anti-MAG activity also react with carbohydrate epitopes on sulfated glucuronic acid-containing glycosphingolipids, i.e., SGPG and its higher-lactosaminyl homologue, SGLPG (2). Another paraproteinemic neuropathy syndrome is chronic large-fiber sensory neuropathy with prominent ataxia (9). The IgM paraprotein reacts with gangliosides bearing NeuNAc(alpha2-8) NeuNAc-linked disialosyl groups, including but not limited to GD3, GD1b, GT1a, GT1b, and GQ1b. The patients may also have cold agglutinin disease by virtue of the presence of sialylated glycoprotein epitopes on human red blood cells with which the IgM paraproteins can cross-react. Ophthalmoplegia is also variably present in this syndrome.

In MMN with demyelinating conduction block, IgM antibodies to the GM1 ganglioside are present in about half of cases (10). A small number of patients have antibodies to GM2. Recently, it was demonstrated that the addition of galactocerebroside to the anti-GM1 antibody assay might improve detection rates; however, this has yet to be applied widely in clinical diagnostic practice (11). Patients with MMN and anti-GM1 antibodies are mostly male and have a clinical picture comprising a chronic asymmetric motor syndrome, usually with distal onset in an upper limb. The average age of onset is in the 4th decade, and the illness runs an indolent course, with patients usually remaining ambulant and physically independent 10 to 20 years after onset. The electrophysiological examination classically shows focal motor conduction block, and intravenous human immunoglobulin is the standard therapy.

In GBS, a wide variety of antiganglioside and antiglycolipid antibodies have been reported for up to 50% of cases in many series (12, 13). Anti-GM1, -GD1a, -GM1b, and -GalNAc-GD1a antibodies mark a form of GBS with prominent motor axonal involvement, now called acute motor axonal neuropathy (AMAN). In MFS, an acute, self-limiting variant of GBS comprising ataxia, areflexia,

doi:10.1128/9781555818722.ch100

TABLE 1 Clinical syndromes associated with specific antiglycolipid autoantibodies

Clinical syndrome	Antibody specificity	Antibody isotype
Chronic sensorimotor demyelinating neuropathy	MAG, SGPG, SGLPG	IgM (monoclonal)
Chronic ataxic neuropathy	NeuNAc(alpha2-8)NeuNAc epitopes on GD1b, GD3, GQ1b, GT1b, GT1a, and GD2	IgM (monoclonal)
MMN	Gal(beta1-3)GalNAc epitopes on GM1, GA1, and GD1b	IgM
Chronic motor neuropathy	GM2, GalNAc-GM1b, GalNAc-GD1a	IgM
AMAN	GM1a, GM1b, GD1a, GalNAc-GD1a	IgG
Demyelinating GBS	GalC, LM1, SGPG, GM1, GM2	IgG
MFS	GQ1b, GT1a, GD3, GD1b	IgG

and ophthalmoplegia, anti-GQ1b and anti-GT1a IgG antibodies are present in over 90% of cases; the antibodies also react with GD1b and/or GD3 in about half of cases (1, 5). Recently, antibodies that bind a combination of two glycolipids that interact with each other to form a heteromeric glycolipid complex were reported (14, 15). Universally recognized methods for detecting these have not yet been incorporated into clinical laboratory practice, although considerable progress towards this is being made (16).

As research into clinical-serological associations between neuropathy phenotypes and antiglycolipid antibodies evolves, it is likely that more requests for clinical testing will enter the diagnostic laboratory. The most commonly sought antibodies at present are those to GM1 and GQ1b gangliosides.

METHODS

Sample Requirements

Antiganglioside antibodies are best measured in serum, although they can also be estimated by using plasma. Cerebrospinal fluid may contain small amounts of antiganglioside antibody (filtered from the systemic circulation), but there is no evidence to indicate any local intrathecal synthesis of antibody, and therefore measurement in cerebrospinal fluid has no advantage over that in serum. Serum antiganglioside antibodies are stable for short periods (days) at standard ambient temperature and can be stored at 4°C for 1 to 2 weeks without adverse effects. Interlaboratory shipping of serum can be conducted at ambient temperature. Repeated freeze-thawing prior to testing should be avoided, as titers will fall. In chronic peripheral neuropathy syndromes, antiganglioside antibodies are usually IgM antibodies, occurring either as paraproteins (often monoclonal gammopathies of undetermined significance) or as polyclonal antibodies. Measurement can be performed at any stage of the clinical illness. For acute-onset, self-limiting neuropathies, such as GBS, the antiganglioside antibodies are usually IgG but may be IgM and IgA. They are at their highest titer at clinical onset and then disappear over the ensuing weeks or months and should therefore be sought immediately after clinical presentation, ideally before any therapeutic intervention. Plasma exchange or intravenous immunoglobulin therapy may substantially reduce or mask titers.

Materials and Reagents

Gangliosides are sialic acid-containing glycosphingolipids composed of a long-chain aliphatic amine, ceramide, attached to one to five hexoses, at least one of which must be sialylated. It is the presence of a sialic acid molecule(s) attached to a galactose residue(s) in the hexose core which defines a glycosphingolipid as a ganglioside. In the human nervous system, the sialic acid is *N*-acetylneuraminic acid (NeuNAc). Common structures are shown in Fig. 1. Ganglioside nomenclature is assigned according to the system of Svennerholm (17), in which the prefix G refers to "ganglio," M, D, T, and Q refer to the number of sialic acid molecules (mono, di, tri, and quad), and arabic numerals and lowercase letters refer to the order of migration of the gangliosides on thin-layer chromatograms (TLC).

Although total chemical or enzymatic synthesis of gangliosides is possible in specialized laboratories, most diagnostic laboratories purchase purified gangliosides from commercial sources or purify them from bovine brains. Chloroform-methanol extraction with DEAE-Sephadex chromatography is one of several commonly used procedures (18). Characterization is aided by chemical and enzymatic derivatization, TLC, and more sophisticated techniques, such as fast atom bombardment mass spectrometry and high-performance liquid chromatography. The major gangliosides in the brain are GM1, GD1a, GD1b, and GT1b, but there are also many minor gangliosides in both the brain and peripheral nerves and in other tissues.

Gangliosides can be purchased from a wide variety of commercial sources. Rare gangliosides should be sought by personal requests to relevant investigators. Many preparations are only partially pure; for example, commercial preparations of GT1a and GT1b may be contaminated by significant amounts of GQ1b and *vice versa*. Care should be taken to control for this in nondiscriminatory immunoassays, such as enzyme-linked immunosorbent assays (ELISAs) or dot blots. Various commercial kits are now available, using either an ELISA-based format or a dot blot or strip assay. Assays are also conducted by commercial companies upon receipt of clinical samples.

Antiganglioside autoantibodies are generally referred to by their specificity, either in terms of individual gangliosides (e.g., anti-GM1 IgG antibodies) or, less often, in terms of the reactive carbohydrate epitope [e.g., anti-Gal(beta1-3) GalNAc or antidisialosyl antibodies]. When generalizing, it is often more appropriate to use the term antiglycolipid antibodies (as opposed to antiganglioside antibodies), since many neuropathy-associated autoantibodies react with glycolipids which are not strictly gangliosides, such as SGPG, LM1, sulfatide, asialo-GM1 (also termed GA1), and galactocerebroside, as these molecules do not contain sialic acid.

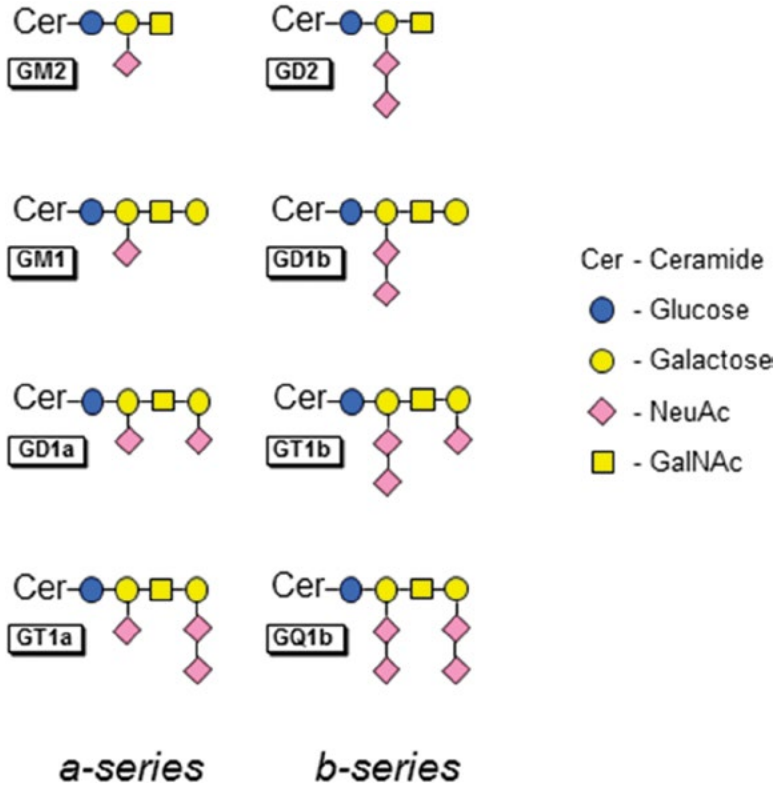

FIGURE 1 Examples of clinically relevant ganglioside structures.

The Current Procedure

The methodology for antibody detection presents difficulties, largely because the physical properties of gangliosides do not lend themselves well to development of uniform assays. Although antiganglioside antibodies can be detected by a variety of different methods, the principal and most commonly used screening method is ELISA (19, 20). A typical ELISA procedure is as follows.

1. Using a standard 96-well ELISA plate selected for high glycolipid binding properties (e.g., Immulon 2 [Dynatech]), coat each well of rows A, C, E, and G with 200 ng of GM1 or GQ1b in 100 μl of 100% ethanol and each well of rows B, D, F, and H with 100 μl of 100% ethanol alone by evaporation to dryness at room temperature and then store the plate for at least overnight at 4°C. Coated plates are stable at 4°C for up to 2 weeks.
2. Block all 96 wells with 200 μl phosphate-buffered saline (PBS)–bovine serum albumin (BSA) (pH 7.4; 1% BSA) for 2 h at 4°C. Discard PBS-BSA by flicking or automated washing.
3. Prepare serum samples by mixing gently and then centrifuge out any fibrin or particulate debris. Dilute the test serum to 1/100 in PBS-0.1% BSA, add samples in duplicate to ganglioside-coated and uncoated wells, and serially dilute the samples from 1/100 to 1/500, 1/2,500, and 1/12,500.
4. Leave the test serum to incubate overnight at 4°C.
5. Wash the plate six times in PBS wash buffer cooled to 4°C by dunking and flicking or using an automated washer.
6. Add 100 μl of peroxidase-conjugated anti-human IgM or IgG, diluted 1/3,000 (dilution optimized by checkerboard analysis) in PBS-0.1% BSA. Incubate for 2 h at 4°C.
7. Wash the plate six times in PBS wash buffer.
8. Develop the plate by adding a substrate solution comprising one 15-mg *o*-phenylenediamine tablet in 60 ml citrate buffer with 20 μl of 30% hydrogen peroxide for 20 min.
9. Stop the peroxidase reaction with 50 μl 3 M H_2SO_4.
10. Read optical densities (ODs) in an automated plate reader at 490 nm.
11. Calculate titers by endpoint dilution analysis as follows.
    (i) Subtract blank well ODs from coated well ODs to obtain working ODs.
    (ii) Obtain the mean of working ODs for duplicate wells.
    (iii) On semilog paper, plot linear OD values (*x* axis) against log test serum dilutions (*y* axis).
    (iv) Draw a best-fit dilution curve and assign the titer to the point at which the dilution curve crosses an OD of 0.1.

There have been some attempts to recommend a standard methodology, although most laboratories have established in-house protocols. In multicenter comparative studies, there has been a fair amount of agreement on clearly positive or negative cases but variable results with borderline samples (21). Important factors in setting up the ELISA include (i) the choice of ELISA plates, including glycolipid binding properties, batch variations, and storage conditions—checks on individual batches of plates are made by using a positive serum sample and calculating the lowest coefficient of variance over the whole plate while

still giving an optimal signal; (ii) the temperature at which the assay is performed, including all incubation and washing steps, with 4°C being the most commonly recommended temperature; (iii) the duration of serum incubation, which should be at least 4 h; and (iv) the presence or absence of Tween 20 as a detergent (gangliosides are soluble in detergent and will therefore be removed from the polystyrene plate). Assay results are usually reported as titers calculated by endpoint analysis.

In addition to ELISA, the TLC overlay technique is widely used (22). TLC overlay involves separating glycolipids on aluminum-backed silica plates in a solvent system and then performing an immuno-overlay with serum and labeled antibodies. Although not readily amenable to quantitative titration, TLC overlay has the advantage of allowing unambiguous identification of a particular glycolipid and is thus considered the gold standard method. This is especially useful when specific glycolipids are not available in pure form. Dot blots are also widely used, but as with TLC, it is harder to obtain readily quantifiable data (16). A technically straightforward and rapid agglutination assay was recently reported (23). Antibodies that react with ganglioside complexes were recently described (24), and the important role of accessory lipids also needs consideration; however, at present, these issues remain outside the remit of a routine diagnostic laboratory.

COST ASSESSMENT

There is no antiganglioside antibody investigation that is absolutely essential for diagnosis of a particular subtype of peripheral neuropathy, since independent investigation, principally electrodiagnostic tests in the context of an appropriate clinical picture and exclusion of other causes, is usually adequate. However, an antiganglioside antibody investigation may be useful (i) to confirm a diagnosis, such as MMN, AMAN, or MFS; (ii) to subclassify an existing diagnosis, such as classifying cases of IgM paraproteinemic neuropathy into those with anti-NeuAc(α2-8)NeuAc activity or anti-SGPG activity; or (iii) to exclude or differentiate between several possible diagnoses, such as between botulism, brain stem demyelinating disease, and MFS (anti-GQ1b antibody testing) or between MMN and amyotrophic lateral sclerosis (anti-GM1 antibody testing).

INTERPRETATION

A normal range of IgG and IgM titers for each glycolipid antigen must be established within a laboratory, since antiglycolipid antibodies form part of the normal autoantibody repertoire and antibodies to some gangliosides may be found at low titers in both normal and disease control sera. The distribution of antiganglioside antibodies in the population does not follow a normal distribution but is skewed, with some control subjects having high antibody levels against some gangliosides (titers of >1/1,000) and most having undetectable levels (titers of <1/100). As a result, defining a clinically meaningful normal range, even using logarithmically transformed data, is problematic. In my laboratory, we set the upper limit of the normal range to 2 standard deviations above the titers obtained using a panel of at least 50 healthy control subjects of all ages and both sexes; for most antiganglioside antibodies, this equates to an antibody titer being positive if it is >1/500 by endpoint dilution analysis (19).

With respect to the sensitivity and specificity of antiganglioside antibodies in particular clinical settings, no clear data are available from large multicenter studies. Some syndromes (e.g., "anti-MAG neuropathy") are defined to an extent by the presence of a particular antiglycolipid antibody. Anti-GQ1b IgG antibodies are a highly sensitive (>90%) and specific (>90%) marker of MFS and related syndromes accompanied by ophthalmoplegia (25). Anti-GM1 IgM antibodies are found in ~50% of cases of MMN (10, 26, 27), although this may rise with the advent of the GM1/galactocerebroside complex assay mentioned above (11). Anti-GM1/GD1a IgG antibodies are very specifically associated with acute motor-dominant forms of GBS, including AMAN, occurring in ~50% of cases (13). Anti-MAG antibodies are found in ~50% of cases of IgM paraproteinemic neuropathy, and a proportion of the remainder react with other glycolipid antigens. Anti-GD1b IgM antibodies are highly specific for a rare form of chronic ataxic neuropathy termed CANOMAD, although the sensitivity is unknown, and anti-GD1b IgG antibodies mark a rare GBS variant termed acute ataxic neuropathy (28).

REFERENCES

1. **Willison HJ, Yuki N.** 2002. Peripheral neuropathies and anti-glycolipid antibodies. *Brain* **125:**2591–2625. PubMed
2. **Latov N.** 1994. Antibodies to glycoconjugates in neuropathy and motor neuron disease. *Prog Brain Res* **101:**295–303. PubMed
3. **Pestronk A.** 1998. Multifocal motor neuropathy: diagnosis and treatment. *Neurology* **51**(Suppl 5)**:**S22–S24. PubMed
4. **Ilyas AA, Willison HJ, Quarles RH, Jungalwala FB, Cornblath DR, Trapp BD, Griffin DE, Griffin JW, McKhann GM.** 1988. Serum antibodies to gangliosides in Guillain-Barré syndrome. *Ann Neurol* **23:**440–447. PubMed
5. **Chiba A, Kusunoki S, Obata H, Machinami R, Kanazawa I.** 1993. Serum anti-GQ1b IgG antibody is associated with ophthalmoplegia in Miller Fisher syndrome and Guillain-Barré syndrome: clinical and immunohistochemical studies. *Neurology* **43:**1911–1917. PubMed
6. **Mizutamari RK, Wiegandt H, Nores GA.** 1994. Characterization of anti-ganglioside antibodies present in normal human plasma. *J Neuroimmunol* **50:**215–220. PubMed
7. **Kissel JT.** 1998. Autoantibody testing in the evaluation of peripheral neuropathy. *Semin Neurol* **18:**83–94. PubMed
8. **Willison HJ, Goodyear CS.** 2013. Glycolipid antigens and autoantibodies in autoimmune neuropathies. *Trends Immunol* **34:**453–459. PubMed
9. **Willison HJ, O'Leary CP, Veitch J, Blumhardt LD, Busby M, Donaghy M, Fuhr P, Ford H, Hahn A, Renaud S, Katifi HA, Ponsford S, Reuber M, Steck A, Sutton I, Schady W, Thomas PK, Thompson AJ, Vallat JM, Winer J.** 2001. The clinical and laboratory features of chronic sensory ataxic neuropathy with anti-disialosyl IgM antibodies. *Brain* **124:**1968–1977. PubMed
10. **Kornberg AJ, Pestronk A, Bieser K, Ho TW, McKhann GM, Wu HS, Jiang Z.** 1994. The clinical correlates of high-titer IgG anti-GM1 antibodies. *Ann Neurol* **35:**234–237. PubMed
11. **Galban-Horcajo F, Fitzpatrick AM, Hutton AJ, Dunn SM, Kalna G, Brennan KM, Rinaldi S, Yu RK, Goodyear CS, Willison HJ.** 2013. Antibodies to heteromeric glycolipid complexes in multifocal motor neuropathy. *Eur J Neurol* **20:**62–70. PubMed
12. **Yuki N.** 1998. Anti-ganglioside antibody and neuropathy: review of our research. *J Peripher Nerv Syst* **3:**3–18. PubMed
13. **Ho TW, Willison HJ, Nachamkin I, Li CY, Veitch J, Ung H, Wang GR, Liu RC, Cornblath DR, Asbury AK, Griffin JW, McKhann GM.** 1999. Anti-GD1a antibody is associated with axonal but not demyelinating forms

of Guillain-Barré syndrome. *Ann Neurol* **45:**168–173. PubMed
14. **Kaida K, Kusunoki S.** 2010. Antibodies to gangliosides and ganglioside complexes in Guillain-Barré syndrome and Fisher syndrome: mini-review. *J Neuroimmunol* **223:**5–12. PubMed
15. **Kusunoki S, Kaida K.** 2011. Antibodies against ganglioside complexes in Guillain-Barré syndrome and related disorders. *J Neurochem* **116:**828–832. PubMed
16. **Rinaldi S, Brennan KM, Willison HJ.** 2012. Combinatorial glycoarray. *Methods Mol Biol* **808:**413–423. PubMed
17. **IUPAC-IUB Commission on Biochemical Nomenclature (CBN).** 1977. The nomenclature of lipids. *Eur J Biochem* **79:**11–21.
18. **Schnaar RL.** 1994. Isolation of glycosphingolipids. *Methods Enzymol* **230:**348–370. PubMed
19. **Willison HJ, Veitch J, Swan AV, Baumann N, Comi G, Gregson NA, Illa I, Zielasek J, Hughes RA.** 1999. Interlaboratory validation of an ELISA for the determination of serum anti-ganglioside antibodies. *Eur J Neurol* **6:**71–77. PubMed
20. **Ravindranath MH, Ravindranath RM, Morton DL, Graves MC.** 1994. Factors affecting the fine specificity and sensitivity of serum antiganglioside antibodies in ELISA. *J Immunol Methods* **169:**257–272. PubMed
21. **Zielasek J, Ritter G, Magi S, Hartung HP, Toyka KV.** 1994. A comparative trial of anti-glycoconjugate antibody assays: IgM antibodies to GM1. *J Neurol* **241:**475–480. PubMed
22. **Willison HJ, O'Hanlon GM, Paterson G, Veitch J, Wilson G, Roberts M, Tang T, Vincent A.** 1996. A somatically mutated human antiganglioside IgM antibody that induces experimental neuropathy in mice is encoded by the variable region heavy chain gene, V1-18. *J Clin Invest* **97:**1155–1164. PubMed
23. **Alaedini A, Wirguin I, Latov N.** 2001. Ganglioside agglutination immunoassay for rapid detection of autoantibodies in immune-mediated neuropathy. *J Clin Lab Anal* **15:**96–99. PubMed
24. **Kaida K, Morita D, Kanzaki M, Kamakura K, Motoyoshi K, Hirakawa M, Kusunoki S.** 2004. Ganglioside complexes as new target antigens in Guillain-Barré syndrome. *Ann Neurol* **56:**567–571. PubMed
25. **Willison HJ, O'Hanlon GM.** 1999. The immunopathogenesis of Miller Fisher syndrome. *J Neuroimmunol* **100:**3–12. PubMed
26. **Adams D, Kuntzer T, Burger D, Chofflon M, Magistris MR, Regli F, Steck AJ.** 1991. Predictive value of anti-GM1 ganglioside antibodies in neuromuscular diseases: a study of 180 sera. *J Neuroimmunol* **32:**223–230. PubMed
27. **van Schaik IN, Bossuyt PM, Brand A, Vermeulen M.** 1995. Diagnostic value of GM1 antibodies in motor neuron disorders and neuropathies: a meta-analysis. *Neurology* **45:**1570–1577. PubMed
28. **Ito M, Matsuno K, Sakumoto Y, Hirata K, Yuki N.** 2011. Ataxic Guillain-Barré syndrome and acute sensory ataxic neuropathy form a continuous spectrum. *J Neurol Neurosurg Psychiatry* **82:**294–299. PubMed

Detection of Antimitochondrial Autoantibodies in Primary Biliary Cholangitis and Liver Kidney Microsomal Antibodies in Autoimmune Hepatitis

PATRICK S. C. LEUNG, MICHAEL P. MANNS,
ROSS L. COPPEL, AND M. ERIC GERSHWIN

101

The immunodetection of autoantibodies in autoimmune liver disease has been technically difficult because of the following: (i) serum autoantibodies from these patients usually react to a broad spectrum of antigens; (ii) some of these autoantibodies may have low titers; (iii) the biochemical nature of these autoantigens is unknown; and (iv) many autoantigens have low concentrations, and their biochemical purification often requires sophisticated procedures. The development and application of immunohistochemical, biochemical, and molecular biological techniques have provided new approaches to the study of autoimmune diseases and, in particular, the immunological detection of autoantigens. This is exemplified by two autoimmune diseases of the liver, namely, primary biliary cholangitis (PBC, formerly known as primary biliary cirrhosis) and autoimmune hepatitis (AIH). This chapter focuses on the detection of antimitochondrial autoantibodies (AMA) in PBC and the detection of liver kidney microsomal (LKM) antibodies in AIH.

PRIMARY BILIARY CHOLANGITIS

PBC is an autoimmune disease of the liver characterized by autoimmune-mediated destruction of intrahepatic bile ducts with progressive inflammatory scarring and eventual liver function failure (1). Immunologically, PBC is characterized by the presence of AMA in the circulation (2) and the infiltration of T cells into the liver (3). AMA can be detected in over 95% of patients with the disease (4, 5). These mitochondrial autoantigens are the E2 subunits of the 2-oxo-acid dehydrogenase complex (6–8) (Table 1). Extensive molecular and immunological studies of PBC, including cloning of mitochondrial autoantigens (9), antigen-specific isotype studies (7, 10), mapping of B and T cell epitopes (3, 11–17), and analysis of human and murine monoclonal antibodies (14, 16, 18–20), have provided valuable information and reagents for an understanding of the immunopathogenesis of PBC as well as for the development of accurate and specific diagnostic reagents with recombinant autoantigens (21–23). Immunohistochemical studies have shown the presence of either PDC-E2 or a cross-reactive molecule at the luminal region of bile duct epithelial cells of PBC patients but not controls (18, 19, 24–26). These data suggest that antibody targeting of bile duct epithelial cells of PBC livers may be pathogenic. Recently, IgG and IgA AMA were detected in the saliva and urine of patients with PBC, suggesting that a locally driven mucosal response is involved in PBC (27, 28).

Detection of AMA

AMA can be detected by the following methods: (i) indirect immunofluorescence (IF) (29), (ii) immunoblotting (13), (iii) enzyme-linked immunosorbent assay (ELISA) (21, 23), and (iv) bead assay (30).

Immunohistochemical Staining for AMA in PBC Sera by IF

Among the various methods of detection of AMA, IF is by far the most commonly used clinical test for AMA, using HEp-2 cells or tissue sections from mice or rats. A detailed protocol is as follows.

1. Prepare smears of HEp-2 cells on a clean glass slide and air dry.
2. Fix cells in cold acetone for 10 min at 4°C and air dry.
3. Place glass slide in phosphate-buffered saline (PBS) for 5 min.
4. Apply diluted patient serum to slide and incubate for 60 min at room temperature.
5. Wash with PBS 3 times for 3 min each.
6. Apply diluted fluorescein isothiocyanate (FITC)-conjugated goat anti-human IgG with Evan's Blue and incubate for 60 min at room temperature.
7. Wash with PBS 3 times for 3 min each.
8. Mount with 90% glycerol in PBS.
9. Examine by fluorescence microscopy.

HEp-2 slides can also be obtained commercially (e.g., Immunoconcepts, Sacramento, CA). Results of a typical IF test of AMA-positive PBC serum on HEp-2 cells are shown in Fig. 1. Alternatively, rat and mouse kidney sections can also be used for immunohistochemical staining for AMA. However, IF lacks the specificity of identifying specific antigens. In addition, background signals caused by nonspecific binding are common. Therefore, accurate detection of AMA by IF requires serial dilutions of sera (usually 1:40, 1:80, 1:160, 1:320, and 1:640) and also an optimal dilution of FITC-labeled anti-human Ig. The precise optimal dilution of the secondary FITC-conjugated antibody may also vary from batch to batch. In addition, thorough washing steps and changes of washing solutions are necessary to reduce the background.

doi:10.1128/9781555818722.ch101

TABLE 1 Summary of 2-oxo-acid dehydrogenase mitochondrial antigens in PBC

Antigen	Molecular mass (kDa)[a]	Frequency (%) in PBC patients[b]
Pyruvate dehydrogenase complex E2 subunit (PDC-E2)	70	>95
Branched chain 2-oxo-acid dehydrogenase complex E2 subunit (BCOADC-E2)	52	53–55
2-Oxo-glutarate dehydrogenase complex, E2 subunit (OGDC-E2)	48	39–88
Pyruvate dehydrogenase complex, E1 alpha subunit (PDC-E1α)	41	41–66
E3BP (protein X)	55	>95

[a]Determined by immunoblotting of beef heart mitochondrial preparations.
[b]Determined from different studies.

Immunoblotting for Detection of Specific AMA against Mitochondrial Antigens

A total mitochondrial homogenate from mammalian tissues is best suited for testing of AMA by immunoblotting. Briefly, mitochondrial preparations from bovine heart, rat liver, human placenta, or other tissues are resolved in an SDS-polyacrylamide gel, transferred to nitrocellulose filters, and probed with sera from patients with PBC. AMA reactivity against mitochondrial antigens is detected by use of enzyme-conjugated or ^{125}I-labeled anti-human Ig.

Preparation of Mitochondria from Mammalian Liver

A convenient method to prepare mitochondria is as follows.

1. Homogenize rat/mouse liver (15 g) in 30 ml of ice-cold buffer I (0.5 M sorbitol, 0.1 mM EDTA, 50 mM Tris, pH 7.4) and centrifuge the homogenate at 250 × *g* for 10 min.
2. Filter supernatant through 4 layers of cheesecloth.
3. Spin supernatant at 250 × *g* for 10 min at 4°C.
4. Take supernatant, and spin it again at 8,000 × *g* for 10 min at 4°C.
5. Resuspend pellet in 15 ml buffer I. Spin it again as in step 4.
6. Repeat step 5.
7. Resuspend pellet in 4 ml of buffer I with 0.05% bovine serum albumin (BSA), and store sample in 1-ml aliquots at −20°C. The final concentration should be approximately 40 to 60 mg/ml.

Test of AMA Reactivity against Mammalian Mitochondria by Immunoblotting

1. Electrophoretically resolve 20 μg of mitochondrial preparation in a 10% SDS-polyacrylamide gel with a preparative comb (Hoefer Scientific, San Francisco, CA). Run molecular weight protein standards in parallel.
2. Stop the gel when the bromphenol blue dye reaches the bottom of the gel, and transfer the resolved protein to a nitrocellulose filter.
3. After transfer, stain the blot with Ponceau S (Sigma, St. Louis, MO) to check for the efficiency of transfer. If the transfer is satisfactory, cut 3-mm strips from the blot by use of a sharp razor blade.
4. Incubate each strip with 1 ml of diluted PBC serum (1:1,000) for 1 h at room temperature. Run positive-control sera and negative-control sera in parallel.
5. After incubation, wash each strip with PBS containing 0.05% Tween 3 times for 10 min each.
6. Incubate each strip with a predetermined optimal dilution of secondary antibody (e.g., enzyme-conjugated secondary antibodies or ^{125}I-labeled anti-human Ig). Wash as in step 5.
7. Detect signals with a substrate for enzyme-conjugated secondary antibodies or expose the strips to X-ray film for ^{125}I-labeled anti-human Ig-treated strips. If horseradish peroxidase-conjugated secondary antibodies are used, the blots can be blocked with milk for 10 min after washing and the signals can be detected by chemiluminescence on X-ray film. Chemiluminescence kits can be obtained from common vendors, such as Pierce.

Figure 2 depicts typical patterns of AMA reactivity against various subunits of the 2-oxo-acid dehydrogenase complex. AMA reactivities are directed against the 70-kDa PDC-E2, 55-kDa E3BP (protein X), 52-kDa BCOADC-E2, 48-kDa OGDC-E2, and 41-kDa PDC-E1α proteins. Note that sera from PBC patients do not necessarily react to all five mitochondrial autoantigens and that the pattern of reactivity may vary from patient to patient (13, 14, 31).

Test for AMA Reactivity in PBC Sera by ELISA with Recombinant Autoantigens

Several studies have demonstrated the successful application of recombinant proteins as test antigens for detection of PBC by ELISA (13, 23, 31, 32). ELISAs using recombinant proteins are versatile, specific, and sensitive. In addition, ELISA is also efficient and allows the testing of multiple sera at several serial dilutions simultaneously. cDNAs encoding PDC-E2, BCOADC-E2, OGDC-E2, and PDC E1α have been cloned and expressed in *Escherichia coli* with IPTG

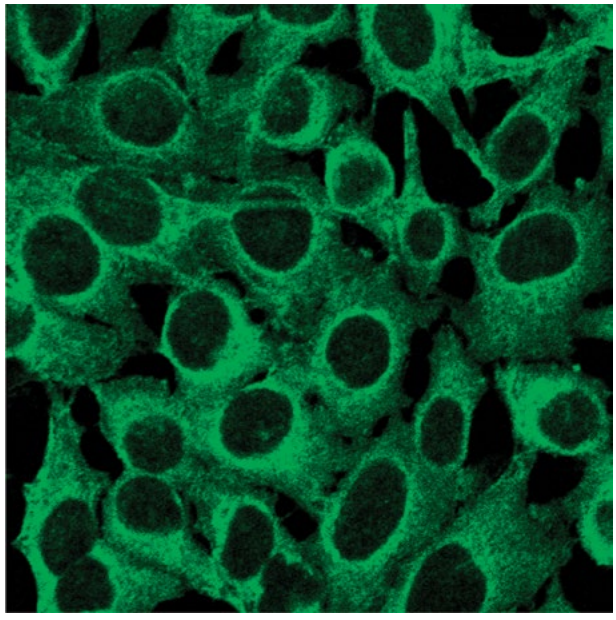

FIGURE 1 Detection of AMA by IF on HEp-2 cells. Note the characteristic mitochondrial staining pattern by PBC sera.

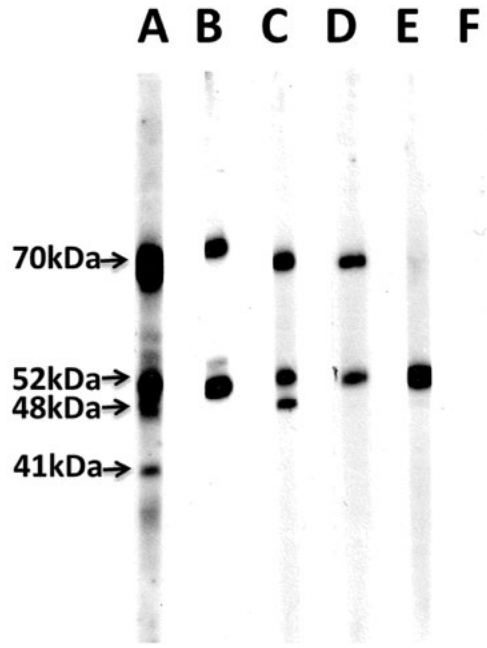

FIGURE 2 Reactivities of PBC sera with bovine heart mitochondria. Bovine heart mitochondria were resolved by SDS-PAGE, transferred to a nitrocellulose filter, and tested for reactivity with PBC sera (lanes A to F). Note the different patterns of AMA reactivities from various patients with PBC to the 70-kDa pyruvate dehydrogenase E2 subunit, the 52-kDa branched-chain 2-oxo-acid dehydrogenase E2 subunit, the 48-kDa 2-oxo-acid dehydrogenase E2 subunit, and the 41-kDa pyruvate dehydrogenase E1alpha subunit.

(isopropyl-β-D-thiogalactopyranoside)-inducible plasmid vectors. Recombinant proteins can easily be purified from IPTG-induced bacterial cultures as described previously (9, 21, 23, 32). Recently, the use of "designer molecules" (22) expressing AMA-reactive epitopes has greatly facilitated the testing of multiple sera for AMA. The availability and application of recombinant proteins clearly provide the cleanest and most specific reagents for AMA assays.

A standard procedure is as follows.

1. Dilute recombinant antigen to 2 to 5 μg/ml in carbonate buffer, pH 9.6.
2. Coat a 96-well ELISA plate with 100 μl/well of recombinant antigen from step 1. Store the plate at 4°C overnight.
3. Wash the plate with 100 μl of PBS containing 0.05% Tween (washing buffer) three times. Shake off the washing buffer between each wash.
4. Block the plate with 100 ml of 1% BSA in PBS; incubate at room temperature for 1 h.
5. Add test sera (serial dilutions) in PBS containing 1% BSA and 0.05% Tween; incubate at room temperature for 1 h.
6. Wash as in step 3, and then add 100 μl of a predetermined dilution of secondary antibody, such as horseradish peroxidase-conjugated anti-human Ig. Incubate at room temperature for 1 h.
7. Wash as in step 3. The presence of bound AMA can be determined by adding 100 μl of substrate for horseradish peroxidase [e.g., 2,2′-azinobis(3-ethylbenzthiazolinesulfonic acid) (ABTS); Sigma]. Incubate for 10 min at room temperature, and stop the reaction by adding 100 μl of 5% SDS. The intensity of color developed can be measured in an ELISA plate reader at 405 nm. Alternatively, 3,3′,5,5′-tetramethylbenzidine (TMB; BD Biosciences) can be used as a substrate for color development.

In ELISA, it is necessary to include a positive serum control, a negative serum control, and a well containing no primary antibody to correct any data or values caused by nonspecific binding of antibodies and background. A test serum is considered positive when the optical density reading is at least 2 times higher than the normal serum reading and the data are reproducible.

Test for AMA by Bead Assay

More recently, the technology of coupling protein antigens to beads was developed to improve the sensitivity associated with spatial presentation, which is essential for conformational epitopes, allowing the detection of multiple antigens at once. This approach of a multiplex bead assay has been applied and validated successfully for the detection of AMA, with specificity directed against three antigens (PDC-E2, BCOADC-E2, and OGDC-E2). The three antigens were chosen to standardize the technique and define applicability, preserving the method's advantages but also reducing potential sources of bias. Notably, an excellent correlation with previous analysis was seen for 100% of patients defined as AMA positive by Western blotting. Strikingly, several sera displayed consistent reactivity at dilutions of up to 1:100,000, 100 times the average dilution for Western blotting, undoubtedly proving the advantages potentially connected to the different spatial presentation allowed by the bead structure. Furthermore, this assay incorporates the advantages of a fully automated procedure that minimizes operator variability and allows a high level of standardization.

Briefly, recombinant antigens (PDC-E2, BCOADC-E2, and OGDC-E2) are initially dialyzed into PBS and conjugated to different nonmagnetic COOH-activated beads according to the manufacturer's recommendations (Bio-Rad). The validity of the assay and baseline fluorescence values are initially determined using specific monoclonal antibodies to the mitochondrial antigens; positive and negative controls are included and tested in quadruplicate. Once the assay is validated, serum samples from either patients or controls are diluted to final concentrations of $1{:}10^{-3}$, $1{:}10^{-4}$, $1{:}10^{-5}$, and $1{:}10^{-6}$ in Blotto blocker (Pierce, Rockford, IL) and added to a premixed bead solution with Luminex beads (1,250 beads/10 ml) in each well of filter microplates (Millipore). After washing, biotinylated IgG, IgA, and IgM detection antibodies are used, followed by a streptavidin R-phycoerythrin (streptavidin-PE) conjugate. The bead suspension is analyzed using a Bio-Plex 200 reader (Bio-Rad) with the default settings. The median fluorescence intensity of the reporter signal is then measured. A detail protocol is as follows.

1. Prewet the filter plate by pipetting 100 μl of assay buffer into each well of the plate. Seal and mix on a plate shaker for 10 min at room temperature.
2. Remove assay buffer by vacuum. Blot excess assay buffer from the bottom of the plate with paper towels.
3. Vortex and add 10 μl of premixed beads to each well.
4. Wash the wells twice by aspiration with the wash buffer (200 μl).
5. Add 30 μl of assay buffer or diluted serum samples to the designated wells.
6. Seal the plate with a plate sealer, and cover it with the lid and aluminum foil. Incubate with mild agitation on a plate shaker for 1 h at room temperature.

7. Gently remove fluid by vacuum.
8. Wash plate 2 times with 200 μl/well of wash buffer, removing wash buffer by vacuum filtration between each wash. Blot excess wash buffer.
9. Add 50 μl of detection antibody (5 μg/ml) to each well. (Allow the detection antibody to warm to room temperature prior to addition.) The detection antibody stock is made up of 1 μl of biotinylated anti-human IgG plus 1,999 μl of detection antibody diluent (1:2,000 dilution).
10. Seal, cover with lid, and incubate with agitation on a plate at room temperature for 30 min. Do not vacuum after incubation.
11. Add 50 μl of streptavidin-PE to each well containing 50 μl of detection Ab. Make up streptavidin-PE by using 100× streptavidin-PE (10 μl) plus assay buffer (990 μl).
12. Seal, cover with lid and aluminum foil, and incubate with agitation on a plate shaker for 30 min at room temperature.
13. Gently remove all contents by vacuum.
14. Wash plate 2 times with 200 μl/well wash buffer, removing wash buffer by vacuum filtration between each wash. Wipe any excess buffer from the bottom of the plate with paper towels.
15. Add 125 μl of assay buffer to each well. Resuspend the beads on a plate shaker (1,100 rpm) for 1 to 3 min.
16. Read the plate with a Bio-Plex 200 reader.

Interpretation of Data

Although AMA are highly reliable for diagnosis of PBC, some limitations and precautions are noted below. First, the high titers of AMA and the sensitivity of the test demand extreme caution to avoid cross-contamination of sera and false-positive results. Second, about 5 to 10% of PBC patients are AMA negative. Other clinical diagnostic features are also critical for differential diagnosis (Table 2). Third, neither the titer nor the specificity of autoantigens is related to the severity of the disease and therefore cannot be used to monitor the clinical course. Most importantly, positive and negative antibody controls should be included in the assays. Despite these limitations, cloned autoantigens and their recombinant proteins are extremely valuable diagnostic tools for the clinician.

AUTOIMMUNE HEPATITIS

Chronic hepatitis is a heterogeneous syndrome characterized by clinical, biochemical, and morphological criteria (33). Hepatitis B and C viruses may cause chronic hepatitis. In contrast, AIH, drug-induced hepatitis, and cryptogenic hepatitis are other subgroups of chronic hepatitis that presumably differ etiologically. AIH is a syndrome of unknown etiology. The loss of tolerance against the patient's own liver is regarded as the main pathogenic mechanism. While hitherto poorly defined defects of the immune system are responsible for chronic viral hepatitis, a hyperreaction of the patient's immune system towards autologous liver tissue is responsible for AIH. AIH was redefined (33, 34). Autoantibodies are the hallmarks of the diagnosis of AIH (Table 3). It is debated whether different patterns of autoantibodies characterize clinically or etiologically distinct subgroups of AIH (35–37). For example, antinuclear antibodies (ANA) are very heterogeneous, and their association with autoimmune liver diseases has not been identified, whereas smooth muscle antibodies in autoimmune liver diseases are particularly directed against F-actin. Recently, significant progress has been achieved in the characterization of microsomal antigens associated with liver diseases (Table 4). Three members of the cytochrome P450 supergene family and two members of the UDP-glucuronosyltransferases have been identified as hepatocellular autoantigens. These antigens are

TABLE 2 Clinical characteristics of primary biliary cholangitis

Characteristic
Clinical symptoms
Skin itching or jaundice appears in some cases
Portal hypertension and ascites or esophageal varices may appear
Osteoporosis according to the insufficiency of vitamin D or calcium may occur
Laboratory data
Presence of AMA
Elevation of serum bile duct-associated enzymes (ALP, g-GTP)
Elevation of serum bile acid
Elevation of total cholesterol
Elevation of serum IgM
Histological parameter
Chronic nonsuppurative destructive cholangitis (CNSDC) in middle-size interlobular or septal bile ducts, vanishing bile ducts, and granuloma
Complications
Skin xanthoma (especially if hypercholesterolemia continues)
Autoimmune diseases, including scleroderma, Sjogren's syndrome, rheumatoid arthritis, and chronic thyroiditis, may coexist.
Diagnosis
The patient is determined to have PBC when one of the following features is recognized.
1. CNSDC is recognized in liver specimen and laboratory data are compatible with PBC. In some cases, the patient is negative for AMA but positive for ANA.
2. AMA or anti-PDC antibody test is positive and liver histology is compatible with PBC, even though CNSDC is not recognized.
3. AMA or anti-PDC antibody test is positive and clinical feature or present history is compatible with PBC, even though liver histology is not checked.

of particular interest because they characterize subgroups of AIH and some forms of drug-induced hepatitis and also occur in a small proportion of patients with chronic viral hepatitis C or D (38).

LKM antibodies have been defined by their typical immunofluorescence staining of liver and kidney tissue. LKM-1 antibodies homogeneously stain the whole liver lobule and the proximal renal tubule (39). They react mainly with human cytochrome P45O 2D6 (40–42). LKM-2 antibodies react with cytochrome P450 IIC9 (43), and LM antibodies react with liver-specific cytochrome P45O IA2 (44). LKM-3 antibodies react with a major autoepitope on family 1 UDP-glucuronosyltransferases, and some sera react in addition with a minor epitope on family 2 UDP-glucuronosyltransferases (45). LKM-1 antibodies are serological markers of AIH type 2 (Table 4), a syndrome that frequently starts in childhood. In AIH, the main epitope is an 8-amino-acid linear epitope that shares sequence homology with the immediate early protein of herpes simplex virus type 1 (IE175). LKM-1 antibodies occur in 0 to 7% of patients with hepatitis C; these microsomal antibodies react with either a larger sequence of P450 IIC9, other epitopes on this protein, or conformational epitopes that are not recognized on immunoblots. Furthermore, hepatitis C sera may react with other microsomal proteins. LKM-2 antibodies did occur in a drug-induced form of hepatitis caused by a diuretic drug called tienilic acid which has only been used in the United States and France. This drug has been withdrawn from the market, and thus these antibodies have been described only in France. LKM-3 antibodies are associated with 5 to 13% of patients with chronic hepatitis D and also occur in some patients with AIH type 2 (Table 4). In rare cases, they may be the only marker of AIH (46). LM antibodies occur in a proportion of patients with AIH type 2 and drug-induced hepatitis caused by dihydralazine. Interestingly, as with LKM-1 antibodies, LKM-3 autoantibodies in autoimmune liver diseases have high titers and a linear and small autoepitope compared to that of low-titer antibodies to conformational epitopes in viral hepatitis. It is unknown whether LKM antibodies are involved in pathogenesis. It is likely that the antibodies themselves do not mediate tissue destruction but rather that tissue damage is mediated by liver-infiltrating T lymphocytes possibly directed against the corresponding cytochrome P450 molecules.

TABLE 3 Diagnostic criteria for AIH[a]

Parameter[b]	Score
Hypergammaglobulinemia	+3
Presence of autoantibodies	
ANA, SMA, LKM-1	+3
SLA, ASGPR, LP	+2
AMA	−2
Female gender	+2
AST or ALT of <3.0	+2
Complete response to immunosuppression	+2
Anti-HAV IgM, HBsAg, anti-HBc IgM	−3
Presence of HCV RNA (PCR)	−2
Other virus infections	−3
Ethanol intake (<35 g/day for males, <25 g/day for females)	+2
Immunogenetics (HLA-B8-DR3 or -DR4)	+1

[a]If the total score is >15 before and >17 after therapy, then AIH is certain; if the total score is 10 to 15 before and 12 to 17 after therapy, then AIH is probable.
[b]SMA, smooth muscle antibodies; SLA, antibodies against soluble liver antigen; ASGPR, antibodies against asialoglycoprotein receptor; LP, anti-liver-pancreas antibodies.

TABLE 4 Heterogeneity of microsomal antigens

Antibody	Molecular mass (kDa)	Target antigen	Disease
LKM-1	50	Cytochrome P450 IID6	AIH type II (hepatitis C)
LKM-2	50	Cytochrome P450 IIC9	Ticrynafen-induced hepatitis
LKM-3	55	Family 1 UGT[a]	Hepatitis D-associated AIH
LM	52	Cytochrome P450 1A2	Dihydralazine hepatitis (AIH)
	56.5	Cytochrome P450 2A6	Autoimmune polyglandular syndrome type-1 (APS-1)[b]
	57	Disulfide isomerase	Halothane hepatitis
	59	Carboxylesterase	Halothane hepatitis
	59	?	Chronic hepatitis C
	64	?	AIH
	70	?	Chronic hepatitis C

[a]UGT, UDP glucuronosyltransferase.
[b]Reference 52.

Detection of LKM Antibodies

LKM autoantibodies can be detected by the following methods: (i) IF (39), (ii) competitive ELISA (47), (iii) immunoblotting with human liver microsomes (48, 49), and (iv) immunoblotting with recombinant antigens (41, 50).

Detection of LKM Autoantibodies in AIH by IF

IF on rat liver and kidney sections (39, 50) is commonly used to detect LKM autoantibodies in patients with AIH. Patient sera are serially diluted 1:40, 1:80, and 1:160. Additionally, the optimal dilution of the FITC-conjugated secondary antibody must be determined for each batch of antibody to avoid strong background fluorescence, which makes the evaluation of LKM-positive sera difficult. The method is described in detail below.

Test for LKM Antibodies by Indirect Immunofluorescence

1. Prepare frozen sections from rat liver and kidney on glass slides and air dry.
2. Apply patient sera to slides at an appropriate dilution and incubate at room temperature for 1 h.
3. Wash 3 times with PBS.
4. Apply FITC-conjugated goat anti-human IgG and incubate for 30 min at room temperature.
5. Wash 3 times with PBS.
6. Mount with 90% glycerol in PBS.
7. Evaluate slides under a fluorescence microscope.

There are some similarities between AMA and LKM antibodies, and these sometimes create problems for inexperienced investigators performing routine immunofluorescence assays. While LKM antibodies do not stain distal renal tubules, LM antibodies do not stain the kidney at all, since they react with a liver-specific antigen. In IF, LKM antibodies stain the whole liver lobule very strongly (Fig. 3A),

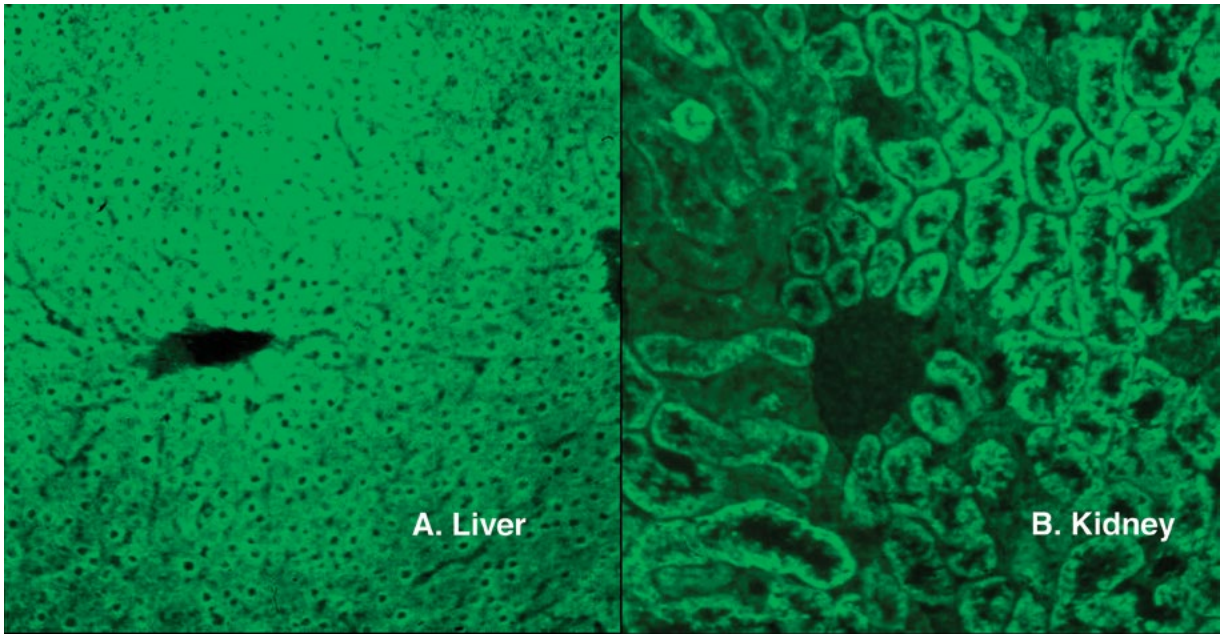

FIGURE 3 Detection of LKM antibodies and AMA by IF on cryostat rat liver and kidney sections. (A) Staining of liver lobule by LKM-1 antibodies. (B) Staining of proximal renal tubules by LKM-1 antibodies.

while in kidney tissue, they stain only the proximal renal tubules (Fig. 3B). In contrast, AMA stain proximal and distal renal tubules. If the medulla of the kidney is not part of the tissue, LKM antibodies may be misdiagnosed as AMA. Since PBC does not occur in childhood, a positive AMA result for children is almost always due to LKM antibody. If in IF only the liver stains and no reaction is seen in the kidney, one must suspect LM antibodies, which are directed against the liver-specific cytochrome P450 IA2.

Detection of LKM Autoantibodies by Competitive ELISA

An additional method to detect and further differentiate LKM autoantibodies in patient serum is by using a competitive ELISA. An Ig fraction, e.g., an LKM-1- or LKM-3-positive serum, is used to coat the plates. At the same time, an aliquot of this Ig fraction is biotinylated.

Preparation of Microsomes from Rat Liver for ELISA

Microsomes from rat liver tissue isolated by differential centrifugation are used as antigens for the competitive ELISA to test for LKM autoantibodies. The procedure is as follows (all steps should be done at 4°C).

1. Remove liver and wash in 0.9% NaCl.
2. Homogenize liver in ice-cold 250 mM sucrose.
3. Centrifuge sample for 10 min at 1,800 × *g*.
4. Centrifuge supernatant for 15 min at 12,000 × *g*.
5. Spin supernatant for 60 min at 200,000 × *g*.
6. Resuspend pellet in a small volume of PBS and determine the protein concentration.

Biotinylation and Preparation of IgG Fraction from Patient Sera for ELISA

An IgG fraction is prepared from LKM-1- or LKM-3-positive patient sera by precipitation with ammonium sulfate. An aliquot of this fraction is biotinylated according to the instructions given by the manufacturer.

Test for LKM Antibodies by Competitive ELISA

1. Dilute the IgG fraction of an LKM-positive patient serum to a concentration of 20 μg/ml in PBS.
2. Coat an ELISA plate with 50 μl/well of the IgG fraction.
3. Wash the plate once with PBS containing 0.1% Tween.
4. Block the plate with 200 μl/well 1% BSA in PBS and incubate it for 24 to 48 h at 4°C.
5. Wash once with PBS-Tween.
6. Dilute liver microsomes to a concentration of 100 μg/ml and place them in an ultrasound water bath for 3 min.
7. Add liver microsomes to the plate (50 ml/well) and incubate the plate at room temperature for 60 min.
8. Wash 2 times with PBS-Tween.
9. Dilute patient serum (1:10) in PBS containing 10 mM EDTA, add 50 μl to each well, and incubate the plate for 60 min at room temperature.
10. Wash as in step 8.
11. Dilute biotin-labeled Ig fraction (1 mg/ml) 1:100 in PBS-BSA, add 50 μl to each well, and incubate the plate for 60 min at room temperature.
12. Wash 3 times with PBS-Tween.
13. Dilute avidin-peroxidase appropriately in PBS-BSA, add 50 μl to each well, and incubate the plate for 60 min; wash as in step 8.
14. Add ABTS (50 μl/well), wait for the color reaction, and then add stop buffer (100 mM citric acid, pH 2) and measure the color intensity at 450 nm in an ELISA reader.

Interpretation

For each test, a positive control with known reactivity and a negative control (normal serum) should be included. Each serum sample should be tested in duplicate. Inhibition is calculated as the percentage of the serum sample value versus the negative-control value, which is defined as 0% inhibition. Serum is considered positive if the optical

density is reduced >40%. Serum samples with 20% to 40% inhibition are considered borderline.

Immunoblotting with Human Liver Microsomes To Test for LKM Antibodies

1. Prepare liver microsomes as described for ELISA. Instead of rat liver, use a small piece of human liver tissue.
2. Resolve 1 mg microsomes in sample buffer by 10% SDS-PAGE. In parallel, run a molecular weight standard.
3. Stop the gel when the bromphenol blue reaches the bottom of the gel, and transfer the proteins to a nitrocellulose filter.
4. Cut the nitrocellulose filter into 3-mm strips, block for 60 min in Tris-buffered saline (TBS)–Tween containing 2% milk powder, and then add patient sera, positive-control sera, and negative-control sera diluted 1:100. Incubate the strips in 1-ml aliquots of diluted sera for 60 min at room temperature.
5. Wash each strip 3 times with TBS-Tween for 5 min.
6. Add 1 ml of an appropriately diluted alkaline phosphatase-conjugated goat anti-human IgG and incubate for 60 min at room temperature.
7. Wash 3 times and then detect the signal by using a substrate for the enzyme-conjugated secondary antibody, such as NBT/BCIP (Nitro Blue Tetrazolium–5-bromo-4-chloro-3-indolylphosphate), or by chemiluminescence.

Interpretation

Characteristic LKM-1 autoantibodies react with a 50-kDa microsomal protein of human liver microsomes. Some sera from patients with AIH type 2 react with a protein of 64 kDa. LKM-1 antibodies in patients with chronic hepatitis C are more heterogeneous (51). They may react with other microsomal proteins, of 59 and 70 kDa. Approximately 50% of hepatitis C sera do not react with human microsomes in immunoblots, since these antibodies react with conformational epitopes.

Immunoblotting with Recombinant Liver Antigens

P450 IIC9 (50) and P450 IA2 (44) cDNAs are expressed in *E. coli*. UGT 1.1 cDNA (45) is expressed in baculovirus. The procedure for immunoblotting with these antigens is as follows.

1. Resolve 50 mg recombinant P450 IID6 or IA2 or 200 mg UGT 1.1 by 10% SDS-PAGE. In parallel, run a molecular weight standard.
2. Stop the gel when the bromphenol blue reaches the bottom of the gel, and transfer the proteins to a nitrocellulose filter.
3. Follow steps 3 to 7 in the protocol described in "Immunoblotting with Human Liver Microsomes To Test for LKM Antibodies."

Interpretation

Since almost all cytochrome P450 enzymes have molecular masses of approximately 50 kDa, a precise differentiation of different cytochrome P450 antibodies may be possible only if recombinant antigens are used. The identification of cytochrome P450 IA2 as a hepatocellular antigen resulted from the observation that a serum reacted with a 50-kDa protein but not with the recombinant cytochrome P450 IID6. In immunoblots with human liver microsomes, a distinction between P450 IID6 and P450 IA2 is not possible.

GENERAL REAGENTS

PBS, pH 7.4: Dissolve 32 g NaCl, 0.8 g KCl, 4.6 g Na_2PO_4 (anhydrous), and 0.8 g KH_2PO_4 (anhydrous) in 4 liters of distilled water. Adjust the pH to 7.2 to 7.4.

TBS-Tween: Dissolve 1.2 g Tris and 8.7 g NaCl in 1 liter of distilled water. Adjust the pH to 8.0 and add 500 μl Tween 20.

3% milk in PBS: Dissolve 3 g of nonfat dry milk in 100 ml of PBS, and adjust the pH to 7.2 to 7.4 by adding a few drops of 2 N NaOH.

Carbonate coating buffer: Dissolve 0.8 g of Na_2CO_3, 1.46 g of $NaHCO_3$, and 0.1 g of NaN_3 in distilled water; adjust to pH 9.6 and a final volume of 500 ml.

5× citrate buffer, pH 5.2: Dissolve 50.0 g of citric acid monohydrate and 7.4 g Na_2HPO_4 in 150 ml of distilled water, and adjust the pH to 5.2. Adjust the final volume to 200 ml.

ABTS substrate: Prepare 1 mM ABTS solution by adding 55 mg of ABTS to 100 ml of citrate buffer. Add hydrogen peroxide to 0.05% immediately before use.

NBT/BCIP substrate: Mix together 33 μl NBT and 16.5 μl BCIP in 5 ml alkaline phosphatase buffer.

Alkaline phosphatase buffer: Dissolve 12.1 g Tris and 1.0 g $MgCl_2$ in 1 liter of distilled water. Adjust the pH to 9.5.

REFERENCES

1. **Kaplan MM.** 1996. Primary biliary cirrhosis. *N Engl J Med* **335:**1570–1580. PubMed
2. **Mackay IR.** 1958. Primary biliary cirrhosis showing a high titer of autoantibody; report of a case. *N Engl J Med* **258:**185–188. PubMed
3. **Van de Water J, Ansari A, Prindiville T, Coppel RL, Ricalton N, Kotzin BL, Liu S, Roche TE, Krams SM, Munoz S, Gershwin ME.** 1995. Heterogeneity of autoreactive T cell clones specific for the E2 component of the pyruvate dehydrogenase complex in primary biliary cirrhosis. *J Exp Med* **181:**723–733. PubMed
4. **Gershwin ME, Coppel RL, Mackay IR.** 1988. Primary biliary cirrhosis and mitochondrial autoantigens—insights from molecular biology. *Hepatology* **8:**147–151. PubMed
5. **Leung PS, Van de Water J, Coppel RL, Gershwin ME.** 1991. Molecular characterization of the mitochondrial autoantigens in primary biliary cirrhosis. *Immunol Res* **10:**518–527. PubMed
6. **Fussey SP, Guest JR, James OF, Bassendine MF, Yeaman SJ.** 1988. Identification and analysis of the major M2 autoantigens in primary biliary cirrhosis. *Proc Natl Acad Sci USA* **85:**8654–8658. PubMed
7. **Van de Water J, Gershwin ME, Leung P, Ansari A, Coppel RL.** 1988. The autoepitope of the 74-kD mitochondrial autoantigen of primary biliary cirrhosis corresponds to the functional site of dihydrolipoamide acetyltransferase. *J Exp Med* **167:**1791–1799. PubMed
8. **Yeaman SJ, Fussey SP, Danner DJ, James OF, Mutimer DJ, Bassendine MF.** 1988. Primary biliary cirrhosis: identification of two major M2 mitochondrial autoantigens. *Lancet* **i:**1067–1070. PubMed
9. **Gershwin ME, Mackay IR, Sturgess A, Coppel RL.** 1987. Identification and specificity of a cDNA encoding the 70 kD mitochondrial antigen recognized in primary biliary cirrhosis. *J Immunol* **138:**3525–3531. PubMed
10. **Surh CD, Cooper AE, Coppel RL, Leung P, Ahmed A, Dickson R, Gershwin ME.** 1988. The predominance of IgG3 and IgM isotype antimitochondrial autoantibodies against recombinant fused mitochondrial polypeptide in patients with primary biliary cirrhosis. *Hepatology* **8:**290–295. PubMed

11. **Dubel L, Tanaka A, Leung PS, Van de Water J, Coppel R, Roche T, Johanet C, Motokawa Y, Ansari A, Gershwin ME.** 1999. Autoepitope mapping and reactivity of autoantibodies to the dihydrolipoamide dehydrogenase-binding protein (E3BP) and the glycine cleavage proteins in primary biliary cirrhosis. *Hepatology* **29:**1013–1018. PubMed
12. **Jones DE, Palmer JM, James OF, Yeaman SJ, Bassendine MF, Diamond AG.** 1995. T-cell responses to the components of pyruvate dehydrogenase complex in primary biliary cirrhosis. *Hepatology* **21:**995–1002. PubMed
13. **Leung PS, Chuang DT, Wynn RM, Cha S, Danner DJ, Ansari A, Coppel RL, Gershwin ME.** 1995. Autoantibodies to BCOADC-E2 in patients with primary biliary cirrhosis recognize a conformational epitope. *Hepatology* **22:**505–513. PubMed
14. **Leung PSC, Krams S, Munoz S, Surh CP, Ansari A, Kenny T, Robbins DL, Fung J, Starzl TE, Maddrey W, Coppel RL, Gershwin ME.** 1992. Characterization and epitope mapping of human monoclonal antibodies to PDC-E2, the immunodominant autoantigen of primary biliary cirrhosis. *J Autoimmun* **5:**703–718. PubMed
15. **Shimoda S, Nakamura M, Ishibashi H, Hayashida K, Niho Y.** 1995. HLA DRB4 0101-restricted immunodominant T cell autoepitope of pyruvate dehydrogenase complex in primary biliary cirrhosis: evidence of molecular mimicry in human autoimmune diseases. *J Exp Med* **181:**1835–1845. PubMed
16. **Surh CD, Ahmed-Ansari A, Gershwin ME.** 1990. Comparative epitope mapping of murine monoclonal and human autoantibodies to human PDH-E2, the major mitochondrial autoantigen of primary biliary cirrhosis. *J Immunol* **144:**2647–2652. PubMed
17. **Tuaillon N, Andre C, Briand JP, Penner E, Muller S.** 1992. A lipoyl synthetic octadecapeptide of dihydrolipoamide acetyltransferase specifically recognized by anti-M2 autoantibodies in primary biliary cirrhosis. *J Immunol* **148:**445–450. PubMed
18. **Cha S, Leung PS, Coppel RL, Van de Water J, Ansari AA, Gershwin ME.** 1994. Heterogeneity of combinatorial human autoantibodies against PDC-E2 and biliary epithelial cells in patients with primary biliary cirrhosis. *Hepatology* **20:**574–583. PubMed
19. **Cha S, Leung PS, Gershwin ME, Fletcher MP, Ansari AA, Coppel RL.** 1993. Combinatorial autoantibodies to dihydrolipoamide acetyltransferase, the major autoantigen of primary biliary cirrhosis. *Proc Natl Acad Sci USA* **90:**2527–2531. PubMed
20. **Fukushima N, Nakamura M, Matsui M, Ikematsu H, Koike K, Ishibashi H, Hayashida K, Niho Y.** 1995. Establishment and structural analysis of human mAb to the E2 component of the 2-oxoglutarate dehydrogenase complex generated from a patient with primary biliary cirrhosis. *Int Immunol* **7:**1047–1055. PubMed
21. **Leung PS, Iwayama T, Prindiville T, Chuang DT, Ansari AA, Wynn RM, Dickson R, Coppel R, Gershwin ME.** 1992. Use of designer recombinant mitochondrial antigens in the diagnosis of primary biliary cirrhosis. *Hepatology* **15:**367–372. PubMed
22. **Moteki S, Leung PS, Coppel RL, Dickson ER, Kaplan MM, Munoz S, Gershwin ME.** 1996. Use of a designer triple expression hybrid clone for three different lipoyl domain for the detection of antimitochondrial autoantibodies. *Hepatology* **24:**97–103. PubMed
23. **Van de Water J, Cooper A, Surh CD, Coppel R, Danner D, Ansari A, Dickson R, Gershwin ME.** 1989. Detection of autoantibodies to recombinant mitochondrial proteins in patients with primary biliary cirrhosis. *N Engl J Med* **320:**1377–1380. PubMed
24. **Joplin R, Wallace LL, Johnson GD, Lindsay JG, Yeaman SJ, Palmer JM, Strain AJ, Neuberger JM.** 1995. Subcellular localization of pyruvate dehydrogenase dihydrolipoamide acetyltransferase in human intrahepatic biliary epithelial cells. *J Pathol* **176:**381–390. PubMed
25. **Migliaccio C, Nishio A, Van de Water J, Ansari AA, Leung PS, Nakanuma Y, Coppel RL, Gershwin ME.** 1998. Monoclonal antibodies to mitochondrial E2 components define autoepitopes in primary biliary cirrhosis. *J Immunol* **161:**5157–5163. PubMed
26. **Tsuneyama K, Van de Water J, Leung PS, Cha S, Nakanuma Y, Kaplan M, De Lellis R, Coppel R, Ansari A, Gershwin ME.** 1995. Abnormal expression of the E2 component of the pyruvate dehydrogenase complex on the luminal surface of biliary epithelium occurs before major histocompatibility complex class II and BB1/B7 expression. *Hepatology* **21:**1031–1037. PubMed
27. **Reynoso-Paz S, Leung PS, Van De Water J, Tanaka A, Munoz S, Bass N, Lindor K, Donald PJ, Coppel RL, Ansari AA, Gershwin ME.** 2000. Evidence for a locally driven mucosal response and the presence of mitochondrial antigens in saliva in primary biliary cirrhosis. *Hepatology* **31:**24–29. PubMed
28. **Tanaka A, Nalbandian G, Leung PS, Benson GD, Munoz S, Findor JA, Branch AD, Coppel RL, Ansari AA, Gershwin ME.** 2000. Mucosal immunity and primary biliary cirrhosis: presence of antimitochondrial antibodies in urine. *Hepatology* **32:**910–915. PubMed
29. **Walker JG, Doniach D, Roitt IM, Sherlock S.** 1965. Serological tests in diagnosis of primary biliary cirrhosis. *Lancet* **i:**827–831. PubMed
30. **Oertelt S, Rieger R, Selmi C, Invernizzi P, Ansari AA, Coppel RL, Podda M, Leung PS, Gershwin ME.** 2007. A sensitive bead assay for antimitochondrial antibodies: chipping away at AMA-negative primary biliary cirrhosis. *Hepatology* **45:**659–665. PubMed
31. **Iwayama T, Leung PS, Rowley M, Munoz S, Nishioka M, Nakagawa T, Dickson ER, Coppel RL, Mackay IR, Gershwin ME.** 1992. Comparative immunoreactive profiles of Japanese and American patients with primary biliary cirrhosis against mitochondrial autoantigens. *Int Arch Allergy Immunol* **99:**28–33. PubMed
32. **Moteki S, Leung PS, Dickson ER, Van Thiel DH, Galperin C, Buch T, Alarcon-Segovia D, Kershenobich D, Kawano K, Coppel RL, Matuda S, Gershwin ME.** 1996. Epitope mapping and reactivity of autoantibodies to the E2 component of 2-oxoglutarate dehydrogenase complex in primary biliary cirrhosis using recombinant 2-oxoglutarate dehydrogenase complex. *Hepatology* **23:**436–444. PubMed
33. **Desmet VJ, Gerber M, Hoofnagle JH, Manns M, Scheuer PJ.** 1994. Classification of chronic hepatitis: diagnosis, grading and staging. *Hepatology* **19:**1513–1520. PubMed
34. **Johnson PJ, McFarlane IG.** 1993. Meeting report: International Autoimmune Hepatitis Group. *Hepatology* **18:**998–1005. PubMed
35. **Czaja AJ, Manns MP.** 1995. The validity and importance of subtypes in autoimmune hepatitis: a point of view. *Am J Gastroenterol* **90:**1206–1211. PubMed
36. **Homberg J-C, Abuaf N, Bernard O, Islam S, Alvarez F, Khalil SH, Poupon R, Darnis F, Lévy V-G, Grippon P, Opolon P, Bernuau J, Benhamou J-P, Alagille D.** 1987. Chronic active hepatitis associated with antiliver/kidney microsome antibody type 1: a second type of "autoimmune" hepatitis. *Hepatology* **7:**1333–1339. PubMed
37. **Manns M, Gerken G, Kyriatsoulis A, Staritz M, Meyer zum Büschenfelde KH.** 1987. Characterisation of a new subgroup of autoimmune chronic active hepatitis by autoantibodies against a soluble liver antigen. *Lancet* **i:**292–294. PubMed
38. **Manns MP.** 1994. Autoantibodies in chronic hepatitis: diagnostic reagents and scientific tools to study etiology, pathogenesis, and cell biology. *Prog Liver Dis* **12:**137–156. PubMed

39. **Rizzetto M, Swana G, Doniach D.** 1973. Microsomal antibodies in active chronic hepatitis and other disorders. *Clin Exp Immunol* **15:**331–344. PubMed
40. **Gueguen M, Yamamoto AM, Bernard O, Alvarez F.** 1989. Anti-liver-kidney microsome antibody type 1 recognizes human cytochrome P450 db1. *Biochem Biophys Res Commun* **159:**542–547. PubMed
41. **Manns MP, Johnson EF, Griffin KJ, Tan EM, Sullivan KF.** 1989. Major antigen of liver kidney microsomal autoantibodies in idiopathic autoimmune hepatitis is cytochrome P450db1. *J Clin Invest* **83:**1066–1072. PubMed
42. **Zanger UM, Hauri HP, Loeper J, Homberg JC, Meyer UA.** 1988. Antibodies against human cytochrome P-450db1 in autoimmune hepatitis type II. *Proc Natl Acad Sci U S A* **85:**8256–8260. PubMed
43. **Beaune P, Dansette PM, Mansuy D, Kiffel L, Finck M, Amar C, Leroux JP, Homberg JC.** 1987. Human anti-endoplasmic reticulum autoantibodies appearing in a drug-induced hepatitis are directed against a human liver cytochrome P-450 that hydroxylates the drug. *Proc Natl Acad Sci U S A* **84:**551–555. PubMed
44. **Manns MP, Griffin KJ, Quattrochi LC, Sacher M, Thaler H, Tukey RH, Johnson EF.** 1990. Identification of cytochrome P450IA2 as a human autoantigen. *Arch Biochem Biophys* **280:**229–232. PubMed
45. **Philipp T, Durazzo M, Trautwein C, Alex B, Straub P, Lamb JG, Johnson EF, Tukey RH, Manns MP.** 1994. Recognition of uridine diphosphate glucuronosyl transferases by LKM-3 antibodies in chronic hepatitis D. *Lancet* **344:**578–581. PubMed
46. **Strassburg CP, Obermayer-Straub P, Alex B, Philipp T, Tukey R, Manns MP.** 1995. Autoepitopes on UDP-glucuronosyl transferases (LKM-3) in autoimmune hepatitis differ from those in hepatitis D. *Gastroenterology* **108:**A1177.
47. **Manns M, Meyer zum Büschenfelde KH, Slusarczyk J, Dienes HP.** 1984. Detection of liver-kidney microsomal autoantibodies by radioimmunoassay and their relation to anti-mitochondrial antibodies in inflammatory liver diseases. *Clin Exp Immunol* **57:**600–608. PubMed
48. **Alvarez F, Bernard O, Homberg JC, Kreibich G.** 1985. Anti-liver-kidney microsome antibody recognizes a 50,000 molecular weight protein of the endoplasmic reticulum. *J Exp Med* **161:**1231–1236. PubMed
49. **Kyriatsoulis A, Manns M, Gerken G, Lohse AW, Ballhausen W, Reske K, Meyer zum Büschenfelde KH.** 1987. Distinction between natural and pathological autoantibodies by immunoblotting and densitometric subtraction: liver-kidney microsomal antibody (LKM) positive sera identify multiple antigens in human liver tissue. *Clin Exp Immunol* **70:**53–60. PubMed
50. **Manns MP, Johnson EF.** 1991. Identification of human cytochrome P450s as autoantigens. *Methods Enzymol* **206:**210–220. PubMed
51. **Durazzo M, Philipp T, Van Pelt FN, Lüttig B, Borghesio E, Michel G, Schmidt E, Loges S, Rizzetto M, Manns MP.** 1995. Heterogeneity of liver-kidney microsomal autoantibodies in chronic hepatitis C and D virus infection. *Gastroenterology* **108:**455–462. PubMed
52. **Obermayer-Straub P, Perheentupa J, Braun S, Kayser A, Barut A, Loges S, Harms A, Dalekos G, Strassburg CP, Manns MP.** 2001. Hepatic autoantigens in patients with autoimmune polyendocrinopathy-candidiasis-ectodermal dystrophy. *Gastroenterology* **121:**668–677.

Cardiovascular Diseases

CHERYL L. MAIER, C. LYNNE BUREK,
NOEL R. ROSE, AND AFTAB A. ANSARI

102

SEROLOGIC DIAGNOSIS AND ASSESSMENT OF ACUTE MYOCARDIAL INJURY

Acute myocardial injury (AMI) most often results from a lack of sufficient blood supply to the myocardium. When patients present with symptoms of chest pain, rapid diagnosis of potential AMI and characterization of the extent of cardiac injury are essential for delivering appropriate treatment, e.g., intervention with thrombolytic therapy or angioplasty. Such interventions are aimed at minimizing the risk of (further) cardiac injury and death. Distinguishing patients with unstable angina from those with AMI is necessary to triage whether patients may be managed in the outpatient setting versus inpatient admission and immediate intervention. Serologic measurements of soluble biomarkers released during myocyte necrosis are used in conjunction with electrocardiograms and with more sophisticated imaging techniques like echocardiography and perfusion scintigraphy. Serum biomarkers have the greater advantage of detecting recent myocardial injury, which is not easily distinguishable by cardiac imaging techniques in patients with clinical evidence of preexisting heart disease (Table 1).

Serological monitoring of myocardial injury relies on the correlation of serum levels of biomarkers with the degree of cardiac myocyte injury and necrosis. Myocardial injury in acute coronary syndrome results from insufficient oxygen during episodes of ischemia. Whether the cellular damage is reversible or irreversible depends on the duration of ischemia. Myocyte necrosis is an example of irreversible injury that results in the rapid and complete release of cytoplasmic proteins of myocyte origin, which then become detectable in the serum. In contrast, proportionally lower levels of myocytic cytoplasmic proteins and macromolecules are released from cardiac myocytes during mild ischemic conditions, and these levels often correlate with reversible myocardial tissue injury.

The earliest conventional serum biomarkers used to assess AMI were enzymes involved in cellular metabolism, including aspartate aminotransferase, lactate dehydrogenase, and creatine kinase MB (CK-MB); however, the sensitivity and specificity of these biomarkers limited their clinical utility in detecting AMI. For example, CK-MB was generally considered a specific biomarker for irreversible myocardial injury; yet vigorous exercise, chronic renal failure, skeletal myopathies, and hypothyroidism can all increase plasma levels of CK-MB. Furthermore, studies of endomyocardial biopsies performed on patients with unstable angina revealed evidence of micronecrosis in the absence of elevated serum levels of CK-MB (1).

Cardiac troponins (cTns) represent a class of serum biomarkers that have become the gold standard for diagnosis of AMI due to their greater specificity and sensitivity for myocardial necrosis. The Tns comprise a group of regulatory proteins uniquely located on the thin filament of striated muscle. The Tn complex is composed of three subunits: (i) TnT, which attaches the Tn complex to tropomyosin; (ii) TnI, which regulates actin-myosin interactions; and (iii) TnC, which binds calcium (2). Immunoassays for cTnT and cTnI were first introduced in the early 1990s and have since then been improved and widely implemented. Tn levels are now included in the Joint European Society of Cardiology/American College of Cardiology Committee's consensus definition of AMI (3). Cardiac-specific isoforms exist for TnI (cTnI) and TnT (cTnT) and can be detected in plasma or serum by specific monoclonal antibodies without detectable cross-reactivity with skeletal muscle Tns. Unlike CK-MB, cTns are not found in the sera of normal patients (i.e., in the absence of cardiac tissue injury), thus providing troponin measurements with a superior signal-to-noise ratio and enhancing their usefulness for risk stratification and for the evaluation of patient response to therapy.

Additional biomarkers have been or are being studied to aid in the diagnosis of AMI, likely to be used in conjunction with cTns and CK-MB. These include myoglobin, copeptin, and heart-type fatty acid-binding protein (4–7). Each of these additional biomarkers has limitations, and their use clinically is not currently recommended for the diagnosis of AMI. It has been suggested that some of these biomarkers might have important prognostic applications or be used in specific clinical settings (8, 9).

SEROLOGIC DIAGNOSIS AND ASSESSMENT OF CHRONIC MYOCARDIAL INJURY

Chronic myocardial injury (CMI) is characterized by a much slower process than the acute myocyte necrosis typically seen in AMI. Slow and progressive myocyte dropout in CMI is usually associated with apoptotic processes involved in the pathogenesis of dilated cardiomyopathy (DCM). DCM results from maladaptive compensatory tissue remodeling responses secondary to reduced cardiac

doi:10.1128/9781555818722.ch102

TABLE 1 Serum biomarkers used for diagnosis of AMI

Plasma/serum biomarker	Specificity/sensitivity (%)					
	2–4 h		6–10 h		18–24 h	
	Sensitivity	Specificity	Sensitivity	Specificity	Sensitivity	Specificity
Enzymes						
Lactate dehydrogenase					95	90
CK-MB activity	40.7	98.8	97.5	96.2	97.9	96.9
CK-MB mass	39.3	98.8	100	90.4	95.7	99.6
CK-MB isoforms	46.4	88.9	96.2	90.2	80.9	89.9
Structural and regulatory proteins						
Cardiac troponins						
cTnT	35.7	98.3	86.5	96.4	78.7	95.7
cTnI	57.5	94.3	92.3	94.6	95.7	93.4
Myosin light chains	75	64.2	78.6	61.1	81.5	52.5

output, which evolve in a complex manner and in the context of different genetic and environmental backgrounds over time. These remodeling responses are mediated by a variety of endogenous stress-induced proteins that act on cardiac myocytes to induce hypertrophy, cytoprotection, and repair, and on nonmyocyte cells to increase vascularization and effect extracellular matrix (ECM) remodeling and fibrosis (10–13).

Left ventricular (LV) hypertrophy and dilatation with reduced ejection fraction is a compensatory response to chronic volume overload that results from myocyte loss and reduced contractile function. Tissue remodeling responses are initiated and directed in part by innate immune cells residing within cardiac tissues, such as cardiac mast cells and dendritic cells. These responses are focused on reorganizing the cardiovascular architecture by degrading ECM components through matrix metalloproteinases (MMPs), promoting replacement fibrosis, developing new ECM and vascular beds, and recruiting and directing adaptive immune cells to remove damaged and necrotic tissues. During this process of remodeling and repair, certain cryptic cardiac antigens, e.g., myosin, mitochrondrial proteins, heat shock proteins, etc., become exposed to immature dendritic cells, which, under the influence of other "danger signals" present, undergo maturation and become capable of initiating subsequent cardiac-specific autoimmune responses. Such responses may or may not contribute significantly to further cardiac tissue injury.

Increases in hemodynamic burden and volume overload can also contribute to cardiomyocyte damage and DCM. Several reports from different laboratories indicate that cardiac hypertrophy is associated with signaling through the Gαq subtype of G proteins (GTP-binding proteins) expressed by cardiac myocytes (14, 15). Molecules such as endothelin-1 and angiotensin II, which are upregulated in response to increased pulmonary pressure and chronic volume overload, signal through Gαq-mediated pathways. This signaling causes reactivation of embryonic genes, such as atrial natriuretic factor, skeletal α-actin, and β-myosin heavy chain, which ultimately results in cardiac myocyte hypertrophy. Excessive hemodynamic stress can alternatively lead to myocyte apoptosis, instead of hypertrophy, resulting in rapid decompensation and DCM.

Chronic overstimulation of the renin-angiotensin-aldosterone system in patients with congestive heart failure (CHF) leads to increases in blood pressure and edema (16). A-type natriuretic peptides are produced by and released from the atria in response to dilatation. C-type natriuretic peptides are produced by cardiovascular endothelial tissues in response to shear stress. B-type natriuretic peptides (BNPs) are released from the ventricles in response to prolonged increases in end-diastolic volume and pressure and thus have emerged as excellent biomarkers for left ventricular dysfunction in DCM. BNP is derived from its high-molecular-weight precursor, pro-BNP (amino acids [aa] 1 to 108), whose expression is genetically regulated and which is not stored preformed in vesicles. The mature form, BNP-32, consists of the 32 C-terminal amino acid residues (aa 77 to 108) of the parent pro-BNP. Elevated plasma levels of the mature BNP or the amino-terminal pro-BNP (Nt-pro-BNP) may be used as indicators of cardiac dysfunction. Increasing concentrations of serum BNP or NT-pro-BNP have been shown to significantly correlate with decreasing ejection fraction ($P < 0.001$) and with increasing New York Heart Association classification of heart failure (17).

Biomarkers that are associated with CMI fall into three overlapping categories: (i) markers of tissue remodeling, (ii) markers of inflammation, and (iii) markers of vascular endothelial activation (Table 2). Myocardial tissue remodeling is triggered by LV dysfunction and is associated with cardiomyocyte hypertrophy and death. Such events in turn lead to remodeling of the ECM with replacement fibrosis. Chronic low, but significant, levels of myocyte dropout induce structural remodeling of LV ECM to compensate for loss of LV function. Increased plasma and tissue expression of MMPs and cardiac mast cell tryptase correlate with evidence of LV remodeling and dysfunction in CHF (18, 19).

Plasma levels of interleukin-6 (IL-6) and related cytokines of the IL-6 family, e.g., cardiotrophin-1, have been shown to increase proportionally with the severity of CHF in both human clinical studies and in experimental animal models (20, 21). Although the exact tissue sources of IL-6-related cytokines have not been identified, vascular endothelium and smooth and cardiac muscle tissues have been implicated. Intracellular signaling on cardiac myocytes is mediated via different multimeric IL-6 family cytokine receptors, which share a common gp130 transmembrane subunit. Homeostatic regulation of IL-6 expression during CHF is complex and appears to be influenced by a larger network of other cytokines and neurohormones, including tumor necrosis factor (TNF), angiotensin II, epinephrine, and norepinephrine. Indeed, angiotensin-converting enzyme inhibitors or β blockers have been shown to have a lowering effect on IL-6 expression during CHF (22). IL-6

TABLE 2 Serum biomarkers for CMI

Markers of tissue remodeling
NT-pro-BNP
BNP
Annexin V
FAS/APO-1
Endothelin-1
Angiotensin-converting enzyme
MMP2
MMP7
MMP9
Transforming growth factor-β
Fibrinogen
Homocysteine
Markers of inflammation
C-reactive protein
CD40 ligand
IL-6
IL-1
TNF
Gamma interferon
Markers of vascular endothelial activation
sICAM-1
Soluble vascular cellular adhesion molecule 1
sE-Selectin
sP-Selectin
Vascular endothelial growth factor
Platelet-derived growth factor
Placental growth factor
Nitric oxide

appears to mediate the detrimental effects of CHF by influencing hypertrophy and apoptosis of cardiac myocytes (23).

Other inflammatory cytokines implicated in the pathogenesis of chronic myocardial injury include TNF and IL-1. TNF promotes LV remodeling by altering the ECM. TNF mediates such structural modifications through its ability to activate proenzyme forms of MMPs in myocardial tissues. TNF also promotes activation of the vascular endothelium. The expression of TNF is triggered by myocardial tissue damage and by inflammation, especially in viral myocarditis. IL-1 expression is also interrelated to the cascade of proinflammatory mediators released during CHF. IL-1 causes a negative inotropic effect in LV function by inducing nitric oxide expression and by promoting the production and release of IL-18.

Inflammation associated with tissue remodeling and the progression toward CHF in DCM results in increases in serum levels of soluble adhesion molecules, e.g., soluble intercellular adhesion molecule 1 (sICAM-1), E-selectin, P-selectin, and vascular cellular adhesion molecule 1, expressed by activated cardiovascular endothelial cells. Research reports have shown that serum levels of sICAM-1, measured by capture enzyme-linked immunosorbent assay, accurately correlated ($P < 0.001$) with intramyocardial expression of ICAM-1 in patients with DCM and correlated with the New York Heart Association classification of DCM (24). Thus, multiple serum biomarkers of tissue remodeling, inflammation, and endothelial activation have been shown to correlate with the development and progression of DCM (Table 3); however, other more invasive procedures involving immunohistochemical characterization of endomyocardial biopsies are required for confirmatory/definitive diagnosis and staging of inflammatory cardiomyopathies.

MOLECULAR DIAGNOSTICS FOR CARDIOMYOPATHIES

The field of molecular diagnostics is rapidly expanding the role of the clinical laboratory in almost all areas of medicine, and is consequently helping to usher in a new era of personalized medicine. Elucidating the genetic mutations and signatures associated with specific cardiomyopathies has fundamentally changed the clinical approach to patients with familial myocardial disorders. Genetic testing enables discrimination between various etiologies of myocardial dysfunction, as well as provides valuable information for family members who might be at increased risk for the development of certain types of cardiac disease. In addition, molecular techniques might provide relevant information about disease progression in a number of cardiomyopathies, including hypertrophic cardiomyopathy (HCM) and DCM.

For cardiomyopathies with well-recognized familial clustering, like HCM, genetic testing has identified key genes and mutations responsible for the disease phenotype. HCM is characterized by myocardial thickening, which interferes with cardiac output by limiting ventricular filling and outflow. More than 900 unique mutations in 13 genes have been identified and reported in patients with HCM (25, 26). Most of these mutations occur within genes encoding for sarcomere (thick and thin filaments) or sarcomere-associated (Z-disc and intercalated disc) proteins, which are important for myocyte contraction. Molecular diagnosis of HCM remains challenging since each family usually has a unique mutation (27); however, improved DNA sequencing techniques continue to evolve and are overcoming this problem. Once identified, pathogenic mutations can be subsequently assessed in relatives more easily and at a lower cost. Although there has not been strong correlation between the different genetic causes of DCM and the degree of cardiac hypertrophy, helpful prognostic information is gleaned from defining the mutation. Specifically, patients with a known sarcomere mutation have significantly worse outcomes than patients with an unknown cause of HCM (28). Finally, and importantly, molecular genetics can distinguish HCM from other genetic causes of cardiac hypertrophy, such as metabolic cardiomyopathy secondary to mutations in *PRKAG2*, *LAMP2*, or *GLA* (29).

In contrast to HCM, DCM is a far more genetically heterogeneous disease. Despite this fact, molecular genetics is emerging as a unique way to uncover important clinical clues in familial cases of DCM. The hallmark feature of DCM is ventricular dilation or enlargement, which impairs both systolic and diastolic function. About half of the cases of DCM are secondary to cardiac ischemia, often with multifactorial contributions from conditions like hypertension, valve dysfunction, and various toxic, metabolic, and immunologic abnormalities. The remainder of DCM cases are unrelated to cardiac ischemia, and of these, up to 50% are familial (30). Such cases of familial HCM result from a single mutation in any of a number of genes that encode various cytoskeletal, nucleoskeletal, mitochondrial, or calcium-handling proteins. In fact, >50 genes have been linked to familial DCM (31). For this reason, genetic testing currently relies on multigene panels that test large numbers of genes simultaneously. The availability of next-generation and whole-exome sequencing in clinical laboratories is rapidly expanding the feasibility of identifying unique index mutations in diseases like DCM (32).

Genetic testing for familial DCM, however, remains challenging given the number of candidate genes and the variable penetrance within family members. Familial DCM is passed down as a single gene mutation, most often with

autosomal dominant inheritance and less often with X-linked recessive inheritance. The latter has been described with several genes, including *DMD*, encoding dystrophin; *TAZ*, encoding tafazzin; and *EMD*, encoding emerin. Maternal inheritance of mitochondrial mutations has also been reported in familial DCM. Not surprisingly, several genes implicated in familial DCM overlap with genes identified in HCM, including genes that encode sarcomere and sarcomere-associated proteins. One such protein is titin, encoded by *TTN*, which plays a role in regulating sarcomere length by serving as a stretch sensor and communicating between the sarcomere and the cardiomyocyte (33). Titin mutations have been estimated to account for a quarter of the cases of DCM (34). While many patients with DCM have been found to have truncating *TTN* mutations, many others have *TTN* coding variants of unknown significance. The role of such variants, especially in patients with cardiac comorbidities like hypertension and valve defects, remains to be fully understood. Nevertheless, studies evaluating the pathogenicity of rare DCM variants through the use of computational prediction alogorithms are under way (35).

PATHOGENESIS AND DIAGNOSIS OF INFLAMMATORY CARDIOMYOPATHIES

Inflammatory cardiomyopathy is defined as myocarditis with cardiac dysfunction resulting from infectious, autoimmune, or idiopathic myocarditis. It represents a subset of DCM unrelated to ischemia, and can be associated with any number of infectious (viral, bacterial, fungal, or parasitic) and/or

TABLE 3 Infectious and noninfectious etiologies of inflammatory cardiomyopathy

Category	Disease or organism	Etiology
Infectious		
Viral myocarditis	Enterovirus	Coxsackie B3, B4 virus
	Herpesvirus	Cytomegalovirus, varicella-zoster virus
	Orthomyxovirus	Influenza virus
	Paramyxovirus	Parainfluenza virus
	Parvovirus	
	Retrovirus	HIV
	Adenovirus	
	Flavivirus	Hepatitis C virus
	Reovirus	
Bacterial myocarditis	*Streptococcus*	Group A strep
	Staphylococcus	*S. aureus*
	Serratia	*S. marcescens*
	Chlamydia	
	Salmonella	
	Aerococcus	*A. urinae*
	Ehrlichia	
	Vibrio	*V. cholerae*
Parasitic/protozoal/spirochetal myocarditis	Chagas' disease	*Trypanosoma cruzi*, *Toxoplasma gondii*
	Lyme disease	*Borrelia burgdorferi*
Rickettsial myocarditis	Q fever	
	Rocky Mountain spotted fever	
	Scrub typhus	
Fungal myocarditis	*Cryptococcus*	*C. neoformans*
	Candidiasis	*Candida albicans*
	Histoplasmosis	
	Aspergillus	
Noninfectious		
Autoimmune myocarditis	Rheumatic fever	
	Systemic lupus erythematosus	
	Sjögren's syndrome	
	Dressler's syndrome	Post-myocardial infarction
	Postpartum cardiomyopathy	
	Kawasaki disease	
	Sarcoidosis	
Drug-induced myocarditis	Cardiotoxic myocarditis	Cocaine 999, catecholamines, doxorubicin
	Hypersensitivity myocarditis	Antibiotics, diuretics, others

TABLE 4 Autoantibodies detected in inflammatory cardiomyopathies

Antigen specificity	Type of mimicry
Cardiac α-actin	Enterovirus
Heat shock protein 60	Enterovirus
β-Adrenergic receptor	*T. cruzi*
M2-cholinergic receptor	*T. cruzi*
Laminin	
Actin	
Myosin	Bacterial, enterovirus
Adenine nucleotide translocator	
Vimentin	
Sarcolemma	Enterovirus
Desmin	
Mitochrondrial antigen	Bacterial, enterovirus
Carnitine	
Laminin	
Myolemma	
Sarcolemma	
DNase B	Bacterial
Hyaluronidase	
Streptozyme	

noninfectious (drugs, genetic background, nutritional status, age, or pregnancy) conditions. These are outlined in Table 3. A list of autoantibodies that may be detected in inflammatory cardiomyopathies is provided in Table 4.

Myocyte damage in infectious myocarditis occurs through both the direct and indirect effects of pathogenic agents (36). Certain cardiotropic viruses, like coxsackie B virus, directly damage myocytes and cause necrosis. Adenoviruses induce apoptosis as a way of escaping immune recognition. Infectious agents can also cause heart disease indirectly by inducing immunologic responses (inflammatory cytokines as well as cell-mediated responses) that injure myocytes. Furthermore, the same immune responses engendered during the infectious phase of myocarditis may persist after viral clearance and develop into autoimmune postinfectious myocarditis. Autoimmune myocarditis can occur from a breakdown of tolerance to self antigens due to epitope mimicry, as in chronic rheumatic fever, or from a breakdown in immunologic ignorance due to exposure of normally cryptic self antigens, which can occur during necrosis.

Diagnosis of myocarditis, inflammatory myocarditis, or lymphocytic myocarditis has traditionally been determined by immunohistochemical analysis of endomyocardial biopsies (EMBs) using the Dallas criteria in conjunction with evidence of a 4-fold increase in virus-specific antibody titers between acute and convalescent sera (37). The Dallas criteria, established in 1986, define active, borderline, and absent myocarditis (38). Active myocarditis is the presence of lymphocytic infiltrates with adjacent myocyte necrosis, while borderline myocarditis is the presence of lymphocytic infiltrates without myocyte necrosis. The absence of infiltrating lymphocytes characterizes absent myocarditis. Collection of EMBs presents several challenges, including the fact that the procedure is relatively invasive. In addition, accurate diagnosis relies on histological evidence of a focal lesion that is often expressed only during the acute phase of infection, when obtaining a biopsy may be clinically contraindicated. Even when biopsies are obtained, they are often limited and lesions may be missed.

Currently, immunohistochemical staining and molecular immunological techniques, e.g., PCR and *in situ* hybridization, are being applied to EMB to enhance the sensitivity and specificity of this procedure for the diagnosis of myocarditis. Enzyme-conjugated monoclonal antibodies are used to distinguish different subsets of infiltrating lymphocytes, macrophages, and neutrophils. Molecular assays, e.g., PCR and *in situ* hybridization, are used to detect specific viral sequences within EMBs. These techniques, which help distinguish between productive and nonproductive infections, are useful in discriminating between active, chronic, and postinfectious cases of myocarditis.

Although the immunohistological characterization of leukocytic infiltrates in EMBs is improving, histological confirmation of myocyte damage has been a greater challenge and a source of interobserver variability in the clinical diagnosis of myocarditis using the Dallas criteria. This difficulty in assessing myocyte damage in EMBs may be one explanation for the low frequency (10%) of Dallas criteria-positive EMBs reported in the results of the 1996 Myocarditis Treatment Trial, which enrolled >2,200 patients with reduced ventricular function and no evidence of coronary artery disease (39). A number of new immunohistochemical and molecular assays are currently available. These include annexin binding assays, terminal deoxynucleotidyltransferase-mediated dUTP-biotin nick end labeling (TUNEL)-based assays, and immunohistochemical assays for the detection of apoptosis-related caspases, all of which may be used clinically to identify and discriminate between apoptotic and necrotic cells. Assays for detection and characterization of inflammatory heart disease are listed in Table 5.

Biomarkers are also showing clinical utility in the assessment of certain types of inflammatory cardiomyopathies. Specifically, a role for biomarkers in peripartum cardiomyopathy (PPCM) is rapidly emerging, especially as the pathophysiologic mechanism of this disease is elucidated. PPCM is defined as the new onset of heart failure in a previously healthy woman during pregnancy or shortly postpartum. A unified hypothesis for the pathogenesis of PPCM was recently proposed whereby any number of factors during pregnancy, whether genetic susceptibility, altered immune response, or infection with cardiotropic viruses, ultimately leads to an imbalance in cytokines and cellular immune mediators that results in inflammatory cardiomyopathy and heart failure (40). Focusing on a common pathway leading to myocarditis in pregnancy, despite the various triggers, may allow for the detection of biomarkers suggestive of PPCM earlier and correlation with recovery outcomes.

Studies of PPCM have illuminated racial and ethnic disparities in disease prevalence. A population-based study of PPCM in the United States revealed a birth prevalence of 1 case for every 4,266 live births among white non-Hispanics, which is 4-fold lower than the birth prevalence of 1 case for every 1,087 live births among black non-Hispanics (41). Although the exact mechanism of disease remains uncertain, current observations support an immune-mediated process. Immune alteration in pregnancy ensures that the maternal immune system tolerates foreign paternal fetal antigens while still providing effective antimicrobial responses. However, studies of patients with PPCM have shown striking imbalances of cytokines and subsets of immune cells as compared to patients without PPCM (42, 43). These include the observation that patients with PPCM have an increase in activated regulatory T cells and a decrease in natural killer cells. A large prospective study, Investigations in Pregnancy

TABLE 5 Clinical immunological assays for detection and characterization of inflammatory heart disease[a]

Specimen	Result	Method	Criteria
EMB	Lymphocytic infiltrates	H&E histology	Cellular morphology
	B-cell infiltrates	IHC/IFA	Detection of CD20 surface antigen
	$CD4^+$ T-cell infiltrates	IHC/IFA	Detection of CD3/CD4 surface antigen
	$CD8^+$ T-cell infiltrates	IHC/IFA	Detection of CD3/CD8 surface antigen
	NK-cell infiltrates	IHC/IFA	Detection of CD56 surface antigen
	Macrophage infiltrates	IHC/IFA	Detection of CD14/CD68 surface antigen
	Infection with specific virus	ISH/PCR	Detection of virus-specific DNA or RNA
	Necrosis	H&E histology	Cellular morphology
	Apoptosis	Cardiac TUNEL assay	Fragmented DNA
Serum	Heart-reactive antibodies	IFA/EIA	Detection of IgG anti-cardiac myosin antibodies
	Cardiac myocyte damage	EIA	Dectection of TnT, TnI, or CK-MB
	Cardiac myocyte damage	Anti-myosin scintigraphy	Nuclear imaging with ^{111}indium–anti-myosin
	Diagnosis of viral myocarditis	ELISA	4-fold rise in specific IgG titer
	Diagnosis of rheumatic myocarditis	Anti-streptolysin O test	

[a]H&E, hematoxylin and eosin; IHC, immunohistochemistry; IFA, immunofluorescence assay; ISH, *in situ* hybridization; EIA, enzyme immunoassay; ELISA, enzyme-linked immunosorbent assay.

Associated Cardiomyopathy (IPAC), is currently under way by the Peripartum Cardiomyopathy Network to assess any correlation between immune system activation and patient outcomes in PPCM.

Several biomarkers believed to play a role in PPCM have been proposed to aid in diagnosis. These include prolactin metabolites, sFLT1, high-sensitivity C-reactive protein (hsCRP), and certain cardiac autoantibodies (44). Investigators have found that prolactin metabolites, called vasoinhibins, generated during pregnancy by oxidative stress can be cardiotoxic and actually drive the PPCM phenotype (45). This has led to studies evaluating the use of the prolactin antagonist bromocriptine for the treatment of PPCM (46). Another candidate biomarker for PPCM is sFLT1, an enzyme in the tyrosine kinase family with known antiangiogenic effects. Plasma sFLT1 appears to be cardiotoxic and is significantly elevated not only in patients with PPCM but also in patients with preeclampsia (47, 48). hsCRP is a nonspecific proinflammatory cytokine; still, its measurement may have utility in PPCM diagnosis and prognosis. Multiple studies, including those being conducted in Haiti, China, and South Africa, have shown that women with PPCM have significantly elevated levels of hsCRP compared to non-PPCM mothers (49–51). Conclusions drawn from the Haitian study implicate a role for hsCRP levels in predicting the chance of disease recovery, since recovered PPCM patients had significantly higher mean serum hsCRP levels compared to nonrecovered PPCM patients. Finally, cardiac autoantibodies are believed to contribute to the pathogenesis of PPCM and may potentially serve as biomarkers, as in other subtypes of inflammatory cardiomyopathy. Evidence comes from reports of cardiac β1-adrenoreceptor antibodies and cardiac myosin heavy chain antibodies in patients with PPCM. Detection of such antibodies early in the disease course may not only aid in diagnostic recognition but also limit their pathogenic contribution later in the disease course (52, 53). Widespread adoption of cardiac biomarker testing for disease diagnosis, prognosis, and monitoring of all types of cardiomyopathy is expected as evidence regarding the clinical utility of biomarker assays becomes increasingly available.

REFERENCES

1. **Gotlieb AI, Freeman MR, Salerno TA, Lichtenstein SV, Armstrong PW.** 1991. Ultrastructural studies of unstable angina in living man. *Mod Pathol* **4:**75–80. PubMed
2. **Levin ER, Gardner DG, Samson WK.** 1998. Natriuretic peptides. *N Engl J Med* **339:**321–328. PubMed
3. **Apple FS, Quist HE, Doyle PJ, Otto AP, Murakami MM.** 2003. Plasma 99th percentile reference limits for cardiac troponin and creatine kinase MB mass for use with European Society of Cardiology/American College of Cardiology consensus recommendations. *Clin Chem* **49:**1331–1336. PubMed
4. **McCord J, Nowak RM, McCullough PA, Foreback C, Borzak S, Tokarski G, Tomlanovich MC, Jacobsen G, Weaver WD.** 2001. Ninety-minute exclusion of acute myocardial infarction by use of quantitative point-of-care testing of myoglobin and troponin I. *Circulation* **104:**1483–1488. PubMed
5. **Khan SQ, Dhillon OS, O'Brien RJ, Struck J, Quinn PA, Morgenthaler NG, Squire IB, Davies JE, Bergmann A, Ng LL.** 2007. C-terminal provasopressin (copeptin) as a novel and prognostic marker in acute myocardial infarction: Leicester Acute Myocardial Infarction Peptide (LAMP) study. *Circulation* **115:**2103–2110. PubMed
6. **Nickel CH, Bingisser R, Morgenthaler NG.** 2012. The role of copeptin as a diagnostic and prognostic biomarker for risk stratification in the emergency department. *BMC Med* **10:**7. doi:10.1186/1741-7015-10-7. PubMed
7. **Seino Y, Ogata K, Takano T, Ishii J, Hishida H, Morita H, Takeshita H, Takagi Y, Sugiyama H, Tanaka T, Kitaura Y.** 2003. Use of a whole blood rapid panel test for heart-type fatty acid-binding protein in patients with acute chest pain: comparison with rapid troponin T and myoglobin tests. *Am J Med* **115:**185–190. PubMed
8. **de Lemos JA, Morrow DA, Gibson CM, Murphy SA, Sabatine MS, Rifai N, McCabe CH, Antman EM, Cannon CP, Braunwald E.** 2002. The prognostic value of serum myoglobin in patients with non-ST-segment elevation acute coronary syndromes. Results from the TIMI 11B and TACTICS-TIMI 18 studies. *J Am Coll Cardiol* **40:**238–244. PubMed
9. **Kilcullen N, Viswanathan K, Das R, Morrell C, Farrin A, Barth JH, Hall AS, EMMACE-2 Investigators.** 2007.

Heart-type fatty acid-binding protein predicts long-term mortality after acute coronary syndrome and identifies high-risk patients across the range of troponin values. *J Am Coll Cardiol* **50:**2061–2067. PubMed

10. **Altieri P, Brunelli C, Garibaldi S, Nicolino A, Ubaldi S, Spallarossa P, Olivotti L, Rossettin P, Barsotti A, Ghigliotti G.** 2003. Metalloproteinases 2 and 9 are increased in plasma of patients with heart failure. *Eur J Clin Invest* **33:**648–656. PubMed
11. **Mann DL.** 2003. Stress-activated cytokines and the heart: from adaptation to maladaptation. *Annu Rev Physiol* **65:**81–101. PubMed
12. **Schwartzkopff B, Fassbach M, Pelzer B, Brehm M, Strauer BE.** 2002. Elevated serum markers of collagen degradation in patients with mild to moderate dilated cardiomyopathy. *Eur J Heart Fail* **4:**439–444. PubMed
13. **Yamazaki T, Lee JD, Shimizu H, Uzui H, Ueda T.** 2004. Circulating matrix metalloproteinase-2 is elevated in patients with congestive heart failure. *Eur J Heart Fail* **6:**41–45. PubMed
14. **Feuerstein GZ, Rozanski D.** 2000. G proteins and heart failure: is Gαq a novel target for heart failure? *Circ Res* **87:**1085–1086. PubMed
15. **Wettschureck N, Rütten H, Zywietz A, Gehring D, Wilkie TM, Chen J, Chien KR, Offermanns S.** 2001. Absence of pressure overload induced myocardial hypertrophy after conditional inactivation of $G\alpha_q/G\alpha_{11}$ in cardiomyocytes. *Nat Med* **7:**1236–1240. PubMed
16. **Suzuki T, Yamazaki T, Yazaki Y.** 2001. The role of the natriuretic peptides in the cardiovascular system. *Cardiovasc Res* **51:**489–494. PubMed
17. **Prontera C, Emdin M, Zucchelli GC, Ripoli A, Passino C, Clerico A.** 2003. Natriuretic peptides (NPs): automated electrochemiluminescent immunoassay for N-terminal pro-BNP compared with IRMAs for ANP and BNP in heart failure patients and healthy individuals. *Clin Chem* **49:**1552–1554. PubMed
18. **Li YY, McTiernan CF, Feldman AM.** 2000. Interplay of matrix metalloproteinases, tissue inhibitors of metalloproteinases and their regulators in cardiac matrix remodeling. *Cardiovasc Res* **46:**214–224. PubMed
19. **Upadhya B, Kontos JL, Ardeshirpour F, Pye J, Boucher WS, Theoharides TC, Dehmer GJ, Deliargyris EN.** 2004. Relation of serum levels of mast cell tryptase of left ventricular systolic function, left ventricular volume or congestive heart failure. *J Card Fail* **10:**31–35. PubMed
20. **Aukrust P, Ueland T, Lien E, Bendtzen K, Müller F, Andreassen AK, Nordøy I, Aass H, Espevik T, Simonsen S, Frøland SS, Gullestad L.** 1999. Cytokine network in congestive heart failure secondary to ischemic or idiopathic dilated cardiomyopathy. *Am J Cardiol* **83:**376–382. PubMed
21. **Tsutamoto T, Hisanaga T, Wada A, Maeda K, Ohnishi M, Fukai D, Mabuchi N, Sawaki M, Kinoshita M.** 1998. Interleukin-6 spillover in the peripheral circulation increases with the severity of heart failure, and the high plasma level of interleukin-6 is an important prognostic predictor in patients with congestive heart failure. *J Am Coll Cardiol* **31:**391–398. PubMed
22. **Gullestad L, Aukrust P, Ueland T, Espevik T, Yee G, Vagelos R, Frøland SS, Fowler M.** 1999. Effect of high- versus low-dose angiotensin converting enzyme inhibition on cytokine levels in chronic heart failure. *J Am Coll Cardiol* **34:**2061–2067. PubMed
23. **Wollert KC, Drexler H.** 2001. The role of interleukin-6 in the failing heart. *Heart Fail Rev* **6:**95–103. PubMed
24. **Noutsias M, Hohmann C, Pauschinger M, Schwimmbeck PL, Ostermann K, Rode U, Yacoub MH, Kühl U, Schultheiss HP.** 2003. sICAM-1 correlates with myocardial ICAM-1 expression in dilated cardiomyopathy. *Int J Cardiol* **91:**153–161. PubMed
25. **Alcalai R, Seidman JG, Seidman CE.** 2008. Genetic basis of hypertrophic cardiomyopathy: from bench to the clinics. *J Cardiovasc Electrophysiol* **19:**104–110. PubMed
26. **Keren A, Syrris P, McKenna WJ.** 2008. Hypertrophic cardiomyopathy: the genetic determinants of clinical disease expression. *Nat Clin Pract Cardiovasc Med* **5:**158–168. PubMed
27. **Watkins H, Ashrafian H, McKenna WJ.** 2008. The genetics of hypertrophic cardiomyopathy: teare redux. *Heart* **94:**1264–1268. PubMed
28. **Olivotto I, Girolami F, Ackerman MJ, Nistri S, Bos JM, Zachara E, Ommen SR, Theis JL, Vaubel RA, Re F, Armentano C, Poggesi C, Torricelli F, Cecchi F.** 2008. Myofilament protein gene mutation screening and outcome of patients with hypertrophic cardiomyopathy. *Mayo Clin Proc* **83:**630–638. PubMed
29. **Wang L, Seidman JG, Seidman CE.** 2010. Narrative review: harnessing molecular genetics for the diagnosis and management of hypertrophic cardiomyopathy. *Ann Intern Med* **152:**513–520, W181. PubMed
30. **Petretta M, Pirozzi F, Sasso L, Paglia A, Bonaduce D.** 2011. Review and metaanalysis of the frequency of familial dilated cardiomyopathy. *Am J Cardiol* **108:**1171–1176. PubMed
31. **McNally EM, Golbus JR, Puckelwartz MJ.** 2013. Genetic mutations and mechanisms in dilated cardiomyopathy. *J Clin Invest* **123:**19–26. PubMed
32. **Gahl WA, Markello TC, Toro C, Fajardo KF, Sincan M, Gill F, Carlson-Donohoe H, Gropman A, Pierson TM, Golas G, Wolfe L, Groden C, Godfrey R, Nehrebecky M, Wahl C, Landis DM, Yang S, Madeo A, Mullikin JC, Boerkoel CF, Tifft CJ, Adams D.** 2012. The National Institutes of Health Undiagnosed Diseases Program: insights into rare diseases. *Genet Med* **14:**51–59. PubMed
33. **LeWinter MM, Wu Y, Labeit S, Granzier H.** 2007. Cardiac titin: structure, functions and role in disease. *Clin Chim Acta* **375:**1–9. PubMed
34. **Herman DS, Lam L, Taylor MR, Wang L, Teekakirikul P, Christodoulou D, Conner L, DePalma SR, McDonough B, Sparks E, Teodorescu DL, Cirino AL, Banner NR, Pennell DJ, Graw S, Merlo M, Di Lenarda A, Sinagra G, Bos JM, Ackerman MJ, Mitchell RN, Murry CE, Lakdawala NK, Ho CY, Barton PJ, Cook SA, Mestroni L, Seidman JG, Seidman CE.** 2012. Truncations of titin causing dilated cardiomyopathy. *N Engl J Med* **366:**619–628. PubMed
35. **Norton N, Robertson PD, Rieder MJ, Züchner S, Rampersaud E, Martin E, Li D, Nickerson DA, Hershberger RE, National Heart, Lung and Blood Institute GO Exome Sequencing Project.** 2012. Evaluating pathogenicity of rare variants from dilated cardiomyopathy in the exome era. *Circ Cardiovasc Genet* **5:**167–174. PubMed
36. **Mason JW.** 2003. Myocarditis and dilated cardiomyopathy: an inflammatory link. *Cardiovasc Res* **60:**5–10. PubMed
37. **Aretz HT.** 1987. Myocarditis: the Dallas criteria. *Hum Pathol* **18:**619–624. PubMed
38. **Aretz HT, Billingham ME, Edwards WD, Factor SM, Fallon JT, Fenoglio JJ Jr, Olsen EG, Schoen FJ.** 1987. Myocarditis. A histopathologic definition and classification. *Am J Cardiovasc Pathol* **1:**3–14. PubMed
39. **Mason JW.** 1996. Immunopathogenesis and treatment of myocarditis: the United States Myocarditis Treatment Trial. *J Card Fail* **2**(Suppl)**:**S173–S177. PubMed
40. **Fett JD, McTiernan CF.** 2011. Towards a unifying hypothesis for the pathogenesis of peripartum cardiomyopathy. *Int J Cardiol* **153:**1–3. PubMed
41. **Harper MA, Meyer RE, Berg CJ.** 2012. Peripartum cardiomyopathy: population-based birth prevalence and 7-year mortality. *Obstet Gynecol* **120:**1013–1019. PubMed
42. **Fett JD, Ansari AA.** 2010. Inflammatory markers and cytokines in peripartum cardiomyopathy: a delicate balance. *Expert Opin Ther Targets* **14:**895–898. PubMed

43. **McTiernan C, Hanley-Yanez K, Pisarcik JE, Morel PA, Cooper LT, Elkayam E, Fett JD, McNamara DM.** 2011. Activation of cellular immunity in peripartum cardiomyopathy: results of the multicenter IPAC Registry. *Circulation* **124:**A14173. https://circ.ahajournals.org/cgi/content/meeting_abstract/124/21_MeetingAbstracts/A14173.
44. **Fett JD.** 2013. Earlier detection can help avoid many serious complications of peripartum cardiomyopathy. *Future Cardiol* **9:**809–816. PubMed
45. **Hilfiker-Kleiner D, Kaminski K, Podewski E, Bonda T, Schaefer A, Sliwa K, Forster O, Quint A, Landmesser U, Doerries C, Luchtefeld M, Poli V, Schneider MD, Balligand JL, Desjardins F, Ansari A, Struman I, Nguyen NQ, Zschemisch NH, Klein G, Heusch G, Schulz R, Hilfiker A, Drexler H.** 2007. A cathepsin D-cleaved 16 kDa form of prolactin mediates postpartum cardiomyopathy. *Cell* **128:**589–600. PubMed
46. **Sliwa K, Blauwet L, Tibazarwa K, Libhaber E, Smedema JP, Becker A, McMurray J, Yamac H, Labidi S, Struman I, Hilfiker-Kleiner D.** 2010. Evaluation of bromocriptine in the treatment of acute severe peripartum cardiomyopathy: a proof-of-concept pilot study. *Circulation* **121:**1465–1473. PubMed
47. **Patten IS, Rana S, Shahul S, Rowe GC, Jang C, Liu L, Hacker MR, Rhee JS, Mitchell J, Mahmood F, Hess P, Farrell C, Koulisis N, Khankin EV, Burke SD, Tudorache I, Bauersachs J, del Monte F, Hilfiker-Kleiner D, Karumanchi SA, Arany Z.** 2012. Cardiac angiogenic imbalance leads to peripartum cardiomyopathy. *Nature* **485:**333–338. PubMed
48. **Rana S, Powe CE, Salahuddin S, Verlohren S, Perschel FH, Levine RJ, Lim KH, Wenger JB, Thadhani R, Karumanchi SA.** 2012. Angiogenic factors and the risk of adverse outcomes in women with suspected preeclampsia. *Circulation* **125:**911–919. PubMed
49. **Fett JD, Sannon H, Thélisma E, Sprunger T, Suresh V.** 2009. Recovery from severe heart failure following peripartum cardiomyopathy. *Int J Gynaecol Obstet* **104:**125–127. PubMed
50. **Huang GY, Zhang LY, Long-Le MA, Wang LX.** 2012. Clinical characteristics and risk factors for peripartum cardiomyopathy. *Afr Health Sci* **12:**26–31. PubMed
51. **Sliwa K, Förster O, Libhaber E, Fett JD, Sundstrom JB, Hilfiker-Kleiner D, Ansari AA.** 2006. Peripartum cardiomyopathy: inflammatory markers as predictors of outcome in 100 prospectively studied patients. *Eur Heart J* **27:**441–446. PubMed
52. **Warraich RS, Sliwa K, Damasceno A, Carraway R, Sundrom B, Arif G, Essop R, Ansari A, Fett J, Yacoub M.** 2005. Impact of pregnancy-related heart failure on humoral immunity: clinical relevance of G3-subclass immunoglobulins in peripartum cardiomyopathy. *Am Heart J* **150:**263–269. PubMed
53. **Mascaro-Blanco A, Alvarez K, Yu X, Lindenfeld J, Olansky L, Lyons T, Duvall D, Heuser JS, Gosmanova A, Rubenstein CJ, Cooper LT, Kem DC, Cunningham MW.** 2008. Consequences of unlocking the cardiac myosin molecule in human myocarditis and cardiomyopathies. *Autoimmunity* **41:**442–453. PubMed

Celiac Disease and Inflammatory Bowel Disease

MELISSA R. SNYDER

103

Celiac disease (CeD) and inflammatory bowel disease (IBD) are chronic inflammatory diseases affecting the gastrointestinal tract. They share certain characteristics, including autoimmune features, the presence of both gastrointestinal and systemic clinical symptoms, and pathogenic contributions by genetic and environmental factors. However, there are several stark differences that must be appreciated. The immunogenic mechanisms of the two diseases are unique, with differing contributions by the innate and adaptive immune responses. Histologically, CeD is distinct from IBD, which is useful diagnostically as well as for gaining insight into disease mechanisms. Lastly, the role of diagnostic laboratory testing, both serologic and genetic, differs greatly between CeD and IBD. The purpose of this chapter is to provide a summary of what is currently known about the pathogenesis, epidemiology, clinical presentation, and diagnostic testing for CeD and IBD.

CELIAC DISEASE

Introduction

CeD results from an inflammatory reaction within the small intestine that is initiated, in genetically predisposed individuals, by ingestion of gluten (1, 2). The incidence of CeD appears to be on the rise in a number of populations throughout the world. Patients may present with gastrointestinal and/or systemic symptoms consistent with malabsorption. The diagnosis of CeD is based on histological evidence of small intestinal villous atrophy and positive antibody serology.

Pathology

For an individual to develop CeD, two criteria must be met: an appropriate genetic background and the necessary environmental exposure. The genetic component of CeD has long been recognized, based on observations that first-degree relatives of patients with CeD have a higher risk of developing the disease compared to the general population (3). At least 50% of the genetic predisposition is associated with HLA-DQ2 and HLA-DQ8. These alleles are closely linked to the second criterion—the environmental exposure—which is dietary gluten.

Gluten is a protein found in wheat, barley, and rye. Gliadin, which is the alcohol-soluble component of gluten, contains large numbers of proline residues, making it particularly resistant to proteolytic degradation (4). As a result, large peptides, some >30 amino acids in length, are produced within the small intestine. Gliadin also contains many glutamine residues, making these peptides attractive substrates for tissue transglutaminase (tTG) (5). tTG converts glutamine residues present in peptides and proteins, specifically in Q-X-P sequences, to glutamic acid, leading to an overall increase in the number of negative charges. HLA-DQ2 and HLA-DQ8 preferentially bind to peptides with negatively charged side chains, particularly deamidated gliadin (DG) peptides (6). The HLA/gliadin complex, present on the surface of antigen-presenting cells, interacts with $CD4^+$ T cells, leading to activation and expansion of DG-specific T cells. These $CD4^+$ T cells then stimulate B cells, resulting in activation of the humoral immune response and production of the anti-DG and anti-tTG antibodies that are characteristic of CeD. In addition, cytotoxic intraepithelial lymphocytes (IELs) are activated and kill enterocytes, which leads to damage of the small intestinal villi, resulting in blunting and atrophy. The only treatment currently available for CeD is strict adherence to a gluten-free diet (GFD). Removal of the inciting antigen downregulates the immune response, resulting in reconstitution of villous structure and decreased production of celiac-specific antibodies.

Epidemiology

In the United States, CeD is estimated to affect 1% of the population, which is similar to the findings of epidemiological studies in northern Europe (7, 8). In some southern European and sub-Saharan African countries, estimates of CeD prevalence are as high as 5 to 6%. In most Asian countries, including China and Japan, CeD is rarely diagnosed and only case reports exist in the literature. Differences in prevalence across geographic areas may reflect genetic diversity, variations in wheat consumption, or a combination. It appears that the prevalence of CeD is increasing in the United States and Europe (8, 9). This can, at least partially, be attributed to improved diagnostic testing and greater awareness of the disease. However, several studies using retrospective sample sets analyzed with current serologic tests have shown that the actual incidence of CeD is increasing (8). The exact reason behind this is unclear, although possibilities include changes in wheat genetics and/or processing,

doi:10.1128/9781555818722.ch103

altered exposure to cereal grains (particularly in childhood), and/or differences in childhood infections.

Clinical Manifestations

The direct consequences of the villous atrophy characteristic of CeD is chronic malabsorption (10). Malabsorption can result in weight loss in adults or "failure to thrive" in children. Ultimately, malabsorption can lead to steatorrhea, abdominal pain, and/or bloating. However, it is estimated that <50% of patients with CeD present to their physician with overt gastrointestinal symptoms (1). Many patients are identified based on more general manifestations of malabsorption, such as iron deficiency anemia, hypoproteinemia, or hypocalcemia/osteoporosis. Patients with CeD may also display liver function abnormalities, such as increased alanine aminotransferase levels. These elevations, however, are usually an incidental finding, with clinically significant liver disease being relatively rare.

CeD is also associated with a number of other immune-mediated diseases. Many of these coexisting conditions have an autoimmune etiology, including type 1 diabetes, autoimmune thyroid disease, and Addison's disease (11). The incidence of CeD in type 1 diabetics ranges from 2 to 8%. Some recommendations suggest that all type 1 diabetics should be routinely screened for CeD, although this remains controversial. Dermatitis herpetiformis (DH) is a relatively uncommon condition that occurs in the context of CeD (12). DH manifests as intensely pruritic lesions, most frequently on the elbows, knees, and forearms. DH is triggered by gliadin peptides and responds to a GFD. In the vast majority of patients with DH, villous atrophy is evident on small intestinal biopsy, although mostly in the absence of gastrointestinal symptoms. Another immune system abnormality, selective IgA deficiency, is also found more frequently in patients with CeD compared to the general population (13). Selective IgA deficiency is defined as low or undetectable concentrations of IgA in the presence of normal IgG and IgM production. Most individuals with selective IgA have no clinical evidence of immunodeficiency. However, because the serological evaluation includes IgA isotypes, selective IgA deficiency must be considered during testing for suspected CeD.

Diagnosis

Biopsy

Atrophy of the small intestinal villi can be visualized histologically. Most recommendations suggest that four to six biopsy samples be obtained during endoscopy in order to avoid false-negative results associated with patchy inflammation. The modified Marsh criteria are frequently used for evaluation of small intestinal biopsies (14). According to these criteria, type 0 is characterized by normal villous architecture; type 1 by increased numbers of IELs; type 2 by increased IELs and crypt hyperplasia; and type 3 by increased IELs, crypt hyperplasia, and villous atrophy (ranging from partial to total). Although often considered the gold standard for diagnosis of CeD, villous atrophy of the small intestine can be observed in a variety of other conditions, including tropical sprue, bacterial overgrowth, and infectious enteritis.

EMAs and Anti-tTG Antibodies

Endomysial antibodies (EMAs) are specific for the tissue that surrounds smooth muscle fibers, known as the endomysium (Fig. 1). EMAs were ultimately shown to be specific for the antigen tTG. EMA testing in the clinical lab is performed by immunofluorescence assays (IFAs), while testing for anti-tTG antibodies is generally performed by some type of solid-phase immunoassay. Testing for IgA and IgG isotypes is frequently available for both EMA and anti-tTG antibodies.

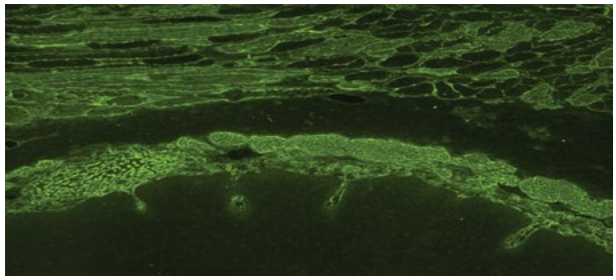

FIGURE 1 EMA by indirect immunofluorescence. The presence of an EMA is identified based on the appearance of latticework staining of the endomysium surrounding the smooth muscle fiber. This photo is a 10× magnification of an indirect immunofluorescence method using monkey esophagus. (Photo courtesy of the Immunodermatology Laboratory, Mayo Clinic, Rochester, MN.)

The specificity of EMA-IgA for CeD approaches 100%, with sensitivities in the range of 90 to 95% (15, 16) (Table 1). Anti-tTG-IgA tends to have very similar diagnostic performance, with sensitivities and specificities as high as 90 to 95% having been reported for CeD. In addition, the anti-tTG-IgA tests overcome some of the limitations of the EMA IFA, including improved quantitation and reduced subjectivity. However, it is important to realize that some variations in anti-tTG-IgA assays exist, related in large part to the source of the antigen (17).

In comparisons of anti-tTG-IgA and anti-tTG-IgG, most data indicate that anti-tTG-IgA has significantly better sensitivity and specificity compared with anti-tTG-IgG (15, 16, 18). However, most studies of this type have been performed in CeD cohorts composed primarily of patients with normal total IgA. For patients with IgA deficiency, testing for anti-tTG-IgG is clearly necessary to avoid false-negative results that would occur in the absence of the IgA isotype.

Anti-Gliadin and Anti-DG Antibodies

Anti-gliadin (GL) antibodies were the first serological marker identified in patients with CeD. However, as EMA and anti-tTG tests were developed, it became clear that these markers offered improved diagnostic sensitivity and specificity compared with anti-GL antibodies (15, 16, 19) (Table 1). Because gliadin is an excellent substrate for tTG, it was hypothesized that antibodies to DG might serve as a better serological marker. Anti-DG-IgA does, in fact, have very similar diagnostic sensitivity and specificity compared to anti-tTG-IgA, especially in adults (20). In children, anti-DG-IgA may offer some improvements in sensitivity (16). In terms of the IgG isotypes, anti-DG-IgG may have better diagnostic utility compared with anti-tTG-IgG, in large part due to improved sensitivity (19). However, these data again come mostly from unselected CeD groups; whether the increased sensitivity of anti-DG-IgG holds true for patients with selective IgA deficiency is still largely unanswered.

HLA Typing

CeD is one of the few chronic inflammatory diseases in which genetic testing, specifically for HLA-DQ2 and HLA-DQ8, plays a role in diagnostic testing. Identification of celiac-associated HLA genotypes requires characterization of both the α and β chains (21). HLA-DQ2.5

TABLE 1 Summary of serologic tests available for evaluation of suspected CeD and IBD

Disease	Antibody	Antigen specificity	Methodology	Isotype	Sensitivity (reference[s])	Specificity (reference[s])	Testing recommendations
CeD	EMA	tTG	Indirect immunofluorescence	IgA	90% (15)	99% (15)	Use as screening test limited by manual methodology; Testing should only be performed in patients on a gluten-containing diet
				IgG	NA[a]	NA	Should be restricted to patients with IgA deficiency
	Anti-tTG	tTG	Solid-phase immunoassay	IgA	78% (18, 19)	98% (18, 19)	Optimal screening test for patients with normal total IgA
				IgG	28% (18, 19)	97% (18, 19)	Should be restricted to patients with IgA deficiency
	Anti-DG	Deamidated gliadin	Solid-phase immunoassay	IgA	74% (18, 19)	95% (18, 19)	May be most useful for diagnosis of CeD in children
				IgG	65% (18, 19)	98% (18, 19)	Should be restricted to patients with IgA deficiency
	Anti-GL	Unmodified gliadin	Solid-phase immunoassay	IgA	63% (18, 19)	90% (18, 19)	No longer recommended for routine testing and should be replaced with anti-tTG and anti-DG
				IgG	42% (18, 19)	90% (18, 19)	
IBD: UC and CD	Atypical pANCA	Unknown	Indirect immunofluorescence	IgG	55% for UC (combined with negative ASCA result) (44)	81% for UC (combined with negative ASCA result) (44)	Not recommended for screening or differentiating IBD from non-IBD, but may be useful, in combination, for subset of patients for whom the diagnosis of UC vs CD is unclear
	ASCA	Cell wall mannan of *S. cerevisiae*	Solid-phase immunoassay	IgA	38% for CD (combined with negative pANCA result) (44)	94% for CD (combined with negative pANCA result) (44)	
				IgG			

[a]NA, not available.

is composed of DQA1*05:xx and DQB1*02:01. A single copy of this genotype is sufficient for predisposing an individual to development of CeD, although homozygosity increases the risk further. HLA-DQ2.2, composed of DQA1*02:01 and DQB1*02:02, also confers some risk for CeD, although generally only in homozygous individuals. Lastly, heterozygosity for DQA1*03:xx and DQB1*03:02, which forms the HLA-DQ8 molecule, also is a substantial risk factor for CeD.

In most populations, 90 to 95% of patients with CeD carry an HLA-DQ2 genotype, with the remaining 5 to 10% being positive for HLA-DQ8 (21). However, in North America and Europe, ~30 to 40% of the total population can be expected to be positive for either allele. Therefore, the presence of HLA-DQ2/DQ8 is necessary, but not sufficient, for the development of CeD.

Testing Recommendations

The multitude of options available for CeD testing can be overwhelming and can cause significant confusion regarding which tests are most appropriate for a given patient. Numerous guidelines and diagnostic algorithms have been published (22–24), based on which it is possible to make several general recommendations:

1. Testing for anti-tTG-IgA is the optimal screening test in patients who have normal concentrations of total IgA.
2. Testing for anti-tTG-IgG and anti-DG-IgG should be restricted to patients with documented selective IgA deficiency.
3. In children, especially those <2 years of age, anti-DG-IgA and anti-DG-IgG testing could be combined with anti-tTG-IgA to improve diagnostic sensitivity.
4. All serologic testing should be performed in patients on a gluten-containing diet.
5. Histological evaluation for villous atrophy is a useful confirmatory test in patients with positive serology or in patients with a high pretest probability of CeD based on clinical evaluation.
6. HLA-DQ2 and HLA-DQ8 typing should only be used to exclude CeD as a diagnosis in certain situations, such as in patients with equivocal biopsy results or in patients on a GFD at the time of serology testing.

Monitoring of Patients with Diagnosed CeD

Following a diagnosis of CeD, monitoring for responses to the GFD is an important part of patient management. Consultation with and guidance from a dietitian is a critical component, not only for exclusion of dietary gluten but also to ensure maintenance of adequate nutrition. Implementation of a successful GFD is accompanied, for most patients, by improvements in clinical symptoms, healing of the small intestinal villi, and decreasing concentrations of gluten-specific antibodies. Serological assessment provides a relatively noninvasive approach to monitoring of the gluten-initiated inflammatory response. The choice of which serological marker depends on which specific antibody the patient was positive for at diagnosis. For most patients, this is likely anti-tTG-IgA or EMA (25–27). Anti-tTG-IgA offers some advantages over EMA for the purposes of monitoring, including numerical quantitation (compared to positive/negative or titer), improved precision, and less subjective interpretation. Although decreasing concentrations of these antibodies are associated with downregulation of the gluten-initiated immune reaction, even conversion to negative serology is not always indicative of complete mucosal healing. Only histological analysis of a small intestinal biopsy can determine if a patient, despite improved clinical symptoms and negative serology, has any remaining degree of villous atrophy.

INFLAMMATORY BOWEL DISEASE

Introduction

IBD encompasses two distinct disorders: ulcerative colitis (UC) and Crohn's disease (CD) (28, 29). UC and CD can be distinguished from one another based on clinical presentation, patterns of inflammation, and, on a limited basis, serologic testing. The pathogenesis of UC and CD involves interactions between the innate immune response and the intestinal microbiome. Epidemiologic studies indicate that IBD is a disease of the developed world. The diagnosis of IBD, and classification as UC or CD, remains challenging due to varied clinical manifestations and lack of sensitive serological biomarkers.

Pathology

IBD results from a complex association between genetic and environmental factors. The genetic component is well recognized, including observations that close to 10% of patients with IBD have an affected first-degree relative (30). Many of the genes identified as risk factors for IBD have a role in the innate immune system. This has led to the hypothesis that disruption of the balance between luminal bacteria and the host immune response may be the initiating event in IBD, ultimately leading to the chronic inflammation characteristic of the disease (31). This is supported indirectly by evidence showing the efficacy of antibiotics and probiotics in the treatment of IBD. In addition, mouse models have demonstrated that experimental colitis can develop only in animals with gastrointestinal biota.

One gene clearly shown to be associated with IBD, specifically CD, is *NOD2/CARD15*. In some populations, homozygosity for certain *NOD2/CARD15* polymorphisms has an odds ratio of >15 for development of CD (30). The *NOD2/CARD15* gene encodes a pattern recognition protein that binds to muramyl dipeptide, a component of bacterial peptidoglycans. It has been suggested that mutations in *NOD2/CARD15* could lead to impaired negative regulation of normal gut biota. Other IBD-related genes also appear to be relevant to the innate immune response (31). *ATG16L1* and *IRGM* are important autophagic factors that play a role in the degradation of microbes and damaged cells. Disruption of autophagy could lead to reduced pathogen clearance, setting the stage for an enhanced inflammatory reaction. *IL23R*, the gene that encodes the interleukin-23 receptor, also plays an important role in several inflammatory pathways, including potentiation of Th17 cellular activation. Polymorphisms in *IL23R* could lead to increased activation of Th17 cells, a mechanism that has been proposed in a number of chronic inflammatory diseases.

Environmental factors are equally important in the pathogenesis of IBD, as highlighted by the observation that concordance in monozygotic twins is only ~20% in UC and ~50% in CD (30). As genetic studies implicate the interaction between the innate immune system and the intestinal microbiota in the development of IBD, one might expect that alterations in the intestinal biota caused by environmental factors could initiate an abnormal immune response in a genetically susceptible individual (32). However, because of the complexity, it has been difficult to demonstrate conclusively that any differences exist between the microbiota of

patients with IBD and control groups. Another piece of evidence suggesting a role of the environment is the observation that IBD is a disease primarily of industrialized populations (33). The reason for this is likely multifactorial. Developed societies tend to have improved sanitation, suggesting that decreased exposure to microbes might prevent development of a normal immune repertoire, predisposing individuals to abnormal immune responses (hygiene hypothesis). However, industrialized societies have additional environmental exposures, along with differences in diet, that could contribute to the risk of IBD. Other environmental factors suggested to have a role in IBD include smoking, breastfeeding as infants, and antibiotic use in children. However, published reports on these various factors are conflicting, which may reflect differences in patient populations or simply the overall complexity of IBD (32).

Epidemiology

Epidemiologic studies of IBD are challenging, primarily because a gold standard diagnostic test for IBD remains elusive. However, most studies have concluded that the highest reported rates are found in North America and Europe, where upper estimates for the incidence of UC are 19.2/100,000 and 24.3/100,000, respectively, compared to 6.3/100,000 in Asia and the Middle East (34). Similar geographic trends are observed for CD. In addition, the incidence of IBD appears to be on the rise, particularly as countries become industrialized. In a recent systematic review, 107 studies were identified in which there were at least three IBD incidence rate estimates over a period of at least 10 years (34). In 75% of the CD studies and 60% of the UC studies, a statistically significant increase in disease incidence was observed. This review also included studies that, collectively, determined that for both UC and CD, the peak age of incidence appears to occur during the third and fourth decades of life. Because IBD strikes at younger ages, and with the increasing incidence of disease, there are concerns that IBD could pose a serious burden to health care resources, particularly in developing countries.

Clinical Characteristics

Patients with UC and CD may present with intestinal and/or extraintestinal symptoms. The gastrointestinal symptoms differ significantly between UC and CD, largely due to differences in affected anatomical sites and patterns of inflammation (35). Most patients with UC have involvement of the rectum, with variations in the degree of proximal colonic involvement. The inflammation in UC is usually restricted to the mucosa, although it tends to be continuous across all affected areas. The most common gastrointestinal symptom in UC is the presence of blood and/or mucus in the stool; patients may also complain of significant cramping in the lower abdomen. CD, in contrast, may affect any part of the gastrointestinal tract. The inflammation often is transmural and is mostly "patchy," with affected areas interspersed with normal tissue. Because of the segmental nature of the inflammation and the more varied localization, the clinical symptoms of CD tend to be subtler in comparison to those of UC. Patients may present with abdominal pain, nausea, epigastric pain, or dysphagia. In addition, because of the transmural inflammation, patients with CD are at risk for the development of fistulas.

Some of the extraintestinal symptoms of IBD, such as weight loss, delayed growth in children, and osteopenia, are a direct result of the gastrointestinal involvement (35). In contrast, for other manifestations, such as fever, the link is less clear. Arthralgias are a common symptom associated with IBD, sometimes even appearing prior to any gastrointestinal symptoms. Patients may also develop oral ulcers or cutaneous symptoms, such as erythema nodosum. Other extraintestinal manifestations of IBD include episcleritis and primary sclerosing cholangitis, primarily in the context of UC. For most patients, the resolution of the extraintestinal symptoms, particularly the arthralgias and oral/skin lesions, parallels successful treatment of the underlying IBD.

Diagnosis

The diagnosis of IBD is based on endoscopic, histologic, imaging, and/or laboratory studies, in conjunction with a comprehensive clinical evaluation (36–39). The clinical evaluation should include assessment of patient history, such as recent travel, medication use, and risk factors. The specific imaging and endoscopy studies are dictated by the clinical presentation of the patient. Endoscopy can be used to characterize the inflammation (patchy or continuous) and to identify its location within the gastrointestinal tract. Biopsies should be obtained from at least five sites, with a minimum of two biopsies per site. In UC, histopathology can be expected to show diffuse mucosal inflammation with distortion of the crypt architecture, which can be distinguished from the transmural inflammation, sometimes with noncaseating granulomas, characteristic of CD. Imaging studies may not be needed to establish a diagnosis of IBD, although there may be some utility in evaluating the extent or severity of the inflammation. Some useful imaging modalities include radiography, ultrasound, computed tomography, and magnetic resonance imaging. Each modality has advantages and disadvantages. However, most guidelines suggest the use of imaging techniques that minimize radiation exposure, as studies may need to be repeated periodically during a patient's disease course.

Laboratory testing for diagnosis of IBD has a more indirect role. Fecal testing is important to rule out the presence of infectious organisms, as well as to assess for occult blood (36–39). In addition, quantitation of fecal calprotectin is increasingly becoming available (40). Calprotectin is an enzyme present in neutrophils. An elevation of calprotectin in stool samples is indicative of localized inflammation within the gastrointestinal tract. Although not specific for IBD, it can be used to rule out noninflammatory conditions, such as irritable bowel syndrome. Also, some publications have shown that routine testing of fecal calprotectin in patients with confirmed IBD may be useful for monitoring for treatment response and disease flares. Other lab testing for IBD, specifically autoantibody serology, is more controversial. The best-characterized antibodies in IBD, and those most frequently used in clinical practice, are anti-neutrophil cytoplasmic antibodies (ANCAs) and anti-glycan antibodies (41, 42) (Table 1). ANCAs associated with IBD produce an atypical perinuclear staining pattern (pANCA) by immunofluorescence using ethanol-fixed neutrophils. This atypical pANCA pattern generally appears as broad, peripheral fluorescence around the nucleus, which contrasts with the perinuclear cytoplasmic fluorescence observed in a pANCA pattern associated with anti-myeloperoxidase antibodies in systemic vasculitis. The specific antigen recognized by pANCAs in IBD is not known. Many candidate antigens have been studied, including elastase, cathepsin, lactoferrin, bactericidal/permeability-increasing protein, enolase, catalase, and high-mobility group 1 and 2 nonhistone chromosomal proteins (43). Unfortunately, significant variability exists across studies in terms of the individual antigen specificities and association with UC or CD, likely due in part to methodological differences and variability in patient cohorts. At this point, it is unclear exactly which antigen specificity

is responsible for the pANCA reactivity associated with IBD, and routine testing is limited to assessment for the pANCA pattern by immunofluorescence. The anti-glycan antibodies are a group of antibodies that are specific for microbial cell wall carbohydrates. Anti-*Saccharomyces cerevisiae* antibodies (ASCAs) bind to terminal mannan groups in the cell wall of the yeast *S. cerevisiae*. In routine clinical labs, testing for IgA and IgG isotypes for ASCAs is generally available. ASCAs tend to be associated with CD, while pANCAs are found more frequently in UC. The specificity of ASCAs and pANCAs for IBD in general is on the order of 80 to 90%. However, the sensitivity is relatively poor, only in the range of 15 to 30% (41, 42). For this reason, neither ASCAs nor pANCAs are considered appropriate for screening or to establish a diagnosis of IBD. However, combined use of ASCAs and pANCAs can be helpful in distinguishing UC from CD, primarily in individuals for whom the specific diagnosis is unclear from endoscopy or histology (43). Other antibodies have been described, including additional anti-glycan, anti-OmpC, anti-I2, and anti-CBir1 antibodies. However, most of these are not widely available, and most testing guidelines discourage their use for diagnostic purposes.

QUALITY ASSURANCE FOR CLINICAL TESTING

Maintaining high-quality testing for CeD and IBD autoantibodies follows principles applicable to any serological analysis. Given the number of assays on the market, most clinical labs elect to use Food and Drug Administration (FDA)-cleared kits for CeD and IBD testing, rather than development of in-house methods. Despite the fact that this classification of kits has undergone review by the FDA, there is little standardization. Different kits have different performance characteristics, often related to differences in the specific capture antigen. The specific kits chosen by a laboratory for either CeD or IBD diagnosis should be dictated by how clinicians intend to use the assay, the specific patient population, and the expertise of the lab.

Even with FDA-cleared reagents, the laboratory must still conduct validation studies prior to implementation. According to regulatory requirements, lab validation of FDA-cleared tests requires assessment of precision, accuracy, reference range, and reportable range. Additional parameters may be necessary, such as documentation of carryover (if using automated pipetting instruments), analyte stability (particularly if specimen transport to a centralized lab within a health system or to a reference lab is necessary), and specimen type (if testing both serum and plasma is desired).

Once the CeD or IBD serology tests are implemented, a robust, ongoing quality assurance program is critical. For both enzyme immunoassay and IFA methods, routine quality control should minimally include a positive and negative sample. For IFAs, if the patient results are reported with a titer, the titer of the positive control should also be monitored. For enzyme immunoassays, the negative control is often a "<" value, limiting its use as a quantitative control. The positive control should be designed to fall within the reportable range of the assay, allowing for the quantitative value to be monitored over time. This is particularly important for analytes, such as anti-tTG-IgA, which are used to monitor patients over the course of their disease. Additionally, labs may find it beneficial to include controls around clinically relevant cutoffs, such as between "indeterminate" and "positive." This should help labs identify any drift in the assay over time, which could result in different interpretations. Although most autoantibody kits include positive and negative controls, labs may want to consider maintaining patient serum pools for use as "in-house controls." These controls, prepared by pooling previously tested patient samples, have the advantage of having the identical matrix as patient samples and being independent of the kit, thereby serving as a bridge when reagent lot changes occur.

Another approach that laboratories might include as part of a quality assurance program is frequency monitoring of patient results. This involves assessing the frequency of positive and negative patient results generated by a laboratory for a given test over time. This approach makes two assumptions—that both the patient population being tested and the prevalence of the disease remain stable. For most autoimmune diseases, including CeD and IBD, these assumptions generally hold true. Even regarding prevalence of disease, although studies have generally concluded that the incidences of these diseases are increasing, the changes are small and are occurring over relatively long time periods. Monitoring of positive and negative frequencies allows laboratories to determine whether a given assay is performing consistently over time, particularly as changes in reagent lots occur.

REFERENCES

1. **Green PH, Cellier C.** 2007. Celiac disease. *N Engl J Med* **357:**1731–1743. PubMed
2. **Di Sabatino A, Corazza GR.** 2009. Coeliac disease. *Lancet* **373:**1480–1493. PubMed
3. **Heap GA, van Heel DA.** 2009. Genetics and pathogenesis of coeliac disease. *Semin Immunol* **21:**346–354. PubMed
4. **Qiao SW, Sollid LM, Blumberg RS.** 2009. Antigen presentation in celiac disease. *Curr Opin Immunol* **21:**111–117. PubMed
5. **Jabri B, Sollid LM.** 2006. Mechanisms of disease: immunopathogenesis of celiac disease. *Nat Clin Pract Gastroenterol Hepatol* **3:**516–525. PubMed
6. **Abadie V, Sollid LM, Barreiro LB, Jabri B.** 2011. Integration of genetic and immunological insights into a model of celiac disease pathogenesis. *Annu Rev Immunol* **29:**493–525. PubMed
7. **Rubio-Tapia A, Ludvigsson JF, Brantner TL, Murray JA, Everhart JE.** 2012. The prevalence of celiac disease in the United States. *Am J Gastroenterol* **107:**1538–1544, quiz 1537, 1545. PubMed
8. **Kang JY, Kang AH, Green A, Gwee KA, Ho KY.** 2013. Systematic review: worldwide variation in the frequency of coeliac disease and changes over time. *Aliment Pharmacol Ther* **38:**226–245. PubMed
9. **Rubio-Tapia A, Kyle RA, Kaplan EL, Johnson DR, Page W, Erdtmann F, Brantner TL, Kim WR, Phelps TK, Lahr BD, Zinsmeister AR, Melton LJ III, Murray JA.** 2009. Increased prevalence and mortality in undiagnosed celiac disease. *Gastroenterology* **137:**88–93. PubMed
10. **Reilly NR, Green PH.** 2012. Epidemiology and clinical presentations of celiac disease. *Semin Immunopathol* **34:**473–478. PubMed
11. **Elli L, Bonura A, Garavaglia D, Rulli E, Floriani I, Tagliabue G, Contiero P, Bardella MT.** 2012. Immunological comorbity in coeliac disease: associations, risk factors and clinical implications. *J Clin Immunol* **32:**984–990. PubMed
12. **Kárpáti S.** 2012. Dermatitis herpetiformis. *Clin Dermatol* **30:**56–59. PubMed
13. **Singh K, Chang C, Gershwin ME.** 2014. IgA deficiency and autoimmunity. *Autoimmun Rev* **13:**163–177. PubMed
14. **Oberhuber G.** 2000. Histopathology of celiac disease. *Biomed Pharmacother* **54:**368–372. PubMed
15. **van der Windt DA, Jellema P, Mulder CJ, Kneepkens CM, van der Horst HE.** 2010. Diagnostic testing for celiac

disease among patients with abdominal symptoms: a systematic review. *JAMA* **303:**1738–1746. PubMed
16. **Rostom A, Dubé C, Cranney A, Saloojee N, Sy R, Garritty C, Sampson M, Zhang L, Yazdi F, Mamaladze V, Pan I, MacNeil J, Mack D, Patel D, Moher D.** 2005. The diagnostic accuracy of serologic tests for celiac disease: a systematic review. *Gastroenterology* **128**(Suppl 1)**:**S38–S46. PubMed
17. **Li M, Yu L, Tiberti C, Bonamico M, Taki I, Miao D, Murray JA, Rewers MJ, Hoffenberg EJ, Agardh D, Mueller P, Stern M, Bonifacio E, Liu E.** 2009. A report on the International Transglutaminase Autoantibody Workshop for Celiac Disease. *Am J Gastroenterol* **104:**154–163. PubMed
18. **Rashtak S, Ettore MW, Homburger HA, Murray JA.** 2008. Combination testing for antibodies in the diagnosis of coeliac disease: comparison of multiplex immunoassay and ELISA methods. *Aliment Pharmacol Ther* **28:**805–813. PubMed
19. **Rashtak S, Ettore MW, Homburger HA, Murray JA.** 2008. Comparative usefulness of deamidated gliadin antibodies in the diagnosis of celiac disease. *Clin Gastroenterol Hepatol* **6:**426–432, quiz 370. PubMed
20. **Lewis NR, Scott BB.** 2010. Meta-analysis: deamidated gliadin peptide antibody and tissue transglutaminase antibody compared as screening tests for coeliac disease. *Aliment Pharmacol Ther* **31:**73–81. PubMed
21. **Dubois PC, van Heel DA.** 2008. Translational mini-review series on the immunogenetics of gut disease: immunogenetics of coeliac disease. *Clin Exp Immunol* **153:**162–173. PubMed
22. **Rubio-Tapia A, Hill ID, Kelly CP, Calderwood AH, Murray JA, American College of Gastroenterology.** 2013. ACG clinical guidelines: diagnosis and management of celiac disease. *Am J Gastroenterol* **108:**656–676, quiz 677. PubMed
23. **Bai JC, Fried M, Corazza GR, Schuppan D, Farthing M, Catassi C, Greco L, Cohen H, Ciacci C, Eliakim R, Fasano A, González A, Krabshuis JH, LeMair A, World Gastroenterology Organization.** 2013. World Gastroenterology Organisation global guidelines on celiac disease. *J Clin Gastroenterol* **47:**121–126. PubMed
24. **Husby S, Koletzko S, Korponay-Szabó IR, Mearin ML, Phillips A, Shamir R, Troncone R, Giersiepen K, Branski D, Catassi C, Lelgeman M, Mäki M, Ribes-Koninckx C, Ventura A, Zimmer KP, ESPGHAN Working Group on Coeliac Disease Diagnosis, ESPGHAN Gastroenterology Committee, European Society for Pediatric Gastroenterology, Hepatology, and Nutrition.** 2012. European Society for Pediatric Gastroenterology, Hepatology, and Nutrition guidelines for the diagnosis of coeliac disease. *J Pediatr Gastroenterol Nutr* **54:**136–160. PubMed
25. **Nachman F, Sugai E, Vázquez H, González A, Andrenacci P, Niveloni S, Mazure R, Smecuol E, Moreno ML, Hwang HJ, Sánchez MI, Mauriño E, Bai JC.** 2011. Serological tests for celiac disease as indicators of long-term compliance with the gluten-free diet. *Eur J Gastroenterol Hepatol* **23:**473–480. PubMed
26. **Basso D, Guariso G, Fogar P, Meneghel A, Zambon CF, Navaglia F, Greco E, Schiavon S, Rugge M, Plebani M.** 2009. Antibodies against synthetic deamidated gliadin peptides for celiac disease diagnosis and follow-up in children. *Clin Chem* **55:**150–157. PubMed
27. **Trigoni E, Tsirogianni A, Pipi E, Mantzaris G, Papasteriades C.** 2014. Celiac disease in adult patients: specific autoantibodies in the diagnosis, monitoring, and screening. *Autoimmune Dis* **2014:**623514. doi:10.1155/2014/623514. PubMed
28. **Kaser A, Zeissig S, Blumberg RS.** 2010. Inflammatory bowel disease. *Annu Rev Immunol* **28:**573–621. PubMed
29. **Abraham C, Cho JH.** 2009. Inflammatory bowel disease. *N Engl J Med* **361:**2066–2078. PubMed
30. **Braus NA, Elliott DE.** 2009. Advances in the pathogenesis and treatment of IBD. *Clin Immunol* **132:**1–9. PubMed
31. **Zhang Y, Li Y.** 2014. Inflammatory bowel disease: pathogenesis. *World J Gastroenterol* **20:**91.99.
32. **Molodecky NA, Kaplan GG.** 2010. Environmental risk factors for inflammatory bowel disease. *Gastroenterol Hepatol (N Y)* **6:**339–346. PubMed
33. **Soon IS, Molodecky NA, Rabi DM, Ghali WA, Barkema HW, Kaplan GG.** 2012. The relationship between urban environment and the inflammatory bowel diseases: a systematic review and meta-analysis. *BMC Gastroenterol* **12:**51. doi:10.1186/1471-230X-12-51. PubMed
34. **Molodecky NA, Soon IS, Rabi DM, Ghali WA, Ferris M, Chernoff G, Benchimol EI, Panaccione R, Ghosh S, Barkema HW, Kaplan GG.** 2012. Increasing incidence and prevalence of the inflammatory bowel diseases with time, based on systematic review. *Gastroenterology* **142:**46–54.e42, quiz e30. PubMed
35. **Hendrickson BA, Gokhale R, Cho JH.** 2002. Clinical aspects and pathophysiology of inflammatory bowel disease. *Clin Microbiol Rev* **15:**79–94. PubMed
36. **Bernstein CN, Fried M, Krabshuis JH, Cohen H, Eliakim R, Fedail S, Gearry R, Goh KL, Hamid S, Khan AG, LeMair AW, Malfertheiner, Ouyang Q, Rey JF, Sood A, Steinwurz F, Thomsen OO, Thomson A, Watermeyer G.** 2010. World Gastroenterology Organization Practice Guidelines for the diagnosis and management of IBD in 2010. *Inflamm Bowel Dis* **16:**112–124. PubMed
37. **Mowat C, Cole A, Windsor A, Ahmad T, Arnott I, Driscoll R, Mitton S, Orchard T, Rutter M, Younge L, Lees C, Ho GT, Satsangi J, Bloom S, IBD Section of the British Society of Gastroenterology.** 2011. Guidelines for the management of inflammatory bowel disease in adults. *Gut* **60:**571–607. PubMed
38. **Kornbluth A, Sachar DB, Practice Parameters Committee of the American College of Gastroenterology.** 2010. Ulcerative colitis practice guidelines in adults: American College of Gastroenterology, Practice Parameters Committee. *Am J Gastroenterol* **105:**501–523, quiz 524. PubMed
39. **Lichtenstein GR, Hanauer SB, Sandborn WJ, Practice Parameters Committee of American College of Gastroenterology.** 2009. Management of Crohn's disease in adults. *Am J Gastroenterol* **104:**465–483, quiz 464, 484. PubMed
40. **Henderson P, Anderson NH, Wilson DC.** 2014. The diagnostic accuracy of fecal calprotectin during the investigation of suspected pediatric inflammatory bowel disease: a systematic review and meta-analysis. *Am J Gastroenterol* **109:**637–645. PubMed
41. **Prideaux L, De Cruz P, Ng SC, Kamm MA.** 2012. Serological antibodies in inflammatory bowel disease: a systematic review. *Inflamm Bowel Dis* **18:**1340–1355. PubMed
42. **Peyrin-Biroulet L, Standaert-Vitse A, Branche J, Chamaillard M.** 2007. IBD serological panels: facts and perspectives. *Inflamm Bowel Dis* **13:**1561–1566. PubMed
43. **Bossuyt X.** 2006. Serologic markers in inflammatory bowel disease. *Clin Chem* **52:**171–181. PubMed
44. **Sandborn WJ, Loftus EV Jr, Colombel JF, Fleming KA, Seibold F, Homburger HA, Sendid B, Chapman RW, Tremaine WJ, Kaul DK, Wallace J, Harmsen WS, Zinsmeister AR, Targan SR.** 2001. Evaluation of serologic disease markers in a population-based cohort of patients with ulcerative colitis and Crohn's disease. *Inflamm Bowel Dis* **7:**192–201. PubMed

Autoantibodies Directed against Erythrocytes in Autoimmune Hemolytic Anemia

R. SUE SHIREY AND KAREN E. KING

104

AUTOIMMUNE HEMOLYTIC ANEMIA

Immune-mediated hemolytic anemia can be broadly divided into two categories: alloimmune and autoimmune (1–4). Autoimmune hemolytic anemia may be further classified according to the immunoglobulin type of the autoantibody and its optimum temperature of reactivity (1–4). Warm autoimmune hemolytic anemia is due to IgG autoantibodies that bind to erythrocytes optimally at 37°C, while cold autoimmune hemolytic anemia is caused by IgM autoantibodies that preferentially react with red cells at low temperatures. A mixed-type autoimmune hemolytic anemia may occur when both warm IgG and cold IgM autoantibodies are implicated in clinical hemolysis. The rarest form of autoimmune hemolytic anemia, paroxysmal cold hemoglobinuria (PCH), is associated with IgG autoantibodies that are biphasic, sensitizing erythrocytes at lower temperatures and activating complement as the temperature increases to 37°C.

The characteristics of these different forms of autoimmune hemolytic anemia are outlined in Table 1. Warm autoimmune hemolytic anemia is the most common of the four types, and may be seen secondary to malignancies, such as chronic lymphocytic leukemia or lymphoma, or it may be idiopathic in nature (1, 2, 5, 6). Some drugs (e.g., α-methyldopa and fludarabine) can induce the production of warm autoantibodies (7). In ~90% of cases, warm autoimmune hemolytic anemia presents with a positive direct antiglobulin test (DAT) due to sensitization of the patient's red cells with IgG and complement or IgG alone (2, 8). An eluate prepared from the patient's red cells typically demonstrates antiglobulin reactivity with all test cells since the IgG autoantibodies usually have a broad specificity (3, 9). However, in ~4% of cases, the eluate may demonstrate an Rh antibody specificity, such as auto-anti-e (9). Detection of IgG warm autoantibodies in the serum or plasma is variable; ~60% have a positive antibody screen at the anti-human globulin (AHG) test phase, depending on the sensitivity of the assay (2, 8).

Cold autoimmune hemolytic anemia, or cold agglutinin disease, may occur acutely secondary to a *Mycoplasma pneumoniae* infection or as a chronic disease in elderly individuals sometimes associated with lymphoma or other malignancies (10, 11). In contrast to warm autoimmune hemolytic anemia, samples from patents with cold autoimmune hemolytic anemia generally demonstrate a high-titer (e.g., ≥1,000 at 4°C) IgM autoagglutinin in the serum (2, 8). Cold autoantibodies implicated in clinical hemolysis have a wide thermal range, reacting optimally at 4°C, but are capable of agglutinating red cells from room temperature (RT) (22 to 25°C) up to 30°C or, in some instances, 37°C (2, 8). The IgM antibodies can directly agglutinate red cells, so anticoagulated blood samples may appear to be clotted due to autoagglutination at ambient RT. IgM autoagglutinins are efficient in activating complement *in vivo*, and thus DATs are positive due to C3 sensitization of the red cells (2, 3, 8).

As is evident from the name, mixed-type (also known as combined-type) autoimmune hemolytic anemia has features of both warm and cold autoimmune hemolytic anemia (2, 8, 12). Usually the patient's red cells are sensitized with both IgG autoantibodies and complement. The serum contains an atypical IgM cold autoantibody that may not have a high titer, but has a high thermal amplitude capable of causing agglutination at temperatures of ≥ 30°C (2, 3, 8). IgG warm autoantibodies may also be detected in the serum reacting at an AHG test phase.

PCH is a very rare, acute illness that is most often seen in pediatric patients following a flu-like illness (13). Because of the biphasic nature of the IgG autoantibodies implicated in PCH, these antibodies are generally not detected in the serum using routine antibody screening methods. The patient's red cells are sensitized with complement alone; IgG is rarely detected on the red cells because the autoantibody dissociates *in vivo* at 37°C. A Donath-Landsteiner (D-L) test, which is designed to detect this unusual biphasic antibody, is diagnostic for PCH (2, 3, 8).

LABORATORY INVESTIGATION

Erythrocyte autoantibodies may cause accelerated intravascular and/or extravascular hemolysis or the autoantibodies may be entirely clinically benign (2). Therefore, the diagnosis of autoimmune hemolytic anemia relies on the clinical presentation and evidence of hemolysis, as well as serologic findings consistent with the presence of autoantibodies (2). The laboratory investigation of suspected autoimmune hemolytic anemia begins with a fundamental DAT using a polyspecific reagent for the detection of *in vivo* IgG and/or complement (C3) sensitization of the patient's red cells (2, 3, 8, 14). DATs should be performed using EDTA-anticoagulated blood, which inhibits complement binding

doi:10.1128/9781555818722.ch104

TABLE 1 Typical serologic characteristics in autoimmune hemolytic anemia (AIHA)

AIHA characteristic	Warm	Cold	Mixed-type	PCH
Immunoglobulin type	IgG	IgM	IgM and IgG	IgG
Optimum temperature	37°C	4°C	4°C and 37°C	Biphasic: 4°C to 37°C
Red blood cell sensitization	IgG alone (30%); IgG and C3 (60%); C3 alone (10%)	C3	IgG and C3	C3
Specificity	Usually broad specificity	Auto-anti-I	Unclear	Auto-anti-P
Serum autoantibody	60% of cases reactive at AHG phase	Cold autoagglutinin; reactive at ≥30°C	IgM cold autoagglutinin; reactive at ≥30°C; possibly IgG autoantibody	Detected only by D-L test

to red cells *in vitro*, ensuring the detection of only *in vivo*-bound complement (14).

Direct Antiglobulin Test

Specimen

Red cells from an EDTA-anticoagulated blood sample

Reagents

Polyspecific AHG reagent
0.9% saline
IgG-coated control red cells (available commercially)

Procedure

1. Prepare a 3 to 4% saline suspension of the patient's red cells from an EDTA-anticoagulated blood sample.
2. Dispense 1 drop of the saline-suspended red cells into a 12- by 75-mm test tube.
3. Wash the test tube three to four times with saline.
4. Completely decant the final wash.
5. Immediately add 2 drops of polyspecific AHG reagent and mix.
6. Centrifuge and immediately read for agglutination.
7. A negative test should be validated by adding 1 drop of IgG-coated control red cells to the tube and recentrifuging.
8. The test is valid if the tube shows agglutination.
9. The test is invalid if the tube shows no agglutination with the IgG-coated control red cells, which may be due to improper washing or failure to add the AHG reagent. The DAT should be repeated starting with step 1.

If the DAT is positive, then a DAT battery or profile is necessary using monospecific AHG reagents, anti-IgG and anti-C3, to specifically identify the sensitizing proteins. The DAT with polyspecific AHG reagent is repeated with the battery as a positive control. A negative (saline) control is included with the DAT battery to rule out the possibility of autoagglutination that may cause false-positive results.

DAT Battery

Specimen

Red cells from an EDTA-anticoagulated blood sample

Reagents

Polyspecific AHG reagent
Monospecific anti-IgG reagent
Monospecific anti-C3 reagent
0.9% saline
IgG-coated control red cells (available commercially)
C3-coated control red cells (available commercially)

Procedure

1. Label four test tubes: PS (polyspecific), IgG, C3, and Control (saline control).
2. Add 1 drop of 3 to 4% saline-suspended red cells into each tube.
3. Wash the tubes three to four times with saline.
4. Immediately add 2 drops of the appropriate AHG reagents to the test tubes and add 2 drops of saline to the control tube.
5. Mix and centrifuge the tubes.
6. Immediately read the tubes for agglutination.
7. The validity of a negative test should be confirmed by adding the appropriate IgG-coated or C3-coated reagent control cells and recentrifuging.
8. The test is valid if agglutination is observed with the control cells. If there is no agglutination with the control cells, then the test is invalid and must be repeated beginning at step 1.

The saline control must be negative to validate the DAT battery results. A positive saline control is usually due to autoagglutination mediated by IgM autoantibodies. In this situation, the patient's saline-suspended red cells should be washed three to six times with warm (37°C) saline to dissociate the IgM antibody. The warm-washed red cells can then be resuspended in saline to a 3 to 4% concentration and the DAT battery can be repeated.

The DAT profile or reaction pattern of IgG alone, IgG and C3, or C3 alone is helpful in determining what additional tests may be indicated for the differential diagnosis of autoimmune hemolytic anemia (Table 2).

Eluate Studies

If the DAT is positive due to IgG sensitization of the red cells (with or without C3), then eluate studies can be performed

TABLE 2 Interpretation of serologic findings in suspected cases of autoimmune hemolytic anemia (AIHA)

Typical serologic reaction pattern	Laboratory test results					Presumptive diagnosis
	DAT profile		Eluate studies	Serum antibody screen		
	Anti-IgG	Anti-C3		Result	Optimum reaction phase	
1	+	+/0	Panagglutinin	+/0	AHG	Warm AIHA
2	0	+	Not applicable	+	RT	Cold AIHA
3	+	+	Panagglutinin	+	RT and AHG	Mixed-type AIHA
4	0	+	Not applicable	0	D-L test positive	PCH

to identify the specificity of the antibodies. Many techniques have been described for eluting or disrupting IgG antibody from red cells (15). Perhaps the most commonly used procedure is the acid elution method, which is available commercially as a kit. A cold acid elution procedure that is also effective in eluting IgG antibodies is described below (15).

Cold Acid Elution Procedure

Specimen

1 ml of red cells from an EDTA-anticoagulated blood sample washed four to six times with large volumes of saline

Reagents

Glycine-HCl (0.1 M, pH 3.0), prepared by dissolving 3.75 g of glycine and 2.922 g of sodium chloride in 500 ml of deionized or distilled water. Adjust the pH to 3.0.

Phosphate buffer (0.8 M, pH 8.2)

0.9% saline kept cold at 4°C

Procedure

1. Place the glycine-HCl and the saline in an ice water bath.
2. Place 1 ml of red cells in a 13- by 100-mm test tube and chill in an ice water bath for 5 min.
3. Add 1 ml of chilled saline and 2 ml of cold glycine-HCl to the red cells.
4. Mix and incubate the tube in an ice water bath for 1 min.
5. Quickly centrifuge the tube at 900 to 1,000 × *g* for 2 to 3 min.
6. Transfer the supernatant eluate into a clean test tube, and test in parallel with the supernatant saline from the final wash ("last wash" control).

The eluate and "last wash" control can be tested in parallel with reagent antibody detection cells or panel cells using standard antibody identification methods. The last wash control should be negative, indicating that all unbound antibodies were removed by the washing process.

Serum or Plasma Studies

Antibody screening of the patient's serum or plasma for antibodies is particularly useful for the detection of cold autoagglutinins that may be implicated in cold or mixed-type autoimmune hemolytic anemia (Table 2). The following procedure is a saline antibody screening procedure by test tube methodology and includes an ambient RT test phase (8, 16).

Antibody Screen

Specimen

0.5 ml of serum or plasma

Reagents

Group O reagent red cells for antibody detection (I and II) (i.e., antibody screening cells) (available commercially)

Monospecific anti-IgG reagent

IgG-coated control red cells (available commercially)

0.9% saline

Procedure

1. Label three 12- by 75-mm tubes: I, II, and Auto.
2. Add 2 drops of serum or plasma into each tube.
3. Add 1 drop of screening cell I to the tube labeled "I" and 1 drop of screening cell II to the tube labeled "II." Add 1 drop of a 3 to 4% saline suspension of the patient's autologous red cells to the tube labeled "Auto."
4. Mix and incubate at RT for 5 min.
5. Centrifuge the tubes and read for agglutination.
6. Place the three tubes in a 37°C incubator for 30 min.
7. Centrifuge and read for agglutination.
8. Wash the tubes three to four times with 0.9% saline.
9. Immediately add 2 drops of anti-IgG reagent to each tube.
10. Centrifuge and immediately read for agglutination.
11. To validate a negative test, add 1 drop of IgG-coated control red cells and recentrifuge.
12. The test is valid if the tube shows agglutination with the IgG-coated control red cells. If the tube shows no reactivity with the control cells, then the test is invalid and must be repeated starting with step 1.

Cold autoagglutinins implicated in autoimmune hemolytic anemia are invariably reactive at the RT phase with the screening cells and the autologous control. However, reactivity at the RT phase does not necessarily indicate that the autoagglutinin is causing *in vivo* hemolysis (2, 8). Although the RT reactivity may persist or "carry over" to the 37°C and AHG test phases in the antibody screening procedure, the actual thermal range of the cold autoantibody would require tests that are performed only in specialized immunohematology reference laboratories. Cold autoagglutinins with a thermal amplitude of ≥30°C have been associated with autoimmune hemolytic anemia (2, 3, 8). Titration of the cold autoagglutinin may provide some additional supportive information, but the titer does not necessarily correlate with clinical significance (8).

IgG autoantibodies in warm or mixed-type autoimmune hemolytic anemia may be detected in the plasma or serum at the AHG test phase.

Antibody identification studies using a commercial panel can be performed using the same method as described above (16).

D-L Test

A D-L test may be indicated when the serologic findings are consistent with PCH, as shown in Table 2. In the D-L test, the patient's serum is incubated with test cells at cold temperatures to allow the antibody to bind to red cells and activate complement when the test is then warmed to 37°C, resulting in hemolysis (8).

Specimen

~1 ml of serum separated from a clotted blood sample that has been maintained at 37°C to prevent loss of antibody from autoadsorption

Reagents

Fresh normal serum as a source of complement. (Complement is added to the test, since patients with PCH may have low levels of complement.)

Group O, P-positive reagent red cells washed and resuspended in 0.9% saline to a 25% concentration. (The autoantibody in PCH is usually directed against the high-frequency P antigen; only very rare individuals are P negative. Reagent antibody screening cells are P positive and can be used as indicator red cells.)

Procedure

1. Label five 12- by 75-mm tubes: Test 1, Control 1, Test 2, Control 2, and Complement Control.
2. Dispense 5 drops of the patient's serum into each of the four tubes labeled Test 1, Control 1, Test 2, and Control 2.
3. Add 5 drops of fresh normal serum to the tubes labeled Test 2, Control 2, and Complement Control.
4. Add 1 drop of 25% group O reagent red cells to each of the five tubes. Gently mix and cork the tubes.
5. Place the patient's control tubes (Control 1 and Control 2) in a 37°C water bath for 90 min.
6. Place the patient's test tubes (Test 1 and Test 2) and the Complement Control tube in a melting ice bath for 30 min.
7. After 30 min, gently mix the tubes in the melting ice and transfer them to the 37°C water bath and incubate for 60 min.
8. Gently mix and centrifuge all tubes.
9. Observe the tubes for hemolysis, comparing the Test tubes with the corresponding Control tubes.

Hemolysis observed in the patient's Test 1 and/or Test 2 tubes when compared to the corresponding Control tubes indicates a positive D-L test. If no hemolysis is observed, the D-L test is negative.

The Complement Control tube is a negative control and should show no hemolysis. Hemolysis observed in the Complement Control tube may be related to the source of fresh complement or technical problems. In this situation, repeat the D-L test using a different source of fresh normal serum.

If hemolysis occurs in both the Test and Control tubes, then there may be a monophasic cold agglutinin present in the serum.

DIFFERENTIAL DIAGNOSIS OF AUTOIMMUNE HEMOLYTIC ANEMIA

Table 2 outlines the serologic findings for the DAT battery, eluate studies, and serum antibody screening tests that are typically seen for each type of autoimmune hemolytic anemia. It is essential that the serologic findings are interpreted in the context of the clinical presentation and medical history of the patient. The interpretation can be complicated by a history of recent blood transfusions, medications that can induce warm autoantibodies or drug-dependent antibodies, and the presence of multiple antibodies that may make it difficult to distinguish allo- from autoantibody activity (2, 7, 17, 18).

Not all cases of autoimmune hemolytic anemia can be categorized into the four types described here. A spectrum of unusual cases has been reported, ranging from DAT-negative autoimmune hemolytic anemia to warm autoimmune hemolytic anemia due to IgM autoantibodies (19–22). However, in the majority of cases of autoimmune hemolytic anemia, a presumptive diagnosis can be made based on the testing outlined in this chapter and clinical correlation.

REFERENCES

1. **Dacie SJ.** 2001. The immune haemolytic anaemias: a century of exciting progress in understanding. *Br J Haematol* **114:**770–785. PubMed
2. **Petz LD.** 2004. Review: evaluation of patients with immune hemolysis. *Immunohematology* **20:**167–176. PubMed
3. **Leger RM.** 2011. The positive direct antiglobulin test and immune-mediated hemolysis, p 497–522. *In* Roback JD, Grossman BJ, Harris T, Hillyer CD (ed), *Technical Manual,* 17th ed. AABB Press, Bethesda, MD.
4. **Klein HG, Anstee DJ.** 2007. *Mollison's Blood Transfusion in Clinical Medicine,* 11th ed, p 253–298. Blackwell Science Ltd, Oxford, United Kingdom.
5. **Sokol RJ, Hewitt S, Stamps BK.** 1981. Autoimmune haemolysis: an 18-year study of 865 cases referred to a regional transfusion centre. *Br Med J (Clin Res Ed)* **282:**2023–2027. PubMed
6. **Das SS, Nityanand S, Chaudhary R.** 2009. Clinical and serological characterization of autoimmune hemolytic anemia in a tertiary care hospital in North India. *Ann Hematol* **88:**727–732. PubMed
7. **Garratty G.** 2010. Immune hemolytic anemia associated with drug therapy. *Blood Rev* **24:**143–150. PubMed
8. **Petz LD, Garratty G.** 2004. *Immune Hemolytic Anemias,* 2nd ed, p 201–230. Churchill Livingstone, New York, NY.
9. **Issitt PD, Anstee DJ.** 1998. *Applied Blood Group Serology,* 4th ed, p 939–993. Montgomery Scientific, Durham, NC.
10. **Bartholomew JR, Bell WR, Shirey RS.** 1987. Cold agglutinin hemolytic anemia: management with an environmental suit. *Ann Intern Med* **106:**243–244. PubMed
11. **Swiecicki PL, Hegerova LT, Gertz MA.** 2013. Cold agglutinin disease. *Blood* **122:**1114–1121.
12. **McCann EL, Shirey RS, Kickler TS, Ness PM.** 1992. IgM autoagglutinins in warm autoimmune hemolytic anemia: a poor prognostic feature. *Acta Haematol* **88:**120–125. PubMed
13. **Wolach B, Heddle N, Barr RD, Zipursky A, Pai KRM, Blajchman MA.** 1981. Transient Donath-Landsteiner haemolytic anaemia. *Br J Haematol* **48:**425–434. PubMed
14. **Zantek ND, Koepsell SA, Tharp DR Jr, Cohn CS.** 2012. The direct antiglobulin test: a critical step in the evaluation of hemolysis. *Am J Hematol* **87:**707–709. PubMed
15. **Judd WJ, Johnson ST, Storry JR.** 2008. *Judd's Methods in Immunohematology,* 3rd ed, p 113–172. AABB Press, Bethesda, MD.
16. **Trudell KS.** 2005. Detection and identification of antibodies, p 242–263. *In* Harmening DM (ed), *Modern Blood*

Banking and Transfusion Practices, 5th ed. F.A. Davis Co, Philadelphia, PA.
17. **Johnson ST.** 2007. Warm autoantibody or drug dependent antibody? That is the question! *Immunohematology* **23:**161–164. PubMed
18. **Svensson AM, Bushor S, Fung MK.** 2004. Case report: exacerbation of hemolytic anemia requiring multiple incompatible RBC transfusions. *Immunohematology* **20:**177–183. PubMed
19. **Kamesaki T, Toyotsuji T, Kajii E.** 2013. Characterization of direct antiglobulin test-negative autoimmune hemolytic anemia: a study of 154 cases. *Am J Hematol* **88:**93–96. PubMed
20. **Palla AR, Khimani F, Craig MD.** 2013. Warm autoimmune hemolytic anemia with a direct antiglobulin test positive for C3 and negative for IgG: a case study and analytical literature review of incidence and severity. *Clin Med Insights Case Rep* **6:**57–60. PubMed
21. **Friedman AM, King KE, Shirey RS, Resar LM, Casella JF.** 1998. Fatal autoimmune hemolytic anemia in a child due to warm-reactive immunoglobulin M antibody. *J Pediatr Hematol Oncol* **20:**502–505.
22. **Arndt PA, Leger RM, Garratty G.** 2009. Serologic findings in autoimmune hemolytic anemia associated with immunoglobulin M warm autoantibodies. *Transfusion* **49:**235–242. PubMed

Immune Thrombocytopenia

THOMAS S. KICKLER

105

GENERAL OVERVIEW

Immune thrombocytopenia (ITP) is an autoimmune disorder characterized by a platelet count of <100,000/μl in the absence of any underlying cause. The incidence of newly diagnosed ITP in adults ranges from 1.6 to 3.9 per 100,000 person-years. The female-to-male ratio ranges from 1.2 to 1.9. The general consensus is that the diagnosis is one of exclusion based on patient clinical history, physical examination, review of medication history, and performance of a complete blood count with review of the peripheral blood smear. One can classify the illness based on duration: (i) newly diagnosed with a duration of up to 3 months, (ii) persistent ITP of 3 months to 1 year, or (iii) chronic ITP of >1 year (1).

ITP can be further defined as either primary or secondary. About 20% of ITP cases are secondary to other illnesses, including autoimmune rheumatologic diseases; lymphoproliferative disorders; and infections including hepatitis C virus, *Helicobacter pylori*, and HIV infection (2).

PATHOPHYSIOLOGY

Antibodies are responsible for the enhanced platelet clearance by the reticuloendothelial system in ITP. The autoantigenic targets are found on the platelet glycoproteins IIb/IIIa, Ib/IX, and Ia/IIa. In some cases no antibodies may be detected. The spleen, being the major site of platelet destruction, is also a major site of autoantibody production (3).

There is a growing body of research that suggests that T-cell abnormalities in ITP are linked to the pathogenesis of the disorder. At the level of T-cell-related cytokine abnormalities, data suggest that interleukin-18 may play an important role in the pathogenesis of ITP. Investigators have shown that levels of interleukin-18 are increased during active disease, whereas in remission these levels fall to those of normal subjects. In addition, T-cell-related abnormalities include Fas-related T-cell apoptosis and deficiencies in T regulatory cell expression (4).

For decades, enhanced platelet destruction was considered the primary pathophysiology in ITP. There are now substantial data showing that autoreactive cytotoxic thymic lymphocytes induce megakaryocyte damage and impaired thrombopoiesis. As a result of these observations, administration of thrombopoietin to stimulate megakaryocytopoiesis is now an important therapeutic modality (4).

DIAGNOSTIC APPROACH TO PATIENTS WITH SUSPECTED ITP

In the majority of ITP cases, reaching the correct diagnosis is possible by taking a complete history, doing a physical examination, and performing a complete blood count with differential and review of the peripheral blood smear. Response to therapy with corticosteroids, high-dose intravenous gamma globulin, or anti-Rh(D) immunoglobulin provides supportive evidence of the immune basis of the thrombocytopenia. It is important to note that additional studies may be necessary to exclude secondary immune thrombocytopenia. Table 1 outlines consensus recommendations for the diagnosis of ITP in both children and adults (5, 6).

Platelet Autoantibody Detection

A variety of methods to measure platelet autoantibodies are available (7). Since the primary antigenic target is platelet glycoproteins, any assay that employs measurement of antibodies to these proteins increases the specificity. It has been noted that the surface of the platelet contains many species of immunoglobulin, so flow cytometric assays or other labeled anti-human globulin tests for platelet-associated immunoglobulin are of low diagnostic utility.

The monoclonal antibody-specific immobilization of platelet antigen assay (MAIPA) is both sensitive and specific (Fig. 1). This test is a laboratory-developed test that is validated by the testing laboratory. The test may be used to measure plasma antibodies or the antibodies that are contained on the surface of the platelet and that are directed toward platelet glycoproteins. When the MAIPA is employed, ~80% of samples will have detectable antibody when a panel of monoclonal antibodies is employed to capture the platelets. The relative sensitivity for plasma antibodies may be as low as 30%.

Test Procedure: MAIPA

Reagents

Coating buffer: 1.6 g of Na_2CO_3, 2.9 g of $NaHCO_3$, and 0.2 g of NaN_3. Add distilled water and adjust pH to 9.6.

TBS (Tris-buffered saline) wash buffer: 3.03 g of Tris, 22 g of NaCl, 12.5 ml of Nonidet P-40, 1.25 ml of Tween 20, and 1.25 ml of 1 M $CaCl_2$. Add distilled water to 2.5 liters.

doi:10.1128/9781555818722.ch105

TABLE 1 International ITP Working Group consensus recommendations for the diagnosis of ITP in children and adults (8)

Basic initial evaluation	Ancillary studies	Tests of unknown utility
Patient history	Antiphospholipid antibodies	Thrombopoietin level
Family history	Thyroid stimulating hormone or antithyroid antibodies	Reticulated platelets
Medication and over-the-counter drug history	Antinuclear antibodies	Platelet-associated immunoglobulin
Complete blood count	Pregnancy test in women of childbearing age	Bleeding time
Quantitative immunoglobulins	Platelet glycoprotein-specific antibodies	Platelet survival and sequestration studies
HIV		
Hepatitis C virus		
Helicobacter pylori		
Bone marrow not necessary in most patients		

Solubilization buffer: 1.21 g of Tris dissolved in 950 ml of saline, pH 7.4. Add 5 ml of Nonidet P-40 and add saline to 1 liter.

Goat anti-mouse IgG (from Jackson ImmunoResearch Laboratories, West Grove, PA). Dilute to 3 μg/ml in coating buffer.

Peroxidase-labeled goat anti-human IgG (Jackson ImmunoResearch). Dilute to 1 in 5,000 to 1 in 25,000 in TBS, as determined by positive and negative control titration.

Substrate. Dissolve four 3.5-mg tablets of 1,2-phenylenediamine dihydrochloride in 12 ml of water in a foil-covered container. Add 10 μl of 30% H_2O_2 before use.

Stop solution. Add 28 ml of 95 to 97% H_2SO_4 to 972 ml of water.

Warning: Use only freshly prepared reagents.

Method

Preparation of Anti-Mouse Antibody-Coated Microtiter Plate

1. Prepare goat anti-mouse IgG as described above and aliquot 100 μl per well into flat-well microplates for duplicate testing and incubate overnight at 4°C. The plates may be stored for up to 14 days.

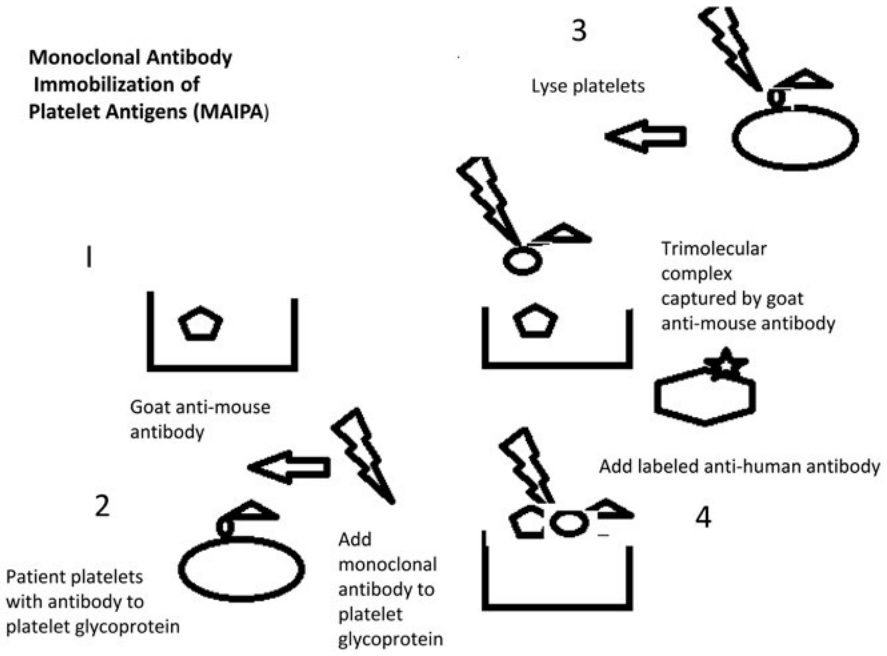

FIGURE 1 The general outline of the MAIPA. Murine monoclonal antibody, such as antibody to glycoprotein IIb/IIIa, is added to the autoantibody-sensitized platelets and the mixture is lysed. The trimolecular complex is captured by goat anti-mouse antibody, enzyme-labeled anti-human antibody is added, and the results are read by adding the appropriate substrate.

2. Before using, wash the plates with TBS wash buffer. Leave the last wash in the well for 30 min to block nonspecific binding of proteins.

Platelet Preparation
1. Take platelets from normal donors for plasma antibody testing. In case of testing patient platelets, collect platelets from blood. Either EDTA or citrate anticoagulant is satisfactory.
2. Prepare platelet-rich plasma using standard centrifugation methodology.
3. Resuspend platelets and adjust final concentration to 200,000/μl.

First Incubation for Plasma Antibody Detection
1. For each sample to be tested, aliquot 100 μl of platelet suspension into a U-well microplate and spin at 1,500 × *g* in a benchtop microplate centrifuge for 3 min. Include two negative controls and a weakly positive control.
2. Decant the supernatant and then suspend the plate pellet in 50 μl of test plasma and incubate at 37°C for 30 min.
3. Wash platelets by adding 200 μl of phosphate-buffered saline-EDTA to each test and centrifuge at 1,500 × *g* for 3 min.
4. Resuspend the platelet pellet using a microplate shaker and wash once more.

Incubation with Monoclonal Antibody

Resuspend platelet pellets in 40 μl of diluted mouse monoclonal antibody (antibodies to IIb/IIIa, Ib/IX, or Ia/IIa; Dako, Carpinteria, CA) and incubate for 30 min, followed by three washes with wash buffer.

Lysis
1. Lyse plates by resuspending each pellet in 130 μl of solubilization buffer.
2. Block the coated microplate with TBS wash buffer.
3. Centrifuge at maximum speed in a benchtop centrifuge. For each test, aliquot 130 μl of TBS wash buffer into each well.
4. Remove 100 μl from each supernatant and dilute in 130 μl of wash buffer.

Attachment to Solid Phase
1. Transfer 100 μl of diluted platelet lysate in duplicate to a precoated and blocked well, and add 100 μl of wash buffer to four reagent blank wells.
2. Incubate at 4°C for 90 min or overnight.
3. Wash microplate wells four times with wash buffer.

Anti-IgG Incubation
1. Add 100 μl of labeled anti-human IgG to each well and incubate at 4°C for 90 min.
2. Wash six times with buffer and blot between washes to dry.

Color Development
1. Add 100 μl of substrate solution to each well and leave at room temperature.
2. Stop the reaction with 100 μl of H_2SO_4.
3. Read the absorbance at 490 nm.

Interpretation

While the diagnosis of ITP is considered one of exclusion without the need for immunologic confirmation, clinicians still find the testing important. We recommend testing in those patients who fail to respond to standard therapy. If the testing is negative, clinicians should be advised to pursue investigation for other, less common causes of thrombocytopenia, especially congenital thrombocytopenia or thrombocytopenia associated with myelodysplasia. Standardization of the testing is demanding and requires expertise in this type of testing. For this reason, this assay is typically only done in platelet reference laboratories.

Calculate the mean optical density for all negative and positive controls and samples. The positive cutoff is the mean of the negative controls plus three standard deviations. The positive control should produce an optical density of least 3 times the negative control.

REFERENCES

1. **Provan D, Stasi R, Newland AC, Blanchette VS, Bolton-Maggs P, Bussel JB, Chong BH, Cines DB, Gernsheimer TB, Godeau B, Grainger J, Greer I, Hunt BJ, Imbach PA, Lyons G, McMillan R, Rodeghiero F, Sanz MA, Tarantino M, Watson S, Young J, Kuter DJ.** 2010. International consensus report on the investigation and management of primary immune thrombocytopenia. *Blood* **115:**168–186. PubMed
2. **Cines DB, Bussel JB, Liebman HA, Luning Prak ET.** 2009. The ITP syndrome: pathogenic and clinical diversity. *Blood* **113:**6511–6521. PubMed
3. **McMillan R.** 2009. Antiplatelet antibodies in chronic immune thrombocytopenia and their role in platelet destruction and defective platelet production. *Hematol Oncol Clin North Am* **23:**1163–1175.
4. **Semple JW.** 2009. Infections, antigen-presenting cells, T cells, and immune tolerance: their role in the pathogenesis of immune thrombocytopenia. *Hematol Oncol Clin North Am* **23:**1177–1192.
5. **Glanz J, France E, Xu S, Hayes T, Hambidge S.** 2008. A population-based, multisite cohort study of the predictors of chronic idiopathic thrombocytopenic purpura in children. *Pediatrics* **121:**e506–e512. doi:10.1542/peds.2007-1129. PubMed
6. **Rodeghiero F, Stasi R, Gernsheimer T, Michel M, Provan D, Arnold DM, Bussel JB, Cines DB, Chong BH, Cooper N, Godeau B, Lechner K, Mazzucconi MG, McMillan R, Sanz MA, Imbach P, Blanchette V, Kühne T, Ruggeri M, George JN.** 2009. Standardization of terminology, definitions and outcome criteria in immune thrombocytopenic purpura of adults and children: report from an international working group. *Blood* **113:**2386–2393. PubMed
7. **Kiefel V, Santoso S, Weisheit M, Müeller-Eckhardt C.** 1987. Monoclonal antibody-specific immobilization of platelet antigens (MAIPA): a new tool for the identification of platelet-reactive antibodies. *Blood* **70:**1722–1726. PubMed
8. **Neunert C, Lim W, Cohen A, Solberg L, Crowther MA, American Society of Hematology.** 2011. Evidence based practice guidelines of immune thrombocytopenia. *Blood* **174:**4190–4207.

Monitoring Autoimmune Reactivity within the Retina

JOHN J. HOOKS, CHI-CHAO CHAN, H. NIDA SEN,
ROBERT NUSSENBLATT, AND BARBARA DETRICK

106

IMMUNE REACTIVITY IN THE EYE

The identification of immune reactivity against self components is a key element in the characterization of autoimmunity and autoimmune diseases. This autoimmune reactivity is most frequently monitored by the detection of specific autoantibodies or the presence of T-cell reactivity to self peptides. Numerous studies have now demonstrated that distinct profiles of autoantibodies are seen in clinically distinct autoimmune syndromes, such as systemic lupus erythematosus, myositis, and insulin-dependent diabetes mellitus. Moreover, the autoantigens are targets of an adaptive immune response.

Despite remarkable features of immune privilege in the eye, inflammatory processes do occur in the eye, and these are frequently referred to as uveitis (1, 2). Uveitis is the fifth-leading cause of vision loss in the world and accounts for 10 to 15% of all cases of total blindness in the United States (3). Most ocular inflammatory processes are associated with a cellular component. Ophthalmologists have a clear advantage in monitoring disease since the severity of the intraocular inflammation can be graded by direct visualization using slit-lamp biomicroscopy and fundoscopy.

Retinal degeneration is a primary cause of visual impairment and vision loss in the world. In the United States alone, there are presently more than 6 million people diagnosed with retinal diseases. This number includes patients with diabetic retinopathy and age-related macular degeneration, as well as patients with the broad diagnosis of retinal degeneration. Immune-mediated vision loss is a rapidly expanding area of research and therapy. It is becoming increasingly clear that retinal degenerative processes can also have an immune component that may be associated with the presence of antiretinal antibodies (4). In fact, several recent studies have focused on the role of antibody-mediated pathology in the retina. The identification of specific antiretinal antibodies may have application in the diagnosis and management of retinal degeneration. This chapter highlights retinal diseases associated with the identification of antiretinal immune reactivity or T-cell immune reactivity. Laboratory assays designed to detect and characterize antiretinal antibody reactivity are reviewed.

CLASSIC EXAMPLES OF AUTOIMMUNE DISEASE IN THE RETINA

Retinal autoimmunity exists as a naturally occurring disease in humans and as an experimentally designed animal model system. In humans, sympathetic ophthalmia and birdshot chorioretinopathy are classic examples of T-cell-mediated autoimmune diseases (5, 6). Sympathetic ophthalmia is an ocular inflammatory (autoimmune) disease that occurs after a perforating injury to one eye. The injured eye undergoes a massive granulomatous infiltration. At any time from the first week to several years following the trauma (peak is second week to 3 months), a spontaneous granulomatous infiltration occurs in the noninjured, "sympathizing" eye. Several studies have shown that the infiltrate consists predominantly of T cells. Birdshot chorioretinopathy is a posterior uveitis that has a strong association with HLA-A29 and the endoplasmic reticulum aminopeptidase (ERAP) 2 gene (7). More recently, this autoimmune disease was shown to be associated with production of Th17 cells (8). Peripheral blood mononuclear cells from patients respond to retinal lysates by producing interleukin-17 (IL-17). This is associated with a significant induction of Th17 cells and not Th1 cells.

Animal model systems have been developed to mimic human retinal diseases. Within the retina, a number of uveitogenic antigens have been identified and characterized. Two of these, retinal S antigen (arrestin) and interphotoreceptor retinal binding protein (IRBP), have been used to develop rodent models of T-cell-mediated autoimmune ocular disease, termed experimental autoimmune uveoretinitis (9). These retinal proteins are now also utilized to monitor human T-cell reactivity to retinal tissue. We have also developed a model of infection-associated retinal autoimmunity, referred to as experimental coronavirus retinopathy (10–12). This degeneration is triggered by the murine coronavirus mouse hepatitis virus and is characterized by genetic predisposition and autoimmune reactivity. Interestingly, the genetic predisposition is correlated with an augmented innate immunity and may be a classic example of innate immunity driving autoimmune responses (13).

doi:10.1128/9781555818722.ch106

RETINOPATHIES ASSOCIATED WITH ANTIRETINAL ANTIBODIES

Human retinopathies associated with the production of antiretinal antibodies can be categorized into three groups: (i) autoimmune retinopathy (AIR), consisting of two subgroups, paraneoplastic disorders and nonparaneoplastic retinopathy; (ii) infection-associated retinopathies; and (iii) retinal degenerative disorders (Table 1).

Autoimmune Retinopathy

AIR is an inflammation-mediated retinopathy characterized by vision loss, scotomas, visual field deficits, photoreceptor dysfunction, and the presence of circulating antiretinal antibodies. AIR is divided into two groups: paraneoplastic and nonparaneoplastic retinopathy. Progressive blindness as a remote effect of cancer was first reported in 1976 (14). The two most frequently observed forms of ocular paraneoplastic disorders are referred to as cancer-associated retinopathy (CAR) and melanoma-associated retinopathy (MAR). Clinical and experimental observations in CAR and MAR probably provide the best evidence for a pathological role of autoreactive antibodies in human retinopathies. First, affected patients suffer from a retinopathy that is characterized by retinal tissue damage and the presence of antiretinal antibodies. Second, some patients respond to plasma exchange and immunosuppressive therapy. Third, in experimental models, retinal cell damage can be induced by the autoreactive antibodies and there is evidence of passive transfer of disease to animals (15, 16).

CAR is most commonly associated with small-cell carcinoma of the lung, but it has also been reported in patients with breast, endometrial, and other cancers (17, 18). In these patients, antibodies develop with reactivity to the retina, and this response is associated with rod and cone dysfunction. Visual loss occurs over months and may even precede the identification of the malignancy. Using immunofluorescent-antibody (IFA) assays on normal retinal tissue sections, it has been demonstrated that sera from CAR patients reacts with the photoreceptor outer segments and ganglion cells. Further analysis of retinal antigens has revealed that a variety of antigens may be involved in this process. The primary antigens identified are a 23-kDa antigen (recoverin); a retinal enolase (46 kDa); and a group of reactivities with retinal antigens identified as 40-, 43-, and 60-kDa molecules. Although >15 retinal antigens have been described in the CAR syndrome, the most common antigen linked to CAR is the 23-kDa recoverin, a calcium-binding protein found in both rods and cones.

MAR is a second paraneoplastic syndrome that occurs in patients with melanoma (1, 19, 20). Progressive visual loss develops over months and is frequently associated with metastatic cutaneous melanoma. Again, IFA technology has been used to identify antibody in MAR patient sera that reacts to bipolar cells in the outer nuclear layer and their dendrites in the outer plexiform layer of the retina. The primary target antigen in MAR has been identified as transient receptor potential melastatin 1 (TRPM1) (21, 22).

TABLE 1 Antibody responses directed against retinal antigens in sera from patients with retinal diseases[a]

Retinal disease	Immunologic reactivity	Antigen
Autoimmune retinopathy (AIR)		
Paraneoplastic		
CAR	Photoreceptor inner and outer segment and ONL	Recoverin (23 kDa), enolase, TULP1, and others
MAR	Outer plexiform layer and INL	Bipolar cells
Nonparaneoplastic	Neuroretina, RPE, and ganglion cell layer	Variety of retina antigens
Infection-associated retinopathy		
Toxoplasmosis	Photoreceptor layer	Not known
Onchocerciasis	Neural retina and RPE	Cross-reactivity between *O. volvulus* Ag (OV39) and RPE Ag (hr44)
Retinal degenerative diseases		
RP	Neural retina	Carbonic anhydrase II (30 kDa) and enolase (45 kDa)
RAR	Photoreceptor	Recoverin
AMD	Photoreceptors	Neurofilaments
Sympathetic ophthalmia	Neural retina	Multiple antigens (T-cell reactivity)
VKH syndrome	Photoreceptors	Unknown
Neurologic disease (stiff man syndrome)	Neural retina	GAD

[a]Ag, antigen; RP, retinitis pigmentosa; RAR, recoverin-associated retinopathy; AMD, age-related macular degeneration; VKH, Vogt-Koyanagi-Harada syndrome; GAD, glutamic acid decarboxylase.

Nonparaneoplastic AIR is a rare disease constituting <1% of all cases of uveitis. The real prevalence of this condition is difficult to determine because of the overlap of clinical features with other retinal degenerative disorders and the lack of standardized laboratory diagnostic criteria. Studies are presently under way to develop standardized laboratory diagnostic criteria. Numerous retinal proteins have been identified as targets for antiretinal antibodies in AIR. These include α-enolase, lens epithelium-derived growth factor, carbonic anhydrase, arrestin, tubby-like protein 1 (TULP1), neurofilament protein, heat shock protein 70, and photoreceptor cell-specific nuclear receptor (23–26).

Infection-Associated AIR

The second group of retinopathies associated with antiretinal antibodies is retinal disorders that are triggered by an infectious agent (11). In humans, onchocerciasis and toxoplasmosis fall into this category. Infection with the nematode parasite *Onchocerca volvulus* can result in severe eye disease, often referred to as river blindness. Humans are infected with the helminth larvae by the bite of a black fly of the *Simulium* genus. It is estimated that ~18 million people in tropical Africa, the Arabian Peninsula, and Latin America are infected with this organism, and of these, ~1 million to 2 million are blind or have severe visual impairment.

Posterior ocular onchocerciasis is characterized by atrophy of the retinal pigment epithelium (RPE), and as lesions advance, subretinal fibrosis occurs. A number of studies indicate that affected patients have antiretinal antibodies in their sera and vitreous (27). Reactivity was observed in the inner retina and photoreceptor layers by IFA analysis. Characterization of the autoantigens revealed that a recombinant antigen in *O. volvulus* showed immunologic cross-reactivity with a component of the RPE. By Western blot analysis, an antibody to a 22,000-molecular-weight antigen (OV39) of *O. volvulus* recognized a 44,000-molecular-weight component (hr44) of the RPE cell. Although OV39 and hr44 are not homologous, they did show limited amino acid sequence identity. Immunizations of Lewis rats with either OV39 or hr44 induce ocular pathology. These studies indicate that molecular mimicry between *O. volvulus* and human RPE protein may contribute to the retinopathy found in patients with onchocerciasis (28, 29).

Toxoplasmosis, which occurs in >500 million humans worldwide, is caused by the obligate intracellular parasite *Toxoplasma gondii*. *T. gondii* is also the most frequently identified infectious agent in posterior uveitis, and *Toxoplasma* retinochoroiditis is an important cause of blindness in young adults. Since the 1980s, several reports have documented a high prevalence of antiretinal antibodies in sera from *T. gondii*-infected patients (30). These antibodies are directed against the photoreceptor layer. Moreover, leukocytes from these patients have been shown to proliferate in response to retinal S antigen (31).

Autoimmunity Associated with Retinal Degenerative Diseases

The third group of retinopathies associated with antiretinal antibodies is classified as the retinal degenerative disorders. These include retinitis pigmentosa with cystoid macula edema, recoverin-associated retinopathy, age-related macular degeneration, idiopathic retinopathies, and retinopathies associated with autoimmune neurologic diseases (32). Table 1 identifies serum antibody responses directed against retinal antigens in patients with retinal diseases. These are described in more detail in reference 16.

LABORATORY MONITORING OF ANTIRETINAL ANTIBODIES

Historically, the detection of autoantibodies has served as an invaluable laboratory tool for the diagnosis, monitoring, and management of patients with autoimmune diseases. Studies to monitor antiretinal antibodies have been performed using one of three assay systems, immunohistochemical assays (such as indirect IFAs and immunoperoxidase assays), enzyme immunoassay (EIA), and Western blot. There is a lack of consensus for the standard screening assay, and thus, there is a need to develop standardized laboratory diagnostic criteria. One such approach has been to use a two-tier testing system consisting of a screening assay, such as an indirect IFA on rodent and/or primate retinal tissue, followed by a second confirmatory test, i.e., an EIA or Western blot. The second-tier test can incorporate known retinal autoantigens, such as recoverin and α-enolase (23). As new retinal autoantigens are identified, they can be incorporated into this test system.

Immunohistochemical Assay System

Standard immunohistochemical assays or immunofluorescent assays are used to identify antibody reactivity within the retina. In addition to human retina, rodent (mouse or rat) or monkey eyes are frequently used as the substrate.

Preparation of Tissue Sections

After enucleation, eyes are immediately placed in OCT and frozen and stored at −70°C. Using a cryostat, whole rodent eye sections can be prepared and placed on SuperFrost slides. When using monkey or human eye tissue as the substrate, the frozen eye must be cut into smaller blocks of tissue before cryosections of the eye are cut. Slides containing the retina are stored at −70°C until used.

Procedure

1. Briefly, the standard procedure consists of fixing and permeabilizing the ocular tissue sections with acetone-methanol (1:1) and rinsing them with phosphate-buffered saline (PBS), pH 7.4. Endogenous peroxidase activity is quenched by incubating the sections in 0.6% H_2O_2 prior to incubating the tissue in a blocking solution. A standard blocking solution is 10% normal goat or rabbit serum in PBS. Bovine serum albumin, glycine, and/or cold-water fish gelatin can be added to the standard blocking solution if necessary to reduce nonspecific binding by the primary antibody.
2. Serial 2-fold dilutions of sera (1:40 to 1:640) from patients with retinal degeneration and healthy controls are incubated with the tissue sections either for 90 min at room temperature or overnight at 4°C.
3. Slides are then washed in PBS with 1% normal goat or rabbit serum, and a dilution of the secondary antibody (horseradish peroxidase-conjugated anti-human IgG) is applied to the tissue for 1 h. For IFA assay, the secondary antibody is labeled with fluorescein isothiocyanate.
4. Detection of bound immunoglobulin molecules is accomplished using a peroxidase substrate such as 3,3′-diaminobenzidine. Instead of horseradish peroxidase, the secondary antibody may be conjugated to alkaline phosphatase. However, the peroxidase substrates produce more-pronounced precipitates and give sharper localization than alkaline phosphatase substrates.
5. Slides are counterstained and dehydrated, and coverslips are mounted prior to examining the tissue sections under a microscope. For IFA assay, the slides are read under a fluorescent microscope.

Interpretation

Studies in our laboratory demonstrate that immunofluorescence or immunocytochemical tests using rodent or primate tissue and serum from individuals without a history of retinal disease are usually negative or reactive only at low serum dilution (<1:80). In contrast, high titers of antibody (>160) are detected in patients with selected retinal degenerative diseases. Sera from 18 healthy individuals demonstrated immunoreactivity to normal mouse ocular tissue in 33% of samples at a 1:40 dilution, in 13% of samples at a 1:80 dilution, and in 3% of samples at a 1:160 dilution, and no reactivity was noted at a dilution of 1:320 or 1:640. In contrast, in selected patients with retinal degenerative disorders, we can detect reactivity in serum samples at dilutions of 1:160 to 1:1,280. We have evaluated 12 patients with primary AIR in this system and have demonstrated a sensitivity of 90% and a specificity of 97% at a serum dilution of 1:160. Based on these data, we have selected 1:160 as the dilution that can discriminate between healthy individuals and patients with retinal degenerative disorders. It is interesting that this is similar to the dilution scheme used to discriminate antinuclear antibody reactivity in patients with systemic lupus erythematosus from positive antinuclear antibody results for healthy individuals (33).

In patients with antiretinal antibodies, the cellular location can be important to report and may provide clues to help distinguish the disease entity. At least five patterns of immunostaining are commonly observed in tissue: photoreceptor inner and outer segments, inner nuclear layer (INL), outer nuclear layer (ONL), ganglion cells, and RPE cells. In CAR patients, reactivity with the outer segment layer of photoreceptors is frequently seen and is associated with antirecoverin antibodies. In MAR patients, staining is frequently observed in bipolar cells of the INL. An example of patterns of immune reactivity in the retina is shown in Fig. 1. This serum was obtained from a patient with AIR and illustrates immune staining at multiple sites in the retina, including ganglion cell layer, INL, ONL, and RPE cell.

LABORATORY MONITORING OF T-CELL REACTIVITY

Procedure

1. Approximately 10 ml of heparinized or EDTA venous blood is needed for T-cell assays. Peripheral blood leukocytes (PBLs) are recovered following Ficoll-Hypaque separation techniques. PBLs are resuspended in RPMI medium supplemented with 5% (vol/vol) fetal bovine serum.
2. Determine the number of viable PBLs by trypan blue exclusion. Adjust the cell concentration to 2×10^6/ml.
3. Deliver 100 μl of the cell suspension into triplicate wells of a 96-well plate.
4. Add 100 μl of stimulant or control as follows: medium (negative control), phytohemagglutinin or concanavalin A (positive control), and retinal antigen (S antigen or IRBP).
5. Incubate the cells at 37°C for 72 h.
6. Assay the response of the stimulated lymphocytes by monitoring cell proliferation or production and release of cytokines. The cell proliferation assay can measure [^{3}H]thymidine incorporation into cellular DNA. Alternatively, one can use the standard EIA methodology to measure the release of gamma interferon or IL-2 in the supernatant fluid.

Interpretation

The appropriate incorporation of controls into these assay systems is essential for interpretation. PBLs from a healthy individual (known nonresponder) should be used each time the test is performed. In addition, in each test a medium control (negative/baseline) and a T-cell stimulant (phytohemagglutinin, concanavalin A, etc.) must be included. When determining cell proliferation by [^{3}H]thymidine assay, the samples are evaluated by stimulation index (SI). The SI is obtained by dividing the counts per minute for retinal antigen-treated cells by those for medium-treated

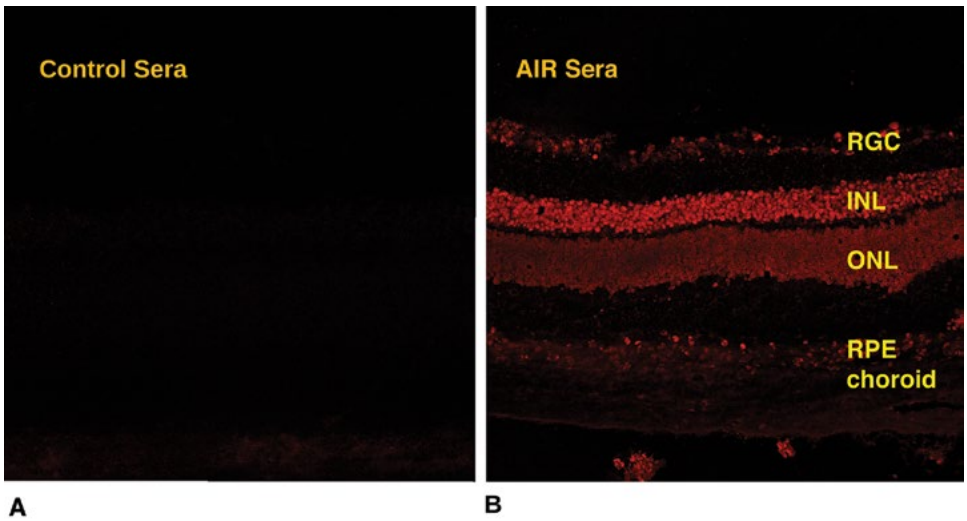

FIGURE 1 Immunofluorescence staining for antiretinal antibodies. Frozen sections of normal mouse retina were incubated with "normal" nonreactive human sera (A) or with sera from a patient with AIR (B). Both sera were tested at a 1:160 dilution. Note reactivity with several marked areas of the retina: retinal ganglia cell layer (RGC), INL, ONL, and RPE.

cells. An SI of > 2.0 is considered positive. An alternative, nonisotope method is the quantification of cell proliferation with Alamar Blue (BioSource, Rockville, MD) (34).

LABORATORY MONITORING OF OCULAR CYTOKINES (IL-6 AND IL-10)

Vitreous biopsies are frequently performed to distinguish between ocular inflammation associated with uveitis and ocular malignancy due to primary vitreoretinal lymphoma (PVRL; previously known as primary intraocular lymphoma) and/or primary central nervous system lymphoma (PCNSL). Cells within the vitreous are collected by cytospin and evaluated by a cytopathologist to identify lymphoma cells. The majority of PVRLs and PCNSLs are diffuse large B-cell lymphomas (24, 27, 35, 36). These tumor cells produce high levels of IL-10, a growth and differentiation factor for B cells. In contrast, the inflammatory cells in uveitis produce high levels of IL-6, a proinflammatory cytokine. We and other investigators have found elevation of vitreal IL-10 with a ratio of IL-10 to IL-6 of >1 in PVRL (37–40). Using this ratio analysis, the sensitivity and specificity of the assay are 85% (41). Evaluation of IL-10 and IL-6 concentrations in vitreous samples is performed using standard EIA methodology.

SUMMARY AND FUTURE DIRECTIONS

Analysis of immune-mediated vision loss is in its infancy. In patients with established retinal disease, the presence of autoantibodies can help define the nature of the disease and provide markers to classify the disease and to monitor therapy. Today, laboratory monitoring of antiretinal antibodies is frequently used to diagnose patients with AIR. Laboratory monitoring of T-cell reactivity to retinal antigens is used to assess uveitic patients undergoing immunomodulatory therapies. Finally, laboratory monitoring of ocular cytokines is frequently used to aid in the differential diagnosis of ocular inflammation and ocular malignancy.

Measurement of antiretinal immune reactivity is difficult to perform in the clinical laboratory. Analysis of immunocytochemical or immunofluorescent staining of retina tissue sections requires special training for interpretation. Nevertheless, with the characterization of specific retinal antigens, the future should include the development of standard EIA methodologies and Western blot assays to monitor patients with this important form of vision loss.

REFERENCES

1. **Hooks JJ, Nagineni CN, Hooper LC, Hayashi K, Detrick B.** 2008. IFN-β provides immuno-protection in the retina by inhibiting ICAM-1 and CXCL9 in retinal pigment epithelial cells. *J Immunol* **180:**3789–3796. PubMed
2. **Nussenblatt RB, Whitcup SM.** 2003. *Uveitis: Fundamentals and Clinical Practice*, 3rd ed. Mosby, Philadelphia, PA.
3. **Resnikoff S, Pascolini D, Etya'ale D, Kocur I, Pararajasegaram R, Pokharel GP, Mariotti SP.** 2004. Global data on visual impairment in the year 2002. *Bull World Health Organ* **82:**844–851. PubMed
4. **Forooghian F, Macdonald IM, Heckenlively JR, Héon E, Gordon LK, Hooks JJ, Detrick B, Nussenblatt RB.** 2008. The need for standardization of antiretinal antibody detection and measurement. *Am J Ophthalmol* **146:**489–495. PubMed
5. **Chan CC, Mochizuki M.** 1999. Sympathetic ophthalmia: an autoimmune ocular inflammatory disease. *Springer Semin Immunopathol* **21:**125–134. PubMed
6. **Chan CC, Nussenblatt RB, Fujikawa LS, Palestine AG, Stevens G Jr, Parver LM, Luckenbach MW, Kuwabara T.** 1986. Sympathetic ophthalmia. Immunopathological findings. *Ophthalmology* **93:**690–695. PubMed
7. **Kuiper JJ, Van Setten J, Ripke S, Van 't Slot R, Mulder F, Missotten T, Baarsma GS, Francioli LC, Pulit SL, De Kovel CG, Ten Dam-Van Loon N, Den Hollander AI, Huis in het Veld P, Hoyng CB, Cordero-Coma M, Martín J, Llorenç V, Arya B, Thomas D, Bakker SC, Ophoff RA, Rothova A, De Bakker PI, Mutis T, Koeleman BP.** 2014. A genome-wide association study identifies a functional *ERAP2* haplotype associated with birdshot chorioretinopathy. *Hum Mol Genet* **23:**6081–6087.
8. **Kuiper JJ, Emmelot ME, Rothova A, Mutis T.** 2013. Interleukin-17 production and T helper 17 cells in peripheral blood mononuclear cells in response to ocular lysate in patients with birdshot chorioretinopathy. *Mol Vis* **19:**2606–2614. PubMed
9. **Caspi RR.** 2011. Understanding autoimmune uveitis through animal models. The Friedenwald Lecture. *Invest Ophthalmol Vis Sci* **52:**1872–1879. PubMed
10. **Detrick B, Hooks JJ.** 2010. Immune regulation in the retina. *Immunol Res* **47:**153–161. PubMed
11. **Detrick B, Hooks JJ, Nussenblatt R.** 2014. Infections associated with retinal autoimmunity, p 943–957. *In* Rose NR, Shoenfeld Y (ed), *Infection and Autoimmunity*, 2nd ed. Elsevier, Amsterdam, The Netherlands.
12. **Hooks JJ, Detrick B, Nussenblatt R.** 2004. Infections associated with retinal autoimmunity, p 691–700. *In* Shoenfeld Y, Rose NR (ed), *Infection and Autoimmunity*. Elsevier, Amsterdam, The Netherlands.
13. **Detrick B, Lee MT, Chin MS, Hooper LC, Chan CC, Hooks JJ.** 2008. Experimental coronavirus retinopathy (ECOR): retinal degeneration susceptible mice have an augmented interferon and chemokine (CXCL9, CXCL10) response early after virus infection. *J Neuroimmunol* **193:**28–37. PubMed
14. **Sawyer RA, Selhorst JB, Zimmerman LE, Hoyt WF.** 1976. Blindness caused by photoreceptor degeneration as a remote effect of cancer. *Am J Ophthalmol* **81:**606–613. PubMed
15. **Adamus G, Machnicki M, Elerding H, Sugden B, Blocker YS, Fox DA.** 1998. Antibodies to recoverin induce apoptosis of photoreceptor and bipolar cells *in vivo*. *J Autoimmun* **11:**523–533. PubMed
16. **Hooks JJ, Tso MO, Detrick B.** 2001. Retinopathies associated with antiretinal antibodies. *Clin Diagn Lab Immunol* **8:**853–858. PubMed
17. **Murphy MA, Thirkill CE, Hart WM Jr.** 1997. Paraneoplastic retinopathy: a novel autoantibody reaction associated with small-cell lung carcinoma. *J Neuroophthalmol* **17:**77–83. PubMed
18. **Thirkill CE, FitzGerald P, Sergott RC, Roth AM, Tyler NK, Keltner JL.** 1989. Cancer-associated retinopathy (CAR syndrome) with antibodies reacting with retinal, optic-nerve, and cancer cells. *N Engl J Med* **321:**1589–1594. PubMed
19. **Lei B, Bush RA, Milam AH, Sieving PA.** 2000. Human melanoma-associated retinopathy (MAR) antibodies alter the retinal ON-response of the monkey ERG in vivo. *Invest Ophthalmol Vis Sci* **41:**262–266. PubMed
20. **Milam AH, Saari JC, Jacobson SG, Lubinski WP, Feun LG, Alexander KR.** 1993. Autoantibodies against retinal bipolar cells in cutaneous melanoma-associated retinopathy. *Invest Ophthalmol Vis Sci* **34:**91–100. PubMed
21. **Dalal MD, Morgans CW, Duvoisin RM, Gamboa EA, Jeffrey BG, Garg SJ, Chan CC, Sen HN.** 2013. Diagnosis of occult melanoma using transient receptor potential melastatin 1 (TRPM1) autoantibody testing: a novel approach. *Ophthalmology* **120:**2560–2564. PubMed
22. **Dhingra A, Fina ME, Neinstein A, Ramsey DJ, Xu Y, Fishman GA, Alexander KR, Qian H, Peachey NS, Gregg RG, Vardi N.** 2011. Autoantibodies in melanoma-associated

retinopathy target TRPM1 cation channels of retinal ON bipolar cells. *J Neurosci* **31:**3962–3967. PubMed

23. **Chin MS, Caruso RC, Detrick B, Hooks JJ.** 2006. Autoantibodies to p75/LEDGF, a cell survival factor, found in patients with atypical retinal degeneration. *J Autoimmun* **27:**17–27. PubMed
24. **Comlekoglu DU, Thompson IA, Sen HN.** 2013. Autoimmune retinopathy. *Curr Opin Ophthalmol* **24:**598–605. PubMed
25. **Ferreyra HA, Jayasundera T, Khan NW, He S, Lu Y, Heckenlively JR.** 2009. Management of autoimmune retinopathies with immunosuppression. *Arch Ophthalmol* **127:**390–397. PubMed
26. **Grange L, Dalal M, Nussenblatt RB, Sen HN.** 2014. Autoimmune retinopathy. *Am J Ophthalmol* **157:**266–272.e1. doi:10.1016/j.ajo.2013.09.019. PubMed
27. **Chan CC, Nussenblatt RB, Kim MK, Palestine AG, Awadzi K, Ottesen EA.** 1987. Immunopathology of ocular onchocerciasis. 2. Anti-retinal autoantibodies in serum and ocular fluids. *Ophthalmology* **94:**439–443. PubMed
28. **Braun G, McKechnie NM, Gürr W.** 1995. Molecular and immunological characterization of hr44, a human ocular component immunologically cross-reactive with antigen Ov39 of *Onchocerca volvulus*. *J Exp Med* **182:**1121–1131. PubMed
29. **McKechnie NM, Gürr W, Braun G.** 1997. Immunization with the cross-reactive antigens Ov39 from *Onchocerca volvulus* and hr44 from human retinal tissue induces ocular pathology and activates retinal microglia. *J Infect Dis* **176:**1334–1343. PubMed
30. **Whittle RM, Wallace GR, Whiston RA, Dumonde DC, Stanford MR.** 1998. Human antiretinal antibodies in toxoplasma retinochoroiditis. *Br J Ophthalmol* **82:**1017–1021. PubMed
31. **Nussenblatt RB, Gery I, Ballintine EJ, Wacker WB.** 1980. Cellular immune responsiveness of uveitis patients to retinal S-antigen. *Am J Ophthalmol* **89:**173–179. PubMed
32. **Morohoshi K, Ohbayashi M, Patel N, Chong V, Bird AC, Ono SJ.** 2012. Identification of anti-retinal antibodies in patients with age-related macular degeneration. *Exp Mol Pathol* **93:**193–199. PubMed
33. **Tan EM, Feltkamp TE, Smolen JS, Butcher B, Dawkins R, Fritzler MJ, Gordon T, Hardin JA, Kalden JR, Lahita RG, Maini RN, McDougal JS, Rothfield NF, Smeenk RJ, Takasaki Y, Wiik A, Wilson MR, Koziol JA.** 1997. Range of antinuclear antibodies in "healthy" individuals. *Arthritis Rheum* **40:**1601–1611. PubMed
34. **Chin MS, Hooper LC, Hooks JJ, Detrick B.** 2014. Identification of α-fodrin as an autoantigen in experimental coronavirus retinopathy (ECOR). *J Neuroimmunol* **272:**42–50. PubMed
35. **Chan CC, Wallace DJ.** 2004. Intraocular lymphoma: update on diagnosis and management. *Cancer Control* **11:**285–295. PubMed
36. **Hormigo A, Abrey L, Heinemann MH, DeAngelis LM.** 2004. Ocular presentation of primary central nervous system lymphoma: diagnosis and treatment. *Br J Haematol* **126:**202–208. PubMed
37. **Cassoux N, Merle-Beral H, Lehoang P, Herbort C, Chan CC.** 2001. Interleukin-10 and intraocular-central nervous system lymphoma. *Ophthalmology* **108:**426–427. PubMed
38. **Chan CC, Whitcup SM, Solomon D, Nussenblatt RB.** 1995. Interleukin-10 in the vitreous of patients with primary intraocular lymphoma. *Am J Ophthalmol* **120:**671–673. PubMed
39. **Whitcup SM, Stark-Vancs V, Wittes RE, Solomon D, Podgor MJ, Nussenblatt RB, Chan CC.** 1997. Association of interleukin 10 in the vitreous and cerebrospinal fluid and primary central nervous system lymphoma. *Arch Ophthalmol* **115:**1157–1160. PubMed
40. **Wolf LA, Reed GF, Buggage RR, Nussenblatt RB, Chan CC.** 2003. Vitreous cytokine levels. *Ophthalmology* **110:**1671–1672. PubMed
41. **Wang Y, Shen D, Wang VM, Sen HN, Chan CC.** 2011. Molecular biomarkers for the diagnosis of primary vitreoretinal lymphoma. *Int J Mol Sci* **12:**5684–5697. PubMed

CANCER

section O

VOLUME EDITOR: ROBERT G. HAMILTON
SECTION EDITORS: DANIEL CHAN AND LORI J. SOKOLL

Introduction

ROBERT G. HAMILTON

107

The National Cancer Institute has defined cancer as a group of diseases in which abnormal cells divide without control and are able to invade other tissues. Cancers can be broadly categorized into five groups depending on their origin: carcinoma (skin), sarcoma (bone, cartilage, fact muscle, and blood vessels), leukemia (blood-forming tissue and bone marrow), lymphoma/myeloma (cells of the immune system), and central nervous system (brain and spinal cord).

The four chapters in the Cancer section of the 8th edition of this *Manual* discuss immunological methods that are used to detect and quantify proven and investigational markers of tumor presence and growth. Since many tumor markers are not elevated under all cancerous conditions and others are elevated under noncancer conditions, this is a challenging area of diagnostic immunology.

The first chapter in this section, by Godbey et al., discusses the design and performance of a number of well-established tumor marker assays that are used in the screening, diagnosis, and management of cancers. The authors provide a detailed description of the assay designs used, validation strategies, and assay interferences. Illustrative tumor markers and algorithms are overviewed, including those for ovarian cancer (CA125, HE4, ROMA, and OVA1), prostate cancer (prostate-specific antigen), and mesothelioma. In chapter 109, Jaffe and Raffeld discuss the classification of the immunologic and molecular tumor markers involved in the diagnosis of lymphomas and nonlymphoid neoplasms that originate from cells involved in antigen presentation and processing. Their chapter describes the current classification system based on the starting lymphoid or mononuclear phagocytic lineage. They then discuss the design and interpretation of molecular assays for clonality or cytogenetic characterization and immunological tests (flow cytometry or immunohistochemistry of paraffin or frozen sections) that are utilized in the diagnosis of lymphomas.

Chapter 110, by Whiteside, provides a comprehensive overview of cellular, humoral, and cytokine assays that use immunologic reagents and are used in the monitoring of immunologic therapies. These involve the quantification of soluble cellular products (immunoglobulin and cytokine levels), phenotypic markers using flow cytometry, and functional (cytotoxicity and chemotaxis) assays. In the final chapter of this section, Danila et al. extend the discussion in the prior chapter to demonstrate how immunological methods are used to identify and quantify circulating tumor cells.

Diagnostic oncology and immunology laboratories employ the methods discussed in these four chapters throughout the world to assist oncologists in making more-accurate diagnoses, assess neoplasm recurrence, and aid in the management of patients with cancer.

doi:10.1128/9781555818722.ch107

Immunoassay-Based Tumor Marker Measurement: Assays, Applications, and Algorithms

ELIZABETH A. GODBEY, LORI J. SOKOLL, AND ALEX J. RAI

108

Tumor markers are molecules derived from patient body fluids or tissues that are measured and can provide information useful for the management of cancer patients. Applications include detection of cancer, monitoring of disease progression, and evaluation of the effectiveness of therapeutic regimens, among others. Henry Bence-Jones discovered the first tumor marker in 1846—a protein seen in acidified urine of patients with multiple myeloma (1). Since that time, many more tumor markers have been described for a variety of other cancers. The Food and Drug Administration (FDA) has approved several of these markers (Table 1), and many more are being investigated and evaluated for clinical use. The goal of this chapter is to review how tumor marker assays are evaluated, describe the applications of tumor markers, provide details on the detection of tumor markers using immunoassays, and then list examples of clinically useful tumor markers that are used in the clinical laboratory today. Although the last few years have witnessed a plethora of developments in molecular testing of tumor markers, these will not be discussed here, as we will restrict our discussion to immunoassay-based detection methods.

EVALUATION OF TUMOR MARKER ASSAYS

Tumor marker assays, as with other laboratory assays, are evaluated based on their performance characteristics, including sensitivity, specificity, positive predictive value, and negative predictive value. These are important concepts that are applied across the laboratory sciences. A few important definitions follow.

Sensitivity: the fraction of all patients *with disease* that a test is able to correctly identify

Specificity: the fraction of all patients *without disease* that a test is able to correctly identify

Positive predictive value: the probability that a patient with a positive test result is *truly disease positive*

Negative predictive value: the probability that a patient with a negative test result is *truly disease negative*

Every lab must carefully select cutoff values for all tests offered. A cutoff value set too low will have many false-positive results but will miss very few truly positive patients. This type of error results in a high sensitivity but low specificity. The positive predictive value of such a test would be lowered, whereas the negative predictive value would be high. On the other hand, if the cutoff value is set too high, true-positive patients will be missed. Such a test would have a low sensitivity and high specificity. The positive predictive value would be higher than expected while the negative predictive value would be lower than expected.

As these two examples indicate, sensitivity and specificity are inversely related, as are positive predictive value and negative predictive value. The sensitivity and specificity for a test are a reflection of the cutoff value. Thus, the cutoff value for a given assay must be selected with the desired sensitivity and specificity in mind. The disease that a particular assay detects determines the balance between sensitivity and specificity: what are the effects of missing a disease-positive person versus incorrectly diagnosing a truly negative patient? Receiver operating characteristic curves graphically depict "[sensitivity]" versus "[1-specificity]." These curves present performance characteristics at multiple thresholds and are used in the selection of ideal cutoff values.

UTILIZATION OF TUMOR MARKERS

As mentioned earlier, tumor markers have a wide range of potential applications. These include cancer screening and detection, evaluation of the effectiveness of cancer therapies, detection of disease recurrence, therapy selection, and other potential uses. These applications are further discussed in this section.

Screening

One of the most desired goals for application of tumor markers is their utilization in screening for cancer. Unfortunately, the vast majority of tumor markers do not have the requisite sensitivity or specificity to be widely used for screening. Some tumor markers (with low sensitivity) are not elevated in all disease cases (this is very common because cancer, by its nature, is a heterogeneous disease), and thus will not detect all patients with a particular cancer. This false-negative result could be quite damaging to a patient, as it will generate false comfort and may allow a case to progress without treatment. Other markers (with low specificity) are elevated in many conditions and do not strictly indicate the presence of cancer, but can also indicate benign conditions. These positive test results may generate false cancer diagnoses, unnecessary follow-up testing, and emotional trauma to patients who are truly cancer negative.

doi:10.1128/9781555818722.ch108

TABLE 1 FDA-approved tumor markers

Cancer type	Tumor marker(s)[a]	Applications	Gene ontology classification
Breast	CA 15-3, CA 27.29	Detection of recurrence; monitoring of therapy and disease progression in metastatic disease	Membrane protein fragment
	HER2/neu	Prognosis; detection of recurrence	Membrane protein, extracellular domain
Prostate	PSA (total, free, and complexed)	Screening; diagnosis; detection of recurrence; as component of *phi*	Secreted protease
Ovarian	CA125	Monitoring of therapy; prognosis; detection of recurrence	Membrane protein fragment
	HE4	Detection of recurrence	Glycosylated protein
	OVA1	Preoperative mass evaluation	Multiple protein components in algorithm: β_2-microglobulin, transferrin, transthyretin, and apolipoprotein A1
	ROMA	Preoperative mass evaluation	Multiple components in algorithm: HE4, CA125, and menopausal status
Colorectal	CEA	Disease stratification—identification of aggressive disease; prognosis; detection of recurrence; monitoring of therapy and response to treatment	Membrane protein fragment
Pancreatic	CA 19-9	Monitoring of therapy and disease progression; detection of recurrence	Membrane protein fragment
Liver	AFP	Screening (in high-risk population, with ultrasound); detection of residual disease; monitoring of therapy; detection of recurrence	Secreted protein
Bladder	NMP-22 (urine)	Detection of residual disease	Nuclear matrix protein
Mesothelioma	SMRP	Monitoring of disease progression	Membrane protein fragment

[a]Abbreviations: CEA, carcinoembryonic antigen; AFP, α-fetoprotein; NMP, nuclear matrix protein.

At this time, prostate-specific antigen (PSA) is the most common tumor marker used for screening (in conjunction with digital rectal exam, or DRE). However, an elevated PSA can result not only from prostate cancer but also from a host of other benign conditions, such as prostatitis or benign prostatic hyperplasia. Although PSA is widely used for screening, this example illustrates that its specificity is lowered at the expense of a higher sensitivity so that the majority of disease-positive patients are identified. However, the disadvantage of this approach is that many men with an elevated PSA are subject to unnecessary workup and potentially unnecessary treatment, resulting in morbidity.

Diagnosis

Another highly desirable goal for tumor marker application is the ability to diagnose cancer. Again, the sensitivity and specificity of most tumor markers cannot accommodate this goal. The gold standard in the diagnosis of cancer is pathologic analysis, most of which is done using histology and immunohistochemistry of biopsy tissues. In the past, one approach to improve the sensitivity and specificity of serum biochemical tumor markers has been to utilize multiple markers instead of single analytes, or to incorporate multiple tumor markers into a more comprehensive algorithm involving other testing modalities. One exception to the general rule, where a tumor marker is diagnostic, is that of the presence of a monoclonal spike (M-spike) in the analysis of serum protein electrophoresis from patients with plasma cell dyscrasias. This test is virtually diagnostic, as the presence of the M-spike indicates an abundance of a particular immunoglobulin clone that is detectable in the γ region of fractionated serum. This situation can occur only in the setting of a plasma cell dyscrasia.

Monitoring of Treatment

Blood, urine, and fluid samples are easily procured from the human body and thus are an ideal way to measure tumor markers and monitor a patient's response to treatment in real time. The measurement of tumor markers should rise and fall with increasing and decreasing disease severity, respectively. Clinicians must remember the importance of establishing a patient's baseline and monitoring tumor marker levels by consistently using the same assay, preferably in the same laboratory. The use of different laboratories and/or different assays could result in falsely rising or falling tumor marker levels; such a result may not be due to a true rise or fall in the marker, but instead may be due to the use of different assays utilizing differing antibodies, instruments, methodologies, and/or reagents. Any one or more of these can result in variation of the detected protein species and can dramatically alter quantitation of the tumor marker of interest. As with other tumor marker applications, lack of sensitivity and/or specificity of a marker may cause misleading results. An example in which different assays measuring the same tumor marker can produce widely discrepant results is that of the CA 19-9 assay. College of American Pathologists proficiency testing summary results (2014; http://www.cap.org/web/home/lab/proficiency-testing) reveal a discrepancy (at certain levels) when the exact same sample is measured on the Architect (Abbott Diagnostics, Lake Forest, IL), ADVIA Centaur (Siemens Healthcare, Erlangen, Germany), AIA (Tosoh Bioscience, South San Francisco, CA), and Access (Beckman Coulter, Brea, CA) assay.

Detection of Disease Recurrence

Patients being evaluated for this purpose have already been diagnosed via pathology and have undergone treatment, so determining the origin of disease is not the major question. Analytical sensitivity, however, is exceedingly important, because rising levels of the tumor marker are interpreted as cancer recurrence. An example of a tumor marker assay that is useful for detecting disease recurrence is PSA, particularly the newer-generation, ultrasensitive PSA assay. Such a test can accurately measure very low levels of the analyte of interest, providing an early indication that the patient's disease has recurred or is no longer responding to treatment.

Therapy Selection

Specific tumor markers may be used to define appropriate therapy for disease. The most common example of this category is the detection of HER2/neu and estrogen receptor in breast cancers to predict disease response to targeted therapy or to cytotoxic agents. HER2 positivity suggests response to HER2-directed therapy, such as trastuzumab. Estrogen receptor positivity suggests response to tamoxifen. Although these tests utilize immunohistochemistry and are not immunoassays *per se*, they are commonly used to direct the treatment of breast cancer patients. Other examples of "predictive biomarkers," i.e., those used to predict response to therapy, include the *EGFR* L858R mutation, which indicates sensitivity to cetuximab in lung cancer patients; and the *BRAF* V600E mutation, which indicates sensitivity to the melanoma drug vemurafenib. These are also molecular assays and not protein-based analyses—DNA sequencing is straightforward and much easier than detection of the encoded protein for these particular applications.

IMMUNOASSAY DESIGN METHODS

Most tumor marker quantification assays are immunoassays based on variations of enzyme-linked immunosorbent assay (ELISA) methods. Antibodies can be used to isolate target molecules in many different clinical sample types, including whole blood, plasma, serum, urine, and other fluids. For an introduction to immunoassays and their utilization, see reference 1.

TYPES OF IMMUNOASSAYS

Immunoassays fall into two large categories, the first of which are limited-reagent assays. In this type of assay, a defined amount of antibody is present on a solid phase. Both labeled antigens and sample antigens compete for binding sites on the antibody. Thus, these are also known as competitive binding assays. Greater concentrations of sample analyte result in decreased binding of the labeled antigen and thus decreased signal. This is illustrated in Fig. 1.

The second category of immunoassays is termed excess-reagent assays. In contrast to the first category, this group of assays involves an excess of antibody that will bind the sample antigen. The "sandwich assay" (also known as a two-site immunometric assay) is one of the most common immunoassay designs, and it falls into the excess-reagent category. A capture antibody, bound to a solid phase, is

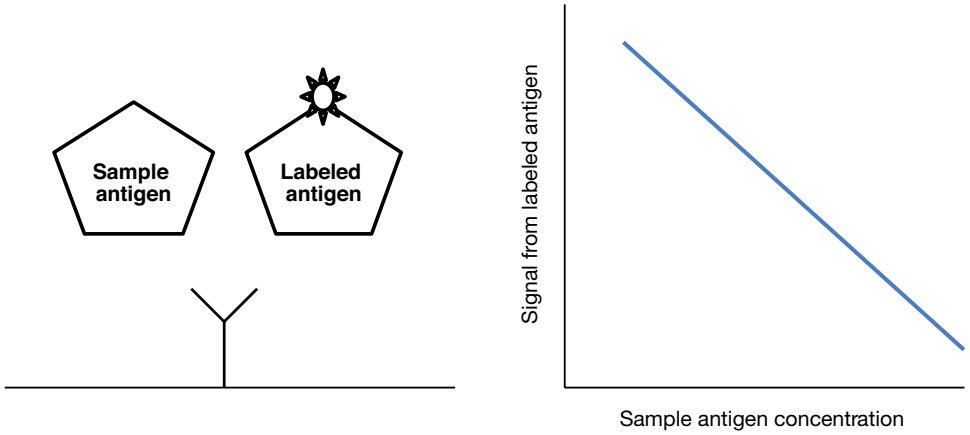

FIGURE 1 (Left) Schematic diagram of a competitive binding (labeled-antigen) immunoassay. In this assay, a limited amount of immobilized antibody binds both labeled and unlabeled forms of the tumor marker antigen of interest. (Right) The higher the concentration of unlabeled tumor marker antigen in the subject's serum, the lower the signal generated by bound labeled antigen.

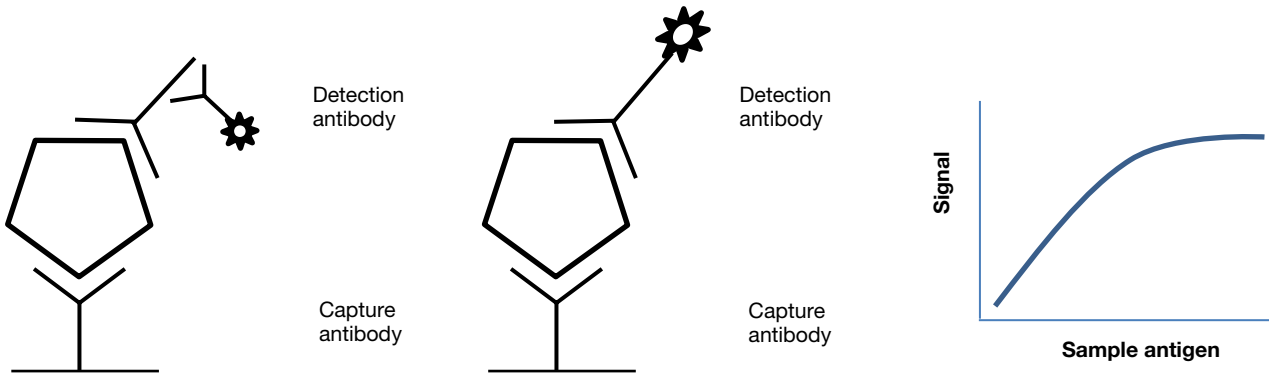

FIGURE 2 Schematic diagram of a noncompetitive binding two-site sandwich immunometric (labeled-antibody) assay. In this assay, molar excess immobilized antibody specific for the tumor marker binds unlabeled forms of the tumor marker antigen in the patient's serum. Bound antigen is then detected with a second antitumor marker antibody that binds to a different antigenic epitope. Either the second antibody can be detected by a third labeled antibody (left) or the second antibody can be directly labeled (middle). The higher the concentration of unlabeled tumor marker antigen in the subject's serum, the higher the signal generated by bound detection antibody (right).

present in excess. The sample antigen is added and allowed to bind to the capture antibody. A second antibody, termed a detection antibody, is added to the mixture. The capture antibody and the detection antibody each target a different epitope of the sample analyte and thus "sandwich" the analyte between them. In contrast to the first category of assays, these assays do not involve a competition among antigens and are thus known as noncompetitive assays. The detection antibody either is directly labeled or is bound by a third labeled antibody. The sample antigen present is measured indirectly by measuring the amount of labeled, bound antibody present. See Fig. 2 for an illustration of this concept.

Two different designs are available to complete a sandwich assay. The first involves a one-step incubation during which both the sample analyte and detection antibody are added simultaneously to the solid-phase capture antibody. While this design minimizes the number of steps and hence the time required to complete the test, the hook effect may interfere with accurate result reporting. See Fig. 3 for a schematic and explanation of the hook effect. The second possible design of a sandwich assay involves a two-step procedure. First, the sample analyte is added to the capture antibody. Then, in a second step, the detection antibody is added. Although this second method is more time-consuming, it may reduce interferences that are present in the single-step method, thus increasing specificity.

CLINICAL TEST DESIGN: IDENTIFICATION OF APPROPRIATE ANTIBODIES

The characteristics of an ideal antibody for use in immunoassays are perhaps intuitive. Antibodies should have low cross-reactivity and should be able to identify analytes at low concentrations. In other words, they should have high specificity and sensitivity. In cases in which an assay requires multiple antibodies (capture and detection), the antibodies should bind different epitopes, be complementary, and also not interfere to target the analyte of interest.

IMMUNOASSAY INTERFERENCES

Immunoassays are a popular laboratory methodology because of their sensitivity and specificity and can be used to quantify targets obtained from minimally invasive procedures such as urine collection or phlebotomy. Unfortunately, as with any laboratory method, interferences may falsely increase or decrease reported analyte values. Several

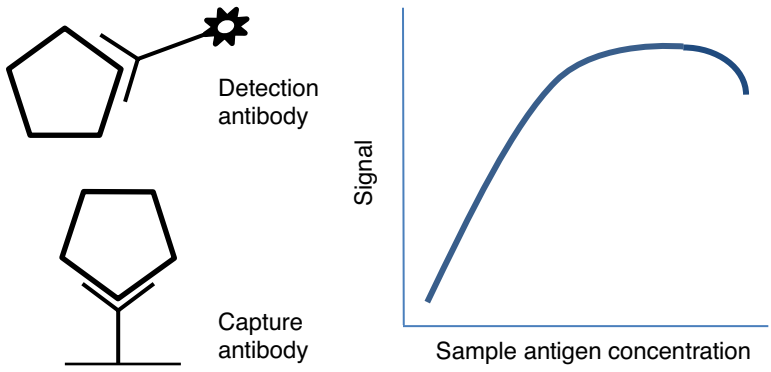

FIGURE 3 In immunometric assays, a hook effect can occur when the capture and detection antibodies bind to different molecules, without the formation of a "sandwich," as shown on the left panel. This results in an erroneous decrease in the measured signal at high concentrations of analyte; the effect on the dose-response curve is shown on the right panel.

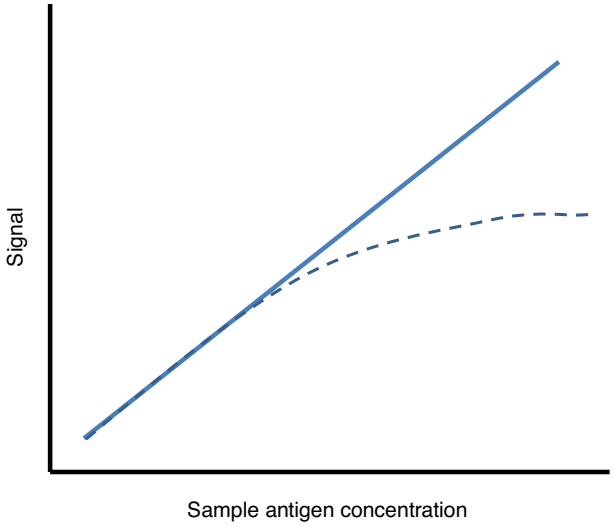

FIGURE 4 Schematic diagram showing result deviation from linearity that may be caused by interference.

interferences can be identified and corrected if proper quality assurance and quality control procedures are upheld. Examples are shown in Table 2. Interferences resulting in altered test values pose a significant problem to patient care. It is important to avoid interferences, identify them when they occur, and correct them (if possible). For example, blocking reagents can be used to avoid negative effects of heterophilic antibodies (see http://scantibodies.com). Endogenous autoantibodies may also interfere with accurate laboratory results. For example, patients with thyroid carcinoma are followed prospectively using serum thyroglobulin measurements. Following thyroidectomy, an increase in thyroglobulin is interpreted as disease recurrence. Endogenous autoantibodies directed against thyroglobulin may be a source of interference and result in a false-negative report (2). This source of interference has obvious negative implications for patient care and outcomes.

If an interference is suspected, serial dilutions should be performed and the samples retested. Samples with interferents often will not dilute linearly. If a linear response does not result, it can be presumed that an interference is affecting results of the test (see Fig. 4). The sample should be further examined, and an appropriate means should be taken to identify the interference. Use of heterophilic blocking preparations and assaying on an alternate method can help solidify the presence of an interference. When applicable, such as for β-human chorionic gonadotropin, testing for the analyte in urine can also be helpful.

EXAMPLES OF TUMOR MARKERS

This section discusses tumor markers and algorithms that incorporate tumor markers utilized in ovarian cancer, prostate cancer, and mesothelioma.

Ovarian Cancer: CA125, HE4, ROMA, and OVA1

CA125 (cancer antigen 125) is used by clinicians to monitor patients with ovarian cancer. The molecule is an antigen present on a large (>200-kDa) glycoprotein that resides on the plasma membrane. The protein antigen for CA125 is encoded by the *MUC16* gene, which is located on chromosome 19. Several different assays are currently available to measure CA125 levels. These make use of different antibodies, all of which target different epitopes of this molecule.

CA125 is FDA approved in its use to monitor the response to therapy in ovarian cancer patients. It is also useful to assess the progression of disease. As tumor burden decreases, so do levels of CA125 in the blood of cancer patients. In contrast, CA125 levels increase in patients with increasing tumor burden.

Although CA125 is often considered a nonspecific indicator of ovarian cancer, it is usually not elevated in nonserous ovarian cancers (other ovarian cancer subtypes include mucinous, endometrioid, and clear cell ovarian cancers). In contrast, the marker is increased in most (>80%) nonmucinous epithelial ovarian cancers. As previously discussed in relation to other markers, several common benign conditions can result in a falsely elevated CA125 level, including pregnancy, menstruation, and endometriosis. Therefore, as with any laboratory test result, CA125 levels must be evaluated in the context of the entire clinical presentation.

HE4 is a glycosylated protein encoded by the *WRDC2* gene localized to chromosome 20q12-13.1. It has been found to be moderately elevated in many types of cancer, but most significantly elevated in ovarian cancer. In a study leading to its FDA approval, HE4 and CA125 were found to have comparable sensitivity (80%) and specificity (95%) when differentiating between patients with and without ovarian cancer (3). The FDA approved HE4 testing in 2009 as a method to evaluate ovarian cancer recurrence. It is not applicable for use in diagnosing ovarian cancer.

Following the discovery of HE4 as a marker for ovarian cancer, investigators began to combine CA125, HE4, and other markers in an effort to improve the performance characteristics over the single markers. As a result of such studies, an algorithm abbreviated as ROMA (Risk of Ovarian Malignancy Algorithm) was developed. ROMA creates a score based on a patient's levels of HE4 and CA125, as well as their menopausal status. In premenopausal patients, a ROMA score of >1.31 favors malignancy. In postmenopausal patients, a ROMA score of >2.77 favors malignancy. Of note, rheumatoid factor serum levels of >250 IU/ml will alter ROMA scores. The ROMA algorithm was approved by the FDA in 2011 for use during preoperative evaluation of pelvic masses along with clinical and/or radiologic studies. In the studies leading to its FDA approval, ROMA was found to have a sensitivity of 88.7% and a specificity of 74.7% (3). For additional information on ROMA, see reference 4.

A separate panel of tumor markers, called OVA1, has also been developed. Four markers (β_2-microglobulin, transferrin, transthyretin, and apolipoprotein A1) were selected via proteomic studies. The OvaCalc software generates a score based on the serum levels of these four markers, as well as the CA125 serum level. In premenopausal patients, a score of ≥5.0 highly favors malignancy. In postmenopausal patients, a score of ≥4.4 highly favors malignancy. OVA1 earned FDA approval in 2009 as an aid in preoperative mass evaluation. The FDA specifies that OVA1 is not to be used for screening or for surgical evaluation. The sensitivity and specificity of OVA1, as reported in clinical trials, were 92.5% and 42.8%, respectively (3). For additional information on OVA1, see references 5 through 7.

Prostate Cancer: PSA and *phi*

PSA, also known as human kallikrein 3 (hK3), is a serine protease of ~28 kDa. As a secreted protein, PSA undergoes maturation during its progression through the secretory

TABLE 2 Assay interferences that cause falsely elevated or decreased tumor marker results

Interference type	Examples and characteristics	Effect on tumor marker results
Sample interferences	Lipemia, hemolysis, or icterous	Usually decrease
Cross-reactivity	More common with polyclonal antibodies	Usually decrease
Antireagent antibodies	Heterophilic antibodies	Either increase or decrease
Rheumatoid factor	Presence of autoantibodies	Usually decrease
Protein complexes	Prolactin, steroids, and troponin	Usually decrease
Hook effect	Presence of excess antigen	Decrease

pathway in prostate epithelial cells. It is initially expressed in a "prepro" form in these cells. This prepro protein contains a 17-amino-acid signal sequence that is later removed to form proPSA, with a 7-amino-acid leader sequence. This proPSA molecule is inactive but is targeted for cleavage by hK2, expressed in the prostate lumen ducts. The hK2 protease cleaves PSA and converts it into its mature, active form of 237 amino acids.

PSA plays an important role in monitoring prostate cancer disease course and response to treatment. Because PSA is produced in the prostate, it is an extremely useful marker for detecting recurrence of disease following definitive therapy. PSA also plays a role in the early detection of prostate cancer. However, although it is prostate gland specific, it is not prostate cancer specific and can be elevated in benign conditions such as benign prostatic hyperplasia and prostatitis. A number of approaches have been proposed to overcome this limitation of PSA and improve its specificity, including measurement of the circulating molecular forms of PSA. The majority of immunoreactive serum PSA is bound to the protease inhibitor α_1-antichymotrypsin, while the remaining 10 to 30% is unbound and is known as free PSA. Men with a higher percentage of free PSA as a function of total PSA have a lower probability of cancer, while men with a lower percentage of free PSA have a higher probability of cancer. The utility of free PSA has subsequently been improved with the knowledge that free PSA consists of cancer-specific (proPSA) and benign (BPSA) isoforms. An automated immunoassay for [−2]proPSA has been developed and approved by the FDA and incorporated into an algorithm with total and free PSA called *phi* (Prostate Health Index) to aid in distinguishing prostate cancer from benign conditions in men with a total PSA between 4 and 10 ng/ml and a negative DRE. In a multicenter trial of 892 men undergoing biopsy with a PSA of 2 to 10 ng/ml and a negative DRE, *phi* had greater specificity than total and percent free PSA for prostate cancer detection and thus potential for reduction in unnecessary biopsies (8). In this and other studies, *phi* also correlated with cancer aggressiveness.

Mesothelioma

Mesothelioma is clinically very difficult to diagnose. In fact, radiology reports often differ significantly from surgical and pathology findings, and 20 to 30% of thoracotomy procedures are aborted due to surgical finding of advanced disease beyond radiologic predictions (9).

There are currently no diagnostic tumor markers approved by the FDA for diagnosis of mesothelioma. A Humanitarian Use Device approval was granted by the FDA several years ago for soluble mesothelin-related peptides (SMRPs) as a method to monitor previously diagnosed mesothelioma, but not to diagnose the disease (although some clinicians utilize the serum ELISA to support a new diagnosis). A Humanitarian Use Device approval from the FDA applies to disorders that occur in <4,000 people in the United States annually. This type of approval requires fewer supportive data. It requires data to support that its benefits outweigh its risks, that its risks are not unreasonable, and that nothing comparable is already available to the patient population (10).

Mesothelin is an adhesion protein produced by mesothelium cells. It is encoded by the *MSLN* gene, the mRNA of which produces a preprotein that is cleaved into two fragments: megakaryocyte-potentiating factor and mesothelin. Mesothelin is a protein involved in cellular adhesion (11). SMRPs are measured in human serum with a quantitative ELISA assay. Many studies have been published on mesothelin, but at a level of 2.00 nmol/liter, studies show large ranges for its sensitivity and specificity, ranging from 19 to 68% and 88 to 100%, respectively (9, 11, 12).

NEW DEVELOPMENTS IN TUMOR MARKER DISCOVERY

An active area of research in the field of tumor markers relates to that of exosomes. Exosomes are extracellular vesicles consisting of lipid bilayers surrounding proteins and nucleic acids. All cells produce exosomes, and these vesicles are present in the circulation (13). Exosomes were first described ~30 years ago, but only in the last decade has there been increasing interest in using exosomes to identify new biomarkers for various diseases. Initially, researchers were able to identify significant increases in exosome markers only after diseases had entered advanced stages (14). Recently, however, exosomes have shown promise in application to early detection and diagnosis, using either protein or nucleic acid markers, and sometimes both. Jakobsen et al. were able to demonstrate that exosome markers have a specificity of 76% by studying expression of 30 different proteins using microarrays (15). Madhavan et al. were able to demonstrate 93% specificity in diagnosing pancreatic cancer using five proteins and four microRNAs (16).

Glypican-1 (GPC1) is a membrane-localized protein found in exosomes. It has been shown to be upregulated in cell lines and mouse models of pancreatic carcinoma. Melo et al. (13) focused their recent studies on GPC1-containing exosomes. They used GPC1-specific antibodies and flow cytometry to show that GPC1 vesicles are upregulated in patients with pancreatic carcinoma but not in patients with other pancreatic diseases. Melo et al. concluded that identification and quantification of GPC1 vesicles was a superior test to CA 19-9 for the early diagnosis of pancreatic cancer. The study was completed with small numbers of patients, and thus additional studies are needed. Such findings are promising and warrant future investigation of exosomes as carriers of early cancer biomarkers. These new methods

hold great potential for early detection of disease and can lead to improved patient outcomes.

THE FUTURE OF TUMOR MARKERS

Advancements in knowledge of the human genome and human proteome, improvements in high-throughput nucleic acid and protein analysis, as well as improved bioinformatics capabilities all contribute to a bright future for tumor marker use, improvement, and discovery. New tumor markers that could be used alone or as part of a larger panel of markers are being studied for a variety of applications related to the management of patients with cancer. Hopefully, these new tests will achieve FDA approval in the near future. Goals for future tumor markers include increased sensitivity and specificity to allow greater diagnosis capability with minimally invasive techniques. Tumor markers with increased sensitivity and specificity will allow for earlier detection and treatment of cancer, and therefore better patient care and improved outcomes for those afflicted with this insidious disease.

REFERENCES

1. **Schrohl AS, Holten-Andersen M, Sweep F, Schmitt M, Harbeck N, Foekens J, Brünner N, European Organisation for Research and Treatment of Cancer (EORTC) Receptor and Biomarker Group.** 2003. Tumor markers: from laboratory to clinical utility. *Mol Cell Proteomics* **2:**378–387. PubMed
2. **Kushnir MM, Rockwood AL, Roberts WL, Abraham D, Hoofnagle AN, Meikle AW.** 2013. Measurement of thyroglobulin by liquid chromatography-tandem mass spectrometry in serum and plasma in the presence of antithyroglobulin autoantibodies. *Clin Chem* **59:**982–990. PubMed
3. **Leung F, Diamandis EP, Kulasingam V.** 2012. From bench to bedside: discovery of ovarian cancer biomarkers using high-throughput technologies in the past decade. *Biomarkers Med* **6:**613–625. PubMed
4. **Montagnana M, Danese E, Ruzzenente O, Bresciani V, Nuzzo T, Gelati M, Salvagno GL, Franchi M, Lippi G, Guidi GC.** 2011. The ROMA (Risk of Ovarian Malignancy Algorithm) for estimating the risk of epithelial ovarian cancer in women presenting with pelvic mass: is it really useful? *Clin Chem Lab Med* **49:**521–525. PubMed
5. **Rai AJ, Zhang Z, Rosenzweig J, Shih IM, Pham T, Fung ET, Sokoll LJ, Chan DW.** 2002. Proteomic approaches to tumor marker discovery. *Arch Pathol Lab Med* **126:**1518–1526. PubMed
6. **Høgdall C, Fung ET, Christensen IJ, Nedergaard L, Engelholm SA, Petri AL, Risum S, Lundvall L, Yip C, Pedersen AT, Hartwell D, Lomas L, Høgdall EV.** 2011. A novel proteomic biomarker panel as a diagnostic tool for patients with ovarian cancer. *Gynecol Oncol* **123:**308–313. PubMed
7. **Bristow RE, Smith A, Zhang Z, Chan DW, Crutcher G, Fung ET, Munroe DG.** 2013. Ovarian malignancy risk stratification of the adnexal mass using a multivariate index assay. *Gynecol Oncol* **128:**252–259. PubMed
8. **Catalona WJ, Partin AW, Sanda MG, Wei JT, Klee GG, Bangma CH, Slawin KM, Marks LS, Loeb S, Broyles DL, Shin SS, Cruz AB, Chan DW, Sokoll LJ, Roberts WL, van Schaik RH, Mizrahi IA.** 2011. A multicenter study of [−2]pro-prostate specific antigen combined with prostate specific antigen and free prostate specific antigen for prostate cancer detection in the 2.0 to 10.0 ng/ml prostate specific antigen range. *J Urol* **185:**1650–1655. PubMed
9. **Pass HI.** 2012. Biomarkers and prognostic factors for mesothelioma. *Ann Cardiothorac Surg* **1:**449–456. PubMed
10. **U.S. Food and Drug Administration.** 2015. Humanitarian device exemption. U.S. Food and Drug Administration, Silver Spring, MD. http://www.fda.gov/MedicalDevices/DeviceRegulationandGuidance/HowtoMarketYourDevice/PremarketSubmissions/HumanitarianDeviceExemption/.
11. **Rai AJ, Flores RM, Mathew A, Gonzalez-Espinoza R, Bott M, Ladanyi M, Rusch V, Fleisher M.** 2010. Soluble mesothelin related peptides (SMRP) and osteopontin as protein biomarkers for malignant mesothelioma: analytical validation of ELISA based assays and characterization at mRNA and protein levels. *Clin Chem Lab Med* **48:**271–278. PubMed
12. **Hollevoet K, Reitsma JB, Creaney J, Grigoriu BD, Robinson BW, Scherpereel A, Cristaudo A, Pass HI, Nackaerts K, Rodríguez Portal JA, Schneider J, Muley T, Di Serio F, Baas P, Tomasetti M, Rai AJ, van Meerbeeck JP.** 2012. Serum mesothelin for diagnosing malignant pleural mesothelioma: an individual patient data meta-analysis. *J Clin Oncol* **30:**1541–1549. PubMed
13. **Melo SA, Luecke LB, Kahlert C, Fernandez AF, Gammon ST, Kaye J, LeBleu VS, Mittendorf EA, Weitz J, Rahbari N, Reissfelder C, Pilarsky C, Fraga MF, Piwnica-Worms D, Kalluri R.** 2015. Glypican-1 identifies cancer exosomes and detects early pancreatic cancer. *Nature* **523:**177–182. PubMed
14. **Peinado H, Alečković M, Lavotshkin S, Matei I, Costa-Silva B, Moreno-Bueno G, Hergueta-Redondo M, Williams C, García-Santos G, Ghajar C, Nitadori-Hoshino A, Hoffman C, Badal K, Garcia BA, Callahan MK, Yuan J, Martins VR, Skog J, Kaplan RN, Brady MS, Wolchok JD, Chapman PB, Kang Y, Bromberg J, Lyden D.** 2012. Melanoma exosomes educate bone marrow progenitor cells toward a pro-metastatic phenotype through MET. *Nat Med* **18:**883–891. PubMed
15. **Jakobsen KR, Paulsen BS, Bæk R, Varming K, Sorensen BS, Jørgensen MM.** 2015. Exosomal proteins as potential diagnostic markers in advanced non-small cell lung carcinoma. *J Extracell Vesicles* **4:**26659. doi:10.3402/jev.v4.26659. PubMed
16. **Madhavan B, Yue S, Galli U, Rana S, Gross W, Müller M, Giese NA, Kalthoff H, Becker T, Büchler MW, Zöller M.** 2015. Combined evaluation of a panel of protein and miRNA serum-exosome biomarkers for pancreatic cancer diagnosis increases sensitivity and specificity. *Int J Cancer* **136:**2616–2627. PubMed

Malignancies of the Immune System: Use of Immunologic and Molecular Tumor Markers in Classification and Diagnostics

ELAINE S. JAFFE AND MARK RAFFELD

109

Malignancies of the immune system are primarily represented by the malignant lymphomas and a smaller number of nonlymphoid neoplasms that originate from cells involved in antigen presentation and processing. The diagnosis and classification of these tumors have benefited enormously from advances in cellular and molecular immunology, as well as from careful dissection of the molecular genetics of the cancers themselves. Our ability to correctly diagnose tumors of the immune system, which in many instances show little morphological variation, requires the careful application of both immunologic tumor markers as well as molecular (DNA- or RNA-based) tumor markers. Therefore, malignancies of the immune system are not only interesting models of normal immune cells but are also excellent examples of the variety of molecular and immunological approaches for assessing cancers.

The classification of the malignant lymphomas and nonlymphoid tumors of immune cells has undergone significant reappraisal over the past 50 years. Early classification systems of malignant lymphomas, such as the Rappaport classification and the Working Formulation, were based on architectural and cytological characteristics of the neoplastic elements. However, with increasing knowledge of the complexity of the immune system, a more functional approach was sought. The next generation of classification schemes (Kiel, and Lukes and Collins) attempted to integrate immunologic function with morphological parameters, with the premise that each of the lymphomas was an expansion of normal cellular counterparts (1, 2). These classification schemes still relied heavily upon the ability to correlate cytological characteristics of tumor cells with the cytological characteristics of normal counterparts. In practice, this proved to be an extremely difficult endeavor, even for experienced hematopathologists, and it became apparent that a more objective and reproducible classification scheme was needed. The decades from the 1970s through the 1990s saw an explosion of basic information in both cellular and molecular immunology and in cancer genetics. The application of monoclonal antibodies, developed in the course of studying the normal immune system, provided one powerful approach for establishing objective diagnostic criteria, while the development of molecular testing based on rapid advances in the molecular genetic understanding of these tumors provided a second approach. By incorporating these technologies into the diagnostic armamentarium, it became possible to develop a more objective classification scheme that would take into account the molecular and immunologic characterization of the tumors.

In 1994, the International Lymphoma Study Group, a consortium of hematopathologists from the United States and Europe, met and concluded that a classification system should consist of a list of agreed-upon disease entities defined by multiple parameters, rather than being driven by a single overriding principle, such as clinical outcome (Working Formulation) or cellular differentiation (Kiel). For the first time, immunophenotype and molecular genotype were recognized as critical elements in establishing a biologically meaningful classification scheme (3). This breakthrough meeting led to the development of the first modern lymphoma classification system based on biological principles, the REAL classification, and its successor, the current World Health Organization (WHO) classification (Table 1) (4, 5).

A major premise underlying the current classification systems was that lineage must be the starting point for a lymphoma classification. The application of modern immunologic techniques and concepts has permitted the development of a conceptual framework that may be used to decipher the morphological diversity of these neoplasms and has shown the relationship of lymphoid and mononuclear phagocytic neoplasms to the normal immune and hematopoietic systems. The development of monoclonal antibodies reactive with lymphoid, monocytic, and myeloid subsets can be used in the classification, primary diagnosis, and staging of hematopoietic malignancies and as adjunctive tools for immunotherapy in both *in vivo* and *in vitro* settings. In addition, many disease entities, particularly among the B-cell lymphomas, have a highly specific immune profile that can aid greatly in differential diagnosis. Other markers associated with lineage and cellular differentiation help to relate the various lymphoproliferative disorders to distinct stages in the development of the normal immune cells, and they are of particular interest in evaluating lymphoblastic neoplasms and in differentiating germinal-center (GC) from post-GC B-cell neoplasms. Monoclonal antibodies to oncogene or tumor suppressor gene products such as cyclin D1, BCL-2, and p53 have also proved useful in diagnosis and prognostication, and in understanding the pathogenetic mechanisms of lymphomagenesis.

The WHO classification system also recognizes the importance of cytogenetic and correlative molecular genetic

doi:10.1128/9781555818722.ch109

TABLE 1 WHO classification of lymphoid neoplasms (2008)

- Precursor lymphoid neoplasms
  - B-cell lymphoblastic leukemia/lymphoma
  - T-cell lymphoblastic leukemia/lymphoma
  - NK-cell lymphoblastic leukemia/lymphoma
- Mature B-cell neoplasms
  - CLL/SLL
    - Monoclonal B lymphocytosis
  - B-cell prolymphocytic leukemia
  - SMZL
  - HCL
  - LPL
  - α heavy-chain disease
  - γ heavy-chain disease
  - μ heavy-chain disease
  - Plasma cell myeloma
    - Heavy- and light-chain deposition diseases
  - Solitary plasmacytoma of bone
  - Extraosseous plasmacytoma
  - Extranodal MZL of MALT type
  - Nodal MZL
    - Pediatric MZL
  - FL
    - Pediatric FL
    - FL *in situ*
    - Primary intestinal FL
  - Primary cutaneous FL
  - MCL
    - MCL *in situ*
  - DLBCL, not otherwise specified
    - T-cell/histiocyte-rich large B-cell lymphoma
    - Primary DLBCL of the central nervous system
    - Primary cutaneous DLBCL, leg type
    - EBV-positive DLBCL of the elderly (provisional)
  - Primary mediastinal (thymic) large B-cell lymphoma
  - Intravascular large B-cell lymphoma
  - Lymphomatoid granulomatosis
  - DLBCL associated with chronic inflammation
  - ALK-positive DLBCL
  - Plasmablastic lymphoma
  - Primary effusion lymphoma
  - Large B-cell lymphoma arising in HHV-8-associated multicentric Castleman's disease
  - Burkitt's lymphoma
  - B-cell lymphoma, unclassifiable, with features intermediate between DLBCL and Burkitt's lymphoma
  - B-cell lymphoma, unclassifiable, with features intermediate between DLBCL and CHL
- Mature T-cell and NK-cell neoplasms
  - T-cell prolymphocytic leukemia
  - T-cell large granular lymphocytic leukemia
  - Indolent large granular NK-cell lymphoproliferative disorder
  - Aggressive NK-cell leukemia
  - Fulminant EBV^+ T-cell lymphoproliferative disorder of childhood
  - ATL
  - Extranodal NK/T-cell lymphoma
  - Enteropathy-associated T-cell lymphoma
  - Hepatosplenic T-cell lymphoma
  - Subcutaneous panniculitis-like T-cell lymphoma
  - Mycosis fungoides
  - Sézary syndrome
  - CD30-positive primary cutaneous T-cell lymphoproliferative disease
    - Lymphomatoid papulosis
    - Primary cutaneous ALCL
  - Primary cutaneous γδ T-cell lymphoma
  - Primary cutaneous aggressive epidermotropic CD8-positive cytotoxic T-cell lymphoma (provisional)
  - Primary cutaneous small/medium CD4-positive T-cell lymphoma (provisional)
  - AILT
  - PTL, unspecified
  - ALCL, ALK positive
  - ALCL, ALK negative

abnormalities in contributing to the pathogenesis of particular entities. Many neoplasms possess recurrent cytogenetic abnormalities involving oncogenes or tumor suppressor genes that play key roles in the pathogenesis of particular tumors. In recent years, with advances in sequencing and improved genetic characterization, the number of lymphoid malignancies with specific genetic alterations has expanded significantly. Some of the earliest translocations identified included the t(8;14) translocation and its variants that involve the *MYC* gene in Burkitt's lymphoma (6), the t(11;14) translocation that involves the *CCND1* (*cyclin D1*) gene in mantle cell lymphoma (MCL) (7), and the t(14;18) translocation that involves the *BCL2* gene in the vast majority of follicular lymphomas (FLs) (8). These associations not only validated the morphological component of the classification scheme but also enabled the further development and refinement of categories of lymphomas that were difficult to separate by morphology alone. The continued molecular dissection of lymphomas has further revealed characteristic cytogenetic and molecular genetic abnormalities in mucosa-associated lymphoid tissue (MALT) lymphomas, in anaplastic large-cell lymphomas (ALCLs), and in plasma cell neoplasms, as well as in many other lymphoma subtypes. The development of molecular technologies, particularly fluorescent *in situ* hybridization (FISH) and PCR, has brought molecular diagnostics into the routine clinical laboratory and has enabled molecular genotyping to increasingly become a part of the classification criteria.

MOLECULAR AND IMMUNOLOGIC TESTS UTILIZED IN LYMPHOMA DIAGNOSTICS

Immunologic Approaches

Lymphoid and histiocytic neoplasms can be studied in fluid phase by flow cytometry or in paraffin or frozen sections by immunohistochemistry. Flow cytometry is particularly useful in assessing cell surface markers and has the advantage of being able to provide semiquantitative information regarding antigen density. Furthermore, advances in fluorescent dye chemistry and in laser technology have made the simultaneous detection of multiple antigens routine (9). The disadvantages of flow cytometry are that *in situ* tissue organization is lost and the detection of cytoplasmic and nuclear antigens is technically challenging, requiring permeabilization of the cells during specimen processing. In addition, cell suspensions may not be representative of the pathological process due to fibrosis or abundant stromal elements, and specimens must be processed at the time of procurement, necessitating careful planning when obtaining the sample.

In contrast to flow cytometry, immunohistochemical techniques allow one to visualize the immunologic phenotype in the context of the *in situ* organization and cellular morphology. This approach is useful when one considers that lymphomas are rarely pure populations of neoplastic cells, and that a variety of normal cell types are invariably present. Moreover, in some situations, such as in Hodgkin's disease and T-cell-rich large B-cell lymphomas, the neoplastic cells represent a minority of the cells present. Such minor populations of cells may be difficult to study by flow cytometry but can be easily identified by the combination of immunohistochemistry and morphology.

In recent years, an increasing number of both murine and rabbit monoclonal antibodies have become available for use in paraffin sections, eliminating the need to perform immunohistochemistry on frozen tissue sections (Table 2). The development of these reagents has not occurred by chance, but rather by targeting the antigenic conformations present in fixed tissues (10). Rabbit monoclonal antibodies generally have a much higher affinity than comparable mouse monoclonal antibodies and have shown great promise for diagnostic applications (11, 12).

Paraffin section immunohistochemistry has also been greatly facilitated by the development of heat-induced antigen retrieval techniques (13, 14). Previous antigen retrieval techniques involving chemicals or proteolytic enzymes had relatively limited success in diagnostic immunohistochemistry, beyond their ability to improve intermediate filament staining. Heat-induced antigen retrieval procedures proved to have broad applicability, allowing for the detection of numerous antigens rendered nonreactive during the fixation and paraffin embedding process. The advances in antigen retrieval techniques eliminated the need for the specialized processing at the time of surgical removal and made

TABLE 2 Recommended immunohistochemical panels for lymphoma diagnosis

Diagnostic panel	Antibodies[a]
Reactive hyperplasia	CD20, IgD, CD3, CD5, BCL-2, κ, λ, *CD21*, *CD123*, *CD138*
Small B-cell lymphomas	CD20, CD79a, IgD, CD3, CD5, CD10, CD23, CD21, MIB-1, cyclin D1, BCL-2, BCL-6, MUM-1/IRF4
DLBCL/Burkitt's lymphoma Aggressive B-cell neoplasms	CD20, CD3, CD79a, BCL-2, BCL-6, CD10, MUM-1/IRF4, p53, MIB-1, MYC, EBER
Plasma cell, plasmablastic neoplasms	CD20, CD79a, CD3, κ, λ, and heavy chains, CD56, CD138, MUM-1/IRF-4, ALK, EMA, EBER
CHL	CD20, CD3, CD30, CD15, PAX5, *Oct-2*, *Bob.1*, EBER, LMP-1
NLPHL	CD20, CD3, IgD, OCT-2, CD21, CD57, PD-1
PTL (nodal)	CD20, CD3, CD5, CD4, CD8, *CD2*, *CD7*, CD10, CD21, CD25, CD30, TIA-1, PD-1, ALK, EBER
PTL (extranodal)	CD20, CD3, CD5, CD4, CD8, *CD2*, *CD7*, CD25, CD30, CD56, TIA-1, granzyme B, β-F1, ALK, EBER
Blastic/blastoid neoplasms	CD20, CD79a, PAX5, CD3, CD4, CD2, *CD34*, CD56, CD68, CD99, CD123, TdT, lysozyme, MPO

[a]Antibodies shown in italics can be added as needed in selected cases. Abbreviations: EBER, EBV-encoded RNA; PAX, paired box; LMP, latent membrane protein; OCT, octamer-binding transcription factor; MPO, myeloperoxidase.

it possible for immunophenotyping to be performed on all diagnostic biopsy specimens. There are excellent reviews of both flow cytometry and immunohistochemistry elsewhere in this *Manual* (see chapters 16, 20, and 40).

Molecular Approaches

The molecular tests that are commonly applicable to tumors of immune cells fall into two categories: assays for clonality and molecular cytogenetic assays. Clonality assays are rarely used in nonlymphoid malignancies; however, there are occasions in which they may be useful. The clinically applicable molecular cytogenetic assays include *in situ* hybridization (ISH) studies and PCR-based assays, which are utilized primarily for translocation detection. The principles behind molecular cytogenetic assays are applicable to both lymphoid and nonlymphoid tumors.

Clonality Assays

By far the most common molecular test used in the assessment of hematologic malignancies is clonality testing. Many reactive conditions simulate lymphomas, and it is critical to distinguish between a self-limited benign lymphoid proliferation caused by an immune response to a drug or virus and an uncontrolled neoplastic proliferation. The basis of clonality testing in lymphoid proliferations lies within the unique molecular biology of antigen receptor genes. When progenitor hematopoietic stem cells become committed to either the B- or T-cell lineage, they undergo a structural change in their DNA encoding their respective antigen receptor genes. This structural change is maintained throughout the life of that cell and is inherited in all daughter cells. Likewise, if a neoplastic event occurs in a lymphoid cell possessing a rearranged antigen receptor gene, all daughter cells will inherit the identical rearrangement, creating a tumor-specific molecular marker. Structural changes of antigen receptor genes have traditionally been evaluated using restriction fragment analysis of genomic DNA followed by Southern blotting (15). In this procedure, DNA is digested by restriction enzymes that cut at known sites in the germ line. The restricted DNA is size fractionated, generally by agarose gel electrophoresis. The fractionated DNA is transferred by Southern blotting to a solid nylon or nitrocellulose matrix, and the position (which is proportional to the size) of the fragment containing the antigen receptor gene of interest is visualized by hybridization with a labeled probe that is directed to the antigen receptor gene. Germ line DNA (i.e., DNA that has not undergone rearrangement) generates a single restriction fragment that reflects the distance between the restriction enzyme sites that encompass the probe sequence. However, DNA that has undergone rearrangement will show an altered restriction fragment, different in size from the germ line fragment, reflecting the structural change that has occurred as a result of the rearrangement. Although this procedure is capable of accurately assessing nearly 100% of all clonal B- or T-cell neoplasms, it is time-consuming and requires a relatively large amount of DNA (>20 μg) and is therefore not as well suited as PCR techniques for clinical laboratory testing.

Unlike restriction fragment analysis, the basis of PCR assays for clonality lies within differences in the sizes of the *junctional* regions that are formed during V-J or V-D-J segment recombinations. The biological basis of these size differences lies primarily with the activity of terminal deoxynucleotidyltransferase (TdT) and exonuclease activities that add and delete nucleotides in a nontemplated manner, generating junctional regions of various lengths. Physiologically this process plays a major role in creating antibody diversity, in combination with somatic mutation of the antigen receptor genes. The junctional "repertoire" can be analyzed using consensus primers that span the junctions (V and J region primers). In a reactive polyclonal population of B or T cells, the junctional sequences generated by PCR will vary from one cell to the next, generating many different-sized PCR fragments visualized as a ladder of bands on an ethidium-stained acrylamide gel. In lymphomas, all daughter tumor cells bear the identical rearranged antigen receptor gene containing identical junctional sequences. In this case, PCR will generate a single-sized product visible on the ethidium-stained gel. This product is specific for and a signature of the tumor from which it was generated.

PCR can be performed with 100 ng or less of DNA, is rapid, and is extremely easy to perform. For these reasons, PCR has become the assay of choice in the clinical laboratory to test for clonality. Detection of the resulting PCR fragments is most frequently assessed by gel or capillary electrophoresis. The disadvantage of PCR is that it typically has a much higher false-negativity rate than the genomic Southern blot approach, approximating 20% or more for B-cell clonality and 10% or more for T-cell clonality, depending on the specific method chosen and the primers used. Recently, a large consortium of European laboratories collaborated in a large study designated as BIOMED-II (16). The consortium developed and tested a multiplex system comprising multiple primer pairs designed to lower the false-negativity rate of the commonly used assays for B- and T-cell clonality. These sets of primers were shown to perform extremely well, approaching detection rates of 100% for both B- and T-cell rearrangements. However, in order to reach this high level of diagnostic sensitivity, >31 primers multiplexed in five separate reactions were required for the assessment of immunoglobulin heavy-chain (IGH) gene rearrangements, and 44 primers multiplexed in five separate reactions were required for the assessment of T-cell receptor (TCR) gene rearrangements. Furthermore, these primer sets were validated primarily for freshly isolated DNA and did not perform as well in paraffin tissue, in which DNA may be partially degraded. Nonetheless, this comprehensive study demonstrates that it is possible to attain high levels of diagnostic sensitivity using PCR assays for clonality. The BIOMED-II primers are available through InVivoScribe Technologies (Carlsbad, CA; www.invivoscribe.com).

Clonality testing is rarely used in nonlymphoid malignancies, but there are occasions in which it can be useful. Simple PCR-based approaches for the assessment of clonality in nonlymphoid malignancies are the HUMARA and related assays that exploit X-linked chromosomal inactivation (17). Since the cells comprising a tumor are descendants of a single progenitor cell, the entire population of tumor cells will carry the identical inactivated maternal or paternal X chromosome that was present in the ancestral progenitor. This phenomenon has been known for many years, and the immunologic assessment of the A and B isoforms of the X-linked glucose-6-phosphate dehydrogenase enzyme, with all of its limitations, was the common method for assessing clonality until the development of molecular technologies (18). A molecular genetic feature of X-linked chromosomal inactivation is promoter hypermethylation of genes located on the inactivated chromosome (19). In a monoclonal population of cells, either 100% of the paternal or 100% of the maternal alleles will be hypermethylated, while in a polyclonal population of cells, 50% of the paternal and 50% of the maternal alleles will be hypermethylated, as a result of random X inactivation in the population. The assessment of hypermethylation is performed through the use of

methylation-sensitive restriction enzymes, in combination with PCR. Prior to PCR, the DNA of interest is cut using a methylation-sensitive restriction endonuclease. Subsequently, PCR is performed using primers that encompass the promoter region. The methylated alleles remain uncut and generate a PCR product, while the nonmethylated alleles are cut by the restriction enzyme, which prevents the generation of a PCR product. In order to assess whether both maternal and paternal alleles have been amplified, the promoter chosen must also contain a highly polymorphic site that allows one to distinguish between the two alleles. The complete loss of one allele (maternal or paternal) indicates the presence of a clonal population. Because the X-linked human androgen receptor (HUMARA) gene contains a highly polymorphic sequence in proximity to its promoter, this locus has become the target of choice for X-linked clonality assays (20). The HUMARA assay can be performed on DNA extracted from formalin-fixed, paraffin-embedded tissue, is relatively simple, and is adaptable to the clinical molecular diagnostics laboratory. As for all assays exploiting X inactivation, the primary disadvantage of the HUMARA assay is that it can only be performed in female patients.

Molecular Cytogenetics

ISH

ISH is a powerful technology that allows for *in situ* visualization of specific chromosomal translocations, chromosome copy number, gene copy number, and mRNA expression. Translocations are assessed through the use of DNA probes that recognize regions of chromosomes involved in translocations. These probes fall into two general categories: so-called break-apart probes, which are generally used singly; and fusion probes, which are used in pairs. Break-apart probes are designed to span a breakpoint region of interest. Therefore, if the targeted chromosome is split by a translocation, three signals will appear, one from the normal nontranslocated chromosome and one from each of the two derivative translocated chromosomes. Break-apart probes can provide information that the targeted region is involved in a translocation; they do not provide information identifying the partner chromosome. Break-apart probes are particularly useful when one does not know one translocation partner, or when multiple partners exist, such as for translocations involving the *BCL6* locus on 3q27 (21). Fusion probes, on the other hand, are designed to recognize both chromosomal regions involved in the translocations, so that one can precisely identify both translocation partners (22). In the case of fusion probes, each member of the differentially labeled probe pair hybridizes with its targeted chromosomal region, generating four signals. In cells containing the targeted translocation, two of the signals from each of the chromosomes involved in the translocation fuse into one, and only three signals are seen. In practice, fusion probes are generally labeled in different colors (green and red), so that the fusion signal generally is a mix of the two different probe colors (yellow). Probes are generally labeled with fluorescent dyes (FISH), but chromogens (CISH) have been used successfully as well for some applications. FISH can be performed on metaphase chromosome spreads, but its greatest success in diagnostic pathology has been its adaptation to interphase nuclei in either frozen or fixed tissues (23). FISH has the highest diagnostic sensitivity of any available test for identifying specific chromosomal translocations and numerical chromosome alterations. However, FISH is labor-intensive and is not available in all diagnostic laboratories due to the high cost of the associated equipment.

FISH overcomes some of the limitations of PCR in the assessment of translocations, since large chromosomal regions can be analyzed, greatly reducing the problem of false negatives due to the focal nature of PCR. As previously mentioned, the disadvantages of FISH are that it is technically challenging when applied to tissue sections, is time-consuming, and requires relatively expensive equipment and an experienced practitioner, preferably a cytogeneticist. Nonetheless, when available, FISH is the method of choice to identify most of the lymphoma-specific translocations. Probes for most of the clinically important translocations are available commercially through Vysis, Inc. (Downers Grove, IL).

PCR

PCR of chromosomal breakpoint junctions is also a popular method for identifying translocations because of its rapidity and simplicity. The translocations that occur in lymphoid neoplasms are of two general types, those that result in the deregulation of normal cellular genes without disrupting the coding sequence (type 1) and those that result in the fusion of two normal cellular genes to create a novel chimeric gene product (type 2). The majority of type 1 translocations involve one of the antigen receptor gene loci. These include translocations such as t(8;14) involving the *MYC* gene on chromosome 8 and the *IGH* locus on chromosome 14, t(11;14) involving the *CCND1* locus on chromosome 11 and the *IGH* locus, and t(14;18) involving the *BCL2* gene and the *IGH* locus. In all of these cases, the translocations deregulate the target gene by disrupting its regulatory elements or by placing it under the control of elements of the involved antigen receptor gene. A minority of the type 1 translocations do not involve an antigen receptor gene, such as some of the variant translocations involving the *BCL6* gene on chromosome 3q27. Nonetheless, the result is similar in that the target gene's coding sequence is left intact, but its regulatory elements are altered through the substitution of control elements from the various genes on the partnering chromosomes. Whereas the type 1 translocations leave the coding sequences of the potential oncogenes intact, type 2 translocations occur between two unrelated genes and result in the creation of a novel mRNA and protein encoded by portions of the two fused genes. Typically both genes are transcription factors and the resulting chimeric proteins display highly aberrant transcriptional activities. Representative of the type 2 translocation is the pre-B-cell acute lymphocytic leukemia (ALL) t(12;21) translocation, which fuses the *TEL* gene on chromosome 12 to the *AML1* gene on chromosome 21.

The molecular detection strategies for the two types of translocations differ in that for the type 1 translocations the targeted template is generally the junctional sequence *within the DNA*, while in the type 2 translocations the primers generally target the junctional sequence *within the message (cDNA)* encoding the novel protein. For both types of translocations, a PCR product will be generated only from the tumor cells bearing the junctional DNA or cDNA sequences created by the translocation, which therefore serves as a tumor-specific marker. Detection is generally carried out either by gel or capillary electrophoresis. Alternatively, PCR and detection may be combined in real-time PCR instruments. These instruments monitor the accumulation of product during the PCR reaction using fluorescent detection technologies (24).

The use of PCR to detect type 1 translocations can be highly effective when the breakpoints on the partnering chromosomes are clustered, as occurs with the t(14;18)

translocations in follicle center lymphomas. However, if the breakpoints are instead spread over a larger area, as they are with the t(11;14) translocation in MCLs, this technique will miss many translocations. While DNA-based PCR assays have a very high analytic sensitivity, capable of identifying 1 in 10^6 abnormal cells, these tests have a much lower diagnostic sensitivity than FISH, since each PCR primer set can target only a few hundred base-pair segments of DNA, while an appropriate FISH probe can identify translocations involving all potential breakpoint regions.

Type 2 translocations occur most frequently in pre-B-cell and B-cell lymphoblastic lymphomas/leukemias, but they also occur in some of the mature B- and T-cell lymphomas, including ALCL and MALT lymphoma. These are extremely interesting events from the biological point of view, as they create chimeric proteins that have novel oncogenic activities. For diagnostic purposes, the chimeric RNA serves as the tumor-specific PCR product. Reverse transcription (RT)-PCR assays targeting the chimeric RNA sequences generally have a much higher diagnostic sensitivity than those that target the corresponding chromosomal breakpoint regions because in most cases, gene splicing events create junctions precisely between the exons of the fused genes, even when the breakpoint sequences themselves may be spread diffusely throughout intronic sequences. For example, 75% of ALCLs possess a t(2;5) translocation joining the nucleophosmin gene (*NPM*) on chromosome 5 to the ALCL tyrosine kinase gene (*ALK*) on chromosome 2. The breakpoints are spread throughout intron 4 of the *NPM* gene and within a single intron of the *ALK* gene, which presents difficulties in the design of a simple DNA-based PCR test. However, splicing events in the novel transcript bring exon 4 of *NPM* into contiguity with a 5′ coding exon of *ALK* in all cases. This allows the design of a simple RT-PCR assay, using only a single primer pair, that can reliably identify all of the t(2;5) translocations.

Other Molecular Tests Used in Lymphoma Diagnostics

PCR is also used to identify the presence of viruses that are associated with different lymphoma subtypes. Section J in this *Manual* discusses viral detection assays in more detail. PCR can be especially helpful in detecting viral DNA and in the diagnosis of human T-cell leukemia virus type 1 (HTLV-1)-associated lymphomas; human herpesvirus 8 (HHV-8)-associated pleural effusion lymphomas; and lymphoproliferations associated with Epstein-Barr virus (EBV), such as EBV posttransplant lymphoproliferative disorders, nasal NK/T-cell lymphoma, angioimmunoblastic T-cell lymphoma (AILT), and Burkitt's lymphoma. However, the identification of a viral product by PCR should be correlated with *in situ* or morphological studies since the presence of these viruses is not tumor specific. For example, HHV-8 may also be found in Kaposi's sarcoma and Castleman's disease and EBV may be identified in nonneoplastic immunoproliferative conditions, particularly when immunosuppression is present. Furthermore, it is important to recognize that because of the extremely high sensitivity of PCR-based tests, nonpathological levels of some viruses that are present at low levels, such as EBV, may be detected.

FISH and the related technique CISH are also well suited for identification of mRNA *in situ* and for identifying viruses such as EBV (25). The advantage of CISH is that it can be assessed using an ordinary light microscope. However, it is limited by the number of chromogens available and by the resolution of the technology. CISH can be used as a secondary technique to assess light-chain exclusion, when exclusion cannot be definitively assessed at the protein level. CISH is commonly used in hematopathology laboratories for the identification of EBV infection and has become an important ancillary test for diagnosing cases of NK/T-cell lymphoma, Burkitt's lymphoma, AILT, and other EBV-associated lymphoproliferative disorders, including posttransplant lymphoproliferative disorders.

cDNA microarray studies have recently been utilized to further the classification of lymphomas. Clinically significant subcategories within morphologically homogeneous lymphoma entities, such as diffuse large B-cell lymphoma (DLBCL), chronic lymphocytic leukemia (CLL), and peripheral T-cell lymphoma, have been identified through the use of this technology (26–28). Recently, these techniques have been adapted to allow analysis of gene expression profiling in routinely processed formalin-fixed, paraffin-embedded sections, making application to the routine clinical laboratory possible in the near future (29). cDNA microarray technology is discussed in detail in chapter 2 of this volume.

INTERPRETATION AND APPLICATION OF IMMUNOLOGIC AND MOLECULAR MARKERS IN THE DIAGNOSIS OF TUMORS OF THE IMMUNE SYSTEM

Precursor Lymphoid Neoplasms

Lymphoblastic malignancies (LBL) are neoplasms of precursor T and B lymphocytes. They may present clinically as either lymphoblastic lymphoma or ALL, and morphologically the T- and B-lineage varieties of LBL are indistinguishable. Virtually 100% of these neoplasms are positive for TdT, which can be detected by immunocytochemical techniques using rabbit antisera or murine monoclonal antibodies directed against TdT.

Precursor T-cell LBL most often present as lymphoma, usually with a mediastinal mass, with or without bone marrow involvement and a leukemic phase. They usually have an immature T-cell phenotype that correlates with different stages of intrathymic maturation (Fig. 1). The earliest T-cell-associated antigen with some lineage specificity is CD7. However, it is also expressed in rare cases of acute myeloid leukemia, where it may represent evidence of lineage infidelity, often seen in primitive hematopoietic malignancies. CD3, linked to the T-cell antigen receptor, is expressed in the cytoplasm prior to its presence on the surface and thus may not be revealed by immunofluorescence techniques on living cells (30). In this situation a T-cell LBL may be CD3 positive in tissue sections but negative by routine flow cytometry. However, techniques that permeabilize the cell membrane are available to detect cytoplasmic antigens by flow cytometry. It should be noted that the normal thymocytes encountered in a lymphocyte-rich thymoma would be phenotypically similar to the cells of a T-cell LBL. Immunohistochemical analysis will be necessary to detect the thymic epithelial cells numerous in the former condition.

T-cell lymphoblastic lymphomas are clonal neoplasms, and most have *TCRβ* or *TCRγ* rearrangements (31). About 20% of T-lymphoblastic lymphomas also have *IGH* rearrangements, a phenomenon known as lineage infidelity (32). Lineage infidelity is common in early-lineage T- and B-cell neoplasms but is rare in mature B- and T-cell neoplasms. Therefore, when assessing clonality in lymphoblastic lymphomas, antigen receptor rearrangements cannot be used to assign B- or T-cell lineage. Up to 50% of T-lymphoblastic lymphomas/leukemias have recurrent translocations most

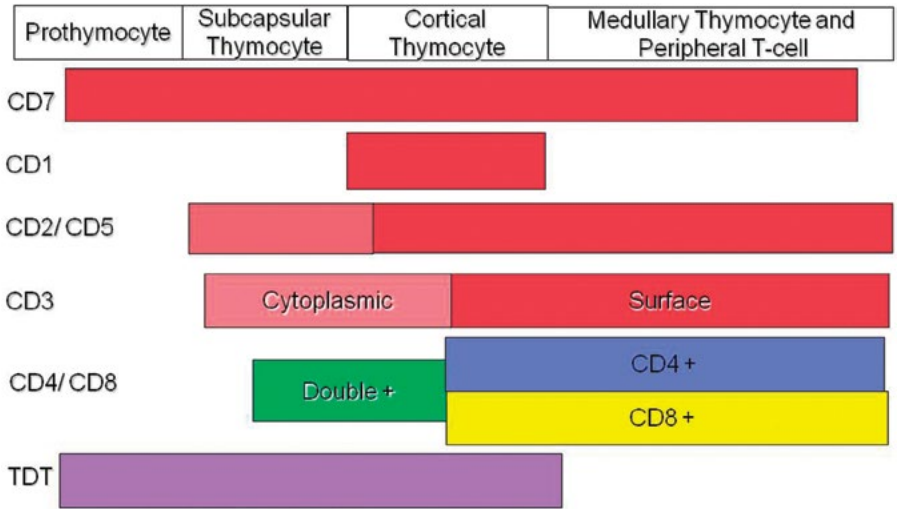

FIGURE 1 Schematic diagram showing stages of T-cell differentiation. Neoplasms can be related to precursor and mature or peripheral T lymphocytes. Antigenic phenotype correlates with maturational stage. Note that CD7 is the earliest T-associated antigen.

frequently involving one of the TCR gene loci (Table 3). These can be detected by FISH and in many cases by PCR.

Precursor B-cell LBL present as leukemia more often than as lymphoma. In cases presenting as lymphoma, common clinical manifestations include skin involvement (often of the scalp or face), lytic bone lesions, or lymphadenopathy. The risk of involvement of the central nervous system is less than for pre-T-cell LBL. Although these precursor B-cell tumors do not normally express immunoglobulin, other markers of B-cell lineage, such as CD19 and CD79a, will be present (Fig. 2) (33). These antigens are expressed at the time of heavy-chain gene rearrangement, usually indicating commitment to the B-cell lineage. In cases of so-called pre-B-cell ALL, the cells contain cytoplasmic μ heavy chains but are still negative for surface immunoglobulin. The CD20 antigen is not acquired until the stage of light-chain gene rearrangement, and it is expressed in ~50% of cases (34). Thus, pre-B-cell LBL are often negative for CD20 in paraffin sections.

All pre-B-cell and B-cell lymphoblastic lymphomas are clonal neoplasms, and the vast majority have *IGH* rearrangements. In some cases *IGH* rearrangements are incomplete, showing only D-to-J segment joining (35). B-cell lymphoblastic lymphomas have an extremely high frequency of lineage infidelity, with 90% of cases having clonal rearrangements of one or more TCR loci (*TCRβ* [35%], *TCRγ* [60%], or *TCRδ* [55%]) (32). About 30% of cases have characteristic chromosomal translocations (Table 3). A high percentage of these involve two nonantigen receptor genes that can be identified by FISH or by RT-PCR.

Both pre-T-cell and pre-B-cell LBL may be negative for the leukocyte common antigen (LCA; CD45). In addition,

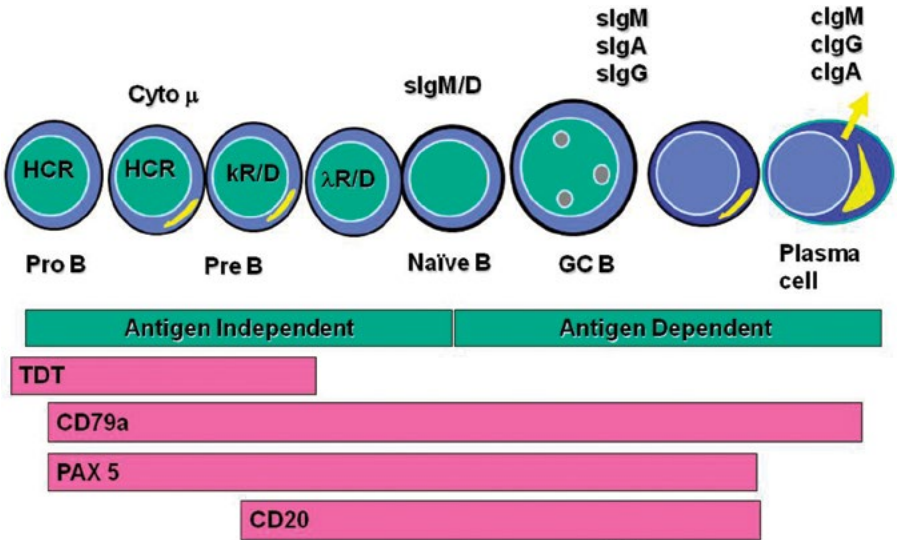

FIGURE 2 Schematic diagram showing stages of B-cell differentiation. Lymphomas can be related to precursor B-cell, mature B-cell, and secretory B-cell (plasma cell) stages of differentiation. Note that CD79a has the broadest range of reactivity, staining precursor, mature, and secretory B cells.

TABLE 3 Chromosomal translocations, involved genes, and detection methods in B- and T-cell lymphomas/leukemias

Translocation	Genes	Tumor[a]	Translocation type	Primary test(s)
B-lymphoblastic leukemias/lymphomas				
t(12;21)(p13;q22)	*TEL-AML1*	B-ALL	2	FISH, RT-PCR
t(1;19)(q23;p13)	*PBX1-E2A*	B-ALL	2	FISH, RT-PCR
t(17;19)(q22;p13)	*HLF-E2A*	B-ALL	2	FISH, RT-PCR
t(9;22)(q34;q11)	*BCR-ABL*	B-ALL	2	FISH, RT-PCR
t(4;11)(q21;q23)	*MLL-AF4*	B-ALL	2	FISH, RT-PCR
t(11;19)(q23;p13.3)	*MLL-ENL*	B-ALL	2	FISH, RT-PCR
Mature B-cell lymphomas				
t(14;18)(q32;q21)	*BCL2-IGH*	FL	1	PCR, FISH
t(11;14)(q13;q32)	*CCND1-IGH*	MCL, MM	1	PCR,[b] RT-PCR,[c] FISH
t(4;14)(p16;q32)	*FGFR3-IGH*	MM	1	FISH
t(6;14)(p16;q32)	*IRF4-IGH*	MM	1	FISH
t(14;16)(q32;q23)	*IGH-MAF*	MM	1	FISH
t(8;14)(q24;q32)	*MYC-IGH*	BL (B-ALL)	1	FISH
t(8;22)(q24;q11)	*MYC-IGλ*	BL (B-ALL)	1	FISH
t(2;8)(p12;q24)	*MYC-IGκ*	BL (B-ALL)	1	FISH
t(11;18)(q21;q21)	*API2-MLT*	MALT	2	FISH, RT-PCR
t(14;18)(q32;q21)	*IGH-MLT*	MALT	1	FISH
t(1;14)(p22;q32)	*BCL10-IGH*	MALT	1	FISH
t(3;14)(q27;q32)	*BCL6-IGH*	DLBCL	1	FISH
t(3;v)(p27;v)[d]	*BCL6*-MPS[e]	DLBCL	1	FISH
t(9;14)(p13;q32)	*PAX5-IGH*	LPL	1	FISH
T-lymphoblastic leukemias/lymphomas				
t(1;14)(p32;q11)	*TAL1-TCRδ*	T-ALL	1	FISH, RT-PCR
t(1;7)(p32;q34)	*TAL1-TCRβ*	T-ALL	1	FISH, RT-PCR
t(1;7)(p34;q34)	*LCK-TCRβ*	T-ALL	1	FISH, RT-PCR
t(11;14)(p15;q11)	*LMO1-TCRδ*	T-ALL	1	FISH, RT-PCR
t(11;14)(p13;q11)	*LMO2-TCRδ*	T-ALL	1	FISH, RT-PCR
t(7;9)(q34;q32)	*TAL2-TCRβ*	T-ALL	1	FISH, RT-PCR
t(7;9)(q34;q34)	*TAN1-TCRβ*	T-ALL	1	FISH, RT-PCR
t(7;11)(q34;p13)	*RHOM2-TCRβ*	T-ALL	1	FISH, RT-PCR
t(7;19)(q34;p13)	*LYL1-TCRβ*	T-ALL	1	FISH, RT-PCR
t(7;10)(q34;q24)	*TCRβ-HOX11*	T-ALL	1	FISH, RT-PCR
t(10;14)(q24;q11)	*HOX11-TCRδ*	T-ALL	1	FISH, RT-PCR
t(8;14)(q24;q11)	*MYC-TCRαδ*	T-ALL	1	FISH, RT-PCR
Mature T-cell lymphomas				
t(2;5)(p23;q35)	*ALK-NPM*	ALCL	2	FISH, RT-PCR, IHC
t(2;v)(p23;v)	*ALK-MPS*[e]	ALCL, ALK+	2	FISH, RT-PCR
t(5;9)(q33;q22)	*SYK-ITK*	AILT, fv-PTCL[f]	2	FISH, RT-PCR
t(6;14)(p25.3;q11.2)	*IRF4-TRA*	PTCL, NOS	1	FISH
t(6;7)(p25.3;q32.3)	*DUSP22-FRA7H*	ALCL, ALK-c-ALCL,[g] LP	2	FISH
inv(3)(q26q28)	*TBL1XR1-TP63*	ALCL, ALK-PTCL, NOS, c-ALCL[g]	2	FISH, RT-PCR
chr 2 locus-specific partial duplication/ fusion	*CTLA4-CD28*	AILT, PTCL, NOS, MF, SS, ATLL	2	FISH, RT-PCR

[a]Abbreviations: B-ALL, pre-B, B-cell acute lymphoblastic lymphoma/leukemia; MM, multiple myeloma; BL, Burkitt's lymphoma; T-ALL, T-cell lymphoblastic lymphoma/leukemia.
[b]Major cluster region primers identify ~35% of translocations.
[c]RT-PCR to the cyclin D1 mRNA will detect close to 100% of cases.
[d]3q27 partners with various (v) chromosomal partners and loci.
[e]MPS, multiple partner genes.
[f]fv-PTCL, follicular variant panniculitis-like T-cell lymphoma.
[g]c-ALCL, cutaneous ALCL.

TABLE 4 Differential diagnosis of small B-cell lymphomas

Disease	CD5	CD10	CD23	CD43	Cyclin D1	Ig class(es)[a]
FL	−	+	±	−	−	IgM, IgG
MCL	+	−	−	+	+	IgM/IgD
CLL/SLL	+	−	+	+	−	IgM/IgD
LPL	−	−	−	±	−	IgM (c)
MALT	−	−	−	±	−	IgM (c, s)
SMZL	−	−	−	−	−	IgM/IgD
HCL	−	−	−	−	±	IgG

[a]Most commonly expressed heavy chain classes. c, cytoplasmic Ig; s, surface Ig.

they both express CD99, the *mic-2* gene product, in a high proportion of cases. This antigen is expressed in Ewing's sarcoma, a nonlymphoid malignancy presenting in children and young adults, often with lytic bone lesions of the distal extremities. Because of potentially overlapping histological and clinical features, an extensive immunohistochemical panel as well as molecular analysis may be required for accurate differential diagnosis (36).

Mature B-Cell Lymphomas

A variety of malignancies composed of small mature B lymphocytes are recognized in the WHO classification. These include small lymphocytic lymphoma (SLL)/B-cell CLL, FL, MCL, extranodal marginal zone lymphoma (MZL) of MALT type, nodal MZL, splenic MZL (SMZL), and hairy cell leukemia (HCL). In most of these neoplasms, the cells are arrested prior to the secretory stage of B-cell development and express pan-B-cell antigens such as CD19, CD20, and CD22. Evidence of plasmacytoid differentiation is most commonly seen in MZL and is a consistent feature of lymphoplasmacytic lymphoma (LPL). Each of the small B-cell malignancies has a characteristic immunophenotypic signature that is highly useful in differential diagnosis (Table 4).

Monoclonal surface immunoglobulin expression is usually readily detected in frozen sections but is generally not evident in paraffin sections. Even in frozen sections, abundant serum immunoglobulins in the interstitial space may result in high background staining, which can obscure cellular staining and make interpretation difficult. This problem is frequently observed in tissues from patients with polyclonal hypergammaglobulinemia. In paraffin sections, cytoplasmic immunoglobulin can be detected, but is usually most evident in cells showing evidence of plasmacytoid differentiation. Positive staining in the perinuclear space is highly reliable and is usually not subject to technical problems.

The ability of the cells to form follicles correlates with the presence of dendritic reticulum cells (DRCs), which can be identified in frozen and paraffin sections by using monoclonal antibodies reactive with CD21, CD23, CD35, or clusterin. DRCs are numerous in FL and intimately associated with the neoplastic nodules, even in extranodal locations. Staining for DRCs will often enhance a vaguely nodular pattern that is difficult to see in routine histological sections. DRCs are rare in SLL but are present with an irregular, vaguely nodular distribution in MCL.

CD5 is very useful in the subclassification of low-grade B-cell lymphomas. This antigen is found on normal T cells but on few normal B cells. Both SLL and MCL are usually positive for CD5, but it is almost never expressed in true FL. Thus, this antigen is useful in the differential diagnosis of MCL with a vaguely nodular growth pattern versus a true FL. CD5 is also useful in the differential diagnosis of SLL and MCL with lymphomas of MALT. MALT lymphomas arise in extranodal sites (e.g., lung, gastrointestinal tract, and salivary gland) and are composed of small round and small-cleaved (centrocyte-like) cells, which may resemble the cells of SLL and MCL. MALT lymphomas are usually CD5 negative (37). CD23 is very useful in the differential diagnosis of SLL/CLL and MCL, since SLL/CLL is nearly always CD23 positive and MCL nearly always CD23 negative (38). The common ALL (cALL) antigen (CD10) is found much more often in FL than in the other small B-cell lymphomas (39). For unknown reasons, MCL and HCL both express λ light chain much more frequently than do the other B-cell lymphomas, which usually express κ.

Cytogenetic and molecular genetic studies are also extremely valuable in differential diagnosis, and monoclonal

TABLE 5 Evaluation of oncogenes and tumor suppressor genes by immunohistochemistry and molecular diagnostic techniques[a]

Antigen	Disease association	Genetic abnormality	Applicable genetic test(s)	Immunohistochemistry result
BCL-2	FL	t(14;18)	GS, PCR, FISH[b]	+, nonspecific
Cyclin D1	MCL	t(11;14)	GS, PCR, FISH[b]	+, specific[b]
	Multiple myeloma (15%)	t(11;14)	RT-PCR[b] (cyclin D1)	+, specific[b]
p53	Progressed lymphomas	17q deletion mutation	LOH, SSCP, FISH	+, probable[b,c]
	Aggressive lymphomas	Mutation	Sequencing[c]	Mutation
BCL-6	DLBCL (GCB > ABC)	t(3;14)	GS, FISH[b]	+, nonspecific
	3q26 variants	Mutation		
ALK	ALCL	t(2;5)	GS, RT-PCR, FISH[b]	+, specific[b]
		2p23 variants		
BRAF	LCH	V600E mutation	Sequencing	+, ab to mutant protein
	Erdheim-Chester disease			
MYC	Burkitt's lymphoma	t(8;14)	FISH, karyotype	+, but not specific

[a]Abbreviations: GS, genomic Southern blot analysis; SSCP, single-strand conformational polymorphism analysis; ab, antibody.
[b]Method(s) of choice for detection of genetic abnormalities in clinical molecular diagnostics laboratory.
[c]p53 overexpression is generally correlated with the presence of mutation; however, lack of expression is poorly correlated with lack of mutation. Sequencing is required for definitive proof of mutation.

antibodies to oncogene products can be used as surrogate markers in some situations (Table 5). FL is characterized by the t(14;18) translocation that juxtaposes the *BCL2* gene with the *IGH* promoter/enhancer, resulting in BCL-2 overexpression (8). While the translocation results in BCL-2 overexpression, BCL-2 expression, however, is not specific for the translocation, as other low-grade lymphomas express this antiapoptotic protein (40). Thus, while the detection of overexpressed BCL-2 by immunohistochemistry is useful in differentiating FL from follicular hyperplasia, it is not helpful in distinguishing FL from other SLLs. PCR assays targeting the most common breakpoint cluster involved in the t(14;18) translocation can identify up to 65% of cases, while FISH analysis is capable of detecting all cases (41).

The t(11;14) translocation is present in nearly all MCLs (42). This translocation involves the cyclin D1 gene, *CCND1*, resulting in the overexpression of the protein, which is not expressed in nonneoplastic lymphoid cells or in other small lymphocytic neoplasms, with the exception of a small percentage of myeloma cases that have the t(11;14) translocation and HCLs that express very low levels of cyclin D1 (43). A very small subset of MCL cases are identical by gene expression profiling but lack cyclin D1 protein, and are negative for the *CCND1* translocation (44). Recent studies have determined that *CCND2* likely substitutes for *CCND1* in these cases, and a high proportion have translocations involving this gene (45).

The development of new mouse and rabbit monoclonal antibodies to cyclin D1 has greatly improved the detection of these aggressive SLLs, and molecular testing for the translocation is generally not necessary (11). PCR analysis for identification of t(11;14) breakpoint sequences has a relatively low yield unless multiple primer pairs are used, and therefore this method is not widely used. However, RT-PCR targeting the overexpressed cyclin D1 transcripts has been successfully employed in diagnostics (46). This assay exploits the fact that normal lymphocytes and other lymphomas do not express cyclin D1 mRNA, except for a minority of myelomas and HCLs at low levels. FISH assays for the t(11;14) translocation will identify 100% of cases. Recently, cDNA microarray analyses have been performed on cases of MCL (47). While these studies have confirmed the homogeneity of this lymphoma, they have also shown that it is possible to stratify cases and predict survival based on the expression of a set of genes associated with cellular proliferation.

The t(11;18) translocation involving *API2/MLT(MALT)* genes is the most common recurring cytogenetic abnormality in MALT lymphomas of gastrointestinal tract and lung, where it is found in about one-third of all cases (48). However, other less common translocations also occur in MALT lymphomas, including the t(14;18) translocation involving the *IGH* gene and *MALT1* and the t(1;14) translocation involving *BCL10* and *IGH* (49). The t(14;18) translocation preferentially involves non-gastrointestinal tract MALT lymphomas such as those in the lung and ocular adnexa, while the t(1;14) translocation tends to be found in advanced-stage MALT lymphoma. It is of interest that these three translocations perturb two genes (*BCL10* and *MALT1*) that are involved in antigen receptor NF-κB activation (49). The most common of these translocations, t(11;18), can be readily assessed using commercially available FISH probes, or by RT-PCR using published primers to the *API2* and *MALT1* genes.

CLL lacks a characteristic recurrent translocation but displays other cytogenetic abnormalities, including deletions of 13q14, trisomy 12, and deletions of 11q and 17p, which are both associated with a more aggressive clinical course (50). The 13q14 deletion occurs in a very high percentage of CLL cases and results in the consistent loss of genes encoding microRNAs (51). MicroRNAs are small antisense RNAs encoded in the genome that appear to regulate the translation of critical proteins (52). The microRNAs that are deleted at 13q14 are miR15 and miR16, which are regulators of the antiapoptotic BCL-2 protein, implicating the loss of these microRNAs in the abnormally high levels of BCL-2 found in CLL (53). FISH analysis tends to underestimate the frequency of microRNA loss because a significant number of the deletions at 13q14 are small.

Over the past several years there have been a number of studies that have clearly shown that there are two distinct clinicopathological subtypes of CLL that can be distinguished by the presence or absence of IGH mutation, CD38 expression, and ZAP70 expression (28, 54). Nonmutated CLL tends to be CD38 positive and ZAP70 positive. Patients with nonmutated CLL have a 5-year survival of about 40 months, compared to 120 months for their counterparts with ZAP70-negative mutated CLL. Gene microarray studies have confirmed the presence of these two clinicopathological subgroups (55). At present, either mutational analysis or ZAP70 expression by immunohistochemistry or flow cytometry is recommended to distinguish these two CLL subtypes (56).

Tumors of fully differentiated B cells synthesize and secrete immunoglobulin, giving rise to monoclonal immunoglobulin spikes that can be detected by serum immunoelectrophoresis. LPL is the histological counterpart of Waldenström macroglobulinemia. In this disease the cell is arrested between the B lymphocyte and the plasma cell. Class switching from IgM to IgG, IgA, etc., has not yet occurred, and clinically the process resembles a low-grade lymphoma with widespread involvement of lymphoid organs. Recent studies have identified a recurrent translocation in *MYD88* at L265P that is found in a high proportion of cases of Waldenström macroglobulinemia, which appears to be a useful marker to distinguish LPL from other low-grade B-cell neoplasms with plasmacytoid differentiation, especially nodal MZLs (57, 58).

Multiple myeloma, which arises from terminally differentiated B cells, may show monoclonal IgG, IgA, IgM, or IgD, in that order of frequency. The cells at this stage of differentiation lose most B-cell markers, such as CD20, CD19, and CD22. However, CD79a is still found (10). All myelomas have clonally rearranged immunoglobulin genes and express monoclonal immunoglobulin, which is mainly cytoplasmic and can be most readily detected in paraffin sections. Of practical significance, it should be noted that normal and neoplastic plasma cells are CD45 (LCA) negative but are positive for epithelial membrane antigen. The pathologist should be alert to these characteristics in the eventual differential diagnosis of anaplastic carcinoma versus multiple myeloma. Multiple myeloma has several characteristic recurrent translocations (Table 3). Interestingly, many of these result in the overexpression of cyclin D, either directly or indirectly, and it has been proposed that overexpression of cyclin D1 is a common pathogenetic mechanism unifying all of the different translocations (59). FISH is the method of choice for detection of the various translocations.

DLBCL is not a single disease entity but a category that includes both primary aggressive B-cell lymphomas and histologically progressed lymphomas. Because there are as yet no immunophenotypic or morphological features that lead to reliable subclassification of these lymphomas, it was deemed most advisable to retain most morphological

variants of DLBCL in a single category, pending further data and delineation of other entities. Notably, some specific entities have been defined, and these include mediastinal or thymic-B-cell lymphoma, primary effusion lymphomas (HHV-8 associated), and intravascular DLBCL (60–63).

Therefore, it is not unexpected that most cases of DLBCL do not display unique phenotypic profiles but express the mature B-cell characteristics seen in diverse low-grade B-cell tumors. For example, expression of CD10 usually correlates with the presence of the t(14;18) translocation (64). In some cases, the presence of CD5 indicates that the process arose in the background of a small lymphocytic malignancy (SLL/CLL), so-called Richter's syndrome, although *de novo* CD5-positive DLBCLs also exist. p53 is commonly expressed and is often an indication of an acquired *p53* mutation associated with histological progression (65). p53 protein expression also is a poor prognostic marker (66). *BCL6* is expressed in the majority of DLBCL cases, in many instances indicating a derivation from the GC. However, both translocations and mutations of *BCL6* occur frequently as well. While translocations of *BCL6* are clearly important pathogenetically, *BCL6* mutations are a normal physiological event in the GC. Recent data from several laboratories using cDNA microarray studies have begun to identify distinct differences within the DLBCLs (67, 68). Mediastinal B-cell lymphomas have been shown to be quite distinct in their gene expression signature from other DLBCLs and, in fact, have a signature closer to that of Hodgkin's disease (68, 69). "Standard" DLBCL has been shown to comprise two major subgroups: a GCB subgroup, simulating the gene expression signature of GC B cells, and an activated B cell (ABC) subgroup, simulating the signature of activated peripheral B cells (26, 67). The ABC subgroup has been shown to have a significantly worse prognosis than the GCB subgroup, demonstrating that the subclassification has clinical relevance. Pathologists have been able to extract from these data a small panel of genes, amenable to immunohistochemical study, that have been shown to be effective in dividing the GCB group (positive for BCL-6, CD10) from the ABC group positive for IRF4 (interferon regulatory factor 4), detecting the protein referred to as MUM1 (multiple myeloma 1) (70).

It also has been shown that ABC and GCB tumors differ pathogenetically and show consistent differences at the genetic level (71). Indeed, mutations involving *MYD88* were first identified in the ABC subset. Evidence of chronic active B-cell receptor signaling is a feature of the ABC subset (72), a finding that has significant therapeutic significance in the use of new targeted agents such as ibrutinib (73).

A morphological variant of DLBCL is so-called T-cell-rich large B-cell lymphoma. The neoplastic cells comprise <5% of the population in these lymph nodes, with most of the infiltrating cells being reactive polyclonal T cells. Staining of paraffin sections with L-26 is especially helpful in the recognition of T-cell-rich B-cell lymphoma and will highlight the large tumor cells. Cell suspensions prepared from such lymph nodes usually contain >75% T cells (up to 90% or more) and may be erroneously diagnosed as T-cell lymphomas with flow cytometric techniques. In many of these cases, the neoplastic cells resemble the L&H cells of nodular lymphocyte-predominant Hodgkin's lymphoma (NLPHL), and a relationship between these entities has been postulated (74). There is as yet no reliable immunohistochemical or molecular test to distinguish these two disease entities, and the diagnosis remains heavily reliant upon clinicopathological parameters.

Another DLBCL variant that has been clearly separated from the vast majority of DLBCLs is the pleural effusion lymphomas associated with HIV infection. Not only do these B-cell lymphomas have the unusual clinical feature of presenting as an effusion, most often without a solid or leukemic phase, but also they have an unusual immunophenotype and contain HHV-8 (62). These lymphomas have a plasmablast-like B-cell phenotype, but paradoxically generally do not display membrane or cytoplasmic immunoglobulin by immunohistochemistry. However, all cases have rearrangement of their immunoglobulin genes as detected by either genomic Southern blotting or PCR. HHV-8 can be easily demonstrated in the tumor cells by specific antibodies to the ORF76 protein or by PCR of involved fluids (75).

Burkitt's lymphoma is a high-grade malignancy that expresses CD20, CD19, and CD22. Surface immunoglobulin is usually of the IgM class, and the cALL antigen (CD10) is nearly always positive. Burkitt's lymphoma can rarely present as acute leukemia. TdT is negative, helping to distinguish Burkitt's lymphoma from LBL, which is always TdT positive. Burkitt's lymphoma is characterized by translocations involving the *MYC* gene (76). Translocations involving *MYC* are best detected by FISH, as the chromosomal breakpoints are not sufficiently clustered to allow simple PCR testing. A monoclonal antibody to the MYC protein is now available for routine immunohistochemistry. While it is highly expressed in cases with a *MYC* translocation, other aggressive lymphomas may also show high levels (77, 78). Burkitt's lymphoma is a highly proliferative tumor, with 100% of the cells in cycle (protein encoded by mindbomb E3 ubiquitin protein ligase 1, or MIB1) and is consistently BCL-2 negative. It is positive for BCL-6, indicating a relationship to the GC. Burkitt's lymphoma also has a characteristic profile by gene expression profiling (79, 80). However, these cases may show overlap with so-called double-hit and triple-hit lymphomas that have *MYC* translocations in conjunction with translocations involving other genes, such as *BCL2* and *BCL6* (81). These double-hit and triple-hit cases have a worse prognosis (82).

Mature T-Cell Neoplasms

Neoplasms of mature or peripheral T-cell origin demonstrate marked cytological heterogeneity. However, in contrast to the case with B-cell lymphomas, cytological features are less useful in defining disease entities. While nearly all cases of peripheral T-cell lymphoma (PTL) possess clonal rearrangements of at least one of the TCR genes, these lymphomas do not display consistent immunophenotypic profiles. In addition, the molecular pathogenesis remains to be defined for most of the T-cell lymphomas. Therefore, at present, clinical parameters play a major role in the classification of T-cell lymphomas, as cytological, immunophenotypic, and molecular features are insufficient to define these neoplasms. As a group they tend to be much more aggressive than B-cell lymphomas (83).

PTL, unspecified, is a category somewhat analogous to DLBCL (84). It is felt to be heterogeneous, and probably contains several yet-to-be-recognized entities. PTLs display a wide morphological spectrum, with cells of diverse sizes and appearances. PTL often has an inflammatory background composed of eosinophils, histiocytes, and plasma cells. This polymorphous cellular composition may lead to difficulty in distinction from classical Hodgkin's lymphoma (CHL). The presence of cytological atypia in the background lymphocytes argues against a diagnosis of CHL. Immunophenotypic markers are also useful in this differential diagnosis.

Immunophenotypic markers for clonality are not readily available in the T-cell system. Therefore, molecular assays for the assessment of clonality are often extremely helpful.

TABLE 6 Immunophenotype in the differential diagnosis of nodal PTLs

Disease	Immunophenotypic features
AILT	$CD10^+$, PD-1 (CD279), mixed CD4/CD8, proliferation of follicular dendritic cells ($CD21^+$ cells), EBV^+ blasts
PTL, unspecified	CD4 > CD8, antigen loss (CD7, CD5, CD2)
ATL	$CD4^+$, $CD25^+$, $CD7^-$, $CD30^{+/-}$, $CD15^-$
ALCL	ALK^+, $CD30^+$, $clusterin^+$, EMA^+, $CD25^+$, $CD4^+$, $CD3^{-/+}$
TCHRLBCL[a]	Large $CD20^+$ blasts in $CD3^+$ background
Reactive	Mixed CD4/CD8, intact architecture, variable CD25, CD30; scattered $CD20^+$

[a]TCHRLBCL, T-cell/histiocyte rich large B-cell lymphoma.

The major subset antigens CD4 and CD8 are not clonal markers analogous to light-chain restriction in the B-cell system. Although most PTLs express only CD4 or CD8, some reactive conditions can also show marked subset restriction, most commonly of the CD4 subset. If a proliferation coexpresses CD4 and CD8 or fails to express either CD4 or CD8, that profile is suggestive of malignancy (85).

Other abnormalities of antigenic phenotype are commonly observed in PTL (Table 6). If a battery of pan-T-cell monoclonal antibodies is used, PTL will often fail to express one or more of the major markers CD7, CD5, CD3, and CD2. The antigen most frequently absent is CD7. However, because this antigen is expressed on only 85% of normal T cells, its absence is not unequivocal evidence of a malignancy. Indeed, some reactive T-cell proliferations will be CD7 negative.

A prominence of postcapillary venules is a feature often noted in PTL. AILT is a specific subtype of PTL characterized by an especially florid proliferation of postcapillary venules (86). The predominant infiltrating cells in AILT are CD4-positive T cells. The neoplastic cells express CD10, programmed death 1 (PD-1; CD279), and CXCR13, suggesting that these tumors originate from T follicular helper (Tfh) cells that normally populate the GC (87, 88). A prominent inflammatory background is present, including polyclonal plasma cells, histiocytes, and eosinophils. A disordered meshwork of CD21-positive reticulum cells distributed around blood vessels is highly characteristic of this lymphoma type (89).

Most cases of AILT show clonal TCRβ or TCRγ gene rearrangement. B cells are variable in frequency and in some cases may be numerous. In addition, some B cells positive for EBV are seen in nearly all cases (90). These EBV-positive cells may be monoclonal as detected by IGH PCR techniques, and in rare cases the EBV-positive B cells may progress to a DLBCL (91). In other rare instances the EBV-positive cells may also simulate Hodgkin's lymphoma morphologically and immunophenotypically (92). It is postulated that the expansion of EBV-positive B cells is secondary to the underlying immunodeficiency so characteristic of this disease. However, EBV-negative B-cell expansions also occur, suggesting that deregulation of B-cell proliferation may be an intrinsic aspect of the disease (93, 94), and likely related to the function of the cells as Tfh. AILT has a characteristic gene expression profile, allowing for inclusion of other forms of T-cell lymphoma with less typical morphological features (95, 96). Recently, recurrent mutations have been identified in AILT and have expanded understanding of its genetic basis (97–99).

Adult T-cell leukemia/lymphoma (ATL) is a unique clinicopathological entity associated with the human retrovirus HTLV-1 (100). The neoplastic cells have a mature T-cell phenotype. They are CD4 positive and strongly express interleukin-2 receptors (CD25). Elevated levels of soluble interleukin-2 receptors may be found in the serum and correlate with disease activity. They have a high proliferative rate with MIB-1, in keeping with the aggressive clinical course. *In vitro* they exhibit suppressor cell function. As with many PTLs, they are CD7 negative. All cases of ATL have clonal *TCR*β and *TCR*γ rearrangements and are associated with clonally integrated HTLV-1 retrovirus. Serologic testing for HTLV-1 as well as the identification of viral genomic sequences by PCR can be of great help in diagnosing this lymphoid neoplasm. However, only a minority of infected patients will develop ATL, and it is important to correlate serologic positivity for HTLV-1 or a positive PCR result with the presence of a clonal T-cell lymphoproliferation. Recurrent translocations are not reported in ATL, but numerical abnormalities and deletions of the long arm of chromosome 6 as assessed by both cytogenetic and loss-of-heterozygosity (LOH) studies are frequent (101).

Extranodal T-cell and NK-cell lymphomas represent a distinctive group and share many histological and immunophenotypic features (102). This observation is in keeping with the close relationship between NK cells and cytotoxic T cells (103). They include intestinal T-cell lymphoma, subcutaneous panniculitis-like T-cell lymphoma, and nasal and extranasal NK/T-cell lymphoma. Most of the extranodal T-cell lymphomas appear to be derived from cytotoxic T cells; they express granzyme B, the cytotoxic-cell-associated granule protein T-cell intracellular antigen 1 (TIA-1; also known as cytotoxic granule-associated RNA binding protein), and perforin (104). CD56, an antigen expressed on NK cells, may also be present, but it is most common in nasal NK/T-cell lymphoma (Table 7). These lymphomas as a group present in and spread to extranodal sites, with infrequent lymph node involvement. They frequently contain extensive necrosis, sometimes associated with angioinvasion. Apoptosis of tumor cells also is prominent, in part related to the cytotoxic features of the neoplastic cells. EBV is universally found in

TABLE 7 Extranodal NK/T-cell lymphomas[a]

Subtype	EBV	CD3	TIA-1	GranB/Per	CD56	TCR	
						Major	Minor
SPTCL	−	+ s	+	+	±	αβ	γδ
EATL	−	+ s	+	+	±	αβ	γδ/NK
Nasal	+	+ c	+	+	+	NK	γδ/αβ?
Hep/spl	−	+ s	+	−	+	γδ	αβ

[a]Abbreviations: SPTCL, subcutaneous panniculitis-like T-cell lymphoma, EATL, enteropathy-associated T-cell lymphoma; Nasal, nasal NK/T-cell lymphoma; Hep/spl, hepatosplenic T-cell lymphoma; GranB/Per, granzyme B/perforin; s, surface CD3; c, cytoplasmic CD3.

nasal and extranasal NK/T-cell lymphoma and may be seen sporadically in intestinal T-cell lymphoma. EBV is generally absent in subcutaneous panniculitis-like T-cell lymphoma. Hepatosplenic T-cell lymphoma also belongs to this broad group of cytotoxic T-cell lymphomas.

Within the extranodal NK/T-cell lymphomas, there is some variation in lineage, a feature that departs from the general principle that lineage is a defining feature of disease entities. For example, nasal NK/T-cell lymphoma is usually of NK-cell derivation, but in rare cases it may be derived from either γδ or αβ T cells. Similarly, intestinal T-cell lymphoma is usually of αβ T-cell derivation, but a minor proportion of cases are derived from γδ T cells.

Nasal NK/T-cell lymphomas express some T-cell-associated antigens but are probably of NK-cell derivation (105). Necrosis is seen in most cases. The midline nasal area is the most common site of involvement, but the disease can also present itself in other extranodal sites. In other sites it is referred to as nasal-type T/NK-cell lymphoma (105). The neoplastic cells generally lack T-cell gene rearrangements. The cells are positive for CD2 and CD7 but negative for surface CD3. However, they usually express CD3ε within the cytoplasm, which can be detected in paraffin sections with both polyclonal and monoclonal antibodies. CD56 is present in virtually all cases. The neoplastic cells are EBV positive, and the EBV genome is monoclonal based on terminal-repeat analysis (106). p53 is overexpressed in nearly all cases, but there have been no confirmatory mutational studies (107). There are few classical cytogenetic studies of these lymphomas, and while numerical abnormalities have been reported, no recurrent translocations have been identified (108). LOH studies show a high frequency of chromosomal loss at 6q, 13q, 11q, and 17p (the site of the p53 gene) (109). Recent studies using spectral karyotyping have identified a cryptic translocation involving Xp21 and 8p23 (110). The genes involved have not been identified.

The hepatosplenic T-cell lymphomas are most often derived from immature γδ T cells (111). The cells express the cytotoxic granule-associated protein TIA-1, but they lack expression of the effector proteins, the granzymes and perforin. This feature may explain the lack of tissue necrosis in these tumors. In addition to expressing TCRγδ, an indication of a γδ cell receptor, the cells are positive for CD56 and either $CD4^-/CD8^-$ or positive for CD8. CD5 is usually absent as well. Recently, it has become possible to detect the antigens associated with the γδ receptor by routine immunohistochemistry, facilitating diagnosis of tumors with a TCRγδ phenotype (112–114). Hepatosplenic T-cell lymphoma, as the name implies, presents with marked hepatosplenomegaly, but occult bone marrow involvement is usually present as well. However, lymph node involvement is absent. This lymphoma is associated with isochromosome 7q and trisomy 8 as consistent cytogenetic abnormalities (115). Interestingly, an identical form of hepatosplenic lymphoma composed of αβ T cells can be encountered in rare cases (116).

A distinctive subtype of T-cell lymphoma is ALCL (117). It can occur at any age but is most common in children and adolescents (118). Although the cells express some T-cell antigens, they usually have a markedly aberrant phenotype, and some cases may appear to be of null cell phenotype (Table 8). However, at the genotypic level, all cases appear to have rearranged TCR genes (119). CD30 is an antigen initially detected on the neoplastic cells of Hodgkin's disease. It is found on Reed-Sternberg (RS) cells, a subset of activated T cells, EBV-infected B cells, and in all cases of ALCL. Other characteristic markers include epithelial membrane antigen (EMA) and clusterin (120). The neoplastic cells also exhibit cytotoxic molecules (121).

Histologically, ALCL most often is composed of large, often lobulated cells that preferentially involve lymph node sinuses, and in the past such lesions were often interpreted as malignant histiocytosis (122). Tissue section immunohistochemistry is helpful in the diagnosis of this entity because the malignant cells may not be numerous and staining for CD30 highlights their sinusoidal distribution. The CD30 antigen can be detected in either paraffin or frozen sections.

ALCL was first recognized based on characteristic histological features (sinusoidal invasion) and a distinctive immunophenotype ($CD30^+$). However, neither sinusoidal invasion nor CD30 positivity proved to be entirely specific. Subsequently, a characteristic cytogenetic abnormality was identified, the t(2;5) translocation, which led to identification of the genes involved in the most common translocation of ALCL (*NPM/ALK*) and insights into the pathogenesis (123, 124). Generation of monoclonal antibodies to the aberrantly expressed ALK can be used diagnostically and has led to improved definition of the diagnostic entity, with important clinical and prognostic implications (125). Utilizing these biological tools, the ultimate histological spectrum of ALCL is both broader and narrower than originally believed. ALK expression can now be considered a defining feature, as ALK-negative cases of ALCL probably represent different entities (126).

In addition to the classical t(2;5) translocation that is found in ~75% of ALCLs, additional variant translocations occur in the remainder of cases (127). All variant translocations involve the *ALK* gene on chromosome 2, but a different partner chromosome. Regardless of the partnering gene involved in the translocation, ALK is activated in all cases and is believed to play a central role in ALCL pathogenesis (128). The diagnosis of ALCL can be assisted by RT-PCR, which will identify the 75% of cases with classical *NPM/ALK* fusion genes, or by FISH, which will detect both classical and variant translocations.

Primary cutaneous ALCL is a different disease and is closely related to lymphomatoid papulosis, a chronic lymphoproliferative disease of the skin (129). These cases do not have a t(2;5) translocation and do not express ALK protein. Notably, although all cases of true ALCL are ALK positive, ALK expression can be detected in other rare entities, such

TABLE 8 Differential diagnosis of ALCL and Hodgkin's disease

Disease	CD30	CD15	LCA	CD3	TIA-1	EMA	Clus	ALK	CD20
ALCL, ALK+	+	−	+	±	+	+	+	+	−
CHL	+	+	−	−	−	−	−	−	±
NLPHL	−	−	+	−	−	±	−	−	+
PTL, unspecified	±	−	+	+	±	−	−	−	−
DLBCL[a]	±	−	+	−	−	±	−	−	+

[a]DLBCL includes T-cell-rich large B-cell lymphoma.

as myofibroblastic tumors, and ALK-positive, CD30-negative large B-cell lymphomas.

Hodgkin's Disease (Hodgkin's Lymphoma)

CHL is an unusual neoplastic disorder because the neoplastic cells represent only a minority of the cells present in the tumor mass. The neoplastic cells, the RS cells and their mononuclear variants, are admixed with normal lymphocytes, histiocytes, eosinophils, neutrophils, and plasma cells. The paucity of RS cells has led to difficulty in their characterization by flow cytometric techniques and has severely impeded the molecular analysis of this neoplasm. The normal lymphocytes within CHL are usually identifiable as T cells, predominantly $CD4^+$. However, the nature of the malignant cell in CHL has taken a long time to unravel.

The tumor cells express CD15, an antigen found in normal granulocytes, histiocytes, and many epithelial cells. They also express the CD30 antigen, first identified on cell lines derived from CHL. LCA (CD45) is frequently absent. The identification of CD20 on at least some of the neoplastic cells led to speculation that CHL was B-cell derived (130). Immunohistochemistry to assess light-chain restriction is also usually not helpful for the assessment of clonality, as the amount of immunoglobulin produced is small, the cells tend to stain nonspecifically, and background staining for immunoglobulin tends to be high. Traditional molecular studies of CHL generally failed to detect clonal *IGH* rearrangements because of the low percentage of tumor cells in the population. The diagnostic sensitivity of IGH PCR is about 2 to 3% tumor cells (of total B cells), and frequently the number of clonal RS cells is below this threshold. However, by enriching RS cells through the use of microdissection techniques, several investigators were able to confirm a clonal B-cell origin in virtually all cases (131, 132). In addition, the cells were shown to have somatic mutations of the IGH genes, indicative of a GC stage of differentiation. Similar to CHL, the nodular lymphocyte-predominant variant (NLPHL) has also been shown to be of B-cell origin; however, because of its distinctive immunophenotypic and clinicopathological characteristics, NLPHL is now considered to be a separate entity (133). There are no characteristic recurrent translocations of significance known in either CHL or in NLPHL, and molecular profiling studies have been difficult to perform due to the difficulty in obtaining pure populations of tumor cells.

NONLYMPHOID TUMORS OF THE IMMUNE SYSTEM: "HISTIOCYTIC" DISORDERS

Normal Histiocytic Subsets

The cells of the histiocytic system consist of two major subsets: the antigen-presenting cells, or dendritic cells; and the antigen-processing cells, or phagocytic cells (134). The follicular DRCs are found in follicles and present antigen to B lymphocytes, but they may not be of hematopoietic origin. They are positive for CD21, CD23, CD35, and clusterin but are CD45 negative. The interdigitating dendritic cells (IDCs) and Langerhans cells (LCs) are bone marrow-derived cells that present antigen to T lymphocytes. LCs are found primarily in the skin but also in other organs. IDCs are found in lymph nodes and other lymphoid organs. Both LCs and IDCs are S100 positive. The relationship between these cells is controversial. Both are CD1a positive, although IDCs show variable expression dependent upon their maturational stage. However, unlike LCs, IDCs do not possess the characteristic Birbeck granule. Fibroblastic reticular cells are involved in transport of cytokines and other mediators (135). In lymph nodes, they ensheathe the postcapillary venules. They are of mesenchymal rather than hematopoietic origin, and they express smooth muscle actin (136).

All of the macrophages of lymph nodes share many enzyme histochemical and immunophenotypic characteristics. They have abundant and diffuse activity for lysosomal enzymes, including acid phosphatase and nonspecific esterase. As stated above, all of these cells can also demonstrate phagocytosis under appropriate conditions. Activity for lysozyme and α1-antitrypsin can be seen in all of the above subtypes but is most prominent in epithelioid histiocytes. Activity for lysozyme decreases abruptly with phagocytosis, presumably because of its loss into lysosomal vacuoles. CD68 is the most useful antigen for detection of macrophages in routine paraffin sections.

A variety of monoclonal antibodies that react with monocytes and macrophages have been derived. Unfortunately, most of these antibodies lack specificity for the mononuclear phagocytic system, and many react with other hematopoietic cells as well: myeloid cells, T cells, or B cells. For example, CD11c is present on monocytes and macrophages and is weak or absent on normal T and B lymphocytes. However, this antigen is found on the cells of HCL (a B-cell lymphoproliferative disorder) and in some cases of B-cell CLL. Cross-reactivities with T cells are present as well. For example, CD4 is found in normal monocytes and macrophages. CD25, in addition to being found on activated T lymphocytes, is found on normal monocytes and macrophages. CD68, strongly positive on histiocytes, also reacts with granulocytic precursors. The CD14 antigen is present on monocytes and macrophages and probably has the greatest specificity for the macrophage lineage among available reagents.

Proliferative Histiocytic Lesions

Proliferative lesions of antigen-presenting cells are relatively rare (137). The principal proliferative lesion of the dendritic cell system is LC histiocytosis (LCH). Recent studies, using the HUMARA method described above, have shown that the cells of LCH are monoclonal, but the disease usually has a self-limited course, especially in older children and adults (138). It may be fatal in infants. The cells of LCH have the characteristics of LCs, including CD1 expression, langerin expression, and Birbeck granules (139). In contrast to normal LCs, the cells also express antigens associated with phagocytic histiocytes, such as CD14 and CD11c. Recently, recurrent mutations of *BRAF* have been identified in a large proportion of cases of LCH, and antibodies to detect the mutant protein may be useful diagnostically (140, 141). Interestingly, Erdheim-Chester disease, another rare histiocytic disorder, also contains *BRAF* mutations (142).

There are rare tumors described that have a derivation from IDCs. These lesions are usually based in lymph nodes and are often associated with an inflammatory background and/or necrosis. There is overlap in histology and phenotype with true histiocytic tumors, and they may have an aggressive clinical course. By contrast, follicular dendritic cell sarcomas usually present with localized lymph node involvement. They may recur locally but usually do not disseminate. These neoplasms are also rare. Rare tumors of fibroblastic reticular cell origin also are seen in lymph nodes. The expression of clusterin, CD21 (DRC sarcomas), S100 (IDC tumors), CD1a (IDC tumors) and actin (fibroblastic reticular cell tumors) can be helpful in distinguishing these three stromal neoplasms of lymph nodes (88, 136). There are no specific cytogenetic abnormalities or molecular tests associated with these tumors.

Malignancies of mononuclear phagocytes include acute monocytic leukemia and histiocytic sarcoma. In rare instances, histiocytic sarcomas may be disseminated, fulfilling criteria for what has been termed in the past "malignant histiocytosis." However, most instances of malignant histiocytosis reported previously represent other entities, such as ALCL (134).

Acute monocytic leukemia relates to a bone marrow-derived monoblast. This malignancy arises in the bone marrow compartment, with secondary involvement of the peripheral blood and usually a markedly elevated leukocyte count. In contrast to acute myeloid leukemia, there is a somewhat higher incidence of involvement of nonhematopoietic sites, with frequent involvement of skin and gingiva.

Histiocytic sarcoma represents a malignancy of the mononuclear phagocytic series at the stage of the fixed-tissue histiocyte. Therefore, the lesions in histiocytic sarcoma represent localized, relatively discrete tumefactions. In addition to the reticuloendothelial system, common sites of involvement include skin and bone. Because there are few, if any, markers with absolute specificity for macrophages, the investigator must rigorously exclude other cell lineages with both immmunophenotypic and molecular means. In the absence of special studies, morphological evidence of phagocytosis by the neoplastic cells, most commonly erythrophagocytosis, had been proposed as a criterion for a derivation from mononuclear phagocytes. However, phagocytosis is inconspicuous in most mononuclear phagocytic malignancies. Moreover, it is not a specific finding and has been described for lymphoid, plasmacytic, and even epithelial tumors. Even if phagocytosis is observed, it is virtually always clinically insignificant. The hemophagocytic syndrome is the most common and clinically significant of the proliferative disorders of macrophages. However, it is not a neoplastic process. It is usually seen in association with immunodeficiency or another hematopoietic malignancy (143, 144). This syndrome appears to be pathogenetically related to an excessive production of cytokines and chemokines capable of stimulating mononuclear phagocytes (145). The cells in hemophagocytic syndromes are morphologically and phenotypically activated macrophages.

CONCLUSIONS

Tumors of the immune system are of interest not only because they represent models of normal immune cells but also because they provide excellent examples of how immunologic and molecular tumor markers may be used in clinical diagnosis. Because the lymphomas simulate normal cellular counterparts, it has been possible to develop modern classification schemes that take advantage of and utilize the large panels of antibodies that were primarily developed to study and characterize normal immune cells. The investigation of the molecular genetic abnormalities found in tumors of the immune system, particularly the translocations that occur in lymphoid neoplasms, has resulted in the discovery of oncogenic classes of genes that have been further exploited for the development of diagnostic testing and tumor classification purposes. The assimilation of both immunologic and molecular approaches has been largely responsible for the current biologically based WHO classification scheme.

The example provided by the WHO classification scheme has not gone unnoticed in the study and classification of other cancers. While many of the other tissues in which cancers arise may not be as complex as the immune system, the classification of nonlymphoid tumors has also benefited from advances in the detection of immunologic and molecular genetics of the tumors. One such example has been the refinements that have occurred in the classification and diagnosis of the so-called small cell tumors of childhood, in which both protein and molecular markers have been used to dissect out the origins and provide the tools to accurately classify these morphologically similar tumors. Small blue cell tumors include neuroblastomas, rhabdomyosarcomas, Ewing's sarcomas, and other rare tumors. Each of these is now known to be associated with characteristic cell surface markers, and tumor-specific translocations. Thus, the same approaches discussed for the lymphomas can be applied to the investigation and classification of these and other cancers. There is little doubt that the next generation of classification schemes developed for both tumors of the immune system and other types of tumors will continue to benefit from and incorporate information from advances in our understanding of the biology of normal cellular counterparts, as well as from the voluminous data being generated from the ongoing molecular dissection of the tumors themselves.

REFERENCES

1. **Gerard-Marchant R, Hamlin I, Lennert K, Rilke F, Stansfeld A, van Unnik J.** 1974. Letter: Classification of non-Hodgkin's lymphomas. *Lancet* **2:**405–408.
2. **Lukes RJ, Collins RD.** 1974. Immunologic characterization of human malignant lymphomas. *Cancer* **34**(Suppl)**:** 1488–1503. PubMed
3. **Harris NL, Jaffe ES, Stein H, Banks PM, Chan JK, Cleary ML, Delsol G, De Wolf-Peeters C, Falini B, Gatter KC, Grogan TM, Isaacson PG, Knowles DM, Mason DY, Muller-Hermelink HK, Pileri SA, Piris MA, Ralfkiaer E, Warnke RA.** 1994. A revised European-American classification of lymphoid neoplasms: a proposal from the International Lymphoma Study Group. *Blood* **84:**1361–1392. PubMed
4. **Swerdlow SH, Campo E, Harris NL, Jaffe ES, Pileri SA, Stein H, Thiele J, Vardiman JW.** 2008. *In* Bosman FT, Jaffe ES, Lakhani SR, Ohgaki H (ed), *WHO Classification of Tumours of Haematopoietic and Lymphoid Tissues*, 4th ed. International Agency for Research on Cancer, Lyon, France.
5. **Campo E, Swerdlow SH, Harris NL, Pileri S, Stein H, Jaffe ES.** 2011. The 2008 WHO classification of lymphoid neoplasms and beyond: evolving concepts and practical applications. *Blood* **117:**5019–5032. PubMed
6. **Rabbitts TH, van Straaten P, Rabbitts PH, Watson J.** 1985. Discussion on the metabolism of c-*myc* mRNA and protein. *Proc R Soc Lond B Biol Sci* **226:**79–82. PubMed
7. **Withers DA, Harvey RC, Faust JB, Melnyk O, Carey K, Meeker TC.** 1991. Characterization of a candidate *bcl-1* gene. *Mol Cell Biol* **11:**4846–4853. PubMed
8. **Tsujimoto Y, Jaffe E, Cossman J, Gorham J, Nowell PC, Croce CM.** 1985. Clustering of breakpoints on chromosome 11 in human B-cell neoplasms with the t(11;14) chromosome translocation. *Nature* **315:**340–343. PubMed
9. **Calvo KR, McCoy CS, Stetler-Stevenson M.** 2011. Flow cytometry immunophenotyping of hematolymphoid neoplasia. *Methods Mol Biol* **699:**295–316. PubMed
10. **Mason DY, Cordell JL, Brown MH, Borst J, Jones M, Pulford K, Jaffe E, Ralfkiaer E, Dallenbach F, Stein H, Pileri S, Gatter KC.** 1995. CD79a: a novel marker for B-cell neoplasms in routinely processed tissue samples. *Blood* **86:**1453–1459. PubMed
11. **Spieker-Polet H, Sethupathi P, Yam PC, Knight KL.** 1995. Rabbit monoclonal antibodies: generating a fusion partner to produce rabbit-rabbit hybridomas. *Proc Natl Acad Sci USA* **92:**9348–9352. PubMed
12. **Rossi S, Laurino L, Furlanetto A, Chinellato S, Orvieto E, Canal F, Facchetti F, Dei Tos AP.** 2005. Rabbit monoclonal

antibodies: a comparative study between a novel category of immunoreagents and the corresponding mouse monoclonal antibodies. *Am J Clin Pathol* **124:**295–302. PubMed
13. **Shi SR, Cote RJ, Taylor CR.** 1997. Antigen retrieval immunohistochemistry: past, present, and future. *J Histochem Cytochem* **45:**327–343. PubMed
14. **Krenacs L, Krenacs T, Raffeld M.** 1999. Antigen retrieval for immunohistochemical reactions in routinely processed paraffin sections. *Methods Mol Biol* **115:**85–93. PubMed
15. **van Dongen JJ, Wolvers-Tettero IL.** 1991. Analysis of immunoglobulin and T cell receptor genes. Part II: possibilities and limitations in the diagnosis and management of lymphoproliferative diseases and related disorders. *Clin Chim Acta* **198:**93–174. PubMed
16. **van Dongen JJ, Langerak AW, Brüggemann M, Evans PA, Hummel M, Lavender FL, Delabesse E, Davi F, Schuuring E, García-Sanz R, van Krieken JH, Droese J, González D, Bastard C, White HE, Spaargaren M, González M, Parreira A, Smith JL, Morgan GJ, Kneba M, Macintyre EA.** 2003. Design and standardization of PCR primers and protocols for detection of clonal immunoglobulin and T-cell receptor gene recombinations in suspect lymphoproliferations: report of the BIOMED-2 Concerted Action BMH4-CT98-3936. *Leukemia* **17:** 2257–2317. PubMed
17. **Diaz-Cano SJ, Blanes A, Wolfe HJ.** 2001. PCR techniques for clonality assays. *Diagn Mol Pathol* **10:**24–33. PubMed
18. **Nurse GT, Jenkins T.** 1973. G.-6-P.D. phenotypes and X-chromosome inactivation. *Lancet* **1:**99–100. PubMed
19. **Robertson KD, Jones PA.** 1999. Tissue-specific alternative splicing in the human INK4a/ARF cell cycle regulatory locus. *Oncogene* **18:**3810–3820. PubMed
20. **Kopp P, Jaggi R, Tobler A, Borisch B, Oestreicher M, Sabacan L, Jameson JL, Fey MF.** 1997. Clonal X-inactivation analysis of human tumours using the human androgen receptor gene (HUMARA) polymorphism: a non-radioactive and semiquantitative strategy applicable to fresh and archival tissue. *Mol Cell Probes* **11:**217–228. PubMed
21. **Pillai RK, Sathanoori M, Van Oss SB, Swerdlow SH.** 2013. Double-hit B-cell lymphomas with *BCL6* and MYC translocations are aggressive, frequently extranodal lymphomas distinct from *BCL2* double-hit B-cell lymphomas. *Am J Surg Pathol* **37:**323–332. PubMed
22. **Barth TF, Floßbach L, Bernd HW, Bob R, Buck M, Cogliatti SB, Feller AC, Hansmann ML, Hartmann S, Horn H, Klapper W, Kradolfer D, Mattfeldt T, Möller P, Rosenwald A, Stein H, Thorns C, Ott G.** 2012. Round robin test for detection of genomic aberrations in non-Hodgkin lymphoma by *in situ* hybridization. *Pathologe* **34:**329–334. (In German.)
23. **Kluin PH, Schuuring E.** 1997. FISH and related techniques in the diagnosis of lymphoma. *Cancer Surv* **30:**3–20. PubMed
24. **Arya M, Shergill IS, Williamson M, Gommersall L, Arya N, Patel HR.** 2005. Basic principles of real-time quantitative PCR. *Expert Rev Mol Diagn* **5:**209–219. PubMed
25. **Kingma DW, Medeiros LJ, Barletta J, Raffeld M, Mann RB, Ambinder RF, Jaffe ES.** 1994. Epstein-Barr virus is infrequently identified in non-Hodgkin's lymphomas associated with Hodgkin's disease. *Am J Surg Pathol* **18:**48–61. PubMed
26. **Rosenwald A, Wright G, Chan WC, Connors JM, Campo E, Fisher RI, Gascoyne RD, Muller-Hermelink HK, Smeland EB, Giltnane JM, Hurt EM, Zhao H, Averett L, Yang L, Wilson WH, Jaffe ES, Simon R, Klausner RD, Powell J, Duffey PL, Longo DL, Greiner TC, Weisenburger DD, Sanger WG, Dave BJ, Lynch JC, Vose J, Armitage JO, Montserrat E, López-Guillermo A, Grogan TM, Miller TP, LeBlanc M, Ott G, Kvaloy S, Delabie J, Holte H, Krajci P, Stokke T, Staudt LM, Lymphoma/Leukemia Molecular Profiling Project.** 2002. The use of molecular profiling to predict survival after chemotherapy for diffuse large-B-cell lymphoma. *N Engl J Med* **346:**1937–1947. PubMed
27. **Iqbal J, Wright G, Wang C, Rosenwald A, Gascoyne RD, Weisenburger DD, Greiner TC, Smith L, Guo S, Wilcox RA, Teh BT, Lim ST, Tan SY, Rimsza LM, Jaffe ES, Campo E, Martinez A, Delabie J, Braziel RM, Cook JR, Tubbs RR, Ott G, Geissinger E, Gaulard P, Piccaluga PP, Pileri SA, Au WY, Nakamura S, Seto M, Berger F, de Leval L, Connors JM, Armitage J, Vose J, Chan WC, Staudt LM, Lymphoma Leukemia Molecular Profiling Project and the International Peripheral T-cell Lymphoma Project.** 2014. Gene expression signatures delineate biological and prognostic subgroups in peripheral T-cell lymphoma. *Blood* **123:**2915–2923.
28. **Wiestner A, Rosenwald A, Barry TS, Wright G, Davis RE, Henrickson SE, Zhao H, Ibbotson RE, Orchard JA, Davis Z, Stetler-Stevenson M, Raffeld M, Arthur DC, Marti GE, Wilson WH, Hamblin TJ, Oscier DG, Staudt LM.** 2003. ZAP-70 expression identifies a chronic lymphocytic leukemia subtype with unmutated immunoglobulin genes, inferior clinical outcome, and distinct gene expression profile. *Blood* **101:**4944–4951. PubMed
29. **Scott DW, Wright GW, Williams PM, Lih CJ, Walsh W, Jaffe ES, Rosenwald A, Campo E, Chan WC, Connors JM, Smeland EB, Mottok A, Braziel RM, Ott G, Delabie J, Tubbs RR, Cook JR, Weisenburger DD, Greiner TC, Glinsmann-Gibson BJ, Fu K, Staudt LM, Gascoyne RD, Rimsza LM.** 2014. Determining cell-of-origin subtypes of diffuse large B-cell lymphoma using gene expression in formalin-fixed paraffin-embedded tissue. *Blood* **123:**1214–1217.
30. **Pittaluga S, Uppenkamp M, Cossman J.** 1987. Development of T3/T cell receptor gene expression in human pre-T neoplasms. *Blood* **69:**1062–1067. PubMed
31. **Szczepański T, Langerak AW, Willemse MJ, Wolvers-Tettero IL, van Wering ER, van Dongen JJ.** 2000. T cell receptor gamma (TCRG) gene rearrangements in T cell acute lymphoblastic leukemia reflect 'end-stage' recombinations: implications for minimal residual disease monitoring. *Leukemia* **14:**1208–1214. PubMed
32. **Szczepański T, Pongers-Willemse MJ, Langerak AW, Harts WA, Wijkhuijs AJ, van Wering ER, van Dongen JJ.** 1999. Ig heavy chain gene rearrangements in T-cell acute lymphoblastic leukemia exhibit predominant DH6-19 and DH7-27 gene usage, can result in complete V-D-J rearrangements, and are rare in T-cell receptor αβ lineage. *Blood* **93:**4079–4085. PubMed
33. **Buccheri V, Mihaljević B, Matutes E, Dyer MJ, Mason DY, Catovsky D.** 1993. mb-1: a new marker for B-lineage lymphoblastic leukemia. *Blood* **82:**853–857. PubMed
34. **Korsmeyer SJ, Arnold A, Bakhshi A, Ravetch JV, Siebenlist U, Hieter PA, Sharrow SO, LeBien TW, Kersey JH, Poplack DG, Leder P, Waldmann TA.** 1983. Immunoglobulin gene rearrangement and cell surface antigen expression in acute lymphocytic leukemias of T cell and B cell precursor origins. *J Clin Invest* **71:**301–313. PubMed
35. **Szczepański T, Willemse MJ, van Wering ER, van Weerden JF, Kamps WA, van Dongen JJ.** 2001. Precursor-B-ALL with D(H)-J(H) gene rearrangements have an immature immunogenotype with a high frequency of oligoclonality and hyperdiploidy of chromosome 14. *Leukemia* **15:**1415–1423. PubMed
36. **Ozdemirli M, Fanburg-Smith JC, Hartmann DP, Shad AT, Lage JM, Magrath IT, Azumi N, Harris NL, Cossman J, Jaffe ES.** 1998. Precursor B-lymphoblastic lymphoma presenting as a solitary bone tumor and mimicking Ewing's sarcoma: a report of four cases and review of the literature. *Am J Surg Pathol* **22:**795–804. PubMed

37. **Ferry JA, Yang WI, Zukerberg LR, Wotherspoon AC, Arnold A, Harris NL.** 1996. $CD5^+$ extranodal marginal zone B-cell (MALT) lymphoma. A low grade neoplasm with a propensity for bone marrow involvement and relapse. *Am J Clin Pathol* **105:**31–37. PubMed
38. **Kumar S, Green GA, Teruya-Feldstein J, Raffeld M, Jaffe ES.** 1996. Use of CD23 (BU38) on paraffin sections in the diagnosis of small lymphocytic lymphoma and mantle cell lymphoma. *Mod Pathol* **9:**925–929. PubMed
39. **Jaffe ES, Raffeld M, Medeiros LJ.** 1993. Histopathologic subtypes of indolent lymphomas: caricatures of the mature B-cell system. *Semin Oncol* **20**(Suppl 5)**:**3–30. PubMed
40. **Gaulard P, d'Agay MF, Peuchmaur M, Brousse N, Gisselbrecht C, Solal-Celigny P, Diebold J, Mason DY.** 1992. Expression of the *bcl-2* gene product in follicular lymphoma. *Am J Pathol* **140:**1089–1095. PubMed
41. **Horsman DE, Gascoyne RD, Coupland RW, Coldman AJ, Adomat SA.** 1995. Comparison of cytogenetic analysis, Southern analysis, and polymerase chain reaction for the detection of t(14; 18) in follicular lymphoma. *Am J Clin Pathol* **103:**472–478. PubMed
42. **Medeiros LJ, Van Krieken JH, Jaffe ES, Raffeld M.** 1990. Association of *bcl-1* rearrangements with lymphocytic lymphoma of intermediate differentiation. *Blood* **76:**2086–2090. PubMed
43. **Raffeld M, Jaffe ES.** 1991. bcl-1, t(11;14), and mantle cell-derived lymphomas. *Blood* **78:**259–263. PubMed
44. **Fu K, Weisenburger DD, Greiner TC, Dave S, Wright G, Rosenwald A, Chiorazzi M, Iqbal J, Gesk S, Siebert R, De Jong D, Jaffe ES, Wilson WH, Delabie J, Ott G, Dave BJ, Sanger WG, Smith LM, Rimsza L, Braziel RM, Müller-Hermelink HK, Campo E, Gascoyne RD, Staudt LM, Chan WC, Lymphoma/Leukemia Molecular Profiling Project.** 2005. Cyclin D1-negative mantle cell lymphoma: a clinicopathologic study based on gene expression profiling. *Blood* **106:**4315–4321. PubMed
45. **Salaverria I, Royo C, Carvajal-Cuenca A, Clot G, Navarro A, Valera A, Song JY, Woroniecka R, Rymkiewicz G, Klapper W, Hartmann EM, Sujobert P, Wlodarska I, Ferry JA, Gaulard P, Ott G, Rosenwald A, Lopez-Guillermo A, Quintanilla-Martinez L, Harris NL, Jaffe ES, Siebert R, Campo E, Beà S.** 2013. *CCND2* rearrangements are the most frequent genetic events in cyclin $D1^-$ mantle cell lymphoma. *Blood* **121:**1394–1402. PubMed
46. **Bijwaard KE, Aguilera NS, Monczak Y, Trudel M, Taubenberger JK, Lichy JH.** 2001. Quantitative real-time reverse transcription-PCR assay for cyclin D1 expression: utility in the diagnosis of mantle cell lymphoma. *Clin Chem* **47:**195–201. PubMed
47. **Wright G, Tan B, Rosenwald A, Hurt EH, Wiestner A, Staudt LM.** 2003. A gene expression-based method to diagnose clinically distinct subgroups of diffuse large B cell lymphoma. *Proc Natl Acad Sci USA* **100:**9991–9996. PubMed
48. **Baens M, Maes B, Steyls A, Geboes K, Marynen P, De Wolf-Peeters C.** 2000. The product of the t(11;18), an API2-MLT fusion, marks nearly half of gastric MALT type lymphomas without large cell proliferation. *Am J Pathol* **156:**1433–1439. PubMed
49. **Wotherspoon AC, Finn TM, Isaacson PG.** 1995. Trisomy 3 in low-grade B-cell lymphomas of mucosa-associated lymphoid tissue. *Blood* **85:**2000–2004. PubMed
50. **Schaffner C, Stilgenbauer S, Rappold GA, Döhner H, Lichter P.** 1999. Somatic *ATM* mutations indicate a pathogenic role of ATM in B-cell chronic lymphocytic leukemia. *Blood* **94:**748–753. PubMed
51. **Calin GA, Dumitru CD, Shimizu M, Bichi R, Zupo S, Noch E, Aldler H, Rattan S, Keating M, Rai K, Rassenti L, Kipps T, Negrini M, Bullrich F, Croce CM.** 2002. Frequent deletions and down-regulation of micro-RNA genes *miR15* and *miR16* at 13q14 in chronic lymphocytic leukemia. *Proc Natl Acad Sci USA* **99:**15524–15529. PubMed
52. **Calin GA, Sevignani C, Dumitru CD, Hyslop T, Noch E, Yendamuri S, Shimizu M, Rattan S, Bullrich F, Negrini M, Croce CM.** 2004. Human microRNA genes are frequently located at fragile sites and genomic regions involved in cancers. *Proc Natl Acad Sci USA* **101:**2999–3004. PubMed
53. **Cimmino A, Calin GA, Fabbri M, Iorio MV, Ferracin M, Shimizu M, Wojcik SE, Aqeilan RI, Zupo S, Dono M, Rassenti L, Alder H, Volinia S, Liu CG, Kipps TJ, Negrini M, Croce CM.** 2005. *miR-15* and *miR-16* induce apoptosis by targeting BCL2. *Proc Natl Acad Sci USA* **102:**13944–13949. PubMed
54. **Tobin G, Rosenquist R.** 2005. Prognostic usage of V_H gene mutation status and its surrogate markers and the role of antigen selection in chronic lymphocytic leukemia. *Med Oncol* **22:**217–228. PubMed
55. **Rosenwald A, Alizadeh AA, Widhopf G, Simon R, Davis RE, Yu X, Yang L, Pickeral OK, Rassenti LZ, Powell J, Botstein D, Byrd JC, Grever MR, Cheson BD, Chiorazzi N, Wilson WH, Kipps TJ, Brown PO, Staudt LM.** 2001. Relation of gene expression phenotype to immunoglobulin mutation genotype in B cell chronic lymphocytic leukemia. *J Exp Med* **194:**1639–1647. PubMed
56. **Wiggers TG, Westra G, Westers TM, Abbes AP, Strunk A, Kuiper-Kramer E, Poddighe P, van de Loosdrecht AA, Chamuleau ME.** 2014. ZAP70 in B-CLL cells related to the expression in NK cells is a surrogate marker for mutational status. *Cytometry B Clin Cytom* **86:**280–287.
57. **Treon SP, Xu L, Yang G, Zhou Y, Liu X, Cao Y, Sheehy P, Manning RJ, Patterson CJ, Tripsas C, Arcaini L, Pinkus GS, Rodig SJ, Sohani AR, Harris NL, Laramie JM, Skifter DA, Lincoln SE, Hunter ZR.** 2012. MYD88 L265P somatic mutation in Waldenström's macroglobulinemia. *N Engl J Med* **367:**826–833. PubMed
58. **Xu L, Hunter ZR, Yang G, Zhou Y, Cao Y, Liu X, Morra E, Trojani A, Greco A, Arcaini L, Varettoni M, Brown JR, Tai YT, Anderson KC, Munshi NC, Patterson CJ, Manning RJ, Tripsas CK, Lindeman NI, Treon SP.** 2013. MYD88 L265P in Waldenström macroglobulinemia, immunoglobulin M monoclonal gammopathy, and other B-cell lymphoproliferative disorders using conventional and quantitative allele-specific polymerase chain reaction. *Blood* **121:**2051–2058. PubMed
59. **Bergsagel PL, Kuehl WM, Zhan F, Sawyer J, Barlogie B, Shaughnessy J Jr.** 2005. Cyclin D dysregulation: an early and unifying pathogenic event in multiple myeloma. *Blood* **106:**296–303. PubMed
60. **Lazzarino M, Orlandi E, Paulli M, Boveri E, Morra E, Brusamolino E, Kindl S, Rosso R, Astori C, Buonanno MC.** 1993. Primary mediastinal B-cell lymphoma with sclerosis: an aggressive tumor with distinctive clinical and pathologic features. *J Clin Oncol* **11:**2306–2313. PubMed
61. **Lamarre L, Jacobson JO, Aisenberg AC, Harris NL.** 1989. Primary large cell lymphoma of the mediastinum. A histologic and immunophenotypic study of 29 cases. *Am J Surg Pathol* **13:**730–739. PubMed
62. **Mesri EA, Cesarman E, Arvanitakis L, Rafii S, Moore MA, Posnett DN, Knowles DM, Asch AS.** 1996. Human herpesvirus-8/Kaposi's sarcoma-associated herpesvirus is a new transmissible virus that infects B cells. *J Exp Med* **183:**2385–2390.
63. **DiGiuseppe JA, Nelson WG, Seifter EJ, Boitnott JK, Mann RB.** 1994. Intravascular lymphomatosis: a clinicopathologic study of 10 cases and assessment of response to chemotherapy. *J Clin Oncol* **12:**2573–2579. PubMed
64. **Fang JM, Finn WG, Hussong JW, Goolsby CL, Cubbon AR, Variakojis D.** 1999. CD10 antigen expression correlates with the t(14;18)(q32;q21) major breakpoint region

in diffuse large B-cell lymphoma. *Mod Pathol* **12:**295–300. PubMed

65. **Sander CA, Yano T, Clark HM, Harris C, Longo DL, Jaffe ES, Raffeld M.** 1993. p53 mutation is associated with progression in follicular lymphomas. *Blood* **82:**1994–2004. PubMed
66. **Wilson WH, Teruya-Feldstein J, Fest T, Harris C, Steinberg SM, Jaffe ES, Raffeld M.** 1997. Relationship of p53, *bcl-2*, and tumor proliferation to clinical drug resistance in non-Hodgkin's lymphomas. *Blood* **89:**601–609. PubMed
67. **Alizadeh AA, Eisen MB, Davis RE, Ma C, Lossos IS, Rosenwald A, Boldrick JC, Sabet H, Tran T, Yu X, Powell JI, Yang L, Marti GE, Moore T, Hudson J Jr, Lu L, Lewis DB, Tibshirani R, Sherlock G, Chan WC, Greiner TC, Weisenburger DD, Armitage JO, Warnke R, Levy R, Wilson W, Grever MR, Byrd JC, Botstein D, Brown PO, Staudt LM.** 2000. Distinct types of diffuse large B-cell lymphoma identified by gene expression profiling. *Nature* **403:**503–511. PubMed
68. **Savage KJ, Monti S, Kutok JL, Cattoretti G, Neuberg D, De Leval L, Kurtin P, Dal Cin P, Ladd C, Feuerhake F, Aguiar RC, Li S, Salles G, Berger F, Jing W, Pinkus GS, Habermann T, Dalla-Favera R, Harris NL, Aster JC, Golub TR, Shipp MA.** 2003. The molecular signature of mediastinal large B-cell lymphoma differs from that of other diffuse large B-cell lymphomas and shares features with classical Hodgkin lymphoma. *Blood* **102:**3871–3879. PubMed
69. **Rosenwald A, Wright G, Leroy K, Yu X, Gaulard P, Gascoyne RD, Chan WC, Zhao T, Haioun C, Greiner TC, Weisenburger DD, Lynch JC, Vose J, Armitage JO, Smeland EB, Kvaloy S, Holte H, Delabie J, Campo E, Montserrat E, Lopez-Guillermo A, Ott G, Muller-Hermelink HK, Connors JM, Braziel R, Grogan TM, Fisher RI, Miller TP, LeBlanc M, Chiorazzi M, Zhao H, Yang L, Powell J, Wilson WH, Jaffe ES, Simon R, Klausner RD, Staudt LM.** 2003. Molecular diagnosis of primary mediastinal B cell lymphoma identifies a clinically favorable subgroup of diffuse large B cell lymphoma related to Hodgkin lymphoma. *J Exp Med* **198:**851–862. PubMed
70. **Hans CP, Weisenburger DD, Greiner TC, Gascoyne RD, Delabie J, Ott G, Müller-Hermelink HK, Campo E, Braziel RM, Jaffe ES, Pan Z, Farinha P, Smith LM, Falini B, Banham AH, Rosenwald A, Staudt LM, Connors JM, Armitage JO, Chan WC.** 2004. Confirmation of the molecular classification of diffuse large B-cell lymphoma by immunohistochemistry using a tissue microarray. *Blood* **103:**275–282. PubMed
71. **Ngo VN, Young RM, Schmitz R, Jhavar S, Xiao W, Lim KH, Kohlhammer H, Xu W, Yang Y, Zhao H, Shaffer AL, Romesser P, Wright G, Powell J, Rosenwald A, Muller-Hermelink HK, Ott G, Gascoyne RD, Connors JM, Rimsza LM, Campo E, Jaffe ES, Delabie J, Smeland EB, Fisher RI, Braziel RM, Tubbs RR, Cook JR, Weisenburger DD, Chan WC, Staudt LM.** 2011. Oncogenically active *MYD88* mutations in human lymphoma. *Nature* **470:**115–119. PubMed
72. **Davis RE, Ngo VN, Lenz G, Tolar P, Young RM, Romesser PB, Kohlhammer H, Lamy L, Zhao H, Yang Y, Xu W, Shaffer AL, Wright G, Xiao W, Powell J, Jiang JK, Thomas CJ, Rosenwald A, Ott G, Muller-Hermelink HK, Gascoyne RD, Connors JM, Johnson NA, Rimsza LM, Campo E, Jaffe ES, Wilson WH, Delabie J, Smeland EB, Fisher RI, Braziel RM, Tubbs RR, Cook JR, Weisenburger DD, Chan WC, Pierce SK, Staudt LM.** 2010. Chronic active B-cell-receptor signalling in diffuse large B-cell lymphoma. *Nature* **463:**88–92. PubMed
73. **Yang Y, Shaffer AL III, Emre NC, Ceribelli M, Zhang M, Wright G, Xiao W, Powell J, Platig J, Kohlhammer H, Young RM, Zhao H, Yang Y, Xu W, Buggy JJ, Balasubramanian S, Mathews LA, Shinn P, Guha R, Ferrer M, Thomas C, Waldmann TA, Staudt LM.** 2012. Exploiting synthetic lethality for the therapy of ABC diffuse large B cell lymphoma. *Cancer Cell* **21:**723–737. PubMed
74. **Delabie J, Vandenberghe E, Kennes C, Verhoef G, Foschini MP, Stul M, Cassiman JJ, De Wolf-Peeters C.** 1992. Histiocyte-rich B-cell lymphoma. A distinct clinicopathologic entity possibly related to lymphocyte predominant Hodgkin's disease, paragranuloma subtype. *Am J Surg Pathol* **16:**37–48. PubMed
75. **Otsuki T, Kumar S, Ensoli B, Kingma DW, Yano T, Stetler-Stevenson M, Jaffe ES, Raffeld M.** 1996. Detection of HHV-8/KSHV DNA sequences in AIDS-associated extranodal lymphoid malignancies. *Leukemia* **10:**1358–1362. PubMed
76. **Boerma EG, Siebert R, Kluin PM, Baudis M.** 2009. Translocations involving 8q24 in Burkitt lymphoma and other malignant lymphomas: a historical review of cytogenetics in the light of todays knowledge. *Leukemia* **23:**225–234. PubMed
77. **Johnson NA, Slack GW, Savage KJ, Connors JM, Ben-Neriah S, Rogic S, Scott DW, Tan KL, Steidl C, Sehn LH, Chan WC, Iqbal J, Meyer PN, Lenz G, Wright G, Rimsza LM, Valentino C, Brunhoeber P, Grogan TM, Braziel RM, Cook JR, Tubbs RR, Weisenburger DD, Campo E, Rosenwald A, Ott G, Delabie J, Holcroft C, Jaffe ES, Staudt LM, Gascoyne RD.** 2012. Concurrent expression of MYC and BCL2 in diffuse large B-cell lymphoma treated with rituximab plus cyclophosphamide, doxorubicin, vincristine, and prednisone. *J Clin Oncol* **30:**3452–3459. PubMed
78. **Green TM, Young KH, Visco C, Xu-Monette ZY, Orazi A, Go RS, Nielsen O, Gadeberg OV, Mourits-Andersen T, Frederiksen M, Pedersen LM, Møller MB.** 2012. Immunohistochemical double-hit score is a strong predictor of outcome in patients with diffuse large B-cell lymphoma treated with rituximab plus cyclophosphamide, doxorubicin, vincristine, and prednisone. *J Clin Oncol* **30:**3460–3467. PubMed
79. **Dave SS, Fu K, Wright GW, Lam LT, Kluin P, Boerma EJ, Greiner TC, Weisenburger DD, Rosenwald A, Ott G, Müller-Hermelink HK, Gascoyne RD, Delabie J, Rimsza LM, Braziel RM, Grogan TM, Campo E, Jaffe ES, Dave BJ, Sanger W, Bast M, Vose JM, Armitage JO, Connors JM, Smeland EB, Kvaloy S, Holte H, Fisher RI, Miller TP, Montserrat E, Wilson WH, Bahl M, Zhao H, Yang L, Powell J, Simon R, Chan WC, Staudt LM, Lymphoma/Leukemia Molecular Profiling Project.** 2006. Molecular diagnosis of Burkitt's lymphoma. *N Engl J Med* **354:**2431–2442. PubMed
80. **Hummel M, Bentink S, Berger H, Klapper W, Wessendorf S, Barth TF, Bernd HW, Cogliatti SB, Dierlamm J, Feller AC, Hansmann ML, Haralambieva E, Harder L, Hasenclever D, Kühn M, Lenze D, Lichter P, Martin-Subero JI, Möller P, Müller-Hermelink HK, Ott G, Parwaresch RM, Pott C, Rosenwald A, Rosolowski M, Schwaenen C, Stürzenhofecker B, Szczepanowski M, Trautmann H, Wacker HH, Spang R, Loeffler M, Trümper L, Stein H, Siebert R, Molecular Mechanisms in Malignant Lymphomas Network Project of the Deutsche Krebshilfe.** 2006. A biologic definition of Burkitt's lymphoma from transcriptional and genomic profiling. *N Engl J Med* **354:**2419–2430. PubMed
81. **Aukema SM, Siebert R, Schuuring E, van Imhoff GW, Kluin-Nelemans HC, Boerma EJ, Kluin PM.** 2011. Double-hit B-cell lymphomas. *Blood* **117:**2319–2331. PubMed
82. **Jaffe ES, Pittaluga S.** 2011. Aggressive B-cell lymphomas: a review of new and old entities in the WHO classification. *Hematology Am Soc Hematol Educ Program* **2011:**506–514.
83. **zur Stadt U, Hoser G, Reiter A, Welte K, Sykora KW.** 1997. Application of long PCR to detect t(8;14)(q24;q32)

translocations in childhood Burkitt's lymphoma and B-ALL. *Ann Oncol* **8**(Suppl 1)**:**31–35. PubMed

84. **Jaffe ES, Krenacs L, Raffeld M.** 1997. Classification of T-cell and NK-cell neoplasms based on the REAL classification. *Ann Oncol* **8**(Suppl 2)**:**17–24. PubMed
85. **Picker LJ, Weiss LM, Medeiros LJ, Wood GS, Warnke RA.** 1987. Immunophenotypic criteria for the diagnosis of non-Hodgkin's lymphoma. *Am J Pathol* **128:**181–201. PubMed
86. **Frizzera G, Kaneko Y, Sakurai M.** 1989. Angioimmunoblastic lymphadenopathy and related disorders: a retrospective look in search of definitions. *Leukemia* **3:**1–5. PubMed
87. **Attygalle A, Al-Jehani R, Diss TC, Munson P, Liu H, Du MQ, Isaacson PG, Dogan A.** 2002. Neoplastic T cells in angioimmunoblastic T-cell lymphoma express CD10. *Blood* **99:**627–633. PubMed
88. **Grogg KL, Macon WR, Kurtin PJ, Nascimento AG, Lae ME, Ahmed I.** 2005. A survey of clusterin and fascin expression in sarcomas and spindle cell neoplasms: strong clusterin immunostaining is highly specific for follicular dendritic cell tumor. *Mod Pathol* **18:**260–266.
89. **Dunleavy K, Wilson WH, Jaffe ES.** 2007. Angioimmunoblastic T cell lymphoma: pathobiological insights and clinical implications. *Curr Opin Hematol* **14:**348–353. PubMed
90. **Weiss LM, Jaffe ES, Liu XF, Chen YY, Shibata D, Medeiros LJ.** 1992. Detection and localization of Epstein-Barr viral genomes in angioimmunoblastic lymphadenopathy and angioimmunoblastic lymphadenopathy-like lymphoma. *Blood* **79:**1789–1795. PubMed
91. **Abruzzo LV, Schmidt K, Weiss LM, Jaffe ES, Medeiros LJ, Sander CA, Raffeld M.** 1993. B-cell lymphoma after angioimmunoblastic lymphadenopathy: a case with oligoclonal gene rearrangements associated with Epstein-Barr virus. *Blood* **82:**241–246. PubMed
92. **Quintanilla-Martinez L, Fend F, Moguel LR, Spilove L, Beaty MW, Kingma DW, Raffeld M, Jaffe ES.** 1999. Peripheral T-cell lymphoma with Reed-Sternberg-like cells of B-cell phenotype and genotype associated with Epstein-Barr virus infection. *Am J Surg Pathol* **23:**1233–1240. PubMed
93. **Nicolae A, Pittaluga S, Venkataraman G, Vijnovich-Baron A, Xi L, Raffeld M, Jaffe ES.** 2013. Peripheral T-cell lymphomas of follicular T-helper cell derivation with Hodgkin/Reed-Sternberg cells of B-cell lineage: both EBV-positive and EBV-negative variants exist. *Am J Surg Pathol* **37:**816–826. PubMed
94. **Jaffe ES, Nicolae A, Pittaluga S.** 2013. Peripheral T-cell and NK-cell lymphomas in the WHO classification: pearls and pitfalls. *Mod Pathol* **26**(Suppl 1)**:**S71–S87. PubMed
95. **Iqbal J, Weisenburger DD, Greiner TC, Vose JM, McKeithan T, Kucuk C, Geng H, Deffenbacher K, Smith L, Dybkaer K, Nakamura S, Seto M, Delabie J, Berger F, Loong F, Au WY, Ko YH, Sng I, Armitage JO, Chan WC, International Peripheral T-Cell Lymphoma Project.** 2010. Molecular signatures to improve diagnosis in peripheral T-cell lymphoma and prognostication in angioimmunoblastic T-cell lymphoma. *Blood* **115:**1026–1036. PubMed
96. **de Leval L, Rickman DS, Thielen C, Reynies A, Huang YL, Delsol G, Lamant L, Leroy K, Brière J, Molina T, Berger F, Gisselbrecht C, Xerri L, Gaulard P.** 2007. The gene expression profile of nodal peripheral T-cell lymphoma demonstrates a molecular link between angioimmunoblastic T-cell lymphoma (AITL) and follicular helper T (TFH) cells. *Blood* **109:**4952–4963. PubMed
97. **Sakata-Yanagimoto M, Enami T, Yoshida K, Shiraishi Y, Ishii R, Miyake Y, Muto H, Tsuyama N, Sato-Otsubo A, Okuno Y, Sakata S, Kamada Y, Nakamoto-Matsubara R, Tran NB, Izutsu K, Sato Y, Ohta Y, Furuta J, Shimizu S, Komeno T, Sato Y, Ito T, Noguchi M, Noguchi E, Sanada M, Chiba K, Tanaka H, Suzukawa K, Nanmoku T, Hasegawa Y, Nureki O, Miyano S, Nakamura N, Takeuchi K, Ogawa S, Chiba S.** 2014. Somatic *RHOA* mutation in angioimmunoblastic T cell lymphoma. *Nat Genet* **46:**171–175. PubMed
98. **Palomero T, Couronné L, Khiabanian H, Kim MY, Ambesi-Impiombato A, Perez-Garcia A, Carpenter Z, Abate F, Allegretta M, Haydu JE, Jiang X, Lossos IS, Nicolas C, Balbin M, Bastard C, Bhagat G, Piris MA, Campo E, Bernard OA, Rabadan R, Ferrando AA.** 2014. Recurrent mutations in epigenetic regulators, *RHOA* and *FYN* kinase in peripheral T cell lymphomas. *Nat Genet* **46:**166–170. PubMed
99. **Odejide O, Weigert O, Lane AA, Toscano D, Lunning MA, Kopp N, Kim S, van Bodegom D, Bolla S, Schatz JH, Teruya-Feldstein J, Hochberg E, Louissaint A, Dorfman D, Stevenson K, Rodig SJ, Piccaluga PP, Jacobsen E, Pileri SA, Harris NL, Ferrero S, Inghirami G, Horwitz SM, Weinstock DM.** 2013. A targeted mutational landscape of angioimmunoblastic T-cell lymphoma. *Blood* **123:**1293–1296. PubMed
100. **Bunn PA Jr, Schechter GP, Jaffe E, Blayney D, Young RC, Matthews MJ, Blattner W, Broder S, Robert-Guroff M, Gallo RC.** 1983. Clinical course of retrovirus-associated adult T-cell lymphoma in the United States. *N Engl J Med* **309:**257–264. PubMed
101. **Hatta Y, Yamada Y, Tomonaga M, Miyoshi I, Said JW, Koeffler HP.** 1999. Detailed deletion mapping of the long arm of chromosome 6 in adult T-cell leukemia. *Blood* **93:**613–616. PubMed
102. **Jaffe ES, Krenacs L, Kumar S, Kingma DW, Raffeld M.** 1999. Extranodal peripheral T-cell and NK-cell neoplasms. *Am J Clin Pathol* **111**(Suppl 1)**:**S46–S55.
103. **Spits H, Blom B, Jaleco AC, Weijer K, Verschuren MC, van Dongen JJ, Heemskerk MH, Res PC.** 1998. Early stages in the development of human T, natural killer and thymic dendritic cells. *Immunol Rev* **165:**75–86. PubMed
104. **de Bruin PC, Kummer JA, van der Valk P, van Heerde P, Kluin PM, Willemze R, Ossenkoppele GJ, Radaszkiewicz T, Meijer CJ.** 1994. Granzyme B-expressing peripheral T-cell lymphomas: neoplastic equivalents of activated cytotoxic T cells with preference for mucosa-associated lymphoid tissue localization. *Blood* **84:**3785–3791. PubMed
105. **Jaffe ES, Chan JK, Su IJ, Frizzera G, Mori S, Feller AC, Ho FC.** 1996. Report of the workshop on nasal and related extranodal angiocentric T/natural killer cell lymphomas: definitions, differential diagnosis, and epidemiology. *Am J Surg Pathol* **20:**103–111. PubMed
106. **Ho FC, Srivastava G, Loke SL, Fu KH, Leung BP, Liang R, Choy D.** 1990. Presence of Epstein-Barr virus DNA in nasal lymphomas of B and 'T' cell type. *Hematol Oncol* **8:**271–281. PubMed
107. **Quintanilla-Martinez L, Franklin JL, Guerrero I, Krenacs L, Naresh KN, Rama-Rao C, Bhatia K, Raffeld M, Magrath IT.** 1999. Histological and immunophenotypic profile of nasal NK/T cell lymphomas from Peru: high prevalence of p53 overexpression. *Hum Pathol* **30:**849–855. PubMed
108. **Wong KF, Zhang YM, Chan JK.** 1999. Cytogenetic abnormalities in natural killer cell lymphoma/leukaemia—is there a consistent pattern? *Leuk Lymphoma* **34:**241–250. PubMed
109. **Siu LL, Wong KF, Chan JK, Kwong YL.** 1999. Comparative genomic hybridization analysis of natural killer cell lymphoma/leukemia. Recognition of consistent patterns of genetic alterations. *Am J Pathol* **155:**1419–1425. PubMed
110. **Wong N, Wong KF, Chan JK, Johnson PJ.** 2000. Chromosomal translocations are common in natural killer-cell

lymphoma/leukemia as shown by spectral karyotyping. *Hum Pathol* **31:**771–774. PubMed

111. **Cooke CB, Krenacs L, Stetler-Stevenson M, Greiner TC, Raffeld M, Kingma DW, Abruzzo L, Frantz C, Kaviani M, Jaffe ES.** 1996. Hepatosplenic T-cell lymphoma: a distinct clinicopathologic entity of cytotoxic γδ T-cell origin. *Blood* **88:**4265–4274. PubMed
112. **Rodríguez-Pinilla SM, Ortiz-Romero PL, Monsalvez V, Tomás IE, Almagro M, Sevilla A, Camacho G, Longo MI, Pulpillo A, Diaz-Pérez JA, Montes-Moreno S, Castro Y, Echevarría B, Trébol I, Gonzalez C, Sánchez L, Otín AP, Requena L, Rodríguez-Peralto JL, Cerroni L, Piris MÁ.** 2013. TCR-γ expression in primary cutaneous T-cell lymphomas. *Am J Surg Pathol* **37:**375–384. PubMed
113. **Pongpruttipan T, Sukpanichnant S, Assanasen T, Wannakrairot P, Boonsakan P, Kanoksil W, Kayasut K, Mitarnun W, Khuhapinant A, Bunworasate U, Puavilai T, Bedavanija A, Garcia-Herrera A, Campo E, Cook JR, Choi J, Swerdlow SH.** 2012. Extranodal NK/T-cell lymphoma, nasal type, includes cases of natural killer cell and αβ, γδ, and αβ/γδ T-cell origin: a comprehensive clinicopathologic and phenotypic study. *Am J Surg Pathol* **36:**481–499. PubMed
114. **Garcia-Herrera A, Song JY, Chuang SS, Villamor N, Colomo L, Pittaluga S, Alvaro T, Rozman M, de Anda Gonzalez J, Arrunategui AM, Fernandez E, Gonzalvo E, Estrach T, Colomer D, Raffeld M, Gaulard P, Campo E, Jaffe ES, Martinez A.** 2011. Nonhepatosplenic γδ T-cell lymphomas represent a spectrum of aggressive cytotoxic T-cell lymphomas with a mainly extranodal presentation. *Am J Surg Pathol* **35:**1214–1225. PubMed
115. **Alonsozana EL, Stamberg J, Kumar D, Jaffe ES, Medeiros LJ, Frantz C, Schiffer CA, O'Connell BA, Kerman S, Stass SA, Abruzzo LV.** 1997. Isochromosome 7q: the primary cytogenetic abnormality in hepatosplenic γδ T cell lymphoma. *Leukemia* **11:**1367–1372. PubMed
116. **Lai R, Larratt LM, Etches W, Mortimer ST, Jewell LD, Dabbagh L, Coupland RW.** 2000. Hepatosplenic T-cell lymphoma of αβ lineage in a 16-year-old boy presenting with hemolytic anemia and thrombocytopenia. *Am J Surg Pathol* **24:**459–463. PubMed
117. **Benharroch D, Meguerian-Bedoyan Z, Lamant L, Amin C, Brugières L, Terrier-Lacombe MJ, Haralambieva E, Pulford K, Pileri S, Morris SW, Mason DY, Delsol G.** 1998. ALK-positive lymphoma: a single disease with a broad spectrum of morphology. *Blood* **91:**2076–2084. PubMed
118. **Falini B, Pileri S, Zinzani PL, Carbone A, Zagonel V, Wolf-Peeters C, Verhoef G, Menestrina F, Todeschini G, Paulli M, Lazzarino M, Giardini R, Aiello A, Foss HD, Araujo I, Fizzotti M, Pelicci PG, Flenghi L, Martelli MF, Santucci A.** 1999. ALK^+ lymphoma: clinico-pathological findings and outcome. *Blood* **93:**2697–2706. PubMed
119. **Foss HD, Anagnostopoulos I, Araujo I, Assaf C, Demel G, Kummer JA, Hummel M, Stein H.** 1996. Anaplastic large-cell lymphomas of T-cell and null-cell phenotype express cytotoxic molecules. *Blood* **88:**4005–4011. PubMed
120. **Wellmann A, Thieblemont C, Pittaluga S, Sakai A, Jaffe ES, Siebert P, Raffeld M.** 2000. Detection of differentially expressed genes in lymphomas using cDNA arrays: identification of clusterin as a new diagnostic marker for anaplastic large-cell lymphomas. *Blood* **96:**398–404. PubMed
121. **Krenacs L, Wellmann A, Sorbara L, Himmelmann AW, Bagdi E, Jaffe ES, Raffeld M.** 1997. Cytotoxic cell antigen expression in anaplastic large cell lymphomas of T- and null-cell type and Hodgkin's disease: evidence for distinct cellular origin. *Blood* **89:**980–989. PubMed
122. **Wright DH.** 1985. Histogenesis of Burkitt's lymphoma: a B-cell tumour of mucosa-associated lymphoid tissue. *IARC Sci Publ* **60:**37–45. PubMed
123. **Rimokh R, Magaud JP, Berger F, Samarut J, Coiffier B, Germain D, Mason DY.** 1989. A translocation involving a specific breakpoint (q35) on chromosome 5 is characteristic of anaplastic large cell lymphoma ('Ki-1 lymphoma'). *Br J Haematol* **71:**31–36. PubMed
124. **Morris SW, Kirstein MN, Valentine MB, Dittmer KG, Shapiro DN, Saltman DL, Look AT.** 1994. Fusion of a kinase gene, ALK, to a nucleolar protein gene, NPM, in non-Hodgkin's lymphoma. *Science* **263:**1281–1284.
125. **Pulford K, Lamant L, Morris SW, Butler LH, Wood KM, Stroud D, Delsol G, Mason DY.** 1997. Detection of anaplastic lymphoma kinase (ALK) and nucleolar protein nucleophosmin (NPM)-ALK proteins in normal and neoplastic cells with the monoclonal antibody ALK1. *Blood* **89:**1394–1404. PubMed
126. **Jaffe ES.** 2001. Anaplastic large cell lymphoma: the shifting sands of diagnostic hematopathology. *Mod Pathol* **14:**219–228. PubMed
127. **Shipp MA, Ross KN, Tamayo P, Weng AP, Kutok JL, Aguiar RC, Gaasenbeek M, Angelo M, Reich M, Pinkus GS, Ray TS, Koval MA, Last KW, Norton A, Lister TA, Mesirov J, Neuberg DS, Lander ES, Aster JC, Golub TR.** 2002. Diffuse large B-cell lymphoma outcome prediction by gene-expression profiling and supervised machine learning. *Nat Med* **8:**68–74. PubMed
128. **Wellmann A, Otsuki T, Vogelbruch M, Clark HM, Jaffe ES, Raffeld M.** 1995. Analysis of the t(2;5)(p23;q35) translocation by reverse transcription-polymerase chain reaction in $CD30^+$ anaplastic large-cell lymphomas, in other non-Hodgkin's lymphomas of T-cell phenotype, and in Hodgkin's disease. *Blood* **86:**2321–2328. PubMed
129. **Willemze R, Beljaards RC.** 1993. Spectrum of primary cutaneous CD30 (Ki-1)-positive lymphoproliferative disorders. A proposal for classification and guidelines for management and treatment. *J Am Acad Dermatol* **28:**973–980. PubMed
130. **Pinkus GS, Said JW.** 1988. Hodgkin's disease, lymphocyte predominance type, nodular—further evidence for a B cell derivation. L & H variants of Reed-Sternberg cells express L26, a pan B cell marker. *Am J Pathol* **133:**211–217. PubMed
131. **Küppers R, Rajewsky K, Zhao M, Simons G, Laumann R, Fischer R, Hansmann ML.** 1994. Hodgkin disease: Hodgkin and Reed-Sternberg cells picked from histological sections show clonal immunoglobulin gene rearrangements and appear to be derived from B cells at various stages of development. *Proc Natl Acad Sci USA* **91:**10962–10966. PubMed
132. **Kanzler H, Küppers R, Hansmann ML, Rajewsky K.** 1996. Hodgkin and Reed-Sternberg cells in Hodgkin's disease represent the outgrowth of a dominant tumor clone derived from (crippled) germinal center B cells. *J Exp Med* **184:**1495–1505. PubMed
133. **Mason DY, Banks PM, Chan J, Cleary ML, Delsol G, de Wolf Peeters C, Falini B, Gatter K, Grogan TM, Harris NL.** 1994. Nodular lymphocyte predominance Hodgkin's disease. A distinct clinicopathological entity. *Am J Surg Pathol* **18:**526–530. PubMed
134. **Jaffe ES.** 1995. Malignant histiocytosis and true histiocytic lymphomas, p 560–593. *In* Jaffe ES (ed), *Surgical Pathology of Lymph Nodes and Related Organs*, 2nd ed. W.B. Saunders Co, Philadelphia, PA.
135. **Gretz JE, Anderson AO, Shaw S.** 1997. Cords, channels, corridors and conduits: critical architectural elements facilitating cell interactions in the lymph node cortex. *Immunol Rev* **156:**11–24. PubMed
136. **Andriko JW, Kaldjian EP, Tsokos M, Abbondanzo SL, Jaffe ES.** 1998. Reticulum cell neoplasms of lymph nodes: a clinicopathologic study of 11 cases with recognition of a new subtype derived from fibroblastic reticular cells. *Am J Surg Pathol* **22:**1048–1058. PubMed

137. **Favara BE, Feller AC, Pauli M, Jaffe ES, Weiss LM, Arico M, Bucsky P, Egeler RM, Elinder G, Gadner H, Gresik M, Henter JI, Imashuku S, Janka-Schaub G, Jaffe R, Ladisch S, Nezelof C, Pritchard J, The WHO Committee On Histiocytic/Reticulum Cell Proliferations, Reclassification Working Group of the Histiocyte Society.** 1997. Contemporary classification of histiocytic disorders. *Med Pediatr Oncol* **29:**157–166. PubMed
138. **Willman CL, Busque L, Griffith BB, Favara BE, McClain KL, Duncan MH, Gilliland DG.** 1994. Langerhans'-cell histiocytosis (histiocytosis X)—a clonal proliferative disease. *N Engl J Med* **331:**154–160. PubMed
139. **Geissmann F, Lepelletier Y, Fraitag S, Valladeau J, Bodemer C, Debré M, Leborgne M, Saeland S, Brousse N.** 2001. Differentiation of Langerhans cells in Langerhans cell histiocytosis. *Blood* **97:**1241–1248. PubMed
140. **Badalian-Very G, Vergilio JA, Degar BA, MacConaill LE, Brandner B, Calicchio ML, Kuo FC, Ligon AH, Stevenson KE, Kehoe SM, Garraway LA, Hahn WC, Meyerson M, Fleming MD, Rollins BJ.** 2010. Recurrent *BRAF* mutations in Langerhans cell histiocytosis. *Blood* **116:**1919–1923. PubMed
141. **Sahm F, Capper D, Preusser M, Meyer J, Stenzinger A, Lasitschka F, Berghoff AS, Habel A, Schneider M, Kulozik A, Anagnostopoulos I, Müllauer L, Mechtersheimer G, von Deimling A.** 2012. BRAFV600E mutant protein is expressed in cells of variable maturation in Langerhans cell histiocytosis. *Blood* **120:**e28–e34. PubMed
142. **Haroche J, Charlotte F, Arnaud L, von Deimling A, Hélias-Rodzewicz Z, Hervier B, Cohen-Aubart F, Launay D, Lesot A, Mokhtari K, Canioni D, Galmiche L, Rose C, Schmalzing M, Croockewit S, Kambouchner M, Copin MC, Fraitag S, Sahm F, Brousse N, Amoura Z, Donadieu J, Emile JF.** 2012. High prevalence of *BRAF V600E* mutations in Erdheim-Chester disease but not in other non-Langerhans cell histiocytoses. *Blood* **120:**2700–2703. PubMed
143. **Risdall RJ, McKenna RW, Nesbit ME, Krivit W, Balfour HH Jr, Simmons RL, Brunning RD.** 1979. Virus-associated hemophagocytic syndrome: a benign histiocytic proliferation distinct from malignant histiocytosis. *Cancer* **44:**993–1002. PubMed
144. **Lane HC, Callihan TR, Jaffe ES, Fauci AS, Moutsopoulos HM.** 1983. Presence of intracytoplasmic IgG in the lymphocytic infiltrates of the minor salivary glands of patients with primary Sjögren's syndrome. *Clin Exp Rheumatol* **1:**237–239. PubMed
145. **Teruya-Feldstein J, Setsuda J, Yao X, Kingma DW, Straus S, Tosato G, Jaffe ES.** 1999. MIP-1α expression in tissues from patients with hemophagocytic syndrome. *Lab Invest* **79:**1583–1590.

Monitoring of Immunologic Therapies

THERESA L. WHITESIDE

110

Immunologic therapies are becoming increasingly widely utilized. The current interest in these therapies is due to considerable successes in treatment outcomes in a broad spectrum of human diseases targeted for biotherapy, including inheritable or acquired immunodeficiencies, autoimmune diseases, cancer, and persistent infections. Many new biologic agents are available for immune therapy, and antibodies, cytokines, activated or genetically modified immune cells, vaccines, and other immunomodulatory drugs are frequently used either as monotherapies or in combination with conventional therapies such as chemotherapy, radiation, surgery, and even behavior-modifying therapies. In cancer, biotherapies are expected to restore dysfunctional antitumor immune responses, activate immune cells, and help immune cells to reacquire normal homeostasis. In addition, tumors resistant to standard therapies are often sensitive to immune interventions, and this offers a promise of combinatorial therapies to overcome drug resistance.

The selection and use of an immunologic therapy usually requires extensive preclinical evaluations. *In vitro* studies with human cells and *in vivo* experiments with animal models of disease are expected to define the presumed mechanism(s) responsible for its therapeutic activity. Animal models are especially useful for studies of dosages, times, frequencies, and sequences of drug delivery and are essential for evaluating the toxicity of immune therapies and their effects on the disease process and overall survival. A clinical protocol design is frequently based on results of experiments performed in animal models. Translation of preclinical *in vitro* and/or *in vivo* results to a clinical protocol design requires close cooperation and collaboration of the laboratory with clinical personnel.

An equally important requirement for implementation of biotherapy in the clinic is the assessment of its direct and/or indirect *in vivo* effects. For this reason, immunologic monitoring has emerged as an advisable, and more recently as a necessary, adjunct to clinical trials with biologics. In the past, immunologic monitoring fell under the "correlative studies" category. Today, it is often a protocol-mandated requirement, and an immunologic response to therapy might be the primary endpoint. Immune monitoring has become an important part of patient assessment in expectation that immune measures could serve as biomarkers or as surrogate endpoints of clinical responses. A series of recommendations for the development and use of immune biomarkers was formulated by a joint International Society for Biological Therapy of Cancer-Society for Immunotherapy of Cancer, US Food and Drug Administration (FDA), and National Cancer Institute task force (1). This document emphasizes the need for development of reliable immune biomarkers and offers guidelines for how to establish, standardize, and evaluate immune assays to see whether they meet a biomarker designation.

CHALLENGES IN MONITORING OF IMMUNE THERAPIES

The immune system is always ready to respond to "danger signals" that originate within or outside the body (2, 3). However, cancer and chronic persistent infections are characterized by local and systemic immune suppression selectively targeting immune cells responding to tumor antigens and infectious agents, respectively. Thus, the host immune system is dysfunctional with respect to the offender and unable to contain tumor growth or infection (4). Biologic therapies are expected to restore the ability of the immune system to respond by activating immune cells, blocking inhibitory signals, and/or removing or silencing suppressor cells (4). While much has been learned about mechanisms responsible for immune dysfunction in cancer and HIV-1, the complexity of cellular signaling and molecular interactions involved and the cross talk ongoing between immune, endocrine, neural, and hormonal networks complicate the interpretation of immune monitoring results and establishment of reliable correlations with clinical outcome. Complex biological interactions of the various immune system components present a landscape in which therapy-associated effects may not always be readily detectable or measurable.

Immune monitoring itself has been often viewed as a particularly complex and poorly controlled task in comparison to conventional clinically used biochemical assays. Although serial monitoring assays (i.e., the "bulk assays") performed at the population level have been largely replaced by more-accurate single-cell technologies allowing for assessments of immune cells *in situ*, these new sophisticated assays have to be considered and interpreted in the context of immune cell and non-immune cell cross talk. Thus, special expertise may be needed to interpret cellular interactions, and the well-known cellular plasticity of immune cells at

doi:10.1128/9781555818722.ch110

tissue sites might further confuse the results. Nevertheless, recent results from, e.g., clinical trials with antibodies to the checkpoint inhibitors cytotoxic-T-lymphocyte-associated antigen 4 (CTLA-4) and programmed cell death ligand 1 (PD-L1) indicate that beneficial clinical results can be linked to measurably reduced immune suppression, and that selected immunologic characteristics can serve as biomarkers of therapeutic response or overall survival (5, 6). Clearly, recent experience with biotherapy provides many examples of the emerging potential of immunologic markers serving as predictors of outcome or response to therapy (7–9).

CLINICAL TRIALS WITH BIOLOGIC AGENTS

Following preclinical evaluations, a therapeutically promising immunologic agent is introduced to the clinic in the form of a phase I protocol. The design of a phase I study is based on the predicted mechanism of action of this agent, as determined in preclinical *in vitro* and *in vivo* experiments. An investigational new drug application, which contains the results of preclinical and animal safety studies as well as the clinical protocol, is filed with the FDA. Agency approval is necessary for clinical evaluations of any experimental biologic agent. Following a review of the application, the FDA might decline to issue approval for opening of the trial and place the study on hold if additional information or clarifications are needed. Clinical trials involving gene therapy need approval by the Recombinant DNA Advisory Committee of the National Institutes of Health. In addition, institutional approvals from the institutional review board and the biosafety committee have to be obtained prior to opening the trial for patient accrual.

Biologic agents are available as natural or recombinant materials that may have potent immunomodulatory activities. When administered systemically in high doses, they often induce considerable toxicities, as is common, e.g., with cytokines such as interferons or interleukin-2 (IL-2). However, the maximal tolerated dose (MTD) for a given biologic agent is not necessarily the dose that produces the desired biologic or therapeutic effect. In fact, low doses of biologics might have greater or different therapeutic effects than high doses without accompanying toxicity. This observation suggests that in contrast to the case for pharmacologic or chemotherapeutic agents, which are usually characterized by a linear dose-response curve, biologic agents have a distinctive bell-shaped response curve. The optimal biologic dose (OBD) for each biologic agent is thus likely to be different from the MTD and needs to be defined in phase I/II clinical trials in order to preserve and optimize its therapeutic benefits and limit its toxicity. The developmental strategy for a therapeutic agent involves determination of the mechanism-specific OBD, that is, the dose that is optimally effective with tolerable toxicity. A clinical trial designed to determine the OBD is referred to as phase Ib, in contrast to a phase Ia trial, in which only the clinical toxicity of a new biologic agent is defined as the MTD (10). It is important to remember that the OBD may be different from the MTD for a given biologic agent. In addition, the same agent might have quite disparate OBDs for different immunologic characteristics. IL-2, for example, a cytokine approved for therapy of renal cell carcinoma and melanoma, has been used at high doses to activate cytolytic and helper T cells and natural killer cells. More-recent studies show that low-dose IL-2 used as therapy enables expansion and upregulates functions of regulatory T cells (Tregs). Thus, IL-2 at low doses can be used as a tolerogenic agent in, e.g., graft-versus-host disease or posttransplant rejection episodes (11–13).

In general, phase Ib trials are intended to measure the pharmacokinetics and biodistribution of a biologic agent, together with selected immunologic parameters that, on the basis of the postulated immune mechanism, are likely to influence the disease process. For example, in a patient with cancer who is treated with IL-2, one postulated mechanism for antitumor effects might be an upregulation of T-cell and/or NK-cell activity in the peripheral circulation (14). In this case, monitoring of the T-cell or NK-cell activation status, e.g., expression of activation markers CD69 or CD154 (CD40L) on the surface of T cells and activation receptors such as NKp30 or NKp46 on the surface of NK cells in the peripheral blood during therapy, might serve as a surrogate measure for the therapeutic effects of IL-2, and the dose of IL-2 resulting in the maximal upregulation of these markers (as percent positive cells and mean fluorescence intensity) with tolerable toxicity would be selected as the OBD. However, it is now known that IL-2, by binding to cells that express the IL-2 receptor (IL-2Rα; CD25), activates $CD4^{+}CD25^{high}$ Tregs, among other cell subsets (15). Tregs downregulate immune responses, including the antitumor activity of effector T cells, which is clearly an undesirable situation in a patient being treated for cancer (15). Further, newer data suggest that stimulatory versus inhibitory *in vivo* effects of IL-2 may be dose dependent, as indicated above (11–13). Hence, it seems important to define the OBD for IL-2 that promotes immune activation in a patient with cancer. On the other hand, for subjects with autoimmune diseases, the OBD for IL-2-based therapy might be different, as inhibitory effects are a desired endpoint. This type of rationale is likely to apply to immune system-based therapy in general, and therefore the goal of establishing the OBD is a critical component of the developmental strategy for biologic agents and their application to various diseases.

In most phase Ib trials performed to date, surrogate immunologic endpoints are achieved much more easily than clinical responses. During IL-2 therapy for renal cell carcinoma, for example, virtually all patients develop high levels of endogenous NK-cell activity, while only a fraction of these patients achieve objective antitumor responses (16). In other words, surrogate immunologic endpoints selected on the basis of preclinical results do not appear to correlate with clinical responses, possibly because these endpoints seldom reflect the entire spectrum of physiologic mechanisms mediated by a biologic agent. In considering the pleiotropic activities of biologic agents, it appears that no single surrogate endpoint is likely to correlate with their therapeutic effects and thus with a clinical response. On the other hand, it is possible that a panel of carefully selected monitoring assays might provide a clue about the *in vivo* effects of an agent. For this reason, the current approaches to monitoring favor multiparameter analyses employing new high-throughput technologies, including genomics and proteomics. The possibilities for multiparameter testing now extend to immunologic monitoring, allowing evaluations of more than one surrogate endpoint in patients treated with biologic agents to identify those that are clinically meaningful.

In view of the difficulties experienced to date in selecting immunologic endpoints for monitoring of phase Ib trials, it could be anticipated that a direct measure of the dose of a biologic agent inducing the best therapeutic, e.g., antitumor or antiviral, effects would be preferable to the use of surrogate biomarkers. However, practical and ethical considerations rule out the direct approach of determining the best therapeutic dose. Since antitumor response rates for single biologic agents generally range between 10 and 30%, dose-finding studies would require excessively large numbers of patients

and would expose many of them to ineffective doses of the agent tested. For this reason, the goal of phase I trials is to determine the toxicity and to define the promising OBD of a biologic agent, with the caveat that this OBD might relate only to one particular biologic activity of this agent and that it may not relate to its therapeutic activity. In fact, it is not uncommon to see few or even no clinical responses in phase I trials. But having obtained evidence of safety and a lack of toxicity, it is then possible to expand the earlier clinical observations in phase II clinical studies and to begin asking questions about the dose and mechanisms of action of a biologic agent. Ultimately, an agent's therapeutic efficacy has to be determined in large-scale randomized phase III clinical trials in which the placebo arm is compared to the experimental arm. It is encouraging that in recent years several biologic therapeutics, including monoclonal antibodies (MAbs), cytokines, and some vaccines, have reached the stage of being evaluated for efficacy in phase III clinical trials (17–19).

A RATIONALE FOR IMMUNOLOGIC MONITORING OF CLINICAL TRIALS WITH BIOLOGIC AGENTS

"Monitoring" refers to serial specimen acquisition and testing. The rationale for immunologic monitoring in clinical trials with biologics is based on the premise that these agents achieve therapeutic effects as a result of their ability to modify one or more components of the patient's immune system. The expectation is that by serially measuring immune markers, which undergo significant changes relative to their pretherapy baseline levels, it might be possible to define the immunologic mechanisms responsible for biologic and possibly also clinical activity of a biologic agent. In addition, the objective is to determine whether the observed changes in the immunologic phenotype or function correlate with clinical responses, toxicity, resistance to other therapies, or any other phenomena likely to influence the therapeutic outcome.

The first step toward rational immunologic monitoring is the selection of the most informative assay(s). This selection cannot be arbitrary and has to be based on a specific hypothesis. It would be best, of course, to formulate the hypothesis on the basis of preclinical data available to the investigator from personal experience and from the current literature. The investigator is obliged to use judgment and collective experience to address the likely mechanisms responsible for therapeutic effects. But since most biologic agents have multiple biologic effects, more than one hypothesis of action can be postulated. Which of these hypotheses is ultimately selected for testing depends on the individual insights and preferences of the clinical investigator. However, it is not advisable to test too many hypotheses at once, for fear of making the design of a clinical trial too complex and the accompanying monitoring too extensive. There is no way to guarantee that the hypothesis selected for testing in a clinical trial is correct; hence, the selection of a hypothesis is the most crucial aspect of the trial design and has to be formulated only after a complete review of all preclinical data. As such, a clinical trial is not different from any other hypothesis-driven scientific experiment.

The next step of the scientific process calls for a design of an experimental plan in which the proposed hypothesis can be tested in the most satisfactory fashion. This includes the selection of assays to be performed and the frequency of monitoring. For phase I clinical trials, it is prudent to begin by considering a broad array of immunologic effects because the biologic activity of the evaluated biologic agent may be incompletely understood. It may be advantageous at this stage to consider alternative explanations for its biologic and, possibly, therapeutic effects. Hence, the selected assays should be sensitive rather than specific in order to detect biologic effects when they are induced by therapy. In phase II and III clinical trials, it might be possible to narrow down the selection of immunologic assays to those that were observed to reflect biologic activity or to correlate with clinical responses in previous clinical trials. In place of sensitive screening assays, more-specialized specific or confirmatory assays could be introduced at this time to better focus on the mechanisms of activity mediated by the biologic agent. While no well-defined criteria exist for the selection of optimal monitoring assays, a general principle may be defined as follows. The choice of immunologic assays to be used for monitoring of phase I trials has to be based on solid preliminary data derived from relevant animal models of disease as well as *in vitro* experiments with human cells. In phase II and III clinical trials, the choice of assays to be used has to depend on previous results derived from phase I trials.

STRATEGY FOR IMMUNOLOGIC MONITORING: A PRACTICAL GUIDE

The choice of a strategy for immunologic monitoring of clinical trials with biologic agents is neither simple nor straightforward. No single assay or experimental approach is appropriate for all therapeutic interventions. The selection of the "right" monitoring assays requires familiarity with immunologic assays, judgment, and a considerable understanding of the biologic and therapeutic effects induced by the biologic agent used. Therefore, clinical investigators are obliged to make a number of well-informed and practical decisions, each of which is likely to influence the overall quality of monitoring and, hence, the final results of the trial. To facilitate assay selection and use in monitoring of clinical trials, several practical guidelines are given below, with the proviso that these are neither comprehensive nor applicable to all situations.

The frequency of immunologic assays to be performed is an important component of the trial design. Clearly, it is essential to establish a pretherapy baseline and posttherapy values. Beyond that, the number of time points selected for monitoring during the course of therapy depends on the characteristics of the biologic agent administered. For example, it is well known that cytokines usually have rapid and often dramatic effects on the total number and functions of cells in the circulation or on the levels of other cytokines or soluble cytokine receptors in the serum. Thus, with IL-2 administered as a bolus, rapid lymphopenia followed by a rebound in the number of circulating lymphocytes is observed (20). In contrast, when low intravenous doses of IL-2 are given continuously over a period of time, a gradual rise in the number of circulating $CD3^{-}CD56^{+}$ NK cells is observed (21). More-recent data suggest that IL-2 delivery may also increase the frequency of Treg cells in the circulation or tissues and promote activation-induced cell death (22). These initial effects of IL-2 are followed by delayed effects due to the induction of secondary cytokines. The well-known result of high-dose IL-2 therapy, i.e., transient hypotension observed 4 to 8 h after IL-2 bolus administration, is induced by the secondary cytokines tumor necrosis factor alpha (TNF-α) and IL-1β, which are released in response to IL-2 (20). In clinical trials with cytokines, it is important to measure the pharmacokinetics of the cytokine used for therapy as well as the levels of secondary cytokines in serum, which might be responsible for toxicity of the therapy.

A well-described effect of long-term therapy with biologics is the development of antibodies (Abs) to the administered biologic agent (23). Such antidrug Abs do not arise in every patient treated, and they may not appear until weeks or months into therapy or until multiple courses of the drug are administered. However, their presence in the plasma of individuals treated with the biologic agent is an important factor for the outcome of therapy, because they may either neutralize the drug or contribute to the development of immune complex disease. Therefore, it seems reasonable to monitor for the appearance of such Abs during the course of therapy. This requirement is obviously necessary when therapy with anti-idiotypic Abs is considered, e.g., for some patients with malignancies. Such patients may be treated with an anti-idiotypic Ab (Ab2) that is an internal image of the antigen and can include the production of Ab1 and Ab3, both of which are able to bind the antigen. Since Ab3 is therapeutic and Ab1 may not be, the presence and levels of Ab1 and Ab3 in serum are crucial for the interpretation of immunologic as well as clinical responses (24).

Another important consideration is the transient nature of some immune responses. For example, in vaccination protocols for patients with cancer or viral infections, the appearance of antigen-specific effector cells in the circulation may be short-lived after single or even multiple vaccinations. In this case, assays for the detection and frequency of such effector cells have to be performed often and soon after vaccination. With other vaccines, however, the appearance in the peripheral circulation of the effector cells may be delayed, so their frequency will not increase until late into the vaccination regimen. It thus appears that a decision to monitor the immediate versus delayed effects of therapy with any biologic agent has to be made with caution, after considering possible implications of these effects on the interpretation of immunologic and therapeutic results of the trial. The relative complexity and cost of the assay often influence the frequency of monitoring. For this reason, simple, robust assays that can be reliably performed on serially collected, cryopreserved samples are necessary for frequent immunologic monitoring.

A decision to select cellular versus humoral immunologic assays for monitoring is directly related to the mechanism of action proposed for the biologic agent. While it may be difficult to prioritize on the basis of the limited understanding of such mechanisms, the consideration of practical aspects of monitoring can help in reaching a reasonable decision. Limitations in the frequency of phlebotomy or the total blood volume obtained from the patient during treatment are an important consideration. The variability of cell yields, day-to-day assay variability, and problems with the functional activity of cryopreserved effector cells often restrict the use of cellular assays. These assays are more difficult and more costly to perform than serum-based assays. It is advisable to consider serum- or plasma-based (hereafter referred to as serum/plasma) assays first, especially when they can substitute for cellular assays. For example, the levels of cytokines released by activated cells, the enzymatic activity known to be induced by a particular biologic agent (e.g., interferon-induced 2′,5′-adenylate synthetase), and the presence of inhibitors or antagonists of biologic agents (e.g., IL-1ra) or products of activated cell subsets (e.g., soluble cytokine receptors, β_2-microglobulin, or neopterin) can be more readily monitored with serum or plasma than with cells.

The only *in vivo* assay available for measurements of cellular immunity in humans, the skin test for delayed-type hypersensitivity (DTH), is often underutilized or misinterpreted, largely because of difficulties in the recording and interpretation of test results. Yet when performed and read according to the guidelines, a DTH assay remains the best available measure of epitope-specific cell-mediated immunity in patients with immunodeficiencies, particularly when it is combined with a biopsy to confirm the nature of cells infiltrating the skin. Reagents for purified protein derivative, tetanus, *Candida*, and other antigens are commercially available. Other antigens, e.g., tumor-derived purified or synthetic peptides that are not yet commercially available or commercially available viral peptides, can also be used, provided that they have passed the safety requirements. A change in the DTH skin test from unreactive to reactive as a result of biotherapy is a significant result.

Monitoring of numbers or functions of mononuclear cells (MNCs) in peripheral blood during therapy often does not adequately reflect immunologic events that take place at the site of disease. Systemic effects of cytokines and certain other biologic agents are generally distinct from their local or locoregional effects, and monitoring of lesions, tissues, or organs involved in a disease is likely to yield more-informative data than will the same assays performed with cells or cell subsets obtained from the peripheral blood. The obvious difficulty with this strategy is that blood is more readily available than tissues. Only superficial lesions or sites accessible to repeated biopsies can be monitored. Nevertheless, during a clinical trial, it might be feasible to obtain serial biopsies for *in situ* studies, and this opportunity should not be overlooked. An alternative possibility is to obtain body fluids (e.g., pleural fluids and ascites), in addition to peripheral blood, to be able to detect longitudinal changes in organ-associated immune cells or their products relative to those in peripheral circulation. This approach is especially recommended when intracavitary therapy with a biologic agent is considered.

Monitoring of immune functions generally requires considerable cell numbers, fairly large volumes of blood or other body fluids, and facilities to process these samples for cell recovery. Vigorous attempts are being made to miniaturize immunologic assays and to perform them with whole blood. Newer, more sensitive technologies, including molecular assessments, flow cytometry, electrochemiluminescence, and more-sophisticated single-cell assays, that are generally performed on whole blood greatly facilitate monitoring, decreasing the required blood volume and dispensing with blood processing. The concept of bringing immunologic monitoring to the bedside, with only drops of blood needed for each assay, is slowly beginning to emerge. This approach must wait for further technical advances and for strong correlations to be established between immunologic biomarkers and clinical endpoints. Meanwhile, it appears that a profile of several immune measures determined in the course of therapy and analyzed using specially created software can provide useful prognostic information (25). These preliminary results are encouraging, and they indicate that immune profiling is likely to be more widely adopted for monitoring in the near future.

In general, a protocol schema specifies the time points for sample collection. These samples must be recovered from the peripheral blood, body fluids, or tissues and either used fresh or preserved for future monitoring. For studies of pharmacokinetics, a special effort has to be made to collect the specimens at the precisely designated time intervals and to process them in accordance with the experimental protocol to avoid degradation, inactivation, or loss of activity. In the planning of immunologic monitoring, not only the timing of specimen collections but also the nature of anticoagulants needs to be considered. For example, to measure

levels of cytokines in body fluids, plasma rather than serum is preferable, since cytokines tend to be trapped in the clot, with subsequently low levels of cytokines measured in the serum (26). While the separation of serum/plasma or MNCs from the peripheral blood is a routine laboratory procedure, the recovery and fractionation of cells from tissues or body fluids containing normal or malignant tissue cells are time-consuming and require special expertise and considerable effort (27). The use of individual separated subsets of tissue-infiltrating or blood MNCs is not recommended for serial monitoring, mainly because of a need for tissue sampling and large blood volumes. Also, the lack of uniformly acceptable procedures for cell separations and unpredictable yields of cells recovered from tissues hamper the use of cell separation techniques for monitoring. Nevertheless, the advantage of studies performed with highly purified subsets of immune cells obtained from the site of disease is obvious. When it is feasible to obtain a biopsy prior to and after therapy and to recover viable cells for monitoring of cellular functions, or even of cellular phenotypes, investigators are encouraged to incorporate such procedures in a protocol schema.

It is often unclear which immunologic assays can be reliably performed with fresh versus cryopreserved cells. From a practical viewpoint, it would be more convenient to use serially harvested frozen aliquots of serum/plasma or batched cryopreserved immune cells instead of freshly harvested specimens for immunologic monitoring. The ability to reliably cryopreserve immune effector cells for future use in retrospective studies or for batching of serially collected specimens to eliminate the interassay variability is highly desirable. In fact, the only reliable way to determine differences between pretherapy and posttherapy assays is to perform them at the same time. This strategy calls for banking of cryopreserved specimens (batching) and for assays that can be routinely performed with cryopreserved cells. However, certain immunologic assays, especially those that measure cell functions, e.g., cytotoxicity, are best performed with freshly harvested samples. Cryopreservation may introduce artifacts, even when a rate-controlled drop in temperature is implemented. Therefore, each laboratory is obliged to compare fresh and frozen cells to ascertain that a test can be reliably performed with either before attempting to use them for monitoring. Assays that can be reliably performed with frozen cells and batched specimens are the best candidates for monitoring, but in situations that require the use of fresh immune cells, it is essential to determine the interassay variability to be able to distinguish spurious from therapy-induced changes.

Immunologic cellular assays performed with whole blood as opposed to separated MNCs are especially useful for serial monitoring. Their advantages include the ability to measure the phenotype and functions of effector cells without separation from other blood cells and plasma. Separation procedures are likely to modulate and alter functions of effector cells. Since phenotypic markers on immune cells are generally assessed in whole blood by flow cytometry, it would seem to be preferable to also monitor functions of these cells in the same way. At the very least, the correlations between the phenotypic and functional immune parameters might improve under these assay conditions. The disadvantage is that whole-blood assays have to be performed with freshly harvested specimens, thus eliminating the possibility of batching serial samples.

Technical advances and new insights into immunologic mechanisms have led to the recent development of new types of immunoassays. As a result, a clinical investigator generally has a choice between phenotypic versus functional, specific versus nonspecific, and direct versus indirect assays. The range of assays currently available for monitoring predicates that careful consideration needs to be given to selection of the optimal assay. Assay validation is expensive and requires special expertise. Monitoring of patients enrolled in clinical trials should only be performed in laboratories with established quality assurance and quality control (QC) measures that meet the standards for good laboratory practice, as defined by the FDA. It is important for clinical investigators to realize that serial immunologic monitoring of clinical trials is more rigorous and demanding than performing a series of research assays. To monitor trials with credibility, the laboratory has to have methods in place to ensure reliable serial data (see "QC in Immunologic Monitoring" below).

In Table 1, assays that are currently in use for immunologic monitoring are divided into two broad categories: serum/plasma assays and cellular assays (phenotypic and functional). The rationale for utilizing serum/plasma assays for monitoring instead of more technically demanding and expensive cell-based measurements was discussed above. In the same vein, among cellular assays, flow cytometry is faster, more accessible, and frequently more reproducible than most other assays, particularly those involving radioactive labels. In addition to monitoring changes in levels of serum immunoglobulins or specific antibodies by routinely available rate nephelometry or enzyme-linked immunosorbent assays (ELISAs), a spectrum of other assays can be used to obtain a longitudinal serum profile reflecting changes in one or more cellular products. Generally referred to as proteomics, these assays are discussed below. In some cases, soluble products can serve as activation markers for a particular subset of immune cells, such as neopterin for monocytes or soluble IL-2Rα chain (CD25) for T helper cells. Body fluids can be readily frozen and banked to allow batch processing of the planned assays or for future studies.

PHENOTYPIC ASSAYS FOR IMMUNOLOGIC MONITORING

In many trials with biologic agents, a priority is given to cell surface-based phenotype assays, which are generally performed with fresh whole-blood specimens or cells separated from the peripheral blood, body fluids, or tissues. Flow cytometry-based assays are now widely and easily accessible and highly accurate. Vast arrays of labeled MAbs suitable for multicolor and multiparameter flow analyses are commercially available, allowing for measurements of the proportions of various immune cell subsets. Percent changes in these subsets as well as alterations in the activation level of the cells can be readily assessed during immunotherapy. In designing a clinical trial, flow cytometry markers should be judiciously selected.

Selection of Markers

There has been a tendency to indiscriminately include large panels of immunologic markers to monitor changes in the proportions of several MNC subsets induced by therapy. However, phenotypic assays, like all other immunologic assays used for monitoring, should be selected in order to test the hypothesis advanced as part of a clinical trial. Through the skillful selection of marker panels, it is possible to focus on a single population of effector cells or on several phenotypically distinct subsets, on cells expressing activation markers, or on cells that express a particular constellation of adhesion molecules. Various receptors for growth factors and cytokines on the cell surface can further be used

TABLE 1 Immunologic assays currently available for monitoring of phase I/II clinical trials with biologic agents

Assay type and parameter	Sample type
Soluble cellular products	
Immunoglobulin levels	Serum, plasma, body fluids
Cytokine and chemokine levels and pharmacokinetics (ELISA, multiplex format)	Serum, plasma, body fluids
Cytokine receptors and antagonists	Serum, plasma, body fluids
Other lymphocyte surface receptors (e.g., CD8, CD25, soluble Fas, HLA molecules)	Serum, plasma, body fluids
Ligands (Fas ligand, TRAIL[a]) and growth factors	Serum, plasma, body fluids
Enzymes (e.g., 2′,5′-adenylate synthetase and terminal deoxynucleotide transferase)	Serum, plasma, body fluids
Neopterin	Serum, plasma, body fluids
β_2-Microglobulin	Serum, plasma, body fluids
Phenotypic markers	
Proportions of cells	Whole blood, tissue biopsy, body fluids
Absolute cell numbers	Whole blood, tissue biopsy, body fluids
Cellular subpopulations (e.g., MHC-restricted vs. nonrestricted T cells; Th1, Th2, effector, memory, or naive T cells; Tregs), percentages of positive cells	Isolated lymphocytes
Single-cell flow cytometry (e.g., CFC, tetramers)	Isolated lymphocytes
Functional assays	
In vivo DTH skin test	Visual inspection or biopsy
Cytotoxicity (ADCC,[b] activated NK-cell, NK-cell, or T-cell specific)	MNCs or subpopulations of MNCs
Cytokine production (ELISA, ELISPOT), Luminex-based technologies	MNCs or subpopulations of MNCs
Proliferation (e.g., CFSE, [^{3}H]thymidine, Ki-67 metabolic changes)	MNCs or subpopulations of MNCs
Chemotaxis	MNCs or subpopulations of MNCs
Signal transduction (phosphorylated signaling molecules, NF-κB pathway; PI3K pathway, ζ-chain expression)	MNCs or subpopulations of MNCs
Superoxide generation	MNCs or subpopulations of MNCs
Apoptosis assays (annexin V binding, caspase activity, TUNEL, survival protein expression)	MNCs or subpopulations of MNCs

[a]TRAIL, TNF-related apoptosis-inducing ligand.
[b]ADCC, antibody-dependent cellular cytotoxicity.

to assign the cells to subsets and to relate their phenotypes to the functional potential of these cells. Thus, phenotypic analysis is a powerful tool for monitoring the effects of therapy on immune cells, and the selection of markers to be monitored on T, B, and NK cells and monocytes or granulocytes for shifts induced by therapy and based on the predicted mechanism of action of a tested biologic agent can be informative. A combination of activation markers, growth receptors, cytokine or chemokine binding sites, etc., on distinct and identifiable subsets of MNCs provides a powerful tool for their characterization. Whole-blood specimens can be shipped by overnight carriers for flow cytometry analysis without compromising their quality. If multiparameter analysis is considered desirable but not feasible within one's own institution, it may be advisable to make arrangements with a flow facility specializing in immunologic monitoring. This alternative is strongly recommended for the monitoring of multicenter or cooperative group trials.

Percentages versus Absolute Numbers of Immune Cells

Surface phenotypic characteristics of immune cells are often utilized for assessments of their absolute numbers in whole blood. The development of single-platform methods, which are performed entirely on a flow cytometer, has significantly improved the assay precision and accuracy. The most popular technique is based on five-color flow cytometry in the presence of counting beads. The identification of lymphocytes by the surface expression of bright CD45 and low side-scatter signals is followed by the quantification of T-cell subsets based on the expression of CD3, CD4, CD8, and CD56 and performed in parallel with counting of fluorescent beads. The number of labeled cells per microliter of blood is obtained as follows: number of counted cells × concentration of beads/number of beads counted. Absolute numbers of $CD3^+$, $CD4^+$, and $CD8^+$ T cells are frequently decreased in the circulation of patients with advanced malignancies (28). In contrast, the percentages of these cells may not be decreased, suggesting that absolute numbers rather than percentages of lymphocyte subsets should be measured in disease. The usually reported cell percentages are misleading because they do not consider a total white blood cell count, which is frequently altered in patients with advanced diseases, particularly after previously administered therapies.

Neutrophil-to-Lymphocyte Ratio

The neutrophil-to-lymphocyte ratio (NLR) has recently emerged as potentially useful predictive measure of outcome in oncology. When measured prior to therapy, elevated NLR, in addition to elevated total white cell blood count, predicted adverse clinical outcome in patients with

lung, breast, renal, ovarian, and head and neck cancers (29). Further, a high NLR is a significant but not yet validated marker of poor response to chemotherapy (29). These observations fit well with previously reported low lymphocyte counts in patients with cancer (28) and suggest that high pretreatment NLR may be a significant independent predictor of poor cancer-specific survival.

Intracellular Staining for Flow Cytometry

Flow cytometry has been widely used to measure intracytoplasmic markers. This method requires cell permeabilization to allow for access of MAbs used for detection of the cytosol components or molecules residing in cellular compartments. Because this method detects intracytoplasmic proteins, such as granzyme B, perforin, antigen-presenting machinery components, caspases and other enzymes, cytokines, signal transduction molecules, and transcription factors, measured in phenotypically defined cells, it can provide useful information about the activation state of individual cells or subsets of cells and about their functional attributes. In performing these assays, use can be made of quantitative flow cytometry, which allows for quantification of the expression level of each protein. By the use of a mixture of four types of beads with known fluorescence intensities and unlabeled blank beads, a standard curve is generated that expresses the fluorescence intensities of each bead set in terms of molecular equivalents of soluble fluorochrome (MESF) units for every assay. The mean fluorescence intensity of each unknown sample can be transformed into MESF units by use of this calibration curve. This minimizes day-to-day variability, thus providing a stable and standardized method for use in clinical laboratories. The method has been applied to assessment of the individual antigen-presenting machinery component expression in human dendritic cells as well as to quantitation of other intracellular molecules such as the T-cell receptor (TCR)-associated ζ chain in human T lymphocytes (30).

Epitope-Specific T Cells

The frequency of peptide-specific T cells present in mixed lymphocyte populations can be determined based on the use of biotin- or streptavidin-labeled complexes containing the peptide linked to HLA class I molecules (31). These complexes, referred to as tetramers, represent oligomeric complexes of HLA molecules with a peptide, which have an increased avidity for T cells expressing the relevant TCR. When tetramers bind to the TCR on T cells able to recognize the peptide, a strong, easily detectable fluorescent signal is generated that can be measured in a flow cytometer. The specificity of tetramers for peptide-specific T cells, which is considered their greatest asset, cannot be taken for granted, however, as nonspecific binding may occur under unfavorable experimental conditions. Nevertheless, tetramers are currently widely used to monitor changes in the frequency of peptide-specific T cells in lymphocyte populations before and after vaccinations (32). Tetramer analysis provides the frequency of epitope-specific T cells with sensitivity of 1/10,000 but gives no information about their function.

Another category of flow cytometry assays that has recently gained wide acceptance is cytokine flow cytometry (CFC) (33). This is another single-cell assay that allows for quantitation of individual cells positive for a cytokine detectable in permeabilized cells by the use of cytokine-specific MAbs. CFC is performed following a brief (4- to 6-h) coincubation of lymphoid cells with an antigen to induce cytokine expression in antigen-responsive cells. CFC has been used to measure the frequency of T cells able to respond to antigens expressed by infectious agents such as cytomegalovirus, Epstein-Barr virus, and HIV-1; tumor-associated antigens such as MUC-1; or melanoma differentiation antigens. CFC can provide the phenotype of epitope-specific responder cells and defines the frequency of cells poised to secrete but not yet secreting the cytokine accumulating in the Golgi apparatus. Its sensitivity is perhaps a little better than that of tetramers, and it lends itself well to serial monitoring. There is also the possibility for the use of a combination of tetramers with CFC for a cytokine of interest to better define the functional potential of peptide-specific T cells.

Subtyping of T Cells

In trials with biologic agents, especially vaccines, that might alter the process of lymphocyte maturation, differentiation or migration from, e.g., the naive to memory pool or the circulation to target tissues, the use of a panel of surface markers such as CCR7, CD45RO or CD45RA, CD27, and CD28 has been found to be informative. This strategy allows for determination of the percentages of naive, central memory, effector, or terminally differentiated T cells. For example, the frequency of $CD8^+CCR7^+$ T cells in the peripheral circulation of patients with cancer at the time of diagnosis not only discriminated cancer patients from healthy subjects but also predicted disease recurrence (34). After up to 4 years of follow-up, disease-free survival was found to be significantly shorter for patients with a circulating $CD8^+CCR7^+$ T-cell frequency of $<28\%$ at diagnosis compared to patients with higher percentages of these cells (34). This result suggests that the $CD8^+CCR7^+$ T-cell subset might play a role in cancer control, and that a simple blood test at diagnosis could have prognostic value for predicting cancer recurrence.

Measuring Cell Death

Still another type of a flow cytometry assay frequently used today provides means for enumerating cells that have initiated apoptosis, i.e., are able to bind annexin V, have an altered mitochondrial membrane potential, express high levels of caspase-3 activity or a high Bax/Bcl2 ratio, show evidence of DNA fragmentation ($TUNEL^+$ cells [terminal deoxynucleotidyl transferase-mediated dUTP-biotin nick end labeling-positive cells]), or have decreased or absent expression of the TCR-associated ζ chain (35). In patients with advanced cancer or with chronic, persistent infections, a considerable proportion of circulating T cells are destined to undergo apoptosis (22), and flow cytometry offers an opportunity to monitor changes in the numbers of these cells before, during, and after immunotherapy. These methods depend on the use of special substrates, chromogens, or MAbs for the detection of proapoptotic or antiapoptotic molecules in the target cell and generally include cell permeabilization as well as a combination of surface and intracellular staining. The availability of reagent kits that are commercially distributed makes measurements of apoptosis relatively simple, with the caveat that freshly harvested cells are required for analyses of annexin binding to cells, as cryopreservation may impair the integrity of cellular membranes.

Multiparameter Flow Cytometry

The ability, using multiparameter flow cytometry, to simultaneously measure numerous (e.g., up to 15 or more) markers on the surface and/or inside the immune cell has greatly expanded opportunities for serial monitoring of therapy-induced changes. It has provided means for following changes in cellular profiles as well as opportunities to measure rare event analysis, including tetramer-based or

cytokine-based detection of peptide-specific T cells. Further, by incorporating calibration beads with different fluorescence intensities, multiparameter flow cytometry has made it feasible to quantitate expression levels of various cellular components. The numerous advantages of flow cytometry have to be counterbalanced by the requirement for special expertise in its performance and in data interpretation. The reproducibility of flow cytometry-based assays is strictly governed by the operator's skills of setting the gates and excluding nonspecific events and is therefore open to considerable subjectivity. However, newer instruments are equipped with automatic compensation strategies facilitating operation. Aside from gating strategies, which can greatly influence results and thus impose a need for a careful and standardized selection of the most appropriate settings, the interpretation of flow cytometry data in serial monitoring requires stringent controls for interassay variability and a great deal of judgment. While daily calibration solves the problem of instrument variability, other challenges exist. For example, some of the lymphocyte subsets encompass only a small proportion of cells in the gate, and to be able to distinguish shifts induced by therapy from daily assay variability, it may be necessary to acquire a large number of cells for such rare event analyses. Changes in the phenotype of effector cells should be interpreted in conjunction with changes observed in functional assays. Specifically, it is important to consider whether changes in function induced during therapy correlate with changes in the number of effector cells or are due to the augmentation of effector function in a small subset of cells. It is also possible that therapy alters both the number and function of effector cells. During therapy, these changes can be dramatic or subtle, and they can simultaneously occur in several subsets of cells. Analyses of these changes and the establishment of correlations between their magnitude and frequency require special statistical approaches, as discussed below. Since alterations in the proportion or absolute number of effector cells and alterations in function may be mediated by entirely different mechanisms (e.g., increased blood vessel permeability and upregulation of NK-cell activity during therapy with IL-2, respectively), it should not be expected that phenotypic and functional data will necessarily correlate with clinical responses. More likely, no significant correlations will be detected, even though significant changes in the immune cell number and/or function may be registered during therapy. This should not be interpreted as evidence that the immune system has no impact on the disease but rather as evidence that despite therapy-mediated immunomodulation, the disease process persists, undoubtedly because of the involvement of factors unrelated to immune system activity.

Immune Score and Monitoring

Phenotypic studies of immune cells need not involve flow cytometry. With the broad availability of excellent Abs, the immunohistochemical evaluation of cells *in situ* is a powerful method for recording therapy-induced changes in the localization, composition, or activation state of infiltrating immune cells. The importance of *in situ* studies cannot be overemphasized. It is well recognized that the tumor microenvironment has a profound impact on immune cells, and the nature, phenotype, localization, and density of immune cells present in the tumor stroma or parenchyma has long been considered to be critical for tumor progression (36). Immune cells accumulating in human tumors have been extensively examined and found to have unique phenotypic and functional characteristics (36). Initially, it was typing of T lymphocytes in human tumors by immunohistochemistry and correlations of $CD8^+$ T-cell infiltrates with prognosis that suggested the role for immune cells as predictors of risk (36). The report on human tumor-infiltrating lymphocytes in colorectal cancer published by Galon and colleagues in 2006 reaffirmed the prognostic significance of tumor-infiltrating T cells (37). Using modern techniques of systems biology and an objective scoring system, these investigators showed that the type, density, and location of immune cells within tumors predicted positive clinical outcome (37). In a series of studies in colorectal cancer, Fridman's group has demonstrated by immunostaining of hundreds of tumor specimens that a strong local immune reaction, including $CD3^+$, $CD8^+$, and memory $CD45RO^+$ T cells, correlates with a favorable prognosis regardless of the local extent of the tumor or the regional lymph node involvement (38). T-cell infiltrates emerged as a stronger independent prognostic factor than the current clinicopathological criteria, which include tumor size, depth of infiltration, differentiation, and nodal status. A number of other laboratories reporting on the nature and cellular composition of immune infiltrates in human tumors have provided additional support to the concept of "immune score" and its role in cancer prognosis. These results have motivated investigators to propose that immune score be considered as a routine part of the standard pathologic examination (39). It is not clear how soon this practice will be embraced by pathologists, pending method standardization and a requirement for automated image analyses. Nevertheless, globally collected data strongly support the merit of the immune score, and it makes sense to evaluate its predictive value, especially in the context of ongoing biotherapy clinical trials. Thus, the immune score emerges as the first immunologic marker of risk in cancer with the potential to be incorporated into prognostically relevant immune classification of human cancer equal to or better than the conventional TNM classification.

Evidence has accumulated indicating that B cells or plasma cells are present in human tumors, especially in breast cancer (40). Recent results validate the B-cell signature as a robust prognostic factor in breast cancer (40). The immunoglobulin κ chain (IGKC) has emerged as a robust immunologic biomarker of prognosis and response to chemotherapy in patients with breast cancer, non-small-cell lung cancer, and colorectal carcinoma (40). The IGKC was microscopically identified as a product of plasma cells present in the tumor stroma and was validated as a prognostic biomarker by RNA- and protein-based expression studies independently performed in thousands of formalin-fixed, paraffin-embedded specimens at 20 centers. Further, the most important feature of IGKC as a biomarker is that it predicts responses to neoadjuvant therapy in breast cancer and thus qualifies as the first immune marker of response to cancer treatment.

FUNCTIONAL ASSAYS IN IMMUNOLOGIC MONITORING

Monitoring the functions of immune effector cells is considered to be necessary, since their phenotypic characteristics may not adequately convey their functional capabilities. Functional assays are usually performed with peripheral blood MNCs and only rarely with effector cells obtained from the site of disease. Thus, functions of "substitute" cells that are easily accessible for monitoring in the circulation are measured instead of those of the effector cells at the sites of disease. This is by far the greatest limitation of monitoring, since systemic effects of biologic agents on immune cells are likely to be different from local or locoregional effects. The surrogate results obtained with peripheral blood lymphocytes

should not be expected to closely reflect the biologic activity of the drug on functions of immune cells *in situ*. Additionally, investigators need to be aware that at any given time point, circulating lymphocytes represent <2% of a total lymphocyte pool, and that the turnover of circulating lymphocytes is responsible for constant changes occurring at the rate determined by the events in the periphery. To overcome these limitations, attempts are being made to study serial tissue biopsies, utilizing immunostaining and/or *in situ* hybridization or reverse transcription-PCR for cellular proteins and/or mRNA coding for the proteins involved in, e.g., cytotoxicity (perforin, granzymes, and TNF), proliferation (growth factors and cytokines), or signal transduction (the ζ chain and protein tyrosine kinases). The field of genomics has greatly facilitated these studies, providing a new set of tools for rapid screening of gene expression, as discussed below. In some cases, it may be possible to recover a limited number of cells from serial biopsies to perform functional studies. Obviously, these studies are very difficult to perform with human tissues, and they are not practical for the monitoring of many patients at multiple time points. Nevertheless, they are extremely valuable because they allow comparisons to be made between local and systemic effects of a biologic agent on immune effector cells and will eventually justify or discredit the common practice of monitoring alterations in cellular functions in the peripheral blood alone.

Antigen-Driven Proliferation

Proliferation of immune cells in response to a biologic agent, an antigen, or a mitogen has been in the monitoring repertoire for a long time. It can be used as a measure of immunocompetence following stimulation with an activating agent and can be performed with banked cryopreserved cells or as a whole-blood assay. In newer, modified versions, it can be nonradioactive. Proliferation assays can require very few cells if performed in Terasaki plates. As discussed above, it is also possible to use a flow cytometer to read the assay and to confirm the phenotype of proliferating cells. Proliferation assays can be used in conjunction with measurements of cytokines and cytotoxicity. These assays are informative, practical, and adjustable to fit the specific trial design or circumstances in a monitoring laboratory. A large variety of proliferation assays, from [^{3}H]thymidine incorporation into cellular DNA to assays based on metabolic changes in proliferating cells, are available, but flow cytometry-based measurements offer special advantages. By using differently labeled responder and stimulator cells, these methods can be adapted to the quantitation of functional responses in individual cells, cell subsets, or entire populations of cells. For example, the proliferative history of fluorescently labeled cells can be established by determining the number of mitoses experienced by these cells. The principle of the method is that the amount of fluorescent dye taken up by the cell is equally partitioned between daughter cells during mitosis and therefore decreased by half at each cell division. Dyes such as carboxyfluorescein diacetate succinimidyl ester (CFSE) diffuse into a cell and are cleaved by intracellular esterases into compounds that are fluorescent and react with amino groups of intracytoplasmic proteins (41). By combining surface marker staining with CFSE, it is possible to monitor a cell or cell subset through successive mitoses and to determine the number of cell divisions. The use of CFSE allows for quantitative resolution of up to eight cell division cycles (41), and by comparing the number of cells that divided with those that did not divide, a precursor frequency as well as the expansion potential of antigen-specific T cells can be calculated with Cell Quest software.

Cytotoxicity Assays

Cytotoxicity measurements have occupied a special place in the monitoring of immune therapies. There is a good rationale for monitoring cytotoxicity in clinical trials with biologics, which often tend to augment this effector function in many different cell types. In oncology protocols, antitumor cytotoxicity, whether mediated by class I major histocompatibility complex (MHC)-restricted antitumor-specific T cells, nonspecific NK cells, monocytes, or FcγR^+ effector cells mediating antibody-dependent cellular cytotoxicity, has been extensively monitored and correlated to outcome. However, tumor progression/regression and metastasis elimination involve multiple mechanisms and cellular interactions, only some of which are mediated by immune cells. Further, the phenomenon known as "epitope spreading" plays an important role in amplification and extension of antitumor responses once the tumor epitope-specific immune activity is induced by biologic therapeutics (32). The process of antitumor cytotoxicity involves not only perforin- or granzyme-mediated lysis, measured *in vitro* by the release of ^{51}Cr from radiolabeled, sensitive targets, but also necrotic or apoptotic cell death. Each of these types of cell death has somewhat different consequences for antitumor immune response, and methods exist that allow for a definition of the mode of cell death. These assays have not yet been used for routine monitoring, and their value as reliable *in vitro* correlates of antitumor immune activity *in vivo* remains to be determined. It is now clear that a classical cytotoxicity assay measuring only the secretory functions of effector cells is not able to adequately reflect the many mechanisms involved in the process of cytotoxicity *in vivo*. It is for this reason that the classical cytotoxicity assay has been largely replaced in monitoring by more-informative, simpler, and cheaper single-cell assays based on multiparameter flow cytometry or image analysis and the enumeration of spots reflecting antigen-specific cytokine production by individual cells (i.e., enzyme-linked immunosorbent spot assay [ELISPOT]). Nevertheless, in some situations, especially when appropriate cellular targets are available, ^{51}Cr-based cytotoxicity may be useful but as a confirmatory rather than monitoring assay. In most viral diseases, the presence of virus-specific cytotoxic T cells is necessary for recovery, and at least one goal of immunotherapy in patients with chronic viral infections is to induce the *in vivo* generation or activation of such virus-specific T cells. Measurements of such responses would be advisable in this case, but the availability of the virus-infected target cells is obligatory for the assay implementation. Also, in a cancer patient immunized with a tumor peptide vaccine in order to induce antigen-specific memory T-cell responses, it might be desirable to monitor for the appearance of tumor-specific cytolytic T lymphocytes (CTLs). Since, however, the number of such cells in the circulation may be very small even after reimmunization, the choice of a specific as well as sensitive assay is critical. The available data indicate that frequencies of single-epitope-specific T cells in non-antigen-primed circulating lymphocyte populations can be as low as 1 in 10^5 to 1 in 10^6. This means that the standard ^{51}Cr-release cytotoxicity assay, even when used after *in vitro* priming of T cells with the relevant peptide, may not be sufficiently sensitive to measure antigen-specific CTL precursors (CTLp). Its sensitivity is estimated to be 1 CTL in 1,000 cells. The frequencies reported in the literature for CTLp specific for some of the well-defined human MHC class I-restricted epitopes in the peripheral circulation of patients with cancer are too low to be detected in classical cytotoxicity assays. Furthermore, cytotoxicity assays measure the activity of the

population of cells and provide no information about the frequency of individual tumor-specific T cells without an additional step of limiting dilution analysis.

The ELISPOT assay for, e.g., T cells that produce gamma interferon or granzyme B when stimulated with a relevant peptide is the assay of choice for monitoring of clinical trials (32). Using synthetic peptides (either individually or as overlapping peptide mixtures) or whole antigens, even cells, total lymphocyte or isolated T-cell subset responses can be assessed either after short-term stimulation or after their expansion during a 10-day culture (cultured ELISPOT). These assays detect different epitope-specific T-cell responses, allowing for the analysis of effector memory T cells and central memory T cells (42). The ELISPOT assay can be used with cryopreserved MNCs and is sufficiently sensitive to detect 1 gamma interferon-secreting T cell among 100,000 plated cells (43). When used with autologous dendritic cells pulsed with cell lysates or individual peptides, for example, the assay can detect not only $CD8^+$ but also $CD4^+$ responses, which is important in view of evidence that $CD4^+$ helper cells play a crucial role in the induction and maintenance of immune responses. The assay can be set up in a variety of formats, allowing for substantial flexibility in the choice of antigen-presenting cells, ratios of responder to stimulator cells, and the use of *in vitro* sensitization for the expansion of antigen-specific T cells (44). ELISPOT assays performed with patients' peripheral blood MNCs without *in vitro* sensitization measure the frequency of epitope-specific precursor cells in the population of responder cells. Like all other assays for the detection of antigen- or peptide-specific T cells, ELISPOT is HLA restricted.

Even with ELISPOT as an assay of choice, monitoring of epitope-specific T-cell cytotoxicity in clinical trials is logistically and practically complex: it requires prior HLA typing of participants and a priori knowledge of the relevant epitope or the use of lysates of cells that express the relevant epitope. To simplify monitoring, non-MHC-restricted cytotoxicity is measured instead to assess lysis mediated by NK cells, activated T cells, NKT cells, monocytes, or granulocytes. The selection of targets (e.g., NK-sensitive K562 versus NK-resistant Daudi cells), length of the assay (4 h for lymphocytes and 18 h for monocytes), and use of targets coated with the target-specific antibody are some of the variables that can be considered.

Cytokine Production and Levels

In addition to proliferation and cytotoxicity, the ability of epitope-sensitized immune cells to produce cytokines or chemokines has been often used as a measure of immunologic activity induced by therapies. Cytokine gene or protein profiling, whether by multiplex immunoassays, microarrays, or proteomics technologies, is especially well suited to evaluations of the functional potential of immune cells in the tumor microenvironment.

The ability to document polarization in the cytokine repertoire or differences in patterns of their production by immune or tumor cells and of relating them to a specific clinical response has tremendous appeal. Also, as systemic and local therapies with cytokines are becoming increasingly common, there is a need for monitoring cytokine levels during therapy in relation to clinical endpoints. Such monitoring has greatly expanded our knowledge of cytokine and chemokine biology and has provided clinically useful information about cytokine involvement in human diseases. In cancer, considered to be a Th2-dominant disease with excess IL-4, IL-5, IL-10, and transforming growth factor beta (TGF-β) production, a therapeutically driven shift back toward the Th1 profile is of interest, as it might correlate with immune and perhaps clinical recovery (45). Indeed, plasma cytokines have been used as prognostic biomarkers in human diseases (46), with individual cytokines emerging as especially promising markers of survival. For example, elevated circulating levels of IL-6 have been associated with decreased survival in patients with cancer. The production of the proinflammatory cytokines IL-1β, IL-6, and TNF-α, all of which facilitate tumor growth, in the tumor microenvironment might be due to STAT3 hyperactivation in both the tumor and immune cells.

Both bioassays and immunoassays are available for assessments of cytokine levels, but only the latter are practical for the monitoring of clinical trials. Body fluids can be frozen and batched for immunoassays. Currently, multiplex-type assays using antibody-coated colored beads for the capture of multiple cytokines in a small (0.5-ml) sample and laser-type detectors to measure the fluorescence intensity of the individual beads have all but replaced traditional ELISAs. Like ELISAs, multiplex cytokine assays are antibody based but have the advantage of providing a profile of 20 to 30 cytokines in a body fluid at a reasonable cost. Assays for Th1- versus Th2-type cytokines, growth-promoting as opposed to inhibitory cytokines, inflammatory cytokines, hematopoietic cytokines, etc., can be selected to profile cytokines associated with a disease process and to assess changes in this profile during or after therapy. A number of problems with the assessment of cytokines in sera exist, including the ability of cytokines to bind to and form complexes with serum proteins and the presence of soluble cytokine receptors or antagonists, natural inhibitors, or anticytokine antibodies (26). Serial, time-course monitoring for cytokines is usually performed with banked serum specimens. Often, samples are banked for extended periods of time before being tested. It has been reported that the length of storage (months, years) in a −80°C freezer profoundly and significantly alters the measured cytokine levels (47). While IL-8 values generally increased after prolonged storage, those for other cytokines tended to decrease, for example. This serves as a reminder that retrospective measurements of cytokines are highly prone to errors resulting from handling of samples, including specimen storage, as also previously emphasized (26). To avoid pitfalls due to long-term storage and sample freezing-thawing, biomarker analyses should be performed with fresh, prospectively collected specimens. The utility of any one cytokine as a candidate biomarker of clinical outcome has to be carefully scrutinized for bias because it is strictly dependent on the sample integrity, rigorous testing, and results interpretation. To be able to accurately assess and interpret alterations of cytokine profiles in biologic fluids, knowledge of cytokine biology is necessary.

Signaling Pathways

In cancer, chronic infections, and certain immunodeficiency diseases, abnormalities in signal transduction have been identified that appear to be responsible for defective functions of immune cells in these diseases (see, e.g., reference 48). Since it might be possible to correct these abnormalities and thus repair immune functions with immunotherapy, monitoring for the presence and extent of signaling defects is indicated, at least before and after such therapy. The TCR-associated ζ chain is one of the key signaling molecules, and its absence or decreased expression in T cells reflects impaired functions (56). Since ζ is also a component of FcγRIII, its lower-than-normal expression in NK cells signifies the presence of signaling defects in these effector cells as well. Today, various components of major signaling

pathways operating in activated immune cells can be measured using Abs specific for phosphorylated proteins by flow cytometry. Commonly, expression of phosphorylated components of the phosphoinositol 3-kinase (PI3K) or mitogen-activated protein kinase pathways, for example, is measured to gauge immune cell activation. Expression of NF-κB or its components and other signaling molecules in MNCs can be measured by Western blotting, but flow cytometry analyses are quantitative and simpler to use for monitoring. Immunostaining *in situ*, which allows for assessment of the signaling molecules in T or NK cells accumulating at the site of disease, is a very useful indirect measure of the functional state of these cells. The expression of signaling molecules in tumor-infiltrating lymphocytes might serve as an important biomarker of survival for patients with cancer, and changes in the mobility of the NF-κB subunits have been related to impaired function of immune cells in some cancers. Thus, monitoring for the expression of signaling molecules in immune cells has biologic as well as clinical significance (35).

Suppressor Cell Functions

Accumulations of $CD4^+Foxp3^+CD25^{high}$ Tregs and myeloid-derived suppressor cells (MDSCs) in human tumors and their increased frequency in the circulation of cancer patients have been widely reported and linked to poor prognosis due to suppression of antitumor responses by the accumulating Tregs (49). However, in colorectal cancer, the presence and density of $Foxp3^+$ Tregs have been reported to predict favorable outcome and better locoregional control of the tumor (49). These conflicting results are based on the prevalent use of Foxp3 transcription factor expression as a marker of human Tregs. However, a comprehensive review of the prognostic significance of $Foxp3^+$ T cells in 16 nonlymphoid cancers suggested that Foxp3 by itself is not a reliable marker of human Tregs and that biologic effects of $Foxp3^+$ Tregs may be regulated by conditions existing at the tumor site. In view of a lack of a definitive phenotypic marker of Tregs, suppressor function remains their only reliable characteristic. Functional assessments of Tregs include (i) coincubation experiments in which responder cells are inhibited in proliferation, cytotoxicity, or cytokine production and (ii) flow cytometry-based detection of surrogate functional markers, such as TGF-β1-associated molecules or IL-10 (50).

MDSC accumulations in the tumor and blood of cancer patients have also been correlated to poor clinical outcome (51). The problems that confound their use as biomarkers of outcome are 2-fold. First, their tremendous phenotypic and functional heterogeneity creates a situation where everyone evaluates a different subset, making it impossible to compare results. Specifically, $HLA\text{-}DR^{neg}Lin^{neg}$ MDSCs present in the human peripheral blood contain cells with monocytic and granulocytic features, which can be subdivided into at least four distinct subsets ($CD33^+$, $CD11b^+$, $CD15^+$, and $CD14^+$) and which differ with respect to mechanisms used for suppression (52). A recently proposed immunophenotyping schema for MDSCs, which utilizes multiparameter flow cytometry, provides a unifying approach to future evaluations of the role these cells play in disease (53). This, however, does not eliminate the second problem of the sensitivity of $CD15^+$ and $CD33^+$ MDSC subsets to cryopreservation (54). Only the frequency of $CD14^+$ and $CD11b^+$ subsets was not significantly decreased after peripheral blood MNC cryopreservation, although their ability to produce reactive oxygen species after *ex vivo* stimulation was lost (54). These findings led to a conclusion that studies of human MDSCs should be performed in fresh blood samples (54). This requirement complicates monitoring of MDSCs in clinical trials and thus their evaluation as potential prognostic biomarkers.

GENOMICS AND PROTEOMICS IN IMMUNOLOGIC MONITORING

Advances in technology now allow for the simultaneous analysis of different genes in cells or tissues by the use of DNA chips or microarrays. Rapid and cost-effective screening for the expression of multiple genes coding for cytokines, activation markers, components of major signaling pathways, etc., offers a powerful new approach to monitoring of cell activation, differentiation, or proliferation in response to biotherapy. The technology involves mRNA extraction from cells or tissues and its subsequent labeling and hybridization to the microarray. The hybridized products are visualized in a phosphorimager and analyzed with software capable of comparing control with test samples to detect differences in the expression of selected genes. In this way, upregulation or downregulation of gene expression in tissues or cells exposed to a biologic agent can be monitored.

Similar to gene arrays, technologies combining two-dimensional PAGE with mass spectrometry allow for simultaneous analysis of many hundreds of proteins in body fluids or tissues. It is expected that pathological changes in tissues or cells are reflected in distinct protein patterns detectable in body fluids or cellular supernatants. Proteomic technologies are able to discriminate between normal and pathological protein patterns and can be used to map protein changes associated with a disease process. The potential of these technologies for capturing distinct protein patterns that could serve as biomarkers or be correlated with clinical responses or prognoses is being actively explored.

Gene and protein profiling, whether by multiplex immunoassays, microarrays, or proteomic detection methods, may be of special importance in relation to cytokine-based therapies. The clinical use of cytokines for therapy of human diseases has been increasing. Discoveries of new cytokines and their availability as recombinant proteins as well as cytokine gene therapies have facilitated the pharmacologic use of cytokines. Systemic or local therapies with these mediators, which induce one another and amplify cytokine circuits, call for careful monitoring of cytokine levels in relation to clinical endpoints. Given the dynamic and rapid progress in cytokine assay development, it appears likely that such monitoring will shortly provide a wealth of clinically useful information about cytokine involvement in human disease.

QC IN IMMUNOLOGIC MONITORING

QC of immunologic assays, particularly cellular assays, is difficult, and QC of serial immunologic measures represents a special challenge. To meet the challenge, a well-designed and rigorously maintained QC program is a requirement in a monitoring laboratory. Such a QC program contains several components, including the definition of standard operating procedures, training of personnel, instrument maintenance, reagent control, review of quality, and proficiency testing. Laboratories performing immunologic monitoring for clinical trials are required to implement their own QC programs to ensure that acceptable data are generated. Currently, no model QC programs exist, but monitoring laboratories are encouraged to follow the good-laboratory practice guidelines defined by various professional groups. A good example is the MIATA program (55). Other proficiency testing programs are becoming available for many

immunologic monitoring assays, and participation in these programs is highly recommended.

An important aspect of serial immunologic monitoring is the documentation of changes from baseline upon treatment. This is possible only when measurements taken over time are assessed accurately. Thus, each assay selected for monitoring has to be vigorously controlled for intra-assay and interassay variability. Also, the reproducibility of the same assay used for individual patients tested at different times has to be ensured (biologic variability).

The process of QC begins with sample collection and processing, which have to be organized to meet the protocol schema and occur at specified times of the day and, presumably, before the next cycle of therapy. Blood samples for immunologic monitoring need to be routinely harvested in the morning to avoid diurnal variability. The flow of specimens and the recording of the collection and arrival times of samples are critical activities in a monitoring laboratory. Although immunologic monitoring assays should be scheduled in advance, times of sample arrival tend to vary. The laboratory is obliged to establish strict guidelines for sample handling and to document problems in accordance with the quality assurance requirements. A precise history of each sample must be maintained. Processing must be uniform and follow standard operating procedures that are available in writing and regularly updated. Frequent checks of reagent quality and equipment performance have to be implemented. The decision to cryopreserve cells or use fresh cells is made prior to the clinical trial and has to be based on preliminary comparative studies using fresh and cryopreserved lots of the same normal MNCs, which need to be performed for every assay. This is a crucial decision for monitoring, because the selection of assays that can be batched (i.e., performed at the same time for all cells collected in the course of the trial) will avoid day-to-day variability and considerably decrease the cost of monitoring.

Regardless of whether cryopreserved or fresh samples are used, standardization of all assays has to be performed prior to the beginning of a clinical trial. The importance of the reproducibility of assays used for longitudinal monitoring cannot be overemphasized. The standardization data are obtained by repeatedly performing the assay with cells obtained from healthy individuals under invariant and previously optimized experimental conditions to establish the mean, median, 80% normal range, and coefficient of variation. The intra-assay variability is also determined. When the standardized assay is ready for monitoring, a set of appropriate controls is selected, and these depend on whether fresh or cryopreserved cells are used. With fresh cells collected at different time points, repeated testing of preserved control samples (e.g., cryopreserved lots of normal MNCs with a predetermined range of reactivity) is necessary to control for day-to-day variability. With fresh cells, it may also be advisable to include fresh control cells obtained from a healthy volunteer. A pool of volunteers repeatedly tested over time can be established for this purpose. A QC program in place will ensure that the values obtained for an individual control sample remain within an acceptable range over time and specify when the assay results are considered out of the normal range. With cryopreserved cells or frozen serum/plasma, it is best to batch and test all serial samples from a patient in one assay. Even in this case, however, it is necessary to control for day-to-day variability to have some assurance that the assay performs equally well for all patients in a protocol. The data obtained from control samples, evaluated in parallel with each patient sample, can help to ensure the validity of the results for a particular day's assay. Whenever universally accepted standards are available (e.g., the World Health Organization standards for cytokines), these should be regularly included in the monitoring of assays. Alternatively, internal controls initially compared with the standards can replace the standards, which are often available in finite quantities, for routine use.

STATISTICAL ANALYSIS OF DATA FROM IMMUNOLOGIC MONITORING

In preparation for final data analysis, the results of immunologic monitoring are "cleaned," i.e., purged of errors made during data entry. We have found it helpful to monitor for such errors at several levels. First, the technologist who performs the test enters the results into the computerized database, after examining the daily controls and finding the assay acceptable. The technologist is least likely to make errors in entering the results of an assay that he or she just performed. Second, prior to the final analysis, a statistician generates summary data sheets, which are screened by the laboratory monitor, often a laboratory supervisor, who is intimately familiar with the assays. All outlier values identified by the computer are checked and verified by the monitor against the laboratory records. Third, all variations from the protocol schema are noted for each patient. It is necessary to confirm that all measurements were made at the time points specified in the original treatment schema. Because of the importance of the timing of samples relative to the treatment, a change in the schedule or dose of therapy or in the sequence of sampling may have profound effects on the results of immunologic monitoring.

The biostatistician performing the analysis of immunologic data should interact closely with the clinical immunologist. The statistician should be consulted with respect to trial design and should be involved in its planning. The statistician's input is vital in determining the number of patients necessary to adequately define an OBD.

Immunologic data are often normalized for analysis with a logarithmic scale. The statistical analysis selected depends on the trial design and hypotheses tested, but since pre- and posttreatment changes are generally measured, the analysis seeks to determine if the changes from baseline are significant. Typically, pretreatment baseline levels are established by computing medians of three pretreatment determinations. Medians are preferable to means, as they are not influenced by extreme data points. Nonparametric tests for differences in posttreatment levels relative to the pretreatment baseline can include tests such as the Wilcoxon signed rank test or analysis of variance with Fisher's protected least-significant-difference method to determine pairwise differences between two specific time points. Comparisons between treatment groups can be accomplished by multiple regression analysis to permit simultaneous contrasts between groups, using a pooled estimate of the variance for all groups. Dose-response analysis utilizes parametric repeated-measure dose-response models that are fitted to posttreatment data, controlling for between-patient differences by including the pretreatment level as a covariate. Repeated-measure analyses are potentially sensitive to occasional extreme data points, and the use of robust fitting methods, which downweigh the influence of extreme data points, is important. The monitoring data are generally presented as a series of time plots, which are adjusted by subtraction of the estimated contribution of each patient's baseline level, so that the plots depict the relationship that would exist if all patients' baseline values were equal to the overall pretreatment average.

ROLE OF THE CLINICAL IMMUNOLOGIST IN IMMUNOLOGIC MONITORING OF CLINICAL TRIALS

The clinical immunologist should play a major role in the design, execution, and analysis of clinical trials that include immunologic monitoring. Many clinicians fail to consult or include the clinical immunologist in the trial design, expecting only to utilize the technical expertise of such an individual. Equally, many clinicians forget that the interpretation of immunologic data is never straightforward and requires special training and considerable experience. The clinical immunologist is likely to be well aware of the preclinical evidence regarding the biologic agent that is being evaluated and can help design a trial based on the agent's mechanism of action. The clinical immunologist can help not only by formulating a correct and rational hypothesis but also by giving advice regarding how best to test this hypothesis by utilizing the assays at hand. The clinician will be best served by working closely with the laboratory staff when monitoring is ongoing, and close daily interactions between the clinical and laboratory teams are necessary for collecting samples and obtaining meaningful data. It is desirable to have the clinical immunologist oversee the performance of assays and be responsible for the QC program in the monitoring laboratory. Equally important responsibilities of the clinical immunologist are the interpretation of results and data analysis, with the latter being performed in conjunction with the statistician. Ongoing discussion between the principal clinical investigator, the immunologist, and the statistician is necessary for the correct analysis and interpretation of immunologic monitoring data.

Immunologic monitoring of clinical trials has entered a new era. Technical developments and molecular insights into interactions of immune cells have expanded the field of opportunities for capturing and analyzing multiple therapy-induced changes in the phenotype and functions of immune cells. The greatest challenge, i.e., relating these changes to clinical endpoints, remains, however, and still requires close and effective teamwork between the clinician, the laboratory immunologist, and biostatistical personnel. Contributions from informatics experts are likely to become equally important. Cooperation and insights provided by each team member will facilitate meaningful monitoring, and the benefits of utilizing combined expertise in all aspects of clinical trials with biologic agents or any other trials monitoring immune responses can be considerable.

REFERENCES

1. **Butterfield LH, Palucka AK, Britten CM, Dhodapkar MV, Håkansson L, Janetzki S, Kawakami Y, Kleen TO, Lee PP, Maccalli C, Maecker HT, Maino VC, Maio M, Malyguine A, Masucci G, Pawelec G, Potter DM, Rivoltini L, Salazar LG, Schendel DJ, Slingluff CL Jr, Song W, Stroncek DF, Tahara H, Thurin M, Trinchieri G, van Der Burg SH, Whiteside TL, Wigginton JM, Marincola F, Khleif S, Fox BA, Disis ML.** 2011. Recommendations from the iSBTc-SITC/FDA/NCI Workshop on Immunotherapy Biomarkers. *Clin Cancer Res* **17:**3064–3076. PubMed
2. **Matzinger P.** 2002. The danger model: a renewed sense of self. *Science* **296:**301–305. PubMed
3. **Huang B, Zhao J, Unkeless JC, Feng ZH, Xiong H.** 2008. TLR signaling by tumor and immune cells: a double-edged sword. *Oncogene* **27:**218–224. PubMed
4. **Whiteside TL.** 2010. Inhibiting the inhibitors: evaluating agents targeting cancer immunosuppression. *Expert Opin Biol Ther* **10:**1019–1035. PubMed
5. **Postow MA, Harding J, Wolchok JD.** 2012. Targeting immune checkpoints: releasing the restraints on anti-tumor immunity for patients with melanoma. *Cancer J* **18:**153–159. PubMed
6. **Brahmer JR.** 2012. PD-1-targeted immunotherapy: recent clinical findings. *Clin Adv Hematol Oncol* **10:**674–675. PubMed
7. **Mellman I, Coukos G, Dranoff G.** 2011. Cancer immunotherapy comes of age. *Nature* **480:**480–489. PubMed
8. **Restifo NP, Dudley ME, Rosenberg SA.** 2012. Adoptive immunotherapy for cancer: harnessing the T cell response. *Nat Rev Immunol* **12:**269–281. PubMed
9. **Topalian SL, Sznol M, McDermott DF, Kluger HM, Carvajal RD, Sharfman WH, Brahmer JR, Lawrence DP, Atkins MB, Powderly JD, Leming PD, Lipson EJ, Puzanov I, Smith DC, Taube JM, Wigginton JM, Kollia GD, Gupta A, Pardoll DM, Sosman JA, Hodi FS.** 2014. Survival, durable tumor remission, and long-term safety in patients with advanced melanoma receiving nivolumab. *J Clin Oncol* **32:**1020–1030. PubMed
10. **Herberman RB.** 1985. Design of clinical trials with biological response modifiers. *Cancer Treat Rep* **69:**1161–1164. PubMed
11. **Kennedy-Nasser AA, Ku S, Castillo-Caro P, Hazrat Y, Wu MF, Liu H, Melenhorst J, Barrett AJ, Ito S, Foster A, Savoldo B, Yvon E, Carrum G, Ramos CA, Krance RA, Leung K, Heslop HE, Brenner MK, Bollard CM.** 2014. Ultra low-dose IL-2 for GVHD prophylaxis after allogeneic hematopoietic stem cell transplantation mediates expansion of regulatory T cells without diminishing antiviral and antileukemic activity. *Clin Cancer Res* **20:**2215–2225. PubMed
12. **Malek TR, Pugliese A.** 2011. Low-dose IL-2 as a therapeutic agent for tolerance induction. *Immunotherapy* **3:**1281–1284. PubMed
13. **Saadoun D, Rosenzwajg M, Joly F, Six A, Carrat F, Thibault V, Sene D, Cacoub P, Klatzmann D.** 2011. Regulatory T-cell responses to low-dose interleukin-2 in HCV-induced vasculitis. *N Engl J Med* **365:**2067–2077. PubMed
14. **Hank JA, Kohler PC, Weil-Hillman G, Rosenthal N, Moore KH, Storer B, Minkoff D, Bradshaw J, Bechhofer R, Sondel PM.** 1988. *In vivo* induction of the lymphokine-activated killer phenomenon: interleukin 2-dependent human non-major histocompatibility complex-restricted cytotoxicity generated *in vivo* during administration of human recombinant interleukin 2. *Cancer Res* **48:**1965–1971. PubMed
15. **Amado IF, Berges J, Luther RJ, Mailhé MP, Garcia S, Bandeira A, Weaver C, Liston A, Freitas AA.** 2013. IL-2 coordinates IL-2-producing and regulatory T cell interplay. *J Exp Med* **210:**2707–2720. PubMed
16. **Gambacorti-Passerini C, Hank JA, Albertini MR, Borchert AA, Moore KH, Schiller JH, Bechhofer R, Borden EC, Storer B, Sondel PM.** 1993. A pilot phase II trial of continuous-infusion interleukin-2 followed by lymphokine-activated killer cell therapy and bolus-infusion interleukin-2 in renal cancer. *J Immunother Emphasis Tumor Immunol* **13:**43–48. PubMed
17. **Hanna MG Jr, Hoover HC Jr, Vermorken JB, Harris JE, Pinedo HM.** 2001. Adjuvant active specific immunotherapy of stage II and stage III colon cancer with an autologous tumor cell vaccine: first randomized phase III trials show promise. *Vaccine* **19:**2576–2582. PubMed
18. **Rosenthal R, Viehl CT, Guller U, Weber WP, Adamina M, Spagnoli GC, Heberer M, Zuber M.** 2008. Active specific immunotherapy phase III trials for malignant melanoma: systematic analysis and critical appraisal. *J Am Coll Surg* **207:**95–105. PubMed
19. **Xu LW, Chow KK, Lim M, Li G.** 2014. Current vaccine trials in glioblastoma: a review. *J Immunol Res* **2014:**796856. doi:10.1155/2014/796856. PubMed

20. **Rosenberg SA, Lotze MT, Yang JC, Aebersold PM, Linehan WM, Seipp CA, White DE.** 1989. Experience with the use of high-dose interleukin-2 in the treatment of 652 cancer patients. *Ann Surg* **210:**474–484, discussion 484–485. PubMed
21. **Caligiuri MA, Murray C, Robertson MJ, Wang E, Cochran K, Cameron C, Schow P, Ross ME, Klumpp TR, Soiffer RJ, Smith KA, Ritz J.** 1993. Selective modulation of human natural killer cells in vivo after prolonged infusion of low dose recombinant interleukin 2. *J Clin Invest* **91:**123–132. PubMed
22. **Whiteside TL.** 2000. Monitoring of antigen-specific cytolytic T lymphocytes in cancer patients receiving immunotherapy. *Clin Diagn Lab Immunol* **7:**327–332. PubMed
23. **Allegretta M, Atkins MB, Dempsey RA, Bradley EC, Konrad MW, Childs A, Wolfe SN, Mier JW.** 1986. The development of anti-interleukin-2 antibodies in patients treated with recombinant human interleukin-2 (IL-2). *J Clin Immunol* **6:**481–490. PubMed
24. **Foon KA, John WJ, Chakraborty M, Das R, Teitelbaum A, Garrison J, Kashala O, Chatterjee SK, Bhattacharya-Chatterjee M.** 1999. Clinical and immune responses in resected colon cancer patients treated with anti-idiotype monoclonal antibody vaccine that mimics the carcinoembryonic antigen. *J Clin Oncol* **17:**2889–2895. PubMed
25. **Manjili MH, Najarian K, Wang XY.** 2012. Signatures of tumor-immune interactions as biomarkers for breast cancer prognosis. *Future Oncol* **8:**703–711. PubMed
26. **Whiteside TL.** 2002. Cytokine assays. *Biotechniques* **33**(Suppl)**:**4–8, 10, 12–15. PubMed
27. **Elder EM, Whiteside TL.** 1992. Processing of tumors for vaccine and/or tumor-infiltrating lymphocytes, p 817–819. *In* Friedman H, Rose NR, deMacario EC, Fahey JL, Friedman H, Penn GM (ed), *Manual of Clinical Laboratory Immunology,* 4th ed. American Society for Microbiology, Washington, DC.
28. **Kuss I, Hathaway B, Ferris RL, Gooding W, Whiteside TL.** 2004. Decreased absolute counts of T lymphocyte subsets and their relation to disease in squamous cell carcinoma of the head and neck. *Clin Cancer Res* **10:** 3755–3762. PubMed
29. **Perisanidis C, Kornek G, Pöschl PW, Holzinger D, Pirklbauer K, Schopper C, Ewers R.** 2013. High neutrophil-to-lymphocyte ratio is an independent marker of poor disease-specific survival in patients with oral cancer. *Med Oncol* **30:**334 doi:10.1007/s12032-012-0334-5. PubMed
30. **Whiteside TL, Stanson J, Shurin MR, Ferrone S.** 2004. Antigen-processing machinery in human dendritic cells: up-regulation by maturation and down-regulation by tumor cells. *J Immunol* **173:**1526–1534. PubMed
31. **Altman JD, Moss PA, Goulder PJ, Barouch DH, McHeyzer-Williams MG, Bell JI, McMichael AJ, Davis MM.** 1996. Phenotypic analysis of antigen-specific T lymphocytes. *Science* **274:**94–96. PubMed
32. **Schaefer C, Butterfield LH, Lee S, Kim GG, Visus C, Albers A, Kirkwood JM, Whiteside TL.** 2012. Function but not phenotype of melanoma peptide-specific $CD8^+$ T cells correlate with survival in a multiepitope peptide vaccine trial (ECOG 1696). *Int J Cancer* **131:**874–884. PubMed
33. **Freer G, Rindi L.** 2013. Intracellular cytokine detection by fluorescence-activated flow cytometry: basic principles and recent advances. *Methods* **61:**30–38. PubMed
34. **Czystowska M, Gooding W, Szczepanski MJ, Lopez-Abaitero A, Ferris RL, Johnson JT, Whiteside TL.** 2013. The immune signature of $CD8^+CCR7^+$ T cells in the peripheral circulation associates with disease recurrence in patients with HNSCC. *Clin Cancer Res* **19:**889–899. PubMed
35. **Boniface JD, Poschke I, Mao Y, Kiessling R.** 2012. Tumor-dependent down-regulation of the ζ-chain in T-cells is detectable in early breast cancer and correlates with immune cell function. *Int J Cancer* **131:**129–139. PubMed
36. **Whiteside TL.** 2010. Immune responses to malignancies. *J Allergy Clin Immunol* **125**(Suppl 2)**:**S272–S283. PubMed
37. **Galon J, Costes A, Sanchez-Cabo F, Kirilovsky A, Mlecnik B, Lagorce-Pagès C, Tosolini M, Camus M, Berger A, Wind P, Zinzindohoué F, Bruneval P, Cugnenc PH, Trajanoski Z, Fridman WH, Pagès F.** 2006. Type, density, and location of immune cells within human colorectal tumors predict clinical outcome. *Science* **313:**1960–1964. PubMed
38. **Fridman WH, Galon J, Pagès F, Tartour E, Sautès-Fridman C, Kroemer G.** 2011. Prognostic and predictive impact of intra- and peritumoral immune infiltrates. *Cancer Res* **71:**5601–5605. PubMed
39. **Galon J, Pagès F, Marincola FM, Angell HK, Thurin M, Lugli A, Zlobec I, Berger A, Bifulco C, Botti G, Tatangelo F, Britten CM, Kreiter S, Chouchane L, Delrio P, Arndt H, Asslaber M, Maio M, Masucci GV, Mihm M, Vidal-Vanaclocha F, Allison JP, Gnjatic S, Hakansson L, Huber C, Singh-Jasuja H, Ottensmeier C, Zwierzina H, Laghi L, Grizzi F, Ohashi PS, Shaw PA, Clarke BA, Wouters BG, Kawakami Y, Hazama S, Okuno K, Wang E, O'Donnell-Tormey J, Lagorce C, Pawelec G, Nishimura MI, Hawkins R, Lapointe R, Lundqvist A, Khleif SN, Ogino S, Gibbs P, Waring P, Sato N, Torigoe T, Itoh K, Patel PS, Shukla SN, Palmqvist R, Nagtegaal ID, Wang Y, D'Arrigo C, Kopetz S, Sinicrope FA, Trinchieri G, Gajewski TF, Ascierto PA, Fox BA.** 2012. Cancer classification using the Immunoscore: a worldwide task force. *J Transl Med* **10:**205. doi:10.1186/1479-5876-10-205. PubMed
40. **Whiteside TL, Ferrone S.** 2012. For breast cancer prognosis, immunoglobulin kappa chain surfaces to the top. *Clin Cancer Res* **18:**2417–2419. PubMed
41. **Givan AL, Fisher JL, Waugh M, Ernstoff MS, Wallace PK.** 1999. A flow cytometric method to estimate the precursor frequencies of cells proliferating in response to specific antigens. *J Immunol Methods* **230:**99–112. PubMed
42. **Calarota SA, Baldanti F.** 2013. Enumeration and characterization of human memory T cells by enzyme-linked immunospot assays. *Clin Dev Immunol* **2013:**637649. doi:10.1155/2013/637649. PubMed
43. **Asai T, Storkus WJ, Whiteside TL.** 2000. Evaluation of the modified ELISPOT assay for gamma interferon production in cancer patients receiving antitumor vaccines. *Clin Diagn Lab Immunol* **7:**145–154. PubMed
44. **Lehmann PV, Zhang W.** 2012. Unique strengths of ELISPOT for T cell diagnostics. *Methods Mol Biol* **792:**3–23. PubMed
45. **Lucey DR, Clerici M, Shearer GM.** 1996. Type 1 and type 2 cytokine dysregulation in human infectious, neoplastic, and inflammatory diseases. *Clin Microbiol Rev* **9:**532–562. PubMed
46. **Lippitz BE.** 2013. Cytokine patterns in patients with cancer: a systematic review. *Lancet Oncol* **14:**e218–e228. PubMed
47. **Butterfield LH, Potter DM, Kirkwood JM.** 2011. Multiplex serum biomarker assessments: technical and biostatistical issues. *J Transl Med* **9:**173. doi:10.1186/1479-5876-9-173. PubMed
48. **Elder ME, Lin D, Clever J, Chan AC, Hope TJ, Weiss A, Parslow TG.** 1994. Human severe combined immunodeficiency due to a defect in ZAP-70, a T cell tyrosine kinase. *Science* **264:**1596–1599. PubMed
49. **Whiteside TL.** 2012. What are regulatory T cells (Treg) regulating in cancer and why? *Semin Cancer Biol* **22:**327–334. PubMed
50. **Schuler PJ, Harasymczuk M, Schilling B, Saze Z, Strauss L, Lang S, Johnson JT, Whiteside TL.** 2013. Effects of adjuvant chemoradiotherapy on the frequency and function

of regulatory T cells in patients with head and neck cancer. *Clin Cancer Res* **19:**6585–6596. PubMed

51. **Marigo I, Dolcetti L, Serafini P, Zanovello P, Bronte V.** 2008. Tumor-induced tolerance and immune suppression by myeloid derived suppressor cells. *Immunol Rev* **222:**162–179. PubMed
52. **Greten TF, Manns MP, Korangy F.** 2011. Myeloid derived suppressor cells in human diseases. *Int Immunopharmacol* **11:**802–807. PubMed
53. **Dumitru CA, Moses K, Trellakis S, Lang S, Brandau S.** 2012. Neutrophils and granulocytic myeloid-derived suppressor cells: immunophenotyping, cell biology and clinical relevance in human oncology. *Cancer Immunol Immunother* **61:**1155–1167. PubMed
54. **Kotsakis A, Harasymczuk M, Schilling B, Georgoulias V, Argiris A, Whiteside TL.** 2012. Myeloid-derived suppressor cell measurements in fresh and cryopreserved blood samples. *J Immunol Methods* **381:**14–22. PubMed
55. **Hoos A, Janetzki S, Britten CM.** 2012. Advancing the field of cancer immunotherapy: MIATA consensus guidelines become available to improve data reporting and interpretation for T-cell immune monitoring. *Oncoimmunology* **1:**1457–1459. PubMed
56. **Boniface JD, Poschke I, Mao Y, Kiessling R.** 2012. Tumor-dependent down-regulation of the zeta-chain in T cells is detectable in early breast cancer and correlates with immune cell function. *Int J Cancer* **131:**129–139.

Circulating Tumor Cells as an Analytical Tool in the Management of Patients with Cancer

DANIEL C. DANILA, HOWARD I. SCHER, AND MARTIN FLEISHER

111

SHEDDING OF CTC AND THE METASTATIC PROCESS

Circulating tumor cells (CTC), first described in 1869 as cells in the blood identical to those of the cancer itself (1), originate from the primary tumor or metastatic deposits after intravasation through the tumor vasculature by mechanisms that are not completely understood (Fig. 1) (2). Although most CTC die in the circulation, a proportion of them have the ability to spread, seed, and proliferate in distant sites to form secondary metastases (3) (estimated to be 0.05%) or to reestablish in the organ of origin to form new tumors (4), as demonstrated in short-term proliferation experiments (3, 5). First described by Paget in 1889, in his "seed and soil" hypothesis (6), the process of metastatic dissemination is driven by chemokines and integrins specific to the tumor type and by the adhesive interactions of the CTC with the vasculature and extracellular matrix components (4, 7–9). As an example, β4 integrin signaling promotes tumor cell adhesion to the endothelium through ErbB2-mediated vascular endothelial growth factor secretion and has been involved in metastatic development (10). Additionally, CTC have the ability to secrete stem cell-like factors to promote proliferation and self-renewal (11, 12). Microembolic clusters of CTC, isolated by a variety of techniques, are associated with a particularly poor prognosis, which may be related to the enhanced activation of survival pathways by cellular contact and to mechanical capture in the microvasculature, further enabling metastasis formation (13, 14).

As a consequence of vascular spread and the microenvironment, tumor cells can be identified in the bone marrow as disseminated tumor cells (DTC). These DTC are in some cases detected more frequently than CTC found concurrently in the blood, and their detection is associated with an increased risk of tumor recurrence (15–20). DTC can also serve as a reservoir organ of CTC for further dissemination (3, 21, 22). At this time, testing for the presence of DTC is not routinely performed for patients with solid malignancies because of the uncertainty of the information provided by the assay; however, they are performed at diagnosis and serially for patients with leukemias and lymphomas (23).

After seeding a potential metastatic site (24), tumor cells have to adapt to a hypoxic, nutrient-deficient, and low-pH environment (25) in order to remain in a viable yet dormant state for extended periods (16, 26). During disease remission, a dormant heterogeneous tumor cell population may undergo a dedifferentiation process, known as the epithelial-mesenchymal transition (EMT), adapt characteristics of stem cells through reprogramming, or selectively enrich for tumor cells with stem cell-like features (27, 28). Eventually, dormant tumor cells are stimulated by intrinsic mechanisms or by the stroma microenvironment to facilitate active proliferation into visible metastases and to promote invasive features and spread hematogenously as CTC again (28).

MORPHOLOGY AND CHARACTERISTICS OF CTC

The range of CTC phenotypes is postulated to recapitulate the heterogenic range of cells found at metastatic sites, such that they can be a source of tumor for profiling to understand the mechanisms of disease progression and to guide treatment selection in an individual patient at the time that treatment decisions are made. Because CTC are shed into the peripheral circulation from both the primary tumor and multiple heterogeneous metastases, they can represent a spectrum of malignant phenotypes, including tumor-initiating cells with stem cell or stem cell-like properties, the full range of undifferentiated to differentiated phenotypes that lack tumor-initiating capabilities, and cells that have undergone an EMT (29, 30). Therefore, there is no single definition of a CTC; rather, there are specific definitions that relate to particular tumor cell types, which are profiled by physical characteristics, such as size or shape, or by molecular markers.

Importantly, the EMT from an epithelial to a fibroblast-like cell morphology is accompanied by decreased expression of epithelial adhesion molecules (e.g., E-cadherin) and increased expression of mesenchymal molecules (e.g., vimentin and N-cadherin), leading to increased mobility and invasiveness (29, 30) and increases in important cancer stem cell properties (31, 32). The EMT phenotypic change is important not only mechanistically but also from the point of view of CTC detection and characterization, because many capture technologies utilize antibodies to epithelial cell adhesion molecule (EpCAM), which, although commonly expressed on the majority of primary tumor cells, may be downregulated or absent on the subsets of CTC that have undergone EMT (33, 34). Similarly, cells with stem

doi:10.1128/9781555818722.ch111

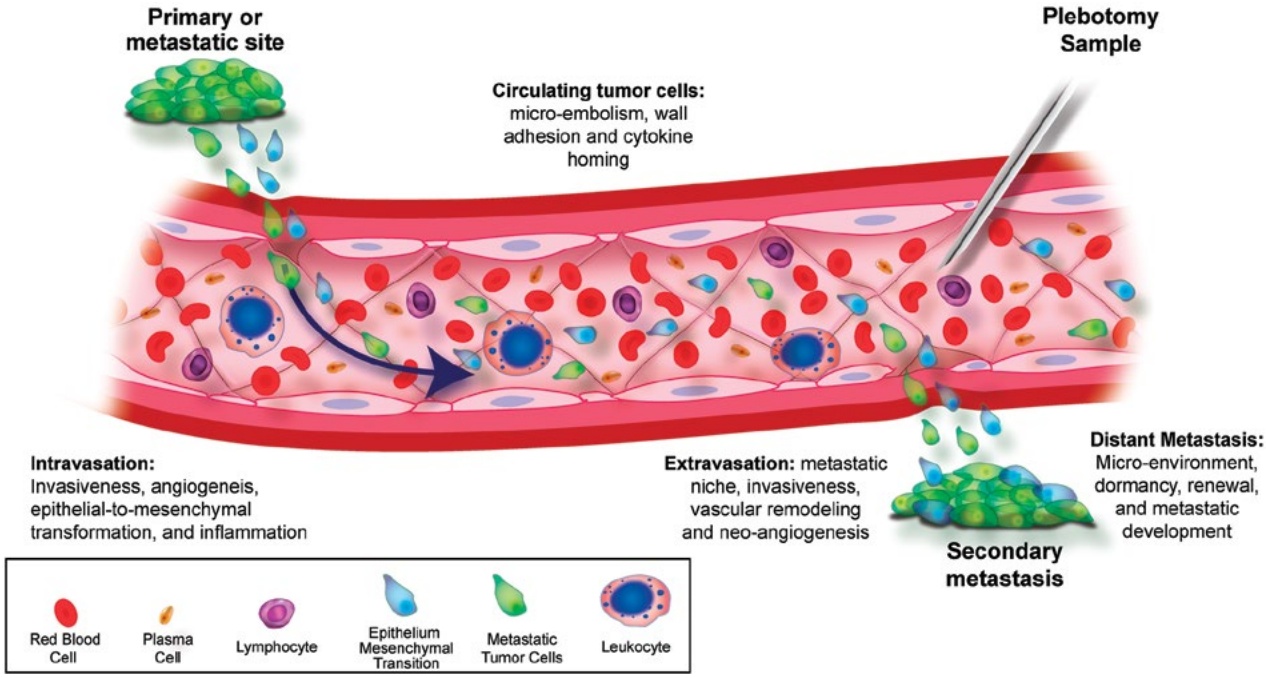

FIGURE 1 CTC in the process of metastatic progression. Tumor cells transition from the primary or metastatic site into the circulation to establish secondary sites. (Reprinted from reference 2 with permission of the publisher.)

cell or stem cell-like properties may also lack EpCAM or cytokeratin expression (35). In addition, DTC in the bone marrow must undergo a reversal of EMT (called MET) to form a solid metastasis. It is therefore possible that cancer cells with a high degree of plasticity to undergo both EMT and MET are the "real" metastasis initiator cells. Different degrees of EMT have been found to occur in solid tumors. Tumor cells with a partial EMT (an "intermediate phenotype" between epithelial and mesenchymal) have shown increased aggressiveness and the ability to survive in suspension as single cells (36).

DETECTION METHODS

CTC are rare in the peripheral blood of patients with a variety of metastatic carcinomas and are currently estimated to account for 1 cell in a billion nucleated cells. In contrast to invasive procedures, such as biopsies, a blood test for CTC or bone marrow aspiration and biopsy for DTC are safe and can be performed with minimal patient discomfort on a repeated basis at low cost (Fig. 2) (37).

Different assays are needed for different contexts of use and different decisions which the test results will be used to inform, whether related to prognosis, prediction, pharmacodynamics, or a measure of patient benefit. For example, these assays may enable a determination of the risk of relapse or the risk of metastasis development or may guide the decision on adjuvant therapy based on posttreatment CTC enumeration.

The definition of a CTC varies with the assay used to isolate, capture, visualize, and/or enumerate cells, and different assays detect different subsets of cells and different biologic determinants in the respective subsets. As such, an individual assay must be evaluated critically from the point of view of which subsets of cells are being captured and/or analyzed, the performance characteristics of the assay that is used for particular types of measurement, and how the results are reported (14, 34, 38, 39).

CellSearch Immunomagnetic Isolation

The CellSearch (Janssen Diagnostics LLC) immunomagnetic isolation technique uses antibodies to EpCAM conjugated to magnetic beads for the immunomagnetic capture of EpCAM-expressing epithelial cells. EpCAM-expressing cells are automatically displayed visually and manually scored as CTC by a trained technologist, based on strict morphologic and immunohistochemical staining characteristics. A captured cell is classified as a CTC if it expresses cytokeratin, displays a nucleus when stained with 4′,6-diamidino-2-phenylindole (DAPI), and is not a white blood cell as determined by a lack of expression of CD45 (40). The results are reported as the number of cells meeting the morphologic and immunohistochemical definition per 7.5 ml of blood, as analytically validated (40) and formally cleared by the FDA as an aid in the monitoring of patients with metastatic breast (41–44), colorectal (45, 46), or prostate (47–49) cancer. Importantly, the number of cells meeting the criteria for CTC is only a small proportion of the EpCAM-positive events displayed (50). Events not counted, for example, include EpCAM-positive cell fragments, cells undergoing apoptosis, necrotic cells, and anucleated cells.

For patients with metastatic prostate cancer, CTC isolated by this method have the biologic determinants unique to prostate cancer, including expression of prostate specific antigen (PSA) and alpha-methylacyl-coenzyme A racemase and prostate-specific genomic abnormalities, such as androgen receptor (AR) gene copy number amplifications, phosphatase and tensin homolog (*PTEN*) deletions, and TMPRSS:ETV fusion products (51, 52). It is underappreciated that the proportion of cells visible in the chamber and meeting the strict criteria defining CTC represents only 1

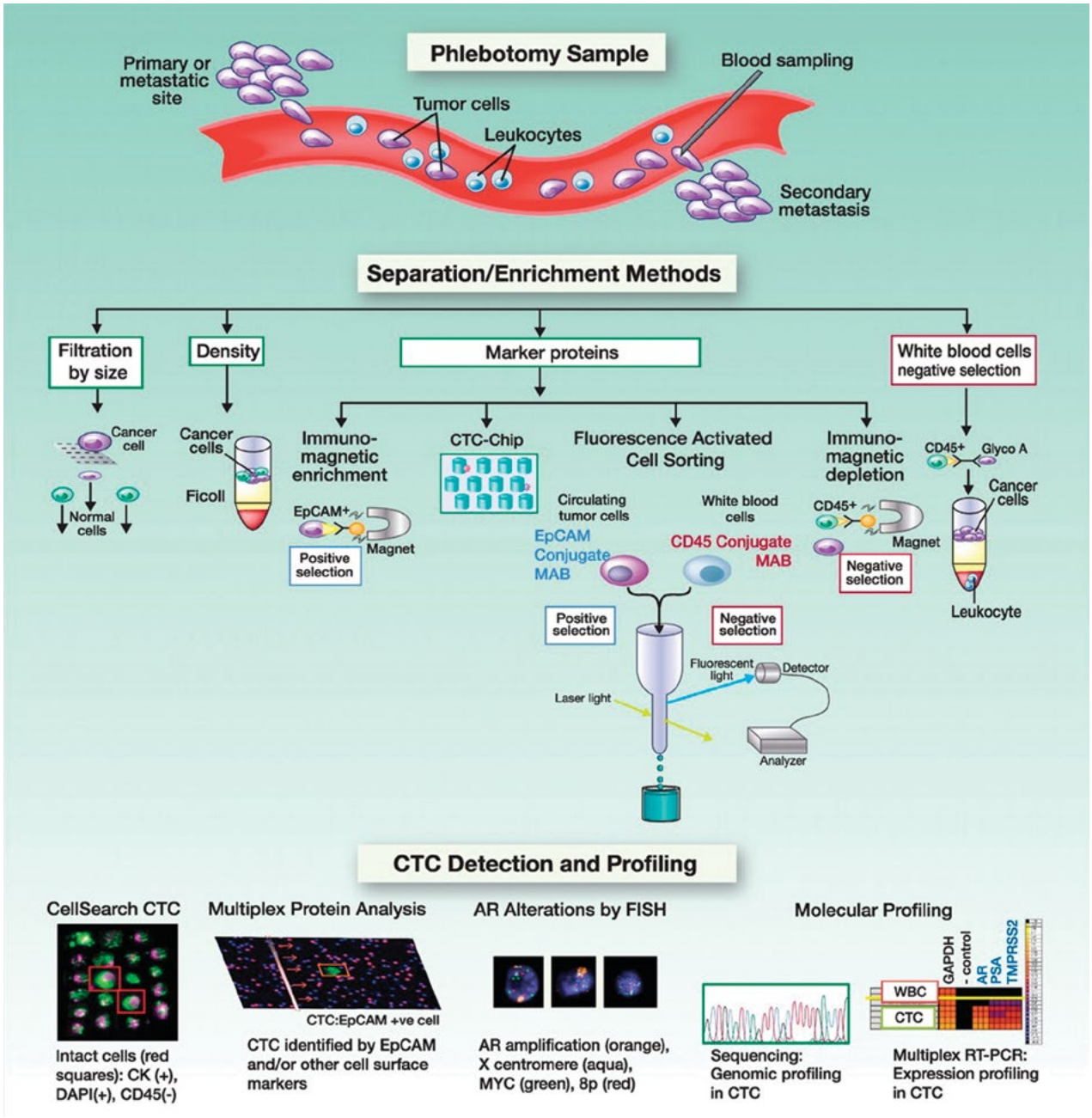

FIGURE 2 CTC in patients with cancer. Sampling of CTC by phlebotomy at the time that treatment is being considered has the potential to provide tumor material for molecular profiling of biomarkers informative of tumor sensitivity to the targeted therapy being considered. FISH, fluorescence *in situ* hybridization. (Reprinted from reference 37 with permission of the publisher.)

to 10% of the cells actually present. The sensitivity of the test can be increased if all $EpCAM^+$ CK^+ $CD45^-$ events are counted, a measurement that is prognostic for survival (50). This finding, however, has not been validated analytically or clinically and is not currently reported routinely.

Because the assay employs positive selection based on immunomagnetic enrichment for tumor cells expressing EpCAM, it is not useful for the isolation of cells from tumors that do not express EpCAM, such as malignant melanoma and renal cell carcinoma. For these tumors, a different "hook" is necessary to capture tumor cells from the circulation. Capture of these cells requires non-EpCAM-based methods, such as negative-depletion strategies that remove leukocytes followed by specific staining of the remaining mononuclear cell fraction with antibodies to markers specific to the tumor under study (11, 12). In an exploratory study of patients with melanoma, the isolation of cells based on the expression of a melanoma-associated chondroitin sulfate proteoglycan allowed the recognition of circulating melanoma cells based on morphology (53).

Flow Cytometry Methods

Flow cytometry methods are used to enrich for more homogeneous and highly purified tumor cell populations separated based on multiple cell surface and intracellular markers. The technique is useful for the evaluation of expression profiles of CTC (54–56), such as the isolation and capture of $EpCAM^+$ $CD45^-$ cells from a mononucleated layer separated from blood through a Ficoll-Hypaque gradient. DAPI is used as a vital stain to exclude permeable and apoptotic cells. Cells isolated by fluorescence-activated cell sorting were shown by multiplex reverse transcription-PCR (RT-PCR) to express tumor-specific mRNAs, indicating that these $EpCAM^+$ events were *bona fide* CTC (37). Another technique uses photoacoustic properties of tumor cells, such as melanoma cells, to enrich for CTC after stimulation by laser light, coupled with flow cytometry for further purification and isolation (57). By isolating CTC with a higher purity, these approaches have the potential to enable in-depth molecular profiling of CTC for a larger cohort of patients, enabling the study of gene signature patterns in the heterogeneous population of CTC. Whole-genome amplification from the cellular events isolated by sorting also enables mutational analyses and studies of copy number alterations at the level of single cells as prognostic and predictive biomarkers (58). Flow cytometry- or fluorescence *in situ* hybridization-based methods to identify sarcoma-specific fusion genes are currently being tested (59–61).

Microfluidic Capture Platforms

Microfluidic capture platforms allow sensitive and selective detection of CTC for enumeration and further molecular profiling at the genomic, transcriptional, and translational levels for CTC isolated from patients with lung, breast, or prostate cancer (5, 14, 62). Reports using this technology have shown CTC isolation and capture rates at points in an illness where the CellSearch assay does not detect cells, such as localized prostate cancer (39). A herringbone configuration designed to create turbulence maximizes gentle cell contact with the surface of the chip while minimizing cell trauma. These platforms allow the isolation and capture of viable cells harboring mutations that predict tumor sensitivity to targeted therapies as well as clinical outcomes, such as the epidermal growth factor receptor T790M activating mutation in non-small-cell lung cancer (63, 64) or the KRAS mutations in colorectal cancer (65). Additional designs stagger obstacles to optimize cell size-dependent flow to increase contact with capture antibody-laden surfaces, where prostate specific membrane antigen-based immunoselection allows enrichment of EpCAM-negative tumor cells (66). Novel generations of this technology allow the isolation of CTC based on inertial focusing-enhanced microfluidic chips or ferrofluidic separation in strategies that are either dependent on or independent of tumor membrane epitopes on CTC from patients with epithelial and nonepithelial cancers, such as lung, prostate, pancreas, and breast cancers and melanoma (67, 68).

Functional Assays

Functional assays allow detection of CTC based on tumor-specific metabolic capabilities. Epithelial immunospot (EPISPOT) assays detect CTC based on the release of full-length CK19 by carcinoma cells of various origins (12). For patients with breast cancer, detection of CK19-releasing cells in blood by EPISPOT assay predicted a lower overall survival rate, and the combination of the EPISPOT and CellSearch assays was the strongest predictor of OS in multivariate regression analysis (69). Tumor antigens mucin 1 and PSA were detected in the majority of patients with metastatic breast and prostate cancers, respectively, whereas the test results were negative for healthy controls or patients with benign prostatic hyperplasia (70). Collagen adhesion matrix assays allow enrichment of CTC based on their ability to ingest and invade connective tissue-like material. Although it is in the initial development phase, this method could allow for a functional separation of more aggressive, invasive types of CTC from patients with prostate or breast cancers (71). Dielectrophoretic array technologies displace blood cells when they pass over microelectrode array configurations designed to separate cells as a function of cell size and electrostatic charges. Cells isolated in this way can be characterized by microscopy or could be analyzed for predictive molecular biomarkers based on relative fluorescence parameters combined with morphology (72–74).

Filtration Assays

Filtration assays capture CTC based on their large size and inflexible biophysical properties relative to those of hematopoietic cells when passed through a porous membrane. Several different pore sizes and shapes have been tested. Advantages of these systems are the ability to perform CTC analysis, including immunocytochemistry, directly on the membrane, as well as the agnostic enrichment of CTC indifferent of EpCAM expression, which allows collection of EMT cells, CTC with stem cell-like features, and circulating cancer-associated macrophage-like cells (75–79). These approaches miss small cells, but in the process of CTC recovery, cancer-associated macrophage-like cell populations have been noted to associate with CTC and provide highly sensitive biomarkers for solid tumors. These tumor-associated giant cells are capable of binding to CTC and facilitate their transport and mobilization through the peripheral circulation of cancer patients (79, 80).

Genome-, Transcription-, and Translation-Based Assays

Genome-, transcription-, and translation-based assays have long been utilized to detect low levels of cancer-specific mRNAs in the mononuclear cell fraction of the blood that are presumed to be from CTC. mRNA for PSA has been tested in the peripheral blood of patients with prostatic cancer (81, 82), and mRNA has been used for detection of CEA, CK, and CD133 in patients with colorectal cancer (83). Additional markers are under investigation for detection of CTC from patients with breast, prostate, lung, melanoma, and head and neck cancers (84–91). An RT-PCR method targeting EWS-FLI-1 or EWS-ERG transcripts was studied for patients with Ewing tumors to detect evidence of occult tumor cells (92). Additional methods isolate CTC from blood by using immunomagnetic methods to preenrich cells for increased detection of tumor-specific mRNAs of breast, prostate, EMT, or stem cell-like cells (93). In some cases, the tumor-specific mRNA detected in the mononuclear cell fraction represents phagocytosed tumor cells in macrophages and does not represent intact tumor cells. To increase the detection sensitivity and tumor-specific molecular profiling of CTC from the blood sample, selection techniques (MagSweeper, AdnaTest, and IsoFlux) have been used to enrich for CTC or to deplete white blood cells before in-depth molecular profiling (68, 94–96).

Agnostic Methods

Agnostic methods to characterize CTC do not enrich for a specific epitope marker or use a physical size-specific capture method; instead, all nucleated blood cells are analyzed

by immunofluorescence and cytometry for tumor-specific markers by use of high-throughput multiparametric imaging systems (Fig. 3) (80). Such technologies have allowed the identification and characterization of tumor cells in relation to their primary tumors in patients with breast, colorectal, and lung cancers (80, 97).

CLINICAL UTILITY OF CTC

Targeted approaches are useful for cohorts of patients with tumors that express the target. A clear unmet need for patients with metastatic cancer is for reliable outcome measures of the clinical benefit at the time of reassessment and treatment selection. Optimal use of these agents for patients with progressive cancer requires new blood-based assays to profile recurrent metastatic disease in a "liquid biopsy" sample to guide treatment selection based on biologic profiles. A biomarker is a characteristic that is objectively measured and evaluated as an indicator of normal biological or pathogenic processes or pharmacologic responses to therapeutic intervention (98). This will ultimately accelerate clinical trials and improve clinical care.

Context of Use

Context of use represents the specific clinical settings in which the results of an assay will be used to inform a medical decision. As drugs are approved for indications, biomarkers are qualified for specific contexts of use as detailed in the FDA Critical Path (99, 100). No single assay can fulfill the requirements for clinical validation or qualification for all contexts of use. The trial designs needed to establish clinical validity and qualification will also differ as a function of which assay, if any, is currently available that addresses the context of use.

The specific contexts of use where qualified biomarkers would influence medical decisions include the following:

1. Detection—use of the biomarker to establish a diagnosis.
2. Prognosis—measuring the probability of a specific clinical outcome, such as recurrence, progression, or survival.
3. Prediction—identifying the chance of response to a specific therapy. Treatment resistance biomarkers define biologic determinants of failure or progression, such as second-site mutations.

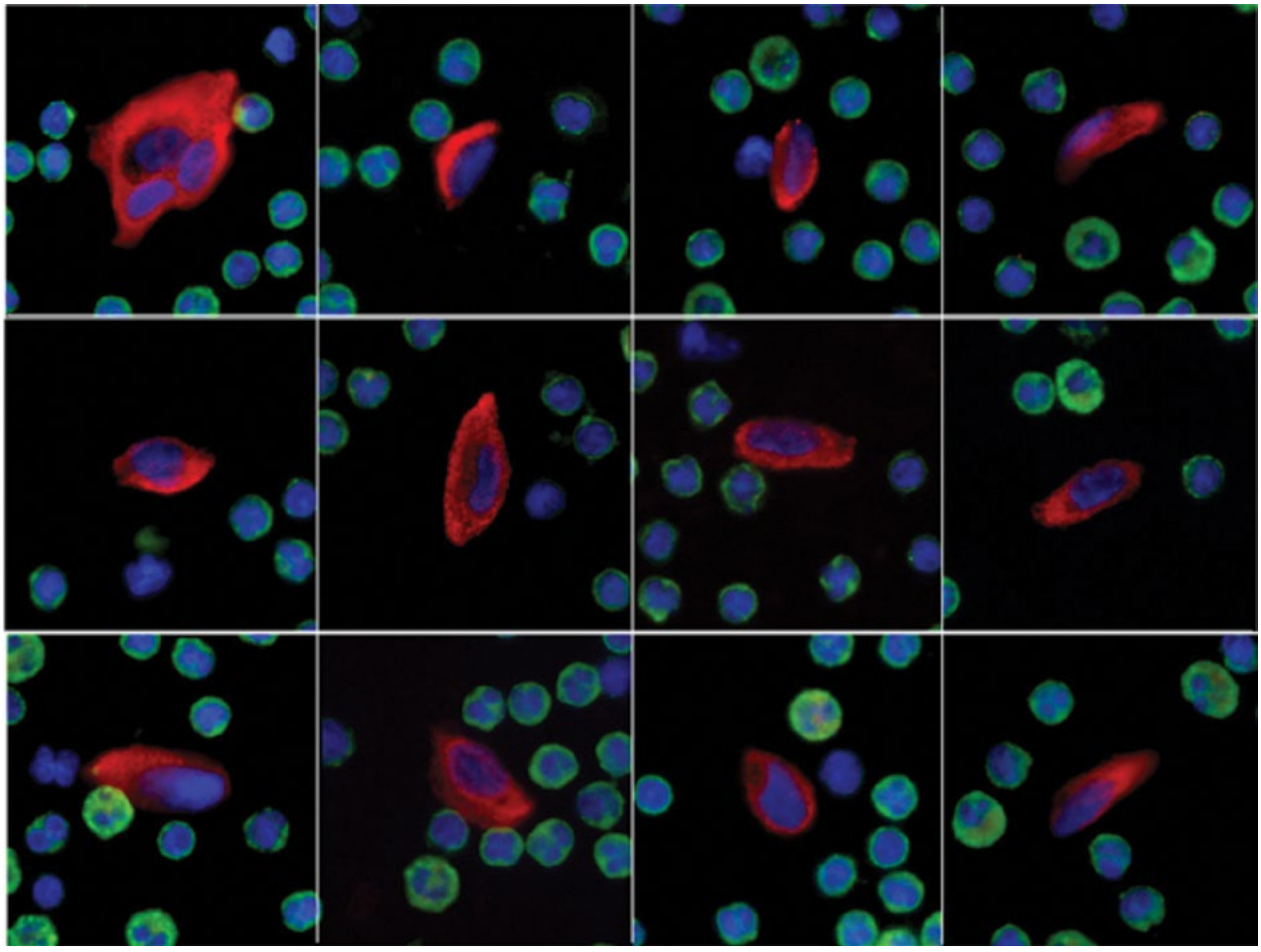

FIGURE 3 Immunofluorescence and cytometry assay by use of high-throughput multiparametric imaging systems for detection of tumor-specific markers in the peripheral blood mononucleated cell fraction for patients with metastatic cancer. Immunostaining for cytokeratin (red) and the nucleus (DAPI; blue) separates morphologically distinct tumor cells from surrounding white blood cells stained by CD45 (green). (Reprinted from reference 80 with permission of the publisher.)

4. Response—response indicator biomarkers demonstrate a pharmacologic or physiologic response to the treatment, which does not necessarily mean that the patient has benefitted from a treatment.
5. Efficacy—efficacy response biomarkers are surrogates for how a patient feels or functions or how long he or she survives and are used to extrapolate the clinical benefit.

Analytical Validation

Analytical validation establishes the performance characteristics of an assay and the range of conditions under which an assay gives reproducible and accurate data. In this process, rigorous performance testing is required to meet Clinical Laboratory Improvement Amendments (CLIA) regulatory requirements. Validation requires a rigorous performance that can be considered in three steps: (i) preanalytical assessment of specimen selection, handling, processing, and storage parameters; (ii) validation of analytical characteristics to meet CLIA regulatory requirements, establishment of the inter- and intra-assay precision, linearity, and analyte recovery, and standardization and development of a comprehensive quality control program; and (iii) assessment of postanalytical parameters requiring data management.

Clinical Qualification

Clinical qualification, distinct from the analytical validation, is the evidentiary process of linking a biomarker with biological processes or clinical endpoints in the context of an intended use to inform a medical decision as described in the FDA Critical Path (99, 100). Because there are more biomarkers than questions, and given the effort and cost to conduct these investigations, it is essential to develop metrics to determine which biomarkers that appear promising warrant prospective testing in large-scale phase III trials to establish qualification.

CTC Enumeration by CellSearch Assay as a Prognosis and Response Indicator Biomarker

CTC enumeration by CellSearch assay as a prognosis and response indicator biomarker was tested in a series of clinical trials of similar design in patients with metastatic breast (41–44), prostate (48, 49), and colorectal (45, 46) cancers about to start a new line of therapy. CTC measured at baseline and at subsequent follow-up visits were used to define patient groups with favorable and unfavorable prognoses based on disease-specific cutoffs (for the favorable group, 4 or fewer CTC per 7.5 ml of blood for breast and prostate cancers and 2 or fewer CTC per 7.5 ml of blood for colorectal cancer). In this context, CTC enumeration was prognostic of median progression-free survival and overall survival (Table 1) (42, 101). Posttreatment CTC enumeration remains prognostic 4, 8, or 12 weeks after initiating treatments in this context (45, 46, 48, 49, 102). These studies resulted in FDA clearance of the CellSearch system to measure CTC as a marker of prognosis in the monitoring of patients with metastatic breast, prostate, and colorectal cancers and as a response indicator biomarker by serial testing for CTC in conjunction with other clinical methods, as described in the 510(K) document (103).

In a head-to-head comparison for patients with metastatic castration-resistant prostate cancer starting a new line of chemotherapy, the posttreatment CTC number was a stronger prognostic factor for survival than a 50% decline in PSA (area under the concentration-time curve for the receiver operating characteristic curve, 0.87 versus 0.62) (48, 49). The discriminatory power of baseline CTC counts for survival was analyzed in a multivariate proportional hazards model with the concordance probability estimate (104). Baseline CTC counts (analyzed with the dichotomous definition of unfavorable versus favorable) had the strongest association with survival time (hazard ratio [HR], 1.58; 95% confidence interval [CI], 1.41 to 1.77) compared to PSA (HR, 1.26; 95% CI, 1.10 to 1.45). Additional baseline factors associated with decreased overall survival included high lactate dehydrogenase levels (HR, 6.44; 95% CI, 4.24 to 9.79) and low hemoglobin levels (HR, 0.72; 95% CI, 0.64 to 0.81).

In a separate analysis, CTC counts were related to survival time as a continuous function by using nonparametric smoothing analysis without a threshold effect (47). This argued against the use of discrete CTC cutoff values in decision-making, a finding confirmed in multiple studies (49).

As a response indicator of treatment outcome, CTC conversion is more associated with survival than is a decline in PSA, as measured at 4, 8, and 12 weeks (48, 49). The most prognostic factors for survival were baseline lactate dehydrogenase levels and the fold change in CTC count from baseline to the follow-up time of measurement (concordance probability estimate, 0.72 to 0.75) (49). A biomarker panel containing CTC number and lactate dehydrogenase levels was demonstrated to be a surrogate for survival at the individual-patient level in a randomized trial with a novel antiandrogen, abiraterone acetate, for patients with metastatic prostate cancer (105). These findings suggest that monitoring the CTC number as early as 4 weeks posttreatment may add clinical data to assist in treatment decisions.

Molecular Characteristics of CTC

Molecular characteristics of CTC observed by PCR-based assays have been tested as prognosis and response indicator biomarkers. The frequency of detection of PSA mRNA in peripheral blood of patients with prostatic cancer correlated with the tumor stage (81, 82). Detection of additional

TABLE 1 Context of use for baseline CTC count as a prognostic biomarker for overall survival for patients with metastatic disease from the Immunicon 38 trials[a]

Type of cancer	Threshold for unfavorable CTC count	No. (%) of patients with unfavorable baseline count	Overall survival based on CTC counts (mo) (mean [95% CI])		Cox HR; log rank *P* value	Reference(s)
			Favorable group	Unfavorable group		
Prostate cancer	<5	219 (43)	21.7 (21.3–>26)	11.5 (9.3–13.7)	3.3; <0.0001	48, 49
Breast cancer	<5	177 (49)	21.9 (20.1–>25)	10.9 (6.4–15.1)	2.45 (1.64–3.65); <0.0001	44
Colorectal cancer	<3	413 (26)	18.5 (15.5–21.2)	9.4 (7.5–11.6)	2.45 (1.77–3.39); <0.0001	45, 46

[a]Reprinted from reference 2 with permission of the publisher.

prostate cancer enriched genes in whole blood collected in PAXgene tubes by a sensitive and analytically validated PCR assay was demonstrated to have predictive value for overall survival in patients with metastatic castration-resistant prostate cancer and was complementary to CellSearch CTC enumeration (91). Detecting CEA, CK19, CK20, and/or CD133 mRNA by RT-PCR was a significant prognostic factor for overall survival (HR, 3.84; 95% CI, 2.41 to 6.22; $P < 0.001$) and disease-free survival (HR, 3.02; 95% CI, 1.83 to 5.00; $P < 0.001$), in particular for patients with Dukes' stage B and C colorectal cancer (83). Serial monitoring by RT-PCR of a multimarker panel for circulating melanoma cells during biochemotherapy may be useful for predicting therapeutic efficacy and disease outcome for patients with metastatic melanoma, although additional studies are necessary (106).

CTC as Biomarkers Predictive of Tumor Sensitivity

As biomarkers predictive of tumor sensitivity, CTC have the potential to provide a snapshot of the molecular makeup of an individual patient's tumor to profile the determinants that predict sensitivity or resistance to treatment at the time of treatment decision. Such a "liquid biopsy" will definitely improve the understanding of tumor growth biology, which can change during the course of disease. Predicting the likelihood that a patient will benefit from a targeted therapy requires a demonstration that the "target" is present in the tumor when treatment is considered. Currently, molecular profiling of heterogeneous tumors is limited by a lack of representative tumor samples in routine clinical practice settings (107).

For prostate cancer, recent reports evaluated alterations in AR at the protein, RNA, and DNA levels (52, 107, 108), IGF-1R expression (109), and TMPRSS2-ETV fusions (52, 94), which have been postulated to increase the likelihood of response to a therapy targeting the specific signaling pathway. AR amplification, although infrequent in primary/diagnostic tumor specimens, is detected in upwards of 50% of castration-resistant lesions (110, 111). AR genomic amplification and copy number gain have been documented for CTC from patients with castration-resistant prostate cancer, with frequencies similar to those reported for late-stage tumors (52, 108).

Detection of a kinase mutation predictive of tumor sensitivity in CTC has potential for clinical application in selecting patients with metastatic colorectal or lung cancer who are most likely to benefit from epidermal growth factor receptor-targeted therapies (64, 112, 113). Combining a microfluidic enrichment system and a mutation assay for KRAS has been proposed to improve the sensitivity of longitudinal tracking of such oncogenic mutational changes, with high success rates (65). The prognostic value of HER2/neu, IGF-1R, and AR splice variants expression in CTC is currently being studied in the context of clinical trials with novel therapies targeting these markers, as a potential tumor sensitivity predictive biomarker, and as a pharmacodynamic measurement for defining the optimal dose, not just the maximum tolerated dose (51, 108, 109, 114).

There are many more potential contexts, and the analytical validation of these assays is ongoing. Although promising, these results still require a rigorous validation across independent cohorts of patients in the appropriate context of proposed use. Since it is not clear which biomarker will be most informative for a medical decision to address a specific context of use, there must be a process for prioritizing biomarker development, first in short efficacy trials in the selected context of use, before beginning full development of a biomarker in large, costly phase III trials.

THE FUTURE OF CTC IN THE CLINIC

Recent work with several tumor types has shown that patients in whom CTC are detected, by use of a variety of different assays, have an inferior prognosis relative to that for patients in whom CTC are not detected and that the "elimination or decrease" of CTC following treatment is associated with improved clinical outcomes (115). The observation in a prostate cancer population that CTC could be detected in patients on hormonal therapy with no measurable PSA suggests that seeding may continue despite seemingly successful therapy and that the continued detection of CTC could provide unique information. Equally intriguing is the potential for the biologic characterization of CTC to provide a profile of an individual patient's tumor that can be used to guide treatment selection, i.e., a liquid biopsy to enable personalized medicine in cases where the potential for point-of-care tests is clear.

The approval of new therapies for patients with cancer based on overall survival requires large cohorts with a lengthy follow-up. Qualified biomarkers for discrete contexts of use have the potential to shorten the drug development process. More significant power to discriminate between low and high risks of a specific outcome could be obtained by combining multiple biomarkers, such as CTC, with additional blood-based as well as radiologic or tissue-based biomarkers, which will ultimately result in a "basket" biomarker meant to influence medical decision-making.

REFERENCES

1. **Ashworth T.** 1869. A case of cancer in which cells similar to those in the tumours were seen in the blood after death. *Aust Med J* **14:**146–149.
2. **Danila DC, Pantel K, Fleisher M, Scher HI.** 2011. Circulating tumors cells as biomarkers: progress toward biomarker qualification. *Cancer J* **17:**438–450. PubMed
3. **Muller V, Stahmann N, Riethdorf S, Rau T, Zabel T, Goetz A, Janicke F, Pantel K.** 2005. Circulating tumor cells in breast cancer: correlation to bone marrow micrometastases, heterogeneous response to systemic therapy and low proliferative activity. *Clin Cancer Res* **11:**3678–3685.
4. **Kim MY, Oskarsson T, Acharyya S, Nguyen DX, Zhang XH, Norton L, Massagué J.** 2009. Tumor self-seeding by circulating cancer cells. *Cell* **139:**1315–1326. PubMed
5. **Stott SL, Hsu CH, Tsukrov DI, Yu M, Miyamoto DT, Waltman BA, Rothenberg SM, Shah AM, Smas ME, Korir GK, Floyd FP Jr, Gilman AJ, Lord JB, Winokur D, Springer S, Irimia D, Nagrath S, Sequist LV, Lee RJ, Isselbacher KJ, Maheswaran S, Haber DA, Toner M.** 2010. Isolation of circulating tumor cells using a microvortex-generating herringbone-chip. *Proc Natl Acad Sci U S A* **107:**18392–18397. PubMed
6. **Paget S.** 1889. The distribution of secondary growths in cancer of the breast. *Lancet* **i:**571–573.
7. **Fidler IJ.** 2003. The pathogenesis of cancer metastasis: the 'seed and soil' hypothesis revisited. *Nat Rev Cancer* **3:**453–458. PubMed
8. **Gupta GP, Massagué J.** 2006. Cancer metastasis: building a framework. *Cell* **127:**679–695. PubMed
9. **Ruoslahti E, Giancotti FG.** 1989. Integrins and tumor cell dissemination. *Cancer Cells* **1:**119–126. PubMed
10. **Fan J, Cai B, Zeng M, Hao Y, Giancotti FG, Fu BM.** 2011. Integrin β4 signaling promotes mammary tumor cell adhesion to brain microvascular endothelium by inducing ErbB2-mediated secretion of VEGF. *Ann Biomed Eng* **39:**2223–2241. PubMed
11. **Alix-Panabières C, Vendrell JP, Pellé O, Rebillard X, Riethdorf S, Müller V, Fabbro M, Pantel K.** 2007. Detection and characterization of putative metastatic precursor cells in cancer patients. *Clin Chem* **53:**537–539. PubMed

12. **Alix-Panabières C, Vendrell JP, Slijper M, Pellé O, Barbotte E, Mercier G, Jacot W, Fabbro M, Pantel K.** 2009. Full-length cytokeratin-19 is released by human tumor cells: a potential role in metastatic progression of breast cancer. *Breast Cancer Res* **11:**R39. PubMed
13. **Krebs MG, Sloane R, Priest L, Lancashire L, Hou JM, Greystoke A, Ward TH, Ferraldeschi R, Hughes A, Clack G, Ranson M, Dive C, Blackhall FH.** 2011. Evaluation and prognostic significance of circulating tumor cells in patients with non-small-cell lung cancer. *J Clin Oncol* **29:**1556–1563. PubMed
14. **Nagrath S, Sequist LV, Maheswaran S, Bell DW, Irimia D, Ulkus L, Smith MR, Kwak EL, Digumarthy S, Muzikansky A, Ryan P, Balis UJ, Tompkins RG, Haber DA, Toner M.** 2007. Isolation of rare circulating tumour cells in cancer patients by microchip technology. *Nature* **450:**1235–1239. PubMed
15. **Riethdorf S, Wikman H, Pantel K.** 2008. Review: biological relevance of disseminated tumor cells in cancer patients. *Int J Cancer* **123:**1991–2006.
16. **Pantel K, Alix-Panabières C, Riethdorf S.** 2009. Cancer micrometastases. *Nat Rev Clin Oncol* **6:**339–351. PubMed
17. **Schindlbeck C, Andergassen U, Hofmann S, Jückstock J, Jeschke U, Sommer H, Friese K, Janni W, Rack B.** 2013. Comparison of circulating tumor cells (CTC) in peripheral blood and disseminated tumor cells in the bone marrow (DTC-BM) of breast cancer patients. *J Cancer Res Clin Oncol* **139:**1055–1062. PubMed
18. **Braun S, Vogl FD, Naume B, Janni W, Osborne MP, Coombes RC, Schlimok G, Diel IJ, Gerber B, Gebauer G, Pierga JY, Marth C, Oruzio D, Wiedswang G, Solomayer EF, Kundt G, Strobl B, Fehm T, Wong GY, Bliss J, Vincent-Salomon A, Pantel K.** 2005. A pooled analysis of bone marrow micrometastasis in breast cancer. *N Engl J Med* **353:**793–802. PubMed
19. **Weckermann D, Polzer B, Ragg T, Blana A, Schlimok G, Arnholdt H, Bertz S, Harzmann R, Klein CA.** 2009. Perioperative activation of disseminated tumor cells in bone marrow of patients with prostate cancer. *J Clin Oncol* **27:**1549–1556. PubMed
20. **Köllermann J, Weikert S, Schostak M, Kempkensteffen C, Kleinschmidt K, Rau T, Pantel K.** 2008. Prognostic significance of disseminated tumor cells in the bone marrow of prostate cancer patients treated with neoadjuvant hormone treatment. *J Clin Oncol* **26:**4928–4933. PubMed
21. **Pierga JY, Bonneton C, Vincent-Salomon A, de Cremoux P, Nos C, Blin N, Pouillart P, Thiery JP, Magdelenat H.** 2004. Clinical significance of immunocytochemical detection of tumor cells using digital microscopy in peripheral blood and bone marrow of breast cancer patients. *Clin Cancer Res* **10:**1392–1400.
22. **Bidard FC, Vincent-Salomon A, Gomme S, Nos C, de Rycke Y, Thiery JP, Sigal-Zafrani B, Mignot L, Sastre-Garau X, Pierga JY.** 2008. Disseminated tumor cells of breast cancer patients: a strong prognostic factor for distant and local relapse. *Clin Cancer Res* **14:**3306–3311.
23. **Scher HI, Pantel K.** 2009. Bone marrow aspiration for disseminated tumor cell detection: a must-have test or is the jury still out? *J Clin Oncol* **27:**1531–1533. PubMed
24. **Hüsemann Y, Geigl JB, Schubert F, Musiani P, Meyer M, Burghart E, Forni G, Eils R, Fehm T, Riethmüller G, Klein CA.** 2008. Systemic spread is an early step in breast cancer. *Cancer Cell* **13:**58–68. PubMed
25. **Bartkowiak K, Wieczorek M, Buck F, Harder S, Moldenhauer J, Effenberger KE, Pantel K, Peter-Katalinic J, Brandt BH.** 2009. Two-dimensional differential gel electrophoresis of a cell line derived from a breast cancer micrometastasis revealed a stem/progenitor cell protein profile. *J Proteome Res* **8:**2004–2014. PubMed
26. **Uhr JW, Pantel K.** 2011. Controversies in clinical cancer dormancy. *Proc Natl Acad Sci U S A* **108:**12396–12400. PubMed
27. **Lin WC, Rajbhandari N, Wagner KU.** 2014. Cancer cell dormancy in novel mouse models for reversible pancreatic cancer: a lingering challenge in the development of targeted therapies. *Cancer Res* **74:**2138–2143. PubMed
28. **Borovski T, De Sousa e Melo F, Vermeulen L, Medema JP.** 2011. Cancer stem cell niche: the place to be. *Cancer Res* **71:**634–639. PubMed
29. **Thiery JP, Sleeman JP.** 2006. Complex networks orchestrate epithelial-mesenchymal transitions. *Nat Rev Mol Cell Biol* **7:**131–142. PubMed
30. **Kalluri R, Weinberg RA.** 2009. The basics of epithelial-mesenchymal transition. *J Clin Invest* **119:**1420–1428. PubMed
31. **Mani SA, Guo W, Liao MJ, Eaton EN, Ayyanan A, Zhou AY, Brooks M, Reinhard F, Zhang CC, Shipitsin M, Campbell LL, Polyak K, Brisken C, Yang J, Weinberg RA.** 2008. The epithelial-mesenchymal transition generates cells with properties of stem cells. *Cell* **133:**704–715. PubMed
32. **Polyak K, Weinberg RA.** 2009. Transitions between epithelial and mesenchymal states: acquisition of malignant and stem cell traits. *Nat Rev Cancer* **9:**265–273. PubMed
33. **Thurm H, Ebel S, Kentenich C, Hemsen A, Riethdorf S, Coith C, Wallwiener D, Braun S, Oberhoff C, Janicke F, Pantel K.** 2003. Rare expression of epithelial cell adhesion molecule on residual micrometastatic breast cancer cells after adjuvant chemotherapy. *Clin Cancer Res* **9:**2598–2604.
34. **Schneck H, Gierke B, Uppenkamp F, Behrens B, Niederacher D, Stoecklein NH, Templin MF, Pawlak M, Fehm T, Neubauer H; Disseminated Cancer Cell Network (DCC Net) Duesseldorf.** 2015. EpCAM-independent enrichment of circulating tumor cells in metastatic breast cancer. *PLoS One* **10:**e0144535. doi:10.1371/journal.pone.0144535.
35. **Mikolajczyk SD, Millar LS, Tsinberg P, Coutts SM, Zomorrodi M, Pham T, Bischoff FZ, Pircher TJ.** 2011. Detection of EpCAM-negative and cytokeratin-negative circulating tumor cells in peripheral blood. *J Oncol* **2011:**252361. PubMed
36. **Huang RY, Wong MK, Tan TZ, Kuay KT, Ng AH, Chung VY, Chu YS, Matsumura N, Lai HC, Lee YF, Sim WJ, Chai C, Pietschmann E, Mori S, Low JJ, Choolani M, Thiery JP.** 2013. An EMT spectrum defines an anoikis-resistant and spheroidogenic intermediate mesenchymal state that is sensitive to e-cadherin restoration by a src-kinase inhibitor, saracatinib (AZD0530). *Cell Death Dis* **4:**e915. PubMed
37. **Danila DC, Fleisher M, Scher HI.** 2011. Circulating tumor cells as biomarkers in prostate cancer. *Clin Cancer Res* **17:**3903–3912.
38. **Yu M, Stott S, Toner M, Maheswaran S, Haber DA.** 2011. Circulating tumor cells: approaches to isolation and characterization. *J Cell Biol* **192:**373–382. PubMed
39. **Stott SL, Lee RJ, Nagrath S, Yu M, Miyamoto DT, Ulkus L, Inserra EJ, Ulman M, Springer S, Nakamura Z, Moore AL, Tsukrov DI, Kempner ME, Dahl DM, Wu CL, Iafrate AJ, Smith MR, Tompkins RG, Sequist LV, Toner M, Haber DA, Maheswaran S.** 2010. Isolation and characterization of circulating tumor cells from patients with localized and metastatic prostate cancer. *Sci Transl Med* **2:**25ra23. PubMed
40. **Allard WJ, Matera J, Miller MC, Repollet M, Connelly MC, Rao C, Tibbe AG, Uhr JW, Terstappen LW.** 2004. Tumor cells circulate in the peripheral blood of all major carcinomas but not in healthy subjects or patients with nonmalignant diseases. *Clin Cancer Res* **10:**6897–6904.
41. **Budd GT, Cristofanilli M, Ellis MJ, Stopeck A, Borden E, Miller MC, Matera J, Repollet M, Doyle GV, Terstappen LW, Hayes DF.** 2006. Circulating tumor cells versus

imaging—predicting overall survival in metastatic breast cancer. *Clin Cancer Res* **12:**6403–6409.
42. **Cristofanilli M, Budd GT, Ellis MJ, Stopeck A, Matera J, Miller MC, Reuben JM, Doyle GV, Allard WJ, Terstappen LW, Hayes DF.** 2004. Circulating tumor cells, disease progression, and survival in metastatic breast cancer. *N Engl J Med* **351:**781–791. PubMed
43. **Cristofanilli M, Hayes DF, Budd GT, Ellis MJ, Stopeck A, Reuben JM, Doyle GV, Matera J, Allard WJ, Miller MC, Fritsche HA, Hortobagyi GN, Terstappen LW.** 2005. Circulating tumor cells: a novel prognostic factor for newly diagnosed metastatic breast cancer. *J Clin Oncol* **23:**1420–1430. PubMed
44. **Hayes DF, Cristofanilli M, Budd GT, Ellis MJ, Stopeck A, Miller MC, Matera J, Allard WJ, Doyle GV, Terstappen LW.** 2006. Circulating tumor cells at each follow-up time point during therapy of metastatic breast cancer patients predict progression-free and overall survival. *Clin Cancer Res* **12:**4218–4224.
45. **Cohen SJ, Punt CJ, Iannotti N, Saidman BH, Sabbath KD, Gabrail NY, Picus J, Morse M, Mitchell E, Miller MC, Doyle GV, Tissing H, Terstappen LW, Meropol NJ.** 2008. Relationship of circulating tumor cells to tumor response, progression-free survival, and overall survival in patients with metastatic colorectal cancer. *J Clin Oncol* **26:**3213–3221. PubMed
46. **Cohen SJ, Punt CJ, Iannotti N, Saidman BH, Sabbath KD, Gabrail NY, Picus J, Morse MA, Mitchell E, Miller MC, Doyle GV, Tissing H, Terstappen LW, Meropol NJ.** 2009. Prognostic significance of circulating tumor cells in patients with metastatic colorectal cancer. *Ann Oncol* **20:**1223–1229. PubMed
47. **Danila DC, Heller G, Gignac GA, Gonzalez-Espinoza R, Anand A, Tanaka E, Lilja H, Schwartz L, Larson S, Fleisher M, Scher HI.** 2007. Circulating tumor cell number and prognosis in progressive castration-resistant prostate cancer. *Clin Cancer Res* **13:**7053–7058.
48. **de Bono JS, Scher HI, Montgomery RB, Parker C, Miller MC, Tissing H, Doyle GV, Terstappen LW, Pienta KJ, Raghavan D.** 2008. Circulating tumor cells predict survival benefit from treatment in metastatic castration-resistant prostate cancer. *Clin Cancer Res* **14:**6302–6309.
49. **Scher HI, Jia X, de Bono JS, Fleisher M, Pienta KJ, Raghavan D, Heller G.** 2009. Circulating tumour cells as prognostic markers in progressive, castration-resistant prostate cancer: a reanalysis of IMMC38 trial data. *Lancet Oncol* **10:**233–239. PubMed
50. **Coumans FA, Doggen CJ, Attard G, de Bono JS, Terstappen LW.** 2010. All circulating EpCAM+CK+CD45− objects predict overall survival in castration-resistant prostate cancer. *Ann Oncol* **21:**1851–1857. PubMed
51. **Shaffer DR, Leversha MA, Danila DC, Lin O, Gonzalez-Espinoza R, Gu B, Anand A, Smith K, Maslak P, Doyle GV, Terstappen LW, Lilja H, Heller G, Fleisher M, Scher HI.** 2007. Circulating tumor cell analysis in patients with progressive castration-resistant prostate cancer. *Clin Cancer Res* **13:**2023–2029.
52. **Attard G, Swennenhuis JF, Olmos D, Reid AH, Vickers E, A'Hern R, Levink R, Coumans F, Moreira J, Riisnaes R, Oommen NB, Hawche G, Jameson C, Thompson E, Sipkema R, Carden CP, Parker C, Dearnaley D, Kaye SB, Cooper CS, Molina A, Cox ME, Terstappen LW, de Bono JS.** 2009. Characterization of ERG, AR and PTEN gene status in circulating tumor cells from patients with castration-resistant prostate cancer. *Cancer Res* **69:**2912–2918. PubMed
53. **Ulmer A, Schmidt-Kittler O, Fischer J, Ellwanger U, Rassner G, Riethmuller G, Fierlbeck G, Klein CA.** 2004. Immunomagnetic enrichment, genomic characterization, and prognostic impact of circulating melanoma cells. *Clin Cancer Res* **10:**531–537.
54. **Racila E, Euhus D, Weiss AJ, Rao C, McConnell J, Terstappen LW, Uhr JW.** 1998. Detection and characterization of carcinoma cells in the blood. *Proc Natl Acad Sci U S A* **95:**4589–4594. PubMed
55. **Scholtens TM, Schreuder F, Ligthart ST, Swennenhuis JF, Tibbe AG, Greve J, Terstappen LW.** 2011. CellTracks TDI: an image cytometer for cell characterization. *Cytometry A* **79:**203–213. PubMed
56. **Bocsi J, Varga VS, Molnár B, Sipos F, Tulassay Z, Tárnok A.** 2004. Scanning fluorescent microscopy analysis is applicable for absolute and relative cell frequency determinations. *Cytometry A* **61:**1–8. PubMed
57. **Weight RM, Viator JA.** 2014. Detection of circulating tumor cells by photoacoustic flowmetry. *Methods Mol Biol* **1102:**655–663. PubMed
58. **Navin N, Kendall J, Troge J, Andrews P, Rodgers L, McIndoo J, Cook K, Stepansky A, Levy D, Esposito D, Muthuswamy L, Krasnitz A, McCombie WR, Hicks J, Wigler M.** 2011. Tumour evolution inferred by single-cell sequencing. *Nature* **472:**90–94. PubMed
59. **Yaniv I, Cohen IJ, Stein J, Zilberstein J, Liberzon E, Atlas O, Grunshpan A, Sverdlov Y, Ash S, Zaizov R, Avigad S.** 2004. Tumor cells are present in stem cell harvests of Ewings sarcoma patients and their persistence following transplantation is associated with relapse. *Pediatr Blood Cancer* **42:**404–409. PubMed
60. **Wong IH, Chan AT, Johnson PJ.** 2000. Quantitative analysis of circulating tumor cells in peripheral blood of osteosarcoma patients using osteoblast-specific messenger RNA markers: a pilot study. *Clin Cancer Res* **6:**2183–2188.
61. **Dubois SG, Epling CL, Teague J, Matthay KK, Sinclair E.** 2010. Flow cytometric detection of Ewing sarcoma cells in peripheral blood and bone marrow. *Pediatr Blood Cancer* **54:**13–18. PubMed
62. **Helzer KT, Barnes HE, Day L, Harvey J, Billings PR, Forsyth A.** 2009. Circulating tumor cells are transcriptionally similar to the primary tumor in a murine prostate model. *Cancer Res* **69:**7860–7866. PubMed
63. **Giordano A, Giuliano M, De Laurentiis M, Arpino G, Jackson S, Handy BC, Ueno NT, Andreopoulou E, Alvarez RH, Valero V, De Placido S, Hortobagyi GN, Reuben JM, Cristofanilli M.** 2012. Circulating tumor cells in immunohistochemical subtypes of metastatic breast cancer: lack of prediction in HER2-positive disease treated with targeted therapy. *Ann Oncol* **23:**1144–1150.
64. **Maheswaran S, Sequist LV, Nagrath S, Ulkus L, Brannigan B, Collura CV, Inserra E, Diederichs S, Iafrate AJ, Bell DW, Digumarthy S, Muzikansky A, Irimia D, Settleman J, Tompkins RG, Lynch TJ, Toner M, Haber DA.** 2008. Detection of mutations in EGFR in circulating lung-cancer cells. *N Engl J Med* **359:**366–377. PubMed
65. **Harb W, Fan A, Tran T, Danila DC, Keys D, Schwartz M, Ionescu-Zanetti C.** 2013. Mutational analysis of circulating tumor cells using a novel microfluidic collection device and qPCR assay. *Transl Oncol* **6:**528–538. PubMed
66. **Gleghorn JP, Pratt ED, Denning D, Liu H, Bander NH, Tagawa ST, Nanus DM, Giannakakou PA, Kirby BJ.** 2010. Capture of circulating tumor cells from whole blood of prostate cancer patients using geometrically enhanced differential immunocapture (GEDI) and a prostate-specific antibody. *Lab Chip* **10:**27–29. PubMed
67. **Ozkumur E, Shah AM, Ciciliano JC, Emmink BL, Miyamoto DT, Brachtel E, Yu M, Chen PI, Morgan B, Trautwein J, Kimura A, Sengupta S, Stott SL, Karabacak NM, Barber TA, Walsh JR, Smith K, Spuhler PS, Sullivan JP, Lee RJ, Ting DT, Luo X, Shaw AT, Bardia A, Sequist LV, Louis DN, Maheswaran S, Kapur R, Haber DA, Toner M.** 2013. Inertial focusing for tumor antigen-dependent and -independent sorting of rare circulating tumor cells. *Sci Transl Med* **5:**179ra47. PubMed

68. **Winer-Jones JP, Vahidi B, Arquilevich N, Fang C, Ferguson S, Harkins D, Hill C, Klem E, Pagano PC, Peasley C, Romero J, Shartle R, Vasko RC, Strauss WM, Dempsey PW.** 2014. Circulating tumor cells: clinically relevant molecular access based on a novel CTC flow cell. *PLoS One* **9:**e86717. PubMed
69. **Ramirez JM, Fehm T, Orsini M, Cayrefourcq L, Maudelonde T, Pantel K, Alix-Panabières C.** 2014. Prognostic relevance of viable circulating tumor cells detected by EPISPOT in metastatic breast cancer patients. *Clin Chem* **60:**214–221. PubMed
70. **Alix-Panabières C, Rebillard X, Brouillet JP, Barbotte E, Iborra F, Segui B, Maudelonde T, Jolivet-Reynaud C, Vendrell JP.** 2005. Detection of circulating prostate-specific antigen-secreting cells in prostate cancer patients. *Clin Chem* **51:**1538–1541. PubMed
71. **Paris PL, Kobayashi Y, Zhao Q, Zeng W, Sridharan S, Fan T, Adler HL, Yera ER, Zarrabi MH, Zucker S, Simko J, Chen WT, Rosenberg J.** 2009. Functional phenotyping and genotyping of circulating tumor cells from patients with castration resistant prostate cancer. *Cancer Lett* **277:**164–173. PubMed
72. **Shim S, Gascoyne P, Noshari J, Hale KS.** 2011. Dynamic physical properties of dissociated tumor cells revealed by dielectrophoretic field-flow fractionation. *Integr Biol (Camb)* **3:**850–862. PubMed
73. **Gel M, Kimura Y, Kurosawa O, Oana H, Kotera H, Washizu M.** 2010. Dielectrophoretic cell trapping and parallel one-to-one fusion based on field constriction created by a micro-orifice array. *Biomicrofluidics* **4:**022808. PubMed
74. **Borgatti M, Altomare L, Abonnec M, Fabbri E, Manaresi N, Medoro G, Romani A, Tartagni M, Nastruzzi C, Di Croce S, Tosi A, Mancini I, Guerrieri R, Gambari R.** 2005. Dielectrophoresis-based 'lab-on-a-chip' devices for programmable binding of microspheres to target cells. *Int J Oncol* **27:**1559–1566. PubMed
75. **Lecharpentier A, Vielh P, Perez-Moreno P, Planchard D, Soria JC, Farace F.** 2011. Detection of circulating tumour cells with a hybrid (epithelial/mesenchymal) phenotype in patients with metastatic non-small cell lung cancer. *Br J Cancer* **105:**1338–1341. PubMed
76. **Lin HK, Zheng S, Williams AJ, Balic M, Groshen S, Scher HI, Fleisher M, Stadler W, Datar RH, Tai YC, Cote RJ.** 2010. Portable filter-based microdevice for detection and characterization of circulating tumor cells. *Clin Cancer Res* **16:**5011–5018.
77. **Zheng S, Lin HK, Lu B, Williams A, Datar R, Cote RJ, Tai YC.** 2011. 3D microfilter device for viable circulating tumor cell (CTC) enrichment from blood. *Biomed Microdevices* **13:**203–213. PubMed
78. **Farace F, Massard C, Vimond N, Drusch F, Jacques N, Billiot F, Laplanche A, Chauchereau A, Lacroix L, Planchard D, Le Moulec S, André F, Fizazi K, Soria JC, Vielh P.** 2011. A direct comparison of CellSearch and ISET for circulating tumour-cell detection in patients with metastatic carcinomas. *Br J Cancer* **105:**847–853. PubMed
79. **Adams DL, Martin SS, Alpaugh RK, Charpentier M, Tsai S, Bergan RC, Ogden IM, Catalona W, Chumsri S, Tang CM, Cristofanilli M.** 2014. Circulating giant macrophages as a potential biomarker of solid tumors. *Proc Natl Acad Sci U S A* **111:**3514–3519. PubMed
80. **Marrinucci D, Bethel K, Kolatkar A, Luttgen MS, Malchiodi M, Baehring F, Voigt K, Lazar D, Nieva J, Bazhenova L, Ko AH, Korn WM, Schram E, Coward M, Yang X, Metzner T, Lamy R, Honnatti M, Yoshioka C, Kunken J, Petrova Y, Sok D, Nelson D, Kuhn P.** 2012. Fluid biopsy in patients with metastatic prostate, pancreatic and breast cancers. *Phys Biol* **9:**016003. PubMed
81. **Ghossein RA, Scher HI, Gerald WL, Kelly WK, Curley T, Amsterdam A, Zhang ZF, Rosai J.** 1995. Detection of circulating tumor cells in patients with localized and metastatic prostatic carcinoma: clinical implications. *J Clin Oncol* **13:**1195–1200. PubMed
82. **Helo P, Cronin AM, Danila DC, Wenske S, Gonzalez-Espinoza R, Anand A, Koscuiszka M, Väänänen RM, Pettersson K, Chun FK, Steuber T, Huland H, Guillonneau BD, Eastham JA, Scardino PT, Fleisher M, Scher HI, Lilja H.** 2009. Circulating prostate tumor cells detected by reverse transcription-PCR in men with localized or castration-refractory prostate cancer: concordance with CellSearch assay and association with bone metastases and with survival. *Clin Chem* **55:**765–773. PubMed
83. **Iinuma H, Watanabe T, Mimori K, Adachi M, Hayashi N, Tamura J, Matsuda K, Fukushima R, Okinaga K, Sasako M, Mori M.** 2011. Clinical significance of circulating tumor cells, including cancer stem-like cells, in peripheral blood for recurrence and prognosis in patients with Dukes' stage B and C colorectal cancer. *J Clin Oncol* **29:**1547–1555. PubMed
84. **Xi L, Nicastri DG, El-Hefnawy T, Hughes SJ, Luketich JD, Godfrey TE.** 2007. Optimal markers for real-time quantitative reverse transcription PCR detection of circulating tumor cells from melanoma, breast, colon, esophageal, head and neck, and lung cancers. *Clin Chem* **53:**1206–1215. PubMed
85. **Reinholz MM, Kitzmann KA, Tenner KS, Hillman DW, Dueck AC, Hobday TJ, Northfelt DW, Moreno-Aspitia A, Roy V, Laplant B, Allred JB, Stella PJ, Lingle W, Perez EA.** 2011. Cytokeratin-19 and mammaglobin gene expression in circulating tumor cells from metastatic breast cancer patients enrolled in North Central Cancer Treatment Group (NCCTG) trials, N0234/336/436/437. *Clin Cancer Res* **7:**7183–7193.
86. **Sieuwerts AM, Mostert B, Bolt-de Vries J, Peeters D, de Jongh FE, Stouthard JM, Dirix LY, van Dam PA, Van Galen A, de Weerd V, Kraan J, van der Spoel P, Ramirez-Moreno R, van Deurzen CH, Smid M, Yu JX, Jiang J, Wang Y, Gratama JW, Sleijfer S, Foekens JA, Martens JW.** 2011. mRNA and microRNA expression profiles in circulating tumor cells and primary tumors of metastatic breast cancer patients. *Clin Cancer Res* **17:**3600–3618.
87. **Zhao S, Liu Y, Zhang Q, Li H, Zhang M, Ma W, Zhao W, Wang J, Yang M.** 2011. The prognostic role of circulating tumor cells (CTCs) detected by RT-PCR in breast cancer: a meta-analysis of published literature. *Breast Cancer Res Treat* **130:**809–816. PubMed
88. **Yoon SO, Kim YT, Jung KC, Jeon YK, Kim BH, Kim CW.** 2011. TTF-1 mRNA-positive circulating tumor cells in the peripheral blood predict poor prognosis in surgically resected non-small cell lung cancer patients. *Lung Cancer* **71:**209–216. PubMed
89. **Ignatiadis M, Kallergi G, Ntoulia M, Perraki M, Apostolaki S, Kafousi M, Chlouverakis G, Stathopoulos E, Lianidou E, Georgoulias V, Mavroudis D.** 2008. Prognostic value of the molecular detection of circulating tumor cells using a multimarker reverse transcription-PCR assay for cytokeratin 19, mammaglobin A, and HER2 in early breast cancer. *Clin Cancer Res* **14:**2593–2600.
90. **Nakagawa T, Martinez SR, Goto Y, Koyanagi K, Kitago M, Shingai T, Elashoff DA, Ye X, Singer FR, Giuliano AE, Hoon DS.** 2007. Detection of circulating tumor cells in early-stage breast cancer metastasis to axillary lymph nodes. *Clin Cancer Res* **13:**4105–4110.
91. **Danila DC, Anand A, Schultz N, Heller G, Wan M, Sung CC, Dai C, Khanin R, Fleisher M, Lilja H, Scher HI.** 2014. Analytic and clinical validation of a prostate cancer-enhanced messenger RNA detection assay in whole blood as a prognostic biomarker for survival. *Eur Urol* **65:**1191–1197. PubMed
92. **Schleiermacher G, Peter M, Oberlin O, Philip T, Rubie H, Mechinaud F, Sommelet-Olive D, Landman-Parker J,**

Bours D, Michon J, Delattre O, Société Française d'Oncologie Pédiatrique. 2003. Increased risk of systemic relapses associated with bone marrow micrometastasis and circulating tumor cells in localized Ewing tumor. *J Clin Oncol* **21:**85–91. PubMed

93. **Aktas B, Bankfalvi A, Heubner M, Kimmig R, Kasimir-Bauer S.** 2013. Evaluation and correlation of risk recurrence in early breast cancer assessed by Oncotype DX(®), clinicopathological markers and tumor cell dissemination in the blood and bone marrow. *Mol Clin Oncol* **1:**1049–1054. PubMed
94. **Danila DC, Anand A, Sung CC, Heller G, Leversha MA, Cao L, Lilja H, Molina A, Sawyers CL, Fleisher M, Scher HI.** 2011. TMPRSS2-ERG status in circulating tumor cells as a predictive biomarker of sensitivity in castration-resistant prostate cancer patients treated with abiraterone acetate. *Eur Urol* **60:**897–904. PubMed
95. **Andreopoulou E, Yang LY, Rangel KM, Reuben JM, Hsu L, Krishnamurthy S, Valero V, Fritsche HA, Cristofanilli M.** 2012. Comparison of assay methods for detection of circulating tumor cells in metastatic breast cancer: AdnaGen AdnaTest BreastCancer Select/Detect™ versus Veridex CellSearch™ system. *Int J Cancer* **130:**1590–1597. PubMed
96. **Talasaz AH, Powell AA, Huber DE, Berbee JG, Roh KH, Yu W, Xiao W, Davis MM, Pease RF, Mindrinos MN, Jeffrey SS, Davis RW.** 2009. Isolating highly enriched populations of circulating epithelial cells and other rare cells from blood using a magnetic sweeper device. *Proc Natl Acad Sci U S A* **106:**3970–3975. PubMed
97. **Wendel M, Bazhenova L, Boshuizen R, Kolatkar A, Honnatti M, Cho EH, Marrinucci D, Sandhu A, Pericone A, Thistlethwaite P, Bethel K, Nieva J, Heuvel M, Kuhn P.** 2012. Fluid biopsy for circulating tumor cell identification in patients with early- and late-stage non-small cell lung cancer: a glimpse into lung cancer biology. *Phys Biol* **9:**016005. PubMed
98. **Biomarkers Definitions Working Group.** 2001. Biomarkers and surrogate endpoints: preferred definitions and conceptual framework. *Clin Pharmacol Ther* **69:**89–95. PubMed
99. **FDA/NCI/CMS Oncology Biomarker Qualification Initiative.** 30 April 2009. *Memorandum of Understanding between the FDA, NCI, and CMS for the FDA/NCI/CMS Oncology Biomarker Qualification Initiative. Document MOU 225-06-8001.* http://www.fda.gov/AboutFDA/PartnershipsCollaborations/MemorandaofUnderstanding MOUs/DomesticMOUs/ucm115681.htm. Accessed 16 March 2011.
100. **Altar CA.** 2008. The Biomarkers Consortium: on the critical path of drug discovery. *Clin Pharmacol Ther* **83:**361–364. PubMed
101. **Botteri E, Sandri MT, Bagnardi V, Munzone E, Zorzino L, Rotmensz N, Casadio C, Cassatella MC, Esposito A, Curigliano G, Salvatici M, Verri E, Adamoli L, Goldhirsch A, Nolè F.** 2010. Modeling the relationship between circulating tumour cells number and prognosis of metastatic breast cancer. *Breast Cancer Res Treat* **122:**211–217. PubMed
102. **Scher HI, Beer TM, Higano CS, Anand A, Taplin ME, Efstathiou E, Rathkopf D, Shelkey J, Yu EY, Alumkal J, Hung D, Hirmand M, Seely L, Morris MJ, Danila DC, Humm J, Larson S, Fleisher M, Sawyers CL, Prostate Cancer Foundation/Department of Defense Prostate Cancer Clinical Trials Consortium.** 2010. Antitumour activity of MDV3100 in castration-resistant prostate cancer: a phase 1-2 study. *Lancet* **375:**1437–1446. PubMed
103. **Veridex LLC.** 2008. *CellSearch Circulating Tumor Cell Kit Premarket Notification—Expanded Indications for Use—Metastatic Prostate Cancer.* http://www.accessdata.fda.gov/cdrh_docs/pdf7/K073338.pdf.
104. **Gonen M, Heller G.** 2005. Concordance probability and discriminative power of proportional hazards regression. *Biometrika* **92:**965–970.
105. **Scher HI, Heller G, Molina A, Attard G, Danila DC, Jia X, Peng W, Sandhu SK, Olmos D, Riisnaes R, McCormack R, Burzykowski T, Kheoh T, Fleisher M, Buyse M, de Bono JS.** 2015. Circulating tumor cell biomarker panel as an individual-level surrogate for survival in metastatic castration-resistant prostate cancer. *J Clin Oncol* **33:**1348–1355.
106. **Koyanagi K, O'Day SJ, Boasberg P, Atkins MB, Wang HJ, Gonzalez R, Lewis K, Thompson JA, Anderson CM, Lutzky J, Amatruda TT, Hersh E, Richards J, Weber JS, Hoon DS.** 2010. Serial monitoring of circulating tumor cells predicts outcome of induction biochemotherapy plus maintenance biotherapy for metastatic melanoma. *Clin Cancer Res* **16:**2402–2408.
107. **Leversha MA, Han J, Asgari Z, Danila DC, Lin O, Gonzalez-Espinoza R, Anand A, Lilja H, Heller G, Fleisher M, Scher HI.** 2009. Fluorescence in situ hybridization analysis of circulating tumor cells in metastatic prostate cancer. *Clin Cancer Res* **15:**2091–2097. PubMed
108. **Antonarakis ES, Lu C, Wang H, Luber B, Nakazawa M, Roeser JC, Chen Y, Mohammad TA, Chen Y, Fedor HL, Lotan TL, Zheng Q, De Marzo AM, Isaacs JT, Isaacs WB, Nadal R, Paller CJ, Denmeade SR, Carducci MA, Eisenberger MA, Luo J.** 2014. AR-V7 and resistance to enzalutamide and abiraterone in prostate cancer. *N Engl J Med* **371:**1028–1038.
109. **de Bono JS, Attard G, Adjei A, Pollak MN, Fong PC, Haluska P, Roberts L, Melvin C, Repollet M, Chianese D, Connely M, Terstappen LW, Gualberto A.** 2007. Potential applications for circulating tumor cells expressing the insulin-like growth factor-I receptor. *Clin Cancer Res* **13:**3611–3616.
110. **Holzbeierlein J, Lal P, LaTulippe E, Smith A, Satagopan J, Zhang L, Ryan C, Smith S, Scher H, Scardino P, Reuter V, Gerald WL.** 2004. Gene expression analysis of human prostate carcinoma during hormonal therapy identifies androgen-responsive genes and mechanisms of therapy resistance. *Am J Pathol* **164:**217–227. PubMed
111. **Scher HI, Kelly WK.** 1993. Flutamide withdrawal syndrome: its impact on clinical trials in hormone-refractory prostate cancer. *J Clin Oncol* **11:**1566–1572. PubMed
112. **Yang MJ, Chiu HH, Wang HM, Yen LC, Tsao DA, Hsiao CP, Chen YF, Wang JY, Lin SR.** 2010. Enhancing detection of circulating tumor cells with activating KRAS oncogene in patients with colorectal cancer by weighted chemiluminescent membrane array method. *Ann Surg Oncol* **17:**624–633. PubMed
113. **Punnoose EA, Atwal SK, Spoerke JM, Savage H, Pandita A, Yeh RF, Pirzkall A, Fine BM, Amler LC, Chen DS, Lackner MR.** 2010. Molecular biomarker analyses using circulating tumor cells. *PLoS One* **5:**e12517. PubMed
114. **Nakazawa M, Lu C, Chen Y, Paller CJ, Carducci MA, Eisenberger MA, Luo J, Antonarakis ES.** 2015. Serial blood-based analysis of AR-V7 in men with advanced prostate cancer. *Ann Oncol* **26:**1859–1865. PubMed
115. **Pantel K, Riethdorf S.** 2009. Pathology: are circulating tumor cells predictive of overall survival? *Nat Rev Clin Oncol* **6:**190–191. PubMed

Transplantation Immunology

section P

VOLUME EDITOR: BARBARA DETRICK

SECTION EDITORS: ELAINE F. REED AND QIUHENG JENNIFER ZHANG

Histocompatibility and Immunogenetics Testing in the 21st Century

QIUHENG ZHANG AND ELAINE F. REED

112

The scope of immunogenetics and histocompatibility testing in transplantation has changed dramatically over the past 50 years. In organ transplantation, outcomes continue to improve as a result of better immunogenetics testing, immune suppression, and patient management; however, acute rejection and chronic rejection remain the biggest obstacles for successful transplantation. Since "crossmatching" was first described by Patel and Terasaki (1), the goal to provide accurate immunological risk assessment for transplant recipients remains unchanged. Histocompatibility and immunogenetics laboratories utilize multiple diagnostic assays to evaluate HLA compatibility between donors and recipients. Furthermore, testing has expanded to include immunogenetics systems other than those using HLA, such as killer immunoglobulin-like receptors (KIR) (2, 3), major histocompatibility complex (MHC) class I chain-related gene A (MICA) (4), angiotensin type 1 receptor (AT1R) (5), and genes encoding cytokines. The application of new state-of-the-art diagnostic tests that inform on the immune status of the transplant recipient has transformed the role of the immunogenetics laboratory from providing tissue-typing and crossmatching services to assessing immunologic risk, donor selection, and presentation of strategies for desensitization and therapeutic intervention. In addition, immunological risk assessment is no longer limited to the pretransplant period but has become increasingly recognized as a noninvasive tool for assessing acute and chronic rejection (6–8).

The MHC, or human leukocyte antigen (HLA), genes are the most polymorphic in the human genome. The highly polymorphic nature of the MHC genes is the foundation of immune responses for both solid-organ transplantation and hematopoietic stem cell transplantation (HSCT). Sanger sequence-based HLA typing has long been considered the "gold standard" for high-resolution typing; however, this method cannot readily distinguish between polymorphisms on the same chromosome (*cis*) or different chromosomes (*trans*), thereby creating ambiguities that are difficult, time-consuming, and expensive to resolve. Recently, a massive parallel sequencing technology, also referred to as next-generation sequencing (NGS), has been developed to sequence the entire HLA gene. Full-length sequencing of a haplotype provides phasing between linked polymorphic sites in both exons and introns, resulting in fewer ambiguities and higher resolution typing results (9, 10). These results will ultimately lead to improved matching and survival. Chapter 113 by Kunkel et al. explains the premises behind various molecular techniques used to differentiate HLA alleles and how to apply one or more of these methods to achieve the degree of typing resolution required for a given clinical application.

Introduced in 1968 by Terasaki (11), the complement-dependent cytotoxicity test became the standard technique for serologic typing, antibody screening, and crossmatching in the 1960s and 1970s. Panel-reactive antibody, or PRA, is used to identify sensitized patients and estimate their likelihood of finding a crossmatch-compatible donor from a panel of healthy blood donors representing the HLA types of the potential organ donor pool. The presence of HLA antibodies at titers sufficient to give a positive cytotoxicity crossmatch has been considered a contraindication for transplantation. Nowadays, cytotoxicity still has an important role in histocompatibility laboratories as a functional assay, and it remains the standard test for antibody crossmatches. Introduction of solid-phase assays in the mid-1990s has allowed for a more comprehensive, sensitive, and cost-effective method for detection of HLA antibodies than the traditional complement-dependent cytotoxicity test. Precise measurement of HLA-specific antibodies permits more accurate risk assessment for patients awaiting transplantation, participating in kidney exchange programs, and undergoing desensitization procedures. Many laboratories have begun to correlate solid-phase test results with cell-based crossmatch test results and have employed this information to develop accurate "virtual" crossmatch predictions to define unacceptable donor HLA antigens for optimizing donor selection for transplantation. A kidney allocation process using calculated PRA (cPRA) was implemented by the United Network for Organ Sharing (UNOS) on 1 October 2009 (12). The cPRA uses the patient's HLA class I and class II antibody specificities to determine the frequency of these unacceptable antigens in the donor population and thereby predicts the probability of a positive crossmatch. A complete review of the patient's sensitization history, including transfusions, pregnancies, and previous transplants, is critically important to accurately define unacceptable HLA antigens for sensitized patients. Increased numbers of unacceptable HLA antigens result in a dramatically diminished potential for receiving organ offers, prolonged wait times, and the death of patients on the wait list.

The demand for organ transplantation has rapidly increased over the past decade. The number of patients on the

doi:10.1128/9781555818722.ch112

wait list at the end of 2014 had risen to over 120,000, while the number of patients receiving deceased-donor transplants remains just over 2,000 annually due to the organ donor shortage. The donor shortage has placed an increased emphasis on attempts to expand live-donor transplants, when possible. However, approximately one-third of kidney transplant candidates who present with a potential living donor(s) will be incompatible owing to blood type or HLA incompatibility. To address this limitation, kidney paired-exchange (KPD) programs have been established to enable kidney transplant candidates with willing but incompatible living donors to join a registry of other incompatible pairs in order to find potentially compatible transplant solutions. To maximize donor-recipient matching and minimize immunologic risk, these multicenter KPD programs use sophisticated algorithms combined with desensitization therapy to identify optimal match potential, with two, three, or more simultaneous complex multiway exchanges. In the United States, KPD has increased dramatically in the past decade (13, 14), from three transplants facilitated in 2000 to 581 in 2013. Clinical protocols using high-dose intravenous immunoglobulin (IVIG) or a combination of IVIG and plasmapheresis with or without rituximab and bortezomib are being used to successfully desensitize and perform transplants on patients who otherwise might have waited years for a compatible deceased-donor organ (15–18). Laboratory support for these innovative clinical protocols is vital and is highly dependent upon timely, complete, and accurate assessment of the levels and specificities of patients' antibodies.

Given that allograft rejection can occur in HLA-identical transplant recipients in the absence of demonstrable donor-specific HLA antibodies, the clinical relevance of non-HLA antibodies is increasingly recognized (19, 20). Non-HLA antibodies can reliably be detected by solid-phase assays (MICA, AT1R, collagen-V, vimentin) and by a flow-crossmatch technique testing for antibodies against donor endothelial progenitors or surrogate endothelial cell lines. In addition, with the advancement of many high-throughput genomics, proteomics, and ProtoArray methods, efforts have been made to understand the mechanisms of graft rejection and identify novel biomarkers for acute rejection, chronic rejection, and tolerance. Five of the chapters in this section focus on the methods that are being used to monitor and evaluate transplant patients. Sikorski and colleagues in chapter 114 compare the various techniques for defining clinically relevant alloantibodies and illustrate the utility of these assays in clinical desensitization protocols, and Jackson and Dale describe current methods for detecting non-HLA antibodies in solid-organ transplantation in chapter 115. In chapter 116, Metes et al. discuss approaches to evaluate cellular sensitization that can be employed in steroid withdrawal protocols and posttransplant monitoring for rejection or tolerance. As summarized by Tan et al. (chapter 117), improved reagents have led to an increased appreciation of the association between complement activation in transplants with poor outcomes (21–23). In addition, the advantages and disadvantages of various reagents to complement used for the diagnosis of different types of rejection in transplants have been discussed. Dadhania et al. (chapter 118) describe molecular and proteomic techniques that permit earlier and more sensitive detection of allograft rejection.

The key factors in predicting survival after bone marrow transplantation or HSCT are the stage of disease and the degree of HLA matching. There is a progressive decrease in survival after HSCT, with each HLA allele mismatch reducing the probability of overall survival at 5 years by approximately 10% (24–26). The availability of suitable donors is problematic for many patients who are candidates for HSCT. The ideal donor for HSCT is an HLA-identical sibling, but only 30% of patients have a suitable matched related donor. Efforts to increase the number of available donors have fostered altruistic donor registries, with more than 50 such registries worldwide. One of the largest registries is the National Marrow Donor Program (NMDP), which presently has more than 10 million typed potential marrow and peripheral blood stem cell donors and more than 185,000 cord blood units. Registry data show that patients receiving transplants from HLA-A, -B, -C, and -DRB1 locus (8/8) allele-matched unrelated donors have outcomes significantly superior to those of patients receiving transplants from donors with one or more mismatches at these loci, while the clinical relevance of matching at the DQB1 locus remains unclear (25). It is estimated that 31 to 75% of patients, depending on ethnic background, are able to find an 8/8 matched unrelated donor in the registry. Recently, retrospective analyses looking at HLA-DPB1 mismatches according to T-cell epitopes showed that nonpermissive mismatches were associated with increased risks of overall mortality, transplant-related mortality, and severe acute graft-versus-host disease (GVHD) compared with permissive mismatches or DPB1 matches (27). Therefore, selecting the best donor, when there are several donors equally matched for HLA-A, -B, -C, and DRB1, may be further narrowed by evaluation of the DPB1 haplotype. Selection of a matched or permissive DPB1 haplotype appears to decrease early nonrelapse mortality but does not impact long-term survival. Alternative sources of stem cells from umbilical cord blood (UCB) serve as a valuable source of hematopoietic stem cells for allogeneic transplantation when a matched sibling or unrelated donor is not available, since UCB requires less stringent HLA matching (28, 29). A major advantage of umbilical cord stem cells is that they can be obtained in less than 4 weeks, which is particularly important for patients with rapidly progressive malignancies. One of the disadvantages of UCB transplantation, however, is that it is associated with a high degree of graft rejection and treatment-related mortality, which appears to be directly associated with UCB cell dose. For transplants with some degree of HLA mismatching, accurate determination of humoral sensitization is required to assess the risk of engraftment failure due to antibody-mediated rejection. The relationship among KIR matching, expression, genotype, and transplantation outcomes has also been an area of intense interest, with rapidly evolving data and insights. In HLA-identical or nearly HLA-identical transplantations, other aspects of KIR physiology may take on a more important role. KIR haplotype A encodes mainly inhibitory receptors and only one activating receptor, while KIR haplotype B encodes more activating receptors. Donors in whom the centromeric B genes were present had a lower rate of relapse and superior rates of survival of acute myeloid leukemia (AML) (2). Compared with homozygous A/A donors, grafts from homozygous centromeric B/B donors resulted in a lower cumulative incidence of relapse. In chapter 119 of this section, Rajalingam et al. focus on the polymorphism of the KIR genes and report that defining KIR alleles and haplotypes is applicable to areas other than HSCT, as KIR genotypes may affect susceptibility to autoimmunity and viral infections.

Graft rejection, disease relapse, and GVHD are major complications after allogeneic HSCT. Short tandem repeats (STRs) are highly polymorphic DNA sequences in the human genome. The basic principle of chimerism detection is based on the differences between donor and recipient

polymorphic genetic markers. Quantitative monitoring of mixed chimerism of self and donor origins after HSCT by STR analysis has become a routine diagnostic tool in the detection of engraftment failure, predicting rejection and disease relapse (30, 31). Baxter-Lowe discusses in chapter 120 the techniques that can be employed to determine both engraftment of donor stem cells and the relative degree of donor-recipient chimerism.

In summary, the following chapters describe the exciting technologies developed during the past 2 decades in histocompatibility and immunogenetics laboratories which advance the care and management of transplant patients using precision-based medicine.

REFERENCES

1. **Patel R, Terasaki PI.** 1969. Significance of the positive crossmatch test in kidney transplantation. *N Engl J Med* **280:**735–739. PubMed
2. **Cooley S, Weisdorf DJ, Guethlein LA, Klein JP, Wang T, Le CT, Marsh SG, Geraghty D, Spellman S, Haagenson MD, Ladner M, Trachtenberg E, Parham P, Miller JS.** 2010. Donor selection for natural killer cell receptor genes leads to superior survival after unrelated transplantation for acute myelogenous leukemia. *Blood* **116:**2411–2419. PubMed
3. **Venstrom JM, Pittari G, Gooley TA, Chewning JH, Spellman S, Haagenson M, Gallagher MM, Malkki M, Petersdorf E, Dupont B, Hsu KC.** 2012. HLA-C-dependent prevention of leukemia relapse by donor activating KIR2DS1. *N Engl J Med* **367:**805–816. PubMed
4. **Terasaki PI, Ozawa M, Castro R.** 2007. Four-year follow-up of a prospective trial of HLA and MICA antibodies on kidney graft survival. *Am J Transplant* **7:**408–415.
5. **Dragun D, Müller DN, Bräsen JH, Fritsche L, Nieminen-Kelhä M, Dechend R, Kintscher U, Rudolph B, Hoebeke J, Eckert D, Mazak I, Plehm R, Schönemann C, Unger T, Budde K, Neumayer HH, Luft FC, Wallukat G.** 2005. Angiotensin II type 1-receptor activating antibodies in renal-allograft rejection. *N Engl J Med* **352:**558–569. PubMed
6. **Amico P, Hönger G, Mayr M, Steiger J, Hopfer H, Schaub S.** 2009. Clinical relevance of pretransplant donor-specific HLA antibodies detected by single-antigen flow-beads. *Transplantation* **87:**1681–1688. PubMed
7. **Hoshino J, Kaneku H, Everly MJ, Greenland S, Terasaki PI.** 2012. Using donor-specific antibodies to monitor the need for immunosuppression. *Transplantation* **93:**1173–1178. PubMed
8. **Wiebe C, Gibson IW, Blydt-Hansen TD, Karpinski M, Ho J, Storsley LJ, Goldberg A, Birk PE, Rush DN, Nickerson PW.** 2012. Evolution and clinical pathologic correlations of de novo donor-specific HLA antibody post kidney transplant. *Am J Transplant* **12:**1157–1167.
9. **Shiina T, Suzuki S, Ozaki Y, Taira H, Kikkawa E, Shigenari A, Oka A, Umemura T, Joshita S, Takahashi O, Hayashi Y, Paumen M, Katsuyama Y, Mitsunaga S, Ota M, Kulski JK, Inoko H.** 2012. Super high resolution for single molecule-sequence-based typing of classical HLA loci at the 8-digit level using next generation sequencers. *Tissue Antigens* **80:**305–316. PubMed
10. **Ozaki Y, Suzuki S, Shigenari A, Okudaira Y, Kikkawa E, Oka A, Ota M, Mitsunaga S, Kulski JK, Inoko H, Shiina T.** 2014. HLA-DRB1, -DRB3, -DRB4 and -DRB5 genotyping at a super-high resolution level by long range PCR and high-throughput sequencing. *Tissue Antigens* **83:**10–16. PubMed
11. **Terasaki P, Mickey MR, Singal DP, Mittal KK, Patel R.** 1968. Serotyping for homotransplantation. XX. Selection of recipients for cadaver donor transplants. *N Engl J Med* **279:**1101–1103.
12. **Cecka JM.** 2010. Calculated PRA (CPRA): the new measure of sensitization for transplant candidates. *Am J Transplant* **10:**26–29.
13. **Montgomery RA, Gentry SE, Marks WH, Warren DS, Hiller J, Houp J, Zachary AA, Melancon JK, Maley WR, Rabb H, Simpkins C, Segev DL.** 2006. Domino paired kidney donation: a strategy to make best use of live non-directed donation. *Lancet* **368:**419–421. PubMed
14. **Rees MA, Kopke JE, Pelletier RP, Segev DL, Rutter ME, Fabrega AJ, Rogers J, Pankewycz OG, Hiller J, Roth AE, Sandholm T, Unver MU, Montgomery RA.** 2009. A nonsimultaneous, extended, altruistic-donor chain. *N Engl J Med* **360:**1096–1101. PubMed
15. **Montgomery RA, Lonze BE, King KE, Kraus ES, Kucirka LM, Locke JE, Warren DS, Simpkins CE, Dagher NN, Singer AL, Zachary AA, Segev DL.** 2011. Desensitization in HLA-incompatible kidney recipients and survival. *N Engl J Med* **365:**318–326. PubMed
16. **Morrow WR, Frazier EA, Mahle WT, Harville TO, Pye SE, Knecht KR, Howard EL, Smith RN, Saylors RL, Garcia X, Jaquiss RD, Woodle ES.** 2012. Rapid reduction in donor-specific anti-human leukocyte antigen antibodies and reversal of antibody-mediated rejection with bortezomib in pediatric heart transplant patients. *Transplantation* **93:**319–324. PubMed
17. **Reinsmoen NL, Lai CH, Vo A, Cao K, Ong G, Naim M, Wang Q, Jordan SC.** 2008. Acceptable donor-specific antibody levels allowing for successful deceased and living donor kidney transplantation after desensitization therapy. *Transplantation* **86:**820–825. PubMed
18. **Stegall MD, Diwan T, Raghavaiah S, Cornell LD, Burns J, Dean PG, Cosio FG, Gandhi MJ, Kremers W, Gloor JM.** 2011. Terminal complement inhibition decreases antibody-mediated rejection in sensitized renal transplant recipients. *Am J Transplant* **11:**2405–2413. PubMed
19. **Opelz G, Collaborative Transplant Study.** 2005. Non-HLA transplantation immunity revealed by lymphocytotoxic antibodies. *Lancet* **365:**1570–1576. PubMed
20. **Zhang Q, Reed EF.** 2010. Non-MHC antigenic targets of the humoral immune response in transplantation. *Curr Opin Immunol* **22:**682–688. PubMed
21. **Mengel M, Sis B, Haas M, Colvin RB, Halloran PF, Racusen LC, Solez K, Cendales L, Demetris AJ, Drachenberg CB, Farver CF, Rodriguez ER, Wallace WD, Glotz D, Banff Meeting Report Writing Committee.** 2012. Banff 2011 Meeting report: new concepts in antibody-mediated rejection. *Am J Transplant* **12:**563–570.
22. **Sacks SH, Zhou W.** 2012. The role of complement in the early immune response to transplantation. *Nat Rev Immunol* **12:**431–442. PubMed
23. **Bartel G, Brown K, Phillips R, Peng Q, Zhou W, Sacks SH, Wong W.** 2013. Donor specific transplant tolerance is dependent on complement receptors. *Transplant Int* **26:**99–108.
24. **Fürst D, Müller C, Vucinic V, Bunjes D, Herr W, Gramatzki M, Schwerdtfeger R, Arnold R, Einsele H, Wulf G, Pfreundschuh M, Glass B, Schrezenmeier H, Schwarz K, Mytilineos J.** 2013. High-resolution HLA matching in hematopoietic stem cell transplantation: a retrospective collaborative analysis. *Blood* **122:**3220–3229. PubMed
25. **Lee SJ, Klein J, Haagenson M, Baxter-Lowe LA, Confer DL, Eapen M, Fernandez-Vina M, Flomenberg N, Horowitz M, Hurley CK, Noreen H, Oudshoorn M, Petersdorf E, Setterholm M, Spellman S, Weisdorf D, Williams TM, Anasetti C.** 2007. High-resolution donor-recipient HLA matching contributes to the success of unrelated donor marrow transplantation. *Blood* **110:**4576–4583. PubMed
26. **Loiseau P, Busson M, Balere ML, Dormoy A, Bignon JD, Gagne K, Gebuhrer L, Dubois V, Jollet I, Bois M, Perrier**

P, Masson D, Moine A, Absi L, Reviron D, Lepage V, Tamouza R, Toubert A, Marry E, Chir Z, Jouet JP, Blaise D, Charron D, Raffoux C. 2007. HLA association with hematopoietic stem cell transplantation outcome: the number of mismatches at HLA-A, -B, -C, -DRB1, or -DQB1 is strongly associated with overall survival. *Biol Blood Marrow Transplant* **13:**965–974.

27. **Fleischhauer K, Shaw BE, Gooley T, Malkki M, Bardy P, Bignon JD, Dubois V, Horowitz MM, Madrigal JA, Morishima Y, Oudshoorn M, Ringden O, Spellman S, Velardi A, Zino E, Petersdorf EW, International Histocompatibility Working Group in Hematopoietic Cell Transplantation.** 2012. Effect of T-cell-epitope matching at HLA-DPB1 in recipients of unrelated-donor haemopoietic-cell transplantation: a retrospective study. *Lancet Oncol* **13:**366–374. PubMed
28. **Delaney C, Bollard CM, Shpall EJ.** 2013. Cord blood graft engineering. *Biol Blood Marrow Transplant* **19**(Suppl 1)**:**S74–S78.
29. **Eapen M, Rubinstein P, Zhang MJ, Stevens C, Kurtzberg J, Scaradavou A, Loberiza FR, Champlin RE, Klein JP, Horowitz MM, Wagner JE.** 2007. Outcomes of transplantation of unrelated donor umbilical cord blood and bone marrow in children with acute leukaemia: a comparison study. *Lancet* **369:**1947–1954. PubMed
30. **Khan F, Agarwal A, Agrawal S.** 2004. Significance of chimerism in hematopoietic stem cell transplantation: new variations on an old theme. *Bone Marrow Transplant* **34:**1–12. PubMed
31. **Lion T.** 2007. Detection of impending graft rejection and relapse by lineage-specific chimerism analysis. *Methods Mol Med* **134:**197–216. PubMed

Molecular Methods for Human Leukocyte Antigen Typing: Current Practices and Future Directions

MARK KUNKEL, JAMIE DUKE, DEBORAH FERRIOLA,
CURT LIND, AND DIMITRI MONOS

113

OVERVIEW

The characterization and clinical assessment of the human leukocyte antigen (HLA) genes has undergone significant advances over the last 50 years. As serological methods have given way to more-advanced molecular methods, our understanding of the complexity and polymorphic nature of the HLA genes has been substantially improved. From its basis in serological and cellular testing in the 1960s (antibody and mixed lymphocyte culture) (1–5), through two-dimensional electrophoresis and restriction fragment length polymorphism analysis in the 1970s and '80s (5, 6), the development of PCR in the mid-1980s revolutionized our molecular understanding of the HLA genes. From PCR, methods utilizing sequence-specific oligonucleotide probes (SSOs) and sequence-specific primers (SSPs) provided the means for more directly evaluating the highly variable sequence motifs within the HLA genes (7–10). Subsequently, in the 1990s, Sanger sequence-based typing (SBT) significantly advanced tissue typing and transplantation genetics (11–14) by providing an unprecedented molecular view of HLA polymorphism in the context of exonic variation. Most recently, next-generation sequencing (NGS) appears to definitively address HLA typing complexity, as it provides entire HLA gene characterization and haploid sequence determination.

From the discovery of the first HLA antigen, MAC (by Jean Dausset in the late 1950s) (15), to the rapid discovery of many more antigens throughout the 1960s (16), the scientific community recognized the need for common reagents, tests, methods, and formal naming conventions for the proteins responsible for self/nonself recognition. The first international HLA workshop in 1964 set the stage for identifying reliable, tested antisera for serological typing and established official nomenclature (17). In conjunction with these workshops, mixed lymphocyte culture testing, developed in the 1960s, quickly demonstrated the inadequacy of serological typing alone, as reactivity (and rejection) was often observed between subjects who were serologically identical (18). At the same time, Rolf Zinkernagel and Peter Doherty in the early 1970s discovered (19, 20) that immunologic effector cells, T cells, recognize and respond to a specific antigen only if a peptide from the antigen is presented in the context of an HLA molecule.

The Role and Polymorphic Nature of HLA Genes

Even with a basic cellular and humoral understanding of HLA protein function, the concept of major histocompatibility complex (MHC) restriction, in light of antigen binding and presentation, wasn't fully understood until the HLA protein structure was determined in the late 1980s (21–23). The identification of the HLA protein's antigen-binding pocket explained how allelic polymorphisms within the pocket create the potentially millions of variable antigen specificities from just a few genes. Therefore, the highly polymorphic nature of the HLA genes is largely related to their necessary immune function, where, as receptors for foreign antigens, the HLA proteins must display a vast repertoire of potential antigen-binding conformations. In the late 1980s and 1990s, as molecular methods like SSO, SSP, and SBT were fully developed (7–14), the HLA genes were recognized as some of the most polymorphic in the human genome and formed the basis for the creation of an HLA allele sequence library, whereby all known HLA alleles could be recorded. The very high variability of the HLA genes and their respective proteins interacting with both self and nonself peptides has implications in organ and bone marrow transplantation, autoimmune disease, response to infectious disease, and even response to medications (pharmacogenomics) (24–29).

Organization of the HLA Genes and the Ensuing Protein Structure

The HLA genes are located on the short arm of chromosome 6 within the MHC region, which encodes many immune response proteins (30, 31). Beyond the standard class I (*HLA-A*, *-B*, and *-C*) and class II genes (*HLA-DRB1/3/4/5*, *-DQA1*, *-DQB1*, *-DPA1*, and *-DPB1*) targeted by HLA typing, there are multiple class I and class II "related" or pseudogenes spread across ~3.5 Mb of the MHC (for a complete list, see Table 1).

The class I molecule is a transmembrane protein made up of a single HLA polypeptide heavy chain (encoded by a single MHC gene) that is associated noncovalently with β-microglobulin (a protein encoded by a nonpolymorphic, non-MHC gene) (Fig. 1). For class I proteins, the antigen recognition site (ARS) is encoded by exon 2 (α1 domain) and by exon 3 (α2 domain). Exon 4 encodes a region (α3 domain) that associates with β-microglobulin and is proximal to the cell membrane. Of most importance to tissue typing, exons 2 and 3 are the most polymorphic and encode the peptide-binding domains involved in antigen presentation, which is why traditionally only polymorphisms in exons 2 and 3 were assessed. More recently, class I HLA typing has

doi:10.1128/9781555818722.ch113

TABLE 1 HLA genes, gene fragments, and pseudogenes[a]

Name	Previous equivalents	Molecular characterization
HLA-A	–	Class I α-chain
HLA-B	–	Class I α-chain
HLA-C	–	Class I α-chain
HLA-E	E, '6.2'	Associated with class I 6.2-kb HindIII fragment
HLA-F	F, '5.4'	Associated with class I 5.4-kb HindIII fragment
HLA-G	G, '6.0'	Associated with class I 6.0-kb HindIII fragment
HLA-H	H, AR, '12.4'	Class I pseudogene associated with 5.4-kb HindIII fragment
HLA-J	cda12	Class I pseudogene associated with 5.9-kb HindIII fragment
HLA-K	HLA-70	Class I pseudogene associated with 7.0-kb HindIII fragment
HLA-L	HLA-92	Class I pseudogene associated with 9.2-kb HindIII fragment
HLA-N	HLA-30	Class I gene fragment associated with 1.7-kb HindIII fragment
HLA-P	HLA-90	Class I gene fragment associated with 9.0-kb HindIII fragment
HLA-S	HLA-17	Class I gene fragment associated with 3.0-kb HindIII fragment
HLA-T	HLA-16	Class I gene fragment associated with 16.0-kb HindIII fragment
HLA-U	HLA-21	Class I gene fragment associated with 2.1-kb HindIII fragment
HLA-V	HLA-75	Class I gene fragment associated with 7.5-kb HindIII fragment
HLA-W	HLA-80	Class I gene fragment associated with 8.0-kb HindIII fragment
HLA-X	HLA-X	Class I gene fragment
HLA-Y	HLA-BEL/COQ/DEL	Class I pseudogene
HLA-Z	HLA-Z1	Class I gene fragment located within the HLA class II region
HLA-DRA	DRα	DR α-chain
HLA-DRB1	DRβI, DR1B	DR β1-chain determining specificities of DR1, DR2, DR3, DR4, DR5, etc.
HLA-DRB2	DRβII	Pseudogene with DR β-like sequences
HLA-DRB3	DRβIII, DR3B	DR β3-chain determining DR52 and Dw24, Dw25, Dw26 specificities
HLA-DRB4	DRβIV, DR4B	DR β4-chain determining DR53
HLA-DRB5	DRβIII	DR β5-chain determining DR51
HLA-DRB6	DRBX, DRBσ	DRB pseudogene found on DR1, DR2, and DR10 haplotypes
HLA-DRB7	DRBψ1	DRB pseudogene found on DR4, DR7, and DR9 haplotypes
HLA-DRB8	DRBψ2	DRB pseudogene found on DR4, DR7, and DR9 haplotypes
HLA-DRB9	M4.2 β exon	DRB pseudogene, isolated fragment
HLA-DQA1	DQα1, DQ1A	DQ α-chain as expressed
HLA-DQB1	DQβ1, DQ1B	DQ β-chain as expressed
HLA-DQA2	DXα, DQ2A	DQ α-chain-related sequence, not known to be expressed
HLA-DQB2	DXβ, DQ2B	DQ β-chain-related sequence, not known to be expressed
HLA-DQB3	DVβ, DQB3	DQ β-chain-related sequence, not known to be expressed
HLA-DOA	DZα, DOα, DNA	DO α-chain
HLA-DOB	DOβ	DO β-chain
HLA-DMA	RING6	DM α-chain
HLA-DMB	RING7	DM β-chain
HLA-DPA1	DPα1, DP1A	DP α-chain as expressed
HLA-DPB1	DPβ1, DP1B	DP β-chain as expressed
HLA-DPA2	DPα2, DP2A	DP α-chain-related pseudogene
HLA-DPB2	DPβ2, DP2B	DP β-chain-related pseudogene
HLA-DPA3	DPA3	DP α-chain-related pseudogene
TAP1	ABCB2, RING4, Y3, PSF1	ABC transporter
TAP2	ABCB3, RING11, Y1, PSF2	ABC transporter
PSMB9	LMP2, RING12	Proteasome-related sequence
PSMB8	LMP7, RING10	Proteasome-related sequence
MICA	MICA, PERB11.1	Class I chain-related gene
MICB	MICB, PERB11.2	Class I chain-related gene
MICC	MICC, PERB11.3	Class I chain-related pseudogene
MICD	MICD, PERB11.4	Class I chain-related pseudogene
MICE	MICE, PERB11.5	Class I chain-related pseudogene

[a]Adapted from reference 35.

expanded to include other exons in high-resolution typing, as exon 4, for example, has been shown to contain polymorphisms that distinguish unique HLA alleles.

The class II molecule is made up of separate α and β protein subunits encoded on separate genes within the MHC that are noncovalently associated posttranslationally (Fig. 1). The ARS is exclusively encoded by exon 2 of both the α- and β-chains (α1 and β1 domains). Exon 3 from both the α- and β-chain (α2 and β2 domains) makes up the region proximal to the cell membrane. Historically, due to its involvement in antigen presentation, only exon 2 of class II proteins was interrogated, but due to known polymorphisms in exon 3, increasingly both exons are included in high-resolution typing.

The Publication of HLA Data

Since 1987, the organization, public accessibility, and distribution of HLA allele data has been provided through the IMGT/HLA database, managed by the Anthony Nolan Research Institute and hosted by the European Bioinformatics Institute (http://www.ebi.ac.uk/ipd/imgt/hla/). Since the introduction of the database, there has been steady growth in the number of alleles, with 14,409 alleles now identified (release 3.23.0, January 2016). The ever increasing number of new alleles, combined with current typing method limitations, poses a challenge to labs that need to identify these alleles for clinical purposes. Identifying new alleles can be costly, time-consuming, and, not infrequently, nearly impossible to do using commercially available products, as the products are often not sufficiently updated to resolve newly described diversity. The immunogenetics community has responded to this challenge by establishing a set of guidelines that determines the extent to which laboratories might resolve HLA ambiguities caused by both the new allele sequence and the unknown phasing of the additional polymorphisms that can lead to additional allele possibilities. These guidelines are based on the frequency of the alleles in a given population and on the polymorphisms located within exons 2 and 3 of class I and exon 2 of class II alleles. Typings that involve common and/or well-documented (CWD) alleles are resolved, while alleles that are extremely rare are not required to be resolved. By definition, "common" alleles are observed at frequencies > 0.001 in reference populations of at least 1,500 individuals and have allele frequency data available. The "well-documented" category includes alleles that have been observed five times in unrelated individuals or have been detected three times via SBT and observed in a specific haplotype in unrelated individuals (32, 33). These guidelines are used for reporting proficiency testing results and have subsequently been adopted by some hematopoietic stem cell donor registries and accreditation organizations. The CWD alleles database is published through a separate consortium and, like the IMGT/HLA database, is also expected to be updated on a regular basis. The most recent publication by this consortium indicates that there are now 1,122 CWD alleles within the HLA-A, -B, -C, -DRB1, -DRB3/4/5, -DQA1, -DQB1, -DPA1, and -DPB1 loci. This represents only 14.3% of the HLA alleles in the IMGT/HLA 3.9.0 database (33).

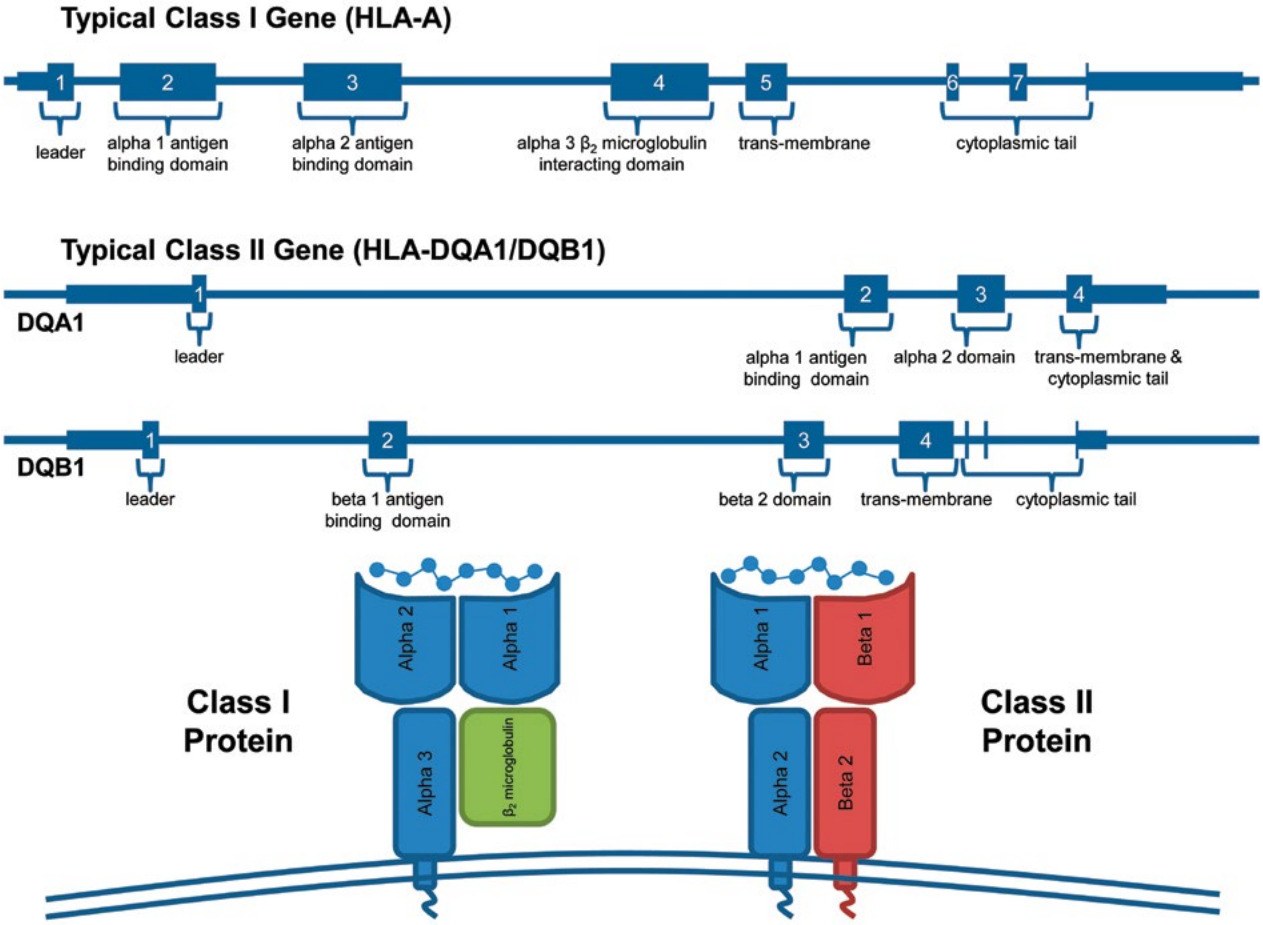

FIGURE 1 Structure of HLA class I and class II genes.

HLA Nomenclature and Recent Changes

The HLA naming convention has undergone substantial iteration, as earlier naming conventions were unable to address the growing numbers and complexity of alleles (e.g., A*02 and B*15 have >100 alleles) (34). At the 15th International Histocompatibility and Immunogenetics Workshop in 2008 (http://ihiws.org/), the WHO Nomenclature Committee for Factors of the HLA System met to determine improvements to the existing nomenclature to address the growing numbers of new alleles being discovered and to reduce naming complexity and confusion (Fig. 2). These changes were implemented in 2010 (35).

Generally, the proposed changes added delimiters (field separators) between each data field in an allele name (e.g., A*01010101 became A*01:01:01:01) to clearly delineate the protein coding and noncoding differences. Three (or more) digit fields are also allowed, providing for allele families that contain >99 alleles. Further changes and details (provided from http://hla.alleles.org) are summarized as follows. The first field following the asterisk in the allele name (**XX**:xx:xx:xx) describes the allele family and generally corresponds to the serological assignment carried by the allotype. HLA typing defined only at the first field is often referred to as low-resolution typing. The second field following the first colon (xx:**XX**:xx:xx) is assigned sequentially as new alleles are determined (e.g., 01, 02, 03 … 101, 102, etc.). Together, these two fields (**XX**:**XX**) indicate one or more nucleotide substitutions that change the HLA protein coding sequence; typing at this level is often referred to as high-resolution typing (the Harmonization of Histocompatibility Typing Terms Working Group recently defined a high-resolution typing result "as a set of alleles that encode the same protein sequence for the region of the HLA molecule called the antigen-binding site and that exclude alleles that are not expressed as cell-surface proteins" [36]). The third field (xx:xx:**XX**:xx) is for designating synonymous nucleotide substitutions within the coding sequence that do not change the amino acids of the protein, while the fourth field (xx:xx:xx:**XX**) identifies sequence polymorphisms in introns, or in the 5′ and 3′ untranslated regions. At the end of the allele name, specific characters have been added (N = null, L = low expression, S = secreted, C = cytoplasm, A = aberrant, Q = questionable) to designate unique characteristics for an allele, such as whether a protein is not expressed (e.g., HLA-A*24:09N) or whether the expression of the protein is unclear (e.g., HLA-A*32:11Q).

HLA TYPING METHODOLOGIES

To meet the growing demand, clinical HLA typing over the past decade has transitioned from a combination of serological and DNA-based methods to a preference for more-direct, faster, more-affordable, and more-informative DNA-based techniques. While serological typing may continue to have a place in clinical or research-based testing in determining the expression of the HLA molecule at the cell surface (a function that DNA-based testing cannot always verify), direct DNA-based typing techniques have all but replaced serological methods in routine HLA typing. This has been driven by advances in commercial HLA typing kits and software using existing SSO, SSP, and SBT methods. With the advent of next-generation and even third-generation sequencing systems, HLA typing is now poised to advance to a level that can truly provide rapid, direct, complete phasing of polymorphic positions throughout an entire gene, with both improved technical performance and reduced overall costs.

DNA-Based Typing Techniques

The most prevalent and well-developed techniques in use today are SSO, SSP, and SBT (Fig. 3). The SSO technique interrogates polymorphic differences using panels of individual DNA oligonucleotide probes that differentially hybridize to the target of interest; the probe either perfectly matches or mismatches the target's polymorphic sites. The hybridization pattern of the oligonucleotides is compared to an expected pattern, based on the sequence database of HLA alleles, and is interpreted as an HLA type. The SSP method uses panels of specific primer sets that overlap polymorphic sites. Perfectly matched primers produce an amplification product, while mismatched primers do not; the pattern of amplification from multiple primer sets determines the HLA allele. In SBT, specific gene regions, usually exons, are amplified and sequenced through a process of polymerase-based extension of specific sequencing primers using fluorescently labeled nucleotides, indicating allelic differences base by base.

Early kits were focused primarily on identifying polymorphisms in exons 2 and 3 of class I genes and exon 2 of class II genes. But as more typings were performed across broader, more ethnically diverse populations, and as more unique HLA alleles were discovered, the ability of these early kits to provide definitive HLA typing decreased. Furthermore, polymorphisms outside of the traditionally tested

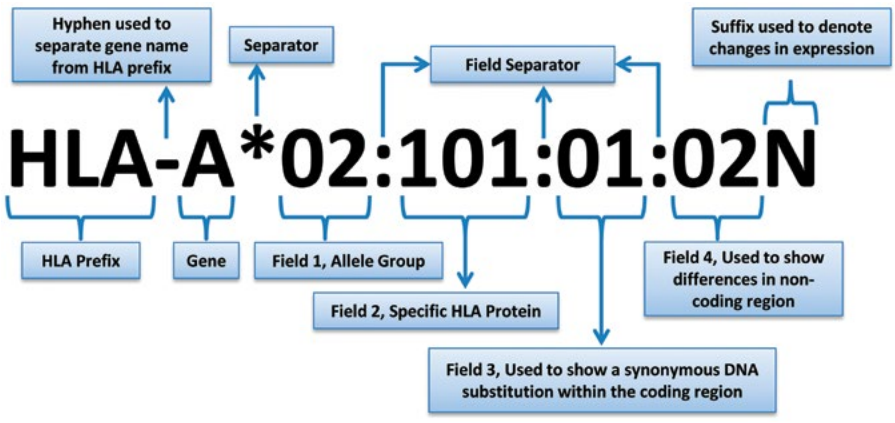

FIGURE 2 HLA nomenclature. Courtesy of Steven G. E. Marsh, Anthony Nolan Research Institute, London, United Kingdom.

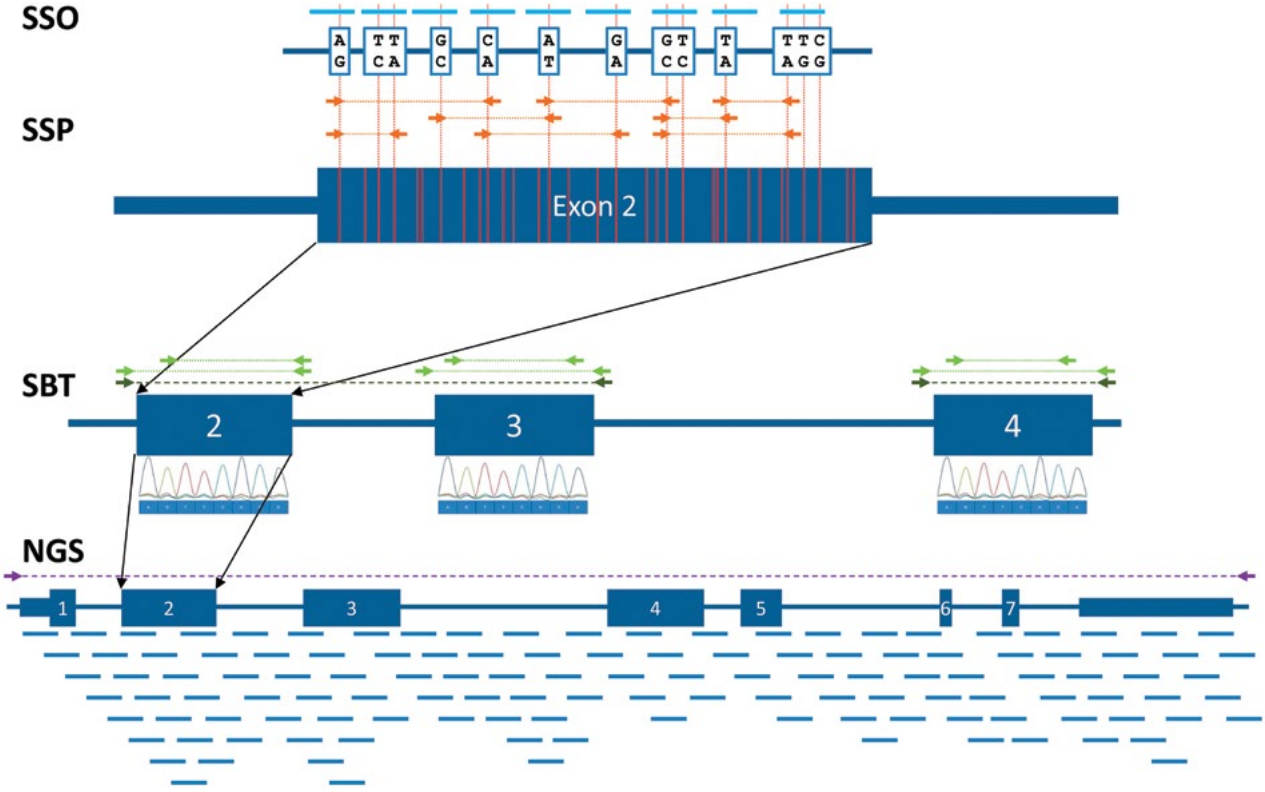

FIGURE 3 Examples of molecular HLA typing techniques and their methods of interrogating the HLA genes. For any given HLA gene (dark blue rectangles), SSOs of ~20 bp (light blue lines) can provide single-nucleotide resolution of haplotype differences (polymorphic differences, red lines in exon 2), but this results in a complex panel of oligonucleotide probes to discern differences between HLA alleles. This probe set is static and therefore cannot adjust to novel alleles. SSPs (orange arrows) can provide haplotype- or allele-specific resolution of nucleotide differences and additionally provide some level of phasing between polymorphic sites. As with SSOs, these oligonucleotide sets are complex and static, limiting their flexibility. SBT provides whole-exon information on the polymorphic content of the HLA allele (amplification primers [dark green] and sequencing primers [light green arrows]) but cannot discern phasing, as this method generally does not rely on allele-specific primers for amplification as a first step. NGS provides whole-gene amplification (amplification primers, purple arrows) and detection of polymorphic content for any HLA allele (known or unknown) and provides significant phasing between polymorphic sites that are within the read lengths of the system being used (usually between 200 and 1,000 bp). This is accomplished through the alignment of thousands of short overlapping reads that are combined to form a single consensus sequence (blue lines).

exons were being described, requiring an expansion into non-ARS regions such as exon 4 for class I and exon 3 for class II. Interrogation of exons that code for transmembrane and intracellular domains was also often required to resolve null alleles that differed only in these exons (e.g., HLA-C*04:09N). Therefore, SSP and SSO kit manufacturers were required to continuously incorporate additional primers and probes to keep up with the growing number of HLA alleles (a problem faced even today). In a further step to provide comprehensive typing, SBT kits began to offer gene amplification with additional sequencing primers (and even allele-specific sequencing primers) as a means to provide expanded coverage of the HLA genes, a practice that is commonplace in SBT kits today.

NGS and Its Potential Impact on HLA Typing

More recently, developments in NGS technology have demonstrated substantial improvements in HLA typing (37–43). Regardless of the platform—Roche 454 GS FLX and GS Junior (Roche Diagnostics, Indianapolis, IN); MiSeq (Illumina, San Diego, CA); Ion Torrent Personal Genome Machine (PGM) (Life Technologies, Thermo Fisher Scientific, Carlsbad, CA), or Pacific Biosciences' (Menlo Park, CA) technology—these systems resolve a number of technological barriers that continue to hamper existing molecular techniques, such as inflexibility in typing and discovering novel alleles and the inability to easily resolve phase ambiguities. While HLA typing by NGS is just now being introduced, it is likely that this new method will transform the way HLA typing is performed in the coming years.

THE PROCESS OF DNA-BASED HLA TYPING

Regardless of the methodology, several processes are required for the implementation of DNA-based HLA typing. Specifically, genomic DNA must be extracted from a sample, the HLA genes amplified, and the resulting products interrogated and analyzed against a library of HLA allele sequences. These processes can be generically broken down into (i) sample preparation, (ii) template amplification,

(iii) interrogation, and (iv) analysis. While template amplification, interrogation, and analysis are often methodology specific, sample preparation is often quite similar and faces similar requirements across all HLA typing methodologies.

Sample Preparation

Genomic DNA should be prepared using well-tested, commercially available DNA preparation kits to ensure consistency of preparation. DNA can be extracted from blood, buccal swabs/brushes, saliva, buffy coat, or blood-spotted filter paper. While ethanol precipitation is generally considered an excellent approach to removing many forms of inhibitors, spin column- and bead-based approaches can provide DNA of sufficient quality and concentration to avoid most problems. The DNA must be free from contaminants that can affect later amplification, hybridization, and sequencing steps (e.g., alcohol, salts, detergents, formaldehyde, and heparin [blood should not be collected in heparinized tubes, and blood samples from patients undergoing heparin therapy and lipemic or hemolyzed samples should not be used]) and should have a 260/280-nm absorbance ratio of ~1.7 to 1.9. Prepared genomic DNA can be used immediately if prepared in nuclease-free water or stored for extended periods at –20°C or lower when properly buffered. Stored DNA should have a concentration of >10 ng/μl and repeated freeze-thaw cycles should be avoided to reduce degradation.

The purity and quality of the genomic and amplified DNA should be validated by spectrophotometric methods. Apart from simple concentration determination (NanoDrop; Thermo Scientific), traditional UV spectrometry can be useful for determining contaminants left over from processing steps, as a number of components (e.g., phenol and chaotropic salts) absorb in the 280-nm and/or 230-nm spectral region. Therefore, visual examination of the absorbance curves can be informative beyond calculating the 260/280-nm ratio. And while the 260/280-nm ratio is useful as a general measure of purity (pure DNA ratio is ~1.8), it is a poor indicator of protein contamination due to its lack of sensitivity (44). Because of potential contaminants, UV methods may not accurately determine concentration. Intercalating dye assays like the Quant-iT PicoGreen dsDNA Assay (Life Technologies) in conjunction with a fluorometer (Qubit; Life Technologies) can provide highly accurate double-stranded DNA concentration determination without interference from potential contaminants. Regardless of the approach, accurate determination of concentration and purity is required for robust assay performance.

Template Amplification

HLA genotyping requires the amplification of the HLA genes by PCR. Depending on the method chosen, the amplification may only include specific exons (exons 2 and 3 of class I genes and exon 2 of class II genes) or may include the entire gene (using multiple amplicons or one single amplicon). Generally, amplification for each HLA locus is performed in a single reaction (one locus per tube) for each sample. Exonic amplification can be performed using standard PCR reagents, while whole-gene amplification generally requires reagents designed for long-range PCR (LR-PCR).

Genotyping

Once DNA is prepared for testing, the process of deriving an HLA genotype can follow several paths depending on the methods and systems installed (described below), the specific need, and the costs involved. While low-resolution typing can typically be obtained with a single test, high-resolution typing is often an iterative process whereby low-resolution testing is followed with additional rounds of high-resolution testing. Historically, low-resolution typing is less costly and higher throughput than high-resolution typing. For bone marrow transplantation, low-resolution typing has been widely used for the initial typing of donors for bone marrow registries, while high-resolution typing is often reserved for bone marrow recipients, is required in selecting final donors for bone marrow transplantation, and, most recently, has also been used for recruitment typing by registries. For solid organ transplantation, low-resolution typing is also performed for donors and recipients, while a second round of high-resolution typing may be required prior to transplantation. This is particularly relevant today as new recombinant single-antigen technology has enabled HLA laboratories to identify anti-HLA antibodies for assessing solid organ transplantation. Therefore, performing allele-level, high-resolution typing can be useful in the context of assessing donor-specific antibodies, as there is now widespread evidence that allele-specific antibodies can impact transplant outcome (45–47).

Analysis

The data generated by the various methods, whether in the form of probe, primer reaction patterns, or sequence information, is typically analyzed with a dedicated software analysis program that accounts for all HLA alleles in the IMGT/HLA database. All software packages available to date use some form of updating service to ensure that the software's internal reference database of known HLA alleles is up to date with the IMGT/HLA database. The level of sophistication, bioinformatics support, and data-handling infrastructure is largely driven by the typing systems being used. SSO- and SSP-based systems have the simplest software requirements and generally require little bioinformatics support, as the amount of raw data is very low and the software automatically converts the raw data (gel images, microparticle fluorescence, and melt curves) into digitized summary data. Interpretation is largely left to the software to assess and determine the HLA alleles present in the sample (or alternative possibilities) based on the presence or absence of assay results (essentially a yes-or-no answer for each probe or primer set). SBT requires significantly more support in terms of both data storage and interpretation of results. Raw sequence reads (electropherograms) are stored and converted by the software into base calls, which are used to determine the presence of specific alleles. With very low noise, robust amplification, and high-quality sequencing, allele calling may produce nonambiguous results. But by the very nature of diploid sequencing, the electropherograms need to be screened visually to determine read quality issues (poor-quality electropherogram), potential contamination issues, miscalled bases (due to low peak height), unexpected homozygosity (from preferential allele amplification), and ambiguous results from unresolvable polymorphism phasing. This review process requires a keen understanding of the biochemistry involved, the operation of the capillary sequencing instrument, and the vagaries of HLA gene sequencing. Therefore, analysis is most often performed by experienced technologists. The introduction of NGS-based HLA typing only increases the bioinformatics support requirements and data analysis needs. NGS systems can generate gigabytes of data per run that need to be processed and supported by well-managed data analysis pipelines. Software packages developed specifically for analyzing HLA NGS data provide automated allele calling but still require manual annotation and review of the results (like SBT).

Review of typing results is critical for detecting problems in the genotyping process and to verify the detection of potential novel alleles. Poor sample quality can result in low or failed amplifications that can skew typing results. Amplification bias, caused by poor primer design, contamination in the reactions, or suboptimal amplification conditions, can lead to spurious typing results even when using commercially available primer sets. A particularly difficult bias arises from imbalanced allele amplification. Due to the complexity of the HLA genes, it is not unusual to have only one of the two alleles present in a sample amplify robustly. This often leads to a strong imbalance in the representation of the two alleles in the amplified material that can mimic a homozygous sample. Imbalances of as much as 90% favoring one allele over the other are not uncommon. Therefore, whichever software is used to analyze the data, the software (and user) must take into account the possibility of allelic imbalance in interpreting the results. While much of the process of analyzing HLA data has been automated, the process of analysis is still sufficiently complex that human oversight and intervention is absolutely required.

REGULATORY OVERSIGHT AND QUALITY CONTROL OF CLINICAL HLA TYPING

Regulatory and Reporting Requirements

Laboratories wanting to establish and perform HLA typing must undergo a process of certification and accreditation. The primary accreditation bodies for HLA typing in the United States are the American Society for Histocompatibility and Immunogenetics (ASHI) and the College of American Pathologists (CAP), while in Europe it is the European Federation for Immunogenetics (EFI). Other countries have chosen to use either ASHI or EFI accreditation. Within the United States, additional accreditation requirements may be imposed by state authorities (e.g., New York or California) in order to perform HLA testing. Organizations like the National Marrow Donor Program and the United Network for Organ Sharing require U.S.-based laboratories to have ASHI or CAP accreditation.

The usual process for accreditation requires that every other year accreditation representatives visit laboratories to physically review procedure documentation (standard operating procedures), quality control and quality assurance practices, and typical typing results (actual patient test records) from organ and bone marrow transplantation testing. These reviews evaluate test results, quality control reports (reagents and instrumentation), maintenance logs, and laboratory staff certifications (training and competency). Generally ASHI and CAP reviews are cycled every other year. In either case, an ASHI reaccreditation application must be filed through online services while a CAP test activity menu is updated online each year. Demonstration of laboratory proficiency is performed through external proficiency testing that can be purchased from CAP or ASHI. This testing service provides blinded sample sets that the laboratory must type accurately in order to pass proficiency.

Quality Control and Quality Assurance

Quality control for HLA typing can be defined as the application of quality processes to ensure correct HLA genotyping, reduce errors, and improve efficiency (driven by standard operating procedures), while quality assurance is the measure of how well those quality control processes are actually working (results from controls, auditing, error correction, and process reviews). Errors in HLA typing can come from multiple sources but are largely driven by people, processes, equipment, or reagents. Validated protocols should be developed, documented, practiced, and updated regularly to reduce errors relating to pipetting mistakes (including cross-contamination), incorrect calculations, and missed steps. The validation process must include rigorous evaluation of the entire process under practical conditions, using both typical and difficult samples to determine the limitations of the assay. Equipment used in any process must be well maintained and checked for performance at least as regularly as specified by the manufacturer. For example, liquid-handling automation must be checked to verify pipetting performance and variance and PCR thermal cyclers must be checked for temperature consistency. Reagent use must be thoroughly documented (with calculations preconfigured for use), and a process should be in place to avoid using expired lots of materials. Negative reactions should be performed to verify that contamination is not present and positive control samples run to verify performance and accuracy over time. The effectiveness of all these quality control processes must also be evaluated over time to ensure that systematic errors are identified and eliminated and that novel errors are reduced as much as possible.

Sample Management and Prevention of Contamination

Barcoding systems for sample tracking and data entry are ideal for avoiding transcription errors and simplifying processing, particularly when samples are stored in 96- or 384-well plates, and when using automation. Irrespective of the size of the laboratory, some degree of automation, whereby manual handling of certain steps and transcription of results is avoided, is strongly recommended and desirable. For large-volume laboratories, the use of liquid-handling automation is absolutely necessary to reduce sample-processing error. Systems from Hamilton (Reno, NV), Tecan (Männedorf, Switzerland), and Beckman Coulter (Brea, CA) have decades of development behind the current commercial products, each with their own advantages and disadvantages (flexibility, capacity, processing speed, operating expense, etc.). While the instruments perform roughly the same function (the automated setup of liquid reagent reactions), the systems have to be assessed in the context of each laboratory's needs and, regardless of the instrument chosen, must be validated for the specific molecular test to be run.

A critical quality control issue is cross-contamination of samples. The possibility of contaminating adjacent samples when loading reactions, removing amplicons for quality control, or even sampling for processing is not trivial. With small reaction volumes and highly sensitive amplification reagents (requiring only nanograms of starting material), even minute droplets of DNA can result in spurious typing. This issue can be partially managed through automated liquid-handling systems. But a thorough quality control program is needed to ensure that samples are clearly and uniquely identified; that processes for selecting, thawing, opening, and plating samples are clear and precise; and that adequate data analysis checks are in place to detect spurious results. Further precautions, such as sequestering the PCR setup process in a separate room from the amplification, cleaning PCR setup surfaces with DNA-degrading cleaners, and performing routine wipe testing to verify lack of contamination, are all required to ensure that erroneous HLA typing results are avoided as much as possible.

CURRENT MOLECULAR METHODS FOR HLA TYPING

Sequence-Specific Oligonucleotide Probes

Principle of the Technology and Its Applications

Typing with SSO probes, commonly referred to as SSO, is a method that uses synthetic oligonucleotides of ~20 to 30 bp to effectively hybridize only to perfectly matched alleles at any given polymorphic site. Large sets of polymorphism-specific oligonucleotides have been designed for each HLA gene to cover a majority of the known HLA alleles. Hybridization conditions are optimized for each oligonucleotide set so that mismatched oligonucleotides do not hybridize efficiently to the target area while perfectly matched oligonucleotides remain stably hybridized.

The original development of the technique in the early 1990s provided a simple test that could easily identify the small number of HLA alleles characterized at that time. PCR primers were developed within conserved regions of the HLA genes with amplification products then bound to a membrane support and denatured to allow the allele-specific oligonucleotides (often labeled with biotin) to hybridize. This "forward" approach of hybridizing the PCR products to the membrane allowed for many samples to be processed on a single membrane, but required the production of the membrane for every sample set.

A simpler method (and the one most commonly used today) was subsequently developed, called reverse SSO (RSSO) typing, in which allele-specific oligonucleotide probes are bound (covalently) to a solid membrane support rather than the amplified products. PCR amplicons, usually labeled using biotin nucleotides, are then denatured and hybridized to the bound probes, washed, and detected by colorimetric or fluorogenic methods. The RSSO method provided a number of advantages, including the ability to preprint membrane strips containing the oligonucleotide probe sets. This allowed vendors to provide test kits ready for detecting amplicons produced by typing laboratories. Today, these membrane strips have largely been replaced by solution-based microparticle assays in which specific capture oligonucleotides are bound to individual microparticles rather than a membrane. In either case, the control of hybridization conditions and the stringency of the washing process greatly affect the pattern of bound versus unbound material and are critical to correctly indicating the alleles present in the sample. SSO typing is still commonly used today (especially in its microparticle form) to provide low-cost, rapid, low- to intermediate-resolution typing.

Strengths and Weaknesses

The primary advantages of SSO typing are its relative simplicity, low cost, and high throughput. RSSO typing based on the Luminex flow cytometry platform enables the interrogation of HLA amplicons by up to 100 or more sequence-specific probes in a single tube. The extent of probe hybridization is measured on the Luminex flow cytometer in an automated manner and through the use of a dedicated software program that translates the probe reaction patterns into HLA genotypes.

Microparticle-based RSSO typing is one of the most widely used methods today but is limited in its resolution. While this method typically delivers low-resolution typing expressed as serological equivalents, it rarely produces unambiguous two-field high-resolution typing, and it requires continual development. As new HLA alleles are discovered, developers of RSSO kits must continually add additional probes and amend the software programs to keep pace with the growing allele library. The technology also suffers from an inability to determine phasing between distal polymorphic sites, leading to unresolved ambiguities. The relatively short oligonucleotide probes can only provide phasing information for polymorphisms underlying the probe, making linkage across an exon difficult, and between exons impossible. For applications like clinical tissue transplantation, where an attempt to reduce ambiguities to an absolute minimum is preferred, an alternative method must be used to supplement the typing results from RSSO (for a summary of strengths and weaknesses, see Table 2).

Analysis of Data and Interpretation of Results

For membrane-based kits, software is now provided to allow automated interpretation of strip results. Membrane strips are either imaged or scanned, allowing the software to automatically detect signals for any specific oligonucleotide on the strip. For the Luminex platform, Luminex-supplied software (and versions of this software modified by each vendor) is provided that detects both the microparticles' fluorescent signature (thereby identifying the specific attached SSO oligonucleotide probe) and the fluorescent hybridization signal generated by the biotinylated HLA PCR product labeled with a streptavidin-phycoerythrin conjugate. The assay result is therefore coordinated with the microparticle signature, and a table of results is created providing oligonucleotide probe identification and allele determination. The software then uses this information to make an HLA genotype call based on expected results from the known oligonucleotide probe set and known HLA alleles. A significant advantage of this system is its real-time determination of assay results (usually within seconds of analyzing a sample). This provides for very rapid downstream analysis of assay results for determination of HLA type.

Troubleshooting and Technical Issues

The Luminex RSSO system is currently the preferred approach for RSSO typing; therefore, this section focuses on troubleshooting specifically for this system. A primary issue for any flow cytometer is proper care and maintenance. Flow cytometers require a sheath buffer for flowing the analytes through the system, and this sheath buffer must be free from contaminants to avoid problems with flow cell clogging and aberrant detection results. Therefore, it is prudent to use the manufacturer's provided sheath buffer. The flow cytometer must also be cleaned regularly, especially after running samples. Failure to do so will result in material trapped within the fluid paths of the system that will obscure results or cause the system to fail entirely.

From an assay perspective, the most critical factor to prevent problems is to ensure proper suspension of the microparticles. Microparticles by nature tend to clump together, and the manufacturer's recommendations for processing the microparticles should be followed. Failing to prepare the microparticles correctly could lead to spurious results and loss of data as clumped microparticles will generally be eliminated from the data set during analysis. As in any hybridization assay, hybridization conditions and reagents must be used and performed exactly as described by the manufacturer. Failure to do so will degrade assay performance or lead to spurious HLA typing results.

Sequence-Specific Priming

Principle of the Technology and Its Applications

Sequence-specific priming relies on the use of primers targeting specific polymorphic sites and has been in use for

TABLE 2 Advantages and disadvantages of molecular methods for HLA typing and of NGS platforms

Methods		Advantages	Disadvantages
Molecular typing methods	(R)SSO	Fast and simple technique Inexpensive Can be performed by hand or with some automation High throughput (SSO); low/high throughput (RSSO)	High frequency of ambiguity Cannot easily identify new alleles Cannot be used for new allele characterization (sequencing) Limited high-resolution typing capability
	SSP	Very fast, simple technique Inexpensive; very little equipment needed Some phasing possible	Not easily automated Cannot easily identify new alleles Ambiguity Kits increase in size as number of alleles in database grows Requires a lot of DNA for full-panel testing
	RT-PCR	Very fast (results in 90 min) Simplified processing (one sample-handling step) Besides the presence/absence of amplicons, analysis accounts for melting temperature features of the particular amplicon	Cannot easily identify new alleles Low throughput (only 1–2 samples per plate) Does not provide high-resolution typing Only one vendor
	SBT	Flexible, from one to dozens of samples per run Accurate, high-resolution typing Robust, validated kits Automatable Can easily handle novel alleles	Takes longer to perform than other methods Relatively expensive (technology is static) Cannot resolve all phasing ambiguities Experienced user required for analysis Low to moderate throughput
	NGS	Single-pass, high-resolution typing Resolves all ambiguities Can be highly automated High throughput	Processing takes 3–5 days Requires complex equipment, skilled technicians Requires batching to be cost-effective Commercial kits are under development Complex data management and analysis Technology development still in flux
NGS platforms	Life Technologies Ion Torrent	Low-cost platform Short run times Semiautomated	Homopolymer inaccuracy contributes to higher error rate
	Illumina MiSeq	Robust sequencing chemistry Least hands-on time Low error rate	Long run time

HLA typing since the early 1990s. In 1995, Bunce et al. (48) developed a comprehensive set of SSPs for all the major HLA genes (A, B, C, DRB1, DRB3, DRB4, DRB5, and DQB1) that could use identical thermal cycling conditions. As with SSOs, most primer sets target exons 2 and 3 of class I genes and exon 2 of class II genes. The basic premise is that one of a pair of unmodified amplification (PCR) primers is designed to overlie a polymorphic site of interest. The primer's 3′ end overlaps the polymorphic site by one to three bases, creating a highly unstable complex when mismatched. A perfectly matched primer pair will produce an amplification product, indicating a positive result, while a mismatched primer pair will not amplify, indicating a negative result. The resulting amplification products are separated and imaged by standard gel electrophoresis or separated by polymer-based capillary separation, allowing HLA typing to be inferred from the pattern of amplification.

Strengths and Weaknesses

The SSP method can be used to provide both low- and high-resolution typing results and can produce results in only 2 to 3 h. This makes it a good choice when immediate results are required, as in the case of deceased donor typing for organ transplantation. Based entirely on standard PCR reagents and gel electrophoresis, the method is also easily accessible and inexpensive to perform. A significant advantage over the SSO method is its ability to provide some phasing information, leading to fewer ambiguities. This is accomplished with PCR primers that overlie polymorphisms on both the

forward and reverse strand, therefore linking the phase of the two polymorphic sites together. Newer kits support preformatted 96-well reaction plates and 96-well gel analysis. More-advanced instruments that can provide capillary-based analysis of the amplicons only simplify this process, albeit for an additional cost.

But the method is not without complication. With primer sets based on known polymorphisms of common HLA alleles, these kits provide limited information in the presence of novel alleles. If the polymorphism that differentiates a novel allele lies within a position targeted by the primers, then the unexpected presence or absence of amplification may indicate the presence of a novel allele. However, like the SSO method, the SSP method does not provide the means to characterize the allele. If there are no primers that target the position differentiating the novel allele, then the allele will go unassigned and may lead to false reporting of the HLA genotype. Therefore, while sufficient for identifying the majority of common alleles, the method does not provide comprehensive coverage of all known and unknown alleles. More problematic is the fact that high-resolution SSP kits can still yield ambiguous results that must be resolved using alternative methods. As the number of allele combinations continues to grow, the ability to resolve ambiguities requires the addition of more and more primer sets, adding to cost and effort. One of the drawbacks of performing high-resolution typing by sequence-specific priming is that the laboratory must maintain a large inventory of kits (as high-resolution kits are most often broken into group-specific assays) that require quality control testing, as many primer sets and even different kits must be independently validated for performance. Yet another constraint of the method is the amount of DNA required. High-resolution typing by SSPs can require hundreds of individual amplification reactions and therefore may require several micrograms of purified DNA. This may limit the method's use when sample availability is restricted. Finally, the amplification requirements to obtain high-resolution typing make this the lowest-throughput method for HLA typing (for a summary of strengths and weaknesses, see Table 2).

Analysis of Data and Interpretation of Results

In the SSP method, a positive reaction is defined as a strong, easily visible, single PCR amplicon of the expected size, while a negative reaction provides no indication of any amplification. Often, kit manufacturers combine an internal control primer set with each allele primer set to provide assurance that amplification conditions were effective and that DNA was added to the well. This control primer set can be targeted to a nonpolymorphic region of the same gene that is being typed and therefore creates no interference with the allele-specific primers. While relatively simple to perform, the manual interpretation of dozens and sometimes hundreds of PCR amplifications quickly becomes burdensome and prone to error. While manufacturers provide visual interpretation tables for determining typings, these worksheets are complex and can be confusing. Therefore, most clinical labs today rely on manufacturer-developed software to interpret the banding patterns expected with any given set of primers.

Troubleshooting and Technical Issues

The consistent amplification of diverse samples as well as the interpretation of the gel electrophoresis result may be complicated by less-than-optimal amplification. A critical quality validation step is the measurement of thermal cycler temperature consistency. Temperature imbalances during cycling can lead to failed reactions and potentially spurious or imbalanced amplification. Therefore, routine (at least quarterly) quality checks of the thermal cyclers are required using calibrated temperature-monitoring equipment that monitors multiple wells in the cycler. Sample quality issues also play a large role in generating spurious results. Impurities accumulated from improperly stored blood or cellular samples can result in reduced amplification efficiency or altered primer behavior. Therefore, the amplification of the internal control must be verified for every reaction. Finally, a clinical laboratory using commercial typing software must make certain to keep the analysis tables or databases used by the software up to date, at least as often as the updates to the IMGT/HLA database. Failure to use updated typing tables or software databases could result in unreported ambiguities.

Real-Time PCR

Principle of the Technology and Its Applications

A relatively new technique for HLA typing was introduced by Linkage Biosciences (South San Francisco, CA) in 2009. Utilizing amplification processes similar to those of the SSP method, allele specificities are evaluated through differences in melting temperature, a predictable physical property. The method utilizes real-time PCR to amplify specific HLA gene regions (overlapping known polymorphic sites) and an intercalating dye to analyze the HLA results, all in the same automated process. This is accomplished through measuring the intercalating dye signal to verify that amplification has occurred and measuring postamplification results through the amplicon's melting curve signature. As the melting temperature of any given amplicon is reached, the double-stranded PCR product denatures and the intercalating dye is released, resulting in a drop in fluorescence. Any differences in base content (different HLA alleles) will cause the amplicon to have a unique melting curve, which is resolvable by the highly precise temperature control provided by the real-time PCR instrument. Linkage Biosciences has spent many years developing its own unique set of SSP assays that can identify the majority of known alleles, including null alleles, at intermediate resolution.

Strengths and Weaknesses

The strengths of real-time PCR HLA typing are the simplicity and speed of the method. Patient DNA is added to reaction buffers and aliquoted into the LinkSeq 96- or 384-well reaction plates. The plates are then sealed and amplified using a standard real-time PCR system. This simplicity translates into the potential for less cross-contamination error due to less sampling handling and reagent transfer.

By performing both amplification and melting curve analysis, the system provides two levels of specificity for positive reactions (endpoint identification of amplification and specific melting curve profile analysis), providing highly accurate results. Overall hands-on and analysis time is purported to be less than 20 min, with a total processing time of just 90 min per sample (one sample per plate). This rapid typing ability is particularly effective for time-critical typing of deceased donors but can also be readily applied to other samples requiring only low-resolution typing. The kits can also be run on several common real-time PCR systems, making the method readily available to many laboratories.

Because the system utilizes melting curve technology with only one manual step and does not require the use of gels or hybridization/washing of probes, it is simple to increase throughput by the addition of standard thermocyclers. Multiple plates can be run in parallel for the amplification step and then transferred to the real-time PCR instrument for a 5-min melting curve analysis. Because the procedure

is straightforward, batching a series of real-time PCR plates takes significantly less effort than running the same number of samples using either SSPs or SSOs. But like the SSO and SSP methods, the company's kits can only account for known HLA alleles. Therefore, this method is not amenable to identifying novel alleles, with spurious results having to be further investigated using other techniques. The system also does not currently provide high-resolution typing, necessitating reflexive testing with alternative methods if high-resolution typing is needed (for a summary of strengths and weaknesses, see Table 2).

Analysis of Data and Interpretation of Results

Analysis of results is automated through the company's SureTyper software. The software is designed to directly accept exported data from supported real-time PCR systems. SureTyper may require specific upgrades to the instrument software for certain models, like Life Technologies' StepOnePlus, which requires software version 2.2 to ensure compatibility. The SureTyper software converts the amplification/melting-curve data into allele calls, which are then used to determine genotype based on expected assay behavior and known IMGT/HLA database alleles. Assay results are provided in a simple +/− format along with the actual allele typing. The software allows manual user intervention and "what if" scenario analysis, providing up to 16 possible allele combination scenarios based on the low-level typing results. Adjusting any result manually forces the software to recalculate its allele calls and provide new scenarios. The software automates the genotype process using embedded allele frequency information and includes some level of linkage analysis between HLA-B and -C, -DRB1 through -DRB3/4/5, and -DRB1 and -DQB1.

Troubleshooting and Technical Issues

All Linkage Biosciences HLA typing kits come with both a negative and positive control. The negative control provides information about contamination of reagents. The positive control is unique in that it both identifies reagent functionality (by producing an amplicon) and provides some measure of sample DNA quality. The positive control is designed to produce a large amplicon that will only amplify optimally with DNA of good integrity (not damaged or fragmented). As with all amplification methods, purity and quality of the DNA sample can impact the quality of the results.

Sequence-Based Typing

Principle of the Technology and Its Applications

Since the advent of Sanger sequencing, SBT has demonstrated itself as a fundamentally improved HLA typing methodology. SBT provides increased flexibility in detecting known and novel alleles and improved accuracy and resolution over SSO and SSP methods with its ability to produce high-resolution typing results (two fields) in a single sequencing reaction. Sequencing in both the forward and reverse directions (bidirectional) for each HLA gene only increases its level of accuracy. Generically, SBT requires two amplification steps: a first amplification that serves to expand the copy number of a particular gene region (exons or an entire gene) and a second amplification to perform the cycle sequencing reactions that produce the fluorescently terminated sequences for subsequent capillary analysis. Historically, the initial process usually amplified only a portion of the HLA gene (exon or exons), while newer strategies generate one or two large amplicons, using long-range PCR to span more of the HLA class I and class II genes. After this initial amplification (and subsequent reaction cleanup), nested primer sets within each gene, specific to one or more exons, are then used for cycle sequencing (e.g., exons 2, 3, and 4 of class I genes). Different kit vendors have developed unique sets of amplification primers that aim to produce balanced amplification for every possible pair of alleles. Designing effective primer sets is quite challenging within the HLA genes, and this critical issue should not be overlooked or minimized, as significant amplification bias can result in spurious typing results.

After initial locus-specific amplification, the PCR reactions are "cleaned" using either a simple enzymatic process (ExoSAP-IT from Affymetrix [Santa Clara, CA], which requires no further purification of the sample) or standard spin preparation- or bead-based kits to remove or inactivate thermal cycling reactants and amplification primers (QIAquick or MinElute spin columns from Qiagen [Venlo, The Netherlands]; Agencourt AMPure XP beads from Beckman Coulter). This cleanup step is essential, as residual PCR reagents (particularly primers) can cause poor sequencing results. The cleaned PCR products are then directly used as a template in subsequent fluorescence-based Sanger sequencing reactions. Sanger sequencing utilizes a method of DNA sequencing called dideoxynucleotide or chain termination sequencing. It is based on the use of 2′,3′-dideoxynucleotides (ddNTPs) in addition to the normal nucleotides (dNTPs) used to synthesize the DNA. These modified nucleotides, when integrated into a sequence, prevent the addition of further nucleotides by DNA polymerase, thus terminating the chain. A sequencing reaction requires the following:

- a template strand to be sequenced (the purified primary PCR product is used as the template)
- forward and reverse sequencing primers (exon specific, used in separate sequencing reactions)
- DNA (Taq) polymerase
- dNTPs: dATP, dCTP, dGTP, and dTTP
- ddNTPs: ddATP, ddCTP, ddGTP, and ddTTP

The concentration of ddNTPs is ~1% of the concentration of dNTPs. The logic behind this ratio is that after DNA polymerase is added, the polymerization will take place and will terminate whenever a ddNTP is incorporated into the growing strand. If the ddNTP is only 1% of the total concentration of dNTP, a whole series of labeled strands of varying length will result. The nucleotide sequence of these fragments is determined using a technique called dye terminator sequencing. In dye terminator sequencing, each of the four dideoxynucleotide chain terminators is labeled with a different dye, each with a unique fluorescent signature. Each terminated fragment has a fluorescent dye on the terminal base that indicates the identity of that base. Once the sequencing reactions are complete, the sequencing products are precipitated with ethanol (to remove unincorporated fluorescent nucleotides), denatured, and loaded onto a sequencer. The sequences of the fluorescently labeled, single-stranded DNA fragments are determined by performing electrophoresis using a capillary genetic analyzer. Briefly, a charge is applied to the sample, which causes the charged DNA fragments to migrate through a polymer-filled capillary and past a detection system (laser and charge-coupled-device [CCD] camera). Smaller fragments migrate faster than larger fragments and thus reach the laser and CCD camera earlier. Each fragment that sequentially passes the laser is one nucleotide longer than the previous fragment. As the fragments pass the laser, the dye attached to the terminal ddNTP is excited and emits

its characteristic wavelength. The CCD camera detects this color, records the fluorescence intensity, and displays the intensity as a colored peak (Fig. 4, top). The color of the peak correlates to the fluorochrome detected, while the peak height correlates to fluorescence intensity (i.e., amount of DNA). It is only the last base in the sequence that is detected since it is the only base to be fluorescently labeled. However, by determining the base at the terminal end of all fragments, the entire DNA sequence can be determined as the pool of fragments, one nucleotide longer than the previous, sequentially reveal their base content (Fig. 4, bottom). The resulting "chromatogram" is used for sequence analysis using specialized genotyping software. In its optimal form, capillary sequencing is performed on an Applied Biosystems (ABI) 3000 series capillary sequencer (Thermo Fisher Scientific).

Strengths and Weaknesses

Sequence-based typing, particularly with the advent of capillary sequencers, is a robust, comprehensive method of determining high resolution HLA typing results, from as few as one to dozens of samples per day. The predominant instrument and sequencing kits from Applied Biosystems provide automated 96/384-well plate handling and sophisticated software to operate the system and collect data. This provides a highly robust and accurate system that is amenable to low and moderate test volumes. Amplification primer sets and related HLA typing software packages provided by commercial vendors have undergone extensive validation testing that confirms both their ability to amplify the region of interest with minimal bias and the ability to derive HLA typing results in a semiautomated fashion.

While Sanger sequencing is considered the gold standard for HLA typing, it has its limitations. Although SBT typically yields higher resolution results than the SSO and SSP methods, it can produce ambiguous results. This is primarily due to the nature of Sanger sequencing itself, whereby both alleles of a given locus are amplified and sequenced together, producing electropherograms that are a combination of the sequences of two alleles present in a sample (heterozygosity). With heterozygous electropherograms, the phase of the polymorphic sites (i.e., which nucleotides are linked together forming an allele) cannot be determined, which is the primary cause of ambiguity in SBT. Ambiguity also arises because of the practice of incompletely sequencing the HLA genes (leaving unsequenced regions that can differentiate one allele from another). Existing SBT kits focus primarily on exons 2, 3, and 4 for class I and exons 2 and 3 for class II. Naturally, alleles that differ (are polymorphic) outside of these sequenced regions cannot be resolved. This requires the reflexive use of alternative technologies like SSO or SSP to resolve these ambiguities. A few companies have developed alternative strategies to provide allele-specific primed sequencing (Abbott Molecular [Des Plaines, IL], Life Technologies, GenDx [Utrecht, The Netherlands], and others) that can help eliminate ambiguities caused by typical heterozygous samples. In this case, allele-specific sequencing primers (similar to SSPs) are used to provide single-allele sequencing results, avoiding *cis*/*trans* effects.

Generally speaking, the process of SBT HLA typing is more complex and time-consuming than either SSO or SSP typing. Primary amplification, cleanup, sequencing reaction setup, and further cleanup steps take a day to perform. Subsequent detection on the capillary sequencer and analysis of results (regardless of the software being used) can take another day. While automation of reaction setup and plate handling by the capillary instrument can help offset the time by reducing hands-on labor, individual sequencing reactions

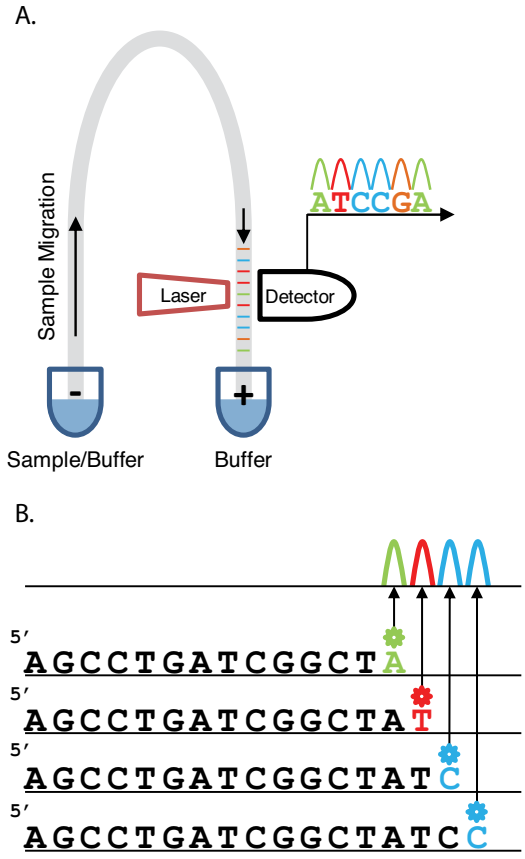

FIGURE 4 (A) Detection of fluorescent terminating nucleotides in a capillary sequencer. (B) Determination of sequence from terminal dideoxy labeling.

are required for each exon in both directions (forward and reverse), making it impossible to type more than four samples on a single 96-well reaction plate. Therefore, SBT is not a rapid methodology and, compared to previously described methods, requires the largest capital expenditure for equipment (for a summary of strengths and weaknesses, see Table 2).

Analysis of Data and Interpretation of Results

HLA typing software is essential for the SBT methodology because the complexity of comparing electropherograms (sequence traces) against a reference library of all HLA alleles makes manual data review impractical. In general, SBT software utilizes HLA sequences published in the IMGT/HLA database, against which sequencing data are compared. This reference set should be updated at least as often as the public updates to the IMGT database itself, and the user should verify this. Each package also provides an automated selection of the most likely candidate alleles from the imported sequencing data. This best match calculation is based on peak calling parameters set by the developers and therefore is not without error. While dedicated software programs facilitate this analysis, manual review of the results is also required because imbalanced allele amplification and poor sequence quality (to name just two issues) can result in incorrect base calls that can confound the HLA typing software's genotype call. Therefore, review of the sequence quality and electropherogram data is crucial to avoid errors.

Individual ABI base quality is measured by a Phred score, a measure of base calling error probability. A Phred score of

30, a common quality cutoff for sequencing, means a base calling error rate of 1 in 1,000 bases, or 99.9% correct base calls. For HLA typing by SBT, bases with Phred scores of <30 should not be used to determine typing results. A second measure of sequence quality is fluorescence intensity/background of each particular trace. Autothresholding found on all ABI sequencing systems adjusts the peak height of each fluorescent channel (base) to normalize the data across the four base channels. But this can lead to artificially high peaks for relatively poor sequencing results, resulting in higher background noise. This high background or "dirty" sequence can lead to incorrect base calling. Finally, all heterozygous positions identified by the sequence traces should be visually confirmed as either indicative of an actual heterozygous position (whether imbalanced or not) or an error. In the case of a suspected error, manually correcting the base call will automatically trigger the reassignment of alleles.

Troubleshooting and Technical Issues

While the abilities of SBT software packages have significantly improved in the last decade, there is still the need for experienced staff in interpreting the eletropherograms and sequencing results. Nonetheless, several issues that can impact automated allele calling should be considered for anyone reviewing SBT HLA typing results.

Amplification bias is a real and complicating factor that can artificially create the absence of heterozygous positions. This can be caused by polymorphic positions underlying primer sites (affecting amplification in an allele-specific manner) but also can be caused simply by difficult-to-amplify regions within the HLA genes (HLA-DQB1 is notorious for allelic imbalance). Despite substantial efforts by vendors developing amplification primer sets, allele bias does occur. Importantly, whether or not bias has occurred cannot be discerned by the results of the amplification step. That is to say, strong amplification is not indicative of balanced amplification any more than poor amplification is indicative of imbalanced amplification.

The quantity of the amplicon can also play a role in the quality of sequencing. Poorly amplified samples will likely generate poor-quality sequencing traces, but this does not mean that sequencing reactions cannot be successful if amplification is weak. Weakly amplifying targets often will sequence with sufficient quality to be HLA typed, if sufficient template is added to the sequencing reaction. Therefore, the issue of whether to sequence weakly performing amplicons is a matter of laboratory preference, quality specifications, and optimization of laboratory costs.

Running a capillary sequencer is generally not a source of problems, so long as the instrument is well maintained and recommended system maintenance is performed on schedule. It is highly recommended that routine system maintenance be performed by a representative of the manufacturer, as indicated in the user manual. From an operational perspective, sequencing quality is generally the first indicator of problems involving the capillary array. Consistently low sequence quality can be caused by either a capillary array that has been used beyond its capacity (the manufacturer stipulates ~150 runs per array), degraded POP6 or POP7 capillary matrix, or both. This problem is different than high background noise. High noise is generally indicative of poor cleanup of the sequencing reactions, leading to free fluorescent nucleotides contaminating the reaction.

Analysis of sequencing results can be highly influenced by the quality and quantity of the input material. In general, a high-quality run will have strong fluorescent signal over background noise, reducing linearly over the course of the run, and have a stable, flat current profile. The electropherogram peaks should be tall, sharp, and nonoverlapping and should not contain artifacts under the peak (from the other bases). Too much DNA loaded into the capillary can cause a truncated (shortened) run with compressed, overlapping peaks. This problem is also identified by an uneven current over the course of the run. Too little DNA caused by poor amplification can lead to peak signals too close to the background noise of the system, leading to poor peak differentiation and thus poor base calling with high inaccuracy. Salt contaminants left over from improper sample processing can elevate the baseline noise, resulting in shorter read lengths and poor-quality reads. A loss of resolution (peak sharpness) can be caused by improper capillary filling or an unexpected sample contaminant (sometimes caused by overloading a spin purification column). Beyond these operational problems, HLA variability can play a direct role in interpreting the electropherogram. In particular, insertions or deletions (indels) within one allele can cause frameshifts that appear as a sudden introduction of overlapping peaks within the electropherogram. Indels, along with difficult-to-sequence regions (regions of high GC content and homopolymers), can present biochemical problems that can also result in overlapping peaks within the electropherogram.

OVERVIEW OF NGS TECHNOLOGIES

Principles of the Technology and Applications

In recent years, new sequencing platforms have been developed that combine novel methods and instrumentation to produce far more sequence than traditional capillary electrophoresis-based Sanger sequencing, at a fraction of the cost. To reflect this advancement, these new methods have been termed next-generation sequencing.

NGS is poised to revolutionize clinical HLA typing by providing the most comprehensive means yet to analyze HLA genes (37–43). The primary advantage of this technology over all other methods is the ability to obtain sequence data from single DNA molecules. Currently, the two most widely used NGS platforms are from Illumina (MiSeq) and Life Technologies (Ion Torrent) (Table 3). It is worth mentioning that the first commercial instrument to be used for HLA typing by NGS was the Roche 454 platform. However, due to a number of limitations, the company decided to withdraw the platform from the market. While the biochemistry of these platforms differs, they are fundamentally similar, as they all combine clonal sequencing with a high level of parallelism. Clonal sequencing is accomplished using methods that enable the isolation of a single DNA molecule, which is subsequently amplified, producing a clonal population of identical DNA fragments. This molecular-level sequencing allows the detection of haploid information directly, resolving many limitations that earlier technologies struggle to resolve. The term "massively parallel" is frequently used to describe NGS technology whereby the simultaneous sequencing of millions of clonal populations is possible.

All NGS workflows consist of the following general steps: template generation, library preparation, clonal amplification, and sequencing.

Template Generation

Within the application of HLA typing, NGS template generation is typically performed by targeted PCR amplification and delivers the specificity and sensitivity required for accurate HLA genotyping. While HLA typing can potentially

TABLE 3 Summary of NGS platform capabilities

Platform	Sequencing chemistry	Library amplification	Read length	Data generation	Run time
Life Technologies Ion Torrent PGM	Ion detection	emPCR	200 or 400 bp	314 Chip: 30–100 Mb 316 Chip: 300 Mb–1 Gb 318 Chip: 600 Mb–2 Gb	314 Chip: 2.3–3.7 h 316 Chip: 3.0–4.9 h 318 Chip: 4.4–7.3 h
Life Technologies Ion Torrent Proton	Ion detection	emPCR	Up to 200 bp	Up to 10 Gb	2–4 h
Illumina MiSeq	Reversible dye terminator	Bridge amplification	1 × 36 bp 2 × 25 bp 2 × 75 bp[a] 2 × 150 bp 2 × 250 bp 2 × 300 bp[a]	500 Mb 800 Mb 3.5 Gb 5.0 Gb (nano: 300 Mb) 8.0 Gb (nano: 500 Mb) 14 Gb	4 h 5.5 h 20 h 24 h (nano: 13 h) 39 h (nano: 22 h) 55 h
Illumina HiSeq 1000	Reversible dye terminator	Bridge amplification	36–101 bp	≤150 Gb	1.5–8.5 days
Illumina HiSeq 2000	Reversible dye terminator	Bridge amplification	36–101 bp	≤300 Gb	2.5–11 days

[a]Uses a version 3 sequencing kit, whereas all other Illumina specs are for version 2 sequencing kits. "nano" indicates the smallest size sequencing chip by Illumina for the MiSeq.

be determined from the sequencing of nonamplified genomic DNA using whole-genome sequencing data, it is not practical to do so. This is primarily due to the low number of reads generated with current technologies for the HLA genes and the absence of adequately tested software analysis tools (see "The Future of HLA Typing" below).

Library Preparation

While library preparation methods vary between platforms, they are conceptually similar in that adaptors are ligated, or integrated through PCR, to the ends of the DNA template. These universal double-stranded DNA adaptors are used throughout the process to capture, amplify, and sequence the DNA. Library preparation is typically performed in one of two ways depending on the size of the DNA region to be sequenced. When the targeted region is relatively small (<500 bases), the regions of interest are amplified using fusion primers that combine or "fuse" region-specific primers with universal adaptor sequences. The resulting PCR amplicon thus incorporates a universal adaptor sequence at its ends. The sequencing approach that uses this type of library preparation method is commonly referred to as amplicon sequencing. For large amplicons (>500 bases in length), an approach called shotgun sequencing is commonly used. In shotgun sequencing, the large PCR amplicon must be fragmented to sizes more appropriate for sequencing on NGS instruments. Breaking large amplicons into smaller fragments is accomplished through nebulization, sonication, or enzymatically. The ends of the fragmented amplicons are then enzymatically blunt-ended (and in some cases 3′ adenylated) in preparation for adaptor ligation. Most, but not all, shotgun sequencing workflows include one or more purification steps to remove enzymes and other reactants between the fragmentation, end repair, and adaptor ligation steps. Purification is typically accomplished with bead-based systems like Beckman Coulter's Agencourt AMPure XP beads. The shotgun approach is typically used for sequencing the full length of HLA genes, while amplicon sequencing characteristically targets specific exons.

Regardless of amplification strategy, a size selection step is necessary to remove adaptors and/or adaptor dimers from the libraries prior to clonal amplification. Failure to remove adaptors and/or adaptor dimers will decrease the availability of library hybridization sites for subsequent clonal amplification due to competitive binding. When using shotgun sequencing, it is also reasonable to specifically select for library sizes that are ideal for clonal amplification on the NGS platforms (500 to 1,200 bp) and for phasing distal polymorphic HLA positions. Commonly used size selection strategies include bead-based technologies such as Beckman Coulter's SPRIselect and Agencourt AMPure XP beads or gel electrophoresis-based technologies like Sage Sciences' (Beverly, MA) Pippin Prep or Life Technologies' E-Gel SizeSelect instruments. Bead-based methods have the advantage of simultaneously concentrating the pools, while electrophoresis-based methods provide better precision.

Indexing

The massively parallel sequencing ability of NGS platforms is best exploited by the sequencing of many samples in a single run through the use of indexed adaptors. An index is a short (6 to 10 bases), unique sequence that is part of the adaptor and is incorporated during library preparation to identify individual samples. These indexes are often referred to as barcodes as they uniquely identify (code) a library. It is the use of indexed adaptors that enables pooling of multiple samples and loci in a single run. There are two primary indexing strategies: indexing by locus or indexing by sample. In the first strategy, a single library is prepared with a unique index for each HLA locus for a single sample. The sequences obtained with this index can then be definitively assigned to a particular locus. The primary benefit of this method is that software programs used to align sequence data and assign HLA genotypes can be aided by this information and can guard against misalignment of reads to an incorrect locus. The second approach, indexing by sample, offers a simplified sample preparation process that also reduces cost. In this approach, amplicons of all loci from a single sample are pooled prior to library preparation; therefore, only one library is prepared per sample. The indexing is simply used to distinguish one sample from the next. This amplicon pooling strategy puts greater pressure on the software programs to accurately identify the source (locus) of the individual reads and align them to the appropriate locus. Given the homology between HLA loci, this approach must be carefully and thoroughly validated.

Quantitation

The concentration of the prepared library must be assessed to ensure that an adequate amount of material is loaded for sequencing. Most importantly, proper library quantitation requires the differentiation of DNA fragments that contain ligated adaptors at both ends from those fragments without adaptors or those that contain only one adaptor (as only those fragments with both adaptors will eventually be sequenced). Most platforms recommend quantitative PCR (qPCR) for library quantitation, as it provides the most accurate assessment of amplifiable material. The qPCR assays can use the ligated adaptor sequence as the priming site for amplification; therefore, only DNA molecules that have successfully incorporated adaptors at both ends will amplify. Nonspecific intercalating fluorescent dyes such as SYBR green are then used to detect the amplification in "real time." Concentration of the library is determined by comparison of fluorescence to that of a standard curve. Currently there are many companies offering qPCR reagents for NGS, such as Kapa Biosystems (Wilmington, MA), Agilent Technologies (Santa Clara, CA), Illumina, and Quanta BioSciences (Gaithersburg, MD). As an alternative, Agilent's Bioanalyzer and TapeStation instruments can determine both size distribution of the library and concentration; however, the concentration measurement from these systems does not accurately represent the library concentration, as it measures all double-stranded DNA that is present and cannot differentiate between completely ligated fragments containing both adaptors and fragments that are missing adaptor sequences.

Clonal Amplification

Each of the NGS technologies described below relies on clonal amplification. However, they do not employ traditional bacterial cloning methods. Instead, they use techniques by which single DNA fragments are isolated and then amplified, producing a population of identical DNA molecules. Clonal amplification can be performed using emulsion PCR (emPCR) (Ion Torrent) or solid-phase amplification on a flow cell (MiSeq).

In emPCR, the DNA library is diluted and stoichiometrically added to capture beads such that a single DNA molecule binds to a single bead. The DNA binds to beads via adaptor sequence with homology to oligonucleotides that are bound to the bead surface. The DNA-bound beads, along with biotinylated primers and other amplification reagents, are placed into an oil emulsion and are shaken in a controlled way such that a single DNA-carrying bead becomes encapsulated in a single micelle droplet. Amplification is thereby performed in isolation within each micelle (microreactor), producing a bead covered with many copies of DNA with identical sequence. After emPCR, the beads are recovered and enriched using streptavidin-coated magnetic microparticles. The DNA-carrying beads are then deposited in a silicon chip (Ion Torrent) possessing microwells in preparation for sequencing. In support of its sequencing systems, Life Technologies has also spent considerable effort in automating the emPCR process. Both semiautomated (Ion OneTouch) and fully automated (Ion Chef) solutions exist that substantially simplify the emPCR and chip-loading process.

Illumina does not use emPCR for clonal amplification; rather, it uses a process called bridge amplification in which DNA fragments are captured onto their chip surface through oligonucleotides prebound at a concentration that allows spatial separation between captured fragments. The capture oligonucleotides also act as amplification primers, priming the DNA fragment for amplification. Repeated cycles of denaturation, annealing to nearby capture oligonucleotides, and extension amplify each fragment, producing localized clonal clusters. These clusters, each produced from different, single DNA fragments, are then sequenced. The clonal generation of clusters is necessary to generate sufficient signals for detecting the sequencing reaction, as a minimum of signal intensity is necessary before it is detected by the camera of the instrument. Using the correct concentration of a particular library is also critical to avoid the overlap of individual clusters on the chip, which can confound the detection of single sequences.

Sequencing

The sequencing methods used by the Ion Torrent and MiSeq platforms are quite different. In Ion Torrent sequencing, following emPCR, DNA-bound beads (Ion Sphere particles) are enriched and loaded into discrete wells on a silicon chip. Nucleotides and polymerases are flowed across the chip in a fixed order, and the incorporation of one nucleotide complementary to the DNA template results in the release of one hydrogen ion. This by-product (H^+) of base incorporation is used to determine sequence. The Ion Torrent detection technology represents a fundamental shift away from fluorescence-based sequencing methodologies, which have been the predominant form of sequencing chemistry for the last 25 years. Using unmodified (i.e., nonfluorescent) nucleotides, the platform's semiconductor chip measures minute changes in pH at the reaction site resulting from the release of the hydrogen ion during base incorporation. The change in pH is proportional to the number of hydrogen ions released, thereby allowing detection of single or multiple base (homopolymer) incorporations. Read lengths on Ion Torrent platforms range from 200 to 400 bases.

Illumina's sequencing method, similar to Sanger sequencing, uses a terminating chemistry in which addition of fluorescently labeled nucleotides is halted following incorporation of a single nucleotide. Unlike Sanger sequencing, however, Illumina's chemistry exclusively uses terminating nucleotides with reversible strand termination. Following fluorescence detection, the dye is cleaved and the terminating 3′ moiety is modified, enabling further nucleotide incorporation. This chemistry may slow the sequencing process, but it provides very accurate base detection, reducing the intrinsic error rate. One of the unique features of the Illumina sequencing chemistry is the simplicity by which both ends of a DNA fragment can be sequenced, commonly referred as "paired-end" sequencing. Single read lengths of 250 to 300 bases are attainable in the paired-end process, producing effective read lengths of 500 to 600 bases and enabling association of paired reads that are distal to each other (depending on insert size). Therefore, fragment sizes up to 1,000 bases can be sequenced on the platform, providing phase information for distant polymorphic positions, a very critical element for eliminating ambiguities in HLA typing.

HLA Gene Coverage Strategies by NGS

Sequencing of the HLA genes has utilized a number of different approaches, from exonic only to whole gene. The choice of approach has largely been driven by the perceived immunologic value versus the complexity, output, and availability of kits to perform the typing. As newer technologies are introduced, more-comprehensive approaches are becoming available to the HLA clinical market.

Exons Only (Amplicon Sequencing)

One of the first methods of HLA typing by NGS, developed by Roche, used short amplicons targeting a limited number

of exons, specifically the exons coding for the ARS. In this protocol, each exon is amplified separately. Non-ARS regions coding exons, introns, and untranslated regions are not sequenced. The primary advantage to this strategy is that the sequence output of the platform is maximally utilized by amplifying and sequencing only those regions that are considered "most relevant." Another advantage to this method is that the universal adaptor sequences can be incorporated through PCR, thereby eliminating the need to fragment DNA and ligate adaptors, as required in LR-PCR shotgun approaches. The disadvantage of the selective exon-only strategy is that ambiguous HLA typing results can be obtained. Non-ARS exons also include polymorphisms, and unless characterized, alleles with otherwise identical sequences will be ambiguously typed. Furthermore, while the sequence obtained within a short amplicon is phased by virtue of its clonal nature, the phase between amplicons is lost. That is, if exons 2 and 3 are amplified separately, it is not possible to phase the sequences from one exon to another unless the intervening intronic sequences are also sequenced and differ between the two alleles. This issue is particularly important, as examples exist of hybrid alleles that have been formed by crossover and exon-shuffling events. For example, discriminating the common alleles B*15:01:01:01 and B*40:01:01 requires the phasing of exon 2 to exon 3 to eliminate the alternative genotype B*40:21 and B*15:212. Therefore, any approach that does not completely sequence the whole gene potentially may generate multiple ambiguities.

A further limitation of this method is that numerous amplifications must be set up for each sample. In an effort to alleviate the burden of preparing numerous reactions, PCR setup has been automated on multiple platforms, including the Fluidigm access array. While the setup of multiple PCRs is simplified through the use of automation, it can be challenging to optimize amplification conditions so that amplification of the numerous exons is equally efficient. Failure to do so leads to nonuniform sequence coverage, which subsequently limits the throughput of the sequencing workflow, as a minimum depth of coverage is necessary for accurate genotype calling.

Whole Gene (Shotgun Sequencing by LR-PCR)

An alternative approach is to sequence the full length of the HLA genes. HLA genes range from 3.2 kb for class I up to 15 kb for class II. While it is possible to amplify the full length of HLA genes through LR-PCR, the current sequence read lengths of second-generation platforms is <1,000 bases. Therefore, in order to sequence the full length of HLA genes, a shotgun sequencing approach is necessary whereby the full gene amplicon is randomly fragmented and sequenced as previously described. The sequences obtained from the fragmented full-gene amplicons are assembled computationally to obtain the full-length sequence of each allele.

Whole Gene (Overlapping Short Amplicon Sequencing)

Yet another approach is a hybrid of the two previously described and is designed to reduce ambiguity through full-gene sequencing while reducing the fragmentation and adaptor ligation steps required of LR-PCR shotgun sequencing. In this approach, numerous amplifications are performed across the full length of the HLA genes with overlapping regions. As each amplicon is designed to overlap its neighbors, it is possible to set the phase from one amplicon to the next given sufficient density of heterozygous positions.

Strengths and Weaknesses of NGS HLA Typing

NGS technology is highly suited for the challenges routinely encountered in HLA genotyping. The two fundamental elements of NGS, clonal sequence and parallelism, can be exploited to develop a typing scheme that delivers high-resolution typing in a single pass. Many of the phase ambiguities encountered in Sanger sequencing are due to the extreme polymorphism of the HLA alleles and the frequently heterozygous nature of our genome. These ambiguities are eliminated by clonal NGS platforms that provide on-phase sequence spanning these regions. In addition, the enormous amount of sequence that can be produced by NGS allows for a new approach to SBT HLA typing that is not limited to a few exons. By expanding the regions that are sequenced, additional ambiguity can be reduced with more-comprehensive data, providing the means to compile a more complete HLA allele library. While current methods of HLA typing have enabled the detection of numerous HLA polymorphisms (14,409 alleles as of January 2016), the majority of these alleles have been only partially sequenced. NGS can be a useful tool for complete characterization of new HLA alleles and for completion of existing, partially sequenced alleles. NGS also offers cost savings when compared to existing high-resolution genotyping methods. Cost savings are achieved primarily through the elimination of reflexive testing (required to resolve ambiguity) and multiplexing (as NGS is highly scalable), allowing many samples to be processed simultaneously in a single run; therefore, the fixed costs can be spread across many samples.

However, as with the introduction of any new technologies, a number of limitations must be considered. NGS-based HLA typing requires a capital investment in equipment. The cost of the sequencer and peripheral equipment can easily exceed $150,000. Another issue is the current limited availability of NGS HLA typing kits. While Roche offers an HLA typing kit based on NGS, the company announced the discontinuation of its 454 sequencing product line by 2016. Meanwhile, a number of commercial vendors have already developed HLA typing products for the two major sequencing platforms including Holotype HLA by Omixon (Budapest, Hungary), MIA FORA by Immucor (Norcross, GA), NGSgo by GenDx (Utrecht, Netherlands), NXType HLA by Thermo Fisher, and TruSight HLA by Illumina.

One of the great challenges in utilizing NGS technology is the analysis of the data. The amount of sequence data produced is immense and therefore requires organized bioinformatics processes and highly sophisticated software programs. Laboratories embarking into NGS are now faced with the need for higher-performance computers and provision for long-term storage of data. Along with expanding bioinformatics requirements, another consideration is the rapid advancement of these technologies as new methods and technologies are continuously being developed, often with different equipment and computational needs. Considering that implementation of any new technology can be costly and time-consuming, laboratories must evaluate the return on this investment to decide if the benefits that NGS offers will translate into better and more cost-effective HLA testing, and to decide at what point in time it makes the most sense to introduce NGS into their workflows (for a summary of strengths and weaknesses, see Table 2).

Current "Clinical" NGS Platforms

The original NGS platforms had throughput capacities that were best suited for high-throughput contract labs but far exceeded the needs of typical clinical HLA labs. Recently, sequencing platform manufacturers have developed

"benchtop" sequencers for the clinical diagnostics market. Illumina's MiSeq and Life Technologies' Ion Torrent PGM systems fall into this category. These smaller versions of the ultra-high-throughput sequencers offer lower per-run cost, shorter sequencing time, and greater ease of use. For targeted applications like HLA typing, these benchtop sequencers are ideal.

Ion Torrent PGM

A primary advantage of the Life Technologies Ion Torrent system is the simplified readout technology provided by the solid-state chip. In contrast to pyrosequencing (Roche 454), none of the complex enzymatic processes and photochemical particles required to generate photoluminescence are required. This directly translates into a much simpler instrument (at much lower cost), as none of the complex and highly sensitive optics of fluorescence-based systems are needed. This also translates into much shorter run times, with sequencing runs taking just a few hours. Additionally, the use of unmodified nucleotides does not result in any chain damage to the growing DNA strand (presumably increasing efficiency). The biochemistry, however, suffers from the same problems as pyrosequencing: the inability to detect homopolymer stretches accurately. Because the sequencing is not terminator based, homopolymer stretches are determined by the proportional proton release from multiple bases added in the same cycle. Taking into account other issues like readout sensitivity, the overall error rate of the system is 1.7%, which is greater than that of the Illumina MiSeq at 0.3% (49). Read lengths are also not as long as for pyrosequencing, with maximum lengths reaching 400 bp. Also, like pyrosequencing, the emPCR process to amplify the template DNA is time-consuming and, in its manual form, difficult. Life Technologies has moderated this problem by introducing semiautomated and now fully automated solutions to the emPCR process (ostensibly alleviating the issue), allowing for the testing of these systems in a clinical environment. The PGM also offers lower per-run costs and shorter sequencing time than the Illumina MiSeq, although the overall time from library preparation to sequencing is comparable between the two systems.

Illumina MiSeq

Illumina's MiSeq has been found to produce the highest-quality sequence data of the existing NGS systems, with reasonable costs and simplified operation. Illumina's reversible terminator sequencing chemistry is very robust and generates accurate base calls. In multiple comparisons between existing systems, Illumina's platform has consistently outperformed all others in terms of sequence quality and low error rate. Also, because Illumina invested heavily in system development, much of the complex chemistry for clonal amplification is performed automatically by the instrument, substantially simplifying the process. From a systems standpoint, the primary disadvantage of the MiSeq system is the relatively long (24 to 39 h, depending on flow cell) run time and onboard data analysis of the instrument. Therefore, the MiSeq is clearly not a system for rapid turnaround of HLA results.

NGS ANALYSIS, INTERPRETATION OF RESULTS, AND TROUBLESHOOTING

After sequencing is completed, the instrument performs base calling on each clonally amplified DNA fragment. The sequence information from each fragment, called a read, is recorded along with the quality scores (the probability of a base calling error quantified using Phred values). Each sequencing platform is unique in how quality scores are calculated and the data storage format used (.sff, .bam). Regardless, all data formats can be converted into the FASTQ format, a standard representation of NGS data, containing entries for each read's haploid DNA sequence and corresponding quality scores (Fig. 5). For paired-end sequencing (Illumina), two FASTQ files are generated, with reads from each end of the DNA fragment placed into separate files and linked through the sequence identifier.

Traditional analysis of NGS data has three main components: (i) alignment of reads to a reference sequence, (ii) identification of variants, and (iii) annotation/interpretation of the identified variants. The first step, alignment, compares the reads to a reference sequence and attempts to locate the proper position of the read, or pairs of reads, given the reference sequence. Typically, the reference sequence selected is a human genome assembly available from a public database (e.g., GRCh37/hg19; UCSC Genome Bioinformatics website [http://genome.ucsc.edu]). After alignment, the variant positions are determined at locations where the aligned sequencing data are different from the reference, and can be either homozygous or heterozygous in nature. In this step, it is important to understand how depth of coverage and the quality score are used to decide whether a position is truly different from the reference. The depth of coverage refers to the number of reads aligned to a given position in the reference sequence (Fig. 6). Aligned bases with lower quality scores indicate lower confidence that the nucleotide call is correct and are down-weighted during variant calling at a given position (with preference given to aligned bases with higher quality scores). A higher number of reads present at a given position (higher depth of coverage) makes it easier to discriminate the signal (actual bases present, high quality scores) from the noise (errors during sequencing, base calling, and alignment, often with lower quality scores) during variant calling. Once the variant positions are identified, these can be fed into various analysis programs for interpretation.

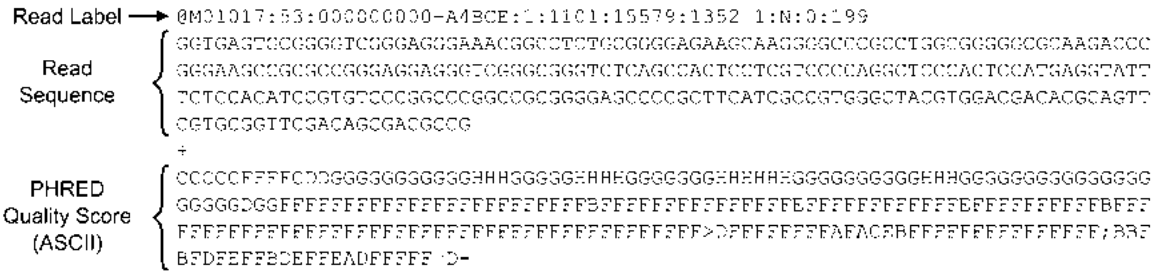

FIGURE 5 NGS read and FASTQ representation.

While it is possible to use a traditional approach to analyze HLA NGS data, methods that rely on alignment against a single reference sequence may be problematic. Widely used alignment programs such as Novoalign, BWA, Bowtie, etc., have limitations or penalties for mapping highly divergent reads to the reference sequence (as would be expected for HLA genes). Given the extreme polymorphism of HLA alleles, it is unlikely that these programs can deliver highly accurate alignment of all HLA alleles. Rather, novel approaches and programs have been developed specifically for HLA sequence data analysis.

Analysis and Interpretation Using Exon-Based and Whole-Gene Strategies

Considering that the two primary methods for sequencing HLA alleles on NGS instruments are the exon-based approach and the whole-gene approach, analysis programs have been developed to match the needs of each sequencing strategy. Exon-based approaches using long reads enable phasing of heterozygous positions within an exon, resolving much of the *cis*/*trans* ambiguity that occurs with the Sanger SBT methodology. However, since exons are amplified separately, these analysis programs cannot resolve all genotyping ambiguities for two reasons: phasing between exons is lost when these regions are amplified separately, and incomplete sequencing of the gene does not allow for resolution of alleles that differ only in regions that have not been included in the amplification strategy (e.g., DRB1*14:01:01/14:54 cannot be resolved without sequencing exon 3). The analysis of the full-length HLA genes is also not without its own challenges. Currently <10% of HLA alleles have been fully sequenced, with the majority of alleles only characterized in regions encoding the ARS (exons 2 and 3 for HLA class I and exon 2 for HLA class II). One of the greatest challenges for developers of analysis programs is accounting for sequence data from the full gene in light of a largely incomplete allele sequence database.

All programs have the capacity to handle NGS data and utilize the IMGT/HLA database genotype assignment, with most of the commercial programs also offering user interfaces that enable the visualization of sequences, coverage, genotype assignment, and mismatch information. While there has been significant development of software programs dedicated to HLA NGS data, these programs continue to evolve alongside the sequencing technology and approaches for HLA template generation. Some of the better-known programs are described below.

Commercial HLA Typing Software Packages

Assign ATF

Assign ATF software (Conexio Genomics, Fremantle, Australia) was developed for use with an exon-based sequencing approach and Roche 454 platform. Assign ATF is similar to the company's Assign software, developed for use in Sanger SBT, and enables the segregation of multiple samples in a single analysis project, providing a graphical user interface for the user to review sequence data and genotype assignment, including mismatch information. Assign ATF also allows manual editing of the data and re-analysis based on user interpretation. While the software has been applied primarily to exon-based sequencing, future versions will

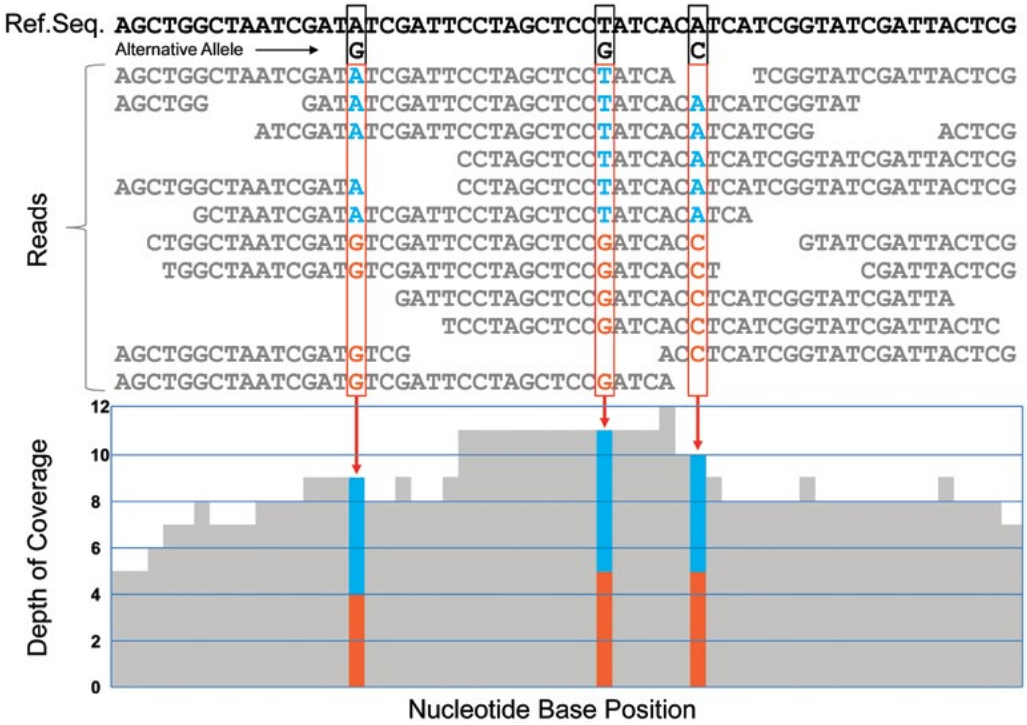

FIGURE 6 Depth of coverage as derived from NGS reads. NGS reads (whether single or paired-end) are aligned to a consensus reference sequence (Ref.Seq.) to form an overlapping, stacked view of the coverage at any given nucleotide position. The number of reads at any given position represents the depth of coverage and is derived by the number of overlapping reads at that nucleotide position. Read depth at polymorphic positions is split between the reference sequence and the alternative allele (blue and orange bars) and indicates allelic representation.

include analysis for full HLA genes with compatibility with additional sequencing platforms.

HLA Twin

HLA Twin (Omixon, Budapest, Hungary) is a highly customizable software program that is able to handle various sequencing platforms (Illumina, Ion Torrent, and Roche 454), gene coverage strategies (exons versus full gene), and data types (targeted, exome, and whole genome). HLA Twin offers two independent genotyping algorithms, a method that aligns the NGS data to the alleles in the IMGT/HLA database, and a second approach using *de novo* assembly of the NGS reads to determine a consensus sequence, which is then compared to the known alleles in IMGT. The combination of the two approaches is a very useful feature that provides a significant degree of confidence for the particular HLA genotyping call. Additional features include the ability to detect novel alleles and their traffic light system to warn users of potential quality issues that may be present in their sample signaling allele imbalance, uneven coverage, exon mismatches, and other statistics. HLA Twin also enables the analysis of mixed data in which sequences from a single sample containing reads from all HLA loci can be parsed to appropriate loci as part of the analysis.

NGSengine

NGSengine (GenDx) has also been developed to handle data from various sequencing platforms (Illumina, Ion Torrent, and Pacific Biosciences) and can analyze data from both exon-based and whole-gene-based sequencing approaches. In an effort to enable full gene alignment of alleles that have not been fully characterized, this software substitutes surrogate sequence for regions not yet characterized, which is obtained from a fully sequenced allele with the fewest differences from the allele in question. After the reads are aligned, the software establishes phase between heterozygous positions. The genotype assignment is based on best-matching alleles and provides mismatch information at the exon and intron level. Additional features include the display of phase across heterozygous positions and the ability to analyze mixed data (multiple loci in a single library). NGSengine also provides statistics about the read length, depth of coverage, and total length of the DNA fragments.

Sequence Pilot

Sequence Pilot (JSI Medical Systems, Ettenheim, Germany) is another commercially available software program for the analysis of HLA NGS data. The SeqNext-HLA module can analyze data from the Illumina, Ion Torrent, and Roche 454 platforms. This program is organized with clinical laboratory operation in mind with the ability to create orders, group files from the same DNA sample, and allow for patient and sample metadata to be stored within the program. This program is able to provide varying precision levels of HLA genotyping, from two-field to full-field resolution, accounting for intronic sequence if provided in the IMGT/HLA database. SeqNext-HLA allows the user to analyze the sequencing data and review, edit, and re-analyze if necessary. Interestingly, while the program was designed for NGS data, it does not provide the user with a view of the sequence read alignment or depth of coverage, but rather displays a simulated electropherogram of the resulting consensus sequence.

Open-Access Software Programs

The development of HLA genotyping programs is not limited to commercial enterprises. Athlates (Broad Institute, Cambridge, MA) is a command line-based application originally developed for HLA genotyping from exome sequencing data. It employs a data-centric approach of identifying reads belonging to HLA genes, assembling the reads into contigs, and creating consensus information for each exon that is compared back to the IMGT/HLA database (with the output of the best pair of alleles that explain the data at each locus identified). Two programs, HLA Caller (an unsupported module for the Genome Analysis Tool Kit, Broad Institute) and SOAP-HLA (Beijing Genomics Institute, Beijing, China), determine HLA genotypes based on alignment of sequencing reads to the human genome. These algorithms are dependent on the accurate alignment of reads and single nucleotide polymorphism determination for making the allele call. While SOAP-HLA works directly with the alignment data, HLA Caller goes one step further in incorporating allele frequencies into its probabilistic algorithm for genotyping. All of the open-access programs listed are restricted to alleles defined in the IMGT/HLA database and cannot handle complicated events, such as allelic imbalance, uncharacterized intronic sequences of alleles, and novel or hybrid alleles, all of which may be encountered in a clinical setting and need to be identified.

The Complexity of HLA Data Analysis—Challenges to Software Programs

All NGS approaches for HLA genotyping have inherent limitations, and the software chosen for analysis should be able to address some, if not all, of the well-known issues with HLA genotyping. Some of the more systematic problems associated with sequencing the HLA genes include nonuniform sequence coverage, allelic imbalance, and coamplification of unintended HLA loci. While it is possible to address these problems during the initial PCR amplification and library preparation steps, the programs should be able to detect events that can lead to incorrect genotype determination. Another event that HLA genotyping programs should be able to detect is the existence of a novel allele. While there are >14,000 known HLA alleles present in the IMGT/HLA database, the number of alleles is increasing rapidly as more sequencing is performed and is only expected to grow as more whole-gene data are characterized. Not only should the programs be able to detect the new alleles that are possible due to novel single nucleotide polymorphisms, but they should also be able to detect and characterize the cases of new alleles that are hybrids of two or more known alleles. Currently, no program is able to handle the detection of hybrid alleles.

THE FUTURE OF HLA TYPING

A plethora of large and small technology companies around the world continue to advance the state of the art in whole- and targeted genome sequencing technologies. Companies like Pacific Biosciences (direct fluorescent sequencing by synthesis) and Oxford Nanopore Technologies (Oxford, United Kingdom) (non-fluorescence, non-polymerase based) are working on more-advanced (true single-molecule) third-generation platforms (Oxford Nanopore has only recently released its first product for commercial evaluation). These third-generation sequencing technologies enable the sequencing of single DNA molecules without the need for clonal amplification and appear promising in regards to supporting more informative HLA typing in the future.

Pacific Biosciences

Pacific Biosciences' technology focuses on using a single, physically anchored DNA polymerase as the driving force

in single-molecule, direct sequencing by synthesis, using fluorescence-tagged, phospholinked nucleotide analogs. This approach allows both the rapid incorporation of nucleotides and very long reads. Initial chemistries produced average read lengths of ~4,500 bp, with newer chemistries today increasing the average to ~10,000 bp (with the longest reads exceeding 30,000 bp). With multi-kilobase reads, ambiguities caused by phasing, even at whole HLA gene distances, can be completely eliminated. A disadvantage of this technology is the Single Molecule Real Time (SMRT) chip itself. Because of the small number of zero-mode waveguides per chip, the system's total output per run (~50 Mbp) is substantially limited. While this level of throughput is insufficient for whole genomes, for targeted approaches, like HLA, this amount of information is entirely sufficient, given the extended read lengths. And while the chemistry suffers from single-pass inaccuracies (median error of ~14%), the base incorporation errors are random and therefore addressable by adequate read depth and appropriate bioinformatics support.

Oxford Nanopore and Similar Nanopore Technologies

Nanopore technology introduces a completely new paradigm in DNA sequencing. Briefly, a single nanoscopic hole (~1 nm) is created in a synthetic membrane within electronically addressable microscopic wells of the application-specific integrated circuit (ASIC) chip, through the addition of a single biological protein nanopore (such as α-hemolysin). A double-stranded DNA template is then prepared by ligating a hairpin to one end and a DNA-unwinding protein at the other. As a single strand of DNA is unwound from the double-stranded target molecule and pulled through the nanopore, an electric potential across the membrane facilitates a unique current signature specific to each type of DNA base as the DNA passes through the pore. These fluctuating electric potentials are then recorded and converted into base calls. The technology enables very long reads, with the additional advantage of simplified sample preparation and reagents. Recent tests of the MinION system demonstrated an average read length of 5.4 kbp, with some reads up to 10 kbp and longer. But the technology is not without problems. Early testing indicates higher error rates than other platforms. The system's low data output (initial chips contain 512 wells, generating only tens of megabases of data per run) and current lack of published data demonstrating the stability, reliability, and accuracy of the technology limit the ability to assess the system's capabilities for HLA typing.

Regardless of current shortcomings, nanopore technology may be a potential sequencing option over the next decade, as a multitude of companies are developing alternative platforms using different nanopore approaches (biological, solid state, and otherwise). Therefore, the technology has the potential to become an extremely inexpensive, very simple, very fast (minutes instead of hours) approach to sequencing any target DNA molecule. From an HLA perspective, this technology has the potential to lead to routine whole-genome sequencing, where HLA typing would naturally result from the overall data.

Alternative Means To Obtain HLA Typing from Whole-Exome or Whole-Genome Sequencing

Besides the approaches described in this chapter for direct HLA typing by NGS, alternative approaches for obtaining HLA typing from whole-exome sequencing (WES) or whole-genome sequencing (WGS) data have recently been attempted (50). Since both WES and WGS data include the HLA sequences, determining the HLA typing from this data is theoretically possible, with the success of these approaches largely dependent on the quality and quantity of the WES or WGS data and the ability of software tools to perform the data analysis.

The challenges associated with HLA genotyping from WGS or WES is inherent to the assay performed. Under the best of circumstances, WES data will be comparable to the exon-based typing strategy, with the known limitations as outlined above [see "Exons Only (Amplicon Sequencing)"] and relatively lower coverage expected for the targeted (HLA) regions. Furthermore, capturing the HLA exons with a standardized set of oligonucleotides for exome sequencing is questionable, since the set of capture oligonucleotides do not change to reflect the increasing diversity (and extensive polymorphism) of the HLA alleles. Therefore, this process may exhibit allelic imbalance or dropouts. So, while WES data may provide sufficient quantity of data, the quality of the sequences remains a challenge. Alternatively, using WGS data (where there is no selection of HLA genomic fragments for sequencing, analogous to shotgun sequencing of the whole HLA genes), the challenge lies in generating a sufficient amount of data to obtain a high enough depth of coverage for accurate HLA genotyping. While WGS is currently cost-prohibitive for HLA typing purposes, it is expected to be possible in the future as NGS technologies are optimized and total throughput increases. But for the foreseeable future (even assuming that throughput is increased and sequencing costs are reduced), it is unlikely that all those who need HLA typing will necessarily have their exome or genome fully sequenced. Therefore, this approach will only be relevant to cases in which WES and WGS data are already available. The computational tools available for WES or WGS HLA analysis, like Omixon's Target HLA, are being tested, and the results suggest that the approach can be successful. However, significant challenges remain, including the considerable time, complexity, and effort for computation and interpretation of results.

REMARKS/CONCLUSIONS

Clinical HLA typing has experienced remarkable technical progress in the last decade that may finally and ultimately resolve several long-standing problems that have hampered HLA testing for the last 60 years. From the inability to determine long-range phasing to the lack of whole-gene information from both coding and noncoding regions to the inability to directly detect novel alleles, HLA typing technologies are poised to rapidly improve our understanding of the role of HLA genes in immune function and transplantation and to provide truly cost-effective, high-volume testing. Equally importantly, these newer technologies can provide high-quality, high-resolution HLA typing for registry donors that will facilitate and expedite organ donor searches while reducing search-related costs. The very fact that non-DNA-based approaches to HLA typing have largely been or are being eliminated from clinical typing laboratories speaks highly of the DNA-based techniques that have replaced antibody- and cell-based screening methods. While SSO and SSP methods will continue to provide simple, economical routine detection of common alleles, methods that can reduce ambiguities and definitively identify HLA alleles will take precedence. This is particularly true when considering the possibility that tissue typing may include even more exons, and possibly introns, in future tissue-matching efforts. Sanger SBT will continue to provide improved high-resolution typing over SSO or SSP methods, but its inability

to resolve phasing ambiguities and its relatively stable and rather high cost will ultimately force its replacement by newer, more advanced sequencing techniques.

With the success of next-generation sequencing platforms and potential advantages of novel third-generation platforms under development, it is clear that single-molecule sequencing may finally resolve all HLA tissue-typing needs. By providing unambiguous, direct haplotype data (within a single gene), the problem of polymorphic phasing is totally eliminated. This is especially true as NGS read lengths continue to increase. By providing whole-gene sequencing, the detection of novel alleles will be facilitated, potentially eliminating all secondary approaches to verify and resolve ambiguities. This whole-gene, full-length allele sequence data will also rapidly improve donor registry databases, providing unprecedented rapidity in evaluating and matching donor and recipient samples.

Even with the current pricing of "personal" sequencing systems, HLA typing by NGS is already possible at costs that are in line with current reimbursement allowances. With sufficient thought and development of the supporting processes, HLA typing by NGS can be both economical and practical. And as NGS continues to advance in technical performance, the ability to apply NGS broadly to clinical HLA typing will only become simpler and more cost-effective for both low- and high-volume laboratories. This is particularly true when considering the interest in HLA typing by leading technology platform companies like Illumina and Thermo Fisher that are actively developing HLA-specific typing kits for their developing platforms. If this trend continues, and if typing by NGS becomes fully supported by these companies, HLA typing will finally advance to the level it has always required but was never quite able to achieve.

Beyond the Molecular Genetics of HLA

While these advanced technologies will provide highly refined approaches for the characterization of HLA genomic sequences, there will remain the need to expand our understanding of the expression of these HLA gene products on the cell surface and the impact of that expression on immune function. Polymorphisms causing alterations in cell surface expression or tissue-to-tissue variability of expression will need to be studied in the context of their significance and impact on tissue transplantation and immune function. For this reason alone, the HLA community should continue to develop new approaches that will match the impressive progress at the genomic level (characterizing genetic variation) with insight into the physiologic relevance and consequences of these genomic differences on HLA protein function.

The authors and volume editors wish to thank Carolyn Katovich Hurley for her excellent review of this chapter and her helpful comments and suggestions.

REFERENCES

1. **Terasaki PI, McClelland JD.** 1964. Microdroplet assay of human serum cytotoxins. *Nature* **204:**998–1000. PubMed
2. **Mittal KK, Mickey MR, Singal DP, Terasaki PI.** 1968. Serotyping for homotransplantation. 18. Refinement of microdroplet lymphocyte cytotoxicity test. *Transplantation* **6:**913–927. PubMed
3. **Biddison WE, Kostyu DD, Strominger JL, Krangel MS.** 1982. Delineation of immunologically and biochemically distinct HLA-A2 antigens. *J Immunol* **129:**730–734.
4. **Mölders HH, Breuning MH, Ivanyi P, Ploegh HL.** 1983. Biochemical analysis of variant HLA-B27 antigens. *Hum Immunol* **6:**111–117. PubMed
5. **Monos DS, Tekolf WA, Shaw S, Cooper HL.** 1984. Comparison of structural and functional variation in class I HLA molecules: the role of charged amino acid substitutions. *J Immunol* **132:**1379–1385. PubMed
6. **Kim SJ, Holbeck SL, Nisperos B, Hansen JA, Maeda H, Nepom GT.** 1985. Identification of a polymorphic variant associated with HLA-DQw3 and characterized by specific restriction sites within the DQ β-chain gene. *Proc Natl Acad Sci USA* **82:**8139–8143. PubMed
7. **Olerup O, Zetterquist H.** 1992. HLA-DR typing by PCR amplification with sequence-specific primers (PCR-SSP) in 2 hours: an alternative to serological DR typing in clinical practice including donor-recipient matching in cadaveric transplantation. *Tissue Antigens* **39:**225–235. PubMed
8. **Bunce M, Taylor CJ, Welsh KI.** 1993. Rapid HLA-DQB typing by eight polymerase chain reaction amplifications with sequence-specific primers (PCR-SSP). *Hum Immunol* **37:**201–206. PubMed
9. **Wordsworth BP, Allsopp CE, Young RP, Bell JI.** 1990. HLA-DR typing using DNA amplification by the polymerase chain reaction and sequential hybridization to sequence-specific oligonucleotide probes. *Immunogenetics* **32:**413–418. PubMed
10. **Scharf SJ, Griffith RL, Erlich HA.** 1991. Rapid typing of DNA sequence polymorphism at the HLA-DRB1 locus using the polymerase chain reaction and nonradioactive oligonucleotide probes. *Hum Immunol* **30:**190–201. PubMed
11. **Cereb N, Maye P, Lee S, Kong Y, Yang SY.** 1995. Locus-specific amplification of HLA class I genes from genomic DNA: locus-specific sequences in the first and third introns of HLA-A, -B, and -C alleles. *Tissue Antigens* **45:**1–11. PubMed
12. **Petersdorf EW, Hansen JA.** 1995. A comprehensive approach for typing the alleles of the HLA-B locus by automated sequencing. *Tissue Antigens* **46:**73–85. PubMed
13. **van der Vlies SA, Voorter CE, van den Berg-Loonen EM.** 1998. A reliable and efficient high resolution typing method for HLA-C using sequence-based typing. *Tissue Antigens* **52:**558–568. PubMed
14. **Kurz B, Steiert I, Heuchert G, Müller CA.** 1999. New high resolution typing strategy for HLA-A locus alleles based on dye terminator sequencing of haplotypic group-specific PCR-amplicons of exon 2 and exon 3. *Tissue Antigens* **53:**81–96. PubMed
15. **Dausset J.** 1958. Iso-leuco-antibodies. *Acta Haematol* **20:**156–166. (In French.)
16. **Park I, Terasaki P.** 2000. Origins of the first HLA specificities. *Hum Immunol* **61:**185–189. PubMed
17. **International Histocompatibility Working Group.** 2016. History. International Histocompatibility Working Group, Seattle, WA. http://www.ihwg.org/about/history.html.
18. **Sengar DP, Mickey MR, Myhre BA, Chen HH, Terasaki PI.** 1971. Mixed leukocyte culture response in HL-A. "Identical individuals". *Transfusion* **11:**251–257. PubMed
19. **Hämmerling GJ.** 1997. The 1996 Nobel Prize to Rolf Zinkernagel and Peter Doherty. *Cell Tissue Res* **287:**1–2. PubMed
20. **Zinkernagel RM, Doherty PC.** 1997. The discovery of MHC restriction. *Immunol Today* **18:**14–17. PubMed
21. **Bjorkman PJ, Strominger JL, Wiley DC.** 1985. Crystallization and X-ray diffraction studies on the histocompatibility antigens HLA-A2 and HLA-A28 from human cell membranes. *J Mol Biol* **186:**205–210. PubMed
22. **Garrett TP, Saper MA, Bjorkman PJ, Strominger JL, Wiley DC.** 1989. Specificity pockets for the side chains of peptide antigens in HLA-Aw68. *Nature* **342:**692–696. PubMed
23. **Bjorkman PJ, Saper MA, Samraoui B, Bennett WS, Strominger JL, Wiley DC.** 1987. The foreign antigen binding site and T cell recognition regions of class I histocompatibility antigens. *Nature* **329:**512–518. PubMed

24. **Trowsdale J, Knight JC.** 2013. Major histocompatibility complex genomics and human disease. *Annu Rev Genomics Hum Genet* **14:**301–323. PubMed
25. **Avidan N, Le Panse R, Berrih-Aknin S, Miller A.** 2014. Genetic basis of myasthenia gravis—a comprehensive review. *J Autoimmun* **52:**146–153. PubMed
26. **Raychaudhuri S, Sandor C, Stahl EA, Freudenberg J, Lee HS, Jia X, Alfredsson L, Padyukov L, Klareskog L, Worthington J, Siminovitch KA, Bae SC, Plenge RM, Gregersen PK, de Bakker PI.** 2012. Five amino acids in three HLA proteins explain most of the association between MHC and seropositive rheumatoid arthritis. *Nat Genet* **44:**291–296. PubMed
27. **Traherne JA.** 2008. Human MHC architecture and evolution: implications for disease association studies. *Int J Immunogenet* **35:**179–192. PubMed
28. **Karlin E, Phillips E.** 2014. Genotyping for severe drug hypersensitivity. *Curr Allergy Asthma Rep* **14:**418. doi:10.1007/s11882-013-0418-0. PubMed
29. **Yip VL, Alfirevic A, Pirmohamed M.** 2015. Genetics of immune-mediated adverse drug reactions: a comprehensive and clinical review. *Clin Rev Allergy Immunol* **48:**165–175. PubMed
30. **Horton R, Wilming L, Rand V, Lovering RC, Bruford EA, Khodiyar VK, Lush MJ, Povey S, Talbot CC Jr, Wright MW, Wain HM, Trowsdale J, Ziegler A, Beck S.** 2004. Gene map of the extended human MHC. *Nat Rev Genet* **5:**889–899. PubMed
31. **Yasukochi Y, Satta Y.** 2013. Current perspectives on the intensity of natural selection of MHC loci. *Immunogenetics* **65:**479–483. PubMed
32. **Cano P, Klitz W, Mack SJ, Maiers M, Marsh SG, Noreen H, Reed EF, Senitzer D, Setterholm M, Smith A, Fernández-Viña M.** 2007. Common and well-documented HLA alleles: report of the Ad-Hoc committee of the American Society for Histocompatiblity and Immunogenetics. *Hum Immunol* **68:**392–417. PubMed
33. **Mack SJ, Cano P, Hollenbach JA, He J, Hurley CK, Middleton D, Moraes ME, Pereira SE, Kempenich JH, Reed EF, Setterholm M, Smith AG, Tilanus MG, Torres M, Varney MD, Voorter CE, Fischer GF, Fleischhauer K, Goodridge D, Klitz W, Little AM, Maiers M, Marsh SG, Müller CR, Noreen H, Rozemuller EH, Sanchez-Mazas A, Senitzer D, Trachtenberg E, Fernandez-Vina M.** 2013. Common and well-documented HLA alleles: 2012 update to the CWD catalogue. *Tissue Antigens* **81:**194–203. PubMed
34. **Marsh SG, Albert ED, Bodmer WF, Bontrop RE, Dupont B, Erlich HA, Geraghty DE, Hansen JA, Hurley CK, Mach B, Mayr WR, Parham P, Petersdorf EW, Sasazuki T, Schreuder GM, Strominger JL, Svejgaard A, Terasaki PI, Trowsdale J.** 2005. Nomenclature for factors of the HLA system, 2004. *Tissue Antigens* **65:**301–369. PubMed
35. **Marsh SG, Albert ED, Bodmer WF, Bontrop RE, Dupont B, Erlich HA, Fernández-Viña M, Geraghty DE, Holdsworth R, Hurley CK, Lau M, Lee KW, Mach B, Maiers M, Mayr WR, Müller CR, Parham P, Petersdorf EW, Sasazuki T, Strominger JL, Svejgaard A, Terasaki PI, Tiercy JM, Trowsdale J.** 2010. Nomenclature for factors of the HLA system, 2010. *Tissue Antigens* **75:**291–455. PubMed
36. **Nunes E, Heslop H, Fernandez-Vina M, Taves C, Wagenknecht DR, Eisenbrey AB, Fischer G, Poulton K, Wacker K, Hurley CK, Noreen H, Sacchi N, Harmonization of Histocompatibility Typing Terms Working Group.** 2011. Definitions of histocompatibility typing terms: Harmonization of Histocompatibility Typing Terms Working Group. *Hum Immunol* **72:**1214–1216. PubMed
37. **Holcomb CL, Höglund B, Anderson MW, Blake LA, Böhme I, Egholm M, Ferriola D, Gabriel C, Gelber SE, Goodridge D, Hawbecker S, Klein R, Ladner M, Lind C, Monos D, Pando MJ, Pröll J, Sayer DC, Schmitz-Agheguian G, Simen BB, Thiele B, Trachtenberg EA, Tyan DB, Wassmuth R, White S, Erlich HA.** 2011. A multi-site study using high-resolution HLA genotyping by next generation sequencing. *Tissue Antigens* **77:**206–217. PubMed
38. **Gabriel C, Danzer M, Hackl C, Kopal G, Hufnagl P, Hofer K, Polin H, Stabentheiner S, Pröll J.** 2009. Rapid high-throughput human leukocyte antigen typing by massively parallel pyrosequencing for high-resolution allele identification. *Hum Immunol* **70:**960–964. PubMed
39. **Bentley G, Higuchi R, Hoglund B, Goodridge D, Sayer D, Trachtenberg EA, Erlich HA.** 2009. High-resolution, high-throughput HLA genotyping by next-generation sequencing. *Tissue Antigens* **74:**393–403. PubMed
40. **Lind C, Ferriola D, Mackiewicz K, Heron S, Rogers M, Slavich L, Walker R, Hsiao T, McLaughlin L, D'Arcy M, Gai X, Goodridge D, Sayer D, Monos D.** 2010. Next-generation sequencing: the solution for high-resolution, unambiguous human leukocyte antigen typing. *Hum Immunol* **71:**1033–1042. PubMed
41. **De Santis D, Dinauer D, Duke J, Erlich HA, Holcomb CL, Lind C, Mackiewicz K, Monos D, Moudgil A, Norman P, Parham P, Sasson A, Allcock RJ.** 2013. 16th IHIW: review of HLA typing by NGS. *Int J Immunogenet* **40:**72–76. PubMed
42. **Wang C, Krishnakumar S, Wilhelmy J, Babrzadeh F, Stepanyan L, Su LF, Levinson D, Fernandez-Viña MA, Davis RW, Davis MM, Mindrinos M.** 2012. High-throughput, high-fidelity HLA genotyping with deep sequencing. *Proc Natl Acad Sci USA* **109:**8676–8681. PubMed
43. **Gabriel C, Fürst D, Faé I, Wenda S, Zollikofer C, Mytilineos J, Fischer GF.** 2014. HLA typing by next-generation sequencing—getting closer to reality. *Tissue Antigens* **83:**65–75. PubMed
44. **Glasel JA.** 1995. Validity of nucleic acid purities monitored by 260nm/280nm absorbance ratios. *Biotechniques* **18:**62–63. PubMed
45. **Ginevri F, Nocera A, Comoli P, Innocente A, Cioni M, Parodi A, Fontana I, Magnasco A, Nocco A, Tagliamacco A, Sementa A, Ceriolo P, Ghio L, Zecca M, Cardillo M, Garibotto G, Ghiggeri GM, Poli F.** 2012. Posttransplant *de novo* donor-specific hla antibodies identify pediatric kidney recipients at risk for late antibody-mediated rejection. *Am J Transplant* **12:**3355–3362. PubMed
46. **Katerinis I, Hadaya K, Duquesnoy R, Ferrari-Lacraz S, Meier S, van Delden C, Martin PY, Siegrist CA, Villard J.** 2011. *De novo* anti-HLA antibody after pandemic H1N1 and seasonal influenza immunization in kidney transplant recipients. *Am J Transplant* **11:**1727–1733. PubMed
47. **O'Leary JG, Kaneku H, Susskind BM, Jennings LW, Neri MA, Davis GL, Klintmalm GB, Terasaki PI.** 2011. High mean fluorescence intensity donor-specific anti-HLA antibodies associated with chronic rejection postliver transplant. *Am J Transplant* **11:**1868–1876. PubMed
48. **Bunce M, O'Neill CM, Barnardo MC, Krausa P, Browning MJ, Morris PJ, Welsh KI.** 1995. Phototyping: comprehensive DNA typing for HLA-A, B, C, DRB1, DRB3, DRB4, DRB5 & DQB1 by PCR with 144 primer mixes utilizing sequence-specific primers (PCR-SSP). *Tissue Antigens* **46:**355–367. PubMed
49. **Duke JL, Lind C, Mackiewicz K, Ferriola D, Papazoglou A, Derbeneva O, Wallace D, Monos DS.** 2015. Towards allele-level human leucocyte antigens genotyping—assessing two next-generation sequencing platforms: Ion Torrent Personal Genome Machine and Illumina MiSeq. *Int J Immunogenet* **42:**346–358.
50. **Major E, Rigó K, Hague T, Bérces A, Juhos S.** 2013. HLA typing from 1000 Genomes whole genome and whole exome Illumina data. *PLoS One* **8:**e78410. doi:10.1371/journal.pone.0078410.

Evaluation of the Humoral Response in Transplantation

PAUL SIKORSKI, RENATO VEGA, DONNA P. LUCAS, AND
ANDREA A. ZACHARY

114

INTRODUCTION

Relevance of Antibody in Transplantation

Antibodies of the IgG class can damage tissues in a variety of ways, including (i) directly through complement activation, (ii) indirectly through the deposition of immune complexes, and (iii) indirectly through the recruitment of cytotoxic or inflammation-inducing cells. Very high levels of antibody result in hyperacute rejection and graft failure, an outcome that can easily be avoided by the performance of a lymphocyte crossmatch test prior to transplantation. In contrast, clear elucidation of the relevance of donor-reactive antibodies of various strengths and specificities and of antibodies that arise after transplantation has been hampered by inadequate technologies and lack of reimbursement for posttransplant monitoring of antibodies. Nonetheless, a deleterious effect of antibody specific for mismatched donor HLA antigens has been demonstrated for nearly every type of organ and tissue that has been transplanted in sufficient numbers, including hematopoietic stem cells and, possibly, composite tissues. There is overwhelming evidence indicating that anti-HLA antibodies are involved in hyperacute, acute, and chronic rejection of organs (1). In mismatched bone marrow transplants, there is a risk of immunocompetent tissues from sensitized patients producing antibody to recipient tissues as well as a risk of recipients making antidonor antibodies. In theory, antibodies specific for any antigen on transplanted tissue should be capable of damaging the transplant. The best-known antibodies that are injurious to allografts are those specific for antigens of the HLA and ABO systems. Potential deleterious effects of other antibodies are being recognized increasingly. A discussion of those is beyond the scope of this chapter, and the interested reader is directed to two excellent reviews on this topic (2, 3). The focus of this chapter will be HLA-specific antibodies, and we will use the term donor-specific antibody (DSA) to refer to antibody(ies) specific for donor HLA antigens.

There are multiple reasons as to why HLA-specific antibodies are so important to detect and monitor. HLA antigens are present on transplanted tissues (class I [HLA-A, -B, -C] antigens are expressed on most nucleated cells, and class II [HLA-DR, -DQ, -DP] antigen expression, although more limited, is likely to be induced at the time of transplantation or inflammation), most transplants involve some degree of HLA mismatch, HLA antigens provoke one of the strongest immune responses, and recipients may become sensitized to HLA antigens prior to transplantation through transfusion, pregnancy, and possibly environmental agents or after transplantation by the graft itself (*de novo*). The risk represented by HLA-specific antibodies is determined by the characteristics of the antibody, including class, specificity, strength, timing, and course (i.e., whether the antibody is increasing or decreasing), and by the characteristics of the tissue (i.e., the extent and type of antigen expression and the resilience of the tissue to antibody-mediated damage). The level of risk, as measured by timing and extent of damage to the graft, is directly proportional to the antibody titer. Regarding immunoglobulin class, IgG antibodies are established risk factors, the data are ambiguous for IgM antibodies, and there are data suggesting that HLA-specific antibodies of the IgA class are beneficial in transplantation (reviewed in reference 1). It has been clearly demonstrated that antibodies to either HLA class I or class II antigens represent a risk and are capable of producing hyperacute rejection. However, the levels of antigen expression vary among HLA loci. Antigens encoded by the HLA-C, -DP, -DQ, -DRB3 (DRw52), -DRB4 (DRw53), and possibly -DRB5 (DRw51) loci are expressed at much lower levels than those encoded by HLA-A, -B, and -DRB1, and there may be a lower risk of rejection associated with their respective antibodies. However, rejection due to antibodies to HLA-Cw, -DQ, and -DP antigens has been reported, including at least one case of a hyperacute rejection resulting from an antibody to donor Cw (4–7). Antibodies that are present at the time of or that develop after transplantation can damage tissues. In contrast, antibodies that were present only historically appear to represent little risk except in two situations: (i) when the current transplant shares a mismatched antigen with a previous transplant and (ii) when a previous graft was lost to an early immunologic rejection. The course of antibodies over time is also an important indicator of the level of risk. Antibodies that are increasing in strength or expanding in specificity may represent a recent or ongoing sensitization, which may include newly developing antibodies to donor antigen; they are potentially of great risk and can be refractory to treatment. Highly sensitive detection assays available now make the determination of these increases in antibody strength and specificity much easier. Conversely, antibodies that are waning in titer or breadth may reflect an active downregulation of the immune response and may be more responsive to intervention. Differences, among organs

doi:10.1128/9781555818722.ch114

and tissues, in HLA antigen expression, extent of exposure to antibody, and impact on the function of antibody-mediated damage are well known. However, a variety of factors, such as certain cytokines and hormones, which can be released in response to trauma, infection, or certain treatments, can affect antigen expression, which, in turn, can provoke a humoral response and provide increased target for antibody binding.

Goals and Aims

When testing for HLA-specific antibody, a laboratory's goal should be to determine the level of risk to the transplanted organ or tissue. Despite the danger represented by HLA antibody, the risk to the transplant can be overcome, in many cases, through appropriate intervention. The data obtained from tests of HLA-specific antibody provide an opportunity to determine what treatment, if any, will overcome the risk associated with any given transplant. Risk exists in the form of existing antibody or an increased probability of making antibody to donor HLA. The most definitive source of information is the detection and characterization of antibodies both prior to and following transplantation. This includes assessing the antibody characteristics, identified above, that are associated with risk: immunoglobulin class, titer, specificity, and trend. However, even routine screening prior to transplantation represents only a small window in the patient's history, and there is a substantial opportunity for undetected sensitization. Therefore, obtaining information about potentially sensitizing events in the patient's history will increase the accuracy of the assessment of risk. This chapter will deal with the technical aspects of obtaining the information necessary to evaluate humoral sensitization to HLA antigens in transplant patients.

The minimal testing requirements for compliance with the Clinical Laboratory Improvement Act (CLIA) of 1988 can be found in the *Code of Federal Regulations* (8). There has been an ongoing expression of concern, by some, regarding the expense of testing for humoral sensitization. A review of the literature provides extensive evidence of the benefit of such testing in prolonging graft and patient survival and reducing injurious rejection episodes. Treatment protocols designed to overcome sensitization, the single largest barrier to transplantation, are being used worldwide to increase opportunities for transplanting sensitized patients. Antibody testing provides a means of identifying the best candidates for these protocols and monitoring treatment efficacy. Given the high cost of treating rejection, of reduced graft survival, and of alternative treatment when transplants fail, testing for antibodies is a very cost-effective investment.

METHODS

Creating a Patient Profile

Certain patient information is useful for quantifying the risk of rejection, assessing how aggressive a responder a patient is, and interpreting results of antibody tests (9). The applicable information is outlined in Table 1. The table is reasonably self-explanatory and merits only a few additional remarks. Information about previous sensitizing events can be used to achieve a gross assessment of how aggressively a patient responds to exposure to HLA. Patients with a previous graft in place have a source of antigen for maintaining sensitization but may have artificially low levels of antibody because the donor tissue is acting like an "immunologic sponge," removing antibody by adsorption onto the antigens expressed on the tissue or by releasing soluble antigens that bind to the antibody. However, the high sensitivity of the multiplexed bead assays in wide use permit detection of HLA antibody even with a graft in place. Following a recent transfusion, samples should be obtained approximately 2 to 4 weeks posttransfusion to optimize detection of a humoral response. Transfusion histories are extremely difficult to obtain, are often inaccurate, and should be supplemented with information about previous surgeries that might have been occasions for transfusion.

Tests

There are two categories of test used to assess a humoral response, crossmatching and the antibody screen, the latter of which may be further subdivided into screens that simply

TABLE 1 Patient information

Item	Information needed	Relevance
Diagnosis	Specific disease	May indicate the likelihood of auto-antibody
Previous transplants	No. and duration	Extent of immunologic exposure
	Type and date of each	Graft duration, organs at risk
	Present or explanted	Allograft in place may absorb antibody
	HLA phenotype of each	Identify mismatched antigens and repeated mismatches
Pregnancy history	No. of pregnacies	Extent of possible sensitization
	No. of births	Extent of possible sensitization
	Identities of paternal antigens	Specificity of possible sensitization
Transfusions	Yes/no/no. and type	Possible sensitization
	Date of most recent	Identification of sera to be tested
Surgeries	Kind and date of each	Possible source of unrecognized transfusions
Medications	Humanized or chimeric antibodies	Test interference not readily resolved
	Xenoantibodies	Test interference, may be adsorbable
	Cytotoxic drugs	Interference in cell-based assays
Proinflammatory events	Infection	Activation of memory, HLA-specific B cells
	Trauma	
	Transfusion	

test for the presence of antibody and those designed to provide antibody characterization.

Crossmatches

The crossmatch test assesses the presence, in the recipient's serum, of antibody reactive with donor antigens. The most commonly used medium for the antigen is donor lymphocytes, which are readily obtainable and express HLA antigens at high levels, although other cells and tissues have been employed in specialized studies. Complement-dependent cytotoxicity and flow cytometry are the techniques most widely used. The advantages of the crossmatch test are that it measures reactivity with donor antigens directly and can be used to track the trend of antidonor reactivity through serum titration. The disadvantages are that (i) when cellular targets are used, the test does not readily differentiate HLA-specific antibodies from other antibodies that bind to lymphocytes; (ii) multiple therapeutic drugs interfere with the crossmatch test and may render the test uninterpretable; and (iii) donor cells are not always available at the necessary time or in sufficient quantity, although it may be possible to use cells from a surrogate donor, as will be discussed later. In HLA-mismatched transplants that include substantial amounts of immunocompetent tissues, such as transplants of bone marrow and possibly lung and small bowel, a reverse crossmatch involving donor serum and recipient cells may also be appropriate since engrafted tissue from a sensitized donor may produce antibody reactive with recipient HLA. Another antibody-mediated problem, transfusion-related acute lung injury (TRALI), can occur when transfused blood contains a substantial amount of antibody specific for the transfusion recipient's HLA antigens (10). Although a reverse crossmatch might identify such situations, it is more efficient and economical to perform screens of plasma units for the presence of HLA-specific antibody, which is now common practice.

Antibody Screens

An antibody screen is simply a crossmatch or series of crossmatches against cells or antigens from individuals selected to represent, collectively, most HLA antigens. There are three types of panels: antigens pooled from hundreds of individuals (a pooled-antigen panel), phenotype panels consisting of cells or antigens from a series of individuals, and single HLA antigens. Pooled-antigen panel tests are considered "yes/no" tests but can provide information about the extent of and changes in antibody breadth and specificity (11). Phenotype and single-antigen panels provide characterization of antibodies with exquisite sensitivity and specificity. The antibody screen has multiple advantages. It can be performed at any time prior to or following transplantation and, thus, prevent unnecessary donor testing and/or shipment of organs. Screening provides information useful in performing and interpreting a crossmatch, such as which sera represent the array of HLA antibodies that the patient has ever had; which sera might contain interfering antibodies, such as autoantibodies or therapeutic antibodies; what is the most appropriate crossmatch technique; and whether or not a positive crossmatch is due to antibodies to the donor HLA antigens. When performed on sequential samples, antibody screens provide information about trends in antibody activity. Finally, antibody screening provides a means of recognizing when sensitizing events or sample switches might have occurred.

The major disadvantages of the antibody screen are that it neither tests actual donor cells nor defines antibody directly. The high polymorphism of the HLA system mandates the use of panels of 50 to 100 phenotypes to be able to determine HLA specificities reliably. However, it is difficult to characterize sera containing multiple antibodies in tests of phenotype panels since antibodies to three or four common antigens can render a serum panreactive. Tests using single, purified antigen targets resolve this problem to some extent, but these panels come with their own attendant problems. Consideration should be given to utilizing a variety of tests in parallel to elucidate the most accurate antibody profile for a given serum. However, this can be cost-prohibitive, and care must be taken when designing testing protocols to test sera in the most cost-effective manner possible, while maintaining a high standard of patient care in relation to antibody characterization.

Techniques for Testing Antibody

General Principles

There are two categories of techniques differentiated by type of target: (i) those that utilize cells as targets, namely, cytotoxicity and flow cytometry, and (ii) those that utilize soluble HLA molecules bound to a solid matrix. The relevant factors for each type of assay and their advantages and disadvantages are summarized in Tables 2 and 3, discussed below.

TABLE 2 Assay characteristics

Characteristic	Outcome of indicated cell-based assay		Outcome of indicated solid-phase assay		
	Cytotoxicity assay	Flow cytometry	ELISA	Beads on a flow cytometer	Beads on a fluoroanalyzer[a]
Sensitivity	Low to moderate	High	High	High	High
HLA specificity	Low	Low	High	High	High
Isotype determination	IgG/IgM via serum manipulation	Yes	Yes	Yes	Yes
Cost	Low	High	Moderate to high	High	High
Automation	No	Partial	Partial	Partial	Partial
Throughput	Limited	Limited	Moderate	Limited	High

[a]Based on results with the Luminex fluoroanalyzer.

TABLE 3 Advantages and disadvantages of different assays

Category	Characteristic of:		
	Cytotoxicity assay	Flow cytometry	Solid-phase immunoassay
Advantages	No additional training needed Sensitivity can be adjusted Has been in use for 40 yr Inexpensive Uses standard laboratory equipment	Has high sensitivity Can test for different Ig isotypes Can test multiple cell types simultaneously	Has high sensitivity Eliminates most non-HLA reactivity Partial automation is possible Commercially available Readily distinguishes between cI and cII antibodies
Disadvantages	Requires manipulation to differentiate cI and cII antibodies Requires an adequate no. of viable lymphocytes Does not distinguish HLA from non-HLA antibodies Has low sensitivity	Requires expensive equipment Requires an adequate no. of viable lymphocytes Does not distinguish HLA from non-HLA antibodies Software may not interface with a lab's database	May require additional training Expensive Subject to interference from immune complexes, IgM, and some therapeutic reagents Yields relative antibody levels but not antibody strength Provides no control over antigen condition or amount

Complement-Dependent Cytotoxicity

Complement-dependent cytotoxicity (CDC) detects antibody through a secondary process: cell lysis by complement which has been activated by antibodies bound to target cells. It usually consists of a sensitization phase in which target cells and serum are incubated together, followed by addition of complement and a subsequent incubation to allow complement to be activated by bound antibody. Microscopic evaluation following addition of a vital stain permits a gross estimation of the percentage of viable cells. The sensitivity of the assay can be modified by altering incubation times and temperatures, performing washes to remove anticomplementary factors, and adding an antiglobulin reagent to enhance complement activation (12). The test is routinely performed on lymphocytes, which are usually further fractionated into T and B lymphocyte populations. Each test uses cells from a single individual.

Flow Cytometry

Cell-based flow cytometry is an indirect assay that measures the binding of antibody to cells through the use of an antiglobulin labeled with a fluorescent marker. The specificity of the antiglobulin reagent permits identification of the immunoglobulin class of cell-bound antibody. Further characterization of the cells can be achieved by gating on cells defined by physical parameters and staining cells with labeled monoclonal antibodies specific for markers that are unique to certain cell types.

Solid-Phase Immunoassays

Solid-phase immunoassays utilize affinity-purified, soluble HLA antigens isolated from culture fluid or human plasma, solubilized from cell membranes, or synthesized via recombinant technology. Initially performed in an enzyme-linked immunosorbent assay (ELISA) format, they are today most commonly performed as a multiplexed assay with soluble antigens bound to beads differentiated fluorescently. Multiplex bead assays can be performed by two means: standard flow cytometry and Luminex immunoassay (13). In standard flow cytometry, a single dye is incorporated into beads in different concentrations to permit differentiation of beads bearing different antigens or antigen combinations. In the Luminex format, two different dyes, each at 10 different dilutions, are incorporated into beads to provide up to 100 different beads differentiated by color. The beads are examined in a dual-laser fluoroanalyzer, where one laser identifies the particular bead and another detects the presence of antigen-specific antibody through use of a fluorochrome-conjugated antiglobulin.

Advantages and Disadvantages

A few of the major advantages of the cytotoxicity assay stem from its use for over 3 decades; (i) it predicts and can prevent hyperacute and acute antibody-mediated rejection; (ii) all the test variables, factors affecting the test, and quality control requirements have been well characterized; (iii) the test utilizes very small volumes of test materials (1 to 2 μl of serum and 2,000 to 2,500 cells per reaction); and (iv) the assay is relatively inexpensive to run. Multiple serum samples can be tested at multiple dilutions, providing information about antibody titers and trends in one or multiple patients. Despite these advantages, however, the test has many shortcomings. It requires an adequate supply of viable lymphocytes, requires separate tests of T and B lymphocytes and removal of class I-specific antibody to identify class II-specific antibodies, depends on the activity of complement, which is a highly variable and labile reagent, requires adequate amounts of the heterophile antibody found in rabbit serum used routinely as the complement source, is not sufficiently sensitive to detect extremely low levels of antibody, and, most importantly, does not readily differentiate between HLA-specific and other lymphocyte-binding antibodies. Antibodies that may interfere in the assay include autoantibodies, therapeutic antibodies that react with all or some subsets of lymphocytes, and

some anti-Lewis antibodies. Spurious reactions with B lymphocytes have been attributed to antiviral antibodies. A gross evaluation of the class of antibody reactive in the assay is possible through inactivation of IgM with reducing reagents or heat aggregation. However, neither technique will completely abrogate the reactivity of high levels of IgM.

Cell-based flow cytometry provides a high degree of sensitivity, permits simultaneous analysis of multiple cell types without the need for separation of cells, and facilitates determination of immunoglobulin class through the selection of antiglobulin specificity. However, like cytotoxicity tests, it requires an adequate number of viable cells and does not readily differentiate between HLA-specific and other lymphocyte-binding antibodies that either are of human origin or have been humanized. Further, it requires expensive equipment and specialized training and utilizes expensive reagents.

Solid-phase immunoassays using purified HLA antigens combine a high degree of sensitivity and specificity. Solid-phase immunoassays readily distinguish between class I- and class II-specific antibodies by using antigens of only one class in a single test. Further, these assays provide a more refined quantification of reactivity with the different phenotypes by scoring reactions on a continuous scale, which enhances the characterization of antibody specificity. The ability to test against pooled antigens represents a potential for substantial cost savings when sera are tested in batches. Further, beads differentiated by color permit multiple tests to be run in a single assay that uses a very small serum volume. Phenotype assays combine the ability to define specificity with an assessment of relative antibody level. However, although some specificities can be determined in even polyreactive sera, not all specificities can be identified in such sera. Single-antigen panels permit detection and identification of all antibody specificities. The disadvantages of the multiplexed bead assays include a potential need for additional equipment and training, increased reagent cost for some of the assays, and a need for extensive quality control. The high sensitivities of these tests contribute to increased variability and necessitate extensive experience to optimize the interpretation and use of the test results. Nonspecific binding of immunoglobulin may occur when the test serum contains immune complexes or aggregated immunoglobulin, rendering the test invalid. We have found that high levels of IgM antibodies can affect test results, even when an IgG-specific antiglobulin is used (14). We and others have also found that some therapeutic agents can interfere with test results (15). In the past, there has not been a uniform amount of antigen among different beads that are each coated with HLA molecules of one specificity. However, manufacturers have made a great effort to provide a more uniform amount of antigen on each bead. HLA molecules may be distorted upon being bound to a solid matrix, resulting in the loss of some epitopes or the creation of others. Naturally occurring antibodies or antibodies to non-HLA epitopes have been found in nonsensitized males. On the one hand, false-positive reactions due to a non-HLA antibody may prevent a compatible transplant, while a false negative that occurs when an HLA antibody fails to react with a distorted molecule may result in a transplant at increased risk for antibody-mediated rejection (16). Finally, in any assay with computer-generated results, there is a potential for a problem in interfacing with the laboratory's existing database.

It is important to note that cell-based and solid-phase immunoassays are complementary—the former assessing the strength of reactivity with donor cells directly and the latter providing determination of the basis for a crossmatch reaction. A conference of experts that took place in 2012 recognized this and made a strong recommendation to use both types of assays in assessing donor-recipient compatibility (17).

Quality Control

Crossmatching

There are three quality control procedures relevant to the crossmatch test. The first is to ensure that the cells being tested are from the right individual. This can be achieved by performing HLA typing in parallel with crossmatching and using the same cells used for the crossmatch. The second is to identify reactivity due to non-HLA-specific antibodies. Some of these antibodies, namely, autoantibody and therapeutic, lymphocyte-reactive antibodies, can be detected by performing an autologous crossmatch. Finally, use of the crossmatch test to track the course of antibody, including with a serum sample that was previously tested by the same technique as a reference, will provide a measure of variability in sensitivity.

Antibody Screen

Even though a positive control is included in all tests, it usually is not adequate to detect small variations in sensitivity. Such variations may result in a failure to detect antibodies present in levels that are at the border of the test's sensitivity. Inclusion of one or more well-characterized sera, diluted to near their endpoint of reactivity, would provide a means of recognizing this degree of variability.

Cytotoxicity Assay

Information about the cytotoxicity assay and relevant quality control measures is available in an excellent source (18), and we mention here only a few items particularly important in tests of antibody.

Frequently, different lymphocyte subsets are used in the cytotoxicity test because of differences in the levels of expression of various antigens. The test should include controls specific for these subsets to estimate the relative purity of the cell preparation and detect contamination with unwanted cell types. These controls are usually monoclonal antibodies specific for a cell surface marker unique to or predominant in a certain cell type and most often are designed to identify T and B lymphocytes and, occasionally, monocytes.

Addition of an antiglobulin reagent is a frequent modification of the cytotoxicity test used for antibody detection. In these cases, it is important to include a control to validate the presence and efficacy of the antiglobulin reagent. This control should be a serum that activates complement only in the presence of the antiglobulin reagent.

Most nonspecific cell death, (i.e., cell death not mediated by HLA-specific antibody) is detected in the negative-control wells. However, there may be occasions, particularly in the crossmatch test, that warrant additional discrimination. In these cases, the question of whether cell death is mediated by antibody or not can be resolved by running a parallel test using heat-inactivated (56°C for 30 min) complement.

Solid-Phase Immunoassays: Reagents

There are a number of factors that can contribute to variability among test reagent lots, including (i) changes in any component that affects test sensitivity, (ii) variability in the preparation of one or more individual phenotypes, (iii) contamination of or absence of antigen on one or more beads, (iv) changes in a cell line used as a source of antigen, and (v) manufacturing differences in the solid-phase media used. In

turn, these factors can affect the threshold value for a positive test result, the background reactivity of an individual phenotype or single antigen bead, and the ability of an individual phenotype or single antigen bead to yield a positive reaction with specific antibody. Some of this variability can be assessed by testing each lot of reagents with a panel of well-characterized sera that includes sera known to contain HLA-specific antibodies as well as some known to lack such antibodies. In addition, each lot of reagents should be monitored throughout the course of its use to determine if the correct value has been selected as the threshold for a positive reaction and to determine if any individual phenotype demonstrates an inordinate number of reactions that are discordant with the assigned antibody specificity (1). Recent reports have shown that normalizing reactions to the amount of antigen present improves the interpretation of the results. It is likely that this sort of normalization is best conducted by the manufacturer on each lot of reagents rather than by each individual user, providing uniform standardization while minimizing the additional cost.

Solid-Phase Immunoassays: Tests

Tests with pooled antigens provide little or no opportunity for detecting slight variations in test sensitivity or operator error, such as sample switch or dilution error. Inclusion of two or more blind, characterized sera serves as a quality control measure of the test system as well as of testing personnel. The sera should vary in strength to provide a meaningful assessment of test sensitivity and should vary from run to run to serve as meaningful unknowns. Background reactivity may be caused by a variety of factors, including high IgM levels, immune complexes, and certain therapeutic agents, among others. Background reactivity can result in false negatives when it occurs in the negative controls and false positives when it occurs in the test well or bead. The high sensitivity of single-antigen beads appears to make this panel more susceptible to interference and variability. There are commercially available blocking agents designed to reduce nonspecific reactivity. We have found that depletion of IgM by hypotonic dialysis effectively removes or reduces interference, providing increased reactivity with test sera and the positive-control bead (14). Drawbacks to this procedure are that it is time-consuming and can introduce some degree of dilution. Certain patients, notably those undergoing hemapheresis or plasmapheresis, have reduced background reactivity. In such cases, computerized analysis may interpret low values as positive. In assays that use beads, the wash technique must be appropriate and consistent to avoid variable loss of beads. Of course, standard quality assurance measures, particularly instrument calibration, are essential to ensure consistent and reproducible results. Quality control factors relevant to tests of antibody are summarized in Table 4.

TEST VALIDATION

The requirements for validation of laboratory assays are described in detail in the *Code of Federal Regulations* (8). Testing for HLA antibodies is confounded by the complexity of the HLA system, the antibody response to HLA antigens, and the lack of reference antibodies. Therefore, test validation can be prolonged and costly. To optimize evaluation of the assays and the clinical utility of the data generated, there should be an ongoing comparison of the results of various tests; can the crossmatch and antibody screen results for a specimen be reconciled? These comparisons reflect the sensitivity and specificity of the various assays. A frequently asked question is "How many sera need to be tested for validation of an antibody screen assay?" This question is impossible to answer with a number because of the thousands of possible combinations of antibodies that can be present in a specimen. The practical answer is that the validation must

TABLE 4 Quality control

Test/method	Factor	QC measure	Purpose
Crossmatching	Cell identity	Performance of serologic typing simultaneously with XM on cells used in XM	To verify identities of cells used in XM test
	Antibody specificity	Autologous XM	To test for the presence of autoantibody
	Titer	Inclusion of a previously tested serum in the XM	To assess the comparability of test sensitivities when comparing changes in antibody strength
Antibody screen	Test sensitivity	Inclusion of a serum tested at the threshold of reactivity	To detect variation in test sensitivity
Cytotoxicity assay	Cell type	Cell-specific antibody	To assess proportions of cell types in the preparation
	Antiglobulin	Inclusion of an antiglobulin-dependent serum in the test	To verify the addition and efficacy of the antiglobulin reagent
	Nonspecific cell death	Inclusion of inactivated complement	To indicate the occurrence and extent of cell death not due to antibody
Solid-phase immunoassays	Nonspecific binding	Antigen-free matrix (bead or well)	To assess nonspecific binding
	Phenotype validation	Panel of sera containing well-characterized HLA antibody	To determine if beads/wells yield expected reactions
	Variability in sensitivity	Normalization of test serum reactivity to that of a positive control	To normalize for variability in sensitivity

generate enough data for the user to be able to interpret the test results reliably. Some aspects of an assay's performance may be detectable only after extensive testing. Therefore, ongoing evaluation of an assay should continue after sufficient testing has been performed to place the test into clinical use with confidence.

INTERPRETATION

Antibody Screen

The data that may be obtained from antibody screens are the antibody level and the specificity. Positive reactions of a serum with a panel of phenotypes may vary in strength because of differences, among phenotypes, in the numbers of antigens to which the serum contains antibodies and, for cell-based assays, because of normal variability in antigen expression among individuals, among cell types, among antigens, and within an individual from day to day. There are abundant data regarding variability in antigen expression on cells. Class I antigens are expressed at higher levels on B cells than on T cells. Among various loci, HLA-Cw antigens are expressed at lower levels than are HLA-A and -B locus antigens, and antigens encoded by DRB3, -4, and (possibly) -5 loci (DR52, -53, and -51, respectively) are expressed at approximately 15 to 20% of the level of the DRB1-encoded antigens (DR1-18) (19). In tests of pooled antigens, differences in reaction scores obtained with different sera from the same individual reflect differences in the breadths of antibody specificities as well as their strengths. In tests of individual phenotypes, stronger reactions are obtained with phenotypes homozygous for a target antigen or having more than one target antigen. This, in turn, may be useful in verifying antibody specificity. Quantification of the strength of reactivity is more refined in solid-phase immunoassays and flow cytometry than in cytotoxicity testing, and this information may be useful in confirming putative assignments of antibody specificity. Determining the molecular equivalents of soluble fluorochromes (MESFs) for flow cytometric or Luminex results permits comparison of test results from specimen to specimen and day to day. To determine MESFs, a standard calibration curve is created using beads labeled with different, known amounts of a fluorochrome. The MESF value for a test serum is then obtained from the standard curve by interpolating the fluorescent channel values of the serum (20).

Immunoglobulin isotype is most precisely defined in adherence assays that use an isotype-specific antiglobulin. When isotype-specific antiglobulins are used, it is important to verify the reagent specificity, as many "monospecific" reagents have been found to cross-react with other isotypes. In cytotoxicity assays, the immunoglobulin class may be approximated by heating serum (63°C for 10 min) or by adding reducing reagents to inactivate IgM. However, both methods have limited efficacy. Titer determination is easily achieved in cell-based assays by testing a serum at multiple dilutions.

Calculated PRA

A major goal of antibody screening is to be able to assess the breadth and strength of a patient's antibodies and to apply that information to crossmatch prediction. Historically, the measure of breadth was the percent panel-reactive antibody (PRA), which is the percentage of a panel of phenotypes with which a serum gives a positive reaction. Obviously, the numeric value obtained is determined by the panel composition, which does not, necessarily, reflect the frequency of phenotypes in the donor population or the likelihood that an unrelated donor will be incompatible. Many transplant programs now use population frequencies to assess the breadth of sensitization more accurately. In 2009, the United Network for Organ Sharing (UNOS) adopted the use of a calculated PRA (CPRA) that applies an algebraic calculation to determine the percentage of the population that is incompatible (21). The patient data used in the calculation are the donor antigens determined to be unacceptable for transplantation. Using the antibody data gathered for any given patient and by establishing a correlation between antibody strength as determined by solid-phase bead-based assays and crossmatching, a CPRA can be generated to calculate the likelihood of achieving a negative flow-cytometric or cytotoxicity crossmatch result. The value can also be applied by setting a very low threshold to encompass all of a patient's antibodies or to avoid previously mismatched antigens, thus giving the likelihood of finding a donor to which the recipient has no HLA antibody. The calculation can be performed readily using the UNOS CPRA calculator, which can be accessed at https://optn.transplant.hrsa.gov/resources/allocation-calculators/. This program uses frequency data from the U.S. population, accounting for the proportions of different races in the population.

Virtual Crossmatching

CPRA is a statistic applied to determining the likelihood of incompatibility of an unspecified donor in the population, while the virtual crossmatch test is applied to assessing the likelihood that a donor of known HLA phenotype is incompatible. The virtual crossmatch test also uses the specificities of antibodies that are at a strength deemed unacceptable for transplantation. When the threshold is a positive crossmatch, one must identify those antibody specificities that, individually, will yield a positive crossmatch. In situations where a patient has antibodies to multiple antigens of a donor, it is important to make an assessment of the collective strength of those antibodies. Data on the relative strengths of antibodies can be obtained from solid-phase assays by correlating the results of those assays with crossmatch results (22). In establishing these correlations, it is important to take into account the variable amounts of different antigens and, in particular, those antigens with greatly increased amounts in bead assays, namely, HLA-Cw, -DQ, and -DP.

Thus, accurate characterization of the HLA-specific antibodies in a serum may provide the most valuable information for transplant purposes. This information can be used to (i) reduce cold ischemia time by preventing the unnecessary shipment of organs and crossmatch testing of patients incompatible with a specific donor, (ii) avoid incorrectly passing over a sensitized patient by recognizing donors to whom the patient has no antibodies, (iii) determine the clinical relevance of a positive crossmatch by recognizing whether the reactivity is due to HLA-specific antibodies or not, (iv) permit preemptive treatment to avoid antibody-mediated rejection by detecting DSA in levels too low to be detected in the crossmatch test and/or formed *de novo* after transplantation, and (v) facilitate accurate and effective paired-exchange programs. While the utility of cell-based assays, such as cytotoxicity and flow-cytometric crossmatches, should never be overlooked, these virtual crossmatches have taken on a larger role in the laboratory.

Phenotype Panel

Most laboratories today use solid-phase assays rather than cell panels. Therefore, we will not deal with interpretation of data from cell panels here. Rather, the reader is referred to previous editions of this *Manual* for a thorough discussion of

that topic. Interpreting antibody specificity from phenotype panels in solid-phase assays is greatly facilitated by ranking reactions in descending order of strength. An example is shown in Fig. 1. It can be seen that DR52-bearing phenotypes are clustered at the top of the results, with the strongest reactions being phenotypes homozygous for DR52. Below that are phenotypes bearing DR8, an antigen strongly cross-reactive with DR52. Note that below these phenotypes, the reaction strength drops off drastically. However, note also that both of the phenotypes immediately below those with DR8 or DR52 have DR4. While this may be a coincidence, it may suggest the presence of very weak antibody, and one should monitor future serum specimens for possible confirmation of that specificity.

Single-Antigen Panel

Solid-phase immunoassays using purified, single HLA molecules as targets have rapidly become the "go-to" test that identifies specificity readily and is the most sensitive of the types of panels available. The advantage of the single-antigen assays is the ease of analysis and the ability to track antibodies to uncommon antigens or antigens that are difficult to detect on phenotype panels. In particular, antibodies to HLA-Cw and -DP are not detected readily on phenotype panels. Furthermore, in the most broadly sensitized individuals, phenotype panels often are panreactive, making it difficult to characterize all HLA antibodies present. However, the high sensitivity of the single-antigen panel also makes it the most susceptible to interference, run-to-run variability, and problems with conformation of the HLA molecules. Attaching soluble HLA molecules to a solid matrix can result in the distortion of the molecule destroying native epitopes and creating nonnative epitopes. The susceptibility to distortion varies among different antigens. It has been demonstrated that antibodies present in males known to be nonsensitized to HLA can react with distorted HLA molecules (16). Thus, a false-positive reaction may occur due to antibody to a nonnative epitope, and a false-negative reaction can result when a native epitope is lost. Precise information about the quantity of each antigen and the extent to which structural conformation may have been compromised is not readily available for these products. Further, when using single-antigen reagents, the determination of the presence or absence of a particular antibody may rely on only a single reaction. In these cases, a technical failure that involves a key antigen may have serious consequences.

Assigned	Raw Val.	Class II Antigens					
Positive	12601	DR18		DR52			DQ4
Positive	12425	DR14	DR17	DR52		DQ5	DQ2
Positive	12148	DR13	DR18	DR52		DQ6	DQ4
Positive	11872	DR18	DR8	DR52		DQ7	DQ4
Positive	11840	DR17		DR52			DQ2
Positive	11342	DR12	DR17	DR52		DQ7	DQ2
Positive	11106	DR12	DR14	DR52			DQ7
Positive	10169	DR11	DR12	DR52			DQ7
Positive	9794	DR17	DR7	DR52	DR53		DQ2
Positive	9638	DR17	DR7	DR52	DR53		DQ2
Positive	9577	DR11		DR52			DQ7
Failed	7138	DR11	DR9	DR52	DR53	DQ7	DQ2
Failed	7024	DR103	DR8			DQ5	DQ4
Positive	6698	DR10	DR11	DR52		DQ7	DQ5
Positive	6647	DR16	DR8	DR51		DQ7	DQ5
Positive	6191	DR1	DR13	DR52		DQ9	DQ5
Positive	6139	DR15	DR8	DR51		DQ6	DQ4
Positive	5665	DR14	DR4	DR52	DR53	DQ8	DQ5
Positive	4410	DR10	DR12	DR52		DQ7	DQ5
Positive	4344	DR10	DR13	DR52		DQ7	DQ5
Positive	271	DR1	DR4	DR53		DQ7	DQ5
Negative	266	DR4		DR53		DQ8	DQ7
Negative	225	DR1					DQ5
Negative	218	DR16	DR9	DR51	DR53	DQ9	DQ5
Negative	200	DR9		DR53			DQ2
Negative	173	DR15	DR7	DR51		DQ9	DQ6
Negative	170	DR15		DR51			DQ6
Negative	164	DR1	DR9	DR53		DQ9	DQ5
Negative	116	DR103	DR15	DR51		DQ7	DQ6
Negative	102	DR7		DR53			DQ2

FIGURE 1 Results of serum tested on a phenotype panel. The specificity of the antibody can readily be discerned by the clustering of DR52 phenotypes. Note that the three phenotypes bearing DR8, an antigen that strongly cross-reacts with DR52, are interspersed among the DR52-bearing phenotypes. Val., value.

Therefore, single-antigen reagents are probably best used as an adjunct to other antibody tests, in particular when other assays do not provide a clear identification of antibody specificities.

As there is a finite amount of antigen present on each bead, there is also a maximum amount of antibody that can be bound. When a bead is saturated with antibody, it will be difficult to assess the relative strength of the antibody or detect changes in antibody strength over time. In such cases, it is necessary to test sera at a dilution. This provides an additional advantage in that diluting a serum often reduces or eliminates interference. However, one should be cautious about testing sera only at dilution, since newly developing antibodies may go undetected until they reach a certain strength.

Crossmatch Tests

There are two levels of interpretation to be considered in the crossmatch test: whether or not the test result is positive and what the test result means clinically. While it is possible to detect cell death and changes in either optical density or fluorescence, the lack of reference reagents has made it impossible to determine what amount of antibody yields what degree of reactivity in any of the assays used. This is further complicated by test variability within and among assays, among laboratories using the same assay, and among treatment protocols and transplant practices. Therefore, most interpretation is based on clinical outcome. Unfortunately, many of the studies performed to correlate crossmatch results with clinical outcome have not controlled for many of the relevant variables, including the (i) timing of the serum specimen relative to transplantation, (ii) immunoglobulin class of the antibody, (iii) antibody specificity, and (iv) antibody titer. Therefore, the conclusions of these studies are frequently in conflict with each other.

Reactivity strength in cytotoxicity assays is measured on a discontinuous scale in which the percentage of dead cells is grouped into five categories, while flow-cytometric assays are measured on a continuous scale. There are a large number of variables that can affect the assessed strength of reactions in a cell-based assay, including day-to-day variability in test conditions and variability among technologists in assessing reaction strength. When using crossmatch tests to monitor changes in antibody over time, it is useful to include a previously tested serum as a means of assessing variability in test sensitivity. Also having a single technologist read sequential tests will eliminate technologist-to-technologist variability.

Dealing with Interference

Autoantibodies

Among the most common interfering antibodies occurring prior to transplantation are autoantibodies. Many of these antibodies are IgM and can be eliminated by heat inactivation or treatment with reducing agents, such as dithiothreitol. However, these techniques will not completely abrogate reactivity when the antibody is at a high titer and are not compatible with testing using solid-phase assays. More-effective techniques to eliminate IgM, such as chromatography or dialysis (14), or tests that use an isotype-specific conjugate may be necessary in order to achieve a meaningful crossmatch or for accurate interpretation of bead-based, solid-phase assays. However, the large IgM molecule may block IgG binding, rendering the use of an isotype-specific conjugate ineffective. Autoantibodies of the IgG class are less common but do occur and are much more problematic in tests. The removal of these antibodies requires adsorption. Periodically, autoantibodies will be present in an otherwise-healthy-appearing donor. This is suggested when tests of donor cells persistently yield positive reactions in the negative controls of cell-based tests despite consistently good pretest viability. When this is suspected, it is worthwhile to do a donor autocrossmatch for confirmation. The reader is advised that adsorption with cells requires a large volume of cells and can lead to dilution when a small quantity of serum is adsorbed.

Therapeutic Antibodies

Therapeutic antibodies can be problematic in both cell-based and solid-phase assays. When the antibodies are of nonhuman origin, they can be removed by adsorption with magnetic beads coated with a species-specific antiglobulin, or the interference can be overcome by performing flow cytometry with antiglobulin reagents that have been adsorbed to remove reactivity with all but human immunoglobulin. The use of therapeutic humanized antibodies, however, is problematic in cell-based and solid-phase bead-based assays. These antibodies may be reactive in cell-based assays for months after cessation of treatment. In some cases, the target antigen may be removed from the cell surface, abrogating antibody activity. For example, pronase treatment of B cells removes CD20, the target of rituximab. However, pronase is a nonspecific protease that may also destroy or distort HLA molecules on the cell surface (23). When the antibody target cannot be removed, adsorption with cells bearing the target antigen but lacking donor HLA antigens becomes the only recourse. In bead-based antibody detection assays, therapeutic antibodies can cause interference. This interference often can be removed by hypotonic dialysis of the serum to remove the interfering agent. Some agents, such as antithymocyte globulin, can yield a pattern of reactivity that appears HLA specific. If the presence of antithymocyte is not known or taken into account, the test results will be misinterpreted as positive for HLA antibody.

Pronase Treatment of Cells

In the flow-cytometric crossmatch, increased background activity is often seen with B cell targets and has been attributed to the nonspecific binding of IgG to Fc receptors present on B cells. Further, the presence of rituximab (Rituxan), which binds to the CD20 molecule on B cells, renders a B cell crossmatch uninterpretable. Pronase, a nonspecific protease, has been used to resolve both problems. Low levels of pronase have been used to reduce or eliminate Fc receptors, while higher doses have been used to cleave CD20. Pronase also affects HLA molecules in a dose-dependent fashion, and selection of the amount of pronase to use should achieve maximum reduction of background with minimal impact on HLA expression. Higher doses of pronase are necessary to reduce CD20 expression sufficiently, and we have shown a significant impact on HLA expression at these higher levels.

Dealing with Interference in Solid-Phase Immunoassays

While autoantibody and certain therapeutic agents (eculizumab, high-dose intravenous [i.v.] immunoglobulin, bortezomib [15]) have been shown to interfere in solid-phase assays, background reactivity, as indicated by high negative-control or low positive-control values, may occur in the absence of these factors. Such interference may be due to the presence of immune complexes, plastic antibodies, or other as-yet-unidentified factors. Several techniques have been

applied to reducing or eliminating interference, including hypotonic dialysis (14), treatment with a reducing agent, dilution, and the addition of EDTA (24) to serum. Hypotonic dialysis is the most labor-intensive and time-consuming of the procedures, but it is also the only procedure that removes interfering substances. Reducing agents have a greater effect on IgM than on IgG; however, monomeric units of IgM with antigen binding capability may remain, and there is some impact on IgG. The benefit of dilution is based on the possibility of a differential effect on the binding of HLA IgG antibodies and the binding of interfering substances. Finally, the use of EDTA is to eliminate the binding of C1q that may block the binding of the antiglobulin reagent.

Assessment of Antibody Function

Based on the assumption that complement activation is the major way in which antibodies damage allogeneic transplants, modifications of the bead-based assays have been developed to assess the binding of C4d (25) and C1q (26). Both of these assays have been shown to correlate with clinical outcomes (25, 27), and at present, the C1q assay is available commercially from One Lambda, Inc. The C4d assay yields very low mean fluorescent intensity (MFI) values that may limit its use as a diagnostic tool. While the MIF values obtained with the C1q assay are high, some have reported that the test results simply correlate with antibody strength (27, 28), although others have reported negative C1q results with sera that yield high MFI values in the unmodified assay for HLA antibody. Further, while complement-mediated injury may be the most severe aspect of antibody-mediated rejection, it is not the only way in which donor-specific antibodies can lead to graft dysfunction and damage.

Application

Whom To Test

Three groups of patients are at high risk for an adverse effect of HLA-specific antibodies: organ transplant recipients, patients receiving platelet and/or leukocyte support, and patients receiving HLA disparate bone marrow transplants. In the case of bone marrow transplants, both the donor and the recipient should be tested. A fourth group of patients are those at risk for TRALI (see above). Although this is a serious condition and responsible for more than 10% of transfusion-related fatalities, the incidence is low (<0.5% of all patients transfused) and can be averted by having plasma screened for HLA and granulocyte-specific antibodies.

When To Test

Conventional wisdom and federal regulations indicate that testing should be performed at regular intervals prior to transplantation and following sensitizing events. Unfortunately, we do not always know about sensitizing events, and it is becoming increasingly apparent that we have not identified all possible routes of sensitization. Clearly, data from apparently nontransfused patients and evidence of similarities between microbial proteins and HLA antigens indicate that there may be a much broader potential for sensitization or reactivation of a humoral response than has been previously appreciated. Further, inflammation itself may generate a polyclonal B cell activation that results in the production of HLA-specific antibodies (29).

It has been suggested that the low rate of sensitization and increasing waiting times dictate testing only when transplantation is imminent. Most historic data on sensitization are based on cytotoxicity testing. With the increased use of the more sensitive and specific solid-phase immunoassays, it has become increasingly apparent that the percentage of patients sensitized may be grossly underestimated (13). Antibody screening can be performed at a low absolute cost, a cost much lower than that of other components of transplantation. Antibody screening provides information important to selecting patients and sera for and interpreting the results of a crossmatch and can provide advance notice of the presence of factors, such as autoantibody, that may adversely affect interpretation of the crossmatch results.

Special considerations apply to patients being treated in a protocol designed to reduce or eliminate humoral sensitization and will be discussed in a separate section below.

Perhaps one of the greatest and most costly deficiencies of the current standard of practice is the lack of adequate posttransplant testing, which results from the lack of financial reimbursement for such testing. Three factors argue in favor of such testing: (i) there are now treatment protocols that produce a durable elimination of DSA, (ii) assays currently available are sufficiently sensitive to detect antibody before a transplanted organ suffers extensive injury, and (iii) prolonging graft survival by avoiding antibody-mediated rejection not only avoids returning a renal transplant patient to costly dialysis but also avoids increasing the number of patients awaiting transplantation.

How To Test

Good management practices dictate applying the minimal number of protocols, uniformly, to maximize cost saving. Having one or a small number of test protocols does save money in the laboratory, which should mean reduced laboratory charges. However, it is quite possible that this approach extracts a much greater cost in rejection, treatment for rejection, and reduced graft survival. Given the complexity of transplantation, it is probably more cost-effective, overall, to customize testing according to the complexity and emergent nature of the case. For patients that are highly sensitized, one method of posttransplant monitoring involves designing individual testing plans for each recipient. Selection of tests appropriate for monitoring a patient's antibodies (phenotype versus single-antigen or class I and/or class II panels) can be done prior to transplantation. Close monitoring during the immediate posttransplant period is advisable, as the trauma of surgery can provoke an increase or recurrence of DSA. It is wise to monitor and reevaluate the effectiveness of the testing schematic over the course of monitoring. Having a variety of tests available in the lab to monitor antibodies and to determine which tests are needed to provide all the necessary information at the lowest possible cost is advisable.

Monitoring for Desensitization Protocols

Patients with HLA-specific antibody have access to transplantation reduced in proportion to the breadth of their sensitization and, as a group, have poorer graft outcomes. Several treatment protocols have been developed to achieve a long-lasting reduction in or elimination of HLA-specific antibodies. Currently, desensitization protocols can be grouped into two general categories: those that utilize high-dose (1 to 2 g/kg of body mass), pooled i.v. Ig and those that use plasmapheresis combined with low-dose (100 mg/kg) cytomegalovirus (CMV) hyperimmune globulin (CMVIg) or i.v. Ig (29–32). The former is used to eliminate some or all HLA-specific antibodies of patients awaiting either live- or deceased-donor organ transplantation, the latter

is used to downregulate antibodies specific for a particular donor's HLA, and both are used for treating antibody-mediated rejection. Both types of protocol require accurate identification of the patient's HLA-specific antibodies prior to treatment.

The goals of monitoring desensitization are to determine the risk of antibody-mediated rejection, monitor treatment efficacy, and generate information that helps guide and fine-tune treatment (30, 31). The pretreatment evaluation of the patient consists of (i) identifying previous potentially sensitizing events and the response to those events, (ii) creating an immunologic profile of the current transplant (i.e., the number of current mismatches, the number to which the patient has antibody, the immunogenicity of the mismatched antigens, and whether or not they are repeat mismatches), and (iii) determining the specificity and strength of the DSA. High-dose i.v. Ig interferes with tests using antiglobulin reagent. Because this protocol usually treats patients monthly, sera obtained prior to each treatment can be used to monitor treatment efficacy. In the plasmapheresis/i.v. Ig protocol, serum samples should be obtained before and after each treatment, immediately prior to transplantation, and 48 to 72 h after treatment is stopped. The extent of treatment (the number of plasmaphereses and additional immunosuppressants) needed correlates most strongly with the titer of the DSA. Therefore, a crossmatch to assess titer should be performed at a time prior to initiation of treatment that is sufficient to allow any needed adjustments in the treatment schedule. Once treatment is started, tests should be performed to monitor the course of the DSA. A cost- and time-efficient way to do this is to test all sera in a solid-phase immunoassay that uses pooled target antigens to chart the general trend of the antibodies and to monitor the strength of DSA by performing crossmatch or antibody identification tests on selected sera. Plasmapheresis removes many substances from the plasma, and background reactivity in solid-phase and flow-cytometric assays usually decreases during treatment. This should be taken into account when interpreting the results of these assays. There is a certain amount of day-to-day and technologist-to-technologist variability in the CDC crossmatch test. This variability can be minimized to a certain extent by having the same technologist perform all crossmatch tests and by including in each round of testing a reference serum which is a historic serum of the patient and has a known titer. Also, normalization of the data through the use of MESFs and other procedures will facilitate a more meaningful interpretation of test results. The data that should be examined are (i) the overall trend of the DSA titer and (ii) the extent of rebound that occurs between treatments. Once the transplant has been performed, a sample should be obtained 48 to 72 h after treatment is completed to check for DSA rebound. Whenever possible, these patients should have antibody monitoring posttransplantation for a minimum of 3 months and following any potentially sensitizing event.

The Whole Picture: the Assessment of Risk

As the opportunities for reducing antibody and modulating the immune response improve, it will become increasingly important to produce a body of information that provides an assessment of risk to the transplant. Our increasing understanding of the role of the humoral response in transplantation indicates the need for certain types of information. (i) Does the patient have antibody? (ii) If so, what is the specificity, titer, and immunoglobulin class? (iii) Is the antibody increasing or decreasing in strength or breadth? (iv) Has the patient had antibody in the past? (v) Has the patient had potentially sensitizing events? Neither the crossmatch nor the antibody screen alone can answer these questions; the tests are complementary, and both are needed to get an accurate assessment of the patient's humoral immune status. The antibody screen may reveal very low levels of antibody, indicating that a very sensitive crossmatch technique, such as flow cytometry, is appropriate, or conversely, it may demonstrate that the antibody levels are such that this expensive technique is overkill. Even when both antibody screening and crossmatch tests are performed, it may not be possible to obtain an adequate picture of the patient's humoral immunity. In these cases, specialized techniques may be appropriate. While use of such *ad hoc* procedures will add to costs, in many cases and particularly where the information is applied to clinical care, the investment will be well worth it.

REFERENCES

1. **Leffell MS, Zachary AA.** 2010. Anti-allograft antibodies: some are harmful, some can be overcome, and some may be beneficial. *Discov Med* **9:**478–484. PubMed
2. **Zhang Q, Reed EF.** 2010. Non-MHC antigenic targets of the humoral immune response in transplantation. *Curr Opin Immunol* **22:**682–688. PubMed
3. **Dragun D, Catar R, Philippe A.** 2013. Non-HLA antibodies in solid organ transplantation: recent concepts and clinical relevance. *Curr Opin Organ Transplant* **18:**430–435. PubMed
4. **Willicombe M, Brookes P, Sergeant R, Santos-Nunez E, Steggar C, Galliford J, McLean A, Cook TH, Cairns T, Roufosse C, Taube D.** 2012. De novo DQ donor-specific antibodies are associated with a significant risk of antibody-mediated rejection and transplant glomerulopathy. *Transplantation* **94:**172–177. PubMed
5. **Gilbert M, Paul S, Perrat G, Giannoli C, Pouteil Noble C, Morelon E, Rigal D, Dubois V.** 2011. Impact of pretransplant human leukocyte antigen-C and -DP antibodies on kidney graft outcome. *Transplant Proc* **43:**3412–3414. PubMed
6. **Rogers NM, Bennett GD, Toby Coates P.** 2012. Transplant glomerulopathy and rapid allograft loss in the presence of HLA-Cw7 antibodies. *Transpl Int* **25:**e38–e40. PubMed
7. **Bachelet T, Couzi L, Guidicelli G, Moreau K, Morel D, Merville P, Taupin JL.** 2011. Anti-Cw donor-specific alloantibodies can lead to positive flow cytometry crossmatch and irreversible acute antibody-mediated rejection. *Am J Transplant* **11:**1543–1544. PubMed
8. **Clinical Laboratory Improvement Act (CLIA).** 1988. Standard: histocompatibility. 42 CFR 493.1278. https://www.gpo.gov/fdsys/pkg/CFR-2015-title42-vol5/pdf/CFR-2015-title42-vol5-sec493-1278.pdf.
9. **Philogene MC, Zachary AA.** 2013. Assessing immunologic risk factors in transplantation. *Expert Rev Clin Immunol* **9:**773–779. PubMed
10. **Vlaar AP, Juffermans NP.** 2013. Transfusion-related acute lung injury: a clinical review. *Lancet* **382:**984–994. PubMed
11. **Zachary AA, Leffell MS.** 2008. Detecting and monitoring human leukocyte antigen-specific antibodies. *Hum Immunol* **69:**591–604. PubMed
12. **Zachary AA, Klingman L, Thorne N, Smerglia AR, Teresi GA.** 1995. Variations of the lymphocytotoxicity test. An evaluation of sensitivity and specificity. *Transplantation* **60:**498–503. PubMed
13. **Earley MC, Vogt RF Jr, Shapiro HM, Mandy FF, Kellar KL, Bellisario R, Pass KA, Marti GE, Stewart CC, Hannon WH.** 2002. Report from a workshop on multianalyte microsphere assays. *Cytometry* **50:**239–242. PubMed
14. **Zachary AA, Lucas DP, Detrick B, Leffell MS.** 2009. Naturally occurring interference in Luminex assays for

HLA-specific antibodies: characteristics and resolution. *Hum Immunol* **70:**496–501. PubMed

15. **Badders JL, Houp JA, Sholander JT, Leffell MS, Zachary AA.** 2010. Considerations in interpreting solid phase antibody data. *Hum Immunol* **71:**18.
16. **El-Awar N, Nguyen A, Almeshari K, Alawami M, Alzayer F, Alharbi M, Sasaki N, Terasaki PI.** 2013. HLA class II DQA and DQB epitopes: recognition of the likely binding sites of HLA-DQ alloantibodies eluted from recombinant HLA-DQ single antigen cell lines. *Hum Immunol* **74:**1141–1152. PubMed
17. **Tait BD, Süsal C, Gebel HM, Nickerson PW, Zachary AA, Claas FH, Reed EF, Bray RA, Campbell P, Chapman JR, Coates PT, Colvin RB, Cozzi E, Doxiadis II, Fuggle SV, Gill J, Glotz D, Lachmann N, Mohanakumar T, Suciu-Foca N, Sumitran-Holgersson S, Tanabe K, Taylor CJ, Tyan DB, Webster A, Zeevi A, Opelz G.** 2013. Consensus guidelines on the testing and clinical management issues associated with HLA and non-HLA antibodies in transplantation. *Transplantation* **95:**19–47. PubMed
18. **Hahn AB, Land GA, Strothman RM.** 2000. *ASHI Laboratory Manual,* 4th ed. ASHI, Lenexa, KS.
19. **Emery P, Mach B, Reith W.** 1993. The different level of expression of HLA-DRB1 and -DRB3 genes is controlled by conserved isotypic differences in promoter sequence. *Hum Immunol* **38:**137–147. PubMed
20. **Schwartz A, Fernández Repollet E, Vogt R, Gratama JW.** 1996. Standardizing flow cytometry: construction of a standardized fluorescence calibration plot using matching spectral calibrators. *Cytometry* **26:**22–31. PubMed
21. **Zachary AA, Braun WE.** 1985. Calculation of a predictive value for transplantation. *Transplantation* **39:**316–318. PubMed
22. **Zachary AA, Sholander JT, Houp JA, Leffell MS.** 2009. Using real data for a virtual crossmatch. *Hum Immunol* **70:**574–579. PubMed
23. **Hetrick SJ, Schillinger KP, Zachary AA, Jackson AM.** 2011. Impact of pronase on flow cytometric crossmatch outcome. *Hum Immunol* **72:**330–336. PubMed
24. **Schnaidt M, Weinstock C, Jurisic M, Schmid-Horch B, Ender A, Wernet D.** 2011. HLA antibody specification using single-antigen beads—a technical solution for the prozone effect. *Transplantation* **92:**510–515. PubMed
25. **Smith JD, Hamour IM, Banner NR, Rose ML.** 2007. C4d fixing, Luminex binding antibodies—a new tool for prediction of graft failure after heart transplantation. *Am J Transplant* **7:**2809–2815. PubMed
26. **Fontaine MJ, Kuo J, Chen G, Galel SA, Miller E, Sequeira F, Viele M, Goodnough LT, Tyan DB.** 2011. Complement (C1q) fixing solid-phase screening for HLA antibodies increases the availability of compatible platelet components for refractory patients. *Transfusion* **51:**2611–2618. PubMed
27. **Sutherland SM, Chen G, Sequeira FA, Lou CD, Alexander SR, Tyan DB.** 2012. Complement-fixing donor-specific antibodies identified by a novel C1q assay are associated with allograft loss. *Pediatr Transplant* **16:**12–17. PubMed
28. **Zeevi A, Lunz J, Feingold B, Shullo M, Bermudez C, Teuteberg J, Webber S.** 2013. Persistent strong anti-HLA antibody at high titer is complement binding and associated with increased risk of antibody-mediated rejection in heart transplant recipients. *J Heart Lung Transplant* **32:**98–105. PubMed
29. **Locke JE, Zachary AA, Warren DS, Segev DL, Houp JA, Montgomery RA, Leffell MS.** 2009. Proinflammatory events are associated with significant increases in breadth and strength of HLA-specific antibody. *Am J Transplant* **9:**2136–2139. PubMed
30. **Montgomery RA, Zachary AA, Racusen LC, Leffell MS, King KE, Burdick J, Maley WR, Ratner LE.** 2000. Plasmapheresis and intravenous immune globulin provides effective rescue therapy for refractory humoral rejection and allows kidneys to be successfully transplanted into crossmatch-positive recipients. *Transplantation* **70:**887–895. PubMed
31. **Sonnenday CJ, Ratner LE, Zachary AA, Burdick JF, Samaniego MD, Kraus E, Warren DS, Montgomery RA.** 2002. Preemptive therapy with plasmapheresis/intravenous immunoglobulin allows successful live donor renal transplantation in patients with a positive cross-match. *Transplant Proc* **34:**1614–1616. PubMed
32. **Tyan DB, Li VA, Czer L, Trento A, Jordan SC.** 1994. Intravenous immunoglobulin suppression of HLA alloantibody in highly sensitized transplant candidates and transplantation with a histoincompatible organ. *Transplantation* **57:**553–562. PubMed

Non-Human Leukocyte Antigen Antibodies in Organ Transplantation

ANNETTE M. JACKSON AND BETHANY L. DALE

115

INTRODUCTION

Clinical Relevance of Non-HLA Antibodies in Transplantation

Transplantation can significantly extend the life of patients with end-stage renal disease and provide a lifesaving treatment for patients with failure of other major organs. Extending the long-term survival of these transplanted organs requires a better understanding of the mechanisms of immune injury, including humoral immunity. Alloantibodies were determined early on to be a contraindication to transplantation, but until recently the primary focus has been on HLA-specific antibodies (1). Historically, the lymphocyte crossmatch was the primary tool used to detect HLA antibodies in the sera of transplant recipients and to assess the risk of antibody-mediated rejection posttransplantation. Now, with the advent of solid-phase immunoassays, we can detect HLA antibodies at very low levels and provide a more accurate characterization of their antigen specificities (2).

As our ability to detect and avoid donor-specific HLA antibodies has improved, the contribution of non-HLA antibodies to allograft injury has become more apparent. Multiple reports have described antibody-mediated allograft rejection in the absence of HLA antibodies or following transplantation with HLA-identical grafts (3, 4). In a large collaborative study, sensitized recipients transplanted with HLA-identical sibling allografts were shown to have reduced long-term graft survival compared with their nonsensitized counterparts, revealing the importance of sensitization to antigens other than ABO or HLA in transplantation (5).

Non-HLA Antigens Implicated in Transplantation

Antigens for non-HLA antibodies associated with rejection in renal, heart, and/or lung transplantation include both polymorphic and nonpolymorphic targets (6, 7). Antibodies specific for autoantigens such as collagen, tubulin, agrin, vimentin, myosin, angiotensin II type 1 receptor (AT1R), perlecan, and protein kinase C-ζ have been implicated in acute and/or chronic allograft injury. Many of these autoantigens are intracellular and are presented to the immune system following tissue damage. Exposure in the presence of inflammation (due to infection, an alloimmune response, or surgical injury) is thought to break self-tolerance and provoke the generation of autoantibodies (8–10). Lung recipients with detectable antibodies toward collagen V and Kα1 tubulin are at increased risk for primary graft dysfunction and the development of bronchiolitis obliterans syndrome, a form of chronic rejection in lung transplantation (6, 7). Vimentin- and myosin-specific autoantibodies have been observed in heart recipients with accelerated, chronic vasculopathy. Antibodies specific for membrane proteins AT1R and major histocompatibility complex class I-related chain A (MICA) have been implicated in acute rejection and reduced allograft survival following kidney transplantation. MICA genes are highly polymorphic and located next to HLA-B within the major histocompatibility complex. Approaches combining proteomics and genomics are uncovering additional tissue-specific non-HLA antigens associated with acute and chronic rejection (11–13). Also of interest are non-HLA antigens expressed on the surface of endothelial cells (ECs), the barrier between the recipient's immune system and the transplanted allograft. EC-reactive antibodies have been eluted from rejected kidney allografts and have been associated with acute rejection and graft failure in kidney and heart recipients (14–16). Reports of hyperacute kidney rejections have also been described in kidney recipients with EC-reactive antibody (17, 18).

Non-HLA Antibody: Mechanisms of Allograft Injury

HLA antibodies are efficient activators of complement, eliciting significant tissue damage and amplification of the immune response through the generation of anaphylatoxins (19). Valenzuela and Reed have also shown a role for HLA antibodies in transplant vasculopathy, an indolent form of chronic heart rejection (20). Mechanisms employed by non-HLA antibodies in allograft injury are diverse, likely due to the heterogeneity of the target antigens. In addition, there may be significant differences in the titer and affinity of non-HLA antibodies that are generated from antigens less immunogenic than HLA. The majority of rejections associated with non-HLA antibodies do not correlate with complement activation as measured by C4d positivity in allograft biopsies (15, 18, 21). Le Bas-Bernardet et al. reported that although EC-reactive antibodies are not cytotoxic, they can induce cell apoptosis independent of complement (22). However, non-HLA antibodies may synergize with donor-specific HLA antibodies to accelerate graft injury, to include complement activation (21, 23). EC-reactive antibodies have been shown to induce activation of vascular endothelium, resulting in the increased expression

doi:10.1128/9781555818722.ch115

of adhesion molecules and leukocyte adhesion (14, 24). Antibodies that bind vimentin on the surface of circulating leukocytes induce the release of prothrombotic factors (fibrinogen, thrombin, and platelet-activating factor) that result in platelet activation and increased risk of thrombosis (25). Non-HLA antibodies, such those directed against AT1R, have also been shown to bind as agonists and initiate downstream effects (26).

Multiple platforms have been used to detect non-HLA antibodies in the sera of transplant recipients. Each has advantages and disadvantages; thus, selecting the optimal assay depends on the nature of the investigation or volume of clinical testing.

METHODS

Selecting a Testing Platform

Detection of Antibody to Unknown Non-HLA Targets

Cell-based crossmatch assays using ECs were the first platform used to identify non-HLA antibodies in the sera of transplant recipients. Advantages include the ability to detect antibodies specific for novel antigens, in particular, polymorphic antigens that may differ between cell donors (27). Cell-based methods also allow the antigens to be presented in their native membrane-bound state with the correct post-translational modifications (e.g., glycosylation) (28). However, one must keep in mind that protein expression may not be the same on cells of the same type (e.g., ECs) isolated from different tissues or on cells that have been immortalized or maintained in long-term culture. Importantly, cell-based methods can identify the presence of non-HLA antibodies in the sera, but the antigen specificity of the bound antibodies is not known. Cell-based methods are less sensitive than solid-phase immunoassays, due to lower protein target densities and higher background reactivity with some cell types. The greatest disadvantage may be expression of HLA antigens on all nucleated cells, precluding the ability to detect non-HLA antibodies in the sera of patients broadly sensitized to HLA. Removing HLA antibodies from the serum prior to testing via cell or platelet adsorptions can eliminate this obstacle, but this is a labor-intensive effort.

Discovery strategies utilizing high-density protein arrays or antigen immunoprecipitation coupled with mass spectrometry also provide a means for identifying novel non-HLA targets (11, 12, 16, 29). Methods using mass spectrometry are robust but labor-intensive and are not suitable for routine clinical testing. Protein arrays are amenable to automation but are costly and have disadvantages such as the use of recombinant proteins that lack certain post-translational modifications, the exclusion of membrane-spanning proteins (e.g., AT1R), and a limited ability to identify highly polymorphic antigens.

Detection of Antibody When Non-HLA Targets Are Known

Enzyme-linked immunosorbent assays (ELISAs) or bead-based immunoassays can be purchased or created when the non-HLA target antigen is known (30; https://www.luminexcorp.com/research/reagents-and-accessories/lumavidin-microspheres/). These platforms can be automated and are most amenable to clinical testing. Both have enhanced sensitivity and specificity compared to cell-based strategies. ELISA methods are less sensitive than flow cytometric or Luminex (Austin, TX) bead-based assays; however, they are less expensive and can utilize cell lysates to allow testing of membrane-spanning proteins. The greatest advantage of Luminex bead assays is the ability to perform multiplex analysis of 100 to 500 antigenic targets simultaneously, using very small amounts of serum.

Optimization of Test Platform

The sensitivity of antibody screening assays is dependent on multiple factors, which include antigen density, signal-to-noise ratio, and the methodology used for signal detection. When using cell-based strategies, the purity and quality of the cells at the time of testing may impact antigen density. Surface protein expression may differ on cells with poor viability, after freezing, following long-term culture, or when isolated from older (>24 h) blood samples. Known surface proteins should be assessed at time of testing to ensure that cells are of good quality. These phenotypic markers can also be utilized in flow cytometric assays as gating parameters to assess cell purity and ensure consistency of cells selected for acquisition. Some studies have activated cells, prior to testing, using cytokines such as tumor necrosis factor alpha or gamma interferon to increase antigen expression on the cell surface (14, 22).

The antigen density in commercial solid-phase immunoassays may be fixed, but variables that affect signal-to-noise ratio may allow some optimization. The optimum antibody-to-antigen ratio is important for maximal detection and to avoid prozone effects. This can be optimized by testing different serum quantities and/or testing serial dilutions of the test serum. In addition, the reaction volume, dilution buffer, temperature, and duration of the serum incubation step can enhance or diminish antibody-antigen interactions. Unlike high-affinity monoclonal antibodies that are used in flow cytometric experiments, serum antibodies are polyclonal, containing antibodies of varying affinities and avidities. Affinity describes the strength of the noncovalent interactions (van der Waals, ionic, and hydrophobic) for each antibody and antigenic epitope. Avidity reflects the overall stability or strength of the antibody-antigen interaction and is impacted by antibody affinity and the valence of both the antibody and the antigen. Therefore, optimal conditions may be different when testing for non-HLA antibodies of different isotypes, which may differ in both affinity and valence. For example, it is well established in blood bank literature that IgM binding is enhanced at colder temperatures (4°C) compared to IgG, which binds across a wider temperature range (4 to 22°C).

Antibody detection assays can also be impacted by interfering substances present in some sera. Steric interference from immune complexes, complement bound to the Fc portion of the antibody, or excess serum IgM can decrease sensitivity by blocking or interfering with binding of the secondary detection antibody (31, 32). Serum dilution, EDTA addition, or treatment to deplete IgM using dithiothreitol, heat, or hypotonic dialysis can reduce this type of interference and increase signal detection.

The type of wash buffer used, the wash volume, and the number of wash steps are also important to reduce background and enhance signal. Wash buffers differ with regard to pH, ionic strength, and detergent and/or protein content (33). Complete removal of residual wash fluid between wash steps and prior to the addition of the detection reagents is also important for increasing sensitivity and reproducibility.

Separate blocking reagents may be included in ELISAs and cell-based assays; these are added prior to the detection antibodies to reduce nonspecific protein-protein interactions (33). Solid-phase immunoassays can also be modified, such that antibody-antigen complexes are formed first (using biotin-labeled antigen), and the volume of mixture is

increased and added to an avidin-coated bead or ELISA plate. This modification takes advantage of the high affinity between avidin and biotin and is used to reduce background signals caused by nonspecific binding of serum proteins to the assay matrix.

Finally, the detection strategy can also influence the sensitivity of the assay. Fluorescent or chemiluminescent detection strategies provide greater sensitivity than colorimetric methods. When using fluorochrome-conjugated detection antibodies, select the brightest fluorochrome and minimize spectral overlap to maximize detection sensitivity (34). These secondary antibodies should be tested at different titers/dilutions to determine optimal detection concentration. Utilization of biotin-conjugated detection antibodies with avidin-conjugated fluorochromes can amplify signal intensity and increase sensitivity.

PROCEDURES

EC Crossmatch

Summary

The EC crossmatch allows for the detection of donor-specific non-HLA antibodies present in the sera of transplant candidates. EC precursors (ECPs) are isolated from donor peripheral blood using anti-Tie2 magnetic nanoparticles (http://www.absorber.se/xm-one) and incubated with test serum. Non-HLA antibody bound to the ECP is detected using a fluorochrome-conjugated anti-IgG detection antibody and flow cytometry.

Assay Procedure

1. **Donor ECP preparation:** Isolate peripheral blood mononuclear cells from 40 ml of acid citrate dextrose using a Ficoll-Hypaque gradient separation. Transfer mononuclear cells into a 50-ml conical tube and wash twice (500 × *g*) with 1× phosphate-buffered saline with 5% heat-inactivated fetal calf serum. Incubate donor mononuclear cells with anti-Tie2 magnetic nanoparticles in 1.5-ml volume of wash buffer in a 5-ml polypropylene tube, rotating at 4°C for 30 min. After incubation, place on magnet for 10 min at 18 to 22°C. Remove supernatant containing mononuclear cells, being careful not to dislodge the cells from the magnet. Add 3 ml of wash buffer to $Tie2^+$ cells, briefly vortex, and apply to magnet for an additional 10 min. Remove and discard wash buffer. Resuspend cells in 1 ml of wash buffer and count using a hemocytometer.
2. **Serum preparation:** Heat-inactivate 100 μl of test/control serum at 63°C for 10 min; then spin in an airfuge for 15 min at 100,000 × *g* to remove IgM and/or immune complexes.
3. **Serum incubation:** Pipette 5×10^5 cells into 12- by 75-mm tubes, add 1.0 ml of wash buffer, and centrifuge (500 × *g*). Remove *all* residual wash buffer by blotting or using a vacuum aspirator. Immediately add 50 μl of test/control serum to each appropriate tube. Add 50 μl wash buffer to one tube in lieu of serum to assess autofluorescence. Briefly vortex and incubate cells and sera for 30 min at 18 to 22°C.
4. **Wash:** Wash cells a total of three times using 1 ml of wash buffer (centrifuge at 500 × *g*). Remove *all* residual wash buffer by blotting or using a vacuum aspirator after final wash.
5. **Detection antibody:** Immediately add fluorochrome-conjugated detection antibody and additional antibodies specific for markers used to determine acquisition gate. Incubate for 30 min at 2 to 8°C in the dark.
6. **Wash:** Wash cells a total of three times using 1 ml of *cold* wash buffer (centrifuge at 500 × *g*). Keeping the cells cold will prevent capping of proteins on the cell membrane.
7. **Detection:** Resuspend in 250 μl of cold wash buffer and immediately acquire on calibrated flow cytometer.

ELISA Procedure

Summary

Test serum is added to an ELISA microtiter plate coated with the target non-HLA protein. Non-HLA antibody bound to the plate is detected using an enzyme-conjugated detection antibody and an enzymatic substrate.

Assay Procedure

1. **Serum and standard preparation:** Dilute serum samples with kit-specific sample diluent. This dilution is generally in the range of 1:100 to 1:200. The standard curve dilutions are normally tested in duplicate.
2. **Serum incubation:** Add 50 to 100 μl of diluted test serum and control sera into appropriate microtiter wells in duplicate. The serum incubation time (from 30 min to 2 h or overnight at 4°C) and temperature (4 to 37°C) may vary.
3. **Wash:** Perform three washes with wash buffer. The number of washes and technique may vary depending on test sensitivity.
4. **Detection antibody:** Add diluted enzyme-conjugated detection antibody and incubate. Time (from 30 min to 2 h or overnight at 4°C) and temperature (18 to 37°C) may vary; shaking (200 rpm) is recommended but optional. Additional wash steps may be performed following the second incubation to remove unbound detection antibody.
5. **Enzymatic reaction:** Add enzymatic substrate and incubate at 18 to 22°C for 20 to 30 min. If fluorescent substrate is used, incubate in the dark.
6. **Detection:** Measure the optical density absorption or fluorescence on an appropriate microtiter plate reader.
7. **Interpretation:** If known standards were run, plot the standard curve graph to determine unknown test serum antibody concentration. If only running a semiquantitation assay, perform calculations using the manufacturer's correction factor.

Luminex Assay

Summary

The Luminex assay includes polystyrene beads coated with purified target protein. The beads are incubated with patient sera to identify the presence of target-specific antibodies using flow cytometry principles. *Note: the beads and secondary detection antibody are light sensitive, and all incubations should be performed in the dark.*

Assay Procedure

1. **Serum incubation:** Add control and test serum at the predetermined dilution with the bead set for 30 min at 18 to 22°C with shaking (200 rpm). This can be performed in a filter plate or a V-bottom plate.
2. **Wash:** If using a V-bottom plate, perform a spin-flick method to wash away unbound antibody. If using a filter plate, perform multiple washes using a vacuum

manifold. The number of washes and technique may vary depending on test sensitivity.

3. **Detection antibody:** Add freshly diluted secondary detection antibody to washed plate. Incubate for 30 min at 18 to 22°C with shaking (200 rpm). An additional wash procedure may be performed following the second incubation to remove unbound detection antibody.
4. **Detection**: Acquire data using a Luminex fluorometer. Results are reported as the mean fluorescence intensity (MFI) values.

Validation

Validation studies are important in both research and clinical settings, to evaluate the final testing conditions and determine negative and positive test thresholds. For cell-based assays, a positive control serum/antibody may not be readily available. In these cases, a commercial antibody or serum containing antibodies specific for an alternate surface protein known to be expressed on the cell of interest can be used as an alternative until a panel of non-HLA antibody-positive sera can be generated. For example, to achieve a positive EC crossmatch test, use sera containing HLA antibodies of different strengths but known to yield positive flow cytometric lymphocyte crossmatch with the cell donor. The range for positivity, what designates a weak, moderate, or strongly positive reaction, should be revisited at regular intervals as more data are compiled. When establishing a positive control serum, it is important to use a serum that yields consistent results but is weak enough to detect suboptimal test conditions or reagents. It is also important to secure a large enough quantity of serum so that it can be utilized over an extended period of time.

Next, and most importantly, the threshold for negativity must be determined. Multiple "negative" sera should be tested to determine a range for negative reactions. Negative control sera can be purchased or generated by screening sera obtained from multiple nontransfused healthy males. The establishment of a valid negative threshold range is vital so that weak positive reactions can be distinguished. The negative range should also be monitored over time as more data are compiled.

The reproducibility of the assay is also important; spending time optimizing each step of the assay will enhance test reproducibility. An acceptable range for test variability (% coefficient of variation) must be determined from replicate testing. Comparisons should be made between sera tested in duplicate within the same assay, on separate days, and by different technologists. Initial reproducibility testing should be performed with positive sera or a positive control antibody.

In ELISAs and some bead-based immunoassays, the concentration of an antibody can be estimated through the use of a standard curve (https://tools.thermofisher.com/content/sfs/brochures/TR0057-Read-std-curves.pdf). Standard curves are constructed by testing a positive control antibody against the antigen (standard) serially diluted across a range of relevant concentrations. Standard curves are generated from at least five points, a blank and four standard concentrations. Each standard data point should be monitored for consistency over time and used to reflect assay reproducibility.

Validation studies should include the development of quality control and quality assurance guidelines. These should describe how new reagents will be evaluated and guidelines for monitoring stored reagents to ensure quality for test consistency. Tracking the positive and negative test control values from each test will provide "real-time" monitoring of reagents and test procedures over time. Determination of the proficiency of each technologist performing the test and performing external proficiencies with other laboratories performing the same test through sera exchanges should also be performed. Additional testing guidelines and regulations can be found for the Code of Federal Regulations, 1988 Clinical Laboratory Improvement Amendments (http://www.gpoaccess.gov/cfr/index.html; search for 42CFR493.1278) and American Society for Histocompatibility and Immunogenetics (http://www.ashi-hla.org).

REFERENCES

1. **McKenna RM, Takemoto SK, Terasaki PI.** 2000. Anti-HLA antibodies after solid organ transplantation. *Transplantation* **69:**319–326. PubMed
2. **Leffell MS, Zachary AA.** 2010. Anti-allograft antibodies: some are harmful, some can be overcome, and some may be beneficial. *Discov Med* **9:**478–484. PubMed
3. **Kalil J, Guilherme L, Neumann J, Rosales C, Marin M, Saldanha L, Chocair PR, Ianhez LE, Sabbaga E.** 1989. Humoral rejection in two HLA identical living related donor kidney transplants. *Transplant Proc* **21:**711–713. PubMed
4. **Grafft CA, Cornell LD, Gloor JM, Cosio FG, Gandhi MJ, Dean PG, Stegall MD, Amer H.** 2010. Antibody-mediated rejection following transplantation from an HLA-identical sibling. *Nephrol Dial Transplant* **25:**307–310. PubMed
5. **Opelz G, Collaborative Transplant Study.** 2005. Non-HLA transplantation immunity revealed by lymphocytotoxic antibodies. *Lancet* **365:**1570–1576. PubMed
6. **Sigdel TK, Sarwal MM.** 2013. Moving beyond HLA: a review of nHLA antibodies in organ transplantation. *Hum Immunol* **74:**1486–1490. PubMed
7. **Zhang Q, Reed EF.** 2010. Non-MHC antigenic targets of the humoral immune response in transplantation. *Curr Opin Immunol* **22:**682–688. PubMed
8. **Fukami N, Ramachandran S, Saini D, Walter M, Chapman W, Patterson GA, Mohanakumar T.** 2009. Antibodies to MHC class I induce autoimmunity: role in the pathogenesis of chronic rejection. *J Immunol* **182:**309–318. PubMed
9. **Thaunat O, Graff-Dubois S, Fabien N, Duthey A, Attuil-Audenis V, Nicoletti A, Patey N, Morelon E.** 2012. A stepwise breakdown of B-cell tolerance occurs within renal allografts during chronic rejection. *Kidney Int* **81:**207–219. PubMed
10. **Chong AS, Alegre ML.** 2012. The impact of infection and tissue damage in solid-organ transplantation. *Nat Rev Immunol* **12:**459–471. PubMed
11. **Li L, Sigdel T, Vitalone M, Lee SH, Sarwal M.** 2010. Differential immunogenicity and clinical relevance of kidney compartment specific antigens after renal transplantation. *J Proteome Res* **9:**6715–6721. PubMed
12. **Dinavahi R, George A, Tretin A, Akalin E, Ames S, Bromberg JS, Deboccardo G, Dipaola N, Lerner SM, Mehrotra A, Murphy BT, Nadasdy T, Paz-Artal E, Salomon DR, Schröppel B, Sehgal V, Sachidanandam R, Heeger PS.** 2011. Antibodies reactive to non-HLA antigens in transplant glomerulopathy. *J Am Soc Nephrol* **22:**1168–1178. PubMed
13. **Otten HG, van den Bosch JM, van Ginkel WG, van Loon M, van de Graaf EA.** 2006. Identification of non-HLA target antigens recognized after lung transplantation. *J Heart Lung Transplant* **25:**1425–1430. PubMed
14. **Lucchiari N, Panajotopoulos N, Xu C, Rodrigues H, Ianhez LE, Kalil J, Glotz D.** 2000. Antibodies eluted from acutely rejected renal allografts bind to and activate human endothelial cells. *Hum Immunol* **61:**518–527. PubMed

15. **Breimer ME, Rydberg L, Jackson AM, Lucas DP, Zachary AA, Melancon JK, Von Visger J, Pelletier R, Saidman SL, Williams WW Jr, Holgersson J, Tydén G, Klintmalm GK, Coultrup S, Sumitran-Holgersson S, Grufman P.** 2009. Multicenter evaluation of a novel endothelial cell crossmatch test in kidney transplantation. *Transplantation* **87:**549–556. PubMed
16. **Qin Z, Zou Y, Lavingia B, Stastny P.** 2013. Identification of endothelial cell surface antigens encoded by genes other than HLA. A combined immunoprecipitation and proteomic approach for the identification of antigens recognized by antibodies against endothelial cells in transplant recipients. *Hum Immunol* **74:**1445–1452. PubMed
17. **Sumitran-Karuppan S, Tyden G, Reinholt F, Berg U, Moller E.** 1997. Hyperacute rejections of two consecutive renal allografts and early loss of the third transplant caused by non-HLA antibodies specific for endothelial cells. *Transpl Immunol* **5:**321–327. PubMed
18. **Jackson AM, Kuperman MB, Montgomery RA.** 2012. Multiple hyperacute rejections in the absence of detectable complement activation in a patient with endothelial cell reactive antibody. *Am J Transplant* **12:**1643–1649. PubMed
19. **Cornell LD, Smith RN, Colvin RB.** 2008. Kidney transplantation: mechanisms of rejection and acceptance. *Annu Rev Pathol* **3:**189–220. PubMed
20. **Valenzuela NM, Reed EF.** 2013. Antibodies in transplantation: the effects of HLA and non-HLA antibody binding and mechanisms of injury. *Methods Mol Biol* **1034:**41–70. PubMed
21. **Taniguchi M, Rebellato LM, Cai J, Hopfield J, Briley KP, Haisch CE, Catrou PG, Bolin P, Parker K, Kendrick WT, Kendrick SA, Harland RC, Terasaki PI.** 2013. Higher risk of kidney graft failure in the presence of anti-angiotensin II type-1 receptor antibodies. *Am J Transplant* **13:**2577–2589. PubMed
22. **Le Bas-Bernardet S, Hourmant M, Coupel S, Bignon JD, Soulillou JP, Charreau B.** 2003. Non-HLA-type endothelial cell reactive alloantibodies in pre-transplant sera of kidney recipients trigger apoptosis. *Am J Transplant* **3:**167–177. PubMed
23. **Cardinal H, Dieudé M, Brassard N, Qi S, Patey N, Soulez M, Beillevaire D, Echeverry F, Daniel C, Durocher Y, Madore F, Hébert MJ.** 2013. Antiperlecan antibodies are novel accelerators of immune-mediated vascular injury. *Am J Transplant* **13:**861–874. PubMed
24. **Florey OJ, Johns M, Esho OO, Mason JC, Haskard DO.** 2007. Antiendothelial cell antibodies mediate enhanced leukocyte adhesion to cytokine-activated endothelial cells through a novel mechanism requiring cooperation between FcγRIIa and CXCR1/2. *Blood* **109:**3881–3889. PubMed
25. **Leong HS, Mahesh BM, Day JR, Smith JD, McCormack AD, Ghimire G, Podor TJ, Rose ML.** 2008. Vimentin autoantibodies induce platelet activation and formation of platelet-leukocyte conjugates via platelet-activating factor. *J Leukoc Biol* **83:**263–271. PubMed
26. **Dragun D, Müller DN, Bräsen JH, Fritsche L, Nieminen-Kelhä M, Dechend R, Kintscher U, Rudolph B, Hoebeke J, Eckert D, Mazak I, Plehm R, Schönemann C, Unger T, Budde K, Neumayer HH, Luft FC, Wallukat G.** 2005. Angiotensin II type 1-receptor activating antibodies in renal-allograft rejection. *N Engl J Med* **352:**558–569. PubMed
27. **Vermehren D, Sumitran-Holgersson S.** 2002. Isolation of precursor endothelial cells from peripheral blood for donor-specific crossmatching before organ transplantation. *Transplantation* **74:**1479–1486. PubMed
28. **Harrison RL, Jarvis DL.** 2006. Protein *N*-glycosylation in the baculovirus–insect cell expression system and engineering of insect cells to produce "mammalianized" recombinant glycoproteins. *Adv Virus Res* **68:**159–191. PubMed
29. **Bilalic S, Veitinger M, Ahrer KH, Gruber V, Zellner M, Brostjan C, Bartel G, Cejka D, Reichel C, Jordan V, Burghuber C, Mühlbacher F, Böhmig GA, Oehler R.** 2010. Identification of non-HLA antigens targeted by alloreactive antibodies in patients undergoing chronic hemodialysis. *J Proteome Res* **9:**1041–1049. PubMed
30. **Drouet C, Nissou MF, Ponard D, Arvieux J, Dumestre-Pérard C, Gaudin P, Imbert B, Massot C, Sarrot-Reynauld F.** 2003. Detection of antiendothelial cell antibodies by an enzyme-linked immunosorbent assay using antigens from cell lysate: minimal interference with antinuclear antibodies and rheumatoid factors. *Clin Diagn Lab Immunol* **10:**934–939. PubMed
31. **Zachary AA, Lucas DP, Detrick B, Leffell MS.** 2009. Naturally occurring interference in Luminex assays for HLA-specific antibodies: characteristics and resolution. *Hum Immunol* **70:**496–501. PubMed
32. **Schnaidt M, Weinstock C, Jurisic M, Schmid-Horch B, Ender A, Wernet D.** 2011. HLA antibody specification using single-antigen beads—a technical solution for the prozone effect. *Transplantation* **92:**510–515. PubMed
33. **Gibbs J.** 2001. Effective blocking procedures. ELISA technical bulletin no. 3. Corning Inc Life Sciences, Acton, MA. http://www.labcluster.com/news4_3/Corning_elisa3_4.pdf.
34. **Baumgarth N, Roederer M.** 2000. A practical approach to multicolor flow cytometry for immunophenotyping. *J Immunol Methods* **243:**77–97. PubMed

Evaluation of the Cellular Immune Response in Transplantation

DIANA METES, NANCY L. REINSMOEN, AND ADRIANA ZEEVI

116

Solid-organ transplantation has become an increasingly important therapeutic modality for patients with various end-stage diseases. Despite improved immunosuppression protocols, most transplant recipients face a variety of complications. Early posttransplant infection and rejection are the major causes of morbidity and mortality. Drug toxicity, chronic rejection, and malignancies are long-term complications.

Many attempts have been made to develop *in vitro* procedures that can assess the immunological status of the allograft reliably and accurately. Immunological monitoring could, in theory, differentiate rejection from other forms of dysfunction, such as infection or primary nonfunction. Furthermore, the ideal tool would be able to gauge accurately a patient's response to antirejection therapy and might help prevent overimmunosuppression. Immunological monitoring could also be important in predicting long-term graft outcome and thereby identify which recipients could have their immunosuppression therapy markedly reduced without increasing the risk of acute or chronic rejection.

Although there is no one ideal immunological test that can accomplish all of the above, there are a number of tests that can be used together to assess the immunological status of the transplant recipient. The most informative approach appears to be performing sequential analyses using assays that measure different immune functions.

MIXED LYMPHOCYTE CULTURE ASSAY

Concept

The mixed lymphocyte culture assay (MLC) is an *in vitro* test of lymphocytes responding to stimulation by disparate HLA class II molecules, including HLA-DR and -DQ and, to a lesser extent, HLA-DP, which are predominantly expressed on B cells and monocytes of the stimulator cell population. Proliferative reactivity to HLA class I molecules has also been reported to play a role in the overall bulk MLC response. The first description of this assay as a measurement of cellular immunity (1, 2) together with the development of a one-way method of stimulation allowed the correlation of proliferative responses between siblings. The conclusion was that a single genetic locus or region, now known as HLA, controlled the MLC reactivity. The recognition of disparate HLA molecules and the resulting T-cell activation (as measured by MLC) are thought to represent an *in vitro* model of the afferent arm of the *in vitro* allograft reaction.

In MLC, stimulator cells have been inactivated, usually by X irradiation, and can no longer divide. The resulting proliferation of responding cells involves the logarithmic expansion of multiple clones of alloactivated T cells. This expansion can be measured by incorporation of the radioisotope-tritiated thymidine into replicating DNA during the logarithmic phase of cellular expansion, usually on the fifth day of culture. The amount of thymidine incorporated into cellular DNA is then assayed by liquid scintillation spectrophotometry. Exogenous tritiated thymidine added to *in vitro* cultures is incorporated during DNA replication via the salvage pathway, in which free purine bases are formed by hydrolytic degradation of nucleic acid and nucleotides. Exogenous tritiated thymidine is added to cultures for a period of time that is longer than the S phase of the cell cycle but shorter than the cell cycle itself, usually 18 h.

The degree of reactivity observed correlates with the degree of antigenic disparity between responding and stimulating cells. MLC has been used clinically for donor selection, predominantly for bone marrow transplantation. With the more recent application of DNA-based HLA typing methods, MLC is not used for donor selection but more often for monitoring of the recipient's posttransplant donor antigen-specific immune status. The difference between posttransplant and pretransplant antidonor MLC responses can be used to define any changes (increases or decreases). Studies have shown that solid-organ recipients who develop a decreased response (i.e., are hyporesponsive) are at low risk for immunological complications, such as late acute-rejection episodes and chronic rejection. Hyporeactivity is defined as at least a 60% decrease in reactivity of the posttransplant antidonor response compared with that of the pretransplant antidonor response, assuming the response to third-party cells remains unchanged (3, 4).

Procedure

Sample Requirements

For collection of specimens, care must be taken throughout the procedure to ensure a sterile specimen. Usually, 20 to 30 ml of sterile heparinized blood is obtained. The specimen may be saved overnight but should be processed within 24 h

doi:10.1128/9781555818722.ch116

of the phlebotomy. It should be maintained at room temperature even if it is being shipped by overnight carrier. Poor cell yields and poor function may result from temperature conditions that are too cold or too warm.

Materials and Reagents

Lymphocyte separation medium (LSM; catalog no. 17084003; Pharmacia Biotechnologies)

Culture medium: RPMI 1640 with HEPES buffer supplemented with 100 U of penicillin per ml, 100 U of streptomycin (Grand Island Biological catalog no. 380-2400AJ) per ml, 10 U of preservative-free heparin (Monoparin heparin; Accurate Chemical & Scientific Corp. catalog no. A6500) per ml, 2 mM L-glutamine, and 10 to 20% pooled human sera

Pooled human sera: sera from 10 to 20 healthy nontransfused male donors, heat inactivated at 56°C for 30 min (see "Pitfalls and Troubleshooting" below for additional specifications)

[^{3}H]thymidine (New England Nuclear catalog no. NEN-027): specific activity of 6.7 Ci/mM. Commonly used amounts are 0.5 to 1.0 mCi per well.

Hanks balanced salt solution (Grand Island Biological catalog no. 310-4170PJ)

Equipment and Instrumentation

Radiation source (usually gamma-emitting radiation source); alternatively, mitomycin (catalog no. M0503; Sigma)

Laminar flow hoods (Baker 60; The Baker Co., Sanford, Maine)

Liquid scintillation counter (1205 Betaplate; Pharmacia LKB)

Rate freezer (model 70014; CryoMed)

Liquid nitrogen refrigeration unit (model CAIIIL; CryoMed)

Mechanics and Controls

Mononuclear cells are isolated by centrifugation of peripheral blood diluted 1:2 with Hanks balanced salt solution over LSM. Peripheral blood mononuclear cells (PBMC) are removed from the LSM interface, diluted with Hanks balanced salt solution, and then centrifuged at 500 × *g* for 10 min. The supernatant is decanted, and the wash steps are repeated two more times. The cells are resuspended in an exact quantity of complete culture medium. A leukocyte count is done, and viability is determined via dye exclusion. The cell suspension is diluted to a final concentration of 5×10^5 PBMC per ml by using the culture medium. Stimulator cells are inactivated either by irradiation at 1,500 to 3,000 rad or by incubation with mitomycin according to the manufacturer's instructions. With a repeating microliter pipette, stimulator and responder cells are added in triplicate to round-bottom microtiter plates (catalog no. 760-042-05; ICN) such that each well receives 100 μl of stimulator cells (5×10^4 PBMC) and 100 μl of responding cells (5×10^4 PBMC).

A complete culture setup includes the following:

1. Allogeneic cultures containing all possible combinations of responder and stimulator cells, including cells from three control cell donors of known HLA phenotypes
2. Autologous cultures containing the responder and stimulator cells from the same cell donor
3. Control wells containing either responder or stimulator cells alone, with an equal volume of complete culture medium
4. Double irradiation control cultures containing stimulator cells from two different cell donors

The cultures are incubated at 37°C in a humidified atmosphere of 5% CO_2 for 5 days, after which 0.5 to 1.0 μCi of tritiated thymidine is added to each well. The cultures are incubated for an additional 18 h. The culture plates can then be harvested immediately or sealed with pressure-sensitive film and placed in the refrigerator until harvesting. A number of different harvesting machines and counting systems are available: the cells can be harvested onto filter disk sheets, or the samples can be counted in vials or cassettes or directly, without the need for scintillation fluid. The manufacturer's instruction manual should describe the appropriate procedures.

Pitfalls and Troubleshooting

1. **Drugs.** If a patient is taking one of the following drugs, the proliferative response may be compromised: prednisone, busulfan (Myleran), hydroxyurea, cyclophosphamide (Cytoxan), or L-asparaginase.
2. **Serum.** One of the most common sources of technical problems in any cellular procedure is a poor serum source. Each individual lot of a serum source, or preferably, each individual serum unit within the lot should be screened for growth support capabilities and possible HLA antibodies. The screen should include a control response to a pool of allogeneic cells to measure maximum response and an autologous control to ensure low backgrounds. If sporadic high backgrounds are observed, an endotoxin test may be advisable.
3. **Tritiated thymidine.** If low counts per minute are observed, the scintillation counter and the shelf life of tritiated thymidine should be checked. The half-life of the tritium is 12.3 years, but the shelf life of the thymidine is considerably shorter.
4. **Frozen cells.** Cells to be used as responder cells in the cell cultures can be bulk frozen by a step-down procedure at 4, −30, and −70°C before use. However, viability and cell recovery are better if the cells are rate frozen and stored in the vapor phase of a liquid nitrogen storage unit.

The *American Society for Histocompatibility and Immunogenetics Procedure Manual* (5) is an excellent source of additional information and details on cellular methods.

Interpretation

Results are usually expressed as raw counts per minute of tritiated thymidine incorporation. The data may be reduced to allow for easier interpretation and comparability from one test to another. The two most common forms of data reduction are the stimulation index and the relative response. The stimulation index is a simple ratio of the counts per minute for an experimental MLC combination to the counts per minute for the autologous control. The relative response is the ratio of the net counts per minute (after subtraction of the autologous control counts per minute for an allogeneic MLC combination) to the counts per minute for a maximally stimulated or control MLC combination (usually the response to a pool of allogeneic cells), multiplied by 100 to obtain a percentage (5).

MLC VARIATIONS

MTT Method

A nonradioactive alternative to detecting proliferation is a colorimetric (3-4,5-dimethylthiazol-2-yl)-2.5 diphenyl

tetrazolium bromide salt (MTT) reduction assay. This assay detects the activity of a mitochondrial enzyme that is proportional to the number of metabolically active cells present in the culture. The MTT, a yellow aqueous solution, is taken up by the viable cells and reduced in the mitochondria to a purple crystal. After solubilization of these crystals, the reaction product is measured with a spectrophotometer. An increase in the measured optical density parallels an increase in mitochondrial enzyme activity, which reflects an increase in the number of cells. This approach can detect increases in an interleukin 2 (IL-2)-sensitive line, CTLL2O. VanBuskirk et al. (6) have demonstrated that colorimetric detection of IL-2 production correlates well with the radioactive detection of T-cell proliferation and can be used interchangeably with the standard MLC.

RELATED METHODS

T-Cell Precursor Frequency Determination by LDA

The frequency of T-cell precursors is determined by limiting dilution assay (LDA). Limiting numbers of responder cells are cultured with a constant number of stimulator cells and assayed for reactivity (cytotoxicity, proliferation, or cytokine release) against additional stimulator cells. In contrast to MLC, which measures a bulk response, LDA is a quantitative tool. It allows the investigator to estimate the frequency of lymphocytes with a given function and antigen specificity. LDA implies that the lysis is a single-hit process; that is, a single precursor cell will initiate the sequence of events that leads, in the case of cytotoxic precursors, to the eventual lysis of the cell. A frequency can be determined if the lymphocyte population is random; that is, the function of the lymphocyte population is not influenced by the presence of another lymphocyte population. The clear distinction between a response and a lack of that response is imperative. Making this distinction is more difficult in the cytotoxicity assay, where an arbitrary threshold that separates the spontaneous release of ^{51}Cr from the release from the lysed targets is set. The frequency of responding cells is determined by a maximum likelihood estimation by using a computer program (7).

LDA of HTL

Helper T lymphocytes (HTL) are detected by their ability to produce IL-2. The murine IL-2-dependent line CTLL2O is used as the indicator line in this bioassay. Adding CTLL2O cells directly to the micrometer wells is a more sensitive method than removing an aliquot of supernatant and adding it to the CTLL2O cells. Before adding the indicator line, the plates are irradiated to inhibit the responder cells from proliferating and incorporating [^{3}H]thymidine. A low dose of irradiation does not block the continued production of IL-2 by the responding cells. In the absence of IL-2, the CTLL2O cells die rapidly. Therefore, any proliferation detected is due to division of the IL-2-stimulated CTLL2O cells.

Method

LDA can be done on fresh or cryopreserved cells. The cells are prepared as described in "Mixed Lymphocyte Culture Assay." Limiting numbers of PBMC (2×10^4, 1.0×10^4, 0.5×10^4, 0.25×10^4, 0.125×10^4, 0.0625×10^4, and 0.03125×10^4) are cultured in round-bottom microtiter plates with constant numbers (10×10^4) of irradiated (3,000 rad) stimulator cells. When HLA-identical pairs are tested, increased numbers of cells are often used such that the highest concentration is 4×10^4, 6×10^4, 8×10^4, or 10×10^4 cells per well. Multiple wells per dilution are necessary to ensure an accurate assessment of the frequency. Usually, 24 wells per dilution are set up. The culture medium is the same as that used in the MLC protocol. Control wells consist of 24 wells containing irradiated stimulator cells alone (for calculation of background activity), responder cells in medium alone (negative controls), and responder and stimulator cells set up separately against HLA-mismatched third-party cells (positive controls). The plates are incubated for 64 h at 37°C in a 5% CO_2 environment. The plates are irradiated with 2,500 rad. CTLL2O cells (1×10^3) are added in 25 ml of medium. The plates are incubated for 8 h with 1 mCi of [^{3}H]thymidine in 25 ml per well. Cultures are reincubated for 16 h. Cultures are harvested and counted as outlined in the MLC protocol. The wells are considered positive if [^{3}H]thymidine incorporation is greater than the mean plus 3 standard deviations of results for the 24 control wells. The frequency of responding cells is determined by maximum likelihood estimation by using a computer program, and the variance is determined by the use of 95% confidence intervals. Regression analysis is used to generate a straight line. Chi-square analysis is used to show that the data obtained are in accordance with single-hit kinetics. A program that does all the necessary calculations for this analysis is listed in reference 7.

Pitfalls and Troubleshooting

The sensitivity of this assay depends on the condition of the IL-2 indicator cells. The proliferation of the CTLL2O line depends on murine or human IL-2 or murine IL-4, without which the cells will die rapidly. The line should be maintained at a concentration of 1×10^4 to 10×10^4 cells per ml in a solution containing RPMI 1640 (with HEPES), 100 U of penicillin/ml, 100 μg of streptomycin/ml, 2 mM L-glutamine, 1% sodium pyruvate (100 mM solution), 1% minimal essential medium amino acids (50×), 0.5% diluted beta mercaptoethanol (diluted 1:57 with phosphate-buffered saline [PBS]), and 10% pooled human serum culture medium, supplemented with 500 U of IL-2. Great care should be taken to subculture this line every 2 to 3 days.

LDA of CTL

As mentioned before, the major advantage of the LDA is the ability to quantitate a particular T-cell function in an antigen-specific manner. The LDA for cytotoxic T lymphocytes (CTL) requires a longer incubation time than that for HTL since the cytotoxic activity must be generated in the presence of growth factors and alloantigen. Thus, the cultures are incubated for 10 days; IL-2 is added on days 3 and 6. The target cells are labeled with ^{51}Cr, which is taken up by the target cells and linked to internal proteins by endogenous enzymes. The unbound ^{51}Cr is washed away. The targets are added to the LDA wells for 4 h. During this time, CTL lyse the targets and ^{51}Cr leaks out of the cell into the culture supernatant. The amount of ^{51}Cr detected in the culture medium is directly related to the number of target cells lysed by the CTL. Although ^{51}Cr does emit gamma rays, it is more efficient to assay for the Auger rays that are also emitted. The Auger rays have an energy level within the same wavelength range as that of tritium and therefore can be detected by the conventional scintillation counting method. Frequency determinations are done in a manner similar to that used for the HTL precursor (HTLp) method.

Reagents

Phytohemagglutinin (PHA), 28.75 U/ml (catalog no. HA-17; Burroughs Wellcome)

RPMI 1640

Method

Limiting numbers of PBMC (5×10^4 to 0.125×10^4) are cultured in round-bottom microtiter plates with constant numbers (5×10^4) of irradiated (3,000 rad) stimulator cells. Multiple wells per dilution are necessary to ensure an accurate assessment of the frequency. Usually, 24 wells per dilution are set up. The culture medium is the same as that used for the MLC method. IL-2 and additional culture medium are added on days 3 and 6 so that the final concentration is 5 U/ml. Target cells are prepared on day 7 by using unirradiated stimulator cells from the initial priming combination. The cell concentration is adjusted to 10^6 cells per ml, and 1 ml of the cells is placed with 1 ml of PHA in 4 to 6 wells of a 24-well microtiter plate and incubated at 37°C in a humidified atmosphere of 5% CO_2 for 3 days. On day 10, the cultures are assayed for cytotoxicity (or other functional assays are used) against ^{51}Cr-labeled target cells. PHA-stimulated target cells (2×10^6) are labeled with 0.5 mCi of ^{51}Cr for 1.5 h, washed, and adjusted to a concentration of 2×10^4 cells per ml. One hundred microliters of the medium is replaced in the priming cultures with 100 μl of labeled target cells, and the plates are spun at $100 \times g$ for 5 min and incubated for 4 h. Supernatants are harvested and tested for released ^{51}Cr by using either a gamma counter to detect the gamma rays or a beta counter to detect the Auger rays released. Wells are scored as positive by determining that the reactivity observed is significantly (>3 standard deviations) greater than the control background. Wells containing irradiated stimulator cells incubated without responder cells are used as background controls. As for the HTLp method outlined above, the frequency of cytotoxic cells is determined by a maximum likelihood estimation by using a computer program and the variance is determined by the use of 95% confidence intervals. A regression analysis is used to generate a straight line, and chi-square analysis is used to show that the data obtained are in accordance with single-hit kinetics. A program that does all the necessary calculations for this analysis is listed in reference 8.

Variation of LDA of CTL

A variation of the target cell labeling procedure for the cytotoxic limiting dilution analysis has been described by Van Besouw et al. (9). In this approach, the T-cell blast target cells are labeled with europium-diethylenetriaminepentaacetate (Fluka [Buchs, Switzerland] and Sigma Chemicals [St. Louis, MO]). The incubation period to measure cytolysis is the same as that previously described. The supernatant (20 μl) is transferred onto a low-background fluorescent 96-well plate (Fluoroimmunoplate; Nunc, Roskilde, Denmark), and 100 μl of enhancement solution (LKB-Wallac, Turku, Finland) is added to each well. Fluorescence of the released europium is measured in a time-resolved fluorometer (Victor 1420 multilabel counter; LKB-Wallac), and results are expressed in counts per second.

Cell Division and Precursor Frequency Analysis Using Multiparameter CFSE-MLC

The ability to visualize specific peripheral blood cell subpopulations dividing during an *in vitro* response to donor alloantigen (allo-Ag) is extremely useful when monitoring alloimmunity in healthy individuals or transplant patients (10, 11). Flow cytometry can efficiently detect and quantify the phenotype, percentage, and precursor frequency of proliferating cells. The fluorescent dye 5(6)-carboxyfluorescein diacetate succinimidyl ester (CFSE) is used to label intracellular responder cells before placing them in the MLC. CFSE is cell permeant and nonfluorescent until cellular esterases cleave carboxyl groups from the molecule, rendering it nonpermeant and fluorescent. The succinimidyl moiety of CFSE covalently attaches to the cytoplasmic amine groups. The covalently bound CFSE is divided equally between the daughter cells, allowing for resolution of up to eight cell division cycles (12). CFSE can be used with or without additional cell surface and/or intracellular fluorochrome-conjugated monoclonal antibody (MAb) staining. This may allow, over a 5-day cell coculture period, the concomitant assessment of the kinetics of cell proliferation, differentiation status, and function. Various subsets of cells such as peripheral blood $CD4^+$ and $CD8^+$ T cells, B cells, and NK cells can be studied in this manner. Therefore, multiparametric CFSE-MLC may be considered a protocol of choice over the classical MLC or LDA assays when assessing allorecognition. In addition, using Modfit software, the number of cell divisions and of precursor frequencies for a given cell subpopulation can be calculated (10). The procedure outlined below is for testing human cells. Procedures for animal models are described in reference 13.

Procedure

Sample Requirements

The collection requirements are the same as those for the MLC procedure.

Materials and Reagents

The lymphocyte separation medium, culture medium, pooled human sera, and Hanks balanced salt solution are the same as those for the MLC procedure.

CFSE is dissolved in dimethyl sulfoxide to the final concentration determined by the investigator. Aliquots can be stored at −20°C in a desiccator and protected from light for up to 1 year.

Instruments

The Fortessa (BD Biosciences) instrument is used for data acquisition, and FlowJo software (Tree Star, Ashland, OR) and ModFit LT software (Verity Software, USA) are used for data analysis. For cell cocultures, an incubator set at 37°C and 5% CO_2 is needed. Refrigerated centrifuges are used.

Mechanics and Controls

1. **Staining procedure.** The responder cell population (1×10^7 lymphocytes/ml) is resuspended in a prewarmed PBS–0.1% bovine serum albumin (BSA) solution and incubated with 2 μM CFSE for 10 min at room temperature. An equal volume of pooled human sera is added, and the mixture is agitated for 1 min to quench the reaction. Cells are then washed three times in PBS and adjusted to the appropriate working concentration in the culture medium. Alternatively, RPMI 1640 containing 10% pooled human sera can be used for the last two washes.
2. **Culture conditions.** CFSE-labeled bulk PBMC (or sorted lymphocyte subsets) used as responders are incubated in a one-way mixed lymphocyte reaction culture (MLC) with γ-irradiated (2,500 rad) allogeneic stimulator PBMC, labeled with PKH-26 dye (according to the manufacturer's protocol) at a 1:1 ratio (10). The stimulators are labeled to allow their discrimination from the responder cells, which have proliferated and undergone CFSE dilution. The positive and negative controls are the same as those for the MLC. The cells are harvested after 5 days, washed, and surface

stained with the appropriate fluorochrome-labeled MAbs for phenotyping as determined by the investigator (e.g., CD3, CD8, CD45RO, CD62L). Intracellular staining (ICS) can be further performed upon permeabilization to identify transcription factors (e.g., T-bet, GATA-3, RORγt, or FOXP3), granzyme B/perforin, or the cytokine of choice (e.g., gamma interferon [IFN-γ], IL-4, IL-17, IL-10), as described in "ICS and Flow Cytometry" below.

3. **Flow cytometry analysis.** After cleavage, CFSE has a peak excitation of 494 nm and a peak emission of 521 nm, characteristics compatible with fluorescein isothiocyanate (FITC) detection systems. PKH26 is a red fluorochrome and has a peak excitation of 551 nm and peak emission of 567 nm, characteristics compatible with phycoerythrin (PE) detection systems. Six to 8 additional fluorochromes can be added to the panel to complete the 10-color panel. A gate defining live lymphocytes and blasts by forward and side scatter properties is used in all analyses, followed by analysis of $CD3^+$ gate and subsequent exclusion of $PKH\text{-}26^+$ stimulator cell gate. Proliferation of the $CD4^+$ (as $CD8^-$) and $CD8^+$ populations is then quantified by CFSE dilution (% $CFSE^{low}$ cells) and by histogram plots of generations of divided cells as determined by ModFit-LT software (10). Proliferating cells may be also assessed for their memory distribution, type 1 lineage commitment (T-bet), and functional capabilities (IFN-γ, granzyme B/perforin) versus type 2, type 17, or Treg commitment.

Pitfalls and Troubleshooting for CFSE-MLC Assay

As in the MLC, the viability of the cells is crucial in the CFSE-MLC assay. The level of CFSE staining must be determined by titration since too-heavy staining can cause problems with cell viability during culture and compensation during acquisition and analysis. Approximately eight division cycles can be identified before the autofluorescence obscures the peaks. If clear division peaks are not seen, optimal proliferating conditions may not have been obtained. It is helpful to start by setting parameters and culture conditions assaying a response obtained by stimulating with an anti-CD3 MAb or a recall antigen. Once reproducible results are obtained, a response to allogeneic cells can be optimized. Using a dump channel to stain for dead cells (Dead cell stain kit-PB; Invitrogen) and CD14-PB (where PB is Pacific Blue stain) helps lower high background noise.

Troubleshooting for Staining and Data Acquisition

For information on Troubleshooting for Staining and Data Acquisition, see "ICS and Flow Cytometry" below.

Data Analysis and Interpretation

For quantitative assessment of the alloresponse, the number of cells within each CFSE fluorescent peak is determined by analysis of the flow cytometric histogram plots. The number of precursors that divided (P_{div}) is determined by analysis of the number of events comprising the various peaks of daughter cells with identical proliferative histories and extrapolated by dividing by $2n$, where n is the division cycle number. The number of precursors that divided makes up the numerator, and the denominator is the total number of cells (P_{tot}). P_{div} is relatively straightforward to calculate; however, the P_{tot} determination is more complex, and several approaches have been reported. To obtain a precursor frequency, the total number of potentially alloreactive cells, including those plated in culture but not recovered, must be considered as representing P_{tot}. Alternatively, the number of cells recovered may be considered to represent P_{tot}. To obtain a responder frequency, the number of cells that were activated but did not proliferate can be considered to represent P_{tot}. Alternatively, the Modfit Software applies deconvolution algorithms to calculate the precursor frequency of cells that divided, reported as the percentage of the parent population. The investigator decides the method of analysis (10). For quantitative assessment of other functions (i.e., cytokine production), see below.

Graft-Infiltrating Cells—Propagation of Lymphocyte Cultures from Allograft Biopsy Specimens

Concept

In solid-organ transplantation, the histological analysis of allograft biopsy specimens remains the "gold standard" for diagnosing rejection. Although many cell types have been implicated in rejecting allografts, including B cells, macrophages, neutrophils, and eosinophils, it is generally accepted that $CD3^+$ T lymphocytes initiate allograft rejection (14, 15). Both $CD4^+$ (helper) and $CD8^+$ (cytotoxic) T cells are present in the graft and express IL-2 receptor and HLA-DR antigens, suggesting the presence of activated lymphocytes. The phenotype studies provide little information about the functional characteristics and their alloreactive specificity.

Another approach is to learn about the functional characteristics of graft-infiltrating cells through *in vitro* propagation in the presence of IL-2 (16–18). Activation of T cells occurs as a result of recipient allorecognition of donor antigens, which leads to the expression of IL-2 receptors on the activated T cells. The lymphocyte growth assay is straightforward. Biopsy specimen fragments are incubated in tissue culture medium supplemented with 5% human serum and 10 to 30 IU of recombinant IL-2. Lymphocyte growth in cardiac transplant recipients correlates with the histological grade of rejection, and positive growth from histologically negative biopsy specimen fragments is associated with subsequent biopsy-proven rejection (19, 20). A persistent lack of growth from biopsy specimen fragments is associated with an increase in rejection-free cardiac allograft survival. These studies indicate that *in vitro* culturing of lymphocytes from endomyocardial biopsy specimen fragments is clinically useful for the early diagnosis of acute cellular rejection. This conclusion may also apply to other organs. For lung transplant recipients, transbronchial biopsy specimen fragments have been cultured to propagate infiltrating alloreactive T cells. Lymphocyte growth is virtually 100% for biopsy specimen fragments with histological diagnosis of acute rejection or active bronchiolitis obliterans, a form of chronic lung rejection, and fewer than 30% of biopsy specimen fragments with no major abnormalities show growth (21). The presence of activated T cells is indicative of a subsequent rejection episode. Lymphocyte growth from renal transplant biopsy specimen fragments also correlates with acute cellular rejection, and the production of IL-2 by the infiltrating cells is associated with irreversible rejection (22). In liver transplant recipients, more culture lymphocyte growth is associated with rejection and less growth is seen for patients on OKT3 treatment for rejection.

A serious complication of heart transplantation is the development of accelerated graft coronary disease (GCD). Persistent growth from biopsy specimen fragments during the first 3 months posttransplant is associated with a higher risk of GCD. More than 40% of patients whose biopsy specimen fragments persistently grew lymphocytes developed

GCD. In contrast, only 6% with nongrower biopsy specimen fragments had subsequent GCD.

This section outlines the basic approach used to propagate cells from biopsy specimen fragments. Other approaches, such as the use of donor or allogeneic cells as feeder cells, may be used at the discretion of the investigator.

Procedure

Sample Requirements

An endomyocardial (or other tissue) biopsy specimen collected in a jar containing sterile physiological saline

Approximately 10 ml of heparinized blood obtained from the patient

Materials and Reagents

LSM Ficoll-Paque (Pharmacia)

500 ml of RPMI 1640 with L-glutamine (Gibco) plus 12.5 ml of HEPES buffer solution 1 M (Gibco) and 2.8 ml of gentamicin reagent solution (10 mg/ml; Gibco)

Pooled human sera type AB (NormIcera-Plus) (Gemini Bio-Products)

Recombinant IL-2 (Hoffmann La-Roche)

Equipment and Instrumentation

Laminar flow biological safety cabinet (NuAire, Inc.)

Beckman centrifuge (model TJ-6)

Olympus biological microscope (model BHTU)

Forma Scientific water jacket incubator (model 3154)

Cesium-137 Gammacell irradiator

Test Procedure

Autologous feeder cells are separated from recipient blood by LSM centrifugation (see description of the MLC method). The biopsy specimens are placed in a small (35- by 10-mm) sterile petri dish by using a sterile transfer pipette, and with a surgical blade or sterile 20-gauge needles, the biopsy specimens are sectioned into three or four small fragments. Each biopsy specimen fragment is transferred onto a 96-well round- (or flat-) bottom plate that contains 100 μl of IL-2-enriched medium (10 to 30 IU of IL-2 in 5% human serum–RPMI 1640). Autologous feeder cells are irradiated (4,000 rad) and added to each well at a concentration of 0.5×10^6/ml. The biopsy cultures are incubated at 37°C and 5% CO_2. Biopsy cultures are monitored for lymphocyte growth regularly. If the investigator wants to monitor rapid lymphocyte growth as a clinical test for rejection, then the biopsy specimen fragments are incubated in IL-2-enriched medium without autologous feeder cells. This procedure allows the identification of graft-infiltrating cells that emigrate from the tissue to the culture well within 24 to 48 h. In the presence of feeder cells, the earliest report of lymphocyte growth is within 5 to 7 days. Once cell growth is observed, the cultures are split and expanded in culture plates with successively larger wells. The cultures are fed with medium containing IL-2 every other day and with autologous feeder cells once a week. All biopsy-derived cell cultures lacking cell growth are discarded after 3 weeks.

Pitfalls and Troubleshooting

When long-term cultures are required to achieve large numbers of cells, the addition of anti-CD3 monoclonal antibody may help expand the activated population without compromising the specificity. In addition, a cocktail of T-cell growth factors such as IL-2 and IL-4 may enhance the growth of graft-infiltrating cells.

Cytokine Measurements

Concept

The conventional assay of T-cell activation is the measurement of cellular proliferation in response to antigen stimulation. More recently, the determination of the frequency of cytokine-expressing cells has been possible through limiting dilution analysis, intracellular cytokine staining, and the enzyme-linked immunospot (ELISPOT) technique. The CD4 T-helper cell polarization has been subdivided into categories according to their cytokine secretion profiles: Th1 cells that secrete IL-2, IFN-γ, and tumor necrosis factor alpha; Th2 cells that secrete IL-4, IL-5, IL-6, and IL-13; and Th17 cells that may secrete IL-17A, IL-17F, IL-22, and IL-21 (21, 23, 24). Many distinct patterns based on differential quantities of expression within the Th1, Th2, and Th17 phenotypes and mixtures of these phenotypes are associated with graft rejection and acceptance.

ELISPOT Assay

The ELISPOT assay was developed in the laboratories of Peter Heeger and Paul Lehmann (25).

Procedure

Sample Requirements

Human peripheral blood collected in three or four green-top Vacutainer tubes with heparin

Antigens (sources are given in parentheses): alloantigen (donor or third-party spleen cells), mitogens (PHA or concanavalin A), or recall antigens (cytomegalovirus or purified protein derivative)

Materials and Reagents

LSM (Isoprep [Robbins Scientific] or Ficoll-Hypaque)

Culture medium: RPMI 1640 containing antibiotics and glutamine with 10% high-quality fetal bovine serum

Blocking solution: PBS–1% BSA–3 g of BSA (Sigma) added to 300 ml of PBS and allowed to sit for 15 min. Filter through a 0.22-mm-pore-size filter and store at 4°C

PBS-Tween-BSA

Red spots: streptavidin-horseradish peroxidase (Dakoo, Carpenteria, CA) diluted 1:2,000 in PBS-Tween-BSA

Buffer for red substrate: 800 ml of 3-amino-g-ethyl carbazole (AEC) added to 24 ml of AEC buffer

AEC buffer (0.1 M sodium acetate buffer, pH 5.0): 0.2 M acetic acid (11.55 ml of glacial acetic acid per liter of distilled water). Add 148 ml of 0.2 M acetic acid to 352 ml of 0.2 M sodium acetate. Bring volume up to 1 liter with distilled water.

AEC: Add 1 g of AEC (ImmunoPure AEC; Pierce; catalog no. 34004) to 100 ml of DMF (*N*,*N*-dimethylformamide; Fisher Scientific catalog no. BP1160-500) using gloves and a mask and working under a fume hood. Wrap the bottle in foil and store at room temperature.

Antibodies from Pharmingen (San Diego, CA):

- Coating antibody-IFN-γ (clone R46A2) at a final concentration of 2 μg/ml or IL-2 (clone JES6-1A12) at a final concentration of 6 μg/ml
- Secondary detection antibodies-IFN-γ (clone XMG1.2 biotin) at a final concentration of 1 μg/

ml and IL-2 (clone JES6-5H4 biotin) at a final concentration of 2 μg/ml

ELISPOT plates (Fisher Scientific, Millipore, or Cellular Technologies Ltd. [Cleveland, OH] catalog no. M200-50)

Equipment and Instrumentation

Laminar flow hood

Incubator set a 37°C and 5% CO_2

Immunospot 2 analyzer from Cellular Technologies Ltd.

Test Procedure

Day 1. Mark the ELISPOT plate and add 100 μl of coating antibody/well diluted to the appropriate concentration in PBS. Wrap the plate in plastic and incubate it in a humid environment at 4°C overnight.

Day 2. In a sterile laminar flow hood, discard the coating antibody by shaking the inverted plate. Block the plate with a sterile solution of PBS–1% BSA at 150 μl/well and incubate the plate for 1 h at room temperature. Discard the liquid from the plate and wash the plate three times with sterile PBS. Until the assay, keep the plates with 200 μl of PBS/well at room temperature. Peripheral blood lymphocytes isolated from the whole blood are diluted to a concentration of 3 million per ml and are plated at 100 μl/well. Stimulator cells (irradiated or mitomycin C treated) are counted and resuspended at 3 million per ml, and 100 μl is used in each well. When needed, T-cell-depleted antigen-presenting cells can be used to control the background. Mitogens (PHA) at a final concentration of 2 μg/ml and soluble protein antigens at different concentrations (0.1 to 50 μM) are added to the plates (final volume of 200 μl/well). The plates are incubated for 24 h at 37°C with 5% CO_2.

Day 3. The secondary antibody is diluted in PBS-Tween-BSA. Discard the fluid from the wells and wash the wells three times with PBS. After each wash, remove the liquid by tapping the plate onto clean towels. Wash the plate four times with PBS-Tween. Leave the last wash in the plate and incubate the plate for 5 min at room temperature. Discard the liquid and add 100 μl of the second detecting antibody/well. The plate is wrapped and incubated overnight at 4°C in a humid atmosphere or for 4 to 5 h at room temperature.

Day 4. Discard the second antibody and wash the plate three times with PBS-Tween. Add 100 μl of streptavidin-horseradish peroxidase/well and incubate for 90 min at room temperature. Near the end of incubation, prepare the reagent for spot development (AEC in AEC buffer plus 12 μl of 30% H_2O_2). Wash the plate four times in PBS (200 μl/well), and add 200 μl of substrate to each well. The spots should develop in 15 to 40 min. Stop the reaction before the background color becomes too strong by washing the plate four times with distilled water. Dry the plate and keep it covered because the spots are light sensitive and fade if exposed to light. The plate can be kept covered in aluminum foil for counting the next day or stored at room temperature for future analysis. When the plate is fully dry, it can be analyzed with a dissecting microscope or with a computer-assisted image analyzer.

Pitfalls and Troubleshooting

The viability of the responder and stimulator cells is very important. Fresh cells are the best; however, frozen specimens can be used if the recovery is sufficient. The sources of fetal calf serum and antibodies are important for the success of the test. Keeping background staining low is crucial, and it is therefore important to stop the reaction in time. Also, the spontaneous release of cytokines from stimulator cells can be diminished by using T-cell-depleted antigen-presenting cells.

Clinical Significance

The ELISPOT assay has a number of advantages over other techniques. The assay is very sensitive and reproducible, and the detection of the secreted molecule occurs directly at the site of the secreting cells. The ELISPOT assay is 100- to 400-fold more sensitive than the enzyme-linked immunosorbent assay performed on culture supernatants. Since this assay can detect antigen-specific cells at the single-cell level, it is more sensitive than intracellular cytokine staining. The analysis is carried out with the help of an automated image analyzer that detects the spots based on predetermined size, shape, and color density characteristics, making the assay very reproducible. The ELISPOT assay may be used to discriminate between *in vitro*-primed alloreactive cells and naive T cells. Antigen-primed T cells produce cytokines in less than 24 h after stimulation, but naive T cells require 3 to 5 days of stimulation *in vitro* to differentiate into effector cells producing Th1, Th2, or Th17 cytokines. Heeger and colleagues have shown that a high frequency of donor-reactive memory T cells producing IFN-γ pretransplant correlates with an increasing risk of posttransplant acute-rejection episodes in living related-donor kidney transplant recipients (25).

ICS and Flow Cytometry

Multiparametric intracellular cytokine staining (ICS) is a widely used flow cytometry-based method to study and quantify cytokine production by memory T cells, including cytokine production by Ag-specific $CD4^+$ and $CD8^+$ T cells. In the field of transplantation, the method may be used on patients' whole blood for *ex vivo* immune monitoring of global T-cell polarization in response to nonspecific stimulation or T-cell immune quiescence, or to detect T-cell activation. In addition, ICS can be used on *in vitro*-activated T cells in a CFSE-MLC, stimulated with allo-Ag by the direct and/or the indirect presentation pathways, to monitor functional donor-specific T cell hyporesponsiveness or to identify patients with donor-reactive T cells that may be at risk of rejection after organ transplantation (11). This method has the advantage over other methods such as ELISPOT or enzyme-linked immunosorbent assay, which allows the simultaneous detection of transcription factors, cytokine production, and surface phenotype of the same cell. Moreover, due to the tremendous progress in knowledge, instrumentation, and reagent development, the method can accommodate assessment of up to 10 to 12 parameters (fluorochrome combinations) at a time, including staining of 3 or 4 intracellular cytokines such as IFN-γ, IL-10, IL-4, and IL-17 per panel (26–28). Most studies in the past have used Ficoll-separated PBMC as a source of staining material, while recently more laboratories have been using whole-blood-based assays (29, 30). Whole-blood staining allows the generation of large sets of data from small volumes of blood and carries *ex vivo* the cellular and biochemical environment maintaining the immunosuppressive drugs during the *in vitro* stimulation.

Procedure

Sample Requirements

Responder cells may consist of human peripheral blood collected in green-top Vacutainer tubes with heparin. Alter-

natively, PBMC isolated by Ficoll density gradient separation, coculture-propagated lymphocytes, tissue-separated cells, or cells from bronchoalveolar lavage fluid can be also used.

To test the responder global nonspecific T-cell cytokine production, phorbol myristate acetate (PMA; catalog no. P-8139; Sigma) and Ca ionophore A23187 (catalog no. C7522; Sigma) can be used as stimulators.

To test the responder T-cell cytokine production stimulated via direct allo-Ag-specific recognition pathway, irradiated donor (or third-party) PBMC or splenocytes can be used as stimulators.

To test the responder T-cell cytokine production stimulated via indirect allo-Ag-specific recognition pathway, donor-derived (or third-party) allo-Ag cell-free lysates can be used. These can be obtained as previously described (30). Briefly, a known number of donor PBMC or splenocytes are lysed by three cycles of freeze/thawing in Tris-EDTA-based buffer containing 1/5,000 NP-40, 0.1 mM phenylmethylsulfonyl fluoride, 1/200 protease inhibitor mixture (Sigma Chemical Co.) and then centrifuged at 1,000 × *g* for 2 minutes, collected, and further centrifuged for 45 minutes at 14,000 × *g*. The pellet is resuspended in assay medium. The equivalent of 1×10^6 intact cells was added per each 1×10^6 responder cells. The absence of whole intact cells should be confirmed by microscopy.

Materials and Reagents

Chemicals for culture and stimulation of cells: intracellular transport inhibitor brefeldin A (catalog no. B-7651; Sigma). Dissolve in 100% dimethyl sulfoxide.

Directly conjugated monoclonal antibodies: from BD Pharmingen, CD3-V500 (clone SP-34-2; catalog no. 560770), CD4-Texas red (clone RPA-T4; catalog no. 555346), CD45RA-APC (clone HI100; catalog no. 550855), CCR4-PE-Cy-7 (clone 1G1; catalog no. 561034), CCR6-PerCP-Cy5.5 (clone 11A9; catalog no. 561752), IL-4-PE (clone MP4-25D2; catalog no. 554485), IFN-γ-AF700 (clone B27; catalog no. 557995), IL-17-FITC (clone N49-653; catalog no. 560489); from eBioscience, CD62L-AF750 (clone DREG-56; catalog no. 47-0629-42), IL-10-eFluor450 (clone JES3-9D7; catalog no. 48-7108-42); and from BioLegend, CXCR3-BV605 (clone G02H7; catalog no. 353727).

Isotype control antibodies each used at concentrations comparable to those of the antibodies of interest.

Staining buffer fluorescence-activated cell sorter (FACS) medium: Dulbecco's PBS (DPBS) without Mg^{2+} or Ca^{2+}, 1% heat-inactivated fetal calf serum, and 0.1% (wt/vol) sodium azide. Adjust buffer pH to 7.4 to 7.6, filter (0.2 μm), and store at 4°C.

Fixation buffer: 2% (wt/vol) paraformaldehyde. Add paraformaldehyde to DPBS and warm in a 50°C water bath (fume hood) until dissolved (1 to 3 h). Adjust pH to 7.4 to 7.6 and store at 4°C.

Permeabilization buffer: DPBS without Mg^{2+} or Ca^{2+}, 1% heat-inactivated fetal calf serum, 0.1% (wt/vol) sodium azide, and 0.1% (wt/vol) saponin (catalog no. S-7900; Sigma). Adjust pH to 7.4 to 7.6 and filter. Fix and Perm permeabilization kit (Caltag Laboratories, Burlingame, CA) for whole-blood assay.

Ficoll-Hypaque gradient

Human AB serum

V-bottom plates (Costar)

12- by 75-mm Polystyrene round-bottom tubes (catalog no. 352008; BD Falcon)

10× PharmLyse buffer (BD catalog no. 555899)

Tubes for whole-blood stimulation polypropylene culture tubes (VWR catalog no. 82-050-140)

Instruments

Fortessa (BD Biosciences) instrument for data acquisition, FlowJo software (Tree Star, Ashland, OR) for data analysis, and an incubator set at 37°C and 5% CO_2.

Nonspecific Stimulation Test Procedure

Cell culture. Responder PBMC or the cells of interest are plated at 50,000 to 250,000 cells in 96-well V-bottom plates in a final volume of 100 μl of 5% AB RPMI 1640. Cells are cultured with or without PMA (50 ng/ml) and Ca ionophore (1 μg/ml) and brefeldin A (1.5 μg/ml). Incubate cells at 37°C in a humidified 5% CO_2 incubator for 4 h for PBMC cultures.

Whole blood. A 100-μl volume of whole blood is stimulated with PMA (50 ng/ml), Ca ionophore (1 μg/ml), and brefeldin A (1.5 μg/ml). Unstimulated whole blood is cultured with RPMI 1640 alone and brefeldin A. Whole-blood cultures are incubated for 4 to 6 h at 37°C in a humidified 5% CO_2 incubator.

AlloAg-Specific Stimulation Test Procedure

Cell culture. Responder PBMC or the cells of interest are plated at 0.3×10^6 cells in 96-well V-bottom plates in a final volume of 100 μl of 5% AB RPMI 1640. Cells are cocultured with or without 100 μl irradiated T-cell-depleted donor (or third-party) PBMC or splenocytes at 1:1 ratio (direct recognition pathway). Alternatively, 0.3×10^6 responder cells are cocultured with a 100-μl equivalent volume of cell free lysates obtained from 0.3×10^6 intact cells (indirect recognition pathway). Incubate at 37°C in a humidified 5% CO_2 incubator for 15 h, and for the last 4 h of incubation add brefeldin A.

Whole blood. Five hundred microliters of whole blood is stimulated or not with 1×10^6 irradiated donor (or third-party) PBMC or splenocytes (direct pathway) or with the equivalent of cell-free lysates obtained from 1×10^6 intact cells (indirect recognition pathway). Whole-blood cultures are incubated for 15 h at 37°C in a humidified 5% CO_2 incubator, and for the last 4 h of incubation brefeldin A is added. Unstimulated whole blood is cultured with RPMI 1640 alone, and brefeldin A is added for the last 4 h of incubation.

Staining Procedure

PBMC cultures.

1. Centrifuge the plate for 5 min at 1,500 rpm (Beckman TJ-6), quickly flick the supernatants, and blot dry the plate.
2. Wash all wells with 150 μl of FACS medium and recentrifuge. Repeat flick, and blot dry.
3. Surface stain with 10 μl (or the titrated amount) of MAb/well. Place the antibodies in the well and gently resuspend cells 8 to 10 times. Wrap the plate in foil and put it in the refrigerator for at least 20 min.
4. Wash wells with 200 μl of FACS medium and centrifuge for 4 min at 1,500 rpm (Beckman TJ-6).

5. Gently flick out the supernatant and fix cells with 150 μl of 2% paraformaldehyde. Incubate overnight in the refrigerator.
6. Centrifuge plates and blot dry. Add 150 μl of permeabilization buffer to each well.
7. Recentrifuge for 4 min, flick the plate, and repeat once. For the unstained wells, use just 10 μl of permeabilization buffer.
8. Stain with intracellular cytokine antibody for each particular cytokine (10 μl of a 1:10 dilution in permeabilization buffer).
9. Place the plate wrapped in foil at 4°C for 30 min.
10. Wash the plate with 200 μl of FACS medium, and centrifuge for 4 min at 1,500 rpm.
11. Flick the plate, add 200 μl of FACS medium, and transfer cells to labeled flow tubes.

Whole blood.

1. Upon harvest, transfer the stimulated whole blood in flow tubes, and add 1 ml of 1× BD PharmLyse lysing buffer (catalog no. 555899) to each tube at room temperature according to the manufacturer's procedure. Vortex to mix, and add 1 ml more of 1× BD PharmLyse buffer to each tube.
2. Incubate for 15 min at room temperature.
3. Wash the cells in 2 ml flow wash.
4. Add 100 μl flow wash/tube.
5. Do the surface marker staining with fluorochrome-labeled MAbs prior to the intracellular staining for 30 min in the dark.
6. Wash cells with 2 ml flow wash/tube.
7. Fix cells by adding 1% PFA for 30 min at room temperature.
8. Wash cells with 2 ml flow wash/tube.
9. Add 2 ml permeabilization buffer and incubate 5 min at 4°C in the dark.
10. Decant liquid, break up pellets, and add 100 μl permeabilization buffer.
11. To block nonspecific binding of intracellular MAbs, add 10 μl mouse serum to each tube, vortex, and incubate tubes for 10 min at 4°C in the dark.
12. Add the intracellular cytokine-specific antibody (10 μl), and incubate the mixture in the dark at room temperature for 30 min.
13. Wash the samples once in permeabilization buffer.
14. Resuspend the samples in 200 μl of FACS medium and analyze them on a FACScan cytometer within 1 hour.

Data Acquisition

Create compensation tubes for each single color used and one unstained as follows:

1. Add 100 μl of flow wash/tube.
2. Add 1 drop of positive beads/tube.
3. Add MAb, incubate at room temperature for 30 min in the dark.
4. Add 2 ml flow wash, centrifuge at 4°C for 5 min.
5. Resuspend in 200 μl flow wash.

After compensation, the experimental tubes are run for data acquisition.

Data Analysis

- Typical forward and side scatter gates are set for lymphocytes, and $CD3^+$ $CD8^+$ or $CD3^+$ $CD8^-$ ($CD4^+$ cells) gates are set to exclude any dead or contaminating nonlymphoid cells. Subsequent gates should be placed close to each population of cells.
- Fifty thousand events per sample are acquired within the specific gate.
- Two-parameter histograms showing memory distribution, chemokine receptors expression, and cytokine staining are created.
- Quadrant statistics are based on the staining of the negative isotype controls.
- The number of cells staining for each cytokine is expressed as a percentage of $CD8^+$ or $CD8^-$, and the total number of cells is expressed per million PBMC. FlowJo (TreeStar, Ashland, OR) or Diva (BD) software is typically used for data analysis.

Troubleshooting for Staining

Always set aside wells for controls and for unstained cells to use in setting the target cell gates. Appropriate Ig isotype controls should be run with each assay, as well as the nonstimulated samples. Initial fluorochrome-conjugated MAb titration should be done to establish the optimal antibody concentration. After fixation, the plates can be kept overnight at 4°C. This step may also lower nonspecific background staining. The intracellular cytokine antibody should be diluted in permeabilization buffer containing saponin. The best results will be obtained when samples are run using the same number of MAb/tube, MAb clones, and fluorochrome conjugation. It is important to choose the optimal color combination especially for >10 color combination panels to avoid significant spillover between channels, which can be achieved by using Spectra Analyser tools (Biolegend).

Troubleshooting for Data Acquisition

The quality of data is highly influenced by the quality of the reagents and by the instrument type and proper setup. Therefore, it is recommended that reagents always be purchased from the same source and data acquisition be performed on the same instrument when possible, paying attention to the voltage and compensation settings, which need to be recorded and checked before every data acquisition experiment.

Troubleshooting for Data Analysis

Due to the complexity of the ICS protocol, with up to 12 color combinations per panel, and the lack of standardized methods for gating, there is a need for experienced personnel to perform data analysis. It is recommended that the same person perform panel-specific analyses, maintaining the same gating strategy and sequence of plots to detect cell subsets (31). Gates should always be placed uniformly after a proper adjustment of bioexponential scaling. Initiatives such as MyFlowCyt and MIATA may be accessed and consulted in order to troubleshoot and improve data analysis and reporting (32, 33).

Intracellular ATP Synthesis Assay: Immune Cell Function Assay

Recently, a method has been developed to measure the cell-mediated (T-cell, or T-lymphocyte) response directly in whole blood (34). The ImmuKnow assay (Cylex, Inc.) has been used to assess the overall basal immune response and to monitor the efficacy of different immunosuppressive protocols posttransplant (26). This whole-blood assay measures increases in intracellular ATP synthesis by $CD4^+$ cells in response to stimulation with PHA in the presence of immunosuppressive drugs. Most immune cell functions

depend directly or indirectly on the production of ATP, and thus, ATP has been used as a marker of lymphocyte activation (15, 35, 36). Reduced ATP levels directly inhibit the cascade of steps required for lymphocyte function, including the transcription of cytokine mRNA, cytokine production, and lymphocyte proliferation. ATP production precedes the appearance of most cytokines measured.

The immune cell function assay measures ATP synthesis that occurs as a result of stimulation with PHA for 15 to 18 h. Whole blood is also incubated in the absence of stimulant to assess basal ATP activity. Anti-CD4 monoclonal antibody-coated magnetic beads are added to immunoselect out CD4 cells from both the stimulated and nonstimulated wells. After washing of the $CD4^+$ cells on a magnet tray, the cells are lysed to release intracellular ATP. Luminescence reagent (luciferin-luciferase) added to the released ATP produces light. The amount of light measured by a luminometer is proportional to the concentration of ATP. The concentration of ATP (in nanograms per milliliter) is calculated from a calibration curve and compared to ATP level ranges to assess the cell-mediated immune function of the sample. The ImmuKnow assay has been approved by the Food and Drug Administration and is commercially available.

Procedure

Sample Requirements

Whole blood is collected into a specimen collection tube containing sodium heparin and stored and transported at room temperature. The assay must be set up within 30 h of specimen collection. Blood should be stored and transported at room temperature only (18 to 28°C). It is recommended that a normal control sample be drawn and run with each test sample.

Materials and Reagents

The Food and Drug Administration-approved assay kit ImmunoKnow (catalog no. 4400; Cylex, Inc.) contains the following materials and reagents.

- Assay plate and cover: 96-well (12- by 8-well strips) plate coated with an inert substance to prevent nonspecific binding. Store at 2 to 28°C, desiccated in the resealable foil pouch.
- Sample diluent: 25 ml. Store at 2 to 8°C.
- Stimulant: PHA-L, 12.5 μg/ml. Store at 2 to 8°C.
- CD4 Dynabeads (Dynal Biotech A.S.A., Oslo, Norway): magnetic beads coated with mouse monoclonal anti-human CD4, supported in buffered saline with BSA and preservative (6.5 ml). Store at 2 to 8°C.
- Wash buffer: buffered saline with BSA (125 ml). Store at 2 to 8°C.
- Lysis reagent: hypotonic basic solution with detergent (50 ml). Store at 2 to 8°C.
- Calibrator panel: ATP concentrations, 0, 1, 10, 100, and 1,000 ng/ml (0.8 ml each). Store at 2 to 8°C.
- Luminescence reagent: luciferin and luciferase in a buffered solution (33 ml). Store frozen upon receipt at −70°C or lower. Thaw at room temperature (18 to 28°C) only. Mix well after thawing. The reagent may be thawed and refrozen up to four times.
- Measurement plate: 96-well (12 8-well strips) black or white opaque plate (two of each plate). Store at 2 to 28°C in the resealable bag.

Reagent and Equipment Requirements

All reagents should be allowed to come to room temperature before use. Luminescence reagent must not be thawed above room temperature (i.e., do not thaw reagent at 37°C). Reagents should be thoroughly mixed immediately before pipetting.

The microtiter plate shaker must provide an adequate mix to fully resuspend settled blood cells following incubation without visible loss of material from the wells (i.e., no visible splashing should be observed on the assay plate cover). Once an appropriate setting is determined, use this setting throughout the assay. A vacuum pump with a strength of 150 to 200 mm Hg is recommended. If a stronger vacuum is used, care should be taken not to aspirate the Dynabeads during the wash steps.

Equipment and Instrumentation

- Luminometer: The luminometer must be formatted for a 96-well microtiter plate, capable of measuring "glow" luminescence, with a maximum emission of 562 nm, and maintain linearity over a measurement range of 5 decades of light output. A computer with Microsoft Excel version 95, 97, or 2000 is needed to support luminometer function.
- Incubator set at 37°C with a 5% CO_2 humidified atmosphere
- Magnet tray (catalog no. 1050; Cylex, Inc.; also available in the Cylex immune cell function assay accessory pack [catalog no. 1004])
- Cylex immune cell function assay data analysis software (catalog no. 1440; Cylex, Inc.; also available in the Cylex immune cell function assay accessory pack [catalog no. 1004])
- Vacuum aspiration system (catalog no. 1040; Cylex, Inc.) or equivalent (also available in the Cylex immune cell function assay accessory pack [catalog no. 1004])
- Eight-channel aspiration manifold with tubing connector (catalog no. 1070; Cylex, Inc.) or equivalent (also available in the Cylex immune cell function assay accessory pack [catalog no. 1004])
- Miscellaneous equipment: vacuum source, vacuum apparatus with disposable tubing and receiving flask, microtiter plate shaker, Vortex mixer, adjustable pipettes and tips capable of delivering 25- to 1,000-μl volumes, eight-channel multichannel pipette(s) and tips capable of delivering 50- to 200-μl volumes, reagent reservoirs, 12- by 75-mm tubes, and a timer.

Mechanics and Controls

Assay part 1: cell stimulation. Gently invert each control and patient whole-blood specimen several times to ensure uniform distribution of blood cells. Prepare a 1:4 dilution of each whole-blood specimen using sample diluent (e.g., 500 μl of whole blood plus 1.5 μl of sample diluent). Assemble the assay plate according to the worksheet supplied by the manufacturer by using one eight-well strip for each specimen and 25 μl of sample diluent in the first four wells. Dispense 100 μl of each diluted patient specimen into eight appropriately labeled wells, according to the worksheet. Replace the plate cover and shake the plate on a plate shaker for 30 s. Incubate the covered assay plate cover and shake the plate on a plate shaker for 30 s. Incubate the covered, assay plate in a 37°C and 5% CO_2 incubator for 15 to 18 h.

Assay part 2: CD4 cell selection and ATP release. Remove the assay plate from the incubator and shake it on a plate shaker for 3 min. Hand mix by gentle inversion the CD4 Dynabeads, and dispense 50 μl into each well. The magnetic beads must be thoroughly suspended to ensure accurate addition to each well. Cover the plate, shake it on the plate shaker for 15 s, and incubate it for 30 min at room temperature (18 to 28°C). Shake the plate for 15 s halfway through the incubation and again at the end of the incubation. Remove the strips from the assay plate and place them onto the assembled magnet tray. Wait 1 to 2 min for the Dynabeads to collect on the sides of the wells to isolate CD4 cells from the whole blood. Carefully aspirate whole blood from each well by using an eight-channel aspiration manifold attached to a vacuum system. Avoid dislodging the Dynabeads. Wash three times to eliminate residual unbound cells and interfering substances from the wells. Wash with 200 μl of wash buffer in each well, wait 1 min, and then aspirate. After the last wash step, remove the strip holder from the magnet base, shake the strips for 1 min on the plate shaker, and then replace the strip holder on the magnet base. Wait 1 min, and then aspirate.

Dispense 200 μl of lysis reagent into each well. Remove the strip holder from the magnet base and shake the strips on the plate shaker for 5 min. Place the strip holder onto the magnet base and wait 1 to 2 min.

Assay part 3: ATP measurement. If there will be a delay of more than 4 h before proceeding to assay part 3, the strips should be frozen at this time. Remove the strips from the strip holder and place them in the assay plate frame. Seal the strips, place the cover on the assay plate, and freeze at −20°C. Frozen strips are stable for at least 1 month. To continue, remove the plate from the freezer, allow it to come to room temperature (18 to 28°C), place the strips in the strip holder of the magnet tray, and dispense into measurement plates as described below.

The measurement plate should include one strip for each patient and two strips for the calibrator panel. Using a multichannel pipette, transfer 50 μl from each well of the magnet tray to the appropriately labeled wells of the measurement plate. Change pipette tips for each strip. Dispense 50 μl of each calibrator into duplicate wells of the measurement plate according to the worksheet. Using a multichannel pipette, dispense 150 μl of luminescence reagent into each well of the measurement plate. Following the luminometer manufacturer's instructions, read the plate between 3 and 10 min after addition of the luminescence reagent.

Calibration

The amount of ATP present in the cell lysate is calculated from an ATP calibration curve generated in each assay run. Relative light units (RLU) for control and patient samples are obtained from the luminometer and converted into nanograms of ATP per milliliter based on comparable RLU signals in the calibrators.

The RLU data from the luminometer are converted and analyzed using the Cylex immune cell function assay data analysis software. Luminometer RLU values provided in Microsoft Excel or tabular formats can be directly copied and exported into the data analysis software spreadsheet. ATP calibrator concentrations versus RLU values are plotted on a log-log scale, and linear regression analysis generates a calibration curve. To assess the linearity of the curve, each calibrator is reanalyzed by plotting RLU values on the curve and calculating corresponding ATP values. In addition, the correlation coefficient (r^2) of the calibration curve is calculated.

Calculation of Results

Calculate the ATP concentrations for the control and patient specimens by using the Cylex immune cell function assay data analysis software. After RLU values and specimen identification are entered into the spreadsheet and the calibration curve is generated, the following data are calculated and displayed in a report: ATP result for each replicate, average ATP value for replicates, standard deviation for replicates, and coefficient of variance of replicates. The coefficient of variance for stimulated wells must be <20%. If not, an analytical method to identify outlier values must be used and the results must be recalculated. Reported ATP values must be limited to the defined range of the calibrator panel. Samples with ATP values above the highest calibrator are reported as having values of >1,000 ng/ml. Samples with ATP values below the lowest calibrator are reported as having values of <1 ng/ml.

Pitfalls and Troubleshooting: Limitations

All of the following criteria must be met for the assay run to be considered valid:

- The ATP result for the nonstimulated control sample must be ≤60 ng/ml.
- The ATP result for the stimulated control sample must be ≥240 ng/ml.
- The ATP level for the nonstimulated sample must be less than the ATP level for the stimulated sample.

If the specimen meets these criteria, proceed with interpretation of the stimulated sample. If the nonstimulated sample does not meet these criteria, the specimen may have nonspecific production of ATP and the results are not valid. A new specimen should be drawn.

The linearity of the calibration curve must be accepted under the following criteria:

- The calculated value for the 1,000-ng/ml ATP calibrator must be 900 to 1,100 ng/ml (refer to the result in the "Average" column in Table IV of the data analysis software report).
- The calculated value for the 100-ng/ml ATP calibrator must be 85 to 115 ng/ml (refer to the result in the "Average" column in Table IV of the data analysis software report).
- The correlation coefficient (r^2) of the ATP calibration curve must be ≥0.97.

Interpretation of Results

The assessment of the cell-mediated immune response of a specimen is made by comparing the ATP concentration for that specimen to fixed ATP level ranges. The ATP concentration for each specimen is calculated from the calibration curve established for the measurement plate in which the sample was run. Assay standardization is maintained by running the calibrator and a freshly drawn specimen from an apparently healthy individual with each assay run. The cutoffs for the ATP level ranges are 225 and 525 ng/ml (Table 1).

The ATP level ranges for the Cylex immune cell function assay were established by testing 155 apparently healthy adults and 127 transplant recipients with the assay. A cumulative frequency of differences was used to select the ATP levels that give the best balance of results between immunosuppressed and nonimmunosuppressed individuals. Note that this is a qualitative assay, and therefore, the results do not directly quantify the level of immunosuppression. Results of the Cylex immune cell function assay should be used

TABLE 1 Interpretation of PHA-stimulated sample

ATP level (ng/ml)	Result	Interpretation
≤225	Low immune cell response	The patient's circulating immune cells are showing low response to PHA stimulation
226–524	Moderate immune cell response	The patient's circulating immune cells are showing moderate response to PHA stimulation
≥525	Strong immune cell response	The patient's circulating immune cells are showing strong response to PHA stimulation

in conjunction with clinical presentation, medical history, and other clinical indicators when establishing the immune status of a patient.

Expected Values

Freshly drawn whole-blood specimens from 155 apparently healthy adults and 127 transplant recipients were evaluated with the ImmuKnow cell function assay. The distribution of results of the assay for these populations is summarized in Table 2.

The population of apparently healthy adults consisted of 37 (24%) females, 105 (68%) males, and 13 (8%) individuals of unknown gender, and the age range was 20 to 60 years. The ethnicity of the population was as follows: 59% (91) African American, 28% (44) Caucasian, and 13% (20) other or unknown. The population of transplant recipients consisted of 55 (43%) females and 72 (57%) males, and the age range was 20 to 64 years. The ethnicity of the population was as follows: 24% (31) African American, 69% (87) Caucasian, and 7% (9) other or unknown. The organs transplanted included kidneys (59% [75]), livers (34% [43]), pancreases (2% [3]), and multiple organs (5% [6]).

VALIDATION OF NEW CELLULAR ASSAY PROCEDURES

Several of the assays outlined in this chapter are being implemented in the clinical laboratory. A few assays, such as the MLC, have written standards (see the *American Society for Histocompatibility and Immunogenetics Procedure Manual* [5]); however, most immune assays do not. Every new test must be validated before being implemented for patient testing, either by running parallel testing with another laboratory with a validated test procedure or by running known samples that have been tested by another validated method. Validation of a new test usually also includes an external quality assessment through a proficiency testing program. Although many agencies and associations offer programs for this purpose, none are available for the cellular immune assays outlined in this chapter.

When proficiency testing is not available, alternative validation procedures must be implemented, including split-sample and audit sample procedures. The split-sample procedure evaluates imprecision and testing errors. For external verification of test results, 5 to 10 samples are aliquoted and distributed to one or several other laboratories for parallel testing. Internal split-sample procedures test intertechnologist variation and operator-dependent variation. To test intertechnologist variation, samples are split and run by two different technologists. Audit samples, aliquots of control samples that are stored and analyzed periodically over time, assess the imprecision of the assay but not the accuracy. The standard deviation and coefficient of variation are statistics used to determine acceptable thresholds.

Analysis of Patient and Healthy Control Subject Data

Tracking of the daily average of patient data has been used extensively for quality control measures. This technique compares the average of 20 consecutive patient values versus an established patient mean value. Optimal application of this method requires an adequate number of patient values obtained using criteria for exclusion of outlying values likely to be from abnormal subjects. In addition, data from two healthy control subjects run with each assay have been used to detect shifts in method performance. Methods to monitor a daily mean or an average for healthy control subjects have been applied as quality control measures for a number of clinical tests. For methods with small population variation, 10 to 100 results are required for valid quality control.

Analysis of Data from Validation Procedures

The laboratory should define the limits of acceptability for each validated procedure either by analysis of internal quality control data (e.g., a standard deviation from the mean of ±2 or 3) or by use of data in the literature.

Statistical Evaluation of Split-Sample Data

The laboratories involved in evaluation of split-sample data must agree on the criteria for validation, including the test methods, numbers of tests, criteria for determining agreement, and procedures to resolve discrepancies. The statistical procedure to determine agreement between laboratories uses a formula to calculate the confidence interval for the difference between two results.

Statistical Evaluation of Patient and Healthy Control Data

The result values are placed in rank order. The central 68% of all values are selected, and the mean is calculated. If the distribution of values is normal, the low and high values of

TABLE 2 Distribution of results of the Cylex immune cell function assay

ATP level (ng/ml)	Immune cell response	No. (%) of transplant recipients with indicated results	No. (%) of healthy adults with indicated results
≤225	Low	51 (40)	9 (6)
226–524	Moderate	66 (52)	102 (66)
≥525	Strong	10 (8)	44 (28)

the central 68% of all values approximately equal 1 standard deviation below and above the mean. The mean and standard deviation provide measures for comparison with other laboratories, previous data from the same laboratory, and published data.

Proficiency Testing

For every test that is performed, the laboratory must participate in external proficiency testing, when available, to ensure quality of testing. The proficiency test samples must be handled in the same manner as the patient samples; that is, they must be introduced into the laboratory system in the same manner. Testing of the proficiency test samples should be rotated among all technologists who routinely perform the assay in question. The relationship between the results must be defined and evaluated. Corrective action must be initiated if a result is found to be unacceptable when compared to the consensus results. The accuracy for external proficiency testing should be >90%. When no commercial proficiency testing programs are available, parallel testing with another laboratory doing the same test must be done at least every 6 months. In-house proficiency testing should also be performed to assess variability between technologists. This comparison testing should be done at least every 6 months.

Quality Assurance for Cellular Assays

Quality assurance is a comprehensive program to ensure quality results from the initiation of a test through the end of result analysis by conforming to established written policies, monitoring compliance to policies, and documenting corrective actions. Each laboratory must have written policies for the requisition and collection of samples, the volume needed, the type of anticoagulant to be used, labeling, and sample storage and transportation for each test done in the laboratory. The policy must include criteria for sample acceptance or rejection. Each written requisition must match the sample and contain the following information: name of patient, identification number, date and time of sample acquisition, specific testing ordered, and referring facility.

Records of the types of problems encountered in sample acquisition should be kept and monitored for trends. Corrective action should be initiated and documented if problems persist. Compliance with requirements should be 95% or better.

Each laboratory should have a comprehensive procedure manual that details the standard operating procedure for each analysis performed, written in the CLSI format. The procedure manual should be reviewed yearly by the director and all technical staff and signed and dated by the director prior to implementation. Minor corrections can be handwritten but need to include the date of revision and the director's approval.

Quality Control Procedures for Cellular Programs

The laboratory shall define and document quality control measures for each test performed. These measures must include written policies outlining the criteria for accepting or rejecting results, evaluating reagents for consistent quality, and documenting equipment performance. All quality control problems must be addressed. The corrective actions must be documented in writing and reported in the quality assurance report.

Each procedure description must indicate quality control measures employed and how they are used in the interpretation of the results. Acceptable ranges must be established, and corrective actions must be documented when the controls do not fall within these ranges. Results of the test are not reported if the quality control for the test procedure exceeds the acceptable limit.

Each laboratory shall have a written policy for labeling reagents with the name, date received, date prepared or expiration date, date opened, technologist's initials, and storage conditions. Written procedures for quality control for each reagent prior to use are required. Descriptions of specific quality control procedures should include the appropriate method for testing each reagent, which may include titration, parallel testing, and measure of cell growth support, as well as documentation of acceptable performance. The date at which the reagent is put into use must also be documented.

Written protocols must be in place for routine equipment performance checks and scheduled preventative maintenance. All maintenance and results must be documented, and such records must be stored. Tolerance limits for each equipment performance check must be established, and compliance must be documented. When acceptable limits are exceeded, corrective action may include a procedure for troubleshooting, criteria for instrument repair, backup procedures or instruments, and a power failure plan.

CLINICAL APPLICATIONS

Currently, cellular assays are used to define donor antigen-specific hyporeactivity, to investigate the function and specificity of graft-infiltrating cells, and to determine T-cell precursor frequencies. The MLC, cell-mediated lympholysis techniques, and CFSE-MLR are currently used to investigate the development of donor antigen-specific hyporeactivity posttransplant (4, 11). These assays may be useful for identifying patients who are good candidates for discontinuing or tapering immunosuppression therapy on the basis of apparent immunoregulation of response to disparate antigens. The development of donor antigen-specific hyporeactivity, as measured by MLC, correlates with improved late solid-organ transplant outcome, as evidenced by fewer late rejection episodes and fewer graft losses (4). Newer multiparameter flow cytometry-based assays provide investigators with enhanced ability to monitor simultaneously numerous analytes of cell-mediated immunity (e.g., phenotype, proliferation, and cytokine production). In order to generate rigorous, reliable, and reproducible results, proficiency panel programs are in place to help investigators optimize their approach and analyses (10, 11, 30).

Propagation of T lymphocytes from kidney, heart, and liver allografts demonstrates a strong correlation between long-term T cell growth and clinical acute cellular rejection (37). The primed lymphocyte test has been used to investigate the specificity of these graft-infiltrating cells. This technique demonstrates functional characteristics of graft-infiltrating cells and provides information on the activation state of the T-cell infiltrate.

Previous studies have suggested a correlation between CTL precursor (CTLp) frequency and the clinical grade of graft-versus-host disease in recipients of bone marrow from unrelated donors (7, 8). Recipients with CTLp frequencies higher than 1:100,000 tended to have more-severe graft-versus-host disease than those with lower CTLp frequencies. Schwarer et al. (38) compared helper and cytotoxic anti-recipient T-cell frequencies in recipients who had received unrelated-donor bone marrow. They found that the HTLp and CTLp assays provided similar predictive information for outcome; however, the HTLp method is more rapid and less labor-intensive and, thus, may be more useful for donor selection in unrelated-donor bone marrow transplantation.

This approach may be useful in predicting graft-versus-host disease in unrelated-donor bone marrow transplant recipients. More recently, VanBuskirk et al. (6) have described the use of the CTLp assay to identify kidney recipients in whom immunosuppressive therapy can be safely reduced. Their data showed that kidney recipients with low or no frequency of donor-specific CTLp could safely have their immunosuppressive drug load tapered. The frequencies of intracellular IL-2- and IFN-γ-producing cells in normal individuals are similar in whole blood and isolated PBMC. However, in transplant recipients on tacrolimus or cyclosporine (CSA), the frequency of IL-2-producing cells may be significantly inhibited in whole blood while little or no inhibition is observed when the cells are isolated prior to the *in vitro* stimulation (26). In addition, the concentration of tacrolimus in blood does not directly correlate with its inhibitory effect on cytokine production in peripheral T-cell subsets (26). Despite these caveats, monitoring the *in vivo* efficacy of tacrolimus or CSA in suppressing cytokine production in T-cell subsets may further improve the posttransplant management of transplant recipients. This approach can also identify patients who are less susceptible to tacrolimus- or CSA-mediated inhibition and who therefore may need other immunosuppression (26).

The immune function assay (ImmuKnow; Cylex, Inc.) is a Food and Drug Administration-approved assay currently being implemented as a clinical test at many transplant centers. The assay has been used to directly assess the immune system, individualize immunosuppressive therapy, monitor drug tapering, conduct vaccine trials, monitor the efficacy of different immunosuppressive regimens, and distinguish rejection from infections such as hepatitis C virus infection in transplant recipients. A recent multicenter study evaluated the Cylex ImmuKnow assay for the measurement of immune response in immunosuppressed transplant recipients (39). Most immunosuppressive drugs are currently administered on the basis of weight. However, the baseline levels of immune response in patients awaiting transplant vary enormously and are not a function of body weight. The investigators in this multicenter trial found that the level of tacrolimus as measured by the conventional immunoassay did not correlate with the degree of biological immunosuppression by the PHA-induced ATP levels (39). They observed that following transplant, recipients' responses were statistically distributed among three levels of reactivity (low, intermediate, and high) based on this assay. Further, the effectiveness of the immunosuppressive therapy appears to increase with time posttransplant since the number of recipients in the low-response-level category increased despite lower dosing of the drugs. Zeevi et al. demonstrated that responses to recall antigen, alloantigen, and PHA were measurable by lymphoproliferation assays in immunosuppressed transplant recipients but were apparently suppressed when measured by the ATP assay. Furthermore, the Cylex assay provides an objective measure of the net state of a patient's immunosuppression while minimizing the drug therapy (40). A systematic review and meta-analysis of the ImmuKnow test in liver transplantation concluded that this assay is a valid tool for determining the risk of infections but not of rejections in adult liver transplant recipients (41).

CONCLUDING REMARKS

The long-term goals of using the cellular assays described in this chapter are to assess accurately the changing immunological statuses of transplant recipients, to predict long-term graft outcome, and to provide the immune response information needed to individualize immunosuppression therapy. By using methods that measure various immune functions in a serial fashion, an accurate assessment of the recipient's immune status can be obtained. Sequential evaluation of a patient's immune status should be considered in any protocols that incorporate modification of the immunosuppression therapy.

REFERENCES

1. **Bach F, Hirschhorn K.** 1964. Lymphocyte interaction: a potential histocompatibility test in vitro. *Science* **143:**813–814. PubMed
2. **Bain B, Vas MR, Lowenstein L.** 1964. The development of large immature mononuclear cells in mixed leukocyte cultures. *Blood* **23:**108–116. PubMed
3. **Reinsmoen NL, Kaufman D, Matas A, Sutherland DE, Najarian JS, Bach FH.** 1990. A new in vitro approach to determine acquired tolerance in long-term kidney allograft recipients. *Transplantation* **50:**783–790. PubMed
4. **Reinsmoen NL, Matas AJ.** 1993. Evidence that improved late renal transplant outcome correlates with the development of in vitro donor antigen-specific hyporeactivity. *Transplantation* **55:**1017–1023. PubMed
5. **Reinsmoen NL, Mickelson EM.** 1994. HLA-DW typing, p II.C.3.1–II.C.3.9 *In* Nikaein A (ed), *American Society for Histocompatibility and Immunogenetics Procedure Manual*. ASHI, Mount Laurel, NJ.
6. **VanBuskirk AM, Adams PW, Orosz CG.** 1995. Nonradioactive alternative to clinical mixed lymphocyte reaction. *Hum Immunol* **43:**38–44. PubMed
7. **Kaminski E, Hows J, Brookes P, Mackinnon S, Hughes T, Avakian O, Sharrock C, Goldman J, Batchelor JR.** 1989. Alloreactive cytotoxic T-cell frequency analysis and HLA matching for bone marrow transplants from HLA matched unrelated donors. *Transplant Proc* **21:**2976–2977. PubMed
8. **Kaminski E, Hows J, Man S, Brookes P, Mackinnon S, Hughes T, Avakian O, Goldman JM, Batchelor JR.** 1989. Prediction of graft versus host disease by frequency analysis of cytotoxic T cells after unrelated donor bone marrow transplantation. *Transplantation* **48:**608–613. PubMed
9. **van Besouw NM, van der Mast BJ, de Kuiper P, Smak Gregoor PJ, Vaessen LM, IJzermans JN, van Gelder T, Weimar W.** 2000. Donor-specific T-cell reactivity identifies kidney transplant patients in whom immunosuppressive therapy can be safely reduced. *Transplantation* **70:**136–143. PubMed
10. **Macedo C, Orkis EA, Popescu I, Elinoff BD, Zeevi A, Shapiro R, Lakkis FG, Metes D.** 2009. Contribution of naive and memory T-cell populations to the human alloimmune response. *Am J Transplant* **9:**2057–2066.
11. **Macedo C, Walters JT, Orkis EA, Isse K, Elinoff BD, Fedorek SP, McMichael JM, Chalasani G, Randhawa P, Demetris AJ, Zeevi A, Tan H, Shapiro R, Landsittel D, Lakkis FG, Metes D.** 2012. Long-term effects of alemtuzumab on regulatory and memory T-cell subsets in kidney transplantation. *Transplantation* **93:**813–821. PubMed
12. **Parish CR, Glidden MH, Quah BJ, Warren HS.** 2009. Use of the intracellular fluorescent dye CFSE to monitor lymphocyte migration and proliferation. *Curr Protoc Immunol* **Chapter 4:**Unit4.9.
13. **Wells AD, Walsh MC, Sankaran D, Turka LA.** 2000. T cell effector function and anergy avoidance are quantitatively linked to cell division. *J Immunol* **165:**2432–2443. PubMed
14. **Fung JJ, Zeevi A, Markus B, Zerbe TR, Duquesnoy RJ.** 1986. Dynamics of allospecific T lymphocyte infiltration in vascularized human allografts. *Immunol Res* **5:**149–163. PubMed

15. **Shearer GM, Clerici M.** 1994. In vitro analysis of cell-mediated immunity: clinical relevance. *Clin Chem* **40:**2162–2165. PubMed
16. **Zeevi A, Fung J, Zerbe TR, Kaufman C, Rabin BS, Griffith BP, Hardesty RL, Duquesnoy RJ.** 1986. Allospecificity of activated T cells grown from endomyocardial biopsies from heart transplant patients. *Transplantation* **41:**620–626. PubMed
17. **Mayer TG, Fuller AA, Fuller TC, Lazarovits AI, Boyle LA, Kurnick JT.** 1985. Characterization of in vivo-activated allospecific T lymphocytes propagated from human renal allograft biopsies undergoing rejection. *J Immunol* **134:**258–264. PubMed
18. **Miceli C, Metzgar RS, Chedid M, Ward F, Finn OJ.** 1985. Long-term culture and characterization of alloreactive T-cell infiltrates from renal needle biopsies. *Hum Immunol* **14:**295–304. PubMed
19. **Kaufman CL, Zeevi A, Kormos RL, Zerbe TR, Keenan RJ, Uretsky BF, Griffith BP, Hardesty RL, Duquesnoy RJ.** 1990. Propagation of infiltrating lymphocytes and graft coronary disease in cardiac transplant recipients. *Hum Immunol* **28:**228–236. PubMed
20. **Weber T, Kaufman C, Zeevi A, Zerbe TR, Hardesty RJ, Kormos RH, Griffith BP, Duquesnoy RJ.** 1989. Lymphocyte growth from cardiac allograft biopsy specimens with no or minimal cellular infiltrates: association with subsequent rejection episode. *J Heart Transplant* **8:**233–240. PubMed
21. **Mosmann TR, Coffman RL.** 1989. Heterogeneity of cytokine secretion patterns and functions of helper T cells. *Adv Immunol* **46:**111–147. PubMed
22. **Kirk AD, Ibrahim MA, Bollinger RR, Dawson DV, Finn OJ.** 1992. Renal allograft-infiltrating lymphocytes. A prospective analysis of in vitro growth characteristics and clinical relevance. *Transplantation* **53:**329–338. PubMed
23. **Del Prete GF, De Carli M, Ricci M, Romagnani S.** 1991. Helper activity for immunoglobulin synthesis of T helper type 1 (Th1) and Th2 human T cell clones: the help of Th1 clones is limited by their cytolytic capacity. *J Exp Med* **174:**809–813. PubMed
24. **Walsh KP, Mills KH.** 2013. Dendritic cells and other innate determinants of T helper cell polarisation. *Trends Immunol* **34:**521–530. PubMed
25. **Heeger PS, Greenspan NS, Kuhlenschmidt S, Dejelo C, Hricik DE, Schulak JA, Tary-Lehmann M.** 1999. Pretransplant frequency of donor-specific, IFN-gamma-producing lymphocytes is a manifestation of immunologic memory and correlates with the risk of posttransplant rejection episodes. *J Immunol* **163:**2267–2275. PubMed
26. **Ahmed M, Venkataraman R, Logar AJ, Rao AS, Bartley GP, Robert K, Dodson FS, Shapiro R, Fung JJ, Zeevi A.** 2001. Quantitation of immunosuppression by tacrolimus using flow cytometric analysis of interleukin-2 and interferon-gamma inhibition in CD8(−) and CD8(+) peripheral blood T cells. *Ther Drug Monit* **23:**354–362. PubMed
27. **Ferry B, Antrobus P, Huzicka I, Farrell A, Lane A, Chapel H.** 1997. Intracellular cytokine expression in whole blood preparations from normals and patients with atopic dermatitis. *Clin Exp Immunol* **110:**410–417. PubMed
28. **Sewell WA, North ME, Webster AD, Farrant J.** 1997. Determination of intracellular cytokines by flow-cytometry following whole-blood culture. *J Immunol Methods* **209:**67–74. PubMed
29. **Jung T, Schauer U, Heusser C, Neumann C, Rieger C.** 1993. Detection of intracellular cytokines by flow cytometry. *J Immunol Methods* **159:**197–207. PubMed
30. **Korin YD, Lee C, Gjertson DW, Wilkinson AH, Pham TP, Danovitch GM, Gritsch HA, Reed EF.** 2005. A novel flow assay for the detection of cytokine secreting alloreactive T cells: application to immune monitoring. *Hum Immunol* **66:**1110–1124. PubMed
31. **McNeil LK, Price L, Britten CM, Jaimes M, Maecker H, Odunsi K, Matsuzaki J, Staats JS, Thorpe J, Yuan J, Janetzki S.** 2013. A harmonized approach to intracellular cytokine staining gating: results from an international multiconsortia proficiency panel conducted by the Cancer Immunotherapy Consortium (CIC/CRI). *Cytometry Part A* **83:**728–738.
32. **Britten CM, Janetzki S, Butterfield LH, Ferrari G, Gouttefangeas C, Huber C, Kalos M, Levitsky HI, Maecker HT, Melief CJ, O'Donnell-Tormey J, Odunsi K, Old LJ, Ottenhoff TH, Ottensmeier C, Pawelec G, Roederer M, Roep BO, Romero P, van der Burg SH, Walter S, Hoos A, Davis MM.** 2012. T cell assays and MIATA: the essential minimum for maximum impact. *Immunity* **37:**1–2. PubMed
33. **Lee JA, Spidlen J, Boyce K, Cai J, Crosbie N, Dalphin M, Furlong J, Gasparetto M, Goldberg M, Goralczyk EM, Hyun B, Jansen K, Kollmann T, Kong M, Leif R, McWeeney S, Moloshok TD, Moore W, Nolan G, Nolan J, Nikolich-Zugich J, Parrish D, Purcell B, Qian Y, Selvaraj B, Smith C, Tchuvatkina O, Wertheimer A, Wilkinson P, Wilson C, Wood J, Zigon R, International Society for Advancement of Cytometry Data Standards Task Force, Scheuermann RH, Brinkman RR.** 2008. MIFlowCyt: the minimum information about a Flow Cytometry Experiment. *Cytometry Part A* **73:**926–930.
34. **Sottong PR, Rosebrock JA, Britz JA, Kramer TR.** 2000. Measurement of T-lymphocyte responses in whole-blood cultures using newly synthesized DNA and ATP. *Clin Diagn Lab Immunol* **7:**307–311. PubMed
35. **Buttgereit F, Burmester GR, Brand MD.** 2000. Bioenergetics of immune functions: fundamental and therapeutic aspects. *Immunol Today* **21:**192–199. PubMed
36. **Schulick RD, Weir MB, Miller MW, Cohen DJ, Bermas BL, Shearer GM.** 1993. Longitudinal study of in vitro CD4+ T helper cell function in recently transplanted renal allograft patients undergoing tapering of their immunosuppressive drugs. *Transplantation* **56:**590–596. PubMed
37. **Zeevi A, Kaufman C, Duquesnoy R.** 1994. Clinical relevance of lymphocyte analysis in cardiac and pulmonary transplantation, p 181–199. *In* Rose ML, Yacoub MH (ed), *Immunology of Heart and Lung Transplantation*. Edward Arnold Publisher, London, United Kingdom.
38. **Schwarer AP, Jiang YZ, Deacock S, Brookes PA, Barrett AJ, Goldman JM, Batchelor JR, Lechler RI.** 1994. Comparison of helper and cytotoxic antirecipient T cell frequencies in unrelated bone marrow transplantation. *Transplantation* **58:**1198–1203. PubMed
39. **Kowalski R, Post D, Schneider MC, Britz J, Thomas J, Deierhoi M, Lobashevsky A, Redfield R, Schweitzer E, Heredia A, Reardon E, Davis C, Bentlejewski C, Fung J, Shapiro R, Zeevi A.** 2003. Immune cell function testing: an adjunct to therapeutic drug monitoring in transplant patient management. *Clin Transplant* **17:**77–88. PubMed
40. **Zeevi A, Britz JA, Bentlejewski CA, Guaspari D, Tong W, Bond G, Murase N, Harris C, Zak M, Martin D, Post DR, Kowalski RJ, Elmagd KA.** 2005. Monitoring immune function during tacrolimus tapering in small bowel transplant recipients. *Transpl Immunol* **15:**17–24. PubMed
41. **Rodrigo E, Lopez-Hoyos M, Corral M, Fabrega E, Fernandez-Fresnedo G, San Segundo D, Pinera C, Arias M.** 2012. ImmuKnow as a diagnostic tool for predicting infection and acute rejection in adult liver transplant recipients: a systematic review and meta-analysis. *Liver Transplant* **18:**1245–1253.

Complement in Transplant Rejection

CARMELA D. TAN, E. RENE RODRIGUEZ, AND WILLIAM M. BALDWIN III

117

Better reagents have led to an increased appreciation of the association between complement activation in transplants and poor outcome (1–4). As diagnostic markers, products of complement activation have two attractive attributes related to the fact that activation of complement proceeds through a series of enzymatic steps resulting in multiple cleavage products. First, each enzymatic step is capable of amplifying the number of molecules that are cleaved. Second, the cleavage process reveals cryptic epitopes that allow the activated products to be distinguished from the unactivated precursors. In addition, activation products from two complement components, namely, C4 and C3, have the unusual property of covalently binding to protein and carbohydrate substrates. All of these properties distinguish complement activation products from some of the molecules that activate complement, such as antibodies. Antibodies themselves are not readily detected in tissue sections because only transient binding of a small number of antibodies to tissue is required to activate exponentially larger amounts of complement.

This chapter examines the advantages and disadvantages of various reagents to complement as applied to the diagnosis of different types of rejection in transplants. In addition, the limitations of complement as a marker of antibody-mediated rejection (AMR) are addressed (5–7).

SELECTION AND INTERPRETATION OF DIAGNOSTIC REAGENTS TO COMPLEMENT IN ALLOTRANSPLANTS

Deposits of Complement in Tissue Biopsy Specimens

Examination of biopsy specimens from organ transplants provides the most direct assessment of pathological processes jeopardizing the transplant. Stains for complement components in the organ transplant offer direct evidence of the location, distribution, and extent of complement activation at the site of injury. The different components of complement that have been used as markers of antibody-mediated rejection in transplants are discussed here in their order of activation by antibodies as shown in Fig. 1.

Polyclonal and Monoclonal Antibodies to C1q

The activation of complement by antibodies is primarily through the classical pathway of complement. Because C1 is the first component of the classical pathway of complement activation, it has long been used as a marker of antibody activation of complement. Polyclonal and monoclonal antibodies are available to detect C1q, the subcomponent of C1 that actually binds to antibodies (Fig. 1). These are frequently applied in renal pathology and dermatopathology to detect immune complexes. There are several drawbacks to C1q as a marker of rejection, however. The most serious drawback relates to sensitivity. In order to bind, one C1q requires at least a pair of IgG antibodies (Fig. 1a). This means that there are actually fewer C1q molecules to detect than IgG molecules. Moreover, the C1q molecules that are bound to antibodies depart when antibodies release from antigen or are shed from a cell surface (Fig. 1c).

In addition to sensitivity, there are theoretical problems of specificity. It is now clear that antibody is not the only ligand that is bound by C1q. C1q can also bind to phosphatidylcholine and sphingomyelin that are exposed on plasma membranes of apoptotic or ischemic cells or to the surface of virally infected cells. The presence of receptors for C1q on endothelial cells raises the possibility that immune complexes containing C1q could result in antigen-independent deposition of C1q on endothelium. However, these reactions are usually less diffuse, and in the case of immune complexes the pattern is usually granular rather than linear.

As predicted by these theoretical considerations, C1q has not proved to be a sensitive marker of antibody-mediated rejection in practice.

Polyclonal and Monoclonal Antibodies to C4d

The tissue-bound split products of C4 are significantly more sensitive than C1q as a marker of antibody-mediated inflammation. Because each activated C1 can enzymatically cleave many C4 molecules, more C4 split products are available to detect. One study found that for each C1 there were about 28 C4b fragments deposited on the cell membrane (8). The covalent binding of C4b and its further split products to tissues results in extended half-lives (Fig. 1c). The result of greater quantities and longer half-lives is that C4b and its further split product C4d are detected more easily than C1q or antibodies in biopsy specimens. Another advantage that results from the enzymatic cleavage of C4 is that neoepitopes are exposed on the split products. Monoclonal antibodies produced to these neoantigens are specific for the activated split product and not the intact precursor.

doi:10.1128/9781555818722.ch117

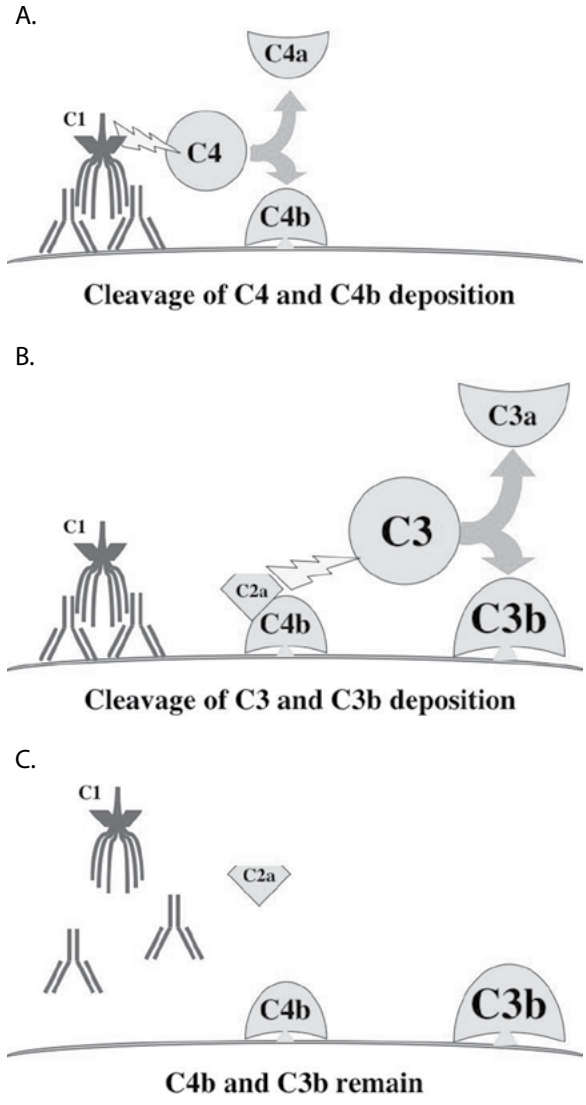

FIGURE 1 Activation of the early complement components by antibodies. (a) A pair of IgG antibodies is bound by C1 through the C1q subcomponent, and the enzymatic C1r and C1s subcomponents are activated to cleave C4 into C4a and C4b. C4b can bind covalently to a membrane protein and provide an anchor for C2, which is then cleaved. (b) The complex of C4bC2a enzymatically cleaves C3 into C3a and C3b. C3b is structurally homologous to C4b and can bind covalently to a membrane protein. (c) The covalently bound split products of C4 and C3 remain attached to the cell membrane after the antibody, C1, and C2a have dissociated from the membrane. The sizes of the symbols for C4b and C3b are intended to reflect the potential for larger quantities of C3 than C4 activation products.

C4d, the final split product of C4, has been the most widely reported marker for humoral immune responses to transplants (1, 2). Therefore, the mechanism that produces C4d is worth reviewing. C4d represents the end product of a regulatory mechanism that evolved to prevent damage to autologous tissues during complement activation. The small C4d fragment results when factor I cleaves C4b twice, once on either side of the covalent bond. Factor I requires a cofactor, such as membrane cofactor protein (MCP; CD46) or complement receptor 1 (CR1), to cleave C4b (Fig. 2). MCP is widely distributed on cells, including leukocytes and vascular endothelial cells. In contrast, CR1 is expressed on erythrocytes and leukocytes, including neutrophils and macrophages. The fluid-phase complement-regulatory protein C4 binding protein (C4bp) can also interact with cell-associated C4b and may also be found in regions of coagulation through its ability to bind to protein S. The rapid enzymatic cleavage of C4b by factor I makes C4d a more stable marker of complement activation than C4b. In fact, the monoclonal antibody used to detect C4d actually detects an epitope expressed on C4b as well as C4d. As a result, both C4d and any remaining C4b are detected by this reagent.

The use of the monoclonal antibodies to C4d has been limited primarily to frozen tissue sections. This limitation has been circumvented by the development of a polyclonal antibody that can be used in formalin-fixed and

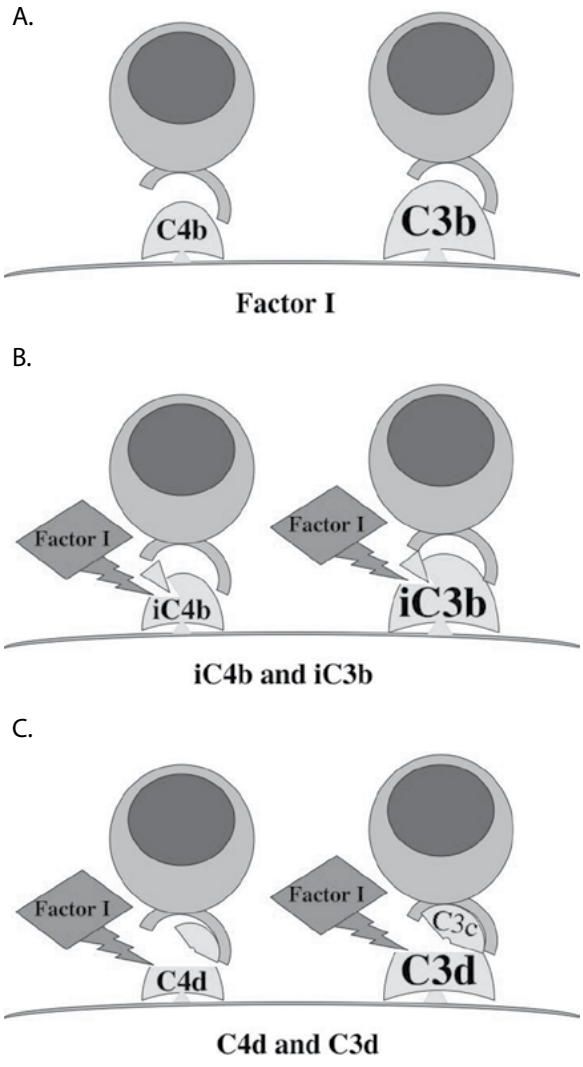

FIGURE 2 Regulation of C4b and C3b by circulating factor I and leukocytes expressing CR1. (a) CR1, which is expressed by leukocytes, associates with C4b or C3b, allowing factor I to cleave C4b and C3b. (b) The first enzymatic cleavage leaves iC4b or iC3b attached to the cell membrane. (c) Factor I then enzymatically cleaves iC4b or iC3b, and C4d and C3d remain covalently bound to the cell membrane. As described for Fig. 1, the sizes of the symbols for C4b and C3b are intended to reflect the potential for larger quantities of C3 than C4 activation products.

paraffin-embedded tissues. The first polyclonal was produced by immunizing a rabbit with a synthetic 15-amino-acid peptide that coincides with a loop segment of C4d that is not shared by the homologous C3d sequence (9). This reagent (available from Biomedica Gruppe, Vienna, Austria, distributed in the United States by Alpco, Salem, NH) has proved to be very useful in the case of biopsy specimens for which no frozen tissue is available. However, detection of C4d in fixed tissues is less sensitive than in frozen sections. In addition, there are difficulties with high background and nonspecific staining of the edges of the biopsy specimens ("edge effects").

The pattern and strength of staining are important for the interpretation of the results (Fig. 3). In biopsy specimens from renal transplants, antibodies to major histocompatibility antigens (HLA in humans) or major blood group antigens are associated with diffuse, linear staining of the peritubular capillaries (2, 10–12). Arterial endothelial cells are variably involved. This pattern may reflect in part the distribution of both the target antigens and the complement regulatory proteins. For example, class II major histocompatibility antigens, such as HLA-DR, are expressed constitutively on capillary and venous endothelium, but not arterial endothelium. However, HLA-DR antigens are upregulated by arterial endothelial cells as well as by tubular epithelial cells in sites of inflammation (13).

A.

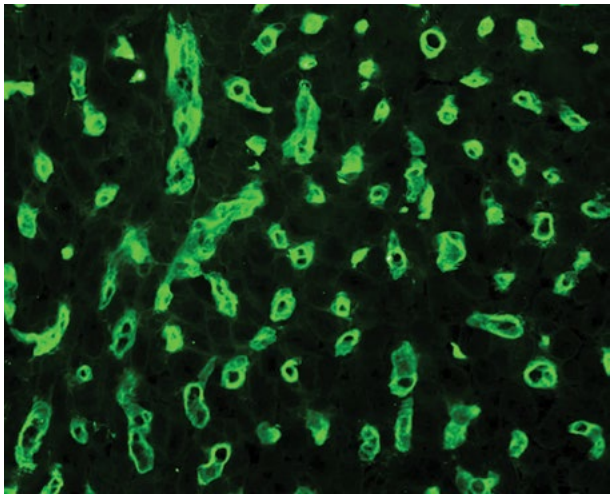

B.

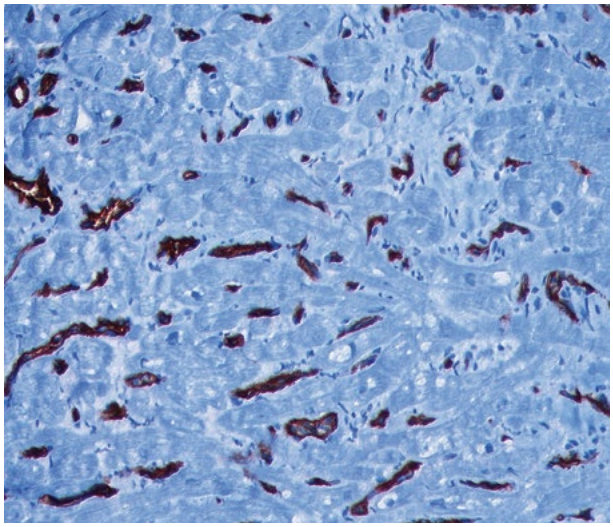

FIGURE 3 C4d staining of a heart transplant biopsy by immunofluorescence (top) and immunohistochemistry (bottom) shows comparable discrete staining of capillaries between myocytes, indicative of antibody-mediated rejection.

Polyclonal and Monoclonal Antibodies to C3 Split Products

Because C3 and C4 are both members of the alpha 2-macroglobulin family (14), the activation and regulation of C3 produce split products that are homologous to C4 split products (Fig. 2). C3d is the final membrane-bound split product of the regulation of C3b by factor I and a cofactor such as factor H, CR1, or MCP. C3d has been compared to C4d as a marker of complement activation (12, 15–18). Like C4d, C3d is covalently bound to tissues. Monoclonal antibodies to C3d are also specific for activated C3 because the epitope recognized is cryptic in uncleaved C3.

There are two major theoretical advantages of C3d as a marker for complement activation. The first advantage is that quantitatively more C3 can be activated than C4 because there is more substrate available and there is an amplification loop that sustains C3 activation. About twice as much C3 as C4 is present normally in the circulation (1.3 and 0.6 mg/ml, respectively), and these levels can be doubled by increased hepatic production in response to acute-phase reactions. In inflammatory sites, macrophages can produce additional C4 and C3. Once C3 is activated by any mechanism, a large supply of C3 is available as a substrate for an amplification loop, in which C3b activates more C3 through factor B.

The second advantage of C3d as a marker is that the split products of C3 have more biological activities than their C4 counterparts. C3b, iC3b, and C3d are the primary ligands for complement receptors 1, 3, and 2 (CR1, CR3, and CR2), respectively. Like CR1, CR3 is expressed on neutrophils, macrophages, and subsets of T lymphocytes. CR2 is part of a major second signaling pathway for antibody production by B lymphocytes. Although C4b is also a ligand for CR1, C4d does not bind CR2 (19). Therefore, the regulation steps for C4b that result in C4d deposition could terminate the complement cascade without activation of C3 or proinflammatory consequences. As a result, cases in which C4d is deposited in the absence of significant activation of C3 would be predicted to be associated with little or no complement-mediated injury (5, 20). In fact, this situation may account for the striking amounts of C4d found in well-functioning major-blood-group-incompatible renal transplants (12, 21, 22). The capacity of renal transplants to function well in the presence of circulating antibodies has been termed "accommodation" (20). The demonstration that C4 is activated indicates that the circulating antibodies do bind to the transplant and initiate activation of complement.

There are practical and theoretical reasons that C4d has been advocated as a better marker for antibody-mediated rejection than C3d. The practical advantage of C4d is that monoclonal and polyclonal antibodies to C4d work well with frozen and formalin-fixed tissue. Interpretation of C3d staining is more problematic with high background staining. In normal kidneys, C3d is also found in the tubular basement membrane and mesangium, particularly in biopsy specimens from older animals or humans.

The theoretical assertion that has been advanced for C4d as a marker for antibody-mediated responses is that it

decreases "false-positive" reactions due to complement activation by the alternative pathway. However, in antibody-mediated immunity, the alternative pathway serves fundamentally as an amplification loop for the classical pathway, and this is one of the reasons that C3 split products can be deposited in larger amounts than C4 split products.

Polyclonal and monoclonal antibodies to other split products of C3 have also been applied in the diagnostic evaluation of tissue biopsy specimens, but these reagents have disadvantages. The intermediate split product, iC3b, has the disadvantage of being short-lived. Moreover, iC3b may be more involved with downregulation of immune responses through its function as the primary ligand for CR3 on T lymphocytes as well as macrophages (reviewed in reference 22).

The use of antibodies to C3c offers even fewer advantages because C3c is the portion of iC3b that is cleaved away to produce C3d (Fig. 2c). As such, C3c does not remain bound to the membrane after being cleaved.

Polyclonal and Monoclonal Antibodies to C5b-C9

The terminal five components of complement attach to each other in succession to form the membrane attack complex (MAC), which increases cell permeability. Polyclonal and monoclonal antibodies have been produced to neoantigens that are created as the complex is formed. The MAC would be the best indicator that enough complement has been activated to exceed the multiple regulatory proteins capable of truncating the complement cascade after C4 or C3 activation. With currently available reagents, however, MAC has proven to be an insensitive indicator (23). This lack of sensitivity is probably related to the fact that MAC is deposited in limited quantities and sublytic amounts of MAC can be cleared rapidly from cell membranes. Regulatory proteins, such as CD59, limit the assembly of MAC on the surface of endothelial cells. Clearance of sublytic amounts of MAC occurs through the endocytic and exocytic response that removes the segments of membrane containing MAC.

Quality Control of Complement Assays Related to Tissue Biopsy Specimens

Quality controls have to be performed on the tissue substrate as well as on the reagents and methods used for the detection of complement. The extremely small tissue samples that are obtained from transplants by percutaneous needle biopsy procedures or bioptomes on catheters can be inadequate quantitatively or qualitatively. The biopsy specimens may provide inadequate amounts of parenchyma or may contain tissue damaged during procurement. Hematoxylin and eosin stains of adjacent tissue sections are useful to control for the quality of the tissue. The use of isotype-matched control antibodies is helpful to determine artifactual staining due to "crushed tissue" or "edge effect." The small size of the transplant biopsy specimens precludes their use as routine controls for the quality or dilution profiles of reagents. Larger specimens from kidneys with deposits of immune complexes can be used to establish optimal dilutions for the primary and secondary antibodies. For this purpose, renal specimens from patients with systemic lupus erythematosus can be useful as positive controls.

Specific Findings in Different Organ Transplants

Detection of activation products of complement is a very useful tool in establishing the diagnosis of AMR and guiding appropriate therapeutic management. The diagnosis of AMR is best made with evidence of histological and immunopathological findings in association with circulating donor-specific antibodies (DSA) and allograft dysfunction. The refinement of these criteria as they pertain to the different solid organ transplants has achieved various degrees of success and consensus, namely because the histopathologic immune response varies in different organs. In general, the presence of histologic alterations and immunopathologic markers for complement activation together with DSA is associated with worse graft survival than the presence of any of these components alone.

Kidney

The deposition of complement split products as a marker of AMR has been most extensively studied in kidney transplants. Recognition of AMR as a cause of graft dysfunction was facilitated by the demonstration of C4d in tissues as a marker of complement-fixing antibodies directed toward the endothelium because antibodies could not be visualized by microscopy in the microvasculature. The 2013 Banff classification of antibody-mediated rejection includes "diffuse or focal C4d staining by IF on frozen sections or any staining by IHC on paraffin sections" as being positive. The immunofluorescence method has been shown to be more sensitive than the immunohistochemical method for C4d staining (24–26). In the interpretation of the C4d stain, it is noteworthy that intrinsic fluorescence of glomerular mesangium and internal elastic lamina of arteries and arterioles is seen with the immunofluorescence method, while artifactual staining of the interstitium, tubular basement membrane, tubular brush border, and plasma in capillaries may be observed in immunohistochemical stains (25). Although C3d correlates with the presence of C4d, staining for C3d added marginal diagnostic value to biopsy specimens that already are positive for C4d and show histologic features of AMR (12). Another study showed no significant correlation of C3d with DSA or graft loss (16). Background staining in the tubular basement membranes may also interfere with accurate interpretation of C3d stains.

Recommendation for C4d staining was first incorporated in the Banff grading system for renal AMR in 2003. Diagnostic criteria for acute AMR include histomorphologic evidence of microvascular injury, C4d deposition in peritubular capillaries, presence of DSA, and allograft dysfunction. A subset of patients with diffuse C4d staining can have microvascular injury and DSA with stable renal function, representing a form of subclinical AMR that appears to be at risk of developing transplant glomerulopathy and graft scarring. The latter histologic changes indicate chronic kidney injury, and a diagnosis of chronic AMR is made if C4d deposition is seen in the presence of these features and DSA (10). Another scenario in which diffuse C4d positivity is commonly seen is in the setting of ABO-incompatible renal transplants with stable function.

Heart

AMR is a well-recognized cause of acute cardiac allograft dysfunction. Immunofluorescence staining, which is considered the gold standard in the evaluation of kidney transplant biopsy specimens, offers a reliable means to evaluate both C4d and C3d in heart biopsy specimens. More importantly, the use of a panel with both C4d and C3d is diagnostically more useful than C4d alone. Concomitant C4d- and C3d-positive staining is significantly correlated with the presence of DSA and cardiac allograft dysfunction (17, 18). Routine C4d and C3d staining of all surveillance biopsy specimens showed that a subset of patients have C4d-only positive

biopsy specimens without evidence of allograft dysfunction, which occurs as single episodes in the majority of cases. It is not clear whether this phenomenon represents subclinical AMR or graft accommodation as seen in ABO-incompatible stable renal allografts (11). Staining of the collagen in the interstitium, endocardium, internal elastic lamina of arteries and arterioles, and myocyte sarcolemma should not be interpreted as positive. Necrotic myocytes, thrombi, and Quilty lesions also exhibit C4d and C3d staining.

Unlike what is recommended for other solid organ transplants, the International Society for Heart and Lung Transplantation working formulation for diagnosis of AMR in heart allografts requires only pathologic evidence of either intravascular macrophages confirmed by CD68 staining or diffuse (>50%) myocardial capillary staining with C4d and/or C3d (27). Most centers utilize immunohistochemical rather than immunofluorescence methods for complement staining in formalin-fixed paraffin-embedded tissue. While C4d staining results using the two methods are comparable, C3d staining by immunohistochemistry has not been standardized, making interpretation less consistent.

Pancreas

The Banff classification of pancreas transplant biopsy requires the presence of histologic evidence of tissue injury, positive C4d staining, and DSA for the diagnosis of acute AMR (28). C4d staining can be seen in interacinar capillaries, interstitial connective tissue, islet capillaries, and small- to medium-sized arteries and veins. However, only C4d deposition in >5% of interacinar capillaries of the pancreatic allograft is correlated with the presence of circulating DSA (29). The presence of C4d staining in interacinar capillaries and DSA has also been shown to correlate with poor graft survival (29, 30). Focal C4d positivity alone is of unknown significance. C3d appears to be less sensitive than C4d as a marker for AMR and does not correlate with DSA. Larger prospective studies are needed to validate these observations and to refine the diagnostic criteria for AMR, which are further hindered by the limited number of surveillance pancreatic biopsies being performed. The feasibility of interpreting biopsy specimens taken from the duodenal segment of a pancreatic graft as a surrogate organ, including evaluation of C4d staining patterns, is beginning to be explored.

Liver

The diagnostic relevance of C4d staining in liver transplantation is not yet clearly established for numerous reasons. Diagnostic criteria for AMR in liver allografts have not been standardized, with only a few cases of reported AMR. The liver allograft is considered quite resistant to AMR, which is thought to be due in part to its capacity to adsorb and neutralize alloantibodies with its large sinusoidal surface area, its ability to secrete soluble HLA molecules, and the presence of Kupffer cells that can phagocytize immune complexes. A major challenge in the interpretation of C4d is the difference in the pattern and sensitivity of C4d staining between immunohistochemical and immunofluorescence methodologies. Most studies have employed immunohistochemical techniques and identified positive staining in portal capillaries and small veins as good markers for AMR (31). Other investigators suggest that diffuse linear C4d staining of sinusoids as detected by immunofluorescence is more reliable. When immunofluorescence and immunohistochemical methods were compared on matched biopsy samples from the same cases, sinusoidal staining was found to be only focal in distribution with much weaker intensity on immunohistochemical staining (32). Nonspecific staining has also been reported in portal tract stroma, internal elastic lamina of arteries, and necrotic hepatocytes. While positive C4d staining is supportive of a diagnosis of AMR, it is also frequently observed in acute cellular rejection, chronic ductopenic rejection, chronic hepatitis, autoimmune hepatitis, and graft-versus-host disease (33).

Lung

AMR in lung transplantation is an infrequent diagnosis, partly because it is not well defined and diagnostic criteria are lacking. Histologic findings of acute lung injury and capillaritis are nonspecific, while C4d deposition is neither a sensitive nor a specific marker of AMR in lung allografts. C4d staining can be seen with acute lung injury patterns, capillary neutrophilic inflammation, high-grade acute cellular rejection, reperfusion injury, and infections (34). In addition, several artifacts make interpretation of C4d staining in the lungs difficult; these include nonspecific staining of vascular and airway elastic fibers, arterial and vein endothelium, peribronchial capillaries, alveolar pneumocytes, hyaline membranes, and macrophage aggregates (35). Only interstitial alveolar capillary staining with C4d is considered positive. A diffuse or multifocal C4d staining is reported as "findings suggestive of AMR," should prompt testing for circulating DSA, and requires clinical correlation to rule out other causes of allograft dysfunction. There is much more limited experience with C3d staining, such that it is currently included only as a secondary antibody panel in the screening for AMR in lung allografts (36).

Small Intestine

Diagnostic criteria for AMR in small intestinal transplantation have not been established. C4d staining currently has not been proven to be of diagnostic utility in small bowel transplantation because of lack of specificity of C4d staining in intestinal mucosa (37, 38).

Composite Tissue Grafts

Compared to other solid organ transplants, composite tissue allografts appear to be less susceptible to AMR. Within the limited experience obtained from the small number of hand and face allotransplantations performed so far, there is no clear evidence that AMR plays an important role in composite tissue grafts because of the lack of detectable DSA, absence of histologic features of microvascular injury, and nonspecific C4d staining (39, 40). The relevance of C4d staining is controversial since it is also observed in inflammatory dermatoses, nonrejecting skin, and mild acute cellular rejection.

Soluble Products of Complement Activation in Serum, Urine, or Bronchoalveolar Lavage Fluid

Activation of the complement cascade produces many split products that do not bind to tissues or that are released from tissues. These fluid-phase products can be detected in plasma, serum, urine, and bronchoalveolar lavage fluids. Enzyme-linked immunosorbent assay kits are available to quantitate soluble split products in fluids (for example, see www.quidel.com/products/product_list.php). C3a, C3c, sC4d, sC3d, and sC5b-8 or -9 are among the most frequently measured soluble complement products. C4a, C3a, and C5a are fluid-phase reactants that are produced by the enzymatic activation of C4, C3, and C5, respectively (Fig. 1b). Regulation of C3b by factor I produces the soluble split product C3c (Fig. 2c). Excess C4b and C3b that fail to bind to protein are hydrolyzed

and can be the source of soluble split products, such as soluble C4d and C3d (sC4d and sC3d). Activation through the amplification loop of the alternative pathway results in the presence of Bb in the plasma. Finally, various forms of MAC that fail to insert into plasma membranes can be detected as soluble C5b-C8 or C5b-C9 (sC5b-8 or -9).

Plasma

Diagnostic tests that require only blood samples are appealing because they are much less invasive than taking biopsy specimens from organ transplants. Theoretically, this approach might also circumvent the sampling error inherent in taking minute pieces of tissue from organs, in which the rejection process may not be diffuse. Finally, avoiding repeated trauma to the transplant could reduce nonspecific inflammation in the organ.

The major disadvantage of testing plasma is the lack of specificity. Many confounding variables can alter the levels of markers in the circulation. In the first decades after transplantation became a successful therapeutic modality, elevated levels of complement split products were detected in the serum as the result of infection as well as rejection (41). More-recent studies have confirmed this finding. One study of patients with renal transplants identified C4b, C4d, C3b, and C3d bound to C-reactive protein in the first days after transplantation (42).

Testing serum can lead to even more sources of artifact. Coagulation enzymes can cleave C3, C4, and C5 and generate excess fragments in a relatively unpredictable fashion (43). Moreover, *ex vivo* activation of complement occurs frequently in samples containing immune complexes, certain drugs, or other contaminants. This is especially true of cryoglobulins, which are barely detectable by other methods. Therefore, it is recommended that samples be collected as EDTA plasma and frozen as soon after centrifugation as possible.

Urine

Urine provides a sample that reflects the inflammatory events in renal transplants more directly. Several reports have indicated that elevated soluble complement split products can be detected in the urine during rejection episodes (23). Obviously, these assays cannot be applied during periods of anuria or oliguria, such as when there is delayed graft function after transplantation. Nonetheless, this is an approach that deserves further investigation.

Bronchoalveolar Lavage Fluids

Currently, most lung transplants are evaluated by periodic bronchoscopic exams that include an infusion and retrieval of saline referred to as bronchoalveolar lavage (usually termed BAL). This procedure is invasive, but the sample is focused on the most susceptible tissue in the transplanted lung. Elevated split products of complement are found during rejection (44). However, the appropriate method of accounting for the effects of dilution have not been established (45).

TYPES OF COMPLEMENT-MEDIATED INJURY IN ALLOTRANSPLANTS

Hyperacute Rejection

Hyperacute rejection is the most unambiguous example of complement-mediated injury to transplants. This type of rejection was first recognized in renal transplants by three groups of investigators between 1966 and 1969 (46–48). This devastatingly rapid type of rejection occurs within minutes to hours after blood flow is restored to the grafted kidney. Immunohistological studies demonstrated that antibodies and complement components were deposited in the transplant. Consequently, hyperacute rejection was quickly attributed to the action of antibodies and complement.

After early reports established a link between antibodies and hyperacute rejection, a "crossmatch test" was devised by Patel and Terasaki to test for the offending antibodies (47). The screening method consisted of mixing leukocytes from the prospective donor with serum from the prospective recipient and then adding a source of complement to demonstrate lysis. After the institution of this test, hyperacute rejection of allografts was almost eliminated.

In hyperacute rejection, complement activation is initiated by large amounts of antibody binding to antigens on the endothelial cells of the transplanted organ. The most characteristic features of hyperacute rejection can be predicted from our knowledge of complement. Prominent inflammatory manifestations of complement activation in hyperacute rejection include (i) recruitment and activation of numerous neutrophils, (ii) disruption of vascular integrity resulting in edema and hemorrhage, and (iii) activation of coagulation leading to fibrin deposition and thrombosis. The relative intensity of these features depends upon the quantities and qualities of the antibodies and their target antigens. Antibodies to both major histocompatibility complex antigens (HLA in humans) and the major blood group antigens (A and B) can cause hyperacute rejection because these antigens are expressed at high concentrations on vascular endothelial cells.

Acute Rejection

Until recently, acute rejection was often cited as an example of pure cell-mediated immunity. This classification was based largely on experimental animal studies, but the vast majority of experimental transplants are performed with young, healthy (even pathogen-free) donor and recipient animals. Unless specifically under study, previous surgical interventions, blood transfusions, trauma, and prolonged ischemia are all avoided or introduced under highly controlled and isolated circumstances. Unfortunately, in clinical transplantation the recipient by definition is suffering from the final stages of organ failure and the organ most often comes from a donor who has died from a traumatic injury. Therefore, the recipient has frequently undergone previous surgical interventions or blood transfusions, the donor has experienced major trauma, and the organ has been subjected to ischemia. All of these variables can affect the function and survival of transplants adversely by increasing the initial recognition of the transplanted organ through complement-mediated processes. More-recent animal experiments have provided evidence to support the clinical observations that complement contributes to the rejection process (49, 50).

Antibodies to major histocompatibility complex antigens can be elicited by previous blood transfusions, pregnancies, or transplants. If this sensitization is below the threshold of the cross-match test used, then hyperacute rejection may be avoided, but the risk of antibody-mediated rejection is increased. Sensitization from previous pregnancies is especially pertinent when a kidney is transplanted to a wife from her husband or to a mother from her child. In these cases, complement deposition can be a prominent feature of the rejection process (51). Obviously, the incidence of antibody-mediated immunity will be related to the composition of the population of patients and the stringency of screening for antibodies before transplantation. In some studies of renal

transplant recipients, a majority of the "steroid-resistant" acute rejections may have an antibody-mediated component. These acute-rejection episodes often occur within the first weeks or months after transplantation in presensitized patients (4). In unsensitized patients, acute-rejection episodes can occur years after transplantation (4, 13, 18).

Chronic Rejection

Chronic loss of graft function is not due solely to immune causes. Instead, the chronic lesions in organ allografts represent repair and remodeling processes that are the final common response to many types of tissue injury. For example, the proliferative vascular lesions that characterize chronic dysfunction of renal and cardiac allografts have some similarities to ordinary arteriosclerosis. The vascular lesions in transplants are generally more extensive and uniform in distribution than ordinary arteriosclerosis, but this may just represent the more widespread injury of the immunologically incompatible tissue. Both types of vascular lesions are currently thought to involve inflammatory processes.

C4d has been associated with chronic rejection in renal transplants. Even in renal transplants, C4d staining often is not strong or diffuse in biopsy specimens with chronic rejection (10). This is not unexpected because the events that initiate chronic repair and remodeling may be resolved and even the covalently bound complement split products can be cleared from the membrane of endothelial cells before the repair processes impair organ function. Moreover, antibodies can initiate vascular changes through mediators independent of complement activation. These include upregulation of adhesion molecules and proliferative signals (52, 53). These changes may be captured by molecular diagnostic techniques (4, 7).

SUMMARY

Complement can be a useful adjunct in diagnosing and directing treatment of rejection, especially for renal and cardiac transplants. Currently, the tissue-associated final split products of C4b and C3b, namely, C4d and C3d, are the most useful markers of antibody-mediated rejection. Both C4d and C3d offer the advantages of being produced in large amounts and binding covalently to tissues. Monoclonal antibodies are available to neoantigens on C4d and C3d that are not accessible in the unactivated precursors. Although these markers have provided significant diagnostic advances for organ transplantation, appropriate interpretation requires additional information, including testing for circulating antibodies to donor antigens and correlation with clinical evidence of graft dysfunction.

REFERENCES

1. **Feucht HE.** 2003. Complement C4d in graft capillaries—the missing link in the recognition of humoral alloreactivity. *Am J Transplant* **3:**646–652. PubMed
2. **Racusen LC, Colvin RB, Solez K, Mihatsch MJ, Halloran PF, Campbell PM, Cecka MJ, Cosyns JP, Demetris AJ, Fishbein MC, Fogo A, Furness P, Gibson IW, Glotz D, Hayry P, Hunsickern L, Kashgarian M, Kerman R, Magil AJ, Montgomery R, Morozumi K, Nickeleit V, Randhawa P, Regele H, Seron D, Seshan S, Sund S, Trpkov K.** 2003. Antibody-mediated rejection criteria—an addition to the Banff 97 classification of renal allograft rejection. *Am J Transplant* **3:**708–714. PubMed
3. **Cohen D, Colvin RB, Daha MR, Drachenberg CB, Haas M, Nickeleit V, Salmon JE, Sis B, Zhao MH, Bruijn JA, Bajema IM.** 2012. Pros and cons for C4d as a biomarker. *Kidney Int* **81:**628–639. PubMed
4. **Mengel M, Sis B, Haas M, Colvin RB, Halloran PF, Racusen LC, Solez K, Cendales L, Demetris AJ, Drachenberg CB, Farver CF, Rodriguez ER, Wallace WD, Glotz D, Banff meeting report writing committee.** 2012. Banff 2011 Meeting report: new concepts in antibody-mediated rejection. *Am J Transplant* **12:**563–570. PubMed
5. **Baldwin WM III, Kasper EK, Zachary AA, Wasowska BA, Rodriguez ER.** 2004. Beyond C4d: other complement-related diagnostic approaches to antibody-mediated rejection. *Am J Transplant* **4:**311–318. PubMed
6. **Sis B, Mengel M, Haas M, Colvin RB, Halloran PF, Racusen LC, Solez K, Baldwin WM III, Bracamonte ER, Broecker V, Cosio F, Demetris AJ, Drachenberg C, Einecke G, Gloor J, Glotz D, Kraus E, Legendre C, Liapis H, Mannon RB, Nankivell BJ, Nickeleit V, Papadimitriou JC, Randhawa P, Regele H, Renaudin K, Rodriguez ER, Seron D, Seshan S, Suthanthiran M, Wasowska BA, Zachary A, Zeevi A.** 2010. Banff '09 meeting report: antibody mediated graft deterioration and implementation of Banff working groups. *Am J Transplant* **10:**464–471. PubMed
7. **Sis B, Jhangri GS, Bunnag S, Allanach K, Kaplan B, Halloran PF.** 2009. Endothelial gene expression in kidney transplants with alloantibody indicates antibody-mediated damage despite lack of C4d staining. *Am J Transplant* **9:**2312–2323. PubMed
8. **Ollert MW, Kadlec JV, David K, Petrella EC, Bredehorst R, Vogel CW.** 1994. Antibody-mediated complement activation on nucleated cells. A quantitative analysis of the individual reaction steps. *J Immunol* **153:**2213–2221. PubMed
9. **Regele H, Exner M, Watschinger B, Wenter C, Wahrmann M, Osterreicher C, Säemann MD, Mersich N, Hörl WH, Zlabinger GJ, Böhmig GA.** 2001. Endothelial C4d deposition is associated with inferior kidney allograft outcome independently of cellular rejection. *Nephrol Dial Transplant* **16:**2058–2066. PubMed
10. **Colvin RB.** 2007. Antibody-mediated renal allograft rejection: diagnosis and pathogenesis. *J Am Soc Nephrol* **18:**1046–1056. PubMed
11. **Haas M.** 2010. The significance of C4d staining with minimal histologic abnormalities. *Curr Opin Organ Transplant* **15:**21–27. PubMed
12. **Haas M, Rahman MH, Racusen LC, Kraus ES, Bagnasco SM, Segev DL, Simpkins CE, Warren DS, King KE, Zachary AA, Montgomery RA.** 2006. C4d and C3d staining in biopsies of ABO- and HLA-incompatible renal allografts: correlation with histologic findings. *Am J Transplant* **6:**1829–1840. PubMed
13. **Nickeleit V, Mihatsch MJ.** 2003. Kidney transplants, antibodies and rejection: is C4d a magic marker? *Nephrol Dial Transplant* **18:**2232–2239. PubMed
14. **Dodds AW, Law SK.** 1998. The phylogeny and evolution of the thioester bond-containing proteins C3, C4 and alpha 2-macroglobulin. *Immunol Rev* **166:**15–26. PubMed
15. **Kuypers DR, Lerut E, Evenepoel P, Maes B, Vanrenterghem Y, Van Damme B.** 2003. C3D deposition in peritubular capillaries indicates a variant of acute renal allograft rejection characterized by a worse clinical outcome. *Transplantation* **76:**102–108. PubMed
16. **Herman J, Lerut E, Van Damme-Lombaerts R, Emonds MP, Van Damme B.** 2005. Capillary deposition of complement C4d and C3d in pediatric renal allograft biopsies. *Transplantation* **79:**1435–1440. PubMed
17. **Rodriguez ER, Skojec DV, Tan CD, Zachary AA, Kasper EK, Conte JV, Baldwin WM III.** 2005. Antibody-mediated rejection in human cardiac allografts: evaluation of immunoglobulins and complement activation products

C4d and C3d as markers. *Am J Transplant* **5:**2778–2785. PubMed

18. **Tan CD, Sokos GG, Pidwell DJ, Smedira NG, Gonzalez-Stawinski GV, Taylor DO, Starling RC, Rodriguez ER.** 2009. Correlation of donor-specific antibodies, complement and its regulators with graft dysfunction in cardiac antibody-mediated rejection. *Am J Transplant* **9:**2075–2084. PubMed
19. **van den Elsen JM, Martin A, Wong V, Clemenza L, Rose DR, Isenman DE.** 2002. X-ray crystal structure of the C4d fragment of human complement component C4. *J Mol Biol* **322:**1103–1115. PubMed
20. **Platt JL.** 2002. C4d and the fate of organ allografts. *J Am Soc Nephrol* **13:**2417–2419. PubMed
21. **Fidler ME, Gloor JM, Lager DJ, Larson TS, Griffin MD, Textor SC, Schwab TR, Prieto M, Nyberg SL, Ishitani MB, Grande JP, Kay PA, Stegall MD.** 2004. Histologic findings of antibody-mediated rejection in ABO blood-group-incompatible living-donor kidney transplantation. *Am J Transplant* **4:**101–107. PubMed
22. **King KE, Warren DS, Samaniego-Picota M, Campbell-Lee S, Montgomery RA, Baldwin WM III.** 2004. Antibody, complement and accommodation in ABO-incompatible transplants. *Curr Opin Immunol* **16:**545–549. PubMed
23. **Bechtel U, Scheuer R, Landgraf R, König A, Feucht HE.** 1994. Assessment of soluble adhesion molecules (sICAM-1, sVCAM-1, sELAM-1) and complement cleavage products (sC4d, sC5b-9) in urine. Clinical monitoring of renal allograft recipients. *Transplantation* **58:**905–911. PubMed
24. **Nadasdy GM, Bott C, Cowden D, Pelletier R, Ferguson R, Nadasdy T.** 2005. Comparative study for the detection of peritubular capillary C4d deposition in human renal allografts using different methodologies. *Hum Pathol* **36:**1178–1185. PubMed
25. **Seemayer CA, Gaspert A, Nickeleit V, Mihatsch MJ.** 2007. C4d staining of renal allograft biopsies: a comparative analysis of different staining techniques. *Nephrol Dial Transplant* **22:**568–576. PubMed
26. **Troxell ML, Weintraub LA, Higgins JP, Kambham N.** 2006. Comparison of C4d immunostaining methods in renal allograft biopsies. *Clin J Am Soc Nephrol* **1:**583–591. PubMed
27. **Berry GJ, Burke MM, Andersen C, Bruneval P, Fedrigo M, Fishbein MC, Goddard M, Hammond EH, Leone O, Marboe C, Miller D, Neil D, Rassl D, Revelo MP, Rice A, Rene Rodriguez E, Stewart S, Tan CD, Winters GL, West L, Mehra MR, Angelini A.** 2013. The 2013 International Society for Heart and Lung Transplantation Working Formulation for the standardization of nomenclature in the pathologic diagnosis of antibody-mediated rejection in heart transplantation. *J Heart Lung Transplant* **32:**1147–1162.
28. **Drachenberg CB, Torrealba JR, Nankivell BJ, Rangel EB, Bajema IM, Kim DU, Arend L, Bracamonte ER, Bromberg JS, Bruijn JA, Cantarovich D, Chapman JR, Farris AB, Gaber L, Goldberg JC, Haririan A, Honsová E, Iskandar SS, Klassen DK, Kraus E, Lower F, Odorico J, Olson JL, Mittalhenkle A, Munivenkatappa R, Paraskevas S, Papadimitriou JC, Randhawa P, Reinholt FP, Renaudin K, Revelo P, Ruiz P, Samaniego MD, Shapiro R, Stratta RJ, Sutherland DE, Troxell ML, Voska L, Seshan SV, Racusen LC, Bartlett ST.** 2011. Guidelines for the diagnosis of antibody-mediated rejection in pancreas allografts-updated Banff grading schema. *Am J Transplant* **11:**1792–1802. PubMed
29. **Torrealba JR, Samaniego M, Pascual J, Becker Y, Pirsch J, Sollinger H, Odorico J.** 2008. C4d-positive interacinar capillaries correlates with donor-specific antibody-mediated rejection in pancreas allografts. *Transplantation* **86:**1849–1856. PubMed
30. **de Kort H, Munivenkatappa RB, Berger SP, Eikmans M, van der Wal A, de Koning EJ, van Kooten C, de Heer E, Barth RN, Bruijn JA, Philosophe B, Drachenberg CB, Bajema IM.** 2010. Pancreas allograft biopsies with positive c4d staining and anti-donor antibodies related to worse outcome for patients. *Am J Transplant* **10:**1660–1667. PubMed
31. **Musat AI, Agni RM, Wai PY, Pirsch JD, Lorentzen DF, Powell A, Leverson GE, Bellingham JM, Fernandez LA, Foley DP, Mezrich JD, D'Alessandro AM, Lucey MR.** 2011. The significance of donor-specific HLA antibodies in rejection and ductopenia development in ABO compatible liver transplantation. *Am J Transplant* **11:**500–510. PubMed
32. **Kozlowski T, Andreoni K, Schmitz J, Hayashi PH, Nickeleit V.** 2012. Sinusoidal C4d deposits in liver allografts indicate an antibody-mediated response: diagnostic considerations in the evaluation of liver allografts. *Liver Transpl* **18:**641–658. PubMed
33. **Ali S, Ormsby A, Shah V, Segovia MC, Kantz KL, Skorupski S, Eisenbrey AB, Mahan M, Huang MA.** 2012. Significance of complement split product C4d in ABO-compatible liver allograft: diagnosing utility in acute antibody mediated rejection. *Transpl Immunol* **26:**62–69. PubMed
34. **Yousem SA, Zeevi A.** 2012. The histopathology of lung allograft dysfunction associated with the development of donor-specific HLA alloantibodies. *Am J Surg Pathol* **36:**987–992. PubMed
35. **Wallace WD, Reed EF, Ross D, Lassman CR, Fishbein MC.** 2005. C4d staining of pulmonary allograft biopsies: an immunoperoxidase study. *J Heart Lung Transplant* **24:**1565–1570. PubMed
36. **Berry G, Burke M, Andersen C, Angelini A, Bruneval P, Calabrese F, Fishbein MC, Goddard M, Leone O, Maleszewski J, Marboe C, Miller D, Neil D, Padera R, Rassl D, Revello M, Rice A, Stewart S, Yousem SA.** 2013. Pathology of pulmonary antibody-mediated rejection: 2012 update from the Pathology Council of the ISHLT. *J Heart Lung Transplant* **32:**14–21. PubMed
37. **de Serre NP, Canioni D, Lacaille F, Talbotec C, Dion D, Brousse N, Goulet O.** 2008. Evaluation of c4d deposition and circulating antibody in small bowel transplantation. *Am J Transplant* **8:**1290–1296. PubMed
38. **Troxell ML, Higgins JP, Kambham N.** 2006. Evaluation of C4d staining in liver and small intestine allografts. *Arch Pathol Lab Med* **130:**1489–1496. PubMed
39. **Hautz T, Zelger B, Brandacher G, Mueller H, Grahammer J, Zelger B, Lee A, Cavadas P, Margreiter R, Pratschke J, Schneeberger S.** 2012. Histopathologic characterization of mild rejection (grade I) in skin biopsies of human hand allografts. *Transpl Int* **25:**56–63. PubMed
40. **Kanitakis J, McGregor B, Badet L, Petruzzo P, Morelon E, Devauchelle B, Dubernard JM.** 2007. Absence of c4d deposition in human composite tissue (hands and face) allograft biopsies: an immunoperoxidase study. *Transplantation* **84:**265–267. PubMed
41. **Fearon DT, Daha MR, Strom TB, Weiler JM, Carpenter CB, Austen KF.** 1977. Pathways of complement activation in membranoproliferative glomerulonephritis and allograft rejection. *Transplant Proc* **9:**729–739. PubMed
42. **Wolbink GJ, Brouwer MC, Buysmann S, ten Berge IJ, Hack CE.** 1996. CRP-mediated activation of complement in vivo: assessment by measuring circulating complement-C-reactive protein complexes. *J Immunol* **157:**473–479. PubMed
43. **Wiggins RC, Giclas PC, Henson PM.** 1981. Chemotactic activity generated from the fifth component of complement by plasma kallikrein of the rabbit. *J Exp Med* **153:**1391–1404. PubMed
44. **Miller GG, Destarac L, Zeevi A, Girnita A, McCurry K, Iacono A, Murray JJ, Crowe D, Johnson JE, Ninan M,**

Milstone AP. 2004. Acute humoral rejection of human lung allografts and elevation of C4d in bronchoalveolar lavage fluid. *Am J Transplant* **4:**1323–1330. PubMed

45. **Dargaville PA, South M, Vervaart P, McDougall PN.** 1999. Validity of markers of dilution in small volume lung lavage. *Am J Respir Crit Care Med* **160:**778–784. PubMed
46. **Kissmeyer-Nielsen F, Olsen S, Petersen VP, Fjeldborg O.** 1966. Hyperacute rejection of kidney allografts, associated with pre-existing humoral antibodies against donor cells. *Lancet* **ii:**662–665. PubMed
47. **Patel R, Terasaki PI.** 1969. Significance of the positive crossmatch test in kidney transplantation. *N Engl J Med* **280:**735–739. PubMed
48. **Williams GM, Hume DM, Hudson RP Jr, Morris PJ, Kano K, Milgrom F.** 1968. "Hyperacute" renal-homograft rejection in man. *N Engl J Med* **279:**611–618. PubMed
49. **Baldwin WM III, Valujskikh A, Fairchild RL.** 2010. Antibody-mediated rejection: emergence of animal models to answer clinical questions. *Am J Transplant* **10:**1135–1142. PubMed
50. **Wehner JR, Morrell CN, Rodriguez ER, Fairchild RL, Baldwin WM III.** 2009. Immunological challenges of cardiac transplantation: the need for better animal models to answer current clinical questions. *J Clin Immunol* **29:**722–729. PubMed
51. **Böhmig GA, Regele H, Säemann MD, Exner M, Druml W, Kovarik J, Hörl WH, Zlabinger GJ, Watschinger B.** 2000. Role of humoral immune reactions as target for antirejection therapy in recipients of a spousal-donor kidney graft. *Am J Kidney Dis* **35:**667–673. PubMed
52. **Zhang X, Reed EF.** 2009. Effect of antibodies on endothelium. *Am J Transplant* **9:**2459–2465. PubMed
53. **Yamakuchi M, Kirkiles-Smith NC, Ferlito M, Cameron SJ, Bao C, Fox-Talbot K, Wasowska BA, Baldwin WM III, Pober JS, Lowenstein CJ.** 2007. Antibody to human leukocyte antigen triggers endothelial exocytosis. *Proc Natl Acad Sci USA* **104:**1301–1306. PubMed

Molecular Characterization of Rejection in Solid Organ Transplantation

DARSHANA DADHANIA, TARA K. SIGDEL,
THANGAMANI MUTHUKUMAR, CHOLI HARTONO,
MINNIE M. SARWAL, AND MANIKKAM SUTHANTHIRAN

118

Improved knowledge of the alloimmune repertoire, development and clinical application of new therapies, advances in surgical techniques, and effective infection prophylaxis have helped to transition transplantation from a high-risk experimental therapy to a safe clinical remedy. Nevertheless, diagnostic and therapeutic challenges remain. Here we provide an outline of the immune cascade implicated in allograft rejection, emphasize molecular protocols for characterizing gene expression strengths and patterns and for high-throughput protein and peptide analyses, and summarize molecular correlates of rejection of human kidney, heart, lung, liver, and pancreas allografts.

The immune cascade culminating in allograft rejection is initiated following the physical interaction between the $CD4^+$ T cells and $CD8^+$ T cells of the allograft recipient and antigen-presenting cells (APCs) of donor origin (direct pathway of allorecognition) or APCs of recipient origin (indirect pathway of allorecognition) (1, 2). The allopeptides displayed on the surfaces of APCs impart antigen specificity and provide the antigenic signal. Costimulatory signals are obligatory for plenary T cell activation (3) and result from the physical contacts between cell surface proteins expressed on the T cell surface (e.g., CD2 antigen) and their counterreceptors displayed on APCs. The antigen-experienced and costimulated T cells then secrete cytokines, such as interleukin 2 and gamma interferon, and recruit and educate cytotoxic $CD8^+$ T cells, antibody-forming B cells, and additional proinflammatory cells, and this highly coordinated immune response results in allograft rejection unless it is restrained by immunosuppressive therapy (2, 4, 5). Major histocompatibility complex class I proteins present donor-derived allopeptides to the recipient's $CD8^+$ T cells, whereas major histocompatibility complex class II molecules present the allopeptides to the recipient's $CD4^+$ T cells. Chemokines and adhesion molecules generate the requisite signals for cell trafficking and transmigration of proinflammatory cells into the allograft (6). Toll-like receptors contribute not only by eliciting innate immunity but also by the amplification of acquired immunity directed at the allograft (7).

With knowledge from preclinical studies, investigators have utilized hypothesis-driven approaches to study targeted gene and protein expression patterns associated with acute and chronic rejection of clinical organ allografts. These initial translational studies led the way in refining our knowledge and in further identification of pathways involved in human allograft rejection. Recently, with advances in technology and bioinformatics, we have seen a shift in translational research from a "hypothesis-driven" approach that studied one gene or protein at a time to a "hypothesis-generating" or "discovery-driven" approach, with the aid of "-omic" methods, that allows researchers to investigate several thousands of genes or proteins simultaneously. Ever-evolving bioinformatic tools have helped in examining thousands of genes and proteins for an understanding of diseases at the cellular and organismal levels. Whereas genomic and transcriptomic methods have been tested for some time, new proteomic methods are actively being developed to garner further insights into the allograft rejection process.

MOLECULAR TECHNIQUES FOR CHARACTERIZATION OF GENE EXPRESSION PROFILES OF ALLOGRAFTS

PCR assays, microarrays, and next-generation sequencing (NGS) tools have enabled the characterization of gene expression strengths and patterns of clinical samples and the development of diagnostic and prognostic biomarkers of allograft rejection.

PCR Assay

PCR is a powerful technique for amplifying a short segment of DNA. PCR methodology relies on alternate heating and cooling cycles allowing for the amplification of a segment of the DNA (8). Automation of PCR was made possible with the discovery of the heat-resistant DNA polymerase from the bacterium *Thermus aquaticus* (9). Reverse transcription-PCR (RT-PCR) is an invaluable variant of PCR used for assessing RNA expression. Since RNA polymerase is inactivated by heat and DNA polymerase cannot amplify RNA, the RNA is first converted (reverse transcribed) to cDNA, which is then used as a target/template in the PCR assay.

To study the transcriptome, obtaining high-quality RNA with minimal degradation is a critical first step (10). RNA is unstable and is prone to degradation by RNases. Hence, adequate precautions should be taken to use RNase-free material. RNA degradation can be minimized with the use of commercially available RNA stabilizing reagents, such as RNAlater (11). The purity of RNA can be assessed by several methods. Measuring the ultraviolet absorbance (*A*) at

doi:10.1128/9781555818722.ch118

260 nm, 280 nm, and 230 nm by use of a spectrophotometer is a commonly used method. An A_{260}/A_{280} ratio of 1.8 to 2.2 and an A_{260}/A_{230} ratio of >1.7 suggest the presence of good-quality RNA that is suitable for downstream applications. Agarose or acrylamide gel electrophoresis is another common method for analyzing RNA integrity (12). Samples are loaded into gels, and as an electrical current is applied, nucleic acid fragments are separated on the basis of size. The fragments in the gels are then stained with nonspecific fluorescent dyes, such as ethidium bromide, SYBR Green, and SYBR Gold. RNA quality is assessed by observing the staining intensities of the major rRNA bands and any degradation products. The use of a Bioanalyzer machine (Agilent Technologies) is another technique for assessing RNA samples. It is similar to the gel system, but in a miniature form. The Bioanalyzer instrument determines the "RNA integrity number" by using a proprietary algorithm that considers the entire electrophoretic traces of the RNA to determine the integrity of RNA and then assigns a number from 1 (worst) to 10 (best) (13). Fluorescent dye-based quantification (e.g., using a Qubit fluorometer) is commonly used to quantify RNA abundance. The dyes used in the fluorometer are specific for RNA or DNA. The RNA concentration is quantified by comparing the relative fluorescence intensities of the RNA bands to those of known RNA standards.

A typical PCR mixture to assay RNA expression consists of target cDNA, free nucleotides, sense and antisense oligonucleotide primers, and thermostable DNA polymerase. A segment of the RNA of interest is amplified exponentially in three sequential steps, i.e., denaturation, annealing of the primers, and primer extension, which are repeated with each PCR cycle. The typical length of the PCR product, the amplicon, is about 90 to 150 bp.

Competitive Quantitative PCR Assay

A PCR assay is an endpoint assay, i.e., the presence or absence of the amplified product is typically determined after the final amplification cycle. In a competitive quantitative PCR assay, a competitive DNA fragment is constructed which is similar to the RNA (converted to cDNA) of interest, with the exception of either a mutation at a specific enzyme restriction site or insertion of a small intron or sequence of DNA (14). The concentration of naturally occurring gene transcript is quantified by measuring the ratio of the cDNA band to the band of the specific competitor on gel electrophoresis by using laser densitometry. This approach was successfully used to quantify urinary cell levels of mRNAs for granzyme B and perforin and to demonstrate their utility as biomarkers of acute rejection of kidney allografts (15).

Kinetic (Real-Time) Quantitative PCR Assay

A real-time quantitative PCR assay incorporates the use of a fluorescence signal that is released in "real time" linearly with the amplification process. DNA-binding fluorescent probes, such as TaqMan probes, are used to detect and measure the amplified products (16). The guiding principle for the development of the probes is the transfer of fluorescence resonance energy from the reporter dye to the quencher dye because of close physical proximity in the intact probe. When the probe is degraded, the reporter dye is no longer in close proximity to the quencher dye, which results in the emission of a fluorescence signal. For a real-time TaqMan PCR assay, the reagent mixture contains the gene-specific probe, sense and antisense primers, cDNA, and *Taq* DNA polymerase. The probe is specific for the target mRNA of interest and is designed to be located downstream from one of the primers. As the primer is extended from the 5′ to the 3′ end by *Taq* polymerase, the exonuclease activity of the enzyme degrades the probe and releases the reporter dye from the quencher. This process is repeated with each PCR cycle, and as the fluorescence signal increases, an amplification plot of the change in fluorescence against the cycle number is created in real time. An arbitrary threshold is chosen where the fluorescence signal is increasing linearly (usually 10 times the standard deviation of the baseline), and the cycle number at this point is reported as the cycle threshold (C_T). The C_T value is used to extrapolate the mRNA quantity by using a relative quantification method ($\Delta\Delta C_T$ method) or for absolute quantification of mRNA abundance by using the standard curve method (17).

Absolute Quantification of mRNA Levels by PCR Assay

The Suthanthiran laboratory optimized absolute quantification by developing a universal standard curve method for the absolute quantification of multiple mRNAs. The method involves design and synthesis of a 73-bp mouse amplicon (Bak amplicon) that is used to generate the standard curve in the PCR assay. It is worth noting that the amplification efficiency of the Bak amplicon is similar to the efficiencies of the mRNAs to be quantified, thereby enabling the use of a single rather than multiple gene-specific amplicons in the standard curve method. The amplicon is generated as a PCR product in a thermal cycler (GeneAmp 9600) by using a specific oligonucleotide primer pair (50 μM [each]; accession no. Y13231) (Bak amplicon sense primer, 5′ CCCACATCTGGAGCAGAGTCA 3′ [positions 192 to 212]; and antisense primer, 5′ CAGATGCCATTTTTCAGGTCTTG 3′ [positions 264 to 242]). The final reaction volume is 100 μl and contains 3 μl cDNA, 1.6 μl of 4× deoxynucleoside triphosphates (dNTPs) (10 mM [each]), 10 μl 10× buffer, 1.6 μl AmpliTaq Gold DNA polymerase (5 U/μl), 6.0 μl $MgCl_2$, and 2.0 μl Bak-specific oligonucleotide primer pair. The PCR product is then separated by electrophoresis on a 2% agarose gel, and the amplicon size is confirmed by using pUC mix marker 8 (Crystalgen) as a DNA size standard. The Bak amplicon is then isolated and purified from the gel by use of a QIAquick gel extraction kit (Qiagen). The absolute quantity of the purified amplicon is measured by determining the A_{260} and converted to the number of copies by using the molecular weight of DNA. A stock solution of the Bak amplicon is created by diluting it to a concentration of 10^7 copies/μl. To establish a standard curve for a PCR assay, the stock solution is diluted over 6 orders of magnitude (10^6, 10^5, 10^4, 10^3, 10^2, and 10^1 copies per μl). To run a PCR plate, 2.5 μl of working solution is used in duplicate wells and amplified with the Bak-specific primer pair and a Bak-specific fluorogenic TaqMan probe (5′ 6-carboxyfluorescein-CAGGTGACAAGTGACGGTGGTCTCCA-6-carboxytetramethylrhodamine 3′ [positions 215 to 240]). The C_T values are then plotted against the log of the initial amount of Bak amplicon (2.5×10^6 to 2.5×10^1) to develop the standard curve (18).

Preamplification-Enhanced Real-Time PCR Assay

The median quantity of total RNA obtained from urinary cells in 50 ml of urine from kidney transplant recipients is about 500 ng. This is less than that obtained from blood cells or biopsy tissue. The Suthanthiran laboratory has modified the PCR assay to minimize the amount of RNA required as starting material to quantify the expression of several mRNAs. When RNA is reverse transcribed to cDNA, the volume is adjusted to yield a final concentration

of 1 μg/100 μl. A typical PCR mixture (in duplicate) to assess the expression of a single mRNA uses 5 μl (50 ng) cDNA. Thus, with 500 ng of RNA in a 50-μl volume, only about 10 mRNAs can be quantified. To overcome this limitation of quantity, a preamplification step to the PCR assay is incorporated, and the real-time PCR assay is modified to be a two-step process (19). In the first step, a preamplification reaction mixture is set up in a thermal cycler, with 3 μl (30 ng) cDNA and 7 μl of dNTPs, PCR buffer, *Taq* DNA polymerase, and a panel of (typically 20 to 25 mRNAs) gene-specific oligonucleotide primer pairs of interest. After a 10-cycle (pre)amplification, the PCR product is diluted and used as a stock solution. In the second step, the expression of each of the preamplified mRNAs is measured using quantitative real-time PCR assays. Thus, this two-step process facilitates measurement of a large number of mRNAs (typically 20 to 25 mRNAs) from 3 μl (30 ng) of cDNA.

Microarray Assays

Microarrays are commonly used platforms for the assessment of global gene expression patterns. The steps involved include (i) development of an expression microarray, (ii) hybridization with a labeled unknown cDNA or cRNA, and (iii) quantification and analysis of the signal resulting from the hybridization of the unknown sample to the probes on the microarray. There are two basic types of microarray platforms: arrays that consist of gene-specific cDNA probes and arrays that consist of synthesized oligonucleotide probes.

cDNA Microarray Assays

In cDNA microarray assays, gene-specific probes are selected based on biological relevance. In addition, each array contains negative controls (plant or bacterial genes), positive controls (housekeeping genes), and key controls (genes with a known pattern of expression in the system being studied). The cDNAs are generally prepared in bacterial colonies, amplified using PCR, and subsequently purified using nucleic acid isolation procedures. The cDNA elements are arrayed using a robotic system onto a glass slide coated with a DNA-binding substrate, such as poly-L-lysine or silane (20). The DNA-binding substrate is inactivated following the arraying process. The unknown sample RNA and reference RNA are labeled with different fluorescent markers, such as Cy4 for the unknown sample and Cy5 for the reference sample. The fluorescent markers are linked to one of the nucleotides and incorporated into the samples individually during RT of RNA to cDNA. Unincorporated nucleotides are removed to minimize background noise, and the labeled reference and unknown samples are mixed in a hybridization solution. The mixture is placed on the array and hybridized for 14 to 16 h. The array is then washed and read in a microarray reader. For oligonucleotide arrays, the oligonucleotide probes are synthesized *in vitro* and subsequently arrayed onto the solid support as in cDNA microarrays, or they can be synthesized *in situ* as in the Affymetrix GeneChip system.

The Affymetrix GeneChip system, the most common platform used to perform microarray studies, is unique in that multiple oligonucleotides of 20 to 25 nucleotides (nt) that are complementary to different regions of the same transcript are synthesized *in situ* for each hybridization unit (20). In addition, the hybridization unit contains a mismatched oligonucleotide probe that differs by one nucleotide for each of the target-specific probes. Hence, a hybridization unit for each gene consists of a series of matched and mismatched probes synthesized in a 24- by 24-μm space. mRNA is reverse transcribed to cDNA, which is then transcribed to cRNA by use of T7 RNA polymerase and biotin-labeled CTP and UTP. The biotinylated cRNA is chemically fragmented into fragments of 35 to 200 bases prior to hybridization. The hybridization cocktail is prepared with a buffer solution, control cRNA, and the biotinylated sample cRNA and is later placed on the chip for hybridization. After hybridization, the biotinylated cRNA is fluorescently labeled with streptavidin-phycoerythrin. The array is scanned on an Affymetrix GeneChip scanner and analyzed using various software packages. The detection of the transcript is based on the degree of binding to the perfectly matched (PM) and mismatched (MM) probes in the hybridization unit. The software program calculates a discrimination score [$R = (PM \times MM)/(PM + MM)$] that is then adjusted, ranked, and assigned a *P* value based on nonparametric testing. The determination of whether a transcript is present, marginally present, or absent is based on the *P* value cutoffs set by the operator.

TaqMan Low Density Array

The TaqMan Low Density Array (TLDA) is a commonly used platform for global profiling of microRNAs (miRNAs) (21). It is a real-time PCR-based assay that measures simultaneously the expression of several hundred miRNAs. Each array is a 384-well plate preloaded with TaqMan miRNA gene expression reaction mixtures that include unique miRNA primers and probe in each well and endogenous control snRNAs. The TaqMan miRNA assay uses a stem-loop structured RT primer (22). In contrast to a linear structure, the stem-loop ensures specificity for mature miRNA target. The stem-loop primer binds to the 3′ end of the miRNA target and is reverse transcribed. First-strand cDNA synthesis with stem-loop primer lengthens the miRNA target from its original ~22 nt to >60 nt, allowing binding of forward and reverse primers as well as the hydrolysis probe, as in a standard real-time PCR assay. The novel design, allowing for increase in the length of first-strand cDNA, overcomes the limitations of primer design for miRNAs, as these small ~22-nt RNA species make primer design challenging. The starting amount of RNA can be as low as 1 ng. The workflow consists of reverse-transcribing the RNA with a pool of stem-loop primers, then an optional preamplification reaction, followed by RT-PCR assay, allowing for simultaneous PCR amplification of unique miRNAs in each of the 384 wells.

Next-Generation Sequencing

NGS is a method for determining the primary structure of the genome. The chain termination method, developed by Frederick Sanger in 1977, is considered the gold standard for determining the order of nucleotide bases in a chain of DNA (23). Recently, massively parallel or NGS technologies have emerged. By overcoming the inherent limitations of Sanger sequencing, these NGS methods allow sequencing of the complete genome, transcriptome (the full complement of expressed genes), and known exomes (parts of the genome specifying the sequences of a portion of proteins) in a relatively short time and at a substantially reduced cost (24, 25). The most commonly used platforms for NGS are those developed by Illumina, Inc. The Illumina NGS protocol consists of DNA fragmentation and the addition of 5′ and 3′ universal adapters to the fragmented DNA. The DNA molecules are then immobilized on a glass slide (flow cell). The flow cell surface is coated with single-stranded oligonucleotides that correspond to the sequences of the adapters. DNA is amplified by solid-phase bridge PCR on the flow cell surface, resulting in an array of clonal clusters. These clusters are then sequenced by successively incorporating fluorescently labeled reversible terminators picked one at a time from a mixture of

4 nt (one base per cycle). Each lane of the flow cell is imaged after each cycle for each nucleotide. The sequence is read in real time by four-channel fluorescence scanning, with each signal corresponding to a single nucleotide at a single position. Usually the forward strand of each cluster is read, and the result is called a single-end read. It is also possible and may even be preferable to read both the forward and reverse templates of each cluster, and this is called paired-end reading. Illumina's HiSeq 2500 machine is able to run two flow cells simultaneously. It can generate up to 2 billion reads (8 billion during paired-end reading) per flow cell, with a read length of up to 150 bp. Depth in deep sequencing refers to the average number of times a given nucleotide is represented in sequence reads. For a reliable base call, the base must be read multiple times. The downsides to the speed and accuracy of the machine are a lower accuracy and shorter sequence length than those with traditional Sanger sequencing. Translating the reads into meaningful information is done in three stages: (i) analyzing the images from the sequencers and converting them into sequence reads, (ii) alignment of reads either by *de novo* assembly or by mapping to a reference database, and (iii) using the mapped and unmapped reads in experiments for specific downstream applications. RNA sequencing is an alternative approach for transcriptome analyses using microarrays. The advantages of this method over microarray technology include a higher resolution, discovery of novel transcripts, and identification of allelic expression, alternate splice variants, posttranscriptional mutations, and isoforms.

MOLECULAR CHARACTERIZATION OF HUMAN ALLOGRAFTS

Quantitative PCR assays have been used successfully to characterize acute rejection of allografts and the presence or absence of allograft fibrosis as well as other complications, such as an inflammatory response to BK virus nephropathy (15, 19, 26–36). The use of competitive quantitative PCR assays to measure levels of mRNA in urinary cells and the discovery that urinary cell mRNA levels of perforin and granzyme B are sensitive and specific noninvasive biomarkers of kidney allograft rejection are summarized in the previous edition of this *Manual* (37).

Clinical Application of Real-Time Quantitative PCR To Characterize Allograft Rejection

At present, real-time RT-PCR assays are utilized to measure mRNA abundance not only in renal allografts but also in heart, lung, liver, pancreas, and small intestine allografts (38).

The Clinical Trials in Organ Transplantation 04 (CTOT-04) study was a prospective nonrandomized observational multicenter study to test the hypothesis that the urinary cell mRNA profile is (i) a sensitive and specific noninvasive diagnostic biomarker for the noninvasive diagnosis of biopsy-confirmed acute rejection of renal allografts and (ii) predictive of an acute rejection episode in the near future. The study was conducted at five different clinical centers, with a targeted enrollment of 495 patients, and urine samples were collected on days 3, 7, 15, and 30 and in months 2, 3, 4, 5, 6, 9, and 12. Of the 497 patients who consented to participate, 485 patients provided 4,300 urine specimens for urinary cell mRNA profiling, and this included 298 biopsy-associated urine specimens from 220 patients (18).

Urine cell pellets were prepared at the transplant sites and shipped to the Weill Cornell Medical College Gene Expression Monitoring Core (WCMC GEM). Absolute levels of prespecified mRNAs—mRNAs for perforin, granzyme B, proteinase inhibitor 9, CD103, CD3ε, interferon-inducible protein 10 (IP-10), CXCR3, and transforming growth factor β1—and 18S rRNA were measured using the preamplification-enhanced real-time quantitative PCR assays developed and validated by the WCMC GEM Core (15, 28, 30, 32).

This large-scale study validated that urinary cell levels of 18S rRNA-normalized perforin, granzyme B, CD3ε, and IP-10 were higher in those with acute rejection than in those without acute rejection or those with stable graft function. A 3-gene signature based on 18S rRNA-normalized measures of CD3ε and IP-10 mRNAs and 18S rRNA emerged as the best-fitting parsimonious model and identified the diagnostic signature for acute rejection as follows: $-6.1487 + 0.8534 \log(\text{CD3}\varepsilon/\text{18S rRNA}) + 0.6376 \log(\text{IP-10/18S rRNA}) + 1.6464 \log(\text{18S rRNA})$. Receiver operator characteristic (ROC) curve analysis of the 3-gene signature yielded an area under the curve (AUC) of 0.85 (95% confidence interval [CI], 0.78 to 0.91; $P < 0.0001$), with a sensitivity of 79% and a specificity of 78%, using a cutoff value of -1.213 for the diagnostic signature.

It is important that the mRNA profile diagnostic of acute rejection may differ depending on whether mRNA levels are normalized to 18S rRNA. Such normalization ensures that the differences in mRNA levels observed between rejection and no-rejection cohorts are not due to differences in RNA integrity and RT efficiency.

The CTOT-04 study also identified that the score of the diagnostic signature increases significantly during the posttransplant period in individuals who are destined to develop biopsy-confirmed acute rejection, while it remains flat below the diagnostic cutoff for acute rejection in individuals who have stable function and do not develop acute rejection. Furthermore, the trajectory of the diagnostic signature starts to separate between those with and without acute rejection approximately 120 to 90 days prior to the rejection biopsy and rise above the diagnostic threshold approximately 20 days prior to the clinical diagnosis of acute rejection (Fig. 1).

The Clinical Trials in Organ Transplantation 01 (CTOT-01) study, a separate prospective multicenter observational study designed to investigate the diagnostic accuracy of urinary biomarkers, measured levels of mRNAs and proteins in urine for the diagnosis and prognostication of acute rejection of renal allografts. In this study, 280 patients were enrolled, 250 completed 6 months of follow-up, and 204 completed the study at 24 months. Patients underwent serial urine and blood sampling weekly 4 times, monthly 5 times, and at 12 and 24 months posttransplantation, and a protocol biopsy was performed at 6 months posttransplantation (39).

The CTOT-01 study utilized the urine collection protocol and the preamplification-enhanced real-time quantitative PCR assay that was developed at WCMC. The mRNAs measured included mRNAs for CCR5, CCL5, interleukin-8, CCR1, perforin, granzyme B, IP-10, CXCR3, and CXCL9. Levels of these mRNAs in urinary cells were compared for individuals with acute rejection diagnosis ($n = 24$), suspicion of rejection diagnosis ($n = 21$), infection ($n = 5$), and other findings ($n = 45$). The authors found that urinary cell mRNA levels for granzyme B (AUC = 0.730; $P = 0.004$), perforin (AUC = 0.701; $P = 0.005$), and CXCL9 (AUC = 0.788; $P = 0.0003$), all normalized to 18S rRNA, were associated with an acute rejection diagnosis. In a multivariable model, a combination of CXCL9 mRNA and CXCL9 protein yielded the highest AUC (0.885), with a sensitivity of 82.6% and a specificity of 86.7% for diagnosing acute rejection in the kidney allograft.

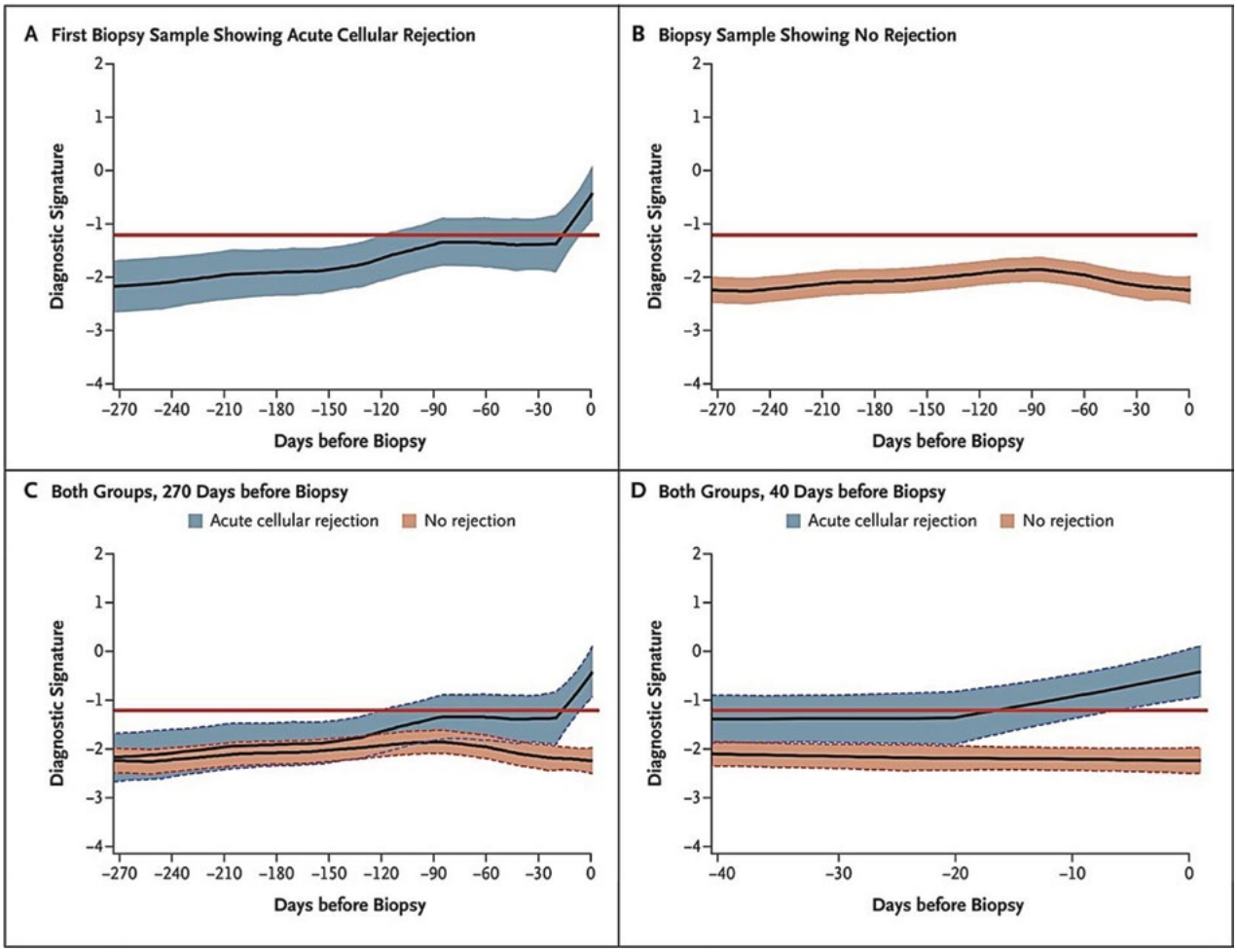

FIGURE 1 CTOT-04 study cohorts and retrospective trajectories of the diagnostic signature. The average within-person retrospective trajectories of the diagnostic signature (i.e., trajectories as a function of the time before biopsy) in urine samples obtained at or before biopsy that passed quality control are shown for the group of 38 patients with first biopsy specimens showing acute cellular rejection (201 urine samples) (A) and the group of 113 patients with specimens showing no rejection (833 urine samples) (B). Only specimens obtained during the first 400 days after transplantation were included. (C) The diagnostic signature remained relatively flat and well below the −1.213 threshold that was diagnostic of acute cellular rejection during the 270 days before biopsy in the group of patients with findings showing no rejection. (D) There was a significant difference in the trajectories between the two groups, with a marked increase in the diagnostic signature during the 20-day period before the first specimen showing acute cellular rejection ($P < 0.001$). In all the panels, the black lines indicate the trajectory, the colored bands indicate the 95% confidence interval, and the red lines indicate the diagnostic threshold. (Reprinted from reference 18 with permission of the publisher.)

Seventy-one samples from the subjects enrolled in the CTOT-01 study were used as an external and independent validation set for the CTOT-04 diagnostic signature. Among the 71 samples, 24 urine samples were from individuals with acute rejection biopsy specimens (from 17 biopsies for cause and 7 protocol biopsies), and 47 urine samples were from individuals with no acute rejection (from 19 biopsies for cause and 28 protocol biopsies). ROC curve analysis of the three-gene (CTOT-04) signature in the validation set yielded an AUC of 0.74 (95% CI, 0.61 to 0.86; $P < 0.0001$) for diagnosis of acute rejection, with a sensitivity of 71% and a specificity of 72%, using the CTOT-04 diagnostic threshold of −1.213 (18).

In addition to serving as diagnostic and prognostic biomarkers, urinary cell mRNA profiles have yielded key insights into the acute rejection process. Existing data from urinary cell mRNA profiling studies suggest the participation of the chemokine signaling pathway (32), costimulatory pathways (26), T cell effector pathways (15), and immune regulatory proteins (19, 30) during an episode of acute rejection in a kidney allograft.

Clinical Application of Microarray Studies To Characterize Allograft Rejection

Interrogation of acute rejection by use of microarrays has helped to elucidate several pathways that are important in acute rejection of solid organ allografts. These studies have also identified prognostic biomarkers of rejection and aided in the development of noninvasive assays for diagnosis of

acute rejection of allografts. Data generated from these studies are also challenging the current diagnostic approach based on histological features alone.

Stanford University has developed a microarray chip, Lymphochip cDNA, containing 28,032 DNA spots representing a large number of selected human genes, to study the rejection of kidney allografts (40). In a study by Sarwal and colleagues, global gene expression profiling of kidney allograft biopsy specimens by use of cDNA microarrays revealed molecular heterogeneity within the acute rejection cohorts. Cluster A (cohort AR-I) demonstrated increased transcripts associated with activated T and B lymphocytes, NK cells, and macrophages; cluster B (cohort AR-II) exhibited increased levels of transcripts associated with the innate immune system, annexin V, and transforming growth factor β1; and cluster C (cohort AR-III) demonstrated increased levels of transcripts associated with cell proliferation and cell cycling (40). Among the acute rejection cohorts, the AR-I cohort was less likely to respond to antirejection therapy and had the highest risk of graft loss. Based on the prominent B cell signature associated with cluster A (AR-I), the authors performed immunostaining for $CD20^+$ cells in kidney biopsy specimens from cases of acute rejection and found that the density of $CD20^+$ cells in the biopsy predicts a poor response to therapy and poor allograft function.

Diagnosis and management of antibody-mediated rejection of kidney allografts remain a challenge and have recently been the focus of many investigations. Microarray analyses of kidney allograft biopsy specimens have provided new insight into the pathways that are upregulated during antibody-mediated rejection. A study of 173 for-cause renal allograft biopsy specimens identified increased expression of endothelial cell-associated transcripts, a group of 119 different transcripts, in the biopsies of patients with acute rejection. The levels of these endothelial cell-associated transcripts were higher in those with antibody-mediated rejection than in those with T cell-mediated rejection (41). Such microarray studies have also questioned the need for positive C4d staining as an absolute requirement for histology diagnosis of antibody-mediated rejection and have facilitated the recent changes in the criteria for diagnosis of acute antibody-mediated rejection.

In an attempt to validate blood gene expression profiles diagnostic of acute rejection across different microarray platforms, Li et al. combined microarray profiles for peripheral blood obtained at the time of for-cause and protocol biopsies from three different platforms: Affymetrix HGU133 Plus 2.0, Agilent, and Lymphochip cDNA (42). From 60 blood samples associated with acute rejection biopsies (AR group) and 62 blood samples associated with normal protocol biopsies in kidney transplant recipients with stable function (stable group), the authors found 32 genes that distinguished the AR group from the stable group, and each gene was present in at least two of the three microarray platforms. These 32 genes were measured in a verification set of 34 samples by use of real-time quantitative PCR, and 15 of the 32 genes (5 previously reported and 10 new genes) distinguished the AR group from the stable group. Among these 10 genes, logistic regression analysis identified 5 genes as the minimal discriminative gene set for the acute rejection diagnosis, and this 5-gene set (DUSP1, PBEF1, PSEN1, MAPK9, and NKTR) was subsequently tested and confirmed to be diagnostic of acute rejection in a single-center training set ($n = 47$). This 5-gene set was later validated with an independent set of 198 biopsy-associated samples obtained from a prospective trial performed at 12 different clinical centers. The 5-gene model distinguished kidney transplant recipients with acute rejection versus stable function with a 91% sensitivity and 94% specificity. The same group measured the 10 genes diagnostic of acute rejection in the kidney transplant recipients in 141 blood samples obtained at the time of biopsy from heart transplant recipients. The samples were split into a discovery set of 32, a validation set for diagnosis of acute rejection ($n = 86$), and a validation set for prediction of acute rejection ($n = 23$) (43). From the 10 genes discovered in kidney transplant recipients, the authors identified a 5-gene signature that was diagnostic of cardiac rejection with 89% accuracy. Furthermore, the measurement of the cardiac 5-gene signature in blood samples obtained 6 months prior to the acute rejection diagnosis predicted the development of biopsy-confirmed acute rejection with an 80% sensitivity.

Microarray studies have also led to the development of noninvasive assay for diagnosis of acute rejection of cardiac allografts. The Cardiac Allograft Rejection Gene Expression Observational (CARGO) study was designed to test the hypothesis that the mRNA profile of peripheral blood mononuclear cells (PBMCs) could discriminate between cardiac rejection with International Society for Heart & Lung Transplantation (ISHLT) grade ≥3A from those with no rejection (ISHLT grade 0) (44). In the CARGO study, the authors designed a custom microarray consisting of 7,370 genes and analyzed mRNA expression patterns of PBMCs from 122 cardiac transplant recipients, 28 with rejection and 94 without rejection. This global gene expression analysis identified 97 genes, and an additional 155 genes were added based on related function and knowledge from the literature. This was followed by diagnostic assay development in which the ability of these genes to distinguish rejection from no rejection in this same cohort was tested using real-time quantitative assays. From this step, 62 genes were found to be informative and many genes were highly correlated. The authors created 20 metagene sets by averaging the gene expression levels of correlated genes and used them in combination with the individual 62 genes to develop a linear discriminant equation that maximized the agreement between the samples and the corresponding biopsy diagnosis. A final equation of 11 genes (5 genes from microarray data and 6 genes based on literature) correctly classified 75% of the samples. This 11-gene signature was tested in two independent sample sets ($n = 63$ and $n = 133$) and was found to accurately diagnose rejection in 84% and 76% and accurately diagnose quiescent (no rejection) in 38% and 41%, respectively.

A prospective randomized multicenter controlled trial compared the use of the 11-gene signature versus endomyocardial biopsies for assessment of cardiac graft function in a cohort of 602 heart transplant recipients. The authors found no difference in the 2-year composite endpoint (14.5% versus 15.3%), consisting of rejection with hemodynamic compromise, graft dysfunction, death, or need for retransplantation, between those monitored using the 11-gene signature and those monitored with endomyocardial biopsies (45). Furthermore, the group monitored with the use of the noninvasive 11-gene signature underwent fewer myocardial biopsies.

The ability to mine data from multiple studies with the use of sophisticated bioinformatic software programs has led to studies focused on identifying a rejection signature that is common across different organs. The Sarwal laboratory performed a meta-analysis of 8 independent data sets obtained from 236 allograft biopsy specimens of different organ types (kidney, lung, heart, and liver) and identified a common rejection module (CRM) consisting of 11 genes (46). The genes associated with CRM, namely, the CD6, CXCL10, CXCL9, brain-abundant membrane-attached signal protein 1

(BASP1), inositol polyphosphate-5-phosphatase (INPP5D), interferon-stimulated exonuclease gene 20 kDa (ISG20), lymphocyte-specific protein tyrosine kinase (LCK), natural killer cell granule protein 7 (NKG7), proteasome subunit beta type 9 (PSMB9), runt-related transcription factor 3 (RUNX3), and TAP1 genes, were also found to be diagnostic of acute rejection in three additional independent data sets consisting of 794 samples. The authors went further and demonstrated that treatment with dasatinib, a potential inhibitor of LCK, and atorvastatin, a modulator of CXCL9 and CXCL10, in an H-2-mismatched mouse heart transplant model resulted in fewer graft-infiltrating cells and reductions in the expression of some of the CRM genes compared to those in controls.

Clinical Application of TaqMan Low-Density Arrays To Characterize Allograft Rejection

miRNAs are recently discovered species of evolutionarily conserved RNA that are not translated into proteins (47). New assays geared towards studies of miRNAs are facilitating the characterization and quantification of miRNAs associated with acute rejection, and these studies may explain the basis for the heterogeneity in the mRNA expression patterns of acutely rejecting allografts.

Sui and colleagues utilized microarray analysis followed by real-time quantitative PCR assay confirmation to study three renal allograft biopsy specimens from patients with acute cellular rejection and three control biopsies from native kidney nephrectomies (48). Twenty miRNAs were differentially expressed (12 downregulated and 8 upregulated).

The Suthanthiran laboratory investigated intragraft expression patterns of miRNAs in seven human kidney grafts (three biopsy specimens showing acute rejection and four with normal results) by using TaqMan low-density arrays containing primers and probes for 365 mature human miRNAs (49). Unsupervised hierarchical clustering and principal component analysis of intragraft miRNA expression patterns correctly differentiated acute rejection from normal biopsy specimens (Fig. 2). There were 17 miRNAs that were differentially expressed ($P < 0.01$) between acute rejection and normal biopsies. Based on their expression patterns and biological relevance, 6 of the 17 differentially expressed miRNAs were evaluated for an independent cohort of 26 kidney graft recipients (9 patients with acute rejection biopsy results and 17 patients with normal biopsies) by use of real-time quantitative PCR assays. In this validation study, five of the six miRNAs were found to be significantly different between patients with acute rejection biopsy results and patients with normal biopsies. As observed in the discovery/training set, intragraft levels of miR-142-5p, miR-155, and miR-223 were higher and the levels of miR-10b, miR-30a-3p, and let-7c were lower in the biopsy specimens showing acute rejection than in those without acute rejection changes. The diagnostic accuracies of intragraft levels of these six miRNAs and four mRNAs (CD3, CD20, NKCC-2, and USAG-1) were evaluated using ROC curve analysis, and the data from ROC curve analysis are summarized in Table 1. Taken together, the data from this study show that (i) miRNAs expressed in high abundance in human PBMCs are present at high levels in acutely rejecting allografts, (ii) a strong positive association exists between intragraft levels of overexpressed miRNAs and mRNAs for T cell CD3 and B cell CD20, and (iii) there is a strong positive relationship between renal tubule-specific NKCC-2 mRNA and the miRNAs miR-30a-3p and miR-10b, expressed in high abundance in human renal tubular epithelial cells. These observations are all consistent with the interpretation that the altered expression of miRNAs during acute rejection is most likely because of the relative proportions of graft-infiltrating immune cells and resident renal parenchymal cells. *In vitro* studies showing that some, but not all, of the differentially expressed miRNAs are also regulated by stimulation raises the possibility that there may be an altered regulation of miRNAs within the cells themselves.

In a recent study of 57 kidney transplant recipients (18 with chronic antibody-mediated rejection, 30 with stable function, and 9 with acute rejection), the level of miR-142-5p in PBMCs was found to be a sensitive and specific biomarker of chronic antibody-mediated rejection (AUC = 0.76; $P = 0.006$) (50).

Future studies focused on the changes in miRNA profiles associated with the course and treatment of acute rejection episodes will improve our understanding of how miRNA profiles can be used to manage transplant recipients and may lead to the development of targeted therapies to improve the long-term function of allografts.

TABLE 1 Diagnostic accuracy of intragraft miRNA/mRNA levels during acute kidney rejection[a]

miRNA or mRNA	Cutoff level	Sensitivity (%)	Specificity (%)	AUC (95% CI)	*P* value
miRNAs					
miR-142-5p	0.11	100	95	0.99 (0.96, 1.02)	<0.0001
miR-155	0.06	100	90	0.98 (0.94, 1.01)	<0.0001
miR-223	0.44	92	90	0.96 (0.90, 1.02)	<0.0001
miR-10b	1.33	100	62	0.83 (0.69, 0.97)	0.002
miR-30a-3p	0.57	67	76	0.79 (0.63, 0.95)	0.007
let-7c	0.64	92	61	0.73 (0.55, 0.92)	0.03
mRNAs					
CD3	4.02	92	86	0.93 (0.85, 1.01)	<0.0001
CD20	1.04	100	80	0.89 (0.77, 1.01)	0.0002
NKCC-2	12.47	67	90	0.77 (0.58, 0.96)	0.01
USA-1	3.04	67	100	0.83 (0.66, 0.99)	0.002

[a]ROC curve analysis was used to determine the optimal cutoff that yields the highest combined sensitivity and specificity. The ratio of miRNA copies to RNU44 copies and the ratio of mRNA copies to 18S rRNA copies were used to perform ROC curve analyses. The levels of the housekeeping miRNA RNU44 and the housekeeping 18S rRNA were not informative individually. The data were obtained from reference 49.

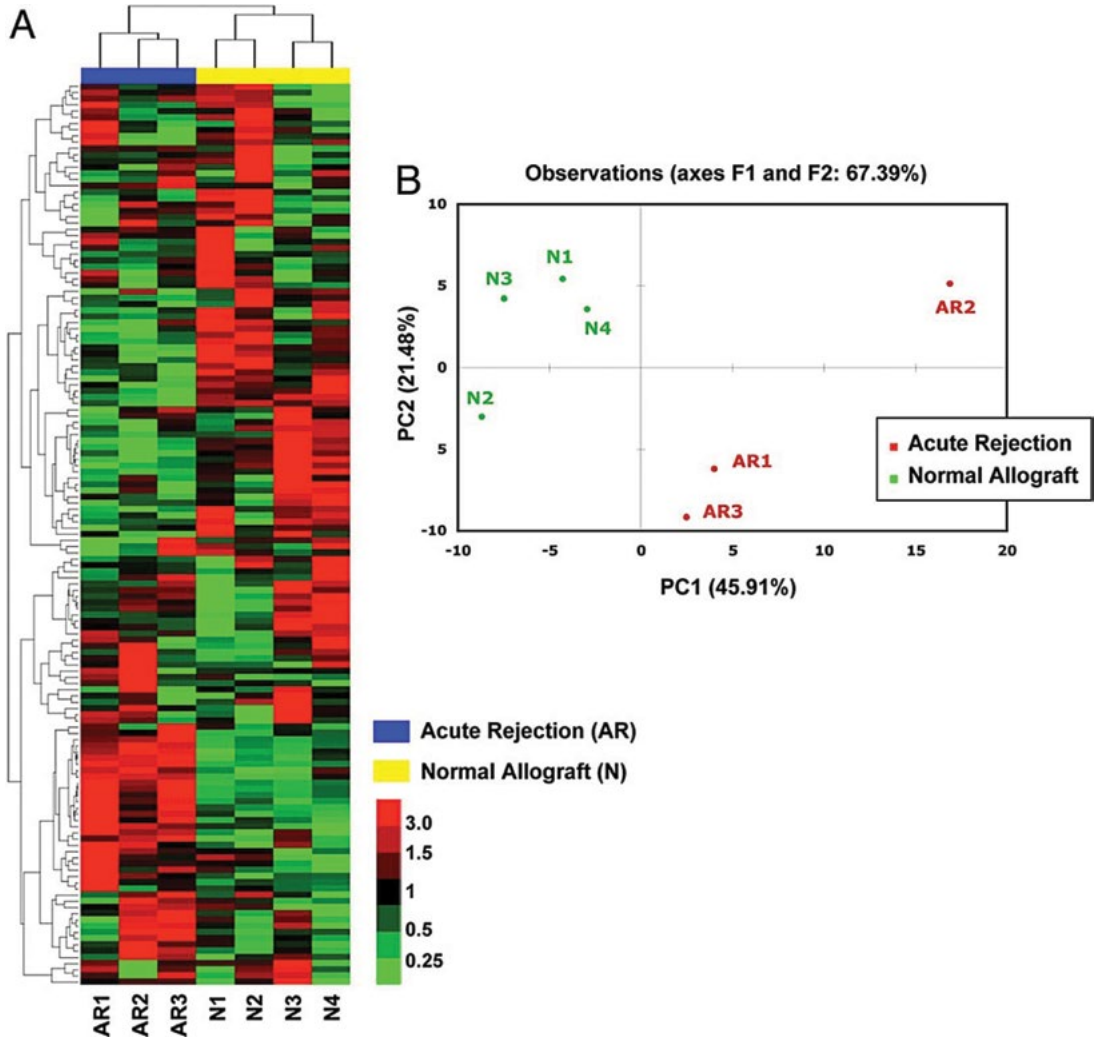

FIGURE 2 Unsupervised hierarchical clustering and principal component analysis of miRNA expression profiles differentiate acute rejection biopsy specimens from normal allograft biopsies of human renal allografts. (A) miRNA expression patterns for seven human kidney allograft biopsy specimens (three with acute rejection [AR] and four with normal allograft biopsy [N]) were examined using TaqMan low-density arrays containing TaqMan probes and primer pairs for 365 human mature miRNAs. A total of 174 ± 7 miRNAs were expressed at a significant level (i.e., C_T of ≥35) in all samples. The biopsy specimens were grouped by unsupervised hierarchical clustering on the basis of similarity in expression patterns, and the degrees of relatedness of the expression patterns of biopsy samples are represented by the dendrogram at the top of the panel. Branch lengths represent the degree of similarity between individual samples (top) or miRNA (left). Two major clusters (top) accurately divided AR biopsy specimens from normal allograft biopsies. Each column corresponds to the expression profile of a renal allograft biopsy, and each row corresponds to a miRNA. The color in each cell reflects the level of expression of the corresponding miRNA in the corresponding sample, relative to its mean level of expression in the entire set of biopsy samples. The increasing intensities of red mean that a specific miRNA has a higher expression in the given sample, and the increasing intensities of green mean that this miRNA has a lower expression. The scale (bottom right) reflects miRNA abundance ratio in a given sample relative to the mean level for all samples. (B) Principal component analysis of seven kidney allograft biopsy specimens based on the expression of 174 small RNAs significantly expressed (i.e., C_T ≥35) in all of the samples. Samples were accurately grouped by PC1, which explained 45.91% of the overall miRNA expression variability, whereas PC2 explained 21.48% of variability and did not classify the samples according to their diagnosis. (Reprinted from reference 49 with permission from the publisher.)

Clinical Application of Sequencing To Characterize Allograft Rejection

Unbiased sequencing of human transcripts can facilitate the identification of novel molecules as well as sequence variants and posttranscriptional modification (PTM) of known transcripts.

A novel bar-coded (multiplexed) sequencing protocol was used successfully for small RNA sequencing of human kidney allograft biopsy specimens, with or without fibrosis. In that study, each RNA sample from human renal allograft biopsies with fibrosis ($n = 4$) and normal ($n = 4$) was labeled using a unique (bar-coded) 3′ adapter, and the pooled RNAs were sequenced (51).

The sequence library contained 2.1 million sequence reads, with ~250,000 unique reads. Reads with miRNA annotation were grouped according to the following three schemes: (i) mature miRNAs with multiple genomic copies were merged into single entries; (ii) reads of mature miRNAs and miRNAs (passenger strands expressed at lower levels), originating from primary miRNA cistronic transcripts, were merged into precursor clusters; and (iii) miRNA reads were grouped by families according to sequence similarities. Among the most abundant miRNAs, miR-21 was more abundant in IFTA (interstitial fibrosis/tubular atrophy) biopsy specimens (2.3-fold increase; false discovery rate of <0.01), while the abundances of miR-30b (3-fold) and miR-30c(2) (2-fold) were higher in normal biopsy specimens (Fig. 3). This differential expression was validated by targeted profiling of an independent cohort of 18 biopsy specimens from 18 patients (10 patients with biopsies showing fibrosis and 8 patients with biopsies showing normal biopsy results).

Importantly, sequencing provided unique information (e.g., nucleotide variations) that could not be gleaned from other platforms. In this first study of miRNA sequencing of human kidney allograft biopsy samples, 33 distinct nucleotide variations that included a single nucleotide polymorphism in miR-196a-2 and RNA editing in the mature sequence of miR-376a/c were identified. Interestingly, variations were noticeably more common in the 3′ end of mature/starred sequences, showing changes compatible with adenylation and uridylation, and these alterations were more frequent in fibrosis samples than in normal biopsy samples.

The application of sequencing to the study of allograft rejection is still in its early stages. Applications of this technique to develop noninvasive biomarkers are limited. Whether the enhanced sensitivity and specificity associated with global sequencing of gene transcripts result in knowledge that explains the clinical heterogeneity and identifies pathways for treatment remains to be resolved fully.

MOLECULAR TECHNIQUES TO CHARACTERIZE THE PROTEOME AND THE PEPTIDOME

The proteome of a cell, an organ, or an organism is defined as the collection of all proteins expressed by the entire genome of the corresponding cell, organ, or organism (52). The publication of the human genome contributed not only to the rapid evolution of molecular profiling and quantification of gene transcripts (mRNA) but also to the identification of protein counterparts of those gene transcripts, with the aid of high-throughput protein profiling and a quantification method termed "proteomics." The central role of proteins in the execution of innumerable biological events makes their analysis on a global scale of prime importance. The traditional one-at-a-time approach utilized tests such as Western blot and immunohistochemistry (IHC), relied on the availability of corresponding antibody, and required relatively larger protein quantities. Currently available proteomic methods help to overcome such issues and provide more analytical strength and capability. Because of this development, the pace of research and our ability to understand molecular mechanisms and to search for more sensitive biomarkers have increased substantially (Fig. 4). Proteomic methods are classified into two types based on how proteins and peptides are prepared for analysis. The first proteomic analysis approach analyzes an unaltered protein or peptide and is called the "top-down" approach. Proteins in a sample are assayed in their intact form by ionization and fragmentation inside a mass spectrometer. This approach does not require proteolytic digestion to generate small peptides. The second approach, the "bottom-up" approach, generates peptides by proteolytically cleaving proteins before they are analyzed by mass spectrometric (MS) methods (53). A list of proteomic analyses and their strengths and weaknesses is given in Table 2.

Proteomic Methods for High-Throughput Protein and Peptide Discovery Biomarker Studies

Gel-Based Methods

Gel-based proteomics utilizes polyacrylamide gels to separate complex protein mixtures of a proteome. There are several gel-based proteomic methods, one of which is traditional one-dimensional SDS-PAGE, which separates proteins in terms of their molecular size. Two-dimensional gel electrophoresis (2DE) was first reported by O'Farrell in 1975 (54) and is a more sophisticated approach to separate proteins, based on their isoelectric points (pIs) as the first dimension of separation and on molecular size-based SDS-PAGE separation in the second. The use of immobilized pH gradient strips contributes to better reproducibility. Two-dimensional difference gel electrophoresis (DIGE) is an advance over conventional 2DE. In this method, two samples are labeled with two different fluorescent dyes (i.e., Cy3 and Cy5) and resolved in a single gel. The assay can be multiplexed in this way, and the ability to use an internal standard is beneficial in terms of gel-to-gel variability and increases reproducibility, with increased statistical confidence (55). In both 2DE and DIGE, the gel is stained and analyzed for significant proteins, and the potential candidates are excised from the gel, digested by

FIGURE 3 miRNA profiles generated by small RNA sequencing. (A) Hierarchical clustering and heat map representation of kidney allograft IFTA biopsy samples (M1, M3, and M4), normal biopsy specimens (M5, M6, M7, and M8), human PBMCs, HDFa cells (primary skin fibroblasts), HEK293 cells (human embryonic kidney cells), and HK2 cells (kidney proximal tubule cells) according to merged miRNA profiles (average linkage, Manhattan distance). miRNAs represented by fewer than 100 reads per sample (average) were collapsed into a single entry ("other mirs"). Brighter shades represent more expression, according to the color scheme shown on the side, in which the numbers correspond to the $\log_2$ values of the normalized read frequencies (e.g., -4 on the scale corresponds to $2^{-4} = 6.25\%$ of all miRNA reads). (B) Multidimensional scaling showing separation of IFTA from normal biopsy specimens by the third factor. (C) MA plot depicting differentially expressed miRNA sequence families, generated using DESeq. miRNA expressed more highly in IFTA samples appear above the horizontal midline. Colored data points represent P values of <0.05 (red points signify false discovery rates of <0.1). (Reprinted from reference 51 with permission of the publisher.)

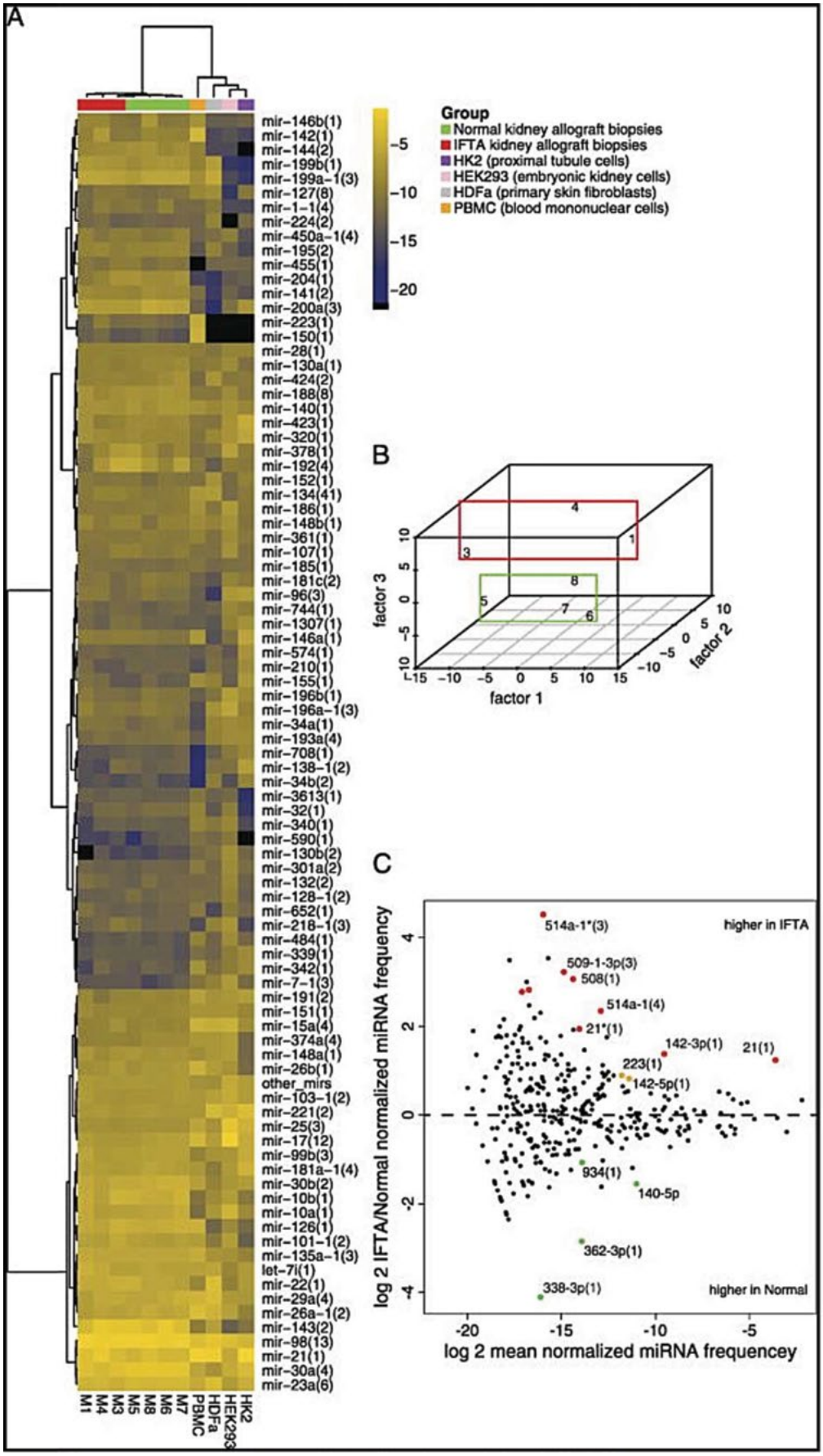
A
Group
Normal kidney allograft biopsies
IFTA kidney allograft biopsies
HK2 (proximal tubule cells)
HEK293 (embryonic kidney cells)
HDFa (primary skin fibroblasts)
PBMC (blood mononuclear cells)
−5
−10
−15
−20
mir−146b(1)
mir−142(1)
mir−144(2)
mir−199b(1)
mir−199a−1(3)
mir−127(8)
mir−1−1(4)
mir−224(2)
mir−450a−1(4)
mir−195(2)
mir−455(1)
mir−204(1)
mir−141(2)
mir−200a(3)
mir−223(1)
mir−150(1)
mir−28(1)
mir−130a(1)
mir−424(2)
mir−188(8)
mir−140(1)
mir−423(1)
mir−320(1)
mir−378(1)
mir−192(4)
mir−152(1)
mir−134(41)
mir−186(1)
mir−148b(1)
mir−361(1)
mir−107(1)
mir−185(1)
mir−181c(2)
mir−96(3)
mir−744(1)
mir−1307(1)
mir−146a(1)
mir−574(1)
mir−210(1)
mir−155(1)
mir−196b(1)
mir−196a−1(3)
mir−34a(1)
mir−193a(4)
mir−708(1)
mir−138−1(2)
mir−34b(2)
mir−3613(1)
mir−32(1)
mir−340(1)
mir−590(1)
mir−130b(2)
mir−301a(2)
mir−132(2)
mir−128−1(2)
mir−652(1)
mir−218−1(3)
mir−484(1)
mir−339(1)
mir−342(1)
mir−7−1(3)
mir−191(2)
mir−151(1)
mir−15a(4)
mir−374a(4)
mir−148a(1)
mir−26b(1)
other_mirs
mir−103−1(2)
mir−221(2)
mir−25(3)
mir−17(12)
mir−99b(3)
mir−181a−1(4)
mir−30b(2)
mir−10b(1)
mir−10a(1)
mir−126(1)
mir−101−1(2)
mir−135a−1(3)
let−7i(1)
mir−22(1)
mir−29a(4)
mir−26a−1(2)
mir−143(2)
mir−98(13)
mir−21(1)
mir−30a(4)
mir−23a(6)
M1
M4
M3
M5
M8
M6
M7
PBMC
HDFa
HEK293
HK2
B
factor 3
factor 1
factor 2
C
log 2 IFTA/Normal normalized miRNA frequency
log 2 mean normalized miRNA frequencey
higher in IFTA
higher in Normal
514a-1*(3)
509-1-3p(3)
508(1)
514a-1(4)
21*(1)
142-3p(1)
21(1)
223(1)
142-5p(1)
934(1)
140-5p
362-3p(1)
338-3p(1)

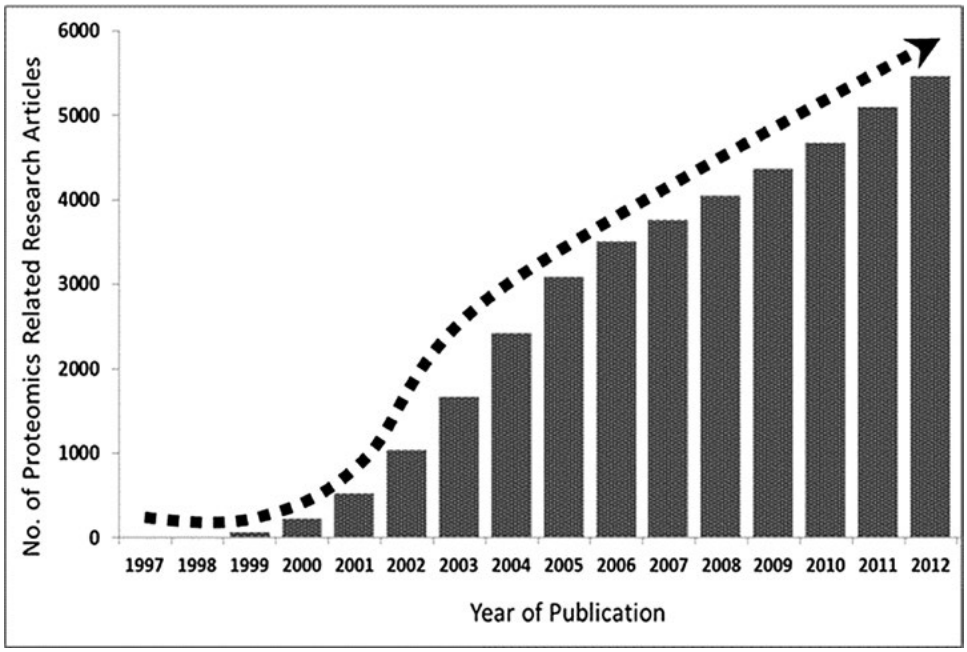

FIGURE 4 Rise in number of published articles on proteomics observed over the last 2 decades. A search of PubMed with the keyword "proteomics" generated a list of research articles and clearly demonstrated a trend of a rise in use of this method for research.

use of proteolytic enzymes (usually trypsin), and analyzed and identified by peptide mass fingerprinting and MS/MS analysis. Since this is a top-down approach and allows for the visualization of intact protein before analysis, this provides an advantage over shotgun proteomics, an approach that does not necessarily provide integrity of the full-length protein. The simple experimental design, the ability to easily assess differential expression or relative abundances of proteins in two biological samples (e.g., samples collected under disease and healthy conditions), and the ease of data analyses are all advantages of the 2DE method. For these reasons, some studies have implemented 2DE-MS in proteomic studies to find markers of rejection. A study published in *Clinical Transplantation* in 2008 used urine samples from healthy control and kidney transplant patients to compare protein preparation methods for biomarker discovery using DIGE (56). Gao et al. (57) and Bañón-Maneus et al. (58) used DIGE to identify proteins as markers of acute and chronic rejection.

Gel-Free Methods

Although gel-based methods such as 2DE and DIGE are useful for assessing proteins in biological samples, they suffer from their inability to resolve proteins with extreme molecular weights and pIs. In addition, these gel-based experiments usually require large sample quantities, have a low-throughput capacity, and are more labor-intensive. Gel-free methods do not use gels but use different methods to analyze the complex proteome in a biological sample.

Capillary Electrophoresis Followed by Mass Spectrometry (CE-MS)

Capillary electrophoresis followed by mass spectrometry (CE-MS) allows for the quick and robust separation of proteins and peptides. In this method, analytes (proteins or peptides) are separated by capillary electrophoresis coupled with mass spectrometry after ionization by either electrospray ionization or matrix-assisted laser desorption ionization. It has applications in basic research in proteomics and quantitative analysis of biomolecules as well as in clinical medicine. Because of low sample consumption and a short analysis time, the CE-MS method provides a powerful alternative for protein and peptide analysis (59). Using urine samples from 29 patients without rejection and 19 with rejection, CE-MS identified distinct urinary biomarkers and patterns in acute rejection or urinary tract infection (60).

Surface-Enhanced Laser Desorption Ionization-Time of Flight Mass Spectrometry

Surface-enhanced laser desorption ionization-time of flight MS (SELDI-TOF MS) combines the strength of different surfaces (reverse phase, anionic exchange, cationic exchange, and immobilized-metal affinity surface) and the use of different binding/washing conditions to resolve a detailed profile of proteins present in the sample. The process involves laser desorption and ionization of proteins from the array surface and detection by TOF MS. This method is limited, however, by the size of the molecules that can be analyzed (>4 kDa to <15 kDa). Because of its commercial availability (Bio-Rad) and available standardized methodology, this platform has been used extensively in biomarker discovery studies, and several studies have been carried out to identify biomarkers for transplantation (61–64).

Liquid Chromatography Coupled with Mass Spectrometry

Liquid chromatography coupled with mass spectrometry (LC-MS) has been used for both top-down and bottom-up approaches. 2D LC separation followed by MS analysis uses strong cation exchange chromatography followed by reverse-phase chromatography. As the name suggests, protein samples are separated by LC before being subjected to MS, by which each fragmented peptide is identified based on its charge and mass (Fig. 5A). Methods based on LC-MS, in general, are able to identify a large number of proteins and peptides in

TABLE 2 Comparison of proteomic methods

Technique	Strengths	Weaknesses	Reference
Gel-based 2DE	Simple experiments and lower cost Easy identification of proteins by Western blotting Ability to analyze full-length proteins	Requirement of larger sample than that for other tests Poor detection of low-abundance proteins Cannot analyze proteins with extreme molecular sizes and pIs Poor reproducibility	54
Gel-based DIGE	Needs smaller sample than 2DE More sensitive than 2DE Lower detection limit and better reproducibility Quantitative and can analyze full-length proteins Can be multiplexed	Requires larger sample than that for LC-MS methods More expensive Cannot analyze proteins with extreme molecular sizes and pIs	97
Gel-free CE-MS and SELDI-TOF MS	Small sample volume Relatively simple procedure	Provides only a signature of peptides and proteins, with difficulty in protein identification	
Gel-free LC-MS (shotgun [no fractionation])	Robust protein identification High throughput compared to other gel-free methods	Suffers from the dynamic range of protein concentration in the sample Exhaustive (once used, samples cannot be revisited)	
Gel-free LC-MS (MudPIT with fractionation)	Very sensitive and easy protein identification Powerful for identifying low-abundance proteins	Suffers from false-positive protein IDs Exhaustive (once used, samples cannot be revisited) Can be very expensive due to the need to analyze multiple fractions from one sample	66
Gel-free LC-MS (top-down approach)	Digestion into peptides is avoided, and protein identification is obtained directly from fragmentation of the intact protein Provides the information for precise identification	More challenging to execute than the bottom-up approach because of the complexity of the data generated and various technical limitations	

biological samples because of their sensitivity and low detection limit (65). In the "bottom-up" approach, protein samples are digested by proteolytic enzymes, such as trypsin, before MS analysis. This kind of strategy is also called "multidimensional protein identification technology" (MudPIT) or shotgun proteomics (66). Fourier transform ion cyclotron resonance (FTICR) MS is another option for the bottom-up approach. It determines the mass-to-charge ratio (m/z) of ions based on the cyclotron frequency of the ions in a fixed magnetic field (67). FTICR MS is particularly beneficial because this method measures peptide and protein masses with a higher accuracy, thereby reducing precursor ion tolerances from the Dalton range to the order of a few subparts per million, reducing the number of peptides initially considered by the peptide spectral matching algorithm. A number of reports on proteomics have reported acute rejection-specific proteins and different transplant injury-specific urine proteins, including those specific for rejection, BK virus nephritis, and chronic allograft injury (68–70).

Top-Down Proteomic Approach with LC-MS

The biggest strength of the bottom-up approach, that it is capable of analyzing hundreds of thousands of peptide fragments to identify parent proteins based on the proteolytic fragments identified, also becomes a weakness because it misses information about the intact protein and its PTM, which is in fact the functioning biological entity. In top-down proteomics (71), proteolytic fragmentation of proteins into peptides is avoided, and detailed information about a protein can be obtained in terms of its exact molecular size and PTMs. However, MS data generated from top-down MS experiments are very complex to interpret because they are different from the data obtained by the bottom-up approach. Because entire sequence coverage is obtained in such experiments, PTMs, N-terminal modifications, and even effects due to single nucleotide polymorphisms need to be considered. Because of its increasing use, more sophisticated software, such as ProSightPC 2.0 (Thermo Scientific), is now available to help researchers in protein identification and analysis (72). Recently, a novel, "middle-down" proteomic approach that utilizes larger proteolytic fragments was introduced. The method uses restricted enzymatic proteolysis using the outer membrane protease T (OmpT) to produce large peptides (>6.3 kDa, on average) for MS-based proteomics (73). A list of studies that have different methodologies for proteomic analyses (gel-based and gel-free) of transplantation specimens is presented in Table 2.

Analysis of PTMs in Biomarker Proteins: A Deeper Look into Disease-Specific Biomarkers

Conventional bottom-up methods usually do not focus on the PTMs of the proteins they identify. PTMs include

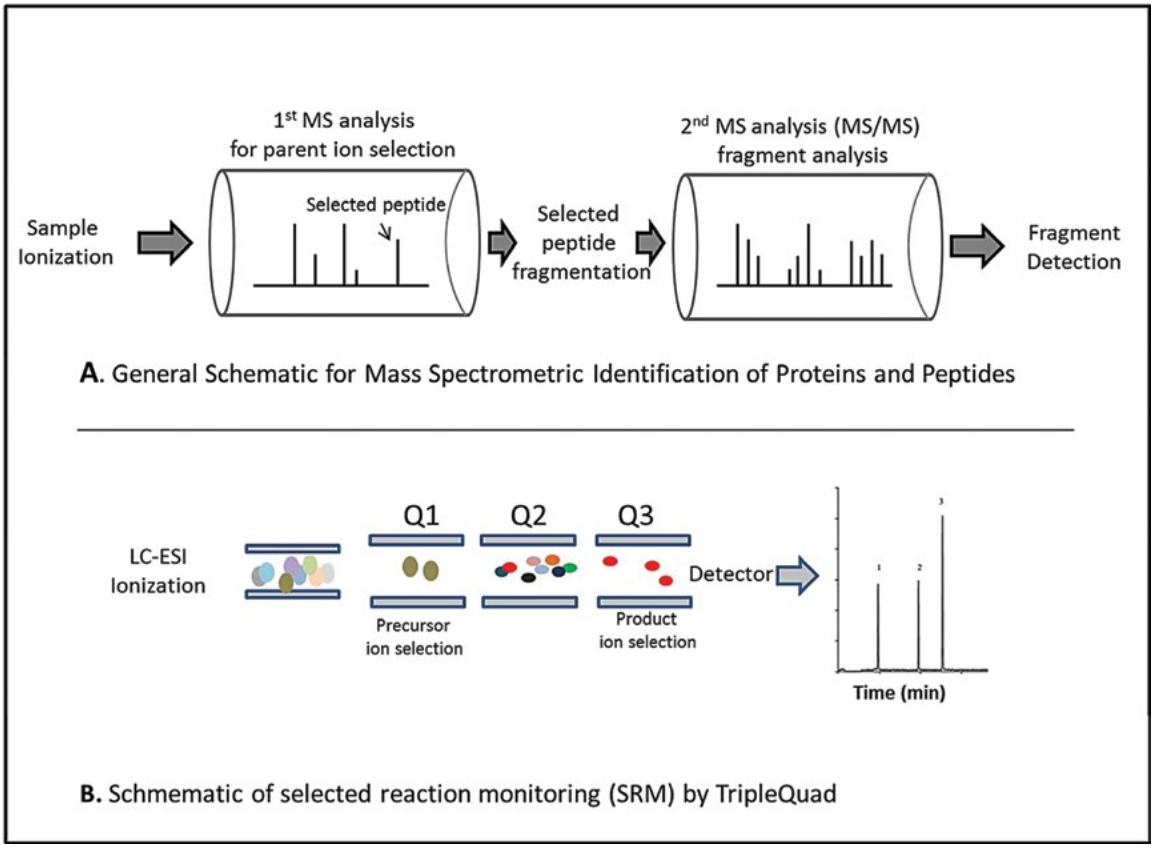

FIGURE 5 MS for proteomic discovery and validation. (A) General schematic for MS identification of proteins and peptides. (B) Schematic of SRM by TripleQuad.

generation of novel protease cleavage sites, isomerization, cross-linking, phosphorylation, nitrosylation, glycosylation, glycation, and hydroxylation, which can be introduced by pathologies and therefore represent potential disease-specific biomarkers (74) as well as novel antigens, as post-translationally modified proteins themselves may be able to activate the immune system (75). The use of recently developed selected reaction monitoring (SRM)-based methods and top-down proteomics makes analysis of PTMs in samples collected from transplant injury and dysfunction possible, which is expected to be a technological feat for biomarker discovery and validation in organ transplantation.

Peptidomics To Screen for "Peptides"

"Peptidomics" is a relatively new term that refers to analysis of the low-molecular-mass proteome, using a technique in which peptides of low molecular mass (<3,000 Da) are analyzed (76). In this method, the low-molecular-mass peptides are isolated, followed by chromatographic separation and MS analysis. Since peptidomic methods identify naturally occurring peptides, this approach also provides invaluable insights into biological processes, such as activation and deactivation of proteases or protease inhibitors. Peptidomic methodologies have been used for the analysis of human samples for the examination of neuropeptides, neurohormones, urothelial cancer, and congenital unilateral ureteropelvic junction in newborns and have been applied to a variety of biofluids, such as blood, cerebrospinal fluid, and urine (77–79). In 2005, Jürgens et al. reported a first-of-its-kind peptidome analysis of urine, using reverse-phase high-pressure liquid chromatography followed by matrix-assisted laser desorption ionization-time of flight analysis (80). More sophistication in peptidomic methods is expected in the future in terms of how to isolate, purify, and analyze the "peptide" fraction. Use of 2,5-dihydroxybenzoic acid for the extraction and purification of small peptides from tissue samples, ranging from cell clusters to brain punches to intact brain regions, was effective for extraction of endogenous peptides from tissue and for long-term preservation of tissue samples and extracts (81). At present, CE-MS (59) and LC-MS are used extensively for peptidomic analysis. A first-of-its-kind report used a novel integrative strategy that utilized peptidomics to identify a 40-peptide panel, including UMOD and collagen peptides, to be acute rejection specific in the urine of kidney transplant patients (82). A list of reports that utilized peptidomics is summarized in Table 2.

Protein Arrays

The ability to print microscopic DNA spots on a solid surface revolutionized DNA microarray technology, but it also evolved to the development of protein microarrays by use of the same biochemical principles, which has greatly facilitated the high-dimensional study of proteins and antibodies (83–85). Currently available protein arrays offer options to measure a large number of proteins or antibodies in a single assay. Protein arrays (Life Technologies) contain approximately 9,500 human antigens to screen for the antibody repertoire against these antigens in the human blood (serum or plasma), and these arrays have been used for the identification of non-HLA antibodies associated with graft

dysfunction and rejection. The current knowledge about non-HLA antibodies in organ transplantation is summarized in recently published reviews (86, 87). Other customized protein/antibody arrays are commercially available from vendors such as RayBiotech (Norcross, GA), Protein Biotechnologies Inc. (Ramona, CA), and Sigma-Aldrich (St. Louis, MO). The application of protein arrays in transplant-related research is summarized in a published review (88).

PROTEIN BIOMARKER VALIDATION PLATFORMS

It is important that a discovery made through any high-throughput method be validated quantitatively on an independent sample set. For a long time, Western blotting was the gold standard not only for protein quantitation but also for the study of PTMs and molecular size estimations. The last decade has seen the evolution of other methodologies for the analysis and quantification of proteins. Similar to how quantitative PCR serves to validate gene expression-related discoveries obtained via microarray platforms, there are two popular methods for quantitative validation for what is discovered through proteomics and peptidomics. These methods are SRM and enzyme-linked immunosorbent assay (ELISA).

Selected Reaction Monitoring

Quantitative proteomic data include the use of $^{16}O/^{18}O$ (89), ICAT (90), and SILAC (91). iTRAQ reagents (Life Technologies) use isobaric labels which, upon fragmentation by MS/MS, give rise to four unique reporter ions (m/z 114 to 117) (92). Second-generation iTRAQ reagents can quantitatively analyze eight samples simultaneously. However, unlike iTRAQ, SRM is a targeted quantitative proteomic method and uses MS to validate the levels of proteins and peptides discovered by high-throughput proteomic and peptidomic methods. This is usually performed by using triple-quadrupole mass spectrometers, a schematic of which is presented in Fig. 5B. In this method, mass-resolving Q1 isolates the precursor, Q2 acts as a collision cell, and Q3 serves for product ion selection. The product ions are detected by an electron multiplier (detector) upon exiting the last quadrupole. Peptides with heavy labels (e.g., D, ^{13}C, or ^{15}N) are used to spike samples to generate a calibration curve, which is often used for the absolute quantification of the peptides being assayed. The ability of this approach to analyze selected peptides quantitatively, with a very low detection limit, makes it the most popular validation platform for proteomic studies (93).

ELISA Validation

ELISA is a popular assay in which the utilized antibody-antigen affinity is used to identify and quantify a substance in the test sample. ELISA is a popular diagnostic tool in medicine. In this method, antigens are first attached to a surface, followed by an antibody linked to an enzyme which acts on a substrate to develop color intensity reflective of the amount of antigen bound to the surface. Because of its simplicity, ELISA has remained a preferred method for validating proteomics-based discoveries (69, 82). Because of the development of better detection systems and with advanced engineering in miniaturizing ELISA plates, new and advanced ELISA platforms are available. One such method involves electrochemiluminescence (ECL) detection, which is highly sensitive. Antibodies, proteins, or peptides can be assayed with the help of ECL. ECL detects analytes with a dynamic range of up to 5 log, which enables the quantification of native levels of biomarker proteins and peptides. Mesoscale Discovery (Rockville, MD) provides this option to researchers through their reagents and kits that can be multiplexed for detection of up to 10 analytes simultaneously (94). This high-throughput analysis of antibodies, proteins, and peptides saves costs and sample volume. The reduced cost and sample volume are very useful, especially for analyzing large sample numbers and when only a limited sample volume is available. Chen et al. utilized publicly available gene expression data sets for screening protein biomarkers for multiple-organ transplants (95). This strategy is summarized in Fig. 6. The use of proteomics and ELISA for discovery and validation of markers in different organ transplants is summarized in previously reported review articles (77, 96).

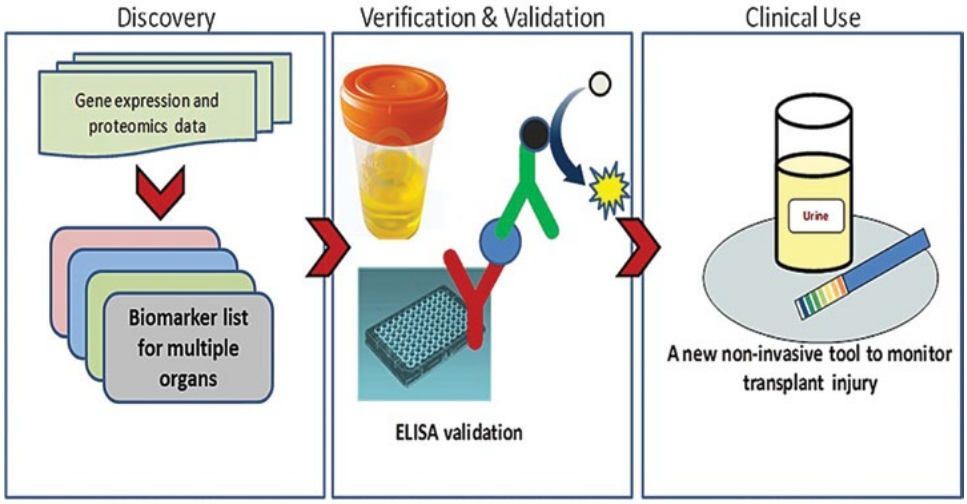

FIGURE 6 Proteomic strategy for biomarker discovery and validation. A strategy that utilizes data sets generated for different organ transplants can be useful for identifying and validating clinically useful protein biomarkers.

CONCLUDING REMARKS

We have presented a summary of molecular profiling methods pertaining to genomics and proteomics in organ transplantation. Whereas nucleic acid-based strategies have proven useful for the detection and quantification of gene expression in the clinic, recent refinements have paved the way for devising noninvasive molecular diagnostic tests for acute rejection of allografts. Protein-, peptide-, and antibody-based methods have further advanced our understanding of underlying molecular mechanisms on the protein level and have provided more potential molecular markers for transplant monitoring. Global expression profiling with technologies such as transcriptome sequencing will add to our knowledge and provide further insights into molecular pathways, and several pathways are likely to be responsible for the rejection process. Future challenges will include sorting through the vast amount of genomic and proteomic data and identifying critical pathways and targetable nodal points. We envision molecular studies to be valuable not only from a diagnostic perspective but also for the development and application of mechanism-based therapeutics. The ultimate objective, personalized medicine for the transplant recipient, is an accomplishable goal.

We are grateful to Deborah Micael and Szu-Chuan Hsieh for their meticulous help in the preparation of the manuscript. We are grateful to our colleagues Ruchuang Ding, Vijay K. Sharma, and Joseph Schwartz for their contributions to gene expression studies in the WCMC GEM laboratory.

The studies from our laboratory were supported in part by awards from the National Institutes of Health (grants R37 AI51652, R01 AI60706, U01 AI 063589, DK083447, and U01 AI63594).

In this focused survey of literature related to molecular correlates of allograft rejection, some of the key and original contributions may not have been cited, and we regret the inadvertent omission.

D.D. and T.S. are co-first authors and M.M.S. and M.S. are co-senior authors of this chapter.

REFERENCES

1. **Heeger PS.** 2003. T-cell allorecognition and transplant rejection: a summary and update. *Am J Transplant* **3:**525–533.
2. **Suthanthiran M.** 1998. Human renal allograft rejection: molecular characterization. *Nephrol Dial Transplant* **13**(Suppl 1)**:**21–24. PubMed
3. **Sayegh MH, Turka LA.** 1998. The role of T-cell costimulatory activation pathways in transplant rejection. *N Engl J Med* **338:**1813–1821. PubMed
4. **Suthanthiran M, Strom TB.** 1994. Renal transplantation. *N Engl J Med* **331:**365–376. PubMed
5. **Lakkis FG, Arakelov A, Konieczny BT, Inoue Y.** 2000. Immunologic 'ignorance' of vascularized organ transplants in the absence of secondary lymphoid tissue. *Nat Med* **6:**686–688. PubMed
6. **Luster AD.** 1998. Chemokines—chemotactic cytokines that mediate inflammation. *N Engl J Med* **338:**436–445. PubMed
7. **Akira S.** 2003. Toll-like receptor signaling. *J Biol Chem* **278:**38105–38108. PubMed
8. **Mullis KB, Faloona FA.** 1987. Specific synthesis of DNA in vitro via a polymerase-catalyzed chain reaction. *Methods Enzymol* **155:**335–350. PubMed
9. **Vosberg HP.** 1989. The polymerase chain reaction: an improved method for the analysis of nucleic acids. *Hum Genet* **83:**1–15. PubMed
10. **Fleige S, Pfaffl MW.** 2006. RNA integrity and the effect on the real-time qRT-PCR performance. *Mol Aspects Med* **27:**126–139. PubMed
11. **Medeiros M, Sharma VK, Ding R, Yamaji K, Li B, Muthukumar T, Valderde-Rosas S, Hernandez AM, Muñoz R, Suthanthiran M.** 2003. Optimization of RNA yield, purity and mRNA copy number by treatment of urine cell pellets with RNAlater. *J Immunol Methods* **279:**135–142. PubMed
12. **Tan SC, Yiap BC.** 2009. DNA, RNA, and protein extraction: the past and the present. *J Biomed Biotechnol* **2009:**574398. PubMed
13. **Schroeder A, Mueller O, Stocker S, Salowsky R, Leiber M, Gassmann M, Lightfoot S, Menzel W, Granzow M, Ragg T.** 2006. The RIN: an RNA integrity number for assigning integrity values to RNA measurements. *BMC Mol Biol* **7:**3. PubMed
14. **Li B, Sehajpal PK, Khanna A, Vlassara H, Cerami A, Stenzel KH, Suthanthiran M.** 1991. Differential regulation of transforming growth factor beta and interleukin 2 genes in human T cells: demonstration by usage of novel competitor DNA constructs in the quantitative polymerase chain reaction. *J Exp Med* **174:**1259–1262. PubMed
15. **Li B, Hartono C, Ding R, Sharma VK, Ramaswamy R, Qian B, Serur D, Mouradian J, Schwartz JE, Suthanthiran M.** 2001. Noninvasive diagnosis of renal-allograft rejection by measurement of messenger RNA for perforin and granzyme B in urine. *N Engl J Med* **344:**947–954. PubMed
16. **Wilhelm J, Pingoud A.** 2003. Real-time polymerase chain reaction. *Chembiochem* **4:**1120–1128. PubMed
17. **Bustin SA.** 2000. Absolute quantification of mRNA using real-time reverse transcription polymerase chain reaction assays. *J Mol Endocrinol* **25:**169–193. PubMed
18. **Suthanthiran M, Schwartz JE, Ding R, Abecassis M, Dadhania D, Samstein B, Knechtle SJ, Friedewald J, Becker YT, Sharma VK, Williams NM, Chang CS, Hoang C, Muthukumar T, August P, Keslar KS, Fairchild RL, Hricik DE, Heeger PS, Han L, Liu J, Riggs M, Ikle DN, Bridges ND, Shaked A, Clinical Trials in Organ Transplantation 04 (CTOT-04) Study Investigators.** 2013. Urinary-cell mRNA profile and acute cellular rejection in kidney allografts. *N Engl J Med* **369:**20–31. PubMed
19. **Muthukumar T, Dadhania D, Ding R, Snopkowski C, Naqvi R, Lee JB, Hartono C, Li B, Sharma VK, Seshan SV, Kapur S, Hancock WW, Schwartz JE, Suthanthiran M.** 2005. Messenger RNA for FOXP3 in the urine of renal-allograft recipients. *N Engl J Med* **353:**2342–2351. PubMed
20. **Casellas P, Peleraux A, Galiegue S.** 2001. Oligonucleotide chips for expression analysis: principles and practical procedures, p 87–101. *In* Jordan BR (ed), *DNA Microarrays: Gene Expression Applications*. Springer-Verlag, New York, NY.
21. **Benes V, Castoldi M.** 2010. Expression profiling of microRNA using real-time quantitative PCR, how to use it and what is available. *Methods* **50:**244–249. PubMed
22. **Chen C, Ridzon DA, Broomer AJ, Zhou Z, Lee DH, Nguyen JT, Barbisin M, Xu NL, Mahuvakar VR, Andersen MR, Lao KQ, Livak KJ, Guegler KJ.** 2005. Real-time quantification of microRNAs by stem-loop RT-PCR. *Nucleic Acids Res* **33:**e179. PubMed
23. **Sanger F, Nicklen S, Coulson AR.** 1977. DNA sequencing with chain-terminating inhibitors. *Proc Natl Acad Sci USA* **74:**5463–5467. PubMed
24. **Schuster SC.** 2008. Next-generation sequencing transforms today's biology. *Nat Methods* **5:**16–18. PubMed
25. **Mardis ER.** 2013. Next-generation sequencing platforms. *Annu Rev Anal Chem* **6:**287–303. PubMed
26. **Afaneh C, Muthukumar T, Lubetzky M, Ding R, Snopkowski C, Sharma VK, Seshan S, Dadhania D, Schwartz JE, Suthanthiran M.** 2010. Urinary cell levels of mRNA for OX40, OX40L, PD-1, PD-L1, or PD-L2 and acute rejection of human renal allografts. *Transplantation* **90:**1381–1387. PubMed
27. **Anglicheau D, Suthanthiran M.** 2008. Noninvasive prediction of organ graft rejection and outcome using gene expression patterns. *Transplantation* **86:**192–199. PubMed

28. **Ding R, Li B, Muthukumar T, Dadhania D, Medeiros M, Hartono C, Serur D, Seshan SV, Sharma VK, Kapur S, Suthanthiran M.** 2003. CD103 mRNA levels in urinary cells predict acute rejection of renal allografts. *Transplantation* **75:**1307–1312. PubMed
29. **Matignon M, Ding R, Dadhania DM, Mueller FB, Hartono C, Snopkowski C, Li C, Lee JR, Sjoberg D, Seshan SV, Sharma VK, Yang H, Nour B, Vickers AJ, Suthanthiran M, Muthukumar T.** 2014. Urinary cell mRNA profiles and differential diagnosis of acute kidney graft dysfunction. *J Am Soc Nephrol* **25:**1586–1597.
30. **Muthukumar T, Ding R, Dadhania D, Medeiros M, Li B, Sharma VK, Hartono C, Serur D, Seshan SV, Volk HD, Reinke P, Kapur S, Suthanthiran M.** 2003. Serine proteinase inhibitor-9, an endogenous blocker of granzyme B/perforin lytic pathway, is hyperexpressed during acute rejection of renal allografts. *Transplantation* **75:**1565–1570. PubMed
31. **Sharma VK, Bologa RM, Xu GP, Li B, Mouradian J, Wang J, Serur D, Rao V, Suthanthiran M.** 1996. Intragraft TGF-beta 1 mRNA: a correlate of interstitial fibrosis and chronic allograft nephropathy. *Kidney Int* **49:**1297–1303. PubMed
32. **Tatapudi RR, Muthukumar T, Dadhania D, Ding R, Li B, Sharma VK, Lozada-Pastorio E, Seetharamu N, Hartono C, Serur D, Seshan SV, Kapur S, Hancock WW, Suthanthiran M.** 2004. Noninvasive detection of renal allograft inflammation by measurements of mRNA for IP-10 and CXCR3 in urine. *Kidney Int* **65:**2390–2397. PubMed
33. **Dadhania D, Muthukumar T, Ding R, Li B, Hartono C, Serur D, Seshan SV, Sharma VK, Kapur S, Suthanthiran M.** 2003. Molecular signatures of urinary cells distinguish acute rejection of renal allografts from urinary tract infection. *Transplantation* **75:**1752–1754. PubMed
34. **Dadhania D, Snopkowski C, Ding R, Muthukumar T, Chang C, Aull M, Lee J, Sharma VK, Kapur S, Suthanthiran M.** 2008. Epidemiology of BK virus in renal allograft recipients: independent risk factors for BK virus replication. *Transplantation* **86:**521–528. PubMed
35. **Dadhania D, Snopkowski C, Ding R, Muthukumar T, Lee J, Bang H, Sharma VK, Seshan S, August P, Kapur S, Suthanthiran M.** 2010. Validation of noninvasive diagnosis of BK virus nephropathy and identification of prognostic biomarkers. *Transplantation* **90:**189–197. PubMed
36. **Dadhania D, Snopkowski C, Muthukumar T, Lee J, Ding R, Sharma VK, Christos P, Bang H, Kapur S, Seshan SV, Suthanthiran M.** 2013. Noninvasive prognostication of polyomavirus BK virus-associated nephropathy. *Transplantation* **96:**131–138. PubMed
37. **Hartono C, Dadhania D, Suthanthiran M.** 2006. Molecular characterization of rejection in solid organ transplantation, p 1244–1259. *In* Detrick B, Hamilton RG, Folds JD (ed), *Manual of Molecular and Clinical Laboratory Immunology,* 7th ed. ASM Press, Washington, DC.
38. **Hartono C, Muthukumar T, Suthanthiran M.** 2010. Noninvasive diagnosis of acute rejection of renal allografts. *Curr Opin Organ Transplant* **15:**35–41. PubMed
39. **Hricik DE, Nickerson P, Formica RN, Poggio ED, Rush D, Newell KA, Goebel J, Gibson IW, Fairchild RL, Riggs M, Spain K, Ikle D, Bridges ND, Heeger PS, CTOT-01 Consortium.** 2013. Multicenter validation of urinary CXCL9 as a risk-stratifying biomarker for kidney transplant injury. *Am J Transplant* **13:**2634–2644.
40. **Sarwal M, Chua MS, Kambham N, Hsieh SC, Satterwhite T, Masek M, Salvatierra O Jr.** 2003. Molecular heterogeneity in acute renal allograft rejection identified by DNA microarray profiling. *N Engl J Med* **349:**125–138. PubMed
41. **Sis B, Jhangri GS, Bunnag S, Allanach K, Kaplan B, Halloran PF.** 2009. Endothelial gene expression in kidney transplants with alloantibody indicates antibody-mediated damage despite lack of C4d staining. *Am J Transplant* **9:**2312–2323. PubMed
42. **Li L, Khatri P, Sigdel TK, Tran T, Ying L, Vitalone MJ, Chen A, Hsieh S, Dai H, Zhang M, Naesens M, Zarkhin V, Sansanwal P, Chen R, Mindrinos M, Xiao W, Benfield M, Ettenger RB, Dharnidharka V, Mathias R, Portale A, McDonald R, Harmon W, Kershaw D, Vehaskari VM, Kamil E, Baluarte HJ, Warady B, Davis R, Butte AJ, Salvatierra O, Sarwal MM.** 2012. A peripheral blood diagnostic test for acute rejection in renal transplantation. *Am J Transplant* **12:**2710–2718.
43. **Li L, Khush K, Hsieh SC, Ying L, Luikart H, Sigdel T, Roedder S, Yang A, Valantine H, Sarwal MM.** 2013. Identification of common blood gene signatures for the diagnosis of renal and cardiac acute allograft rejection. *PLoS One* **8:**e82153. PubMed
44. **Deng MC, Eisen HJ, Mehra MR, Billingham M, Marboe CC, Berry G, Kobashigawa J, Johnson FL, Starling RC, Murali S, Pauly DF, Baron H, Wohlgemuth JG, Woodward RN, Klingler TM, Walther D, Lal PG, Rosenberg S, Hunt S, CARGO Investigators.** 2006. Noninvasive discrimination of rejection in cardiac allograft recipients using gene expression profiling. *Am J Transplant* **6:**150–160. PubMed
45. **Pham MX, Teuteberg JJ, Kfoury AG, Starling RC, Deng MC, Cappola TP, Kao A, Anderson AS, Cotts WG, Ewald GA, Baran DA, Bogaev RC, Elashoff B, Baron H, Yee J, Valantine HA, IMAGE Study Group.** 2010. Gene-expression profiling for rejection surveillance after cardiac transplantation. *N Engl J Med* **362:**1890–1900. PubMed
46. **Khatri P, Roedder S, Kimura N, De Vusser K, Morgan AA, Gong Y, Fischbein MP, Robbins RC, Naesens M, Butte AJ, Sarwal MM.** 2013. A common rejection module (CRM) for acute rejection across multiple organs identifies novel therapeutics for organ transplantation. *J Exp Med* **210:**2205–2221. PubMed
47. **Lee RC, Feinbaum RL, Ambros V.** 1993. The C. elegans heterochronic gene lin-4 encodes small RNAs with antisense complementarity to lin-14. *Cell* **75:**843–854. PubMed
48. **Sui W, Dai Y, Huang Y, Lan H, Yan Q, Huang H.** 2008. Microarray analysis of microRNA expression in acute rejection after renal transplantation. *Transpl Immunol* **19:**81–85. PubMed
49. **Anglicheau D, Sharma VK, Ding R, Hummel A, Snopkowski C, Dadhania D, Seshan SV, Suthanthiran M.** 2009. MicroRNA expression profiles predictive of human renal allograft status. *Proc Natl Acad Sci U S A* **106:**5330–5335. PubMed
50. **Danger R, Paul C, Giral M, Lavault A, Foucher Y, Degauque N, Pallier A, Durand M, Castagnet S, Duong Van Huyen JP, Delahousse M, Renaudin K, Soulillou JP, Brouard S.** 2013. Expression of miR-142-5p in peripheral blood mononuclear cells from renal transplant patients with chronic antibody-mediated rejection. *PLoS One* **8:**e60702. PubMed
51. **Ben-Dov IZ, Muthukumar T, Morozov P, Mueller FB, Tuschl T, Suthanthiran M.** 2012. MicroRNA sequence profiles of human kidney allografts with or without tubulointerstitial fibrosis. *Transplantation* **94:**1086–1094. PubMed
52. **Ali-Khan N, Zuo X, Speicher DW.** 2003. Overview of proteome analysis. *Curr Protoc Protein Sci* **Chapter 22:**Unit 22.1.
53. **Bogdanov B, Smith RD.** 2005. Proteomics by FTICR mass spectrometry: top down and bottom up. *Mass Spectrom Rev* **24:**168–200. PubMed
54. **O'Farrell PH.** 1975. High resolution two-dimensional electrophoresis of proteins. *J Biol Chem* **250:**4007–4021. PubMed

55. **Rozanas CR, Loyland SM.** 2008. Capabilities using 2-D DIGE in proteomics research: the new gold standard for 2-D gel electrophoresis. *Methods Mol Biol* **441:**1–18. PubMed
56. **Sigdel TK, Lau K, Schilling J, Sarwal M.** 2008. Optimizing protein recovery for urinary proteomics, a tool to monitor renal transplantation. *Clin Transplant* **22:**617–623. PubMed
57. **Gao Y, Wu K, Xu Y, Zhou H, He W, Zhang W, Cai L, Lin X, Fang Z, Luo Z, Guo H, Chen Z.** 2009. Characterization of acute renal allograft rejection by human serum proteomic analysis. *J Huazhong Univ Sci Technol Med Sci* **29:**585–591. PubMed
58. **Bañón-Maneus E, Diekmann F, Carrascal M, Quintana LF, Moya-Rull D, Bescós M, Ramírez-Bajo MJ, Rovira J, Gutierrez-Dalmau A, Solé-González A, Abián J, Campistol JM.** 2010. Two-dimensional difference gel electrophoresis urinary proteomic profile in the search of nonimmune chronic allograft dysfunction biomarkers. *Transplantation* **89:**548–558. PubMed
59. **Herrero M, Ibañez E, Cifuentes A.** 2008. Capillary electrophoresis-electrospray-mass spectrometry in peptide analysis and peptidomics. *Electrophoresis* **29:**2148–2160. PubMed
60. **Wittke S, Haubitz M, Walden M, Rohde F, Schwarz A, Mengel M, Mischak H, Haller H, Gwinner W.** 2005. Detection of acute tubulointerstitial rejection by proteomic analysis of urinary samples in renal transplant recipients. *Am J Transplant* **5:**2479–2488. PubMed
61. **Wang LY, Chakraborty A, Comaniciu D.** 2005. Molecular diagnosis and biomarker identification on SELDI proteomics data by ADTBoost method. *Conf Proc IEEE Eng Med Biol Soc* **5:**4771–4774. PubMed
62. **Issaq HJ, Veenstra TD, Conrads TP, Felschow D.** 2002. The SELDI-TOF MS approach to proteomics: protein profiling and biomarker identification. *Biochem Biophys Res Commun* **292:**587–592. PubMed
63. **El Essawy B, Otu HH, Choy B, Zheng XX, Libermann TA, Strom TB.** 2006. Proteomic analysis of the allograft response. *Transplantation* **82:**267–274. PubMed
64. **Schaub S, Wilkins J, Weiler T, Sangster K, Rush D, Nickerson P.** 2004. Urine protein profiling with surface-enhanced laser-desorption/ionization time-of-flight mass spectrometry. *Kidney Int* **65:**323–332. PubMed
65. **Qian WJ, Jacobs JM, Liu T, Camp DG II, Smith RD.** 2006. Advances and challenges in liquid chromatography-mass spectrometry-based proteomics profiling for clinical applications. *Mol Cell Proteomics* **5:**1727–1744. PubMed
66. **Wolters DA, Washburn MP, Yates JR, III.** 2001. An automated multidimensional protein identification technology for shotgun proteomics. *Anal Chem* **73:**5683–5690. PubMed
67. **Marshall AG, Hendrickson CL, Jackson GS.** 1998. Fourier transform ion cyclotron resonance mass spectrometry: a primer. *Mass Spectrom Rev* **17:**1–35. PubMed
68. **Sigdel TK, Salomonis N, Nicora CD, Ryu S, He J, Dinh V, Orton DJ, Moore RJ, Hsieh SC, Dai H, Thien-Vu M, Xiao W, Smith RD, Qian WJ, Camp DG II, Sarwal MM.** 2014. The identification of novel potential injury mechanisms and candidate biomarkers in renal allograft rejection by quantitative proteomics. *Mol Cell Proteomics* **13:**621–631. PubMed
69. **Sigdel TK, Kaushal A, Gritsenko M, Norbeck AD, Qian WJ, Xiao W, Camp DG II, Smith RD, Sarwal MM.** 2010. Shotgun proteomics identifies proteins specific for acute renal transplant rejection. *Proteomics Clin Appl* **4:**32–47. PubMed
70. **Konietzny R, Fischer R, Ternette N, Wright CA, Turney BW, Chakera A, Hughes D, Kessler BM, Pugh CW.** 2012. Detection of BK virus in urine from renal transplant subjects by mass spectrometry. *Clin Proteomics* **9:**4. PubMed
71. **Gauci VJ, Padula MP, Coorssen JR.** 2013. Coomassie blue staining for high sensitivity gel-based proteomics. *J Proteomics* **90:**96–106. PubMed
72. **Garcia BA.** 2010. What does the future hold for top down mass spectrometry? *J Am Soc Mass Spectrom* **21:**193–202. PubMed
73. **Wu C, Tran JC, Zamdborg L, Durbin KR, Li M, Ahlf DR, Early BP, Thomas PM, Sweedler JV, Kelleher NL.** 2012. A protease for 'middle-down' proteomics. *Nat Methods* **9:**822–824. PubMed
74. **Karsdal MA, Henriksen K, Leeming DJ, Woodworth T, Vassiliadis E, Bay-Jensen AC.** 2010. Novel combinations of post-translational modification (PTM) neo-epitopes provide tissue-specific biochemical markers—are they the cause or the consequence of the disease? *Clin Biochem* **43:**793–804. PubMed
75. **Papini AM.** 2009. The use of post-translationally modified peptides for detection of biomarkers of immune-mediated diseases. *J Pept Sci* **15:**621–628. PubMed
76. **Tammen H, Peck A, Budde P, Zucht HD.** 2007. Peptidomics analysis of human blood specimens for biomarker discovery. *Expert Rev Mol Diagn* **7:**605–613. PubMed
77. **Sigdel TK, Gao X, Sarwal MM.** 2012. Protein and peptide biomarkers in organ transplantation. *Biomarkers Med* **6:**259–271. PubMed
78. **Bauca JM, Martinez-Morillo E, Diamandis EP.** 2014. Peptidomics of urine and other biofluids for cancer diagnostics. *Clin Chem* **60:**1052–1061. PubMed
79. **Ling XB, Sigdel TK, Lau K, Ying L, Lau I, Schilling J, Sarwal M.** 2010. Integrative urinary peptidomics in renal transplantation identifies biomarkers for acute rejection. *J Am Soc Nephrol* **21:**646–653.
80. **Jürgens M, Appel A, Heine G, Neitz S, Menzel C, Tammen H, Zucht HD.** 2005. Towards characterization of the human urinary peptidome. *Comb Chem High Throughput Screen* **8:**757–765. PubMed
81. **Romanova EV, Rubakhin SS, Sweedler JV.** 2008. One-step sampling, extraction, and storage protocol for peptidomics using dihydroxybenzoic acid. *Anal Chem* **80:**3379–3386. PubMed
82. **Ling XB, Sigdel TK, Lau K, Ying L, Lau I, Schilling J, Sarwal MM.** 2010. Integrative urinary peptidomics in renal transplantation identifies biomarkers for acute rejection. *J Am Soc Nephrol* **21:**646–653. PubMed
83. **Cheung VG, Morley M, Aguilar F, Massimi A, Kucherlapati R, Childs G.** 1999. Making and reading microarrays. *Nat Genet* **21**(Suppl)**:**15–19. PubMed
84. **Bertone P, Snyder M.** 2005. Advances in functional protein microarray technology. *FEBS J* **272:**5400–5411. PubMed
85. **Li L, Wadia P, Chen R, Kambham N, Naesens M, Sigdel TK, Miklos DB, Sarwal MM, Butte AJ.** 2009. Identifying compartment-specific non-HLA targets after renal transplantation by integrating transcriptome and "antibodyome" measures. *Proc Natl Acad Sci U S A* **106:**4148–4153. PubMed
86. **Sigdel TK, Li L, Tran TQ, Khatri P, Naesens M, Sansanwal P, Dai H, Hsieh SC, Sarwal MM.** 2012. Non-HLA antibodies to immunogenic epitopes predict the evolution of chronic renal allograft injury. *J Am Soc Nephrol* **23:**750–763. PubMed
87. **Dragun D, Catar R, Philippe A.** 2013. Non-HLA antibodies in solid organ transplantation: recent concepts and clinical relevance. *Curr Opin Organ Transplant* **18:**430–435. PubMed
88. **Sigdel TK, Sarwal MM.** 2013. Moving beyond HLA: a review of nHLA antibodies in organ transplantation. *Hum Immunol* **74:**1486–1490. PubMed
89. **Yao X, Freas A, Ramirez J, Demirev PA, Fenselau C.** 2001. Proteolytic 18O labeling for comparative proteomics: model studies with two serotypes of adenovirus. *Anal Chem* **73:**2836–2842. PubMed

90. **Gygi SP, Rist B, Gerber SA, Turecek F, Gelb MH, Aebersold R.** 1999. Quantitative analysis of complex protein mixtures using isotope-coded affinity tags. *Nat Biotechnol* **17:**994–999. PubMed
91. **Oda Y, Huang K, Cross FR, Cowburn D, Chait BT.** 1999. Accurate quantitation of protein expression and site-specific phosphorylation. *Proc Natl Acad Sci U S A* **96:**6591–6596. PubMed
92. **Ross PL, Huang YN, Marchese JN, Williamson B, Parker K, Hattan S, Khainovski N, Pillai S, Dey S, Daniels S, Purkayastha S, Juhasz P, Martin S, Bartlet-Jones M, He F, Jacobson A, Pappin DJ.** 2004. Multiplexed protein quantitation in Saccharomyces cerevisiae using amine-reactive isobaric tagging reagents. *Mol Cell Proteomics* **3:**1154–1169. PubMed
93. **Picotti P, Aebersold R.** 2012. Selected reaction monitoring-based proteomics: workflows, potential, pitfalls and future directions. *Nat Methods* **9:**555–566. PubMed
94. **Sloan JH, Siegel RW, Ivanova-Cox YT, Watson DE, Deeg MA, Konrad RJ.** 2012. A novel high-sensitivity electrochemiluminescence (ECL) sandwich immunoassay for the specific quantitative measurement of plasma glucagon. *Clin Biochem* **45:**1640–1644. PubMed
95. **Chen R, Sigdel TK, Li L, Kambham N, Dudley JT, Hsieh SC, Klassen RB, Chen A, Caohuu T, Morgan AA, Valantine HA, Khush KK, Sarwal MM, Butte AJ.** 2010. Differentially expressed RNA from public microarray data identifies serum protein biomarkers for cross-organ transplant rejection and other conditions. *PLoS Comput Biol* **6:**e1000940. PubMed
96. **Sigdel TK, Lee S, Sarwal MM.** 2011. Profiling the proteome in renal transplantation. *Proteomics Clin Appl* **5:**269–280. PubMed
97. **Unlü M, Morgan ME, Minden JS.** 1997. Difference gel electrophoresis: a single gel method for detecting changes in protein extracts. *Electrophoresis* **18:**2071–2077. PubMed

Killer Cell Immunoglobulin-Like Receptors in Clinical Transplantation

RAJA RAJALINGAM, SARAH COOLEY, AND JEROEN VAN BERGEN

119

Both in hematopoietic stem cell transplantation (HSCT) and in solid-organ transplantation (SOT), T and B cell-mediated immunity toward nonshared HLA alleles can have a detrimental outcome. In the past decade, many studies have investigated whether natural killer (NK) cell-mediated immunity might also play a role in clinical transplantation. This work has focused on killer cell immunoglobulin-like receptors (KIRs), as these NK cell receptors interact with HLA class I molecules in an allele-specific manner. In this chapter, we describe the genetics and functions of KIRs and discuss their role in HSCT and SOT.

OVERVIEW OF NK CELLS AND KIRs

NK Cells Contribute to Innate Immunity

NK cells are a subset of lymphocytes representing 10 to 20% of peripheral blood mononuclear cells that contribute to the host defense against virally infected and malignantly transformed cells. NK cells have a highly specific and complex target cell recognition receptor system arbitrated by the integration of signals triggered by a multitude of inhibitory and activating receptors, which trigger cytotoxicity and the secretion of chemokines and cytokines (1). The principal function of NK cells is to respond quickly to infection and tumor transformation, soon after it begins. By such action, NK cells can either terminate infection/transformation without the need for the adaptive immune response or keep it in check until the effector responses of adaptive immunity are brought into play. Because NK cells circulate in a state that can rapidly deliver effector functions, it is critical that they do not attack healthy cells of the body. To prevent such detrimental autoreactivity, NK cells carry inhibitory receptors that engage HLA class I determinants of healthy cells. An essential part of NK cell development is that each functionally competent NK cell expresses at least one inhibitory receptor for a self-HLA class I determinant. As a consequence of this self-tolerance mechanism, NK cells can attack cells in which HLA class I expression is downregulated or otherwise perturbed, common properties of cells that are virally infected or malignantly transformed, a concept originally termed the "missing-self" hypothesis (2) (Fig. 1). Other pathological perturbations of human cell surfaces might also trigger NK cell attack through the activating receptors that recognize either the "induced self" (such as major histocompatibility complex class I chain-related genes MICA and MICB), "altered self" (HLA class I molecule loaded with a foreign peptide), or "nonself" (either pathogen-encoded HLA class I-like molecules or the allogeneic HLA class I molecule). In humans, receptors for the induced self (NKG2D) and allogeneic nonself (KIR2DS1) have been identified, but receptors for the altered self or pathogen-encoded nonself have not.

NK Cell Receptors

Unlike T and B lymphocytes, NK cells do not express receptors that require somatic gene rearrangements to generate receptor diversity and specificity. Instead, NK cells express a wide array of conventional germ line-encoded receptor families with inhibitory or activating functions, including (i) KIRs, (ii) killer cell lectin-like receptors, such as CD94/NKG2, (iii) leukocyte immunoglobulin-like receptors, and (iv) natural cytotoxicity receptors, such as NKp46, NKp44, NKp30, and 2B4. Most of these receptors are expressed in stochastic, variegated combinations of activating and inhibitory receptors, resulting in many subsets of functionally distinct NK cells (3). In addition to receptor-mediated regulation, NK cell functions are enhanced by type I IFNs, interleukin 2 (IL-2), IL-18, and IL-15, which are secreted by dendritic cells and macrophages, as well as pathogen-infected tissue. The integration of signals via inhibitory NK cell receptors, activating NK cell receptors, and cytokine receptors determines the response of an NK cell to a given target. For example, the activating receptor NKG2D is important in the response to acute myeloid leukemia (AML) stem cells, and the expression of class I HLA has been correlated with the relative resistance of some tumors, such as primary pre-B cell acute lymphocytic leukemia (ALL) blasts, to lysis by NK cells.

Killer Cell Immunoglobulin-Like Receptors

KIRs were identified just 2 decades ago and are absent in rodents, so KIR genes likely originated recently, after the split of humans and mice. Fourteen KIRs triggering either inhibition (KIR3DL1 to -3, -2DL1 to -3, -2DL5) or activation (KIR3DS1, -2DS1 to -5), or both (KIR2DL4) have been identified (Fig. 2). HLA-C is the prominent ligand for inhibitory KIRs. Half of the HLA-C allotypes (Cw*02, Cw*04, Cw*05, Cw*06, and Cw*15, collectively called C2) have a lysine residue at position 80 that is recognized

doi:10.1128/9781555818722.ch119

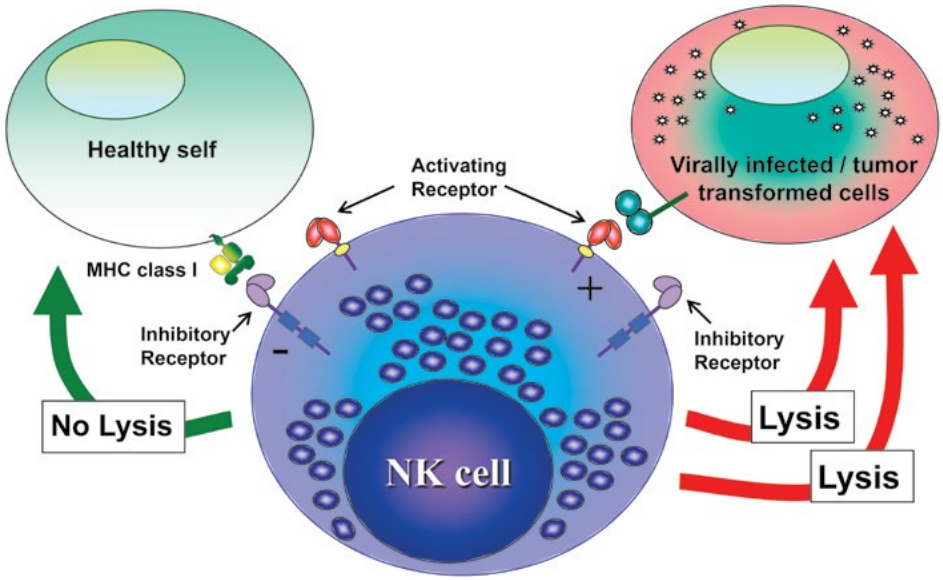

FIGURE 1 NK cell recognition. NK cells are fast-acting effector lymphocytes that provide the first line of defense against an array of viral pathogens by their ability to spontaneously kill infected cells, as well as to rapidly secrete proinflammatory cytokines. Because NK cells circulate in a state that can rapidly deliver effector functions, NK cells express multiple inhibitory receptors that engage specific HLA class I molecules of healthy cells to prevent harmful autoreactivity. By expressing HLA-A, -B, and -C molecules, the healthy cells become resistant to NK cell surveillance. An essential part of NK cell development is that each functionally competent NK cell expresses at least one inhibitory receptor for a self-HLA class I determinant. As a consequence of this self-tolerance mechanism, NK cells can attack cells in which HLA class I expression is downregulated, a common property of cells that are virally infected or malignantly transformed, a phenomenon first described as the missing-self hypothesis. Other pathological perturbations of human cell surfaces might also trigger NK cell attack through the activating receptors that recognize either induced-self (such as MICA and MICB), altered-self (HLA class I molecule loaded with a foreign peptide), or nonself (either pathogen-encoded HLA class I-like molecules or allogeneic HLA class I).

by KIR2DL1. The remaining half of the HLA-C allotypes (Cw*01, Cw*03, Cw*07, and Cw*08, collectively called C1) have an asparagine at position 80 that is bound by KIR2DL2 and -2DL3. In addition to binding C1, KIR2DL2/3 can interact with several C2 allotypes with lower affinity, notably C*05:01 and C*02:02. KIR3DL1 binds to the Bw4 serological epitope, defined by amino acid residues 77 to 83 in the α1 domain, present on 40% of the HLA-B allotypes and certain HLA-A allotypes (HLA-A23, -A24, -A25, and -A32). KIR3DL2 has been shown to recognize certain HLA-A allotypes (HLA-A3 and -A11) loaded with Epstein-Barr virus-derived peptides, as well as HLA-B27 homodimers. The KIR2DL4 receptor probably binds to the trophoblast-specific nonclassical class I molecule HLA-G. The specificities of KIR2DL5 and KIR3DL3 are unknown.

Although the specificities of most inhibitory KIRs have been characterized extensively, very little is known about the ligands for the activating KIRs. Certain activating KIRs are predicted to bind to the same HLA class I ligands as their structurally related inhibitory KIRs. Indeed, the activating receptor KIR2DS1, like KIR2DL1, binds HLA-C2 epitopes. Furthermore, activating receptor KIR3DS1, which differs by less than 10 amino acids from the inhibitory receptor KIR3DL1 in its extracellular Ig domain, may bind to HLA-Bw4. However, KIR2DS2, unlike KIR2DL2, does not seem to bind HLA-C1 epitopes, and KIR2DS3, KIR2DS4, and KIR2DS5 do not have obvious inhibitory receptor counterparts.

KIRs Are Considerably Varied between Individuals

The KIRs are encoded by a family of polymorphic but homologous genes located in the leukocyte receptor complex (LRC), which maps to chromosome 19q13.4 (4). The numbers and types of KIR genes differ substantially between haplotypes (Fig. 3). Nearly 30 distinct KIR haplotypes with distinct gene content have been characterized to date. They are broadly classified into two groups: groups A and B. Group A haplotypes have a fixed gene content comprising KIR3DL3-2DL3-2DP1-2DL1-3DP1-2DL4-3DL1-2DS4-3DL2 but are diversified through allelic polymorphism of the individual genes. In contrast, group B haplotypes have varied gene contents comprising several genes and alleles that are not part of the A haplotype. Particularly, KIR2DS1, -2DS2, -2DS3, -2DS5, -2DL2, -2DL5, and -3DS1 are associated only with group B haplotypes, and thus B haplotypes generally encode more activating KIRs than A haplotypes. The gene contents vary dramatically between group B haplotypes. Only four KIR genes (KIR2DL4, -3DL2, -3DL3, and -3DP1) are present invariably on all KIR haplotypes, and thus they are referred to as framework genes (4). Inheritance of paternal and maternal haplotypes comprising different KIR gene contents generates diversity between humans. For example, homozygotes for group A haplotypes have only 6 or 7 functional KIR genes, while heterozygotes for group A and group B haplotypes may have all 14 functional KIR genes. Group A homozygotes (AA carriers), who

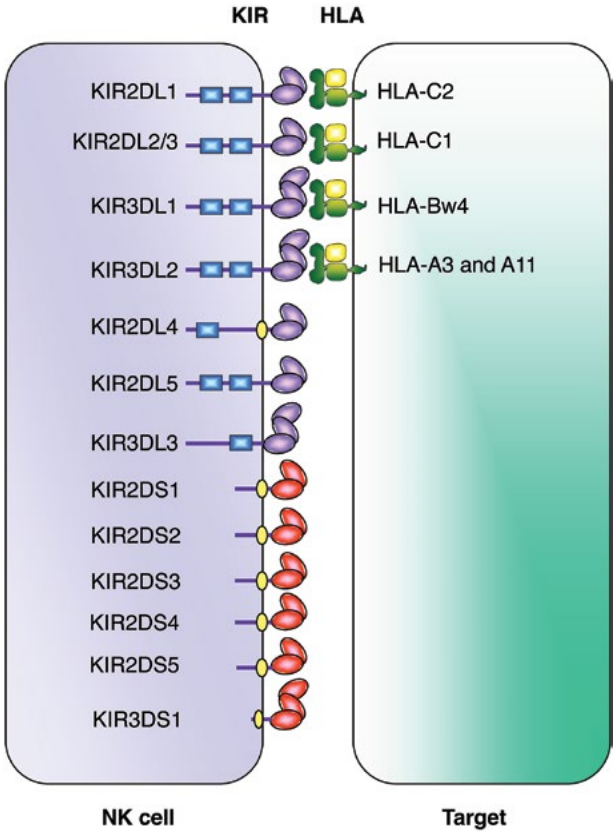

FIGURE 2 Killer cell immunoglobulin-like receptors (KIRs). Fourteen distinct KIRs have been characterized in humans that comprise either two or three (2D or 3D) extracellular Ig-like domains and either a long (L) or short (S) cytoplasmic tail. Six KIRs are activating types, and the remaining KIRs are inhibitory types. The immunoreceptor tyrosine-based inhibition motifs in the cytoplasmic tails of inhibitory KIRs are shown as blue boxes, and positively charged residues in the transmembrane regions of activating KIRs are shown as yellow circles. The inhibitory KIRs bind to distinct HLA class I allotypes, and the ligands for the activating KIRs are not known.

are common in most populations (38% of Asians, 27% of Hispanics, 31% of Caucasians, and 31% of Africans), have a single activating KIR2DS4. Approximately 50% of them were homozygous for the 2DS4 deletion variants, and therefore, 13.4% of human populations do not express any activating KIRs (5).

Nature of KIR Sequence Polymorphism

Each KIR gene exhibits considerable sequence polymorphism in addition to haplotypic diversity. The most abundant allelic polymorphism was reported for KIR3DL1 (6). The KIR3DL2 and -3DL3 framework genes are relatively more polymorphic, while the activating KIR genes are generally conserved. The amino acid substitutions that distinguish the allelic diversity of KIR3DL1 are rich in the region where the receptor contacts the polymorphic HLA-Bw4 ligands (6). The sequence polymorphism of KIR3DL1 is shown to influence their expression, ligand binding, and cytolytic and cytokine secretion functions. Some nucleotide mutations affect the cell surface expression of KIRs. For example, some of the frequently occurring KIR2DS4 sequences have a 22-bp deletion in exon 5, which shifts the reading frame and results in a premature stop codon causing KIR2DS4 to be nonexpressed at the cell surface. Furthermore, chain-terminating frameshift deletions were reported for KIR2DL4. Similarly, sequence variation in the promoter region is associated with the lack of KIR2DL5 expression, and amino acid polymorphism is largely responsible for the intracellular retention of KIR3DL1*004 and -2DL2*004. The synergistic combination of allelic polymorphism and varied gene contents individualizes KIR genotypes to the extent that unrelated individuals almost always have different KIR types. This level of diversity likely reflects a strong pressure from pathogens on the human NK cell response.

Human Populations Differ Substantially in KIR Gene Content Diversity

A stretch of 14 kb enriched with L1 repeats upstream of KIR2DL4 divides the KIR haplotype into halves (4) (Fig. 3). The centromeric half is delimited by KIR3DL3 at the 5′ end and -3DP1 at the 3′ end, while the telomeric half is delimited by -2DL4 at the 5′ end and -3DL2 at the 3′ end. These four framework genes are present on all KIR haplotypes and thus occur in 100% of all populations. In contrast, the existence of the other 12 KIR genes is considerably variable. The inhibitory receptors KIR2DL2 and -2DL3 segregate as alleles of a single locus in the centromeric half. Similarly, inhibitory KIR3DL1 and activating KIR3DS1 behave as alleles of the same locus at the telomeric half. Almost all haplotypes contain these two loci, such that virtually everyone has either -2DL2 or -2DL3 and -3DL1 or -3DS1 within their KIR genome. KIR2DL1, -2DL2, -2DL3, and -2DS2 are specific to the centromeric half, while KIR3DL1, -3DS1, -2DS1, and -2DS4 are specific to the telomeric half. Three KIR genes, -2DL5, -2DS3, and -2DS5, are found in both the centromeric and telomeric locations. For genes within each half, there is significant linkage disequilibrium, but the disequilibrium is much less for genes in the different halves.

Multiple reciprocal recombination events at the center of the KIR complex, between -3DP1 and -2DL4, presumably diversify gene content for KIR haplotypes across individuals and populations. Most of the KIR gene content haplotypes published to date can be explained by the recombination of 10 centromeric and 10 telomeric gene content motifs (7). Recombination events also are reported outside the region between -3DP1 and -2DL4. These are generally nonallelic crossovers generating several unusual haplotypes, including truncated haplotypes that are missing some framework genes or elongated haplotypes that contain duplicated genes. It is important to remark here that the current genotyping methods used to detect the presence and absence of individual KIR genes will not identify the copy number of each KIR gene within a given individual. In recent years, more-advanced typing methods that determine KIR gene copy numbers and that allow allele-level KIR typing have been developed, but these have not yet been implemented in most clinical tissue typing laboratories.

Populations Differ in Their Constellations of KIR-HLA Compound Genotypes

All human populations have both group A and B haplotypes, but their frequencies vary considerably (8). Individuals carrying homozygous group A KIR genotypes (AA genotypes) are common in Northeast Asians (Chinese, Japanese, and Koreans). Conversely, individuals carrying AB/BB genotypes are common in the natives of America, Australia, and India (9). The NK cells from AA-homozygous individuals can express a maximum of four inhibitory KIRs

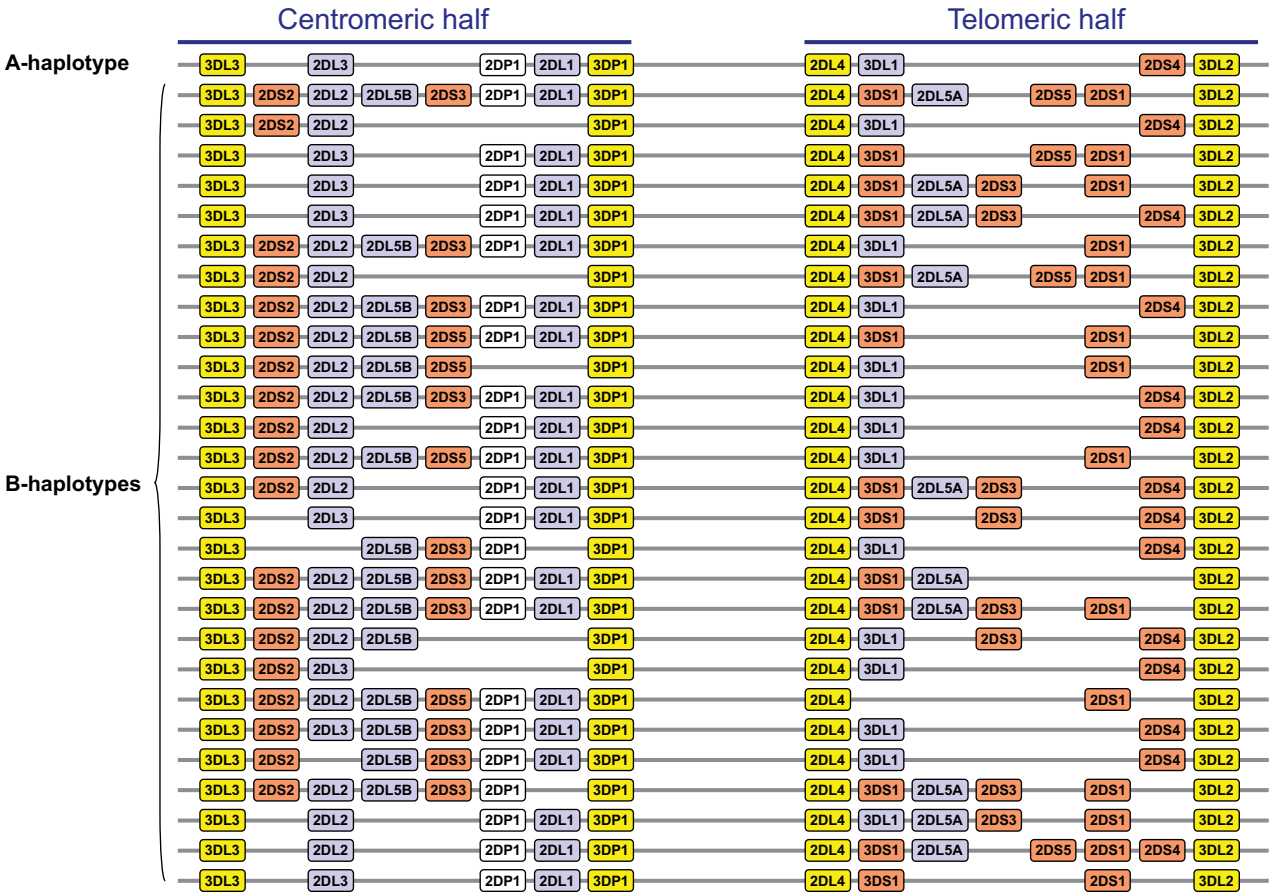

FIGURE 3 KIR haplotypes have varied gene contents. Map of KIR haplotypes as determined by family segregation analyses. The first haplotypes on the top represent the group A KIR haplotype, and the remainder represent the group B haplotype. A stretch of 14 kb enriched with L1 repeats upstream of KIR2DL4 divides the KIR haplotype into halves. The centromeric half is delimited by 3DL3 and 3DP1, while the telomeric half is delimited by 2DL4 and 3DL2. Multiple reciprocal meiotic recombination events between 3DP1 and 2DL4 shuffled the centromeric and telomeric motifs and thus diversified gene content KIR haplotypes across individuals and populations. The framework genes, present in all haplotypes, are shown in yellow, genes encoding activating KIRs are in orange, and those for inhibitory receptors are in blue. KIR2DP1 and -3DP1 are pseudogenes that do not express a receptor.

(KIR2DL1, -2DL3, -3DL1, and -3DL2) and one activating KIR (KIR2DS4). In contrast, individuals carrying AB/BB genotypes can express a maximum of six inhibitory KIRs (KIR2DL1 to -3, -2DL5, -3DL1, and -3DL2) and two to six activating KIRs (KIR3DS1, -2DS1 to -5). The function of the inhibitory KIRs depends on the availability of their specific cognate HLA class I ligands. Given that KIR genes at chromosome 19q13.4 and HLA genes at chromosome 6p21.3 are polymorphic and display significant variations, the independent segregation of these unlinked gene families produces diversity in the number and type of KIR-HLA pairs inherited in individuals (5), which might influence the health and disease status of a given individual. Consistently with this theory, combinations of certain KIR-HLA genes have been associated with diseases as diverse as autoimmunity, infection, cancer, and reproductive failure (10).

Clonal Expression of KIRs and Acquisition of NK Cell Tolerance/Competence/Responsiveness

KIRs are clonally expressed on NK cells, so that each NK cell clone expresses only a portion of the genes within the gene profile (3). Stochastic expression of different combinations of receptors by NK cells results in this repertoire of NK clones with a variety of ligand specificities. Once a given KIR is expressed on an NK cell clone or T cell, it is stably maintained in the progeny of the clone. This pattern of expression appears to be regulated by the methylation of the silent KIR loci.

The majority of NK cells in peripheral blood express at least one inhibitory receptor for self-major histocompatibility complex (MHC) class I and are functionally competent to recognize and eliminate target cells that have downregulated the respective MHC class I ligands (3). However, a subpopulation of NK cells lacks inhibitory receptors for self-MHC class I and is generally hyporesponsive to target cells that are deficient in MHC class I expression (11). In line with this, NK cells from MHC class I-deficient mice and humans, lacking inhibitory receptors for self-MHC class I by definition, are similarly hyporesponsive and defective in target killing (11). Finally, NK cells expressing an activating receptor recognizing a self-ligand are also hyporesponsive (12). Thus, the acquisition of functional competence correlates with the presence of inhibitory and the absence of activating NK cell receptors recognizing self-HLA ligands.

This phenomenon has been referred to as "licensing," "arming/disarming," or "education" (11). NK cell education is not an on-off phenomenon but rather functions like a rheostat. For example, expression of progressively higher numbers of inhibitory KIRs for self-HLA-B and HLA-C molecules is correlated with an increased effector capacity (13). The result is a diverse NK cell repertoire, in which each NK cell has tuned its responsiveness so that the net signaling input from autologous cells is just insufficient to induce activation. This ensures optimum NK cell responsiveness to infected or transformed cells that have upregulated ligands for activating receptors or downregulated ligands for inhibitory receptors.

NK Cell Alloreactivity and Clinical Transplantation

As described above, an NK cell's reactivity pattern is shaped by the interactions between its KIR and autologous HLA, both encoded by highly polymorphic gene families. As a result of this education by autologous HLA, NK cells can respond to allogeneic cells. In an HLA-Cw4+ (C2) individual, for example, an NK cell expressing KIR2DL1 as its only inhibitory receptor depends on KIR2DL1-C2 interactions for self-tolerance, and this NK cell will respond to C1-homozygous (C2-negative) allogeneic cells, as these fail to provide a ligand for KIR2DL1. Had this NK cell been raised in a C1-homozygous individual, however, it would be hyporesponsive and also nonresponsive to C1-homozygous allogeneic cells. A small fraction of the population lacks the KIR2DL1 gene and therefore lacks NK cells with the ability to respond to "missing C2." These considerations make it possible to predict with reasonable accuracy whether NK cells exist in one individual that will attack cells from another individual, based on KIR and HLA class I typing of the former and HLA class I typing of the latter. In the example described above, a KIR-ligand mismatch requires the presence of KIR2DL1 and a C2 HLA-C allele in the responder and the absence of a C2 HLA-C allele from the target. Other KIR-ligand mismatches are based on the interaction between KIR2DL2 or KIR2DL3 and C1, KIR3DL1 and Bw4, and KIR3DL2 and HLA-A3/A11.

Many retrospective studies of SOT and of HSCT have attempted to correlate the results of KIR and HLA genotyping with outcome. This genotyping yields information on the presence or absence of 14 KIR genes and at least 3 HLA-encoded KIR ligands in donors and recipients. For such studies, usually relatively small cohorts (100s of patients) are available for sufficient statistical power, and the typing results have to be analyzed using models that translate such complex outcomes into a smaller number of variables. In most cases, the above-described KIR-ligand mismatch model has been applied, as it reflects current knowledge about NK cell biology and translates the typing outcome into a single binary variable: alloreactivity is either expected (≥1 KIR-ligand mismatch) or not (0 KIR-ligand mismatches). A drawback of this approach is that any potential information on the magnitude of the NK cell alloresponse is lost.

Several variations on this definition of KIR-ligand mismatches have been used in genetic-association studies on transplantation. First, since the phenotype frequencies of the relevant KIRs range from 95 to 100%, taking into account only the HLA genotype of the donor and recipient appears to be sufficient for a reliable prediction of NK cell alloreactivity (14). The "missing KIR ligand" model examines only the responder's KIR and the stimulator's HLA, thereby disregarding the educating impact of the responding party's HLA. Recent evidence suggests that there is a biological foundation for this model as well (15). It is important to note that all transplantations with a KIR-ligand mismatch by definition fall into the "missing KIR-ligand" category and that they may make up such a large fraction of it that it becomes difficult to distinguish between them in statistical analyses.

Another way to analyze the data is to translate the KIR genotyping results into A and B KIR haplotypes. The first studies of this kind classified the individual as either AA or Bx. At the time, it was not possible to distinguish between BB and BA individuals, because A haplotypes are defined by the absence of B haplotype-specific KIR genes (KIR2DL2, KIR2DL5, KIR2DS1, KIR2DS2, KIR2DS3, KIR2DS5, and KIR3DS1). More recently, genotyping methods determining KIR copy numbers or KIR alleles have allowed the translation of the genotyping results into AA, AB, and BB. As a meiotic recombination hotspot is located in the center of the locus, just upstream of KIR2DL4, follow-up studies then attempted to map KIR haplotype effects to either the centromeric or the telomeric portion of the haplotypes (centromeric A and B haplotypes [Cen-A, Cen-B] and telomeric A and B haplotypes [Tel-A, Tel-B]).

In the following two sections, the results of the various types of analyses in HSCT and SOT will be discussed. In HSCT, one of the main questions is whether NK cell alloreactivity in the graft-versus-host direction has an impact on the patient's fate after transplantation. Therefore, HSCT studies generally examine the effects of donor KIR and HLA and patient HLA genotypes. In SOT, NK cell alloreactivity in the host-versus-graft direction is most relevant. Solid-organ transplantation studies therefore mostly determine patient KIR and HLA and donor HLA genotypes.

KIRs IN HEMATOPOIETIC STEM CELL TRANSPLANTATION

Determination of Donor NK Cell Alloreactivity

NK cells are the first lymphocyte population to reconstitute after HSCT. Engrafted alloreactive NK cells may (i) protect against graft-versus-host disease (GvHD) by depleting host antigen-presenting cells, (ii) facilitate engraftment by production of cytokines and elimination of host immune barriers, (iii) kill residual host tumor to protect against relapse, and (iv) decrease infectious complications. Allogeneic HSCT provides the opportunity to induce NK cell alloreactivity by selecting donors who express inhibitory KIRs for which the donor expresses class I HLA ligand, but the recipient does not express that ligand, thus mimicking missing self. The clinical efficacy of this strategy was first demonstrated in 2002 by the Perugia group, who used predicted KIR-ligand mismatching or incompatibility to select haploidentical donors for HSCT (14). They used donor and recipient HLA typing to predict donor NK cell alloreactivity in the graft-versus-host direction when recipients lacked C2, C1, or Bw4 alleles that were present in the donor. In line with this KIR-ligand mismatch concept, prior to transplantation, *in vitro* graft-versus-host NK cell reactivity was indeed detected in all KIR-ligand-mismatched transplantations (14). A related strategy, referred to as "missing ligand," focuses only on the HLA type of the recipient to assess for KIR ligand absence, where alloreactive potential is based entirely on the number of KIR ligands that the recipient lacks. Initial studies did not include KIR genotyping, as the phenotype frequencies of the relevant KIRs are between 95 and 100%. The incorporation of KIR genotyping has allowed a more accurate prediction of receptor-ligand interactions between donor inhibitory KIRs and their corresponding class I HLA ligands in the recipient. The high degree of allelic polymorphism in the KIR

gene family with associated variability in levels of receptor expression and in the strengths of interactions with different HLA alleles has led to a more recent push to incorporate KIR allelic-level typing into models to predict the magnitude of potential NK cell alloreactivity.

It is important to note that all of these models to predict NK cell alloreactivity assume that they be functionally competent (educated) and present in sufficient numbers to mediate beneficial effects in the recipient. Many groups have demonstrated that despite their high numbers, NK cells reconstituting after HSCT have decreased effector functions, such as CD107a degranulation and IFN-γ production, compared to those in their donors (15). Variables such as stem cell source (umbilical cord blood [UCB], unrelated donors, and siblings), T cell depletion, and graft processing, and the strength of the preparative regimen can affect the kinetics of NK and T cell reconstitution after transplantation, which may have an impact on clinical outcomes. In addition, high levels of stimulation by inflammatory cytokines that are triggered by preparative chemotherapy or GvHD can overcome the rules of NK cell education and receptor-ligand-based determinants of alloreactivity. This may allow graft-versus-host NK cell reactivity in HLA-identical transplants if self-tolerance of donor NK clones expressing KIR for which they lack the ligand is broken in the posttransplant setting, providing a potential rationale for the missing-ligand model.

Role of NK Cells in Hematopoietic Stem Cell Transplantation

The first report of a successful strategy to manipulate NK cell alloreactivity to improve outcome after HSCT came from Velardi's group in Perugia. They demonstrated that patients with AML but not ALL had higher rates of engraftment, less GvHD, and durable remission after T cell-depleted haploidentical transplantation from donors, with graft-versus-host NK cell alloreactivity predicted on the basis of KIR-ligand mismatches deduced from HLA typing results (14). However, in a long-term follow-up of 112 patients, KIR-ligand-mismatched donors were associated with decreased relapse and improved disease-free survival only in patients transplanted while in complete remission (16). Subsequent analyses of the effect of KIR-ligand mismatching and KIR-ligand absence have produced mixed results depending on the clinical setting. In a large cohort of unrelated-donor (URD) transplants, Davies et al. (17) did not observe a benefit to KIR-ligand mismatching, whereas in a T cell-depleted cohort, Giebel et al. (18) demonstrated an association between KIR-ligand mismatching and overall survival. A subsequent study of over 1,500 URD transplants reported higher incidences of GvHD and treatment-related mortality and shorter leukemia-free survival associated with KIR-ligand mismatching (19). In 1,700 URD transplants, Yu et al. reported a beneficial effect of HLA-B and -C mismatches corresponding to recipient KIR ligand absence, but these mismatches did not necessarily correlate with a prediction of donor NK alloreactivity (13). Another large analysis of 2,000 URD transplant recipients found that the absence of one or more KIR ligand in the recipient was associated with less relapse in patients with AML and chronic myeloid leukemia (CML) (20). The effect of KIR-ligand mismatching after transplantation with UCB grafts appears to depend on the intensity of the regimen and the amount of T cell depletion. Willemze et al. (21) reported an association between KIR-ligand mismatching and protection from relapse and improved overall survival, whereas Brunstein et al. (22) observed an increase in acute GvHD and increased risk of death in the presence of KIR-ligand mismatching. The inconsistent benefit reported for KIR-ligand mismatch and KIR-ligand absence strategies is likely related due to key differences among the cohorts, including differences in the stem cell source, conditioning regimen, degree of T cell depletion and type of post-HCT immunosuppression, all of which can affect NK cell development, education, and function.

Donor Selection Based on KIR Genotype

The development of methods to measure the presence or absence of KIR genes to determine the KIR genotype allowed for analysis of the impact of donor and recipient KIRs on outcome after HSCT. In the haploidentical setting, a study of 86 nonmyeloablative, T cell-replete transplants demonstrated protection from relapse and transplant-related mortality as well as improved disease-free survival and overall survival associated with KIR-ligand mismatching or when KIR A/A recipients received grafts from donors with at least one KIR B haplotype. McQueen et al. (23) studied a cohort of HLA-identical sibling transplant recipients, and they observed improved survival in KIR B haplotype recipients receiving grafts from KIR A haplotype donors. Another group reported a beneficial association between donors with the KIR B haplotype genes KIR2DS1, KIR3DS1, and KIR2DL5A and both reduced levels of relapse and improved overall survival after T cell-depleted HLA-matched sibling transplants in 246 patients with AML. In a cohort of 1,087 URD transplants with mixed diseases matched for 9 or 10 HLA loci, donors with KIR3DS1 were associated with reduced acute GvHD and showed increased protection from donors with two copies of the gene (24). The same group published that donors with KIR2DS1 conferred protection from AML relapse but only when the donors expressed at least one copy of HLA-C1 antigens. Cooley et al. demonstrated that patients with AML had reduced relapse and a 30% improvement in disease-free survival after receiving transplants from HLA-matched or -mismatched unrelated donors with at least one B haplotype (25). A subsequent analysis of 1,086 AML and 323 ALL patients evaluated the relative effects of the Cen-B versus Tel-B motifs on transplant outcomes. Donors with Tel-B were associated with relapse protection, whereas donors homozygous for the Cen-B haplotype motif conferred significant reduction in leukemic relapse and improved overall disease-free survival in AML but not in ALL patients.

The general picture emerging from these studies is that the presence of KIR B haplotypes in the donor appears to be beneficial in HSCT and that this effect maps mainly to the centromeric portion of the B haplotype (Cen-B), with a smaller contribution from Tel-B. Therefore, an algorithm was constructed to classify URDs based on KIR genotype in which donors with 0 to 1 KIR B motif were defined as "neutral," donors with ≥2 KIR B motifs were defined as "better," and donors with ≥2 KIR B motifs, including Cen-B/Cen-B, were defined as "best." A publicly available calculator to determine this stratification is available online (http://www.ebi.ac.uk/ipd/kir/donor_b_content.html). A prospective trial incorporating KIR genotyping into unrelated-donor selection for patients with AML facilitated via the National Marrow Donor Program is ongoing. Therefore, it is increasingly accepted that in addition to HLA matching, donor selection for KIR genes is a promising strategy to improve outcome after HCT.

Control of Viral Infection

NK cells play an important role in controlling infections, including those which contribute to morbidity after allogeneic HSCT. Virally infected cells express decreased HLA

and increased stress-induced ligands, which are recognized by NK cell inhibitory and activating receptors, respectively. The KIR genotype of donor NK cells appears to also play an important role in the control of infections after HSCT. A 65% reduction in cytomegalovirus (CMV) reactivation was observed with donors who had more than one activating KIR gene after HLA-matched sibling transplants where both donor and recipient were CMV seropositive. In humans, CMV has been shown to play a unique role in shaping the NK cell receptor repertoire. Recently, it has been proposed that CMV infection may drive the development of a population of $NKG2C^+$ memory-like NK cells (26) in parallel with the $Ly49H^+$ response to murine CMV. These $NKG2C^+$ cells express more self-KIR and have enhanced IFN-γ production after HCST compared to cells from recipients of UCB or allogeneic-sibling transplants who did not reactivate CMV cells. An analysis of KIR repertoires in 200 healthy donors determined that skewing toward expression of self-specific inhibitory KIR was observed only in CMV-seropositive individuals. This observation may be of particular importance in understanding KIR and HLA responses after transplantation. The role of the CMV-induced memory-like NK cells in mediating outcome after HSCT is unknown, but several groups have reported that posttransplant reactivation of CMV is associated with protection against relapse. This supports a model where CMV reactivation early after transplantation may promote expansion of functionally competent $NKG2C^+$ NK cells, which may better mediate antileukemic protection.

Methods To Augment NK Cell-Mediated Benefits after HSCT

Expanded access to KIR genotyping and, increasingly, KIR allelic-level typing is supporting efforts to optimize donor selection to exploit the beneficial effects of NK cells engrafting after allogeneic HSCT. However, many other therapeutic strategies are being perused to be used alone or in conjunction with HSCT. Blockade of inhibitory KIR signaling has been tested using an antibody directed against KIR2DL1, KIR2DL2, and KIR2DL3, which is currently in phase 1 and phase 2 clinical trials (27). Alternatively, enhanced NK cell-mediated antibody-dependent cellular cytotoxicity (ADCC) can be achieved by coating targets with antibodies such as the anti-CD20 agent rituximab to induce signaling via CD16. Autologous NK cells from cancer patients are poor antitumor effectors because they are exposed to cancer-induced immune-suppressive mechanisms (regulatory T cells) and are likely to be inhibited by self-class I HLA ligands. Thus, many groups are testing adoptive transfer of *ex vivo-* or *in vivo*-expanded haploidentical adult NK cells to increase the frequency of alloreactive subsets. Others are testing the manufacture of NK cell products from UCB stem cells or NK cell lines. The safety and clinical efficacy of adoptive haploidentical NK cell infusions given with subcutaneous IL-2 to treat refractory/relapsed AML have been assessed, and complete remissions correlated with *in vivo* NK expansion and higher proportions of circulating (and functional) NK cells.

Although significant heterogeneity in clinical cohorts renders the literature about the beneficial effects of NK cells after HSCT rather confusing, there is a strong consensus that NK cells can play an important role in improving posttransplant outcomes. Many groups are studying the mechanisms of NK cell education and function, defining the effects of the interactions between activating and inhibitory receptors and their ligands and investigating the immunoregulatory roles of NK cells and their interactions with other immune cells. Ultimately, the success of NK cell-based approaches to enhance graft-versus-leukemia and improve outcome after HSCT will require optimization for the specific disease, the type of transplant, donor and recipient immunogenetic factors, and combination with other therapeutic interventions.

KIRs IN SOLID-ORGAN TRANSPLANTATION

Kidney Transplantation

NK cells infiltrate human kidney allografts shortly after transplantation, and this is accompanied by the presence in the blood of NK cells responding to cells from the donor. Yet, when the collaborative transplant study (CTS) examined thousands of kidney transplantations, they detected no effect of KIR-ligand mismatches on graft survival (28). In this case, the presence of KIR-ligand mismatches was derived from HLA typing results, on the usually correct assumption that the corresponding KIR would be present in the patient. Subsequent, often smaller, studies also failed to detect any effect of KIR-ligand mismatches on the occurrence of acute rejection after the reduction of immunosuppression or on acute rejection after kidney transplantation. Taken together, these studies indicated that the presence of KIR-ligand mismatches, predictive of NK cell alloreactivity in the host-versus-graft direction, was not associated with adverse outcome. However, the majority of the transplantations in these studies were incompatible for HLA-A, HLA-B, and/or HLA-DR. Alloreactive T cells may therefore have dominated the allo-immune response, possibly obscuring the negative effects of NK cell-mediated rejection suggested by the mouse experiments. Alternatively, as in the mouse models, NK cell-mediated deletion of graft antigen-presenting cells may have hindered T cells attacking the kidney, thus balancing negative NK cell effects.

In HLA-A-, -B-, and -DR-compatible transplantations, the role of T and B cells in graft rejection is relatively small, potentially revealing detrimental effects of alloreactive NK cells. A retrospective two-center study ($n = 137$) in such HLA-compatible transplantations reported that the presence of KIR-ligand mismatches was associated with a significant reduction in long-term graft survival (29). However, a recent multicenter study by the CTS ($n = 605$) found no such effect (30), not even in separate subset analyses of four larger centers (60 to 80 transplants each). Thus, the consequences of KIR-ligand mismatches in kidney transplantation are currently unclear.

Many studies tested other models, including those with no immediately obvious foundation in NK cell biology (Fig. 4), and reported several, sometimes conflicting, associations. Multiple studies reported an effect of the presence of specific KIR genes in the patient. For example, in one study, KIR2DL1, KIR2DL2/S2, and more inhibitory receptors protected against acute rejection, while in another, KIR2DS5 protected against graft rejection. KIR2DS4, on the other hand, was associated with graft rejection. Another study examined the influence of KIR differences between donor and patient, which may effectively translate into KIR-derived minor antigens on NK cells that might be recognized by T cells in an HLA-restricted fashion. In contrast with the results of studies on HSCT, patient KIR haplotypes (A and B) do not seem to influence graft survival. Finally, the presence HLA-C2 in patients was associated with significantly lower graft survival.

CMV Infection after Kidney Transplantation

Cytomegalovirus infection and reactivation can cause serious complications after kidney transplantation. Patients

	Number of transplant cases studied	KIR-ligand mismatch		Missing ligand				KIR repertoire		
Recipient		KIR HLA	HLA	KIR		HLA	KIR	Single KIR	Ratio act/inh KIR	A/B haplotypes
Donor		HLA	HLA	HLA	HLA		KIR			
ref (28)	2757	-								
ref (46)	69	-		-			-	-		-
ref (47)	224	-		-	-			+	-	
ref (29)	137	+								
ref (30)	608	-						-	-	
ref (48)	760					+				
ref (49)	283							+		
ref (50)	339									-

FIGURE 4 KIR-HLA effects on kidney transplantation. + indicates the presence and − indicates the absence of a particular genetic association. act, activator; inh, inhibitor.

carrying at least one KIR B haplotype had a significantly reduced incidence of CMV reactivation/infection (31). This effect mapped to the telomeric end of these B haplotypes, which contains one or more of the following genes: KIR2DS1, KIR3DS1, KIR2DL5A, and KIR2DS5. In the same vein, Hadaya et al. observed an association between the number of patients activating KIR and a reduced incidence of posttransplant CMV infection (32). As most of the ligands for these KIRs are unknown, the mechanistic basis for this association can only be speculated upon. The findings are reminiscent of a study of HSCT in which a 65% reduction in CMV reactivation was observed with donors who had more than one activating KIR gene (33). Also, as in HSCT, in kidney transplantation, CMV infection is also associated with an expansion of $NKG2C^+$ memory-like NK cells (32). In conclusion, KIR B haplotypes may help combat CMV infections in immunosuppressed HSCT and SOT patients, and this effect is likely to involve $NKG2C^+$ NK cells.

Liver Transplantation

In contrast to kidney transplants, liver transplants are not usually matched for HLA. Despite this, graft survival is usually considerably better than for kidneys, suggesting that immune-mediated rejection plays only a minor role in liver transplantation. In line with this, in one study, the presence of KIR-ligand mismatches did not appear to be correlated with graft survival or rejection (34). Yet, another study reported that the presence of HLA-C-based KIR-ligand mismatches was associated with more rejection episodes (35). Several studies investigated the effect of donor HLA-C group 2 (C2), a high-affinity ligand for KIR2DL1. In two of these studies (35, 36), the presence of C2 in the donor was beneficial. However, this trend was not replicated by the CTS (37), and another study reported that donor C2 was associated with more-acute rejection and worse survival (38).

Hepatitis C after Liver Transplantations

In hepatitis C patients with low HCV infectious doses, the presence of KIR2DL3 and a C1 allele is associated with increased HCV clearance (39). This effect is likely to be absent in liver transplantations in HCV-positive patients, as recipient KIR2DL3 is associated with more-aggressive recurrent liver disease (40).

KIR GENOTYPING

Uhrberg et al. developed the first KIR genotyping method in 1997 using sequence-specific-primer-based PCR (PCR-SSP) (41). Since then, various KIR genotyping technologies have been developed using multiplex PCR-SSP (42, 43), real-time PCR assays, sequence-specific oligonucleotide probe hybridization, reverse-sequence-specific oligonucleotide hybridization, matrix-assisted laser desorption ionization–time of flight mass spectrometry, and direct DNA sequencing.

The most commonly used method is SSP analysis, which utilizes gene-specific primers to perform PCR amplification of 16 distinct KIR genes (44). Each primer carries a 3′ residue matching a unique position conserved on all known sequences of a given KIR gene. Primer lengths are adjusted to result in annealing temperatures between 59°C and 67°C to enable PCR amplification of all KIR genes under the same thermal-cycling conditions. An internal positive-control primer specific to a conserved housekeeping gene is coamplified to confirm the success of each PCR.

KIR genotyping is performed in a reaction volume of 15 μl, with a final concentration of 1× PCR buffer II (10 mM Tris-HCl, 50 mM KCl), 200 μM each deoxynucleoside triphosphate (dNTP), 1.0 μM each forward and reverse primer to a given KIR gene, 3.0 mM MgCl2, 0.5 U of AmpliTaq DNA polymerase, and 100 ng of genomic DNA (Applied Biosystems, Foster City, CA). For KIR gene-specific PCRs, an additional set of primers (PIC-F and PIC-R, 0.1 μM each) specific to the polyposis coli gene is included to serve as an internal positive control. For KIR2DS4 subtyping reactions, the internal positive-control primers (GH1F and GH1R, 0.3 μM each) are targeted to human growth hormone gene 1. Thermal cycling is performed using an ABI 9700 GeneAmp PCR system (Applied Biosystems) according to the following conditions: an initial denaturation for 3 min at 95°C and then 5 cycles of 94°C for 20 s, 65°C for 20 s, and 72°C for 90 s; 32 cycles of 94°C for 20 s, 61°C for 20 s, and 72°C for 90 s; and a final extension at 72°C for 10 min. Ten microliters of the PCR-amplified product is electrophoresed on ethidium bromide-prestained 2% agarose gel and examined for the presence and absence of gene-specific PCR products of appropriate sizes.

Under strictly controlled PCR conditions, perfectly matched primer pairs result in the amplification of target sequences (i.e., a positive reaction), while mismatched

primer pairs do not result in amplification (i.e., a negative reaction). Each PCR mixture includes, in addition to KIR gene-specific primers, a positive internal control primer pair which amplifies a 256-bp fragment from a conserved polyposis coli gene. The presence of the 256-bp positive internal control band is used to confirm the success of each PCR. In the presence of a positively typing band, the product of the internal control primer pair may be weak or absent due to the differences in concentrations and melting temperatures between the specific primer pairs and the internal control primer pair. Interpretation of the PCR-SSP typing results is relatively simple and straightforward and is done basically by detecting an amplified product of the correct size by gel electrophoresis. Determine the approximate molecular weight of each PCR product by comparing its mobility against the DNA ladder.

CONCLUSIONS

Taken together, the studies described in this chapter indicate involvement of KIR-HLA interactions in both HSCT and kidney transplantation, most likely mediated by NK cells. These interactions can regulate engraftment and relapse in HSCT, graft survival, and CMV pathology in both HSCT and SOT. However, only in the case of CMV is there a clear consensus between studies: B haplotypes protect both in HSCT and in SOT (45).

Many studies include data from multiple centers, thus increasing statistical power but introducing variation between centers as an additional variable. In HSCT, different transplant centers use different stem cell sources, different conditioning regimens, different degrees of T cell depletion, and different types of post-HCT immunosuppression, all of which can affect NK cell development, education, and function. Increased international standardization of HSCT protocols would greatly facilitate any studies attempting to perform genetic association studies. Another vulnerability of the studies described in this chapter is that they were all retrospective in nature. An exciting development on this front is the prospective trial incorporating KIR genotyping into unrelated-donor selection for patients with AML, facilitated via the National Marrow Donor Program.

REFERENCES

1. **Lanier LL.** 2003. Natural killer cell receptor signaling. *Curr Opin Immunol* **15:**308–314. PubMed
2. **Ljunggren HG, Kärre K.** 1990. In search of the 'missing self': MHC molecules and NK cell recognition. *Immunol Today* **11:**237–244. PubMed
3. **Valiante NM, Uhrberg M, Shilling HG, Lienert-Weidenbach K, Arnett KL, D'Andrea A, Phillips JH, Lanier LL, Parham P.** 1997. Functionally and structurally distinct NK cell receptor repertoires in the peripheral blood of two human donors. *Immunity* **7:**739–751. PubMed
4. **Wilson MJ, Torkar M, Haude A, Milne S, Jones T, Sheer D, Beck S, Trowsdale J.** 2000. Plasticity in the organization and sequences of human KIR/ILT gene families. *Proc Natl Acad Sci USA* **97:**4778–4783. PubMed
5. **Du Z, Gjertson DW, Reed EF, Rajalingam R.** 2007. Receptor-ligand analyses define minimal killer cell Ig-like receptor (KIR) in humans. *Immunogenetics* **59:**1–15. PubMed
6. **Norman PJ, Abi-Rached L, Gendzekhadze K, Korbel D, Gleimer M, Rowley D, Bruno D, Carrington CV, Chandanayingyong D, Chang YH, Crespí C, Saruhan-Direskeneli G, Fraser PA, Hameed K, Kamkamidze G, Koram KA, Layrisse Z, Matamoros N, Milà J, Park MH, Pitchappan RM, Ramdath DD, Shiau MY, Stephens HA, Struik S, Verity DH, Vaughan RW, Tyan D, Davis RW, Riley EM, Ronaghi M, Parham P.** 2007. Unusual selection on the KIR3DL1/S1 natural killer cell receptor in Africans. *Nat Genet* **39:**1092–1099. PubMed
7. **Norman PJ, Abi-Rached L, Gendzekhadze K, Hammond JA, Moesta AK, Sharma D, Graef T, McQueen KL, Guethlein LA, Carrington CV, Chandanayingyong D, Chang YH, Crespí C, Saruhan-Direskeneli G, Hameed K, Kamkamidze G, Koram KA, Layrisse Z, Matamoros N, Milà J, Park MH, Pitchappan RM, Ramdath DD, Shiau MY, Stephens HA, Struik S, Tyan D, Verity DH, Vaughan RW, Davis RW, Fraser PA, Riley EM, Ronaghi M, Parham P.** 2009. Meiotic recombination generates rich diversity in NK cell receptor genes, alleles, and haplotypes. *Genome Res* **19:**757–769. PubMed
8. **Ashouri E, Farjadian S, Reed EF, Ghaderi A, Rajalingam R.** 2009. KIR gene content diversity in four Iranian populations. *Immunogenetics* **61:**483–492. PubMed
9. **Rajalingam R, Du Z, Meenagh A, Luo L, Kavitha VJ, Pavithra-Arulvani R, Vidhyalakshmi A, Sharma SK, Balazs I, Reed EF, Pitchappan RM, Middleton D.** 2008. Distinct diversity of KIR genes in three southern Indian populations: comparison with world populations revealed a link between KIR gene content and pre-historic human migrations. *Immunogenetics* **60:**207–217. PubMed
10. **Khakoo SI, Carrington M.** 2006. KIR and disease: a model system or system of models? *Immunol Rev* **214:**186–201. PubMed
11. **Kim S, Poursine-Laurent J, Truscott SM, Lybarger L, Song YJ, Yang L, French AR, Sunwoo JB, Lemieux S, Hansen TH, Yokoyama WM.** 2005. Licensing of natural killer cells by host major histocompatibility complex class I molecules. *Nature* **436:**709–713. PubMed
12. **Fauriat C, Ivarsson MA, Ljunggren HG, Malmberg KJ, Michaëlsson J.** 2010. Education of human natural killer cells by activating killer cell immunoglobulin-like receptors. *Blood* **115:**1166–1174. PubMed
13. **Yu J, Heller G, Chewning J, Kim S, Yokoyama WM, Hsu KC.** 2007. Hierarchy of the human natural killer cell response is determined by class and quantity of inhibitory receptors for self-HLA-B and HLA-C ligands. *J Immunol* **179:**5977–5989. PubMed
14. **Ruggeri L, Capanni M, Urbani E, Perruccio K, Shlomchik WD, Tosti A, Posati S, Rogaia D, Frassoni F, Aversa F, Martelli MF, Velardi A.** 2002. Effectiveness of donor natural killer cell alloreactivity in mismatched hematopoietic transplants. *Science* **295:**2097–2100. PubMed
15. **Yu J, Venstrom JM, Liu XR, Pring J, Hasan RS, O'Reilly RJ, Hsu KC.** 2009. Breaking tolerance to self, circulating natural killer cells expressing inhibitory KIR for non-self HLA exhibit effector function after T cell-depleted allogeneic hematopoietic cell transplantation. *Blood* **113:**3875–3884. PubMed
16. **Ruggeri L, Mancusi A, Burchielli E, Capanni M, Carotti A, Aloisi T, Aversa F, Martelli MF, Velardi A.** 2008. NK cell alloreactivity and allogeneic hematopoietic stem cell transplantation. *Blood Cells Mol Dis* **40:**84–90. PubMed
17. **Davies SM, Ruggieri L, DeFor T, Wagner JE, Weisdorf DJ, Miller JS, Velardi A, Blazar BR.** 2002. Evaluation of KIR ligand incompatibility in mismatched unrelated donor hematopoietic transplants. Killer immunoglobulin-like receptor. *Blood* **100:**3825–3827. PubMed
18. **Giebel S, Locatelli F, Lamparelli T, Velardi A, Davies S, Frumento G, Maccario R, Bonetti F, Wojnar J, Martinetti M, Frassoni F, Giorgiani G, Bacigalupo A, Holowiecki J.** 2003. Survival advantage with KIR ligand incompatibility in hematopoietic stem cell transplantation from unrelated donors. *Blood* **102:**814–819. PubMed
19. **Farag SS, Bacigalupo A, Eapen M, Hurley C, Dupont B, Caligiuri MA, Boudreau C, Nelson G, Oudshoorn M, van**

Rood J, Velardi A, Maiers M, Setterholm M, Confer D, Posch PE, Anasetti C, Kamani N, Miller JS, Weisdorf D, Davies SM, KIR Study Group, Center for International Blood and Marrow Transplantation Research. 2006. The effect of KIR ligand incompatibility on the outcome of unrelated donor transplantation: a report from the center for international blood and marrow transplant research, the European blood and marrow transplant registry, and the Dutch registry. *Biol Blood Marrow Transplant* **12:**876–884. PubMed

20. **Miller JS, Cooley S, Parham P, Farag SS, Verneris MR, McQueen KL, Guethlein LA, Trachtenberg EA, Haagenson M, Horowitz MM, Klein JP, Weisdorf DJ.** 2007. Missing KIR ligands are associated with less relapse and increased graft-versus-host disease (GVHD) following unrelated donor allogeneic HCT. *Blood* **109:**5058–5061. PubMed
21. **Willemze R, Rodrigues CA, Labopin M, Sanz G, Michel G, Socié G, Rio B, Sirvent A, Renaud M, Madero L, Mohty M, Ferra C, Garnier F, Loiseau P, Garcia J, Lecchi L, Kögler G, Beguin Y, Navarrete C, Devos T, Ionescu I, Boudjedir K, Herr AL, Gluckman E, Rocha V, Eurocord-Netcord and Acute Leukaemia Working Party of the EBMT.** 2009. KIR-ligand incompatibility in the graft-versus-host direction improves outcomes after umbilical cord blood transplantation for acute leukemia. *Leukemia* **23:**492–500. PubMed
22. **Brunstein CG, Wagner JE, Weisdorf DJ, Cooley S, Noreen H, Barker JN, DeFor T, Verneris MR, Blazar BR, Miller JS.** 2009. Negative effect of KIR alloreactivity in recipients of umbilical cord blood transplant depends on transplantation conditioning intensity. *Blood* **113:**5628–5634. PubMed
23. **McQueen KL, Dorighi KM, Guethlein LA, Wong R, Sanjanwala B, Parham P.** 2007. Donor-recipient combinations of group A and B KIR haplotypes and HLA class I ligand affect the outcome of HLA-matched, sibling donor hematopoietic cell transplantation. *Hum Immunol* **68:**309–323. PubMed
24. **Venstrom JM, Gooley TA, Spellman S, Pring J, Malkki M, Dupont B, Petersdorf E, Hsu KC.** 2010. Donor activating KIR3DS1 is associated with decreased acute GVHD in unrelated allogeneic hematopoietic stem cell transplantation. *Blood* **115:**3162–3165. PubMed
25. **Cooley S, Trachtenberg E, Bergemann TL, Saeteurn K, Klein J, Le CT, Marsh SG, Guethlein LA, Parham P, Miller JS, Weisdorf DJ.** 2009. Donors with group B KIR haplotypes improve relapse-free survival after unrelated hematopoietic cell transplantation for acute myelogenous leukemia. *Blood* **113:**726–732. PubMed
26. **Lopez-Vergès S, Milush JM, Schwartz BS, Pando MJ, Jarjoura J, York VA, Houchins JP, Miller S, Kang SM, Norris PJ, Nixon DF, Lanier LL.** 2011. Expansion of a unique CD57^{+}NKG2Chi natural killer cell subset during acute human cytomegalovirus infection. *Proc Natl Acad Sci USA* **108:**14725–14732. PubMed
27. **Benson DM Jr, Hofmeister CC, Padmanabhan S, Suvannasankha A, Jagannath S, Abonour R, Bakan C, Andre P, Efebera Y, Tiollier J, Caligiuri MA, Farag SS.** 2012. A phase 1 trial of the anti-KIR antibody IPH2101 in patients with relapsed/refractory multiple myeloma. *Blood* **120:**4324–4333. PubMed
28. **Tran TH, Mytilineos J, Scherer S, Laux G, Middleton D, Opelz G.** 2005. Analysis of KIR ligand incompatibility in human renal transplantation. *Transplantation* **80:**1121–1123. PubMed
29. **van Bergen J, Thompson A, Haasnoot GW, Roodnat JI, de Fijter JW, Claas FH, Koning F, Doxiadis II.** 2011. KIR-ligand mismatches are associated with reduced long-term graft survival in HLA-compatible kidney transplantation. *Am J Transplant* **11:**1959–1964. PubMed
30. **Tran TH, Unterrainer C, Fiedler G, Döhler B, Scherer S, Ruhenstroth A, Adamek M, Middleton D, Opelz G.** 2013. No impact of KIR-ligand mismatch on allograft outcome in HLA-compatible kidney transplantation. *Am J Transplant* **13:**1063–1068. PubMed
31. **Stern M, Elsässer H, Hönger G, Steiger J, Schaub S, Hess C.** 2008. The number of activating KIR genes inversely correlates with the rate of CMV infection/reactivation in kidney transplant recipients. *Am J Transplant* **8:**1312–1317. PubMed
32. **Hadaya K, de Rham C, Bandelier C, Bandelier C, Ferrari-Lacraz S, Jendly S, Berney T, Buhler L, Kaiser L, Seebach JD, Tiercy JM, Martin PY, Villard J.** 2008. Natural killer cell receptor repertoire and their ligands, and the risk of CMV infection after kidney transplantation. *Am J Transplant* **8:**2674–2683. PubMed
33. **Cook M, Briggs D, Craddock C, Mahendra P, Milligan D, Fegan C, Darbyshire P, Lawson S, Boxall E, Moss P.** 2006. Donor KIR genotype has a major influence on the rate of cytomegalovirus reactivation following T-cell replete stem cell transplantation. *Blood* **107:**1230–1232. PubMed
34. **Moroso V, van der Meer A, Tilanus HW, Kazemier G, van der Laan LJ, Metselaar HJ, Joosten I, Kwekkeboom J.** 2011. Donor and recipient HLA/KIR genotypes do not predict liver transplantation outcome. *Transpl Int* **24:**932–942. PubMed
35. **Bishara A, Brautbar C, Zamir G, Eid A, Safadi R.** 2005. Impact of HLA-C and Bw epitopes disparity on liver transplantation outcome. *Hum Immunol* **66:**1099–1105. PubMed
36. **Hanvesakul R, Spencer N, Cook M, Gunson B, Hathaway M, Brown R, Nightingale P, Cockwell P, Hubscher SG, Adams DH, Moss P, Briggs D.** 2008. Donor HLA-C genotype has a profound impact on the clinical outcome following liver transplantation. *Am J Transplant* **8:**1931–1941. PubMed
37. **Tran TH, Middleton D, Döhler B, Scherer S, Meenagh A, Sleator C, Opelz G.** 2009. Reassessing the impact of donor HLA-C genotype on long-term liver transplant survival. *Am J Transplant* **9:**1674–1678. PubMed
38. **Legaz I, López-Álvarez MR, Campillo JA, Moya-Quiles MR, Bolarín JM, de la Peña J, Salgado G, Gimeno L, García-Alonso AM, Muro M, Miras M, Alonso C, Álvarez-López MR, Minguela A.** 2013. KIR gene mismatching and KIR/C ligands in liver transplantation: consequences for short-term liver allograft injury. *Transplantation* **95:**1037–1044. PubMed
39. **Khakoo SI, Thio CL, Martin MP, Brooks CR, Gao X, Astemborski J, Cheng J, Goedert JJ, Vlahov D, Hilgartner M, Cox S, Little AM, Alexander GJ, Cramp ME, O'Brien SJ, Rosenberg WM, Thomas DL, Carrington M.** 2004. HLA and NK cell inhibitory receptor genes in resolving hepatitis C virus infection. *Science* **305:**872–874. PubMed
40. **de Arias AE, Haworth SE, Belli LS, Burra P, Pinzello G, Vangeli M, Minola E, Guido M, Boccagni P, De Feo TM, Torelli R, Cardillo M, Scalamogna M, Poli F.** 2009. Killer cell immunoglobulin-like receptor genotype and killer cell immunoglobulin-like receptor-human leukocyte antigen C ligand compatibility affect the severity of hepatitis C virus recurrence after liver transplantation. *Liver Transpl* **15:**390–399. PubMed
41. **Uhrberg M, Valiante NM, Shum BP, Shilling HG, Lienert-Weidenbach K, Corliss B, Tyan D, Lanier LL, Parham P.** 1997. Human diversity in killer cell inhibitory receptor genes. *Immunity* **7:**753–763. PubMed
42. **Gómez-Lozano N, Vilches C.** 2002. Genotyping of human killer-cell immunoglobulin-like receptor genes by polymerase chain reaction with sequence-specific primers: an update. *Tissue Antigens* **59:**184–193. PubMed

43. **Ashouri E, Ghaderi A, Reed EF, Rajalingam R.** 2009. A novel duplex SSP-PCR typing method for KIR gene profiling. *Tissue Antigens* **74:**62–67. PubMed
44. **Rajalingam R, Ashouri E.** 2013. Gene-specific PCR typing of killer cell immunoglobulin-like receptors. *Methods Mol Biol* **1034:**239–255. PubMed
45. **Horowitz A, Strauss-Albee DM, Leipold M, Kubo J, Nemat-Gorgani N, Dogan OC, Dekker CL, Mackey S, Maecker H, Swan GE, Davis MM, Norman PJ, Guethlein LA, Desai M, Parham P, Blish CA.** 2013. Genetic and environmental determinants of human NK cell diversity revealed by mass cytometry. *Sci Transl Med* **5:**208ra145. PubMed
46. **Kreijveld E, van der Meer A, Tijssen HJ, Hilbrands LB, Joosten I.** 2007. KIR gene and KIR ligand analysis to predict graft rejection after renal transplantation. *Transplantation* **84:**1045–1051.
47. **Kunert K, Seiler M, Mashreghi MF, Klippert K, Schonemann C, Neumann K, Pratschke J, Reinke P, Volk HD, Kotsch K.** 2007. KIR/HLA ligand incompatibility in kidney transplantation. *Transplantation* **84:**1527–1533.
48. **Nowak I, Magott-Procelewska M, Kowal A, Miazga M, Wagner M, Niepieklo-Miniewska W, Kaminska M, Wisniewski A, Majorczyk E, Klinger M, Luszczek W, Pawlik A, Ploski R, Barcz E, Senitzer D, Kusnierczyk P.** 2012. Killer immunoglobulin-like receptor (KIR) and HLA genotypes affect the outcome of allogeneic kidney transplantation. *PLoS One* **7:**e44718. doi:10.1371/journal.pone.0044718
49. **Hanvesakul R, Kubal C, Moore J, Neil D, Cook M, Ball S, Briggs D, Moss P, Cockwell P.** 2011. KIR and HLA-C interactions promote differential dendritic cell maturation and is a major determinant of graft failure following kidney transplantation. *PLoS One* **6:**e23631. doi:10.1371/journal.pone.0023631
50. **Stern M, Hadaya K, Honger G, Martin PY, Steiger J, Hess C, Villard J.** 2011. Telomeric rather than centromeric activating KIR genes protect from cytomegalovirus infection after kidney transplantation. *Am J Transplant* **11:**1302–1307.

Chimerism Testing

LEE ANN BAXTER-LOWE

120

Chimerism testing is routinely used after allogeneic hematopoietic stem cell transplantation (HSCT) to monitor engraftment, detect relapse, identify patients with increased risk for graft-versus-host disease or graft loss, and monitor the effectiveness of therapeutic interventions. Chimerism testing can also be useful in other settings, such as detecting engraftment of donor lymphocytes after organ transplantation and determining sample identity (e.g., investigating suspected sample exchanges).

There are many methods for chimerism testing, but the predominant method for monitoring patients after HSCT measures relative quantities of donor and recipient alleles at loci with short tandem repeats (STR) or variable-number tandem repeats (VNTRs). STR/VNTR loci have alleles that differ in their numbers of tandemly repeated sequence motifs, which are identified by differences in size. The PCR is used to amplify an STR/VNTR locus, and the resultant fluorescently labeled amplicons are separated and quantified using automated capillary electrophoresis instruments. Other methods in use include well-established methods, such as fluorescence *in situ* hybridization (FISH), and novel approaches which take advantage of new technology. This chapter will focus on the use of STR/VNTR methods for HSCT because this represents the majority of chimerism testing conducted in clinical laboratories today. Examples of the alternative methods and other applications will be briefly described.

STR/VNTR METHODS

STR and VNTR alleles differ in number of repeat units and sequence (1). The repeat units can be simple repeats, compound repeats, or complex repeats. Simple repeats have multiple copies of the same sequence motif (Fig. 1), compound repeats have two or more adjacent sequence motifs of the same length but different sequences (an example is AGAT AGAT AGAT TTAA TTAA TTAA), and complex repeats have varied lengths and compositions (an example is AGAT AGAT AGGAT AGAT AGAT TTAACGGCCAT). Although the majority of reference sequences for STR/VNTR loci in the Genome DataBase are simple repeat units, careful sequencing has shown that many of these loci have variability within the repeats (1). The term STR is usually defined as loci with repeat units that are 2 to 6 bp long. These loci are sometimes called microsatellites due to their characteristic banding pattern in DNA centrifugation studies. The term VNTR is usually used to refer to loci with longer repeat units; these loci are sometimes referred to as minisatellites due to their distinctive banding patterns.

DNA Templates

DNA concentration and quality are important factors for STR/VNTR methods because the template influences the amount of PCR product, which in turn can affect several other parameters, including electrophoretic migration of DNA, signal strength, and background fluorescence. For chimerism tests, the amount of genomic DNA in each reaction mixture also affects the sensitivity (i.e., limits of detection) and technical variation (2, 3). Many procedures for chimerism testing recommend 50 to 100 ng template in each reaction mixture, which corresponds to approximately 7,500 to 15,000 cells. A EuroChimerism Consortium reported that under their assay conditions, 10 ng DNA template (equivalent to approximately 1,500 cells) resulted in sensitivities ranging from 0.8 to 1.6% in 90% of tests and showed acceptable technical variation (3). Although they could obtain results using 1 ng of the DNA template, the sensitivity and reproducibility were inferior to those observed for reaction mixtures containing 10 ng DNA. With the 1-ng DNA template, the sensitivity was more likely to be 3 to 5% (3). Although it is technically feasible to generate PCR products using extremely small quantities of DNA, this is not desirable for chimerism testing because sensitivity is affected by the number of cells represented in the reaction. For example, 1 ng genomic DNA represents DNA from approximately 150 cells. If the minority population is 1% of the cells and only 1 ng of the DNA template is added to each reaction mixture, some reactions will not have any detectable signal from the minority population due to sampling variation and stochastic events during PCR.

Each laboratory should establish methods for DNA isolation and acceptance criteria for DNA templates that are appropriate for their procedures and specimens. Acceptance criteria for DNA templates are usually determined using optical density at 260 nm (OD_{260}) and OD_{280} measurements. A EuroChimerism Consortium compared four procedures for isolation of DNA from small samples and reported the best results for an approach using detergents and proteinase K (4). Many labs use commercial kits which have a solid support that binds DNA.

doi:10.1128/9781555818722.ch120

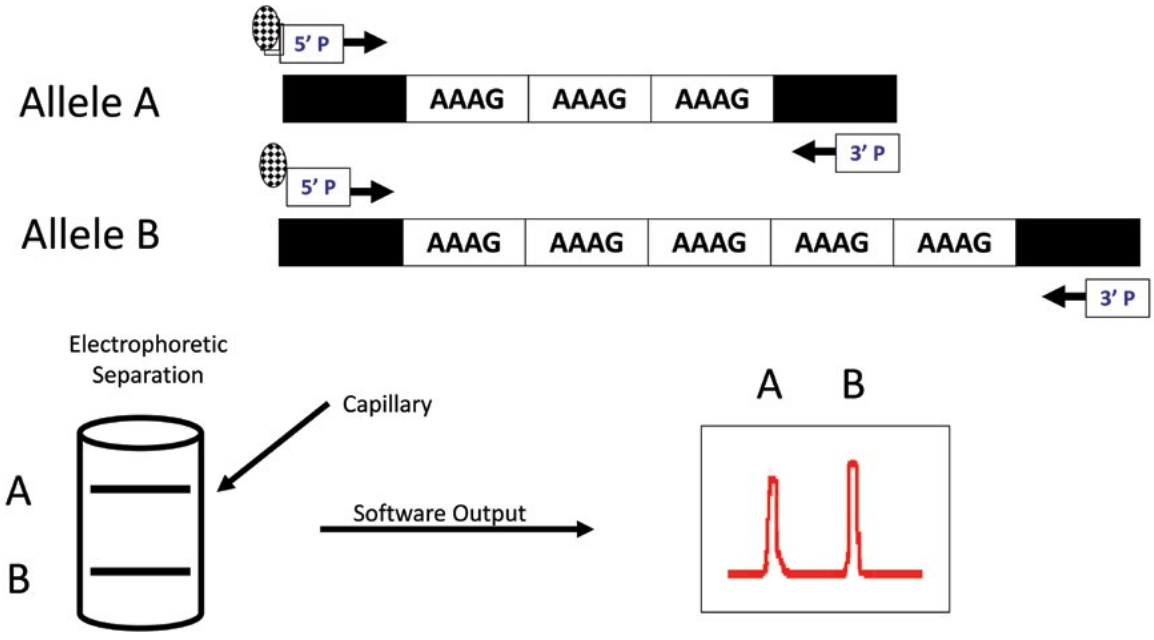

FIGURE 1 STR alleles differ in their lengths due to differences in the numbers of tandemly repeated sequence motifs. This figure shows a simple STR, which is referred to as a tetranucleotide repeat because there are 4 nucleotides in the motif. STRs used for chimerism testing are usually dinucleotide, trinucleotide, tetranucleotide, or pentanucleotide repeats.

Posttransplant specimens are usually peripheral blood or bone marrow. Pretransplant specimens from the donor and recipient are also important to provide control material for posttransplant chimerism assays. If a pretransplant specimen from the recipient is not available, DNA can be isolated from the recipient's hair, nail clippings, and biological material remaining after pathology studies (e.g., paraffin blocks). DNA can be isolated from buccal mucosa or skin, but these sources must be used with caution because contamination with donor lymphocytes is sometimes observed. If donor or recipient DNA is available but extremely limited, whole-genome amplification can be used to generate DNA for control material (5), but this DNA should be used with caution because the use of amplified DNA for the template for STR/VNTR testing has been reported to cause unbalanced reactions, allele dropouts, and allele additions (6).

PCR and Electrophoresis

Multiplex or single primer pairs can be used for PCR. The advantages of multiplex reactions include efficient use of consumables and the opportunity to average the results of several markers in an effort to improve accuracy. However, these advantages are offset by a loss of sensitivity caused by overlapping peaks, limitations in correction for overlapping signals from several different fluorescent dyes, and other factors that influence amplification efficiency. In general, the sensitivity for optimized single reactions is approximately 1%, while multiplex reactions have about 5% sensitivity (3, 7). Since sensitivity is important for determining donor chimerism after HSCT, this chapter will describe methods using a single primer pair in each PCR for measuring donor chimerism.

There is considerable variation in the methods that are used for STR/VNTR-based chimerism testing; most labs either use laboratory-developed tests or adapt commercial kits that were designed for identity (i.e., forensic or parentage) testing (7–10). Panels of PCR primers for 8 to 16 STR/VTNR loci are commonly used, but the loci, primer sequences, and assay conditions are extremely variable. A EuroChimerism Consortium recently proposed a standardized approach for chimerism testing for HSCT which includes methods for preparing DNA templates, primers, and amplification conditions, quality control procedures, criteria for selecting STR markers for each donor-recipient pair, and descriptive nomenclature for reporting the results (3, 4).

STR/VNTR amplicons are detected using capillary electrophoresis capable of resolving single nucleotide differences (e.g., a model 3130XL or 3500 genetic analyzer). The amount of PCR product, injection time, and voltage should be optimized to achieve minimal background fluorescence and strong signals that are not off the scale. Fragment analysis software (e.g., GeneScan/GeneMapper) is used to determine the size and area under the curve for each peak, and data are visualized as a chromatogram (Fig. 2). Each laboratory should establish acceptance criteria, which include signal strength, background fluorescence, and peak resolution. If any peaks are off the scale, it is not possible to accurately determine the relative quantities of each allele.

There are several factors which can adversely affect results, but many problems can easily be prevented or resolved. Signal strength can be improved by changing injection parameters and/or voltage. Fluorescent dyes are susceptible to photobleaching, and signals can be affected if labeled primers or amplicons are exposed to light. This problem can be avoided by ensuring that all fluorescent molecules are protected from light. If this problem is suspected, new reagents (primers) or PCR amplifications (amplicons) should be obtained. Intercapillary bleed-through can cause false-positive signals or confound interpretation of the data. This problem can be prevented by careful instrument setup (e.g., spectral and spatial calibrations). It is best to avoid any possibility of spectral overlap by judicious selection of dyes and primers. Dye-associated peaks caused by template-independent events can confound results when they migrate within the

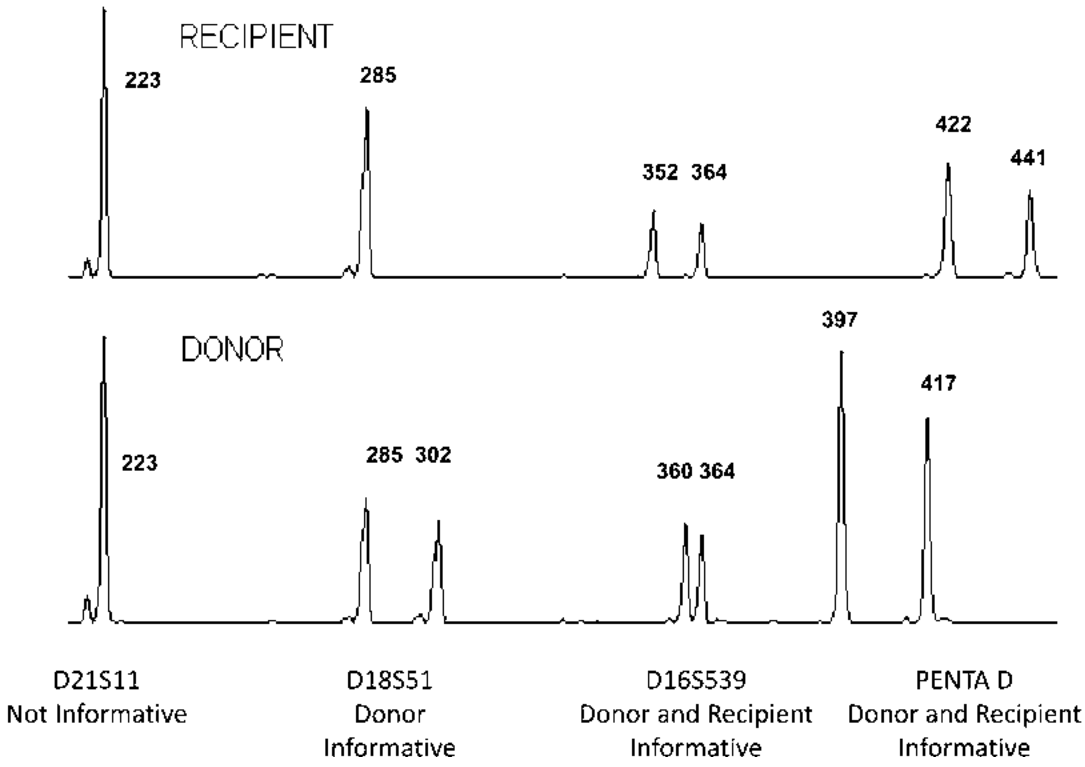

FIGURE 2 Identifying informative STR loci. Electropherograms of a multiplex PCR for four STR loci are shown for an HSCT recipient (top) and donor (bottom). For D21S11, the donor and recipient are homozygous for alleles of the same length (223 bp). For D18S51, the recipient is homozygous for an allele that is 285 bp. The donor shares this allele and has an additional allele that is 302 bp. Thus, D18S51 is a donor-informative locus. For D16S539, the donor and recipient share an allele that is 364 bp, and there are informative alleles for the donor (360 bp) and recipient (352 bp). For Penta D, there are two informative alleles for the recipient (422 and 441 bp) and the donor (394 and 417 bp).

range of STR alleles (11). If this problem occurs, it can be resolved by changing dyes and/or markers. If amplicons appear as split peaks, the DNA polymerase may be adding a single nucleotide to the 3′ ends of amplicons in a template-independent manner. This problem can usually be avoided by including a 30-min incubation at 60°C to allow extra time for the polymerase to catalyze the nontemplate addition of a nucleotide to all amplicons. Another factor that can affect the results is that the templates can slip during DNA synthesis and the resultant PCR products can appear as small peaks surrounding the main peak at intervals corresponding to the size of the repeat unit. This problem can be avoided through locus selection, reaction conditions, and technical factors. If stutter peaks are unavoidable and the area under the peak is used for calculations (see "Donor Chimerism Calculations" below), it is possible to make corrections for overlapping peaks.

Selecting Informative Loci

Loci with at least one allele unique to the donor or recipient are referred to as informative loci. The ideal locus has at least one allele that is informative for the donor and at least one allele that is informative for the recipient (bidirectional informative loci). In Fig. 2, D16S539 and Penta D are bidirectional informative loci. If unique alleles are limited to either the donor or the recipient, the locus is referred to as donor informative or recipient informative, respectively. In Fig. 2, D18S51 is an example of a donor-informative locus. If all alleles are shared, the locus is not informative (D21S11 in Fig. 2).

The likelihood of informative alleles at a particular locus is correlated with the degree of heterozygosity for that locus, not the number of alleles in the population. Thiede et al. compared the frequencies of 27 STR/VNTR markers in 203 recipients and their HLA-matched related donors and reported that Penta E, SE33, D2S1338, and D18S51 were most frequently informative for both recipient and donor (25 to 50% of pairs) (12). A panel of 13 primers was selected by the EuroChimerism Consortium because it provided bidirectional informative alleles for >99% of their donor-recipient pairs (3). Since the heterozygosity index and numbers of alleles for each locus can vary in different racial and ethnic populations, the likelihood of identifying an informative locus using a particular panel of STR/VNTR loci is dependent upon the laboratory's patient population.

To select optimal STR/VNTR loci for posttransplant monitoring, control DNA from the donor and recipient is used to determine the sizes and characteristics (e.g., presence of stutter peaks) of donor and recipient alleles for the lab's panel of STR/VNTR loci (Fig. 2). For this step, multiplex PCR is usually used because it provides efficient use of reagents and resources without compromising the ability to select informative loci. It is desirable to select at least two informative loci for posttransplant testing because averaging the results of multiple loci can increase accuracy. Loci located on different chromosomes are recommended to detect

a loss of heterozygosity which would cause false-negative results (13). The relative sizes of donor and recipient alleles are a very important consideration. If the alleles are within 1 to 3 repeat units in size, analysis can be confounded by stutter peaks, which appear as small peaks surrounding the main peak at intervals corresponding to the size of the repeat unit (see examples in D21S11 and D18S51 in Fig. 2). Stutter peaks are caused by template slippage during DNA synthesis, and the likelihood for stutter peaks is a characteristic of each locus. If possible, loci with stutter peaks that might confound analysis should be avoided. If it is necessary to use loci with stutter peaks, accuracy can be improved by making adjustments for the stutter peaks when the percentage of donor chimerism is calculated.

It is also beneficial to avoid informative loci that have substantial differences in the sizes of alleles because small alleles can be preferentially amplified over larger alleles. For example, Fig. 2 shows that the donor's Penta D 397 allele is amplified more efficiently than the donor's 417 allele. The recipient's 422 allele is amplified more efficiently than the 441 allele. Preferential amplification occurs because amplification efficiency is affected by the amplicon's size and, in some cases, sequence. Technical factors have also been reported to contribute to preferential amplification, including the PCR setup, the amount of template DNA, and the number of cycles used for thermal cycling (3). If there is evidence for preferential amplification of informative alleles, it is possible to correct for differences in amplification efficiency by making adjustments based upon a standard curve consisting of artificial mixtures of donor and recipient DNA (9).

The EuroChimerism Consortium proposed a descriptive nomenclature system for informative alleles named the Recipient-Shared-Donor (RSD) code (14), which incorporates relative allele sizes and the presence of stutter peaks. "D" indicates donor informative, "R" indicates recipient informative, and "S" indicates shared alleles. Alleles with stutter peaks are indicated with the corresponding lowercase letters (i.e., "d," "r," and "s"). Subscripts show the number of nucleotides separating the alleles. For example, $r_8D_{12}S$ is a code for a recipient allele with stutter peaks that is 8 nucleotides smaller than a donor allele that does not have stutter peaks. This donor allele is 12 nucleotides smaller than another allele that is shared.

The optimal informative loci can change during the posttransplant course. For example, if a patient has shown 100% donor chimerism in prior specimens, selecting a locus with an informative recipient allele that is preferentially amplified can improve sensitivity for detecting reemergence of recipient cells. STR/VNTR instability can result in mutations after transplant, particularly if there are malignant cells (13, 15, 16). If this occurs, these loci should be avoided. Loss of heterozygosity can also occur during the posttransplant course, particularly for patients transplanted for hematological malignancy (13). Loci showing loss of heterozygosity cannot be used for determining percentage donor chimerism.

Donor Chimerism Calculations

If the primary data meet the lab's criteria for reporting (e.g., signal strength and background), the areas under each of the informative peaks for the donor and recipient can be used to calculate the percent donor using the equation % donor chimerism = (D1 + D2)/(D1 + D2 + R1 + R2), where D1 and D2 are the areas under each of the donor's informative peaks and R1 and R2 are the areas under each of the recipient's informative peaks. If the donor and recipient share an allele, that allele can be eliminated from the equation. Some laboratories use peak heights rather than area under the peak. Both methods can achieve accurate results. Methods for calculating donor chimerism using many other possible combinations of informative alleles are described elsewhere (3, 8).

Since many factors can affect electrophoresis and sensitivity, it is optimal to include controls using DNA from the donor and recipient in each assay. Donor and recipient DNA is used to confirm alleles, and mixtures of donor and recipient DNA are used to determine sensitivity. The control DNA should have the same concentration as that in unknown samples because sensitivity is influenced by DNA concentration. For example, if an assay that typically achieves 1 to 5% sensitivity with 10 ng genomic DNA template, the mixtures of donor and recipient DNA might be 0%, 1%, 2%, 5%, 95%, 98%, 99%, and 100% donor added in mixtures totaling 10 ng DNA.

In clinics, descriptive terms are often used to describe donor chimerism. Detection of only donor is described as full donor chimerism. Some centers also consider ≥95% donor to be full donor chimerism. Detection of both donor and recipient is termed mixed chimerism. If chimerism is determined for cell lineages and some lineages are only donor while others are only recipient, the term "split chimerism" is used.

Cell Subsets

Determining donor chimerism in cell subsets can provide information that is extremely beneficial for monitoring and managing patients (2, 17–19). Testing of subsets can be used to substantially increase sensitivity. For example, if 8% of T cells are recipient derived, 10% of leukocytes are T cells, and all other cells are donor derived, testing of peripheral blood will show 100% donor because recipient cells represent less than 1% of nucleated cells in peripheral blood. If detection of persistent recipient cells might be critical for optimal management of this patient, sensitivity can be improved by testing a T cell subset where 8% recipient would be readily detected. When subsets that are frequently analyzed are taken into consideration, sensitivity for STR/VNTR-based tests becomes 0.1 to 0.01% of nucleated cells in peripheral blood (20).

Numerous reports have shown that testing of cell subsets can be useful for optimal patient management. For example, engraftment kinetics for T and NK cells has been reported to identify patients at increased risk for rejection and graft-versus-host disease (21–25). For patients that have hematological malignancies, detecting cells in the disease-associated subset can be indicative of impending recurrence, particularly when recipient cells are increasing in longitudinal samples (18–20, 26–29).

Cell subsets are usually isolated using immunomagnetic particles or sorting by flow cytometry to select cells with appropriate CD markers. CD markers that are frequently employed include CD3 (T cells), CD56 (NK cells), and CD19 (B cells). If immunomagnetic particle separation is used, confirming the purity of the subset with analytic flow cytometry can be extremely important to identify preparations that are compromised by contaminating cells (2, 30).

OTHER METHODS

Fluorescence *In Situ* Hybridization

FISH is a long-standing and well-established method that is still used by many laboratories for chimerism testing. Probes for X and Y chromosomes are usually used, but autosomal markers can also be used (31). This method achieves high precision and sensitivity if large numbers of cells are counted

(32). One of the advantages of this method is that it can be used for relatively small numbers of sorted cells, which would be difficult to reliably test using STR/VNTR methods (33); however, sensitivity is compromised if the number of cells that are counted is relatively small.

Quantitative PCR

Conventional real-time PCR methods have also been utilized for chimerism testing but have not achieved widespread use. Many markers have been used for this approach, including single nucleotide polymorphism, HLA, and insertion/deletion mutations (indels) (34–36). Advantages of real-time PCR include excellent sensitivity and avoidance of some of the limitations of STR/VNTR methods. Real-time PCR methods can be very accurate when the minority population is relatively small (<10%). However, technical variation increases when mixed chimerism is in the midrange. The coefficient of variation for real-time PCR methods has been reported to be 30 to 50% (35, 37), in comparison to <5% for STR/VNTR methods (9, 38, 39).

One of the challenges for real-time PCR methods is that they are influenced by relatively small differences in amplification efficiency. A 10% decrease in efficiency over 30 cycles would result in a 4-fold decrease in the estimation of a target sequence. For accurate results, it is important to include controls for amplification efficiency, replicates of each sample to minimize the effects of technical variation in threshold cycle, and calibration curves for the target sequence. Inclusion of these controls for a relatively large number of target sequences can be cumbersome. Although this method has some drawbacks, the high levels of sensitivity are advantageous when it is important to detect extremely low levels of chimerism, such as detection of recipient cells as an indicator for minimal residual disease and determining the presence of microchimerism (18, 19, 40–42).

Droplet digital PCR is a third-generation quantitative PCR method which overcomes many of the drawbacks of conventional real-time PCR methods and provides an absolute measure of target nucleic acid with unrivaled accuracy, precision, and sensitivity (43). Early reports of droplet digital PCR for chimerism testing are very encouraging (44, 45). In this method, target DNA is partitioned into nanodroplets (e.g., emulsion PCR) that contain on average one target molecule. The PCR is performed and each droplet is scored for the presence or absence of an amplicon. Poisson statistics are used to determine the number of copies of the target sequence in the starting material if TaqMan probes are used to differentiate alleles and the relative proportion of each allele can be calculated. Since this method uses endpoint PCR (in contrast to real-time methods), small differences in amplification efficiency do not affect the results and calibration curves are not necessary. Droplet digital PCR overcomes many of the limitations of other methods that are currently in use and has the potential to become a mainstream method for chimerism testing.

Nucleotide Sequencing

Pyrosequencing, which is a rapid and quantitative sequencing method, has been applied to chimerism testing, but early reports showed sensitivity that is inferior to those of STR/VNTR methods (46, 47). Next-generation sequencing technology utilizing pyrosequencing or other platforms is currently being explored for chimerism testing (48, 49). As this technology becomes readily available in clinical laboratories, next-generation sequencing may become an attractive option due to its high sensitivity and accuracy and its potential for lower costs.

Flow Cytometry

There have been several reports showing that flow cytometry using antibodies against proteins that are unique to the donor and recipient can be used for chimerism testing. Major advantages include determining if single cells are of donor or recipient origin, along with fast and convenient analysis of subpopulations. Although these are appealing features, flow cytometry is not widely used for chimerism testing. Antibody reagents that can reliably distinguish cells from a large number of donor/recipient pairs are likely to be one of the limiting factors. Several groups have reported using HLA antibodies, but this approach is not useful when the donor and recipient are HLA matched or there are no reagents to distinguish a small number of HLA mismatches (50, 51). Additionally, many HLA antibodies demonstrate cross-reactivity, which can confound chimerism analysis.

OTHER CLINICAL APPLICATIONS

Chimerism testing is routinely used following HSCT and is sometimes useful in other transplant settings. After solid-organ transplantation, donor microchimerism in peripheral blood has been detected, but the clinical significance is controversial. Some tolerance protocols combine HSCT and solid-organ transplantation and have reported that transient donor chimerism in peripheral blood can be associated with tolerance (52). Detection of donor chimerism can also aid in the assessment of risk for and diagnosis of graft-versus-host disease caused by lymphocytes carried by a solid-organ graft (53). When patients develop malignant disease after transplantation, chimerism testing can be used to determine if the tumor is of donor or recipient origin (15).

Microchimerism is widespread due to maternal-fetal cell exchange (54). Persistent microchimerism has also been reported after blood transfusion (55, 56). Microchimerism that is not caused by transplantation has been implicated in many diseases, including scleroderma, inflammatory bowel disease, Alzheimer disease, allergies, and certain cancers (41). Availability of new technology to aid investigation of microchimerism in health and disease may lead to new discoveries that increase demand for clinical microchimerism testing.

Finally, chimerism tests can also be extremely useful in the laboratory for investigating sample exchanges and confirming the identities of samples sent to the laboratory. For example, chimerism tests can be used to determine if a sample delivered to the laboratory was drawn from the correct individual. It can also be used to investigate suspected sample exchanges within the laboratory.

SUMMARY

Chimerism testing is currently routine for monitoring patients after allogeneic HSCT. Chimerism testing can be useful for other applications, including solid-organ transplantation and diseases associated with microchimerism. Numerous methods for chimerism testing have been reported, but STR/VNTR-based methods currently predominate. It is possible that new technologies that improve sensitivity and accuracy will ultimately supplant current methods.

REFERENCES

1. **Tilanus MG.** 2006. Short tandem repeat markers in diagnostics: what's in a repeat? *Leukemia* **20:**1353–1355. PubMed
2. **Willasch A, Eing S, Weber G, Kuçi S, Schneider G, Soerensen J, Jarisch A, Rettinger E, Koehl U, Klingebiel T, Kreyenberg H, Bader P.** 2010. Enrichment of cell

subpopulations applying automated MACS technique: purity, recovery and applicability for PCR-based chimerism analysis. *Bone Marrow Transplant* **45:**181–189. PubMed

3. **Lion T, Watzinger F, Preuner S, Kreyenberg H, Tilanus M, de Weger R, van Loon J, de Vries L, Cavé H, Acquaviva C, Lawler M, Crampe M, Serra A, Saglio B, Colnaghi F, Biondi A, van Dongen JJ, van der Burg M, Gonzalez M, Alcoceba M, Barbany G, Hermanson M, Roosnek E, Steward C, Harvey J, Frommlet F, Bader P.** 2012. The EuroChimerism concept for a standardized approach to chimerism analysis after allogeneic stem cell transplantation. *Leukemia* **26:**1821–1828. PubMed
4. **van der Burg M, Kreyenberg H, Willasch A, Barendregt BH, Preuner S, Watzinger F, Lion T, Roosnek E, Harvey J, Alcoceba M, Díaz MG, Bader P, van Dongen JJ, EU-Supported EuroChimerism Consortium Project QLRT-2001-01485.** 2011. Standardization of DNA isolation from low cell numbers for chimerism analysis by PCR of short tandem repeats. *Leukemia* **25:**1467–1470. PubMed
5. **Khan F, Liacini A, Arora E, Wang S, Assad M, Doulla J, Faridi RM, Berka N.** 2012. Assessment of fidelity and utility of the whole-genome amplification for the clinical tests offered in a histocompatibility and immunogenetics laboratory. *Tissue Antigens* **79:**372–379. PubMed
6. **Nagy M, Rascon J, Massenkeil G, Ebell W, Roewer L.** 2006. Evaluation of whole-genome amplification of low-copy-number DNA in chimerism analysis after allogeneic stem cell transplantation using STR marker typing. *Electrophoresis* **27:**3028–3037. PubMed
7. **Thiede C, Florek M, Bornhäuser M, Ritter M, Mohr B, Brendel C, Ehninger G, Neubauer A.** 1999. Rapid quantification of mixed chimerism using multiplex amplification of short tandem repeat markers and fluorescence detection. *Bone Marrow Transplant* **23:**1055–1060. PubMed
8. **Nollet F, Billiet J, Selleslag D, Criel A.** 2001. Standardisation of multiplex fluorescent short tandem repeat analysis for chimerism testing. *Bone Marrow Transplant* **28:**511–518. PubMed
9. **Scharf SJ, Smith AG, Hansen JA, McFarland C, Erlich HA.** 1995. Quantitative determination of bone marrow transplant engraftment using fluorescent polymerase chain reaction primers for human identity markers. *Blood* **85:**1954–1963. PubMed
10. **Thiede C, Bornhäuser M, Ehninger G.** 2004. Evaluation of STR informativity for chimerism testing—comparative analysis of 27 STR systems in 203 matched related donor recipient pairs. *Leukemia* **18:**248–254. PubMed
11. **Schraml E, Lion T.** 2003. Interference of dye-associated fluorescence signals with quantitative analysis of chimerism by capillary electrophoresis. *Leukemia* **17:**221–223. PubMed
12. **Thiede C, Bornhäuser M, Ehninger G.** 2004. Strategies and clinical implications of chimerism diagnostics after allogeneic hematopoietic stem cell transplantation. *Acta Haematol* **112:**16–23. PubMed
13. **Pereira S, Vayntrub T, Hiraki DD, Cherry AM, Arai S, Dvorak CC, Grumet FC.** 2011. Short tandem repeat and human leukocyte antigen mutations or losses confound engraftment and typing analysis in hematopoietic stem cell transplants. *Hum Immunol* **72:**503–509. PubMed
14. **Watzinger F, Lion T, Steward C, Eurochimerism Consortium.** 2006. The RSD code: proposal for a nomenclature of allelic configurations in STR-PCR-based chimerism testing after allogeneic stem cell transplantation. *Leukemia* **20:**1448–1452. PubMed
15. **Lipshutz GS, Baxter-Lowe LA, Nguyen T, Jones KD, Ascher NL, Feng S.** 2003. Death from donor-transmitted malignancy despite emergency liver retransplantation. *Liver Transplant* **9:**1102–1107.
16. **Much M, Buza N, Hui P.** 2014. Tissue identity testing of cancer by short tandem repeat polymorphism: pitfalls of interpretation in the presence of microsatellite instability. *Hum Pathol* **45:**549–555. PubMed
17. **Antin JH, Childs R, Filipovich AH, Giralt S, Mackinnon S, Spitzer T, Weisdorf D.** 2001. Establishment of complete and mixed donor chimerism after allogeneic lymphohematopoietic transplantation: recommendations from a workshop at the 2001 Tandem Meetings of the International Bone Marrow Transplant Registry and the American Society of Blood and Marrow Transplantation. *Biol Blood Marrow Transplant* **7:**473–485.
18. **Kroger N, Bacher U, Bader P, Bottcher S, Borowitz MJ, Dreger P, Khouri I, Macapinlac HA, Olavarria E, Radich J, Stock W, Vose JM, Weisdorf D, Willasch A, Giralt S, Bishop MR, Wayne AS.** 2010. NCI First International Workshop on the Biology, Prevention, and Treatment of Relapse after Allogeneic Hematopoietic Stem Cell Transplantation: report from the Committee on Disease-Specific Methods and Strategies for Monitoring Relapse following Allogeneic Stem Cell Transplantation. Part I. Methods, acute leukemias, and myelodysplastic syndromes. *Biol Blood Marrow Transplant* **16:**1187–1211.
19. **Kroger N, Bacher U, Bader P, Bottcher S, Borowitz MJ, Dreger P, Khouri I, Olavarria E, Radich J, Stock W, Vose JM, Weisdorf D, Willasch A, Giralt S, Bishop MR, Wayne AS.** 2010. NCI First International Workshop on the Biology, Prevention, and Treatment of Relapse after Allogeneic Hematopoietic Stem Cell Transplantation: report from the Committee on Disease-Specific Methods and Strategies for Monitoring Relapse following Allogeneic Stem Cell Transplantation. Part II. Chronic leukemias, myeloproliferative neoplasms, and lymphoid malignancies. *Biol Blood Marrow Transplant* **16:**1325–1346.
20. **Lion T, Daxberger H, Dubovsky J, Filipcik P, Fritsch G, Printz D, Peters C, Matthes-Martin S, Lawitschka A, Gadner H.** 2001. Analysis of chimerism within specific leukocyte subsets for detection of residual or recurrent leukemia in pediatric patients after allogeneic stem cell transplantation. *Leukemia* **15:**307–310. PubMed
21. **Breuer S, Preuner S, Fritsch G, Daxberger H, Koenig M, Poetschger U, Lawitschka A, Peters C, Mann G, Lion T, Matthes-Martin S.** 2012. Early recipient chimerism testing in the T- and NK-cell lineages for risk assessment of graft rejection in pediatric patients undergoing allogeneic stem cell transplantation. *Leukemia* **26:**509–519. PubMed
22. **Matthes-Martin S, Lion T, Haas OA, Frommlet F, Daxberger H, König M, Printz D, Scharner D, Eichstill C, Peters C, Lawitschka A, Gadner H, Fritsch G.** 2003. Lineage-specific chimaerism after stem cell transplantation in children following reduced intensity conditioning: potential predictive value of NK cell chimaerism for late graft rejection. *Leukemia* **17:**1934–1942. PubMed
23. **Lawler M, McCann SR, Marsh JC, Ljungman P, Hows J, Vandenberghe E, O'Riordan J, Locasciulli A, Socié G, Kelly A, Schrezenmeier H, Marin P, Tichelli A, Passweg JR, Dickenson A, Ryan J, Bacigalupo A, Severe Aplastic Anaemia Working Party of the European Blood and Marrow Transplant Group.** 2009. Serial chimerism analyses indicate that mixed haemopoietic chimerism influences the probability of graft rejection and disease recurrence following allogeneic stem cell transplantation (SCT) for severe aplastic anaemia (SAA): indication for routine assessment of chimerism post SCT for SAA. *Br J Haematol* **144:**933–945. PubMed
24. **Baron F, Maris MB, Storer BE, Sandmaier BM, Panse JP, Chauncey TR, Sorror M, Little MT, Maloney DG, Storb R, Heimfeld S.** 2005. High doses of transplanted CD34+ cells are associated with rapid T-cell engraftment and lessened risk of graft rejection, but not more graft-versus-host disease after nonmyeloablative conditioning and unrelated hematopoietic cell transplantation. *Leukemia* **19:**822–828. PubMed

25. **Lion T.** 2007. Detection of impending graft rejection and relapse by lineage-specific chimerism analysis. *Methods Mol Med* **134:**197–216. PubMed
26. **Bader P, Kreyenberg H, Hoelle W, Dueckers G, Handgretinger R, Lang P, Kremens B, Dilloo D, Sykora KW, Schrappe M, Niemeyer C, Von Stackelberg A, Gruhn B, Henze G, Greil J, Niethammer D, Dietz K, Beck JF, Klingebiel T.** 2004. Increasing mixed chimerism is an important prognostic factor for unfavorable outcome in children with acute lymphoblastic leukemia after allogeneic stem-cell transplantation: possible role for pre-emptive immunotherapy? *J Clin Oncol* **22:**1696–1705. PubMed
27. **Bader P, Kreyenberg H, Hoelle W, Dueckers G, Kremens B, Dilloo D, Sykora KW, Niemeyer C, Reinhardt D, Vormoor J, Gruhn B, Lang P, Greil J, Handgretinger R, Niethammer D, Klingebiel T, Beck JF.** 2004. Increasing mixed chimerism defines a high-risk group of childhood acute myelogenous leukemia patients after allogeneic stem cell transplantation where pre-emptive immunotherapy may be effective. *Bone Marrow Transplant* **33:**815–821. PubMed
28. **Horn B, Soni S, Khan S, Petrovic A, Breslin N, Cowan M, Pelle-Day G, Cooperstein E, Baxter-Lowe LA.** 2009. Feasibility study of preemptive withdrawal of immunosuppression based on chimerism testing in children undergoing myeloablative allogeneic transplantation for hematologic malignancies. *Bone Marrow Transplant* **43:**469–476. PubMed
29. **Ozyurek E, Cowan MJ, Koerper MA, Baxter-Lowe LA, Dvorak CC, Horn BN.** 2008. Increasing mixed chimerism and the risk of graft loss in children undergoing allogeneic hematopoietic stem cell transplantation for non-malignant disorders. *Bone Marrow Transplant* **42:**83–91. PubMed
30. **Hanson V, Adams B, Lord J, Barker A, Poulton K, Lee H.** 2013. Assessment of the purity of isolated cell populations for lineage-specific chimerism monitoring post haematopoietic stem cell transplantation. *Tissue Antigens* **82:**269–275. PubMed
31. **Ruiz ADS, Chauffaille MDLF, Alves ST, Oliveira JS.** 2009. Prevalence of chimerism after non-myeloablative hematopoietic stem cell transplantation. *Sao Paulo Med J* **127:**251–258.
32. **Buño I, Nava P, Simón A, González-Rivera M, Jiménez JL, Balsalobre P, Serrano D, Carrión R, Gómez-Pineda A, Díez-Martín JL.** 2005. A comparison of fluorescent in situ hybridization and multiplex short tandem repeat polymerase chain reaction for quantifying chimerism after stem cell transplantation. *Haematologica* **90:**1373–1379. PubMed
33. **Cotteret S, Belloc F, Boiron JM, Bilhou-Nabera C, Dumain P, Boyer C, Lacombe F, Reiffers J, Bernard P.** 1998. Fluorescent in situ hybridization on flow-sorted cells as a tool for evaluating minimal residual disease or chimerism after allogenic bone marrow transplantation. *Cytometry* **34:**216–222. PubMed
34. **Lee TH, Chafets DM, Reed W, Wen L, Yang Y, Chen J, Utter GH, Owings JT, Busch MP.** 2006. Enhanced ascertainment of microchimerism with real-time quantitative polymerase chain reaction amplification of insertion-deletion polymorphisms. *Transfusion* **46:**1870–1878. PubMed
35. **Alizadeh M, Bernard M, Danic B, Dauriac C, Birebent B, Lapart C, Lamy T, Le Prisé PY, Beauplet A, Bories D, Semana G, Quelvennec E.** 2002. Quantitative assessment of hematopoietic chimerism after bone marrow transplantation by real-time quantitative polymerase chain reaction. *Blood* **99:**4618–4625. PubMed
36. **Gendzekhadze K, Gaidulis L, Senitzer D.** 2013. Chimerism testing by quantitative PCR using Indel markers. *Methods Mol Biol* **1034:**221–237. PubMed
37. **Maas F, Schaap N, Kolen S, Zoetbrood A, Buño I, Dolstra H, de Witte T, Schattenberg A, van de Wiel-van Kemenade E.** 2003. Quantification of donor and recipient hemopoietic cells by real-time PCR of single nucleotide polymorphisms. *Leukemia* **17:**621–629. PubMed
38. **Hancock JP, Goulden NJ, Oakhill A, Steward CG.** 2003. Quantitative analysis of chimerism after allogeneic bone marrow transplantation using immunomagnetic selection and fluorescent microsatellite. PCR *Leukemia* **17:**247–251. PubMed
39. **Kreyenberg H, Hölle W, Möhrle S, Niethammer D, Bader P.** 2003. Quantitative analysis of chimerism after allogeneic stem cell transplantation by PCR amplification of microsatellite markers and capillary electrophoresis with fluorescence detection: the Tuebingen experience. *Leukemia* **17:**237–240. PubMed
40. **Baxter-Lowe LA, Busch MP.** 2006. Tracking microchimeric DNA in plasma to diagnose and manage organ transplant rejection *Clin Chem* **52:**559–561. PubMed
41. **Nelson JL.** 2003. Microchimerism in human health and disease. *Autoimmunity* **36:**5–9. PubMed
42. **Reed WF, Lee TL, Trachtenberg E, Vinson M, Busch MP.** 2001. Detection of microchimerism by PCR is a function of amplification strategy. *Transfusion* **41:**39–44. PubMed
43. **Hindson CM, Chevillet JR, Briggs HA, Gallichotte EN, Ruf IK, Hindson BJ, Vessella RL, Tewari M.** 2013. Absolute quantification by droplet digital PCR versus analog real-time PCR. *Nat Methods* **10:**1003–1005. PubMed
44. **Beck J, Bierau S, Balzer S, Andag R, Kanzow P, Schmitz J, Gaedcke J, Moerer O, Slotta JE, Walson P, Kollmar O, Oellerich M, Schütz E.** 2013. Digital droplet PCR for rapid quantification of donor DNA in the circulation of transplant recipients as a potential universal biomarker of graft injury. *Clin Chem* **59:**1732–1741. PubMed
45. **George D, Czech J, John B, Yu M, Jennings LJ.** 2013. Detection and quantification of chimerism by droplet digital PCR. *Chimerism* **4:**102–108. PubMed
46. **Hochberg EP, Miklos DB, Neuberg D, Eichner DA, McLaughlin SF, Mattes-Ritz A, Alyea EP, Antin JH, Soiffer RJ, Ritz J.** 2003. A novel rapid single nucleotide polymorphism (SNP)-based method for assessment of hematopoietic chimerism after allogeneic stem cell transplantation. *Blood* **101:**363–369. PubMed
47. **Wu CJ, Hochberg EP, Rogers SA, Kutok JL, Biernacki M, Nascimento AF, Marks P, Bridges K, Ritz J.** 2003. Molecular assessment of erythroid lineage chimerism following nonmyeloablative allogeneic stem cell transplantation. *Exp Hematol* **31:**924–933. PubMed
48. **Rieneck K, Bak M, Jønson L, Clausen FB, Krog GR, Tommerup N, Nielsen LK, Hedegaard M, Dziegiel MH.** 2013. Next-generation sequencing: proof of concept for antenatal prediction of the fetal Kell blood group phenotype from cell-free fetal DNA in maternal plasma. *Transfusion* **53**(Suppl 2)**:**2892–2898. PubMed
49. **Bentley G, Higuchi R, Hoglund B, Goodridge D, Sayer D, Trachtenberg EA, Erlich HA.** 2009. High-resolution, high-throughput HLA genotyping by next-generation sequencing. *Tissue Antigens* **74:**393–403. PubMed
50. **Schumm M, Feuchtinger T, Pfeiffer M, Hoelle W, Bethge W, Ebinger M, Kuci S, Handgretinger R, Lang P.** 2007. Flow cytometry with anti HLA-antibodies: a simple but highly sensitive method for monitoring chimerism and minimal residual disease after HLA-mismatched stem cell transplantation. *Bone Marrow Transplant* **39:**767–773. PubMed
51. **Metes D, Logar A, Rudert WA, Zeevi A, Woodward J, Demetris AJ, Abu-Elmagd K, Eghtesad B, Shapiro R, Fung JJ, Trucco M, Starzl TE, Murase N.** 2003. Four-color flow cytometric analysis of peripheral blood donor cell chimerism. *Hum Immunol* **64:**787–795. PubMed

52. **Kawai T, Sachs DH.** 2013. Tolerance induction: hematopoietic chimerism. *Curr Opin Organ Transplant* **18:**402–407. PubMed
53. **Domiati-Saad R, Klintmalm GB, Netto G, Agura ED, Chinnakotla S, Smith DM.** 2005. Acute graft versus host disease after liver transplantation: patterns of lymphocyte chimerism. *Am J Transplant* **5:**2968–2973.
54. **Nelson JL.** 2012. The otherness of self: microchimerism in health and disease. *Trends Immunol* **33:**421–427. PubMed
55. **Lee TH, Paglieroni T, Ohto H, Holland PV, Busch MP.** 1999. Survival of donor leukocyte subpopulations in immunocompetent transfusion recipients: frequent long-term microchimerism in severe trauma patients. *Blood* **93:**3127–3139. PubMed
56. **Utter GH, Owings JT, Lee TH, Paglieroni TG, Reed WF, Gosselin RC, Holland PV, Busch MP.** 2004. Blood transfusion is associated with donor leukocyte microchimerism in trauma patients. *J Trauma* **57:**702–708. PubMed

Laboratory Management

section Q

VOLUME EDITOR: ROBERT G. HAMILTON
SECTION EDITOR: RONALD J. HARBECK

Clinical Immunology Laboratory Accreditation, Licensure, and Credentials

LINDA COOK AND RONALD J. HARBECK

121

Today's clinical immunology laboratories have emerged from research laboratories as new assays became available to researchers and clinician-scientists. However, in today's hospital and reference laboratory environment, many governmental regulations and professional guidelines mandate defined education levels of individuals who oversee and perform patient testing, recommend test procedures, and define acceptable ordering, result reporting, and billing practices. Among these organizations is the Centers for Medicare and Medicaid Services (CMS), previously known as the Health Care Financing Administration (HCFA). CMS is a federal agency within the U.S. Department of Health and Human Services (DHHS) that administers the Medicare program and works in partnership with state governments to administer Medicaid. CMS also regulates billing practices and has a significant impact on the manner in which laboratories must be structured and managed. Today's successful clinical immunology laboratory practitioners must be knowledgeable about current guidelines and regulations and keep abreast of the constant changes in order to ensure compliance and professionalism in all areas of the laboratory. This chapter provides a broad overview of the major governmental agencies and regulations that impact on clinical laboratory practices. Various agencies and regulations are discussed in this chapter. To assist the reader, a list of their abbreviations is provided. In addition, an extensive list of websites is given in Table 1 to enable the reader to obtain further information regarding specific agencies, regulations, and programs.

Abbreviations.

AAAAI, American Academy of Allergy, Asthma and Immunology; **ACAAI,** American College of Allergy, Asthma and Immunology; **AACC,** American Association of Clinical Chemistry; **AABB,** American Association of Blood Banks; **ABB,** American Board of Bioanalysts; **ABCC,** American Board of Clinical Chemistry; **ABMG,** American Board of Medical Genetics; **AOA,** American Osteopathic Association; **ASCP,** American Society of Clinical Pathologists; **ASHI,** American Society for Histocompatibility and Immunogenetics; **ASM,** American Society for Microbiology; **ASO,** anti-streptolysin O; **ASR,** analyte-specific reagents; **CAP,** College of American Pathologists; **CCSQ,** Center for Clinical Standards and Quality; **CDC,** Centers for Disease Control and Prevention; **MPEP,** CDC Model Performance Evaluation Program; **CLEP,** Clinical Laboratory Evaluation Program; **CLIA,** Clinical Laboratory Improvement Amendments; **CLSI,** Clinical and Laboratory Standards Institute (formerly National Committee for Clinical Laboratory Standards, **NCCLS**); **CMS,** Centers for Medicare and Medicaid Services (formerly the Health Care Financing Administration [**HCFA**]); **COLA,** Commission on Office Laboratory Accreditation; **COMACC,** Commission on Accreditation in Clinical Chemistry; **ABFT,** American Board of Forensic Toxicology; **CPA,** Clinical Pathology Accreditation Ltd.; **CPT,** Current Procedural Terminology; **DHEW,** Department of Health, Education and Welfare; **DRG,** diagnosis-related group; **CEN,** European Committee for Standardization; **EA,** European Accreditation; **FESCC,** Forum of European Societies of Clinical Chemistry; **EFLM,** European Federation of Clinical Chemistry and Laboratory Medicine; **FDA,** Food and Drug Administration; **GLP,** Good Laboratory Practice; **HCPCS,** HCFA Common Procedure Coding System; **HMO,** health maintenance organization; **ICD,** International Classification of Diseases; **ISO,** International Organization for Standardization; **NRCC,** National Registry of Certified Chemists; **TJC,** The Joint Commission (formerly known as the Joint Commission on Accreditation of Healthcare Organizations [**JCAHO**]); **LAP,** Laboratory Accreditation Program; **LOINC,** Laboratory Observation Identifier Names and Codes; **LDT,** laboratory-developed tests; **OIG,** Office of the Inspector General; **PPM,** provider-performed microscopy; **WHO,** World Health Organization.

REGULATORY ISSUES AND AGENCIES OF THE FEDERAL GOVERNMENT

The Clinical Laboratory Improvement Amendment

In 1965, the U.S. federal government enacted Public Law 89-97, which created Medicare and Medicaid under the Social Security Act of 1939. As a result of this law, the Department of Health, Education and Welfare developed standards for clinical laboratories operating in inpatient and outpatient settings. DHEW appointed The Joint Commission (TJC), formerly known as the Joint Commission on Accreditation of Healthcare Organizations (JCAHO), to set standards and survey the laboratories for accreditation. However, Congress became concerned that significant problems existed in the quality of laboratory testing for Medicare recipients provided by laboratories engaged in interstate

doi:10.1128/9781555818722.ch21

commerce. Therefore, in 1967, Congress passed the Clinical Laboratory Improvement Amendment (CLIA '67) mandating licensure for laboratories providing testing on more than 100 out-of-state specimens per year in major testing categories such as microbiology, immunology, chemistry, general serology, and hematology. A letter of exemption could be obtained from the CDC for those laboratories receiving fewer than 100 out-of-state specimens per year.

In 1987, the *Wall Street Journal* published an article that again raised concerns among the public about the quality of laboratory testing, especially cytology (1, 2). This prompted Congress and many state health departments to closely review the operations of the nation's clinical laboratories. This review resulted in Congress passing Public Law 100-578 or the Clinical Laboratory Improvement Amendment of 1988 (CLIA '88) (3). In 1992, the final rules for CLIA '88 were published (4, 5, 8). CLIA '88 replaced CLIA '67 and the separate Medicare/Medicaid regulations that were in effect up until this time. CLIA '88 required that all facilities performing examinations on materials obtained from the human body for the purpose of providing information for the diagnosis, prevention, or treatment of any disease or impairment or for the assessment of the health of human beings be subject to CLIA regulations. The sites included in these new regulations were doctor's offices, clinics, health departments, hospitals, and reference laboratories. The primary aim and authority of CLIA is to ensure the accuracy, reliability, and timeliness of test results regardless of where the test was performed. These requirements mandated additional procedures, reviews, and proficiency testing for all laboratories whether or not they were directly associated with a health care institution. Laboratories exempt from CLIA '88 include those that are subject to the rules published and enforced by the Department of Veterans Affairs and by the Department of Defense (for personnel drug surveillance and enforcement purposes). In addition, laboratories licensed by approved state licensure programs, law enforcement agencies that determine the legal status of individuals, laboratories performing forensic testing, and those performing research testing for which the results are not reported for clinical use are also exempt from CLIA '88 regulations.

As part of CMS's (HCFA's) mandates, it is responsible for the administration of the Medicare and Medicaid programs. The Division of Laboratory Services under the Center for Clinical Standards and Quality (CCSQ) is responsible for implementing the CLIA program. It is the responsibility of the Division of Outcomes and Improvement within CMS to ensure that medical laboratories provide quality testing results. This is achieved through a survey and certification program (6). As of January 2016, there were 254,650 laboratories and 122,617 physician office laboratories currently registered with CLIA. The majority of these are located in the United States. Funding of the CLIA program is maintained by user fees collected from these laboratories. There are 10 regional offices located throughout the United States with at least one laboratory consultant in each office who has experience and formal training as a medical technologist and is responsible for ensuring that the laboratories within that region are in compliance with the regulations.

Many medical laboratories may not be directly affected by the CMS surveys. CMS has granted "deemed" status to several organizations. In other words, CMS has the authority to establish and oversee a program that allows private, national accreditation organizations to "deem" that a laboratory is in compliance with Medicare requirements. These organizations include the College of American Pathologists (CAP), The Joint Commission (TJC), the American Association of Blood Banks (AABB), the American Osteopathic Association (AOA), the American Society for Histocompatibility and Immunogenetics (ASHI), and the Commission on Office Laboratory Accreditation (COLA). In addition, two states, Washington and New York, are exempt from CLIA regulations since their programs were found to be equal to or exceed Medicare compliance requirements. As of 2016, 7,796 laboratories had been certified by the CAP while over 3,000 have been certified by TJC.

CLIA has established four categories of testing, i.e., waived, moderate complexity, provider-performed microscopy, and high complexity. The waived tests are those considered simple laboratory examinations and procedures that have insignificant risk of an erroneous result. Laboratories with a certificate of waiver are not subject to inspection for certification. However, it is expected that the laboratory will follow the manufacturer's instructions and perform quality control measures as specified by the manufacturer of the kits in use. CLIA '88 waived tests include those performed in bacteriology, endocrinology, general chemistry, hematology, toxicology and therapeutic drug monitoring (TDM), and urinalysis. The following clinical immunology laboratory tests have been approved as waived tests: HIV-1 and -2 antibodies, influenza virus A/B, Lyme disease antibodies, bladder tumor-associated antigen, and antibodies against *Helicobacter pylori*, Epstein-Barr virus (EBV; infectious mononucleosis), and respiratory syncytial virus (RSV). The FDA maintains a website, which contains frequent updates of waived tests (Table 1). Moreover, waived tests are not completely foolproof. Some waived tests have the potential for serious health impacts if not performed correctly.

For moderate- and high-complexity tests, the FDA evaluates each new commercial test system during the premarket approval process by scoring seven criteria as described in the CLIA regulations. The criteria for categorization include (i) knowledge, (ii) training and experience, (iii) reagent and materials preparation, (iv) characteristics of operational steps, (v) calibration, quality control, and proficiency testing materials, (vi) test system troubleshooting and equipment maintenance, and (vii) interpretation and judgment.

Tests included in the "moderately complex" category require basic scientific and technical knowledge in the various analytical phases of the test. In addition, basic training and experience are required to perform the test. The tests may not be fully automated and may require monitoring, timing, or simple calculations. Independent technical skill decision making or intervention by the analyst may be required. Before the results of a moderately complex test are released, interpretation and judgment may be required by the analyst. There are also requirements for quality control (QC) and quality assurance (QA) processes, for enrollment in a proficiency testing (PT) program, personnel requirements, and accreditation by an approved agency.

The "moderately complex" testing category contains one subcategory of provider-performed microscopy (PPM). Tests included in this category are procedures that utilize a microscope and in which the test specimen is labile or, if testing is delayed, could compromise the accuracy of the results. Some of the tests included in this category are wet mounts, including preparations of vaginal, cervical, or skin specimens, pinworm examinations, microscopic urinalysis, and urinalysis by dipstick or tablet reagent for bilirubin, glucose, hemoglobin, ketones, leukocytes, nitrite, pH, protein, specific gravity, and urobilinogen. Tests included in this category must be performed during a patient's visit only by

TABLE 1 Website addresses of governmental and private agencies that establish regulations and guidelines for clinical laboratories

Agency or organization	Website[a]
Federal regulations and guidelines	
Agency for Healthcare Research and Quality	www.ahcpr.gov/
Centers for Disease Control and Prevention	www.cdc.gov
Centers for Disease Control and Prevention (waived tests)	http://wwwn.cdc.gov/CLIA/Resources/WaivedTests/default.aspx
Centers for Medicare and Medicaid Services (CMS)	www.dhhs.gov
CMS CLIA information	http://www.cms.gov/Regulations-and-Guidance/Legislation/CLIA/index.html?redirect=/CLIA/
CMS Lab Diagnostic Fee Schedules (yearly file)	http://www.cms.gov/Medicare/Medicare-Fee-for-Service-Payment/ClinicalLabFeeSched/index.html?redirect=/ClinicalLabFeeSched
College of American Pathologists	www.cap.org/apps/cap.portal
College of American Pathologists ISO15189	http://www.cap.org/apps/cap.portal?_nfpb=true&cntvwrPtlt_actionOverride=%2Fportlets%2FcontentViewer%2Fshow&_windowLabel=cntvwrPtlt&cntvwrPtlt%7BactionForm.contentReference%7D=laboratory_accreditation%2F15189%2Fabout.html&_pageLabel=cntvwr
Department of Health and Human Services	http://www.hhs.gov/
Food and Drug Administration (FDA)	www.fda.gov
FDA Good Laboratory Practice Document 21 Part 58	http://www.accessdata.fda.gov/scripts/cdrh/cfdocs/cfcfr/CFRsearch.cfm?CFRPart=58
Good Laboratory Practices Online	http://www.accessdata.fda.gov/scripts/cdrh/cfdocs/cfcfr/CFRsearch.cfm?CFRPart=58
Medicare, glossary of terms	http://www.medicare.gov/glossary/a.html
National Institutes of Health	www.nih.gov
National Institute of Occupational Safety and Health	www.cdc.gov/niosh/homepage.html
Office of Inspector General (Federal Register Notices/Compliance)	http://oig.hhs.gov/authorities/docs/cpglab.pdf
Society of Quality Assurance	www.sqa.org
State regulations and guidelines	
California Department of Health Services, Division of Laboratory Science, Laboratory Field Services	http://www.cdph.ca.gov/programs/lfs/Pages/default.aspx
New York State Clinical Laboratory Evaluation Program	http://www.wadsworth.org/regulatory/clep
Oregon	https://public.health.oregon.gov/LaboratoryServices/ClinicalLaboratoryRegulation/Pages/index.aspx
Washington State	http://www.doh.wa.gov/LicensesPermitsandCertificates/FacilitiesNewReneworUpdate/LaboratoryQualityAssurance/Licensing/Applications
International regulations and guidelines	
European Communities Confederation of Clinical Chemistry and Laboratory Medicine	www.e-c4.org
External Peer Review Techniques	http://www.ncbi.nlm.nih.gov/pubmed/10894188
Institute for Standardization and Documentation in Medical Laboratory	www.instand-ev.de/
International Federation of Clinical Chemistry and Laboratory Medicine	www.ifcc.org
International Organization for Standardization (ISO)	http://www.iso.org/iso/home.html
ISO clinical laboratory testing and *in vitro* diagnostic test systems	http://www.iso.org/iso/catalogue_ics
The Clinical Pathology Accreditation Ltd.	http://www.ukas.com/services/accreditation-services/clinical-pathology-accreditation/
World Health Organization	www.who.int/en/
Other	
American Association of Blood Banks (AABB)	www.aabb.org/
American Medical Association (AMA)	www.ama-assn.org/
AMA CPT Coding	http://www.ama-assn.org/ama/pub/physician-resources/solutions-managing-your-practice/coding-billing-insurance/cpt.page
American Osteopathic Association	www.aoa-net.org/
American Society for Histocompatibility and Immunogenetics	www.ashi-hla.org/
Clinical and Laboratory Standards Institute (formerly National Committee for Clinical Laboratory Standards)	http://www.clsi.org/
The Joint Commission	http://www.jointcommission.org/

[a]See the text for abbreviations.

licensed physicians, dentists, podiatrists, or mid-level practitioners including nurse practitioners, nurse-midwives, and physician assistants.

The "highly complex" category of tests includes a manual procedure with multiple steps in the sample or reagent processing or automated procedures requiring significant operator intervention. These tests require specialized scientific and technical knowledge as well as appropriate training and experience in order to perform all phases of the analytical process optimally. Reagents used in these tests may be labile and may require special handling or preparation. The operational steps involved in performing highly complex tests may require manual manipulation and monitoring. A high level of troubleshooting ability, decision making, intervention, interpretation, and judgment is required. Many tests performed in the clinical immunology laboratory as well as more than 50 general tests or procedures have been categorized as high complexity. Table 2 provides a list of pertinent Clinical and Laboratory Standards Institute (CLSI) documents that aid immunology laboratories in establishing and reviewing procedures.

CLIA '88 specifies the training required by individuals based on the complexity of the testing. For a laboratory performing moderately complex testing, the directors may include pathologists, medical doctors (M.D.s) doctors of osteopathic medicine (D.O.s), or persons holding a doctoral degree (Ph.D.s) with appropriate laboratory experience and training or individuals with a master's or bachelor's degree in science with appropriate experience and training. For high-complexity laboratories, a pathologist, other M.D., or D.O. with 1 year of laboratory training during residency or 2 years' experience directing or supervising high-complexity testing may direct the laboratory. In addition, the laboratory director may hold an earned doctoral degree in a chemical, physical, biological, or clinical laboratory science from an accredited institution and be certified and continue to be certified by a board approved by DHHS. The current approved boards are listed on the CMS website (Table 1), and they include the following: American Board of Bioanalysis (ABB), ABB public health microbiology certification, American Board of Clinical Chemistry (ABCC), ABCC 24-month Commission on Accreditation in Clinical Chemistry (COMACC) accredited program, American Board of Forensic Toxicology (ABFT) (limited to individuals with a doctoral degree), American Board of Histocompatibility and Immunogenetics (ABHI), American Board of Medical Genetics (ABMG), American Board of Medical Laboratory Immunology (ABMLI), American Board of Medical Microbiology (ABMM), and National Registry of Certified Chemists (NRCC) (limited to individuals with a doctoral degree). These Boards are recognized by federal and state government agencies as a significant component toward meeting licensure requirements to direct clinical laboratories engaged in the diagnosis of human disease. Board certification in some cases is recognized not only by CLIA but also in other states that require licensure, e.g., Florida, Georgia, Hawaii, Louisiana, Montana, Nevada, New York, North Dakota, Rhode Island, Tennessee, and West Virginia.

As of 24 February 2003, an individual may serve as a laboratory director under a grandfather clause with at least 2 years of laboratory training or experience. At the end of the 2 years, such an individual must (i) become board certified, (ii) be serving as a laboratory director and previously qualified on or before 24 February 2003, (iii) be qualified under 14 March 1990 CLIA '67, or (iv) be qualified under state law to direct a laboratory in the state on or before 24 February 2003. In addition to the laboratory director, specific qualifications are required for technical supervisors, general supervisors, clinical consultants, and cytotechnologists.

The CLIA regulations require that the laboratory employ one or more individuals who are qualified by education and either training or experience to perform the responsibilities of a technical supervisor. For the clinical immunology laboratory, the requirements range from board-certified pathologists to a bachelor's degree in science with 4 years of training in high-complexity testing. For histocompatibility

TABLE 2 Immunology standardization documents available from CLSI

Document/ status[a]	Title
I/LA02-A2	*Quality Assurance of Laboratory Tests for Autoantibodies to Nuclear Antigens: (1) Indirect Fluorescence Assay for Microscopy and (2) Microtiter Enzyme Immunoassay Methods.*
I/LA18-A2	*Specifications for Immunological Testing for Infectious Disease*
I/LA20-A2	*Analytical Performance Characteristics and Clinical Utility of Immunological Assays for Human Immunoglobulin E (IgE) Antibodies and Defined Allergen Specificities*
I/LA21-A2	*Clinical Evaluation of Immunoassays*
I/LA23-A	*Assessing the Quality of Immunoassay Systems: Radioimmunoassays and Enzyme, Fluorescence, and Luminescence Immunoassays*
I/LA26-A2	*Performance of Single Cell Immune Response Assays*
I/LA29-A	*Detection of HLA-Specific Alloantibody by Flow Cytometry and Solid Phase Assays*
I/LA30-A	*Immunoassay Interference by Endogenous Antibodies*
I/LA34-A	*Design and Validation of Immunoassays for Assessment of Human Allergenicity of New Biotherapeutic Drugs*
NBS06-A	*Newborn Blood Spot Screening for Severe Combined Immunodeficiency by Measurement of T-cell Receptor Excision Circles*
I/LA1-A2	*Assessing the Quality of Radioimmunoassay Systems* (2nd ed.)
H42-A2	*Enumeration of Immunologically Defined Cell Populations by Flow Cytometry*
H43-A2	*Clinical Flow Cytometric Analysis of Neoplastic Hematolymphoid Cells*
M53-A	*Criteria for Laboratory Testing and Diagnosis of Human Immunodeficiency Virus Infection*

[a]A, approved.

and clinical cytogenetics, individuals must be an M.D., D.O., or Ph.D. with 4 years of training or experience. The CLIA requirements for a general supervisor are to be an M.D. or D.O. or hold a Ph.D. or master's or bachelor's degree in science with 1 year of training or experience in high-complexity testing. Alternatively, the general supervisor must have an associate degree in laboratory science or medical laboratory technology and 2 years of training or experience in high-complexity testing. One should refer to the CMS website for additional requirements on education and training for laboratory directors, supervisors, and testing personnel (Table 1).

Good Laboratory Practices

Clinical laboratories have been increasingly involved with pharmaceutical and diagnostic companies in the evaluation of new drugs or diagnostic products. In the 1970s, the FDA published regulations governing the conduct of the safety tests on regulated products, and these have been updated regularly [*Good Laboratory Practice (GLP) Regulations, 21 CFR Part 58*]. Compliance with these regulations is intended to ensure the quality and integrity of the safety data prior to the marketing and/or clinical testing of the regulated product. Products that must have evidence of safety include human and animal drugs, human biological products, medical devices, and diagnostic products. The regulations address such issues as the protocol, personnel, facilities, equipment, operations, testing, and controls. The FDA conducts regular inspections and data audits to monitor a laboratory's compliance with GLP requirements. This process is rather detailed and thorough. Before undertaking a GLP project, it would be important to consult with a quality assurance professional who has familiarity with GLP regulations. Table 1 lists websites that provide more detailed information on GLP licensing.

Analyte-Specific Reagents

In 1997, the FDA issued a Final Rule regulating "Analyte specific reagents (ASR)" that are sold for clinical diagnostic applications. The latest revision was in 2007 ("Labeling for in vitro diagnostic products," FDA Guidance Document, 21, CFR 809.10, 2007). These products are defined by the FDA as "antibodies, both polyclonal and monoclonal, specific receptor proteins, ligands, nucleic acid sequences, and similar reagents which, through specific binding or chemical reactions with substances in a specimen, are intended for use in a diagnostic application for identification and quantification of an individual chemical substance or ligand in biological specimens" (7) (Table 1). FDA regulations require that manufacturers of ASRs include only a general description concerning the quantity, proportion, or concentration of the product and information about the manufacturer. They are further prohibited from making claims regarding the analytical or clinical performance of the ASR. The FDA has noted that some laboratories have used products or devices that lack FDA clearance and that can be lawfully used only for research or for investigational purposes, outside the context of research or clinical investigations. To address this situation, the FDA issued guidance stating that the manufacturers should not sell "research use only" or "investigational use only" products to laboratories that they know will use the products for nonpermitted purposes such as clinical patient testing, and the manufacturers should halt sales to those laboratories that they discover use the products for nonpermitted purposes, or the manufacturer should comply with FDA requirements for premarket review. This rule made it easier for manufacturers of diagnostic products to develop and market products. The burden of responsibility for the performance of an ASR in an assay thus rests on the clinical laboratory that offers a test using the reagent. Clinical laboratories that use products designated ASRs must be qualified to perform high-complexity testing. This regulation mandates that on each report generated by a clinical laboratory in which an ASR was used, it state, "This test was developed and its performance characteristics determined by (*laboratory name*). It has not been cleared or approved by the U.S. Food and Drug Administration." A laboratory may elect to include additional, clarifying information along with this statement, and the CAP has developed some sample statements to go along with the required statement (7). For example, the following additional statements may be added: (i) "The FDA has determined that such clearance or approval is not necessary"; (ii) "This test is used for clinical purposes. It should not be regarded as investigational or for research"; (iii) "Analyte specific reagents (ASR) are used in many laboratory tests necessary for standard medical care and generally do not require U.S. Food and Drug Administration (FDA) approval or clearance"; and (iv) "This laboratory is certified under the Clinical Laboratory Improvement Amendments of 1988 (CLIA) as qualified to perform high-complexity clinical testing. Pursuant to the requirements of CLIA, this laboratory has established and verified the test's accuracy and precision."

Laboratory-Developed Tests

In the context of personalized medicine, diagnostic tests have an increasingly important role in clinical decision making and disease management. However, the FDA is concerned that some LDTs have not been properly validated for their intended use and thus may put patients at risk for a missed or wrong diagnosis or failure to receive appropriate treatment. In 2010, the FDA announced its intention to begin regulating LDTs, and it planned to release a draft guidance in 2011. However, in 2012, those opposed to LDT regulation convinced Congress to pass a law that requires the FDA to give Congress 60 days' notice before issuing a draft guidance on LDTs. Since that time, there has been no activity in Congress to regulate LDTs; however, it is a process that will likely come to fruition in the future.

STATE CERTIFYING PROGRAMS

CMS has recognized certain states as being exempt from their certifying program. These states can carry out their own laboratory surveillance and issue their own certification. These states currently include Washington and New York.

Washington State

In 1989, the Washington State legislature passed the Medical Test Site Licensure law, which allowed the state to regulate clinical laboratory testing. In 1993, Washington's program was judged to be equivalent to that of the CLIA, and it became the first state in the country to be granted deemed status. In 1997 HCFA (CMS) extended Washington State's exempt status under the CLIA program for all laboratories. Washington State retains its regulatory activity at the state level, where it is claimed that the process is more accessible and responsive to local needs.

Washington State surveys the various testing facilities and examines their quality control and patient records, test performance and reporting data, management policies, and quality assurance programs. Although the state does not offer its own proficiency testing program, testing sites must participate in a program that is approved by CMS. The state monitors proficiency test results for acceptability.

New York State

In 1996, New York state received exempt status under the CLIA program for independent and hospital laboratories. Prior to this time, New York became the first state in 1965 to initiate a certification and licensing program for clinical laboratories operating within the state. Since then, the program has been expanded, and now, through the Clinical Laboratory Evaluation Program (CLEP), it monitors the quality of testing from all clinical laboratories and blood banks within the State of New York as well as all out-of-state facilities that accept clinical specimens obtained from within New York State. In very rare situations, an unusual test can be granted an exception and performed in a laboratory without a license. CLEP issues permits on an annual basis to over 1,000 laboratories across the nation and 900 patient service centers in New York State. On a biennial basis, CLEP grants over 3,000 certificates of qualification to individuals to serve as directors/assistant directors of these clinical laboratories and blood banks. The three objectives of the CLEP program are (i) to monitor, improve, and broaden the clinical capabilities of participating laboratories and blood banks; (ii) to provide guidelines, quality control standards, and procedures to be used by permit-holding clinical facilities; and (iii) to expand the clinical and educational background of medical technologists, laboratorians, and other personnel involved in the operation of clinical laboratories through training and remediation programs.

Standards for New York State accreditation can be found on their website (Table 1). To obtain a New York State laboratory permit, the laboratory must complete an application, submit the required fees, designate a laboratory director and assistant directors, if applicable, and obtain Certificates of Qualification (CQ) in all permitted categories for which the laboratory has applied. In addition, the laboratory must successfully participate in two successive New York State proficiency testing (PT) events for all applied categories and subcategories and for all analytes for which New York State proficiency testing is offered, submit standard operating procedures and validation data for Department review and approval, complete a successful on-site inspection, and submit an acceptable plan of correction for any deficiencies cited during the inspection. An out-of-state laboratory seeking a New York State permit shall pay to the NYS Department of Health an on-site survey fee which shall consist of a transportation expense and a *per diem* expense. Details concerning certification of laboratories and tests and a request form for a nonlicensed exemption can be found on their website.

California

The California Department of Public Health, section of Laboratory Field Services (LFS), is responsible for licensing clinical laboratories and personnel, including clinical laboratory scientists (formally titled clinical laboratory technologists), bioanalysts, specialty directors, specialty scientists, and cytotechnologists, through an application process and examination. The program also approves training schools for clinical laboratory personnel, including schools that provide instruction in phlebotomy. LFS also conducts complaint investigations, which may include on-site inspection processes.

California requires all laboratories to participate in proficiency testing programs that have been approved by the California Department of Health Services and the federal government. Other states in which a permit must be obtained, especially if testing is performed in an out-of-state laboratory, include Maryland, Rhode Island, Florida, and Pennsylvania.

ACCREDITATION AND LICENSURE OF LABORATORIES

The CLIA '88 regulations issued by the federal government mandate that all laboratories performing clinical testing must undergo regular inspections by an agency or organization with deemed status, e.g., CAP, TJC, and New York State. These agencies all have detailed requirements, which include acceptable education and training for all personnel, content of procedure manuals, documentation of quality control and preventive maintenance procedures, verification of new procedures, ordering, and result reporting procedures, and many other details that are necessary for documentation of appropriate laboratory practices. The requirements by these agencies are equal to or, in most cases, greater than those mandated by CLIA.

College of American Pathologists

The Laboratory Accreditation Program (LAP) of the CAP has been in existence since 1962. Since that time, it has developed into the world's largest single voluntary clinical laboratory improvement program. The LAP has been granted deemed status by CMS, and it is recognized by the TJC as an equivalent program in TJC-accredited institutions. There are currently over 7,000 laboratories accredited by CAP in the United States and abroad. The focus of the LAP is the use of educational, peer-review inspection processes using teams of laboratory professionals as inspectors. The CAP gives working laboratorians an opportunity to participate in the inspection process. By visiting and inspecting peer laboratories, a significant educational component is added to the accreditation process. The CAP selects a team of inspectors of practicing pathologists, laboratory scientists, and medical technologists who are matched to the laboratory's profile as closely as possible. All aspects of the laboratory's operation are evaluated in this process, from sample acquisition to general laboratory management.

The process of becoming accredited by the CAP begins with the submission of an application. The CAP then forwards to the laboratory "checklists" for each of the laboratory sections. The checklists are developed and approved by CAP committees, and they address each laboratory discipline. There are frequent revisions to the checklists, and most are customized based on the laboratory's activity menu. It is advisable to check the CAP website to review the current checklists. For the immunology laboratory, the checklists that are relevant depend on the menu of tests in the laboratory. They include (i) flow cytometry, (ii) immunology, (iii) general chemistry, and (iv) special chemistry (if such tests as measurement of immunoglobulin and complement levels or electrophoretic techniques are performed), (v) molecular pathology, and (vi) histocompatibility. Since the checklists that are sent to the laboratories are the same ones that the inspectors use during the on-site visit, the laboratory can review all items and address any deficiencies or problem areas prior to their inspection. The major areas that are covered in the checklist include proficiency testing, quality control, and quality improvement (e.g., supervision, procedure manuals, specimen collection and handling, reporting of results, reagents, calibration, controls and standards, instruments and equipment), personnel, physical facilities, and laboratory safety. During the inspection, there are two types of deficiencies that can be noted by the inspectors, phase I and phase II. Phase I deficiencies require a written response indicating that corrective action is taken, while phase II deficiencies require a written response and supporting documentation demonstrating compliance. As of 2006, the CAP conducts unannounced inspections. The

inspection should occur within 90 days of the anniversary date unless it is the laboratory's first inspection.

During the inspection process, the inspectors conduct a thorough inspection of each phase of the laboratory's operation using the checklists as guides. Recently, the CAP implemented the "ROAD" (*R*ead, *O*bserve, *A*sk, *D*iscover) inspection process. This process involves *R*, reading and reviewing documents; *O*, observing laboratory practices, noting if practice deviates from the documented policies or procedures; *A*, asking open-ended, probing questions; and *D*, discovering or following a representative specimen through the lab from collection to reporting.

After the inspection, the inspectors meet with the laboratory staff for a summation conference to review the findings. The inspectors leave a copy of the final summation report, and the laboratory must correct any deficiencies within 30 days and provide any requested documents to the CAP. If the deficiencies are corrected to the satisfaction of the CAP, the laboratory is accredited for a 2-year period. However, the laboratory must conduct a self-inspection at the 1-year mark using the most current checklists.

The Joint Commission

The mission statement for TJC is " To continuously improve health care for the public, in collaboration with other stakeholders, by evaluating health care organizations and inspiring them to excel in providing safe and effective care of the highest quality and value." More than 20,000 health care organizations are accredited by TJC, an independent, not-for-profit organization in the United States and in several foreign countries. TJC began evaluating hospital laboratory services in 1979. In 1995, TJC standards were deemed to be certifiable under CLIA '88. A medical technologist surveyor is assigned to review the laboratory's activities and policies. During the on-site survey, the surveyor looks at administrative, technical, safety, and infection control policies and procedures as well as proficiency testing records. In addition, surveyors meet with laboratory directors and managers to determine their involvement in the operation of the organization. Specifically, they seek information on the communication between the clinical staff, administrators, and other departments, reviewing in-services, evaluating the oversight of the laboratory testing and quality assessment and improvement activities. While visiting each laboratory section, the surveyor reviews section-specific policies and procedures, infection control and safety practices, preventive maintenance, quality control, and proficiency testing results. The surveyor also visits patient care areas to assess the processes for testing, specimen collection, and requesting and reporting of results and blood transfusions.

American Society for Histocompatibility and Immunogenetics

The American Society for Histocompatibility and Immunogenetics (ASHI) has set standards for histocompatibility testing for years. The standards include the following areas: general policies, personnel qualifications, quality assurance, HLA antigens, serological typing (HLA class I and II antigens), mixed leukocyte culture tests, antibody screening, renal transplantation, nonrenal organ transplantation, marrow transplantation, platelet and granulocyte transfusion, disease association, parentage testing, nucleic acid analysis, flow cytometry, and enzyme-linked immunosorbent assays. ASHI maintains these standards and conducts inspections of laboratories for licensing as well as assisting in the certification of technologists and directors. ASHI information is available on their website (Table 1).

Proficiency Testing

A significant ongoing requirement of all accrediting agencies is the regular performance of testing on masked samples. Laboratories must show evidence that they are enrolled and participate in a regular proficiency testing process. Moreover, they must regularly review results and make corrections to problems and errors discovered in the process of the testing. Subsets of tests are "regulated analytes," in which a continuing good performance is necessary in order for the laboratory to be able to bill Medicare and Medicaid for these tests. Regulated tests in the immunology laboratory include a number of assays that are performed by nephelometry (IgG, IgA, IgM, C-reactive protein (CRP), C3, C4, haptoglobin, alpha-1 antitrypsin), venereal disease research laboratory test (VDRL), rapid plasma reagin (RPR), and a few serology tests including alpha-fetoprotein, HIV, HBsAg, anti-HBc, HBeAg rheumatoid factor, quantitative anti-streptolysin O, infectious mononucleosis, rubella, and anti-nuclear antibodies.

Any tests performed by laboratories in which proficiency testing is unavailable must be shown to be performing correctly in some other manner. This may include trading split samples with other laboratories that offer the same test, regular review of clinical appropriateness or correlation, or other strategies. The laboratory director is responsible for reviewing the results for acceptability and taking corrective actions if necessary.

The College of American Pathologists is the proficiency supplier with the largest range of test samples. Details of the surveys available and the analytes contained in each survey are available on the CAP Proficiency website (Table 1). Many other organizations including ASHI, American Association of Bioanalysts, the CDC Model Performance Evaluation Program (MPEP), and certain state programs also supply proficiency materials, e.g., New York. A variety of manufacturers of reagents and instruments also produce proficiency testing or quality control materials in which results from laboratories are compared to each other.

INTERNATIONAL ISSUES AND AGENCIES

While the U.S. medical laboratories are required to follow guidelines established by CLIA, laboratories outside the United States have, in many cases, developed systems for the assessment of quality that follow international standards. One such organization is the International Organization for Standardization (ISO), headquartered in Geneva, Switzerland. ISO is a nongovernmental federation of national standards bodies from over 100 countries worldwide. Established in 1947, the mission of ISO "is to promote the development of standardization and related activities in the world with a view to facilitating the international exchange of goods and services, and to developing cooperation in the spheres of intellectual, scientific, technological and economic activity." During the 1970s and 1980s, with an increase in the global economy, companies found extensive variation in the quality of the goods and services that they purchased from sources all over the world. The ISO has developed internationally accepted standards to ensure product quality. In 1987, the ISO published the ISO 9000 series of international standards and guidelines on quality management and quality assurance. For clinical laboratories, document ISO/TC 212, CD 15189 addresses standardization and guidance in the field of laboratory medicine and *in vitro* diagnostic test systems. Currently, ISO 15189 accreditation is offered in 44 countries. Although this is not yet the case in the United States, in some countries it is the standard by which laboratories are reimbursed.

For medical laboratories, ISO 15189 supports the goals of a laboratory that is working to achieve best practices in quality management systems and specifies requirements for competency and quality. It also addresses the continuum of care directly connected with improving patient safety, risk mitigation, and operational efficiency. In addition to the quality management areas discussed in this document, pre- and postanalytical procedures, analytical performance, laboratory safety, reference systems, and quality assurance are included. Certification by the ISO is a voluntary activity. Since the fall of 2008, CAP launched the program based on the ISO 15189:2007 standard (Table 1). This process reinforces the ISO goals and standards while supporting CAP's mission of advocating excellence in the practice of pathology and laboratory medicine. The CAP was also a significant contributor to the development of the ISO 15189 standard. As of April 2014, there were 29 clinical laboratories accredited by CAP ISO 15189.

In addition to the ISO, other nongovernmental organizations are involved in laboratory quality assurance at the international level (9). These include the International Federation of Clinical Chemistry and Laboratory Medicine and the World Health Organization. The IFCC interacts with several international professional organizations involved in laboratory medicine including the International Union of Immunological Societies (IUIS) and the World Association of Societies of Pathology and Laboratory Medicine (WASPALM). Among the national organizations are the Clinical and Laboratory Standards Institute (formerly National Committee for Clinical Laboratory Standards [NCCLS]) in the United States and the Institute for Standardization and Documentation in Medical Laboratory (INSTAND) in Germany. Regional organizations include the Asian Pacific and Latin American Federation of Clinical Biochemists. In addition to Germany, many other countries in Europe and several clinical laboratory professional organizations have been actively involved in addressing quality systems and accreditation issues. Among these are the European Communities Confederation of Clinical Chemistry and Laboratory Medicine (10, 11) and External Peer Review Techniques (ExPeRT). Further information about the activities of these organizations can be found on their websites (Table 1).

A peer review system for the accreditation of pathology laboratory services in the United Kingdom was inaugurated in 1992. The Clinical Pathology Accreditation (UK) Ltd (CPA) is a nonprofit company associated with incorporating the Royal College of Pathologists, the Association of Clinical Pathologists, the Association of Clinical Biochemists, and the Institute of Biomedical Science. The operation functions in a manner similar to that of the CAP in the United States. There are Advisory Committees that define and review standards, assess applications, recommend inspectors, and advise on decisions after inspection. Survey teams of voluntary inspectors, each with expertise in the laboratory's specific disciplines, conduct on-site inspections. The inspectors are drawn from practicing pathologists and clinical/biomedical scientists (12).

TABLE 3 Credentialing agencies and programs[a]

Level	Certifying agency or program	Organization	Education level required	Website
Director	American Board of Medical Laboratory Immunology (ABMLI)	ASM	Ph.D. or M.D. and appropriate experience	https://www.asm.org/index.php/abmli-cert
Director	American Board of Medical Microbiology (ABMM)	ASM	Ph.D. or M.D. and appropriate experience	https://www.asm.org/index.php/abmm-cert
Director	American Board of Histocompatibility and Immunogenetics (ABHI)	ASHI	Ph.D. or M.D. and appropriate experience	http://www.ashi-hla.org/lab-center/director-training-review/
Director	American Board of Clinical Chemistry (Molecular Diagnostics) (ABCC)	ABCC	Ph.D. and appropriate experience	http://www.abclinchem.org/mold_chem/Pages/default.html
Medical laboratory professionals	American Society for Clinical Pathology (ASCP)	ASCP	Multiple levels and educational requirements	http://www.ascp.org/certification#tabs-1
1. Certified Histocompatibility *Associate:* CHA(ABHI) 2. Certified Histocompatibility *Technologist:* CHT(ABHI) 3. Certified Histocompatibility *Specialist:* CHS(ABHI)	Clinical Histocompatibility	ASHI	B.S. and appropriate experience	www.ashi-hla.org

[a]See the text for abbreviations.

For a laboratory to become accredited, the process begins with the laboratory assessing itself against the relevant CPA standards, filing an application, and being subjected to an on-site inspection in order to determine compliance with the standards. After the relevant advisory committee has reviewed the inspectors' assessment, a report is sent back to the laboratory. If there are no problems with the on-site inspection of the laboratory, the Board issues a 12-month certificate. If deficiencies are found, accreditation is withheld until the deficiencies have been corrected to the satisfaction of the CPA. When the laboratory has major deficiencies, approval is withheld until the deficiencies have been corrected and reapplication is required. Accreditation is valid for 4 years, with CPA reserving the right to reinspect at any time without notice. There is a requirement for an annual reregistration and a self-declaration stating continuing compliance with the standards. European Federation of Clinical Chemistry and Laboratory Medicine (EFLM) was formed in June 2007 at the Euromedlab Congress in Amsterdam, Netherlands, by the merger of the Forum of European Societies of Clinical Chemistry (FESCC) and the European Communities Confederation of Clinical Chemistry (EC4). In order to better serve the public interest in health care, EFLM connects National Societies of Clinical Chemistry and Laboratory Medicine and provides European leadership in clinical chemistry and laboratory medicine to national professional societies, the diagnostic industry, and governmental and nongovernmental organizations. It also represents the International Federation of Clinical Chemistry and Laboratory Medicine (IFCC) in Europe. The Quality and Regulations Committee supports the establishment of effective accreditation schemes and quality management systems in all European countries and liaises with ISO, European Committee for Standardization (CEN), and the European Accreditation body (EA). The Committee currently has two working groups. One focuses on influencing ISO/CEN standards and harmonization of accreditation and on setting European procedures for accreditation. The second working group, the "IVD Directive," focuses on guidance documents in the application of laboratory practices and accreditation.

CREDENTIALING

A number of organizations are involved in issuing credentials or licenses for individuals who demonstrate technical and management skills in clinical immunology. These programs generally include two components, one that establishes guidelines for training programs and another that creates and administers the examination process. It is important for all the individuals involved in clinical immunology laboratory practice to obtain appropriate certification. These programs encourage professionalism for their members and provide core groups of exceptionally qualified leaders in laboratory immunology. A list of professional societies that provide credentialing programs is shown in Table 3.

REFERENCES

1. **Bogdanich W.** 2 February 1987. Medical labs, trusted as largely error-free, are far from infallible, p 1. *Wall Street Journal*, New York, NY.
2. **Bogdanich W.** 2 November 1987. The Pap test misses much cervical cancer through labs' errors, p 1. *Wall Street Journal*, New York, NY.
3. **U.S. Department of Health and Human Services.** 1988. *The Clinical Laboratory Improvement Amendments of 1988. Public law no. 100-578*. U.S. Department of Health and Human Services, Washington, DC.
4. **U.S. Department of Health and Human Services, Office of Inspector General.** 1998. Publication of the OIG compliance program guidance for hospitals—OIG. Notice. *Fed Regist* **63:**8987–8998. PubMed
5. **Wanamaker V.** 1999. Health Care Financing Administration/clinical laboratory improvement amendments of 1988. *Arch Pathol Lab Med* **123:**478–481. PubMed
6. **U.S. Department of Health and Human Services.** 1980. *Survey Procedures and Interpretative Guidelines for Laboratories and Laboratory Services. HCFA State Operations Manual*. Health Care Financing Administration and Food and Drug Administration, Baltimore, MD, and Rockville, MD.
7. **Federal Register.** 1997. Medical devices; classification/reclassification; restricted devices; analyte specific reagents. 21 CFR 809. Final rule. 1997. *Fed Regist* **62:**62243–62260.
8. **U.S. Department of Health and Human Services.** 1992. Medicare, Medicaid and CLIA programs; regulations implementing the Clinical Laboratory Improvement Amendments of 1988 (CLIA)—HCFA. Final rule with comment period. *Fed Regist* **57:**7002–7186.
9. **McQueen MJ.** 1997. Laboratory quality assurance at the international level: the role of nongovernmental organizations. *J Int Fed Clin Chem* **9:**144–146, 148, 150. PubMed
10. **Jansen RT, Blaton V, Burnett D, Huisman W, Queraltó JM, Zérah S, Allman B.** 1997. Essential criteria for quality systems in medical laboratories. *Eur J Clin Chem Clin Biochem* **35:**121–122. PubMed
11. **Sanders GT, Jansen RT, Beastall G, Gurr E, Kenny D, Kohse KP, Zérah S.** 1999. Recent activities of EC4 in the harmonization of clinical chemistry in the European Union. *Clin Chem Lab Med* **37:**477–480. PubMed
12. **Burnett D, Blair C, Haeney MR, Jeffcoate SL, Scott KWM, Williams DL.** 2002. Clinical pathology accreditation: standards for the medical laboratory. *J Clin Pathol* **55:**729–733. PubMed

Validation and Quality Control: General Principles and Application to the Clinical Immunology Laboratory

VIJAYA KNIGHT AND TERRI LEBO

122

Clinical laboratories provide vital services to physicians and patients, public health agencies, and medicolegal entities. Because laboratory test results influence patient care and medical decisions rely on accurate and timely laboratory results, clinical laboratories must ensure that the *right* results are obtained at the *right* time and for the *right* patient. The ability to ensure accuracy of patient results rests on developing a quality program that governs all functional aspects of the clinical laboratory.

Quality, as defined by the Oxford Dictionary, is "a degree of excellence of something," and in the laboratory, it encompasses both internal quality control (IQC) and external quality assessment (EQA). IQC comprises processes that ensure precise and accurate results and focuses on monitoring the day-to-day precision and accuracy of assays, whereas EQA focuses on the comparison of various methods and examination of concordance in testing across a number of facilities. EQA also serves an educational purpose and assists with the evaluation of testing platforms, the comparison of methodologies, and benchmarking a laboratory's performance against peer groups.

Ensuring a quality laboratory from the analytical perspective requires that all assays be validated. This means that they have been thoroughly examined for both robust performance and appropriateness for clinical use. Moreover, it makes sure that there are procedures in place to ensure accurate performance of the assay, as well as detect errors in performance, reagents, or instrumentation as early in the process as possible so as to minimize any impact on patient care. In addition, a well-validated assay also establishes and documents any assay performance limitations, particularly for the more esoteric laboratory-developed tests (LDTs) that are not cleared by federal regulators.

Total quality encompasses all aspects of a clinical laboratory including adequate facilities and infrastructure, trained and qualified personnel, and vendor and instrument qualification and is beyond the scope of this chapter. Additional information regarding total quality programs may be obtained from a number of sources (1, 2). The scope of this chapter is to discuss (i) general guidelines for robust assay validation and quality control and (ii) challenges faced by clinical immunology laboratories performing assays that do not have well-defined guidelines for validation or are LDTs for infrequently encountered immunological disorders.

GUIDELINES FOR ASSAY DEVELOPMENT AND VALIDATION

Guidelines for the development of clinical diagnostic assays are provided by various organizations of which the most widely recognized is the Clinical Laboratory Standards Institute (CLSI). Originally known as National Committee for Clinical Laboratory Standards (NCCLS), the CLSI was started in the 1960s by a group of clinicians and laboratorians with the intention of developing a formal, consensus process for standardization of processes impacting patient care, including laboratory testing. Since then, CLSI has evolved into a global organization that is actively involved in education and global harmonization of standards through collaborative efforts with organizations involved in developing standards and standard material for laboratory testing (see chapter 121). While CLSI guidelines are most commonly used for development and validation of clinical testing, the Centers for Disease Control and Prevention (CDC) (3) and the International Clinical Cytometry Society (ICCS) also provide consensus guidelines for several flow cytometry based assays (4–6). More recently, the International Council for Standardization in Hematology (ICSH) and the ICCS convened a working group to develop comprehensive guidelines on all aspects of development and validation of flow cytometric assays encompassing preanalytical, analytical, and postanalytical stages (7). Additionally, several key publications have emerged to address the development, optimization, and validation of assays for biomarker analysis during immune monitoring studies for new therapeutics that involve challenging methodologies such as flow cytometry, single cell analysis such as the ELISpot and various antibody- and ligand-binding immunoassays, that are also making their way into the arena of diagnostic testing (8–12).

CLASSIFICATION OF ASSAYS

Diagnostic assays may be classified according to their regulatory status or according to their technical performance characteristics. Validation or verification requirements depend on the classification of the assay.

Regulatory Status

For information regarding regulatory status, see http://www.cms.gov/Regulations-and-Guidance/Legislation/CLIA.

doi:10.1128/9781555818722.ch122

FDA-Approved Assays

Food and Drug Administration (FDA)-approved assays have undergone rigorous testing by the kit or device manufacturer, and assay performance characteristics have been defined and deemed acceptable for clinical use. Clinical studies have been conducted to establish the diagnostic utility of the assay, and reference intervals have been established. When a laboratory is considering offering an FDA-approved assay, a *verification* of assay performance characteristics claimed by the manufacturer must be performed (per Clinical Laboratory Improvement Amendments [CLIA] standard 493.1253) (Table 1).

FDA-Approved, Modified Assays

These assays have been approved in their commercially available format for diagnostic testing. Any modification to the assay (e.g., change in volume of a reagent, sample type [plasma versus serum], length of incubation, anticoagulant [EDTA versus heparin], or other parameters) must be *validated* prior to use for diagnostic purposes. It must be noted here that assays for nonstandard body fluids (e.g., pleural fluid, cerebrospinal fluid, and in general, fluids other than blood or urine) are considered FDA-modified assays because nonstandard body fluids are regarded as an alternate matrix and are not interchangeable with serum or plasma (14). For such assays, the effects of the matrix on the performance characteristics of the assay must be evaluated. The criteria to be fulfilled to establish a modified FDA assay as a validated, clinical assay are defined in Table 1.

Lab-Developed Tests

LDTs are prevalent in clinical immunological laboratories and present the greatest challenges for successful validation. In general, the criteria that must be fulfilled to establish an LDT for clinical use are detailed in Table 1 and are similar to those required for an FDA-approved, modified test. However, it must be noted here that depending on the technical nature of the assay, not all validation parameters may be applicable.

Classification According to Performance Characteristics

Diagnostic tests fall into four categories depending on the nature of the result (15): qualitative, quasiquantitative, semiquantitative, and quantitative.

Qualitative Assays

These assays have a binary answer: present/absent, positive/negative, or reactive/nonreactive. While these assays do not provide a numerical value but an absolute descriptive result, they may employ a numerical cutoff value that determines whether a result is positive or negative. Analysis of gene mutations, microbiological assays, infectious disease screening serological tests, flow cytometry tests for leukemia or lymphoma, and the majority of LDTs for the analysis of immune cellular function such as the dihydrorhodamine assay for neutrophil oxidative burst (16) fall into this category.

Quasiquantitative Assays

These assays do not employ a calibration standard but have a continuous response that can be expressed as a numeric value. Examples of quasiquantitative assays include enzyme-linked immunosorbent assays (ELISAs) that employ a single positive control. The absorbance of the test sample is compared with that of the control sample, and a numerical result is calculated as a function of the control sample's absorbance. Flow cytometry assays such as analysis of lymphocyte subsets, DNA content, immunogenicity assays for antidrug antibodies, and functional assays such as lymphocyte proliferation assays also fall into this category (7).

Semiquantitative or Relative Quantitative Assays

Semiquantitative or relative quantitative assays employ calibration standards that do not fully represent the analyte or biomarker. The matrix of the standard may differ from that of the test samples, and a direct quantitative comparison is not possible. While these assays provide a numeric value, this value is often related to a range that describes a qualitative result. Immunological assays for detection of autoantibodies and ligand-binding assays fall into this category, as do flow cytometry-based assays such as CD34 enumeration, which relies on fluorescent calibration beads (7, 15, 17). Precision for semiquantitative assays tends to be much more variable than that of quantitative assays and can be as high as 25% at the upper and lower limits of quantitation for soluble analytes (17) and as high as 45% for flow cytometry-based assays designed to detect rare cell populations (18).

Quantitative Assays

Quantitative assays make use of characterized standards with known numerical values and utilize a regression curve to determine, accurately, the numeric value of an analyte. Reference standards employed in these assays are fully characterized and are representative of the analyte or biomarker. The majority of analytes encountered in chemistry laboratories fall into this category, whereas few immunological assays can truly be considered to be quantitative assays.

TABLE 1 Assay validation or verification requirements per CLIA standard 493.1253

Validation or verification requirement	FDA-cleared, unmodified assays	FDA modified or LDT	Reference document
Accuracy	Required	Required	CLSI EP-12A
Precision	Required	Required	CLSI EP-12A
Reportable range	Required	Required	CLSI MM6-A
Linearity	Required initially and every 6 months thereafter	Required	CLSI EP6-A
Reference interval	Required	Required	CLSI C28-A2
Analytical sensitivity	Not required, verify with 20 results spanning the analytical range	Required	CLSI EP17A
Analytical specificity	Not required	Required	CLSI MM6-A

Based on the nature of the assay, not all assay performance criteria are required to be fulfilled during validation. For instance, an LDT with a qualitative readout will not require studies for linearity, and the limit of detection for a qualitative assay may not be necessary if the result does not depend on a numeric value. Thus, the assay must be fully understood prior to undertaking validation, so that only parameters that are truly representative of the assay's performance are examined and validated.

DEVELOPMENT AND VALIDATION

Validation and quality control of immunological assays can be challenging due to the complex nature of the analyte (autoantibodies, cellular function) as well as the complexity of the analytical methods. Furthermore, in many cases there is little to no standardization of these assays. Assay variability can be introduced at a number of levels, including reagents (antigen preparation, antibody source, cell extract, cells or tissue sources, recombinant or native protein preparations), detection systems (nature of the detection antibody, i.e., monoclonal versus polyclonal; nature of conjugation, i.e., enzyme or fluorophore), variation in method (incubation time, reaction volume, method of readout), and data analysis. Cellular function assays are particularly challenging because they are inherently much more complex than serum-based assays and less robust in their reproducibility. All of these variables influence the assay and must be tested rigorously in order to develop a robust, reproducible, and reliable assay suitable for patient care.

The following section discusses general development and validation guidelines for the four types of assays. The definition of "validation" according to the Oxford Dictionary is to "demonstrate or support the truth or value of..." something. In the context of a clinical diagnostic assay, validation implies the ability of the assay to demonstrate certain predetermined criteria that establish the assay to be "fit-for-purpose." The term "fit-for-purpose" is commonly used in biomarker assay development for therapeutics (15), but similar concepts can be applied to diagnostic testing. The International Organization for Standardization (ISO) defines validation of a method as "the confirmation by examination and the provision of objective evidence that the particular requirements for a specific intended use are fulfilled" (19, 20). This concept may be extended to fit-for-purpose validation, whereby the suitability of a diagnostic test must be evaluated scientifically and clinically based on the literature or alternate existing methods. In parallel, an analytical validation plan must be developed describing preset performance criteria for the assay, which if fulfilled, yield results appropriate for diagnostic use. A validation study is then undertaken using suitable clinical samples, and if the performance criteria are met, then the assay is considered fit-for-purpose. Although the relation of a test result to the clinical status of the patient should determine whether the test is fit-for-purpose, clinical information linked to samples is generally not available in most laboratories, making it challenging to perform *clinical* validation of the assay. It is therefore important to evaluate a new test or platform alongside an FDA-approved or predicate method, when available (21), or a method currently employed by the laboratory when considering an alternate method or platform. While these approaches are suitable for FDA-approved kits or methods or when developing an alternate method for a preexisting assay, *de novo*-developed tests are far more challenging since there may be no other method in existence. In such cases, information regarding the suitability of an assay for diagnostic purposes is gathered from prior documented or published research.

Prior to Validation

Prior to commencing test validation, several factors should be taken into consideration. In addition to providing relevant information to the clinician to support diagnosis, a clinical test must be technically feasible and financially viable both for the laboratory and for the patient. Accordingly, the test must be researched thoroughly, and data must be gathered and analyzed prior to commencing validation. Table 2 includes some questions that must be considered prior to test development.

Following an analysis of these factors, if the decision is made to offer the diagnostic test, an optimization protocol must then be developed. The optimization protocol takes into consideration the technical variables that must be examined and optimized before the assay can move into further validation. Optimization protocols are required mainly for LDTs and for modifications of FDA-approved tests. Unmodified FDA-approved tests are performed according to the protocols determined by the manufacturer and should not require any further optimization. The optimization protocol considers variables such as sample type and stability, optimal concentration of reagents (e.g., antibodies for immune assays or flow cytometry), compatible reagents (examination of buffer systems, antibody pairs or combinations), incubation times, substrates, instrumentation, and data processing algorithms.

Depending on the assay or technical platform, there may be other parameters that must be examined and characterized prior to proceeding to validation (e.g., effect of anticoagulant on cellular phenotype or function, sample stability, particularly for cell-based assays, or the effect of transport temperature on the stability of the analyte).

Once all variables are optimized, the assay can proceed to validation as described below. Figure 1 provides a summary of the steps required to develop and validate a test.

TABLE 2 Considerations prior to development or validation studies

1. Clinical considerations
   a. What is the diagnostic value of the test?
   b. Is the test result actionable, and will it influence clinical decisions?
2. Technical considerations
   a. Will Institutional Regulatory Board (IRB) approval be required to develop and validate the test?
   b. On what technical platform will the test be offered?
   c. If the test is a *de novo* lab-developed test, are reagents available?
   d. What quality control parameters must be instituted?
3. Financial considerations
   a. What is the cost of developing the test?
   b. What is the reimbursement for the test?
   c. If the test is to be validated on a new platform, what is the cost of instrumentation?
   d. Is staff available to validate the test?
4. Physician and/or patient interface considerations
   a. How will the test be reported: quantitative, semiquantitative, or qualitative result?
   b. How will results be made available to the physician or patient (laboratory information system interfaces)?

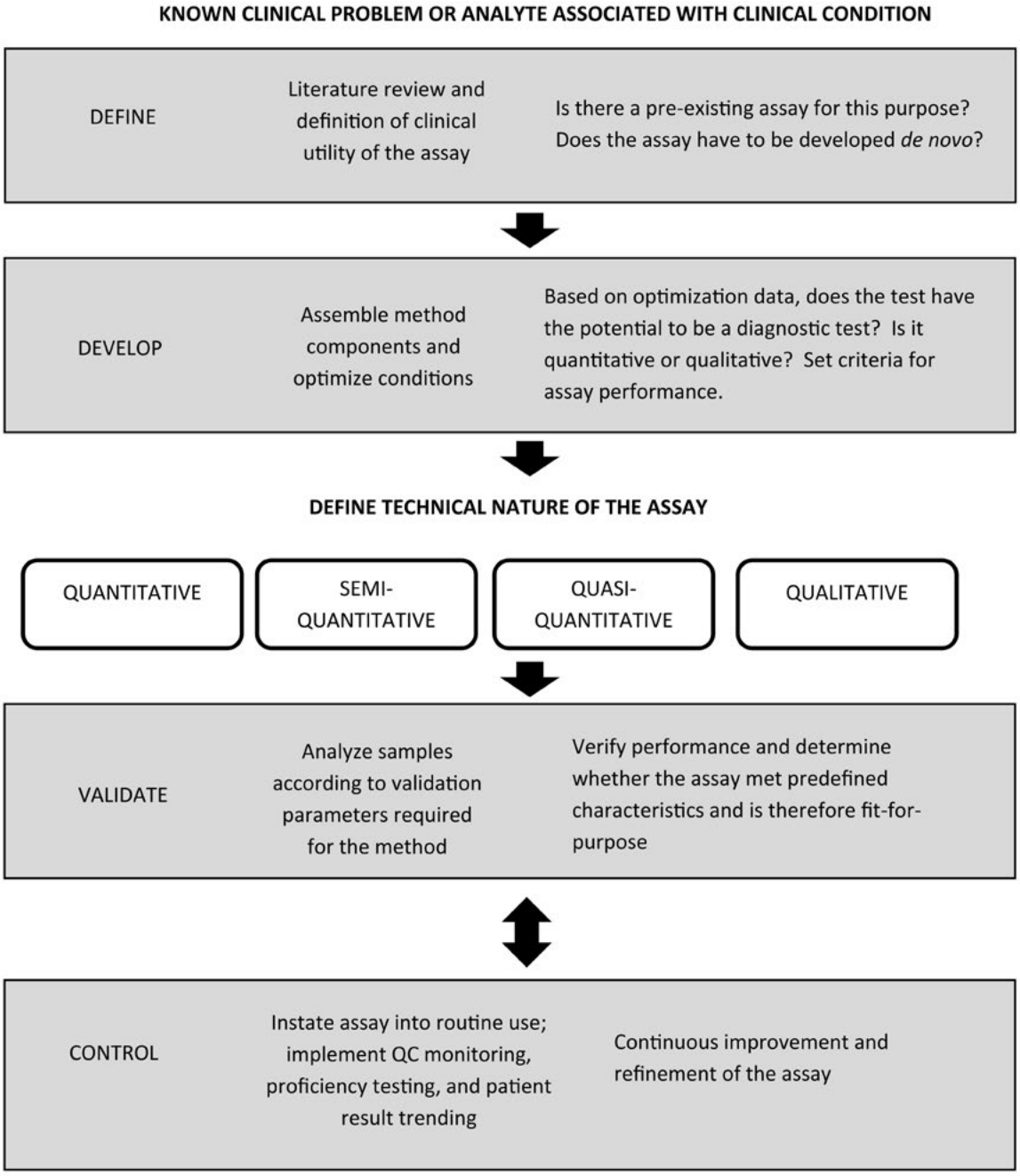

FIGURE 1 Stages in assay development and validation. The flowchart illustrates the four stages of assay development required to scientifically evaluate a potential diagnostic assay, develop and validate the method, and implement continuous quality monitoring of the assay.

Validation Parameters

Validation or verification of an assay determines its performance characteristics. As detailed in Table 1, assay validation examines the accuracy and precision, the analytical range, the limit of detection and linearity, and the analytical sensitivity and specificity of the assay and establishes reference values for diagnostic or clinical monitoring purposes. The following paragraphs examine each of these parameters.

Accuracy

Accuracy is defined as the closeness of agreement to the actual, expected value. *Diagnostic accuracy* of a test refers to the extent of agreement of the test result with the clinical condition associated with the test. When assessing diagnostic accuracy, a relevant patient population must be available. While assessment of diagnostic accuracy is ideal, it is generally beyond the scope of most diagnostic laboratories.

Instead, most laboratories perform studies to demonstrate *agreement* of the diagnostic test with an established method or verify the manufacturer's claims to accuracy using well-characterized samples. To establish agreement, proficiency testing samples, previously assayed patient samples, or reference panels can be used. CLSI EP12-A2 recommends testing at least 50 positive and 50 negative samples for a qualitative assay (22). For quantitative assays, samples chosen to represent the analytical range of the assay are analyzed by the reference method and test method and are compared for agreement using Bland-Altman plots or comparison plots (23; see also www.westgard.com). While these methods are suitable for verification of the manufacturer's claims for a commercially available assay or when comparing a new method with an established method, it is far more challenging to assess accuracy for an LDT. Accuracy for LDTs may be assessed by splitting samples with another laboratory performing the test, by comparing test results with clinical data, or by analyzing previously characterized samples where possible. Flow cytometry- and cell-based functional assays pose additional challenges in that samples utilized in these assays have limited stability and true standard reference material is not available. Furthermore, cellular functions such as lymphocyte proliferative responses to mitogenic or antigenic stimulation can vary widely from person to person and are dependent on seasonal or even diurnal influences. Accordingly, establishing accuracy for such assays can be difficult. Accuracy for flow cytometry assays may be documented by correlation with clinical phenotype where possible. *Analytical accuracy* can be demonstrated by comparison with an alternate methodology (e.g., a protein's phosphorylation status may be detected by flow cytometry or by Western blotting). Such comparisons are not perfect since differences in methodology may affect results. However, laboratories developing esoteric tests must document attempts to assess accuracy and provide reasonable explanations for discrepancies found between methods (7).

Precision

Precision is the ability to obtain the same result on repeated analyses under the same conditions. Precision is expressed as the coefficient of variation (CV) where %CV = SD/mean × 100, where SD is standard deviation. During validation studies, precision of the assay must be analyzed in a single run (intra-assay precision), across multiple runs (interassay precision), and among multiple operators or laboratories (interoperator variability) to determine the total variability of the assay. Qualitative assays with a binary answer do not require precision studies, unless the result is based on a numerical value. In such cases, precision must be examined around the numerical decision point at which a result transitions from negative to positive or normal to abnormal. CLSI EP12-A2 provides detailed guidance on examining precision around a numerical cutoff value for qualitative assays (22). Quantitative assays require examination of at least three levels of the analyte that cover the reportable range of the assay. Twenty replicate values are obtained during a single analytical run for intra-assay precision, whereas 20 values are accumulated over 20 separate analytical runs over several days and involve several operators to estimate inter- and intra-assay precision (25). When validating a commercially available assay, precision (%CV) must correlate with the manufacturer's claim. CLSI EP05-A2 provides further guidance for precision studies for quantitative assays (25).

As with accuracy, defining precision for flow cytometry assays that report a numerical value (percentage of cells) or the ELISpot that is designed to assess cellular function (e.g., cytokine-producing cells) or lymphocyte proliferation assays for antigen-specific responses is challenging. This is because these assays are often developed to detect rare antigen-specific T or B cell populations, which tend to be present in very low numbers and are often close to the detection limit of the assay. Additionally, lymphocyte proliferative responses are known to vary due to biological variation within and between individuals, diurnal variation, and variation due to differences in activation pathways triggered by different stimuli (26). Cell-based assays are inherently less precise than serum-based assays because of greater variability in preparation of cells, stability of samples (27), staining methods, and instrument settings for flow cytometry and assessment of cytokine-positive spots and data analysis for ELISpot assays. Because a flow cytometry result is derived from several thousand individual, simultaneous measurements of cellular parameters such as light scatter and fluorescence, all of which are transformed into numeric values for mean fluorescence or percentages of gated populations, large numbers of replicate samples as for chemistry-based analytes are not required to establish imprecision, nor is it feasible to obtain large numbers of samples with limited stability (28). In general, intra-assay precision studies may be performed with as few as five samples in triplicate within a single run. While a desirable %CV for flow cytometry assays is 10%, precision can be much more variable for less abundant populations. When the frequency of the population is less than 0.1%, as in analysis of low-frequency tetramer-specific T cells or in minimal residual disease, a CV of 20% may be acceptable. Imprecision for functional assays such as the ELISpot assay may be as high as 20 to 25% (18).

The lymphocyte proliferation assay has been widely used as a measure of general immune function and immunological memory. In HIV infection, in particular, loss of lymphocyte responses has been shown to correlate with advancing immune deficiency and has been utilized as a correlate of progression to AIDS (29, 30). The AIDS Clinical Trial Group (ACTG) has therefore established protocols and quality control measures for the lymphocyte proliferation assay in order to establish acceptable parameters for the assay across multiple testing sites (31).

In general, when %CV varies widely, an attempt must be made to analyze larger numbers of samples to develop as stringent precision criteria as possible (7) or to establish that the variability in precision does not have a significant impact on the interpretation of the assay result.

Precision for semiquantitative or quasiquantitative antibody assays can show wide variation as well (10). For instance, immunofluorescence techniques for the detection of autoantibodies can show a variation as high as 20%, or ±2 dilutions when a titer is reported (32), and this is well illustrated by the results of proficiency testing surveys conducted by the College of American Pathologists for autoantibody assays. In many cases, assays that show large variations in precision tend to be semiquantitative in nature, where the result is qualitative. Precision studies should be conducted around the lower discrimination point or medical decision point, particularly at the point where a result transitions from negative to positive, and it is necessary to determine that this wide variation in precision does not impact clinical decisions. It must be noted here that assays with larger imprecision around clinical decision points may require a "grey area" of interpretation, indicating that the numeric cutoff value is not an absolute transition point from a negative to a positive result. Excellent examples of this situation are the interferon gamma release assays that support the diagnosis

of latent tuberculosis infection. Both the ELISpot method (33) and the ELISA method (34) have been shown to have CVs as high as 30% for results at or near the cutoff value for a positive result, whereas imprecision of the assay is much lower for subjects with higher levels of reactivity to tuberculosis antigens. This variability can cause a negative result to turn positive or a positive one to turn negative when the patient's test results are close to the clinical decision point. Because clinical decisions such as isoniazid therapy or the necessity for a chest X ray to rule out tuberculosis may depend on these results, it is advisable to define a "grey area" that encompasses the coefficient of variation around the mean clinical decision point value and recommend repeat testing rather than define an absolute cutoff value, which then defines an absolute, qualitative positive or negative result. Such "indeterminate" result categories are useful for immunological assays when imprecision around the clinical decision point is large.

Measurement of imprecision for cell-based assays includes biologic and clinical variability and must also be considered in light of the clinical interpretation as illustrated earlier. Although cell-based assays tend to be much less precise than serum-based assays, they do provide the physician with useful information. Therefore, it is critical for the physician to consult with the laboratory director regarding the interpretation of such test results and determine whether the results correlate with the patient's clinical information, rather than rely exclusively on a numerical result.

Once interassay, intra-assay, and intraoperator variability is determined, total precision of the assay can be calculated. The precision of the assay can then be used to set acceptable criteria to qualify reagent performance or for acceptable proficiency testing performance.

LoB, LoD, and LoQ

For quantitative, semiquantitative, and qualitative assays that utilize a numeric value to discriminate positive from negative results, it is necessary to determine the lowest concentration of analyte that can be reliably measured by the assay (35). Qualitative assays that yield a binary answer, such as organism identification or confirmation of the expression of a cell surface molecule, do not require these studies.

The three values that are required to establish the lowest reliably measured concentration are (i) limit of blank (LoB), defined as the *highest apparent* concentration of the analyte that can be measured when replicates of a blank sample (vehicle alone) are tested. LoB is determined by the equation $\text{LoB} = \text{mean}_{\text{blank}} + 1.645(\text{SD}_{\text{blank}})$, where $\text{mean}_{\text{blank}}$ is the mean of several replicate measurements of blank (vehicle alone) samples. Limit of detection (LoD) is the *lowest* analyte concentration that can be reliably distinguished from the LoB. LoD is determined by using both the LoB and replicate test samples known to contain a low concentration of the analyte and is defined by the equation $\text{LoD} = \text{LoB} + 1.645(\text{SD}_{\text{low concentration sample}})$. Limit of quantitation (LoQ) is the lowest concentration at which the analyte is reliably detected based on predefined goals or clinical criteria and may equal or be higher than LoD. Further information and studies for the determination of LoD, LoB, and LoQ are defined in CLSI EP17-A (36).

To establish LoB and LoD for soluble analytes, the general recommendation is to use 100 low-positive and 60 negative samples, analyzed over several days (36). While this process is suitable for stable sample types such as serum, it poses problems for cell-based assays such as flow cytometry due to reasons stated earlier, e.g., limited sample stability or unavailability of abnormal samples. LoD is relevant in quasiquantitative flow cytometry assays, where rare populations with dim fluorescence must be detected accurately (e.g., minimal residual disease) or in relative quantitative flow cytometry that employs fluorescent beads as a calibration standard (7). Because of limited sample stability for cell-based assays, it is not possible to analyze several replicates over several days as can be done for soluble analytes. Instead, a limited number of replicates may be analyzed to confirm LoD and LoQ. The ICCS and ICSH guidelines recommend analyzing fewer numbers of samples (e.g., 5 low-positive and negative samples analyzed in 5 replicates over 3 days) (7). LoB is confirmed if 95% of blank replicates fall below the expected low-positive sample value and LoD is confirmed in 95% of the positive samples falling at or above the target value. Other means to establish LoD for flow cytometry-based assays are to use the fluorescence-minus-one (FMO) method, where all antibodies required to identify the population of interest with the exception of the antibody directed against the analyte of interest are included in the assay. This setup can then serve as a blank for the analyte of interest (7).

LoDs for functional cell-based assays such as the ELISpot assay or tetramer analysis by flow cytometry make use of spiking studies to determine the lowest number of antigen-specific cells that can be detected above a background response (18).

Linearity

A quantitative analytical method is said to be linear when the observed value of the analyte from a series of samples with varying concentrations of the analyte is linearly proportional to the true or actual concentration of the analyte in those samples. The linear range of the assay is defined by upper and lower limits of the analytical measurement range that fit a straight line. Assays that measure serum chemistry analytes are generally quantitative and require assessment of linearity when the assay is first initiated and at 6-month intervals thereafter. The general method for linearity assessment requires evaluation of at least five concentrations of the analyte spanning the analytical measurement range and determination of the correlation between the expected versus measured values. It is important to ensure that the matrix of samples used to establish or verify linearity match the matrix of samples used for clinical testing. CLSI EP6-A provides detailed guidance on the establishment and assessment of linearity for quantitative assays (37).

Some immunoassays, such as competitive ELISA, do not have a linear relationship between the instrument response and the analyte concentration. In such cases, the parabolic or sigmoidal curve that describes the mathematical relationship between the instrument's response and the analyte concentration can be transformed into a linear comparison using a four-parameter logistic model (38), allowing test results to then be extrapolated from the linear curve.

Linearity studies for flow cytometry may be performed in the context of both instrument and assay performance. Instrument-specific linearity studies compare the signal detected and the actual fluorescence over an established dynamic range and are performed using hard dyed calibrated beads of known fluorescence intensity. The measured geometric mean fluorescence intensity of the beads is then plotted against the manufacturer's reference values and the linear relationship determined. A coefficient of variation of 1 ($r^2 = 1$) indicates that matched observed and expected data points lie on a straight line. Linearity can vary from instrument to instrument but is generally stable for a

particular instrument and does not have to be checked on a daily basis (39).

Since the vast majority of flow cytometry assays are either qualitative or quasiquantitative, assessment of linearity of the assay is not necessary, except in the case of relative quantitative assays such as the quantitation of surface CD64, recognized as a correlate of sepsis (40, 41). Linearity of the assay can be established using fluorescence calibration beads in which fluorescence intensity is reported in quantitative terms such as molecules of equivalent soluble fluorochrome or antibody binding capacity. The fluorescence intensity of the test sample can then be extrapolated to either molecules of equivalent soluble fluorochrome or antibody binding capacity units from the linear regression curve.

Reference Range or Reference Interval

In order to provide the clinician with information that supports medical decision making, a laboratory test result must be compared with what is considered to be "normal." Determination of the expected normal is the responsibility of clinical laboratories and diagnostic test manufacturers and is termed "reference range" or "reference interval."

Reference intervals are generally defined as the range of values that lie between an established upper and lower limit for the analyte of interest and include the upper and lower limits. However, depending on the type of assay, the reference interval may be a numerical range (quantitative assay), a set of numerical ranges that are assigned to a qualitative result (semi- or quasiquantitative), or simply a qualitative, binary result. In some cases, the reference interval may require only one value (any value above a certain limit is considered abnormal, or values below a certain level are determined to be low). Reference intervals are expected to be characteristic of 95% of healthy subjects (preferably comprising 50% male and 50% female subjects) tested for the particular analyte and should be developed using a clinically relevant population.

CLSI C28-A3c provides detailed guidance on the establishment of reference intervals. Reference intervals do not necessarily have to be established for all analytes. In some cases, national or international consensus determines decision limits (e.g., the reference range for glycated hemoglobin, HbA1c, has been standardized (42) and is accepted and utilized universally). In these cases, the laboratory does not have to establish or even verify the reference interval. Instead, the onus for ensuring accuracy of the reference interval falls to manufacturers of diagnostic kits or instrumentation used to measure the analyte, and the clinical laboratory must ensure the accuracy and precision of the method and implement quality measures to ensure optimal performance of the test. For assays that have an established reference interval, the laboratory *verifies* the interval using at least 20 clinically representative or previously analyzed samples.

Analytes reported as or based on numerical values that do not have established decision limits require the establishment of a reference interval. The recommended method to establish a reference interval is to collect data from 120 samples (from 60 male and 60 female subjects) that are representative of the population normally encountered by the clinical laboratory. In practice, however, it is often not possible for individual clinical laboratories to collect 120 samples. CLSI-C28-A2c recommends, instead, that the laboratory can *verify* the reference interval established elsewhere, for example, in a published study with adequate numbers of subjects. When reference intervals are adopted from published studies, the relevant study or studies must be cited on the laboratory report. Sources for reference interval determination include samples from normal, healthy volunteers. However, patient samples may be used as well, particularly when a reference interval is under verification and not establishment. In some cases, patient samples may be included in the development of a reference interval when they are deemed to be "relatively healthy" as in patients who are undergoing elective surgery or routine health screening or are blood donors.

The accuracy of a reference interval is dependent on the robustness of the method, since analytical variability such as intra-assay and interassay precision, linearity, and sensitivity of performance as well as controls, calibrators, and equipment can all affect the test result and thereby the reference interval. Therefore, for LDTs, parameters such as accuracy, precision, linearity, and limit of detection must be established prior to proceeding to normal range studies. Furthermore, when verifying a reference interval from previously published data, it is critical to ensure that methods and reagents (e.g., antibody clone or fluorophores, antibody concentrations, or buffer systems) are comparable since changes in reagents and methodology can affect test values and therefore the reference interval.

Pediatric reference intervals also pose challenges for the laboratory, since unlike adult samples pediatric samples are not easily available. When possible, efforts should be made to determine the comparability of adult values to pediatric values in a smaller subset of pediatric samples. These data may be acquired from pediatric samples that have undergone routine clinical testing but have values that are considered normal. Reference intervals may also be adapted from published studies and cited on the laboratory report. An alternate is to consider reporting pediatric test results qualitatively, rather than quantitatively, when developing a reference interval is not feasible.

Analytical Sensitivity and Specificity

Analytical sensitivity refers to the ability of a test to detect the smallest concentration of the analyte that can be reliably measured by the assay. Analytical specificity refers to the ability of the assay to accurately measure the particular analyte under consideration, to the exclusion of other analytes. Both these terms relate to the technical aspect of the assay and are not necessarily related to clinical sensitivity and specificity (defined below). It is important to make this distinction because clinical laboratory validation most often refers to sensitivity and specificity relating to the technical performance of the assay.

Clinical (Diagnostic) Sensitivity

Clinical sensitivity is defined as the percentage of subjects with the clinical status as determined by the diagnostic accuracy of the test (in other words, the percentage of subjects with disease who test positive). Sensitivity is calculated as $100 \times$ true positives/(true positives + false negatives) (43). True clinical sensitivity can be calculated only when a study is performed on a relevant clinical population and is often beyond the scope of a clinical laboratory.

Laboratories assess analytical sensitivity instead, which is the ability of the assay to detect low quantities of the analyte and is similar to determining the LoD and LoQ (35). Sensitivity for cell-based assays such as flow cytometry or ELISpot assays is especially challenging to determine and relates to the ability of the assay to identify rare or dimly fluorescent populations. As previously described, sensitivity is assessed by determining the LoD and LoQ of the assay using the FMO approach. In addition, unlabeled samples (whole blood or peripheral blood mononuclear cells) may be spiked with serial dilutions of labeled, fixed cells, and the

lower limit of quantitation can be determined (7). Assay sensitivity for low-frequency populations, such as tetramer-positive cells, can be improved by collecting larger numbers of events on the cytometer. However, this has to be balanced with a practical workflow and the volume of sample available for analysis.

Analytical sensitivity for the ELISpot assay is dependent on the numbers of cells included in the assay. Unlike flow cytometry, increasing the number of cells in the ELISpot assay can lead to lower resolution of individual cytokine-producing spots, making it difficult to obtain an accurate count of antigen-specific cytokine-producing cells. Additionally, since the analytical sensitivity of an ELISpot assay is defined by the denominator or total number of cells per well, a lower number of cells may produce a number of spots similar to that obtained with a higher number of cells but can cause the assay to appear to be less sensitive (18). As with flow cytometry, defining sensitivity of the ELISpot assay must be balanced with optimal numbers of cells for optimal production and resolution of cytokine-producing spots.

Clinical (Diagnostic) Specificity

Clinical specificity of a diagnostic test is the ability to detect true negatives or the number of subjects without disease whose test values are negative. Specificity is calculated as 100 × true negatives/(false positives + true negatives) (43). As with sensitivity, defining clinical or diagnostic specificity of a laboratory test requires a study of the relevant clinical population and is generally not within the scope of most clinical laboratories.

Laboratories instead determine analytical specificity, which is the ability of the assay to detect the analyte to the exclusion of all other analytes or potentially interfering substances. Specificity is often determined by conducting studies to examine the potential for interfering substances to hinder the detection of the analyte. Specificity for serum-based analytes may be determined by spiking hemolyzed, icteric, or lipemic samples with known positive samples or controls. In flow cytometry-based assays, analytical specificity is defined as the ability of the assay to distinguish the cell population or the antigen from all other populations. Strategies that may be employed to demonstrate analytical specificity include (i) use of the FMO approach, (ii) depletion of the cell population of interest with magnetic beads and demonstration of a loss of staining, (iii) use of isotype controls and demonstration of a specific shift over the background fluorescence of the isotype control, or (iv) gating on a population that does not express the molecule of interest as an internal control for specificity (e.g., CD19, a B lymphocyte lineage-specific phosphoglycoprotein, is expressed exclusively on B lymphocytes; therefore, gating on T lymphocytes to demonstrate lack of expression defines specificity of CD19 expression on B lymphocytes). Assay specificity for low-frequency tetramer-positive populations may be determined by using an irrelevant tetramer. Similarly, ELISpot assay specificity for antigen-specific T cell populations may be established by lack of a response to irrelevant peptides along with a positive response to the specific peptide(s) under consideration (18).

QUALITY CONTROL

Once an assay is either verified or validated, it is ready to be put into clinical use. However, prior to including the assay in routine clinical testing, it is necessary to implement quality control procedures. Why control the quality of the assay? Quality control is not merely required to satisfy regulatory requirements but is the means to ensure consistent performance of the assay and detect errors as early as possible, preferably prior to any impact on patient results. As with validation, quality control in the immunology laboratory can be quite challenging due to lack of standardization of control material, quality control guidelines, defined expected values, and the plethora of LDTs that are often exclusively performed in a single laboratory (44). The burden of establishing robust quality control therefore rests with the individual laboratory and requires robust IQC and EQA.

In order to control the quality of an assay, its performance characteristics must be established. This is done at the validation stage, where the accuracy and precision of the assay are established, the LoD is determined, and if a standard curve is used, its performance is documented. Day-to-day quality of the assay can then be assessed by including control material in the assay and monitoring and benchmarking the control values according to the performance characteristics of the assay.

Quality Control Material

Characterized control materials are used to monitor the performance of assays (see www.westgard.com). It is important for control material to be as similar as possible to the clinical samples being tested since differences in sample and control matrices may affect results. Although manufacturers provide control material included in assay kits, this material is often identical to the standards provided for calibration. Any effect on the stability of the standard material may also be observed in the controls, and any changes in the calibration curve may not be detected for a considerable length of time, leading to erroneous results. Controls purchased from another manufacturer or prepared by the laboratory by pooling known positive and negative samples are acceptable alternatives. When pooling known positive or negative samples, it is important to maintain documentation of the samples and original results in order to provide traceability to the origin of the control pool and as a resource to troubleshoot technical issues.

Controls, whether purchased or prepared in the laboratory, must undergo a qualification process prior to being placed in use. Such processes are necessary to document the expected performance of control material such that any changes, e.g., shift or drift trends in values, are detected early and prior to release of patient results. In order to qualify control material, the numeric values of the test material as well as the tolerance limits must be known. The tolerance limits for the control material cannot exceed those established for the assay from precision studies during the validation phase. For example, if the total precision of an assay is ±5%, a control that falls outside these limits is by definition always out of control and therefore invalidates all results. To qualify a control, a minimum of 20 values must be obtained on several independent runs. The recommendation is that 20 values be collected over 2 weeks or 10 working days, and preferably over at least 4 weeks or 20 working days (46). The mean and SD of these values are then utilized to generate a Levey-Jennings (L-J) chart to monitor the assay's performance (see www.westgard.com).

While it is possible to establish controls for stable sample types such as serum, controlling cell-based assays in a similar manner is much more problematic. Functional cellular assays such as lymphocyte proliferation assays for immune competence, neutrophil oxidative burst, or cytokine release assays utilize date-matched samples from healthy volunteers, and the performance of these cells is compared with the test subject's response. For these assays, it is also important to

note that the date-matched control is utilized to control the technical aspects of assay performance, e.g., appropriate distribution of immune cell subsets or a proliferative response to mitogenic or antigenic stimulation, and is therefore only a methodological control. A date-matched control sample's test results may occasionally fall outside the established reference range for the assay. This does not necessarily invalidate the technical performance of the assay since these results may be characteristic of the date-matched control sample and not a reflection of a technical problem with the assay. Maintaining documentation of expected assay results for a pool of donors utilized as date-matched controls can address these situations.

Quality control material for flow cytometry assays is also challenging due to the lack of long-term stability of samples. Stabilized control cells are commercially available for commonly used lymphocyte markers and can be used to monitor instrument and assay performance. However, for the majority of flow cytometry-based LDTs, commercial controls are not available and date-matched normal control samples are generally used to monitor assay performance. An alternative is to use commercially available anti-immunoglobulin-coated beads that have the capacity to bind mouse anti-human labeled antibodies, which can be stained with assay-specific antibody combinations to monitor assay-specific instrument settings and assay performance. However, since beads do not possess the characteristics of live cells and do not react to changes in pH or other reagent parameters as cells would, they are not ideal controls for light scatter settings, nor do they address interference from autofluorescence inherent to certain cell populations.

Tools To Monitor Quality

Levey-Jennings Charts

In the clinical laboratory, the daily documentation and evaluation of quality control is critical for timely detection of errors. The most commonly used method to evaluate quality control is the Levey-Jennings (L-J) control chart. The L-J chart is based on the Shewart control chart, proposed in 1931 by Walter Shewart at the Bell Telephone Laboratories, as a statistics-based graphical representation to monitor industrial manufacturing processes. In 1950, S. Levey and E. R. Jennings adapted this method for the clinical laboratory (48).

The L-J chart provides visual indication of the performance of a laboratory test. The general principle of the L-J chart is that the distance of the observed value from the expected mean value of the control material provides an indication of any perturbation to the test system (48). In practice, control material for which the mean and SD are established is analyzed at an established time during an analytical run (at the beginning, in the middle, and at the end), and the values obtained are plotted on a chart as shown in Fig. 2. The value of the control material for a particular assay run is noted in relation to the mean. The standard L-J chart includes limits at the 1 SD, 2 SD, and 3 SD levels. If the control material shows a Gaussian distribution, 68.2% of the values will be within ±1 SD of the mean, 95.5% of the results will be within ±2 SD of the mean, and 99.7% will be within ±3 SD. Thus, if a control value varies within 1 SD, it is likely due to random chance, and while the laboratory must be aware of a minor shift, it is generally not actionable. However, if a control value falls outside 2 or 3 SD, it is statistically unlikely to be due to random chance and must be investigated. James O. Westgard defined a set of rules, "Westgard rules," to determine whether an analytical run is in control or out of control (49). Figure 2 illustrates the utility of L-J charts to monitor control values and the implementation of Westgard rules to determine whether the analytical run is in or out of control. Several instances of out-of-control runs are indicated. Point A indicates a control value greater than 3 SD from the mean, which must be investigated, and the analytical run must be rejected until troubleshooting has been performed. Points B and C are

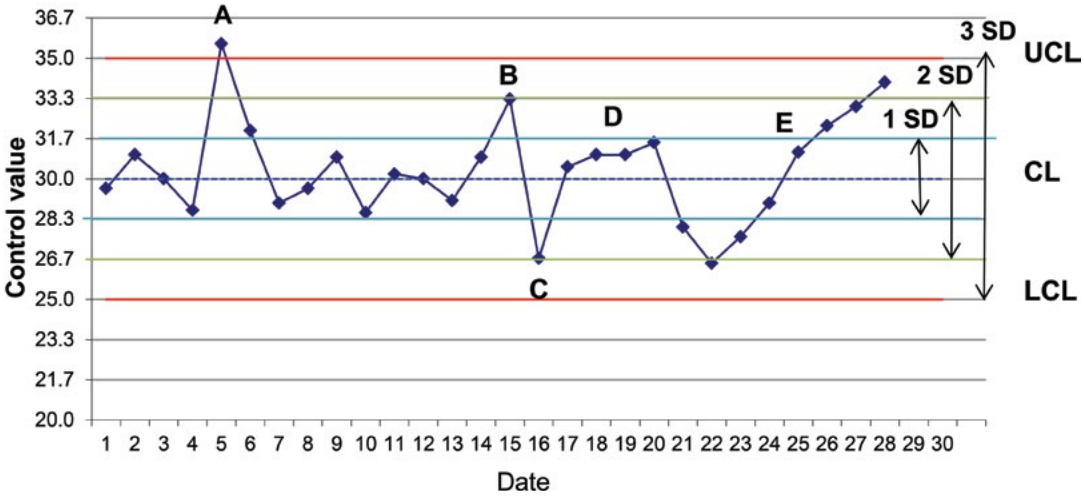

FIGURE 2 Tracking control performance using a Levey-Jennings chart. The chart shows daily values of a hypothetical control with a mean value of 30.0. The upper limit and lower limit of the control are set at +3 SD and −3 SD from the mean value, respectively. The positions of 1 and 2 SD from the mean are indicated. The chart illustrates several instances of out-of-control analytical runs as described by the Westgard rules, indicated by letters A through E: A, violation of 1_{2S} rule (control value exceeds mean + 2 SD); B and C, violation of 2_{2S} rule (two consecutive control values are either plus or minus 2 SD from the mean); D, violation of 4_{1S} rule (four consecutive measurements exceed the mean by 1 SD); E, violation of 7_{T} rule (seven consecutive measurements trend upwards). CL, control limit; UCL, upper control limit; LCL, lower control limit.

consecutive runs where the control value is either +2 SD or −2 SD from the mean and must be investigated. Although the four data points indicated in D are within 1 SD, they all fall on one side of the mean, resulting in a trend requiring investigation. When controls show either a negative or positive trend compared with the mean, assay performance is biased and can potentially affect patient results similarly. Similarly, when the control value consistently trends either upwards (Fig. 2E) or downwards over seven or more consecutive runs, the analytical run must be rejected and troubleshooting of the assay commenced. Detailed use and interpretation of L-J charts and the use of Westgard rules to evaluate an analytical run are available through the Westgard basic QC course (46).

While L-J charts are useful for monitoring quantitative or semiquantitative assays (such as immunoassays for detection of antibodies) when numerical values are known, they are not useful for qualitative and quasiquantitative assays. In these assays, a qualitative positive/negative or known reactive/nonreactive control is analyzed along with test samples to ensure that the assay is performing accurately.

Control material for cell-based assays is particularly challenging due to the limited stability of samples. Flow cytometry assays can be controlled with commercially available stabilized cells. However, only a limited set of surface markers are currently commercially available. In most other assays, a normal control sample is utilized or, in the case of leukemia and lymphoma panels, internal control populations may be employed.

Internal Controls

For some assays, internal controls may be used to verify results and assay performance. For example, when analyzing serum immunoglobulin G (IgG) subclasses, the sum of the concentrations of the four subclasses (IgG_1, IgG_2, IgG_3, and IgG_4) must be equal to total IgG concentration, or when analyzing lymphocyte subsets by flow cytometry, the sum of T, B, and NK (natural killer) cells must be within 5% of the $CD45^+$ lymphocyte population. These internal controls are a good indicator for assay performance and accuracy of test results.

Delta Checks

Delta checks are built into laboratory quality systems to identify discrepant patient results during sequential testing. Delta checks compare current laboratory results to previous results. If the two values differ by predetermined criteria and within a specific time interval, they must be investigated further. Discrepant results may be caused by sample integrity, stability issues, or mislabeling, all of which cannot be detected by QC methods that evaluate assay performance. Discrepant results may also occur due to therapeutic intervention or a genuine change in the patient's clinical status.

Result Trending

For any clinical laboratory, it is necessary to understand the general trend of results for a particular test. Trending patient results can be very informative in detecting potential analytical errors or changes in the patient population. A hypothetical trending chart over the course of 12 months is shown in Fig. 3. The general trend in the laboratory is for negative samples to be at about 90%. During the summer months, a spike in positive samples was observed. Such trends must be investigated to determine if the change was due to an assay error, a change in reagent, shipping conditions during extreme summer temperatures, or a genuine change in patient demographics and epidemiology.

Laboratory result trends also provide valuable information for surveillance programs for communicable diseases. For instance, essential components of HIV surveillance programs include CD4 counts and viral load test results, both of which are used not only to identify cases of HIV, classify disease stage at the time of diagnosis, and monitor disease progression but also to evaluate HIV prevention efforts (3, 50, 13).

AUTOMATED LIQUID-HANDLING SYSTEMS

A number of immunological techniques (ELISA, ELISpot assay, flow cytometry, and cell-based assays such as lymphocyte proliferation assays) have been moved to automated platforms, or liquid-handling robotic systems have been integrated into some of the steps of the assays. Automated liquid-handling systems improve throughput and pipetting accuracy,

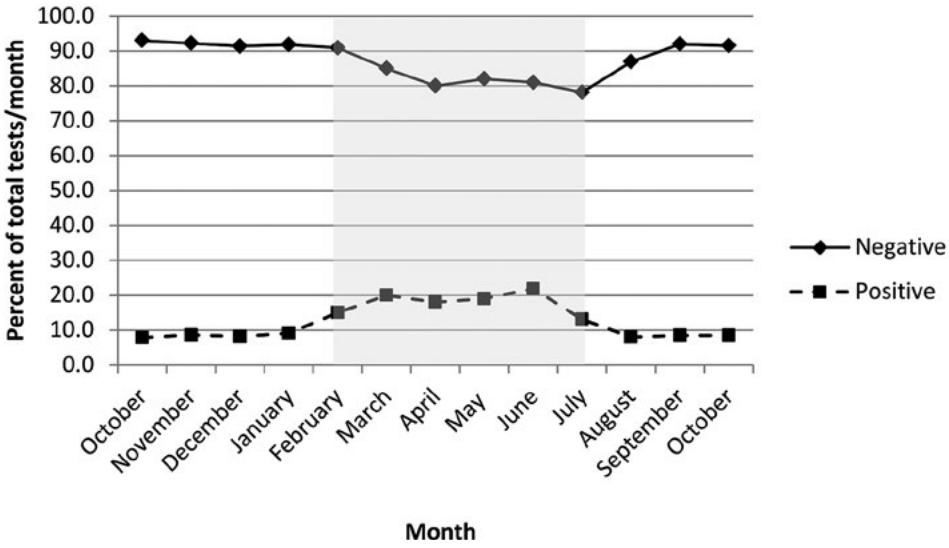

FIGURE 3 Monthly trending of assay results. Assay results were trended over the course of 12 months. The shaded region spanning months March through June shows an abnormally elevated percentage of positive results, which require further investigation.

prevent injuries due to repetitive manual pipetting, and are therefore a significant technical component for the clinical immunology laboratory. Automated systems for serum-based assays such as immunofluorescence assays or ELISA for autoantibodies have been available for a number of years, similar to the automated robotic systems employed in chemistry or molecular laboratories. More recently, liquid-handling systems are being adapted to handle the more complex cell-based assays such ELISpot, lymphocyte proliferation, and flow cytometry assays and are becoming increasingly common in immunological laboratories. It is therefore necessary to implement procedures to initially verify the performance of the instrument relative to its application, as well as establish a quality control program that ensures periodic evaluation of the pipetting accuracy and performance of the instrument.

Validation of an automated liquid-handling system requires evaluation of both the accuracy of the amount of fluid dispensed and the precision or reproducibility of the instrument's performance and, per ISO 17035 guidelines, requires that actual volumes transferred by the automated system be verified and optimized if necessary. The performance of automated liquid-handling systems can be validated and optimized using a number of methods including gravimetric, colorimetric, or fluorometric methods or combinations of these methods for volumes as low as 1 μl. Gravimetric methods, described in ISO 8655-6 (24), utilize weight to confirm the accuracy of dispensed volumes. The uncertainty of gravimetrically verified volumes increases in regions of low humidity and for small volumes (1 μl or lower). In such cases, photometric or fluorimetric methods may be employed (45). Both of these methods employ a linear regression curve generated using a calibrated, verified pipette and compare the instruments' actual to the expected performance (47). The performance of automated liquid handling systems, as with manual pipettes, must be verified periodically. Verification of automated liquid handling systems' performance every 6 months is the generally accepted practice. However, the frequency of a performance check also depends on the frequency of usage, the volume and type of samples handled by the instrument, and the frequency of maintenance or technical troubleshooting procedures.

CONCLUDING REMARKS

Assay validation and quality control, particularly in the area of LDTs, is an evolving process. As an understanding of the differences between chemistry-based and immunological assays continues to develop, guidelines and procedures will continue to be established for esoteric immunological assays to enable laboratories to continue to expand the field of specialized immunological assays that inherently depart from the rigorous, well-established world of chemistry-based testing but are nevertheless key components that aid the diagnosis of immunological disorders. Evolution of immunological testing is and will continue to be a collaborative effort among diagnostics manufacturers, physicians, and directors of clinical immunological laboratories.

REFERENCES

1. **Daley AT, Allen M, Carlson JM, Flaherty C, Gillard L, Granade SE, Grindle KA, Kuehl D, Padley LM, Walker K.** *CLSI GP22-A3. Quality Management System: Continual Improvement; Approved Guideline*, 3rd ed. Clinical and Laboratory Standards Institute, Wayne, PA.
2. **Berte LM.** 2007. Laboratory quality management: a roadmap. *Clin Lab Med* **27:**771–790, vi. PubMed
3. **Centers for Disease Control and Prevention.** 1997. 1997 revised guidelines for performing CD4+ T-cell determinations in persons infected with human immunodeficiency virus (HIV). *MMWR Recommend Rep* **46**(RR-2)**:**1–29. PubMed
4. **Borowitz MJ, Craig FE, Digiuseppe JA, Illingworth AJ, Rosse W, Sutherland DR, Wittwer CT, Richards SJ, Clinical Cytometry Society.** 2010. Guidelines for the diagnosis and monitoring of paroxysmal nocturnal hemoglobinuria and related disorders by flow cytometry. *Cytometry B Clin Cytom* **78:**211–230. PubMed
5. **Wood BL, Arroz M, Barnett D, DiGiuseppe J, Greig B, Kussick SJ, Oldaker T, Shenkin M, Stone E, Wallace P.** 2007. 2006 Bethesda International Consensus recommendations on the immunophenotypic analysis of hematolymphoid neoplasia by flow cytometry: optimal reagents and reporting for the flow cytometric diagnosis of hematopoietic neoplasia. *Cytometry B Clin Cytom* **72**(Suppl 1)**:**S14–S22. PubMed
6. **Davis BH, Foucar K, Szczarkowski W, Ball E, Witzig T, Foon KA, Wells D, Kotylo P, Johnson R, Hanson C, Bessman D.** 1997. U.S.-Canadian Consensus recommendations on the immunophenotypic analysis of hematologic neoplasia by flow cytometry: medical indications. *Cytometry* **30:**249–263. PubMed
7. **Wood B, Jevremovic D, Béné MC, Yan M, Jacobs P, Litwin V, ICSH/ICCS Working Group.** 2013. Validation of cell-based fluorescence assays: practice guidelines from the ICSH and ICCS—part V—assay performance criteria. *Cytometry B Clin Cytom* **84:**315–323. PubMed
8. **Cai XY, Thomas J, Cullen C, Gouty D.** 2012. Challenges of developing and validating immunogenicity assays to support comparability studies for biosimilar drug development. *Bioanalysis* **4:**2169–2177. PubMed
9. **O'Hara DM, Xu Y, Liang Z, Reddy MP, Wu DY, Litwin V.** 2011. Recommendations for the validation of flow cytometric testing during drug development: II assays. *J Immunol Methods* **363:**120–134. PubMed
10. **U.S. Department of Health and Human Services, Food and Drug Administration Center for Drug Evaluation and Research (CDER), Center for Biologics Evaluation and Research (CBER).** 2009. *Guidance for Industry—Assay Development for Immunogenicity Testing for Therapeutic Proteins*. U.S. Department of Health and Human Services, Washington, DC.
11. **Lee JW, Devanarayan V, Barrett YC, Weiner R, Allinson J, Fountain S, Keller S, Weinryb I, Green M, Duan L, Rogers JA, Millham R, O'Brien PJ, Sailstad J, Khan M, Ray C, Wagner JA.** 2006. Fit-for-purpose method development and validation for successful biomarker measurement. *Pharm Res* **23:**312–328. PubMed
12. **Landay AL, Fleischer TA, Kuus-Reichel K, Maino VC, Reinsmoen NL, Weinhold KJ, Whiteside TL, Altman JD.** 2012. *Performance of Single Cell Immune Response Assays—Approved Guideline. Clinical and Laboratory Standards Institute I/LA26-A*. CLSI, Wayne, PA.
13. **Schneider E, Whitmore S, Glynn KM, Dominguez K, Mitsch A, McKenna MT, Centers for Disease Control and Prevention.** 2008. Revised surveillance case definitions for HIV infection among adults, adolescents, and children aged <18 months and for HIV infection and AIDS among children aged 18 months to <13 years—United States, 2008. *MMWR Recommend Rep* **57:**1–12.
14. **McPherson RA, Bidkorpeh EK, Castellani WJ, Glasser L, Griesmacher A, Hartmann AE, Ingram K, Knight JA, Rosen MA, Sadek W, Slickers KA.** 2007. *Analysis of Body Fluids in Clinical Chemistry: Approved Guideline*. CLSI Document C49-A. Clinical and Laboratory Standards Institute, Wayne, PA.
15. **Cummings J, Ward TH, Dive C.** 2010. Fit-for-purpose biomarker method validation in anticancer drug development. *Drug Discov Today* **15:**816–825. PubMed
16. **O'Gorman MR, Corrochano V.** 1995. Rapid whole-blood flow cytometry assay for diagnosis of chronic granulomatous disease. *Clin Diagn Lab Immunol* **2:**227–232. PubMed

17. **Viswanathan CT, Bansal S, Booth B, DeStefano AJ, Rose MJ, Sailstad J, Shah VP, Skelly JP, Swann PG, Weiner R.** 2007. Quantitative bioanalytical methods validation and implementation: best practices for chromatographic and ligand binding assays. *Pharm Res* **24:**1962–1973. PubMed
18. **Xu Y, Theobald V, Sung C, DePalma K, Atwater L, Seiger K, Perricone MA, Richards SM.** 2008. Validation of a HLA-A2 tetramer flow cytometric method, IFNgamma real time RT-PCR, and IFNgamma ELISPOT for detection of immunologic response to gp100 and MelanA/MART-1 in melanoma patients. *J Transl Med* **6:**61. PubMed
19. **International Organization for Standardization.** 2005. *General Requirements for the Competence of Testing and Calibration Laboratories. 17025 1.1.* ISO, Geneva, Switzerland. http://www.iso.org/iso/catalogue_detail.htm?csnumber=39883.
20. **International Organization for Standardization.** 2005. *Quality Management Systems—Fundamentals and Vocabulary. ISO 9000:2005.* ISO, Geneva, Switzerland.
21. **U.S. Food and Drug Administration.** 2011. *Draft Guidance for Industry and Food and Drug Administration Staff—The 510(k) Program: Evaluating Substantial Equivalence in Premarket Notifications [510(k)].* U.S. Food and Drug Administration, Rockville, MD.
22. **Garrett PE, Laskey FD, Meier KL.** 2008. *User Protocol for Evaluation of Qualitative Test Performance; Approved Guideline—2nd ed. CLSI EP12-A2.* CLSI, Wayne, PA.
23. **Dewitte K, Fierens C, Stockl D, Thienpont LM.** 2002. Application of the Bland-Altman plot for interpretation of method-comparison studies: a critical investigation of its practice. *Clin Chem* **48:**799–801; author reply, 801–792.
24. **International Organization for Standardization.** 2002. *Piston-Operated Volumetric Apparatus. Gravimetric Methods for the Determination of Measurement Error. BS EN ISO 8655-6:2002.* ISO, Geneva, Switzerland.
25. **Daniel W, Tholen AK, Kennedy JW, Krouwer JS, Meier K.** 2012. *Evaluation of Precision Performance of Quantitative Measurement Methods; Approved Guideline, 2nd ed. CLSI EP5-A2.* CLSI, Wayne, PA
26. **Froebel KS, Pakker NG, Aiuti F, Bofill M, Choremi-Papadopoulou H, Economidou J, Rabian C, Roos MT, Ryder LP, Miedema F, Raab GM.** 1999. Standardisation and quality assurance of lymphocyte proliferation assays for use in the assessment of immune function. European Concerted Action on Immunological and Virological Markers of HIV Disease Progression. *J Immunol Methods* **227:**85–97. PubMed
27. **Weinberg A, Betensky RA, Zhang L, Ray G.** 1998. Effect of shipment, storage, anticoagulant, and cell separation on lymphocyte proliferation assays for human immunodeficiency virus-infected patients. *Clin Diagn Lab Immunol* **5:**804–807. PubMed
28. **Davis BH, McLaren CE, Carcio AJ, Wong L, Hedley BD, Keeney M, Curtis A, Culp NB.** 2013. Determination of optimal replicate number for validation of imprecision using fluorescence cell-based assays: proposed practical method. *Cytometry B Clin Cytom* **84:**329–337. PubMed
29. **Roos MT, Miedema F, Koot M, Tersmette M, Schaasberg WP, Coutinho RA, Schellekens PT.** 1995. T cell function in vitro is an independent progression marker for AIDS in human immunodeficiency virus-infected asymptomatic subjects. *J Infect Dis* **171:**531–536. PubMed
30. **Schellekens PT, Roos MT, De Wolf F, Lange JM, Miedema F.** 1990. Low T-cell responsiveness to activation via CD3/TCR is a prognostic marker for acquired immunodeficiency syndrome (AIDS) in human immunodeficiency virus-1 (HIV-1)-infected men. *J Clin Immunol* **10:**121–127. PubMed
31. **ACTG Laboratory Technologist Committee.** 2000. Lymphocyte Proliferation Assay (LPA), Version 1.0. Duke Human Vaccine Institute, Durham, NC. http://iqa.center.duke.edu/files/documents/29-ALM-Lymphocyte-Proliferation-Assay.pdf.
32. **Clinical and Laboratory Standards Institute.** 2008. *Quality Assurance of Laboratory Tests for Autoantibodies to Nuclear Antigens: (1) Indirect Fluorescence Assay for Microscopy and (2) Microtiter Enzyme Immunoassay Methods—Approved Guideline*, 2nd ed. CLSI ILA-A2. CLSI, Wayne, PA.
33. **Tuuminen T, Tavast E, Väisänen R, Himberg JJ, Seppälä I.** 2010. Assessment of imprecision in gamma interferon release assays for the detection of exposure to Mycobacterium tuberculosis. *Clin Vaccine Immunol* **17:**596–601. PubMed
34. **Tuuminen T.** 2013. It is high time to reevaluate QuantiFERON-TB gold for clinical practice. *Clin Vaccine Immunol* **20:**1778. PubMed
35. **Armbruster DA, Pry T.** 2008. Limit of blank, limit of detection and limit of quantitation. *Clin Biochem Rev* **29**(Suppl 1)**:**S49–S52. PubMed
36. **Tholen DW, Linnet K, Kondratovich M, Armbruster DA, Garrett PE, Jones RL, Kroll MH, lequin RM, Pakratz TJ, Scassellati GA, Schimmel H, Tsai J.** 2012. *Protocols for Determination of Limits of Detection and Limits of Quantitation; Approved Guideline. CLSI EP17-A.* CLSI, Wayne, PA.
37. **Tholen DW, Kroll M, Astles JR, Caffo AL, Happe TM, Krouwer J, Laskey F.** 2012. *Evaluation of Linearity of Quantitative Measurement Procedures: A Statistical Approach; Approved Guideline CLSI EP6-A.* Clinical and Laboratory Standards Institute, Wayne, PA.
38. **Jhang JS, Chang CC, Fink DJ, Kroll MH.** 2004. Evaluation of linearity in the clinical laboratory. *Arch Pathol Lab Med* **128:**44–48. PubMed
39. **Donnenberg A, Donnenberg VS.** 2008. Understanding clinical flow cytometry, p 181. *In* O'Gorman MRG, Donnenberg AD (ed), *Handbook of Human Immunology.* CRC Press, Boca Raton, FL.
40. **Qureshi SS, Lewis SM, Gant VA, Treacher D, Davis BH, Brown KA.** 2001. Increased distribution and expression of CD64 on blood polymorphonuclear cells from patients with the systemic inflammatory response syndrome (SIRS). *Clin Exp Immunol* **125:**258–265. PubMed
41. **Davis BH, Olsen SH, Ahmad E, Bigelow NC.** 2006. Neutrophil CD64 is an improved indicator of infection or sepsis in emergency department patients. *Arch Pathol Lab Med* **130:**654–661. PubMed
42. **Miedema K.** 2005. Standardization of HbA1c and optimal range of monitoring. *Scand J Clin Lab Invest Suppl* **240:**61–72. PubMed
43. **Florkowski CM.** 2008. Sensitivity, specificity, receiver-operating characteristic (ROC) curves and likelihood ratios: communicating the performance of diagnostic tests. *Clin Biochem Rev* **29**(Suppl 1)**:**S83–S87. PubMed
44. **Lock RJ.** 2006. My approach to internal quality control in a clinical immunology laboratory. *J Clin Pathol* **59:**681–684. PubMed
45. **International Organization for Standardization.** 2005. *Piston-Operated Volumetric Apparatus—Part 7: Non-Gravimetric Methods for the Assessment of Equipment Performance. ISO 8655-7:2005.* ISO, Geneva, Switzerland.
46. **Westgard JO.** 2010. *Basic QC Practices*, 3rd ed. Westgard QC, Madison, WI.
47. **Stangegaard M, Hansen AJ, Frøslev TG, Morling N.** 2011. A simple method for validation and verification of pipettes mounted on automated liquid handlers. *J Lab Autom* **16:**381–386. PubMed
48. **Levey S, Jennings ER.** 1950. The use of control charts in the clinical laboratory. *Am J Clin Pathol* **20:**1059–1066. PubMed
49. **Westgard JO.** 1994. Selecting appropriate quality-control rules. *Clin Chem* **40:**499–501. PubMed
50. **Konrad S, Skinner S, Kazadi GB, Gartner K, Lim HJ.** 2013. HIV disease progression to CD4 count <200 cells/μL and death in Saskatoon, Saskatchewan. *Can J Infect Dis Med Microbiol* **24:**97–101. PubMed

Author Index

Subject Index